

ANALYTICAL CHEMISTRY IN THE SOVIET UNION

YU. A. ZOLOTOV

V. I. Vernadsky Institute of Geochemistry and Analytical Chemistry of the USSR Academy of Sciences,
Moscow, 117975, USSR

(Received 15 October 1985. Accepted 8 August 1986)

Summary—The history of the development of analytical chemistry in the Soviet Union is briefly outlined. Organizations co-ordinating research in this field, and the leading scientific centres, are indicated. Achievements in various analytical techniques are reviewed. Analytical services in some branches of the economy, and the analysis of most important materials are considered. Major publications are pointed out and international contacts of Soviet experts are discussed.

The assay of ores and noble metals has been practised in Russia for many centuries. In all probability, the first assay laboratories appeared there in the 16th century and the analysts made use of an assay balance. The description of the assaying procedures may be found in a number of manuals dating back to the 18th century, *e.g.*, in G. V. de Guennin's "Description of Works in the Ural and Siberia".

The first treatises on analytical chemistry also appeared in the 18th century. The famous Russian scientist M. V. Lomonosov (1711–1765) used weighing of initial and final reaction products systematically; he experimentally confirmed the law of conservation of matter (1756), which had been stated in general form by philosophers in antiquity. Lomonosov established the first chemical laboratory in Russia (1748) and used a microscope for chemical studies two years before Markgräff. Unfortunately, not all of his remarkable achievements were known outside the country. V. I. Klementyev, Lomonosov's student, wrote a thesis "On Increase in Weight of Some Metals on Precipitation" in 1754. He dissolved a certain amount of iron or copper in a certain amount of nitric acid, precipitated the metal with an alkali and separated the precipitate, which he dried and weighed. This method was thus completely based on weighing before and after the reaction.

T. E. Lovitz (1757–1804), a naturalized German who had lived in St. Petersburg since childhood, initiated the microcrystalloscopic method. He undertook a microscopic study of crystals of many salts and proposed using the shape of crystals for salt identification. Lovitz reported this work in the St. Petersburg Academy of Sciences in 1798; the paper was published in 1804 and was entitled "Demonstration of a New Way to Test Salts". The studies on the form of crystals for analytical purposes were furthered by the prominent crystallographer E. S. Fedorov (1853–1919).

V. M. Severgin (1765–1826), a chemist and mineralogist, determined concentrations of solutions by comparing the intensity of their colour with that of solutions containing definite amounts of the analyte.

This was essentially the colorimetric technique. He also wrote several manuals on assaying and testing of mineral waters and drugs. In the 19th century Academician G. I. Hess (1802–1880), known as one of the founders of thermochemistry, Professor K. K. Klaus (1756–1864) from Kazan', who discovered ruthenium in 1844, and A. A. Voskresensky (1809–1880), who determined the composition of quinone and undertook the analysis of the coals of the Donetsk basin, were the leading analytical chemists of the day. Discovery of the Periodic Law by D. I. Mendeleev (1834–1907) and the theory of the structure of organic compounds developed by A. M. Butlerov (1828–1886) were major advances in the development of chemistry.

In the 18th century analytical chemistry was introduced into the curriculum of St. Petersburg Mining School (later Mining Institute) founded in 1773. Students were taught fire assay and other techniques. V. M. Severgin was on the staff of this school; the department of chemistry there was set up in 1808. From 1832 to 1850 the department was chaired by G. I. Hess, who introduced qualitative and quantitative analysis into the syllabus. In 1849 Hess's student N. A. Ivanov published a textbook "Basics of Analytical Chemistry". The chair of analytical chemistry in the Mining Institute was most likely established in 1899, and was headed by the prominent chemist N. S. Kurnakov. In Moscow University, founded in 1755, analytical chemistry was taught at the Medical Faculty. The chair was held by A. A. Iovsky from 1827. His book "Chemical Equations with the Descriptions of Various Methods to Determine Chemical Substances Quantitatively" was published in the same year. At the Physico-Mathematical Faculty a course of analytical chemistry was taught from 1861. In 1867 a division of analytical and organic chemistry was created and the chair of analytical chemistry in 1929. In St. Petersburg University (founded in 1819) the course of inorganic and analytical chemistry was given by A. A. Voskresensky from 1839. Some time between 1867 and 1886 the department of technological and analytical chemistry

was formed and was headed by N. A. Menshutkin. An independent chair was created as late as in 1947.

Some of the first textbooks on analytical chemistry have already been mentioned. Of later textbooks the most popular was Menshutkin's "Analytical Chemistry", the first edition of which was printed in 1871. The book ran into 16 editions and was translated and published in Germany, the U.S.A. and Great Britain.

Among the scientific advances in this period several deserve special mention. M. I. Ilyinsky discovered the reaction of nitrosonaphthols with cobalt in the 1880s, and F. F. Beilstein used electrolysis for the separation of metals. In 1903 M. S. Tsvet suggested chromatography, a contribution which is very well known. L. A. Chugaev discovered the selective reaction of nickel with dimethylglyoxime in 1905, and later developed the theory of chelate formation; he demonstrated, in particular, that 5- and 6-member cycles are the most stable.

After the October Socialist Revolution of 1917 a great number of research and educational centres was established. Extensive research in the field of analytical chemistry was initiated in a number of new institutes, the Institute of Reagents, Radium Institute, Institute for the Study of Platinum and other Precious Metals among them. Production of analytical equipment, reagents and standard reference materials was organized, and training of analytical chemists was stepped up.

Professor N. A. Tananaev of Kiev Polytechnicum proposed a drop-test technique simultaneously with F. Feigl. Thin-layer chromatography was first described by two scientists from the town of Kharkov, N. A. Ismailov and M. S. Shreiber, in 1938. Plasma sources for atomic-emission analysis were proposed in the 1940s; the ICP method originated from an article published in the USSR in 1942. Vast experience has been accumulated in the analysis of mineral raw materials and metals (I. P. Alimarin *et al.*).

After World War II, the analysis of nuclear and electronic materials became an important objective of applied analytical chemistry. A. K. Babko and his colleagues in the Ukraine initiated the investigation and subsequent analytical application of various mixed-ligand complexes. The theory of the effects of organic analytical reagents has been consistently developed by many researchers, V. I. Kuznetsov, L. M. Kulberg and S. B. Savvin in particular. Many highly sensitive and selective reagents have been synthesized: dipicyrlamine (N. S. Poluektov, 1935), thoron (V. I. Kuznetsov, 1942), stilbazo (V. I. Kuznetsov, 1950), beryllon II (A. M. Lukin, 1950), diantipyrylmethane (S. I. Gusev, 1950), lumogallion (A. M. Lukin, 1960), arsenazo III (S. B. Savvin, 1959), sulphochlorophenol S (S. B. Savvin, 1964), picramine E. (Yu. M. Dedkov, 1970) and others. B. V. L'vov was the first to apply electrothermal atomization in atomic-absorption spectrometry. Later he was awarded the Talanta gold medal for this work.

The development of analytical chemistry has significantly promoted scientific and technological progress. It has helped solve the problems of analytical monitoring in industry and contributed to technological advance in the production of new materials and substances. Some analytical techniques such as methods of separation and preconcentration have been introduced on an industrial scale.

CO-ORDINATING ORGANIZATIONS

Analytical chemists work under the auspices of the Scientific Council for Analytical Chemistry of the USSR Academy of Sciences. The system of scientific councils was formed in the Academy in the 1960s. The councils were set up as public bodies designed to provide guidance and co-ordinate fundamental research on a national scale, regardless of departmental chains-of-command. The importance of the councils was considerably augmented by the government decision to entrust the Academy of Sciences with complete authority over the problems of control and co-ordination of fundamental research in the country. The network of scientific councils that had been established by that time proved to be the tool for implementation of these goals. Many councils functioned as interdepartmental bodies of experts and maintained close ties with related ministries and offices. They were cognizant of the situation in various branches of the economy and thus proved to be in a position to provide guidelines for co-ordinated research. The Scientific Council for Analytical Chemistry was one of these.

An analytical chemistry commission dealing mainly with the problems of platinum metals was set up in Leningrad as early as the 1920s. It was affiliated to one of the institutes of the Academy. Before World War II it was renamed the Committee of Analytical Chemistry. In 1939 this committee sponsored the 1st All-Union conference on analytical chemistry. After the war the committee worked under the auspices of the V. I. Vernadsky Institute of Geochemistry and Analytical Chemistry, organized in 1947. It was headed by Academician A. P. Vinogradov, who was later elected vice-president of the Academy. The scope of the Committee's activities had been considerably broadened by that time and it provided guidance for many branches of analytical chemistry. Such distinguished scholars as Academicians I. P. Alimarin and I. V. Tananaev, Corresponding Member D. I. Ryabchikov, Academician of the Ukrainian Academy A. K. Babko, and others were active on the Committee. The Committee issued its own publications. In the early 60s the Committee was reorganized into the Scientific Council for Analytical Chemistry of the Academy of Sciences. Since that time it has been chaired by I. P. Alimarin.

The scope and importance of the Council have grown continuously. Prominent analytical chemists of the All-Union and Republic Academies, from

research and educational establishments, sit on the Council. The members of the Council are ranking analytical chemists and physicists, scientists of different generations from various regions of the country. Within the framework of the Council there is a bureau, 30 special committees and 7 regional branches.

The Council defines the policies and strategies of analytical chemistry research and development. To this end planning forecasts are developed every 5 years to help organize 5-year co-ordination plans. While forecasts are largely developed by the higher echelons of the Council, co-ordination plans are based on suggestions of the institutions and individual experts. Co-ordinated research planning in analytical chemistry is an important tool for channelling the collective effort of scientific teams, experts and the national economy managers to achieve planning objectives. Integration of research conducted in educational establishments into the co-ordinated plan ensures local recognition and support for such endeavours. Co-ordination provides for the possibility of problem-oriented assessment of results and prospects of research carried out by scientific teams on the local and regional scale. Besides all this, the Scientific Council defines the scope and range of research and co-ordinates scientific effort through other forms of activity such as annual sessions, meetings and regular correspondence, which are probably no less important.

Much attention is given to such important means of co-ordination and data collection as conferences, seminars and workshops. Efforts towards organization of seminars in large urban centres have yielded good results. These seminars are many, and among them the seminars on analytical chemistry in Moscow, Leningrad, Kiev and Odessa and on organic analysis in Moscow deserve special mention. Annual sessions of the Council attended by various other agencies, and workshops run by leading analytical chemists, are quite popular. Various arrangements are made to promote research in various branches of analytical chemistry. The Council has repeatedly rendered assistance to educational institutions in the organization of fundamental research laboratories and secured managerial support of the appropriate bodies for promising research trends.

Another function of the Council is to provide for the logistics of research and analytical monitoring in various branches of the economy. This involves the problems of equipment, laboratory apparatus and materials, reagents, standard samples and, to a certain extent, the problem of metrological standardization. This is the province of the joint committee on analytical equipment and complexes, which is sponsored both by the Scientific Council and by the scientific and technical council of the Ministry of Instrument Engineering. The Council maintains contacts with the State Standardization Committee (Gosstandart) as regards metrology of analysis. It

also issues recommendations and guidelines for securing rational employment of trained research personnel and deals with educational programs in higher educational institutions. It also concerns itself with terminology. The Council's committee on terminology deals with dissemination of the IUPAC nomenclature rules through *Zhurnal Analiticheskoi Khimii*.

Organization of conference sessions and bureau meetings is another aspect of the many-faceted activities of the Council. In recent years, these have been organized in Leningrad, Tashkent, Nalchik and Riga. The Council carries on extensive correspondence and organizes numerous meetings, yet it basically functions through its sections, committees and departments.

The section of analytical chemistry of the All-Union Mendeleev Chemical Society is the second co-ordinating body. In addition, several ministries (non-ferrous metallurgy, geological survey, etc.) have their own councils on analytical monitoring.

SOME SCIENTIFIC CENTRES

Three groups of establishments pertaining to analytical chemistry as a science may be distinguished: (1) research institutes of the All-Union and Republic Academies, (2) universities and other educational establishments, (3) branch research institutes of industrial ministries and other state bodies, the number of establishments and the strength of research staff increasing in that order, *i.e.*, branch institutes are the most numerous. This, however, does not signify that their contribution to analytical chemistry is strictly proportional to their number. The bulk of fundamental research is done in the laboratories of the Academy and they yield the greatest results. There are however, several branch institutes where analytical research is first-rate.

The Vernadsky Institute of Geochemistry and Analytical Chemistry in Moscow is the major academic institution. Here the research involves all basic trends and techniques of analytical chemistry. Of note, is the research on determination of gases in metals by use of organic analytical reagents, preliminary concentration of traces, and the analytical chemistry of actinides and precious and rare metals. The Institute serves as a home base for both the Scientific Council for Analytical Chemistry of the USSR Academy of Sciences and the editorial board of *Zhurnal Analiticheskoi Khimii*. It organizes numerous conferences and meetings and a considerable share of international contacts is channelled through the offices of the Council and the Institute. Among other academic establishments the Dumansky Institute of Colloids and Chemistry of Water, of the Ukrainian Academy in Kiev, the Nesmeyanov Institute of Organoelement Compounds, of the USSR Academy in Moscow, the Tashkent Institute of Nuclear Physics, of the Uzbek Academy, and the Institute of Inorganic Chemistry, of the Siberian Branch

of the USSR Academy in Novosibirsk, should be mentioned. Research is also conducted in the field of photometric analysis (Kiev), analysis of organic substances (Moscow), nuclear physics analytical methods (Tashkent), and analysis of ultrapure substances (Novosibirsk).

Among universities and educational establishments the uppermost place is occupied by Moscow University. The department of analytical chemistry is engaged in photometric studies with organic reagents, laser- and atomic-emission spectroscopy, ion and extraction chromatography, solvent extraction, voltammetry, kinetic methods of analysis, *etc.* Analytical studies are also conducted by some other departments. The universities of Kiev, Kharkov and Uzhgorod are renowned for their work on photometry; research on ion-selective electrodes, fluorescence and extraction of metals is done in Leningrad University; studies on ion-selective electrodes are performed in Byelorussian University (Minsk). A great contribution to atomic-absorption spectrometry has been made in Leningrad Polytechnical Institute. Potentiometry is developed in the Moscow Mendeleev Chemico-Technological Institute. Voltammetry is widely practised in Tomsk Polytechnical Institute and the Sverdlovsk Institute of the People's Economy; chromatography receives much attention in Kuybyshev University. Kinetic methods for determination of noble and other metals are developed in the Moscow Institute of Fine Chemical Technology. Atomic-emission analysis is practised in the Urals Polytechnical Institute, Tadjik University, and many other institutions.

Among industrial scientific institutes the State Scientific Research and Project Institute of Rare Metals Industry (Moscow) should be mentioned. Vast experience has been accumulated here in the analysis of semiconductors and other ultrapure substances. This is one of the largest scientific centres in the field of analytical chemistry in the country; it is affiliated to the Ministry of Non-Ferrous Metallurgy. Several other institutes of this ministry are engaged in analytical research. The All-Union Institute of Chemical Reagents and Ultrapure Substances (Moscow), affiliated to the Ministry of Chemical Industry, deals with analysis of ultrapure substances. Geological materials are studied in the All-Union Institute of Mineral Raw Materials, of the Ministry of Geology (Moscow). The All-Union Scientific-Research Institute of Metrology in Leningrad, and the Institutes of Analytical Instrument Engineering in Leningrad, Kiev and Tbilisi should also be mentioned.

ANALYTICAL METHODS

Extensive research is conducted in the field of photometric analysis. Organic reagents proposed in the USSR and mentioned above are used for photometric elemental determinations. Their mechanism is

being elucidated by application of conformational analysis and quantum-chemical calculations on the molecules of reagents and their metal complexes. The potential of the photometric method for metal determination has grown considerably with application of surface-active substance and non-aqueous solutions. Differential (derivative) spectrophotometry has been initiated.

Another field of research is atomic-emission spectrometry. Along with the Scientific Council on Analytical Chemistry this research is co-ordinated by the Scientific Council of the Academy on Spectroscopy of Atoms and Molecules. New sources of spectrum excitation are studied, particularly inductively-coupled plasmas. The studies concern the effects of inert atmospheres, carriers and other admixtures, and their rational combination with preliminary concentration of elements under study. The so-called spill method of analysis of powder samples of geological and other materials, developed in the All-Union Institute of Mineral Raw Materials, has been introduced. A number of combined methods of analysis involving trace concentration by extraction, sorption, distillation and co-precipitation have been developed. Computer-assisted analysis is undertaken in the Central Scientific Research Institute of Non-Ferrous Metallurgy (Moscow). Atomic-emission spectrometry is an important means of mass analysis, particularly semi-quantitative analysis employed in the USSR Geological Survey, and analysis of ultrapure materials such as semiconductors (with preliminary concentration of microelements). It is also important in the analysis of natural and industrial samples of platinum, with prior concentration, by assaying or other techniques. Atomic-emission analysis with photoelectric recording and multichannel detectors is an important technique for determination of trace impurities in metals and alloys. There are many types of such instruments, largely produced in Leningrad.

Many scientific teams work in the field of atomic-absorption spectrometry. Thus, research on electrothermal AAS is conducted in Leningrad Polytechnical Institute; the platform method proposed by B. V. L'vov is used all over the world. Of note is the research on the theory of processes in electrothermal atomizers. Atomic-absorption analysis of powder samples is done in the Institute of Geochemistry and Analytical Chemistry; new atomizers have been suggested. The "cold vapour" mercury determination initially developed in the Odessa Physico-Chemical Institute is now very extensively applied. Multi-channel analysers designed in Moscow and Leningrad are used for atomic-absorption and atomic-emission analysis and can determine 24 elements simultaneously; a xenon lamp is used as light-source. Many atomic-absorption techniques for elemental analysis, combined with prior extractive concentration in particular, have been developed.

Laser spectroscopy is being developed on a large scale, including the atomic-ionization technique

based on stepwise ionization of atoms with multi-mode dye lasers; the technique is developed in two modifications for vacuum and air (Moscow University, Institute of Spectroscopy and Institute of Chemistry of the Academy of Sciences *etc.*). The thermoluminescence method and laser atomic-fluorescence technique are being developed in the Novosibirsk Institute of Inorganic Chemistry. Both methods are at the stage of laboratory research; their introduction is hindered by a number of methodological and metrological problems.

The Universities of Rostov and Irkutsk are important centres of X-ray spectrometry, as is the "Burevestnik" pilot enterprise in Leningrad, which produces the necessary equipment. The X-ray fluorometric method is used for the analysis of silicate geological materials for rock-forming elements. This method is especially widely applied in ferrous and non-ferrous metallurgy and mining. X-Ray quantumometers are used in these industries as the main components of automated analytical control systems. A new electron-probe X-ray fluorescence technique has been developed. Application of synchrotron radiation in X-ray fluorometric analysis and X-ray combination dispersion has been initiated. The latter technique helps determine low atomic-number elements up to lithium.

Electron paramagnetic resonance spectroscopy has proved to be an original and, to a certain extent, universal technique. Analytical reagents that are stable free radicals containing complexing and radical groups have been obtained. In complexes with metals the concentration of this latter may be determined through the paramagnetism of the organic part of the molecule.

Since similar complexes may be obtained for practically any element, the technique is virtually universal. Research of this kind is conducted in the Vernadsky Institute of Geochemistry and Analytical Chemistry and in the Institute of Chemistry of the Tadjik Academy.

Fundamental research in the field of solid-state mass spectroscopy, particularly in spark-source mass spectroscopy is conducted. The principal goal of the research is to increase the precision of the analysis through better understanding of the physical and chemical mechanisms in the vacuum spark discharge. The data obtained have helped in the development of a multipurpose probe technique for the analysis of both solid (including non-conducting) and liquid materials. Spark-source mass spectroscopy for micro and layer analysis of metals, alloys, semiconductors, and epitaxial films of silicon and germanium, with resolution of $0.1 \mu\text{m}$ in depth, has been developed. In ferrous metallurgy mass spectroscopy is used for quality control in the converter process. A new time-of-flight mass spectrometer has been developed in the Leningrad Physico-Technical Institute of the USSR Academy of Sciences.

Radioactivation analysis is widely used both in the

instrumental version and in isolation of radioisotopes of elements in studies on their radiochemical purification. Various activation methods are used, including activation by fast and slow neutrons, gamma-rays, photons and charged particles. The particle-activation methods are predominantly used for determination of gas-generating impurities. Neutron activation is widely used for mass determination of gold in rocks and ores.

Besides nuclear reactors, neutron generators and neutron sources of the ^{252}Cf and Sb-Be types are used for this purpose. Purely scientific research concerns the application of resonance neutrons, analysis of strong neutron absorbers, computerization of activation analysis, new methods of radiochemical isolation of radioisotopes, and development of new analytical techniques for new materials, including biological ones. Research of this kind is conducted in the Institute of Nuclear Physics of the Uzbek Academy of Sciences in Tashkent, the Institute of Nuclear Physics of the Latvian Academy in Riga and many other scientific establishments.

Many electrochemical methods are being developed, as well as the theory and application of voltammetric methods. The number of elements that may be determined has been considerably increased through the application of various solid electrodes, organic reagents and masking agents, and analysis in non-aqueous media. Especially successful are the studies of inverse (stripping) voltammetry theory for various electron processes. The kinetics of formation and dissociation of intermetallic and complex compounds has been studied (Tomsk, Sverdlovsk, Moscow). The high sensitivity and speed of inverse voltammetry account for its wide practical application, particularly in the analysis of ultrapure materials, pure water and films and application of the method may be extended even further. New ion-selective electrodes, particularly those with liquid membranes, have been developed. Highly selective extraction systems are used for this purpose. Coulometry with controlled potential is at present being examined for high-precision determination of components of materials; precision coulometers are being designed to determine macro-components in samples.

Kinetic methods for determination of micro-elements are being developed in several centres such as Moscow University, the Moscow Institute of Fine Chemical Technology, Kiev Institute of Physical Chemistry and Ivanovo Chemico-Technological Institute. Several highly sensitive catalytic techniques have been described; some of them are used for mass analysis. The latter include techniques for determination of iodine, silver, rhenium and platinum. Thus, traces of ruthenium and osmium are determined in this way at the Norilsk metallurgical plant. In Moscow University kinetic methods are widely used for determination of biologically active organic compounds. Several monographs devoted to this subject have been published in Russian.

Chromatographic techniques are being intensively developed. Some modifications of gas chromatography have been proposed (A. A. Zhukhovitsky *et al.*); chromatography helps in study of the structure of organic compounds. Reaction gas chromatography and capillary gas chromatography are used. Thin-layer chromatography for the purposes of inorganic analysis has been further developed. Of interest is the work on application of the chromatographic method for organoleptic studies on foodstuffs. This work is conducted in the Nesmeyanov Institute of Organoelement Compounds (Moscow). Moscow University is the centre of research in the field of ion chromatography.

Synthesis of selective sorbents, which may have other uses beside analytical ones, is actively pursued. Heterochain sulphur- and nitrogen-containing sorbents $(-\text{CH}_2-\text{S}-)_n$ and $[(-\text{CH}_2-\text{CH}_2)_3-\text{N}]_n$ have been proposed. They are effective for concentration of heavy metals, platinum and gold. After the concentration the solvent may be analysed for noble metals by such techniques as atomic-absorption, atomic-emission and X-ray fluorescence.

Important advances have been made in the thermodynamics and kinetics of extraction; some new extractants have been synthesized and studied. Among these *O*-isopropyl-*N*-methylthiocarbamate has proved useful for selective extraction of silver and is widely applied in geological survey and non-ferrous metallurgy; substituted thioureas are proposed for the group concentration of platinum metals, and organotin compounds are the best known extractants for arsenic and phosphorus ions. Diantiprylmethane is very effective in determination of titanium and other elements. 8-Mercaptoquinoline and its numerous derivatives have been studied systematically. These works have been performed mostly by Yu. A. Bankovsky.

ANALYSIS OF INORGANIC SUBSTANCES AND CONTROL OF PROCESSES

Many laboratories deal with analysis of metals, alloys and raw materials, and control of metallurgical processes.

Chemical analysis in ferrous metallurgy may in some respects set an example for other branches of industry. It is characterized by extensive use of advanced equipment, a high level of automation, and prompt introduction of new physical and physicochemical techniques, these being important means of increasing production and improving its quality (*e.g.*, high-precision control of poisoning and alloying microcomponents of steels). Automated analytical systems comprising devices for taking and conveying samples, combined with quantummeters and computers, are used at large metallurgical works. Sampling of molten metal to determine gas-generating impurities—carbon, hydrogen, sulphur, oxygen—is

particularly important. To speed up the determination of carbon and sulphur the corresponding equipment is installed near the steel-making units. The economic effects of the seconds and minutes thus saved in analysis in the course of a heat are quite appreciable. Automation of sampling presents certain difficulties, however.

A sufficiently high level of analytical control has been achieved in non-ferrous metallurgy. Here attention is focused on provision of automated control based on multichannel X-ray spectrometers. Introduction of the automated information search system "Analytica" is under way in the industry.

Ultrapur inorganic substances constitute a special group of materials for analysis. Vast experience has been accumulated in this field and many complex problems have been solved. Atomic-emission spectroscopy (with chemical concentration) and, to some extent, atomic-absorption spectrometry and spectrophotometric methods, serve for analytical purposes in industry. Neutron activation and spark-source mass spectroscopy are largely used in research laboratories. Many studies deal with determination of microelements in semiconductors, pure chemical reagents and other high-purity substances. The problems under study include further increase in sensitivity of determination, correct procedures for reference tests, and problems of calibration, since standard samples are often unavailable. It is necessary to develop methods ensuring the determination of 15–20 impurities constituting 10^{-8} – $10^{-9}\%$ w/w, *i.e.*, down to 10 pg/g or less. Laser spectroscopy, mentioned above, appears promising in this respect. Increase of the neutron flux in nuclear reactors to 10^{15} neutrons. $\text{cm}^{-2}.\text{sec}^{-1}$ is another possibility, that is particularly advantageous for the analysis of matrices difficult to activate, *e.g.*, silicon or graphite. Problems to be solved in the analysis of ultrapur substances provide an excellent opportunity to hone the capabilities of an analyst. This type of analysis is performed in many scientific establishments but most extensively in the Institute of Inorganic Chemistry in Novosibirsk, the State Institute of Rare Metals in Moscow, Institute of Chemistry in Gorky, and Institute of Chemical Reagents in Moscow.

Geological materials make up another important group of inorganic substances to be analysed. Their analysis is essential for geological survey, the mining industry and some branches of science, primarily geochemistry. Experience in this field covers a wide range of large-scale analysis for rockforming and trace elements as well as phase analysis. The geological survey has 250 large laboratories which employ a wide range of techniques, including chemical, spectroscopic and nuclear-physical methods. Thus X-ray fluorescence is widely used for determination of components of rocks and ores, and an X-ray radiometric modification is quite widespread and is used in field conditions. About 200–300 million elemental determinations are carried out for the geological survey

annually. An extensive network of laboratories and monitoring stations monitors levels of inorganic substances (heavy metals, toxic anions, dissolved oxygen) in the environment.

ORGANIC ANALYSIS

Analysis of organic substances is a constituent part of analytical chemistry. This statement is not as trite as it may appear. In this country there still exists a deep-rooted tendency to treat organic analysis as a part of organic chemistry or the chemistry of high molecular-weight compounds, bio-organic chemistry or some other branches of the chemicobiological realm. The argument underlying this notion is perfectly logical. The proponents of this approach hold that to analyse minutely it is necessary to know the nature of an organic substance and take into account the specificity of the material. Yet all objects of analytical chemistry are specific and sound analysis should be based on knowledge of the specificity of the sample anyway. The same is true of geological materials, environmental samples, ultrapure substances, archaeological artefacts and many other objects.

If we assume the viewpoint that organic analysis is a part of organic chemistry and extend this approach to other objects of analysis and other sciences and human activities generally, we would have to do away with analytical chemistry altogether, yet nobody seems to harbour such plans. Such an approach would inflict gross and, with time, irreparable damage on many branches of chemical analysis, perceived in strictly utilitarian terms, and on organic chemistry proper. The importance of organic analysis is self-evident. It is a vast and important field of analytical chemistry.

On the other hand, organic analysis is highly specific. The spectrum of analytical techniques needed is significantly at variance with the set of analytical approaches to inorganic materials, at least in terms of priorities. In inorganic analysis the hierarchy of methods in terms of diminishing importance and applicability is apparently as follows: elemental > phase, molecular > isotopic > structural-group analysis. In modern organic analysis the sequence is different: molecular (analysis of mixtures) > structural (functional) group, elemental > isotopic > phase analysis.

Many research bodies in this country are engaged in organic studies. In the field of elemental analysis efficient means of decomposition of complex organic and organometallic substances, including plasma techniques, have been developed. Methods of determining the empirical formulae of compounds, without analytical weighing, have been elaborated. Automation of elemental analysis is being put into effect with the use of CHN-analysers. New methods of heteroelement determination have been worked out,

including those based on X-ray fluorescence. Of note are the works on identification of individual compounds with the help of computers (V. A. Koptuyg) and artificial intelligence (L. A. Gribov).

To analyse complex mixtures of organic compounds chromatographic methods are very widely used. These, gas chromatography in particular, are very important in monitoring processes for production of polymers and other organic products in the petrochemical industry.

Besides the centres of organic analysis mentioned above, the Institute of Organic Semiproducts and Dyes (Moscow), Institute of High-Molecular Compounds of the USSR Academy (Leningrad), and the State Institute of the Nitrogen Industry (Moscow) should be noted. Analytical methods for the chemical, petrochemical and pharmaceutical industries are developed in their own branch research institutes as well as in academic and educational establishments. These last most frequently sign contracts with industrial enterprises, usually on mutually profitable terms. The same concerns the sphere of inorganic analysis.

The diversity of products of the chemical industry generates numerous methodological problems. The number of different products runs into tens of thousands and each must be provided with analytical means. For a long time the strategy adopted was to develop individual techniques and analysers for the most important substances, but this approach is too laborious. Even now, almost every tenth worker in the chemical industry is engaged in analysis. Obstacles linked with difficulties arising in monitoring may sometimes impede introduction of new processes. While requirements for the quality of products become more stringent, the quality indicators often depend on the reliability of analytical techniques. To overcome this limitation a new concept of a "universal system of chemical analysis" is being developed (*Zh. Analit. Khim.*, 1982, **37**, 1104). It envisages the transition from single-purpose analysers to universal analytical systems with multi-indicator detectors. Thus, correlated simultaneous readings from several detectors are used as an analytical indicator of a substance.

PUBLICATIONS

Zhurnal Analiticheskoi Khimii (Journal of Analytical Chemistry) is the major periodic publication in Russian. It has been published by the Academy of Sciences since 1946. Along with original contributions, it carries reviews, letters to the editor, and information items on conferences, books and equipment. Two other publications that give much space to analytical chemistry are the *Zavodskaya Laboratoriya* (Plant Laboratory) and *Zhurnal Prikladnoi Spektroskopii* (Journal of Applied Spectroscopy). Many communications are published in other all-union and regional magazines, e.g., *Doklady Akade-*

miya Nauk (Reports of the Academy of Sciences) and *Ukrainskii Khimicheskii Zhurnal* (Ukrainian Chemical Journal).

Four series of monographs and collections of papers are published. They are "Analytical Chemistry of the Elements", "Analytical Reagents", "Problems of Analytical Chemistry", and "Methods of Analytical Chemistry". Textbooks are published by the publishing houses "Vysshaya Shkola" and "Khimiya" and translations by "Mir" and "Khimiya".

INSTRUMENT ENGINEERING FOR ANALYTICAL PURPOSES

New equipment is developed in research laboratories and design offices. Some original devices have been mentioned above. In addition such devices as the microcolumn liquid chromatograph "Mili-khrom", ion chromatograph "Tsvet 3006", various types of gas chromatographs, the precision coulometer PKU-1, and atomic-absorption spectrometer "Saturn-2" should be mentioned. Polarographs, pH-meters, gas chromatographs and X-ray fluorometric spectrometers are produced on a large scale.

Home supply, however, does not meet the demand, because of insufficient quantity of production of instruments such as Fourier infrared spectrometers, gas chromatograph-mass spectrometers and X-ray microanalysers. International co-operation within the framework of the Socialist Economic Community helps solve this problem. Thus we traditionally buy polarographs in Hungary and Czechoslovakia, some spectral equipment in the GDR, precision balances in Poland. Trade in this field involves some other countries. Thus Perkin-Elmer atomic-absorption instruments and Leco and Balzer instruments for gas determination in metals are widely used.

INTERNATIONAL CONTACTS

There are several fields in which the leading position of Soviet analytical chemistry is unanimously recognized. These are spectrophotometry in the ultraviolet and visible regions, particularly with organic reagents, electrothermal atomic-absorption spectrometry, inverse voltammetry and some other electrochemical methods, concentration of microelements (including extraction concentration), analysis of mineral raw materials and ultrapure substances, and the analytical chemistry of noble and rare metals. Soviet analysts working in these and other fields are invited to make reports at international conferences and give lectures in universities abroad. Soviet analytical chemists are on the editorial boards and advisory committees of 25-30 international or national journals of analytical chemistry and related disciplines. Ten scientists are elected members of IUPAC. Professor I. P. Alimarin is an honorary member of many scientific societies and a doctor *honoris causa* of a number of universities, including those of Birmingham and Göteborg. He has been awarded the Talanta gold medal and the Emich, Hevesy and Purkyně medals.

A biennial Soviet-Japanese symposium on analytical chemistry is regularly convened. The first took place in 1982 in Kyoto, the second was held in Moscow and Kiev in 1984.

Joint scientific projects are carried out in collaboration with chemists from the GDR, Hungary, Bulgaria and Czechoslovakia; for example, standard samples are being developed. The Vernadsky Institute has carried out a number of joint projects in the field of spectroscopic methods of analysis together with the Karl-Marx University of Leipzig. Many foreign analysts come to visit our country, and international co-operation and exchange of ideas and information are always welcome as they are throughout the scientific fraternity of the world.

ANALYTICAL CHEMISTRY TEACHING IN THE USSR

YE. N. DOROKHOVA

Moscow State University, Lenin Hills, Moscow, USSR

(Received 15 October 1985. Accepted 4 August 1986)

Summary—The paper reviews the state of analytical chemistry teaching at Soviet higher educational establishments, discussing specifics of teaching techniques at various schools of higher learning, *viz.* universities and technological and non-chemical institutes*. It describes the curricula and methods of continuous assessment. Particular attention is paid to the subject matter of courses in analytical chemistry and its future improvement, with special focus on problems related to training specialists in analytical chemistry at universities and other institutions of higher education. The paper also deals with facilities and opportunities offered for research projects, and finally touches on the problem of text books.

Scientific progress is impossible without highly competent research workers. Analytical chemistry is an ancient science, yet it may also be regarded as one of the youngest sciences; that is to say, it is in the process of rebirth, overstepping its old boundaries. It is not incidental that scientists all over the world are paying great attention to analytical chemistry as a science. The broader range of samples and scope of methods, the extensive use of electronics, and the automation, computerization and instrumentation of analysis all influence the requirements for university and technological institute graduates. "To solve unconventional problems in studying the composition and structure of new natural and synthetic substances and materials, to analyse standard and reference samples, to investigate unique samples of small mass, to evaluate results and to work out recommendations, will call for specialists with a high degree of experience and a profound knowledge of physics, mathematics, programming and computer electronics".¹ This prompts the necessity of far-reaching planning for higher education. Under-rating the role of analytical chemistry teaching (as well as of any other science) may have disastrous consequences for the successful progress of science, technology and the economy.¹⁻⁸

In the Soviet Union the serious and comprehensive

approach to analytical chemistry teaching has deep roots. Many outstanding chemists who have made great contributions to the development of the theory and practice of chemical analysis were also educators: D. I. Mendeleev, whose thesis dealt with analytical chemistry; N. A. Menshutkin, who wrote Russia's first textbook on analytical chemistry; L. A. Chugaev, the founder of the use of organic reagents for analysis, and many others, taught at universities and institutes, and were talented lecturers and educators. This tradition is being preserved and will be maintained in the future. About 40% of the members of the Scientific Council of the USSR Academy of Sciences, in the branch of analytical chemistry (the chief co-ordinational and scientific advisory body), are heads of departments and institutes of higher education, as well as teachers, and in certain sections and commissions this representation reaches 60%. Academician I. P. Alimarin, Head of the Scientific Council, is also Head of the Analytical Chemistry Faculty at Moscow University, and his deputy, Corresponding Member of the USSR Academy of Sciences, Yu. A. Zolotov, heads a laboratory of the same faculty. Many scientist members of the Council combine their research work with teaching (Academician A. T. Pilipenko, Corresponding Member of the USSR Academy of Sciences, Yu. A. Zolotov, Professors Yu. A. Karpov, O. M. Petrukhin and many others). Outstanding scientists who are not educators maintain contacts with higher educational institutions by delivering lectures to students and teachers. Thus most analytical scientists understand the tasks and problems facing analytical chemistry teaching.

On the whole a sufficient number of analytical scientists is being trained for service in industry and research, but the continuous development and perfection of programmes, updating of textbooks and improvement of teaching standards make it possible

*Universities are higher educational establishments which do not grant degrees in technology, but prepare their students for scientific and research work in various sciences—exact, natural and social, as well as the humanities. Institutes are more specialized schools of higher learning, training specialists for a particular field of science and technology. Thus, graduates of chemical and technological institutes will be granted degrees in technology and work as chemical engineers, while graduates of medical institutes will devote themselves to the medical profession, and those of pedagogical institutes will work as teachers.

to train better qualified graduates. Unfortunately, a certain number of scientists (particularly non-chemical) and those in high administrative posts are inclined to regard analytical chemistry as a subsidiary science. This results in the reduction or even exclusion of analytical chemistry courses at institutes and non-chemical university departments. In some cases this is justifiable, *e.g.*, cancellation of the course on classical qualitative analysis, at chemico-technological and technological institutes, as well as courses of analytical chemistry at certain faculties of aviation, building and metallurgical institutes. Reduction of courses at agricultural, medical and food institutes causes great concern, however. Sometimes analytical scientists themselves are to blame because they have failed to perceive and keep pace with the new trends in chemical analysis and to alter the courses accordingly. At such institutes the teaching of physicochemical and physical methods of analysis has been transferred to other faculties (such is the case, for instance, at metallurgic institutes). Biochemical and clinical analysis is at present almost an exclusive prerogative of organic chemistry faculties. In this connection it would seem appropriate to quote the answer of Kellner and Malissa to the question "Will analytical chemistry be done in the future by analytical chemistry?"—"Most likely, yes, if chemistry departments realize the new trends! If they do not, someone else will come up and solve the problems for us as was demonstrated already in the past".⁷

According to the Working Party on Analytical Chemistry of the Federation of European Chemical Societies a teacher must be well versed in the following subjects: chemical analysis, biochemical analysis, chemometrics, analytical strategy, materials analysis, clinical analysis, analysis of environmental samples, *etc.*⁷ Can we maintain that most of our teachers fit the description? Do our curricula fully correspond to these requirements? Apparently, not. Before covering the problems of analytical chemistry teaching and possible solutions to them let us dwell upon the present state of teaching, including certain formal

aspects (curricula, arrangement of courses, co-ordination of efforts aimed at raising teaching standards, *etc.*).

CURRICULA

Analytical chemistry is taught at 700 higher and secondary educational institutions of the USSR. There are three groups of higher educational establishments with different curricula: (1) universities, (2) chemical and technological, technological, and poly-technic institutes, (3) non-chemical institutes (medical, pharmaceutical, food, agricultural, oil, *etc.*).

Universities

Of the 60 universities training chemists, about 60% have Departments of Analytical Chemistry (including the Universities of Moscow, Leningrad, Kazan, Saratov and other big cities, as well as the capitals of the Republics). Some universities (mainly those orientated to training school teachers) have united departments of, for example, inorganic and analytical chemistry, biology and analytical chemistry, and so on. At certain universities analytical scientists are trained by specialized departments, such as the Department of Chemical Metrology at Kharkov University, the Department of Rare Elements at Kazakh University. Analytical chemistry teaching is conducted at three levels: a general course for all students majoring in chemistry, a general course for students of some non-chemical faculties, and special courses for analytical graduates.

The first three and a half years at Soviet universities are devoted to mastering the fundamentals of chemistry, physics, and mathematics. In the opinion of Soviet scientists, a solid physical and mathematical basis is prerequisite for the education of a modern chemist. That is why a considerable amount of time is devoted to the study of mathematical and physical sciences (Fig. 1). The elements of programming are introduced as early as the first year. Much attention is paid to foreign languages. A modern graduate

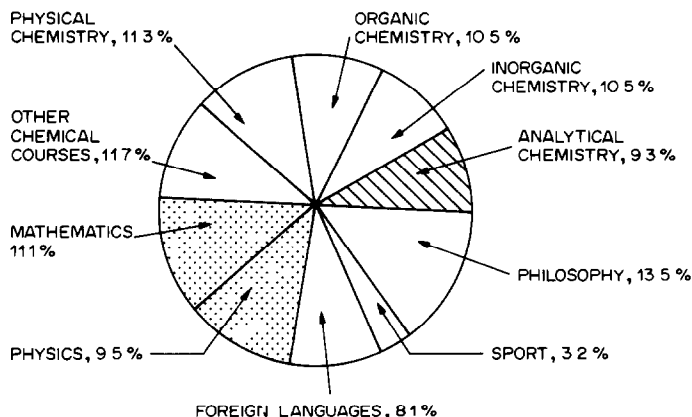


Fig. 1. Proportions of different disciplines in university curricula.

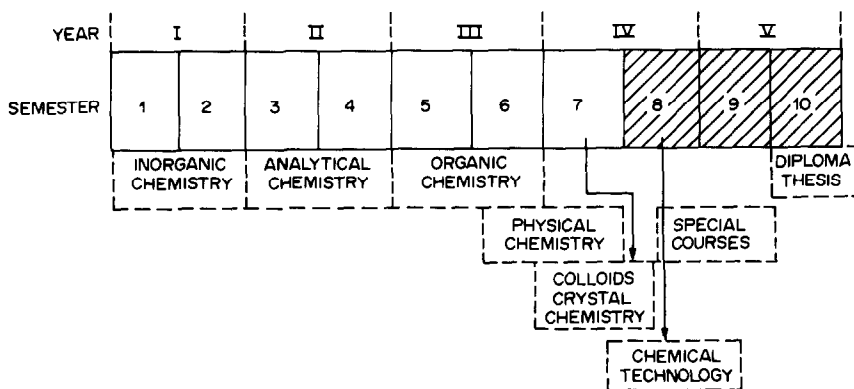


Fig. 2. Order of study of chemical disciplines at universities.

majoring in natural sciences should be a confirmed materialist, a conscientious citizen, a patriot, and know the basic Soviet laws. That is why the curricula ensure a profound study of social and political sciences, philosophy, political economy and chemical history. Physical training and sports are compulsory components of the curricula.

The curricula of certain institutes include pedagogics and psychology (for would-be school teachers). Besides the compulsory courses above, the curricula include optional courses (radio-electronics, for instance). Each year is devoted to the study of a basic chemical science (inorganic, analytical, organic and physical chemistry) (Fig. 2). At the end of the aca-

Table 1. Curriculum for chemical faculties of Soviet Universities

	Hours per week	Assessment		Hours per week	Assessment
<i>Semester 1</i>			<i>Semester 5</i>		
Inorganic chemistry	14	Examination	Organic chemistry	14	Examination
Mathematical analysis	5	Examination	Radiochemistry	2	Credit
Analytical geometry	3	Credit	Quantum mechanics	3	Credit
Programming	1	Credit	Molecular structure	4	Examination
Foreign language	4	Credit	Foreign language	4	Credit
History of the Communist Party	4	Examination	Philosophy	4	Examination
Physical training	2	Credit	<i>Semester 6</i>		
<i>Semester 2</i>			Organic chemistry	12	Examination
Inorganic chemistry	12	Examination	Physical chemistry	10	Examination
Mathematical analysis	6	Examination	Substance structure	2	Credit
Physics	6	Examination	Foreign language	4	Examination
Programming	2	Examination	Political economy	4	Examination
Foreign language	4	Credit	<i>Semester 7</i>		
Physical training	2	Credit	Physical chemistry	10	Examination
History of the Communist Party	3	Credit	Colloid chemistry	5	Examination
<i>Semester 3</i>			Crystal chemistry	3	Examination
Analytical chemistry	11	Credit with a mark	High molecular-weight compounds	3	Credit
Mathematical analysis	4	Examination	Political economy	4	Examination
Physics	8	Examination	Law	2	Credit
Mathematical physics equations	3	Credit	Specialization	3	Credit
Foreign language	2	Credit	<i>Semester 8</i>		
Physical training	2	Credit	Chemical engineering	8	Examination
<i>Semester 4</i>			High molecular-weight compounds	4	Examination
Analytical chemistry	12	Examination	Specialization	12	
Mathematical analysis	4	Examination	Practical work	1½ months	
Linear algebra	3	Credit	<i>Semester 9</i>		
Theoretical mechanics	3	Examination	Specialization	12	
Probability theory	3	Credit	History and methodology of chemistry	2	Credit
Philosophy	4	Examination	Environmental protection	2	Credit
Foreign language	2	Credit	Philosophy	5	Credit
Physical training	2	Credit	Pre-diploma practical work		

Table 2. Course (hours) in analytical chemistry at Moscow University

	Lectures	Seminars	Practicals
<i>Semester 1</i>			
Theoretical basis of analytical chemistry			
Introduction	2		
Equilibrium theory	22	12	
Methods of separation	10	4	
Methods of separation and detection			140
Total:	34	16	140
<i>Semester 2</i>			
Metrological aspects of analytical chemistry	6	—	—
Quantitative methods of analysis			
Gravimetric	6	—	18
Titrimetric	8	—	36
(visual and potentiometric)			
Electrochemical	12	—	30
Optical	12	—	30
Course paper (thesis)	—	—	32
Total:	44	—	146

demic year students take an experimental course based on one of the chemical sciences, and also take shorter courses dealing with some other less time-consuming fundamentals of chemistry.

Table 1 lists, as an example, a standard curriculum adopted at Moscow University and (with minor modifications in stratification) at other universities of the Soviet Union.

At some universities one or two groups (comprising 20–40 students) work according to individual programmes. At Moscow University, for example, graduates with a profound knowledge of mathematics (theoreticians) and programming (computer experts) have been trained for several years. Such graduates are especially valuable since they combine a profound knowledge of the chemical sciences and mathematics.

Fourth-year students major in a chosen field, with special courses and practical classes recommended by the corresponding departments. Fifth-year students (undergraduates) are engaged in their graduation examinations, which are preceded by practice sessions (more detailed information on specialization is presented below).

As is seen, analytical chemistry is an essential component of the curricula, taking up much time and effort. How is this time distributed? The whole course of 350–390 hr of teaching time consists of lectures, practicals and seminars, run in parallel. Table 2 lists, as an example, the analytical chemistry curriculum adopted at Moscow University.

Analytical chemistry at non-chemical departments

is taught according to a similar, but less complicated scheme, with inevitably shorter courses, optional lectures, no course papers and examinations only in certain studies (Table 3).

Chemical and technological, technological and polytechnic institutes (chemical specialities)

Chemical engineers in the USSR are trained at 70 institutes. Almost all of them have departments of analytical chemistry, drawing all the students into studying this science.

The analytical chemistry course at these institutes is divided into two parts. Second-year students study chemical methods of quantitative analysis, fourth-year students (after studying physical chemistry and engineering sciences) master physicochemical and physical methods of analysis (Table 4). The choice of analytical methods depends on the kind of facilities at the disposal of the departments. Usually these are electrochemical and optical methods, but some institutes are better at teaching chromatography, others kinetic methods of analysis, and still others organic analysis. Much of the aforesaid is also true of similar higher educational establishments, *i.e.*, comprehensive mathematical training, a rather considerable period of time allotted to chemical sciences, and attention devoted to socio-political and philosophical sciences. The number of teaching hours envisaged for chemical sciences at such institutes is almost 40% less than at universities, as most of the time is consumed by engineering sciences, radio-electronics, industrial economics, *etc.* In general there is more time allotted

Table 3. Distribution of hours in non-chemical faculties of universities

Speciality/Department	Semester 2	Semester 3	Assessment
Biological	42–72	36–64	Credit
Soil	36–48	90	Examination
Geological	72	—	Credit
Geochemical	72	48	Examination
Geographical	42	36	Credit

Table 4. Distribution of hours in chemicotechnological and technological institutes

	Lectures	Seminars	Practicals
<i>Semester 3</i>			
Chemical methods of analysis (gravimetry and titrimetry)	17	8	100
<i>Semester 7</i>			
Physicochemical and physical methods	32	—	85
Environmental protection (Learning and research work)	2	—	—
Personal research projects			

to physical, mathematical and engineering studies than to chemistry. Only a very few of these departments of analytical chemistry are engaged in training analytical graduates.

Non-chemical institutes

This is the most numerous group of higher educational establishments. Some of them have analytical chemistry departments (these are normally pharmaceutical institutes and pharmaceutical faculties of medical institutes, and of food and certain agricultural institutes). Of late, analytical chemistry as a course has been excluded from the curricula of

some non-chemical institutes, but elements of analysis are included in the programmes of other chemical courses (usually general chemistry).

The number of teaching hours and curricula greatly depends on the type of institute and speciality. Usually second-year students are taught analytical chemistry during one or two terms (semesters). At other establishments of higher education with a larger group of classes for analytical chemistry, the course lasts 3 semesters. Tables 5 and 6 list, as an example, the curricula of two educational institutions. Regrettably, at some non-chemical institutes there is no room for the course of instrumental methods of

Table 5. Distribution of hours at the pharmaceutical faculty of the Sechenov 1st Moscow Medical Institute

	Lectures	Practicals	Assessment
<i>Semester 2</i>			
Methods of identification and separation	38	114	2 Tests
<i>Semester 3</i>			
Quantitative chemical analysis (gravimetry and titrimetry)	36	54	Credit with a mark
<i>Semester 4</i>			
Instrumental methods of analysis (spectrophotometry, coulometry, potentiometry, chromatography)	18	36	
Total:	92	204	

Table 6. Distribution of hours at the Gubkin Moscow Petrochemical Institute

	Lectures	Seminars	Practicals	Assessment
<i>Semester 3</i>				
Theoretical basis of analytical chemistry	17	6		Credit with a mark
Qualitative analysis	—	—	48	
<i>Semester 4</i>				
Theoretical basis of analytical chemistry	17	6		Credit with a mark
Chemical methods of quantitative analysis	—	—	48	
<i>Semester 8 (or 11)</i>				
Physicochemical methods of analysis	14	—	48	Credit with a mark
Total:	48	12	144	

analysis, and its inclusion in curricula depends on personal decisions by Department Heads. This is particularly true of the agricultural institutes.

Part-time departments

Many institutes and universities of the USSR have set up part-time departments training graduates according to the curricula of the full-time departments, but envisaging 10–25% less attendance time than in full-time departments, with some acquisition of knowledge entrusted to the students' own efforts. Since the requirements and methods of assessment are the same as in full-time departments, part-time education makes greater demands on the students' perseverance and self-discipline.

CO-ORDINATION OF ACTIVITIES IN ANALYTICAL CHEMISTRY TEACHING

Higher and secondary educational institutions work under the supervision of the USSR Ministry for Higher and Specialized Secondary Education, as well as the Ministries of Higher Education of the Union Republics. Non-chemical institutes are also subordinate to the Educational Methodological Departments of the corresponding branch Ministries, *e.g.*, medical and pharmaceutical institutes to the Ministry of Public Health, agricultural institutes to the Ministry of Agriculture. Methodological and organizational activities are co-ordinated by the Scientific and Methodological Council of the Ministry for Higher Education, composed of outstanding Soviet scientists and pedagogues, *viz.* Rectors of institutes, Deans of faculties, Heads of departments. The Council consists of sections considering problems of one particular course, *e.g.*, chemistry. Within the framework of the section for chemistry there are subsections for analytical chemistry, for universities (Chairman—

Academician I. P. Alimarin), chemical institutes (Chairman—Professor O. M. Petrukhin), non-chemical institutes (Chairman—Professor D. A. Knyazev).

In 1981 the Scientific Council for Analytical Chemistry of the USSR Academy of Sciences set up a Commission for Analytical Chemistry Teaching (Chairman—Dr I. I. Alexeeva) which comprises members of the subsections for analytical chemistry of the Scientific and Methodological Council of the USSR Ministry for Education (Fig. 3). The Commission is called upon to solve methodological and organizational problems of teaching. The activities of the Commission are guided by perspective plans worked out once every five years, which reflect major trends and tendencies in teaching. Every year the Commission draws up detailed programmes. Once a year the Commission meets to discuss methodological and organizational problems and account for its work to the Scientific Council for Analytical Chemistry. The major aspects of the work of the Commission can be formulated as follows: it determines the contents and objectives of courses (programmes); improves curricula and brings them up to date; promotes new specialities; supervises compilation and publication of textbooks, *etc.*; collects information and statistics on the state of teaching standards at various higher educational establishments; sponsors briefings and conferences on problems of analytical chemistry teaching, as well as seminars for teachers on methodological problems; its members also participate in international meetings, co-operation, etc.

Contents of courses

The development of courses plays a big part in improving teaching standards. Correctly determined objectives and contents of courses serve as a basis for perspective planning of education. Methodological problems figure largely at briefings and conferences

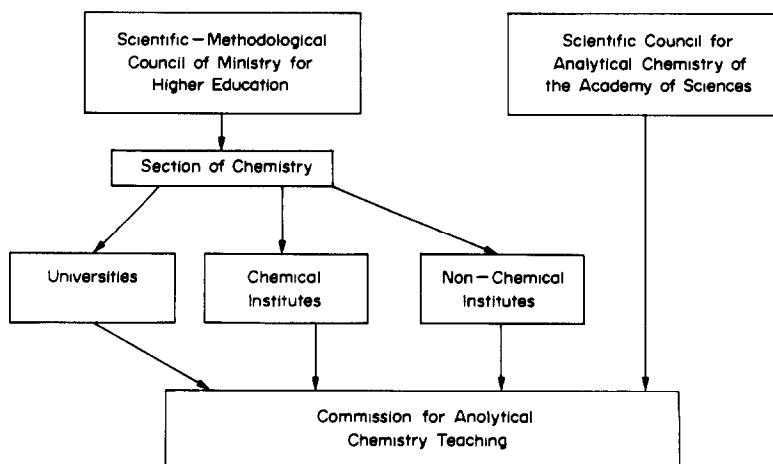


Fig. 3. Scheme of the co-ordinating bodies for analytical chemistry teaching.

on teaching, being the main concern of the methodological commissions of departments and of the Commission for Teaching.

The contents of courses are reflected in programmes compiled every five years by the leading institutes at the request of the Ministry for Higher Education and/or branch Ministries (for non-chemical institutes). Such standard programmes are subjected to close discussion and criticism, and are then approved by the Scientific and Methodological Council for Chemistry. Programmes for non-chemical institutes are bound to reflect their specific interests, which is why the number of such programmes exceeds 100.

The programmes are meant to reflect the present state and trends of development in analytical chemistry, and the ratios between different methods of analysis; they determine the objectives for analysis and recommend the necessary (accompanying) literature. The programmes of general courses for universities should not overlap the programmes of the special courses.

To answer the question of what to teach, it is necessary to define analytical chemistry as a science and formulate its objectives. The original objective was to find out what a given substance consists of, *i.e.*, to determine its chemical composition, but this has now been extended to include the nature and distribution of the individual substances present. This objective is attained by methods which are constantly brought up to date and modified.¹ According to Professor Zolotov⁴ neither time nor effort should be spared in conveying to students a knowledge of the general problems of analytical chemistry and a feeling for the correct approach to their solution in formulating the philosophy of the science, determining its place among other natural sciences and establishing a fundamental principle for analytical chemistry. This principle, according to Professor Moskvina (Leningrad University), might be the determination of the characteristic properties of a substance, *i.e.*, any manifestations ensuring identification and determination of the substance. There are other opinions, of course, but it is essential that the programmes should make it clear that analytical chemistry is a science dealing with measurement. This introduces the importance of the metrological aspects. The student must be taught how to select and prepare a sample, and how to work out a scheme of analysis and choose the right methods.⁴

The theoretical basis of analytical chemistry is still a focus of attention, but the depth of study of certain issues may vary. Previously the courses gave a formal approach to the reactions used for detection and determination, while now much more attention is paid to reaction mechanism, the role of solvents, and processes in plasma, *etc.*

A drawback of the old programmes was the neglect of automated analysis and use of computers.

Of particular importance is the ratio between cer-

tain methods of analysis. There used to be a great deal of disproportion between classical and modern methods in the old programmes. In the new programmes the proportion of physicochemical and physical methods has increased; chromatography is now regarded not only as a separation method, but also as a determination method. Even so, the classical chemical methods of analysis cannot be altogether ruled out. "A lot of analysts overestimate the inexhaustible possibilities of physical methods to such an extent, that these have come to the point of ousting chemistry from chemical control".¹ The progress achieved in analytical chemistry should not mean complete renunciation of the experience accumulated.

The old courses put the main emphasis on analysis of inorganic substances. This is no longer acceptable. The analysis of therapeutic drugs, foodstuffs, and environmental samples is part and parcel of analytical chemistry, and should find reflection in modern courses.

These concepts have been voiced more than once¹⁻⁶ in the press and at different conferences, and have been taken into consideration, to a certain extent, in the compilation of programmes for universities and chemotechnological institutes for 1985-90. For example, the programme for universities compiled by the Analytical Chemistry Department of Moscow University (Editor-in-Chief—I. P. Alimarin; Head of the Department of the Methodological Commission—Dr V. I. Fadeeva) contains sections dealing with general problems of analytical chemistry, metrological aspects, and analysis of organic substances. The programme recommends the following distribution of lectures and laboratory classes:

theoretical basis	46%
separation methods	12%
physicochemical and physical methods	30%
gravimetric and titrimetric methods	12%

Methods of assessment

Several methods of assessment are accepted at higher educational establishments of the USSR, *viz.* examination, credit for attendance (with a mark assigned), and credit for attendance. Continuous assessment during the term is made by means of written and oral tests. The latter, known as colloquia, are also of educational value for the student since the direct contact and animated discussion with the teacher, which reveal his/her personality and expertise, cannot but contribute to moulding and fostering the young chemist.

Technical teaching aids, such as test programs, and testing and teaching machines are extensively (although, so far insufficiently) used during such assessments. Much attention is attached to technical teaching aids at Byelorussian University (Head of the Department—Professor G. L. Starobinets) and at Saratov University (Head of the Department—

Professor R. K. Chernova), as well as at some other higher educational establishments.

TRAINING OF ANALYTICAL GRADUATES

As mentioned above, analytical chemists are trained only at universities. Specialization starts from the fourth year. Senior students who have decided to major in analytical chemistry attend special courses and perform laboratory assignments (for a total of 550 hr). The courses are designed to deepen the students' knowledge in the theory and practice of chemical analysis, so that they can independently plan and complete investigations, and develop schemes and methods of analysis. The contents of these courses should correspond to the current theoretical and practical achievements of analytical chemistry. The spirit of research should permeate laboratory classes. The students should learn how to use the latest analytical devices, and master the ways of processing measurement results, as well as graphical and numerical calculation. They should learn how to write reports based on the results obtained and become experienced in using the appropriate reference literature.

Each department is free to choose special courses. The choice of a course largely depends on the scientific interests of the department, and the availability of the necessary equipment. For example, electrochemical methods are being developed at Kazan University, analysis of organic substances at Omsk University, chromatography at Leningrad University.

The Commission for analytical chemistry teaching recommends the following courses.

- Introduction to modern analytical chemistry.
- Metrological methods of analysis.
- Complex compounds and organic reagents used for analysis.
- Separation and concentration methods.
- Chromatographic methods of analysis.
- Optical methods of analysis:
 - atomic-emission spectroscopy
 - atomic-absorption spectroscopy
 - atomic-fluorescence spectroscopy
 - molecular-absorption spectroscopy (ultraviolet, visible, infrared, microwave)
 - luminescence
- Physical methods of analysis:
 - X-ray spectral methods and electron spectroscopy
 - mass-spectrometry
 - activation analysis
 - NMR, ESR, Mössbauer spectroscopy
 - Electrochemical methods of analysis.
 - Kinetic methods of analysis.
 - Analysis of the most important materials, including environmental samples.

It is certainly often impossible to deliver all the courses, and the choice should rest with the de-

partments concerned, but no tendency to narrow specialization can be tolerated. A modern graduate should know various methods of analysis, their possibilities and limitations. From this point of view, the course "Introduction to Modern Analytical Chemistry" delivered at Moscow University by Yu. A. Zolotov is of interest as it gives a comprehensive coverage of all the methods above.

The demand for analytical scientists with higher or secondary qualifications is great, and is not being fully met by the universities. Analytical laboratories often employ graduates from chemical and non-chemical institutes who do not have a specialized analytical education. Most of the analytical graduates work at universities, research institutes and secondary schools. University graduates are seldom appointed to industrial, plant, agrochemical or clinical laboratories. A typical example of this situation is the following list of staff at two large analytical laboratories.

Research Institute of Metallurgy and Beneficiation Kazakh Academy of Sciences

Total staff	42
With higher education	34
Graduates from: universities	25
institutes	9
pharmaceutical	1
pedagogical	3
polytechnic	1
technological	2
food	1
biological department	1
With no specialized education	8

Central Plant Laboratory of the Ust-Kamenogorsk Integrated Lead and Zinc Works

Total staff	100
With higher education	24
University graduates	10
Technological institute graduates	10
Non-chemical institute graduates	4

The small number of university graduates working at industrial laboratories appear insufficiently trained for their work, as they often know little or next to nothing of the production procedure they are engaged in. Graduates from technological and non-chemical institutes are often to be found in such laboratories. The analytical methods now in use have become very complicated. Their correct and effective application and perfection is impossible without special background training, specialized knowledge of their theoretical basis, and dexterity in apparatus handling. It is important to master the essentials of general analytical methodology, including the ability to compare different methods, select a scheme or method for solving particular tasks, and knowledge of chemical analysis metrology. Learning all this is a time and labour consuming task. Chemicotechnological and technological institutes grant no such

training, nor is it available to graduates from such institutes who are working at branch institutes and laboratories (agrochemical, clinical, geological and others). The vital interests of their work make them raise their qualification standards by themselves. In the course of time they become experienced analytical scientists, and even heads of laboratories and services. This is not the solution to the problem as a whole, however. A possible way out might be to offer specialist training at technological and some non-chemical institutes (pharmaceutical, agricultural, oil and food). Some experience has been gained in this respect. Analytical engineers are trained by the Ural Polytechnical Institute (Head of Department—Professor V. N. Muzgin) and the Leningrad Polytechnic Institute (Head of Department—Professor B. V. L'vov).

IMPROVING TEACHING STANDARDS

Even the most experienced and qualified teachers and laboratory staff should constantly raise their professional level. A teacher finds it difficult to do this because of the heavy time-table during the semester. Hence the Ministry for Education grants every lecturer the opportunity to go on study leave once every five years to improve his/her teaching standard, at special departments set up by leading institutes. The teachers attend compulsory courses on pedagogics, psychology, and programming, as well as lectures delivered by outstanding scientists on certain problems of analytical chemistry. Another approach is attendance at analytical chemistry schools, which attract a great number of teachers, especially the younger ones.

STUDENT RESEARCH WORK

The involvement of students in research work under the supervision of teachers and departmental staff is an old custom in the higher educational institutions of the Soviet Union.

There are the following levels of student research work.

(1) Participation in students' research societies. This form is particularly widespread at universities: long before specialization, undergraduates come to the research laboratories to try themselves out in experimental work. On entering the university a student does not know what speciality to choose. In this he finds assistance and advice rendered by lecturers, teachers, senior students or postgraduates of the Department. The personality of a lecturer or teacher, and his/her ability to present the achievements and problems of analytical chemistry in a vivid and exciting manner at the very first classes are most important factors in helping students choose their future speciality. Students working in research laboratories belong to the students' research societies and an incentive is that the best research papers are

rewarded. Every year the Ministry for Higher Education and other organizations sponsor contests of students' research achievements, and the winners are awarded medals. The most interesting papers are published in scientific journals. In 1983, for example, 12 student articles were published by Moscow University, and in 1984 the number rose to 13. Typical themes are: "A study of the kinetics of formation of the palladium PAR complex in aqueous organic media", "Extraction of copper by oxygen-containing macrocyclic compounds", "The effect of noise on the results of flame-photometric determination of boron".

(2) Course and diploma theses. These forms of research work are included in university curricula. Second-year students write a course thesis. This might be a literature review or a simple experiment in a narrow field, taking four or five practical sessions to accomplish at the end of the laboratory practical course. The students report the results of their work in the presence of teachers and other students. This approach helps an undergraduate to acquire useful habits, *viz.* to work with the reference literature, to formulate the results in a proper manner, to present the gist of the problem briefly and clearly, and to speak in public.

A graduation thesis is a serious research piece of work, normally involving specific analytical applications. Not infrequently it is associated with the scientific adviser's research or a postgraduate thesis. In working on his graduation thesis the student must display independent approaches to the experimental work and the interpretation of the results obtained.

(3) Students' research projects. This method is practised for good students in chemicotechnological institutes where the laboratory practical course covers only uncomplicated experiments. It might consist in developing a new methodology or verifying an already existing one, perfecting practical work, *etc.* Such students study a lot of reference literature on the problem and write a review. Examples of such reviews presented at the Moscow Institute of Chemical Engineering are "Methods of determining arsenic in semiconductor materials", "Detection of sulphur in rubber", "Kjeldahl determination of nitrogen in organic substances", the reviews being complemented by an appropriate practical investigation.

At non-chemical institutes, where this method is not envisaged by the curriculum, research elements are introduced into practical tasks (at the initiative of the teachers). Thus, at the First Moscow Medical Institute (Professor B. A. Rudenko) the final task is analysis of a therapeutic drug or some other substance, which a student must analyse independently, using literature information and his own judgement and experience.

An interesting method of student research work has been suggested at the Moscow Petrochemical Institute (Professor E. I. Isaev), namely, that students in the prospectors' department analyse natural waters

under field conditions as their analytical practical work.

Such methods are very useful because non-chemical graduates begin to take much greater interest in analytical chemistry and become aware of its importance.

MANUALS

Manuals meeting the requirements of modern science are an indispensable element of education.

For years Soviet students have been using the notable textbooks "A Course of Qualitative Semimicroanalysis" and "Quantitative Analysis", written by V. N. Alexeev in the 1940s in a logical, interesting and comprehensible manner. They have been translated into many languages and are still popular (with later amendments) with both students and teachers. In addition, other textbooks are issued for use in different types of higher institutions of the Soviet Union, namely universities,⁹ agricultural institutes,¹⁰ and pedagogical institutes.¹¹

However, these manuals no longer conform to the present level of analytical chemistry, *i.e.*, theoretical problems are expounded from obsolete standpoints (for example, acid-base equilibrium, complex-formation, *etc.*); there are no metrological aspects (except for brief information on the statistical processing of measurements); they lack modern methods of analysis. To some extent the drawback concerning modern methods of analysis has been rectified in Kreshkov's book on fundamentals.¹² Some modern manuals on the theoretical basis of analytical chemistry have appeared,¹³⁻¹⁵ but they expound only the issues of ionic solution equilibria in the same way as in problem books.¹⁶⁻¹⁸ Certain physicochemical and physical methods are expounded in a number of textbooks that came out in the 1970s.¹⁹⁻²⁴ Undergraduates also use other books on certain issues that are not covered in the manuals.^{2,25-27} A book on demonstration experiments in analytical chemistry has been written²⁸ to help lecturers.

However, no manual which could meet the present-day level of analytical chemistry has so far been compiled in the USSR.

Foreign manuals translated into Russian are widely used in higher educational institutions of the Soviet Union.²⁹⁻³⁶ These manuals meet the demand of modern analytical chemistry but their relatively small circulation (6000-10000 copies) does not permit them to be recommended as basic manuals. Also, they often deal insufficiently with, or neglect altogether, certain aspects traditionally emphasized in the USSR, namely organic reagents for analysis, and luminescence analysis.

Higher educational establishments are trying to compensate for the lack of manuals by issuing methodological synopses. This is praiseworthy, but such an approach will hardly solve the problem; moreover, the quality of some of them leaves much to be desired

since they are not always seriously criticised and edited.

Students taking special courses use many other monographs (both Soviet and foreign), reviews and scientific articles, in addition to the manuals above.

Soviet pedagogues are well aware of the necessity of compiling an adequate analytical chemistry manual. Such a manual must reflect the philosophy of the science, and the place of analytical chemistry among other sciences, and contain analytical strategy and the metrological basis of analytical chemistry. The theoretical treatment should not be confined to ionic equilibria, which should be expounded on the basis of thermodynamics and kinetics. Physical and physicochemical methods should be generously dealt with. Such a fundamental manual would not preclude the publication of a laboratory practical manual reflecting the specific interests of a particular institute.

CONCLUSION

One article can hardly touch upon all the problems concerning analytical chemistry teaching, such as teaching at technical schools, availability of equipment for laboratory practice, modern teaching aids, active methods of teaching students, and chemical olympiads. The author has endeavoured only to cover generally the state of teaching and the tasks facing teachers.

REFERENCES

1. I. P. Alimarin, *Zh. Analit. Khim.*, 1983, **38**, 540.
2. Yu. A. Zolotov, *Vestn. Vyssh. Shk.*, 1985, No. 8, 33.
3. *Idem*, *Essays on Analytical Chemistry*, Khimiya, Moscow, 1977.
4. *Idem*, *Actual Problems of Analytical Chemistry*, Znanie, Moscow, 1980.
5. I. P. Alimarin, *Period. Polytechn., Chem. Eng., Budapest*, 1970, **14**, 163.
6. G. E. Baiulescu, C. Patroescu and R. A. Chalmers, *Education and Teaching in Analytical Chemistry*, Horwood, Chichester, 1982.
7. R. Kellner and H. Malissa, *Z. Anal. Chem.*, 1984, **319**, 1.
8. *Z. Anal. Chem.*, 1979, **297**, 241-340; 1981, **305**, 97-129.
9. A. K. Babko and I. V. Pyatnitsky, *Quantitative Analysis*, Mir, Moscow, 1969.
10. I. K. Tsitovich, *Textbook of Analytical Chemistry*, Vyssh. Shk., Moscow, 1977.
11. N. Ya. Loginov, A. G. Voskresenski and I. S. Solodkin, *Analytical Chemistry*, Prosvetshenie, Moscow, 1979.
12. A. P. Kreshkov, *Fundamentals of Analytical Chemistry*, Khimiya, Moscow, 1970.
13. I. V. Pyatnitsky, *Theory of Analytical Chemistry*, Vyssh. Shk., Kiev, 1978.
14. E. Yu. Yanson and Ya. K. Putnin, *Theory of Analytical Chemistry*, Vyssh. Shk., Moscow, 1980.
15. N. N. Ushakova, *Textbook of Analytical Chemistry*, MGU, Moscow, 1984.
16. V. P. Vasiljev (ed.), *Exercises and Problems in Analytical Chemistry*, Vyssh. Shk., Moscow, 1976.
17. V. F. Toropova (ed.), *Problems in Analytical Chemistry*, KGU, Kazan, 1978.
18. Ye. N. Dorokhova and G. V. Prokhorova, *Problems and Exercises in Analytical Chemistry*, MGU, Moscow, 1984.

19. V. M. Peshkova and M. I. Gromova, *The Methods of Absorption Spectroscopy in Analytical Chemistry*, Vyssh. Shk., Moscow, 1976.
20. M. I. Bulatov and I. P. Kalinkin, *Practical Guide in Photometric and Spectrophotometric Methods of Analysis*, Khimiya, Leningrad, 1972.
21. A. P. Golovina and L. V. Levshin, *Chemical Luminescence Analysis of Inorganic Substances*, Khimiya, Moscow, 1978.
22. B. V. Ivazov, *Introduction to Chromatography*, Vyssh. Shk., Moscow, 1983.
23. I. P. Alimarin (ed.), *Detection and Separation of Elements*, MGU, Moscow, 1984.
24. N. I. Tarasevich, K. A. Semenenko and A. D. Khlystova, *Methods of Spectral and Chemospectral Analysis*, MGU, Moscow, 1973.
25. Yu. A. Zolotov and N. M. Kuzmin, *The Concentration of the Microelements*, Khimiya, Moscow, 1982.
26. B. V. L'vov, *Atomic-Absorption Spectral Analysis*, Nauka, Moscow, 1966; Hilger, London, 1970.
27. A. K. Charykov, *The Processing of Chemical Analysis Data*, Khimiya, Leningrad, 1984.
28. I. P. Alimarin, V. I. Fadeeva and Ye. N. Dorokhova, *Lecture Experiments in Analytical Chemistry*, Mir, Moscow, 1976.
29. D. A. Skoog and D. M. West, *Fundamentals of Analytical Chemistry*, Mir, Moscow, 1979.
30. A. Hulanicki, *Acids and Bases in Analytical Chemistry*, Mir, Moscow, 1975.
31. H. A. Laitinen and W. E. Harris, *Chemical Analysis*, Khimiya, Moscow, 1979.
32. *Analytikum*, Mir, Moscow, 1975.
33. J. S. Fritz and G. H. Schenk, *Quantitative Analytical Chemistry*, Mir, Moscow, 1978.
34. D. G. Peters, J. M. Hayes and G. M. Hieftje, *Chemical Separation and Measurements*, Khimiya, Moscow, 1978.
35. P. Bonchev, *Introduction to Analytical Chemistry*, Khimiya, Leningrad, 1978.
36. L. Meites, *An Introduction to Chemical Equilibrium and Kinetics*, Mir, Moscow, 1984.

ARTIFICIAL INTELLIGENCE SYSTEMS FOR MOLECULAR SPECTRAL ANALYSIS

M. E. ELYASHBERG, V. V. SEROV and L. A. GRIBOV

Vernadsky Institute for Geochemistry and Analytical Chemistry, USSR Academy of Science,
19 ul. Kosygina, 117975, Moscow V-334, USSR

(Received 15 October 1985. Accepted 26 July 1986)

Summary—A brief survey is given of the most recent publications on development of artificial-intelligence systems for molecular spectral analysis. A new approach to solution of the problems of qualitative molecular spectral analysis is based on an applied logical calculus developed by the authors for fuzzy predicates. It is suggested that spectral-structural knowledge should be specified in the language of fuzzy predicates, and mechanical theorem-proving procedures used for solving qualitative problems of spectral analysis, the initial information being considered as a set of axioms. System-oriented matters are given consideration. The formalism suggested is a basis for the development of an artificial-intelligence dialogue system capable of solving various problems in molecular spectral analysis while maintaining a dialogue with a research worker using a professionally-restricted natural language.

The problem of identification of organic compounds from their spectra through the use of computers had become fully comprehended in the late 60s. At present, the problem is the focus of attention for research workers in organic and analytical chemistry, because the number of known chemical substances is approaching 10 million,¹ and what is more, some 100,000 new compounds are synthesized every year.

The necessity of developing computer-aided identification of organic substances from their spectra has led to a new branch of analytical chemistry, which can be called analytical mathematical spectrochemistry (AMS). AMS has emerged at the interface between chemistry, spectroscopy and discrete mathematics, these disciplines being amalgamated in the provision of algorithms realized in the form of programs for computers. There are three major aspects of AMS: (a) development of information-retrieval systems (IRS) for molecular spectral analysis; (b) utilization of pattern-recognition theory; (c) design of automated artificial-intelligence systems (AIS). In this review we shall deal with the last of these and shall confine ourselves to those publications which are mainly concerned with optical and resonance spectroscopy.

A specific feature of the artificial intelligence systems is that they are based on mathematical simulation of the chemist's lines of reasoning in the identification of an unknown substance with the aid of correlations between spectra and structure. The identification procedure has three stages: (1) structure-group analysis (SGA); (2) generation of structural formulae from the sets of molecular fragments sorted out in the course of the SGA; (3) checking the structural formulae and finding the most probable ones by comparing the predicted spectra with those obtained experimentally.

The first publications on the development of AIS appeared in 1968²⁻⁴ in which we were the first to elaborate SGA theory^{2,3} on the basis of symbolic logic. By now, advances in AIS as applied to molecular spectroscopy have been summarized in two monographs^{5,6} and in a number of surveys,⁷⁻¹⁰ and further set out in a great many papers. Here we offer a brief survey of the most recent publications, and a description of our new approach to solving the problems of qualitative spectral analysis within the framework of an artificial-intelligence system.

TYPES OF ARTIFICIAL INTELLIGENCE SYSTEMS

Several research teams have been working on intelligence systems oriented to molecular structure elucidation from spectra. The DENDRAL project group⁶ is developing the strategy of heuristic search based on the exhaustive generation of structural formulae satisfying various imposed constraints and the empirical formula of the substance. One of the most recent advances made by this team is the program GENOA,¹¹ the major distinction of which is that it is capable of handling fragments having overlapping atoms. Such a situation appears quite often when several independent spectral methods are used in detecting the fragments. Because the structures are always generated from fragments having no atoms in common, provisions are made in the GENOA program for the fact that for generating the structures, the fragments are constructed by a computer operating in an interactive mode. Another distinction of the system is that it can efficiently take into account alternative substructures, *i.e.*, different fragments implied by one and the same spectral feature. A substantial role in the GENOA program is played by the use of constraints introduced by the chemist, in the

form of a set of non-overlapping fragments. The primary constraints can be given in the form of the molecule skeleton and fragments constructed from different sources (spectra, chemical experiments). The program makes up all the paths by which every newly introduced constraint can be satisfied, making sure that the previously imposed constraints are also satisfied. Each path represents a separate "case"—generally an incomplete structure including such fragments and atoms which are not associated with one another. An avalanche growth in the number of "cases" is eliminated by the continuous control exercised by the chemist, who cuts off undesirable paths. The results of imposing constraints are checked visually with the aid of a display unit or graph plotter. The final result ensured by the program is a structural formulae satisfying all of the imposed constraints.

The structures singled out by the GENOA program can be further investigated for the purpose of finding possible stereoisomers, which is done with the aid of the program STEREO,¹² worked out by the same group. To solve the problem of recognizing molecular structures, a generator of stereoisomerism is employed as a source of additional constraints imposed on the structures. The particular type of these constraints can be established from stereochemical data obtained from NMR spectra or by chirality-optical methods. The notion of the configuration symmetry group^{13,14} has been taken as a basis for the algorithm generating all the stereoisomers and calculating their number. First, the program determines the symmetry group of a chemical group, which reflects the structure, and after that this group is converted into the configuration symmetry group, which in turn is used for generating all of the distinguishable stereoisomers, and finding a theoretical value (without generation) for the number of configurational stereoisomers. Stereochemical constraints are used both for averting the generation of forbidden stereoisomers and for weeding out the set of already generated structural isomers, the maximum effect being achieved by imposing those constraints which eliminate the strained structures.

The DENDRAL group is paying much attention to the problem of predicting the spectra of conceivable structures for the purpose of checking their validity. They have suggested methods and programs for interpretation and prediction of mass spectra,¹⁵ ¹³C NMR spectra¹⁶⁻¹⁹ and ¹H NMR spectra.²⁰ Prediction of the ¹³C NMR spectra is made from the database comprising structures of organic molecules and their interpreted spectra. In doing this, use is made of the fact that the chemical shift of the carbon atom carries information on the spatial environment of this atom and on the influence of substituents spaced 1-4 bonds apart. To forecast a spectrum, the fragments of the structure under investigation are searched in the database, and the accuracy of prediction is determined by the extent of similarity of the

carbon atom environment; the maximum accuracy is obtained when the coincidence extends to a depth of 4 bonds. The structures under investigation are ranked according to the degree of agreement between the predicted and experimental spectra. Prediction and interpretation of the PMR spectra²⁰ are based, to a large extent, on similar considerations. The DENDRAL programs were originally oriented towards structure analysis, but now, owing to the inclusion of data banks into the system, they are becoming a powerful tool in analytical chemistry.

A lot of publications are concerned with description of various stages in the development of the CHEMICS system.²¹⁻²⁵ The most recent version of the system²⁵ is capable of recognizing compounds containing C, H, N, O, S and halogen atoms, with the aid of NMR, infrared and mass spectra. The molecular formula of an unknown substance is presented by the researcher or it can be found automatically from ¹³C NMR and mass spectra. To define the structure, use is made of a library of fragments (components) and of their features in ¹³C NMR, PMR and infrared spectra. Class CHO is represented by 189 components, and a further 572 components have had to be included to handle samples which also contain N, S and halogens. The system establishes the sets of fragments consistent with the empirical formula and spectral data, followed by the generation of the structural candidate-formulae. In doing this, known or conceivable fragments and constraints on the size of the cycles can be deliberately introduced. To reduce the number of candidates use is made of prediction of the number of signals within the ¹³C NMR spectra (but not of the spectra *per se*) and calculation of the strain-energy index. Comparison of the calculated with the experimental values allows certain structures to be discarded from consideration. The authors furnish examples of recognizing molecules of class CHO comprising 10-13 skeletal atoms.

The CASE system²⁶⁻³¹ is oriented primarily to the recognition of the structure of natural compounds, the spectra being interpreted with the participation of the chemist, who detects the constitutional characteristics of the substance under investigation by using programs for the analysis of infrared spectra^{26,27} and ¹³C NMR spectra.^{28,29} Selection of the most probable isomers from those generated is done with the aid of a program designed to predict the number of signals within the ¹³C NMR spectra.²⁹ A special characteristic of the approach utilized in these publications is that the functional groups are detected from the infrared spectra according to the rules specified for each chemical group. A similar approach has been used in developing the PAIRS system designed for interpreting the infrared spectra of condensed^{32,33} and gaseous³⁴ phases. A language for description of the interpretation rules for infrared spectra in the PAIRS system has been developed and described.^{35,36}

The SEAC system³⁷ is capable of recognizing the structures of compounds containing C, H, N, O, Cl,

Br, I and obeying certain constraints. Use is made of a machine library comprising spectra-structure correlations for the infrared and PMR spectra taken separately, as well as fragments with combination features. Spectra of each kind are interpreted by special-purpose programs, the choice of which is determined by the elemental constitution of the substance. Generation of structures is based on a vector-division operation introduced by the authors. Some structures (having no more than 10 skeletal atoms) that have been thus recognized are given as examples.

The STRUCTURE system³⁸ is capable of identifying substances with C, H, N, O, S and halogen constituents, from the infrared PMR and ¹³C NMR spectra. Use is made of a library comprising 32 microfragments. The program establishes sets of microfragments which can constitute a molecule, building various versions of the structures from each of the sets. Finally, those structures are chosen which are not inconsistent with the experimental data, and the number of solutions is not high for a molecule containing 10-12 skeletal atoms.

Various programs have been adapted to detection of fragments from ¹³C NMR spectra³⁹⁻⁴¹ or from a combination of spectra. Thus the ASSIGNER system^{42,43} is intended for finding functional groups from the infrared and ¹³C NMR spectra. Each type of spectrum is provided with its own associated library of fragments and their spectral features. The fragments are encoded with the aid of a numerical identifier or descriptor reflecting their elemental constitution. The fragments selected on the basis of one type of spectrum (for example, ¹³C NMR) are subjected to validation against the infrared spectra. The fragments are also divided into classes according to the informational content of the spectral features. Despite the fact that the number of fragments distinguished by the program is usually 1.5-2.5 times that really comprised by a molecule, the real groupings can always be found among those provided by the program.

Our own artificial intelligence system STREC (STRUCTURE RECOgnition) has been described in detail.^{5,44,45} The empirical formula and infrared, ultraviolet, PMR and mass spectra of a substance, as well as a machine library of the spectra-structure correlations are used as starting information in the STREC system. Its own library of typical fragments (LTF) has been produced for each type of spectrum, the primary role being played by infrared spectroscopy. The infrared-library consists of an active file used in making a structure-group analysis (SGA), and a passive file used as a filter in validating the candidate structures. First the SGA is made by using the infrared spectrum. SGA logic equations are automatically derived and solved, followed by generation of the structural formulae from the selected sets of fragments. In so doing, account is taken of the non-equivalence of atoms having free valencies, and the possibility of repeated occurrence of a fragment

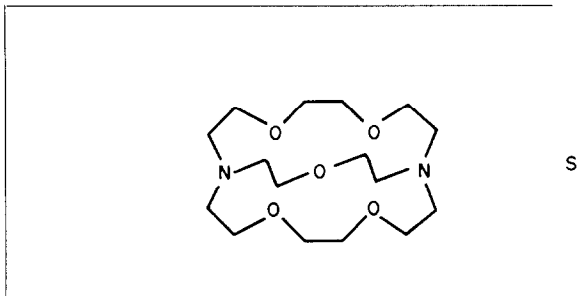
within the structure. After that, all the isomers are passed through a system of filters represented by the fragment libraries of the types of spectra used. Upon detection of a fragment within the structure, the characteristic features of the fragment are compared with the experimental spectra. Should the presence of all of the fragments found in the structure be substantiated by the spectra, then the structure is included in the file of answers. Selection of the most probable structures and elucidation of their spatial constitution is done on the basis of the conformational analysis and calculations of the infrared spectra.⁴⁵ The trial operation of the system has shown that it is quite capable of confidently coping with the identification of compounds having 10-15 skeletal atoms.

As a result of further research we have developed a dialogue system STREC-2^{46,47} capable of handling large structures including as many as 40 skeletal atoms, and identifying compounds from their infrared, PMR and ¹³C NMR spectra.

To improve the discrimination capability of the system, each of the fragments from the LTF is assigned, in addition to its valency and empirical formula, the ranges of values of the spectral feature in the infrared, PMR and ¹³C NMR spectra. Such an approach eliminates the necessity of having separate special-purpose libraries for the SGA for each type of spectrum. The features in infrared spectra are the frequency ranges and half-widths of bands, as well as the expected intensities on a five-value scale. Those of the NMR spectra are the ranges for the chemical shifts, spin-spin interaction constants and expected multiplicities. Each fragment is assigned, in addition to the spectral features, the descriptors—one for each atom having free valencies. A descriptor indicates the possibility for a given atom to add hetero-atoms, aromatic rings, multiple bonds, hydrogen atoms. If there is more than one free valency at a given atom, the descriptor will show whether or not a multiple bond can be formed. The possibility of occurrence of a fragment within a cycle is also marked. Descriptors enable quite accurate specification of the allowed position of a fragment within a molecule, a possibility which is used for eliminating structures failing to satisfy these requirements. The fragments included in the LTF can comprise as many as 15 skeletal atoms. At the first stage, an SGA is made in a dialogue mode, ensuring an intimate relationship between the operator and the program. Data-exchange between the operator and computer is done by use of a display unit or a typewriter. The program interrogates the researcher, providing him at the same time with explanations as to the form in which the answers are expected to be given. In the course of a dialogue the empirical formula of a substance and all its available spectra are introduced into the computer. The program makes up and delivers to a display unit the logic relationships (implications) which bring the frequencies and chemical shifts in the experimental spectra into correspondence with the fragments

included in the LTF, the occurrence of these fragments being not unlikely in the compound under investigation. Using *a priori* knowledge relating to a sample, an expert can introduce corrections into the computer's "reasoning": he can eliminate the library fragments from the implications or add them thereto, introduce any new ("chemical") fragments, alter the possible sets of fragments found by the program, form various sets by using his own judgement, and so on.

At the second stage, a set of fragments approved by the expert is used for generating the structural formulae of all the isomers having a given constitution, with additional constraints imposed on the structures, in a dialogue mode of operation. In so doing, it is possible to preset both indispensable and forbidden fragments (for both types of the fragments it is allowed to have atoms common to the fragments taken from the LTF and the new fragments derived in the course of the SGA), as well as the maximum multiplicity r_m of bonds formed when mathematically synthesizing the structures. This last facility allows



suppression of the mathematical synthesis of structures comprising $r > r_m$, which offers indubitable savings in machine time. If the minimal size of cycles is preselected, generation of the strained structures including small cycles can be averted, provided that the chemist possesses the pertinent information.

The fragments (new, indispensable and forbidden) are introduced into the computer by representing their constitutional formulae on the screen of a video display unit, in the form customary for the chemist. Generation of isomers takes place with due account taken of the descriptor requirements, thus avoiding the handling of a lot of unnecessary structures.

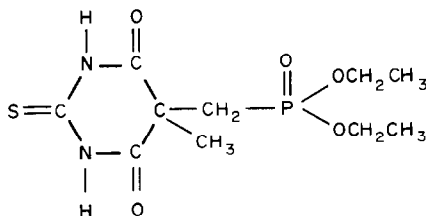
The third stage is used to disclose the constitution of the fragments included in the structural formulae as "macroatoms", and by screening of all the fragments, taken from the filter library, through each of the structures, the isomers can be checked for consistency with the experimental spectra. Here, an additional filtration of the structures is done with a specialized PMR-LTF including 270 fragments. The filter library can be further filled up with other special purpose LTF (infrared, ^{13}C NMR, ultraviolet, MS). Drawings of the structural formulae which completely satisfy the machine knowledge and the constraints introduced and utilized in making the identification, are printed out; it should be mentioned

here that the program can easily handle images of rather complex molecules, including bridged polycyclic molecules.

A preferred structure is selected on the basis of prediction of the number of signals and their multiplicities within the ^{13}C NMR spectrum, by a specialized program. Further discrimination between structures can be obtained by predicting the infrared spectra of the candidates.

It is worth noting that the STREC-2 system can be operated in the filtration mode for verifying the conformity between the filter libraries and various structural formulae suggested by the chemist himself.

The efficiency of the STREC-2 system has been substantiated by the solution of a great number of spectro-analytical problems, a substantial fraction of which is represented by the problems of identifying organophosphorus compounds on the basis of the specialized infrared-LTF for phosphorus-containing fragments. The following are examples of the structures recognized with aid of "prompting" on the part of the chemist:



FUNDAMENTALS OF THE THEORY OF SOLVING QUALITATIVE PROBLEMS IN MOLECULAR SPECTRAL ANALYSIS

As can be seen from the foregoing, artificial-intelligence systems deal with qualitative spectral problems of the following four types: (1) elucidation of molecular structures, (2) interpretation of spectra, (3) prediction of spectra from a given structure, (4) derivation of information from systematized knowledge. These problems *per se* are the most common types of problems in molecular spectroscopy and spectral analysis. That is why we have made an attempt⁴⁸ to build an applied theory for solving qualitative problems in molecular spectroscopy on the basis of the logical calculus of fuzzy predicates. Within the framework of this theory, spectrochemical knowledge is specified with the aid of predicates.

Let us now consider some of these, taking infrared spectroscopy as an example.

1. *Predicates characterizing the infrared spectrum.*
 $I_1(a, b, x_1, y_1, z_1)$ —the spectrum comprises the mode a vibration band, of chemical group b , with frequency x_1 , intensity y_1 , half-width z_1 .
 $I_2(a, b, x_2, n)$ —the spectrum comprises n bands of vibration mode a , of chemical group b , within the frequency range

specified by a fuzzy variable x_2 . The notion of fuzziness will be discussed below.

Both the intensity and half-width are estimated qualitatively by integers from 0 to 5, and the values of the frequency by positive integers. Variable a has the traditional notations (ν_s —stretching vibrations, δ_p —deformation planar vibrations, and so on).

2. Predicates characterizing molecular constitution.

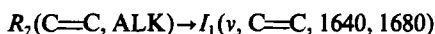
$R_1(r_1)$ —the molecule comprises fragment r_1 . $R_2(r_1, r_2, n_1)$ —the molecule comprises fragment r_1 and fragment r_2 separated from r_1 by n_1 bonds. $R_3(r_3, n_3)$ —the molecule comprises n_3 structural elements r_3 . $R_5(r_5, j)$ —there is a cycle of size j , which includes fragment r_5 .

3. Predicates characterizing additional conditions.

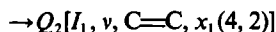
$T_1(l)$ —the pure substance is in aggregate state l (1—solid, 2—liquid, 3—gaseous). $T_2(m)$ —the pure substance is dissolved in a solvent of type m (1—basic, 2—acidic, 3—neutral).

4. *Second order predicates used for specifying data variations.* $Q_1[P, s_1(l_1), s_2(l_2) \dots]$ —the values of variables, s_1, s_2, \dots described by predicate P are replaced by new values l_1, l_2, l_3, \dots . $Q_2[P, s_1(d_1), s_2(d_2), d_3) \dots]$ —the values of variables s_1, s_2, \dots described by predicate P are being changed, and the nature of these changes is determined by the value of variables $d_1, d_2, d_3, \dots d_i \dots$ (1—increasing, 2—decreasing, 3—disappearing, 4—split into d_{i+1} components).

By using the system of predicates and ordinary logic operations we can already formalize a large portion of declarative knowledge. For example, the phrase “compounds with a single double bond and alkyl substituents (ALK) absorb within the range 1640–1680 cm^{-1} ” is associated with the expression



The expression



corresponds to the phrase “conjugation of two alkyl-substituted $\text{C}=\text{C}$ bonds results in the splitting of the stretching vibration band into two lines”.

Empirical knowledge in the field of infrared spectroscopy has been ordered in the literature according to the types of the structural fragments and modes of vibrations.⁴⁹ In the theory above for solving qualitative problems, a more detailed data structuring has been introduced. Proceeding from the nature of knowledge it can be divided into facts (expressions comprising constants) and regularities (expressions comprising variables, even only one). Now let us distinguish a class of general regularities which describe knowledge true for all the polyatomic molecules or at least for many of them. The main fragments having characteristic features ($\text{C}=\text{C}$, $\text{C}\equiv\text{C}$, Ar , $\text{C}=\text{O}$ and so on) will be taken as the structural units for the rest of the knowledge. Every major fragment is specified as a whole, and then the sur-

rounding atoms are successively added to it, thus forming fragments of the 1st, 2nd, 3rd and higher levels, and so on, up to the boundaries of our knowledge. The hierarchy of knowledge thus produced is represented by a graph in the form of a tree. Let us call it a network of objective knowledge. Specification of the network node includes data as follows.

1. Number and structure of a fragment, list of possible vibration modes and so on.
2. Regularities and facts common for a given fragment.
3. Regularities and facts for every vibration mode.

A special characteristic of empirical knowledge in spectroscopy, as presented in natural language, is its fuzziness, which occurs, for example, in such phrases as “the spectrum includes a rather intense band at around 965 cm^{-1} ”, or “alkyl-substituted $\text{C}=\text{C}$ double bonds absorb most often in the range 1640–1660 cm^{-1} ”.

To describe the uncertainty of knowledge we will employ a body of the fuzzy set theory.⁵⁰

Let M be a set, and x an element or member of set M , then fuzzy subset A of set M is defined as a set of ordered pairs $\{[x, \mu_A(x)]\}$, where $\mu_A(x)$ is a characteristic assignment or membership function, which varies within the range from 0 to 1, indicating the extent or degree of membership of member x in a subset A . For the first example above, $\mu(965) = 1$. There are boundaries, for example 955 and 975 cm^{-1} , beyond which $\mu(x) = 0$. Assume that $\mu(x)$ represents a set of functions that are linear over narrow intervals, and that to specify these functions it is sufficient to have a pair of numbers which would show the interval where $\mu(x) = 1$, and another pair of numbers to indicate the minimal departure from the left and right boundaries of that interval for $\mu(x)$ to be zero. The function can be symmetrical, or it can happen that the region where $0 < \mu(x) < 1$ is missing, and so forth. The numbers carrying no information can be discarded. For example, to write 1650, 1660 {10, 20} means that in the range 1650–1660 cm^{-1} function $\mu(x) = 1$, whilst over the regions 1650–1640 cm^{-1} and 1660–1680 cm^{-1} $\mu(x)$ is decreasing in a linear fashion and reaches zero at the extreme points (1640 and 1680 cm^{-1}); to write 965 {10} predetermines a function $\mu(x)$ which is equal to 1 at $x = 965 \text{ cm}^{-1}$, and decreases linearly to zero over the regions 965–955 and 965–975 cm^{-1} .

Each n -place predicate symbol is assigned with mapping M^n into a set of values of the characteristic membership function, which will be referred to here as a truth function μp , $0 \leq \mu p \leq 1$.

Logic formula G and predicate symbol P are assigned a set of exterior values of the truth function μe , $0 \leq \mu e \leq 1$. An exterior value of function μe reflects a quantification of knowledge (“often”, “sometimes”, “in some cases” and the like). To find the value of the truth function of an elementary

(comprising no logic operations) formula we multiply an exterior value of μ_e by the values of the truth functions of the fuzzy constants and variables of this formula.

Consider an elementary formula [0.8] I_1 (ν , C=C, 1640, 1660 {10}), which corresponds to the proposition "where group C=C is present in a molecule, band ν (C=C) is most often observed in the range 1640–1660 cm^{-1} ". In this case $\mu_e = 0.8$, and if an absorption frequency observed within the spectrum equals 1665 cm^{-1} , then $\mu(x) = 0.5$, whence the truth value for the elementary formula is $\mu_t = 0.5 \times 0.8 = 0.4$.

Now, with reference to two formulae G and F , define the fuzzy logic operations as follows:

$$G \wedge F = \text{MIN}(G, F)$$

$$G \vee F = \text{MAX}(G, F)$$

$$\bar{G} = 1 - G$$

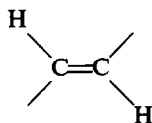
$$G \rightarrow F = \bar{G} \vee F$$

$$G \sim F = (\bar{G} \vee F) \wedge (G \vee \bar{F})$$

It can be shown that, with few exceptions, the formulae in classical predicate logic and in applied theory have the same set of equivalent transformations.

Here is an example of specifying knowledge in the field of infrared spectroscopy.

The basic fragment C=C is associated with the zero hierarchical level. Consider group



(TRS) related to the first level.

1. Possible vibration modes: stretching ν (C=C); stretching ν (=CH), non-planar deformation δ (=CH), planar deformation δp (=CH).

2. Group TRS-ALK usually has the stretching vibration band ν (C=C) at 1665–1680 cm^{-1} , with low intensity: [0.8] R_2 (TRS, ALK) $\rightarrow I_1$ (ν , C=C, 1665, 1680, 1, 2).

3. TRS shows a single band ν (=CH) in the region 3000–3040 cm^{-1} : R_2 (TRS, ALK) $\rightarrow I_1$ (ν , =CH, 3000, 3040).

4. TRS gives absorption δ (=CH) in the range 965–990 cm^{-1} , with intensity from medium to high: R_2 (TRS, ALK) $\rightarrow I_1$ (δ , =CH, 965, 990, 3, 5).

5. Addition of groups or atoms C=N, OH, O-ALK, Cl, Br, I to an α -atom at TRS, has no influence upon the position of δ (=CH): R_2 (TRS, CN \vee OH \vee O-LAK \vee Cl \vee Br \vee I, 2) $\rightarrow I_1$ (δ , =CH, 965, 990).

6. When TRS is conjugated with the group C=O, we can observe a tiny shift of δ (=CH) towards high frequencies: R_2 (TRS, C=O) $\rightarrow I_1$ (δ , =CH, 970, 1000, 3, 5).

7. The group TRS generally gives rise to a δp (=CH) planar vibration band of medium or high intensity in the region 1290–1310 cm^{-1} : [0.9] R_2 (TRS, ALK) $\rightarrow I_1$ (δp , =CH, 1290, 1310, 3, 5).

Let us consider declarative knowledge as a system of axioms of an applied theory, and qualitative problems as theorems. Now let us take it that the task of theorem proving is to elucidate the question of a certain formula G logically following from a given set of formulae $\{F_1, F_2, \dots, F_n\}$; in other words to establish the validity of a formula $(F_1 \wedge F_2 \wedge \dots \wedge F_n) \rightarrow G$.

It has been proved by Church that there can be found no general decision procedure to check the validity of formulae, even of the first-order predicate logic.⁵¹ However, it follows from the Herbrand theorem⁵¹ that if a formula is indeed valid, there can be found a proof procedure for verifying its validity. Practically, it is much more convenient to establish non-validity than validity. To establish inconsistency of a formula $F_1 \wedge F_2 \wedge \dots \wedge F_n \wedge \bar{G}$ in an applied logic calculus, it is necessary to prove that no such interpretation exists for which the truth values of formulae $F_1, F_2, \dots, F_n, \bar{G}$ are simultaneously non-zero. Several methods for theorem proving are now in existence, the most common of which are based on the Robinson resolution principle.⁵¹

Within the frame of the first-order predicate calculus, the notion of substitution is specified as a finite set γ of type $\gamma = \{t_1/x_1, \dots, t_n/x_n\}$, where x_i is a variable and t_i a term, *i.e.*, a variable or a constant. A set of formulae $\{G_\gamma\}$ is called a unifiable set if there exists a substitution γ such that $G_{1\gamma} = G_{2\gamma} = \dots = G_{n\gamma}$ (the values of x_i are replaced by t_i).

In applied logic calculus x_i and t_i are terms such that if x_i is a constant, then t_i is also a constant. In the general case, x_i and t_i are sets of fuzzy subsets, with the assignment functions $\{\mu_i(t_i)\}$ and $\{\mu_{x_i}(x_i)\}$. A substitution is then referred to as a finite set of pairs of the type $\alpha = \{(t_1/x_1), [\mu_{x_1}(t_1) \cdot \mu_{t_1}(t_1) / \mu_{x_1}(x_1)], \dots, (t_n/x_n), [\mu_{x_n}(t_n) \cdot \mu_{t_n}(t_n) / \mu_{x_n}(x_n)]\}$. A set of formulae G_α is termed a unifiable set if there exists a substitution α such that $g_1 \cdot G_{1\alpha} = g_2 \cdot G_{2\alpha} = \dots = g_n \cdot G_{n\alpha}$, where g_i represents non-zero coefficients which equalize the truth values of the formula. A substitution is called degenerate if only a single product $\mu_{x_i}(t_i) \cdot \mu_{t_i}(t_i)$ is zero.

For example, if we substitute frequency 1635{5} in the formula [0.8] I_1 (ν , C=C, 1640{10}), then $\mu_x(t) \cdot \mu_t(t) = 0.5$ (1635{5}), and the result will be [0.4] I_1 (ν , C=C, 1635{5}).

Suppose that $\{L_i\}$ and $\{M_i\}$ are two clauses having no common variables, $\{l_i\}$ and $\{m_i\}$ are subsets such that $\{l_i\} \subseteq \{L_i\}$, $\{m_i\} \subseteq \{M_i\}$ and for $\{l_i\}$ and $\{m_i\}$ there exists a substitution α such that $\{m_i\}_\alpha$ and $\{l_i\}_\alpha$ are complementary. Given that, a new clause, referred to as a resolvent, can be inferred from the starting clauses: $[\{L_i\} - \{l_i\}]_\alpha \cup [\{M_i\} - \{m_i\}]_\alpha$.

For example, if

$$\{L_i\} = I_1(\delta, =\text{CH}, x_1) \vee I_2(\delta, =\text{CH}, x_1, x_2)$$

$$\{M_i\} = I_1(\delta, =\text{CH}, 980) \vee R_1(\text{C}=\text{C});$$

$$\{l_i\} = I_1(\delta, =\text{CH}, x_1),$$

$$\{m_i\} = I_1(\sigma, =\text{CH}, 980); \alpha = 980/x_1$$

we obtain a resolvent $I_2(\delta, =\text{CH}, 980, x_2) \vee R_1(\text{C}=\text{C})$.

A resolution is an inference rule which generates resolvents from a set of clauses S . Let us designate as $D(S)$ an amalgamation of S with a set of all the resolvents which can be produced from S . Then $D_0(S) = S$, $D_{n+1}(S) = D[D_n(S)]$.

If S is an arbitrary finite set of clauses, then S is not satisfiable if, and only if, an empty clause occurs in $D_n(S)$ for a certain $n \geq 0$.

To illustrate the solving of the interpretation problem for bands 970, 1313, 1670 and 3030 cm^{-1} in an infrared spectrum of a compound of TRS-ALK type, convert into clauses expressions 2, 3, 6, 7 given in an example of knowledge specification:

1. $[0.8] \bar{R}_2(\text{TRS}, \text{ALK}) \vee I_1(v, \text{C}=\text{C}, 1665, 1680, 1, 2)$.
2. $\bar{R}_2(\text{TRS}, \text{ALK}) \vee I_1(v, =\text{CH}, 3000, 3040)$.
3. $\bar{R}_2(\text{TRS}, \text{C}=\text{O}) \vee I_1(\delta, =\text{CH}, 970, 1000, 3, 5)$.
4. $[0.9] \bar{R}_2(\text{TRS}, \text{ALK}) \vee I_1(\delta p, =\text{CH}, 1290, 1310, 3, 5)$.

So far as the spectral interpretation problems are concerned we know both the molecular structure and its spectrum. Assume that structural distinctions are specified by type R predicates, and a spectrum by type I_1 predicates. Unknown variables are a_i and b_i which characterize the vibration mode and chemical group. Now add a clause characterizing a molecular constitution:

5. $R_2(\text{TRS}, \text{ALK})$.

In this case, and according to what has been said above, it is necessary to prove that clauses which specify the spectrum cannot be satisfied:

6. $\bar{I}_1(a_1, b_1, 1670, 1) [I_1(a_1, b_1, 1670, 1)]$
7. $\bar{I}_1(a_2, b_2, 3030, 2) [I_1(a_2, b_2, 3030, 2)]$
8. $\bar{I}_1(a_3, b_3, 1312, 4) [I_1(a_3, b_3, 1312, 4)]$
9. $\bar{I}_1(a_4, b_4, 970, 3) [I_1(a_4, b_4, 970, 3)]$.

Given in square brackets are the "answering" clauses produced by negation of a starting clause. These take no part in the resolving process; however, the same substitutions are used for them as those for a set of clauses. Should an empty clause be obtained as a result, this would mean that the "answering" clause includes the sought-for variables. By successively resolving (1), (6), (5) we arrive at an empty clause; an answering clause includes the values of variables a_1, b_1 and a truth function μ_i :

10. $[0.8] I_1(v, \text{C}=\text{C}, 1670, 1)$

By resolving (2), (7), (5) we obtain:

11. $I_1(v, =\text{CH}, 3030, 2)$

By resolving (4), (8), (5) we find:

12. $[0.54] I_1(\delta p, =\text{CH}, 1312, 4)$.

The value of the truth function 0.54 is obtained by multiplying the exterior value [0.9] by [0.6], the latter figure being found as a result of the substitution $(1312\{5\}/1310\{5\})$.

Resolving of (3), (9), (5) can be effected only as a result of a degenerate substitution, since $\text{C}=\text{O}$ does not classify with ALK:

13. $[\mu_i] I_1(\delta, =\text{CH}, 960, 1100, 2, 5)$.

A singular substitution leads to unpredictable changes in the values of the truth functions.

Self-learning of declarative knowledge is effected by solving interpretation problems, whereby facts and regularities are verified, the values of the characteristic membership functions are varied, and new facts and regularities are revealed, resulting in the declarative knowledge network being extended in depth. Knowledge dynamics automatically reflects the specific features of classes of the problems being solved.

SYSTEM-ORIENTED PROBLEMS

When constructing a theory of solving qualitative problems in molecular spectroscopy, in addition to the content-oriented aspects of the problem (methods of solving problems and formalization of knowledge), consideration should also be given to system-oriented matters, which will be treated below.

Let us treat problem solving as a process of interaction (dialogue) between the operator and computer. We will consider both the operator and the computer as resolving systems (RS). Then the operator is solving problems on a conscious (reflexive) level, in other words, the operator represents a reflexive resolving system (RRS). A computer accommodating a collection of formalized knowledge is solving problems on a formal level, thus representing a formal resolving system (FRS).

So far as molecular spectroscopy is concerned, let us distinguish between the following three levels of knowledge, which differ in the manner of their gathering and use.

The first level is object-oriented knowledge K_0 . This includes spectral curves, external conditions, spectral instrument specifications, experimental technique and the like.

The second level is conscious (reflexive) knowledge K_r , possessed by the operator. This includes notions and ideas, theories, methods for computing and solving problems, known relationships and empirical regularities.

The third level is formalized knowledge K_f , used in solving problems with the aid of a computer. Within the frame of the applied theory under consideration,

K_r includes data on the relationship between the molecular structures and their spectral features, presented in the form of expressions in applied logic calculus, procedures (programs) of solving specific problems, and declarative and procedural knowledge ensuring communication between the RRSs and FRSS.

Let us distinguish between the following categories within knowledge: object, property, operation, relationship.

We identify object A_i as an entity which can be given a name, can be presented, perceived, utilized. An object can be found in various states, each of which is determined by a set of values of its properties $\{H_i\}$. Entities and properties of the object world are reflected in the names, notions, representations of reflexive and formal knowledge. On a reflexive level, entities and their properties are generalized and roughened. On a formal level, entities and properties are presented by sets of variables and constants.

We define a change as a process of transition of an entity from one state to another. The operation D_i will be identified as any action upon an entity which results in a change in this entity.

Both objects and operations are in different relationships with one another. These relationships can be formal or informal. Now, let us define a system as a set of concurrently considered sets of entities, properties, operations, relationships, *i.e.*, $S = \{\{A_i\}, \{H_i\}, \{D_i\}, \{R_i\}\}$, and identify a procedure P as a system wherein sets of operations and the relationships between them have been specified, as well as sets of relevant entities and their properties. An operation can then be considered as a subsystem of a procedure.

We define the domain of "molecular spectroscopy" as a threefold set of numbers $K = (K_o, K_r, K_f)$. The knowledge for each of the three knowledge levels can be defined as a fourfold set $K_i = (\{A_i\}, \{H_i\}, \{P_i\}, \{R_i\})$, where $\{A_i\}, \{H_i\}, \{P_i\}, \{R_i\}$ are the sets of entities, properties, procedures and relationships for the i th member of the set $\{o, r, f\}$.

A problem in the realm of molecular spectroscopy is identified as a triplet $T = (K^{\text{in}}, K^{\text{act}}, K^{\text{res}})$, where K^{in} and K^{res} are initial and resultant states of the domain, and K^{act} is an activated subset of knowledge, which includes not only the members of sets $\{A_i\}, \{H_i\}, \{P_i\}, \{R_i\}$, the values of which in the initial state are unknown, having been determined in the resultant state, but also all the members of the above-discussed sets necessary for solving the problem.

Interaction between the operator or expert (user) and the computer is effected in the form of exchange of messages, whereby each of the resolving systems undergoes changes directed towards the solving of the problem, *i.e.*, transformation of K^{in} into K^{res} .

As a means of communication take a communication language of a formal resolving system (CLF), and a limited subset of the expert's professional language, *i.e.*, a reflexive communication lan-

guage (RCL). From the communication languages let us separate the following three types of propositions: (a) narrative, which will be termed here informative propositions, (b) question propositions, (c) peremptory, referred to here as imperatives.

As a basis for constructing a CLF we take the language of an applied logic calculus (ALC) for fuzzy predicates, discussed above. ALC syntax will be used with the addition of the operators of a question mark "?", imperative "!", transition $\Rightarrow, \Rightarrow, \Rightarrow$.

Operator "?" defines which of the objects of the CLF is under question, operator "!" defines which actions must be accomplished and with which objects. The result of accomplishing the "?" operator is an answer, and a report is the result of using operator "!".

Questions can be direct or indirect. For example, the expression $(? 1650, 4, 2) (R_2 (C=C, ALK) \rightarrow I_1 (v, C=C, 1650, 4, 2))$ means a direct question: "whether or not a narrow strong band with the frequency 1650 cm^{-1} can be considered as a result of the presence of the group C=C in a molecule?". Expression $(?x) I_1 (\delta, =CH, x)$ means an indirect question of the second type: "what is the frequency of the deformation vibrations of the group =CH?". Expression $(?\forall y) I_1 (y, C=C, 1650, y, z)$ means an indirect question of the second type: "whether or not the stretching vibrations of the group C=C can have any intensity?".

In the examples above, the correct answers are presented by the informatives $[R_2 (C=C, ALK) \rightarrow I_1 (v, C=C, 1650, 4, 2)] \wedge R_4 (C=C, 2)$ —"yes, if C=C is not far from the α -atom"; $I_1 (\delta, =CH, 965) \wedge R_2 (=CH, ALK)$ —"deformation vibration frequency for the group =CH equals 965 cm^{-1} , if the immediate environment is of type ALK"; $I_1 (y, C=C, 1650, \forall y, z) \wedge R_4 (C=C, K)$ —"vibration of the group C=C can have any intensity within the IR spectrum depending upon how far the group C=C is from the centre of symmetry".

Now let us consider two types of imperatives—imperatives of finding and imperatives of object. The imperative of finding is equivalent, syntactically and semantically, with the indirect questions of the first type. An example of an imperative of object is the expression $!INTRPR (I_1(a_1, b_1, 690) \wedge I_1(a_2, b_2, 760) \wedge I_1(a_3, b_3, 830) \wedge I_1(a_4, b_4, 965) \wedge I_1(a_5, b_5, 1080) \wedge I_1(a_6, b_6, 1450) \wedge I_1(a_7, b_7, 1510) \wedge I_1(a_8, b_8, 1600) \wedge I_1(a_9, b_9, 1675) \wedge I_1(a_{10}, b_{10}, 3040) \wedge R_1(r_o))$ —"interpret an infrared spectrum including bands $690, 760, \dots, 3040 \text{ cm}^{-1}$, provided that the molecule has the structure r_o ". In a similar fashion we can introduce imperatives of prediction, generation of structural formulae, structure-group analysis, checking, comparison and so forth.

As already mentioned, it is the informatives that are the correct answers to a question or imperative, *i.e.*, narrative sentences in the communication language of a formal resolving system CLF. The informatives can be transferred from one resolving

system to another (external level), or used for bringing information to new questions and imperatives (inner level in the FRS). Transmission of any expressions can similarly be effected. Let U be an informative, question or imperative. Then the expressions $U \Rightarrow$ and $\Rightarrow U$ mean "transmission of U from RRS to FRS", "receiving of U from RRS in FRS", respectively, and $U \rightrightarrows$ and $\rightrightarrows U$ mean "transmission and receiving of U at the inner level of the FRS".

An expression will be identified as a specification of a process in a CLF if the expression is composed of a set of expressions $\{U_i\}$ separated by the transition operators (\Rightarrow , \rightrightarrows , \rightrightarrows or by enumeration symbols (:).

Specification of a process of solving a qualitative problem by using the CLF is identified as a problem solving frame. An FRS contains standard declarative frames for solving qualitative problems. When we have to solve a problem in a non-standard sequence, e.g., in the course of solving one problem we shift to the solving of another problem and so forth, we are thus making corrections in the declarative frame.

As an example, consider a declarative form for the generation of structural formulae:

$$\Rightarrow [R_{3_1}(r_{3_1}, r_{3_1}) \wedge \dots \wedge R_{3_m}(r_{3_m}, r_{3_m})] \wedge [R_{2_1}(r_{1_1}, r_{2_1}) \wedge \dots \wedge R_{2_k}(r_{1_k}, r_{2_k})] \wedge [R_{2_1}(r_{4_1}, r_{5_1}) \wedge \dots \wedge R_{2_e}(r_{4_e}, r_{5_e})] \rightrightarrows !\text{GENER} \rightrightarrows !\text{COMP} [R_1(r_0), [R_{2_1}(r_{1_1}, r_{2_1}) \wedge \dots \wedge R_{2_k}(r_{1_k}, r_{2_k})], [R_{2_1}(r_{4_1}, r_{5_1}) \wedge \dots \wedge R_{2_e}(r_{4_e}, r_{5_e})] \rightrightarrows R_1(r_0)$$

Data on the constituent atoms in the molecule, and necessary and forbidden fragments are introduced into the FRS, making generation of the structural formulae and comparison of these with the starting or initial conditions (imperatives !GENER and !COMP), the results being transferred to the FRS.

Of primary importance in the communication of the resolving systems is the sense of a phrase and the goals of those participating in the communication. We assume that understanding is achieved between an FRS and an RRS if every statement and message delivered by a resolving system which displays initiative, is brought into association, by the other resolving system, with one of the possible goals, and the correctness of such an association is substantiated. Solution to a qualitative problem can be considered as achievement of one of the goals or of a series of goals of the resolving systems.

We now briefly characterize the procedures taking place in a formal resolving system. In an applied calculus of fuzzy predicates, information is presented through a system of expressions, considered as axioms, whilst the problems represent theorems. As a method for solving theorems, we are using the resolution procedure modified for use with clauses formed by fuzzy predicates. A procedure realizing the adopted method of theorem proof is a major basic procedure in an FRS.

Each of the object imperatives is being realized as a separate specialized procedure (or a series of procedures). Achievement of the objects of the resolving systems, i.e., obtaining the results of solving quali-

tative problems, requires an FRS to ensure ordering, and to provide for the utilization of specialized procedures in conformity with the declarative frames (standard frames or those formed by the RRS). To that end, use is made of a procedure which will be referred to here as a planner (PLAN).

As a separate procedure (or group of procedures), self-learning algorithms for an FRS are also realized.

Still another group of procedures comprises those for the transformation linguistic information (in the explanatory presentation these are the operators \Rightarrow , \rightrightarrows), which ensure the translation of the phrases and messages in the resolving systems, and mutual understanding between them.

The principles and concepts above provide sufficient grounds for confidence that on the basis of our theory we will manage to develop a self-learning artificial intelligence system capable of solving the most varied spectro-analytical problems by a dialogue with a researcher using a professionally-restricted natural language.

REFERENCES

1. J. T. Clerc and G. Szekely, *Trends Anal. Chem.*, 1983, 2, 50.
2. M. E. Elyashberg and L. A. Gribov, *Zh. Prikl. Spektroskop.*, 1968, 8, 296.
3. M. E. Elyashberg, *ibid.*, 1968, 8, 648.
4. S. Sasaki, H. Abe, T. Ouki, M. Sakamoto and S. Ochiai, *Anal. Chem.*, 1968, 40, 2020.
5. M. E. Elyashberg, L. A. Gribov and V. V. Serov, *Molecular Spectral Analysis and the Computer*, Nauka, Moscow, 1980.
6. R. K. Lindsay, B. G. Buchanan, E. A. Feigenbaum and J. Lederberg, *Applications of Artificial Intelligence for Organic Chemistry—The DENDRAL Project*, McGraw-Hill, New York, 1980.
7. L. A. Gribov and M. E. Elyashberg, *CRC Crit. Rev. Anal. Chem.*, 1979, 8, 111.
8. Z. Hippe and R. Hippe, *Appl. Spectrosc. Rev.*, 1980, 16, 135.
9. N. A. Gray, *Prog. NMR Spectrosc.*, 1982, 15, 201.
10. Z. Hippe, *Anal. Chim. Acta*, 1983, 150, 11.
11. R. E. Carhart, D. H. Smith, N. A. B. Gray, J. G. Nourse and C. Djerassi, *J. Org. Chem.*, 1981, 46, 1708.
12. J. G. Nourse, D. H. Smith, R. E. Carhart and C. Djerassi, *J. Am. Chem. Soc.*, 1980, 102, 6289.
13. J. G. Nourse, *ibid.*, 1979, 101, 1210.
14. J. G. Nourse, R. E. Carhart, D. H. Smith and C. D. Djerassi, *ibid.*, 1979, 101, 1216.
15. N. A. B. Gray, R. E. Carhart, A. Lavanchy, D. H. Smith, T. Varkony, B. G. Buchanan, W. C. White and L. Creary, *Anal. Chem.*, 1980, 52, 1095.
16. D. H. Smith, N. A. B. Gray, J. G. Nourse and C. W. Crandell, *Anal. Chim. Acta*, 1981, 133, 471.
17. N. A. B. Gray, J. G. Nourse, C. W. Crandell, D. G. Smith and C. Djerassi, *Org. Magn. Reson.*, 1981, 15, 375.
18. N. A. Gray, C. W. Crandell, J. G. Nourse, D. H. Smith, M. L. Dagefordes and C. Djerassi, *J. Org. Chem.*, 1981, 46, 703.
19. C. W. Crandell, N. A. Gray and D. H. Smith, *J. Chem. Inf. Comput. Sci.*, 1982, 22, 48.

20. H. Egli, D. H. Smith and C. Djerassi, *Helv. Chim. Acta*, 1982, **65**, 1898.
21. S. Sasaki, H. Abe, Y. Hirota, Y. Ishida, Y. Kudo, S. Ochiai, K. Saito and T. Yamasaki, *Sci. Rep. Tohoku Univ. Ser. I*, 1978, **60**, 153.
22. S. Sasaki, I. Fujiwara, H. Abe and T. Yamasaki, *Anal. Chim. Acta*, 1980, **122**, 87.
23. T. Oshima, Y. Ishida, K. Saito and S. Sasaki, *ibid.*, 1980, **122**, 95.
24. I. Fujiwara, T. Okuyama, T. Yamasaki, H. Abe and S. Sasaki, *ibid.*, 1981, **133**, 527.
25. H. Abe, L. Fujiwara, T. Nishimura, T. Okuyama, T. Kida and S. Sasaki, *Comp. Enhanced Spectrosc.*, 1983, **1**, 55.
26. H. B. Woodruff and M. E. Munk, *J. Org. Chem.*, 1977, **42**, 1761.
27. *Idem*, *Anal. Chim. Acta*, 1977, **95**, No. 1/2, 13.
28. C. A. Shelley and M. E. Munk, *Anal. Chem.*, 1982, **54**, 516.
29. *Idem*, *ibid.*, 1978, **50**, 1522.
30. *Idem*, *Anal. Chim. Acta*, 1981, **133**, 507.
31. M. E. Munk, C. A. Shelley, H. B. Woodruff and M. O. Trulson, *Z. Anal. Chem.*, 1982, **373**, 473.
32. H. B. Woodruff and G. M. Smith, *Anal. Chem.*, 1980, **52**, 2321.
33. *Idem*, *Anal. Chim. Acta*, 1981, **133**, 543.
34. S. A. Tomellini, J. M. Stevenson and H. B. Woodruff, *Anal. Chem.*, 1984, **56**, 67.
35. G. M. Smith and H. B. Woodruff, *J. Chem. Inf. Comput. Sci.*, 1984, **24**, 33.
36. S. A. Tomellini, R. A. Hartwick, J. M. Stevenson and H. B. Woodruff, *Anal. Chim. Acta*, 1984, **162**, 227.
37. B. Debska, J. Duliban, B. Guzowska-Swider and Z. Hippe, *ibid.*, 1981, **133**, 303.
38. G. P. Gurinovich and V. P. Suboch, *Zh. Prikl. Spektrosk.*, 1983, **38**, 26.
39. J. E. Dubois, M. Carabedian and I. Dagane, *Anal. Chim. Acta*, 1984, **158**, 217.
40. L. G. Melkozerova, V. P. Suboch and G. P. Gurinovich, *Zh. Prikl. Spektrosk.*, 1980, **32**, 1060.
41. I. V. Gritsenko, T. F. Bogdanova, O. V. Toropov, K. S. Chmutina and V. N. Piottukh-Peletsy, 6th All-Union Conference, "Utilization of computers in molecular spectroscopy and chemical research", Novosibirsk, 1983, p. 16.
42. M. Farkas, J. Markos, P. Szepesváry, I. Bartha, G. Szalontai and Z. Simon, *Anal. Chim. Acta*, 1981, **133**, 19.
43. G. Szalontai, Z. Simon, Z. Csapó, M. Farkas and Gy. Pfeifer, *ibid.*, 1981, **133**, 31.
44. L. A. Gribov, M. E. Elyashberg and V. V. Serov, *ibid.*, 1977, **95**, 75.
45. L. A. Gribov, M. E. Elyashberg and M. M. Raikhshtat, *J. Mol. Struct.*, 1979, **53**, 81.
46. M. E. Elyashberg, L. A. Gribov, V. N. Koldashov and I. V. Pletnjov, *Dokl. Akad. Nauk SSSR*, 1983, **268**, 112.
47. L. A. Gribov, M. E. Elyashberg, V. N. Koldashov and I. V. Pletnjov, *Anal. Chim. Acta*, 1983, **148**, 159.
48. V. V. Serov, L. A. Gribov and M. E. Elyashberg, *J. Mol. Struct.*, 1985, **129**, 183.
49. L. J. Bellamy, *The Infra-red Spectra of Complex Molecules*, (in Russian), Izdat. inostr. lit., Moscow, 1963.
50. A. Kofman, *Vvedenie v teoriu nechetkikh mnozhestv (Introduction to Fuzzy Set Theory)*, Radio i svyaz, Moscow, 1982.
51. Ch.-L. Chang and R. Lee, *Symbolic Logic and Mechanical Theorem Proving*, (in Russian), Nauka, Moscow, 1983.

RECENT ADVANCES IN THE ANALYTICAL CHEMISTRY OF THE TRANSPLUTONIUM ELEMENTS

B. F. MYASOEDOV

V.I. Vernadsky Institute of Geochemistry and Analytical Chemistry, the USSR Academy of Sciences,
Moscow, USSR

(Received 15 October 1985. Accepted 10 August 1986)

Summary—A survey is given of current developments in the determination of the transplutonium elements, and of the properties useful in their analytical chemistry.

The recent development of the analytical chemistry of the transplutonium elements (TPE) is mainly connected with the rapid growth of nuclear energetics and the increasing use of TPE. Two principal directions of progress can be noted. In the one, methods of analysis with record low determination limits have been established to solve problems in environmental control and the determination of TPE in various natural samples; these are mainly radiometric methods used in conjunction with preliminary chemical isolation and concentration. The other trend is the working out of simple and reliable, precise and selective techniques for determination of the elemental and nuclide composition of irradiated targets, and technological solutions and products, on the basis of various analytical methods.

Some problems of the analytical chemistry of TPE have been systematized in monographs^{1,2} and surveys.^{3,4} This paper is a review of recently developed new methods of isolation and determination of TPE, with special attention given to the methods using various oxidation states of TPE.

SEPARATION METHODS

Modern analytical methods, such as radiometric, neutron-activation, spectral, electrochemical and others, particularly when used in combination with computer data-processing, make it possible to directly determine individual isotopes of TPE in various materials. Preliminary isolation, preconcentration and separation from other elements is required to solve numerous practical problems in the determination of TPE. Extraction and chromatography, extraction-chromatography, precipitation and co-precipitation, paper chromatography, sublimation and electrophoresis are used for these purposes. The best separation is obtained by using the methods based on various oxidation states of TPE.

Transplutonium elements are characterized by a much larger number of oxidation states than the analogous *4f* elements—the lanthanides (Table 1). In

aqueous solutions most TPE are in the trivalent state in the absence of oxidants or reductants. However, Am, Cm, Bk and Cf may exist in higher oxidation states, and Md can be rather easily reduced to Md²⁺. The most stable state for No in aqueous solutions is No²⁺. Recently the existence of Am(VII),⁵ Cm(VI),⁶ Cf(V),⁷ Cf(IV),⁸ and Md(I)⁹ under different conditions has been established.

The practical use of TPE in unusual oxidation states for their isolation and determination depends mainly on the stability of these oxidation states in solution. The thermodynamic stability of M^{Z+} ions in aqueous solution is primarily defined by the direction and completeness of the redox reactions of these ions and by the solution components: water molecules, H⁺ and OH⁻ ions. We have estimated the thermodynamic stability of TPE ions of types M²⁺, M³⁺, M⁴⁺, MO₂²⁺ in aqueous solutions (Table 2). An ion is deemed to be stable if at equilibrium it is the predominant form of the element (*i.e.*, at least 90% of the element present is in that form). Under this condition M²⁺ ions will be stable if the oxidation potential of the M^{Z+}/M^{(Z-1)+} couple is less than 1.10 V in aqueous solutions (hence no reduction by water) and the M^{(Z-1)+} ions will be stable if the potential is more than 0.16 V *i.e.*, no oxidation by water). Ions for which the oxidation potential of a higher oxidation-state couple is higher than that for a lower oxidation-state couple are stable to disproportionation. Table 2 shows that MO₂⁺, M³⁺ (except No³⁺) and MO₂²⁺ ions are stable in dilute acid solutions. The stability of M⁴⁺ and MO₂²⁺ increases appreciably in solutions containing strongly complexing anions, whereas marked complexation and increased acidity will decrease the stability of MO₂⁺ ions (which disproportionate noticeably) and M²⁺ ions. In order to increase the stability of the M²⁺ ions it is necessary to use some specific complexing agents which give more stable complexes with M²⁺ than with M³⁺ ions. A study of these regularities allows us to choose the "necessary" oxidation states of TPE for their separation and determination, and find the correct conditions for their use.

Table 1. Oxidation states and standard redox potentials of TPE

Oxidation states	Am	Cm	Bk	Cf	Es	Fm	Md	No	Lr
+7	±								
+6	+								
	+1.7								
+5	+								
	+1.1								
+4	+	±	+	±	±				
	+2.45	+3.1	+1.67	+3.1	+4.5				
+3	⊕	⊕	⊕	⊕	⊕	⊕	⊕	+	⊕
	-2.6	-3.8	-2.8	-1.7	-1.2	-0.65	-0.15	+1.45	
+2	±	±	±	±	±	±	+	⊕	
+1							±		

⊕ The most stable oxidation state in aqueous solutions.

+ Relatively stable oxidation state.

± Unstable oxidation state.

Redox potentials are in volts (*vs.* normal hydrogen electrode) and refer to vertically neighbouring couples of ions.

Table 2. Types of instability of the TPE ions in acidic aqueous solution (at 298 K)

Ion	Am	Cm	Bk	Cf	Es	Fm	Md	No
M ²⁺	ox; d	ox; d	ox; d	ox	ox	ox	ox	
M ³⁺								red
M ⁴⁺	red; d	red; d	red; d	red; d	red	red	red	red
MO ₂ ⁺		?	?		?	?	?	?
MO ₂ ²⁺	red	red	?	?	?	?	?	?

ox—oxidation by water;

red—reduction by water;

d—disproportionation (in the case of M²⁺-ions, with formation of M³⁺ and M);

?—estimation of stability is impossible because of deficiency of data.

A number of methods for practical production and stabilization of such states as Am(IV), Am(V), Am(VI), Bk(IV), Fm(II) and Md(I) have been developed as a result of methodical studies of the properties of TPE in unusual oxidation states in solution, and enlarge their field of application in analytical practice and technology.

Using Am(V) is the most effective way to separate americium from other TPE. Am(V) is usually produced in acid solutions in two stages: Am(III) is first oxidized to Am(VI), which is then reduced to Am(V). Persulphate ions and heating are most often used for the oxidation, but lately more convenient oxidation methods have been proposed: use of a mixture of persulphate and silver ions at room temperature, and electrochemical methods. In the latter Am(III) is oxidized at a platinum anode at a potential of 2 V, in presence of phosphate ions in slightly acid perchlorate medium. The Am(VI) is then easily reduced to Am(V) by decreasing the potential to 1.27 V.¹⁰ In practice there is no necessity to specially reduce the Am(VI), since an extractant or a sorbent can later function as a reducing agent.

The conditions for quantitative extraction of Am(V) with 1-phenyl-3-methyl-4-benzoylpyrazolone-5 (PMBP),¹¹ di(2-ethylhexyl)phosphoric acid (HDEHP)¹² and ammonium pyrrolidinedithiocarbamate (PDTC)¹³ have been found. Table 3 shows

that Am(V) is extracted well by different extractants at pH 5 and Fig. 1 shows that extraction of tervalent actinide ions may be suppressed by complexing agents such as acetate and potassium phosphotungstate. Am(V) (both micro and macro amounts) can be extracted by HDEHP from acetate buffer at pH 4–5, with a distribution coefficient as high as 30. The separation factor of Am from Cm by extraction of Am(V) with PMBP or HDEHP is (3–6) × 10³.^{12,14} Quinquevalent americium can be separated from other actinides and lanthanides by extraction with mixtures of picrolonic acid (PA) and sulphoxides in methyl isobutyl ketone from nitric acid since Am(V) is extracted significantly under these conditions.¹⁵

Sexivalent americium at concentrations ≥ 2 mg/ml is extracted by solutions of HDEHP,^{16–19} TOPO,¹⁹ di(2,6-dimethyl-4-heptyl) phosphoric acid²⁰ and by mixtures of HDEHP and TBP²¹ or TOPO¹⁸ in cyclohexane. Extraction with mixtures of PMBP with TOPO²² and of TTA with TOPO²³ in cyclohexane will separate Am and Cm. The americium is first oxidized to the sexivalent state, and during the extraction step is reduced to the unextractable quinquevalent state; curium and the other tervalent ions with high distribution coefficients are transferred into the organic phase (Fig. 2). The method provides quantitative separation of americium and a high degree of its

Table 3. Conditions for Am(V) separation from transplutonium elements

Aqueous phase composition	Organic phase composition	Distribution ratio		Separation factor, Am(V)/Me(III)	Reference
		Am(V)	Me(III)		
0.01M NH ₄ NO ₃ , pH 5	0.06M NH ₄ PDTC in isopentanol-ethanol mixture	30	0.02	1.5 × 10 ³	13
0.1M NH ₄ NO ₃ , pH 5 (acetate buffer + 0.001M PW*)	0.05M PMBP in isopentanol	12.7	0.002	6.4 × 10 ³	12
0.1M NH ₄ NO ₃ , pH 5 (acetate buffer + 0.001M PW)	0.5M HDEHP in octane	30	0.01	3.0 × 10 ³	14
0.1M HClO ₄ + 0.01M H ₃ PO ₄	0.05M PMBP + 0.025M TOPO in cyclohexane	0.02	900	4.5 × 10 ⁴ †	22
0.1 M HNO ₃	0.16M PA in methyl isobutyl ketone	0.26	194	7.3 × 10 ² †	15

*PW = potassium phosphotungstate.

†Me(III)/Am(V).

purification from curium (separation factor > 10³) and fission products.²² If radiometric determination is used, electrochemical oxidation gives better precision than persulphate oxidation does.

Recently the conditions for extraction of quadrivalent americium have been established for the first time.²⁴ Am(IV) is extracted quantitatively by 3% dioctylamine in dichloroethane from 0.5–1.0N sulphuric acid (Fig. 3). The presence of Am(IV) in the organic phase was proved spectrophotometrically (Fig. 4).

For the selective isolation of berkelium, a number of methods for extraction of Bk(IV) have been worked out. The most effective oxidant for berkelium is a mixture of ammonium persulphate and silver

nitrate, which oxidizes Bk(III) to Bk(IV) at room temperature in nitric or sulphuric acid media of various concentrations³¹ (Table 4). Electrochemical oxidation or bromate or dichromate can also be used. The conditions for extraction of Bk(IV) with HDEHP^{25,26} and its stripping from the organic phase have been studied in detail.²⁷ TOPO and TBPO solutions extract Bk(IV) quantitatively from 1–12M nitric acid²⁸ and TBP solutions extract it from 8–12M nitric acid.²⁹ The extraction of Bk(IV) by TOPO from sulphuric acid media is less effective and TBP practically does not extract it at all. The use of the high molecular-weight amines to extract berkelium is most promising.^{30,32} Bk(IV) is well extracted by 0.4M tri-

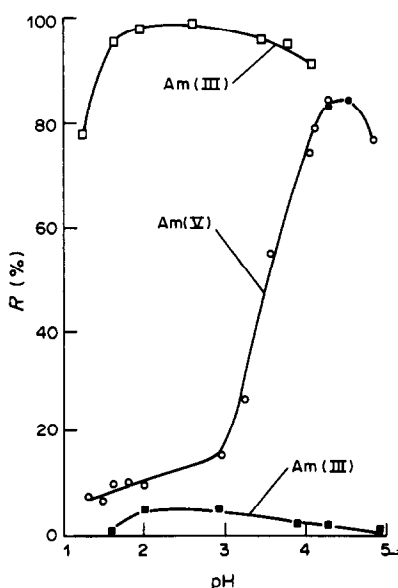


Fig. 1. Dependence of the extraction of Am(III) (Curves 1,3) and Am(V) (Curve 2) by 0.5M HDEHP in octane from acetic acid solutions (□ and ○) and in the presence of 10⁻³M potassium phosphotungstate (■ and ●) on the pH.¹²

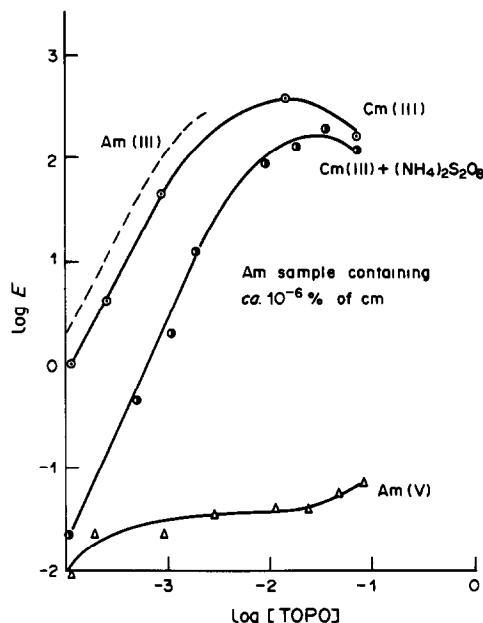


Fig. 2. Extraction of Am(V) and Cm(III) by a mixture of 0.05M PMBP and TOPO in cyclohexane.²² 1—Cm(III) from 0.1M HNO₃; 2—Cm(III) from 0.1M HNO₃ containing 5 mg/ml (NH₄)₂S₂O₈; 3—Am, after oxidation, from 0.1M HNO₃ containing 50 mg/ml (NH₄)₂S₂O₈.

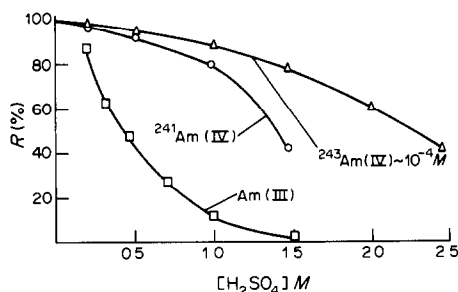


Fig. 3. Extraction of americium by dioctylamine from H_2SO_4 solutions containing $10^{-3}M$ $K_{10}P_2W_{17}O_{61}$.
1— $10^{-4}M$ Am(IV); 2— $^{241}Am(IV)$; 3— $10^{-4}M$ Am(III).

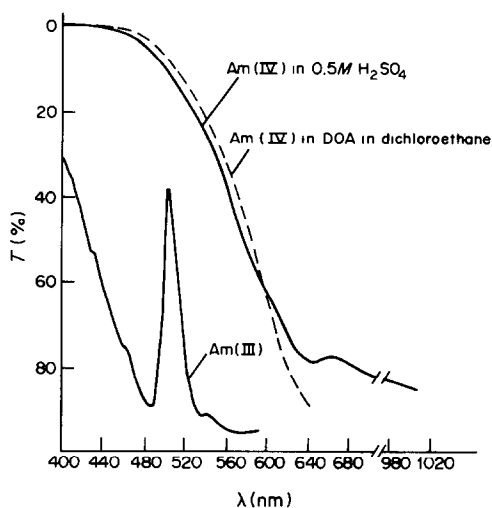


Fig. 4. Solution absorption spectra of $10^{-3}M$ Am(III) and Am(IV).²⁴ 1—Am(III); 2—Am(IV) in $0.5M$ H_2SO_4 containing $10^{-2}M$ $K_{10}P_2W_{17}O_{61}$; 3—Am(IV) in the organic extract (DOA in dichloroethane).

octylamine solution in carbon tetrachloride from 6–10M nitric acid (after oxidation by potassium dichromate). Use of the silver nitrate and persulphate mixture as oxidant before extraction with TOA makes it possible to separate berkelium from cerium, since in these conditions berkelium is reduced to the trivalent state and remains in the aqueous phase.³⁰ By extraction of berkelium with 30% Aliquat solution

in carbon tetrachloride from 10–12M nitric acid after oxidation with dichromate, a separation from the other TPE and the lanthanides is achieved.³² In the presence of heteropoly acid anions Bk(IV) is quantitatively extracted from nitric acid (Fig. 5) and sulphuric acid (Fig. 6) by primary, secondary or tertiary amines and quaternary ammonium bases. Heteropoly anions not only stabilize the berkelium(IV) but also form part of the extracted species.³³

One of the more efficient methods of TPE separation is extraction chromatography. HDEHP is most often used as the extractant on various supports. New methods for separation of americium and curium^{16,34} and selective isolation of Bk(IV)^{25,35} have been worked out in this way. The separation factor of Am(VI) from Cm is 200 and that of Cm from Am is 100. If Am(V) is used the purification factor from Cm is 5×10^3 but the purification factor for Cm from Am is worse (~ 60).¹⁶ A mixture of TTA (thenoyltrifluoroacetone) and TBP has been used as a stationary phase for the rapid separation of a complex mixture including Am, Cm, Cf, U, Th and other elements.³⁶

The use of so-called solid sorbents (TVEX) in

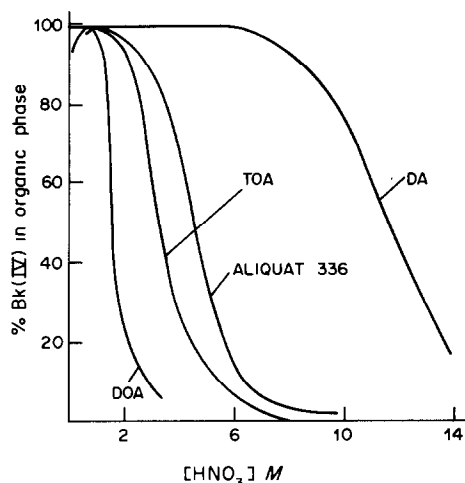


Fig. 5. Dependence of the extraction of berkelium(IV) by amines on the concentration of nitric acid containing $4 \times 10^{-5}M$ $K_{10}P_2W_{17}O_{61}$.³³ 1—3% decylamine in chloroform; 2—3% dioctylamine in dichloroethane; 3—1% tri-octylamine in CCl_4 ; 4—5% Aliquat-336-S in CCl_4 .

Table 4. Methods of complete oxidation of Bk(III) to Bk(IV)

Method of oxidation	Medium	Conditions*
Electrochemical	H_2SO_4 1–10M	+1.7 V
	H_3PO_4 4–9M	+1.5 V
	HCO_3 9M	+1.8 V
Ag^+ ($10^{-2}M$) + $S_2O_8^{2-}$ (0.1M)	HNO_3 0.5–10M	$\tau = 1$ min
	H_2SO_4 0.1–1M	
$KBrO_3$ (0.3M)	HNO_3 0.5–10M	$\tau = 1$ min
	H_2SO_4 0.5–2M	$\tau = 15$ min
$K_2Cr_2O_7$ (0.2M)	HCl 0.5–2M	$\tau = 15$ min
	HNO_3 1–10M	$\tau = 15$ min, $90^\circ C$

* τ = reaction time.

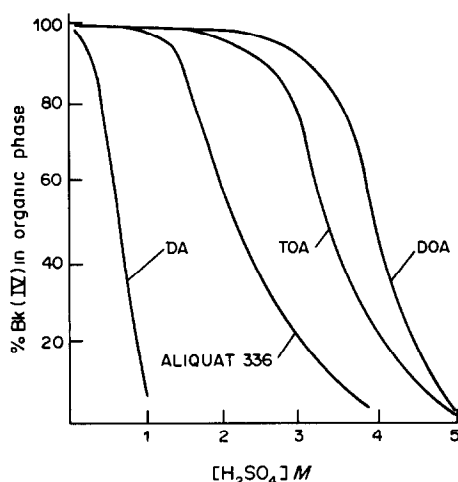


Fig. 6. Dependence of the extraction of berkelium(IV) by amines on the concentration of sulphuric acid containing $4 \times 10^{-3} M$ $K_{10}P_3W_{17}O_{61}$.³³ 1—3% decylamine in chloroform; 2—3% dioctylamine in dichloroethane; 3—1% tri-octylamine in CCl_4 ; 4—5% Aliquat-336-S in CCl_4 .

extraction chromatography opens up new possibilities. Such sorbents have good reproducibility of properties and can be used repeatedly^{37,38} because of the firm fixation of the extractants which are introduced into the sorbent during its synthesis. The application of such sorbents for the separation of TPE in unusual oxidation states has not been investigated up to now.

The behaviour of TPE in the higher oxidation states during their sorption on organic mixtures and inorganic sorbents has been insufficiently studied. The separation of Am(V) and Cm(III) on a Dowex-A1 \times 8 resin has been studied.³⁹ It was shown that the separation coefficient of Am and Cm increases strongly with increasing pH (from pH 2.5 to 3.2),

decreasing temperature and increasing quantity of resin. Anion-exchangers give selective isolation and purification of berkelium(IV) (Fig. 7).⁴⁰ The separation of TPE in the tervalent state on ion-exchange resins with aqueous organic solutions has given the most interesting results.^{41,42} In aqueous alcohol solutions and the presence of α -hydroxybutyric acid the separation factor of americium and curium on Dowex-1 \times 8 resin is ~ 6 .⁴¹

Zirconium phosphate is the most widely used of the inorganic sorbents which separate TPE. It has been used to separate Am(IV),⁴⁴ Am(V)^{45,46} and Am(VI)⁴⁷ from Cm, and for selective isolation of Bk(IV) from a mixture of actinide elements and fission products⁴⁸ (Fig. 8).

To separate TPE in different oxidation states the methods of precipitation and co-precipitation are also useful. The co-precipitation of Am(III, V, VI) with lanthanum, thorium and cerium fluorides or bismuth and zirconium phosphates has been investigated.⁴⁹ All the precipitates studied, except zirconium phosphate, fully carry down Am(III), and Am(VI) remains in the solution. Am(V) is partially carried down by lanthanum and thorium fluorides. Am(V) can be separated from Am(III) and Am(IV) in acetate solutions by co-precipitation with a pyrrolidinedithiocarbamate.¹³

For the separation of fermium from Cf and lanthanides an efficient method has been suggested which is based on the co-crystallization of Fm, reduced with Yb(II) in the presence of sodium chloride from aqueous ethanol solution. When practically quantitative extraction of Fm is attained the degree of purification from most accompanying elements is 10^3 – 10^4 .⁵⁰ In the presence of bivalent europium, Md(II) is reduced to Md(I) which can be co-crystallized with potassium or sodium chlorides from ethanol; the purification factor from the other actinides and lanthanides reaches $\sim 5 \times 10^2$.⁵¹

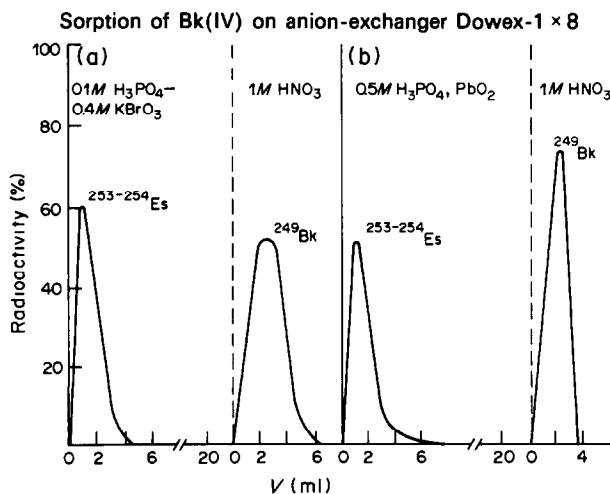


Fig. 7. Separation of ^{249}Bk from $^{253,254}\text{Es}$ by H_3PO_4 solutions on an anion-exchanger in the presence of an oxidant:⁴⁰ (a) $0.1 M \text{H}_3\text{PO}_4 + 0.4 M \text{KBrO}_3$; (b) $0.5 M \text{H}_3\text{PO}_4$, Dowex-1 \times 8 + PbO_2 (10:1), column 0.3×3 cm.

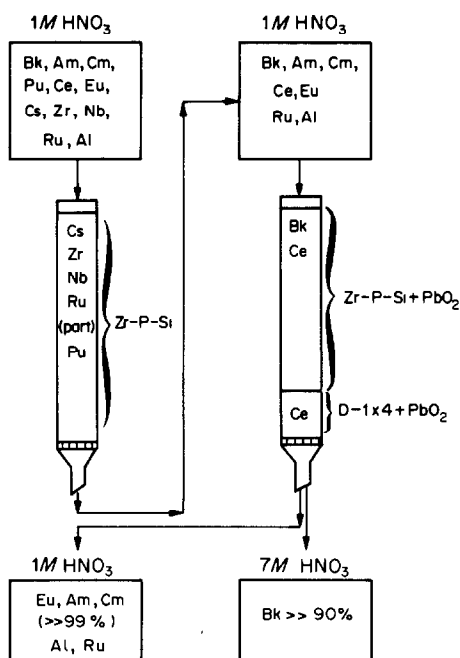


Fig. 8. Scheme of Bk(IV) isolation with zirconium phosphate.⁴⁶

METHODS OF TPE DETERMINATION

As mentioned in the introduction, there have been two trends in development of methods for TPE determination: methods of determination of relatively large amounts of TPE (\sim several mg) with high precision (0.05–0.1%), and methods with record low detection limits (10^{-8} – 10^{-9} g) but much poorer precision (several per cent).

Gravimetric, coulometric and titrimetric methods belong to the first group. They are used primarily for the accurate determination of a bulk element in metals, salts, oxides, and pure solutions, during precision studies. The coulometric methods are the most intensively developed.

The coulometric methods for americium determination with high sensitivity and accuracy have been developed on the basis of the reversible electrochemical couples Am(VI)/Am(V) and Am(IV)/Am(III) (Table 5).^{52,53} The possibility of electrochemical oxidation of Am(III) to Am(IV) and Am(VI) and the high stability of the higher oxidation

states of americium under certain conditions underlie these methods. Am(IV) has been established as stable not only in 10–15M phosphoric acid solutions but also when formed by electrochemical oxidation of Am(III) in 0.3–2.0M phosphoric acid in acetonitrile.⁵³ The equipment available allows determination of 5–10 μ g of americium with an error of 1–2%.

It is possible to determine 5–100 μ g of americium by coulometry of the Am(IV)/Am(III) couple in 0.1M perchloric acid in the presence of 6×10^{-3} M potassium phosphotungstate.⁵² In this solution Am(III) is completely oxidized to Am(IV) in 15 min at a potential of 1.7 V, and the coulometric determination is carried out by reducing Am(IV) to Am(III) at 1.17 V. Am(IV) is very stable in potassium phosphotungstate solution, so tenfold ratio of curium does not interfere. Many elements oxidizable under these conditions (Pu, Ce and others) also do not interfere, since they are not reduced at a potential of 1.17 V. The measurement error does not exceed 3% even in the presence of 100-fold ratios (to Am) of other metals.⁵²

Coulometric determination of americium by means of the Am(IV)/Am(III) couple can also be done in an acetonitrile solution of phosphoric acid, in which Am(III) is electrochemically oxidized rapidly and reversibly to Am(IV). Microgram amounts of americium can be determined with measurement error of 1–2%, for example, in 0.5M phosphoric acid in acetonitrile.⁵³

An indirect coulometric method of americium determination with high accuracy has been suggested,⁵⁴ based on displacement of Hg^{2+} from its EDTA complex by americium, with subsequent coulometric determination of the mercury (reduction to the metal). The determination takes 1 hr, and the determination error for 0.3–0.7 mg of Am is only 0.1–0.2%. This method can be recommended only for the standardization or analysis of pure solutions of americium, since it has very poor selectivity; all the lanthanides, the actinides in oxidation states +3 and +4, many bivalent and trivalent cations (Pb^{2+} , Zn^{2+} , Cd^{2+} , Cu^{2+} , etc.) will give the displacement reaction and thus interfere, and anions which form stable complexes with Am^{3+} will also interfere.

An analogous method has been used for the accurate determination of $\sim 100 \mu$ g of ^{248}Cm in nitric acid solution.⁵⁵ In this case a known quantity of EDTA (in excess) is added to the solution of curium in an

Table 5. Selective coulometric determination of americium

Couple	Composition of the solutions	Oxidation time, hr	Detection limits, μ g	Relative standard deviation, %
Am(VI)/Am(V)	2M H_3PO_4 + 0.1M $HClO_4$	1.5	5	1.5
Am(IV)/Am(III)	0.5M H_3PO_4 in CH_3CN	0.5	5	2
Am(IV)/Am(III)	0.1M $HClO_4$ + 6×10^{-3} M PW*	0.25	6–70	3
Am(IV)/Am(III)	1–2M Na_2CO_3 (pH 10)	0.5	5	2.5

*PW = potassium phosphotungstate.

acetate buffer, and the uncomplexed EDTA is titrated with Hg^{2+} electrochemically generated from mercury metal. The curium content is calculated from the quantity of electricity needed for generation of the Hg^{2+} . The measurement error does not exceed 1%.

The reversible electrochemical Bk(IV)/Bk(III) couple is theoretically suitable for the coulometric determination of berkelium, but until recently attempts to use it failed to show good results.^{56,57} However, a fairly precise method for coulometric determination of several milligrams of berkelium has now been worked out; the measurement error is 1–2%.⁵⁸

The TPE are most often determined by complexometric titration. Americium and curium are known to form very stable complexes with the complexones usually used—EDTA and DTPA. By spectrophotometric EDTA titration with Xylenol Orange as indicator it is possible to determine about 1 mg of americium and curium in a sample, with an error of about 1.4 μg .⁵⁹ Methods of determination of microgram amounts of americium and curium by titration with DTPA have been developed.^{60,61} With potentiometric indication of the end-point the measurement error is $\sim 2\%$; for spectrophotometric titration it is 0.5%.⁶⁰ In another version of this method, an electrochemically generated complex of Fe(II) with DTPA serves as titrant. This makes it possible to conduct the analysis with the help of an automatic coulometric titrator.⁶² The measurement error of 20–200 μg of americium is 3–5%.⁶¹

The second group of methods, characterized by high sensitivity, selectivity, and adequate rapidity, is mainly used for the determination of TPE in various natural and technological samples, and irradiated targets. These methods are used to study TPE and for many other purposes, and include the radiometric methods.

Thanks to a considerable improvement in measuring equipment and knowledge of the half-lives, the radiometric methods of TPE determination now achieve good precision. This is particularly the case for the α -activity methods, in which the best measurement characteristics (low detection limit, high

efficiency and small errors) are obtained with the silicon semiconductor detectors and liquid scintillators. An alpha-spectrometer with a semiconductor detector (area 1–3 cm^2) can have an efficiency of nearly 50% and a detection limit of 10^{-3} Bq (in a sample) (Table 6).^{63,64} As the energy resolution of such detectors is 20–30 keV, it is possible to determine americium and curium without a preliminary separation. If a separation is required (electrochemical oxidation of the americium (instead of persulphate oxidation) before extraction, makes the radiometric determination more precise.¹⁰

In the case of complex α -spectra, various mathematical processing methods are used.^{65,66} The determination of one nuclide is impoverished by the presence of another which has higher α -particle energy and intensity. In some cases the method of α - γ coincidence is used. Such a method allows determination of up to 1% of ^{243}Am in a mixture with ^{244}Cm (detection limit $3 \times 10^{-3}\%$ ^{243}Am by α -activity), even in the presence of fission products with γ -activity.⁶⁷ The method of α - γ coincidence is also used to measure the absolute α -activity of nuclides, e.g., ^{241}Am , with a very small error (0.1–0.2%).^{68,69}

Recently, for the determination of α -active TPE directly in solutions, an "immersed" Si(Li) detector has become widely used.^{70,71} Such a detector has a low counting efficiency and is convenient for measuring high α -activities. The presence of non-volatile macro impurities in the solution usually prevents the preparation of samples with a thin layer for α -counting, but practically does not effect measurement with an "immersed" detector. In combination with a multi-channel analyser the "immersed" detector makes it possible to conduct an α -spectrometric analysis: a determination of α -active nuclides in solutions containing such mixtures as ^{244}Cm , ^{252}Cf , ^{253}Es ,⁷² or ^{241}Am , ^{243}Am , ^{242}Cm , ^{244}Cm ,^{70,71} has been described. The energy resolution of such an α -spectrometer is usually 50–100 keV,^{71,72} and may even be 18–20 keV.⁷² Determination is possible in solutions containing sodium nitrate up to 7M concentration.⁷¹

The problem of counting β -particles with low

Table 6. Radiometric determination of transuranium elements

Method	Elements	Main features
α - γ Coincidence	Am	Up to $10^{-3}\%$ Am by radioactivity in presence of Cm and fission products
Liquid scintillation counting	Bk Pu, Am	Measuring ^{249}Bk in solutions of various compositions; detection limit ~ 0.1 Bq; error $\sim 0.1\%$
α -Spectrometry ("immersed" detectors)	Am, Cm	Determination in solutions in the presence of 5–10M salt back-ground; detection limit 10 Bq
γ -Spectrometry with automatic spectrum processing	Am, fission products	Solid and liquid samples 0.1–100 ml in volume; determination time 10 min
α -Spectrometry with automatic spectrum processing	Am, Cm	Determination limit 10^{-3} Bq

energy arises in the analytical chemistry of TPE in connection with analysis of samples containing ^{249}Bk . As a rule, a proportional-flow counter (the counting efficiency is 50–100%, background about 1 cps) or a liquid scintillator (LS) counter is used for this purpose. The use of the LS method for ^{249}Bk determination is complicated by the fact that most substances quench the relatively weak scintillations induced by the β -particles of ^{249}Bk .

A convenient method for determination of nuclides which are spontaneously fissile is to measure the neutron activity. The even mass-number isotopes of curium and californium belong to the nuclides with high neutron activity. The neutron-counting method makes it possible to determine the content of the nuclides in samples of various configurations without destroying them. The influence of α -active nuclides must be taken into account, however, since they can give an additional flux of neutrons by (α , n) nuclear reactions with light nuclides. Neutron–neutron coincidence counters are the most useful. They exclude the background from (α , n)-reactions and provide identification of individual neutron-active nuclides through the value of the average number of neutrons per fission.^{73,74} The determination of microgram quantities of ^{244}Cm , with the help of these devices, has been described for samples containing only this nuclide^{73,74} and for mixtures with ^{240}Pu .⁷³ The error measurement of neutron-active nuclides by this method is 1–2%, and the detection limit for ^{244}Cm is 3 ng. In the analysis of a mixture of neutron-active nuclides rather precise results are obtained if the specific neutron activity of all the nuclides is nearly equal.⁷³

Sensitive techniques for mass-spectrometric determination of TPE in samples of uranium, plutonium, americium, curium, berkelium and californium have been developed.^{75,76} With a 0.1–10 μg sample, it is possible to determine 0.01% of americium in curium, and 0.5% of plutonium, americium and curium in berkelium and californium. In this case the measurement error is 10–20%, but for a higher content of determinand the error can be reduced to 4–5%. Am and Cm are simultaneously determined together with La, Ce, Pr, Nd, Sm and Eu. With a 5–10 μg Am sample, Cm and the lanthanides can be determined at the $10^{-3}\%$ level and in 0.1 μg of Bk, Cf can be determined at the 0.03% level. The measurement error is 10–20%.⁷⁶

A sensitive neutron-activation method for berkelium determination in a mixture of curium and californium has recently been worked out.⁷⁷ ^{250}Bk , with half-life 3.32 hr and intense γ -radiation, is produced during the irradiation of ^{249}Bk by thermal neutrons. The sample is irradiated by thermal neutrons at a flux of 1×10^{13} n.cm⁻².sec⁻¹ for several hours, and a short time later the intensity of the 989-keV γ -line is measured on a γ -spectrometer with a semiconductor detector. The absolute measurement error for berkelium in a 2 μg sample is $1.8 \times 10^{-4}\%$.

The emission-spectrometry method for berkelium determination is especially useful. Until recently the only useful spectrographic method known for TPE analysis was detection of americium by use of a combustible cathode.⁷⁸ A new direct spectrographic method of determination of microamounts of Am in Cm, with a detection limit of 0.01% in a sample containing up to 20 μg of curium, with a relative standard deviation of 25%, has been developed. The solid residue from evaporation of the sample solution containing curium is excited in an alternating current arc.⁷⁹

The emission spectra of berkelium and californium over the range 250–336 nm, excited in an alternating current arc, have been investigated in detail. A semi-quantitative method of berkelium determination in solutions containing large amounts of curium, cerium and other elements has been developed on the basis of that study. The detection limit for berkelium is 3×10^{-8} g over the concentration range 1–100 $\mu\text{g}/\text{ml}$.

CONCLUSIONS

A survey of the principal trends in the analytical chemistry of the transplutonium elements in the last five years shows that there have been considerable advances in the field.

Some perspectives for further progress in modern radiochemistry are as follows. First of all there is an urgent need to investigate the chemical properties of TPE in unusual oxidation states, and to study the composition and structure of their complexes in solution. It is also necessary to search for and use new complexing media, such as carbonate solutions, to stabilize Cm, Bk, Cf, and perhaps Es in higher oxidation states. For extraction, it is attractive to use multiphase systems, including aqueous ones, and to study the kinetics of interphase equilibria. It may be expected that such further studies in the chemical properties of TPE in unusual oxidation states and the application of new extractants and sorbents will provide the basis for effective methods of isolation and separation of radioactive elements and for more reliable techniques for control work in the radiochemical industry.

REFERENCES

1. C. F. Metz and G. R. Waterbury, in *Treatise on Analytical Chemistry*, I. M. Kolthoff and P. J. Elving (eds.), Part II, Vol. 9, p. 189. Interscience, New York, 1962.
2. B. F. Myasoedov, L. I. Guseva, I. A. Lebedev *et al.*, *Analiticheskaya khimiya transplutoniyevykh elementov (Analytical Chemistry of the Transplutonium Elements)*, Nauka, Moscow, 1972.
3. I. A. Lebedev and B. F. Myasoedov, *Radiokhimiya*, 1982, **24**, 700.
4. B. F. Myasoedov and I. A. Lebedev, *Radiochim. Acta*, 1983, **32**, 55.
5. N. N. Krot, A. D. Gel'man, M. P. Mefodieva *et al.*,

- Semivalentnoe sostoyanie neptuniya, plutoniya, ameritsiya (Septavalent State of Neptunium, Plutonium, Americium)*, Nauka, Moscow, 1977.
6. V. F. Peretrukhin, E. A. Erin, V. I. Dzyubenko, V. V. Kopytov, V. G. Polyukhov, V. Ya. Vasil'ev, G. A. Timofeev, A. G. Rykov, N. N. Krot and V. I. Spysyn, *Dokl. Akad. Nauk SSSR*, 1978, **242**, 1359.
 7. V. N. Kosyakov, E. A. Erin, V. M. Vityutnev, V. V. Kopytov and A. G. Rykov, *Radiokhimiya*, 1982, **24**, 551.
 8. V. N. Kosyakov, G. A. Timofeev, E. A. Erin, V. V. Kopytov and V. I. Andreev, *ibid.*, 1977, **19**, p. 82.
 9. N. B. Mikheev, A. N. Kamenskaya, V. I. Spitsyn, Ya. Mikul'skii, T. Petryna and N. A. Konovalova, *ibid.*, 1981, **23**, 736.
 10. V. Ya. Frenkel, YU. M. Kulyako, I. A. Lebedev and B. F. Myasoedov, *Zh. Analit. Khim.*, 1979, **34**, 330.
 11. B. F. Myasoedov and N. P. Molochnikova, *Radiochem. Radioanal. Lett.*, 1974, **18**, No. 1, 33.
 12. N. P. Molochnikova, B. F. Myasoedov and V. Ya. Frenkel, *ibid.*, 1983, **59**, No. 1, 25.
 13. B. F. Myasoedov, N. P. Molochnikova and A. V. Davydov, *Radiokhimiya*, 1979, **21**, 400.
 14. N. P. Molochnikova, V. Ya. Frenkel, B. F. Myasoedov and I. A. Lebedev, *ibid.*, 1982, **24**, 303.
 15. B. F. Myasoedov, N. P. Molochnikova, Yu. G. Kutavov and Yu. E. Nikitin, *ibid.*, 1981, **23**, 43.
 16. V. N. Kosyakov, N. G. Yakovlev and G. M. Kazakova, *ibid.*, 1979, **21**, 262.
 17. G. A. Timofeev, B. I. Levakov and N. A. Vladimirova, *ibid.*, 1975, **17**, 124.
 18. G. A. Timofeev, B. I. Levakov and V. I. Andreev, *ibid.*, 1977, **19**, 525.
 19. C. Musicas, M. Germain and G. Bathellier, in *Actinide Separations*, J. D. Navrotil and W. W. Schulz (eds.), p. 157. American Chemical Society, Washington D.C., 1980.
 20. G. W. Mason, A. F. Bollmeier and D. F. Peppard, *J. Inorg. Nucl. Chem.*, 1970, **32**, 1011.
 21. M. Zangen, *ibid.*, 1966, **28**, 1693.
 22. B. F. Myasoedov, N. P. Molochnikova and I. A. Lebedev, *Zh. Analit. Khim.*, 1971, **26**, 1984.
 23. R. P. Bernabee, D. R. Percival and F. D. Hindman, *Anal. Chem.*, 1980, **52**, 2351.
 24. B. F. Myasoedov, M. S. Milyukova and E. V. Kusovkina, *Dokl. Akad. Nauk SSSR*, 1985, **283**, 640.
 25. G. M. Kazakova, V. N. Kosyakov and E. A. Erin, *Radiokhimiya*, 1975, **17**, 311.
 26. V. N. Kosyakov, N. G. Yakovlev, G. M. Kazakova, E. A. Erin and V. V. Kopytov, *ibid.*, 1977, **19**, 486.
 27. E. A. Erin, V. M. Vityutnev, V. V. Kopytov and V. Ya. Vasilyev, *ibid.*, 1979, **21**, 560.
 28. M. S. Milyukova, D. A. Malikov, E. V. Kusovkina and B. F. Myasoedov, *ibid.*, 1983, **23**, 305.
 29. P. K. Khopkar and J. N. Mathur, *J. Radioanal. Chem.*, 1980, **60**, 131.
 30. M. S. Milyukova and B. F. Myasoedov, *Radiokhimiya*, 1978, **20**, 378.
 31. M. S. Milyukova, D. A. Malikov and B. F. Myasoedov, *Radiochem. Radioanal. Lett.*, 1977, **29**, 93.
 32. *Idem*, *Radiokhimiya*, 1980, **22**, 352.
 33. B. F. Myasoedov, M. S. Milyukova and D. A. Malikov, *Solvent Extr. Ion Exch.*, 1984, **2**, 61.
 34. M. Hara and S. Suzuki, *Bull. Chem. Soc. Japan*, 1974, **47**, 635.
 35. E. A. Erin, V. M. Vityutnev, V. V. Kopytov and V. Ya. Vasilyev, *Radiokhimiya*, 1979, **21**, 100.
 36. Yu S. Korotkin, *ibid.*, 1981, **23**, 181.
 37. K. V. Barsukova, N. Yu. Kremliakova and B. F. Myasoedov, *Radiochem. Radioanal. Lett.*, 1981, **48**, 373.
 38. N. Yu. Kremliakova, K. V. Barsukova and B. F. Myasoedov, *ibid.*, 1983, **57**, 293.
 39. F. El-Sweify and S. A. Aly, *J. Radioanal. Chem.*, 1980, **60**, 353.
 40. L. I. Guseva, V. V. Stepushkina and G. S. Tikhomirova, *Solvent Extr. Ion Exch.*, 1985, **3**, 501.
 41. L. I. Guseva, I. A. Lebedev, B. F. Myasoedov and G. S. Tikhomirova, *J. Radioanal. Chem.*, 1976, **38** (Suppl.), 55.
 42. I. A. Lebedev, B. F. Myasoedov and L. I. Guseva, *Radioanal. Chem.*, 1974, **21**, 259.
 43. L. I. Guseva and G. S. Tikhomirova, *J. Radioanal. Chem.*, 1979, **52**, 369.
 44. E. A. Erin, A. I. Shafiev and G. N. Yakovlev, *Radiokhimiya*, 1975, **17**, 93.
 45. F. L. Moore, *Anal. Chem.*, 1971, **43**, 487.
 46. A. I. Shafiev, Yu. V. Efremov and G. N. Yakovlev, *Radiokhimiya*, 1975, **17**, 498.
 47. A. I. Shafiev, Yu. V. Efremov, V. M. Nikolaev and G. N. Yakovlev, *ibid.*, 1971, **13**, 129.
 48. B. F. Myasoedov and K. V. Barsukova, *Radiochem. Radioanal. Lett.*, 1971, **7**, 269.
 49. M. Hara and S. Suzuki, *Bull. Chem. Soc. Japan*, 1975, **48**, 1431.
 50. N. B. Mikheev, A. N. Kamenskaya, N. A. Konovalova, I. A. Rumer and S. A. Kalyukhin, *Radiokhimiya*, 1983, **25**, 158.
 51. N. B. Mikheev, A. N. Kamenskaya, J. Mikulski *et al.*, *ibid.*, 1981, **23**, 927.
 52. Yu. M. Kulyako, T. I. Trofimov, V. Ya. Frenkel, L. A. Lebedev and B. F. Myasoedov, *Zh. Analit. Khim.*, 1981, **36**, 2343.
 53. Yu. M. Kulyako, S. A. Perevalov, V. Ya. Frenkel, I. A. Lebedev, B. F. Myasoedov and P. L. Khizhnyak, *Radiochem. Radioanal. Lett.*, 1983, **59**, 235.
 54. C. Bergey and L. Fouchard, *Talanta*, 1979, **26**, 445.
 55. J. E. McCracken, J. R. Stokely, R. D. Baybarz, C. E. Bemis, Jr. and R. Eby, *J. Inorg. Nucl. Chem.*, 1971, **33**, 3251.
 56. J. R. Stokely, R. D. Baybarz and W. D. Shultz, *Inorg. Nucl. Chem. Lett.*, 1969, **5**, 877.
 57. R. C. Propst and M. L. Hyder, *J. Inorg. Nucl. Chem.*, 1970, **32**, 2205.
 58. V. M. Barinov, V. I. Konovalov and E. A. Erin, *Second All-Union Conf. on Chemistry of Transplutonium Elements*, Dimitrovgrad, 21–23 June 1983, *Abstracts of Papers*, p. 95.
 59. K. Buijs and W. Bartscher, *Anal. Chim. Acta*, 1977, **88**, 403.
 60. G. A. Timofeev, G. A. Simakin, P. F. Baklanova, G. F. Kuznetsov and V. I. Ivanov, *Zh. Analit. Khim.*, 1976, **31**, 2337.
 61. G. A. Simakin, G. A. Timofeev and N. A. Vladimirova, *Radiokhimiya*, 1977, **19**, 560.
 62. G. A. Simakin, P. F. Baklanova, G. F. Kuznetsov and A. V. Chernov, *Zh. Analit. Khim.*, 1974, **29**, 1585.
 63. E. Holm and R. Fukai, *Talanta*, 1976, **23**, 853.
 64. *Idem*, *ibid.*, 1977, **24**, 659.
 65. B. G. Basova, A. D. Rabinovich, V. G. Polyachov and G. A. Timofeev, *Radiokhimiya*, 1979, **21**, 430.
 66. S. K. Aggarwal, A. T. Almaula, P. M. Shah, P. A. Ramasubramanian, A. R. Parals and H. C. Jain, *Radiochem. Radioanal. Lett.*, 1980, **45**, No. 1, 73.
 67. B. F. Myasoedov, G. M. Chernov, A. P. Myagkov and I. A. Lebedev, *Zh. Analit. Khim.*, 1973, **28**, 294.
 68. F. Amoudry, *Analysis*, 1980, **8**, 463.
 69. F. M. Karavaev, *Izmereniya aktivnosti nuklidov (Measurements of Nuclide Activity)*, Standard, Moscow, 1972.
 70. M. I. Krapivin, I. A. Lebedev, B. F. Myasoedov, V. G. Udina, A. A. Yakobson and V. Ya. Frenkel, *Zh. Analit. Khim.*, 1978, **33**, 1911.
 71. M. I. Krapivin, I. A. Lebedev, B. F. Myasoedov, V. G.

- Yudina, A. A. Yakobson and V. Ya. Frenkel, *Radio-khimiya*, 1979, **21**, 321.
72. V. V. Pevtsov and G. A. Timofeev, *ibid.*, 1977, **19**, 450.
73. A. A. Voronkov, N. M. Kazarinov, A. G. Korenkov and V. A. Maevsky, *ibid.*, 1978, **20**, 924.
74. V. V. Berdikov, N. G. Triumphov and O. S. Tsvetkov, *ibid.*, 1979, **21**, 289.
75. V. V. Tikhomirov, V. Ya. Gabeskiriya and A. P. Chetverikov, *ibid.*, 1981, **23**, 595.
76. V. V. Tikhomirov, A. P. Chetverikov and V. Ya. Gabeskiriya, *ibid.*, 1981, **23**, 896.
77. O. I. Ivanov, E. V. Krainov and A. F. Sviridov, *At. Energ.*, 1978, **45**, 231.
78. E. A. Zacharov, B. F. Myasoedov and I. A. Lebedev, *Zh. Analit. Khim.*, 1975, **30**, 1344.
79. T. Ya. Verechagina, Yu. I. Korovin and G. A. Timofeev, *Second All-Union Conf. on Chemistry of Transplutonium Elements*, Dmitrovgrad, 21-23 June 1983, *Abstract of Papers*, p. 98.

ADVANCES IN VOLTAMMETRY

KH. Z. BRAININA

Sverdlovsk Institute of National Economy, Sverdlovsk, USSR

(Received 15 October 1985. Accepted 28 July 1986)

Summary—The possibilities of voltammetry as a source of information in bioelectrochemistry, electrochemistry, solid-state chemistry and analytical chemistry are reviewed. Attention is drawn to the use of catalytic currents and adsorption, inverse voltammetry, and solid and modified electrodes. The review mainly covers papers published in 1983 and 1984, especially those in the Soviet literature.

Analytical chemistry as a whole, and voltammetry in particular, are connected with many fields of natural science and technology.^{1,2} This makes it necessary to consider two aspects of voltammetry: its development as a technique in the context of progress in cognate fields, and its application in various areas of science and technology. Because of the wide range of these topics, this review will be limited to the aspect of voltammetry as a source of information on the concentration and some properties of substances, the fundamental problems of electrochemical theory and methodology having been adequately dealt with in books,³⁻⁵ and those of mathematical methods and instrumentation in reviews.^{6,7}

Orient and co-workers,^{8,9} from analysis of the journals and the citation index of papers on analytical chemistry, have shown that more papers feature electrochemical methods than any other topic, owing to the rapid development of the theory,¹⁰⁻¹⁵ deeper understanding of the mechanism and kinetics of electrode processes, development of instrumentation,^{10,11} evolution of modified electrodes^{10,16} and substantial broadening of the fields of application. This is because polarography and voltammetry supply information inaccessible by other methods, for example, in medicine, biochemistry and molecular biology, monitoring of waters,¹⁷⁻¹⁹ and investigation of solids.^{12,20,21}

Electrochemical detectors²² are important in various rapidly developing hybrid analytical methods¹ such as liquid chromatography and flow-injection analysis. Comparison of the detection limits is often in favour of voltammetry, and especially of stripping voltammetry.²³

In recent years several books on polarography^{4,14,15,24} and voltammetry^{4,12,13,15} have been published. *Analytical Chemistry* publishes biennial reviews^{10,11,16} of dynamic electrochemical methods of analysis. Specialist reviews cover voltammetric analysis of waters,¹⁷⁻¹⁹ and polarographic and voltammetric methods used in biochemistry and molecular biology.²⁶⁻²⁹ Use of inverse voltammetry (IV) for investigation of biologically active substances³⁰ and in phase analysis and in the investigation of solids^{12,20,21}

has been reviewed, and so has the use of organic reagents in inverse voltammetry.³¹ Several reviews are devoted to new ideas³² and prospects,³³ advances,^{34,35} electrodes,³⁶ feasibility of use of voltammetry in inorganic³⁷ and pharmaceutical³⁸ analysis, and specification of the physicochemical forms of metals in solutions.¹⁹ Nevertheless, a simple comparison of the literature cited by Soviet and foreign authors shows that there is a language and information barrier; as a rule, most of the Soviet papers escape mention by the foreign authors. This review will attempt to fill the information gap and to make recent developments in the Soviet Union more accessible to the rest of the world. It will therefore mainly cite reviews and papers of the last two years (1983-4) and touch only on the trends which seem the most important and promising. It should be borne in mind, however, that the choice made is arbitrary and in no way lays claim to give a complete picture. Thus, many developments in determination of the elements will not be discussed in detail, and the reader will simply be referred to the original papers.

KINETIC CURRENTS AND COMPLEX FORMATION IN VOLTAMMETRY

Important contributions to the understanding of the mechanism of electrode processes, including chemical and adsorption stages, have been made by Mairanovsky³⁹ and Turian.¹⁴ Mairanovsky has shown, in particular, that protonation of adsorbed metabisaccharin proceeds with the participation of two protons simultaneously.⁴⁰ He has also detected an unusual effect of the nature of the cation on the rate of protonation of double-charged anions,⁴¹ and was the first to investigate purely surface chemical reactions and the influence of the electrode field on their course.^{42,43} Further papers⁴⁴⁻⁴⁶ were devoted to hydrogen catalytic waves and to the kinetics of protonation of pachicarpine adsorbed on a dropping mercury electrode (dme). The mechanism and kinetics of protonation of aromatic aldehydes and ketones,⁴⁷ and the solubility and adsorption of acetophenone⁴⁸ have also been investigated.

Turian¹⁴ has summarized the results of investigations on the application of chemical reactions in polarographic analysis. In recent papers Turian and Ruvinsky have continued to develop the theory of kinetic currents arising at the dme in solutions of organic compounds,⁴⁹⁻⁵¹ and their practical applications.^{52,53}

Catalytic hydrogen-ion reduction at the dme in solutions of metal complexes with organic reagents has been studied by several workers.⁵⁴⁻⁵⁹

Two groups of processes, including the catalytic reduction of hydrogen ions, can be distinguished, depending on the oxidation state of the central ion. In the first group (usually with central ions in oxidation state II) the preceding stage is protonation. The second group, of electrochemical reactions occurring at more negative potentials (mainly in alkaline medium), is characteristic of complexes of transition metals and sulphur-containing ligands, and the catalytic waves follow reduction of the central ion.⁵⁴ The hydrogen evolution is catalysed by the adsorbed complexes. This effect is exhibited on mercury, graphite and carbon-paste electrodes.

Catalytic hydrogen currents can be used for determination of metal ions⁵⁵⁻⁵⁸ and organic compounds.⁵⁶ Rhodium has been used as the central metal ion in a comparison of the hydrogen catalytic currents obtained in solutions of its complexes with a number of polyfunctional ligands.⁵⁹ A review of determination of platinum metals⁵⁵ dealt in particular with hydrogen catalytic currents obtained with buffered solutions of the metal complexes with organic ligands containing donor atoms capable of protonation.

The polarographic behaviour and adsorption of 1,10-phenanthroline and its metal complexes⁵⁷ and of 2,2'-bipyridyl metal complexes⁵⁸ have been investigated. 2,2'-Bipyridyl was used to determine cobalt in the presence of large amounts of nickel.⁵⁸ The catalytic currents obtained with iodate ions in the presence of unithiol and glutathione⁶⁰ and their use in analysis have been examined. The anodic voltammetry of *N*-benzoylphenylhydroxylamine and its analogues on solid electrodes, and the polarographic behaviour of organic reagents and organic extracts of their metal complexes have been reviewed.⁶¹

Ulakhovich and co-workers have examined the extraction polarography (on mercury electrodes) and voltammetry (on solid electrodes) of complexes of metals and derivatives of dithio-acids,^{62,63} and the polarographic behaviour of Co(II), Ni(II), Cu(II) and Zn(II) complexes with diethyldithiophosphoric acid, 2,2'-bipyridyl, 1,10-phenanthroline, α -aminopyridine and ethylenediamine in dimethylformamide medium.⁶⁴ They have also successfully used mixed-ligand complexes in polarography⁶⁵ and voltammetry with platinum and glassy-carbon electrodes⁶⁶⁻⁶⁸ to study the extraction and determination of Mn(II), Fe(II), Ni(II)^{65,69} and Pb(II).⁷⁰ The extraction of alkyl-substituted mercaptoquinolines of metals by molten naphthalene has been used in the polarographic

determination of Pb(II), and Mg(II),⁷¹ and the thiooxinate complex of molybdenum has been employed for layer-by-layer phase analysis of titanium alloys.⁷²

These papers were preceded by a monograph⁷³ summarizing the results in the field of the electrochemistry of metal chelates in non-aqueous media, special attention being paid to the effect of the oxidation state of the metal in complexes on the mechanism of catalytic evolution of hydrogen, and to the types of extraction polarography systems, and use of extraction voltammetry in inorganic analysis.

VOLTAMMETRY IN BIOELECTROCHEMISTRY

Voltammetry is one of the few techniques which can supply information on the changes in the structure and properties of macromolecules in their interaction with a charged surface,²⁹ which is of great importance in living organisms. The methods of voltammetry and polarography can be applied not only to determination of the concentration of low molecular-weight substances in solution²⁸ but also to the structural analysis of macromolecules.²⁹

Consideration has been given to the scope of polarography in analytical biochemistry (analysis of metabolites, coenzymes, metalloenzymes, proteins and nucleic acids), as well as to the polarographic determination of the electrochemical characteristics of substances participating in electron transfer in the respiration cycle and in photosynthesis,²⁷ the mechanism of electron transfer at active enzyme centres⁷⁴ and through the adsorption layers of membranes.⁷⁵ Kuznetsov and co-workers have investigated the conformational changes of proteins on stationary and dropping mercury electrodes, by cyclic voltammetry. They have shown^{76,77} that egg albumin, in which in the native state all the SS- and SH-groups are found inside the globule, is flattened on the electrode surface and have examined⁷⁸ the effect of denaturation of proteins containing coenzyme groups and metals, on the course of electrode processes and on their inhibition by unfavourable orientation of the molecules on the surface. Some natural cobalamins have been investigated by polarographic and cyclic voltammetry methods,^{79,80} and the feasibility of their identification⁷⁹ and determination of impurities in them has been demonstrated.

Electrochemical measurements are also used in the study of immune reactions. The use of In(III) as a label⁸¹ and of differential pulse anodic stripping voltammetry (DPASV) as the determination technique forms the basis for the development of non-radiometric investigation methods.

Catalytic waves in solutions containing proteins and metal ions, in particular Co(II) or Ni(II) (Brdička waves) are widely used for diagnosis in clinical work. They are described in detail in a number of reviews, e.g., that by Paleček.²⁹ The effect of the background electrolyte composition has been studied and the role of protein adsorption in the formation of these waves

stressed. It has been shown that the Brdička current decreases with decrease in the stability constants of the complexes in the order: cysteine ethyl ether > cysteine > cysteinamine or mercaptosuccinic acid > thioglycollic acid > 2-mercaptopropionic acid. Alexander *et al.*⁸² have suggested a new catalytic protein reaction with considerably higher sensitivity. A corresponding wave arises in the presence of *trans*-dichloro-bis(*N,N'*-dimethylethylenediamine) rhodium(III) chloride. Recently, automated continuous-flow determination of serum albumin by means of differential pulse polarography (DPP) has been devised.⁸³ However, the mechanism of these catalytic reactions has not yet been fully elucidated. For example, Shinagawa and Kakumoto,⁸⁴ from a study of the emergence of hydrogen catalytic waves for suspensions of a number of simple and complex semiconductors, have come to the conclusion that the reaction has a semiconductor nature.

Several papers and monographs devoted to bio-electrochemistry are mentioned in the review by Johnson *et al.*¹⁰ New information is being provided by use of spectroelectrochemical and electrochemiluminescence methods,⁸⁵ of a combination of electrochemical and ESR methods,⁸⁶ and of electrodes with immobilized enzymes.¹⁰

INVERSE (STRIPPING) VOLTAMMETRY

This technique is a rapidly growing branch of electroanalytical chemistry.^{4,5,12,13,87} It can be used in electrochemistry, where the polarization curves are a source of information on the character of the interactions in the system investigated, on the initial stages of electrocrystallization, and on the kinetics of anodic reactions. In analytical chemistry it is a very valuable means of trace analysis, monitoring of natural waters, and speciation of the forms of the elements in them. In solid-state chemistry it is being used for the investigation of solid-phase reactions, non-stoichiometry and adsorbability. Unfortunately, this field of electroanalytical chemistry deserves the comment by Kissinger⁴ (p. 5): "So much nomenclature, so much jargon". The most widely used term, "stripping voltammetry", does not reflect all the present-day variants of the method, inasmuch as the substance is not always stripped from the surface of the electrode in the process of measurement.^{12,20,30,31} The term "inverse" reflects the essence of the method more exactly than does "stripping", since the system response (analytical signal) recorded is determined not by the solution composition, but by that of the electrode¹⁵ (p.13). Hence, we shall hereafter use the term inverse voltammetry (IV), distinguishing two branches: IV of solutions^{12,13,87} and IV of solids,^{12,20,21} and noting that in certain cases the electrochemical concentration stage is not necessary.

IV has been applied to reactions of the following types:^{12,13,87} (1) anodic oxidation of metals, with and without accompanying chemical reactions or inter-

action with the electrode surface; (2) formation and dissolution of chemical compounds on the electrode surface, including processes having adsorption stages; (3) electrochemical transformations of solids and adsorption processes on their surfaces.

Reactions of the first and second type form the basis of IV of solutions; those of the third type open up possibilities for the analysis and investigation of solid compounds.

Inverse voltammetry of solutions

For the implementation of reactions of the first two types use is made of stationary mercury-drop and mercury-film electrodes and glassy-carbon or impregnated graphite electrodes, including those coated with mercury *in situ*.^{12,88,89} In certain cases the electrode surface is modified by adsorption of a reagent *in situ*^{31,87} either in advance, or as a result of a chemical reaction.^{10,11} The diversity of reactions, electrodes and measuring techniques makes it possible to establish a rational procedure for analysis of materials of rather complex composition without preliminary separation and concentration of the components to be determined.^{12,13} Two of the main problems in using the reactions of the first type are (1) "delay" in (or even the impossibility of) deposition of an element on the electrode surface, and (2) interaction of the deposited elements to form solid solutions or intermetallic compounds. Digital simulation of the discharge and subsequent ionization of the analyte metals on the electrode surface has been used to explore the conditions (differences in electron work-functions for the metal being deposited and the electrode, the potential and duration of electrolysis, optimal concentration range) for the formation of metal deposits in different energy states and for catalysis by adsorbed atoms.

The processes of formation and dissolution of the metal nuclei have been examined,⁹⁰⁻⁹² and deposition and reduction of mercury salts described.⁹³

The results of various investigations of the mutual influence of metals deposited on an electrode are given in detail in a monograph¹² and appropriate papers.⁹⁴⁻⁹⁶ Consideration has been given to using formation of intermetallic compounds to develop an analytical signal when the elements in the pure form do not produce one, and to methods of eliminating metal interaction (effect of a third element on carbon electrodes coated with mercury *in situ*) whenever these distort the analytical signal.¹²

A number of papers have been devoted to the study of the conditions for coating carbon (graphite) electrodes with mercury *in situ*. Delays have been revealed in the deposition of mercury on the electrode surface.¹² This leads to a change in time of analytical signals registered in succession, and to a higher detection limit for mercury itself. It has been shown that the introduction of ions of electronegative elements into the solution catalyses the evolution of mercury on a solid surface.⁹⁷ Thus, graphite elec-

trodes coated with mercury *in situ* by joint electro-deposition of metals and mercury differ from other mercury electrodes as regards the specific dynamics of formation¹² (p. 126). A preliminary deposition of mercury on the electrode surface eliminates the "delay" effect and reduces the interaction between metals in the early stages of the electrolysis.¹²

It has been found that the metal oxidation current is directly proportional to the metal concentration only if the ratio of concentration of added mercury to concentration of determinand metal exceeds a certain limiting value.^{12,98-100}

Zebreva *et al.* have analysed the processes of oxidation of the homogeneous and heterogeneous amalgams formed during the joint discharge of mercury and metal ions,^{99,100} and have shown that there is direct proportionality between the peak oxidation current for the metal and the concentration of its ions in the original solution. They also found that formation of a heterogeneous amalgam leads to greater sensitivity,⁹⁹ which is in agreement with the ideas developed earlier⁸⁷ on the process of stripping metals from the surface of a foreign solid electrode.

The feasibility has been shown of investigating the mechanism and kinetics of electrode processes complicated by chemical reactions, of determining the composition and kinetics of transformation of short-lived complex ions participating in the electrode process, of investigating rapid subsequent chemical reactions, and of detecting kinetic currents,¹² and of the speciation of the forms of metal ions in natural waters.^{19,34}

Adsorption processes are used to concentrate certain elements and organic substances.^{12,30,31,101} This expands the field of application of IV to include some elements that cannot be concentrated as the metal or as insoluble compounds. On the other hand, the adsorption of organic compounds allows determination of their concentration from measurement of their oxidation or reduction currents^{101,102} or tensametric peaks.²⁸⁻³⁰ A third possibility is to use an indirect method of detecting various substances, including non-electroactive ones, by registering the decrease in signal from surface-active materials which react with them. Use of adsorption concentration for determination of inorganic components of solutions with the help of organic reagents has been treated in detail in reviews,^{31,101} monographs,^{12,13} and papers.¹⁰³⁻¹⁰⁶ Adsorption processes and electrochemical transformations of biologically active compounds have been employed for the investigation of their state and conformational changes in the electrical field of the electrode,^{26-30,77,107,108} and of their concentration in solution.^{28,29,109-111} Biocatalytic concentration has been used for the determination of lactate, glucose and hypoxanthine.¹¹²

Recently a new variant of IV has been suggested which uses ion-induced adsorption¹¹³⁻¹¹⁶ for determination of arsenic^{114,115} and tellurium¹¹⁶ in iodide solutions.

It should be noted that in processes involving adsorption of the reagent, the electrode surface should be considered as modified *in situ*.

A further variant of IV is being developed, in which an element is concentrated by means of a chemical oxidation-reduction reaction on the electrode surface¹¹⁷ or by the usual electrochemical accumulation of the metal,¹¹⁸ and then the catalytic currents arising in the presence of oxidants are registered.

Extraction and voltammetric determination of bismuth and antimony with preliminary chemical concentration in non-aqueous solutions has been described by Toropova *et al.*¹¹⁹⁻¹²² Karbainov and Mamaeva¹²³ are working on the IV of extracts, with electrochemical concentration. Tanaka and Yoshida¹²⁴ have suggested an original method of concentrating cysteine as its complex with copper, formed on a copper amalgam electrode.

Pulse voltammetry (and polarography) is the theme of a thorough monograph by Kaplan.¹⁵ The present state of alternating current (a.c.) voltammetry is considered in a book by Kaplan *et al.*²⁵ In recent years Kaplan and co-workers have made a series of investigations on the IV of selenium,¹²⁵ tellurium,¹²⁵ arsenic,¹²⁶ cadmium¹²⁷ and thallium.¹²⁸ They have used a.c. voltammetry with the hanging mercury-drop electrode,^{125,128} and a graphite electrode coated with mercury *in situ*.^{126,127}

A multi-element consecutive IV analysis has been described by Kaplin and Pichugina.¹²⁹

Such important questions as the preparation of samples and the elimination of the influence of organic substances and interfering elements on the results of IV analysis have discussed, and programmed electrolysis proposed.¹³⁰ Ultraviolet irradiation has been used to deactivate dissolved oxygen.¹³¹

Inverse voltammetry in phase analysis and investigation of the defect structure of solids

One of the special features of modern electro-analytical chemistry, and in particular of voltammetry, is the penetration of its methods into solid-state chemistry. In the last decade or so noticeable progress has been achieved in the electrochemical investigation of the phase composition, oxidation state of components, adsorbability, catalytic activity and defect structure of solid substances.^{12,20,132,133}

Information is provided by the potentiodynamic or *i-E* curves, recorded during the electrochemical transformations of the compounds under investigation or of the adsorption layers (mainly of oxygen) on their surface. Various experimental techniques are used to investigate solid substances in the form of single crystals, polycrystalline specimens, thin films, or powders dispersed in carbon-paste electroactive electrodes (CPEE) or deposited on their surfaces.^{12,20,21} A connection between the character of the electrochemical transformations and the types of crystalline and defect structures has been noted in

the investigation of several systems. The work in this field has been dealt with in a review²⁰ and a monograph.¹²

In recent years Zaharchuk and co-workers.¹³³⁻¹³⁸ have studied the electrochemical behaviour of compounds in the In-Sb-O system (Sb , α and β Sb_2O_3 , α and β Sb_2O_4 , Sb_6O_{13} , $\text{Sb}_2\text{O}_5 \cdot x\text{H}_2\text{O}$, In_2O_3 , InSbO_4 , InSb) with a CPEE. Differences in the oxidation potentials of amorphous and crystalline arsenic and antimony and the reduction potentials of oxides in various crystalline modifications have been revealed. The techniques developed by these authors have been used to investigate the phase and elemental composition of dielectric layers.¹³³ The electrochemical-transformation potential spectra for antimony and oxides of indium and antimony were recorded.¹³³ The elemental composition of the oxide layers has been determined by IV of the etching solution. These investigations enabled the authors to establish the phase composition of films on semiconductors of A^{III}B^V type.

A series of papers by Vidrevich and co-workers¹³⁹⁻¹⁴⁵ showed the possibilities for the phase analysis of powders and films of chalcogenide semiconductor compounds: CdS , ZnS , PbS , HgS , CuS , Cu_2S , Ag_2S , Bi_2S_3 . The peak potential of the electrochemical transformation depends on the nature of the substance, whereas the magnitude of the current at this potential depends on the quantity of the substance investigated. The composition of solid binary solutions such as CdS-ZnS , CdS-PbS was determined by comparing the quantities of electricity used for oxidation of the metals formed by preliminary cathodic reduction of the solid solutions. It was found possible to determine the nature, and in certain cases the quantity, of impurities such as CuS , Cu_2S , Cu_{2-x}S , Ag_2S , in CdS . A method was also worked out for the electrochemical phase analysis of films and powders of cadmium sulphide containing impurity phases of cadmium cyanamide, sulphate and oxide.

Inverse voltammetry with a rotating disc electrode has been used to examine corrosion in alloys.¹⁴⁶ A phase analysis method for nickel-aluminium catalysts has been developed by Matakova *et al.*,¹⁴⁷ who used a CPEE containing the substance investigated.

The investigations begun by Kuzmina *et al.*¹⁴⁸ have been reviewed.^{12,21} These authors designed a cell to be laid on an electroplated surface, and suggested a new electrochemical method for determining the thickness, composition and protective properties of the coating. They have also shown the possibility of phase and elemental analysis of thermic alloys and galvanic coatings.

Determination of composition of metal powders with a pellet electrode and a Kuzmina-type cell has also been investigated.^{149,150}

Recently^{12,20} much attention has been paid to the feasibility of using electrochemical transformations of chemisorbed oxygen as a source of information on the defect structure of solid substances. Two ap-

proaches to this problem have been taken, differing in the indicator signal used. In the first, use is made of the reduction current of oxygen chemisorbed from the gaseous phase or from solution (non-electrochemically sorbed oxygen). This is called a signal of the first kind and is usually observed at potentials near to 0.0 V *vs.* a saturated silver chloride electrode. The second uses electrochemical transformation of the chemisorbed products of an anodic reaction (electrochemically chemisorbed oxygen). The corresponding cathodic and anodic currents are recorded,^{12,20,151} and are called signals of the second kind. The advantages of the second method are the greater coverage of the surface by the adsorbate, the considerably higher signals obtained, compared with those of the first kind, and the possibility of more precise adjustment of the "effective partial oxygen pressure", by presetting a certain potential or current.

The connection between the adsorption of oxygen (and the corresponding reduction currents) and the defect structure of compounds has been demonstrated.^{152,153} It was shown¹⁵² that the quantity of electricity required for the reduction of chemisorbed oxygen depends linearly on the logarithm of the concentration of quasi-free electrons in specimens of ZnO doped with Ga_2O_3 . The increase in the reduction current of oxygen chemisorbed in the course of anodic polarization of V_2O_5 , with increase in y , leads to the same relation. In the reduction of V_2O_5 to V_4O_9 , the oxygen vacancy concentration increases, and there is correspondingly a rise in the oxygen chemisorption and a growth in the signal of the second kind.¹⁵³

The connection between signals of the second kind and the thermodynamic characteristics of oxide compounds has also been discussed.¹⁵⁴ The values of signals of the first and second kinds are also influenced by the degree of perfection of the crystal structure. It has been shown that the degree of ordering of the structure by annealing is accompanied by a drop in the signal of the second kind. This is most clearly exhibited by vanadium oxide bronzes with a wide region of homogeneity.²⁰ The signals, as expected, increase sharply at the homogeneity boundary and decrease as a result of ordering of the structure.

A number of papers^{12,20,153} record non-uniformity in the energy of oxygen adsorption on the surface. This non-uniformity is represented by current maxima on the potential *vs.* time curves recorded at different electrode potentials. A significant correlation has been shown to exist between signals of the second kind and the catalytic activity of compounds, an example being the system $\text{V}_2\text{O}_5\text{-MoO}_3$.¹⁵¹

Thus, the signals due to electrochemical transformations and chemisorbed layers may supply very valuable, perhaps unique, information on the phase composition, non-stoichiometry, crystal and defect structure of solid substances.

Nevertheless, in view of the "infancy" of the

method, the complexity of the signals and of the materials under investigation, it is necessary to proceed very cautiously in interpreting the results. Evidently what is required is further electrochemical investigation of model materials, and the establishment of unambiguous relationships between the results and the properties of the models.

INSTRUMENTATION

A wide range of instruments is commercially available^{4,10,13,37} for all variants of voltammetry. Computerization of the systems has now reached a high level of perfection, the use of computers has become routine, and the number of new publications on the subject is decreasing.¹⁰¹ Further developments, mainly in the field of IV, are aimed at finding ways of compensating the residual current,^{155,157} and improving subtractive polarographs,^{158,159} circulation electrolytic cells,¹⁶⁰ and solid electrodes with renewable surfaces.¹⁶¹ New approaches, methods and devices for enhancing quality control by IV are being examined.^{162,163} In particular, attention is being paid to voltammetry with stepwise potential scanning,¹⁶⁴ which greatly improves the response speed and the signal-to-noise ratio, and reduces the limit of detection by an order of magnitude.

New possibilities for enhancing selectivity and signal resolution, shortening the analysis time and increasing the amount of information obtained, are provided by combination of chemometrics and voltammetry.^{6,7} An analytical method can be chosen rationally according to which gives the better resolution: chemical separation or signal separation by means of mathematical information processing.⁷ Combined methods are being developed, such as spectroelectrochemistry,^{10,165} voltammetry in conjunction with photoelectron spectroscopy or ESR measurements,⁸⁶ and differential electrochemical mass-spectrometry.¹⁶⁶

Electrodes

The electrodes currently used in voltammetry may be subdivided into three groups: non-reactive, modified, and those having protective membranes. This subdivision is conventional, inasmuch as it is not always possible to explain the mechanism of the electrode process for a particular electrode. For example, the glassy-carbon and impregnated-graphite electrodes were traditionally considered to be non-reactive, but in the process of mercury deposition in the presence of Cd(II), Tl(I) or Pb(II) they behave like one modified by adsorbed atoms, and in solutions of surface-active substances operate like one modified by the surfactant. Nevertheless, for convenience of discussion we shall use the subdivision above.

Non-reactive electrodes. The classical hanging mercury drop electrode is being modified in construction. Capillaries have been made of Teflon and

polyethylene-coated glass.¹⁶ Designs include forced supply of mercury, and the static mercury electrode can be operated in both dropping and stationary modes.¹⁶⁷ Various mercury film electrodes have been compared.¹⁶⁸ For the fabrication of solid electrodes the most widely used materials are carbon-based: glassy carbon, impregnated graphite, carbon paste, pyrolytic graphite, and in certain cases "carbositall".¹⁶⁹⁻¹⁷¹ Requirements have been set forth for strict adherence to the carbonization process for fabrication of glassy carbon and the correct orientation of pyrolytic graphite when it is used as an electrode.¹⁶⁹ The orientation must be such that the exposed surface plane is parallel to the graphite layers, and this creates substantial difficulties in the machining of the material. In this regard two papers^{172,173} are of interest: they recommend coating glassy-carbon electrodes with a film of pyrolytic graphite. Deposition of a film of graphite on a metal substrate has also been suggested,¹⁷⁴ with a view to obtaining an electrode with an energy-uniform surface. Carbon-fibre electrodes are being used for *in vivo* analysis.^{175,176}

Doronin *et al.*¹⁷⁰ have shown that "carbositall" has better metrological characteristics than glassy carbon. Electrodes made of spectroscopic graphite and impregnated with wax,¹⁶⁹ a mixture of paraffin and polyethylene,¹² or epoxy resins^{12,177} are widely used. Carbon-paste electrodes are utilized for analysis of solutions, but more often for the investigation and phase analysis of solid compounds.^{12,20,21} A review has recently been published on the voltammetric characteristics of carbon electrodes.¹⁷⁸

Inverse voltammetry employs various film electrodes, especially those coated with mercury *in situ*,^{12,88,89} (usually made of impregnated graphite^{12,87,172} or glassy carbon).^{13,19,89}

An important role is played by the treatment of the electrode surface prior to measurements. Various techniques have been proposed, such as grinding, spalling, polishing, treatment with detergents, renewal of paste layers, *etc.*^{36,169}

Various methods of electrochemical regeneration of the surface between measurements have also been suggested. It has been shown¹⁷⁰ that minimal background currents on a "carbositall" electrode are obtained after an anodic-cathodic polarization cycle in perchloric acid medium, and that a preliminary cathodic polarization at potentials at which hydrogen is evolved reduces the capacitive current of the paste electrode.¹⁷⁸

Mercury electrodes of all types can be treated by polarization at potentials several tens of mV more negative than the potential for oxidation of mercury¹⁷⁹ or by multiple linear voltage pulses.¹⁸⁰ More complex programmes of electrochemical surface regeneration have been suggested,¹⁸¹ depending on the nature of the reactions and solutions used.

During its electrochemical preparation the electrode surface may sometimes be modified by the

carbon oxidation products.^{182,183} This may result in a substantial increase in the sensitivity and resolution of determination of hydrazine and its derivatives¹⁸⁴ and of copper.¹⁸² These authors recommend not to polarize the electrode at potentials at which hydrogen is evolved, which differs from the technique suggested by Urbaniczky.¹⁷⁸ The electrode reactions on electrodes treated by various techniques have been investigated.¹⁸⁵

Detailed procedures have been given for preparing glassy-carbon electrodes for voltammetry¹⁸⁶ and graphite electrodes for IV.¹² Despite the great experience acquired in the use of various methods of electrode regeneration, this problem cannot be considered to be fully solved.^{186,187}

Modified electrodes. Following the work by Murray in the mid-seventies, there has been great interest in electrodes with surfaces modified by chemical reaction, adsorption, or formation of a polymer film.^{11,16} Unfortunately, no mention has been made in Western literature of the first papers in this field,^{31,188,189} describing the use of organic compounds (Rhodamine C,¹⁸⁸ triphenylmethane dyes,¹⁸⁹ nitrosonaphthols¹⁸⁸) for the determination of low concentrations of a number of elements. The organic reagent was shown to be adsorbed on the surface of the graphite electrode,¹⁸⁹ which was therefore what would now be called an electrode modified *in situ*. The electrodes utilized by Monien and co-workers^{31,190,191} evidently belong to the same group. Modified electrodes are now widely used in electrocatalysis¹⁹² and are gaining recognition in voltammetric analysis.^{10,11,16} The electrode surfaces may be modified by adsorbed metal atoms,^{12,97,192} immobilized enzymes,¹⁹³ or membranes.¹⁹⁴ Membranes of various types are used to protect the surface of non-reactive electrodes from contamination by surface-active materials.¹⁹⁴

Flow-through electrochemical detectors

Electrochemical detectors are widely used in flow-through analytical control systems,^{22,184,195-202} on account of their selectivity, low detection limit and low cost. Depending on the complexity of the materials being analysed, electrochemical detectors are used either after a chromatographic separation or directly in flow-through systems. A wide range of electrodes and methods is available.

Glassy-carbon electrodes,^{184,200} carbon-paste electrodes,¹⁹⁵ modified electrodes,²² porous electrodes,¹⁰ wall-jet electrodes,¹⁰ and wall-jet detectors of the ring-disc type¹⁰ are all in use. Interference due to organic substances is eliminated by protecting the electrodes with special membranes.^{10,22} In flow-injection analysis (FIA) rapid linear sweep and cyclic sweep voltammetry has been used.¹⁰ IV techniques are also considered suitable for FIA.^{195,200,202}

Techniques have been suggested for subtracting the background current in voltammetric detection in FIA.²⁰ A new variant of subtractive anodic inverse

voltammetry for FIA, based on use of two identical flow-through injection systems, has been described.²⁰²

CONCLUSION

The increasing number of publications devoted to voltammetry testifies to the growing use of this method. Its success has been due to advances in cognate sciences: the deeper understanding of theoretical concepts in electrochemistry, *e.g.*, those concerning the mechanism and kinetics of electron transfer, adsorption and electrocatalysis; the development of computers and digital simulation of electrode processes; the development of new methods for discriminating between the useful signal and the background current. The feedback is also plain to see: voltammetry provides acquisition of information on the structure and properties of substances, for example, in organic chemistry and biochemistry, on the initial stages of electrodeposition, on electrocatalysis, and on the phase composition and defect structure of solid substances. There is also the possibility of solving a number of analytical problems without the need for time-consuming chemical separation and concentration of the determinands. In return, measurement automation, data processing, modified electrodes and microelectrodes for *in vivo* analysis, and chemometrics methods will all contribute to the further progress of voltammetry.

REFERENCES

1. Yu. A. Zolotov, *Essays on Analytical Chemistry*, Khimia, Moscow, 1977.
2. I. M. Orient, *Zh. Analit. Khim.*, 1981, **36**, 578.
3. V. E. Kazarinov (ed.), *Double Layer and Electrode Kinetics*, Nauka, Moscow, 1981.
4. P. T. Kissinger and W. R. Heineman (eds.), *Laboratory Techniques in Electro-Analytical Chemistry*, Dekker, New York, 1984.
5. A. M. Bond, *Modern Polarographic Methods in Analytical Chemistry*, Dekker, New York, 1980.
6. M. F. Delaney, *Anal. Chem.*, 1984, **56**, 261.
7. S. A. Borman, *ibid.*, 1981, **53**, 703A.
8. I. M. Orient and B. A. Markusova, in *Electrochemical Methods of Materials Analysis*, p. 95. *Metallurgiya*, Moscow, 1972.
9. A. G. Stromberg, I. M. Orient and T. M. Kameneva, *Zh. Analit. Khim.*, 1982, **37**, 2245.
10. D. C. Johnson, M. D. Ryan and G. S. Wilson, *Anal. Chem.*, 1984, **56**, 7R.
11. M. D. Ryan and G. S. Wilson, *ibid.*, 1982, **54**, 20R.
12. Kh. Z. Brainina and E. Ya. Neiman, *Solid Phase Reactions in Electroanalytical Chemistry*, Khimia, Moscow, 1982.
13. F. Vydra, K. Štulík and E. Juláková, *Electrochemical Stripping Analysis*, Horwood, Chichester, 1976.
14. Ya. I. Turian, *Chemical Reactions in Polarography*, Khimia, Moscow, 1980.
15. B. Ya. Kaplan, *Pulse Polarography*, Khimia, Moscow, 1978.
16. W. Heineman and P. Kissinger, *Anal. Chem.*, 1980, **52**, 139R.
17. M. J. Fishman, D. E. Erdmann and T. P. Steinhelmer, *ibid.*, 1981, **53**, 182R.
18. Kh. Z. Brainina, L. I. Roitman, R. M. Khanina and N. A. Gruzukova, *Khim. i Tekhnol. Vody*, 1985, **7**, 27.

19. T. M. Florence, *Anal. Proc.*, 1983, **20**, 552.
20. Kh. Z. Brainina and M. B. Vidrevich, *J. Electroanal. Chem.*, 1981, **121**, 1.
21. *Idem*, *Zavodsk. Lab.*, 1985, **51**, No. 1, 3.
22. P. T. Kissinger, in *Laboratory Techniques in Electroanalytical Chemistry*, P. T. Kissinger and W. R. Heineman (eds.), Dekker, New York, 1984.
23. O. G. Koch, F. D. Lafer and J. Morrison, *Pure Appl. Chem.*, 1982, **54**, 1565.
24. J. Doležal and I. Musil, *Polarographic Analysis of Mineral Raw Materials*, Mir, Moscow, 1980.
25. B. Ya. Kaplan, R. G. Patz and R. M.-F. Salikhdzanova, *A.C. Voltammetry*, Khimia, Moscow, 1985.
26. G. Berg, in *Polarography: Problems and Perspectives*, p. 308. Zinatne, Riga, 1977.
27. B. A. Kuznetsov, in *Polarography: Problems and Perspectives*, p. 293. Zinatne, Riga, 1977.
28. J. Kuta and E. Paleček, *Topics in Bioelectrochemistry and Bioenergetics*, 1983, **5**, 1.
29. E. Paleček, *ibid.*, 1983, **5**, 65.
30. Kh. Z. Brainina, *Bioelectrochem. Bioenerg.*, 1981, **8**, 479.
31. *Idem*, *Z. Anal. Chem.*, 1982, **312**, 428.
32. *Idem*, *Zavodsk. Lab.*, 1981, **47**, No. 12, 1.
33. P. K. Agasyan, V. P. Gladyshev and B. Ya. Kaplan, *ibid.*, 1982, **48**, No. 2, 16.
34. T. M. Florence, *J. Electroanal. Chem.*, 1984, **168**, 207.
35. R. Kalvoda, *Ann. Chim. (Ital.)*, 1983, **73**, 239.
36. I. Tenygl, *Zavodsk. Lab.*, 1982, **48**, No. 6, 4.
37. S. I. Zhdanov, V. A. Zarinskii and R. M.-F. Salikhdzanova, *Zh. Analit. Khim.*, 1982, **37**, 1682.
38. M. A. Brooks, in *Laboratory Techniques in Electroanalytical Chemistry*, P. T. Kissinger and W. Heineman (eds.), p. 569. Dekker, New York, 1984.
39. S. G. Mairanovsky, *Catalytic and Kinetic Waves in Polarography*, Nauka, Moscow, 1966.
40. *Idem*, in *Voltammetry of Organic and Inorganic Compounds*, P. K. Agasyan (ed.), Nauka, Moscow, 1985.
41. S. G. Mairanovsky, G. G. Kryukova and O. S. Kozlova, *Elektrokhimiya*, 1982, **18**, 1542.
42. *Idem*, *ibid.*, 1983, **19**, 1255.
43. *Idem*, *Stadia Biophysica*, 1983, **94**, 127.
44. S. G. Mairanovsky, G. K. Bishimbaeva and M. Zh. Zhurimov, *Elektrokhimiya*, 1984, **20**, 719.
45. S. G. Mairanovsky, G. K. Bishimbaeva, L. V. Odnoral and Yu. M. Loshkarev, *ibid.*, 1985, **21**, 216.
46. S. G. Mairanovsky and G. K. Bishimbaeva, *ibid.*, 1985, **21**, 5.
47. S. G. Mairanovsky, *ibid.*, 1983, **19**, 838.
48. S. G. Mairanovsky, N. P. Klochko and V. V. Orekhova, *ibid.*, 1984, **20**, 690.
49. O. E. Ruvinsky and Ya. I. Turian, *ibid.*, 1984, **20**, 699.
50. Ya. I. Turian, *ibid.*, 1984, **20**, 455.
51. *Idem*, *ibid.*, 1984, **20**, 139.
52. Ya. I. Turian, N. P. Vinyukova and K. M. Kardashova, *Izv. Vyssh. Ucheb. Zaved., Pisch. Tekhnol.*, 1984, No. 3, 99.
53. I. A. Tikhonova, Ya. I. Turian and N. K. Strizhov, *ibid.*, 1984, No. 2, 23.
54. V. F. Toropova, H. C. Budnikov, N. A. Ulakhovich and E. P. Medyantseva, *J. Electroanal. Chem.*, 1983, **144**, 1.
55. N. A. Ezerskaya and I. N. Kiseleva, *Zh. Analit. Khim.*, 1984, **39**, 1541.
56. N. A. Ulakhovich, E. P. Medyantseva, V. P. Frolova and O. N. Romanova, *ibid.*, 1983, **38**, 1963.
57. E. A. Osipova, I. V. Osipov, G. V. Prokhorova, P. K. Agasyan and I. A. Rodionov, *ibid.*, 1981, **36**, 2350.
58. E. A. Osipova, G. V. Prokhorova, P. K. Agasyan and S. V. Rudometkin, *ibid.*, 1983, **38**, 689.
59. N. A. Ezerskaya, I. N. Kiseleva, I. L. Kazakevitch, N. B. Gerbeleu and L. K. Shubochkin, *ibid.*, 1984, **39**, 654.
60. V. F. Toropova, Yu. N. Polyakov, N. I. Movchan and O. E. Bobyleva, *Izv. Vyssh. Ucheb. Zaved., Khim. i Khim. Tekhnol.*, 1982, **25**, 1192.
61. Z. A. Gallai, N. V. Shvedene and N. M. Sheina, *Zh. Analit. Khim.*, 1981, **36**, 1828.
62. V. F. Toropova, H. C. Budnikov and N. A. Ulakhovich, *Talanta*, 1978, **25**, 263.
63. N. A. Ulakhovich, G. K. Budnikov and G. A. Kutuyev, *Zh. Analit. Khim.*, 1983, **38**, 671.
64. N. A. Ulakhovich, I. V. Postnova and G. K. Budnikov, *Zh. Organ. Khim.*, 1983, **53**, 736.
65. N. A. Ulakhovich and I. V. Postnova, *Zavodsk. Lab.*, 1982, **48**, No. 8, 17.
66. N. A. Ulakhovich, I. V. Postnova and G. K. Budnikov, *Zh. Analit. Khim.*, 1983, **38**, 245.
67. *Idem*, *ibid.*, 1982, **37**, 2212.
68. H. C. Budnikov, N. A. Ulakhovich and I. V. Postnova, *J. Electroanal. Chem.*, 1983, **154**, 171.
69. N. A. Ulakhovich, G. K. Budnikov and I. V. Postnova, *Zh. Analit. Khim.*, 1982, **37**, 203.
70. N. A. Ulakhovich, G. A. Kutuyev, A. B. Lygin and L. F. Ibragimov, *ibid.*, 1984, **39**, 52.
71. N. A. Ulakhovich, G. K. Budnikov, A. P. Sturis, T. S. Gorbunova and E. Yu. Evstigneeva, *ibid.*, 1983, **38**, 974.
72. N. A. Ulakhovich, N. E. Naida, T. S. Gorbunova, I. R. Akhmetzyanova, A. P. Sturis and G. K. Budnikov, *Zavodsk. Lab.*, 1984, **50**, No. 3, 3.
73. G. K. Budnikov, T. V. Troepolskaya and N. A. Ulakhovich, *Electrochemistry of Metal Chelates in Non-aqueous Media*, Nauka, Moscow, 1980.
74. A. I. Archakov, B. A. Kuznetsov, M. V. Izotov and I. I. Karuzina, *Dokl. Akad. Nauk SSSR*, 1981, **258**, 216.
75. B. A. Kuznetsov, E. E. Emnova, N. M. Barabanova, V. I. Biryuzova, N. A. Kostrikin and A. K. Romanova, *Biokhimiya*, 1984, **49**, 230.
76. G. P. Shumakovich and B. A. Kuznetsov, *Elektrokhimiya*, 1984, **20**, 448.
77. B. A. Kuznetsov and G. P. Shumakovich, *Izv. Akad. Nauk SSSR, Ser. Khim.*, 1982, **10**, 2282.
78. B. A. Kuznetsov, N. M. Mestechkina and G. P. Shumakovich, *Bioelectrochem. Bioenerg.*, 1977, **4**, 1.
79. B. A. Kuznetsov and S. A. Eliseev, *Prikl. Biokhim. Mikrobiol.*, 1983, **19**, 840.
80. *Idem*, *ibid.*, 1984, **20**, 139.
81. M. J. Doyle, H. B. Halsall and W. R. Heineman, *Anal. Chem.*, 1982, **54**, 2318.
82. P. W. Alexander, R. Hoh and L. E. Smythe, *J. Electroanal. Chem.*, 1977, **81**, 151.
83. P. W. Alexander and M. H. Shah, *Anal. Chem.*, 1980, **52**, 1896.
84. M. Shinagawa and S. Kakumoto, *J. Heyrovský Memorial Congress on Polarography, Proceedings, II*, Prague, Czechoslovakia. 25–29 August 1980.
85. H. Tachikawa and L. R. Faulkner, in *Laboratory Techniques in Electroanalytical Chemistry*, P. T. Kissinger and W. R. Heineman (eds.), p. 637. Dekker, New York, 1984.
86. F. B. Goldberg and T. M. McKinney, in *Laboratory Techniques in Electroanalytical Chemistry*, P. T. Kissinger and W. R. Heineman (eds.), p. 675. Dekker, New York, 1984.
87. Kh. Z. Brainina, *Inverse Voltammetry of Solid Phases*, Khimia, Moscow, 1972; *Stripping Voltammetry in Chemical Analysis*, Halsted Press, New York, 1974.
88. E. M. Roizenblat and Kh. Z. Brainina, *Elektrokhimiya*, 1969, **5**, 396.
89. T. M. Florence, *J. Electroanal. Chem.*, 1970, **27**, 273.
90. S. Fletcher, C. S. Halliday, D. Gates, M. Westcott, T.

- Lwin and G. Nelson, *J. Electroanal. Chem.*, 1983, **159**, 267.
91. A. I. Mamaev, B. F. Nazarov and A. G. Stromberg, *Zh. Fiz. Khim.*, 1983, **57**, 197.
 92. V. V. Pnev, *Elektrokhimiya*, 1983, **19**, 1540.
 93. K. S. Parubochnaya, M. S. Zakharov and N. M. Khlynova, *Zh. Analit. Khim.*, 1983, **38**, 405.
 94. A. G. Stromberg and T. I. Katyukhina, *Zh. Fiz. Khim.*, 1981, **55**, 2145.
 95. A. A. Kaplin, V. A. Kolpakov and G. V. Klimachev, *Zh. Analit. Khim.*, 1981, **36**, 441.
 96. A. I. Kamenev, I. Mustafa and P. K. Agasyan, *ibid.*, 1984, **39**, 1242.
 97. E. M. Roizenblat, L. F. Manueva and G. N. Veretina, *ibid.*, 1973, **28**, 33.
 98. E. Ya. Neiman and Kh. Z. Brainina, *ibid.*, 1975, **30**, 1073.
 99. A. I. Zebrev, R. N. Matakova and M. S. Sharipova, *ibid.*, 1978, **33**, 2085.
 100. A. I. Zebrev, R. N. Matakova and R. V. Zholdybaeva, *Izv. Akad. Nauk Kaz. SSR, Khim.*, 1981, No. 3, 83.
 101. R. Kalvoda, *Anal. Chim. Acta*, 1982, **138**, 11.
 102. J. Wang and B. A. Freiha, *Talanta*, 1983, **30**, 837.
 103. J. Wang and M. Metzger, *Z. Anal. Chem.*, 1984, **318**, 321.
 104. M. Schnurrbusch, K.-H. Lubert and A. Thomas, *Z. Chem.*, 1983, **23**, 194.
 105. N. K. Lam, R. Kalvoda and M. Kopanica, *Anal. Chim. Acta*, 1982, **154**, 79.
 106. A. Meyer and R. Neeb, *Z. Anal. Chem.*, 1983, **315**, 118.
 107. V. Brabec and I. Schindlerová, *Bioelectrochem. Bioenerg.*, 1981, **8**, 451.
 108. V. Brabec, V. Glezers and V. Kadysch, *Collection Czech. Chem. Commun.* 1983, **48**, 1257.
 109. U. Forsman, *Anal. Chim. Acta*, 1984, **156**, 43.
 110. V. Stará and M. Kopanica, *Anal. Chim. Acta*, 1984, **159**, 105.
 111. L. Ramaley, J. A. Dalziel and Wee Tee Tan, *Can. J. Chem.*, 1981, **59**, 3334.
 112. J. J. Kulyš, M. K. Čėnas, G.-J. S. Švirmickas and V. P. Švirmickienė, *Anal. Chim. Acta*, 1982, **132**, 19.
 113. Kh. Z. Brainina, A. V. Chernysheva and N. Yu. Stozhko, *Zh. Analit. Khim.*, 1982, **37**, 1790.
 114. N. I. Stenina, A. V. Chernysheva, N. A. Zabugornaya and Kh. Z. Brainina, *Zavodsk. Lab.*, 1980, **46**, 1085.
 115. Kh. Z. Brainina, R. P. Lesunova, N. I. Stenina and N. A. Gruzskova, *ibid.*, 1980, **46**, 1076.
 116. Kh. Z. Brainina, A. V. Chernysheva and N. Yu. Stozhko, *ibid.*, 1984, **50**, No. 4, 3.
 117. V. F. Toropova, Yu. N. Polyakov, E. A. Naumova and O. V. Kopylova, *Zh. Analit. Khim.*, 1980, **35**, 296.
 118. M. Reigner and C. Buess-Herman, *Z. Anal. Chem.*, 1984, **317**, 257.
 119. V. F. Toropova, Yu. N. Polyakov and G. N. Zhdanova, *Zh. Analit. Khim.*, 1983, **38**, 238.
 120. *Idem*, *ibid.*, 1984, **39**, 1455.
 121. *Idem*, *Zavodsk. Lab.*, 1984, **50**, No. 1, 4.
 122. V. F. Toropova, Yu. N. Polyakov, G. N. Zhdanova and A. R. Garifyanov, *Zh. Analit. Khim.*, 1984, **34**, 1238.
 123. Yu. A. Karbainov and V. A. Mamaeva, *ibid.*, 1982, **37**, 359.
 124. S. Tanaka and H. Yoshida, *J. Electroanal. Chem.*, 1983, **149**, 213.
 125. I. N. Shvedova, B. Ya. Kaplan and T. N. Varavko, *Zavodsk. Lab.*, 1983, **49**, No. 10, 6.
 126. I. B. Berengard and B. Ya. Kaplan, *Proc. "Giredmet" Institute*, 1980, 100, 67.
 127. *Idem*, *Zavodsk. Lab.*, 1983, **49**, No. 11, 27.
 128. *Idem*, *ibid.*, 1984, **50**, No. 4, 8.
 129. A. A. Kaplin and V. M. Pichugina, *Zh. Analit. Khim.*, 1984, **39**, 664.
 130. Kh. Z. Brainina, R. M. Khanina, N. Yu. Stozhko and A. V. Chernysheva, *ibid.*, 1984, **39**, 2068.
 131. E. A. Zakharova and V. N. Volkova, *ibid.*, 1984, **39**, 636.
 132. E. Ya. Sapozhnikova, A. G. Davidovich, E. M. Roizenblat, M. A. Zinovik, E. V. Markovsky and L. V. Kosheleva, *Zh. Neorgan. Khim.*, 1982, **27**, 2888.
 133. V. I. Belyi, N. F. Zakharchuk, T. P. Smirnova and I. G. Yudelevich, *Electronics Industry*, 1980, No. 11-12, 35.
 134. N. F. Zakharchuk, T. P. Smirnova, V. I. Belt and I. G. Yudelevich, *Growth of Semiconductor Crystals and Films*, Part 2, p. 143. Novosibirsk, 1984.
 135. N. F. Zakharchuk, N. A. Valisheva, N. R. Vitsina, T. P. Smirnova, K. P. Le'l'kin, I. G. Yudelevich and I. S. Illarionova, *Izv. Sib. Otd. Akad. Nauk SSSR, Ser. Khim.*, 1984, No. 2, 83.
 136. T. P. Smirnova, V. N. Shpurik, V. I. Belyi, N. F. Zakharchuk, *ibid.*, 1982, No. 3, 93.
 137. T. P. Smirnova, V. I. Belyi and N. F. Zakharchuk, *Surface, Sect. Physics, Chemistry, Mechanics*, 1984, No. 2, 94.
 138. V. I. Belyi, T. P. Smirnova and N. F. Zakharchuk, *Thin Solid Films*, 1984, **113**, 157.
 139. M. B. Vidrevich, M. V. Slinkina, G. A. Kitaev, V. M. Zhukovsky and M. Ya. Khodos, *Izv. Akad. Nauk SSSR, Neorgan. Mater.*, 1983, **19**, 1257.
 140. M. B. Vidrevich, T. A. Drozdova and G. A. Kitaev, *Zavodsk. Lab.*, 1983, **49**, No. 10, 7.
 141. M. B. Vidrevich, A. A. Uritskaya, G. A. Kitaev, E. Ya. Mellikov and M. I. Krunka, *ibid.*, 1984, **50**, No. 1, 17.
 142. G. A. Kitaev, A. A. Uritskaya and M. B. Vidrevich, *Izv. Akad. Nauk SSSR, Ser. Neorgan. Mater.*, 1984, **20**, 17.
 143. M. B. Vidrevich, A. A. Uritskaya, I. M. Khaimova and G. A. Kitaev, *ibid.*, 1983, **19**, 16.
 144. M. B. Vidrevich, M. V. Slinkina, G. A. Kitaev, V. M. Zhukovsky and M. Ya. Khodos, *ibid.*, 1983, **19**, 1257.
 145. M. B. Vidrevich, A. A. Uritskaya, T. A. Drozdova and G. A. Kitaev, *ibid.*, 1984, **20**, 17.
 146. V. V. Zhdanov and B. K. Filanovsky, *Elektrokhimiya*, 1984, **20**, 225.
 147. R. N. Matakova, R. F. Yulmetova and A. I. Zebrev, *Zh. Analit. Khim.*, 1984, **39**, 1200.
 148. N. N. Kuzmina, V. I. Runtov and O. A. Songina, *Zavodsk. Lab.*, 1969, **35**, 274.
 149. V. V. Slepushkin and T. A. Nikulaeva, *Zh. Analit. Khim.*, 1984, **39**, 232.
 150. B. M. Stifatov, L. V. Kolzov and M. G. Yartsev, *Izv. Vyssh. Ucheb. Zaved. Khim. i Khim. Tekhnol.*, 1984, **27**, 314.
 151. M. Ya. Hodos, E. V. Bazarova, A. P. Palkin and Kh. Z. Brainina, *J. Electroanal. Chem.*, 1984, **164**, 121.
 152. D. M. Shub, V. P. Pakhomov, G. A. Ivanov and V. I. Veselovsky, *Elektrokhimiya*, 1969, **5**, 1448.
 153. Kh. Z. Brainina, E. V. Bazarova and M. Ya. Khodos, *ibid.*, 1984, **20**, 613.
 154. M. Ya. Khodos, G. M. Belysheva and M. B. Vidrevich, in *VIII All-Union Meeting on Polarography: Development and Application of Polarography and Related Methods*, Part 1, p. 95. Dnepropetrovsk Chem.-Technol. Inst., Dnepropetrovsk, 1984.
 155. Yu. A. Ivanov, A. I. Zinov'ev and E. I. Chubakova, *Zavodsk. Lab.*, 1983, **49**, No. 5, 21.
 156. A. I. Zinov'ev, A. P. Mazur and Yu. A. Ivanov, *ibid.*, 1983, **49**, No. 8, 10.
 157. J. Wang and B. Greene, *Anal. Chim. Acta*, 1982, **144**, 137.
 158. A. I. Zinov'ev, L. P. Mazur, Yu. A. Ivanov and A. G. Stromberg, *Zavodsk. Lab.*, 1983, **49**, No. 7, 11.
 159. Yu. A. Ivanov, S. S. Shumilin and L. D. Svintsova, *ibid.*, 1983, **49**, No. 8, 8.

160. A. G. Stromberg, V. A. Kosukhin and V. I. Kuleshov, *ibid.*, 1983, **49**, 24.
161. Yu. B. Kletenik, R. Yu. Bek, V. N. Kiryushov, A. P. Zamyatin, L. Yu. Polyakin and I. I. Burenkov, *Zh. Analit. Khim.*, 1982, **37**, 534.
162. R. M.-F. Salikhdzanova and G. I. Ginzburg, in *Chemico-Analytical Check As a Means of Product Quality Enhancement*, p. 108. Moscow, 1984.
163. M. R. Vyaselev, *Zh. Analit. Khim.*, 1983, **38**, 373.
164. *Idem*, *ibid.*, 1983, **38**, 382.
165. V. E. Norvell and G. Mamantov, in *Molten Salt Techniques*, D. G. Lovering and R. J. Gale (eds.), Vol. 1, p. 151. Plenum Press, New York, 1983.
166. O. Wolter and J. Heitbaum, *Ber. Bunsenges. Phys. Chem.*, 1984, **88**, 1.
167. L. S. Zaretsky, B. I. Varnovsky and M. I. Pidovich, in *VIII All-Union Meeting on Polarography: Development and Application of Polarography and Related Methods*, Part 2, p. 49. Dnepropetrovsk Chem.-Technol. Inst., Dnepropetrovsk, 1984.
168. K. Wikieł and Z. Kublik, *J. Electroanal. Chem.*, 1984, **161**, 269.
169. G. Dryhurst and D. D. McAllister, in *Laboratory Techniques in Electroanalytical Chemistry*, P. T. Kissinger and W. R. Heineman (eds.), p. 289. Dekker, New York, 1984.
170. A. N. Doronin, S. M. Veniaminova and O. L. Kabanova, *Zh. Analit. Khim.*, 1982, **37**, 1619.
171. V. V. Gaditskü, A. I. Ozerov and E. P. Kratsberg, *Zavodsk. Lab.*, 1984, **50**, No. 6, 20.
172. I. Gustavsson and K. Lundström, *Talanta*, 1983, **30**, 959.
173. *Idem*, *Z. Anal. Chem.*, 1984, **317**, 388.
174. J.-M. Kauffmann, Th. Montener, J. L. Vandenbalck and G. J. Patriarche, *Mikrochim. Acta*, 1984 **I**, 95.
175. A. N. Doronin and G. G. Muntyanu, *Zh. Analit. Khim.*, 1984, **39**, 607.
176. R. Yu. Bek, A. I. Maslii and T. I. Lavrova, *Izv. SO Akad. Nauk SSSR, Ser. Khim.*, 1972, No. 1, 25.
177. E. M. Roizenblat, in *Analysis Methods for Electronics Materials*, p. 187. Moscow, 1983.
178. C. Urbaniczky, *Acta Univ. Upsal. Abstr. Uppsala Diss. Fac. Sci.*, 1984, No. 736.
179. T. M. Florence, *Anal. Chim. Acta*, 1980, **119**, 217.
180. N. A. Gruzskova, *Zavodsk. Lab.*, 1982, **48**, No. 1, 12.
181. Kh. Z. Brainina, N. A. Gruzskova and L. I. Roitman, *ibid.*, 1983, **49**, 11.
182. T. E. Edmonds and J. Guoliang, *Anal. Chim. Acta*, 1983, **151**, 99.
183. R. C. Engstrom and V. A. Strasser, *Anal. Chem.*, 1984, **56**, 136.
184. K. Ravichandran and R. P. Baldwin, *ibid.*, 1983, **55**, 1782.
185. J. F. Rusling, *ibid.*, 1984, **56**, 575.
186. M. Cross and J. Jordan, *Pure Appl. Chem.*, 1984, **56**, 1096.
187. G. Farsang, W. Klunda, K. Lundström, U. Palm, E. Pungor, T. Ryan and J. D. R. Thomas, *Modern Trends Anal. Chem.*, Parts A-B, *Budapest*, 1984, A415.
188. Kh. Z. Brainina, *Zh. Analit. Khim.*, 1966, **31**, 529.
189. Kh. Z. Brainina and A. V. Tchernysheva, *Talanta*, 1974, **21**, 287.
190. H. Monien and K. Linke, *Z. Anal. Chem.*, 1970, **250**, 178.
191. B. Lenderman, H. Monien and H. Specker, *Anal. Lett.*, 1972, **5**, 837.
192. N. N. Kim, Yu. B. Vasiliev and I. V. Kudryashov, *Zh. Fiz. Khim.*, 1984, **58**, 226.
193. G. K. Budnikov, E. P. Medyantseva, A. V. Volkov and S. S. Aronzon, *Zh. Analit. Khim.*, 1983, **38**, 1283.
194. E. E. Stewart and R. B. Smart, *Anal. Chem.*, 1984, **56**, 1131.
195. J. Wang and B. A. Frelhs, *ibid.*, 1983, **55**, 1285.
196. A. M. Bond and G. G. Wallace, *ibid.*, 1984, **56**, 2085.
197. K. Štulík and V. Pacáková, *CRC Crit. Rev. Anal. Chem.*, 1984, **14**, 297.
198. E. Pungor and K. Tóth, *Anal. Proc.*, 1983, **20**, 562.
199. J. Wang, *Am. Lab.*, 1983, **15**, No. 7, 14.
200. J. Wang, H. D. Dewald and B. Greene, *Anal. Chim. Acta*, 1983, **146**, 45.
201. J. Wang and H. D. Dewald, *Talanta*, 1984, **31**, 387.
202. *Idem*, *Anal. Chem.*, 1984, **56**, 156.

DETERMINATION OF VOLATILE COMPONENTS OF SYSTEMS NOT IN THERMODYNAMIC EQUILIBRIUM

R. V. GOLOVNYA

N.A. Nesmeyanov Institute of Organoelement Compounds, USSR Academy of Sciences, Moscow, USSR

(Received 15 October 1985. Accepted 12 December 1985)

Summary—A review is given of the literature on the analysis of complex mixtures of organic compounds and a procedure proposed for the separation and identification of the components of such mixtures. Retention data obtained with several chromatographic columns are combined with information from mass and Fourier-transform infrared spectra and identifications made with the aid of a computer.

The combination of methods of investigation and determination of the composition of a mixture of volatile compounds evolved from a sample into its environment is known as "head-space" analysis. This method is extensively used in studies of natural materials.

THERMODYNAMIC APPROACH TO CLASSIFICATION OF HEAD-SPACE ANALYSIS

From texts on the topic¹⁻³ two variants of head-space analysis can be distinguished.⁴

The first is realized when the sample is a system in thermodynamic equilibrium. We are then dealing with vapour-phase analysis, since the vapour of each component is in direct contact with its condensed (liquid or solid) phase present in the sample. The vapour phase can then be analysed under either equilibrium or non-equilibrium conditions.^{5,6} In systems in thermodynamic equilibrium the composition of the vapour phase over a sample depends on the partition coefficients, concentration and structure of the components, and on the temperature and pressure, but is independent of the mass of the analysed sample.

The second variant is the determination of volatile compounds in samples that do not form systems in thermodynamic equilibrium. All biological samples, from micro-organisms to higher animals and plants, natural foods, animal and insect glands, various parts of plants, *etc.*, produce volatile substances. The study of phytocides and pheromones, as well as some ecological problems, is realized under thermodynamically non-equilibrium conditions, and so is the determination of volatile substances in urban air. In such circumstances the volatile compounds are not in contact with a condensed liquid or solid phase of the corresponding composition in the sample taken. Moreover they are frequently the products of chemical or enzymatic transformations occurring in the

sample and changing with time, and the material under investigation may not contain the analytes, but only their precursors. Thus when analysing the volatiles from such a non-equilibrium system we obtain the qualitative and quantitative composition of the mixture of components over the sample, but cannot judge the amount of these substances in the sample itself.

Hence there are at least three distinguishing features of the head-space analysis of these non-equilibrium systems: the dependence of the results on the mass of the sample and on the time needed to prepare the sample for analysis, and the absence of direct proportionality between the amounts of the volatile substances in the gas phase and their content in the specimen.

It is clear that the head-space analysis of the non-equilibrium systems requires a special methodology.

The head-space analysis of complex mixtures of volatile organic substances of biogenic origin generally includes four stages: concentration, gas-chromatographic (GC) separation, biological tests (organoleptic in the case of foods), and identification.

METHODOLOGICAL ASPECTS OF IDENTIFICATION

The development of a general methodology for the analysis of complex mixtures of organic substances⁷ opens the possibility of solving most efficiently the problems related to determination of environmental pollution, key components of food flavour, pheromones, *etc.*

In the early 70s work was started in the USSR on use of computers for identification in trace chemical analysis of natural organic substances.⁸⁻¹⁰ The main ideas proposed retain their significance despite the great progress in development of instrumental analysis, and are as follows.

1. A complex mixture of natural organic compounds should be separated into classes or fractions, because even the most modern chromatographic systems do not provide complete separation into the individual components, because of the large number of components that may be present and their wide range of concentrations. Further, substances in a natural mixture belong to different classes, so it is impossible to avoid overlapping of chromatographic zones, *i.e.*, to get one chromatographic peak for each particular compound. It is therefore logical to separate the mixture into fractions that will reduce to the minimum the overlaps in the subsequent analyses. Each of the fractions has to be analysed on 3 or 4 columns of different polarity. The choice of fractions for a detailed study is made by biological testing, for example, or by a sensory method in odour investigation.

2. To establish the structure of the components in the mixture it is necessary to use a wide variety of information, including the sorption characteristics, because no single technique, such as gas chromatography (GC) coupled with a detector or with mass spectrometry (GC-MS) or Fourier-transform infrared spectrometry (GC-FTIR), can supply enough information for complete interpretation of the composition of complex natural mixtures.

3. It is necessary to study the mathematical interrelation of the sorption characteristics with the structure of the individual compounds, and to use this in working out computerized identification programs, since deciphering complex natural mixtures only by use of reference substances is impossible because of the enormous number of standards required and the instability of many of them.

CURRENT EQUIPMENT FOR SEPARATION AND IDENTIFICATION

There are three methods combining "on line" the processes of separation of mixtures of organic substances and of obtaining data for identification: gas chromatography with a set of detectors (GC), gas chromatography/mass spectrometry (GC-MS), and the system combining a gas chromatograph with a Fourier-transform infrared spectrometer (GC-FTIR).

In all these systems the organic compounds are separated in either packed or capillary columns, which must be easy to prepare reproducibly and stable over long periods of operation. The retention parameters should be reproducible to within 1-2%. The column material should be glass or fused silica to minimize the decomposition and adsorption of the sample. A low carrier-gas flow-rate in capillary columns allows them to be combined directly with mass spectrometric and infrared detection. On the other hand, the low capacity of ordinary capillary columns with a stationary phase 0.2-0.3 μm thick is one of the

reasons for the lower sensitivity of the GC-MS and GC-FTIR systems. The development of thick-film capillary columns with an immobilized phase 1.0-5.0 μm thick has considerably increased the potential of these methods. Such columns have been described by Grob¹¹ and Ettre.¹²

Stable and reproducible capillary and packed columns

Thanks to a specially designed apparatus¹³ it is now possible to use the high-pressure static method to prepare reproducible glass capillary columns capable of sustaining reliable operation for up to 7 years, with retention indices constant within 1-2%. For instance,¹⁴ the following columns have been prepared by simultaneous application of the stationary phase and the salt: PEG-40M + Na₃PO₄, Triton X-305 + Na₃PO₄, PEG-40M + KF. By the same technique with application of a plasticizer, reproducible columns of OV-101, OV-25, SP-2300, OV-17 and OV-225 have been obtained.¹⁵

These capillary columns are convenient for the analysis of organic substances in natural mixtures. An example is given in Fig. 1, where chromatograms of two types of aroma¹⁶ are shown. Chromatograms of the volatile nitrogen bases of Antarctic krill¹⁷ are shown in Fig. 2.

Gas chromatography

Gas-liquid chromatography with suitable detectors has high selectivity and sensitivity, for example, as low as 10⁻¹⁶ g for the photoionization detector, and 10⁻¹⁴ g for thermionic and electron-capture detectors. Specific detectors are available for detection of compounds containing N, P, S, or halogen atoms. Their sensitivity to such compounds is several orders better than for hydrocarbons. By use of GC with a high-sensitivity detector, the sorption and structure characteristics of a substance can be obtained simultaneously. The sorption characteristics on a number of columns of different polarity are used for elucidation of the structure of substances.

GC-MS. Gas chromatography/mass spectrometry instruments make it possible to obtain a molecular fragmentation picture that is specific for every substance analysed. Mass spectra always contain information on the structure of molecules, though it is not so easy to interpret this information.¹⁸ New GC-MS systems include fast-scanning instruments capable of rapid change of operational mode from 70-eV electron impact (EI) to chemical ionization (CI). The CI spectra always show a high abundance of the molecular ion. The combination of EI and CI mass spectra for a molecule gives valuable information on the molecular structure and provides identification at ppm concentration levels and below. The system has a high rate (several hundred per run) of primary spectra output. The treatment of these spectra becomes a serious problem. For effective use of gas chromatograph/mass spectrometers expensive com-

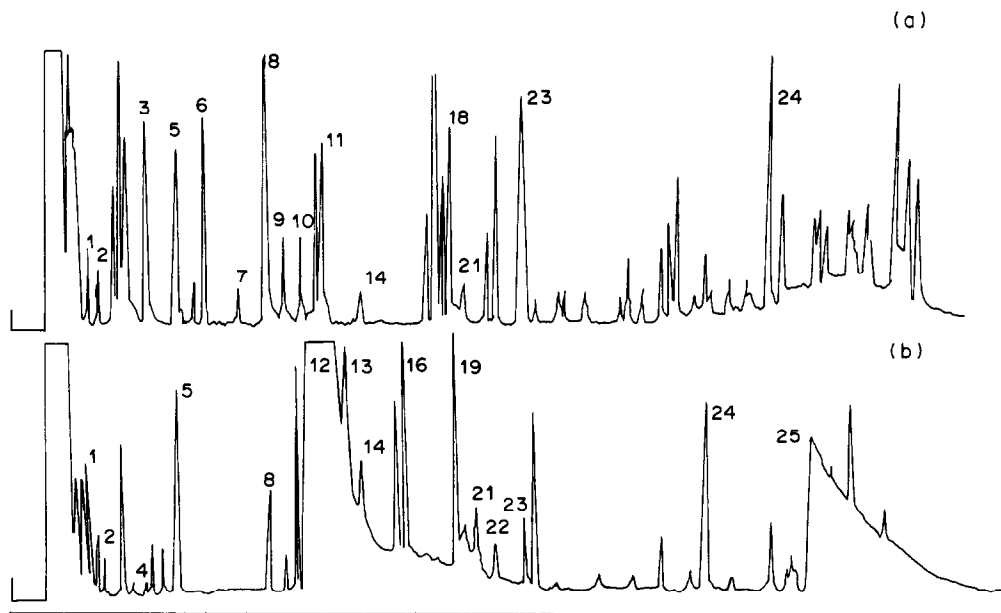


Fig. 1. Chromatograms for the components of natural broth and meat aroma.⁷⁰ Glass capillary column 50 m × 0.25 mm coated with OV-101; temperature programme 40° for 2 min and then 4°/min to 250°. 1, 2-Methylfuran; 2, 2,3-pentanedione; 3, hexanal; 4, vinyl-tert-butyl sulphide; 5, 2-methylfuran-3-thiol; 6, heptanal; 7, furanol; 8, benzaldehyde; 9, 2-methylthiophen-3-one; 10, diethyl sulphide; 11, 2-pentylfuran; 12, 2-methyl-3-mercaptopropan-1-ol; 13, 4-methyl-1-oxa-2-thiolane; 14, phenylacetaldehyde; 15, 2-acetylthiophene; tert-butyl n-butyl sulphide; 16, 3-acetylthiophene; isobutyl butyl sulphide; 17, 18, 3,5-dimethyl-1,2,4-trithiolane; 19, methyl butyl disulphide; 20, 2,6-dimethyl-1-oxo-3-thiane; 21, 2-methylfuryl 3-methyl disulphide; 22, 2,6-dimethyl-1,4-dithiane; 23, 2-methylacetylthiophene; 24, bis(2-methylfuryl) disulphide; 25, bis[3-(2-methylpropan-1-ol)] disulphide.

puters with special programs are needed.^{2,18} For identification, the mass spectrum of the fragmentation products of the molecule is compared with the spectra of standard substances available in a reference library. However, the experimental spectra frequently differ from those in the library; this is related to the change in the ratio of mass spectral line intensities because of the distortions in the analysis of complex mixtures in the dynamic mode (in flow), on account of fast recording of the spectrum and of "memory" effects in the instrument, since we are dealing with concentrations differing by several orders of magnitude. Thus, the fragment-ion peak heights cannot be determined with good accuracy and that complicates the identification.

There are also several limitations imposed by structural factors. For instance, it is sometimes impossible to establish from the mass spectra the structure of substituted aromatics, *cis* and *trans* isomers, positional isomers, or homologues with a long carbon chain. It is therefore usual to utilize subsidiary chemical reactions in determination of the structure of substances in natural mixtures by GC-MS. In turn it is then necessary to take into account and investigate the artifacts accompanying almost every chemical transformation. These problems are widely discussed in the literature.^{3,18-20}

The application of relative retention parameters to identification from mass spectral data has been substantiated.²¹

GC-FTIR. The GC-FTIR systems seem to be quite promising. The first such system was demonstrated by Low and Freeman²² but for a long time the low sensitivity prevented its wide use in head-space analysis. It took more than 10 years to improve the system. In the last few years, several reports on identification of components in complex mixtures of volatile organic compounds with the use of a new generation of GC-FTIR systems have appeared.^{18,23-26} The performance of the system depends to a large extent on the efficiency of the glass or fused-silica capillary column and on the thickness of its immobilized stationary phase coating. Substances eluted from the column by the carrier gas reach a gold-plated light-pipe cell made of a capillary restricted by salt windows and having a volume of 0.1–0.6 μl . The temperature in the light-pipe during spectral measurements is maintained at 200–250°. The spectrum output for every peak is produced within 0.3–0.5 sec by summation of 6–12 interferograms. At the outlet of the light-pipe the substance is detected with a flame-ionization or other suitable detector. Thus, the GC-FTIR system delivers the infrared spectra for all the substances eluted

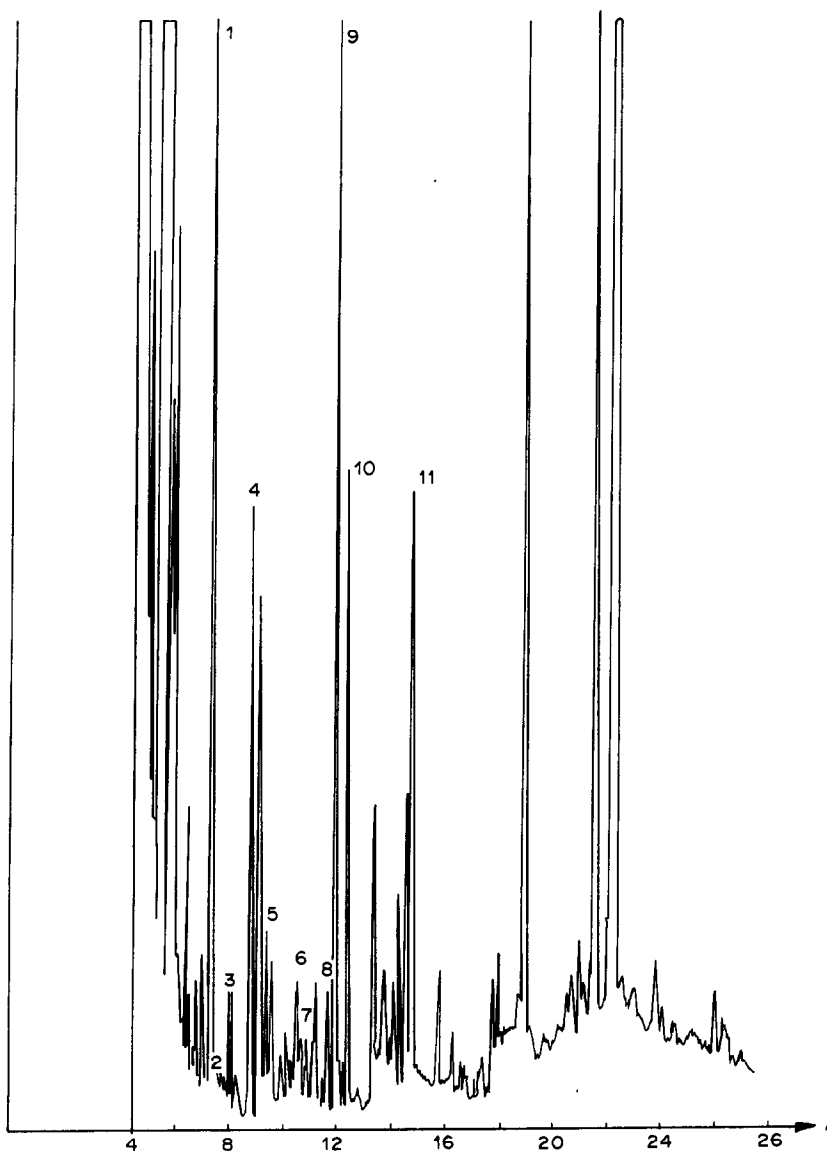


Fig. 2. Chromatogram of volatile nitrogen bases from the Antarctic krill *E. superba Dana*⁴⁴ on a glass capillary column coated with PEG-40M KF (40 m \times 0.28 mm). Temperature programme 4°/min from 80° to 160°. 1, Pyridine; 2, *N*-ethylpyrrole; 3, 2-picoline; 4, methylpyrazine; 5, tributylamine; 6, 2,5-dimethylpyrazine; 7, 2,3-dimethylpyrazine; 8, 2-methoxy-3-methylpyrazine; 9, 4-ethylpyridine; 10, trimethylpyrazine; 11, tetramethylpyrazine.

from the column (calculated by computer²⁴), and also the chromatogram recorded with an ordinary GC-detector.

The GC-FTIR system makes it possible to determine the structural features of a molecule, such as the functional groups present, double bonds and *cis-trans* isomerism. It also distinguishes between the isomers producing identical mass spectra and having close retention indices, as has been shown by analysis of a mixture of five butyl butanoates: 2-butyl isobutanoate, 2-butyl *n*-butanoate, *n*-butyl *n*-butanoate, isobutyl *n*-butanoate, and isobutyl isobutanoate.²³ An important property of the method is that the substances analysed do not undergo destruction, and

may be determined by other techniques, including mass spectrometry.

A major restraint on identification of substances by GC-FTIR is the shortage of data in the libraries of infrared spectra for organic substances in the gas phase at 200–250°. The banks of data usually contain the infrared spectra for substances in the liquid phase at room temperature, from which the gas-phase spectrum may differ considerably, complicating the identification. Nevertheless, GC-FTIR appears to be the most promising system for the present; its detection limits are rapidly decreasing and the spectra libraries are widening.

Ettré²⁵ used "on the fly" GC-FTIR for

identification of components in a petroleum sample preliminarily separated into groups of substances by liquid chromatography. He managed to identify 75% of the few hundred components by their infrared spectra. Note that in this case there was an unlimited amount of sample available and a large spectrum library for hydrocarbons in the gas-phase.

For head-space analysis, however, even systems as informative as GS-MS and GC-FTIR are still not sensitive enough, and cannot identify all the natural material components which can be detected by gas chromatography. Only the components present at concentrations above about 10^{-7} – 10^{-5} g/ml are determined, and the results of application of these systems to trace analysis of organic compounds in natural mixtures are rather modest. The upper detection limit in GC-FTIR is set by the capacity of the capillary column and the lower one by the sensitivity of the detector, which is proportional to the molar extinction coefficient. Thus, for example, only 15% of 200 flavour components of the African fruits cherimoya and guava were identified in this way; the components present at 1 ng/g concentration or lower did not produce interpretable infrared spectra.^{26,27}

Specialists in GC-FTIR believe that the instruments are very convenient for the routine analysis of flavour components, especially in the case of suspected adulteration of natural extracts^{24,28} as well as for detection of the functional groups of the key odour components.

Because a GC-FTIR system can be combined with a mass spectrometer, it is interesting to compare the performance of these systems. For example, in the analysis of hazardous-waste soil by fused-silica capillary GC-FTIR and GC-MS systems operated in parallel,²⁹ of the 44 major peaks obtained by separation on identical columns, 28 were identified, 15 predicted and 1 unidentified by GC-FTIR, the corresponding numbers being 13, 23 and 8 for GC-MS. It is seen that GC-FTIR is superior in identification power.

Wilkins *et al.*³⁰ compared the results for identification of volatile components of mint oil and of an industrially produced lacquer thinner, using the GC-FTIR-MS system "on-the-fly". The mixtures of volatiles, after separation on a capillary column, contained 30 major components each. Mass spectra were recorded both in EI mode at 50 eV and after CI (with methane) at 12 eV. The MS library contained 32000 substances. All data-processing was done by computer. For the mint oil, the isomers which could not be distinguished by MS were fairly identified by infrared, for example, the barely separable α - and β -pinenes, *d*-isomentone and *l*-mentone. However, if the content of a substance in the mixture was less than 0.5%, its infrared spectrum could not be interpreted. All 30 mint components were identified. In the analysis of the lacquer thinner only 18 out of 30 volatile compounds were identified, and the

presence of certain functional groups or structural fragments was deduced for 10 of the rest.

SORPTION-STRUCTURE CORRELATIONS AND THEIR APPLICATION TO IDENTIFICATION

In our opinion, too little attention is still being paid to the possibilities for identifying compounds in complex natural mixtures by means of the sorption parameters (Fig. 3), which have been successfully used in the analysis of isomeric unsaturated hydrocarbons,³¹ of saturated, unsaturated and polycyclic hydrocarbons,³² and of odour components.^{10,33} The sorption-structure characteristics are especially useful for determination of aliphatic compounds in natural mixtures.

In homologous series, there are regular changes in the retention parameters with increasing carbon chain-length, depending on the nature of the functional groups, the sorbent and the conditions of analysis. Methods of computer-identification from gas chromatographic data without use of standards have been developed.^{10,34}

Identification without use of standards uses a specially selected system of either packed or capillary columns for a particular mixture of substances having similar functional groups or structural fragments, to provide optimal separation and make it possible to express mathematically the dependence of the retention indices on the structures of the substances and their physico-chemical properties. The identification is done by computer with a special program.^{9,10,34}

Productive use of the method depends on knowledge of the sorption thermodynamics for the substances under consideration, on stationary phases of different structure. Studies on this have been made for some years.³⁵⁻⁴⁰

Universal equation for calculation of sorption characteristics of homologues

As a result of a series of studies^{36,37,40-42} on the thermodynamics of sorption, a general type of mathematical dependence of the retention index values on the carbon number in a homologous series was found to exist. For the first time, universal equations are available which permits the sorption characteristics to be calculated with good accuracy for all the homologues, including the first members of a series.^{41,43-45}

$$I = A + Bm + C \frac{\log m}{m} + \frac{D}{(m-2)^2 + 0.1} \quad (1)$$

$$\Delta G = -2.3RT \left[\alpha + \beta m + \gamma \frac{\log m}{m} + \frac{\xi}{(m-2)^2 + 0.1} + \log \frac{T\rho}{273} \right] \quad (2)$$

where I is a retention index or may be $\log V_g$, or $\log i'$, m is the homologue's carbon number, ΔG is the partial free energy of sorption, A , B , C , D , α , β , γ , ξ

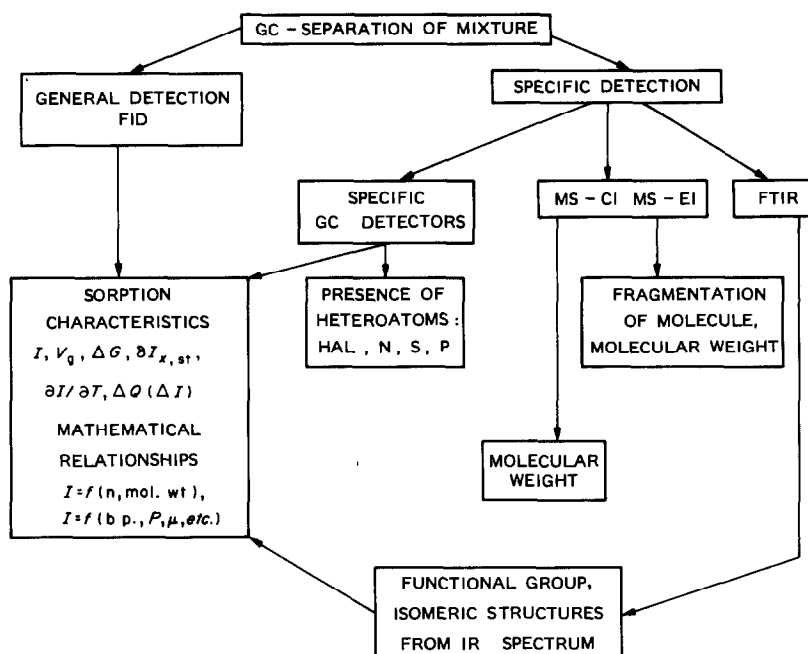


Fig. 3. Set of analytical data to be used in identification of organic substances in natural mixtures. I —retention index; V_g —specific retention volume; G —partial free energy of sorption; $\delta I_{x,stand}$ —difference in retention indices of substance and standard; $\delta I/\delta T$ —temperature dependence of the retention index; ΔQ —thermodynamic equivalent of ΔI .

are coefficients in the equations, ρ is the density of the stationary phase and T is the absolute temperature of the column.

Thus, instead of the eight known correlation equations⁴⁶⁻⁵³ used in calculation of retention indices for the members of homologous series, we have now one general equation (1) based on the principle of non-additive change in the sorption energy of homologues with increasing chain length. The equation takes account of the non-linear nature of the van der Waals energy change in a homologous series on chromatography. Under the conditions of gas-liquid chromatography, the validity of the equation has been affirmed for 74 homologous series and 10 stationary phases of different polarity.

The gas-solid chromatography retention indices and thin-layer chromatography R_f -values for homologues also obey equation (1), and so do the logarithms of the partition coefficients for the distribution of homologues between water and organic solvents.⁴²

The sorption characteristics are calculated by equation (1) with an accuracy sufficient for identification purposes, but accuracy can be improved by increasing that of experimental determination of the retention values.⁵⁴ Equation (1) is convenient for computer-assisted identification of aliphatic compounds.

GC/computer identification algorithm

In spite of the large number of studies on the use of computers in chromatography there are only a few

reports on automated identification of organic substances in a mixture.⁵⁵⁻⁶¹ In these, samples containing generally not more than 20 known compounds were analysed. With such a small number of components, complete separation of the mixture was achieved by using only one (or sometimes two) gas chromatographic columns. In analysis of complex multi-component mixtures, such as those of volatile substances of biogenic nature, it is impossible to obtain complete resolution on any of the existing types of GC-columns, either packed or capillary, and such examples were not considered earlier from the viewpoint of computer-identification. The programming of the recognition process was based on the idea of library comparison of GC retention parameters, which is suitable in a search for known compounds in comparatively simple mixtures, e.g., analysis of the amino-acid composition of peptides.⁵⁷ In addition, the early methods of computer-identification dealt, as a rule, with the retention parameters for only one column, with a chosen stationary phase. This information is not sufficient for the analysis of natural mixtures containing several hundred chemical compounds of different classes, the retention parameters of which frequently coincide. Hence, none of the algorithms suggested earlier⁵⁵⁻⁶¹ for mathematical identification has been applied to deciphering the composition of natural mixtures of substances.

The first methodological approach to identification of natural mixtures of substances was based on chromatographic separation of organic compounds

with the same type of functional group, with a system of 3 or 4 columns of different polarity which provided maximum resolution of components with minimum overlap of the chromatographic zones.^{8,9} Later it was shown^{57,60,62} that the reliability of identification increases under these conditions. The universal expression (1) and the thermodynamic criterion^{38,39} determining the nature of the functional group and the number of carbon atoms in a homologue, are incorporated in the computer programs designed for identification of aliphatic compounds without use of standards. A flow-sheet for computer-identification of odour components from GC data is shown in Fig. 4. According to the scheme, the GC retention

indices for the sample are determined on 3 or 4 columns of different polarity, and input to the computer, which utilizes the linear equation to determine the thermodynamic criterion characterizing a functional group (or molecular fragment) and the number of carbon atoms in a homologue, the hyperbolic equation for the dependence of the retention index on the boiling point of the substance, and the general equation (1) describing the dependence of the index value on the number of carbon atoms. The computer memory needed in deciphering the composition of odour components is not less than 16 kbytes. The computer displays the components identified, and their retention indices, boiling points and expected

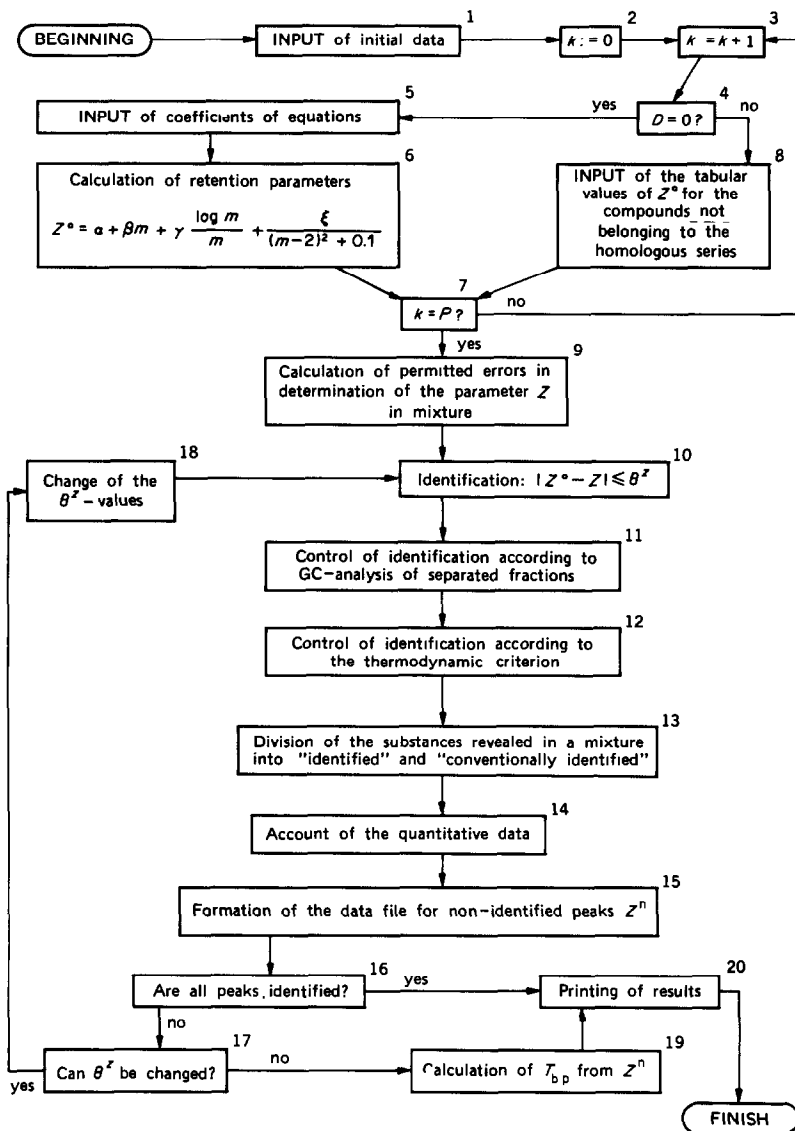


Fig. 4. Schematic representation of a computer program for investigation of composition of complex mixtures by use of GC-data. D —parameter indicating method of identification: $D = 0$ —without a standard; $D = 1$ —use of table of standards; Z° and Z —retention indices of standard and compound sought, respectively; θ^z —permitted error in determination of Z in a mixture; m —homologue carbon number; k —number of the homologous series $k = 1, 2, \dots, P$; $T_{b,p}$ —boiling point calculated from the retention index Z for a non-identified peak on a non-polar column; $\alpha, \beta, \gamma, \xi$ —coefficients of the equations.

number of carbon atoms, and the probable type of functional group for tentatively identified compounds.

The GC/computer method is limited by the need to use chemical reactions for extraction and concentration of organic substances with identical functional groups, and to the difficulties in identification of isomeric derivatives of aromatic and heterocyclic compounds. In this case the computer performs identification by comparison of the retention indices on 3 or 4 columns with the standard values. For example, in the GC/computer identification of sulphur-containing components of meat flavourings, 37 compounds were identified,³³ but isomeric *S*-substituted furans and thiophenes were also found. The problem was successfully solved only by gas chromatography/mass spectrometry of derivatives of the furans and thiophenes, a subtraction operation on the mass spectra before and after the derivative formation, and comparison of the results with the library values of *I* and ΔI . In this way, 8 compounds from the furan and thiophene series were identified and certain information on the structure of some heterocyclic substances was additionally obtained.⁶³ This example shows the complexity of identification of odour components.

Identification by GC/computer technique

This technique of GC/computer identification has been successfully used for interpretation of the odours of meat,⁶⁴⁻⁶⁶ salmon,⁶⁷ krill,¹⁷ bread,⁶⁸ sherry,⁶⁹ and volatile compounds from the Maillard reaction simulating meat and chicken flavour.³³

The correctness of the GC/computer identification of odour components was verified for the carbonyl

compounds in a concentrate of natural meat flavour.⁶⁵ The analysis was done by three methods simultaneously *viz.* by chromatography of free organic bases under GLC conditions, separation of their 2,4-dinitrophenylhydrazones by liquid chromatography with refractometric detection, and gas chromatography/mass spectrometry. The fair agreement between the results obtained shows the GC/computer-identification method to be quite reliable for determination of aliphatic compounds. A second example, for determination of sulphur-containing compounds by two methods,⁷⁰ is given in Table 1.

The study of food flavour components has produced some practical results. Flavour additives imitating the natural aromas have been created for sturgeon and salmon caviare, salmon fillet,⁹ and meat.^{33,66,70,71} The cause of odour production appearing on storage of casein and its co-precipitate has been determined.^{72,73} Volatile amines were shown to be a taxonomic sign of micro-organisms.⁷⁴ The production of nitrogenous bases during sherry fermentation has been estimated.⁷⁵ A procedure for determination of chocolate compositions has been suggested,⁷⁶ and it has been shown that the composition of bread flavour components depends on the methods of baking and dough making.⁷⁷

SCHEME FOR HEAD SPACE ANALYSIS OF NATURAL SYSTEMS NOT IN THERMODYNAMIC EQUILIBRIUM

In conclusion we propose the following system for determination of the composition of trace organic substances in complex mixtures. A concentrate from the sample is separated into fractions or classes,

Table 1. Substances identified in the vapour of a meat flavour composition made from autolysine⁷⁰

No.	Compound	Analytical procedure	No.	Compound	Analytical procedure
ALIPHATICS					
1	Hydrogen sulphide	GC	22	1,2-Dithiane	GC
2	Methanethiol	GC	23	3,6-Dimethyl-1,2-dithiane	GC,MS
3	Ethanethiol	GC	THIOPHENES		
4	1-Propanethiol	GC	24	Thiophene	GC,MS
5	2-Methylpropanethiol	GC	25	2-Methylthiophene	GC,MS
6	2,3-Dithiabutane	GC,MS	26	2-Formylthiophene	GC,MS
7	2,3-Dithiapentane	GC,MS	27	3-Methyl-2-formylthiophene	GC,MS
8	3,4-Dithiahexane	GC,MS	28	Dimethylformylthiophene	MS
9	3,4-Dithiaheptane	GC	29	3-Acetylthiophene	GC,MS
10	2,7-Dimethyl-4,5-dithiooctane	GC	30	Methylacetylthiophene	MS
11	3,5-Dithiaheptane	GC	31	2-Methylthiophen-3-thiol	MS
12	2,4,6-Trimethyl-3,5-dithiaheptane	GC	FURANS		
13	4-Ethyl-3,5-dithiaheptane	GC	32	2-Methylfuran-3-thiol	GC,MS
14	2,4-Dimethyl-3-thiapentane	GC	33	Methylfuranthiol	MS
15	3-Mercaptobutan-2-one	MS	34	Furylmercaptan	GC,MS
16	4-Mercaptopentan-3-one	MS	35	2-Methyldihydrofuran-3-thiol	MS
17	3-Mercaptopentan-2-one	MS	36	Furyl methyl sulphide	GC,MS
18	2-Thiapentanal	GC,MS	37	2-Furyl methyl disulphide	MS
CYCLICS					
19	1,3-Dithiolane	GC	38	3-(2-Methylfuryl) methyl disulphide	MS
20	2-Methyl-1,3-dithiolane	GC	39	Bis[3-(2-methylfuryl)]disulphide	GC,MS
21	2-Methylthiophen-3-one	MS	40	Bis-(2-methylfuryl)disulphide	MS
			41	Bis(furyl) disulphide	MS
			42	12-Methyldihydrofuryl)disulphide	MS

which are analysed with a GC-FTIR-MS system. The components are separated on 3 or 4 capillary columns. The data for identified and tentatively identified compounds are obtained by use of a special computer program operating with sorption-structure correlations and simulating the experimenter's reasoning. The data obtained from the sorption characteristics are juxtaposed by the computer with the data obtained from spectra-structure correlations on the basis of infrared and MS characteristics. The methodology of identification by use of infrared spectra is rapidly developing and can be utilized in the creation of the "artificial intelligence" programs⁷⁹ for identification by gas-phase infrared spectra and chromatography.

The list of components of the mixture, with specified reliability of the identification, and predicted physicochemical properties and structure for tentatively identified substances, is obtained after computer processing of the whole of the data from the GC-FTIR-MS system. For complete identification of minor components in the mixture, the system has to give recommendations for an optimal version of the analysis, involving subsidiary chemical and physical methods. The major difficulties in implementation of the scheme consist in obtaining the necessary data library and in working out the "artificial intelligence" algorithm.

REFERENCES

- G. Charalambous (ed.), *Analysis of Food and Beverages: Headspace Techniques*, p. 245. Academic Press, New York, 1978.
- P. Schreier (ed.), *Analysis of Volatiles*, p. 320. De Gruyter, Berlin, 1984.
- H. Maarse and R. Belz, *Isolation, Separation, and Identification of Volatile Compounds in Aroma Research*, p. 280. Akad. Verlag, Berlin, 1981.
- R. V. Golovnya, in *Prikl. Kromatografi*, p. 253. K. I. Sakodinskii (ed.), Nauka, Moscow, 1984.
- A. G. Vitenberg and B. V. Ioffe, *Gasovaya Ekstraksiya in Khromatograficheskoy Analize*, Khimiya, Leningrad, 1982.
- B. Kolb, *Angewandte Gas-Chromatographie*, Vol. 15, Perkin-Elmer, Überlingen, 1972.
- L. A. Gribov, Yu. A. Zolotov, V. I. Kalmanovskii, L. L. Kunin, Yu. Lukhskov, A. A. Popov and V. S. Torontsev, *Zh. Analit. Khim.*, 1982, **37**, 1104.
- R. V. Golovnya, in *Letuchie Biologicheski Aktivnye Soedineniya Biogennogo Proiskhozhdeniya*, M. Telitchenko and A. Tambiev, (eds.), p. 731. MGU, Moscow, 1971.
- Idem*, *Usp. Khim.*, 1976, **45**, 1895.
- Idem*, *J. Chromatog.*, 1982, **251**, 249.
- R. Grob and G. Grob, *J. High Resol. Chromatog., Chromatog. Commun.*, 1983, **6**, 133.
- L. S. Ettre, G. L. McClure and F. D. Walter, *Chromatographia*, 1983, **17**, 1.
- R. V. Golovnya, A. L. Samusenko and E. A. Mistryukov, *J. High-Resol. Chromatog., Chromatog. Commun.*, 1979, **2**, 609.
- A. L. Samusenko, R. V. Golovnya, V. B. Khabarov and A. F. Aerov, *USSR Patent*. 1111101; *Chem. Abstr.*, 1984, **101**, 183210q.
- R. V. Golovnya, A. L. Samusenko, A. V. Vasil'ev and T. E. Kuz'menko, *USSR Patent* 1132227; *Chem. Abstr.*, 1985, **102**, 178390q.
- T. V. Mikhailova, A. I. Gren, L. E. Vysotskaya, T. A. Misharina, S. V. Vitt and R. V. Golovnya, *Nahrung*, 1985, **29**, 671.
- N. I. Svetlova, R. V. Golovnya, I. L. Zhuravleva, D. N. Grigoryeva and A. L. Samusenko, *ibid.*, 1985, **29**, 143.
- R. Flath, in *Flavour Research—Recent Advances*, R. Tekanishi, R. Flath, and H. Sagisawa (eds.), p. 83. Dekker, New York, 1981.
- L. Nykänen and H. Suomalainen, *Aroma of Beer, Wine and Distilled Alcoholic Beverages*, p. 412. Akad. Verlag, Berlin, 1983.
- D. Rosenthal, *Anal. Chem.*, 1982, **54**, 63.
- B. N. Golby, P. N. Ryan and I. E. Wilkinson, *J. High Resol. Chromatog., Chromatog. Commun.*, 1983, **6**, 72.
- M. I. Law and S. K. Freeman, *Anal. Chem.*, 1967, **39**, 194.
- W. Herres in *Analysis of Volatiles*, P. Schreier (ed), p. 183. De Gruyter, Berlin, 1984.
- D. N. Hanna, G. Hangac, B. A. Hohne, G. W. Small, R. C. Wieboldt and T. L. Isenhour, *J. Chromatog. Sic.*, 1979, **17**, 423.
- L. S. Ettre, *Chromatographia*, 1983, **17**, 519.
- P. Schreier and H. Idstein in *Analysis of Volatiles*, P. Schreier (Ed.), p. 294. De Gruyter, Berlin, 1984.
- W. Herres, H. Idstein and P. Schreier, *J. High Resol. Chromatog., Chromatog. Commun.*, 1983, **6**, 590.
- G. L. McClure, *Chromatog. Newsl.*, 1983, **11**, 3.
- K. H. Schafer, T. L. Hayes, J. W. Brasch and R. J. Jakobsen, *Anal. Chem.*, 1984, **56**, 237.
- C. L. Wilkins, G. N. Giss, R. L. White, G. M. Brissey and E. C. Onyiriuka, *ibid.*, 1982, **54**, 2260.
- L. Soják, E. Král'ovičová, I. Ostrovský and P. A. Leclercq, *J. Chromatog.*, 1984, **292**, 241.
- T. B. Gavrilova, A. V. Kiselev and T. M. Roshchina, *ibid.*, 1980, **192**, 323.
- R. V. Golovnya, T. A. Misharina, V. G. Garbuzov and F. A. Medvedev, *Prikl. Biokhim. i Mikrobiol.*, 1983, **19**, 681.
- D. N. Grigoryeva, R. V. Golovnya, I. L. Zhuravleva, N. I. Svetlova and G. V. Sergeev, *Zh. Analit. Khim.*, 1979, **34**, 2434.
- R. V. Golovnya and T. A. Misharina, *Usp. Khim.*, 1980, **49**, 172.
- R. V. Golovnya and D. N. Grigoryeva, *Izv. Akad. Nauk SSSR, Ser. Khim.*, 1983, 995.
- Idem*, *ibid.*, 1984, 1240.
- Idem*, *J. Chromatog.*, 1984, **290**, 275.
- Idem*, *Chromatographia*, 1984, **18**, 449.
- R. V. Golovnya and T. A. Misharina, *J. High Resol. Chromatog., Chromatog. Commun.*, 1980, **3**, 1.
- R. V. Golovnya and D. N. Grigoryeva, *Chromatographia*, 1983, **17**, 613.
- Idem*, *Sb. Dokl. Mezhdunarod. Konf. Stran SEV*, Bratislava, Czechoslovakia, 1982, p. 61.
- Idem*, *Zh. Analit. Khim.*, 1985, **40**, 316.
- R. V. Golovnya, I. L. Zhuravleva, N. I. Svetlova, M. B. Terenina, D. N. Grigoryeva and S. B. Gudnik, *ibid.*, 1981, **36**, 748.
- R. V. Golovnya, I. L. Zhuravleva, M. B. Terenina and D. N. Grigoryeva, *ibid.*, 1981, **36**, 968.
- V. M. Sakharov, Yu. N. Bogoslovsky and K. I. Sakodinsky, *J. Chromatog.*, 1971, **58**, 103.
- D. E. Diskina, L. S. Soyak, B. V. Roiz and M. S. Vigdergauz, in *Uspekhi Gazovoi Khromatografii*, p. 14. Kazany, Vypusk 3, 1973.
- G. J. Nelson, *Lipids*, 1974, **9**, 254.
- A. Orav and K. Kuningas, *Izv. Akad. Nauk SSSR, Ser. Khim.*, 1980 **29**, 174.
- M. S. Vigdergauz and V. I. Semkin, *Zh. Fiz. Khim.*, 1972, **46**, 948.

51. F. J., Heeg, R. Zinburg, H. J. Neu and K. K. Ballschmiter, *Chromatographia*, 1979, **12**, 452.
52. R. V. Golovnya, V. G. Garbuzov and T. A. Misharina, *Izv. Akad. Nauk SSSR, Ser. Khim.*, 1976, 2266.
53. F. S. Calixto and A. Garcia-Raso, *Chromatographia*, 1981, **14**, 143.
54. R. V. Golovnya and D. N. Grigoryeva, *J. High Resol. Chromatog., Chromatog. Commun.*, 1983, **5**, 269.
55. V. D. Shvarts, A. A. Abots, A. M. Kofman and Ya. Ya. Silis, *Zh. Analit. Khim.*, 1975, **30**, 2306.
56. K. Yabumoto, W. G. Jennings and M. Yamaguchi, *Anal. Biochem.*, 1977, **78**, 244.
57. B. M. Nair, *J. Chromatog.*, 1978, **155**, 249.
58. K. R. Betty and F. W. Karasek, *ibid.*, 1978, **166**, 111.
59. B. E. Blaisdell, S. C. Gates, F. E. Martin and C. C. Sweeley, *Anal. Chim. Acta*, 1980, **117**, 35.
60. L. V. Semenchenko, F. I. Lapteva, V. G. Brezhneva, *Zh. Analit. Khim.*, 1978, **33**, 2244.
61. H.-J. Stan and H. Goebel, *J. Chromatog.*, 1983, **268**, 55.
62. J. Ševčík, *Advan. Chromatog.*, 1979, 157.
63. S. V. Vitt, V. M. Belikov, T. A. Misharina and R. V. Golovnya, *Tezisy v Vsesoyuznoi Konferentsii po Analiticheskoi Khimii Organicheskikh Soedinenii*, p. 189. Nauka, Moscow, 1984.
64. V. G. Garbuzov, G. Rehfeld, G. Wölm, R. V. Golovnya and M. Rothe, *Nahrung*, 1976, **20**, 235.
65. V. P. Urälets and R. V. Golovnya, *ibid.*, 1980, **24**, 155.
66. R. V. Golovnya, V. G. Garbuzov, I. Ya. Grigoryeva, S. L. Zharich and A. S. Bolshakov, *ibid.*, 1982, **26**, 89.
67. T. A. Misharina, R. V. Golovnya and S. V. Vitt, *Prikl. Biokhim. i Mikrobiol.*, 1985, **21**, 107.
68. R. V. Golovnya, N. G. Enikeeva, I. L. Zhuravleva and A. S. Sjuzko, *Nahrung*, 1974, **18**, 143.
69. Z. N. Kishkovskii, N. G. Enikeeva, G. F. Dremucheve, R. V. Golovnya and I. L. Zhuravleva, *Prikl. Biokhim. i Mikrobiol.*, 1977, **13**, 773.
70. T. V. Mikhailova, A. I. Greny, L. E. Vysotskaya, T. A. Misharina, S. V. Vitt and R. V. Golovnya, *VINITI*, Dep. No. 5644-83, 1983, 1.
71. R. V. Golovnya, N. I. Svetlova, I. L. Zhuravleva and D. N. Grigoryeva, *Prikl. Biokhim. i Mikrobiol.*, 1983, **19**, 277.
72. R. V. Golovnya, N. I. Svetlova, V. A. Obelets, N. K. Rostrosa and P. F. Dyachenko, *ibid.*, 1979, **15**, 93.
73. R. V. Golovnya, *Nahrung*, 1982, **26**, 603.
74. R. V. Golovnya, I. L. Zhuravleva and M. B. Terenina, *Prikl. Biokhim. i Mikrobiol.*, 1985, **21**, 16.
75. Z. N. Kishkovskii, L. P. Palamarchuk, R. V. Golovnya, I. L. Zhuravleva, *ibid.*, 1980, **16**, 446.
76. L. M. Bogod, T. P. Ermakova, I. L. Zhuravleva, D. N. Grigoryeva and R. V. Golovnya, *Khlebopek. i Konditer. Prom.*, 1984, No. 2, 29.
77. N. G. Enikeeva, T. T. Kichaeva, L. I. Pushkova, R. V. Golovnya and B. M. Terenina, *Tezisy v Vsesoyuznoi Konferentsii po Analiticheskoi Khimii Organicheskikh Soedinenii*, p. 69. Nauka, Moscow, 1984.
78. M. E. Elyashberg, L. A. Gribov and V. V. Serov, *Molekulyarnyi Spektralnyi Analiz i EVM*, p. 307. Nauka, Moscow, 1980.
79. P. G. Barker, *Computers in Analytical Chemistry*, p. 488. Pergamon Press, Oxford, 1983.

PERSPECTIVES IN THE DEVELOPMENT OF THE THEORY OF SPARK-SOURCE AND LASER-PLASMA SOURCE MASS-SPECTROMETRY

G. I. RAMENDIK, B. M. MANZON and D. A. TYURIN

Vernadsky Institute of Geochemistry and Analytical Chemistry, USSR Academy of Sciences,
Moscow, USSR

N. E. BENYAEV and A. A. KOMLEVA

All-Union Scientific Research Institute for Medical Engineering, Moscow, USSR

(Received 15 October 1985. Accepted 14 August 1986)

Summary—The processes of substance evaporation and atom ionization under different conditions of spark discharge or laser radiation are considered. It is shown that the dependence of the relative sensitivity coefficients on the properties of an element can be presented as the product of two exponents with parameters proportional to the atomization energies and first ionization potentials of the element. Differences in matrix composition and conditions influencing a sample in the ion source are considered by means of introducing two fitting parameters—atomization and ionization “temperatures”—into these exponents. Experiments carried out with the help of mass-spectrometers with spark and laser ion sources have corroborated the validity of the suggested quasi-equilibrium model and shown the possibility of its application for the improvement of the accuracy of analysis without use of standards as well as for checking the stability of experimental conditions in the process of analysis with standard samples.

Mass-spectrometry with spark¹⁻⁶ and laser-plasma^{1,7,8} ion-sources is more and more widely used in analytical practice. Many authors have studied the mechanisms of ion and ion-beam formation, with two main objectives.

(1) A purely scientific one—to study the laws of ion formation and detection in the important group of physical methods of analysis.

(2) A practical one—to improve the precision and accuracy of the methods and, in particular to find quantitative methods that do not require use of standards. Solution of this problem could give mass-spectrometry extraordinary advantages over other methods of inorganic analysis.

Attempts to work out “standardless” (absolute) methods on the basis of purely empirical expressions have been made in spark-source mass-spectrometry for more than 20 years, though without any success (as shown in a critical review of the literature¹⁰). In laser-source mass-spectrometry a very simplified qualitative model of ion-formation has been advanced,¹¹ which led the authors to the conclusion that at an energy flux $q = 2 \times 10^9$ W/cm² the relative sensitivity coefficients (RSC) for all elements would be equal to unity, but this approach has been criticised.¹² It has been found that the RSC values depend on the interaction conditions as well as on the sample matrix composition.

In the general case the task of determining the composition of the ion-beam by calculation from the sample composition and the interaction conditions is extremely difficult, since several complex, inter-

connected and not fully studied processes occur simultaneously in the vacuum spark discharge or laser-plasma cloud. If a solution to the problem could be found either by mathematical analysis or by means of computer modelling, it would be possible to apply it only to substances with similar chemical composition. If, as happens in the majority of cases, the matrix composition is not known with enough precision, it is necessary to solve the even more complicated inverse problem of determination of the sample composition from the mass-spectrum. At present no real progress seems to have been made in this field.

Thus, to create a complete enough theory of spark-source and laser-plasma mass-spectrometry it is necessary to exert a great deal of effort. This paper puts forward what we think is sufficiently well-founded, semi-empirical model allowing more systematic further investigation of ion-formation mechanisms as well as direct calculation of the RSC values from the experimental results with a precision acceptable for quantitative analysis.

1 PHYSICAL ASPECTS OF ATOMIZATION, IONIZATION AND RECOMBINATION IN PLASMA SOURCES

Many papers and some reviews on the physics of spark discharge in a vacuum^{13,14} and on the effect of laser radiation on a sample^{9,15} have recently been published. In our work we have used the results of these investigations, as well as a number of assumptions.

(1) We have assumed that when a sample is subjected to a spark discharge or laser radiation some similar processes occur and the parameters of the plasma formed are similar.^{10,16}

(2) We have conditionally divided the process of mass-spectrum formation into a number of stages:^{16,17} sample evaporation and atomization, atom ionization, plasma expansion, ion-beam formation, mass-analysis, ion-detection. In this paper we will discuss the influence of the first three stages on the mass-spectrum and the RSC values, since the influence of the other stages can be assessed with the help of appropriate mass-spectrometer calibration.¹⁸

(3) To a first approximation we assume there is thermodynamic equilibrium between the components of the medium. Such an assumption was put forward earlier for secondary-ion mass-spectrometry¹⁹ and laser mass-spectrometry,²⁰ but was related only to the ionization process. At the same time it was tacitly assumed that the atomization and plasma-expansion processes do not affect the RSC values.

When a spark discharge or laser radiation is applied to a solid, one of two effects can result.

(1) There is no energy absorption by the vapour or plasma. This occurs when the laser radiation flux density q is $\leq 10^8$ – 10^9 W/cm² (depending on the target substance). For spark discharge this corresponds to initiation of the breakdown stage, *i.e.*, the first few nanoseconds after the voltage applied to the electrodes reaches the breakdown value.

(2) A sufficient amount of energy is absorbed by the vapour. When a spark discharge is applied, strong energy absorption by the vapour occurs shortly after the beginning of the evaporation process. Plasma appears in the interelectrode gap and electric breakdown occurs there. Similarly, with laser excitation the change to energy-absorption by the vapour occurs very rapidly.¹⁶

Evaporation and atomization

The character of the evaporation depends on the energy flux ϵ and the specific energy of sublimation A . If the energy flux in a layer with thickness d is equal to ϵ , heat conduction will reduce it to ϵ' given by

$$\epsilon' = \epsilon \frac{d}{d'} = \epsilon \frac{d}{d + d_h} \quad (1)$$

where d_h is the thickness of the layer heated by heat conduction, and $d' = d + d_h$ is the total thickness of the warmup layer.

If the energy release time t is small compared to the expansion time t_e of the absorbing layer,¹⁵ then $d_h = \sqrt{\chi t_e}$, where $t_e \approx d/\sqrt{\epsilon}$, and χ is the thermal diffusivity coefficient. If t is long enough to establish a stationary evaporation regime, $d_h = \chi/u$, where u is the velocity of the evaporation front.

When a short (about 10 nsec) laser radiation pulse with $q = 10^8$ – 10^{10} W/cm² acts on metals, $d \approx 10^{-6}$ – 10^{-5} cm, and $d_h \approx 10^{-4}$ – 10^{-3} cm. Thus, the heat conduction significantly decreases the energy

flux. For opaque dielectrics $d \approx d_h \approx 10^{-5}$ cm and the energy flux is decreased by only a factor of ~ 2 .

The flow of atoms (j_i) of a given element (i) from unit area of sample surface (solid or molten) heated by radiation can be determined according to the Hertz-Knudsen relation:

$$j_i = n_i v_i = (1 - \eta) n_i^\circ v_i = (1 - \eta) n_{ic} v_i \exp\left(-\frac{B_i}{kT}\right) \quad (2)$$

where $v_i = \sqrt{kT/2\pi m_i}$ is the mean thermal velocity of the atoms, k is Boltzmann's constant, m_i is the atomic weight of the given element, and n_{ic} , n_i , n_i° are the concentrations of the element in the condensed phase, the vapour and the saturated vapour respectively, η is the return ratio of vapour atoms ($\eta < 1$), and B_i is the bond energy between atoms of the element in the solid sample.

To satisfy relation (2) it is necessary that the decrease in atom concentration in the condensed phase near the evaporation surface is compensated by the diffusion flow $j_{iD} = D_i \nabla n_{ic}$ where D_i is the diffusion coefficient and ∇n_{ic} the gradient of the component concentration in the condensed phase. From the condition $j_{iD} = j_i$ we obtain

$$D_i \nabla n_{ic} = (1 - \eta) n_{ic} v_i \exp\left(-\frac{B_i}{kT}\right) \quad (3)$$

A typical thickness for the layer of substance, r_D , from which atoms diffuse to the surface is given by

$$r_D = \frac{n_{ic}}{\nabla n_{ic}} \leq \frac{D_i}{(1 - \eta) v_i} \exp\left(\frac{B_i}{kT}\right) \quad (4)$$

For molten alkali metals $D_i \approx 5 \times 10^{-5} \exp(-A_i/kT)$, where the activation energy of diffusion, A_i , is about 0.5 eV. Hence

$$r_D \leq \frac{5 \times 10^{-5}}{(1 - \eta) v_i} \exp\left(\frac{B_i - A_i}{kT}\right) \quad (5)$$

If we take into account that $T \leq T_c \approx (0.1-0.2)B_i$ (T_c is the critical temperature for the given substance), and at $T \approx T_c$ the value of v_i is $\sim 10^4$ cm/sec, we obtain from (5) $r_D \leq 10^{-5}$ cm. This parameter is comparable with the absorption depth d of laser radiation in metals and opaque dielectrics, as well as with the depth of sample warm-up by electrons in a spark discharge.²¹ If $d' \leq r_D$ and $\epsilon' < A$ the heated layer will partially evaporate, and the evaporation will be selective with regard to the sample elements, and dependent on their binding energies [see equation (2)].

The concentration of atoms of element i in the vapour phase, n_i , will be related to its concentration in the sample (n_{ic}) by the expression

$$n_i \sim n_{ic} \exp(-B_i/kT) \quad (6)$$

If $d' > r_D$ (a large depth of warm-up in metals by heat conduction, or large depth of absorption in dielectrics) the selectivity of transfer of atoms of different elements to the plasma is reduced. This effect can be taken into account by introducing into

equation (6) the atomization temperature T_A instead of the real temperature of the process (T), and in general $T_A > T$.

When the energy flux is big enough but does not exceed the specific sublimation energy, the liquid layer may be ejected in the form of drops. Boiling of the liquid phase (in the stationary evaporation regime) is also possible. In both cases the evaporation area S_{ev} increases significantly and correspondingly the effective thickness of the evaporating liquid layer decreases: $d_{ev} = V/S_{ev}$ where V is the heated layer volume. If $d_{ev} < r_D$ the selectivity of evaporation of different elements will be maintained.

If the energy flux ϵ' exceeds the specific sublimation energy Λ , the temperature of the heated layer will exceed the critical temperature and all the components of the layer will evaporate without discrimination. Formally this means that $T_A \rightarrow \infty$.

During transfer to the vapour energy-absorption regime the character of the evaporation and atomization process will change. The flow of energy onto the surface will decrease owing to the energy absorption by the plasma and the pressure will increase owing to the additional heating of the expanding vapour. All this will lead to the evaporation velocity being lower than that when the vapour does not absorb the laser energy, and hence to increased selectivity for different elements if the energy flux does not exceed Λ .

Ionization of atoms

In the regime without absorption of energy by the vapour, the degree of ionization of the vapour can be approximately determined from the Saha-Langmuir equation for surface ionization:

$$\frac{n_i^1}{n_i^0} = \frac{g_i^1}{g_i^0} \exp\left(\frac{\psi - \phi_i^1}{kT}\right) \quad (6)$$

where n_i^1 and n_i^0 are the numbers of singly-charged ions and atoms of the given element in unit volume of vapour, g_i^1 and g_i^0 are the statistical weights of the singly-charged ions and atoms of the i th element, respectively, ϕ_i^1 is its first ionization potential, ψ is the electron work function for the sample surface, and T is the absolute temperature of this surface. When the vapour absorbs laser energy, however, the resulting heating of the plasma leads to additional ionization. In the initial moment (before expansion) the plasma is in local thermodynamic equilibrium owing to its high initial density, and the ion distribution in the plasma according to degree of ionization is determined by the Saha equation:²²

$$\frac{n_e n_i^{z+}}{n_i^{(z-1)}} = \frac{g_i^z}{g_i^{(z-1)}} A T^{3/2} \exp\left(-\frac{\phi_i^z}{kT}\right) \quad (7)$$

where $A = 6.06 \times 10^{21} \text{ cm}^{-3} \cdot \text{eV}^{-3/2}$ and g_i^z and $g_i^{(z-1)}$ are the statistical weights of the ions with charges z and $(z-1)$ respectively.

Let us note that only that part of the sample substance which has evaporated immediately during

the radiation process experiences strong additional ionization. According to our estimates, laser pulses with $q = 10^9 - 10^{10} \text{ W/cm}^2$ and a duration of about 10 nsec will make about 10% of an irradiated metal surface evaporate, and about 50% of the irradiated surface of a highly absorptive dielectric. Strong sample evaporation after the spark discharge pulse is over is also possible in the vacuum spark method.²³ The portion of substance evaporating after the pulse is over is weakly ionized, its ionization being described by equation (6), as for the case of heating without energy absorption by the vapour.

Recombination of ions with electrons during plasma expansion

In the process of expansion, at a certain moment of time t_1 the typical relaxation time will exceed the typical ionization times. In this case the thermodynamic equilibrium distribution between degrees of ionization will be violated,²² and the equilibrium recombination will change to a slower non-equilibrium state which will continue till the moment t_2 when recombination ceases (freezing of the ionization state).

If the degree of plasma ionization at t_1 is less than 1, recombination during expansion will not change the relative concentration of ions of different elements until the system is frozen. The recombination coefficient b_z is given by

$$b_z = b_0 \frac{n_e^2 z^3}{T^{9/2}} \quad (8)$$

where $b_0 = 8.75 \times 10^{-27} \text{ cm}^6 \cdot \text{eV}^{9/2} \cdot \text{sec}^{-1}$.

For ions with charge $z = 1$ the recombination coefficient does not depend on the specific properties of elements. In this case $n_i^0 \approx n_i$, and the final degree of ionization is

$$n_i^1/n_i \sim \exp\left(-\frac{\phi_i^1}{kT}\right) \quad (9)$$

If the degree of ionization at t_1 is > 1 , the process of recombination will depend on the relation between the initial plasma radius R_0 and the characteristic separation distance for recombination of electrons with ions with charge z , which is $l_z = v_h/b_z$ where v_h is the thermal velocity of the ions. If R_0 is higher than the characteristic length of recombination for doubly charged ions l_2 , but smaller than the characteristic length for singly-charged ions l_1 , then the majority of the ions will be singly-charged. In this case the dependence of the degree of ionization on the first ionization potential is weaker and this can be taken into account by introducing into equation (9) the temperature of ionization T_1 instead of the actual temperature T , T_1 being $> T$. In the limiting case, if in the process of expansion all the multi-charged ions have recombined with electrons to form singly-charged ions but the recombination of singly-charged ions with electrons is negligible, the dependence of

the singly-charged ion function on the ionization potential ceases, which is equivalent to $T_1 \rightarrow \infty$.

Dependence of the RSC values on the main parameters of the elements to be determined and on the experimental conditions

Summing up the discussion above, we come to the conclusion that there are some general laws applicable to different matrices and experimental conditions. First, if we neglect energy losses during expansion, the final state of the plasma after the expansion is over is determined mainly by the energy flux and the mass of the heated substance, irrespective of the method of heating. Secondly, the relative sensitivity coefficients are proportional to the exponents of the atomization energies and the first ionization potentials:

$$\text{RSC}_i \sim \exp\left(-\frac{B_i}{kT_A}\right) \exp\left(-\frac{\phi_i^1}{kT_1}\right) \quad (10)$$

When an internal standard is used, equation (9) can be written in the form

$$\text{RSC}_i = \exp\left(-\frac{B_i - B_h}{kT_A}\right) \exp\left(\frac{\phi_i^1 - \phi_h^1}{kT_1}\right) \quad (11)$$

If the atomization and ionization are equilibrium processes that are in equilibrium with one other and recombination does not change the relation between the concentrations of singly-charged ions of different elements, then $T_A = T_1 = T$.

In other cases, for example, when the diffusion rate is low, in a liquid medium, or there is non-equilibrium recombination, and so on, the parameters T_A and T_1 turn out to be higher than temperatures which could be detected in reality if the processes were in equilibrium. Under certain conditions already discussed above, the value of T_A or T_1 tends towards infinity. In the particular case when $T_A = T_1 = \infty$ the conditions for analysis without use of standards, with $\text{RSC} = 1$ for all elements, are realized. It is this particular case that corresponds to the data reported by Bykovskii *et al.*¹¹

EXPERIMENTAL

To check the model, experiments with spark and laser ion-sources have been conducted for inorganic and organic samples containing elements which vary in atomization energy, ionization potential and atomic weight.

An SM-602 spark-source mass-spectrometer (Thomson CSF, France) and a laser EMAL-2 mass-spectrometer ("Electron", USSR) were used. The international geological standard GM, into which from 35 to 300 ppm of lutetium had been introduced (as the nitrate), was analysed with the spark-source mass-spectrometer by the counter-electrode technique²⁴ under the following conditions:

vacuum gap breakdown voltage—5 kV
pulse length—50 μsec (frequency 1 MHz)
frequency of pulse repetition—100 Hz.

Experiments with the laser ion-source have been done on a model sample, with dried rat liver as matrix, doped with the oxides of Li, Al, V, Cr, Mn, Fe, Co, Cu, Zn, Zr, Cd, Cs, Ce and Pb in concentrations corresponding to 0.1–10 g of

the element per kg of matrix, very much greater than the natural content in the matrix. The biological samples were analysed directly in the mass-spectrometer without preliminary ashing. Experimental conditions for the laser mass-spectrometer were:

radiation wavelength—1060 nm
frequency of pulse repetition—25 Hz
diameter of the spot on the target—50–100 μm .

The radiation flux was changed by use of neutral filters within the limits 3×10^8 – 7×10^9 W/cm² and controlled by an IMO-2M power meter.

The samples for use with both mass-spectrometers were homogenized and pressed as described earlier.¹⁰

The mass-spectra were recorded on Ilford Q2 photoplates, and the intensities of the mass-spectrum lines were evaluated by Hull's method.²⁵

The selectivity of the ion-beam formation, mass division and ion detection were individually assessed by means of the instrument calibration.¹⁸

The RSC values were determined with respect to the internal standard: lutetium has been used as the standard for GM and carbon for the rat liver. The results were processed by computer. For the set of RSC values determined in each experiment, the system of equations:

$$\ln(\text{RSC}) = -\left(\frac{B_i - B_h}{kT_A}\right) - \left(\frac{\phi_i^1 - \phi_h^1}{kT_1}\right) \quad (12)$$

was solved to obtain the atomization temperature T_A and ionization temperature T_1 , by the method of least squares.

The atomization energy of the pure compounds of the elements added to the samples was used as the binding energy B_i .

RESULTS

The dependence of the RSC values on the ionization potentials and atomization energies, calculated for one of the experiments with the spark-source mass-spectrometer, is given in Fig. 1, and the corresponding relations for experiments with laser ion-sources at different power densities are shown in Fig. 2.

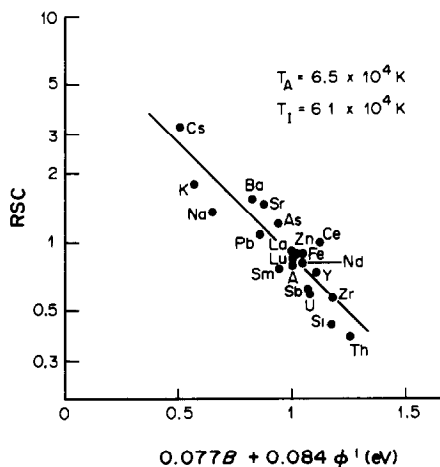


Fig. 1. The dependence of the RSC values on $(B_i/kT_A) + (\phi_i^1/kT_1)$ for spark-source mass-spectrometry: (●) experimental points; (—) the best approximation by the proposed model.

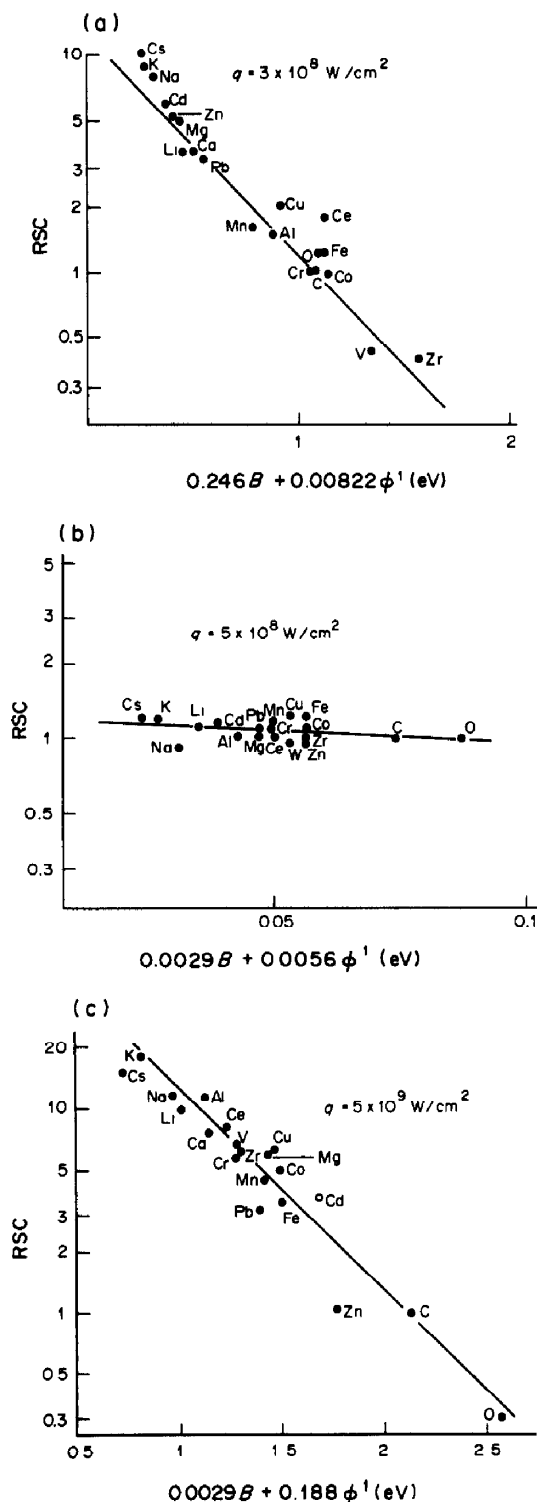


Fig. 2. The dependence of the RSC values on $(B_i/kT_A) + (\phi_i^1/kT_i)$ in laser mass-spectrometry at different values of the laser radiation flux: (●) experimental points; (—) the best approximation by the proposed model.

Table 1 presents the values of T_A and T_i determined by analysis with the spark ion-source, with one standard under similar experimental conditions on different days, and with the laser ion-source at

different values of the power density of laser radiation on the sample surface. The mean deviations of the $(RSC_i)_c$ values calculated by means of equation (12), from the experimental $(RSC_i)_{exp}$ values, were calculated by means of the expression

$$\bar{\Delta}_c = \exp \left[\frac{1}{n} \sum_{i=1}^n \left| \ln(RSC_i)_{exp} - \ln(RSI_i)_c \right| \right] \quad (13)$$

where n is the number of elements being determined here.

The mean deviations of the experimental RSC values from unity were calculated by the expression

$$\bar{\Delta} = \exp \left[\frac{1}{n} \sum_{i=1}^n \left| \ln(RSC_i)_{exp} \right| \right] \quad (14)$$

and are given for comparison.

DISCUSSION

It is clear from Figs. 1 and 2 that the proposed model approximates the RSC values in all the experiments quite well. From Table 1 it follows that the mean relative systematic error of the analysis without standards, calculated by means of equation (13), is reduced to 7–30%, which is comparable with the precision of the determination of the RSC values (about 20%). In contrast, if it is assumed that the RSC values are all equal to unity, the mean error for the same set of results will be very much greater. This is the case for $q > 2 \times 10^9 \text{ W/cm}^2$ with the laser ion-source, given as optimal in the paper by Bykovskii *et al.*¹¹

For both ion-sources T_A and T_i are higher than the real temperatures of the molten sample¹⁴ (by about 1 eV) and the initial plasma temperature¹⁶ (5000–15000 K). The reasons for this overestimation have already been discussed.

From the experiments on the effect of different laser radiation intensities on biological samples it is clear that at low intensities ($q = 3 \times 10^8$ – 10^9 W/cm^2) the RSC values are dependent on the atomization energies B , and the values of T_A and T_i change with q (Fig. 3). The effect of q on T_i differs from that known for metals, where increase in q leads to stronger plasma heating and correspondingly to higher ionization temperature growth.¹⁵ In our opinion, the dependence observed here can be explained by considering the possible contribution of the evaporation of sample after the laser pulse is over. Owing to its relatively weak absorption in the plasma, part of the radiation energy heats the sample to the depth d' , which, as mentioned earlier, can be much bigger than the thickness of the layer evaporated during the pulse. Perhaps one of the specific features of dried and pressed biological samples is that at $q \leq 10^9 \text{ W/cm}^2$ this additionally heated layer of the sample practically does not evaporate, but at higher q the energy flux (ϵ) in it becomes comparable with the sublimation energy or exceeds it. This part of the substance is then additionally evaporated and ion-

Table 1. The values of T_A and T_I and the mean deviations of the RSC experimental values from those calculated for laser and spark ion-sources

Type of source	Power density (q), W/cm^2	T_A , $10^3 K$	T_I , $10^3 K$	Mean deviations	
				Equation (13)	Equation (14)
Spark	—	65	60	1.21	1.46
	—	66	56	1.19	1.51
	—	54	47	1.16	1.48
	—	55	48	1.22	1.55
Laser	3×10^8	20	613	1.19	2.68
	5×10^8	170	900	1.12	1.17
	8×10^8	540	5800	1.07	1.07
	1×10^9	960	1300	1.11	1.15
	2×10^9	179	53	1.26	2.38
	5×10^9	1700	27	1.26	4.77
	7×10^9	89	20	1.30	10.91

ized, though rather weakly, since the evaporation occurs after the laser pulse is over. If the contribution of such a weakly ionized plasma is considerable, this will lead to the dependence of the RSC value on the ionization potentials.

To calculate the RSC values by means of the proposed model it is necessary to determine T_A and T_I according to three elements—used as internal standards. These can be the main components of the sample (when analysing rocks and minerals it is usually easy to obtain the necessary data on their contents by chemical analysis, *i.e.*, by independent methods) or elements specially introduced into the sample. The solution of the equation system (12) forms a plane with the co-ordinates $\ln RSC$, B , ϕ^1 . To make the plane formed by the values for three elements approximate most closely the results of the experiment, it is necessary that the values B_i , ϕ_i^1 corresponding to these 3 elements, on the plane B , ϕ^1 , are located at the corners of a triangle with maximum area. The concentrations of the remaining elements can then be found without the use of other standards. For example, in the case illustrated in Fig. 1, we can choose silicon, caesium and lutetium as internal

standards. In this case the $\bar{\Delta}_c$ is 1.25, which is not much worse than the value obtained when the dependence $\ln RSC = f(B, \phi_i^1)$ is formed by means of all 21 points, as done in Fig. 1.

CONCLUSION

At present it is impossible to build a complete theory of the spark-source and laser mass-spectrometry which would allow us to determine the RSC values needed for analysis without standards.

This paper shows the possibility of a universal approach to investigation of the mechanisms of ion formation in the plasma of the spark vacuum discharge and in the laser plasma. The calculations and experiments performed allow us to put forward a quasi-equilibrium model based on a semiempirical description of the mechanisms of atomization and ionization, with the use of two parameters—the temperatures of atomization and ionization. Such an approach is a new step compared to the previous purely empirical approach. It allows us (a) to consider the influence of the composition of the sample matrix and the conditions for the spark discharge or laser radiation; (b) to offer a method of calculating the RSC according to the results of a calculation based on the data for at least three elements used as internal standards; (c) on this basis to work out methods of quantitative analysis without use of standards (with errors of less than 30%) by means of spark-source and laser mass-spectrometry.

Acknowledgements—The authors express their gratitude to Professor Yu. A. Shukolyukov (Vernadskii Institute of Geochemistry and Analytical Chemistry, USSR Academy of Sciences) for constant attention and valuable recommendations.

REFERENCES

1. A. J. Ahearn (ed.), *Trace Analysis by Mass Spectrometry*, Academic Press, New York, 1972.
2. M. S. Chupakhin, O. I. Kryuchkova and G. I. Ramendik, *Analytical Capabilities of Spark Source Mass Spectrometry*, Atomizdat, Moscow, 1972.
3. Working Group on Spark-Source Mass Spectrometry, *Z. Anal. Chem.*, 1982, **309**, 257.

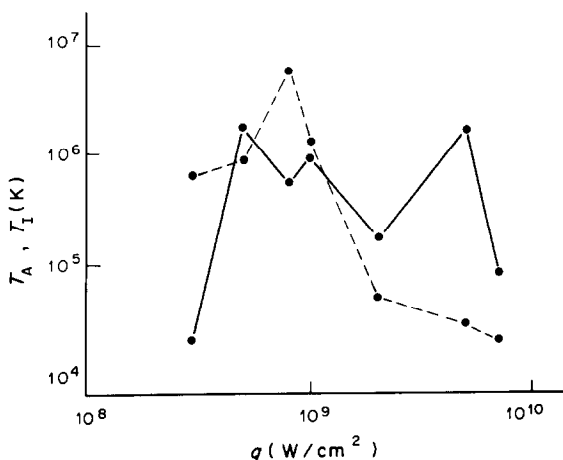


Fig. 3. The dependence of T_A (—) and T_I (---) on the laser radiation flux.

4. F. Adams, *Phil. Trans. Roy. Soc. Lond.*, 1982, **305A**, 509.
5. G. I. Ramendik, *J. Anal. Chem. USSR*, 1983, **38**, 1570 (Transl. from *Zh. Analit. Khim.*, 1983, **38**, 2036).
6. J. R. Bacon and A. M. Ure, *Analyst*, 1984, **109**, 1229.
7. I. D. Kovalev, G. A. Maksimov, A. I. Suchkov and N. V. Larin, *Int. J. Mass Spectrom. Ion Phys.*, 1978, **27**, 101.
8. R. J. Conzemius and J. M. Capellen, *ibid.*, 1980, **34**, 197.
9. V. I. Belousov, *J. Anal. Chem. USSR*, 1984, **39**, 734 (Transl. from *Zh. Analit. Khim.*, 1984, **39**, 909).
10. G. I. Ramendik, O. I. Kryuchkova, D. A. Tyurin, T. R. Mchedlidze and M. Sh. Kaviladze, *Int. J. Mass Spectrom. Ion Phys.*, 1985, **63**, 1.
11. Yu. A. Bykovskii, G. I. Zhuravlev, V. I. Belousov, V. M. Gladskoi, V. G. Degtyarev and V. N. Nevolin, *Zavodsk. Lab.*, 1978, **48**, 701.
12. G. I. Ramendik, O. I. Kryuchkova, D. A. Tyurin, T. R. Mchelidze and M. Sh. Kaviladze, *J. Anal. Chem. USSR*, 1983, **38**, 1393 (Transl. from *Zh. Analit. Khim.*, 1983, **38**, 1749).
13. I. N. Slivkov, *Electrical Insulation and Discharge in Vacuum* (in Russian), Atomizdat, Moscow, 1972.
14. G. A. Mesjats and D. I. Proscurovskii, *Impulse Electrical Discharge in Vacuum* (in Russian), Nauka, Novosibirsk, 1984.
15. T. F. Ready, *Effects of High-Power Laser Radiation*, Academic Press, New York, 1971.
16. G. I. Ramendik, *Advan. Mass Spectrom.*, 1980, **8A**, 408.
17. G. I. Ramendik, in *Euroanalysis IV, Reviews on Analytical Chemistry*, L. Niinisto (ed.), p. 57. Akadémiai Kiadó, Budapest, 1982.
18. G. I. Ramendik, D. A. Tyurin, O. I. Kryuchkova and G. I. Chernoglasova, *Zh. Analit. Khim.*, 1985, **40**, 1210.
19. C. A. Andersen and J. R. Hinthorne, *Anal. Chem.*, 1973, **45**, 1421.
20. J. M. Beusen, P. Surkin, R. Gijbels and F. Adams, *Spectrochim. Acta*, 1983, **38B**, 813.
21. G. I. Ramendik and V. I. Derzhiev, *J. Anal. Chem. USSR*, 1977, **32**, 1197 (Transl. from *Zh. Analit. Khim.*, 1977, **32**, 1508).
22. Ya. B. Zeldovich and Yu. P. Raiser, *Impact Waves and High Temperature Hydrodynamic Phenomena Physics*, (in Russian), Nauka, Moscow, 1966.
23. G. I. Ramendik, M. S. Chupakhin and M. A. Potapov, *Zh. Analit. Khim.*, 1975, **30**, 669.
24. C. W. Hull, *10th Ann. Conf. Mass Spectrom. All. Top. Com. E-14*, p. 404. ASTM, New Orleans, 1962.
25. G. I. Ramendik, M. S. Chupakhin, Yu. G. Tatsii and V. I. Derzhiev, *J. Anal. Chem. USSR*, 1974, **29**, 202 (Transl. from *Zh. Analit. Khim.*, 1974, **29**, 238).

CATALYTIC KINETIC METHODS FOR THE DETERMINATION OF PLATINUM METALS

K. B. YATSIMIRSKII and L. P. TIKHONOVA

L. V. Pisarzhevsky Institute of Physical Chemistry of the Ukrainian SSR Academy of Sciences,
Kiev, USSR

(Received 15 October 1985. Accepted 1 July 1986)

Summary—A review is given of developments over the last two decades in the determination of platinum metals by catalytic kinetic methods.

The application of kinetic methods of trace analysis,^{1,2} particularly the catalytic variants, is now well established. The advantages include high sensitivity, simple instrumentation and simplicity,^{3,4} all of which attract the interest of workers in the field of the analytical chemistry of platinum metals, where it is frequently necessary to analyse samples for very small amounts of these metals. The platinum metals and their compounds are also an attractive subject for the development of sensitive, and in some cases selective, methods for their determination, owing to the wide range of their chemical reactions.

Numerous examples have been published of methods for the determination of micro and submicro quantities of platinum metals, based on their catalytic action in various indicator reactions. To keep within reasonable limits a discussion of the voluminous literature on catalytic methods for the determination of platinum metals,^{8,9} this paper will deal only with methods that use mainly homogeneous catalytic reactions in solution. Methods based on the measurement of luminescence during a catalysed reaction, or on the measurement of a catalytic polarographic wave, will not be discussed here.

Even so, we do not pretend to give a full coverage of the literature on these methods, since in many papers the main emphasis is on the indicator reaction or its kinetics and mechanism, and not on the application, but important papers and reviews are referred to where appropriate. The main attention is given to the publications that have appeared in the past 20 years, since a practically complete bibliography of earlier papers has been given elsewhere.¹

PLATINUM METAL COMPOUNDS AND IONS IN HOMOGENEOUS CATALYTIC REACTIONS

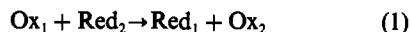
The catalytic properties of transition metal compounds and ions in homogeneous reactions are usually associated with their repeated interaction with a component of the indicator reaction, bringing about a change in the reaction mechanism, manifested as a corresponding change in the reaction rate.^{1–4,10} Such

an interaction may involve formation of an active intermediate between the catalyst and one of the reacting components, further transformation of which leads to the formation of reaction products and release of the catalysts.

The indicator reactions used for platinum metal determinations are almost always redox reactions and the catalysis mechanism usually involves cycling of the platinum metal between two oxidation states, and occasionally formation of intermediates between the reaction components and the catalyst in different oxidation states. Other types of reaction are seldom used, and will not be discussed here.

The solution chemistry of the platinum metal ions is essentially the chemistry of their co-ordination compounds, including polynuclear species.^{5–7} It is characteristic of the platinum metals (especially osmium and ruthenium) that they exhibit different oxidation states, and it is usually the interaction of a platinum metal complex with a complex of a transition metal to form a reaction intermediate which makes the catalytic reaction possible.

A necessary (but not sufficient) requirement for involvement of a platinum metal complex in such a system is that its standard redox potential (E_{cat}°) should lie between those (E_1° and E_2°) of the components of the indicator reaction



Tables 1 and 2 list the standard potentials for the redox pairs used in the most common indicator reactions, and for some platinum metals. In connection with Table 2 it should be pointed out that the standard potentials for platinum metal bromide complexes are close to those for the chloride complexes. The potentials of the corresponding $\text{Me}^{4+}/\text{Me}^{3+}$ redox pairs in perchloric and sulphuric acid media seem, judging from the source literature data,⁷ to range from 0.90 to 1.40 V.

The values listed in Tables 1 and 2 suggest that many of the platinum metals should be able to catalyse the various oxidation–reduction systems shown in Table 1, *i.e.*, to increase the reaction rate.

Table 1. Oxidation potentials of redox reactions for indicator reactions used in the determination of platinum metals in solution^{11,12}

Oxidant		Reductant*	
Reaction	E°, V	Reaction	E°, V
$\text{BrO}_3^- + 6\text{H}^+ + 6e^- \rightarrow \text{Br}^- + 3\text{H}_2\text{O}$	1.45	$2\text{Hg}^{2+} + 2e^- \rightarrow \text{Hg}_2^{2+}$	0.907
$\text{HBrO} + \text{H}^+ + 2e^- \rightarrow \text{Br}^- + \text{H}_2\text{O}$	1.34	$\text{Cl}_2 + 2e^- \rightarrow 2\text{Cl}^-$	1.36
$\text{IO}_4^- + 2\text{H}^+ + 2e^- \rightarrow \text{IO}_3^- + \text{H}_2\text{O}$	1.38	$\text{Cu(III)} + e^- \rightarrow \text{Cu(II)}$	1.1
$\text{IO}_3^- + 6\text{H}^+ + 6e^- \rightarrow \text{I}^- + 3\text{H}_2\text{O}$	1.38	$\text{MnO}_4^- + 8\text{H}^+ + 5e^- \rightarrow \text{Mn(II)} + 4\text{H}_2\text{O}$	1.51
$\text{HClO}_2 + 3\text{H}^+ + 4e^- \rightarrow \text{Cl}^- + 2\text{H}_2\text{O}$	1.56	$\text{I}_2 + 2e^- \rightarrow 2\text{I}^-$	0.62
$\text{H}_2\text{O}_2 + 2\text{H}^+ + 2e^- \rightarrow 2\text{H}_2\text{O}$	1.77	$\text{H}_3\text{AsO}_4 + 2\text{H}^+ + 2e^- \rightarrow \text{HAsO}_2 + 2\text{H}_2\text{O}$	0.56
$\text{NO}_3^- + 3\text{H}^+ + 2e^- \rightarrow \text{HNO}_2 + \text{H}_2\text{O}$	0.94	$\text{C}_6\text{H}_4\text{O}_2 + 2\text{H}^+ + 2e^- \rightarrow \text{C}_6\text{H}_4(\text{OH})_2$	0.68
$\text{Ce(IV)} + e^- \rightarrow \text{Ce(III)}$ (in H_2SO_4)	1.44	$\text{Fe(II)} + e^- \rightarrow \text{Fe(III)}$	0.77
$\text{Mn(III)} + e^- \rightarrow \text{Mn(II)}$	1.51		
$\text{VO}_3^- + 4\text{H}^+ + e^- \rightarrow \text{VO}_2^{2+} + 2\text{H}_2\text{O}$	1.0-1.3		

*For many organic compounds used as reductants in indicator reactions, oxidation potentials are unknown. But it seems that oxidation potentials for benzidine derivatives are near 0.76 V.

The rate of a redox reaction between an oxidant and a reductant of like charge is likely to be low owing to electrostatic hindrance, but can be increased by a catalyst which can form an intermediate of opposite charge with one of the redox-system components or can serve as a bridge in a ternary oxidant-catalyst-reductant intermediate. It has been found¹³⁻¹⁵ that platinum metals readily form such intermediate complexes, in which electron or atom transfer can occur. The retention of OH^- groups in the co-ordination sphere of the catalyst (even in an acidic medium), which is characteristic of platinum metal complexes, contributes to the formation of suitable intermediates since the OH^- groups can serve as bridging ions or favour the approach of other interacting species through hydrogen-bond formation.

Platinum metal complexes can also increase the rate of an indicator reaction by removing the kinetic hindrance that may arise when the indicator reaction half-cells involve different numbers of electrons. The complexes of elements such as osmium and ruthenium, which exhibit several different oxidation states, are able to take part in processes involving the transfer of different numbers of electrons, e.g., to interact alternately with a one-electron oxidant and a two-electron reductant. The reaction between cerium(IV) and arsenic(III) is one of the best-known indicator reactions: osmium and ruthenium catalyse

this reaction by being alternately oxidized by cerium(IV), in two one-electron steps, and reduced by arsenic(III) in a 2-electron step.¹⁶⁻²²

A very different mechanism involving platinum metal compounds depends on the possibility of reducing their ions to the metal with a strong reductant and utilizing the high catalytic activity of the colloidal metal thus produced. The reduction step may precede²³ or accompany the indicator reaction. The number of such reactions, involving reductants such as formic acid (determination of platinum¹), tetrahydroborate (determination of osmium²⁴), hypophosphite (determination of palladium^{25,26}) and tin(II) chloride (determination of palladium²⁷) is small. Since these reactions are not entirely homogeneous, the reproducibility of the results depends on achieving complete reduction of the platinum metal to be determined. This fact and the low selectivity of the methods limits the use of such reactions.

The oxidation of tin(II) chloride by iron(III) stands, to some extent, by itself among the indicator reactions used for determining platinum metals. The catalytic activity of platinum metal complexes in this reaction may be accounted for by the possibility of the formation of readily oxidizable complexes between the platinum metal and complex chloro-tin(II) anions.⁷

INDICATOR REACTIONS FOR CATALYTIC DETERMINATION OF PLATINUM METALS

Table 2. Oxidation potentials for redox-pairs of some platinum metal compounds^{7,11}

Reaction	E°, V
Acid medium	
$\text{RuCl}_6^{2-} + e^- \rightarrow \text{RuCl}_6^{3-}$	1.2
$\text{OsCl}_6^{2-} + e^- \rightarrow \text{OsCl}_6^{3-}$	0.85
$\text{RhO}^{2+} + 2\text{H}^+ + e^- \rightarrow \text{Rh}^{3+} + \text{H}_2\text{O}$	1.40
$\text{IrCl}_6^{2-} + e^- \rightarrow \text{IrCl}_6^{3-}$	0.93
$\text{PdCl}_6^{2-} + 2e^- \rightarrow \text{PdCl}_4^{2-} + 2\text{Cl}^-$	1.30
$\text{PtCl}_6^{2-} + 2e^- \rightarrow \text{PtCl}_4^{2-} + 2\text{Cl}^-$	0.708
Alkaline medium	
$\text{RuO}_4^- + e^- \rightarrow \text{RuO}_4^{2-}$	0.595
$\text{RuO}_4 + e^- \rightarrow \text{RuO}_4^-$	1.00
$\text{HOsO}_5^- + 2e^- + \text{H}^+ \rightarrow \text{OsO}_4^{2-} + \text{H}_2\text{O}$	0.30

Though many catalytic methods have been developed for the determination of platinum metals in solution, the number proposed for each of the platinum elements is very different, being largest for osmium and ruthenium, smaller for iridium, and very small for rhodium and palladium, and only one homogeneous catalytic reaction has been proposed for the determination of platinum. Tables 3-5 list the main indicator reactions used for determination of osmium, ruthenium and iridium; Table 6 lists those for rhodium, palladium and platinum. Most of the oxidants [cerium(IV), oxyhalogen compounds, hy-

Table 3. Indicator reactions* for the determination of osmium

Reaction	Detection limit, ng/ml	Interfering platinum metals	References
Ce(IV) + As(III)	2.5×10^{-5}	Ru†	17-22, 28
Ce(IV) + Sb(III)	4×10^{-4}	Ir, Pt, Pd	28
BrO ₃ ⁻ + I ⁻	4×10^{-5}	—	29, 30
BrO ₃ ⁻ + <i>p</i> -phenetidine	2.8×10^{-3}	Ru	31
BrO ₃ ⁻ + As(III)	10^{-4} - 10^{-6}	—	32-35
BrO ₃ ⁻ + azo-dyes	—	—	36
ClO ₂ ⁻ + I ⁻	10^{-3}	—	30-37
IO ₄ ⁻ + I ⁻	10^{-4}	—	30
IO ₄ ⁻ + As(III)	6×10^{-7}	Ru	30, 38
IO ₃ ⁻ + I ⁻	10^{-4}	—	30
IO ₃ ⁻ + As(III)	10^{-4}	Ru	30
H ₂ O ₂ + oxyaminobenzosulphonic acid	0.53	?	39
H ₂ O ₂ + I ⁻	10^{-5}	Ru	30, 40
H ₂ O ₂ + <i>p</i> -phenylenediamine	4×10^{-5}	Ru	41
HNO ₃ + α -naphthylamine	2×10^{-3}	Ru†	42, 45
Fe(III) + Sn(II)	10^{-3}	Pt, Ru	46
Fe(II) + Ag(I)	4×10^{-4}	Ru, Ir, Pt, Pd, Rh	47
K ₃ [Fe(CN) ₆] + NaBH ₄	1.7×10^{-3}	Ru	24

*In Tables 3-6 only the reagents for the indicator reactions are shown, because the products of many reactions are unknown.

†Under some conditions these reactions become specific.

drogen peroxide] and reductants [iodide, arsenic(III), aromatic amines] are also widely used in indicator reactions for the catalytic determination of other transition metals.¹⁻⁴ For instance, the oxidation of manganese(II) by hypobromite was used earlier to determine copper(II)¹ and proposed later as an indicator reaction for the determination of iridium(IV) and rhodium(III).^{73,78} Some indicator reactions for the determination of platinum metals were known long ago, but more recent studies have made it possible to improve them considerably. Examples

include the determination of osmium and ruthenium by use of the arsenic(III)-cerium(IV)²⁸ and α -naphthylamine-nitrate⁴²⁻⁴⁵ reactions.

Particular attention should be given to methods based on new indicator reactions. For example, the oxidation of arsenite by halate ions has turned out to be very interesting: the oxidation by bromate is specific for the determination of osmium,³²⁻³⁵ and the oxidation of arsenic(III) by iodate or periodate is used for determining osmium^{30,38} and ruthenium.⁵⁶ In these reactions, the detection limits are very low

Table 4. Indicator reactions for the determination of ruthenium

Indicator reaction	Limit of detection, $\mu\text{g/ml}$	Interfering platinum elements	Reference
Ce(IV) + As(III)	2×10^{-3}	Ir, Os*	18, 28
Ce(IV) + Hg(I)	10^{-3}	*	48
Ce(IV) + diphenylamine	5×10^{-3}	—	—
Ce(IV) + Sb(III)	4×10^{-4}	Ir, Pt, Pd	49
Mn(III) + Hg(I)	10^{-3}	Ir	49
Mn(III) + <i>p</i> -anisidine	10^{-3}	—	49, 50
Mn(III) + <i>p</i> -quinone	10^{-3}	—	51
IO ₄ ⁻ + <i>o</i> -dianisidine	10^{-5}	Ir, Pd	52
IO ₄ ⁻ + Fe(phen) ₃ ⁺	5×10^{-6}	—	53
IO ₄ ⁻ + Methyl Red	5×10^{-6}	Ir	54
IO ₄ ⁻ + Tropaeolin-00	2×10^{-6}	—	55
IO ₄ ⁻ + As(III)	5×10^{-7}	—	56
IO ₄ ⁻ + diphenylamine	5×10^{-2}	Ir, Os	57
IO ₄ ⁻ + Cu(II)	4×10^{-4}	—	58
BrO ₃ ⁻ + Ce(III) + CH ₂ (COOH) ₂	5×10^{-3}	—	59
BrO ₃ ⁻ + Mn(II) + CH ₂ (COOH) ₂	5×10^{-3}	—	59
H ₂ O ₂ + I ⁻	5×10^{-4}	Os	60
H ₂ O ₂ + benzidine	2×10^{-3}	Os	61
H ₂ O ₂ + Direct Blue	($10^{-4}\%$)	?	62, 63
NH ₄ VO ₃ + <i>N</i> -methyl-diphenyl-4-sulphonic acid	4×10^{-5}	—	64
HNO ₃ + α -naphthylamine	5×10^{-2}	Os	43-45
Fe(III) + Sn(II)	1.7×10^{-2}	Os, Pt	65
Fe(III) + S ₂ O ₃ ²⁻	2×10^{-2}	?	66
Ag(I) + Fe(II)	4×10^{-2}	Os, Ir, Pt, Pd, Ru	47

*See text for comment on the selectivity of this method.

Table 5. Indicator reactions for the determination of iridium

Indicator reaction	Limit of determination, $\mu\text{g/ml}$	Interfering platinum elements	Reference
Ce(IV) + As(III)	2×10^{-3}	Os, Ru*	18, 67
Ce(IV) + H ₂ O	10^{-2}	Rh	68
Ce(IV) + Hg(I)	10^{-3}	Ru†	69
Ce(IV) + diphenylamine	10^{-2}	Ru	70
Ce(IV) + Sb(III)	4×10^{-3}	—	67
Mn(III) + Hg(I)	10^{-3}	Ru	49, 71
IO ₄ ⁻ + <i>o</i> -dianisidine	10^{-5}	Ru, Pd	9
IO ₄ ⁻ + Direct Blue	($10^{-4\%}$)	?	63
IO ₄ ⁻ + murexide	2×10^{-4}	Ru, Os	72
BrO ⁻ + Cu(II)	5×10^{-4}	Rh	74
BrO ⁻ + Mn(II)	10^{-4}	Ru	73
NH ₄ VO ₃ + <i>N</i> -methyl-diphenyl-4-sulphonic acid	2×10^{-4}	Ru	75

*This reaction is specific for iridium if followed fluorometrically.

†See text for comment on the selectivity of this method.

Table 6. Indicator reactions for the determination of rhodium, palladium and platinum

Indicator reaction	Element determined	Limit of determination, $\mu\text{g/ml}$	Interfering platinum elements	Reference
IO ₄ ⁻ + Cu(II)	Rh	10^{-4}	—	76
BrO ₃ ⁻ + Cu(II)	Rh	2×10^{-3}	—	77
BrO ⁻ + Mn(II)	Rh	10^{-4}	Ir, Pd	78
Ce(IV) + Hg(I)	Pd	9×10^{-3}	Ir, Ru	79
Mn(III) + Cl ⁻	Pd	10^{-3}	—	80
I ₂ + N ₃ ⁻	Pd	10^{-2}	—	81
NaH ₂ PO ₂ + Toluidine Blue	Pd	?	?	25
NaH ₂ PO ₂ + phenosafranine	Pd	?	?	26
As(III) + Sn(II)	Pd			27
NaH ₂ PO ₂ + Ni(II)	Pd	4×10^{-4}	Os, Ir, Ru, Pt, Rh	82
Fe(III) + Sn(II)	Pt	2.5×10^{-2}	Os, Ru	83

(10^{-7} – 10^{-6} $\mu\text{g/ml}$), and they are fairly tolerant towards other metals.

Many new methods have been based on indicator reactions involving components that had not been used before; some of these have been proposed for the determination of osmium, ruthenium and iridium. For instance, the catalytic action of platinum metals on the oxidation of mercury(I),^{28,69} diphenylamine,⁷⁰ antimony(III)^{28,67} and even water⁶⁸ by cerium(IV) has been used as the basis of analytical procedures. Copper(II) has been employed as reductant in indicator reactions with periodate or hypobromite as oxidant, where the reaction producing stable coloured copper(III) complexes is catalysed by ruthenium(III,IV), iridium(IV) and (very important) rhodium(III) compounds. These are the only homogeneous reactions for the determination of rhodium which are very sensitive and selective.

New oxidants have also been proposed, in particular manganese(III) in sulphuric acid medium.^{49-51,71,80} The determination of ruthenium(IV) by its catalytic action on the oxidation of *p*-anisidine or of *p*-

quinone by manganese(III)⁴⁹⁻⁵¹ tolerates the presence of the other platinum metals.

An advantage of these and other oxidations by manganese(III) is the extremely low rate of the uncatalysed process, which allows omission of a blank run. The oxidation of chloride by manganese(III), catalysed by palladium(II) and used for its determination,⁷⁸ is easy and has good reproducibility. Manganese(III) serves as the indicator species in these reactions: the rate of the reaction is determined from the decrease in its absorbance.

A new selective indicator reaction involving chlorite ions as oxidant has been proposed for determining osmium(VIII).^{30,37}

A new catalytic determination of ruthenium(III) and ruthenium(IV) makes use of Belousov-Zhabotinskii oscillating chemical reactions involving bromate, cerium(III,IV)* and malonic acid, or bromate, manganese(II,III) and malonic acid. These reactions produce periodic changes in the concentration ratio of the oxidized and reduced metal ion species and in the concentrations of bromide and some intermediates. These changes are followed potentiometrically, photometrically or by some other instrumental method. Ruthenium(III,IV) sulphate complexes catalyse some of the oscillating reaction stages, resulting

*Here and elsewhere, the two oxidation states within the brackets are those involved in the catalysed reaction.

in a shorter induction period and higher oscillation frequency. The method compares favourably with others in terms of its sensitivity (detection limit = 5 ng/ml), and gives relative errors of <5%.

LIMITATIONS AND POSSIBILITIES OF CATALYTIC METHODS FOR DETERMINATION OF PLATINUM METALS

Tables 3–6 indicate the very low detection limit in catalytic methods for the determinations of platinum metals; they can be as low as 10^{-7} – 10^{-6} $\mu\text{g/ml}$. Such a sensitivity can only be attained when certain experimental conditions, which are necessary for obtaining the most catalytically active form of the element to be determined, are fulfilled. Whereas the co-existence in solution of co-ordination complexes of platinum metals such as osmium and ruthenium in different oxidation states and with different combinations of ligands is to some extent an advantage, it can also make it more difficult to control the experimental conditions, since the catalytic activities of the various complexes of one and the same metal co-existing in the solution to be analysed may be different. To establish the conditions for the highest reproducibility of a catalytic method for the determination of a platinum metal, it is important to know precisely which complex ion is most catalytically active. Investigations of the catalytic properties of platinum metal complexes at microgram and submicrogram levels in solution have shown complexes of Os(VIII)–Os(VI) and Ru(VIII)–Ru(VI),^{14,84–88} and the oxo and hydroxo complexes of Ir(IV)–Ir(III) and Rh(IV)–Rh(III)^{14,87} to have highest activity in alkaline solution. In acid solution, the higher oxidation states of the platinum metals are unstable.

It has also been found that the catalytic activity of osmium, ruthenium, iridium and rhodium complexes in solution increases with increasing number of hydroxo groups in the inner co-ordination sphere of the compounds,^{14,87–89} which should be taken into account in determining the optimum analysis conditions. On the other hand, the presence of hydroxo groups in the complex restricts the upper limit of the concentrations which can be determined, since hydrolysis and condensation to yield polynuclear species occurs at quite low concentrations of the platinum metals.^{7,68,90}

Since the catalytic activity can vary from one co-ordination compound to another of the same central metal ion, measurements of rates of catalysed reactions can be used to investigate the nature of the different complex species. This approach is especially useful in investigation of equilibria in aqueous solutions of platinum metals in the predominance region of their mononuclear forms, since polynuclear compounds of these metals are formed at concentrations as low as 10^{-5} M .^{7,68,90} at which the application of most other methods of investigation is no longer possible. Catalytic methods made possible the first

characterization of mononuclear osmium, ruthenium and iridium species in aqueous mineral acid and alkali solutions,^{84–86,88–91} and this led to recommendations concerning the standardization of solutions of these elements, and establishment of conditions for their determinations,^{84–86} with highest sensitivity and good reproducibility.

One of the disadvantages of kinetic methods of analysis is considered to be their poor selectivity. It should be pointed out that a number of quite specific indicator reactions have been proposed in recent years for determining osmium,^{32–35} ruthenium^{49–51,55} and palladium.⁸⁰ However, most of the indicator reactions which are convenient to use are catalysed by several platinum metals, and the methods based on them are not selective enough. In such a case the investigator may attempt to improve the tolerance for (a) other platinum metals and (b) other elements generally. The usual approach is to separate the noble metals as a group from other metals in the sample and then to use conditions that increase the selectivity for the platinum metals in particular. The selectivity may be improved by including further separation of the platinum metals or exploiting the peculiarities of the kinetics of the catalytic reaction and differences in the chemical properties of the catalytically active substances. For example, osmium and ruthenium are usually determined after selective distillation of their tetroxides. The indicator reaction involving oxidation of α -naphthylamine by nitrate may then be used for the determination of both ions.⁴³ Alternatively, the same reaction can be used to determine osmium and ruthenium without prior separation; a differential method is used, based on the difference in the dependence of the catalytic reaction rates on the reductant concentration.^{44,45} An earlier similar differential method for the determination of osmium and ruthenium was based on their catalysis of the oxidation of arsenite by cerium(IV).²²

The same approach to increasing the selectivity may be adopted in the determination of other platinum metals, though in this case there are usually more than two of them present in the solution to be analysed. Most commonly, to determine one platinum metal in the presence of another that catalyses the same reaction, use is made of the fact that the highest catalytic activity of each will be obtained under different conditions. Thus there are indicator reactions which are catalysed by several of the platinum metals but can, nevertheless, be made selective. For example, the oxidation of copper(II) by periodate may be made specific for determination of ruthenium or rhodium since their catalytic activities show different pH-dependence: catalysis by ruthenium(IV) is most effective at pH 12.5 and that by rhodium(III) at pH 8.0.^{58,76} In the oxidation of diphenylamine by cerium(IV), which is an indicator reaction for the determination of iridium or ruthenium, the catalytic action of ruthenium(IV) compounds is retained at higher acid concentrations,

whereas iridium(IV) compounds completely lose their catalytic activity under these conditions, allowing determination of the ruthenium.⁴⁸

The determination of iridium in a mixture of platinum metals in solution is rather a knotty problem. Such solutions usually contain much less iridium than other metals, and a completely specific indicator reaction for this element is not yet known. The oxidation of mercury(I) by cerium(IV), which is very simple to use and has good reproducibility, tolerates all the noble metals except ruthenium, and practically all the commonly occurring metals. This indicator reaction has been applied to the determination of iridium after its separation by paper chromatography.^{92,93} It has been found recently that this reaction may prove to be specific for the determination of iridium if ruthenium(IV) is converted into inactive nitroso complexes by pretreating the solutions to be analysed,⁹⁴ or if the iridium is determined in perchloric acid medium.⁹⁵

CONCLUSIONS

The material considered in this paper shows that catalytic methods are now available for determining all the platinum metals in solution. As follows from Table 7, however, the number of homogeneous indicator reactions for the determination of each element is very different. The sensitivity of the methods is extremely high, with detection limits as low as 10^{-7} – 10^{-6} $\mu\text{g/ml}$. For each element (except platinum), specific indicator reactions are available. The application of catalytic methods directly to the analysis of "real" samples makes it possible to reduce the amount of sample required compared with that required for other methods and in many cases the procedures can be automated. Continuous progress in this field faces some problems, but the most important needs, in our opinion, are as follows.

1. Search for indicator reactions and development of selective methods for the determination of platinum, palladium and rhodium at trace levels.

2. Wider use of modern instrumental methods to allow the range of indicator reactions to be widened and their sensitivity to be increased.

3. Systematic search for activators^{9,96,97} to increase the sensitivity of the catalytic methods for determining platinum metals.

Table 7. A summary of the catalytic methods for the platinum metals based on homogeneous indicator reactions

Element	No. of methods	Determination limit, $\mu\text{g/ml}$
Ru	23	5×10^{-7}
Rh	2	10^{-4}
Pd	4	10^{-3}
Os	17	6×10^{-7}
Ir	11	10^{-5}
Pt	1	2.5×10^{-2}

4. Investigation of the catalytic properties of platinum metal compounds in other types of reaction besides redox reactions.

REFERENCES

1. K. B. Yatsimirskii, *Kinetic Methods of Analysis*, Pergamon Press, Oxford, 1966.
2. H. B. Mark and G. O. Rechnitz, *Kinetics in Analytical Chemistry*, Interscience, New York, 1968.
3. H. Müller, M. Otto and G. Werner, *Katalytische Methoden in der Spurenanalyse*, Akad. Verlag, Leipzig, 1980.
4. S. Yu. Kreingold, *Katalimetriya v analize reaktivov i veschestv osoboy chistoti*, Khimia, Moscow, 1983.
5. F. E. Beamish, *The Analytical Chemistry of the Noble Metals*, Pergamon Press, Oxford, 1966.
6. W. Griffith, *The Chemistry of Rarer Platinum Metals*, Interscience, London, 1967.
7. S. I. Ginzburg, N. A. Ezerskaya, I. V. Prokof'eva, N. V. Fedorenko, V. I. Shlenskaya and N. K. Belskii, *Analiticheskaya khimia platinovykh metallov*, Nauka, Moscow, 1972.
8. V. I. Shlenskaya, V. P. Khvostova and G. I. Kadirova, *Zh. Analit. Khim.*, 1973, **28**, 779.
9. K. B. Yatsimirskii and L. P. Tikhonova, in *Uspekhi analiticheskoi khimii*, p. 779. Nauka, Moscow, 1974.
10. P. R. Bonchev, *Kompleksoobrazovane i katalitichna aktivnost*, Nauka i izkustvo, Sofia, 1972.
11. W. M. Latimer, *Oxidation Potentials*, 2nd Ed., Prentice-Hall, Englewood Cliffs, 1952.
12. A. Berka, J. Vulterin and J. Zýka, *Vybrané oxydacne redučni odmerne metody*, SNTL, Prague, 1961; *Newer Redox Titrants*, Pergamon Press, Oxford, 1965.
13. K. B. Yatsimirskii and L. P. Tikhonova, in *Voprosy kinetiki i kataliza*, p. 11. Ivanovo, 1974.
14. V. E. Kalinina and K. B. Yatsimirskii, in *Voprosy kinetiki i kataliza*, p. 43. Ivanovo, 1974.
15. L. P. Tikhonova and K. B. Yatsimirskii, in *Metallokompleksny kataliz*, p. 107. Naukova dumka, Kiev, 1979.
16. R. L. Habig, H. L. Pardue and J. B. Worthington, *Anal. Chem.*, 1967, **39**, 600.
17. R. D. Sauerbrunn and E. B. Sandell, *Mikrochim. Acta*, 1953, 22.
18. A. C. Gillet, Jr., *ibid.*, 1970, 855.
19. P. A. Rodriguez and H. L. Pardue, *Anal. Chem.*, 1969, **41**, 1369.
20. J. B. Worthington and H. L. Pardue, *ibid.*, 1970, **42**, 1157.
21. H. Weisz and H. Ludwig, *Anal. Chim. Acta*, 1972, **60**, 385.
22. H. Ludwig and H. Weisz, *ibid.*, 1974, **72**, 315.
23. A. T. Pilipenko, L. V. Markova and T. S. Maksimenko, in *Analiz i tekhnologia blagorodnykh metallov*, p. 115. Metallurgiya, Moscow, 1971.
24. V. S. Khain, A. A. Volkov and E. V. Fomina, *Zh. Analit. Khim.*, 1976, **31**, 1500.
25. C. Sánchez-Pedreño, M. Hernandez-Cordoba and G. Martinez Tudela, *Anal. Quim.*, 1979, **75**, 536.
26. C. Sánchez-Pedreño, I. Albero Quinto and M. Hernandez-Cordoba, *Afinidad*, 1980, **37**, 313.
27. T. I. Fedorova and L. V. Shvedova, *Zh. Analit. Khim.*, 1970, **25**, 307.
28. O. D. Injutina, D. P. Shcherbov and A. I. Ivankova, in *Issledovaniya v oblasti khim. i fiz. metodov analiza mineralnogo syr'ya*, p. 21. Alma Ata, 1972.
29. I. I. Alekseeva, I. B. Smirnova and K. B. Yatsimirskii, *Zh. Analit. Khim.*, 1970, **25**, 539.
30. I. I. Alekseeva, N. K. Ignatova, A. P. Rysev, I. B. Smirnova and A. I. Yakshynskii, in *Khimia i khim. tekhnologia*, p. 291. Moscow, 1972.

31. A. P. Filippov, V. M. Ziatkovskii and K. B. Yatsimirskii, *Zh. Analit. Khim.*, 1970, **25**, 1769.
32. I. I. Alekseeva, N. K. Ignatova, A. P. Rysev and A. I. Yakshynskii, *Zavodsk. Lab.*, 1972, **38**, 919.
33. D. R. Bhattarai and J. M. Ottaway, *Talanta*, 1972, **19**, 793.
34. I. I. Alekseeva, A. D. Gromova, A. P. Rysev, N. A. Khvorostukhina and A. I. Yakshynskii, *Zh. Analit. Khim.*, 1974, **29**, 1017.
35. A. E. Burgess and J. M. Ottaway, *Talanta*, 1975, **22**, 401.
36. N. V. Rao and P. V. Ramana, *Mikrochim. Acta*, 1981 **II**, 269.
37. I. I. Alekseeva, N. K. Ignatova, A. P. Rysev and A. I. Yakshynskii, *Zh. Analit. Khim.*, 1974, **29**, 335.
38. E. S. Khomutova, N. A. Khvorostukhina and I. O. Moskvina, *ibid.*, 1983, **38**, 170.
39. R. Z. Gregorowicz and S. Suwińska, *Mikrochim. Acta*, 1967, 546.
40. I. I. Alekseeva, A. P. Rysev, N. K. Ignatova and A. I. Yakshynskii, *Zh. Analit. Khim.*, 1972, **27**, 1566.
41. G. A. Konishevskaya, V. F. Romanov and K. B. Yatsimirskii, *ibid.*, 1973, **28**, 1154.
42. V. P. Khvostova, V. I. Shlenskaya and G. I. Kadyrova, *ibid.*, 1973, **28**, 328.
43. G. I. Kadyrova, V. P. Khvostova and V. I. Shlenskaya, *ibid.*, 1974, **29**, 1389.
44. H. Müller and M. Otto, *Z. Chem.*, 1974, **14**, 159.
45. *Idem*, *Mikrochim. Acta*, 1975 **I**, 519.
46. I. I. Alekseeva and L. N. Zhir-Lebed, *Izv. Vysh. Uchebn. Zavedeniya, Khim. i Khim. Tekhnol.*, 1970, **13**, 1260.
47. A. T. Pilipenko, L. V. Markova and T. S. Maksimenko, *Zh. Analit. Khim.*, 1973, **28**, 1544.
48. L. P. Tikhonova, K. B. Yatsimirskii, I. P. Svarkovskaya and L. N. Zakrevskaya, *ibid.*, 1973, **28**, 561.
49. K. B. Yatsimirskii, L. P. Tikhonova, V. P. Goncharik and G. V. Kudina, *Chem. Anal. Warsaw*, 1972, **17**, 798.
50. V. P. Goncharik, K. B. Yatsimirskii and L. P. Tikhonova, *Zh. Analit. Khim.*, 1972, **27**, 1348.
51. H. Müller, L. P. Tikhonova, K. B. Yatsimirskii and S. N. Borkovets, *ibid.*, 1973, **28**, 2012.
52. V. E. Kalinina, K. B. Yatsimirskii and T. S. Zimina, *ibid.*, 1969, **24**, 1178.
53. I. I. Alekseeva, A. P. Rysev, N. M. Sinitsyn, L. P. Zhytenko and A. I. Yakshynskii, *ibid.*, 1974, **29**, 1859.
54. A. P. Rysev, I. I. Alekseeva, S. F. Koriavova, L. P. Zhytenko and A. I. Yakshynskii, *ibid.*, 1976, **31**, 508.
55. A. P. Rysev, L. P. Zhytenko and I. I. Alekseeva, *ibid.*, 1979, **34**, 1132.
56. I. I. Alekseeva, N. A. Khvorostukhina, A. P. Rysev and E. G. Khomutova, *ibid.*, 1980, **35**, 505.
57. R. P. Morozova, L. P. Nishchenkova and L. N. Blinova, *ibid.*, 1981, **36**, 2356.
58. G. R. Rozovskii, Z. A. Poshkute and A. Yu. Propokhik, *ibid.*, 1974, **29**, 512.
59. L. P. Tikhonova, L. N. Zakrevskaya and K. B. Yatsimirskii, *ibid.*, 1978, **33**, 1991.
60. I. I. Alekseeva, A. P. Rysev, A. I. Yakshynskii and N. K. Ignatova, *ibid.*, 1973, **28**, 1368.
61. R. P. Morozova and K. B. Yatsimirskii, *ibid.*, 1969, **24**, 1183.
62. S. Suwińska, Z. Gregorowicz and D. Matysek-Majewska, *Zesz. Nauk., Politech. Śląsk., Chem.*, 1980, **96**, 235; *Chem. Abstr.*, 1982, **96**, 115090d.
63. Z. Gregorowicz, S. Suwińska and D. Matysek-Majewska, *ibid.*, 1979, **88**, 182; *Chem. Abstr.*, 1980, **92**, 87479j.
64. N. N. Gusakova and S. P. Mushtakova, *Zh. Analit. Khim.*, 1981, **36**, 317.
65. V. I. Vershynin, B. E. Reznik and V. P. Statsenko, *ibid.*, 1974, **29**, 380.
66. I. I. Alekseeva and L. N. Zhir-Lebed, *Izv. Vysh. Uchebn. Zaved., Khim. i Khim. Tekhnol.*, 1970, **13**, 1260.
67. D. P. Shcherbov, O. D. Iniutina and A. I. Ivankova, *Zh. Analit. Khim.*, 1973, **28**, 1372.
68. S. I. Ginzburg and M. I. Yuzko, *ibid.*, 1966, **21**, 79.
69. L. P. Tikhonova and K. B. Yatsimirskii, *ibid.*, 1968, **23**, 1413.
70. L. P. Tikhonova, K. B. Yatsimirskii and I. P. Svarkovskaya, *ibid.*, 1970, **25**, 1766.
71. L. P. Tikhonova, K. B. Yatsimirskii and G. V. Kudina, *ibid.*, 1972, **27**, 1331.
72. V. E. Kalinina, Yu. A. Zhukov, P. G. Velasko and G. A. Ivanova, *Izv. Vysh. Uchebn. Zaved., Khim. i Khim. Tekhnol.* 1984, **27**, 791.
73. M. P. Volynets, R. P. Morozova, A. N. Ermakov, I. V. Pankratova and T. V. Dubrova, *Zh. Analit. Khim.*, 1973, **28**, 555.
74. V. E. Kalinina, V. M. Liakushyna and N. V. Petrova, *ibid.*, 1978, **33**, 959.
75. N. N. Gusakova, S. P. Mushtakova and N. S. Frumina, *ibid.*, 1979, **34**, 2213.
76. L. P. Tikhonova, S. N. Borkovets and L. N. Pevenko, *Ukr. Khim. Zh.*, 1976, **42**, 869.
77. V. E. Kalinina, V. M. Liakushyna and A. E. Rybina, *Zh. Analit. Khim.*, 1978, **33**, 125.
78. R. P. Morozova, K. B. Yatsimirskii and I. T. Egorova, *ibid.*, 1970, **25**, 1954.
79. E. T. Gaynullina, I. P. Ivanov and O. V. Chebotarev, *Zh. Vses. Khim. Obsch. im Mendeleeva*, 1971, **16**, 105.
80. K. B. Yatsimirskii, L. P. Tikhonova and S. N. Borkovets, *Zh. Analit. Khim.*, 1976, **31**, 339.
81. Z. Kurzawa and H. Matusiewicz, *Chem. Anal. Warsaw*, 1975, **20**, 465.
82. A. S. Segeda, *Zh. Analit. Khim.*, 1969, **24**, 1058.
83. V. E. Kalinina and N. A. Moiseeva, *ibid.*, 1971, **26**, 1973.
84. I. I. Alekseeva, A. D. Gromova, I. V. Dermeleva and N. A. Khvorostukhina, *ibid.*, 1975, **35**, 1017.
85. A. P. Rysev, L. P. Zhytenko and I. I. Alekseeva, *Zh. Neorgan. Khim.*, 1977, **22**, 2481.
86. E. G. Khomutova, N. A. Khvorostukhina and I. I. Alekseeva, *Zh. Analit. Khim.*, 1984, **39**, 1099.
87. V. E. Kalinina, K. B. Yatsimirskii, V. M. Liakushyna and L. P. Tikhonova, *Zh. Neorgan. Khim.*, 1977, **22**, 2488.
88. B. E. Kalinina, L. V. Shvedova and K. B. Yatsimirskii, *ibid.*, 1971, **16**, 1377.
89. L. P. Tikhonova and V. Ya. Zayats, *ibid.*, 1976, **21**, 2154.
90. L. P. Tikhonova, V. Ya. Zayats and I. P. Svarkovskaya, *ibid.*, 1979, **24**, 2706.
91. N. N. Massley, B. I. Nabivanets and E. A. Yantso, *Ukr. Khim. Zh.*, 1976, **42**, 1314.
92. G. M. Varshal, L. P. Tikhonova, L. S. Shulik and V. A. Sychkova, *Zh. Analit. Khim.*, 1970, **25**, 2427.
93. N. N. Nikolskaya, L. P. Tikhonova, Z. A. Yezhkova and I. Yu. Davydova, *ibid.*, 1979, **34**, 171.
94. L. P. Tikhonova, V. P. Goncharik, I. P. Svarkovskaya, S. K. Kalinin and L. V. Kikina, *ibid.*, 1981, **36**, 1982.
95. I. I. Alekseeva, G. N. Latysheva, L. E. Romanovskaya and L. P. Tikhonova, *Zavodsk. Lab.* 1984, **50**, 5.
96. P. R. Bonchev, *Talanta*, 1972, **19**, 675.
97. *Idem.*, *Wiss. Z. Karl-Marx-Univ., Leipzig, Math.-Naturwiss. Reihe*, 1975, **24**, 409.

SELECTIVITY AND SENSITIVITY OF METAL DETERMINATION BY CO-ORDINATION COMPOUNDS

A. T. PILIPENKO* and L. I. SAVRANSKY

A. V. Dumansky Institute of Colloid and Water Chemistry, Ukrainian Academy of Sciences, Kiev and
T. G. Shevchenko Kiev State University, Kiev, USSR

(Received 15 October 1985. Accepted 8 September 1986)

Summary—Quantum chemical structure calculations for metal co-ordination compounds with various organic ligands allow choice of generalized parameters of chelate electronic structures, to form a basis for systematization and prediction of analytical properties. The extent of the co-ordinative saturation of a metal is measured as the sum of the covalent bonding energies of the two-centre metal interactions with the ligand atoms. The concept of “valence state of the ligand” is considered and characterized by the energy sum of the covalent components of two-centre interactions in the ligand. It is shown that the ligand structure can be correlated with the complex stability and this provides a new mechanism for assessing the influence of substituents in ligands. The calculated data make it possible to predict compound stability in solutions and synergic action, and therefore such analytical properties as sensitivity and selectivity. For the azo dyes as an example, it is shown that quantum chemical calculations can explain many of the experimental data on the use of azo dyes in photometry, and suggest directions of search for new analytical reagents.

The search for new analytical reagents and new reactions for simultaneous determination of trace components, especially metals, is at the centre of analytical chemistry. Problems not yet solved include group concentration and separation of trace components, separation of traces from macro-components, and development of methods for multi-component analysis, especially photometric procedures. To resolve these problems it is necessary to utilize all our knowledge about the structure of compounds and their formation reactions. The study of co-ordination compounds, their properties and formation reactions is therefore very important for analytical chemical research.

This paper gives the results of our quantum chemical calculations of the structure and properties of various reagents and their co-ordination compounds with metals. The quantitative parameters of the complex electronic structures determined have enabled us to model qualitatively or semiquantitatively some analytical properties of the compounds.

STABILITY OF METAL CO-ORDINATION COMPOUNDS IN SOLUTION AND SELECTIVITY OF COMPLEX FORMATION

Theoretical calculations of the thermodynamic complex-formation energy in the gas phase and in

solutions are not yet possible.^{1,2} The main approach (mathematical model), to prediction of complex stability (formation constants) in solutions is the use of semi-empirical dependences between some ligand properties and complex physical properties such as spectral characteristics and stability constant values.³⁻⁵ A special case of this approach is the use of the free-energy linearity principle to predict the effect of different substituents in a ligand on the values of the stability constants, as shown, *e.g.*, by Ovchinnikov *et al.*,⁶ but the semi-empirical equations published allow only prediction of stability constants for one metal and a narrow class of ligands.

The work described in this paper was an attempt to establish a relationship between the parameters of the electronic structure and the stability constant of the co-ordination compound, and the related analytical properties. The quantum chemical calculations were done in approximation of CNDO/2 with the parameter chosen by Clack *et al.*⁷ Compound structure analysis was done in terms of charge distribution and the energy of two-centre interactions. The energies of the covalent contribution to two-centre interactions (covalent-part energies, CPE)† are the most interesting for compound stability analysis.⁸

Donor atoms

The effect of ligand donor atoms on the stability of co-ordination compounds has been considered many times. It is well known that the stability of heavy metal compounds increases in a set of ligands containing different donor atoms, in the order O < N < S. However, this is not always true,

*Author for correspondence.

†The absolute values of the calculated energies depend on the parameters used in the semi-empirical methods. Thus, the energy values given here should be used only for comparison purposes.

Table 1. The values of donor-atom charges (q_x) and metal-donor-atom two-centre interaction energies (E_{M-X} , arbitrary units) in Co(II), Ni(II) and Cu(II) complexes

Complex*	Donor atom (X)	Co(II)		Ni(II)		Cu(II)	
		$-q_x$	$-E_{Co-X}$	$-q_x$	$-E_{Ni-X}$	$-q_x$	$-E_{Cu-X}$
M(py)(H ₂ O) ₅	N	0.05	0.982	0.04	1.054	—	—
	O	0.18	0.825	0.18	0.865	—	—
M(py) ₂ (H ₂ O) ₄	N	0.04	0.984	0.03	1.042	—	—
	O	0.19	0.785	0.18	0.825	—	—
M(py) ₄ (H ₂ O) ₂	N	0.03	0.923	0.02	0.978	—	—
	O	0.20	0.732	0.19	0.768	—	—
M(phen)(H ₂ O) ₄	N	0.07	0.967	0.06	1.024	—	—
	O	0.18	0.810	0.18	0.848	—	—
M(phen) ₂ (H ₂ O) ₂	N	0.06	0.942	0.05	0.996	0.07	1.038
	O	0.18	0.764	0.18	0.789	0.20	0.812
M(acac)(H ₂ O) ₄	O	0.32	0.926	0.32	0.966	0.33	1.006
	O _{H₂O}	0.17	0.807	0.16	0.828	0.18	0.869
M(acac) ₂ (H ₂ O) ₂	O	0.30	0.878	0.30	0.919	0.31	0.956
	O _{H₂O}	0.15	0.770	0.14	0.813	0.16	0.852
M(dbm) ₂ (H ₂ O) ₂	O	0.30	0.895	0.29	0.937	0.30	0.976
	O _{H₂O}	0.17	0.633	0.17	0.659	0.17	0.683
M(oxine)(H ₂ O) ₄	O	0.38	1.000	0.37	1.043	0.38	1.076
	N	0.04	0.981	0.04	1.036	0.06	1.085
M(oxine) ₂ (H ₂ O) ₂	O _{H₂O}	0.17	0.790	0.17	0.830	0.18	0.870
	O	0.35	1.017	0.38	0.963	0.40	0.996
M(oxine) ₂ (H ₂ O) ₂	N	0.08	1.061	0.00	0.997	0.02	1.041
	O _{H₂O}	0.18	0.743	0.15	0.781	0.17	0.799
M(thiox)(H ₂ O) ₄	S	0.15	1.411	0.14	1.479	0.16	1.547
	N	0.03	0.941	0.03	0.992	0.05	1.047
M(thiox) ₂ (H ₂ O) ₂	O _{H₂O}	0.17	0.766	0.17	0.780	0.18	0.832
	S	0.19	1.318	0.18	1.384	0.20	1.450
M(thiox) ₂ (H ₂ O) ₂	N	0.00	0.871	0.00	0.922	0.02	0.964
	O _{H₂O}	0.16	0.653	0.16	0.691	0.17	0.727
M(dtp) ₂	S	0.20	1.327	0.20	1.327	0.20	1.458
M(dtc) ₂	S	0.09	1.249	0.06	1.364	0.12	1.296

Phen—1,10-phenanthroline, acac—acetylacetonate anion, dbm—dibenzoylmethane anion, oxine—8-hydroxyquinoline anion, thiox—8-mercaptoquinoline anion, py—pyridine, dtp—dimethyldithiophosphoric acid anion, dtc—diethyldithiocarbamic acid anion. The energies of $ML_2(H_2O)_2$ complexes, where L is a bidentate ligand, were calculated by modelling the square-plane co-ordination of two bidentate ligands with a trans-axial arrangement of two water molecules.

especially for IVth series transition metals with oxidation state + II. In Pearson's well-known classification they are assigned to an intermediate group. Calculated charges on the ligand donor atoms and the CPE of the metal-donor-atom bonds are listed in Table 1. The CPE values may give a quantitative measure of preference for bond formation between a metal and one or other donor atom. The charges on the donor atoms are less useful, and do not correlate with metal-complex stability. The CPE values give interesting information. The following conclusions may be drawn.

(1) In the metal series Co(II), Ni(II), Cu(II), for a given type of complex, the CPE (absolute value) increases in most cases. This agrees with the experimental stability constants.

(2) Analysis of the relative stability of complexes of the $ML_n(H_2O)_m$ type shows that the individual bond formation energies are not additive, because of ligand interactions. In most cases, increasing the number of ligands, by replacing water molecules in the inner sphere of complexes, leads to an energy

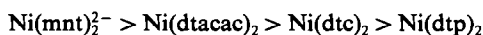
decrease in the metal bonds with all the donor atoms. Other examples, illustrating the role of co-ordinated water molecules in the energy of complex formation are given in an earlier paper.⁹

(3) The comparison of CPE values for M-O and M-N bonds in $M(oxine)(H_2O)_4$ and $M(oxine)_2(H_2O)_2$ complexes shows that in the first complex the metal-oxygen bonds are more favourable for Co(II) and Ni(II), whereas in the dioxinates the metal-nitrogen bonds are more favourable for all metals. Also, the metal-oxygen bond in the mono-oxinate is more favourable than, e.g., the metal-nitrogen bonds in the mono- and bis-phenanthroline complexes. Thus, the preference of a metal for interactions with donor atoms (such as nitrogen and oxygen) depends on the composition and structure of the ligand, and also on the specific composition of the metal co-ordination sphere. The most stable bond is metal-sulphur in all the examples considered. Many examples have been given previously.¹ These showed that, although metal-donor atom interactions make the main contribution to the energy

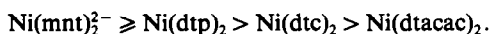
Table 2. The sum values of metal–ligand atom two-centre interaction energies (CPE, arbitrary units) as metal free valence indices in complexes

Metal (M)	M(dtp) ₂	M(dtc) ₂	M(oxine) ₂	M(thiox) ₂	M(acac) ₂
Co	−6.234	−5.460	−5.424	−5.834	−4.560
Ni	−6.124	−6.040	−5.606	−6.030	−4.698
Cu	−6.956	−5.748	−5.780	−6.256	−4.854

of the metal–ligand bond, the interaction of metal atoms with other ligand atoms close to the metal may change the order of complex stability. For example, for Ni(II) complexes with dithioacetylacetone (dtacac), dimethyldithiocarbamate (dtc), dimethyldithiophosphate (dtp) and maleonitriledithiol (mnt) the order of CPE values for the metal–donor-atom bond is



The order for the metal–ligand interaction energy is



This order of complex stability may be explained¹ by spatial tension in the Ni(dtc)₂ and Ni(dtp)₂ four-membered chelate rings, which results in low-energy metal–sulphur interaction, being compensated by the abundance of trans-annular interactions. The latter make the Ni(dtc)₂ and Ni(dtp)₂ complexes, which have four-membered rings, more stable than Ni(dtacac)₂, which has a six-membered chelate ring.

Co-ordinative saturation

“Free valence” as an index of reaction ability has been used in quantum organic chemistry for many years. It was introduced to allow comparison of co-ordinative saturation of various atoms in molecules. The atom which has the largest sum of the bond orders with neighbouring atoms is less able to form additional bonds. Evidently such an index would be useful in analysis of the properties of co-ordination compounds. It is well known that some ligands form inert stable complexes in which the metal has a low co-ordination number. Compounds such as bis(dithiocarbamate)M(II), bis(dithiophosphato)M(II), and others, form stable compounds which show no tendency to oligomer or stable adduct formation. On the other hand, compounds such as bis(acetylacetonato)M(II) (with M = Fe, Co, Ni) exist either as oligomers or as adducts, such as M(acac)₂ · 2L (L = monodentate ligand) or M(acac)₂L (L = bidentate ligand). This illustrates the fact that

two bidentate anions of acetylacetonate do not saturate the metal co-ordination sphere; hence the ease of formation of compounds in which the metal co-ordination number increases to six. Thus any quantitatively calculated criterion for metal co-ordinative saturation should be able to make predictions about adduct formation. Table 2 gives CPE values for metal-atom bonds with all ligand atoms, which may be used as the free valence index of a metal (FV). It is evident from Table 2, that FV correlates with complex stability, and that the higher the FV value, the less is the possibility of the metal forming bonds with additional ligands. The possibility of predicting these properties is very important for analytical chemistry, because it can explain the synergic action of various active additives (amines, phosphine oxides and others) in metal extraction.^{10–12} Unfortunately, there are not enough data in the literature to allow quantitative correlation of the suggested FV values with the stability of ML₂A or ML₂A₂ compounds (L = bidentate ligand, A = monodentate base). For a qualitative correlation, we can compare Yordanov's order¹³ for the affinity of copper(II) bis-chelates (with ligands containing various donor atoms) for attachment of a molecule of base, with our calculated FV indices. Yordanov's order is

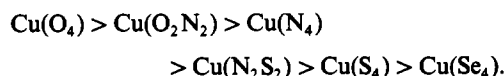


Table 3 gives the calculated FV values for a number of bis-chelates having the same general structure but differing in the type of donor atoms:

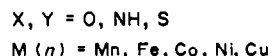
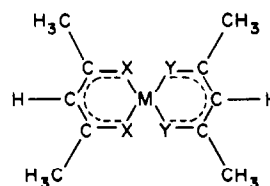


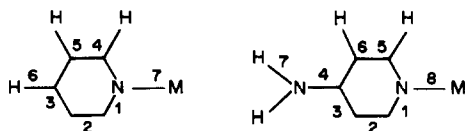
Table 3. The sum values of metal–ligand atom two-centre interaction energies (CPE, a.u.) as metal free valence indices in complexes of the form

Metal	X ₁ O	Y ₁ O	X ₁ N	Y ₁ N	X ₁ S	Y ₁ S	X ₁ O	Y ₁ N	X ₁ O	Y ₁ S	X ₁ N	Y ₁ S
Mn	−4.072	−4.880	−5.056	−4.448	−4.576	−4.928						
Fe	−4.386	−5.292	−5.476	−4.802	−4.960	−5.336						
Co	−4.560	−5.500	−5.710	—	—	—						
Ni	−4.698	−5.686	−5.930	−5.148	−5.356	−5.756						
Cu	−4.854	−5.874	−6.136	−5.324	−5.540	−5.954						

Table 4. The covalent contribution (CPE) to the two-centre interaction energies in co-ordinated and free molecules of pyridine and 4-aminopyridine

Compound	Bond* number								$\Sigma \Delta E$
	1	2	3	4	5	6	7	8	
Py	-1.710	-1.750	-1.740	-0.950	-0.950	-0.950	—	—	—
Ni(py)(H ₂ O) ₅ †	-0.081	0.012	-0.014	-0.018	-0.003	-0.005	-1.054	—	-0.213
Co(py)(H ₂ O) ₅	-0.082	0.011	-0.013	-0.020	-0.003	-0.005	-0.997	—	-0.219
4-NH ₂ py	-1.700	-1.770	-1.700	-1.450	-0.950	-0.980	-0.980	—	—
Ni(4-NH ₂ py)(H ₂ O) ₅	-0.087	0.016	-0.027	0.048	-0.019	-0.001	-0.006	-1.068	-0.200
Co(4-NH ₂ py)(H ₂ O) ₅	-0.088	0.016	-0.027	0.048	-0.021	-0.001	-0.006	-1.011	-0.206

*Bond numbers in reagents and complexes:



†The values of $\Delta E = E_{CPE}^{free} - E_{CPE}^{lig}$ calculated for each bond are shown.

The data of Table 3 agrees with Yordanov's order and enables us to generalize this order for Mn(II), Fe(II) and Ni(II) complexes and in a number of cases for Co(II) complexes.

Ligand valence state

Metal and reagent electron shells are rearranged when a co-ordination compound is formed. The energy of rearrangement of the metal electron shell, *i.e.*, the energy needed to change the oxidation state of the metal atom or ions is called the "valence state energy". Transitions between valence states often demand considerable promotion in energy. That is why the metal valence-state energy is significant in the energy balance for a compound. The question of analogous values for polyatomic ligands has not been raised in the literature. As far as we are aware, quantitative analysis of energy promotion for ligand transition in the valence state has not been discussed. Two-centre interaction energies for pyridine and 4-aminopyridine, and for the corresponding metal aqua complexes are listed in Table 4. These data give a vivid picture of reagent destabilization on complex

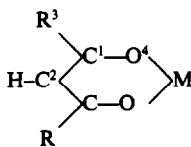
formation. The destabilization energy is 20% of the metal-ligand bond energy. It is most interesting to follow the effect of hydrogen substitution on the amino group on changing from pyridine to 4-aminopyridine. The data show that the 4-amino group stabilizes the quinonoid form of the pyridine ring. The destabilization energy of the reagent on its conversion from the free state into the co-ordinated one, was determined as the difference between the two-centre interactions sums in the two states. For both metals, the pyridine and 4-aminopyridine destabilization energy difference is equal to 0.013 a.u. (arbitrary units), and the metal-ligand bond energy difference is 0.014 a.u. Thus, the influence of the amino group is similar for the pyridine-ring nitrogen donor properties, and for the ligand valence-state stabilization.

Table 5 lists the two-centre interaction energies for bis(β -diketonato)Ni(II). These data show that replacement of a methyl group in acetylacetonate by phenyl leads to ligand bond stabilization ($\Delta E_{lig} = -0.24$) which is higher by a factor of 10 than the metal-ligand bond energy change ($\Delta E_{M-O} = -0.024$).

Table 5. Two-centre interaction energies (arbitrary units) in Ni(II) complexes with acetylacetonate and dibenzoylmethane M(L)(H₂O)₄

L	Bond number				$\Sigma_{1,2,3}^*$
	1	2	3	4	
CH ₃ (Me)	-1.701	-1.675	-1.338	-0.966	-4.714
C ₆ H ₅ (Ph)	-1.689	-1.672	-1.413	-0.972	-4.774

* $\Sigma_{1,2,3} = E_1 + E_2 + E_3$

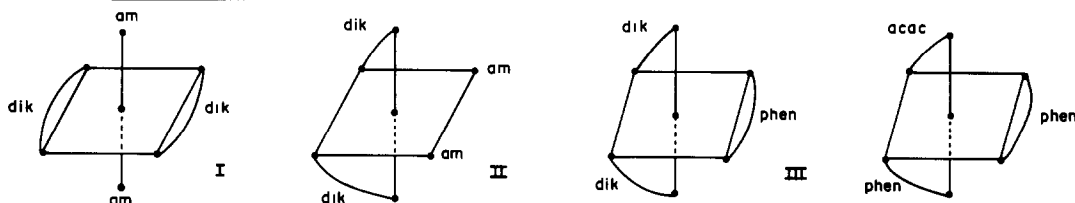


$$\Delta E_{Lig} = 4(\Sigma_{1,2,3}^{Ph} - \Sigma_{1,2,3}^{Me}) = -0.24$$

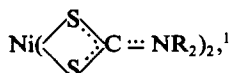
$$\Delta E_{M-O} = 4(E_4^{Ph} - E_4^{Me}) = -0.024.$$

Table 6. Two-centre interaction energies for $\text{Cu}(\text{dik})_2(\text{am})_2$ type complexes in two conformations (I and II) and $\text{Cu}(\text{dik})_2(\text{phen})$ and $\text{Ca}(\text{acac})(\text{phen})_2$ (III) (acac—acetylacetonone, hfa—hexafluoroacetylacetonone, py—pyridine, apy—4-aminopyridine, phen—1,10-phenanthroline)

	acac, apy		hfa, apy		hfa, py		acac phen	hfa phen	$\text{Cu}(\text{acac})(\text{phen})_2$
	I	II	I	II	I	II	$\text{Cu}(\text{dik})_2(\text{phen})$		
$-E_{\text{Cu-O}}$	0.922	0.916	0.908	0.901	0.911	0.905	0.909	0.893	0.894 (0.913)
$-E_{\text{Cu-N}}$	0.839	0.842	0.858	0.861	0.850	0.853	0.967	0.986	0.989
$-E_{\text{Cu-L}}$	6.560	6.552	6.547	6.540	6.549	6.541	6.862	6.851	7.350



From this point of view we considered the influence of the radicals in complexes of the type



and showed that as in the above-mentioned example with acetylacetonone and dibenzoylmethane, the radical substitution effect on complex stability should not be caused by the change in electron density on the donor atoms. The radical influence is primarily the valence-state energy change of ligands and therefore determines the relative complex stability.

Thus, quantitative data on the ligand valence-state energies give us a new understanding of the role of substituents and ligand structure in determining the complex-formation energy.

Mutual ligand influence and mixed-ligand complex stability

Our data can also illustrate mutual influences between ligands. Substitution of water molecules in the metal inner sphere changes the energies of the metal bonds with any other water molecules and other ligands (Table 1). It is evident that the place of a particular ligand in the complex stability order may change with the inner sphere composition. Table 6 gives electron structure parameters for copper(II) compounds of the $\text{Cu}(\text{dik})_2(\text{am})_2$ type, where dik is acetylacetonone or hexafluoroacetylacetonone and am is pyridine or 4-aminopyridine. The data for $\text{Cu}(\text{dik})(\text{phen})_2$ or $\text{Cu}(\text{dik})_2(\text{phen})$ are also given, where phen is 1,10-phenanthroline.

Complexes of the $\text{Cu}(\text{dik})_2(\text{am})_2$ type were analysed in two conformations: (I) a coplanar arrangement of the two chelate rings and a transaxial arrangement of the two amine molecules; (II) a non-coplanar arrangement of the chelate rings. From these data, we may conclude the following.

(1) Irrespective of the diketone and amine, the metal–ketone bond is more stable in conformation I,

and the metal–amine bond is less stable. Since the conformational change is more substantial for metal bonds with β -diketones, conformation I is more stable.

(2) Metal bonds with β -diketones are more stable, and bonds with amine molecules less stable in the acetylacetonone complexes than in the hexafluoroacetylacetonone complexes.

(3) For a given β -diketone, 4-aminopyridine is bonded more strongly than pyridine. The nature of the β -diketone is very important, in that 4-aminopyridine is bonded more weakly with the acetylacetonone complex than pyridine is with the hexafluoroacetylacetonone complex.

(4) The metal–nitrogen bond in mixed-ligand complexes with phenanthroline is more stable than the metal–nitrogen bond with pyridine and 4-aminopyridine monodentate ligands. This illustrates the difference between ligand basicity (*i.e.*, proton affinity) and ability to make bonds with metals. In the above-mentioned mixed-ligand complexes (MLC) with monodentate amines, the amines form weaker bonds with the metal than the β -diketone does. In MLC with phenanthroline, the reverse is true.

There are data in the literature for formation of transition-metal MLC, containing a β -diketone and various bidentate reagents. The energy characteristics of a number of complexes are given in Table 7. Comparison of the metal–ligand bond energies in these complexes illustrates the bond polarization.¹⁴ For example, oxine forms more stable bonds with nickel(II) than acetylacetonone does in the corresponding homo-ligand (HLC) bis-chelates. The nickel(II)–oxine bond is stabilized, and the nickel(II)–acetylacetonone bond destabilized, in MLC in comparison with HLC.

These data are in accordance with the well-known stabilities of homo- and mixed-ligand complexes with β -diketones. Our approach allows prediction of the relative complex stability from the β -diketone substituent properties.

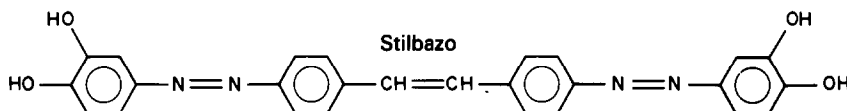
Table 7. Metal-donor atom two-centre interaction energies in Ni(II) complexes

Complex	Ligand	Donor atom	$-E_{M-x}$ (arbitrary units)
Ni(oxine) ₂ (H ₂ O) ₂	oxine	O	0.963
		N	0.997
Ni(acac) ₂ (H ₂ O) ₂	acac	O	0.919
		N	0.992
Ni(acac)(oxine)(H ₂ O) ₂	oxine	O	0.992
		N	0.994
	acac	O	0.894

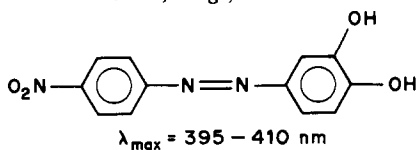
SPECTRAL CONTRAST

Let us consider the properties of azo dyes that make them suitable as reagents for photometric determination of metals. The difference between the positions of the absorption bands of the free reagent and the metal complex depends on the structure of the complex and on the chemical equilibria of the reagent in solution. The following groups of azo dyes can be distinguished.

(1) Reagents that form complexes with metals with the help of functional groups that are remote from the azo groups. The metals are not bonded directly with the nitrogen atoms of the azo groups in complexes with such reagents. Examples of such reagents and their photometric characteristics have been given.^{15,16} To construct a reagent of this type, reagents that form colourless complexes with many metals are modified to give reagents that form coloured ones. For example, the azo coupling reaction with salicylic acid, pyrocatechol and other hydroxy- and carboxy derivatives of benzene yields coloured reagents that form coloured complexes with metals. Typical reagents are:



The nature of the colour of the compound and the spectral contrast on complexation has been considered in depth.¹⁷ Since metals are bonded with these reagents either by two hydroxyl groups, or by hydroxyl and carboxyl groups, and are not connected directly with the nitrogen atoms of the azo group, the maximum possible colour contrast on reaction is determined by the absorption maxima of the corresponding acid-base forms,¹⁸ e.g.,

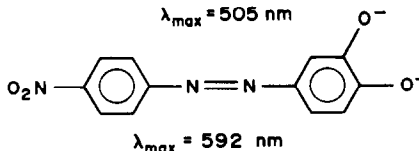
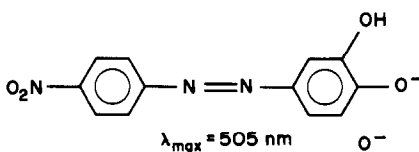
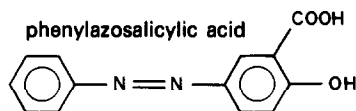
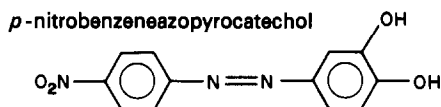
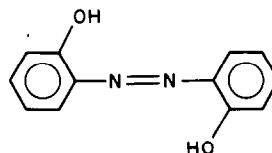


Examples^{15,16} show that the colour contrast in reactions with such reagents is fully determined by the acid-base properties of the reagent.¹⁷

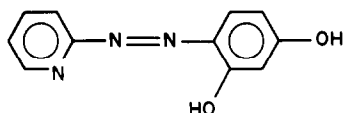
(2) Chelate-forming reagents, in which the metals are directly bonded with the nitrogen atoms of the azo group.

This group of reagents is widely used in analytical practice. From the point of view of the nature of the absorption spectra, it is expedient to divide these compounds into three subgroups.

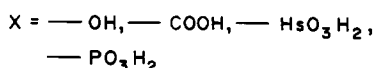
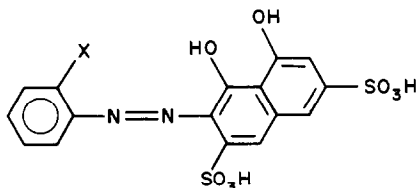
(a) Hydroxyazo compounds in which hydroxy groups are bonded only to benzene nuclei, e.g., 2,2'-dihydroxyazobenzene and its numerous derivatives



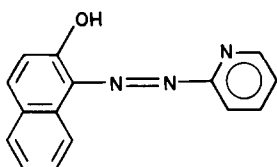
and 4-(2-pyridylazo)resorcinol (PAR)



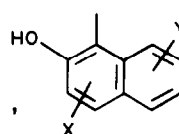
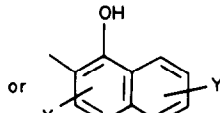
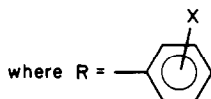
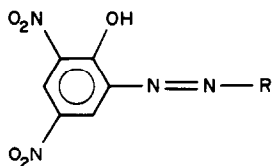
(b) Hydroxyazo compounds in which hydroxy groups are also (or only) bonded with naphthalene nuclei, *e.g.*, numerous mono- and bis-azo derivatives of chromotropic acid



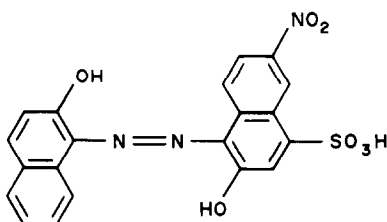
and 1-(2-pyridylazo)-2-naphthol



(c) Hydroxyazo compounds containing a nitro group in the aromatic nucleus, *e.g.*, compounds derived from picramine

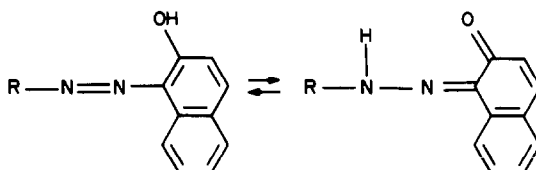


with different substituents X, Y, and Eriochrome Black T



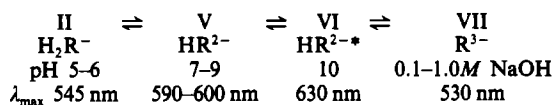
A characteristic feature of the compounds of subgroups 2a is that they exist in solution, mainly in azo forms. Metal complex formation is usually characterized by a considerable shift of the longest-wavelength absorption maximum of the reagent, $\Delta\lambda \geq 100$ nm. By choice of certain reaction conditions, such as solvent and acid-base parameters, it is possible to

achieve more contrast. For example, formation of the PAR complex of Pd(II) in sulphuric acid followed by extraction into an organic phase leads to a band shift of >200 nm. In many similar spectrophotometric procedures used for metal determination with this group of reagents, the contrast has not been optimized. This optimization of conditions has been discussed in several papers.^{1,2,18,19} The peculiarity of hydroxyazo compounds with hydroxy groups on the naphthalene nucleus is the possibility of the azohydrazone tautomeric equilibrium in solution.



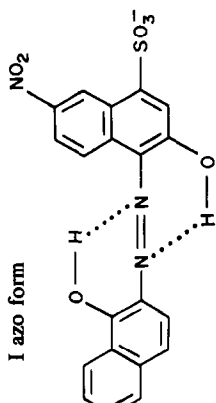
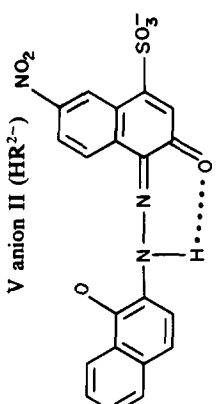
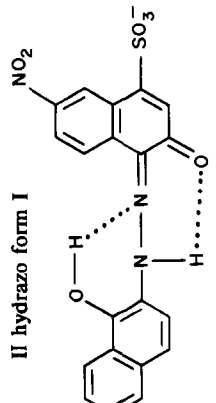
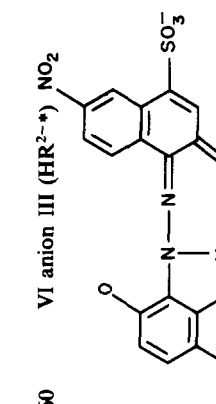
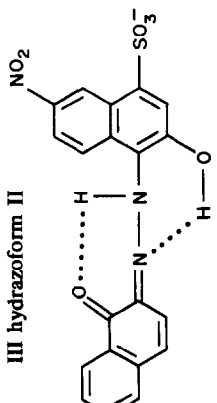
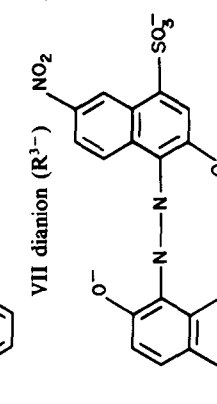
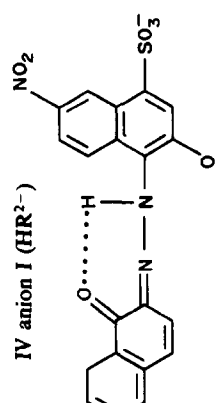
The change from azo to hydrazone form is usually accompanied by a large red shift of the absorption band (see Table 8). From evidence in the literature,²⁰ confirmed by the calculations shown in Table 8, the absorption spectra of these compounds in water and other polar solvents show the presence of mainly the hydrazone form, but in less polar media it may be possible to see both the azo and hydrazone forms. The comparison of the experimentally observed spectra of two reagents, Eriochrome Black T (ECB-T) and Calcon, with the calculated band position for the different forms of these reagents shows that it is

possible to characterize and identify the forms of a reagent in solution, and also shows the insufficiency of traditional methods for characterizing acid-base and tautomeric equilibria. From our research, we suggest that the equilibria of ECB-T aqueous solutions are as follows (numbering as in Table 8)

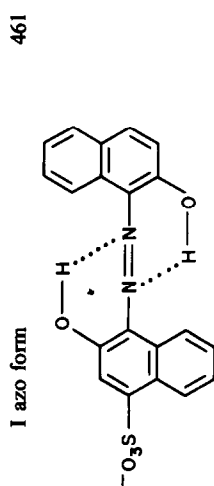


If the reagent H_3R can exist only as the single non-charged form or as the anions H_2R^- , HR^{2-} and R^{3-} , it is impossible to understand the appearance of three new bands and not two between pH values 7 and 14. Each species is assumed to be characterized by its own absorbance maximum. The calculations show that the species with $\lambda_{max} = 590-600$ and 630 nm

Table 8. Calculated and experimental values of maximum absorption bands for Eriochrome Black T and Calcon

State of dye	Calculated λ_{max} , nm	Experimental λ_{max} , nm	State of dye	Calculated λ_{max} , nm	Experimental λ_{max} , nm
<i>Eriochrome Black T</i>					
I azo form 	442		V anion II (HR ²⁻) 	606	
II hydrazo form I 	538	pH 5-6 $\lambda = 530-560$	VI anion III (HR ^{2-*}) 	634	pH 10 $\lambda = 630$
III hydrazoform II 	506		VII dianion (R ³⁻) 	516	0.1-1.0M NaOH $\lambda = 530$
IV anion I (HR ²⁻) 	563	pH 7-9 $\lambda = 590-600$			

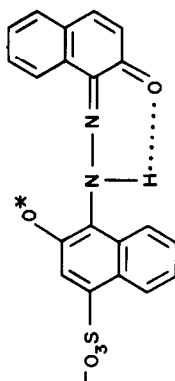
Calcon



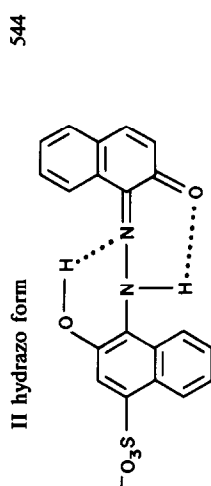
pH 5-7
 $\lambda = 520$

604

IV anion II (HR^{2-})



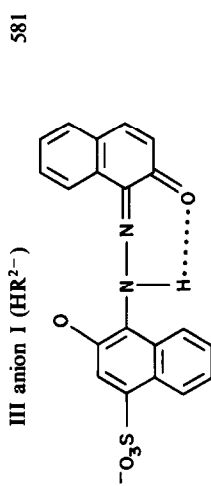
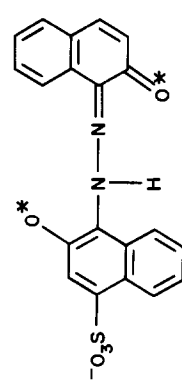
pH 8-9
 $\lambda = 600$



pH 10
 $\lambda = 650$

636

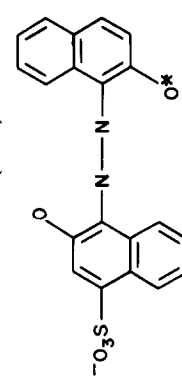
V anion III (HR^{2-})



pH 8-9
 $\lambda = 600$

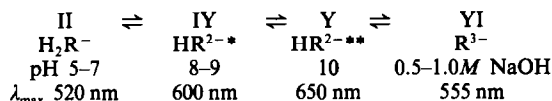
561

VI anion (R^{3-})



0.5-1.0M NaOH
 $\lambda = 540-565$

are doubly charged anions that differ in the degree of preservation of the strong hydrogen bonds of hydrogen ions with the oxygen atoms of the hydroxyl groups.^{21,22} Thus, the normal picture of an acid-base equilibrium, in which only a single species with a particular charge, is not correct. For example (see Table 8) there are two forms of the anion HR^{2-} for Eriochrome Black T at pH 7–10. These forms differ in the position of the maximum absorptivity. In the scheme above and Table 8, the form VI differs from form V by weakening of the hydrogen bond formed by the oxygen atom of one of the reagent hydroxyl groups. An analogous picture is observed for the spectra of Calcon solutions. The new absorption band at pH 10 cannot be explained by a normal acid-base equilibrium. The forms IV and V of Calcon (see Table 8) are both HR^{2-} and differ, like the forms V, VI of ECB-T, in the degree of preservation of strong hydrogen bonds with the oxygen atoms of hydroxyl groups. The most probable forms of Calcon in water solutions appear to be:



The absorption maxima for metal complexes are rather close to those of the hydrazo forms of the reagent, which explains why reactions with reagents present in the azo form in solution give the greatest contrast. Subgroup 2a reagents exist in the azo form in solution, and offer potentially the highest colour contrast in reactions with metals. Reagents that have a substituent $-\text{NO}_2$ group form a special group (2c), since they differ in the nature of the chromophore from hydroxyazo compounds.¹⁷ The presence of the nitro group leads to additional intramolecular charge-transfer bands.

CONCLUSIONS

The comparison of electron structure parameter values with experimental stability-constant data shows the potential for use of semi-empirical mathematical models for quantitative description and prediction of analytical properties. The lack of

quantitative experimental data on compound stability means that we have found only qualitative correlations between the orders of relative stability of compounds in solutions and electron structure parameter values. Our research on the spectra of azo dyes gives a key to the understanding of reagent colour contrast.

REFERENCES

1. A. T. Pilipenko, L. I. Savransky, A. I. Zubenko, V. L. Sheptun and O. N. Miroshnikov, *Zh. Analit. Khim.*, 1984, **39**, 997.
2. A. T. Pilipenko and L. I. Savransky, *ibid.*, 1977, **32**, 421.
3. V. N. Kumok, *Zakonomernosti v ustoychivosti koordinatsionnykh soedineniy v rastvorakh*, Tomskii Universitet, Tomsk, 1977.
4. S. Yamada, T. Kido and M. Tanaka, *Inorg. Chem.*, 1984, **23**, 2990.
5. A. B. Lever, P. Paoletti and L. Fabbrizzi, *ibid.*, 1979, **18**, 1324.
6. V. V. Ovchinnikov, A. P. Gariphzyanov, P. A. Cherkasov and V. F. Toropova, *Zh. Obshch. Khim.*, 1983, **53**, 1262.
7. D. W. Clack, N. S. Hush and J. R. Yandle, *J. Chem. Phys.*, 1972, **57**, 3503.
8. H. Fischer and H. Kollmar, *Theor. Chim. Acta*, 1970, **16**, 163.
9. A. T. Pilipenko, L. I. Savransky and O. N. Miroshnikov, *Dokl. Akad. Nauk SSSR*, 1984, **275**, 1126.
10. Yu. A. Zolotov, O. M. Petrukhin and L. G. Gavrilova, *J. Inorg. Nucl. Chem.*, 1970, **32**, 1679.
11. N. N. Kazanova, I. I. Antipova-Karataeva, O. M. Petrukhin and Yu. A. Zolotov, *Izv. Akad. Nauk SSSR, Ser. Khim.*, 1974, 15.
12. *Idem, ibid.*, 1973, 1716.
13. N. D. Yordanov, *J. Mol. Structure*, 1978, **47**, 107.
14. A. T. Pilipenko, L. I. Savransky, A. I. Zubenko and V. P. Kobylashny, *ibid.*, 1981, **86**, 155.
15. O. M. Vilkoval, V. M. Ivanov and A. I. Busev, *Zh. Analit. Khim.*, 1978, **33**, 716.
16. V. M. Ivanov, *Geterotsiklicheskie azotsoderzhashchie azosodineniya*, Nauka, Moscow, 1982.
17. A. T. Pilipenko and L. I. Savransky, *Talanta*, 1978, **27**, 451.
18. *Idem., Izv. Vysch. Uchebn. Zaved., Khim. Khim. Tekhnol.*, 1973, **16**, 32.
19. A. T. Pilipenko, L. I. Savransky and E. G. Skorokhod, *Zh. Analit. Khim.*, 1972, **27**, 1080.
20. I. Ya. Bershtein and O. F. Ginzburg, *Uspekhi Khim.*, 1972, **41**, 172.
21. L. I. Savransky, *Zh. Prikl. Spektrosk.*, 1971, **15**, 336.
22. A. T. Pilipenko and L. I. Savransky, *ibid.*, 1970, **13**, 918.

5-AZO DERIVATIVES OF RHODANINE AND ITS ANALOGUES IN THE ANALYTICAL CHEMISTRY OF THE NOBLE METALS

S. B. SAVVIN and R. F. GUR'eva

V. I. Vernadskii Institute of Geochemistry and Analytical Chemistry, Academy of Sciences of the USSR, Moscow, USSR

(Received 15 October 1985. Accepted 8 August 1986)

Summary—Progress in the synthesis and theoretical study of the 5-azo derivatives of rhodanine, thiorhodanine, 3-aminorhodanine, thiohydantoin, pseudothiohydantoin, thiopropiorhodanine, and seleniorhodanine is discussed. Emphasis is placed on peculiarities in the interaction of this series of reagents with noble metals and their practical application in analytical chemistry.

Azo compounds based on rhodanine, thiorhodanine, and isorhodanine were synthesized for the first time at the L'vov Medical Institute as potential medicinal preparations. Their qualitative reactions with some elements were also reported.¹⁻³

The 5-azo derivatives of rhodanine and its analogues based on aromatic amines containing salt-forming groups, the hydroxyl group in particular, which have been synthesized by us, have proved to be valuable analytical reagents for noble metals (NM).⁴⁻⁶ In contrast to the 5-substituted derivatives of rhodanine (e.g., *p*-dimethylaminobenzylidenerhodanine) which have found application largely for the determination of gold and silver, the 5-azo compounds react in acid and strongly acid media with all NM except osmium. The reactions have high sensitivity and selectivity. The 5-azo compounds of rhodanine are also distinguished by their rather good solubility and stability in strongly acid media.

Systematic study of the properties of the 5-azo derivatives of rhodanine has proved these reagents to be quite promising in the analytical chemistry of NM, including spectrophotometry, differential spectrophotometry, precipitation, identification of chro-

matographic and electrophoretic zones, separation of NM as coloured complexes, extractive enrichment, and enrichment and separation on chelate sorbents involving azorhodanine and azothiopropiorhodanine. Owing to the exceptional ability of these reagents to react with NM in strongly acid media, methods were developed for the first time for the determination of NM as various acid complexes. These not only enlarged the range of analytical methods available but in some cases gave improved analytical characteristics (sensitivity, selectivity, reaction kinetics). This group of reagents also seemed promising for the determination of non-ferrous and heavy metals.

SYNTHESIS OF REAGENTS

A series of reagents was obtained, which are based on the following heterocyclic azo compounds: rhodanine, thiorhodanine, thiohydantoin, pseudothiohydantoin, 3-aminorhodanine, *N*-substituted 3-aminorhodanine, seleniorhodanine, and a six-membered analogue of rhodanine, thiopropiorhodanine (Table 1).⁴⁻⁶

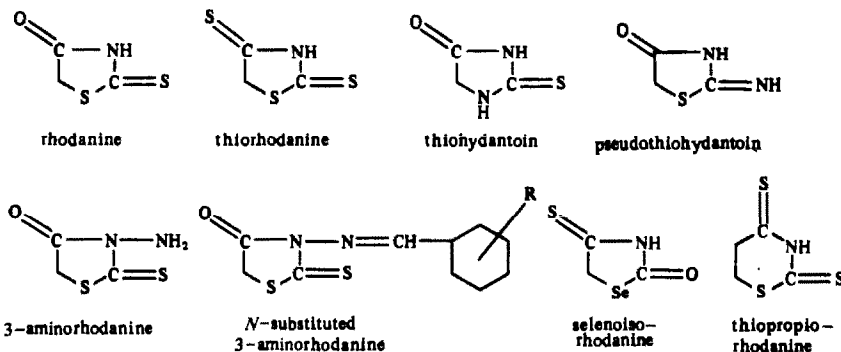


Table 1. 5-Azo derivatives of rhodanine and its analogues

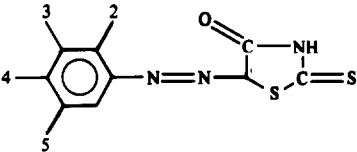
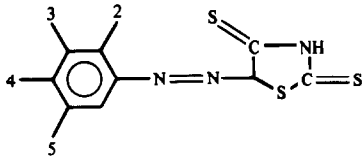
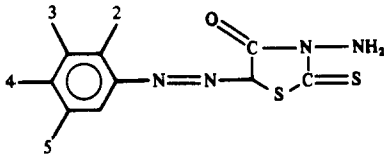
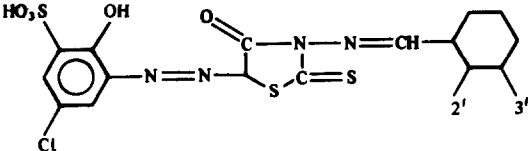
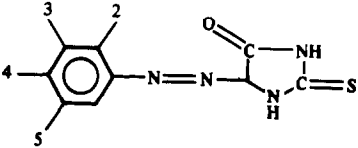
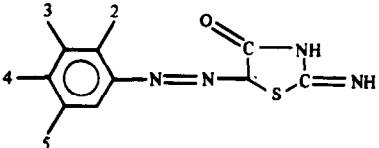
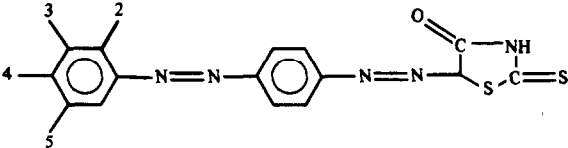
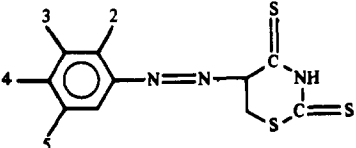
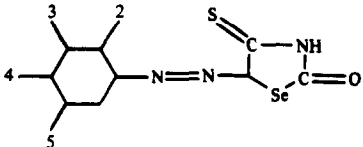
No.	Substituents in diazocomponent	Name of reagent
5-Azo derivatives of rhodanine		
		
1.	2—OH, 3—SO ₃ H, 5—Cl	Sulphochlorophenolazorhodanine
2.	2—OH, 3—SO ₃ H, 5—NO ₂	Sulphonitrophenolazorhodanine
3.	2—OH	<i>o</i> -Phenolazorhodanine
4.	2—OH, 3—COOH, 5—SO ₃ H	Carboxysulphophenolazorhodanine
5.	2—OH, 3,5—SO ₃ H	Disulphophenolazorhodanine
6.	2—OH, 3,5—NO ₂	Picraminazorhodanine
7.	4—OH	<i>p</i> -Phenolazorhodanine
8.	3—OH	<i>m</i> -Phenolazorhodanine
9.	2—COOH	Carboxybenzenazorhodanine
10.	2—SO ₃ H	<i>o</i> -Sulphobenzenazorhodanine
11.	3—SO ₃ H	<i>m</i> -Sulphobenzenazorhodanine
12.	4—SO ₃ H	<i>p</i> -Sulphobenzenazorhodanine
13.	4—NO ₂	<i>p</i> -Nitrobenzenazorhodanine
14.	2—AsO ₃ H ₂	Arsonobenzenazorhodanine
15.	No substituents	Benzenazorhodanine
5-Azo derivatives of thiorhodanine		
		
16.	2—OH, 3—SO ₃ H, 5—Cl	Sulphochlorophenolazothiorhodanine
17.	2—COOH	Carboxybenzenazothiorhodanine
18.	2—AsO ₃ H ₂	Arsonobenzenazothiorhodanine
5-Azo derivatives of 3-aminorhodanine		
		
19.	2—OH, 3—SO ₃ H, 5—Cl	Sulphochlorophenolazo-3-aminorhodanine
20.	2—OH, 3—SO ₃ H, 5—NO ₂	Sulphonitrophenazo-3-aminorhodanine
21.	4—OH	<i>p</i> -Phenol-3-aminorhodanine
22.	2—COOH	Carboxybenzene-3-aminorhodanine
23.	3—SO ₃ H	<i>m</i> -Sulphobenzenazo-3-aminorhodanine
5-Azo derivatives of <i>N</i> -benzylidene-3-aminorhodanine		
		
24.	2',3'—H	Sulphochlorophenol- <i>N</i> -(benzylidene)-3-aminorhodanine
25.	2'—OH	Sulphochlorophenol- <i>N</i> -(2'-hydroxybenzylidene)-3-aminorhodanine
26.	2'—OH, 3'—OCH ₃	Sulphochlorophenol- <i>N</i> -(2'-hydroxy-3'-methoxybenzylidene)-3-aminorhodanine

Table 1—continued

No.	Substituents in diazocomponent	Name of reagent
5-Azo derivatives of thiohydantoin		
		
27.	2—OH	<i>o</i> -Phenolazothiohydantoin
28.	2—OH, 3—SO ₃ H, 5—NO ₂	Sulphonitrophenolazothiohydantoin
5-Azo derivatives of pseudothiohydantoin		
		
29.	2—OH, 3—COOH, 5—SO ₃ H	Carboxysulphophenolpseudothiodantoin
30.	2—OH, 3—SO ₃ H, 5—NO ₂	Sulphonitrophenolazopseudothiohydantoin
31.	2—OH, 3,5—SO ₃ H	Disulphophenolazopseudothiohydantoin
32.	2—OH, 3—SO ₃ H, 5—Cl	Sulphochlorophenolazopseudothiohydantoin
5-Bisazo derivatives of rhodanine		
		
33.	No substituents	Benzenazobenzenazorhodanine
34.	3—SO ₃ H, 4—OH	Sulphophenolazobenzenazorhodanine
5-Azo derivatives of thiopropiorhodanine		
		
35.	2—OH, 3—SO ₃ H, 5—Cl	Sulphochlorophenolazothiopropiorhodanine (thiorhodine)
36.	2—OH, 3—SO ₃ H, 5—NO ₂	Sulphonitrophenolazothiopropiorhodanine
37.	2—OH, 3—COOH, 5—SO ₃ H	Carboxysulphophenolazothiopropiorhodanine
38.	2—COOH	Carboxybenzenazothiopropiorhodanine
5-Azo derivatives of selenisorhodanine		
		
39.	2—COOH	Carboxybenzenazoselenisorhodanine
40.	4—NO ₂	<i>p</i> -Nitrobenzenazoselenisorhodanine
41.	2—OH, 3—SO ₃ H, 5—Cl	Sulphochlorophenolazoselenisorhodanine
42.	2—OH, 3—SO ₃ H, 5—NO ₂	Sulphonitrophenolselenisorhodanine

Aromatic amines containing largely hydroxyl and other salt-forming groups ($-\text{SO}_3\text{H}$, $-\text{COOH}$, $-\text{AsO}_3\text{H}_2$) were employed as diazo components.

The heterocyclic azo compounds were synthesized as described elsewhere. Rhodanine was prepared by condensation of monochloroacetic acid with ammonium thiocyanate by heating.⁷ Thiorhodanine was prepared from rhodanine by replacing the carbonyl group by thiocarbonyl by the action of P_2S_5 .⁴ Thiohydantoin was obtained by the reaction of potassium thiocyanate with the hydrochloride of glycyl ethyl ether. Pseudothiohydantoin was obtained by condensation of urea with monochloroacetic acid by heating.⁸ 3-Aminorhodanine was prepared by condensation of sodium monochloroacetate with hydrazine dithiocarbazine.^{9,10}

3-Aminobenzylidenerhodanine was prepared by condensation of 3-aminorhodanine with benzaldehyde in acetic acid. Thiopropiorhodanine (2,4-dithione-1,3-thiazane) was prepared by treating propiorhodanine with P_2S_5 in anhydrous dioxan.¹¹ Propiorhodanine (2-thione-4-oxo-1,3-thiazane) was obtained by condensation of 2-chloroacetic acid with freshly prepared ammonium dithiocarbamate, followed by heating with acetic anhydride.¹² Selenisorhodanine (4-thione-1,3-selenazolid-2-one) was obtained by the reaction of 1,3-selenazolidine-2,4-dione with P_2S_5 in anhydrous dioxan.¹³ The 1,3-selenazolidine-2,4-dione was synthesized by condensation of monochloroacetic acid with selenourea by heating.

Azo compounds based on heterocyclic azo components were synthesized by the action of the corresponding diazotized amine on the heterocyclic component under appropriate conditions for each reaction (nature of solvent, reaction pH, duration of the reaction). This provided the reagents in high yield with the least possible amounts of by-products. The conditions for the synthesis of azorhodanines are as follows: pH 8.9, $\text{CH}_3\text{COOH}/\text{NaOH}$ mixture, 1–2 hr; those for azothiorhodanines: pH 5–7, $\text{CH}_3\text{COOH}/\text{NaOH}$ or $\text{CH}_3\text{COOH}/\text{NH}_3$ mixture, 1 hr; for azo-3-aminorhodanines: pH 8–10, $\text{C}_2\text{H}_5\text{OH}/\text{CH}_3\text{COOH}/\text{NaOH}$ mixture; for azothiopropiorhodanines: pH 7.8, dimethylformamide/ $\text{C}_2\text{H}_5\text{OH}/\text{NaOH}$ mixture, 30 min; for azothiohydantoins and azopseudothiohydantoins: pH 10, NaHCO_3 , 1.2 hr; for azoselenisorhodanines: pH 6–8, Na_3PO_4 , 30 min; for bisazo compounds based on rhodanine: pH 8–10, $\text{C}_2\text{H}_5\text{OH}/\text{CH}_3\text{COOH}/\text{NaOH}$. The reactivity of the heterocyclic components in the azo-combination reactions with aromatic amines increases in the series

The azo compounds based on *p*-nitroaniline, aniline, and anthranilic acid were precipitated as diazonium salts. Other reagents, besides those based on aminophenols and selenisorhodanine, were isolated by acidification with hydrochloric acid to pH 2–4. The precipitates were filtered off, washed with water or alcohol, and air-dried. The products obtained contained 60–85% of the main compound, with the remainder being water of crystallization and mineral salts, which did not affect the analytical properties of the reagents. Reprecipitation was occasionally used for better purification, although it caused considerable loss of the reagent. The synthesis of the reagents in the presence of salts of some metals (Ca, Pb) resulted in purer reaction products and higher yields, but the solubility of the reagents decreased. The azo compounds based on aminophenols and selenisorhodanine could not be isolated. Acidification or salting-out resulted in tarry reaction products.

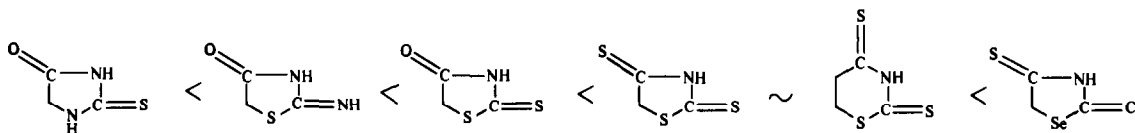
The azo compounds obtained (Table 1) were identified by chromatography, and electrophoresis with various buffer systems,⁵ as well as by the typical absorption spectra of the reagents (in concentrated sulphuric acid and neutral and alkaline solutions) and their metal complexes. The content of the main product was established by potentiometric and high-frequency titration with alkali, and spectrophotometric titration with metal salt solutions.^{5,6,14,15}

PROPERTIES OF THE REAGENTS

5-Azo derivatives of rhodanine and thiorhodanine

The azo derivatives of rhodanine are yellow, orange, or red-orange powders. The reagents containing salt-forming groups (besides carboxyl) are soluble in water, dioxan, and dimethylformamide. The solubility increases in alkaline and strongly acid media. The reagents based on anthranilic acid, *p*-nitroaniline, and aniline are soluble in alcohol and acetone. The azothiorhodanine derivatives are deeper in colour, more soluble in water, more stable in alkaline and less stable in acid media, than the corresponding azorhodanines. Neutral and acid solutions of the reagents are stable for several days. The solid reagents are stable for more than three years.^{4,5,14,15}

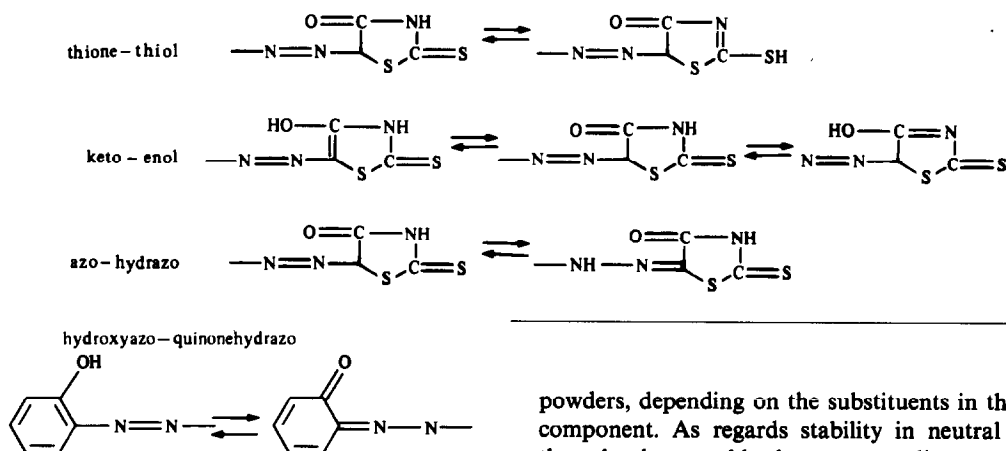
The state of the reagents in solution is one of the essential factors that determine the reactivity, the mechanism of complex-formation, and the nature of their colour reactions with metals. When the pH is



changed the reagents solutions sharply change their colour, owing to dissociation of acidic groups or protonation of basic groups, and various tautomeric conversions. For the azo derivatives of rhodanine which contain a hydroxyl group, several coloured forms can be distinguished, *e.g.*, red-orange (concentrated sulphuric acid), yellow (pH 14), orange (pH 4–8), red-orange (pH 8–10), and violet (pH 11). The colour of the reagents with no hydroxyl groups develops from lemon-yellow (acid and neutral media) to yellow-orange (alkaline solutions) and red (strongly alkaline solutions). For azothiorhodanines with a hydroxyl group three coloured forms can be distinguished, *viz.* dark-red (acid-neutral media), violet (weakly alkaline media), and blue (strongly alkaline media). The azothiorhodanines are unstable in strongly acid media.

The data on potentiometric and high-frequency titration, and analysis of the absorption spectra at the pH values corresponding to the potential jumps allowed us to establish pH-values and sequence for ionization of the acid groups of the reagents.^{5,6,14,15} The nature of the hetero-atom (O, S) affects the pK of dissociation of the NH group. The NH group of azothiorhodanines is titrated at lower pH values. At the same time, the nature of substituents in the diazo component affects the pK of the hydroxyl group on the benzene ring. For example, for sulphochlorophenolazorhodanine $pK = 10$, while for picraminazorhodanine $pK = 6$. For most azorhodanines $pK_{NH} < pK_{OH}$. However, in the case of disulphophenolazorhodanine the NH and OH groups are titrated simultaneously, while in picraminazorhodanine, which contains two strong electron-acceptor substituents, the hydroxyl group of the benzene ring dissociates at lower pH the NH group.

Four types of tautomerism can be suggested for the azo derivatives of rhodanine, *viz.*



the last arising when the benzene ring carries a hydroxyl group.

For all 5-azo derivatives of rhodanine in concentrated sulphuric acid there is a shift of the long-

wavelength absorption band ($\Delta\lambda$ 70 nm) from that in neutral solutions. According to calculated data¹⁴ the bathochromic shift is due to protonation of the reagents. Since the hetero-atoms of the rhodanine ring carry the largest negative charge, it is these atoms that are protonated, and not the hydroxyl group of the benzene ring or the nitrogen atom of the azo or hydrazo group.

In neutral form the azo derivatives of rhodanine exist largely as their azodiketo tautomers. Complex formation shifts the equilibrium to the enolic form. This is confirmed by the observed data on the number of protons liberated in complex-formation between copper and sulphochlorophenylazorhodanine (SC-PAR). Formation of the 1:1 complex produces two protons.⁵ The concentration of the azothiol tautomer is quite low. The only exception is picraminazorhodanine, which has roughly equal content of the diketo and thiol forms. For the reagents containing a hydroxyl group the first bathochromic shift (pH 6–10) results from the transition of the azo form of the reagent into the quinonehydrazo one. Strongly alkaline media shift the thione-thiol equilibrium to the side of the azothiol tautomer, which results in the bathochromic shift of the long-wavelength absorption band. The presence of electron-acceptor substituents in the benzene ring shifts the thione-thiol transition to lower pH (as is the case for picraminazorhodanine and sulphonitrophenolazorhodanine).

5-Azo compounds based on 3-aminorhodanine and its N-substituted derivatives⁶

Like the 5-azo derivatives of rhodanine, the reagents based on 3-aminorhodanine and N-benzylidene-3-aminorhodanine are yellow, orange, or red

powders, depending on the substituents in the diazo component. As regards stability in neutral media, they closely resemble the corresponding azo derivatives of rhodanine. At the same time, the reagents based on 3-aminorhodanine are less stable in concentrated mineral acid, and concentrated alkaline solutions. They are also characterized by poorer solubility than the azorhodanines. The NH_2 and

$\text{N}=\text{CH}-\text{C}_6\text{H}_5$ type substituents at position 3 of rhodanine do not essentially affect the spectral features. The same regularities in the influence of substituents in the diazo component on the spectral features and acid-base properties are observed for these reagents. The sequence of dissociation of the acid groups is the same but there is an increase in the acidity of the hydroxyl group of the benzene ring. For example, for sulphochlorophenolazorhodanine $pK_{\text{OH}} = 8.5$, while for sulpho-3-aminorhodanine $pK_{\text{OH}} = 7.0$. The bathochromic effect in concentrated sulphuric acid is less pronounced than for the 5-azo derivatives of rhodanine.

5-Azo derivatives of thiohydantoin and pseudo-thiohydantoin

These are the least studied reagents. They are pale-yellow powders. In solution azothiohydantoins and azopseudothiohydantoins are less deeply coloured than the azorhodanines. The solids are stable, especially in salt form. In solution the reagents are less stable than the azorhodanines and azo-3-aminorhodanines. The sequence of ionization of the acid groups is retained. In contrast to azorhodanines and azo-3-aminorhodanines, the reagents in concentrated sulphuric acid solutions are pale in colour.

5-Bisazo derivatives of rhodanine

These are stable dark powders. The reagents containing hydroxyl and sulpho groups are well soluble in water, while those containing no such groups are soluble in polar organic solvents and water-organic solvent mixtures. The reagents sharply change colour with change in pH. The presence of a second arylazo group affects the state of the reagents in acid media. While for azorhodanines protonation, accompanied by deepening in colour (420–500 nm), is observed in 10–15*M* sulphuric acid, the rhodanine-based bisazo compound is protonated even in 1–2*M* sulphuric acid. The protonation of the bisazo compounds is accompanied by a deeper change in colour (420–560 nm). For the bisazo compounds thermochromism is observed, *i.e.*, a sharp deepening in colour on heating in acid media.

5-Azo-derivatives of thiopropiorhodanine

These are powders, dark red in colour, well soluble in water and water-organic solvent mixtures. As is the case for azothiorhodanines, the substitution of S for O in the heterocycle enhances the solubility of the azo compounds obtained. The reagents are unstable in hydrochloric acid solutions. In neutral and alkaline solutions the reagents are more deeply coloured than the corresponding azorhodanines. For azothiopropiorhodanines the sequence of dissociation of the NH and OH groups is reversed, *i.e.*, the OH group of the benzene ring dissociates at lower pH values than the NH group. This may be caused by both the difference in acid properties of the individual azo components (for rhodanine $pK_{\text{NH}} = 5.8$, for thio-

propiorhodanine $pK_{\text{NH}} = 8.1$), and by the different nature of the tautomeric conversions. No deepening in the reagent colour is observed for azothiopropiorhodanines in strongly acid media, in contrast to azorhodanines and azo-3-aminorhodanines. The yellow colour of the reagents in weakly acid media, which is characteristic of the neutral form, is unaffected even in concentrated sulphuric acid. Surface-active compounds affect the colour of azothiopropiorhodanines and the corresponding bisazo compounds over a wide range of pH.

5-Azo derivatives of selenisorhodanine

The reagents based on anthranilic acid and nitroaniline are brown powders, stable in the dry state, but unstable in solution. Aminophenol-based azoselenisorhodanines failed to be isolated in the solid state. Changing the pH affects the colour of the reagent solutions. The nature of the heteroatom (Se) enhances the acid properties of the selenisorhodanines. These reagents are protonated in more dilute solution of acids, and the process is accompanied by greater deepening in colour, compared to the azorhodanines.

INTERACTION WITH METAL IONS

5-Azorhodanines

The aminophenol-based reagents provide the most sensitive and contrasting colour reactions. Three regions for the interaction with metal ions can be distinguished. Co, Ni, Cd, Pb, Zn, Ag, Cu give colour reactions at pH 6–10, changing the colour from orange (480 nm) to violet (530–550 nm). The molar absorptivity (ϵ , 1. mole⁻¹.cm⁻¹) is about 2×10^4 .

Cu, Pd, and Ag give colour reactions at pH 1–6, changing from yellow (430 nm) to red-orange (480–500 nm), ϵ 1.5–3.0 $\times 10^4$. Noble metals (Pt, Pd, Rh, Ir, Ru, Au, Ag) and mercury give colour reactions in acid and strongly acid media (λ 500–530 nm; ϵ 2–12 $\times 10^4$). The reactions in strongly acid media are slow and need 30–50-fold excess of reagent. Heating increases the reaction rate with NM but in some cases reduces the yield. For example, platinum gives a slow reaction (20 hr, ϵ 3.3 $\times 10^4$) with sulphochlorophenolazorhodanine in the presence of reductants in 3*M* HCl and in HCl/H₂SO₄ or HCl/H₃PO₄ mixtures (4 hr, ϵ = 1.0 $\times 10^5$, for the latter mixture).

Rhodium and iridium give colour reactions with the azorhodanines in 10–15*M* H₃PO₄ (2–7*M* H₂SO₄). The presence of CH₃COOH enhances the sensitivity, Heating at 70° and 90°, respectively, increases the reaction rate.

Gold reacts with azorhodanines in HCl media at room temperature in 5–10 min. The presence of H₂SO₄ or H₃PO₄ does not affect the sensitivity and reaction rate, but presence of H₃PO₄ increases the solubility of the complexes and extends the range of acidity for maximum absorption.

Like palladium, silver reacts differently in weakly acid-neutral and in strongly acid media, to give coloured compounds which differ in composition, solubility, *etc.* In neutral and weakly acid solutions palladium and silver give well soluble 1:1 complexes, and only 2–3-fold excess of reagent is needed. The best azorhodanines to use are those existing largely as the diketo-tautomers in acid and neutral media, *e.g.*, sulphochlorophenolazorhodanine, *o*-phenolazorhodanine, carboxyphenolazorhodanine ($\epsilon \ 2 \times 10^4$). The reagents that produce comparable amounts of the diketo and thiol forms in weakly acid solutions usually give lower ϵ (0.7×10^4), *e.g.*, picraminazorhodanine, sulphonitrophenolazorhodanine. According to quantum chemical calculations¹⁴ high sensitivity is expected for the reaction of silver with benzeneazorhodanines which contain electron-donor substituents in the benzene ring. The presence of the *o*-hydroxy group improves the colour contrast, owing to the hydroxyazoquinone-hydrazone tautomerism. In strongly acid media the reactions of Ag, Pd, Rh, Ir, Ru and Pt are slow and need considerable excess of reagent.

In strongly acid media the selectivity towards the common non-ferrous metals is higher, and towards the platinum-group metals lower, than in weakly acid-neutral solutions.

Table 2 presents the characteristics of the reactions of noble metals with sulphochlorophenolazorhodanine and sulphochlorophenolazothiopropiorhodanine (thiorhodine), which have the best combination of analytical characteristics (solubility and stability of individual reagents and their reaction products, sensitivity and selectivity of determination) of all the reagents of this type synthesized and studied by us.

5-Azothiorhodanines

These reagents react with gold, platinum, and palladium in 1–6*N* HCl, changing the colour from red to blue-violet ($\epsilon \ 2\text{--}5 \times 10^4$). Silver reacts at pH 1.5 with low sensitivity. 5-Azothiorhodanines do not give a colour reaction with rhodium and iridium.⁴

5-Azothiopropiorhodanines

These reagents do not react with rhodium and iridium, but in acid and strongly acid media give highly sensitive reactions with Pt, Pd, and Au, changing colour from yellow to red. The reactions for platinum and gold are slow. Heating increases the reaction rates, while decreasing the yields. The presence of HCl has an adverse effect on the reactions for gold and platinum. An $\text{H}_3\text{PO}_4(\text{H}_2\text{SO}_4)/\text{CH}_3\text{COOH}$ mixture is best for the reaction with platinum and gold. The presence of reducing agents increases the rate and yield of the reaction with platinum.^{6,26}

Silver reacts with azothiopropiorhodanines in neutral (pH 5–9, $\lambda_{\text{max}} \ 565 \text{ nm}$, $\Delta\lambda \ 30 \text{ nm}$, $\epsilon \ 1.5 \times 10^4$) and acid media (10*M* $\text{CH}_3\text{COOH}/2\text{M}$ H_3PO_4 mixture,

$\lambda_{\text{max}} \ 535 \text{ nm}$, $\Delta\lambda \ 75 \text{ nm}$, $\epsilon \ 5.3 \times 10^4$). The reaction with azothiopropiorhodanines in acid media is of practical interest. The formation of a coloured compound of silver in strongly acid media was observed for the first time with the azorhodanines.¹⁵ The interaction of silver with azothiopropiorhodanines has several differences from that with azorhodanines, despite the similarity in structure of the reagents. The azothiopropiorhodanines give their most sensitive reaction with silver in concentrated solutions of CH_3COOH , H_3PO_4 , or their mixtures, whereas with the azorhodanines silver not only gives no colour reaction in CH_3COOH , but even small amounts of this acid mask the reaction. This difference appears to be due to the azothiopropiorhodanine silver complexes being more stable than the azorhodanine complexes. The reaction with the azothiopropiorhodanines is also faster, being complete in 3–5 min, and needs only 2–3-fold excess of reagent, whereas a 20–50-fold excess of azorhodanines is required. The azothiopropiorhodanines are characterized by high selectivity for silver with respect to copper and other non-ferrous metals.^{6,26}

5-Azo derivatives of 3-aminorhodanine

For Pt, Pd, Au, and Ag the derivatives of 3-aminorhodanine have analytical characteristics (sensitivity and contrast of colour reactions, colour-development rate) close to those of the corresponding azorhodanines. Like the azothiorhodanines and azothiopropiorhodanines, they do not react with rhodium and iridium; this seems to result from the instability of these compounds in strongly acid media, especially on heating, *i.e.*, under the conditions in which kinetically inert elements, such as rhodium and iridium, undergo reaction.

Applications

A comparative study of the colour reactions of metals with the azoderivatives of rhodanine and its analogues has shown these reagents to be of practical value, especially for the determination of noble metals. The aminophenol-based azo compounds are recognized as the best, and of these sulphochlorophenolazorhodanine and sulphochlorophenolazothiopropiorhodanine (thiorhodine) prove to be the most advantageous. The reactions of noble metals with these reagents are highly sensitive ($\epsilon \ 2\text{--}12 \times 10^4$) with good colour contrast, and take place in acid and strongly acid media. The presence of a considerable excess of alkali, alkaline-earth, and non-ferrous metals does not interfere. Some platinum-group metals can be determined in the presence of others, owing to differences in the reaction rates, the conditions used for the determination (concentration and nature of the acid, acid-mixture composition), the spectral features of the complexes, and the effect of auxiliary ligands on the reactivity of the noble metals.

Table 2. Analytical characteristics of NM complex compounds with sulphochlorozorhodamine and thiorhodine

Initial form of NM*	Reaction conditions	λ_{max} , nm	ϵ , $10^4 l. mole^{-1}. cm^{-1}$	Tolerance limits (mg) in determination of NM (20-30 $\mu g/25$ ml)	References
Sulphochlorozorhodamine (SCPAR)					
Pt(II)	3M HCl + asc. acid, 20 hr, 20° asc. acid, 4 hr, 20°	500	3.2 10.0	Ni, Co, Fe (1); Ca, Mg, Ba, Al (3); Zn (2); Th (3); Mo, Hg (0.5); Fe (5); Ni, V, Zn, Pb, La (3); Co, Bi (2); Cd, Os (1); Mo, Zr (0.5); Cu, Hg, Ag (0.2) Ir, Rh (0.3)	4, 16-19
Pt(III)	2M H ₂ SO ₄ + 10.8M H ₃ PO ₄ , 30 min, 50°	500	10.0	Cu (30); Fe (25); Zn (6); Co, Ni (3); Mg (2); Ca (0.4); Th (13); Ir (1); Ru, Hg (0.03)	
Pt(III)	12-15M H ₃ PO ₄ , asc. acid, 50 min, 50°	500	10.0	Rh (2); Ir (1)	
Pd(II)	8M H ₃ PO ₄ + 5M H ₂ SO ₄ 1M HCl, 1-2 hr	520 520	120 5.0	in 8M H ₃ PO ₄ + 0.5M HCl: Fe, Ni, V, Zn, Sn (25); Mo, Co, Pb, Rh (10); Nb, Cu (2); Th, Zr (0.25); Pt, Rh (0.025)	16, 20, 21
Pd(II)	Sulphate Phosphate			Sensitivity identical to chlorides; reaction rate increases	
Rh(III)	7M H ₂ SO ₄ + 6M CH ₃ COOH 60 min, 70°	510	6.5	Ni (112); Co, Zn (30); Hg (2.5); Cu (0.5); Pt (0.3); Au, Ir (0.04)	5, 16, 17
Rh(III)	7M H ₃ PO ₄ + 6M CH ₃ COOH	510	3.5	Fe, (15); Cu (13); Ni (4); Co (2.5)	
Rh(III)	14M CH ₃ COOH + asc. acid 60 min, 70°	510	8	Ir (1)	
Rh(III)	Sulphate Sulphate				
Rh(II)	7M H ₂ SO ₄ + 6M CH ₃ COOH 10 min, 70°	510	1.7		
Rh(III)	7M H ₂ SO ₄ + 6M CH ₃ COOH 10 min, 70°	510	1.1		
Rh(II)	7M H ₂ SO ₄ + 6M CH ₃ COOH 20 min, 20°	510	4.5		
Ir(II)	5M H ₂ SO ₄ + 6M CH ₃ COOH Weak reaction	510	4.0	Ni (2); Zn, Co (10); Fe, Hg (0.6); Pt, Au (0.1)	4, 16, 22
	Sulphate Phosphate				

Ru(III) Ru(II)	Chloride, Chloride	2M HCl + 10M CH ₃ COOH	500	1.6	Cu, Ni, Co (5); Fe (7.5); Hg (0.2); Be, Mg (2); Bi, Pb, Ir (0.6); Ag, Rh (0.2); Os (2.5)	18, 19, 23, 24
Ru(II, III) Ru(II, III)	Phosphate Sulphate					
Au	Chloride	1M HCl, min	530	5.3	Pt, Pb, Al, Ba, Ca, Mg (1); Ni, Cu, Co (7); Fe (5); Hg (2); Os (0.5); Ir (0.2); Rh (0.04)	4, 25
Ag	Nitrate	pH 2-6	480	1.6	pH 2; Ni, Co (0.5); Cu (0.3); Bi, Pb, Ca, Zn (1) Trilon B: Co, Ni, Bi (3); Cu (1); Pb, Zn (10); Ca (30)	4
		1-6M H ₂ SO ₄ (H ₃ PO ₄) 30 min	500	4.0 (4.5M) H ₂ SO ₄ 1.5 (3M H ₃ PO ₄)	1M H ₂ SO ₄ ; Ni, Co, Bi, Cu (10) 3M H ₃ PO ₄ ; Pb (20); Cu, Ni, Co, Bi (1)	15
Thiorhodine						
Pt(II)	Chloride	3-4 hr	510	6.5	Cu (60); Fe, Ni (6); Co (4); Ir (0.2); Rh (0.1); Pb, Be, Mg (1); Ag, Au, Pd interfere	6, 19
Pt(III) Pt(III)	Sulphate Phosphate	20-30 min 20-40 min	510 510	6.5 5.5	Cu (0.1); Fe, Ni (6); Co (4); Ir (0.4); Rh (0.2) Pb, Be, Mg (1); Ag, Au, Pd interfere	
Ag	Nitrate	1M H ₃ PO ₄ + 10M CH ₃ COOH	535	5.3	Cu, Zn (150); Co, Ni (30); Fe (15); Mg, Ba, Ca (2.5); Pb (1.5); Ir, Rh (0.3); O, Pt (2)	6, 26
Au	Chloride	3M H ₃ PO ₄ + 3.5M CH ₃ COOH 15-30 min	510	2.5		6

*Pt(III) implies a binuclear complex, which may be Pt(II)-Pt(IV) or Pt(III)-Pt(III).

REACTIONS OF VARIOUS OXY-ANION COMPLEXES
OF PLATINUM GROUP METALS WITH
AZORHODANINES AND AZOTHIOPROPORHODANINES

Most methods for the determination of platinum-group metals are applicable only to the chloro-complexes. Analysis of systems containing platinum-group metals in other forms involves, as a rule, the additional step of converting the initial complexes into the chloride ones. A study of the reactivity of the complexes of platinum-group metals with the anions of various oxy-acids (such as H_2SO_4 , $HClO_4$, H_3PO_4 , CH_3COOH), would be of significant practical value, since it is these acids that are frequently employed in different stages of manufacture and purification of chemicals. A study of the reactivity of the dimeric complexes of platinum-group metals involving metal-to-metal bonds would also be of practical significance. The oxygen-containing ligands in the dimeric complexes seem to stabilize the metal-to-metal bond.²⁷ Such compounds manifest specific thermodynamic and kinetic properties. They are readily aquated and prove more active than the chlorides in substitution reactions. This provides new possibilities for development of the analytical chemistry of the platinum-group metals and their practical application. These compounds are expected to display new specific features of platinum-group metals.

The difficulties in the development of photometric methods for the determination of platinum-group metals in forms other than that of the chloride complexes (*e.g.*, the sulphate and phosphate forms) are known to result from the easy hydrolysis of these forms and the formation of non-reactive polymeric forms in dilute acid solutions. The distinguishing feature of azorhodanines and their analogues is their highly sensitive colour reaction with noble metals in strongly acid media, in which the easily hydrolysed forms of the platinum-group metals retain their reactivity.

The reactivity of the sulphate (Pt, Pd, Rh), phosphate (Pt, Pd, Rh, Ir), acetate (Rh), and nitrate (Pd) complexes with sulphochlorophenolazorhodanine and sulphochlorophenolazothiopropiorhodanine (thiorhodine) has been studied (Table 2) along with a spectrophotometric study of the behaviour of oxy-anion complexes of platinum-group metals in various media (effect of nature and concentration of the acid, heating, reducing agents and organic solvents). These studies have revealed the nature of the active forms of the platinum-group metals, the factors defining their yields, and suggested methods for stabilizing the active forms, and in some cases for converting the initial forms into the active ones.^{17-19,23,24,28,29}

Platinum

The binuclear phosphate and sulphate complexes of platinum(III), together with the chloride forms react with sulphochlorophenolazorhodanine and sulphochlorophenolazothiopropiorhodanine to give

intensely coloured compounds (λ_{max} 500–510 nm). The nature of the ligand and the oxidation number of the central atom of the initial complex affect the kinetics, sensitivity and selectivity of these colour reactions. Platinum phosphate and sulphate complexes interact with organic reagents in more acid media and display higher kinetic activity. Reducing agents show quite a distinctive effect on the colour reactions of platinum complexes, sharply increasing the rate of reaction between the chloride complexes and organic reagents, whereas the colour reactions of the sulphates and phosphates are practically unaffected. The absorption spectra of the platinum complexes with organic reagents are independent of the initial form of the platinum. The colour reactions of the dimeric complexes of platinum sulphate and phosphate have similar properties. The complexes are more soluble and more stable on heating. For the chloride complexes heating even to only 40–50° decreases the yield of the coloured compound (although the reaction rate increases), whereas for the sulphate and phosphate complexes the reaction mixture can be heated to 50–70° to reduce the reaction time from 4 hr to 30–60 min.

It has been shown that irrespective of the nature of the ligand in the initial complex, reduction from Pt(IV) to Pt(II) precedes the reaction with the organic reagent. For the sulphate and phosphate complexes of Pt(III) the Pt–Pt bond seems to break initially to give Pt(II) and Pt(IV), and then the Pt(IV) is reduced to Pt(II). Platinum sulphate and phosphate are reduced more quickly than the chlorides and with lower concentration of the reducing agent. One of the reasons for these considerable distinctions in reactivity may lie in the difference in the rates and conditions of reduction and activation of the initial forms. The resemblance in the behaviour of the platinum sulphate and phosphate complexes, and in the features of their colour reactions with sulphochlorophenolazorhodanine and sulphochlorophenolazothiopropiorhodanine results, evidently, from the similar structure of the complexes.

The reactions of the binuclear sulphate and phosphate complexes of platinum are characterized by high sensitivity and selectivity, and high kinetic activity. All this allows these reactions to be considered most promising in the analytical chemistry of platinum. The sulphate and phosphate forms have similar selectivity to that of the chloride forms towards alkali and alkaline-earth metals, but higher selectivity towards Cu, Fe, and other transition metals, as well as towards rhodium and iridium. The selectivity towards silver and mercury is, however, higher for the chloride forms. From a practical viewpoint it is important that the conditions under which the sulphates and phosphates are stable and retain their reactivity for a long period of time, have been established and that analytical amounts of the kinetically inert chloride complexes can be converted into these more labile complexes.

Palladium^{17,18,28}

The sulphate, phosphate, nitrate, and chloride complexes of Pd(II) interact with sulphochlorophenolazorhodanine under roughly similar conditions. Their spectrophotometric characteristics are also similar. However, the kinetic activity of the sulphate, phosphate, and nitrate complexes is higher than that of the chloride complexes. The reaction products of the sulphate, phosphate, and nitrate complexes are more soluble than those derived from the chloride complexes.

Iridium^{17,28}

The sulphate and phosphate complexes of iridium are less active than the chloride complexes in reactions with organic reagents, but on prolonged heating react with sulphochlorophenolazorhodanine in strong acid media.

Ruthenium

The sulphate, phosphate and chloride complexes of ruthenium(III, IV) form coloured sulphochlorophenolazorhodanine complexes with similar spectrophotometric characteristics (λ_{\max} 500 nm, ϵ_{HCl} 0.6×10^4 , $\epsilon_{(\text{HCl} + \text{CH}_3\text{COOH})}$ 1.7×10^4). The reactions of ruthenium sulphate and phosphate complexes with the reagent are preceded by transition into the chloride form which has been characterized as $[\text{Ru}_2\text{OCl}_{10}]^{4-}$.

Irrespective of the nature of the ligand and the oxidation state of ruthenium in the initial complex, it is the aquochloro-complex of ruthenium(III) that seems to react with the organic reagent. The conditions for the colour reaction, the HCl/CH₃COOH medium used, and the reducing properties of the reagent ensure the transition of the initial forms of ruthenium into the active form.^{23,24}

In the presence of an organic solvent, *e.g.*, CH₃COOH, the formation of the chloride form from the initial phosphate or sulphate form proceeds in more dilute hydrochloric acid solution, *e.g.*, 0.5–2*M* instead of 5–7*M*, because the organic solvent appears to decrease the degree of hydrolysis of the chloride form. The organic reagent plays the role of a stabilizing additive. The reaction is also faster at the lower HCl concentrations, and this enhances the selectivity.

In the absence of chloride, ruthenium gives no colour reactions with sulphochlorophenolazorhodanine in H₂SO₄ and H₃PO₄ media, because of formation of the non-reactive hydrolysed forms of ruthenium. In the presence of chloride, however, the colour reaction is selective and the presence of Os, Hg, Ag, Ir, Rh, Pb, Bi, and some other metals can be tolerated. The reaction products are stable and have good solubility. The reaction can be used in spectrophotometric and differential-spectrophotometric versions for the analysis of solutions containing the individual forms of ruthenium alone or in mixtures.

This is important for analysis of the sulphate-chloride solutions used in ruthenium production technology, and in complex processing of copper-nickel ores.

Rhodium^{5,17,28}

The sulphate, phosphate and acetate complexes of Rh(II) and Rh(III), and the chloride complexes of Rh(III) react with sulphochlorophenolazorhodanine to give coloured compounds all characterized by an absorption maximum at 510 nm irrespective of the nature of the ligand and the oxidation state of the central atom in the initial complexes. The dependence of the yield on the nature and concentration of the acid used for the reaction and on the reagent concentration is also similar for all these initial complex forms, so presumably the active form of rhodium involved is the same (Table 2). The only differences lie in the kinetics and sensitivity of the reactions. The binuclear acetate and sulphate complexes of Rh(II) are more active in the ligand-substitution reaction, the acetate complex being the most active. The rate of formation of the coloured complex from Rh(II) acetate is extremely high. The colour develops at room temperature in 10–20 min and is characterized by high sensitivity. The high kinetic activity of the binuclear Rh(II) complexes, compared to the corresponding Rh(III) complexes, is attributed to the higher ability of Rh(II) to form labile aquo-complexes which accelerate many processes, including the ligand-substitution reactions.

In the case of the sulphate, phosphate, and chloride complexes of Rh(III) it can be suggested that one of the intermediate steps in formation of the sulphochlorophenolazorhodanine complex is transition of the initial forms into the more reactive binuclear acetate and acetate-sulphate complexes of Rh(II). This suggestion is prompted by the fact that the conditions for the colour reactions (7*M* H₂SO₄/6*M* CH₃COOH mixture, heating to 60–70°, excess of reducing agent) are practically the same as those for preparation of these binuclear complexes. Under specific conditions the acetate and sulphate complexes retain their reactivity towards sulphochlorophenolazorhodanine for a long period of time. The high kinetic activity of the binuclear complexes, especially the Rh(II) acetate complex, and the high sensitivity of the colour reaction could form the basis for new fast methods for determination of rhodium.

FIELDS OF APPLICATION OF AZO DERIVATIVES OF RHODANINE AND ITS ANALOGUES

Spectrophotometry

Methods have been developed for the spectrophotometric determination of Pt [Pt(II) and Pt(IV) chlorides, Pt(III) phosphates and sulphates], Rh [Rh(III) chlorides, acetates, and phosphates, Rh(II) acetates and sulphates], Ir [Ir(IV) chlorides], Pd [Pd(II) chlorides, sulphates, phosphates and nitrates],

Au and Ag with sulphochlorophenolazorhodanine. Thiorhodine has been used for the determination of Pt [Pt(IV) chlorides, Pt(III) phosphates and sulphates], and silver (Table 3). The methods for the photometric determination of noble metals with these two reagents are characterized by high sensitivity and selectivity, possibility of the direct determination of platinum-group metals when these are present as their different complexes with mineral acid anions (or acetate) in the presence of other metals, and high speed of determination. These methods have found application for the analysis of natural and industrial samples. Lead can be determined with thiorhodine, and mercury with *p*-hydroxy-3-aminorhodanine.

Differential spectrophotometry

The use of organic acids, acetic acid in particular, in the reactions of platinum with thiorhodine increases the solubility of the reagent and reaction products, as well as the stability of the solutions as a function of time. The high kinetic activity of the sulphate and phosphate complexes of platinum, and the possibility of activating the chloride complexes with ascorbic acid or copper salts,²⁹ provides fast and direct differential-photometric methods for the determination of platinum with thiorhodine in $H_2SO_4 + CH_3COOH$ medium. Combination of the photometric and differential-photometric versions allows determination of platinum with thiorhodine over a Pt range of 0.04–20 $\mu g/ml$.

Ruthenium can be determined with sulphochlorophenolazorhodanine in $HCl + CH_3COOH$ medium over an Ru range of 0.2–40 $\mu g/ml$ by combination of photometric and differential-photometric methods. The methods are versatile since both different ruthenium complexes (*e.g.* the sulphates and chlorides) can be determined individually or as their sum, under identical conditions. These methods have found application for the analysis of alloys, composites, *etc.* (Table 3). Silver can similarly be determined at pH 1.5–5, over the range 0.2–60 $\mu g/ml$. The selectivity for silver can be enhanced by extraction of the Ag-sulphochlorophenolazorhodanine-tributyl phosphate system from 0.1M HNO_3 with cyclohexanone.^{44,45}

A differential-photometric method can be used for determination of rhodium in alloys with *p*-sulphobenzeneazorhodanine in $H_2SO_4 + CH_3COOH$ medium.³⁷

Precipitation

Gold, platinum and palladium can all be precipitated quantitatively with a small excess of sulphochlorophenolazorhodanine, Au at room temperature, Pt and Pd on heating (Table 3). Precipitation of platinum is done in the presence of a reducing agent.

Detection and identification

Methods have been developed for use of sul-

Table 3. Applications of 5-azo derivatives of rhodamine and its analogues

Analytical application	Reagent	Element	Conditions for determination	Sample	References
Spectrophotometric determination	Sulphochlorophenolazorhodanine	Pd	$9M H_3PO_4 + 0.5M HCl$	Electrolytes, ores, ceolith-based catalysts	20, 21, 30
		Au	$1M HCl$, after separation by extraction	Ores and tailings	31
		Au	$1M HCl$	Industrial solutions and water	32–34
		Pt	$1M HCl + 2M H_3PO_4$	Ceolith-based catalysts Copper-based standard samples	21, 30–35
		Pt	$2M H_2SO_4 + 10M H_3PO_4$	Alumino-platinum catalysts, wastes	
	Rh	$7M (H_2SO_4 + CH_3COOH)$	Copper-based standard samples	35	

	Ag	pH 1.5-3	Halides, scrap, waste	31
Thiorhodine	Ag Pb	10M CH ₃ COOH + 1M H ₃ PO ₄ pH 3	River and sea-water	36
<i>p</i> -Hydroxy-3-amino-rhodanine	Hg	4M H ₃ PO ₄	Environmental samples, alloys	
Differential spectrophotometric determination	Ag	pH 1.5-5	Alloys	
	Ru	2M HCl + 5M CH ₃ COOH	Composites	
Thiorhodine	Pt	3M H ₃ PO ₄ + 7M CH ₃ COOH	Alloys	
<i>p</i> -Sulphobenzeneazorhodanine	Rh	5M H ₂ SO ₄ + 5M CH ₃ COOH	Alloys	37
Precipitation	Au Pt (sulphates, phosphates) Pt (chlorides) Pd	1M HCl 6M H ₂ SO ₄ 2M HCl, ascorbic acid 1-8M H ₂ SO ₄		
Detection and identification on chromatograms	Pt, Pd, Rh, Ir (chlorides, sulphates, phosphates) and Au, Ag Au and Pt Pt	0.2% reagent solution in 5-8M H ₃ PO ₄ 1-3M HCl 15M CH ₃ COOH (ascorbic acid)	Alloys	22, 38, 39
Separation of coloured complexes	Pt and Ag Pt and Au Pd and Ag Pd and Au	pH 1.7 pH 8.6		40
Enrichment and separation	Pt(II), Pd(II), Rh(III), Au(III) Ag, Hg		Ores, mineral raw material, industrial solutions, river and sea water	32, 33, 41-43

phochlorophenolazorhodanine to detect and identify chromatographic and electrophoretic zones of both individual and total NM (except Os) as different complexes, including those with chloride, sulphate and phosphate. The reagent colours the zones bright crimson, against its own yellow background on the chromatogram. The limit of visual detection is 0.01–0.5 μg of a metal in a zone. This method of detection is superior to that for *p*-nitrosodimethylaniline and *p*-aminobenzylidenerhodanine, in sensitivity of visual detection, stability of colour with time, and the possibility of identifying the zones for various mineral acid anion complexes. Methods have been proposed for electrophoretic and chromatographic separation on paper and thin layers for Pd–Ir, Pd–Rh, Ir–Rh, Pd–Pt–Au, Pd–Pt–Ir, Pd–Pt–Rh, Pd–Au, and Pt–Rh mixtures. These methods have found application in the analysis of alloys.^{22,39,40}

Separation of NM complexes with azorhodanines

The electrophoretic mobility and characteristics of the noble metals as their coloured complexes with azo derivatives of rhodanine have been studied in buffer systems based on formic, acetic and oxalic acids (pH 1.5–1.7), acetic and boric acids (pH 2), pyridine and oxalic acid (pH 5.9). Distinct separation of zones was observed for Pd–Ag, Pt–Ag, Pd–Au, Pt–Au binary mixtures as their complexes with sulphochlorophenolazorhodanine and sulphonitrophenolazorhodanine.⁴⁰

Enrichment and separation on chelating sorbents

Chelating sorbents based on rhodanine, azorhodanine, and azothiopropiorhodanine have been synthesized.^{32,33,41–43} Cellulose, the styrene–divinylbenzene copolymers, and Sephadexes were used as the matrix. The sorbents are of interest mainly for the enrichment and separation of noble metals. These sorbents interact with the noble metals under roughly the same conditions and with the same selectivity as the free rhodanine reagents. The methods have found application to the analysis of ores, industrial solutions and natural waters (Table 3).

REFERENCES

1. N. M. Turkevich and B. N. Turkevich, *Ukr. Khim. Zh.*, 1950, **16**, 558.
2. A. P. Grishchuk and S. N. Baranov, *Zh. Obshch. Khim.*, 1958, **28**, 916; 1959, **29**, 1665.
3. I. D. Komaritsa, S. N. Baranov and A. P. Grishchuk, *Khim. Geterotsikl. Soed.*, 1967, **4**, 664.
4. R. F. Propistsova, S. B. Savvin and Yu. G. Rozovskii, *Zh. Analit. Khim.*, 1971, **26**, 2424.
5. R. F. Propistsova and S. B. Savvin, *ibid.*, 1973, **28**, 1768.
6. R. F. Gur'eva, L. M. Trutneva and S. B. Savvin, *ibid.*, 1978, **33**, 632.
7. L. M. Kul'berg, *Sintezy organicheskikh reaktivov (Syntheses of Organic Reagents)*, Goskhimizdat, Moscow, 1947.
8. E. V. Vladimirskaia, *Zh. Obshch. Khim.*, 1955, **25**, 2255.
9. C. L. Lapiere, *J. Pharm. Belg.*, 1959, **24**, 126.
10. M. M. Turkevich, A. S. Konivich and L. I. Petlichna, *Tr. L'vovsk. Med. Inst.*, 1967, **24**, 22.
11. A. P. Grishchuk, G. I. Roslaya and S. N. Baranov, *Khim. Geterotsikl. Soed.*, 1967, **4**, 661.
12. A. P. Grishchuk and I. R. Barilyak, *Zh. Obshch. Khim.*, 1963, **33**, 3972.
13. N. I. Busev, *Sintez novykh organicheskikh reagentov dlya neorganicheskogo analiza (Synthesis of New Organic Reagents for Inorganic Analysis)*, p. 124. MGU, Moscow, 1972.
14. R. F. Propistsova, S. B. Savvin, L. A. Gribov and N. B. Teplyakova, *Zh. Analit. Khim.*, 1975, **30**, 250.
15. R. F. Bur'eva, S. B. Savvin and N. B. Shcheglova, *ibid.*, 1976, **31**, 660.
16. R. F. Propistsova and S. B. Savvin, *ibid.*, 1974, **29**, 2097.
17. R. F. Gur'eva, S. B. Savvin, N. N. Chalisova, M. I. Yuz'ko and T. A. Fomina, *ibid.*, 1977, **32**, 1394.
18. R. F. Gur'eva, S. B. Savvin, L. M. Trutneva, N. N. Chalisova, T. A. Fomina and L. K. Shubochkin, *ibid.*, 1983, **37**, 667.
19. R. F. Gur'eva, S. B. Savvin, L. M. Trutneva and N. N. Chalisova, *ibid.*, 1983, **38**, 881.
20. N. N. Basargin, Yu. G. Rozovskii, V. A. Sychkova, N. N. Nikol'skaya and Z. A. Ezhova, in *Metody khimicheskogo analiza gornykh porod i mineralov (Methods for Chemical Analysis of Ores and Minerals)*, p. 10. Nauka, Moscow, 1973.
21. N. N. Basargin and Yu. G. Rozovskii, *Zavodsk. Lab.*, 1973, **39**, 3.
22. M. P. Volynets, A. N. Ermakov, S. I. Ginzburg, N. N. Chalisova, R. F. Gur'eva, T. V. Dubrova, M. I. Yuz'ko and T. A. Fomina, *Zh. Analit. Khim.*, 1977, **32**, 914.
23. S. B. Savvin, R. F. Gur'eva, L. M. Trutneva, N. N. Chalisova, T. A. Fomina and L. K. Shubochkin, *ibid.* 1982, **37**, 654.
24. R. F. Gur'eva, L. M. Trutneva, S. B. Savvin and N. N. Chalisova, *ibid.*, 1984, **39**, 1653.
25. S. B. Savvin, R. F. Propistsova and Yu. G. Rozovskii, *ibid.*, 1972, **27**, 1554.
26. S. B. Savvin, R. F. Propistsova and L. M. Trutneva, *ibid.*, 1979, **34**, 1493.
27. I. B. Baranovskii and R. N. Shchelokov, *Zh. Neorgan. Khim.*, 1978, **23**, 3.
28. S. B. Savvin and R. F. Gur'eva, *Zh. Analit. Khim.*, 1980, **35**, 1818.
29. S. B. Savvin, R. F. Gur'eva, L. M. Trutneva and N. N. Chalisova, *ibid.*, 1983, **38**, 132.
30. Yu. G. Rozovskii, T. A. Ekimenkova and N. F. Budyak, *Sravnitel'noe izuchenie spektrofotometricheskikh metodov opredeleniya palladiya s nekotorymi organicheskimi reagentami (Comparative Study of Spectrophotometric Methods for the Determination of Palladium with some Organic Reagents)*, in *IX All-Union Conference on Chemistry, Analysis and Technology of Noble Metals, Abstracts*, Krasnoyarsk, 1973, p. 77.
31. N. N. Basargin, Yu. G. Rozovskii, V. A. Volchenkova and L. S. Zubkova, in *Teoreticheskie i prakticheskie voprosy primeneniya organicheskikh reagentov v analize mineral'nykh ob'ektov (Theoretical and Practical Topics in Application of Organic Reagents for the Analysis of Minerals)*, p. 96. Nauka, Moscow, 1976.
32. G. V. Myasoedova, O. P. Eliseeva, S. B. Savvin and N. I. Uryanskaya, *Zh. Analit. Khim.*, 1972, **27**, 2004.
33. G. V. Myasoedova, L. I. Bol'shakova, S. P. Shvedova and S. B. Savvin, *ibid.*, 1973, **23**, 1550.
34. G. V. Myasoedova, I. I. Antokol'skaya, L. I. Bol'shakova, O. P. Shvedova and S. B. Savvin, *ibid.*, 1974, **29**, 2104.
35. F. I. Danilova, V. A. Orobinskaya, B. G. Parfenova, R. F. Propistsova and S. B. Savvin, *ibid.*, 1974, **29**, 2150.
36. O. P. Shvedova, N. I. Shcherbinina, G. V. Myasoedova, A. M. Sorochan, M. M. Senyavin and S. B. Savvin, *ibid.*, 1983, **38**, 221.

37. L. E. Drozd, F. I. Danilova, N. V. Shcheglova and G. V. Mechetkina, *Referat Zh. Khim.*, 1982, 10G187 Dep.
38. T. G. Akimova, R. F. Propistsova and S. B. Savvin, *Zh. Analit. Khim.*, 1974, **29**, 2365.
39. M. P. Volynets, L. I. Pavlenko, T. V. Dubrova, L. B. Simakova and S. M. Pirogov, in *Metody vydeleniya i opredeleniya BM (Methods for Isolation and Determination of Noble Metals)*, p. 53. GEOKhI AN SSSR, Moscow 1981.
40. T. G. Akimova, R. F. Propistsova and S. B. Savvin, *Zh. Analit. Khim.* 1973, **28**, 2005.
41. G. V. Myasoedova, and S. B. Savvin, *Khelatobrazuyushchie sorbenty (Chelate-Forming Sorbents)*, Nauka, Moscow, 1984.
42. N. N. Basargin, Yu. G. Rozovskii and V. M. Zharova, in *Organicheslie reagenty i khelatnye sorbenty v analize mineral'nykh ob'ektov (Organic Reagents and Chelate Sorbents for the Analysis of Minerals)*, p. 82. Nauka, Moscow, 1980.
43. G. V. Myasoedova, M. P. Volynets, T. A. Koveshkina, Yu. I. Belyaev and T. V. Dubrova, *Zh. Analit. Khim.*, 1974, **29**, 2253.
44. N. N. Basargin, Yu. G. Rozovskii, V. A. Volchenkova and L. S. Zubkova, in *Teoreticheslie i prakticheskie voprosy primeniya organicheskikh reagentov v analize mineral'nykh ob'ektov (Theoretical and Practical Topics in Application of Organic Reagents for the Analysis of Minerals)*, p. 132. Nauka, Moscow, 1976.
45. *Idem*, in *Organicheskie reagenty v analiticheskoi khimii (Organic Reagents in Analytical Chemistry)*, IV All-Union Conference, Abstracts, Kiev, 1976, Part 2, p. 63.

CONCENTRATION, SEPARATION AND DETERMINATION OF SCANDIUM, ZIRCONIUM, HAFNIUM AND THORIUM WITH A SILICA-BASED SULPHONIC ACID CATION-EXCHANGER

I. P. ALIMARIN, V. I. FADEEVA, G. V. KUDRYAVTSEV, I. M. LOSKUTOVA
and T. I. TIKHOMIROVA

Department of Chemistry, N. V. Lomonosov State University, Moscow 119899, USSR

(Received 15 October 1985. Revised 3 February 1986. Accepted 1 August 1986)

Summary—A study has been made of the dependence of the sorption of scandium, zirconium, hafnium and thorium from aqueous solutions with a silica-based sulphonic cation-exchanger (SCE-SiO₂) on the concentration and nature of the acid medium, time of contact, concentration of the element, and the ionic strength. The selectivity decreases in the order Zr ≈ Hf > Th > Sc > Fe(III). The sorption characteristics of silica gel and SCE-SiO₂ have been compared, and the sorption mechanism is discussed. The SCE-SiO₂ exchanger has been used for 100-fold concentration of scandium, zirconium, hafnium and thorium from their 10⁻⁸–10⁻⁷ M solutions, and a spectrophotometric method has been developed for their determination with a detection limit of 0.5 ng/ml for Zr and Sc and 0.1 ng/ml for Hf and Th. Zirconium and hafnium have been determined in the solvent phase by X-ray fluorescence and atomic-emission methods.

Silica-based bonded phases with attached ionogenic and complex-forming groups are being increasingly used in inorganic analysis¹⁻⁴ owing to their high mass-exchange characteristics, low swelling, and a number of other valuable properties. Though the sorption capacities of such modified silicas are smaller than those of organic polymeric exchange resins, this has little effect on the extraction of micro-amounts of inorganic ions.

The strong-acid sulphonic cation-exchanger (SCE-SiO₂), which contains arenesulphonic acid molecules attached to the silica surface is by far the most universal sorbent for cation separation and is used in the analysis of organic⁵ and inorganic⁶ substances by HPLC. It is also doubtless suitable for concentration of metal ions and their separation by column chromatography, but there is practically no published information on the topic. We have investigated the possibility of using SCE-SiO₂ for sorption of scandium, zirconium, hafnium and thorium.

These elements were chosen for several reasons. First, the sorbent matrix—silica—has a higher affinity for ions of easily-hydrolysed elements, notably for zirconium and hafnium, which can contribute to the bonding of these ions on the SCE-SiO₂ sorbent. Secondly, there is a need for fast and efficient methods of concentration and separation of metal ions from natural materials and alloys which have complex compositions. Although a large number of polymeric organic ion-exchange and chelating sorbents is known, the problem of selective extraction of scandium, zirconium, hafnium and thorium from materials with complex composition has not yet been fully solved.⁷⁻⁹

EXPERIMENTAL

Apparatus

Spectrophotometric measurements were made with an SP-26 spectrophotometer. X-Ray fluorescence determination of elements in the sorbent matrix was performed with an EGG-ORTEC TEFA-III X-ray fluorescence energy-dispersive analyser equipped with an X-ray tube with a double Mo/W anode. The standard-background method was used, in which the analytical parameter is the ratio of fluorescence intensity to the peak area of the Compton-scattered radiation of the anode material. The sample was prepared by grinding the air-dried sorbent-concentrate with silica in an agate mortar to 50-μm particle size, and placing the mixture in a polyethylene cuvette (32 mm diameter), the bottom of which was a polystyrene film 4 μm in thickness. The weight of the prepared sample was 1.5 g.

For atomic-emission analysis of the sorbent a DFS-13 diffraction spectrograph was used, with the ZrII 327.305 nm and HfI 286.637 and 307.288 nm lines as the analytical lines. The sample was prepared by drying the sorbent-concentrate in a glassy-carbon crucible over a sand-bath, and then grinding it in an agate mortar and mixing the powder with high-purity graphite powder (1:1); 20 mg of the resultant mixture was placed in a "wine-glass" electrode soaked with 1M barium chloride solution.

Reagents

The sorbent was synthesized¹⁰ from "Silochrome C-80" silica (specific surface area 80 m²/g, mean pore diameter 50 nm, particle-size fraction 0.16–0.25 mm) by reaction with benzenetrichlorosilane, followed by sulphonation with chlorosulphonic acid. The amount of sulphonic groups attached was determined by potentiometric titration and found to be 0.20 mmole/g.

All reagents used were of analytical reagent grade and were prepared by dissolution in demineralized and distilled water. Standard solutions of the elements were prepared by dissolving the metals, oxides or salts in a suitable acid (perchloric, hydrochloric, nitric, sulphuric).

Sorption by the batch method

The required amount of solution containing the metal ions to be studied, and a calculated amount of mineral acid or sodium hydroxide solution, was diluted with water to 10 ml in a 20-ml vessel fitted with a ground-in stopper; 0.01 or 0.1 g of sorbent was added and the vessel was shaken on a mechanical vibrator for 30 min. The sorbent was then filtered off, and the equilibrium concentration of metal ions in the aqueous phase was determined in a suitable aliquot by established methods,¹¹⁻¹³ zirconium, hafnium and thorium with Arsenazo III, scandium with Xylenol Orange, and titanium with diantipyrylmethane. To eliminate nitrite formed in nitric acid oxidation of organic reagents in the determination, 2 ml of 2.5% urea solution were added per 25 ml of reaction mixture. In the scandium determination after sorption from hydrochloric acid media (0.2–2M acid), the aqueous phase was evaporated to remove the acid. In the zirconium determination with Arsenazo III in the presence of oxalic acid, a corresponding amount of oxalic acid was added to the zirconium standards used for the calibration.

Concentration and determination

A 0.3-g portion of SCE-SiO₂ sorbent was packed in a 5 mm bore tube to give a 5-cm long chromatographic column and washed with a solution of the same acidity as the test solution. Then 300–600 ml of test solution were passed at a linear velocity of 25 cm/min through the column and the column was washed with 5 ml of 0.1M hydrochloric acid. The acidity of the test solution for the concentration step was as follows: Sc pH 2–3; Zr and Hf 0.1–0.3M hydrochloric acid; Th 0.1–0.2M hydrochloric acid. Sc was eluted with 1M hydrochloric acid, Zr with 0.05M oxalic acid, Hf with 0.5M sulphuric acid, Th with saturated ammonium oxalate solution. The eluent volume in all experiments was 5 ml. The elements eluted were determined by spectrophotometry and those retained in the sorbent phase were determined by X-ray fluorescence or atomic-emission. The relative standard deviation S_r was calculated for the results of 4 or 5 measurements.

Sample dissolution

Approximately 1 g of sample (cast iron or alloy steel) for 10⁻⁴–10⁻³% content of the element(s) of interest, or 0.1 g for 10⁻³–10⁻²%, was placed in a borosilicate glass beaker (100 ml), and dissolved by heating with 10–20 ml of 5M hydrochloric acid, followed by oxidation with 5–8 drops of concentrated nitric acid. The solution was evaporated to dryness, 5 or 6 drops of concentrated hydrochloric acid were added and the acid was evaporated (this treatment was repeated twice). The residue was dissolved by heating with 20–30 ml of water and 5 or 6 drops of concentrated hydrochloric acid. The solution was filtered, and the filter with residue was placed in a platinum crucible, dried, and ignited at 900–1000°. The crucible was cooled, and the residue treated with 3 or 4 drops of concentrated sulphuric acid, and 2–3 ml of concentrated hydrofluoric acid, followed by evaporation until fuming ceased. After this removal of silicon, the residue was fused with 0.5 g of sodium potassium carbonate at 900–1000° for 15–20 min, then the cooled melt was dissolved in 25 ml of 2M hydrochloric acid. This solution was added to the filtrate which was then diluted with water to 200–300 ml; the hydrochloric acid concentration should be 0.2–0.3M.

RESULTS AND DISCUSSION

Influence of nature and concentration of the acid

As already mentioned, silica—the base of the studied sorbent—has increased affinity for easily hydrolysed elements, which makes it possible for the residual silanol groups on the surface of the SCE-SiO₂

sorbent to participate in bonding of metal ions. In this connection, we have studied ion sorption on "Silochrome C-80" silica, which is the base for the SCE-SiO₂ sorbent.

A comparison of the dependence of sorption of metal ions on SCE-SiO₂ and on silica on hydrochloric acid concentration (Fig. 1) shows that the sorption curves for SCE-SiO₂ are shifted into the acidic region relative to those for silica. This can serve as proof that ion sorption on SCE-SiO₂ mostly takes place at the sulphonate groups. The distribution coefficients on SCE-SiO₂ are as high as 3 × 10³ cm³/g for Sc, 6 × 10³ cm³/g for Zr and Hf, and 1 × 10⁴ cm³/g for Th. The reduction in sorption with higher acidity is explained, on the one hand, by formation of metal chloride and hydroxychloride complexes, and on the other by competitive sorption of H₃O⁺ ions. As seen from Fig. 1, titanium(IV) ions are not sorbed on

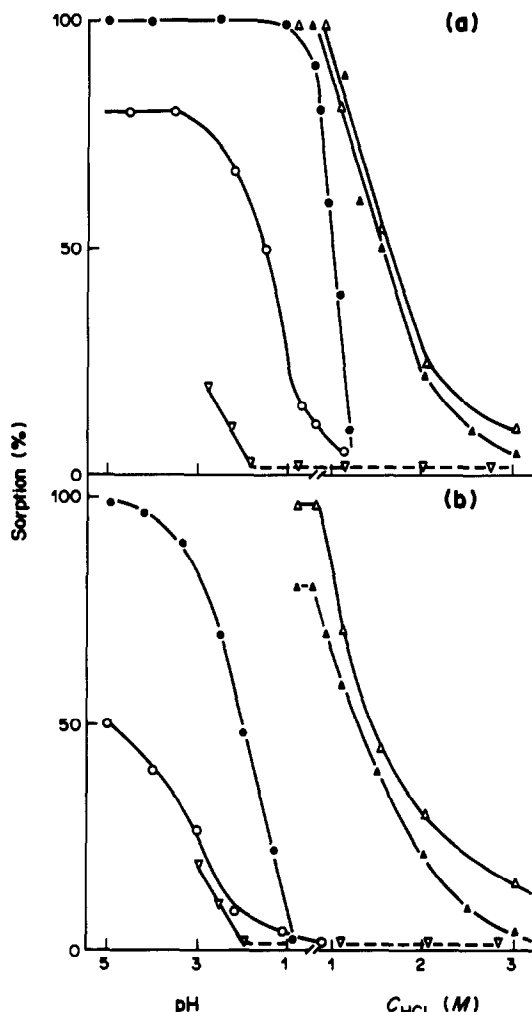


Fig. 1. Dependence of scandium (O), titanium (∇), zirconium (Δ), hafnium (▲) and thorium (●) sorption on SCE-SiO₂ (a) and on silica (b), on concentration of hydrogen ions: 1.3 × 10⁻⁴ M Sc; 1.1 × 10⁻⁴ M Ti; 2.2 × 10⁻⁵ M Zr; 1.1 × 10⁻⁵ M Hf; 8.6 × 10⁻⁶ M Th; sorbent mass 0.1 g (Zr, Hf, Th, Ti) and 0.01 g (Sc).

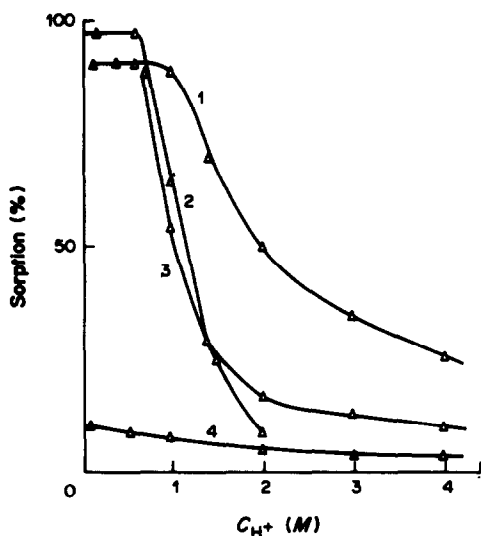


Fig. 2. Dependence of zirconium sorption on SCE-SiO₂ on acid type nature and concentration: $2.2 \times 10^{-5} M$ Zr; sorbent mass 0.1 g; 1, HClO₄; 2, HCl; 3, HNO₃; 4, H₂SO₄.

SCE-SiO₂ or silica in the acidity interval from pH 2 to 4M hydrochloric acid. At pH > 2, titanium is sorbed but as the colloidal hydroxide.

The influence of the nature of the acid used was studied with perchloric, hydrochloric, nitric and sulphuric acids, the anions of which decrease in complexing ability in the order $SO_4^{2-} > NO_3^- \approx Cl^- > ClO_4^-$. The results for zirconium sorption with SCE-SiO₂ are in agreement with this series (Fig. 2). Similar results were obtained for hafnium, but the sorption of thorium is practically unaffected by the type of acid. Scandium sorption is reduced in the presence of high sulphate concentrations, owing to complex formation.

Influence of duration of phase contact

The high rate of sorption-desorption equilibration is among the major advantages of modified silicas. For instance, when Zr is sorbed from solutions with $C_{Zr} = 2.2 \times 10^{-5} M$, the degree of extraction becomes constant in under 2 min (Fig. 3).

In most cases, the rate of sorption increases with metal concentration in solution, but as seen from Fig. 3, Zr sorption on SCE-SiO₂ from hydrochloric acid follows the reverse trend, with equilibrium being reached only after 30 min for $C_{Zr} = 4.4 \times 10^{-4} M$. The corresponding effect for silica is even more drastic; at $C_{Zr} = 4.4 \times 10^{-4} M$, it takes more than 8 hr for equilibrium to be reached (Fig. 3).

Differences in the behaviour of silica and SCE-SiO₂ also become manifest in the dependence of equilibration rate on acidity. Thus, with hydrochloric acid concentration increasing from 0.3 to 0.7M, the rate of sorption on SCE-SiO₂ remains unchanged, whereas for silica the equilibration time increases from 1 to 4 hr.

These results can be explained in the following way. It is known that at $C_{Zr} > 10^{-4} M$ in aqueous solutions and an acidity of 0.1–1.0M hydrochloric acid, polynuclear complexes are formed, and equilibration between the various ionic forms is slow.¹⁴ It may therefore be supposed that mononuclear zirconium hydroxy complexes are sorbed, and the rate-limiting step of the process at high zirconium concentrations is depolymerization of the polynuclear species. Analogous trends in sorption kinetics are also observed for hafnium, but are absent for the metals which do not form polynuclear species in solution.

A study of sorption of scandium on SCE-SiO₂ has shown that for $C_{Sc} = 2.2 \times 10^{-5}$ – $1.8 \times 10^{-3} M$, the sorption rate increases with C_{Sc} . At $C_{Sc} > 2 \times 10^{-3} M$, 70% of the scandium is extracted from the solution in 15–20 min.

Sorption isotherms and reversibility

Isotherms for zirconium and hafnium sorption on SCE-SiO₂ are presented in Fig. 4, and those for scandium in Fig. 5. Two things are worth mentioning in connection with these isotherms. First, because the element concentration has a strong influence on sorption speed, the contact time was increased with element concentration in accordance with the data found previously. Secondly, very small sorbent samples were used (0.01 g) in order to lower the initial element concentration and thereby avoid complications due to formation of polynuclear species.

The sorption capacity of SCE-SiO₂ for Zr and Hf in 0.3M hydrochloric acid is 4.3 and 8.9 mg/g respectively, or 0.05 mmole/g for both elements. With increasing acid concentration, both the strength of metal ion-sorbent bonding and the sorption capacity are reduced. SCE-SiO₂ has substantially greater (approximately 2.5-fold) capacity than silica for Zr and Hf and provides stronger bonding of the metal ions.

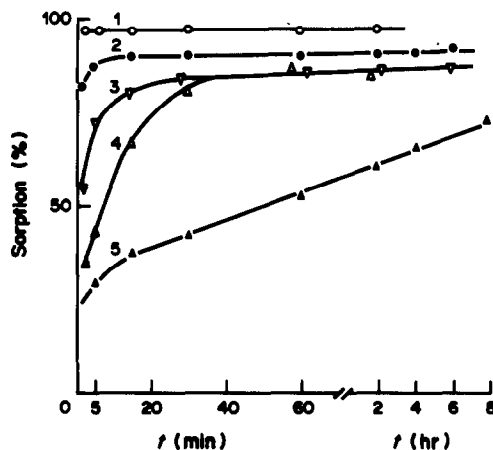


Fig. 3. Dependence of zirconium sorption on SCE-SiO₂ (1–3) and silica (4, 5) on duration of phase contact. C_{Zr} , $10^{-4} M$: 0.2 (1), 1.1 (2, 4), 4.4 (3, 5); sorbent mass 0.1 g; C_{HCl} 0.3M.

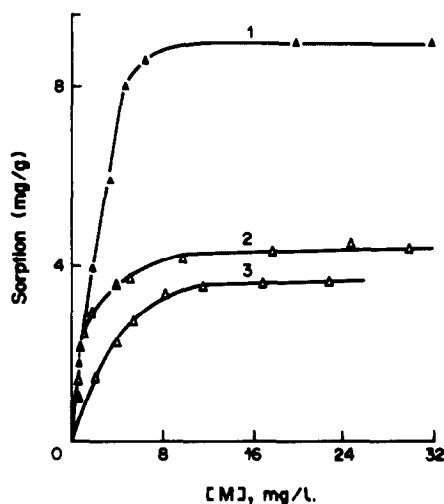


Fig. 4. Isotherms of hafnium (1), zirconium (2, 3) sorption on SCE-SiO₂ from 0.3M HCl (1, 2) and 0.7M HCl (3); Δ and ▲ are points for sorption and desorption, respectively.

The isotherms for scandium sorption on SCE-SiO₂ have an unusual form (Fig. 5). At scandium concentrations up to 30 mg/l., the sorption isotherm is described by the Langmuir equation; at higher concentrations the isotherm has an inflection point and takes the form of a polymolecular sorption isotherm. It can be assumed that at high scandium concentrations polynuclear species are formed and sorbed, which explains the greater degree of sorption.

Sorption reversibility is of great practical and theoretical importance. It is evinced by the distribution coefficient being independent of the direction from which equilibrium is approached. To examine this, a solution containing zirconium in 0.3M hydrochloric acid was shaken with SCE-SiO₂ for the length of time needed for equilibrium to be reached; the zirconium content in both phases was then determined, the aqueous phase was removed and 0.3M hydrochloric acid added and the mixture was shaken until equilibrium was again attained, and the zirconium content in both phases was determined once more. As seen from Fig. 4, the "sorption" and "desorption" points are satisfactorily accommodated by a single curve. Moreover, it was found that the equilibration time was the same for both "sorption" and the "desorption" experiments. The combined data indicate reversibility of the sorption process.

Reversibility of sorption on SCE-SiO₂ determines the possibility of ion desorption and sorbent regeneration. Elution conditions can be chosen according to the dependence of the element sorption on acidity of the medium. Figure 1a shows that zirconium and hafnium can be eluted with 3–5M hydrochloric acid, scandium with the 1M acid and thorium with 2M acid. Quantitative desorption of 5–200 μg of these elements from 0.3 g of sorbent in the dynamic mode

can be achieved with quite small eluent volumes (5–40 ml). We have also studied the possibility of zirconium, hafnium and thorium elution with oxalic acid and sulphuric acid (Zr, Hf), and saturated ammonium carbonate or oxalate solutions (Th). Since sulphate and oxalate form stable complexes with zirconium and hafnium, it is possible to use 5 ml of 0.05M oxalic acid and 5 ml of 0.5M sulphuric acid for elution of 5 μg of zirconium and hafnium respectively. Using dilute acids as eluents preserves the sorption characteristics of the sorbent, and makes the work easier. Our experiments have shown that the sorbent can be used at least 10 times, with regeneration.

Influence of ionic strength on sorption

The SCE-SiO₂ sorbent studied belongs to the class of strong acid cation-exchangers, and the degree of sorption depends markedly on the ionic strength of the solution. In the series of elements studied, the dependence of sorption on concentration of background electrolyte (sodium perchlorate) is strongest for scandium (Fig. 6). Since perchlorate has little tendency to complex metal ions, the decrease in

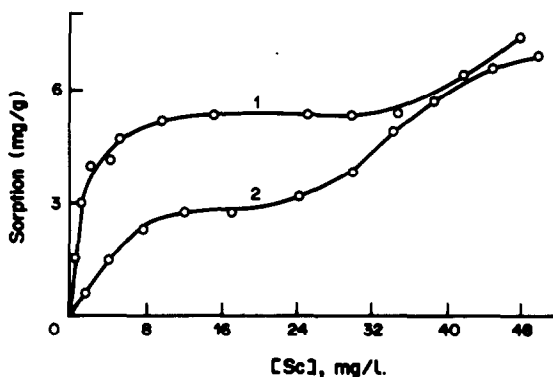


Fig. 5. Isotherms of scandium sorption on SCE-SiO₂ at pH 2 (1) and pH 1 (2).

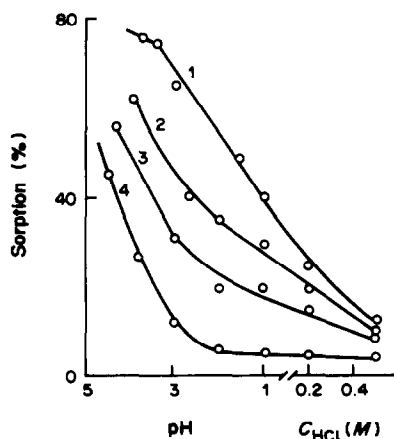


Fig. 6. Dependence of scandium sorption on SCE-SiO₂ on pH at different NaClO₄ concentrations. C_{Sc} = 1.3 × 10⁻³ M, sorbent mass 0.01 g, C_{NaClO₄}: 0M (1), 0.1M (2), 0.5M (3), 1.0M (4).

Table 1. Zirconium and hafnium sorption on SCE-SiO₂ in the presence of 5 × 10⁴-fold amounts of alkali and alkaline-earth metal ions

Macrocomponent	Zr(Hf) added, μg	Zr(Hf) found, μg	S_r , %
Na ⁺	7.8	7.7	7
Ca ²⁺	7.8	7.8	4
Mg ²⁺	7.8	7.6	5

scandium sorption is probably due to a shift of the ion-exchange equilibrium to sorption of low-charge ions (Na⁺), the concentration of which is very much greater than that of the scandium.

The influence of sodium perchlorate and chloride on sorption of zirconium and hafnium on SCE-SiO₂ in the batch mode is practically the same—increasing the salt concentration up to 1M decreases the degree of extraction from 95 to 80%. Despite this decrease in extraction in the batch mode, sorption in the dynamic mode still gives quantitative extraction of these elements in the presence of 5 × 10⁴-fold amounts of sodium, calcium and magnesium ions (Table 1). Analogous results have also been obtained for thorium.

The sorption mechanism

In our earlier investigation of scandium sorption¹⁵ on a number of chemically modified silicas containing various ionogenic and complex-forming groups, we proved that, depending on the nature of the attached group, the metal ions can be sorbed at either the attached group, or at residual silanol groups. Analysis of the data obtained for sorption of the studied metal ions on SCE-SiO₂ indicates that for a sorbent with sulphonate groups, the interaction is principally by substitution of the sulphonic acid proton. However, further analysis shows that it is difficult to explain the experimentally observed trends solely in terms of bonding of the ion to the sulphonate-group. Use of the ion-potentials and pH-values corresponding to precipitation of the metal hydroxides leads to the following theoretical series of cation-exchanger affinity for easily-hydrolysed elements sorbed from acidic solutions: Ti(IV) > Zr(IV) > Hf(IV) ≈ Fe(III)

> Th(IV) > Sc(III). The selectivity series found in the present work, Zr(IV) ≈ Hf(IV) > Th(IV) > Sc(III) > Fe(III) ≫ Ti(IV), is different, but can be understood by assuming that in the sorption process the affinity of ions for the sorbent is determined, along with electrostatic factors, by additional donor-acceptor interaction that increases the covalency of the metal-sulphonate bond.

Comparison of the sorption behaviour of scandium and thorium with reference data on their state in hydrochloric acid media leads to the conclusion that scandium and thorium are sorbed as aquo-complexes at pH < 3, and hydroxy-complexes at pH > 3. For zirconium, mathematical modelling has been used to show that sorption occurs with formation (on the sorbent surface) of a complex having the composition Zr(OH)₃R, where R is the sorbent sulphonate group.

The sorption behaviour of titanium(IV) deserves special mention. Theoretically, titanium should be sorbed by silica and other cation-exchangers better than zirconium, hafnium and thorium are, but our experimental data testify to the opposite.

Sorption of titanium(IV) on SCE-SiO₂ and silica occurs only in the presence of complex-forming agents, notably salicylhydroxamic acid. Mathematical modelling has shown that mixed-ligand uncharged complexes Ti(OH)₃L and Ti(OH)₂L₂ (L is the anion of salicylhydroxamic acid) are the species sorbed. Extraction of these complexes from the solution is explained by physical adsorption at the sorbent surface.

Concentration and separation

Combined separation and concentration first of all removes complications connected with multielement sample composition, and provides for a substantially lower detection limit. Organic ion-exchangers are very seldom used for concentrating the elements studied here, owing to the large solution volumes needed for desorption. Results pertaining to element concentration are given in Table 2. The concentration coefficient was calculated according to the equation $K = q_2 V_1 / q_1 V_2$, where q_1 is the element content in the sample solution and q_2 that in the eluate, and V_1 is

Table 2. Scandium, zirconium, hafnium and thorium concentration on SCE-SiO₂

Element	Volume of test solution, ml	Added, μg	Found, μg	S_r , %	Concentration factor
Sc	300	13.7	13.5	4	58
	600		13.0	3	113
Zr	300	5.8	5.7	4	58
	600		5.7	4	117
Hf	300	8.0	8.0	2	60
	600		7.8	4	116
Th	300	5.0	5.0	2	60
	600		4.9	4	117

Table 3. Zirconium (hafnium) separation from other elements on SCE-SiO₂

Element	M: Zr(Hf), w/w	Zr(Hf) added, μg	Zr(Hf) found, μg	S _r , %
Sc	1 × 10 ³	5.8	5.7	5
	2 × 10 ³		5.5	5
Ti	1 × 10 ³	9.9	10.0	6
	2 × 10 ³		9.7	5
Al	2 × 10 ³	7.8	7.9	4
	6 × 10 ³		7.8	5
Ni(Co)	1 × 10 ²	5.8	5.7	5
	1 × 10 ³		5.6	6
Cr	1 × 10 ²	7.4	7.4	6
	1 × 10 ³		7.2	8
Fe	2 × 10 ³	8.0	7.9	7
	1 × 10 ⁴		7.7	7
La	5 × 10 ²	8.0	7.9	4
	1 × 10 ³		7.7	5
Nb	1 × 10 ²	7.6	7.4	8
	2 × 10 ²		7.2	10
Mo(W)	1 × 10 ²	5.8	5.7	8
	2 × 10 ²		5.5	9
Re	1 × 10 ²	5.8	5.7	7
	2 × 10 ²		5.4	9

the volume of sample solution and V_2 the eluate volume. Table 2 shows that the elements studied can be concentrated 100-fold; the detection limit can be lowered proportionately.

We have used spectrophotometric methods for the determination of the elements in the concentrates. For determination of Zr, Hf and Th in the concentrates with Arsenazo III, detection limits of 5×10^{-5} μg/ml for Zr, and 1×10^{-4} μg/ml for Hf and Th were attained; for Sc, determined with Xylenol Orange, the limit was 5×10^{-4} μg/ml. The corresponding limits for the direct spectrophotometric determinations without concentration are 5×10^{-3} μg/ml for Zr, 1×10^{-2} μg/ml for Hf and Th¹¹ and 5×10^{-2} μg/ml for Sc.¹²

The high affinity of SCE-SiO₂ for zirconium and hafnium and the differences (Fig. 1a) between the optimal sorption conditions for these elements on the one hand, and for Sc and Ti on the other, make it possible to separate zirconium and hafnium from macroamounts of Sc and Ti (Table 3). Moreover, metal ions such as nickel, cobalt(II), iron(III), aluminium, lanthanum and chromium(III) are not sorbed from 0.1–0.3M hydrochloric acid, and have little influence on the degree of Zr and Hf extraction (Table 3). Zr and Hf can be separated from niobium,

Table 4. Zirconium determination in cast iron by the sorption-spectrophotometric method

Sample	Zr added, %	Zr found, %	S _r , %
1	0.0	1.5×10^{-3}	15
	2.0×10^{-3}	3.3×10^{-3}	13
2	0.0	2.0×10^{-3}	14
	2.0×10^{-3}	3.9×10^{-3}	12
3	0.0	4.5×10^{-4}	28
	5.0×10^{-4}	9.3×10^{-4}	21

molybdenum, tungsten and rhenium in the presence of hydrogen peroxide; 6×10^4 -fold amounts of peroxide have no effect on sorption of Zr and Hf.

By use of selective zirconium extraction on SCE-SiO₂, with a concentration factor of 100, we have developed a sorption-spectrophotometric method for the determination of 10^{-4} – 10^{-3} % zirconium in cast iron (Table 4).

The SCE-SiO₂ sorbent has also been used for the separation of thorium from large amounts of scandium, lanthanum, aluminium, iron(III) and titanium by sorption from 0.2M hydrochloric acid (Table 5).

However, attempts to separate scandium and iron(III) by using SCE-SiO₂ at pH 1–3 failed even at a 1:1 concentration ratio. To improve the sorption selectivity, the system was made 0.02M in sulphosalicylic acid. At pH ≈ 4 iron(III) forms anionic complexes with sulphosalicylic acid, and is not sorbed on SCE-SiO₂ (Table 6). Run 1 shows that the separation is complete at 20:1 Fe:Sc w/w ratio, but at higher ratios the scandium extraction is incomplete (runs 2 and 3).

Determination of zirconium and hafnium in the sorbent phase

Atomic-emission determination. Atomic-emission spectroscopy is one of the possible methods for determination of Zr and Hf when both are present. Sorption and atomic-emission determination of these elements with preconcentration on sorbents with an organic polymer base has its flaws. For instance, chelate-forming sorbents on an organic polymer base, used for extraction of zirconium and hafnium from highly-mineralized water and alloy steel, have to be subjected to ashing prior to atomic-emission determination.⁷ Otherwise, intense ejection of sample occurs in the initial stage of the arcing.

Table 5. Separation of 5 μg of thorium from other elements on SCE-SiO₂

Element	M: Th	Th found,	
		μg	S _r , %
Sc	2 × 10 ²	5.1	5
	1 × 10 ³	4.8	6
La	1 × 10 ³	4.5	5
	2 × 10 ³	4.0	5
Al	1 × 10 ³	4.9	6
	2 × 10 ³	4.7	5
Fe	1 × 10 ³	4.9	4
	5 × 10 ³	4.7	6
Ti	1 × 10 ³	5.0	4
	2 × 10 ³	4.8	5

Table 6. Separation of 13.6 μg of scandium from iron(III) in the presence of sulphosalicylic acid on SCE-SiO₂

Fe added, mg	Sc found, μg	S _r , %
0.3	13.5	6
0.8	11.3	7
1.0	10.1	10

Table 7. Sorption and atomic-emission determination of zirconium and hafnium in alloy steels

Sample	Added, %		Zr found, %	S_r , %	Hf found, %	S_r , %
	Zr	Hf				
1	0	0	2.3×10^{-2}	14	1.8×10^{-1}	07
	2.0×10^{-2}	2.0×10^{-1}	4.1×10^{-2}	11	3.7×10^{-1}	05
2	0	0	2.0×10^{-3}	23	1.4×10^{-2}	16
	2.0×10^{-3}	2.0×10^{-2}	3.8×10^{-3}	23	3.2×10^{-2}	18

Interference from the sorbent base is eliminated when zirconium and hafnium are extracted with SCE-SiO₂, and the concomitant concentration lowers the detection limits. Moreover, the replacement of a complex base by a unified matrix—the sorbent—simplifies standardization and unifies the analysis techniques.

The detection limits of the direct atomic-emission determination, calculated according to Rusanov,¹⁶ are 1.5 µg/ml for Zr and 1.8 µg/µl for Hf. Owing to a concentration coefficient of 10³, the detection limit was lowered to 1 ng/ml for Zr and 2 ng/ml for Hf.

The method developed has been used to determine zirconium and hafnium in alloy steels containing boron, aluminium, titanium, chromium, cobalt, molybdenum, tungsten, rhenium and rare-earth elements. All these elements, which are macro-components, have multiline spectra, which makes the choice of analytical lines difficult and raises the detection limits of direct atomic-emission determination of zirconium and hafnium. Moreover, the interelement effects in this case may lead to shifts in calibration graphs and an increasingly high systematic error in the determination.

The results of spectral Zr and Hf determination in the concentrate were checked by the spiking method. The overall error S_r for Zr and Hf determination in alloy steels is composed of errors pertaining to the sorption concentration, and to the spectral determination (Table 7).

X-Ray fluorescence (XRF) determination. This method is widely used for determining ions sorbed on the surface of modified silica.^{1,17} One source of error in XRF determination is unsuitable chemical composition and physicochemical properties of the test solutions and standards. Selective extraction of Zr on SCE-SiO₂ yields a concentrate suitable for XRF analysis without further treatment. The detection limit for zirconium in the sorbent phase is 30 µg/g. Since a concentration factor of 2×10^3 is attained by

sorption on 0.3 g of sorbent from 600 ml of solution, the relative zirconium detection limit is 15 ng/ml in the sample solution. The XRF method with sorption on SCE-SiO₂ has been used for zirconium determination in synthetic mixtures containing 10⁴-fold amounts of alkali and alkaline-earth metal ions, and 100-fold amounts of tungsten and molybdenum, *i.e.*, those elements that interfere with zirconium determination. The mixtures also included hafnium in 10–100-fold amounts (Table 8).

CONCLUSION

As seen from the data above, the strong acidic cation-exchanger based on silica possesses the following major advantages as compared to other sorbents, notably silica and sorbents with a polymer matrix:

- high rate of attainment of equilibrium;
- high distribution coefficients;
- quantitative elution of sorbed ions with small volumes of eluent.

These features determine the value of SCE-SiO₂ for concentrating, separating and determining scandium, zirconium, hafnium and thorium. Direct element determination in the sorbent phase by various methods, particularly X-ray fluorescence and atomic-emission, looks very promising from the point of view of speed and sensitivity.

REFERENCES

- D. E. Leyden and G. H. Luttrell, *Anal. Chem.*, 1975, **47**, 1612.
- I. P. Alimarin, P. N. Nesterenko and V. M. Ivanov, *Dokl. Akad. Nauk SSSR*, 1983, **271**, 627.
- V. M. Ivanov, G. N. Gorbunova, G. V. Kudryavtsev, G. V. Lisichkin and T. I. Shurupova, *Zh. Analit. Khim.*, 1984, **39**, 504.
- G. V. Lisichkin, G. V. Kudryavtsev and P. N. Nesterenko, *ibid.*, 1983, **38**, 1684.
- K. K. Unger, *Porous Silica*, Elsevier, Amsterdam, 1975.
- J. S. Fritz, D. Gjerde and C. Pohlandt, *Ion Chromatography*, Hüttig Verlag, Heidelberg, 1982.
- S. B. Savvin and G. V. Myasoedova, *Khelatoobrazuyushchie Sorbenty (Chelating Sorbents)*, Nauka, Moscow, 1984.
- M. M. Senyavin (ed.), *Ionny Obmen (Ion Exchange)*, Nauka, Moscow, 1981.
- K. I. Sakodinskii (ed.), *Prikladnaya Khromatografiya (Applied Chromatography)*, Nauka, Moscow, 1984.
- S. Z. Bernadyuk, G. V. Kudryavtsev, S. V. Markin and G. V. Lisichkin, *Zh. Vses. Khim. Obshchest. (USSR)*, 1982, **27**, 586.

Table 8. Sorption and X-ray-fluorescence determination of 100 µg of zirconium in synthetic mixtures

Hf added, µg	Zr found, µg	S_r , %
2×10^2	105	10
1×10^3	95	11
1×10^4	110	15

*Na, Ca, Mg, 2 g; Mo, W, 20 mg.

11. S. B. Savvin, *Organicheskie Reagenty Gruppy Arsenazo III (Organic Arsenazo III Group Reagents)*, Atomizdat, Moscow, 1971.
12. Z. Marczenko, *Spectrophotometric Determination of Elements*, Horwood, Chichester, 1976.
13. A. I. Busev, V. G. Tiptsova and V. M. Ivanov, *Rukovodstvo po Analiticheskoi Khimii Redkikh Elementov (Manual for Analytical Chemistry of Rare Elements)*, 2nd Ed., Khimiya, Moscow, 1978.
14. V. A. Nazarenko, V. P. Antonovich and E. M. Nevskaya, *Gidroliz Ionov Metallov v Razbavlennykh Rastvorakh (Hydrolysis of Metal Ions in Dilute Solutions)*, Atomizdat, Moscow, 1979.
15. T. I. Tikhomirova, I. M. Loskutova, V. I. Fadeeva, I. R. Zmievskaya and G. V. Kudryavtsev, *Zh. Analit. Khim.*, 1984, **39**, 1630.
16. A. K. Rusanov, *Osnovy Kolochestvennogo Spectral'nogo Analiza Rud i Mineralov (Principles of Quantitative Spectral Analysis of Ores and Minerals)*, 2nd Ed., Nedra, Moscow, 1978.
17. D. E. Leyden, G. H. Luttrell, M. K. Nonidez and D. B. Werho, *Anal. Chem.*, 1976, **48**, 67.

ION-SELECTIVE ELECTRODES FOR GOLD AND SILVER DETERMINATION

O. M. PETRUKHIN, E. N. AVDEEVA, YU. V. SHAVNYA
D. I. Mendeleev Moscow Chemical Technology Institute, Moscow, USSR

V. P. YANKAUSKAS, R. M. KAZLAUSKAS
V. Kapsukas Vilnius State University, Vilnius, USSR

A. S. BYCHKOV and YU. A. ZOLOTOV
V. I. Vernadsky Institute of Geochemistry and Analytical Chemistry, Moscow, USSR

Summary—Some new ion-selective electrodes for silver and gold are described. They are based on the ion-associate species formed by the cyanide, chloride or thiourea complexes of the metals, with hydrophobic anions or cations, as appropriate. The electrodes have been applied to the determination of gold and silver in various technological process solutions in industry.

The development of new methods and improvement of the existing ones for determining gold and silver in solutions is still a topical problem. It is particularly necessary to develop selective methods for determining these elements in technological solutions, e.g., those formed in the course of extractive and sorptive recovery of gold, or used in electrolytic baths. One method is to use ion-selective electrodes and is characterized by simplicity, speed and sufficiently high accuracy.

In the present work liquid and film electrodes reversible to complex ions have been investigated. These electrodes have a number of advantages: (1) they can be used to determine metals that form relatively stable complexes; (2) by control of the degree of complexation it is possible to determine the total metal concentration, and not just the concentration of one of its individual forms; (3) converting highly-charged metal aquo-cations into complex anions makes it possible to decrease the ionic charge and thus raise the precision of the potentiometric determination. When choosing complex gold and silver compounds for the electrode-active membranes and the conditions for metal determination we proceeded from the relationships between the analytical characteristics of the electrodes and the factors determining the extraction of the metals as ion-association compounds of their complex ions. This allowed us to use the available data on the extraction of gold and silver complexes, as well as the more general data accumulated in extraction chemistry. Moreover, the choice of complex ions was determined by practical objectives: the need for methods of determining gold(I) and (III) in cyanide, chloride and thiourea solutions and silver(I) in cyanide and thiourea solutions.

In this way we have developed new ion-selective electrodes with respect to $\text{Au}(\text{CN})_2^-$, AuCl_4^- , $\text{Au}(\text{TU})_2^+$, $\text{Ag}(\text{CN})_2^-$ and $\text{Ag}(\text{TU})_n^+$ ions, where TU is thiourea. Silver forms $\text{Ag}(\text{TU})_n^+$ complexes, with overall stability constants $\log \beta_1 = 7.11$, $\log \beta_2 = 10.61$, $\log \beta_3 = 11.73$, $\log \beta_4 = 13.57$, so the composition of a solution containing silver and thiourea will depend on their relative concentrations. It is therefore important to adhere strictly to the conditions specified in this paper, under which the predominant species will be $\text{Ag}(\text{TU})_n^+$; for generality, however, the species will be designated $\text{Ag}(\text{TU})_n^+$. These complex gold and silver ions were combined as ion-associates with hydrophobic cations and anions, such as tetraphenylarsonium (TPA), tetradecylphosphonium (TDP), Crystal Violet (CV), tetranitrodiaminocobaltate (TNDC) and 2,4,6-trinitrophenolate (picrate, Pic).

EXPERIMENTAL

Reagents

Gold(III) chloride solution was prepared by dissolving an accurately weighed quantity of AuCl_3 in 0.1M hydrochloric acid. Solutions of gold and silver cyanide complexes were prepared by dissolving accurately weighed quantities of $\text{KAu}(\text{CN})_2^-$ or $\text{KAg}(\text{CN})_2^-$ in 0.45M sodium sulphate. Gold(I) thiourea solution was prepared by dissolving a weighed quantity of high-purity metallic gold in *aqua regia*, adding concentrated sulphuric acid and heating until a moist residue was left (this step being repeated), the residue being dissolved in 1M sulphuric acid and the corresponding amount of thiourea added. Silver(I) thiourea solution was obtained by dissolving a weighed quantity of chemically pure silver in 6M nitric acid, evaporating the solution to dryness, dissolving the residue, and adding the required amount of thiourea.

Solutions of lower concentration were obtained by appropriate successive dilution. All solutions were prepared in a

background electrolyte of 0.45M sodium sulphate, the salt background and ionic strength of solutions being maintained constant throughout, which made it possible to plot electrode potential *vs.* logarithm of the potential-determining ion concentration for the calibration graphs.

Solutions of potassium chloride, ammonium TNDC, 2,4,6-trinitrophenol (TNP), TDP bromide, TPA chloride, as well as the salts of iron, copper, nickel, zinc and other materials were prepared from accurately weighed quantities of the corresponding compounds. Organic solvents were purified by conventional techniques.¹ All aqueous solutions were prepared with doubly distilled water. Solutions of the following surface-active substances (SAS) were prepared: "Sulphanol" (sodium alkylbenzenesulphonates based on kerosene, $C_nH_{2n+1}C_6H_4SO_3Na$, where $n = 12-18$); "Progress" (sodium sec.-alkylsulphates based on α -olefins of the 320° fraction, $C_nH_{2n+1}CH(CH_3)OSO_3Na$, where $n = 6-16$); highly sulphurized castor oil (HCO) based on the disodium salt of 1-carboxy-8-heptadecen-11-ylsulphuric acid, $CH_3(CH_2)_5CHOSO_3NaCH_2CH=CH(CH_2)_7COONa$, synthesized according to Dauyotis *et al.*, "Nekal", a mixture of dibutyl-naphthalenesulphonates $[(C_6H_5)_2C_{10}H_6SO_3Na]$. Turkey Red oil (TRO), known as alizarin oil, was also used; the most widely used raw material for it is castor oil, consisting of the esters of ricinoleic acid, $CH_3(CH_2)_3CHOHCH_2CH=CH(CH_2)_7COOH$. On treatment with sulphuric acid the castor oil forms an ester, or H_2SO_4 is added across the double bond; in addition to this, the triglycerides are partially or completely saponified and the ricinoleic acid yields formed products of different composition. The SAS concentrations in the solutions, mg/ml, were: "Sulphanol" 2; "Progress" 2; "Nekal" 0.34; HCO 3.9; TRO 10.

Preparation of liquid membranes

Membrane species were prepared by substoichiometric extraction, with the metal concentration exceeding the reagent concentration by an order of magnitude. Gold and silver thiourea complexes were extracted from aqueous solutions of $Au(TU)_2^+$ (pH 4.0) and $Ag(TU)_n^+$ (pH 2.0) in 0.15M sodium sulphate/0.3M thiourea. The acidity was adjusted with 0.1M sulphuric acid. When $[Au(TU)_2^+ - TNDC^-]$ solutions were prepared the aqueous phase contained, besides $Au(TU)_2^+$, the TNDC salt. Extraction was conducted in separating funnels, and after phase-separation the organic phase was filtered through a filter paper and used as the liquid membrane.

Preparation of the plasticized membranes

$TPA^+AuCl_4^-$, $TDP^+Au(CN)_2^-$ and $TDP^+Ag(CN)_2^-$ ionic associates were used as the electrode-active compounds. The ion-associate solution in chloroform was thoroughly stirred with a 10% solution of poly(vinyl chloride) (PVC) in cyclohexanone (CH) or tetrahydrofuran (THF), and dibutyl phthalate (DBP) was added as the plasticizer. After plasticization an elastic film 0.5–0.8 mm thick was glued to the end face of a vinyl plastic or poly(vinyl chloride) tube with PVC solution in CH. The membrane contained the following quantities of components (wt.%): electrode-active substances 0.2–0.5, DPB 68.3–69.8, PVC 29.2–29.9.

Protective films for the $Ag(CN)_2^-$ -selective electrode

To protect the electrode from the action of SAS we used 2-cm diameter discs cut from films of cellophane [lavsan (d-acron), brand XE-56, pore diameter 1.4 μ m]; cellulose acetate, pore size 0.55 and 0.85–0.95 μ m; nitrocellulose, pore diameter 0.4 μ m; "Serva" dialysis bags (FRG), pore size 4.8 nm. To seal the gap between the plasticized membrane and the protective film the latter was fixed on the electrode with a ring.

Measurements of potential

Type pH-121 and pH-340 high impedance pH-meter/voltmeters and an EV-74 universal ion-meter were used for

measuring the e.m.f. of the following galvanic cells.

Ag/AgCl Comparison Liquid Investigated External
solution membrane solution comparison
electrode

Ag/AgCl Comparison Plasticized Investigated External
solution membrane solution comparison
electrode

Solid Plasticized Investigated External
contact membrane solution comparison
electrode

An EVL-IM flow-type Ag/AgCl electrode served as the external comparison electrode. Comparison solutions were: for the $AuCl_4^-$ -selective electrode, a 0.001M gold(III)/0.1M hydrochloric acid/0.6M lithium chloride solution; for the $Au(CN)_2^-$ -selective electrode, a 0.001M solution of $Au(CN)_2^-$ in 0.45M sodium sulphate; for the $Ag(CN)_2^-$ -selective electrode, a 0.001M solution of $Ag(CN)_2^-$ in 0.45M sodium sulphate. The function of a solid contact in the case of the cell without internal comparison solution, was performed by a graphite rod 6 mm in diameter, or a 3 × 3 mm platinum or copper plate. A thoroughly polished end face of the graphite rod or a cleaned platinum or copper surface was brought into direct contact with the plasticized membrane. The response time of membrane potential was studied with a KSP-4 automatic recording potentiometer. A pH-340 millivoltmeter was used as the amplifier. The scheme made it possible to record E *vs.* t 5–10 sec after immersion of the electrodes in the solution investigated. The $K_{m/m}^{pot}$ coefficients were determined graphically by the method of mixed solutions.³

RESULTS AND DISCUSSION

Development of ion-selective electrodes

Choice of the systems. Distribution of the complex ion between the organic phase of the membrane and the aqueous phase is associated with charge-transfer and a potential arising at the interface. That is why the following requirements are imposed on an electrode-active substance: (1) the complex ion must be sufficiently stable in water and in the organic phases; (2) this ion must predominate both in the membrane phase and in the aqueous solution; it is desirable that the ion should have a low charge; (3) the ion distribution coefficient must be sufficiently high, which usually means the ion hydration energy must be low; (4) equilibrium at the interface must be rapidly established when potential measurements are performed.

In their complexing capacity gold and silver behave as soft acids, forming stable complexes with soft bases: CN^- , I^- , SCN^- , thiourea, and others.⁴ In technological solutions gold and silver exist, as a rule, in the form of cationic and anionic complexes with cyanide, thiourea, and halides. "Inactive" solvents, such as nitrobenzene, chloroform, 1,2-dichloroethane and chlorobenzene, extract them with sufficient specificity and high distribution coefficients, in the form of ion-associates with large organic cations or anions. The extraction conditions, *e.g.*, the acidity of the medium, corresponding to predominance of the electrode-active form of the metal ions, determine to a considerable extent the selectivity and efficiency of

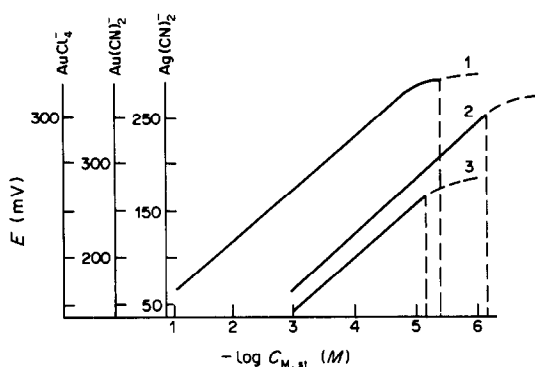


Fig. 1. Electrode function of plasticized electrodes selective for dicyanoargentate (1), tetrachloroaurate (2) and dicyanoaurate (3).

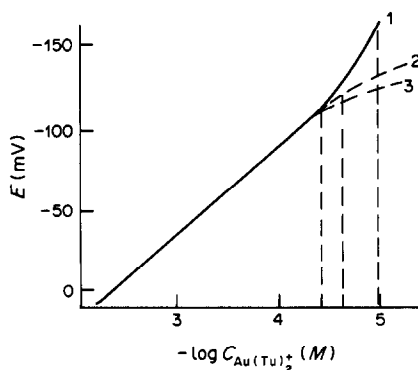


Fig. 3. Solvent effect on detection limit of electrode selective to $Au(TU)_2^+$ ion. Membranes: $1 \times 10^{-3} M [Au(TU)_2^+ Co(NH_3)_2(NO_2)_4^-]$ in nitrobenzene (1), 1,2-dichloroethane (2), chloroform (3). Comparison solution: $[Au(TU)_2]_2SO_4$ in $0.45 M Na_2SO_4$.

the membrane. In these conditions the extent of side-reactions in the aqueous phase is low, and the electrode potential is a function of the total concentration of the metal in solution.

We used the following ion-associates as the electrode-active compounds: $(C_{10}H_{21})_4PAu(CN)_2$, $(C_{10}H_{21})_4PAg(CN)_2$, $(C_6H_5)_4AsAuCl_4$, $(C_6H_5)_4AsAu(CN)_2$, $(C_6H_5)_4AsAg(CN)_2$, $CVAu(CN)_2$, $Au(TU)_2Co(NH_3)_2(NO_2)_4$, $Ag(TU)_nPic$, and others. Chloroform, 1,2-dichloroethane and nitrobenzene served as solvents.

The detection limits of the metals were determined in accordance with IUPAC recommendations.⁵

The principal potentiometric characteristics. The electrode functions $E = f(\log C_m)$ were found to be linear for all the systems, over a broad range of metal concentrations, with close to Nernstian slope (Fig. 1). The increase in e.m.f. with increase in overall metal concentration shows that the electrodes react to complex species. The detection limit depends on the nature of the solvent used for the liquid electrodes, and decreases in the series chloroform > 1,2-dichloroethane > nitrobenzene (Figs. 2 and 3). The

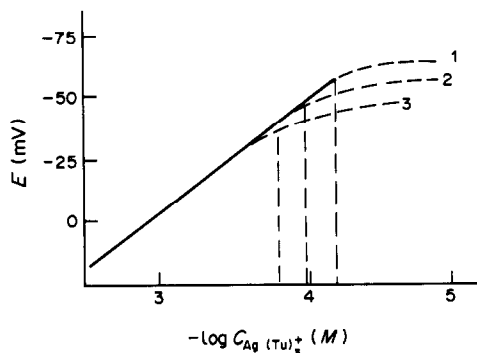


Fig. 2. Solvent effect on detection limit of the electrode selective for $Ag(TU)_n^+$ ion. Membrane: $1 \times 10^{-3} M [Ag(TU)_n^+ Pic^-]$ in nitrobenzene (1), 1,2-dichloroethane (2), chloroform (3). Comparison solution: $[Ag(TU)_n^+]_2SO_4$ in $0.45 M Na_2SO_4$.

distribution coefficients of the metals (extracted as their complex anions) increase in this series. All other things being equal, the detection limit for gold is lower than that for silver, owing to the higher distribution coefficients of the gold complexes. The detection limit also depends on the nature of the organic cation, and for a given solvent decreases in the order $Fe(phen)_3^{2+} > CV^+ > Fe(bphen)_3^{2+} > (C_6H_5)_4As^+ > CH_3(C_8-C_{10})_3N^+$ (Fig. 4), which is the opposite of the order for the cation extractive capacity. A decrease in the electrode-active compound concentration in a liquid membrane results in a decrease in the detection limit. There is, however, a lower limit of liquid ion-exchanger concentration imposed by the increasing time taken for the equilibrium potential to be established, and the growing ohmic resistance of the membrane. The optimum liquid ion-exchanger concentration is $5 \times 10^{-4} - 1 \times 10^{-3} M$.

The detection limit is thus associated with the parameters characterizing the extraction. Deviation of the function from linearity at relatively low con-

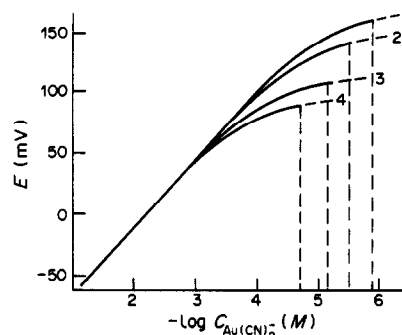


Fig. 4. Effect of the nature of ion-exchanger organic cation on detection limit of electrode selective to $Au(CN)_2^-$ ion. Membrane: $1 \times 10^{-3} M$ Cationⁿ⁺ $[Au(CN)_2^-]_n$ solution in 1,2-dichloroethane. Cations: $CH_3(C_8-C_{10})_3N^+$ (1), $Fe(bphen)_3^{2+}$ (2), Crystal Violet (3), $Fe(phen)_3^{2+}$ (4); (bphen = bathophenanthroline; phen = 1,10-phenanthroline).

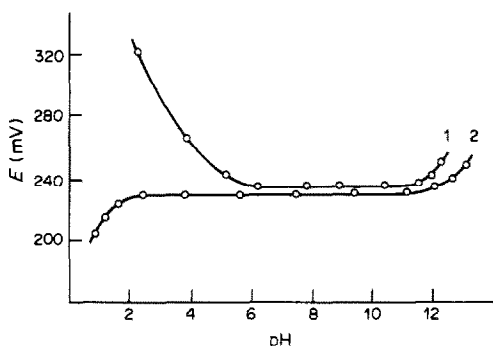


Fig. 5. Effect of pH on the e.m.f. of galvanic cell with electrodes for $\text{Ag}(\text{CN})_2^-$ and $\text{Au}(\text{CN})_2^-$. Membrane: $[\text{TDP}^+\text{Ag}(\text{CN})_2^-]$ (1) or $[\text{TDP}^+\text{Au}(\text{CN})_2^-]$ (2) in poly(vinyl chloride) matrix. Concentration in solutions: silver— $1 \times 10^{-4} M$ (1), gold— $5 \times 10^{-4} M$ (2).

centrations of the potential-determining ions is caused by the ion-exchanger distribution between the organic (electrode membrane) and the aqueous phase, and by its dissociation in the aqueous phase, resulting in an increase in the concentration of the metal-containing ions in the test solution.

The effect of the acidity of the test solution on the e.m.f. of the electrochemical cell with $\text{M}(\text{TU})_n^+$ - and $\text{M}(\text{CN})_2^-$ -selective electrodes is associated with a change in the concentration of the potential-determining ions. The upper limit of the working pH-range is determined by the region of existence of the complex ion in the aqueous phase. The higher stability of gold thiourea and cyanide complexes ($\log \beta_{\text{Au}(\text{TU})_n^+} = 25.3$; $\log \beta_{\text{Au}(\text{CN})_2^-} = 56$), compared to that of the silver complexes ($\log \beta_{\text{Ag}(\text{TU})_n^+} = 13.57$; $\log \beta_{\text{Ag}(\text{CN})_2^-} = 21.1$), causes a wider pH-range within which the e.m.f. of the electrochemical cell remains constant (Figs. 5 and 6). The lower stability of the silver complexes leads to the working pH-interval for the $\text{Ag}(\text{TU})_n^+$ - and $\text{Ag}(\text{CN})_2^-$ -selective electrodes increasing with increase in the concentration of thiourea and cyanide ions in solution. The increase in the e.m.f. of the electrochemical cell in highly acid solutions seems to be explained by the destruction of the electrode-active compounds and a change in the diffusion potential at the test solution/external comparison interface. It is thus seen that, depending on the nature of the complex ion, the electrodes can be used in different media: the electrodes for gold and silver thiourea complexes can be used in solutions with a high concentration of hydrogen ions; the electrodes for cyanide complexes can be used in alkaline solutions.

The electrode systems studied have a high selectivity. An interfering effect is exerted by metals forming stable complexes with the ligands in question and capable of being extracted by the membrane organic phase with high distribution coefficients (Fig. 7). It has been established that the poten-

tiometric selectivity series coincides with the extractability series. The interfering effect decreases in the same order as the extractability of the complexes. Solvent replacement leads to a change in the numerical value of the selectivity coefficients, but the selectivity series remains the same. Potentiometric selectivity is not affected by the nature of the organic cation (anion) and the concentration of ion-exchanger in the membrane. The interfering effect of urea and cyanide ions can be reduced by varying the concentration of hydrogen ions.

The response time of the electrodes depends on the concentration of the potential-determining ions and varies from 5–7 min in the most dilute solutions to 10–20 sec in the solutions of highest concentration. All other things being equal, the response time increases in multi-component solutions, particularly in technological solutions, presumably because of concurrent reactions taking place or a change in the formation rate of the double electrical layer at the interface (Fig. 8).

Comparison of the analytical and performance characteristics of film and liquid electrodes (Table 1) has shown that the detection limits for the metals, slope of the calibration graph, potentiometric selectivity and working pH-range are practically the same for both types of electrodes. The film electrodes, however, have the advantages of ease of handling and manufacture.

Effect of surface-active substances. Numerous technological solutions, in particular those containing silver, include SAS which hinder the analysis.⁶⁻⁸ On prolonged immersion in "Sulphanol", "Progress", "Nekal" and other SAS solutions, the electrode becomes unfit for use. The SAS are slowly desorbed from a plasticized membrane by soaking in $\text{Ag}(\text{CN})_2^-$ solution, but even after prolonged treatment the initial characteristics of the electrode are not completely restored. The strong negative shift of the $\text{Ag}(\text{CN})_2^-$ -selective electrode potential seems to be explained by the fact that the SAS organic anion has

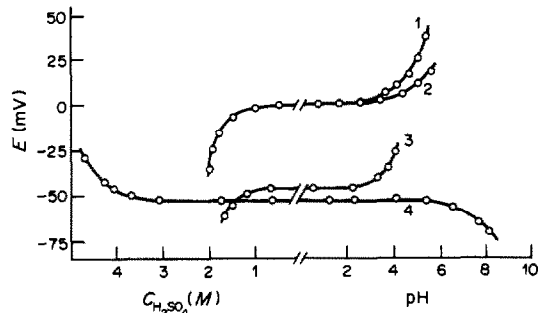


Fig. 6. Effect of pH on the e.m.f. of galvanic cell with electrodes for $\text{Ag}(\text{TU})_n^+$ and $\text{Au}(\text{TU})_2^+$. Membrane: $1 \times 10^{-3} M$ $[\text{Ag}(\text{TU})_n^+ \text{Pic}^-]$ (1–3) or $[\text{Au}(\text{TU})_2^+ \text{Co}(\text{NH}_3)_2(\text{NO}_2)_4^-]$ (4) in nitrobenzene. Concentration in solutions: silver— $1 \times 10^{-3} M$ (1, 2), $1 \times 10^{-4} M$ (3); gold— $5 \times 10^{-4} M$ (4); thiourea— $0.1 M$ (1, 3) and $0.3 M$ (2).

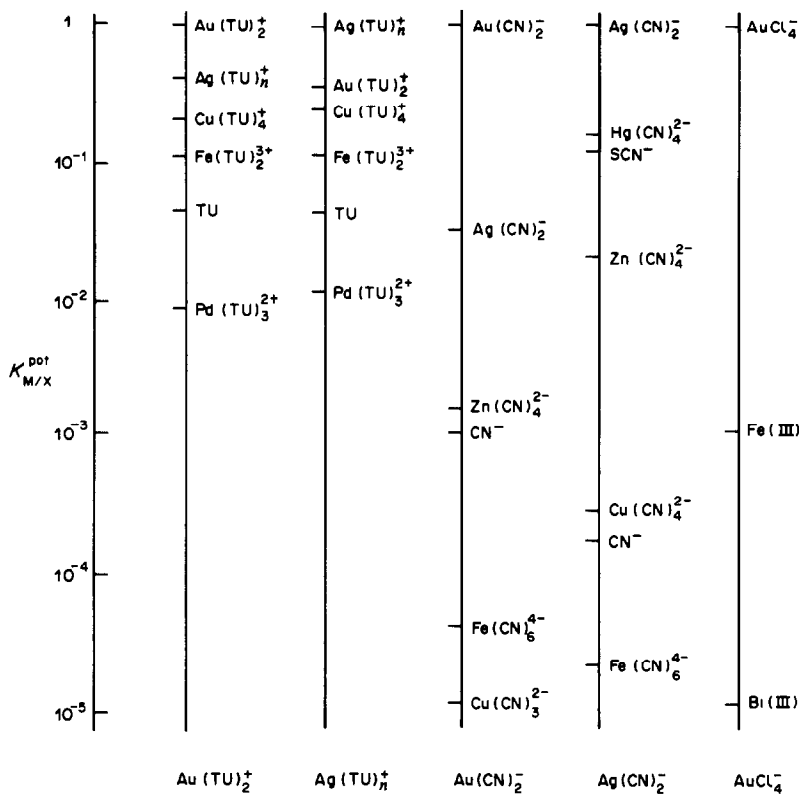


Fig. 7. Selectivity coefficients of AuCl_4^- , $\text{Ag}(\text{CN})_2^-$, $\text{Au}(\text{CN})_2^-$, $\text{Ag}(\text{TU})_n^+$ and $\text{Au}(\text{TU})_2^+$ -selective electrodes, determined by the method of mixed solutions. Conditions of measurement: $\text{Au}(\text{TU})_2^+$ -SE, Ag, Cu, Fe, Pd 0.1M, TU 0.3M, pH 3; $\text{Ag}(\text{TU})_n^+$ -SE, Au, Cu, Fe, Pd 0.1M, Tu 0.3M, pH 2; $\text{Au}(\text{CN})_2^-$ -SE, Ag 0.01M, Zn, Fe, Cu 0.1M, CN^- 0.1M; $\text{Ag}(\text{CN})_2^-$ -SE, Hg, Zn 0.01M, Cu, Fe 0.1M, SCN^- 0.01M, CN^- 0.01M, pH 5-12; AuCl_4^- -SE, Bi, Fe 0.1M, Ce^- 6M, pH 1.

high affinity for the solvent and the membrane electrode-active compound, penetrates into the membrane surface layer, and becomes competitive with $\text{Ag}(\text{CN})_2^-$ ions.

The interfering effect of SAS can be eliminated in two ways: (1) extraction of the SAS from the electro-

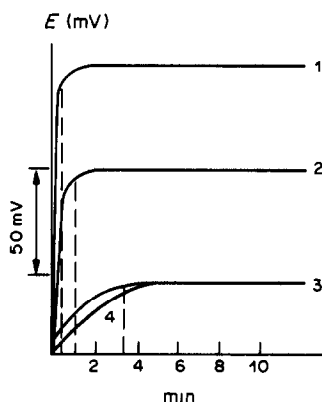


Fig. 8. Time for the establishment of the potential of the plasticized electrode for $\text{Au}(\text{CN})_2^-$ ions in standard (1-3) and process (4) cyanide solutions. Gold concentration (M): 1×10^{-3} (1), 1×10^{-4} (2) and 1×10^{-5} (3, 4).

lyte with coagulants, e.g., calcium aluminate or activated charcoal;⁹ (2) the use of protective films. Calcium aluminate has been shown to precipitate SAS slowly and incompletely, and the time for silver determination increases to 1 hr. Activated charcoal adsorbs $\text{Ag}(\text{CN})_2^-$ as well as SAS. Having decided to use protective films, we first established their influence on the detection limit and response time of the $\text{Ag}(\text{CN})_2^-$ -selective electrode. The hydrophilic properties of the films used decrease in the order cellophane > dialysis bag > nitrocellulose > cellulose acetate > lavsan (dacron). Before work the plasticized electrode together with the protective film was soaked in 0.01M $\text{KAg}(\text{CN})_2$ solution for 1 hr. The protective properties of the films were investigated at a constant SAS concentration and a variable concentration of the potential-determining ion.

The protective properties of the films can be tentatively explained on the basis of current concepts of the structure of electrolyte solutions, and of the capillary-filtration model for separating mixtures of substances by reverse osmosis and ultrafiltration.¹⁰ On the surface and inside the pores of a lyophilic membrane immersed in electrolyte solution a layer of bound water is formed, which, not being a solvent for

Table 1. Properties of ion-selective electrodes

Ion determined	Ion-exchanger	Solvent*	Lower detection limit, <i>M</i>	Operating range of acidity or pH
Liquid electrodes				
Au(TU) ₂ ⁺	Au(TU) ₂ ⁺ Co(NH ₃) ₂ (NO ₂) ₄ ⁻	CB	3.2 × 10 ⁻⁵	4 <i>M</i> H ₂ SO ₄ -pH 4.0
		DCE	5.5 × 10 ⁻⁵	4 <i>M</i> H ₂ SO ₄ -pH 4.0
		NB	1.0 × 10 ⁻⁵	4 <i>M</i> H ₂ SO ₄ -pH 4.0
Ag(TU) _n ⁺	Au(TU) ₂ ⁺ Pic ⁻	NB	9.9 × 10 ⁻⁴	4 <i>M</i> H ₂ SO ₄ -pH 4.0
		CB	2.8 × 10 ⁻⁴	1 <i>M</i> H ₂ SO ₄ -pH 3.0
		DCE	1.2 × 10 ⁻⁴	1 <i>M</i> H ₂ SO ₄ -pH 3.0
Au(CN) ₂ ⁻	(C ₆ H ₅) ₄ As ⁺ Au(CN) ₂ ⁻	NB	7.2 × 10 ⁻⁵	1 <i>M</i> H ₂ SO ₄ -pH 3.0
		NB	1.0 × 10 ⁻⁶	2.5-11.5
		DCE	6.8 × 10 ⁻⁶	2.5-11.5
Ag(CN) ₂ ⁻	(C ₆ H ₅) ₄ As ⁺ Ag(CN) ₂ ⁻	CL	1.0 × 10 ⁻⁵	2.5-11.5
		NB	3.0 × 10 ⁻⁶	6.0-11.0
		DCE	1.8 × 10 ⁻⁵	6.0-11.0
AuCl ₄ ⁻	(C ₆ H ₅) ₄ As ⁺ AuCl ₄ ⁻	CL	4.8 × 10 ⁻⁵	6.0-11.0
		DCE	8.2 × 10 ⁻⁶	2.3-3.5
		CL	8.4 × 10 ⁻⁵	2.3-3.5
Film electrodes				
Au(CN) ₂ ⁻	(C ₁₀ H ₂₁) ₄ P ⁺ Au(CN) ₂ ⁻	DBP	9.9 × 10 ⁻⁶	2.5-11.5
AuCl ₄ ⁻	(C ₆ H ₅) ₄ As ⁺ AuCl ₄ ⁻	DBP	1.1 × 10 ⁻⁶	1.0-3.5
Ag(CN) ₂ ⁻	(C ₁₀ H ₂₁) ₄ P ⁺ Ag(CN) ₂ ⁻	DBP	5.2 × 10 ⁻⁶	6.5-12.0

*CB—chlorobenzene, DCE—1,2-dichloroethane, NB—nitrobenzene, CL—chloroform, DBP—dibutylphthalate.

the substances in question, prevents their penetration into the membrane, and hence determines its selectivity. Moreover, at the film-solution interface the SAS molecules are orientated as a result of the surface activity of the dissolved molecules. The hydrophobic part of the molecule, directed towards the membrane surface, and its hydrophilic part, directed into the solution under the influence of hydration forces, form an additional SAS layer playing a significant part in the SAS penetration. The amount of SAS in the hydrophilic surface of the film reaches its maximum when the equilibrium solution concentration approaches the critical concentration for

micelle formation. The surface hydroxyl groups of the protective films form hydrogen bonds with water molecules, with an energy close to 20–22 kJ/mole.¹¹ This value exceeds the decrease of molar free energy on dispersive interaction of the hydrocarbon moieties of the SAS ions with the atoms of the surface of the hydrophilic films, and so the SAS hydrocarbon chains cannot be sorbed at the sites on the surface occupied by hydroxylic groups.

Figure 9 presents the data on the electrode performance with and without use of a protective film. The effectiveness of using films was estimated from the ratio of the detection limits in the presence of

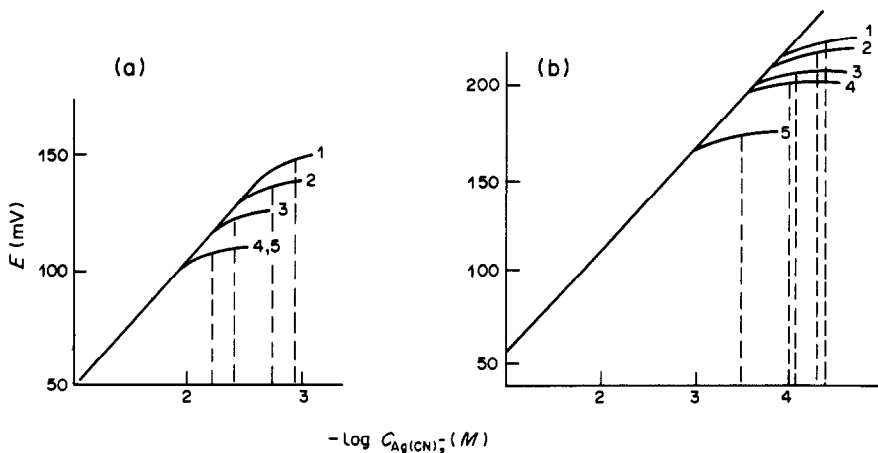


Fig. 9. SAS effect on the electrode function of electrode for Ag(CN)₂⁻ without (a) and with a protective film (b). (a)—SAS concentration, mg/ml: 1—0.25 (Sulphanol), 2—0.39 (HCO), 3—2.0 (RTO), 4—0.034 (Nekal), 5—0.05 (Progress). (b)—Sulphanol; film: 1—cellulose acetate, 2—nitrocellulose, 3—cellophane, 4—lavsan, 5—dialysis bag.

Table 2. Ratio of electrode detection limits for $\text{Ag}(\text{CN})_2^-$ in the presence of SAS without use of a protective film to those found by use of a protective film

SAS	Cellophane	Lavsan	Cellulose acetate (0.55 μm)	Cellulose acetate (0.9 μm)	Nitrocellulose	Dialysis bag
"Sulphanol"	12.1	9.1	22.9	14.5	18.4	2.9
"Progress"	21.6	34.8	21.0	12.3	4.4	13.2
HCO	10.0	1.5	10.5	8.3	2.0	5.0
"Nekal"	8.3	1.3	17.4	4.2	5.0	7.3
TRO	19.9	12.6	2.0	1.6	4.4	4.5

SAS, with and without the protective films. The results are listed in Table 2. Films made of cellophane, lavsan and cellulose acetate proved to be effective. When choosing the protective film, to eliminate the interfering action of SAS it is necessary to take into account, apart from the sieving effect, the interaction of the film with the SAS.

New electrodes. The investigations served as the basis for the development of new ion-selective electrodes. The following electrodes have good performance characteristics.

1. Electrode with a liquid membrane based on tetraphenylarsonium dicyanoaurate in 1,2-dichloroethane, selective with respect to the $\text{Au}(\text{CN})_2^-$ ion.

2. Film electrode based on tetradecylphosphonium dicyanoaurate, selective with respect to the $\text{Au}(\text{CN})_2^-$ ion.

3. Electrode with a liquid membrane based on tetraphenylarsonium tetrachloroaurate in 1,2-dichloroethane, selective with respect to the AuCl_4^- ion.

4. Film electrode based on tetraphenylarsonium tetrachloroaurate, selective with respect to the AuCl_4^- ion.

5. Electrode with a liquid membrane based on the ion-associate $\text{Au}(\text{TU})_2^+ \text{Co}(\text{NH}_3)_2(\text{NO}_2)_4^-$ in nitrobenzene, selective with respect to the $\text{Au}(\text{TU})_2^+$ ion.

6. Film electrode based on tetradecylphosphonium dicyanoargentate, selective with respect to the $\text{Ag}(\text{CN})_2^-$ ion.

7. Electrode with a liquid membrane based on the ion-associate $\text{Ag}(\text{TU})_n^+ \text{Pic}^-$, selective with respect to the $\text{Ag}(\text{TU})_n^+$ ion.

DETERMINATION OF GOLD AND SILVER

These electrodes have been used to develop techniques for determining gold and silver in a broad concentration range in solutions of complex composition: citrate and cyanide gilding electrolytes, technological and waste thiourea and cyanide solutions from gold-extraction plants, chloride gold solutions, cyanide and dicyanoargentate-thiocyanate silvering solutions. The accuracy and precision satisfy technological control requirements and the methods have been introduced into practice at numerous plants. Some of them are described below.

Determination of gold in citrate gilding electrolytes

The electrode with a liquid membrane based on 0.001M tetraphenylarsonium dicyanoaurate in 1,2-dichloroethane was used for gold determination in citrate gilding electrolytes. These electrolytes comprise $\text{KAu}(\text{CN})_2$ solutions in a mixture of potassium citrate (75 g/l. $\text{K}_3\text{C}_6\text{H}_5\text{O}_7 \cdot \text{H}_2\text{O}$) and citric acid (20 g/l. $\text{H}_3\text{C}_6\text{H}_5\text{O}_7 \cdot \text{H}_2\text{O}$), and containing as impurities Na, Mg, Ag, Mn, Fe, Cu, Bi, Al (10^{-3} – 10^{-4} M). The concentration of gold, impurities and base electrolyte changes in the course of cell operation. The analysis was performed by the calibration graph method.⁵ Standard gold solutions (20 mg/ml) were prepared in pH 5.05 citrate buffer.

To determine gold, 0.5 ml of test solution was transferred into a 25-ml standard flask and diluted to the mark with citrate buffer solution. After equilibrium had been established the e.m.f. was measured.

When gold was determined in gilding electrolytes that had been used for a long time the results were improved by adding small quantities of oxalic acid (0.2 g per 25 ml) to the flask prior to sample dilution.

Replicate analyses of samples with different gold concentrations gave a relative standard deviation of 2–3% (Table 3), and the results were in good agreement with those of gravimetric determination by reduction with thioglycolic acid in 6M hydrochloric acid medium, cupellation, and weighing as the metal. The potentiometric method is much simpler and

Table 3. Results of gold determination in citrate gilding electrolytes, mg/ml

$\bar{X} \pm \frac{t_p S^\dagger}{\sqrt{n}}$	Potentiometric method ($n = 9$; $P = 0.95$; $t_p = 2.31$)		Gravimetric method ($n = 3$)
	$S_r, \%$	$S_r, \%$	
3.90 \pm 0.05	2	3.96	
5.46 \pm 0.09	2	5.46	
6.30 \pm 0.13	3	6.17	
7.09 \pm 0.09	2	7.03	
8.17 \pm 0.14	2	8.17	
8.40 \pm 0.13	2	8.37	
9.96 \pm 0.19	3	9.87	
10.08 \pm 0.14	2	10.02	
10.28 \pm 0.13	2	10.36	
13.38 \pm 0.22	2	13.30	
16.69 \pm 0.32	3	16.38	

$^\dagger S$ = standard deviation.

$^\S S_r$ = relative standard deviation.

Table 4. Results of gold and silver determination ($\mu\text{g/ml}$) in the liquid phase of cyanide pulps ($n = 5$, $P = 0.95$, $t_p = 2.78$)

Quantity of gold found			Quantity of silver found		
Potentiometric method Electrode for $\text{Au}(\text{CN})_2^-$			Potentiometric method		
$\bar{X} \pm \frac{t_p S}{\sqrt{n}}$	$S_r, \%$	Atomic-absorption method	$\bar{X} \pm \frac{t_p S}{\sqrt{n}}$	$S_r, \%$	Atomic-absorption method
1.45 ± 0.30	25	1.35	5.6 ± 0.5	30	5.8
1.85 ± 0.32	20	2.10	8.9 ± 1.0	28	11.0
2.00 ± 0.20	20	1.75	5.8 ± 0.5	25	5.2
2.40 ± 0.28	24	2.50	13.5 ± 0.8	30	15.2
2.70 ± 0.20	17	3.20	19.8 ± 1.5	20	23.4

faster, and has satisfactory accuracy and reproducibility.

Determination of gold and silver in cyanide solutions. To determine gold and silver in cyanide solutions one $\text{Au}(\text{CN})_2^-$ -selective film electrode was used. The silver concentration was determined by the difference between the e.m.f. values of two measurements:

$$C_{\text{Ag}} = \frac{C_{\text{Au}}}{K_{\text{Au/Ag}}} (10^{\Delta E/s} - 1),$$

where $\Delta E = E_2 - E_1$, E_1 and E_2 being the e.m.f. before (E_1) and after (E_2) acidification of the sample, $K_{\text{Au/Ag}}$ is a constant* depending on the pH of the solutions and s is the slope of the calibration graph.

A 25-ml portion of sample solution was placed in a polyethylene measuring cell, sodium sulphate was added to give 0.45M concentration and dissolved, and E_1 was measured. The solution was then acidified to pH 3.5 by addition of concentrated sulphuric acid and E_2 was measured. The value of E_2 gave the gold concentration, and the silver concentration was found from the equation above. The e.m.f. readings were taken 5 min after immersion of the electrodes in the test solution.

The results thus obtained for gold and silver in the liquid phase of the pulp formed in sorptive extraction of the metal had relative standard deviations (S_r) of 17–25% and 20–30%, respectively, and were in agreement with the results of atomic-absorption analysis (Table 4). The proposed method satisfies the requirements of production control at the low levels concerned.

Determination of gold in cyanide solutions of gold-extracting plants. The electrode with 0.01M tetraphenylarsonium dicyanoaurate solution in nitrobenzene as the liquid membrane was used to determine gold in the process and waste solutions of gold-extracting plants. At such plants it is necessary to control the gold content at several points of the

process: (1) in the liquid phase of the pulp during cyanide complexation and sorption, (2) in the solutions after elution or stripping, and (3) in the waste solutions. The wide range of gold concentrations in these solutions (2×10^{-5} –1 g/l.) requires the use of different methods of potentiometric control.

To determine gold, a known volume of test solution, acidified with concentrated sulphuric acid to pH 3, was placed in a measuring cell, and sodium sulphate solution was added till the Na_2SO_4 concentration was 0.45M. The e.m.f. was measured 3 min after immersion of the electrodes in the solution. The results for gold have good reproducibility (Table 5, $S_r = 2$ –6%) and show satisfactory agreement with the atomic-absorption analysis results. However, when gold is determined in the liquid phase of the pulp in the cyanide treatment, a large discrepancy is observed between the results of potentiometric and atomic-absorption analysis, and the reproducibility becomes much poorer ($S_r = 14$ –27%), but even in this case the proposed method satisfies the requirements of production control.

To improve the reproducibility of gold determination in the liquid phase of the pulp, two variants of the method of standard additions were used.

(1) Two equal portions (0.04 ml of each) of standard $5 \times 10^{-3}M$ $\text{NaAu}(\text{CN})_2$ solution (method of double additions) were successively added, with constant stirring, to 25 ml of test solution. The gold concentration (C_x) was found with the help of tables of $R = f(C_x/\Delta C)$. The value of R was calculated from the equation

$$R = \frac{E_2 - E}{E_1 - E} = \frac{\log \left(\frac{C_x + 2\Delta C}{C_x} \right)}{\log \left(\frac{C_x + \Delta C}{C_x} \right)},$$

where E , E_1 and E_2 are the e.m.f. values for the sample and after the introduction of the first and the second addition, respectively; ΔC is the increment in gold concentration due to the addition.

(2) Portions of 0.04–0.1 ml of standard $5 \times 10^{-3}M$ $\text{NaAu}(\text{CN})_2$ solution were added to the test solution with constant stirring. Each addition (ΔC) caused a

* $K_{\text{Au/Ag}}$ is the selectivity coefficient $K_{\text{Au}(\text{CN})_2^-/\text{Ag}(\text{CN})_2^-}$, the value of which depends on pH [which affects the conditional stability of the $\text{Ag}(\text{CN})_2^-$ complex].

Table 5. Results of gold determination in process solutions of gold-extraction plants, mg/ml

Substance analysed	Potentiometric method ($n = 10, P = 0.95, t_p = 2.26$)		
	$\bar{X} \pm \frac{t_p S}{\sqrt{n}}$	$S_r, \%$	Atomic-absorption method
Liquid phase of pulp during cyanide complexation	$(1.20 \pm 0.23) \times 10^{-3}$	27	1.0×10^{-3}
	$(1.46 \pm 0.15) \times 10^{-3}$	14	1.9×10^{-3}
	$(1.62 \pm 0.35) \times 10^{-3}$ *	17	2.0×10^{-3}
	$(1.95 \pm 0.32) \times 10^{-3}$	14	2.6×10^{-3}
	0.91 ± 0.02	4	0.82
Solutions after stripping	1.09 ± 0.03	4	1.13
	1.24 ± 0.09 *	6	1.27
	1.36 ± 0.06	6	1.38
	1.38 ± 0.03	3	1.32
	1.52 ± 0.04	2	1.60

*Mean values for results of five measurements ($n = 5, P = 0.95, t_p = 2.78$).

change (ΔE) in the e.m.f. of 7–10 mV. Additions were continued until the total e.m.f. change reached 40 mV (which required less than 1 ml of standard solution). The gold concentration (C_x) and the electrode function slope (s) were found by calculating

$$E = f(\Delta C) = S \log \left(\frac{C_x + \Delta C}{C_x} \right)$$

by the least-squares method on a computer.

The results obtained by both variants had better reproducibility ($S_r \leq 8\%$) and agreed well. The analysis took about 30 min. The method of standard additions not only improves the reproducibility but also makes it possible to use the $\text{Au}(\text{CN})_2^-$ -selective electrode without preliminary calibration with standard solutions.

For the $\text{Au}(\text{CN})_2^-$ waste solutions the selective electrode was used only to indicate whether the concentration was above or below a preselected level.

The $\text{Au}(\text{CN})_2^-$ -selective electrode can be used for laboratory and continuous automatic control of the gold content in the process and waste solutions of gold-extracting plants.

Determination of gold(III) in chloride solutions. With the plasticized AuCl_4^- -selective electrode

gold(III) was determined in chloride solutions containing copper(II), nickel, platinum(II) and palladium. Such problems arise in the analysis of gold concentrates and alloys. Known volumes of solutions with a known concentration of copper, nickel, platinum and palladium were added to standard AuCl_3 solutions in 0.1M hydrochloric acid. The $\text{TPA}^+\text{AuCl}_4^-$ ion-associate served as the electrode-active compound in the AuCl_4^- -selective electrode. The correctness of analysis was estimated by the t -criterion; S_r was 2–6% (Table 6).

Determination of gold and silver jointly present in thiourea solutions. Since gold has a large interfering effect on silver determination in thiourea solutions, direct silver determination is possible only with the use of some calculations, which fortunately are rather simple. The method is based on measuring simultaneously the potentials of $\text{Au}(\text{TU})_2^+$ [electrode-active compound the $\text{Au}(\text{TU})_2^+\text{Co}(\text{NH}_3)_2(\text{NO}_2)_4^-$ ion-associate dissolved in benzene], $\text{Ag}(\text{TU})_3^+$ - and TU-selective electrodes in the sample and standard solutions [the TU-selective electrode¹² is used because the TU concentration limits the range of the $\text{Ag}(\text{TU})_3^+$ -selective electrode and needs to be measured]. In the general form the e.m.f. of a cell with such ion-selective electrodes can be described by the

Table 6. Results of gold determination in model solutions (mg/ml) ($n = 9, P = 0.95, t_p = 2.31$)

Molar ratio of metals in solutions	Gold introduced, $10^2 x$	Gold found, $\left(\bar{x} \pm \frac{t_p S}{\sqrt{n}} \right) 10^2$	$S_r, \%$	t_{exp}
Au:Cu = 1:10	1.97	1.93 ± 0.07	4	1.29
Au:Cu = 1:10	0.20	0.20 ± 0.00	2	1.15
Au:Cu = 1:10	0.02	0.02 ± 0.00	5	1.66
Au:Cu:Ni = 1:10:10	1.97	1.88 ± 0.06	4	0.26
Au:Cu:Ni = 1:10:10	0.20	0.21 ± 0.01	3	0.03
Au:Cu:Ni = 1:10:10	0.02	0.02 ± 0.00	6	0.26
Au:Pt = 1:1	1.97	1.96 ± 0.04	3	0.52
Au:Pt = 1:10	1.97	1.97 ± 0.06	4	0.05
Au:Pt = 1:10	1.97	1.92 ± 0.08	5	1.42

Table 7. Results of silver and potassium thiocyanate determination (mg/ml) in silvering electrolytes containing $\text{Ag}(\text{CN})_2^-$

Silver			Thiocyanate		
Potentiometric method ($n = 9$)		Thiocyanate method ($n = 3$)	Potentiometric method ($n = 9$)		Reverse titration ($n = 3$)
$\bar{x} \pm \frac{t_p S}{\sqrt{n}}$	$S_r, \%$		$\bar{x} \pm \frac{t_p S}{\sqrt{n}}$	$S_r, \%$	
26.8 ± 0.5	2.5	27.2	143.7 ± 2.4	2.1	135.2
18.5 ± 0.6	3.4	18.2	84.4 ± 1.6	2.4	80.3
22.7 ± 0.5	2.7	22.0	100.1 ± 1.5	2.0	97.2

following set of linear equations:

$$Y_{\text{Au}(\text{TU})_2^+} = C_{\text{Au}(\text{TU})_2^+} + \Sigma K_{\text{Au}/\text{M}_i^+}^{\text{pot}} + C_{\text{M}_i^{1/2+}}^{1/2+}$$

$$Y_{\text{Ag}(\text{TU})_n^+} = C_{\text{Ag}(\text{TU})_n^+} + \Sigma K_{\text{Ag}/\text{M}_i^+}^{\text{pot}} + C_i^{1/2+}$$

where $Y_{\text{M}(\text{TU})_n^+} = C_{\text{M}(\text{TU})_n^+, \text{st}} \exp[\Delta E/n]$, and ΔE is the difference in potential of the $\text{M}(\text{TU})_n^+$ -selective electrode, measured in the test solution and standard solutions of similar composition.

The $\Sigma K^{\text{pot}} C^{1/2+}$ values depend on the number of interfering ions. The potential of the $\text{M}(\text{TU})_n^+$ -selective electrode depends on both the $\text{M}(\text{TU})_n^+$ concentration and the concentration of extraneous M_i^{z+} ions. The maximum value of the deviation of concentrations ($\Delta C_{\text{M}_i}^{z+}$) from the average $\bar{C}_{\text{M}_i}^{z+}$ can be estimated from

$$\Delta C_{\text{M}_i}^{z+} = \frac{C_{(+)} - C_{(-)}}{2}$$

where $C_{(+)}$ and $C_{(-)}$ are the upper and lower limits of the extraneous ion concentration in the solution. The number and admissible concentration of interfering ions are determined by the analytical accuracy required. It has been established that errors caused by the presence of Zn(II), Fe(III) and Fe(II) are insignificant, at least within the range of their concentration in the process solutions. The expressions for the apparent concentrations in solutions at pH 2–3 are

$$C'_{\text{Au}(\text{TU})_2^+} = C_{\text{Au}} + 0.38C_{\text{Ag}(\text{TU})_n^+} + 0.18C_{\text{Cu}(\text{TU})_2^+}$$

$$C'_{\text{Ag}(\text{TU})_n^+} = C_{\text{Ag}} + 0.53C_{\text{Au}(\text{TU})_2^+} + 0.30C_{\text{Cu}(\text{TU})_2^+}$$

Solution of the set of equations for the boundary conditions makes it possible to find mutually consistent values of the coefficients and use them in formulae to calculate the gold and silver concentrations when they are present together:

$$C_{\text{Au}} = Y_{\text{Au}(\text{TU})_2^+} + 0.219 Y_{\text{Ag}(\text{TU})_n^+}$$

$$C_{\text{Ag}} = Y_{\text{Ag}(\text{TU})_n^+} + 0.470 Y_{\text{Au}(\text{TU})_2^+} + 0.0182$$

The results have satisfactory reproducibility and the proposed technique is sufficiently selective.

Determination of silver and thiocyanate in dicyanoargentate–thiocyanate silvering electrolytes. The total concentration of dicyanoargentate and

thiocyanate ions is determined with the help of the $\text{Ag}(\text{CN})_2^-$ -selective film electrode. The dicyanoargentate complex is then broken up with sodium sulphide, and the thiocyanate ions are determined with an SCN^- -selective electrode (NPO "Analitpribor", Tbilisi). The concentration of $\text{Ag}(\text{CN})_2^-$ ions is then calculated from

$$C_{\text{Ag}(\text{CN})_2^-} = C_{\text{Ag}(\text{CN})_2^- + \text{SCN}^-} - K_{\text{Ag}(\text{CN})_2^- / \text{SCN}^-} C_{\text{SCN}^-},$$

where $K_{\text{Ag}(\text{CN})_2^- / \text{SCN}^-}$ is the $\text{Ag}(\text{CN})_2^-$ -selective electrode selectivity co-efficient, equal to 0.128 ± 0.01 .

Standard silver solution (0.1M) was prepared by dissolving $\text{KAg}(\text{CN})_2$ in 0.45M sodium sulphate and adding a standard potassium thiocyanate solution to give 0.1M thiocyanate concentration. The salt content and ionic strength of the solutions were kept constant.

One ml of tenfold diluted electrolyte was placed in a 50-ml standard flask, 25 ml of 0.9M sodium sulphate were added and then water up to the mark. The solution was transferred to a beaker and stirred, and the $\text{Ag}(\text{CN})_2^-$ -selective electrode and a reference electrode were immersed in it. Three minutes later the e.m.f. was measured and $C_{\text{Ag}(\text{CN})_2^- + \text{SCN}^-}$ was found from a calibration graph. Then 0.1 ml of 1M sodium sulphide was added and the concentration of thiocyanate was determined with the SCN^- -selective electrode and a calibration graph, and $C_{\text{Ag}(\text{CN})_2^-}$ was calculated as shown above. The analysis of a single sample takes 20 min. Results are given in Table 7. The method can serve as the basis for continuous automatic control of the content of silver and thiocyanate.

REFERENCES

1. A. Weissberger, E. Proskauer, G. Riddick and E. Toops, *Organic Solvents: Physical Properties and Methods of Purification*. Interscience, New York, 1955.
2. V. E. Dauyotis, R. S. Martinkus, T. Yu. Yankauskas and P. P. Dobrovolskis, *Auth. Cert. USSR No. 690010, Bullizobr.*, 1979, No. 37.
3. K. Srinivasan and G. A. Rechnitz, *Anal. Chem.*, 1969, **41**, 1203.
4. J. Inczedy, *Analytical Applications of Complex Equilibria*, Horwood, Chichester, 1976.
5. K. Cammann, *Das Arbeiten mit Ionenselectiven Elektroden*, 2nd Ed., Springer, Berlin, 1977.
6. S. V. Timofeev, Ye. A. Materova, L. K. Arkhangelskii and Ye. V. Chirkova, *Vestn. Leningr. Univ., Fiz. Khim.*, 1978, **16**, No. 3, 139.

7. R. A. Llenado, *Anal. Chem.* 1975, **47**, 2243.
8. A. Craggs, G. I. Moody, J. D. R. Thomas and B. I. Birch, *Analyst*, 1980, **105**, 426.
9. A. M. Kochanovskii and N. A. Klimenko, *Physico-Chemical Fundamentals of Extracting Surface-Active Substances from Aqueous Solutions and Effluents*, p. 176. Naukova dumka, Kiev, 1978.
10. Yu. I. Dytnerskii, *Reversed Osmosis and Ultrafiltration*, p. 352. Khimiya, Moscow, 1978.
11. N. I. Nikolayev, *Diffusion in Membranes*, pp. 232. Khimiya, Moscow, 1980.
12. A. V. Gordiyevskii, O. V. Zemskaya, N. I. Savvin, V. S. Shterman and A. Ya. Syrchenkov, *Zh. Analit. Khim.*, 1974, **29**, 164.

THE ANALYSIS OF SOLID AND LIQUID HIGH-PURITY SUBSTANCES

G. G. DEVYATYKH

Institute of Chemistry, USSR Academy of Sciences, Gorky, USSR

YU. A. KARPOV

All-Union Institute Giredmet, Moscow, USSR

(Received 15 October 1985. Revised 3 February 1986. Accepted 14 August 1986)

Summary—This paper reviews the problems of atomic-spectrometry, mass-spectrometry and activation methods in elemental analysis of high-purity substances. The specific techniques of sample preparation, preconcentration of impurities and the determination of gas-forming trace elements are discussed.

High-purity substances have been attracting the attention of scientists for more than half a century. The chemical purity of materials is often the main criterion for their applicability in new fields of science and engineering. The purity required is constantly increasing. In the '40s the limiting impurity level was 10^{-4} – $10^{-3}\%$, in the '50s 10^{-5} – $10^{-4}\%$, in the '60s 10^{-7} – $10^{-6}\%$ and nowadays a number of materials require an individual impurity content of not more than 10^{-8} – $10^{-7}\%$ and sometimes even less (down to $10^{-11}\%$), with a total impurities level of 10^{-7} – $10^{-5}\%$.

Analytical control is an integral part of preparation of high-purity substances since the total impurity content is generally taken as the main criterion of purity, mainly because of the practical impossibility of achieving a precision of even 1 part in 10^6 in determination of the matrix material. Attempts to measure purity by means of physical properties, such as the residual electrical resistance of metals at low temperatures,¹ have failed to give the results hoped for, owing to the dependence of these properties not only on composition but also on the perfection of the sample crystalline structure, on impurity inclusions, and on the chemical form of impurities.

The impurity composition of a substance is usually determined by several methods of analysis, one being of multi-element or survey nature and the others chosen for their selectivity and sensitivity or to detect components not found by the survey method.² Procedures for estimating total impurity concentration in a sample by means of an incomplete analytical data set are being developed.³

Proof of the precision of a determination is the main problem in the analysis of high-purity substances. An analysis is often performed at the limits of detection of the methods used, and even a slight departure from the correct procedure may lead to appreciable error. Specific methods are applied for precision control. In particular, in the methods based on recovery of known amounts of added materials,

preference is given to use of the radioactive and less-common stable isotopes of the analytes, which makes it possible to introduce a very small amount of the impurity of interest without the danger of contamination. To introduce a trace of an analyte into the sample the ion implantation method is generally used, but even in this case there is a high probability of error. Therefore it is recommended to use several techniques simultaneously. Table 1 shows the results of analysis for the iron content of germanium dioxide by different methods. Comparatively high reproducibility is obtained.

Multi-element methods of analysis

Multi-element methods include spark-source mass-spectrometry, atomic spectrometry and activation analysis; single-element methods include electrochemical, spectrophotometric and kinetic methods.⁴⁻⁹ Let us consider the trends in development of the most widely used multi-element methods. Some aspects of this problem are discussed in a number of monographs¹⁰⁻¹³ and reviews.^{14,15}

Atomic-spectrometry methods—emission, absorption and fluorescence spectrometry—are widely used to detect the impurities in high-purity substances. The application of atomic-emission methods with an arc source and of atomic-absorption methods with electrothermal atomizers is especially effective in conjunction with preconcentration of impurities; in this case preference is given to physicochemical methods which do not require chemical reagents^{16,17} or use them in minimum (stoichiometric) amount.¹⁸ Concentration of impurities on a collector (most often on graphite powder) or directly in a graphite-electrode crater, makes it possible to use spectral reference samples (standards) prepared from metal salt solutions in acids or water. Another advantage of preconcentration is that it decreases the fluctuation in results that arises from inhomogeneous distribution of the impurities in the sample. The drawbacks are

Table 1. Comparative results for the iron content in high-purity germanium dioxide samples, $10^{-5}\%$ w/w

No.	Method of analysis	Sample No.	
		1	2
1.	Extraction colorimetric method	2.6	4.2
2.	Atomic-emission method with concentration in open system	1.8	3.5
3.	Atomic-absorption method with electrothermal atomization from solid sample	2.0	5.1
4.	Extraction photometric method	2.7	3.7
5.	Atomic-emission method with excitation in direct current arc after vapour-phase autoclave concentration	2.5	4.8
6.	Atomic-emission method with electrothermal atomization from solution after vapour-phase autoclave concentration	3.1	5.4
7.	Atomic-emission method with excitation in inductively-coupled plasma after vapour-phase autoclave concentration	3.0	5.5
8.	Atomic-emission method with excitation in inductively-coupled plasma after concentration in open system	2.0	5.0
9.	Spark-source mass-spectrometry	2.2	4.1
10.	Instrumental neutron-activation	2.0	5.0
	Average value	2.4 ± 0.6	4.6 ± 0.9

the possible distortion of results owing to loss of impurities and sample contamination during the pre-concentration and also loss of possible information about the homogeneity of the material.

The progress in lowering the limits of detection in atomic spectrometry is primarily related to development of more effective excitation sources. The advances made in the period 1966–1981 have been reviewed.¹⁹ During this period the limit of detection for many elements was lowered by about 3 orders of magnitude.¹⁹ The use of the inductively coupled plasma (ICP) makes possible the multi-element analysis of many high-purity liquid substances without preconcentration, with limits of detection in the range 10^{-7} – $10^{-5}\%$ w/w. However, the potentialities of the method for analysis of solids are sharply reduced by the need to bring the sample into solution. To overcome this shortcoming “combined sources” are used, *i.e.*, two separate high-temperature units, one for atomization and the other for excitation and observation and are coupled “on-line”.²⁰

A substantial lowering of the limits of detection for individual impurities down to $10^{-9}\%$ is achieved in atomic-emission analysis by application of a hollow-cathode discharge as an excitation source.^{16,21,22} The current potentialities of the method have been comprehensively surveyed.^{22,23} Although the precision is not very high, the method seems rather promising in atomic-absorption and mass-spectrometry analysis.

Spectroscopic analysts place their main hopes on use of lasers.^{24–28} The progress in analytical laser spectrometry is mainly related to the development of frequency-tuned lasers which may drastically lower the limits of detection impurities. The most promising applications of lasers in the analytical chemistry of high-purity substances are to atomic-fluorescence,

intracavity-type absorption and photoionization methods.

In atomic-fluorescence analysis with laser excitation^{29–31} the sample vapours are exposed to laser radiation tuned to the absorption-line frequencies of the analyte atoms. In this case it is often possible to saturate the quantum transition, so about half the atoms irradiated are excited. The fluorescence at a frequency-shifted line is usually recorded, which simplifies the detection of the signal against the background of scattered exciting radiation. The linear range of calibration covers 3–6 orders of magnitude. The extrapolated limits of detection for a number of metal impurities in reference water solutions are as low as 10^{-14} – 10^{-13} g/ml.^{30,31} For cobalt determination in high-purity silicon dioxide, after preconcentration a limit of detection of $10^{-7}\%$ w/w has been obtained.³²

In laser stepwise-photoionization analysis^{33,34} the sample is atomized in a vacuum chamber and a directed atom flux is formed. The radiation pulses of two or three lasers, with wavelengths tuned to resonance transitions of the impurity atoms, excite the atoms stepwise to the Rydberg state. The highly excited atoms are ionized by an electric field. The ions generated are forced out from the ionization region and detected. The method of laser stepwise-photoionization has the highest selectivity among the methods of laser atomic-spectrometry analysis but only a few methods have been developed.^{33,35} For aluminium and sodium determination in high-purity germanium³³ without preconcentration a limit of detection of 2×10^{-9} atom% has been obtained.

Great problems are encountered in sample atomization when methods of micro-impurity determination in high-purity substances are being devel-

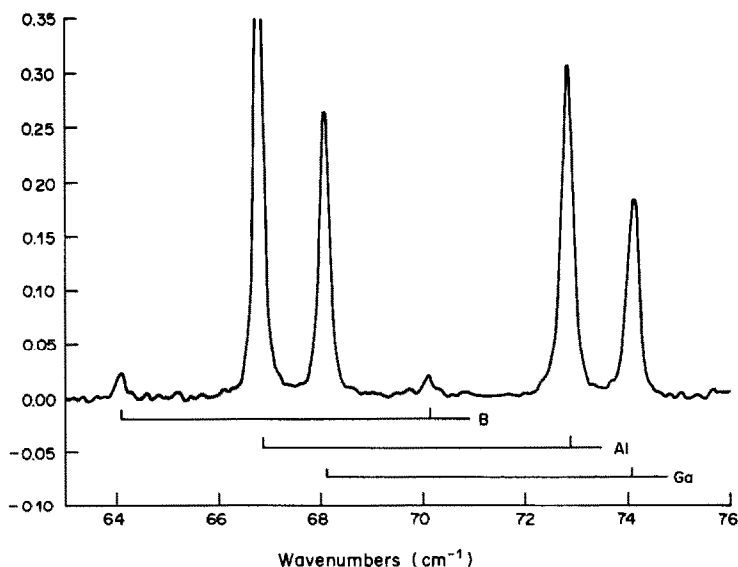


Fig. 1. Impurity spectrum range in high-purity germanium. Contactless spectrum recording. Ordinate: photocell response, arbitrary units. [B] = 2×10^{-12} atom%; [Al] = 5×10^{-11} atom%; [Ga] = 3×10^{-11} atom%.

oped. One of the ways to overcome this problem is the formation of a directed atom flux of high intensity. It eliminates chemical preparation of the sample, and hence lowers the blank level. In atom-flux fluorescence excitation deactivation effects are practically absent, which gives this atomization method an advantage over the others.

Photothermal ionization spectroscopy in the infrared range³⁶⁻³⁸ is one of the most sensitive methods of semiconductor analysis, and provides the determination of donor and acceptor impurities of chemical elements and complexes, directly in the semiconductor crystal bulk. The measurements are done at liquid-helium temperatures. A contactless technique of recording photothermal ionization spectra has been worked out,³⁹ which eliminates sample contamination from ohmic contacts, and broadens the range of semiconductor materials that can be analysed. In this method surface contamination does not influence the analysis results and makes it possible to determine electroactive impurities at the level of 10^{-12} atom% and less (see Fig. 1).

Mass spectrometry methods are among the most informative methods of high-purity substance analysis. Spark-source mass-spectrometry (SSMS) is the most important, and provides data on the content of up to 70 impurity elements in a sample, in a single determination, with a limit of detection of 10^{-7} – 10^{-5} % w/w with a 10-mg sample.^{40,41} Unfortunately, the precision is not very high (40–45%), though attempts to improve it continue.⁴² The analysis may be done without reference samples, the matrix element being used as internal standard. The impurity content is determined with an accuracy dictated by the relative sensitivity coefficient (RSC).

There are reasons to believe that the RSC of an element does not depend on concentration, and the RSC values of different elements generally differ by not more than a factor of 5. The potentialities of SSMS have led to this method becoming in essence the main means for multi-element analysis of high-purity substances. The universal nature of SSMS makes it possible to conduct a survey analysis of most solids and many liquids without time-consuming methodological developments. It should be pointed out that the first 25 years of development of SSMS did not greatly increase the potentialities of the method. Only a few improvements were made. However, modern instruments have high resolution, which lowers the limit of detection for some impurities and they are equipped with devices for automatic maintenance of the spark gap as well as with a recording system for ion current. With application of the systems for additional evacuation of the ion-source, techniques for carbon, nitrogen and oxygen determination at 10^{-6} – 10^{-4} % w/w levels have been worked out.⁴³ Computer techniques of spectra processing are being developed,⁴⁴ which greatly reduce the time of mass-spectra identification and improve the reproducibility of results. The trends in development of SSMS are mainly connected with improvement of the ion-source and techniques for impurity concentration.⁴¹ The impurity concentrates can be analysed with sufficiently intense and stable ion current by the "frozen drop"⁴⁵ and "thin layer" methods.⁴⁶ The combined application of SSMS as a survey method together with atomic-absorption spectrophotometry for precision determination of individual technology important impurities is of interest.⁴⁷ The current state of SSMS and the application

of the ICP as a mass-spectrum ion-source in the analysis of solutions have been discussed.^{48,49}

In the USSR, mass spectrometers with laser ion-sources are being manufactured⁵⁰ and corresponding analysis techniques have been developed.⁵¹ The application of laser mass-spectrometry (LMS) for the determination of trace impurities has been discussed.^{52,53} In general, LMS is equivalent to SSMS with respect to limits of detection but has certain advantages in layer analysis as well as in analysis of non-conducting material. The work on mass-spectral laser microanalysis of high-purity substances is continuing.^{54,55}

Secondary-ion mass-spectrometry (SIMS) finds wider and wider application owing to its high sensitivity and ability to give data on distribution of sample components. A specific feature of secondary-ion emission is a high yield of polynuclear ions and, as a consequence, a superposition of lines in the mass spectrum. Various methods have been suggested for dealing with such interference lines; but the use of high-resolution mass analysers (resolution 5000–10000) remains the most reliable way for lowering the limit of detection. Secondary-ion emission differs considerably between various elements and depends on the sample material. That is why in survey analysis of high-purity materials SIMS is inferior to spark-source and laser mass-spectrometry except for some advantages in determination of alkali metals.

SIMS is certainly more advantageous than the other methods of analysis for investigation of element distribution in thin surface layers, as it provides a low limit of detection with high depth-resolution (to several nm). Most research on element distribution in ion-implanted, diffusion and thin epitaxial layers of semiconductor materials is done by SIMS. To obtain a reliable concentration profile it is necessary to develop a special technique.

SIMS may also be used to determine the surface contamination composition, but generally high-resolution instruments must be used because in surface atomization there is a large yield of polynuclear ions.

Various models for secondary-ion emission have been suggested.⁵⁶ The techniques for determination of element content from the secondary-ion current, based on these models, give results which vary from the mean by a factor of ~ 3 , which is why it is necessary to use reference samples to improve the precision of SIMS analysis. Great problems are encountered in making and using reference samples, owing to the dependence of the secondary-ion yield on the form of the element in the sample. It seems that one of the most reliable techniques is introduction of a predetermined quantity of analyte into the surface layer of the sample by ion implantation. The results are calculated either from the total dose of the implant or the maximum of its distribution profile.⁵⁷ Good results have been obtained for the

distribution of oxygen in selenium⁵⁸ and of impurities in gallium arsenide.⁵⁹

Activation analysis remains one of the most sensitive methods. The low absolute and relative limits of detection, and the possibility of completely precluding the influence of surface contamination, the environment and reagent purity, make activation methods indispensable for analysis of high-purity substances. Like SSMS among mass-spectral methods, neutron-activation analysis (NAA) plays the leading part among activation methods, as it provides simultaneous determination of more than 60 elements with high precision.

There have been no basic changes in NAA in the last decade, and the main improvements of NAA have been in the development of new high-efficiency methods of radiochemical separation.⁶⁰ Thanks to the development of such methods the range of materials analysed has been substantially expanded, and now includes such "difficult" subjects for NAA as mercury.⁶¹ Great attention has been paid to the development and application of reference samples specific to NAA.⁶² To further increase the sensitivity of NAA, research has been done on the potential of using a high-flux nuclear reactor (flux 1×10^{14} n. cm⁻². sec⁻¹). As follows from Table 2, the limit of detection for the impurities in silicon has been lowered by an order of magnitude. Further improvement of the technique is expected to lower the limit of detection by two orders of magnitude. It is interesting that with improvement of the sensitivity the number of detected impurities has greatly increased. It may be expected that the use of charged particles^{63,64} and the methods of nuclear microanalysis⁶⁵ will provide considerable progress in activation analysis of high-purity substances.

Sample preparation and concentration of impurities

The analysis of ever purer substances demands not only the development of highly sensitive methods of analysis but also imposes strict requirements on the cleanliness of all chemical operations, and the reduction and control of surface contamination, and the background signals from the environment and equipment. A considerable amount of research is devoted to these problems. We may point out the necessity to work in specialized "clean" rooms,⁶⁶ control reagent purification,⁶⁷ clean the sample surface, and use efficient and sterile methods of sample decomposition.¹⁵

Automation of all operations—from sampling to producing the results—should preclude contamination of the substance by human contact. Current interest is in sample decomposition in autoclaves or other sealed pressure vessels, to minimize contamination, prevent the loss of volatile components, and accelerate the decomposition process.^{13,15,18,67} It has been shown¹⁵ that the development of special microtechniques for all preliminary chemical operations—from reagent purification prior to de-

Table 2. Detection limits (L) for impurities in high-purity silicon by the NAA method with high-flux reactor, % w/w

Element	Traditional technique, L_1	With high-flux reactor, L_2	Attainable value with high-flux reactor and improved technique, L_3	Expected gain, L_1/L_3
Na	6×10^{-9}	2×10^{-9}	5×10^{-10}	12
Sc	5×10^{-10}	5×10^{-11}	1×10^{-11}	50
Cr	5×10^{-8}	2×10^{-8}	5×10^{-9}	10
Fe	2×10^{-6}	1×10^{-7}	4×10^{-8}	50
Cu	2×10^{-8}	2×10^{-9}	1×10^{-9}	20
Ni	2×10^{-5}	5×10^{-7}	1×10^{-7}	200
Co	5×10^{-9}	2×10^{-10}	5×10^{-11}	100
Zn	2×10^{-7}	6×10^{-9}	3×10^{-9}	70
Gd	2×10^{-9}	4×10^{-10}	2×10^{-10}	10
As	2×10^{-9}	1×10^{-10}	5×10^{-11}	40
Br	2×10^{-9}	4×10^{-10}	2×10^{-10}	10
Ag	5×10^{-8}	2×10^{-9}	5×10^{-10}	100
Cd	5×10^{-8}	4×10^{-9}	1×10^{-9}	50
Sb	1×10^{-9}	1×10^{-10}	5×10^{-11}	20
Cs	1×10^{-8}	5×10^{-10}	1×10^{-10}	100
La	1×10^{-9}	1×10^{-10}	5×10^{-11}	20
Eu	5×10^{-10}	4×10^{-11}	3×10^{-12}	220
Lu	1×10^{-9}	1×10^{-10}	3×10^{-11}	33
Hf	5×10^{-9}	2×10^{-10}	5×10^{-11}	100
Ta	1×10^{-8}	8×10^{-10}	2×10^{-10}	50
W	3×10^{-9}	5×10^{-10}	1×10^{-10}	30
Ir	5×10^{-10}	9×10^{-12}	3×10^{-12}	170
Au	1×10^{-10}	7×10^{-12}	2×10^{-12}	50
Hg	1×10^{-7}	1×10^{-8}	5×10^{-9}	20

composition and concentration, to introduction of the concentrate into the instrument for the final analysis—makes it possible to reduce the blank by several orders of magnitude. This combination of relatively simple devices and chemical operations minimizes the most common types of analytical error, and allows the introduction of the impurity concentrate into the analyser without substantial losses or contamination, and thereby lowers the detection limits. A number of new concentration techniques in trace analysis have been described.⁶⁹⁻⁷²

In recent years gas-phase methods of detecting and concentrating micro-impurities have been developed.⁷³⁻⁷⁵ The traditional conversion of a sample into the liquid state before concentration of the impurities is often far from the best solution. The dissolution process may lead to substantial increase in the blank, and decrease in the analyte concentration owing to dilution with solvent *etc.* Transfer of the impurities into the gas phase by reaction gas extraction (RGE) is a more efficient solution of the problem. In RGE the analytes are converted into gaseous compounds which can be identified and determined directly in the gas phase. These methods provide a new limit of detection owing to the efficiency of concentration in the gas phase and the use of minimum (often stoichiometric) quantities of reagent. RGE methods are especially promising in determination of non-metal micro-impurities (primarily silicon, phosphorus and arsenic) which are difficult to determine. High-

temperature extraction for the determination of gas impurities (oxygen, hydrogen, and nitrogen) may be preferred to RGE methods.^{76,77} In the last few years there has been a rapid increase in research on the determination of arsenic, selenium, tellurium, tin, germanium, *etc.* as their volatile hydrides.⁷⁸⁻⁸⁰ Atomic emission and absorption spectrometers are now equipped with volatile-hydride generators. Analysis with extraction of volatile halides is being developed in two directions—the search for highly efficient halogenation agents and optimal conditions for transfer of the analyte into the gas phase, and the choice of a rational analytical technique.^{81,82}

Determination of gas-forming impurities

Oxygen, nitrogen, carbon and hydrogen are commonly called gas-forming impurities, because in their determination by high-temperature extraction they are isolated in gas form from the samples. Many other elements are now isolated and determined by this method.⁷⁵ This aspect makes the term "gas-forming" ambiguous, but it is convenient to combine these four elements into one group and retain the existing terminology. The gas-forming elements are widely spread in the environment and are of high reactivity. These characteristics impede the purification of substances and materials on the one hand, and considerably complicate the analytical determination on the other. Despite intensive efforts by analysts, the methods for determining the gas-

Table 3. Oxygen and carbon determination with activation by 10-MeV helium-3 ions

Analysed material	Method of determination	Lower boundaries of detected content, % w/w
Al, Si, Hf, Ta, W, Re	Instrumental	10^{-7} – 10^{-6}
Al, Si, SiC, Sc, Ti, V, Cu, Ge, Ga, P, GaAs, Y, Zr, Nb, Mo, Ag, In, Sb, La, Hf, Ta, W, Re	Radiochemical separation of analytical isotopes	
Lanthanides	^{18}F and ^{11}C	

forming elements in pure substances remain the most difficult, mainly because of sample-surface contamination and the high background. Activation and high-temperature extraction are the most widely used methods of analysis.

The activation methods used for the determination of gas-forming impurities differ both in the type of radiation used for activation and in the type of products of the nuclear reactions.⁶⁴

Fast neutrons are used for rapid determination of oxygen and nitrogen, with lower limits of determination of 10^{-5} – 10^{-4} % w/w. For the determination of oxygen and carbon at concentrations of 10^{-6} – 10^{-4} % w/w deuterons may be used. Protons are used to determine nitrogen at 10^{-8} % w/w levels. Helium-3 ions provide oxygen and carbon determination at concentrations of 10^{-7} % w/w. The same high level of sensitivity is achieved in oxygen determination with α -particles. Bremsstrahlung from linear accelerators or microtrons of 25–30 MeV power is used to determine oxygen, carbon and nitrogen with detection limits of 10^{-6} – 10^{-5} % w/w.

Up till now, techniques have been developed and used for the determination of oxygen, carbon and nitrogen by activation with helium-3 ions and protons, for more than 30 different pure materials (Tables 3 and 4). To preclude any influence of the impurity composition on the results a universal technique for isolation and purification of the analyte isotopes has been developed, based on distillation of volatile compounds containing these isotopes. The technique is applicable to all the materials in Tables 3 and 4 with minor changes in the purification system for the gases distilled.

High-temperature extraction is the most well-known and widespread method of determination of gas-forming impurities. In the USSR new modifications of the vacuum extraction method have been developed: oxidative melting in vacuum for carbon determination, "neutral" melting for nitrogen determination, and techniques for removal of surface contamination.^{83,84}

Carbon is usually determined by combustion in oxygen. In analysis of high-purity substances this method has considerable limitations due to sample surface contamination and high blanks due to the carbon content of the ceramic crucibles and oxygen used. That is why oxidative fusion in vacuum is used to determine carbon contents $<10^{-3}$ % w/w;⁸ a blank of $0.06 \pm 0.02 \mu\text{g}$ has been achieved, two orders of magnitude lower than that for the combustion method. Such sensitivity may be gained by reducing the influence of "surface" carbon on the analysis results. For this purpose the sample surface is scavenged with oxygen before the analysis.

The application of reductive vacuum-fusion in graphite crucibles in the analysis of pure metals (especially refractory and less-common metals) has led to problems as the degree of nitrogen extraction is low and variable. That is why "neutral" vacuum-fusion, *i.e.*, extraction of nitrogen from a melt which does not contain appreciable amounts of oxygen and carbon, has been used.⁸³

For oxygen determination a crucible made of high-purity graphite has been used, and a blank of $0.1 \mu\text{g}$ obtained. To reduce the surface contamination a high-temperature interaction of methane with surface oxides was applied before the analysis.⁸⁴

Table 4. Nitrogen determination with 6.5–10-MeV proton activation

Analysed material	Method of determination	Lower boundaries of detected content, % w/w
Al, Si, V, Nb, La, Ce, Nd, Eu, Tb, Ho, Ta, Re	Instrumental	10^{-8} – 10^{-6}
Al, Si, SiC, Sc, Ti, V, Cu, Ge, GaP, GaAs, Y, Zr, Nb, Mo, Hf, Ta, W, Re	Radiochemical separation of analytical isotopes	
Lanthanides	^{11}C	

Table 5. Results of oxygen, carbon and nitrogen determination in pure metals by vacuum-extraction methods, $X \pm S$, $\mu\text{g/g}$, $n = 4$

Material analysed	Traditional treatment of sample surface	Direct surface cleaning in the plant	Detected impurity
Copper	4 ± 0.5	1.2 ± 0.1	Oxygen
Nickel	4 ± 1	1 ± 0.1	
Molybdenum	7.5 ± 2	2.1 ± 0.3	
Rhenium	15 ± 2	2.8 ± 0.3	
Iridium	10 ± 2	3.5 ± 0.5	
Niobium	6 ± 1	1.2 ± 0.3	
Copper	3.5 ± 1	0.2 ± 0.1	Carbon
Nickel	5 ± 0.5	0.4 ± 0.1	
Molybdenum	1.2 ± 0.2	0.02 ± 0.01	
	2.8 ± 0.2	0.2 ± 0.05	
Nickel	0.9 ± 0.2	0.2 ± 0.05	Nitrogen
Molybdenum	1.2 ± 0.2	0.2 ± 0.03	
Silicon	1.4 ± 0.4	0.6 ± 0.2	

The results for oxygen, nitrogen and carbon determinations in pure metals are given in Table 5. The data show the efficiency of oxygen removal from the surface by methane, and of nitrogen and carbon by oxidation. The accuracy of analysis is confirmed by comparison of the results obtained with those found by other methods (Table 6). Table 7 shows the lower limits for determination of oxygen, carbon and nitrogen. These values are substantially lower (by an order of magnitude or more) than those for traditional methods. The blank due to "surface" oxygen does not exceed $0.1 \mu\text{g/g}$, and that for carbon and nitrogen is $0.02 \mu\text{g/g}$ and these do not limit the analysis sensitivity as a whole.

The variants of high-temperature vacuum extrac-

tion shown bring the performance of this method nearer to that of the nuclear methods of analysis, and need only relatively simple operations and equipment. The analysis of low-melting and especially of highly volatile substances demands new approaches, however. For high-purity materials used in modern engineering, such as phosphorus, arsenic, mercury, tellurium, selenium, cadmium and their compounds, reliable methods of determination of gas-forming impurities are lacking, and on the whole, analysis for oxygen, carbon, nitrogen and hydrogen traces remains one of the main problems in the analytical chemistry of high-purity substances.

The determination of suspended particles in high-purity substances should be considered as an individ-

Table 6. Comparative results for oxygen, carbon, and nitrogen determination in pure metals, $X \pm S$, $\mu\text{g/g}$

Sample	Vacuum-extraction method	Comparative analysis	Comparative method
		Oxygen	
Nickel-1	1 ± 0.2	0.6	Accelerated ion activation
Nickel-2	0.7 ± 0.2	0.4	
Molybdenum-1	2.1 ± 0.3	2.1	
Molybdenum-2	< 0.2	0.03	
Niobium-1	1.2 ± 0.3	1.3	Fast-neutron activation
Niobium-2	2 ± 0.2	2	
Niobium-3	0.2	0.1	
Molybdenum-3	4 ± 1	4.4	
		Carbon	
Silicon-1	1.8 ± 0.3	2	Accelerated ^3He -ion activation
Silicon-2	$< 0.5 \pm 0.05$	0.5	
Niobium-4	0.2 ± 0.05	0.3	Deuteron activation with radiochemical separation
Niobium-5	0.4 ± 0.1	0.2	
Niobium-6	0.3 ± 0.1	0.4	
		Nitrogen	
Nickel-3	1.5 ± 0.1	1.5 ± 0.1	Isotope dilution
Nickel-4	0.2 ± 0.03	0.3 ± 0.05	
Molybdenum-1	0.2 ± 0.03	0.3 ± 0.05	
Niobium-1	0.4 ± 0.1	0.5 ± 0.2	

Note: each result obtained by the vacuum-extraction method is the average of 5-10 parallel determinations; by the other methods the average of 3-5 parallel determinations.

Table 7. Detection limits for oxygen, carbon and nitrogen in various materials by vacuum-extraction methods, $\mu\text{g/g}$

Material analysed	Oxygen	Carbon	Nitrogen
Cu, Ag, Au and their alloys	0.2	0.1	0.2
Fe, Co, Ni and their alloys	0.4	0.1	0.2
Pd, Pt, Rh, Ru, Ir	0.5	0.1	0.2
Mo, W, Re and their alloys	0.5	0.1	0.2
Nb, Ta and their alloys	0.6	0.2	0.4
In, Ga, Sn	3	1	—
Si, Ge	—	0.2	0.3
V, Hf and their alloys	5	0.5	1
Ti, Zr	100	1	1
Rare-earth metals	50	1	1
Rare-earth metal fluorides	10	1	—

ual problem. Particles of sub- μm size are hard to remove by traditional methods of purification so their contribution to the total impurity content increases with increasing purity of the substance. Methods for determination of particle size and concentration need further development.

To put things into perspective we may state that there are all the possibilities for development of analysis techniques with limits of detection of 10^{-10} – 10^{-8} % w/w for a large group of impurity elements in a wide range of solid and liquid high-purity materials, but in some cases there is still a need for determination of even lower contents. Development of the necessary techniques and ancillary equipment needs special attention.

REFERENCES

- G. G. Devyatykh, V. M. Il'in, N. V. Larin, G. A. Maksimov and A. N. Moiseev, *Izv. Akad. Nauk SSSR, Neorgan. Mater.*, 1979, **15**, 1735.
- O. G. Koch, P. D. La Fleur, G. N. Morrison, E. Jackwerth, A. Townshend and G. Tölg, *Pure Appl. Chem.*, 1982, **54**, 1565.
- G. G. Devyatykh, V. M. Stepanov and K. K. Malyshev, *Dokl. Akad. Nauk SSSR*, 1985, **283**, 144.
- P. L. Buldini, D. Ferri and P. Lanza, *Anal. Chim. Acta*, 1980, **113**, 171.
- P. Lanza, *ibid.*, 1983, **146**, 61.
- A. A. Kaplin and V. M. Pichugina, *Zh. Analit. Khim.*, 1984, **39**, 664.
- P. Buldini and D. Sandrini, *Anal. Chim. Acta*, 1978, **98**, 401.
- T. M. Maljutina, V. A. Orlova and B. Ya. Spivakov, *Zh. Analit. Khim.*, 1974, **29**, 790.
- S. U. Kreingold, *Katalimetriya v analize reaktivov i veshchestv osoboi chistoty*, Khimiya, Moscow, 1984.
- Yu. A. Zolotov and N. M. Kuz'min, *Kontsentrirovaniye mikroelementov*, Khimiya, Moscow, 1982.
- I. G. Yudelevich, L. M. Budnova and I. R. Shelpakova, *Khimikospektral'nyi analiz veshchestv osoboi chistoty*, Nauka, Novosibirsk, 1980.
- I. R. Shelpakova, I. G. Yudelevich and B. M. Ayunov, *Posloyniy analiz materialov elektronnoi tekhniki*, Nauka, Novosibirsk, 1984.
- M. S. Chupakhin, A. I. Sukhanovskaya, V. Z. Krasil'shchik, S. U. Kreingol'd, L. A. Demina, V. I. Bogomolov, E. V. Dobizha, M. Przhibyl, Z. Slovak, I. Borak and M. Smrz, *Metody analiza chistykh khimicheskikh reaktivov*, Khimiya, Moscow, 1984.
- Yu. A. Karpov and I. P. Alimarin, *Zh. Analit. Khim.*, 1979, **34**, 1402.
- G. Tölg, *Pure Appl. Chem.*, 1983, **55**, 1989.
- G. G. Devyatykh, V. N. Shishov, V. G. Pimenov, A. N. Egorochkin and Yu. V. Revin, *Zh. Analit. Khim.*, 1978, **33**, 464.
- A. N. Kirgintsev, V. A. Isaenko, I. I. Kasil' et al., *Upravlyaemaya kristallizatsiya v trubchatom konteinere*, Nauka, Novosibirsk, 1978.
- V. G. Pimenov, P. E. Gaivoronskii, V. N. Shishov and G. A. Maksimov, *Zh. Analit. Khim.*, 1984, **39**, 1072.
- M. L. Parsons, S. Major and R. Forster, *Appl. Spectrosc.*, 1983, **37**, 411.
- T. Kántor, *Spectrochim. Acta*, 1983, **38B**, 1483.
- N. K. Rudnevskii, D. E. Maksimov, A. N. Tumanova and T. M. Shabanova, *Zh. Prikl. Spektrosk.*, 1982, **37**, 722.
- S. Caroli, *Prog. Anal. Atom. Spectrosc.*, 1983, **6**, 253.
- Improved Hollow Cathode Lamps for Atomic Spectroscopy*, S. Caroli (ed.), Horwood, Chichester, 1985.
- Analiticheskaya lazernaya spektroskopiya*, N. Omenetto (ed.), (translation from English by N. B. Zorov, edited by Yu. Ya. Kuz'kov), Mir, Moscow, 1982.
- V. I. Grishko and I. G. Yudelevich, *Zavodsk. Lab.*, 1982, **48**, No. 4, 1.
- N. B. Zorov, Yu. Ya. Kuzyakov and O. I. Matveev, *Zh. Analit. Khim.*, 1982, **37**, 520.
- J. C. Wright, *Tech. Chem. (New York)*, 1982, **17**, 35.
- N. Omenetto and H. G. Human, *Spectrochim. Acta*, 1984, **39B**, 1333; H. G. Human, N. Omenetto, P. Cavalli and G. Rossi, *ibid.*, 1984, **39B**, 1345.
- L. M. Fraser and J. D. Winefordner, *Anal. Chem.*, 1971, **43**, 1693.
- M. A. Bol'shov, A. V. Zybin and V. G. Koloshnikov, *Kvant. Elektronika*, 1980, **7**, 1808.
- M. A. Bol'shov, A. V. Zybin and J. J. Smirenkina, *Spectrochim. Acta*, 1981, **36B**, 1143.
- M. A. Bol'shov, I. B. Gornushkin, H. I. Zil'bershtein, A. V. Zybin, Yu. B. Kiselev and I. I. Smirenkina, *II Vsesoyuz. konf. po metodam poluch. i analiza vysokochistykh veshchestv: Tez. Dokl. V 2-ku ch. Gorkii: Institut Khimii AN SSSR*, 1985, **2**, 17.
- R. Akilov, G. I. Bekov, G. G. Devyatykh, V. S. Letokhov, G. A. Maksimov, V. N. Radaev, V. N. Shishov and E. M. Shcheplyagin, *Zh. Analit. Khim.*, 1984, **39**, 31.
- I. M. Beterov, V. L. Kurochkin and I. G. Yudelevich, *Zh. Prikl. Spektrosk.*, 1985, **42**, 17.
- S. Mayo, T. B. Lucatorto and G. G. Luter, *Anal. Chem.*, 1982, **54**, 553.
- Sh. M. Kogan, and T. M. Lifshits, *Phys. Stat. Solidi*, 1977, **39A**, 11.
- E. E. Haller, W. L. Hansen and F. S. Goulding, *Advan. in Phys.*, 1981, **30**, 93.

38. B. A. Andreev, V. A. Gavva, A. V. Gusev, A. V. Ivashin, V. B. Ikonnikov, G. A. Maksimov and V. B. Shmagin, *VII Vsesoyuz. konf. po metodam poluch. i analiza vysokochistyykh veshchestv: Tez. dokl. V 2-kh ch. Gorkii: Institut Khimii AN SSSR*, 1985, 2, 63.
39. B. A. Andreev, L. I. Gershtein, V. B. Ikonnikov and V. B. Shmagin, *Prib. Tekh. Eksp.*, 1985, No. 3, 172.
40. M. S. Chupakhin, O. I. Kruchkova and G. I. Ramendik, *Analiticheskie vozmozhnosti iskrovoy mass-spektrometrii*, Atomizdat, Moscow, 1972.
41. *Trace Analysis by Mass Spectrometry*, A. J. Ahearn (ed.), Academic Press, New York, 1972.
42. G. I. Ramendik, B. M. Manzon, D. A. Tyurin, N. E. Benyayev and A. A. Komleva, *Talanta*, 1987, 34, 61.
43. D. C. Walters, D. S. Look and T. O. Terman, *Anal. Lett.* 1983, 16, 1427.
44. A. Pilate and F. Adams, *Anal. Chim. Acta*, 1980, 122, 57.
45. I. G. Yudelevich, I. R. Shelpakova, L. N. Shabanova, V. A. Gerasimov and T. M. Korda, *Zh. Analit. Khim.*, 1976, 31, 561.
46. A. I. Saprykin, I. R. Shelpakova, T. A. Chapysheva and I. G. Yudelevich, *ibid.*, 1983, 38, 1238.
47. P. Murugaiyan P. *Pure Appl. Chem.*, 1982, 54, 835.
48. H. E. Beske, *Int. J. Mass Spectrom. Ion Phys.*, 1981, 45, 173.
49. F. Adams, *Spectrochim. Acta*, 1983, 38B, 1379.
50. A. S. Brukhanov, A. V. Boriskin, Yu. A. Bykovskii and V. M. Eriomenko, *Int. J. Mass Spectrom. Ion Phys.*, 1983, 47, 351.
51. Yu. A. Bykovskii, G. I. Zhuravlev, V. I. Belousov, V. I. Gladskoi, V. G. Degtyarev and V. N. Nevolin, *Zavodsk. Lab.*, 1978, 44, 701.
52. I. D. Kovalev, G. A. Maksimov, A. I. Suchkov and N. V. Larin, *Int. J. Mass Spectrom. Ion Phys.*, 1978, 27, 101.
53. S. Shankai, R. J. Conzemius and H. J. Svec, *Anal. Chem.*, 1984, 56, 382.
54. H. J. Heinen, S. Meier, H. Vogt and R. Wechsung, *Int. J. Mass Spectrom. Ion Phys.*, 1982, 47, 19.
55. I. D. Kovalev, N. V. Larin, A. I. Potapov and A. I. Suchkov, *Zh. Analit. Khim.*, 1985, 40, 1971.
56. Z. Iurela, *Int. J. Mass Spectrom. Ion Phys.*, 1981, 45, 25.
57. D. P. Leta and G. H. Morrison, *Anal. Chem.*, 1980, 52, 277.
58. T. Obata, B. Tsijimura and O. Oda, *Surface Sci.*, 1983, 135, 110.
59. A. E. Morgan and J. B. Clegg, *Anal. Chim. Acta*, 1980, 35B, 281.
60. G. V. Verevkin, E. N. Gil'bert, V. A. Mikhailov and E. G. Obrazovskii, *Khimiya ekstraktii*, Nauka, Novosibirsk, 1984, 215.
61. E. N. Gil'bert, G. V. Verevkin, V. A. Mikhailov and N. A. Korol', *Zh. Analit. Khim.*, 1980, 35, 2300.
62. R. Delfanti, M. Di Casa, M. Gallorini and E. Orvini, *Mikrochim. Acta*, 1984 I, 239.
63. E. A. Schweikert, *Some Selected Nucl. Techn. Res. and Developments, Proc. Adv. Group Meet., San Jose 1977* p. 1. I.A.E.A., Vienna, 1978.
64. P. Albert, *Pure Appl. Chem.*, 1982, 54, 689.
65. K. Bethge, H. Baumann, H. Jex and F. Rauch, *Nuclear Physics Methods in Material Research*, Vieweg, Braunschweig, 1980.
66. V. L. Sabatovskaya, G. I. Zhuravlev and T. A. Bibikova, *Zavodsk. Lab.*, 1983, 49, No. 9, 43.
67. M. Z. Hasan, *Metal Miner. Rev.*, 1982, 21, No. 10, 242.
68. T. M. Malyutina, E. G. Namvrina and O. A. Shiryayeva, *Zavodsk. Lab.*, 1981, 47, No. 9, 8.
69. E. Jackwerth and S. Gomišček, *Pure Appl. Chem.*, 1984, 56, 479.
70. V. G. Pimenov, P. E. Gaivoronskii and V. N. Shishov, *Poluch. i Analiz Chistyykh Veshchestv, Gorkii*, 1983, 47.
71. B. Lersmacher, E. Bart van der Brock and P. Rommers, *DBR Ang.* 3149634; *Referat Zh. Khim.*, 1984, No. 7, 7D24P.
72. M. Sager, *Mikrochim. Acta*, 1984 I, 461.
73. G. G. Devyatykh and Yu. A. Karpov, *Analiz neorganicheskikh gasov*, Nauka, Leningrad, 1983, 58.
74. K. Bächmann, *Talanta*, 1982, 29, 1.
75. Yu. A. Karpov, L. B. Kuznetsov and V. N. Belyaev, *Zavodsk. Lab.*, 1981, 47, No. 3, 3.
76. *Determination of Gaseous Elements in Metals*, L. M. Melnich, L. L. Lewis and B. D. Holt (eds.), Wiley, New York, 1975.
77. A. M. Vasserman, L. L. Kunin and Yu. N. Surovoi, *Opredelenie gasov v metallakh*, Nauka, Moscow, 1976.
78. H. Bonbach, B. Luft, E. Weinholt and F. Mohr, *Neue Huette*, 1984, 29, 233.
79. T. Nakahara, *Appl. Spectrosc.*, 1983, 37, 539.
80. R. W. Ward and P. B. Stockwell, *J. Autom. Chem.*, 1983, 5, 193.
81. Yu. A. Karpov, L. B. Kuznetsov and V. N. Belyaev, *Proc. 2nd USSR-Japan Symp. Anal. Chem.*, pp. 116-128. *Geokhim*, Moscow, 1984.
82. L. B. Kuznetsov, V. N. Belyaev and V. P. Baluda, *Zh. Analit. Khim.*, 1984, 39, 215.
83. P. N. Petrov, Yu. A. Karpov, K. Yu. Natanson and O. V. Zav'yalov, *Zavodsk. Lab.*, 1980, 46, 484.
84. P. N. Petrov and Yu. A. Karpov, *ibid.*, 1981, 47, No. 9, 40.

LASER-ULTRAMICROSCOPIC METHOD OF DETERMINING SUSPENDED PARTICLES IN HIGH-PURITY LIQUIDS

G. G. DEVYATYKH, YU. A. KARPOV, V. A. KRYLOV and O. P. LAZUKINA
Institute of Chemistry, USSR Academy of Sciences, Gorky, USSR

(Received 15 October 1985. Revised 14 April 1986. Accepted 15 August 1986)

Summary—Two main types of impurities in high-purity liquids have been determined. One consists of suspended particles of sub- μm size, and optical counters are the most suitable for their determination. Their main characteristics are given. The errors of suspended particle determination are discussed. The data on particles dispersion composition and concentration in some high purity liquids as well as on their nature are given.

High-purity substances play an important part in scientific and engineering progress. It is safe to say that the development of some fields of modern science, such as the physics of semiconductors and superconductors, optics and materials technology, is directly related to achievements in the preparation of increasingly pure substances. In the last few years some branches of science have needed substances which are practically free from all impurities. Hence extensive research on impurity composition is an urgent problem in the chemistry of high-purity substances. A set of data on impurity composition has been accumulated within the framework of the All-Union Permanent Exhibition of high-purity substances.¹ The Permanent Exhibition comprises about 70 samples of liquid substances: inorganic volatile halides and hydrides, organometallic compounds, and some organic substances. On the basis of the analyses of these samples it is possible to obtain the concentration distribution of the impurities. This relation is bimodal in nature.² Figure 1 shows the concentration distribution of impurities for germane. The first maximum of the distribution curve refers to the dissolved impurities. The second is related to the presence of suspended particles. Thus, there are two kinds of impurities in high-purity liquid substances, which differ in their solubility in the matrix. Classification of impurities according to solubility is of vital importance, since each type demands a different approach in choice of sampling and concentration technique as well as of method of detection.

The soluble impurities are usually detected by gas chromatography, infrared spectrometry, mass-spectrometry and atomic-emission methods and have been comprehensively reviewed in monographs.³⁻⁷ The determination of the suspended particles has so far not been sufficiently considered, though this type of impurity determines many important properties of liquids and the substances obtained from them. It should be pointed out that high blank values, which limit the accuracy of solid substances analysis, may

also be related to the presence of suspended particles in liquid reagents.⁸

Of all the characteristics determining the behaviour of particles, size is the most important, closely followed by the nature of the particle. That is why the particle analysis demands the determination of the particle size distribution and of the nature of the particles.

Particle detection by light-scattering

High-purity liquids may be considered as highly diluted disperse systems, which is why the methods of suspended particle determination may be used for their analysis. The method used should meet the following requirements. It should, if possible, be non-destructive and use small sample volumes in a sealed system. It should also have low limits of detection with respect to size and concentration, the two main characteristics in the ultramicroscopic analysis of high-purity liquids. Application of techniques such as electron and optical microscopy,^{9,10} conduc-

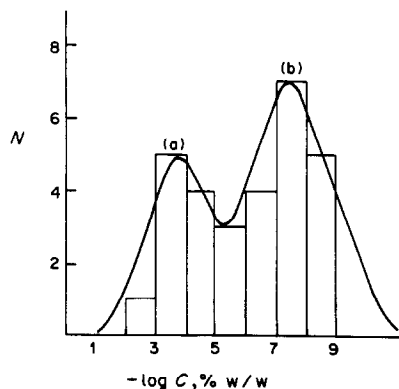


Fig. 1. Distribution of (a) dissolved impurities and (b) impurities in the form of suspended particles in germane; C —impurity concentration; N —number of impurities in the given concentration range.

timetry,¹¹ Auger-spectroscopy,¹² atomic-emission spectroscopy,¹³ and gravimetry¹⁴ is problematic. These methods assume the collection of particles on substrates and filters. The change of medium in the process of sample preparation may influence the particle composition. Also, incomplete particle extraction and aerosol contamination may occur during sample preparation. Non-destructive techniques provide the determination of particles directly in the sample volume by radiation probes. Among non-destructive methods the light-scattering methods¹⁵⁻²¹ are the most highly developed at the present time and their application makes it possible to achieve low limits of detection with respect to size and concentration.

The integral light-scattering methods register the radiation scattered by the disperse system as a whole and provide the determination of mean particle size down to 5 Å and the polydispersion index.²²⁻²⁶ However, these methods require that the content of suspended particles is not less than 10⁻³% w/w and thus are not applicable for the analysis of high-purity liquids. Particle counters which register light scattered by individual particles^{17,27-30} are the most suitable for that purpose and provide simultaneous determination of the size-distribution and concentration of the suspended particles.

The method of individual particle registration by scattered light is termed ultramicroscopy. A flow ultramicroscope for the analysis of liquids has been developed by Deryagin and Kudryavtseva,³¹ and has served as the basis for several models of counters, including counters with automatic registration.^{32,33}

Filament lamps were initially used as the radiation source, which prevented attainment of a low limit of detection with respect to size. Substantial reduction of the limit becomes possible when the laser is used as the source of radiation.

The advantages of lasers are: the small spatial divergence of the light flux, which drastically lowers the level of background noise and does not require complicated collimation; monochromatic radiation, so background light can be precluded by filters; high density of radiation power attained by simple beam focusing.^{30,31} The application of lasers also greatly improves the signal/noise ratio at the photodetector output. Application of multimode lasers provides the most uniform energy distribution in the beam,³⁰ which reduces the drawbacks caused by non-uniformity of illumination of the volume examined.¹⁷

Various counter designs differ in the angle at which the scattered light is recorded.³⁵⁻³⁸ Some devices register the light scattered at small angles to the direction of incidence. This design is chosen on account of the asymmetry of light-scattering by individual particles; the scattering is maximal in the direction of the incident beam,¹⁶ and the symmetry diminishes with decrease in particle size. On the other hand, with recording of the light scattered at 90° the contribution of background noise is minimal³⁰ and the

instrumentation is simpler. Hence most apparatus makes measurements at 90° to the incident beam.

Most counters are equipped with flow-cells, but their use is not convenient for the analysis of liquids available only in small quantity. Application of convective flow to provide directed movement of the particles in the cell makes it possible to use only 5-10 ml of liquid for the analysis and to analyse high-purity liquids, including corrosive liquids, in a sealed non-flow cell.³⁹ Use of refrigerated cells permits the analysis of volatile inorganic hydrides in the liquid state.⁴⁰

The main problem of dispersion analysis is the correct determination of particle size from the intensity of the scattered light. The intensity is dependent not only on the particle size, but also on the particle shape and relative refractive index, and the intensity and wavelength of the incident radiation.¹⁶ The analytical signal also depends on the characteristics of the photodetector and the recorder. Two main approaches are used to plot the analytical curve which relates the signal to the particle size. The first uses a number of monodisperse colloidal systems (synthetic samples) which contain particles of known size and refractive index.^{30,34,35,41} In the other the analytical curve is explicitly based on the laws of the electromagnetic radiation theory of scattering.

The Rayleigh approximation of the theory of scattering is applicable for the analysis of high-purity liquids.¹⁶ In this approximation the intensity of light scattered at 90° by a spherical isotropic particle and received by a photodetector is given by the expression

$$I = 0.125 I_0 B K d^6 \left(\frac{\pi n_0}{\lambda} \right)^4 \left(\frac{m^2 - 1}{m^2 + 2} \right)^2 \quad (1)$$

where I_0 is the power of the incident radiation, B the solid angle in which the scattered light is collected, K the light-transmission factor of the focusing system positioned in front of the photodetector, d the particle diameter, λ the wavelength of the incident radiation, n_0 the refractive index of disperse medium, and m the relative refractive index of the particle.

The intensity of the scattered light depends on the sixth power of the particle diameter, and the data on the particle nature are contained in the term $[(m^2 - 1)/(m^2 + 2)]^2$. The Rayleigh approximation is valid for $\pi d n_0 / \lambda \leq 2$.⁴² Thus, with He-Ne lasers ($\lambda = 630$ nm) the application of an analytical curve based on equation (1) is possible for particles with size down to about 0.3 μm. According to the Kaiser criterion⁴³ the limit of detection for particle size is that corresponding to an analytical signal which is three times the standard deviation of the background noise.

Table 1 gives some performance characteristics of commercial and laboratory counters for particles in liquids. As follows from the data given, these counters provide determination of particles with sizes down to 0.04-0.08 μm in liquids. It is also shown that under the same conditions the determination of low

Table 1. Optical-counter characteristics

Radiation source	Registering unit	Scattering geometry	Size range, μm	Concentration range, cm^{-3}	References
He-Ne laser, 2 mW $\lambda = 630 \text{ nm}$	Photomultiplier, recorder	90°	>0.5	up to 5×10^3	[44]
He-Ne laser	Photomultiplier, multichannel pulse analyser	0°	0.5–25	up to 1.2×10^4	Royco-346 description
He-Ne laser 50 mW	Photomultiplier, amplifier, multichannel pulse analyser	light collection in solid angle from 3° to 13°	0.3–30	$10\text{--}10^7$	[45]
He-Ne laser, 2.5 mW	Photomultiplier, multichannel pulse analyser	$30^\circ, 20^\circ$	0.2–20	—	[38]
1 amp	Photomultiplier, multichannel pulse analyser	90°	0.1–30	$10^4\text{--}10^7$	[32]
He-Ne laser, 5 mW	Photomultiplier, high-speed recorder	3.5°	0.08–10	—	[36, 37]
He-Ne laser, 20 mW	Photomultiplier, high-speed recorder	90°	0.04–0.3	$10^4\text{--}5 \times 10^7$	[46]

Table 2. Suspended-particle concentrations in some high-purity liquids

Substance	Concentration, cm^{-3}
SiCl_4	$< 10^4$
SiHCl_3	5×10^4
CCl_4	7×10^5
GeCl_4	5×10^6
HNO_3	4×10^6
$i\text{-C}_3\text{H}_7\text{OH}$	9×10^5
PCl_3	3×10^5
$\text{Ga}(\text{CH}_3)_3$	1×10^5
$\text{Ta}(\text{OC}_2\text{H}_5)_5$	$> 5 \times 10^7$
$\text{Cd}(\text{CH}_3)_2$	$> 5 \times 10^7$
H_2O	3×10^5

number concentrations is possible only for relatively large particles. This is because it is necessary to increase the counter volume, which lowers the incident radiation power and thus degrades the limits of size detection.

On the other hand, the determination of very small particles requires a high radiation power and low particle velocity to reduce the bandwidth of the recorder and increase the signal/noise ratio. Reduction of both the minimum detectable concentration and particle size is possible only by changing the independently acting parameters of wavelength, radiation power and observation time.

Table 2 gives the content of suspended particles in some high-purity liquids.⁴⁶ The average content of particles of size $\geq 0.04 \mu\text{m}$ is $10^5\text{--}10^6/\text{cm}^3$. Figure 2 shows typical histograms of suspended-particle distribution with respect to size. Such histograms may be approximated by functions of two types: (a) a function with a maximum which is usually near the lower boundary of determinable size, and (b) a monotonically decreasing function. It follows from the figure that there are no particles with a size of more than $0.3 \mu\text{m}$.

Sources of error

The operation of particle counters is characterized by a number of errors.^{17,19,30,47–50} The random error in measurement of particle concentration is due to errors in the determination of the scattering volume, observation time, the time needed for particles to cross the scattering volume and number of detected particles. The relative standard deviation is 30%.⁴⁶

Systematic errors may be instrumental and methodological in origin. The latter errors are due to incompatibility between the model used for the objects measured and the shape of actual particles. Instrumental errors are due to non-uniform radiation

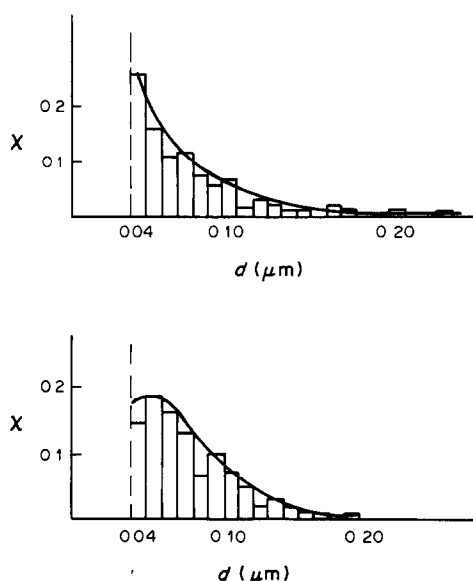


Fig. 2. Typical histograms of suspended particle distribution with respect to size in high-purity liquids: d —particle diameter; χ —fraction of particles in each histogram interval.

distribution in the measurement volume, vignetting (*i.e.*, unsharpness of the edge of the beam), and coincidence. The influence of vignetting increases with reduction in measurement volume. The probability of the simultaneous presence of two or more particles in the scattering volume (coincidence) increases with concentration, and leads to distortion of the values for both the particle concentration and size. The systematic error of instrumental origin can be estimated by analysis of synthetic samples which contain particles corresponding to the model used for the objects measured. The ultramicroscopic analysis of synthetic samples based on isopropyl alcohol and germanium powders of different dispersion has been performed.⁵⁰ The powders consisted of spherical particles with a diameter of 0.08–0.2 μm ; the particle size was determined by electron microscopy.⁵¹ The results are given in Table 3. A *t*-test showed that the discrepancy between the two sets of concentration values was not statistically significant.

Methodological systematic error in the analysis of samples is related to possible incompatibility in the refractive index values for the suspended particles and the model used for the system. To assess the influence of methodological errors on the accuracy of particle-size determination possible values of the term $[(m^2 - 2)/(m^2 + 2)]^2$ have been estimated for suspended particles in carbon, silicon, germanium, and tin tetrachlorides on the basis of the data for the nature of the particles found in these materials.⁵² Its range is 0.03–0.1, which means that the corresponding relative systematic error does not exceed 70%. The accuracy of particle determination in liquids may also be affected by gas bubbles, which in the ultramicroscopy method are interpreted as solid particles of the same size. These gas bubbles are thermo-

dynamically unstable and may exist only if stabilized by factors which reduce the interfacial surface tension, such as surface-active agents or by stabilizing ions. Surface-active agents manifest a stabilizing effect at concentration of 0.1%.⁵³ High-purity liquids may contain similar impurities of considerably lower concentrations. Estimation of the possible surface concentration of ions adsorbed by gas bubbles, on the basis of electrophoretic measurements,⁵⁴ has shown that the charge on the bubble is far less than the critical value. Thus, gas bubbles are unstable in high-purity liquids and should instantly dissolve.⁵⁵

The comparison of results of ultramicroscope analysis of the chlorides mentioned with those of spectral analysis of the particles isolated with nuclear filters, indicates that the discrepancy does not exceed 50%.⁵²

The problem of the stability of suspended-particle aggregates is of importance for analytical measurements. The presence of water micro-impurities in high-purity chlorides produces ionic stabilization of particles in germanium and tin tetrachlorides.⁵⁴ The particles in silicon tetrachloride are stabilized by polysiloxanes. In carbon tetrachloride both stabilizing factors are absent. The suspended particles are stable in silicon tetrachloride for months, in germanium and tin tetrachlorides for days, and in carbon tetrachloride for hours.

Chemical composition

As already pointed out, the high-purity liquids contain high concentrations of suspended particles. The problem of the chemical composition of the suspended particles is of great importance. Investigation of the elemental composition of aerosols has shown that the particle composition is as follows: calcium up to 10%, iron up to 3%, aluminium 1.5%,

Table 3. Results of triplicate determinations of powder concentration in synthetic samples

Synthetic Sample	Powder concentration (<i>C</i>) known from synthesis technique, g/cm^3	Mean value of powder concentration (\bar{C}), g/cm^3	Standard deviation of powder concentration (S_c), g/cm^3	$t = \frac{ C - \bar{C} \sqrt{n}}{S_c}$
1	$(1 \pm 0.1) \times 10^{-6}$	1.32×10^{-6}	4.6×10^{-7}	1.20
2	$(1 \pm 0.15) \times 10^{-7}$	7.6×10^{-8}	2.2×10^{-8}	1.89
3	$(1 \pm 0.2) \times 10^{-8}$	9.7×10^{-9}	3.3×10^{-9}	0.16
4	$(1 \pm 0.2) \times 10^{-9}$	8.7×10^{-10}	3.3×10^{-10}	0.68
5	$(1 \pm 0.2) \times 10^{-10}$	8.5×10^{-11}	3.2×10^{-11}	0.81

Table 4. Composition of total suspended particles in inorganic volatile hydrides, %

Impurity	Silane	Germane	Ammonia	Phosphine	Arsine	Stibine
NaCl	1.2	18.1	—	1.5	2.2	26.0
CuO	11.2	11.0	0.5	3.5	0.8	2.4
B ₂ O ₃	6.6	11.5	27.7	1.5	4.2	24.0
SiO ₂	52.1	44.0	61.5	39.0	32.1	38.0
Fe ₂ O ₃	11.2	0.5	5.6	2.0	8.2	2.6
MnO ₂	2.2	0.3	0.2	0.6	0.2	2.9
NiO	2.2	—	—	0.2	0.1	0.3
MgO	3.0	14.2	2.3	30.2	10.2	—
Al ₂ O ₃	10.3	0.4	2.2	21.5	42.0	4.8

copper 0.5%, silicon 5%, nickel 1.5%, potassium 1%, magnesium 1%, manganese 0.5% and traces of other elements.^{56,57} The same common elements may be present in the particles in liquids.

The elemental composition of suspended particles in inorganic volatile hydrides has been determined by spectral and electron micrograph methods.⁵⁸ The results are shown in Table 4. The determination of the nature of the suspended particles in these volatile chlorides is complicated by the fact that metals and silicon may be present in these substances in the dissolved state.^{59,60} The total impurities content in these chlorides has been determined by the atomic-emission method with preconcentration of the impurities on a carbon collector.⁶¹ The elemental composition of the suspended particles has been determined by spectral analysis of deposits separated by filtration of the chlorides through porous membranes (nuclear filters).⁵² Table 5 gives the total content of metals and suspended particles. It follows from these values that the concentrations of impurities which are present in the form of particles in these chlorides are at the level of 10^{-6} % w/w, the main contribution being from iron and silicon. Comparison of the concentration data obtained by filtration and distillation methods shows that the fraction of metal and silicon impurities present in the form of suspended particles is high and approaches 10% of their total content in these chlorides. It is seen from Tables 4 and 5 that though the particles in high-purity liquids and in aerosols contain the same common elements, the relative content of these elements is different, probably owing to specific features in preparation of the high-purity liquids.

Conclusions

The application of lasers as light-sources and of sealed cells makes it possible to determine particles with sizes down to $0.04 \mu\text{m}$ even in corrosive liquids.⁴⁶ Lowering the detection limit to this value is achieved owing to the low speed with which the particles cross the scattering volume of 10^{-8}cm^3 , but leads to degradation of the detection limit with respect to concentration, increasing up to $10^4/\text{cm}^3$. However, the investigations showed the validity of the approach—in most cases high-purity liquids contain sub- μm particles at concentrations of 10^5 – $10^6/\text{cm}^3$.⁴⁶ In analysis of aerosols a sharp increase in particle concentration with decrease in particle size has been observed.⁶² This impels a search for ways to further reduce the limit of detection for particles with respect to size. A certain reduction (down to $0.01 \mu\text{m}$) may be obtained by application of powerful short-wave lasers. Another way to reduce the limit of detection is to examine the particles in supersaturated vapour, which by condensing on the particles enlarges them and makes it possible to determine the particles of smaller size. For an aerosol the particles of size down to 1 nm have thus been determined.⁶³ The particles with size of about 1 nm may also be

Table 5. Metal and silicon content in high-purity chlorides (C, % w/w) ($n = 5, P = 0.95$)

Si	1×10^{-5}	6.0×10^{-6}	2×10^{-7}	0.10	1×10^{-5}	6.0×10^{-6}	2×10^{-7}	0.10	1×10^{-5}	6.0×10^{-6}	1×10^{-6}	0.15
Total content	1.6×10^{-5}	6.0×10^{-6}	1.5×10^{-6}	0.10	4×10^{-5}	8.0×10^{-6}	1.8×10^{-6}	0.10	3×10^{-5}	8.0×10^{-6}	4×10^{-6}	0.15
Mg	3×10^{-6}	1.3×10^{-6}	1×10^{-7}	0.27	7×10^{-6}	3.0×10^{-6}	$< 1 \times 10^{-7}$	3×10^{-6}	3×10^{-6}	1.3×10^{-6}	5×10^{-7}	0.2
Al	1×10^{-7}	5.6×10^{-8}	5×10^{-8}	0.27	5×10^{-6}	3.0×10^{-6}	$< 4 \times 10^{-8}$	5×10^{-7}	6×10^{-6}	2.8×10^{-7}	2×10^{-7}	0.2
Ca	1×10^{-7}	4.5×10^{-8}	$< 2 \times 10^{-7}$		3×10^{-6}	1.3×10^{-6}	$< 2 \times 10^{-7}$	4×10^{-6}	4×10^{-6}	2.7×10^{-6}	$< 2 \times 10^{-7}$	
Cr	$< 3 \times 10^{-8}$		1×10^{-6}		1×10^{-6}	3.7×10^{-7}	$< 1 \times 10^{-7}$		4×10^{-6}	1.5×10^{-6}	$< 1 \times 10^{-7}$	
Mn	3×10^{-8}	9.0×10^{-9}	$< 1 \times 10^{-8}$		1×10^{-7}	3.0×10^{-8}	2×10^{-8}	0.15	7×10^{-8}	2.1×10^{-8}	8×10^{-8}	0.2
Fe	3×10^{-7}	1.6×10^{-7}	4×10^{-7}	0.24	1×10^{-6}	5.3×10^{-7}	6×10^{-7}	0.15	5×10^{-6}	2.6×10^{-6}	7×10^{-7}	0.2
Co	$< 6 \times 10^{-9}$		$< 2 \times 10^{-7}$		3×10^{-6}	1.0×10^{-6}	$< 2 \times 10^{-7}$		$< 6 \times 10^{-9}$		$< 2 \times 10^{-7}$	
Ni	3×10^{-9}		$< 1 \times 10^{-7}$		2×10^{-6}	5.4×10^{-7}	$< 1 \times 10^{-7}$		$< 6 \times 10^{-8}$		$< 1 \times 10^{-7}$	
Cu	3×10^{-9}	1.4×10^{-9}	$< 8 \times 10^{-9}$		1×10^{-6}	4.7×10^{-7}	$< 8 \times 10^{-9}$		3×10^{-8}	1.4×10^{-8}	$< 8 \times 10^{-9}$	
Ag	$< 3 \times 10^{-9}$		$< 6 \times 10^{-9}$		8×10^{-8}	2.0×10^{-8}	$< 6 \times 10^{-9}$		$< 3 \times 10^{-9}$		$< 6 \times 10^{-9}$	
Cd	$< 1 \times 10^{-8}$		$< 2 \times 10^{-8}$		2×10^{-6}	6.1×10^{-7}	$< 2 \times 10^{-8}$		$< 1 \times 10^{-8}$		$< 2 \times 10^{-8}$	
Sb	$< 1 \times 10^{-7}$		5×10^{-6}	0.17	5×10^{-6}	1.5×10^{-6}	$< 4 \times 10^{-9}$		$< 1 \times 10^{-7}$		3×10^{-7}	0.17
Pb	3×10^{-9}	1.2×10^{-9}	$< 1 \times 10^{-7}$		2×10^{-7}	8.0×10^{-8}	$< 1 \times 10^{-7}$		6×10^{-8}	2.4×10^{-8}	$< 1 \times 10^{-7}$	
Bi	2×10^{-6}	7.4×10^{-7}	$< 1 \times 10^{-8}$		1×10^{-6}	3.7×10^{-7}	$< 1 \times 10^{-8}$		5×10^{-7}	1.9×10^{-7}	$< 1 \times 10^{-8}$	
Si	1×10^{-5}	6.0×10^{-6}	2×10^{-7}	0.10	1×10^{-5}	6.0×10^{-6}	2×10^{-7}	0.10	1×10^{-5}	6.0×10^{-6}	1×10^{-6}	0.15
Total content	1.6×10^{-5}	6.0×10^{-6}	1.5×10^{-6}	0.10	4×10^{-5}	8.0×10^{-6}	1.8×10^{-6}	0.10	3×10^{-5}	8.0×10^{-6}	4×10^{-6}	0.15

* S_y = standard deviation of the mantissa of the logarithms of analysis results, assumed to have log-normal distribution.

recorded by the use of the cavitation chamber.⁶⁴ Irradiation of a liquid with a powerful laser pulse produces gas bubbles on the particles, by means of which the particles can be determined.

The determination of particles of nm size is also possible by electron microscopy. The application of electron microscopy with X-ray spectral analysis alongside electron-energy analysis spectroscopy provides determination of both particle size and composition. However, the application of this destructive method demands that sample preparation and analysis be done in isolation from the environment, with special apparatus.

REFERENCES

- G. G. Devyatykh, *Vestn. Akad. Nauk SSSR*, 1982, 7, 25.
- G. G. Devyatykh, V. M. Stepanov, M. F. Churbanov, V. A. Krylov and S. V. Yan'kov, *Dokl. Akad. Nauk SSSR*, 1980, 254, 670.
- G. G. Devyatykh and I. L. Agafonov, *Mass-spektrometricheskii analiz gazov i parov osoboi chistoty*, Nauka, Moscow, 1980.
- N. Omenetto, *Analytical Laser Spectroscopy*, Wiley, New York, 1979.
- O. P. Bochkova and E. Ya. Shreder, *Spektral'nyi analiz gazovykh smesei*, Fizmatgiz, Moscow, 1963.
- V. G. Berezkin and V. S. Tatarinsky, *Gazokhromatograficheskie metody analiza primesei*, Nauka, Moscow, 1970.
- V. M. Nemets, A. A. Petrov and A. A. Solov'ev, *Zavodsk. Lab.*, 1984, 50, No. 1, 22.
- G. G. Devyatykh and Yu. A. Karpov, *Talanta*, 1987, 34, 123.
- P. W. Hawkes, *Electron Optics and Electron Microscopy*, Taylor and Francis, London, 1972.
- L. Ya. Gradus, *Rukovodstvo po dispersionnomu analizu metodom mikroskopii*, Khimiya, Moscow, 1979.
- F. M. Rabinovich, *Konduktometricheskii metod dispersionnogo analiza*, Khimiya, Leningrad, 1970.
- A. Ioshi, L. E. Davis and P. W. Palmberg, in *Methods of Surface Analysis*, A. W. Czanderna (ed.), p. 159. Elsevier, Amsterdam, 1975.
- G. G. Devyatykh, V. N. Shishov, V. V. Balabanov, N. V. Larin, V. I. Zvereva and V. I. Rodchenkov, *Zh. Analit. Khim.*, 1977, 32, 1578.
- Ya. B. Chertkov, K. V. Rybakov and V. N. Zrel'ov, *Zagryazneniya i metody ochistki neftyanykh topliv*, Khimiya, Moscow, 1970.
- Yu. I. Petrov, *Fizika malykh chastits*, p. 215. Nauka, Moscow, 1982.
- H. C. van de Hulst, *Light Scattering by Small Particles*, p. 79. Wiley, New York, 1957.
- A. P. Klimenko, *Metody i pribory dlya izmereniya kontsentratsii pyli*, Khimiya, Moscow, 1978.
- G. F. Bolshakov, V. F. Timofeev and M. N. Novichkov, *Opticheskie metody opredeleniya zagryaznennosti zhidkikh sred*, Nauka, Novosibirsk, 1984.
- S. P. Belyaev, N. K. Nikiforova, V. V. Smirnov and G. I. Shchelchikov, *Optiko-elektronnye metody izucheniya aerozolei*, Energoizdat, Moscow, 1981.
- R. A. Mavliev, A. N. Ankilov and K. P. Kutsenogii, *Kolloidn. Zh.*, 1981, 43, 1089.
- A. Lieberman, *Laboratorio*, 1975, 20, 10.
- V. I. Klenin, S. Yu. Shchegolev and L. G. Lebedeva, *Opt. Spektrosk.*, 1973, 35, 1161.
- S. Egusa, *J. Colloid Interface Sci.*, 1982, 86, 135.
- L. W. Caspersen, *Appl. Opt.*, 1977, 16, 3183.
- M. Hansen, *ibid.*, 1980, 19, 3441.
- E. Trakhovskiy, S. G. Lipson and A. D. Devir, *ibid.*, 1982, 21, 3005.
- P. G. Liroy, D. Rimberg and F. G. Haughey, *J. Aerosol Sci.*, 1975, 6, 183.
- C. Roth, G. Gebhart and G. Heigwer, *J. Colloid Interface Sci.*, 1976, 54, 265.
- E. D. Hirleman and H. K. Moon, *ibid.*, 1982, 87, 124.
- K. Suda, *Rev. Sci. Instrum.*, 1980, 51, 1049.
- B. V. Deryagin and N. M. Kudryavtseva, *Kolloidn. Zh.*, 1964, 26, 61.
- E. I. Akopov, M. A. Karabegov and A. G. Ovanesyan, *Prib. Sist. Upravl.*, 1973, 5, 42.
- M. L. Mikhel'son, *Kolloidn. Zh.*, 1977, 39, 302.
- Yu. V. Zhulanov, B. F. Sadovskii, I. A. Nevskii and I. B. Petryanov, *ibid.*, 1977, 39, 1064.
- N. Buske, H. Gedan, H. Lichtenfeld, W. Katz and H. Sonntag, *Colloid Polym. Sci.*, 1980, 258, 1303.
- W. Kaye, *J. Colloid Interface Sci.*, 1973, 44, 384.
- Idem*, *Anal. Chem.*, 1973, 45, 221A.
- D. J. Walsh, J. Anderson, A. Parker and M. J. Dix, *Colloid Polym. Sci.*, 1981, 259, 1003.
- Metody analiza chistykh khimicheskikh reaktivov*, p. 265. Khimiya, Moscow, 1984.
- V. V. Balabanov, V. A. Eremina, V. N. Liverko, V. A. Krylov, O. P. Lazukina, *Poluch. Anal. Chist. Veshchestv*, 1982, 87.
- P. G. Cummins, E. J. Staples, L. G. Thompson, A. L. Smith and L. Pope, *J. Colloid Interface Sci.*, 1983, 92, 189.
- W. J. Pangonis, V. Heller and N. A. Economou, *J. Chem. Phys.*, 1961, 34, 960.
- H. Kaiser, *Two Papers on the Limit of Detection of a Complete Analytical Procedure*, A. C. Menzies (transl.), Hilger, London, 1968.
- G. G. Devyatykh, M. S. Chupakhin, V. A. Krylov, O. P. Lazukina, S. U. Kreyngold, G. G. Vinogradov and E. M. Yutal, *Zavodsk. Lab.*, 1980, 46, 921.
- S. V. Kuzmin, S. A. Saunin, Yu. A. Sprizhitskii and M. S. Bezruchko, *Prib. Tech. Eksp.*, 1983, 1, 165.
- V. A. Krylov, O. P. Lazukina, A. V. Golubev and S. U. Kreyngold, *Fiziko-khimicheskie metody analiza*, p. 72. GGU, Gorkii, 1982.
- S. V. Kuzmin, *Kolloidn. Zh.*, 1984, 46, 355.
- A. N. Ankilov, A. I. Borodulin, B. M. Goldman, K. P. Kutsenogii, Yu. F. Chankin, V. P. Grivin and A. B. Semenov, *ibid.*, 1978, 40, 735.
- A. N. Ankilov, A. I. Borodulin, K. P. Kutsenogii, Yu. A. Grishin and A. G. Semenov, *ibid.*, 1978, 40, 426.
- A. F. Shchurov, T. V. Grachova, V. A. Krylov, V. A. Shipunov, O. P. Lazukina and A. V. Golubev, *Poluch. Anal. Chist. Veshchestv*, 1982, 66.
- G. G. Devyatykh, A. V. Gusev and V. M. Vorotyntsev, *Teor. Osn. Khim. Tekhnol.*, 1976, 10, 614.
- V. A. Krylov, O. P. Lazukina, A. V. Golubev, V. N. Shishov and O. P. Struchkova, *Zh. Analit. Khim.*, 1984, 39, 678.
- G. G. Devyatykh, S. G. Krasnova and L. I. Osipova, *Zh. Fiz. Khim.*, 1981, 55, 750.
- G. G. Devyatykh, V. A. Krylov, O. P. Lazukina, L. N. Doronina and A. V. Golubev, *Kolloidn. Zh.*, 1984, 46, 1019.
- K. E. Perepelkin and V. S. Matveev, *Gazovye emulsii*, Khimiya, Leningrad, 1979.
- P. W. Morrison (ed.), *Contamination Control in Electronic Manufacturing*, p. 241. Van Nostrand-Reinhold, New York, 1973.
- J. Růžička and J. Starý, *Substoichiometry in Radiochemical Analysis*, p. 54. Pergamon Press, Oxford, 1968.
- G. G. Devyatykh, V. V. Balabanov, V. I. Zvereva, V. N. Shishov and V. I. Rodchenkov, *Dokl. Akad. Nauk SSSR*, 1976, 230, 342.

59. Yu. M. Martynov and I. G. Syrkina, *Zh. Neorgan. Khim.*, 1965, **10**, 943.
60. G. V. Seryakov and L. A. Niselson, *Zh. Prikl. Khim., Leningrad*, 1962, **35**, 482.
61. N. V. Larin, V. N. Shishov, V. A. Krylov and E. I. Mishina, *Zh. Analit. Khim.*, 1976, **31**, 2193.
62. C. E. Junge, *Air Chemistry and Radioactivity*, Academic Press, New York, 1963.
63. L. Herrebaut and G. J. Madelaine, *Chauf.-Vent. Cond.*, 1975, **51**, 31.
64. A. V. Butenin and B. Ya. Kogan, *Prib. Tekhn. Eksp.*, 1974, **5**, 175.

THE EFFECT OF THERMAL SAMPLE PRETREATMENT ON THE ABSORPTION SIGNAL IN GRAPHITE FURNACE AAS

B. V. L'VOV, L. K. POLZIK and L. F. YATSENKO
Analytical Chemistry Department, Polytechnic Institute, Leningrad, USSR

(Received 15 October 1985. Accepted 20 July 1986)

Summary—The origin of the unusual maxima observed in the decomposition curves for pure solutions of some elements has been investigated theoretically and experimentally. An increase in the atom residence time caused by longitudinal redistribution of the analyte in the tube during the pyrolysis step was found to be responsible. The effect can be observed only if the sample is atomized under gas-flow conditions. To prevent any influence on analytical results, atomization should be done in the gas-stop mode.

Graphite-furnace atomic-absorption (AA) analysis of samples of complex composition includes, as a rule, a stage of thermal pretreatment of the sample prior to its atomization. The purpose of this is to remove as completely as possible the volatile material released in the thermal decomposition of the matrix. The charring temperature chosen is the maximum temperature at which no loss of the analyte is observed. To determine it, the absorption signal is measured as a function of the charring temperature. There is a wealth of data on the thermal pretreatment of samples.¹⁻³ In the book by Lindsjo and Riekkola,² for example, there are decomposition curves for 42 elements. For some of these (Be, Bi, Na, La, Si, etc.) the fall-off in the curve corresponding to the start of loss of analyte is preceded by a noticeable increase in the signal.^{2,3}

The present work was undertaken in an attempt to explain this effect, which at first glance might seem anomalous, by considering the longitudinal distribution of the sample in the furnace.

THEORY

Formulation of the problem

The technique of finding the optimal thermal sample pretreatment regime involves maintaining the sample in the furnace at a chosen temperature for a given time, with subsequent determination by AAS of the amount of analyte remaining, under standard conditions. The temperature dependence of the ratio of the absorbances measured with (Q_A) and without $(Q_A)_0$ thermal pretreatment is called the decomposition curve.

Let us consider possible causes of variations in the absorption signal at the atomization stage. It is well known⁴ that the integrated absorbance (Q_A) is pro-

portional to the amount of analyte in the sample and the mean residence time (τ) of atoms in the analytical volume. If the sample vaporization conditions at the atomization stage are the same, variations in the absorption signal may be due either to analyte losses in the course of the thermal pretreatment or to a change in the residence time of the atoms in the furnace. In the first case, the signal can only diminish, and decrease in $Q_A/(Q_A)_0$ can then be readily related to the extent of sample loss during the thermal pretreatment. In the second case both an increase and decrease of the absorption signal can be observed, depending on the actual change of the magnitude of τ .

Consider the factors affecting the magnitude of τ . For a tube furnace, τ depends on the rates of diffusional transfer of the analyte vapour through the sample-injection hole and side openings and of convective transfer of the atoms by the purge gas. When the purge-gas flow is stopped (the gas-stop mode), the analyte vapour can escape from the furnace volume only by diffusion, whereas if the furnace is purged with an inert gas, convective transfer predominates. Let us now consider how variations in the dimensions and longitudinal position of the sample spot can affect the residence time of the atoms in the furnace volume in the two cases.

Effect of sample position on τ in the gas-stop mode

Earlier publications^{5,6} dealing with models of diffusional transfer of the vapours from the furnace considered the sample as a point source of atoms located at the centre of an isothermal furnace. Gilmutdinov and Fishman^{7,8} have proposed a diffusional transfer model for a sample with finite dimensions along the furnace axis, taking into account the longitudinal temperature gradient. The treatment was limited, however, to consideration of atom removal

only through the open tube ends, and a Gaussian temperature distribution. For HGA furnaces such a distribution is appropriate only at low temperatures; at high temperatures the distribution is nearly trapezoidal.⁹ The model in question^{7,8} implies that the atom residence time in the furnace should decrease monotonically with increasing length of the atom source.

Let us now evaluate the importance of taking into account the diffusional escape of vapours through the injection hole. In this simulation of the process, only the case of a point atom-source will be considered, and, to further simplify the model, the non-uniformity of the atom distribution over the furnace cross-sectional area will be neglected. Then, from symmetry considerations, the problem of the diffusional vapour transfer through the open tube ends and the injection hole for a furnace of length l may be reduced to that of diffusional transfer of vapour out of a tube of the same diameter and length $l/2$ with one end open and the other stoppered by a plug having a channel of cross-sectional area half that of the injection hole, and of length equal to the furnace wall thickness (Fig. 1a).

In the steady state, the diffusion flux J of atoms through a hole is determined by Fick's equation

$$J = -\frac{SD}{RT} \frac{dp}{dx} \quad (1)$$

where S is the hole cross-sectional area, D the vapour diffusion coefficient in the purge gas, R the gas constant and dp/dx the partial pressure gradient of the diffusing vapour along the x -axis.

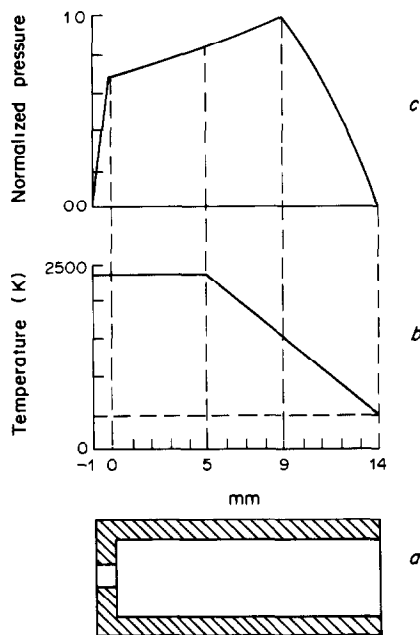


Fig. 1. (a) An equivalent model of the furnace, (b) longitudinal temperature distribution, (c) calculated longitudinal vapour distribution, for the atom source at $x = 9$ mm.

Integration of equation (1) yields $p(x)$ distributions for various source positions along the furnace axis. Figure 1c presents such a distribution for a particular source position. The calculation included vapour transfer through both holes, their cross-sectional-area ratio being 25. The plug channel was assumed to be 1 mm long for a tube length of 14 mm. The furnace temperature profile (Fig. 1b) was approximated (in accordance with the results of Slavin *et al.*⁹) by: $T = 2300$ K for x from -1 to $+5$ mm, and $T = [2300 - 200(x - 5)]$ K for $5 \text{ mm} \leq x \leq 14$ mm. The temperature-dependence of the diffusion coefficient was assumed to be¹⁰

$$D = D_0(T/273)^{1.75} \quad (2)$$

the boundary conditions for $p(x)$ being obviously $p(-1 \text{ mm}) = p(14 \text{ mm}) = 0$.

The $p(x)$ distributions found for different atom-source positions in the furnace were then used to calculate from equation (1) the two diffusion fluxes (J_1 and J_2), and also the total number of the atoms in the furnace

$$N = \int_0^{l/2} \frac{p(x)}{RT} S dx. \quad (3)$$

From the obvious relationship

$$\tau(x) = N/(J_1 + J_2), \quad (4)$$

the function of interest

$$f(x) = \tau(x)/\tau(0) \quad (5)$$

can now be calculated. This characterizes the relative variation of the atom residence time in the furnace and, hence, of the absorption signal *vs.* atom source position with respect to the furnace centre ($x = 0$).

Figure 2 illustrates the calculations of the function $f(x)$ with and without taking into account the vapour diffusional transfer through the injection hole. As seen from the data, neglect of the latter process leads, just as in the previous model,^{7,8} to a monotonic decrease in $f(x)$ to 18% at $x = 8$ mm. If the vapour diffusional transfer through the injection hole is included, then the quantity $f(x)$ exhibits first a slight increase (by 10%) followed by a fall-off starting from $x = 5$ mm. The quantity $f(x)$ approaches 1 at 8.5 mm from the furnace centre. Thus, the diffusive transfer

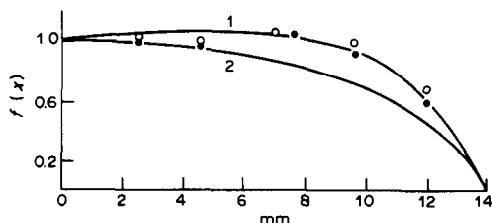


Fig. 2. Relative variation of the absorption signal *vs.* atom source position for the gas-stop mode with diffusional transfer through the injection hole (1) taken into account, (2) neglected. The points are the experimental data (●—Be; ○—Bi).

of vapour through the injection hole should favour stabilization of the mean atom residence time in the furnace as the atom-source position is varied along the furnace axis. It must be noted that this conclusion assumes use of the gas-stop mode.

Effect of sample position on τ in the gas-flow mode

In the gas-flow mode, the diffusional vapour transfer for a sample at the centre of the furnace may be neglected, to a first approximation. It is further assumed that the vapours escape from the furnace at a constant rate and over the shortest path, of length d , for the atom source at the furnace centre. If the source is at a distance x from the centre, the length of the escape path is $(x^2 + d^2)^{1/2}$. Then as the atom source is moved along the furnace axis the relative atom residence time in the furnace should increase according to

$$f(x) = \sqrt{1 + (x/d)^2}. \quad (6)$$

Naturally, as x increases, the diffusional vapour transfer through the tube ends will play an ever increasing role, so that beyond a certain value of x , the atom residence time in the furnace will start to decrease.

Sample redistribution at the thermal pretreatment stage

Variations in the dimensions and position of the atom source at the thermal pretreatment stage may result from a redistribution of the analyte in the course of gas-phase thermochemical processes. One of the possible mechanisms is the thermal reduction of oxides by carbon. This mechanism has been shown¹¹ to consist of transfer of carbon by the gaseous metal-carbide molecules to oxide particles. If, at a given temperature, the partial pressure of analyte in the gas phase greatly exceeds the saturated vapour pressure, the reduced metal should condense near the oxide particles. In this case, little or no sample transfer occurs. If, however, the partial vapour pressure of analyte reached in the course of the thermal reduction of oxides by carbon is close to the saturated vapour pressure of the metal, the sample may become redistributed over a fairly large area of furnace surface.

Another possible process starting at the thermal pretreatment stage is the thermal dissociation of oxides. Since the metal vapour pressure reached here is less than the saturated vapour pressure of the analyte in question, the decomposition curves should exhibit a fall-off of absorbance. Only at low temperatures can the metal condense at the furnace walls, because there is a greater longitudinal temperature gradient from the furnace centre to the ends at low temperature. The temperature gradient in the central part of the furnace at low temperatures should favour condensation not only of metal vapours but also of gaseous compounds which vaporize at

low temperatures without decomposition (e.g., alkali metal chlorides).

This leads to the following conclusions. The position of the atom source can change during the sample thermal-pretreatment stage, as a result of gas-phase thermochemical processes. If atomization is performed under gas-flow conditions, this may cause an increase in the residence time of atoms in the furnace volume, and hence an increase in the absorption signal. If a sample is atomized in the gas-stop mode, variations in the atom-source position (for $x \leq 8$ mm) should not affect the absorption signal.

EXPERIMENTAL

The experimental investigation of the possible causes of enhanced absorption signals in the decomposition curves included, first, a study of the effect of the purge-gas flow conditions on the absorption signal with the atom source shifted from the furnace centre toward the tube end, second, a study of the dependence of $Q_A/(Q_A)_0$ on furnace temperature at the charring stage for different purge-gas flow conditions at the atomization stage, for a number of elements (Be, Bi, Na, Si).

Perkin-Elmer models 603 and 5000 atomic-absorption spectrometers fitted with models HGA-76 and HGA-500 electrothermal atomizers, respectively, were used, with standard pyro-coated tubes. The purge gas was high-purity argon (oxygen content $< 10^{-3}\%$). The lines used were Be 234.9 nm, Bi 221.1 nm, Na 330.2 nm, and Si 251.6 nm.

The variation of the absorption signal with longitudinal position of the sample for different purge-gas flow-rates was studied for bismuth and beryllium. The experiments were performed in the following way. A hole was drilled in the 1.5-mm thick wall of a ring of outer diameter 6 mm and length 3 mm, fabricated from a carbon rod. A shallow indentation was made in the inner surface of the ring opposite the hole. The ring was placed inside the furnace so as to bring the ring hole in line with the injection hole of the furnace. A 10- μ l sample was injected into the indentation on the ring with an Eppendorf pipette. After drying of the solution the ring was moved to the desired position in the furnace, and the absorption signal Q_A was measured under standard conditions¹² (without the thermal pretreatment stage).

The effect of purge-gas flow at the atomization stage on the shape of the decomposition curves was studied for beryllium, bismuth, sodium and silicon. A 10- μ l sample was deposited on the inner surface of the furnace. Beryllium and bismuth were introduced into the furnace as nitrate solutions, silicon as a solution of sodium silicate and sodium as sodium chloride solution. The nitrates decompose at about 400–500 K with the formation of the oxides. Sodium silicate also decomposes into sodium and silicon oxides. Thus the compounds actually studied were BeO (10^{-8} g), Bi₂O₃ (10^{-8} g), SiO₂ (10^{-7} g), and NaCl (10^{-7} g). The thermal pretreatment was applied at the maximum argon flow-rate (300 ml/min), for 40 sec. Atomization was in the "gas-stop" or "full-flow" mode.

DISCUSSION

Figures 2 and 3 present the experimental curves showing the dependence of the absorption signal for beryllium (3 ng) and bismuth (10 ng) on the sample position, varied from the centre to the end of the tube, as obtained in the gas-stop and full-flow modes. In the gas-stop mode the absorption signal remains

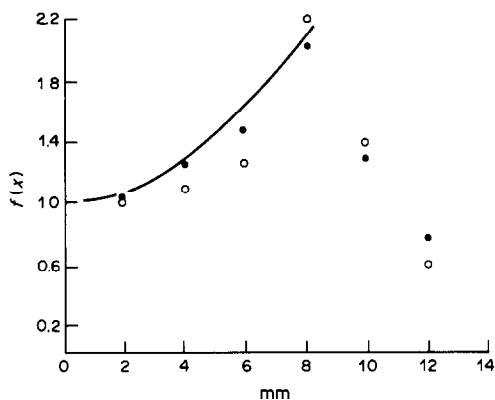


Fig. 3. Relative variation of the absorption signal as a function of atom source position for the full-flow mode (with $d = 4.5$ mm). The points are the experimental data (●—Be; ○—Bi).

practically constant up to $x = 8$ mm, after which it drops off monotonically (Fig. 2). When the tube is purged with argon at a flow-rate of 300 ml/min, the $f(x)$ vs. x plot reveals a strongly pronounced maximum (Fig. 3) corresponding to the ring with the sample being placed at a distance of 8 mm from the furnace centre. In both cases the experimental data were found to agree with the theoretical estimates. This supports our suggestion that the increase in the absorption signal in the thermal decomposition curves originates from a change in the atom-source position and from using the gas-flow mode at the atomization stage.

The magnitude of the effect observed in the decomposition curves (Figs. 4 and 5) depends on the actual extent of sample redistribution. This, in its turn, depends on several factors, namely the mechanism and rate of the process involved, the metal vapour pressure, and the character of the longitudinal tem-

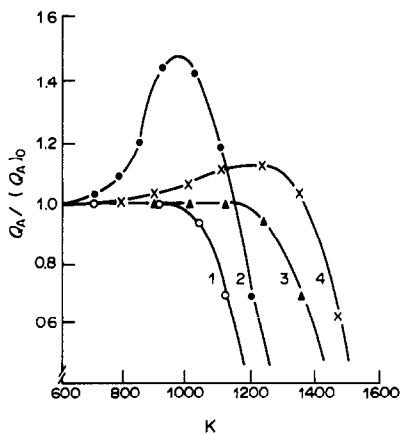


Fig. 4. Decomposition curves for 500 ng of NaCl (1, 2) and 80 ng of BeO (3, 4) for different sample atomization conditions: 1, 3—argon flow stopped; 2, 4—full argon flow.

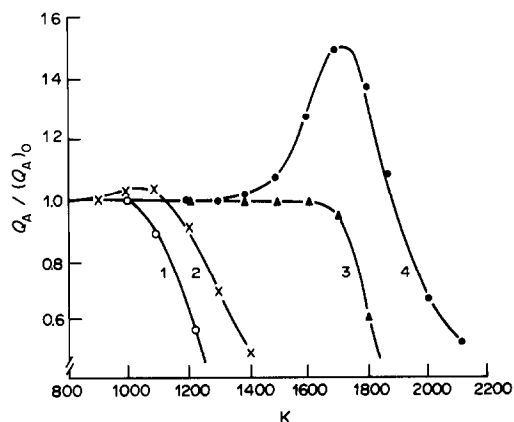


Fig. 5. Decomposition curves for 15 ng of Bi_2O_3 (1, 2) and 250 ng of SiO_2 (3, 4) for different sample-atomization conditions: 1, 3—argon flow stopped; 2, 4—full argon flow.

perature distribution during the pretreatment stage. As seen from Figs. 4 and 5, the increase in the absorbance is different for beryllium and bismuth oxides, although in both cases the effect is seen at similar temperatures. This may result from the differing decomposition processes—for beryllium, thermal reduction of the oxide by carbon,¹³ and for bismuth, thermal dissociation of the oxide.¹⁴

In the case of silicon oxide (Fig. 5) the sample redistribution again results from thermal reduction of the oxide by carbon, since the calculated temperature of the initiation of this process (around 1400 K)¹³ is in accord with the beginning of the rise in the absorption signal. Transfer of sodium (Fig. 4) results from the sodium molecules being transported to the colder tube ends owing to the noticeable temperature gradient present (at < 1000 K) in the central part of the furnace.

Thus, in all the cases considered, the rise in the absorption signal in the decomposition curves results from sample redistribution occurring at the thermal pretreatment stage. To prevent this process from affecting the analytical results, atomization should be done under gas-stop conditions. This recommendation conforms to the conditions favouring interference-free analysis by use of platform furnaces.^{15,16}

REFERENCES

1. B. Welz, *Atomic Absorption Spectroscopy*, Verlag Chemie, Weinheim, 1976.
2. O. Lindsjo and M. Riekkola, *Atomabsorptionsspektrometria*, Teknillisten Tieteiden Akatemia, 1976.
3. G. Müller-Vogt and W. Wendl, *Anal. Chem.*, 1981, **53**, 651.
4. B. V. L'vov, *Zh. Prikl. Spektrosk.*, 1968, **8**, 517.
5. B. V. L'vov, *Atomic Absorption Spectrochemical Analysis*, Hilger, London, 1970.
6. B. V. L'vov and L. K. Polzik, *Zh. Analit. Khim.*, 1978, **33**, 1461.
7. A. Kh. Gilmudtinov and I. S. Fishman, *Zh. Prikl. Spektrosk.*, 1982, **37**, 541.

8. *Idem*, *Spectrochim. Acta*, 1984, **39B**, 171.
9. W. Slavin, S. A. Myers and D. C. Manning, *Anal. Chim. Acta*, 1980, **117**, 267.
10. *Tables of Physical Constants* (in Russian), ed. I. K. Kikoin, Moscow, 1976.
11. B. V. L'vov, A. S. Savin and L. F. Yatsenko, *Zh. Prikl. Spektrosk.*, 1985, **43**, 887.
12. *Analytical Methods for Furnace AAS*, Perkin-Elmer, Bodenseewerk, 1980.
13. B. V. L'vov, *Izv. Vuz. (Chern. Metallurg.)*, 1986, No. 1, 4.
14. B. V. L'vov and L. F. Yatsenko, *Zh. Analit. Khim.*, 1984, **39**, 1773.
15. W. Slavin and G. R. Carnrick, *Spectrochim. Acta*, 1984, **39B**, 271.
16. B. V. L'vov, E. A. Norman and L. V. Masaltseva, *Zh. Analit. Khim.*, 1985, **40**, 275.

ATOMIC-ABSORPTION METHODS FOR ANALYSIS OF HIGH-PURITY SUBSTANCES

I. G. YUDELEVICH, L. V. ZELENTOVA and N. F. BEISEL

Institute of Inorganic Chemistry, Siberian Division, USSR Academy of Sciences, Novosibirsk, USSR

(Received 25 October 1985. Revised 20 March 1986. Accepted 14 August 1986)

Summary—A review is given of the use of atomic-absorption methods for determining the trace impurities in high-purity metals.

Atomic-absorption spectrometry (AAS) is one of the most promising methods of modern analytical chemistry and is used for analysis of a great variety of materials. The low detection limits and sufficiently high accuracy provided by AAS with electrothermal atomization serve as the basis for application of this method for analysis of high-purity substances. The ability of AAS to compete successfully with emission spectrometry (ES) and spark-source mass-spectrometry (SSMS) methods for this purpose is shown in Table 1, which shows the detection limits for a wide range of elements, for the three methods being compared. In many instances AAS gives detection limits as low as those of SSMS but with better accuracy and precision: the relative standard deviation is in most cases 4–20% for AAS and 20–30% for ES and SSMS. The analysis time for 10–15

micro-impurities is nearly the same for all three methods, but AAS is more convenient for running reagent blanks and especially for using the standard-additions method to deal with matrix effects.

We have used AAS with electrothermal atomization for development of methods for analysis of some high-purity metals (Ag, As, Au, Ga, In, Re, Sn).

DIRECT ATOMIC-ABSORPTION ANALYSIS OF HIGH-PURITY MATERIALS

The potential of AAS is not always realizable, because of the matrix effects on the analytical signals, especially when they result in strong degradation of the sensitivity. Hence development of any atomic-absorption procedure starts with an investigation of matrix effects and ways of eliminating any un-

Table 1. Absolute detection limits of impurities by ES,¹ AAS and SSMS² methods

Detection limits, g	ES*	AAS†	SSMS "thin layer"‡
10^{-13} – 10^{-12}	—	Ag, Cd, Mg, Zn	Be, Mn, V
10^{-12} – 10^{-11}	—	Be, Cd, Cr Cu, K, Li, Mn, Na, Yb	Ag, As, Co, Cr, Cs, Cu, Ga, Hf, In, Ni, Rb, Re, Rh, Ru, Sb, Se, Sn, Sr, Te, Zn, Zr, REE
10^{-11} – 10^{-10}	—	Al, Au, Bi, Co, Cs, Fe, Ga, In, Mo, Ni, Pb, Pd, Rb, Rh, Sb, Si, Sn, Sr, Ta	Al, Ba, Ca, Cd Fe, Ir, K, Mg, Mo, Na, P, Pb, S, Pt, Se, Ti, Tl, W
10^{-10} – 10^{-9}	Ag, B, Be, Cd, Cu, Ga, Mn, Pb, Zn	As, Ba, Eu, Ru, Sc, Se, Te, V	Au, Bi, Nb
10^{-9} – 10^{-8}	Au, Ba, Bi, Co, Cr, Fe, In, Mg, Mo, Ni, Pd, Se, Sn, Ti, Tl, V, Y, Zr	B, Dy, Hg, Ho, Ir, Pt, Y	—
10^{-8} – 10^{-7}	Al, As, Ca, Hf, La, Nb, Pt, Sb, Te, W	—	—
10^{-7} – 10^{-6}	Ir, P, Ta	—	—

*Sample matrix—graphite powder (20 mg) + 0.5% NaCl.

†Aqueous solutions of salts of elements.

‡Impurities on the surface (area 1 cm²) of a polished silicon plate.

desirable ones. It often becomes in many cases necessary to remove major elements in a preliminary chemical separation.

Analysis of tin and arsenic

When readily volatile matrices are analysed it is possible to remove the interfering matrix by distilling it off from the graphite furnace at pre-atomization stages. We did this when developing methods for analysis of high-purity tin³ and arsenic:⁴ tin was volatilized as the tetrabromide and arsenic as the chloride and oxide. Much attention was given to optimizing this step. It was established that as the drying temperature was increased to 250–300° and the ashing temperature to 900–1000°, no more than 1% of the As and 1–5% of the tin remained in the furnace. At lower ashing temperature these quantities were higher and liable to interfere in determination of the trace analytes, but on the other hand, losses of these analytes may occur during matrix distillation, making a compromise necessary. In consequence of this we checked the change in the analytical signals of trace impurities as different quantities of the main components were distilled off. All the impurities were determined under the optimal conditions previously chosen (in the absence of matrix). It was shown that when the test solutions contained up to 20 mg of As or Sn per ml, Ag, Ba, Be, Ca, Co, Cr, Cu, Ni, Sr, V and Yb could be determined without interference. However, up to 10–22% of any Cd, Fe, Mg or Mn present could be lost during the matrix distillation so they were determined by making appropriate corrections. It was possible to determine Al, Ca, Co, Cr, Cu, Fe, Li, Mg, Mn, Ni, Sr in solutions containing As up to 20 mg/ml, and Cd, Pb, Zn in solutions containing As up to 10 mg/ml. There were losses of up to 90% of microimpurities of Al, Bi, Ca, Pb, Sb, Zn during distillation of Sn, and of Au, Sb, Si and Ga during distillation of As. These impurities cannot be determined by this method.

On the basis of these investigations the following procedures for analysis of high-purity tin and arsenic are suggested. The tin sample (100 mg) is placed in a PTFE beaker, 1.5 ml of concentrated hydrobromic acid and 0.05 ml of bromine are added, and the tin is dissolved by heating at 65–68° for 4–5 hr in a thermostat. Demineralized water is then added to bring the volume to 5 ml, and the solution is analysed directly. The arsenic (200 mg) is dissolved in a mixture of 1.5 ml of 6*M* hydrochloric acid and 0.5 ml of 12*M* nitric acid by heating at 70° for 3–4 hr in a thermostat. The solution is diluted accurately to 10 ml with demineralized water and analysed directly for all the impurities except Pb, Cd and Zn, for which an additional dilution is required.

Ag, Ba, Be, Ca, Cd, Co, Cr, Cu, Fe, Mg, Mn, Ni, Sr, V and Yb are determined in tin, and Ag, Al, Ca, Cr, Cd, Co, Cu, Fe, Li, Mg, Mn, Ni, Pb, Sr, Zn in arsenic, with detection limits of 10^{-7} – $10^{-5}\%$, and relative standard deviation of 2–3%.

Analysis of rhenium

The opposite method—fractional evaporation of impurities from a very involatile matrix—was used for analysis of high-purity rhenium.^{5,6} The perrhenic acid obtained by dissolution of rhenium in hydrogen peroxide or nitric acid can be reduced to rhenium (m.p. 3167°, b.p. 5370°) in the graphite furnace. To ensure this, programmed thermal decomposition was used; under the optimal conditions used (Table 2) rhenium does not even melt, and micro-impurities of Ag, Al, Bi, Ca, Cd, Cr, Cu, Fe, Mg, Mn, Ni, Pb, Zn can be determined with detection limits in the range 10^{-7} – $10^{-4}\%$. However, rhenium slightly depresses the signal from some of the impurities and considerably decreases the signal for Bi. An attempt to lower the detection limits through extractive separation of the matrix with 0.3*M* tri-*n*-octylamine oxide in toluene decreased the detection limits for Cd, Cr and Pb by one order of magnitude, for Ni by two orders, and for Bi by three orders, but limits for Al, Ca, Fe, Mg, Mn, Zn either did not decrease or sometimes grew, because of an increase in the blank signal, due to the large quantities of reagents used and additional operations necessary. Thus it is expedient to employ two methods for analysis of rhenium: the direct method for the determination of Ag, Al, Ca, Cu, Fe, Mg, Mn, Zn with detection limits ranging from 5×10^{-7} to $2 \times 10^{-5}\%$, and the extraction method for the determination of Bi, Cd, Cr, Ni, Pb with detection limits in the range 4×10^{-8} – $1 \times 10^{-6}\%$.

ATOMIC-ABSORPTION ANALYSIS OF HIGH-PURITY METALS WITH CONCENTRATION OF IMPURITIES

As noted above, the direct AAS analysis of pure substances is not always possible because of strong depression of the analytical signal by the main component. To eliminate this effect, the matrix must be

Table 2. Conditions for determination of impurities in rhenium*

Element	Ashing		
	Time of temperature increase, sec	Final temperature, °C	Atomization temperature, °C
Ag	70	600	2500
Al	60	1450	2700
Bi	70	600	1900
Ca	60	1400	2340
Cd	70	600	1900
Cu	75	1000	2550
Cr	45	1200	2700
Fe	35	1150	2530
Mg	80	1150	2500
Mn	75	1000	2600
Ni	35	1150	2560
Pb	85	700	2100
Zn	85	700	1900

*Drying for 20–60 sec at 100°.

separated from the analytes and this is usually done by extraction of the matrix or the impurities.

Analysis of indium and gallium

Because of the matrix effect, only Al, Ca, Cu, Mg and Mn can be directly determined in gallium with sufficiently low detection limits (5×10^{-6} – $1 \times 10^{-5}\%$). The extractive separation of In and Ga by β,β' -dichlorodiethyl ether (chlorex) has been employed for widening the number of determinable impurities. It is necessary to reduce the quantity of matrix metal in the aqueous phase to not more than 50 μg . In and Ga can be most completely removed by extraction with freshly distilled chlorex at $\text{pH} \leq 1$. The aqueous phase must contain no nitrate, as gallium nitrate is not extracted by chlorex. The procedure recommended is as follows. Metallic gallium (1 g) is dissolved in a mixture of 3 ml of 12M hydrochloric acid and 1 ml of 14M nitric acid by heating at 95° for 16–18 hr in a thermostat. The solution is evaporated to a syrup, 1 ml of 12M hydrochloric acid is added and the solution evaporated again, to give more complete conversion of gallium nitrate into the chloride complexes. The residue is transferred into a separating funnel with 10 ml of 12M hydrochloric acid and Ga extracted with three 10-ml portions of chlorex. The aqueous phase is evaporated at 80° and the residue dissolved in 2 ml of 0.3M hydrochloric acid, and this solution analysed. Metallic indium (1 g) is dissolved in 4 ml of 8M hydrobromic acid at 60–70°. The solution is evaporated to dryness, and the residue is taken up in 5 ml of 8M hydrobromic acid and transferred into a fused-silica separating funnel. In is separated by extraction with three 10-ml portions of chlorex at the phase-ratio org:aq = 2:1. The temperature control during the dissolution and the use of small volumes of the acids minimize the content of impurities in the blank run. The methods make it possible to determine 23 impurities in Ga and 21 impurities in indium with detection limits of 10^{-8} – $10^{-5}\%$ and relative standard deviations of 4–30%.^{7,8}

Analysis of gold and silver^{9,10}

An initial study of the mutual effects of the analytes in hydrochloric and nitric acid media showed that 50-fold w/w ratio of each of the other impurity elements does not affect the determination of As, Cd, Co, Cr, Cu, Fe, Ir, Ni, Mn, Mo, Pd, Rh, Sb, Zn in nitric acid medium, and As, Cd, Co, Cr, Cu, Fe, Ir, Mn, Mo, Ni, Pd, Rh, Zn in hydrochloric acid medium, but considerable interfering effects are found for Ag, Sb, Fe, Bi, Pb, Pt and Se in hydrochloric acid medium and for Bi, Pb, Se and Te in nitric acid medium. To eliminate the interfering effects buffering with copper sulphate (5-mg/ml Cu) can be used. Matrix effects are caused by 100- $\mu\text{g}/\text{ml}$ Ag and 1-mg/ml Au for all the impurities being determined. To eliminate the matrix effects an extractive separation of the matrix was used: silver

was extracted with a solution of *O*-isopropyl-*N*-methylthiocarbamate in chloroform, and gold with a solution of di-*n*-butylsulphide in chloroform. All the micro-impurities except Pd remain completely in the aqueous phase. Pd was therefore determined in a separate sample: in gold after extractive separation of the gold with diethyl ether, and in silver by extraction of the Pd with 0.3M dioctylsulphoxide in toluene.

Sample preparation is as follows. Gold (1–10 g) is dissolved in a mixture of nitric and sulphuric acids (1:3) with addition of hydrogen peroxide, then the nitric acid is removed by repeated evaporations with concentrated hydrochloric acid. Gold is then extracted from 2M hydrochloric acid with 1M di-*n*-butylsulphide in chloroform, and the aqueous phase is evaporated to give a moist residue. This is dissolved in 5–25 ml (accurately measured) of 0.1M hydrochloric acid and aliquots are analysed for Ag, As, Bi, Cd, Pb, Pt, Se and Te after addition of copper sulphate. Silver (0.5 g) is dissolved in 1.8 ml of 6M nitric acid and the solution diluted to 5 ml with demineralized water. Silver is then extracted with an equal volume of 2M *O*-isopropyl-*N*-methylthiocarbamate in chloroform. The aqueous phase, after washing with a 0.2M chloroform solution of the extractant is evaporated, the residue is dissolved in 0.1M nitric acid and the solution obtained is analysed for As, Bi, Cd, Pb, Sb, Se, Te with copper sulphate added as buffer. Use of the buffer improves the sensitivity and precision for all these elements, whether they are subject to mutual interference or not.

To bring Rh and Ir completely into solution, a.c. electrolytic dissolution of a separate sample is used. The detection limits for impurities in Ag and Au are 1×10^{-9} – $2 \times 10^{-6}\%$.

Silver and gold can be analysed for P and Si by an indirect method based on atomic-absorption determination of the molybdenum in phosphomolybdic acid (PMA) and silicomolybdic acid (SMA) formed from these elements. Gold is first separated by extraction with diethyl ether then PMA is formed with ammonium molybdate and extracted with a mixture of *n*-butanol and carbon tetrachloride (1:3), and the molybdenum is stripped with 3M ammonia and determined by AAS. Because silicon may be lost by conversion into inactive silica during the decomposition of the sample, the silicon was co-precipitated on AgCl as carrier and subsequently converted into an active form by heating the AgCl with sodium hydroxide, filtering, and adding the filtrate to the main solution for analysis. PMA was extracted first with a mixture of *n*-butanol and carbon tetrachloride (1:3) from nitric acid, then SMA was extracted from sulphuric acid medium with isoamyl ether. To determine silicon, the absorption of the molybdenum in the organic phase was measured; phosphorus was determined by stripping the PMA and measuring molybdenum in the aqueous phase. The detection limit for P and Si in silver and for P in gold was $5 \times 10^{-7}\%$, the relative standard deviation $\leq 6\%$.¹¹

Table 3. Detection limits for flameless atomic-absorption determination of trace impurities in pure metals (%)

Impurity	Metal analysed						
	As	Sn	Re	In	Ga	Au	Ag
Ag	2×10^{-6}	2×10^{-6}	9×10^{-7}	5×10^{-8}	2×10^{-8}	4×10^{-8}	—
Al	9×10^{-6}	—	2×10^{-5}	5×10^{-6}	2×10^{-6}	—	—
As	—	—	—	—	5×10^{-7}	2×10^{-7}	2×10^{-7}
Ba	—	6×10^{-5}	—	2×10^{-6}	2×10^{-6}	—	—
Be	—	3×10^{-7}	—	5×10^{-8}	5×10^{-8}	—	—
Bi	—	—	2×10^{-7}	5×10^{-7}	2×10^{-7}	2×10^{-8}	2×10^{-8}
Ca	3×10^{-5}	2×10^{-5}	2×10^{-5}	5×10^{-5}	4×10^{-5}	—	—
Cd	5×10^{-7}	3×10^{-7}	4×10^{-8}	3×10^{-8}	2×10^{-9}	2×10^{-9}	2×10^{-9}
Co	5×10^{-6}	5×10^{-6}	—	2×10^{-7}	2×10^{-7}	2×10^{-7}	2×10^{-7}
Cr	1×10^{-6}	1×10^{-6}	3×10^{-7}	3×10^{-7}	4×10^{-8}	8×10^{-8}	8×10^{-8}
Cu	2×10^{-6}	2×10^{-6}	7×10^{-6}	1×10^{-7}	1×10^{-7}	1×10^{-7}	1×10^{-7}
Eu	—	—	—	1×10^{-6}	1×10^{-6}	—	—
Fe	9×10^{-6}	6×10^{-6}	8×10^{-6}	—	—	8×10^{-7}	8×10^{-7}
In	—	—	—	—	1×10^{-7}	—	—
Ir	—	—	—	—	—	4×10^{-6}	4×10^{-7}
Li	2×10^{-6}	—	—	6×10^{-8}	6×10^{-8}	—	—
Mg	5×10^{-6}	5×10^{-6}	6×10^{-7}	9×10^{-6}	4×10^{-6}	—	—
Mn	8×10^{-7}	1×10^{-6}	6×10^{-7}	9×10^{-7}	1×10^{-7}	6×10^{-8}	6×10^{-8}
Mo	—	—	—	—	—	4×10^{-7}	4×10^{-7}
Ni	7×10^{-6}	7×10^{-6}	1×10^{-6}	9×10^{-7}	4×10^{-6}	2×10^{-7}	2×10^{-7}
Pb	4×10^{-6}	—	1×10^{-7}	9×10^{-7}	1×10^{-7}	2×10^{-7}	2×10^{-7}
Pd	—	—	—	—	—	1×10^{-6}	1×10^{-6}
Pt	—	—	—	—	—	4×10^{-7}	—
Rh	—	—	—	—	—	2×10^{-7}	2×10^{-7}
Sb	—	—	—	—	—	4×10^{-7}	4×10^{-7}
Sc	—	—	—	2×10^{-6}	2×10^{-6}	—	—
Se	—	—	—	—	—	2×10^{-6}	2×10^{-6}
Sr	6×10^{-6}	5×10^{-6}	—	2×10^{-7}	2×10^{-7}	—	—
Te	—	—	—	—	—	1×10^{-6}	1×10^{-6}
V	—	1×10^{-5}	—	3×10^{-6}	3×10^{-6}	—	—
Yb	—	2×10^{-6}	—	4×10^{-8}	4×10^{-8}	—	—
Zn	5×10^{-6}	—	6×10^{-7}	3×10^{-5}	9×10^{-6}	2×10^{-8}	2×10^{-8}

The possibility was also examined of determining platinum metals in Ag and Au by direct analysis of solid samples in a graphite furnace,¹² which eliminates the time-consuming sample pretreatment and significantly reduces the interelement effects. A 10-mg sample was placed in the hollow of a L'vov platform installed in the central part of the graphite furnace. Standards were made of artificial alloys made from Ag and Au of 99.9999% purity. For analysis of silver the heating conditions chosen made it possible to distil off as much as 80–90% of the matrix before atomization of the analytes began. A two-stage temperature programme was used: stage I—distilling off the matrix at 2100° for 1–1.5 min; stage II—atomization of impurities at 2650° for 15–20 sec. The detection limits for Pt, Pd and Rh in silver are $(2-5) \times 10^{-9}$ g, relative standard deviation <10%, and the limits for Pd and Rh in gold are 6×10^{-9} and 2×10^{-8} g, respectively. Under the optimum conditions for determining Pd and Rh in gold (stage I—1100–1200° for 30 sec; stage II—2650° for 15–20 sec) only 30–40% of the gold is distilled off, so a control sample is used to correct for the residual matrix effect. No interelement effects have been detected.

DISCUSSION

Application of electrothermal AAS has allowed us to develop sensitive methods for analysis of some high-purity metals for a wide range of elements. The detection limits for the impurities in all the metals tested are summarized in Table 3. AAS also makes it possible to determine the impurities that give poor sensitivity in emission spectrometry. These include P, Si and Hg. The "cold vapour" technique can be used to determine Hg in pure Cd, Ge, In and Te, with a detection limit of $\sim 10^{-6}\%$.¹³

There are still possibilities for lowering the detection limits for some impurities, particularly the common ones by better optimization of the experimental conditions and greater purification of reagents.

Problems arise however, when concentration techniques are used. As a rule, a 1-g sample is used with extractive concentration. Electrothermal AAS for 15–20 micro-impurities requires about 1 ml of solution, so the impurity concentration (w/w) in the solution analysed is about the same as in the original material. With larger sample weights (up to 10 g) a higher concentration can be achieved in the same

volume of solution, as shown above for gold. However, this frequently leads to an increase in the content of impurities in the reagent blank and hence in the detection limits. Consequently it is preferable to use those methods of enrichment which use large sample weights but with minimum consumption of reagents. These include distillation, precipitation and so on. The advantages of such methods are illustrated by the analysis of high-purity tin by combination of electrothermal AAS determination of impurities with distillation of the matrix as tin tetrabromide, the detection limits for determining Ag, Ca, Co, Cr, Fe, In, Mg, Mn, Ni, Pb, Zn then being as low as 1×10^{-9} – $5 \times 10^{-8}\%$.

REFERENCES

1. I. R. Shelpakova, I. G. Yudelevich, T. A. Chanysheva, *Metody spektral'nogo analiza mineral'nogo syrya*, pp. 63–68. Nauka, Novosibirsk, 1984.
2. I. R. Shelpakova, A. I. Saprykin, T. A. Chanysheva and I. G. Yudelevich, *Zh. Analit. Khim.*, 1983, **38**, 581.
3. L. V. Zelentsova, I. G. Yudelevich and G. Emrich, *ibid.*, 1982, **37**, 789.
4. L. V. Zelentsova and I. G. Yudelevich, *ibid.*, 1983, **38**, 1404.
5. L. V. Zelentsova, I. G. Yudelevich and V. P. Shaburova, *ibid.*, 1977, **32**, 1166.
6. I. G. Yudelevich, L. V. Zelentsova, N. F. Beisel, T. A. Chanysheva and L. Vechernish, *Anal. Chim. Acta*, 1979, **108**, 45.
7. L. V. Zelentsova, I. G. Yudelevich and T. A. Chanysheva, *Zh. Analit. Khim.*, 1980, **35**, 515.
8. *Idem*, *Izv. Sib. Otd. Akad. Nauk SSSR, Ser. Khim.*, 1982, No. 1, 132.
9. E. A. Startseva, N. M. Popova and I. G. Yudelevich, *ibid.*, 1980, No. 4, 127.
10. E. A. Startseva, N. M. Popova, I. G. Yudelevich, N. G. Vanifatova and Yu. A. Zolotov, *Z. Anal. Chem.*, 1980, **300**, 28.
11. E. A. Startseva, N. M. Popova, V. P. Khrapai and I. G. Yudelevich, *Izv. Sib. Otd. Akad. Nauk SSSR, Ser. Khim.*, 1979, No. 6, 139.
12. I. G. Yudelevich, E. A. Startseva and N. M. Popova, *ibid.*, 1981, No. 5, 90.
13. L. V. Zelentsova, I. G. Yudelevich and T. A. Chanysheva, *ibid.*, 1982, No. 1, 130.

DETERMINATION OF OXYGEN IN FUSIBLE METALS BY USE OF SOLID ELECTROLYTE CELLS

L. L. KUNIN, A. A. BOGDANOV and V. I. RODIONOV

V. I. Vernadsky Institute of Geochemistry and Analytical Chemistry of the USSR Academy of Sciences,
Moscow, 117975, USSR

(Received 11 November 1985. Revised 10 May 1986. Accepted 9 August 1986)

Summary—A new method has been devised for determination of oxygen in fusible metals and compounds based on them, *viz.*, by electrochemical extraction of oxygen with the help of a specially designed solid electrolyte cell. The physicochemical conditions for the method to be used, and the analytical characteristics, are discussed. Results are given for determination of oxygen in a number of high-purity fusible metals. The relative standard deviation is inversely proportional to the mean oxygen concentration in the sample.

High-purity fusible metals are widely used as components of semi-conducting materials.¹ Many studies have stressed the great influence of oxygen on some galvanometric and optical properties of semi-conducting compounds,²⁻⁵ but this influence cannot be examined quantitatively until reliable methods for determining elemental oxygen in these materials are available.

Many workers have tried to determine the oxygen content of fusible metals and the experience gained has been summarized.⁶⁻¹¹ The existing methods are as follows: high-temperature extraction, chemical, nuclear-physical, mass-spectrometric and molecular and electron spectroscopic. The last three can sometimes provide information on the surface content of oxygen in the sample. In spite of some progress, the problem of determining oxygen concentrations at the level of $10^{-5}\%$ w/w in such materials as cadmium, antimony, gallium, tellurium and their combinations is yet to be completely solved. When high-temperature extraction methods are used, the analysis is difficult owing to the high vapour pressures of these elements. The use of molecular spectroscopy methods is restricted because it is difficult to identify the spectra. Also, like the nuclear-physical methods they call for special procedures and precision equipment. Implementation of the existing methods is faced with the problem of calibrating the equipment, since standard samples of fusible metals or reference gaseous mixtures are practically unavailable.

This paper partially summarizes our long experience in using solid electrolytic cells (SECs) for practical analysis with a view to determining oxygen in fusible metals. A new method of analysis, electrochemical extraction of oxygen with the help of SECs has been described.¹² This method is devoid of the shortcomings listed above and requires no calibration. The sample to be analysed is dissolved in a fusion mixture in an inert atmosphere, and as this takes place, the oxygen present in the sample passes

into the melt and is removed from it with help of an SEC immersed in the melt and working in a coulometric mode. The quantity of electricity required to remove the oxygen gives the initial content of the latter in the sample analysed.

The factors to be taken into account when the new method is used are as follows: the electrophysical characteristics of the SEC, the type of bath for fusing the sample, the oxidation potential of oxygen in the gaseous phase above the bath, the electrochemical deoxidation of the melt, and selection of the optimum analysis conditions. Further interpretation of the results for high-purity substances (containing 10^{-4} – $10^{-5}\%$ w/w oxygen) requires the background concentration of oxygen in the bath to be taken into account and the corresponding calculation formulae to be derived.

PHYSICOCHEMICAL PRINCIPLES OF THE METHOD

Electrophysical characteristics of SECs

The key problems are to find the temperature range in which the SECs possess practically uni-polar oxygen-ion conductivity adequate for efficient electrochemical extraction and to select SEC electrodes that will provide high exchange currents and reversibility. In our work, we used the well-known electrolytes based on ZrO_2 doped with the oxides of bi- or trivalent metals: calcium, yttrium and scandium. In the 400–800° temperature range the ion transport number of these SECs is close to 1, the electric conductivity being 10^{-3} – 10^{-1} ohm⁻¹.cm⁻¹.^{13,14} This is sufficient for efficient mass transfer of oxygen. The electrochemical aspects of SECs have been well studied and discussed.^{15,16} Thus, analysis of literature sources and experimental investigations helped us to choose platinum–air SEC electrodes for purification of the inert gas and measuring its potential. In the reactor, the oxygen solution in liquid

metal is used as the cathode and platinum–air or silver–air electrodes as anodes.

Type of fusion bath

The type of bath is selected with a view to serving three purposes simultaneously:

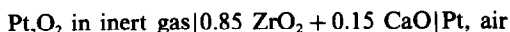
(a) the bath is the SEC cathode, and the oxygen dissolved in it has a certain activity and its electrical conductivity should not be lower than that of the SEC;

(b) the bath is a solvent for the sample being analysed and should have low vapour pressure;

(c) the bath is a reservoir for the oxygen present in the sample; it must be possible for oxygen to be introduced into it or removed from it, without risk of oxygen loss into the gaseous phase and binding in a chemical compound that is not susceptible to dissociation under the experimental conditions.

Analysis of the literature data with due regard to all these requirements helped us to select as optimal the melts of fusible metals, tellurium-based compositions and of alkali-metal halides. Some of the recommended bath compositions are given in Table 1.

The oxidation potential in the gaseous phase above the melt is preset with a view to preventing oxidation of the melt. Inert gases, argon or helium, are used as the gaseous phase. The procedure involves electrochemical removal of oxygen from the inert-gas flow by means of the SEC working in coulometric mode. The electrochemical cell is



By application of an electromotive force to the SEC electrodes, mass transfer of oxygen from the inert gas

Table 1. Recommended fusion baths

Sample	Bath	Electrical connection
Tin, lead, cadmium, silver	Tin, lead	Molybdenum
Bismuth, antimony, copper		
Gallium	Gallium	Platinum
Tellurium	Tellurium	Platinum
Zinc	Zinc, tin	Molybdenum
Magnesium	Tin	Molybdenum

Salt melts are used for selective desorption of surface-sorbed oxygen into the melt.

into the air is ensured (through the SEC). The oxidation potential is kept under control by a similar SEC working in potentiometric mode.¹⁷ A schematic diagram of the apparatus is given in Fig. 1. Electrochemical removal of oxygen from the inert gas flow is done in block 1 and P_{O_2} is controlled in block 3 located after the reaction chamber 2. Provision is made for switching the gas flow from block 1 directly into the oxidation-potential control block 3, and by-passing block 2. Curves of the SEC e.m.f. in block 3, and the corresponding P_{O_2} levels, *vs.* time, are shown in Fig. 2. In section *a* the P_{O_2} in the inert gas is measured, without introduction of purification. Section *b* corresponds to electrochemical purification of the inert gas in block 1 to remove oxygen. P_{O_2} levels as low as 10^{-15} Pa may be achieved. Section *c* corresponds to the gas flow being switched over to the inlet of the reaction chamber 2. Section *d* characterizes the removal of oxygen from the reaction chamber. Curves 1, 2 in this section correspond to different inert gas-flow rates. At high flow-rate, oxygen is carried through block 1 too rapidly for complete reaction, resulting in inadequate purification of the inert gas. Curve 3 corresponds to instances of

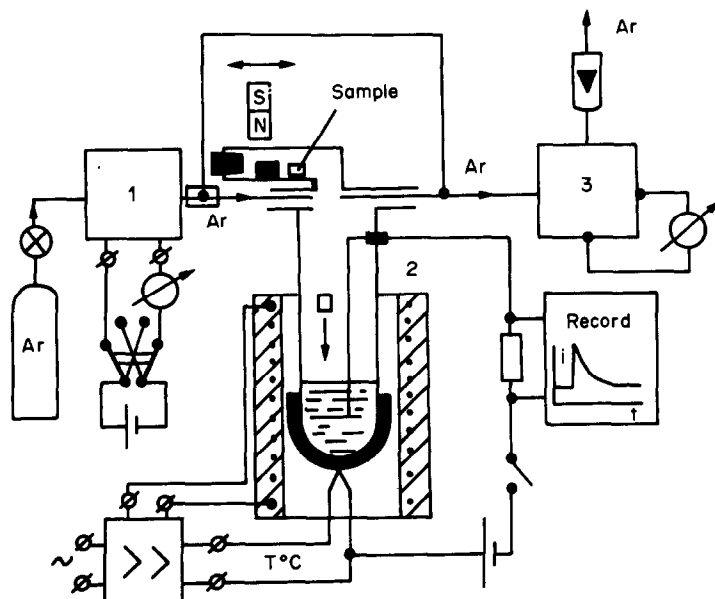


Fig. 1. Schematic diagram of experimental installation: 1—block for experimental removal of oxygen from the gaseous phase; 2—the reaction chamber; 3—block for control of P_{O_2} in the gas phase.

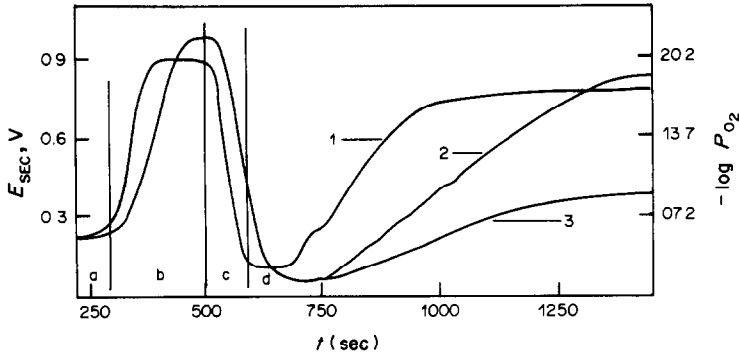


Fig. 2. Curves of P_{O_2} in block 3 vs. time: a— P_{O_2} in Ar without purification; b— P_{O_2} in Ar after switching to purification in block 1; c—gas-flow switched over to the inlet of the reaction chamber; d—removal of oxygen from the reaction chamber. Curves 1, 2 correspond to 12 and 4 ml/sec inert-gas flow respectively; curve 3 shows the effect of leaks in the gas lines.

large quantities of oxygen accumulating in the reaction chamber (owing to leaks in the gas lines). The shape of these curves is determined by the volume of the reaction chamber and gas lines. The oxidation potential values in block 3 are adjusted by altering the P_{H_2}/P_{H_2O} ratio in the inert gas during electrochemical removal of oxygen in block 1.

Electrochemical deoxidation of the baths

This is done in order to make the oxygen concentration in the melt much lower than the equilibrium concentration. A simplified diagram of the electric circuit for switching on the SEC in the reaction chamber is shown in Fig. 3. For the open circuit, E_{SEC} can be written as

$$E_{SEC} = \left(\frac{RT}{2F} \ln \frac{(P_{O_2}^{Ref})^{1/2}}{[O]f} - \frac{\Delta G}{2F} \right) \quad (1)$$

where R is the gas constant, F the Faraday constant, $P_{O_2}^{Ref}$ is 0.21 atm, $[O]$ is the oxygen concentration in the bath, % w/w, f is the oxygen activity coefficient, and ΔG is the Gibbs free energy of oxygen dissolution in a given melt.

On application of an impressed e.m.f. $E_{imp} = 1.3-1.5$ V to the SEC electrodes and closing the key K (Fig. 3), oxygen is electrochemically removed from the bath. Here, the current flowing through the SEC is

$$i = \frac{(E_{imp} - E_{SEC} - E_\eta)}{\Omega} \quad (2)$$

where Ω is the overall electric circuit resistance and

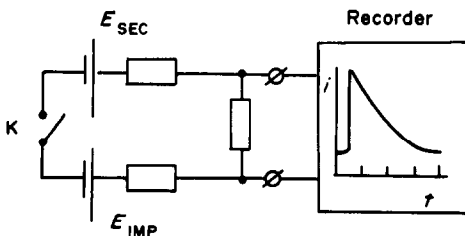


Fig. 3. Electrical circuit scheme.

E_η is the SEC polarization voltage when the current i is passed through it. On the other hand, owing to convective stirring of the melt and cathodic concentration polarization of the SEC, the current corresponding to the stabilized stationary oxygen flow through the diffusion layer at the melt/SEC interface is given by

$$i = \alpha([O] - [O]_s) = \frac{SDF\rho}{\epsilon\delta_{100}} [O]; ([O]_s \approx 0) \quad (3)$$

where α is a proportionality constant, S is the electrode surface area (cm^2), D is the oxygen diffusion coefficient (cm^2/sec), δ is the thickness of the melt/SEC interface diffusion layer (cm), $[O]$ is the oxygen concentration in the bath (% w/w) $[O]_s$ is the oxygen concentration in the melt/SEC interface (% w/w) ϵ is the electrochemical equivalent of the O^{2-} ion (g), and ρ is the density of the melt (g/ml). Typical melt deoxidation curves are shown in Fig. 4.

There is a dynamic equilibrium between the oxygen flow accumulating in the melt from the gaseous phase or due to dissociation of oxygen-containing phases on the bath surface and the flow of oxygen removed

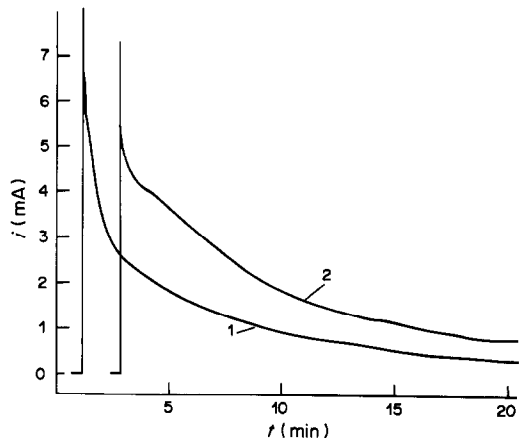


Fig. 4. Typical melt deoxidation curves: curve 1—Te melt, mass of melt 3.724 g, $T = 570^\circ$, $E_{imp} = 1.51$ v; curve 2—Pb melt, mass of bath = 6.923 g, $T = 586^\circ$, $E_{imp} = 1.49$ V.

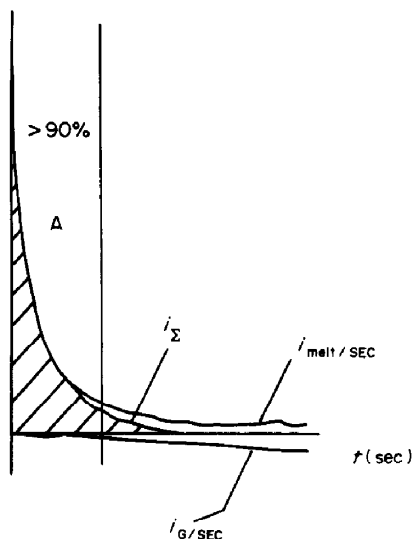


Fig. 5. Correlation between flow of oxygen from the gaseous phase to the melt and flow of oxygen removed from the melt by the SEC during the deoxidation—schematic presentation (section A is responsible for removal of more than 90% of the initial oxygen content).

from the bath through the SEC, and this equilibrium corresponds to the ultimate value of the oxygen removal current i_ϕ . With this in mind, and taking into account the fact that initially the oxygen flow from the gaseous phase into the melt is zero (the melt and the gaseous phase are in equilibrium), the conclusion can be drawn that as the melt is deoxidized the oxygen flow from the gaseous phase into the melt varies from 0 to its peak value of $i_\phi \epsilon / F$. Figure 5 explains this schematically. The oxygen removal curves (see Fig. 4) show that the initial value of the

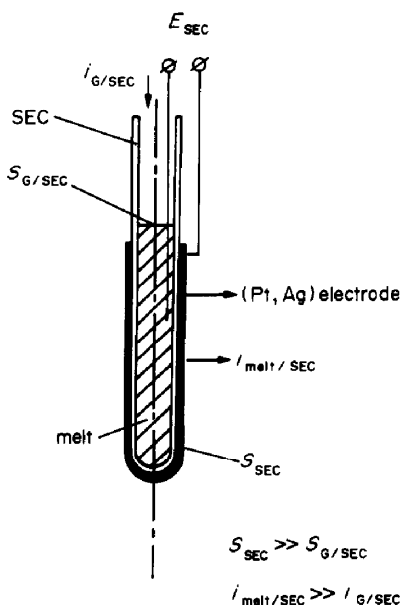


Fig. 6. The optimal geometry of the SEC for deoxidation.

oxygen removal current (i_0) exceeds its final value (i_ϕ) by one or two orders of magnitude.

Therefore, it can be said that during electrochemical removal of the bulk oxygen from the non-deoxidized melt (section A in Fig. 5) the contribution of oxygen accumulation in the bath is negligible. Experiment has shown that it is section A (Fig. 5) that is responsible for more than 90% reduction of the oxygen concentration from the saturation level to the background concentration. Thus, equation (4) can be used to describe the oxygen removal in this section:

$$\ln \frac{i - i_\phi}{i_0 - i_\phi} = -\frac{SD\rho t}{m_{\text{bath}}\delta}, \quad (4)$$

where i_0 is the current corresponding to the oxygen saturation concentration in the bath. By finding the oxygen mass transfer coefficient (D/δ) from equation (4) it is easy to evaluate the oxygen concentration in the bath from the value of the current flowing through the SEC.

$$[O] = K\delta Si_i/D \quad (5)$$

where K is a constant and the ion transfer number is about 1. To create conditions for equation (4) to be satisfied, the oxygen flow from the gaseous phase into the melt and on to the SEC must be co-ordinated. The P_{O_2} in the gaseous phase is made almost equal to P_{O_2} for equilibrium with Me_xO_y in the bath. In this case, the oxygen concentration in the melt/gaseous phase interface is close to that of saturation and no oxygen leakage from the bath into the gaseous phase takes place. The deoxidation effect can be enhanced by selecting the correct shape for the SEC, making the oxygen-removal flow through the SEC much greater than that of oxygen accumulation in the melt from the gaseous phase. This is achieved by making $S_{SEC} \gg S_{\text{melt/gaseous phase}}$ (see Fig. 6).

Determination

Dumping the sample into the melt results, as a rule, in greater oxygen activity in the bath, owing to the oxygen introduced into the melt by the sample. According to equation (1), this causes the SEC e.m.f. to decrease, and consequently the analytical signal to appear (the current passing through the SEC increases) [see equation (2)]. As oxygen is removed from the bath, the current passing through the SEC will tend to acquire its original background value. From the material balance of oxygen in the system we obtain for the oxygen concentration in the sample (c):

$$C = \left\{ \frac{100\epsilon}{Fm_{\text{samp}}} \int (i_t - i_\phi) dt \right\} + C_{\text{bath}}^{\circ} \% \text{ w/w} \quad (6)$$

where C_{bath}° is the background oxygen concentration in the bath, % w/w. Experience has shown that C_{bath}° is in the range 10^{-6} – 10^{-5} % and can generally be neglected in comparison with C values of 10^{-4} – 10^{-3} % w/w.

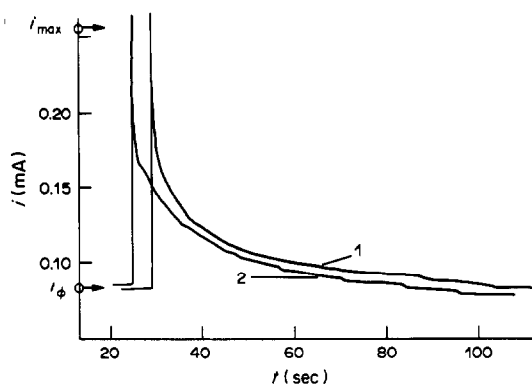


Fig. 7. Typical analytical signals; curve 1—mass of Pb sample = 0.039 g, $Q = 0.139 \times 10^{-2}$ C, $G = 1.1 \times 10^{-7}$ g, $C = 2.9 \times 10^{-4}$ % w/w; bath Pb (7.210 g); curve 2—mass of Te sample = 0.042 g, $T = 560^\circ$, $G = 0.99 \times 10^{-7}$ g, $Q = 0.121 \times 10^{-2}$ C, $C = 2.4 \times 10^{-4}$ % w/w, $E_{\text{imp}} = 1.52$ V.

If necessary, C_{bath}° is determined by either equation (5) or (7):

$$C_{\text{bath}}^{\circ} = \frac{100Gi_{\phi}}{\Delta i(m_b + m_{\text{samp}})} \% \text{ w/w} \quad (7)$$

where $G = \epsilon Q/F$ and $\Delta i = i_{\text{max}} - i_{\phi}$. Both formulae yield results that agree satisfactorily. The spread of results from formulae (5) and (7) is characterized by a relative standard deviation S_R of about 12–15%. This spread is due to the approximation in modelling the convectively stirred melt as a series of standard-depth diffusion layers. Also, when the sample is dumped into the melt the conditions corresponding to the initial sections of the curve for $\ln(i - i_{\phi})/(i_0 - i_{\phi}) = f(t)$ are disturbed.

The experimental system was assembled according to Fig. 1. Partial oxygen pressures were built up to the level of 10^{-15} Pa in the gaseous phase. The pre-chosen bath was deoxidized to 10^{-6} – 10^{-5} % w/w residual oxygen concentrations. The current yield through the SEC for the background level indicated when the system was ready for operation.

The analyses done showed that dry mechanical machining of the sample surface with a scalpel or chipping-off the sample from the bulk of the material were the most efficient means of sampling. The samples were weighed to ± 1 mg, which was sufficient precision for the overall sample mass of 50–100 mg.

Typical analytical signals and the results of determination of oxygen in a number of high-purity fusible metals are shown in Fig. 7 and Table 2. The

Table 2. Determination of overall oxygen content (C) in samples (volume + surface; dry machining of sample surfaces; n replicates)

Element	$(C \pm 2S)$, 10^{-4} % w/w	n	Sample No.
Tellurium-1	28.6 ± 8.4	18	1
Bismuth	7.5 ± 1.6	16	2
Lead-1	6.3 ± 1.6	23	3
Lead-2	5.3 ± 1.3	18	4
Tin-1	5.0 ± 1.0	19	5
Tellurium-2	4.6 ± 1.9	7	6
Tin-2	3.7 ± 0.7	15	7
Lead-3	3.2 ± 0.9	12	8
Cadmium-1	3.0 ± 0.6	18	9
Antimony	2.5 ± 0.5	18	19
Cadmium-2	2.1 ± 0.6	13	11
Gallium	1.4 ± 0.7	10	12
Tellurium-3	1.3 ± 0.3	18	13
Tellurium-4	0.9 ± 0.2	14	14
Tellurium-5	0.4 ± 0.2	6	15
Tellurium-6	0.3 ± 0.2	6	16
Tellurium-7	0.2 ± 0.2	7	17

Samples 13–17 were prepared by chipping-off from the bulk of the material.

correctness of the determinations for lead, tin, cadmium, copper and indium samples was established by the analysis of samples with a weighed oxygen content and by analyses with control methods (see Table 3). The limit of detection was assessed by the $2S$ criterion. The spread of data observed is due to heterogeneous oxygen distribution in the sample volume and to surface contamination of the samples. Table 4 gives the detailed results for determination of oxygen in cadmium. Analyses of bismuth ($n = 16$) and antimony ($n = 18$) samples gave mean oxygen contents of $(7.5 \pm 1.6) \times 10^{-4}$ % and $(2.5 \pm 0.5) \times 10^{-4}$ % w/w (95% confidence limits), respectively. A tin sample ($n = 30$) gave $(5.3 \pm 1.0) \times 10^{-4}$ % and two tellurium samples ($n = 18$) gave $(2.9 \pm 0.8) \times 10^{-3}$ % and $(1.3 \pm 0.3) \times 10^{-4}$ %.

Sources of error

The main sources of error are in weighing the sample and determining the amount of electricity required to reduce the oxygen. From the law of propagation of independent random errors we can write

$$S_R = \left\{ \sqrt{\frac{Q^2(dm)^2}{m^4 C^2} + \frac{(dQ)^2}{m^2 C^2}} \right\} 100\epsilon/F \% \quad (8)$$

Table 3

Metal	$(C \pm 2S)$, % w/w	S_R , %	n	$(C \pm 2S)$, comparison % w/w	Method of comparison
Lead	$(3.2 \pm 1.1) \times 10^{-4}$	10	12	$(4 \pm 1) \times 10^{-4}$	neutron activation
Tin	$(4.4 \pm 0.8) \times 10^{-4}$	10	19	$(4 \pm 1) \times 10^{-4}$	neutron activation
Cadmium	$(2.1 \pm 0.6) \times 10^{-4}$	10	13	$(1.4 \pm 0.7) \times 10^{-4}$	isotopic dilution
Copper	$(4.5 \pm 0.4) \times 10^{-2}$	5	16	$(4.9 \pm 0.7) \times 10^{-2}$	vacuum fusion
Cu-10	$(8.1 \pm 0.7) \times 10^{-4}$	10	10	$(8.0 \pm 0.6) \times 10^{-4}$	copper standard
In VHP-90	$(1.0 \pm 0.7) \times 10^{-4}$		10	$(0.91 \pm 0.05) \times 10^{-4}$ $(1.1 \pm 0.4) \times 10^{-4}$	γ -activation analysis reduction fusion

Table 4. Determination of oxygen* in cadmium

No.	Sample weight, g	$Q, 10^{-2} C$	$G, 10^{-7} g$	$C, 10^{-4}\% w/w$	$T, ^\circ C$
1	0.040	0.124	1.0	2.5	610
2	0.020	0.083	0.7	3.5	610
3	0.033	0.125	1.6	4.9	610
4	0.026	0.130	1.1	4.2	610
5	0.115	0.423	3.5	3.1	610
6	0.013	0.024	0.2	1.6	602
7	0.016	0.076	0.6	3.9	602
8	0.014	0.050	0.4	3.0	602
9	0.045	0.079	0.6	1.4	602
10	0.058	0.086	0.7	1.2	602
11	0.109	0.522	4.3	4.0	598
12	0.086	0.180	1.5	1.7	598
13	0.034	0.160	1.3	3.9	598
14	0.031	0.161	1.3	4.3	598
15	0.019	0.068	0.6	3.0	596
16	0.095	0.131	1.1	1.1	598
17	0.122	0.731	6.0	5.0	598
18	0.145	0.248	2.1	1.4	598

*95% confidence limits: $C = (2.9 \pm 0.6) \times 10^{-4}\% w/w$.

where (dm) and (dQ) are the precisions of measuring mass and charge respectively. With (dm) = 0.001 g, (dQ) = 1.2×10^{-5} , $Q = 4 \times 10^{-4} C$, $m = 0.100 g$, w/w, which are typical values, we get $S_R = 5\%$ for an oxygen content C_{samp} of $5 \times 10^{-5}\% w/w$, and 20% for $C_{\text{samp}} = 3 \times 10^{-5}\% w/w$. The practical range for S_R can be taken as 20–5% for $C_{\text{samp}} = (1-10) \times 10^{-5}\% w/w$.

One of the systematic errors is binding of some of the oxygen from the sample dissolved in the bath, to form an Me_xO_y -type compound which does not dissociate under the conditions used. Traces of elements such as Al, Ti, Zr, Hf, V, Nb, Ta, present in the bath or in the sample, would cause such an effect. However, by making the baths from pure metals produced by zone-refining with a residual aluminium (or similar metal) content of about 10^{-7} – $10^{-6}\% w/w$, we can disregard irreversible losses of oxygen caused by its binding as M_xO_y in the bath metal. The presence of such a metal in the sample, however, would simply result in determination of the dissociable oxygen content, and not the total oxygen content.

Another systematic error is due to the SEC ion transfer number not being equal to 1. Nevertheless, this need be kept in mind only in analysis of high-purity substances when the overall oxygen content in the sample is determined against the background oxygen concentration in the bath. In other cases, the differential signal is integrated. In baths deoxidized with help of the SEC the background oxygen concentration is $10^{-6}\% w/w$, so in the majority of cases it can be disregarded and the error caused by the non-ionic component of the conductivity in the SEC is not great (the ion transfer number is approximately 1).

In special cases, the ion transfer number is determined beforehand by one of the known methods.¹⁵

Surface contamination of the sample is the main source of systematic error. Experiments have shown that if the surface is cleaned in the dry state with a

scalpel in air, C_{surf} is at the level of 10^{-5} – $10^{-4}\% w/w$ or 0.1–0.01 $\mu\text{g}/\text{cm}^2$. Judging by the order of magnitude, this conforms to the data obtained from the literature.¹⁸

Thus, the main limitations of the method are: the impossibility of completely deoxidizing the metallic melts containing aluminium and similar refractory oxide-forming elements as impurities and, consequently, failure to determine all oxygen in the sample; the necessity for correct estimation of oxygen-containing compounds sorbed on the sample surface.

We feel that the future of the method is subject to these shortcomings and limitations being overcome and to expansion of the range of materials to be analysed.

REFERENCES

1. *Great Soviet Encyclopaedia*, Vol. 20, pp. 270–271. *Poluprovodnikovye materialy*, Sovetskaya Entsiklopediya, Moscow, 1975.
2. A. Ya. Nashelsky, *Proizvodstvo poluprovodnikovykh materialov*, pp. 66–67. Metallurgiya, Moscow, 1982.
3. G. B. Abdullaev, G. M. Aliev, Kh. G. Barkinkhoev, Ch. M. Askerov and L. S. Larionkina, *Fiz. Tverd. Tela*, 1964, 6, 1018.
4. V. T. Butkevich, O. R. Niyazova, A. M. Susova, S. F. Tkachenko and Yu. V. Zaikin, *Elektronnaya Tekhnika, Ser. 2, Poluprovodnikovye Pribory*, 1983, 5, 11.
5. A. M. Gaskov, A. A. Goldenveizer, I. N. Sokolov, V. P. Zlomanov and A. V. Novoselova, *Dokl. Akad. Nauk, SSSR*, 1983, 269, 607.
6. L. M. Melnik, L. L. Lewis and B. O. Holt, *Determination of Gaseous Elements in Metals*, Wiley, New York, 1974.
7. A. M. Vasserman, L. L. Kunin and Yu. N. Surovoi, *Opreделение газов в металлах*, Nauka, Moscow, 1976.
8. Z. M. Turovtseva and L. L. Kunin, *Analiz gazov v metallakh*, Izdat. AN SSSR, Moscow, 1959.
9. L. L. Kunin, E. D. Malikova and B. A. Chapyzhnikov, *Opreделение kisloroda, ugleroda, azota i vodoroda v shelochnykh i shelochno-zemelnnykh metallakh*, Atomizdat, Moscow, 1972.

10. *Analysis of Non-Metals in Metals*, G. Kraft (ed.), de Gruyter, Berlin, 1981.
11. *Gases in Metals*, Proceedings Deutsche Gesellschaft für Metallkunde, Oberursel, 1979, 1982, 1984.
12. L. L. Kunin, G. M. Murzin, R. L. Pinkhusovich, V. I. Rodionov and D. P. Podrugin, *USSR Patent*, SU 1160295, 1985; *Chem. Abstr.*, 1985, **103**, 226690g.
13. V. V. Osiko, A. L. Shimkevich and B. A. Shmatko, *Dokl. Akad. Nauk SSSR*, 1982, **267**, 351.
14. V. I. Aleksandrov, R. G. Belyanina, V. A. Blokhin, Zh. I. Ievleva, V. V. Osiko, A. L. Shimkevich and B. A. Shmatko, *Izv. Akad. Nauk SSSR, Neorgan. Mater.*, 1979 **15**, 1619.
15. V. N. Chebotin and M. V. Perflyev, *Elektrokhimiya tverdykh elektrolitov*, Khimiya, Moscow, 1978.
16. E. A. Ukshe and N. G. Bukun, *Tverdye elektrolity*, Nauka, Moscow, 1977.
17. V. I. Rodionov, A. A. Bogdanov and L. L. Kunin *Tezisy Dokl.*, Leningrad, 1983, p. 224.
18. L. Quaglia, G. Webe, D. David, J. Triffaux, J. Geerts, J. Van Audenhove and J. Pauwells, *Comm. Eur. Communities Rep. EUR*, 1979, EUR 6602.

DETERMINATION OF MOLECULAR-WEIGHT DISTRIBUTION AND AVERAGE MOLECULAR WEIGHTS OF BLOCK COPOLYMERS BY GEL-PERMEATION CHROMATOGRAPHY

V. V. NESTEROV, O. I. KURENBIN, V. D. KRASIKOV and B. G. BELENKII

Institute of Macromolecular Compounds of the Academy of Sciences of the USSR, Leningrad, USSR

(Received 15 October 1985. Accepted 8 August 1986)

Summary—The problem of preparation of a block copolymer of precise molecular-weight distribution (MWD) and with heterogeneous composition on the basis of gel-permeation chromatography (GPC) data has been investigated. It has been shown that in MWD calculations the distribution $f(p)$ of the composition p in individual GPC fractions should be taken into account. The type of the $f(p)$ functions can be simultaneously established by an independent method, such as use of adsorption-column or thin-layer chromatography sensitive to the composition of the copolymer. It has also been shown that the actual $f(p)$ may be replaced by a corresponding piecewise distribution, of simple form, without decrease in the precision of calculation of the MWD and average molecular weights of most known block copolymers.

Gel-permeation chromatography (GPC) has long been a powerful tool for analysis of polymer samples, because calibration of the chromatographic system by various methods¹⁻⁴ makes it possible to obtain easily the most important characteristic of the polymer under analysis, its molecular-weight distribution (MWD), from the gel chromatogram.

Right from its inception, GPC was used not only for the analysis of homopolymers but also for that of copolymers.⁵⁻⁷ However, the information obtained was only qualitative, mainly because adequate calibration was not available.

Almost all modern plastics are copolymers or polymer composites. Hence, the application of GPC to the determination of their molecular heterogeneity as well as to the specific problem of their compositional heterogeneity is one of the most important tasks in characterizing the physics and chemistry of polymers.

The present paper is concerned with investigation of the molecular characteristics of block copolymers with heterogeneous composition, by use of GPC.

THEORY

Proceeding from the segregated conformation of components of most BC in a dilute solution, and using the principle of universal calibration in GPC, we have proposed^{8,9} a method for the calculation of their molecular-weight distribution (MWD) and compositional distribution by using the equation

$$I = M_{BC} \{ (\bar{p}^{\alpha_1 + 1} K_1 M_{BC}^{\alpha_1})^{2/3} + [(1 - \bar{p})^{\alpha_2 + 1} K_2 M_{BC}^{\alpha_2}]^{2/3} \}^{3/2} \quad (1)$$

where M_{BC} is the molecular weight of the two-component block copolymer (BC), \bar{p} is the average value for the first component determining the average composition of the BC, K_1 , K_2 , α_1 and α_2 are the Mark-Kuhn-Houwink constants for components 1 and 2 respectively (as indicated by subscript) and I is the universal calibration parameter related to the hydrodynamic volume V_h of the corresponding BC molecules by the equation $I = 5 V_h N_A / 2$ (N_A is Avogadro's number).

Equation (1) may be written in another form more suitable for the subsequent calculations

$$M'_2 = (B \bar{p}^{\alpha_1} M_{BC}^{\alpha_1} + (1 - \bar{p})^{\alpha_2} M_{BC}^{\alpha_2})^{1/\alpha_2} \quad (2)$$

where M'_2 is the molecular weight of component 2, the molecules of which are eluted at the same retention volume as the BC molecules, $\alpha_1 = 2(\alpha_1 + 1)/3$; $\alpha_2 = 2(\alpha_2 + 1)/3$; $B = (K_1/K_2)^{2/3}$.

However, BC fractions corresponding to a narrow retention-volume range in the GPC and hence containing molecules of the same size, may have a compositional distribution p given by a certain function $f(p)$. The function $f(p)$ may be in correlation with the overall compositional distribution of the BC, $F(p)$. The specific type of $F(p)$ and $f(p)$ is dependent on the method of BC synthesis and is difficult to predict *a priori*, with the exception of BCs obtained by ionic polymerization according to the "living" chain mechanism.^{10,11} These BCs are characterized by a relatively narrow compositional distribution, and their compositional inhomogeneity is in agreement with their MWD.

These facts show that the precision of the determination of MWD by GPC depends on the com-

positional inhomogeneity of the BC. Let us analyse the problem.

The molecular weight of the BC, M_{BC} , corresponding to a given narrow retention-volume range, is defined as the average value over the whole composition:

$$M_{BC} = \int_0^1 f(p) M_{BC}(p) dp \quad (3)$$

In a particular case $f(p) = \delta(p - \bar{p})$, where $\delta(p - \bar{p})$ is Dirac's delta function, we have $\bar{M}_{BC} = M_{BC}(\bar{p})$ and the correct value of M_{BC} may be directly determined from equations (1) and (2).

The most promising method for determination of the function $f(p)$ is the combination of GPC with adsorption liquid chromatography sensitive to the composition of the block copolymer, under both "off-line" conditions, *e.g.*, by TLC,¹² and "in-line" conditions with the aid of so-called orthogonal chromatography.¹³ The average composition \bar{p} is determined by using dual-detector GPC^{8,14} or by analysing the composition of GPC fractions, by pyrolysis gas chromatography for example.^{11,15} This composition \bar{p} is used in equations (1) and (2) and in this case we have, according to definition,

$$\bar{p} = \int_0^1 pf(p) dp \quad (4)$$

In principle it is possible not only to determine \bar{p} as the mathematical expectation (E) of distribution $f(p)$ but also to evaluate the width d of this distribution. In the latter case $f(p)$ may be most simply approximated by the piecewise function of the form

$$f(p) = \begin{cases} 1/d, p \in [\bar{p} - d/2, \bar{p} + d/2] \\ 0 \text{ at other } p \text{ values} \end{cases} \quad (5)$$

Function (5) is symmetrical around \bar{p} and characterizes equal probability of existence of BC molecules of identical size having the composition greater than \bar{p} and less than \bar{p} . It may be said that if $f(p)$ is represented not by equation (5) but by any other type of distribution, this will not result in any considerable error in the calculation of the MWD of the BC. The greatest width of distribution (5) exists at $\bar{p} < 1/2$, $d = 2\bar{p}$ and at $p > 1/2$, $d = 2(1 - \bar{p})$.

If we have $a_1 = a_2 = 0.5$, *i.e.*, if θ -conditions exist for both components, then it is possible to integrate the right-hand side of equation (3) in the analytical form obtained by applying equations (2) and (5), the resulting expression for M_{BC} being

$$M_{BC} = \frac{M'_2}{d(B-1)} \ln \frac{(B-1)(\bar{p} + d/2) + 1}{(B-1)(\bar{p} - d/2) - 1} \quad (6)$$

Comparison of M_{BC} found according to equation (6) with that determined from equation (2) makes it possible to evaluate the error ϵ_p , in the calculated molecular weight, introduced because the compositional distribution of the GPC fractions of BC for a fixed retention volume was not taken into

account. The value of ϵ_p is given by the equation

$$\epsilon_p = \frac{|M_{BC} - M_{BC}(\bar{p})|}{M_{BC}(\bar{p})} \quad (7)$$

where $M_{BC}(\bar{p})$ is calculated according to equations (1) and (2).

In practice we almost always have $a_1 \neq a_2$. In this case the value of M_{BC} and hence that of ϵ_p may be calculated by numerical integration of the corresponding expressions on the right-hand side of equation (3). These calculations can be done with a microcomputer.

RESULTS AND DISCUSSION

Figure 1 shows the dependence of ϵ_p on the range-width d for the case $a_1 = a_2 = 0.5$. It is clear that at $\bar{p} = 0.5$ and $K_1/K_2 = 2.82$, which corresponds to $B = 2$, ϵ_p does not exceed 4%. At $K_1/K_2 = 11.28$, $B = 5$, ϵ_p may increase to 20%.

The results of the calculation of ϵ_p at different values of d are shown in Fig. 2. It is clear (Fig. 2a) that at a limited distribution width, $d = 0.6$, the maximum error for the case $a_1 = a_2 = 0.5$ at $B = 2$, and in particular for $B = 5$, corresponds to $p = 0.3$. However, for $a_1 = a_2 = 0.7$ the type of dependence of ϵ_p on d at $B = 2$ and $B = 5$ is quite different (Fig. 2b).

If ϵ_p is calculated for various changes in the constants K and a of the BC components (either in the same direction or in opposite directions), then, as can be seen from Fig. 3a, at $a_1 = 0.6$, $a_2 = 0.8$ (*i.e.*, $a_1 < a_2$), the maximum value of ϵ_p , even at $B = 5$, does not exceed 1.5%. If $a_1 > a_2$ ($a_1 = 0.7$, $a_2 = 0.6$) then at $B = 2$ the error increases to 5% and at $B = 5$ to 17% (Fig. 3b).

Let us compare the theoretical data with experimental results for some BCs.^{8-10,16} The maximum value of B (and hence of K_1/K_2), is observed for a BC

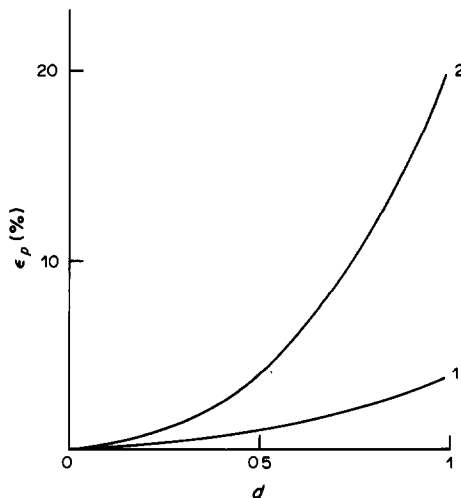


Fig. 1. Dependence of ϵ_p on the width of the distribution range for the case $a_1 = a_2 = 1$ and $\bar{p} = 0.5$ (1) $B = 2$ ($K_1/K_2 = 2.83$); (2) $B = 5$ ($K_1/K_2 = 11.08$).

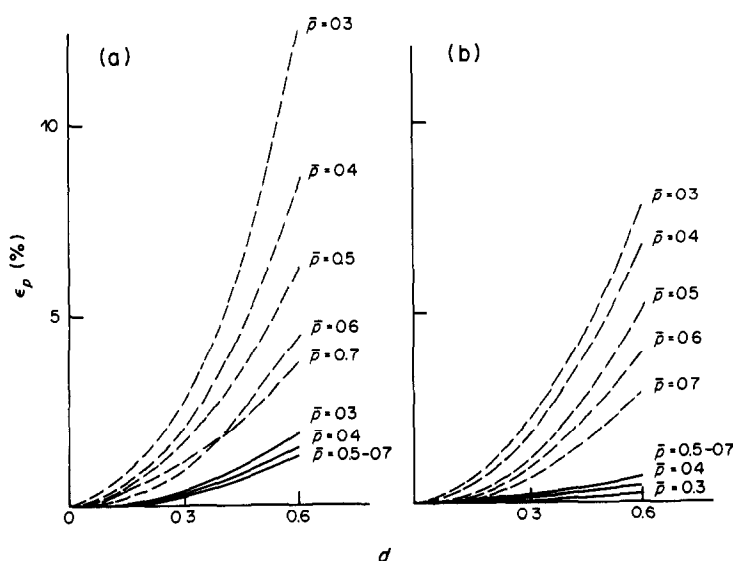


Fig. 2. Dependence of ϵ_p on d for various conditions, (a) $a_1 = a_2 = 0.5$; (b) $a_1 = a_2 = 0.7$; $B = 2$ (solid lines); $B = 5$ (broken lines).

of polystyrene (PS) and polybutadiene (PB) in tetrahydrofuran (THF). As a result, the corresponding calibration curves for PS and PB (Fig. 4) show maximum divergence. It is noteworthy that the plot in Fig. 4 corresponds to a real chromatographic system with linear calibration.¹⁷ In contrast, the calibration curves for PS and poly(methyl methacrylate) (PMMA) almost coincide. Both cases are interesting because the BCs of PS and PB are characterized by low compositional inhomogeneity ($d \approx 0.2$)^{10,11} and BCs consisting of PS and PMMA exhibit high compositional inhomogeneity, according to the TLC data ($d \sim 1$).¹⁸

The dependence of ϵ_p on d at different \bar{p} values is

shown in Fig. 5 for BCs consisting of PS and PB and in Fig. 6 for BCs consisting of PS and PMMA. It is clear that the maximum possible error due to the fact that compositional inhomogeneity of the GPC fractions was not taken into account does not exceed 1% in both cases. Since the calibration curves for PS and PB are virtually parallel and those for PS and PMMA coincide, the error in the calculation of \bar{M}_w , \bar{M}_n and other average molecular weights of these BCs, arising from neglect of compositional inhomogeneity of GPC fractions, does not exceed 1% either. This error may be neglected because the usual error (arising from various sources) in the calculation of \bar{M}_w and \bar{M}_n according to GPC data, is 5–8%.⁴ In particular,

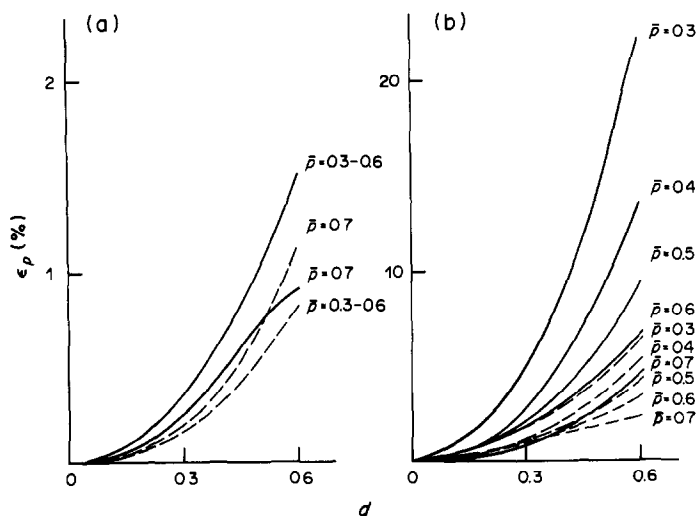


Fig. 3. Dependence of ϵ_p on d for changes in the ratio of the constants in the same direction and in the opposite direction for BC components; (a) $a_1 = 0.6$, $a_2 = 0.8$; (b) $a_1 = 0.7$, $a_2 = 0.6$. $B = 2$ (solid lines); $B = 5$ (broken lines).

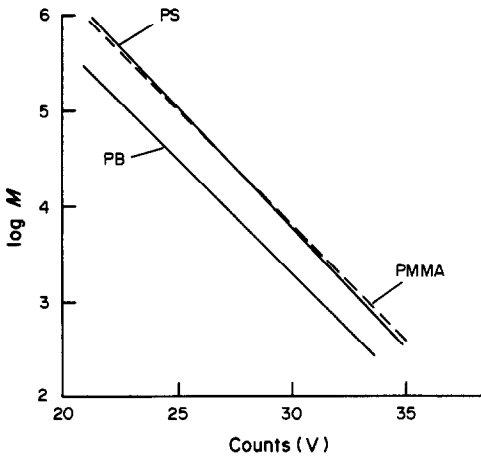


Fig. 4. Molecular-weight calibration dependences for PS, PMMA and PB in THF. Two columns 30 cm in length, bore 0.4 cm, packed with silica sorbent, giving linear calibration.¹⁷

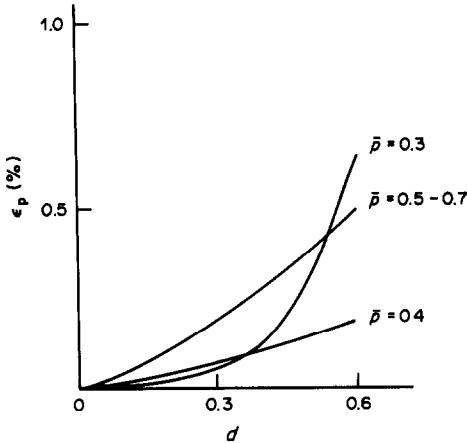


Fig. 5. Dependence of ϵ_p on d for BCs consisting of PS and PB in THF. $K_{PB}/K_{PS} = 1.28$, $a_{PB} = 0.78$, $a_{PS} = 0.71$.

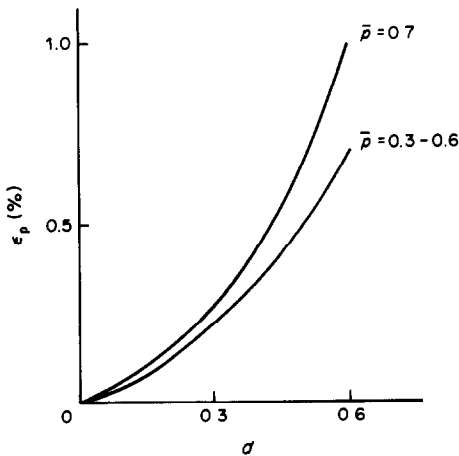


Fig. 6. Dependence of ϵ_p on d for BCs consisting of PS and PMMA in THF; $K_{PMMA}/K_{PS} = 1.368$, $a_{PMMA} = 0.67$, $a_{PS} = 0.71$.

Table 1. Comparison of molecular weights of BCs consisting of PS and PMMA, calculated according to equations (1) and (8) and measured independently

Solvent	Molecular weight		100 Δ, M/M, %	
	$K_{BC} \times 10^4$	a_{BC}	from eq. (1)	from eq. (8)
THF	$0.640^{(a)}$	$0.76^{(a)}$	$1.251^{(b)}$	$1.7^{(d)}$
	10^5	$0.717^{(b)}$	$1.28^{(c)}$	$0.69^{(e)}$
	10^6	$0.69^{(d)}$	1.12×10^6	1.05×10^6
Toluene	$1.318^{(a)}$	$0.69^{(a)}$	1.10×10^5	1.09×10^6
	10^4	$0.71^{(d)}$	1.025×10^4	9.48×10^3
	10^6	$0.73^{(d)}$	1.18×10^6	1.02×10^6
			eq. (1)	eq. (8)
			+5	-3
			-0.5	-10
			+12	+5
			+2.5	-3
			+10	+2
			+18	+9

(a) According to Kotaka *et al.*¹⁹
 (b) G. Kraus and C. J. Stacy, *J. Polym. Sci., Polym. Phys. Ed.*, 1972, 10, 657.
 (c) W. W. Yau, J. J. Kirkland and D. D. Bly, In *Modern Size-exclusion Liquid Chromatography*, p. 253 Interscience, New York, 1979.
 (d) *Polymer Handbook*, J. Brandrup and E. H. Immergut (eds.) p. iv-1. Interscience, New York, 1966.

this may explain the good agreement between the values of \bar{M}_n and the intrinsic viscosity calculated for these BCs from GPC data, and measured by other methods.⁸⁻¹⁰

The values of constants K_{BC} and a_{BC} have been determined experimentally¹⁹ for BCs consisting of PS and PMMA with azeotropic composition ($\bar{p} = 0.5$) in solvents of different thermodynamic strengths with respect to BC components. It is of interest to compare the values of the molecular weights (MW) of these BCs established experimentally and calculated according to equation (1) and according to the equation

$$V_h = 2 \left[\sum_i \omega_i (K_i M_{BC}^{a_i+1})^{2/3} \right]^{3/2} \quad (8)$$

Equation (8) has recently been proposed for the calculation of the MW of block copolymers by Goldwasser and Rudin²⁰ and derived by these authors on the basis of slightly different premises than equation (1). Equation (8) coincides with equation (1) at $i = 2$ and $a_1 = a_2 = 0.5$ and is close to this equation at other values of a_1 and a_2 .

The data obtained are given in Table 1 for two solvents: THF and toluene. The values of constants K and a for PS and PMMA are taken from earlier work.^{8-10,16} The values $MW = 10^4$, 10^5 and 10^6 were substituted into equations (1) and (8), and the corresponding values of V_h were calculated with the given constants K and a . These values were inserted into the left-hand side of equation (9).

$$V_h = 2K_{BC} M_{BC}^{a_{BC}+1} / 5N_A \quad (9)$$

The corrected MW of the BC was calculated with the aid of equation (9), and the relative divergence between the values of MW for the BC and PMMA found from GPC data and determined according to equations (1) and (8) was calculated. Table 1 shows that the average divergence between the experimental and calculated data is 5–8% for THF and 8–10% for toluene solutions. Leaving aside discussion of the correctness of equations (1) or (8) (they are virtually equally adequate) we can see that the divergences in the MW values greatly exceed the errors caused by the fact that the compositional inhomogeneity of the GPC fractions was not taken into account.

CONCLUSIONS

In order to obtain a precise MWD for a block copolymer with heterogeneous composition from GPC data, the compositional distributions in the GPC fractions should be taken into account in the

calculations. These distributions may be established independently, for example by using adsorption-column or thin-layer chromatography sensitive to copolymer composition, for the analysis.

However, our investigations have shown that in order to calculate the MWD of most known types of block copolymers the function $f(p)$ can be used successfully. This function is determined from equation (5) at maximum dispersion ($d = 2\bar{p}$, $\bar{p} < 1/2$) of the distribution, or with a limited dispersion value with its dependence on the retention volume taken into account.

If any real distribution function $f(p)$ is simulated by the right-hand side of equation (5), the errors arising in the calculations of the MWD and average MW of a BC are small compared to those arising from other sources when GPC is used.

REFERENCES

1. J. C. Moore, *J. Polym. Sci., A*, 1964, **2**, 835.
2. Z. Grubisič, P. Kempf and H. Benoit, *J. Polym. Sci., B*, 1967, **5**, 753.
3. A. Rudin and R. A. Wagner, *J. Appl. Polym. Sci.*, 1976, **20**, 1483.
4. B. G. Belenkii and L. Z. Vilenchik, *Modern Liquid Chromatography of Macromolecules*, Elsevier, Amsterdam, 1983.
5. D. D. Bly, *J. Polym. Sci., C*, 1968, **21**, 13.
6. J. R. Urwin and J. M. Stearne, *Makromol. Chem.*, 1964, **78**, 194.
7. D. N. Cramond, J. M. Hammond and J. R. Urwin, *Eur. Polym. J.*, 1968, **4**, 451.
8. V. V. Nesterov, V. D. Krasikov, E. V. Chubarova, L. D. Turkova, E. S. Gankina and B. G. Belenkii, *Vysokomol. Soedin.*, 1980, **A20**, 2320.
9. V. V. Nesterov, V. D. Krasikov, E. V. Chubarova and B. G. Belenkii, *ibid.*, 1982, **A24**, 1330.
10. V. V. Nesterov, V. D. Krasikov, V. N. Zgonnik, E. Yu. Melenevskaya, I. V. Kosheleva and B. G. Belenkii, *ibid.*, 1983, **A25**, 2568.
11. J. Stejskal and P. Kratochvil, *Polym. J.*, 1982, **14**, 603.
12. H. Inagaki and T. Tanaka, *Pure Appl. Chem.*, 1982, **54**, 309.
13. G. Glöckner, *ibid.*, 1983, **55**, 1553.
14. S. Mori and T. Suzuki, *J. Liq. Chromatog.*, 1981, **4**, 1685.
15. Y. Tanaka, H. Sato, Y. Nakafutami and Y. Kashiwazaki, *Macromolecules*, 1983, **16**, 1925.
16. V. V. Nesterov, L. V. Zamoiskaya, V. D. Krasikov and G. P. Martianova, *Vysokomol. Soedin.*, 1983, **A25**, 2561.
17. V. V. Nesterov, V. D. Krasikov, S. P. Zhdanov, B. J. Venzel, I. Z. Vilenchick, O. I. Kurenbin, T. P. Zhmakina and B. G. Belenkii, *ibid.*, 1984, **B26**, 163.
18. T. Kotaka, T. Uda, T. Tanaka and H. Inagaki, *Makromol. Chem.*, 1975, **176**, 1273.
19. T. Kotaka, T. Tanaka, H. Ohsuma, Y. Muramaki and H. Inagaki, *Polym. J.*, 1970, **1**, 245.
20. J. M. Goldwasser and A. Rudin, *J. Liq. Chromatog.*, 1983, **6**, 2433.

IDENTIFICATION OF BLOCK COPOLYMERS AND DETERMINATION OF THEIR PURITY BY THIN-LAYER CHROMATOGRAPHY

E. S. GANKINA, I. I. EFIMOVA, J. J. KEVER and B. G. BELENKII
Institute of Macromolecular Compounds of the Academy of Sciences of the USSR,
Leningrad, USSR

(Received 15 October 1985. Accepted 8 August 1986)

Summary—The application of adsorption, precipitation and extraction thin-layer chromatography to the identification of block copolymers, determination of their homogeneity (mixtures of homopolymers), and evaluation of their compositional homogeneity by one- and two-dimensional, multistage and gradient methods, is described. To detect the polymers on the thin-layer plate, various methods of detection are used, including those specific for each component of the block copolymer. Examples of analysis of the following block copolymers by thin-layer chromatography are reported: PS-PMMA, PS-PB, PS-PAN, PS-PBG, PI-PMS-PI, PMMA-PBMA, PMMA-PBG, PS-PEO*.

Analysis of block copolymers (BC) involves their identification (the decision whether they are copolymers or a mixture of homopolymers, and the determination of their purity and homogeneity), the determination of the molecular-weight distribution (MWD), compositional inhomogeneity (CI), and structure (whether they are A-B or A-B-A copolymers), and the composition of admixtures of homopolymers and other components.

Unfortunately, the methods of fractional precipitation and dissolution are not very suitable for these purposes, because they seldom make it possible to obtain fractions that are homogeneous with respect to composition or molecular weight (MW).^{1,2} Without such fractionation, the methods of light scattering, turbidimetric titration, equilibrium sedimentation and diffusion^{3,4} require a long and laborious experimental procedure, and the quantitative interpretation of the results is difficult.

In recent years liquid chromatography has been widely applied^{5,6} to the study of polydispersity of BCs because it provides ample possibilities for selective separation and effective fractionation. It has been shown that it is possible to determine the MWD and compositional distribution according to MW with the aid of exclusion liquid chromatography (ELC).^{7,8} Thin-layer, adsorption, precipitation and extraction chromatography (TLC, AC, PC, EC respectively) make it possible to fractionate BCs according to

composition, to distinguish between two- and three-block BCs and to separate BCs and accompanying homopolymers.^{2,9,10}

To obtain the complete BC characteristics (the MWD of the BC and the blocks of which it consists, the CI of the BC and the MWD of homopolymer admixtures) various chromatographic methods (ELC, LLC, and pyrolysis gas chromatography)^{2,7,9-11} and a combination of chromatographic and non-chromatographic methods (ELC and ozonolysis¹²) have been used.

The most important analytical problem in the investigation of BCs is the identification and determination of their primary characteristic, their purity (homogeneity). It should be noted that this field of BC analysis has not been discussed in detail in the literature, but it has been pointed out that the application of classical methods of polymer analysis for this purpose is not very effective.^{1,2} Presumably, the best method for identification of BCs involves the application of adsorption TLC (ATLC), which is characterized by its simplicity of performance and the well defined results. An advantage of this method is the difference between the adsorption characteristics of A and B homopolymers. Not only are homopolymers separated from BCs but in many cases BCs with different structures (A-B and A-B-A) are also separated from each other.

With the aid of ATLC it is possible not only to identify the BCs but also to determine the content of A and B homopolymers. For these purposes the chromatographic system should ensure that one homopolymer, for example A (even that with the lowest MW) should remain at the start, whereas the other (homopolymer B, even that with the highest MW)

*The following abbreviations are used: polystyrene—PS, poly(methylmethacrylate)—PMMA, poly(ethylene oxide)—PEO, polyisoprene—PI, polyacrylonitrile—PAN, poly(γ -benzyl glutamate)—PBG, poly(α -methylstyrene)—PMS, poly(butyl methacrylate)—PBMA.

should migrate with the eluent front. It is then always possible to remove the BC from the start and distribute it along the plate with the same eluent, or with an eluent of different composition.

However, when homopolymers A and B exhibit similar adsorption characteristics, the application of ATLC to this problem does not always lead to the desired effect. In this case variations of TLC may be used, based on another principle of polymer separation: dissolution-precipitation, *i.e.*, precipitation chromatography (PC) and extraction chromatography. When this method is used, the product containing a BC can also be separated into three fractions: the BC proper, homopolymer A and homopolymer B. If AC and PC are applied, the BC can only be separated from the homopolymers when their adsorption activities or solubilities are sufficiently different, and this can only be attained for a BC containing the two components in a ratio of not less than 1/20–1/50, because if the content of one component is too low, the BC will behave like the other homopolymer. If the adsorption activities of solubilities of the homopolymers are very different, this limiting ratio range may be widened.

Hence, apart from this restriction which in practice is not important in most cases, it is always possible to propose a chromatographic system consisting of AC and PC for the identification of BCs and determination of the content of homopolymers. It should be noted that the TLC method of identification of BCs is based on fundamental physical differences between the BC and the homopolymers that are due to their chemical structure and MW, and exhibited in the difference between their solubilities and adsorbabilities.

Another restriction on the application of chromatographic identification of BCs may be complexation of the BC with one of the homopolymers, for example, in the case of stereoblock and stereoregular homopolymers.^{13,14} Hence, it is desirable to employ two or more chromatographic systems for the solution of this analytical problem with the aid of AC and PC.

This paper describes the results of our investigations on the identification of BCs with the aid of TLC, and the determination of their purity, *i.e.*, the content of the corresponding homopolymers.

As indicated above, TLC is the simplest and most convenient chromatographic method for qualitative analysis, particularly because the open surface of the sorbent makes it possible to use various detection procedures, including those specific for each BC component. The mechanism of polymer separation according to the adsorption or the precipitation method may change if the ratio of the components of the eluent is varied. This fact can be clearly seen if we take as an example the TLC of PMMA in a chloroform-methanol system. If pure chloroform is used, PMMA, whatever its MW, remains at the start. To move PMMA from the start and distribute it

along the plate according to its MW, it is necessary to add methanol to the chloroform in 5–20% v/v proportion. In contrast, if a 1:4 v/v methanol-chloroform mixture is used as eluent from the very beginning, then as the methanol is gradually adsorbed on the adsorbent, its content in the eluent decreases and hence PMMA fractions of increasing molecular weight will be successively retained on the plate. In both cases we evidently deal with ATLC. On the other hand, if the methanol content is increased from 20 to 70%, PMMA is not adsorbed at all and its R_f value is unity. At a methanol content above 70%, PMMA does not dissolve, and remains at the start; if a gradient concentration of chloroform in methanol from 90% to lower values is fed to the plate, fractions of gradually increasing molecular weight appear on the plate (precipitation TLC; PTLC).

The process of BC adsorption has been studied in detail, both theoretically and experimentally.^{9,10,15} Skvortsov and Gorbunov¹⁵ considered the adsorption theory for a BC consisting of blocks A and B (with the numbers of segments N_A and N_B , respectively) interacting with the surface of the adsorbent at different energies ($-\epsilon_A$ and $-\epsilon_B$). When $-\epsilon_A$ and $-\epsilon_B$ are lower than the critical energy for the corresponding homopolymers A and B, the BC is not adsorbed and migrates along the plate in accordance with the laws of exclusion chromatography (on a plate unsaturated with the solvent, the BC migrates with the eluent front). At $-\epsilon_A$ and $-\epsilon_B$ higher than the critical energy for the homopolymers A and B, the BC remains at the start. If the energy $-\epsilon_A$ for one of the blocks is higher than the critical value and $-\epsilon_B$ for the other block is lower than that value, then starting from a certain critical composition of BC, $\xi = \xi_{\text{crit}}$ where $\xi = N_A/(N_A + N_B)$, the macromolecules with $\xi > \xi_{\text{crit}}$ are predominantly located inside the pores of the adsorbent, whereas those with $\xi < \xi_{\text{crit}}$ are preferentially located outside them, which permits the separation of the BC fractions according to composition. Moreover, ξ_{crit} depends on both the energy of interaction between the "adhesive" segment and the adsorbent surface, $-\epsilon_A$ (ξ_{crit} in turn determines the $-\epsilon_{\text{crit}}$ value for the BC) and on the pore radius r . The efficiency of BC separation according to composition increases with decreasing r . (Skvortsov and Gorbunov¹⁵ assumed that the optimum pore diameter for BC separation is in the range 100–200 Å). Hence, the separation of BC according to composition (ξ) is made possible by varying both $-\epsilon$ (by changing the composition of the eluent or the temperature) and r , since these parameters determine ξ_{crit} . On the other hand, it has been shown that at $-\epsilon_B (= -\epsilon_B^{\text{crit}})$ and under the critical conditions for block A ($-\epsilon = -\epsilon_A^{\text{crit}}$), in which the molecule of homopolymer A is energetically indifferent to being located inside or outside the pores, the BC can be separated according to the exclusion effect of block B, *i.e.*, according to its length (MW). In this case it is

possible to separate a BC of homogeneous composition according to its MW. The critical conditions for homopolymer A are observed when its R_f value is independent of MW.⁹ In TLC this effect is observed when homopolymer B migrates with the eluent front and homopolymer A and the BC leave the start and are located in the upper third of the plate, which is saturated with the solvent vapour. On the other hand, it is natural that in order to separate the BC according to its composition, ζ , it is necessary to use stepwise chromatography or a continuous gradient of eluent composition, or else, which is more complicated, a gradient of the adsorbent layer according to pore size.

Distribution of the "adhesive" homopolymer along the plate ($R_f < 1$) and the R_f value for the BC being higher than that for this homopolymer (up to $R_f = 1$) are the criteria for this mechanism of BC fractionation. As indicated above, the choice of the components of the eluent for the identification of the BC and their ratio are based on the necessity to adsorb homopolymer A of any, even the lowest, MW, and the absence of adsorption of homopolymer B of the highest molecular weight. The problem may be simplified by successive chromatography on the same plate with different eluents, first an eluent in which homopolymer has $R_f = 1$ and BC and homopolymer A have $R_f = 0$, then in an eluent in which homopolymer B has $R_f = 1$, BC has $R_f = 0.2-0.8$ and homopolymer A has $R_f = 0$, and finally in an eluent in which homopolymer B and BC have $R_f = 1$ and homopolymer A has $R_f = 0$. This step-wise chromatography in analysis of BCs is especially effective when two-dimensional TLC is used.

Experimental results show that in the ATLC of BCs, eluents consisting of two or more components should be used. They should contain a solvent for the BC, the adsorption activity of which is insufficient to prevent the adsorption of the BC, and a displacer, the adsorption-active component of the eluent. This displacer may be a solvent or, at high concentrations, a precipitant for BC. In the latter case PTLC takes place. Naturally, in the former case there are no restrictions on the composition of the eluent but there are in the latter case. It can be pointed out that

solvent systems exist (although they have not yet been used for BCs), in which a polymer is soluble at a certain solvent composition, even though both components of the mixture are precipitants for it.⁵

EXPERIMENTAL

TLC was performed on 6×9 cm glass plates coated with KSKG silica gel (pore diameter ~ 120 Å, particle diameter $8-12$ μm), with a stable silicic acid sol¹⁶ or gypsum¹ as adhesive. The TLC procedure has already been described. The following reagents were used for detection of the polymers. (a) A 3% KMnO_4 solution in concentrated sulphuric acid with subsequent heating at 180° for 5-10 min;¹⁷ the polymer zones developed as black spots on a white background; the detection sensitivity was 0.2 μg for PS. (b) A modified Dragendorff reagent,¹⁸ prepared by dissolving 1.7 g of bismuth nitrate (with heating) in 80 ml of distilled water, and adding 20 ml of glacial acetic acid (solution I), dissolving 40 g of potassium iodide in 100 ml of water (solution II), mixing solutions I and II, adding 200 ml of glacial acetic acid and diluting to 1 litre with water (solution A). A 20% solution of barium chloride in water was also prepared (solution B). Solutions A and B were mixed in a ratio of 2:1 by volume to give the reagent used for spraying. PEO developed as orange-reddish spots on a yellow background. The sensitivity of detection was $0.05-0.1$ μg . Subsequent treatment of the zones with reagent (a) led to disappearance of the yellow colour of the background, and the colour contrast of the zones became more pronounced. (c) A 10% aqueous solution of potassium hydroxide was used with subsequent heating at $\sim 150^\circ$ for 10-15 min. PAN zones acquired a yellow-orange colour. The lower limit of detection for PAN was ~ 1 μg .¹⁹ The characteristics of the homopolymers and BCs used in these experiments are given in Table 1.

RESULTS AND DISCUSSION

Adsorption thin-layer chromatography of BCs

First, it should be noted that the greater the difference in the polarity of the homopolymers, the easier it is to separate the less polar homopolymer from the BC (even from one containing $>90\%$ of the polar homopolymer) and the other homopolymer. For example, in chloroform or benzene, the PS homopolymer is separated from such BCs as PS-PAN, PS-PEO, PBG, etc. A characteristic example of ATLC is the investigation of the PS-PMMA BC, which can be performed by several methods. (A)

Table 1. Samples used

No.	Samples	MW	No.	Samples	MW
1	PS-PMMA	1.26×10^5	7	PS-PEO	1.00×10^5
2	PS _{init.}	2.6×10^4		PS _{init.}	5.0×10^4
2	PS-PB	6.2×10^4	8	PBG-PS-PBG	1.38×10^5
	PS _{init.}	1.2×10^4		PS _{init.}	5.0×10^4
3	PS-PB-PS	9.0×10^4	9	PS-PAN	5.3×10^4
	PB _{init.}	3.0×10^4		PS _{init.}	3.6×10^4
4	PI-PMS-PI	1.85×10^5	10	PS-PMMA	8.0×10^4
	PMS _{init.}	8.5×10^4		PS _{init.}	6.0×10^4
5	PMMA-PBMA	7.5×10^4	11	PS-PAN	—
	PMMA _{init.}	2.5×10^4		PS _{init.}	5.0×10^4
6	PMMA-PBG	1.50×10^5			
	PMMA _{init.}	4.0×10^4			

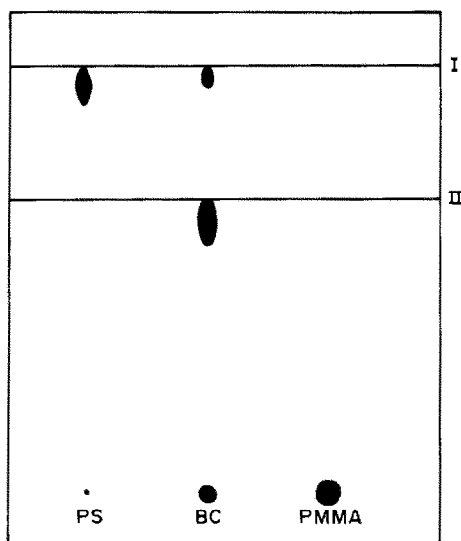


Fig. 1. Stepwise TLC of PS-PMMA (No. 1 in Table 1). The eluent fronts are for (I) benzene, (II) chloroform-MEK (6:3) mixture. Detection with reagent (a). MW: PS 1.11×10^5 ; PMMA 4.0×10^4 .

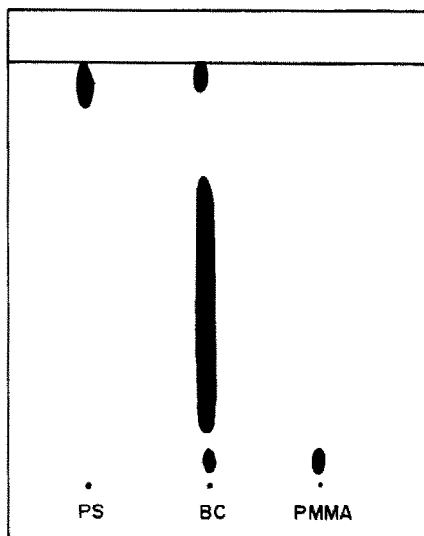


Fig. 2. Gradient TLC of PS-PMMA BC (No. 1 in Table 1). Chloroform-MEK (6:1) with the addition of 6 ml of MEK for 12 min. Detection with reagent (a). MW: PS 1.11×10^5 ; PMMA 4.0×10^4 .

As can be seen from Fig. 1, in order to separate PS from the BC it is convenient to use benzene, since the PS with the highest MW migrates with the eluent front, whereas the BC and even the PMMA with the lowest molecular weight remain at the start. (B) In a chloroform-methyl ethyl ketone (MEK) mixture, the BC is separated from the PMMA. As the MEK content increases, the BCs with increasing PMMA content begin to be separated from the starting spot. It is advisable to increase the MEK content in the eluent until that concentration is attained at which PMMA with the MW corresponding to that of the PMMA block of the BC remains at the start. If the chromatography of the PS-PMMA BC is done in a chloroform-MEK mixture with programmed MEK content, it is reasonable to use a gradient at which PS

migrates with the front, PMMA remains near the start and the BC is distributed along the plate according to its composition (*i.e.*, according to the MW of the PMMA block), (Fig. 2). (C) Interesting possibilities are provided by the application of a chloroform-methanol mixture to the analysis of the PS-PMMA BC. Figure 3 shows the changes in the R_f value of PS and PMMA of various MW, occurring when the methanol content in the mixture with chloroform is increased. It is clear that at a certain methanol content it becomes a displacer for these homopolymers (for PS this content is 30-70% and for PMA and for PMMA it is 20-70%). At a methanol content less than 20%, PS is completely displaced and PMMA is separated according to MW. Hence, for example in a 97:3 v/v chloroform-

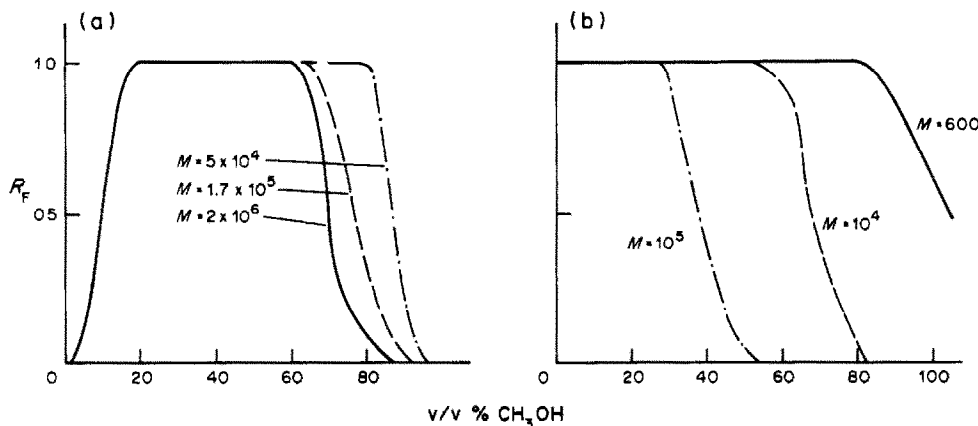


Fig. 3. Dependence of the R_f value of (a) PMMA and (b) PS of different MW in TLC, on the composition of the chloroform-methanol eluent.¹¹ (Reprinted by permission of the copyright holders, Elsevier Scientific Publishing Co.)

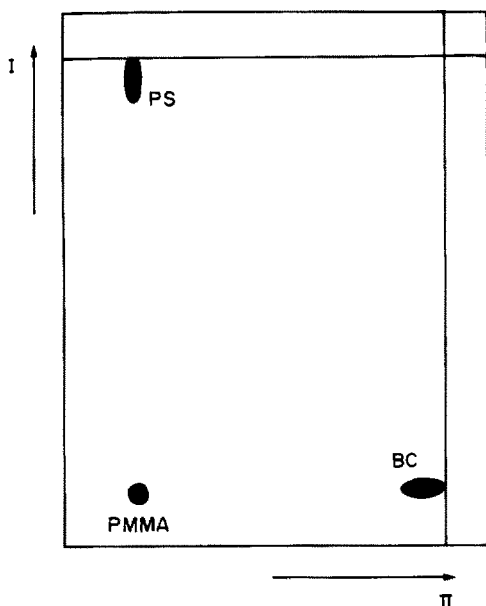


Fig. 4. Two-dimensional TLC of the PS-PMMA BC (No. 1 in Table 1) in benzene (direction I) and chloroform-methanol (97:3) mixture (direction II). Detection with reagent (a). MW: PS 1.11×10^5 ; PMMA 4.0×10^4 .

methanol mixture, a BC containing more than 10% of PS migrates with the eluent, whereas PMMA remains at the start. In this case, if PS has previously been removed by passing benzene along the plate in one direction, all three components of the mixture are separated after chromatography with the chloroform-methanol mixture in the second direction (Fig. 4).

As already indicated, when BCs containing components of similar polarity are analysed, it is more difficult (but nevertheless possible) to select eluents that permit the separation of all three components of the BCs by ATLC. This is particularly important if a selective solvent for one of the homopolymers cannot be found. PS and PB as well as PS and PMS are pairs of homopolymers exhibiting similar polarities. Figure 5 shows analysis of the PS-PB BC by ATLC. A cyclohexane-toluene mixture is a good solvent for both PS and PB. In this mixture toluene is the displacer for both homopolymers but the displacement of PB requires a much lower toluene concentration in the eluent. Hence, by increasing the toluene content in the mixture, it is possible to select conditions under which PB migrates with the eluent front, whereas the BC and PS remain at the start (eluent containing 30% of toluene). When the toluene content is increased to 40%, the BC also migrates with the eluent front and PS remains at the start. The cyclohexane-toluene mixture with increasing toluene content can be used for gradient TLC of the PS-PB BC. It is clear that the BC being investigated exhibited different composition distributions. For analysis of the PI-PMS-PI BC a chloroform-hexane (7:12) mixture is used. PI migrates with the eluent

front, BC is distributed in the middle of the plate and PMS remains near the start. It is possible to displace BC and PI completely to the eluent front by increasing the chloroform content. In this case PMS is distributed in the R_f range 0.1-0.4 according to molecular weight.

Precipitation thin-layer chromatography of BCs

The PTLC of BCs has not been investigated in detail theoretically. However, the solubility of the BCs and their capacity for precipitation are doubtless determined by the overall solubility characteristics of both blocks, *i.e.*, they depend on the MW and hence on the composition of the BC.

Three variations of chromatographic systems may be used for the PTLC and ETLC of BC. They comprise (a) an adsorption-active solvent and precipitant, (b) an adsorption-active solvent and an adsorption-inactive precipitant, (c) an adsorption-inactive solvent and an adsorption-active precipitant. The last variation may evidently be used only with a certain concentration range of the precipitant. The difference between PTLC and ETLC is as follows: in PTLC a sample is spotted on the plate and chromatographed with an eluent of constant composition, in which all the BC fractions are soluble. The eluent composition changes, however, as a result of the evaporation or adsorption of the solvent and the resulting enrichment of the eluent with the precipitant. Hence, the BC fractions are precipitated and distributed along the plate according to their solubility, which is determined by the MW and the component ratio. In ETLC, the eluent should have variable composition, with gradual decrease in precipitant content. In this case BC fractions appear on

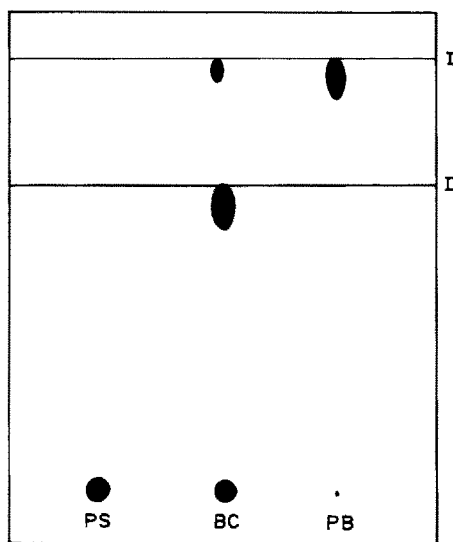


Fig. 5. Stepwise TLC of PS-PB BC (No. 2 in Table 1). The eluent fronts are for cyclohexane-toluene (7:3) (I) and (7:5) (II). Detection with reagent (a). MW: PS 1.0×10^4 ; PB 5.0×10^4 .

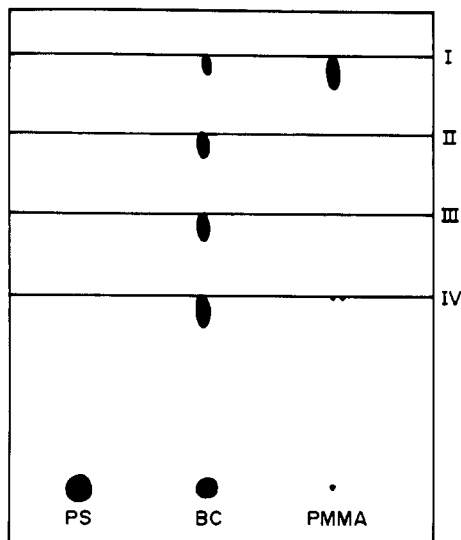


Fig. 6. Stepwise TLC of the PS-PMMA BC (No. 1 in Table 1). The solvent fronts correspond to acetone containing I 50%, II 40%, III 30%, IV 20% of methanol. Detection with reagent (a). MW: PS 1.11×10^5 ; PMMA 1.00×10^5 .

the plate in order of gradually decreasing solubility (resulting from increase in the MW of the BC or a change in its composition). Hence, in the ETLC a mixed type of separation of BC fractions takes place, according to both composition and MW. Let us demonstrate the application of PTLC and ETLC to BC analysis by taking a few examples. For analysis of the PS-PMMA BC we can use a chloroform-methanol (1:1) eluent which is a solvent for PMMA and a precipitant for B and PS. In this system, PMMA (of any MW) is separated from BC and PS and migrates with the eluent front, whereas PS and BC remain at the start. A mixture of acetone and methanol is also a good system for the PTLC separation of PMMA from BC and PS. An effective procedure for preparative separation of PMMA from the PS-PMMA BC is by extraction with a 10% methanol solution in acetone. In a typical separation a TLC check showed that the BC in the residue did not contain free PMMA, even though the initial BC contained 10% of PMMA. Figure 6 shows stepwise fractionation of a PS-PMMA BC on a thin-layer plate with an acetone-methanol eluent with decreasing methanol content. At 50% methanol content both BC and PS remain at the start and PMMA migrates with the front. When the methanol content decreases, BC fractions with a gradual increase in PS content begin to migrate with the eluent front. For the PTLC of the PMMA-PBMA BC, acetonitrile is used as an adsorption-active solvent for PMMA, which migrates with the front, and as a precipitant for BC and PBMA, which remain at the start. Subsequent addition of the eluent displaces the BC and the PBMA remains at the start. For the PMMA-PBG BC, MEK is an adsorption-active solvent for PMMA and a precipitant for PBG and the BC

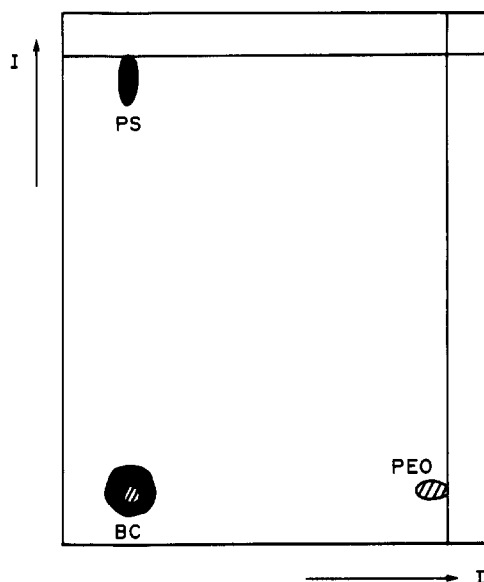


Fig. 7. Two-dimensional TLC of the PS-PEO BC (No. 7 in Table 1) in benzene (direction I) and pyridine-water (3:9) mixture (direction II). Successive detection by methods (b) and (a). MW: PS 1.11×10^5 ; PEO 1.00×10^5 .

(PMMA migrates with the eluent front, the BC and PBG remain at the start). When dioxan is added to give a 7:3 MEK-dioxan mixture as eluent, the BC is displaced, and PBG remains at the start.

Figures 7-9 show examples of the ETLC of the PS-PEO, PS-PBG and PS-PAN BCs, in which one component of the eluent is an adsorption-active solvent for one homopolymer and the second component is a selective and adsorption-active solvent for the other homopolymer (but not for the BC).

An additional possibility for identification of BC

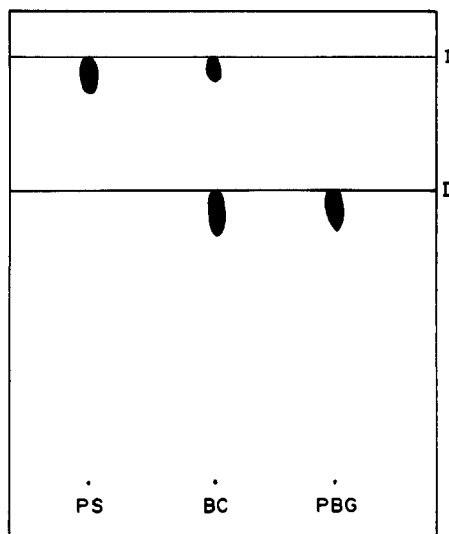


Fig. 8. Stepwise TLC of the PBG-PS-PBG BC (No. 8 in Table 1). The eluent fronts are for (I) chloroform, (II) tetrahydrofuran. Detection by method (a). MW: PS 1.11×10^5 ; PBG 5.0×10^4 .

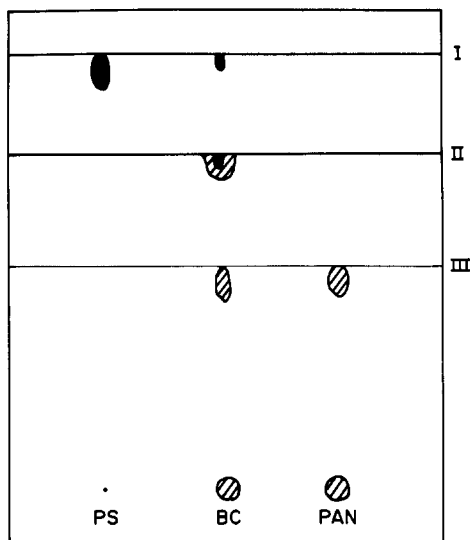


Fig. 9. Stepwise TLC of the PS-PAN BC (No. 9 in Table 1). The eluent fronts are for (I) chloroform, (II) chloroform-DMF (18:2) mixture, (III) DMF. Detection with reagents (a) and (c). MW: PS 1.11×10^5 ; PAN 1.7×10^4 .

components by TLC is specific staining with the detecting reagents. Thus, in the TLC of the PS-PEO BC the Dragendorff reagent stains only PEO (red), ensuring its detection with very high sensitivity, and the $\text{KMnO}_4/\text{H}_2\text{SO}_4$ reagent stains only PS (black). hence, use of both reagents in succession for staining the chromatographic spot remaining at the start after the separation of both homopolymers, will establish that this spot contains the BC. The same detection principle can be used for the PS-PAN BC, PAN being specifically stained yellow by potassium hydroxide solution.

In BC analysis it may be required to evaluate the MW of the homopolymer admixture and compare it with that of the precursor homopolymer. These problems have been studied in greater detail for BCs based on PS, by using our method for separation of PS according to MW by ATLC.⁹ Taking as an example the PS-PMMA BC (Fig. 10) it becomes clear that the PS admixture is separated into two components, the less adsorption-active of which corresponds to the PS precursor. Investigations showed that the PS-admixtures in BCs may differ in nature and may be (a) PSs of different MW, (b) PSs containing or not containing the adsorption-active end-groups, or (c) BCs with a small content of the second homopolymer.

If two PS-components with different adsorbabilities appear on the plate, it is possible to decide by PTLC whether this difference results from the MW effect or from the presence of different numbers of adsorption-active end-groups in one of these PSs, since the PTLC is not sensitive to the content of end-groups but readily reveals the difference between polymers according to MW.

Hence, if one component is observed in PTLC and several components are detected by ATLC, then the PS consists of molecules of the same MW but containing different numbers of adsorption-active groups. If the same number of components is observed in both the PTLC and ATLC, then the PS components present in the BC differ only in MW. In order to identify a PS containing adsorption-active end-groups, ATLC may also be used. If the elution strength of the eluent is increased (by increasing the content of the adsorption-active solvent component), the R_f value of the components in the sample does not obey the ATLC relationships for standard linear PS, so if the R_f value of the PS-components (in contrast to that of the standard PS) exhibits little dependence on the elution strength of the solvent, then the PS admixture evidently contains adsorption-inactive end-groups.

Thus by TLC of the PS-PAN BC, the existence of an admixture of PS-components with a much higher adsorption activity than for the precursor PS was revealed. Moreover, the adsorption activity of this admixture was different in the two BCs (BC_1 and BC_2) under investigation (Fig. 11). The application of a detecting reagent specific for PAN (10% aqueous solution of potassium hydroxide) showed that the admixture was not pure PS: it was a BC consisting of PS with a small amount of PAN. Moreover, a larger amount of PAN was contained in BC_2 than in BC_1 .

CONCLUSION

A method for the identification of block copolymers and the determination of the presence of

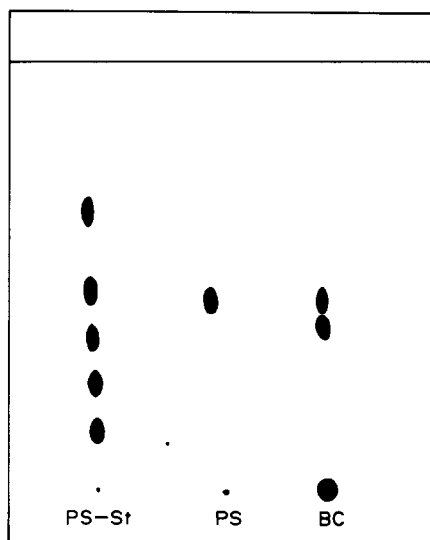


Fig. 10. TLC of the PS-PMMA BC (No. 10 in Table 1) with cyclohexane-toluene-MEK (91:10:8) eluent. Detection with reagents (a) and (c). The reference mixture contained PSs with MW 2.0×10^4 , 5.1×10^4 , 1.11×10^5 , 2.00×10^5 and PS No. 11 (in Table 1).

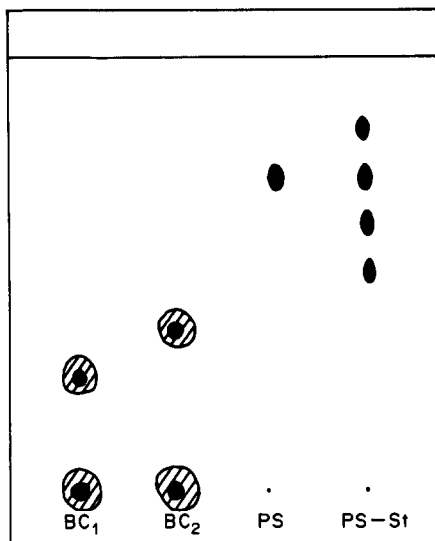


Fig. 11. TLC of the PS-PAN BC (No. 11 in Table 1) with cyclohexane-benzene-acetone (120:40:9) eluent. Detection with reagents (a) and (c). The reference mixture contained PSs with MW 2.0×10^4 , 5.1×10^4 , 1.11×10^5 , 2.00×10^5 and PS No. 11 (in Table 1).

other polymer components in them has been developed on the basis of ATLC and PTLC. This method may be used for determination of the MW and end-group content for the homopolymers present, and the composition of the BC. This method is also useful for selecting the conditions for preparative fractionation of BCs and checking the resulting fractions. It has been successfully used for the investigation of PS-PB, PS-PEO, PS-PBG, PMMA-PBMA, PI-PMS-PI, PMMA-PBG and PS-PAN block copolymers.

Acknowledgement—The authors should like to express their gratitude to V. N. Zgonnik, L. V. Zamoiskaya, E. P.

Skvortsevich, G. D. Rudkovskaya and L. A. Ovsianikova for supplying the samples.

REFERENCES

1. R. J. Ceresa, *Block and Graft Copolymers*, Butterworths, London, 1962.
2. A. Noshay and J. E. McGrath, *Block Copolymers*, Academic Press, New York, 1977.
3. V. N. Tsvetkov, V. E. Eskin and S. Ya. Frenkel, *Struktura makromolekul v rastvorakh*, Nauka, Moscow, 1964.
4. H. Inagaki and T. Tanaka, *Pure Appl. Chem.*, 1982, **54**, 309.
5. W. W. Yau, J. J. Kirkland and D. D. Bly, *Modern Size-Exclusion Liquid Chromatography*, Wiley, New York, 1979.
6. B. G. Belenkii and L. Z. Vilenchik, *Modern Liquid Chromatography of Macromolecules*, Elsevier, Amsterdam, 1983.
7. V. V. Nesterov, V. D. Krasikov, L. D. Turkova, E. S. Gankina and B. G. Belenkii, *Vysokomol. Soedin.*, 1978, **A20**, 2320.
8. V. V. Nesterov, L. V. Zamoiskaya, V. D. Krasikov and G. P. Matianova, *ibid.*, 1983, **A25**, 2561.
9. B. G. Belenkii and E. S. Gankina, *J. Chromatog.*, 1977, **141**, 13.
10. H. Inagaki, T. Kotaka and T.-I. Min, *Pure Appl. Chem.*, 1976, **46**, 61.
11. B. G. Belenkii, E. S. Gankina, P. P. Nefedov, M. A. Lasareva, T. S. Savitskaya and M. D. Volchikhina, *J. Chromatog.*, 1975, **108**, 61.
12. V. V. Nesterov, V. D. Krasikov, V. N. Zgonnik, E. Yu. Melenevskaya, I. V. Kosheleva and B. G. Belenkii, *Vysokomol. Soedin.*, 1983, **A25**, 2568.
13. H. Inagaki and F. Kamiyama, *Macromolecules*, 1973, **6**, 107.
14. N. Donkai, N. Murayama, T. Miyamoto and H. Inagaki, *Macromol. Chemie*, 1974, **175**, 187.
15. A. M. Skvortsov and A. A. Gorbunov, *Vysokomol. Soedin.*, 1979, **A21**, 339.
16. B. G. Belenkii, E. S. Gankina, L. S. Litinova, I. I. Efimova, V. E. Vaskovsky, S. V. Khotimchenko and V. P. Dikarev, *Bioorgan. Khim.*, 1984, **10**, 224.
17. E. S. Gankina, S. I. Gancheva, V. M. Baliaev, J. J. Kever and B. G. Belenkii, *J. Chromatog.*, 1981, **208**, 381.
18. K. Burger, *Z. Anal. Chem.*, 1967, **224**, 42.
19. I. G. Krasnoselskaya, E. S. Gankina, B. G. Belenkii and B. L. Erusalimsky, *Vysokomol. Soedin.*, 1977, **A19**, 999.

LIQUID-LIQUID EXTRACTION OF ELEMENTS BY ANTIPYRINE AND DIANTIPYRYLMETHANE SALTS FROM NON-AQUEOUS SOLUTIONS OR IN SYSTEMS WITHOUT AN ORGANIC SOLVENT

B. I. PETROV and V. P. ZHIVOPISTSEV

Department of Chemistry, A.M. Gorky State University, Perm, USSR

(Received 15 October 1985. Accepted 12 August 1986)

Summary—The liquid-liquid extraction method for inorganic compounds has been developed and further improved by using different types of multiphase systems involving pyrazolone derivatives. The degree of concentration of elements by use of three-phase liquid systems has been increased by 1-2 orders of magnitude, and a universal method for preconcentration of elements in non-aqueous media has been suggested. The development of extraction systems based on a single liquid component—water—and not requiring an organic solvent at all, has increased the safety of extraction methods and improved the working conditions. A new variant of spectrochemical analysis without mineralization of an extract has been developed. Its main advantage is that it reduces the analysis time by a factor of 6 or 8. The liquid-liquid extraction of elements in purely aqueous two-phase systems without an organic solvent can be combined with titrimetric, photometric and polarographic determination in hybrid analytical procedures.

In spite of its wide use, the method of liquid-liquid extraction for separation and preconcentration of inorganic compounds has some drawbacks. The low concentration factor is one of them, since in most cases the phase-volume ratio (organic solvent:aqueous phase) is in the range from 1:1 to 1:10. Further, aqueous solutions are very seldom used for the extraction of elements although many of the solvents and diluents used are flammable (sometimes explosively), fairly volatile, toxic and often very disagreeable in odour.

For twenty years we have been systematically studying the multiphase liquid systems involving pyrazolone derivatives. On the basis of the information obtained we are able to suggest some techniques for overcoming some of the drawbacks of liquid-liquid extraction and to develop and improve it.

For extraction by diantipyrylmethane, which is a weak base, chloroform is usually used as solvent,¹ but when the reagent is present as a simple or complex salt the use of a mixture of chloroform with an inert diluent such as kerosene or an aromatic hydrocarbon results in the formation of a liquid three-phase system.² In one of the two organic phases—the so-called “third phase”—the elements extracted are obtained in 93-98% yield. The concentration factor thus obtained is not determined by the initial volume ratio between the aqueous solution and extracting solvent but by the ratio between the aqueous phase and the third phase in equilibrium with it. According to our extraction procedures for Pd(II),³ Pt(IV)⁴ and Re(VII),⁵ these elements can be concentrated from 1

litre of aqueous solution into 1 ml of third phase. Thus the concentration factor is 10^3 , which is 1-2 orders of magnitude greater than for conventional two-phase systems.

The advantages of three-phase extraction for the preconcentration of trace elements have been fully realized in a new variant of spectrochemical analysis.⁶⁻⁹ The third-phase volume, which depends on the quantity of the appropriate diluent in the solvent mixture, can be reduced to a few drops. Transfer of drops of the viscous third phase onto the flat surface of 3-10 carbon electrodes and direct atomic-emission analysis of the air-dried concentrate, reduces the analysis time by a factor of 6-8. Some 30 trace elements have now been determined by this technique of spectrochemical analysis without mineralization of the extract.

In three-phase systems³⁻⁵ the volumes of aqueous, organic and third phase decrease successively. The element passes from a greater volume into a smaller volume twice, giving in effect a double concentration step. The same effect can be achieved if we divide the procedure into distribution between the aqueous phase and a one-component organic phase first, and then between the two organic phases. Such a scheme envisages extraction of the elements from aqueous solution with a solution of diantipyrylmethane in chloroform, separation of the extract, and its division into two phases by addition of an inert diluent (petroleum ether, kerosene, etc.). We recommend using this two-step scheme for very large volumes of aqueous solution, or when extraction is slow, there is a low distribution ratio, or a precipitate is present.¹⁰⁻¹²

In the second step, the inert diluent produces a second phase which is similar to the third phase of the three-phase systems in composition and properties. Owing to its small volume it has been called the micro-phase. It can be regarded as being in effect an "extractant" for non-aqueous solutions. The diantipyrylmethane salts which form 40–50% of the whole mass of the micro-phase are its active component. The extraction of trace elements from aqueous solutions is done with a very large excess of diantipyrylmethane, so the phase equilibria in the second extraction stage are determined by the properties of the ternary system diantipyrylmethane salt–polar solvent–inert diluent. The data available on the solubility isotherms of such systems have been widely used in choosing the optimal amounts of the components for the extraction.

It further occurred to us to replace the group extractant—the solution of diantipyrylmethane in chloroform—by more selective extractants and at the second stage to split the extract by means of direct addition of diantipyrylmethane salts. Diantipyrylmethane thiocyanate and iodide, the cheapest and most easily available of the antipyrine derivatives, give the best technical characteristics of the micro-phase, as shown by a study of the extraction of Ag(I), Au(III), Ge(IV) and Tl(III) as a function of the nature of the salt used. As expected, the procedures developed^{13,16} give high selectivity and concentration factors.

The possibility of group preconcentration of elements from non-aqueous solutions is exemplified by the metal dithizonates.¹⁷ In spite of their stability, these chelates decompose in the presence of diantipyrylmethane salts, and the metals pass into the micro-phase.

The number of elements transferable into the microphase is increased by the use of a mixture of diantipyrylmethane salts—the thiocyanate and iodide. It is easy to predict the result of the preconcentration process since the elements extracted into the micro-phase are only those having thiocyanate and iodide complexes which can be separated from aqueous solutions by a solution of diantipyrylmethane in chloroform. From our point of view the production of a liquid concentrate in the form of the micro-phase is preferable to other ways of preparation of organic solutions for trace element analysis. It is highly important in the case of very volatile compounds such as GeCl_4 or explosive ones such as perchlorates, and also in the case of solvents with high boiling point (kerosene, etc.) or of difficulty in stripping because of formation of very stable complexes with reagents such as organic sulphides.

A study of the solubility of diantipyrylmethane in trichloroacetic acid solutions has shown that the acid and diantipyrylmethane become concentrated in the same phase. On the other hand many trichloroacetates are extracted from aqueous solutions into chloroform by diantipyrylmethane, although the

components of the compounds extracted come from different phases: protons and trichloroacetate ions from the aqueous phase, diantipyrylmethane from the organic one. These facts led one of us¹⁸ to suggest using systems containing pyrazolone derivatives and water as a single liquid component for the extraction of elements. A systematic study of the distribution of elements in the system water–antipyrine–monochloroacetic acid has now been completed. The advantages of the use of such systems for the development of hybrid methods of analysis has been established.^{19,20}

This paper presents some new data about extraction of elements from organic solutions and, *vice versa*, in systems without an organic solvent.

EXPERIMENTAL

Reagents

All the chemicals (Souzglavreaktiv) were of analytical-reagent grade. Standard 0.1M solutions of Cd(II), Mo(VI), V(V) in redistilled water, Hg(II), In(III) in 1M sulphuric acid, Au(III), Tl(III) in 1M hydrochloric acid, and 0.05M solutions of Nb(V) in 25% tartaric acid solution and W(VI) in 0.1M sodium hydroxide were prepared from $\text{CdCl}_2 \cdot 2.5\text{H}_2\text{O}$, $\text{Na}_2\text{MoO}_4 \cdot 2\text{H}_2\text{O}$, NH_4VO_3 , HgSO_4 , $\text{In}_2(\text{SO}_4)_3$, $\text{HAuCl}_4 \cdot 2\text{H}_2\text{O}$, Ti_2O_3 , NbBr_5 and $(\text{NH}_4)_4\text{W}_3\text{O}_{17} \cdot 2.5\text{H}_2\text{O}$ respectively. The Cd(II), Hg(II), In(III), Tl(III), Mo(VI), V(V) concentrations were checked by EDTA titration [the Mo(VI) and V(V) were reduced to Mo(V) and V(VI) beforehand]. The Au(III), Nb(V) and W(VI) concentrations were checked gravimetrically. More dilute (10^{-6} – 10^{-3} M) metal salt solutions were prepared dilute from the 0.1M standard solutions.

Diethyl ether, chloroform and antipyrine were of medical and pharmaceutical grade. Pyrocatechol was purified by distillation, with an air condenser.

Diantipyrylmethane iodide was produced from the third phase of a system containing 100 ml of 1M sulphuric acid, 10 ml of chloroform, 40 ml of benzene, 15 g of potassium iodide and 20 g of diantipyrylmethane. Treating the third phase with several portions of diethyl ether gives a solid product corresponding to the formula $(\text{LH})\text{I}$, where L is diantipyrylmethane, established by two-phase titration with sodium hydroxide.

Procedures

Preconcentration of Au(I), Cd(II), Hg(II), In(III) and Tl(III) in non-aqueous medium. The elements were extracted from 20 ml of aqueous 1M potassium iodide/1M sulphuric acid solution with an equal volume of diethyl ether. A 10-ml aliquot of the ether extract was transferred to a dry separatory funnel and 7 ml of 4% diantipyrylmethane iodide solution in chloroform were added to split the phase. After separation of the two layers the viscous lower micro-phase, several drops in volume, was transferred to the flat surfaces of 6 graphite electrodes. After drying, the electrodes were arced in succession, and the spectra were recorded in exactly the same position on the photoplate.

The calibration graphs were plotted as logarithm of the relative intensity of the analytical line-pair (corrected for background) vs. logarithm of amount of element taken (μg). The background was measured at the least possible distance to the right from the element line. Cadmium (10 μg) was added as reference element.

The completeness of preconcentration in the micro-phase was checked by analysis of the aqueous and ether phases. For this purpose the ether phase was again split by additional of diantipyrylmethane iodide. The elements

Table 1. Distribution of 100 μg of elements between the phases in the two-stage preconcentration

Ion determined	Extraction from aqueous solution, %	Extraction into micro-phase, %	Analytical line, nm
Au(I)	99	98	267.5
Cd(II)	98	95-96	228.0
Hg(II)	99	99	253.6
In(III)	98	94-96	303.9
Tl(III)	95	99	276.7

remaining in the aqueous phase were extracted with two 10-ml portions of diethyl ether, and the metals were removed from the combined extract into a micro-phase as before. Both micro-phases were then analysed spectrographically.

Distribution of Mo(VI), Nb(V), V(V) and W(VI) in the water-antipyrine-pyrocatechol system. The influence of various parameters on the phase-volume ratio was examined by performing the extractions in test-tubes graduated in 0.1-ml divisions, and the distribution ratios of the elements were determined by extraction in separatory funnels at 30-35°.

RESULTS AND DISCUSSION

The results of the two-stage extraction, first from aqueous solution then from the ether extract, are shown in Table 1. Quantitative preconcentration of the elements takes place in the micro-phase. The volume ratio of aqueous phase to micro-phase is 20:0.5 hence the overall concentration factor is 40, compared with 1 for the first stage of the process. To study the effect of various matrices on the results, appropriate calibration graphs were plotted. The influence of 10⁵-fold (10⁶-fold in the case of gold) ratio of Al, Co, Cr, Fe, Li, Mg, Mn, Ni to analyte metal is negligible. Calibration graphs obtained with synthetic standards can therefore be employed for determinations. A rapid spectrochemical procedure for determining 1-10 μg of Au, 2-40 μg of In and 3-80 μg of Hg and Tl has been developed. The relative standard deviation for 5 determinations of 2.5 μg of Au and 10 μg each of Hg, In and Tl was between 4 and 22%. The method of standard additions was used to establish the accuracy.

With the ternary system water-antipyrine (Ant)-pyrocatechol (PC), increasing the temperature to 30-35° accelerates the separation of the phases, decreases the viscosity of the organic phase, and

Table 2. Effect of pH on organic phase volume in the 0.01M antipyrine/0.01M pyrocatechol system (20 ml total volume)

1M HCl,		Organic phase,		1M NaOH,		Organic phase,	
ml	pH	ml	ml	pH	ml	ml	ml
5.0	1.65	0.0	0.0	6.10	1.9		
4.0	1.50	0.5	0.01	6.65	2.2		
3.0	1.70	1.0	0.05	7.75	2.2		
2.0	1.80	1.4	0.2	8.40	1.8		
1.0	2.15	1.6	0.4	8.75	1.8		
0.4	2.60	1.7	0.6	9.00	1.8		
0.2	2.90	1.7	0.8	9.10	1.7		
0.1	3.15	1.8	1.0	9.20	1.7		
0.0	6.10	1.9	2.0	9.45	1.5		

prevents its crystallization. When the total volume of the system is 20 ml and the antipyrine concentration (0.01M) is kept constant, the organic phase forms at a PC/Ant molar ratio of 0.2; with further increase in pyrocatechol content the organic phase volume gradually approaches 3 ml, and, finally, as a PC/Ant molar ratio of 2.6 crystallization takes place. At PC/Ant = 1.0 the organic phase volume is 1.9 ml, quite sufficiently for use for absorbance measurement in a 3-mm cell.

The effect of the pH of the medium is also important. As Table 2 shows, the organic phase volume changes slightly, from 1.6 to 2.2 ml, with increase in pH from ~2 to ~8, but outside this range the mutual solubility of the phases increases, giving homogenization at pH \approx 1.6. The increase in mutual solubility of the phases on introduction of acid or alkali is due to protonation of the antipyrine by the strong acid and by dissociation of the phenolic group(s) of pyrocatechol at high pH. The homogenization of the system is due to the different properties of these products.

The blue, green or yellow colour of the organic phase produced on the introduction of V(V), Mo(VI), Nb(V) or W(VI) salts into the aqueous layer, proves the extraction of these elements. Beer's law is obeyed at the optimum pH 4.5, 2.1, 2.6 and 2.3 for V, Nb, Mo and W respectively.

Inert electrolytes affect the organic phase volume owing to the salting out of antipyrine and pyrocatechol from the aqueous phase. To avoid consequent errors the conditions used for analysis of samples and for calibration must be as similar as possible.

Table 3. Spectrophotometric methods based on liquid-liquid extraction in the water-antipyrine-pyrocatechol system

Species extracted	Optimum pH	λ_{max} , nm	ϵ , l. mole ⁻¹ cm ⁻¹	Amount determined, μg
V(V)	3.5-5.5	650	1.4×10^5	2-30
Nb(V)	1.9-2.2	350	1.5×10^5	3-50
Mo(VI)	1.9-3.1	350	5×10^4	7-100
		640		
W(VI)	1.8-2.6	340	3×10^4	20-550

Because the optimum pH and λ_{\max} values for the Nb, Mo and W complexes differ considerably from those for the vanadium complex, the latter can be determined in the presence of the others. Vanadium may also be determined in the presence of alkali, alkaline earth and rare-earth metals, Al, Be, Cd, Ga, Mn, Sc, and Zr. Although coloured, Co, Cr, Cu and Ni cations do not affect the analyses. Fe(III) and Ti(IV) are extracted as coloured complexes and hence interfere.

Table 3 shows the main characteristics of the extraction-spectrophotometric procedures. The extracts obtained can be analysed titrimetrically, spectrophotometrically, or polarographically.

REFERENCES

1. B. I. Petrov, *Zh. Analit. Khim.*, 1983, **38**, 2051.
2. T. P. Yakovleva, V. P. Zhivopistsev, K. I. Mochalov and B. I. Petrov, *Diantipyrylmethane and its Derivatives as Analytical Reagents*, pp. 46-56. Perm University Press, 1974.
3. B. I. Petrov, V. N. Vilisov, I. N. Ponosov and V. P. Zhivopistsev, *USSR Patent*, 446797, 15 October 1974.
4. B. I. Petrov, V. P. Zhivopistsev, I. N. Ponosov and V. N. Vilisov, *USSR Patent*, 446801, 15 October 1974.
5. B. I. Petrov, V. P. Zhivopistsev, M. I. Degtev and Yu. A. Makhnev, *USSR Patent*, 446803, 15 October 1974.
6. V. P. Zhivopistsev, Yu. A. Makhnev and B. I. Petrov, *Zh. Prikl. Spektrosk.*, 1969, **11**, 779.
7. V. P. Zhivopistsev, Yu. A. Makhnev, B. I. Petrov and O. I. Savina, *Zavodsk. Lab.*, 1969, **35**, 902.
8. A. I. Busev, V. P. Zhivopistsev, B. I. Petrov and Yu. A. Makhnev, *Talanta*, 1972, **19**, 173.
9. A. I. Busev, V. P. Zhivopistsev, B. I. Petrov and M. I. Degtev, *Anal. Lett.*, 1972, **5**, 265.
10. Yu. A. Makhnev, B. I. Petrov, V. P. Zhivopistsev and I. N. Ponosov, *USSR Patent*, 446799, 15 October 1974.
11. B. I. Petrov, Yu. A. Makhnev, V. P. Zhivopistsev and I. N. Ponosov, *USSR Patent*, 446800, 15 October 1974.
12. B. I. Petrov, K. G. Galinova and V. P. Zhivopistsev, *Zh. Prikl. Spektrosk.*, 1975, **23**, 486.
13. B. I. Petrov, K. G. Galinova, Yu. A. Makhnev and V. P. Zhivopistsev, *Zavodsk. Lab.*, 1977, **43**, 923.
14. B. I. Petrov, V. P. Zhivopistsev and K. G. Galinova, *The Use of Pyrazolone Derivatives in Analytical Chemistry*, pp. 70-74. Perm University Press, 1977.
15. B. I. Petrov and K. G. Galinova, *Zh. Analit. Khim.*, 1978, **33**, 1481.
16. B. I. Petrov, K. G. Galinova, V. P. Zhivopistsev and Yu. A. Shchurov, *ibid.*, 1981, **36**, 1918.
17. B. I. Petrov and A. P. Oshchepkova, *ibid.*, 1984, **39**, 1577.
18. B. I. Petrov, *VII All-Union Conference on Extraction Chemistry*, p. 44. Nauka, Moscow, 1984.
19. B. I. Petrov and S. I. Rogozhnikov, *Zh. Analit. Khim.*, 1984, **39**, 1848.
20. *Idem*, *ibid.*, 1985, **40**, 247.

PRECONCENTRATION OF MICROAMOUNTS OF ELEMENTS IN NATURAL WATERS WITH 8-MERCAPTOQUINOLINE AND BIS(8-QUINOLYL) DISULPHIDE FOR THEIR ATOMIC-ABSORPTION DETERMINATION

YU. A. BANKOVSKY, M. V. VIRCAVS, O. E. VEVERIS, A. R. PELNE
and D. K. VIRCAVA

Institute of Inorganic Chemistry of the Academy of Sciences of the Latvian SSR, Miera 34,
Salaspils, 229021, USSR

(Received 15 October 1985. Revised 14 May 1986. Accepted 9 August 1986)

Summary—A method has been developed for the group concentration of microamounts of metals (Fe, Co, Ni, Mn, Cu, Zn, Cd, Hg, Pb, Bi, Sb, Mo, W, V, Cr, Ga, In, Sn, Ag, Au, Pd, Pt) in the form of their 8-mercaptoquinolinates co-precipitated on bis(8-quinolyl) disulphide as collector, the latter being an oxidation product of 8-mercaptoquinoline. The collector is formed during the co-precipitation process, which is the reason for its high co-precipitating power. The elements thus concentrated are determined by atomic-absorption spectrometry after dissolution of the precipitate in dilute nitric acid.

Organic co-precipitants were proposed in the 1950s by Kuznetsov^{1,2} and his investigations of the theoretical principles of their behaviour began a new stage in the analytical chemistry of microamounts of elements.^{1,2} Despite the fact that concentration of elements by organic collectors has considerable advantages over concentration by extraction (a higher concentration coefficient is attained and the procedure is more convenient for field work) the technique has not been applied as widely as extraction. Perhaps the basic reason for this is that a large weight of the organic collector is required (from 1 to 4 g per litre of solution to be analysed). Mineralization of so massive a precipitate is time-consuming and there is a risk of loss of the elements to be determined. The large mass of collector is required because of the inefficiency of collection. When an alcohol or acetone solution of the organic collector is mixed with the aqueous solution to be analysed there is almost complete local precipitation of nearly all the collector in a small fraction of the total volume of sample solution.

It is considerably more efficient to form the organic collector simultaneously throughout the volume of solution to be analysed. The efficiency is then greatly increased because the collector particles possess their greatest sorption power during their growth. Especially efficient are those chelating agents which bind metals in highly stable chelate compounds and can themselves be turned into compounds that are only slightly soluble in water and can thus act as co-precipitants for the metal complexes. Typical chelating agents of this type are those organic reagents which contain an —SH group in the molecule, e.g., 8-mercaptoquinoline, and its derivatives, di-

thiocarbamates (ammonium pyrrolidinedithiocarbamate and sodium diethyldithiocarbamate, xanthates (potassium ethylxanthate), dithiocarboxylic acids, dialkyl- and diaryldithiophosphoric acids, thionalide, 2-mercaptobenzothiazole, and dithiol.

The —SH group in these reagents is easily oxidized to the disulphide group by aerial oxygen, hydrogen peroxide and other suitable oxidizing agents. If hydrophilic groups are absent in the reagent molecule the disulphide compounds formed are practically insoluble in water and can be highly efficient co-precipitants of metal chelates, particularly if these have been formed by the reagent itself.

Thus, the proposed method is based on the application of —SH-containing organic reagents for binding metals into chelate compounds and obtaining efficient co-precipitation of the metal chelates by oxidizing the excess of reagent to the disulphide form.

In the present paper we propose use of 8-mercaptoquinoline as the chelating agent and its oxidation product bis(8-quinolyl)disulphide as collector.³

EXPERIMENTAL

Reagents

A 1% solution of sodium 8-mercaptoquinolate dihydrate ($C_9H_6NSNa \cdot 2H_2O$) in doubly distilled water. Though the reagent manufactured in the Soviet Union is sufficiently pure with regard to heavy metals, its purification is advisable, according to the following procedure. The reagent solution is left to stand for 1 hr and is then filtered twice through the same dense filter. The bis(8-quinolyl) disulphide resulting from aerial oxidation of the 8-mercaptoquinoline remains on the filter together with the co-precipitated complexes of any heavy metals present. The reagent solution is slowly oxidized by air and becomes

turbid (though this does not interfere with the determination) and is best used when fresh (in 18 hr about 20% of the reagent becomes oxidized).

Highly pure nitric acid, aqueous ammonia solution (purified by isothermal distillation), hydrogen peroxide (1% solution), doubly distilled water.

During development of the concentration procedure, artificial sea-water was used.

The following radionuclides, in microgram and sub-microgram amounts, were used during the research: ^{59}Fe , ^{57}Co and ^{60}Co , ^{125}Sb , ^{116m}In , ^{198}Au , ^{210}Pb , ^{65}Zn , ^{48}V , ^{54}Mn , ^{64}Cu , ^{115m}Cd and ^{109}Cd , $^{110m} + ^{110}\text{Ag}$, ^{203}Hg , ^{51}Cr , ^{207}Bi , ^{72}Ga , ^{99}Mo , ^{109}Pd , ^{197}Pt , ^{187}W , ^{65}Ni , ^{113}Sn .

Apparatus

The activity of the radionuclides used was measured by scintillation-counting and γ -spectrometry.

The degree of co-precipitation of a metal was determined by measuring the activity of its radionuclide in the material collected on the filter.

Filtration was done by suction with a specially constructed plexiglas apparatus.

Very dense filters prevent loss of the precipitate through the pores of the filter, but filtration with them is very slow. Whatman No. 42 or Filtrak No. 390 filter papers and also Nuclepore or nuclear lavsan filters⁴ with pore diameter 0.42–0.45 μm , are recommended; they permit fast enough filtration (2 litres per hr) and are not penetrated by the precipitate if the filtration is done as described for the concentration method. The diameter of the filter is 46 mm for 1 litre of sample, or 18 mm for 200 ml. The paper filters are used if the concentrate is to be analysed by the neutron-activation method, since the filters are more stable towards radioactivity. The nuclear filters are more useful for atomic-absorption analysis.

Concentration procedure

Adjust 1 litre of the water to be analysed (filtered through an appropriate filter to remove particulate matter) to pH 1 with concentrated nitric acid. Add 10 ml of 1% sodium 8-mercaptoquinolate solution. After 15 min add 10% ammonia solution dropwise with stirring to adjust the pH to 4–6. After 30 min add 2 ml of 1% hydrogen peroxide solution, with stirring. After another 30 min transfer the mixture to the beaker of the filtration apparatus, rinsing with three 30-ml portions of doubly distilled water.

In the filtration it is essential to prevent the precipitate from passing through the filter. Therefore, start the filtration without suction, and apply suction only when about 100 ml of the mixture has been filtered. Failure to do so leads to penetration of the precipitate through the filter and considerable loss of the elements to be concentrated. When the filtration is complete, wash the walls of the beaker and the precipitate on the filter with small amounts of doubly distilled water. If the solution to be analysed contains a high concentration of sodium salts, 150–200 ml of water will be needed to wash all the sodium from the concentrate on the filter (which is necessary if neutron-activation is to be used). Run a reagent blank determination with 1 litre of doubly distilled water. *Note.* Quantitative formation of the complexes proceeds at room temperature except for chromium and platinum, for which heating at 90° for 2–3 min (chromium) or 30 min (platinum) is needed after addition of the reagent and neutralization to pH 4–6, followed by cooling before addition of the hydrogen peroxide.

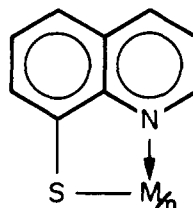
Atomic-absorption determination of metals in the concentrates

Immerse the concentrate and nuclear lavsan filter for several min in 3 ml of 5M nitric acid. Dilute the resulting solution with doubly distilled water to 10 ml. Do not subject the nuclear-type filters to treatment with concentrated nitric

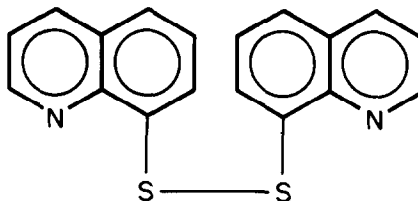
acid (the filter would disintegrate and its fragments interfere in the determination). Analyse the solution by standard atomic-absorption methods.

RESULTS AND DISCUSSION

8-Mercaptoquinoline and its derivatives containing hydrophobic substituents are particularly useful organic reagents for binding microamounts of metals into chelate compounds and their subsequent co-precipitation. These reagents form five-membered rings with the metal ion to yield highly stable inner-complex compounds (which are insoluble in water) with transition and non-transition *d*-elements (Cu, Ag, Au, Zn, Cd, Hg, Ga, In, Tl, Ge, Sn, Pb, As, Sb, Bi, Se, Te, V, Cr, Mo, W, Mn, Tc, Re, Co, Ni, Ru, Rh, Pd, Os, Ir, Pt)³. This allows the group concentration of these elements in the presence of high concentrations of all other cations.



These complex compounds are not oxidized even with 1000-fold ratio of hydrogen peroxide, but the excess of 8-mercaptoquinoline in the solution is readily oxidized by aerial oxygen, hydrogen peroxide, sodium hypochlorite, *etc.*, to bis(8-quinolyl) disulphide.



In contrast to 8-mercaptoquinoline, this oxidation product is practically insoluble in water (0.026 mg/l.), or feebly acid and alkaline solutions, and precipitates in a state of fine dispersion, thus being an efficient co-precipitant of metal 8-mercaptoquinolates because of its large surface area.

The oxidation with hydrogen peroxide takes place over the pH range 2.5–12, and is complete within 5 min at pH 4–11. The oxidation is slower at lower pH, taking about 1 hr for completion at pH 2–3. At pH 2.5 the bis(8-quinolyl) disulphide begins to dissolve because of protonation. Oxidation of 8-mercaptoquinoline and its derivatives proceeds only to the disulphide stage even with a large excess of oxidizing agent. Excess of oxidant and increased temperature (up to 85°) do not affect the completeness of co-precipitation.

Table 1. pH-interval and degree of maximum co-precipitation of metal 8-mercaptoquinolinates with bis(8-quinolyl) disulphide

Complex	pH interval of quantitative co-precipitation	Degree of co-precipitation %	Complex	pH interval of quantitative co-precipitation	Degree of co-precipitation %
Fe(C ₉ H ₆ NS) ₃	2.8-11	98	MoO ₂ (C ₉ H ₆ NS) ₂	3-5	96
Co(C ₉ H ₆ NS) ₃	2.3-10	98	WO ₃ (C ₉ H ₆ NS) ₂	2.2-5.3	95
Ni(C ₉ H ₆ NS) ₂	2.3-13	98	VO(C ₉ H ₆ NS) ₂	4-6.4	98
Mn(C ₉ H ₆ NS) ₂	5.8-10	97	Cr(C ₉ H ₆ NS) ₃ *	3.8-5.2	94
Cu(C ₉ H ₆ NS) ₂	2-13	98	Ga(C ₉ H ₆ NS) ₃	3.7-6.8	93
Zn(C ₉ H ₆ NS) ₂	4-10	97	In(C ₉ H ₆ NS) ₃	3-8.7	95
Cd(C ₉ H ₆ NS) ₂	2.4-10	98	Sn(C ₉ H ₆ NS) ₄	2.5-9.5	95
Hg(C ₉ H ₆ NS) ₂	2.4-10	98	Ag(C ₉ H ₆ NS)	3.6-11	97
Pb(C ₉ H ₆ NS) ₂	4.8-9	95	Au(C ₉ H ₆ NS) ₃	2.3-8.4	97
Bi(C ₉ H ₆ NS) ₃	2.5-12	97	Pd(C ₉ H ₆ NS) ₂	2-12	98
Sb(C ₉ H ₆ NS) ₃	2.5-7.6	93	Pt(C ₉ H ₆ NS) ₂ *	3.5-12	98

*On heating.

Presumably the co-precipitation is due to adsorption of the metal complex molecules on the growing particles of bis(8-quinolyl) disulphide and formation of occlusive compounds, possibly clathrates of the metal complex in the crystal lattice of the disulphide. That is suggested by the fact that if the disulphide is crystallized from its saturated solution in toluene in the presence of platinum 8-mercaptoquinolate (blue in solution) or palladium 8-mercaptoquinolate (pink) at 10^{-4} - $10^{-3}M$ level, the transparent crystals of the disulphide formed acquire the colour of the corresponding metal complex. Crystallization of the disulphide extracts the palladium and platinum complexes quantitatively from the toluene solution.

The pH interval for quantitative co-precipitation

Table 2. Atomic-absorption determination of elements in artificial seawater after concentration by co-precipitation

Element	Introduced, μg	Found, μg
Zn	2	2.0
	3	2.9
	5	5.2
	20	20.6
Cu	0.8	0.81
	5	4.8
	10	8.9
	20	20.6
	30	29.3
Cr	2	1.8
Pb	2	1.9
Ni	4	3.9
	5	4.8
	10	9.6
	20	18.6
Cd	5	4.8
	10	8.3
Fe	8	8.2
Co	5	4.8
	10	9.7

of the element of interest from solution depends on the stability constant of the metal complex formed as well as on certain other factors. For instance, metal diethyldithiocarbamates are considerably less stable than the corresponding 8-mercaptoquinolinates, and co-precipitation of a diethyldithiocarbamate with tetraethylthiuram disulphide proceeds over only a very narrow pH interval (5-7), in comparison to that for the 8-mercaptoquinoline systems (Table 1).

For quantitative extraction of microamounts of metals from natural waters and salt solutions, in most cases 30 ml of 1% sodium 8-mercaptoquinolate solution is sufficient for 1 litre of the solution to be analysed. However, for safety we recommend using 100 mg of sodium 8-mercaptoquinolate (which would yield 73 mg of the disulphide on oxidation). This amount is considerably smaller than that recommended for other organic collectors reported in the literature. This comparatively low weight of collector makes it unnecessary to mineralize the precipitate before its analysis. A further advantage is that the filtration is much faster.

When solvent extraction is used, the concentration coefficient seldom exceeds 100 (ratio of aqueous to organic phase volume), whereas co-precipitation by the proposed method gives a concentration coefficient of 14000 (ratio of weight of solution to be analysed, to weight of disulphide collector).

Table 1 shows that the pH-interval for quantitative co-precipitation of microamounts of metal 8-mercaptoquinolinates with bis(8-quinolyl) disulphide lies mostly within the pH-interval for maximum formation of the disulphide.

At pH 4-6 simultaneous concentration of most of the metals listed in Table 1 is possible.

The high stability of the 8-mercaptoquinoline complexes enables microamounts of heavy metals to be concentrated in the presence of high concentrations of masking agents. For example, the co-precipitation of even submicrogram amounts of many metals is at least 95% complete in the presence of 1-3M fluoride, chloride, bromide, iodide or thiocyanate or 1M citrate.

Numerous experiments have indicated that the higher the concentration of inorganic salts (not reacting with 8-mercaptoquinoline) in the test solution, the faster and more reliable is the co-precipitation process. The reason for this is that electrolytes increase the rate of coagulation of the bis(8-quinolyl) disulphide. It is possible that under such conditions the disulphide is formed in a more finely dispersed state and hence will have greater adsorption power.

The method is applicable to natural waters containing not more than 5 mg/l., total concentration of heavy metals, or to purification of salts.

Table 2 gives results for determination of micro amounts of some elements in concentrates obtained

by co-precipitation of the elements with bis(8-quinolyl) disulphide from 1 litre of artificial seawater.

REFERENCES

1. V. I. Kuznetsov, *Zh. Analit. Khim.*, 1954, 9, 199.
2. V. I. Kuznetsov and T. G. Akimova, *Concentration of Actinides by Co-precipitation with Organic Co-precipitants*, Atomizdat, Moscow, 1968.
3. Yu. A. Bankovskii, *The Chemistry of the Mercaptoquinoline Chelates and their Derivatives*, Zinatne, Riga, 1978.
4. Yu. S. Zam'yatin, in *3rd Conference on Application of New Nuclear-Physical Methods to Solution of Science Technology and Industrial Problems*, Dubna, 1979, pp. 153-163.

THIN-LAYER CHROMATOGRAPHY WITH MOBILE PHASES OF LOW VOLATILITY

V. G. BEREZKIN and S. L. BOLOTOV

Institute of Petrochemical Synthesis, Academy of Sciences of the USSR, Lenin, Av. 29,
Moscow, V-71, USSR

(Received 11 November 1985. Accepted 10 August 1986)

Summary—The analytical possibilities and specific features of a variation of thin-layer chromatography with mobile phases of low volatility (which may be organic liquids or melts of organic solids) are discussed.

Thin-layer chromatography (TLC) is currently enjoying wide popularity as an analytical technique¹ which is universal, highly effective and simple, yet its history is relatively short. As a matter of record, the first publication on TLC appeared in 1938.² A major contribution to the development of this technique has been made by Stahl,^{3,4} who proposed standardizing the sorbents, instrumentation, and experimental procedure in order to render it as widely applicable as possible. In recent years, major advances have been made in the new modification of TLC known as high-performance thin-layer chromatography (HPTLC).⁵ An important advantage of TLC, in our opinion, is the fact that in spite of the development of highly sophisticated and expensive equipment (intended primarily for quantitative detection), TLC remains one of the simplest and least costly analytical methods. TLC is broadly employed for analysis of a great variety of mixtures in the chemical, pharmaceutical and food industries, in agriculture, and so forth.^{6,7}

The mobile phases used in traditional TLC are generally composed of volatile low-boiling solvents such as methanol, acetone, benzene, chloroform, and so on,⁸ so that they can quickly be removed from the sorbent layer once the separation is over. Therefore, the chromatographic system also contains mobile phase components in the gas phase. With this in mind, Niederwieser and Honneger⁹ proposed that TLC should be regarded as a process occurring in a three-phase gas-liquid-solid system. The validity of this proposition is obvious if it is borne in mind that the presence of the gas phase strongly influences the separation, although it is not involved in the transport and distribution of the separated substances.

A serious drawback of TLC is the poor reproducibility of the chromatographic conditions, which manifests itself quantitatively in inadequate reproducibility¹⁰ of the retention values R_f which serve as a major characteristic in the identification of the separated components. As a consequence, the experimentally found values of R_f vary widely from one laboratory to another.¹¹ The reproducibility in

TLC depends on a number of factors that are difficult to control, including the reproducibility of the porous layer characteristics and the effect of the gas phase.¹² Now that TLC procedures have become standardized and commercial plates with adequately reproducible sorbent layers are commonly used, the poor reproducibility in TLC stems, in our opinion, primarily from the effect of the gas phase on the chromatographic process.¹³ The chromatographic conditions constantly change during the separation and are difficult to reproduce because of exchange interaction between the liquid phase, gas phase, and the dry sorbent on the plate. To stabilize the separation conditions various types of chromatographic chambers have been used but then the separation results become heavily dependent on the type of chamber used.¹⁴

The effect of the vapour phase can be minimized, in principle, by resorting to:

- (1) complete standardization of the experimental procedure (use of special chambers, temperature control, etc.);
- (2) uninterrupted running of the chromatogram;¹⁵
- (3) forced mobile-phase flow;¹⁶
- (4) use of mobile phases of low volatility.

Since it is desirable to maintain the inherent simplicity of the technique, variants (2) and (4) seem to hold the most promise. Variant (2), however, calls for a much longer duration of the analysis.

The basic idea behind the two new variants of TLC known under the common name "TLC with low-volatility mobile phases",¹⁷ is that the mobile phase is an organic liquid of low volatility or a melt of an organic compound that is solid at room temperature. The first variant can be run at room temperature, but the other needs a temperature above the melting point of the mobile phase. We have prepared a classification of the variants of TLC, based on the volatility and type of mobile phase (Fig. 1). It should be pointed out that melts of inorganic salts and their eutectic mixtures were widely used in the fifties and sixties as mobile phases in thin-layer chromatography

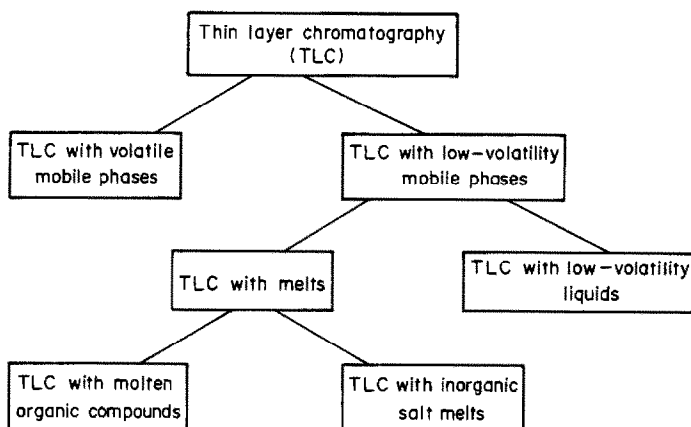


Fig. 1. Classification of TLC variants.

and in electrophoresis.^{18,19} However, TLC with melts of organic compounds differs from TLC with melts of inorganic salts in area of application, mechanism of separation, and experimental conditions, which gives us every reason to regard it as an independent variant of TLC with melts.²⁰

The TLC variant with melts of organic compounds has been used by Szekely and Baumgartner²¹ for separation of low-volatility natural dyes.

This review covers the analytical potential and specific features of TLC with low-volatility mobile phases.

SPECIFIC FEATURES OF TLC WITH LOW-VOLATILE MOBILE PHASES

Reproducibility of separation

A distinctive feature of TLC with low-volatility mobile phases is that the separation is conducted under conditions in which the effect of the gas phase on the chromatographic process is negligible, thus eliminating its contribution to irreproducibility of the chromatogram. We are therefore dealing essentially with a two-phase chromatographic system: liquid-solid. The higher separation temperature when melts are used is an additional stabilizing factor, since the preliminary conditioning of the plate removes adsorbed water from the sorbent layer. This is another reason for the good reproducibility of separation in TLC with molten mobile phases.

To estimate the reproducibility of the separation

conditions we have examined the reproducibility of the rate of advance of the front of a hexadecanol melt at 120° on Merck 60 F-254 TLC plates. The relative standard deviation (rsd) of the time needed for the front to advance the first 1.5 cm was found to be 5.4% ($n = 10$) at the 95% confidence level. According to the literature, the corresponding value for a volatile mobile phases exceeds 10%.¹³ Under the same conditions, the rsd for an advance of 5.5 cm was 3.7%, which is indicative of high stability of the mobile-phase flow in TLC with melts.

For assessment of the overall separation we have studied the reproducibility of the R_f values of Sudan dyes on Silufol plates under traditional TLC conditions and those of TLC with low-volatility mobile phases (Table 1).

When application of the sample onto the plate was carefully replicated, the rsd of the R_f values on Merck 60 F-254 TLC plates with a hexadecanol melt at 120° was found to be 1.3–1.6%. Under similar conditions but on Anasil G plates, the rsd of the R_f values was 1.9–2.8%. In traditional TLC with volatile mobile phases the reproducibility is 5%, provided the separation parameters are in strict compliance with the experimental conditions.⁸

An important consideration is that the type and dimensions of the chromatographic chamber do not affect the reproducibility of separation in TLC with low-volatility mobile phases, whereas they produce a tangible effect on the R_f values and separation reproducibility in traditional TLC.²²

Table 1. Relative standard deviations of R_f values for Sudan Dyes on Silufol plates

Dyes	Relative standard deviation, %		
	Benzene	Triethanolamine	Tetradecanol
Sudan Orange P	7.3	2.7	2.4
Sudan Orange	6.9	3.0	3.1
Sudan III	6.4	3.1	3.0
Sudan Black B	9.5	3.3	2.9

Specific features of chromatograms in TLC with low volatility mobile phases

The specific features of chromatographed TLC plates in TLC with low-volatility mobile phases stem from the fact that after the separation the mobile phase remains in the sorbent layer, without being evaporated as in traditional TLC. The mobile phase also continues slowly advancing after the separation is over and the plate has been withdrawn from the chamber, as a result of the even distribution of the mobile phase throughout the layer, and the zones undergo additional broadening as a consequence of molecular diffusion. The relative chromatographic zone-broadening data are presented in Table 2. Therefore, detection in TLC with low-volatility mobile phases should preferably be performed immediately after the separation in order to avoid distortion of the chromatogram. Should the need arise, however, the chromatographed plate may be stored in a refrigerator at a temperature below the freezing point of the mobile phase. Alternatively, as shown by Alt and Szekely,²³ the low-volatility mobile phase may be removed from the sorbent layer by heating under reduced pressure.

After the separation in TLC with melts is over and the plate has been chilled, the mobile phase freezes within the sorbent layer. At the same time, if the chromatography is conducted on a loose layer, the portion of the latter covered by the mobile phase becomes attached to the support. Binding of the layer to a glass support has been observed in experiments with loose silica gel, alumina, and cellulose layers. The mobile phases were melts of alcohols (tetradecanol, hexadecanol, octadecanol), acids (stearic and capric), and of amyl stearate.

Another consequence of solidification of the mobile-phase melt is preservation of the chromatogram as the solid mobile phase protects the chromatographic zones against interaction with the surrounding medium, as illustrated by the following example. When Sudan dye zones separated on Merck 60 F-254 TLC plates with benzene and with octadecanol as mobile phases were exposed to light of wavelength 254 nm, the dye zones on the plate chromatographed with benzene became completely decolorized after 3 hr, whereas the zones on the plate with solidified octadecanol retained their intensity of colour. Another example is assay of commercially produced tetraethylthiuram disulphide for

pharmaceutical-grade purity. In traditional TLC with hexane-ethyl acetate mixture the zones of the impurities disappeared completely from the plate 3-5 days after separation. With separation by a tetradecanol melt, the impurity zones persisted on the plate without change in the course of time. It should also be pointed out that the solidified mobile phase substantially enhances the mechanical strength of the sorbent layer, which, in combination with the preservation, creates favourable conditions for long-term storage of chromatograms, and permits direct comparison of the analytical results after long periods of time.

Detection and determination of zones of colourless components

Colourless substances are detected on a TLC chromatogram by exposure to ultraviolet light or by obtaining coloured zones by spraying with a dye,^{8,24} and both methods can be used in TLC with low-volatility mobile phases. For example, the colourless zones of tetraethylthiuram disulphide and its impurities on Merck 60 F-254 plates are detected with ultraviolet light at 254 nm, in the form of dark blotches against a fluorescent background. Pyruvic, salicylic, benzoic, succinic, and α -ketoglutaric acids can be detected on Silufol UV-254 plates after chromatography with tetradecanol, octadecanol, and amyl stearate melts, by exposure to ultraviolet light or by spraying with an alcohol solution of Bromocresol Green, which gives bright yellow spots on a pale green background.

Quantitative measurement in TLC may be done either directly on the plate or after removal of the substance from the sorbent layer.^{24,25} Direct photometric and fluorimetric methods are currently indispensable in quantitative thin-layer chromatography,²⁵ and are fully applicable in TLC with low-volatility mobile phases. In our work, all determinations in TLC with such phases are done with a thin-layer scanning spectrophotometer. The techniques including removal of the separated compounds from the TLC plates are much more time-consuming and arduous, and are less accurate than the direct detection methods, and consequently have become obsolete. However, as shown by Alt and Szekely,²³ they can still be used in TLC with low-volatility mobile phases.

Separation techniques in TLC with low-volatility mobile phases

Samples are applied exactly as in traditional TLC. The separation step is different in that TLC with melts is conducted at elevated temperature. Most convenient for the purpose are air thermostats with a fan, in which there is virtually no temperature gradient and temperature changes are quickly corrected. There is no need to employ airtight chromatographic chambers, and the separation results are practically independent of the chamber type and size.

Table 2. Relative broadening of the Sudan Red zone 20 hr after analysis

Mobile phase	Relative broadening, %
Hexanol	203
Octanol	127
Decanol	82

Table 3. Liquid alcohol saturated vapour pressures

Mobile phase	Temperature, °C			
	1 mmHg	10 mmHg	40 mmHg	100 mmHg
Ethanol	-31.3	-2.3	19.0	34.9
Butanol	-1.2	30.2	53.4	70.1
Hexanol	24.4	58.2	33.7	102.8
Octanol	54.0	88.3	115.2	135.2
Decanol	69.5	111.3	142.1	165.8

Thus, all variants of TLC with low-volatility mobile phases retain the simplicity of the TLC technique in general and do not require special equipment.

Silica gel, alumina and cellulose thin-layer plates are all suitable.

THE MOBILE-PHASE FLOW

TLC with low-volatility liquids

To compare mobile phases of different volatility we have studied the flow of liquid alcohols at room temperature (20°). The volatility of the alcohols is shown in Table 3. The chromatography was conducted in closed cylindrical chambers after a 12-hr period during which equilibrium was established in the system. The curves in Fig. 2 represent the velocity coefficient of the solvent front as a function of time. It can be seen that the velocity coefficient varies with time, the change being much more pronounced for ethanol than for butanol, which is consistent with published data.²² For hexanol, octanol and decanol, the velocity coefficient is virtually invariable with time. Consequently (Fig. 2 and Table 3) it can be assumed that during chromatography at room tem-

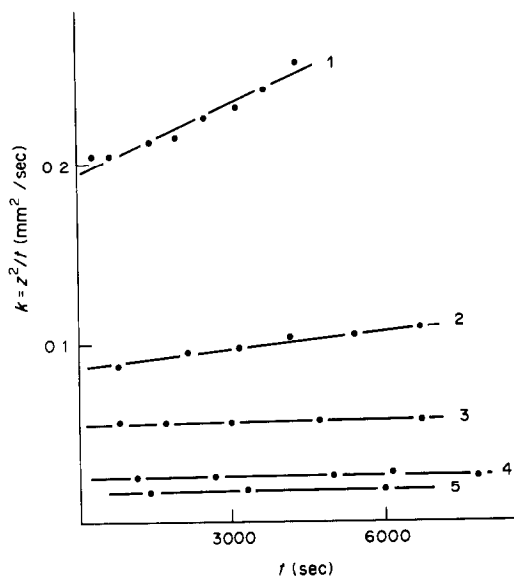


Fig. 2. Variation of the velocity coefficient of the front (k) for liquid alcohols with time (t) on Merck 60 F-254 TLC plates: 1—ethanol, 2—butanol, 3—hexanol, 4—octanol, 5—decanol.

perature the effect of the vapour phase is nil for liquid mobile phases with a saturated vapour pressure less than 1 mmHg.

TLC with melts

What sets TLC with melts apart from other chromatographic techniques is that the separation is performed at temperatures above the melting point of the mobile phase. As the viscosity and surface tension vary with temperature, the latter influences the mobile-phase velocity.

The relationship between the velocity coefficient for the front and the analysis time at different temperatures has been studied for alcohol melts on Merck 60 F-254 plates characterized by a narrow particle size distribution and good reproducibility of sorbent layer properties. The plates were preconditioned by storage in a thermostat at the analysis temperature, then transferred into the chromatographic chamber without cooling. Figure 3 shows how the velocity coefficient for a hexadecanol melt varies with time at different temperatures. At analysis temperatures up to 140° the velocity coefficient remains practically invariable. This may be due to the low vapour pressure of the melt, which is less than 1 mmHg at these temperatures, and determines to a first approximation the evaporation and adsorption rates in the chromatographic chamber.

When the experiments were repeated on plates that had not been preconditioned, the velocity coefficient increased initially, the increase being the greater, the higher the analysis temperature. It was established

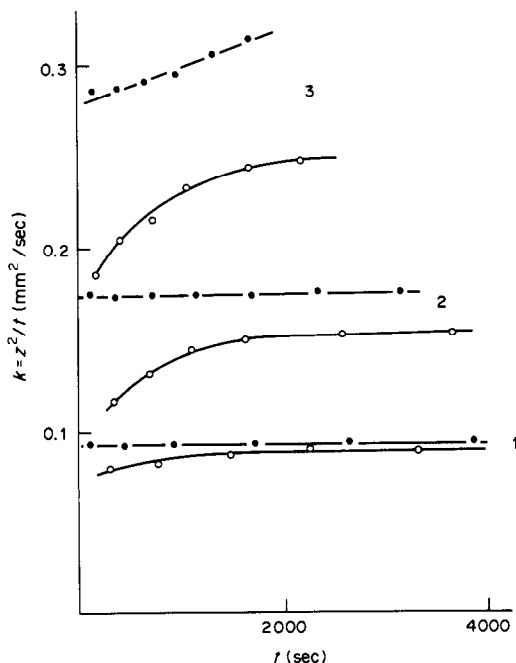


Fig. 3. Variation of the velocity coefficient of the front (k) for a hexadecanol melt with time (t) on conditioned (●) and unconditioned (○) Merck 60-254 TLC plates at different temperatures: 1—80°C, 2—140°C, 3—180°C.

that the initial increase in the velocity coefficient was caused by the plate temperature changing from the ambient level to that for the analysis.

Specific pattern of flow in TLC with melts

It is now of particular interest to use porous layers of a sorbent with uniform particle size in TLC, since this enhances the separation efficiency considerably.²⁶ The mobile phase flow in thin layers of this type can be described with due account taken of the sorbent particle size.

Guiochon and Siouffi²⁷ proposed the following equation for the velocity coefficient of the front, k , ($k = z^2/t$, where z is distance travelled in time t):

$$k = 2k_0 d_p \gamma / \eta \cos \theta, \quad (1)$$

in which k_0 is the specific permeability of the porous layer, γ/η is the ratio of the surface tension to the viscosity of the mobile phase, d_p is the sorbent particle size, and θ is the wetting angle (usually close to 180°).

In the present study, the values of specific permeability were calculated from the experimental values of the velocity coefficient for alcohol melts at different temperatures on Merck 60 F-254 TLC plates. As in the work cited,²⁷ the calculation was based on the assumption of complete wetting ($\cos \theta = 1$) in view of the insignificant variations of the wetting angle in the homologous alcohol series.²⁸ The calculated data are given in Table 4. The specific permeability for TLC with melts is only about half that reported by Guiochon and Siouffi²⁷ for volatile mobile phases in a saturated chamber. This difference can be explained by the fact that the molten mobile phase flows across a sorbent layer free from adsorbed liquid. As is known, all of the physically adsorbed water is removable from silica gel at temperatures of up to 120° ,²⁹ whereas adsorption of the molten mobile phase vapours is, as shown previously, either zero or negligible.

For the general analytical case an equation can be

Table 4. Specific permeability values (k_0) for alcohol melts on Merck 60 F-254 TLC plates

Temperature, °C	γ/η , m/sec	k , mm ² /sec	k_0 , mm ² /sec
Tetradecanol			
100	1.13	1.10	4.42
120	1.63	1.45	4.04
140	2.32	2.00	3.92
160	3.13	2.75	3.99
Hexadecanol			
80	0.58	0.65	5.09
100	0.91	0.94	4.69
120	1.38	1.21	3.99
140	2.00	1.75	3.98
160	2.60	2.27	3.97
180	3.27	2.88	4.00
Octadecanol			
120	1.16	1.05	4.13
140	1.60	1.41	4.01
160	1.98	1.75	4.02

proposed similar in all ways to equation (1) except that it contains an additional factor taking into account the filling of the porous layer as a result of adsorption:

$$k = 2k_0^\circ \left(\frac{\epsilon_T}{\epsilon_T - \epsilon_V} \right) d_p \gamma / \eta \cos \theta, \quad (2)$$

where k_0° is a constant determined by the size of the pores inside the layer, ϵ_T is the total porosity of the layer (ratio of the total volume of external and internal pores to the layer volume), and ϵ_V is the ratio of the adsorbed liquid volume to that of the layer. A mean value of k_0° , of $(4.00 \pm 0.05) \times 10^{-2}$, calculated from the data in Table 4 except for the values derived at analysis temperatures below 120° , is the constant for Merck 60 silica gel plates.

Determination of the mobile-phase content in a porous thin layer

The mobile phase traverses a thin porous layer that is not previously saturated with it, so there is a gradient of the mobile phase content in the layer from the source toward the front. This gives rise to a systematic error in the experimental determination of the R_f values because true or thermodynamic retention values presuppose presaturation of the sorbent with the mobile phase.¹⁷

In an attempt to study the mobile-phase content profiles we have proposed and used for the first time photometric scanning of the TLC plate containing solidified mobile phase. The content profiles for Merck 60 F-254 plates are illustrated in Fig. 4.

Irrespective of the mobile phase used, its content profile on Merck 60 F-254 TLC and HPTLC plates will take the form shown in Fig. 4. Note that the profile resulting from the photometric scanning of the Merck 60 F-254 plates matches well that derived by

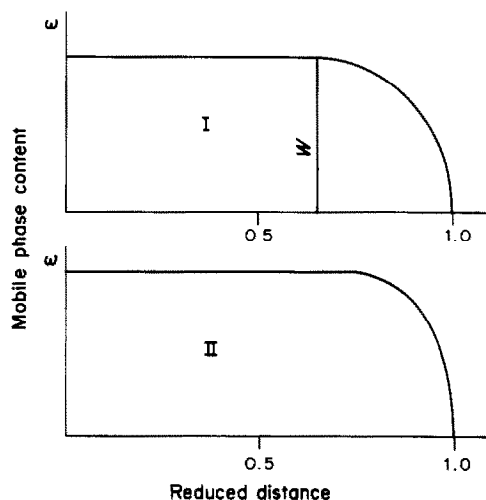


Fig. 4. Reduced content profiles for TLC^(I) and HPTLC^(II) Merck 60 F-254 plates. Reduced distance = (distance from source to measurement position)/(distance from source to solvent front).

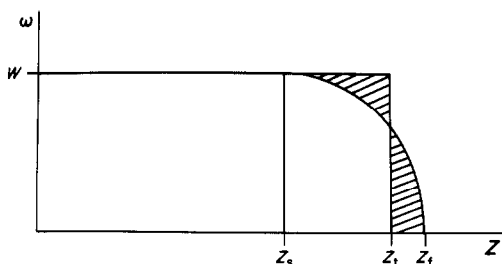


Fig. 5. Correction of the mobile phase front position.

the gravimetric method for Merck TLC plates with an aluminium support.³⁰

We now propose a method for correction of the position of the unsaturated flow front, necessary to determine the ratio between the experimental and true R_f values. It is based on the premise that corresponding to the real unsaturated flow of the mobile phase there is an idealized saturated flow, with a different position of the mobile phase front. This position will be that required to make the hatched areas in Fig. 5 equal. Equalization of these areas gives the following analytical expression for the idealized saturated-flow front position Z_t :

$$Z_t = \frac{1}{W} \int_{Z_s}^{Z_t} \omega(Z) dZ + Z_s \quad (3)$$

where Z_f is the position of the real unsaturated-flow front, Z_s is the position corresponding to the saturated portion of the real flow, and W is the content of mobile phase in the saturated flow and is a function $\omega(Z)$ of Z . It has been empirically determined that the unsaturated portion of the flow profile for Merck 60 F-254 TLC plates in Fig. 4 is given by an elliptic equation. Having substituted the elliptic equation into (3), and performed the necessary integration and simple transformations, we have determined the numerical ratios between the experimental (R_f) and true ($R_{f,t}$) retention values for Merck 60 F-254 TLC plates.

When the chromatographic zone is in the saturated portion of the mobile phase flow ($R_f \leq 0.65$),

$$R_{f,t} = \frac{R_f}{0.924} = 1.08R_f \quad (4)$$

If the chromatographic zone is in the unsaturated portion, a correction for the zone position is introduced similarly to that for the front position, which gives, for $R_f \geq 0.65$,

$$R_{f,t} = 0.85R_f + 0.15 \quad (5)$$

THE ROLE OF TEMPERATURE IN TLC WITH LOW-VOLATILITY MOBILE PHASES

As mentioned above in connection with mobile-phase flow, temperature affects the flow velocity of low-volatility mobile phases. Moreover, temperature may be instrumental in controlling the retention and separation in TLC with these mobile phases.

In traditional TLC, the effect of temperature on retention is insignificant.³¹ According to Geiss,³⁰ this is due to the fact that two things happen when the temperature rises: first, the adsorbed water evaporates and the sorbent becomes more active, and, second, the mobile liquid phase is transferred onto the sorbent layer through the vapour phase, as a result of evaporation and adsorption. Therefore, the overall temperature effect in traditional TLC is insignificant.

TLC with melts of organic compounds permits separation within a broad range of analytical temperatures and under conditions in which the adsorption of mobile phase vapours is virtually nil, as was shown in the study on the mobile-phase flow. On the other hand, according to De Boer and Vleeskens,^{32,33} all of the physically adsorbed water is removed from the silica gel layer at temperatures of up to 120°, whereas at temperatures ranging from 80 to 120° the water content changes insignificantly.²⁹ Consequently, TLC with melts brings about a systematic increase in the R_f values as the temperature is raised.

Figure 6 is a logarithmic plot showing the capacity factor determined for true retention values, as a function of the reciprocal of absolute temperature for analysis on Merck 60 F-254 TLC plates. The curves in Fig. 6 are close to linear, which is indicative of analysis under conditions with constant qualitative and quantitative phase compositions.³⁰

Significantly, the intersection of the curves in Fig. 6 corresponds to a temperature-induced variation in the relative retention of the mixture components. Greater detail concerning the effect of temperature on

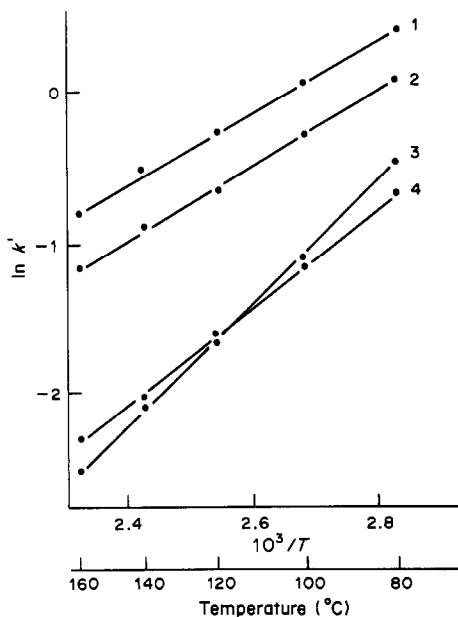


Fig. 6. Plot of $\ln k'$ vs. $1/T$ for a mixture of dyes on Merck 60-254 plates; mobile phase n-hexadecanol. 1—Sudan R, 2—Dimethyl Yellow, 3—Victoria Blue, 4—Sudan III.

retention in TLC with low-volatility mobile phases has been published elsewhere.³⁴

CONCLUSION

The use of low-volatility mobile phases gives better reproducibility of the separation conditions and R_f values and also broadens the scope of TLC. The use of molten organic compounds as the mobile phase offers several advantages, including better stability of the chromatograms and the possibility of extended storage. The technique retains all the simplicity of traditional TLC.

REFERENCES

1. V. G. Berezkin, T. Yu. Chernysheva and S. L. Bolotov, *J. Chromatog.*, 1982, **253**, 227.
2. N. A. Izamailov and M. S. Shraiber, *Farmatsiya*, 1938, 1.
3. E. Stahl, *Dünnschichtchromatographie*, Springer, Berlin, 1962.
4. *Idem*, *J. Chromatog.*, 1968, **33**, 273.
5. D. C. Fenimore and C. M. Davis, *Anal. Chem.*, 1981, **53**, 252A.
6. R. Amos, *Talanta*, 1973, **20**, 1231.
7. S. A. Kibardin and K. A. Makarov, *Thin-Layer Chromatography in Organic Chemistry*, Khimiya, Moscow, 1978.
8. J. C. Kirchner, *Thin-Layer Chromatography*, Wiley, New York, 1978.
9. A. Niederwieser and C. C. Honegger, *Advan. in Chromatog.*, 1966, **2**, 123.
10. M. S. J. Dallas, *J. Chromatog.*, 1968, **33**, 58.
11. F. Geiss, *ibid.*, 1968, **33**, 9.
12. D. Janchen, *ibid.*, 1968, **33**, 195.
13. *Idem*, in *High Performance Thin Layer Chromatography*, A. Zlatkis and R. E. Kaiser (eds.), p. 129. Elsevier, Amsterdam, 1976.
14. M. Brenner, A. Niederwieser, G. Pataki and R. Weber, in *Dünnschichtchromatographie*, E. Stahl (ed.), p. 79. Springer, Berlin, 1962.
15. V. G. Berezkin, R. G. Vinogradova, O. A. Rusaev, V. N. Chechivichkin and F. I. Romanov, *J. High. Resol. Chromatog., Chromatog. Commun.*, 1982, **5**, 93.
16. E. Tyihák, E. Mincsovcics and F. Körmendi, *Hung. Sci. Instrum.*, 1983, **55**, 33.
17. V. G. Berezkin and S. L. Bolotov, *J. High Resol. Chromatog., Chromatog. Commun.*, 1981, **4**, 398.
18. G. Alberti and S. Allulli, *Chromatogr. Rev.*, 1968, **10**, 99.
19. S. Abbe and L. F. Druding, *Sepn. Sci.*, 1969, **4**, 217.
20. V. G. Berezkin and S. L. Bolotov, *Kontaktie*, 1982, No. 3, 9.
21. G. Szekely and P. Baumgartner, *J. Chromatog. Sci.*, 1979, **186**, 575.
22. H. Halpaap and J. Rippahhn, in *High Performance Thin Layer Chromatography*, E. Zlatkis and R. E. Kaiser (eds.), p. 95. Elsevier, Amsterdam, 1976.
23. K. O. Alt and G. Szekely, *J. Chromatog.*, 1980, **202**, 151.
24. J. Blome, in *High Performance Thin Layer Chromatography*, A. Zlatkis and R. E. Kaiser (eds.), p. 51. Elsevier, Amsterdam, 1976.
25. E. J. Shellard (ed.), *Quantitative Paper and Thin-Layer Chromatography*, Academic Press, New York, 1968.
26. A. Zlatkis and R. E. Kaiser (eds.), *High Performance Thin Layer Chromatography*, Elsevier, Amsterdam, 1976.
27. G. Guiochon and A. Siouffi, *J. Chromatog. Sci.*, 1978, **16**, 598.
28. A. W. Adamson, *Physical Chemistry of Surfaces*, Wiley, New York, 1976.
29. R. P. Scott, *J. Chromatog. Sci.*, 1980, **18**, 297.
30. F. Geiss, *Die Parameter der Dünnschichtchromatographie*, Vieweg, Braunschweig, 1972.
31. J. Blome, in *High Performance Thin Layer Chromatography*, A. Zlatkis and R. E. Kaiser (eds.), p. 39. Elsevier, Amsterdam, 1976.
32. J. H. de Boer and J. M. Vleeskens, *Koninkl. Ned. Akad. Wetenschap. Proc. Ser. B*, 1957, **60**, 234.
33. *Idem*, *ibid.*, 1958, **61**, 85.
34. V. G. Berezkin and S. L. Bolotov, *J. High Resol. Chromatog., Chromatog. Commun.*, 1983, **6**, 203.

DETERMINATION OF ALKALI METALS BY LASER-INDUCED ATOMIC-IONIZATION IN FLAMES

V. I. CHAPLYGIN, YU. YA. KUZYAKOV, O. A. NOVODVORSKY
and N. B. ZOROV

Department of Chemistry, Lomonosov State University, V-234 Moscow, 119899, USSR

(Received 15 October 1985. Accepted 15 August 1986)

Summary—The technique of laser-induced atomic-ionization (AI) in flames has been used for direct determination of Na, K, Rb, and Cs in samples such as water, high-purity alkali metals and their salts and polymeric organosilicon compounds. Different procedures for sample introduction into the flame were studied: (a) the sample was placed onto the cathode of the detector (this gave limits of detection for Na and Cs of 4×10^{-16} and 2×10^{-15} g, respectively), (b) electrothermal vaporization and (c) aspiration of the sample into the flame. To reduce the interference of SiO_2 in the AI determination of K in polymeric organosilicon compounds (at the level of 10^{-3} – $10^{-5}\%$), a procedure involved additional electrical heating of the FID cathode was developed. The efficiency of certain schemes for the laser stepwise and two-photon excitation of atoms was compared for determination of Na.

Laser-induced atomic-ionization¹ or laser-enhanced ionization² in flames, based on the optogalvanic effect, is a new highly sensitive analytical method undergoing intensive development. It relies on detection of the changes in an electrical current passed through a flame by application of a high voltage across electrodes. The current changes arise from production of additional charges due to selective resonance ionization of analyte atoms by dye-laser radiation.

Most studies on AI analysis have been done with sample atomization in flames, since flame spectrometric techniques have much to offer. They are simple, inexpensive to operate, and have good reproducibility and high speed of analysis. For trace detection of more than 30 elements AI spectrometry is certainly competitive with, and often superior to, other flame spectrometric methods (atomic emission, atomic absorption, atomic fluorescence).³ Stepwise laser excitation⁴ is highly advantageous for determination of most elements with high ionization potentials,⁵ because of its high sensitivity and selectivity.

The AI method is free from certain interferences inherent in techniques using optical detection of the signal, for example, those caused by scattered laser radiation, which is a severe problem in laser-induced atomic fluorescence. However, some ionization interferences occur when the sample matrix contains large amounts of elements of low ionization potential;⁶ these have been studied in detail^{7,8} and ways to avoid or eliminate them discussed.⁹⁻¹¹ The ionization mechanisms and the theory of processes resulting in AI signal formation in flames have also been considered.¹²⁻¹⁴

The present work demonstrates the application of

AI to direct determination of Na, K, Rb, and Cs in different water samples, Rb and Cs in high-purity alkali metals and their salts, and K in organosilicon compounds. The limits of detection (LODs) for these elements (0.1–0.001 ng/ml) are among the lowest attained with the AI techniques,¹⁵⁻¹⁶ and are two orders of magnitude better than the best obtained by other flame techniques (for K, Rb and Cs about 1 ng/ml and for Na about 0.1 ng/ml).^{17,18} The AI determination of Li has been studied;¹⁹ the LOD of 0.001 ng/ml attained is close to the theoretically ultimate value calculated for the flame.^{20,21}

The efficiency of some stepwise and two-photon schemes of excitation of atoms has been compared, with determination of Na as an example. Different procedures for introducing the sample into the flame in the AI analysis have been studied.

EXPERIMENTAL

Reagents

Stock solutions of alkali metals (concentration 1 and 10 mg/ml) were prepared from the chlorides of "high purity" grade and water purified by being twice distilled in a fused-silica still and then demineralized with a "Milli-Q" system (water resistivity $\sim 20 \text{ M}\Omega \cdot \text{cm}$). The organic solvents, ethanol, methyl isobutyl ketone (MIBK), toluene and n-octane, were purified by double distillation in a fused-silica still. In the analysis of organosilicon compounds, stock solutions of potassium were prepared from its 1:1 stoichiometric complex with 18-crown-6 ether, $[(\text{CH}_2\text{CH}_2\text{O})_6\text{K}^+]\text{OH}^-$, containing 15.3% K.

Laser dyes were of a special grade "for quantum electronics".

Apparatus

In determination of K, Rb, and Cs the AI spectrometer was based on a 300-kW nitrogen-laser (repetition rate 5 Hz)

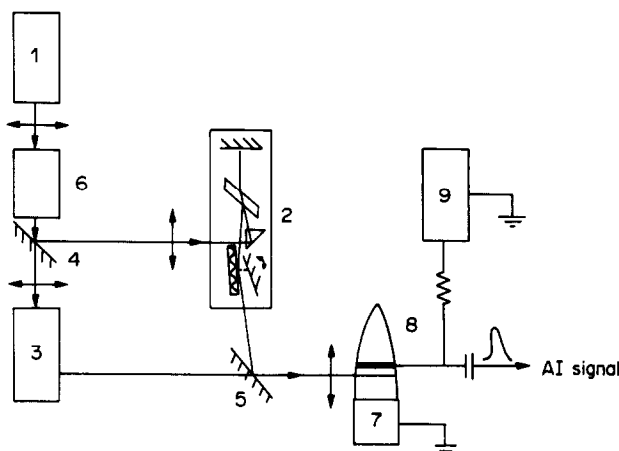


Fig. 1. Block scheme of the experimental apparatus: 1—Nd:YAG laser; 2,3—pulsed dye-lasers; 4,5—dichroic mirrors; 6—KDP frequency-doubler crystal; 7—burner; 8—cathode; 9—high-voltage source.

and a transverse pumped dye-laser with grazing incidence. The dye-laser power was 2–20 kW at 400–460 nm, pulse duration, about 10 nsec. The AI spectrometer has been described elsewhere.²²

The determination of Na was done with the spectrometer shown in Fig. 1. The 2nd harmonic emission of an Nd:YAG laser ($\lambda = 532$ nm) with power up to 800 kW per pulse, pulse length 14 nsec and repetition rate of 10 Hz (1) was used for longitudinal pumping of one or two dye-lasers (2,3) arranged to give grazing incidence. The first experiments on longitudinal pumping of the dye-cell in a resonator of that type were performed by Novodvorsky *et al.*,²³ who emphasized the high oscillation performance of the laser. Upon pumping, the peak power of one of the dye-lasers approached 180 kW (546–600 nm band, Rhodamine 6G), the efficiency of radiant power transformation was $\sim 24\%$ and the line-width 0.003 nm. For synchronous pumping of both dye-lasers the 2nd harmonic radiation of the Nd:YAG laser was divided into two equal parts by means of a dichroic mirror (4). The radiation of the two dye-lasers (the beam diameters were 1 mm) was directed co-linearly to the flame of a circular Méker-type premix burner (7). The burner used was the one from the assembly of a Zeiss AAS-1 atomic-absorption spectrophotometer (solution uptake rate 4 ml/min). The optical path-length was the same for the two lasers. A cathode (8) (at -600 V) was inserted in the flame over the laser beams and parallel to them: the burner served as the anode. The cathode was made of 0.6 mm diameter stainless-steel rod or iridium wire.

The ionization signal from the cathode was amplified by a broad-band amplifier and processed with an analogue-to-digital converter unit which integrated a gated part of the signal pulse. The output signal was the average response of 10 pulses and was shown on a digital display.

In determination of Cs, in addition to the Méker burner, a burner with electrothermal sample vaporization²⁴ was also used, providing a micro-method of AI analysis. The vaporizer (a loop of 0.5-mm thick tungsten wire, with a diameter of 4 mm) was heated by means of a Varian-Techtron CRA-90 power-supply unit with temperature-programming control.

Tuning of the dye-lasers to the analytical lines of K, Rb, Na, and Cs and to excite the Na ($3s \rightarrow 3p$) resonance was done by resonance-changing of the impedance of electrodeless discharge lamps.²⁵ In the determination of Na, the dye-laser of the second step was tuned with a monochromator and then, more accurately, by maximizing the amplitude of the AI signal.

Procedure

A propane-butane-air flame was used. The maximum AI signals for the Méker-type burner were obtained with fuel-gas and air flow-rates of 0.6 and 6 l./min, respectively. The optimal distance of the cathode from the burner head was 18–20 mm.

It should be noted that in the determination of very low concentrations of K and Na, precautions were taken to decrease the background level, *viz.* stock solutions and samples were prepared in polytetrafluoroethylene (Teflon), standard flasks, and the support gas (air) was purified by pumping through a special filter before it entered the burner.

The general procedure for measurement with the burner with electrothermal vaporizer was as follows. A 5- μ l sample of solution was put on the vaporizer loop by micropipette, and dried at 100–120° for 20–25 sec. The argon flow required for sample transfer to the flame was then passed through the vaporizer passage (isolated from the fuel gas and air), the flame was ignited, and the loop temperature was raised to 1300° within 3 sec. The sample was evaporated from the loop and entered the flame, where it was atomized and the analyte atoms were selectively ionized. The integrated AI signal was recorded until its value fell to the noise level of the detection system. One measurement took less than 25–30 sec. The optimal flow-rates of the gases were argon 0.2–0.3 l./min, propane-butane 0.6 l./min, air 6 l./min. The optimum distance between cathode and burner head was 50 mm.

RESULTS AND DISCUSSION

Determination of alkali metals in aqueous solutions of their salts

The calibration graphs obtained on aspiration of stock solutions of Na, K, Rb, and Cs into the flame were linear over 3–4 orders of magnitude of concentration. The excitation schemes and detection limits attained are shown in Table 1. The limits of detection of K, Rb and Cs in aqueous solutions were determined by the noise from the recording unit, since the background signal in the determination of K, Rb and Cs in demineralized water did not exceed the noise level. The lower level of detection of Na in its

Table 1. Determination of alkali metals in pure aqueous solutions

Element	Ionization potential, eV	Excitation mode	Wavelength (λ), nm	Dye	Limit of detection, ng/ml*	
<i>One-step</i>						
K	4.34	$4s^2 S_{1/2} \rightarrow 5p^2 P^{\circ}_{3/2}$	404.4	PBBO	0.1	
Rb	4.18	$5s^2 S_{1/2} \rightarrow 6p^2 P^{\circ}_{3/2}$	420.2	POPOP	0.1	
Cs	3.89	$6s^2 S_{1/2} \rightarrow 7p^2 P^{\circ}_{3/2}$	455.5	Coumarin 47	0.004	
<i>Stepwise</i>						
Na	5.14	$3s^2 S_{1/2} \xrightarrow{\lambda_1} 3p^2 P^{\circ}_{3/2} \xrightarrow{\lambda_2} 4d^2 D_{5/2}$	λ_1 589.0	Rhodamine 6G	0.002	
			λ_2 568.8	Rhodamine 110		
			λ_1 589.0	Rhodamine 6G	0.01	
			λ_2 616.0	Rhodamine C		
<i>Two-photon</i>						
Na	5.14	$3s^2 S_{1/2} \rightarrow 5d^2 D_{5/2}$	540.0	Rhodamine 110	74	
			$3s^2 S_{1/2} \rightarrow 6s^2 S_{1/2}$	550.0	Rhodamine 110	2.9
			$3s^2 S_{1/2} \rightarrow 4d^2 D_{5/2}$	578.7	Rhodamine 6G	0.86

*The limit of detection is the analyte concentration which corresponds to a signal equal to three times the standard deviation of the blank signal (calculated from 20 replicates of the blank).

determination by stepwise excitation was limited by the Na content of the demineralized water (48 pg/ml). The relative standard deviation at the 1.0–0.1 ng/ml level ($n = 10$) was 5–6%.

Besides the determination of K, Rb and Cs with the one-step excitation scheme we tested stepwise schemes, utilizing as the second source a fraction of the nitrogen laser radiation ($\lambda_2 = 337.1$ nm, power = 150 kW). Under these conditions, the AI signals were no higher than those for one-step excitation, which indicated the high efficiency of ionization of K, Rb and Cs by the one-step excitation scheme. Of these three elements, sodium has the highest ionization potential (5.14 eV), so for comparison of efficiency Na was determined with the use of stepwise and two-photon excitation schemes. The best detection limit for the stepwise scheme was obtained by the excitation of Na to its 4D level. Assuming a photoionization mechanism for ionization of the excited atoms, this can be explained as due to the larger photoionization cross-section of the D-level with respect to the S-state.²⁶ The laser powers at 568.8 and 616.0 nm were approximately equal. Comparison of the LODs for Na with the two-photon

excitation scheme shows that excitation to a higher level results in loss in sensitivity. In addition to the difference in the photoionization cross-sections, this may be due to different effects of the matrix element on the two-photon transition.¹⁴

The LODs attained enabled the direct determination of alkali metals at the ng/ml level in water samples, by either the calibration-graph or the standard-additions method. The results are listed in Table 2. The accuracy of the determinations of Na and K in distilled water and K in tap water was verified by flame emission spectroscopy, the results agreeing within the limits of measurement error.

When a sample is aspirated into the flame, the transfer efficiency is rather low. The positioning of the cathode of the detector directly in the flame made it possible to determine very small absolute amounts of Na and Cs by placing the sample on the cathode, thus creating a high concentration of the analyte atoms in the excitation zone. A sample (2–5 μ l of solution) was placed by micropipette in a wire loop 3 mm in diameter attached to the cathode. The water was evaporated by radiant heating and the flame was ignited, and the AI signal was recorded. The laser

Table 2. Determination of Na, K, Rb, and Cs (ng/ml) in water samples ($n = 10$, $p = 0.95$)

	Element	Tap water	Distilled water	Demineralized water (Milli-Q™ system)
Calibration graph method	Na	—	30 ± 2	0.048 ± 0.005
	K	950 ± 40	52 ± 3	< 0.1
	Rb	7.0 ± 0.5	1.0 ± 0.1	< 0.1
	Cs	0.60 ± 0.05	0.11 ± 0.01	< 0.004
Standard-additions method	Na	—	30	—
	K	1100 ± 6	58 ± 4	—
	Rb	8.0 ± 0.5	1.2 ± 0.1	—
	Cs	1.0 ± 0.1	0.10 ± 0.01	—

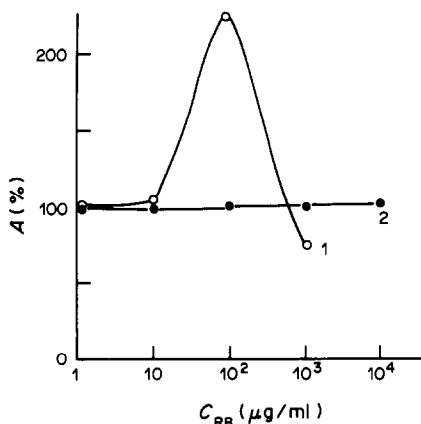


Fig. 2. Dependence of AI signal for Cs (% of nominal signal A) on concentration of Rb: 1-sample nebulization into the flame ($C_{Cs} = 0.01 \mu\text{g/ml}$); 2-atomizer with electrothermal sample vaporization into the flame ($C_{Cs} = 1 \mu\text{g/ml}$).

beam was directed 1 mm above the cathode. The sample was completely vaporized within about 1 min and the analytical signal was the integral of the AI signal amplitudes over this period. The calibration curves were plotted and the absolute LODs for Na and Cs were calculated to be equal to 4×10^{-16} and 2×10^{-15} g, respectively. The relative standard deviation at the 10^{-13} g level was 25–30% ($n = 5$).

Determination of Rb and Cs in high-purity alkali metals and their salts

The most important and complicated problem arising in the analysis of "real" samples is determination of trace elements in the presence of large amounts of elements very similar to them in their properties; for example, the determination of one alkali metal in compounds of the others.

The ionization interferences in AI determination by sample aspiration into the flame are known to be essentially lower when the cathode is placed directly in the flame.²⁷ Nevertheless, as shown previously,²² there are ionization interferences in the AI signal for Cs as analyte even at Rb concentrations as low as $10 \mu\text{g/ml}$ in the sample matrix (Fig. 2, curve 1). The nature of these interferences had been explained.²⁷ A similar effect is exhibited by Cs in the determination of Rb. Also, when K, Rb or Cs solutions with concentrations $> 1 \text{ mg/ml}$ are aspirated into the flame, there is a considerable increase of the noise from the AI signal recording system, caused by the increased conductivity of the flame (arcing effect); this complicates the problem of reliable detection of the AI signal. Hence, Rb and Cs were determined by the standard-additions method, solutions with matrix concentrations of 0.2–0.4 mg/ml being used in the determinations. The samples to be analysed were pure Cs and Rb metals (5-mg samples) and K_2CrO_4 (3-mg samples).

The samples of Rb and Cs were transferred into Teflon beakers and dissolved in distilled ethanol

(10 ml). The K_2CrO_4 samples were dissolved in purified water. These solutions were quantitatively transferred to 25-ml standard flasks and diluted to volume with water. Cs and Rb in the final solutions were determined by aspiration of the sample solution into the flame. The additions were made so that the signals were in the linear region of the calibration curves. The amount of element to be determined was calculated from the average AI signal for each solution (10 independent measurements) according to the equation:

$$C = \frac{BA_1}{A_2 - A_1}$$

where B is the standard-addition concentration (ng/ml) and A_1 and A_2 are the AI signals for the sample alone and for the sample plus added standard, respectively, corrected for the background.

The results presented in Table 3 are the average values for determination of Rb and Cs from three identical samples. To verify the accuracy of the results, the Rb and Cs were determined by AAS with a Varian-Techtron AA875 spectrophotometer by the standard-additions method, in solutions containing 2–10 mg/ml of the alkali metals. To prepare these samples it was necessary to combine 10–20 specimens of Cs or Rb, whereas the sensitivity of the AI technique allowed the content of Rb and Cs to be monitored in each individual specimen. The data in Table 3 show good enough agreement between the results obtained by the two methods.

Application of micro-methods seems promising as a means of eliminating ionization interferences.¹¹ The determination of Cs in high-purity RbCl and Rb_2CO_3 was done with the use of a flame atomizer with electrothermal vaporization of sample from the tungsten loop. We first studied the effect of Rb on the AI signal of Cs, with solutions containing 1 mg/ml Cs and different concentrations of Rb. It was found that even at the 10 mg/ml level Rb did not interfere in the determination of Cs (see Fig. 2, curve 2) whereas with sample aspiration into the flame strong interference resulted, and the AI signal for Cs in the presence of 10-mg/ml Rb solutions could not be detected at all.

The determination of Cs in 10-mg/ml Rb solutions with use of the electrothermal atomizer was done by the calibration-graph method (linear region

Table 3. Results of AI and AAS determinations of Rb and Cs in high-purity materials ($n = 10$, $p = 0.95$)

Sample	Element	Content, $\left(\bar{x} \pm \frac{t_{p,n}S}{\sqrt{n}}\right)$, $10^{-3}\%$	
		AI technique	AA technique
Cs 1	Rb	3.3 ± 0.6	3.3
Cs 2	Rb	6.1 ± 1.2	4.0
Cs 3	Rb	2.2 ± 0.3	1.8
Cs 4	Rb	8.4 ± 1.1	8.0
Rb	Cs	0.8 ± 0.1	1.1
K_2CrO_4 1	Cs	2.7 ± 0.2	—
K_2CrO_4 2	Cs	5.2 ± 0.3	—

Table 4. Determination of Cs in high-purity salts of Rb ($n = 5, p = 0.95$)

Sample	Content, $\left(\bar{x} \pm \frac{t_{p,n} S}{\sqrt{n}}\right), 10^{-4}\%$		Content certified by GOST*, $10^{-4}\%$
	Electrothermal vaporizer-flame	Pneumatic nebulizer-flame	
RbCl	13 ± 1	12 ± 1	<20
Rb ₂ CO ₃	7.2 ± 0.3	7.0 ± 0.4	<20

*Soviet Union Standards.

5×10^{-4} – $10 \mu\text{g/ml}$). To verify the results, $100\text{-}\mu\text{g/ml}$ solutions of the same salts were analysed by sample aspiration into the flame. The results are presented in Table 4.

Determination of K in organosilicon compounds

In analytical practice, samples containing substances which produce refractory compounds such as SiO₂, Al₂O₃, etc. are often encountered. If the cathode is placed directly in the flame, its temperature is lower than the temperature of the flame itself and compounds of that kind are deposited on the electrode surface, thus resulting in a break in the circuit of AI signal detection and, hence, to a dramatic decrease of the signal, and even its complete elimination.²⁸ This effect would be even stronger if the water-cooled cathode were used.⁹

We have worked out a procedure for direct trace determination of K at the level of 10^{-4} – $10^{-6}\%$ in samples of polymeric organosilicon compounds. Use of the acetylene-air flame and out-of-flame arrangement of the cathode turned out to be ineffective as far as deposition of SiO₂ was concerned. To prevent the deposition of SiO₂ on the cathode surface we applied additional electrical heating, using a d.c. source (a 12-V 6-A .hr storage battery), a switch and a 100-W variable resistor (0–2 Ω).

The organosilicon samples were rather viscous substances, soluble in non-polar solvents. The analysis was done by the standard-additions method, the added standards being ethanolic solutions of the potassium complex with 18-crown-6 ether; 50 mg of the complex was dissolved in 50 ml of ethanol (solution 1) so that the K concentration was about 150 mg/ml. Solution 1 was more precisely standardized by means of a calibration graph prepared by use of an aqueous reference solution of high-purity KCl containing 1% v/v ethanol. One ml of solution 1 was diluted 100-fold with water (solution 2) and the potassium content of solution 2 found by AAS, with the aid of the calibration graph.

To find a solvent which would support the combustion, dissolve the samples and be miscible with the K-18-crown-6 ethanolic solution, we tried toluene, n-octane and MIBK. The last turned out to be the best. We diluted aliquots of solution 1 with MIBK to obtain solutions with K content ranging from 0.5 to 50 $\mu\text{g/ml}$. These solutions were used as additives in preparing mixtures with organosilicon polymers.

In the AI determinations with additional heating of the cathode, the latter was made of iridium wire (m.p. 2450°). The temperature of the cathode surface on nebulization of MIBK in the flame was 1180–1230°; that with the additional heating applied was 1700–1750° (as measured with an optical pyrometer) and there was no SiO₂ deposition at this temperature. In the determination of 1 $\mu\text{g/ml}$ K in MIBK stock solutions with and without additional cathode heating the signal to noise ratio was found to deteriorate by a factor of about 2 owing to the increased noise level.

The samples of polymers (~2 g) were placed in preweighed graduated test-tubes, which were then weighed again. A known quantity of K was introduced and the mixture was diluted to fixed volume with MIBK. The determination was done by aspiration of the mixtures into the flame. The cathode heating was switched on for a short time (5–10 sec) while the AI signal was measured. Three independent determinations of K were made for each of the samples. The results are presented in Table 5.

It will be seen that application of additional electrical heating for the cathode (inserted directly into the flame) has good prospects for the trace analysis of elements in samples that form refractory compounds in the flame.

CONCLUSIONS

The present study has shown the application of a new method of analytical atomic flame spectrometry—laser atomic-ionization analysis—to

Table 5. AI determination of K in organosilicon compounds ($n = 3, p = 0.95$)

Sample	1	2	3	4
K content, $\left(\bar{x} \pm \frac{t_{p,n} S}{\sqrt{n}}\right), 10^{-4}\%$	0.25 ± 0.03	5.1 ± 0.7	12 ± 2	15 ± 1

some real samples. Different excitation modes can be used: one-step, stepwise, multiphoton. This makes the technique flexible for "real" sample analysis (it is possible to reduce matrix spectral interferences). To solve different problems of analysis (improvement of LODs or to reduce the matrix interferences) it is profitable to study various ways of introduction of the sample into the flame. Investigations of other ways of sample introduction (for example, by solid sample vaporization and atomization in the flame by laser) are under way. Refractory matrix interferences can sometimes be reduced by additional electrical heating of the cathode of the detector system.

REFERENCES

1. N. B. Zorov, Yu. Ya. Kuzyakov and O. I. Matveev, *Zh. Analit. Khim.*, 1982, **37**, 520.
2. J. C. Travis, G. C. Turk and R. B. Green, *Anal. Chem.*, 1982, **54**, 1006A.
3. G. C. Turk, J. C. Travis and J. R. DeVoe, *J. Phys. Colloq.*, 1983, **C7**, 301.
4. A. S. Gonchakov, N. B. Zorov, Yu. Ya. Kuzyakov and O. I. Matveev, *Anal. Lett.*, 1979, **12**, 1037.
5. G. C. Turk, J. R. DeVoe and J. C. Travis, *Anal. Chem.*, 1982, **54**, 643.
6. J. C. Travis, G. C. Turk and R. B. Green, In *New Applications of Lasers to Chemistry*, G. M. Hieftje (ed.), p. 91. American Chemical Society. Washington D.C., 1978.
7. R. B. Green, G. J. Havrilla and T. O. Trask, *Appl. Spectrosc.*, 1980, **34**, 561.
8. G. J. Havrilla and R. B. Green, *Anal. Chem.*, 1980, **52**, 2376.
9. G. C. Turk, *ibid.*, 1981, **53**, 1187.
10. T. O. Trask and R. B. Green, *Spectrochim. Acta*, 1983, **38B**, 503.
11. V. I. Chaplygin, *Ph. D. Thesis*, Moscow State University, 1984.
12. J. C. Travis, G. C. Turk, J. R. DeVoe, P. K. Schenck and C. A. van Dijk, *Progr. Anal. Atom. Spectrosc.*, 1984, **7**, 199.
13. O. Axner, T. Berglund, J. L. Heully, I. Lindgren and H. Rubinsztein-Dunlop, *J. Appl. Phys.*, 1984, **55**, 3215.
14. O. A. Novodvorsky, *Ph. D. Thesis*, Moscow State University, 1984.
15. V. I. Chaplygin, Yu. Ya. Kuzyakov and N. B. Zorov, *Spectrochim. Acta*, 1983, **38B**, Supplement (Abstracts 23 CSI, Amsterdam, 1983), 386.
16. I. V. Bykov, A. B. Skvortsov, Yu. G. Tatsii and N. B. Chekalin, *J. Phys. Colloq.*, 1983, **C7**, 345.
17. S. J. Weeks, H. Haraguchi and J. D. Winefordner, *Anal. Chem.*, 1978, **50**, 360.
18. Z. Grobanski, D. Weber, B. Welz and J. Wolff, *Analyst*, 1983, **108**, 925.
19. G. C. Turk, J. C. Travis, J. R. DeVoe and T. C. O'Haver, *Anal. Chem.*, 1979, **51**, 1890.
20. N. B. Zorov, Yu. Ya. Kuzyakov, O. I. Matveev and V. I. Chaplygin, *Zh. Analit. Khim.*, 1980, **35**, 1701.
21. J. C. Travis, *J. Chem. Educ.*, 1982, **59**, 909.
22. V. I. Chaplygin, N. B. Zorov and Yu. Ya. Kuzyakov, *Talanta*, 1983, **30**, 505.
23. O. A. Novodvorsky, G. Korn, N. B. Zorov, Yu. Ya. Kuzyakov and S. Poltze, *Kvantovaya Elektronika*, 1983, **10**, 1997.
24. V. I. Chaplygin, N. B. Zorov, Yu. Ya. Kuzyakov and O. I. Matveev, *Zh. Analit. Khim.*, 1983, **38**, 802.
25. L. E. Salsedo Torres, N. B. Zorov, Yu. Ya. Kuzyakov, O. I. Matveev and O. A. Novodvorsky, *Zh. Prikl. Spektrosk.*, 1982, **37**, 488.
26. A. N. Klucharev and N. N. Bezuglov, *Excitation and Ionization of Atoms by Absorption of Light*, p. 272. Leningrad University Ed., Leningrad, 1983.
27. Yu. Ya. Kuzyakov, N. B. Zorov, V. I. Chaplygin and O. A. Novodvorsky, *J. Phys. Colloq.*, 1983, **C7**, 335.
28. V. I. Chaplygin, N. B. Zorov, Yu. Ya. Kuzyakov and O. I. Matveev, *Vestn. Mosk. Univ., Ser. Khim.*, 1983, **24**, 168.

ELECTROTHERMAL ATOMIC-ABSORPTION AND ATOMIC-FLUORESCENCE SPECTROMETRY WITH A TUNGSTEN-COIL ATOMIZER

V. N. MUZGIN, YU. B. ATNASHEV, V. E. KOREPANOV and A. A. PUPYSHEV
Kirov Urals Polytechnical Institute, Sverdlovsk, USSR

(Received 15 October 1985. Revised 20 February 1986. Accepted 10 August 1986)

Summary—A pulsed electrothermal atomizer of the tungsten-coil type and apparatus for its application in atomic-absorption and atomic-fluorescence spectrometry are described. A tungsten-coil atomizer is shown to be just as good as commercial electrothermal atomizers with regard to sensitivity and reproducibility, but to have better operating characteristics. A theoretical model for formation of the atom cloud is given. Mechanisms for atomization of different groups of element in an atmosphere of pure argon and in the presence of reductants (hydrogen and carbon) are proposed.

Atomic-absorption analysis with electrothermal atomization (ETA) has found wide application in industry, geology, agriculture, medicine, *etc.*^{1–3} The Massmann-type graphite furnaces⁴ are widely used for ETA. However, the commercial equipment for ETA has some shortcomings (comparatively short furnace lifetime, slower analysis than with flame atomization, considerable matrix effects, need for high-power sources). To eliminate some of these drawbacks, various workers have proposed coating the graphite tube with pyrolytic carbon, modifying the tube surface with carbides and oxides, lining the tube with refractory metal foil,^{5,6} using the L'vov platform,^{7,8} changing the furnace shape, automating the sampling operation, and so on.

Much attention has been given to the investigation of open electrothermal atomizers in the form of filaments,^{9,10} ribbons,^{11,12} rods¹³ or loops,^{14,15} these are simple to make and provide sufficiently high heating rates and good sensitivity.

Metal-coil atomizers of low mass (3–5 mg) and power input (10–20 W) have a larger radiation area and heated space volume than filament atomizers do,¹⁶ and in our opinion are of special interest. Moreover, atomizers of this kind have long lifetimes and can be used as high-precision samplers.^{17,18} The analytical and operating characteristics of the tungsten-coil atomizer (TCA) are of undoubted interest for analytical chemistry.

An investigation of the fundamental analytical characteristics of atomic-absorption and atomic-fluorescence analysis with a tungsten-coil atomizer is described here.

EXPERIMENTAL

Apparatus

A block diagram of a spectrometer fitted with a TCA is shown in Fig. 1. The atomizer is made in the form of a coil 1.3 mm in diameter and 1.5 mm long (10 turns of a tungsten

or tungsten-rhenium wire 0.08 mm in diameter). For atomic-absorption, the atomizer is placed in the centre of a light-beam 2–4 mm in diameter emitted by a hollow-cathode lamp (HCL). A deuterium lamp is used for background correction.

For atomic-fluorescence, an electrodeless-discharge lamp (EDL) is used as the light-source, with its radiation directed at right angles to the optical axis of the coil and monochromator system. The coil is protected from atmospheric oxidation by a laminar flow of purified argon (flow-rate 1–2 l./min), supplied through a nozzle 2–3 mm below the coil. To create a reducing atmosphere, up to 10% of hydrogen or methane is introduced into the argon. Liquids are sampled by filling a coil with the test solution by surface tension. For this purpose an automatic sampler is used, incorporating a mechanism for raising and lowering a sample cup, carried on a turntable sample magazine (Fig. 1). The autosampler works as follows: when the control motor is switched on, the argon-supply on the nozzle is drawn aside, the sample cup is lifted up until the coil just touches the solution, then the cup and nozzle are returned to their original positions. The moment of contact of the coil with the solution is determined automatically through the accompanying change in the electrical characteristics of the coil. The volume of sample is determined by the size of the coil. The precision of autosampling is better than 2%.

For the analysis of solid conducting materials a sample table is substituted for the liquid-sample holder, and the sample is introduced onto the coil by means of a low-powered electric pulse-discharge between the coil and the solid sample in an atmosphere of argon. The discharge power-supply consists of a high-voltage power supply (1000–1500 V), resistor (100–500 Ω) and a condenser (0.1–10 mF), connected in series. The coil is the negative electrode and the solid sample the positive electrode, connected in parallel with the condenser. The gap between the electrodes is 0.1–1 mm, and the discharge frequency is 0.01–50 kHz. The mass of sample thus transferred to the coil is 10^{-12} – 10^{-7} g, depending on the duration and other parameters of the discharge.

Drying, ashing and carbon-modification cycles (if required) are performed by passage of current from a d.c. supply (the voltages being in the ranges 0.5–0.9, 1–5 and 5–10 V, respectively). To reduce the analysis time and increase the lifetime of the atomizer, a sensor is used which automatically detects the end of the solution drying cycle. Atomization is achieved by current impulses produced by a battery of 20-mF condensers charged to 18–20 V. The

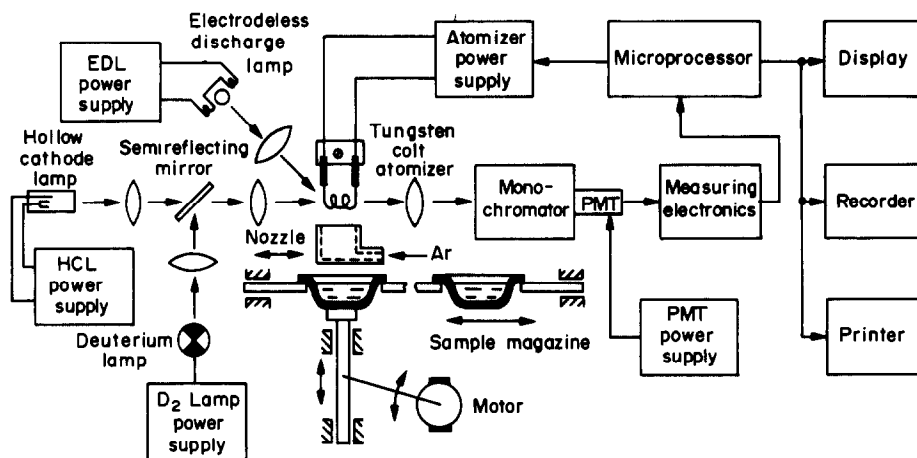


Fig. 1. Block diagram of the spectrophotometer.

atomizer is thus heated at a rate as high as 3×10^5 K/sec, and the maximum coil temperature is 3100 K.

The apparatus incorporates a monochromator of Ebert-Fasty type (spectral range 190–800 nm, dispersion 0.5 nm/mm). Single-beam optics are used, without rotary mechanical modulators (choppers). The radiation from the light-sources is electronically modulated at different frequencies (20 kHz for the HCL or EDL and 12.5 kHz for the deuterium lamp) and combined with the aid of the half-silvered mirror (Fig. 1). The signal from the photomultiplier is separated by means of frequency selectors and then goes to the double-channel measuring device. The absorption of the HCL radiation is measured in the first channel, and that of the deuterium lamp radiation is measured in the second. The output signal is the difference between the signals in the channels. The intensities of the two light-sources are also measured directly before the atomization and their values stored in the microprocessor, to provide the equivalent of a reference beam.

There is feedback between the output of the measurement system and the atomizer-current regulator to fix the maximum absorption automatically, and the absorption signal is integrated. This automatic temperature control widens the range of linear response.

An 8080A microprocessor is used to control the operation of the spectrophotometer and process the signal. The results can be displayed on a VDU, recorded or printed out. The time-constant is adjustable from 0.25 to 25 msec for variation of the electronics band-pass.

Reagents

Standard and developmental test solutions were made from the high-purity nitrates, chlorides or sulphates of the metals of interest, and demineralized water. The stock solutions had a metal content of 10 mg/ml and were diluted as required. To minimize adsorption losses, Teflon and polyethylene vessels were used and to prevent hydrolysis the solutions were acidified with high-purity nitric acid (to an acid concentration of 0.1M). A sample volume of 2 μ l was used. In the analysis of conductive solids, the sample surface was cleaned by preliminary sparking before the sampling discharge proper.

RESULTS AND DISCUSSION

The absorption peak given by use of the TCA is similar in shape to that obtained with other types of atomizers, but is very much shorter in duration. Its shape is determined by the heating rate of the atomizer. Over the range investigated (10^3 – 10^5 K/sec) the

peak height increases linearly but the integral value (peak area) remains constant (Fig. 2).

A theoretical model of formation of the atom cloud from the TCA can be based on the assumptions that (1) the sample is deposited as a monolayer on the tungsten coil, (2) all the atoms can participate equally in the absorption process, (3) the degree of atomization is constant over the temperature range corresponding to the absorption peak, and (4) the rate of removal of atoms from the absorption zone is much greater than the rate of their arrival from the surface of the atomizer. The rate of arrival, V_{ar} , can then be obtained from the differential equation

$$V_{ar} = \frac{dN_{at}}{dt} = kN_{at} \quad (1)$$

where N_{at} is the number of atoms on the surface of the atomizer at time t , and k is the evaporation-rate constant. Since k will depend on the temperature of the atomizer and hence on time, we can define the number of atoms (N_t) in the absorbing zone at time t as

$$N_t = N_0 B p(t) \exp \left[- \int_0^t p(t) dt \right] \tau \quad (2)$$

where N_0 is the initial number of atoms on the atomizer, B is a coefficient taking account of the diffusion rate of the atoms, the geometry of the

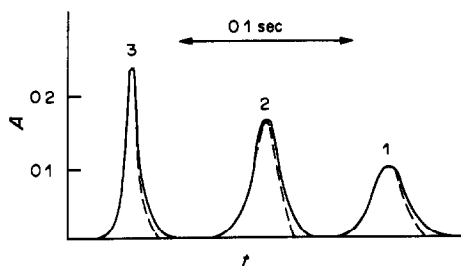


Fig. 2. Experimental (—) and theoretical (---) peak shapes for Pb. Heating rates: (1) 9.5×10^3 , (2) 1.35×10^4 , (3) 2.20×10^4 K/sec.

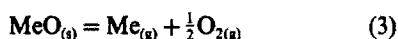
atomizer, and Boltzmann's constant (an increase in temperature of 1500 K increases B by a factor of only 2–3), $p(t)$ is the partial vapour pressure at time t (and increases by 2–4 orders of magnitude when the temperature is increased by 1500 K), and τ is the mean residence time of the atoms in the atomization zone.

From a known or assumed mechanism for atomization of the element, and reference data concerning $p(t)$ for the metal or its compounds, we can calculate the form of the $p(t)$ function for the atomizer heating-rate selected, $T = f(t)$, and hence from equation (2) calculate the shape of the absorption peak.

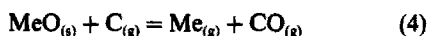
The results given by this theoretical model are in very good agreement with the experimental results (Fig. 2), especially with regard to constancy of the peak area and linear increase in peak height with increase in heating rate. Also, the final temperature of the atomizer is found not to be important, provided it is 300–500 K higher than the appearance temperature of the absorption peak. The model given can be used for other types of ETA. In this connection it should be noted that it is more correct to characterize the atomization process by means of the heating rate of the atomizer [in general by the form of the function $T = f(t)$], than by the atomization temperature as is usually done.

Mechanism of atomization

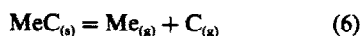
Depending on the conditions of atomization a few processes for free-atom formation can be singled out for the TCA. Thus, for atomization in an argon atmosphere thermal dissociation of oxides is considered to prevail:



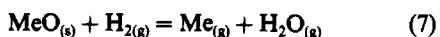
If the TCA is modified with carbon (by preliminary heating at 1600 K in an argon–methane atmosphere) the detection limits for Co, Fe, Mn, Ni and especially for Al, Be, Sr, Si (Table 1) are lowered; this can be explained as due to the reaction



However, for the carbide-forming elements (Cr, Ti, V, rare-earth elements) the detection limits are higher owing to the formation of the carbides, which are more difficult to dissociate:



The use of an argon–hydrogen mixture as the protective atmosphere for the coil lowers the detection limits for the elements forming refractory oxides and carbides, since the following reduction reaction is then operative:



Linearity of calibration graphs

The narrow linear range of calibration, which does

not exceed 1.5–2 orders of concentration magnitude, is considered to be one of the drawbacks of the atomic-absorption method. Application of the atomic-fluorescence method, besides lowering the detection limits, increases the linear response range to 2–3 orders of magnitude.

Application of the automatic temperature control (ATC) method with graphite furnace ETA also widens the linear range of calibration (Fig. 3),¹⁶ but considerably decreases the lifetime of the furnaces as well as increasing the analysis time (the atomization process may take several minutes). Application of the ATC method to the TCA considerably widens the linear response range [up to 3–5 orders of magnitude on a log–log plot (Fig. 3)] though with some increase in atomization time (to some scores of seconds). Thus, the combination of impulse atomization and the ATC method in one device provides both very low detection limits and a wide calibration range, prospects which appear to brighten the future for atomic absorption.

Analytical applications

The high heating rate of the TCA produces a very high density of atomic vapour, resulting in the very low detection limits in spite of the comparatively small volume of the analytical zone and the high rate of atom removal from it. Table 1 presents the values of the characteristic mass for the elements tested,

Table 1. Characteristic masses of analyte (μg) for a peak absorbance of 0.0044 and type of atomization reaction shown in brackets

Element and wavelength at line, nm	Argon atmosphere		
	TCA	TCA modified with carbon	TCA, Ar + H ₂ (10:1)
Ag 328.1	0.3 (3)	0.3 (3)	0.3 (3)
Al 309.2	100 (3)	1 (4)	6 (7)
Au 242.8	0.4 (3)	0.4 (3)	0.4 (3)
Be 234.9	40 (3)	0.06 (4)	0.6 (7)
Bi 223.1	4 (3)	4 (3)	4 (3)
Ca 422.7	30 (3)	30 (30)	0.7 (7)
Cd 228.8	0.08 (3)	0.08 (3)	0.08 (3)
Co 240.7	2 (3)	1 (4)	0.3 (7)
Cr 357.9	4 (3)	3 (6)	0.06 (7)
Cu 324.8	0.5 (3)	0.5 (3)	0.5 (3)
Eu 459.4	—	—	1 (7)
Fe 248.3	0.7 (3)	0.3 (4)	0.5 (7)
Ga 287.4	10 (3)	10 (3)	10 (3)
La 550.1	—	—	900 (7)
Mg 285.2	0.1 (3)	0.1 (3)	0.03 (7)
Mn 279.5	0.2 (3)	0.1 (4)	0.05 (7)
Mo 313.3	—	—	40 (7)
Ni 232.0	2 (3)	1 (4)	2 (7)
Pb 283.3	2 (3)	2 (3)	2 (3)
Sc 391.2	—	6 (6)	10 (7)
Si 251.6	—	6 (4)	—
Sm 429.7	—	—	10 (7)
Sn 286.3	20 (3)	20 (3)	20 (3)
Ti 364.3	—	6000 (6)	20 (7)
V 318.5	—	1000 (6)	8 (7)
Y 410.2	—	—	70 (7)
Zn 213.8	0.2 (3)	0.2 (3)	0.2 (3)

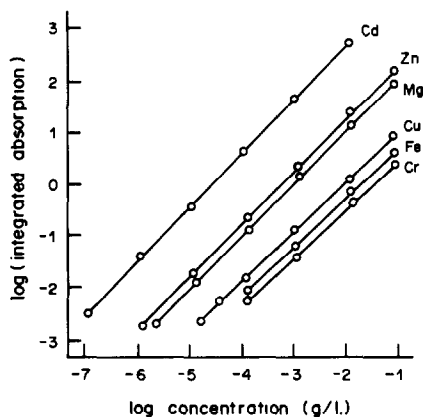


Fig. 3. Calibration graphs for cadmium, zinc, magnesium, copper, iron and chromium with automatic temperature control.

since it is this quantity that shows the analytical possibilities of the atomizer. The detection limit (DL) for elements depends on the type of hollow-cathode lamp used, and the operating and recording conditions. To obtain a low DL with only a narrow absorption peak, it is imperative to choose the measuring electronics band-pass that will give the optimum signal to noise ratio. With the optimum band-pass for the spectrometer described, the DL is about 2–5 times the characteristic mass. This ratio is much poorer than that for flame methods or ETA with graphite furnaces, by reason of the short duration of the peak and the consequently wider band-pass. However, the DL values obtained for the TCA appear, in general, to be better than those for commercial ETA equipment.

TCA with small volumes (2 μ l) of selected samples provides acceptable precision. Thus for most elements tested, the relative standard deviation is 2–4% for an absorbance of 0.1–0.3. Furthermore, most of this error seems due to the sampling process; this was established by measuring the weight of selected sample-volumes of solutions with a wide range of viscosity and surface tension. However, the sampling error is no worse than that obtained with microsyringes.

For sampling of solid conductive materials by means of an electric spark the relative standard deviation is much higher, 5–15%.

In spite of the high heating rate of the TCA, the anionic composition of liquid samples can influence the results, and the matrix effects characteristic of other types of ETA will also occur. A chloride matrix interferes seriously (starting at the 1–100 μ g/ml chloride level) in determination of metals forming relatively volatile chlorides. However, use of the automatic temperature control noticeably reduces matrix effects (Table 2).

To reduce or compensate for matrix and anionic composition effects, the usual techniques such as

Table 2. Effect of sample macrocomponents on integrated manganese absorption (Mn 0.1 μ g/ml, λ = 285.2 nm)

Macro-component (M)	(Mn absorption in presence of M)/ (Mn absorption in absence of M)		
	M = 1 μ g/ml	M = 10 μ g/ml	M = 100 μ g/ml
Fe	0.88	0.72	0.74
Al	0.99	1.07	1.04
Cd	1.09	1.04	0.98

the standard-addition method, matrix modification, matrix-matched standards, matrix-swamping, and dilution to below matrix-interference concentrations, can all be used.

The apparatus and procedures described can be successfully used for the analysis of sewage and natural waters, determination of lead in urine, gold and silver determination in geological samples, and in industry for process-solution control, and in coating and thin-film analysis.

The low cost and long lifetime of the atomizer as well as the good performance and analytical characteristics of the spectrophotometer fitted with the TCA allow us to hope for its further wide application both for determining traces of elements and for analysis of samples widely varying in analyte concentration, without the need for preliminary dilution.

REFERENCES

1. C. K. Ramamurty, G. Kaiser and G. Tölg, *Mikrochim. Acta*, 1980 **I**, 79.
2. S. Levi, R. C. Fortin and W. C. Purdy, *Anal. Chim. Acta*, 1981, **127**, 103.
3. I. Atsaya, K. Ito and M. Otomo, *ibid.*, 1983, **147**, 185.
4. H. Massmann, *Spectrochim. Acta*, 1968, **23B**, 215.
5. G. D. Renshaw, C. A. Pounds and E. F. Pearson, *At. Abs. Newslett.*, 1973, **12**, 55.
6. C. D. Wall, *Talanta*, 1977, **24**, 755.
7. B. V. L'vov, L. A. Pelieva and A. I. Sharnopolskii, *Zh. Prikl. Spektrosk.*, 1977, **27**, 395.
8. W. Slavin and D. C. Manning, *Spectrochim. Acta*, 1980, **35B**, 701.
9. W. Lund and B. V. Larsen, *Anal. Chim. Acta*, 1974, **72**, 57.
10. T. Maruta and T. Takeuchi, *ibid.*, 1973, **66**, 5.
11. T. Hasegawa, M. Yanagisawa and T. Takeuchi, *ibid.*, 1977, **89**, 217.
12. R. L. Warren, *Analyst*, 1980, **105**, 227.
13. J. E. Cantle and T. S. West, *Talanta*, 1973, **20**, 459.
14. M. P. Newton and D. G. Davis, *Anal. Chem.*, 1975, **47**, 2003.
15. M. H. West, J. F. Molina, C. L. Yuan, D. G. Davis and J. V. Chauvin, *ibid.*, 1979, **51**, 2370.
16. M. Williams and E. H. Piepmeier, *ibid.*, 1972, **44**, 1342.
17. S. Mushi, M. Munemori and H. Matsuoka, *Bunseki Kagaku*, 1971, **20**, 1177.
18. Yu. B. Atnashev, V. N. Muzgin, Yu. P. Lyashenko, V. E. Korepanov and E. P. Pilepenko, *Zh. Analit. Khim.*, 1980, **35**, 2156.
19. V. B. Atnashev, V. N. Muzgin and Yu. B. Atnashev, *ibid.*, 1982, **37**, 1590.
20. D. A. Katskov and I. G. Burtzeva, *ibid.*, 1981, **36**, 1895.

ASSAY OF ENZYME EFFECTORS

I. F. DOLMANOVA, T. N. SHEKHOVTSOVA and V. V. KUTCHERYAEVA
Lomonosov Moscow State University, Moscow, USSR

(Received 15 October 1985. Accepted 16 August 1986)

Summary—The effects of various classes of organic compounds and of metal ions on the catalytic activity of horseradish peroxidase in hydrogen peroxide-catalysed *o*-dianisidine oxidation and, on the activity of alkaline phosphatase in *p*-nitrophenyl phosphate hydrolysis have been studied. Enzymic methods have been developed for determination of sulphur compounds at 10^{-5} – $10^{-4}M$, nitrogen compounds at 2×10^{-7} – $3 \times 10^{-5}M$ mercury at $3 \times 10^{-7} \mu\text{g/ml}$ and lead at $6 \times 10^{-4} \mu\text{g/ml}$ concentration.

Enzyme assays are highly selective and sensitive. These properties together with simplicity, speed, and ease of automation make the methods highly promising for use in pharmacology, agriculture, the food industry and environmental protection. Enzymic methods can be used to determine the enzymes themselves, their substrates and effectors (substances affecting enzyme catalytic activity). Most literature methods are concerned with enzyme-substrate assays. Little attention has been paid to methods for determination of the metals and organic compounds that act as enzyme activators or inhibitors, although these methods for effectors are often highly sensitive,¹ (but less selective than those for substrates). Besides, enzyme effectors are much more numerous than enzyme substrates, so the number of compounds that can be determined by enzymic methods is increased.

This paper is concerned with the possibilities for use of enzymic methods for determination of enzyme effectors by consideration of two enzymes of differing classes, horseradish peroxidase and alkaline phosphatase. Various organic compounds and a number of metal ions have been studied as effectors.

EXPERIMENTAL

The horseradish peroxidase was a product of Reanal (Hungary) ($RZ = A_{403}/A_{287} = 3.28$). The enzyme solutions were obtained by dissolving the commercial enzyme preparation in borate buffer (pH 7.0), containing 0.1M sodium nitrate to maintain a constant ionic strength. The lyophilized alkaline phosphatase from chicken intestinal mucosa (activity $0.4 \mu\text{M} \cdot \text{mg}^{-1} \cdot \text{min}^{-1}$) was purchased from "Reanal". The enzyme solutions were obtained by dissolving a precisely weighed sample of the commercial enzyme preparation in 0.05M tris(hydroxymethyl)amino-methane buffer. The solutions of organic compounds, enzyme substrates and effectors were prepared by dissolving in demineralized water or ethanol, reagents from "Soyuz Reaktiv", USSR, being used. The solutions of metal salts were prepared by dissolving weighed amounts in demineralized water. Absorbances of solutions were measured with an Sph-26 spectrophotometer (USSR).

The experiments with effectors were done as follows: to the spectrophotometric cell were added in succession the necessary amounts of buffer, enzyme and effector. In the case of phosphatase, the substrate was added last, and in the case of peroxidase, peroxide was the last to be added. The

total volume of mixture was 2.5–3.0 ml. After rapid mixing, the absorbance of the solution was measured every 15 sec for 2–3 min at 460 or 400 nm. The rate of the reaction was characterized by the slope of the kinetic curves plotted as absorbance *vs.* time.

RESULTS AND DISCUSSION

The effectors for peroxidase were studied by using the oxidation of *o*-dianisidine by hydrogen peroxide as the tracer reaction. This reaction was chosen because, unlike the peroxidase oxidation of other substrates, its kinetics and mechanism have been fairly well studied.^{2,3} The reaction was monitored at 460 nm.

Effect of some nitrogenous organic compounds on the rate of oxidation of o-dianisidine

It has been reported that some nitrogenous compounds (including heterocyclics) activate peroxidase. We have tried to use peroxidase to assay imidazoles, triazoles, pyridines and other nitrogenous heterocyclic compounds. It is usually difficult to determine these by routine functional group analysis, and it is difficult to develop assays for them not involving preliminary mineralization.

According to the literature,⁴ nitrogenous nucleophiles do not activate peroxidase *o*-dianisidine oxidation at pH 5.0–6.0 (the pH for maximum enzyme activity), but only at pH > 6.5. For this reason, pH 8.5 (borate buffer) was taken as optimal, since the enzyme is still active and the activating effect of the nitrogenous compounds is fairly high. The influence of nitrogenous compounds on the rate of the tracer reaction has been studied for a wide range of concentrations (up to $10^{-3}M$).

Most of the compounds studied enhanced the enzyme catalytic activity. The greatest effect was shown by imidazoles, aminopyridines and triazoles. The activation increased with basicity of the compounds, since basicity determines the influence of the activator on the protein ionogenic group limiting the enzyme activity⁵ (Table 1). Exploration of the influence of substituted benzimidazoles has shown

Table 1. Concentration ranges and lower limits of determination (C_1) for nitrogenous organic compounds ($n = 3$, $P = 0.95$)

Compound	C_1, M	Concentration range, M
Imidazole	$(2.0 \pm 0.6) \times 10^{-6}$	$(2-15) \times 10^{-6}$
2-Methylbenzimidazole	$(1.3 \pm 0.4) \times 10^{-5}$	$(1.3-15.0) \times 10^{-5}$
1-Hydroxymethylbenzimidazole	$(2.0 \pm 0.6) \times 10^{-5}$	$(2-30) \times 10^{-5}$
1,2,4-Triazole	$(4 \pm 1) \times 10^{-5}$	$(4-30) \times 10^{-5}$
1,2,3-Benzotriazole	$(2.0 \pm 0.5) \times 10^{-6}$	$(0.2-20.0) \times 10^{-5}$
4-Aminopyridine	$(2.0 \pm 0.6) \times 10^{-7}$	$(2-20) \times 10^{-7}$
2-Methylindole	$(3 \pm 1) \times 10^{-7}$	$(0.3-3.0) \times 10^{-6}$
5-Methoxyindole	$(6 \pm 2) \times 10^{-6}$	$(0.6-3.0) \times 10^{-5}$

that the enzyme is activated least by sterically hindered imidazoles. Thus, 2-methylbenzimidazole was a better activator than 1-hydroxymethylbenzimidazole, whereas 2,2'-pyridylbenzimidazole did not affect the rate of the tracer reaction. From the results obtained, we concluded that highly basic nitrogenous heterocyclic compounds that are not sterically hindered, can be fairly effective activators for peroxidase *o*-dianisidine oxidation.

Among the compounds tested indoles were of particular interest. They have no basic properties, and were included because they are physiologically active, and are often used as ingredients in drugs. Indoles were found to decelerate the tracer reaction, probably not because of any direct influence on the enzyme, but as a result of interaction with intermediates of the *o*-dianisidine oxidation. In favour of this supposition is the fact that many substituted indoles (such as 2-methylindole) are easily oxidized in air.

The presence of linear portions on the graphs of rate of oxidation *vs.* concentration of nitrogenous compound permits the development of enzymic assay methods. For the compounds listed in Table 1 the

optimum concentrations were shown to be peroxidase $9 \times 10^{-10}M$; *o*-dianisidine $5 \times 10^{-6}M$ and hydrogen peroxide $2 \times 10^{-4}M$. The concentration ranges and lower limits of determination are listed in Table 1.

Enzymic methods for determination of sulphur-containing organic compounds

A major problem of analytical chemistry is the determination of sulphur-containing organic compounds present as impurities in various industrial materials and forming part of many pesticides. As test substances, we chose some heterocyclic compounds containing the groups —S, —SH and heterocyclic sulphur. Saunders⁶ reported that almost all these compounds should inhibit peroxidase.

The effect of the compounds on peroxidase activity was studied at pH 5.0, where the enzyme activity is maximal. First, the influence of buffer on the tracer reaction rate was studied. The rate proved to depend on the type of buffer and was maximal in phthalate buffer. Also, the organic compounds had the greatest inhibitory effect in that buffer. The optimum concentrations of the reaction components were peroxidase

Table 2. Mode of action, concentration ranges and lower limits of determination (C_1) for sulphur-containing organic compounds ($n = 3$, $P = 0.95$)

Compounds	Mode of action on enzyme	C_1, M	Concentration range, M
Thiophenol	Linear dependence of tracer reaction rate on inhibitor concentration	$(2.0 \pm 0.6) \times 10^{-8}$	$(0.2-3.0) \times 10^{-7}$
Rubeanic acid		$(1.0 \pm 0.3) \times 10^{-6}$	$(1-16) \times 10^{-6}$
Phenylthiourea		$(1.0 \pm 0.3) \times 10^{-4}$	$(0.1-2.0) \times 10^{-3}$
Pyridylthioamide		$(5 \pm 1) \times 10^{-5}$	$(0.5-12.0) \times 10^{-4}$
Allylthiourea	Linear dependence of logarithm of tracer reaction rate on inhibitor concentration	$(3.0 \pm 0.8) \times 10^{-4}$	$(3-10) \times 10^{-4}$
Acetylthiourea		$(5 \pm 1) \times 10^{-4}$	$(0.5-7.0) \times 10^{-3}$
Dithiothreitol		$(1.0 \pm 0.3) \times 10^{-6}$	$(1-8) \times 10^{-6}$
1,2,4-Triazolethiol		$(8 \pm 2) \times 10^{-7}$	$(0.8-9.0) \times 10^{-6}$
Thiourea	Time-dependent enzyme inhibition	$(1.0 \pm 0.3) \times 10^{-4}$	$(1-10) \times 10^{-4}$
2-Mercaptoethanol		$(5.0 \pm 0.9) \times 10^{-7}$	$(0.5-8.0) \times 10^{-6}$
Bismuthiol I	Linear dependence of induction period on inhibitor concentration	$(2.0 \pm 0.5) \times 10^{-6}$	$(2-30) \times 10^{-6}$
Benzylbismuthiol		$(1.3 \pm 0.4) \times 10^{-6}$	$(1.3-20.0) \times 10^{-6}$
Thionalide		$(4 \pm 1) \times 10^{-7}$	$(0.4-5.0) \times 10^{-6}$
Thiosalicylic acid		$(2.0 \pm 0.3) \times 10^{-6}$	$(2-30) \times 10^{-6}$
Sodium diethylthiocarbamate		$(1.0 \pm 0.3) \times 10^{-6}$	$(0.1-3.0) \times 10^{-5}$

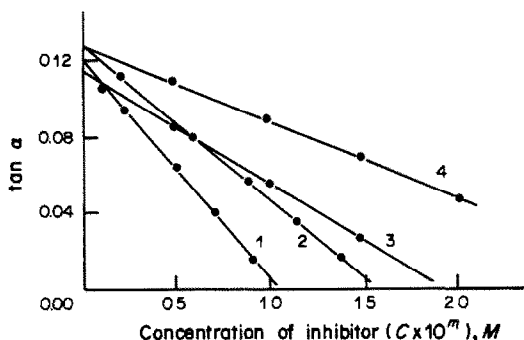


Fig. 1. Dependence of the rate of the peroxidase-catalysed oxidation of *o*-dianisidine on the concentration of pyridylthioamide (1, $m = 3$), rubeanic acid (2, $m = 5$), phenylthiourea (3, $m = 3$), thiophenol (4, $m = 7$); (pH 5.0, phthalate buffer, peroxidase $3 \times 10^{-11}M$, *o*-dianisidine $6 \times 10^{-5}M$, peroxide $1 \times 10^{-3}M$); m replicates.

$4 \times 10^{-10}M$, *o*-dianisidine $6 \times 10^{-5}M$ and hydrogen peroxide $1 \times 10^{-3}M$.

All the compounds tested were found to inhibit peroxidase. In dependence on the extent and mode of inhibition, they can be arbitrarily divided into four groups (Table 2).

Thiophenol, rubeanic acid, phenylthiourea and pyridylthioamide lower peroxidase catalytic activity in such a way that the tracer reaction rate is inversely proportional to the amount of compound (Fig. 1). The dependence of the rate on concentration of allylthiourea, acetylthiourea, 1,3-dithiothreitol and 1,2,4-triazolethiol is rather complicated, but the rate of the reaction again decreases with increasing amount of inhibitor (Fig. 2). Thiourea and 2-mercaptoethanol also lower the tracer reaction rate but this interaction has a particular pattern. When peroxidase is incubated with them, the enzyme activity decreases with time, the rate of the activity attenuation being proportional to inhibitor concentration (Fig. 3).

In the presence of bismuthiol I and sodium diethyldithiocarbamate, the kinetic curves show an induction period, the length of which is proportional to

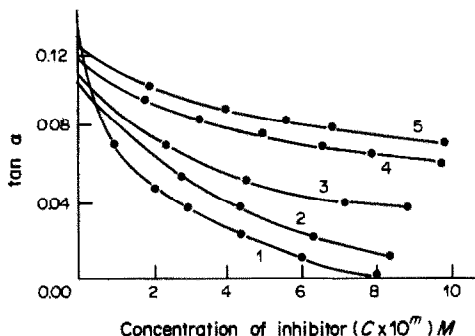


Fig. 2. Dependence of the rate of the peroxidase-catalysed oxidation of *o*-dianisidine on the concentration of thiourea (1, $m = 3$), 1,2,4-triazole (2, $m = 6$), acetylthiourea (3, $m = 3$), dithiothreitol (4, $m = 6$), allylthiourea (5, $m = 4$); (pH 5.0, phthalate buffer, peroxidase $3 \times 10^{-11}M$, *o*-dianisidine $6 \times 10^{-5}M$, peroxide $1 \times 10^{-3}M$).

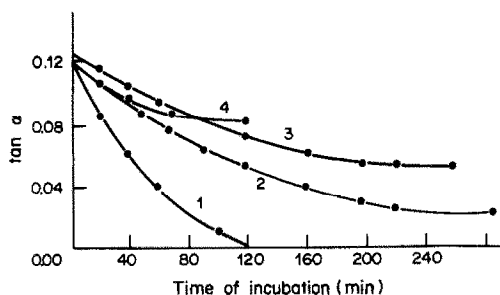


Fig. 3. Dependence of the rate of the peroxidase-catalysed oxidation of *o*-dianisidine on incubation time of peroxidase with thiourea (1, 2, 3) and 2-mercaptoethanol (4); (pH 5.0, phthalate buffer, peroxidase $3 \times 10^{-11}M$, *o*-dianisidine $6 \times 10^{-5}M$, peroxide $1 \times 10^{-3}M$, thiourea $2.5 \times 10^{-5}M$ (1), $4 \times 10^{-6}M$ (2), $2 \times 10^{-6}M$ (3), 2-mercaptoethanol $5 \times 10^{-7}M$).

the concentration of the sulphur-containing compound (Fig. 4). The rate of *o*-dianisidine oxidation starting after the induction period decreases with increasing concentration of compound.

From our kinetic study of peroxidase *o*-dianisidine oxidation in the presence of sulphur-containing compounds, and from study of some model systems, we have suggested^{7,8} reasons for the various effects of the compounds on the reaction rate. The compounds of the first and second groups (Table 2) were found to be reversible competitive inhibitors for peroxidase. The mechanism of the effect of compounds of the third group, thiourea in particular, is more intricate and involves two steps: a rapid reversible competitive inhibition and an irreversible enzyme inactivation with time.⁷ The kinetic features of *o*-dianisidine oxidation in the presence of compounds of the fourth group can be explained by the scheme suggested as a result of the kinetic study of a combined oxidation of *o*-dianisidine and bismuthiol I, the latter acting as the peroxidase substrate. This scheme involves the competitive reactions of individual oxidation of each substrate by the enzyme as well as interaction of bismuthiol I with the intermediate of *o*-dianisidine oxidation.⁸

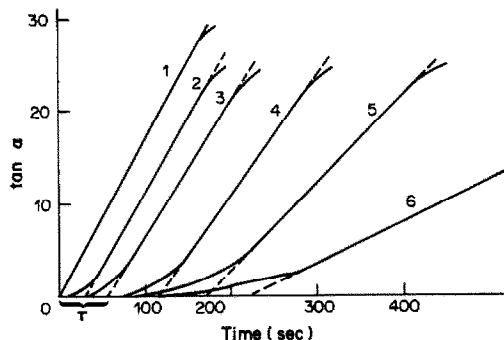


Fig. 4. Dependence of the rate of the peroxidase-catalysed oxidation of *o*-dianisidine in the presence of bismuthiol I, on time; [pH 5.0, phthalate buffer, peroxidase $5 \times 10^{-11}M$, *o*-dianisidine $3 \times 10^{-4}M$, peroxide $1 \times 10^{-3}M$, bismuthiol I O (1), $1 \times 10^{-3}M$ (2), $2 \times 10^{-3}M$ (3), $4 \times 10^{-3}M$ (4), $6 \times 10^{-3}M$ (5), $1 \times 10^{-4}M$ (6)].

Table 3. Lower limits of detection, C_{\min} , of metal ions by peroxidase *o*-dianisidine oxidation in the presence and absence of thiourea and dithiothreitol ($n = 3$, $P = 0.95$)

Metal ions	C_{\min} , $\mu\text{g/ml}$ in the absence of effector	C_{\min} , $\mu\text{g/ml}$ in the presence of thiourea	C_{\min} , $\mu\text{g/ml}$ in the presence of dithiothreitol
Ag(I)	—	1×10^{-2}	2×10^{-2}
Zn(II)	1	1×10^{-1}	5×10^{-1}
Pb(II)	1×10^{-1}	1×10^{-2}	5×10^{-2}
Bi(III)	—	1×10^{-3}	2×10^{-4}
Cd(II)	—	6×10^{-4}	3×10^{-3}
Hg(II)	5×10^{-2}	1×10^{-5}	3×10^{-4}

The linear dependence of the tracer reaction rate (or the induction time) on the concentration of sulphur-containing compounds allows enzyme assay methods to be developed for these compounds (Table 2). The methods are non-selective, and allow determination of only a single substance, but the sensitivity is comparable with that of the most sensitive current electrochemical and fluorescence methods for sulphur-containing compounds. The sulphur does not have to be converted into SO_2 , SO_3 or H_2S (by mineralization), as it does in most methods for determination of sulphur in organic compounds. The methods are simple and require little equipment.

We have also observed that the sulphur-containing effectors thiourea and dithiothreitol exhibit not only their own inhibitory action, but enhance or promote emergence of the inhibitory action of metals such as mercury, silver, cadmium, bismuth, zinc and lead. Enzymic assay methods have been developed for these metals (Table 3). The assay is done at pH 4.8–5.0 (phthalate buffer). The optimum concentrations for determination of mercury, bismuth and cadmium are $4 \times 10^{-11}M$ peroxidase, $8 \times 10^{-5}M$ *o*-dianisidine and $10^{-3}M$ hydrogen peroxide. The optimum concentrations of thiourea for determination of mercury and cadmium are $5 \times 10^{-3}M$ and $5 \times 10^{-7}M$, respectively.

The inhibitory action of cadmium and mercury is enhanced only when the mixed enzyme–thiourea solution, preincubated for 4 hr, is used.⁹ The concentration of dithiothreitol for determination of bismuth is $4 \times 10^{-6}M$.

To try to enhance the sensitivity of the assay methods for peroxidase effectors, we tested other potential substrates for the enzyme. The literature reports rather a limited number of peroxidase substrates used in analyses.^{10–17} We also studied some organic compounds: amidol, *o*- and *p*-phenylenediamine, diaminodiphenylmethane, α -naphthylamine, aminoacetanilide and 3,3',5,5'-tetramethylbenzidine (TMB). TMB gave the highest rate and lowest substrate concentration.

The optimum conditions of the reaction were borate–phosphate buffer (pH 7.0); $3 \times 10^{-10}M$ peroxidase; $2 \times 10^{-5}M$ TMB and $2 \times 10^{-4}M$ hydrogen peroxide. Under these conditions, the possibility of determining a nitrogenous peroxidase effector,

1,2,3-benzotriazole, and also mercury in the presence of thiourea, was investigated. TMB, as substrate, markedly decreased the lower limit of the concentration range for determination of 1,2,3-benzotriazole [$C_1 = (8 \pm 2) \times 10^{-8}M$, $P = 0.95$, $n = 3$] compared with the method based on peroxidase *o*-dianisidine oxidation. The least detectable amount of mercury with use of TMB oxidation in the optimum conditions above and at a thiourea concentration of $10^{-6}M$ was $(3.0 \pm 0.5) \times 10^{-7} \mu\text{g/ml}$ ($n = 3$; $P = 0.95$).

Thus, the use of TMB as peroxidase substrate gave a useful enhancement of sensitivity of the enzyme effector assays.

The usefulness of a systematic study of potential enzyme effector methods is illustrated by our current exploration of the effects of various compounds on the activity of alkaline phosphatase. We began by choosing a substrate with which alkaline phosphatase gave a high catalytic activity; hydrolyses of *p*-nitrophenyl phosphate, glucose-6-phosphate, 1-glycerophosphate and phosphoethanolamine showed the catalytic activity to be greatest with *p*-nitrophenyl phosphate. The optimum conditions for this reaction are pH 9.8 [tris(hydroxymethyl)aminomethane–HCl buffer]; $4 \times 10^{-7}M$ phosphatase and $3 \times 10^{-4}M$ *p*-nitrophenyl phosphate.

Only a few methods have been described in the literature for determining alkaline phosphatase effectors;^{18–26} metal ions, and less often organic compounds, were studied as the effectors. We have studied the influence of some metal ions on alkaline phosphatase activity and shown that the enzyme is activated by aluminium (1–10 $\mu\text{g/ml}$). Using the inhibitory effect, we have developed enzymic methods for determining magnesium (10^{-3} – $10^{-1} \mu\text{g/ml}$), cadmium (10^{-3} – $10^{-2} \mu\text{g/ml}$), calcium and barium (10^{-3} – $10^{-2} \mu\text{g/ml}$) in the presence of strontium. We were the first to find the inhibitory effect of magnesium in the concentration range 10^{-3} – $1 \mu\text{g/ml}$. A method for determination of lead has also been developed; its lower limit of determination is $(6 \pm 2) \times 10^{-4} \mu\text{g/ml}$, and its sensitivity exceeds that of previous enzymic methods for lead^{15,27} and is comparable with the most sensitive atomic-fluorescence methods.

During our studies on alkaline phosphatase, the effects of organic compounds of various classes, over

Table 4. Effect of organic compounds on the rate of *p*-nitrophenyl phosphate hydrolysis in the presence of alkaline phosphatase

Compound	Minimum concentration with inhibitory effect, <i>M</i>
<i>Phosphorus-containing organic compounds</i>	
Ethylenediaminetetramethylenephosphonic acid	8×10^{-6}
Hydroxyethylidenediphosphonic acid	1×10^{-5}
Iminodimethylenephosphonic acid	8×10^{-4}
Nitrilotrimethylenephosphonic acid	1×10^{-4}
Isobutyrylphosphonic acid	3×10^{-6}
Adenosine 5'-triphosphate	9×10^{-5}
Uridine 5'-triphosphate	2×10^{-5}
Guanosine 5'-triphosphate	1×10^{-5}
<i>Sulphur-containing organic compounds</i>	
Thiophenol	2×10^{-4}
Thionaphthol	8×10^{-5}
<i>o</i> -Thiocresol	1×10^{-3}
<i>p</i> -Thiocresol	1×10^{-6}
<i>o</i> -Ethylthiophenol	1×10^{-4}
Decamethylenedimercaptan	7×10^{-5}
β -Phenylethylmercaptan	7×10^{-4}
Thionalide	1×10^{-5}
Bismuthiol I	1×10^{-5}

a wide concentration range (up to $10^{-2}M$), on the rate of enzymic hydrolysis of *p*-nitrophenyl phosphate were tested. We did not find any organic compounds that acted as activators for alkaline phosphatase. The majority of sulphur-containing heterocyclic and nitrogenous compounds did not alter the rate of the tracer reaction. Amino-acids at 10^{-4} – $2 \times 10^{-3}M$ concentration inhibited the enzyme. Phosphorus complexones, natural esters of phosphonic acids and mercaptans were the inhibitors of alkaline phosphatase of the greatest analytical interest (Table 4). It seems likely that fairly sensitive and selective assays can be developed for a limited number of these compounds.

REFERENCES

- G. G. Guilbault and M. M. Sadar, *Proc. Anal. Div. Chem. Soc.*, 1977, **14**, 302.
- K. M. Möller and P. Ottolenghi, *Compt. Rend. Trav. Lab. Carlsberg*, 1966, **35**, 369.
- O. V. Lebedeva, N. N. Ugarova and I. V. Berezin, *Biokhimiya*, 1977, **8**, 1372.
- N. N. Ugarova, O. V. Lebedeva, T. A. Kurilina and I. V. Berezin, *ibid.*, 1977, **42**, 1577.
- O. V. Lebedeva, V. A. Dombrovsky, N. N. Ugarova and I. V. Berezin, *ibid.*, 1978, **43**, 1024.
- B. C. Saunders, A. G. Solmes-Siedle and B. P. Stark, *Peroxidase: The Properties and Use of a Versatile Enzyme and of some Related Catalysts*, Butterworths, Washington, 1964.
- N. N. Ugarova, I. M. Popova, I. F. Dolmanova and T. N. Shekhovtsova, *Biokhimiya*, 1981, **46**, 1026.
- Idem, ibid.*, 1980, **45**, 2243.
- I. F. Dolmanova, E. V. Ershova, V. U. Nad and T. N. Shekhovtsova, *Zh. Analit. Khim.*, 1979, **34**, 1644.
- M. Takayama, S. Iton, T. Nagasaki and J. Tanimisi, *Clin. Chim. Acta*, 1977, **79**, 93.
- R. C. Trivedy, L. Rebal, E. Berta and L. Strong, *Clin. Chem.*, 1978, **24**, 1908.
- G. Weinryb, *Biochemistry*, 1966, **5**, 2003.
- G. G. Guilbault and D. H. Kramer, *Anal. Chem.*, 1964, **36**, 2494.
- G. G. Guilbault and P. I. Brignac, *ibid.*, 1968, **40**, 1256.
- G. G. Guilbault, P. I. Brignac and M. Zimmer, *ibid.*, 1968, **40**, 180.
- T. T. Ngo and H. M. Lengoff, *Anal. Biochem.*, 1980, **108**, 389.
- R. E. Childs and W. G. Bardsley, *Biochem. J.*, 1975, **145**, 93.
- M. Gottessman, R. T. Simpson and B. L. Vallee, *Biochemistry*, 1979, **8**, 3776.
- A. Townshend and A. Vaughan, *Talanta*, 1969, **16**, 929.
- R. A. Thomas and J. P. Kirsch, *Biochemistry*, 1980, **19**, 5328.
- D. J. Plocke and B. L. Vallee, *ibid.*, 1962, **1**, 1039.
- H. Neumann, *J. Biol. Chem.*, 1968, **243**, 1671.
- G. G. Guilbault, M. H. Sadar and M. Zimmer, *Anal. Chim. Acta*, 1969, **44**, 361.
- M. A. Grocet, G. L. Kramer and D.-L. Carberst, *Biochem. Pharm.*, 1979, **28**, 1227.
- H. Van Belle, *Biochem. Biophys. Acta*, 1972, **289**, 158.
- P. Kumar, *Enzyme*, 1979, **24**, 152.
- E. C. Toren and F. I. Burger, *Mikrochim. Acta*, 1968, 1049.

FLUORESCENCE DETERMINATION OF TRACE AMOUNTS OF URANIUM(VI) IN VARIOUS MATERIALS BY A REPETITIVE LASER TECHNIQUE

G. I. ROMANOVSKAYA*, V. I. POGONIN and A. K. CHIBISOV

V.I. Vernadsky Institute of Geochemistry and Analytical Chemistry, Academy of Sciences of the USSR,
Moscow 117975, USSR

(Received 15 October. Revised 28 January 1986. Accepted 30 July 1986)

Summary—A laser-induced fluorescence method (LFM) is described for determination of trace amounts of uranium(VI), with a detection limit of 4×10^{-11} g/ml. A repetitive pulsed laser, time discrimination and an averaging technique are used. The optimum time discrimination is obtained when the uranyl ion is complexed with phosphoric acid or sodium polysilicate. LFM does not need a preconcentration step or separation of uranium from interfering elements. The time needed for analysis is only 1–2 min.

It is well known that the luminescence method is widely used for determination of low concentrations of uranium in solutions and solid materials.¹ The method does not need a preconcentration step or even a separation from interfering elements,² which may act as quenchers of the uranium fluorescence or exhibit a luminescence of their own that overlaps that of the uranium but these interferences are the reason for the high detection limit for uranium (*ca.* 10^{-8} g/ml). Reduction of this detection limit is of prime importance for solving many geochemical problems, as well as for determination of uranium in natural waters. A lower detection limit may be attained by using new principles, involving elimination of the background emission and increasing the signal-to-noise (S/N) ratio.

With this in mind a new laser-induced fluorescence method was developed for uranium determination with a low detection limit,^{3,4} based on use of a repetitive pulsed laser as an intense excitation source, time discrimination with a gated detection system for suppressing the background emission, and an averaging technique to increase the S/N ratio.

In this paper we summarize our results for application of the laser-induced fluorescence method (LFM) for determination of trace amounts of uranium(VI) in various materials.

EXPERIMENTAL

Synthesis of reagents

$(\text{CN}_2\text{H}_6)_4[\text{UO}_2(\text{CO}_3)_3]$, $\text{UO}_2(\text{NO}_3)_2 \cdot 6\text{H}_2\text{O}$ and $\text{UO}_2(\text{H}_2\text{PO}_4)_2 \cdot 4\text{H}_2\text{O}$ were synthesized as previously described.^{5,6} Sodium polysilicate was synthesized according to Sokolov *et al.*⁷

Reagents and solutions

All reagents were used as 4×10^{-11} – 2×10^{-7} g/ml solutions in doubly distilled water at pH 2 (nitric acid). All solvents and reagents were of analytical grade. The elements in the salts present in sea-water were used as quenchers of the uranium fluorescence.⁸

Apparatus

Fluorescence measurements were made with a Jobin Yvon 3CS spectrofluorimeter. Laser-induced fluorescence measurements were performed by means of a laser fluorimetric system (Fig. 1). A ЛГН-21 nitrogen laser was used as the excitation source, with wavelength 337 nm, pulse width 10 nsec, repetition rate 100 Hz and power 1.6 kW. The laser beam was directed onto the sample cell. The fluorescence of a solution in the cell was detected by a photomultiplier tube (PMT) operated both in an analogue mode (PMT type ФЭУ-38) and in a photon counting mode (PMT type ФЭУ-79). To protect the PMT from scattered laser light and organic fluorescence a green-transmitting

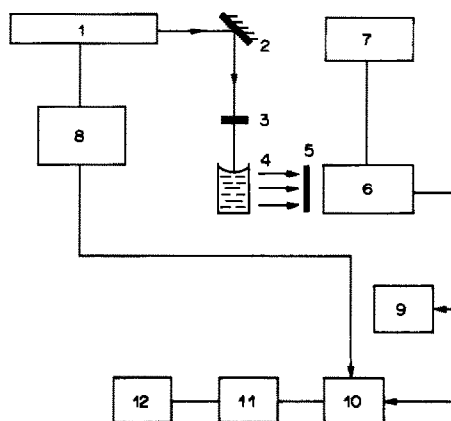


Fig. 1. Schematic diagram of the instrumentation: 1—laser ЛГН-21, 2—mirror, 3—UV-light filter, 4—sample cell, 5—green filter, 6—photomultiplier ФЭУ-38 or ФЭУ-79, 7—power supply, 8—pulse generator, 9—pulse counter, 10—transient recorder, 11—averager, 12—x-y plotter.

*Author for correspondence.

filter was placed between the cell and the PMT. When the PMT was operated in the analogue mode the PMT output was coupled to a transient-recorder (Bruker BC-104), averager (Fabri-Tek 1074) and x-y plotter. When the PMT was operated in the photon-counting mode the output was coupled to a photon-counter (home-made).

The sampling gate was used to suppress the scattered light and electrical noise from the laser pulse, as well as the intense short-lived organic fluorescence. The fluorescence signal was averaged over 1000 laser pulses and normally three runs were measured under identical conditions. Measurements were made at ambient temperature with the sample in a special cylindrical cell made from non-fluorescent glass.

RESULTS AND DISCUSSION

Some features of the laser-induced fluorescence method (LFM)

The detection limit of uranyl fluorescence depends on several factors such as the intensity of the excitation source, intensity of background emission, and noise level. The background emission originates both as a result of scattered laser radiation and the luminescence of impurities when the luminescence spectra of uranium(VI) and the impurities overlap.

To find the optimal values of time delay and sampling gate time the decay kinetics of the uranyl fluorescence and impurities emission was measured. It was found that the difference between the life-time of the uranyl fluorescence and the background emission is greatest when the uranium(VI) is complexed with phosphoric acid³ or sodium polysilicate (SPS).⁷ Moreover SPS has some unique properties. When complexed with uranium(VI) the SPS protects the long-lived intense fluorescence of the uranyl complex from the quenching caused by certain anions. The

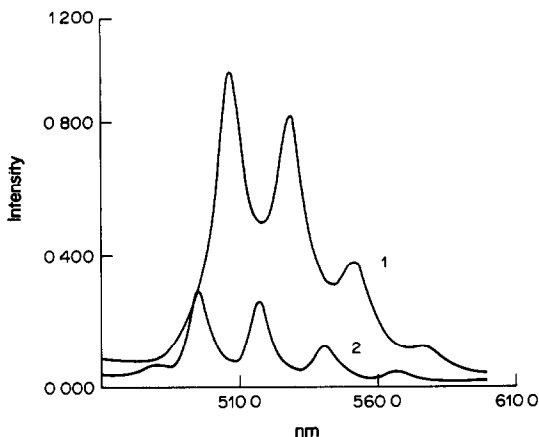


Fig. 2. Fluorescence spectra of uranyl polysilicate (1) and uranyl phosphate complexes (2) ($C_{\text{uranyl}} = 10^{-7}$ g/ml) at $\lambda_{\text{ex}} = 337$ nm.

fluorescence spectra of the uranyl polysilicate and uranyl phosphate complexes are presented in Fig. 2. The fluorescence intensity of the uranyl polysilicate complex is maximal at pH 7–10.⁹

Fig. 3 show schematically the time course of the long-lived uranyl fluorescence and the intense short-lived background emission. The uranyl concentration can readily be measured after complete decay of the short-lived background emission. When the fluorescence measurements were made in the analogue mode the intensity of the uranyl emission was recorded 50 μ sec after the laser pulse. The detection limit for uranyl was 10^{-9} g/ml.

When the uranyl concentration was less than 10^{-9} g/ml the measurements were made in the

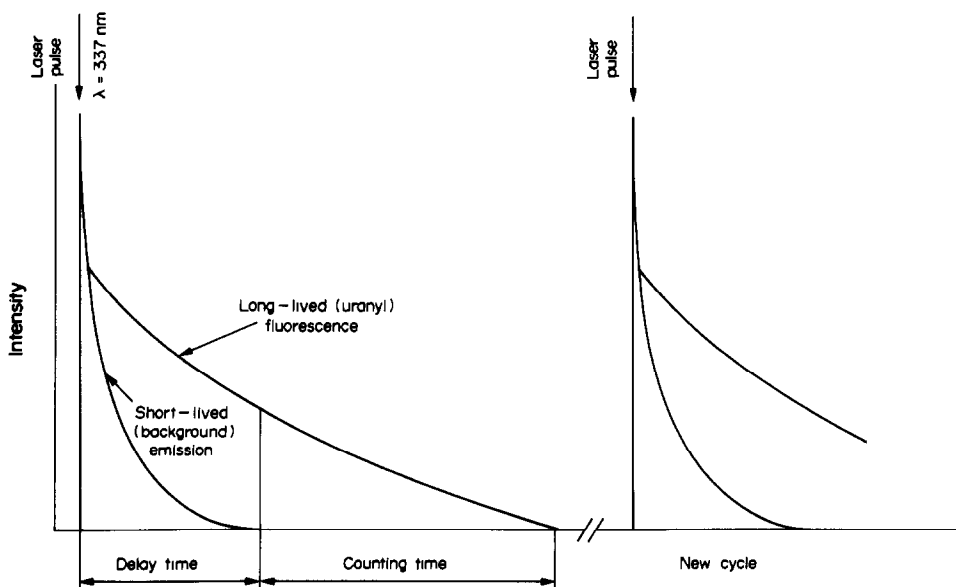


Fig. 3. Time course of short-lived and long-lived fluorescence intensity of impurities and uranyl ion respectively (see text).

Table 1. The tolerance limits for inorganic ions in determination of 3 ng/ml uranium(VI) in 1 M H₃PO₄

Ion	Limits, g/ml	Ion	Limits, g/ml
Mg ²⁺	1 × 10 ⁻²	Sr ²⁺	2 × 10 ⁻²
SO ₄ ²⁻	1 × 10 ⁻¹	H ₂ BO ₃ ⁻	6 × 10 ⁻²
Ca ²⁺	5 × 10 ⁻²	F ⁻	2 × 10 ⁻²
Br ⁻	7 × 10 ⁻⁷	Cu ²⁺	7 × 10 ⁻⁴
HCO ₃ ⁻	3 × 10 ⁻⁴	Co ²⁺	4 × 10 ⁻⁴

photon-counting mode. The delay time and sampling gate time were adjusted to 100 and 300 μsec, respectively when the fluorescence measurements were made with uranyl ion in 1M phosphoric acid, and 300–400 μsec for measurements of uranyl fluorescence in the presence of SPS. The detection limit for the uranyl ion in phosphoric acid or in the presence of SPS is 4 × 10⁻¹¹ g/ml.

Factors affecting the detection limit for uranium(VI)

The detection limit of uranium depends not only on the ligands affecting the lifetime of the excited uranyl ions but also on the quenching of uranyl fluorescence by certain interfering impurities.

Table 1 gives the tolerance limits for certain inorganic ions¹⁰ in determination of uranium(VI) at the 3-ng/ml level* in 1M phosphoric acid medium. The maximal concentration of Cl⁻ and Br⁻ as impurities must not exceed 10⁻⁷ g/ml, assuming that the fluorescence quenching of uranyl by these ions is governed by their diffusion rate.

It was established previously^{11,12} that the quenching of uranyl fluorescence by inorganic ions can occur by both electron and energy transfer. It was found that the complexation of uranyl ions with different ligands facilitates the electron transfer process if the electron donors are metal ions, and makes the transfer difficult if the electron donors are anions.

When the concentration of anions as impurities is higher than the limit of interference (Table 1) the determination of uranium(VI) should be done in the presence of SPS⁷. The tolerance limits for interferences in the determination of uranium as its complex with SPS are summarized in Table 2. From comparison of the data presented in Tables 1 and 2 it follows that the determination of uranium(VI) in presence of Ca²⁺, Mg²⁺ and Cu²⁺ ions should preferentially be done in 1M phosphoric acid medium, and this probably also applies to other metal ions except those of the alkali metals.

Analysis of natural waters

Determination of uranium(VI) in natural waters is performed with sodium polysilicate (4% vol.) added to the samples. Natural water is known to contain a

Table 2. The tolerance limits for inorganic ions for determination of 3 ng/ml uranium(VI) in presence of sodium polysilicate

Ion	Limits, g/ml	Ion	Limits, g/ml
Na ⁺	1.0 × 10 ⁻²	Ni ²⁺	5.1 × 10 ⁻⁵
K ⁺	1.0 × 10 ⁻²	Ce ⁴⁺	2.8 × 10 ⁻⁵
Cl ⁻	1.0 × 10 ⁻²	Pb ²⁺	2.1 × 10 ⁻⁵
F ⁻	1.0 × 10 ⁻²	Cu ²⁺	1.9 × 10 ⁻⁵
NO ₃ ⁻	1.0 × 10 ⁻²	Co ²⁺	1.8 × 10 ⁻⁵
SO ₄ ²⁻	1.0 × 10 ⁻²	Fe ²⁺	1.7 × 10 ⁻⁵
HPO ₄ ²⁻	1.0 × 10 ⁻²	Mn ²⁺	1.6 × 10 ⁻⁵
HCO ₃ ⁻	1.8 × 10 ⁻³	Cr ³⁺	1.6 × 10 ⁻⁵
CO ₃ ²⁻	1.8 × 10 ⁻³	H ₂ BO ₃ ⁻	6.6 × 10 ⁻⁵
Cd ²⁺	3.3 × 10 ⁻⁴	SCN ⁻	5.8 × 10 ⁻⁶
Al ³⁺	2.7 × 10 ⁻⁴	I ⁻	3.8 × 10 ⁻⁶
Sr ²⁺	2.6 × 10 ⁻⁴	Cr(VI)	1.6 × 10 ⁻⁷
Mg ²⁺	2.4 × 10 ⁻⁴	Hg(I)	1.2 × 10 ⁻⁷
Br ⁻	2.3 × 10 ⁻⁴	Tl ⁺	2.0 × 10 ⁻⁸
Zn ²⁺	2.0 × 10 ⁻⁴	Ag ⁺	1.1 × 10 ⁻⁸
Ca ²⁺	1.2 × 10 ⁻⁴		

relatively large amount of organic substances (humic and fulvic acids) and inorganic ions. The organic compounds may quench the uranyl fluorescence, and the ions Ca²⁺, Mg²⁺ (> 10⁻⁴ g/ml), Na⁺, Cl⁻ (> 10⁻² g/ml) result in coagulation of the SPS. That is why the water samples need tenfold dilution. Organic matter can be destroyed by treatment with perchloric acid.⁷ The concentration of uranium(VI) in the sample is calculated from the formula:

$$U(IV) = \frac{6.25n}{[(N_3 - N_2)/(N_1 - N_2)] - 1} \text{ ng/ml}$$

where N_1 = number of fluorescence pulses for the sample, N_2 = number of pulses of background emission, N_3 = number of fluorescence pulses for the sample plus 6.25 × 10⁻⁹ g/ml (CN₃H₆)₄[UO₂(CO₃)₃], and n = degree of dilution.

The time needed for a uranium analysis is only 1–2 min. The relative standard deviation is 5%. Table 3 gives the results of analysis of water samples from different areas of the Pacific Ocean by LFM and a conventional spectrophotometric method.¹³ The results are in reasonable agreement. It should be noted that determination of the uranyl ion by LFM needs only dilution of the water samples, whereas the determination by spectrophotometry requires a pre-concentration step.

Analysis of solid samples

Rock samples were finely ground and decomposed by treatment with nitric and hydrofluoric acids,¹⁴

Table 3. Concentration of uranium(VI) found in different areas of Pacific Ocean (mean of 5 analyses)

Area	Found by LFM, ng/ml	Found by spectrophotometry, ¹³ ng/ml
I	3.4	3.6
II	3.4	3.3
III	3.3	3.3

*The average concentration of uranium(VI) in sea-water.⁸

Table 4. Concentration of uranium(VI) in rocks

Sample	Found by LFM, 10 ⁻⁴ %	Found by γ -spectrometry, ¹⁴ 10 ⁻⁴ %
Granite, international standard	7.2	6.8
Albitized granite, native standard	60	65
Granite	102	100

followed by evaporation to dryness and dissolution of the nitrates in 0.01M nitric acid. SPS was added before the fluorescence was measured. The results obtained by LFM are in good agreement with those obtained by γ -spectrometry¹⁴ (Table 4).

REFERENCES

1. T. S. Dobrolubskaya, *Luminescence Methods for Determination of Uranium* (in Russian), Nauka, Moscow, 1968.
2. W. Campen and K. Bächmann, *Mikrochim. Acta*, 1979 II, 159.
3. V. I. Pogonin, G. V. Zakharova, G. I. Romanovskaya and A. K. Chibisov, *Zh. Analit. Khim.*, 1979, **34**, 1779.
4. J. Robbins, *CIM Bull.*, 1978, **71**, 61.
5. I. I. Chernyaev, V. A. Golovnya and G. V. Ellert, *Zh. Neorgan. Khim.*, 1961, **6**, 790.
6. G. I. Sergeeva, *The Study of Photochemical Reactions of Uranyl Ion in Aqueous Solution by Flash Photolysis* (in Russian), Candidate Thesis, Moscow, 1974.
7. A. K. Sokolov, M. M. Sokolov and V. K. Titov, *Zh. Analit. Khim.*, 1982, **37**, 1466.
8. I. N. Lepeshkov and B. Ya. Rozen, *Mineral Gifts of the Sea* (in Russian), Nauka, Moscow, 1972.
9. G. I. Romanovskaya, G. V. Zakharova and A. K. Chibisov, *Zh. Analit. Khim.*, 1984, **39**, 930.
10. G. I. Romanovskaya, V. I. Pogonin and A. K. Chibisov, *ibid.*, 1980, **35**, 70.
11. *Idem*, *Zh. Prikl. Spektrosk.*, 1980, **33**, 850.
12. G. I. Romanovskaya, L. S. Atabekyan and A. K. Chibisov, *Teoret. Exper. Khim.*, 1981, **17**, 282.
13. L. V. Ryzhova, G. V. Myasoedova, L. M. Khitrov, O. V. Stepanets and L. Khakimchodzhaev, *Radio-khimiya*, 1980, **22**, 284.
14. M. A. Kremneva, O. F. Mironova and G. I. Romanovskaya, *Zh. Analit. Khim.*, 1984, **39**, 847.

STERIC AND HYDROPHOBIC EFFECTS OF SUBSTITUENTS IN EXTRACTION OF METAL COMPLEXES WITH *O,O*-DIALKYLDITHIOPHOSPHORIC ACIDS

V. F. TOROPOVA, A. R. GARIFZYANOV and I. E. PANFILOVA

Faculty of Chemistry, U.I.Ul'yanov-Lenin State University, Lenina, 18 Kazan, 420008, USSR

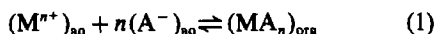
(Received 15 October 1985. Revised 25 March 1986. Accepted 9 August 1986)

Summary—The two-phase stability constants (equilibrium constants) of metal complexes MA_n [$M^{n+} = Ni(II), Zn(II), Cd(II), Pb(II), Tl(I), In(III)$] with a series of *O,O*-dialkyldithiophosphoric acids in the system water-organic solvent have been determined. By use of correlation analysis the role of the steric and hydrophobic effects of the substituents at the phosphorus atom on the stability constant β_n and distribution constant P of the complexes has been elucidated. The data obtained are of use for determining the relationships in the influence of structure of a reagent on its extraction properties and on the conditions for practical application of *O,O*-dialkyldithiophosphoric acids for metal extraction.

A great many organic compounds are suitable for extraction of metals from aqueous solution, but the search for new extractants continues, owing to the growing role of extraction methods in analysis and technology. In this context data on the interrelation between the structure of organic reagents and their extraction properties acquire especial significance.¹

The *O,O*-dialkyldithiophosphoric acids (DTPA), first proposed by Busev and Ivaniutin² as analytical reagents, have found wide application in various methods of analyses. The availability of a wide variety of dithiophosphoric acid derivatives leads to choice of these compounds as an ideal model system for investigation of the influence of substituents in ligand molecules on the stability and distribution of the corresponding metal chelates. To examine the possibility of applying the principle of linear free-energy change for the quantitative estimation of substituent effects on the extraction properties of DTPA, the extraction of metal ions by a series of DTPA of different structure was investigated.

In extraction in a two-phase system of water and organic solvent there exists the equilibrium:



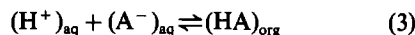
where $M = Ni(II), Zn(II), Cd(II), Pb(II), Tl(I), In(III)$; $A^- =$ anion of DTPA, $(RO)_2P(S)S^-$.

The equilibrium constant (or two-phase stability constant) is equal to the product of the stability constant of the complex MA_n in the aqueous phase, β_n and the distribution constant P :

$$P\beta_n = \frac{[MA_n]_{org}}{[M^{n+}]_{aq}[A^-]_{aq}^n} \quad (2)$$

When the extraction proceeds in acid solutions, the distribution of DTPA must also be taken into ac-

count:



The equilibrium constant of this process (extraction constant of DTPA) is equal to K_d/K_a , where K_d is the distribution constant of HA between the aqueous and organic phases and K_a is the acid dissociation constant of HA in the aqueous phase.

EXPERIMENTAL

Reagents

O,O-Dialkyldithiophosphoric acids were synthesized and purified by a literature method.³ Heptane, benzene, toluene, carbon tetrachloride and chloroform were used as the solvents.

Procedure

Extraction was performed in test-tubes at constant temperature ($25 \pm 0.2^\circ$) by shaking for 1 hr equal volumes (8 ml) of the aqueous and organic phases, the concentration of metal in the aqueous phase being 5×10^{-4} – $10^{-3}M$. The ionic strength and acidity of the solutions were maintained by adding the appropriate amounts of perchloric acid and sodium perchlorate or, in the case of Pb(II) and Cd(II), hydrochloric acid and sodium chloride. The equilibrium concentration of free metal ions in the aqueous phase was determined by complexometric titration or polarographically.

RESULTS AND DISCUSSION

The values of K_d/K_a were obtained by the method of Wingefors.⁴ The values of $P\beta_n$ were calculated by using the equation

$$\log D = n \log[A^-] + \log(P\beta_n) \quad (4)$$

where D is the distribution ratio for the metal.

The dependence of $\log D$ on $\log[A^-]$ is a straight line with slope equal to the charge on the metal ion

Table 1. Logarithms of the two-phase stability constants ($\log P\beta_n$) of complexes $M[S(S)P(OR)_2]_n$ in the systems $1M$ $HClO_4/NaClO_4$ -organic solvent, at $25 \pm 0.2^\circ$ (the error in $\log P\beta_n$ is estimated to be ± 0.05)

R	$\log P\beta_n$											
	Ni(II)					Zn(II) CCl ₄	In(III) CCl ₄	Cd(II) ^a toluene	Ti(I)		Pb(II) ^b	
	C ₇ H ₁₆	CCl ₄	toluene	C ₆ H ₆	CHCl ₃				toluene	CHCl ₃	CCl ₄	toluene
Me	—	0.18	0.59	—	1.58	0.09	2.75	2.51	1.61	1.69	3.55	—
Et	1.68	3.34	3.73	4.06	4.45	2.70	6.88	5.22	2.90	3.00	6.33	8.84
Pr	4.17	5.93	6.34	6.87	7.11	5.13	10.80	7.55	4.22	4.28	9.15	11.62
i-Pr	4.82	6.65	6.97	7.43	7.98	5.44	11.92	7.95	4.14	4.20	9.34	11.78
Bu	6.93	8.68	9.14	9.41	9.97	7.72	14.78	10.32	5.50	5.62	11.93	14.37
i-Bu	6.53	8.20	8.62	9.07	9.32	7.49	14.36	10.03	5.29	5.38	11.58	13.83
s-Bu	7.90	9.32	10.08	10.52	10.92	8.29	15.55	10.56	5.53	5.60	12.30	14.52
t-Bu	—	—	—	11.49	11.99	8.85	—	11.78	—	—	13.81	16.36
n-C ₅ H ₁₁	9.50	11.08	11.77	12.02	12.59	10.37	19.00	12.83	6.36	6.48	14.55	17.17
i-C ₅ H ₁₁	9.13	10.38	11.06	11.69	12.02	10.04	17.81	12.48	6.40	6.77	14.30	16.69
(C ₂ H ₅) ₂ CH	10.56	12.08	12.31	—	—	10.88	19.44	13.01	6.52	—	14.80	—
n-C ₆ H ₁₃	—	—	—	14.63	15.07	13.06	23.19	15.58	—	8.11	17.29	19.96

^aThe ionic strength of the aqueous phase ($\mu = 1$) were maintained with HCl and NaCl.

^b $\mu = 2$ (HCl/NaCl).

(n). Since the total concentration of metal in the solution did not exceed $5 \times 10^{-4}M$, any possibility of forming polynuclear complexes could be disregarded. The values found for $\log K_d/K_a$ and $\log P\beta_n$ are given in Tables 1 and 2.

As can be seen, the two-phase stability constants depend on the length and the branching of the alkyl groups. In all cases the values of $P\beta_n$ increase with increase in the carbon atom number of the substituents. The dependence on the branching is more complicated. Since $P\beta_n$ is a composite value, the interpretation of the results obtained requires consideration of the substituent effects on both the stability constant and the distribution constant.

Since the generally accepted opinion^{5,6} is that the induction effect of alkyl groups is constant, it may be supposed that changing an alkyl substituent should not seriously affect the energy of the metal-ligand bond. It might then be concluded that any change in the stability constants would be mainly due to steric effects. The influence of alkyl groups on the value of P is connected to a considerable degree with the solvent effects: the influence of substituents on the solvation of the ligand and of the complex. It is well

known that an increase in anion size leads to an increase in solvation free energy. The effect on the solvation of the neutral chelates will largely depend, as a rule, on the entropy effects: increasing the size of the alkyl groups and, consequently, the size of the complex molecules, results in destruction of the water structure and thus in a free energy gain. In this case, both factors will promote increase of the stability constants with increase in alkyl group size. As regards the influence of substituents on the distribution constant of the complex, a large number of data on the distribution of homologous series of organic compounds are present in the literature.⁷ As a rule, the higher members of a series are more easily transferred into the organic phase. Since it was shown in our previous communication⁸ that the influence of substituents on the stability constant of DTPA complexes can be described by a one-parameter correlation equation using Taft E_s constants, characterizing the steric effects of substituents,

$$\log \beta_n = a_0 + a_1 \Sigma E_s \quad (5)$$

and as the hydrophobic constants⁹ (π) can be applied for description of the influence of substituents on the

Table 2. Logarithms of the extraction constants (K_d/K_a) of O,O -dialkyldithiophosphoric acids $(RO)_2P(S)SH$ in the systems $1M$ $HClO_4/NaClO_4$ (or $HCl/NaCl$)—organic solvent (estimated uncertainty ± 0.02)

R	$\log K_d/K_a$					$-\Sigma E_s$	$\Sigma \pi$
	CCl ₄	C ₆ H ₆	toluene	CHCl ₃	C ₇ H ₁₆		
Pr	1.71	1.99	1.88	2.40	—	0.78	1.06
i-Pr	1.99	2.22	2.11	2.71	—	1.86	0.86
Bu	3.03	3.22	3.15	3.66	2.10	0.80	2.06
i-Bu	2.96	3.14	3.03	3.56	2.00	0.70	1.86
s-Bu	3.39	3.56	3.44	4.01	2.48	1.94	1.86
t-Bu	4.11	—	4.16	—	—	3.48	1.66
n-C ₅ H ₁₁	4.23	4.49	4.42	—	3.36	0.80	3.06
i-C ₅ H ₁₁	4.02	4.19	4.11	4.66	3.10	0.80	2.86
(C ₂ H ₅) ₂ CH	4.64	4.71	4.68	5.27	3.80	1.94	2.86
c-C ₆ H ₁₁ *	4.68	—	4.70	—	—	1.96	2.82

*Cyclohexene.

Table 3. Parameters of the correlation equations $\log P\beta_n = a_0 + n(a_1\Sigma E_s + a_2\Sigma\pi)$

M ²⁺	Organic solvent	a ₀	-a ₁	a ₂	R*	s†
Ni(II)	CHCl ₃	3.65	0.54 ± 0.04	1.28 ± 0.03	0.9980	0.26
Ni(II)	C ₆ H ₆	3.30	0.54 ± 0.04	1.29 ± 0.03	0.9978	0.23
Ni(II)	toluene	2.99	0.46 ± 0.06	1.30 ± 0.04	0.9983	0.24
Ni(II)	CCl ₄	2.52	0.50 ± 0.04	1.27 ± 0.03	0.9992	0.16
Ni(II)	C ₇ H ₁₆	0.80	0.50 ± 0.05	1.30 ± 0.03	0.9985	0.18
Zn(II)	CCl ₄	2.16	0.34 ± 0.03	1.27 ± 0.02	0.9991	0.18
Cd(II)	toluene	4.61	0.36 ± 0.05	1.26 ± 0.04	0.9973	0.29
In(III)	CCl ₄	6.09	0.37 ± 0.04	1.30 ± 0.02	0.9987	0.32
Tl(I)	CHCl ₃	2.83	0.19 ± 0.09	1.25 ± 0.04	0.9972	0.16
Tl(I)	toluene	2.78	0.16 ± 0.07	1.22 ± 0.03	0.9975	0.14
Pb(II)	toluene	8.17	0.44 ± 0.06	1.34 ± 0.04	0.9964	0.37
Pb(II)	CCl ₄	5.76	0.43 ± 0.06	1.32 ± 0.04	0.9965	0.36

*Regression coefficient

†Standard deviation.

distribution constant P , we use a two-parameter correlation equation accounting for both the steric and hydrophobic effects of the substituents:

$$\log(P\beta_n) = a_0 + n(a_1\Sigma E_s + a_2\Sigma\pi) \quad (6)$$

where ΣE_s is the sum of the steric constants of the substituents on the phosphorus atom, $\Sigma\pi$ is the sum of the hydrophobic constants of the substituents, and n is the stoichiometric coefficient in equation (1).

It turns out that equation (6) well describes the influence of alkyl groups on $P\beta_n$ for DTPA complexes and on K_d/K_a for DTPA. The parameters of the correlation equation are given in Tables 3 and 4.

The coefficient a_2 , which reflects the sensitivity of the series to the hydrophobic effects of the substitu-

ents, is virtually independent of the central ion and of the organic solvent, whereas the coefficient a_1 , which reflects the sensitivity of the series to the steric effects of the substituents, shows an appreciable dependence on the nature of the metal ion. Hence, it follows that by variation of the substituents, the conditions for preconcentration and separation of metals can be optimized to a certain degree with DTPA as the extracting agent.

The separate determination of the P and β_n values is difficult, as the equilibrium concentration of the complex in the aqueous phase is very low, owing to the high value of P . At the same time, the stability constants of the DTPA complex in aqueous solutions cannot readily be determined, owing to their low

Table 4. Parameters of correlation equations $\log K_d/K_a = a_0 + a_1\Sigma E_s + a_2\Sigma\pi$

Organic solvent	a ₀	-a ₁	a ₂	R	s
C ₇ H ₁₆	-0.90	0.42 ± 0.05	1.30 ± 0.03	0.9978	0.09
CCl ₄	-0.11	0.41 ± 0.02	1.28 ± 0.02	0.9912	0.08
C ₆ H ₅ CH ₃	0.06	0.50 ± 0.03	1.27 ± 0.02	0.9955	0.07
C ₆ H ₅	0.18	0.55 ± 0.02	1.26 ± 0.01	0.9993	0.04
CHCl ₃	0.59	0.58 ± 0.03	1.26 ± 0.02	0.9992	0.05

Table 5. Logarithms of stability constants ($\log \beta_2$) in the water-propan-2-ol solutions and of the distribution constants ($\log P$) in the system 1M HClO₄/NaClO₄-CCl₄ for the nickel *O,O*-dialkyldithiophosphates Ni[S(S)P(OR)₂]₂ at 25 ± 0.2°

R	25% H ₂ O	40% H ₂ O	60% H ₂ O	100% H ₂ O (extrapol.)	log P
Me	2.04	0.76	-0.28	-1.62	1.80
Et	2.73	1.49	0.47	-0.88	4.22
Pr	3.01	2.06	1.01	-0.47	6.40
i-Pr	4.71	3.59	2.49	1.09	5.56
Bu	3.19	2.11	1.13	-0.37	9.05
i-Bu	3.44	2.40	1.49	0.13	8.07
s-Bu	5.51	4.47	3.65	2.08	7.24
t-Bu	8.90	7.65	6.49	5.23	—
n-C ₃ H ₁₁	3.20	1.93	1.11	-0.37	11.45
i-C ₃ H ₁₁	3.27	2.12	1.42	0.03	10.35
(C ₂ H ₅) ₂ CH	6.51	5.35	4.37	2.93	9.15
n-C ₆ H ₁₃	3.20	2.00	—	-0.39	—

solubility. The only way to solve this problem consists in determining the β_n values in aqueous organic solutions containing different concentrations of water, and extrapolating the results to 100% water. In that way, we have determined the β_2 values of nickel-DTPA complexes in water-propan-2-ol solutions containing 20, 40 and 60% v/v water. For all cases investigated, the change in β_2 from one medium to another is approximately the same, and the equilibrium constant of the complexation reaction ($K = \beta_2[\text{H}_2\text{O}]^6$) is only slightly affected by the composition of the aqueous alcohol solvent, *i.e.*, the change observed for a series of solvents is considered to be due to the dilution effect.⁹ The values of β_2 found by extrapolation to purely aqueous medium are presented in Table 5.

It is interesting that the influence of alkyl groups on the distribution constants P of the complexes examined can also be described by a two-parameter correlation equation

$$\log P = 4.53 + 2(0.49 \Sigma E_s + 1.25 \Sigma \pi) \quad (7)$$

with a standard deviation of 0.4 and regression coefficient 0.995. The coefficient a_1 has a positive value, *i.e.*, unlike the stability constants, the P values

decrease with increase in the steric effect of the alkyl groups.

In conclusion, it should be noted that there is a possibility of using these data in analytical chemistry. Knowledge of the extraction equilibrium constants and correlations between the extraction properties of DTPA and their structure allows a quantitative approach to the choice of proper reagents and estimation of the optimal conditions for preconcentration or separation of different metal ions.

REFERENCES

1. V. S. Shmidt, *Usp. Khim.*, 1978, **47**, 1755.
2. A. I. Busev and M. I. Ivaniutin, *Tr. Komiss. po Analit. Khim. Akad. Nauk SSSR*, 1960, **11**, 172.
3. P. S. Pishchimuka, *Zh. Russ. Fiz.-Khim. Obshchest.* 1912, **44**, 1406.
4. S. Wingefors, *Acta Chem. Scand.*, 1980, **A34**, 289.
5. D. F. DeTar, *J. Am. Chem. Soc.*, 1980, **102**, 7988.
6. M. Charton, *ibid.*, 1979, **99**, 5687.
7. A. Leo, C. Hansch and D. Elkins, *Chem. Rev.*, 1971, **71**, 525.
8. V. V. Ovchinnikov, A. R. Garifzyanov and V. F. Toropova, *Zh. Obshch. Khim.*, 1983, **53**, 1262.
9. V. I. Belevantsev and V. A. Fedorov, *Koord. Khim.*, 1977, **3**, 638.

PHOTOMETRIC DETERMINATION OF TUNGSTEN IN ROCKS WITH TRIHYDROXYFLUORONES

V. A. NAZARENKO, V. P. ANTONOVICH and N. A. VESCHIKOVA

A. V. Bogatsky Physico-Chemical Institute, Academy of Sciences of the Ukrainian SSR, Odessa, USSR

(Received 15 October 1985. Revised 20 December 1985. Accepted 9 August 1986)

Summary—The interaction of tungsten(VI) with a series of 2,3,7-trihydroxyfluorones in the presence of cationic and non-ionic surfactants has been studied. Optimal conditions for the formation of the complexes and their spectrophotometric determination have been found. Possible mechanisms for the effect of the surfactants are suggested. The method developed has been applied to determination of trace tungsten in rocks and silts.

Various techniques have been proposed for determination of tungsten in magmatic and sedimentary rocks.¹⁻³ Thiocyanate and toluene-3,4-dithiol have been used as photometric reagents. Preliminary concentration of tungsten is often necessary by ion-exchange,³ or extraction or precipitation with α -benzoinoxime or dithiol,² owing to the low sensitivity and selectivity of some methods, and rather a large sample is taken for the analysis. To improve the sensitivity and selectivity of photometric determination of tungsten in rocks it would seem profitable to examine the use of more sensitive reagents than thiocyanate or dithiol. We have found that 2,3,7-trihydroxyfluorone and 3,4,5-trihydroxyfluorone derivatives give very sensitive reactions with tungsten in the presence of surfactants, with an accompanying extension of the reaction conditions towards higher acidity.⁴⁻⁷ However, the 2,3,7-trihydroxyfluorones are the more sensitive reagents, and we have extended their investigation to include some further derivatives, in the presence of cetylpyridinium (CP) and cetyltrimethylammonium (CTMA) ions as representative cationic surfactants, and syntanol, Triton X-100 and OC-20 as representative non-ionic surfactants. The trihydroxyfluorones tested were:

EXPERIMENTAL

Reagents

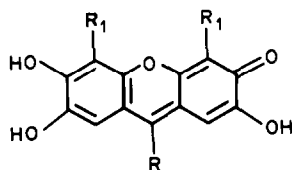
A $1 \times 10^{-3}M$ solution of sodium tungstate in 0.5M sodium hydroxide was used. The PF, SF and DSPF solutions ($1-2 \times 10^{-3}M$) were prepared in 0.06M hydrochloric acid in ethanol, and $5 \times 10^{-4}M$ solutions of DBPF and TBSF were prepared in a 1:1 v/v mixture of water and ethanol; solutions were made on the day of use. A 1% solution of gelatin was prepared as well as 0.01M solutions of the cationic surfactants, 1 and 10% solutions of the non-ionic surfactants, and 0.01M sodium citrate solution. The pH was adjusted with hydrochloric acid, sulphuric acid, ammonia, and ammonium acetate buffer solutions.

Procedure

The required quantities of acid or buffer solution, ethanol, sodium citrate, surfactant or gelatin were placed (in that order) in a 25-ml standard flask, followed by the trihydroxyfluorone solution and the tungsten solution. Sodium citrate was added to prevent hydrolysis of the tungsten. The combining ratio of tungsten and trihydroxyfluorone was determined spectrophotometrically by the isomolar series, molar ratio and isobestic point methods. The interaction between the binary tungsten-trihydroxyfluorone complexes and the surfactant was examined by the equilibrium shift method.

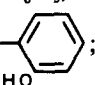
Procedure for rock analysis

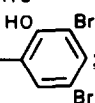
Decompose the sample (0.25-0.50 g) in a platinum dish with concentrated sulphuric acid (2.0-2.5 ml) and concen-

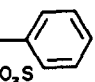


R = $-C_6H_5$, R₁ = H (phenylfluorone, PF);

R = $-C_6H_5$, R₁ = Br (dibromophenylfluorone, DBPF);

R = ; R₁ = H (salicylfluorone, SF);

R = ; R₁ = Br (tetrabromosalicylfluorone, TBSF);

R = ; R₁ = H (disulphophenylfluorone, DSPF).

trated hydrofluoric acid (10 ml). Before the decomposition samples containing carbonates should be treated with hydrochloric acid followed by evaporation to dryness, and shales and silts should be ignited at 450–500°. Evaporate the acid mixture till fumes of SO_3 appear, cool, add water (2–3 ml) and evaporate again to yield the moist salts. Cool, take up in water, oxidize with hydrogen peroxide, then filter if necessary through a sintered glass filter (porosity 4), neutralize with ammonia to pH 5–7, add concentrated hydrochloric acid (5 ml), evaporate to 10 ml, add 1 ml of 2.5% solution of titanium(III) chloride in concentrated hydrochloric acid and boil for 5–10 min. To the cooled solution add 1 ml of 0.4% suspension of zinc dithiolate complex in ethanol, adjust the hydrochloric acid concentration to 6*M* and heat on a water-bath for 10 min. Cool, and shake with 5 ml of chloroform for 2 min. Separate the extract and evaporate it to dryness in a platinum dish, then ignite in a muffle furnace at 500° for 10–15 min. Cool, add 2 ml of 1% sodium carbonate solution and 3 drops of saturated potassium chlorate solution, evaporate to dryness and fuse at 750–800° for 2–3 min. Leach the cooled fusion cake with water (5–7 ml), add 2.5 ml of 20% hydrazine hydrochloride solution, 5 ml of 5% mannitol (or sorbitol) solution and 2.5 ml of 10% EDTA solution. Boil for 3–4 min to reduce the volume to 10–12 ml, and cool. Add 0.5 ml of 0.01*M* sodium citrate, 4 ml of 6*M* hydrochloric acid, 0.5 ml of 5% ascorbic acid solution, 1 ml of 1% ammonium fluoride solution, 1.5 ml of 0.002*M* salicylfluorone and 2 ml of 0.01*M* CP or CTMA and dilute to volume with water, in a 25-ml standard flask. Measure the absorbance 20 min later, at 518 nm, in a 5-cm cell against a reagent blank carried through the entire procedure. Construct a calibration graph from the absorbances for known quantities of tungsten (0–10 μg) and the amounts of hydrazine hydrochloride, mannitol, EDTA, sodium citrate, hydrochloric acid, ascorbic acid, ammonium fluoride, salicylfluorone and CP or CTMA used in the procedure for samples.

RESULTS

Study of the reactions of tungsten(VI) with the trihydroxyfluorones, in presence of gelatin as stabilizing agent, showed as in previous work⁴ that in acid medium a single coloured complex is formed; with PF and DBPF as reagent (R) the W:R ratio is 1:2 and with SF and TBSF it is 1:1. The reagents brominated in the xanthene ring react at greater acidity (pH 2–2.5 for PF and SF and pH 0.5–1.0 for DBPF and TBSF). To stabilize the gelatin systems the addition of up to 30% ethanol is necessary. A higher ethanol content decreases the absorbance. The surfactant systems require a lower ethanol content.

Introduction of a cationic surfactant instead of gelatin as stabilizing agent shifts the complex formation into a still more acid region, this effect being considerable for sulphate solutions and DBPF and TBSF. Use of the non-ionic surfactants gives a smaller shift into the acid region, but the effect of the cationic and non-ionic surfactants on the spectrophotometric characteristics is similar. The use of non-ionic surfactant produces an unusual tungsten-trihydroxyfluorone combining ratio in some cases.

Figure 1 shows the absorption spectra of the tungsten-PF complex in the presence of CP at different acidities. Introduction of surfactants into the system results in a hyperchromic shift in the

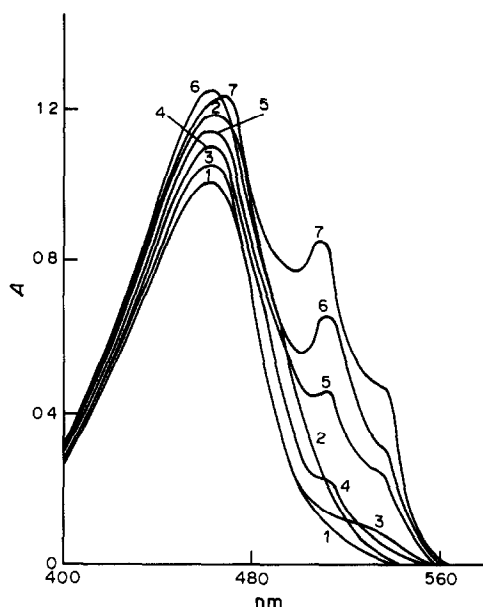


Fig. 1. Absorption spectra of tungsten phenylfluoronate in the presence of CP at different acidities: 2×10^{-6} *M* W; 1×10^{-5} *M* PF; 1×10^{-3} *M* CP; 1×10^{-4} *M* sodium citrate; 10% of ethanol; 2-cm cell. Curves 1 and 2, reagent blank; 1, 1*M* H_2SO_4 ; 2, pH 1.3. Curves 3–7, complexes; $[\text{H}_2\text{SO}_4]$, *M*: 3, 1.0; 4, 0.75; 5, 0.5; 6, 0.4; 7, 0.1.

spectra, and the appearance of the band at 505–515 nm and the shoulder at 540 nm, the intensity of which depends on the solution pH and the ethanol and surfactant concentrations. Similar results were obtained for all the trihydroxyfluorones and surfactants studied.

The absorption spectra do not in general change with surfactant concentration except for the band at 505–515 nm, which increases in intensity with surfactant concentration up to the critical micelle concentration (CMC) and then becomes constant and independent of surfactant concentration. Figure 2 shows the dependence of the surface tension and absorbance of the solution on the surfactant concentration for the system W–DSPF–CP. Maximum absorbance and minimum surface tension occur for CP concentrations greater than the CMC.

To stabilize the tungsten-trihydroxyfluorone-surfactant systems the addition of ethanol is necessary. The maximum absorbance is obtained with 2–10% v/v ethanol.

In acid medium up to pH 3 the systems give only one coloured complex, except for the W–SP–CTMA and W–SP–CP systems in sulphate medium, which yield a mixture of complexes. In most of the systems studied there is no evidence, over a wide range of surfactant concentrations, of formation of stoichiometric ternary complexes. The conditions for complex formation in the systems studied, and the spectrophotometric characteristics of the complexes, are summarized in Table 1.

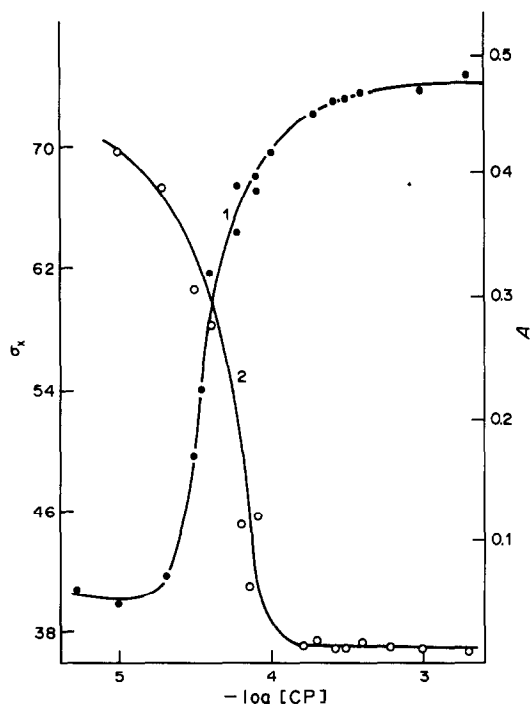


Fig. 2. Dependence of absorbance (1) and surface tension (2) of the system W-DSPF-CP on CP concentration in solution: $2 \times 10^{-6}M$ W; $1 \times 10^{-3}M$ DSPF; $1 \times 10^{-4}M$ sodium citrate; 1% of ethanol; pH 1.0 (HCl).

DISCUSSION

From comparison of the experimental results with the literature data it may be concluded that the mechanisms of formation of tungsten and molybdenum complexes with 2,3,7-trihydroxyfluorones are similar.⁸⁻⁹ As for molybdenum, optimal effects on the light-absorption characteristics of the tungsten trihydroxyfluoronates appear at surfactant concen-

trations at CMC level and above. This proves the decisive role of the surfactant micelles in stabilization of the complexes. Presumably the micelles react with the trihydroxyfluorone molecules through acid groups which do not take part in co-ordination of the metal ion. The tungsten ions react with the fluorone molecules fixed on the micelles. That is why the spectra of the complexes formed in the presence of any stabilizing agents (gelatin, cationic surfactants, non-ionic surfactants) are analogous. Since this fixation of the trihydroxyfluorone prevents aggregation of the tungsten complexes and promotes the production of finely-dispersed light-absorbing particles within the solution, hyperchromic shifts are observed in the absorption spectra. The extraordinary variation in tungsten-trihydroxyfluorone ratio from 1:1 to 1:4 for different trihydroxyfluorones and different surfactants is due to a variety of interactions that we have not yet fully elucidated. The sizes and hydrophobic properties of the trihydroxyfluorones and surfactant micelles studied are different, and the form, structure, and "capacity" of the surfactant micelles also differ, which determines the possibilities of co-ordination of different numbers of trihydroxyfluorone ions by the tungsten(VI). It is possible that the Triton X-100 micelles interact not just with single PF and SF molecules but also with their hydrogen-bonded aggregates, which could account for the 1:4 complexes observed. This is perhaps substantiated by the observation that the complexes of composition 1:4 are not the most intensely coloured, *i.e.*, the increase in the molar absorptivity of the complex in the presence of surfactants is not due to increased co-ordination capacity of the metal ion. The tungsten trihydroxyfluoronates can be stabilized both by cationic surfactants (CP, CTMA) and non-ionic ones (Triton X-100, OC-20). Tungsten salicylfluoronate formed in the presence of these

Table 1. Characteristics of tungsten complexes with trihydroxyfluorones in the presence of surfactants

Trihydroxyfluorone + surfactant	λ , nm reagent	λ , nm complex	pH _{opt} /acidity _{opt}	Ethanol, W: trihydroxyfluorone %	ϵ , 10 ⁴ l. mole ⁻¹ . cm ⁻¹	
PF + CP	464	510	0.7-0.9 (H ₂ SO ₄)	6-18	1:1	10.1
PF + CTMA	480	508; 540	0.9-1.2 (H ₂ SO ₄)	2-20	1:1	8.4
PF + Triton X-100	472; 496	512	1.6-2.0 (0.1M H ₂ SO ₄)	8-20	1:4	5.6
DBPF + CP	472; 496	518; 546	1M H ₂ SO ₄ -pH 1.4	4-10	1:1	7.5 (518) 5.0 (546)
DBPF + CTMA	480	528; 550	0.5-1.0M H ₂ SO ₄	2-20	1:2	7.8
DBPF + Triton X-100	480	530	0.1-0.3M H ₂ SO ₄	2-16	1:2	5.5
SF + CP	472	518; 536	0.4-1.0M HCl	2-6	1:1	12.4
SF + CP	470	512; 534	0.3-0.6M H ₂ SO ₄	2-6	1:1 (512) 1:2 (534)	
SF + CTMA	470	512; 532	0.4-0.7M H ₂ SO ₄	2-6	1:2 (512) 2:3 (532)	13.6
SF + Triton X-100	480	512	1.4-1.6 (H ₂ SO ₄)	5-15	1:4 (512)	13.2
SF + syntanol	472	517	1.0-2.0 (HCl)	2-4	1:4	7.4
SF + OC-20	470	514	1.6-2.2 (H ₂ SO ₄)	2-4	1:2	13.6
TBSF + CP	480; 512	564	1.2-2.2 (H ₂ SO ₄)	5-15	1:2	7.7
TBSF + CTMA	480; 512	528; 552	1M H ₂ SO ₄ -pH 1	2-6	1:2 (552)	5.5
TBSF + Triton X-100	480; 512	540; 560	0.8-1.6 (H ₂ SO ₄)	2-20	1:2	1.6
DSPF + CP	464	500	1.0-1.4 (HCl)	1	1:1	6.7

Table 2. Results for 8 parallel determinations of tungsten in geological samples

Sample type	Sample reference mark	W found,* 10 ⁻⁴ %	Relative std. devn., %
Alkaline granite	CF-3	1.0 ± 0.07	10
Metamorphized shale	CCJ-1	1.51 ± 0.14	11
Dolomitic stromalitic limestone	CH-2	0.22 ± 0.07	11
Dolomitic limestone containing feldspar	CH-3	3.28 ± 0.05	2
Carbonate-silicate rocks	CGXM-1	0.90 ± 0.04	1
Aluminium silicate rocks	CGXM-2	0.85 ± 0.05	1
Carbonate-silicate rocks	CGXM-3	3.03 ± 0.09	1
River silt	CGX-1	2.41 ± 0.06	7
River silt	CGX-3	2.58 ± 0.06	7
River silt	CGX-5	12.5 ± 0.2	2

*95% confidence limits.

surfactants is one of the most sensitive of the complexes of this metal with organic analytical reagents known today.

Unfortunately, the selectivity is rather poor. Nb, Ta, Ti, Zr, Hf, Mo, Sb, Sn and Fe all interfere. The effect of some of these elements can be eliminated by preliminary extraction of the tungsten with α -benzoinoxime or dithiol, and several of them, molybdenum in particular, can be masked by a mixture of EDTA, hydrazine hydrochloride and mannitol (or sorbitol). Ascorbic acid and ammonium fluoride are finally added to mask any traces of iron(III) introduced with the masking mixture. The tolerance limits (μg) in the determination of 0.2–1 μg of tungsten are Nb (20), Ta (30), Mo (250), Sn (200) and (mg) Zr (0.5), V (0.5), Cr (>1), Fe (>4), Cu, Ni, Zn, Mn (10–20).

The method has been used to determine traces of tungsten in nickel-based alloys and alkali metal halides and perrhenates.¹⁰ We have used the technique for determination of tungsten in a number of rocks and silts intended as standard samples for issue by the Institute of Geochemistry, Siberian Branch of the USSR Academy of Sciences (Table 2). The validity of the method has been established by analysis of a standard sample of albitized granite,

CF-1A, [certified value $2.3 \pm 0.4 \times 10^{-4}$ % W; tungsten content found $2.28 \pm 0.06 \times 10^{-4}$ % (95% confidence limits), $n = 21$; relative standard deviation 6%] and of a nickel alloy (certified W content 0.035%; content found 0.0335 ± 0.0004 %).

REFERENCES

1. A. I. Busev, V. M. Ivanov and T. A. Sokolova, *Analytical Chemistry of Tungsten* (in Russian), Nauka, Moscow, 1976.
2. N. A. Stepanova and G. A. Yakunina, *Zh. Analit. Khim.*, 1962, 17, 858.
3. K. Kawabuchi and R. Kuroda, *Talanta*, 1970, 17, 67.
4. V. A. Nazarenko and V. P. Antonovich, *Trioksisfluorony*, Nauka, Moscow, 1973.
5. V. A. Nazarenko, G. I. Ibragimov, E. N. Poluektova and G. G. Shitareva, *Zh. Analit. Khim.*, 1978, 33, 938.
6. V. P. Antonovich, G. I. Ibragimov, E. M. Nevskaya, E. I. Shelikhina and M. A. Chernysheva, *ibid.*, 1979, 34, 81.
7. V. P. Antonovich, M. M. Novoselova and V. A. Nazarenko, *ibid.*, 1984, 39, 1157.
8. V. A. Nazarenko, M. M. Novoselova, Yu. M. Chernoberezhsky, E. V. Golikova and V. P. Antonovich, *ibid.*, 1980, 35, 2331.
9. M. M. Novoselova, E. V. Golikova, Yu. M. Chernoberezhsky and V. P. Antonovich, *ibid.*, 1981, 36, 914.
10. V. A. Nazarenko, N. A. Veschikova, V. P. Antonovich and M. M. Novoselova, *Zavodsk. Lab.*, 1984, 50, No. 2, 7.

ELECTROCHEMICAL INVESTIGATION OF PALLADIUM COMPLEXES WITH ORGANIC SULPHIDES AND THEIR USE IN EXTRACTION DIFFERENTIAL PULSE POLAROGRAPHY

H. C. BUDNIKOV*

Faculty of Chemistry, V.I. Ul'yanov-Lenin State University, Lenina 18, Kazan, 420008, USSR

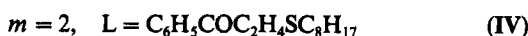
V. N. MAYSTRENKO and Yu. I. MURINOV

Faculty of Chemistry, Bashkirian State University, Frunze 32, Ufa, USSR

(Received 15 October 1985. Accepted 1 February 1986)

Summary—Dialkyl-, amino-, keto- and ketoaminosulphide complexes of palladium(II) are shown to undergo one- or two-step reduction in a mixed acetonitrile-toluene solvent containing Bu_4NClO_4 at 0.1M concentration. The half-wave potentials of the complexes show a certain dependence on the ligand structure, a positive shift of the potentials being caused by an increase in the π -acceptor ability of the ligands. The limiting currents are proportional to the concentration of the complex, according to the Ilkovič equation. Fast-scan differential pulse polarography was applied to the determination of palladium(II) in the organic phase after extraction of its complex with dihexylsulphide.

There are a number of papers and reviews dealing with the co-ordination chemistry of ligands and chelates containing the thio-ether group in their structure.¹ These organic compounds are of some importance on account of their biological activity and also their usefulness as extraction reagents for the concentration and determination of metal ions.² The analytical application of organic extractants for the separation and determination of metals, in particular palladium, in the presence of the other platinum metals, is of special interest. This paper reports on the electrochemical reduction of palladium(II) complexes with organic sulphides, with composition PdL_mCl_2 , where



in an acetonitrile-toluene mixture at the dropping mercury electrode, and discusses the possibility of determining palladium(II) by fast-scan differential pulse polarography (FSDPP) with dihexylsulphide (DHS) as an extractant. The general principles of extraction polarography used in the investigation have been described in a review.³

EXPERIMENTAL

Apparatus

The electrochemical experiments were done with a PU-1 polarograph (USSR) for recording d.c. and a.c. polarograms, a dropping mercury electrode (d.m.e.) with $m = 1.96$ mg/sec at zero potential and controlled drop time $t = 0.21$ sec. Cyclic and FSDPP voltamperograms were obtained with a PA-3 polarograph and a stationary mercury drop electrode of type SMDE-1 (Czechoslovakia). All voltammetric measurements were made with a three-electrode cell at $25 \pm 0.1^\circ$ with $\text{Ag}/0.1M \text{AgNO}_3$ in acetonitrile as a reference electrode, and a platinum wire as an auxiliary electrode.

Reagents

The organic sulphides and palladium complexes were prepared as described in the literature.⁴⁻⁶ Their purity was checked by infrared spectroscopy and elemental analysis. Organic solvents were purified by the methods recommended in the literature⁷ and were kept over 4A molecular sieves. Tetrabutylammonium perchlorate (0.1M) was used as background electrolyte. The solutions were deoxygenated by a stream of argon. The purity of the electrolyte was checked by recording blank polarograms with the d.m.e. The base-line for the solvent mixture was run as a check on electrochemical purity.

Solutions

Measurements were made on a 2:3 v/v mixture of the extracting and ionizing solvents: 0.15M Bu_4NClO_4 in acetonitrile as ionizing solvent and 0.05M DHS in toluene as the extractant. Stock solutions of organic sulphides were prepared by accurate direct weighing. The buffer solutions for the extraction were prepared from reagents of high purity.

Extraction procedure

A 5-ml portion of 0.05M DHS in toluene and a 25-ml portion of 10^{-5} – $10^{-7}M$ aqueous solution of palladium(II) in 1M hydrochloric acid were shaken together in a separating funnel for 10 min. After separation of the phases by

*Author to whom correspondence should be addressed.

centrifuging, a 2-ml portion of the extract was transferred to a polarographic cell and 3 ml of 0.15M Bu_4NClO_4 in acetonitrile were introduced. The FSDPP voltamperogram was recorded after deaeration of the solution.

RESULTS AND DISCUSSION

Palladium(II) complexes with the ligands mentioned above show one reduction step in acetonitrile at the d.m.e. in the concentration range 10^{-5} – $5 \times 10^{-5}M$ (Fig. 1a), but those with the ligands II–IV, containing the keto-group, give a second reduction wave at more negative potentials, from -2.1 to -2.3 V. The experimental data indicate that this step arises from reduction of free ligand released during reduction of the complexed metal ion at less negative potentials. A number of electrochemical characteristics of some palladium(II) complexes are given in Table 1. Microcoulometric measurements indicate that two electrons react with one molecule of palladium(II) complex to give elemental palladium.

Cyclic voltamperograms show a pair of cathodic (i_{pc}) and anodic (i_{pa}) peaks corresponding to the d.c. waves. The peak current ratio (i_{pa}/i_{pc}) tends towards unity as the scan-rate is increased within the range 0.01–0.5 V/sec. Decrease of this ratio with decrease in scan-rate is thought to be due to degradation of the two-electron reduction product within the period from one scan to the next. Alternating current voltamperograms show one symmetric peak. Both the half-width of the a.c. peak (46–48 mV) and the slope of the plot of E_p vs. $\log(i_{lim} - i)/i$ (Table 1) indicate that the electrode process is close to being completely reversible. The reduction scheme may be as follows:



Comparison of the half-wave potentials for the reversible reduction of Pd(II) complexes (Table 1) and PdCl_2 ($E_{1/2} = -0.105$ V) shows the contribution of the metallic atomic orbitals to the localized valency molecular orbital energy to be essential. Therefore the fast degradation of the negatively charged product of the two-electron reduction, $[\text{PdL}_m\text{Cl}_2]^{2-}$, produces Pd and free ligand, this being noticeable at slow scan-rate. The reduction may also proceed by a one-electron transfer and simultaneous cleavage of a metal–ligand bond, owing to the relatively low atomic orbital energy of the central ion. The second

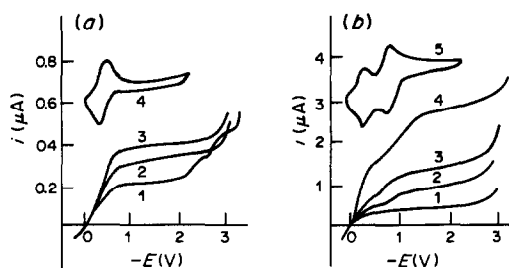


Fig. 1. a—Voltamperograms (d.c., curves 1–3; cyclic, curve 4) for palladium(II) complexes at $5 \times 10^{-5}M$ concentration in 0.1M Bu_4NClO_4 solution in acetonitrile, at the d.m.e.: 1—ligand II; 2—ligand V; 3 and 4—ligand I. b—Voltamperograms (d.c., curves 1–4; cyclic, curve 5) for the complex with ligand I in 0.1M Bu_4NClO_4 solution in acetonitrile at the d.m.e. Concentrations: 1— $5 \times 10^{-5}M$; 2— $1 \times 10^{-4}M$; 3— $1.5 \times 10^{-4}M$; 4 and 5— $3 \times 10^{-4}M$.

electron transfer occurs at potentials close to the $E_{1/2}$ values for the complexes, depending on the strength of the metal–ligand bond. Examples of analogous reduction mechanisms of metal complexes with organic ligands have been reviewed.⁷

If the concentration of the complexes is higher than $5 \times 10^{-5}M$, new waves appear at more negative potentials ($E_{1/2}$ from -0.58 to -0.67 V) on the voltamperograms, and the sum of the wave-heights corresponds to a two-electron reduction (Fig. 1b). The cyclic and a.c. voltamperograms both contain peaks in the potential range under discussion. The parameters of the peaks show the electrode process to be not fully reversible. Increasing the complex concentration increases the half-width of the a.c. peaks to 78–82 mV and decreases the current ratio i_{pa}/i_{pc} on the cyclic curves to 0.17–0.23. A second scan of the cyclic voltamperogram at the stationary mercury electrode shows only the second peak.

Figure 2a illustrates the dependence of the limiting currents of the complex with ligand V on its concentration. When the concentration is increased the diffusion current of the first wave reaches a limit when $C > 5 \times 10^{-3}M$. The height of the second wave is also dependent on the concentration, and the sum of the wave-heights is a linear function of concentration. The limiting current of the first step increases linearly with the height of the mercury column and

Table 1. Electrochemical data for the reduction of palladium(II) complexes at the d.m.e. in 0.1M Bu_4NClO_4 solution in acetonitrile; palladium concentration $5 \times 10^{-5}M$

Ligand	$-E_{1/2}$, V	i_{lim} , μA	$\Delta E/\Delta \log(i_{lim} - i)/i$, mV	i_{pa}/i_{pc} *	$\Delta \log i_{pc}/\Delta \log V$
I	0.255	0.36	35	0.92	0.54
II	0.270	0.24	35	0.87	0.57
III	0.360	0.30	37	0.84	0.58
IV	0.225	0.20	33	0.95	0.52
V	0.205	0.32	31	0.97	0.48
VI	0.200	0.30	32	0.98	0.49

*Scan-rate 0.5 V/sec.

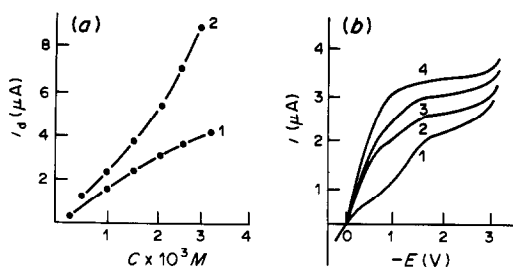


Fig. 2. *a*—The relationship between the limiting current of the reduction steps of the complex with ligand V, and the concentration; 1—the first step; 2—the second step. *b*—Polarograms of the palladium complex with ligand VI in 0.1M Bu_4NClO_4 solution in acetonitrile at the d.m.e. at various temperatures: 1—15°; 2—25°; 3—35°; 4—45°.

with temperature, at any concentration in the range $1-5 \times 10^{-5} M$.

The temperature coefficient is about 6–8% per degree, a value characteristic for reduction of adsorbed species. When the temperature reaches 45° the second waves for the complexes with ligands V and VI practically vanish (Fig. 2*b*) and only one step is recorded on the voltamperograms. The appearance of the second waves at high concentration indicates that the first reduction step is inhibited by the adsorbed film of the reduction product. The first wave corresponds to a process at the clean electrode surface and the second to one at the surface covered with electrolysis products. Adsorption of reduction products of Pd(II) complexes at the mercury electrode has been reported before.^{8,9} Interestingly, PdCl_2 has been shown to undergo a two-step reduction identical to the one described for the complexes.

The reversibility of the first reduction and its occurrence at the free electrode surface indicates that the $E_{1/2}$ values should be close to the standard reduction potentials (E_0). Hence, the shifts in $E_{1/2}$ may be considered to be a measure of the ligand effect on the electron transfer. The $E_{1/2}$ values for the complexes studied become more negative, for the following sequence of ligands: V, VI > IV > I > II > III. The data are in accordance with the idea that the properties of organic sulphides

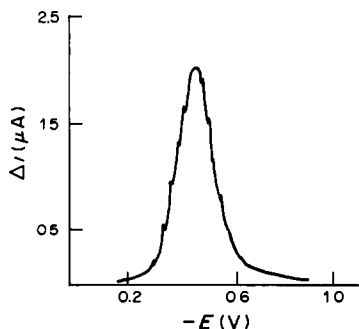


Fig. 3. The differential pulse polarogram of $10^{-6} M$ palladium(II) complex in 0.02M DHS/0.1M Bu_4NClO_4 solution in toluene-acetonitrile mixture (2:3), initial potential +0.3 V; pulse magnitude -50 mV; scan-rate 20 mV/sec.

Table 2. Determination of palladium in solutions with 1000-fold excess of Pt, Rh, Ru and Ir; 0.1M Bu_4NClO_4 solution in 2:3 toluene-acetonitrile mixture (extraction reagent 0.05M DHS in toluene)

Taken, $\mu\text{g/ml}$	Found, $\mu\text{g/ml}$
0.063	$0.059 \pm 0.003^*$
0.128	0.123 ± 0.004
0.250	0.240 ± 0.006
0.500	0.479 ± 0.010

* \pm Confidence limits ($n = 5$, $p = 0.95$).

as π -acceptors affect the reduction potentials of the complexes.¹⁰ Strengthening the π -acceptor properties of the ligand shifts the reduction potential of the palladium(II) complexes in general. However this relationship is not too clear: it is possible that the first three complexes are in *cis*-form, and the others in *trans*-configuration.

A linear relation between the limiting current and the concentration of the complexes (for concentrations below $5 \times 10^{-5} M$) was also found with the 3:2 acetonitrile-toluene mixture, which is of practical importance for the extraction-polarographic determination of Pd(II) in the presence of other platinum group metals. The usefulness of this method of analysis is based on the selectivity of the extraction of palladium dialkylsulphides from hydrochloric acid solution.² To lower the limit of detection the FSDPP method of determination was used. The relation between Δi_{max} and the concentration of palladium(II) in the organic phase is linear over the range 10^{-5} – $10^{-7} M$. Figure 3 shows the differential pulse voltamperogram of a $10^{-6} M$ Pd(II) solution in the 3:2 acetonitrile-toluene mixture in the presence of DHS. The limit of detection is 0.01 $\mu\text{g/ml}$.

To select the optimum conditions for the determination of palladium the influence of different factors on the limiting current of the extract was investigated. Artificial mixtures were used to show that Δi_{max} is practically constant for extraction from 1–4M hydrochloric acid. Extraction times greater than 10 min did not further improve the extraction efficiency, which was >98%. The optimum extraction conditions are listed in the experimental section. Results for the determination of palladium in the presence of 1000-fold excesses of platinum, rhodium, ruthenium and iridium are summarized in Table 2.

REFERENCES

- S. G. Murray and F. R. Hartley, *Chem. Rev.*, 1981, **81**, 365.
- N. G. Vanifatova, I. V. Seryakova and Yu. A. Zolotov, *Extraction of Metals by Neutral Sulphur-Containing Compounds*, p. 13. Nauka, Moscow, 1980.
- H. C. Budnikov and N. A. Ulakhovich, *Usp. Khim.*, 1980, **49**, 147.
- E. F. Challenger, *Aspects of the Organic Chemistry of*

- Sulphur*, p. 12. Butterworths, London, 1959.
5. V. P. Krivonogov, R. M. Shayakhmetova, V. I. Dronov, R. S. Enikeeva, Yu. E. Nikitin, N. L. Egutkin, A. S. Bodrova and L. V. Spirkin, *Zh. Prikl. Khim.*, 1981, **54**, 2505.
 6. B. E. Aires, J. E. Fergusson, D. T. Howarth and J. M. Miller, *J. Chem. Soc. A*, 1971, 1144.
 7. H. C. Budnikov, T. V. Troepolskaya and N. A. Ulakhovich, *Electrochemistry of Metal Chelates in Non-Aqueous Media*, Nauka, Moscow, 1980.
 8. V. I. Kravtsov and I. I. Shereshevskaya, *Elektrokhimia*, 1971, **7**, 618.
 9. A. A. Pozdeeva, G. A. Tolstikov, V. A. Chernova, S. I. Zhdanov and Yu. M. Yemilev, *Izv. Akad. Nauk SSSR (Ser. Khim.)*, 1983, 2241.
 10. Yu. N. Kukushkin, *Koord. Khim.*, 1981, **7**, 335.

LIQUID CHROMATOGRAPHY OF PALLADIUM AND NON-FERROUS METAL CHELATES WITH 1-(2-PYRIDYLAZO)-2-NAPHTHOL

YU. S. NIKITIN, N. B. MOROZOVA, S. N. LANIN, T. A. BOL'SHOVA,
V. M. IVANOV and E. M. BASOVA

Department of Analytical Chemistry, M. V. Lomonosov Moscow State University, Lenin Hills,
Moscow, USSR

(Received 15 October 1985. Revised 14 February 1986. Accepted 9 August 1986)

Summary—1-(2-Pyridylazo)-2-naphthol has been used for extraction concentration of palladium, copper, cobalt and nickel from aqueous solutions and subsequent separation of the chelates obtained, by means of high-pressure liquid chromatography. A technique for determining microamounts of palladium in aqueous solutions in the presence of 100-fold ratio of copper and 80-fold ratio of cobalt has been developed.

The rapid development of high-pressure liquid chromatography (HPLC) in recent years has considerably expanded the area of its application in science, technology and industry. In addition to the traditional fields, such as separation and determination of organic compounds and biologically active substances, and in environmental pollution monitoring, HPLC is widely used for inorganic systems for the separation and determination of metals both in the ionic state and in the form of organometallic and complex compounds.^{1,2} Chelates appear to be convenient species for the determination of some metals by HPLC,¹ since the structures and properties of chelates are close to those of organic compounds, which makes possible the direct transfer of the wide experience obtained in organic HPLC.

A combination of preliminary extractive concentration of chelates followed by chromatographic analysis of the extracts makes it possible to combine in a single technique the main advantage of HPLC, namely, fast and effective separation of complex multi-component mixtures, with the selectivity of complexation and extraction.

The high molar absorptivity of chelates in the ultraviolet and visible regions of the spectrum allows the use of the detector most widely used in liquid chromatography, the spectrophotometer. The main principles for selecting the chelating agents for use in HPLC are well known. The requirements are that each element should form only one complex with the reagent, and that the chelates should be stable in the conditions for the chromatographic separation (medium, pH, temperature), and have high molar absorptivity at the absorption maxima.¹

All the possible types of interaction of chelate complexes with silica gels have been identified,^{3,4} and mechanisms proposed for the separation of diethyl-dithiocarbamates⁵ and β -diketonates^{6,7} of metals by

thin-layer chromatography. Owing to the similarity of the adsorption process in two-dimensional and three-dimensional layers of a sorbent, these mechanisms can be used for interpretation of the chelate retention in HPLC.

At present HPLC is mainly being developed in terms of choosing the optimal chelating systems for metal separation.¹ Detection of platinum metals in the presence of non-ferrous metal impurities represents one of the important and not yet completely solved problems of the analytical chemistry of these metals. Separation and determination of the platinum metals in the form of their chelates holds a great deal of potential for solution of the problem. Use has been made⁸⁻¹¹ of the chromatographic behaviour of palladium chelates with quadridentate ligands (various substituted β -ketoimines and salicylaldehyde) to separate palladium from copper and nickel, but the palladium was not determined quantitatively. The most promising class of organic reagents for platinum metals, palladium in particular, since these tend to form complexes with donor S- and N-atoms, appears to be that of the heterocyclic azo-compounds which are widely used for their spectrophotometric determination.¹² 1-(2-Pyridylazo)-2-naphthol (PAN-2), one of this class of compounds, complies with all the requirements listed above for chelating agents useful in HPLC. PAN-2 has already been used for the separation and determination of iron, nickel, cobalt and copper by both normal-phase¹³ and reversed-phase¹⁴ HPLC.

This paper deals with a study of the chromatographic properties of the palladium, copper, nickel and cobalt chelates with PAN-2 and the development of an HPLC method which would combine preliminary extractive concentration of palladium with its determination in the presence of larger amounts of copper, nickel and cobalt.

EXPERIMENTAL

Palladium solution (0.935 mg/ml) was prepared by dissolving PdCl₂ (analytical grade) in 0.1M hydrochloric acid, and standardized gravimetrically with dimethylglyoxime.¹⁵ Palladium solutions of lower concentration were prepared by dilution with 0.01M hydrochloric acid. Copper, cobalt and nickel solutions were made from the pure nitrates and standardized complexometrically. Inorganic salts were removed from the PAN-2 reagent (Reanal, Hungary) by recrystallization from ethanol,¹⁶ and the absence of PAN-1 in the initial PAN-2 was checked by HPLC.¹⁷ The palladium(II) chelate was made according to an established procedure.¹⁸ Dimethylformamide (DMF) solutions of PAN-2 (10⁻³ or 10⁻²M) were used for complexation, the optimal pH values being attained by addition of hydrochloric acid and sodium hydroxide solution, and monitored potentiometrically. The conditions for separating Pd(II), Cu(II), Ni(II) and Co(III) by HPLC were chosen by use of the PAN-2 chelates of these metals obtained under the conditions optimal for formation of the Pd(II) chelate.

The chelates was separated with a Varian-5000 liquid chromatograph equipped with a spectrophotometric detector (200–700 nm), and stainless-steel columns (250 × 5 mm) packed with Silasorb-600 silica gel (Lachema, CSSR) with an average particle size of 10 μm. Acetone, benzene, propan-2-ol, chloroform and their mixtures of various composition were used as eluents. All the organic solvents used were analytically pure.

The capacity factors were determined in the usual way, with quinalizarin as the model non-adsorbed substance. The resolution (*R_s*) for adjacent peaks was also calculated in the usual way.¹⁹

Calibration graph

Since the chromatographic peaks of the palladium chelate with PAN-2 have the form of Gauss curves, the peak height can be plotted against amount of palladium for calibration.

Solutions containing 1.86–186 μg of palladium are each mixed with 5 ml of 10⁻³M PAN-2 solution in DMF and diluted with water to 25 ml after pH adjustment to 2.9–3.2. After mixing, the solutions are heated for 1–2 min in a boiling water bath and then cooled. Next, 1 ml of chloroform is added to each, the mixtures are shaken for 1 min, and the extracts are separated. For chromatographic analysis, a 10-μl aliquot part of the chloroform extract is injected by sample-loop into the HPLC column and chromatographed with acetone as eluent at a flow-rate of 2 ml/min, at 25°. The absorbance of the eluate at 620 nm is monitored. The calibration graph is linear over the palladium range 1.86–186 μg in the initial solution.

Procedure

Five ml of 0.1M PAN-2 solution in DMF are added to a known volume of sample solution containing 3–180 μg of palladium and not more than 2.5 mg of copper and 1.8 mg of cobalt. After adjustment of the pH to 2.9–3.2, the mixture is diluted to 25 ml with water, and then heated, extracted *etc.*, as in the procedure above for calibration.

RESULTS AND DISCUSSION

The absorption spectra of the chelates studied have their absorption maxima in the visible region of the spectrum (Table 1), where they differ from the PAN-2 spectrum ($\lambda_{\max} = 470$ nm). They coincide with the PAN-2 spectrum in the ultraviolet region. Because of the overlap of their major spectral bands, there is mutual interference between the palladium, cobalt, copper and nickel complexes, so a separation is needed. Because of the large excess of PAN needed

Table 1. Optical characteristics of metal chelates with PAN-2²⁰

Central ion	λ_{\max} , nm	ϵ , 10 ⁴ l.mole ⁻¹ .cm ⁻¹ (λ , nm)
Pd(II)	620; 675	1.60 (620)
Ni(II)	530; 565	4.96 (565)
Cu(II)	550	2.50
Co(III)	580; 630	2.31 (580) 1.95 (630)

for the complexation reaction, the chromatographic detection of all the chelates was performed at 620 nm to avoid the background signal of PAN-2. At 620 nm the PAN-2 signal is not significant, and the palladium complex exhibits maximum absorption.

To choose the best conditions for the separation, the nature and the composition of the mobile phase were varied, chloroform, acetone, benzene, propan-2-ol and their mixtures being used as eluents. The palladium and nickel PAN-2 complexes are eluted with chloroform and acetone to give sharp and symmetrical peaks and exhibit comparatively short retention times (Fig. 1). The retention volumes for these compounds do not depend on the size of the sample, which indicates that the chromatography of these chelates occurs in the linear region of their adsorption isotherms. Therefore, these components can be identified in a mixture by measuring the retention volumes. With acetone as eluent, the copper and cobalt chelates with PAN-2 are strongly retained, and their elution peaks, though symmetrical, are very broad. Although a mixture of the PAN-2 chelates of Pd(II), Cu(II) and Co(III) can be readily separated and palladium detected, the resolution is not good enough for complete separation of the palladium and nickel chelates.

A weaker eluent, chloroform, also did not allow chromatographic separation of the four chelates, the cobalt chelate being so strongly retained that

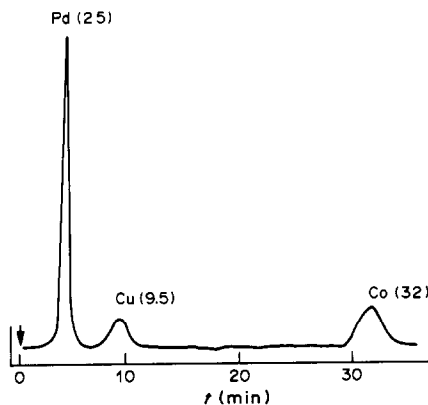


Fig. 1. Chromatogram of a mixture of the PAN-2 chelates of palladium, copper and cobalt. Eluent acetone, flow-rate 2 ml/min, adsorbent 10-μm Silasorb-600, *P* = 28 atm, temperature 25°. The retention volumes (ml) corresponding to the peak maxima are given in parentheses.

Table 2. Retention parameters of PAN-2 chelates of palladium, nickel, copper and cobalt with the benzene-propan-2-ol 1:1 v/v mixture

Central ion	Retention time, t_R	Capacity factor, K'	Peak resolution, R_s	Plate number, N
Ni(II)	1 min 22 sec	0	1	100
Pd(II)	4 min	1.67	6.4	50
Cu(II)	28 min	17.67	1.5	2×10^3
Co(III)	31 min 40 sec	20.11		2×10^3

it was not eluted even with a very large volume of eluent, and the palladium and nickel peaks were not well separated, the resolution factor being only 0.6 (Fig. 2).

Complete separation of all four components was attained with a 1:1 v/v mixture of propan-2-ol and benzene (Fig. 3, Table 2). The copper and cobalt chelates have considerable retention times, and their separation requires greater consumption of eluent, and gradient elution with increasing polarity of the mobile phase is recommended for practical application.

The column used in this work has been operated continuously for two months without change in the retention parameters or deterioration in the reproducibility of the peak heights.

In the triplicate determination of 23.25 μg of palladium in the presence of 2.33 mg of copper and 1.86 mg of cobalt 23.1 \pm 0.5 μg of palladium were found, showing that copper and cobalt do not interfere in the determination.

The detection limit for palladium (with a 10- μl injection) is 19 ng in the initial sample, the concen-

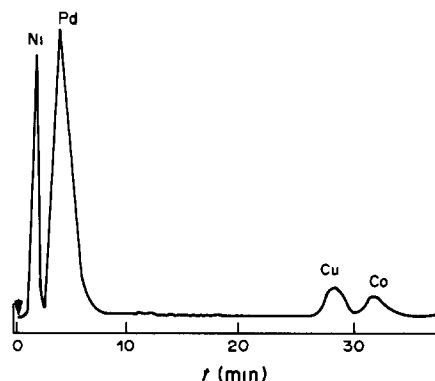


Fig. 3. Separation of palladium, nickel, copper and cobalt PAN-2 chelates. Eluent 1:1 v/v mixture of benzene and propan-2-ol, $P = 32$ atm. Other conditions as for Fig. 1.

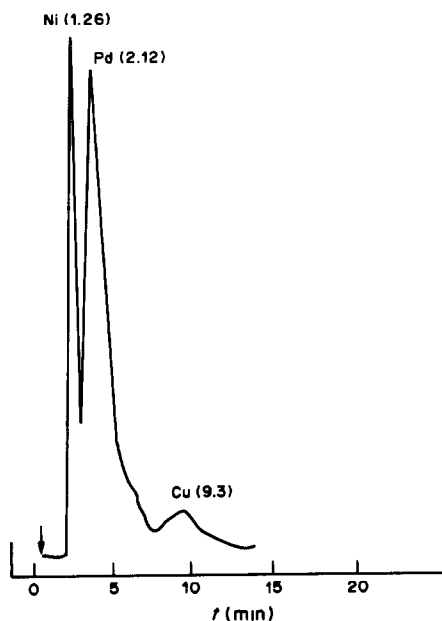


Fig. 2. Chromatogram of a mixture of nickel, palladium and copper PAN-2 chelates. Eluent chloroform, $P = 32$ atm, other conditions as for Fig. 1.

tration coefficient being 25. However, the detection limit can be decreased further by use of extractive chromatographic concentration. The method for palladium with PAN-2 solution in pentan-2-ol on polytetrafluoroethylene (Teflon-4) is characterized by a concentration coefficient of 100;²¹ this should enable us to develop a new combination method involving the preliminary extractive chromatographic concentration of palladium from dilute solution, and its subsequent determination by the HPLC method.

REFERENCES

1. A. R. Timerbaev, O. M. Petrukhin and Yu. A. Zolotov, *Zh. Analit. Khim.*, 1981, **36**, 1160.
2. J. W. O'Laughlin, *J. Liquid Chromatog.*, 1984, **7**, Suppl. 1, 127.
3. A. R. Timerbaev, O. M. Petrukhin and Yu. A. Zolotov, *Zh. Analit. Khim.*, 1982, **37**, 581.
4. K.-H. König, G. Schneeweis and B. Steinbrech, *Z. Anal. Chem.*, 1983, **316**, 13.
5. A. R. Timerbaev, O. M. Petrukhin and Yu. A. Zolotov, *Zh. Analit. Khim.*, 1982, **37**, 1360.
6. A. R. Timerbaev and O. M. Petrukhin, *ibid.*, 1984, **39**, 1177.
7. *Idem*, *Anal. Chim. Acta*, 1984, **159**, 229.
8. E. Gaetani, C. F. Laureri, A. Mangia and G. Perolari, *Anal. Chem.*, 1976, **48**, 1725.
9. P. J. Clark, I. E. Treble and P. C. Uden, *Polyhedron*, 1982, **1**, 785.
10. F. H. Walters, *Anal. Lett.*, 1982, **15**, 1031.
11. P. C. Uden, D. M. Parees and F. H. Walters, *ibid.*, 1975, **8**, 795.

12. V. M. Ivanov, *Heterocyclic Nitrogen-containing Azo-compounds*, (in Russian), p. 229. Nauka, Moscow, 1982.
13. S. V. Galushko, I. P. Shishkina and Yu. I. Usatenko, *Zh. Analit. Khim.*, 1982, **37**, 1833.
14. G. Schwedt and R. Budde, *Chromatographia*, 1982, **15**, 527.
15. F. Beamish, *Analytical Chemistry of Noble Metals* (in Russian). Part 2, p. 41. Mir, Moscow, 1969.
16. V. M. Ivanov, *op. cit.*, p. 21.
17. S. N. Lanin, N. B. Morozova, V. M. Ivanov and E. M. Basova, *Tezisy Dokl. Vses. Konf. po Analit. Khim. Organich. Soedineni*, Moscow, 1984, 151.
18. V. M. Ivanov, *op. cit.*, p. 55.
19. H. Engelhardt, *High-Pressure Liquid Chromatography* (in Russian), p. 20. Mir, Moscow, 1980.
20. V. M. Ivanov, *op. cit.*, p. 51.
21. T. A. Bol'shova, N. B. Morozova and V. M. Ivanov, *Tezisy Dokl. VII Vses. Konf. po Khim. Ekstrakt.*, Moscow, 1984, 147.

PULSE CIRCULATION GAS CHROMATOGRAPHY ON CAPILLARY COLUMNS

V. P. CHIZHKOV, S. S. PAVLOV, N. V. STERKHOV, V. M. RAVIKOVICH,
E. F. LITVIN and E. A. VARYVONCHIK

Zelinsky Institute of Organic Chemistry, USSR Academy of Sciences, Moscow, USSR

(Received 15 October 1985. Accepted 11 July 1986)

Summary—The method and equipment for pulse circulation high-resolution gas chromatography on glass capillary columns have been developed. The separation of a mixture of C_6H_6 , C_6H_5D , $C_6H_3D_3$ and C_6D_6 on carbonized columns coated with squalane has been taken as an example to show the advantages of the method. An efficiency of about 5×10^6 theoretical plates has been achieved with a capacity factor of $k = 1$.

The method of pulse circulation gas chromatography^{1,2} provides an efficiency of up to 1.2×10^5 theoretical plates² with standard packed columns, as shown by the separation of isotopically-substituted organic compounds. However, even this high efficiency is insufficient to solve certain analytical and physicochemical problems. For this reason capillary columns are frequently used in such schemes.³⁻⁸

auxiliary gas flow into the detector. The required gas pressure at the outlet^{1,11} is maintained by means of the pressure regulator.

In the main mode of operation there is bleed of a part of the gas flow between the columns. The bleeding velocity^{1,2} is controlled by feeding an auxiliary gas flow into the bleeding line *via* an additional line supplied with the pressure regulator. In the other mode of operation there is no bleeding of the gas flow.

EXPERIMENTAL

Experiments were done with the BIOCHROM-27 capillary gas chromatograph. The chromatograph is supplied with an electro-pneumatic eight-way valve for switching columns^{5,6,9} and a time-programming switching unit with two programme channels.¹⁰

The circulation scheme is given in Fig. 1. The apparatus has a line with a pressure regulator for providing an

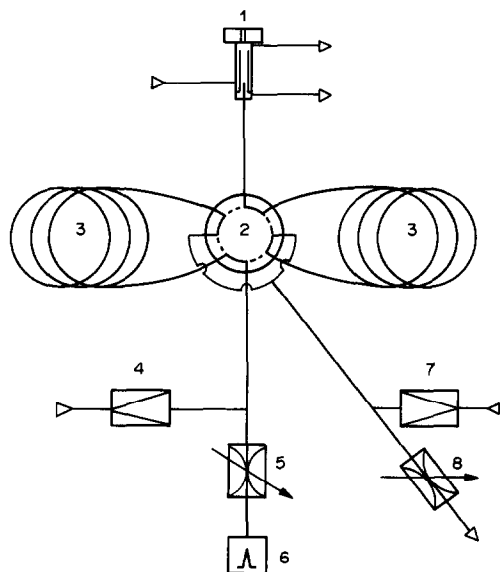


Fig. 1. Circulation scheme of the BIOCHROM-27. 1, injector; 2 eight-way valve with microchannels; 3, capillary columns; 4, 7, pressure regulators; 5, 8, flow restrictors; 6, flame-ionization detector.

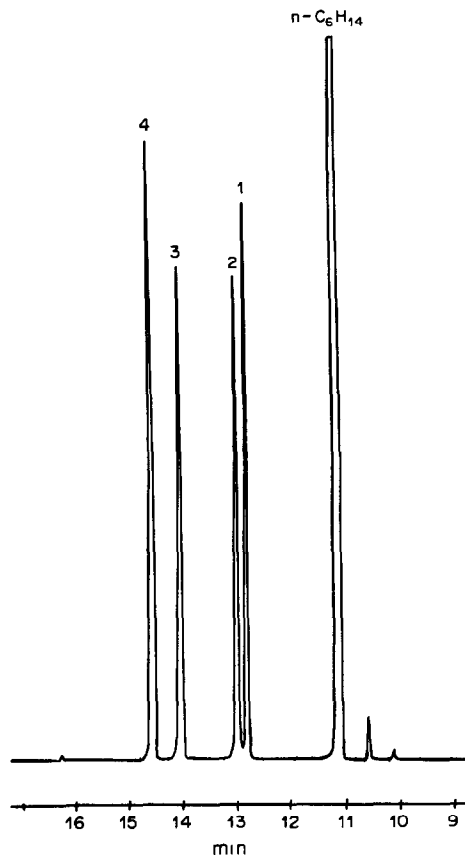


Fig. 2. Chromatogram of a mixture of hexadeuterobenzene (1), benzene (2), dodecadeuterocyclohexane (3) and cyclohexane (4).

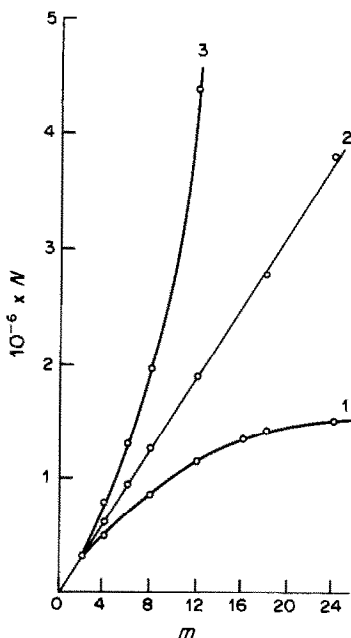


Fig. 3. Relationship between the number of theoretical plates N (for cyclohexane) and number of semi-cycles m (1, without gas bleeding between columns; 2, 3, with gas bleeding).

Two carbonized glass capillary columns (37.5 m × 0.028 cm) coated with squalane were used. To carbonize the inner surface of the column, methyl bromide was pyrolysed at 500°; the carbonized surface was coated with the liquid phase by the static method.¹² The columns were connected to the circulation valve by platinum-iridium capillaries.^{3,6} The joints were coated with a special glue for quartz and glass capillaries,¹³ which practically excluded uncontrolled gas bleeding.

Experiments were performed at 65° and gauge pressures of 0.4 and 0.25 mPa at the inlet and outlet of the system, respectively. Under these conditions the linear velocity of the carrier gas (helium) was 16.8 cm/sec, and the column efficiency measured for benzene ($k = 0.81$) was 4700 theoretical plates per metre.

RESULTS AND DISCUSSION

Figure 2 illustrates the high resolution obtained with these columns without switching the circulation

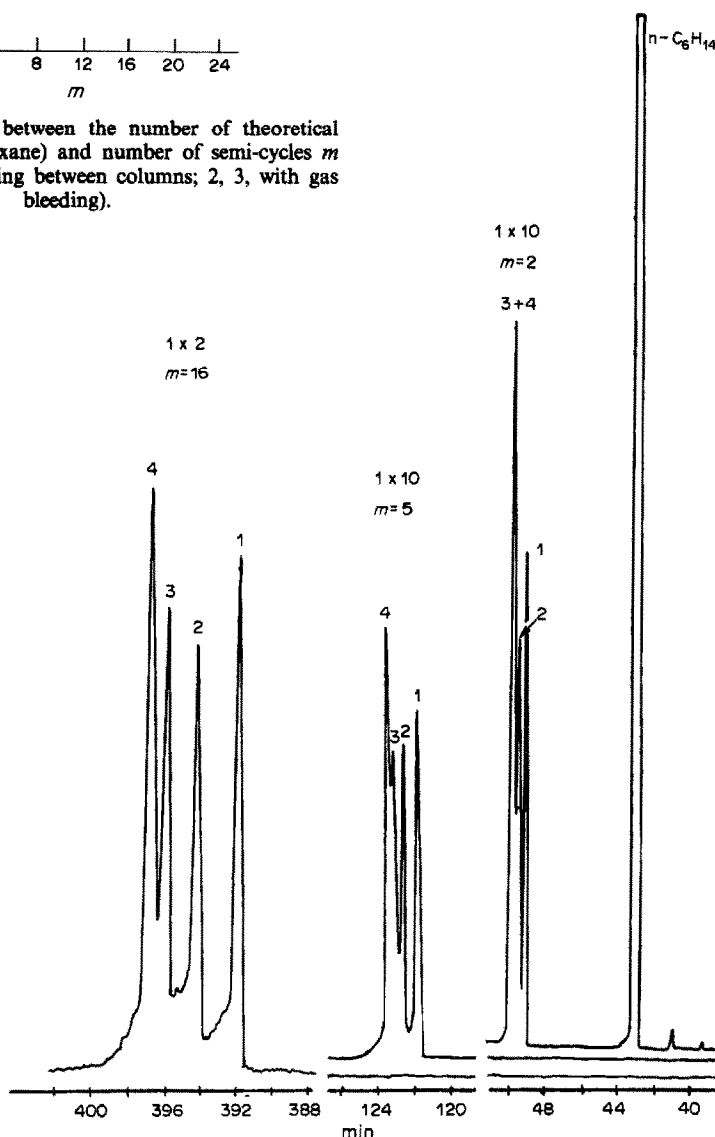


Fig. 4. Circulation chromatograms of a mixture of deuterobenzenes and benzene (1, C_6D_6 ; 2, C_6H_5D ; 3, $C_6H_4D_2$; 4, C_6H_6).

valve. Figure 3 shows the number of theoretical plates N (for cyclohexane) as a function of the number of semi-cycles m , obtained by switching the circulation valve. Curve 1 was obtained with no bleeding of the gas flow between the columns. Under these conditions ($k = 1.00$), a non-linear increase of efficiency was observed. With bleeding of a given fraction of the gas flow between the columns of the circulation scheme we obtained a linear dependence of N on m (curve 2 on Fig. 3) over a wide range of m values (up to 24 semi-cycles). A further increase in the bleeding velocity leads to a non-linear dependence of N on m (curve 3 on Fig. 3), characterized by a more rapid rise in N . The data agree with earlier results for packed columns^{1,2}.

The separation efficiency of capillary columns in circulation gas chromatography of isotopically-substituted compounds was studied by using a mixture of deuterobenzenes (C_6D_6 , C_6H_5D , $C_6H_3D_3$) and benzene. Two carbonized glass capillary columns (75×0.028 cm) with squalane as the liquid phase¹⁴ were used (Fig. 1). The separation was done in a pulse mode at 65° and gauge pressures of 0.4 and 0.25 mPa at inlet and outlet, respectively. Under these conditions the mean velocity of the gas flow (nitrogen) was 9.0 cm/sec, the dependence of N on m was close to linearity, and the mean column efficiency for benzene was 4500 theoretical plates per metre.

Chromatograms obtained after a certain number of semi-cycles (m) are presented in Fig. 4. A separation characterized by the criterion $R \cong 1$ for the solute pair most difficult to separate was achieved

at $m = 16$, which corresponds to a 1.2-km column length and an efficiency of about 5×10^6 theoretical plates.

The BIOCHROM-27 instrument can also be used for back-flush of capillary columns and multi-dimensional chromatography^{9,15}.

REFERENCES

1. M. P. Zabokritsky, V. P. Chizhkov and B. A. Rudenko *J. High Resol. Chromatog., Chromatog. Commun.*, 1983, **6**, 460.
2. V. P. Chizhkov and L. A. Sinitsina, *J. Chromatog.*, 1975, **104**, 327.
3. H. Pauschmahn, *Z. Anal. Chem.*, 1967, **228**, 39.
4. V. P. Chizhkov and G. A. Yushina, *ibid*, 1976, **31**, 16.
5. W. Jennings, J. A. Settlege and R. J. Miller, *J. High Resol. Chromatog., Chromatog. Commun.*, 1979, **2**, 441.
6. W. Jennings, J. A. Settlege, R. J. Miller and O. G. Raabe, *J. Chromatog.*, 1979, **186**, 189.
7. C. D. Chriswell, *J. High Resol. Chromatog., Chromatog. Commun.*, 1982, **5**, 210.
8. N. V. Sterkhov, V. M. Ravikovich, E. F. Litvin and V. P. Chizhkov, *Zh. Fiz. Khim.*, 1983, **57**, 2897.
9. R. J. Miller, S. E. Stearns and R. R. Freeman, *J. High Resol. Chromatog., Chromatog. Commun.*, 1979, **2**, 55.
10. R. M. Lambrecht, R. Withnell and A. P. Wolf, *Chem. Instrum.*, 1976, **7**, 157.
11. R. E. Pauls, A. T. Shepard, J. E. Phelps, J. E. Devis and L. B. Rogers, *Sepr. Sci.*, 1977, **12**, 289.
12. E. L. Ilkova and E. A. Mistrykov, *J. Chromatog. Sci.*, 1971, **9**, 569.
13. P. Sandra, M. Schefaut and M. Verzele, *J. High Resol. Chromatog., Chromatog. Commun.*, 1982, **5**, 50.
14. F. Bruner and G. P. Cartoni, *J. Chromatog.*, 1963, **10**, 396.
15. D. E. Willis, *Anal. Chem.*, 1978, **50**, 827.

THE EFFECT OF INORGANIC PARTICULATES ON THE ASV SIGNALS OF Cd, Pb AND Cu

T. U. AUALIITIA and W. F. PICKERING

Chemistry Department, University of Newcastle, N.S.W. 2308, Australia

(Received 23 June 1986. Revised 24 July 1986. Accepted 18 September 1986)

Summary—The potential influence of inorganic particulates on the ASV response of $<100\text{-}\mu\text{g/l}$. levels of Cd, Pb and Cu, at a thin film mercury electrode, was examined by adding various weights of the solids to the acetate background electrolyte solution. Materials added included the hydrous oxides of Mn(IV), Fe(III) or Al(III), clay minerals (kaolinite, illite, montmorillonite) and some contaminated sediments. Abrasion of the mercury film was minimized by deaerating the turbid solutions before their transfer to the measuring cell. The hydrous oxides specifically sorbed all three metal ions, resulting in peak-size changes that varied in magnitude with pH. With the clays, only sorption of Pb by illite or montmorillonite was detected. The presence of the solids had little effect on the peak position or half-peak breadth of the Cd or Pb signals, but the Cu peak parameters changed, indicating some hydroxy-species formation at higher pH. Some contaminated sediment samples released a significant fraction of their total metal content into acetate buffer solutions. Shielding the mercury film with a semipermeable membrane had a similar effect to filtering the suspension before analysis, but diffusion equilibrium was only slowly achieved (>12 hr).

In water analysis, it is traditional to isolate particulate matter (by using a $0.45\text{-}\mu\text{m}$ membrane) before determining the metal content of the aqueous phase. Analysis by techniques such as plasma emission spectrometry or atomic-absorption spectrometry yields total metal contents, whereas anodic stripping voltammetry (ASV) provides an estimate of the "labile" metal fraction, which may be regarded as a better estimate of the fraction "available" to biota.

The preliminary filtration may result in an underestimation of the total "available" fraction, since part of the metal content of the particulate matter can be loosely bound, and available for redistribution. It has been noted,¹ for example, that surface association phenomena involving colloidal suspended matter are an integral part of metal transport in natural waterways. The sorption process can control the fraction of total metal ion present in labile (or available) forms in the waters and their associated sediments.

It would thus be more appropriate to analyse unfiltered water samples by ASV, but before adopting this approach it is desirable to have some understanding of the effect of suspended colloids on electrode response.

Various groups²⁻⁴ have investigated the effect of colloidal organic matter on the ASV parameters (i_p and E_p) of several metal ions. The influence of inorganic suspensions is less well understood, although a recent voltammetric study of lead(II) solutions containing hydrous oxide suspensions yielded results which support the view that metal ions adsorbed on particulate surfaces are essentially non-labile.⁵

The aim of our study was accordingly an examination of the influence of different inorganic particulates on the ASV response for low levels of cadmium, lead and copper. It was expected that the study would also provide some information in respect to sorption behaviour and modes of bonding.

ulates on the ASV response for low levels of cadmium, lead and copper. It was expected that the study would also provide some information in respect to sorption behaviour and modes of bonding.

EXPERIMENTAL

Reagents and equipment

Voltammetric measurements were made with an ESA Model 2014 Anodic Stripping Analyser, which uses thin (~ 150 nm) mercury films deposited on wax-saturated graphite rods. Comparison tests were restricted to a single cell, since differences in cell geometry contribute to the variance of the peak current. The $4\text{-}\mu\text{mole}$ mercury coating on the electrode was renewed regularly, and with different films the reproducibility (relative standard deviation, R.S.D.) of the peak currents for $100\text{-}\mu\text{g/l}$. cadmium and lead was usually 2-4%. In this analyser, a nitrogen stream (flowing at 40 ml/min) is used to deoxygenate and stir the assay solution in the test-cell.

Test samples containing particulates were deaerated for 5 min away from the cell system, because it has been shown⁶ that pre-analysis abrasion of the mercury film by particles can cause enhancement of cadmium and lead peak currents. After deaeration, the sample vials were transferred to the electrode unit, where metal was deposited for 3 min, at an applied potential of -900 mV. The amalgam was then stripped at a scan-speed of 50 mV/sec to a cut-off potential between -10 and -50 mV (the value required to resolve the copper peak from dissolution of mercury varied according to the ligands present). Five analytical cycles were run for each test solution, and the ASV traces were recorded on a fast-response Rickadenki Chart Recorder (Model B-181H).

The background electrolyte solutions (usually sodium acetate/acetic acid, pH 5.5) were purified by electrolysis with an ESA Model 2014 P Reagent Cleaning System. The standard metal-ion solutions were prepared from analytical grade salts and demineralized distilled water (Elga Model B116 Cartridge De-ioniser). After dilution with base solution, the test solutions contained up to $100\text{ }\mu\text{g/l}$. lead, cadmium and/or copper.

In one series of studies, the mercury electrode was protected by a perforated glass tube covered with dialysis tubing (Visking) which has a nominal molecular-weight cut-off of 1000–1200. Before use, the membrane was treated by a procedure described by Smart and Stewart,⁷ to remove the sodium benzoate preservative and prevent attack by cellulytic micro-organisms when the membrane was thoroughly wet. Fresh tubing was used in each new study.

Colloidal particulates

Amorphous hydrous iron oxide [HFO, "Fe(OH)₃"] suspensions were prepared by adding ~22 mmoles of sodium hydroxide to 7 mmoles of iron(III) nitrate in a total volume of 500 ml. The suspension (pH 5–6.5) was stirred for several hours before withdrawal of the aliquots (4 ml, ~8 mg of HFO) used in the test studies.

Amorphous hydrous aluminium oxide [HAO, "Al(OH)₃"] suspensions were prepared by adding ~50 mmoles of sodium hydroxide to a vigorously stirred solution containing 17 mmoles of aluminium nitrate (equilibrium pH ~7). Dilution to 600 ml yielded a suspension containing ~2 mg of colloid per ml.

Procedures described in the literature were used to prepare goethite (FeOOH),⁸ hydrous manganese(IV) oxide (HMO)⁹ and cryptomelane (α MnO₂).¹⁰

The three clay minerals used were commercial products: a kaolinite (Carlo Erba), an illite [Morris, Illinois] and a montmorillonite [Parkville, Mississippi].

The organic particles used in comparison studies included two humic acids. One [HA(F), Fluka, ash content 13.2%] required pH 8 for dissolution; the other (Tas-4, extracted from a forest soil) had a lower ash content (7.1%), and dissolved at pH > 6. An acid-soluble fulvic acid (FA, m.w. < 1000) was obtained from Contech Ltd., Ottawa.

A series of contaminated estuarine sediments, calcine and jarosite residue were kindly supplied by the Sulfide Corporation Laboratory, Boolaroo.

Particulate effects

Aliquots (4.0 ml) of the inorganic suspensions (~8 mg of solid) were transferred into clean acid-washed 30-ml glass vials which contained acetate buffer (adjusted to a pH in the range 4–8), a metal loading of 100 μ g/l. cadmium, lead and copper, and enough purified water to give a final volume of 20.0 ml with an acetate concentration of 0.13M.

The vials were sealed and mechanically shaken overnight to ensure equilibration between the phases. Just before analysis each vial was purged for >5 min with a flow of nitrogen, which was continued during the transfer to the ASV unit. Each sample was subjected to five deposition/stripping cycles. The mean peak heights were used to assess the effect of pH.

The experimental parameters varied in different test sequences included the nature of the particulate matter, the solid density, and the metal ion concentration. In some studies with cadmium and goethite, the background electrolyte was loaded with 10⁻²M sodium chloride or ammonium acetate.

In another study sequence, a series of metal ion–colloid mixtures was dialysed against 5 ml of pH-5 background electrolyte contained in a perforated glass tube covered with dialysis tubing. All analyses were performed after an equilibration time of >15 hr. The variables examined included type of solid [HA(F), Tas-4, FA and FeOOH], particulate level (0.1, 0.3, 0.5 mg/ml), and supporting base electrolyte (0.13M sodium acetate, chloride or nitrate). To determine the optimum dialysis time for the metal ions of interest, solid-free metal solutions (100 μ g/l.) were dialysed for times ranging from 10 min to 14 hr.

In a final study, weighed amounts of contaminated sediments were equilibrated with background electrolyte.

RESULTS

Comparison of the peak sizes obtained with those for standard solutions (100 μ g/l. metal ion, no solids) clearly indicated that the particles were adsorbing part of the cadmium, lead and copper content, the extent varying with pH, metal-ion involved, and the chemical nature of the suspended matter. The dependence of uptake on pH was also found to depend on the weight of solid present and the initial ion concentration. In general, the higher the solid:ion ratio, the lower the pH required for onset of sorption, except for hydrous Mn(IV) oxide, which gave virtually total sorption under all conditions studied.

In the clay studies, the loading with solid was varied between 0.1 and 1.4 mg/ml, but no significant change in cadmium or copper peak size was observed. Some lead(II) was retained by illite (*cf.* Fig. 1, *, I') and montmorillonite suspensions, with uptake increasing with pH (5.3–8.1) and weight of solid present. Retention decreased in the presence of higher acetate concentrations.

Only in the case of copper was peak position (E_p) or shape influenced by the presence of particulate matter (*cf.* Fig. 3). Comparison with the responses for the solid-free systems indicated that the E_p and half-breadth ($b_{1/2}$) values for the cadmium and lead

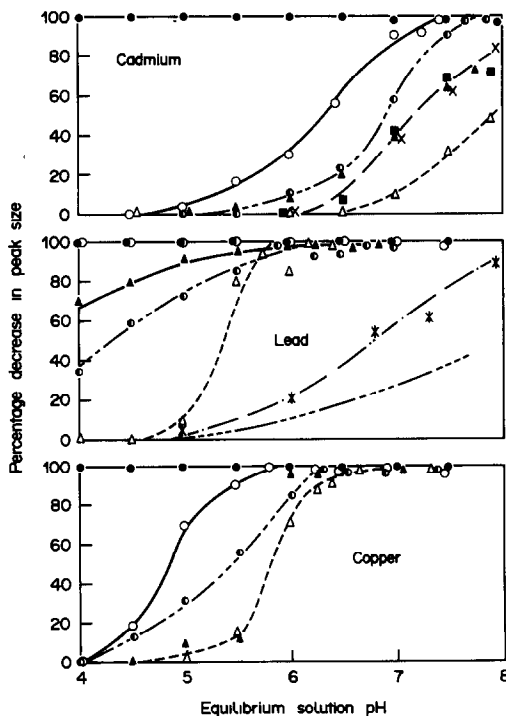


Fig. 1. Effect of pH on the percentage decrease in peak size for Cd, Pb and Cu, in the presence of various hydrous oxide particles. Total initial M^{2+} concentration, 100 μ g/l.; solid 8 mg/20 ml, background electrolyte solution, 0.13M CH_3COONa , pH 5.5. Substrate code: ●, MnOOH; ○, α MnO₂; △, HAO; ▲, HFO; ○, FeOOH [■, 10⁻²M NaCl present, X, 10⁻²M CH_3COONH_4 present]; *, illite [I', 0.5M acetate base].

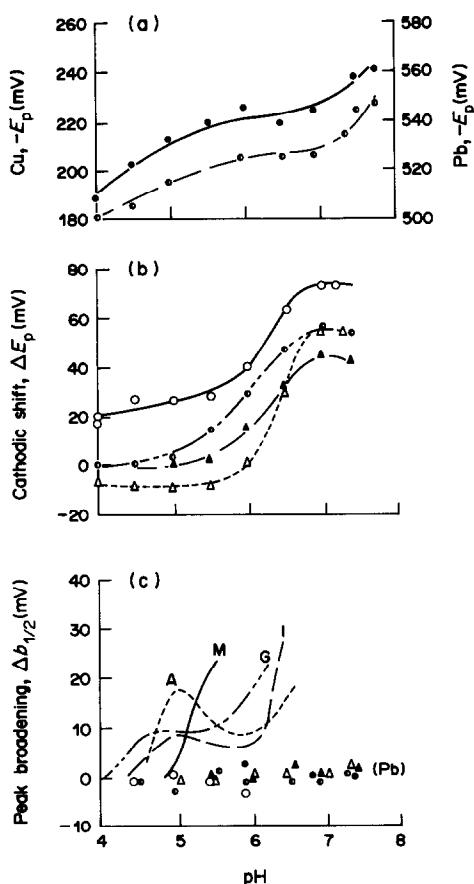


Fig. 2. Diagram showing the effect of pH and 0.4 mg/ml of solids on ASV peak parameters. (a) E_p (mV), for Cu (●) and Pb (●) present at 100 μ g/l. level with no solid present. (b) Cu peak cathodic shifts, in presence of α MnO₂ (○), FeOOH (○), HFO (△) or HAO (△). (c) Cu peak broadening (expressed as $\Delta b_{1/2}$ values) in presence of A, HAO; G, FeOOH; I, HFO, or M, α MnO₂. Coding for Pb response, same as (b).

peaks not affected (within the precision limits) by the presence of colloidal suspensions, but the lead peaks did shift with increasing pH, owing to hydroxy-species formation (cf. Fig. 2a; ●).

For copper, the presence of suspended matter caused peaks attributable to hydroxy-species formation to appear at lower pH values. With the exception of the α MnO₂ systems, most peak-position changes closely reflected the observed increases in the amount of metal ion sorbed (cf. Figs. 1 and 2b). As shown in Fig. 2c, the formation of an "ASV-labile" hydroxy-bonded species led to peak broadening, and in the case of HAO gels, this broadening at low pH contributed to an apparent anodic shift in E_p . The anodic shift could also have arisen from adsorption of colloid on the mercury film. The $\Delta b_{1/2}$ values recorded in Fig. 2c are the differences in half-breadth values ($b_{1/2}$) observed in the presence and absence of particulates.

Figure 3 shows some typical voltamperograms;

Fig. 3b shows how the peak area for copper and lead varied with pH in the presence of inorganic particulates.

Shielding the mercury film electrode with a dialysis membrane mounted on a perforated glass support was found to have an effect similar to filtration of the suspension before the ASV analysis. A minimum diffusion period of 9 hr was required for migration of dialysable metal species (cf. Fig. 4D).

The full lines in Figs. 4 and 5 show how the metal-ion signal decreased with increasing solid level, in the absence of the dialysis membrane. The dotted lines indicate the ratio of the signal observed for the dialysate to that observed with solid in contact with the electrode. With organic acids present, the ratio was less than unity (indicating <100% recovery) and its value was influenced by the introduction of chloride ions (cf. ○ and □, Fig. 5).

When polluted-sediment samples were suspended in the same background electrolyte (0.13M acetate buffer) and subjected to ASV analysis, measurable

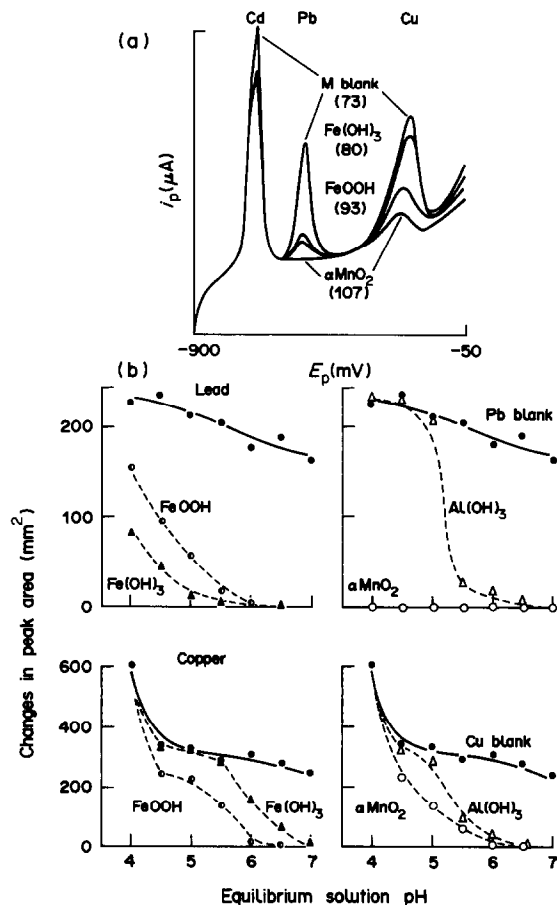


Fig. 3. (a) Voltamperograms of assay solutions in the presence of 0.4 mg/ml inorganic particulates at pH 5.5. Values in parentheses indicate broadening of the Cu peak [expressed as $b_{1/2}$ (mV) values]. (b) Diagrams showing how the peak area of Cu and Pb curves varied with pH in the presence of inorganic particulates. Experimental conditions and substrate coding, as for Fig. 1.

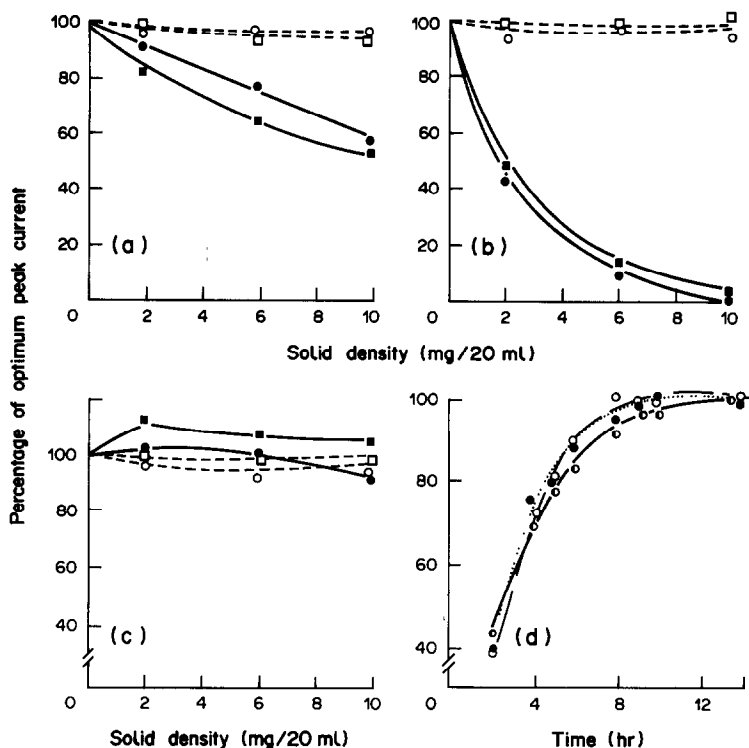


Fig. 4. A–C: diagrams showing the effect of suspended FeOOH density on (i) the amount of metal ion sorbed from 100 $\mu\text{g/l}$. solutions (full lines) and (ii) the percentage of residual "ASV-labile" metal ion found to diffuse through dialysis tubing (dashed lines). ●, ○, 0.13M CH_3COONa buffer, pH 5; ■, □, background electrolyte 0.13M in NaCl. A, Cu; B, Pb; C, Cd. 4D: rate curve for the diffusion of Cu (●), Pb (■) and Cd (○) ions (initially 100 $\mu\text{g/l}$) through the electrode-shielding membrane. Background electrolyte 0.13M CH_3COONa , pH 5.

amounts of Cd, Pb and Cu were released, as shown in Table 1.

DISCUSSION

The signal loss caused by the presence of the added solids could have arisen from electrode passivation (*i.e.*, colloid attraction to the surface) but the effect of pH and the protective film more strongly supports the concept of specific sorption of metal ions by the particulate matter.

The use of acetate background electrolyte solutions in ASV studies has been recommended^{11,12} because acetato-metal complexes are highly labile, but it also has to be recognized that the inclusion of acetate at high concentration (*e.g.*, 0.13M) results in 99.9% conversion of low concentrations of metal ions into the acetato-complexes. With the free metal ion concentrations thus reduced to low $\mu\text{g/l}$. levels, the tendency to form hydrolysed metal species is reduced and they are formed in higher pH regions. With such low metal ion concentrations, there should also be minimal sorption by solids. The presence of 0.1M sodium from the buffer salt should also minimize metal-ion retention by ion-exchange, and in any case traces held by electrostatic attraction are normally labile in ASV.

The decreases in peak height shown in Fig. 1 thus imply that the affinity of metal ions for some sites on the colloidal particles was sufficiently high to promote dissociation of acetato-metal complexes.

With most systems, the uptake increased steadily with increasing pH (*cf.* Fig. 1), and in only a few cases [*e.g.*, Pb and Cu on HAO; Cu on HFO and αMnO_2] did the sorption values increase rapidly over a narrow (1–2 unit) pH range, though this is the more widely observed response at higher free metal-ion levels (*e.g.*, mg/l.).

Mn(IV) oxides are considered¹³ to be better scavengers of metal ions than are other inorganic particulates, and it can be seen from Fig. 1 that this trend persists even when only traces of metal ion are present. Relative uptake values decreased in the sequence $\text{MnOOH} > \alpha\text{MnO}_2 > \text{FeOOH} > \text{HFO} > \text{HOA}$ (with the exception of Pb, for which the positions of FOA and FeOOH were reversed).

The affinity order for each of the oxides studied followed the sequence $\text{Pb} > \text{Cu} \gg \text{Cd}$, which bears some relationship to the relative magnitudes of the respective hydrolysis constants, but it can be modified by substrate crystal structure and metal complex formation.

Complex formation applied in these specific sorption studies, as shown by the effect of adding $10^{-2}M$

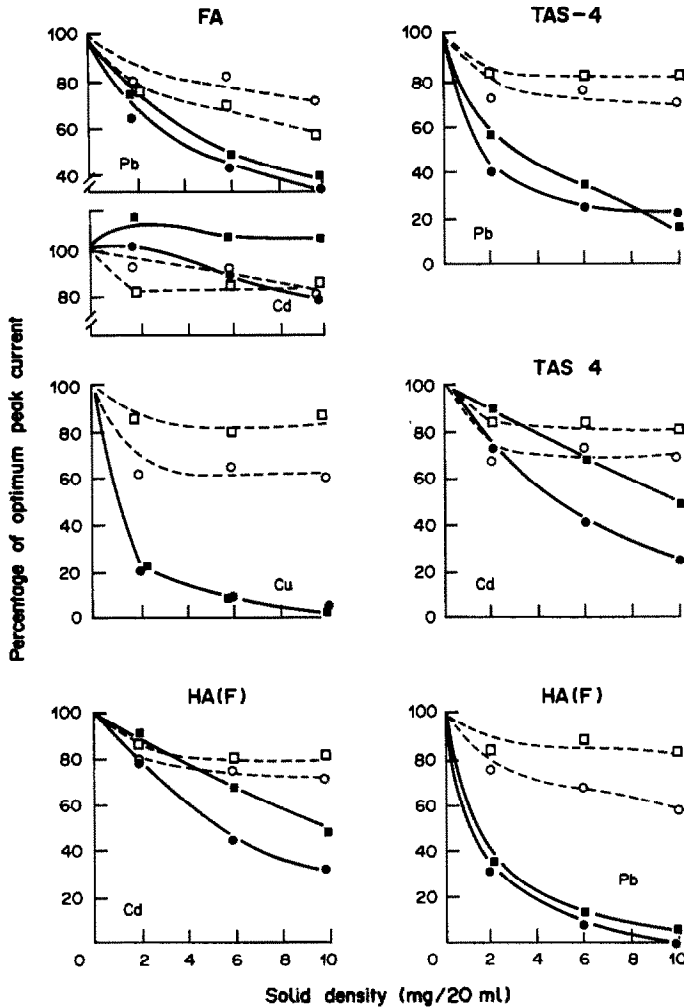


Fig. 5. Diagrams showing the effect of added organic acids on (i) the amount of metal ion rendered not "ASV labile" (e.g., sorbed), with initial ion levels of $100 \mu\text{g/l}$. (full lines) and (ii) the percentage of residual "ASV labile" metal ion found to diffuse through a semipermeable membrane film (dashed lines). Coding: FA, fulvic acid added; HA (F), Fluka brand humic acid; Tas-4, forest soil humic acid. ●, ○, $0.13M \text{ CH}_3\text{COONa}$ buffer, pH 5; ■, □, background electrolyte $0.13M$ in NaCl.

Table 1. Weakly bonded metal ions on contaminated sediments

Sediment material	Total metal, <i>mg/kg</i>			"ASV labile" metal,* <i>mg/kg</i>		
	Cu	Pb	Cd	Cu	Pb	Cd
Calcine residue	4000	13000	70	1410	6460	14
Jarosite residue	1200	15000	250	190	146	60
Estuarine sediment: A	4000	15000	900	1700	11800	539
B	3800	13000	1000	1610	8940	680
C	480	2000	60	70	1790	20
D	70	170	5	8	87	ND
E	40	270	10	ND	ND	ND
F	40	90	5	1	12	ND
G	40	60	10	ND	ND	ND

*10 mg of solid equilibrated overnight with $0.13M \text{ CH}_3\text{COONa}$ (pH 5) prior to deaeration and ASV analysis; ND = none detected.

sodium chloride or ammonium acetate to cadmium solutions in the presence of goethite (*cf.* Fig. 1, points ■ and X).

The specific sorption of Cu, Pb and Cd by these inorganic particulates, as observed in the ASV studies, will be described in more detail in a later publication. The sorption of metal ions by colloids has been examined extensively but few publications are directly comparable with the ASV approach, owing to differences in initial concentration or the chemical form of the solute species (*e.g.*, hydrated ions and acetato-complexes).

Displacement of acetate ions from the metal complex by other ligands (*e.g.*, Cl^- , OH^-) in the solution, with the formation of different metal species, tends to lead to changes in stripping peak potential values (E_p) and peak shape (*e.g.*, width at half peak-height, $b_{1/2}$).

In this study, the formation of hydroxo lead or copper species on increasing the system pH was the most obvious species change (*cf.* Fig. 2), but other ligand effects have been considered in some detail in earlier papers.^{4,6,14}

Half-wave potential shifts, in the presence of excess ligand, have been used to determine the stability of metal complexes,¹⁵ and this approach has been applied to ASV determinations of hydroxo or carbonate complexes of metal ions,^{3,16} but doubts about the validity of the measurements can arise where there is electrochemical irreversibility or adsorption onto the electrode surface.^{3,17}

The peak broadening and potential shift observed for copper(II) systems may be due to a suspension and/or sedimentation effect on potential,¹⁸ but the changes are equally indicative of non-specifically sorbed metal ion being present (at higher pH) as hydroxo-species (*e.g.*, $[\text{Cu}(\text{OH})_x]^{2-x}$).

The results for lead confirmed the responses reported⁵ in a study which used MnO_2 , FeOOH and SiO_2 suspensions and a.c. polarography to assess colloidal effects on the capacity of the double layer. Reversibility was examined by constructing pseudopolarograms.

The presence of dispersed aluminosilicate clays caused no significant change in peak position or peak half-widths, but at pH < 6 the peak currents observed tended to be larger than those observed in control runs (by < 15%). This suggests that some dispersed colloids may behave in a similar fashion to those surfactants which form adsorbed layers that attract M^{2+} ions by electrostatic attraction and so promote a higher rate of electro-reduction at the mercury film.¹⁹

Electrode activation or passivation due to abrasion of the film surface by moving particles or adsorption effects can be a problem in ASV studies^{3,17} but it has been proposed recently⁷ that this limitation may be minimized by shielding the mercury film with a semipermeable membrane. In our studies, the ASV signals recorded with a shielded electrode in the

presence of FeOOH differed little from the values recorded without the shield (provided ample time was allowed for dialysis), as shown by the dashed lines in Fig. 4, A–C. It was concluded that the change in peak height for copper and lead in the presence of the particulates (full lines, Fig. 4, A, B) was due to specific sorption of these metal ions. The presence of chloride ions (■) resulted in some cadmium peak enhancement (Fig. 4C), but this was attributed to an anion effect, rather than particulate intervention, because the changes were small when acetate base electrolyte was used.

In contrast, in the presence of humic or fulvic acids, insertion of the dialysis membrane resulted in decrease in peak size, in some cases to only 60% of the value obtained for the mercury electrode immersed in the suspension (*cf.* Fig. 5). Such results imply that part of the "ASV labile" content consists of entities too large to permeate through the membrane (*i.e.*, metal-ion loosely bound to particulates or dispersed as large metal-bearing molecules). The magnitude of this "restrained" fraction varied with the metal ion, composition of background electrolyte, and solid added.

Similar (though smaller) differences in response were observed in a previous study⁴ when organic acid suspensions were filtered through a 0.45- μm membrane before re-analysis. The differences have been attributed to the smaller pore size of the dialysis tubing.

The membrane tubing used in our experiment had a molecular weight cut-off of 1000–1200, hence it was predicted that monomeric metal fulvate species should diffuse through, while humate species should be excluded. In the event, somewhat similar results were obtained with a fulvic acid sample and two different humic acids. This suggests that part of the "labile metal content" determined by direct analysis of suspensions is present as complexes having a molecular weight > 1200 (either as small dispersed entities or electrostatically bound to single functional groups on the solid surface). Alternatively, it can be proposed that diffusion of the larger molecules proceeds far more slowly (*i.e.*, longer equilibration time is required).

As shown by the results listed in Table 1, a significant fraction of the metal ion present in contaminated environmental samples proved to be "ASV labile", when suspended in acetate buffer solution. The percentage released varied with total loading, a trend to be expected in samples of poorly defined composition and possessing a range of sorption sites having different affinities for metal ions. With low total contents, the more active sites are involved and specific sorption predominates.

ANALYTICAL AND ENVIRONMENTAL IMPLICATIONS

Combination of anodic-stripping voltammetry with preliminary separation steps has been used by a

number of groups to subdivide the metal-ion content of waters into several different categories, and it has been demonstrated, *inter alia*, that significant fractions can be associated with colloidal matter.²⁰⁻²⁵

This study has confirmed that inorganic particulates are capable of specifically sorbing a high proportion of any lead, copper or cadmium ions present in an aqueous phase, particularly in the pH range covered by natural waters. The high affinity, which persists down to ng/l. level, also explains why only a small fraction (<1%) of the total metal content of a water system is usually present as soluble species.

In natural systems, the specifically sorbed fraction would normally be complemented by some exchangeable metal ion, with the magnitude of the latter reflecting the overall salt content of the waters.

The size of the displaceable fraction is indicated by the results listed in Table 1. These were preliminary studies which utilized a background electrolyte solution recognized²⁶ as being capable of displacing metal ions that are held by ion-exchange, weakly adsorbed, or associated with carbonate minerals.

In future studies, modifications of these procedures will be used to characterize the lability of the differently bonded forms of metal ion assumed to be present in natural-system suspended matter.

Provided turbid solutions are deaerated before contact with the mercury film electrode, so that abrasive effects (if any) are restricted to the time period associated with the ASV deposition cycle, protection of the electrode with a membrane is considered to be a precaution that can be time-consuming and an extra source of error. It is considered that direct analysis of turbid solutions (*i.e.*, the preliminary filtration step is eliminated) probably yields a more valid estimate of "available" metal-ion levels.

Our investigation has also indicated that ASV analysis of suspensions could be used to ascertain the adsorption capacities of fine particles in different chemical environments, at the metal-ion concentrations likely to exist in natural waters.

Eventually it should prove possible to utilise ASV analysis of suspensions as a new approach to "speciation" of soil/sediment systems.

REFERENCES

1. W. Salomons and U. Forstner, in *Metals in the Hydro-cycle*, Chapter 1, Springer-Verlag, Berlin, 1984.
2. P. Sagberg and W. Lund, *Talanta*, 1982, **29**, 457.
3. R. Ernst, H. E. Allen and K. H. Mancy, *Water Res.*, 1975, **9**, 969.
4. T. U. Aualiitia and W. F. Pickering, *ibid.*, 1986, **20**, 1397.
5. M. de L. S. Goncalves, L. Sigg and V. V. Stumm, *Environ. Sci. Technol.*, 1985, **19**, 141.
6. T. Ugapo and W. F. Pickering, *Talanta*, 1985, **32**, 131.
7. R. B. Smart and E. E. Stewart, *Environ. Sci. Technol.*, 1985, **19**, 137.
8. R. J. Atkinson, A. M. Posner and J. P. Quirk, *J. Inorg. Nucl. Chem.*, 1968, **39**, 2371.
9. R. R. Gadde and H. A. Laitinen, *Anal. Chem.*, 1974, **46**, 2022.
10. R. M. McKenzie, *Min. Mag.*, 1971, **38**, 493.
11. I. Sinko and J. Doležal, *J. Electroanal. Chem.*, 1970, **25**, 299.
12. Y. K. Chau and Lum-Shue-Chan, *Water Res.*, 1974, **8**, 383.
13. T. T. Chao and P. K. Theobald, *Econ. Geol.*, 1976, **71**, 1560.
14. E. A. Schonberger and W. F. Pickering, *Talanta*, 1980, **29**, 1.
15. D. R. Crow, in *Polarography of Metal Complexes*, Academic Press, New York, 1969.
16. H. Bilinski, R. Huston and W. Stumm, *Anal. Chim. Acta*, 1976, **84**, 157.
17. S. A. Wilson, J. C. Huth, R. E. Arndt and R. K. Skogerbee, *Anal. Chem.*, 1980, **52**, 1515.
18. D. P. Brezinski, *Analyst*, 1983, **108**, 425.
19. V. S. Krylov and I. F. Fishtik, *Elektrokhimiya*, 1981, **17**, 787.
20. G. E. Batley and T. M. Florence, *Mar. Chem.*, 1976, **4**, 347.
21. G. E. Batley and D. Gardiner, *Estuarine Coastal Mar. Sci.*, 1978, **7**, 59.
22. D. Gardiner, *Water Res.*, 1974, **8**, 157.
23. K. K. Turekian, *Geochim. Cosmochim. Acta*, 1977, **41**, 1139.
24. T. M. Florence and G. E. Batley, *CRC Crit. Rev. Anal. Chem.*, 1980, **9**, 219.
25. *Idem*, *Talanta*, 1977, **24**, 151.
26. W. F. Pickering, *Oregeol. Revs.*, 1986, **1**, 83.

ENHANCEMENT OF SENSITIVITY OF ION-EXCHANGER ABSORPTIOMETRY BY USING A THICK ION-EXCHANGER LAYER

KAZUHISA YOSHIMURA

Chemistry Laboratory, College of General Education, Kyushu University, Ropponmatsu, Chuo-ku,
Fukuoka 810, Japan

HIROHIKO WAKI

Department of Chemistry, Faculty of Science, Kyushu University, Hakozaki, Higashiku,
Fukuoka 812, Japan

(Received 9 January 1985. Revised 3 September 1986. Accepted 17 September 1986)

Summary—Enhancement of the sensitivity of ion-exchanger absorptiometry by the use of much thicker ion-exchanger layers than those previously employed has been investigated. Because the background attenuation due to light-scattering from the solid particle layer increases only moderately, whereas the net absorbance of the sorbed sample species increases greatly when the cell length is increased, a cell with at least 10-mm path-length may be effectively used without difficulty in most commercial spectrophotometers, giving at least ten times the sensitivity obtainable with a 1-mm cell. Since the background attenuation depends on the optical geometry, it can be lowered to some extent by using a particular type of spectrophotometer, and by placing a cylindrical mirror between the cell and the light-detector window or by setting the cell as close as possible to the window. The use of such long cells has been found to improve the sensitivity in the chromium-diphenylcarbazide, iron-1,10-phenanthroline, nickel-PAN, cadmium-PAR, bismuth-chloride and uranium-thiocyanate systems. Other methods may be similarly improved.

Since the new technique of solid-phase photometry ("ion-exchanger colorimetry") was proposed in 1976,¹ a large number of applications have been made for the determination of trace metal ions in water samples,²⁻⁹ and have been reviewed.¹⁰ Recently the method was extended to the ultraviolet absorption region.¹¹ The advantages of this method are (a) the sensitivity is much higher than that of the corresponding conventional spectrophotometric method since the light-absorption measurement is made directly on the ion-exchanger phase without stripping of the coloured component and (b) species interfering in ordinary solution spectrophotometry can be excluded from the ion-exchanger through equilibration under proper conditions and thus the spectrophotometric selectivity may often be increased. It has already been stated briefly¹⁰ that the sensitivity can be still further enhanced by using a much thicker ion-exchanger layer than those previously employed. The present paper will treat this in detail.

EXPERIMENTAL

The ion-exchangers, reagents, procedures and conditions used were in principle the same as those in the literature, unless otherwise stated.

Light-measurements were made with a Hitachi EPS-3T double-beam spectrophotometer (automatic recording analogue type) or a Nippon Bunko UVIDEC-320 (digital type) at room temperature.

The thickness of the ion-exchanger layer was varied by using fused-silica cells of different light-path lengths or a

combination of a 10-mm path-length fused-silica cell and fused-silica spacers of different thickness. A narrow black-sided cell (Fujihara Factory, 4 mm width and 10 mm path-length) or a wedge-shaped acrylic spacer (Fig. 1) was employed in some cases to reduce the volume occupied by the ion-exchanger layer, but not the light-path length. The shape of the spacer was determined by the geometry and the shape of the light-beam of the spectrophotometer. The spacer was easily made with acrylic resin plates.

An externally silvered fused-silica tube (12 mm internal diameter and 40 mm long for the Nippon Bunko spectrophotometer) was placed between the cell holder and the light-detector window to partly recover the light scattered from the ion-exchanger layer (Fig. 2). Otherwise, the cell was set as close as possible to the detector window, to give the best geometry for light-collection, but in any case the ion-exchanger layer was set closest to the detector when spacers were used to reduce the path-length.

RESULTS AND DISCUSSION

Theoretical background of solid-phase absorptiometry

The net ion-exchanger phase absorbance due to the sample component sorbed (A_{RC}) can be represented by

$$A_{RC} = A - A_{ref} = \epsilon_{RC} l_R C_0 \frac{V}{mv(1 + V/mD)} \quad (1)$$

if the sample and reference ion-exchanger layers have practically the same background attenuation under the same conditions. Here A is the sample layer

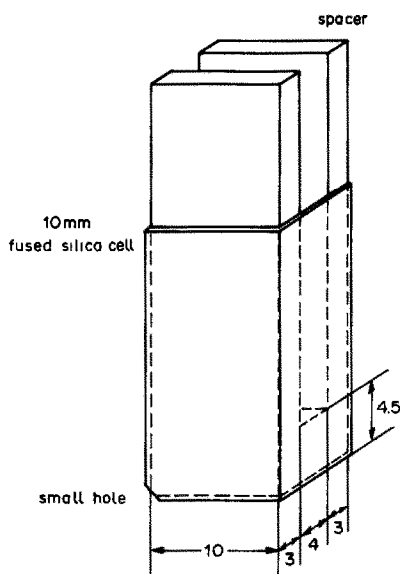


Fig. 1. The acrylic resin spacer for a 10-mm cell. The cell is for the Nippon Bunko spectrophotometer.

attenuance,* A_{ref} the reference layer attenuance, ϵ_{RC} the molar absorptivity of the sample species in the ion-exchanger phase, l_R the actual path-length of the light penetrating through the ion-exchanger layer (in general not equal to the cell length), C_0 the sample component concentration in the initial solution to be analysed, V the sample solution volume taken for the equilibration, m the weight of ion-exchanger, v the volume of equilibrated ion-exchanger per unit weight

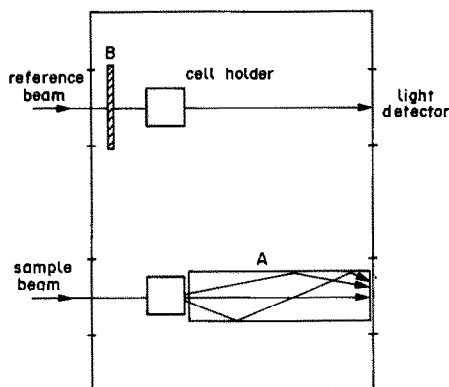


Fig. 2. The cell compartment furnished with special accessories. A: a cylindrical mirror tube (15 mm outer diameter, 12 mm inner diameter). A thin silver layer deposited by the silver-mirror reaction was fixed on the outer surface of a fused-silica tube with a synthetic glue. B: a commercial perforated metal disc (Hitachi).

*Attenuance = $\log I_0/I$, for the case in which light is scattered as well as absorbed by the system.

taken, and D the distribution ratio of the sample component (ml/g).¹²

As shown in equation (1), an effective way to enhance the sensitivity is undoubtedly to use a longer cell, since the increase in cell length leads to an increase in the actual light-path length through the ion-exchanger layer, though a direct proportionality between these two quantities cannot necessarily be expected. On the other hand, the use of a very long cell results in light loss by scattering and/or absorption to such an extent that the light intensity to be detected may be below the limit of detection by the light-detector used. Therefore we first examined the correlation between the background attenuance of the ion-exchanger layer and the cell length, to find the maximum cell length for reliable and sensitive measurements.

Background attenuance and cell length

Figure 3 demonstrates typical examples of the attenuance spectra of long ion-exchanger layers, in which no light-absorbing species are sorbed, measured against air as reference. A perforated metal disc of attenuance 1.0 or 2.0 was used to balance the light intensities. The increase in cell length caused only a moderate increase in background attenuance (curves D, E and F), unlike the case for a liquid medium (Lambert's law) and the attenuance was found to be a linear function of the logarithm of the cell length, in all cases studied, at wavelengths where only light scattering is involved (Fig. 4). This relationship is empirical and has not been derived from first principles, but can be understood by considering the following. If the light-source passes through the centre of a layer of large dimensions consisting of fine

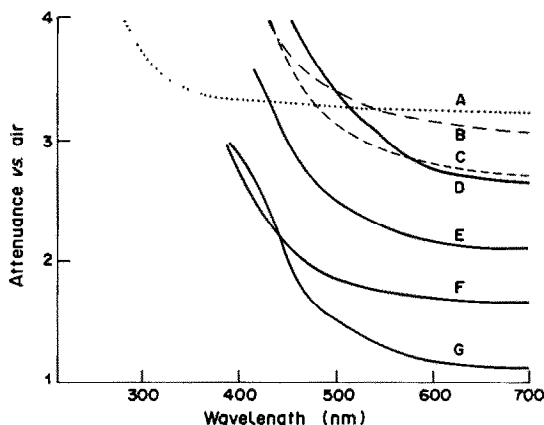


Fig. 3. Attenuance spectra of an ion-exchanger layer at long cell length. A: QAE-Sephadex A-25, Cl^- form, Hitachi, 10 mm. B: Dowex 1-X2, Cl^- form (100-200 mesh), Hitachi, 10 mm. C: AG 50W-X2, H^+ form (100-200 mesh), Hitachi, 10 mm. D-G: AG50W-X2, H^+ form (100-200 mesh), Nippon Bunko, 20 mm (D), 10 mm (E), 5 mm (F), 10 mm with cylindrical mirror (G). Light measurements were conveniently made with use of a perforated metal disc of $A = 1.0$ or 2.0. The ordinates in the figure are taken as measured against air for mutual comparison.

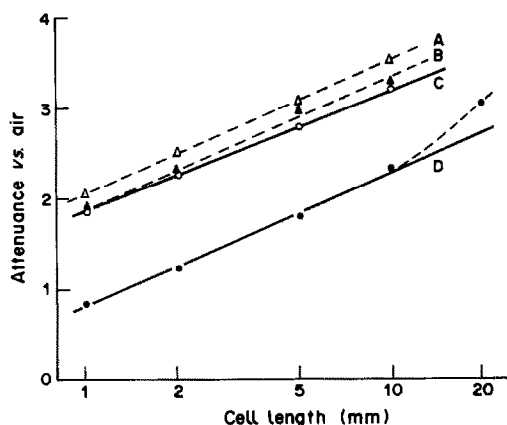


Fig. 4. The cell-length dependence of the ion-exchanger layer background attenuation. A and B: QAE-Sephadex A-25, Cl^- form, in H_2O , at 330 nm (A), and 600 nm (B). C: Dowex 1-X2, Cl^- form (100–200 mesh), in H_2O , at 600 nm. D: AG 50W-X2, H^+ form (100–200 mesh) in H_2O , at 550 nm. Instrument: Hitachi EPS-3T (A, B and C), Nippon Bunko UVIDEC-320 (D).

ion-exchanger particles and water, the light intensity at any point inside this layer should be inversely proportional to the square of its distance from the centre, if no light-absorption takes place, as the light intensity will be the result of multiple reflection and refraction inside the layer.

In practical measurements with an ordinary square-type cell of path-length l , the relationship between the intensities of the incident (I_0) and detected (I) light may be written in approximate form as

$$I = I_0 \frac{(1-r)Sf}{2\pi l^{(2-a)}} \quad (2)$$

where r is the fraction reflected at the irradiated layer surface (which is a constant for a thick solid layer), S is the area of the front surface facing the light-detector window, f is the intensity ratio of the light reaching the layer front to that detected by the detector, which depends on the geometry of the cell-detector system (Fig. 5), and a is a directionality parameter which should usually be somewhat larger than zero, because the incident light enters the ion-exchanger layer only in the direction from the light source to the detector and this directionality cannot be completely destroyed even by a long cell length, because the partially directional reflectance at particles and the cell wall is still forwards towards the detector. Equation (2) can be written in logarithmic form,

$$A = \log I_0/I = (2-a) \log l + k \quad (3)$$

where k is a constant. Equation (3) is consistent with the results in Fig. 4, when $a = 0.5-0.7$ in the conditions studied. A similar relation was found for milk samples, but a was approximately zero.

The attenuation of a layer consisting of fine solid

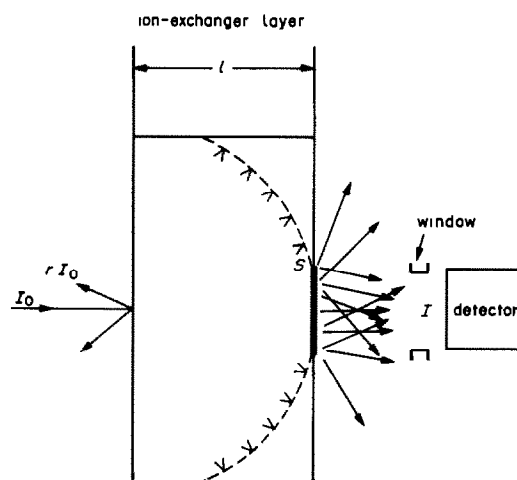


Fig. 5. A schematic model of the behaviour and detection of a light beam passed through an ion-exchanger particle layer.

particles depends on the geometry for the cell and the detector, and therefore on the instrument employed. For instance the Nippon Bunko UVIDEC-32 spectrophotometer gave significantly lower background attenuation than the Hitachi instrument (curves C and E in Fig. 3), indicating that the geometry is optically more favourable in this instrument. A further lowering of the background attenuation could be accomplished by placing a cylindrical mirror parallel to the light beam and covering the optical path from the cell to the detector window (curves E and G). Setting the cell as closely as possible to the light-detector window lowers the background attenuation by about 0.5. A cell length of 10 mm seems to be a practical limit, for use with an ordinary commercial spectrophotometer with a measurable absorbance limit of 3–4, though it may sometimes be possible to use a 20-mm cell with longer wavelengths in the visible region (curve D).

For the ultraviolet region, aromatic ion-exchange resins cannot be used, because of the strong absorptivity of the aromatic matrix, whereas Sephadex ion-exchangers can safely be employed with 10 mm cell length even at wavelengths near the ultraviolet (curve A in Fig. 3).

Enhancement of sensitivity by use of long cells

Next we examined the relation between the measured net absorbance due to the sample component sorbed and the cell length. As shown by the examples in Fig. 6, a direct proportionality was observed in some cases between the two quantities, while in other cases, especially with the Sephadex ion-exchanger in the ultraviolet region, the increase in cell length produced a non-linear increase in the absorbance. Taking all these facts into account, it can be concluded that the use of cell lengths of about 10 mm is very advantageous for the determination of sample components present at low levels.

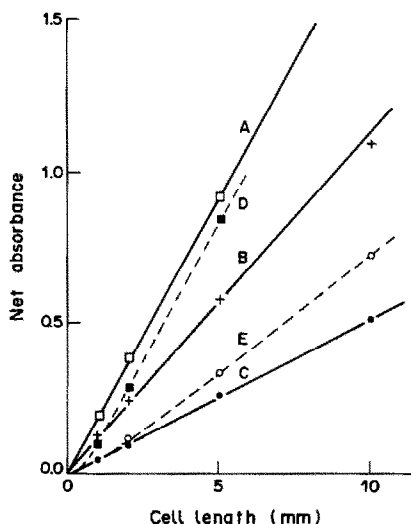


Fig. 6. The effect of cell length on the net absorbance of an ion-exchanger layer with a sample component sorbed on it. A: solution, $2 \times 10^{-7} M$ Ni (pH 6.0); ion-exchanger, AG 50W-X2 (100–200 mesh) with presorbed PAN; $V/m = 400$. B: solution, $2 \times 10^{-7} M$ Cr, 0.006% diphenylcarbazine + 0.025 M H_2SO_4 ; ion-exchanger, AG 50W-X2 (100–200 mesh); $V/m = 400$. C: solution, $2 \times 10^{-7} M$ Fe, $2.5 \times 10^{-4} M$ 1,10-phenanthroline + 0.25% hydroxylamine (pH 5); ion-exchanger, AG 50W-X2 (100–200 mesh); $V/m = 400$. D: solution, $4 \times 10^{-7} M$ U, 1 M NH_4SCN + 0.1 M HCl + ascorbic acid; ion-exchanger, QAE-Sephadex A-25; $V/m = 1000$. E: solution, $3 \times 10^{-7} M$ Bi, 0.2 M HCl + 50% 2-propanol; ion-exchanger, QAE-Sephadex A-25; $V/m = 200$.

Figure 7 gives calibration graphs for various metal elements with long cells. A much higher sensitivity, roughly in proportion to the cell length, was attained in every case, without an appreciable lowering of the accuracy in comparison with that obtainable with a 1-mm cell. This suggests that use of longer cells would significantly enhance the sensitivity for all systems usable in ion-exchanger spectrophotometry.

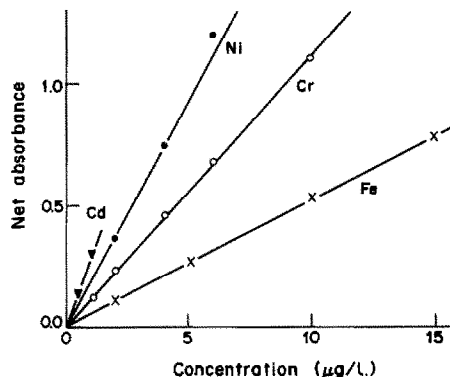


Fig. 7. The calibration curves for ion-exchanger absorptiometry with a 10-mm cell ($V/m = 400$). Colouring agent: Fe, 1,10-phenanthroline;¹ Cr, diphenylcarbazine;¹ Ni, PAN;⁶ Cd, PAR.⁴

REFERENCES

1. K. Yoshimura, H. Waki and S. Ohashi, *Talanta*, 1976, **23**, 449.
2. K. Yoshimura and S. Ohashi, *ibid.*, 1978, **25**, 103.
3. K. Yoshimura, H. Waki and S. Ohashi, *ibid.*, 1978, **25**, 579.
4. K. Yoshimura and S. Ohashi, *Mem. Fac. Sci., Kyushu Univ., Ser. C*, 1978, **11**, 181.
5. Y. Toshimitsu, K. Yoshimura and S. Ohashi, *Talanta*, 1979, **26**, 273.
6. K. Yoshimura, Y. Toshimitsu and S. Ohashi, *ibid.*, 1980, **27**, 693.
7. K. Yoshimura, S. Nigo and T. Tarutani, *ibid.*, 1982, **29**, 173.
8. K. Ohzeki, T. Sakuma and T. Kambara, *Bull. Chem. Soc. Japan*, 1980, **53**, 2878.
9. H. Ishii, *Z. Anal. Chem.*, 1984, **319**, 23.
10. K. Yoshimura and H. Waki, *Talanta*, 1985, **32**, 345.
11. H. Waki and J. Korkisch, *ibid.*, 1983, **30**, 95.
12. H. Waki, in D. Naden and M. Streat (eds.), *Ion Exchange Technology*, p. 595. Ellis Horwood, Chichester, 1984.

INTERFACING AN ANALOGUE INFRARED SPECTROMETER TO A MICROCOMPUTER*

M. J. ADAMS and G. J. EWEN

Department of Spectrochemistry, Macaulay Institute for Soil Research, Craigiebuckler,
Aberdeen, Scotland

(Received 17 August 1986. Accepted 12 September 1986)

Summary—An Apple microcomputer has been interfaced to a Perkin-Elmer model 577 infrared spectrometer. The spectral data are digitized with the aid of an in-house designed 12-bit analogue-to-digital interface unit. Control and status signals are obtained from the spectrometer and an optical encoder unit is used to provide an accurate wavenumber marker for the conversion and data recording. The digital data are formatted by the microcomputer and then can be manipulated by programs already developed for handling spectral data recorded from digital spectrometers.

In recent years the integration of microprocessor technology into the construction of spectrometers by manufacturers has produced major advances in the move to more automated and computerized laboratory instrumentation and procedures. Today analytical apparatus having a significant electronic component is invariably supplied with a digital output for computer interfacing or, with the larger instruments, an integral computer or workstation is available. There has also been an acceptance of some necessary standardization in digital interfacing schemes. Possibly the most common is the asynchronous serial data-transfer protocol, the RS232C. Originally intended for data transfer rather than instrument control, the serial interface can provide a simple yet effective link between a computer and laboratory equipment.^{1,2} Higher rates of data transfer can be achieved with a parallel interface, and one sophisticated and popular arrangement is the general-purpose interface bus (GPIB), often referred to as the IEEE488 interface, originally conceived by the Hewlett-Packard Corp. These developments in modern analytical instrumentation have produced changes in laboratory practice and management. The basic principles and advantages of an integrated laboratory data-acquisition and manipulation system using a network of linked microcomputers are now widely appreciated and a modern instrumentation laboratory would not be designed without some thought to computerized communications and laboratory information management.

The transition of the instrumental analytical laboratory from manual to computerized and automated work cannot be achieved overnight, and in most laboratories there is the need to integrate into the newer digital system the older, but still functional and

respected, spectrometers. In such cases the more traditional techniques of analogue interfacing of the apparatus to the computer system are employed and, unlike the digital interfacing schemes, there are rarely "off-the-shelf" solutions.

In our spectrometry laboratories Apple microcomputers are employed for the acquisition and manipulation of spectral data. A research-grade infrared spectrometer is controlled by a serial RS232C digital link^{1,2} and the data produced by EPR and AAS spectrometers are accessed by analogue interface links.^{3,4} In this communication we report the modification of an analogue infrared spectrometer and its interfacing to an Apple microcomputer for data-logging. The techniques and procedures employed are relevant to the integration of any similar analogue instrument into a more modern and computerized laboratory information network.

INSTRUMENTATION AND INTERFACING

The Perkin-Elmer Model 577 infrared spectrophotometer is a double-beam instrument typical of many analogue spectrometers still in routine use. It provides a continuous record of the infrared transmittance of a sample, as a function of frequency, by means of a chart driven in synchronization with the monochromator. The wavenumber (frequency) scanning motor drives both the recorder and the grating monochromator, and as both are directly coupled, this ensures that the wavenumber settings are accurately reproduced. As well as the chart recorder, an analogue read-out signal obtainable from one of two external sockets can be connected to a logging device. The magnitude of the read-out voltage (10 mV and 1 V full-scale deflection) is indicative of the sample transmittance. The 0-1 V range output signal is employed for interfacing and data-logging by the microcomputer.

*© The Macaulay Institute for Soil Research, 1986.

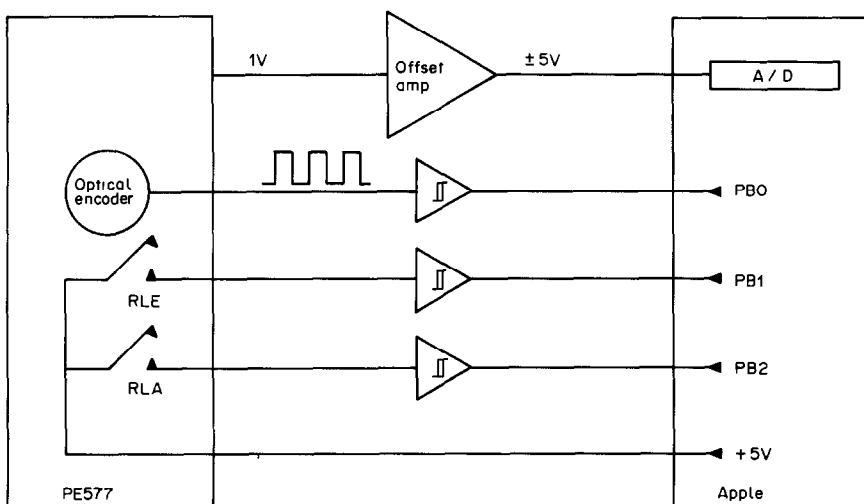


Fig. 1. Schematic representation of the computer-spectrometer interface, illustrating the trigger, status and control signals employed in the digitization of the spectral data.

The acquisition of spectral data from the spectrometer and their subsequent digitization and formatting were achieved with an Apple microcomputer system. This type of microcomputer is employed extensively in many laboratories for instrument control and data-logging and has been demonstrated to be of considerable value in laboratory applications. The Apple microcomputer's internal architecture and interfacing capabilities have been recently reviewed by Karanassios and Horlick.⁵ Briefly, the computer is based on an 8-bit 6502 microprocessor having direct access to 64 kbyte of digital memory, of which up to about 48 kbyte may be used for program and data storage in a typical system. The most common language employed with this computer, as with most microcomputers, is BASIC, although a wide range of "higher" languages is available. Interfacing of external devices to the Apple computer is achieved through the backplane bus arrangement used in this computer. A series of six directly addressable edge-connector slots is provided within the computer. The provision of these expansion ports provides the Apple computer with the flexibility needed for the general-purpose interfacing tasks required of a laboratory microcomputer and has been a major factor in this computer's popularity for laboratory use and application.

A diagram of the general scheme for interfacing the Model 577 spectrometer and the Apple microcomputer is given in Fig. 1. The 0–1 V analogue transmittance signal from the spectrometer is linked to the computer by a $\times 10$ offset amplifier unit necessary for the ± 5 V bipolar analogue-to-digital (A/D) computer interface. The design, construction and use of the high-speed 12-bit A/D unit have been described in detail elsewhere.⁶ By use of the technique of successive approximations a complete 12-bit data conversion is accomplished in about 25 μ sec. For use

with the Apple computer, all the A/D components were mounted on a single circuit board for direct connection to the computer by one of the input/output slots. No external power supply is necessary. To use an A/D interface in the laboratory for data acquisition a trigger signal is required to initiate a conversion and control the data-logging operations. The provision of these control signals, Fig. 1, required modifications and additions to the spectrometer.

It is important in infrared spectrometry that transmission measurements be recorded at reproducible and accurately known frequency intervals. The accuracy and precision were attained in this application with the aid of an optical rotary encoder mounted on the monochromator-grating drive shaft. Optical encoders are commonly employed in many servo loops requiring accurate positional information, e.g., plotters, automatic handlers, robots *etc.*, and are widely available. The device employed was a high-resolution 1000 counts/rev, two-channel (quadrature) kit (Hewlett-Packard type HEDS 6000), the 5-V operating supply being derived from the Apple computer. The TTL-compatible outputs from the encoder were linked to the computer through a buffer gate. The resolution of the encoder provided a trigger pulse at every wavenumber, in the region from 4000 to 2000 cm^{-1} , and two pulses per wavenumber from 2000 to 200 cm^{-1} , *i.e.*, 5600 data points per complete spectrum. As well as this trigger signal it was necessary to derive (from the spectrometer) signals to indicate a start-of-scan condition and to monitor the positions during a scan when the grating and filter changes occur. During these latter periods no data should be recorded. Actuation of the start button on the spectrometer caused a relay (RLA) to be energized and spare contacts on this relay were used to switch a 5-V line to indicate to the computer a start-of-scan. The dead periods of a scan were indicated by means of a

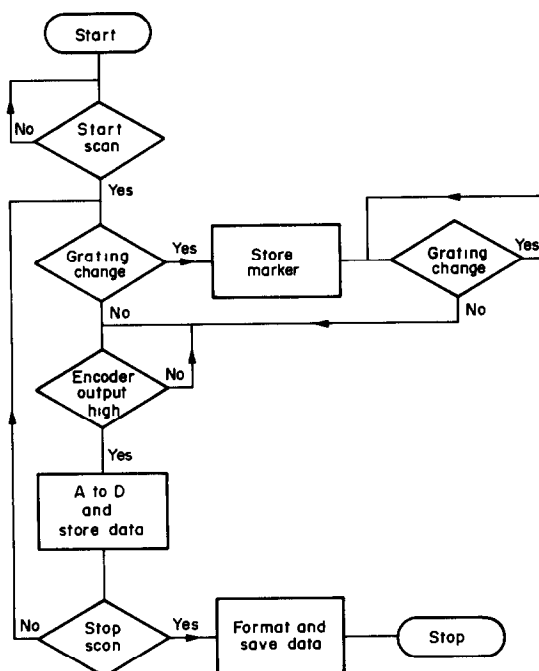


Fig. 2. A flowchart of the data-acquisition algorithm coded in machine assembly language within the computer.

5-V line switch by a relay mounted in parallel with the relay (RLE) which the spectrometer employs to disengage the pen recorder during a grating change.

As well as the expansion slots the Apple computer provides a useful but simple interfacing facility by means of a "games" socket which permits the computer to monitor the status of TTL signal lines directly. The scan-start and grating-change signals, as well as the optical encoder input, were all connected to this peripheral socket (PB0, PB1 and PB2) by TTL buffer amplifiers, as indicated in Fig. 1.

Data acquisition

The general scheme for logging the data from the spectrometer is provided in flowchart form in Fig. 2, and to take advantage of its high operating speed was coded in the Apple microcomputer in assembly language. The timing diagram shown in Fig. 3 illustrates the status of the various control and trigger signals during a spectral scan. The status of the start-scan button is monitored and once it is activated the output signals from the spectrometer are digitized by use of the trigger signal supplied by the optical encoder, until the end-of-scan (START-SCAN) signal is recorded. During a scan the status of the monochromator gratings is monitored continuously and, within the indicated dead periods when a grating is changed, no digitizing is performed. The spectral data, as 12-bit integer values, are recorded sequentially in RAM within the computer with the position of the grating changes marked with a suitable flag value (Hex FFFF). After the spectrum has been recorded, the computer automatically proceeds to format the spectral data. The accurate assignment of spectral frequency is achieved by reference to the internal flag markers in the data. To ensure compatibility of the data with similar spectra recorded from other instruments, the spectra were reduced to 2820 data points of 11-bit resolution. By this means the data recorded from the type 577 spectrometer could be stored, examined and manipulated by software developed for use with the model 580B research infrared spectrometer.¹

Conclusion

With the increasing use of microcomputer systems in analytical laboratories, there is frequently the demand that instrumentation be linked directly to the computer for recording data. Where no suitable digital interfaces are available with the instrument,

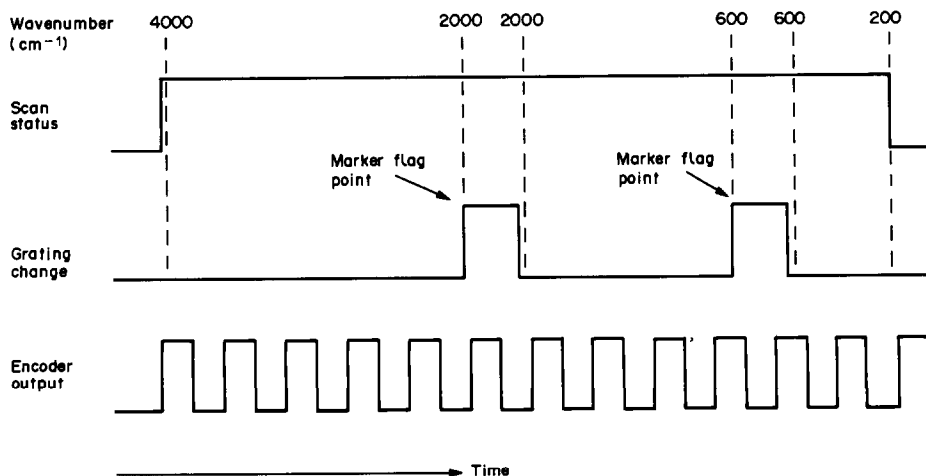


Fig. 3. The trigger, status and control signals during a spectral scan.

analogue interfacing techniques can be efficiently employed. As described here, a common type of double-beam infrared spectrometer can be connected to a microcomputer with relatively minor additions to the spectrometer mechanics to provide suitable control, trigger and status signals for the data digitization. The use of an inexpensive, but high-precision, rotary optical encoder mounted directly on the monochromator drive shaft ensured accurate frequency assignment of the spectral data. The 12-bit analogue-to-digital conversion process was performed by a specially designed interface board. The total interface system required no external power

supplies, was inexpensive to construct and has been demonstrated to be of value in providing greater integration of analytical spectrometers in the laboratory.

REFERENCES

1. M. J. Adams and I. Black, *J. Auto. Chem.*, 1983, **5**, 9.
2. *Idem*, *Anal. Proc.*, 1982, **19**, 470.
3. M. J. Adams and G. J. Ewen, *J. Auto. Chem.*, 1984, **6**, 202.
4. M. J. Adams, M. C. Mitchell and G. J. Ewen, *Anal. Chim. Acta*, 1983, **149**, 1011.
5. V. Karanassios and G. Horlick, *Talanta*, 1985, **32**, 601.
6. G. J. Ewen and M. J. Adams, *Lab. Pract.*, 1984, **33**, 116.

ADSORPTIVE STRIPPING VOLTAMMETRIC MEASUREMENTS OF TRACE LEVELS OF URANIUM FOLLOWING CHELATION WITH MORDANT BLUE 9

JOSEPH WANG* and JAVAD M. ZADEH

Department of Chemistry, New Mexico State University, Las Cruces, NM 88003, U.S.A.

(Received 14 August 1986. Accepted 12 September 1986)

Summary—The chelate of uranium with the azo dye Mordant Blue 9 is shown to be adsorbed and then reduced on the hanging mercury drop electrode. These properties have been exploited in developing a highly sensitive stripping voltammetric procedure for trace determination of uranium. With controlled adsorptive accumulation for 5 min, a detection limit near $2 \times 10^{-10} M$ uranium is obtained. Cyclic voltammetry has been used to characterize the interfacial and redox behaviour. The effect of various operational parameters on the stripping response is discussed. Experimental conditions include use of $1 \times 10^{-6} M$ Mordant Blue 9 in 0.05M acetate buffer (pH 6.5), an accumulation potential of $-0.43 V$, and a linear potential scan. The response is linear up to $1.2 \times 10^{-7} M$ uranium, and the relative standard deviation at $4.2 \times 10^{-8} M$ is 3.2%. The effects of possible interferences from organic surfactants or metal ions have been investigated.

Because of the importance of uranium, a simple, rapid and highly sensitive method for its determination is required. Atomic-absorption spectroscopy, neutron-activation analysis, X-ray fluorescence, and other techniques can be used, but with various difficulties, often insufficient sensitivity, and expensive instrumentation.¹⁻³

Voltammetric techniques have frequently been used for the determination of uranium in various matrices. At mercury electrodes uranium yields a number of reduction steps which can be used for polarographic measurements. Modern polarographic methods—based on alternating current, differential pulse or square wave techniques—permit convenient and rapid determination of uranium down to the submicromolar level.^{3,4} Even lower levels of uranium can be measured by using the recently developed adsorptive stripping voltammetric approach^{5,6} based on interfacial accumulation of the uranium-catechol complex on the hanging mercury drop electrode, followed by reduction of the adsorbed species. While the method permits measurement down to the $3 \times 10^{-10} M$ level, it suffers from a narrow linear range and interferences by iron, lead and copper ions.

The present paper describes a highly sensitive adsorptive stripping procedure for determining uranium by adsorptive accumulation and reduction of its chelate with the dihydroxyazo dye Mordant Blue 9 (Colour Index 14855). The polarographic behaviour of the uranium/Mordant Blue 9 chelate has been described by Ishibashi *et al.*⁷ The chelate produces a distinct cathodic response, attributed to reduction of the azo bond involved in the co-ordination. The polarographic procedure enables uranium to be de-

termined down to the $2 \times 10^{-6} M$ level. The interfacial properties of the uranium/Mordant Blue 9 chelate are exploited in the present study to achieve a substantial lowering of the detection limit, by use of a stripping voltammetric measurement at the hanging mercury drop electrode. Conditions for enhancing the surface concentration of the chelate have been carefully optimized. The proposed method offers a similar detection limit to that of the catechol-based adsorptive approach,⁶ but with shorter accumulation times. Other advantages of the present method are its extended linear range and reduced interferences from lead, copper, and iron. A number of sensitive adsorptive stripping procedures for measuring other trace metals, such as titanium,⁸ aluminium,⁹ manganese¹⁰ and yttrium,¹¹ based on chelation with dihydroxyazo dyes, have also been developed recently in our laboratory.

EXPERIMENTAL

Apparatus

The instrumentation used, a PAR 264A voltammetric analyser with a PAR 303 static mercury drop electrode, has already been described in detail.^{8,9}

Reagents

The uranium stock solution (1000 ppm) was obtained from Aldrich, and diluted as required for making standard additions. A $1 \times 10^{-4} M$ stock solution of Mordant Blue 9 (Aldrich) was prepared daily. The supporting electrolyte was a 0.05M acetate buffer (pH 6.5). All solutions were prepared from doubly distilled water.

Procedure

Transfer 10.0 ml of $1 \times 10^{-6} M$ Mordant Blue 9 solution in the supporting electrolyte into the cell, and purge with nitrogen for 8 min. Switch on the accumulation potential (usually $-0.43 V$) while the solution is still being stirred. After the accumulation step, stop the stirring, and after 15

*Author for correspondence.

sec record the voltamperogram by applying a linear scan terminating at -1.0 V. This gives the background curve. Introduce an aliquot of the uranium sample or standard solution, stir (while purging with nitrogen) for 6 min to allow chelate formation, then go through the deposition and stripping steps as before. All the results in this paper were obtained at room temperature, with a nitrogen atmosphere maintained over the solution surface.

RESULTS AND DISCUSSION

Figure 1 shows voltamperograms obtained with a hanging mercury drop electrode immersed in a stirred $2\text{-}\mu\text{g/l.}$ ($8.4 \times 10^{-9} M$) uranium solution, containing $1 \times 10^{-6} M$ Mordant Blue 9, for increasing periods of time. The uranium/Mordant Blue 9 chelate yields a well defined reduction peak at -0.56 V, the peak width at half-height being 55 mV. The longer the accumulation time, the more the amount of chelate adsorbed onto the mercury surface, and the larger the peak current. For a 120-sec accumulation period (curve e), the response obtained is 20 times that attained without accumulation (curve a). Hence, convenient measurements at the $\mu\text{g/l.}$ level are feasible following short accumulation periods. Also shown in Fig. 1 are current *vs.* accumulation-time plots for 2 (A) and 4 (B) $\mu\text{g/l.}$ uranium. At both levels the peak rises rapidly at first and then more slowly. Obviously, a compromise between sensitivity and speed is advisable when optimizing the accumulation period, with 10 and 60 sec sufficing for convenient measurements at the 10 and 1 $\mu\text{g/l.}$ levels, respectively.

The interfacial and redox behaviour of the uranium/Mordant Blue 9 chelate can be evaluated from cyclic voltammetric experiments. For example, Fig. 2A shows repetitive cyclic voltamperograms for $1 \times 10^{-6} M$ Mordant Blue 9, obtained after accumulation at -0.20 V for 60 sec. The first scan (labelled 1) exhibits a distinct cathodic peak at -0.43 V, related to the reduction of the adsorbed dye. Subsequent scans result in a sharp decrease of the dye peak, to a stable response associated with the dissolved species (*i.e.*, rapid desorption of the reduced form of the dye). No peaks are observed on scanning in the positive direction. When the same experiment is repeated after the addition of $25 \mu\text{g}$ of uranium per litre (Fig. 2B), an additional cathodic peak, due to reduction of the adsorbed chelate, is observed at -0.56 V. Desorption of the product is indicated by subsequent scans. Accumulation at -0.43 V results in a single chelate reduction peak (Fig. 2C). With $25 \mu\text{g/l.}$ uranium, $1 \times 10^{-6} M$ Mordant Blue 9 and stirring at -0.43 V, maximum adsorption density was attained after 240 sec. The maximum charge, obtained by integrating the area under the chelate stripping peak ("cut and weigh" method), was found to be $0.69 \mu\text{C}$. Division of the charge by the conversion factor (nFA) yields an adsorbed-layer density of 1.2×10^{-10} mole/ cm^2 ($n = 4$). A plot of $\log(\text{peak-current})$ *vs.* $\log(\text{scan-rate})$ for the adsorbed chelate was linear, with a slope of 1.12, over the 10–200 mV/sec range (other conditions as in Fig. 2C). A slope of 1.0 would be expected for an ideal redox couple immobilized on an electrode sur-

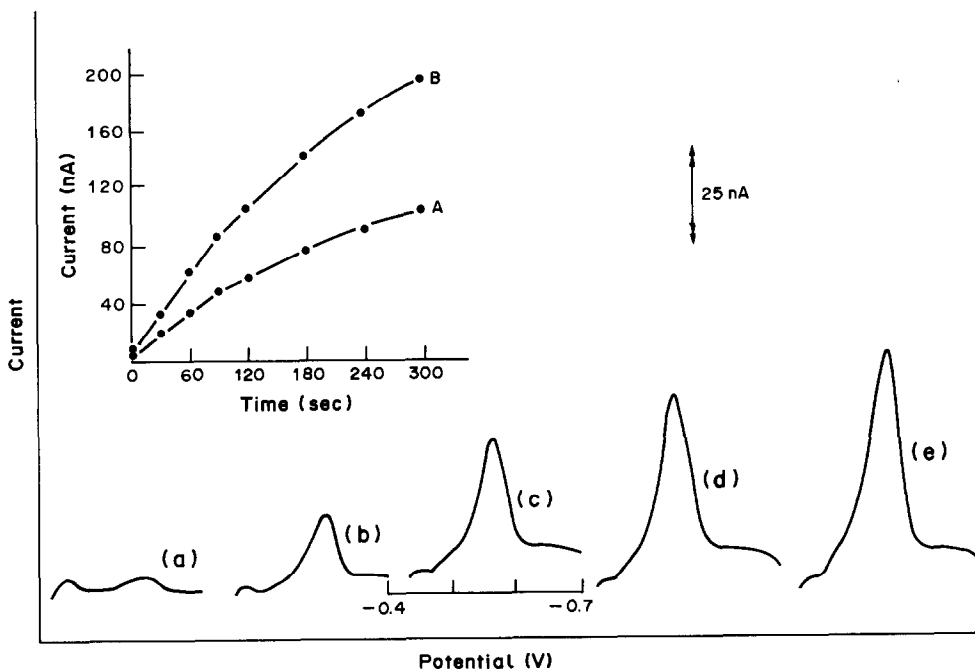


Fig. 1. Voltamperograms for $2 \mu\text{g/l.}$ ($8.4 \times 10^{-9} M$) uranium following different accumulation periods: (a) 0, (b) 30, (c) 60, (d) 90, (e) 120 sec. Also shown are current *vs.* accumulation-time plots for the 2 (A) and 4 (B) $\mu\text{g/l.}$ uranium levels. Accumulation potential, -0.43 V; scan-rate, 50 mV/sec, $0.05 M$ acetate buffer (pH 6.5) solution, containing $1 \times 10^{-6} M$ Mordant Blue 9.

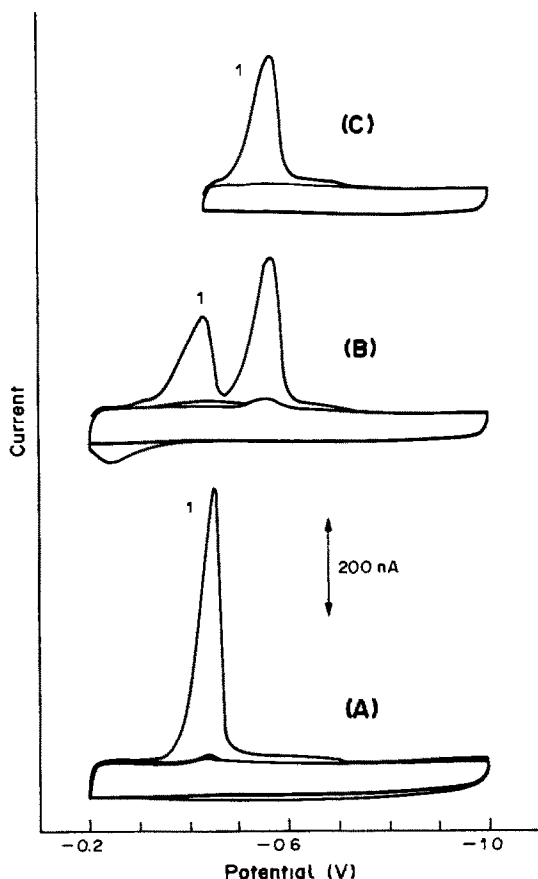


Fig. 2. Repetitive cyclic voltamperograms following 60 sec accumulation in the absence (A) and the presence (B, C) of 25 $\mu\text{g/l}$. uranium. Accumulation potential, -0.2 (A, B) and -0.43 (C) V. Other conditions as for Fig. 1.

face. A negative shift in the peak potential, from -0.65 to -0.73 V, was observed upon increasing the scan-rate from 10 to 200 mV/sec. The resulting plot of peak-potential *vs.* log (scan-rate) was linear, with a correlation coefficient of 0.999.

Various experimental variables affecting the adsorptive stripping response were evaluated and optimized. For example, Fig. 3A shows the dependence of the uranium/Mordant Blue 9 chelate peak on the dye concentration. The peak height rapidly increases with the dye concentration up to $6 \times 10^{-7} M$, after which it starts to level off. The dye-to-metal ratio is 1:1.¹² All subsequent work used the dye at a concentration of $10^{-6} M$. The dependence of the peak height on the accumulation potential is shown in Fig. 3B. Potentials ranging from 0 to -0.30 V yielded similar stripping peaks; larger peaks were obtained over the range from -0.40 to -0.43 V. The peak current decreased rapidly at potentials more negative than -0.43 V. The best results, judged from the overall signal-to-background characteristics, were obtained at an accumulation potential of -0.43 V. At this potential, the peak is not affected by the base-line current associated with the preceding dye peak.

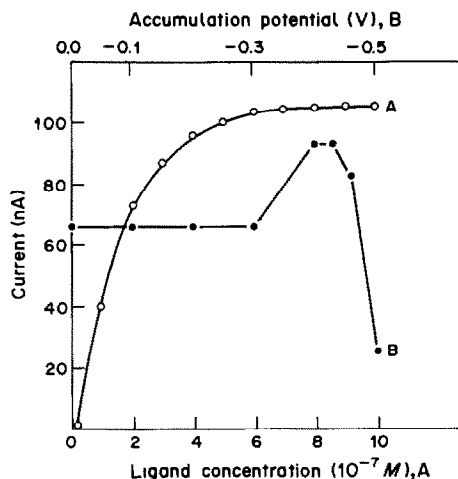


Fig. 3. Effect of Mordant Blue 9 concentration (A) and accumulation potential (B) on the stripping peak current. Accumulation for 60 sec in the presence of 10 $\mu\text{g/l}$. uranium. Other conditions as for Fig. 1.

Accordingly, this potential was used in all further work. Earlier polarographic measurements on the uranium/Mordant Blue 9 chelate required the pH-5.3 acetate buffer solution to be heated to assist chelate formation.^{7,12} In contrast, the best adsorptive stripping results were obtained when the solutions were kept at room temperature, with 6 min allowed for chelate formation. The present approach uses a pH-6.5 acetate supporting electrolyte.

Mass-transport during the accumulation step also affects the magnitude of the uranium/Mordant Blue 9 stripping peak. For example, a stirring rate of 400 rpm resulted in 3.5-fold enhancement of the response, compared to that obtained in a quiescent solution (10 $\mu\text{g/l}$. uranium, 1-min accumulation). Such mass-transport control indicates a fast rate of chelate adsorption. The linear-scan stripping mode offered slightly better signal-to-background characteristics than the differential pulse mode. As a result of its response characteristics and speed advantage, the linear-scan mode was used throughout this study.

The adsorptive stripping peak for the uranium/Mordant Blue 9 chelate yields a well-defined concentration dependence. Figure 4 shows voltamperograms for solutions of increasing uranium concentration, 2–10 $\mu\text{g/l}$. ($8.4 \times 10^{-9} M$ – $4.2 \times 10^{-8} M$, a–e), after 45 sec accumulation. Sharp and well defined peaks are observed. Also shown as an inset in Fig. 4 are calibration plots, over the 2–28 $\mu\text{g/l}$. ($8.4 \times 10^{-9} M$ – $1.2 \times 10^{-7} M$) concentration range, following 0 (A), 15 (B), and 45 (C) sec accumulation times. For 15-sec accumulation the response is linear over the entire range examined (slope, $5.1 \text{ nA} \cdot \mu\text{g}^{-1}$; correlation coefficient, 0.999). With 45-sec accumulation the response is linear up to 16 $\mu\text{g/l}$. ($6.7 \times 10^{-8} M$; slope of the initial linear portion, $12.6 \text{ nA} \cdot \mu\text{g}^{-1}$; correlation coefficient; 0.999). Analogous uranium measurements, based on the

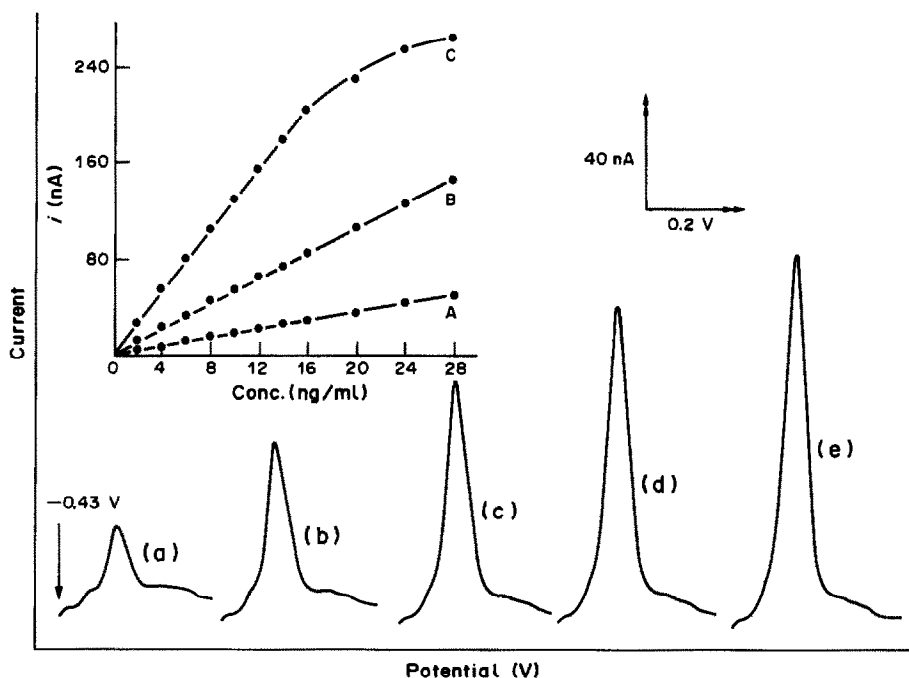


Fig. 4. Stripping voltamperograms obtained after increasing the uranium concentration in steps of $2 \mu\text{g/l}$, (a-e). Accumulation for 45 sec, other conditions as for Fig. 1. Also shown are calibration plots over the 2–28 $\mu\text{g/l}$. range, following 0 (A), 15 (B) and 45 (C) sec accumulation.

uranium–catechol complex, result in a linear response up to $5 \times 10^{-8} M$.⁶

The inherent sensitivity of the method is apparent from a comparison with adsorptive stripping measurements of the uranium–catechol complex.^{5,6} Figure 5 compares voltamperograms for $10 \mu\text{g/l}$. uranium in the presence of Mordant Blue 9 (a) and catechol (b) as complexing ligands. Optimized conditions were employed for both ligands, in conjunction with 60-sec accumulation. While convenient determination at the $\mu\text{g/l}$. level is feasible in the presence of both ligands, the use of Mordant Blue 9 offers improved sensitivity and sharper peaks. Detection

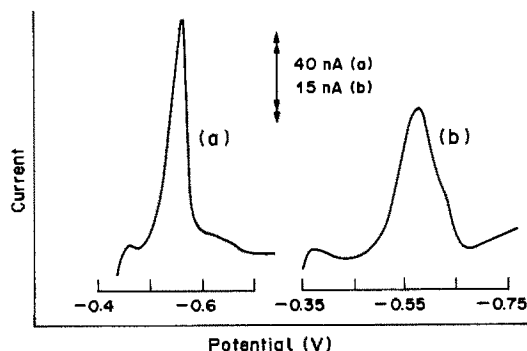


Fig. 5. Stripping voltamperograms for $10 \mu\text{g/l}$. uranium in the presence of Mordant Blue 9 (a) and catechol (b). Accumulation for 1 min, 50 mV/sec scan-rate. Other conditions: (a) as for Fig. 1; (b) $2 \times 10^{-3} M$ catechol in 0.008M PIPES solution (pH 6.8) with accumulation at -0.35 V .

limits were estimated from the base-line noise characteristics ($S/N = 3$) of the $2\text{-}\mu\text{g/l}$. ($8.4 \times 10^{-9} M$) uranium solution (conditions as for Fig. 1). For 120 and 300-sec accumulation periods the limits found were $3 \times 10^{-10} M$ and $2 \times 10^{-10} M$, respectively. A detection limit of $3 \times 10^{-10} M$ was reported for the catechol-based procedure, with accumulation for 150 sec.⁶ The adsorptive accumulation of the uranium/Mordant Blue 9 chelate results in reproducible stripping peak currents. For ten successive measurements of $10 \mu\text{g/l}$. uranium, the mean peak current was 102 nA with a range of 98–106 nA and a relative standard deviation of 3.2% (conditions as for Fig. 1c).

The major sources of interference in adsorptive stripping measurements are likely to be organic surfactants that compete with the chelate for space on the mercury surface, and other metal ions that form chelates with Mordant Blue 9. Interferences by organic surfactants were tested by addition of two model compounds (conditions as for Fig. 1c, with $10 \mu\text{g/l}$. uranium). The signal for uranium/Mordant Blue 9 chelate was decreased by 11, 27, 31 and 42% in the presence of 2, 4, 5 and 100 mg/l. respectively, of the representative colloidal protein gelatin. Even larger depressions, ca. 32, 80 and 93%, of the chelate peak were observed on adding 2, 4 and 6 mg/l., respectively, of the anionic surfactant dodecyl sodium sulphate. Hence, destruction of organic surfactants by ultraviolet irradiation is advisable for samples suspected to contain high levels of these materials. Similar measurements on $10 \mu\text{g/l}$. uranium were not

affected by the addition of 10 $\mu\text{g/l}$. Cu(II), Zn(II), Pb(II), Cd(II), Hg(II), Ca(II), Th(IV), Sb(III) and Fe(III). Similar additions of Ti(IV) and Al(III) resulted in 26 and 27% enhancements of the uranium/Mordant Blue 9 peak, respectively; 4, 16 and 20% diminutions of the 10- $\mu\text{g/l}$. uranium peak were observed on adding 10 $\mu\text{g/l}$. Bi(III), Ga(III) and Ni(II), respectively. The addition of Fe(III), Ni(II), and Ga(III) resulted in the appearance of new peaks (at 0.13 and 0.11 V more negative, and 0.07 V more positive than the uranium peak, respectively) associated with reduction of their corresponding chelates with Mordant Blue 9. On the basis of these peak separations, it is possible to measure uranium simultaneously with nickel or iron. The results quoted indicate an advantage of the proposed method over the catechol-based stripping scheme⁶ as far as interferences due to copper, lead or iron are concerned. In contrast, a separation step is required for samples "rich" in titanium, aluminium or gallium. Hence, the use of Mordant Blue 9 for adsorptive stripping measurements of uranium offers a useful alternative to the use of catechol, and each ligand

may have advantages over the other under certain conditions.

Acknowledgement—This work was supported in part by the National Institutes of Health Grant No. GM 30913-03.

REFERENCES

1. J. Holzbecher and D. E. Ryan, *Anal. Chim. Acta*, 1980, **119**, 405.
2. M. D. Amos and J. B. Willis, *Spectrochim. Acta*, 1966, **22**, 1325.
3. A. M. Bond, V. S. Biskupsky and D. A. Wark, *Anal. Chem.*, 1974, **46**, 1551, and references cited therein.
4. R. Keil, *Z. Anal. Chem.*, 1978, **292**, 13.
5. N. K. Lam, R. Kalvoda and M. Kopanica, *Anal. Chim. Acta*, 1983, **154**, 79.
6. C. M. G. van den Berg and Z. Q. Huang, *ibid.*, 1984, **164**, 209.
7. M. Ishibashi, T. Fujinaga and K. Izutsu, *J. Electroanal. Chem.*, 1959/60, **1**, 26.
8. J. Wang and J. Mahmoud, *ibid.*, 1986, **208**, 383.
9. J. Wang, P. A. M. Farias and J. S. Mahmoud, *Anal. Chim. Acta*, 1985, **172**, 57.
10. J. Wang and J. Mahmoud, *ibid.*, 1986, **182**, 147.
11. J. Wang and J. Zadeii, *Talanta*, 1986, **33**, 321.
12. G. W. Latimer, *ibid.*, 1968, **15**, 1.

AN APPARATUS FOR THE EMISSION SPECTROMETRIC DETERMINATION OF NITROGEN RELEASED INTO AN ARGON GAS STREAM BY CHEMICAL REACTIONS IN SOLUTION

G. T. ABOU ZEID, J. B. HEADRIDGE and C. WHITE
Department of Chemistry, The University, Sheffield, England

(Received 20 June 1986. Accepted 12 September 1986)

Summary—An apparatus has been constructed primarily for determination of nitrogen released from steels on reaction with organic solvent-halogen mixtures. The nitrogen is collected in a coil and then flushed with argon through a spectroanalyser that is selective to nitrogen and coupled to a recorder and integrator. The integrated signal is linearly related to the mass of nitrogen produced. The apparatus has been tested by determining the yield of nitrogen produced by reaction of hydrazine with a large excess of hypobromite in aqueous solution. For ten 57- μg amounts of hydrazine the average yield of nitrogen was 99%, with a relative standard deviation of 2.4%.

Nitrogen, which is present in almost all steels, usually at concentrations in the range 10–500 $\mu\text{g/g}$, can have profound effects on the mechanical properties of the steels, and the manner in which the nitrogen is distributed is very important.¹ The nitrogen can be present in different forms, depending on the elements in the steels and the heat treatments to which they have been subjected. Some of it may be present as atomic nitrogen, some may be bound as less stable nitrides such as manganese silicon nitride and some may be combined in more stable or very stable nitrides such as aluminium nitride or titanium nitride respectively. Organic solvent-halogen mixtures have long been used to isolate inclusions such as aluminium nitride from steels.² It is known that the more stable nitrides are not decomposed by some of these mixtures whereas less stable nitrides are dissolved.^{3,4} The ability of the mixtures to dissolve nitrides and other non-metallic phases is least if the halogen is iodine and greatest if it is chlorine. The oxidizing power can also be modified by using interhalogen compounds such as iodine trichloride instead of a single halogen.⁴ It has been stated that when steels are dissolved in appropriate organic solvent-halogen mixtures, the atomic nitrogen and the nitrogen from less stable nitrides is released as molecular nitrogen but very little work has been done on determining the nitrogen released under different conditions and relating it to the concentrations of the various forms of nitrogen in steel.⁵ For progress to be achieved in this area an apparatus was required for collecting the nitrogen released by such chemical reactions and determining it conveniently.

Such an apparatus is described in this paper. The nitrogen released is flushed into a collection coil by a stream of pure argon. After collection the nitrogen/argon mixture is flushed through a BOC

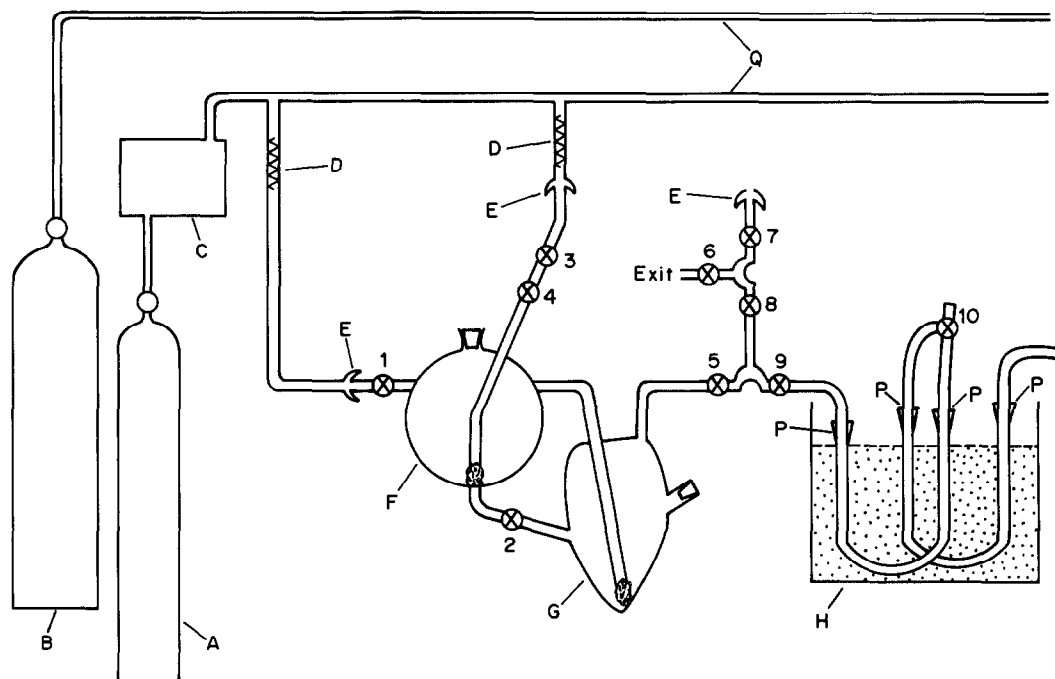
Spectroanalyser, in which the nitrogen molecules are excited and produce a molecular emission spectrum on relaxation. The radiation at 337 nm is measured with a photomultiplier tube, the current from which is processed and then registered on a potentiometric recorder fitted with an integrator. For standard nitrogen/argon mixtures the integrated signal is a linear function of the mass of nitrogen. The apparatus has been thoroughly tested by investigating the yield of nitrogen produced by reaction of hydrazine with excess of hypobromite.

EXPERIMENTAL

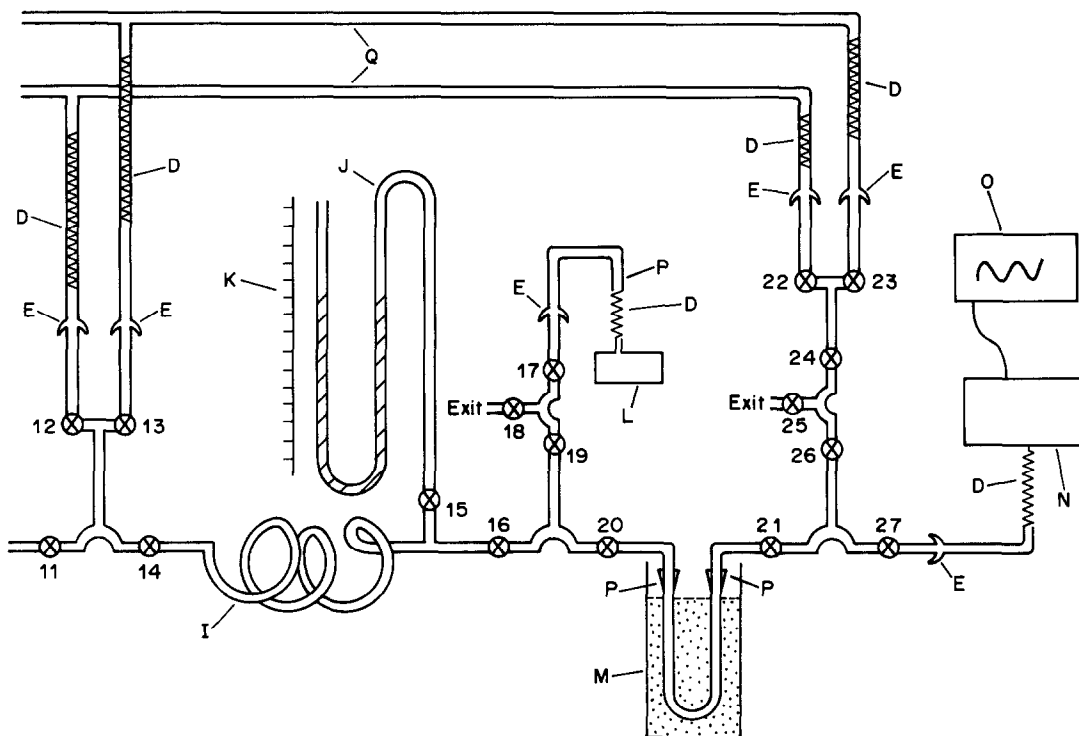
Apparatus

This is shown in Fig. 1 and incorporates the following components.

- (i) A cylinder of high purity argon (A).
- (ii) A cylinder of nitrogen in argon, Gold Star standard, BOC Special Gases (Deer Park Road, London SW19 3UF), certified to contain 40 ± 0.08 ppm v/v nitrogen (B).
- (iii) A BOC Rare Gas Purifier (RGP-4) supplied by the British Oxygen Company (C), operated according to the manufacturer's instructions; the argon from the purifier contained less than 1 ppm v/v of total impurities.
- (iv) A BOC Spectroanalyser Mark II (N), which was kept permanently switched on with argon continuously passing through it. The argon flow-rate was kept low overnight, for economy. The equipment was operated according to the manufacturer's instructions. The Span potentiometer for the range 0–100 was adjusted so that the meter read zero when the purified high-purity argon (7 psig) was flowing through it at 2.0 l./min, and read 40 for passage of the standard gas mixture at the same pressure and flow-rate.
- (v) Cylinder gauges—Spectrol Model 40B/BS3/GG Regulators from BOC Special Gases.
- (vi) Vacuum pump (L), Leybold-Heraeus, Type D2A.
- (vii) Potentiometric chart recorder with integrator (O), JJ Instruments, type CR604. This was connected to the output from the BOC Spectroanalyser (100 mV).



(a)



(b).

Fig. 1. The apparatus. A, high-purity argon gas cylinder; B, standard nitrogen-in-argon gas cylinder; C, BOC rare gas purifier; D, stainless-steel bellows; E, ball and socket glass joints with clips; F, reagent flask; G, "pear-shaped" reaction flask; H, cold trap 1; I, collecting volume (coil); J, mercury manometer; K, measuring ruler; L, vacuum pump; M, cold trap 2; N, BOC Spectroanalyser; O, potentiometric chart-recorder; P, Quickfit glass joints fitted with springs; Q, stainless-steel tubes.

(viii) SHLS stainless-steel tube, A 269–321 grade, outside diameter 0.25 in., wall thickness 0.032 in. Seven metres were used in construction of the gas lines.

(ix) Eight SS-400-6 straight connectors, four SS-400-3 tees and three SS-400-7 elbows, all $\frac{1}{4}$ -in. size, Swagelok type, were used to join the various parts of the gas lines.

(x) Seven stainless-steel bellows (D) overall length 12 in., 0.455 in. outside diameter, with $\frac{1}{4}$ -in. termination at each end, supplied by FTL Engineering Systems (6–11 Riley St., Willenhall, England), were used in the construction of the gas lines.

(xi) PTFE greaseless high-vacuum taps.

(xii) PTFE greaseless Rotaflor high-vacuum stopcocks were used as exit taps at the end of a branch to void gases to atmosphere when desired.

(xiii) Glass-to-metal seals (Jencons Scientific) were used for the connection of stainless-steel tubes to glass tubes.

(xiv) All glass-to-glass tube connections were by Quickfit joints.

The apparatus contains a glass reaction flask (G) (volume about 200 ml) connected to a glass reagent flask (F) (volume about 400 ml) by means of tap 2. Both flasks have Quickfit female joints (B19 and B14 for flasks F and G respectively) for the introduction of solids or solutions; normally these joints are closed with well greased Quickfit stoppers, secured with two pairs of springs and hooks. Each flask has an inlet tube ending in a fine sinter; introduction of argon through these tubes efficiently deaerates solutions in the flasks. An exit tube from flask G leads through taps 5 and 9 to cold-trap H which consists of two U-tubes, one filled with glass beads to aid in the condensation of solvent vapours arising from the solution in flask G. The second U-tube contains anhydrous magnesium perchlorate (8–20 mesh), a very efficient desiccant. The exit tube from H passes through taps 11 and 14 to a 27-turn collection coil (I) with an internal diameter of about 12 mm, coil diameter about 15 cm and volume of 1.64 litres. The other end of the coil is connected to a manometer (J) through tap 15 and through taps 16 and 20 to cold-trap M which consists of a U-tube filled with glass beads to condense any mercury vapour arising from the manometer. The exit tube from M leads to the Spectroanalyser through taps 21 and 27.

The manometer is used to measure the pressure of the standard gas within the coil and to adjust the pressure of nitrogen/argon mixtures before they are flushed into the Spectroanalyser. The volume of gas in the manometer was always less than 1% of that in the coil. Between taps 16 and 20, a side-arm is connected to the vacuum pump L through taps 19 and 17. The vacuum pump stands on 2 in. thick stiff sponge and is connected to the gas line through a stainless-steel bellows (D) and a ball and socket glass joint (E). The output from the Spectroanalyser is displayed on the recorder.

The lower stainless-steel gas line in Fig. 1 is connected to the high-purity argon cylinder through the Rare Gas Purifier. There are five entrances to the glass parts of the apparatus from this argon line, into the reagent flask F, into the reaction flask G, immediately before the cold-trap H, immediately before the collection coil I and just before the spectroanalyser N. The third of these is used only occasionally and is connected to the flexible steel bellows when required, the bellows normally being connected to the entrance tube to the reagent flask F.

The upper stainless-steel line in Fig. 1 is connected to the standard gas mixture. There are two entrances to the glass parts of the apparatus from this gas line, namely immediately before the collection coil I and just before the Spectroanalyser N. The stainless-steel lines and glass lines and apparatus are clamped to a rigid stand fixed to the work-bench.

Calibration graph

This is obtained by plotting the peak area obtained from

the integrator of the recorder vs. mass of nitrogen. The mass of nitrogen is obtained from its partial pressure (P_{N_2}) in the collecting coil, by using the equation of state:

$$n \text{ (moles)} = \frac{P_{N_2} \text{ (atm)} \times V \text{ (litres)}}{R \times T \text{ (kelvin)}}$$

where $R = 0.0821 \text{ l. atm. K}^{-1} \text{ mole}^{-1}$.

Since $P_{N_2} = (40 \times 10^{-6}) P$, where P is the pressure (in the coil) of the nitrogen-in-argon mixture containing 40 ppm v/v nitrogen, and $V = 1.64$ litres, the equation reduces to:

$$\begin{aligned} \text{Amount of nitrogen} &= 7.99 \times 10^{-4} P/T \text{ moles} \\ &= 2.24 \times 10^4 P/T \mu\text{g} \end{aligned}$$

where T is the temperature of the apparatus (K).

(a) Raise the pressure of argon (from the overnight minimum) to 7 psig on the cylinder head gauge. Adjust the flow-rate so that the Spectroanalyser flowmeter reads 2.0 l./min. Switch on the gas purifier and wait about 20 min for the temperature to reach 700° and become steady. Put a mixture of acetone and solid carbon dioxide into the Dewar vessel around cold-trap M to give a temperature of about -78°. Open the standard-gas cylinder and adjust the pressure to 6 psig. Allow argon to flow through the coil into the Spectroanalyser with taps 12, 14, 15, 16, 20, 21, 24, 26 and 27 open and the others closed. Maintain this flow for about 10 min.

(b) Check that the argon pressure and flow-rate are 7 psig and 2.0 l./min respectively, adjusting if necessary. If necessary, adjust the Spectroanalyser meter to read zero. Note the reading on the manometer.

(c) Close taps 12 and 20 and quickly open tap 22. Check that the reading on the Spectroanalyser meter is still zero.

(d) Switch on the vacuum pump and open taps 17 and 19. When the manometer reading is steady, close tap 19 and switch off the pump. Note the manometer reading.

(e) Open tap 13 and allow a certain amount of standard gas mixture to pass through to the coil. Note the manometer reading and close tap 13 when the required pressure has been reached.

(f) Close tap 22, quickly open tap 12, which introduces argon into the coil, and observe the mercury level. When the manometer reaches the level previously observed in step (b), close taps 12 and 15. Open tap 22 to allow the Spectroanalyser meter to settle down to zero again.

(g) Close tap 22 and quickly open taps 12 and 20, thus allowing the argon to push into the Spectroanalyser the gas mixture already collected in the coil. A signal due to molecular nitrogen is produced on the chart recorder along with the integrated signal.

(h) Repeat operations (b)–(g) with different pressures of gas in the coil to ensure that data for about 8 points on the calibration graph have been obtained.

(i) Convert the manometer readings (in cm) into pressure of gas mixture in the coil (atmospheres) by using the equation

$$P = \frac{2[(\text{manometer reading for gas}) - (\text{reading for vacuum})]}{76.0}$$

(j) Calculate the mass of nitrogen in the coil from the equation derived above, namely mass of nitrogen = $2.24 \times 10^4 P/T \mu\text{g}$.

Determination of the yield of nitrogen from reaction of hydrazine with a large excess of hypobromite

Use analytical-grade chemicals whenever possible.

Sodium hypobromite solution. Dissolve 11 g of sodium hydroxide in 500 ml of water and add 20 g of bromine slowly with vigorous shaking. Dilute to 2 litres with water and store in a dark cupboard. Prepare a fresh batch every two weeks.

Ammonia-free water. Pass distilled water through a column of Amberlite IR-120 ion-exchange resin in the hydrogen form.

Stock solution of hydrazine sulphate (nitrogen 1 mg/ml). Dissolve 4.644 g of $N_2H_4 \cdot H_2SO_4$ in ammonia-free water and make up accurately to 1 litre. Dilute 20-fold to obtain hydrazine sulphate solution A (nitrogen 50 $\mu\text{g/ml}$) with ammonia-free water.

Dilute solution A 10-fold with ammonia-free water to obtain hydrazine sulphate solution B (nitrogen 5 $\mu\text{g/ml}$).

Hydrazine sulphate solutions for reaction flask G. Dilute 0, 10, 20, 40, 60 and 80 ml of solution B to 100 ml with ammonia-free water in six separate standard flasks. These solutions have nitrogen concentrations of 0, 0.5, 1, 2, 3 and 4 $\mu\text{g/ml}$. In a similar way prepare 500 ml of a hydrazine sulphate solution containing 2.5 μg of nitrogen per ml. The eighth standard is solution B.

Procedure

(i) Carry out steps (a)–(c) in the procedure for obtaining a calibration graph.

(ii) Fill the Dewar vessel around cold trap H with a mixture of acetone and solid carbon dioxide.

(iii) Rinse flask F and G thoroughly with water. Suck out the water by means of a syringe tip fitted in the end of a plastic tube joined to a water suction-pump.

(iv) Rinse the flasks with acetone from a wash-bottle and pass argon through the sinters of flasks F and G until the flasks are thoroughly dry.

(v) Close tap 2 and introduce a mixture of 20 ml of hypobromite solution together with 5 ml of 1M potassium bicarbonate into flask F. The pH of the mixture should be adjusted beforehand to 7.3–7.5 by dropwise addition of 5M hydrochloric acid. Deaerate the solution by passage of argon through it for about 15 min.

(vi) Pipette into flask G, through the side-arm, 20 ml of one of the eight standard hydrazine sulphate solutions (nitrogen 0–5 $\mu\text{g/ml}$) and deaerate with argon for about 15 min.

(vii) Stopper the side-arm of flask G and secure the stopper with springs. Open taps 6, 8 and 5 to flush out any air remaining in the tube between flask G and tap 5. Close taps 5, 8 and 6.

(viii) Close tap 4 and open tap 2. The argon will now pass through tap 2 and bubble through the hypobromite solution in flask F.

(ix) Stopper flask F, securing the stopper with springs, close tap 1 and open tap 4. The hypobromite rushes into flask G. Close taps 4 and 2. The reaction producing nitrogen is now in progress.

(x) After about 10 min, evacuate the volume between taps 5 and 20 with tap 15 open. Close tap 22 to stop the argon flow through the Spectroanalyser, and open taps 1 and 5. The argon now bubbles through the reaction mixture, carrying the released nitrogen and filling the volume up to tap 20. Let the pressure in the manometer rise until the reading is the same as that noted in step (b) of the calibration. Then close tap 1.

(xi) Pass argon through the Spectroanalyser via taps 22, 24, 26 and 27 for about 30 sec to stabilize the meter reading at zero. Then close tap 22 and allow argon to pass through taps 12 and 14 and flush through the Spectroanalyser the gas collected from the reaction.

(xii) Obtain the peak area from the recorder and read off the corresponding mass of nitrogen from the calibration graph.

(xiii) Empty flask G by suction.

(xiv) Repeat steps (iii)–(xi) with the other seven standard hydrazine sulphate solutions and then ten times more with 2.5 $\mu\text{g/ml}$ nitrogen solution.

RESULTS

Calibration graphs

Calibration graphs of peak area *vs.* mass of nitrogen (up to 110 μg) were very good straight lines with an intercept of 0.46–0.77 cm^2 on the ordinate, equivalent to 0.9–1.5 μg of nitrogen. The slopes of the graphs were very consistent, varying by only $\pm 0.4\%$.

The small intercept is an instrumental effect caused by a temporary decrease in flow-rate when tap 22 is closed moments before taps 12 and 20 are opened.

Determination of the yield of nitrogen in the hydrazine–hypobromite reaction

The masses of nitrogen obtained from the increasing amounts of hydrazine sulphate taken are shown in Table 1. The amount of nitrogen found was read from a calibration graph with a slope of 0.496 $\text{cm}^2/\mu\text{g}$ and intercept of 0.46 cm^2 on the ordinate.

Plotting “nitrogen found” against “nitrogen taken” (Table 1) yields a straight line with a slope of 0.980 (s.d. 0.003), intercept of 0.11 $\mu\text{g N}_2$ on the *y*-axis (s.d. 0.16 μg) and a correlation coefficient of 0.9999. The average yield of nitrogen from this reaction is thus 98% and the reagent blank 0.11 μg of nitrogen.

Analysis of ten 20-ml aliquots of hydrazine sulphate solution (nitrogen 2.5 $\mu\text{g/ml}$) with correction for the blank, gave a mean of 49.6 μg with a relative standard deviation (rsd) of 2.4%. From the data in Table 1, an rsd of 0.6% would be expected at this level. Three of the results were 47.9, 51.6 and 51.8 μg , and if these are treated as outliers, the rsd for the remaining results (mean 49.4 μg) is 0.8%, in better agreement with expectation.

DISCUSSION

For very low masses of nitrogen (<5 μg), the recorder tracings are sharp peaks. With increasing mass, these rise sharply, approach a constant height and broaden. This pattern arises because when argon is introduced to bring the pressure within the coil up to the normal pressure, the nitrogen-in-argon mixture is compressed into the right-hand section of the collection volume. However, there is no problem in measuring the peak areas. Typical peaks are shown in Fig. 2.

The collection volume, which is mainly that of the coil, was determined by filling it with a standard gas mixture and pushing this volume through the Spectroanalyser with high-purity argon at flow-rates

Table 1. Nitrogen yield from the hydrazine–hypobromite reaction

Nitrogen taken, μg	0	10.00	20.0	40.0	50.0	60.0	80.0	100
Peak area, cm^2	0.48	5.26	10.4	19.9	24.8	29.9	39.3	49.1
Nitrogen found, μg^*	0.04	9.68	20.0	39.2	49.1	59.4	78.3	98.1

*Uncorrected for the blank.

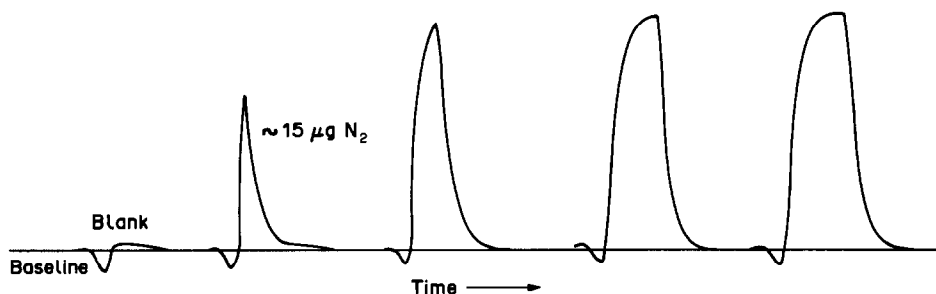


Fig. 2. Peaks recorded for increasing masses of nitrogen.

of 1.00, 1.50, 2.00 and 2.50 l./min. The times taken for the volumes of gas to pass through the Spectro-analyser were obtained from the recorder tracings of potential (light intensity) *vs.* time. Four determinations of the volume were made at each flow-rate. The overall average volume found was 1.64 litres, with a relative standard deviation of 2.3%.

Because of the compression effect (referred to above) when high-purity argon is added to the coil to bring the pressure to the required level, a small amount of nitrogen will be lost in the manometer (above tap 15). This will be proportionately greater when low pressures of standard gas are used for constructing the calibration graph. However, the volume of gas in the manometer above tap 15 is always less than 1% of the total collection volume, and a study of all the calibration graphs obtained shows no detectable loss of nitrogen at levels below 25 μg . This effect would appear to be negligible but could be completely prevented by reducing the pressure in the collection volume, containing high-purity argon, not to a vacuum but to say 50 mmHg, before adding the standard gas. It would then be pure argon that is compressed into the manometer. This minor adjustment in operating conditions should ensure that no nitrogen released in reactions in flask G is lost in the manometer.

Riley *et al.*,⁶ in studying the reaction between hydrazine and hypobromite by using the tracer ^{15}N and mass spectrometric analysis of the product, reported that the oxidation of hydrazine yields nitrogen as the main product, together with a very small

amount of nitrous oxide. The results of our study show conclusively that hydrazine is 98–99% oxidized to nitrogen by a large excess of hypobromite at pH 7.3–7.5. It has been established in our laboratory that nitrous oxide, nitric oxide and nitrogen dioxide are not detected by the BOC Spectroanalyser.

The apparatus works well and will be used to study the reactions between organic solvent–halogen mixtures and steels containing nitrogen. Because it does not respond to oxides of nitrogen, it could also be employed to investigate the exact yields of nitrogen produced from other reactions in aqueous solution, which produce high yields of nitrogen, such as the ammonia–hypobromite reaction.

Acknowledgements—We thank the Science and Engineering Research Council for a grant to purchase equipment and materials for the apparatus, the Lebanese University for a studentship (for G.T.A.Z.) and Dr. D. A. Leathard of Sheffield City Polytechnic for valuable discussions.

REFERENCES

1. A. A. Baker, J. B. Headridge, S. R. Keown, G. D. Long, P. A. Vergnano and M. I. Wilson, *Anal. Chim. Acta*, 1979, **107**, 339.
2. H. F. Beeghly, *Anal. Chem.*, 1949, **21**, 1513.
3. I. S. Busheina and J. B. Headridge, *Analyst*, 1981, **106**, 221.
4. G. T. Abou Zeid and J. B. Headridge, *ibid.*, 1982, **107**, 200.
5. T. K. Willmer and K. Zimmermann, *Arch Eisenhüttenwes.*, 1971, **42**, 877.
6. R. F. Riley, E. Richter, M. Rotheram, N. Todd, L. S. Myers and R. Nusbaum, *J. Am. Chem. Soc.*, 1954, **76**, 3301.

STUDIES OF ATOMIZATION FROM A GRAPHITE PLATFORM IN GRAPHITE-FURNACE ATOMIC-ABSORPTION SPECTROMETRY

C. L. CHAKRABARTI,* S. B. CHANG, P. W. THONG, T. J. HUSTON and SHAOLE WU
Department of Chemistry, Carleton University, Ottawa, Ontario, Canada

(Received 27 August 1985. Revised 5 September 1986. Accepted 12 September 1986)

Summary—A theoretical model has been proposed for the transient characteristics of an atomic-absorption pulse generated by atomization from a graphite platform in a pulse-heated graphite-furnace atomic-absorption spectrometer. The model has been used (with the aid of a computer program) to predict the effects of various factors on analyte atom populations as a function of time. The various factors studied were heating rate, initial temperature of the graphite tube wall, platform mass and thickness, and activation energy for the rate-determining step in the reaction sequence leading to atom formation. The results predicted by the model are in reasonable agreement with the experimental results obtained by using lead as the analyte element.

Transient atomic-absorption signals generated by rapid atomization of an analyte element in a pulse-heated electrothermal atomizer provide a temporal history of the analyte atom population. Several dynamic models for interpretation of the transient signal generated by various types of electrothermal atomizers have been proposed.¹⁻¹¹ Holcombe has reported the effect, on the atomic-absorption signal, of gas expulsion resulting from the heating of the tube.¹²

Paвери-Fontana and Tessari¹³ have developed a model to describe atomization of an analyte element from a graphite platform in a pulse-heated graphite furnace, assuming a linear, slow increase in the temperature of the platform.

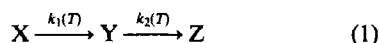
Assuming that the graphite platform is heated primarily by radiation emitted from the heated graphite tube wall, Chakrabarti *et al.*¹⁴ have proposed a model to describe the non-linear heating characteristics of the platform under various chosen conditions.

In the present study a simplified model to describe atomization of an analyte element from a graphite platform is advanced. The atomization process and model for prediction of platform temperature proposed by Chakrabarti and co-workers,^{11,14} are used to study the effect of some chemical, physical and instrumental parameters on the analyte atom population as a function of time. The predictions of the model have been tested qualitatively by comparing them with experimental results obtained with lead as the test analyte.

THEORY

The time-dependence of the atom population in a graphite tube furnace can be described by a

first-order, or pseudo first-order, consecutive rate process^{11,15}



where X is the pre-atomization analyte species, Y is the absorbing analyte atomic vapour formed, Z is the analyte species that is lost from the analysis volume, and $k_1(T)$ and $k_2(T)$ are the first-order rate constants for the formation and loss of the observable atomic species, Y, respectively, as a function of the absolute temperature, T . Since the temperature of a pulse-heated graphite furnace is a function of time, t , the expressions $k_1(T)$ and $k_2(T)$ should be replaced by $k_1[T(t)]$ and $k_2[T(t)]$, respectively. However, to simplify the notation for the rate constants, $k_1(t)$ and $k_2(t)$ will be used in the following text to stand for $k_1[T(t)]$ and $k_2[T(t)]$, respectively.

Assuming that the rate constant for the formation of atoms, $k_1(t)$, is determined by an Arrhenius-type equation, and the rate constant for the atom loss, $k_2(t)$, is determined solely by diffusion, Chakrabarti *et al.*¹¹ have expressed the rates of change for each species in equation (1) by a set of differential equations as follows:

$$\frac{dX_t}{dt} = -k_1(t)X_t = -A \exp[-E_a/RT(t)]X_t \quad (2)$$

$$\begin{aligned} \frac{dY_t}{dt} &= k_1(t)X_t - k_2(t)Y_t \\ &= A \exp[-E_a/RT(t)]X_t - \frac{8D_0}{l^2} \left[\frac{T(t)}{T_0} \right] Y_t \end{aligned} \quad (3)$$

$$\frac{dZ_t}{dt} = k_2(t)Y_t = \frac{8D_0}{l^2} \left[\frac{T(t)}{T_0} \right]^n Y_t \quad (4)$$

where $k_1(t)$ and $k_2(t)$ have units of sec^{-1} ; X_t , Y_t and Z_t are numbers of atoms of species X, Y and Z; A ,

*Author to whom correspondence should be addressed.

E_a , D_0 , l and n are the frequency factor, activation energy of the rate-determining step, diffusion coefficient at T_0 (273 K) and 1 atm, length of the graphite tube, and gas combination factor, respectively.

At $t = 0$, X_i is the amount of analyte introduced, i.e., $X_{i=0} = X_0$, and Y_i and Z_i are zero. With these as initial conditions in equations (2)–(4), a numerical integration method, the Adams–Bashforth method, was employed to compute the instantaneous amount of each species inside the furnace.^{11,16}

When a graphite platform is used inside a pulse-heated graphite furnace, the sample is usually deposited on the platform through the sample injection hole. It is reasonable to assume that the rate of atom formation depends on the temperature of the atomization surface; hence, the temperature of the platform, and not that of the tube wall, is the determining factor. In addition, loss by diffusion is a gas-phase mass-transport process. The rate of analyte loss by diffusion is therefore considered to be determined by the gas temperature inside the graphite tube. This treatment of analyte atom loss as solely due to diffusion is admittedly an over-simplification as it

experimentally studied by Chakrabarti *et al.*¹⁴ and Falk.¹⁷ Although the electrical resistive (Joule) heating of the graphite platform has some effects on the temperature profiles because of the contact between the tube and the platform, these effects have not been taken into account, in order to keep the mathematical formulation of the theoretical model simple. In the present model, the platform is regarded as heated primarily by radiation heat transfer from the tube wall, and the platform temperature, $T_{pl}(t)$, is expressed by¹⁴

$$\frac{dT_{pl}(t)}{dt} = \frac{\sigma a \mathcal{F}_{2-1} [T_w^4(t) - T_{pl}^4(t)]}{mc_p} \quad (7)$$

where m , c_p , \mathcal{F}_{2-1} , a and σ are the mass of the platform (g), specific heat of the platform ($J \cdot g^{-1} \cdot K^{-1}$), total radiation interchange factor between the platform and the furnace wall¹⁴ (dimensionless), effective surface area of the platform (cm^2), and the Stefan–Boltzmann constant ($5.67 \times 10^{-12} W \cdot cm^{-2} \cdot K^{-4}$), respectively.

To develop a digital computer solution for the temperature transient of the platform, equation (7) is expressed¹⁴ in a finite-difference form:

$$T_{pl}(t + \Delta t) = T_{pl}(t) + \frac{\sigma a \mathcal{F}_{2-1} \{ [T_w(t + \Delta t)]^4 - [T_{pl}(t)]^4 \} \Delta t}{mc_p} \quad (8)$$

does not take into account analyte atom loss by expulsion, especially in tube-wall atomization and at high tube-wall heating rates.¹⁰

Platform temperature

When the temperature of the graphite tube wall is increased linearly from the charring temperature (T_c) to a predetermined final atomization temperature (T_f) at a certain heating rate, α , the instantaneous temperature of the tube wall, $T_w(t)$, can be described by the equations:

$$T_w(t) = T_c + \alpha t; \quad 0 < t < \frac{T_f - T_c}{\alpha} \quad (5)$$

$$T_w(t) = T_f; \quad t > \frac{T_f - T_c}{\alpha} \quad (6)$$

The temperature of a graphite platform inside a pulse-heated graphite tube has been theoretically and

where $t + \Delta t$ is the time expressed explicitly in terms of the previous time, t , plus a finite increment of time, Δt .

Because of the large temperature ranges encountered in the furnace, an accurate analysis requires that the temperature-dependence of various properties of the materials be taken into account (Table 1).

Approximation of the gas-phase temperature in the graphite tube with the platform

As mentioned earlier, the rate of loss of species Y by diffusion is dependent on the temperature of the gas-filled space inside the graphite tube. It is therefore important to know this temperature.

Two-dimensional Cartesian co-ordinates can be used to describe the gas-filled space in the graphite tube with the platform inside it, and hence the gas-phase temperature distribution. However, in the present study, the nodal geometry of the system is

Table 1. Properties of anisotropic pyrolytic graphite and argon as a function of temperature

Material	Property	Unit	Function	Ref.
Anisotropic pyrolytic graphite	Density, ρ	g/cm^3	$\rho(T) = 2.20$	
	Heat capacity, c_p	$J \cdot g^{-1} \cdot K^{-1}$	$c_p(T) = 0.816 + 9.59 \times 10^{-4}T$	14
	Emissivity, ϵ		$\epsilon(T) = 0.7 + 8.36 \times 10^{-3}T$	14
Argon*	Density, ρ	g/cm^3	$\rho(T) = 1.784 \times 10^{-3}(273.15/T)$	
	Heat capacity, c_p	$J \cdot g^{-1} \cdot K^{-1}$	$c_p(T) = 0.52$	18
	Thermal conductivity, κ		$\kappa(T) = 1.774 \times 10^{-4}(T/303.15)^{0.68}$	19

* $c_v = (c_p - R)$ where R is the gas constant.

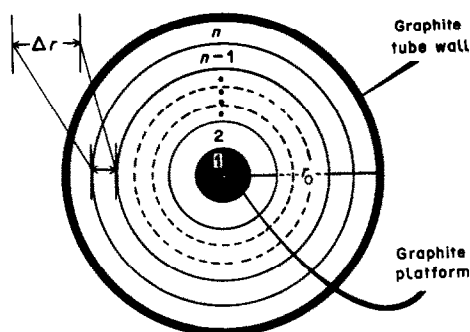


Fig. 1. Nodal geometry of the cross-sectional plane of the graphite tube. The filled circle at $n=1$ represents the graphite platform.

described more simply by use of one-dimensional radial co-ordinates, as shown in Fig. 1. In particular, the platform is considered as a cylindrical rod at the centre of the tube, shown as a filled circle at the centre of the diagram. Although the actual position of the graphite platform is off-centre, calculations made for this position by use of two-dimensional Cartesian co-ordinates yield results of the weighted-average gas temperature (not shown here) which are not significantly different from those obtained by using the simplified model in Fig. 1. The simplified model shortens the computational time considerably. The real platform is a rectangular plate and not a cylindrical rod. However, a cylindrical rod has been used in the model because the cylindrical symmetry of the rod inside the cylindrically symmetrical graphite tube considerably simplifies the model's mathematical complexity without seriously impairing the validity of the results obtained.

With this simplification, the temperature at the centre of the tube is that of the platform [equation (8)]. The temperature of the tube wall is given by equations (5) and (6). Assuming that heat is transferred from both the tube wall and the platform to stagnant argon inside the tube by conduction alone, the rate of heat transfer inside the gas-filled space of any node is then expressed by:²⁰

$$\frac{\kappa}{r} \frac{\partial}{\partial r} \left(r \frac{\partial T}{\partial r} \right) = \rho c_v \frac{\partial T}{\partial t} \quad (9)$$

$$r = 0; \quad T = T_{pl}$$

$$r = r_0; \quad T = T_w$$

where κ , ρ , r and c_v are the thermal conductivity of the gas ($\text{W} \cdot \text{cm}^{-1} \cdot \text{K}^{-1}$), density of the gas (g/cm^3), radial distance from the centre of the tube, and heat capacity of argon at constant volume, respectively. The reason for the use of c_v instead of c_p has been given by Chakrabarti *et al.*¹⁰ If equation (9) is put into finite difference form, the temperature of the vapour in each annular node, T_u , after a finite time in-

crement, can be expressed as:

$$T_u(t + \Delta t) = Fo_u(t) \left[T_{u+1}(t) \left(1 + \frac{\Delta r}{2r} \right) + T_{u-1}(t) \times \left(1 - \frac{\Delta r}{2r} \right) \right] + T_u(t) [1 - 2Fo_u(t)] \quad (10)$$

where

$$\Delta r = \frac{r_0}{n}; \quad 2 \leq u \leq n-1; \quad Fo_u(t) = \left(\frac{\kappa \Delta t}{\rho c_v (\Delta r)^2} \right)'_u;$$

$$T_{u=1} = T_{pl} \text{ and } T_{u=n} = T_w$$

The subscript u in the equation above represents the annular node, Fo is the Fourier number and r_0 is the internal radius of the graphite tube. The mathematical stability criterion for the equation is $Fo < 0.5$. The gas temperature is considered to be the weighted-average gas temperature (of all annular nodes inside the tube), defined by

$$T_{\text{avg}} = \frac{\sum_{u=2}^n m_u T_u}{\sum_{u=2}^n m_u} \quad (11)$$

where m_u is the mass of gas in the volume of node u .

Rate expressions for atom formation and loss in the platform atomization technique

The set of differential equations for calculating the rates of atom formation and loss in atomization from the platform can now be written as follows:

$$\frac{dX_i}{dt} = -A \exp[-E_a/RT_{pl}(t)] X_i \quad (12)$$

$$\frac{dY_i}{dt} = A \exp[-E_a/RT_{pl}(t)] X_i - \frac{8D_0}{l^2} \left(\frac{T_{\text{avg}}}{T_0} \right)^n Y_i \quad (13)$$

$$\frac{dZ_i}{dt} = \frac{8D_0}{l^2} \left(\frac{T_{\text{avg}}}{T_0} \right)^n Y_i \quad (14)$$

EXPERIMENTAL

Apparatus

Computation was done with a Honeywell CP-6 computer. The program was written in FORTRAN IV.

A Perkin-Elmer heated graphite atomizer, model HGA-2100, equipped with a laboratory-made power supply, was used. This power supply provided furnace heating rates varying from 1 to 10 K/msec. Atomic-absorption signals were measured with a Varian-Techtron 0.5 m Ebert-mount monochromator (50×50 mm grating, ruled with 638 lines/mm), fitted with a Hamamatsu R955 photomultiplier tube. Signals from the photomultiplier tube were passed through a laboratory-made amplifier which had a time-constant variable from 4 to 104 msec. A time-constant of 8 msec was used.

Perkin-Elmer pyrocoated graphite tubes (part No. 091504) were used. Rectangular platforms (of various dimensions and masses specified later) made of anisotropic pyrolytic graphite and reported in earlier papers^{14,21} from this laboratory were used. The platforms were cut away to a depth of 0.5 mm along their lower lateral edges, between the corners, to prevent physical contact between the sides of the platforms and the tube wall except at four corners.

Temperatures below 1300 K were measured with an automatic optical pyrometer, Ircon series 300, model 300 (Ircon Inc., Skokie, IL, USA). Higher temperatures were measured through the sample injection hole with another automatic optical pyrometer, Ircon series 1100, model 11 × 30.

In the atomization stage, the output voltages from the optical pyrometer and spectrophotometer were recorded simultaneously with a Nicolet model 2090-III dual-channel digital oscilloscope, fitted with a model 201 plug-in unit and a disk recorder. The output voltage of the optical pyrometer was converted into temperature by means of the calibration curves provided by the manufacturer.

Reagents and procedure

A stock 1000- $\mu\text{g/ml}$ solution of lead was prepared by dissolving lead nitrate in 1% ULTREX™ nitric acid (J. T. Baker Chemical Co.). The test solutions were prepared immediately before determination by serial dilution of the stock solution with ultrapure water obtained direct from a Milli-Q2 water-purification system (Millipore Corporation). A 5- μl aliquot of test solution was deposited through the sample injection hole onto either the tube wall or the graphite platform with an Eppendorf microlitre pipette fitted with a disposable plastic tip.

RESULTS AND DISCUSSION

The instantaneous absorbance value is assumed to be proportional to the number of analyte atoms in the analysis volume. Analytical information is usually obtained from the peak height or the integrated absorbance. It would be interesting to study, at least qualitatively, the effect of physical, chemical and instrumental parameters on the analyte atom population as a function of time.

The platform is primarily heated by radiation emitted by the heated tube wall. Chakrabarti *et al.*¹⁴ have theoretically shown that the characteristics of a non-linear temperature *vs.* time curve for a graphite platform is determined by the initial temperature, final temperature and heating rate of the graphite tube wall, as well as the geometry of the graphite platform.

Effect of heating rate of the graphite tube wall

Figure 2 shows curves for analyte atom population *vs.* time, calculated by means of the model, for tube-wall heating rates of 10, 5, 2 and 1 K/msec, respectively. In Fig. 2 (I–IV), curves A represent the analyte atom population as a function of time, simulated by using equations (2)–(4), for the analyte element atomized from the tube wall,¹¹ and curves B represent the analyte atom population as a function of time, simulated by using equations (12)–(14), for the analyte element atomized from the platform. Curve c is the weighted-average gas temperature inside the gas-filled space of the graphite tube, simulated by using equations (10) and (11). As can be seen from Fig. 2, an increase in the heating rate of the tube wall increases the peak height. When the analyte element is atomized from the platform, the peak height remains nearly constant at heating rates > 2 K/msec under the conditions used.

As shown in Fig. 2, at the beginning of the heating

cycle the predicted platform temperature increases more slowly than the temperature of the tube wall. Also, the instantaneous heating rate of the platform is lower than that of the tube wall if the tube wall heating rate is > 5 K/msec. However, no significant change in the heating rate of the platform with increasing rate of heating of the tube wall is observed between 1500 and 2600 K when the heating rate of the tube wall is > 2 K/msec. Since atomization of an analyte element from the platform is determined by the platform temperature, the delay in the rise of the platform temperature causes a later appearance time of the analyte atom from platform atomization. If the appearance temperature of the analyte element from platform atomization is > 1500 K, the peak height of the analyte atom population *vs.* time curve is not affected by the heating rate of the tube wall if that is > 2 K/msec. However, for appearance temperatures < 1500 K, the different instantaneous heating rates of the platform at different tube-wall heating rates may affect the rate of atomization, and hence, the peak height.

As Fig. 2 shows, the weighted-average gas temperature, T_{avg} , follows the tube wall temperature closely. However, there is as much as 1000 K difference between T_{pl} (platform temperature) and T_{avg} during the heating of the platform. The resulting temperature gradient in the gas phase may have a significant effect on the loss of analyte atoms by diffusion and convection.

In the model considered here, atom loss by diffusion is the only process which has been taken into account. The gas temperature experienced by the analyte element will generally be higher for platform atomization than for tube-wall atomization. This higher gas temperature increases the rate of diffusional loss of the analyte element. A combination of relatively low platform heating rate and higher gas temperature results in lower peak height and peak area of the analyte signal for platform atomization than for tube-wall atomization.

However, as shown in Fig. 2 (IV), at a relatively low heating rate of the tube wall, the heating rate of the platform is higher than that of the tube wall over most of the analyte atom-population *vs.* time curve. Since the diffusion coefficient, D , is a power function of temperature,¹ [$D = D_0(T/273)^n$] where n is 1.5–2.0, and the rate constant for analyte atom formation is an exponential function of temperature, $k_f(t) \propto \exp[-E_a/RT(t)]$, the rate of analyte atom loss by diffusion is not as sensitive to temperature as the rate of analyte atom formation is. Hence, in platform atomization at low platform heating rates, for analyte species having appearance temperatures below about 1500 K the rate of analyte atom formation may be greater than that of diffusional loss, resulting in the peak height of the analyte being higher for platform atomization than for tube-wall atomization.

Curves A and B in Fig. 3 show the experimentally observed atomic-absorption signals for lead atomized

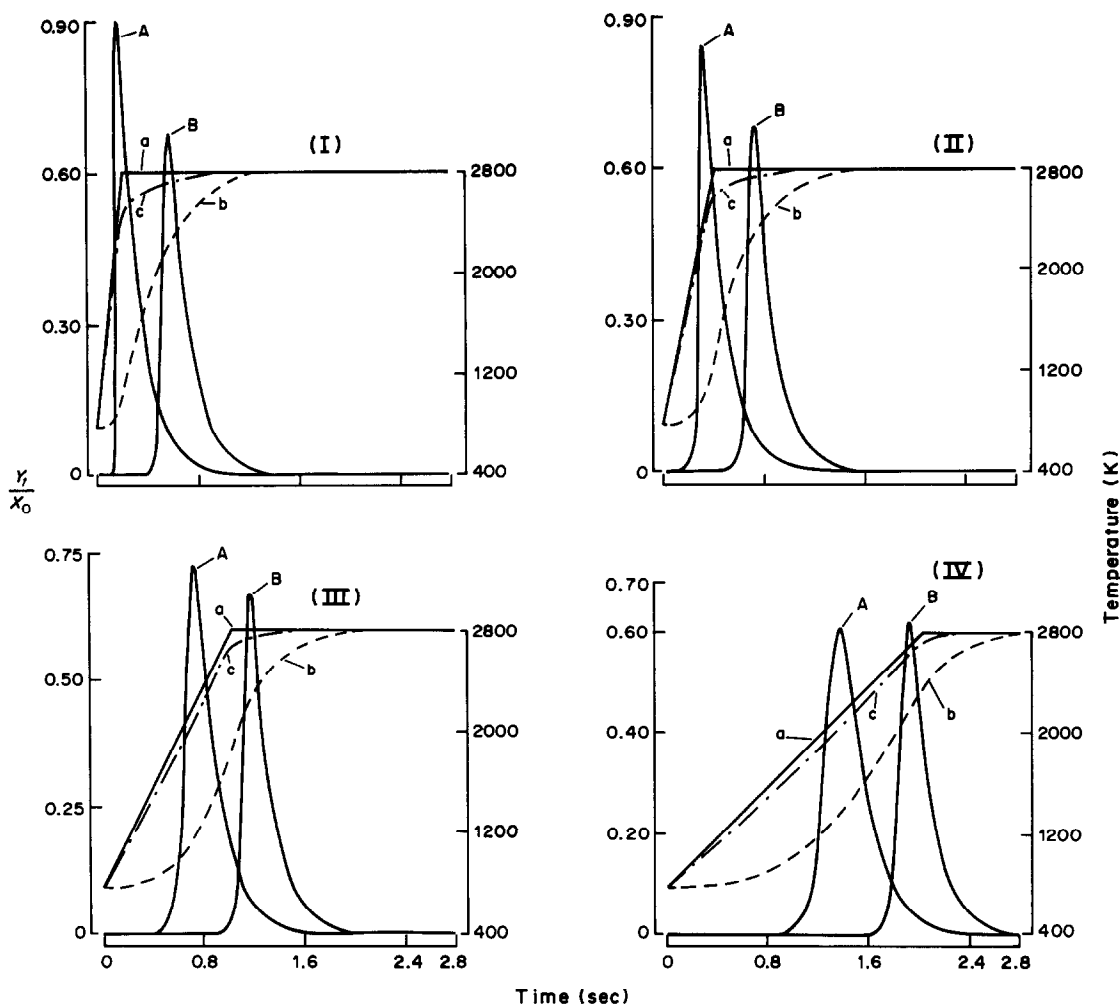


Fig. 2. Theoretical analyte atom population vs. time curves for tube-wall and platform atomization at various heating rates of the tube wall: A, tube-wall atomization; B, platform atomization; a, tube-wall temperature; b, platform temperature; c, weighted-average gas temperature with the platform inside the graphite tube. General parameters: $E_a = 430$ kJ/mole, $A = 1.0 \times 10^{12}$ sec $^{-1}$, $D_0 = 0.10$ cm 2 /sec, $n = 1.8$, graphite tube length = 2.8 cm, graphite tube internal diameter = 0.60 cm, platform length = 1.8 cm, platform width = 0.43 cm, platform thickness = 0.03 cm, initial wall temperature = 773 K, final wall temperature = 2800 K. Tube-wall heating rate, K/msec: (I) 10, (II) 5, (III) 2, (IV) 1.

from the tube wall (A) and the platform (B), respectively, at tube-wall heating rates of 4.5, 1.8 and 1.3 K/msec. The peak heights and peak areas of the Pb atomic-absorption signals in Fig. 3 are compared in Table 2. Curves a represent the tube-wall temperature used to calculate the theoretical platform temperature, shown as curves b. Curves c (mainly coincident with curves a) represent the tube-wall temperature measured by optical pyrometry. The relative positions of curves A and B in Fig. 3 agree qualitatively with predictions from the model. Also, both the theoretical and experimental values indicate that increase in the heating rate of the tube wall results in more of the platform-atomization signal arising when the tube wall has reached constant temperature.

Table 2 shows that for wall-atomization the peak

height of the lead signal first increases slightly with heating rate, then decreases, whereas the peak area decreases approximately linearly with increase in heating rate. These decreases are not predicted by the model, and may be due to other processes occurring during atomization, e.g., analyte loss by expulsion,¹⁰ which is not taken into account by the theoretical model. Since the furnace is open to the ambient atmosphere through the sample injection hole, the pressure inside the furnace is constant (1 atm). According to the ideal gas law, $pV = nRT$, an increase in temperature results in expansion of the gas. The amount of gas thus expelled from the furnace depends only on the initial and the final temperature, but the rate of expansion and hence of expulsion depends on the rate of change of temperature.²² Any analyte vaporized from the tube wall during the rapid

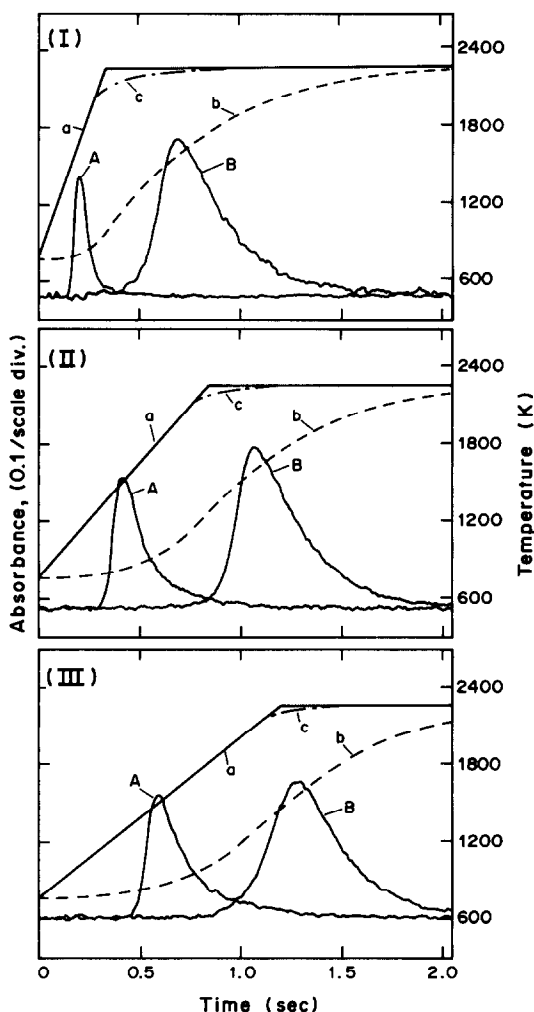


Fig. 3. Experimental atomic-absorption pulses for 1.0 ng of Pb (taken as the nitrate) for (A) tube-wall and (B) platform atomization at various heating rates of the tube wall; a and b are the theoretical temperatures of the tube wall and platform, respectively; c is the measured tube-wall temperature. Initial tube-wall temperature = 773 K, final tube-wall temperature = 2273 K, platform mass = 51.0 mg. Tube-wall heating rate, K/msec: (I) 4.5, (II) 1.8, (III) 1.3.

heating of the furnace may be partially lost with the gas expelled. Thus, expansion of the purge gas in the furnace plays an important role in the loss of analyte element during fast heating of the furnace, especially if the analyte is vaporized or atomized concurrently.¹⁰

Atomization from the platform generally results in

the analyte signal appearing at a relatively high gas temperature. As shown in Fig. 3, even at the lowest heating rate used, 1.3 K/msec, with platform atomization ~70% of the peak area of the Pb signal is obtained at constant temperature of the tube wall, whereas the corresponding fraction is only ~9% for wall atomization. Appearance of the analyte signal pulse at high and nearly constant gas temperature eliminates loss of the analyte element by expulsion along with expanding internal purge gas. The increased residence time of the analyte atoms in the tube makes the peak area for platform atomization greater than that for wall atomization. Table 2 shows that with platform atomization the peak area for lead is practically independent of wall heating rate, and that peak area measurement with platform atomization is the most reliable method of determination, fulfilling all the conditions required for the use of integrated absorbance.²³ The slight increase in the peak height with the initial increase in the heating rate of the tube wall agrees with the predictions of the model.

Effect of initial wall temperature

Figure 4 shows the simulated analyte atom population *vs.* time curves obtained for initial wall temperatures of 773, 1073 and 1373 K, with a final temperature of 2800 K and a wall heating rate of 2 K/msec. As the radiational energy emitted is proportional to the fourth power of the temperature,²⁴ a low initial wall temperature results in a longer delay in the rise of the platform temperature.

As seen in Fig. 4, change in the initial wall temperature has no effect on the peak-height, -shape or -temperature for wall atomization. However, for platform atomization, decreasing the initial wall temperature shifts the analyte atom concentration profile further into the constant wall-temperature region and slightly increases its peak height. Although diffusional losses increase with increasing gas temperature, use of a lower initial wall temperature results in a higher platform heating rate at the appearance time for analyte atoms. As explained earlier, the rate of analyte atom loss by diffusion is not as sensitive as the rate of atom formation to change in temperature, so for platform atomization the peak height should be higher for lower initial tube wall temperatures.

Figure 5 shows the experimental results for the effect of initial tube wall temperature. The values of

Table 2. Values of the peak height and the peak area of the Pb atomic-absorption signal pulses shown in Fig. 3 (Abs. = absorbance)

Plot	Curve A		Curve B	
	Peak height, Abs.	Peak area, Abs.msec	Peak height, Abs.	Peak area, Abs.msec
I	0.313	28.2	0.410	163.1
II	0.334	71.4	0.412	162.1
III	0.319	87.6	0.348	160.1

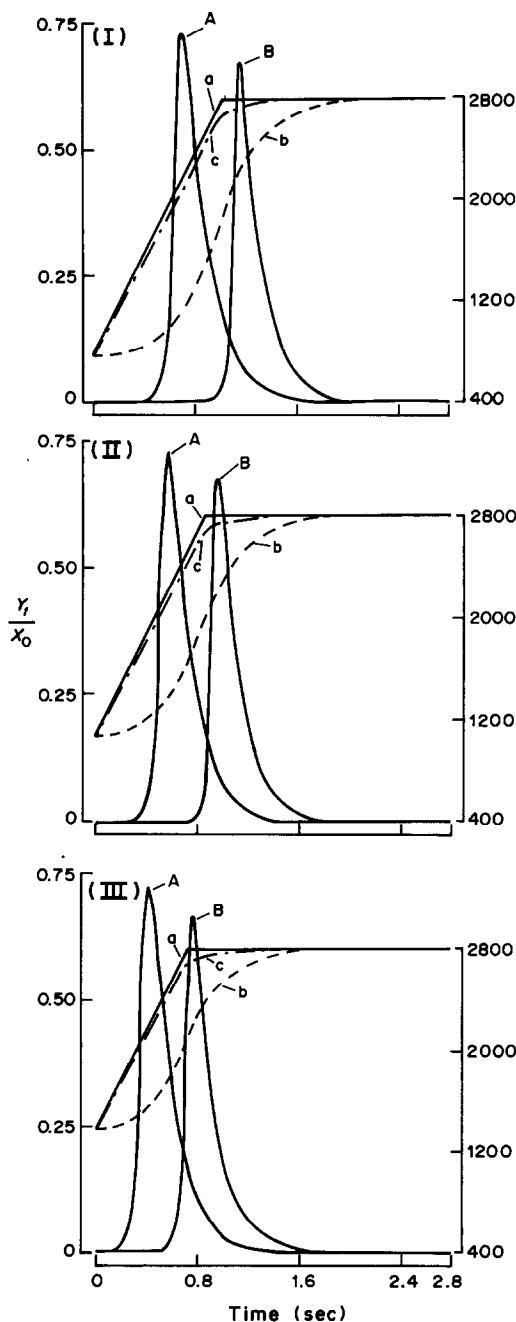


Fig. 4. Theoretical analyte atom population vs. time curves for tube-wall and platform atomization at various initial tube-wall temperatures. Heating rate of tube wall = 2 K/msec; initial tube-wall temperatures: (I) 773 K, (II) 1073 K, (III) 1373 K; other conditions and symbols as for Fig. 2.

peak heights and peak areas of the signals in Fig. 5 are compared in Table 3. At initial tube-wall temperatures of 473, 673 and 873 K, the measured average heating rates of the tube wall were 2.00, 1.95, and 1.90 K/msec, respectively. However, these slight differences between the average heating rates should not affect the significance of the results. For the

platform atomization, the effect of initial tube-wall temperature agrees qualitatively with the effects predicted by the model, except for the decrease in the peak height with decreasing initial tube-wall temperature. This decrease may be due to a temperature gradient that develops along the length of the end-contacted graphite tube, which is not accounted for in the model. Falk *et al.*²⁵ have reported that there is a significant drop in the temperature at the tube ends with time after the tube centre attains the preset temperature for the atomization step. An increasing temperature gradient along the tube length after attainment of the preset atomization temperature by its centre may make the instantaneous rate of heating of the platform predicted by the model too high, since for calculating the platform temperature the model

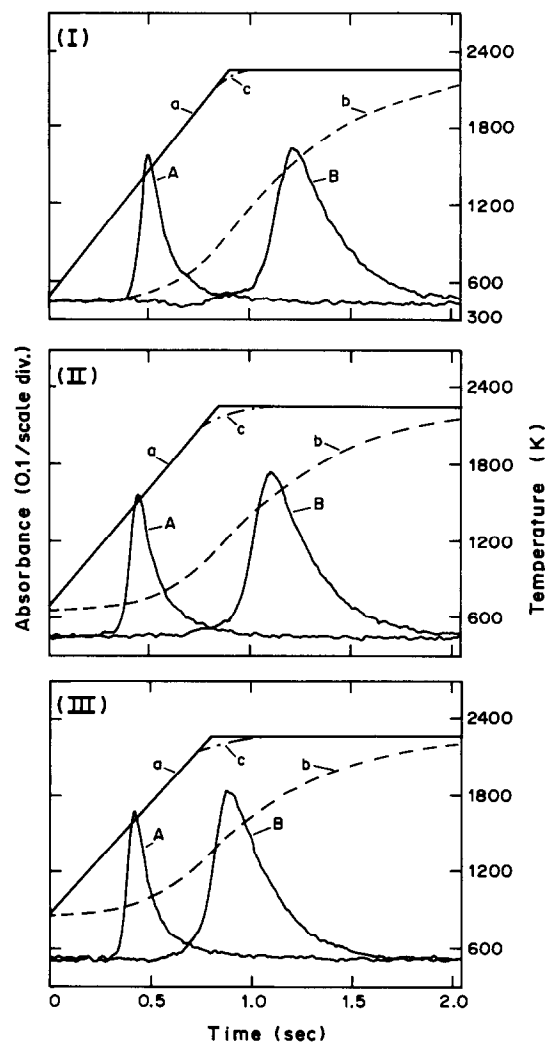


Fig. 5. Experimental atomic-absorption pulses for 1.0 ng of Pb (taken as the nitrate) for (A) tube-wall and (B) platform atomization at various initial tube-wall temperatures. Final tube-wall temperature = 2273 K, platform mass = 51.0 mg. Initial tube-wall temperatures, K, (I) 473, (II) 673, (III) 873; heating rates of the tube wall, K/msec, (I) 2.0, (II) 1.95, (III) 1.90; other symbols and conditions as for Fig. 3.

Table 3. Values of the peak height and the peak area of the Pb atomic-absorption signal pulses shown in Fig. 5

Plot	Curve A		Curve B	
	Peak height, Abs.	Peak area, Abs.msec	Peak height, Abs.	Peak area, Abs.msec
I	0.373	61.2	0.395	155.3
II	0.372	62.3	0.428	160.2
III	0.378	59.7	0.438	150.3

assumes there is a uniform temperature along the tube length. A lower initial tube-wall temperature results in a further delay in the atomization from the platform, and hence in a further shift of the Pb atomic-absorption pulse into the constant-temperature region of the temperature *vs.* time curve (the temperature being measured at the centre of the tube); this further delay results in a greater cooling at the tube ends. Thus, in Table 3, for the platform atomization, the observed slight decrease in the peak height absorbance of lead with decreasing initial tube-wall temperatures may be attributable to a decrease in the actual heating rate of the platform by an increased temperature gradient along the tube length.

Effect of the platform mass

For a given type of graphite, a change in the geometry of the platform may result in a change in

the mass. Only the top and bottom surfaces of the platform are used in equation (8) as the effective surface area for receiving radiational energy from the tube wall.¹⁴ According to equation (8) the platform temperature is directly proportional to the effective surface area and inversely proportional to the mass of the platform. A change in the length and/or width of the platform (with other dimensions being held constant) does not affect the heating characteristics of the platform, because it results in the same fractional change in the effective surface area and mass, and these effects, being in opposite directions, cancel. However, a change in the thickness of the platform results in a change in the mass but not the effective surface area, and hence would affect the heating characteristics.

Figure 6 shows the tube-wall (curve a) and platform temperature profiles superimposed on the simulated analyte atom population profiles for graphite

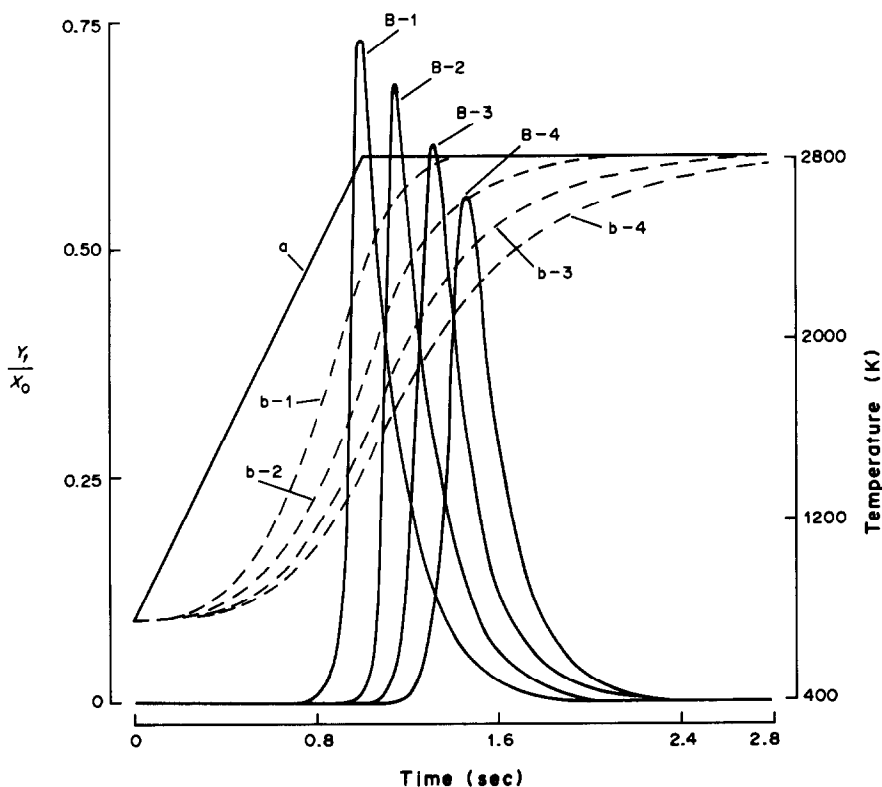


Fig. 6. Theoretical analyte atom population *vs.* time curves for atomization from platforms of different thicknesses: a, tube-wall temperature-time curve; B-1, B-2, B-3 and B-4, analyte atom population *vs.* time curves; b-1, b-2, b-3 and b-4, platform temperatures for platform thickness 0.015, 0.030, 0.045 and 0.060 cm, respectively. Wall heating rate 2 K/msec; other parameters as for Fig. 2.

platforms of different masses. With increasing platform mass, a decrease in the heating rate of the platform and a longer delay in commencement of the platform heating is expected from equation (8), and the greater the platform mass, the greater is the shift of the analyte atom population *vs.* time curve towards the constant-temperature region. Increase in the platform mass also results in decrease in the peak height of the population *vs.* time curve, because of the lower heating rate of the platform.

Figure 7 shows experimental results for the effect of the platform mass. The peak heights and peak areas are compared in Table 4. Figure 7 shows that increase in the platform mass shifts the lead signal towards the constant-temperature region of the tube-wall temperature curve and decreases the peak height, in agreement with the model. Table 4 shows that the peak area for platform atomization is nearly constant and independent of the platform mass but the peak height is significantly decreased by a relatively large change in mass above a certain critical value.

Effect of activation energy

Figure 8 shows the effect of activation energy on the analyte atom population *vs.* time curves. Once the platform geometry, initial temperature, final temperature and heating rate of the tube wall are fixed, the characteristics of the temperature-time profile of the platform become invariant. Equation (3) shows that for a given temperature, the rate constant for

atom formation, $k_1(t)$, is governed by both the frequency factor and the activation energy. A high activation energy makes $k_1(t)$ relatively small, so an atomization reaction having a high activation energy requires a high temperature for its initiation. For platform atomization, when the activation energy is high the platform takes a relatively long time to reach the required temperature, as seen in Fig. 8, which also shows that an increase in activation energy results in a decrease in the peak height of the analyte atom population curve. Since the gas temperature closely follows the tube-wall temperature, and since curves B-2 and B-3 are both located in the constant-temperature region of the tube-wall temperature curve, the rate constant for diffusional loss should be the same for both curves. However, although the heating rate of the platform is nearly the same at the appearance temperatures for curves B-2 and B-3, it decreases at temperatures above the appearance temperatures for curve B-3 and the consequent lower rate

Table 4. Values of the peak height and peak area of the Pb atomic-absorption signal pulses shown in Fig. 7

Curve	Peak height, Abs.	Peak area, Abs.msec
A	0.395	77.8
B-1	0.435	162.2
B-2	0.440	168.3
B-3	0.387	160.0

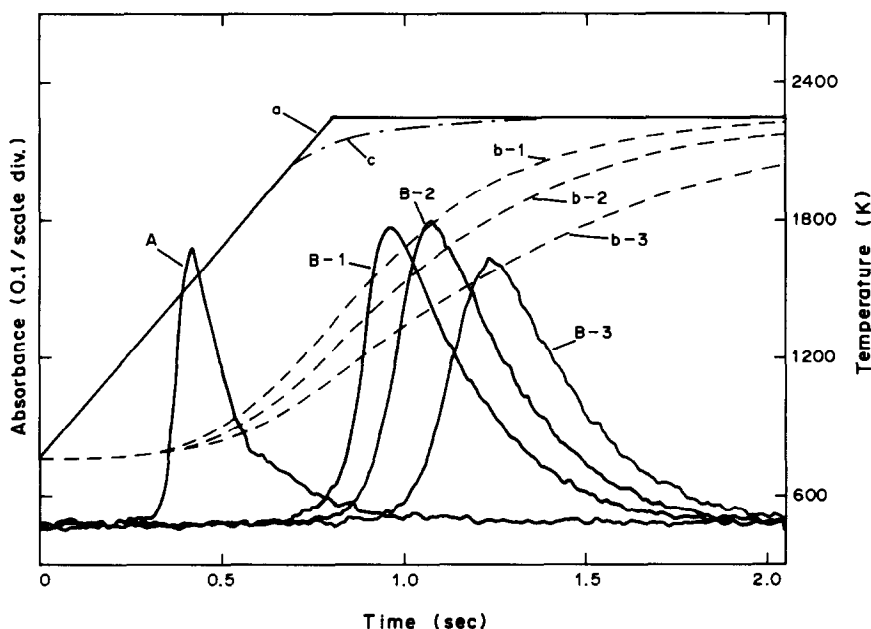


Fig. 7. Experimental atomic-absorption pulses for 1.0 ng of Pb (taken as the nitrate) for wall atomization and platform atomization from platforms of different masses: a, the measured tube-wall temperature-time curve used for calculation of the platform temperature; c, measured tube-wall temperature; A, atomic-absorption pulse from wall atomization; B-1, B-2 and B-3, atomic-absorption pulses for atomization from platforms of masses 39.0, 50.0 and 76.5 mg (thickness 0.23, 0.30, 0.45 mm), respectively; b-1, b-2 and b-3, corresponding platform temperature curves.

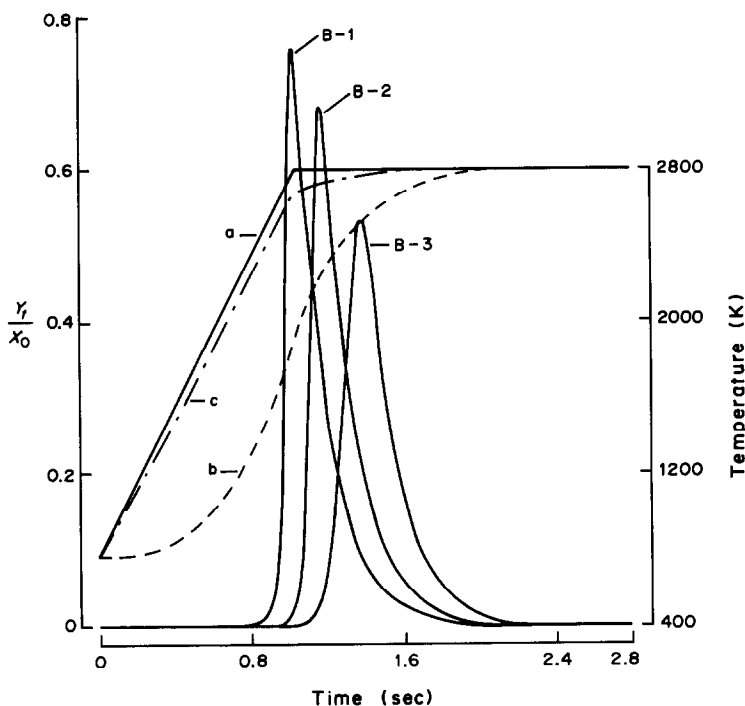


Fig. 8. Theoretical analyte atom population *vs.* time curves for platform atomization and various activation energies: B-1, B-2 and B-3, curves for activation energies of 350, 430 and 510 kJ/mole, respectively. Wall heating rate 2 K/msec; other symbols and parameters as for Fig. 2.

of atom formation decreases the peak height, but the peak area is much less affected.

CONCLUSIONS

The simple model presented has some limitations which stem largely from the simplifying assumptions and oversimplified treatment of the atom loss processes. However, such limitations do not seriously impair its usefulness, which lies not so much in its predictive power as in its ability to offer a theoretical framework for understanding the effect of various experimental parameters on the analytical signals arising from atomization from graphite platforms in atomic-absorption spectrometry.

A relatively high heating rate and a relatively low initial temperature of the tube wall result in a shift of the atomic-absorption signal from platform atomization towards the region of constant temperature of both the tube wall and the gas phase. The advantage of this shift is a large decrease in the loss of the analyte by expulsion with the expanding internal purge gas. Relatively high heating rates of the tube wall maximize the heating rate of the platform at the appearance time of the atomic-absorption signal, and hence result in an increase in the rate of atomization of the analyte element.

Since a low initial temperature of the tube wall

results in a shift of the analyte absorption pulse towards the constant wall-temperature region and an increase in the platform heating rate, a cooling step before the atomization stage is suggested for optimizing experimental conditions for platform atomization.¹⁴ The activation energy is also an important factor. For an atomization reaction having a high enough activation energy, the whole signal pulse will arise when the heated tube wall has reached constant temperature. A platform of relatively high mass will have a relatively slow heating rate, which results in a decrease in peak height. However, for an analyte element having a low activation energy for the atomization reaction, a platform of relatively high mass is necessary to shift the analyte atomic-absorption pulse into the constant-temperature region of the tube-wall-temperature curve. Although use of a relatively heavy platform, desirable for elements with low activation energy (such as relatively volatile elements), may result in a decrease in peak height, a concurrent decrease in matrix interferences may result from the high gas temperature during sample atomization; the net result will be an advantage for platform atomization over tube-wall atomization.

Acknowledgement—The authors are grateful to the Natural Sciences and Engineering Research Council of Canada for financial support of this research project.

REFERENCES

1. B. V. L'vov, *Atomic Absorption Spectrochemical Analysis*, Hilger, London, 1970.
2. B. V. L'vov, P. A. Bayunov and G. N. Ryabchuck, *Spectrochim. Acta*, 1981, **36B**, 396.
3. W. M. G. T. van den Broek and L. de Galan, *Anal. Chem.*, 1977, **49**, 2176.
4. G. Torsi and G. Tessari, *ibid.*, 1973, **45**, 1812.
5. S. L. Paveri-Fontana, G. Tessari and G. Torsi, *ibid.*, 1974, **46**, 1032.
6. G. Tessari and G. Torsi, *ibid.*, 1979, **51**, 2039.
7. H. Falk, *Spectrochim. Acta*, 1978, **33B**, 695.
8. J. A. Holcombe and G. D. Rayson, *Prog. Anal. Atom. Spectrosc.*, 1983, **6**, 225.
9. A. Kh. Gilmudinov and I. S. Fishman, *Spectrochim. Acta*, 1984, **39B**, 171.
10. C. L. Chakrabarti, S. Wu, R. Karwowska, J. T. Rogers and R. Dick, *ibid.*, 1985, **40B**, 1663.
11. C. L. Chakrabarti, S. B. Chang, S. R. Lawson and S. M. Wong, *ibid.*, 1983, **38B**, 1287.
12. J. A. Holcombe, *ibid.*, 1983, **38B**, 609.
13. S. L. Paveri-Fontana and G. Tessari, *Prog. Anal. Spectrosc.*, 1984, **7**, 243.
14. C. L. Chakrabarti, S. Wu, R. Karwowska, J. T. Rogers, L. Haley, P. C. Bertels and R. Dick, *Spectrochim. Acta*, 1984, **39B**, 415.
15. C. L. Chakrabarti, C. C. Wan, R. J. Teskey, S. B. Chang, H. A. Hamed and P. C. Bertels, *ibid.*, 1981, **36B**, 427.
16. C. F. Gerald, *Applied Numerical Analysis*, 2nd Ed., Addison-Wesley, Don Mills, Ontario, 1978.
17. H. Falk, *31st Canadian Spectroscopy Symposium*, Gray Rocks, Canada, 1984, Paper A2.
18. Y. S. Touloukian and C. Y. Ho, *Properties of Non-metallic Fluid Elements*, McGraw-Hill, New York, 1981.
19. J. C. Bailar, H. J. Emelius, R. S. Nyholm and A. F. Trotman-Dickenson, *Comprehensive Inorganic Chemistry*, Vol. 1, Pergamon Press, New York, 1973.
20. J. P. Holman, *Heat Transfer*, 5th Ed., McGraw-Hill, New York, 1981.
21. C. L. Chakrabarti, S. Wu and P. C. Bertels, *Spectrochim. Acta*, 1983, **38B**, 1041.
22. S. B. Chang and C. L. Chakrabarti, *Prog. Anal. Atom. Spectrosc.*, 1985, **8**, 83.
23. Reference 1, p. 120.
24. P. W. Atkins, *Physical Chemistry*, 2nd Ed., Oxford University Press, Oxford, 1982.
25. H. Falk, A. Glismann, L. Bergann, G. Minkwitz, M. Schubert and J. Skole, *Spectrochim. Acta*, 1985, **40B**, 533.

ULTRATRACE MOLYBDENUM DETERMINATION IN BIOLOGICAL SAMPLES BY GRAPHITE-FURNACE ATOMIC-ABSORPTION SPECTROMETRY

SCOTT P. ERICSON and MICHAEL L. McHALSKY

Travenol Laboratories, 6301 Lincoln Ave., Morton Grove, IL 60053, U.S.A.

BRUNO JASELSKIS

Department of Chemistry, Loyola University of Chicago, IL 60626, U.S.A.

(Received 28 April 1986. Revised 30 July 1986. Accepted 10 September 1986)

Summary—A method is described for molybdenum determination in human serum at sub-ng/ml levels by graphite-furnace atomic-absorption spectrometry. Sample preparation involves a nitric acid digestion, chelation with benzohydroxamic acid and extraction into hexanol. A detection limit of 0.1 ng/ml and a characteristic concentration of 0.18 ng/ml for 1% absorption can be achieved. The effectiveness of the method has been demonstrated by analysis of unspiked and spiked human serum, standard reference materials, and comparison with the results obtained by inductively-coupled plasma atomic-emission spectroscopy.

Molybdenum has been shown to be an essential trace element in man.¹ Its clinical importance presents an analytical challenge for chemists. For instance, the recent practice of supplementing diets with trace elements has created a need for monitoring the serum of patients receiving such treatment.^{2,3} To date, neutron-activation analysis (NAA) is the only technique that has been reported to be successful for determination of molybdenum in human serum at normal sub-ng/ml levels.⁴ It is unlikely that NAA can be applied for routine testing.

This study was performed to develop an accurate and precise method for determining molybdenum in human serum by graphite-furnace atomic-absorption spectrometry (GFAAS). The adoption of a digestion/chelation/extraction method was necessary owing to the nature of the matrix interference effects in molybdenum determination by GFAAS. Molybdenum is considered a refractory element in that it can form thermally stable molybdenum carbides.^{5,6} This property effectively limits application of the technique as for many instruments it necessitates running at the maximum temperature attainable. Tube life is shortened under those conditions and carry-over between injections is often a problem.⁷⁻⁹ Carbon deposits in the furnace tube from undigested serum samples magnify the effect of molybdenum carbide formation. Some instrument systems allow introduction of oxygen or air during one of the steps in the heating programme to reduce carbon build-up in the tube, but our experience is that this also tends to degrade the furnace cones.

Digestion techniques may be used to remove the organic components from the samples, leaving the

molybdenum in an inorganic matrix, but the salt components may depress the molybdenum signal.¹⁰ Extraction of the molybdenum from the sample digest with a chelating agent removes the element from the interfering serum matrix.

EXPERIMENTAL

Apparatus

Atomic-absorption measurements were made with a Perkin-Elmer Zeeman/5000 spectrophotometer. The system included an HGA 500 furnace with magnet and optical pyrometer, an AS-40 autosampler, a Data 10 station, a Hewlett-Packard 7470 plotter and an Alanthus Decwriter III. Atomic-emission measurements were made on an Instruments SA JY38P sequential inductively-coupled plasma spectrophotometer. The instrument was equipped with a Plasma-Therm 2500 torch box, peristaltic pump and MAK nebulizer with a Matheson mass-flow controller.

All sample and reagent preparations were performed with plastic or Teflon ware. Glassware was used only for pipetting the hexanol for the extraction. All other pipetting was performed with Eppendorf micropipettes with disposable plastic tips. Digestions were performed in 30-ml Teflon centrifuge tubes with Teflon screw-caps (Nalgene cat. # 3114-0030). The tubes were heated in aluminium blocks inside a portable class-100 air laminar-flow hood placed in a fume hood.

Reagents

Benzohydroxamic acid, Eastman Kodak No. 8262; 1-hexanol, Eastman Kodak No. 825; nitric acid, J. T. Baker Ultrex® grade; nitric acid, reagent grade (for cleaning); magnesium nitrate, recrystallized Fisher ACS grade; ammonium nitrate, recrystallized Fisher ACS grade; ammonium heptamolybdate tetrahydrate, Johnson-Matthey Puratronic® grade; NRS-250 detergent concentrate, Norrel, Inc. (for cleaning).

A stock solution of molybdenum(VI) was prepared by dissolving 1.8398 g of the ammonium heptamolybdate

Table 1. Temperature programme, HGA 500 furnace

Step	1	2	3	4	5	6	7
Temperature, °C	110	180	1300	20	2700	2700	20
Ramp time, sec	20	5	20	1	0*	1	1
Hole time, sec	10	10	10	10	5	2	5
Argon, ml/min	300	300	300	300	0†	300	300

*Engages "Max Power" option.

†Changed to 20 ml/min for higher molybdenum concentrations.

tetrahydrate in 1000 ml of demineralized distilled water. This standard was stored in a plastic screw-cap bottle and used for up to one year.

Cleaning of laboratory ware

The vessels used in reagent and sample preparation were cleaned by soaking for at least 2 hr in a solution of NRS-250 detergent, rinsing with distilled water, soaking for at least 2 hr in a polyethylene bin containing a 10% v/v solution of reagent grade nitric acid in distilled water, thorough rinsing with demineralized distilled water (DDW), and drying face down on rubber matting, then were stored in plastic bags. A final DDW rinse was performed immediately before use. The Teflon digestion vessels were cleaned by refluxing for at least 1 hr with 1 ml of concentrated Ultrex® nitric acid, followed by a thorough DDW rinse. The Teflon caps for the vessels were cleaned by soaking overnight in a 10% v/v solution of Ultrex® nitric acid in DDW, then thorough rinsing with DDW.

Sample identification

Method-development work was performed on Sera Chem Normal Clinical Chemistry Control Serum (Human) Unassayed, obtained from Fisher Scientific Company. Sufficient quantities of the lyophilized serum were reconstituted with DDW, on the day of use, in polyethylene bottles. Reference materials investigated included NBS SRM 1577a Bovine Liver, NBS RM 8419 Bovine Serum, and NBS SRM 1572 Citrus Leaves.

Instrument conditions

Zeeman-corrected absorbances were taken in the peak area mode for the 313.3 nm line, with a 0.7-nm band-width and 5-sec integration time. Table 1 gives the temperature program used for the hexanol extracts. ICP emission intensities were recorded for observation at 15 mm above the coil, with an incident RF power of 1.5 kW, an argon coolant flow-rate of 16 l/min and an auxiliary coolant flow-rate of 0.8 l/min. Sample flow-rates were 0.6 ml/min into the MAK nebulizer, which was operated with an argon flow-rate of 0.50 l/min. The molybdenum emission line at 202.07 nm was used in the analysis, with the carbon line at 199.36 nm as a reference.

Extraction procedure

Samples. Serum (2.0 ml) and Ultrex® nitric acid (2.0 ml) were pipetted into a 30-ml Teflon centrifuge tube. The sample was refluxed at 130° by heating in an aluminium block inside a class-100 air laminar-flow hood, until the volume was reduced to about 0.1 ml (approximately 4 hr). The tube was removed from the block and allowed to cool, then 2.0 ml of 2M hydrochloric acid, 0.2 ml of 0.2 g/ml magnesium nitrate solution and 2.0 ml of 0.1M benzo-hydroxamic acid (BHA) solution were added. Finally 1.0 ml of hexanol was pipetted into the tube and the mixture was shaken for 2 min. The hexanol layer was analysed by graphite-furnace atomic-absorption spectrometry (GFAAS). The entire procedure was similarly applied to 2-ml portions of nitric acid as digestion blanks.

Standards. Into each of four 30-ml Teflon centrifuge tubes were pipetted 0 (standard blank), 50 µl, 100 µl and 150 µl

of a 20-ng/ml intermediate molybdenum standard. To the tubes were added 100 µl of nitric acid, 2.0 ml of 2.0M hydrochloric acid and 0.2 ml of 0.2-g/ml magnesium nitrate solution. The molybdenum was then extracted from the standards with BHA as described above for samples. The standards had molybdenum concentrations equivalent to 0, 0.5, 1.0 and 1.5 ng/ml (in a 2-ml initial volume).

Sample concentrations were calculated from the results of linear regression analysis of the calibration standards.

RESULTS

Five samples containing molybdenum at a concentration of about 1 ng/ml were analysed in triplicate to establish the precision of the technique at this level. The results obtained are shown in Table 2. Validation experiments were performed by applying the digestion/BHA-hexanol extraction to unspiked serum and serum spiked with 1, 2, 3 and 4 ng/ml molybdenum. Each level was run in quadruplicate, including digestion blanks. Calibration standards of 0, 2, 4 and 6 ng/ml were used in these experiments. Table 3 contains results for trials performed on three separate days. Bovine serum was evaluated by applying the technique to four 0.5-ml aliquots. Portions of the solid reference materials (0.2 g of bovine liver and 1.0 g of citrus leaves) were weighed, digested and extracted as for the serum samples. Data obtained for the reference material samples are listed in Table 4. The experiment comparing the GFAAS technique with ICP-AES was designed to compensate for the lower sensitivity of the latter method, the serum being spiked at 100, 200 and 300 ng/ml levels, each in triplicate. GFAAS determinations were made on the hexanol extracts remaining after the ICP analysis, diluted to bring them into the concentration range of the working standards. Table 5 gives the results of the comparison.

Table 2. Extraction of unspiked serum (triplicate results)

Sample	Mean, ng/ml	R.S.D., %
A	0.92	0.6
B	0.95	5.5
C	1.00	1.6
D	1.06	4.8
E	1.03	3.2

Table 3. BHA/hexanol validation experiment results

	Mean, ng/ml	R.S.D. (N = 12), %	Average spike recovery, %
Unspiked serum	0.80	7.8	
Serum + 1 ng/ml	1.81	6.7	101.1
Serum + 2 ng/ml	2.78	4.3	99.0
Serum + 3 ng/ml	3.69	6.0	96.3
Serum + 4 ng/ml	4.68	5.2	97.4

Table 4. Molybdenum in reference materials

NBS Bovine Liver, certified value $3.5 \pm 0.5 \mu\text{g/g}$
ICP 3.14 (S.D. 0.19) $\mu\text{g/g}$
GFAAS 2.19 (S.D. 0.06) $\mu\text{g/g}$
NBS Citrus Leaves, certified value $0.17 \pm 0.09 \mu\text{g/g}$
GFAAS 0.08 (S.D. 0.003) $\mu\text{g/g}$
NBS Bovine Serum, reference value $16 \pm 4 \text{ ng/ml}$
GFAAS 19.0 (S.D. 1.3) ng/ml

Table 5. ICP/GFAAS Comparison

	Recovery, %	
	ICP	GFAAS
Serum + 100 ng/ml	92.2	86.3
Serum + 200 ng/ml	92.0	94.3
Serum + 300 ng/ml	91.3	95.7
Mean	91.8	92.1

DISCUSSION

Instrument optimization

Studies have shown that heating rate has a significant effect on the signal from refractory elements.^{11,12} As shown by Fig. 1, use of the "max power" mode of the Perkin-Elmer instrument (which

allows an atomization temperature of 2700°) has a dramatic effect on the molybdenum signal. Pyrolytically coated tubes were used in the course of this study, had a useful lifetime of only 40 firings at an atomization temperature of 2800°. Use of the 2700° atomization temperature increased the lifetime to 100 firings for acidified aqueous solutions and 150 firings for organic extracts, but reduced the signal by about 30%.

Selection of charring temperature was based on the

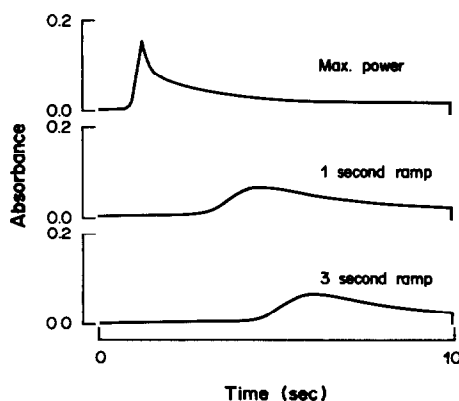


Fig. 1. Effect of heating rate for 0.5-ng molybdenum injections.

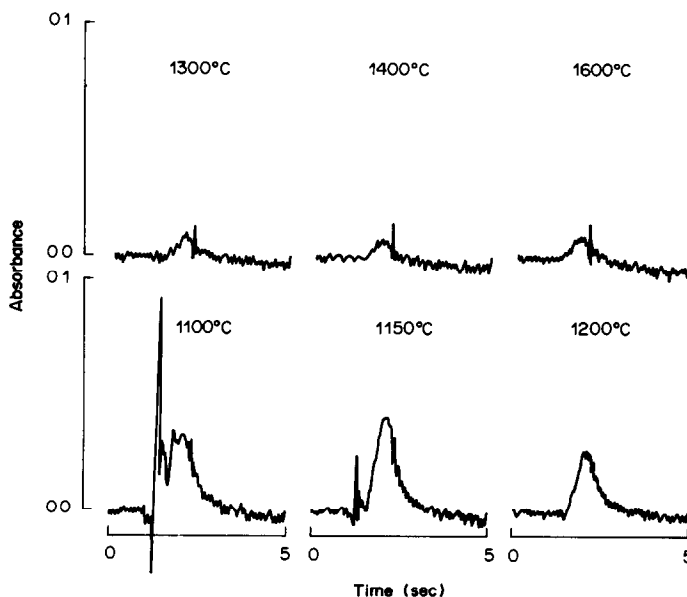


Fig. 2. Effect of charring temperature on digested-serum absorbance profiles.

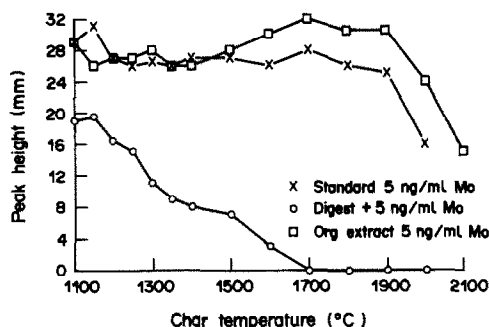


Fig. 3. Effect of charring temperature on peak-height signals for a simple acid matrix, digested serum, and a hexanol extract of digested serum.

data illustrated in Figs. 2 and 3. The salt matrix interference is not removed by charring at 1100°. Charring at 1300° removes the interference, but most of the molybdenum signal is lost as well. Figure 3 compares the effect of charring temperature for molybdenum in a simple acid matrix, a serum digest supplemented with molybdenum, and hexanol extract of digested serum supplemented with molybdenum. It is apparent that the extraction is successful in removing molybdenum from the signal-suppressing components of the serum digest. Since it was not necessary to char at above 1300°, this temperature was chosen for the method.

Sample-injection size and argon flow-rate at atomization were adjusted to accommodate the working standard range. For unspiked serum samples containing approximately 1 ng/ml molybdenum, 30- μ l injections were used, with the argon flow interrupted at atomization. The signal to noise ratio is illustrated in Fig. 4. Samples at normal physiological levels of 0.6 ng/ml should fall within the working standard

range. The low value for the digestion blank should allow for quantitative measurements in serum. Under these conditions, a detection limit of 0.1 ng/ml (defined as the concentration equivalent to 3 times the standard deviation of the blank) and a characteristic concentration of 0.18 ng/ml (for 1% absorption) were obtained. Standards up to 1.5 ng/ml may be injected without carry-over problems. The validation experiments with standards up to 6 ng/ml required reduction of the sample size to 20 μ l and introduction of argon at 20 ml/min at atomization. These changes raised the characteristic concentration to 0.34 ng/ml, but maintained a detection limit of 0.1 ng/ml. Even with introduction of argon at atomization, the 6-ng/ml standard has a carry-over of approximately 5%. This carry-over was completely removed by using a 2-sec manually controlled burn-out step at 2800° between injections. This short cleaning step was not observed to affect tube life.

Method development

Four chelating agents were investigated for effectiveness in determination of molybdenum in serum. Besides benzohydroxamic acid (BHA), experiments were run with ammonium pyrrolidinedithiocarbamate (APDC), acetylacetone (ACAC) and trifluoroacetylacetone (TFAA). Chelation of molybdenum with APDC and extraction into MIBK (methyl isobutyl ketane) lacked sufficient precision. Acetylacetone, which chelates molybdenum at acidity up to 3.0M sulphuric acid,¹³ requires no pH adjustment after the digestion. However, extraction of molybdenum from serum digests with ACAC/MIBK or ACAC/CHCl₃ gave recoveries with a high positive bias. The high solubility of ACAC in aqueous solution also made use of this reagent a questionable

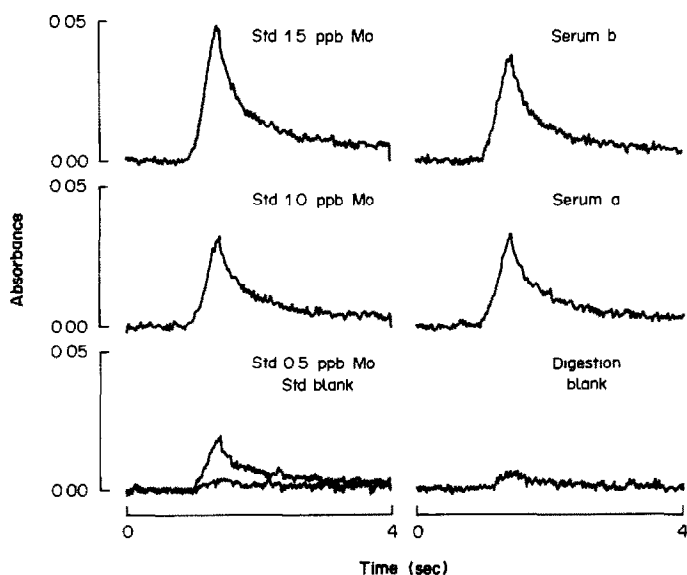


Fig. 4. Hexanol extract absorbance profiles for molybdenum standards, a digestion blank and two digested serum samples.

choice. Trifluoroacetylacetone was investigated in the hope that the fluorine environment would improve the efficiency of molybdenum transport in a way similar to that given by the addition of trifluoromethane to the argon purge-gas, as reported by Kirkbright and Snook.¹⁴ However, the molybdenum-TFAA extract gave the same appearance temperature as that for the ACAC extract, and the recovery of molybdenum was poor.

The first experiments with the BHA/hexanol extraction system included attempts to duplicate the work of Agrawal.¹⁵ The colorimetric method was not sufficiently sensitive for determinations at ng/ml serum concentrations of molybdenum. A nitric acid digestion prior to chelation/extraction was adopted in order to recover all of the molybdenum from the samples. Experiments were performed with 3 ml of serum, 10 ml of 2M hydrochloric acid, 4 ml of 0.1M BHA and 2 ml of hexanol. Spike recoveries were approximately 90% and a value of 3.57 $\mu\text{g/g}$ was obtained for NBS Bovine Liver.

These encouraging results led to validation experiments in which the sample and reagent volumes were reduced to those described in the procedure. These changes were made to reduce sample requirements and achieve a concentration factor of 2 in the extraction. Apparently, the new experimental conditions magnified the matrix effects in the method, recovery values for spiked serum samples being 160–180%. The source of the bias was thought to be some electrolyte remaining after the digestion step. Investigations were made of the effect of various salts on the extraction procedure. It was found that magnesium nitrate caused a significant signal enhancement. Potassium nitrate at similar concentrations caused signal suppression, indicating that the magnesium was the cause of the enhancement, rather than the nitrate. Increasing amounts of magnesium nitrate were added to 5-ng/ml molybdenum standards which were then extracted. The results are illustrated in Fig. 5. This graph was used to modify the extraction procedure for serum digests. The magnesium nitrate effect begins to level off at addition of about 200 μl of 0.2-g/ml solution. This volume of the reagent was

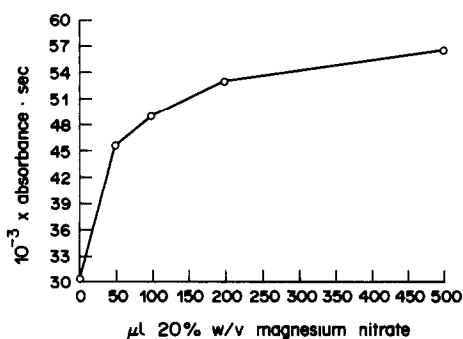


Fig. 5. Plot of magnesium nitrate addition vs. absorbance for extracted 5-ng/ml molybdenum standards.

added, before the extraction, to all subsequent standards and samples, the data for which are reported in Tables 2–5.

The positive bias, due to magnesium, in the GFAAS determinations was not found in the ICP results for similar solutions. Standards extracted with and without prior addition of magnesium nitrate gave virtually identical ICP emission intensities. Extraction efficiency was evaluated by GFAAS and ICP-AES through comparison of the molybdenum signals for the aqueous and organic phases. In both cases the signal for the aqueous phase was the same as the baseline noise. The organic layers were analysed for magnesium content. The hexanol was found to contain 0.5 mg/l. magnesium when 50 μl of magnesium nitrate solution were added before the extraction, and 1.0 mg/l. when 200 μl were added. These values are consistent with the signal enhancement effect shown in Fig. 5. Thus, the bias is not due to an effect on extraction efficiency, but to a matrix effect in the graphite tube.

Statistical evaluation

The results summarized in Tables 2–5 suggest that the BHA/hexanol technique can reliably determine molybdenum in serum at concentrations close to normal physiological levels. Precision of 5% or better can be expected for replicate samples at approximately 1 ng/ml molybdenum content. The 12 determinations in the validation experiment had a precision of 8% at a molybdenum concentration of 0.8 ng/ml. This slight decrease in precision may partly be attributed to the poorer sensitivity under the instrument conditions used in the experiment.

Analysis of variance calculations were performed on the data of the validation experiments. No effects were observed for the 12 determinations on unspiked serum over the three trials, at the 95% confidence level. This shows consistency of the technique for samples at 0.8 ng/ml molybdenum concentration. There were also no significant difference between spiking-level or between-determination effects within quadruplicate groups. A significant effect was found when comparing between-trial data for spiked samples. This effect was due to a somewhat higher average spike recovery on day 1 as opposed to days 2 and 3. The magnitude of this error was estimated to be 0.1 ng/ml.

The experiment comparing ICP with GFAAS data was performed to validate the technique by two methods based on dissimilar principles. The results in Table 5 are very close. Analysis of variance calculations on these data showed no significant effects at the 95% confidence level.

Evidence of matrix effects in the GFAAS can be found in the values for reference materials presented in Table 4. Addition of magnesium nitrate can compensate for these effects in serum samples, as the bovine serum falls within the recommended concentration range.¹⁶ However, bovine liver definitely

shows a negative bias when the GFAAS technique is used. The value of 3.57 $\mu\text{g/g}$ for the sample in an earlier experiment suggests that simple modifications to the procedure, such as increasing reagent volumes, might overcome such interferences. The results for bovine liver in Table 4 show that the ICP method of detection is not prone to matrix effects. For samples with molybdenum concentrations in the $\mu\text{g/g}$ range, ICP would be the method of choice for determination.

CONCLUSIONS

The practical usefulness of the BHA/hexanol technique in terms of routine analyses has been demonstrated. The GFAAS method presented is far cheaper and simpler than NAA. Careful laboratory technique and a class-100 air laminar-flow hood are essential to the success of the method. However, even a moderate commitment to contamination control should be sufficient for reliable results to be obtained. The laboratory where this work was performed did not have clean-room conditions, yet the results on unspiked serum samples at the 0.8 ng/ml concentration level, over three days, contained no outliers. The procedure itself takes 4–5 hr for sample digestion (2 ml serum sample size) and approximately 4 hr for extraction and analysis of 25 samples. The digestion does not require constant operator attention. The extracted samples are stable for at least one week in snap-top polyethylene vials, and the hexanol is relatively involatile, minimizing variation due to

evaporation losses. These features make the method convenient for the analyst. The method as described provides an option for monitoring of blood serum for molybdenum and may also be useful for analysis of other types of biological samples.

REFERENCES

1. G. H. Morrison, *CRC Crit. Rev. Anal. Chem.*, 1979, **8**, 287.
2. Expert Panel for Nutrition Advisory Group, *JAMA*, 1979, **241**, 2051.
3. R. E. Burch and H. K. Hahn, *Med. Clin. N. Am.*, 1979, **63**, 1057.
4. J. Versieck, *CRC Crit. Rev. Clin. Lab. Sci.*, 1985, **22**, 97.
5. J. Sneddon, J. M. Ottaway and W. B. Rowston, *Analyt.*, 1978, **103**, 776.
6. G. Muller-Vogt, W. Wendl and P. Pfundstein, *Z. Anal. Chem.*, 1983, **314**, 638.
7. S. Henning and T. L. Jackson, *At. Abs. Newslett.*, 1973, **12**, 100.
8. W. S. Wan Ngah, L. L. Sarkissian and J. F. Tyson, *Anal. Proc.*, 1983, **20**, 597.
9. D. R. Neuman and F. F. Munshower, *Anal. Chim. Acta*, 1981, **123**, 325.
10. G. E. Bentley, L. Markowitz and R. R. Meglen, *Adv. Chem. Surv.*, 1979, **172**, 33.
11. D. Littlejohn and J. M. Ottaway, *Anal. Chim. Acta*, 1978, **98**, 279.
12. N. G. Zhou, W. Frech and L. de Galan, *Spectrochim. Acta*, 1984, **39B**, 225.
13. J. P. McKaveney and H. Freiser, *Anal. Chem.*, 1957, **29**, 290.
14. G. F. Kirkbright and R. D. Snook, *ibid.*, 1979, **51**, 1938.
15. Y. K. Agrawal, *Anal. Lett.*, 1980, **13**, 357.
16. C. Veillon, S. A. Lewis, K. Y. Patterson, W. R. Wolf, J. M. Harnly, J. Versieck, L. Vanballenberghe, R. Cornelis and T. C. O'Haver, *Anal. Chem.*, 1985, **57**, 2106.

DETERMINATION OF ULTRATRACE AMOUNTS OF COBALT BY CATALYSIS OF THE TIRON-HYDROGEN PEROXIDE REACTION WITH AN IMPROVED CONTINUOUS-FLOW ANALYSIS SYSTEM

KENJI ISSHIKI

Department of Chemistry, Faculty of Science, Kyoto University, Kyoto, 606 Japan

EIICHIRO NAKAYAMA

Research Center for Instrumental Analysis, Faculty of Science, Kyoto University, Kyoto, 606 Japan

(Received 28 May 1986. Accepted 6 September 1986)

Summary—An improved continuous-flow analysis method has been designed and applied to the determination of ultratrace amounts of cobalt(II) by the catalysis of the tiron-hydrogen peroxide reaction in basic medium. From 3 to 5000 pg of cobalt(II) in 1 ml of acidified sample can be determined at a sampling rate of 40 samples/hour. The relative standard deviations (10 replicates) are 1% at the 100 pg/ml level and 3% at 10 pg/ml.

The need for methods for the determination of cobalt at pg/ml-levels is increasing in industrial and environmental analysis. Hence, kinetic methods based on a catalytic reaction have received considerable attention in those fields because of their great sensitivity.¹ It is well known that cobalt(II) catalyses the oxidation of *o*-dihydroxybenzene derivatives in a basic medium, and many workers have applied this phenomenon to the determination of cobalt; a number of reagents such as tiron (disodium 1,2-dihydroxybenzene-3,6-disulphonate),²⁻⁸ catechol,⁹ quinizarin,¹⁰ quinalizarin,¹¹ Alizarin Red S,¹² chromotropic acid¹³ and its derivatives,^{14,15} galloxyaniline¹⁶ and pyrocatechol Violet¹⁷ have been investigated. Among them, the method using tiron is especially sensitive; moreover, its reaction mechanism has been investigated and the oxidation product identified.^{5,6}

In spite of their high sensitivity, these reactions have not been used for routine analyses because of defects such as poor reproducibility and complicated procedures. These difficulties, however, can be eliminated by means of a flow system. There are two types of continuous-flow analysis, the air-segmented flow type,¹⁸ and the unsegmented flow type (flow-injection analysis, FIA),¹⁹ which has been used for catalytic analysis.^{8,13,14} One of the advantages of the latter is its higher throughput rate because of the shorter residence time of the sample in the flow system. For its use with catalytic reactions, however, a longer residence time may be needed, and can be achieved by using the stopped-flow mode.²⁰ In such a case the sampling rate can be improved by use of a rotating-drum parallel flow-injection system.²¹ The segmented-flow method has an inherently longer residence time, however, and may offer a simpler flow system.

We decided to use a segmented-flow system, but found it necessary to modify the conventional type of

manifold to overcome certain problems encountered in its use for determination of cobalt by its catalysis of the tiron-hydrogen peroxide system, as described below.

EXPERIMENTAL

Reagents

A standard cobalt(II) solution was prepared by diluting a commercial standard for atomic-absorption spectrometry (Nakarai Chemicals). The tiron solution was prepared from a commercial reagent (Dotite) without further purification. Hydrogen peroxide solution was prepared by diluting a commercial 30% solution for atomic-absorption spectrometry (Wako Chemicals). Hydrochloric acid was prepared by purifying analytical-reagent grade acid by a rapid isothermal distillation method we had developed. All other chemicals were of analytical-reagent grade and were checked for contaminants. The water used was prepared by purifying distilled water with a Millipore Milli-Q system.

Apparatus

A Shimadzu UV-240 spectrophotometer with a flow-cell (light-path 10 mm, cell volume 18 μ l) was used for all absorbance measurements; pH measurements were made with a Hitachi-Horiba F-7 pH-meter.

The flow system used is shown in Fig. 1. A Technicon proportioning pump and a Sampler II were used. The pump tubes were made of Tygon and all other flow lines and 3-way mixing joints were made of Teflon. A Teflon home-made debubbling unit was inserted immediately before the flow-cell.

An IL Video 12 atomic-absorption spectrometer equipped with an IL 755 graphite-furnace atomizer and an IL Fastac II automatic sample injector was used for cross-checking the analyses.

RESULTS AND DISCUSSION

The flow system

The samples were made 0.1M in hydrochloric acid to prevent the adsorption of cobalt on container walls. Sample solutions and blank solution were

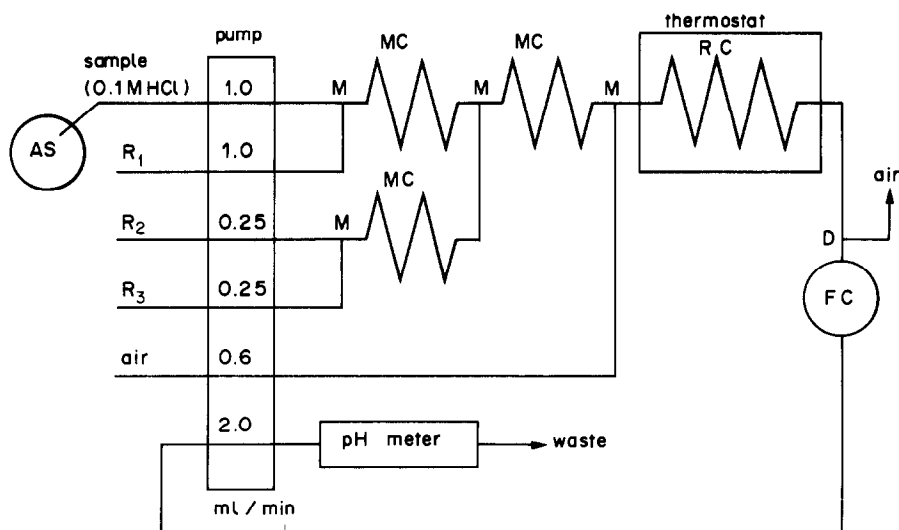


Fig. 1. Schematic diagram of the improved continuous-flow system for the catalytic determination of cobalt(II). AS, automatic sampler; MC, mixing coil (1 mm bore \times 0.5 m, Teflon); RC, reaction coil (1 mm bore \times 12 m, Teflon); M, mixing joint (Teflon); FC, flow-cell (volume 18 μ l). R₁, 0.05M sodium carbonate-sodium bicarbonate/0.1M sodium hydroxide; R₂, 0.01M tiron; R₃, 0.005M H₂O₂.

alternately introduced into the sample flow line, neutralized and buffered, and then mixed with the reagent solutions. In a conventional segmented-flow system the sample solution is segmented with air before mixing with other solutions. However, when this mode was used in the catalytic determination of cobalt, undesired peaks appeared at both ends of the air segments, because of the irregular mixing of the reagents with liquid segments at air-liquid interface, and the baseline fluctuated somewhat owing to the slight difference in the volume of each liquid segment. These effects were successfully eliminated by mixing the sample solution with the buffer solution and the reagent solutions before segmenting the flow with air. To avoid carry-over between samples in the mixing coils before they were segmented with air, each sample solution zone was separated from the contiguous blank solution zones by introduction of a small air segment when the sampling arm was moved from one cup to another on the automatic sampler. It was found that if glass tubes and joints were used in the flow-line, the absorption signals were deformed, probably because of adsorption of the oxidation product on the walls of the flow lines. This was eliminated by using Teflon tubes and joints.

The effect of air segmentation on the dispersion of a sample zone was checked by using a dye solution. The dispersion, D , of the whole flow system is defined as A_0/A , where A_0 is the absorbance corresponding to the fully developed colour reaction and A is the absorbance at the peak obtained by introducing sample over a period of 30 sec. In a completely unsegmented system D was 2.45. When the individual sample flow was segmented with air only at the reaction coil, D was 1.40. For the finally-designed flow system, D was 1.25. Further experiment indi-

cated that a sample introduction time of at least 60 sec was required for a flat-topped signal to be obtained with the final flow system.

The chemical system

Tiron is oxidized by an oxidizing reagent such as dissolved oxygen or hydrogen peroxide in basic medium and forms a yellow product.²² This reaction is accelerated in the presence of trace amounts of cobalt(II). From an e.s.r. spectroscopic study, Otto *et al.*⁵ deduced that the oxidation product is the tiron radical (semiquinone), which is stable for several hours. It has an absorption maximum at around 440 nm, as shown in Fig. 2, and the maximum shifts from 440 to 426 nm on increase in the pH from 9 to

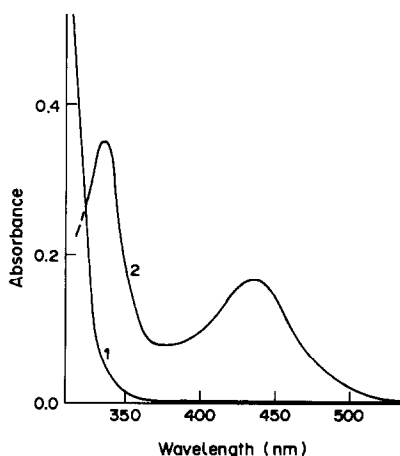


Fig. 2. Absorption spectra of tiron oxidized in basic medium (pH 10.5). (1) Spectrum of a solution without cobalt(II). (2) Spectrum of a solution containing 100 pg/ml of cobalt(II), measured against a solution without cobalt(II).

12, owing to formation of different products at low and high pH.⁵ As shown in Fig. 2, the spectrum of the oxidation product has another absorbance maximum at 336 nm. Kucharkowski *et al.*⁴ used monitoring at this wavelength to determine cobalt, but did not refer to the absorption maximum at around 440 nm. In our preliminary experiments, the stability of the baseline and the reproducibility of the signals were much better at 440 nm than at 336 nm though the sensitivity at 336 nm was about twice that at 440 nm. Further, the absorbance was much less sensitive to change in wavelength when the 440-nm maximum was used, so this wavelength was used for monitoring the oxidation product in the present work, as it was as in earlier work.⁶⁻⁸

Effect of pH. Phosphate, ammonium, borate and carbonate buffers were tested. When phosphate buffer or no buffer was used, the reproducibility of the signals was not so good because the pH was unstable in the region around 11. Both ammonium buffer and borate buffer were unsuitable because a small amount of ammonium and a large amount of borate interfered with the catalytic action of cobalt(II) (see Table 1). However, carbonate up to a concentration of 0.05M, did not interfere with the reaction, and the pH of the solution in the reaction coil could be maintained within ± 0.05 by use of 0.05M carbonate buffer. The effect of pH on the catalysed reaction was examined over the range 8.5–12. The maximum signal was obtained at a pH around 11.2; pH 10.3–12 was reported as the optimum pH by other workers.^{2-4,7,8}

Effect of reagent concentrations. In most methods based on catalytic reactions, the reagent concentrations must be kept strictly constant to obtain good reproducibility because the rate of catalytic reactions is strongly dependent on them. The effect of varying the reagent concentration from $10^{-4}M$ to 0.1M was examined. The signal for 100 pg/ml cobalt was maximal with 0.010M tiron and 0.005M hydrogen peroxide, and changed little over the ranges 0.010–0.015M tiron and 0.004–0.007M hydrogen peroxide.

Effect of reaction time and temperature. Since the coloured oxidation product gradually turns into a colourless species on further oxidation with hydrogen peroxide,⁶ the absorbance curve is typical for an intermediate reaction and passes through a maximum. Both the maximum absorbance and the reaction time at which it is obtained vary with the reaction temperature. From the response surface contours of absorbance as a function of reaction time and temperature, the optimum values of the reaction time and temperature were found to be 210 sec and 30°, respectively. In addition, at temperatures $> 40^\circ$ the peak shapes were somewhat deformed.

Calibration graphs, sensitivity and reproducibility

In catalytic analysis reaction rate plots are often used to obtain a linear relation to catalyst concen-

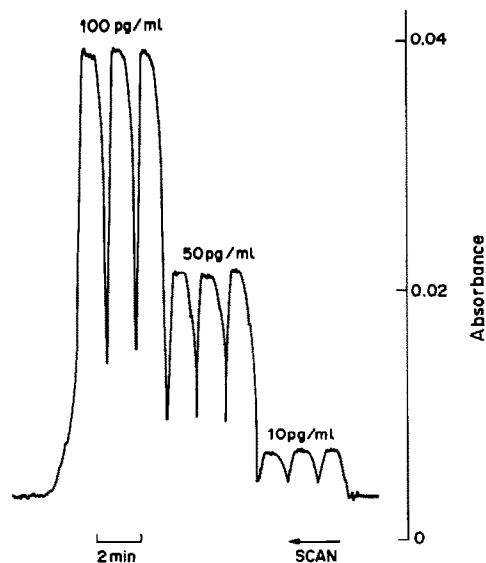


Fig. 3. Typical signal traces for various concentrations of cobalt(II). Sampling time 60 sec, sampling interval 30 sec, pH 11.2, tiron 0.01M, H₂O₂ 0.005M, reaction time 210 sec, reaction temperature 30°.

tration. However, in the tiron reaction system, a linear calibration graph was obtained by using the fixed-time method for cobalt concentrations less than 500 pg/ml. At cobalt concentrations > 500 pg/ml, a curved fixed-time graph was obtained because the catalysed reaction could not be regarded as pseudo zero-order with respect to the reagent concentrations. For example, by using the reported value of the molar absorptivity of the oxidation product (3.5×10^3 l.mole⁻¹.cm⁻¹)⁵ it was calculated that 28% of the tiron added was oxidized in the presence of 5000 pg/ml cobalt.

The detection limit depends on the background signal arising from impurities in the reagents, mainly the sodium hydroxide and sodium carbonate. Although the baseline was raised to a level equivalent to 10 pg/ml cobalt in a sample by the impurities contained in the buffer reagents, the fluctuation of the absorbance baseline was < 0.0005 over a period of several hours. Therefore, the effect of the impurities was almost negligible. The cobalt detection limit, for a signal-to-noise ratio of 3, was 3 pg/ml, and from the dilution of the sample in the flow-cell with the reagent solutions and the buffer solution, the apparent molar absorptivity for cobalt was calculated to be 6×10^7 l.mole⁻¹.cm⁻¹ in the linear response region of the calibration graph. According to earlier investigations of the tiron–hydrogen peroxide reaction, the detection limit for cobalt obtained by manual operation was 600 pg/ml (at 336 nm)⁴ and 50 pg/ml (at 440 nm),⁷ and that obtained by FIA with an on-line concentrator was 2 pg/ml (at 440 nm).⁸ In the present study, a lower or comparable value was obtained.

Figure 3 shows typical absorbance signals obtained with the flow system (Fig. 1) under the selected

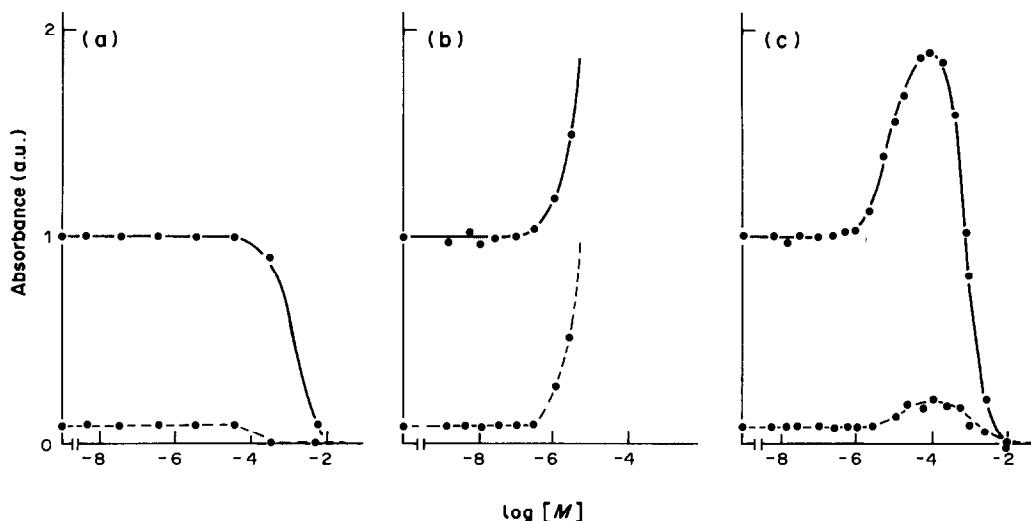


Fig. 4. Typical interference curves in the catalytic determination of cobalt(II). Solid lines, with 100 pg/ml cobalt(II); broken lines, without cobalt(II). (A) Effect of magnesium, (B) effect of iron(III), (C) effect of calcium.

conditions. When each sampling time was set at 60 sec and each sampling interval at 30 sec, the volume of each sample was 1 ml and the throughput rate was 40 samples/hour. The relative standard deviations ($n = 10$) were 1% at 100 pg/ml and 3% at 10 pg/ml with this flow system, whereas they were 6% at 1000 pg/ml and 15% at 100 pg/ml by manual operation.

Interferences

Although most catalytic analytical methods suffer interference from foreign species, the tiron-peroxide reaction is little affected, because of the specificity of the catalytic action of cobalt(II). In the present work, the interferences were investigated in presence and

absence of 100 pg/ml cobalt at various concentrations of foreign species, and classified into three types as shown in Fig. 4 and Table 1. The first type, A in Table 1, inhibits the catalytic reaction of cobalt(II). As a typical case, the interference of magnesium is shown in Fig. 4(A). Further, this type of the interference generally occurs in the presence of species, *e.g.*, EDTA and ammonia, which form stable complexes with cobalt(II). The second type, B, occurs when a coloured complex is formed between tiron and the foreign species, *e.g.*, iron(III) as shown in Fig. 4(B), and/or the foreign species catalyses the oxidation of tiron. Although manganese(II) and nickel catalyse the reaction,⁶ their catalytic activity is far less than

Table 1. Interference levels of foreign species in the catalytic determination of cobalt(II) at 100 pg/ml ($1.69 \times 10^{-9}M$) level

Species	Type*	Tolerance limit, † M	Species	Type*	Tolerance limit, † M
Al(III)	A	5×10^{-6}	ammonia	A	5×10^{-4}
Ca(II)	C	2×10^{-6}	borate	A	1×10^{-3}
Cr(III)	B	1×10^{-6}	citrate	A	1×10^{-3}
Cr(VI)	B	1×10^{-5}	EDTA	A	1×10^{-7}
Cu(II)	B	1×10^{-5}	fluoride	B	1×10^{-2}
Fe(II)	B	2×10^{-6}	nitrate	A	1×10^{-1}
Fe(III)	B	5×10^{-7}	nitrite	A	5×10^{-4}
Mg(II)	A	5×10^{-4}	perchlorate	A	1×10^{-1}
Mn(II)	B	2×10^{-7}	phosphate	A	5×10^{-2}
Mo(VI)	—	§	silicate	A	5×10^{-6}
Ni(II)	C	1×10^{-6}	sulphate	A	1×10^{-1}
Pb(II)	—	§	tartrate	A	1×10^{-2}
Sr(II)	A	1×10^{-5}			
Ti(IV)	B	2×10^{-5}			
V(IV)	B	2×10^{-5}			
V(V)	—	§			
Zn(II)	A	5×10^{-6}			

*Interference type indicated in Fig. 4.

†The concentration giving 10% deviation.

§No effect at concentration of $2 \times 10^{-4}M$.

Table 2. Determination of cobalt in various waters

Sample	Cobalt found, ng/l.	
	Catalytic method	GFAAS
Distilled water	5.0	5.1
Purified water*	0.35	ND†
Sea-water; depth	0 m	1.7
	50 m	3.4
	100 m	5.3

*Purified with a Millipore Milli-Q system.

†Not determined.

that of cobalt(II). The third type, C, enhances the catalytic activity of cobalt(II). As shown in Fig. 4(C), calcium acts an enhancer at 2×10^{-6} – $10^{-3}M$ concentration and an inhibitor at concentrations $>10^{-3}M$. Although a similar effect of magnesium on the catalytic oxidation of galloxyanin by hydrogen peroxide has been reported,¹⁶ it is not clear why inorganic ions such as calcium specifically enhance the catalytic oxidation. Furthermore, some synergic effects are found: zinc acts as a suppressor in the absence of calcium, but as an activator in its presence. The interferences are summarized in Table 1. The tolerance limit was defined as the concentration causing a 10% deviation in determination of 100 pg/ml cobalt.

Applications

The system has been applied to the determination of cobalt in purified waters and sea-water. Samples (100 ml) of distilled water and of water purified with a Milli-Q system were evaporated to dryness in a ventilated clean box and the residues were dissolved in 1 ml of 0.1M hydrochloric acid. The sea-water was collected during a cruise of R.V. Ryohu Maru (Japan Meteorological Agency) in spring 1984, and filtered through a 0.4- μ m Nuclepore filter immediately after collection. Cobalt(II) was selectively concentrated by a factor of 10 for the catalytic method and of 50 for graphite-furnace atomic-absorption spectrometry (GFAAS), by chelate formation with 4-(2-thiazolyl-azo)resorcinol (TAR) and adsorption on XAD-4 resin (details will be published elsewhere). In the analysis of sea-water, the catalytic determination required at least 10 ml of sample, whereas the determination with GFAAS required at least 250 ml. The results are shown in Table 2. The values obtained were checked by the standard-addition method for type A and type C interferences and by replacement of hydrogen peroxide by water for type B interferences. The reproducibility of the measurement of each preconcentrated sample by the catalytic method was better than 3% ($n = 3$) and that with GFAAS was

about 10% ($n = 5$). In view of these values, the agreement of the results in Table 2 is acceptable.

CONCLUSION

The results of this work indicate that more than 3 pg of cobalt(II) in 1 ml of acidified sample can be determined by the catalytic method based on the oxidation of tiron by hydrogen peroxide. By use of the improved continuous-flow analysis system in which air segmentation is introduced after mixing the reagent solutions, good mixing, long residence time and little carry-over were achieved. Maximum throughput rate was 40 samples/hour. The investigation of interferences indicates that many species interfere when present in 100-fold ratio to cobalt, and need to be eliminated before the determination.

Acknowledgment—This research was supported in part by a grant from the Nissan Science Foundation.

REFERENCES

- H. A. Mottola, *CRC Crit. Rev. Anal. Chem.*, 1977, **4**, 229.
- J. Bognár and O. Jelinek, *Magy. Kem. Foly.*, 1961, **67**, 73.
- J. Bognár, *Microchim. Acta*, 1961, 901.
- R. Kucharkowski and H. G. Döge, *Z. Anal. Chem.*, 1968, **238**, 241.
- M. Otto, J. Stach, R. Kirmse and G. Werner, *Talanta*, 1981, **28**, 345.
- M. Otto and G. Werner, *Anal. Chim. Acta*, 1983, **147**, 255.
- M. Otto, J. Rentsch and G. Werner, *ibid.*, 1983, **147**, 265.
- C. Maekoya, F. Mizuniwa, K. Usami and K. Osumi, *Nippon Kagaku Kaishi*, 1983, 1023.
- A. A. Alexiev and M. G. Angelova, *Microchim. Acta*, 1980 **II**, 187.
- R. P. Igov and M. D. Jaredic, *Glas. Hem. Drus., Beograd*, 1979, **44**, 711.
- Gh. Ionescu, A. Duca and F. Matei, *Microchim. Acta*, 1980 **I**, 329.
- G. E. Batley, *Talanta*, 1971, **18**, 1225.
- T. Yamane, *Nippon Kagaku Kaishi*, 1982, 93.
- Idem*, *Anal. Chim. Acta*, 1981, **130**, 65.
- D. Costache, *Farmacia (Bucharest)*, 1972, **20**, 545.
- K. Hirayama and N. Unohara, *Nippon Kagaku Kaishi*, 1978, 1498.
- T. J. Janjic and G. A. Milovanovic, *Glas. Hem. Drus., Beograd*, 1972, **37**, 173.
- L. T. Skeggs, *Am. J. Clin. Pathol.*, 1957, **28**, 311.
- J. Růžička and E. H. Hansen, *Anal. Chim. Acta*, 1975, **78**, 145.
- Idem*, *ibid.*, 1979, **106**, 207.
- Idem*, *Flow Injection Analysis*, pp. 65–71. Wiley, New York, 1981.
- G. F. Atkinson and W. A. E. McBryde, *Can. J. Chem.*, 1957, **35**, 477.

HYDROGENATION ENTHALPIMETRY—I

MICROCOMPUTER-ASSISTED CALIBRATION AND DATA-ACQUISITION

D. W. ROGERS and B. J. SIEDMAN

Chemistry Department, Long Island University, Brooklyn, New York 11201, U.S.A.

(Received 11 April 1986. Revised 12 June 1986. Accepted 6 September 1986)

Summary—A calorimetric device is described which permits enthalpimetric determination of unsaturated hydrocarbons through the enthalpy change for their catalytic hydrogenation. Samples with weights from <1 to about 20 mg can be analysed with a mean error of about 2%. The method makes extensive use of digital electronics and is well suited to routine automated determination of unsaturation. The principal drawback is lack of specificity.

Enthalpy, like all thermodynamic properties, is an extensive variable

$$q = n\Delta H_m \quad (1)$$

where q is the heat of reaction at constant pressure, n is the number of moles of reactant and ΔH_m is the molar enthalpy change. This means, among other things, that if a reaction selective to one component of a mixture (the analyte) can be conducted at constant pressure, the heat produced or absorbed is directly dependent upon the number of moles of analyte present. Catalytic hydrogenation of a single alkene, polyalkene or alkyne in an alkane or mixture of alkanes, is such a reaction. Determining the amount of reactant in an unknown by measuring its heat of reaction at constant pressure is a well-established analytical technique called enthalpimetry.¹⁻⁴ To distinguish the method from thermometric titration,⁵⁻⁷ in which the end-point is indicated by cessation of heat-production when all the analyte has been used up, the method is called direct enthalpimetry. A favoured technique in direct enthalpimetry is to inject the sample into an excess of reagent, and for this the term direct injection enthalpimetry (DIE) is used.

Instrumental factors having been optimized, the sensitivity of an enthalpimetric method is ultimately limited by the enthalpy change per mole of analyte, which determines the slope of the calibration graph of measured heat output *vs.* moles of analyte taken. Hydrogenation has one of the highest known molar enthalpy changes at room temperature.⁸⁻¹⁰ The molar enthalpy change for hydrogenation of a typical alkene is more than twice the enthalpy change for neutralization of a strong acid with a strong base. Hydrogenation of polyalkenes and alkynes is even more exothermic than that of alkenes.

We have developed an automated microcalorimeter that represents a considerable advance on previous designs.¹¹⁻¹⁶ It uses a single-board microcomputer for precise electrical calibration, and

collects and treats digitized data under the control of a second, independent microprocessor. The device will be used for enthalpy measurements in various analytical investigations, *e.g.*, direct injection hydrogenation enthalpimetry.

THEORY

Some time ago, we described a method of hydrogenation enthalpimetry that depended on chemical calibration.¹¹⁻¹⁶ A known amount of an appropriate standard was injected into a suitable calorimeter and the temperature rise on hydrogenation was noted. The temperature rise for injection of an analyte sample into the same calorimeter under identical conditions was also measured. The ratio of the molar enthalpies of hydrogenation of the analyte and the standard was used to calculate the number of moles of analyte.

There are some drawbacks to chemical calibration for hydrogenation enthalpimetry. For example, the method is not applicable to styrene even though that can be quantitatively hydrogenated to ethylbenzene over 5% Pd-charcoal catalyst under 2 atm pressure of hydrogen at room temperature.¹⁷

Augustine¹⁸ has described differences in interactions between some commonly-used heavy metal catalysts and various reactants and their hydrogenation products. Although the aromatic ring is not hydrogenated under these conditions, it does interact with the catalyst surface, probably by π -complex formation. Aromatic molecules shield the catalyst surface and prevent approach by less electron-rich molecules such as the 1-hexene frequently used as the chemical standard in hydrogenation calorimetry¹⁰ and enthalpimetry.⁴ Though not generally regarded as catalyst poisons, aromatic analytes severely retard hydrogenation of the standard, and the method of chemical calibration breaks down.

Aromatic molecules, notably styrene itself, are not hindered in this way. Even in the presence of its

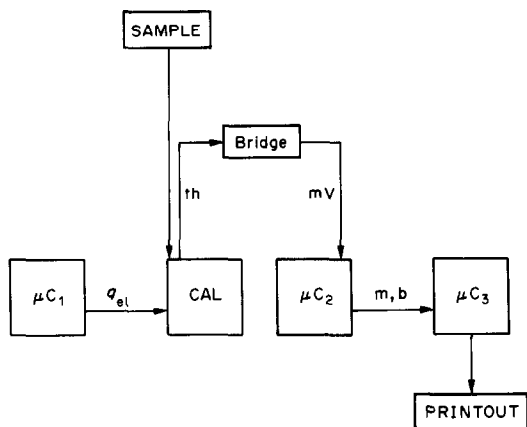


Fig. 1. Block diagram of tandem microcomputers and solution calorimeter (th = thermistor; m and b are the slope and intercept of dT/dt as calculated by μC_2).

hydrogenation product, ethylbenzene, styrene is evidently successful in competing for the catalyst surface and reacts cleanly and rapidly. One scheme for hydrogenation enthalpimetry might be to use a known solution of styrene as the standard for measuring the styrene content of analyte solutions. Because of its proclivity for polymerization, however, styrene is not a good standard. The pure reagent and its solutions in an inert solvent pose storage problems.

The same difficulties are encountered in the hydrogenation thermochemistry of free fatty acids, and their methyl esters and triglycerides.¹⁹⁻²¹ All of these compounds are in some degree chemically unstable and all associate more strongly with palladium catalysts than do stable, commonly-used thermochemical standards.

We have, therefore, chosen electrical calibration of the enthalpimetric calorimeter for these studies. The coulomb is, perhaps, the most fundamental chemical standard of all and has been measured very accurately.²² The fundamental thermochemical unit, the joule, is 1 volt-coulomb. Electrical standardization is commonplace in classical thermochemistry and most other enthalpimetric methods, but has not been reported for hydrogenation enthalpimetry. In this series of papers, we propose to develop methods for enthalpimetric determination of a number of analytes, including styrene, simple lipids and simple lipid mixtures, for which chemical standardization is not well-suited.

The method of electrical standardization is based on the relation

$$J = VQ = VI t = I^2 R t \quad (2)$$

where V is the voltage across a resistance of R ohms, I is the current in amperes and t the time in seconds. Because the method is microanalytical, intended for the determination of milligram quantities of analyte, it uses short calibration times t and employs a digital data-gathering scheme. Some sophistication is re-

quired in the electrical apparatus; the classical knife-switches and potentiometer have been replaced by microcomputers and microelectronic interface circuits which are programmable, more accurate and much faster.

EXPERIMENTAL

In recent years, our enthalpimetric apparatus has been brought under microcomputer control. Figure 1 is a block diagram of the apparatus in its present form. A control microcomputer μC_1 sends current for a very precise time t through the heating circuit of the calorimeter CAL.¹⁰⁻¹⁶ The temperature within the reaction flask is transduced by a thermistor-bridge combination into a voltage in mV and sent to microcomputer μC_2 which digitizes and stores the mV values obtained at regular time intervals. After storage of the digitized heating curve as $mV = f(t)$, the slope and intercept of the heating curve before and after the heating pulse are calculated by μC_2 and stored in microcomputer μC_3 . Microcomputer μC_3 is programmed to calculate the temperature rise, ΔT , due to electrical heating, that would ideally have been observed if there had been instant heating, no heat leak and no instrumental lag. The heat generated electrically is q_{el} .

The procedure is repeated for injection of a sample, which generates a heat of hydrogenation q_h . The new heating curve is stored in digital form and treated by μC_2 in the same way as the curve for q_{el} . The ratio of the temperature change for hydrogenation to the temperature change for electrical calibration yields a precise heat of reaction in joules. The molar enthalpy of hydrogenation of the analyte, $\Delta H_{h,m}$, having previously been entered into it, microcomputer μC_3 completes the calculation of the number of moles of analyte present, from equation (1), and prints the result.

Details of the components in Fig. 1 are as follows.

Microcomputer μC_1 . The single-board microcomputer (MMD-1, E & L Instruments Inc.) is programmed to control a switching circuit SW so as to send a precise energy pulse of $I^2 R t$ joules to the calorimeter. The circuit²³ and the machine-language program²⁴ are described elsewhere. The voltage at the microcomputer output port is used to drive a DIP reed relay (Mauser Electronics) having a maximum operating time of 0.2 msec. The relay, in turn, places a regulated voltage of 12.54 V across a 199.3-ohm resistor within the reaction flask to deliver $J = I^2 R t$ joules of heat. In this work, calibration pulses covering the range 1-15 J were used, with heating times of 1.318-10.545 sec. The current was read from a digital milliammeter and was the least accurately known electrical operating variable, being about 60.0 ± 0.2 mA.

CAL. The reaction vessel is a thermally isolated 25-ml Erlenmeyer flask fitted with a rubber septum through which pass the heating resistor, a hydrogen inlet needle and a steel-jacketed thermistor probe (YSI 406, Cole-Parmer Instrument Co., 8436, time-constant 2.5 sec). The temperature change occurring within the reaction flask is monitored by using the thermistor probe as part of a 1.5-V d.c. bridge circuit, BR, (Leeds & Northrup 4775), which communicates the bridge imbalance (mV) to an analogue-to-digital converter A/D and thence to a second microcomputer μC_2 .

The reaction flask contains 20 ml of hexane, 300 mg of 5% Pd-charcoal catalyst (Aldrich) and a magnetic stirring bar. Hydrogen is admitted to the flask before a series of experiments and is maintained at a constant pressure of 2 atm. The stirring rate is about 400 rpm. Thermal insulation is achieved by using a combination of foam blankets and concentric styrofoam boxes. Injections are made with a microsyringe (Hamilton) with a mechanical stop set at 40 μ l (calibration of the syringe used showed its mean delivery volume to be within 0.2% of the nominal value, with reproducibility 0.6%). Solutions of 1-heptene were made up

Table 1. Enthalpimetric determination of 1-heptene in amounts from 3.4 to 16.5 μmol

Number of determinations	Amount taken, mg	Amount found, mg	Difference, %	Standard deviation, mg
12	16.5	16.3	-1.2	0.22
9	8.34	8.31	-0.4	0.09
13	8.30	8.40	1.2	0.06
9	5.67	5.69	0.4	0.05
11	5.47	5.57	1.8	0.03
11	5.38	5.43	0.9	0.04
12	4.33	4.35	0.5	0.07
14	4.24	4.27	0.7	0.07
12	4.08	4.16	2.0	0.04
9	3.07	3.19	3.9	0.04
9	1.49	1.45	-2.7	0.09
10	1.49	1.42	-4.7	0.06
10	1.35	1.46	8.1	0.07
5	0.723	0.738	2.1	0.02
9	0.679	0.644	-5.2	0.03
10	0.339	0.334	-1.5	0.03

in n-hexane so that the amount of analyte in a 40- μl sample varied from <0.4 mg to >16 mg, as shown in Table 1. The sum of reaction time plus instrumental response time was about 10 sec.

Microcomputer μC_2 . The second microcomputer (Bascom-Turner, Model 3110) gathers 500 points for the bridge output as a function of time, by means of a 12-bit A/D converter. One point is stored every 200 msec and a continuous curve is drawn concurrently with the data-gathering. This is essentially a temperature-time curve except that the temperature is measured in mV units.

Having collected the data set, μC_2 performs a linear least-squares treatment on segments of the temperature-time curve just before the thermal event, e.g., electrical heating, and immediately after it. In these experiments, 150 points were treated before the thermal event and their least-squares slope and intercept calculated and entered into microcomputer μC_3 . Immediately after the thermal event, a sharp temperature rise was noted. The point of vertical inflection²³ of the temperature-time curve was estimated visually from the recorder plot and entered in μC_3 . After a thermal steady-state had been re-established, 150 points were subjected to least-squares treatment to obtain a second slope and intercept which were entered into μC_3 . Of the 500 data points collected in a typical run time of 100 sec, 150 were used to establish a linear function $T = f(t)$ before the thermal event, 200 were discarded during the period immediately after the thermal event, except that the time when the curve passed through its vertical inflection t_i was noted, and 150 were used to establish $T = g(t)$ after the thermal event.

Microcomputer μC_3 . This is a commercial microcomputer (Tandy TRS-80 Model III) which accepts the data and treats them according to an accepted procedure²⁴ to find the ideal ΔT for the electrical heating, free of thermal and instrumental drift. The first linear function $f(t)$ was extrapolated forward to t_i to obtain one point T_1 on a vertical line drawn through the inflection point and the second function $g(t)$ was extrapolated back to t_i to obtain a second point T_2 on the vertical. The temperature difference $T_2 - T_1$ is the idealized temperature rise ΔT (in units of mV) and is proportional to the heat released in the thermal event, q_{el} or q_h . Once the ratio of the ΔT values for electrical heating and hydrogenation is known, q_h is also known because $q_{el} = I^2 R t$. The number of moles of analyte follows from $\Delta H_{h,m}$ for the analyte.

Microcomputer μC_3 is programmed (in BASIC) to compute and print the number of milligrams of analyte in the sample. Minor changes can be made in the programming,

to obtain the enthalpy of hydrogenation for temperature ratios obtained for hydrogenation of a known amount of alkene having an unknown $\Delta H_{h,m}$, equation (1).

RESULTS AND DISCUSSION

A series of 12 heating pulses q_{el} was sent to the calorimeter and the individual ΔT values were recorded. After each pulse, the bridge had to be reset to restore the base-line (bridge output voltage) to its original value. The bridge output and the thermistor response differed in their temperature coefficients, and an upward trend in mV output was found, for constant q_{el} . Non-linearity over a temperature range of a few mK is expected to be very small, however, and agreement between successive calibration pulses is expected to be good, as indeed it must be for the method to work.

The mean ratio of successive pulses for $q_{el} = 3.67 \pm 0.01$ J is expected to be 1.000 and was found to be 1.004 with a standard deviation of 0.016. A ratio that is slightly larger than expected is consistent with a slight upward trend in measured q_{el} . The uncertainty of 0.3% in the heating pulse is due mainly to uncertainty in measurement of I . The relative standard deviation of 1.6% is the total uncertainty contributed by all instrumental elements of the calibration and data-gathering circuitry. It is due mainly to uneven heat leak from the calorimeter and temperature-sensing apparatus. Slight variations in heat leak are magnified by the extrapolation procedure. This source of error is thought to be the main limitation on the accuracy of the present method. The standard deviation of instrumental response is close to the total uncertainty given in Table 1 for the experiments in which 4–5 mg of analyte were taken. The remaining known source of error is sample delivery.

1-Heptene has a molecular weight of about 100 and $\Delta H_{h,m}$ is -126.6 kJ/mole, so 1 mg of analyte is

equivalent to about 0.8 J. Both electrical calibration errors, uncertainty in I and the 0.4% upward trend due to non-linear bridge and thermistor response, are minor components of the total error. All these sources of error have obvious remedies and we do not think that the limits of accuracy or sensitivity have been reached.

The results for 16 series of determinations over a 40-fold (0.34–16.5 mg) variation in sample size are shown in Table I for 1-heptene dissolved in *n*-hexane. The mean of the relative deviations (irrespective of sign) is 2.3%, and there is a slight positive bias, *i.e.* the mean of the signed deviations is +0.37%, but this is not significant in the light of the 2.3% dispersion of the data set. The $\Delta H_{h,m}$ calibration value could have been selected so as to get rid of the positive systematic deviation but there is, at present, no thermochemical justification for doing so.^{26,27}

Acknowledgements—The authors wish to acknowledge funding from the Petroleum Research Fund of The American Chemical Society, and the Minority Access to Research Careers programme of the National Institutes of Health. Long Island University provided released time for doing this work.

REFERENCES

1. J. C. Wasilewski, P. T-S. Pei and J. Jordan, *Anal. Chem.*, 1964, **36**, 2131.
2. J. Jordan in *Treatise on Analytical Chemistry*, 1st Ed., I. M. Kolthoff and P. J. Elving (eds.), Part I, Vol. 8, Ch. 91, Wiley-Interscience, New York, 1968.
3. G. W. Ewing, *Instrumental Methods of Chemical Analysis*, 5th Ed., pp. 440–442. McGraw-Hill, New York, 1985.
4. D. W. Rogers, *Am. Lab.*, 1981, **13**, No. 1, 63.
5. G. W. Ewing, *op. cit.*, pp. 438–440.
6. N. Jespersen, in *Instrumental Analysis*, H. H. Bauer, G. D. Christian and J. E. O'Reilly (eds.), Section 17.5. Allyn and Bacon, Boston, 1978.
7. A. J. C. L. Hogarth and J. D. Stutts, *Am. Lab.*, 1981, **13**, No. 1, 18.
8. J. B. Conant and G. B. Kistiakowsky, *Chem. Rev.*, 1937, **20**, 181.
9. J. L. Jensen, *Prog. Phys. Org. Chem.*, 1976, **12**, 189.
10. D. W. Rogers, *Am. Lab.*, 1982, **14**, No. 1, 15.
11. *Idem*, *Anal. Chem.*, 1971, **43**, 1468.
12. D. W. Rogers and R. J. Sasiela, *Mikrochim. Acta*, 1973, 33.
13. *Idem*, *Talanta*, 1973, **20**, 232.
14. *Idem*, *Anal. Biochem.*, 1973, **56**, 480.
15. L. A. Williams, B. Howard and D. W. Rogers, *Anal. Calorimetry*, 1974, **3**, 207.
16. A. Goldberg and D. W. Rogers, *ibid.*, 1975, **4**, 125.
17. H. E. Davis, D. W. Rogers and N. L. Allinger, unpublished data.
18. R. L. Augustine, *Chemalog*, 1985, November, 3.
19. D. W. Rogers and N. A. Siddiqui, *J. Phys. Chem.*, 1975, **79**, 574.
20. D. W. Rogers, O. P. A. Hoyte and R. K. C. Ho, *J. Chem. Soc. Faraday I*, 1978, **74**, 46.
21. D. W. Rogers and D. N. Choudhury, *ibid.*, 1978, **74**, 2868.
22. W. F. Koch and H. Diehl, *Talanta*, 1976, **23**, 509.
23. D. W. Rogers, B. Munoz-Hresko and R. R. Mandra, *Mikrochim. Acta*, 1984 **II**, 417.
24. P. R. Rony, *Introductory Experiments in Digital Electronics and 8080A Microcomputer Programming and Interfacing*, pp. 96–97. Sams, Indianapolis, 1977.
25. W. Hemminger and G. Hohne, *Calorimetry, Fundamentals and Practice*, Section 6.2. Verlag Chemie, Weinheim, 1984.
26. D. W. Rogers, *J. Phys. Chem.*, 1979, **83**, 2430.
27. R. B. Williams, *J. Am. Chem. Soc.*, 1942, **64**, 1395.

SHORT COMMUNICATIONS

SPECTROPHOTOMETRIC AND FLUORIMETRIC DETERMINATION OF NOMIFENSINE MALEATE

ABDEL-AZIZ M. WAHBI, MOHAMMAD A. ABOUNASSIF, EL-RASHEED A. GAD-KARIEM
and HASSAN Y. ABOUL-EINEIN

Pharmaceutical Chemistry Department, College of Pharmacy, King Saud University, P.O. Box 2457,
Riyadh-11451, Saudi Arabia

(Received 30 November 1985. Revised 30 August 1986. Accepted 10 September 1986)

Summary—Three methods have been developed for the determination of nomifensine maleate alone and in capsules: a spectrophotometric, an iodine charge-transfer, and a spectrofluorimetric method. All three give linear calibration graphs, over the ranges 20–100, 1–5 and 0.1–0.5 $\mu\text{g/ml}$, respectively, with coefficients of variation of 0.8, 1.3 and 1.3%, respectively.

Methods reported for the determination of nomifensine maleate include polarographic and amperometric,¹ TLC^{2,3} and HPLC and GC^{4,5} procedures. The polarographic method is non-specific since it is based on electroreduction of the maleate ion. The amperometric method involves titration with silicotungstic acid. The chromatographic methods deal mainly with the separation and determination of nomifensine in presence of its metabolites in human urine and serum.

This paper deals with the determination of nomifensine maleate alone and in capsules by (i) a spectrophotometric method, (ii) a charge-transfer method with iodine, and (iii) a direct spectrofluorimetric method.

EXPERIMENTAL

Reagents

Spectroscopic grade methanol was used, and other solvents were analytical reagent grade.

Iodine solution. A 10-mg/ml solution freshly prepared in dry chloroform.

Standard solutions of nomifensine maleate. For the ΔA method prepare accurately a 1-mg/ml solution in 0.1M hydrochloric acid. For the spectrofluorimetric method prepare accurately a 0.25-mg/ml solution in 0.1M hydrochloric acid; using appropriate standard flasks, dilute 20 ml of this solution to 50 ml with 0.1M hydrochloric acid and then 5 ml of that solution to 100 ml with 0.1M sodium hydroxide to give a final concentration of 5 $\mu\text{g/ml}$. For the iodine method transfer an accurately weighed quantity of nomifensine maleate equivalent to 20 mg of nomifensine base to a separating funnel containing 10 ml of water, add 5 ml of 0.1M sodium hydroxide and mix, then extract with four 20-ml portions of chloroform, washing each extract with the same three 15-ml portions of water and filtering each extract through anhydrous sodium sulphate into a 100-ml standard flask; wash the filter with three 5-ml portions of dry chloroform and dilute to volume with dry chloroform. Dilute 25 ml of this solution to volume with dry chloroform in a 100-ml standard flask to give a final concentration (free base) of 50 $\mu\text{g/ml}$.

Calibration graphs

Spectrophotometric method. Into one set of 100-ml standard flasks pipette 1, 2, ..., 9, 10 ml of the 1-mg/ml standard solution and dilute to volume with 0.1M hydrochloric acid. Into a second set of 100-ml standard flasks pipette corresponding volumes of the same standard solution and dilute to volume with 0.1M sodium hydroxide. Measure each solution at 283 nm against the appropriate blank, and plot the absorbance difference (ΔA) for each pair against concentration.

Spectrofluorimetric method. Pipette 1, 2, 3, 4 and 5 ml of the 5- $\mu\text{g/ml}$ standard solution into 50-ml standard flasks, and add 4, 3, 2, 1 and 0 ml of 0.1M sodium hydroxide, as appropriate, to make a total volume of 5 ml of 0.1M alkali in each flask. Complete to volume with spectroscopic grade methanol. Read the fluorescence at 340 nm, using 292 nm as the excitation wavelength. Plot fluorescence intensity against concentration.

Charge-transfer method. Pipette 1, 2, 3, 4 and 5 ml of the 50- $\mu\text{g/ml}$ standard in dry chloroform into 50-ml standard flasks. Add 5.0 ml of 10-mg/ml iodine solution to each. Dilute to volume with dry chloroform, mix and allow to stand for 15 min at room temperature. Measure the absorbance at 293 or 366 nm against a reagent blank. Plot absorbance against concentration.

Procedures for capsules

Weigh the contents of 20 capsules of nomifensine maleate (e.g., Merital capsules, 20 and 50 mg) and find the average weight per capsule. For the ΔA method weigh accurately an amount of the capsule contents equivalent to about 50 mg of nomifensine maleate and transfer it to a 100-ml standard flask. Add 80 ml of 0.1M hydrochloric acid, shake the flask for 15 min, dilute to volume with 0.1M hydrochloric acid, mix and filter through a dry paper. Reject the first portion of filtrate. Into each two 100-ml standard flasks, pipette 10 ml of the filtrate. Dilute to volume in one flask with 0.1M hydrochloric acid and in the other with 0.1M sodium hydroxide, and measure the absorbance at 283 nm against the appropriate blank. Use the calibration graph to find the concentration corresponding to ΔA .

Spectrofluorimetric method. Weigh accurately an amount of the capsule contents equivalent to about 10 mg of nomifensine maleate. Transfer to a 100-ml standard flask, add 80 ml of 0.1M hydrochloric acid, shake the flask for 15 min, complete to volume with 0.1M hydrochloric acid, mix,

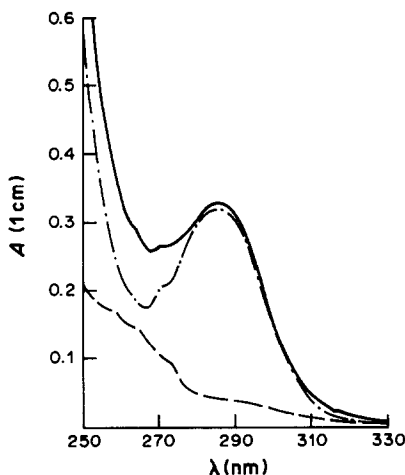


Fig. 1. Absorption spectra of 65- $\mu\text{g/ml}$ nomifensine maleate in 0.1M sodium hydroxide (—) and 0.1M hydrochloric acid (---), and the ΔA curve (-·-·).

filter (dry paper), reject the first portion of filtrate, pipette 5 ml of filtrate into a 100-ml standard flask and dilute to volume with 0.1M sodium hydroxide. Pipette 3 ml of this solution into a 50-ml standard flask, add 2 ml of 0.1M sodium hydroxide and dilute to volume with spectroscopic grade methanol. Read the fluorescence intensity at 340 nm, with excitation at 292 nm. Read the concentration from the standard graph.

Charge-transfer method. Weigh accurately a quantity of the capsule contents equivalent to about 10 mg of nomifensine base into a separating funnel containing 10 ml of water. Add 5.0 ml of 0.1M sodium hydroxide and mix. Proceed as for the standard solution preparation, starting with the chloroform extraction. Transfer 6 ml of the final chloroform solution to a 5-ml standard flask and continue as for preparation of the calibration graph. Read the concentration from the standard graphs.

RESULTS AND DISCUSSION

Nomifensine maleate contains a primary aromatic amino-group and in 0.1M sodium hydroxide exhibits an absorbance peak at 283 nm which is absent for the compound in 0.1M hydrochloric acid, owing to protonation of the aromatic amino-group (Fig. 1). The absorbance difference (ΔA) is maximal at 283 nm, and can be used^{6,7} to correct for the absorption of any interferents that have spectra which are not dependent on pH. The calibration graph is linear from 20 to 100 $\mu\text{g/ml}$. The molar absorptivity calculated from ΔA at 283 nm is $1.12 \times 10^3 \text{ l. mole}^{-1} \cdot \text{cm}^{-1}$.

Nomifensine base in alkaline methanol is fluorescent, and has maximum emission at 340 nm

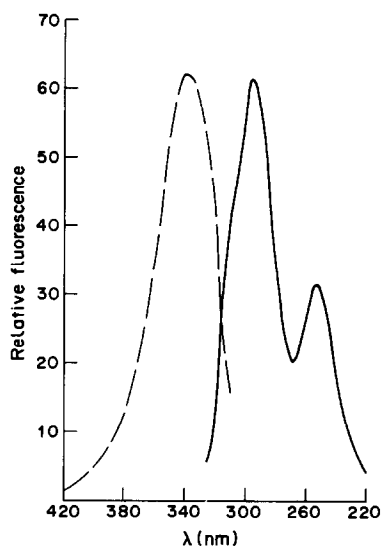
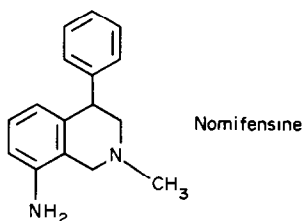


Fig. 2. Relative fluorescence excitation (---) and emission (—) spectra of 0.02- $\mu\text{g/ml}$ nomifensine maleate in methanol:0.1M sodium hydroxide (90:10) mixture.

when excited at 292 nm (Fig. 2). The intensity of fluorescence is linearly related to concentration over the range 0.1–0.5 $\mu\text{g/ml}$. At the normal instrumental gain setting used, the method is about 200 times more sensitive than the ΔA method and can be recommended for determination of nomifensine in biological fluids after a suitable separation; a higher instrumental gain setting can be used if needed. The volume of 0.1M sodium hydroxide in the total 50 ml of final solution must be kept constant for the samples and standards, and spectroscopic grade methanol must be used or fluorescence quenching may occur. The fluorescence is very weak if purely aqueous 0.1M sodium hydroxide is used, but greatly increases in the methanolic medium.

The immediate change of the violet colour of iodine in chloroform to lemon yellow on reaction with nomifensine in dry chloroform suggests charge-transfer complex formation, and two new absorption maxima are found to occur at 293 and 366 nm (Fig. 3). For quantitative reaction the use of 5 ml of

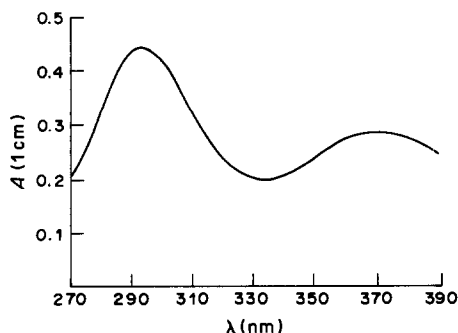


Fig. 3. Absorption spectrum of 3- $\mu\text{g/ml}$ nomifensine complex with iodine in dry chloroform.

Table 1. Spectrophotometric and fluorimetric determination of nomifensine maleate

Sample	Found*, % \pm s.d.			
	ΔA method, 283 nm	Iodine method		Fluorimetric method $\lambda_{ex} = 292$; $\lambda_{em} = 340$ nm
		293 nm	366 nm	
Authentic (<i>n</i>)	99.7 \pm 0.84 9	99.7 \pm 1.25 8	99.5 \pm 1.30 8	99.6 \pm 1.29 12
<i>F</i> -test (0.05)	2.39 (3.50)			
<i>t</i> -test (0.05)	0.38 (2.13)			
Capsules (25 mg each) (<i>n</i>)	101.7 \pm 0.60 6	100.8 \pm 1.27 6	101.5 \pm 1.02 6	100.9 \pm 0.85 6
<i>F</i> -test (0.05)	4.48 (5.05)			
<i>t</i> -test (0.05)	1.89 (2.23)			
Capsules (50 mg each) (<i>n</i>)	99.4 \pm 0.96 6	99.5 \pm 0.75 6	99.1 \pm 0.72 6	98.9 \pm 0.57 6
<i>F</i> -test (0.05)	2.84 (5.05)			
<i>t</i> -test (0.05)	1.56 (2.23)			

*Relative to amount taken or nominal content.

Figures in parentheses show significance levels. (*n*) = number of experiments.

10-mg/ml iodine solution is found to be adequate. The absorbances at 293 and 366 nm should be measured 15 min after the addition of the reactants, for stable readings to be obtained. Beer's law is obeyed over the concentration range 1–5 μ g/ml. The apparent molar absorptivities are 3.47×10^4 at 293 nm and 2.29×10^4 l.mole⁻¹.cm⁻¹ at 366 nm.

The iodine charge-transfer method is only about a tenth as sensitive as the fluorimetric method but about 20 times more sensitive than the ΔA method. It is non-specific, however, since many basic nitrogenous compounds form charge-transfer complexes with iodine under the same conditions.

The results obtained by using the three methods (Table 1) have been statistically analysed with regard to accuracy and precision. The variance ratio (*F*) test was applied to the highest and lowest variance in each row and the *t*-test to the highest and lowest means.

The results in Table 1 show that the three methods have similar accuracy and precision. The methods are reproducible, accurate, and easy to automate for routine analysis.

REFERENCES

1. K. Nikolić, L. Arsenijević and M. Medenica, *Acta Pharm. Jugosl.*, 1984, **34**, 69.
2. E. J. Baltova and A. Shishkov, *Folia Medica*, 1983, **25**, 36.
3. N. Sistovaris, *J. Chromatog.*, 1983, **276**, 139.
4. E. Bailey, M. Fenoughty and L. Richardson, *ibid.*, 1977, **131**, 347.
5. R. L. P. Lindberg, J. S. Salonen and E. I. Iisale, *ibid.*, 1983, **276**, 85.
6. G. Aulin-Erdtman, *Chem. Ind. (London)*, 1955, 581.
7. A. M. Wahbi and A. M. Farghaly, *J. Pharm. Pharmacol.*, 1970, **22**, 848.

A GRAPHITE-TUBE FURNACE FOR USE IN LASER-EXCITED ATOMIC-FLUORESCENCE SPECTROMETRY*

D. GOFORTH and J. D. WINEFORDNER†

Department of Chemistry, University of Florida, Gainesville, FL 32611, U.S.A.

(Received 30 June 1986; Accepted 6 September 1986)

Summary—The construction and performance of a graphite-tube furnace for use in laser-excited atomic-fluorescence spectrometry are evaluated. The graphite-tube furnace gives better detection limits than a cup-furnace does for the non-volatile elements.

In most research on atomic-fluorescence spectrometry with atomization in a graphite furnace,¹⁻⁷ an open furnace, such as a graphite cup, has been used. A tube furnace has been utilized most often in atomic-absorption spectrometry. The semi-enclosed design of the tube provides better conditions for atomization than does the graphite cup. The difficulty in using a tube furnace for atomic-fluorescence is observation of the fluorescence. Dittrich and Stark⁸ used passage of the laser beam through holes in the sides of a graphite tube and viewed the fluorescence through the end of the tube. However, they only reported improved sensitivities (slope of calibration curve) and did not discuss any other figures of merit.

Because of the poorer atomization conditions in the graphite cup, many of the refractory elements have not been studied by atomic-fluorescence generated in a graphite furnace. The refractory elements generally require very high temperatures for atomization, owing to the formation of involatile carbides with the graphite. In previous work from this laboratory,⁷ atomic-fluorescence was excited by a laser beam in a graphite-cup furnace placed in an argon atmosphere. Poor results were obtained for aluminium, the least volatile of the elements studied. To improve on those results, better atomization conditions were needed. This communication describes a tube furnace to be used with laser-excited atomic-fluorescence spectrometry.

EXPERIMENTAL

The laser system, the argon furnace system, the detection electronics, and the experimental procedure, were as described earlier.⁷ Figure 1 shows the tube-furnace system. The laser beam passed through a $\frac{1}{4}$ -in. hole in the tilted mirror and then excited the atoms in the channel through the graphite tube. The fluorescence radiation travelling in the opposite direction to the propagating laser beam was

reflected off the mirror and focused (without magnification) by a lens (diameter 2 in., focal length 3 in.) into the monochromator. The tube furnace was placed in an enclosed argon atmosphere; a glass dome covered the tube furnace, and both the laser beam and the fluorescence had to pass through a quartz window in it, placed between the tube furnace and the mirror. One change made from the previous design⁷ was that the glass arm holding the window was cut at an angle of 45° to the incident beam. Consequently, the small (~5%) laser reflection from the window was directed upwards rather than back towards the mirror, where it might have been directed into the monochromator, causing a large scatter signal. The graphite tube (Fig. 2) was held between two spring-loaded graphite electrodes. For practical reasons, the graphite tube was not pyrolytically coated. Two power supplies (TCR 3φ, Electronics Measurements) were connected in parallel to provide rapid heating of the graphite tube.

The mirror and the graphite tube system were aligned by placing the mirror so that the laser beam would pass axially through the hole in the mirror and the graphite tube. The monochromator was set in the visible wavelength region and the output from the photomultiplier tube was connected directly to a chart recorder. The graphite tube was then heated for a long period of time while the mirror and lens were aligned to give the largest signal from the graphite emission. This alignment ensured that the image of the centre of the graphite tube was focused onto the monochromator slit.

RESULTS AND DISCUSSION

In Table 1, the detection limits obtained for several elements by use of the tube furnace are given. Figure 3 shows the calibration curves. In comparison with the results obtained with the graphite cup previously described,⁷ the detection limit for Cu was poorer and that for Al was better. Also, it should be noted that Mo and V were not even measurable with the previous graphite-cup system but were readily detectable with the tube furnace.

The results for copper were poorer because the metal is relatively volatile and atomizes more easily in the graphite cup. When the graphite tube was used, the amount of fluorescence collected was significantly

*This research was supported by AFOSR-86-0015.

†Author to whom correspondence should be sent.

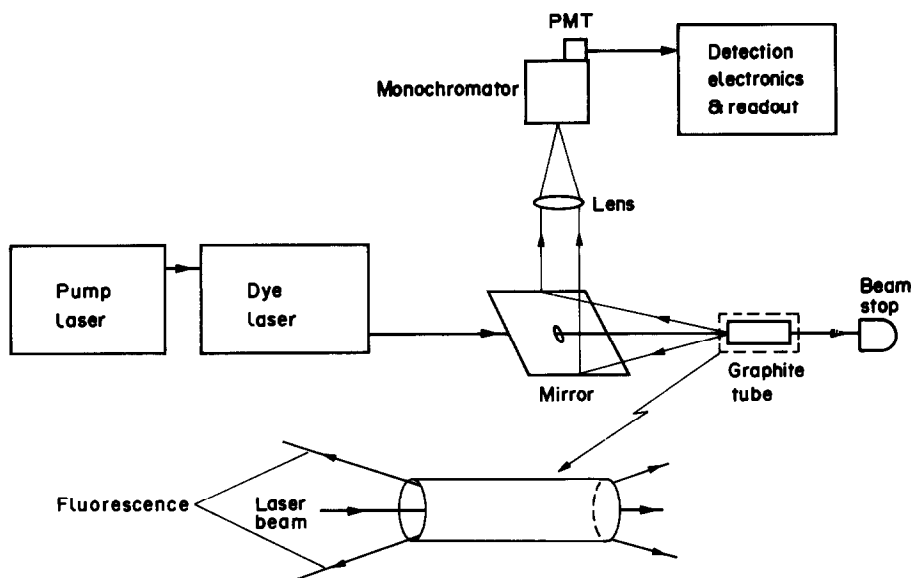


Fig. 1. Optical arrangement of tube furnace system for laser-excited atomic-fluorescence.

less than with the cup furnace. In the tube furnace, there were light losses due to fluorescence escaping through the hole in the mirror. Also, the graphite tube limited the solid angle of the light leaving it. For these reasons, the tube furnace did not work as well as the plain graphite cup for the more volatile elements.

The improved results for Al, Mo, and V showed that the graphite tube was more effective than the graphite cup for atomizing these elements. The semi-enclosed furnace was necessary for atomizing Mo and V. However, the detection limits were still significantly worse than those obtained by electrothermal atomic-absorption, especially for V. The results from this work could have been improved by using a pyrolytic coating on the tube furnace, to minimize carbide formation. However, because of the bulkiness of the furnace, *in situ* coating of the graphite tube

with pyrolysed methane was not possible. Also, the limiting noise of a blank run was due to scatter of laser radiation into the monochromator by particles within the furnace. A pyrolytic coating should minimize this scatter. Another problem was the laser scatter caused by the front of the quartz window. Even though most of the scatter was deflected upward, a small fraction would still be measured by the photomultiplier tube. In most cases, a neutral density filter cutting off at least 99% of the radiation had to be used in front of the monochromator so that the detection electronics would not be overloaded. Placing the front quartz window at the Brewster angle¹⁰ should minimize such scatter and probably improve the detection powers by 1–2 orders of magnitude.

The other major problem was the light loss through the hole in the mirror. A $\frac{1}{8}$ -in. hole was

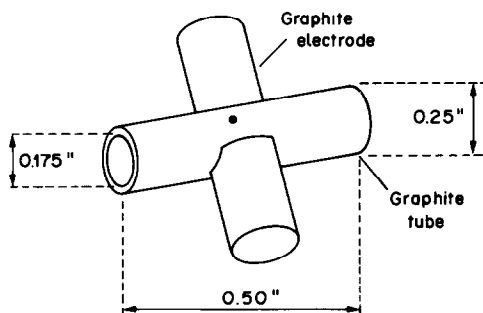


Fig. 2. A graphite-tube furnace for laser-excited atomic-fluorescence.

Table 1. Limits of detection by laser atomic-fluorescence spectroscopy*

Element	Wavelength, nm		Limits of detection, pg		
	Exc	Fl	Tube†	Cup ⁷	GFASS ⁹
Al	394.4	396.2	1×10^2	5×10^2 §	1
Cu	324.8	327.4	8	2	2
Mo	313.3	317.0	1×10^2	NS‡	1×10^2
V	385.6	411.2	2×10^5	NS‡	2×10^1

*Defined as $3\sigma/m$, where σ = standard deviation of the blank and m = slope of calibration curve; 5- μ l volumes were used.

†This work.

§Hydrogen-argon atmosphere.

‡No signal.

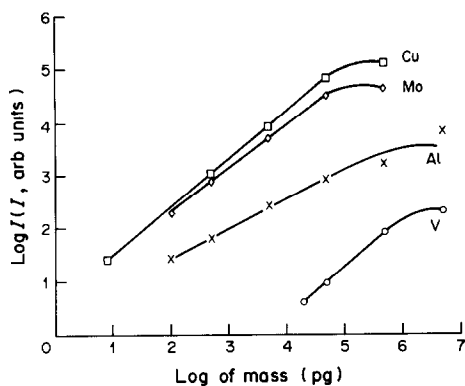


Fig. 3. Log intensity *vs.* log mass for the graphite-tube furnace method. Slopes: Cu 0.90; Mo 0.80; Al 0.55; V 0.95.

originally used but alignment was much more difficult, and there was more scatter as the laser beam passed through the hole. Such scatter was worse when a frequency-doubled beam was used since it had a much larger diameter. Modifications of the tube furnace are currently being made to improve the detection powers. However, the tube furnace design

described in this paper should be of interest to those workers requiring high detection powers and wide analytically useful ranges.

REFERENCES

1. S. Neuman and M. Kriese, *Spectrochim. Acta*, 1974, **29B**, 127.
2. J. P. Hohimer and P. J. Hargis, Jr., *Appl. Phys. Lett.*, 1977, **30**, 344.
3. M. A. Bolshov, A. V. Zybin and I. I. Smirenkina, *Spectrochim. Acta*, 1981, **36B**, 1143.
4. A. W. Miziolek and R. J. Willis, *Opt. Lett.*, 1981, **6**, 528.
5. H. G. C. Human, N. Omenetto, P. Cavalli and G. Rossi, *Spectrochim. Acta*, 1984, **39B**, 345.
6. J. Tilch, H. Falk, H. J. Paetzold, P. G. Mon and K. P. Schmidt, *Colloquium Spectroscopicum Internationale XXIV*, FRG, 15–25 September 1985.
7. D. Goforth and J. D. Winefordner, *Anal. Chem.*, 1986, **58**, 2598.
8. K. Dittrich and H. J. Stark, *J. Anal. At. Spectrom.*, 1986, **1**, 237.
9. *The Guide to Techniques and Applications of Atomic Spectroscopy*, Perkin-Elmer Technical Publication, 1983.
10. C. A. Sacci and O. Svelto, in *Analytical Laser Spectroscopy*, N. Omenetto (ed.), Wiley, New York, 1979.

A SELECTIVE SPECTROPHOTOMETRIC METHOD FOR DETERMINATION OF COPPER WITH FERRON

S. P. ARYA,* J. L. MALLA and VEENA SLATHIA
Department of Chemistry, University of Jammu, Jammu 180001, India

(Received 25 March 1985. Revised 19 July 1986. Accepted 6 September 1986)

Summary—A selective spectrophotometric determination of copper is based on extraction of the copper–ferron complex with tribenzylamine in chloroform at low acidity, and measurement of the absorbance of the yellow extract at 410 nm. Beer's law is found to hold up to 8 $\mu\text{g/ml}$ copper concentration. Of 30 elements tested, only molybdenum interferes. The ratio copper:ferron:tribenzylamine in the extracted species is 1:2:2.

Over 1000 methods are available for the spectrophotometric determination of copper¹ but only a few are sufficiently selective to be useful.² Although ferron (7-iodo-8-hydroxyquinoline-5-sulphonic acid) is used for determination of several metals,² and might therefore be regarded as an unsuitable reagent for copper, its copper complex is extractable from slightly acidic solutions by tribenzylamine solution in chloroform. Most of the transition elements do not form extractable coloured complexes under the conditions used for the copper extraction, and those that do can be masked by suitable complexing agents.

EXPERIMENTAL

Reagents

Stock solution of copper (5 mg/ml). Prepared from the sulphate, standardized by the cuprous thiocyanate method,³ and further diluted as required.

Stock solutions of other elements (10 mg/ml). Prepared by dissolving suitable salts in water or dilute hydrochloric acid.

Tribenzylamine (TBA) solution in chloroform, 10 mg/ml.
Aqueous ferron solution, 1 mg/ml.

Decomposition of samples

Steels. Dissolve a 0.1-g sample in ~ 15 ml of 2M sulphuric acid with gentle heating. Add 0.5 ml of concentrated nitric acid and evaporate nearly to dryness. Cool, take up the residue in ~ 5 ml of water, add dilute ammonia solution until the appearance of a slight precipitate, then just clear the solution by addition of dilute sulphuric acid. Dilute the solution to volume in a 25-ml standard flask. Determine the copper content in a suitable aliquot.

White metals. Place a 0.15-g sample in a 100-ml beaker covered with a watch-glass and dissolve it in the minimum amount of concentrated nitric acid. Add 2–3 ml of concentrated sulphuric acid, evaporate nearly to dryness, cool, dilute to 10 ml with water, evaporate to fumes of sulphur trioxide, cool and dilute to ~ 30 ml with water. Filter

(Whatman No. 41 paper) and wash the residue twice with hot water. Add dilute ammonia solution to the combined filtrate and washings until a slight precipitate appears, clear the solution with dilute sulphuric acid, cool, dilute to volume in a 50-ml standard flask, and analyse a suitable aliquot for copper.

Procedures

To a nearly neutral solution containing less than 200 μg of copper, in a 100-ml separatory funnel, add 12 ml of ferron solution, 1 ml of 1M sulphuric acid and enough distilled water to make up to ~ 20 ml. Extract the copper(II)–ferron complex with two 10-ml portions of TBA solution in chloroform, shaking each time for 1 min. Combine the extracts in a 25-ml standard flask, make up to the mark with chloroform, and measure the absorbance at 410 nm in 1-cm glass cells against a similarly prepared reagent blank. Prepare a calibration curve in the same way with known quantities of copper.

Samples containing iron. After the reagents, add 100 mg of hydrazine sulphate and heat until the green colour of the iron(III) complex is completely discharged. Cool, transfer to the separatory funnel and pass carbon dioxide through the solution for at least 1 min before performing the extraction. Use a third extraction with 5 ml of TBA solution.

Samples containing titanium, zirconium and/or tin. Before adding the ferron, mask these elements with up to 100 mg of sodium fluoride.

Samples with vanadium and/or chromium. Add up to 500 mg of ascorbic acid to the solution before the ferron.

Samples containing antimony and/or tungsten. Add up to 100 mg of tartaric acid before the ferron.

RESULTS AND DISCUSSION

When ferron is added to an acidic solution of copper(II) a yellow complex is formed which is extractable into isopentyl alcohol or butan-1-ol but not into benzene, chloroform, carbon tetrachloride, carbon disulphide, isopentyl acetate, ethyl acetate or methyl isobutyl ketone. Tertiary amine solutions in chloroform also extract the complex readily to give maximum absorbance at 410–415 nm (Fig. 1). Of those tested, tribenzylamine gives the highest absorb-

*Present address—Department of Chemistry, Kurukshetra University, Kurukshetra-132119, Haryana, India.

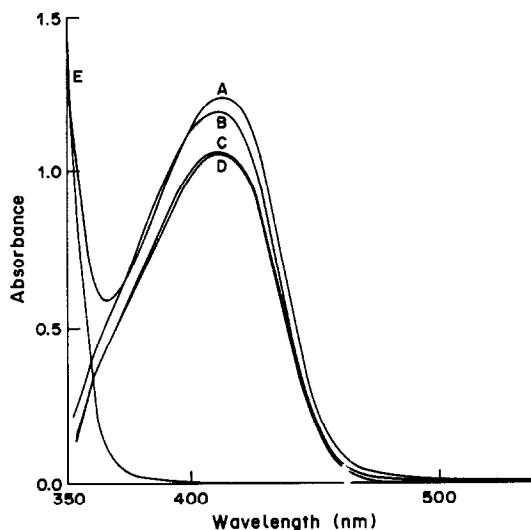


Fig. 1. Absorption spectra of copper(II)-ferron complex in amine-chloroform solution (1%): A—tribenzylamine; B—tributylamine; C—tri-n-hexylamine; D—tri-n-octylamine; E—reagent blank measured against chloroform.

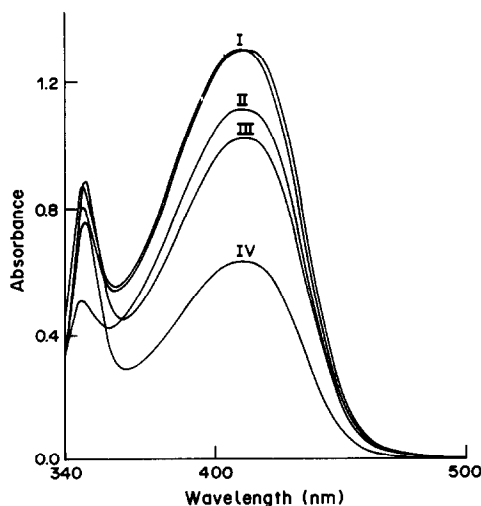


Fig. 2. Influence of acidity (sulphuric acid concentration) on the absorbance of the complex: I—0.01M and 0.05M H_2SO_4 ; II—0.0025M H_2SO_4 ; III—0.2M H_2SO_4 ; IV—0.4M H_2SO_4 .

ance, and is preferred. The reagent blank absorbs strongly at 340 nm but very little at 410–415 nm.

Composition of the complex

Copper(II) is reported^{4,5} to form a 1:2 complex

Table 2. Effect of anions and other complexing agents on the absorbance of Cu(II)-ferron complex

Ion*	Concentration, mg/20 ml	Absorbance†
None	—	1.260
Cl^-	200	1.234
SO_4^{2-}	200	1.260
NO_3^-	100	1.256
CH_3COO^-	100	1.172
$H_2PO_4^-$	100	1.258
Br^-	200	1.234
I^-	100	1.057
F^-	50	1.257
Tartrate	100	1.265
Citrate	100	1.177
$C_2O_4^{2-}$	100	0.807
EDTA	100	0.000
	100	1.262
	500	1.260

*All anions and complexing agents were added before the ferron.

†After a single extraction with 10 ml of TBA- $CHCl_3$ solution.

with ferron in aqueous solution. Job's method⁶ showed that the copper(II):ferron:tribenzylamine ratio in the extracted complex is 1:2:2.

Optimization of conditions

Figure 2 shows the absorption spectra of the complex at different acidities. There is no shift in wavelength of maximum absorption over the range 0.0025–0.4M sulphuric acid, but the absorbance is maximal and constant over the range 0.02–0.1M sulphuric acid. The effect of other conditions is shown in Table 1. The optimum conditions for maximum extraction are 12–16 ml of 1-mg/ml ferron solution, 10–20 mg/ml TBA solution in chloroform, and shaking for at least 1 min for extraction.

Beer's law and molar absorptivity

The complex is quite stable and the absorbance remains unchanged for at least 24 hr. The calibration graph is linear and passes through the origin and Beer's law is obeyed for copper concentrations up to 8 $\mu g/ml$ in the extract. The molar absorptivity is $9.1 \times 10^3 l. mole^{-1}. cm^{-1}$.

Interferences

The effect of various anions and complexing agents on the absorbance of the complex was studied, as shown in Table 2. High concentrations of even

Table 1. Influence of different parameters on the absorbance of the Cu(II)-ferron-TBA complex (4 $\mu g/ml$ Cu in the organic phase)

Ferron (1 mg/ml), ml	0.5	2	4	8	12–16
Absorbance	0.130	0.707	1.099	1.260	1.296
[TBA] in $CHCl_3$, mg/ml	2	5	10–20	40	
Absorbance	1.129	1.254	1.296	1.280	
Shaking time, min	0.5	1–5			
Absorbance	1.290	1.296			

Table 3. Tolerance limits for various ions in the determination of copper by the proposed method

Ion	Concentration, mg/20ml	Masking agent
Mg(II)	50	—
Ca(II)	10	—
Sr(II)	20	—
Ba(II)	10	—
Zn(II)	20	—
Cd(II)	10	—
Hg(II)	10	—
Co(II)	30	—
Ni(II)	20	—
Mn(II)	20	—
Al(III)	30	—
Tl(I)	20	—
As(V)	10	—
Ag(I)	20	—
U(VI)	5	—
Ce(IV)	1	—
Bi(III)	2	—
Be(II)	20	—
Si(IV)	20	—
Th(IV)	5	—
Pb(II)	10	—
Fe(III)	20	Reduced with hydrazine sulphate
Cr(VI)	10	Ascorbic acid (0.2 g)
V(V)	0.1	Ascorbic acid (0.1 g)
W(VI)	1	Tartaric acid (0.1 g)
Zr(IV)	5	NaF (50 mg)
Ti(IV)	2	NaF (50 mg)
Sn(II)	1	NaF (50 mg)
Sb(III)	2	Tartaric acid (50 mg)

Table 4. Determination of copper in various samples

Cu taken, µg	Foreign ions added, mg	Cu found, µg
100	Zn(II)	15
	Cd(II)	10
	Hg(II)	5
50	Al(III)	20
	Ag(I)	10
	Mg(II)	20
150	Co(II)	25
	Ni(II)	10
	Mn(II)	20
70	Cr(VI)	8
	V(V)	0.1
80	Ti(IV)	2
	Zr(IV)	4
	Fe(III)	15
175	Ni(II)	10
	Ce(IV)	1
NBS Steel	0.072%*	0.069%, 0.070%
BS 8d white metal	3%*	2.96%

*Reported value.

common anions decrease the absorbance but moderate amounts of these ions can be tolerated. The tolerances for complexing ions are lower, only 50 mg

each of acetate, citrate and fluoride or 10 mg of oxalate being tolerated, but ascorbic acid (0.5 g), sulphosalicylic acid (0.1 g) and tartaric acid (0.1 g) have no effect on the extraction of the complex. EDTA and thiourea inhibit the copper extraction completely.

The tolerance limits for various cations in the determination of 125 µg of copper are given in Table 3. Lead, calcium, strontium and barium give the insoluble sulphates, which need not be filtered off. Iron(III), which forms an extractable green complex with ferron, is reduced to iron(II) with hydrazine sulphate, and is not reoxidized during the extraction if air is purged from the separatory funnel and solution by passage of carbon dioxide. When iron is present, three extractions with 10, 10 and 5 ml of TBA-chloroform solution are needed for complete recovery of copper. Chromium(VI) and vanadium(V) are masked by reduction with ascorbic acid. Tungsten(VI) forms a cream emulsion on shaking with TBA-chloroform solution, but this is prevented by adding tartaric acid. Interference by titanium, zirconium and tin is avoided by addition of fluoride. Of the 30 metals studied, only molybdenum is found to interfere.

Applications

The recommended procedure is highly selective for determination of copper and is sufficiently sensitive for analysis of some natural samples as well as a variety of copper-containing alloys. The method is simple and rapid, and requires no prior separation of the elements generally associated with copper. Its utility is shown by the satisfactory analysis of various synthetic samples and of a steel and a white metal (Table 4).

Acknowledgements—The authors wish to express their sincere thanks to Professor V. Yatirajam, Chemistry Department, Kurukshetra University, for helpful discussion and providing some samples for analysis, also to the authorities of Jammu University for laboratory facilities.

REFERENCES

1. F. J. Welcher and E. Boschmann, *Organic Reagents for Copper*, Krieger, Huntington, NY, 1979.
2. Z. Marczenko, *Spectrophotometric Determination of Elements*, Ellis Horwood, Chichester, 1976.
3. A. I. Vogel, *Quantitative Inorganic Analysis*, 3rd Ed., Longmans, London, 1961.
4. M. A. Azizov, E. Kh. Khudaiberdiev and M. K. Alyaviya, *Koord. Khim.*, 1981, 7, 1209.
5. E. G. Chikryzova and V. T. Meryan, *Fiz.-Khim. Metody Anal.*, 1971, 96.
6. P. Job, *Ann. Chim. Paris*, 1928, 9, 113.

MICRODETERMINATION OF OXPRENOLOL HYDROCHLORIDE AND METOPROLOL TARTRATE WITH AMMONIUM METAVANADATE

SAEED AHMAD, R. D. SHARMA and I. C. SHUKLA

Department of Chemistry, University of Allahabad, Allahabad 211002, India

(Received 11 December 1984. Revised 7 August 1986. Accepted 6 September 1986)

Summary—A micro method has been developed for the determination of oxprenolol hydrochloride and metoprolol tartrate in pure form and in pharmaceutical preparations, with vanadium(V) in acidic medium.

Oxprenolol and metoprolol are beta-blocker agents widely used for the treatment of hypertension, cardiac arrhythmia and angina pectoris. Oxprenolol has been determined by gas chromatography¹ and high-pressure liquid chromatography (HPLC).^{2,3} The British Pharmacopoeia method⁴ for the assay of oxprenolol hydrochloride tablets involves a double extraction followed by evaporation of the organic solvent, dissolution of the residue in dilute hydrochloric acid and then spectrophotometric determination. Metoprolol has been determined by HPLC³ and gas chromatography,^{5,6} but no method for its determination is given in the most recent edition of the British Pharmacopoeia. Here, we describe a convenient method for determination of both drugs in pure form and in pharmaceutical preparations.

EXPERIMENTAL

Reagents

Analytical reagent grade chemicals were used whenever possible, unless otherwise stated.

Ammonium metavanadate solution, 0.30M. Prepared by dissolving 3.50 g in 20 ml of 10% v/v sulphuric acid and making up to 100 ml with distilled water.

Ferrous ammonium sulphate solution, 0.025M. Prepared by dissolving 2.45 g of the analytical grade salt in about 100 ml of 10% v/v sulphuric acid and diluting to volume in a 250-ml standard flask with distilled water, and standardized by titration with 0.02M standard potassium dichromate solution (accurately prepared from primary-standard material), using diphenylaminesulphonic acid as indicator.

Indicator solution. *N*-Phenylanthranilic acid (0.2 g) was dissolved in 30 ml of 5% sodium carbonate solution and diluted to 150 ml with distilled water.

Sample solutions

Pure drugs. Accurately weighed 50-mg amounts of oxprenolol and metoprolol were dissolved in the minimum amount of concentrated sulphuric acid and diluted to volume with distilled water in a 50-ml standard flask.

Tablets. Ten tablets were ground and a known weight of the powder, equivalent to about 50 mg of the pure drug, was dissolved and accurately diluted to 50 ml in the same way as for the pure drugs.

Injections (ampoules). The contents of the ampoule were dissolved in the minimum of concentrated sulphuric acid and

diluted to known volume with distilled water to give a solution with a drug concentration of about 1 mg/ml.

Procedure

Aliquots of sample solution containing 1-5 mg of the drug were taken in 100-ml conical flasks, and 5 ml of 4M sulphuric acid and 1 ml of 0.3M vanadate reagent (accurately measured) were added to each. The reaction mixtures were shaken and kept for 15 min at room temperature (27°), then the unconsumed vanadate was back-titrated with 0.025M ferrous ammonium sulphate, with 2 drops of *N*-phenylanthranilic acid as indicator. A blank was run in the same way. The drug content was calculated from

$$\text{mg of drug} = \frac{(B - S) MW}{n}$$

where *B* = volume of Fe(II) solution consumed in the blank titration, *S* = volume of Fe(II) solution consumed in the test-sample titration, *W* = molecular weight of the drug, *M* = molarity of the Fe(II) solution, *n* = number of moles of vanadate consumed per mole of drug.

Determination of reacting ratio and minimum reaction time

Aliquots containing 1-5 mg of the drug were allowed to react with a known and excessive volume of ammonium metavanadate reagent for various lengths of time, and the unconsumed reagent was back-titrated. The reacting ratio (moles of vanadate per mole of drug) was calculated for each test and plotted against reaction time. It was found that both drugs require 15 min reaction time and the reacting ratios are 20 and 10 for oxprenolol hydrochloride and metoprolol tartrate respectively.

The reaction products were determined as follows. Carbon dioxide was determined by passage of the gases from the reaction vessel over soda-lime. Care was taken to eliminate the presence of atmospheric carbon dioxide from the reaction vessel. This determination showed the presence of 3.5-3.9 moles of carbon dioxide liberated per mole of oxprenolol and 1.5-1.8 moles of carbon dioxide per mole of metoprolol. Acetone was determined by distilling the reaction mixture at 56°, collecting the distillate, adding a known amount of hydroxylamine hydrochloride (neutralized to Methyl Red), letting stand for 10-15 min, then titrating the unconsumed hydroxylamine hydrochloride with alkali. The amount of acetone found corresponded to about 0.8 mole of acetone per mole of oxprenolol or metoprolol. The ammonium ion was determined as described earlier,⁷ about 1 mole being produced per mole of drug.

The other product in each case was extracted with diethyl ether and analysed for methoxy group content, about 2 groups per molecule being found.

Table 1. Results obtained by the standard-addition method (means of 5 determinations)

Preparation	Added, mg	Found, mg	Recovery, %	
			Present method	B.P. method
<i>Oxprenolol hydrochloride</i>				
Tablets* (40 mg)	15.0	14.9	99.3	98.5
	30.0	39.8	99.3	98.0
	45.0	44.9	99.8	98.5
Injection* (2-mg dry ampoule)	15.0	15.1	100.6	(-)
	30.0	29.9	99.6	(-)
	45.0	44.3	99.5	(-)
<i>Metoprolol tartrate</i>				
Tablets† (100 mg)	15.0	14.9	99.3	(-)
	30.0	30.1	100.3	(-)
	45.0	44.9	99.7	(-)
Injection† (1 mg/ml)	15.0	14.9	99.3	(-)
	30.0	29.9	99.6	(-)
	45.0	44.8	99.5	(-)

*Ciba-Geigy.

†Astra-IDL.

(-) No B.P. methods available.

Tartaric acid and hydrochloric acid do not react under the reaction conditions used.

RESULTS AND DISCUSSION

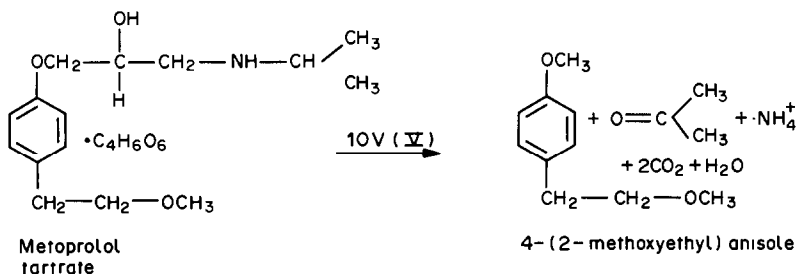
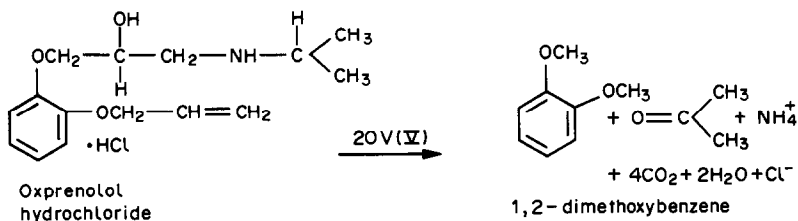
Assay of pure samples of oxprenolol hydrochloride and metoprolol tartrate, and their pharmaceutical preparations, *viz.* tablets and injections, was achieved by the recommended procedure with an error not exceeding $\pm 1\%$ (Tables 1 and 2). It was observed

that the reaction was best done with the recommended concentration of vanadate at room temperature. Lower temperature gives low results and slow reaction, and higher temperature gives no improvement in the precision. Since the reaction is not instantaneous, direct titration cannot be used. An acidic medium is essential for quantitative results to be obtained.

Possible reaction schemes are proposed below on the basis of the reacting ratios and determination of the reaction products.

Table 2. Microdetermination of oxprenolol hydrochloride and metoprolol tartrate in pure form and in their pharmaceutical preparation (10 replicates)

Sample	Amount taken, mg	Amount found, mg	Standard deviation, μg	Relative std. devn., %
1. Oxprenolol (pure sample)	1.00	0.99	4	0.4
	3.00	2.99	5	0.2
	5.00	4.99	6	0.1
(a) Oxprenolol tablet (Ciba-Geigy) (40 mg)	1.00	0.99	4	0.4
	3.00	2.99	6	0.2
	5.00	5.00	3	0.1
(b) Oxprenolol injection (Ciba-Geigy) (2-mg dry ampoule)	1.00	1.00	4	0.4
	3.00	3.00	10	0.3
	5.00	4.99	21	0.4
2. Metoprolol (pure sample)	1.00	0.99	3	0.3
	3.00	3.00	11	0.4
	5.00	4.99	21	0.4
(a) Metoprolol tablet (Astra-IDL) (100 mg)	1.00	0.99	6	0.6
	3.00	2.99	16	0.5
	5.00	5.02	0.8	0.02
(b) Metoprolol (Astra-IDL) (1 mg/ml)	1.00	0.99	5	0.5
	3.00	3.02	2	0.1
	5.00	5.01	24	0.5



Common excipients in pharmaceutical preparations, e.g., starch, calcium carbonate, sodium citrate, magnesium trisilicate, tricalcium phosphate, gum acacia, if present, do not interfere in the determination.

REFERENCES

1. D. DeBruyne, H. Kinsun, M. A. Mouline and M. C. Bigot, *J. Pharm. Sci.*, 1979, **68**, 511.
2. S. E. Tsuei, J. Thomas and R. G. Moore, *J. Chromatog.*, 1980, **181**, 135.
3. M. Ervik, *Acta Pharmacol. Toxicol., Suppl.*, 1975, **36** (V), 136.
4. *British Pharmacopoeia 1980*, p. 797. H. M. Stationery Office, London, 1980.
5. C. D. Kinney, *J. Chromatog.*, 1981, **225**, 213.
6. A. C. Mehta, *Analyst*, 1982, **107**, 1379.
7. R. D. Tiwari, J. P. Sharoma and I. C. Shukla, *Talanta*, 1966, **13**, 499.

SOFTWARE SURVEY SECTION

Software package TAL-001-86

DATABANK

Contributors: L. VINCZE and S. PAPP, Department of General and Inorganic Chemistry, Veszprém University of Chemical Engineering, H-8200 Veszprém, Schönherz Z. u. 10, HUNGARY.

Brief description: Often, literature values for the stability constants that describe complex equilibrium systems have been measured at different ionic strengths, temperatures, etc., and consequently show much scatter. DATABANK was written to allow an optimum value to be selected. Literature data are fitted to the Davies equation: the function minimized is

$$U(\log \beta_t, b) = \sum (\log \beta_{md} - \log \beta_{calc})^2$$

The program contains data (from the well-known compilations) for the iron(II) and iron(III) complexes of formate, oxalate, acetate, sulphate and hydroxide. For a chosen complex, the log beta values can be plotted on the screen as a function of ionic strength, and the literature references printed. Optimal log beta and b values can be found, and the theoretical dependence plotted. Experimental values that differ from the general trend can be eliminated. A flashing point can be moved around the screen; its log beta and ionic strength co-ordinates are printed on the screen continually. It would be easy to update the data if new measurements became available, and it would also be easy to amend the program for use with other equilibrium systems.

Potential users: workers in the stability constant field.

This application program for stability constant work has been developed to run on a Sinclair ZX Spectrum 48K computer, and is written in Spectrum BASIC. It is available on audio cassette tape.

Distributed by the contributors.

The program is self-documenting, but partly in Hungarian. The source code is available.

The package is fully operational. The contributors are available for user enquiries.

Software package TAL-002-86

LABMASTER

Contributor: Dr. A.G. Rowley, Geolab Nor A/S, Hornebergveien 5, P.O. Box 1581, 7001 Trondheim, Norway.

Brief description: Turns a BBC micro into a laboratory data logger for use with chromatographs and autoanalysers. The collected data can be displayed as a displacement - time plot, and interrogated for retention time, peak height, etc. Chromatographic peaks can be integrated. All data can be archived to disc.

Potential users: Analytical chemists, chromatographers.

Fields of interest: Analytical and environmental chemistry.

This application program in the area of laboratory data capture has been developed for an Acorn BBC Model B or B+ with OS 1.2 or later, and fitted with a twin disc drive. It is written in BASIC/machine code. It is available on 40- or 80-track 5.25-inch floppy discs.

Distributed by UnivEd Technologies Ltd., 16 Buccleuch Place, Edinburgh EH8 9LN, Scotland.

The memory required is 32K. There is extensive external documentation. The source code is not available.

The package has been fully operational for 2 years, and is in use at 20 sites. The contributor is willing to deal with enquiries.

Software package TAL-003-86

LABROM

Contributor: Dr. A.G. Rowley, Geolab Nor A/S, Hornebergveien 5, P.O. Box 1581, 7001 Trondheim, Norway.

Brief Description: A self-contained ROM which lets a BBC B microcomputer, with no disc drives, stand alone and collect data from autoanalysers or chromatographs. The data can be redisplayed and retention times and peak heights measured. Plots can be dumped to a dot-matrix printer.

Potential users: Teaching Laboratories.

Fields of interest: Chromatography, Autoanalysers.

This application program in the area of laboratory data logging has been developed for the Acorn BBC B, B+, or Master 128 (OS 1.2 or later), in machine code and BASIC. It is available on ROM.

Distributed by UnivEd Technologies Ltd., 16 Buccleuch Place, Edinburgh EH8 9LN, Scotland.

The minimum hardware required is a standard BBC-B with 32K of memory. The program is easy to use in conjunction with the external documentation provided. The source code is not available.

The package has been fully operational for 1 year, and is in use at 2 sites. The contributor is available for enquiries.

Software package TAL-004-86

NUMBERMASTER

Contributor: Dr. A.G. Rowley, Geolab Nor A/S, Hornebergveien 5, P.O. Box 1581, 7001 Trondheim, NORWAY.

Brief description: This is a general purpose simple statistics package. It calculates means, standard deviations and confidence limits. A second module carries out least squares on data sets and determines all parameters. A screen plot of the best straight line is available, and can be dumped to a printer. Facilities are also provided for the direct reading of data from the BBC's analogue-to-digital port.

Potential users: Any science.

Fields of interest: Wet chemical analysis, solution chemistry.

This utility program in the field of calibration and statistics has been developed in BASIC for the Acorn BBC-B microcomputer, to run under OS 1.2 or later. It is available on single-sided 5.25-in disc. The memory required is 32K.

Distributed by UnivEd Technologies Ltd., 16 Buccleuch Place, Edinburgh EH8 9LN, Scotland.

The minimum hardware configuration is a BBC-B with 1 disc drive. There is extensive external documentation. The source code is not available.

The package has been fully operational for two years, and is in use at twenty sites. The contributor is available for user enquiries.

Software package TAL-005-86

SIGNWRITER

Contributor: Dr. Anthony Durham, Wight Scientific, 44 Roan Street, London SE10 9JT, England. (Tel. 01-858-2699).

Brief Description: SIGNWRITER gives instant display lettering by computer. It prints letters, numbers, punctuation, symbols, pictures, etc., any size, anywhere on paper, horizontally or vertically. Scientists use it

for poster displays at conferences, laboratory notices, and for printing and publishing with unusual technical symbols. SIGNWRITER treats character outlines as a series of straight lines and circle arcs, and hence prints each character accurately to the nearest printer dot position. The sign-inputting program is a specialized typographical word processor that takes care of layout (centring, justification, etc.). In contrast with other "presentation graphics" packages, the quality of SIGNWRITER's output improves with increasing size, and can rival typesetting or dry-transfer lettering after photoreduction. A ready-to-use font of over 120 characters is provided and other fonts are becoming available. Users can alter characters and create their own new ones using the on-screen design program, which is a powerful CAD tool in its own right.

Potential users: All scientists and administrators.

Fields of interest All branches of science, scholarship, and business.

This utility program has been developed for IBM PC, Apricot, BBC and Amstrad, in compiled BASIC and Assembler, to run under PCDOS, MSDOS, BBC DFS, CP/M3, and is available on floppy disc as appropriate for the computer. The memory required is 128K (for the IBM PC).

Distributed by Wight Scientific (and local distributors). Price: £80 + VAT or \$120 (IBM PC and Apricot), £49.95 including VAT (Amstrad), £29.95 including VAT (BBC).

The IBM PC requires a graphics card.

The package has been fully operational for 9 months, and is in use at over 100 sites. There is extensive external documentation. The contributor is available for user enquiries.

Software package TAL-006-86

PAPERBASE De Luxe

Contributor: Dr. Anthony Durham, Wight Scientific, 44 Roan Street, London SE10 9JT, England. (Tel. 01-858-2699).

Brief description: PAPERBASE De Luxe enables a scholar or small research group to manage (store, edit, interrogate, sort, format) a database of several thousand references on a personal computer. It can also help construct reference lists for manuscripts by producing a list of all the probable citations in a text, looking them up in the database, and laying them out in any target journal's preferred format. It scores over other bibliographic database programs in these ways:

- No practical limit to amount of information per reference (abstracts too);
- Compact, flexible storage of information as ASCII files for data portability and compatibility with other programs;
- Truly international - accepts non-English language, sold world-wide;
- Versions for most makes of computer;
- No instruction manual - menu-driven, on-screen help, just one disc;
- Fast and helpful on entry;
- Continual upgrades and prompt support by letter or phone;
- Most sales now generated by word-of-mouth recommendation by users;
- Exceptional value for money.

Potential users: Researchers, students, teachers, librarians.

Fields of interest: All branches of science and scholarship.

This utility program is available in compiled BASIC for most MSDOS and CP/M computers. It is available on floppy disc as appropriate for the computer. The memory required is 64K.

Distributed by Wight Scientific. Price £90 or \$175.

The minimum hardware configuration is any typical personal computer. The program is self-documenting. The source code is not available (parts by special arrangement).

The package has been fully operational for ca. 2 years, and is in use at over 200 sites. The contributor is available for user enquiries.

STUDY ON THE SYNERGISTIC EXTRACTION OF COBALT(II) WITH LOWER FATTY ACIDS IN THE PRESENCE OF HETEROCYCLIC AMINES AND SOME METAL ION SEPARATIONS

S. K. GOGIA, D. SINGH, O. V. SINGH and S. N. TANDON*

Department of Chemistry, University of Roorkee, Roorkee 247 667, India

(Received 29 March 1984. Revised 28 August 1986. Accepted 6 November 1986)

Summary—The synergistic extraction of cobalt(II) with a chloroform solution of propionic, butyric or valeric acid in the presence of β -picoline, pyridine or quinoline has been investigated. The effect of different variables, such as pH of the aqueous phase, and concentration of metal ion, acid and amine, is reported. On the basis of slope analysis the species extracted were generally found to be $\text{CoA}_2 \cdot 2\text{HA} \cdot 2\text{B}$ where HA is the acid and B the base, but $\text{CoA}_2 \cdot \text{HA} \cdot 2\text{B} \cdot \text{H}_2\text{O}$ for the butyric acid-quinoline system. The extraction constants were used to assess the relative effectiveness of the amines as synergists. From the extraction data, methods for separation of Co(II) from Mn(II), Cr(III), Fe(III), Zn(II), Cd(II) and Hg(II), with fairly high separation factors, have been worked out.

Synergism in the extraction of metal ions has been observed in a wide variety of systems. Nitrogenous organic bases can act as synergists in the extraction of metal carboxylates; they not only extend the pH range of effective extraction but also reduce the tendency to emulsification, thereby increasing the utility of carboxylic acids as extractants. Most such studies have been made on caproic, enanthic and capric acids and their derivatives. Comparatively little work with the lower aliphatic monocarboxylic acids ($<C_5$) in the presence of amines has been reported.¹⁻⁷ Here we present a study on the extraction of Co(II) with propionic, butyric and valeric acids in the presence of some aliphatic and heterocyclic amines. The heterocyclic amines significantly enhanced the extraction but the aliphatic amines did not. The extraction of Mn(II), Cr(III), Fe(III), Zn(II), Cd(II) and Hg(II) was also studied and conditions for their separation from Co(II) are proposed.

EXPERIMENTAL

Materials

Stock solutions of metal ions were prepared by dissolving the sulphates or nitrates (of analytical purity) in distilled water and adding a few drops of the appropriate mineral acid to prevent hydrolysis. The solutions were standardized by EDTA titration. The distribution studies were done with radioactive isotopes; the ⁵⁸Co, ⁵⁵Mn, ⁵¹Cr, ⁵⁵⁺⁵⁹Fe, ⁶⁵Zn, ^{115m}Cd and ²⁰³Hg used were procured from Bhabha Atomic Research Centre, Bombay. The acids used were standardized by acid-base titration and the amines by non-aqueous titrimetry. All chemicals used were of analytical purity. The pH of aqueous phases was adjusted with perchloric acid and sodium hydroxide.

The activities of all the radioisotopes except ^{115m}Cd were measured with a well-type NaI(Tl) scintillation counter; for ^{115m}Cd a GM counter was used.

Procedure

Equal volumes (10 ml) of radiolabelled aqueous metal-ion solution and the organic phase containing the organic acid and amine were shaken at room temperature ($25 \pm 2^\circ$) for about 5 min. After separation of the phases, equal volumes of each were removed and their activities counted. Each experiment was run in duplicate, and the precision was about $\pm 1\%$ (for 60% extraction) for the gamma-counting and $\pm 2\%$ for the beta-counting.

The partition coefficients of the acids and amines were determined at room temperature for the solvent system used. That for the acids (P_{HA}) was determined by acid-base titration to the phenolphthalein end-point, and that of the base (P_{B}) in the presence of acid was determined by titrating the equilibrated organic phase with perchloric acid in glacial acetic acid, with Methyl Violet in chlorobenzene as indicator.⁸ The average P_{HA} values found were 0.26, 1.41 and 16.5 for propionic, butyric and valeric acid, respectively. The partition coefficient for quinoline was so high ($P_{\text{B}} > 100$) that it was assumed that all the amine added was present in the organic phase.

The nmr spectra of valeric acid in deuteriochloroform in the presence and absence of heterocyclic amines were recorded with TMS ($\tau = 10$ ppm) as internal standard.

RESULTS AND DISCUSSION

The distribution ratios of propionic, butyric and valeric acids between chloroform and water gradually increase with increase in initial acid concentration. This may be ascribed to polymerization of the acids in the chloroform phase. The distribution (between organic and aqueous phase) of a monocarboxylic acid that dimerizes in the organic but not the aqueous phase can be described by



*To whom correspondence should be addressed.

where P_{HA} is the partition coefficient of the monomeric acid and K_D is the dimerization constant ($K_D = [H_2A_2]_o/[HA]_o^2$). If the first term on the right-hand side is negligible compared to the second, this relation can be approximated to

$$\log([HA]_o + [H_2A_2]_o) = \log 2K_D P_{HA}^2 + 2 \log [HA]_o$$

or

$$\log C_o = \log 2K_D P_{HA}^2 + 2 \log C_a$$

Plots of $\log C_o$ vs. $\log C_a$ gave straight lines of slopes approximating to 2, suggesting that the dimerization of propionic, butyric and valeric acids in chloroform is more or less complete. Moreover, the values of the arbitrary distribution ratio $[H_2A_2]_o/[HA]_o^2$ remained constant over a wide range of acid concentration, confirming the dimerization in chloroform.

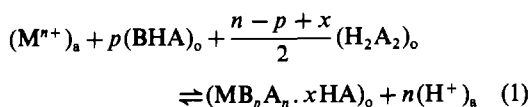
A chloroform solution of the amine is able to extract Co(II) only to the extent of about 10%. Chloroform solutions of propionic, butyric and valeric acids are also poor extractants for cobalt in the pH range 2–8. Pietsch and Sinic⁹ reported a similar observation.

Addition of the amine to the chloroform solution of the acid generally enhanced the extraction of these metal ions. This may be ascribed to the formation of a less hydrophilic species by the amine removing water molecules from the co-ordination sphere of the metal ion.

It can be assumed that the amine forms a salt with the organic acid in chloroform medium. Although the acid would be practically completely undissociated in chloroform solution because of the low dielectric constant and polarity of the solvent, the same solvent properties would favour formation of ion-pairs of the protonated amine and the acid anion if the amine were sufficiently basic. The possibility of the absence of any reaction between the acid proton and the amine in chloroform solution was ruled out by consideration of the nuclear magnetic resonance (nmr) spectra of deuteriochloroform solutions of valeric acid in the absence and presence of amines. The presence of an equimolar amount of amine shifted the signal for the carboxyl group proton to an extent dependent on the basicity of the amine, indicating salt-formation. Similar evidence (for amines and enanthic acid in chloroform) has been given by Pyatnitskii *et al.*¹⁰

Equilibrium treatment

It can be assumed that in the organic phase the excess of the acid (HA) mostly exists as the dimer H_2A_2 and the amine (B) as its salt BHA. The equilibrium between an aqueous metal ion solution (M^{n+}) and a chloroform solution of the carboxylic acid and amine, can be represented in general, as:



the equilibrium constant for which is

$$K_{ex} = \frac{[MB_pA_n \cdot xHA]_o [H^+]_a^n}{[M^{n+}]_a [BHA]_o^p [H_2A_2]_o^{(n-p+x)/2}} \quad (2)$$

and hence

$$\log D = \log K_{ex} + npH + \left(\frac{n-p+x}{2}\right) \log [H_2A_2]_o + p \log [BHA]_o \quad (3)$$

where the distribution coefficient, D , is given by

$$D = [MB_pA_n \cdot xHA]_o / [M^{n+}]_a \quad (4)$$

assuming that the metal ion does not form any other complex with the excess of acid.

Differentiation of equation (3) with respect to pH at constant acid and amine concentration gives

$$\left(\frac{\delta \log D}{\delta pH}\right) = n \quad (5)$$

and the slope of a plot of $\log D$ vs. pH at constant acid and amine concentration in the organic phase will give the value of n . Similarly, a plot of $\log D$ vs. the logarithm of the total amine concentration, at constant free acid concentration in the organic phase, will give p . A plot of $\log D$ vs. the logarithm of the dimeric acid concentration at constant pH and amine concentration will have a slope of $(n-p+x)/2$, from which x can be calculated.

Effect of pH of the aqueous phase

The degree of extraction of Co(II) increases with increase in pH and reaches a maximum near the pH at which the metal ion starts to hydrolyse. The extraction starts from pH ~ 5 and becomes more or less constant in the pH range 6.5–8.0. Therefore, subsequent studies on Co(II) were all done at pH 6.8. The plots of $\log D$ vs. pH at constant metal ion, acid and amine concentrations gave straight lines with slopes close to 2, indicating release of two protons per metal ion to give an uncharged extracted metal species.

Effect of metal ion concentration

Varying the cobalt concentration in the range 10^{-6} – $10^{-3}M$ changed the distribution coefficient by not more than $\pm 3\%$, ruling out the possibility of extraction of polymeric species in this concentration range. A cobalt concentration of $1.0 \times 10^{-4}M$ was used for further investigations.

Choice of solvent

Solvents with varied dielectric constants, *e.g.*, n-heptane, benzene, 1,2-dichloroethane, n-butanol and nitrobenzene, were tested, but no correlation was found between the degree of extraction and the dielectric constant of the solvent. Of the solvents tested, chloroform gave the highest extraction and was used for all further work.

Table 1. Number of heterocyclic amine molecules (p) co-ordinated with Co(II) in the extracted species and number of acid molecules (x) required for solvation of the species

Amine	Propionic acid			Butyric acid			Valeric acid		
	Slope	Slope	x	Slope	Slope	x	Slope	Slope	x
	p	$\frac{n-p+x}{2}$		p	$\frac{n-p+x}{2}$		p	$\frac{n-p+x}{2}$	
β -Picoline	1.7	1.1	1.9	1.8	1.0	1.8	1.8	1.2	2.2
Pyridine	1.9	1.0	1.9	2.3	1.0	2.3	1.8	1.2	2.2
Quinoline	—	—	—	2.0	0.60	1.2	2.3	1.0	2.3

Effect of amine concentration

Plots of $\log D$ vs. $\log [\text{amine}]_0$ for constant pH, [Co(II)] and large and effectively constant excess of acid, gave straight lines with slopes near to 2, indicating that two molecules of amine were present for each molecule of extracted species (i.e., $p = 2$).

Effect of acid concentration

It was found that at constant pH and amine concentration the degree of extraction increased with acid concentration. The extraction efficiency increased with the number of carbon atoms in the acid.

Plots of $\log D$ vs. $[\text{H}_2\text{A}_2]_0$ at constant pH, [Co(II)] and large and effectively constant excess of amine, gave straight lines with slopes corresponding to $(n - p + x)/2$. From the values of n and p already found, the numbers of acid molecules (x) solvating the extracted species were calculated, and are given in Table 1. It is clear that the value of x is two except for the butyric acid-quinoline system where it is one.

On the basis of these results the composition of the extracted species can be represented as $\text{CoA}_2 \cdot 2\text{HA} \cdot 2\text{B}$ except in the butyric acid-quinoline system, for which it is considered to be $\text{CoA}_2 \cdot \text{HA} \cdot 2\text{B} \cdot \text{H}_2\text{O}$, on the assumption that a water molecule would be needed to satisfy the co-ordination number requirement.

Pyatnitskii *et al.*¹⁰ reported the incorporation of two molecules of quinoline in the Co(II) species extracted in the quinoline-enanthic acid system. Also, in a study on the extraction study of Cu(II) with butyric and α -bromobutyric acids in presence of pyridine or quinoline, the extracted species was found to contain two molecules of the amine per copper atom.³

Calculation of extraction constants

Equation (3) was used to calculate the extraction constants from results obtained at constant acid and varied amine concentration and the results are given in Table 2. The relative effectiveness of the amines as synergists follows the order β -picoline \geq pyridine $>$ quinoline.

Pyatnitskii *et al.*³ have reported that pyridine is a better synergist than quinoline for the extraction of Cu(II) with butyric and α -bromobutyric acids, and a similar order of effectiveness was observed by earlier workers¹¹⁻¹³ for some other acid systems.

Separations

The extraction behaviour of Mn(II), Cr(III), Fe(III), Zn(II), Cd(II) and Hg(II) was studied under similar experimental conditions and the variables such as nature and concentration of amine and acid and pH of the aqueous phase were explored to achieve optimum conditions for separations. The extraction of Mn(II) and Cr(III) was found negligible ($< 2\%$) with 1.0M propionic, butyric and valeric acids in the presence of different aliphatic and heterocyclic amines in the pH range 2-8. The extraction of Co(II) was almost quantitative in the pH range 6.5-8.0 with valeric and butyric acids in combination with β -picoline or pyridine. Thus Co(II) can be separated from Mn(II) and Cr(III) under these experimental conditions with fairly high separation factors. Cobalt(II) can also be separated from Fe(III), Zn(II) and Cd(II) when valeric acid and *n*-butylamine or dibutylamine are used as extractants, the Co(II) showing negligible extraction whereas the others are almost quantitatively extracted.

Table 2. Extraction constants for cobalt with various amines and carboxylic acids

Acid	Amine					
	β -Picoline		Pyridine		Quinoline	
	$\log K_{ex}$	Mean	$\log K_{ex}$	Mean	$\log K_{ex}$	Mean
Propionic	-12.92		-13.99			
	-12.76	-12.79	-13.97	-13.97		
	-12.68		-13.95			
Butyric	-12.28		-12.82		-14.17	
	-12.30	-12.31	-12.80	-12.76	-14.05	-14.07
	-12.35		-12.67		-14.00	
Valeric	-11.36		-11.44		-13.56	
	-11.56	-11.49	-11.44	-11.43	-13.53	-13.56
	-11.56		-11.42		-13.62	

Table 3. Some metal ion separations from Co(II) in carboxylic acid-amine extraction systems

No.	Metal ion(s) separated	Acid	Amine	Aqueous phase pH	Separation factor
1	Mn(II) and Cr(III)	Butyric (1.5M) or valeric (1.0M)	β -Picoline (1.5M) or pyridine (1.5M)	6.5-8.0	$\geq 10^4$
		Butyric (2.5M)	β -Picoline (1.5M) or pyridine (1.5M)	6.5-8.0	$\geq 10^5$
2	Zn(II) and Cd(II)	Valeric (1.0M)	Dibutylamine (1.0M) or tributylamine (1.5M)	6.0-8.0	$\geq 10^4$
3	Hg(II)	Valeric (1.0M)	Dibutylamine (1.0M) or tributylamine (1.5M)	5.5-7.5	$\geq 10^4$
		Propionic (1.0M)	Quinoline (1.5M)	3.0-5.5	$> 10^4$
		Valeric (1.0M)	β -Picoline (1.0M) or pyridine (1.0M)	3.5-5.0	$\geq 10^5$
4	Fe(III)	Valeric (1.0M)	Dibutylamine (1.0M) or tributylamine (1.5M)	3.0-7.0	$\geq 10^4$
		Butyric (1.0M) or valeric (1.0M)	β -Picoline (1.0M) or pyridine (1.0M)	3.0-5.0	$\geq 10^5$

In general the extraction of the metal ion increases with acid concentration. The extraction of Co(II) in the butyric acid and β -picoline or pyridine system increases from 90% to almost 99% when the acid concentration is increased from 1.0 to 2.5M, but Mn(II) and Cr(III) still show negligible extraction even at the higher acid concentration.

The degree of extraction also increases with concentration of the synergist. Mercury(II) is almost quantitatively extracted with 1.5M quinoline at 1.0M propionic acid concentration and pH 3.0-5.5. Under these conditions the extraction of Co(II) is very poor. This offers an effective separation of Co(II) from Hg(II). Hg(II) can also be effectively separated from Co(II) in the valeric acid and β -picoline or pyridine system at pH 3.5-5.0. Co(II) can be conveniently separated from Fe(III) by use of butyric or valeric acid (1.0M) and β -picoline or pyridine (1.0M). The extraction of Fe(III) starts at around pH 2 and is almost quantitative at pH \sim 3, but the extraction of Co(II) starts only at pH \sim 5.

The metal ions can be stripped from the organic phase with nitric acid. The optimum conditions for separations are given in Table 3. Since no strong complexing agent is involved in the carboxylic acid-amine system, there is the additional advantage over many other systems that the subsequent determination of metal ion is easier.

Acknowledgement—The financial assistance of Council of Scientific and Industrial Research (CSIR), New Delhi, India, is gratefully acknowledged.

REFERENCES

1. I. V. Pyatnitskii, A. Omode, V. V. Sukhan and V. A. Frankovskii, *Zh. Analit. Khim.*, 1973, **28**, 50.
2. V. V. Sukhan, I. V. Pyatnitskii and A. G. Sakhno, *ibid.*, 1973, **28**, 541.
3. I. V. Pyatnitskii, A. Omode and V. V. Sukhan, *ibid.*, 1973, **28**, 2317.
4. I. V. Pyatnitskii, V. V. Sukhan and V. B. Ischenko, *Ukr. Khim. Zh.*, 1977, **53**, 411.
5. I. V. Pyatnitskii and V. I. Simonenko, *ibid.*, 1972, **43**, 203.
6. I. V. Pyatnitskii, V. V. Sukhan, V. B. Ischenko and V. A. Frankovskii, *ibid.*, 1979, **45**, 246.
7. S. K. Gogia, D. Singh, O. V. Singh and S. N. Tandon, *Intern. Solv. Extn. Conf., Colorado (USA)*, 1983, 367.
8. J. S. Fritz, *Anal. Chem.*, 1950, **22**, 1028.
9. R. Pietsch and B. Sinic, *Anal. Chim. Acta*, 1970, **49**, 51.
10. I. V. Pyatnitskii, V. M. Sidorenko and V. V. Sukhan, *Zh. Analit. Khim.*, 1975, **28**, 42.
11. J. M. Singh, O. V. Singh and S. N. Tandon, *Indian J. Chem.*, 1978, **16A**, 1083.
12. V. P. R. Rao and V. V. R. Sastri, *J. Inorg. Nucl. Chem.*, 1974, **36**, 415.
13. B. Gupta, J. M. Singh, R. N. Goyal and S. N. Tandon, *Can. J. Chem.*, 1980, **58**, 1958.

SPECIATION OF MANGANESE IN FRESH WATER—I USE OF EPR STUDIES

BARRY CHISWELL and MAZLIN BIN MOKHTAR

Department of Chemistry, University of Queensland, St Lucia, Queensland 4067, Australia

(Received 9 July 1986. Accepted 31 October 1986)

Summary—The process of standardization of the use of electron paramagnetic resonance (EPR) spectrometry in the determination of Mn(II) species in aqueous solution by comparison with atomic absorption spectrometry (AAS) is discussed. It is shown that EPR signals obtained from standardized aqueous solutions of manganese(II) perchlorate and nitrate in the concentration range of 0.05–2 mg/l. do not vary significantly over the pH range 2.1–7.0. Study of the effect (on the manganese EPR signals) of the addition of inorganic ions commonly found in significant concentrations in natural waters, *viz.* chloride, sulphate and bicarbonate, has shown that such ions, at the levels reported to occur in surface fresh waters, will not complex manganese(II); however, evidence is obtained that humic acid/manganese complexes could be present in such waters. The EPR signals are not affected by ionic strengths of the levels found in fresh waters.

Much of the work on the speciation of metal ions in natural waters has been done by electrochemical methods.¹ Although results from such work have been valuable in the study of manganese species,² it is of importance to develop alternative methods of determining the speciation and to compare the results obtained by different techniques.

Electrochemical methods invariably require the addition of various electrolyte/buffer solutions, and these may disturb the natural equilibrium of the species in the solution under study. We have therefore applied the non-intrusive analytical technique of EPR spectrometry, which has been used by Carpenter³ and in this laboratory⁴ for study of the speciation of manganese in sea-water, and assessment of the manganese species present in storage-dam waters.⁵ We are currently assessing the results obtained by EPR studies with those from anodic-stripping voltammetry, and this paper deals with the methods of establishing EPR spectrometry standards for work to be reported at a later date.

Dilute aqueous solutions of simple manganese(II) salts give a sharp six-peak first-derivative EPR spectrum; the fourth of these peaks from the low-field side of the spectrum is typically used for quantitative work. Three different changes in the parameters of this peak have been used⁴ to assess manganese(II) concentration and speciation in solution: (i) change in peak height; (ii) change in peak width; (iii) change in peak area.

Earlier workers who have used EPR spectrometry to determine manganese(II) in aqueous solution do not appear to have studied the possibility of a variation of EPR signal with change of pH. As the signal is sensitive to changes in the ligand field about the manganese(II) ion, we thought

that a change from pH < 3 to pH 7 in solutions of a simple Mn(II) salt might lead to EPR changes, as the species $[\text{Mn}(\text{H}_2\text{O})_6]^{2+}$, which is stable in solutions of pH < 3.5,⁶ is hydrolysed to species such as $[\text{Mn}(\text{H}_2\text{O})_5\text{OH}]^+$ and the dihydroxy-bridged $[(\text{H}_2\text{O})_4\text{Mn}(\text{OH})_2\text{Mn}(\text{H}_2\text{O})_4]^{2+}$ as the pH increases to that found in dam waters.

The need to clarify this situation is obvious since a particular EPR peak parameter is correlated with manganese concentration by use of solutions which have been standardized by atomic-absorption spectrometry. Such solutions, particularly if prepared by the recommended method of dissolving pure manganese metal in acid, have a very low pH value.

Analysis of EPR work on manganese in sea-water has been claimed³ to indicate that the common inorganic anions, chloride, sulphate and bicarbonate, can complex Mn(II) to a combined extent of ~20%, though there is some debate about the extent of complexation of the metal by these anions in freshwaters, in which both the manganese and anion concentrations are much lower. Work by Turekian⁷ and Callender and Bowser⁸ indicates that there is some possibility of such complexation, but there is little conclusive evidence.

This same situation arises in natural organic acid (humic and fulvic) complexation of manganese in fresh waters, although Gamble *et al.*⁹ claim from proton nuclear magnetic resonance work that such complexation is outer-sphere in character, even at its strongest.

EXPERIMENTAL

Reagents

Manganese atomic-absorption standard solution (1 g/l.) in 2% v/v nitric acid was obtained from Aldrich Chemical

Table 1. Normalized fourth EPR peak heights (mm) and AAS signals (arbitrary units) for aqueous manganese solutions at pH 2, 5 and 7

Manganese, mg/l.	pH 2.1 ± 0.1		pH 5.0 ± 0.1		pH 7.0 ± 0.1	
	AAS signal	EPR peak	AAS signal	EPR peak	AAS signal	EPR peak
0.050	0.010	6.3	0.010	6.2	0.010	6.3
0.100	0.028	12.7	0.025	12.7	0.023	12.7
0.150	0.040	20.8	0.038	20.8	0.033	20.8
0.200	0.054	25.5	0.048	25.8	0.044	25.0
0.400	0.108	51.0	0.103	51.0	0.097	51.0
0.600	0.156	73.6	0.150	73.6	0.143	73.6
0.800	0.213	104.0	0.201	105.0	0.213	104.0
1.400	0.366	184.1	0.360	185.7	0.353	177.8
2.000	0.482	252.5	0.478	257.5	0.479	260.0

Co. Manganese(II) perchlorate (pulum p.a.) was from Fluka, Switzerland, as was the humic acid, No. 53680, molecular weight 600–1000. BDH AnalaR perchloric acid was used.

Instrumental

EPR work was undertaken on a Bruker ER200D spectrometer with a microwave frequency of 9.26 ± 0.02 GHz. The spectrometer and cell were tuned by adjusting the microwave frequency and iris screw until the dip on the oscilloscope was flat at its minimum and centred on the cross-hair of the oscilloscope screen. After tuning, the microwave power was raised to 100 mW, the detector current brought to 200 μ A by turning the iris screw, and the frequency error adjusted to zero. The absence of power-saturation phenomena at 100 mW power was determined. Centre field was then set at 3310 G with a scan range of 375 G each side of centre. The modulation frequency was 100 kHz, and the modulation amplitude was 8 G.

The first-derivative scans were made for each sample. The first scan, which covered all six peaks, used a time constant of 200 msec and a sweep time of 200 sec, and the second scan, which covered only the fourth peak from the low-field side, had a time constant of 1000 msec and a sweep time of 1000 sec. These latter scans were used for quantitative calculations.

The three peak parameters measured were:

(i) height of fourth peak; to allow direct comparison of peaks recorded with different gain, the peak-height was normalized by measuring the height in mm, multiplying by 10^6 and dividing by the gain.

(ii) width of fourth peak; this was obtained as the difference between the maximum and the minimum of the peak scan, which were read from the nmr gaussmeter probe.

(iii) area of fourth peak; this was calculated from the Lorentzian equation: area = (peak width)² × height.

All EPR spectra were run at a controlled room temperature of $20 \pm 2^\circ$. The samples were placed in fused-silica tubes (Wilmad Glass Co., U.S.A.).

Atomic-absorption measurements for manganese were made with a Varian AA 875 spectrometer, a lamp wavelength of 279.5 nm, and an air/acetylene flame.

The pH-measurements were made with a Metrohm 632 pH-meter and a Metrohm 9100 combined glass electrode.

Procedures

Variation of EPR and AAS signals with pH. A manganese(II) perchlorate stock solution of manganese concentration ~100 mg/l. was prepared by dissolving 0.0740 g of $Mn(ClO_4)_2 \cdot 6H_2O$ in 100 ml of distilled water and filtering through a 0.45- μ m membrane filter. The concentration of this stock solution was determined at pH 7 and pH 2 (after acidification with perchloric acid) by atomic-absorption with calibration by means of standards prepared from the Aldrich 1-g/l. stock standard manganese solution. The

absorption signal of the perchlorate stock solution at both pH values was the same (within experimental error, see Table 1).

Suitable dilution of the stock solution yielded 250-ml portions of $Mn(ClO_4)_2$ solutions containing 0.050, 0.100, 0.150, 0.200, 0.400, 0.600, 0.800, 1.400 and 2.000 mg/l. manganese at pH 7.0 ± 0.1 . These solutions were adjusted to pH 5.0 ± 0.1 and 2.1 ± 0.1 with perchloric acid.

Atomic-absorption measurements and EPR spectra of all solutions were obtained on the day of their preparation, so that the instrumental conditions were not altered during the measurements.

EPR signal and ionic strength. A manganese(II) nitrate solution of manganese concentration 0.200 mg/l. at pH 3.0 ± 0.1 was prepared from the Aldrich atomic-absorption standard solution, and a manganese(II) perchlorate solution of the same concentration was obtained by dilution of the stock perchlorate solution and adjusted to the same pH with perchloric acid.

The sodium perchlorate and nitrate solutions used for ionic strength adjustment were obtained by dilution of 100 g/l. stock solutions of the analytical grade salts in distilled water.

EPR signal and anionic complexing agents. The manganese(II) perchlorate stock solution was diluted and mixed with solutions of analytical grade sodium chloride, sulphate, or bicarbonate or of humic acid, to yield the required manganese concentrations and ionic strengths for the solutions studied by EPR.

RESULTS AND DISCUSSION

Variation of AAS and EPR signals with change in pH

The change of atomic-absorption signal with manganese concentration at pH 2.1 is linear up to about 1.4 mg/l., and then shows slight convexity up to 2.0 mg/l.; the perchlorate and nitrate solutions yield identical signals for the same concentration of manganese. The variation of the height of the fourth EPR peak with manganese concentration at pH 2.1 is linear over the range 0.05–10.0 mg/l. at pH 2.1; again there is no significant difference between the signals from the perchlorate and the nitrate for the same concentrations of manganese.

Plots of the peak area and peak width of the fourth EPR signal against manganese concentration over the range 0.05–10.0 mg/l. for solutions of manganese(II) nitrate at pH 2.1 show that the peak width is constant and that the peak area is a linear function of manganese concentration over the range tested.

Carpenter³ has already indicated that for the concentrations of manganese of interest in our work on fresh waters (normally <2 mg/l.), there is no association of perchlorate and metal ion; the EPR spectrum at low pH values is attributable to the $[Mn(H_2O)_6]^{2+}$ ion alone, with the perchlorate anion having no effect on the spectrum. This claim is substantiated by our observation (reported above), that the EPR peak heights of manganese(II) nitrate solutions at pH 2.1 are the same as those for the same concentrations of manganese(II) perchlorate.

The AAS signals and EPR peak heights for various concentrations of manganese at three different pH values are summarized in Table 1. Each value is the mean of three readings. The EPR peak height varies

Table 2. Normalized fourth EPR peak heights (mm) for solutions containing 0.200 mg/l. manganese and varying amounts of nitrate and perchlorate ions (pH 3.0 ± 0.1)*

Added anion concn., g/l.	Nitrate		Perchlorate	
	I^\dagger, M	Peak height	I^\dagger, M	Peak height
0	1.09×10^{-5}	27.6	1.09×10^{-5}	30.1
12.5	0.176	27.6	0.126	30.1
25.0	0.352	27.3	0.251	30.1
50.0	0.704	24.5	0.503	30.7
75.0	1.056	22.6	0.754	31.0
100.0	1.408	19.8	1.006	31.0

*Note that the EPR peak height for a given concentration of manganese must be obtained by standardization each time the spectrometer is turned on. The nitrate and perchlorate values were obtained on different days.

†Ionic strength.

Table 3. Normalized fourth EPR peak heights (mm) for various concentrations of manganese(II) perchlorate* at pH 6.9 ± 0.2 with addition of various amounts of sodium chloride

[Cl ⁻], mg/l.	Peak height		
	A	B	C
0	9.9	108.0	6.04×10^3
50	9.9	108.0	—
500	9.9	108.0	5.96×10^3
2000	8.7	105.2	5.88×10^3
4000	—	103.4	5.68×10^3
6000	7.7	103.4	5.48×10^3

*[Mn²⁺], mg/l.—A, 0.083; B, 0.880; C, 48.6.

Table 5. Normalized fourth EPR peak heights (mm) for various concentrations of manganese(II) perchlorate* at pH 7.0 ± 0.2 with addition of various amounts of sodium bicarbonate

[HCO ₃ ⁻], mg/l.	Peak height		
	A	B	C
0	8.9	109.9	6.55×10^3
50	8.9	106.8	6.50×10^3
500	7.2	101.2	5.22×10^3
1000	6.2	84.9	4.85×10^3
1900	3.6	76.4	3.35×10^3

*[Mn²⁺], mg/l.—A, 0.076; B, 0.895; C, 52.76.

by no more than 3% with change in pH from 7.0 to 2.1. On the other hand, the AAS signals vary significantly with pH for manganese concentrations below 1.4 mg/l., the greatest decrease in signal intensity being obtained for the less concentrated solutions at the highest pH.

We can find no reference in the literature to such a decrease in AAS signal for manganese with increase in solution pH. However, Singh¹⁰ has reported that in the concentration range 2–6 mg/l., cadmium in soil

samples produces a lower atomic-absorption signal in non-acidified solution than it does in acid solution, the reduction in signal varying from 18.2% at the lower concentration to 3.6% at the higher. He suggests that, at higher pH, hydrous cadmium oxides adhere to the atomizer surface, thus yielding low analytical results. Cresser and Hargitt¹¹ have reported a similar effect for chromium(III) solutions, which at

Table 4. Normalized fourth EPR peak heights (mm) for various concentrations of manganese(II) perchlorate* at pH 6.9 ± 0.2 with addition of various amounts of sodium sulphate

[SO ₄ ²⁻], mg/l.	Peak height		
	A	B	C
0	8.8	122.2	6.35×10^3
50	8.7	120.7	6.26×10^3
500	7.9	113.7	6.10×10^3
2000	6.4	96.2	4.86×10^3
4000	5.5	76.2	3.90×10^3
6000	—	62.7	3.42×10^3

*[Mg²⁺], mg/l.—A, 0.075; B, 0.992; C, 51.15.

Table 6. Normalized fourth EPR peak heights (mm) for various concentrations of manganese(II) perchlorate* at neutral pH with addition of various amounts of humic acid

[Humic acid], mg/l.	Peak height		
	A	B	C
0	5.9	106.8	6.68×10^3
1	4.2	—	—
5	1.0	—	—
10	0.0	67.8	—
20	—	47.4	—
50	—	16.6	6.15×10^3
100	—	5.7	5.84×10^3
200	—	—	5.55×10^3
500	—	—	3.52×10^3

*[Mn²⁺], mg/l.—A, 0.051 (pH 7.5 ± 0.3); B, 0.853 (pH 6.8 ± 0.1); C, 53.79 (pH 6.9 ± 0.1).

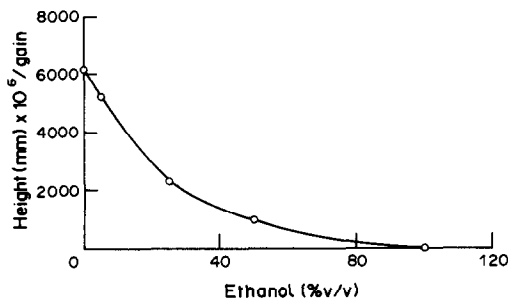


Fig. 1. Normalized fourth EPR peak height vs. percentage volume of ethanol for manganese concentration of 50 mg/l.

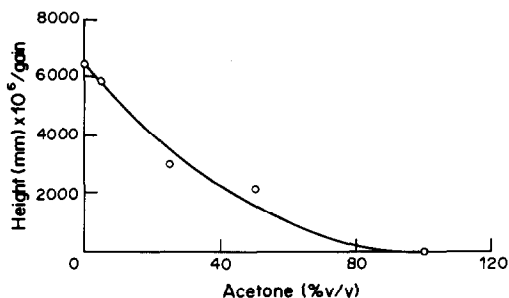


Fig. 2. Normalized fourth EPR peak height vs. percentage volume of acetone for manganese concentration of 50 mg/l.

pH > 6 give low absorbance readings if allowed to stand. They attribute this to deposition of the hydrous metal oxide.

Other workers^{12,13} have connected reduction in absorbance-signal for zinc, as the pH is increased, with adsorption of hydrous zinc oxides on the container walls, but some of these results have been disputed.¹⁴ Lowering of the absorbance signal with increase in pH has also been noted by Danielson *et al.*¹⁵ in their work on calcium and magnesium in serum.

If it is accepted that the lowering of the absorbance signal with increase in pH, in our work, is due to the production of hydrous metal oxide adsorbed on the vessel walls, it is of interest that the EPR signal does not change with increase in pH. This suggests that no oxidation occurs, as this would lower the EPR signal, which derives from the Mn(II) species.

Variation of EPR signal with change in ionic strength

Previous workers³ studying speciation of manganese in sea-water by use of EPR spectrometry have found it necessary to adjust the ionic strength of the test solutions. However, Millero and Schreiber¹⁶ have estimated that river water has an ionic strength of $2.09 \times 10^{-3}m$ whereas that of sea-water³ is $7.23 \times 10^{-1}m$, and we have found that for solutions of manganese(II) nitrate and perchlorate containing 0.200 mg/l. manganese at pH 3.0 ± 0.1 , the addition of up to 25 g/l. nitrate (as sodium nitrate) or perchlorate (as sodium perchlorate) produces no change in the EPR signal (Table 2). Although higher concentrations of either salt do lead to a change in the EPR peak signal, such concentrations are vastly in excess of those in freshwaters, and we conclude that ionic strength adjustments are not required for use of the EPR spectrum of $[Mn(H_2O)_6]^{2+}$ as a manganese concentration probe for fresh waters.

Variation of EPR signal with addition of possible complexing anions

Tables 3–5 indicate that the presence of inorganic anions capable of forming complexes with manganese has no appreciable effect on the EPR peak height (or width) at neutral pH, and at the levels at which

such anions are found in fresh waters, such as those in the water storage dams which we are studying in the vicinity of Brisbane, which have chloride and sulphate concentrations of ~ 30 and 5 mg/l., respectively.

The results also indicate that the presence of large amounts of chloride, sulphate and bicarbonate are required at neutral pH to change the EPR spectrum of manganese. As might be expected from the work of Callender and Bowser,⁸ sulphate is the anion most likely to form complexes (Table 4).

By comparison, the addition of humic acid to aqueous manganese perchlorate solutions produces a major change in EPR peak height (Table 6). Although our studies on dam storage waters to date support the contention of Gamble⁹ that humic acid complexation of manganese in fresh waters does not appear to be strong, its possibility is clearly demonstrated by these results. The disappearance of all six EPR peaks of manganese solutions on addition of sufficient humic acid is similar to the results obtained when aqueous solutions of manganese perchlorate are made up with progressively increasing amounts of ethanol or acetone. Figures 1 and 2 demonstrate the decrease in signal as the water molecules around the manganese(II) ion are replaced by organic solvent molecules.

Acknowledgement—The authors would like to thank the Queensland Department of Local Government for financial support of this work.

REFERENCES

1. T. M. Florence and G. E. Batley, *CRC Crit. Rev. Anal. Chem.*, 1980, **9**, 219.
2. H. Eskilsson and D. R. Turner, *Anal. Chim. Acta*, 1984, **161**, 293.
3. R. Carpenter, *Geochim. Cosmochim. Acta*, 1983, **47**, 875.
4. B. Chiswell and M. Bin Mokhtar, *Talanta*, 1986, **33**, 669.
5. B. Chiswell and G. Rauchle, *Proc. Roy. Soc. Queensl.*, 1986, **97**, 53.
6. C. F. Wells and M. A. Salam, *J. Inorg. Nucl. Chem.*, 1969, **31**, 1083.
7. K. K. Turekian, *Handbook of Geochemistry*, Vol. 1, K. H. Wedepohl (ed.), p. 297. Springer-Verlag, Berlin, 1978.

8. E. Callender and C. J. Bowser, *Freshwater Ferromanganese Deposits*, in *Handbook of Strata-bound and Stratiform Ore Deposits*, K. H. Wolf (ed.), p. 371. Elsevier, Amsterdam, 1976.
9. D. S. Gamble, C. H. Langford and J. P. K. Tong, *Can. J. Chem.*, 1976, **54**, 1239.
10. S. S. Singh, *Comm. Soil Sci. Plant Anal.*, 1977, **8**, 177.
11. M. S. Cresser and R. Hargitt, *Talanta*, 1976, **23**, 153.
12. B. V. L'vov, N. A. Orlov and E. K. Mandrazhi, *Zh. Analit. Khim.*, 1980, **35**, 894.
13. A. E. Dong, *Appl. Spectrosc.*, 1973, **27**, 124.
13. G. E. Bentley and M. L. Parsons, *ibid.*, 1974, **28**, 71.
14. B. G. Danielson, E. Pallin and M. Sohtell, *Upsala J. Med. Sci.*, 1982, **87**, 43.
16. F. J. Millero and D. R. Schreiber, *Am. J. Sci.*, 1982, **282**, 1508.

UNTERSUCHUNGEN ZUR ANWENDUNG TERNÄRER KOMPLEXE IN DER PHOTOMETRIE—IV

DAS CHELAT FeY^- ($\text{H}_4\text{Y} = \text{EDTE}$) ALS REAGENS FÜR PHENOLE

S. KOCH und G. ACKERMANN

Bergakademie Freiberg, Sektion Chemie, Lehrstuhl für Analytische Chemie, 9200 Freiberg, DDR

(Eingegangen am 6. Mai 1986. Revidiert am 5. August 1986. Angenommen am 29. Oktober 1986)

Zusammenfassung—Auf Grund theoretischer Überlegungen zur Komplexbildung phenolischer OH-Gruppen mit Metallionen und der experimentellen Untersuchung zahlreicher Reaktionsvarianten wird das Reagens FeY^- ($\text{H}_4\text{Y} = \text{EDTE}$) für Phenole empfohlen. Das Chelat FeY^- bildet mit Phenolen je nach deren Struktur farbige ternäre aber auch binäre Komplexe, welche die Ausarbeitung spektralphotometrischer Verfahren gestatten. Wie Untersuchungen zur Empfindlichkeit, Selektivität sowie Genauigkeit zeigen, handelt es sich dabei um analytisch wertvolle Reaktionen.

Summary—Both theoretical considerations and experimental investigations have shown the iron(III)-EDTA complex to be a useful reagent for phenols, many of which form strongly-coloured ternary complexes with the proposed reagent, as well as weaker binary complexes with iron(III) alone. The sensitivity, selectivity (towards phenols as a group) and reproducibility of the proposed method are such that it can be firmly recommended.

Auch in der organischen Analyse haben chemische Methoden neben der instrumentellen Analytik nach wie vor ihre Bedeutung, wobei sich wegen der außerordentlichen Vielzahl organischer Verbindungen beide Möglichkeiten in vielen Fällen nahezu ideal ergänzen. Die Spektralphotometrie nimmt in der organischen Analyse bei chemischen, klinischen bzw. biologischen Untersuchungen einen festen Platz ein, und naturgemäß finden dabei organische sowie anorganische Reagenzien—auch in Kombination—Verwendung.

Sehr häufig findet man mit anorganischen Reagenzien Oxydations- bzw. Komplexbildungsreaktionen, wobei bei letzteren von Vorteil ist, daß unter optimalen Bedingungen ein einheitliches Reaktionsprodukt auftritt. Die Anwendung von Komplexbildungsreaktionen in der organischen Analyse ist jedoch begrenzt, weil ein Großteil organischer Verbindungen keine zur Komplexbildung geeigneten Ligandatome aufweist. Folgende funktionelle Gruppen sind z.B. zur Bildung von Koordinationsverbindungen geeignet: $-\text{OH}$, $-\text{COOH}$, $-\text{NH}_2$, $-\text{SO}_3\text{H}$, $-\text{SH}$. Von den angegebenen Funktionen tritt die OH-Gruppe am häufigsten auf; sie kann bekanntlich aliphatischer, heterocyclischer oder aromatischer Natur sein.

In der vorliegenden Arbeit soll über Farbreaktionen der aromatischen Hydroxyl-Gruppe mit Eisen(III) in Gegenwart eines geeigneten Zweitliganden unter Bildung ternärer Komplexe berichtet werden. Wie die Untersuchungen zeigen, ist diese Variante vom analytischen Standpunkt aus den bisherigen Reaktionen mit einfachen binären Kom-

plexen überlegen. In diesem Zusammenhang ist interessant, daß im Gegensatz zur anorganischen Analyse¹⁻⁴ in der organischen Analyse,⁵⁻⁷ ternäre Komplexe bisher kaum Anwendung gefunden haben.

EXPERIMENTELLER TEIL

Die spektralphotometrischen Messungen erfolgten mit einem Beckman Spektralphotometer DU bzw. Zeiss Specord M40 gegen Lösungsmittel. Zur Einstellung der pH-Werte (MV 87, VEB Präcitronic Dresden) dienten Perchlorsäure sowie Ammoniak geeigneter Konzentrationen.

Alle Messungen erfolgten in Wasser bei Zimmertemperatur und $I = 0,1$ (Natriumperchlorat). Die Proben wurden in der Reihenfolge $\text{Na}_2\text{H}_2\text{Y}$, NaClO_4 , $\text{pH} \approx 10$, Fe(III) , Phenol hergestellt und sofort gemessen.

Chemikalien

Für die Metalle standen gravimetrisch kontrollierte Stammlösungen (1M) zur Verfügung. Alle verwendeten Chemikalien waren handelsübliche Produkte. Die Reinheit der unkristallisierten Phenole wurde durch Schmelzpunkt bzw. Elementaranalyse überprüft.

Farbreaktionen der aromatischen OH-Gruppe

Phenole bilden mit sehr vielen Reagenzien farbige Reaktionsprodukte, welche zwar empfindliche, aber wenig selektive Reaktionen gestatten.⁸ Bei der photometrischen Bestimmung mit Hilfe organischer Reagenzien⁹ treten die Phenole hauptsächlich als Kupplungskomponente bei Diazotierungsreaktionen auf, wobei eine große Zahl an Diazoniumsalzen vorgeschlagen wird. Umfangreiche systematische Untersuchungen¹⁰ mit vier zumeist benutzten organischen Reagenzien machen jedoch deutlich, daß es bis jetzt kein universelles Reagens für die funktionelle OH-Gruppenanalyse gibt.

Bei den anorganischen Phenol-Reagenzien¹¹ dominieren neben einigen weniger bedeutsamen Reaktionstypen wie Oxydation, Nitrosierung, Nitrierung und Alkalisierung eindeutig Komplexbildungsreaktionen. Zur analytischen Charakterisierung von Phenolen haben praktisch nur Koordinationsverbindungen mit Fe(III), Ti(IV) und U(VI) aus verschiedenen Gründen Bedeutung erlangt. Dabei beruhen die bekanntgewordenen Reaktionen meistens auf Komplex- bzw. Chelatbildung mit Eisen(III)-Salzen. Die Farbreaktion von Eisen(III) mit phenolischen Verbindungen wurde von Runge^{12,13} schon im Jahre 1834 beschrieben und wird seitdem sehr häufig zum Nachweis sowie zur photometrischen Bestimmung verschiedener Phenolverbindungen angewandt.^{11,14,15}

Bei der sogenannten Eisenchloridreaktion handelt es sich um eine wenig selektive Farbreaktion mit den meisten ein- und mehrwertigen Phenolen bzw. Naphtholen. Ebenfalls reagieren unter anderem Enole, Hydroxamsäuren, Oxime, Hydroxyderivate von 5,6-gliedrigen *N*-Heterocyclen, aliphatische OH-Gruppen, Carbonsäuren sowie Aminosäuren. Störungen treten weiterhin durch Anwesenheit von Reduktionsmitteln bzw. Komplexbildnern auf, und auch das Medium kann einen deutlichen Einfluß auf die Farbreaktionen ausüben.

Aufgrund eingehender Untersuchungen^{16,17} liegen in Systemen Eisen(III)/Phenol komplizierte Mechanismen vor. Bei der isolierten OH-Gruppe laufen nach der schnellen Komplexbildung langsame Hydrolyse- und Polykondensationsvorgänge ab, welche zu unerwünschten polymeren Eisen(III)-Species führen. Hinzu kommt noch, daß Polyphenole—insbesondere mit *o*-Position—durch Eisen(III) leicht zu unbekanntem Oxydationsprodukten reagieren. Nachgewiesen ist in diesem Zusammenhang¹⁸ der oxydative Zerfall von 1:1-Chelaten einiger *o*-Diphenole unter Bildung von Eisen(II).

Genannte Störungen müssen zwangsläufig dazu führen, daß die klassische Eisenchlorid-Reaktion keine streng reproduzierbaren Ergebnisse liefert. Wie man der Literatur entnehmen kann, hat es in der Vergangenheit nicht an Versuchen gefehlt, die oben gezeigten Schwierigkeiten durch systematische Untersuchungen,¹⁹ oder neue Reaktionsvarianten zu umgehen. Die Bemühungen führten zwar zur Verbesserung einiger Verfahren prinzipiell konnten aber die Probleme so nicht gelöst werden.

UNTERSUCHUNGSERGEBNISSE

Phenole, besonders mit der *o*-Dihydroxy-Gruppierung, reagieren mit einer großen Zahl von Metallkationen,²⁰ wobei polare M—O-Bindungen bevorzugt werden. Farbige Komplexe entstehen dabei nur dann, wenn es sich um Metalle mehrerer Valenzmöglichkeiten mit nicht vollständig besetzten *d*-Orbitalen handelt.²¹

Man findet nur für Fe(III), U(VI) sowie Ru(III) universelle Komplexbildung, d.h., nur diese drei Ionen reagieren mit ein- und mehrwertigen Phenolen. Da bei Ru(III) aber wenig intensive Farbreaktionen auftreten, kommen zur Anwendung praktisch nur die Kationen Fe³⁺ und UO₂²⁺ in Frage.

Zur Ausschaltung der bereits diskutierten Störungen (Hydrolyse und Oxydation) sind ternäre Komplexbildungsreaktionen geeignet. Aus komplexchemischen Gesichtspunkten bieten sich dafür von vielzähligen Chelatbildnern besonders α -Aminopolycarbonsäuren (APC) an, weil sie wegen der Ligatortome O und N universelle Chelatbildner darstellen und die entsprechenden Chelate "freie" Koordinationstellen aufweisen können. Als nächstes sollen deshalb Ergebnisse zur Komplexbildung von Fe³⁺ und UO₂²⁺ mit Phenol (isolierte OH-Gruppe) sowie Tiron (*o*-OH-Gruppe) in Gegenwart der Aminopolycarbonsäuren NTE (H₃X, vierzählig $z = 4$) bzw. EDTE (H₄Y, sechszählig, $z = 6$) beschrieben werden.

Das Eisen(III)-Ion reagiert in Lösung mit den Anionen der NTE oder EDTE zu äußerst stabilen Chelaten FeX bzw. FeY⁻.^{22,23} Die pH-Kurven $E = f(\text{pH})$ der Systeme Fe(III)/NTE (EDTE)/Phenol (rote Lösungen, $C_{\text{Fe}} = 10^{-3}M$, $p = C_{\text{R}}/C_{\text{Fe}} = 80$, $s = C_{\text{APC}}/C_{\text{Fe}} = 1$, $\lambda = 490 \text{ nm}$) weisen bei pH = 5,5 (NTE) und pH = 8,6 (EDTE) Maxima auf, wo optimale Komplexbildung vorliegt.²⁴ Aus den pH-Kurven^{25,26} der Systeme Fe(III)/NTE (EDTE)/Tiron [blaue (violette) Lösungen, $C_{\text{Fe}} = 2 \times 10^{-4}M$ ($5 \times 10^{-4}M$), $p = 50$ (40), $s = 1$, $\lambda = 570$ (555) nm] findet man bei pH = 4,1 (NTE) bzw. pH = 4,3 (EDTE) optimale Komplexbildung. Weiterhin liegt in beiden Systemen bei pH > 7 ein einheitliches rotes Chelat ($\lambda_{\text{max}} = 480 \text{ nm}$) vor.

Zur Charakterisierung der einzelnen Species dienen Absorptionsspektren der Systeme im sichtbaren Bereich. Folgende Beziehungen gelten dabei:

$$\lambda_{\text{max}} \left(\text{Fe/APC/Phenol} \right) < \lambda_{\text{max}} \left(\text{Fe/Phenol} \right)$$

490 nm 560 nm

ternärer Komplex

$$\lambda_{\text{max}} \left(\text{Fe/APC/Tiron} \right) > \lambda_{\text{max}} \left(\text{Fe/Tiron} \right)$$

570 (555) nm 560 nm

(<) ternärer Komplex

$$\lambda_{\text{max}} \left(\text{Fe/APC/Tiron} \right) = \lambda_{\text{max}} \left(\text{Fe/Tiron} \right)$$

480 nm 480 nm

binärer Komplex
(pH = 8,0)

Auf Grund der angegebenen Kriterien⁴ existieren in der Lösung mit beiden Phenolen ternäre APC-Komplexe. Mit dem zweizähligen Ligand Tiron kommt es im alkalischen Milieu auch in Gegenwart einer APC noch zur Bildung binärer Systeme.

Uranylionen bilden in wäßriger Lösung mit Aminopolycarbonsäuren wenig stabile Chelate,²⁷ wobei für hohe Ligandenüberschüsse verschiedene Species nachgewiesen werden konnten.²⁸ Nach den

Untersuchungen der entsprechenden Systeme liegen trotz der hohen Koordinationszahl für UO_2^{2+} von $K_z = 6$ nur binäre Uraniumkomplexe mit Phenol (Tiron) vor.

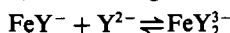
Die experimentellen Ergebnisse zur Komplexbildung von Fe^{3+} und UO_2^{2+} mit Phenolen in Gegenwart von APC machen deutlich, daß Eisen(III) als analytisches Reagens besonders geeignet ist. Mit dem Eisen(III)-Ion (hohe Ladungsdichte, unvollständig gefüllte d -Orbitale, $K_z = 6$) existieren ternäre Teilchen, welche analytisch wertvolle Reaktionen versprechen. Bei dem Chelat FeX ist wegen der zwei "freien" Koordinationsstellen von Nachteil, daß schon in schwach saurer Lösung Stufenkomplexbildung (FeX_n) sowie starke Komplexhydrolyse [$\text{FeX}(\text{OH})_n$] auftritt ($n = 1, 2$).²² Außerdem sind hier auch—wie orientierende Versuche zeigen—wenig selektive Reaktionen zu erwarten.

Andere hochzählige Zweitliganden wie 1,2-Diaminocyclohexantetraessigsäure ($z = 6$) und Diethylentriaminpentaessigsäure ($z = 8$) bilden zwar auch ternäre Species.²⁹ Unter optimalen Bildungsbedingungen ($\text{pH}_{\text{max}} \approx 10$) kommt es jedoch mit vielen Phenolen zur Oxydation durch Luftsauerstoff.

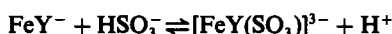
Nach den hier vorliegenden Ergebnissen muß man somit das Eisen(III)-Chelat $\text{FeY}(\text{H}_2\text{O})$, das eine freie Carboxylatgruppe hat ($\text{EDTE} = \text{H}_4\text{Y}$), als analytisches Reagens für ein- und mehrwertige Phenole ansehen. Das Teilchen stellt dabei eine offene Chelatstruktur mit fünfzählig wirksamen Liganden dar, wo eine durch Wasser besetzte Koordinationslücke auftritt.^{30,31} Auf Grund der großen Stabilität des Chelates treten Zersetzungsreaktionen erst bei $\text{pH} > 10$ und Protolyse vorwiegend nach



erst im alkalischen Milieu auf.²³ Eine eventuelle Blockierung der Koordinationslücke durch Carboxylatgruppen überschüssiger EDTE-Liganden kann ausgeschlossen werden, da die Bildung von FeY_2^{3-} zwar möglich ist, das Gleichgewicht



mit $K_1 = 11,6$ aber praktisch vollständig auf der Seite von FeY^- liegt.³² Bei dem Teilchen FeY^- handelt es sich nach Pearson um eine bevorzugt harte Säure,³³ was die Reaktionen mit phenolischen Liganden als harte Basen begünstigt. Von Vorteil ist weiterhin, daß FeY^- ($\text{FeY}^{2-} \rightleftharpoons \text{FeY}^- + e$, $E^0 = 0,117 \text{ V}^{23}$) gegenüber $\text{Fe}^{3+} = 0,77 \text{ V}$) aufgrund der Abschirmung durch Y^{4-} nur ein äußerst schwaches Oxydationsmittel darstellt. Diese Tatsache macht es möglich, in der praktischen Analyse Reduktionsmittel zur Verhinderung einer Oxydation der Phenole durch Luftsauerstoff einzusetzen. Als besonders geeignet dafür erweist sich Natriumsulfit,³⁴ welches FeY^- nicht reduziert, sondern einen Verschieden-Ligand-Komplex nach



bildet.

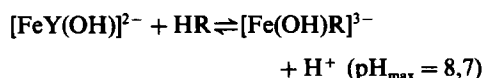
Wie aus den Eigenschaften dieses Teilchens abzuleiten ist, wird die Komplexbildung mit Phenolen durch kleine Überschüsse an Natriumsulfit nicht gestört. Schließlich läßt sich nachweisen, daß Lösungsmiteleinflüsse durch Methanol bis 50 Vol.% auf die ternäre Komplexbildung unbedeutend sind. Neben einer geringen bathochromen Verschiebung von λ_{max} findet man eine leichte Erhöhung für pH_{max} .

Reaktionsgleichgewichte

Im folgenden soll die Komplexbildung von FeY^- mit einigen typischen Phenolen (R) näher beschrieben werden. Die Charakterisierung der Systeme $\text{Fe}(\text{III})/\text{EDTE}/\text{R}$ erfolgt mit Hilfe spektralphotometrischer und elektrophoretischer Methoden, wobei experimentell ermittelte Kurven $E = f(\text{pH})$ sowie $E = f(C_R)$ nach speziellen Programmen LITRAFAL³⁵ analysiert werden. Zur Ermittlung der Komplexladungen dient hierbei die Papierelektrophorese.³⁶ Die nachstehenden Gleichgewichte gelten für Systeme mit Ligandenüberschuß ($C_{\text{Fe}} = 10^{-3} \text{ M}$, $C_R/C_{\text{Fe}} = 100$, $C_Y/C_{\text{Fe}} = 5$).

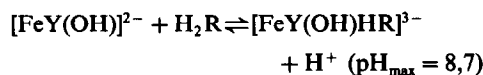
Einwertige Phenole

Phenol (HR)³⁷

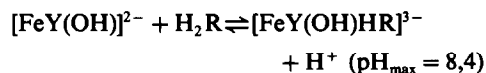


Zweiwertige Phenole

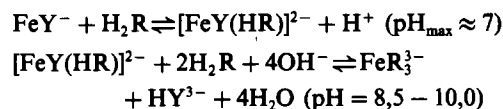
Hydrochinon (H_2R)³⁸



Resorcinol (H_2R)³⁸

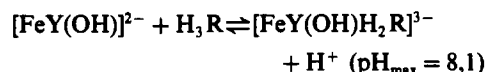


Brenzcatechin (H_2R)³⁹



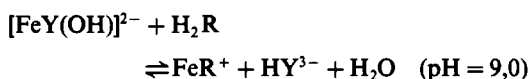
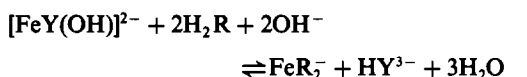
Dreiwertige Phenole

Phloroglucinol (H_3R)⁴⁰



Bei der Bildung der ternären Komplexe mit isolierter OH-Gruppe (Phenol, Hydrochinon, Resorcinol sowie Phloroglucinol) und der Hydrolyseform $[\text{FeY}(\text{OH})]^{2-}$ handelt es sich um eine innerkomplexe Verdrängungsreaktion, dabei wird eine Carboxylatgruppe des Y^{4-} durch den Ligand R-O^- aus der Koordinationsphäre verdrängt. Wie die Untersuchungen zeigen, bilden sich die Species $[\text{FeY}(\text{OH})\text{H}_n\text{R}]^{3-n}$ ($n = 0, 1, 2$) auch in äquimolaren Lösungen sowie in Systemen mit FeY^- -Überschuß.

Die Bildung des ternären Komplexes mit der *o*-OH-Gruppierung (Brenzcatechin) stellt eine Anlagerungsreaktion unter Verdrängung von Wasser dar. Genanntes Teilchen existiert aber nur in einem sehr engen pH-Bereich, und schon in schwach alkalischer Lösung kommt es zur Abspaltung von Y^{4-} . Da der ternäre Komplex außerdem zeitlich wenig stabil ist, kommen hier zur analytischen Nutzung nur die entsprechenden binären Chelate in Frage. Wie die Untersuchungen zeigen, liegen dann in Lösungen mit FeY-Überschuß folgende Reaktionen vor:



Empfindlichkeit

Die Absorptionsbanden der ternären Eisen(III)-Komplexe im sichtbaren Spektralbereich stellen Charge-Transfer-Banden dar, weil die Spektren durch Liganden- bzw. Zentralion-Übergänge nicht erklärbar sind und die Extinktionskoeffizienten in der dafür typischen Größenordnung liegen. Durch die Abschirmung des Kationenfeldes vom Zweitliganden kommt es zur hypsochromen Verschiebung von λ_{max} gegenüber den entsprechenden binären Species FeR. Das bedeutet aber, durch die ternäre Komplexbildung tritt keine Erniedrigung des Extinktionskoeffizienten und damit der Empfindlichkeit auf. In Tabelle 1 sind dazu die optischen Eigenschaften zusammengestellt. Wie die Werte der molaren Extinktionskoeffizienten ($\epsilon_{\text{max}} \approx 2 \times 10^3 \text{ l.mole}^{-1} \text{ cm}^{-1}$) deutlich machen, sind somit empfindliche analytische Reaktionen zur Bestimmung von Phenolen möglich.

Selektivität

Bei den hier beschriebenen Reaktionen mit dem Reagens $[\text{FeY}(\text{H}_2\text{O})]^-$ unter Bildung ternärer Komplexe findet man gegenüber der klassischen Eisenchloridreaktion eine höhere Selektivität, weil die Anlagerung des mehrzähligen Zweitliganden eine deutliche Änderung der Koordinationsverhältnisse (Neutralisation von Ladungen, weniger "freie" Koordinationsstellen) mit sich bringt. Im weiteren soll nun über die Ergebnisse zur Selektivität der FeY-Gruppe ausführlicher berichtet werden. Die Charakterisierung der Farbreaktionen erfolgt hierbei vi-

suell für Systeme ($C_{\text{Fe}} = 10^{-3} \text{ M}$, $p = 100$, $s = 5$) mit Ligandenüberschuß im pH-Bereich 2 bis 10, und zum spektralphotometrischen Nachweis ternärer Komplexbildung dienen die entsprechenden Kriterien.

Phenole. Die Komplexbildung ist hierbei an negative Liganden R-O^- gebunden. Bei veresterten Verbindungen (Anisol, Brenzcatechindiethylester) treten deshalb keine Farbreaktionen auf.

Für die isolierte OH-Gruppe findet man bei vielen Verbindungstypen (Kresole, Xylenole, halogensubstituierte Produkte u.a.) ternäre Komplexbildung, wobei das Absorptionsmaximum je nach der Art und Zahl der Substituenten verschoben ist. Untersuchungen an Nitroverbindungen (*o*-Nitrophenol, 2,4-Dinitrophenol, Pikrinsäure) zeigen dagegen, daß mit diesen Liganden keine Farbreaktionen auftreten. Offensichtlich bewirken hier durch die Nitrogruppen hervorgerufene Induktionseffekte eine deutliche Schwächung der Fe-O-Bindung. Bei *p*-Nitrophenol tritt aufgrund der Struktur eine abgeschwächte Positivierung des Ligatoratoms auf, weshalb diese Verbindung ternäre Komplexbildung zeigt. Interessant sind in diesem Zusammenhang einige Liganden, welche in *o*-Position zur OH-Gruppe einen Substituenten aufweisen. Während *m*-Aminophenol sowie *p*-Aminophenol ternäre Komplexe bilden, beobachtet man mit *o*-Aminophenol (zweizählig mit "freiem" *N*-Ligatoratom) eine Verdrängung von Y^{4-} unter Bildung farbiger binärer Chelate. Phenole mit der Carboxylgruppe in *o*-Stellung (Salicylsäure, 3,5-Dinitrosalicylsäure, 5-Sulfosalicylsäure) zeigen dagegen keine Farbreaktionen. Die Ursache dafür dürfte in der Blockierung der komplexbildenden R-O^- Gruppe durch ein Wasserstoffion liegen, welches wegen einer Wasserstoffbrückenbindung zur Carboxylatgruppe sehr fest gebunden ist.

Auch andere phenolische Verbindungen mit der *o*-OH-Gruppierung (Pyrogallol, Gallussäure, Pyrogallolcarbonsäure) reagieren nach dem für Brenzcatechin angegebenen Mechanismus unter Bildung ternärer und binärer Species. Ist aber eine der R-O^- -Gruppen durch Veresterung blockiert (Guajacol), so ist die Verdrängung des Zweitliganden nicht mehr möglich und man findet nur noch ternäre Komplexbildung. Bei Verbindungen mit stark elektrophilen Substituenten (Brenzcatechin-3,5-disulfonsäure, 4-Nitrobrenzcatechin) treten dagegen praktisch nur die entsprechenden binären Komplexe FeR_3 auf. Wegen der Natur dieser Substituenten kommt es zur leichten Abspaltung der Protonen des *o*-Diphenols, woraus eine frühzeitige Abspaltung des Y^{4-} und Anlagerung des Erstliganden resultiert.

Naphthole. Naphthole als Träger aromatischer Hydroxylgruppen geben unter geeigneten Bedingungen Farbreaktionen, wobei die bereits beschriebenen Prinzipien Gültigkeit haben. Die isolierte OH-Gruppe zeigt in schwach alkalischer Lösung die Bildung ternärer Komplexe. Auch hier üben die in Nachbarstellung befindlichen "freien" Ligatoratome einen Einfluß auf den Mechanismus aus. Mit dem

Tabelle 1. Optische Eigenschaften von ternären Komplexen mit EDTE als Zweitligand

Erstligand	λ_{max} , nm	ϵ_{max} , $\text{l.mole}^{-1} \cdot \text{cm}^{-1}$
Phenol	495 (rot)	$2,0 \times 10^3$
Hydrochinon	545 (lila)	$1,8 \times 10^3$
Resorcinol	500 (rot)	$2,0 \times 10^3$
Brenzcatechin	540 (lila)	$2,0 \times 10^3$
Phloroglucinol	505 (rot)	$1,7 \times 10^3$

zweizähligen Ligand 8-Hydroxychinolin beispielsweise kommt es schon in schwach saurer Lösung zur Abspaltung des Y^{4-} , und die Bildung eines ternären Komplexes ist so ausgeschlossen. Bei der *o*-OH-Gruppierung liegt in neutraler Lösung zunächst ternäre Komplexbildung vor, im alkalischen Milieu kommt es wie bei *o*-Diphenolen zur Zersetzung des Komplexes unter Bildung eines binären Chelates FeR_3 .

Enole. Ascorbinsäure aus der Gruppe der Endiole zeigt im Neutralen eine schwache blaugrüne Färbung, welche innerhalb weniger Minuten verblaßt. Im Falle von aliphatischen Enolen (Acetessigester, Acetylaceton) kann wegen der Keto-Enol-Tautomerie die saure Enolgruppe nach Abspaltung eines Protons koordinativ wirksam werden. Acetessigester gibt keine Farbreaktion, obwohl Eisen(III) im Sauren rote Komplexe bildet. Offensichtlich ist hier die wirksame Konzentration der Enolform zu gering, um mit FeY^- zu reagieren. Mit Acetylaceton findet man dagegen wegen der leichteren Enolisierung in alkalischer Lösung orangefarbene Species ($\lambda_{max} = 445$ nm). Wie die Untersuchungen zeigen, handelt es sich hierbei um einen komplizierten Reaktionsmechanismus unter gleichzeitiger Bildung verschiedener Komplexe. Auch bei heterocyclischen Verbindungen mit Keto-Enol-Tautomerie (Barbitursäure, Antipyrin) zeigt sich ein Selektivitätszuwachs. Während mit Eisen(III) Farbreaktionen auftreten, können sie mit FeY^- nicht beobachtet werden.

Hydroxamsäuren. Hydroxamsäuren (Acetyl-, Capronylhydroxamsäure) reagieren mit FeY^- gegenüber Fe^{3+} erst in alkalischer Lösung mit Verzögerung unter Bildung orangefarbener Lösungen. Wie zu erwarten, kommt es aufgrund der Ligandenstruktur mit einem zusätzlichen "freien" Ligandatom unter Verdrängung des Y^{4-} zur Bildung von stabilen 5-gliedrigen Chelaten.

Oxime. Bei der Reaktion von Eisen(III) mit Oximen (Diacetyldioxim, Benzoinoxim, Cyclohexanonoxim) treten farbige Reaktionsprodukte auf. Die analytische Gruppe FeY^- reagiert dagegen nicht mit Oximen, so daß hier keine Störung vorliegt.

Heterocyclen. Mit Heterocyclen, welche ungeladene Heteroatome als Donator aufweisen (Pyridin, Furan, Thiophen), beobachtet man keine Reaktionen. Erst wenn eine Verbindung mit quasiaromatischer OH-Gruppe vorliegt, treten Farbreaktionen auf. Am Beispiel der Kojisäure [5-Hydroxy-2-(hydroxymethyl)-4-pyron] läßt sich zeigen, daß in schwach alkalischer Lösung eine unvollständige Verdrängungsreaktion abläuft, wobei sich das binäre Chelat FeR_3 ($\lambda_{max} = 460$ nm, gelb-orange) bildet. Die Ursache liegt auch hier wieder in einem "freien" Ligandatom, welches sich am γ -Pyrin in *o*-Stellung zur Hydroxylgruppe befindet.

Aliphatische OH-Gruppen. Es ist seit langem bekannt, daß aliphatische Hydroxylverbindungen mit Eisen(III)-chlorid eine gelbe Farbreaktion zeigen.

Zum Mechanismus dieser Reaktion findet man jedoch in der Literatur keine Angaben. Da bei den experimentellen Bedingungen Oxydations- und Komplexbildungsreaktionen mit der OH-Gruppe ausgeschlossen werden können, bilden sich hierbei unter dem Einfluß der organischen Verbindungen durch Abnahme der Dielektrizitätskonstante wahrscheinlich verstärkt Komplexe der Art $FeCl_2^n$. Dafür spricht die Beobachtung, daß mit Eisen(III)-sulfat die besprochene Farbreaktion nicht auftritt und andere organische Verbindungen (Essigsäureethylester, Aceton u.a.) ähnlich wirken. Wie die Untersuchungen weiterhin zeigen, gibt FeY^- mit der aliphatischen OH-Gruppe (Methanol, Butanol, Benzylalkohol, Glycerin u.a.) keine Farbreaktionen.

Carbonsäuren und Aminosäuren. Zu einer häufigen Störung der Eisenchlorid-Reaktion kommt es in Anwesenheit von Carbonsäuren bzw. Aminosäuren. In Gegenwart genannter Verbindungen laufen Komplexbildungsreaktionen mit farbigen Species ab. Auch in diesem Fall bleiben die entsprechenden Reaktionen (Essigsäure, Benzoesäure, Glykokoll u.a.) mit FeY^- wegen der schon beschriebenen Gründe aus.

Weitere Verbindungen. Neben den besprochenen Verbindungen gibt es noch einige, welche die Eisenchlorid-Reaktion aufgrund einer Redox-Reaktion stören. So werden z.B. viele aromatische Amine von Eisen(III) zu dunklen Produkten oxydiert. All diese Störungen sind mit FeY^- aufgehoben, weil es sich hierbei nur um ein sehr schwaches Oxydationsmittel handelt.

Schließlich soll noch etwas zur Reaktion organischer Schwefelverbindungen gesagt werden, da auch durch diese Substanzen erhebliche Störungen bei der klassischen $FeCl_3$ -Reaktion auftreten können. Das Teilchen FeY^- bildet mit Neutralliganden des Typs $R-S-R'$ keine farbigen Species. Bei Verbindungen $R-SH$ treten dagegen Farbreaktionen auf.³³

Außer Thiophenol bilden die Thioliganden zeitlich wenig stabile Komplexe, welche sich nach einem Redoxmechanismus zu farblosen Reaktionsprodukten zersetzen.

Präzision

Es wurde schon darauf hingewiesen, daß die klassische Eisenchlorid-Reaktion durch Konkurrenzreaktionen (Hydrolyse, Oxydation) gestört wird und somit wenig reproduzierbare Ergebnisse liefert. Durch ternäre Komplexbildung lassen sich dagegen beide Störungen ausschalten. Die im weiteren mitgeteilten experimentellen Ergebnisse sollen das veranschaulichen.

System Eisen(III)/Phenol

$$C_{Fe} = 10^{-3} M, p = 100,$$

$$pH = 2,30, \lambda = 560 \text{ nm}$$

Tabelle 2. Eichfunktionen ($d = 1$ cm) $A = bc + a$ (c in mole/l.) zur Bestimmung von Phenolen

Analyt	pH _{max}	λ_{max} , nm	b	a	r
Phenol	8,0	520	68,8	0,025	1,000
Hydrochinon	8,0	560	175,8	-0,002	0,999
Resorcinol	7,8	520	143,0	0,040	0,998
Brenzcatechin	9,0	610	1275	0,014	0,996
Phloroglucinol	7,4	515	192,4	0,002	0,999

System Eisen(III)/EDTE/Phenol

$$C_{\text{Fe}} = 10^{-3} M, p = 100,$$

$$s = 5, \text{pH} = 8,70, \lambda = 495 \text{ nm}$$

Wie Extinktions- sowie Potentialmessungen an den entsprechenden Lösungen zeigen, ist das System Eisen(III)/Phenol gegenüber Eisen(III)/EDTE/Phenol zeitlich sehr instabil. Aus Wiederholungsmessungen der Extinktion ($f = 10$ Freiheitsgrade) ergeben sich dazu folgende Variationskoeffizienten: $V(\text{Fe}/\text{Phenol}) = 12,6\%$; $V(\text{Fe}/\text{EDTE}/\text{Phenol}) = 0,2\%$. Der sehr gute Wert von $0,2\%$ macht deutlich, daß mit dem Reagens FeY^- Bestimmungen mit hoher Präzision möglich sind. Nach den vorliegenden Untersuchungen trifft das auch auf zwei- und dreiwertige Phenole zu.

Zur praktischen Anwendung

Bei der analytischen Anwendung von FeY^- sind noch einige praktische Hinweise von Bedeutung, welche an dieser Stelle kurz behandelt werden sollen.

Als Eisen(III)-Reagens ist eine $1 M$ Stammlösung [$\text{Fe}(\text{NO}_3)_3$, $0,1 M$ an HClO_4] geeignet. Nach UV-spektroskopischen Untersuchungen an Modelllösungen ($C_{\text{R}} = 8 \times 10^{-4} M$, $C_{\text{NaNO}_3} = 4 \times 10^{-2} M$) können dabei eventuelle Nitrierungsreaktionen mit Phenolen (isolierte OH-Gruppen sowie o -OH-Gruppierung) ausgeschlossen werden.

Für das Reagens FeY^- ist von Bedeutung, daß Systeme mit EDTE-Überschuß $s = 5$ gegenüber verdünnter Natronlauge (pH-Einstellung) noch stabil sind. Die einzelnen Proben werden deshalb am besten in der Reihenfolge $\text{Na}_2\text{H}_2\text{Y}$ (pH = 10), Eisen(III), Analyt hergestellt, wobei $s = 5$ einzuhalten ist. Während nun für die qualitative Analyse besonders Systeme mit Phenol-Überschuß ($p > 1$) geeignet sind, kommen für die photometrische Bestimmung Systeme mit FeY^- ($p < 1$) und auch Analyt-Überschuß in Frage. Die erste Variante ergibt eine lineare Abhängigkeit $A = bc + a$ der Extinktion A von der Konzentration c und ist für kleine Gehalte geeignet. Für einige typische Phenole sind die durch Regression erhaltenen Eichfunktionen in Tabelle 2 enthalten. Man sieht an den linearen Korrelationskoeffizienten r sofort, daß bei allen Verbindungen eine strenge lineare Verbundenheit vorliegt.

Bei der zweiten Variante, welche zur Bestimmung hoher Gehalte geeignet ist, liegt wegen des Überschusses an Analyt kein linearer Zusammenhang vor.

Die Eichfunktionen $E = f(c)$ stellen gekrümmte Kurven dar und lassen sich am besten durch ein Polynom zweiten Grades, $P = a_0 + a_1c + a_2c^2$, beschreiben.

LITERATUR

1. A. K. Babko, *Talanta*, 1968, **15**, 721.
2. I. P. Alimarin und V. I. Shlenskaya, *Pure Appl. Chem.*, 1970, **21**, 461.
3. A. T. Pilipenko und M. M. Tananaiko, *Talanta*, 1974, **21**, 501.
4. S. Koch, *Z. Chem.*, 1982, **22**, 317.
5. A. J. Nazarenko und I. V. Pyatnitski, *Zh. Analit. Khim.*, 1978, **33**, 1860.
6. V. F. Toropova, S. G. Selyaunva und L. A. Anisurova, *ibid.*, 1983, **38**, 1066.
7. N. Burger und V. Karas-Gašporec, *Talanta*, 1984, **31**, 169.
8. P. Buryan, J. Mitera, V. Kubelka und J. Macák, *Chem. Listy*, 1979, **73**, 161.
9. Z. J. Vejdělek und B. Kakáč, *Farbreaktionen in der spektralphotometrischen Analyse organischer Verbindungen*, Band I, Fischer Verlag, Jena, 1969.
10. P. Koppe, F. Dietz, J. Traud und Ch. Rübelt, *Z. Anal. Chem.*, 1977, **285**, 1.
11. Z. J. Vejdělek und B. Kakáč, *Farbreaktionen in der spektralphotometrischen Analyse organischer Verbindungen*, Band II, Fischer Verlag, Jena, 1973.
12. F. F. Runge, *J. Prakt. Chem.*, 1834, **1**, 22.
13. *Idem*, *Pogg. Ann.*, 1834, **31**, 65.
14. S. Veibel, *The Determination of Hydroxyl Groups*, S. 13, Academic Press, New York, 1972.
15. *Idem*, *Analytik organischer Verbindungen*, S. 56, Akademie-Verlag, Berlin, 1960.
16. G. Ackermann und D. Hesse, *Z. Anorg. Allgem. Chem.*, 1969, **367**, 243.
17. L. Sommer, *Z. Anal. Chem.*, 1962, **187**, 7.
18. G. Ackermann und D. Hesse, *Z. Anorg. Allgem. Chem.*, 1969, **368**, 25.
19. P. H. Gore und P. J. Newman, *Anal. Chim. Acta*, 1964, **31**, 111.
20. P. Pfeiffer, *Angew. Chemie*, 1940, **53**, 93.
21. L. Sommer, *Acta Chim. Acad. Sci. Hung.*, 1962, **33**, 23.
22. G. Schwarzenbach und J. Heller, *Helv. Chim. Acta*, 1951, **34**, 1889.
23. *Idem*, *ibid.*, 1951, **34**, 576.
24. S. Koch und G. Ackermann, *Z. Anorg. Allgem. Chem.*, 1976, **420**, 85.
25. *Idem*, *ibid.*, 1973, **400**, 21.
26. *Idem*, *ibid.*, 1973, **400**, 29.
27. G. Schwarzenbach und H. Flaschka, *Die komplexometrische Titration*, S. 183. Enke Verlag, Stuttgart, 1965.
28. S. Koch und G. Ackermann, *Z. Anorg. Allgem. Chem.*, 1982, **494**, 196.
29. *Idem*, *Z. Chem.*, 1976, **16**, 196.
30. G. Schwarzenbach, *Helv. Chim. Acta*, 1949, **32**, 839.
31. R. H. Nuttall und D. M. Stalker, *Talanta*, 1977, **24**, 355.
32. S. Koch und G. Ackermann, *Z. Anorg. Allgem. Chem.*, 1986, **537**, 219.

33. *Idem, ibid.*, 1985, **520**, 203.
34. *Idem, Z. Chem.*, 1984, **24**, 265.
35. S. Koch, P. Weber und G. Ackermann, *Chem. Anal. (Warsaw)*, 1978, **23**, 563.
36. S. Koch und G. Ackermann, *Z. Chem.*, 1976, **16**, 237.
37. *Idem, ibid.*, 1983, **23**, 231.
38. *Idem, ibid.*, 1985, **25**, 444.
39. *Idem, ibid.*, 1986, **26**, 181.
40. *Idem, ibid.*, 1983, **23**, 436.

KINETIC SPECTROPHOTOMETRIC DETERMINATION OF NANOGRAM LEVELS OF MANGANESE BY USE OF THE SALICYLALDEHYDE GUANYLHYDRAZONE-HYDROGEN PEROXIDE SYSTEM

F. SALINAS, J. J. BERZAS NEVADO and P. VALIENTE

Department of Analytical Chemistry, Faculty of Sciences University of Extremadura, 06071 Badajoz, Spain

(Received 26 March 1986. Revised 22 July 1986. Accepted 22 October, 1986)

Summary—A kinetic method is described for determining trace amounts of manganese(II), based on its catalytic effect on the oxidation of salicylaldehyde guanylhydrazone by hydrogen peroxide. The reaction is followed spectrophotometrically by measuring the rate of change of absorbance at 505 nm. The calibration graph is linear in the range 8–80 $\mu\text{g/l}$. with a relative error of $\pm 1\%$. The method has been applied to the determination of manganese in various samples.

In recent years, many kinetic methods have been described for the determination of manganese(II), based on its catalytic effect on the oxidation of organic compounds by hydrogen peroxide. Several Schiff's bases, including thiosemicarbazones¹⁻⁵ and pyridilhydrazones⁶ have been used for this purpose.

Guanylhydrazones have not received extensive study as analytical reagents, but dimedone bisguanylhydrazone has been used for the kinetic spectrophotometric determination of copper.⁷ In the present work, salicylaldehyde guanylhydrazone (SAG) is employed for the first time in a kinetic system, based on its oxidation by hydrogen peroxide, catalysed by manganese(II). The analytical properties of SAG and a spectrophotometric method for determining iron(II) were described earlier.⁸

Manganese(II) reacts with SAG in basic medium to give a yellow complex, which is probably an Mn(III) complex because the colour is slow to appear and the reaction is not observed when SAG and Mn(II) solutions are mixed under an atmosphere of nitrogen. The absorption spectrum of the yellow complex shows one absorption band between 380 and 440 nm, with $\lambda_{\text{max}} = 400$ nm.

The rate of complex formation is increased by the addition of hydrogen peroxide, but a new reaction is observed. SAG undergoes oxidation by hydrogen peroxide [catalysed by manganese(II)], producing a red colour. This reaction is suitable for a spectrophotometric kinetic determination of trace amounts of manganese, in which the rate of change of absorbance at 505 nm is measured. This paper describes a new, sensitive and selective kinetic method for determining manganese at nanogram levels. The method has been applied to the determination of manganese in natural water, Portland cement, basic slag, Lincolnshire iron ore and lead concentrates.

EXPERIMENTAL

Apparatus

A Beckman DU 50 spectrophotometer (equipped with a Soft-Pac Module for kinetic studies) and a Zeiss DMR 11 spectrophotometer were used, both having constant-temperature cell-holders and 1.0-cm glass or fused-silica cells.

Solutions

All solvents and reagents were of analytical-reagent grade.

Salicylaldehyde guanylhydrazone was synthesized according to the procedure of Thiele and Bihan.⁹ A 0.1% solution was prepared by dissolving 1.0 g of SAG in 50 ml of dimethylformamide (DMF) and making up to 1 litre with demineralized water.

Standard manganese(II) solution was prepared from the nitrate (Merck) and standardized by titration with EDTA; it was diluted as required, just before use.

Buffer solution, pH 9.5, was prepared by dissolving 80 g of ammonium nitrate and 127 ml of concentrated ammonia in water and diluting to 1 litre.

Procedure

To a solution containing up to 2 μg of Mn(II), in a 25-ml standard flask, add 5 ml of 0.1% SAG solution, 1.5 ml of DMF, 5 ml of pH-9.5 buffer and 1 ml of 0.3% v/v hydrogen peroxide solution, and start the stop-clock. Make up to the mark with water, mix well, then transfer a portion to a 1.0-cm cell at $25 \pm 0.1^\circ$ and follow the reaction by recording the absorbance (against water) at 505 nm as a function of time, beginning the measurements 45 sec after addition of the last reagent. The reaction rate is calculated by the initial-rate method applied to the data obtained in the first 60 sec of reaction.

Preparation of samples

Portland cement. Take about 0.25 g of the sample and 0.5 g of ammonium chloride and add 5 ml of concentrated hydrochloric acid. Heat on a steam-bath for 30 min. Add 20 ml of hot water to the solution for complete dissolution of the soluble components of the cement sample. Filter, and wash the precipitate with hot water. Cool the filtrate and dilute it to volume in a 100-ml standard flask.

Basic slag. Take about 0.1 g of sample and dissolve it in a few ml of concentrated perchloric acid. Heat on a steam-

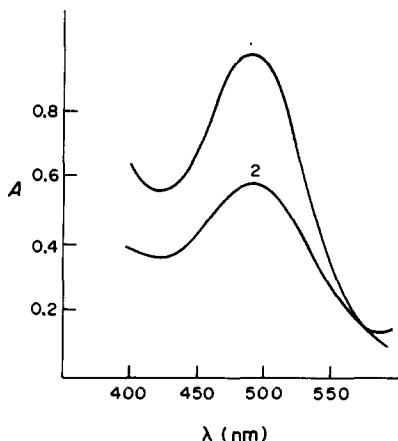


Fig. 1. Absorption spectra of the oxidation product of SAG in the presence of (1) H_2O_2 and 40 ng/ml Mn(II) and (2) $1.5 \times 10^{-4} \text{M IO}_4^-$.

bath to a white residue of silica. Add a few ml of water, filter, and wash the precipitate with hot water. Cool the filtrate and dilute it to volume in a 100-ml standard flask.

Lincolnshire iron ore. Use the procedure for basic slag.

Lead concentrates. Take about 0.25 g of the sample and dissolve it in a few ml of concentrated perchloric acid. Heat until dissolution is complete. If a white precipitate of lead sulphate is observed, filter it off and wash it with hot water. Cool the filtrate and dilute it to volume in a 100-ml standard flask.

Natural waters. Take a sample (with or without prior dilution) such that the amount of manganese in it is within the determination range of the method.

RESULTS

Catalytic effect of manganese(II)

The oxidation of SAG is instantaneous in the presence of periodate, giving a red precipitate soluble in DMF. In the presence of persulphate it is not as fast. When hydrogen peroxide is used as the oxidizing agent, a weak red colour is observed but only when $\geq 33\%$ v/v H_2O_2 is used. The reaction speeds up considerably if small amounts of manganese(II) are present, owing to its catalytic effect. Because the colour obtained (in DMF-water) is the same as that produced by the other oxidizing agents, it is concluded that oxidation of SAG takes place, and that the reaction is catalysed by manganese ions. The catalytic action of manganese(II) is favoured in a buffered ammoniacal solution. The absorption spectra of the oxidation products of SAG with periodate and hydrogen peroxide-Mn(II) are shown in Fig. 1. The absorption spectrum of the oxidation product and its variation with time are shown in Fig. 2. The reaction rate can be calculated by linear regression analysis of the initial straight portions of the kinetic curves (obtained by measuring the rate of change of absorbance at 505 nm). The uncatalysed reaction rate is negligible in all cases, under the conditions in which the curves were obtained.

Effect of reaction variables

The oxidation of SAG is influenced by the reagent, hydrogen peroxide and manganese(II) concentrations, pH, buffer composition and temperature. The effects of all these variables on both the catalysed and uncatalysed reactions, were investigated, by means of evaluating $\tan \alpha = \Delta A / \Delta t$ for the initial straight-line portions of the absorbance vs. time plots.

In preliminary studies it was observed that the temperature has a slight effect on the reaction rate. We therefore first studied all the other variables, keeping the temperature at 25° , and once the optimum chemical conditions were identified we kept them constant and studied the effect of the temperature.

The effect of pH and buffer composition was studied simultaneously, by use of mixtures of ammonia and ammonium nitrate. Ammonium chloride was also tried, but chloride decreases the reaction rate, whereas nitrate does not. Two solutions, one of ammonia and the other of ammonium nitrate were prepared, and with these, two series of samples were made: in one the concentration of ammonia was kept constant, and in the other the concentration of ammonium nitrate. Taking into account that the other reagent concentrations remain constant, the following relationships should be valid:⁷

$$\log (\tan \alpha / [\text{NH}_4^+]^n) = K - x \text{pH} \quad (1)$$

$$\log (\tan \alpha / [\text{NH}_3]^m) = K' - x \text{pH} \quad (2)$$

The variation of the initial rate of reaction for $[\text{NH}_3] = \text{constant}$ and $[\text{NH}_4^+] = \text{constant}$ is shown in Fig. 3. The partial reaction orders with respect to hydrogen and ammonium ions were calculated by plotting equations (1) and (2), for different m and n values and the pH interval 9–10. The values $x = -1$, $m = -1$ and $n = 1$ were obtained. The uncatalysed reaction rate was negligible.

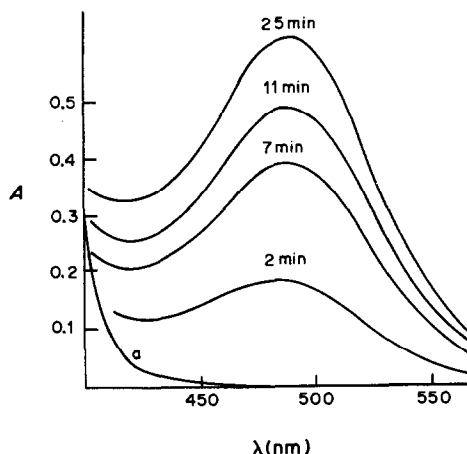


Fig. 2. Variation of absorption spectrum of SAG in the presence of H_2O_2 and 18 ng/ml Mn(II). (a) Uncatalysed reaction after 10 min.

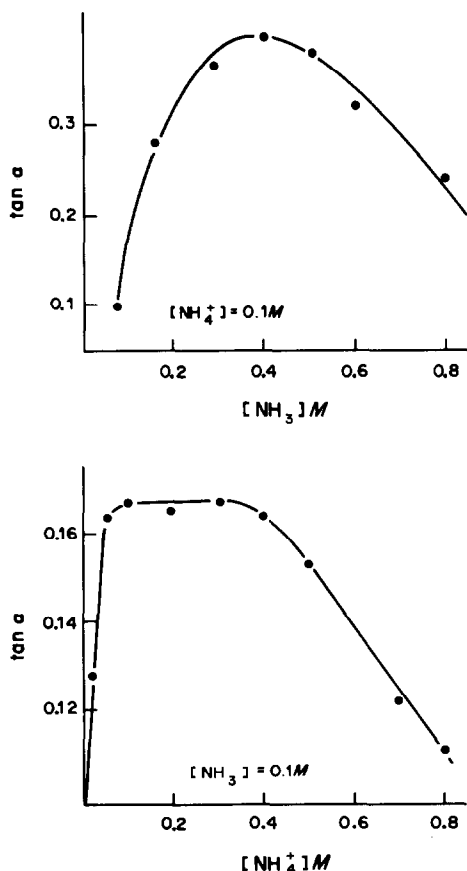


Fig. 3. Variation of reaction rate for $[\text{NH}_4^+] = \text{constant}$ and $[\text{NH}_3] = \text{constant}$. $[\text{Mn(II)}] = 200 \text{ ng/ml}$. Samples contained 5 ml of DMF.

The effect of SAG concentration on the reaction rate was studied in the range $0.18\text{--}4.22 \times 10^{-3} \text{ M}$. A logarithmic plot showed that the reaction rate was independent of the SAG concentration in the range $0.75\text{--}1.50 \times 10^{-3} \text{ M}$. A $0.83 \times 10^{-3} \text{ M}$ SAG concentration was chosen for subsequent studies.

The effect of hydrogen peroxide concentration was studied for solutions containing 60 ng/ml manganese(II). A logarithmic plot showed that the reaction rate was independent of the hydrogen peroxide concentration in the range $3.2\text{--}5.0 \times 10^{-3} \text{ M}$. A $3.9 \times 10^{-3} \text{ M}$ peroxide concentration was chosen for

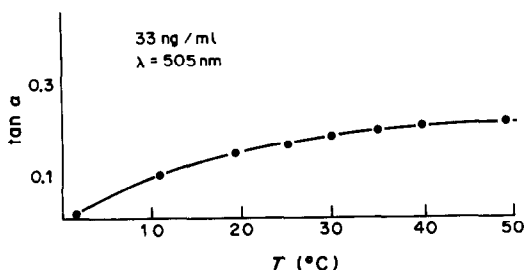


Fig. 4. Variation of the rate of the catalysed reaction with temperature.

subsequent studies; this concentration was obtained by use of 1 ml of 0.3% hydrogen peroxide solution per 25 ml of final solution.

The oxidation reaction rate decreased with increasing volume of DMF added to the sample; however, addition of DMF is necessary to keep the oxidation product in solution, and use of 1.5 ml is recommended. The order of addition of the reagents has no influence on the oxidation reaction rate.

The effect of temperature on both the catalysed and uncatalysed reactions was studied in the range $3\text{--}50^\circ$. The uncatalysed reaction rate was negligible in the temperature range examined. The catalysed reaction rate increased slowly with temperature (Fig. 4). A temperature of 25° was judged to be the optimum for the final procedure. The activation energy calculated from the reaction rates by using the Arrhenius equation over the $10\text{--}40^\circ$ range is 14.4 kJ/mole.

Rate equation and calibration graphs

The absorbance vs. time curves for solutions containing different amounts of Mn(II) were recorded. On their basis, the following equation is suggested for the manganese(II)-catalysed oxidation of SAG at pH 9.5 in the concentration range $0.75\text{--}1.50 \times 10^{-3} \text{ M}$:

$$d[\text{SAG}]_{\text{ox}}/dt = k \frac{[\text{NH}_4^+][\text{Mn(II)}]}{[\text{NH}_3][\text{H}^+]}$$

which can be written as

$$d[\text{SAG}]_{\text{ox}}/dt = kk'[\text{Mn(II)}] = K[\text{Mn(II)}]$$

where k' is the apparent equilibrium constant for $\text{H}^+ + \text{NH}_3 \rightleftharpoons \text{NH}_4^+$.

Table 1. Influence of foreign ions on the kinetic determination of Mn(II) (40 ng/ml)

Tolerated ratio to Mn, w/w	Ions
$> 10^5$	$\text{Na}^+, \text{SO}_4^{2-}, \text{NO}_3^-$
10^5	K^+
7.5×10^4	F^-
1.8×10^4	$\text{C}_2\text{O}_4^{2-}$
1.2×10^4	$\text{PO}_4^{3-}, \text{As(V)}, \text{tartrate}$
8.5×10^3	Cl^-
2×10^3	$\text{Mo(VI)}, \text{Ag}^+, \text{Ca}^{2+}$
10^3	Mg^{2+}
500	$\text{In}^{3+}, \text{As(III)}, \text{Sb(III)}, \text{Ba}^{2+}, \text{Y}^{3+}$
250	$\text{Pb}^{2+}, \text{Bi(III)}, \text{Be}^{2+}, \text{W(VI)}, \text{Pd(II)}$
125	$\text{Cd}^{2+}, \text{Zn}^{2+}, \text{Al}^{3+}, \text{Co}^{2+}$ *
75	V(V)
50	Hg(II)
40	Fe(III)^\dagger
25	Cu^{2+}
12.5	Cr^{3+}
10	Ni^{2+}
6	$\text{Ti}^{4+}, \text{Sn(II)}, \text{CN}^-$
0.25	EDTA

*A constant error of +7% is produced when the Co(II) concentration range is 50–5000 ng/ml.
†7 ml of 0.1% SAG added.

Table 2. Determination of Mn(II) in diverse samples

Sample	Certified % composition	Mn certified, %	Mn* found, %
Portland cement BCS-372	SiO ₂ (21.3); TiO ₂ (0.33) CaO (65.8); Al ₂ O ₃ (5.35) MgO (1.30); Na ₂ O (0.21) K ₂ O (0.62); SO ₃ (2.35) P ₂ O ₅ (0.19)	0.046	0.045
Basic slag BCS-381	P ₂ O ₅ (15.7); SiO ₂ (8.78) FeO (3.69); Fe total (13.3) Al ₂ O ₃ (0.67); V ₂ O ₅ (0.94) TiO ₂ (0.35); Cr ₂ O ₃ (0.33) CaO (49.0); MgO (1.03) S (0.19)	2.45	2.39
Lead concentrate BAS-426	Zn (3.40); S (14.2) Fe (1.35); Pb (75.6) Cu (0.14); As (0.32) Sb (0.15); Bi (0.020) Ag (0.074); Au (0.016)	0.210	0.203
Lincolnshire iron ore BCS-301/1	Fe (23.8); SiO ₂ (7.40) Al ₂ O ₃ (4.26); TiO ₂ (0.16) CaO (22.6); MgO (1.73) Na ₂ O (0.07); K ₂ O (0.32) S (0.040); P (0.35)	0.970	1.01

*Mean of 3 separate determinations.

Table 3. Determination of Mn(II) in water samples by the standard-additions procedure

Sample	Manganese		
	Added, ng/ml	Found,* ng/ml	Recovery, %
Running water A	—	6.6	—
	8.2	14.0	95
	24.6	31.7	102
	41.0	47.3	99
Running water B	—	3.5	—
	8.2	12.4	106
	24.6	29.5	105
	41.0	47.4	106
Running water C	—	7.5	—
	8.2	16.2	103
	24.6	32.0	100
	41.0	47.0	97
Guadiana river	—	86	—
	134†	230	104
	402†	470	96

*Mean of 3 separate determinations.

†Added prior to dilution of the sample.

The value of $\tan \alpha = \Delta A / \Delta t$ for the initial straight-line portions was determined from the absorbance *vs.* time curves. The calibration graph of initial rate *vs.* Mn(II) concentration is linear over the range 8–80 ng/ml. The relative error (95% confidence level) is 1% for 40 ng/ml.

The fixed-time method was also used and the calibration graph was linear over the range 8–65 ng/ml and 8–50 ng/ml when the fixed time was 2 and 4 min respectively.

Interferences

The influence of foreign ions was examined and the results are summarized in Table 1. The proposed kinetic method is reasonably selective. The most important interference is from EDTA which acts as an inhibitor since it forms a complex with manganese(II) at the pH used.

Applications

The proposed method has been used to determine manganese in a variety of samples and the results are shown in Table 2. Results for the determination of manganese in natural water samples by the standard-additions method are given in Table 3.

Acknowledgement—We thank the Comisión Asesora de Investigación Científica y Técnica del Ministerio de Educación y Ciencia de España for supporting this study (Project No. 2903–83).

REFERENCES

1. D. Pérez Bendito, M. Valcárcel, M. Ternero and F. Pino, *Anal. Chim. Acta*, 1977, **94**, 405.
2. T. Raya Saro and D. Pérez Bendito, *Analyst*, 1983, **108**, 857.
3. A. Moreno, M. Silva, D. Pérez Bendito and M. Valcárcel, *Talanta*, 1983, **30**, 107.
4. D. Pérez Bendito, J. Peinado and F. Toribio, *Analyst*, 1984, **109**, 1297.
5. J. Vázquez Ruiz, A. García de Torres and J. M. Cano Pavón, *Talanta*, 1984, **31**, 29.
6. S. Rubio, A. Gómez Hens and M. Valcárcel, *Analyst*, 1984, **109**, 717.
7. F. Salinas, J. J. Berzas Nevado and A. Espinosa Mansilla, *Talanta*, 1984, **31**, 325.
8. J. J. Berzas Nevado, A. Espinosa Mansilla and P. Valiente González, *Microchem. J.*, 1984, **30**, 380.
9. J. Thiele and R. Bihan, *Annalen*, 1898, **302**, 278.

SIMULTANEOUS DETERMINATION OF HISTIDINE AND HISTAMINE BY SECOND-DERIVATIVE SYNCHRONOUS FLUORESCENCE SPECTROMETRY

M. C. GUTIERREZ, S. RUBIO, A. GOMEZ-HENS and M. VALCARCEL

Department of Analytical Chemistry, Faculty of Sciences, University of Córdoba, Córdoba, Spain

(Received 24 June 1986. Accepted 10 October 1986)

Summary—Simultaneous direct determination of histidine and histamine in mixtures is described. The method is based on the formation of fluorescent condensation products with *o*-phthalaldehyde in a basic medium in the presence of 2-mercaptoethanol. Both the conventional and synchronous fluorescence spectra of these condensation products completely overlap, making determination by either of these techniques impossible. However, the determination can be performed by second-derivative synchronous fluorescence spectrometry. The method is simple, rapid and inexpensive and the measurements are performed in a single scan. Calibration graphs are linear in the range 0.1–4.0 $\mu\text{g/ml}$ for histidine and 0.06–5.0 $\mu\text{g/ml}$ for histamine. Mixtures of histidine and histamine in ratios between 12:1 and 1:8 have been satisfactorily resolved.

The analysis of mixtures of compounds which have similar fluorescence characteristics is usually troublesome owing to spectral overlap. Generally, these compounds are determined by using a prior separation step, which is rather time-consuming for routine analysis and in some cases requires special and expensive instrumentation. For this reason, the development of techniques allowing the direct determination of related compounds through careful selection of the instrumental variables is of great interest. Derivative-synchronous fluorescence spectrometry is one such technique. It was introduced by John and Soutar¹ and is a combination of synchronous^{2,3} and derivative fluorescence spectrometry.⁴ Its analytical applications have recently been reviewed.⁵ This technique has been used for direct analysis of several mixtures of related compounds, such as epinephrine and norepinephrine,⁶ and pyridoxal, pyridoxal-5-phosphate and pyridoxic acid.⁷ These mixtures are usually resolved by tedious chromatographic separations unsuitable for routine analytical work.

A similar problem is encountered in the determination of histidine and histamine, which is usually done by electrophoresis^{8,9} and paper¹⁰⁻¹² or thin-layer¹³⁻¹⁶ chromatography. Both compounds form fluorescent condensation products with *o*-phthalaldehyde, and these have very similar characteristics. When only histamine is to be determined, the fluorimetric determination is done in an acid medium, where the fluorescence signal yielded by the histamine derivative is more intense¹⁷ than that obtained in a basic medium, and that due to the fluorescent derivative of histidine is decreased. However, when both compounds are determined together, the corresponding analytical signals must be roughly of the same magnitude if adequate results are to be obtained. Roth¹⁸ showed that the addition of

2-mercaptoethanol in a basic medium improves the fluorescence intensity of both condensation products with *o*-phthalaldehyde, owing to the formation of *N*-substituted 1-(2-hydroxyethyl)thioisindoles, as proposed by Simons and Johnson.^{19,20}

In the method described here, histidine and histamine are determined directly and simultaneously by Roth's reaction.¹⁸ However, as the conventional and synchronous spectra of the fluorescent products of both analytes completely overlap, the determination is done by second-derivative synchronous fluorescence spectroscopy, and provides a clear example of the high resolving power of this technique. The method is simple, rapid and inexpensive since no sophisticated detection equipment is necessary: in fact, any conventional modern spectrofluorimeter is suitable.

EXPERIMENTAL

Reagents

Stock L-histidine and histamine solutions, 1 mg/ml. Prepared from L-histidine and histamine dihydrochloride (Aldrich), respectively, in distilled water, and stored at 0–4°. Lower concentrations of both histidine and histamine solutions were prepared daily by dilution with distilled water.

***o*-Phthalaldehyde (OPT) solution, 1 mg/ml.** Prepared by dissolving 25 mg of reagent (Merck) in 5 ml of ethanol and diluting to 25 ml with distilled water.

2-Mercaptoethanol solution, 0.1%. Prepared by dissolving 0.1 ml of reagent (Merck) in 100 ml of distilled water.

Borate buffer solution, approx. 0.05M. A 0.05M sodium tetraborate solution adjusted to pH 10.1 with concentrated sodium hydroxide.

Reagent-grade chemicals and pure solvents were used.

Apparatus

A Perkin-Elmer fluorescence spectrophotometer, model MPF-43A, with 1-cm fused-silica cells and a xenon source, was used. The cell compartment was kept at 25° by circulating water from a thermostat. A spectral band-pass of

5 nm was set for the excitation and emission monochromators. For synchronous fluorescence measurements, both monochromators were interlocked and scanned simultaneously at 2 nm/sec. Derivative spectra were obtained by electronic differentiation of the signal from a Perkin-Elmer derivative accessory, model H 200-0507. Of the six differential time-constants available from the mode switch, position 6 was selected for all measurements. The spectrofluorimeter response (time-constant) was set to 1.5 sec. A series of fluorescent polymer samples was used daily to adjust the spectrofluorimeter to compensate for changes in source intensity.

Procedure

To a sample solution containing 1.0–40.0 μg of histidine and 0.6–50 μg of histamine, in a 10-ml standard flask, were added 3 ml of 0.05M borate buffer (pH 10.1), 0.25 ml of OPT solution and 0.25 ml of 2-mercaptoethanol solution. The mixture was made up to the mark with distilled water and allowed to stand for 5 min. The second-derivative synchronous fluorescence spectrum was recorded by scanning both monochromators together, while maintaining a 120 nm constant difference between their wavelengths. The excitation monochromator was scanned from 280 to 400 nm and the emission monochromator from 400 to 520 nm. The instrumental parameters were as detailed above. Second-derivative measurements were made from peak to trough,²¹ *i.e.* by measuring the difference between the derivative signal at two wavelengths, corresponding to an adjacent maximum and minimum, given as relative fluorescence intensity and expressed as ΔI . The derivative signal obtained between the minimum at 464 nm and the maximum at 470 nm (ΔI_1) is directly related to the histidine concentration. The value measured between 476 and 490 nm (ΔI_{2+3}) is contributed to by both histidine and histamine. A previous calibration (ΔI_2 *vs.* histidine concentration) allowed the determination of the individual contribution of histidine to this derivative signal. The difference between the total ΔI_{2+3} and ΔI_2 , attributed to the action of histamine, is thus directly related to the histamine concentration (ΔI_3). The net fluorescence for each peak was obtained by subtracting the corresponding signal for a blank solution.

RESULTS AND DISCUSSION

Fluorescence spectra

Histidine and histamine react with OPT in a basic medium in the presence of a reductant such as 2-mercaptoethanol,¹⁸ yielding strongly fluorescent compounds having very similar properties. The analysis of mixtures of histidine and histamine by conventional fluorimetry is not feasible because, as Fig. 1 shows, the emission spectra of both reaction products ($\lambda_{\text{ex}} = 345$ nm) consist of broad spectral bands overlapping one another. The synchronous scanning approach produces spectra with a much smaller bandwidth, but does not permit a more precise determination for any value of $\Delta\lambda$ so far tested (Fig. 2). The determination is also impossible by the use of the second-derivative of the conventional emission spectra. Therefore, the possibility of direct analysis of this mixture by applying derivative synchronous fluorescence spectrometry without resorting to separation steps, is of great interest.

Figure 3 (A,B) shows the individual second-derivative synchronous fluorescence spectra ($\Delta\lambda = 120$ nm) of the condensation products of

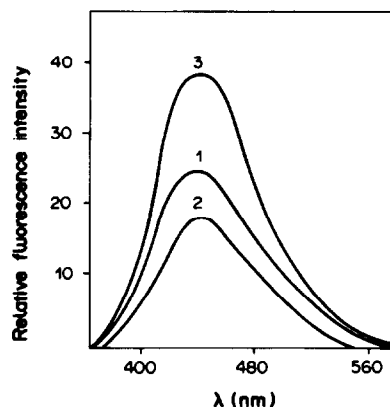


Fig. 1. Emission spectra ($\lambda_{\text{ex}} = 360$ nm) of the condensation products of OPT with histidine (curve 1) and histamine (curve 2), and of their mixture (curve 3) in a basic medium.

histidine and histamine with OPT. The derivative spectrum of the reaction product of histidine shows two ΔI values ($\Delta I_{464-470}$ and $\Delta I_{476-490}$) which can be related to the histidine concentration. The spectrum of histamine shows that the signal $\Delta I_{476-490}$ also depends on the histamine concentration. The spectrum of the mixture of both analytes (Fig. 3, C) shows

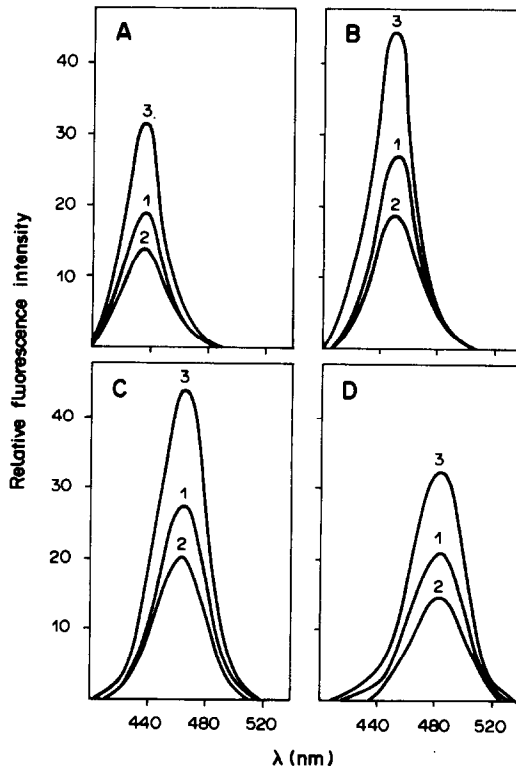


Fig. 2. Synchronous fluorescence spectra of the condensation products of OPT with histidine (curve 1) and histamine (curve 2), and of their mixture (curve 3) at different $\Delta\lambda$ values: (A) 80 nm; (B) 100 nm; (C) 120 nm; (D) 140 nm.

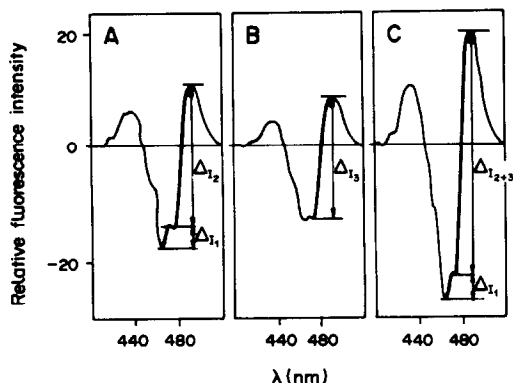


Fig. 3. Second-derivative synchronous fluorescence spectra of the condensation products of OPT with histidine (A) and histamine (B), and of their mixture (C); $\Delta\lambda = 120$ nm.

that the signal $\Delta I_{464-470}$ is not affected by the presence of histamine and that the signal $\Delta I_{476-490}$ is the sum of those due to both compounds.

Owing to the fact that the reaction product of histamine gives a greater fluorescence intensity than that of the histidine product, the resolution of this mixture was studied with solutions containing 0.30 $\mu\text{g/ml}$ histidine and 0.15 $\mu\text{g/ml}$ histamine.

Optimization

The system was optimized by changing one variable at a time while keeping all others constant. The instrumental variables, including wavelength difference between excitation and emission monochromators ($\Delta\lambda$), wavelength scanning speed, differentiation constant and spectrofluorimeter time-constant, affect the intensity, number and distribution of maxima and minima on the derivative synchronous fluorescence spectra and, therefore, have a critical effect on the sensitivity and selectivity of the method. The chemical variables only affect the intensity of the analytical signals and, therefore, influence the sensitivity of the method. The optimum value taken for each variable was that at which the following requirements were met: (1) the fluorescence signal $\Delta I_{464-470}$ should not depend on the histamine concentration; (2) the fluorescence signal $\Delta I_{476-490}$ should be additive for the histidine and histamine concentrations; (3) both fluorescence signals should be as intense as possible.

Second-derivative synchronous fluorescence spectra show red shifts as $\Delta\lambda$ increases. This variable also affects the shape of these spectra, so that only in the $\Delta\lambda$ interval 110–140 nm does the histidine concentration correlate with the signal $\Delta I_{464-470}$, and do both histidine and histamine concentrations correlate with the signal $\Delta I_{476-490}$. The best intensity values are obtained for $\Delta\lambda = 120$ nm.

The intensity of the bands and the spectral distribution are also strongly affected by the wavelength scanning rate (Fig. 4). An increase in this variable results in increased ΔI , but also in decreased spectral

resolution. At rates higher than 2 nm/sec the spectra overlap, while at lower rates they are very diffuse.

The differentiation constant is another variable modifying the shape of the derivative spectra. The best results are obtained when the response speed is at a minimum, *i.e.*, when the spectral resolution is adequate for the determination, and the analytical signals are at a maximum.

The spectrofluorimeter time-constant (0.3, 1.5 and 3.0 sec) has a minor effect on the derivative spectra. However, the peak intensity decreases slightly as this variable increases and, for a value of 0.3 sec, the signal corresponding to histidine is also dependent on the histamine concentration. For a value of 1.5 sec this signal is dependent only on the histidine concentration.

The analytical signals corresponding to both analytes are independent of pH over the range 9.2–10.5. Outside this range the fluorescence intensity decreases. A borate buffer was used to adjust the pH of the samples to 10.1. The concentration of this buffer in the range 10^{-3} – $2.5 \times 10^{-2} M$ does not affect the fluorescence intensity. The effect of temperature was studied over the range 10–60°. The peak intensity

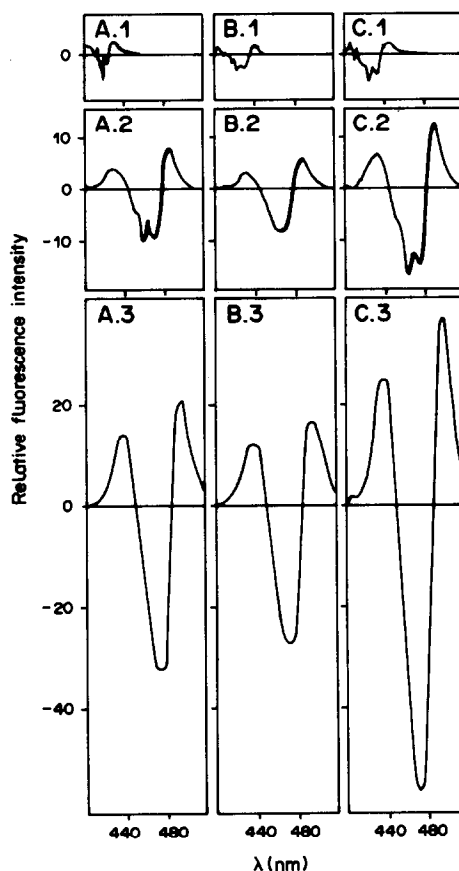


Fig. 4. Effect of the wavelength scanning speed on the second-derivative synchronous fluorescence spectra of the condensation products of OPT with histidine (A) and histamine (B), and of their mixture (C). (1) 1 nm/sec; (2) 2 nm/sec; (3) 4 nm/sec.

Table 1. Effect of various species on the determination of 0.3 $\mu\text{g/ml}$ of histidine and histamine

Tolerance ratio, species/analyte	Species added
100:1	1-Methyl-4-imidazole acetic acid, Ca^{2+} , Mg^{2+}
50:1	NAD
25:1	Cu^{2+}
10:1	Fe^{3+}
5:1	Spermidine, cysteine, epinephrine
2:1	Spermine, putrescine
1:1	Cadaverine
Interfere at the same level as the analyte	1-Methylhistidine, 3-methylhistidine, 1-methylhistamine, norepinephrine, glycine

Table 2. Resolution of histidine-histamine mixtures

Histidine/histamine ratio	Histidine, $\mu\text{g/ml}$		Histamine, $\mu\text{g/ml}$	
	Taken	Found*	Taken	Found*
12:1	1.20	1.18	0.10	0.11
9:1	0.90	0.93	0.10	0.12
1:1	0.30	0.30	0.30	0.31
3:4	0.30	0.29	0.40	0.42
3:5	0.30	0.31	0.50	0.47
1:2	0.30	0.28	0.60	0.58
2:5	0.30	0.28	0.75	0.77
1:3	0.30	0.30	0.90	0.88
1:8	0.15	0.17	1.20	1.23

*Average of three determinations.

does not change with temperature up to 40° , but starts to decrease above this value. This behaviour parallels that of conventional emission spectra. A temperature of 25° was selected.

The concentrations of OPT and 2-mercaptoethanol in the ranges 1.5×10^{-4} – $7.4 \times 10^{-4} M$ and

3.6×10^{-4} – $2.0 \times 10^{-3} M$, respectively, do not affect the ΔI values. Decreasing the dielectric constant of the solution by addition of ethanol exerts no influence on the signal $\Delta I_{476-490}$, but when the ethanol content is higher than 8%, a loss of correlation between the signal $\Delta I_{464-470}$ and the histidine concentration occurs. Variation of the ionic strength with potassium chloride (0–0.5M), and the order of addition of the reagents, exert almost no influence on the fluorescence of these systems.

Features of the proposed methods

The signals $\Delta I_{464-470}$ and $\Delta I_{476-490}$ vary linearly with histidine concentration in the range 0.1–4.0 $\mu\text{g/ml}$. Similarly, the calibration graph obtained by measuring the variation of the signal $\Delta I_{476-490}$ with the histamine concentration is linear in the range 0.06–5.0 $\mu\text{g/ml}$. By using these calibration graphs, it is possible to analyse mixtures of histidine and histamine with a single scan.

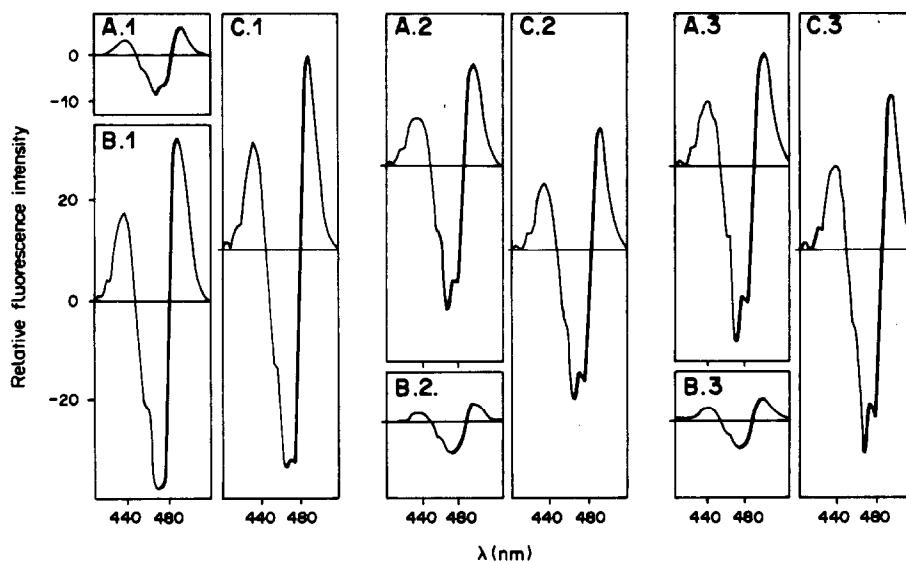


Fig. 5. Second-derivative synchronous fluorescence spectra of several mixtures of histidine and histamine. (A) histidine; (B) histamine; (C) mixture. Histidine concentration ($\mu\text{g/ml}$): (1) 0.5; (2) 0.9; (3) 1.2. Histamine concentration ($\mu\text{g/ml}$): (1) 1.2; (2) 0.1; (3) 0.1.

The relative standard deviations (r.s.d.) ($P = 0.05$, $n = 11$) for 0.3 $\mu\text{g/ml}$ histidine at $\Delta I_{464-470}$ and $\Delta I_{476-490}$ were 8.3% and 3.9%, respectively, and for 0.2 $\mu\text{g/ml}$ histamine at $\Delta I_{476-490}$ the r.s.d. was 3.7%.

The effect of foreign species on the determination of 0.3 $\mu\text{l/ml}$ of each analyte is summarized in Table 1. Methyl derivatives of histidine and histamine interfere at the same concentration level as the analytes because they form condensation products with OPT similar to those of histidine and histamine. However, many amines which also react with OPT are tolerated at the same concentration levels as the analytes.

Simultaneous determination of histidine and histamine

The second-derivative synchronous fluorescence spectrometric technique has been applied to the analysis of several synthetic mixtures of histidine and histamine. Table 2 summarizes the results obtained and Fig. 5 shows the spectra of some of these mixtures.

In view of the results, it can be inferred that the combination of second-derivative spectrometry and synchronous fluorimetry has a great potential in developing an efficient, fast and straightforward method for the simultaneous analysis of mixtures. The equipment needed is inexpensive, as the derivative technique requires only the incorporation of a

simple "outboard" circuit to an unmodified instrument, and the synchronous technique merely calls for a simple switch for simultaneous scanning of both monochromators.

REFERENCES

1. P. John and I. Soutar, *Anal. Chem.*, 1976, **48**, 520.
2. J. B. F. Lloyd, *Nature*, 1971, **231**, 64.
3. T. Vo-Dinh, *Anal. Chem.*, 1978, **50**, 396.
4. G. L. Green and T. C. O'Haver, *ibid.*, 1974, **46**, 2191.
5. S. Rubio, A. Gómez-Hens and M. Valcárcel, *Talanta*, 1986, **33**, 633.
6. *Idem*, *Clin. Chem.*, 1985, **31**, 1790.
7. A. Petidier, S. Rubio, A. Gómez-Hens and M. Valcárcel, *Anal. Biochem.*, 1986, **157**, 212.
8. K. Fuecker, R. Meyer and H. P. Pietsch, *Nahrung*, 1974, **18**, K1.
9. M. Ferenčík, *Chem. Listy*, 1962, **56**, 289.
10. J. Seto, *Bunseki Kagaku*, 1961, **10**, 25.
11. J. E. McNeal, *J. Assoc. Off. Anal. Chem.*, 1976, **59**, 570.
12. L. Y. Foo, *ibid.*, 1977, **60**, 183.
13. L. Edvinsson, R. Hakanson, A. L. Roennberg and F. Sundler, *J. Chromatog.*, 1972, **67**, 81.
14. S. Lee and S. Yin, *ibid.*, 1976, **129**, 482.
15. H. Nakamura, *ibid.*, 1977, **131**, 215.
16. E. R. Lieber and S. L. Taylor, *ibid.*, 1978, **153**, 143.
17. P. A. Shore, *Methods Enzymol.*, 1971, **17**, 842.
18. M. Roth, *Anal. Chem.*, 1971, **43**, 880.
19. S. S. Simons Jr. and D. F. Johnson, *J. Am. Chem. Soc.*, 1976, **98**, 7098.
20. *Idem*, *Anal. Biochem.*, 1978, **90**, 705.
21. T. C. O'Haver, *Clin. Chem.*, 1979, **25**, 1548.

EXTRACTION OF ZIRCONIUM AND HAFNIUM THIOCYANATE WITH POLYURETHANE FOAM

LIU JIN-CHUN* and ARTHUR CHOW

Department of Chemistry, University of Manitoba, Winnipeg, Manitoba, Canada

(Received 6 June 1986. Accepted 10 October 1986)

Summary—Conditions for the extraction of zirconium and hafnium thiocyanate by polyether-type polyurethane foam were studied in detail. The composition of the extractable species was found to be dependent on both the thiocyanate and metal-ion concentrations. The extraction efficiency for zirconium and hafnium depended on the size of the counter-cation as well as on the type of anion.

The separation of zirconium and hafnium is one of the more difficult to achieve, but the usefulness of zirconium in metallurgy and in the nuclear industry makes this separation of practical importance. Methods for preconcentration and separation of zirconium and hafnium by solvent extraction¹⁻⁴ with benzene, chloroform or cyclohexanone in the presence of thiocyanate ions are widely known, but the use of polyurethane foam as a solid extractant for these has not been reported.

Compared with liquid-liquid extraction, solid-liquid extraction with polyurethane foam offers the following features: low solubility of the extractant, which does not interfere with the determination; easy separation of the phases; easy use of larger phase ratios; possible synergistic extraction effect due to polyfunctional groups on the foam.

The purpose of the present work was to study the optimum conditions for the preconcentration and separation of zirconium and hafnium, and to investigate the mechanism of extraction of their thiocyanates by polyether-type polyurethane foam.

EXPERIMENTAL

Apparatus

A Varian 634S spectrophotometer and a Coleman 38A pH-meter were used. A thermostatically-controlled multiple automatic squeezer was used as previously described.^{2,6}

Reagents

All chemicals were of reagent grade and reverse-osmosis water was purified with a Barnsted Nanopure IITM system before use.

A standard solution of $1.1 \times 10^{-3} M$ (100 ppm) zirconium was prepared⁷ by fusing 0.1351 g of zirconium dioxide in a porcelain crucible with 4 g of potassium pyrosulphate at 750° for 10-15 min. After cooling, the solidified melt was heated with 100 ml of 2M hydrochloric acid until it was completely dissolved. The solution was then diluted to 1 litre with 2M hydrochloric acid. A standard solution of $5.6 \times 10^{-4} M$ hafnium was prepared by dissolving 0.1000 g

of the metal in a platinum crucible with about 1 ml of concentrated hydrofluoric acid and cautious addition of concentrated nitric acid, drop by drop, until dissolution was complete. Two ml of concentrated sulphuric acid were added to the solution, which was then heated until white fumes appeared, and then for 5 min more. After cooling, the solution was diluted to 1 litre with 2M hydrochloric acid.

Polyether-type polyurethane foam (# 1338 from G. N. Jackson Ltd., Winnipeg, Canada) was cut into pieces 2.0 cm in diameter and 4.6 cm long, which were then washed as described previously.⁵

Procedure

An aliquot of zirconium or hafnium solution was placed in a 100-ml standard flask along with the appropriate amount of thiocyanate and water; the pH was adjusted with concentrated hydrochloric acid or sodium hydroxide solution as required, and the solution made up to volume. The extraction was done by placing 95 ml of the sample in a 250-ml glass cell containing the desired amount of foam. The foam was squeezed by means of a glass plunger in order to bring fresh solution into contact with it. The plunger was operated by an automatic squeezer^{5,6} consisting of an eccentric cam turned by a heavy-duty motor giving a 5-cm stroke at a rate of 24 strokes/min.

Zirconium and hafnium were determined by spectrophotometry with Arsenazo III.^{8,9} The sensitivity was found to be improved by 25% by the presence of 6% v/v n-butanol. The degree of extraction of the metals (*E*) was calculated by measuring the concentration before and after the extraction,

$$E = \frac{[\text{metal}]_{\text{initial}} - [\text{metal}]_{\text{final}}}{[\text{metal}]_{\text{initial}}} \times 100\%$$

The distribution ratio (*D*) for the extraction process was calculated from the ratio of the concentration of the metal in the foam to that left in solution at equilibrium.

$$D = \frac{\% \text{ metal in foam}}{\text{weight of foam (g)}} \times \frac{\text{volume of solution (ml)}}{\% \text{ metal left in solution}}$$

RESULTS AND DISCUSSION

Effect of pH

The pH of $1.1 \times 10^{-5} M$ zirconium or $1.12 \times 10^{-5} M$ hafnium solution containing 2.0M ammonium thiocyanate was adjusted with hydrochloric acid or sodium hydroxide as required. After the

*Permanent address: Department of Chemistry, Wuhan University, Wuhan, China.

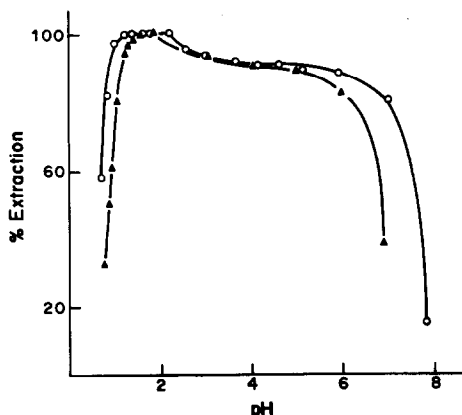


Fig. 1. Effect of pH on extraction of zirconium and hafnium. Conditions: 0.250 g of foam; 100 ml of solution in 2.0M NH_4SCN ; \blacktriangle — $1.1 \times 10^{-5}M$ Zr; \circ — $1.12 \times 10^{-5}M$ Hf.

initial pH measurement the solutions were equilibrated with 0.250 g of foam for up to 24 hr, and the pH was redetermined. The results given in Fig. 1. show that the sorption of zirconium and hafnium was quite sensitive to the pH of the aqueous phase at $\text{pH} < 1$ or > 6 , hafnium being much more extractable than zirconium at the higher and lower acidities. The extraction was relatively insensitive to pH in the range 2–6, but there was a gradual decrease in extraction of both metals with increasing pH. At an acidity greater than 1M hydrochloric acid, a yellow solution or precipitate was formed as indicated previously.⁵ Therefore, the optimum pH range should be 1.5–2.0 for zirconium and 1.2–2.2 for hafnium and pH 1.8 was used for further studies.

Effect of thiocyanate

The effect of thiocyanate on the extraction is shown in Fig. 2. The extraction of zirconium increased from 13% at 0.25M thiocyanate concentration to 99.8% at 3.0M and then remained constant.

Zirconium and hafnium ions react with thiocyanate to form multi-ligand complexes, the composition of which depends on the thiocyanate concen-

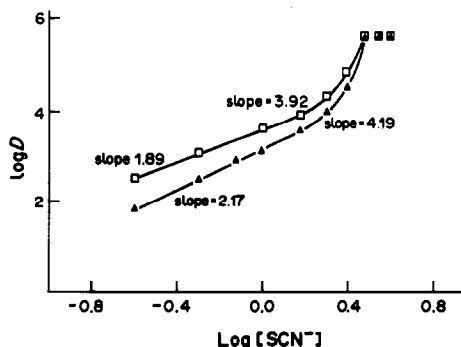


Fig. 2. Effect of thiocyanate concentration on sorption of zirconium and hafnium. Conditions: 0.250 g of foam; 100 ml of solutions at pH 1.8; time for extraction 24 hr; \blacktriangle — $1.1 \times 10^{-5}M$ Zr; \square — $1.12 \times 10^{-5}M$ Hf.

tration and the acidity of the solutions. Figure 2 shows that the number of thiocyanate ions in the extractable species increased with increasing thiocyanate concentration. If a mononuclear complex is assumed, the slope of about 2 for the range 0.25–1.0M thiocyanate suggests that two thiocyanate ligands are involved in the extractable species, and the slope of about 4 over the range 1.5–2.5M thiocyanate indicates that four thiocyanate ligands may be involved.

The extractable forms of zirconium or hafnium thiocyanate have been described as $[\text{Zr}(\text{SCN})_4] \cdot \text{S}$, $[\text{Zr}(\text{SCN})_6] \cdot \text{S}$,¹⁰ $[\text{Zr}(\text{OH})_2(\text{SCN})_2] \cdot \text{S}^4$ or $[\text{M}(\text{OH})_2(\text{SCN})_2] \cdot 2(\text{HSCN} \cdot \text{S})$ ¹¹ where $\text{M} = \text{Zr}$ or Hf and $\text{S} = \text{solvent}$. Therefore it is reasonable to suggest from the results above, and those described later in this paper, that the zirconium and hafnium thiocyanates are extracted by the foam in the form of an ion-association complex with the general formula $\text{M}'_z[\text{M}(\text{OH})_y(\text{SCN})_z] \cdot x\text{SCN}$ where $\text{M}' = \text{H}^+$, NH_4^+ or an alkali metal ion; $\text{M} = \text{Zr}$ or Hf ; $y = 0$ or 2; $z = 2$ or 4.

Time dependence

The rate of extraction of the zirconium and hafnium thiocyanates was studied by varying the time of contact from 5 min to 24 hr, for $1.1 \times 10^{-5}M$ zirconium or $1.12 \times 10^{-5}M$ hafnium with various ammonium thiocyanate concentrations at pH 1.8. The results shown in Fig. 3 indicate that the time needed to reach equilibrium for maximum extraction depended strongly on the thiocyanate concentration, with longer times required for lower concentrations. The extraction equilibrium was established after 30 min with 3.5M ammonium thiocyanate and after 1 hr with 2.0M ammonium thiocyanate for both zirconium and hafnium thiocyanates. The degree of extraction of both species increased gradually with longer contact time in 0.2M thiocyanate. In the presence of potassium chloride the degree of extraction of both zirconium and hafnium increased somewhat, but the time needed to reach equilibrium was even longer.

Effect of zirconium concentration

The effect of metal-ion concentration on the sorption behaviour of the metal- SCN^- complexes is shown in Figs. 4 and 5. In order to study the extraction mechanism, solutions containing initial zirconium concentrations from 5.5×10^{-6} to $1.1 \times 10^{-4}M$ with 3.5M ammonium thiocyanate at pH 1.8 were equilibrated with 0.1000 g of foam for 1 hr.

Figure 4 shows that the initial zirconium concentration affected the distribution ratio only slightly from $\log[\text{Zr}] = -5.3$ to $\log[\text{Zr}] = -4.5$ and then caused a more marked decrease. In Fig. 5 the data used for Fig. 4 are restructured to show the relationship between the concentration of zirconium on the foam to that of the zirconium left in solution at

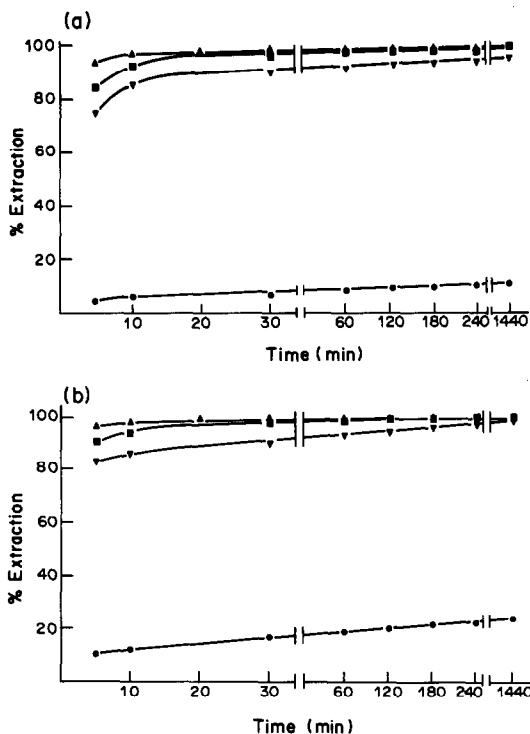


Fig. 3. Time dependence of (a) sorption of zirconium, (b) sorption of hafnium. Conditions: 0.250 g of foam; 100 ml of solution $1.1 \times 10^{-5}M$ in Zr or $1.12 \times 10^{-5}M$ in Hf at pH 1.8; \blacktriangle — $3.5M$ NH_4SCN ; \blacksquare — $2.0M$ NH_4SCN ; \bullet — $0.2M$ NH_4SCN ; \blacktriangledown — $1.0M$ NH_4SCN + $1.0M$ KCl .

equilibrium. The slope of about 0.85 in section *a* in Fig. 5 suggests that the metal is extracted predominantly in the form of a mononuclear complex. The slope of about 0.52 in section *b* indicates that some other phenomenon must occur at these zirconium concentrations. It is likely that some degree of polymerization occurs and that Zr^{4+} , ZrO^{2+} and various polymerized species are present together in the solution. Whether different species are extracted or the solution chemistry is changed or a different extraction mechanism is involved was not determined.

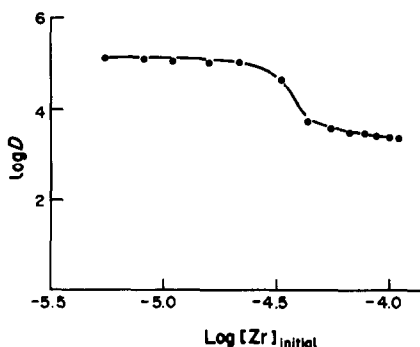


Fig. 4. Effect of zirconium concentration on the distribution ratio. Conditions: 0.100 g of foam; 100 ml of solution at pH 1.8; 5.5×10^{-6} – $1.1 \times 10^{-4}M$ Zr.

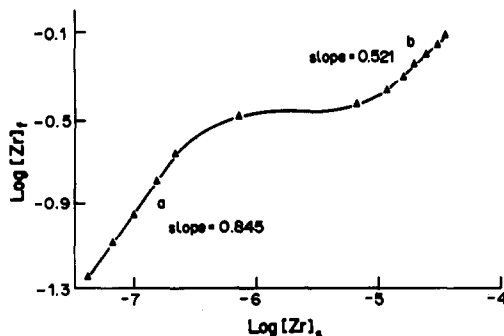


Fig. 5. Effect of zirconium concentration on extraction of $Zr-SCN^-$ complex. Conditions as for Fig. 4. $[Zr]_f$ = equilibrium concentration on foam, mole/kg; $[Zr]_i$ = equilibrium concentration in solution, M .

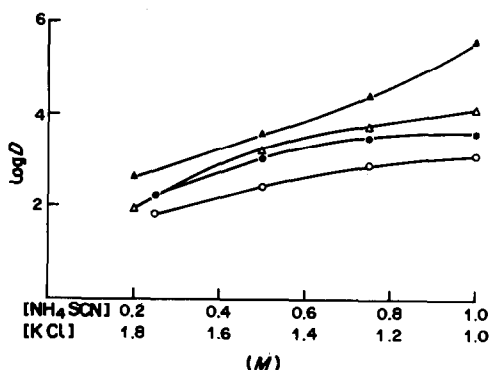


Fig. 6. Effect of NH_4SCN and KCl concentration on the distribution ratio for Zr and HF thiocyanates. Conditions: 0.250 g of foam; 100 ml of solution $1.1 \times 10^{-5}M$ in Zr or $1.12 \times 10^{-5}M$ in Hf at pH 1.8; \blacktriangle —Hf in presence of KCl ; \triangle —Zr in presence of KCl ; \bullet —Hf in absence of KCl ; \circ —Zr in absence of KCl .

Effect of cations

Solutions of $1.1 \times 10^{-5}M$ zirconium or $1.12 \times 10^{-5}M$ hafnium at pH 1.8 and various ammonium thiocyanate and cation concentrations were used to study the effect of cations on the sorption of

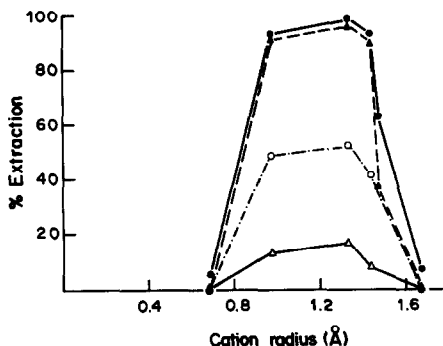


Fig. 7. Effect of cation size on extraction of Zr and Hf. Conditions: 0.250 g of foam; 100 ml of solution $1.1 \times 10^{-5}M$ in Zr or $1.12 \times 10^{-5}M$ in Hf at pH 1.8; extraction time 24 hr; \triangle —Zr with $0.2M$ NH_4SCN + $1.8M$ cation; \circ —Hf with $0.2M$ NH_4SCN + $1.8M$ cation; \blacktriangle —Zr with $1.0M$ NH_4SCN + $1.0M$ cation; \bullet —Hf with $1.0M$ NH_4SCN + $1.0M$ cation.

Table 1. The effect of anions on zirconium and hafnium sorption

Anion	Source	Concentration, M	D_{Zr} , l./kg	D_{Hf} , l./kg	$\alpha = \frac{D_{Hf}}{D_{Zr}}$
Cl ⁻	KCl	1.0	1.23×10^4	4.0×10^5	32.5
Br ⁻	KBr	1.0	4.43×10^3	4.26×10^4	9.61
I ⁻	KI	1.0	1.49×10^3	5.38×10^3	3.61
NO ₃ ⁻	KNO ₃	1.0	4.25×10^3	4.84×10^3	1.14
CH ₃ COO ⁻	CH ₃ COOK	1.0	52	59.5	1.14
SO ₄ ²⁻	K ₂ SO ₄	0.5	6.1	31.5	5.16
HPO ₄ ²⁻	K ₂ HPO ₄	0.5	0	0	—

zirconium and hafnium thiocyanates. The results of one experiment in which the total concentration of ammonium thiocyanate and potassium chloride was kept constant at 2.0M are shown in Fig. 6. In the presence of potassium chloride, the distribution ratio of both zirconium and hafnium increased markedly. When the concentrations of ammonium thiocyanate and potassium chloride were equal, more than 97% of the zirconium or 99% of the hafnium was extracted by the foam. The effect of various univalent cations on the extraction was studied and the results are given in Fig. 7. The degree of extraction for zirconium is generally lower, but the same pattern can be seen for both metals; the extraction changes with the size of the added cation, increasing with increasing size to potassium and then decreasing with further increases in cation radius. The order is $K^+ > Na^+ \approx NH_4^+ > Rb^+ > Cs^+ > Li^+$.

Chow *et al.*¹² proposed a "cation chelation" mechanism for the sorption of anionic metal complexes and used this to explain the extraction of palladium thiocyanate.¹³ In this mechanism the sorption occurs in two steps. First, an ion-association complex of the anionic metal complex and the cation is formed, then the complex dissociates so that the cation occupies a cavity in the foam and the anionic complex acts as a counter-ion to balance the charge of the chelated cation. The size of the cation and of the cavity in the foam is important in determining the extent of extraction of the cation; those cations with a larger or smaller radius will be less efficiently extracted. The order of extraction of zirconium and hafnium thiocyanates in the presence of the cations shown in Fig. 7 can be explained by the cation chelation mechanism, and the selectivity for K^+ is consistent with previous studies.^{12,13}

Effect of anions

To investigate the effects of other anions on the extraction of zirconium and hafnium thiocyanates, and to simplify the interpretation of the results, both the ammonium thiocyanate and potassium concentrations were kept constant at 1.0M and $1.1 \times 10^{-5}M$ zirconium or $1.12 \times 10^{-5}M$ hafnium solutions at pH 1.8 were extracted with 0.250 g of foam for 24 hr.

Table 1 shows the effect of anions on the distribution ratio of zirconium and hafnium. The anions affect the stability of the complexes and D decreases with anion in the order $Cl^- > Br^- > NO_3^- >$

$I^- > acetate > SO_4^{2-} > HPO_4^{2-}$ for zirconium and $Cl^- > Br^- > I^- > NO_3^- > acetate > SO_4^{2-} > HPO_4^{2-}$ for hafnium. The highest distribution ratio and separation factor for zirconium and hafnium are obtained with solutions containing chloride. The lower values for the other anions may result from competitive reactions between the ligands and thiocyanate for the metal, to form unextractable complexes or precipitates, as in the case of HPO_4^{2-} which decreases the distribution ratio to zero.

CONCLUSION

Polyether-type polyurethane foam is highly effective for the preconcentration of zirconium and hafnium from thiocyanate solutions containing only hydrochloric acid, and from those containing potassium chloride at pH 1.8. The composition of the extractable species depends on both the thiocyanate and metal-ion concentrations. The extraction process can be explained in terms of the cation chelation mechanism previously proposed. The separation of zirconium and hafnium under the conditions examined still appears to be very difficult, but some success might be expected if the pH is kept at < 1 or > 6 .

Acknowledgement—This work was supported by the Natural Sciences and Engineering Research Council of Canada.

REFERENCES

1. Z. Kh. Sultanova, L. K. Chuchalin, B. Z. Iofa and Yu. A. Zolotov, *J. Anal. Chem. USSR*, 1973, **28**, 369.
2. T. M. Moroshina, A. M. Serbina, G. A. Petrova and I. I. Sadkovskaya, *Zh. Analit. Khim.*, 1979, **34**, 872.
3. L. T. Gvelesiani, V. K. Akimov, G. Rudzitis and S. Pastare, *Latv. PSR Zint. Akad. Vestis, Khim. Ser.*, 1980, 212.
4. A. I. Orlova, I. V. Vinarov, L. P. Grigoreva and L. I. Iichenko, *Ukr. Khim. Zh.*, 1980, **46**, 548.
5. R. F. Hamon and A. Chow, *Talanta*, 1984, **31**, 963.
6. R. F. Hamon, *Ph.D. Thesis*, University of Manitoba, 1981.
7. *Laboratory Handbook of Teaching and Research in Analytical Chemistry*, Zhong Nan Mineral-Metallurgical Institute, Ke Xue Publishing House, Beijing, China, 1984.
8. A. I. Busev, V. G. Tiptsova and V. M. Ivanov, *Handbook of the Analytical Chemistry of Rare Elements*, Ann Arbor-Humphrey, Ann Arbor, Michigan, 1970.
9. A. A. Nemodruk and A. N. Boganova, *Zh. Analit. Khim.*, 1976, **31**, 854.

10. I. V. Vinarov, A. I. Orlova, G. I. Byk and N. F. Kislitsa, *Ukr. Khim. Zh.*, 1964, **30**, 758.
11. O. A. Sinegribova and G. A. Yagodin, *Zh. Neorgan. Khim.*, 1965, **10**, 1250.
12. R. F. Hamon, A. S. Khan and A. Chow, *Talanta*, 1982, **29**, 313.
13. S. J. Al-Bazi and A. Chow, *ibid.*, 1983, **30**, 487.

EXTRACTION AND PRECONCENTRATION OF SELENIUM FROM AQUEOUS SOLUTIONS AND ITS DETERMINATION IN WATER AND HAIR SAMPLES BY ATOMIC-ABSORPTION SPECTROPHOTOMETRY

M. EJAZ

Department of Chemical Engineering, College of Engineering King Abdulaziz University,
P.O. Box 9027, Jeddah-21413, Saudi Arabia

M. A. QURESHI*

Pakistan Institute of Nuclear Science and Technology, Nilore, Rawalpindi, Pakistan

(Received 16 October 1984. Revised 16 September 1986. Accepted 10 October 1986)

Summary—Several organic solvents, including benzene, xylene, toluene, nitrobenzene, chloroform, carbon tetrachloride, chlorobenzene and high molecular-weight pyridines such as 4-(5-nonyl)pyridine, 2-hexylpyridine and benzylpyridine have been investigated as components of systems for the extraction and preconcentration of selenium from nitric acid solutions containing iodide. The results are discussed in terms of choice of reagents and the acid and iodide concentrations, and of several other parameters affecting the extraction. The utility of the method for separation of selenium from aqueous solution has been evaluated. The method has been used for preconcentration of trace levels of selenium from water and hair samples for determination by atomic-absorption spectrophotometry.

In our investigations on the use of high molecular-weight pyridines in extraction of selenium, we have found that when benzene is used as diluent it enhances the extraction under certain experimental conditions. The present work was therefore devoted to study of the distribution of selenium between several common organic solvents (in addition to various new nitrogen-donor compounds) and nitric acid containing iodide. There seems to be no published information concerning solvent extraction of selenium(IV) with the solvents and aqueous conditions reported here, although chloride complexes of selenium have been extracted¹⁻³ with liquid-anion exchangers, solvating solvents, and chelating extractants. The method is rapid and selective, and the reaction conditions have wide tolerance; it has been used for determination of the element in water and hair samples by atomic-absorption spectrophotometry (AAS). Selenium can be determined without preconcentration, by using hydride generation and silica-tube AAS,⁴ but this is prone to several interferences.⁵⁻⁷

EXPERIMENTAL

Reagents

Standard 1000- $\mu\text{g/ml}$ stock solution of selenium(IV) was prepared by dissolving 0.5 g of pure selenium pellets in a mixture of 2 ml of concentrated sulphuric acid and 3 ml of concentrated nitric acid and making up to volume in a 500-ml standard flask with demineralized distilled water. All

other reagents used were Merck analytical grade. 4-(5-Nonyl)pyridine (Npy), 2-hexylpyridine (Hpy), and benzylpyridine (Bpy) were obtained from K & K Laboratories Inc., Plainview, N.Y. Their characteristics have been reported elsewhere.^{8,9}

Apparatus

A Zeiss F M D-3 atomic-absorption spectrophotometer equipped with a Perkin-Elmer graphite-furnace atomizer unit (HGA-74), a Servogor S RE/541 recorder and a deuterium lamp for background compensation, was used. The selenium hollow-cathode lamp was operated at 20 mA and the wavelength selector was set at 392.1 nm for monitoring the 196-nm line, in accordance with the instruction manual for the atomic-absorption spectrometer. Eppendorf pipettes were used for injecting the sample (10 μl) into the graphite tube of the HGA unit. The heating programme was 60 sec drying at 150°, 60 sec ashing at 600°, 5 sec atomization at 2650°, 10 sec cleaning at 2650°, in the gas-stop mode, with background correction.

Tracers

Selenium-75 ($t_{1/2} = 120.4$ days) tracer was obtained by neutron-activation of SeO_2 in the PARR-1 research reactor of the Pakistan Institute of Nuclear Science and Technology. The concentration of selenium in the original aqueous solutions was $<10^{-6}M$. All other tracers used were obtained by (n, γ) reactions, or by separation of daughter nuclides from the parents without a carrier,¹⁰ or were obtained from the Radiochemical Centre, Amersham. The equipment used for the radioassay has been described in earlier papers.^{9,11}

Extraction procedure

The distribution coefficients of selenium(IV) and the other elements were determined by procedures analogous to those used for zinc¹² and copper.¹³ One ml of 0.1M benzene solution of ligand, or of the pure ligand, was shaken vigorously for 5 min with 1 ml of an aqueous solution of

*Present address: Research Institute, University of Petroleum and Minerals, Dhahran, Saudi Arabia.

nitric acid containing potassium iodide and the radioisotope of the test element ($\sim 10^5$ counts/100 sec/ml). The phases were then separated by centrifugation. Aliquots (500 μ l) were removed from each phase and the concentration of the test element determined radiometrically.

Preparation of calibration graph

Standard aqueous solutions of selenium in the range 0.1–4.0 μ g/ml were prepared by dilution of the stock solution and used for calibration by extraction of the selenium with toluene, and its determination by AAS.

Analysis of hair samples

A representative sample of hair was taken in an acid-washed polyethylene tube and washed with detergent, then rinsed three times with distilled, demineralized water, dried at $\sim 40^\circ$ and cooled. Part of it was then immersed in 20 ml of 1- μ g/ml selenium standard solution for 90 hr.

A 0.5-g portion of each hair sample (selenium-treated and untreated) was added to 4 ml of concentrated nitric acid and left to stand in it overnight to prevent foaming on subsequent heating. The samples were then heated at 60–70° until a clear solution was obtained. The reliability of the decomposition method was checked by adding radiotracer to samples and standards before the digestion.

The clear solution was evaporated (at 60–70°) nearly to dryness, and the residue was taken up in 0.5M nitric acid, made 0.2–0.5M in potassium iodide, and extracted. Standard selenium solutions and a reagent blank were prepared and treated in the same way. The selenium in the extract was determined by AAS.

About 0.5 g of the hair sample which had been dipped in selenium solution was weighed into a narrow quartz tube and irradiated for 30 hr in the PINSTECH reactor at a neutron flux of 2×10^{13} n.cm⁻².sec⁻¹, with a selenium standard taped alongside. The irradiated samples were allowed to decay for 4 weeks. The 265-keV peak was then used for measurement with a Ge(Li) detector coupled with a charge-sensitive preamplifier (Canberra Model 970D) and a spectroscopic amplifier (Octec Model 451). The pulses from the amplifier were analysed by a Nuclear Data NCD-4410 computerized multichannel analyser. The resolution of the detector was 2.9 keV at the 1332 keV gamma-ray of ⁶⁰Co.

Analysis of water samples

Water samples were not given any prior treatment and the amount of selenium was determined by the standard-addition method. A 10-ml water sample, made 0.5M in potassium iodide and containing known added amounts of selenium, was equilibrated with 1 ml of toluene. The digestion procedure used for the hair samples had been found not to be necessary for water samples.

RESULTS AND DISCUSSION

In preliminary experiments, the partition behaviour of selenium between nitric acid and 0.1M 4-(5-nonyl)pyridine (Npy) in benzene was investigated but the distribution coefficients (D) were very low. In line with some of our previous investigations^{12–14} these experiments were repeated with 0.02M potassium iodide in the aqueous phase, and it was found that selenium(IV) could be quantitatively extracted from 1M nitric acid/0.02M potassium iodide by 0.1M Npy in benzene. It was also found that even with only 10^{-4} M Npy in benzene the value of D was 40, suggesting that benzene itself had some solvent action. This led to investigation of the extraction of selenium by benzene and several other common solvents, as shown in Fig. 1. Xylene and heptane were also investigated but gave relatively poor extraction. In general, with increasing acid concentration the D values passed through a maximum at 0.5–1M nitric acid concentration. The decrease at higher acidity is probably due to decrease in the iodide concentration by oxidation to molecular iodine, as shown by most of the organic phases becoming dark red at >4 M nitric acid concentration. The efficiency of the extraction systems ranks in the order 0.1M Npy/benzene > carbon tetrachloride > benzene \geq cyclohexane > chloroform \geq nitrobenzen

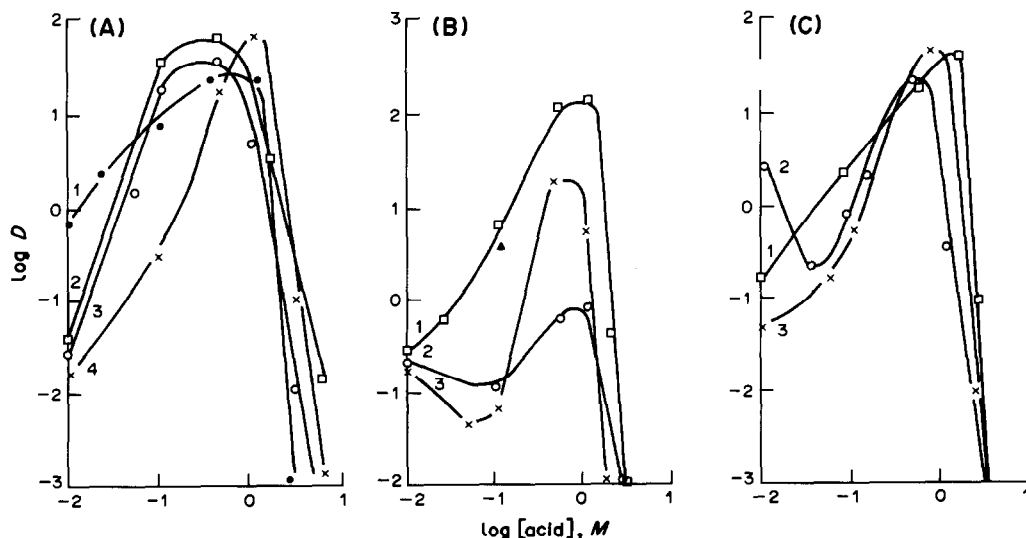


Fig. 1. Dependence of the distribution coefficient of selenium on the concentration of nitric acid solutions which were 0.02M with respect to iodide, with various solvents. A: (1) toluene; (2) carbon tetrachloride; (3) cyclohexane; (4) benzene. B: (1) 0.0M Npy/benzene; (2) Hpy; (3) Bpy. C: (1) nitrobenzene; (2) chlorobenzene; (3) chloroform.

> chlorobenzene > toluene > benzylpyridine > 2-hexylpyridine.

The high efficiency of the Npy/benzene system may be due to synergism. Carbon tetrachloride gives high extraction efficiency over a wider acidity range than the other systems, and this may be associated with its low dielectric constant, presumably because extraction of ion-association complexes is less favourable with solvents of relatively high dielectric constant.

The effect of the iodide concentration on the benzene, 0.1M Npy/benzene and toluene systems was investigated as a function of nitric acid concentration (Fig. 2). There is generally a linear increase in $\log D$ with increasing iodide concentration up to 0.2M, and then a levelling off. In general the efficiency is highest with an acid concentration of $\sim 0.5M$.

The effect of chloride, oxalate, acetate, citrate and ascorbate on extraction of selenium(IV) at 0.5M nitric acid and 0.5M iodide concentrations was found to be generally insignificant up to concentrations of about 0.1M, but in some cases (depending on the combination of anion and solvent system) the degree of extraction was decreased at higher concentrations, offering convenient stripping systems.

The mechanism of the extraction of selenium by the pure solvents is not known. The extraction of nitric acid with aromatic hydrocarbons (Ar) has been attributed to formation of a species such $Ar \cdot H_2O \cdot HNO_3$.¹⁵ It is possible that a species of the type H_2SeI_6 could be formed and extracted in this way, but it seems more likely that a species such as SeI_4 is extracted. The similarity of the extraction curves certainly suggests a common mechanism for all the systems. The increased extraction with pure

Bpy or with benzene containing Npy could be due to the additional formation of an ion-association complex of the type $SeI_5^- \cdot NpyH^+$. We have found that several solvents give quantitative extraction, including benzene, toluene, carbon tetrachloride, cyclohexane and Npy. Of these we examined Npy/benzene and toluene more extensively, with 0.01M nitric acid–1M potassium iodide and 0.5M nitric acid–0.5M potassium iodide respectively. For the Npy/benzene system, the conditions chosen were those giving simultaneous extraction of selenium and common toxic metal ions.^{12,16}

Table 1 shows the distribution coefficients obtained for both systems. The toluene system is much the more selective, but still allows co-extraction of mercury, the halide complexes of which are soluble in a variety of inert solvents.^{17,18} The methods can thus be used for the preconcentration of certain toxic elements in solutions.

At this stage in the work our stock of Npy became exhausted and the suppliers had stopped making it, so for investigation of applications we had to use the toluene system.

Atomic-absorption measurements

Selenium was extracted into toluene from aqueous solutions and determined at 392 nm by AAS. Extraction of selenium is highest in benzene, toluene, carbon tetrachloride and cyclohexane, but toluene was preferred because of its higher boiling point.

The calibration graph was very convex (Fig. 3). When water samples spiked with known amounts of selenium were extracted with toluene as described in

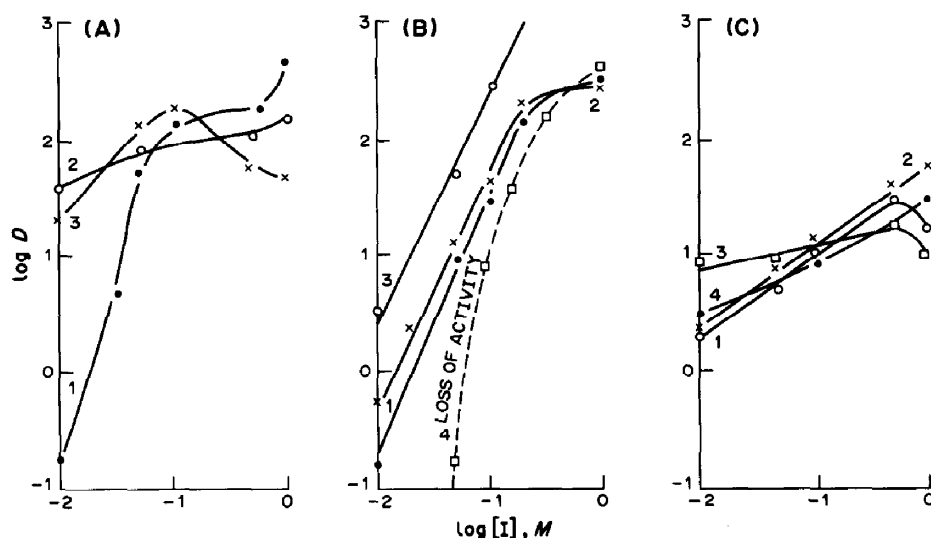


Fig. 2. Dependence of the distribution coefficient of selenium on aqueous iodide concentration for extraction by different solvents from nitric acid media. A, Benzene: (1) 0.1M HNO_3 ; (2) 0.5M HNO_3 ; (3) 1M HNO_3 . B, 0.1M Npy in benzene: (1) 0.05M HNO_3 ; (2) 0.1M HNO_3 ; (3) 0.5M HNO_3 ; (4) 1M HNO_3 . C, Toluene: (1) 0.02M HNO_3 ; (2) 0.1M HNO_3 ; (3) 0.5M HNO_3 ; (4) 1M HNO_3 .

Table 1. Distribution coefficients of various metal ions with respect to selenium

Species	Concentration, <i>M</i>	Distribution coefficients*	
		A	B
Se(IV)	10 ⁻⁶	418	30
Tc(VII)	C.F†	1.57	3.2
Mo(VI)	10 ⁻⁵	1.26	0.21
Cr(VI)	C.F	1.09	—
Mo(V)	10 ⁻⁵	1.21	—
Hf(IV)	10 ⁻⁷	0.0	0.0
Zr(IV)	10 ⁻⁷	0.0	0.0
Sn(IV)	10 ⁻⁸	43	—
	10 ⁻⁷	—	0.15
Cr ³⁺	C.F	0.0	0.0
La ³⁺	10 ⁻⁷	—	0.05
Nd ³⁺	10 ⁻⁷	0.9	0.08
Ce ³⁺	10 ⁻⁸	0.0	0.0
Fe ³⁺	10 ⁻⁶	0.0	—
	10 ⁻⁷	—	0.0
Ir ³⁺	10 ⁻⁸	1.6	—
In ³⁺	10 ⁻⁸	32	0.1
Pm ³⁺	10 ⁻⁸	0.0	0.0
Sr ²⁺	10 ⁻⁸	0.0	—
	10 ⁻⁷	—	0.0
Co ²⁺	10 ⁻⁷	0.2	0.0
Hg ²⁺	10 ⁻⁷	1400	907
Zn ²⁺	10 ⁻⁶	910	—
	10 ⁻⁵	—	0.02
Cd ²⁺	10 ⁻⁸	640	0.03
Pb ²⁺	10 ⁻⁶	33.2	1.0
Mn ²⁺	10 ⁻⁸	0.0	—
	10 ⁻⁷	—	0.0
UO ₂ ⁺	10 ⁻³	0.16	—
Cu ²⁺	10 ⁻⁵	91	—
	10 ⁻⁶	—	0.98
Cs ⁺	10 ⁻⁸	0.0	0.0
Ag ⁺	10 ⁻⁷	0.0	0.0

*A: 0.1M HNO₃/1M KI (0.1M Npy/benzene); B: 0.5M HNO₃/0.5M KI (toluene).

†C.F = Carrier-free.

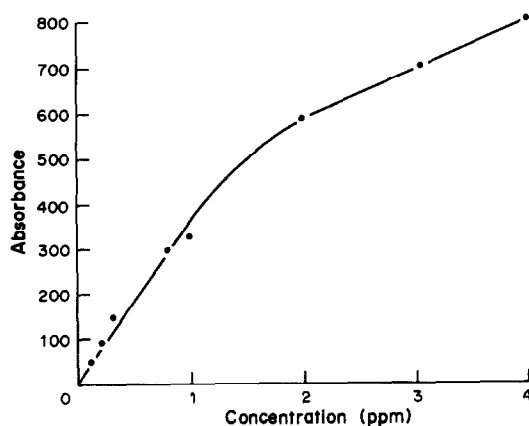


Fig. 3. Calibration curve.

Table 2. AAS determination of selenium in water

Se added to 10 ml of H ₂ O, μg	Se found in 1-ml toluene extract, μg
0.10	0.09 \pm 0.00
0.20	0.18 \pm 0.02
0.30	0.30 \pm 0.02

the procedure, the results shown in Table 2 were obtained. It was further found that the extraction is > 90% even with 100:1 aqueous phase/toluene volume ratio.

Triplicate AAS analysis of the hair sample gave selenium contents of 0.04, 0.03, 0.04 $\mu\text{g/g}$. For the hair sample impregnated by immersion in 1- $\mu\text{g/g}$ selenium solution triplicate AAS analysis gave 0.22, 0.19, 0.21 $\mu\text{g/g}$, and neutron-activation analysis give 0.21–0.25 $\mu\text{g/ml}$, in good agreement with the AAS result.

Acknowledgements—The authors are grateful to Dr. Shamim A. Chaudri and Miss W. Dil for their useful contribution to certain atomic-absorption measurements.

REFERENCES

1. C. Fisher, K. Gloe, P. Muhl and V. V. Bagreev, *J. Inorg. Nucl. Chem.*, 1978, **40**, 1793.
2. Y. Marcus, *Co-ord. Chem. Rev.*, 1967, **2**, 195.
3. N. Jordanov and L. Futekov, *Talanta*, 1965, **12**, 371.
4. G. A. Cutter, *Anal. Chim. Acta*, 1978, **98**, 59.
5. F. C. Pierce and H. R. Brown, *Anal. Chem.*, 1976, **48**, 693.
6. *Idem, ibid.*, 1977, **49**, 693.
7. R. M. Brown, Jr., R. C. Fry, J. L. Moyers, S. J. Northway, M. B. Denton and G. S. Wilson, *ibid.*, 1981, **53**, 1560.
8. M. Ejaz and M. Iqbal, *ibid.*, 1975, **47**, 936.
9. M. Ejaz, M. Iqbal, S. A. Chaudri and R. Ahmed, *Sepr. Sci.*, 1976, **11**, 255.
10. M. S. Fadeeva, O. N. Panlov and V. V. Bakunina, *Zh. Neorgan. Khim.*, 1958, **3**, 165.
11. M. Ejaz, *Anal. Chem.*, 1976, **48**, 1158.
12. M. Ejaz and Shamus-ud-Zuha, *ibid.*, 1978, **50**, 740.
13. M. Ejaz, Shamus-ud-Zuha, D. Wasim and S. A. Chaudri, *Talanta*, 1981, **28**, 441.
14. M. Ejaz, S. Ahmed, D. Wasim and S. A. Chaudri, *ibid.*, 1979, **26**, 503.
15. A. P. Bobylev and L. N. Komissarova, *Russ. J. Inorg. Chem.*, 1978, **23**, 1186, and references therein.
16. M. Ejaz, M. A. Qureshi and Shamus-ud-Zuha, *Sepr. Sci Technol.*, 1981, **16**, 291.
17. I. Eliezer, *J. Chem. Phys.*, 1965, **42**, 3625.
18. *Idem, ibid.*, 1965, **41**, 3276.

DETERMINATION OF GERMANIUM BY GRAPHITE-FURNACE ATOMIC-ABSORPTION SPECTROMETRY

YOSHIKI SOHRIN, KENJI ISSHIKI and TOORU KUWAMOTO

Department of Chemistry, Faculty of Science, Kyoto University, Kyoto 606, Japan

EIICHIRO NAKAYAMA

Research Center for Instrumental Analysis, Faculty of Science, Kyoto University, Kyoto 606, Japan

(Received 22 May 1986. Accepted 9 October 1986)

Summary—The premature loss of germanium as volatile GeO results in low sensitivity and poor reproducibility in the determination of germanium by graphite-furnace atomic-absorption spectrometry. This interference can be eliminated by suppressing the premature reduction of GeO₂ to GeO during the ashing step, and dissociating the germanium oxides into the atoms simultaneously with their vaporization during the atomization step. The premature reduction of GeO₂ to GeO has been successfully prevented by several approaches: (1) diminishing the reducing activity of the graphite furnace by (a) oxidizing the graphite surface and intercalating oxygen into the graphite lattice with oxidizing acids, such as nitric or perchloric, in the sample solution, or (b) using a tantalum-treated graphite furnace; (2) keeping the analyte as germanium (IV) by addition of sodium or potassium hydroxide to the sample solutions.

The determination of germanium by graphite-furnace atomic-absorption spectrometry (GFAAS) can suffer from low sensitivity and poor reproducibility. This is often attributed to part of the analyte being lost as volatile GeO without undergoing atomization. A mechanism for this interference has been reported by Johnson *et al.*,¹ who pointed out that (1) reduction of GeO₂ to GeO occurs on heating in the presence of carbon (graphite), and GeO begins to sublime at *ca.* 1000°; (2) since germanium atoms are not produced below *ca.* 3000°, because of the large dissociation energy of the Ge–O bond, it is important that the time taken for the tube temperature to rise from 1000° to 3000° is as short as possible to prevent loss of the analyte as GeO; (3) in order to prolong the residence time of GeO, a tube furnace rather than a filament furnace should be used. However, they did not attempt to suppress the formation of GeO by matrix modification or by surface treatment of the furnace.

We have found that the nature of the sample matrix, the surface condition of the graphite and the atomization conditions all play a role in determining the magnitude of the error caused by the formation of GeO. In this paper, we show how the premature formation of GeO can be noticeably suppressed by modifying the sample matrix with an oxidizing acid or an alkali, and by tantalum-treatment of the furnace.

EXPERIMENTAL

Apparatus

A Nippon Jarrel-Ash model AA-8200 atomic-absorption spectrometer and a model FLA-100 electrothermal atomizer

were used. Argon was used as the purge gas, at 2.0 l/min flow-rate during all steps unless otherwise stated. Nippon Jarrel-Ash graphite tubes were used. Tantalum-treated graphite furnaces were made from new tubes by Zatká's method.² A Hamamatsu Photonics germanium hollow-cathode lamp was used as the spectral source. The unresolved 256.118–265.158 nm resonance line-pair of germanium was employed for all analyses. Samples were injected with a 20- μ l Eppendorf micropipette.

The heating power of the FLA-100 was supplied by a current-regulated sequential control system. The temperatures shown below (in parentheses after the currents) were taken from the current–temperature table in the user's manual for the FLA-100.

Reagents

Demineralized distilled water (Millipore Milli-Q) and chemicals of reagent-grade quality or better were used. A 1000 μ g/ml germanium standard solution was made by dissolving 0.1439 g of pure germanium dioxide in 25 ml of 1M sodium hydroxide and diluting to 1000 ml with demineralized distilled water. This solution, when further diluted with only demineralized distilled water, will be referred to as an aqueous solution of germanium.

RESULTS AND DISCUSSION

Heating conditions

An atomization study showed that the maximum peak height for germanium was obtained with currents greater than 280 A (2890°) in the "FLASH" mode with untreated furnaces. Under such optimum atomization conditions, the peak height is considerably affected by the ashing conditions, as shown in Fig. 1. The peak height increases with increase in ashing current, attaining a maximum value at *ca.* 70 A (1050°) and decreasing abruptly above 75 A (1115°). Although, the higher the ashing temperature,

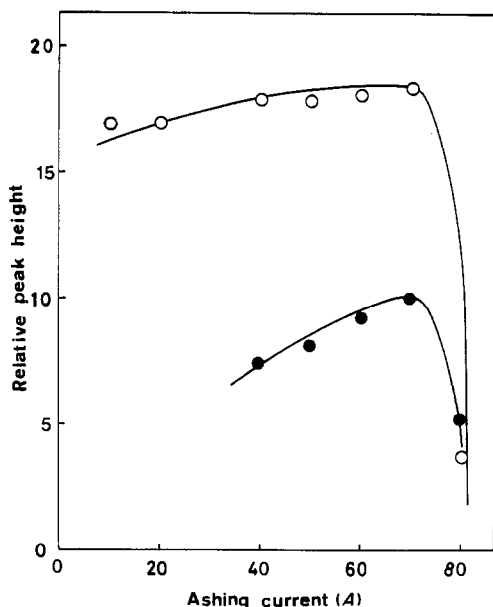


Fig. 1. Effect of ashing current on the relative peak height for 200 ng/ml germanium with the untreated furnace. Dry 22 A, 20 sec. Ash, 50 sec. Atomize, 300 A ("FLASH"), 7.5 sec. Ar flow 2.0 l./min. ○, 0.1M KOH; ●, 0.1M HNO₃.

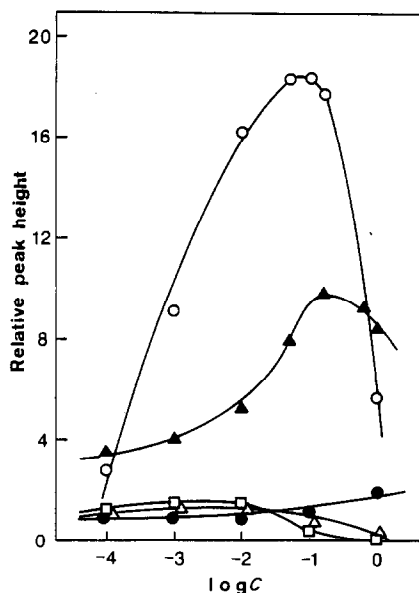


Fig. 2. Relative peak height for 200 ng/ml germanium in acidic solutions with the untreated furnace. C is the molarity of the acids. ○, HClO₄; ▲, HNO₃; ●, CH₃COOH; △, HCl; □, H₂SO₄.

the shorter the time required to achieve atomization, producing increasing efficiency of atomization up to 70 A (1050°) ashing current, loss of the analyte as GeO was significant above 75 A (1115°). Table 1 shows the optimum heating conditions with untreated furnaces. Subsequent studies were conducted under these conditions unless otherwise stated.

However, when tantalum-treated furnaces are used these currents should be reduced by 15% to obtain maximum peak height for germanium, because the electrical resistance of the furnaces is altered by the tantalum treatment.

Effects of coexisting materials

Johnson *et al.*¹ reported that other salts, such as sodium chloride or magnesium sulphate, present in the sample, interfere in the determination of germanium, by either molecular absorption or light scattering and that addition of zinc nitrate improves the sensitivity of the determination. We have studied extensively the effect of other species in the sample solution and found that the atomization efficiency for germanium is affected much more than that for most of the other heavy metals.

Acids. The effects of various acids on the germanium absorption peak are illustrated as a function of

their concentrations in Fig. 2. The results are shown as relative peak heights normalized with respect to the peak height obtained with the aqueous solution of germanium. The relative peak heights are unity for hydrochloric, sulphuric and acetic acid concentrations less than 10⁻²M, but interferences are observed for the first two acids at concentrations greater than 10⁻²M. However, for nitric and perchloric acid solutions, the peak heights increase significantly with acid concentration. When an aliquot of the aqueous germanium solution was fired in a furnace which had been previously heated with an aliquot of 0.1M perchloric or nitric acid up to the ashing temperature, the peak height was greater than would otherwise have been expected. Since almost all of the perchloric and nitric acid in the graphite furnace should be lost on heating during the ashing step, it is considered that the increase in the peak height is attributed to a change in the condition of the graphite furnace. That is, oxidation of the graphite surface and intercalation of oxygen into the graphite lattice by these oxidizing acids² counteracts the reducing activity of the graphite, suppressing the premature reduction of GeO₂ to GeO by the graphite. The effect of perchloric acid is more remarkable than that of nitric acid, showing that perchloric acid intercalates oxygen more effectively into the graphite lattice.

Bases. The effects of several bases on the germanium absorption peak are illustrated as a function of their concentrations, in Fig. 3. The relative peak heights remain at unity for all ammoniacal solutions, whereas the peak heights for alkali-metal hydroxide solutions increase significantly with alkali concentration. This indicates that the molten alkali-metal

Table 1. Optimum heating programme

	Dry	Ash	Atomize
Current, A	22	70	300*
(Temp., °C)	(250)	(1050)	(3020)
Time, sec	20	50	7.5

*"FLASH" mode.

Sample volume, 20 μl.

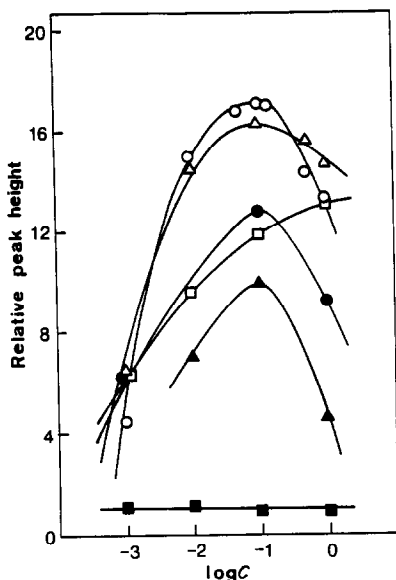


Fig. 3. Relative peak height for 200 ng/ml germanium in basic solutions with the untreated furnace. C is the molarity of bases. ○, KOH; △, NaOH; □, LiOH; ●, RbOH; ▲, CsOH; ■, NH₃.

hydroxides keep GeO₂ as germanium(IV), suppressing its premature reduction by the graphite during the ashing step. However, ammonia is vaporized during the drying step, thus showing no effect.

Salts. The effects of various salts on the germanium signal are tabulated in Table 2 along with those of acids and alkali-metal hydroxides. The relative peak heights are higher in the presence of alkali-metal or alkaline-earth metal nitrates, nitrites, carbonates or acetates, which change to the oxides on heating during the drying and ashing steps. Of these salts, the nitrates are the most effective. All of these salts are likely to show the same magnitude of effect as the alkali-metal hydroxides, especially the nitrates, which enhance the effect of oxidation of the graphite. However, the effects of magnesium nitrate and sodium perchlorate on the relative peak heights are about the same as those of nitric and perchloric acids respectively. This shows that these salts act only as

Table 3. The relative peak heights for 200 ng/ml germanium with tantalum-treated furnaces, in the presence of various salts, acids and bases

Anion	Cation, present at 0.1M			
	Na ⁺	K ⁺	NH ₄ ⁺	H ⁺
OH ⁻	16.4	17.5	14.5	14.0
NO ₃ ⁻	20.5	19.3	—	13.8
CH ₃ COO ⁻	18.1	—	—	—
ClO ₄ ⁻	18.4	—	—	18.9
Cl ⁻	8.2	—	—	10.8
SO ₄ ²⁻	0.2	—	—	1.7

oxidizing agents for graphite on heating, due to the formation of inert magnesium oxide from the nitrate and sodium chloride from the perchlorate. Halides, sulphate and phosphate decrease the peak height to the same extent as do their respective acids. Since these salts do not change to oxides on heating during the ashing step, they evaporate unchanged during the atomization step. This is consistent with the high background absorption observed during the atomization step when these salts are present. Although ammonium peroxydisulphate is an oxidizing agent, it does not increase the peak height, presumably because of its facile thermal decomposition.

Tantalum-treated furnaces

The effects of acids, alkali-metal hydroxides and salts on the germanium atomic-absorption peak when tantalum-treated furnaces are used are given in Table 3. The peak height for the aqueous solution is 14 times that observed with the untreated furnaces. This is probably due to the fact that the tantalum carbide layer on the graphite furnace prevents the analyte from coming into contact with the graphite, suppressing the premature reduction of GeO₂ to GeO.

However, the effects of materials which increase the peak height (relative to that for aqueous solution), such as nitric acid, perchloric acid and alkali-metal hydroxides, are almost the same as those observed with untreated furnaces. The interference of hydrochloric acid and sulphuric acid and their salts

Table 2. The relative peak heights for 200 ng/ml germanium with the untreated furnace in the presence of various salts, acids and bases

Anion	Cation, present at 0.1M					
	Na ⁺	K ⁺	Mg ²⁺	Ca ²⁺	NH ₄ ⁺	H ⁺
OH ⁻	16.2	17.0	—	—	1.1	(1)
NO ₃ ⁻	20.5	19.9	13.2	20.1	12.0	10.0
NO ₂ ⁻	18.3	—	—	—	—	—
CO ₃ ²⁻	—	18.0	—	—	1.0	—
CH ₃ COO ⁻	17.7	—	—	—	—	1.1
ClO ₄ ⁻	18.5	—	—	—	—	18.4
Cl ⁻	0.9	0.5	—	—	—	0.7
Br ⁻	—	0.5	—	—	—	—
I ⁻	—	1.0	—	—	—	—
H ₂ PO ₄ ⁻	—	0.7	—	—	—	—
SO ₄ ²⁻	—	0.5	—	—	—	0.4
S ₂ O ₈ ²⁻	—	—	—	—	0.8	—

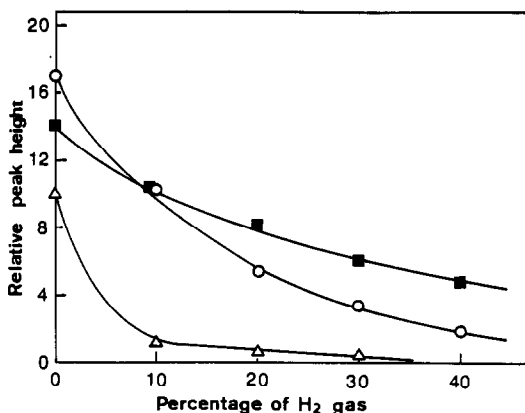


Fig. 4. Effect of hydrogen (added to the argon purge gas) on the relative peak height for 200 ng/ml germanium. Total flow-rate of the gas mixture was 2.0 l./min. ○, untreated furnace, 0.1M KOH; △, untreated furnace, 0.1M HNO₃; ■, tantalum-treated furnace, aqueous germanium solution.

is much more pronounced than for the untreated tubes, however.

Effects of gases in the furnace

The effects of gases in the furnace were studied to examine the validity of the argument stated above.

First, the effect of atmospheric oxygen was tested with a furnace that had been previously heated at ca. 70 A (1050°) without passage of argon purge gas. With this furnace, an increase of three times in the peak height was observed for the aqueous solution. This shows that the reducing activity of the graphite furnace is reduced by oxidation of its surface. The magnitude of the increase in the peak height was less than that observed for nitric and perchloric acid solutions because oxygen intercalation into the graphite lattice probably does not occur with atmospheric oxygen.

Secondly, the effect of hydrogen (added to the purge gas) on the peak heights was tested with untreated and tantalum-treated furnaces. With both furnaces, the peak heights decreased with an increase in the amount of hydrogen in the purge gas, as shown in Fig. 4. The peak heights also decreased when

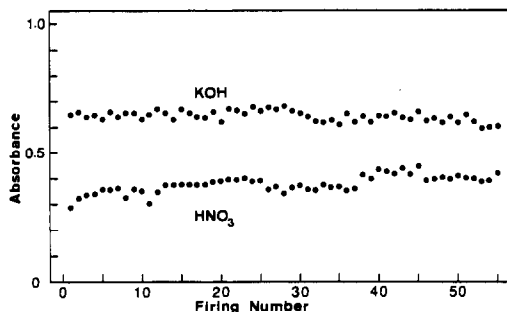


Fig. 5. Repetitive measurements for 200 ng/ml germanium in 0.1M HNO₃ and 0.1M KOH.

hydrogen was added only during the drying and ashing steps. Consequently, this decrease in the peak height is most likely caused by reduction of GeO₂ by the hydrogen during the ashing step. With untreated furnaces, the peak height decreased more abruptly than with tantalum-treated furnaces. This indicates that germanium dioxide is reduced not only by the hydrogen but also by the graphite, when other species added in the sample solution, such as nitric acid, are reduced by the hydrogen.

Reproducibility and sensitivity

The reproducibility of the measurements for germanium solutions in 0.1M nitric acid and 0.1M potassium hydroxide was tested with a new untreated furnace. Figure 5 shows that the fluctuation of absorbance was smaller when the potassium hydroxide solution was used. The relative standard deviations were 3.5% for the alkali system and 8.6% for the acid system. Moreover, though the absorbance peak increases with addition of nitric acid and decreases with addition of potassium hydroxide as the number of firings increases, the magnitude of the absorbance change for the acid is larger than that for the base. Consequently, it is apparent that the use of 0.1M potassium hydroxide is preferable for the determination of germanium by GFAAS.

When germanium in 0.1M potassium hydroxide was determined with an untreated furnace, the detection limit for S/N = 2 was 60 pg in 20 μl and the characteristic weight was 28 pg for 1% absorption. These values represent an improvement by a factor of five over the results reported by Johnson *et al.*¹

CONCLUSION

The interference caused by the formation of GeO can be eliminated by optimizing the heating programme, modifying the matrix in the sample solution and using the tantalum-treated furnace. To obtain high sensitivity and good reproducibility in results, it is recommended that samples be prepared in 0.1M potassium hydroxide. However, other types of chemical interferences, caused by chloride or sulphate for example, are still serious (as shown in Tables 2 and 3). These interferences can only be eliminated by a preliminary separation of the germanium from the sample matrix. A suitable procedure for this will be discussed in forthcoming reports.

Acknowledgement—This research was supported in part by a grant from the Nissan Science Foundation.

REFERENCES

1. D. J. Johnson, T. S. West and R. M. Dagnall, *Anal. Chim. Acta*, 1973, **67**, 79.
2. V. J. Zátka, *Anal. Chem.*, 1978, **50**, 538.
3. W. Slavin, G. R. Carnrick and D. C. Manning, *Anal. Chim. Acta*, 1982, **138**, 103.

NON-AQUEOUS FLUORIMETRIC DETERMINATION OF SCANDIUM IN SILICATE ROCKS

F. GARCIA SANCHEZ and C. CRUCES BLANCO

Department of Analytical Chemistry, Faculty of Sciences, The University, 29071 Málaga, Spain

A. HEREDIA BAYONA

Department of General Chemistry, Faculty of Sciences, The University, 29071 Málaga, Spain

(Received 27 January 1986. Revised 24 September 1986. Accepted 8 October 1986)

Summary—A method for the fluorimetric determination of scandium with 1,2,7-trihydroxyanthraquinone in dimethylformamide medium is described. The calibration graphs obtained by the normal, synchronous, and synchronous first and second derivative techniques are linear between 12 and 225 ng/ml, and the detection limit is 2 ng/ml. The method is applied to the determination of Sc(III) in two simulated and two naturally occurring rocks.

As a general rule, inorganic spectrofluorimetry has been traditionally done in aqueous or ethanolic media, with no systematic search for the most suitable solvent. However, many changes in the position, relative intensity, shapes and Stokes shifts of the fluorescence and absorption bands can be induced by solvents.¹ Hence proper study of these effects on the characteristics of the reagent and complex could give data useful for designing a more sensitive and selective spectroscopic determination.²⁻⁴

The fluorescence usually arises solely from the organic ligand, and the cation in the complex only modifies the spectral characteristics. For that reason, knowledge of the ligand behaviour permits better design of the analytical procedure.

Scandium has been determined by both fluorimetry and photometry,⁵⁻⁷ but the use of anthraquinone derivatives as ligands has been restricted to photometric methods. For example, Alizarin Red⁸ and anthrapurine⁹ have been used in the determination of scandium at $\mu\text{g/ml}$ levels, whereas until now no anthraquinone dye has been used as a fluorogenic ligand for scandium determination.

Generally, the ligands used in the determination of scandium have a functional hydroxy group and the co-ordination takes place in alkaline media. This limits the use of hydroxyanthraquinones because of their instability in these media.

In the present work, use of a non-aqueous medium (*N,N*-dimethylformamide, DMF) permits the determination of scandium with 1,2,7-trihydroxyanthraquinone. The selectivity is poor, but this is always a problem with scandium and the lanthanides, because of the similar chemical and physical properties of these elements, necessitating a separation procedure. Fractional crystallization, liquid-liquid extraction, ion-exchange and gas-liquid chromatography

have all been used with success but are time-consuming and complicated. Emission, absorption and fluorescence measurements in the X-ray, ultraviolet and visible regions are all subject to spectral interference. A prior separation is also needed with the procedure described, to improve the selectivity.

EXPERIMENTAL

Apparatus

Fluorescence measurements were made with a Perkin-Elmer MPF-43A spectrofluorimeter equipped with a 150-W Osram XBO lamp, excitation and emission monochromators, 1×1 cm fused-silica cells, an R-777 Hamamatsu photomultiplier, and a Perkin-Elmer 023 recorder. Instrument sensitivity was adjusted daily, with a Rhodamine B bar as reference standard. The Perkin-Elmer model DCSU-2 unit, connected to the spectrofluorimeter, was used to obtain the derivative spectra.

Reagents

1,2,7-Trihydroxyanthraquinone (THAn) solution, $1 \times 10^{-3}M$, in DMF, was prepared weekly. Diluted solutions were prepared from this stock solution daily, with DMF.

A 0.015M stock solution of scandium was prepared by dissolving the oxide in 7M nitric acid and standardized complexometrically. Solutions of $1 \times 10^{-3}M$ concentration were prepared by dilution with DMF.

All solvents used were of analytical reagent grade.

General procedures

Place 0.5 ml of $1 \times 10^{-3}M$ 1,2,7-THAn solution in DMF and an aliquot of the sample solution in DMF [containing 0.34-2.55 μg of Sc(III)] in a 10-ml standard flask. Dilute to volume with DMF. Record the first and second derivative ($\Delta\lambda = 10$ nm) of the synchronous spectrum ($D\lambda = 30$ nm), with a response-time of 0.3 sec, and a scan-speed of 120 nm/min. Measure the derivative values as the vertical distance from the peak to the trough, and from the right-hand peak to the trough, for the first and second derivatives, respectively.

Sample preparation

Vermiculite. Accurately weigh approximately 0.1 g of the finely powdered vermiculite into a graphite crucible and add 0.6 g of anhydrous lithium metaborate. Insert (on a silica tray) into a muffle (1000°), then withdraw it after 15 min. Transfer the cooled fusion cake from the crucible to a 1500-ml polythene beaker containing 950 ml of water and 15 ml of concentrated hydrochloric acid and leave it for 2–3 hr to dissolve. Transfer the solution to a 1-litre standard flask and dilute to volume with water. Store the solution in a clean dry polythene bottle.

Montmorillonite. Accurately weigh approximately 0.1 g of the finely powdered rock. Add 10 ml of concentrated hydrofluoric acid and 2 ml of 9M sulphuric acid, and evaporate to dryness. Dissolve the final residue with 5 ml of 6M hydrochloric acid. Transfer to a 50-ml standard flask and dilute to the mark with demineralized water.

Simulated samples. Two samples were prepared, corresponding to a diatomite and steatite according to the compositions given by the British Ceramic Research Association.¹⁰

RESULTS AND DISCUSSION

Fluorescence spectra and effect of experimental variables

Figure 1 shows the fluorescence excitation and emission spectra of 1,2,7-THAn and its complex with scandium in DMF medium. A considerable increase in the fluorescence intensity at 565 nm (excitation at 465 nm) is observed to be caused by the chelation.

The fluorescence and absorption spectra of both reagent and complex in eight different solvents were studied to evaluate the solvent–solute interaction. The most relevant characteristics found are summarized in Table 1. An increase in the dielectric constant causes a decrease in the relative fluorescence intensity (RFI) in both reagent and complex, so acetone, acetonitrile and dioxan give the highest RFI and water the lowest. The fluorescence intensity of the complex was greater than that of the reagent only in acetonitrile and DMF, and the increase was larger for DMF as medium.

The absorption maxima of the reagent and complex are generally shifted to longer wavelengths with increasing solvent polarity, but some solvents give

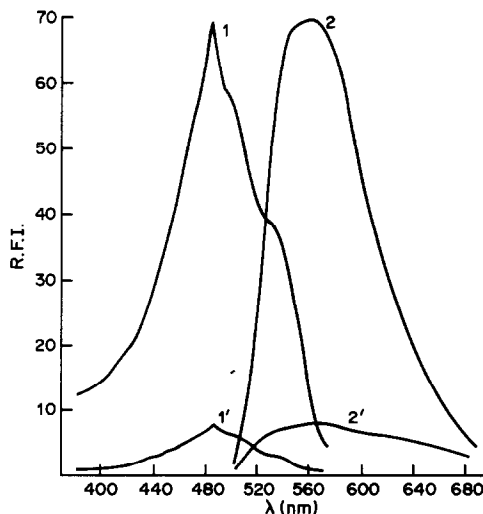


Fig. 1. Excitation (1,1') and emission (2,2') spectra of Sc(III)-1,2,7-THAN complex and the reagent at a concentration of 0.22 $\mu\text{g/ml}$; $\lambda_{\text{exc}} = 465 \text{ nm}$, $\lambda_{\text{em}} = 565 \text{ nm}$. Sensitivity: coarse 0.3, fine 0, slit band-passes 10 nm.

anomalous behaviour which cannot be explained in terms of polarity or dielectric constant, and other aspects have to be taken into account.

The charge-transfer nature of the long-wavelength absorption band of hydroxyanthraquinones has been studied for various organic solvents with different donor numbers¹¹ and in general the solvent–anthraquinone interaction appears to be charge-transfer complexation with strong electron-pair donor solvents.^{12,13}

From the analytical point of view, there are three aspects of the results in Table 1 that need further explanation. First, the unusual blue-shift observed for the DMF solutions. Owing to the charge-transfer nature of the reaction, and the fact that DMF is a polar solvent with high dielectric constant and solvating ability, the reagent dissociates in the ground state to give an ionic species which cannot occur in other solvents. When scandium is present in the

Table 1. Spectral characteristics of the reagent (R) and complex (C) in different solvents

Solvent	λ_a , nm		λ_f , nm		$D\lambda$,* nm		RFI		$\log \epsilon \dagger$		$\Delta\text{RFI} \S$
	R	C	R	C	R	C	R	C	R	C	
Ethanol	518	520	570	565	52	45	73	28	4.0	3.8	-45
Methanol	515	516	570	560	55	44	56	42	4.1	3.8	-14
Acetone	480	480	555	565	75	85	130	113	3.9	3.9	-17
Acetonitrile	485	478	560	560	75	82	85	118	3.8	3.8	33
Dioxan	478	480	565	565	87	85	100	80	3.8	3.9	-20
DMF	525	485	587	565	62	80	6	62	4.0	3.9	56
Water	480	518	565	565	85	47	5	4	3.8	3.8	-1
Water:dioxan (10:90)	504	482	565	570	61	88	63	62	3.9	3.8	-1

*Stokes shift, $D\lambda = \lambda_f - \lambda_a$; λ_f = wavelength of fluorescence maximum; λ_a = wavelength of maximum absorbance.

$\dagger \epsilon$ expressed in $\text{l. mole}^{-1} \cdot \text{cm}^{-1}$.

$\S \Delta\text{RFI} = \text{RFI}_C - \text{RFI}_R$.

solution, the charge on this anion is minimized by the reagent-cation interaction and the absorption maximum is blue-shifted to a wavelength indicating acidic character ($\lambda = 480$ nm).

Secondly, the large difference between the RFI of the reagent and of the complex is due to the reagent anion in the excited state being less stabilized than the complex, and hence having more rapid deactivation. This causes the factor of 10 increase in RFI which makes possible this fluorimetric determination of Sc(III).

Thirdly, the effect of water required examination. Even as little as 1% water greatly decreased the fluorescence of the complex, indicating that when water is present, a rapid deactivation of the excited state take place owing to the strong interaction of hydrogen bonds. Hence the method must be applied in anhydrous DMF medium. Use of this solvent increases the sensitivity, and the photodecomposition of the reagent which occurs in aqueous medium is avoided, allowing longer storage of standard solutions and giving a more reliable analytical method.

The effect of reagent concentration was tested at constant Sc(III) concentration of $2.5 \times 10^{-6}M$ and showed a linear increase in signal up to $5 \times 10^{-5}M$ reagent concentration, and further linear increase (but of lower slope) at higher concentrations. A $5 \times 10^{-5}M$ reagent concentration was selected for use, but because at least 10:1 reagent:metal concentration ratio is needed for the complex formation, this limits the Sc(III) concentration to $5 \times 10^{-6}M$. The RFI is a linear function of Sc(III) concentration from $6.2 \times 10^{-7}M$ up to this limit.

Under the selected experimental conditions, no changes in RFI were observed when the order of reagent addition was changed or the temperature was varied from 10 to 70°. The stability of the complex was tested by exposing the solutions to daylight and the RFI was found to remain stable for 2 hr, after which a decrease occurred.

Selection of instrumental parameters

The application of the derivative technique to the determination of metal ions by chelating agents has been recently developed.^{14,15} However, the fluorescence spectra of these metallic chelates are characteristically wide and poorly structured bands (see Fig. 1), leading to very weak derivative signals and poor detection limits. This is because the amplitude of the derivatives is inversely related to the band-width of the normal spectrum, so the band-narrowing effect of the synchronous scanning technique is very valuable.

When these two techniques are used, the instrumental parameters such as the time-constant (t_r), scan-speed of the monochromators (V_{scan}), differential wavelength interval ($\Delta\lambda$), and the difference in wavelength between the two monochromators ($D\lambda$) must be optimized. This last parameter, $D\lambda$, can

considerably modify the spectrum shape, as shown in Fig. 2.

For selection of the appropriate $D\lambda$ value, various synchronous spectra from $D\lambda = 30$ nm to $D\lambda = 100$ nm (Stokes shift) were recorded. A red shift and a decrease in the RFI is observed (Fig. 2) for change from the highest to the smallest $D\lambda$. Although a better signal-to-noise ratio (SNR) would be obtained by using $D\lambda = 100$ nm, we have selected $D\lambda = 30$ nm for the experimental work, because of the symmetry and the narrow peak half-width (38 nm) of the synchronous spectrum at $D\lambda = 30$ nm compared to that of the normal spectrum (90 nm).

Consequently, the application of the synchronous and synchronous derivative techniques, in this particular case, gives a much more selective method, despite the sacrifice in sensitivity and detection limit.

To register both the synchronous first and second derivatives, and to obtain a good SNR, a combination of 120 nm/min scan-speed, 0.3 sec time-constant and 10 nm $\Delta\lambda$ was found to be optimal.

Calibration graphs, sensitivity and precision

The calibration graphs prepared by plotting the normal, and synchronous first and second derivative values against scandium concentrations were linear over the range 34–225 ng/ml. The synchronous first and second derivative spectra used for this calibration graph are shown in Fig. 3; there is good correlation between signal and concentration.

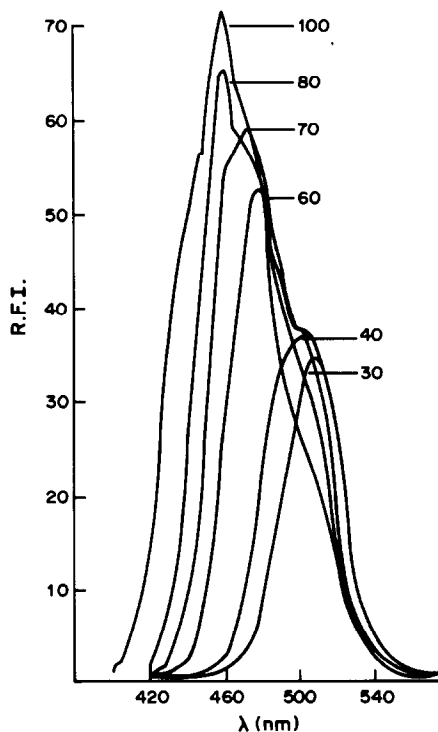


Fig. 2. Synchronous spectra at different $D\lambda$ of a $0.22 \mu\text{g/ml}$ solution of the complex in DMF. Conditions as for Fig. 1.

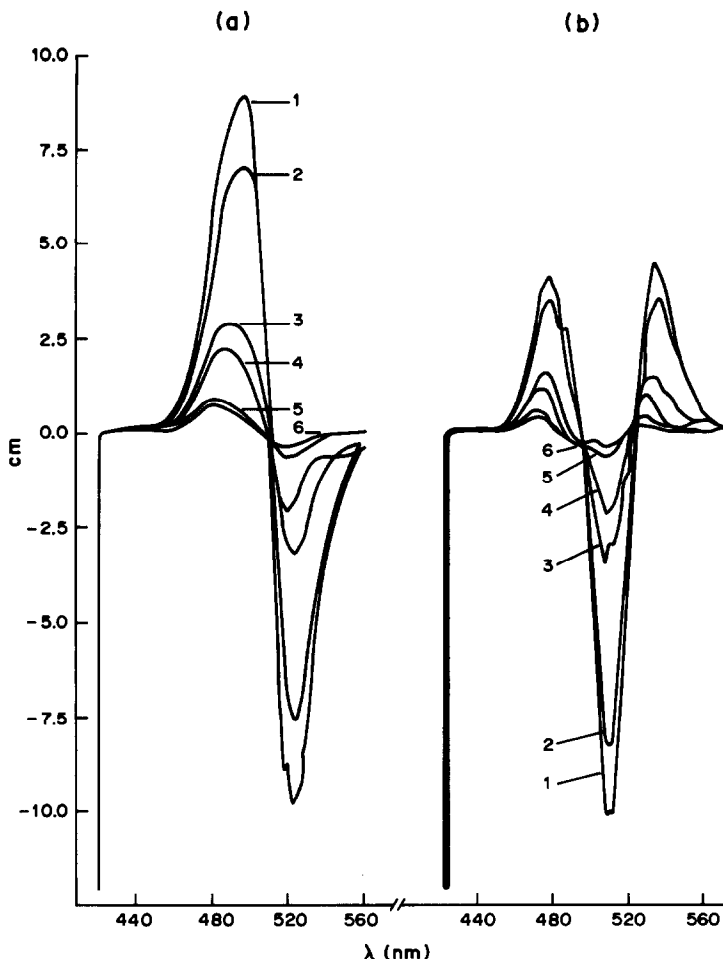


Fig. 3. Synchronous first (a) and second (b) derivative spectra used for the calibration graph: Sc (1) 50, (2) 75, (3) 112.5, (4) 170, (5) 225 ng/ml, (6) reagent blank. Sensitivity: coarse 3, fine 5. Scan-speed 120 nm/min, time-constant 0.3 sec, $\Delta\lambda = 10$ nm.

The limits of detection, c_L , and of quantification, c_Q , (used as the lower point of the analytical graph), of all the methods were established according to the IUPAC definitions.^{16,17} The sensitivity, s_A , was calculated as previously defined.¹⁸

For a series of ten measurements of 112.5 ng/ml Sc(III), the concentrations found and standard deviations, together with other details related to the analytical methods are shown in Table 2. Although the data for c_L and c_Q are very similar for the three techniques investigated, there is a considerable reduction in s_A , c_L and relative standard deviation by the synchronous method, making this, together with the

synchronous first derivative method, the most appropriate choice for the determination of scandium.

Effect of diverse ions

In the determination of 112.5 ng/ml Sc(III) various ions were tested to check the selectivity of the methods. Because of the water effect on the fluorescence signal, $1 \times 10^{-3} M$ solutions of each ion in DMF were prepared from concentrated aqueous solutions. The results are shown in Table 3. The tolerance criterion is based on the RSD of the methods, and taken as a deviation of the fluorescence intensity (or derivative values) of $\bar{x} \pm 2t_{s_s}$, where \bar{x} is the mean value for

Table 2. Characteristics of the analytical methods

Method	Sensitivity, s_A , ng/ml	c_L , ng/ml	Linear dynamic range, ng/ml	Concentration found, ng/ml	R.S.D., %
Fluorimetric	9	4	12-225	135	7.0
Synchronous	6	2	8-225	106	5.3
Synchronous (first deriv.)	8	3	9-225	104	4.7
Synchronous (second deriv.)	7	3	10-225	131	5.3

Table 3. Interference study [Sc(III) = 112.5 ng/ml]

Fluorimetric	Synchronous	Synchronous (first deriv.)	Synchronous (second deriv.)	Tolerance ratio, [ion]: [Sc(III)]
Fe(III), Mg(II)	Al(III), Fe(III), Mg(II),	Fe(III), Al(III), Mg(II)	Fe(III), Al(III), Mg(II)	100
SO ₄ ²⁻	SO ₄ ²⁻	SO ₄ ²⁻	SO ₄ ²⁻	50
Al(III)		Gd(III), F ⁻	Gd(III), F ⁻	25
F ⁻	F ⁻			10
Cu(II), Gd(II)	Cu(II), Gd(II)	Cu(II), Sm(III), Y(III), Ga(III)	Sm(III), Y(III)	5
Sm(III), Y(III)	Sm(III)			2
Ga(III)	Y(III), Ga(III)			
Pr(III), La(III)	Pr(III), La(III)	Pr(III), La(III)	Pr(III)	1
				0.5

Table 4. Recoveries (%) of scandium in four silicate rocks

Type of silicate rock	Sc(III) taken*	Fluorimetric	Synchronous	Synchronous (first deriv.)	Synchronous (second deriv.)
Vermiculite	1	101	97	106	101
	2	104	103	101	100
	3	113	100	98	108
Montmorillonite	1	105	94	102	98
	2	111	102	100	103
	3	117	95	106	103
Steatite†	1	107	96	103	99
	2	116	98	106	107
	3	113	97	99	100
Diatomite†	1	109	97	105	101
	2	120	101	111	111
	3	114	99	101	101

* (1) 225, (2) 112.5, (3) 50 ng/ml.

† Simulated samples prepared according to Bennett and Reed.¹⁰

scandium alone, s_s the standard deviation of the analytical signals, and t is "Student's" t for 10 measurements.

It can be deduced from Table 3 that the tolerance for serious interferences such as that of Al(III) can be raised by a factor of 10 by employing the synchronous and synchronous derivative techniques, and by a factor of 2 for SO₄²⁻, F⁻, Gd(III), Sm(III), Y(III) and Ga(III) with the synchronous derivative approach. This illustrates that with a little extra instrumentation, real advantages in terms of selectivity are obtained with these techniques.

Where high tolerance ratios appear to be obtained for some ions with the normal fluorescence method, this is due to the high imprecision (high s_s) and lack of sensitivity of the analytical method.

Stoichiometry

The ratio of scandium to 1,2,7-THAn in the chelate was established by both the molar-ratio and continuous-variations methods. The results indicated a scandium to 1,2,7-THAn ratio of 1:3.

Analysis of silicate rocks

To verify the utility of the methods they were applied to the determination of scandium in silicate rocks (two "real", vermiculite and montmorillonite, and two simulated, steatite and diatomite).

To 0.5 ml of the sample solution, 0.68, 0.34 and

0.15 ml of the stock solution of Sc(III) were added. The solutions were diluted with DMF to a final volume of 10 ml, to obtain spiked samples containing 45, 22 and 9.85 µg/ml Sc(III). These samples were used for analysis by the general procedure. The final scandium concentrations to be determined were 225, 112.5 and 50 ng/ml, respectively, obtained by adding 0.5 ml of $1 \times 10^{-3} M$ 1,2,7-THAn solution to 50 ml of sample and diluting to 10 ml with DMF.

Recovery data for five replicates of each sample are indicated in Table 4. It can be seen that a positive error was obtained at the three scandium levels with the conventional fluorimetric method, whereas recoveries near to 100% were obtained by application of the synchronous and synchronous derivative approaches, confirming their advantages.

Although sulphate interferes at 50:1 ratio to Sc(III) and sulphuric acid was used in decomposition of the montmorillonite, the triple dilution step reduced the sulphate concentration to below the tolerance level.

Acknowledgement—We thank the Comision Asesora de Investigación Científica y Técnica for supporting this study (Project No. 3007/83 C02-02).

REFERENCES

1. M. J. Wirth, *Trends Anal. Chem.*, 1982, 1, 383.
2. M. Román Ceba, C. Cruces Blanco and F. García Sánchez, *J. Photochem.*, 1985, 30, 353.

3. C. Cruces Blanco and F. García Sánchez, *Anal. Chim. Acta*, 1984, **166**, 277.
4. A. L. Ramos Rubio, C. Cruces Blanco and F. García Sánchez, *Z. Anal. Chem.*, 1986, **323**, 153.
5. A. I. Busev, V. G. Tiptsova and V. M. Ivanov, *Handbook of the Analytical Chemistry of the Rare Elements*, p. 52. Ann Arbor-Humphrey, Ann Arbor, Michigan, 1970.
6. F. D. Snell, *Photometric and Fluorimetric Methods of Analysis*, Part I, p. 535. Wiley, New York, 1978.
7. A. Fernandez Gutierrez and A. Muñoz de la Peña, in *Molecular Luminescence Spectroscopy: Methods and Applications*, Part I, S. G. Schulman (ed.), p. 371. Wiley, New York, 1985.
8. A. W. Ashbrook, *Analyst*, 1963, **88**, 113.
9. J. C. MacDonald and J. H. Yoc, *Anal. Chim. Acta*, 1963, **28**, 264.
10. H. Bennett and R. A. Reed, *Chemical Methods of Silicate Analysis*, p. 255. British Ceramic Research Association and Academic Press, London, 1971.
11. S. H. Etaiw, M. M. Abou Sekkina, G. B. El-Hefnawey and S. S. Assau, *Can. J. Chem.*, 1982, **60**, 304.
12. C. Reichardt, *Solvent Effects in Organic Chemistry*, Verlag Chemie, Weinheim, 1979.
13. R. S. Mulliken and W. B. Pearson, *Molecular Complexes*, Wiley-Interscience, New York, 1969.
14. H. Ishii, T. Odashima and T. Imamura, *Analyst*, 1982, **107**, 885.
15. R. B. Singh, T. Odashima and H. Ishii, *ibid.*, 1983, **108**, 1120.
16. *Spectrochim. Acta*, 1978, **33B**, 242.
17. *Anal. Chem.*, 1980, **52**, 2242.
18. F. García Sánchez and C. Cruces Blanco, *ibid.*, 1986, **58**, 73.

KINETIC DETERMINATION OF IODIDE, BASED ON THE CHLORPROMAZINE-BROMATE REACTION

P. VIÑAS, M. HERNANDEZ CORDOBA and C. SANCHEZ-PEDREÑO*

Department of Analytical Chemistry, Faculty of Chemistry, University of Murcia, Murcia, Spain

(Received 16 May 1986. Revised 17 July 1986. Accepted 18 September 1986)

Summary—A kinetic method based on the catalytic effect of iodide on the chlorpromazine-bromate reaction is described. The reaction was followed spectrophotometrically by measuring the increase in the absorbance at 525 nm. Under optimal experimental conditions ($10^{-4}M$ chlorpromazine hydrochloride, $1.5M$ phosphoric acid, $5 \times 10^{-4}M$ potassium bromate, 40°), iodide was determined between 5 and 70 ng/ml by the tangent method. The influence of reaction variables, the precision and accuracy of the method and the effect of foreign ions were studied. The procedure was applied to the determination of iodide in iodinated salts and in rat thyroid.

In recent years, there has been an increasing interest in determination of iodide in foods and animal tissues because of the advantages of including iodide in the human diet. The use of iodinated salt in the diet is the most frequent way to obtain an additional supply of iodide, which is metabolised in the thyroid for the synthesis of hormones. Absence of iodide in the diet produces several diseases with well-known clinical symptoms.

Current techniques used for iodide determination include activation and catalytic methods. Most catalytic methods use the well-known Ce(IV)-As(III) reaction.^{1,2} Other reactions catalysed by iodide have also been described.³⁻¹⁵

The oxidation of chlorpromazine, a tranquillizing drug, currently employed in medicine, has been used in the present study. In a previous paper,¹⁶ we reported for the first time the use of this substance in catalytic analysis. The oxidation of chlorpromazine by bromate is a slow process which is catalysed by the iodide anion. This effect is described here, and a new method for the determination of iodide in the range 5-70 ng/ml is proposed. The procedure has been applied to the determination of iodide in iodinated salts and rat thyroid, with excellent results.

EXPERIMENTAL

Reagents

All chemicals used were of analytical grade and the solutions were prepared with doubly distilled water.

Chlorpromazine hydrochloride solution, $10^{-3}M$. Prepared from the commercial product (Sigma) by dissolving 0.0888 g in 250 ml of water. The solution is stable if kept in an amber-coloured bottle in the cold.

Potassium iodide stock solution 0.01M. Prepared by dis-

solving 0.415 g of potassium iodide in 250 ml of water. The solution was standardized by a recommended procedure.¹⁷ Working solutions were prepared by dilution just before use.
Potassium bromate solution, $5 \times 10^{-3}M$.

Apparatus

A Pye Unicam SP8-100 double-beam spectrophotometer with 1-cm cells and constant-temperature cell-holder was used for recording spectra and absorbance-time curves.

General procedure

In a 10-ml standard flask place 1 ml of $10^{-3}M$ chlorpromazine hydrochloride (CPH), 1.5 ml of $10M$ phosphoric acid, the appropriate volume of diluted iodide solution to keep the final concentration of the anion between 5 and 70 ng/ml, and distilled water up to 8.5 ml. Keep the flask in a thermostat at $40.0 \pm 0.5^\circ$ for 15 min, then add 1 ml of $5 \times 10^{-3}M$ potassium bromate and dilute to volume with water (both heated to $40.0 \pm 0.5^\circ$ in the thermostat). Turn on the recorder, mix the solution by vigorous shaking, transfer it to the spectrophotometer cell (kept at $40.0 \pm 0.5^\circ$) and record the absorbance-time curve for measurement at 525 nm. Obtain the slope from the initial straight-line portions of these curves. Prepare a blank in the same way but in the absence of iodide, and obtain the calibration graph by plotting $\tan \alpha$ vs. iodide concentration.

Determination of iodide in common iodinated salt

Weigh accurately 0.1 g of the iodinated salt, dissolve it in doubly distilled water and dilute to volume in a 25-ml standard flask. Determine iodide in a 1-ml aliquot, according to the general procedure, but with a new calibration graph for iodide in the presence of the same amount of chloride as that in the sample. Add the chloride in the form of potassium chloride solution prepared by reaction of iodide-free hydrochloric acid and potassium hydroxide.

Determination of iodide in rat thyroid

Place the rat thyroid in a fused-silica crucible and decompose it as follows.¹⁸ Add 0.2 ml of 1-g/ml potassium hydroxide solution and evaporate to dryness in an oven at about 100° . Place the crucible in a muffle furnace at 600° for 2.5 hr. The residue should be white. Cool, wash down the sides of the crucible with water and dilute the solution to volume in a 25-ml standard flask. Determine iodide in a suitable aliquot according to the general procedure. Prepare a blank by the same treatment.

*To whom correspondence should be addressed.

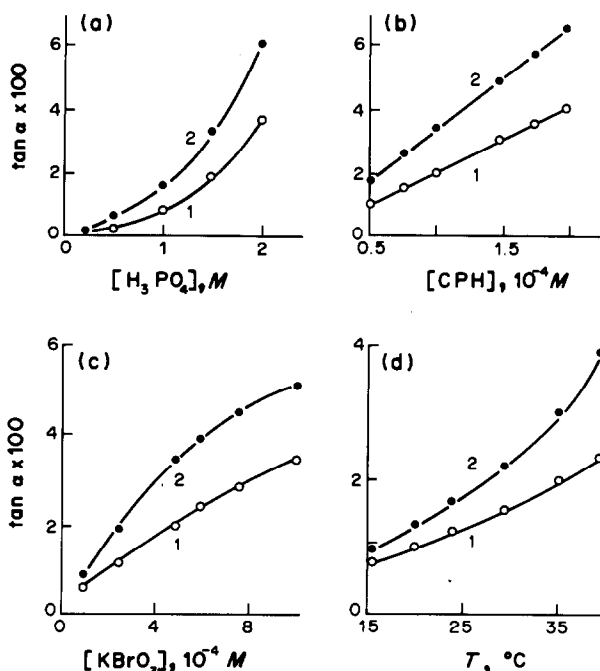


Fig. 1. Influence of variables on reaction rate. (1) Uncatalysed reaction; (2) 40 ng/ml iodide. (a) Influence of acidity; (b) influence of CPH concentration; (c) influence of potassium bromate concentration; (d) influence of temperature.

RESULTS AND DISCUSSION

Chlorpromazine hydrochloride (CPH) has a sulphur atom which is susceptible to oxidation. The oxidation product is a red free radical^{19,20} having an absorption maximum at 525 nm. The iodide-catalysed oxidation of CPH by bromate was followed spectrophotometrically by measuring the increase in the absorbance of the red free radical of CPH at 525 nm. The slope of the absorbance-time graph was used as a measure of the reaction rate.

Influence of acidity

The free radical obtained from the oxidation of CPH is stable only in acidic media. Therefore, the catalysed reaction was exclusively studied in different acidic media.

It was not possible to study the reaction in perchloric acid because a white precipitate appears in this medium. Hydrochloric acid was also unsuitable

because the rate of the uncatalysed reaction was too fast. Phosphoric acid gives lower blanks than sulphuric acid and was chosen for this reason.

As can be seen in Fig. 1a, the rate of both the catalysed and uncatalysed reactions increases with phosphoric acid concentration. A 1.5M phosphoric acid medium was selected. Acid concentrations lower than 0.5–1.0M are not advisable because the red colour of the free radical is less stable.

Influence of reagent concentrations

Figure 1b shows the effect of varying the CPH concentration between 5×10^{-5} and $2 \times 10^{-4}M$ on reaction rate. Both the catalysed and uncatalysed reactions increase their rate with CPH concentration, showing a kinetic order of +1 in the range studied. A $10^{-4}M$ CPH concentration, which gives a convenient value of absorbance at 525 nm, was chosen.

As Fig. 1c demonstrates, increase in the potassium bromate concentration in the range 10^{-4} – $10^{-3}M$

Table 1. Kinetic data for the iodide-catalysed chlorpromazine-bromate reaction

Variable	Uncatalysed reaction		Catalysed reaction	
	Concentration range, M	Kinetic order	Concentration range, M	Kinetic order
Phosphoric acid	0.2–1.0	+1	0.2–1.0	+1
	1.0–2.0	+2	1.0–2.0	+2
Chlorpromazine	5×10^{-5} – 2×10^{-4}	+1	5×10^{-5} – 2×10^{-4}	+1
Bromate	10^{-4} – 10^{-3}	+1	10^{-4} – 6×10^{-4}	+1
			6×10^{-4} – 10^{-3}	$+\frac{1}{2}$

Table 2. Interference of foreign ions in the determination of $4 \times 10^{-7}M$ iodide

Limiting molar ratio [ion]/[I ⁻]	Foreign ion
2000*	ClO ₄ ⁻ , SO ₄ ²⁻ , NO ₃ ⁻ , ClO ₃ ⁻ , Cl ⁻ , F ⁻ , EDTA, tartrate, oxalate, citrate, acetate, As(V), Ca(II), Sr(II), Ba(II), Mg(II), Tl(I), Al(III), Zn(II), Co(II), Ni(II), Cr(III), Cd(II), Ce(III), Th(IV), La(III)
500	Pb(II), Fe(III)
200	Mn(II), Mo(VI)†, Cu(II)†
100	W(VI), Bi(III)
20	Br ⁻ †, Se(IV)
5	SCN ⁻ , IO ₃ ⁻ †
2	IO ₃ ⁻ †, Ce(IV)†, Ru(III)†
1	Ag(I)
<1	V(V)†, Hg(II), Pd(II)

*Maximum ratio tested.

†Ions which increase the reaction rate.

produces an increase in reaction rate. Furthermore, the stability of the red colour depends on the bromate concentration in the solution. When this concentration is higher than $10^{-3}M$, the red colour disappears quickly, leaving a colourless solution. The red radical is therefore oxidized irreversibly by the excess of oxidant to a colourless sulphoxide, with the loss of one more electron.¹⁹ A $5 \times 10^{-4}M$ bromate concentration was selected for the kinetic study.

The dependence of the reaction rate on temperature was studied between 15 and 40° for the uncatalysed reaction and in the presence of 40 ng/ml iodide. Both reactions increase their rates with temperature, but this effect is more pronounced for the catalysed reaction, as shown in Fig. 1d. A temperature of 40° was selected as optimal. The kinetic data obtained for the reaction variables are summarized in Table 1.

Calibration graph and effect of foreign ions

By use of the tangent method and under the optimal experimental conditions previously established ($10^{-4}M$ CPH, $1.5M$ H₃PO₄, $5 \times 10^{-4}M$ KBrO₃, $40.0 \pm 0.5^\circ$), a calibration graph linear between 5 and 70 ng/ml iodide was obtained.

The standard deviation of the method for 40 ng/ml iodide (10 determinations) was ± 1.5 ng/ml, with a mean relative error of $\pm 3.9\%$.

Interference by foreign ions in the system was studied with a $4 \times 10^{-7}M$ iodide solution containing the foreign ion. The tolerance limit was taken as the concentration causing an error of no more than $\pm 5\%$ in the iodide concentration. Results are summarized in Table 2.

Determination of iodide in common iodinated salts

The results are compared with those obtained by the iodide-catalysed Ce(IV)–As(III) reaction.¹² Chloride ions are known to exert a weak catalytic action on the cerium(IV)–arsenic(III) system and we have

found that high chloride concentrations also affect the rate of the chlorpromazine–bromate reaction. For this reason, the standard samples used when constructing the calibration graph must contain the same amount of chloride as the samples. The main problem lies in finding an iodide-free chloride for preparing the calibration curve; most of the usual reagent-grade chloride salts were unsuitable. The use of a potassium chloride solution prepared from reagent-grade hydrochloric acid and potassium hydroxide was adopted.²¹

The results obtained for three determinations of each sample are given in Table 3 and are in good agreement with those obtained by the cerium(IV)–arsenic(III) reaction.

Determination of iodide in rat thyroid

The procedure has also been applied to the determination of iodide in rat thyroid and the results are summarized in Table 4. We have proved that, under

Table 3. Determination of iodide in common iodinated salts

Sample	Iodide, $\mu\text{g/g}$	
	Ce(IV)–As(III)	CPH–BrO ₃ ⁻
1	39	40
2	54	57
3	56	58
4	67	66

Table 4. Determination of iodide in rat thyroid

Sample	Iodide, $\mu\text{g/gland}$	
	CPH–bromate	Ce(IV)–As(III)
1	11.3	10.8
2	11.0	10.1
3	10.6	10.5
4	7.8	8.6
5	8.0	8.4

the experimental conditions chosen, the recovery of iodide was 100%.

CONCLUSIONS

The proposed method allows the determination of iodide down to the 5 ng/ml level and is one of the more sensitive catalytic methods for this anion. The method is very selective because only V(V), Hg(II) and Pd(II) interfere at a molar ratio (to iodide) < 1 . The procedure is widely applicable and two different natural samples, in which the determination of iodide is actually very important, have been chosen as examples.

REFERENCES

1. E. B. Sandell and I. M. Kolthoff, *J. Am. Chem. Soc.*, 1934, **56**, 1426.
2. *Idem*, *Mikrochim. Acta*, 1937, **1**, 6.
3. V. F. Toropova and L. M. Tamarchenko, *Zh. Analit. Khim.*, 1967, **22**, 576.
4. H. Ballczo, *Monatsh. Chem.*, 1968, **99**, 2480.
5. *Idem*, *Z. Anal. Chem.*, 1969, **245**, 20.
6. J. M. Ottaway, C. W. Fuller and W. B. Rowston, *Anal. Chim. Acta*, 1969, **45**, 541.
7. S. Funahashi, M. Tabata and M. Tanaka, *ibid.*, 1971, **57**, 311.
8. H. Weisz and K. Rothmaier, *ibid.*, 1974, **68**, 93.
9. E. Jasinskiene and O. Umbraziunaite, *Zh. Analit. Khim.*, 1975, **30**, 1590.
10. M. A. Koupparis and T. P. Hadjiioannou, *Anal. Chim. Acta*, 1978, **96**, 31.
11. *Idem*, *Mikrochim. Acta*, 1978 **II**, 267.
12. S. U. Kreingol'd, L. I. Sosenkova, A. A. Pan-teleimonova and L. V. Lavrelashvili, *Zh. Analit. Khim.*, 1978, **33**, 2168.
13. R. P. Igov, M. D. Jaredic and T. G. Pecev, *Mikrochim. Acta*, 1979 **II**, 171.
14. T. Nomura, *J. Electroanal. Chem. Interfacial Electrochem.*, 1982, **139**, 97.
15. K. Sriramam, B. S. R. Sarma, A. R. K. V. Prasad and K. Kalidas, *Analyst*, 1983, **108**, 543.
16. M. Hernández Córdoba, P. Viñas and C. Sánchez-Pedreño, *ibid.*, 1985, **110**, 1343.
17. F. Sierra Jiménez and C. Sánchez-Pedreño, *An. Quim. Ser. B*, 1958, **54**, 541.
18. K. Lauber, *Anal. Chem.*, 1975, **47**, 769.
19. I. S. Forrest, F. M. Forrest and M. Berger, *Biochim. Biophys. Acta*, 1958, **29**, 441.
20. G. Dusinsky and O. Liskova, *Chem. Zvesti*, 1958, **12**, 213.
21. R. Malvano, G. Buzzigoli, M. Scarlattini, G. Cenderelli, C. Gandolfi and P. Grosso, *Anal. Chim. Acta*, 1972, **61**, 201.

PHARMACOKINETICS AND THE ANALYTICAL CHEMIST

ANIL C. MEHTA

Department of Pharmacy, The General Infirmary, Leeds, Yorkshire, England

(Received 2 May 1986. Revised 27 August 1986. Accepted 12 September 1986)

Summary—A prerequisite in pharmacokinetic studies is the development of analytical methods to assay the parent drug and its metabolites in biological fluids. For method development and application, a detailed knowledge of pharmacokinetics is not essential, but familiarity with its fundamental principles and terminology is necessary and helps in interpreting assay results and in interacting more effectively with colleagues who may be specialists in medical or related fields. The purpose of this article is to introduce the basic concepts of pharmacokinetics and some of the biological processes associated with it. Areas relevant to the needs of analytical chemists are discussed.

Anyone engaged in drug determination in biological fluids should realize that the drug concentration is a result of the interaction of a wide variety of biological processes. These include, among others, drug absorption, distribution, metabolism, and excretion. All these processes are interrelated, each playing a part in determining the drug concentration achieved after a given dose. The study of these processes forms the basis of pharmacokinetics.

Pharmacokinetics is the study of the time course of absorption, distribution, metabolism, and elimination of drugs, the relationships among these processes, and the observed pharmacological, therapeutic, or toxic effects in animals and man.¹⁻⁵ It involves quantifying drug and/or metabolite levels in appropriate body fluids or tissues at any point in time following drug administration. Advances in analytical techniques have now made it possible to measure very low concentrations of drugs in biological fluids.⁶ The most commonly sampled body fluid is plasma or serum, because a good correlation between drug concentration and therapeutic effect is usually found. Urine analysis for drugs is used in connection with urinary excretion and bioavailability studies. Other body fluids and tissues are also utilized for pharmacokinetic drug analysis but less frequently. Plasma concentration-time curves are constructed to determine various pharmacokinetic parameters with a view to studying the fate of drugs in the body. Pharmacokinetics is increasingly utilized in clinical practice for the safe and effective therapeutic management of patients. This application, which is emphasized in this article, is termed clinical pharmacokinetics.⁷⁻⁹

Metabolites of certain drugs (e.g., nortriptyline from amitriptyline, *N*-acetylprocainamide from procainamide) are pharmacologically active. They may have different modes of action or different potencies. Under such circumstances knowledge of metabolite kinetics is also necessary, especially if the metabolite

is present in a sufficiently high concentration to produce a pharmacological effect.⁹⁻¹¹

ABSORPTION AND OTHER PROCESSES

The term absorption is used to describe the transfer of the drug from the site of administration to the general circulation. When a drug is given orally in a form of a tablet, capsule, or suspension, it is absorbed from the gastrointestinal (GI) tract into the portal system of veins. It then passes through the liver before reaching the general circulation and the site of action. If the drug is rapidly metabolised on the first pass through the gut wall and/or the liver, a large portion of it may be inactivated before it reaches the site of action. The net result is incomplete bioavailability of the drug administered. This phenomenon is known as first pass metabolism. The metabolites may be pharmacologically active or inactive substances. Drugs subject to the first pass effect include imipramine, propranolol, pethidine and many more. Intravenous administration of a drug avoids the absorption step since the drug is injected directly into the systemic circulation and is unaffected by the potential rate-limiting and metabolic factors associated with drug absorption in extravascular routes. High first pass metabolism sometimes prevents oral administration of a drug or results in use of an oral dose much larger than the equivalent parenteral dose (e.g., propranolol).

When a drug is administered to the patient orally, its concentration in the plasma increases owing to rapid absorption in the blood from the site of administration. Generally, the faster the rate of absorption, the higher the peak concentration attained. After a drug has been absorbed, it is distributed non-uniformly throughout the body. When the peak concentration is reached, the rate of drug absorption equals the rate of distribution and elimination. Absorption continues after the peak but at a rate

exceeded by the rate of elimination, and consequently the drug concentration in the plasma falls exponentially. For a given drug, the post-absorptive decline of plasma concentration is the same irrespective of the route of administration. It takes about 6 half-lives for 99% of the drug to be completely eliminated. When a drug is administered in fixed doses and at fixed intervals and if drug intake exceeds elimination, the plasma concentration increases until it reaches a plateau or steady-state. It is the concentration at steady-state that relates best to pharmacological effect. The time required to attain the steady-state is about 4 plasma half-lives. When the dose is discontinued, the plasma concentration decreases in much the same manner as it does after a single dose administration.

It is usual to find intersubject differences in drug plasma levels from the same dose, even in healthy individuals. The variation tends to be greater with drugs showing a first pass effect. Factors that cause variation in plasma levels after a standard dosage regimen are shown in Table 1. All these factors can be taken into account to adjust drug dosage to an individual patient's needs.^{12,13} Even after dosage adjustment, there is usually often sufficient variation remaining to require careful monitoring of drug response and, in many cases, of plasma concentration.^{14,15} It is expensive and time-consuming to monitor drug levels routinely, and the reasons for doing so are carefully examined before the task is undertaken. Indications for routine drug monitoring are shown in Table 2. In recent years, plasma concentrations of many drugs have been measured during their therapeutic use; the measurements are of either total drug concentrations,¹⁶⁻²¹ or in some cases free (*i.e.*, unbound) drug concentrations.^{22,23}

Distribution of the drug to various sites in the body is reversible, *i.e.*, the drug in the plasma exists in a distribution equilibrium with the drug in other body fluids and tissues. As a result of this equilibrium, changes in the concentration of the drug in plasma often reflect changes in its levels in other tissues, including the receptor site. Following distribution, the drug is eliminated from the body either unchanged (excretion) or as metabolites (biotransfor-

Table 2. Rationale for undertaking routine drug level monitoring

1. Considerable inter-individual pharmacokinetic variation (theophylline)
2. Narrow therapeutic index with serious side-effects in the toxic range (digoxin, aminoglycosides)
3. Pharmacological and toxic effects not readily measurable (anticonvulsants, antiarrhythmics)
4. Non-linear (saturation) kinetics (phenytoin)
5. Special circumstances, such as
 - (a) treatment of infants
 - (b) presence of hepatic or renal disease
 - (c) patient non-compliance
 - (d) drug interactions
 - (e) drug overdose or abuse
 - (f) clinical trial of a new drug

mation) or both. The drug is mainly excreted by means of biliary and renal excretion, since the liver and kidneys are the two important eliminating organs for most drugs. Distribution and elimination are sometimes referred to collectively as disposition.

Some or all of the drug excreted in the bile and subsequently into the intestine may be re-absorbed from the intestine into the portal circulation and back to the liver. This process is called enterohepatic recirculation or biliary recycling. Compounds which are not re-absorbed from the intestine are excreted in the faeces. In some cases, highly polar metabolites such as glucuronides, which cannot be re-absorbed, undergo deconjugation by biliary enzymes or by GI bacteria in the intestine, and the liberated parent drug is then readily re-absorbed. Secretion into the bile and intestinal re-absorption may continue until the drug is completely eliminated by metabolism and by renal and faecal excretion.

The enterohepatic recirculation can lead to a late surge in drug plasma concentration as the drug is re-absorbed. Rises in plasma concentrations (secondary peaks) have been observed for several drugs such as diazepam, chlorpromazine, and indomethacin as a result of this phenomenon. Also the action of the drug is prolonged by this mechanism, owing to its unusually long persistence in the body.

COMPARTMENT MODELS

The most common method used to describe the pharmacokinetic behaviour of a drug in the body is by use of models depicting the body as composed of one or more units or compartments. These compartments have no precise physiological or anatomical definition, but visualization of the body in this way helps to explain the disposition characteristics of a drug and allows interpretation of drug concentrations in the body as a function of time, dose, and route of administration. Experimental data (plasma level *vs.* time curves) are used to fit compartment models. In general, for a given drug the one-compartment model is first examined for a fit to the data. If no correlation is obtained, the two-

Table 1. Factors that cause intersubject variation in plasma levels

1. Physicochemical properties of the drug and the dosage form, including their disintegration/dissolution characteristics
2. Dosage regimen: the route and the rate of administration
3. Age, weight, and other pertinent patient data
4. Physiological status: metabolic capacity, changes in protein binding, pH of stomach and intestine, distribution of the drug between plasma and blood cells
5. Substances in GI tract, *e.g.*, food
6. Competition for binding sites between two drugs (drug interactions)
7. Disease state in particular hepatic and/or renal failure
8. Patient compliance

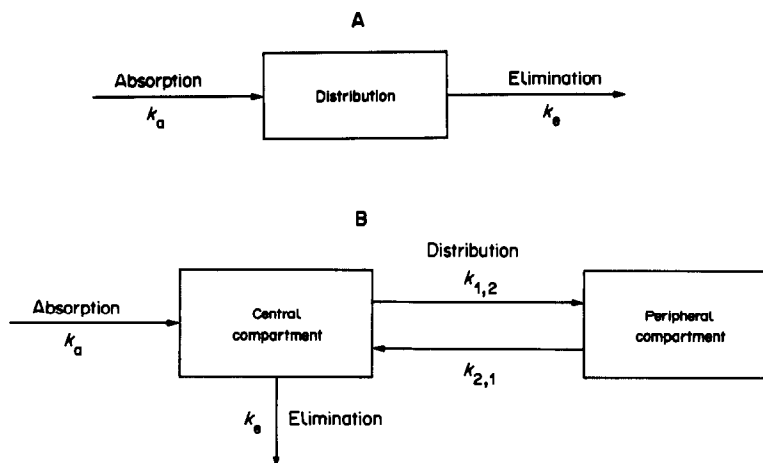


Fig. 1. One- and two-compartment models.

compartment model is tried. Whenever possible, the validity of the model is tested against further data to establish the closeness of fit. A certain type of model is not necessarily specific for a particular drug.

One-compartment model

The simplest pharmacokinetic model, the one-compartment model, assumes that the drug entering the body is distributed (equilibrated) instantaneously throughout the body fluids and tissues (Fig. 1A). This assumption does not necessarily mean that the concentration of the drug in the plasma and other body fluids and tissues is the same at the same time. Indeed it is rarely the same. It does mean, however, that changes in plasma drug concentration quantitatively reflect changes occurring in the drug concentration in other body fluids and tissues.

Two-compartment model

The two-compartment model is useful when the drug goes through an initial distribution phase. The

model separates the body into a central and a peripheral compartment (Fig. 1B). The drug enters the central compartment either by absorption from the GI tract (oral dose) or by the intravenous or other route. The drug then equilibrates with the peripheral compartment and is eliminated via the central compartment. During distribution the drug enters much more rapidly into highly perfused tissues (*e.g.*, liver, kidneys) than into poorly perfused tissues (muscle, skin, or fat). The transfer of the drug from one compartment to another is associated with a specific rate constant (*k*) for that particular transfer. Both the transfer of drug between compartments and the drug elimination from the central compartment are assumed to obey first-order kinetics. This means that the rate at which a drug is removed from a compartment is proportional to the drug concentration in that compartment.

Application of pharmacokinetic models becomes increasingly complicated as the number of compartments increases. Multicompartment models have been suggested but their increased complexity may reduce their clinical usefulness. For most drugs the one- and two-compartment models are adequate to describe the pharmacokinetic profiles.

PHARMACOKINETIC CONSTANTS

Area under the curve, and bioavailability

Three important parameters can be derived from the plasma concentration–time curve (Fig. 2) following oral administration of a drug, namely, peak concentration, the time of peak concentration, and the area under the concentration–time curve (or area under the curve, AUC). The AUC is expressed in $\text{mg}\cdot\text{l}^{-1}\cdot\text{hr}$. The bioavailability of a dose, *i.e.*, the fraction (*F*) of drug absorbed as such into the general circulation, is reflected by the AUC, which can be estimated by use of the trapezoidal rule.⁷⁻⁹ Absorption of the drug is assumed to be complete from an intravenous injection, *i.e.*, $F = 1$. For non-

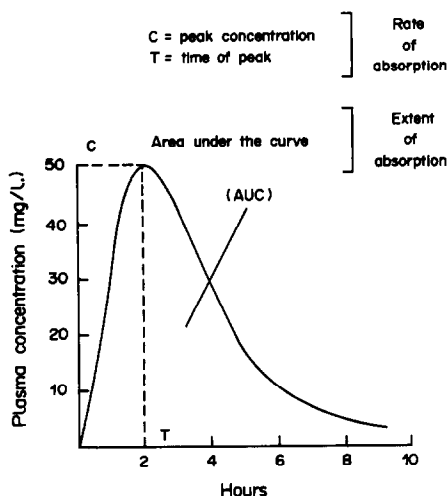


Fig. 2. Plasma drug concentration–time profile after oral administration of a drug.

intravenous routes, the bioavailability of a drug may be less than 100% ($F < 1$) owing to incomplete absorption, since part of the drug may be metabolised before reaching the systemic circulation. The bioavailability of a drug may be evaluated by comparison of its AUC with that of an equivalent dose of a standard.

$$F = \frac{[\text{AUC}] \text{ drug product}}{[\text{AUC}] \text{ standard}} \quad (1)$$

The standard may be an intravenous injection, in which case absolute bioavailability is obtained, or it may be an oral solution or another well established formulation of the same drug, in which case relative bioavailability is obtained. Bioavailability is usually assessed by plasma concentration measurements, but other body fluids such as urine or saliva may be used. The assessment of bioavailability is useful not only in the control of therapy but also in the evaluation of alternative dosage forms (bioequivalence studies). Differences in bioavailability are of greater concern for coated and sustained-release preparations and for drugs with a steep dose-response relationship, narrow therapeutic index (*i.e.*, the difference between therapeutic and toxic levels is small), and poor solubility in water.⁷

Clearance

Clearance is used to describe quantitatively the removal of a drug from the body. It is the volume of plasma (or blood) from which the drug is completely removed per unit time. The total body clearance is the sum of the individual clearances of that drug by the various organs and tissues of the body. For example, if a drug is eliminated by metabolism in the liver and excretion by the kidneys, the total body clearance is the sum of the hepatic and renal clearances. It is worth repeating that clearance does not indicate how much drug is being removed but, rather, the hypothetical volume of biological fluid that could be completely cleared of the drug in unit time. Experimentally it is calculated by dividing the systemically available dose of the drug by the AUC produced by that dose.

Total body clearance

$$= \frac{\text{Dose or amount absorbed}}{\text{AUC}} \quad (2)$$

In pharmacokinetic terms, total body clearance (Cl) can be related to volume of distribution (V_d) and elimination rate constant (k_{el}):

$$Cl = V_d k_{el} \quad (3)$$

Clearance is influenced by liver and renal functions and by a number of variables such as blood flow to the liver and kidneys, age, metabolic capacity of liver enzymes, plasma concentration and protein binding, urine flow-rate and urine pH. The concept of clearance can be applied in clinical work in establishing and maintaining drug dosage regimens.

Volume of distribution

The apparent volume of distribution relates the amount of the drug in the body to the concentration of the drug in the blood or plasma, depending on the fluid measured. It is defined as the volume of body water which would be required to account for the amount of drug in the body if it were uniformly present throughout the body in the same concentration as that found in the plasma. The concept of volume of distribution is often difficult to grasp. It does not relate to any physiological volume (it rarely corresponds to a real volume) but it gives an estimate of drug distribution in the body. Mathematically it is simply a proportionality constant which, when multiplied by the concentration of the drug in the plasma (C), gives the amount of drug in the body (A).

$$A = V_d C \quad (4)$$

Alternatively, V_d can be assessed from the ratio A/C when distribution equilibrium has been attained. For the oral route, however, the dose must be corrected for bioavailability (F) since the absorption may be incomplete. There are different methods of calculating volume of distribution,⁹ and they may give different results. It is therefore necessary to specify the method used for calculation and the fluid used for measurement.

The magnitude of volume of distribution for a man may vary from a few litres to several hundred litres, as shown in Table 3. Variation in volume of distribution can occur in a disease state and as a result of changes in physiological factors (age, body weight, protein binding *etc.*). Drugs that are water-soluble, extensively bound to plasma proteins, or exhibit little tissue uptake, have a small volume of distribution, which means most of the drug may be confined to blood and extracellular fluid. Such drugs (*e.g.*, penicillins) are present in relatively large amounts (microgram levels) in plasma and analytical problems in determining them are minimized. A large volume of distribution (up to several hundred litres) may be observed with drugs that are lipid-soluble or

Table 3. Average volume of distribution in a normal (70 kg) man

Drug	Volume of distribution, litres
Amitriptyline	600
Amoxycillin	21
Amphetamine	300
Digoxin	760
Frusemide	11
Haloperidol	1200
Lignocaine	100
Nortriptyline	1400
Pethidine	300
Phenytoin	50
Procainamide	140
Propranolol	180
Theophylline	35
Tolbutamide	10

extensively bound to adipose tissues. Drugs with a relatively small dose and large volume of distribution (e.g., β -blockers) are left in only a very small amount (nanogram or even picogram levels) in the plasma, and consequently their determination requires more sensitive and elaborate techniques.

Though hypothetical, the volume of distribution of a drug is a useful concept because it allows estimation of the dose required to achieve a given concentration, and conversely the concentration achieved on administering a given dose. It is also useful in calculating a loading dose.

Elimination rate-constant and half-life

When the plasma concentrations are plotted against time on semilogarithmic paper following oral or intramuscular dose, the type of curve shown in Fig. 3 is obtained. After the peak, the graph shows a linear portion corresponding to the post-absorptive phase. A straight line on a semilogarithmic graph is indicative of a first-order process. The nature of the graph suggests the one-compartment model, and the slope of the line represents the rate of elimination of the drug from the body. Although it is possible to calculate the elimination rate constant (k_{el}) from the slope of the line, it is much easier to determine it by making use of the relationship

$$k_{el} = \frac{0.693}{t_{1/2}} \quad (5)$$

where $t_{1/2}$ is the half-life, i.e., the time required for the plasma concentration to be reduced to half its original value. This parameter is determined directly from the graph. Equation (5) indicates that the units of k_{el} are reciprocal time (e.g., hr^{-1}).

The half-life can be very short (e.g., 20 min for nitrofurantoin) or very long (e.g., 4 days for phenobarbitone). It is independent of dose, the initial plasma concentration, and the rate of administration, but it can vary between subjects as a function of sex, age, and environment. Variation in half-life as a function of dose suggests non-linear kinetics and/or prolonged absorption owing to biliary recycling.

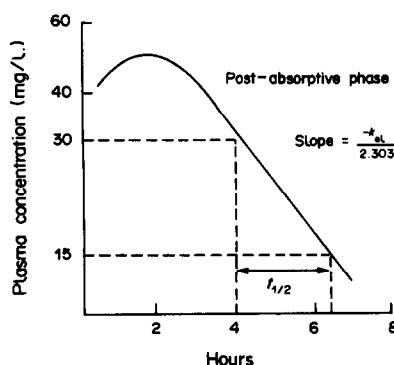


Fig. 3. Semilogarithmic plot of plasma drug concentrations vs. time after oral or intramuscular administration for a drug characterized by the one-compartment model.

It is apparent from equations (3) and (5) that the half-life is related to the volume of distribution and the clearance

$$t_{1/2} = \frac{0.693V_d}{Cl} \quad (6)$$

Hence changes in these two parameters can change the half-life. For example, the half-life of a drug may differ between children and adults because of differences in size and weight (different volumes of distribution) and the half-life in elderly subjects may be increased owing to a decreased rate of metabolism and excretion (decreased clearance). It should be pointed out that although the half-life is influenced by clearance and volume of distribution, these two parameters are independent of each other and independent of half-life.

From the analyst's point of view, the half-life is a more important parameter than the elimination rate constant, and fortunately, it is more common to refer to the half-life rather than to the elimination rate constant of a drug. Knowledge of the half-life gives the analyst some idea of how long a single-dose bioavailability or pharmacokinetic study should be continued in terms of assaying the samples. For clinicians, knowledge of half-life or elimination rate constant is very useful because it provides a good indication of the survival of drug in the body, which can be related to the duration of clinical effect and to the frequency of dosing.

Figure 4 shows the semilogarithmic plot of an intravenously administered drug distributed in a two-compartment model. The nature of the curve represents two processes. Initially there is a rapid decrease in plasma concentration, owing to distribution of the drug into the tissues. The first slope represents the initial distribution process (α -phase), which is followed by the elimination process (β -phase), which involves both metabolic reactions and the excretion of the drug. In general the α -phase is much more rapid than the β -phase and usually lasts approxi-

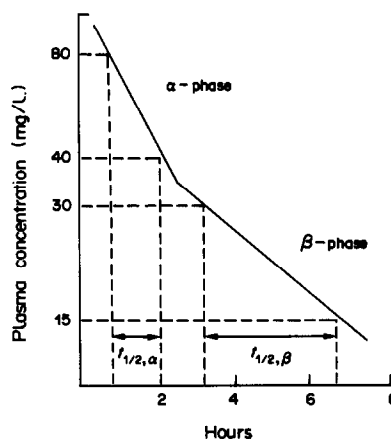


Fig. 4. Semilogarithmic plot of plasma drug concentrations vs. time after intravenous administration for a drug distributed within two compartments.

mately 30–120 min for most drugs, but may continue for 6 hr or longer for certain drugs such as digoxin. The half-life of the β -phase is often referred to as the elimination half-life or biological half-life. In considering the timing of blood sampling in drug monitoring, sampling during the α -phase is avoided, especially when the drug is given intravenously, otherwise an erroneously high plasma level (not representative of the level at the receptor site) may be obtained.

A number of computer programs are available²⁴ which, for given plasma concentration–time data, will estimate the pharmacokinetic parameters and the concentration that can be achieved following a given dose.

NON-LINEAR KINETICS

Generally the drug elimination process is assumed to obey first-order kinetics. This means that the rate of elimination is proportional to the drug concentration in the body. It also means that the drug dosage is related directly to plasma concentration. This assumption is valid for most drugs, but certain drugs show non-linear kinetics, *i.e.*, a small increase in maintenance dosage results in a disproportionate increase in the steady-state plasma concentration and, in some cases, toxicity. The commonest cause of this is saturation of hepatic drug metabolizing systems. If the enzymes responsible have a limited capacity to metabolize the drug, a large fraction of the drug survives first passage through the liver, resulting in a clinically significant elevation in the plasma concentration. Fortunately, for most drugs the plasma concentrations achieved at therapeutic dosages are low relative to the concentration necessary to saturate the particular enzyme system involved. Changes in protein binding or hepatic blood flow can also alter the kinetics of a drug. For a drug exhibiting non-linear characteristics, the plasma concentration–time plot is linear and a semi-logarithmic plasma concentration–time plot is curvilinear. This is in marked contrast to a first-order process, where, as mentioned earlier, an exponential decline in plasma concentration is observed, resulting in a linear semilogarithmic plot. Non-linear kinetics has been observed within the therapeutic range of certain drugs such as phenytoin and salicylate. Drugs with non-linear characteristics have to be treated differently, for example, by using Michaelis–Menten kinetics.^{4,5,7,8}

CONCLUSION

Studies of pharmacokinetics have greatly added to our knowledge of drug disposition and therapy. As a result of this it has been possible to use pharmacokinetic principles in a clinical setting in initiating and monitoring drug therapy and in providing the optimum dosage regimens for patients to achieve maximum benefit. In industry, pharmacokinetics is

routinely applied during various stages of drug development, *e.g.*, in animal toxicity studies, formulation design (evaluation of bioavailability), and in clinical trials of new drugs. Analytical chemists have already made and will continue to make a significant contribution to these areas by providing analytical information and methods of analysis for the drugs under investigation.

Acknowledgement—I thank Dr. R. T. Calvert for valuable comments on the manuscript. Thanks are also due to Pratik Mehta for drawing the figures.

REFERENCES

1. S. H. Curry, *Drug Disposition and Pharmacokinetics*, 3rd Ed., Blackwell, Oxford, 1980.
2. S. A. Kaplan and M. L. Jack, in *Progress in Drug Metabolism*, J. W. Bridges and L. F. Chasseaud (eds.), Vol. 4, p. 1. Wiley, New York, 1980.
3. B. Clark and D. A. Smith, *An Introduction to Pharmacokinetics*, Blackwell, Oxford, 1981.
4. D. W. A. Bourne, E. J. Triggs and M. J. Eadie, *Pharmacokinetics for the Non-mathematical*, MTP Press, Lancaster, 1986.
5. W. J. Tilstone and A. H. Stead, in *Clarke's Isolation and Identification of Drugs*, A. C. Moffat (ed.), 2nd Ed., p. 276. Pharmaceutical Press, London, 1986.
6. M. Lesne, *J. Pharm. Biomed. Anal.*, 1983, 1, 415.
7. M. Gibaldi, *Biopharmaceutics and Clinical Pharmacokinetics*, Lea and Febiger, Philadelphia, 1984.
8. R. E. Notari, *Biopharmaceutics and Clinical Pharmacokinetics: An Introduction*, 3rd Ed., Dekker, New York, 1980.
9. M. Rowland and T. Tozer, *Clinical Pharmacokinetics: Concepts and Applications*, Lea and Febiger, Philadelphia, 1980.
10. J. B. Houston and G. Taylor, *Br. J. Clin. Pharmacol.*, 1984, 17, 385.
11. T. R. Marten, *Chem. Br.*, 1985, 21, 745.
12. J. E. Knoben and P. O. Anderson (eds.), *Handbook of Clinical Drug Data*, Drug Intelligence Publications, Hamilton, 1983.
13. F. Bochner, G. Carruthers, J. Kampmann and J. Steiner, *Handbook of Clinical Pharmacology*, 2nd Ed., Little Brown, Boston, 1983.
14. A. Richens and S. Warrington, *Drugs*, 1979 17, 488.
15. C. E. Pippenger, in *Therapeutic Drug Monitoring and Toxicology by Liquid Chromatography*, S. H. Y. Wong (ed.), p. 11. Dekker, New York, 1985.
16. W. Sadee and G. C. M. Beelen (eds.), *Drug Level Monitoring: Analytical Techniques, Metabolism and Pharmacokinetics*, Wiley, New York, 1980.
17. A. Richens and V. Marks (eds.), *Therapeutic Drug Monitoring*, Churchill Livingstone, Edinburgh, 1981.
18. B. Widdop (ed.), *Therapeutic Drug Monitoring*, Churchill Livingstone, Edinburgh, 1985.
19. *Drug Level Monitoring*, Special Volume, *J. Chromatog.*, 1985, 340.
20. S. H. Y. Wong (ed.), *Therapeutic Drug Monitoring and Toxicology by Liquid Chromatography*, Dekker, New York, 1985.
21. V. Marks, in *Clarke's Isolation and Identification of Drugs*, A. C. Moffat (ed.), 2nd Ed., p. 101. Pharmaceutical Press, London, 1986.
22. R. H. Levy and T. A. Moreland, *Clin. Pharmacokinet.*, 1984, 9, (Supplement 1), 1.
23. T. C. Kwong, *Clin. Chim. Acta*, 1985, 151, 193.
24. L. P. Balant and E. R. Garrett, in *Drug Fate and Metabolism: Methods and Techniques*, E. R. Garrett and J. L. Hirtz (eds.), Vol. 4, p. 1. Dekker, New York, 1983.

SOME ION-EXCHANGE RESINS FOR ANION-CHROMATOGRAPHY

ALI S. AL-OMAIR and SAMUEL J. LYLE

The Chemical Laboratory, The University of Kent, Canterbury, Kent, England

(Received 28 April 1986. Accepted 4 September 1986)

Summary—The quaternary ammonium salts, n-butyltrimethylammonium iodide, 1,1,3,3-tetramethylbutyltrimethylammonium iodide, n-octadecyltrimethylammonium iodide and tri-n-dodecylmethylammonium iodide were synthesized from commercially available amines and together with n-hexadecyltrimethylammonium bromide tested for retention by a series of macroreticular resins (XAD-2, XAD-4, XAD-7, XAD-8 and XAD-11) for use as "surface" ion-exchangers in the chromatography of anions. Exchange-capacity studies of the coated resins showed that the non-polar XAD-2 and XAD-4 resins had retention characteristics superior to those of the polar resins and that pore size in the resin was more important than surface area per unit weight of resin. Tri-n-dodecylmethylammonium salts in XAD-2 gave the highest exchange capacity, with best retention under elution conditions. Columns prepared from this anion-exchanger were used to separate and analyse simple mixtures of anions (chloride, nitrate and sulphate) each within the 1-30 ppm range, by single-column operation with indirect photometric detection and also by conductivity detection with background-ion suppression. Though of use for the determination of anions in simple mixtures, the resolution and performance were generally poorer than those displayed by a commercial (Dionex) column. This is at least partly attributable to the inferior column-packing properties of the granular XAD-resin.

Ion-exchange chromatography assumed a new role in chemical analysis with the introduction of the two-column technique by Small *et al.*¹ The first of the two columns, which are in series, performs the separation, while the second, the suppressor column, removes the ionic contribution from the eluting medium, enabling a conductivity detector, placed after the second column, to act as a sensitive universal detector for the ions in the original sample. A single-column version which operates without a suppressor and uses conductivity detection was introduced by Fritz *et al.*² Both techniques have undergone modifications, the most important of which are probably the replacement of the suppressor column by a self-regenerating membrane system based on hollow fibres³ and of indirect photometric detection⁴ in the single-column technique. Chromatographs with background suppression and conductivity detectors have been developed commercially by the Dionex Corporation, Sunnyvale, California.

As was shown by Small *et al.*¹ a "surface" ion-exchanger of low exchange capacity is desirable for use in the separator column. Entirely satisfactory anion-exchangers have proved difficult to produce yet it is in the separation and determination of anions that the technique has had its greatest impact. Quaternary ammonium groups on a hydrocarbon chain chemically bonded to pellicular silica can be used, but such materials are expensive to produce. Cassidy and Elchuk^{5,6} prepared exchangers conveniently by dynamically coating commercial reversed phases (used in HPLC) with quaternary ammonium salts, which

are apparently strongly held by the hydrocarbon chemically bonded to the silica substrate. However, by their nature, these silica-based materials lack durability when used with alkaline eluents.⁷ Gjerde *et al.*^{2,8} introduced the quaternary ammonium group, which is the best available for general anion-exchange purposes, into polystyrene cross-linked with divinylbenzene. Though a good ion-exchange material is thus produced, the synthesis is lengthy and it is difficult to achieve a reproducible exchange capacity.

Recently^{9,10} it has been found that macroreticular resins prepared from various cross-linked organic polymers, available commercially (Amberlite XAD-resins, Rohm and Haas, Philadelphia), have the ability to retain long-chain quaternary ammonium salts, presumably with the hydrocarbon component of the molecule incorporated within the resin pores and the ionic group exposed at the surface. This provides a very simple and convenient means of producing a low-capacity anion-exchanger.

In the work described here, several quaternary ammonium salts (n-octadecyltrimethylammonium iodide, 1,1,3,3-tetramethylbutyltrimethylammonium iodide, n-butyltrimethylammonium iodide and tri-n-dodecylmethylammonium iodide) have been synthesized and, together with the commercially available n-hexadecyltrimethylammonium bromide, tested by exchange-capacity measurements for retention in the pores and/or surfaces of a range of XAD-resins. The most promising preparation was tested in single- and dual-column chromatography, with indirect optical and conductivity detection, respectively. The best

column thus produced was compared in performance with that of a commercial column in a Dionex instrument.

EXPERIMENTAL

Apparatus

The ion-chromatography for indirect photometric detection was home-made. It consisted of a solvent reservoir, a Milton Roy (Laboratory Data Control) pump model 396-74, a pulse-damper made from Teflon tubing (0.25 mm bore, 50 m long), an injection septum, glass column and fittings obtained from Omnifit (Cambridge, England) and a Pye-Unicam (Cambridge, England) model LC3 photometric detector fitted with an 8- μ l flow-cell. The detector output signal was fed to a Smith's Servoscribe pen-recorder.

A Dionex QIC IonChrom Analyser was used in the direct detection method. It was fitted with a 50- μ l injection loop, an ion-concentration column (2.0 mm bore, 50 mm long), a separator column (2.0 mm bore, 250 mm long), a membrane-type suppressor unit and a conductivity detector.

A Hitachi Perkin-Elmer model 139 spectrophotometer was used for the turbidimetric measurements of resin exchange-capacity.

Reagents

Hexadecyltrimethylammonium bromide was used as received from the suppliers (Aldrich Chemical Co.). The other quaternary ammonium salts were prepared by refluxing 5-g quantities of 1,1,3,3-tetramethylbutylamine, n-butylamine, n-octadecylamine (all from Aldrich Chemical Co.) and tri-n-dodecylamine (from Rhone-Poulenc, Paris, France) with an excess of methyl iodide (about 25 ml for each amine). The first two were refluxed for 3 hr and each of the others overnight. Excess of methyl iodide and any hydrogen iodide produced were removed by distillation. The quaternary ammonium salts were dissolved or dispersed in water and the equivalent weight determined gravimetrically by precipitation of silver iodide. However, the n-octadecyltrimethylammonium salt needed purification by ether extraction from aqueous ammoniacal solution, followed by precipitation with aqueous hydrochloric acid. The purities found were 99.1, 98.7, 91.3 and 98.7% for the quaternary ammonium salts derived from the amines in the order listed above.

Solutions of potassium hydrogen phthalate and mixtures of sodium bicarbonate and carbonate were prepared from reagent grade salts in demineralized water for use in the column elution studies. In the indirect photometric method, the columns were eluted with dilute phthalate solution, monitored at 264 nm. Unless specified, other chemicals used were of reagent grade.

The XAD-resins (BDH Chemicals Ltd. or Rohm and Haas) listed in Table 1 were washed well with water, then ground, while wet, into fine particles. The dried fraction in the particle size range 60–100 μ m was isolated for use in preparing the ion-exchanger.

Preparation of resins

In the preparation of the ion-exchanger, 3 g of XAD resin, previously dried for 2 hr at 80°, were added to 30 ml of 10⁻²M quaternary ammonium salt solution in 1:1 v/v aqueous acetonitrile and the mixture was agitated for 15 min. Water (100 ml) was added and after gentle mixing, the coated resin was filtered off. About 0.7 g of it was slurried into an Omnifit column (3.5 mm bore, 250 mm long). Each column was washed successively with 500 ml of water, 1 litre of 10⁻³M potassium hydrogen phthalate, 100 ml of 10⁻²M sodium chloride and 300 ml of water, at 2.1 ml/min flow-rate. The column was considered to be ready for exchanger retention and other studies after this treatment, provided it retained sufficient quaternary ammonium salt to warrant such studies.

Ion-exchange capacity

For capacity measurements, the chloride was displaced from the resin in the column by pumping 200 ml of 10⁻³M phthalate solution through at a flow-rate of 1 ml/min. The eluate was collected in 50-ml batches and it was generally found that all the chloride was eluted in the first batch. The chloride content was determined turbidimetrically by the method of Puphal *et al.*¹¹ In the subsequent studies of retention of quaternary ammonium salts, after each litre of phthalate solution had been pumped through the column the exchanger was converted back into the chloride form, as described above for the capacity measurement.

RESULTS AND DISCUSSION

According to the manufacturer's data, XAD-2 and XAD-4 provide non-polar resin frameworks, XAD-7 and XAD-8 have structures of intermediate polarity, and XAD-11 has a polar structure. The quaternary ammonium salts showed variable retention on these resins. The relatively low molecular-weight tetramethylbutyl-, trimethyl- and butyltrimethylammonium salts were released totally from each XAD resin by the preliminary treatment described above, but retention, although inadequate for practical purposes, was highest on the XAD-4 resin. Octadecyltrimethylammonium chloride and hexadecyltrimethylammonium bromide had better retention on the resins, particularly on XAD-2 and XAD-4, but they were slowly removed by further washing with 10⁻³M phthalate, as shown in Figs. 1 and 2. It may be noted that the former salt gave an exchange capacity that was only about one half of that of the latter with XAD-2 and XAD-4. Both of these resins gave coated products with better exchange capacities than those obtained with the more polar XAD-7 and XAD-8. The retention of all the above-mentioned quaternary ammonium salts on XAD-11 was very poor. Thus it is evident that retention is best on the non-polar type of XAD resin, with marked deterioration in this property as the polarity of the resin framework increases. This general trend is supported by the observations on the retention of tridodecylmethylammonium chloride (Fig. 3). The exchange capacity is higher for each XAD resin preparation than the capacities recorded for the corresponding XAD resin in Figs. 1 and 2. Furthermore, the tridodecylmethylammonium salt gives a higher exchange capacity when incorporated in XAD-2 than in XAD-4, the opposite of the behaviour found for the quaternary ammonium salts carrying only one long-chain alkyl group. Since the average pore diameter (Table 1) in XAD-2 is almost twice that in XAD-4 and the surface area per unit weight is roughly greater by a factor of two in XAD-4 than in XAD-2, it can be concluded that pore size in these non-polar resins plays a part in incorporation and retention of alkylammonium salts. Thus compatibility of the hydrocarbon framework with the alkyl chains of the ammonium salt, the presence of at least one long alkyl chain in the salt, and the pore-size of the resin appear to be key

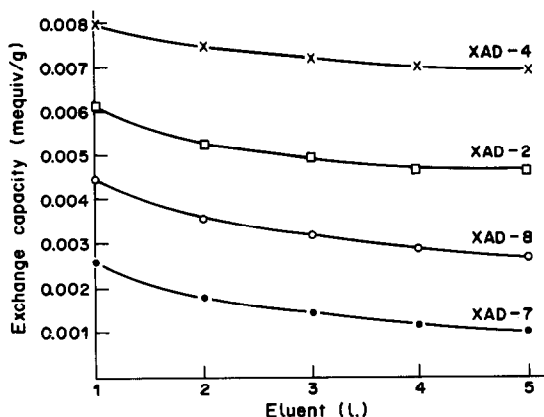


Fig. 1. The exchange capacities of XAD-resins treated with *n*-octadecyltrimethylammonium salt, as a function of the volume of $10^{-3}M$ phthalate solution pumped through the column (3.5 mm bore, 250 mm long) at 2.1 ml/min.

factors in securing relatively high capacity and good retention properties.

It is clear from Figs. 1–3 that on repeated elution with phthalate solution, after an initial decrease in column capacity, the tri-*n*-dodecylmethylammonium salt in XAD-2 shows the best retention of all the systems tested and gives the highest exchange capacity. Consequently, it was used in the chromatographic studies. The capacity is comparable with that of hexadecylpyridinium chloride and and slightly higher than that of tetraoctylammonium chloride, both incorporated into XAD-8.¹⁰

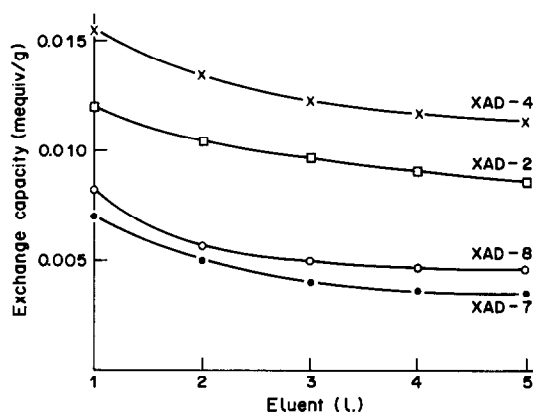


Fig. 2. The exchange capacities of XAD-resins treated with hexadecyltrimethylammonium salt, as a function of the volume of $10^{-3}M$ phthalate solution pumped through the column, as described in Fig. 1 and the text.

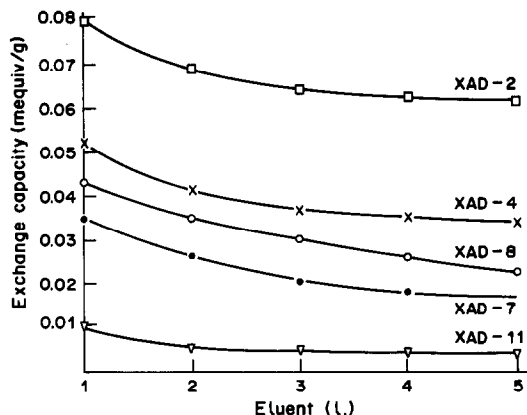


Fig. 3. Capacities of XAD-resins incorporating tri-dodecylmethylammonium salt as a function of volume of $10^{-3}M$ phthalate solution pumped through the column, as described in Fig. 1 and the text.

In testing the indirect method with the Omnitit column, the calibration graphs for chloride, nitrate and sulphate were linear over the concentration range 1–20 ppm for each ion. For injection of 8 samples each of $25 \mu\text{l}$ of 5 ppm chloride solution, the relative error was 2.4%; that for nitrate was similar, and that

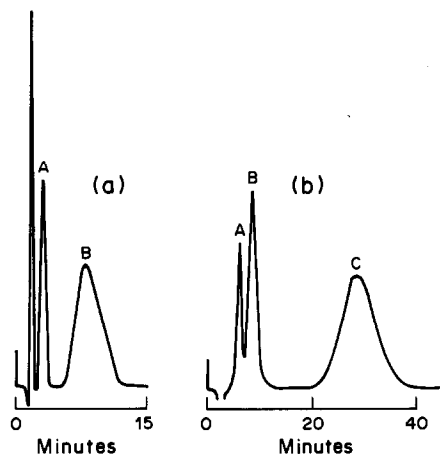


Fig. 4. Typical chromatograms for the elution of chloride, nitrate and sulphate by phthalate solution from a column (3.5 mm bore, 250 mm long) filled with XAD-2 coated with tri-*n*-dodecylmethylammonium salt; ultraviolet detection. (a) The separation of 6 ppm chloride (A) from 17 ppm sulphate (B) in a $25 \mu\text{l}$ sample with $3 \times 10^{-4}M$ phthalate, pH 4.12, at a flow-rate of 1.5 ml/min. (b) The chromatogram for 5 ppm chloride (A), 25 ppm nitrate (B) and 40 ppm sulphate (C) in a $30 \mu\text{l}$ sample, eluted with $5 \times 10^{-3}M$ phthalate at a flow-rate of 0.8 ml/min.

Table 1. Information supplied by the manufacturer, on Amberlite XAD-resins

	Polymer type	Porosity volume, %	Wet density, g/cm^3	Area, m^2/g	Mean pore diameter, \AA
XAD-2	Polystyrene	42	1.02	330	90
XAD-4	Polystyrene	51	1.02	750	50
XAD-7	Acrylic ester	55	1.05	450	80
XAD-8	Acrylic ester	52	1.09	140	250
XAD-11	Polyamide	41	1.07	170	210

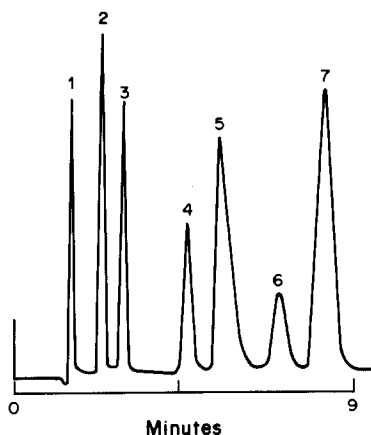


Fig. 5. Separation on the QIC IonChrom Analyser of 50 μ l of a mixture containing 3 ppm fluoride (1), 4 ppm chloride (2), 7 ppm nitrite (3), 9 ppm bromide (4), 18 ppm nitrate (5), 15 ppm phosphate (6) and 22 ppm sulphate (7). The eluting medium was $2.1 \times 10^{-3}M$ $Na_2CO_3/6.0 \times 10^{-4}M$ $NaHCO_3$ and the flow-rate 2.0 ml/min.

for sulphate was around 3% (5 ppm levels). Typical chromatograms are presented in Fig. 4. They show that good separations of chloride and sulphate are readily achieved but chloride and nitrate are not so well separated in the ternary mixture.

The QIC IonChrom Analyser was used with a sodium bicarbonate/carbonate eluent. Good linear calibration graphs were obtained from about 1 to at least 30 ppm for chloride, nitrate and sulphate. For 9 injections, each 50 μ l, of a 7-ppm chloride solution the mean relative error was 1.2%. The superiority of the commercial separator column can be gauged by comparison of the chromatogram (Fig. 5) for the separation of 7 anions with those shown in Fig. 6 for 2 and 3 anions. The chromatograms shown in Fig. 6 were obtained by substitution of the Omnifit column containing tridodecylmethylammonium chloride in XAD-2 for the commercial separator column in the instrument. The resolutions calculated for the chloride and sulphate peaks in the chromatograms shown in Fig. 6a and Fig. 5 were 1.6 and 9.8 respectively. It is likely that the ion-exchange capacity is somewhat greater and the resin particles are more nearly spherical and uniform in size in the commercial column.¹² The poorer performance of the XAD-based columns described here relates largely to the greater particle-size range and the relatively uneven packing of the granular particles. (Unfortunately, small spherical particles of XAD resins are not available.) Column overloading is not considered to be a significant factor in the disparity in performance. Thus the use of the columns so readily prepared from a quaternary am-

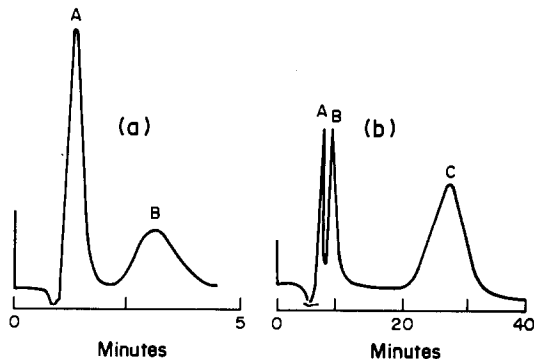


Fig. 6. Chromatograms obtained for the column filled with XAD-2 coated with tri-n-dodecylmethylammonium salt and used as separator column in the QIC IonChrom Analyser. (a) Separation of 10 ppm chloride (A) from 10 ppm sulphate (B) in a 50- μ l sample. The eluting solution and flow-rate are the same as for Fig. 5. (b) Chromatogram for 5 ppm chloride (A), 40 ppm nitrate (B) and 90 ppm sulphate (C) in a 50- μ l sample; developed with $5.0 \times 10^{-4}M$ $Na_2CO_3/6.0 \times 10^{-4}M$ $NaHCO_3$ at a flow-rate of 0.9 ml/min.

monium salt and an XAD resin is likely to remain limited to separations and determination of a restricted number of ions in a sample. These inexpensive exchangers can, however, be regenerated readily after prolonged use, by treatment with fresh solutions of quaternary ammonium salt.

Acknowledgements—The authors thank Dionex (UK) Ltd. for the loan of the QIC IonChrom Analyser, and one of them (A.S.A.) thanks the Kuwait Institute for Scientific Research for a Scholarship.

REFERENCES

1. H. Small, T. S. Stevens and W. C. Bauman, *Anal. Chem.*, 1975, **47**, 1801.
2. D. T. Gjerde, J. S. Fritz and G. Schmuckler, *J. Chromatog.*, 1979, **186**, 509.
3. T. S. Stevens, J. C. Davis and H. Small, *Anal. Chem.*, 1981, **53**, 1488.
4. M. Dreux, M. Lafosse and M. Pequignot, *Chromatographia*, 1982, **15**, 653.
5. R. M. Cassidy and S. Elchuk, *Anal. Chem.*, 1982, **54**, 1558.
6. *Idem*, *J. Chromatog. Sci.*, 1983, **21**, 454.
7. D. P. Lee, *ibid.*, 1984, **22**, 327.
8. J. S. Fritz, D. T. Gjerde and C. Pohlandt, *Ion Chromatography*, Hüthig Verlag, Heidelberg, 1982.
9. T. K. Al-Jorani and S. J. Lyle, *Anal. Proc. Roy. Soc. Chem.*, 1983, **20**, 111.
10. D. L. Duval and J. S. Fritz, *J. Chromatog.*, 1984, **295**, 89.
11. K. W. Pupal, G. L. Booman and J. E. Rein, *U.S. At. Energy Comm. Rept.*, IDO-14389, 1956; *Chem. Abstr.*, 1957, **51**, 5631c.
12. T. S. Stevens and M. A. Langhorst, *Anal. Chem.*, 1982, **54**, 950.

SHORT COMMUNICATIONS

SPECTROPHOTOMETRIC DETERMINATION OF CLOFIBRATE

Y. K. AGRAWAL and D. R. PATEL

Pharmacy Department, Faculty of Technology and Engineering, M.S. University of Baroda,
Kalabhavan, Baroda 390 001, India

(Received 30 August 1985. Revised 6 August 1986. Accepted 1 November 1986)

Summary—A sensitive method for the rapid and accurate determination of clofibrate by hydroxamic acid formation is described. Hydroxylamine hydrochloride is reacted with clofibrate in alkaline medium to give 4-chlorophenoxyisobutyrohydroxamic acid, which forms a purple complex with iron(III) in acidic medium. Common excipients do not interfere.

Clofibrate is a relatively new anti-hyperlipidaemic drug of both clinical and theoretical interest.^{1,2} The ester is readily absorbed, but it is rapidly hydrolysed, and the free acid is presumed to be the active agent *in vivo*.^{3,4} Clofibrate causes a hypocholesterolaemic effect which may be related in part to its ability to block cholesterol biosynthesis.⁵ It may be contaminated with *o*-chlorophenol, from which it is prepared. Hence most of the methods for its determination, which are based on ultraviolet and infrared spectrometry, required a prior separation by ion-exchange.⁶⁻¹⁰ The BP qualitative test for clofibrate is based on formation of the iron(III) complex of the 4-chlorophenoxyisobutyrohydroxamic acid produced by reaction of clofibrate with hydroxylamine in alkaline medium,¹¹ and we have examined this reaction with a view to its quantitative use.

EXPERIMENTAL

Reagents

All general chemicals used were of B.D.H. AnalaR or Merck G.R. grade. Clofibrate (B.P.) was used, without further purification, as a 500 mg/l. solution in ethanol.

The alkaline hydroxylamine solution used was prepared by mixing equal volumes of 4.0M hydroxylamine hydrochloride and 5.5M sodium hydroxide solutions. The mixture has limited stability and should not be used more than a few hours after it has been prepared. A stock 4.0M hydroxylamine hydrochloride solution is stable for several weeks at room temperature.

The 0.5M ferric chloride solution used was prepared in 0.1M hydrochloric acid.

Procedures

Calibration graph. Portions of standard 500-mg/l. clofibrate solution ranging from 0.5 to 3.5 ml were each mixed with 5 ml of alkaline hydroxylamine solution in 25-ml standard flasks, then 5 ml of ethanol, 5 ml of water, 1 ml of 5M hydrochloric acid and 2 ml of 0.5M ferric chloride were added to each and the mixtures diluted to volume with

0.1M hydrochloric acid. The absorbances were measured at 530 nm against a reagent blank, similarly prepared. The standards thus prepared covered the concentration range 10–70 µg/ml clofibrate in the final solution measured.

Analysis of synthetic mixtures. Mixtures containing clofibrate and common excipients such as propylene glycol, glycerine, talc, starch, dextrose, lactose, gum acacia, etc., were prepared. A portion of mixture equivalent to 50 mg of clofibrate was weighed accurately. The clofibrate was extracted with four 15-ml portions of ethanol, each extract being decanted through Whatman No. 40 filter paper. The residue on the filter paper was washed with 20 ml of ethanol. The filtrate and washings were collected in a 100-ml standard flask and diluted to volume with ethanol. A 2-ml aliquot of this solution was treated as described for preparation of the calibration graph.

Analysis of clofibrate capsules. Twenty capsules were emptied and their contents mixed and weighed. An amount of powder equivalent to 50 mg of clofibrate was weighed accurately and analysed as in the preparation of the calibration graph.

RESULTS AND DISCUSSION

Spectral characteristics

The purple ferric 4-chlorophenoxyisobutyrohydroxamate complex has maximum absorbance at 530 nm. The reagent blank has no absorption between 450 and 600 nm.

Reaction variables

Maximum colour intensity for 25 µg/ml final clofibrate concentration (in 25 ml) was found to be obtained with 2–5 ml of 2M hydroxylamine solution; higher concentrations of hydroxylamine gave precipitation. Maximum colour intensity was obtained with 0.5–2.5 ml of 0.5M ferric chloride, and the optimum pH range was 1.0–1.5. The colour was stable for 2 hr at room temperature.

Beer's law was found to hold over the clofibrate range 10–70 µg/ml in the final solution.

Determination of clofibrate in pharmaceuticals

The results for the synthetic mixtures are given in Table I. Analysis of five samples of clofibrate capsules (nominal content 500 mg per capsule) gave mean values (8 replicates) ranging from 499 to 502 mg per capsule (standard deviations ranging from 1 to 2.5 mg).

Table I. Analysis of synthetic samples

Clofibrate taken, mg	Clofibrate found, mg	
	Proposed method*	USP method ¹⁰
20.0	19.9 ± 0.3	20.0
30.0	30.1 ± 0.2	30.0
40.0	39.6 ± 0.5	39.0
60.0	59.4 ± 0.8	59.5
70.0	69.8 ± 0.5	69.0

*Mean ± standard deviation (10 replicates).

REFERENCES

1. J. M. Thorp, *Lancet*, 1962, **1**, 1323.
2. N. S. Waring, *Nature*, 1962, **194**, 948.
3. D. T. Witiak and M. W. Whitehouse, *Biochem. Pharmacol.*, 1969, **18**, 971.
4. B. U. Mussa, J. T. Ogilvie and J. T. Dowling, *Metabolism*, 1968, **17**, 909.
5. P. J. Nestal, E. Z. Mirsch and E. A. Couzens, *J. Clin. Invest.*, 1969, **44**, 891.
6. T. D. Bjornsson and T. F. Blaschke, *J. Chromatog.*, 1977, **137**, 145.
7. S. Silvestri, *Farmaco Ed. Prat.*, 1970, **25**, 197.
8. H. Aftalion, R. Siminovi and F. M. Albert, *Rev. Roum. Chim.*, 1968, **13**, 1195.
9. K. Florey, *Analytical Profiles of Drug Substances*, Vol. 11, Academic Press, New York, 1982.
10. *United States Pharmacopeia*, 20th Revision; *The National Formulary*, 15th Ed., p. 157. United States Pharmacopeial Convention, Rockville, MD, 1980.
11. *British Pharmacopoeia 1980*, p. 116. HMSO, London, 1980.

SPECTROPHOTOMETRIC DETERMINATION OF COBALT IN IRON-, COBALT- AND NICKEL-BASE ALLOYS

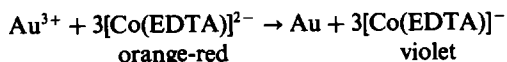
B. V. RAO,* V. G. RADHA MENON† and K. C. SAROJAM‡

Defence Metallurgical Research Laboratory, P.O. Kanchanbagh, Hyderabad 500 258, India

(Received 10 January 1985, Revised 23 September 1986, Accepted 10 October 1986)

Summary—A spectrophotometric method has been developed for the accurate determination of cobalt at milligram level, based on oxidation of the cobalt(II)–EDTA complex with gold(III) chloride at pH 4.0–6.5 and 100° and measurement of the absorbance of the resultant violet cobalt(III)–EDTA complex at 535 nm. The precision is not affected by the presence of several metal ions; including coloured ones such as Cu(II), Ni(II) and Fe(III). However, chromium(III) interferes since it also forms a violet complex with EDTA, but can be removed by separation with pyridine. Practical application of the method is illustrated by the determination of cobalt in alloys based on iron, cobalt and nickel. Over the cobalt range 8–52% the error ranges from 0.1 to 0.3%.

The analytical chemistry of cobalt continues to be of interest since cobalt is increasingly used in modern metallurgical products. Gravimetric,¹ titrimetric^{2–4} and colorimetric^{5–7} procedures have been developed, but most of these methods have disadvantages. Silverstone and Bach⁸ have described a spectrophotometric method for determination of major amounts of cobalt in nickel alloys by use of EDTA and hydrogen peroxide at elevated temperatures. In a previous investigation⁹ in this laboratory, it was shown that gold(III) can be reduced to the metal quantitatively with cobalt(II) nitrate in the presence of EDTA in weakly acidic medium:



The redox potential of the Co(III)/Co(II) system is reduced from ~ +1.8 V to ~ +0.6 V by complex formation with EDTA; the redox potential of the Au(III)/Au couple is +1.4 V. This enables gold(III) to oxidize cobalt(II)–EDTA quantitatively to violet cobalt(III)–EDTA under appropriate conditions. The experimental parameters for the formation of the violet cobalt(III)–EDTA complex to be measured spectrophotometrically have been studied for determining cobalt over a wide concentration range in different types of alloys.

EXPERIMENTAL

Reagents

Cobalt(II) nitrate standard solution (Co 1 mg/ml). Prepared by dissolving 1.000 g of cobalt (purity 99.99%) in nitric acid (1 + 2) and diluting the solution to exactly 1 litre.

*Author for correspondence.

†Present address: Defence Bio-Engineering and Electro-Medical Laboratory, Bangalore 560 075, India.

‡Present address: Naval Chemical and Metallurgical Laboratory, Naval Dockyard, Bombay 400 023, India.

Gold(III) chloride solution, 0.01M. Prepared by dissolving 1.97 g of gold metal (purity 99.9%) in *aqua regia*, slowly evaporating the solution nearly to dryness, adding 10 ml of concentrated hydrochloric acid and diluting to 1 litre.

EDTA solution, 0.25M.

Iron(III) chloride solution. Prepared by dissolving 4.00 g of pure iron in hydrochloric acid, oxidizing with the minimum of concentrated nitric acid and diluting to 100 ml.

Acid mixture. A mixture of 25 ml of concentrated nitric acid, 75 ml of concentrated hydrochloric acid and 50 ml of distilled water.

Solutions of the following species (5 mg/ml) were prepared from analytical grade reagents: copper(II), nickel(II), zinc(II), manganese(II), iron(III), aluminium(III) and chromium(III) sulphates, lead and zirconium nitrates, titanium(IV) chloride, and sodium vanadate, molybdate and tungstate.

Procedure for determination of cobalt in alloys

Weigh 0.1–0.5 g of sample into a 100-ml beaker and dissolve it in 5–15 ml of acid mixture. Add 1 ml of iron(III) chloride solution if the alloy contains chromium. Evaporate the solution nearly to dryness, cool, add 5 ml of hydrochloric acid (1 + 1) and warm gently to dissolve the salts. Boil the solution, cool, transfer to a 100-ml standard flask, dilute to about 75 ml with water, add 15 ml of pyridine, mix, make up to volume with water and mix. After 15 min filter the solution through a dry Whatman No. 41 filter paper in a dry funnel into a dry beaker. If the alloy does not contain chromium, omit the addition of iron(III) chloride and pyridine, but dilute the sample solution to 100 ml as described.

Pipette 10 ml of the sample solution, containing between 4 and 8 mg of cobalt, into a 100-ml beaker, add 3 ml of 0.25M EDTA, 10 ml of 0.1M sodium acetate–acetic acid buffer (pH 5) and 6 ml of gold(III) chloride solution. Boil the solution for 15 min, cool, transfer it to a 50-ml standard flask and make up to the mark with water. Centrifuge the solution to remove elemental gold and, using 1-cm cells, measure the absorbance of the violet cobalt(III)–EDTA complex at 535 nm against a reference solution similarly prepared but without the gold(III) chloride.

Prepare a calibration graph with 1.0–8.0 ml of standard 1-mg/ml cobalt(II) solution processed in the same way as the 10-ml sample solutions. The graph is linear over the range 1–8 mg of cobalt, but the slope is slightly lower when the pyridine treatment is used.

Table 1. Spectrophotometric determination of cobalt in iron-, cobalt- and nickel-base alloys

Type of alloy	Cobalt, %		Absolute standard deviation, %
	Present	Mean found (5 replicates)	
<i>Iron-base</i>			
Permanent magnet alloy (BCS 365)	24.7*	24.6	0.1
Permanent magnet alloy (BCS 233)	23.72*	23.7	0.2
Kovar alloy	18.0†	18.1	0.1
Cobalt steel (NBS 153a)	8.47*	8.5 ₆	0.08
<i>Cobalt-base</i>			
Vicalloy	52.0†	52.2	0.2
Co-base alloy (NBS 168)	41.2*	41.2	0.2
<i>Nickel-base</i>			
Nimonic-90 (BCS 310/1)	17.0*	17.1	0.2
Waspaloy (NBS 349)	13.95*	13.8	0.04

*Certified values.

†Values obtained by the method of Vydra and Přibil.⁴

RESULTS AND DISCUSSION

The experimental conditions were optimized in a series of preliminary investigations. One ml of 0.01M gold(III) solution will oxidize 1.768 mg of cobalt(II), and the excess of gold(III) is reduced to the metal by excess of EDTA present. Hence excess of both gold(III) and EDTA must be added or low results will be obtained. The quantities specified in the procedure are sufficient for 40 mg of sample. Increase in the pyridine concentration decreases the absorbance, but small variations in the quantity of pyridine have no significant effect.

The oxidation of the cobalt(II)-EDTA complex is slow at room temperature but complete in 10 min when the solution is boiled. Longer boiling does not affect the absorbance. Once the complex has been completely formed, its absorbance is constant for at least 24 hr.

Of the ions from the elements Mn, Cr, Ti, Al, V, Mo, Fe, Cu and Ni, commonly present in the alloys, only chromium(III) causes serious interference, because it also forms a violet complex with EDTA, so any chromium(III) present must be removed beforehand. In presence of a sufficient amount of iron(III), chromium(III) is precipitated quantitatively as a mixture of chromium and iron hydroxides by means of pyridine; Al(III), Ti(IV) and Zr(IV) are also precipitated, leaving Co(II), Ni(II), Cu(II), Mn(II), V(V) and Mo(VI) in solution. The cobalt(III)-EDTA complex has maximum absorption at 535 nm whereas the EDTA complexes of Cu(II) and Ni(II) have only slight absorption at that wavelength. Hence measuring the absorbance of the cobalt(III)-EDTA complex against a reference solution containing the same

concentration of the EDTA complexes of Cu(II) and Ni(II) will eliminate any interference due to these species. The unoxidized reference solution will obviously contain the cobalt as the cobalt(II)-EDTA complex but this also has negligible absorbance at 535 nm, and even this will be automatically compensated for in the calibration procedure.

The results in Table 1 show the method to be accurate and to have good reproducibility. The results compare well with the certified values or those obtained by the redox method of Vydra and Přibil.⁴ The method is not expensive, since the gold can be recovered and converted into the gold(III) chloride reagent solution for further work.

Acknowledgements—The authors thank Dr. D. P. Lahiri, Deputy Director, Defence Metallurgical Research Laboratory, Hyderabad for constant encouragement in the work and for suggestions and help in preparation of the manuscript.

REFERENCES

1. A. I. Vogel, *Quantitative Inorganic Analysis*, 2nd Ed., pp. 529-530. Longmans, London, 1959.
2. *Idem*, *op. cit.*, pp. 955-956.
3. F. Vydra and R. Přibil, *Collection Czech. Chem. Commun.*, 1961, **26**, 2169.
4. *Idem*, *Talanta*, 1960, **5**, 92.
5. E. C. Pigott, *Ferrous Analysis: Modern Practice and Theory*, p. 176. Chapman & Hall, London, 1941.
6. F. J. Welcher, *The Analytical Uses of Ethylenediamine Tetraacetic Acid*, pp. 280-281. Van Nostrand, New York, 1958.
7. W. J. Williams, *Talanta*, 1958, **1**, 88.
8. N. M. Silverstone and B. B. Bach, *Metallurgia*, 1961, **63**, 205.
9. S. Raoot, K. N. Raoot, B. V. Rao, S. L. N. Acharyulu and R. V. Tamhankar, *Chim. Anal. (Paris)*, 1971, **53**, 584.

SYNTHESIS OF 2-(3,5-DICHLORO-2-PYRIDYLAZO)-5-DIMETHYLAMINOPHENOL AND ITS APPLICATION TO THE SPECTROPHOTOMETRIC DETERMINATION OF COBALT

MASAAKI NAKAMURA, YUTAKA SAKANASHI, HIROAKI CHIKUSHI and FUMIAKI KAI
Department of Chemistry, Faculty of Science, Kumamoto University, Kumamoto 860, Japan

SHIGEYA SATO,* TOSHIE SATO and SUMIO UCHIKAWA
Faculty of Education, Kumamoto University, 2-40-1, Kurokami, Kumamoto 860, Japan

(Received 9 April 1986. Revised 10 June 1986. Accepted 7 November 1986)

Summary—2-(3,5-Dichloro-2-pyridylazo)-5-dimethylaminophenol (3,5-diCl-DMPAP) has been synthesized and its analytical application investigated. It reacts with cobalt in aqueous solution at pH 2.2–6.0 and room temperature to form a water-soluble ML_2 complex with absorption maximum at 590 nm, and molar absorptivity 8.4×10^4 l. mole⁻¹. cm⁻¹. Interference from other transition metals can be eliminated by their solvent extraction with 8-hydroxyquinoline. The method has been successfully applied to determination of cobalt in mild steels.

Many studies have been made of organic reagents for cobalt since Liu reported synthesis of PAN. Many of them are based on the reactions of cobalt with suitable colour-producing reagents²⁻¹⁰ and the ion-pair extraction of anionic cobalt-complexes with quarternary ammonium salts.^{11,12} Some of these methods have disadvantages such as low sensitivity and selectivity, absorption maxima in the ultraviolet range, and need to remove excess of reagent. The need for extraction has been eliminated by use of a non-ionic surfactant (Triton X-100),¹³⁻¹⁵ but although these methods are simple, they have some defects with respect to sensitivity and removal of interferences.

In our laboratories, a study has been made of some pyridylazo compounds with two chlorine atoms at the 3- and 5-positions of the pyridine ring, and the use of 4-(3,5-dichloro-2-pyridylazo)-1,3-diaminobenzene for determination of palladium(II) has already been reported.¹⁶ In the present work 2-(3,5-dichloro-2-pyridylazo)-5-dimethylaminophenol (3,5-diCl-DMPAP) was synthesized as a new reagent and its analytical application to determination of 3d transition metal ions investigated. It was found that this reagent reacts with cobalt to form a water-soluble complex in weakly acidic medium.

EXPERIMENTAL

Apparatus

Hitachi 181 and 624 digital spectrophotometers were used for absorbance measurements with 10-mm glass cells. An Iwaki V-DN type KM shaker, a Hitachi 03P centrifuge and a Hitachi-Horiba M-8 pH-meter were also used.

Preparation of 3,5-diCl-DMPAP

The reagent was prepared by coupling *m*-dimethylaminophenol with 3,5-dichloro-2-pyridyldiazotote synthesized according to the previous paper.¹⁶ *m*-Dimethylaminophenol (1.3 g, 9.47 mmole) and diazotote (2.0 g, 9.35 mmole) were dissolved in 50 ml of methanol, then carbon dioxide was bubbled through the solution for 5 hr at 10–20°, and the red brown crystals precipitated were filtered off and washed with water. The product was recrystallized from chloroform to give red needles, m.p. 189–191°. Infrared: 1625 cm⁻¹ (—N=N—). ¹H-NMR (CDCl₃): δ = 3.22 (6H, s, 2 × CH₃), 6.05 (1H, d, J = 2.4 Hz, H-6), 6.60 (1H, dd, J = 10.2 and 2.4 Hz, H-4), 7.62 (1H, d, J = 10.2 Hz, H-3), 7.86 (1H, d, J = 3.0 Hz, H-3'), 8.47 (1H, d, J = 3.0 Hz, H-6'), and 16.11 (1H, br, s, OH). Found: C, 49.9% H, 4.0%; N, 17.8%. C₁₃H₁₂N₄OCl₂ requires C, 50.18%; H, 3.99%; N, 18.01%. Acid dissociation constants obtained were pK_{a2} [corresponding to deprotonation of the conjugate acid of —N⁺H(CH₃)₂] = 1.1 and pK_{a3} (dissociation of phenolic proton) = 10.9 in 30% v/v dioxan–water at 25°, ionic strength 0.1 (KNO₃); pK_{a1}, corresponding to deprotonation of the conjugate acid of the pyridine nitrogen atom, was not obtained because deprotonation occurred in a strongly acidic region.

Reagents

3,5-diCl-DMPAP standard solution. Recrystallized 3,5-diCl-DMPAP (m.w. 311) was dissolved in ethanol to give a $1.0 \times 10^{-3} M$ solution; working solutions were prepared by dilution with ethanol. The solution was stable for several months if stored in an amber bottle.

Standard cobalt(II) solution. A stock solution ($1.0 \times 10^{-2} M$; 590 mg/l) was prepared by dissolving cobalt(II) chloride in water; working solutions were prepared by suitable dilution with water.

8-Hydroxyquinoline (oxine) solution. Oxine (4.0 g) was dissolved in 5 ml of glacial acetic acid and the solution diluted to 100 ml with water.

Demineralized water was used throughout. All other reagents were of analytical-reagent grade, used as received.

Recommended procedure

Take 1.0 ml of 0.1M acetate buffer (pH 4.0) and an aliquot of cobalt(II) solution containing up to 1.3 μg of

*Author for correspondence.

cobalt, in a stoppered graduated 10-ml test-tube. Add 0.5 ml of 3,5-diCl-DMPAP solution ($1.0 \times 10^{-4}M$) and dilute to 3.0 ml with water. After 60 min, add 4 ml of benzene and shake the mixture for 5 min. After phase separation, measure the absorbance of the aqueous phase at 590 nm against water.

Preparation of steel sample solution

Weigh up to 0.2 g of sample into a 100-ml beaker, dissolve it in 20 ml of sulphuric acid (1 + 6) by heating, then gradually add 5 ml of 30% hydrogen peroxide solution, and boil the solution for about 10 min to completely remove residual hydrogen peroxide. Cool, adjust to pH 1.8–2.0 with 8M sodium hydroxide, then make up to volume in a 100-ml standard flask with water.

Removal of interfering ions

Take 1.0 ml of steel solution in a stoppered graduated 10-ml test-tube. Add 1.0 ml of acetate buffer and 1.0 ml of oxine solution, and dilute to 4.0 ml with water (the pH of the solution will be ~ 2.6). Shake the solution with 4.0 ml of benzene for 5 min, then separate the phases. Analyse 0.5 or 1.0 ml of the aqueous phase by the recommended procedure.

RESULTS AND DISCUSSION

Colour reaction with metal ions

Ions that do not give a detectable colour at room temperature include Be(II), Mg(II), Ca(II), Sr(II), Ba(II), B(III), Ce(IV), Sn(II), Sn(IV), Pb(II), As(III), As(V), Sb(V) and Cr(III). Fe(III), Mn(II), Mo(VI), Pr(III), Sm(III) and Nd(III) give colour reactions but the molar absorptivities are very low ($\epsilon < 5.0 \times 10^3$ l.mole $^{-1}$.cm $^{-1}$). Cd(II) and Hg(II) give a colour reaction in weakly alkaline solution, followed by rapid precipitation. Details of useful colour reactions are given in Table 1. The reagent is superior for the determination of 3d-type transition metals, and several differential methods can be based on the difference in reaction rate, optimum pH and absorption maximum.

When aqueous solutions of the complexes are shaken with benzene, only the Co and Ti complexes remain in the aqueous phase, the other complexes and the reagent being extracted. Ti ($5.0 \times 10^{-4}M$) does not react with 3,5-diCl-DMPAP in the presence of fluoride ($1.5 \times 10^{-2}M$). Under proper conditions, the selectivity for cobalt is thus greatly improved.

Absorption spectra

Figure 1 shows the spectrum of the reagent is independent of pH in the range from 1M hydro-

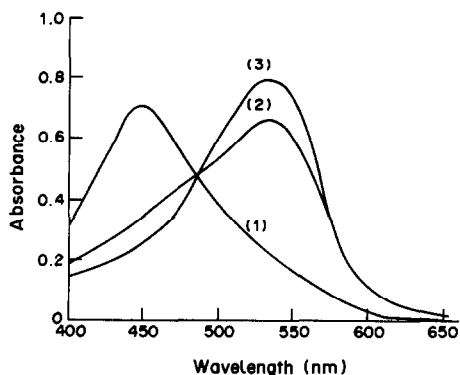


Fig. 1. Absorption spectra of 3,5-diCl-DMPAP in water at various pH values. $[3,5\text{-diCl-DMPAP}] = 1.67 \times 10^{-5}M$. (1) 1M HCl-pH 10; (2) pH 12; (3) 1M NaOH.

chloric acid to pH 10 and the molar absorptivity at 450 nm is 4.20×10^4 l.mole $^{-1}$.cm $^{-1}$. Above pH 10 the absorption maximum shifts to longer wavelength and the spectra have an isosbestic point at 485 nm and absorption maxima at 530 nm ($\epsilon = 4.74 \times 10^4$ in 1M sodium hydroxide).

The spectrum of the cobalt complex in the aqueous phase after the extraction with benzene has absorption maxima at 555 ($\epsilon = 8.25 \times 10^4$) and 590 nm ($\epsilon = 8.40 \times 10^4$). There is no reagent blank absorbance in the range 400–650 nm, because the reagent is completely removed from the aqueous phase by the benzene extraction.

Experimental variables

The absorbance of the cobalt complex in the aqueous phase is constant and maximal over the pH range 2.2–6.0. The minimum time for complete colour development of the complex is 60 min at room temperature, and heating at 45° does not significantly change the reaction time. The absorbance is stable for at least 10 days.

When dichloroethane, dichloromethane, or chlorobenzene is used as the washing solvent, the cobalt complex is partly extracted. Toluene, carbon tetrachloride, n-hexane and cyclohexane do not completely extract the copper complex, so would cause a positive error if used in determination of cobalt. Benzene is the preferred solvent. Shaking with 3 ml of benzene for 3 min is enough to eliminate the other metal complexes from the aqueous phase. The ab-

Table 1. Reactions between 3,5-diCl-DMPAP and metal ions

Metal ion	pH	Standing time, min	λ_{\max} , nm	ϵ , 10^4 l. mole $^{-1}$. cm $^{-1}$	[DMPAP]
					[Co]
Ti(IV)	1.4–3.0	60	540	6.3	1
V(IV)	0.5M H $^{+}$ –1.6	60	600	7.2	1
V(V)	3M H $^{+}$ –2.0	60	600	6.8	1
Co(II)	2.2–6.0	60	590	8.8	2
Ni(II)	4.0–10.0	20	530	12.0	2
Cu(II)	1.2–5.0	0	560	5.8	1
	7.6–10.0	0	560	9.3	2
Zn(II)	5.6–11.0	0	559	12.1	2

Table 2. Determination of cobalt in carbon steel

Steel (certified value, %)*	Sample weight, † g	Cobalt‡	
		µg	%
NBS 362 (0.3%)	0.1001	0.368	0.29 ₄
	0.1004	0.378	0.30 ₁
	0.1025	0.391	0.30 ₅
	0.1504	0.553	0.29 ₄
JSS 172-3 (0.049%)	0.1001	0.122	0.048 ₈
	0.1000	0.118	0.047 ₂
	0.1503	0.189	0.050 ₃
	0.1486	0.185	0.049 ₈
JSS 175-3 (0.011%)	0.2001	0.061	0.012 ₂
	0.2014	0.055	0.010 ₆
	0.2006	0.053	0.010 ₆

*Other components. NBS: C, 0.16; Mn, 1.04; Si, 0.39; V, 0.04; Mo, 0.068; W, 0.20; Sn, 0.016; Al, 0.09; Zr, 0.19; Sb, 0.013; Cu, 0.50; Ni, 0.59; Cr, 0.30; As, 0.09%. JSS 172-3: C, 0.047; V, 0.010; Al, 0.014; B, 0.0022; Nb, 0.052; Zr, 0.010; Sb, 0.0020%. JSS 175-3: C, 0.038; V, 0.093; Al, 0.054; B, 0.0091; Nb, 0.011; Zr, 0.031; Sb, 0.0196%.

†1.0 ml of the 100 ml of steel solution was extracted with oxine, and 0.5 ml (NBS) or 1.0 ml (JSS) of the resulting aqueous phase was analysed for cobalt.

‡Mean of five determinations.

sorbance of the cobalt complex is unaffected by continuing the shaking with benzene for up to 60 min.

Calibration graph

Beer's law is obeyed up to $7.5 \times 10^{-6} M$ cobalt (corresponding to 1.3 µg in 3 ml), and the molar absorptivity is 8.4×10^4 l.mole⁻¹.cm⁻¹. The coefficient of variation was 1.3% for eight runs at $5.0 \times 10^{-6} M$ cobalt.

Composition of the cobalt complex

The continuous-variation and mole-ratio methods indicated a 1:2 metal:reagent mole ratio. When the complex was treated with benzene in the presence of a bulky anion such as perchlorate or thiocyanate ($1.7 \times 10^{-3} M$), it was completely removed from the aqueous phase, but remained in it in the presence of tetra-alkylammonium cations. Consequently, it was concluded that the cobalt is present as Co(III) in the complex.

Determination of cobalt in steels

The proposed method was applied to the determination of cobalt in carbon steels. The iron(III) and other potentially interfering ions present in relatively high concentrations in the steel sample, must be removed prior to the determination step. These ions, in up to 0.01M concentration, can be removed by extraction at pH < 4 as the oxinates into benzene without loss of cobalt.

Examination of any residue from the acid/peroxide treatment (dissolved as described previously¹⁷) showed the absence of any significant amount of cobalt so such a residues step can be discarded in the procedure.

Table 2 shows that the values obtained are in good agreement with the certified values. Recovery tests by the standard-addition method showed recoveries of 98–101%. The relative standard deviation for the determination of cobalt in NBS 362 was 1%.

Though too slow for production control, the method should be suitable for quality control and investigational purposes.

REFERENCES

1. J. C. I. Liu, *Ph.D. Thesis*, University of Illinois, 1951.
2. K. L. Cheng and R. H. Bray, *Anal. Chem.*, 1955, **27**, 782.
3. R. Püschel, E. Lassner and K. Katzengruber, *Z. Anal. Chem.*, 1966, **223**, 414.
4. R. Lundquist, G. E. Markle and D. F. Boltz, *Anal. Chem.*, 1955, **27**, 1731.
5. K. J. McNaught, *Analyst*, 1942, **67**, 97.
6. J. Adam and R. Přibil, *Talanta*, 1971, **18**, 733.
7. S. Shibata, M. Furukawa, Y. Ishiguro and S. Sasaka, *Anal. Chim. Acta*, 1971, **55**, 231.
8. S. Shibata, *Bunseki Kagaku*, 1972, **21**, 551.
9. S. Shibata, M. Furukawa and E. Kamata, *Anal. Chim. Acta*, 1974, **73**, 107.
10. E. Kiss, *ibid.*, 1975, **77**, 320.
11. S. Motomizu and K. Toei, *Talanta*, 1982, **29**, 89.
12. K. Ueda, *Bull. Chem. Soc. Japan*, 1979, **52**, 1215.
13. H. Watanabe, *Talanta*, 1974, **21**, 295.
14. S. Okawa, B. Kominami and A. Kawase, *Bunseki Kagaku*, 1982, **31**, 373.
15. K. Hayashi, Y. Sasaki, S. Tagashira, K. Ito and M. Suzuki, *ibid.*, 1978, **27**, 204.
16. F. Kai, Y. Sakanashi, S. Sato and S. Uchikawa, *Anal. Lett.* 1983, **16**, 1013.
17. S. Sato and S. Uchikawa, *Talanta*, 1986, **33**, 115.

SPECTROPHOTOMETRIC DETERMINATION OF SOME INSECTICIDES WITH 3-METHYL-2-BENZOTHAZOLINONE HYDRAZONE HYDROCHLORIDE

C. S. P. SASTRY and D. VIJAYA

Food and Drug Laboratories, School of Chemistry, Andhra University, Waltair 530 003, India

(Received 13 February 1986. Revised 1 July 1986. Accepted 1 November 1986)

Summary—A simple, rapid and sensitive spectrophotometric method is described for determining carbaryl, propoxur, fenitrothion and methyl parathion, based on reaction of their hydrolysis or reduction products (as appropriate) with 3-methyl-2-benzothiazolinone hydrazone hydrochloride in the presence of an oxidant (Ce^{4+} or Fe^{3+}) to give coloured species.

Several spectrophotometric methods for assay of carbamate¹⁻¹¹ and organophosphorus insecticides¹²⁻²² are cited in the literature.

This paper describes the use of 3-methyl-2-benzothiazolinone hydrazone hydrochloride (MBTH) in the presence of an oxidant for the determination of carbamates and organophosphorus insecticides, based on hydrolysis of the former to phenols and reduction of the latter to amines, and reaction of these products with MBTH and oxidants as reported by Umeda²⁴ and Sawicki *et al.*²⁵

EXPERIMENTAL

Reagents

All chemicals were analytical grade.

Standard solutions of carbaryl and propoxur (500 µg/ml). To 50 mg of the insecticide dissolved in 25 ml of methanol, 2 ml of 1M sodium hydroxide were added and after 5 min the solution was made up to volume in a 100-ml standard flask with distilled water.

Standard solutions of fenitrothion and methylparathion (500 µg/ml). To 50 mg of the insecticide were added 10 ml of methanol, 10 ml of distilled water, 1.6 ml of 2.5M sulphuric acid and 0.5 g of zinc dust, and the mixture was gently boiled for 5-6 min, then cooled, filtered into a 100-ml standard flask and made up to the mark with distilled water.

Working solutions of the insecticides were prepared by dilution with distilled water as required.

MBTH solution in distilled water, 2%.

Ceric ammonium sulphate solution, 1%, in 0.7M sulphuric acid.

Ferric chloride hexahydrate solution, 0.8%, freshly prepared in distilled water.

Triethanolamine, 50% solution in distilled water.

General procedures

For carbamates. Into 10-ml graduated test-tubes, transfer 0.25-2.5 ml portions of standard carbaryl (10 µg/ml) solution or 0.35-3.5 ml portions of standard propoxur (10 µg/ml) solution and 1 ml of MBTH solution and set aside for 5 min. Add 0.5 ml of ceric ammonium sulphate solution and allow to stand for another 5 min, then make alkaline with 1 ml of triethanolamine and dilute to 10 ml with methanol. Measure the absorbance of the coloured species at 500 nm after 5-120 min, against a reagent blank.

Compute the amount of carbamate from a calibration graph.

For organophosphorus insecticides. Transfer 0.2-2.25 ml portions of standard fenitrothion (10 µg/ml) solution or 0.4-4.0 ml portions of standard methylparathion (25 µg/ml) solution into 10-ml graduated test-tubes. Add to each tube 1 ml of MBTH solution and 2 ml of ferric chloride solution, allow to stand for 15 min and dilute to volume with methanol. Measure the absorbance at 560 nm against a corresponding reagent blank after 5-180 min.

For formulations. Weigh an amount of well-mixed formulation, equivalent to 50 mg of the insecticide, treat it with 15 ml of methanol and centrifuge for 5 min. Filter the supernatant liquid by decantation, into a 100-ml standard flask. Wash the residue with 10 ml of methanol, make up the filtrate and washings with methanol and analyse as for the standard solutions.

Residue analysis. A 50-mg sample of vegetable or fruit free from insecticide was uniformly mixed with 10 ml of methanol containing various amounts of the insecticide, and left for 24 hr to give closer simulation of environmental samples. The insecticidal residues were extracted according to the procedure of Deshmukh and Sidhu.²¹ The extracts were treated in the manner given for standard solution preparation and determination.

RESULTS AND DISCUSSION

The optimum conditions were established in the usual way by altering one variable at a time.

The absorbance maximum was at 500 nm for carbamates and 560 nm for organophosphorus insecticides. Beer's law was found valid over the concentration ranges presented in Table 1. The molar absorptivities, and regression equations obtained by linear least-squares treatment of the results, are also given in Table 1.

The insecticidal residues in simulated samples were extracted according to Deshmukh and Sidhu,²¹ and appropriate volumes of the extracts were analysed (Table 2). The method works well for analysis of commercial insecticide formulations (Table 3).

Mechanism

The hydrolysis products of the carbamate (1-naphthol from carbaryl; *o*-isopropoxyphenol

Table 1. Optical characteristics, precision and accuracy

Compound	Carbaryl	Propoxur	Fenitrothion	Methylparathion
Concentration range, $\mu\text{g/ml}$ (C)	0.25–2.5	0.35–3.5	0.2–2.25	1.0–10
Regression equation*	$0.0011 + 0.197C$	$-0.0014 + 0.15C$	$0.0035 + 0.236C$	$0.0002 + 0.0473C$
Molar absorptivity ($l.\text{mole}^{-1}.\text{cm}^{-1}$)	4.02×10^4	3.14×10^4	6.65×10^4	1.26×10^4
Relative standard deviation, %	0.8	0.7	0.7	1.4
Error, %	0.4	0.4	0.4	0.6

*Found in this work; must be determined independently by users of the method.

Table 2. Estimation of insecticidal residues in vegetables and fruits

Substrate		Insecticide	
		Added, μg	Recovered, μg
Cabbage	C	15	14.9
	P	15	14.4
	F	5	4.9
	MP	15	14.4
Tomato	C	5	4.8
	P	15	14.4
	F	5	4.8
	MP	15	14.4
Potato	C	5	4.6
	P	15	13.8
	F	5	4.6
	MP	15	13.7

C, carbaryl; P, propoxur; F, fenitrothion; MP, methylparathion.

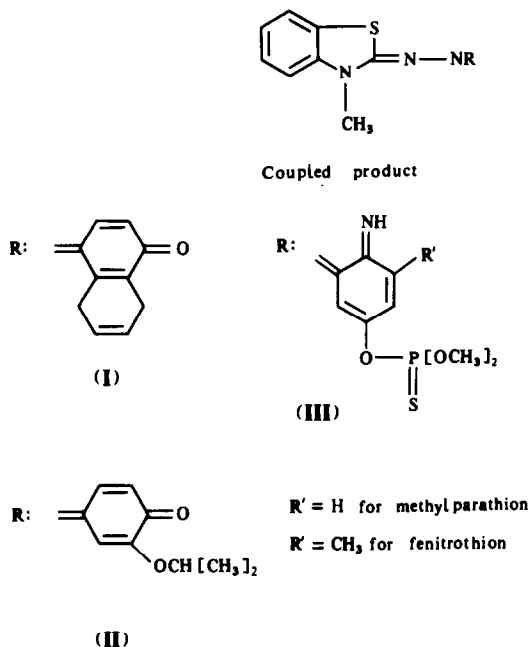
Table 3. Determination of carbamate and organophosphorus insecticides in formulations

Technical grade sample	Indicated on label, %	Found,* %	Reference method, ^{1,12} %
Carbaryl			
I (dust)	85	83.8	83.6
II (dust)	5	4.9 ₂	4.8 ₈
Propoxur			
I (spray)	1	0.97	0.92
II (dust)	2	1.97	1.96
Fenitrothion			
Sumithion 50E	50	49.6	49.3
Sumithion 30E	30	29.4	29.2
Methylparathion			
Devithion 50E	50	49.0	48.7
Devithion 30E	30	29.2	29.1

*Mean of three determinations.

from propoxur) and the reduction products of the thiophosphate (*O, O*-dimethyl-*O*-3-methyl-4-aminophenylthiophosphate from *O, O*-dimethyl-*O*-3-methyl-4-nitrophenylthiophosphate; *O, O*-dimethyl-*O*-4-aminophenylthiophosphate from *O, O*-dimethyl-*O*-4-nitrophenylthiophosphate) insecticides, containing a phenolic or aromatic amine group, can react with MBTH in presence of an oxidizing agent to form coloured coupling products (I–III), similar to those of MBTH and phenols²³ or aromatic amines.²⁴ Under the reaction conditions MBTH loses two electrons and one proton on oxidation, forming the electrophilic intermediate which has been postulated to be the active coloured species. The intermediate under-

goes electrophilic substitution with phenol or amine to form the coupled product. Phenols or aromatic amines react in the *p*-position or *o*-position (if the *p*-position is blocked) to the hydroxyl or amine group, which is quite usual in such oxidative coupling reactions. The nature of the coloured species formed from the insecticides mentioned may be represented as follows.



Scheme 1

REFERENCES

- K. M. Appaiah, R. Ramakrishna, K. R. Subba Rao and K. Omprakash, *J. Assoc. Offic. Anal. Chem.*, 1982, **65**, 32.
- P. Bracha, *J. Agric. Food Chem.*, 1964, **12**, 461.
- S. K. Handa and A. K. Dikshit, *Analyst*, 1979, **104**, 1185.
- W. H. McDermott and A. H. DuVall, *J. Assoc. Offic. Anal. Chem.* 1970, **53**, 896.
- G. Mukherjee, A. K. Mukherjee and B. R. Roy, *J. Food Sci. Tech.*, 1975, **12**, 96.
- J. R. Rangaswamy and S. K. Majumdar, *J. Assoc. Offic. Anal. Chem.*, 1974, **57**, 592.
- M. Ramaswamy, *Pestic Sci.*, 1974, **5**, 381.
- M. Syoyama, J. Miyachi and J. Sakakibara, *Bunseki Kagaku*, 1975, **24**, 30.
- W. F. van Gils, *Analyst*, 1970, **95**, 88.

10. E. E. Vonesch and M. H. C. K. Riveros, *J. Assoc. Offic. Anal. Chem.*, 1971, **54**, 128.
11. S. H. Yuen, *Analyst*, 1965, **90**, 569.
12. P. R. Averell and M. V. Norris, *Anal. Chem.*, 1948, **20**, 753.
13. R. C. Blinn and F. A. Gunther, *ibid.*, 1950, **22**, 7219.
14. A. I. Biggs, *Analyst*, 1955, **80**, 279.
15. E. Hjelt and A.-L. Mukule, *ibid.*, 1958, **83**, 283.
16. R. Buckley and J. P. Colthurst, *ibid.*, 1954, **79**, 285.
17. N. Ramakrishna and B. V. Ramachandran, *ibid.*, 1976, **101**, 528.
18. J. A. R. Bates, *ibid.*, 1965, **90**, 453.
19. D. E. Coffin and W. P. McKinley, *J. Assoc. Offic. Anal. Chem.*, 1963, **46**, 223.
20. D. K. Das, T. V. Mathew, A. K. Mukherjee and Mitra, *J. Food Sci. Tech.*, 1970, **7**, 62.
21. S. N. Deshmukh and T. S. Sidhu, *ibid.*, 1974, **11**, 81.
22. J. C. Gage, *Anal. Chim. Acta*, 1957, **17**, 291.
23. J. Gasparič, D. Svobodová and M. Pospisilová, *Mikrochim. Acta*, 1977 **I**, 241.
24. E. Sawicki, T. W. Stanley, T. R. Hauser, W. Elbert and J. L. Noe, *Anal. Chem.*, 1961, **33**, 722.
25. M. Umeda, *J. Pharm. Soc. Japan*, 1963, **83**, 951.

ANALYTICAL DATA

ELECTROMIGRATION OF CARRIER-FREE RADIONUCLIDE IONS

BISMUTH COMPLEXES IN AQUEOUS SOLUTIONS OF OXALIC, FUMARIC AND SUCCINIC ACIDS

F. RÖSCH, TRAN KIM HUNG, M. MILANOV and V. A. KHALKIN
 Joint Institute for Nuclear Research, Dubna, P.O. Box 79, 101000 Moscow, USSR

(Received 23 June 1986. Accepted 12 September 1986)

Summary—The overall ion mobilities \bar{u} of carrier-free radiobismuth have been measured in aqueous solutions of some dicarboxylic acids (H_2L)—oxalic, fumaric and succinic—by means of a new version of the electromigration method in electrolytes consisting of $HClO_4/H_2L$, 0.20*m* H^+ , $\mu = 0.20m$; $Na(H)ClO_4/H_2L$, 0.05*m* H^+ , $\mu = 0.20m$; $Na(H)ClO_4/H_2L$, 0.05*m* H^+ , $\mu = 0.25m$; at 298.15 K. Mathematical processing of the experimental functions $\bar{u} = f([L^{2-}])$ allowed calculation of the mean individual stability constants K_n and ion mobilities u° of the complex ions $[BiL_n]^{3-2n}$, $n = 1, 2$: $[Bi(C_2O_4)]^+$, $\log K_1 = 7.65$ (8), $u^\circ = +2.26$ (5) $\times 10^{-4}$ $cm^2 \cdot sec^{-1} \cdot V^{-1}$; $[Bi(C_2O_4)_2]^-$, $\log K_2 = 4.81$ (2), $u^\circ = -1.63$ (64) $\times 10^{-4}$ $cm^2 \cdot sec^{-1} \cdot V^{-1}$; $[Bi(C_4O_4H_2)]^+$, $\log K_1 = 6.90$ (20); $[Bi(C_4O_4H_4)]^+$, $\log K_1 = 8.76$ (48).

The electromigration method, used to measure the ion mobilities of elements in a constant electric field, is very suitable for determination of stability constants for metal-ion complexes in solution, especially for carrier-free radionuclide concentrations of the elements.¹⁻³ In earlier work⁴ we investigated hydrolysis of Bi(III) in acidic and alkaline sodium perchlorate solutions, using a special horizontal electrophoresis technique. This modified version of the electromigration method, which avoids use of finely divided inert materials such as quartz sand for hydrodynamic stabilization of the electrolyte, has been developed in our laboratory.⁵⁻⁷ A new design of the electromigration cell ensures stability of the chemical composition of electrolytes and also temperature stability during prolonged measurements. It also excludes the occurrence of liquid fluxes in the tube along which the ions are moving.

The results of the first radiobismuth experiments showed that it is reasonable to use this technique for studying not only hydrolysis, but also formation of metal-ion complexes with various ligands.

The aim of the work described in this paper was to determine the stability constants of the mononuclear bismuth complexes with dicarboxylic (oxalic, fumaric, succinic) acids. Bismuth complexes of this type are poorly studied, compared with those of other metals. This is evidently due to difficulties in processing and interpreting the experimental results, since the investigations are performed in slightly acidic or neutral solutions where two processes occur at the same time: complex formation and hydrolysis of the bismuth cation Bi^{3+} . The available literature data, obtained with only one analytical technique for one ligand, seemed to us to be worth checking.

Table 1 lists the available data on the stability constants of bismuth complexes with dicarboxylic acids.

EXPERIMENTAL

The investigations were performed with carrier-free ^{205,206}Bi radionuclides.

Table 1. Stability constants of bismuth complexes with dicarboxylic acids H_2L

Acid (H_2L)	<i>T</i> , K	μ ; electrolyte; pH	Equilibrium reaction	$\log K_1$	$\log K_2$	$\log K_3$	Ref.
Oxalic	293.1	0.01; $HClO_4$; 2.0	$Bi^{3+} + L^{2-} \rightleftharpoons BiL^+$	6.1			8
Oxalic	298.1	1.0; KNO_3 ; 2.33	$Bi_2L_3 + 2L^{2-} \rightleftharpoons BiL_2^- + BiL_3^{3-}$		($\log \beta_2 = 8.38$) ($\log \beta_3 = 8.15$)		8
Malic	298.1	3.0; Na_2SO_4 ; 4.5	$Bi^{3+} + 5HL^- \rightleftharpoons Bi(HL)_3^{3-}$			($\log \beta_3 = 16.53$)	9
Tartaric	298.1	3.0; Na_2SO_4 ; 3.0	$Bi^{3+} + HL^- \rightleftharpoons Bi(HL)^{2+}$	7.56			9
Aspartic	298.1	0.1; $NaClO_4$; 2.6-9.0	$Bi^{3+} + nL^{2-} \rightleftharpoons BiL_n^{3-2n}$	10.47	8.65	3.67	10
Glutamic	298.1	0.1; $NaClO_4$; 2.6-9.0	$Bi^{3+} + nL^{2-} \rightleftharpoons BiL_n^{3-2n}$	10.47	8.28	3.50	10

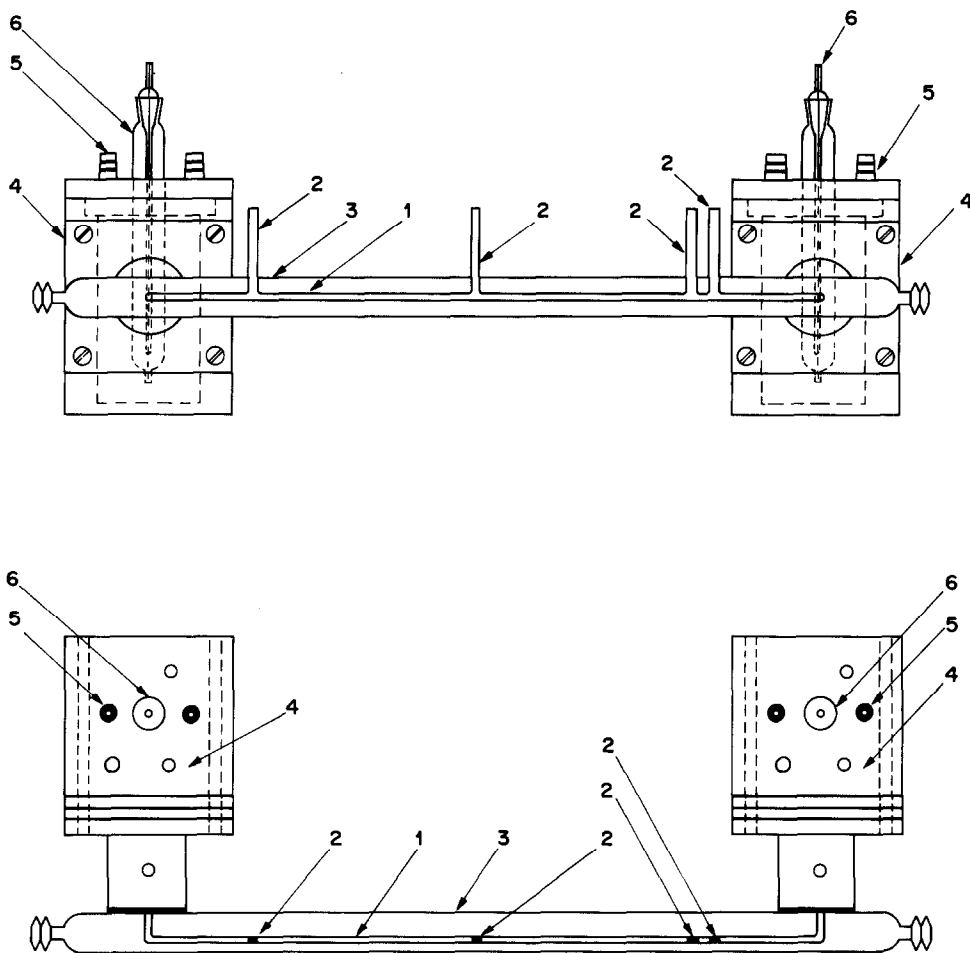


Fig. 1. Lay-out of the electromigration cell: 1—electromigration tube of glass; 2—outlets to insert a thermosensor and voltage-measuring electrodes and inject radionuclide solutions; 3—thermostatic casing; 4—electrode chambers; 5—tubes to supply water for cooling electrode chambers; 6—platinum electrodes.

Radiobismuth was obtained by exposure of natural lead to 65-MeV protons in the isochronous cyclotron U-240, INR Academy of Sciences of the Ukrainian SSR (Kiev). Radiobismuth was separated from lead, then purified and concentrated by known techniques.¹² The specific activity of the final ^{205,206}Bi solution in 0.1*m* nitric acid was about 10 GBq/ml.

The electromigration cell is schematically shown in Fig. 1. A detailed description of the experimental procedure is given in our previous papers.⁴⁻⁷

The overall ion mobilities of bismuth were measured at 298.15(10) K in the following electrolyte systems, containing oxalic, fumaric and succinic acids (H₂L): (I) HClO₄/H₂L, 0.200*m* H⁺, $\mu = 0.200$ (2); (II) Na(H)ClO₄/H₂L, 0.050*m* H⁺, $\mu = 0.200$ (5); (III) Na(H)ClO₄/H₂L, 0.050*m* H⁺, $\mu = 0.250$ (5). The L²⁻ concentrations varied from 0 to 2×10^{-4} *m*, 7.5×10^{-7} *m* and 4×10^{-8} *m* for C₂O₄²⁻, C₄O₄H₂²⁻ and C₄O₄H₄²⁻, respectively. Electrolyte solutions were prepared in doubly distilled water with chemically pure and analytical grade reagents.

The electromigration tube and the electrode chambers were filled with electrolyte of given composition, and 1–2 μ l of the ^{205,206}Bi stock solution was injected.

The electromigration of radiobismuth, building up equilibrium systems corresponding to the electrolyte com-

position, was monitored by detecting the gamma-radiation of ^{205,206}Bi by means of a gliding scintillation detector. The electric field-strength gradient was kept constant in all experiments: $\Delta E = 10.00$ (5) V/cm. The experimental set-up allowed continuous measurement of the radiobismuth velocity (cm/sec) along the tube. These values were then used for calculation of the overall ion mobilities (u , 10^{-4} cm²·sec⁻¹·V⁻¹) in the given systems.

RESULTS AND DISCUSSION

Formation of Bi(III) complexes with oxalate

Figure 2 shows the results obtained for the experimental dependence of the overall bismuth ion mobility $\bar{u}_{\text{Bi(III)}}$ on C₂O₄²⁻ concentration in 0.200 and 0.050*m* solutions of H⁺ at constant overall ionic strength $\mu = 0.200$ (electrolyte systems I and II). Concentrations of oxalate were calculated on the basis of the oxalic acid dissociation constants $pK_{01} = 1.31$, $pK_{02} = 3.81$.¹¹

To simplify the calculation of the stability constants we assumed that the complex formation occurs

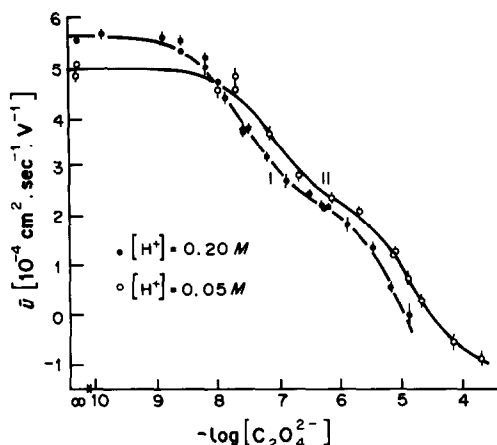
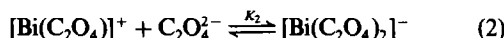
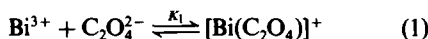


Fig. 2. Overall ion mobility of carrier-free radiobismuth in aqueous solutions of oxalic acid/H(Na)ClO₄; $\mu = 0.200$, $T = 298.15$ (10) K. (I, $[H^+] = 0.200m$; II, $[H^+] = 0.050m$; solid lines are the calculated curves).

only according to reactions (1) and (2):



We also assumed that other ions in the systems under investigation, as well as protonated oxalate species, do not markedly affect the radiobismuth electromigration. These assumptions allowed formulation of equation (3), which takes into account the influence of both of the complex formation reactions and of the Bi(III) hydrolysis on the overall ion mobility \bar{u} of Bi(III):

$$\bar{u} = \frac{u_1^{\circ}[H^+]^3 + u_2^{\circ}K_1'[H^+]^2 + u_3^{\circ}K_1'K_2'[H^+] + u_4^{\circ}K_1[L^{2-}][H^+]^3 + u_5^{\circ}K_1K_2[L^{2-}]^2[H^+]^3}{[H^+]^3 + K_1'[H^+]^2 + K_1'K_2'[H^+] + K_1'K_2'K_3' + K_1[L^{2-}][H^+]^3 + K_1K_2[L^{2-}]^2[H^+]^3} \quad (3)$$

Table 2. Values of complex formation parameters in equation (4) obtained after mathematical processing of experimental dependences $\bar{u} = f([C_2O_4^{2-}])$ in the electrolyte systems I and II [here and elsewhere in the paper, the numbers in brackets are the standard deviations of the results and refer to the last figure(s) quoted]

Parameter	Electrolyte system		Mean values
	I (0.200m H ⁺)	II (0.050m H ⁺)	
log K_1	7.67 (2)	7.40 (7)	7.65 (8)
log K_2	4.92 (2)	4.81 (7)	4.81 (2)
log β_2	12.59 (34)	12.21 (13)	12.46 (5)
$u_{[Bi(C_2O_4)]^+}^{\circ}$ (10^{-4} cm ² .sec ⁻¹ .V ⁻¹)	+2.26 (4)	+2.24 (11)	+2.26 (5)
$u_{[Bi(C_2O_4)_2]^-}^{\circ}$ (10^{-4} cm ² .sec ⁻¹ .V ⁻¹)	-2.55 (21)	-1.18 (15)	-1.63 (64)
C_1 (10^{-4} cm ² .sec ⁻¹ .V ⁻¹)	6.66 (4)	10.33 (8)	
C_1^* (10^{-4} cm ² .sec ⁻¹ .V ⁻¹)	6.34	7.90	
C_2	1.184 (8)	2.064 (18)	
C_2^*	1.205	1.902	

At $[L^{2-}] = 0$, $\bar{u}_{Bi(III)} = +5.64$ (4) $\times 10^{-4}$ cm².sec⁻¹.V⁻¹ (I), and $+5.00$ (5) $\times 10^{-4}$ cm².sec⁻¹.V⁻¹ (II), respectively. C_1^* and C_2^* are calculated from the hydrolysis data given earlier.⁴

where u_i° and K_i' ($i = 1, 2, 3$) are the individual ion mobilities and individual stoichiometric hydrolysis constants for $[Bi(OH)_i]^{3-i+}$ species and u_4° , u_5° , K_1 and K_2 are the individual ion mobilities and stoichiometric complex formation constants of $[BiL_n]^{3-2n}$ ions with ligands L^{2-} and $n = 1, 2$. Equation (3) can be reduced to a more compact form (4).

$$\bar{u} = \frac{C_1 + u_4^{\circ}K_1[L^{2-}] + u_5^{\circ}K_1K_2[L^{2-}]^2}{C_2 + K_1[L^{2-}] + K_1K_2[L^{2-}]^2} \quad (4)$$

where C_1 and C_2 represent the bismuth hydrolysis data:

$$C_1 = u_1^{\circ} + u_2^{\circ}K_1'[H^+]^{-1} + u_3^{\circ}K_1'K_2'[H^+]^{-2}$$

$$C_2 = 1 + K_1'[H^+]^{-1} + K_1'K_2'[H^+]^{-2}$$

$$+ K_1'K_2'K_3'[H^+]^{-3}$$

Equation (4) allows calculation of the individual ion mobilities and stability constants of bismuth complexes without knowledge of the Bi(III) hydrolysis data in the electrolyte systems I and II, since these data can be treated as unknowns to be evaluated in the data-processing. This equation was used for mathematical processing of the experimental results by the least-squares method with the minimizing program MINUIT,¹³ its six unknown parameters being calculated on a CDC-6500 computer. The calculation results are listed in Table 2.

The solid lines in Fig. 2 show the curves calculated by means of the parameters obtained. They fit well with the experimental points.

It follows from the data of Table 2 that the values of K_1 and K_2 and the individual ion mobility of the $[Bi(C_2O_4)]^+$ complex cation were similar for electrolytes I and II, but the individual ion mobility of the

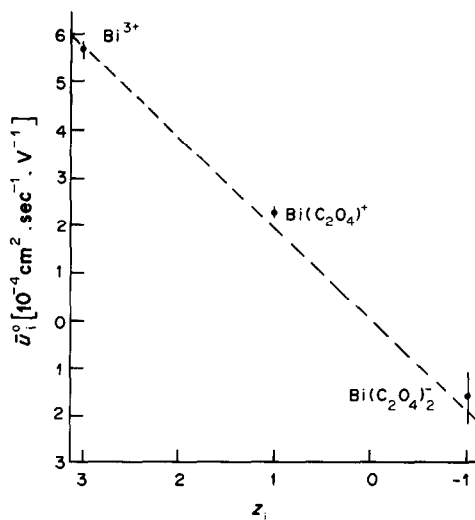


Fig. 3. Individual ion mobilities of Bi^{3+} , $[\text{Bi}(\text{C}_2\text{O}_4)]^+$ and $[\text{Bi}(\text{C}_2\text{O}_4)_2]^-$ as a function of ion charge ($u_{\text{Bi}^{3+}}$ from previous work⁴).

$[\text{Bi}(\text{C}_2\text{O}_4)_2]^-$ anion is only half as large in system II as in system I. The value from system II is probably the more reliable, since the maximum concentration of $\text{C}_2\text{O}_4^{2-}$ is one order of magnitude higher than in system I: $1.99 \times 10^{-4} m$ and $1.24 \times 10^{-5} m$, respectively.

Table 2 also lists values of parameters C_1^* and C_2^* calculated on the basis of the data previously obtained for the hydrolysis constants and individual ion mobilities for Bi(III) hydrolysis in perchlorate solutions with $\mu = 0.250 m$.⁴ It is seen that the two sets of results for electromigration of radiobismuth in solutions of different chemical composition are in good agreement. This allows the conclusion that the calculated individual ion mobilities and stability constants

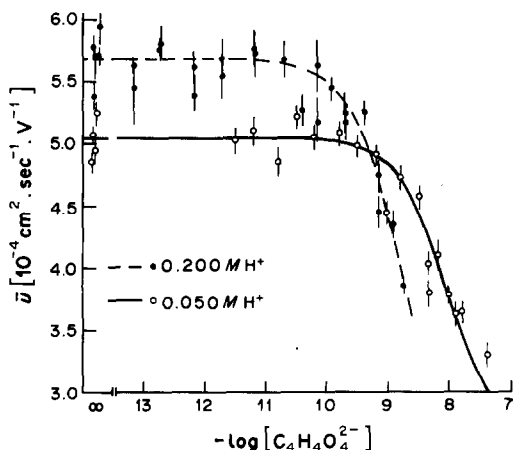


Fig. 4. Overall ion mobility of carrier-free radiobismuth in aqueous solutions of succinic acid/ $\text{H}(\text{Na})\text{ClO}_4$; $\mu = 0.200$, $T = 298.15 (10) \text{ K}$. (I, $[\text{H}^+] = 0.200 m$; II, $[\text{H}^+] = 0.050 m$; solid lines are the calculated curves).

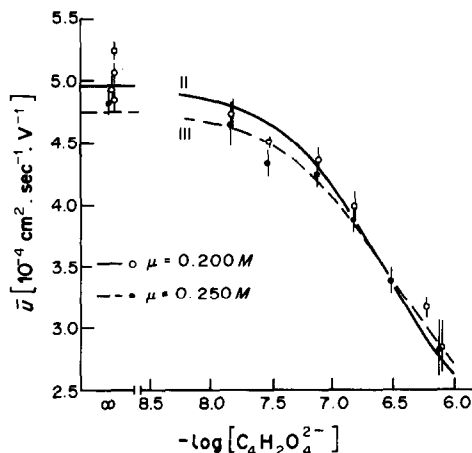


Fig. 5. Overall ion mobility of carrier-free radiobismuth in aqueous solutions of fumaric acid/ $\text{H}(\text{Na})\text{ClO}_4$; $[\text{H}^+] = 0.050 m$, $T = 298.15 (10) \text{ K}$. (II, $\mu = 0.200 m$; III, $\mu = 0.250 m$; solid lines are the calculated curves).

for the complex $[\text{Bi}(\text{C}_2\text{O}_4)_n]^{3-2n}$, $n = 1, 2$, are probably close to the real values, despite the simplification of the model chosen for processing the experimental data.

On the other hand, the results of the present paper can be treated as confirmation of the fact that the data on bismuth hydrolysis obtained earlier by the electromigration method⁴ are correct.

The individual ion mobilities of Bi^{3+} , $[\text{Bi}(\text{C}_2\text{O}_4)]^+$ and $[\text{Bi}(\text{C}_2\text{O}_4)_2]^-$ calculated in the present paper—and for $\text{Bi}(\text{OH})_n^{3-n}$ ions with $n = 0, 1, 3, 4$, calculated in the previous work⁴—show a distinct linear dependence on the charges of the ions (Fig. 3), which is close to the Stokes law. The correlation can be written as

$$u_{[\text{Bi}(\text{C}_2\text{O}_4)_n]^{3-2n}}^{\circ} = \text{const.} \times z_{[\text{Bi}(\text{C}_2\text{O}_4)_n]^{3-2n}}, \quad (5)$$

where $n = 0, 1, 2$. This allows the assumption that the ions under consideration have similar radii and electrolyte micro-viscosity in aqueous solutions. Similar experimental dependences have been discussed by other authors.^{2,14}

Formation of Bi(III) complexes with fumarate and succinate

The experimentally measured overall ion mobilities of Bi(III) in electrolytes I and II containing different concentrations of $\text{C}_4\text{O}_4\text{H}_4^{2-}$ (succinate) and electrolyte systems II and III containing $\text{C}_4\text{O}_4\text{H}_2^{2-}$ (fumarate) are shown in Figs. 4 and 5. In calculating the stability constants for the succinate and fumarate complexes, we assumed the complex formation mechanism was similar to that adapted for oxalate as ligand. Mathematical processing was again done by means of the program MINUIT, according to equation (4).

As both fumaric and succinic acids are weak (the $\text{p}\beta_2$ values are 7.41 and 9.08 respectively^{15,16}), it is

Table 3. Values of $\log K_1$ and $\bar{u}_{\text{Bi(III)}}$ (at $[L^{2-}] = 0$), calculated by the mathematical processing of experimental dependences $\bar{u} = f([L^{2-}])$, where L^{2-} represents succinate ($C_4O_4H_4^{2-}$) and fumarate ($C_4O_4H_2^{2-}$) in the electrolyte systems I, II, III

Acid	Parameter	Electrolyte system			Mean value
		I	II	III	
Succinic	$\log K_1$	9.07 (7)	8.27 (9)	—	8.67 (48)
	$\bar{u}_{\text{Bi(III)}} (10^{-4} \text{ cm}^2 \cdot \text{sec}^{-1} \cdot \text{V}^{-1})$	+5.68 (10)	+5.04 (10)	—	—
Fumaric	$\log K_1$	—	6.94 (10)	6.82 (20)	6.90 (20)
	$\bar{u}_{\text{Bi(III)}} (10^{-4} \text{ cm}^2 \cdot \text{sec}^{-1} \cdot \text{V}^{-1})$	—	+4.96 (10)	+4.74 (10)	—

evident that changes in the bismuth overall ion mobility in the electrolytes used were mainly determined by formation of the complex cations $[\text{BiL}]^+$.

Therefore, in performing the calculations, we cannot keep the quantities $u_{[\text{BiL}_n]^{3-2n}}^{\circ}$, $n = 1, 2$, as unknowns in equation (4) and, consequently, have to give them fixed values: $u_{[\text{BiL}]^+}^{\circ} = +2.25(25) \times 10^{-4} \text{ cm}^2 \cdot \text{sec}^{-1} \cdot \text{V}^{-1}$ and $u_{[\text{BiL}_2]^-}^{\circ} = -2.0(1.0) \times 10^{-4} \text{ cm}^2 \cdot \text{sec}^{-1} \cdot \text{V}^{-1}$. These values were chosen on the assumption that complex ions of bismuth with dicarboxylic acid anions have similar individual ion mobility values in aqueous electrolytes with the same (or almost the same) overall ionic strength and the same temperature.

The results are given in Table 3. First it should be noted that similar values of $\log K_1$ were obtained for electrolyte systems of different composition, *i.e.*, of different pH or overall ionic strength, for both the succinate and fumarate complexes. The overall ion mobilities of Bi(III) obtained at $[L^{2-}] = 0$ were practically the same as those for the oxalic acid solutions, or calculated on the basis of our earlier work.⁴

The solid lines in Figs. 4 and 5 show $\bar{u} = f([L^{2-}])$ calculated by equation (4) with parameters obtained in the mathematical processing of the experimental data. As is seen, the curves satisfactorily coincide with the experimental points.

The complex formation of bismuth with fumarate was investigated in two solutions of constant acidity (0.05M H^+) but different values of overall ionic strength (electrolytes II and III). As could be expected, the bismuth overall ion mobilities tended to decrease in electrolyte III ($\mu = 0.250m$).

CONCLUSION

Measurement of the electromigration values of carrier-free radiobismuth in aqueous solutions of dicarboxylic (oxalic, fumaric, succinic) acids at 298.15(10) K has yielded the experimental dependence of the overall ion mobility of bismuth on ligand concentration, $\bar{u} = f([L^{2-}])$. The mathematical (computer) processing of these functions by the least-squares method was based on simplified models of the equilibrium processes of bismuth complex formation and hydrolysis of Bi(III) in the systems under investigation. Mean values of the first and second individual stability constants and the individ-

ual ion mobilities of bismuth oxalate complexes were calculated: $\log K_1 = 7.65(8)$ and $\log K_1 = 4.81(2)$; $u_{[\text{Bi}(\text{C}_2\text{O}_4)]^+}^{\circ} = +2.26(5) \times 10^{-4} \text{ cm}^2 \cdot \text{sec}^{-1} \cdot \text{V}^{-1}$ and $u_{[\text{Bi}(\text{C}_2\text{O}_4)_2]^-}^{\circ} = -1.63(64) \times 10^{-4} \text{ cm}^2 \cdot \text{sec}^{-1} \cdot \text{V}^{-1}$; ($\mu = 0.200$).

The first stability constants of the succinate and fumarate complexes of bismuth are $\log K_1 = 8.67(48)$; ($\mu = 0.200$) and $\log K_1 = 6.90(20)$; ($\mu = 0.200$ and 0.250), respectively.

None of these values was determined earlier, except K_1 for oxalate complexes. Our value for it is almost two orders of magnitude larger than the one in Table 1. Such a significant difference is probably due to improper allowance for bismuth hydrolysis in the earlier work.⁸

The individual ion mobilities u° of Bi^{3+} and its oxalate complexes show a linear dependence on the ionic charge. The dependence can be described by

$$u_{[\text{Bi}(\text{C}_2\text{O}_4)_n]^{3-2n}}^{\circ} = 1.9(3 - 2n)$$

where $n = 0, 1, 2$, and suggests that the radii and micro-viscosities of the bismuth species are close in value for these ions in the electrolyte systems used.

Acknowledgements—The authors are thankful to V. A. Ageev who very kindly provided lead targets irradiated by protons, and to A. M. Akimova and V. I. Sobolev for their great technical assistance in preparing and performing the experiments.

REFERENCES

- V. P. Shvedov, *Elektromigratsionnyi metod v fiziko-khimicheskikh issledovaniyach*, Atomizdat, Moscow, 1971.
- A. V. Stepanov and E. K. Kortshemnaja, *Elektromigratsionnyi metod v neorganicheskom analysie*, Khimiya, Moscow, 1979.
- T. P. Makarova and A. V. Stepanov, *Radiokhimiya*, 1977, **19**, 125.
- M. Milanov, F. Rösch, V. A. Khalkin, J. Henniger and Tran Kim Hung, *JINR*, E12-86-144, Dubna, 1986.
- M. Milanov, W. Doberenz, R. Dreyer, M. Noak and V. A. Khalkin, *Radiokhimiya*, 1982, **24**, 520.
- M. Milanov, W. Doberenz, A. Marinov and V. A. Khalkin, *J. Radioanal. Nucl. Chem.*, 1984, **82**, 101.
- M. Milanov, A. Marinov, Tran Kim Hung, W. Doberenz and V. A. Khalkin, *JINR*, 6-83-209, Dubna, 1983.
- H. Ladzinska-Kulinska, *Chemia*, 1975, **31**, 35.
- E. G. Tshirkesova and I. I. Vataman, *Zh. Neorgan. Khim.*, 1970, **15**, 424.

10. M. K. Singh and M. N. Srivastava, *J. Inorg. Nucl. Chem.*, 1972, **34**, 2067.
11. G. M. Armitage and H. S. Sunsmore, *ibid.*, 1973, **35**, 817.
12. V. P. Erlitchenko, V. G. Vinogradova and Yu. G. Sevast'yanov, *Atom. Energiya*, 1969, **27**, 349.
13. F. James and M. Roos, *MINUIT Program*, CERN Computer Centre, Program Library, Long-Write-Up, D-506, D-596 (1971).
14. R. Lundqvist, *Acta Chem. Scand.*, 1981, **A35**, 31.
15. P. G. Manning and S. Ramamoorthy, *J. Inorg. Nucl. Chem.*, 1973, **35**, 1571.
16. Yu. Yu. Lurye, *Spravochnik po analiticheskoy khimii*, Khimiya, Moscow, 1979.

DESIGN OF SOFTWARE FOR THERMAL TITRATIONS*

RICHARD C. GRAHAM

Science Research Laboratory, US Military Academy, West Point, New York 10996, U.S.A.

(Received 21 August 1985. Revised 12 November 1986. Accepted 28 November 1986)

Summary—A set of computer programs has been written in FORTRAN and in BASIC to allow automation of data acquisition from a TRONAC titration calorimeter and calculation of the concentration of titrant or titrand in an acid-base reaction; the heat capacity of a solution and enthalpies of reaction may also be calculated. The enthalpy change of a reaction and equilibrium constant can also be determined under certain conditions.

Thermometric titration has long been used for analytical purposes¹ and calculation of the enthalpy change of a reaction. A major advantage of the technique is that it is applicable to many titration reactions that cannot be monitored by potentiometric methods, e.g., titration of weak acids or bases in aqueous solutions.

There are occasions also where the equivalence point obtained is not well-defined, such as the titration of *o*-bromoaniline with hydrochloric acid monitored thermometrically.² The fact that the *o*-bromoaniline is not stoichiometrically protonated can be used to advantage, allowing the enthalpy change and the equilibrium constant to be evaluated simultaneously,² because the titration trace becomes curved and the equilibrium position is continually changing during the addition of more titrant. By appropriate mathematical modelling of the reactions occurring in the titration vessel, both the equilibrium constant and the enthalpy change of the reaction may be calculated. From these two values other thermodynamic quantities may then be obtained.

EXPERIMENTAL

Apparatus

A TRONAC 450 isoperibol (adiabatic) titration calorimeter with a TRONAC PTC40 precision temperature controller was used for all experiments (see Fig. 1 for a schematic diagram). A Digital Equipment Corporation MINC-11/23 laboratory with clock, preamplifier, and analogue-to-digital converter was used to convert the analogue signal from the calorimeter into digital form. The data acquired were then stored on magnetic media for use in subsequent calculations. The interface between the MINC-11 and the TRONAC was a twisted pair of 18-gauge copper wires. The analogue-digital converter was run in the differential mode to avoid the possibility of a difference in

the ground potential of the calorimeter and the laboratory computer.

COMPUTATION

BASIC programs

The BASIC programs are executed in chain fashion since the DEC RT-11 operating system allows addressing of only 64K of memory, which is insufficient for the simultaneous retention in memory of all the subroutines and data arrays. The operator-interactive initial subroutine, TITINP.BAS, allows the analyst to enter the values (such as the factor for conversion of mV into °C) required in later calculations. The variables defined and input in response to prompts from the program are carried through the set of subroutines by a common block in the memory. TITINP.BAS also converts the calorimeter analogue data into digital form and calls a subroutine to store the digitized data on disc. The digitized data are displayed on the video terminal in graphic form as they are acquired.

The data must be smoothed to remove superimposed noise. Walraven³ has given several formulae for that purpose. We chose to use a low-frequency band-pass filter, giving the effect of a moving box-car average. The transfer function, for a seven point moving box-car average, was:

$$H(f) = \frac{(1 + 2 \cos 2\pi ft + 2 \cos 4\pi ft + 2 \cos 6\pi ft)}{7} \quad (1)$$

as derived by Graham *et al.*⁴ where f is frequency and t is time.

This transfer function essentially transfers all signals with ft values less than 0.20 and eliminates all ft values greater than 0.20 by a four-pass filter, i.e., the seven-point box-car smoothing is applied four times. Each successive smoothing is applied in a different direction, which has the effect of eliminating the phase shift often associated with a simple box-car averaging technique.³

*Publication does not signify that the contents necessarily reflect the views and policies of Department of Army and the US Military Academy, nor does mention of trade names or commercial products constitute endorsement or recommendation for use. Not subject to copyright restrictions, work of US Government.

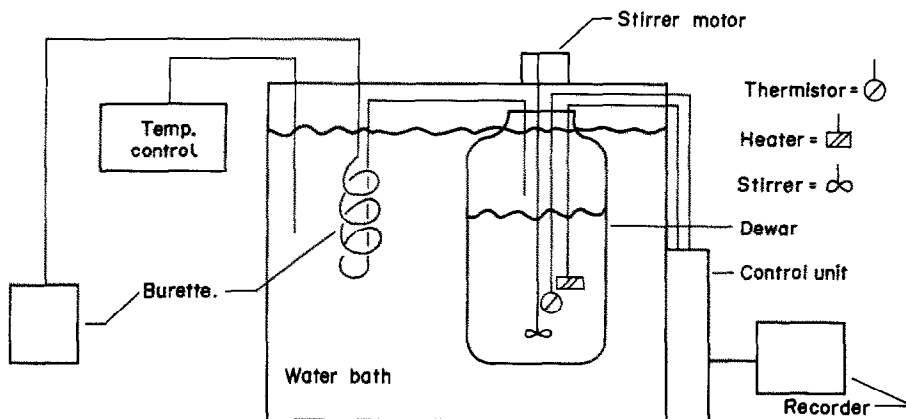


Fig. 1. Schematic of TRONAC 450 titration calorimeter.

The course of a typical calorimetric titration is shown in Fig. 2. The initial heat capacity of the titrand is determined first, then the amount of titrant added and the resulting temperature rise from the titration reaction are determined. The heat capacity of the titrand must be determined only if it is desired to calculate the enthalpy of the reaction in addition to the concentration of analyte. This heat capacity of the titrand is determined by using Joule heating of the titrand, and the equation:

$$q = V_h i_h t \quad (2)$$

where q = total electrical heat applied to the system (J); V_h is the voltage drop (V) across the Joule heater (a 100.00- Ω resistor); i_h is the current (A) through the resistor; and t is the heating time (sec).

The temperature in the reaction vessel is monitored with a calibrated thermistor in a Wheatstone bridge. It is necessary to monitor the temperature changes before and after the heat capacity determination and the titration, to take account of any departure from adiabatic conditions and because the stirrer imparts

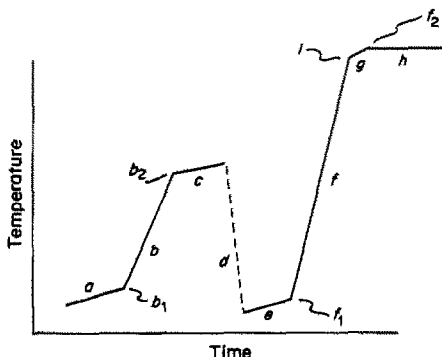


Fig. 2. Typical acid-base titration with thermometric detection. *a*, Initial stir slope— C_p determination. *b*, Heating— C_p determination; b_1 heater on; b_2 heater off. *c*, Final stir slope— C_p determination. *d*, Cool to 25°C. *e*, Initial stir slope—titration. *f*, Titration; f_1 burette on; f_2 burette off. *g*, Addition of excess of titrant. *h*, Final stir slope—titration. *i*, Equivalence point.

sufficient frictional energy to change the temperature significantly.

The subroutine HTCAP.BAS calculates the slope, dV/dt , for initial and final stirring, and the total temperature rise due to stirring and Joule heating, this being corrected for heat leaks *etc.* by using equation (3):

$$\Delta T_C = \Delta T - [(S_i + S_f)/2]t]B \quad (3)$$

where ΔT_C is the corrected temperature rise (°C) ΔT is the emf (V) corresponding to the total temperature rise, S_i and S_f are the initial and final stirring slopes, respectively, t is the heating time (sec) and B is a conversion constant (°C/V). The initial heat capacity (C_p , J/deg) is then given by:

$$C_p = q/\Delta T_C \quad (4)$$

After calculation of the titrand heat capacity, the operator is prompted by the computer to allow the reaction vessel to cool to the original starting temperature before the titration is begun. After acquisition of the titration data, three linear equations are derived from them, the first and third for the initial and final stirring slopes, and the second for the titration data. The burette is turned off after the equivalence point is reached. Figure 2 shows that a change of slope occurs at the equivalence point, the position of which is calculated as the intersection between portions *f* and *h* of the titration plot (Fig. 2). Theoretically, the equivalence point should be calculated as the intersection between portions *f* and *g* of the curve, but in practice portions *g* and *h* cannot be distinguished. The intersection of portions *a* and *f* gives the time at which addition of titrant begins. The time at which the burette is switched on cannot be used as the initial point of titrant addition since a small air-bubble is always left in the titrant delivery tube to preclude premature delivery of titrant to the reaction vessel.

The time elapsed between the start of the titration and the equivalence point is used to calculate the concentration of the unknown solution. The corresponding temperature rise is used in equation (3), to

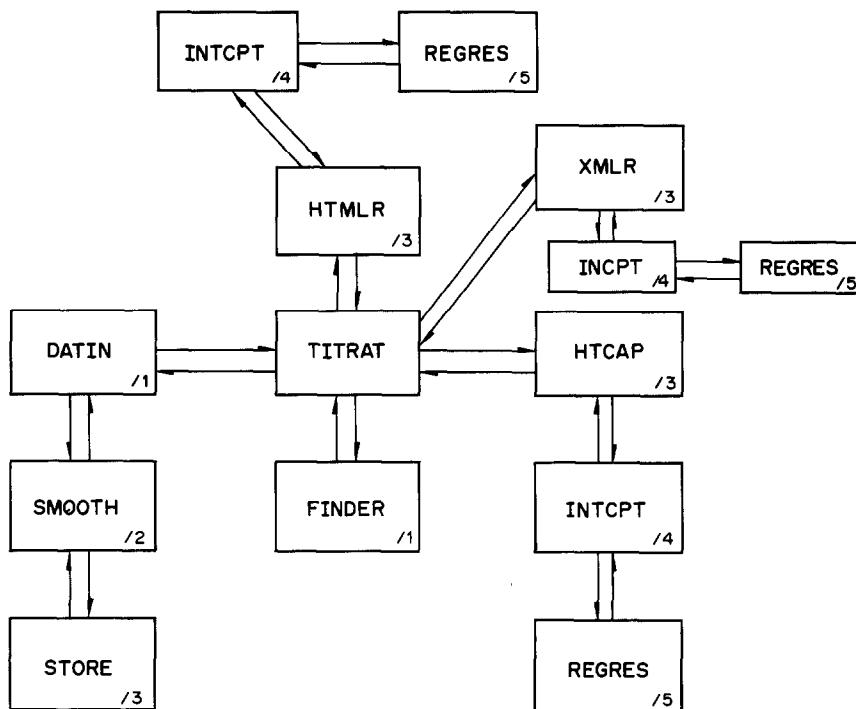


Fig. 3. Interrelationship of FORTRAN subroutines.

calculate ΔT_C , which in turn is used with equation (4) to calculate q , the heat released in the reaction. The temperature rise is also corrected for the heat of ionization of the titrant. The heat capacity used is, however, the sum of that of the titrand and that of the titrant added, which can be calculated from the volume added and literature values of C_p for the titrant.

The enthalpy change of the reaction is then calculated from:

$$\Delta H_{\text{neut}} = q/n \quad (5)$$

where ΔH_{neut} is the standard enthalpy of neutralization, q is the heat released in the titration and n is the number of moles of water formed in the reaction. It is assumed that the titration system gives a well-defined equivalence point such as that for an acid-base titration. The same equations should be usable for calculating concentrations and enthalpies of reaction for those complexometric reactions for which ΔH is not too close to zero.

FORTRAN programs

The FORTRAN programs are very similar to the BASIC programs except for a few modifications, but the FORTRAN programs are more interactive, having a menu-type selection of operations to be performed. The BASIC programs allow calculation of the enthalpy change of a reaction with a well-defined equivalence point and/or calculation of the analyte concentration. The FORTRAN program allows in addition the calculation of the heat capacity of

solutions. It also provides for simultaneous calculation of the enthalpy and equilibrium constant of a reaction, but the user has to supply the necessary subroutine, such as the one written by Eatough *et al.*,⁴ since the interpretation of the data depends upon the reaction system being studied.

The relation of the set of FORTRAN subroutines is shown in Fig. 3. An overlay execution scheme must be used because of memory space limitations in the RT-11 operating system. Although the computer system has 256 kbytes of memory, the RT-11 will allow access to only 64 kbytes at a time. The /1 etc. in the corner of each block indicates the overlay segment which contains the subroutines. The main program, TITRAT, controls the overall execution of the program and is always resident in memory as the root segment of the overlay scheme. The subroutine FINDER is the menu of the program and also acquires such information as the names of files, data acquisition channels and values for constants used in several other subroutines. The rest of the subroutines will be discussed in terms of a typical flow stream.

The initial heat capacity of the reaction vessel and contents must be determined before any other calculations can be performed. Subroutine DATIN acquires the necessary data. During the execution of DATIN, subroutines SMOOTH and STORE are called. SMOOTH filters the data by the seven-point moving box-car average, using a transfer function with the same form and characteristics as that used in the BASIC routines. STORE writes the smoothed data onto disc for access in subsequent subroutines.

After DATIN, TITRAT calls subroutine HTCAP which calculates C_p . HTCAP is similar to HTCAP.BAS of the BASIC program except that the break points b_1 and b_2 in Fig. 2 are determined by criteria based upon the value of the derivative at four consecutive points. Intersection co-ordinates are found by Kramer's rule for the solution of two simultaneous equations. The heat capacity is then calculated by equations (2)–(4), and is returned to the main program for use in other subroutines. At this point, the menu is again written on the screen. To perform titration calculations, DATIN is once again called to acquire data from the titration run (after the reaction vessel has cooled to the original starting temperature). The data are again smoothed and stored on magnetic disc. Only the routine HTMLR will be discussed in detail, since XMLR is a subset of HTMLR and calculates only the normality of a solution.

HTMLR allows calculation of the concentration of analyte and also the enthalpy change of the reaction. In general, its use is limited to acid–base reactions or other reactions in aqueous solution which exhibit a well-defined thermometric equivalence point. A typical use is determination of the concentration of ammonia in household cleaners.⁵ Although we have not tested the point, the precision and accuracy of the technique may allow identification of the analyte from tabulated enthalpies of reaction.² The co-

ordinates of f_1 and f_2 (Fig. 3) are again calculated by Kramer's rule and the derivative algorithm described above. The normality of the solution is then calculated from the time co-ordinates; and the enthalpy change from the temperature co-ordinates. Corrections for stirring, heat loss through the reaction vessel walls, dilution of the titrant, and other side-effects are taken into account in the calculation of the enthalpy change.

Conclusion

The two sets of programs have been tested for data acquisition and limited data reduction and perform well. The FORTRAN set, as expected, is more efficient and faster. Copies of the programs may be obtained from the author.

REFERENCES

1. J. Jordan, in *Treatise on Analytical Chemistry*, I. M. Kolthoff and P. J. Elving (eds.), Part 1, Vol. 4, pp. 5175–5242. Wiley-Interscience, New York, 1968.
2. D. Eatough, J. J. Christensen and R. Izatt, *Thermometric Titrations and Titrimetric Calorimetry*, p. 79. Brigham Young University Press, Provo, UT, 1974.
3. R. Walraven, *Proc. Symposium Digital Equipment Computer User's Society*, San Diego, CA, November, 1908, p. 827.
4. R. C. Graham, H. Hacker and J. K. Robertson, *Comput. Appl. Lab.*, 1983, 1, 281.
5. R. C. Graham and S. Depew, *J. Chem. Educ.*, 1983, 60, 765.

ETUDE DE LA FORMATION DES COMPLEXES EN SOLUTION AQUEUSE—III¹

NOUVELLE METHODE D'AFFINEMENT DES CONSTANTES DE STABILITE DES COMPLEXES ET DES AUTRES PARAMETRES DES TITRAGES PROTOMETRIQUES

ROBERT FOURNAISE et CHRISTIAN PETITFAUX

Laboratoire de Chimie de Coordination, Université de Reims Champagne-Ardenne, B.P. 347,
51062 Reims, France

(Reçu le 4 juin 1986. Révisé le 13 octobre 1986. Accepté le 28 novembre 1986)

Résumé—Cet article expose les fondements théoriques d'un nouveau programme d'affinement des constantes de stabilité des complexes conjointement aux autres paramètres des différents titrages protométriques. La méthode utilisée est basée sur la minimisation de la somme pondérée des carrés des résidus sur les variables expérimentales: volume de réactif et E ou pH. Un principe original de traitement des relations mathématiques permet d'affiner simultanément les différents paramètres et les concentrations des ions libres inconnues. Après convergence, le programme PROTAF permet également de connaître les valeurs ajustées des variables expérimentales.

Summary—This paper describes the theoretical basis of a new program for refinement of complex stability constants together with the other parameters of various protometric titrations. The method is based on minimization of the sum of the weighted squares of the residuals of the experimental variables reagent volume and E or pH. A new exploitation of mathematical relations allows simultaneous refinement of the various parameters and unknown free ion concentrations. After convergence, the program PROTAF also provides the adjusted values of experimental variables.

A la suite des premières publications²⁻⁶ concernant les algorithmes de calcul des constantes de stabilité, de nombreux autres programmes ont été élaborés. Plusieurs articles⁷⁻¹¹ consacrés à leur analyse montrent qu'ils offrent des possibilités d'utilisation très diverses. Toutefois, ce domaine étant en évolution constante, d'autres algorithmes¹²⁻²⁶ ont vu le jour depuis la dernière de ces mises au point.

De ce vaste ensemble, il ressort que les programmes les plus généraux et les plus employés semblent être LETAGROP VRID,²⁷ SCOGS,²⁸ MINQUAD,^{29,30} MUCOMP¹⁶ et ACREF 3 AM.¹⁷ La majorité de ces algorithmes reposent sur la méthode des moindres carrés,³¹⁻³⁵ qui consiste à minimiser une somme pondérée de carrés de résidus. Les variables sur lesquelles sont calculés ces résidus peuvent être soit les variables directement mesurées (par exemple, le volume comme dans SCOGS) soit des variables auxiliaires déduites des données expérimentales (par exemple, le nombre moyen de protons fixés par mole de coordinat comme dans ACREF 3 AM). Quant à la pondération des résidus, elle n'est que rarement employée puisque la plupart des auteurs mènent leurs calculs avec des poids égaux à l'unité.

Deux principales variantes de la méthode des moindres carrés ont été surtout utilisées. L'une, qui ne nécessite que le calcul de dérivées premières, est la méthode de Gauss-Newton.^{32,36} Elle est la plus fréquemment rencontrée car la plus simple à mettre en

oeuvre et elle constitue le fondement de programmes tels que SCOGS, MINQUAD ou MUCOMP. L'autre, qui en plus des dérivées premières fait appel à des dérivées secondes est connue sous le nom de méthode de Newton-Raphson.^{9,37,38} Cette méthode équivalente à celle du "pit-mapping" de Sillén³ est la base de programmes comme LETAGROP VRID ou ACREF 3 AM. Les caractéristiques essentielles de la plupart des programmes majeurs traitant les mesures potentiométriques sont regroupées dans les tableaux comparatifs des articles de Gaizer¹⁰ et de Wozniak et Nowogrocki.¹⁵

A la suite de l'examen des différents principes adoptés par chacun des programmes les plus généraux publiés jusqu'à présent, nous avons entrepris de mettre au point une nouvelle méthode qui, d'une part, essaye de rassembler les aspects les plus essentiels de chacun d'eux et, d'autre part, tente de présenter un traitement original des mesures potentiométriques.

SYMBOLISME

- AH_N, A Formes neutre et basique du complexant
V*, C* Volume et concentration d'une des solutions mères employées pour réaliser le mélange initial
V_i Volume de réactif ajouté au point i
I_i Valeur indiquée par le potentiomètre au point i

C_M, C_A Concentrations analytiques en ion métallique et en complexant
 C_H Concentration analytique en protons.
 $C_H = C_A(N + x_H - x_{OH})$ avec x_H et x_{OH} les nombres de moles de H^+ et OH^- ajoutés par mole de complexant
pH = -\log[H]
 γ_H Activité de H^+
 $\beta_{m,a,h}$ Constante de stabilité d'une espèce:

$$\beta_{m,a,h} = \frac{[M]_m [A]_a [H]_h}{[M]^m [A]^a [H]^h} \text{ avec } m + a \neq 0$$

Pour les espèces hydroxylées, h est négatif
D, E, F Fonctions implicites exprimant les bilans respectifs de l'ion métallique, du complexant et des protons

K_e Produit ionique de l'eau
 ψ Fonction implicite reliant $[H]$ à la valeur I indiquée par le potentiomètre
 ϕ Equation fondamentale déduite des équations conditionnelles D, E et F et de la fonction ψ

σ_0^2 Variance d'une fonction de poids unitaire
 σ_Y^2 Variance de la grandeur Y
 $\sigma_{X,Y}$ Covariance entre les grandeurs X et Y
 $\rho_{X,Y}$ Coefficient de corrélation entre les grandeurs X et Y :

$$\rho_{X,Y} = \frac{\sigma_{X,Y}}{\sigma_X \sigma_Y}$$

Y^e Valeur expérimentale de la variable Y
 \hat{Z} Valeur ajustée ou estimateur de la grandeur Z

R_Y Résidu sur la variable Y : $R_Y = Y^e - \hat{Y}$
 W_Y Poids du résidu sur la variable Y :
 $W_Y = \sigma_0^2 / \sigma_Y^2$

W_i Poids global de la mesure i
 S Somme pondérée des carrés des résidus
 Z^s Valeur grossière de la grandeur Z

Z^0 Valeur initiale de la grandeur Z
 ΔZ^0 Correction à apporter à Z^0 pour obtenir Z^0 :
 $\Delta Z^0 = Z^0 - Z^s$

$\Delta \hat{Z}$ Correction à apporter à Z^0 pour obtenir \hat{Z} :
 $\Delta \hat{Z} = \hat{Z} - Z^0$

λ Multiplicateur de Lagrange
 P Paramètres à affiner: constantes de stabilité et autres paramètres des titrages

Dans un but de clarté, les charges sont volontairement omises.

PRINCIPE GENERAL

Par souci de simplification, nous nous limiterons intentionnellement au cas des mélanges où interviennent trois constituants M, A et H. Il serait facile de généraliser à des systèmes plus compliqués, par exemple à quatre constituants M, A, B et H.

Soit un mélange initial réalisé en additionnant successivement:

—un volume V_M^* d'une solution mère d'ion métallique de concentration C_M^* contenant un acide fort de concentration C_{AM}^* ;
—un volume V_A^* d'une solution mère de complexant (AH_N sous la forme neutre) de concentration C_A^* contenant un acide fort de concentration C_{AA}^* ;
—un volume V_F^* d'acide fort de concentration C_F^* ;
—un volume V_B^* d'eau et un volume V_E^* d'une solution d'électrolyte indifférent pour aboutir à la dilution et à la force ionique désirées.

Ce mélange est dosé en ajoutant des volumes V_i d'une base forte de concentration C_B^* . Le volume total pour chaque mesure est alors:

$$V_{Ti} = V_A^* + V_M^* + V_F^* + V_D^* + V_E^* + V_i$$

Chaque point de la courbe de titrage acido-basique du mélange ion métallique-complexant est alors défini par trois équations conditionnelles, chacune d'elle correspondant au bilan d'un constituant:

$$C_{Mi} = [M]_i + \sum_{m,a,h} m \beta_{m,a,h} [M]_i^m [A]_i^a [H]_i^h \quad (1)$$

$$C_{Ai} = [A]_i + \sum_{m,a,h} a \beta_{m,a,h} [M]_i^m [A]_i^a [H]_i^h \quad (2)$$

$$C_{Hi} = [H]_i - \frac{K_e}{[H]_i} + \sum_{m,a,h} h \beta_{m,a,h} [M]_i^m [A]_i^a [H]_i^h \quad (3)$$

Ces équations conditionnelles exprimées en fonction des caractéristiques choisies du dosage deviennent:

$$V_M^* C_M^* - V_{Ti} \left([M]_i + \sum_{m,a,h} m \beta_{m,a,h} [M]_i^m [A]_i^a [H]_i^h \right) = D_i = 0 \quad (4)$$

$$V_A^* C_A^* - V_{Ti} \left([A]_i + \sum_{m,a,h} a \beta_{m,a,h} [M]_i^m [A]_i^a [H]_i^h \right) = E_i = 0 \quad (5)$$

$$NV_A^* C_A^* + V_A^* C_{AA}^* + V_M^* C_{AM}^* + V_F^* C_F^* - V_i C_B^* - V_{Ti} \left([H]_i - \frac{K_e}{[H]_i} + \sum_{m,a,h} h \beta_{m,a,h} [M]_i^m [A]_i^a [H]_i^h \right) = F_i = 0 \quad (6)$$

La f.e.m. de la chaîne de mesures utilisée peut s'écrire:^{39,40}

$$E = E' + s \frac{RT}{F} \ln \gamma_H [H] + \epsilon_{ja} [H] + \epsilon_{jb} [OH] \quad (7)$$

avec s le facteur correctif de la pente de l'électrode, et $\epsilon_{ja} [H]$ et $\epsilon_{jb} [OH]$ les potentiels de la jonction liquide. En posant $r = sRT(\ln 10)/F$, on obtient:

$$\log [H] + \frac{E'}{r} + \log \gamma_H - \frac{E}{r} + \frac{\epsilon_{ja}}{r} [H] + \frac{\epsilon_{jb}}{r} K_e / [H] = 0 \quad (8)$$

Si l'on appelle I la valeur indiquée par le potentiomètre, cette relation peut encore s'écrire:

$$\log[H] + \omega + \theta I + J_a[H] + J_b K_c/[H] = 0 \quad (9)$$

avec $J_a = \epsilon_{ja}/r$ et $J_b = \epsilon_{jb}/r$; soit de manière condensée:

$$\psi(I, [H], \omega, \theta, J_a, J_b, K_c) = 0 \quad (10)$$

Suivant le mode d'utilisation du potentiomètre, on obtient respectivement pour les valeurs de I , ω et θ :

(i) en potentiométrie:

$$I = E; \quad \omega = \frac{E'}{r} + \log \gamma_H; \quad \theta = -\frac{1}{r}$$

(ii) en protométrie avec étalonnage à l'aide de deux tampons de la série des tampons de Bates:^{41,42}

$$I = \frac{E' - E}{r} = -\log \gamma_H[H]; \quad \omega = \log \gamma_H; \quad \theta = 1$$

(iii) en protométrie avec étalonnage à l'aide de deux tampons à la même force ionique que la solution étudiée:

$$I = \frac{E' - E}{r} + \log \gamma_H = \text{pH}; \quad \omega = 0; \quad \theta = 1$$

Quel que soit le type de mesures envisagé (protométrie ou potentiométrie), la détermination préalable des quatre constantes ω , θ , J_a et J_b du couple d'électrodes grâce à des expériences spécifiques (dosage acide fort-base forte par exemple) permet à partir de la mesure I d'en déduire la valeur de $[H]$ en résolvant l'équation (9) par approximations successives.

En chaque point, les trois équations conditionnelles (4), (5) et (6) doivent être vérifiées simultanément. Parmi les quatre variables V_i , $[M]_i$, $[A]_i$ et $[H]_i$, seuls le volume V_i et la concentration $[H]_i$ sont effectivement déterminés expérimentalement lors des dosages protométriques. On est donc en présence de deux types d'inconnues à affiner. D'une part, des paramètres $P_l (l = 1, 2, \dots, p)$ communs ou non aux différents titrages: constantes de stabilité β , paramètres du couple d'électrodes, concentrations C^* , produit ionique de l'eau K_c ... D'autre part, les concentrations libres $[M]_i$ et $[A]_i$ variables d'un point à l'autre d'une courbe de neutralisation. Par la suite, contrairement à la plupart des algorithmes existants, ces deux types d'inconnues seront traitées au même niveau. En d'autres termes, les concentrations libres $[M]_i$ et $[A]_i$ seront affinées conjointement aux paramètres P_l , d'une manière analogue à celle employée par Sabatini et Vacca.³⁸

Sous forme condensée, les équations conditionnelles (4), (5) et (6) peuvent alors s'écrire respectivement:

$$D_i = D(V_i, [H]_i, [M]_i, [A]_i, P_l) = 0 \quad (11)$$

$$E_i = E(V_i, [H]_i, [M]_i, [A]_i, P_l) = 0 \quad (12)$$

$$F_i = F(V_i, [H]_i, [M]_i, [A]_i, P_l) = 0 \quad (13)$$

avec

$$\psi_i = \psi(I_i, [H]_i, \omega, \theta, J_a, J_b, K_c) = 0 \quad (14)$$

On dispose donc d'un système de $3n$ équations à $(2n + p)$ inconnues. Par la suite, nous symboliserons par $[M]_i$, $[A]_i$ et $[H]_i$ les estimateurs des concentrations libres, par \hat{P}_l les estimateurs des paramètres, ainsi que par \hat{V}_i et \hat{I}_i les valeurs ajustées du volume expérimental V_i^c et de la mesure expérimentale I_i^c indiquée par le potentiomètre.

Les résidus sur les variables expérimentales sont définis par:

$$R_{V_i} = V_i^c - \hat{V}_i \quad (15)$$

$$R_{I_i} = I_i^c - \hat{I}_i \quad (16)$$

et les poids correspondants par:

$$W_{V_i} = \frac{\sigma_0^2}{\sigma_{V_i}^2} \quad (17)$$

$$W_{I_i} = \frac{\sigma_0^2}{\sigma_{I_i}^2} \quad (18)$$

Comme il n'y a aucune corrélation entre les variables expérimentales, la méthode des moindres carrés³¹⁻³⁵ consiste alors à minimiser la somme pondérée des carrés des résidus, définie par:

$$S = \sum_q \sum_i (W_{V_{q,i}} R_{V_{q,i}}^2 + W_{I_{q,i}} R_{I_{q,i}}^2) \quad (19)$$

Dans cette formule, l'indice q est relatif à l'une des expériences et l'indice i à l'un des points de chacune d'elles. Afin d'alléger la formulation ultérieure, le raisonnement sera limité par la suite au cas d'une seule expérience. Dans ces conditions, l'expression de la somme S se réduit à:

$$S = \sum_i (W_{V_i} R_{V_i}^2 + W_{I_i} R_{I_i}^2) \quad (20)$$

Cette recherche du minimum de S est assortie d'une contrainte concernant les équations conditionnelles. En effet, celles-ci doivent être satisfaites par les estimateurs des concentrations libres et des paramètres ainsi que par les valeurs ajustées des variables. En tout point on doit donc avoir:

$$\hat{D}_i = D(\hat{V}_i, [\hat{H}]_i, [\hat{M}]_i, [\hat{A}]_i, \hat{P}_l) = 0 \quad (21)$$

$$\hat{E}_i = E(\hat{V}_i, [\hat{H}]_i, [\hat{M}]_i, [\hat{A}]_i, \hat{P}_l) = 0 \quad (22)$$

$$\hat{F}_i = F(\hat{V}_i, [\hat{H}]_i, [\hat{M}]_i, [\hat{A}]_i, \hat{P}_l) = 0 \quad (23)$$

avec

$$\hat{\psi}_i = \psi(\hat{I}_i, [\hat{H}]_i, \hat{\omega}, \hat{\theta}, \hat{J}_a, \hat{J}_b, \hat{K}_c) = 0 \quad (24)$$

Nous avons préféré utiliser la formulation (20) de la somme S à minimiser plutôt que celle employée dans la plupart des programmes les plus récents,¹⁶⁻²⁶ c'est à dire:

$$S = \sum_i W_i (y_{i, \text{exp}} - y_{i, \text{calc}})^2$$

avec $y = E$ ou V suivant les cas. En effet, à notre connaissance, la formulation (20) est la seule qui

permette d'accéder directement aux résidus R_{V_i} et R_{I_i} et par conséquent aux valeurs ajustées \hat{V}_i et \hat{I}_i des variables expérimentales V_i^e et I_i^e .

VALEURS APPROXIMATIVES DES INCONNUES

La minimisation de la somme S ne peut s'effectuer qu'à condition de disposer de valeurs approximatives initiales des paramètres et des concentrations libres inconnues. En ce qui concerne les constantes de stabilité, il est généralement possible d'obtenir d'assez bonnes approximations $\beta_{m,a,t}^0$ par diverses méthodes numériques ou graphiques comme, par exemple, la méthode CILS.¹

Dans le cas particulier des valeurs initiales $[M]_i^0$ et $[A]_i^0$, elles sont calculées en considérant qu'elles vérifient les équations conditionnelles (11) et (12) dans lesquelles les paramètres P_i sont remplacés par leurs valeurs approchées P_i^0 et les valeurs théoriques V_i et $[H]$, par la valeur expérimentale V_i^e et la valeur initiale $[H]_i^0$, soit:

$$D(V_i^e, [H]_i^0, [M]_i^0, [A]_i^0, P_i^0) = D_i^0 = 0 \quad (25)$$

$$E(V_i^e, [H]_i^0, [M]_i^0, [A]_i^0, P_i^0) = E_i^0 = 0 \quad (26)$$

avec

$$\psi_i^0 = \psi(I_i^e, [H]_i^0, \omega^0, \theta^0, J_a^0, J_b^0, K_c^0) = 0 \quad (27)$$

Si l'on dispose d'approximations grossières $[M]_i^g$ et $[A]_i^g$ des concentrations libres, la méthode de Newton-Raphson pour les équations simultanées non linéaires conduit à:

$$-D_i^g = \frac{\partial D_i^g}{\partial \ln[M]_i^g} \frac{\Delta[M]_i^0}{[M]_i^g} + \frac{\partial D_i^g}{\partial \ln[A]_i^g} \frac{\Delta[A]_i^0}{[A]_i^g} \quad (28)$$

$$-E_i^g = \frac{\partial E_i^g}{\partial \ln[M]_i^g} \frac{\Delta[M]_i^0}{[M]_i^g} + \frac{\partial E_i^g}{\partial \ln[A]_i^g} \frac{\Delta[A]_i^0}{[A]_i^g} \quad (29)$$

avec

$$D_i^g = D(V_i^e, [H]_i^0, [M]_i^g, [A]_i^g, P_i^0) \quad (30)$$

et

$$E_i^g = E(V_i^e, [H]_i^0, [M]_i^g, [A]_i^g, P_i^0) \quad (31)$$

Il est préférable d'employer des différentielles logarithmiques dans les équations (28) et (29) afin d'obtenir une matrice mieux conditionnée. Après résolution de ce système d'équations, les valeurs grossières $[M]_i^g$ et $[A]_i^g$ sont corrigées pour aboutir aux valeurs initiales, selon:

$$[M]_i^0 = [M]_i^g (1 + \Delta[M]_i^0/[M]_i^g) \quad (32)$$

$$[A]_i^0 = [A]_i^g (1 + \Delta[A]_i^0/[A]_i^g) \quad (33)$$

Ce processus doit être réitéré jusqu'à convergence, celle-ci étant obtenue lorsque les corrections relatives sont toutes inférieures à une valeur fixée arbitrairement, le plus souvent 10^{-5} . En pratique, il suffit généralement de disposer d'approximations grossières des concentrations libres uniquement pour le premier point. Pour les autres points, les approxi-

mations grossières seront considérées comme étant égales aux valeurs initiales du point précédent.

ELIMINATION DES CORRECTIONS SUR LES CONCENTRATIONS LIBRES INCONNUES

Sabatini *et al.*^{29,38} ont proposé la résolution d'un système de $3n$ équations à $(2n + p)$ inconnues analogue à celui décrit précédemment, les p inconnues étant constituées uniquement par les constantes de stabilité. Leur résolution conduit à la manipulation de matrices de très grandes tailles et, en particulier, d'une matrice des équations normales de dimension $(2n + p) \times (2n + p)$ dont l'inversion n'est pratiquement pas réalisable directement. Ils ont donc été amenés à utiliser une méthode indirecte relativement complexe nécessitant l'emploi de matrices auxiliaires afin de transformer cette matrice en une hypermatrice diagonale. Dans le but d'éviter la manipulation de matrices de tailles aussi considérables, nous avons élaboré une méthode qui permet d'éliminer les $2n$ corrections sur les concentrations libres du métal et du complexant et, par conséquent, d'obtenir un système beaucoup plus simple dans lequel ne subsistent plus que p inconnues. Symbolisons par $\Delta\hat{P}_i/P_i^0$ les corrections relatives sur les paramètres et, d'une manière générale, par $\Delta[\hat{X}]_i/[X]_i^0$ celles sur les concentrations libres. Le développement de l'équation (24) en série de Taylor en utilisant des différentielles logarithmiques sauf pour les variables expérimentales conduit à:

$$\hat{\psi}_i = 0 = \psi_i^0 - \frac{\partial \psi_i^0}{\partial I_i^e} R_{I_i} + \frac{\partial \psi_i^0}{\partial \ln[H]_i^0} \frac{\Delta[\hat{H}]_i}{[H]_i^0} + \sum_i \frac{\partial \psi_i^0}{\partial \ln P_i^0} \frac{\Delta\hat{P}_i}{P_i^0} \quad (34)$$

On peut alors en déduire:

$$\frac{\Delta[\hat{H}]_i}{[H]_i^0} = -\psi_i^0 / \left[\frac{\partial \psi_i^0}{\partial \ln[H]_i^0} \right] - \frac{\partial \ln[H]_i^0}{\partial I_i^e} R_{I_i} + \sum_i \frac{\partial \ln[H]_i^0}{\partial \ln P_i^0} \frac{\Delta\hat{P}_i}{P_i^0} \quad (35)$$

Après développement en série de Taylor des deux premières équations conditionnelles (21) et (22), on obtient:

$$\hat{D}_i = 0 = D_i^0 - \frac{\partial D_i^0}{\partial V_i^e} R_{V_i} + \frac{\partial D_i^0}{\partial \ln[H]_i^0} \frac{\Delta[\hat{H}]_i}{[H]_i^0} + \frac{\partial D_i^0}{\partial \ln[M]_i^0} \frac{\Delta[\hat{M}]_i}{[M]_i^0} + \frac{\partial D_i^0}{\partial \ln[A]_i^0} \frac{\Delta[\hat{A}]_i}{[A]_i^0} + \sum_i \frac{\partial D_i^0}{\partial \ln P_i^0} \frac{\Delta\hat{P}_i}{P_i^0}$$

$$\hat{E}_i = 0 = E_i^0 - \frac{\partial E_i^0}{\partial V_i^e} R_{V_i} + \frac{\partial E_i^0}{\partial \ln[H]_i^0} \frac{\Delta[\hat{H}]_i}{[H]_i^0}$$

$$\begin{aligned}
 & + \frac{\partial E_i^0}{\partial \ln[M]_i^0} \frac{\Delta[\hat{M}]_i}{[M]_i^0} + \frac{\partial E_i^0}{\partial \ln[A]_i^0} \frac{\Delta[\hat{A}]_i}{[A]_i^0} \quad \text{et} \\
 & + \sum_i \frac{\partial E_i^0}{\partial \ln P_i^0} \frac{\Delta \hat{P}_i}{P_i^0}
 \end{aligned}$$

En reportant l'expression (35) de $\Delta[\hat{H}]_i/[H]_i^0$ dans ces deux développements, on aboutit après modification à :

$$\begin{aligned}
 & -D_i^0 + \frac{\partial D_i^0}{\partial \ln[H]_i^0} \left[\frac{\partial \psi_i^0}{\partial \ln[H]_i^0} \right]^{-1} \psi_i^0 \\
 & + \frac{\partial D_i^0}{\partial V_i^0} R_{V_i} + \frac{\partial D_i^0}{\partial \ln[H]_i^0} \frac{\partial \ln[H]_i^0}{\partial I_i^0} R_{I_i} \\
 & - \sum_i \left(\frac{\partial D_i^0}{\partial \ln P_i^0} + \frac{\partial D_i^0}{\partial \ln[H]_i^0} \frac{\partial \ln[H]_i^0}{\partial \ln P_i^0} \right) \frac{\Delta \hat{P}_i}{P_i^0} \\
 & = \frac{\partial D_i^0}{\partial \ln[M]_i^0} \frac{\Delta[\hat{M}]_i}{[M]_i^0} + \frac{\partial D_i^0}{\partial \ln[A]_i^0} \frac{\Delta[\hat{A}]_i}{[A]_i^0} \quad (36)
 \end{aligned}$$

$$\begin{aligned}
 & -E_i^0 + \frac{\partial E_i^0}{\partial \ln[H]_i^0} \left[\frac{\partial \psi_i^0}{\partial \ln[H]_i^0} \right]^{-1} \psi_i^0 \\
 & + \frac{\partial E_i^0}{\partial V_i^0} R_{V_i} + \frac{\partial E_i^0}{\partial \ln[H]_i^0} \frac{\partial \ln[H]_i^0}{\partial I_i^0} R_{I_i} \\
 & - \sum_i \left(\frac{\partial E_i^0}{\partial \ln P_i^0} + \frac{\partial E_i^0}{\partial \ln[H]_i^0} \frac{\partial \ln[H]_i^0}{\partial \ln P_i^0} \right) \frac{\Delta \hat{P}_i}{P_i^0} \\
 & = \frac{\partial E_i^0}{\partial \ln[M]_i^0} \frac{\Delta[\hat{M}]_i}{[M]_i^0} + \frac{\partial E_i^0}{\partial \ln[A]_i^0} \frac{\Delta[\hat{A}]_i}{[A]_i^0} \quad (37)
 \end{aligned}$$

En adoptant une écriture matricielle, ce système devient :

$$\mathbf{C}_{K_{2,1}} - \mathbf{M}_{R_{2,2}} \mathbf{C}_{R_{2,1}} + \mathbf{M}_{P_{2,p}} \mathbf{C}_{P_{p,1}} = \mathbf{M}_{C_{2,2}} \mathbf{C}_{C_{2,1}}$$

avec :

$$\begin{aligned}
 \mathbf{C}_{K_{2,1}} &= \begin{vmatrix} -D_i^0 + \frac{\partial D_i^0}{\partial \ln[H]_i^0} \left[\frac{\partial \psi_i^0}{\partial \ln[H]_i^0} \right]^{-1} \psi_i^0 \\ -E_i^0 + \frac{\partial E_i^0}{\partial \ln[H]_i^0} \left[\frac{\partial \psi_i^0}{\partial \ln[H]_i^0} \right]^{-1} \psi_i^0 \end{vmatrix} \\
 \mathbf{M}_{R_{2,2}} &= - \begin{vmatrix} \frac{\partial D_i^0}{\partial V_i^0} \frac{\partial D_i^0}{\partial \ln[H]_i^0} \frac{\partial \ln[H]_i^0}{\partial I_i^0} \\ \frac{\partial E_i^0}{\partial V_i^0} \frac{\partial E_i^0}{\partial \ln[H]_i^0} \frac{\partial \ln[H]_i^0}{\partial I_i^0} \end{vmatrix} \\
 \mathbf{M}_{P_{2,p}} &= - \begin{vmatrix} \frac{\partial D_i^0}{\partial \ln P_i^0} + \frac{\partial D_i^0}{\partial \ln[H]_i^0} \frac{\partial \ln[H]_i^0}{\partial \ln P_i^0} \cdots \frac{\partial D_i^0}{\partial \ln P_p^0} + \frac{\partial D_i^0}{\partial \ln[H]_i^0} \frac{\partial \ln[H]_i^0}{\partial \ln P_p^0} \\ \frac{\partial E_i^0}{\partial \ln P_i^0} + \frac{\partial E_i^0}{\partial \ln[H]_i^0} \frac{\partial \ln[H]_i^0}{\partial \ln P_i^0} \cdots \frac{\partial E_i^0}{\partial \ln P_p^0} + \frac{\partial E_i^0}{\partial \ln[H]_i^0} \frac{\partial \ln[H]_i^0}{\partial \ln P_p^0} \end{vmatrix} \\
 \mathbf{M}_{C_{2,2}} &= \begin{vmatrix} \frac{\partial D_i^0}{\partial \ln[M]_i^0} \frac{\partial D_i^0}{\partial \ln[A]_i^0} \\ \frac{\partial E_i^0}{\partial \ln[M]_i^0} \frac{\partial E_i^0}{\partial \ln[A]_i^0} \end{vmatrix} \quad \mathbf{C}_{R_{2,1}} = \begin{vmatrix} R_{V_i} \\ R_{I_i} \end{vmatrix} \\
 \mathbf{C}_{P_{p,1}} &= \begin{vmatrix} \Delta \hat{P}_1 / P_1^0 \\ \vdots \\ \Delta \hat{P}_p / P_p^0 \end{vmatrix} \quad \mathbf{C}_{C_{2,1}} = \begin{vmatrix} \Delta[\hat{M}]_i / [M]_i^0 \\ \Delta[\hat{A}]_i / [A]_i^0 \end{vmatrix}
 \end{aligned}$$

Les matrices M_R , M_P et M_C ainsi que le vecteur colonne C_K sont facilement calculables. Par contre, les vecteurs colonnes C_R des résidus sur les variables expérimentales, C_P des corrections relatives sur les paramètres et C_C des corrections relatives sur les concentrations libres en métal et en complexant sont inconnus.

On peut alors exprimer C_C en fonction de C_R et de C_P . En effet, en multipliant à gauche par la matrice inverse M_C^{-1} , on obtient:

$$M_{C_{2,2}}^{-1} C_{K_{2,1}} - M_{C_{2,2}}^{-1} M_{R_{2,2}} C_{R_{2,1}} + M_{C_{2,2}}^{-1} M_{P_{2,p}} C_{P_{p,1}} = C_{C_{2,1}} \quad (38)$$

D'autre part, en utilisant l'équation (35), le développement en série de Taylor de la dernière des équations conditionnelles (23) conduit à:

$$\begin{aligned} \hat{F}_i = 0 = F_i^0 - \frac{\partial F_i^0}{\partial \ln[H]_i^0} \left[\frac{\partial \psi_i^0}{\partial \ln[H]_i^0} \right]^{-1} \psi_i^0 \\ - \frac{\partial F_i^0}{\partial V_i^c} R_{V_i} - \frac{\partial F_i^0}{\partial \ln[H]_i^0} \frac{\partial \ln[H]_i^0}{\partial I_i^c} R_{I_i} \\ + \frac{\partial F_i^0}{\partial \ln[M]_i^0} \frac{\Delta[\hat{M}]_i}{[M]_i^0} + \frac{\partial F_i^0}{\partial \ln[A]_i^0} \frac{\Delta[\hat{A}]_i}{[A]_i^0} \\ + \sum_i \left(\frac{\partial F_i^0}{\partial \ln P_i^0} + \frac{\partial F_i^0}{\partial \ln[H]_i^0} \frac{\partial \ln[H]_i^0}{\partial \ln P_i^0} \right) \frac{\Delta \hat{P}_i}{P_i^0} \quad (39) \end{aligned}$$

avec $F_i^0 = F(V_i^c, [H]_i^0, [M]_i^0, [A]_i^0, P_i^0)$.

Sous forme matricielle, l'équation (39) s'écrit encore:

$$F_i^0 - \frac{\partial F_i^0}{\partial \ln[H]_i^0} \left[\frac{\partial \psi_i^0}{\partial \ln[H]_i^0} \right]^{-1} \psi_i^0 - L_{R_{1,2}} C_{R_{2,1}} + L_{C_{1,2}} C_{C_{2,1}} + L_{P_{1,p}} C_{P_{p,1}} = 0$$

avec:

$$\begin{aligned} L_{R_{1,2}} &= \left\| \frac{\partial F_i^0}{\partial V_i^c} \quad \frac{\partial F_i^0}{\partial \ln[H]_i^0} \frac{\partial \ln[H]_i^0}{\partial I_i^c} \right\| \\ L_{C_{1,2}} &= \left\| \frac{\partial F_i^0}{\partial \ln[M]_i^0} \quad \frac{\partial F_i^0}{\partial \ln[A]_i^0} \right\| \\ L_{P_{1,p}} &= \left\| \frac{\partial F_i^0}{\partial \ln P_i^0} + \frac{\partial F_i^0}{\partial \ln[H]_i^0} \frac{\partial \ln[H]_i^0}{\partial \ln P_i^0} \right\| \dots \left\| \frac{\partial F_i^0}{\partial \ln P_p^0} + \frac{\partial F_i^0}{\partial \ln[H]_i^0} \frac{\partial \ln[H]_i^0}{\partial \ln P_p^0} \right\| \end{aligned}$$

Si l'on remplace C_C par son expression (38) et que l'on réunit les termes qui se correspondent, on obtient:

$$\begin{aligned} \left(F_i^0 - \frac{\partial F_i^0}{\partial \ln[H]_i^0} \left[\frac{\partial \psi_i^0}{\partial \ln[H]_i^0} \right]^{-1} \psi_i^0 + L_{C_{1,2}} M_{C_{2,2}}^{-1} C_{K_{2,1}} \right) \\ - (L_{R_{1,2}} + L_{C_{1,2}} M_{C_{2,2}}^{-1} M_{R_{2,2}}) C_{R_{2,1}} \\ + (L_{P_{1,p}} + L_{C_{1,2}} M_{C_{2,2}}^{-1} M_{P_{2,p}}) C_{P_{p,1}} = 0 \end{aligned}$$

soit encore:

$$\phi_i^0 - \phi_{R_{1,2}} C_{R_{2,1}} + \phi_{P_{1,p}} C_{P_{p,1}} = 0$$

Sous forme détaillée, cette équation fondamentale

pour les développements ultérieurs s'écrit:

$$\begin{aligned} \phi \left(R_{V_i}, R_{I_i}, \frac{\Delta \hat{P}_i}{P_i^0} \right) = \phi_i^0 - \phi_{V_i} R_{V_i} \\ - \phi_{I_i} R_{I_i} + \sum_i \phi_{i,i} \frac{\Delta \hat{P}_i}{P_i^0} = 0 \quad (40) \end{aligned}$$

Dans cette équation, les termes ϕ_i^0 , ϕ_{V_i} , ϕ_{I_i} et $\phi_{i,i}$ sont calculables. Seules subsistent comme inconnues les corrections relatives sur les paramètres $\Delta \hat{P}_i / P_i^0$ ainsi que les résidus R_{V_i} et R_{I_i} sur les variables puisque les corrections relatives sur les concentrations libres $\Delta[\hat{M}]_i / [M]_i^0$ et $\Delta[\hat{A}]_i / [A]_i^0$ ont été éliminées. Cette équation permettra donc la manipulation ultérieure d'une matrice des équations normales de taille $p \times p$, contrairement à LEAST³⁸ ou MINQUAD²⁹ qui emploient une matrice de taille $(2n + p) \times (2n + p)$.

EQUATIONS NORMALES

La somme pondérée des carrés des résidus S , dont l'expression est donnée par la formule (20), est minimum lorsque:

$$\frac{1}{2} dS = \sum_i W_{V_i} R_{V_i} dR_{V_i} + \sum_i W_{I_i} R_{I_i} dR_{I_i} = 0 \quad (41)$$

De plus, la différentiation de l'équation (40) conduit à:

$$\begin{aligned} d(-\phi_i^0) = 0 = -\phi_{V_i} dR_{V_i} \\ - \phi_{I_i} dR_{I_i} + \sum_i \phi_{i,i} d \frac{\Delta \hat{P}_i}{P_i^0} \quad (42) \end{aligned}$$

Il existe une équation de ce type pour chaque mesure i , soit au total n équations. Multiplions chacune d'elles par une valeur arbitraire λ_i appelée multiplicateur de Lagrange et ajoutons ces n équations à

l'équation (41):

$$\begin{aligned} \sum_i (W_{V_i} R_{V_i} - \lambda_i \phi_{V_i}) dR_{V_i} + \sum_i (W_{I_i} R_{I_i} \\ - \lambda_i \phi_{I_i}) dR_{I_i} + \sum_i \left(d \frac{\Delta \hat{P}_i}{P_i^0} \sum_i \lambda_i \phi_{i,i} \right) = 0 \quad (43) \end{aligned}$$

Cette équation (43) contient $(3n + p)$ inconnues: λ_i , R_{V_i} , R_{I_i} et $\Delta \hat{P}_i / P_i^0$. De plus, elle doit être vérifiée quelles que soient les valeurs de ces inconnues, ce qui exige que les coefficients des éléments différentiels soient nuls simultanément. On obtient ainsi $(2n + p)$ équations:

$$W_{V_i} R_{V_i} - \lambda_i \phi_{V_i} = 0 \quad i = 1, 2, \dots, n \quad (44)$$

$$W_i R_i - \lambda_i \phi_i = 0 \quad i = 1, 2, \dots, n \quad (45) \quad \text{et}$$

$$\sum_l \lambda_l \phi_{l,i} = 0 \quad l = 1, 2, \dots, p \quad (46)$$

D'après (44) et (45), les résidus sur les variables expérimentales s'expriment donc par:

$$R_{v_i} = \frac{\lambda_i \phi_{v_i}}{W_{v_i}} \quad (47)$$

et

$$R_i = \frac{\lambda_i \phi_i}{W_i} \quad (48)$$

Reportons ces valeurs dans l'équation (40):

$$-\phi_i^0 = -\lambda_i \left(\frac{\phi_{v_i}^2}{W_{v_i}} + \frac{\phi_i^2}{W_i} \right) + \sum_l \phi_{l,i} \frac{\Delta \hat{P}_l}{P_i^0} \quad (49)$$

On obtient ainsi n équations de cette forme qui, avec les p équations (46), fournissent alors un système de $(n + p)$ équations à $(n + p)$ inconnues: n multiplicateurs de Lagrange λ_i et p corrections relatives sur les paramètres $\Delta \hat{P}_i / P_i^0$.

Il est donc possible de résoudre ce système et d'en déduire à la fois les valeurs des multiplicateurs de Lagrange et celles des corrections relatives sur les paramètres. En pratique, on peut se ramener à un système beaucoup plus simple en combinant les n équations (49) avec les p équations (46). En effet, d'après (49), on obtient:

$$\lambda_i = W_i \left(\phi_i^0 + \sum_l \phi_{l,i} \frac{\Delta \hat{P}_l}{P_i^0} \right) \quad (50)$$

avec

$$W_i = \frac{W_{v_i} W_i}{\phi_{v_i}^2 W_i + \phi_i^2 W_{v_i}} = \left(\frac{\phi_{v_i}^2}{W_{v_i}} + \frac{\phi_i^2}{W_i} \right)^{-1} \quad (51)$$

W_i peut être appelé le poids global de la mesure i et, en fonction des expressions (17) et (18) des poids des résidus, il est encore égal à:

$$W_i = \frac{\sigma_0^2}{\phi_{v_i}^2 \sigma_{v_i}^2 + \phi_i^2 \sigma_i^2}$$

Maintenant reportons λ_i dans les p équations (46):

$$\sum_i W_i \left(\phi_i^0 + \sum_l \phi_{l,i} \frac{\Delta \hat{P}_l}{P_i^0} \right) \phi_{j,i} = 0 \quad \text{avec } j = 1, 2, \dots, p$$

On obtient ainsi le système dit des "équations normales", système de p équations à p inconnues:

$$-\sum_i W_i \phi_i^0 \phi_{j,i} = \sum_i \left(\frac{\Delta \hat{P}_i}{P_i^0} \sum_l W_l \phi_{l,i} \phi_{j,i} \right) \quad \text{avec } j = 1, 2, \dots, p \quad (52)$$

Sous forme matricielle ce système des "équations normales" s'écrit:

$$\mathbf{Y} = \mathbf{B}\mathbf{A} \quad (53)$$

avec

$$b_{j,i} = \sum_l W_l \phi_{l,i} \phi_{j,i}$$

$$y_j = -\sum_i W_i \phi_i^0 \phi_{j,i}$$

Lors de la généralisation du raisonnement précédent à l'analyse simultanée de plusieurs titrages, la matrice \mathbf{B} est de la forme représentée sur la figure 1, l'exemple choisi étant relatif à trois dosages. Si certains paramètres sont communs à deux ou plusieurs dosages, il faut alors en tenir compte et modifier la matrice \mathbf{B} en conséquence. Un exemple de la matrice résultante est représenté sur la figure 2. Les corrections relatives sur les paramètres sont obtenues par l'intermédiaire de la relation:

$$\mathbf{A} = \mathbf{B}^{-1} \mathbf{Y} \quad (54)$$

On en déduit ensuite les estimateurs \hat{P}_i des paramètres. En pratique, comme les développements en série de Taylor (36), (37) et (39) sont limités aux différentielles premières, les corrections relatives ainsi obtenues ne sont pas exactes. Le processus devra donc être réitéré jusqu'à convergence, celle-ci étant atteinte lorsque les corrections relatives sur les paramètres sont toutes inférieures à une valeur prédéterminée, en général 10^{-5} .

OBTENTION DES VALEURS AJUSTÉES DES VARIABLES EXPERIMENTALES ET DES CONCENTRATIONS LIBRES INCONNUES

Lorsque la convergence est obtenue, les dernières valeurs des corrections relatives sur les paramètres sont reportées dans l'équation (50). On détermine ainsi les valeurs des n multiplicateurs de Lagrange λ_i . Ces valeurs de λ_i sont ensuite utilisées pour calculer les résidus R_{v_i} et R_i par l'intermédiaire des relations (47) et (48). Enfin, on en déduit les valeurs ajustées \hat{V}_i et \hat{I}_i à l'aide des équations (15) et (16) ainsi que $[\hat{H}]_i$ grâce à la relation (24).

Théoriquement, pour calculer les corrections relatives $\Delta[\hat{M}]_i/[M]_i^0$ et $\Delta[\hat{A}]_i/[A]_i^0$ à apporter aux concentrations libres, il faut alors appliquer la relation (38) puisque le vecteur colonne \mathbf{C}_R des résidus sur les variables expérimentales et celui \mathbf{C}_P des corrections relatives sur les paramètres sont maintenant connus. On peut ensuite en déduire les valeurs de $[\hat{M}]_i$ et $[\hat{A}]_i$ par l'intermédiaire de relations analogues aux équations (32) et (33). En pratique, il est plus simple d'utiliser la méthode de Newton-Raphson selon le principe exposé précédemment, les relations (25) et (26) étant remplacées par les équations conditionnelles (21) et (22) alors que les expressions (30) et (31) deviennent:

$$D(\hat{V}_i, [\hat{H}]_i, [M]_i^0, [A]_i^0, \hat{P}_i) = \hat{D}_i^0$$

$$E(\hat{V}_i, [\hat{H}]_i, [M]_i^0, [A]_i^0, \hat{P}_i) = \hat{E}_i^0$$

MATRICE DES VARIANCES-COVARIANCES ET MATRICE DE CORRELATION DES PARAMETRES

On peut démontrer²¹⁻²³ qu'un estimateur non biaisé de la variance d'une fonction de poids unitaire est

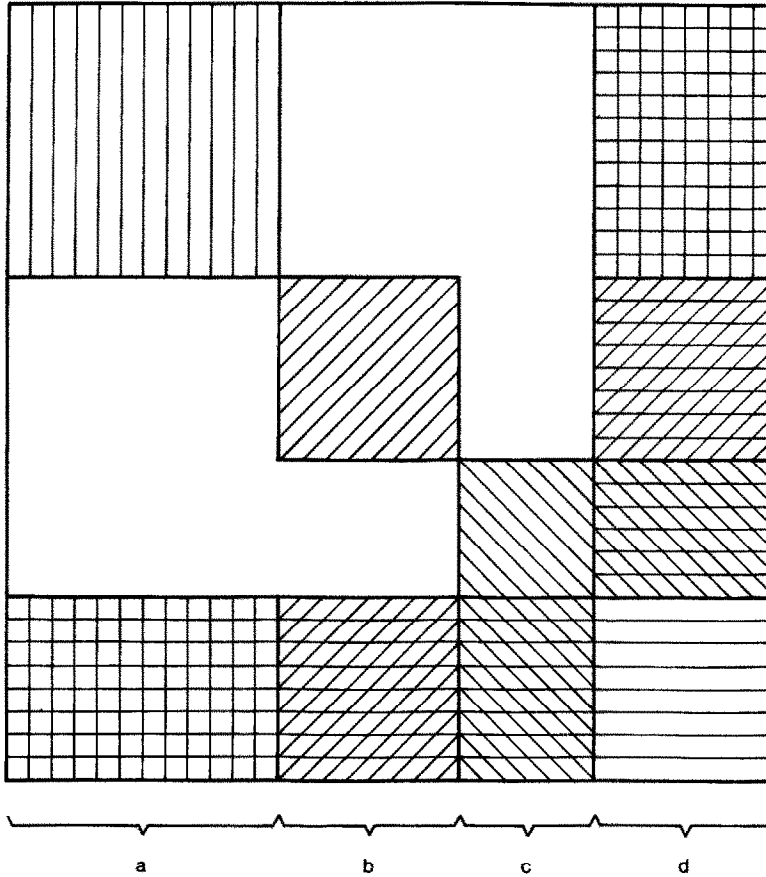


Fig. 1. Forme de la matrice B: (a) paramètres du premier titrage, (b) paramètres du second titrage, (c) paramètres du troisième titrage, (d) constantes de stabilité.

donné par la formule:

$$\hat{\sigma}_0^2 = \frac{S}{n - p} \tag{55}$$

Cette grandeur est fondamentale pour juger les résultats de l'affinement. En effet, si le schéma de pondération retenu et le modèle mathématique envisagé sont cohérents avec les valeurs expérimentales, cet estimateur $\hat{\sigma}_0^2$ doit être proche de la valeur σ_0^2 utilisée dans le calcul des poids par l'intermédiaire des formules (17) et (18). Si l'affinement est valable, on doit donc avoir le rapport $\hat{\sigma}_0^2/\sigma_0^2$ qui tend vers 1.

Un estimateur de la matrice des variances-covariances des paramètres dont les éléments diagonaux sont les variances $\hat{\sigma}_{i,i} = \hat{\sigma}_i^2$ des paramètres \hat{P}_i et les éléments hors-diagonaux sont les covariances $\hat{\sigma}_{j,i}$ des paramètres \hat{P}_j et \hat{P}_i est fourni par:

$$\hat{\sigma}_0^2 \mathbf{D} \mathbf{B}^{-1} \mathbf{D} \tag{56}$$

avec **D** la matrice diagonale des paramètres.

Ces variances et covariances sont utiles lors du calcul de la variance d'une constante d'équilibre. Par exemple, lorsqu'on veut calculer la variance de la constante de l'équilibre $\text{MA} + \text{A} \rightleftharpoons \text{MA}_2$, avec une écriture simplifiée on a $K_2 = \beta_2/\beta_1$. D'après la règle de

propagation de la variance,⁴³ on aboutit alors à:

$$\sigma_{K_2}^2 = \frac{\beta_2^2}{\beta_1^4} \sigma_{\beta_1}^2 + \frac{1}{\beta_1^2} \sigma_{\beta_2}^2 - 2 \frac{\beta_2}{\beta_1^3} \sigma_{\beta_1, \beta_2}$$

soit encore:

$$\sigma_{\log K_2}^2 = \sigma_{\log \beta_1}^2 + \sigma_{\log \beta_2}^2 - 2\sigma_{\log \beta_1, \log \beta_2}$$

Connaissant la matrice des variances-covariances, on peut alors facilement en déduire la matrice de corrélation^{32,33} dont les éléments sont les coefficients de corrélation définis par:

$$\hat{\rho}_{j,i} = \frac{\hat{\sigma}_{j,i}}{\hat{\sigma}_j \hat{\sigma}_i} \tag{57}$$

Ces coefficients indiquent la plus ou moins forte dépendance positive ou négative des paramètres vis à vis les uns des autres.

PROTECTION CONTRE LA DIVERGENCE

Lorsque les estimations initiales des paramètres sont assez éloignées des valeurs réelles, le processus peut parfois diverger car les développements en série de Taylor deviennent trop approximatifs puisqu'ils sont limités aux différentielles premières. Parmi les diverses méthodes⁹ envisagées pour se protéger contre une telle divergence, celle proposée par Hartley⁴⁴ est

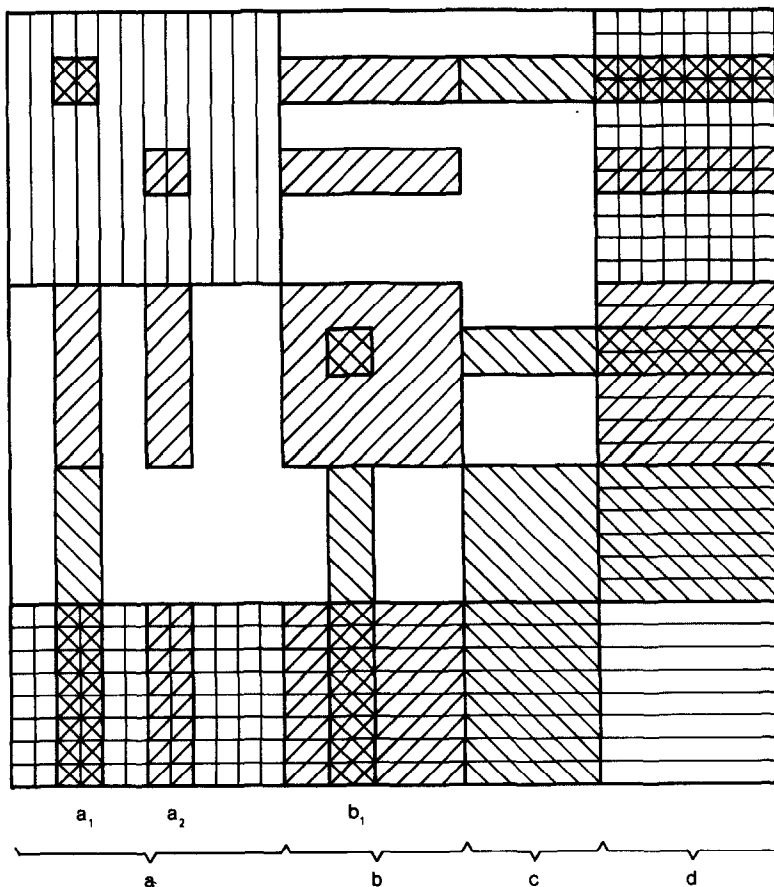


Fig. 2. Forme de la matrice B lorsqu'il existe des paramètres communs; (a₁) un paramètre est commun aux trois titrages, (a₂) un paramètre est commun aux premier et second titrages, (b₁) un paramètre est commun aux second et troisième titrages.

l'une des plus simples à mettre en oeuvre. Son principe repose sur l'optimisation des corrections relatives à apporter aux paramètres. Dans l'expression (20) de la somme pondérée des carrés des résidus S, remplaçons les résidus par leurs valeurs données par les formules (47) et (48):

$$S = \sum_i \lambda_i^2 \left(\frac{\phi_{v_i}^2}{W_{v_i}} + \frac{\phi_{l_i}^2}{W_{l_i}} \right)$$

soit encore d'après (51):

$$S = \sum_i \lambda_i^2 W_i^{-1}$$

En remplaçant les multiplicateurs de Lagrange λ_i par leur expression (50), on obtient:

$$S = \sum_i W_i \left(\phi_i^0 + \sum_l \phi_{l,i} \frac{\Delta \hat{P}_l}{P_i^0} \right)^2 \quad (58)$$

Or si les développements en série de Taylor sont trop approximatifs, les corrections relatives sur les paramètres ne sont pas optima, c'est à dire qu'elles n'assurent pas la décroissance la plus rapide de la somme S. On peut alors considérer que de meilleures valeurs des corrections relatives seront obtenues en multipliant celles-ci par un facteur d'optimisation t.

Dans ces conditions la somme S devient, d'après (58):

$$S = \sum_i W_i \left(\phi_i^0 + \sum_l \phi_{l,i} t \frac{\Delta \hat{P}_l}{P_i^0} \right)^2$$

La somme S est donc une fonction quadratique de t:

$$S = x_0 + 2x_1 t + x_2 t^2$$

Selon les relations (52) et (53), on obtient alors le minimum de S pour:

$$t = -\frac{x_1}{x_2} = \frac{\Delta^T Y}{\Delta^T B \Delta} \quad (59)$$

Malgré cette optimisation, dans certains cas il peut également être nécessaire de fixer un seuil maximum aux corrections relatives successives, par exemple 50%.

CONCLUSION

La méthode originale exposée précédemment est à la base du programme PROTAF d'analyse des mesures protométriques, programme mis au point et testé depuis plusieurs années dans notre laboratoire. Il rassemble plusieurs aspects essentiels, quelques uns étant déjà présents dans divers algorithmes décrits antérieurement, les autres étant nouveaux.

Nous avons choisi de minimiser les résidus pondérés sur les variables expérimentales, à savoir le volume de réactif ajouté et la valeur indiquée par le potentiomètre (E ou pH). En effet, il nous semble préférable, pour plusieurs motifs, d'utiliser les données effectivement mesurées plutôt que des variables auxiliaires déduites de celles-ci. Tout d'abord, le calcul des ces fonctions auxiliaires (\bar{n} , \bar{h} , ...) cumule inévitablement les erreurs, qu'elles soient aléatoires ou systématiques, puisque ces fonctions dépendent de l'ensemble des facteurs: concentrations analytiques, E ou pH , volume de réactif... Ensuite, ces fonctions auxiliaires n'étant plus indépendantes, le choix des poids à leur affecter devient un problème crucial. Il faut tenir compte à la fois de leurs variances, mais également de leur covariance, termes qui deviennent assez difficilement appréhendables. Enfin, les résidus sur ces fonctions auxiliaires sont beaucoup moins facilement interprétables que ceux sur les variables effectivement mesurées. Dans la plupart des programmes existants, les dérivées, qu'elles soient premières ou secondes, sont calculées numériquement par incrémentation des paramètres. Selon ce procédé, on obtient par exemple:

$$\frac{\partial^2 F(x, y)}{\partial x^2} = \frac{F(x + \Delta x, y) - 2F(x, y) + F(x - \Delta x, y)}{(\Delta x)^2}$$

Si cette méthode de calcul à l'avantage d'être très générale et particulièrement simple à programmer, elle présente toutefois le grave inconvénient d'aboutir parfois à des dérivées trop approximatives. En effet, des essais de minimisation de la fonction de Rosenbrock:⁴⁵ $f(x, y) = 100(y - x^2)^2 + (1 - x)^2$ à l'aide de dérivées calculées de cette manière prouvent que la convergence vers le minimum est très largement tributaire du choix judicieux de l'incrément, choix particulièrement délicat conditionnant la plus ou moins bonne approximation des dérivées. Ces essais montrent également qu'avec des dérivées calculées analytiquement la convergence est à la fois meilleure et plus rapide. Par conséquent, à l'instar de quelques autres auteurs,^{16,20,21,24-26,29} nous avons décidé d'opter pour un calcul analytique des dérivées plus efficace que le calcul numérique bien que sa programmation soit nettement plus longue.

A notre connaissance, parmi les programmes les plus généraux, seuls MUCOMP,^{15,16} MICMAC,²³ SUPERQUAD²⁶ et, dans de moindres proportions, TITFIT²⁰ et LETAGROP VRID⁴⁶ sont en mesure d'affiner d'autres paramètres que les constantes de stabilité des complexes. Pour notre part, nous avons conçu le programme PROTAF de telle manière qu'il soit possible d'affiner non seulement les constantes de stabilité, mais aussi tous les autres paramètres des différents dosages que nous appellerons "paramètres secondaires": concentrations C^* des solutions mères ayant servi à réaliser les mélanges initiaux, paramètres du couple d'électrodes, ... Suivant les cas, ces

"paramètres secondaires" peuvent être communs ou non à plusieurs ou à l'ensemble des titrages. En particulier, l'innovation consistant à employer les concentrations C^* permet de tenir compte des concentrations communes ou non. Par exemple, lors de l'analyse de plusieurs expériences à concentrations en complexant différentes, mais dont les mélanges initiaux ont été effectués à l'aide de la même solution mère de complexant, la concentration C_A^* est un paramètre commun à l'ensemble des dosages. Inversement, si différentes solutions mères d'ion métallique ont dû être utilisées, les concentrations C_M^* sont propres à chaque expérience et s'il est nécessaire de les affiner elles le seront indépendamment les unes des autres.

Il faut, toutefois, être très prudent lors de l'emploi de ces "paramètres secondaires". En effet, leur affinement évite souvent d'introduire dans le modèle retenu des espèces chimiques irréalistes, n'ayant d'autre rôle que la compensation d'erreurs systématiques négligées. Mais inversement, l'affinement de ces "paramètres secondaires" (en particulier les concentrations) risque également de compenser artificiellement d'autres erreurs systématiques,²⁶ voire des espèces chimiques minoritaires. L'affinement de ces "paramètres secondaires" ne doit donc être employé qu'avec beaucoup de circonspection et surtout ne doit pas être considéré comme un moyen de se dispenser de protocoles expérimentaux rigoureux. Enfin, il est à noter que de nombreux essais du programme PROTAF effectués sur des exemples simulés montrent qu'il est pratiquement impossible d'affiner simultanément l'ensemble des paramètres car certains coefficients de corrélation sont très proches les uns des autres, entraînant ainsi la divergence du processus d'affinement.

Ce programme présente également l'originalité de pouvoir traiter ensemble des titrages de buts différents. Par exemple, il peut analyser simultanément des dosages du complexant seul et en présence d'ion métallique. En effet, dans ce cas il tient compte des deux types de constantes de stabilité: d'une part, les constantes de protonation du complexant communes à l'ensemble des dosages, d'autre part, les autres constantes intervenant uniquement dans les expériences en présence d'ion métallique.

A l'instar de MINQUAD, qui était jusqu'à présent le seul à présenter cette particularité, notre programme PROTAF affine simultanément les différents paramètres et les concentrations libres $[M]$, et $[A]$, car ces deux types d'inconnues sont traitées au même niveau. Cependant, contrairement à MINQUAD, la méthode matricielle que nous avons adoptée nécessite uniquement la manipulation de matrices de tailles beaucoup plus raisonnables et conduit, alors, à un traitement pratique nettement plus succinct.

Enfin, la méthode utilisée permet, pour la première fois, de calculer conjointement les valeurs ajustées des variables expérimentales que sont le volume de réactif

et E ou pH , et, par voie de conséquence, les valeurs exactes des résidus sur ces variables.

Ces différentes améliorations ont été exploitées avec succès lors de l'analyse d'exemples expérimentaux variés dont certains seront publiés ultérieurement. Le programme PROTAF, mis en œuvre sur ordinateur CII Mini 6, est écrit en langage FORTRAN et en mode conversationnel. Il est structuré de manière à pouvoir utiliser éventuellement la technique de recouvrement ("overlay"). Dans sa version actuelle, il est capable de traiter simultanément dix séries de cent mesures chacune faisant intervenir au maximum trois ions métalliques et trois complexants différents, le nombre de constantes de stabilité étant limité à vingt. Le programme PROTAF est disponible sur demande auprès de R. Fournaise.

LITTÉRATURE

1. Partie I—R. Fournaise et C. Petitfaux, *Talanta*, 1986, **33**, 499; II—R. Fournaise, C. Petitfaux et J. C. Emond, *J. Chem. Research*, (S), 1986, 372.
2. J. C. Sullivan, J. Rydberg et W. F. Miller, *Acta Chem. Scand.*, 1959, **13**, 2023.
3. R. S. Tobias et Z. Z. Hugas, Jr., *J. Phys. Chem.* 1961, **65**, 2165.
4. R. S. Tobias et M. Yasuda, *Inorg. Chem.*, 1963, **2**, 1307.
5. L. G. Sillén, *Acta Chem. Scand.*, 1962, **16**, 159.
6. N. Ingri et L. G. Sillén, *ibid.*, 1962, **16**, 173.
7. C. W. Childs, P. S. Hallman et D. D. Perrin, *Talanta*, 1969, **16**, 1119.
8. F. J. C. Rossotti, H. S. Rossotti et R. J. Whewell, *J. Inorg. Nucl. Chem.*, 1971, **33**, 2051.
9. P. Gans, *Coord. Chem. Rev.*, 1976, **19**, 99.
10. F. Gaizer, *ibid.*, 1979, **27**, 195.
11. P. Gans, *Adv. Mol. Relaxation Interact. Process.*, 1980, **18**, 139.
12. A. Avdeef, S. R. Sofen, T. L. Bregante et K. N. Raymond, *J. Am. Chem. Soc.*, 1978, **100**, 5362.
13. F. Gaizer, *Acta Chim. Acad. Sci. Hung.*, 1980, **103**, 397.
14. M. Wozniak et G. Nowogrocki, *Talanta*, 1978, **25**, 633.
15. *Idem*, *ibid.*, 1978, **25**, 643.
16. M. Wozniak, J. Canonne et G. Nowogrocki, *J. Chem. Soc., Dalton Trans.*, 1981, 2419.
17. M. Cromer-Morin, J. P. Scharff et R. P. Martin, *Analisis*, 1982, **10**, 92.
18. R. J. Motekaitis et A. E. Martell, *Can. J. Chem.*, 1982, **60**, 168.
19. *Idem*, *ibid.*, 1982, **60**, 2403.
20. A. D. Zuberbühler et T. A. Kaden, *Talanta*, 1982, **29**, 201.
21. J. Kostrowicki et A. Liwo, *Comput. Chem.*, 1984, **8**, 101.
22. M. Meloun et J. Čermák, *Talanta*, 1984, **31**, 947.
23. A. Laouenan et E. Suet, *ibid.*, 1985, **32**, 245.
24. G. Arena, E. Rizzarelli, S. Sammartano et C. Rigano, *ibid.*, 1979, **26**, 1.
25. C. Rigano, A. De Robertis et S. Sammartano, *Transition Met. Chem. (Weinheim)*, 1985, **10**, 1, 36.
26. P. Gans, A. Sabatini et A. Vacca, *J. Chem. Soc., Dalton Trans.*, 1985, 1195.
27. L. G. Sillén, *Acta Chem. Scand.*, 1964, **18**, 1085.
28. I. G. Sayce, *Talanta*, 1968, **15**, 1397.
29. A. Sabatini, A. Vacca et P. Gans, *ibid.*, 1974, **21**, 53.
30. P. Gans, A. Sabatini et A. Vacca, *Inorg. Chim. Acta*, 1976, **18**, 237.
31. Y. V. Linnik, *Méthode des Moindres Carrés*, Dunod, Paris, 1963.
32. W. C. Hamilton, *Statistics in Physical Science*, Ronald Press, New York, 1964.
33. W. E. Deming, *Statistical Adjustment of Data*, Dover Publications, New York, 1964.
34. W. E. Wentworth, *J. Chem. Educ.*, 1965, **42**, 96.
35. H. G. Mendelbaum, F. Madaule et M. Desgranges, *Bull. Soc. Chim. France*, 1973, **5**, 1619.
36. R. H. Moore et R. K. Zeigler, *Los Alamos Scientific Laboratory Rept.*, LA-2367, March 1960.
37. T. G. Strand, D. A. Kohl et R. A. Bonham, *J. Chem. Phys.*, 1963, **39**, 1307.
38. A. Sabatini et A. Vacca, *J. Chem. Soc., Dalton Trans.*, 1972, 1693.
39. N. Ingri, G. Lagerström, M. Frydman et L. G. Sillén, *Acta Chem. Scand.*, 1957, **11**, 1034.
40. H. S. Rossotti, *Talanta*, 1974, **21**, 809.
41. R. G. Bates, *Determination of pH*, Wiley, New York, 1964.
42. A. K. Covington, R. G. Bates et R. A. Durst, *Pure Appl. Chem.*, 1983, **55**, 1467.
43. H. H. Ku, *J. Res. Natl. Bur. Stand.*, 1966, **70c**, 263.
44. H. O. Hartley, *Technometrics*, 1961, **3**, 269.
45. H. H. Rosenbrock, *Comput. J.*, 1960, **3**, 175.
46. P. Brauner, L. G. Sillén et R. Whiteker, *Arkiv Kemi*, 1969, **31**, 365.

DETERMINATION OF SULPHATE BY pH TITRATION

BÉLA NOSZÁL and MÁRIA JUHÁSZ

Department of Inorganic and Analytical Chemistry, L. Eötvös University, 1088 Budapest,
 Múzeum krt. 4/B, Hungary

(Received 20 August 1985. Revised 28 July 1986. Accepted 15 November 1986)

Summary—A simple and inexpensive method has been developed for the determination of sulphate and other very weak bases and acids. It utilizes the partial protonation of the weak base or the partial dissociation of the weak acid, which has not been exploited for analytical purposes thus far. The procedure consists of three pH titrations: one with a test solution of known sulphate content, the second with the sulphate sample, and the third with a blank. This method can be used in the presence of several inorganic ions and organic matrices, including non-aqueous solvents. In aqueous medium sulphate contents above $10^{-3}M$ can be determined. The use of solvent mixtures may increase the sensitivity of the method by two orders of magnitude.

Most analytical methods for the determination of sulphate (gravimetry, chelatometry, potentiometry, conductometry, amperometry *etc.*) are based on the formation of its barium or lead salts.¹ Besides these, several classical or instrumental analytical methods have been developed in which organic reagents are used to form a sulphate precipitate. However, there is no report on the analytical exploitation of the equilibrium interaction between the sulphate and hydrogen ions. The obvious reason is the low basicity of sulphate, which does not allow its determination by normal direct acidimetric titration.

Here a method, and its application to sulphate, will be introduced, which utilizes the partial protonation of very weak bases (or dissociation of fairly strong acids). The best known method for evaluating potentiometric titrations of weak bases and acids is the classical Gran plot.² Preconditions for its use are knowledge of the equilibrium constant valid under the given circumstances, and of the pH and the titrant concentration. The procedure of Ivaska and Nagypál³ needs considerable mathematical apparatus, but can be used even for analysis of mixtures. The recent method by Burger *et al.*,⁴ based on measurement of the amount of bound reagent, applies when protonation or deprotonation is practically complete.

The present method does not require knowledge of the equilibrium constant, the pH or the titrant concentration, and furthermore is satisfactory even if the reaction takes place only to the extent of 20–30%; thus it is suitable for the determination of very weak acids and bases.

Protonation of bases

The proportion of the conjugated acid (HB^+) formed in the protonation equilibrium $B + H^+ \rightleftharpoons BH^+$ of a monoacidic base (B) can be calculated from the formation function well known in

co-ordination chemistry:⁵

$$\bar{n} = \frac{[HB^+]}{[B] + [HB^+]} \quad (1)$$

The formation constant (B) for BH^+ is:

$$\beta = \frac{[HB^+]}{[B][H^+]}. \quad (2)$$

Combining (1) and (2) gives:

$$\bar{n} = \frac{\beta[H^+]}{1 + \beta[H^+]}. \quad (3)$$

The equivalent relation for a polyacidic base (yielding BH_m^{m+} on complete protonation) is:

$$\bar{n} = \frac{\sum_{i=1}^m i\beta_i[H^+]^i}{\sum_{i=0}^m \beta_i[H^+]^i}. \quad (4)$$

Dissociation of acids

The extent of dissociation of an acid HA is given by the function:

$$H = \frac{[A^-]}{[A^-] + [HA]} \quad (5)$$

which can be expressed in terms of $[H^+]$ and protonation constant of A^- :

$$H = \frac{1}{1 + \beta[H^+]}. \quad (6)$$

For a polybasic acid (H_mA):

$$H = \frac{m + \sum_{i=1}^{m-1} (m-i)\beta_i[H^+]^i}{\sum_{i=0}^m \beta_i[H^+]^i}. \quad (7)$$

It is a common property of (3) and (4) as well as of (6) and (7), that \bar{n} and H depend only on the

equilibrium constant and the hydrogen-ion activity, and are independent of the total (analytical) concentrations. Accordingly, \bar{n} and \bar{H} are intensive attributes of the material (acid or base) in question. Their actual value at a given pH are as characteristic of them in pH titrations as the molar absorption coefficient at a given wavelength is in spectrophotometry. Nevertheless, it does not make sense to introduce the term "molar protonation coefficients", since the term \bar{n} has long been familiar in equilibrium chemistry.

Experimental determination of \bar{n} and \bar{H}

From (3), (4), (6) and (7), \bar{n} and \bar{H} can be calculated from the equilibrium constants and hydrogen-ion activities. However, the equilibrium constants are only valid for the ionic strength, temperature, medium and circumstances under which they were determined. Furthermore, they are subject to the experimental error of their determination, which is especially significant, when the glass electrode is used, at the pH values at which the weakest bases or acids are protonated or deprotonated (as the case may be). Moreover, there are several substances for which the protonation constants are not known (e.g., polypeptides, proteins, nucleic acids, compounds of unknown structure), or cannot even be determined unambiguously (for example in non-aqueous medium). Consequently their \bar{n} or \bar{H} values cannot be calculated.

More reliable and strictly valid \bar{n} or \bar{H} values can be obtained by determinations made with a known amount of pure test substance. This can be done by two potentiometric titrations. In a blank titration sodium hydroxide (or simply water) is titrated potentiometrically with an acid titrant, and in the second titration an identical amount of hydroxide (or water) plus a known amount of weak base is titrated under the same conditions, to the same pH value. In this way the number of extra moles of titrant needed in the presence of the weak base, divided by the number of moles of weak base present, yields the \bar{n} value:

$$\bar{n} = \frac{\text{number of extra moles of acid}}{\text{number of moles of weak base}} \quad (8)$$

Figure 1 shows three titration curves, where in each case sodium hydroxide was accompanied by a weak base, the bases differing in strength. It is remarkable that the strongest of these bases, cyanide, can be well determined, whereas the less basic acetate, even in high concentration, can only be determined with much ambiguity by traditional evaluation methods, owing to its incomplete protonation during the second pH "break". The very weak base sulphate cannot be determined at all by simple evaluation methods, because it is only partially protonated, even at the lowest pH which can be reached by using 1M strong acid as the titrant. Nevertheless, from (8) and a third titration the number of moles of sulphate can be obtained from the measured extra number of moles

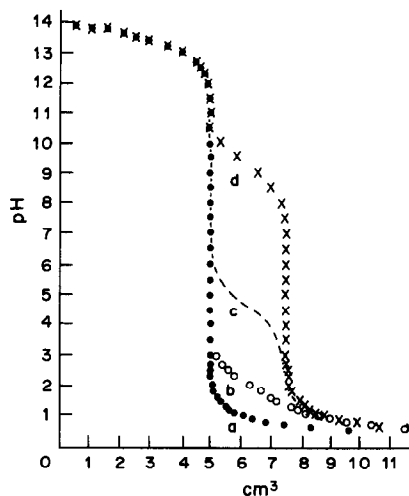


Fig. 1. Calculated titration curves for 5.0 of solution titrated with 1.0M HCl. a, 1.0M NaOH alone; b, 1.0M NaOH + 0.5M K_2SO_4 ; c, 1.0M NaOH + 0.5M CH_3COONa ; d, 1.0M NaOH + 0.5M KCN. The basicities of cyanide,⁶ acetate⁷ and sulphate⁸ were taken from the literature values recommended by Martell and Smith.⁹

of titrant needed and previously determined \bar{n} data as a function of pH. It is recommended to use a high ionic strength medium (e.g., 2M sodium perchlorate) for all three titrations, to eliminate matrix effects.

Determination of very weak acids can be done in an analogous manner by titrations with a base.

EXPERIMENTAL

We have developed a microtitration technique with a combined microelectrode suitable for pH determination in an initial volume of 0.6–1.0 ml. Accordingly, with 2.0M acid (HNO_3 , HCl, $HClO_4$) as titrant, as little as 0.02 g of sodium sulphate can be determined. If the amount of sulphate in the sample is approximately known, it is recommended to use as similar an amount of reference material as possible for the \bar{n} determination. Since different pH regions of the titration curves do not provide equally undistorted data, it is also advisable to check these \bar{n} values against known amounts of sulphate in one or two preliminary experiments. Normally the best parts of the titration curves to use for the analysis are those where the protonation of sulphate is already significant (10% or more), but the titration curves have not yet become horizontal. The amount of analyte can be calculated most conveniently by means of the equation

$$m_T = \frac{D_T}{D_S} m_S \quad (9)$$

where m_T and m_S are the numbers of moles of sulphate in the test sample and the reference standard respectively, and D_T and D_S are the corresponding distances of their titration curves from the sulphate-free titration curve at a given pH. D_T and D_S can be measured in the same arbitrary units (ml or mm on a graph) since only their ratio is significant.

Since the ratio D_S/m_S is a form of \bar{n} , equation (9) is also a simple, practical derivative of equation (8). It can be seen that by means of this equation the determination of sulphate is reduced to measurement of the titrant volumes. For accurate measurements of small volumes and their differences a Radiometer ABU 12 automatic burette was used.

All the potentiometric titrations were done by with use of an Orion Research 801-2 pH-meter with Ingold 104053059

Table 1. Experimental results for sulphate determinations under different conditions. A, B and C refer to the blank, standard and sample titration curves, respectively

Sulphate taken, g/100 ml		Found,* g/100 ml	Number of titration curves			Number of different pH values	pH	Medium
Standard	Sample		A	B	C			
7.1021	8.5221	8.6 ₀	1	1	1	1	0.4	NaCl, 2M
7.1021	8.5221	8.3 ₄	1	1	1	1	0.65	NaCl, 2M
7.1021	7.8122	7.8 ₀ ± 0.0 ₃	1	1	1	9	0.47-1.10	NaCl, 2M
2.8400	8.5206	8.4 ₀ ± 0.2 ₃	1	1	1	10	1.6-1.9	NaClO ₄ , 2M
8.5700	11.6680	11.7 ₄ ± 0.1 ₆	1	1	1	10	1.7-2.1	NaNO ₃ , 2M
4.3760	8.5742	8.6 ₂ ± 0.2 ₈	1	1	1	10	1.2-1.55	NaOOCCH ₃ , 0.12M NaNO ₃ , 2M
4.3500	2.7250	2.6 ₀ ± 0.1 ₂	1	1	1	10	0.07-0.92	NaNO ₃ , 2M
3.1188 } 4.9900 }	3.7425	3.7 ₄ ± 0.0 ₉	1	2	1	15	0.74-0.96	NaNO ₃ , 2.6-3.1M

*Mean ± 95% confidence limits.

combined electrode. The method requires neither temperature-control nor calibration of the cell, but the \bar{n} determination and the analytical measurements have to be made under strictly identical conditions. For approximate pH standardization, Radiometer pH 7.0 buffer was used.

All the chemicals were of analytical-reagent grade (Reanal, Hungary) and used without further purification.

RESULTS AND DISCUSSION

It can be seen in Fig. 1, that the sulphate and blank titration curves are identical above pH 3, owing to the negligible protonation of the sulphate, so this part of the titration is of no value for our purpose.

Table 1 shows experimental results for determination of sulphate in the presence of accompanying electrolytes at high concentrations. It can be seen that the sulphate determination is feasible in solutions of not only the less basic chloride, nitrate and perchlorate ions, but also in the presence of the significantly more basic acetate (and of course hydroxide) ions.

Since the acetate protonation is more than 99% complete below pH 2.7, this effect can be quantitatively taken into account at pH 0.1-1.9, where the evaluation of the sulphate content is best. The use of two standards, at greater and lower sulphate concentration than that of the sample, is recommended when the ionic strength is unknown or cannot be kept constant.

It is obvious from theoretical considerations that sulphate can be determined by this simple method without interference in the presence of all the halides and perhalates, carbonate, permanganate, sulphide and so on. Of the other common inorganic anions, phosphate, chromate and thiosulphate definitely interfere. In general, those bases with protonation constants ($\log K$) outside the range $\log K_{\text{SO}_4^{2-}} \pm 3$ do not interfere, the others do. Ions with $\log K > 4.5$ are protonated practically completely by the acid titrant before the sulphate is protonated, and nitrate and the other anions of very low basicity do not even begin to be protonated. Since SO_4^{2-} , $\text{S}_2\text{O}_3^{2-}$ and H_2PO_4^- are all protonated in a similar pH range, $\text{S}_2\text{O}_3^{2-}$ and

H_2PO_4^- seriously interfere. However, sulphate can still be determined in the presence of ions of similar basicity by potentiometric mixture analysis, which is an improved version of this evaluation method.¹⁰ Table 1 shows that even a single determination at one pH value (arbitrarily chosen) gives satisfactory results.

Interfering ions can be detected by the use of the titration data for several pH-values. Accurate measurements in the absence of interferents give the same, pH-independent, analytical results from different points over a wide pH range. If the protonation properties of the interfering ions are not identical to those of sulphate, they will cause a definite pH-dependence of the analytical data.

The protonation constant of sulphate decreases with increase in ionic strength.⁸ Accordingly, the lower the salt concentration in the titrated solution, the lower the concentration of sulphate that can be determined. Similarly, if the protonation of sulphate is promoted by a decrease in the dielectric constant of the medium (e.g., by use of a non-aqueous or partly aqueous solvent), the sensitivity of the method can be increased, by as much as two orders of magnitude.

The classical gravimetric methods for sulphate determination are certainly more accurate and precise, but simplicity, cheapness and rapidity are advantageous characteristics of this titrimetric type of determination of sulphate (and other very weak bases and acids).

REFERENCES

1. W. J. Williams, *Handbook of Anion Determination*, Butterworths, London, 1979.
2. G. Gran, *Analyst*, 1952, **77**, 661.
3. A. Ivaska and I. Nagypál, *Magy. Kém. Foly.*, 1980, **86**, 84.
4. K. Burger, G. Pethő and B. Noszál, *Anal. Chim. Acta*, 1980, **118**, 93.
5. N. Bjerrum, *Z. Anorg. Chem.*, 1921, **119**, 179; J. Bjerrum, *Metal Ammine Formation in Aqueous Solution*, Haase, Copenhagen, 1941.

6. K. P. Ang, *J. Chem. Soc.*, 1959, 3822.
7. I. Feldman and L. Koval, *Inorg. Chem.*, 1963, 2, 145.
8. C. W. Davies, H. W. Jones and C. B. Monk, *Trans. Faraday Soc.*, 1952, 48, 921.
9. R. M. Smith and A. E. Martell, *Critical Stability Constants*, Vol. 4, Plenum Press, New York, London, 1977.
10. B. Noszál and M. Juhász, in preparation.

SEPARATION OF BISMUTH FROM GRAM AMOUNTS OF THALLIUM AND SILVER BY CATION-EXCHANGE CHROMATOGRAPHY IN NITRIC ACID

E. MEINTJES, F. W. E. STRELOW and A. H. VICTOR

National Chemical Research Laboratory, Council for Scientific and Industrial Research,
P.O. Box 395, Pretoria 0001, Republic of South Africa

(Received 29 October 1986. Accepted 8 November 1986)

Summary—Traces and small amounts of bismuth can be separated from gram amounts of thallium and silver by successively eluting these elements with 0.3M and 0.6M nitric acid from a column containing 13 ml (3 g) of AG50W-X4, a cation-exchanger (100–200 mesh particle size) with low cross-linking. Bismuth is retained and can be eluted with 0.2M hydrobromic acid containing 20% v/v acetone, leaving many other trace elements adsorbed. Elution of thallium is quite sharp, but silver shows a small amount of tailing (less than 1 µg/ml silver in the eluate) when gram amounts are present, between 20 and 80 µg of silver appearing in the bismuth fraction. Relevant elution curves and results for the analysis of synthetic mixtures containing between 50 µg and 10 mg of bismuth and up to more than 1 g of thallium and silver are presented, as well as results for bismuth in a sample of thallium metal and in Merck thallium(I) carbonate. As little as 0.01 ppm of bismuth can be determined when the separation is combined with electrothermal atomic-absorption spectrometry.

The separation of bismuth from other elements by ion-exchange chromatography has received considerable attention during the past few decades. A method was described by Lurje *et al.*¹ who showed that bismuth is eluted by 0.05M sulphuric acid, containing 1% of potassium iodide, from a cation-exchange column, while copper and lead are retained; this was probably the first of the numerous methods published. One of the most generally applicable methods originates from the work of Nelson *et al.*² who showed that bismuth is retained by strongly basic anion-exchange resins from hydrochloric acid over practically the whole acid concentration range. Lead can be eluted with 8M hydrochloric acid, followed by elution of iron(III) and most other elements with 0.5M hydrochloric acid, bismuth being retained; it can be eluted with 1M sulphuric acid. Cadmium, zinc and indium are not effectively eluted with 0.5M hydrochloric acid. Numerous applied and adapted versions of this method have appeared in the literature. Furthermore, in hydrochloric acid–ammonium fluoride mixtures, elements such as tin, germanium, arsenic and antimony can be separated from bismuth.³

Probably the most selective method, which separates bismuth from almost all other elements, is anion-exchange in nitric–hydrobromic acid mixtures.⁴ By elution with 0.03M hydrobromic acid in 2M nitric acid, even gram amounts of cadmium can be separated from traces of bismuth, with only a very small column. This separation is not possible in pure hydrochloric or hydrobromic acid solutions by anion-exchange because both elements are very strongly retained down to very low acid concen-

trations and show only small differences in their anion-exchange behaviour.

Aqueous hydrohalic acids and their mixtures with other acids or with organic solvents are not suitable for the separation of bismuth from large amounts of thallium and silver because thallium(I) chloride and bromide are only sparingly soluble, the silver compounds are insoluble, and thallium(III) is very strongly retained over the whole acid concentration range (similarly to bismuth). In the nitric–hydrobromic acid mixtures described above,⁴ separation of thallium(I) from bismuth could become possible provided that the formation of bromine through oxidation by nitric acid, leading to the formation of thallium(III) (which is very strongly adsorbed), could be suppressed by addition of a suitable reducing agent such as sulphur dioxide. However, only limited amounts of thallium(I) could be handled because of precipitate formation. The separation of silver would once again not be possible. Furthermore, it has been shown that bismuth is selectively sorbed from ammonium nitrate solutions by anion-exchange resins,⁴ but the distribution coefficient for bismuth (about 90 in 8M ammonium nitrate medium) is not very high. The high salt concentration could cause problems, and the behaviour of thallium and silver does not seem to have been investigated. A better separation with a larger distribution coefficient for bismuth can be obtained when nitric acid–methanol mixtures are used instead of ammonium nitrate, and co-sorbed thorium, lanthanides and lead are eluted with hydrochloric acid–methanol mixtures before the final elution of bismuth with 1M nitric acid.⁵ Unfortunately, the

exchange rates with the 8% cross-linked resin used are rather low with the nitric acid-methanol mixtures. In addition, the nitrates of thallium(I) and silver have only limited solubility in methanol and ethanol.

This paper presents an alternative approach which can be used to separate traces and also small amounts of bismuth from gram amounts of thallium and silver, with only small resin columns. It has been shown recently that the cation-exchange separation of indium and silver in nitric acid can be considerably improved by using a resin with low cross-linking (AG50W-X4) instead of the usual AG50W-X8 resin.⁶ The improved separation is due to the fact that with the lower cross-linking all cations are somewhat less strongly sorbed and the exchange rates are considerably faster and more favourable, especially for strongly sorbed univalent elements such as silver and thallium, which tend to tail considerably with the AG50W-X8 resin. As a result, silver and thallium should be eluted quantitatively at considerably lower nitric acid concentrations. Because the distribution coefficients of univalent elements decrease linearly with increase in hydrogen-ion concentration, while those of trivalent elements decrease in proportion to the third power of increasing hydrogen-ion concentration, elution with a lower concentration of nitric acid considerably enhances the separation factor between uni- and trivalent cations.

According to published data⁷ thallium is only slightly more strongly sorbed than silver by the 8% cross-linked resin. Bismuth is somewhat less strongly sorbed than indium, but the distribution coefficient of 379 in 0.5M nitric acid is still sufficiently large (the coefficient given in reference 7 was in error). No experimentally determined coefficients seem to be available for a 4% cross-linked resin, though our own experience indicates that the same pattern should be followed, with coefficient values around 60% of those obtained with the AG50W-X8 resin.

This seems to suggest favourable conditions for a separation of bismuth from large amounts of thallium and silver. The quantitative aspects of such a separation have been investigated and are described here.

EXPERIMENTAL

Reagents and apparatus

Analytical reagent grade chemicals were used. Water was distilled and then demineralized. The resin used was the AG50W-X4 strongly acid sulphonated polystyrene cation-exchanger, 100-200 mesh particle size, in the hydrogen form. Borosilicate glass tubes (14.6 mm bore and 200 mm long) joined to a wider upper part (20 mm diameter and 100 mm long) served as columns. The columns were fitted with a porosity-1 sintered-glass disc and a burette tap at the bottom and a B19 ground-glass socket at the top to hold a dropping funnel as a reservoir. The columns were filled with a slurry of resin until the settled resin reached a mark corresponding to 13.0 ml (\approx 3.0 g of dry resin). The resin was washed with 100 ml of 3.0M nitric acid (to remove

traces of chloride impurities) and then equilibrated with 50 ml of 0.2M nitric acid.

Atomic-absorption measurements were made with a Varian-Techtron AA-5 instrument. An automatic Aimer Central Fractionator was used to collect fractions for the preparation of the elution curves.

Elution curves

Separation of Tl(I) from Bi(III). A mixture containing 2 g of thallium and 10 mg of bismuth in 200 ml of 0.2M nitric acid was prepared and passed through an equilibrated resin column. The elements were washed onto the resin with five 10-ml portions of 0.3M nitric acid. Elution was done with 200 ml of 0.6M nitric acid for thallium and 100 ml of 0.2M hydrobromic acid-20% v/v acetone for bismuth. A flow-rate of 4.0 ± 0.5 ml/min was maintained throughout. Fractions of 20 ml were collected from the beginning of the sorption step, by use of the automatic fractionator. The amounts of the elements in each fraction were determined by atomic-absorption spectrometry, with the air-acetylene flame, at the 276.8 and 223.1 nm lines for thallium and bismuth, respectively. Larger amounts of thallium were determined by complexometric titration of thallium(III) (after oxidation with bromine) with EDTA at pH 9.0, with Methylthymol Blue (sodium salt) as indicator.⁸ The experimental curve is shown in Fig. 1.

Separation of Ag(I) from Bi(III). A mixture containing 1.3 g of silver and 2 mg of bismuth in 200 ml of 0.2M nitric acid was prepared and passed through an equilibrated resin column. The elements were washed onto the resin with five 10-ml portions and one 50-ml portion of 0.3M nitric acid. Elution was done with 250 ml of 0.6M nitric acid for silver and 100 ml of 0.2M hydrobromic acid-20% v/v acetone for bismuth. A flow-rate of 4.0 ± 0.5 ml/min was maintained throughout. Fractions of 20 ml were collected from the beginning of the sorption step, with the automatic fractionator. The amounts of the elements in each fraction were determined by atomic-absorption spectrometry, with the air-acetylene flame, and the 328.1 and 223.1 nm lines for silver and bismuth, respectively. Larger amounts of silver were determined by titration with potassium thiocyanate, with ferric iron solution as indicator. The experimental curve is shown in Fig. 2.

Quantitative separations of synthetic mixtures

A series of columns containing 13.0 ml of AG50W-X4 resin was prepared as described above. Appropriate volumes of standard solutions of bismuth and thallium nitrates in dilute nitric acid were measured out accurately in triplicate, mixed, and adjusted to give a final volume of 200 ml with 0.2M nitric acid concentration. Three extra portions of each standard solution were measured out and kept separately for comparison. The mixtures were passed through the resin columns, which had been equilibrated with 0.2M nitric acid. The elements were washed onto the resin with five 20-ml portions of 0.3M nitric acid. Thallium was eluted with 200 ml of 0.6M nitric acid, and collected from the beginning of the sorption step. Bismuth was eluted with 100 ml of 0.2M hydrobromic acid-20% v/v acetone. The bismuth eluates were evaporated to dryness on a water-bath and the organic matter oxidized by heating with 2 ml of concentrated nitric acid and 0.5 ml of concentrated perchloric acid and evaporation to small volume. The residue was taken up in enough nitric acid to give a final concentration of 0.2M when made up to the appropriate volume. Blanks were run through the whole procedure. The amounts of the elements in the eluates and in the standard solutions were determined. When necessary, thallium was determined by complexometric titration with EDTA, and traces of thallium and the amounts of bismuth in the bismuth fractions were determined by atomic-absorption spectrometry as described above. Table 1 presents the results obtained.

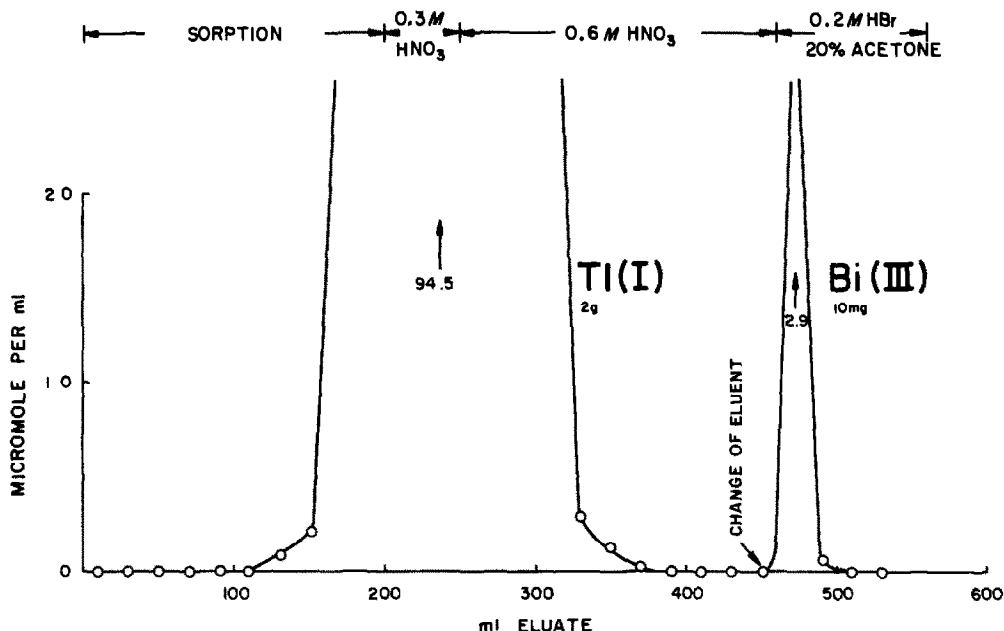


Fig. 1. Elution curve for Bi(III)-Tl(I): 13 ml (3 g) of AG50W-X4 resin, 100-200 mesh; column length 80 mm, diameter 14.6 mm; flow-rate 4.0 ± 0.5 ml/min.

Quantitative separations of bismuth and silver were performed in the same manner except that five 20-ml portions and one 50-ml portion of 0.3M nitric acid were used to wash the elements onto the resin and 250 ml of 0.6M nitric acid were used to elute the silver. Large amounts of silver were determined by titration with potassium thiocyanate as described above. Table 1 gives the results.

Determination of bismuth in analytical-grade reagents

Thallium metal (14.2204 g) or thallium(I) carbonate (22.9363 g) was dissolved by heating with a calculated

amount of nitric acid (enough to form the nitrate and to give a final concentration of 0.2M nitric acid in 500 ml). The solutions were diluted to 500 ml and 50-ml aliquots were measured out in quadruplicate. Each was diluted to 200 ml and enough nitric acid added to give 0.2M concentration. The bismuth was then separated on 3-g resin columns as described above. Duplicate blanks were run through the whole procedure and the results were corrected accordingly. The bismuth-containing fractions were evaporated to dryness and the organic matter oxidized as described above. The solutions were finally made up to 10 ml in volume with

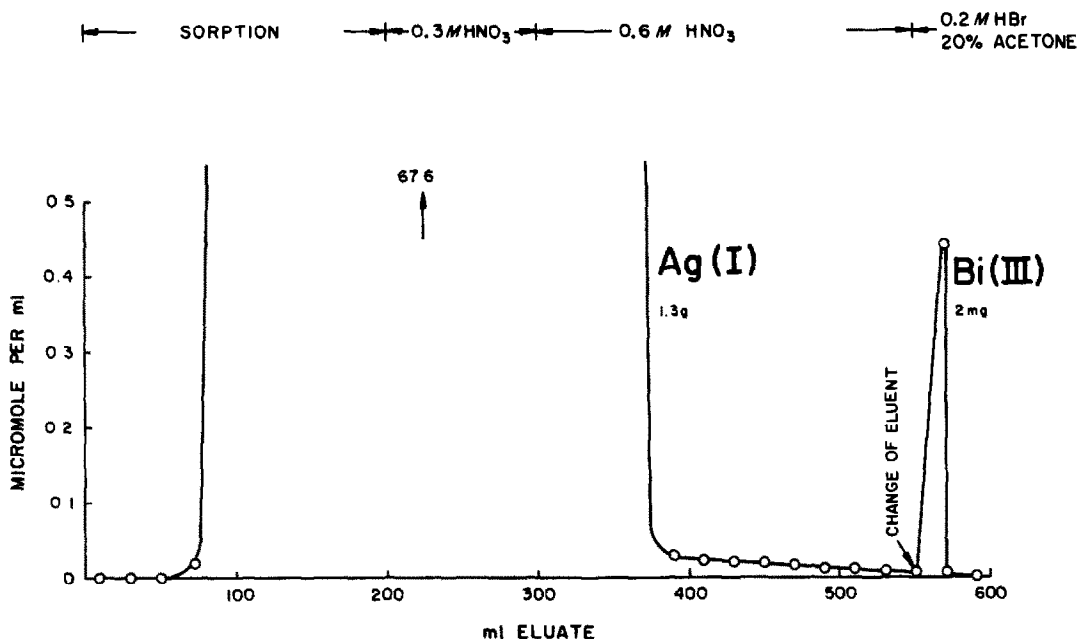


Fig. 2. Elution curve for Bi(III)-Ag(I). Column, resin and flow-rate as for Fig. 1.

Table 1. Quantitative separations of synthetic mixtures

Amount taken, mg			Amount found,* mg		Amount of other ion found in Bi fraction, μg
Other	ion	Bi	Other ion	Bi	
Tl(I)	2000	10.40	n.d.†	10.42 \pm 0.03	
Tl(I)	199.0	9.89	198.9 \pm 0.8	9.85 \pm 0.03	0
Tl(I)	2000	0.1980	n.d.	0.1985 \pm 0.0007	12-17
Tl(I)	2000	0.0495	n.d.	0.0495 \pm 0.0001	11-17
Ag(I)	1300	10.00	n.d.	10.01 \pm 0.01	43-78
Ag(I)	130.28	10.00	130.08 \pm 0.09	10.02 \pm 0.02	6-45
Ag(I)	1300	0.198	n.d.	0.197 \pm 0.001	26-79
Ag(I)	1300	0.0495	n.d.	0.0491 \pm 0.0014	20-78

*Results are the means of at least triplicate runs.
†n.d., not determined.

Table 2. Determination of bismuth in analytical grade chemicals

Chemical	Source	Amount taken, g	Bismuth content
Thallium metal puriss	Fluka	1.4220	2.37 \pm 0.11 $\mu\text{g/g}$
Tl ₂ CO ₃ , analytical reagent grade	Merck	2.2936	12 \pm 3 ng/g

0.2M nitric acid. Bismuth was determined by electrothermal atomic-absorption spectrometry as described below. The results are presented in Table 2.

Electrothermal atomic-absorption spectrometry

A Perkin-Elmer model 4000 atomic-absorption spectrometer with a deuterium arc background corrector was used in conjunction with a Perkin-Elmer HGA-500 graphite furnace. Pyrolytically coated graphite tubes (6 mm bore, 28 mm in length) were obtained from Pyrocarbo, Pretoria. The bismuth hollow-cathode lamp was operated at 7 mA and monitored at 223.0 nm, with a band-pass of 0.2 nm. Samples were dispensed into the graphite tube with a Perkin-Elmer AS-40 autosampler, capable of delivering 20- μl samples with a precision of $\pm 1\%$. Argon (African Oxygen Ltd, spectrographic grade) was used as sheath gas.

Aliquots (20 μl) of standards and samples, each containing 50 $\mu\text{g/ml}$ Ni were analysed under the operating conditions described in Table 3. The presence of 50 $\mu\text{g/ml}$ nickel in the standard bismuth solutions increased the sensitivity by an average of about 30%, and the reproducibility was also considerably improved (coefficient of variation less than 1%). A minimum of four analyses was performed on each solution. As the absorbance values tend to vary according to the condition of the tube, the readings for standards and samples were taken alternately during the same run, the standard chosen being the one which gave a reading nearest to that of the unknown.

DISCUSSION

The results obtained after the quantitative sep-

arations of binary synthetic mixtures are presented in Table 1 and those from some analytical grade chemicals in Table 2. The method described provides a useful means for the quantitative separation of bismuth from large amounts of strongly retained univalent cations such as thallium(I) and silver(I) and demonstrates that only by use of a resin with a low cross-linking does such a separation become relatively easy. With the usual 8% cross-linked resin, both thallium(I) and silver tail considerably, even when eluted with 1.0M nitric acid, while the distribution coefficient of bismuth is considerably lower at this acid concentration and longer columns are required. This makes the separation problematical. Most other elements, including indium, gallium, zinc, lead(II) and iron(III) are still retained when bismuth is eluted from the AG50W-X4 resin with 0.2M hydrobromic acid containing 20% v/v acetone. The accurate determination of bismuth in thallium metal and compounds thus becomes possible even when it occurs at very low trace levels.

Separations of bismuth from thallium are sharp and recoveries quantitative, as indicated by the elution curve (Fig. 1) and the results for the determination in the synthetic mixtures containing amounts ranging from 50 μg to 10 mg of bismuth (Table 1). When the separation is combined with a method of determination which is of sufficient sensitivity such as electrothermal (furnace) atomic-absorption spectrometry, even bismuth at concentrations as low as a few ng/g in solid samples can still be separated and determined successfully, as indicated by results obtained for bismuth in analytical grade thallium(I) carbonate (Table 2), although the reproducibility of the results is somewhat poorer. It was found that when the furnace method was used for determination, the presence of 50 $\mu\text{g/ml}$ nickel in

Table 3. Operating conditions for the graphite furnace

Step	Temperature, $^{\circ}\text{C}$	Ramp time, sec	Hold time, sec	Internal gas flow, ml/min
1	110	40	20	300
2	500	15	5	300
3	2300	0	5	20
4	2600	2	5	300

the solutions leads to an increase of about 30% in the sensitivity for bismuth and a considerable improvement in reproducibility. The amounts of thallium found in the bismuth fraction were always below 20 μg when 2 g were present originally. These amounts did not interfere with the determinations.

When bismuth was separated from silver a small amount of tailing at a level of less than 1 $\mu\text{g}/\text{ml}$ silver in the eluate was observed and between 20 and 80 μg of silver was found in the bismuth fractions. The tailing did not disappear completely even after 700 ml of 0.6M nitric acid had been passed through the column. However the amount of silver found in the bismuth fraction did not interfere significantly with the determination of bismuth by flame atomic-absorption spectrometry.

REFERENCES

1. J. J. Lurje and N. A. Filipova, *Zavodsk. Lab.*, 1948, **14**, 159; *Chem. Abstr.*, 1948, **42**, 8696.
2. F. Nelson and K. A. Kraus, *J. Am. Chem. Soc.*, 1954, **76**, 5916.
3. F. Nelson, R. M. Rush and K. A. Kraus, *ibid.*, 1960, **82**, 339.
4. F. W. E. Strelow and T. N. van der Walt, *Anal. Chem.*, 1981, **53**, 1637.
5. S. S. Ahluwalia and J. Korkisch, *Z. Anal. Chem.*, 1965, **208**, 414.
6. T. N. van der Walt, F. W. E. Strelow and R. J. N. Brits, *Int. J. Appl. Radiat. Isot.*, 1985, **6**, 501.
7. F. W. E. Strelow, R. Rethemeyer and C. J. C. Bothma, *Anal. Chem.*, 1965, **37**, 106.
8. F. W. E. Strelow and F. Von S. Toerien, *Anal. Chim. Acta*, 1966, **36**, 189.

BEHAVIOUR OF A CHALCOCITE COPPER ION-SELECTIVE ELECTRODE IN SOLUTIONS OF IRON(III) IONS

ADAM HULANICKI and TADEUSZ KRAWCZYŃSKI VEL KRAWCZYK
Department of Chemistry, Warsaw University, Warsaw, Poland

(Received 9 June 1986. Accepted 8 November 1986)

Summary—The effect of iron(III) ions on the potential of the chalcocite electrode was investigated. Linear graphs were obtained for $p\text{Fe(III)} = 2-4$, and were suitable for analytical purposes. The effect of ligands complexing iron(III) was studied, and the potential shown to be due to the concentration of free iron(III) ions only. The pH effect is mainly connected with solution reactions. A mechanism of potential response, based on a redox reaction, has been postulated, but the response does not depend on the redox potential in the bulk of the solution.

Copper(I) is nominally the primary ion for the chalcocite membrane electrode, but in many analytical conditions its concentration can be neglected in comparison to that of other potential-influencing ions. Such ions include copper(II), for determination of which the chalcocite electrode is usually applied. Another important interferent is iron(III). The selectivity coefficient $K_{\text{Cu}^+, \text{Fe(III)}}^{\text{pot}}$ is as high as 20.¹ Some authors^{2,3} indicate that the potential of the copper-selective electrode is influenced by iron(III) even when copper is present in tenfold ratio to it. It has also been observed⁴ that the membrane dissolves in the presence of iron(III). To avoid the harmful effect of iron(III) on copper(II) determinations the interferent should be masked by fluoride^{3,5-7} or citrate⁸ or precipitated as the hydrous oxide.^{9,10} The last procedure can, however, lead to co-precipitation errors.¹⁰ The aim of this study was to elucidate the mechanism of the iron(III)-response of the copper ion-selective electrode. Understanding of the electrode behaviour in various conditions may be useful in practical applications for analytical determination of iron.

EXPERIMENTAL

Reagents

All reagents were of analytical grade, and their solutions were prepared with triply distilled water.

Standard solutions of iron(III), 0.980 and 0.985M, as the nitrate and sulphate, respectively, were acidified with the appropriate acids. Working solutions were prepared by dilution with water. A standard solution of iron(II) was kept under argon to prevent its aerial oxidation.

Apparatus

The chalcocite copper ion-selective electrode was of our own construction and its properties were investigated earlier.¹¹⁻¹³ For potential and pH measurements, Beckman model 4500 and Orion model 701 pH-meters were used with the chalcocite electrode and a Beckman 39301 glass electrode. As reference, an Orion 90-02 double-junction electrode was used.

Procedure

The working curve of potential as a function of Fe(III) concentration was prepared by addition of standard iron(III) solution to a solution containing 5 ml of 2M sodium nitrate or 0.5M magnesium sulphate, and 95 ml of distilled water. The pH was adjusted to 1-2 by addition of concentrated nitric or sulphuric acid. The solution was stirred continuously with a magnetic stirrer and deaerated with a stream of argon for 30 min. The potential was read when the drift was not more than 0.1 mV/min. The electrode surface was polished with emery paper wetted with 1% ascorbic acid solution.

RESULTS AND DISCUSSION

Dependence of electrode potential on $\log [\text{Fe}^{3+}]$

The working curve for determination of iron(III) was determined for the $p\text{Fe(III)}$ range 2-5. The standard solutions were prepared by addition of iron(III) nitrate to a solution of pH 2.00. The pH was corrected with sodium hydroxide solution after each addition (Fig. 1, curve 1). Transient formation of Fe(OH)_3 was observed. The slope of the curve was 28.5 mV/ $p\text{Fe(III)}$, less than that for solutions without pH correction (Fig. 1, curve 2) for which the final pH was 1.78 at $p\text{Fe(III)} = 2$, and the slope was 31 mV/ $p\text{Fe(III)}$. It is probable that formation of inert polynuclear hydroxide complexes during the pH-adjustment may be responsible for this behaviour; however, the conditioning of the electrode before measurements also has an effect on the electrode characteristics. The behaviour described was found for electrodes which were kept dry before measurements. When an electrode was conditioned in 1M copper nitrate, the slope was 27 mV/ $p\text{Fe(III)}$ (Fig. 1, curve 3). The linear ranges also differed for these curves, the shortest being that for the electrode treated in copper solution. The reproducibility of the slope [1 mV/ $p\text{Fe(III)}$] and the constancy of E° (5 mV) were worst when the electrode surface was freshly

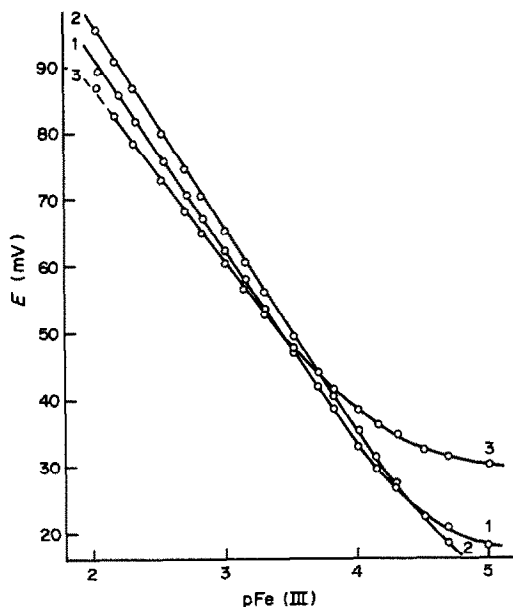


Fig. 1. Working curves for the chalcocite electrode in iron(III) nitrate solution, with various electrode pretreatments (see text).

polished. It has been stated that polishing is in general not necessary, especially when the iron(III) concentration is less than $10^{-2}M$, and this indicates that at pH 2 the membrane corrosion is negligible, which is not the case at pH 1.

Electrode response at various pH values

Increasing the pH above 2 has a disadvantageous effect on the solution conditions, because of formation of hydroxide complexes of iron(III), and the possibility of forming polynuclear species.

The formation constant of $Fe(OH)^{2+}$ is $\log \beta_1 = 11.8$,¹⁴ so at pH 2 and 1, the side-reaction coefficients $\alpha_{Fe(OH)}$ are 1.64 and 1.06, respectively.

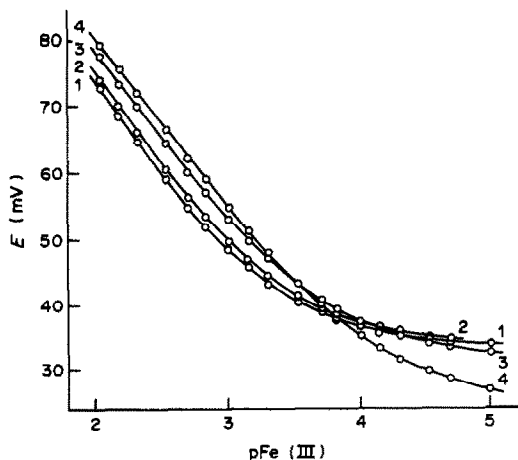


Fig. 2. Working curves for the chalcocite electrode at various pH values. 1, pH 1.0; 2, pH 1.3; 3, pH 1.7; 4, pH 2.0.

This suggests that the working curve should shift toward more positive potentials by approx. 6 mV. The experimental curves, however, show a reverse shift of 10 mV (Fig. 2). This is most probably caused by a change of the liquid-junction potential when the double-junction reference electrode is used. This change, measured *vs.* a chloride ion-selective electrode, is -20 mV, which swamps the change due to the side-reaction. A difference of 4 mV can be attributed to corrosion processes at pH 1.

Effect of complexation and redox potential

Hydroxide complexation does not explain completely the effect of decreasing the concentration of Fe(III), because of accompanying effects due to the pH change. A better insight is obtained when measurements in nitrate solutions are compared with measurements in sulphate solutions, with magnesium sulphate to keep the ionic strength constant (Fig. 3). At $pFe(III) = 3$, the potential is 15 mV lower in sulphate medium than in nitrate, because the iron(III)-sulphate complex is stronger.

In the presence of strong complexing agents (phosphate, citrate) the potential of the electrode is independent of the iron(III) concentration, but depends only on the pH and ligand concentration. The iron(III) is presumably completely complexed by strong ligands, and the potential governed by the residual copper(II) interactions, which are activated by the presence of oxygen in the solution.

When the solution contains higher levels of iron(III), the deaeration with argon has little effect on

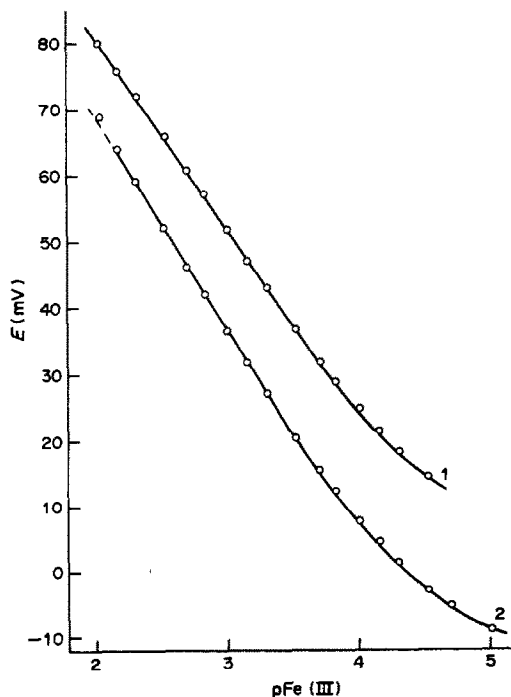


Fig. 3. Comparison of working curves in potassium nitrate (curve 1), and magnesium sulphate (curve 2) media.

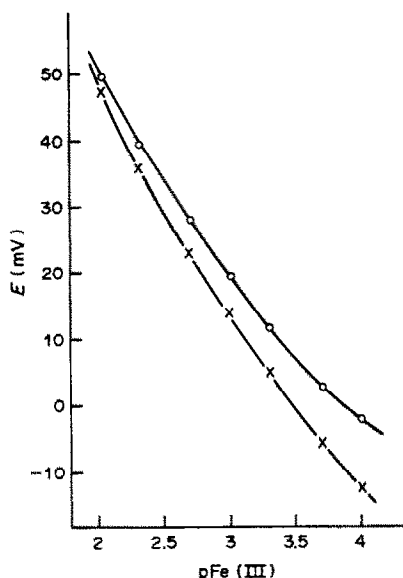


Fig. 4. Potential of the chalcocite electrode in the presence of iron(II). The ratio $C_{\text{Fe}^{2+}}/C_{\text{Fe}^{3+}} = 5:4$ is constant; pH = 1; ○—electrode without polishing, solution not deaerated; ×—electrode polished before measurements, deaerated solution.

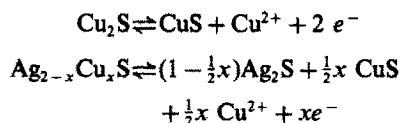
the electrode response. A series of measurements was performed in the presence of both components of the Fe(III)/Fe(II) redox couple at a constant ratio of 5:4 (Fig. 4), and therefore of constant redox potential. In this case, the presence of iron(II) had a small effect on the electrode response and the electrode potential was a function of only the iron(III) concentration. A small difference observed between readings in the presence and absence of oxygen was probably caused by slight oxidation of iron(II) to iron(III) when the solution was not deaerated. The iron(II) ions alone exert an effect similar to or weaker than that of other bivalent transition-metal ions. These experiments indicate that only the iron(III) is responsible for the electrode behaviour.

Mechanism of electrode function

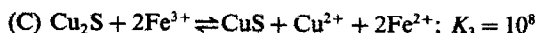
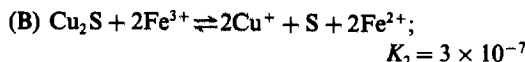
There has been some controversy concerning the mechanism of the iron(III) interaction with copper ion-selective electrodes. Although different types of copper electrodes differ in initial composition, it has been stated by several investigators, who used various techniques (including X-ray diffraction),^{15,16} that they all contain jalpaite ($\text{Ag}_{1.5}\text{Cu}_{0.5}\text{S}$), which is largely responsible for the electrode properties.

Savvin *et al.*,¹⁷ using the Cu_2S electrode, have postulated a simple exchange mechanism, which they base on the values of the solubility products of corresponding salts. Smith and Manahan³ and Fung and Fung¹⁸ have suggested oxidation of the sulphides in the $\text{Ag}_2\text{S} + \text{CuS}$ membrane. Zhukov *et al.*¹⁹ have presented similar suggestions for Cu_{2-x}Se and Cu_{2-x}Te membranes, which also contain the corresponding silver salts. On the basis of their experi-

ments, Heijne *et al.*^{15,20} suggest the occurrence of the oxidation reactions:



Taking into account all these suggestions, three different mechanisms may be responsible for the iron(III) interference and the iron(III) function of the copper electrode:



for which the equilibrium constants were calculated from data given in Table 1.

For chalcocite membrane electrodes, the potential depends on the concentrations of copper(I) and copper(II) according to the equations

$$E = E^0 + 59.2 \log [\text{Cu}^+] \quad (1)$$

$$E = E^0 + 29.6 \log [\text{Cu}^{2+}] \quad (2)$$

If the concentration of copper(I) is calculated from the equilibrium constant of reaction (A) then

$$[\text{Cu}^+] = \sqrt[6]{K_1[\text{Fe}^{3+}]^2} = \sqrt[6]{K_1[\text{Fe}^{3+}]^{1/3}} \quad (3)$$

Substitution into equation (1) shows the electrode slope should be 59.2/3 mV/pFe(III) which is close to 20 mV/pFe(III), which is in disagreement with the experimental value.

When scheme (B) is assumed, the concentration of copper (I) is given as:

$$[\text{Cu}^+] = \frac{[\text{Fe}^{3+}]K_2}{[\text{Fe}^{2+}]} \quad (4)$$

Two cases can be discussed here. In the first, the iron(II) ions originate only from the indicated reaction. Then

$$[\text{Cu}^+] = [\text{Fe}^{2+}] \quad (5)$$

and

$$[\text{Cu}^+]^2 = K_2[\text{Fe}^{3+}] \quad (6)$$

or

$$[\text{Cu}^+] = \sqrt{K_2[\text{Fe}^{3+}]} \quad (7)$$

Table 1. Constants used in calculations

Constant	Value	Ref.
$K_{s0}(\text{Cu}_2\text{S})$	10^{-48}	14
$K_{s0}(\text{CuS})$	10^{-36}	14
$K_{s0}(\text{Fe}_2\text{S}_3)$	10^{-88}	17, 21
$K_1(\text{H}_2\text{S})$	$10^{-13.9}$	14
$K_2(\text{H}_2\text{S})$	$10^{-7.02}$	14
$E_{\text{Fe}^{3+}/\text{Fe}^{2+}}^0$	749 mV	22
$E_{\text{Cu}^{2+}/\text{Cu}^+}^0$	158.6 mV	22
$E_{\text{S}/\text{S}^{2-}}^0$	-476.3 mV	22

This would be confirmed by a slope of 30 mV/pFe(III), which agrees with the experimental data. However, if an excess of iron(II) is added and kept at a constant level, then

$$[\text{Cu}^+] = \frac{[\text{Fe}^{3+}]K_2}{\text{const}} \quad (8)$$

and the slope should be 59.2 mV/pFe(III), which is not observed experimentally. The addition of large amounts of iron(II) influences neither the response slope nor the potential values. The validity of mechanism (B) requires also that the addition of $10^{-3}M$ iron(II) to $10^{-3}M$ iron(III) should decrease the concentration of copper(I) at the membrane surface from $5.2 \times 10^{-4}M$ to $3.0 \times 10^{-4}M$, leading to a potential change of 7–8 mV, which was not experimentally observed. It is also difficult to imagine why an equilibrium constant of the order of 10^{-7} could give an experimental selectivity coefficient in the range 0.1–1.0.

The most probable mechanism seems to be (C). The reaction should be strongly shifted to the right and consequently the concentration of copper(II) at the membrane surface would be equal to half the iron(III) concentration in the bulk solution. Thus

$$[\text{Cu}^{2+}]_0 = \frac{1}{2}[\text{Fe}^{3+}] \quad (9)$$

and the expected slope should be close to 29.6 mV/pFe(III). The potential values of the electrode for given iron(III) concentrations should be about 9 mV more positive than for copper(II) under similar experimental conditions. This is within 1 mV of the measured values. The concentration of copper(I) at the membrane surface calculated from the equilibrium constants should be independent of iron(II) concentration, which is in fact observed. The large value of the equilibrium constant for mechanism (C) also suggests that the value of the selectivity coefficient should be close to units. In such a case, a rapid establishment of a stationary state must be assumed, as is the case for the iodide ion-selective membrane used for cyanide measurements. In that case, the CuS layer forms a diffusion barrier.

Mechanism (C) is also supported by Pomianowski,²³ who postulates similar reactions in his study of the corrosion of certain minerals, including chalcocite.

CONCLUSIONS

The chalcocite copper ion-selective electrode may be used as an iron(III) electrode. The response slope

is close to 29.6 mV/pFe(III), and the response is thought to be due to the reaction:



The electrode may be used for determination of iron(III) and has been successfully applied to analysis of the acid solutions used for desulphuration of coal-gas, for iron(III) at concentrations $> 10^{-4}M$.²⁴

Acknowledgements—This work was supported through the project MR-I-32 and CPBP-01.17. The authors are grateful to Dr. Andrzej Lewenstam and mgr Tomasz Sokalski for fruitful discussions.

REFERENCES

1. M. Neshkova and J. Havas, *Anal. Lett.*, 1983, **16**, 1567.
2. T. Aomi, *Denki Kagaku*, 1978, **46**, 259.
3. M. J. Smith and S. E. Manahan, *Anal. Chem.*, 1973, **45**, 836.
4. M. Neshkova and H. Sheytanov, *J. Electroanal. Chem.*, 1979, **102**, 189.
5. A. Hulanicki, M. Trojanowicz and T. Krawczyński vel Krawczyk, *Water Res.*, 1977, **11**, 627.
6. Y. S. Fung and K. W. Fung, *Analyst*, 1978, **103**, 149.
7. M. Taddia and P. Lanza, *Ann. Chim. (Rome)*, 1975, **65**, 719.
8. A. Hulanicki, T. Krawczyński vel Krawczyk and M. Trojanowicz, *Chem. Anal. Warsaw*, 1979, **24**, 435.
9. A. Varma, *Talanta*, 1981, **28**, 785.
10. G. K. Rice and R. J. Jasiński, *NBS Special Publ. No. 422*, 1976, 899.
11. A. Hulanicki, M. Trojanowicz and M. Cichy, *Talanta*, 1976, **23**, 47.
12. A. Hulanicki, T. Krawczyński vel Krawczyk and A. Lewenstam, *Anal. Chim. Acta*, 1984, **158**, 343.
13. A. Lewenstam, in *Ion Measurements in Physiology and Medicine*, M. Kessler, D. K. Harrison and J. Hoepfer (eds.), p. 24. Springer-Verlag, Berlin, 1985.
14. R. M. Smith and A. E. Martell, *Critical Stability Constants*, Vol. 4, Plenum Press, New York, 1975.
15. G. J. M. Heijne and W. E. van der Linden, *Anal. Chim. Acta*, 1977, **93**, 99.
16. S. Ikeda, N. Matsuda, G. Nakagawa and K. Ito, *Denki Kagaku*, 1980, **48**, 16.
17. N. I. Savvin; V. S. Shterman, A. V. Gordievskii and A. Ya. Syrchenkov, *Zavodsk. Lab.*, 1971, **37**, 1025.
18. Y. S. Fung and K. W. Fung, *Anal. Chem.*, 1977, **49**, 497.
19. A. F. Zhukov, A. V. Vishnyakov, Yu. I. Urusov, A. V. Kopytin and A. V. Gordievskii, *Zavodsk. Lab.*, 1980, **46**, 13.
20. G. J. M. Heijne, W. E. van der Linden and G. den Boef, *Anal. Chim. Acta*, 1978, **98**, 221.
21. *Poradnik Fizykochemiczny (Physico-chemical Handbook)*, WNT, Warsaw, 1974.
22. L. G. Sillén and A. E. Martell, *Stability Constants of Metal-Ion Complexes*, Special Publication No. 17, Chemical Society, London, 1964.
23. A. Pomianowski, *Proc. Intern. Symp. Electrochemistry in Mineral and Metal Processing*, Cincinnati, Ohio 6–11 May 1984.
24. A. Hulanicki, T. Krawczyński vel Krawczyk and M. Biesaga, *Chem. Anal. Warsaw* (in press).

DETERMINATION OF PROTONATION CONSTANTS BY COULOMETRIC TITRATION

STANISŁAW GZAB, ELŻBIETA SKRZYDLEWSKA* and ADAM HULANICKI
Department of Chemistry, University of Warsaw, Warsaw, Poland

(Received 14 April 1986. Revised 4 September 1986. Accepted 8 November 1986)

Summary—Application of coulometric titration to the determination of the protonation constants of acids and bases offers several advantages because of its simplicity, precision and accuracy. This procedure is rapid and requires only one calibration solution of strong acid in the same solvent and at the same ionic strength as the solution of acid (or base) being investigated. The procedure seems to be especially advantageous in the case of non-aqueous or mixed solvents having amphiprotic character. The validity of the method has been checked with several substances in water, 95% ethanol and ethylene glycol.

The most common procedure for determining protonation constants is based on titration of the investigated acid with strong base, or titration of the investigated base with a strong acid.¹ The changes in hydrogen-ion activity are followed with a glass electrode calibrated with appropriate standards. In the procedure used by Budevsky *et al.*² for studies of non-aqueous equilibria, no preliminary calibration of the cell with pH standards is needed. The potential evaluation is based on the so-called " E° -titration",³ in which a strong acid of known concentration is titrated with a strong base. At constant ionic strength the e.m.f. of the cell is linearly dependent on the logarithm of the hydrogen-ion concentration.

Knowledge of protonation constants in non-aqueous or mixed solutions is interesting for analytical chemistry, but several experimental difficulties hinder the measurements. The coulometric titration technique can easily be adapted to investigation of autoprotolytic equilibria in various amphiprotic solvents⁴ and this paper extends the study to protonation equilibria. Well-known equilibria were studied so that the results would be compared with literature data.

The main advantage expected in this procedure is simplicity, because it is not necessary to prepare titrant solutions (the titrant is generated electrolytically). This eliminates standardization, but requires 100% generation efficiency. An additional advantage is possible in the titration of acids, because a single-compartment cell can be used, providing that the silver error in a given solvent is sufficiently small.⁵ This advantage arises from the elimination of diffusion between the two parts of the cell. The advantages of both types of cell have been discussed elsewhere.^{4,5}

EXPERIMENTAL

Reagents

Analytical grade chemicals were used with further purification in the following cases. Ethylene glycol was additionally dried with anhydrous sodium sulphate and distilled at 1.3 kPa (10 mmHg) pressure. Mono-, di- and triethanolamines were distilled at normal pressure. Nitrophenols were recrystallized from water. Sodium perchlorate and bromide were recrystallized from water.

Apparatus

The amperostat was a PAR model 173 with a model 179 integrator. A Radiometer PHM-64 pH-meter was used with a G202B Radiometer glass electrode and a silver-silver bromide reference electrode. The generating circuit consisted of a platinum electrode with a surface area of about 0.6 cm², and a platinum auxiliary electrode with surface area of about 3 cm². With the single-compartment cell a silver anode with surface area of about 25 cm² was used. All measurements were made at 25° in deaerated solutions.

Procedure

In the two-compartment cell the anode and cathode were separated by two sintered-glass diaphragms (porosity 4) with the intermediate space filled with 3% agar-agar solution. The generating electrode was placed in the 100-ml compartment and used as the cathode in titrations of acids or the anode in titrations of bases. In titrations of acids this compartment was filled with 40–60 ml of 0.05M sodium perchlorate/0.05M sodium bromide solution in an appropriate solvent. The same electrolyte was used in titrations in the single-compartment cell. In titration of bases the solution contained only 0.1M sodium perchlorate. The second compartment of the cell was filled with 0.1M sodium perchlorate in water or methanol.

The indicator glass electrode was placed directly in the generating compartment. In titrations of acids the reference electrode was also directly immersed in this compartment, whereas for titrations of bases it was placed in a 0.09M sodium perchlorate/0.01M sodium bromide solution connected to the cell by an electrolyte bridge. The sample solutions contained from 0.04 to 0.2 mmole of acid or base. The current density at the generating electrode was approximately 10 mA/cm².

The titration end-point was evaluated by means of the Gran function⁶ in the form modified for coulometric titrations without volume change. The electrode slope factor

*Present address: School of Medicine, Białystok, Poland.

Table 1. Current efficiency of base generation in different solvents

Solvent	HClO ₄ taken, mmole	Theoretical charge, C	Charge found, C	Error, %
Water	0.0420	4.052	4.050 ± 0.003	0.05
Ethylene glycol	0.0510	4.921	4.930 ± 0.006	0.18
Ethanol 95%	0.0620	5.982	5.993 ± 0.005	0.18

was assumed to have the theoretical value for aqueous solutions, *i.e.*, -59.16 mV/pH at 25°.

RESULTS AND DISCUSSION

For evaluation of the cell calibration constant in the E° -titration, the Nernst equation was used in the form given by Johansson and Johansson⁷

$$E = E^\circ + j(\text{H}^+) + \frac{RT}{nF} \ln [\text{H}^+] \quad (1)$$

where E° is the constant for the acid, E_a° , and $j(\text{H}^+)$ represents the liquid-junction potential. In the acid titrations $j(\text{H}^+) = 0$ because the reference electrode was placed directly in the solution titrated. When bases were titrated with anodically generated protons, the solutions did not contain bromide ions and the reference electrode made contact through the electrolyte bridge. In such cases $j(\text{H}^+)$ was assumed to be constant throughout the experiment.

The E° -titrations were carried out in the cell (SH = solvent):



The E_a° value (mV) was then calculated from

$$\begin{aligned} E_a^\circ &= E - 59.16 \log [\text{SH}_2^+] \\ &= E - 59.16 \log \left(\frac{Q_{\text{EP}} - Q}{FV} \right) \quad (2) \end{aligned}$$

where V is the volume of solution, Q the charge generated at e.m.f. E , and Q_{EP} the end-point charge. Points from the titration curve between titration-fraction 0.2 and 0.8 were used for the calculations. In a similar manner, for the titration-fraction between 1.2 and 2.0,

$$\begin{aligned} E_b^\circ &= E - 59.16 \log [\text{S}^-] \\ &= E - 59.16 \log \left(\frac{Q - Q_{\text{EP}}}{FV} \right) \quad (3) \end{aligned}$$

The constancy of E_a° and E_b° along the titration curves indicates proper functioning of the indicator electrode and the validity of the assumptions.

The values of E_a° and E_b° were determined for water, ethylene glycol and 95% ethanol in electrolyte solutions containing 0.05M sodium bromide and

0.05M sodium perchlorate. For titration series on different days E° varied by up to 2-3 mV, but the difference $E_a^\circ - E_b^\circ$ remained constant within 0.5 mV, indicating the constancy of the autoprotolysis constants. For ethylene glycol and 95% ethanol these constants were $10^{-14.89}$ and $10^{-15.42}$, respectively. The 0.5 mV difference corresponds to an error of 0.01 in the logarithm of the autoprotolysis constant. With standard perchloric acid solutions, 100% generation efficiency was confirmed for the solvents tested. With water the error was less than 0.1%, and for non-aqueous solutions less than 0.2% (Table 1). These results refer to a two-compartment cell. In the case of a one-compartment cell the error is mainly connected with the silver error.⁷

For calculation of protonation constants the usual equation

$$\begin{aligned} \log K_{\text{H}} &= \text{pH} + \\ &\log \frac{C_{\text{T}} V_{\text{EP}} - C_{\text{T}} V_{\text{T}} - (V_0 + V_{\text{T}})([\text{H}^+] - [\text{OH}^-])}{C_{\text{T}} V_{\text{T}} + (V_0 + V_{\text{T}})([\text{H}^+] - [\text{OH}^-])} \quad (4) \end{aligned}$$

must be rewritten in the form appropriate for coulometric titrations:

$$\log K_{\text{H}} = \text{pH} + \log \frac{Q_{\text{EP}} - Q - FV_0([\text{H}^+] - [\text{OH}^-])}{Q + FV_0([\text{H}^+] - [\text{OH}^-])} \quad (5)$$

These formulae indicate two principal advantages of coulometric determination of equilibria. According to the general formula (5), only two charge values, Q_{EP} and Q , and the initial volume, V_0 , are needed, whereas when the volumetric procedure is used, not only the equivalence point volume, V_{EP} , titrant volume, V_{T} , and initial volume, V_0 , are necessary, but also the exact concentration of titrant, C_{T} , or the concentration of the titrated acid sample.

The next advantage results from the better precision of charge measurement compared with the measurement of volume. A precision of 0.1% can easily be attained in coulometry, and with special care even 0.01% can be reached. The proper measurement of charge or volume is of special importance when calculating differences.

An important practical advantage results from the possibility of better protection of solutions against

Table 2. Comparison of two procedures for calculating protonation constants from coulometric titration data (benzoic acid in aqueous 0.05M NaClO₄-0.05M NaBr)

Charge (<i>Q</i>), <i>C</i>	e.m.f. (<i>E</i>), <i>mV</i>	<i>Q</i> × 10 ^{<i>E</i>/5} × 10 ⁻³	-log [SH ₂ ⁺]	log <i>K</i> _H , [Eq. (5)]	<i>Q</i> + <i>A</i>	[SH ₂ ⁺](<i>Q</i> + <i>A</i>) × 10 ⁴
						[Eq. (6)]
9.001	189.9	14.20	4.02	3.98	9.445	8.718
10.00	183.9	12.74	4.12	3.99	10.36	7.718
11.01	178.2	11.31	4.22	3.99	11.30	6.803
12.10	171.4	9.56	4.34	3.99	12.32	5.693
12.50	168.8	8.92	4.38	3.99	12.70	5.296
13.00	165.3	8.09	4.44	3.99	13.18	4.796
13.50	161.4	7.22	4.50	3.98	13.65	4.273
14.00	157.2	6.36	4.58	3.99	14.13	3.758
15.00	147.3	4.63	4.74	3.99	15.09	2.731

V = 50 ml; *E*₀ = 427.4 mV; *Q*_{EP} = 17.75. mean log *K*_H = 3.99 ± 0.004 [equation (5)], mean log *K*_H = 3.98 ± 0.01 [equation (6)].

the access of carbon dioxide. In coulometric titration of acids no dilute solutions of base are needed at all, so changes of the titrant concentration or distortion of the titration curve do not occur. For studies of equilibria in non-aqueous solutions, coulometric titration eliminates the cumbersome preparation of the solution of the base. Thus only one solution in the solvent studied must be prepared and its concentration is determined in the course of examination of the protonation constant.

Coulometric data can be used also in protonation constant calculations according to Chakarova and Budevsky,⁸ where the end-point charge *Q*_{EP} and the protonation constant *K*_H are calculated as parameters of the straight line from the equation

$$[\text{SH}_2^+](Q + A) = Q_{\text{EP}}/K_{\text{H}} - (Q + A)/K_{\text{H}} \quad (6)$$

where *A* = *FV* { [SH₂⁺] - *K*₁/[SH₂⁺] }, *K*₁ = 10 (*E*₀ - *E*_a⁰)/59.16 is the ion-product of the solvent, and *E* is expressed in mV.

Table 3. Protonation constants (log *K*_H) of acids and bases determined by coulometric titration at *I* = 0.1 and 25°C

Acid or base	Amount taken, mmole	log <i>K</i> _H [†]		log <i>K</i> _H (literature)	Ref.
		TCC ^a	SCC ^b		
Solvent: water					
Acetic acid	0.1618	4.57 ± 0.01	4.57 ± 0.01	4.55	11
Benzoic acid	0.1846	3.99 ± 0.01	4.01 ± 0.01	4.01	12
Succinic acid	0.1431	4.00 ± 0.02	4.01 ± 0.03	4.00	13
Tartaric acid	0.0962	5.17 ± 0.01	5.30 ± 0.03	5.28	14
		2.80 ± 0.02	2.81 ± 0.02	2.80	
Phthalic acid	0.1212	4.00 ± 0.01	4.02 ± 0.03	3.96	15
		2.86 ± 0.02	2.80 ± 0.01	2.76	
<i>p</i> -Nitrophenol	0.1019	4.96 ± 0.03	4.95 ± 0.03	4.92	16
		6.98 ± 0.02	6.99 ± 0.01	7.02	
<i>o</i> -Nitrophenol	0.1064	7.01 ± 0.01	7.04 ± 0.02	7.06	16
<i>m</i> -Nitrophenol	0.0926	8.06 ± 0.03	8.07 ± 0.02	8.04	16
Solvent: 95% ethanol					
Acetic acid	0.0571	6.74 ± 0.01	6.80 ± 0.02	5.33 ^c	2
				9.44 ^e	17
Benzoic acid	0.0482	6.54 ± 0.01	6.58 ± 0.01	9.14 ^e	17
Solvent: ethylene glycol					
Acetic acid	0.0456	7.50 ± 0.02	7.52 ± 0.02	7.69 ^e	18
Benzoic acid	0.0596	7.39 ± 0.02	7.46 ± 0.02	7.54 ^e	18
Solvent: water					
Monoethanolamine	0.0755	9.26 ± 0.01		9.25 ^e	19
Diethanolamine	0.1330	8.87 ± 0.01		8.87 ^e	20
Triethanolamine	0.1109	7.76 ± 0.02		7.83 ^e	20

[†]Mean from 4 titrations.

^aTwo-compartment cell.

^bSingle-compartment cell.

^cData for 45% ethanol—55% water.

^dData for 100% ethanol.

^eCorrected to *I* = 0.1 by equation (10).

Good agreement between calculations done with the two procedures was found for benzoic acid (Table 2).

For determination of constants of diprotic acids we have used the procedure given by Britton⁹ modified for coulometric titrations. The protonation constants are expressed as

$$K_{H1} = \frac{X_1 Y_1 - X_2 Y_2}{Y_1 Z_1 - Y_2 Z_2} \quad (7)$$

$$K_{H2} = \frac{Y_1 Z_2 - Y_2 Z_1}{X_1 Z_2 - X_2 Z_1} \quad (8)$$

where

$$X_i = \left(\frac{2Q - Q_{EP}}{2FV_0} \right) [H^+] + [H^+]^2$$

$$Y_i = \left(\frac{Q_{EP} - Q}{FV_0} \right) - [H^+]$$

$$Z_i = [H^+]^2 \left(\frac{Q}{FV_0} + [H^+] \right)$$

and Q_{EP} corresponds to titration of both protons.

The protonation constants of several acids and bases in three solvents were determined by this technique and compared with the literature data (Table 3). The values for bases were calculated by using an appropriate modification of equation (5) in the form

$$\log K_H = \frac{E_a^0 - E}{59.16} + \log \left(\frac{Q}{Q_{EP} - Q} \right) \quad (9)$$

When the literature data were given for other conditions of ionic strength, they were corrected to $I = 0.1$, by using the Debye-Hückel equation

$$-\log f_{\pm} = Az^2 \sqrt{I} / (1 - Ba \sqrt{I}) \quad (10)$$

with $a = 5$.¹⁰ In most cases the results agreed with the literature data within the limits of experimental error.

CONCLUSIONS

The coulometric titration procedure was adapted for determination of protonation constants of acids and bases in water and organic or mixed solvents. This procedure simplifies the determination,

especially in the case of non-aqueous solvents, because preliminary preparation of only one solution is required, and its concentration is easily evaluated by using coulometric base generation with potentiometric detection. It seems that this procedure can be applied to amphiprotic solvents in which the strong acid and base are sufficiently dissociated, and no parasitic reduction or oxidation reactions occur during cathodic or anodic (base or acid) generation, respectively. The precision and accuracy of the determination of protonation constants are satisfactory for most analytical purposes.

Acknowledgement—This work was supported through the project CPBP-01.17.

REFERENCES

1. A. Albert and E. P. Serjeant, *The Determination of Ionization Constants*, Chapman & Hall, London, 1971.
2. J. Tencheva, G. Velinov and O. Budevsky, *J. Electroanal. Chem.*, 1974, **68**, 65.
3. L. Persson, F. Ingman and A. Johansson, *Talanta*, 1976, **23**, 76.
4. S. Glab and A. Hulanicki, *ibid.*, 1981, **28**, 183.
5. A. Hulanicki, S. Glab and W. Jedral, *Analyst*, 1986, **111**, 335.
6. G. Gran, *ibid.*, 1952, **77**, 661.
7. A. Johansson and S. Johansson, *ibid.*, 1978, **103**, 305.
8. P. Chakarova and O. Budevsky, *J. Electroanal. Chem.*, 1976, **73**, 369.
9. H. T. Britton, *Hydrogen Ions*, Chapman & Hall, London, 1955.
10. R. A. Robinson and R. H. Stokes, *Electrolyte Solutions*, 2nd Ed., p. 230. Butterworths, London, 1968.
11. R. S. Kolat and J. E. Powell, *Inorg. Chem.*, 1962, **1**, 293.
12. M. Yasuda, K. Yamasaki and M. Ohtaki, *Bull. Chem. Soc. Japan*, 1960, **33**, 1067.
13. E. Campi, *Ann. Chim. (Rome)*, 1963, **53**, 96.
14. C. F. Timberlake, *J. Chem. Soc.*, 1964, 1229.
15. M. Yasuda, K. Suzuki and K. Yamasaki, *J. Phys. Chem.*, 1956, **60**, 1649.
16. K. E. Jabalpurwala and R. M. Milburn, *J. Am. Chem. Soc.*, 1966, **88**, 3224.
17. G. Charlot and B. Trémillon, *Chemical Reactions in Solvents and Melts*, p. 278. Pergamon Press, Oxford, 1969.
18. K. K. Kundu and M. M. Das, *J. Chem. Eng. Data*, 1964, **82**, 9.
19. L. Cockrell and M. F. Walton, *J. Phys. Chem.*, 1962, **66**, 75.
20. G. Douheret, *Bull. Soc. Chim. France*, 1965, 2915.

THE EFFECT OF TEMPERATURE ON SINGLE-COLUMN ION-CHROMATOGRAPHY OF METAL IONS

NANCY E. FORTIER and JAMES S. FRITZ

Ames Laboratory and Department of Chemistry, Iowa State University, Ames, Iowa 50011, U.S.A.

(Received 1 September 1986. Accepted 7 November 1986)

Summary—Temperature is shown to be a valuable parameter for optimizing single-column ion-chromatographic separations of metal ions. With a perchloric acid eluent, retention times of bivalent metal ions decrease with an increase in system temperature, but with doubly protonated amines as eluents the retention times increase with an increase in temperature. Consequently, increasing the system temperature improves separations of bivalent metal ions when *p*-phenylenediamine dihydrochloride is used as the eluent. Both conductivity detection and post-column reaction followed by spectrophotometric detection are suitable detection methods at above-ambient temperatures.

Although temperature is a major experimental variable in gas chromatography, the use of above-ambient temperatures in liquid chromatography, and especially in ion-exchange chromatography, is much less common. Several research groups have investigated the effect of temperature on ion-exchange equilibria, including classical ion-exchange separations.¹⁻²³ Selectivity coefficients were found to increase or decrease as a function of temperature, depending on the exchange reaction.^{1,3,5-9,14} Changes in separation factors with temperature have been noted.^{2-4,6,9} In addition, elevated temperature has been shown to speed up the equilibrium between complexing eluents and metal ions, thus yielding peaks of better shape.^{20,22}

The thermodynamic functions ΔH^* , ΔG^* , and ΔS^* have been calculated for ion-exchange reactions as a function of temperature,^{1,5-9} and found to differ substantially, even for chemically similar ions.^{1,7,8} The ΔG° term is due to several factors. One is the difference in the energy of interaction between the exchanged ions and the resin functional groups. Another is the relative energy and entropy contribution from the dehydration of ions entering the resin and the hydration of ions initially present in the resin. Metal ions are hydrated to different extents at room temperature and the changes in hydration spheres as the temperature is raised vary from one ion to another.

Stress has been laid on solvation effects in ion-exchange.^{14,24} For the exchange of X and Y ions when the differences in activity coefficients are negligible in comparison to swelling effects, Gregor gives the equation

$$\ln K_Y^X = \frac{\pi}{RT} (Z_X V_Y - Z_Y V_X) \quad (1)$$

where K_Y^X is the selectivity coefficient, π is the swelling pressure, R is the gas constant, T is the absolute

temperature, Z is the absolute value of the ion charge, and V is the solvated molar volume.²⁴ Gregor and Bregman¹⁴ confirmed that the selectivity coefficient is approximately constant with change in temperature for ions of similar hydration, but changes with temperature when X and Y are hydrated to different extents.

Amino-acids are often separated by ion-exchange chromatography at temperatures between 25° and 80°.^{15,16,25} Operating at an elevated temperature has been shown to improve the resolution, although no explanation is usually offered. Partridge and Brimley¹⁶ noted a change in the order of elution of amino-acids from a cation-exchange column at elevated temperatures.

In the present work the effect of elevated temperatures on the ion-chromatographic separation of metal ions is examined. Depending on the eluent used, the retention times of metal ions can be changed substantially by increasing the temperature. In some cases the temperature effects can be used to improve the resolution.

EXPERIMENTAL

Apparatus

The instrument used consisted of a model 302 Gilson single-piston pump, a model 1116 Eldex column-heater, a model 7125 Rheodyne injector equipped with a 20- μ l sample loop, a Li-Chroma-Damp II coil-type pulse-dampener, a model 269-004 Wescan catex column (capacity 0.03 meq/g, 12-16 μ m particle size, 5% cross-linked sulfonated polystyrene-divinylbenzene gel, 25 cm long, 2 mm bore), and a Curken strip-chart recorder. Two modes of detection were used. A model 213A Wescan conductivity detector was used for conductivity detection, and a Spectroflow 783 Kratos UV-visible spectrophotometric detector was used with the post-column reaction system. The post-column mixer consisted of a bored-out stainless-steel tee as described by Elchuk and Cassidy.²⁶ The post-column colour-forming reagent was delivered with a Gilson Minipuls 2 peristaltic pump. A model PD-60-LF Fluid Metering Inc. pulse-dampener was placed in the line between the

peristaltic pump and mixing tee. The eluent was preheated and kept at constant temperature with a Haake A80 waterbath. All connecting tubing was insulated by wrapping it with sheets of styrofoam packing material. The conductivity cell was also insulated with styrofoam.

Eluents and colour-forming reagents

Reagent grade *p*-phenylenediamine, *p*-phenylenediamine dihydrochloride, ethylenediamine, tartaric acid, perchloric acid, 4-(2-pyridylazo)resorcinol (PAR), Arsenazo I, ammonia, and ammonium acetate were used without further purification. The *p*-phenylenediamine eluent was prepared by dissolving the solid in perchloric acid, diluting with demineralized water (NANOpure II system, Barnstead), and adjusting the pH to 3 to ensure complete protonation of the amine. The ethylenediamine/tartaric acid eluent was prepared by dissolving appropriate amounts of ethylenediamine and tartaric acid in demineralized water, diluting to volume, and adjusting the pH with aqueous sodium hydroxide. The *p*-phenylenediamine dihydrochloride eluent was prepared by dissolving the solid and diluting the solution with demineralized water; the perchloric acid eluent was prepared by diluting 70% perchloric acid. The amine eluents were freshly prepared each day, and stored under a helium atmosphere and protected from light to prevent decomposition. All eluents were filtered through a 0.45- μ m membrane and degassed with suction.

The Arsenazo I solution was prepared by dissolving 3 mmoles of Arsenazo I and 3 moles of ammonia in 1.0 litre of demineralized water. The PAR solution was prepared by dissolving 0.56 mmoles of PAR and 9 mmoles of ammonia in about 400 ml of demineralized water, then adding a solution of 1 mole of ammonium acetate in about 350 ml of demineralized water, and diluting to 1.0 litre. All post-column reagent solutions were filtered through a 0.45- μ m membrane prior to use.

Sample solutions

All metal-ion solutions were prepared by using reagent-grade salts, concentrated perchloric acid, and demineralized water; the pH was adjusted to approximately 3 with perchloric acid to prevent hydrolysis.

Chromatographic conditions

All chromatography was done at a flow-rate of 0.6 ml/min. Additional eluent degassing was carried out on-line by continually sparging the eluent in the reservoir with helium. With each change of temperature or eluent, the system was allowed to equilibrate overnight (for at least 5 hr).

With amine eluents, conductivity detection was employed. When perchloric acid was the eluent, post-column reaction combined with spectrophotometric detection was used. Magnesium and calcium were detected at 585 nm with Arsenazo I as the post-column reagent, and other metal ions were detected at 520 nm with PAR.

RESULTS AND DISCUSSION

For an eluent ion, E, of charge x , and a sample metal ion, M, of charge y , the exchange reaction



can be written, where R_x and R_y represent the number of resin exchange sites occupied by E and M ions, respectively. This exchange reaction can be either exothermic or endothermic, depending on the ions involved. Consequently, the equilibrium can be shifted in either direction as the temperature is increased, resulting in a change in the capacity factor, k , for the metal ion.

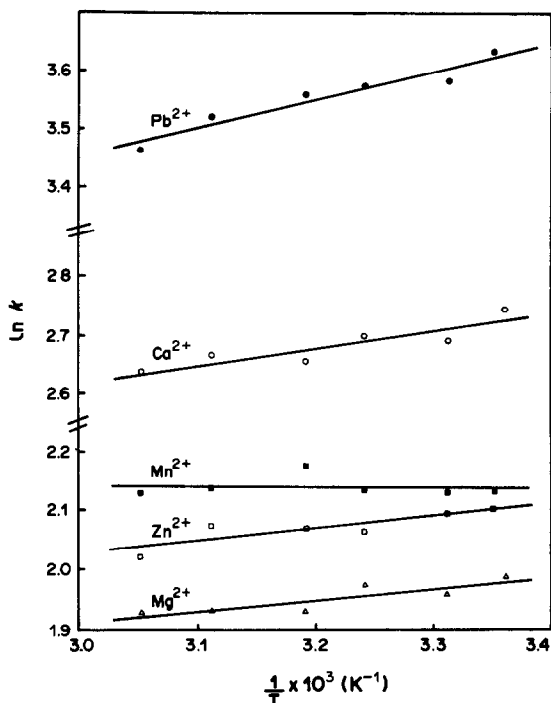


Fig. 1. Plot of $\ln k$ for bivalent metal ions as a function of reciprocal of the system temperature. Eluent 0.12M perchloric acid.

The relationship between capacity factor, k , and system temperature, T , is mathematically represented by:

$$\ln k = \frac{-\Delta H^\circ}{RT} + \frac{\Delta S^\circ}{R} + \ln \phi \quad (3)$$

where ΔH° is the enthalpy change for the exchange reaction (3), ΔS° is the corresponding change in standard entropy, and ϕ is the column phase-ratio, a characteristic constant for a given column.^{27,28} A plot of $\ln k$ vs. the reciprocal of the temperature should have a slope equal to $-\Delta H^\circ/R$.

Figure 1 shows a plot of $\ln k$ vs. $1/T$ for several metal ions eluted from a cation-exchange column with a perchloric acid eluent. The exchange reactions are exothermic, except for that of manganese(II), which is slightly endothermic. Figure 2 shows that the situation is reversed when a *p*-phenylenediamine dihydrochloride eluent is used; in this case the exchange reactions are all endothermic. Two trivalent rare-earth ions were also chromatographed at various temperatures with these two eluents, both of which gave strongly endothermic exchange reactions. The results of the runs with the perchloric acid eluent are summarized in Table 1 and those with the *p*-phenylenediamine dihydrochloride eluent are given in Table 2.

It should be mentioned that the protonated *p*-phenylenediamine eluent first used was prepared from *p*-phenylenediamine and perchloric acid, but though this proved to be a stable and satisfactory

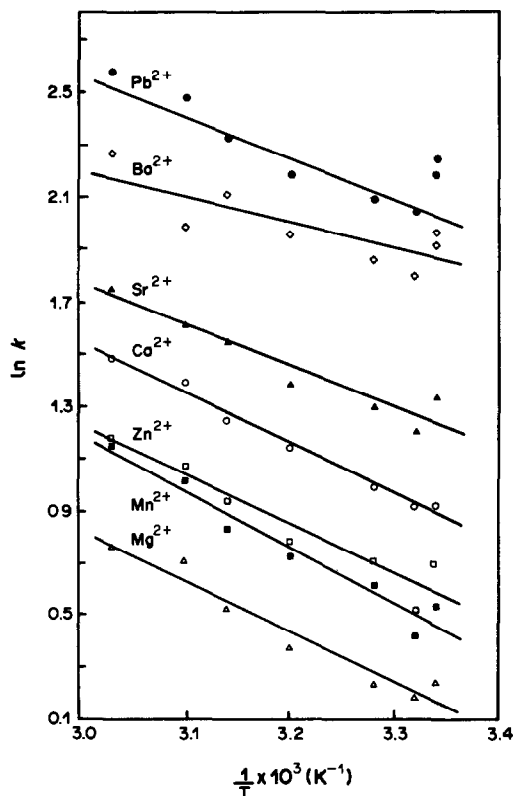


Fig. 2. Plot of $\ln k$ for bivalent metal ions as a function of reciprocal of the system temperature. Eluent 3.0mM *p*-phenylenediamine dihydrochloride.

Table 1. Linear regression data for plot of $\ln k$ vs. $1/T$ for a perchloric acid eluent; the eluent concentration was 0.12M for the bivalent metal ions and 0.29M for the rare-earth cations

Cation	Slope = $-\Delta H^\circ/R^*$	Correlation coefficient	ΔH , kcal/mole
Mg ²⁺	185	0.851	-0.37
Zn ²⁺	216	0.870	-0.43
Mn ²⁺	-18	-0.115	0.04
Ca ²⁺	295	0.901	-0.59
Pb ²⁺	489	0.970	-0.98
Lu ³⁺	-572	-0.980	1.14
Dy ³⁺	-994	-0.978	1.99

* $R = 2.0 \text{ cal. deg}^{-1} \cdot \text{mole}^{-1}$.

Table 2. Linear regression data for plot of $\ln k$ vs. $1/T$ for a *p*-phenylenediamine dihydrochloride eluent; the eluent concentration was 3.0mM for the bivalent metal ions and 7.8mM for the rare-earth cations

Cation	Slope = $-\Delta H^\circ/R$	Correlation coefficient	ΔH° , kcal/mole
Mg ²⁺	-1945	-0.971	3.87
Mn ²⁺	-2161	-0.976	4.29
Zn ²⁺	-1870	-0.952	3.72
Ca ²⁺	-1924	-0.993	3.82
Sr ²⁺	-1575	-0.954	3.13
Ba ²⁺	-965	-0.794	1.92
Pb ²⁺	-1318	-0.855	2.62
Lu ³⁺	-3068	-0.975	6.10
Dy ³⁺	-3300	-0.985	6.56

Table 3. Adjusted retention times (min) for some bivalent and trivalent metal ions at two system temperatures (flow-rate 0.6 ml/min; for the bivalent ions the concentration of *p*-phenylenediamine dihydrochloride was 3.0mM; for the trivalent ions 7.8mM was used)

	27.9°C	56.9°C	25.4°C	55.8°C
Mg ²⁺	0.97	1.73		
Mn ²⁺	1.23	2.55		
Zn ²⁺	1.36	2.63		
Ca ²⁺	2.03	3.59		
Sr ²⁺	2.71	4.66		
Ba ²⁺	4.92	7.82		
Pb ²⁺	6.26	10.63		
Lu ³⁺			11.72	30.28
Dy ³⁺			14.61	40.94

eluent at room temperature,²⁹ it was found to decompose too quickly at higher temperature to be useful. However, the corresponding eluent prepared from *p*-phenylenediamine dihydrochloride was found to be entirely stable and satisfactory at the higher temperatures. This may have been because the dihydrochloride salt was purer than the free base used earlier.

The retention times of metal ions eluted with the *p*-phenylenediamine dihydrochloride eluent are considerably longer at higher temperatures, as shown by Table 3. In some cases the difference between the retention times of two metal ions is larger at a higher temperature. This can be useful in obtaining better chromatographic separations. Figure 3 shows the improved resolution for calcium and manganese(II) obtained by chromatography at 54° instead of 25°. Figure 4 shows that the separation of calcium and zinc is also much better at the higher temperature.

It is worth noting that conductivity detection of the

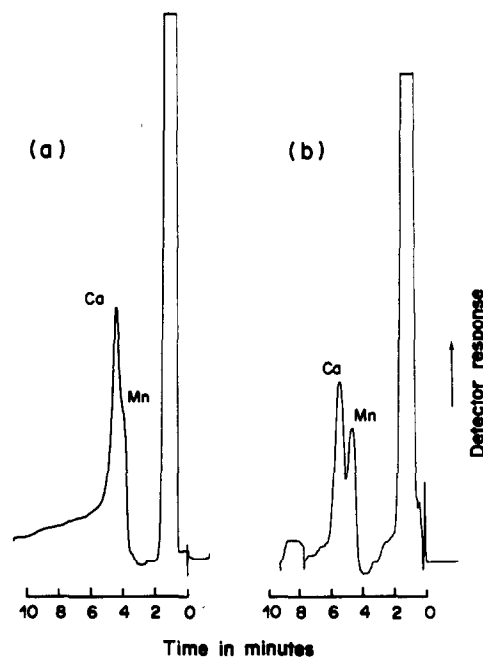


Fig. 3. Separation of Mn²⁺ and Ca²⁺. Eluent 1.0mM ethylenediamine, 2.0mM tartaric acid, pH 4.5. (a) 25°C, (b) 54°C.

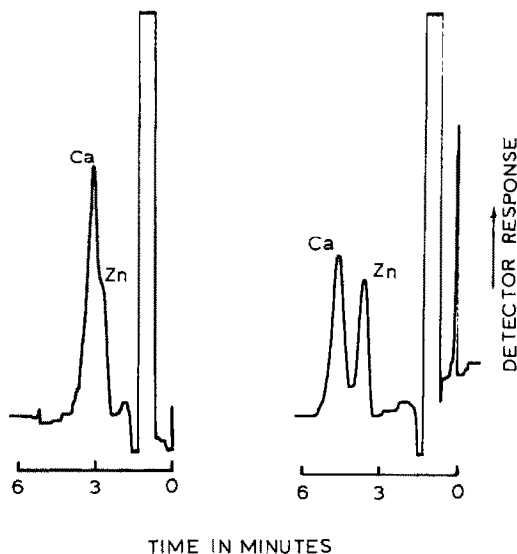


Fig. 4. Separation of Zn^{2+} and Ca^{2+} . Eluent 3.0mM *p*-phenylenediamine dihydrochloride. (a) 27°C, (b) 57°C.

metal ions works well at temperatures up to at least 60° when either an ethylenediamine/tartaric acid eluent or a *p*-phenylenediamine dihydrochloride eluent is used.

Acknowledgements—The authors thank Wescan for the gift of the column used in this work. One of the authors (NEF) thanks J. P. van Alstyne, N. K. Kildahl and G. J. Sevenich for continued encouragement throughout the course of this study.

Ames Laboratory is operated for the U.S. Department of energy under Contract No. W-7405-ENG-85. This work was supported by the Director of Energy Research, Office of Basic Energy Sciences.

REFERENCES

1. R. Dybczyński, *Roczniki Chem.*, 1967, **41**, 1689.
2. *Idem*, *Nukleonika*, 1967, **12**, 869.
3. *Idem*, *J. Chromatog.*, 1972, **71**, 507.
4. *Idem*, *ibid.*, 1967, **31**, 155.
5. K. A. Kraus and R. J. Raridon, *J. Phys. Chem.*, 1959, **63**, 1901.
6. R. Dybczyński, *J. Chromatog.*, 1964, **14**, 79.
7. *Idem*, *Roczniki Chem.*, 1963, **37**, 1411.
8. R. Dybczyński and L. Wódkiewicz, *J. Inorg. Nucl. Chem.*, 1969, **31**, 1495.
9. R. Dybczyński, H. Polkowska-Motrenko and R. M. Shabana, *J. Chromatog.*, 1977, **134**, 285.
10. R. Dybczyński, *Anal. Chim. Acta*, 1963, **29**, 369.
11. Y. Baba, N. Yoza and S. Ohashi, *J. Chromatog.*, 1985, **348**, 27.
12. *Idem*, *ibid.*, 1985, **350**, 119.
13. R. Pecina, G. Bonn, E. Burtcher and O. Bobleter, *ibid.*, 1984, **287**, 245.
14. H. P. Gregor and J. I. Bregman, *J. Colloid Sci.*, 1951, **6**, 323.
15. S. Moore and W. H. Stein, *J. Biol. Chem.*, 1951, **192**, 663.
16. S. M. Partridge and R. C. Brimley, *Biochem. J.*, 1951, **48**, 313.
17. P. B. Hamilton, D. C. Bogue and R. A. Anderson, *Anal. Chem.*, 1960, **32**, 1782.
18. B. H. Ketelle and G. E. Boyd, *J. Am. Chem. Soc.*, 1947, **69**, 2800.
19. L. W. Holm, G. R. Choppin and D. Moy, *J. Inorg. Nucl. Chem.*, 1961, **19**, 251.
20. E. K. Hulet, R. G. Gutmacher and M. S. Coops, *ibid.*, 1961, **17**, 350.
21. M. Schädel, N. Trautmann and G. Herrmann, *Radiochim. Acta*, 1977, **24**, 27.
22. J. P. Surls Jr. and G. R. Choppin, *J. Inorg. Nucl. Chem.*, 1957, **4**, 62.
23. M. Schädel, W. Brüchle, B. Haefner, J. V. Kratz, W. Schorstein, N. Trautmann and G. Herrmann, *Radiochim. Acta*, 1978, **25**, 111.
24. H. P. Gregor, *J. Am. Chem. Soc.*, 1951, **73**, 642.
25. R. E. Pfeifer, R. Karol, J. Korpi, R. Burgoyne and D. McCourt, *Am. Lab.*, 1983, **15**, No. 3, 78.
26. S. Elchuk and R. M. Cassidy, *Anal. Chem.*, 1979, **51**, 1434.
27. C. Horváth, W. Melander and I. Molnár, *J. Chromatog.*, 1976, **125**, 129.
28. W. Melander, D. E. Campbell and C. Horváth, *ibid.*, 1978, **158**, 215.
29. N. E. Fortier and J. S. Fritz, *Talanta*, 1985, **32**, 1047.

EXTRACTION AND SPECTROPHOTOMETRIC DETERMINATION OF MOLYBDENUM(VI) WITH MALACHITE GREEN AND *p*-CHLOROMANDELIC ACID

SHIGEYA SATO, MARI IWAMOTO and SUMIO UCHIKAWA

Faculty of Education, Kumamoto University, 2-40-1, Kurokami, Kumamoto 860, Japan

(Received 26 April 1986. Accepted 7 November 1986)

Summary—Molybdenum(VI) reacts with *p*-chloromandelic acid to form a complex extractable into chlorobenzene with Malachite Green, from aqueous solution at pH 2.0–4.0 at room temperature, and can then be determined indirectly by measuring the absorbance of the Malachite Green in the extract, at 630 nm. The calibration graph is linear for molybdenum over the range $0.26\text{--}10.0 \times 10^{-6}M$ ($0.10\text{--}4.0 \mu\text{g}$); the apparent molar absorptivity is $1.06 \times 10^5 \text{ l. mole}^{-1} \cdot \text{cm}^{-1}$. The method has been applied to the determination of molybdenum in mild steels with satisfactory results.

Several methods have been reported for the extraction and spectrophotometric determination of molybdenum in various complex materials.^{1,2} Of these, the classical thiocyanate–stannous chloride method is the most commonly used, in spite of its drawbacks. The methods based on other reagents^{3–16} also suffer from various disadvantages.

We have found that α -hydroxy acids are very useful complexing agents, especially for metals which form oxo-ions in solution, and highly sensitive and selective methods for their determination have been reported.^{17–21} Molybdenum(VI) can easily be extracted as an ion-association complex with Malachite Green into chlorobenzene, but the sensitivity is very low. Addition of *p*-chloromandelic acid, however, produces a molybdenum complex which forms a very stable and readily extractable ion-association complex with Malachite Green, which is highly suitable for determination of molybdenum. Interference from antimony(III) and tungsten(VI) can be effectively eliminated by the use of citrate, and from titanium(IV) by addition of fluoride or *trans*-1,2-cyclohexanediaminetetra-acetic acid (DCTA).

EXPERIMENTAL

Reagents

All reagents and solvents used were of analytical grade. All aqueous solutions were prepared with demineralized water.

Standard molybdenum(VI) solution. A commercially available molybdenum standard solution (1000 ppm Mo) was diluted as required.

Malachite Green (MG) solution. $5.0 \times 10^{-3}M$. Prepared from guaranteed grade MG oxalate.

***p*-Chloromandelic acid (*p*-MACI) solution.** $1.0 \times 10^{-3}M$.

Sodium acetate buffer (pH 3.0). Prepared from 0.1M sodium acetate and 0.5M sulphuric acid.

DCTA solution 0.1M.

Sodium citrate solution, 0.1M.

Potassium fluoride solution, 0.2M.

Standard procedure

Take an aliquot of standard molybdenum(VI) solution containing up to $4.0 \mu\text{g}$ of molybdenum, in a 10-ml test-tube equipped with a stopper. Add 1.0 ml of sodium acetate buffer, 0.4 ml of *p*-MACI solution and 0.2 ml of MG solution. Dilute to 4.0 ml with water and shake the solution with 4.0 ml of chlorobenzene for 5 min. Separate the phases and measure the absorbance of the organic phase at 630 nm, in a 1-cm glass cell, with chlorobenzene as reference.

Procedure for steel analysis

Weigh the steel sample (up to 0.1 g) into a 100-ml fused silica beaker, and dissolve it in 20 ml of sulphuric acid (1 + 6) by heating, and then gradually add 5 ml of 35% hydrogen peroxide solution. When the sample has dissolved, boil the solution on the hot-plate for about 10 min to destroy the surplus hydrogen peroxide. Adjust the solution to pH 1.8–2.0 with 8M sodium hydroxide, transfer the solution to a 100-ml standard flask and make up to volume with water. Apply the standard procedure to 1.0 ml of this solution after addition of 0.4 ml of DCTA solution, 0.5 ml of potassium fluoride solution and 0.1 ml of sodium citrate solution.

RESULTS AND DISCUSSION

Selection of complexing agent, cationic dye and extraction solvent

We have examined the reactions between molybdenum(VI) and 2-hydroxy-2-methylbutyric acid, 2-hydroxyisocaproic acid, mandelic acid and *p*-chloromandelic acid, and extraction of the products into chloroform, chlorobenzene, benzene, toluene, carbon tetrachloride and cyclohexane, with the dyes Ethyl Violet, Methyl Violet, Crystal Violet, Brilliant Green and Malachite Green as counter-ions. Chloroform is unsuitable as the solvent owing to the high extractability of the cationic dyes themselves. Carbon tetrachloride and cyclohexane do not extract the ion-association complexes at all. Chlorobenzene was the solvent of choice, because the sensitivity was greater than with benzene or toluene. Table I shows that the MG–*p*-MACI–chlorobenzene system is the most

Table 1. The reagent blank absorbance (A) and the apparent molar absorptivity (ϵ , l. mole⁻¹. cm⁻¹) for molybdenum complexes with α -hydroxy acids and dyes, extracted into chlorobenzene

Complexing reagent	Ethyl Violet		Methyl Violet		Crystal Violet		Brilliant Green		Malachite Green	
	A	ϵ	A	ϵ	A	ϵ	A	ϵ	A	ϵ
2-Hydroxy-2-methylbutyric acid	0.39	6.2×10^4	0.17	1.2×10^4	0.19	1.0×10^4	0.13	4.0×10^3	0.16	2.0×10^4
2-Hydroxyisocaproic acid	0.43	2.2×10^4	0.15	2.6×10^4	0.14	6.1×10^4	0.16	3.2×10^4	0.26	2.9×10^4
Mandelic acid	0.48	2.9×10^4	0.17	9.8×10^3	0.20	3.2×10^4	0.15	1.2×10^4	0.24	4.4×10^4
<i>p</i> -Chloromandelic acid	0.65	4.3×10^4	0.16	2.4×10^4	0.23	3.3×10^4	0.12	5.3×10^4	0.06	1.06×10^5

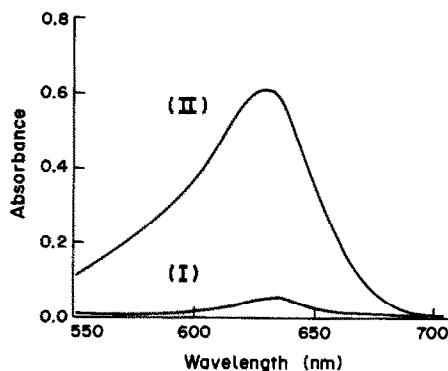


Fig. 1. Absorption spectra. (I) Reagent blank. (II) $5.2 \times 10^{-6}M$ Mo(VI) (2.0 μg). MG $2.5 \times 10^{-4}M$. pH 3.0. *p*-Chloromandelic acid $1.0 \times 10^{-4}M$. Reference, chlorobenzene.

suitable for determination of micro amounts of molybdenum(VI). The absorption spectra of the complex and reagent blank are shown in Fig. 1. MG is not extracted.

Experimental variables

Maximum and constant absorbance of the organic phase was obtained over the pH range 2.0–4.0, and pH 3.0 was chosen as optimal. Phosphate buffer (0.1M, pH 3) can be used instead of acetate buffer, but tartrate or citrate buffer can not, owing to the lower sensitivity ($\epsilon = 2.38 \times 10^4$ l. mole⁻¹. cm⁻¹ for tartrate and 1.91×10^4 for citrate).

The absorbance of the reagent blank increases with increase in MG concentration, but the net absorbance for a fixed molybdenum concentration is constant for MG concentrations exceeding $1.8 \times 10^{-4}M$ in the aqueous solution extracted. The concentration of MG was fixed at $2.5 \times 10^{-4}M$. Figure 2 shows that maximal and constant net absorbance is obtained with more than $0.3 \times 10^{-4}M$ *p*-MACl in the aqueous phase extracted. The concentration of *p*-MACl was therefore fixed at $1.0 \times 10^{-4}M$.

A shaking time of about 3 min is adequate, but 5 min is recommended.

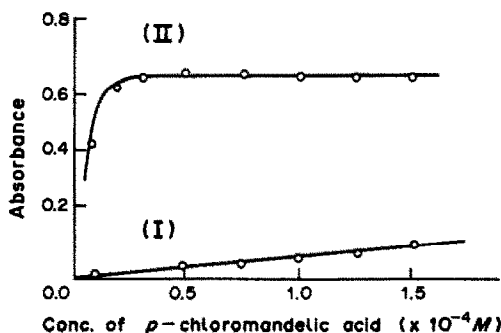


Fig. 2. Effect of *p*-chloromandelic acid concentration. (I) Reagent blank. (II) Net absorbance (Mo = $5.2 \times 10^{-6}M$) MG $2.5 \times 10^{-4}M$. pH 3.0.

Table 2. Effect of diverse ions on the determination of 2.00 μg of molybdenum in 4 ml

Ion	Added as	Amounts added, * μg	Mo recovery, %	Ion	Added as	Amounts added, * μg	Mo recovery, %
F ⁻	KF	1000	97	As(III)	As ₂ O ₃	1600	103
Cl ⁻	KCl	4000	103	As(V)	Na ₂ HAsO ₄	1600	98
Br ⁻	NaBr	500	103	Sb(III)	SbCl ₃	0.16	103
I ⁻	NaI	5.2	103	Sb(V)	K[Sb(OH) ₆]	400	102
ClO ₄ ⁻	KClO ₄	0.4	103	Se(IV)	H ₂ SeO ₃	1600	97
SCN ⁻	KSCN	0.2	104	B(III)	H ₃ BO ₃	8.6	103
NO ₃ ⁻	NaNO ₃	10	104	Cr ³⁺	CrCl ₃	750	96
SO ₄ ²⁻	Na ₂ SO ₄	20000	102	Mn ²⁺	MnCl ₂	1200	103
H ₂ PO ₄ ⁻	KH ₂ PO ₄	10000	97	Fe ³⁺	Ferric alum	30	95
Be ²⁺	BeSO ₄	100	95	Co ²⁺	CoCl ₂	600	97
Mg ²⁺	MgCl ₂	1000	103	Ni ²⁺	NiCl ₂	600	95
Ca ²⁺	CaCl ₂	1000	101	Cu ²⁺	CuSO ₄	1500	99
Sr ²⁺	SrCl ₂	1800	103	Zn ²⁺	ZnCl ₂	1500	97
Ba ²⁺	BaCl ₂	1400†	100	Sn(II)	SnCl ₂	0.6	105
Al ³⁺	Potassium alum	150	96	Sn(IV)	SnCl ₄	100	104
Pb ²⁺	PbCl ₂	1000†	96	Ti(IV)	TiOSO ₄	0.04	103
				W(VI)	Na ₂ WO ₄	0.25	103

*Amounts added per 4 ml.

†Acetate buffer solution adjusted with HCl was taken.

Composition of the complex

The molar absorptivity of MG in aqueous solution is *ca.* 6.8×10^4 l.mole⁻¹.cm⁻¹, and the apparent molar absorptivity for molybdenum in the extract is about 1.6 times that of MG. It is suggested that the mole ratio of MG and molybdenum in the complex is 2:1. The composition of the extracted species cannot be determined by the continuous-variations or mole-ratio methods, because of the large excess of *p*-MACl and MG required for its formation. However, it is suggested that $[\text{MoO}_x(\textit{p}\text{-MACl})_2]^{2-}$ is formed and extracted as its ion-association complex with MG.

Calibration graph

The calibration graph obtained by the standard procedure was linear over the range $0.26\text{--}10.4 \times 10^{-6}M$ (0.10–4.00 μg) molybdenum in the aqueous phase. The apparent molar absorptivity calculated from the slope of the graph was 10.6×10^4 l.mole⁻¹.cm⁻¹, and the absorbance of the reagent blank was 0.057. These figures were independent of temperature in the range 10–25°. The coefficient of variation was 1.8% for eight replicates at the $5.2 \times 10^{-6}M$ level of molybdenum. The absorbance of the organic phase remained constant for at least 60 min.

Effect of diverse ions

The effect of various ions on the determination of 2.00 μg of molybdenum was examined (Table 2). Iodide, perchlorate and thiocyanate, which are bulky and of low surface-charge density, cause positive errors at low levels, whereas chloride, sulphate and phosphate do not interfere even at high concentrations. Most cations tested do not interfere when present in 500-fold ratio to the amount of molyb-

denum. The permissible amounts of foreign metal ions which strongly interfere with the determination of molybdenum are shown in Table 3. The cause of the interference by iron(III) is not known. Antimony(III), titanium(IV), tin(II) and tungsten give positive errors because they react with *p*-MACl to form extractable complex anions, whereas antimony(V) does not interfere, owing to its slow reaction rate at room temperature. Boron does not interfere strongly, probably because of the low concentration of *p*-MACl.

Determination of molybdenum in steel samples

The proposed method was applied to the determination of molybdenum in carbon steels (NBS 362, JSS 169-3 and 171-3). As the presence of certain ions leads to less satisfactory results, we examined masking of these ions. Addition of masking agents decreased the sensitivity for molybdenum, but this could be counterbalanced by using more MG solution (0.5 ml), though the absorbance of the reagent blank was then 0.168. The tolerance limits are given in Table 3. The iron(III) and any titanium(IV) from

Table 3. Permissible amounts* of interfering ions in the determination of molybdenum (2.00 μg per 4 ml) in the presence of masking agents

Ion	Masking agent			
	None	KF, 0.025M	DCTA, 0.01M	Citrate, 0.0025M
Ti(IV)	0.04	158	0.28	0.04
Sb(III)	0.16	3.8	0.22	1.9
W(VI)	0.25	0.53	0.25	2.8
Fe(III)	30	—	1200	—

*Amounts (μg per 4 ml) that give not more than +3% error.

Table 4. Determination of molybdenum in steel

Sample* (certified value, %)	Sample weight, g	Molybdenum found†	
		µg	%
NBS 362 (0.068)	0.0503	0.335	0.066 ₆
	0.0529	0.364	0.068 ₈
	0.0987	0.665	0.066 ₅
	0.1001	0.676	0.067 ₅
	0.1004	0.678§	0.067 ₅
JSS 169-3 (0.064)	0.0514	0.324	0.063 ₀
	0.0987	0.641	0.064 ₉
	0.1024	0.648	0.063 ₃
JSS 171-3 (0.035)	0.0974	0.341	0.0350
	0.1003	0.347	0.0346
	0.1041	0.371	0.0356

Other components: NBS 362: C, 0.16; Mn, 1.04; Si, 0.39; V, 0.04; Ti, 0.084; W, 0.20; Sn, 0.016; Al, 0.09; Zr, 0.19; Sb, 0.013; Cu, 0.50; Ni, 0.59; Cr, 0.30; Co, 0.30; As, 0.09%. JSS 169-3: Ti, 0.013; As, 0.005; Ni, 0.050; Sn, 0.011; Cr, 0.095; Al, 0.045; Ca, 0.0006%. JSS 171-3: Ti, 0.036; As, 0.045; Ni, 0.11; Sn, 0.034; Cr, 0.067; Al, 0.040; Ca, 0.0013%.

*1.0 ml of the 100 ml of sample solution was analysed.

†Mean of six determinations.

§Standard deviation 0.012 µg.

the steel can be masked with DCTA and potassium fluoride respectively, and any antimony(III) and tungsten(VI) with citrate. Any residue from the sulphuric acid-hydrogen peroxide treatment was dissolved as described earlier^{20,21} and analysed for molybdenum. No significant amounts were found to be present, so any residue from the dissolution step can safely be discarded. Table 4 shows that the values obtained are in good agreement with the certified

values. Recoveries of 98–102% were obtained by the standard addition method.

REFERENCES

1. E. B. Sandell, *Colorimetric Determination of Traces of Metals*, 3rd Ed., Interscience, New York, 1959.
2. Z. Marczenko, *Spectrophotometric Determination of Elements*, Horwood, Chichester, 1976.
3. K. Kawabuchi and R. Kuroda, *Anal. Chim. Acta*, 1969, **46**, 23.
4. J. E. Wells and R. Pemberton, *Analyst*, 1947, **72**, 185.
5. K. Tanaka and N. Takagi, *Bunseki Kagaku*, 1970, **19**, 790.
6. K. Motojima, H. Hashitani, H. Yoshida and K. Izawa, *ibid.*, 1962, **11**, 47.
7. E. Sudo, *Nippon Kagaku Zasshi*, 1957, **77**, 1451.
8. H. Kohara, N. Ishibashi and K. Abe, *Bunseki Kagaku*, 1970, **19**, 48.
9. S. Maekawa, K. Kato and A. Sasaki, *ibid.*, 1970, **19**, 1275.
10. A. G. Fogg, J. L. Kumar and D. T. Burns, *Analyst*, 1975, **100**, 311.
11. T. J. Koralewski and G. A. Parker, *Anal. Chim. Acta*, 1980, **113**, 389.
12. A. M. Wilson and O. K. McFarland, *Anal. Chem.*, 1966, **36**, 2488.
13. R. Přibil and J. Adam, *Talanta*, 1971, **18**, 349.
14. K. S. Patel and R. K. Mishra, *ibid.*, 1982, **29**, 791.
15. K. S. Patel, H. Khatri and R. K. Mishra, *Anal. Chem.*, 1983, **55**, 1823.
16. A. Ahmand, F. I. Nwabue and G. E. Ezeife, *Talanta*, 1984, **31**, 265.
17. S. Sato, *Anal. Chim. Acta*, 1983, **151**, 465.
18. S. Sato, S. Uchikawa, E. Iwamoto and Y. Yamamoto, *Anal. Lett.*, 1983, **16**, 827.
19. S. Sato, *Talanta*, 1985, **32**, 341.
20. *Idem*, *ibid.*, 1985, **32**, 447.
21. S. Sato and S. Uchikawa, *ibid.*, 1986, **33**, 115.

CONSTANT CALCEIN BLUE: AN INDICATOR FOR SPECTROFLUOROMETRIC CALCIUM DETERMINATION

GERALDINE M. HUITINK

Department of Chemistry, Indiana University at South Bend, South Bend, Indiana 46615, U.S.A.

(Received 6 June 1986. Accepted 6 November 1986)

Summary—A new fluorescent indicator for metal ions, called Constant Calcein Blue, has been synthesized by condensing 7-hydroxy-2,3-dimethylchromone, iminodiacetic acid and formaldehyde. The indicator exhibits extraordinary resistance to alkaline hydrolysis and is recommended for spectrofluorometric determinations of metal ions, such as calcium, that must be performed at pH 10.5 and higher.

Since its introduction by Diehl and Ellingboe¹ in 1956, Calcein has found widespread use as a metallofluorescent indicator in spite of problems posed by its instability. In aqueous alkaline solution it decomposes at an appreciable rate and loses all indicator function within a few days. Though this is not a serious problem when Calcein is used to mark the end-point of EDTA titrations of metal ions, the decomposition complicates direct fluorometric determinations of metal ions and necessitates frequent checks of calibration plots of fluorescence as a function of metal ion concentration. Attempts to reduce the rate of decomposition have included dissolution of Calcein in an aqueous alkaline medium with subsequent pH adjustment to 7,² freezing and storage in the dark,³ and use of propylene glycol⁴ rather than water as the solvent. Though these approaches extend the life of Calcein stock solutions, decomposition persists and most analysts prefer to prepare stock solutions of Calcein daily or to use it in a 1% solid mixture with an inert salt such as potassium chloride.

Because determinations of metal ions are often performed in alkaline medium, attack on metal ion-indicator complexes by hydroxide ion must also be considered. Jaselskis and Hefley⁵ report that the relative fluorescence of the cadmium-Calcein complex in 0.5M potassium hydroxide decreases by 7% within 2 hr. Such rapid deterioration requires that fluorescence measurements be made within 15 min of solution preparation.

Schepers⁶ attempted to solve the problem of indicator instability by employing fluorescent compounds more resistant to alkaline hydrolysis than fluorescein, the fluorescent moiety of Calcein, in condensation with iminodiacetic acid and formaldehyde. The compounds he produced were indeed more resistant to alkaline hydrolysis than Calcein, but were insufficiently fluorescent to serve as indicators. A series of 7-hydroxybenzo-4-pyrones differing in substituents at positions 2- and 3- of the benzo-4-pyrone ring was subsequently investigated by the present author.⁷ Substitution patterns favour-

ing both a high degree of fluorescence and resistance to alkaline hydrolysis were discovered. This study led to selection of 7-hydroxy-2,3-dimethylchromone for condensation with iminodiacetic acid and formaldehyde. The indicator resulting from that condensation is described below.

EXPERIMENTAL

Reagents

Respropiofenone was prepared by an adaptation of the synthesis of resacetophenone found in *Organic Syntheses*.⁸ To 199 g (202 ml, 2.7 mole) of propionic acid and 40.4 g (40 ml, 0.3 mole) of propionic anhydride in a 1-litre beaker was added 165 g (1.2 mole) of anhydrous zinc chloride, which was dissolved with the aid of heat. To this hot mixture 110 g (1 mole) of resorcinol was added with constant stirring. Heating was continued until small bubbles appeared. The beaker was removed from the hot-plate and left until the reaction was complete. After standing overnight, the solution was diluted with 500 ml of hydrochloric acid (1 + 1) and the dark reddish brown solution was placed in an ice-bath. The resulting precipitate was filtered off and washed free from zinc salts with five 200-ml portions of hydrochloric acid (1 + 3). The solid was dissolved in 1.8 litres of hot dilute hydrochloric acid (1 + 11) and the hot solution was filtered and cooled. The product obtained was 16 g (9.6% yield) of pale yellow crystals, m.p. 101–102°, and 105 g (63.3% yield) of oil which solidified on cooling, m.p. 97–100° (literature value 101.5°).

7-Hydroxy-2,3-dimethylchromone was synthesized by the procedure of Canter *et al.*⁹ by reacting the respropiofenone with sodium acetate and acetic anhydride at 170–180°, and treating the resulting acetyl derivative with warm dilute potassium hydroxide.

Standard $3.11 \times 10^{-3}M$ calcium solutions were prepared by dissolving primary standard calcium carbonate in hydrochloric acid and diluting with water.

Stock $3.11 \times 10^{-3}M$ solutions of Constant Calcein Blue were prepared by dissolving the material in 0.1M triethanolamine, pH = 9.0

The 0.7M potassium hydroxide used contained sufficient EDTA to sequester any potentially interfering metal ions present.

Buffer solutions were prepared by the method of Bates¹⁰ and were of the same ionic strength.

All reagents used were of analytical grade. All water was distilled and demineralized by passage through Amberlite MB-1 ion-exchange resin.

All glassware was cleaned with alcoholic potassium hydroxide containing EDTA and was rinsed three times with distilled water and five times with demineralized water.

Synthesis of Constant Calcein Blue

To 50 ml of water were added 0.06 mole (3.36 g) of potassium hydroxide, 0.045 mole (5.99 g) of iminodiacetic acid and 0.03 mole (5.71 g) of 7-hydroxy-2,3-dimethylchromone. The pH was adjusted to 8 by dropwise addition of dilute hydrochloric acid (1 + 3). To this mixture was added 0.045 mole (4.44 ml) of 37% formaldehyde solution. The temperature was raised to 60° and the reaction allowed to proceed overnight with stirring. The resulting mixture was filtered while warm. The filtrate, adjusted to pH 4.0 by addition of dilute hydrochloric acid (1 + 3), was reduced to near dryness by freeze-drying in vacuum. The white precipitate was separated by filtration and the yellow filtrate was stirred for 10 min with 200 ml of acetone. The upper liquid layer was decanted and discarded, then 200 ml of fresh acetone were added to the lower layer and stirred, this process being repeated three more times. The white solid produced by this procedure was combined with the solid obtained earlier and was recrystallized three times by dissolving it in the minimum amount of water by adding potassium hydroxide pellets, filtering, and readjusting the pH to 2.8 by dropwise addition of dilute hydrochloric acid. Analysis by Galbraith Laboratories, Inc. yielded C, 52.0%; H, 5.6%; N, 3.7%. The values calculated for $C_{16}H_{17}NO_7 \cdot 2H_2O$, molecular weight 371.31 are: C, 51.75%; H, 5.70%; N, 3.77%.

Apparatus and procedures

Measurements of pH were made with a Corning Model 10 pH-meter equipped with glass and calomel electrodes. Potentiometric titrations were done in 0.1M potassium chloride, with 0.1072M potassium hydroxide made up in 0.1M potassium chloride. Back-titrations were performed with 0.0760M hydrochloric acid made up in 0.1M potassium chloride.

A Micrometric Model SB2 microburette and Model S5Y syringes were used to deliver all microlitre volumes of reagents.

Absorbance study

Absorbance spectra of solutions at pH intervals of 0.5 over the range 3.5–12 were obtained with a Cary Model 219 spectrophotometer. The solutions were prepared by delivering 375 μ l of Constant Calcein Blue stock solution and 15 μ l of $1.46 \times 10^{-2}M$ EDTA into 25-ml standard flasks and diluting to the mark with appropriate buffers all of the same ionic strength. Acid dissociation constants were determined from the absorbances of additional solutions with pH values equal to the estimated $pK_{a2} \pm 0.0, 0.2, 0.4, \text{ and } 0.6$, by means of the equation

$$pK_{a2} = pH - \log \frac{(A_{\text{mix}} - A_{\text{HA}})}{(A_{\text{A}^-} - A_{\text{mix}})}$$

where A_{HA} is the absorbance of the acid form of the indicator, A_{A^-} is the absorbance of the base form of the indicator and A_{mix} is the absorbance of a mixture containing both forms of the indicator.

Fluorescence study

Fluorescence excitation and emission spectra of solutions at pH intervals of 0.5 over the range 3.5–12 were obtained by means of an Aminco-Bowman spectrofluorometer equipped with a Mosely XY Recorder. The spectra were uncorrected for variations in the emission characteristics of the lamp and response characteristics of the photomultiplier. The solutions were prepared by delivering 50 μ l of indicator stock solution and 15 μ l of $1.46 \times 10^{-2}M$ EDTA into 25-ml standard flasks and diluting to the mark with appropriate buffers, all of the same ionic strength. Acid dissociation constants were determined from the

fluorescence data by measuring the fluorescence of solutions with pH values equal to the estimated $pK_{a2} \pm 0.0, 0.2, 0.4, \text{ and } 0.6$ and calculating pK_{a2} by using the equation

$$pK_{a2} = pH - \log \frac{(F_{\text{mix}} - F_{\text{HA}})}{(F_{\text{A}^-} - F_{\text{mix}})}$$

Other measurements of fluorescence were made on a Turner Model 110 fluorometer. The filters used were: primary, 110-811 (7-60); secondary, 110-816 (2A), plus a 1% neutral density filter.

Stability studies

Constant Calcein Blue stock solution. The fluorescence of 0.7M potassium hydroxide containing Constant Calcein Blue and calcium in a molar ratio of 1:10 was measured approximately 1 hr after preparation. Identical solutions were prepared periodically over a seven-month period, with the same indicator stock solution. The decrease in fluorescence with time was used to determine the rate of hydrolysis of the stock solution. The apparent first-order rate constant was calculated by the method described in an earlier paper.⁷ The study was repeated three times and at different concentrations of indicator. No attempt was made to keep the indicator stock solution at constant temperature or to protect it from light.

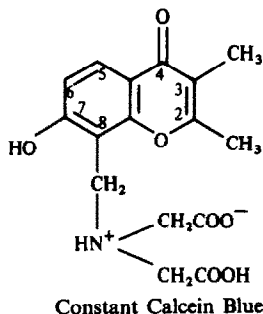
Constant Calcein Blue in 0.7M potassium hydroxide. Solutions of Constant Calcein Blue in 0.7M potassium hydroxide were prepared and kept in a water-bath at 25.5° for 2½ months. Aliquots were removed periodically and mixed with sufficient calcium stock solution to provide a tenfold molar excess of calcium. The fluorescence which developed was measured approximately 1 hr after solution preparation. The decrease in fluorescence with time was used to determine the rate of hydrolysis of Constant Calcein Blue in 0.7M potassium hydroxide. The study was repeated seven times and at different concentrations of indicator. No attempt was made to shield the solutions from light. The data were treated in the same manner as those for the stability study on the Constant Calcein Blue stock solution.

Calcium-Constant Calcein Blue in 0.7M potassium hydroxide. Solutions containing indicator and calcium ion in 1:10 molar ratio were made up in 0.7M potassium hydroxide and kept in a water-bath at 25.5°. Aliquots were removed periodically for fluorescence measurement. The decrease in fluorescence with time was used to determine the rate of hydrolysis of the calcium-Constant Calcein Blue complex. The study was repeated nine times and at different concentrations of indicator. The hydrolyses were, in most instances, followed for 5½ half-lives.

The fluorescence of solutions containing sufficient calcium to provide 0–0.35:1 calcium:indicator molar ratios was monitored for 32 hr. The solutions were prepared by adding calcium stock solution in 20- μ l (6.22×10^{-8} mole) increments to a series of 100 ml standard flasks and diluting to the mark with $1.24 \times 10^{-2}M$ indicator solutions in 0.7M potassium hydroxide. Solutions were made up in Pyrex and in polypropylene flasks. No attempt was made to control the temperature or protect the solutions from light.

RESULTS AND DISCUSSION

Constant Calcein Blue, H_2In , is regarded as being 7-hydroxy-2,3-dimethylchromone-8-methyleneiminodiacetic acid. The methyleneiminodiacetic acid group has been assigned to position 8- in keeping with established substitution patterns found for 7-hydroxybenzo-4-pyrones.^{6,11} In titration of the material with potassium hydroxide, end-points occur at pH values of approximately 5.02 and 8.90 and correspond to formation of H_2In^- and $HIIn^{2-}$, respect-



ively. The value for pK_{a_2} , determined by titration with potassium hydroxide and attributed to dissociation of the phenolic proton, is 6.75; pK_{a_1} , the dissociation constant of the carboxylic proton, could not be determined by titration with potassium hydroxide, as the material did not fully dissolve until just before the first end-point. Back-titration with hydrochloric acid yielded values of 3.07 and 6.76 for pK_{a_1} and pK_{a_2} , respectively. The first acid dissociation constant could be determined by back-titration with hydrochloric acid because the material remained in solution until well past the middle of the second half of the back-titration curve.

In weakly acidic solution Constant Calcein Blue exhibits maximum absorbance at 298 nm (at pH 4.0, $\epsilon = 1.50 \times 10^4$ l.mole⁻¹.cm⁻¹). On neutralization of the phenolic proton the wavelength of maximum absorbance shifts to 333.1 nm (at pH 10.0, $\epsilon = 1.39 \times 10^4$ l.mole⁻¹.cm⁻¹). Absorbance measurements yield 6.80 ± 0.09 for pK_{a_2} .

In acid solution the indicator, present as H_2In^- , is weakly fluorescent. The wavelength of maximum excitation at pH 4.0 is 302 nm and the wavelength of maximum emission is 475 nm. Above pH 6.0 the fluorescence emission increases dramatically, the wavelength of maximum excitation shifts to 333 nm, and the wavelength of maximum emission shifts to 450 nm. The fluorescence emission reaches a maximum at pH 8.90, at which point the material is in the form HIn^{2-} (Fig. 1). Changes in the fluorescence intensity at 450 nm are the result of changes in absorbance at 333 nm and yield a value of 6.69 ± 0.04 for pK_{a_2} , a ground-state constant. This value agrees with the pK_{a_2} values obtained from potentiometric titration and absorbance measurement. With additional increase in pH, the imino hydrogen atom dissociates and the fluorescence is lost, the data yielding a value of 11.30 ± 0.02 for pK_{a_1} . At pH 13 and higher, addition of calcium and cadmium and, to

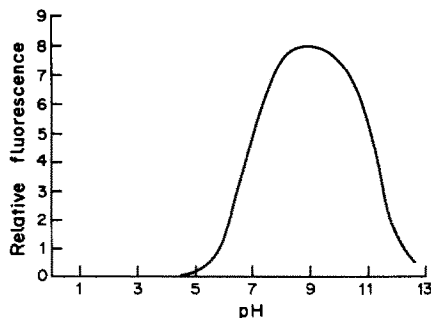


Fig. 1. Fluorescence of Constant Calcein Blue as a function of pH. Excitation monochromator set at 333 nm, emission monochromator set at 450 nm.

a lesser extent, addition of barium and strontium, restores the fluorescence.

The phenolate ion is responsible for the absorbance and fluorescence at pH 6.0 and above. Upon addition of a proton, the wavelength of maximum absorbance shifts from 333.1 nm to 298 nm. This shift to shorter wavelength is consistent with protonation of a phenolic oxygen atom. Simultaneously, the wavelength of maximum emission shifts from 450 nm to 475 nm. This shift to longer emission wavelength with increasing acidity suggests that the fluorescent species has undergone tautomerization and in the excited state it is the carbonyl oxygen atom, not the phenolic oxygen atom, that is protonated.

Hydroxide ion attacks position 2- of the benzo-4-pyrone ring,¹² causing ring opening and concomitant loss of the fluorescence of the calcium-Constant Calcein Blue complex. In 0.7M potassium hydroxide and at 25.5°, the fully deprotonated form of the indicator, In^{3-} , and its calcium complex, $CaIn^-$, decompose according to pseudo-first-order kinetics; see Table 1 for the apparent first-order rate constants and half-lives.

In^{3-} decomposes more slowly than $CaIn^-$, a charge of -3 being more effective than a charge of -1 in retarding nucleophilic attack by hydroxide ion. Under the same conditions of solvent and temperature, 7-hydroxy-2,3-dimethylchromone, the parent fluorescent molecule, carries a charge of -1 and has an apparent first-order rate constant of 0.0704 ± 0.0007 day⁻¹ and a half-life of 9.80 ± 0.09 days,⁷ values similar to those of $CaIn^-$.

Stock solutions of Constant Calcein Blue made up in 0.1M triethanolamine, pH = 9.0, decompose with a half-life of 73.8 ± 1.7 days (apparent first-order rate constant, 0.00935 ± 0.00009 day⁻¹). The lower hydroxide ion concentration accounts for the slower rate of hydrolysis of the stock solutions.

Before 0.7M potassium hydroxide can be used in spectrofluorometric determinations of metal ions, sufficient EDTA must be added to sequester any potentially interfering metal ion impurities. These impurities are present at a level ($3 \times 10^{-6}M$) equal to and higher than the metal-ion levels generally deter-

Table 1. Apparent first-order rate constants and half-lives for Constant Calcein Blue and its calcium complex in 0.7M potassium hydroxide at $25.5 \pm 0.1^\circ$

Compound	k, day^{-1}	$t_{1/2}, \text{days}$
In^{3-}	0.0360 ± 0.0012	19.26 ± 0.66
$CaIn^-$	0.0743 ± 0.0011	9.30 ± 0.13

Table 2. Relative fluorescence of calcium-Constant Calcein Blue in 0.7M potassium hydroxide as a function of time; concentration of indicator, $1.25 \times 10^{-5}M$; Pyrex flasks

Time after solution preparation, hr	[Ca ²⁺], μM	0.00	0.62	1.24	1.87	2.49	3.11	3.73	4.35
	[Ca ²⁺]/[In ³⁻]	0.00	0.05	0.10	0.15	0.20	0.25	0.30	0.35
1.0		15.7	22.1	34.0	47.2	59.4	72.9	86.3	98.3
1.5		14.7	22.9	34.3	47.5	60.7	73.7	88.0	98.6
4.0		14.4	22.1	35.5	48.1	60.2	74.7	87.3	99.2
5.5		15.9	23.3	35.5	47.8	61.1	74.5	86.3	99.1
7.0		15.7	24.5	36.4	48.1	60.6	74.1	86.5	98.2
10.5		14.8	23.2	37.3	48.3	61.6	73.3	86.1	98.1
32.0		14.7	23.9	34.9	48.3	60.8	72.9	83.9	96.0

Table 3. Relative fluorescence of calcium-Constant Calcein Blue in 0.7M potassium hydroxide as a function of time; concentration of indicator, $1.25 \times 10^{-5}M$; polypropylene flasks

Time after solution preparation, hr	[Ca ²⁺], μM	0.00	0.62	1.24	1.87	2.49	3.11	3.73
	[Ca ²⁺]/[In ³⁻]	0.00	0.05	0.10	0.15	0.20	0.25	0.30
1.0		14.2	23.1	35.8	49.8	62.9	74.3	93.2
1.5		14.3	23.1	36.1	50.0	63.3	75.1	93.3
4.0		14.1	22.9	35.9	49.8	62.4	74.8	93.3
5.5		14.3	23.0	35.8	49.7	62.3	74.0	92.7
7.0		14.1	22.9	35.8	49.8	62.7	75.2	93.1
10.5		14.1	22.8	35.7	49.3	61.3	73.8	91.9
32.0		14.7	23.0	35.2	48.7	61.1	72.1	89.5

mined fluorometrically. The amount of EDTA required is obtained from fluorometric titration of 0.7M potassium hydroxide containing Constant Calcein Blue, the relative fluorescence being plotted as a function of the volume of EDTA added.

Calcium combines with Constant Calcein Blue in 1:1 ratio as determined by the mole-ratio method. The fluorescence of CaIn⁻ in 0.7M potassium hydroxide remains unchanged over a period of 10½ hr (see Tables 2 and 3). Similar results are obtained in both Pyrex and polypropylene flasks provided the Pyrex flasks are cleaned with alcoholic potassium hydroxide containing EDTA and thoroughly rinsed with demineralized water. Without this treatment the fluorescence increases dramatically and irregularly from flask to flask and with time, and this is attributed to calcium contamination from the glass itself.

Light apparently does not affect the rate of decomposition of solid H₃In, 0.1M triethanolamine solutions of HIn²⁻, aqueous solutions of In³⁻, or aqueous solutions of CaIn⁻, as no evidence for this was detected.

Because of its unexcelled resistance to alkaline hydrolysis, Constant Calcein Blue is recommended as a substitute for Calcein and Calcein-like indicators in fluorometric determinations of metal ions at pH 13 and higher.

Acknowledgements—Support from Indiana University in the form of Summer Faculty Fellowships, and Grant-in-Aid of Research funds, is gratefully acknowledged. The author also wishes to thank Professor Harvey Diehl for providing bench space and making instruments available to her during a sabbatical leave.

REFERENCES

- H. Diehl and J. L. Ellingboe, *Anal. Chem.*, 1956, **28**, 882.
- W. C. Hoyle and H. Diehl, *Talanta*, 1972, **19**, 206.
- D. F. H. Wallach and T. L. Steck, *Anal. Chem.* 1963, **35**, 1035.
- B. L. Kepner and D. M. Hercules *ibid.*, 1963, **35**, 1238.
- A. J. Hefley and B. Jaselskis, *ibid.*, 1974, **46**, 2036.
- G. J. Scheppers, *The 7-hydroxy-8-(N,N-bis(carboxymethyl)aminomethyl)benzo- γ -pyrones as metallofluorescent indicators*, Ph.D. Dissertation, Iowa State University, Ames, Iowa, 1967.
- G. M. Huitink, *Talanta*, 1980, **27**, 977.
- Organic Syntheses, Collective Volume III*, 1964, 761.
- F. W. Canter, F. H. Curd and A. Robertson, *J. Chem. Soc.*, 1931, 1262.
- R. G. Bates, *Determination of pH; Theory and Practice*, pp. 156-162, Wiley, New York, 1964.
- D. V. Joshi, J. R. Merchant and R. C. Shah, *J. Org. Chem.*, 1956, **21**, 1004.
- R. C. Elderfield (ed.), *Heterocyclic Compounds*, Vol. 2, p. 258. Wiley, New York, 1951.

DETERMINATION OF RUBIDIUM, STRONTIUM AND BARIUM IN BARITE BY ATOMIC-ABSORPTION SPECTROMETRY AFTER DISSOLUTION IN DISODIUM ETHYLENEDIAMINETETRA-ACETATE*†‡

J. G. SEN GUPTA

Geological Survey of Canada, Ottawa, Ontario, Canada

(Received 9 June 1986. Accepted 31 October 1986)

Summary—A simple and rapid method is described for determining up to 50% of barium, ~350 µg/g or more of strontium and ~1 µg/g or more of rubidium in barite samples. The method involves dissolution of the barite by refluxing with an ammoniacal disodium EDTA solution. For the determination of total strontium and rubidium, the silicate residue remaining is filtered off and decomposed with hydrofluoric and sulphuric acids to recover residual strontium and rubidium. Barium and strontium are subsequently determined by flame atomic-absorption spectrometry and rubidium is determined by graphite-furnace atomic-absorption spectrometry. Results obtained for barium and strontium in several barites by the proposed method are compared with those obtained by wavelength-dispersive and energy-dispersive X-ray fluorescence spectrometry, respectively. The method is reliable and more rapid than conventional methods.

Barite (BaSO_4) which is a principal source of barium compounds, occurs in nature mainly as a gangue mineral in hydrothermal vein deposits, in sedimentary and igneous rocks, and in clay and hot spring deposits. Because celestine (SrSO_4) is isostructural with barite, barium in barite can be replaced by strontium to yield a continuous series of solid solutions ranging from barite to celestine,¹ which explains why the strontium content of barites varies from several hundred to several thousand µg/g. Studies on the distribution of strontium and variations in the $^{87}\text{Sr}/^{86}\text{Sr}$ ratio have been applied in elucidating the genesis of barites.²⁻⁵ Besides being a stable natural isotope, ^{87}Sr is also a decay product of radioactive ^{87}Rb and, consequently, the measurement of rubidium and strontium concentrations plays an important role in determining the age and mineralization process of barites in various geochemical environments.²⁻⁵ To aid in these studies reliable methods are required for the determination of small amounts of strontium and rubidium and major and minor levels of barium in barite samples.

Procedures recently recommended for opening out barite involve fusion with sodium carbonate³ or lithium metaborate,⁴ leaching of the sample with sodium carbonate solution,⁶ and high-pressure heating at 1000° with graphite.⁷ However, none of these methods was considered suitable for the present

work. Complete decomposition of barium sulphate is not always obtained with sodium carbonate even after a double fusion step, and lithium metaborate also decomposes any associated barium feldspar, which would give erroneous results for determination of barium combined as sulphate. The sodium carbonate leaching method has only been recommended for 5-mg samples, which would not be adequate for the determination of µg/g concentrations of rubidium, and the graphite method results in loss of rubidium by volatilization. Because disodium EDTA has been recommended for the dissolution of traces of barium sulphate in diagnostic meals⁸ and calcium carbonate⁹ its applicability for dissolution of barite was investigated in this work.

The proposed method involves the dissolution of barite with an ammoniacal solution of disodium EDTA, the recovery of strontium and rubidium in the silicate residue and the ultimate determination of barium and strontium by flame AAS and of rubidium by graphite-furnace AAS.

EXPERIMENTAL

Apparatus

A Techtron model AA-3 spectrometer, fitted with a water-cooled burner and some model AA-3 accessories,¹⁰ was used for flame atomic-absorption measurements. Nitrous oxide-acetylene and air-acetylene flames were employed for the determination of barium and strontium, respectively, and absorbance peaks were recorded on a Varian model 9176 strip-chart recorder at a chart speed of ~8 cm/min.

A Varian model GTA-95 graphite-tube atomizer, equipped with a programmable sample dispenser and memory storage for 8 operating-parameter programmes, and coupled with a Varian model AA-475 spectrometer

*Presented at 1986 Congress on Advances in Spectroscopy and Laboratory Science, held in Toronto, 6-9 October, as an invited paper.

†Government of Canada copyrights reserved.

‡Geological Survey of Canada Contribution 13786.

Table 1. Operating parameters and characteristic concentrations for barium, strontium and rubidium

Element	Wavelength, nm	Spectral bandwidth, nm	Lamp current, mA	AAS mode	Characteristic concentration*
Ba	553.6	0.5	10†	N ₂ O-C ₂ H ₂ flame	0.57
Sr	460.7	0.5	5†	Air-C ₂ H ₂ flame	0.14
Rb	780.0	0.2	10‡	Graphite furnace	2

*Concentration of the element, in $\mu\text{g/ml}$ for flame AAS or weight of the element in pg for electrothermal AAS, which produces a change, compared with a pure solvent or blank, of 0.0044 absorbance units.

†Varian hollow-cathode lamp.

‡Cathodeon hollow-cathode lamp.

fitted with IEEE communication, was used for the graphite-furnace AAS determination of rubidium. An Epson model MX-82 Type III printer with IEEE interface was employed for recording absorbances and temperature-absorption peak profiles, and pyrolytically-coated graphite tubes and argon gas (99.999% pure) were used throughout the work. The spectrometer was operated in the single-beam and peak-height mode and a 1-sec integration-time was used in setting zero absorbance on the instrument.

Characteristic concentrations and instrumental operating parameters for barium, strontium and rubidium are given in Tables 1-3.

Reagents

A standard 500- $\mu\text{g/ml}$ barium solution was prepared by dissolving 0.0850 g of pure barium sulphate powder as described in the procedure, followed by dilution of the resulting solution to 100 ml with water. This solution contains 30 mg of disodium EDTA per ml (equivalent to 3.71 mg of sodium per ml).

A 100- $\mu\text{g/ml}$ strontium solution was prepared by appropriate dilution of a commercial 1000- $\mu\text{g/ml}$ solution and a 100- $\mu\text{g/ml}$ rubidium solution was prepared by dissolving 0.1415 g of pure rubidium chloride in water and diluting to 1 litre. A 1- $\mu\text{g/ml}$ rubidium solution was prepared by appropriate dilution of the stock solution with water.

A 10-mg/ml sodium (spectroscopic buffer) solution was prepared by dissolving 25.4 g of pure sodium chloride in water and diluting to 1 litre.

Carbonate-free ammonia was prepared by passing ammonia gas into a plastic bottle containing ~ 500 ml of water (cooled in ice-water) until the volume of the resulting solution was ~ 750 ml.

A 120-mg/ml disodium ethylenediaminetetra-acetate (EDTA) solution was prepared by dissolving 60 g of the pure salt in boiling water and diluting at room temperature to 500 ml. This solution contains 14.84 mg of sodium per ml.

Demineralized water was used throughout and the solutions were stored in tightly stoppered Nalgene bottles.

Calibration solutions

Barium. Prepare 50-, 100-, 150- and 200- $\mu\text{g/ml}$ barium solutions by adding 1, 2, 3 and 4 ml of 500- $\mu\text{g/ml}$ standard barium solution to four 10-ml standard flasks, together with sufficient 120-mg/ml disodium EDTA solution and 10-mg/ml sodium buffer solution in each flask for the final solutions to contain 12 mg/ml disodium EDTA and a total of ~ 3000 $\mu\text{g/ml}$ sodium, then dilute each solution to volume with water. Prepare a blank calibration solution containing 12 mg/ml disodium EDTA and a total of ~ 3000 $\mu\text{g/ml}$ sodium.

Strontium and rubidium. Transfer 3 g of disodium EDTA to each of four 50-ml beakers, add 15 ml of water and heat to dissolve the salt. Add 2.5, 3.75, 5 and 6.25 ml of 100- $\mu\text{g/ml}$ standard strontium solution and 0.25, 0.5, 1 and 1.5 ml of 1- $\mu\text{g/ml}$ rubidium solution to give final solutions containing 10, 15, 20 and 25 $\mu\text{g/ml}$ strontium and 10, 20, 40 and 60 ng/ml rubidium. If necessary, evaporate the solutions to ~ 20 ml, cool to room temperature, then transfer them to 25-ml standard flasks and dilute to volume with water. Prepare a blank calibration solution containing 120 mg/ml disodium EDTA (Note 1).

Procedure

Transfer 0.1 g of powdered barite sample to a 150-ml borosilicate beaker and add 60 ml of freshly prepared carbonate-free ammonia solution and 3 g of disodium EDTA. Place a glass rod in the solution, cover the beaker with a watch glass and boil the solution on a hot-plate for 3-4 hr (Note 2). Stir the solution periodically and rub the solid sample against the bottom of the beaker to aid the dissolution. Add sufficient carbonate-free ammonia solution as required during the boiling step to keep the volume of the solution at ~ 60 ml. Wash down the cover and the sides of the beaker with water, add 2 ml of carbonate-free ammonia solution, cover the beaker, allow it to stand on a steam-bath overnight (Note 3), then, if necessary, filter the solution (5.5-cm Whatman No. 40 paper) into a 100-ml beaker and wash the paper thoroughly with hot 5% ammonia solution.

Table 2. Operating parameters for rubidium in a pyrolytically-coated graphite furnace

Step number	Temperature, °C	Time, sec	Argon gas flow, l./min
1	75	15	3
2	90	60	3
3	120	10	3
4	600	10	3
5	850	10	0
6	2000	1	0*
7	2000	2	0*
8	2000	1	3

*Read command initiated.

Table 3. Auto sample-dispenser parameters for rubidium

Type	Samples and standards		
	Location	Volume, μl	Blank* volume, μl
Blank	—	—	10
STD 1	46	10	10
STD 2	47	10	10
STD 3	48	10	10
STD 4	49	10	10
Samples†	—	10	10

*Demineralized water.

†Location 1 was used for disodium EDTA (3 g/25 ml) blank, and locations 2-45 were used for samples.

Reserve the residue. Evaporate the solution to ~20 ml and, if necessary, add several drops of carbonate-free ammonia and warm the solution to remove turbidity. Transfer the hot solution (Note 4) to a 25-ml standard flask (Note 5), make up the volume nearly to the mark with water, cool the flask under running cold tap water and dilute to volume with water (solution A).

Transfer the residue to a 30-ml platinum crucible, burn off the paper at ~450° and ignite the residue at ~800°. Cool the crucible, add 2 ml of concentrated hydrofluoric acid and several drops of 50% v/v sulphuric acid and evaporate the solution to dryness on a sand-bath. Cool, add exactly 10 ml of solution A to the crucible, then heat the solution gently on a sand-bath, stirring periodically with a short glass rod. Filter the solution as described above and collect the filtrate in a 20-ml beaker. Evaporate the solution to ~8 ml, cool it to room temperature, transfer it to a 10-ml standard flask and dilute to volume with water (solution B). Carry a blank (10 ml of 120-mg/ml disodium EDTA solution) through the procedure for treatment of the residue, to obtain a calibration blank for solution B.

For the determination of barium, transfer a 1-ml aliquot of solution A to a 10-ml standard flask, add 1.5 ml of 10-mg/ml sodium buffer solution and dilute to volume with water. Using the conditions described under *Apparatus* and in Table 1, measure the absorbance at 553.6 nm, when this solution is sprayed into an appropriately adjusted nitrous oxide-acetylene flame. Determine the barium content of the sample solution by reference to a calibration graph obtained with standard barium solutions containing approximately the same concentrations of EDTA and sodium as the sample solution.

Using the conditions described under *Apparatus* and in Table 1, measure the strontium absorbance of sample solutions A and B, at 460.7 nm, in an appropriately adjusted air-acetylene flame. Utilizing the conditions given under *Apparatus* and in Tables 1-3, and using a 10- μ l aliquot (Note 6), measure the rubidium absorbance of both solutions at 780.0 nm, by graphite-furnace AAS. Determine the strontium and rubidium contents (Note 7) of both solutions by reference to calibration graphs obtained with standard solutions containing the same concentration of disodium EDTA as the sample solutions. Calculate the total strontium and rubidium contents of the sample by adding the amounts found in solutions A and B. Correct the rubidium result obtained for the sample by subtracting that obtained for the blank.

Notes

1. This blank is the calibration blank for the determination of strontium and rubidium in solution A only. For solution B, use the blank carried through the whole procedure.

2. For routine analysis of a large number of samples it is convenient to use a hot-plate in the dissolution step. However, BaSO₄ and barite dissolve more rapidly in ammoniacal EDTA solution if the beaker is placed on an asbestos-covered wire gauze supported by a tripod stand and heated directly with a Bunsen burner. In this case the disodium EDTA should be added gradually in ~1-g portions in the presence of an excess of ammonia solution, and the solution should be stirred periodically with a glass rod.

3. Pure barium sulphate and pure barite give clear solutions under these conditions.

4. This step is to prevent any separation of solid salts on the sides of the beaker on cooling.

5. If only strontium and rubidium are to be determined, the final solution obtained after treatment of the residue, as described in the next part of the procedure, should be combined with the initial solution (solution A).

6. This volume was found to be optimum; greater volumes result in excessive background signals because of

the longer time necessary to burn off the EDTA. The capillary tube of the automatic sample dispenser was rinsed with 10 μ l of water after injection of each 10- μ l sample solution.

7. If dilution of solution B is necessary, particularly for samples containing >5 μ g/g of rubidium, use 120-mg/ml disodium EDTA solution for the dilution.

RESULTS AND DISCUSSION

Effectiveness of disodium EDTA for dissolution of barite

Preliminary work showed that pure barium sulphate and pure barite completely dissolved when 0.1-g samples were heated with a strongly ammoniacal solution containing 3 g of disodium EDTA as described in the proposed method. However, some insoluble material, which was found from its X-ray powder-diffraction pattern to contain quartz, feldspar, pyrite and celsian (BaAl₂Si₂O₈), remained when impure barite samples (e.g., from Hemlo, Ontario) were treated in the same way. Some additional tests with various barium silicate minerals of the feldspar group, which may be associated with barite, viz. hyalophane (BaNaKAl₄Si₄O₁₆), celsian and paracelsian, confirmed that only barium sulphate is dissolved under these conditions.

Because barite does not incorporate rubidium in its structure, most of the rubidium in barite is probably present as silicate in the associated silicate gangue minerals. Although strontium is mostly present as SrSO₄ in solid solution with barite, small amounts may also be present as silicate in the gangue minerals, particularly as radiogenic ⁸⁷Sr. Consequently, to determine total strontium and rubidium for use in geochronological studies, it is necessary to recover these two elements from the silicate residue remaining after the dissolution of barite with ammoniacal EDTA solution. In the proposed method, the insoluble residue is decomposed with hydrofluoric and sulphuric acids and the resulting strontium and rubidium sulphates are leached out of any remaining residue by treatment with an aliquot of the initial EDTA solution.

Atomic-absorption finishes

Flame AAS finishes were chosen for the determination of both barium and strontium because of the high levels of these elements in barite and because of the high sensitivity (particularly for strontium, Table 1) at the most sensitive resonance lines. Because it was found that sulphate suppresses the absorbance of barium in a nitrous oxide-acetylene flame at barium concentrations >150 μ g/ml, barium sulphate, rather than chloride, was used to prepare the standard barium solution to keep the matrix approximately the same in both sample and calibration solutions, although the expected sulphate concentration would be below this level.

Tests showed that up to ~30 mg of disodium EDTA per ml has no significant effect on the deter-

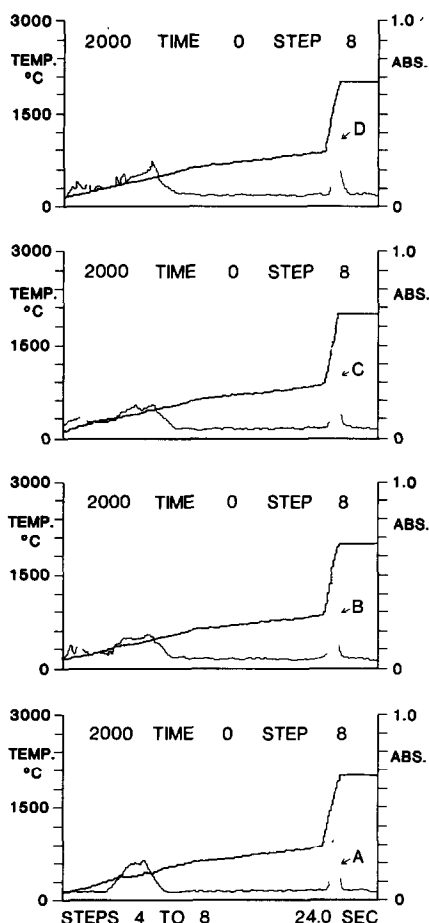


Fig. 1. Temperature-absorbance profiles (video display) for rubidium in the presence of disodium EDTA. A, Blank; B, 10-ng/ml Rb; C, 20-ng/ml Rb; D, 0.1 g of barite/25 ml. All solutions contained 120 mg of disodium EDTA per ml; 10- μ l aliquots taken.

mination of barium in a nitrous oxide-acetylene flame. However, the absorbance decreases if the concentration of sodium, which acts as an ionization suppressant, is less than ~ 2 or more than ~ 4 mg/ml. Consequently, the concentration of sodium in the sample and calibration solutions was kept at ~ 3 mg/ml. In the determination of strontium in an air-acetylene flame, any possible interference from

Table 5. Comparison of flame AAS and energy-dispersive XRF results for strontium in barites

Sample	Sr found, $\mu\text{g/g}$	
	FAAS	EDXRF
D	900	1036
E	4125	3816
F	4500	4154
G	4450	4426

Table 6. Determination of rubidium in some international reference rocks by graphite-furnace AAS

Sample	Rb found, $\mu\text{g/g}$	
	GFAAS	Other values ¹⁴
Gabbro MRG-1	8	8
Basalt BHVO-1 (Hawaiian)	11	10
Norite NIM-N	6	6?*
Basalt BE-N	48	47
Basalt BCR-1	48	47

*"Usable value" reported by Abbey.¹⁴

EDTA and sodium was avoided by keeping the concentration of disodium EDTA the same (~ 120 mg/ml) in both the sample and calibration solutions.

Although the characteristic concentration for rubidium, at 780.0 nm, in an air-acetylene flame is almost the same ($0.13 \mu\text{g/ml}$ for 0.0044 absorbance units) as that for strontium, rubidium was determined by graphite-furnace AAS because of its low level, usually $< 10 \mu\text{g/g}$, in most barite samples. Figure 1(B-D) shows the instrumental video-display of the temperature-absorbance profiles for rubidium in the presence of 120 mg of disodium EDTA per ml, with use of a pyrolytically-coated graphite tube and argon as purge gas. The results show that essentially all the EDTA is removed in the ash steps at 600–850° before the atomization of rubidium at 2000° and that rubidium can be readily determined under these conditions after correction for a suitable reagent blank (Fig. 1A) containing the same concentration of disodium EDTA. The disodium EDTA used was found to contain $\sim 0.2 \mu\text{g/g}$ rubidium, which is considerably

Table 4. Comparison of flame AAS and wavelength-dispersive XRF results for barium in barites

Sample	Ba found, %		S, %	
	FAAS*	WDXRF	Calculated from BaSO ₄	Found by combustion method
A	50.0	49.9	11.7	12.1
	50.0			
B	36.3	36.2	8.5	8.5
	36.3			
C	26.5	26.1	6.2	6.0
	26.5			

*Results shown are for duplicate determinations.

less than the rubidium content of most barite samples.

Applications

Table 4 shows that the results obtained for barium in three barite samples by the proposed method were reproducible and agreed well with those obtained for the same samples by wavelength-dispersive X-ray fluorescence spectrometry. The sulphur values, calculated as the amount of sulphur in the sulphate equivalent to the barium found by AAS, were also in good agreement with the sulphur results obtained by a combustion method.^{12,13}

Table 5 shows that the results obtained for total strontium in four other barite samples were also in reasonably good agreement with those obtained for the same samples by energy-dispersive X-ray fluorescence spectrometry, considering that the error in the latter method is ~10%.

Although no barite samples of known rubidium content were available, Table 6 shows that the results obtained for rubidium in some international reference samples by the graphite-furnace method were in excellent agreement with previously reported values.¹⁴ Samples A, B and C in Table 4 were found to contain 4, 9 and 60 $\mu\text{g/g}$ of rubidium, respectively. Twenty-five other barite samples were found to contain from 1 to 6 $\mu\text{g/g}$ rubidium.

Acknowledgements—The author is indebted to R. F. Rouseau for the XRF determination of barium and strontium in the barite samples, to R. N. Delabio for X-ray diffraction powder-pattern identification of the residues of some barites after disodium EDTA dissolution, to H. G. Ansell for supplying some barium feldspars for study and to Elsie M. Donaldson and G. R. Lachance for critical reading of the manuscript.

REFERENCES

1. W. Grahmann, *Neues Jahrb. Min.*, 1920, 1, 1.
2. E. D. Goldberg, B. L. K. Somayajulu, J. Galloway, I. R. Kaplan and G. Faure, *Geochim. Cosmochim. Acta*, 1969, 33, 287.
3. M. Barbieri, U. Masi and L. Tolomeo, *Chem. Geol.*, 1982, 35, 351.
4. S. Lange, S. Chaudhuri and N. Clauer, *Econ. Geol.*, 1983, 78, 1255.
5. R. Hofmann and A. Baumann, *Miner. Deposita*, 1984, 19, 166.
6. G. N. Breit, E. C. Simmons and M. B. Goldhaber, *Chem. Geol.*, 1985, 52, 333.
7. M. P. Cecile, M. A. Shakur and H. R. Krouse, *Can. J. Earth Sci.*, 1983, 20, 1528.
8. R. A. Sharp and A. M. Knevel, *J. Pharm. Sci.*, 1971, 60, 458.
9. F. J. Bano, *Analyst*, 1973, 98, 655.
10. J. G. Sen Gupta, *Talanta*, 1984, 31, 1045.
11. W. A. Deer, R. A. Howie and J. Zussman, *Rock-forming Minerals*, Vol. 4, *Framework Silicates*, p. 166. Longmans, London, 1963.
12. J. G. Sen Gupta, *Anal. Chim. Acta*, 1970, 49, 519.
13. J. L. Bouvier, J. G. Sen Gupta and S. Abbey, *Geol. Surv. Can. Paper*, 1972, 72-31.
14. S. Abbey, *ibid.*, 1983, 83-15.

SHORT COMMUNICATIONS

ANION-EXCHANGE ENRICHMENT AND SPECTROPHOTOMETRIC DETERMINATION OF URANIUM IN SEA-WATER

ROKURO KURODA, KOICHI OGUMA, NORIKO MUKAI and MASATOSHI IWAMOTO
Laboratory for Analytical Chemistry, Faculty of Engineering, University of Chiba, Yayoi-cho,
Chiba, Japan

(Received 28 April 1986. Revised 12 September 1986. Accepted 15 November 1986)

Summary—A method is proposed for the determination of uranium in sea-water. The uranium is strongly sorbed on a strongly basic anion-exchange resin (Cl^- form) from acidified sea-water containing sodium azide (0.3M) and is easily eluted with 1M hydrochloric acid. Uranium in the effluent can be determined spectrophotometrically with Arsenazo III. The combined method allows easy and selective determination of uranium in sea-water without using a sophisticated adsorbent. The overall recovery and precision are satisfactory at the 3 $\mu\text{g/l}$. level.

The determination of uranium in sea-water generally entails a concentration step, even when the highly sensitive fluorometric and neutron-activation methods are used, almost the only exception being the direct determination by stripping voltammetry.^{1,2} A number of preconcentration techniques, including co-precipitation,³ co-crystallization,⁴ extraction,^{5,6} froth flotation,⁷⁻⁹ and sorption on chelating^{10,11} or anion-exchange resins^{12,13} or of a uranium chelate on lipophilized silica gel,¹⁴ have been used. Use of exchangers based on cellulose and polystyrene containing 2-hydroxyphenyl-(2)-azonaphthol (Hyphan) as anchor group^{15,16} and of an anion-exchange resin with thiourea groups on a polystyrene-divinylbenzene matrix¹⁷ has also been reported for the preconcentration of uranium in sea-water.

Conventional ion-exchange has seldom been used, since the high concentration of sodium chloride in sea-water usually makes it difficult to achieve quantitative recovery of the uranium. We have found that uranium is strongly sorbed from saline water by a strongly basic anion-exchange resin in the presence of azide ion (N_3^-). This behaviour of uranium prompted us to develop a simple enrichment and spectrophotometric procedure for traces of uranium in sea-water.

EXPERIMENTAL

Reagents

A stock solution (5.7 mg/ml) of uranium was prepared by converting uranyl nitrate into the chloride, dissolving it in demineralized water and standardizing by back-titration with thorium nitrate after addition of excess of EDTA. Unless otherwise mentioned, reagents of analytical grade were used throughout. The strongly basic anion-exchange resin Bio-Rad AG 1, X-8 (100-200 mesh), in the chloride form was used. A slurry of 3.0 g of the resin in water was

poured into a conventional ion-exchange tube (1.5 cm diameter) to make a bed 3.2 cm long.

Measurements of distribution coefficients

The distribution coefficients of uranium(VI) were determined by the batch equilibrium method. Weighed portions of dried resin (1.0 g each) were mixed with 40-ml portions of 0.1M hydrochloric acid-0.5M sodium chloride solution containing various concentrations of sodium azide and 4.2 μmole of uranium(VI). The mixtures were shaken for 5 hr at 25° and the weight distribution coefficients determined as described earlier.¹⁸

Procedure

Ion-exchange enrichment. Filter the sea-water sample (previously acidified to 0.1M in hydrochloric acid to stabilize it) through a membrane filter (0.45 μm Millipore filter). Take a 1-litre fraction of the filtrate and add 19.5 g of sodium azide to it. Pass the mixture through the ion-exchange column at a flow-rate of 5 ml/min. Wash the column with a total of 30 ml of 0.1M hydrochloric acid-0.3M sodium azide solution. Discard the effluent. Strip the uranium with 50 ml of 1M hydrochloric acid.

Spectrophotometric determination.¹⁹ Evaporate the stripings to dryness on a hot-plate. Take up the residue with 5 ml of 8M hydrochloric acid and 0.6 ml of 1% ascorbic acid solution. Add 0.7 g of metallic zinc and let stand for 15 min. Transfer the solution to a 25-ml standard flask, add 1.0 ml of 0.1% Arsenazo III solution and dilute to the mark with 8M hydrochloric acid. Measure the absorbance at 665 nm against a reagent blank, using 2-cm cells.

RESULTS AND DISCUSSION

Hydrazoic acid is a weak acid ($\text{p}K_a = 4.77$ at 25°), which can form complexes with uranium and has been used for its spectrophotometric determination,²⁰ though with low sensitivity. Oguma *et al.*²¹ have already reported the sorption behaviour of uranium on the anion-exchanger Bio-Rad AG 1 (azide form) in hydrazoic acid solutions ranging 0.05 to 0.5M in

Table 1. Distribution coefficients of U(VI) on Bio-Rad AG 1 (Cl⁻ form) in 0.1M HCl-xM NaN₃-0.5M NaCl

NaN ₃ , M	pH	K _d
0	1.05	2 ~ 3*
0.10	2.80	14
0.15	4.06	2160
0.20	4.35	8110
0.25	4.55	15,800
0.30	4.70	14,900
0.40	4.88	12,200
0.50	5.00	6220

*Estimated by column method.

Table 2. Determination of uranium in sea-water (1 litre samples)

Sample	U added, μg	U found, μg
A	0	3.18, 3.07, 2.94
B	0	3.26, 3.39, 3.24
	3.43	6.93, 6.85, 6.87
C	0	3.13, 3.16, 3.13

A: collected at Inage Yacht Harbour, Tokyo Bay, Japan, on 28 November 1985, salinity 30.19‰. B: collected at 1.5 km off the shore of Amatsukominato, Chiba, Japan, on 31 January 1986, salinity 34.51‰. C: collected on the shore at Tokawa, Choshi, Japan, 31 January 1986, salinity 33.57‰.

concentration. However, there is little information about the sorption of uranium from saline azide media. The distribution coefficients of uranium(VI) on Bio-Rad AG 1 (chloride form) in acidified 0.5M sodium chloride (0.1M in hydrochloric acid) are listed in Table 1 as a function of azide concentration. The distribution coefficient increases rapidly with increasing concentration of azide, reaching a maximum at 0.25M concentration. In a solution of hydrazoic acid alone, the distribution coefficient increases sharply with increasing concentration of the acid, reaching about 10⁴ at 0.5M concentration. The presence of 0.5M sodium chloride apparently favours the sorption of uranium, the distribution coefficient being much higher than that with hydrazoic acid alone over the azide concentration range from 0.2 to 0.4M. This behaviour is favourable for the determination of uranium in highly saline water such as sea-water.

It is, in fact, very difficult to recover uranium from saline solutions which contain simple ligands. For example, we have found that the presence of sodium chloride (0.5M) greatly decreases sorption of uranium(VI) on AG 1 in bicarbonate (0.1-1.0M), sulphuric acid (0.01-0.50M), and 0.01-0.05M oxalic acid/0.01-0.5M hydrochloric acid media. The high degree of sorption of uranium from the azide-chloride media is probably due to the formation of mixed-ligand complexes, as is the case for thiocyanate-chloride media.²² The sorbed uranium can be very easily stripped by elution with 1M hydrochloric acid.

To test application of the anion-exchange azide system for the determination of uranium in water

samples, an artificial sea-water (28 g of NaCl, 5.5 g of MgCl₂·6H₂O, 6.9 g of MgSO₄·7H₂O and 1.5 g of CaCl₂ per litre) was prepared, spiked with 3.4 μg of uranium per litre, and analysed according to the procedure above. Recoveries were satisfactory, being 98.3 and 99.6% for duplicate analyses.

Sorption of uranium on AG 1 from hydrazoic acid media is comparatively selective; Be, Mg, Al, Ca, Sc, Cr(III), Mn(II), Co(II), Ni, Ge, As(III), Sr, Y, Zr, Te(IV), Ba, La, Sm, Yb, Hf and Th are not retained on the AG 1 column from 0.5M hydrazoic acid. V(V), Fe(III), Cu(II), Zn, Mo(VI), Pd(II), In(III), W(VI), Re(VII), Ir(IV), Pt(IV), Au(III), and Hg(II) are sorbed more or less firmly from hydrazoic acid media, but even when these metals behave the same as uranium in the anion-exchange concentration and elution steps, they do not interfere with the spectrophotometric determination of uranium with Arsenazo III. The metals that interfere seriously with that determination are zirconium and thorium, but these are not retained on the column from sea-water, and therefore do not affect the determination. The results of repeated determination of uranium in three sea-water samples are given in Table 2 together with those for some spiking tests. The overall recoveries and precision (r.s.d. 0.7-4%) are satisfactory.

REFERENCES

1. K. Izutsu, T. Nakamura and T. Ando, *Anal. Chim. Acta*, 1983, **152**, 285.
2. C. M. G. van den Berg and Z. Q. Huang, *ibid.*, 1984, **164**, 209.
3. M. Fujinami, K. Nagashima and Y. Sugitani, *Bunseki Kagaku*, 1979, **28**, 616.
4. H. Bem and D. E. Ryan, *Anal. Chim. Acta*, 1984, **158**, 119.
5. Y. Shijo and K. Sakai, *Bunseki Kagaku*, 1982, **31**, E395.
6. S. Degetto, M. Faggini, A. Moresco and L. Baracco, *Bull. Chem. Soc. Japan*, 1983, **56**, 904.
7. G. Leung, Y. S. Kim and H. Zeitlin, *Anal. Chim. Acta*, 1972, **60**, 229.
8. K. Sekine, *Mikrochim. Acta*, 1975 **I**, 313.
9. R. S. S. Murthy and D. E. Ryan, *Anal. Chem.*, 1983, **55**, 682.
10. P. Pakalns, *Anal. Chim. Acta*, 1980, **120**, 289.
11. E. S. Gladney, R. J. Peters and D. R. Perrin, *Anal. Chem.*, 1983, **55**, 976.
12. J. Korkisch and I. Steffan, *Anal. Chim. Acta*, 1975, **77**, 312.
13. R. J. N. Brits and M. C. B. Smit, *Anal. Chem.*, 1977, **49**, 67.
14. A. Prange, A. Knöchel and W. Michaelis, *Anal. Chim. Acta*, 1985, **172**, 79.
15. K. H. Lieser and B. Gleitsmann, *Z. Anal. Chem.*, 1982, **313**, 289.
16. P. Burba, M. Cebulč and J. A. C. Broekaert, *ibid.*, 1984, **318**, 1.
17. M. Ochsenkühn-Petropulu and G. Parissakis, *ibid.*, 1985, **321**, 581.
18. T. Kiriya and R. Kuroda, *Talanta*, 1983, **30**, 261.
19. H. Onishi and Y. Iida, *Bunseki Kagaku*, 1965, **14**, 1141.
20. F. G. Sherif and A. M. Awad, *Anal. Chim. Acta*, 1962, **26**, 235.
21. K. Oguma, T. Maruyama and R. Kuroda, *ibid.*, 1975 **74**, 339.
22. H. Hamaguchi, R. Kuroda, K. Aoki, R. Sugisita and N. Onuma, *Talanta*, 1963, **10**, 153.

SEQUENTIAL COLLECTION OF SELENIUM(IV) AND SELENIUM(VI) BY THE USE OF AN ANION-EXCHANGE RESIN LOADED WITH BISMUTHIOL-II SULPHONIC ACID

MORIO NAKAYAMA

Department of Applied Chemistry, Kumamoto University, Kurokami, Kumamoto 860, Japan

TOMOO TANAKA and MOTOKO TANAKA

Meiji College of Pharmacy, Nozawa, Setagaya, Tokyo 154, Japan

MASAHIKO CHIKUMA

Osaka University of Pharmaceutical Sciences, Kawai, Matsubara, Osaka 580, Japan

KAZUO ITOH

Environmental Pollution Research Institute, City of Nagoya, Minami-ku, Nagoya 457, Japan

HIROMU SAKURAI

Faculty of Pharmaceutical Sciences, University of Tokushima, Shomachi, Tokushima 770, Japan

HISASHI TANAKA and TERUMICHI NAKAGAWA

Faculty of Pharmaceutical Sciences, Kyoto University, Sakyo-ku, Kyoto 606, Japan

(Received 4 January 1986. Revised 29 October 1986. Accepted 28 November 1986)

Summary—A new ligand-loaded anion-exchange resin has been developed which allows determination of Se(VI) and Se(IV) in mixtures of the two. The ligand is a sulphonic acid derivative of bismuthiol-II.

We have developed a versatile method for the preparation of functional resins by a simple treatment of an ion-exchange resin with appropriate reagents.¹⁻³ These reagents should have three functional properties, namely selective reaction with the determinant of interest, an ion-exchange reaction with the resin and strong physical sorption on the ion-exchange resin matrix. Selenium, which has become of interest because of the small difference between its essential and toxic levels, has been selectively collected with some functional resins made in this way. Ion-exchange resins loaded with azothiopyrine sulphonic acid or bismuthiol-II (abbreviated as bis-II), which bear a thiol group, have been found useful for collection of selenium(IV), through formation of stable selenotrisulphide, which forms an —S—Se—S— linkage with the resin.⁴⁻⁶

Determination of both selenium(VI) and selenium(IV) is necessary for elucidation of the distribution of the oxidation states of selenium in environmental waters.⁷ Selenium(VI) can be determined as selenium(IV) after reduction by refluxing with concentrated hydrochloric⁸ or hydrobromic acid,⁹ but in practice this is inconvenient for determination of the trace amount of selenium(VI) in environmental samples. Several methods based on reduction to selenium(IV) have been proposed for the pre-concentration of selenium(IV) and (VI),¹⁰⁻¹⁵ but the amount of selenium(VI) has to be estimated indirectly

by determination of the selenium(IV). These methods are also unsatisfactory for treatment of large volumes of environmental samples. A method for direct isolation and determination of selenium(VI) is highly desirable.

In an attempt to develop a simple method for the separation and selective collection of selenium(VI) and (IV), we have examined the use of sulphonated bismuthiol II (bis-IIS, Fig. 1) loaded on an anion-exchange resin. We have synthesized bis-IIS from 4-hydrazinobenzenesulphonic acid and carbon disulphide with high yield. The anion-exchange resin can be loaded simply by mixing it with an aqueous solution of bis-IIS. There is practically no release of bis-IIS from the resin, even with 0.1M sodium chloride or 2.0M hydrochloric acid. In these electrolyte solutions the resin loaded with bis-IIS is more stable than that loaded with bis-II. The sorption of selenium(IV) by the bis-IIS resin is complete from

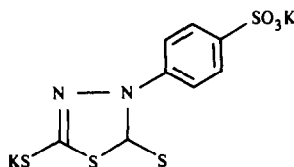


Fig. 1. Bismuthiol-II sulphonic acid, potassium salt (bis-IIS).

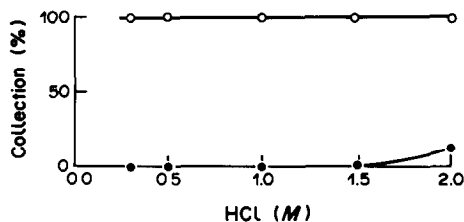


Fig. 2. Collection of selenium(IV) and (VI) on bis-IIS loaded resin. Batch method (shaking time 8 hr; temperature 30°). Bis-IIS loaded resin (0.2 mmole/g), 0.1 g. ○ Se(IV), 10 μ g. ● Se(VI), 10 μ g. Total volume 50 ml.

0.3–2.0M hydrochloric acid medium, as shown in Fig. 2, the ratio of selenium(IV) to bis-IIS on the resin being approximately 1:4, as in the case of the bis-II resin,⁵ but selenium(VI) is hardly sorbed on the bis-IIS resin from 0.3–1.8M hydrochloric acid. The selenium can be eluted from the resin with cysteine or penicillamine solution and subsequently determined by spectrofluorimetry. An attempt was then made to find a reagent able to form the selenotrisulphide of bis-IIS from selenium(VI) under mild conditions. Various reagents, including thiols, were examined. As shown in Fig. 3, only the addition of thiourea gave satisfactory collection of selenium(VI) on the bis-IIS resin. It seems likely that selenium(VI) is reduced to a lower oxidation state by thiourea and forms a selenotrisulphide first with thiourea, and then with bis-IIS, the latter being the more stable. In this reaction, the function of thiourea may not simply be the reduction of selenium(VI). The mechanism of this reaction is now under study. Sorption equilibrium was reached after shaking for 12 hr in 2M hydrochloric acid. As shown in Fig. 4, the degree of selenium(VI) collection increased (up to 98%) with an increase in the amount of bis-IIS loaded on the resin. These results indicate that the method is reasonably effective for preconcentration of selenium(VI), when a large volume of environmental water sample is treated. Similar use of the bis-II resin did not give satisfactory results, because oxidation of the thiol group to disulphide in the acid solution took place too rapidly. We have developed a procedure,

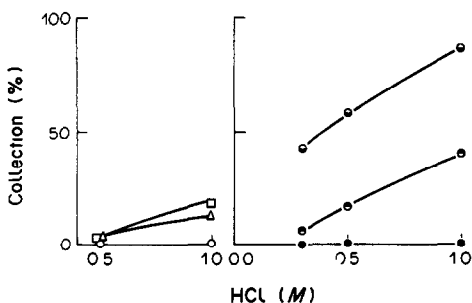


Fig. 3. Collection of selenium(VI). Bis-IIS loaded resin (0.2 mmole/g), 0.1 g, Se(IV) 10 μ g (50 ml). Reagents (0.1M): ○ NaBH₄, △ ascorbic acid, □ (NH₂)₂H₂SO₄, ● thiourea, ● thiosemicarbazide, ● cysteine.

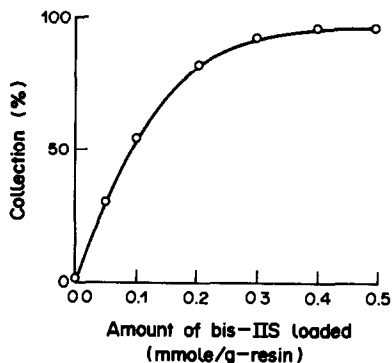


Fig. 4. Effect of amount of bis-IIS loaded, on the collection of selenium(VI). Bis-IIS resin 0.1 g. Se(VI) 10 μ g. Thiourea 0.1M. HCl 2M. Shaking time 15 hr.

described below, for the separation and determination of selenium(IV) and (VI), based on use of the bis-IIS resin.

A mixture of selenium(IV) and (VI) in 0.3–0.5M hydrochloric acid was applied to a column packed with bis-IIS resin, and selenium(IV) was collected on the resin (resin 1). The effluent, containing the selenium(VI), was made 0.1M in thiourea, bis-IIS resin (100–200 mesh) was added and the acidity of the solution was adjusted to 2M hydrochloric acid. The mixture was stirred very vigorously for 15 hr at 30°. The bis-IIS resin with selenium(VI) sorbed on it (resin 2) was collected and packed in a minicolumn. The selenium sorbed on the two resins was eluted with 0.02M cysteine or penicillamine, and determined spectrofluorimetrically after digestion with nitric acid and perchloric acid. The amounts of selenium recovered from resins 1 and 2 respectively correspond to the selenium(IV) and (VI) in the sample. The method was found to be applicable to the determination of selenium at levels of about 10–20 μ g/ml. The method should be useful for field work, because the selenium(IV) and (VI) can be collected from the water immediately after sampling, and the selenium sorbed on the resin is stable and can be determined later at any convenient time.

REFERENCES

1. H. Tanaka, M. Chikuma and M. Nakayama, in *Analytical Techniques in Environmental Chemistry 2*, J. Albaiges (ed.), pp. 381–388. Pergamon Press, Oxford, 1982.
2. M. Nakayama, M. Chikuma, H. Tanaka and T. Tanaka, *Talanta*, 1982, **29**, 503.
3. M. Chikuma, M. Nakayama, J. Kunimasa, Y. Suzuki, Y. Kurisaka and H. Tanaka, *Reactive Polymers*, 1985, **3**, 163.
4. M. Nakayama, M. Chikuma, H. Tanaka and T. Tanaka, *Talanta*, 1983, **30**, 455.
5. M. Nakayama, K. Itoh, M. Chikuma, H. Sakurai and H. Tanaka, *ibid.*, 1984, **31**, 269.
6. K. Itoh, M. Nakayama, M. Chikuma and H. Tanaka, *Z. Anal. Chem.*, 1985, **321**, 56.

7. H. Robberecht and R. Van Grieken, *Talanta*, 1982, **29**, 823.
8. D. R. Roden and D. E. Tallman, *Anal. Chem.*, 1982, **54**, 307.
9. G. R. Desai and J. Paul, *Microchem. J.*, 1977, **22**, 176.
10. O. Yoshii, K. Hiraki, Y. Nishikawa and T. Shigematsu, *Bunseki Kagaku*, 1977, **26**, 91.
11. Y. Shimoishi and K. Toei, *Anal. Chim. Acta*, 1978, **100**, 65.
12. K. Subramanian and J. C. Meranger, *ibid.*, 1981, **124**, 131.
13. K. W. Michael Siu and S. S. Berman, *Anal. Chem.* 1984, **56**, 1806.
14. Y. Sugimura and Y. Suzuki, *J. Oceanog. Soc. Japan*, 1977, **33**, 23.
15. H. J. Robberecht and R. E. Van Grieken, *Anal. Chem.*, 1980, **52**, 449.

DIRECT FLUORESCENT DETECTION OF CHROMATOGRAPHICALLY SEPARATED AMINO-ACIDS BY MEANS OF 9-ISOTHIOCYANATOACRIDINES

C. SĂRBU

Faculty of Mechanical Technology, Polytechnic Institute, 3400 Cluj-Napoca, Romania

C. MĂRUTOIU and M. VLASSA

Institute of Chemistry, 3400 Cluj-Napoca, Romania

C. LITEANU

Department of Chemistry, Babeş-Bolyai University, 3400 Cluj-Napoca, Romania

(Received 24 November 1985. Revised 8 April 1986. Accepted 15 November 1986)

Summary—A new method is presented for fluorescent detection of amino-acids separated on silica gel R plates, by spraying with a 0.1% solution of 9-isothiocyanatoacridine derivatives in dichloromethane or benzene, heating and examining in ultraviolet light at 254 and 336 nm. This method is useful for routine analysis owing to its selectivity and sensitivity.

Isothiocyanates react easily with amino-acids and amines,¹⁻³ and fluorescein isothiocyanate,⁴ phenyl isothiocyanate,⁵ the trifluoroacetate salt of nitrofluorescein isothiocyanate⁶ and optically-active fluorescent isothiocyanates^{7,8} have been used as reagents for amino groups of amino-acids.

For detection of primary and secondary amines, the isothiocyanates of acridine⁹⁻¹¹ or of polycyclic aromatic derivatives¹⁰⁻¹² have been successfully used.

In the work described here we used various 9-isothiocyanatoacridine derivatives as spray reagent for fluorescent detection of amino-acids separated by TLC. The method is simple, rapid and much more selective than other procedures, allowing visual detection of amino-acids separated on silica gel R plates, with a detection limit of 0.1 µg/spot at 254 and 366 nm wavelengths.

EXPERIMENTAL

Glass plates 20 × 20 cm, covered with a 0.5-mm thick layer of silica gel R containing a 1:1 starch:agar-agar mixture as binder were used. Standard amino-acid solutions (1 mg/ml) were applied to the plates by micropipette.

Ascending development over a distance of 10 cm was done in an unsaturated N-chamber with n-butanol-acetic acid-water (4:1:5).

After development, the plates were dried first in an air stream and then in an oven at 100° for 15 min, and finally sprayed with a 0.1% solution of 9-isothiocyanatoacridine derivative in dichloromethane or benzene. They were then heated in an oven at different temperatures for various times and examined in ultraviolet light of 254 and 336 nm wavelength (Camag type lamp).

The 9-isothiocyanatoacridine derivatives were prepared by a phase-transfer catalysis method.¹³

RESULTS AND DISCUSSION

Because the fluorescence of the spots appears only on heating, the influence of temperature and heating time on fluorescence intensity were examined by

visual inspection after the plates had been heated at 80, 100, 120, 150 and 180° for 15 or 30 min. The heating temperature did not influence the fluorescence, but increasing the temperature reduced the heating time needed. Heating the plates at 100–120° for 15 min is enough to produce maximum fluorescence.

The colours obtained under ultraviolet light differ according to the particular amino-acid and isothiocyanatoacridine derivative used, and are listed in Table 1.

The 2-methoxy-9-isothiocyanatoacridine derivative gives a green fluorescence on the plate before heating and a blue fluorescence after it. The amino-acid spots show up more distinctly against a blue background. 2-Methyl-9-isothiocyanatoacridine gives a greenish-yellow fluorescence on the plate whereas the halogenated derivatives give a blue fluorescence before and after heating.

It is known that fluorescein isothiocyanate derivatives react with amino-acids to yield, under acid conditions, thiohydantoin derivatives, which can be separated by TLC¹⁴ or by high-speed liquid chromatography.¹⁵

If the heating time is too short or the temperature not high enough dark spots are observed against the brightness of the plate. Presumably, under these conditions analogous thiohydantoin derivatives are not formed. With proper selection of experimental conditions (heating time and/or temperature) the thiohydantoin derivatives are formed and the fluorescence appears under ultraviolet light. This postulate is supported by the fact that cyclization reactions with formation of hydantoin derivatives have been observed to occur at room temperature on neutral alumina.¹⁶ Spraying with hydrochloric acid has no influence on the fluorescence of the spot.

Table 1. Use of 9-isothiocyanatoacridine derivatives for detection of amino-acids separated on silica gel R by TLC

Amino-acid	R_f	9-isothiocyanatoacridine derivative				
		2-methoxy-*	2-methyl-†	2-fluoro-‡	2-chloro-‡	2-bromo-‡
L-Proline	0.26	brownish-yellow	yellowish-green	yellowish-green	brown	yellowish-green
DL-Serine	0.28	greenish-yellow	yellowish-green	light yellow	light green	light yellow
DL-Methionine	0.50	pale yellow	brownish-yellow	intense yellow	intense green	greenish-yellow
DL-Aminobutyric acid	0.32	pale yellow	brownish-yellow	yellowish-green	pale green	yellowish-green
DL-Threonine	0.28	greenish-yellow	brownish green	brown	light green	light yellow
L-Lysine	0.11	pale yellow	dark blue	yellowish-green	pale green	yellowish-green
DL-Alanine	0.31	pale yellow	brownish-yellow	light yellow	dark green	light green
L-Asparagine	0.21	yellow	yellow	yellowish-green	yellowish-green	dark green
L-Leucine	0.60	light green	yellowish-green	yellowish-green	greenish-yellow	yellow
L-Glutamic acid	0.30	pale green	violet	light yellow	greenish-yellow	light green
L-Valine	0.45	yellowish-green	light yellow	yellowish-green	light blue	brown
Glycine	0.26	yellowish-green	greenish-yellow	dark green	light blue	greenish-yellow
Aspartic acid	0.23	blue	yellowish-green	dark green	blue	greenish-yellow
L-Tryptophan	0.64	dark blue	light yellow	dark yellow	brown	greenish-yellow
L-Izoleucine	0.58	green	light yellow	light yellow	greenish-yellow	greenish-yellow
D-Arginine	0.17	yellowish-green	brownish-yellow	yellowish-green	greenish-yellow	light blue
Cystine	0.15	dark blue	brown	blue	greenish-yellow	greenish-yellow
L-Phenylalanine	0.59	yellowish-green	brown	greenish-yellow	light yellow	light yellow

Background colour: *blue, †greenish-blue, ‡pale blue.

Triethanolamine solution in 2-propanol, which has been used to intensify fluorescence,¹⁷ had no effect except for the yellow fluorescence of the L-asparagine spot.

The most efficient of the 9-isothiocyanatoacridine derivatives studied, judged in terms of colour contrast and brightness of fluorescence, are the 2-methoxy and the halogenated (especially the 2-chloro) compounds.

CONCLUSIONS

Because its selectivity is greater than that of other detection methods (the 2-methoxy derivative is highly selective for aspartic acid, cystine and L-tryptophan, which give blue spots, in contrast to the other amino-acids) this new method can be very useful for routine analyses. A further advantage is that as amino-acids are not soluble in dichloromethane or benzene, the shape of the spots is not changed, thus affording extension of the method to quantitative analysis *in situ*.

REFERENCES

1. P. Kristian, *Chem. Zvesti*, 1961, **15**, 641.
2. L'. Drobnica and J. Augustin, *Collection Czech. Chem. Commun.*, 1965, **30**, 99.
3. *Idem, ibid.*, 1965, **30**, 1221.
4. H. Maeda, N. Ishida, H. Kawauchi and K. Tuzimura, *J. Biochem. (Tokyo)*, 1969, **65**, 777; *Chem. Abstr.*, 1969, **71**, 45949.
5. P. Edman, *Acta Chem. Scand.*, 1950, **4**, 283.
6. H. Kawauchi and K. Tuzimura, *Agric. Biol. Chem.*, 1971, **35**, 150; *Chem. Abstr.*, 1971, **75**, 20961.
7. A. J. Sedman and J. Gal, *J. Chromatog.*, 1983, **278**, 199.
8. J. Gal and A. J. Sedman, *ibid.*, 1984, **314**, 275.
9. J. E. Sinsheimer, D. D. Hong, J. T. Stewart, M. L. Fink and J. H. Burckhalter, *J. Pharm. Sci.* 1971, **60**, 141.
10. A. De Leenheer, J. E. Sinsheimer and J. H. Burckhalter, *ibid.*, 1973, **62**, 1370.
11. J. E. Sinsheimer, V. Jagodic, Lj. Polak, D. D. Hong and J. H. Burckhalter, *ibid.*, 1975, **64**, 925.
12. H. Ichikawa, T. Tanimura, T. Nakajima and Z. Tamura, *Chem. Pharm. Bull.*, 1970, **18**, 1493; *Anal. Abstr.*, 1971, **20**, 4169.
13. M. Vlassa, M. Kezdi and M. Bogdan, *J. Prakt. Chem.*, in the press.
14. H. Kawauchi, K. Tuzimura, H. Maeda and N. Ishida, *J. Biochem. (Tokyo)*, 1969, **66**, 783; *Chem. Abstr.*, 1970, **72**, 44095.
15. K. Muramoto, H. Kawauchi, Y. Yamamoto and K. Tuzimura, *Agric. Biol. Chem.*, 1976, **40**, 85; *Anal. Abstr.*, 1976, **31**, 5D102.
16. M. Vlassa and F. Hodoşan, *Rev. Roum. Chim.*, 1977, **22**, 1111.
17. S. Uchiyama and M. Uchiyama, *J. Liq. Chromatog.*, 1980, **3**, 681.

NEW DERIVATIVES OF *N*-NITROSAMINES

O. R. IDOWU and O. O. P. FABOYA

Department of Chemistry, University of Ibadan, Ibadan, Nigeria

(Received 9 July 1986. Accepted 1 November 1986)

Summary—Two new derivatives are proposed for determination of nitrosamines by GLC. One is formed by reaction with di(2-chloroethyl) phosphochloridate and the other by reaction with *m*-trifluorotoluene sulphonyl chloride.

Considerable interest in the determination of *N*-nitrosamines has been generated since Magee and Barnes¹ first discovered that dimethylnitrosamine caused malignant tumours in the rat, and the subsequent reports by other workers of the presence of *N*-nitrosodimethylamine and many other carcinogenic *N*-nitrosamines in various foodstuff, biological and environmental samples.²⁻⁹

An IARC review of methods¹⁰ for the determination of *N*-nitrosamines states that basic methodology now exists for determining volatile *N*-nitrosamines in a variety of substrates at the 1–10 µg/kg level but there is still a need for the development of methods which can be used in laboratories where expensive equipment is not available.

Gas chromatographic methods based on the measurement of derivatives of *N*-nitrosamines with an electron-capture detector can be used when sufficiently clean extracts can be achieved. In general there have been two approaches to making derivatives of *N*-nitrosamines. The less attractive and more time-consuming approach involves a two-stage procedure in which either the nitrosamine is denitrosated and the resulting amine is reacted with a polyfluorinated anhydride^{11,12} or the nitrosamine is reduced to the hydrazine, which may then be reacted with a polyfluorinated 2,4-diketone.¹³ The alternative one-step procedures involve either the oxidation of *N*-nitrosamines to the nitramines with peroxytrifluoroacetic acid^{14,15} or direct reaction with fluorinated anhydrides in presence of pyridine as catalyst.¹⁶⁻¹⁸ Preparation of the peroxy acid requires the use of concentrated hydrogen peroxide (50–90% aqueous solution) which is not readily available and may be hazardous to handle. The reaction with polyfluorinated anhydrides with pyridine as catalyst is unpredictable, different types of product being obtained for different *N*-nitrosamines. Furthermore, even when both are highly purified, the pyridine and the anhydride often react to give an unidentified compound, which makes the subsequent gas chromatographic work problematic.

Because of the inadequacies of the existing derivatives, simple reactions of *N*-nitrosamines are

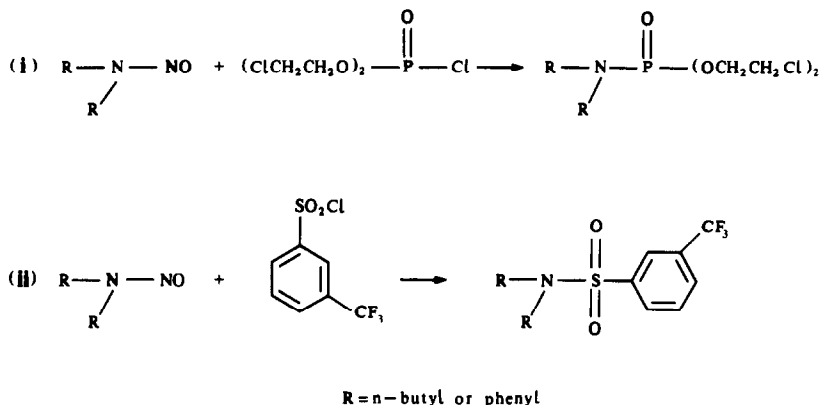
required, yielding products which may serve as the basis for the routine determination of *N*-nitrosamines not only by gas chromatography but also by other methods such as liquid chromatography (with ultraviolet or fluorimetric detection) and spectrophotometry. The following is a report on two such reactions.

Following a study of the mechanism of denitrosation of *N*-nitrosoureas in buffers containing acetic acid,¹⁹ it was thought that treatment of nitrosoureas and nitrosamines with acid chlorides or other compounds in which a labile chlorine atom is attached to an electrophilic centre, as in sulphonyl chlorides, chloroformates and dialkylphosphorochloridates, should result in the liberation of the nitroso group as nitrosyl chloride and formation of the corresponding amide from the denitrosated amine.

EXPERIMENTAL

N-Nitrosodibutylamine and *N*-nitrosodiphenylamine were chosen for the present study as representatives of aliphatic and aromatic nitrosamines respectively. Di(2-chloroethyl) phosphorochloridate was prepared according to the method of McCombie *et al.*²⁰ for the preparation of diethyl phosphorochloridate, and was purified by distillation twice under reduced pressure. *m*-Trifluorotoluene sulphonyl chloride (m.p. 120–121°) was prepared from chlorosulphonic acid and trifluorotoluene at 5° and recrystallized from chloroform. *o*-Chlorobenzoyl chloride was prepared from *o*-chlorobenzoic acid, and ethyl chloroformate was obtained from British Drug Houses Ltd. The usual handling precautions for work with nitrosamines were taken throughout.

The *N*-nitrosamine was warmed with di(2-chloroethyl) phosphorochloridate on a water-bath in a well-ventilated fume cupboard for 1 hr. The excess of reagent was removed by warming the reaction mixture briefly with 1M sodium hydroxide. The mixture was then extracted with chloroform and the chloroform removed after drying over anhydrous sodium sulphate. A light yellow viscous liquid was obtained from the reaction involving *N*-nitrosodibutylamine. A black viscous liquid with a nauseating smell was the initial product from the reaction involving *N*-nitrosodiphenylamine. A yellow semi-solid was, however, obtained from the chloroform extract. Thin-layer chromatography (TLC) of the reaction products was performed on silica gel with hexane:ether (1:1 v/v) as solvent.



Scheme 1

The reaction of the *N*-nitrosamines with *m*-trifluorotoluene sulphonyl chloride was done by warming (water-bath) a mixture of the *N*-nitrosamine and the reagent in chloroform for 1 hr. Excess of reagent was removed as before and the product extracted into chloroform. TLC examination of the product was performed on silica gel with hexane:chloroform (5:2 v/v) as solvent.

A similar procedure was adopted for reaction of the *N*-nitrosamines with *o*-chlorobenzoyl chloride and ethyl chloroformate.

All the products were examined by gas chromatography with a Varian model 3700 gas chromatograph equipped with an 8-mCi ^{63}Ni electron-capture detector and a 2-m glass column packed with 1% OV-1 on Chromosorb W (80-100 mesh). The nitrogen carrier-gas flow-rate was 40 ml/min, and the column, injection port and detector temperatures were 150, 290 and 300° respectively. The substances were dissolved in ethyl acetate for chromatography.

All the reaction products were subjected to microanalysis for carbon, nitrogen and hydrogen.

RESULTS AND DISCUSSION

Thin-layer and gas chromatographic analysis confirmed the formation of new compounds in the reaction between the *N*-nitrosamines and the phosphorochloridate and between the *N*-nitrosamines and *m*-trifluorotoluene sulphonyl chloride. The retention time for the product of the reaction between *N*-nitrosodibutylamine and the phosphorochloridate was 3.5 min and that for the product of the reaction between *N*-nitrosodiphenylamine and the same reagent was 4 min. The retention times for the products of the reaction of *N*-nitrosodibutylamine and *N*-nitrosodiphenylamine with *m*-trifluorotoluene sulphonyl chloride were 2.0 and 2.5 min respectively. The reagents and the *N*-nitrosamines were eluted with the solvent front.

The results of microanalysis for carbon, nitrogen and hydrogen are consistent with the expectation that the products of the reactions were the respective phosphoramides and sulphonamides. Thus the reaction of the *N*-nitrosamines with these two reagents may be represented as shown in Scheme 1.

No reaction was observed between the

N-nitrosamines and chlorobenzoyl chloride. The results of microanalysis showed that the white solid obtained in each case was *o*-chlorobenzoic acid, resulting from the hydrolysis of the acid chloride. The lack of reaction between the *N*-nitrosamines and *o*-chlorobenzoyl chloride is contrary to an earlier observation in a separate but related study in which 1-*N*-nitroso-4-diethylcarbamyloxy-piperazine was found to react readily with chloroacetyl chloride to give the amide derivative. The lack of reaction between *o*-chlorobenzoyl chloride and the nitrosamines may have been due to the facile hydrolysis of the acid chloride before it could react with the *N*-nitrosamines.

There was no reaction between the *N*-nitrosamines and ethyl chloroformate, the *N*-nitrosamines being recovered unchanged.

From this study we consider the reactions of *N*-nitrosamines with phosphorochloridates and with sulphonyl chlorides may provide suitable derivatives of *N*-nitrosamines for routine analysis.

REFERENCES

1. P. N. Magee and J. M. Barnes, *Brit. J. Cancer*, 1956, **10**, 114.
2. W. Linjinsky and S. S. Epstein, *Nature*, 1970, **225**, 21.
3. N. P. Sen, B. Donaldson, J. R. Iyengar and T. Panalaks, *ibid.*, 1973, **241**, 473.
4. N. T. Crosby, J. K. Foreman, J. F. Palframan and R. Sawyer, *ibid.*, 1972, **238**, 342.
5. T. Fazio, R. H. White, L. R. Dusold and J. W. Howard, *J. Assoc. Off. Anal. Chem.*, 1973, **56**, 919.
6. N. D. McGlashan, C. L. Walters and A. E. M. McClean, *Lancet*, 1968, **2**, 1017.
7. L. Hedler and P. Marquardt, *Food Cosmet. Toxicol.*, 1968, **6**, 341.
8. T. Panalaks, J. R. Iyengar and N. P. Sen, *J. Assoc. Off. Anal. Chem.*, 1973, **56**, 621.
9. J. Sakshaug, E. Soggen, M. A. Hansen and N. Koppang, *Nature*, 1965, **260**, 1261.
10. E. A. Walker, L. L. Griquite, M. Castegnaro and M. Borzsonyi (eds.), *N-Nitroso Compounds: Analysis, Formation, Occurrence*, IARC, Lyons, 1980.
11. G. Eisenbrand, *N-Nitroso Compounds: Analysis, For-*

- tion, *Proc. Work. Conf.*, P. Bogovski (ed.), pp. 64–70. IARC, Lyons, 1972.
12. T. G. Alliston, G. B. Cox and R. S. Kirk, *Analyst*, 1972, **97**, 915.
 13. A. E. Wasserman, *N-Nitroso Compounds: Analysis, Formation, Proc. Work. Conf.*, P. Bogovski (ed.), pp. 10–15. IARC, Lyons, 1972.
 14. N. P. Sen, *J. Chromatog.*, 1970, **51**, 301.
 15. J. Althorpe, D. A. Goddard, D. J. Sissons and G. M. Telling, *ibid.*, 1970, **53**, 371.
 16. J. B. Brooks, C. C. Alley and R. Jones, *Anal. Chem.*, 1972, **44**, 1881.
 17. T. A. Gough, K. Sugden and K. S. Webb, *ibid.*, 1975, **47**, 509.
 18. T. A. Gough, M. A. Pringuer, K. Sugden and K. S. Webb, *ibid.*, 1976, **48**, 583.
 19. O. R. Idowu, *Ph.D. Thesis*, University of Strathclyde, Glasgow, 1980.
 20. H. McCombie, B. C. Saunders and G. J. Stacey, *J. Chem. Soc.*, 1945, 380.

ANALYTICAL DATA

STABILITY ORDER OF THE LANTHANIDE CHELATES OF TWO DISUBSTITUTED 3-HYDROXY-4*H*-PYRAN-4-ONES IN AQUEOUS SOLUTION

RAIJA PETROLA and PAULA LAMPÉN

Division of Analytical Chemistry, University of Helsinki, Vuorikatu 20, SF-00100 Helsinki, Finland

SEPPO LINDROOS

Division of Inorganic Chemistry, University of Helsinki, Vuorikatu 20, SF-00100 Helsinki, Finland

(Received 2 April 1986. Revised 12 September 1986. Accepted 28 November 1986)

Summary—The stability constants of the 1:1 chelates formed by trivalent lanthanides with 2-bromo-3-hydroxy-6-(hydroxymethyl)-4*H*-pyran-4-one and 3-hydroxy-6-(hydroxymethyl)-2-iodo-4*H*-pyran-4-one were determined by spectrophotometric titration in aqueous potassium chloride solution at 25°. The determinations were done at two different ionic strengths near 0.1 and the value at $I = 0.1$ was interpolated. The $\log \beta_{101}$ values of both complex series exhibit the same trend; the stability increases gradually with decrease in the ionic radius and shows a break at Gd and Lu.

Complex formation between 3-hydroxy-4*H*-pyran-4-ones (maltol, kojic acid and chlorokojic acid) and rare earth(III) ions has been studied by several authors.¹⁻⁴ Also there are a few publications describing the isolation and characterization of these complexes.^{5,6}

In the present work the chelate formation between two halo-substituted kojic acid analogues [2-bromo-3-hydroxy-6-(hydroxymethyl)-4*H*-pyran-4-one and 3-hydroxy-6-(hydroxymethyl)-2-iodo-4*H*-pyran-4-one] and lanthanide(III) ions was examined under conditions where metal ions were present in large excess. The measurements were made by the spectrophotometric titration technique in aqueous solution at 25°. The main objectives were to determine the stability sequence of the chelates and to observe the changes in the ultraviolet absorption spectra of the ligand anions, caused by the lanthanide co-ordination.

EXPERIMENTAL

Reagents

The preparation and purification of the 6-bromo and 6-iodo derivatives of kojic acid have been reported elsewhere.⁷ The cerium salt was $\text{Ce}(\text{NO}_3)_3 \cdot 6\text{H}_2\text{O}$ (Fluka, *puriss.*). All the other lanthanide salts were the metal(III) perchlorates prepared from the corresponding oxides (Fluka or B.D.H., labelled 99.9% purity). The stock solutions were analysed for total cation concentrations (Ln^{3+} and H^+) by running aliquots through a column of Amberlite IR-120 resin in the hydrogen form and titrating the eluted hydrogen ions with standard sodium hydroxide. The exact lanthanide ion concentrations were determined by EDTA titrations with Xylenol Orange as indicator.

The ionic strength was maintained by addition of suitable amounts of potassium chloride.

Apparatus and methods

The absorptometric titrations were done with a Radiometer PHM 64 Research pH-meter equipped with a Beckman N 40495 glass electrode and an open liquid-junction saturated calomel reference electrode system connected by a Masterflex peristaltic pump and Tygon tubing to a Perkin-Elmer Model 554 recording and printing double-beam spectrophotometer. During the measurements, the titration vessel was immersed in a water thermostat ($25.0 \pm 0.1^\circ$) and the flow-through cell holder in the spectrophotometer was kept at the same temperature by an external thermostatic circulator. The solutions were protected by an atmosphere of purified nitrogen.

The initial volume of the solution to be titrated was 107 ml. The total concentration of the ligand (C_L) was $1.0 \times 10^{-4} M$ and the ratio $C_M : C_L$ (C_M = the total concentration of lanthanide) was about 10.

The emf and absorbance measurements were performed for 10–20 different solutions of each ligand–lanthanide(III) system at two different ionic strengths near 0.1.

The program SQUAD⁸ was used in calculating the overall stability constants of the complexes, $M_p H_q L_r$:

$$\beta_{par} = [M_p H_q L_r] / [M]^p [H]^q [L]^r \quad (1)$$

The thermodynamic stability constant at 25° for the 1:1 samarium complex of 6-bromokojic acid was resolved by application of a least-squares calculation to the following Debye-Hückel equation:

$$\log \beta_{101} = \log \beta_{101}^\circ - 0.509z^2 I^{1/2} / (1 + \alpha I^{1/2}) + BI \quad (2)$$

RESULTS AND DISCUSSION

The effects on the ultraviolet absorption and protolysis of kojic acid when bromo and iodo substituents are introduced in the position *ortho* to the hydroxyl group have been described in a recent report from our laboratory.⁷ The studies on protolysis suggested that bromine and iodine, as electron-withdrawing substituents, increase the acid strength of kojic acid. The

Table 1. The $\log \beta_{101}$ values of the lanthanide complexes of 2-bromo-3-hydroxy-6-(hydroxymethyl)-4*H*-pyran-4-one at two different ionic strengths and interpolated to ionic strength 0.1 at 25°C; standard deviations are given in parentheses; $\beta_{101} = K(\text{Ln}^{3+} + \text{L}^- = \text{LnL}^{2+})$, $K_1 = K(\text{Ln}^{3+} + \text{HL} = \text{LnL}^{2+} + \text{H}^+)$

Metal	<i>I</i>	$\log \beta_{101}$	<i>I</i>	$\log \beta_{101}$	$\log \beta_{101}$ (<i>I</i> = 0.1)	pK_1 (<i>I</i> = 0.1)
La	0.085	4.703(0.002)	0.105	4.671(0.001)	4.68	1.64
Ce	0.086	4.935(0.002)	0.106	4.889(0.003)	4.90	1.42
Pr	0.086	5.051(0.002)	0.106	5.005(0.002)	5.02	1.30
Nd	0.085	5.114(0.001)	0.105	5.062(0.002)	5.08	1.24
Sm	0.085	5.291(0.002)	0.105	5.260(0.002)	5.27	1.05
Eu	0.086	5.325(0.001)	0.106	5.283(0.002)	5.30	1.02
Gd	0.085	5.289(0.002)	0.105	5.271(0.002)	5.27	1.05
Tb	0.084	5.440(0.001)	0.104	5.392(0.002)	5.40	0.92
Dy	0.085	5.496(0.002)	0.105	5.459(0.001)	5.47	0.85
Ho	0.084	5.516(0.001)	0.104	5.484(0.001)	5.49	0.83
Er	0.087	5.539(0.005)	0.107	5.491(0.002)	5.51	0.81
Tm	0.087	5.619(0.002)	0.107	5.596(0.002)	5.60	0.72
Yb	0.087	5.717(0.002)	0.107	5.658(0.005)	5.68	0.64
Lu	0.093	5.668(0.001)	0.113	5.596(0.004)	5.64	0.68

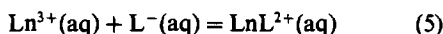
Debye-Hückel equations describing the dependence of the protonation constants on ionic strength

$$\log K_1 = 6.54 - 1.018I^{1/2}/(1 + 1.33I^{1/2}) + 0.16I \quad (3)$$

$$\log K_1 = 6.73 - 1.018I^{1/2}/(1 + 1.38I^{1/2}) + 0.13I \quad (4)$$

showed the logarithm of the thermodynamic protonation constant of kojic acid ($\log K_1^0 = 7.91$) to decrease by 1.37 for substitution with bromine and 1.18 for substitution with iodine. Both equations are valid in the ionic strength range $0 \leq I \leq 1.6$.

In the present work we have determined the stability constants for the reactions between trivalent lanthanides (except promethium) and the ligand anions



Since the measurements were performed under experimental conditions where metal ions were present in large excess, it could be assumed that only 1:1 chelates were formed. The stability constants at two different ionic strengths are given, together with the

standard deviations in Tables 1 and 2. As could be expected from the protonation constants of the ligands, the chelates of the iodo derivatives exhibit slightly higher stability. The stability constants of the LnL^{2+} chelates are plotted as a function of atomic number in Fig. 1, and, as can be seen, the stability sequence is reasonably similar in the two series. The orders obtained here are also more or less parallel with the sequences reported for the lanthanide chelates with kojic acid, chlorokojic acid and maltol.¹⁻⁴

It is generally agreed that the bonding in lanthanide(III) chelates between the lanthanide and oxygen donor atoms is mainly electrostatic in nature. This being so, according to Moeller *et al.*⁹ there should be a linear increase in the $\log \beta_{101}$ values with $1/r$ (r = ionic radius of the lanthanide ion). In the present case the stability does indeed increase with decrease in ionic size, but not linearly: the slope of the plot of $\log \beta_{101}$ vs. the reciprocal of the ionic radius is distinctly greater for the elements at the beginning of the series (up to Eu) than for the heavier lan-

Table 2. The $\log \beta_{101}$ values of the lanthanide complexes of 3-hydroxy-6-(hydroxymethyl)-2-iodo-4*H*-pyran-4-one at two different ionic strengths and interpolated to ionic strength 0.1 at 25°C

Metal	<i>I</i>	$\log \beta_{101}$	<i>I</i>	$\log \beta_{101}$	$\log \beta_{101}$ (<i>I</i> = 0.1)	pK_1 (<i>I</i> = 0.1)
La	0.085	4.725(0.002)	0.105	4.701(0.002)	4.71	1.79
Ce	0.086	4.969(0.002)	0.106	4.908(0.003)	4.92	1.58
Pr	0.086	5.072(0.003)	0.106	5.036(0.003)	5.05	1.45
Nd	0.085	5.120(0.003)	0.105	5.090(0.003)	5.10	1.40
Sm	0.085	5.349(0.002)	0.105	5.297(0.003)	5.31	1.19
Eu	0.086	5.411(0.004)	0.106	5.372(0.006)	5.38	1.12
Gd	0.086	5.403(0.004)	0.106	5.357(0.003)	5.37	1.13
Tb	0.086	5.536(0.007)	0.106	5.497(0.007)	5.51	0.99
Dy	0.086	5.625(0.002)	0.106	5.576(0.002)	5.59	0.91
Ho	0.086	5.628(0.001)	0.106	5.573(0.004)	5.59	0.91
Er	0.086	5.638(0.002)	0.106	5.601(0.002)	5.61	0.89
Tm	0.086	5.712(0.002)	0.106	5.664(0.002)	5.68	0.82
Yb	0.086	5.752(0.002)	0.106	5.711(0.003)	5.72	0.78
Lu	0.086	5.751(0.002)	0.106	5.690(0.002)	5.71	0.79

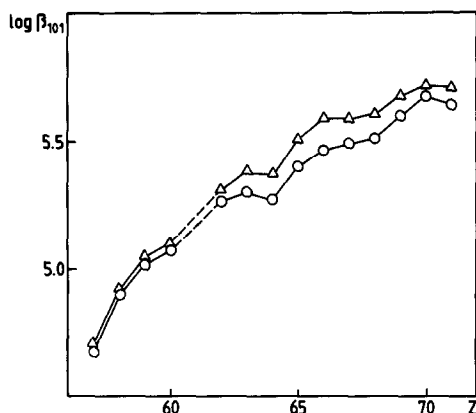


Fig. 1. The $\log \beta_{101}$ values of the lanthanide chelates of 6-bromokojic acid (\circ) and 6-iodokojic acid (Δ) as a function of atomic number, at $I = 0.1$ and 25°C .

thanides. This implies that there are also other factors influencing the stability. One factor could be a small amount of interaction between the well-shielded 4f-orbitals of the lanthanides and the ligand orbitals.⁵

A trend of this type, with a break at Gd, and often also at Lu, is not uncommon among the lanthanide chelates. A perusal of the literature reveals that perhaps more than half of the ligands investigated to date yield a stability sequence approximately like this. Such ligands include EDTA,¹⁰ NTA,¹¹ Tiron,¹² tropolone¹³ and acetylaceton,¹⁴ though no obvious similarities exist between all of these.

Figure 2 shows the ultraviolet absorption spectra of the different species of 6-bromokojic acid (HL and L^-) and the spectrum of the holmium chelate (HoL^{2+}) of the same ligand in the wavelength range 230–380 nm. Table 3 contains spectral data for the chelates formed with the lightest (La) and the heaviest (Lu) member of the lanthanide series. The blue-shifts caused by the metal co-ordination (3–6 nm for the chelates of the bromo derivative and 5–8 nm for those of the iodo derivative) vary over the same range (3 nm) in the two series, the values for the Lu chelate being the greatest. Accordingly, the weaker the chelate the less its absorption maximum differs from that of the corresponding ligand anion. The wavelength of the very well defined isobestic point remained nearly invariable along the series, differing by not more than 2 nm for any pair of chelates.

The effect of ionic strength on the stability was examined for the SmL^{2+} chelate of 6-bromokojic acid. The data in Table 4 were fitted to equation (2), with the results (\pm standard deviation) $\log \beta_{101}^\circ = 5.91 \pm 0.01$, $\alpha = 1.52 \pm 0.10$, $B = 0.16 \pm 0.12$.

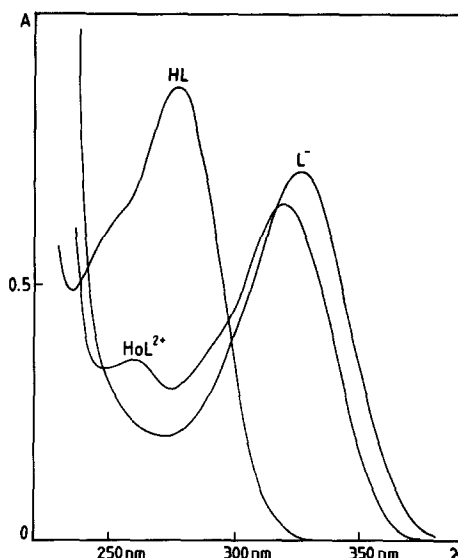


Fig. 2. The ultraviolet absorption spectra of the ligand species (HL and L^-) and the holmium chelate (HoL^{2+}) of 6-bromokojic acid in aqueous solution at 25°C . $I = 0.104$, $C_L = 1.00 \times 10^{-4} M$, $C_M = 9.72 \times 10^{-4} M$.

Recalculation of $\log \beta_{101}$ with these parameters reproduced the observed values within ± 0.01 in all cases.

Stability constants for the lanthanide chelates formed with the two ligands examined are not available in the literature. However, a few values for other metal chelates of these ligands can be found. Kotani *et al.*¹⁵ have reported the values $\log \beta_{101}(\text{CuL}^+) = 5.71$ and $\log \beta_{101}(\text{CdL}^+) = 3.61$ for the chelates of 6-bromokojic acid at ionic strength 0.1 (NaCl) and 25° . The constants $\log \beta_{101}(\text{NiL}^+) = 4.48$ and $\log \beta_{101}(\text{ZnL}^+) = 4.59$ at $I = 0.1$ (KCl) and 25° for the chelates of the same ligand and $\log \beta_{101}(\text{NiL}^+) = 4.61$ and $\log \beta_{101}(\text{ZnL}^+) = 4.67$ for the chelates of 6-iodokojic acid were determined earlier

Table 4. The $\log \beta_{101}$ values (and standard deviations) at different ionic strengths for the samarium chelate of 6-bromokojic acid at 25°C

I	$\log \beta_{101}$ (observed)	$\log \beta_{101}$ (calculated)
0.0053	5.723 (0.003)	5.71
0.0452	5.419 (0.001)	5.42
0.0852	5.291 (0.002)	5.30
0.105	5.260 (0.002)	5.26
0.197	5.128 (0.001)	5.13
0.381	5.008 (0.002)	5.00
0.941	4.856 (0.001)	4.86

Table 3. Spectral data (wavelengths, nm) for the ligand species (HL and L^-) and for the lanthanum and lutetium chelates of the same ligands at 25°C

Ligand	$\lambda_{\text{max}}^{\text{HL}}$	$\lambda_{\text{max}}^{\text{L}^-}$	$\lambda_{\text{max}}^{\text{LaL}^{2+}}$	$\lambda_{\text{max}}^{\text{LuL}^{2+}}$	Isobestic points	
					HL/LaL ²⁺	HL/LuL ²⁺
6-Bromokojic acid	278	326	323	320	241, 300	241, 299
6-Iodokojic acid	285	334	329	326	242, 306	240, 304

in our laboratory.^{16,17} As can be seen, all these chelates except that of copper are slightly weaker than the corresponding lanthanide chelates under similar conditions.

REFERENCES

1. H. Yoneda, G. R. Choppin, J. L. Bear and J. V. Quagliano, *Inorg. Chem.*, 1964, **3**, 1642.
2. N. K. Dutt and U. V. M. Sharma, *J. Inorg. Nucl. Chem.*, 1970, **32**, 1035.
3. N. K. Dutt, S. Sanyal and U. U. M. Sharma, *ibid.*, 1972, **34**, 2261.
4. R. Stampfli and G. Choppin, *J. Coord. Chem.*, 1971, **1**, 173.
5. R. C. Agarwal, S. P. Gupta and D. K. Rastogi, *J. Inorg. Nucl. Chem.*, 1974, **36**, 208.
6. N. K. Dutt and U. U. M. Sharma, *ibid.*, 1975, **37**, 1801.
7. R. Petrola, *Finn. Chem. Lett.*, 1985, 201.
8. D. Leggett and W. McBryde, *Anal. Chem.*, 1975, **47**, 1065.
9. T. Moeller, D. F. Martin, L. C. Thompson, R. Ferrús, G. R. Feistel and W. J. Randall, *Chem. Revs.*, 1965, **65**, 1.
10. E. J. Wheelwright, F. H. Spedding and G. Schwarzenbach, *J. Am. Chem. Soc.*, 1953, **75**, 4196.
11. T. Moeller and R. Ferrús, *Inorg. Chem.*, 1962, **1**, 49.
12. L. H. J. Lajunen, *Finn. Chem. Lett.*, 1976, 31.
13. H. Hirai and Y. Oka, *Bull. Chem. Soc. Japan*, 1970, **43**, 778.
14. A. Dadgar and G. Choppin, *J. Coord. Chem.*, 1971, **1**, 179.
15. T. Kotani, I. Ichimoto, C. Tatsumi and T. Fujita, *Agr. Biol. Chem.*, 1976, **40**, 765.
16. R. Petrola and L. Repetti, *Finn. Chem. Lett.*, 1985, 213.
17. R. Petrola, *ibid.*, 1985, 219.

POTENTIOMETRIC STUDY OF SILVER ION CO-ORDINATION BY AZO DYES

J. KATONA-BALÁZS, G. MOLNÁR, ZS. NEMES-VETÉSSY
and K. BURGER

Department of Inorganic and Analytical Chemistry, A. József University, H-6701 Szeged,
P.O. Box 440, Hungary

(Received 21 February 1986. Revised 3 September 1986. Accepted 28 November 1986)

Summary—The stability constants of the silver(I) complexes of five azo dyes have been determined by means of potentiometric equilibrium measurements with silver electrodes in 75% v/v acetone–water solution. Each azo dye molecule was shown to co-ordinate at most three silver ions. The sequence of the stepwise stability constants indicated an effect stabilizing complexes with high silver content.

In spite of the fact that azo dyes are widely used in analytical chemistry and chemical technology, where the reactions of their metal complexes are of considerable importance, little is known about their complexation characteristics.

Complex formation between azo dyes and copper(II), nickel(II), zinc(II), cadmium(II), aluminium(III), iron(III), magnesium(II), gallium(III), chromium(III) and lanthanides has been studied by spectrochemical^{1,2} and electroanalytical³⁻⁶ methods. Equilibrium studies have revealed that azo dyes form metal complexes with 1:1, 1:2 and 2:1 metal-to-ligand ratios. In the last case, both nitrogen atoms of the azo group act as donor atoms.

Some of the complexes serve as the basis for the spectrometric^{1,7} or polarographic^{3,5} determination of the metal ions. They are also used in separations involving solvent extraction.⁸

Despite the lack of any quantitative information about their interaction with silver ions, azo dyes have been used as indicators in argentometric titrations.⁹

The present paper reports the results of an equilibrium study of complex formation between silver ions and five azo dyes. The work was done to obtain additional information on the donor ability of azo nitrogen atoms, and to investigate the role of the N=N double bond in the interaction with the typically "soft" silver ion.¹⁰ The results may contribute to the theory of the use of azo dyes as argentometric indicators.

The equilibrium study utilized potentiometric measurements with a silver electrode of the first kind. Azo dyes free from contamination were required for this investigation, and this limited the number of model compounds available and consequently the selection of a coherent series (Fig. 1).

EXPERIMENTAL

Reagents

All reagents used were of analytical purity. For preparation of the solutions, doubly distilled water and acetone dried with Klinosorb 4 molecular sieve were used.

The azo dyes were checked for purity by standard chromatographic methods^{11,12} and were found to be homogeneous compounds. Solutions were freshly prepared for each experiment.

Standard 0.0500M silver(I) solution was prepared by dissolving silver nitrate in a 75% v/v acetone–water mixture and standardized by potentiometric titration with potassium chloride.

Preparation of chloride-free Variamine Blue

For comparison, the indicator Variamine Blue was studied analogously. Since the commercial form of this dye is a chloride salt, the indicator was converted into its nitrate salt by dissolving it in distilled water and adding an excess of ammonia solution to precipitate the free base. This was filtered off, and washed free from chloride with distilled water. Subsequently, it was dissolved in dilute nitric acid and recrystallized.

Potentiometric equilibrium measurements

Because of the low water-solubility of azo dyes, the equilibrium studies were performed with solutions in a 75% v/v acetone–water mixture. Azo dye solutions with concentrations of 5×10^{-4} – $10^{-3}M$ were titrated with standard 0.0500M silver nitrate until a silver excess of $2.5 \times 10^{-2}M$ was achieved. The ionic strength of all solutions used was adjusted with potassium nitrate to 0.15M. During the measurements, the temperature of each system was kept constant at $20 \pm 0.1^\circ$. In every case, measurements were made on three solutions with different concentrations, in the concentration range mentioned above.

Both indicator and reference electrodes were silver electrodes of the first kind, prepared by electrolytic deposition of silver on platinum electrodes. The electrodes were calibrated before each experiment. To decrease the diffusion potential and keep it at a constant small value, the reference silver electrode was placed in a Wilhelm salt bridge. Titrant was added from a computer-operated Radelkis OP-930 automatic burette (reproducibility ± 0.001 ml). The emf values were recorded with a Radelkis OP-208/1 precision digital pH-meter (reproducibility ± 0.1 mV). The experimental data were evaluated by computer; 30 experimental points per titration were used in the calculations.

Both the calibration and titration curves showed that although the silver electrodes were being used in solutions with a high organic solvent content, the silver-ion activity could be measured potentiometrically with high accuracy.

Computer evaluation

The potentiometric data were evaluated by computer on the basis of Bjerrum's complex formation function, by a

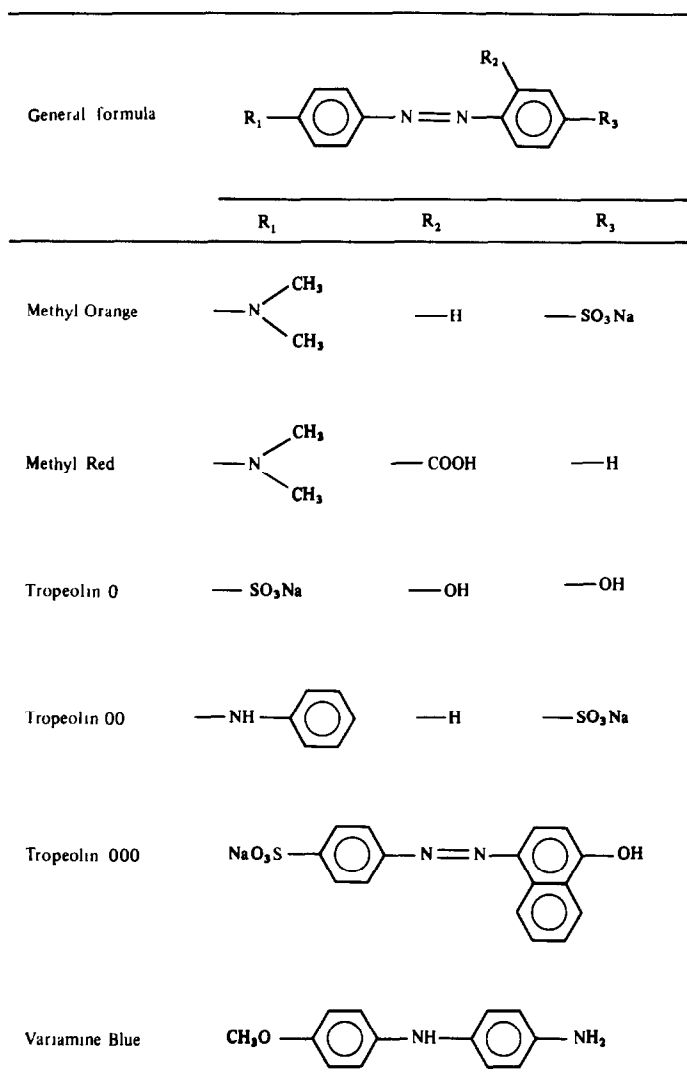


Fig. 1. Structural formulae of five azo dyes and of Variamine Blue.

non-linear least-squares method. The reciprocal values of the squares of the experimental data served as statistical weights in the sums of squares. The reproducibility of the complex stability constants calculated from the results of three or more titrations is illustrated in Table 1. The precision of the stability constants is seen to correspond to that of the experimental procedure, indicating the reliability of the constants.

RESULTS AND DISCUSSION

The five azo dyes investigated are presented in Fig. 1. The average number (\bar{n}) of silver ions bound by one dye molecule was determined in each system from the data from the potentiometric titrations. The curves of \bar{n} vs. $\log[\text{Ag}^+]$ demonstrate that, in solutions containing excess of silver, polynuclear complexes are formed. Figure 2 shows a typical curve of \bar{n} vs. $\log[\text{Ag}^+]$ for Methyl Orange. Similar curves were obtained for the other four ligands, indicating that the maximum number of silver ions bound by

one dye molecule is 3.0 in each system. Table 1 shows the logarithms of the stability constants determined from the experimental data by computer. The data show that there is an anomalous sequence in the successive stepwise stability constants: $K_3 > K_1$ in all cases, and $K_3 > K_2$ for Methyl Orange, Tropeolin 00 and Tropeolin 000.

This indicates that there must be some effect stabilizing the complexes with high silver content.

Table 1. Stepwise stability constants of the silver complexes of azo dyes

Azo dye	$\log K_1$	$\log K_2$	$\log K_3$
Methyl Orange	1.73 ± 0.02	0.47 ± 0.14	3.66 ± 0.09
Methyl Red	1.31 ± 0.09	1.96 ± 0.16	1.81 ± 0.07
Tropeolin 0	0.77 ± 0.04	2.76 ± 0.07	1.89 ± 0.04
Tropeolin 00	1.78 ± 0.04	0.50 ± 0.12	4.69 ± 0.03
Tropeolin 000	3.31 ± 0.15	0.04 ± 0.20	4.47 ± 0.07

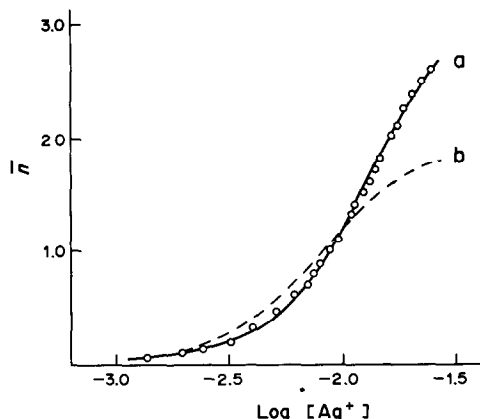


Fig. 2. Complex formation curve for Methyl Orange; circles denote experimental \bar{n} vs. $\log[\text{Ag}^+]$ values, while full lines are computer-calculated formation curves assuming (a) maximum $\bar{n} = 3$, (b) maximum $\bar{n} = 2$.

As a check on the evaluation method, the computer was used to calculate simulated \bar{n} vs. $\log[\text{Ag}^+]$ curves and the data of the original potentiometric titrations, and compare them with the corresponding experimental plots. The good agreement points to the reliability of the equilibrium constants.

The results of the equilibrium studies did not reveal the exact binding sites of the silver ions in the complexation process.

Figure 1 shows that, besides the azo group, each dye molecule contains two potential donor atoms: either an amino nitrogen atom and a sulphonate or carboxylate oxygen atom, or sulphonate and hydroxyl oxygens atoms together (the co-ordination of silver by hydroxyl is, however, improbable).

The ligands examined can be divided into two groups: (a) those with $K_3 > K_2$, and (b) those with $K_3 < K_2$. Ligands in group (a) (Methyl Orange, Tropeolin 00 and Tropeolin 000) do not contain any substituents *ortho* to the azo moiety, while those in group (b) (Methyl Red and Tropeolin 0) have a carboxyl or a hydroxyl group in this position. This indicates that both nitrogen atoms of the azo group co-ordinate silver ions, as found for the copper and nickel¹ complexes. The equilibrium data suggest that, in ligands not containing *ortho* substituents, silver ions are co-ordinated to the two azo nitrogen atoms practically simultaneously, the two equilibrium reactions not being distinguishable. Thus, $K_3 > K_2$.

In Methyl Red and Tropeolin 0, one of the azo nitrogen atoms is sterically hindered by the *ortho* substituent, which hinders co-ordination of the third silver ion, and accordingly, $K_2 > K_3$. In this respect, complex formation for silver differs from that for

transition metals, which do form chelates with azo dyes containing *ortho* donor groups, resulting in an increased stability. Silver complexes have linear co-ordination, so substituents which could lead to five or six-membered chelate rings do not co-ordinate to silver, but rather sterically hinder the co-ordination of one of the azo nitrogen atoms.

For the unambiguous assignment of the three binding sites, structural study of the complexes in solution is necessary. This could also lead to clarification of the factor stabilizing the complexes with maximum silver content. At present, we have no obvious explanation for the results; π back-donation to low-energy π^* orbitals is frequently assumed to be the reason for anomalous stabilization effects, but such a hypothesis is hard to reconcile with a model involving the co-ordination of silver by sp^2 -type orbitals of the azo-group nitrogen atoms, since in this case the coalescence of the metal filled d -orbitals with the azo group π^* orbitals is not favoured.

For comparison, an analogous equilibrium study was performed on co-ordination of silver by Variamine Blue. This dye is a diphenylamine derivative and does not contain an azo group. Its structure is shown in the last row of Fig. 1. In accordance with expectations, the measurements revealed that only two silver ions are co-ordinated by one Variamine Blue molecule, which contains two donor nitrogen atoms. The values $\log K_1 = 2.23 \pm 0.06$ and $\log K_2 = 1.95 \pm 0.07$ demonstrate the usual sequence of the stepwise stability constants, $K_1 > K_2$. Thus, the stabilization effect assumed to be due to π back-donation does not appear in the system not containing the azo group.

The affinity of azo nitrogen atoms for silver ions seems to explain the applicability of compounds of this type as argentometric indicators.⁹

REFERENCES

1. M. Pesavento and F. T. Soldi, *Analyst*, 1983, **108**, 1128.
2. R. C. Bertoglio, M. Pesavento and F. T. Soldi, *Ann. Chim. (Rome)*, 1978, **68**, 651.
3. G. W. Latimer, *Talanta*, 1968, **15**, 1.
4. E. Coates and B. Riggs, *J. Soc. Dyers Colourists*, 1956, **72**, 332.
5. G. F. Reynolds, *Z. Anal. Chem.*, 1960, **173**, 24.
6. O. Yamauchi, H. Tanaka and T. Uno, *Talanta*, 1968, **15**, 177.
7. K. Saxena and A. K. Dey, *Anal. Chem.*, 1968, **40**, 1280.
8. A. J. Nazarenko and T. A. Stolyarchuk, *Zh. Neorgan. Khim.*, 1982, **27**, 443.
9. E. Singh, *Z. Anal. Chem.*, 1977, **283**, 299.
10. R. C. Pearson, *J. Chem. Educ.*, 1968, **45**, 581.
11. E. Stahl, *Dünnschichtchromatographie*, p. 592. Springer, Berlin, 1967.
12. P. Wollenweber, *J. Chromatog.*, 1962, **7**, 557.

APPLICATION OF A METALLIZED MEMBRANE ELECTRODE FOR THE DETERMINATION OF GASEOUS SULPHUR COMPOUNDS AFTER REDUCTIVE PYROLYSIS

JAN LANGMAIER and FRANTIŠEK OPEKAR

UNESCO Laboratory of Environmental Electrochemistry, J. Heyrovský Institute of Physical Chemistry and Electrochemistry, Czechoslovak Academy of Sciences, Jilská 16, 110 00 Prague 1, Czechoslovakia

VĚRA PACÁKOVÁ

Department of Analytical Chemistry, Faculty of Sciences, Charles University, Albertov 2030, 128 40 Prague 2, Czechoslovakia

(Received 25 July 1986. Revised 22 December 1986. Accepted 12 January 1987)

Summary—Sulphur-containing gases are converted by non-catalytic reductive pyrolysis into an equivalent amount of H₂S, which is determined by electrochemical oxidation at a gold-plated porous membrane electrode. The calibration for H₂S is linear up to 18 ml/m³ with a slope of 1.12 μA · m³ · ml⁻¹. The relative standard deviation for the determination of 3.7 ml/m³ H₂S was 1.0% and the detection limit 4 μl/m³. About 60 samples can be determined per hour. The method has been employed for the determination of total sulphur and individual gases after separation on a chromatographic column.

The determination of the sulphur content of various media is important in a number of technological and environmental applications. The determination of sulphur compounds in technological gases (e.g., fuel gases) and in the atmosphere is especially important.

In addition to methods employing flame photometric detectors (FPD), electrochemical methods are useful in these determinations; coulometry has been extensively employed,¹⁻³ but potentiometry with ISEs⁴ and polarography (differential pulse, differential pulse cathodic stripping voltammetry)⁵ have been used less often. In all these methods, the sulphur-containing compounds are converted by oxidative or reductive pyrolysis into electrochemically determinable SO₂ or H₂S. After pyrolysis the gaseous sample is absorbed in a suitable electrolyte solution in which the pyrolysis products are determined.

Both SO₂ and H₂S can be determined directly in the gas phase by amperometry with a metallized membrane electrode.⁶ The gas leaving the pyrolyser is led directly to the unmetallized side of the membrane, through which it permeates (for non-porous membranes) or diffuses through the pores (for porous membranes) to the metallic layer, which acts as the working electrode of the amperometric system. This approach prevents vaporization loss of the component to be determined, and in the case of H₂S it also avoids losses through reaction with traces of heavy metals in the electrolyte. The use of a porous membrane electrode usually greatly decreases the response time of the system, as would be expected from a comparison of the diffusion coefficients of

substances in solution ($\approx 10^{-5}$ cm²/sec) and of gases in the gaseous phase filling the membrane pores ($\approx 10^{-1}$ cm²/sec).

Metallized porous membrane electrodes have so far been used primarily for the determination of substances in solution after these have been transferred into the gaseous phase (pneumatometry),⁷ or after subsequent separation of the mixture of electrochemically active gases on a chromatographic column.^{8,9}

This paper describes a method employing a gold-plated porous membrane electrode (AuPME) for the determination of gaseous sulphur-containing compounds after their conversion by reductive pyrolysis into hydrogen sulphide. The rapid response of the AuPME permits determination not only of the total sulphur content but also of the individual components of the mixture, after separation on a column, followed by pyrolysis. Reductive pyrolysis is employed because the conversion is stoichiometric under suitable conditions for most sulphur compounds¹ and because only one gas is required—hydrogen, which acts as both reagent and carrier gas. In principle, oxidative pyrolysis could also be employed, as the required electrochemical data for the oxidation of SO₂ at an AuPME are also available.¹⁰

EXPERIMENTAL

Apparatus

The apparatus employed (Fig. 1) consists of three basic parts—the input system, the pyrolyser and the detection system.

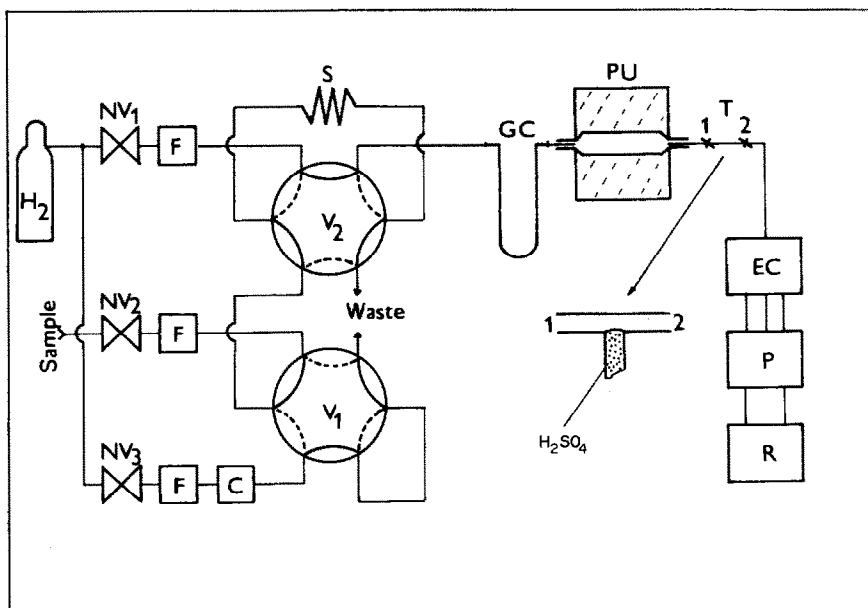


Fig. 1. Schematic diagram of the experimental apparatus: NV—needle valves, C—calibrator, F—flowmeters, V—six-way valves, S—sample loop, GC—chromatographic column, PU—pyrolysis unit, EC—electrochemical cell (see Fig. 2), P—potentiostat and current measurement, R—recorder, T—tube with a meniscus of concentrated H_2SO_4 .

The input system consists of two PTFE six-way valves. The first (V_1) controls the filling of the sample loop (S) with either the sample gas (position depicted) or a calibration mixture of hydrogen and H_2S from the calibrator (C). The second valve (V_2) feeds the content of the sample loop into the hydrogen stream and thus to the other parts of the apparatus. Pure hydrogen passes through the apparatus during filling of the sample loop (depicted position for V_2). Hydrogen was taken from a cylinder and its flow-rate was controlled by needle valves (NV) and measured by flowmeters (F). The working flow-rate of hydrogen as a carrier and reagent gas was 2 ml/sec; the hydrogen flow-rate through the calibration apparatus was set so as to give the required H_2S concentration in the calibration mixture.

The H_2S source for calibration (C) was a tempered H_2S permeation tube (Dynacal Permeation Tubes, Metronic Assoc., Palo Alto, USA), producing 27.2 ng of H_2S per sec ($\pm 2\%$) at 35° .

Periodic calibration was employed to verify the functioning of the pyrolysis unit and detection apparatus. Other gases employed to test the method were also obtained from permeation tubes from the same company—the gases tested are listed in Table 1. The required concentrations of these gases were attained by suitable choice of the temperature and diluent gas flow-rate.

Sample loop (S) consisted of a PTFE tube with a bore of 3 mm and a volume of 1.57 ml.

The pyrolysis unit (PU) was a silica tube 300 mm long, bore 4 mm, fitted with a helical resistance heating wire over a length of 150 mm. The tube was fitted coaxially in a steel casing (220 mm long, 50 mm internal diameter) filled with heat-resistant aluminosilicate wool ("Termovit", Vítkovice Iron and Machine Works, Czechoslovakia). The temperature was adjusted by varying the heating current by a regulating transformer and was measured with a Pt-Pt/Rh thermocouple. The zone with a working temperature of 800° was about 100 mm long. The tube did not contain any packing and there was no need for activation. A fused silica tube was selected as the basis for the pyrolysis system.^{11,12}

It, and other parts of the apparatus, were connected by careful fitting of PTFE fitted joints into the narrowed ends of the tubes, and casing in thick-walled silicone rubber tubing.

The total sulphur content was determined by passing the sample directly into the pyrolysis unit. The individual components in the mixture were determined after passage through a chromatographic column (GC) consisting of a PTFE tube 700 mm long, 2.5 mm bore, packed with Porapak QS 100–120 mesh (Waters Associates, Inc., U.S.A.), heated to $180 \pm 1^\circ$.

The detection system consisted of an electrochemical cell (Fig. 2), with a working electrode consisting of an AuPME (3) constructed from a sheet of porous PTFE membrane, Gore Tex No. S 10363 (W. L. Gore and Assoc., Inc., U.S.A.) vacuum-plated with gold. The membrane was fixed between the polished ends of the two Plexiglas parts of the cell, (1) and (2), and sealed with 0.5-mm thick polyethylene foil (4). The sample gas from the pyrolysis unit was fed to the unmetallized side of the AuPME by a PTFE tube (5), the length of which (500 mm) also ensured cooling of the gas. The metallized side of the membrane was immersed in a supporting electrolyte solution (6) containing the auxiliary electrode—a gold wire (7)—and the reference electrode (SCE) (8). The geometric active surface area of the AuPME was 0.2 cm^2 . Contact to the AuPME was made through a strip of aluminium foil (9). The two parts of the cell were held together by four screws (not shown).

The newly prepared AuPME was cyclically polarized in 0.1M sulphuric acid in the potential range from +1.6 to -0.4 V (scan-rate 100 mV/sec, hydrogen flow-rate to the unmetallized side, 4 ml/sec) for a period of about 20 min. This electrode required no activation over several months of use. After termination of the measurement, the AuPME was rinsed with water and stored dry, in air.

The supporting electrolyte was aqueous 10^{-2} M potassium sulphate. The electrochemical determination of H_2S is more often done with use of a solution of alkali to prevent losses of H_2S from solution;⁵ it was found here, however, that the

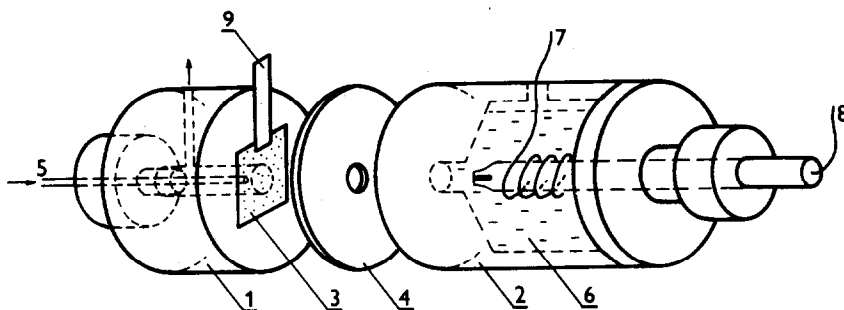


Fig. 2. Scheme of the electrochemical cell: 1, 2—body of the cell, 3—AuPME, 4—polyethylene seal, 5—PTFE inlet tube, 6—electrolyte compartment, 7—Au auxiliary electrode, 8—SCE, 9—contact to the AuPME.

responses of the AuPME in $10^{-2}M$ sodium hydroxide and $10^{-2}M$ potassium sulphate are similar. A lower background current was obtained with the latter (< 50 nA) and the response was not dependent on electrolyte concentration in the range 10^{-3} – $10^{-1}M$. Oxygen need not be removed from the supporting electrolyte.

It was found from the polarization curve of the AuPME in $10^{-2}M$ potassium sulphate + $10^{-3}M$ sodium sulphide that inorganic sulphides are oxidized at potentials more positive than -0.35 V. A potential of $+0.1$ V was chosen as the working potential.⁹

All connections in the apparatus were made of PTFE tubing with a bore of 0.5 mm. The connections between the source of the sample gas, the column and the pyrolysis unit should be as short as possible.

The chemicals employed were of analytical grade purity and water was doubly distilled in a silica apparatus.

Working procedure

The hydrogen flow-rate was adjusted to 2 ml/sec with valve NV_1 . The cell was filled with the supporting electrolyte solution; the background current attained a constant value after about 5 min. The sample loop was filled with a mixture of H_2S and hydrogen from the calibration apparatus (ca. 4 ml/m³ H_2S) and the mixture passed through the cell. The AuPME response became reproducible after passage of about five sample volumes.

Determination of total sulphur content. The chromatographic column was disconnected and the sample gas fed into the pyrolysis unit at regular intervals of about 30 sec, alternating as required with the H_2S calibration mixture from the calibration unit. A calibration graph was prepared; in the linear region (see below) the sample response can be compared directly with that for the standard sample from the calibration unit. The analysis time (sample + standard) is not greater than 1 min.

Determination of individual components of a mixture. The chromatographic column is connected between the sample loop and the pyrolysis unit.

RESULTS AND DISCUSSION

Pyrolysis conditions

Utilization of the dynamic properties of the AuPME requires that the pyrolysis be quantitative during the residence time of the substance in the pyrolysis tube, which is controlled by the flow-rate of the carrier gas (without flow interruption). The silica tube was found to be quite satisfactory for this purpose provided that certain experimental conditions were fulfilled.

(i) The dependence of the pyrolysis efficiency on temperature was tested in the range 20–1000°. The response of the AuPME to a known H_2S concentration (6.6 ml/m³) fed directly to the AuPME without passage through the pyrolysis unit was compared with that for the same concentration of H_2S passing through the pyrolysis unit. The concentrations of other test gases passing through the pyrolysis unit were recalculated to yield the equivalent H_2S content.

Figure 3 depicts this dependence for electroactive H_2S and 2-propanethiol and electro-inactive dimethyl sulphide. In Fig. 3, it can be seen that in the temperature range 300–600° H_2S is lost by decomposition, sulphur being deposited on the walls of the connecting tube. Nonetheless, reductive pyrolysis begins to take place at these temperatures and is

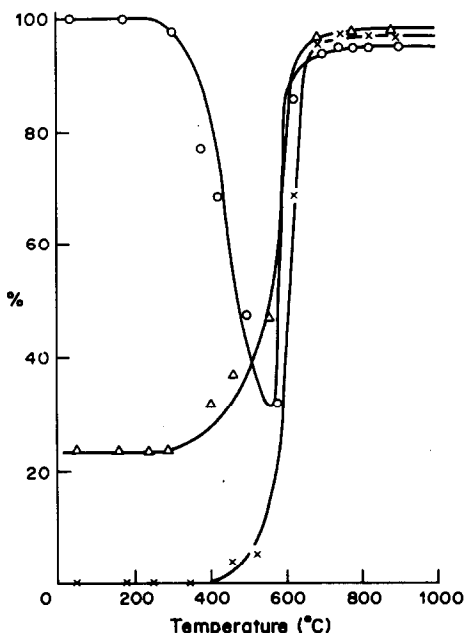


Fig. 3. Dependence of the pyrolysis efficiency on temperature: ○—6.6 ml/m³ hydrogen sulphide, △—3.9 ml/m³ 2-propanethiol, ×—13.2 ml/m³ dimethylsulphide. H_2 flow-rate 2 ml/sec, pyrolysis tube bore 4 mm, length of heated zone, 100 mm.

practically complete above 700°. A temperature of 800° was employed for subsequent measurements. Thus pyrolysis occurs at lower temperatures than that reported by Drushel¹² (1125°), probably because gaseous compounds are being pyrolysed, whereas liquid samples were analysed by Drushel. The use of a lower working temperature prolongs the lifetime of the pyrolysis tube.

(ii) The effect of the geometry of the silica tube and of the hydrogen flow-rate on the pyrolysis efficiency was studied for tubes with various internal diameters (1, 1.75 and 4 mm) at various flow-rates of hydrogen gas (0.5–2 ml/sec). Figure 4 shows the effect for dimethyl sulphide. The pyrolysis efficiency decreases with decreasing flow-rate and decreasing internal diameter of the tube. This is because the silica tube has zones at a transition temperature of 300–600° before and after the zone that is at the working temperature of 800°, and the H₂S can be decomposed in the first of these (see Fig. 3). If the tube diameter is decreased and the hydrogen flow-rate kept constant, the area of the transition region per unit volume of gas passed increases and the overall conversion efficiency decreases. If the hydrogen flow-rate is increased at a given tube diameter, the contact time in the transition band decreases and the overall efficiency increases. Subsequent measurements were made with use of a tube of 4 mm bore and a hydrogen flow-rate of 2 ml/sec. The low flow-rate (compared to that used by others,^{11,12} viz. 24 and 10 ml/sec respectively) was

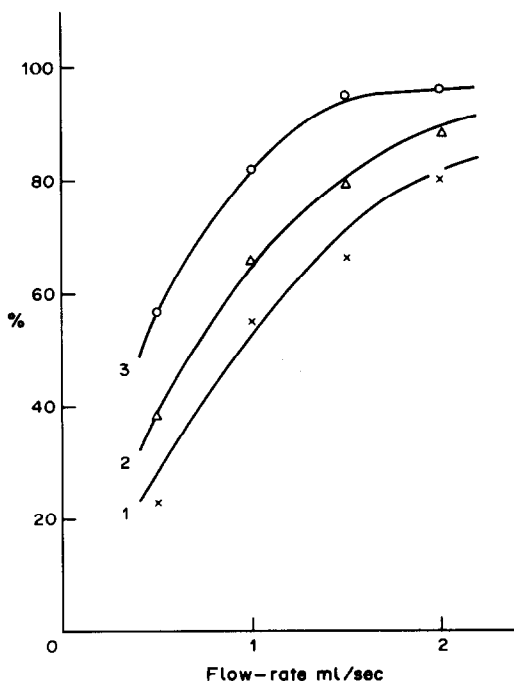


Fig. 4. Dependence of the pyrolysis efficiency on the hydrogen flow-rate and internal diameter of the pyrolysis tube: 1—1 mm, 2—1.75 mm, 3—4 mm; 12 ml/m³ dimethylsulphide, pyrolysis temperature 800°.

chosen because of the presence of the chromatographic column in front of the pyrolysis unit.

The effect of the length of the heated zone on the pyrolysis efficiency was studied for 2-propanethiol (20 ml/m³). The decrease in efficiency on shortening the zone from 100 to 20 mm was only 5%; the length of the pyrolysis zone is thus not critical for complete conversion.

(iii) The pyrolysis efficiency for the individual sulphur compounds was determined in two ways. The method described in (i) was employed, both for dosage of discrete samples, and also for continuous monitoring, in which the test gas was passed continuously through the pyrolysis unit over a period of 30 min and the pyrolysis products were absorbed in 10 ml of 0.1M sodium hydroxide. The amount of H₂S absorbed was determined pneumato-amprometrically.⁹ The pyrolysis efficiency determined by the two methods was comparable and values are listed in Table 1.

The pyrolysis efficiency for 2-propanethiol was tested as a function of concentration in the range 0.44–17 ml/m³ according to the procedure for the determination of total sulphur. In this range the AuPME response is linear with a slope of 1.10 $\mu\text{A} \cdot \text{m}^3 \cdot \text{ml}^{-1}$; comparison with the concentration dependence for H₂S (see below) thus indicates 98% conversion. The relative standard deviation for 10 measurements of 3.7 ml/m³ 2-propanethiol was 1.0%.

Detection of hydrogen sulphide

The conversion of sulphur-containing gases into H₂S renders the dependence of the AuPME response (peak height) on H₂S concentration the only calibration necessary.

The concentration dependence was determined without a chromatographic column by adding various concentrations of H₂S to the hydrogen. The concentration range from 0.44 to 65 ml/m³ was tested (*i.e.*, volumes of 1.57 ml in the sulphur concentration range 0.57–85.0 ng/ml were employed). In the range from 0.44 to *ca.* 18 ml/m³ this dependence is linear; the regression straight line $I = ac + b$ was determined from 20 points in this interval, where I is the peak height in μA , $a = (1.12 \pm 0.02) \mu\text{A} \cdot \text{m}^3 \cdot \text{ml}^{-1}$, c is the H₂S concentration in ml/m³ and $b = (0.07 \pm 0.10) \mu\text{A}$; the standard deviation was 0.18 μA and the correlation coefficient 0.9993. The dependence of the peak area on the concentration is also linear in this concentration range, the factor being 1.4 $\mu\text{C} \cdot \text{m}^3 \cdot \text{ml}^{-1}$. At higher H₂S concentrations this dependence becomes non-linear (Fig. 5). Twelve determinations of 3.7 ml/m³ H₂S yielded a relative standard deviation of 1.0%. The detection limit for H₂S, 4 $\mu\text{l/m}^3$, was taken as the concentration corresponding to three times the peak-to-peak background noise ($3 \times 1.5 \text{ nA}$). The linear dynamic range thus extends over more than 4 orders of magnitude.

The peak height increases linearly with increasing

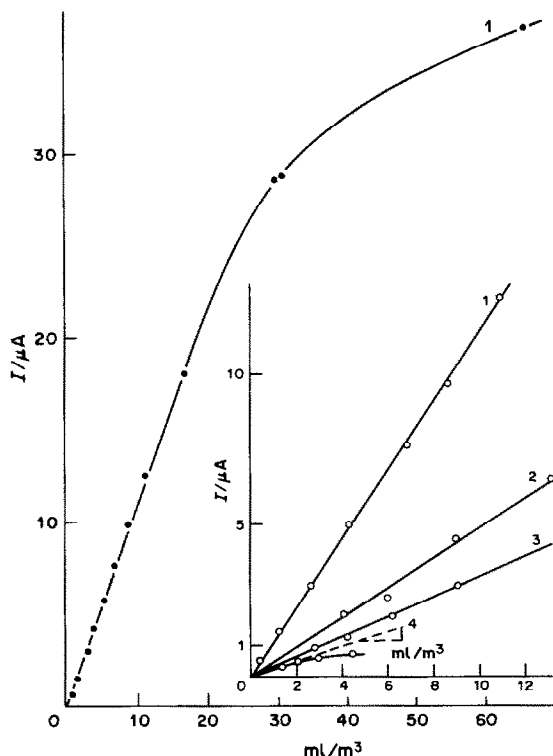


Fig. 5. Dependence of the AuPME on the H_2S concentration—curve 1. Inset—dependence of the AuPME response on concentration for lower thiols: 2—methylmercaptan, 3—ethylmercaptan, 4—2-propanethiol; the curvature for 2-propanethiol is a result of condensation on the walls of the apparatus.

flow-rate of the carrier gas (in the range tested, 0.5–2 ml/sec), and the peak area (electrolysis efficiency) is inversely proportional to the square root of the flow-rate. Electrolysis efficiency values of 21.5 and 11.2% were found for flow-rates of 0.5 and 2 ml/sec respectively.

The response rate of the AuPME was evaluated by measuring the time of the exponential AuPME response for direct injection of the H_2S sample into the detector. Time-constant values of 250 and 80 msec, respectively, were found for hydrogen flow-rates of 0.5 and 2 ml/sec. The AuPME peak disappears after about 10 sec.

In addition to hydrogen as diluent gas for samples to be analysed, nitrogen and, to increase the safety (the pyrolysis unit was placed in a wire mantle), air were also employed. The AuPME response to H_2S in nitrogen was about 4% higher and, in air about 8% higher, than that for the sample in hydrogen. When the total sulphur was determined for samples in air, the sulphur compounds produced were separated from oxygen on a column (PTFE tube, bore 3 mm, packed with Porapak QS to a length of about 5 mm), placed between the sampling valve and the pyrolysis unit. The water formed was collected in the meniscus of concentrated H_2SO_4 formed in a T-tube (bore 3 mm) placed after the pyrolysis unit (see Fig. 1, T). If the water is not removed, it absorbs H_2S , leading

to a dramatic decrease in the AuPME response. This removal of water becomes unnecessary in the determination of the individual components of a mixture on a chromatographic column, where the oxygen is completely separated from the sulphur-containing components.

Direct detection of thiols without conversion into H_2S is possible only for the lowest members of the series. However, the AuPME response is much lower and decreases with increasing thiol molecular size (see Fig. 5 and Table 2). Direct detection could be important for the identification of substances leaving the chromatographic column. Conversion into H_2S is preferable for quantitative determination.

The problem of interferences in reductive pyrolysis has been discussed by Wallace *et al.*¹ Because of the nature of the detection system and the experimental conditions employed in this work, HCN is the only potential interferent; this substance is formed in the reductive pyrolysis of nitrogen-containing substances. At a potential of +0.1 V, the AuPME has the same sensitivity for HCN as for H_2S . According to Cedergren and Sundén,¹³ HCN is formed at a temperature of about 1125° from about 2–3% of the nitrogen content and the conversion decreases with decreasing temperature. The platinum catalysts commonly used in reductive pyrolysis participate in HCN formation.¹ It was assumed that the amount of HCN formed under conditions of uncatalysed pyrolysis at the temperatures employed in the proposed method would be minimal. The effect of nitrogen-containing substances was not studied. Hydrogen halides formed from halogen-containing gases do not interfere as they undergo an electrochemical reaction at the AuPME at a more positive potential.

The proposed method for determining total sulphur was tested on a model mixture of 6.6 ml/m³ H_2S + 12.9 ml/m³ $(\text{CH}_3)_2\text{S}$ + 2.5 ml/m³ $(\text{CH}_3)_2\text{CHSH}$ + 2.4 ml/m³ $(\text{CH}_3)_2\text{S}_2$ in hydrogen. The theoretical sulphur content was 55.1 ng per injection; 52.8 ng of sulphur was found by use of a calibration graph (Fig. 5).

Table 1. Experimentally determined efficiency of reductive pyrolysis

Compound	Concentration added, ml/m ³	Pyrolysis efficiency, %*
$\text{H}_2\text{S}^\dagger$	6.7	96 ± 2
CH_3SH	0.5	92 ± 2
$\text{C}_2\text{H}_5\text{SH}$	0.6	92 ± 4
$(\text{CH}_3)_2\text{CHSH}$	8.7	96 ± 6
$(\text{CH}_3)_2\text{S}$	7.0	98 ± 4
$\text{C}_2\text{H}_5\text{SCH}_3$	8.4	98 ± 2
$(\text{CH}_3)_2\text{S}_2$	2.3	96 ± 4
SO_2	0.4	105 ± 2
CS_2	1.2	94 ± 3
Tetrahydrothiophene	6.3	103 ± 3

*Mean and s.d. from 6 measurements.

†Less than 100% efficiency as a result of decomposition of H_2S in the silica tube in the first transition temperature region.

Table 2. Direct detection of thiols at the AuPME

Compound	Concentration range, ml/m^3	Sensitivity, $\mu A \cdot m^3 \cdot ml^{-1}$	Relative sensitivity compared to H_2S , %
CH_3SH	4.1–13.5	0.48	43
C_2H_5SH	2.1–9.1	0.33	30
$(CH_3)_2CHSH$	1.4–4.5	0.28	25

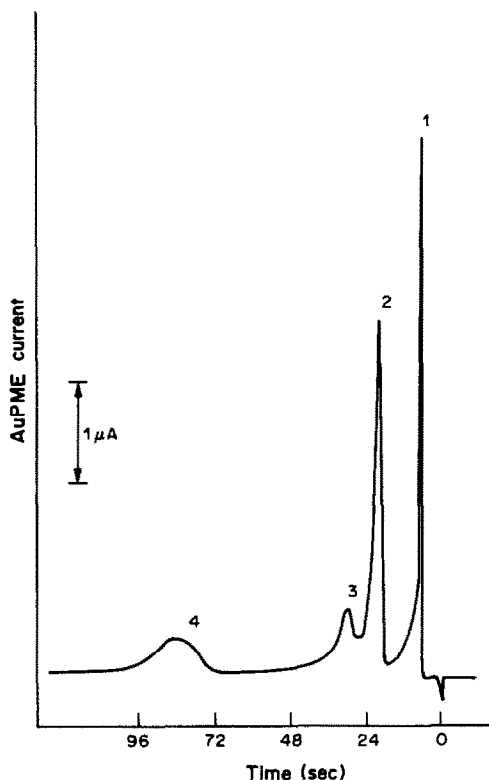


Fig. 6. AuPME detection of sulphur-containing compounds after separation on a column of Porapak QS (see Table 3). H_2 flow-rate 2 ml/sec, pyrolysis tube bore 4 mm, length of heated zone 100 mm, 800° .

Detection after separation on a column

A chromatographic column was placed between the sampling valve and the pyrolysis unit and the AuPME was tested as a gas chromatographic detector. The AuPME response to the individual gases in the model mixture (the same as that used for the determination of total sulphur) is depicted in Fig. 6;

see also Table 3. It is obvious from the results that the AuPME with post-column reductive pyrolysis can be used as a detector for the determination of sulphur-containing compounds. Separation of the individual components can be improved by optimization of the chromatographic process.¹⁴

Conclusions

The AuPME can be used in combination with reductive pyrolysis for the sensitive determination of the total sulphur content in gases. The detection limit of $4 \mu l/m^3$ for H_2S ($S \sim 5 \text{ pg/ml}$) is only one order of magnitude higher than that given for the FPD determination of sulphur (0.5 pg/ml).¹⁵ Because of the character of the calibration graph, the AuPME is more suitable for the determination of low concentrations up to *ca.* 20 ml/m^3 , where the concentration dependence is linear.

The response rate and sensitivity permit use of the AuPME as a detector of sulphur-containing compounds in gas chromatography. The different electrochemical behaviour of various sulphur-containing compounds permits combination of direct detection and detection after pyrolysis to obtain information for identification of substances separated on the column.

The AuPME can thus be used as a universal detection system that can be combined with reductive pyrolysis for the determination of sulphur in liquid samples as well as in the air. As in differential pulse polarography,⁵ the sensitivity of the determination of total sulphur can be increased by using the cathodic stripping voltammetry method with a silver-plated membrane electrode.¹⁶

Acknowledgements—The authors wish to thank Dr J. Mizera and Dr Z. Lukáš (Transgas Control Laboratory of Gas Quality, Prague) for providing most of the permeation tubes.

Table 3. Detection of individual sulphur-containing gases after separation on the column (see Fig. 6)

Peak No.	Compound	Uncorrected retention time, sec	Concentration, ml/m^3	Amount of sulphur, ng	Peak area, μC	Conversion efficiency relative to H_2S , %
1	H_2S	6	6.6	13.6	9.2	100
2	$(CH_3)_2S$	20	12.9	26.5	17.3	97
3	$(CH_3)_2CHSH$	30	2.5	5.1	3.3	96
4	$(CH_3)_2S_2$	85	2.4	9.9	6.2	93

REFERENCES

1. L. D. Wallace, D. W. Kohlenberg, R. J. Joyce, R. T. Moore, M. E. Riddle and J. A. McNulty, *Anal. Chem.*, 1970, **42**, 387.
2. G. de Groot, P. A. Greve and R. A. A. Maes, *Anal. Chim. Acta*, 1975, **79**, 279.
3. R. T. Moore, P. Clinton and V. Barger, *Anal. Chem.*, 1980, **52**, 760.
4. T. Kojima, Y. Seo and J. Sato, *Bunseki Kagaku*, 1974, **23**, 1389; 1975, **24**, 772.
5. R. E. Reim and D. D. Hawn, *Anal. Chem.*, 1981, **53**, 1088.
6. I. Bergman, *J. Electroanal. Chem.*, 1983, **157**, 59.
7. F. Opekar, *Chem. Listy*, 1985, **79**, 703.
8. P. R. Gifford and S. Bruckenstein, *Anal. Chem.*, 1980, **52**, 1208.
9. F. Opekar and S. Bruckenstein, *Anal. Chim. Acta*, 1985, **169**, 407.
10. F. Opekar, Z. Večeřa and J. Janák, *Intern. J. Environ. Anal. Chem.*, 1986, **27**, 123.
11. J. K. Fogo and M. Popowsky, *Anal. Chem.*, 1949, **21**, 734.
12. H. V. Drushel, *ibid.*, 1978, **50**, 76.
13. A. Cedergren and T. Sundén, *Anal. Chim. Acta*, 1977, **88**, 25.
14. T. L. C. de Souza, D. C. Lane and S. P. Bhatia, *Anal. Chem.*, 1975, **47**, 543.
15. R. M. Harrison, *CRC Crit. Rev. Anal. Chem.*, 1984, **15**, 1.
16. F. Opekar and S. Bruckenstein, *Anal. Chem.*, 1984, **56**, 1206.

A SUB-MICROLITRE TWO-PHOTON IONIZATION DETECTOR FOR HIGH-PERFORMANCE LIQUID CHROMATOGRAPHY

S. YAMADA,* C. SAKANE and T. OGAWA†

Department of Molecular Science and Technology, Kyushu University, Kasuga-shi, Fukuoka 816, Japan

(Received 25 June 1986. Revised 11 August 1986. Accepted 20 December 1986)

Summary—A simple sub-microlitre two-photon ionization detector for high-performance liquid chromatography has been constructed; it basically consists of a pulsed laser, a falling-jet cell, and a boxcar detection system. The performance of the cell has been evaluated; the cell is windowless and its volume is about 14 nl. A dye laser is applicable as excitation light-source.

The development of sensitive, selective and widely applicable detectors for high-performance liquid chromatography (HPLC) is of great interest in clinical, environmental and biological analysis. Lasers have opened up new frontiers in spectroscopy because of their high photon flux, monochromaticity, and excellent spatial and temporal coherence. Recently, laser two-photon ionization spectrometry has proved to be a sensitive and practical technique for the determination of various kinds of organic molecules in solution.¹⁻⁸ Its application for detection in HPLC has also received substantial attention.⁹⁻¹³

A few different photoionization cells for detecting components of HPLC effluents have been developed. Voigtman and Winefordner constructed a flowing droplet cell (cell volume 6 μ l)^{2,9} and a crystalline quartz cell (9 μ l).¹⁰ For use of an excimer laser (wavelength 308 nm), they reported a detection limit of 80 ng/ml ($S/N = 3$) for *N*-ethylcarbazole in 70:30 v/v acetonitrile/water mixture.¹⁰ We constructed a cuvette cell (5 μ l),¹¹ with which a double-beam method using a nitrogen laser (337.1 nm) achieved a detection limit of 0.2 ng/ml ($S/N = 2$) for pyrene in hexane;¹² it is as sensitive as a laser-induced fluorescence detector¹⁴ and is superior to a commercial ultraviolet absorbance detector¹¹ or a one-photon ionization detector.¹⁵

The cell volume of an HPLC detector should be kept small in order to minimize band broadening. Two-photon ionization is a non-linear process and tight focusing of the laser beam is desirable for higher efficiency. In such a case, the limit of the cell volume arises from the flow design and not from the light source.¹⁶ Thus, there is still considerable scope for reducing the cell volume in this technique. Quite recently, we reported a sub-microlitre windowless

flow-cell (14 nl) for two-photon ionization detection,¹⁷ which was based on the free-falling jet principle.¹⁸

Although the nitrogen laser is compact, reliable, reasonable in price, and convenient in operation, its wavelength is not tunable. Thus, a tunable dye laser may enhance the practical analytical utility in the two-photon ionization technique. An excimer laser-pumped dye laser would offer a higher sensitivity because of its higher power.

In this paper, we have modified the falling-jet cell¹⁷ for detecting HPLC effluents and have applied it with a dye laser as well as a nitrogen laser as excitation light-source.

EXPERIMENTAL

Instrumentation

The schematic diagram of the experimental system is shown in Fig. 1. Excitation illumination was provided either by a nitrogen laser (Molelectron UV-12, pulse duration 10 nsec, repetition rate 10 Hz) or by a dye laser (Molelectron DL-14P, 6-8 nsec, 10 Hz) pumped by a nitrogen laser (Molelectron UV-24). A quartz lens (focal length 10 cm) focused the laser beam into a photoionization cell. The resultant photoionization current was converted into a voltage by a current-to-voltage converter (10^7 V/A).^{7,8}

The converter output was fed into a high-pass filter with a cut-off frequency of 3 kHz.¹⁷ The output signal was averaged by a boxcar integrator and recorded by a strip-chart recorder.

Photoionization cell

The effluent from an HPLC column was arranged as a free-falling jet, which was produced by a small-bore capillary (Fig. 1). The capillary consisted of two tubes; one end of a stainless-steel tube (outer diameter 1.6 mm, bore 0.25 mm, length 150 mm; a in Fig. 1) was drilled out to take another stainless-steel tube (outer diameter 0.33 mm, bore 0.15 mm, length 7 mm; b in Fig. 1). This device gave a fine free-falling jet of HPLC effluent at flow-rates down to 1.1 ml/min. A fine liquid column was formed between the capillary end and a conical brass electrode placed just below the capillary end (c in Fig. 1). The capillary also served as an electrode and was electrically grounded. The conical electrode was attached to a high-voltage BNC connector which was fixed to a micrometer-driven carrier to adjust the

*Present address: Laboratory of Chemistry, College of General Education, Kyushu University, Ropponmatsu, Fukuoka 810, Japan.

†Author to whom correspondence should be addressed.

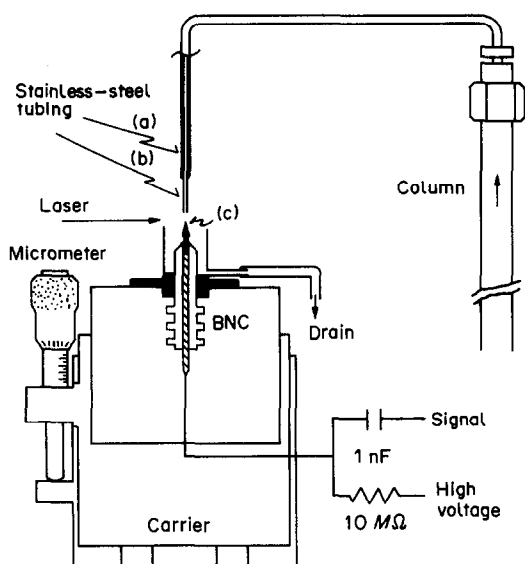


Fig. 1. Schematic diagram of the experimental system. The falling jet stream was formed from a capillary consisting of wide (a) and narrow (b) stainless-steel tubes. The fine liquid column was produced between the two electrodes (b, c): b, narrow tubing; c, conical electrode.

electrode spacing between the conical electrode and the capillary end; the spacing could be varied in the range 0–12 mm. The conical electrode carried a current-limiting resistor (10 M Ω) and a capacitor (1 nF, 3 kV). A stabilized dc power supply (Kikusui 1041) gave a voltage of 1.5 kV across the electrodes.

Chromatography

The chromatographic system consisted of a pump (Hitachi 655A-11), an injector (Hitachi, 20- μ l loop), and a column (4.6 \times 150 mm, packed with 5- μ m Shodex Silikapack E-411). The effluent from the column was monitored with a commercial ultraviolet absorbance detector or the falling-jet cell. The injected volume was 10 μ l and the flow-rate was in the 1–2 ml/min range. Since our purpose was to demonstrate the feasibility of the present system as a detector for HPLC, no attempt was made to optimize the chromatographic conditions.

Reagents

Pyrene (Nakarai Chemicals) was purified as described previously.⁵ Other analytes (reagent grade) were commercially obtained and used without further purification. Laser dyes (Exciton), BBQ for 374 nm and coumarin 440 for 434 nm, were used as received. Iso-octane (Kishida Chemicals, special reagent grade for HPLC) was deaerated by ultrasonic irradiation for 5–10 min. Sample solutions were prepared from stock solutions (10⁻²–10⁻³ M) in iso-octane.

RESULTS AND DISCUSSION

Formation of the fine liquid column

The present photoionization cell is based on the free-falling jet principle.¹⁸ Formation of the liquid column between the electrodes depended both on the electrode spacing and on the flow-rate, as shown in Fig. 2. A fine liquid column of iso-octane solution was formed down to a flow-rate of 1.1 ml/min. Turbulence or droplet formation appeared under

conditions corresponding to the unshaded area in Fig. 2. The liquid column was more stable at higher flow-rate, and this allowed use of a closer electrode spacing. In photoionization detection, the electrode spacing should be made as narrow as possible, but avoiding direct illumination of the electrodes and electrical breakdown.^{3,6} In this study, the electrode spacing and the flow-rate were set at 0.8 mm and 1.5 ml/min, respectively.

Sensitivity

To compare the new detector with previous ones, the chromatographic detection limit for anthracene was evaluated as before,¹¹ the results are summarized in Table 1. The new system is slightly worse than the ultraviolet detector and substantially worse than the previous cell, if the comparison is made in terms of concentration and the same excitation wavelength (337.1 nm). However, the cell volume of the new detector (14 nl) is more than two orders of magnitude smaller than that of the ultraviolet detector cell (17.7 μ l) or the previous cell (5 μ l), and the new system is more sensitive than the others if the comparison is made in terms of detectable amount in the cell. Thus, the detectability with the new system is better than that with the others. The method is as sensitive as laser fluorimetry and is superior to the laser photoacoustic method. With photoionization detection, the sensitivity is better for non-polar solvents, owing to the lower leakage currents.^{2,7,13}

Chromatographic measurements

Figure 3 shows photoionization and ultraviolet detection chromatograms of an equimolar (1.4 \times 10⁻⁶ M) mixture of seven aromatic molecules (anthracene, pyrene, 2-methylanthracene, 9-methylanthracene, 9,10-dimethylanthracene, benz(a)anthracene, and perylene) measured at an excitation wavelength of 337.1 nm. The photoionization detection gave five peaks, assigned as (a) anthracene,

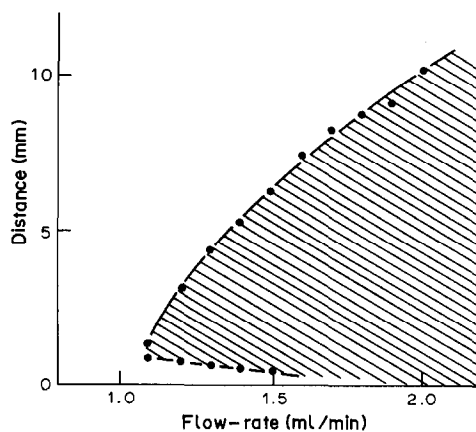


Fig. 2. Formation of the falling jet. The fine liquid column was formed when the distance between the two electrodes and the flow-rate were in the shaded region.

Table 1. Chromatographic detection limits ($S/N = 3$) for anthracene

Method	Excitation wavelength, nm	Solvent	Cell volume, μl	Detection limit		Reference
				Concn., ng/ml	Amount, pg	
UV absorption	337.1	iso-octane	17.7	50	880	This work
	254	hexane	17.7	2.6	45	11
Laser photoionization	337.1	iso-octane	0.014	81	1.1	This work
	337.1	hexane	5	0.8	4	11
	308	acetonitrile/water, 70/30	9	100	900	10
Laser fluorometry	308	acetonitrile/water, 70/30	6	40	240	9
Laser photoacoustic spectrometry	308	acetonitrile/water, 70/30	6	3.0×10^3	1.80×10^4	9

(b) overlap of pyrene and 2- and 9-methylanthracene, (c) 9,10-dimethylanthracene, (d) benz(a)anthracene, and (e) perylene. In contrast, the ultraviolet detection showed only two peaks.

The sensitivity of the ultraviolet detector should be approximately proportional to the molar absorptivity of the analyte. The sensitivity of photoionization detection tends to increase with increasing molar absorptivity of the analyte at the excitation wavelength,⁶⁻⁸ so both chromatograms should be similar. However, Fig. 3 indicates that the photoionization signals of anthracene, 9,10-dimethylanthracene and perylene are relatively larger than those expected from their molar absorptivities at 337.1 nm.⁷ The two-photon ionization spectra of pyrene,¹⁹

fluoranthene²⁰ and N,N,N',N' -tetramethyl-*p*-phenylenediamine,²⁰ which were obtained by monitoring the photoionization current as a function of the excitation wavelength, showed deviations from their one-photon absorption spectra; the photoionization spectra are broader at each peak and more intense in the shorter wavelength region than the absorption spectra. These findings show that the efficiency of photoionization depends not only on the efficiency of one-photon excitation from the ground state but also on other physical properties of the molecule such as the molar absorptivity of the intermediate state(s), the ionization potential, and the deactivation pathways of photoexcited states.

Figure 4 shows photoionization chromatograms of an equimolar ($1.4 \times 10^{-5} M$) mixture of the seven aromatic molecules, with excitation at 337.1, 374 and

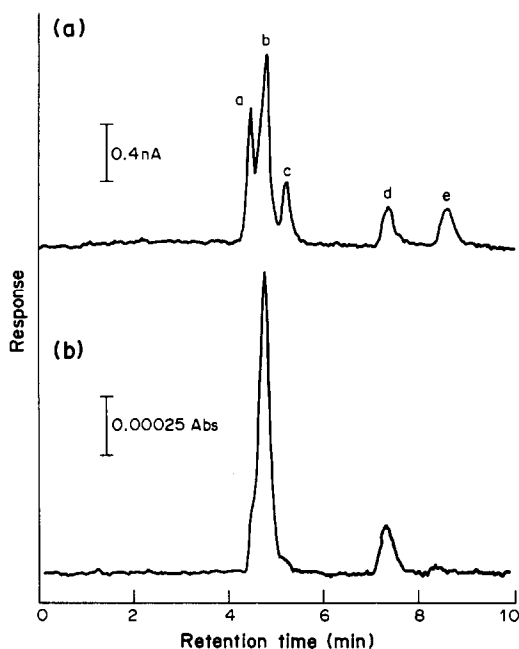


Fig. 3. Photoionization (a) and ultraviolet (b) chromatograms of an equimolar ($1.4 \times 10^{-6} M$) mixture of seven aromatic molecules eluted with iso-octane. Peaks: (a) anthracene, (b) pyrene, 2- and 9-methylanthracene, (c) 9,10-dimethylanthracene, (d) benz(a)anthracene, (e) perylene. Excitation at 337.1 nm.

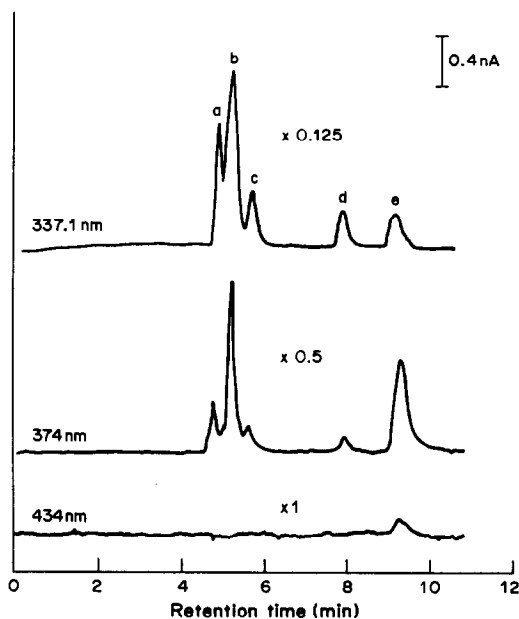


Fig. 4. Photoionization chromatograms of an equimolar ($1.4 \times 10^{-5} M$) mixture of the seven aromatic molecules (excitation at 337.1, 374 and 434 nm), eluted with iso-octane. See Fig. 3 for identity of peaks.

434 nm. The photoionization signal was strongest and the *S/N* ratio was best for excitation at 337.1 nm, mainly because the nitrogen laser had higher power than the dye laser. Anthracene, 9,10-dimethylanthracene and benz(*a*)anthracene showed relatively more intense signals than perylene in the shorter wavelength region. Only perylene showed a peak on excitation at 434 nm, mainly because it had the largest molar absorptivity.

Comparison of photoionization cells

The use of the free-falling jet principle¹⁸ has substantially reduced the cell volume compared with that of previously reported cells.⁹⁻¹³ In the present cell, the shape of the liquid column is almost independent of the physical properties of the solvent. A cell with windows and/or walls is inconvenient for optical adjustment. The laser power should be kept low in order to avoid damage at a quartz/liquid interface in such a photoionization cell,¹⁰ although high laser power gives a high photoionization signal. The present cell has no such drawbacks, since it has neither windows nor walls; it is also free from possible contamination and memory effects from windows and walls.

Acknowledgements—The authors thank H. Kawazumi, N. Sato and T. Matsumoto for their co-operation in the measurements. The work was partially supported by a Grant-in-Aid for Scientific Research (Grant No. 60470067) and for Special Project Research (Grant No. 61227019, from the Ministry of Education of Japan, and by a grant from Shimazu Science Foundation.

REFERENCES

1. E. Voigtman, A. Jurgensen and J. D. Winefordner, *Anal. Chem.*, 1981, **51**, 1921.
2. E. Voigtman and J. D. Winefordner, *ibid.*, 1982, **52**, 1834.
3. *Idem*, *Talanta*, 1983, **30**, 75.
4. K. Fujiwara, E. Voigtman and J. D. Winefordner, *Spectrosc. Lett.*, 1984, **17**, 9.
5. S. Yamada, K. Kano and T. Ogawa, *Bunseki Kagaku*, 1982, **31**, E247.
6. S. Yamada, A. Hino, K. Kano and T. Ogawa, *Anal. Chem.*, 1983, **53**, 1914.
7. S. Yamada, T. Ogawa and P.-H. Zhang, *Anal. Chim. Acta*, 1986, **183**, 251.
8. T. Ogawa, S. Yamada, P.-H. Zhang, S. Yoshida and C. Sakane, *Repts. Asahi Glass Found. Ind. Tech.*, 1985, **46**, 65.
9. E. Voigtman and J. D. Winefordner, *J. Liq. Chromatog.*, 1982, **5**, 2113.
10. *Idem*, *ibid.*, 1983, **6**, 1275.
11. S. Yamada, A. Hino and T. Ogawa, *Anal. Chim. Acta*, 1984, **156**, 273.
12. *Idem*, *Bunseki Kagaku*, 1984, **33**, E37.
13. A. Hino, S. Yamada, T. Nagamura and T. Ogawa, *ibid.*, 1984, **33**, 393.
14. J. H. Richardson, K. M. Larson, G. R. Haugan, D. C. Johnson and J. E. Clarkson, *Anal. Chim. Acta*, 1981, **116**, 407.
15. D. C. Locke, B. S. Dhingra and A. D. Baker, *Anal. Chem.*, 1982, **54**, 447.
16. E. S. Yeung, in *Lasers in Chemical Analysis*, G. M. Hieftje, J. C. Travis and F. E. Lytle (eds.), Chap. 14, p. 273, Humana Press, Clifton, N.J., 1981.
17. S. Yamada and T. Ogawa, *Anal. Sci.*, 1986, **2**, 199.
18. S. Folestad, L. Johnson, B. Josefsson and B. Galle, *Anal. Chem.*, 1982, **54**, 925.
19. K. Siomos and L. G. Christophorou, *Chem. Phys. Lett.*, 1980, **72**, 43.
20. K. Siomos, G. Kourouklis and L. G. Christophorou, *ibid.*, 1981, **80**, 504.

ELECTROTHERMAL ATOMIC-ABSORPTION SPECTROMETRIC ANALYSIS OF LAKE WATERS FOR Mn, Fe, Pb AND Cd

STUART J. NAGOURNEY,* MERRILL HEIT and DONALD C. BOGEN

Environmental Measurements Laboratory, U.S. Department of Energy, 376 Hudson Street, New York, NY 10014, U.S.A.

(Received 4 March 1985. Revised 17 November 1986. Accepted 18 December 1986)

Summary—Analyses have been made for trace metals in surface waters from lakes known to be sensitive to inputs of acidic deposition. Electrothermal atomic-absorption spectrometry was used for direct measurement of the low metal concentrations. The studies revealed non-spectral interferences resulting from small amounts of inorganic material in the sample matrix that prevent accurate measurements of Mn and Pb. Several types of interferences were identified by means of a computer coupled to the atomic-absorption spectrometer and procedures to overcome them were evaluated. Matrix modification with nitric acid is required for the determination of Mn. Atomization from a platform inserted within the graphite tube is necessary for interference-free Pb determination.

The determination of trace metals in environmental samples such as natural waters, rain and airborne particulates is an important component in studies assessing the impact of energy-related pollutants on natural ecosystems. Mn, Fe, Pb and Cd are among the many trace elements of interest. The Pb and Cd present are recognized as being anthropogenic; Mn has both natural and man-made sources; and Fe is of interest since it can be used to measure the input from crustal sources.¹ These metals are utilized to evaluate temporal trends in deposition and the extent of transport of materials from distant sources. Accurate measurements are vital to such interpretations.

There are several analytical techniques that can be used to determine the trace metal content in environmental samples. The most commonly applied is atomic-absorption spectrometry (AAS). Since the concentrations of metals such as Mn, Fe, Cd and Pb in natural water samples are often below 10 ng/ml, flame AAS does not provide adequate limits of detection. Electrothermal AAS (ETAAS), which is 100–1000 times more sensitive than the flame technique, has become a widely used alternative.

Chemical interferences resulting from the interaction of the analyte and the inorganic sample matrix have minimal effects on the flame AAS response of trace metals. These interferences are well understood and can be easily controlled. In contrast, the ETAAS signals for several metals can be dramatically affected by small amounts of inorganic salts that compose the sample matrix.² The mechanisms of interaction between the analyte and matrix are not completely understood, and have been studied only for individual elements or compounds at high salt concen-

trations. These matrix effects can either increase or decrease the measured ETAAS response and the interferences differ for each element and matrix. The effect of the sample matrix on ETAAS analyses of environmental samples has not been considered in depth. The aim of our study was to examine this problem. Without such information, the values obtained for trace metals in environmental samples, e.g., atmospheric deposits and natural waters, may be erroneous, resulting in misleading conclusions being drawn for significant environmental questions such as the impact of acidic precipitation on natural ecosystems.

These interferences can alter the magnitude, shape and temporal position of an ETAAS response that is only several seconds in duration. To characterize these rapid signals fully, it is necessary to acquire the data at high speed, while ensuring that they are unaffected by signal damping, and to store, present and manipulate this information as the analyst requires. These objectives have been accomplished by interfacing a computer with the AA spectrometer and developing the software necessary to process the data. The information obtained can be used to assess the effects of the interferences and evaluate techniques to overcome them.

A variety of methods are available to correct for these interferences. One is to prepare the standards with the same matrix as the samples, but is not useful when diverse sample types must be analysed. Another is the method of standard additions, which requires the preparation of numerous spiked solutions and can result in contamination, especially at low metal concentrations. Procedures for chemical separation of the analytes from the matrix are time-consuming, prone to contamination and often not quantitative. Techniques that require minimal sample handling and/or chemical treatment are better able to provide accurate data at ng/ml concentration levels.

*Author for correspondence. Present address: Witco Chemical Corporation, 633 Court St., Brooklyn, NY 11231-2193, U.S.A.

We have used ETAAS to measure Mn, Fe, Cd and Pb in atmospheric deposition and natural surface-water samples, including samples from several lakes and reservoirs in the Adirondack region of New York State, an area known to be sensitive to inputs of acidic precipitation. Data obtained from our AAS-computer system have been used to identify interferences that seriously affect these measurements, and have enabled us to determine their possible causes and the analytical conditions required to compensate for their effect and obtain accurate results.

EXPERIMENTAL

Apparatus

AAS analyses were made with a Perkin-Elmer (PE) Model 5000 spectrometer. Flame measurements were performed with a 10.5-cm single-slot burner head and an air-acetylene flame. ETAAS measurements were made with a PE Model 500 heated graphite atomizer and a PE Model AS-1 autosampler; pyrolytically-coated graphite tubes and solid pyrolytic graphite platforms were used throughout. The AAS-computer system used to acquire and process the ETAAS data has already been described in detail.³

Measurements of chloride, nitrate and sulphate were made by ion-chromatography on a Dionex Model 2020 unit equipped with a 50- μ l sample loop, an HPIC AG-4 anion guard-column, HPIC AS-4 separator column and a fibre suppressor-unit. The results were used along with the Na, Mg, Ca and K values determined by flame AAS to determine the composition of the major-ion matrix.

Reagents

"Ultrex" nitric acid (J. T. Baker Chemical Co.) and doubly-demineralized water (DDW, 2 M Ω resistance) were used exclusively for all cleaning procedures and preparation of standards. Standard solutions (1000 μ g/ml) of the metals were obtained from the Fisher Scientific Company. The salts used to prepare the major cation and anion standards were Fisher ACS reagent grade.

Procedures

To minimize problems associated with the sampling and manipulation of natural water samples containing low concentrations of trace metals, plasticware was used throughout. Conventional polyethylene vessels are practical containers, since they are inexpensive, can be easily cleaned, have a low rate of loss of water vapour, and low levels of trace metal contamination.⁴

In addition to its role in preventing loss of trace metals from aqueous samples by adsorption on the container, nitric acid has been shown to have a major effect on the ETAAS response of many trace metals.⁵ To study this factor, duplicate samples were collected at each location. One duplicate was acidified with 10 ml of concentrated nitric acid per litre, and the other (which was also to be used for major-ion analyses), was left unacidified. Comparison of the positions of the ETAAS peaks for the acidified and unacidified fractions under various analytical conditions can be used to identify the causes of the non-spectral interferences and determine what corrective measures need to be applied.

Bottles for trace-metal analysis samples were cleaned by first rinsing and then leaving filled with 1% v/v nitric acid for 48 hr. They were then rinsed with DDW and left filled with DDW for 48 hr. This cleaning cycle was repeated three times.

The bottles for major-ion analysis samples were submitted to three cycles of rinsing and then left standing for 48 hr filled with DDW. All bottles were filled with DDW for transport to the field.

Sampling

Grab samples were collected at two sites at each lake or reservoir. At each site, a conventional polyethylene bottle was rinsed thoroughly with demineralized water. The bottle was then filled with lake material about 0.5 m below the surface and emptied, this rinsing being repeated three times. The sample was then collected at the same depth.

The sample was immediately filtered by use of a polystyrene filter funnel containing a 0.45- μ m Millipore filter, a polystyrene filter flask, and a polyvinyl hand-operated vacuum pump equipped with Tygon tubing.

Two sets of filtration apparatus were used. The set used for trace metal samples was cleaned by rinsing the filter funnel and flask three times with 1% v/v nitric acid, followed by DDW, and that for major-ion samples was rinsed only with water. After filtration, 2-5 ml of concentrated nitric acid was added to each sample for trace metal analyses. Field blanks were filtered identically to the samples.

Analysis

Standard solutions covering the concentration range of the samples were prepared daily by serial dilution from the 1000 μ g/ml stock solutions. The trace metal concentrations were calculated by use of calibration graphs generated by measurement of these standard solutions. Both laboratory reagent blanks and field blanks were processed identically. The analytical conditions used for the AAS measurements have been listed elsewhere.⁶

Two types of reference materials were concurrently analysed. Trace metal standards were obtained from the Environmental Protection Agency (EPA) Environmental Monitoring and Support Laboratory and prepared according to their instructions.⁷ These solutions contain ng/ml concentrations of various trace metal nitrates in dilute nitric acid, with no other alkali or alkaline-earth metals or anions present. Also analysed was National Bureau of Standards standard reference material 1643, "Trace Elements in Water." This solution contains ng/ml concentrations of trace metals in a major-ion matrix that simulates fresh water.

RESULTS AND DISCUSSION

There are several types of interference that hinder ETAAS analysis of environmental samples. Non-spectral interferences directly affect the analyte signal by altering the time-dependent concentrations of metal atoms. There are two types of non-spectral interference. Solute-volatilization or condensed-phase interferences result from interactions between the analyte, matrix and/or sample tube prior to atomization. This type of interference is indicated by the atomization time of the analyte being different for the sample from that for an aqueous solution. Vapour-phase interferences result from interactions between the metal and matrix in the gas phase after vaporization.⁸

If the sample is vaporized after being deposited on the wall of the graphite tube, the metal vapour is introduced into an environment where the temperature is rapidly changing. If condensed-phase matrix interferences then cause the temperature of atomization of an analyte in the samples to differ from that for the aqueous standards of the same metal, calculations based upon calibration graphs will give incorrect results. These interferences can be identified by comparing peak parameters such as

appearance time and peak time for samples with those of standards, as measured by the AAS-computer system.

There are several direct approaches to alleviating these effects. One is matrix modification,⁹ by addition of chemical reagents that interact with the matrix to render it incapable of interfering with the analyte atomization. This interaction may enable the modified matrix material to be removed during the char state. Its success in correcting for condensed-phase interferences can be demonstrated by comparing standard and sample peak parameters before and after modification.

Another approach, suggested by L'vov,¹⁰ is to atomize the sample at constant temperature, by putting it on a graphite platform inserted in the graphite tube. Under these conditions, the tube reaches maximum temperature before the platform reaches the volatilization temperature of the analyte, and changes in atomization time due to condensed-phase interferences will have no effect on the calculated metal concentrations because the effective atomization temperatures of samples and standards will be the same. Also, the atomization occurs at higher temperatures, so vapour-phase interference effects are minimized because of more complete dissociation of analyte-matrix species that would otherwise be non-absorbing and would deplete the amount of metal available for atomic absorption.

Manganese

We have demonstrated the importance of the effect of small amounts of sample matrix on the ETAAS response of trace metals in wet, dry and bulk depositions, collected at American Samoa.¹¹ The major ionic matrix for all samples at this site has been

shown to be diluted sea-spray aerosol, with the major-ion concentrations in the samples varying over more than three orders of magnitude.¹² The most desirable analytical approach is one that avoids such procedures as the method of additions, matrix-matching or removal of the major-ion salts. Procedures such as matrix modification were therefore evaluated to see whether they would permit sample measurement by use of similarly treated aqueous standards.

As shown in Fig. 1a, for 0.2 ng of manganese in artificial sea-water solutions the response increases asymptotically with salinity, whereas for sodium chloride solutions of corresponding concentrations (Fig. 1b) there is a very broad and shallow maximum in manganese response.

We believe that with the sea-water matrix the manganese is entrained at the charring stage in a magnesium oxide matrix arising from the magnesium in the sea-water.¹³ Since wall-sampling is used, the manganese is placed in a non-isothermal environment where the rapidly changing atomization temperature results in changes in observed response. The results for the sodium chloride solutions, where no magnesium is present, support this conclusion. The mean peak-times for the two types of solution are shown in Table 1. The decrease in response for both types of solution at higher salt concentrations is attributed to vapour-phase binding of some of the manganese by the increasingly large amount of chloride present, resulting in lower atomic manganese concentration.

These effects can be eliminated by matrix modification with nitric acid. The acid treatment results in volatilization of hydrogen chloride from the sample matrix, leaving the more readily decomposed nitrate species, which are therefore converted into the oxides

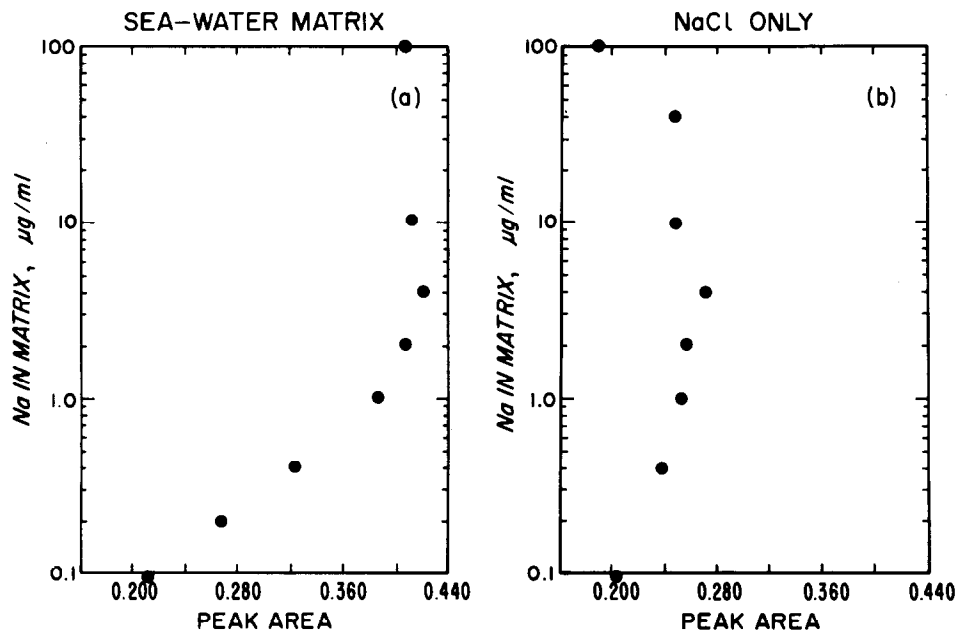


Fig. 1 Mn—wall atomization, 0.2 ng. Each value is the mean of duplicate measurements.

Table 1. Mean peak times for 0.2 μg of Mn in sea-water matrix and pure sodium chloride solutions, *sec*

Na concentration in solution, $\mu\text{g/ml}$	Sea-water matrix	NaCl solution
0	1.99 \pm 0.05	1.98 \pm 0.01
0.2	2.04 \pm 0.01	—
0.4	2.07 \pm 0.01	2.03 \pm 0.01
1.0	2.15 \pm 0.03	2.06 \pm 0.01
2.0	2.20 \pm 0.03	2.02 \pm 0.01
4.0	2.29 \pm 0.02	2.01 \pm 0.01
10.0	2.32 \pm 0.06	2.04 \pm 0.01
40.0	—	2.07 \pm 0.05
100.0	2.45 \pm 0.03	2.12 \pm 0.04

in the char stage, irrespective of the medium, presumably without entrainment by magnesium. After this treatment, we can measure any of the modified samples directly against similarly acidified aqueous standards by using wall sampling. Atomization from a platform is not required.

In our analyses of lake waters we have used these concepts to identify matrix interferences and explore corrective measures. Separate samples from each lake site were analysed, one acidified with 10 ml of concentrated nitric acid per litre and the other not. Analyses of these samples by flame AAS and ion-chromatography showed that except for nitrate the major-ion matrix in the two samples was the same. Comparison of trace metal concentrations in the two fractions was not meaningful, because of differences in the leaching or adsorption patterns for these elements. However, the ETAAS peak parameters for the two sets of samples could be compared to evaluate matrix interferences. This is illustrated for manganese in Table 2.

A condensed-phase interference similar to that for manganese in saline samples is evident for the lake water samples. Since the same interference occurs in analyses performed with and without maximum power heating, this shows that an increased rate of analyte volatilization provides no analytical advantage in this instance. No vapour-phase effects are evident, confirming earlier conclusions for the determination of manganese in natural solutions containing chloride concentrations below 20 $\mu\text{g/ml}$.³

Various corrective measures were studied. As shown in Table 2, atomization from a platform delays the peak as expected, but the large difference in mean peak time between standards and samples without acidification shows that use of the platform alone does not provide the complete remedy; matrix modification with nitric acid is sufficient to eliminate

Table 2. Mean peak times, *sec*, for ETAAS analyses for Mn in lake waters, maximum power heating

Matrix	Method of atomization	Standards	Lake waters
H ₂ O	Wall	0.21 \pm 0.01	0.33 \pm 0.02
H ₂ O	Platform	0.92 \pm 0.03	1.22 \pm 0.04
1% HNO ₃	Wall	0.30 \pm 0.01	0.30 \pm 0.01
1% HNO ₃	Platform	1.30 \pm 0.05	1.35 \pm 0.06

Table 3. Mean peak times, *sec*, for ETAAS analyses for Fe in lake waters maximum power heating

Matrix	Method of atomization	Standards	Lake waters
H ₂ O	Wall	0.41 \pm 0.02	0.41 \pm 0.03
H ₂ O	Platform	1.67 \pm 0.12	1.66 \pm 0.12
1% HNO ₃	Wall	0.55 \pm 0.02	0.54 \pm 0.02
1% HNO ₃	Platform	1.05 \pm 0.05	1.00 \pm 0.07

the condensed-phase interferences, and use of a platform is then not necessary.

Iron

Our previous experience with the determination of iron in rain-water samples indicated the use of ascorbic acid as a matrix modifier. The role of the ascorbic acid is not clear; by some it is believed to act as a flux, improving the thermal contact between the sample and the graphite tube, thus aiding in the decomposition of the matrix, whereas others may regard it as reducing iron(III) to iron(II), facilitating further reduction by the graphite. In any case, it has been used successfully for determination of iron in sea-water.¹⁴ We found there were no matrix interferences in the determination of iron in the lake water samples, as shown in Table 3.

Lead

The determination of lead by ETAAS has been studied extensively.¹⁵ The primary cause of halide-rich matrix interference is vapour-phase formation of lead halides, resulting in incomplete atomization.¹⁶ The magnitude of this effect has been shown to vary greatly, depending on the quantity and composition of the matrix and on the atomization temperature.¹⁷ Another factor is that halide from the sample matrix may lead to shorter atomization times for the lead.¹⁸ The matrix may also convert the lead into a compound that is atomized at a slightly lower temperature than PbO.¹⁹ The presence of anions, such as sulphate, has also been shown to suppress the response for lead when it is atomized from the tube wall.²⁰ The anion measurements made on the unacidified fractions of the lake water samples show mg/l. concentrations of both chloride and sulphate to be present.

Many of these investigations were originally concerned with analyses by wall sampling and matrix modification. Ammonium nitrate was generally used as the matrix modifier, to remove chloride from the matrix by volatilization of hydrogen chloride in the char cycle, and the interior surface of the graphite tube was generally coated with molybdenum to increase the precision of the response.²¹ We have successfully used this method to determine lead in Samoan rainfall.²² However, this procedure involves the addition of several chemicals that can complicate analyses at low concentrations. The platform approach is an attractive alternative since the higher and constant temperature environment that it pro-

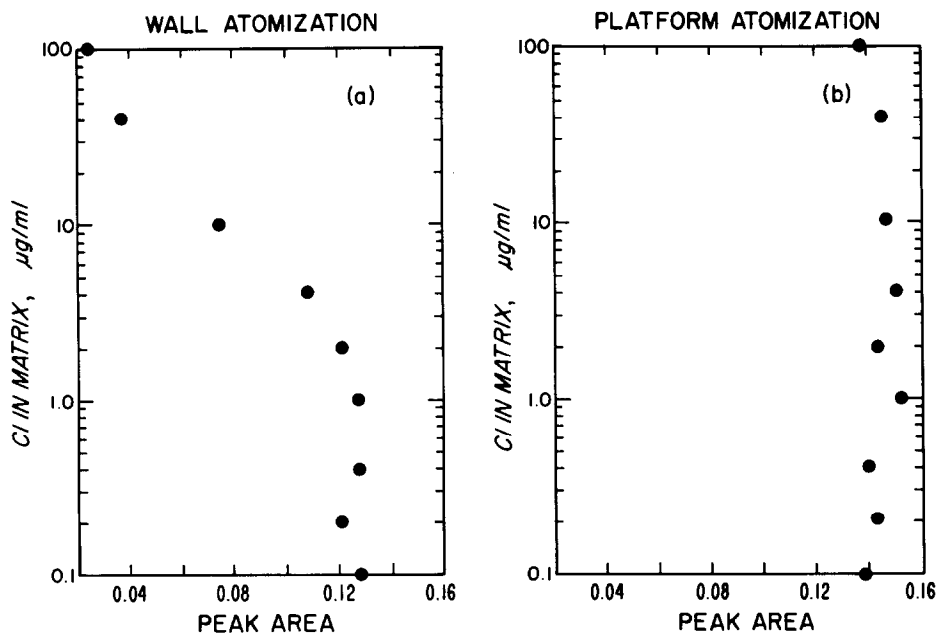


Fig. 2. Pb—sea-water matrix, 0.8 ng. Each value is the mean of duplicate measurements.

vides for analyte atomization will serve to dissociate the Pb—Cl species that would otherwise decrease the measured Pb response.

After our measurements of lead in Samoan rainfall, we examined the response of lead at the 40 ng/l. level in a series of saline solutions that corresponded to the major-ion matrix of the samples. The results from the AAS—computer system for analyses with atomization from the tube wall are shown in Fig. 2a. The extremely rapid decrease in response at higher salinities is due to vapour-phase binding of a portion of the lead by the increasing quantity of chloride in the matrix. We observed no significant change in the lead peak-signal time or appearance time with increasing amounts of sea-salt matrix. Similar results were observed for solutions containing only sodium chloride as matrix component.²³ When these solutions are atomized from the platform, the results (shown in Fig. 2b) indicate that the higher temperature environment provided by the platform eliminates the chemical vapour-phase interference by dissociating the Pb—Cl species. This implies that use of platform analysis alone without any matrix modification would have been a useful method for the determination of lead in

these samples, permitting use of aqueous standards without chemical modifiers. Platform techniques are also effective in minimizing sulphate and phosphate interferences in ETAAS analyses.²⁴

With these results as a guide, we measured the response for lead in the acidified and unacidified fractions of the lake-water samples, with test aliquots placed on the wall and on the platform. The mean values for the appearance and peak times for both fractions, with atomization at both normal and maximum heating rates, are shown in Table 4. These results suggest that for wall analysis the presence of the matrix in lake-water samples results in faster atomization, *i.e.*, atomization at a lower temperature than for the standards. Nitric acid has been reported to be an ineffective matrix modifier for the determination of lead in complex sample matrices that include sulphate.²⁵ Our results in Table 4 agree with this observation.

Table 4 also shows that with maximum-power heating there is a delay in response when the platform is used, indicating the time needed for the platform to reach the volatilization temperatures for the lead compounds on it. The higher constant temperature

Table 4. Mean appearance times and peak times for ETAAS analysis for Pb in lake waters, sec

Matrix	Method of atomization	Atomization ramp	Standards	Lake waters
<i>Appearance times</i>				
H ₂ O	Wall	1	1.30 ± 0.16	1.21 ± 0.10
1% HNO ₃	Wall	0	0.20 ± 0.03	0.13 ± 0.03
<i>Peak times</i>				
H ₂ O	Wall	1	2.43 ± 0.05	2.09 ± 0.15
1% HNO ₃	Wall	0	0.33 ± 0.02	0.29 ± 0.04
1% HNO ₃	Platform	0	1.24 ± 0.02	1.17 ± 0.04

Table 5. Mean appearance times and peak times for ETAAS analysis for Cd in lake waters, *sec*

Matrix	Method of atomization	Atomization ramp	Standards	Lake waters
<i>Appearance times</i>				
H ₂ O	Wall	1	0.87 ± 0.08	0.87 ± 0.06
1% HNO ₃	Wall	1	0.91 ± 0.07	0.98 ± 0.09
1% HNO ₃	Platform	0	0.46 ± 0.04	0.41 ± 0.06
<i>Peak times</i>				
H ₂ O	Wall	1	1.43 ± 0.08	1.48 ± 0.03
1% HNO ₃	Wall	1	1.80 ± 0.13	1.71 ± 0.17
1% HNO ₃	Platform	0	1.26 ± 0.06	1.17 ± 0.07

environment provided by use of the platform serves to reduce the analytical interferences from the anions in the sample matrix, as discussed by Hageman *et al.*²⁵ The use of a platform for the analysis of these lake waters is necessary for direct analysis without matrix modification.

Cadmium

The mean ETAAS peak parameters for determination of cadmium in both aqueous and acidified solutions by atomization from wall and platform are presented in Table 5. No matrix interferences are observed, demonstrating that nitric acid acts only as a preservative and not as a matrix modifier, and that wall analysis gives accurate cadmium results for these samples.

Results

The values for the acidified samples range from 3 to 65 µg/l. for Mn, 10 to 150 µg/l. for Fe, 0.5 to 8.0 µg/l. for Pb, and 0.05 to 70 µg/l. for Cd, and are shown in Tables 6–9. Since 80% of the Mn and Fe values are more than 10 times the detection limits of flame AAS, the flame AAS and ETAAS results for these elements can be compared. No comparisons between flame and ETAAS data can be made for Pb and Cd since their values are below the flame AAS detection limits.

The values for Mn, Fe, Pb and Cd in the field blanks and laboratory reagent blanks, measured by ETAAS, are at the limit of detection.

The mean values for the data obtained by flame

Table 6. Mn—all values in µg/l.*

Lake	ETAAS (wall)	ETAAS (platform)	Flame AAS
Sacandaga	3.9 ± 1.0	3.7 ± 1.1	< 15
Dart	78 ± 3	79 ± 11	78 ± 3
Big Moose	71 ± 1	71 ± 7	68 ± 3
Moss	12 ± 1	11 ± 1	< 15
Hinkley	14 ± 1	16 ± 1	< 15
Cranberry	34 ± 6	33 ± 1	35 ± 2
Sagamore	51 ± 1	49 ± 6	53 ± 3
Carry Falls	4.1 ± 0.1	4.5 ± 0.4	< 15
Stillwater	55 ± 1	53 ± 6	53 ± 3
North	62 ± 1	63 ± 3	63 ± 3
South	60 ± 1	62 ± 13	65 ± 1

*Limits of detection: flame AAS 15 µg/l., ETAAS 0.1 µg/l.

Table 7. Fe—all values in µg/l.*

Lake	ETAAS (wall)	ETAAS (platform)	Flame AAS
Sacandaga	43 ± 5	43 ± 5	40 ± 5
Dart	36 ± 1	32 ± 2	35 ± 5
Big Moose	26 ± 2	25 ± 1	25 ± 5
Moss	16 ± 1	17 ± 1	15 ± 8
Hinkley	43 ± 11	38 ± 1	45 ± 5
Cranberry	55 ± 6	53 ± 2	55 ± 5
Sagamore	108 ± 1	115 ± 6	115 ± 5
Carry Falls	105 ± 12	105 ± 3	110 ± 5
Stillwater	101 ± 14	107 ± 1	102 ± 5
North	56 ± 8	53 ± 6	55 ± 5
South	33 ± 5	34 ± 3	30 ± 5

*Limits of detection: flame AAS 10 µg/l., ETAAS 0.2 µg/l.

Table 8. Pb—all values in µg/l.

Lake	ETAAS (wall)	ETAAS (platform)
Sacandaga	0.8 ± 0.1	0.9 ± 0.1
Dart	1.1 ± 0.1	1.5 ± 0.1
Big Moose	1.4 ± 0.1	1.6 ± 0.2
Moss	1.6 ± 0.1	2.3 ± 0.2
Hinkley	0.5 ± 0.2	0.8 ± 0.1
Cranberry	0.7 ± 0.1	1.4 ± 0.1
Sagamore	0.9 ± 0.1	1.5 ± 0.1
Carry Fall	0.6 ± 0.1	1.4 ± 0.3
Stillwater	1.0 ± 0.1	1.3 ± 0.1
North	0.9 ± 0.1	1.8 ± 0.3
South	0.9 ± 0.1	1.8 ± 0.3

AAS, and wall and platform ETAAS for manganese and iron are compared in Table 10. As discussed above, small amounts of matrix do not affect flame AAS. For manganese there is little difference

Table 9. Cd—all values in µg/l.

Lake	ETAAS (wall)	ETAAS (platform)
Sacandaga	0.18 ± 0.01	0.22 ± 0.02
Dart	0.26 ± 0.01	0.27 ± 0.04
Big Moose	0.42 ± 0.08	0.41 ± 0.10
Moss	0.61 ± 0.06	0.55 ± 0.01
Hinkley	0.16 ± 0.01	0.16 ± 0.02
Cranberry	1.4 ± 0.4	1.2 ± 0.4
Sagamore	0.28 ± 0.09	0.34 ± 0.08
Carry Falls	0.13 ± 0.01	0.20 ± 0.01
Stillwater	0.25 ± 0.07	0.27 ± 0.02
North	0.70 ± 0.06	0.85 ± 0.10
South	69 ± 1	68 ± 1

Table 10. Comparison of analytical methods for the ETAAS determination of Mn and Fe in lake waters ($\mu\text{g}/\text{l}$.)

Element	Wall/platform	Flame/wall	Flame/platform
Mn	1.02 ± 0.08	1.03 ± 0.10	1.07 ± 0.10
Fe	1.03 ± 0.07	0.98 ± 0.10	1.02 ± 0.13

between the results from the three techniques, supporting the conclusions that nitric acid is an effective matrix modifier for ETAAS, and that the platform offers no additional analytical advantage for these samples. All three techniques give similar values for iron, and, as shown in Table 3, nitric acid is not needed as a matrix modifier.

The results for lead show that the platform method is required if accurate values are to be obtained. The mean wall/platform ratio for Pb is 0.66 ± 0.18 . This lower response for volatilization from the tube wall suggests that two different interference mechanisms may be affecting these data. There is clearly a vapour-phase interference, indicating that the chloride in the matrix is binding some of the available Pb, resulting in lower responses. Since the wall analyses are being conducted in a non-isothermal environment, the shift to lower temperatures suggested in Table 4 may also contribute to the lower results for the set of data obtained by wall sampling. The higher values for the platform measurements are due to isothermal higher-temperature atomization resulting in dissociation of the Pb-Cl species. Equivalent atomization temperatures are indicated for both sample and standard measurements.

The Cd sample data show a wall/platform ratio of 0.91 ± 0.07 , demonstrating that sample analyses from the tube wall are sufficient to generate accurate data for this element in these samples.

Analysis of standards

The results for determination of Mn, Fe, Pb and Cd in the EPA and NBS reference materials by both wall and platform ETAAS are shown in Table 11. The EPA reference values and our results show good agreement for both the wall and platform methods for all four metals, as expected since the EPA sol-

utions contain no matrix to cause interferences. The comparison is complicated, however, by the large standard deviations associated with some of the EPA values. Comparison of our results (obtained by use of acidified aqueous standards) with the certified values for NBS SRM 1643 (which contains matrix material) supports the conclusions drawn above from the interference studies. Mn, Fe, and Cd can also be measured successfully by both the wall and platform techniques, whereas the wall method produces low values for Pb, indicating interference. The platform technique gives good agreement with the NBS certified value for lead, indicating that the higher temperature environment obtained by use of the platform eliminates the interference.

CONCLUSIONS

The ETAAS determination of Mn and Pb in environmental samples such as lake water and rain-water is complicated by non-spectral interference by relatively small amounts of inorganic matrix material in these samples. These interferences are element-specific and due to particular components, and unless corrected for can result in positive or negative errors. For Mn, matrix modification with nitric acid, and for Pb, constant-temperature atomization by use of a graphite platform, can eliminate these interferences.

Acknowledgement—The authors wish to thank Camille C. Torquato of the Environmental Measurements Laboratory for the ion-chromatography data.

REFERENCES

1. M. Heit, *A Review of Current Information on Some Ecological and Health Related Aspects of the Release of Trace Metals into the Environment Associated with the Combustion of Coal*, U.S. Res. and Develop. Admin. Environmental Rept. HASL-320, New York, 1977.
2. J. Smeyers-Webeke, Y. Michotte, P. Van der Winkel and D. L. Massart, *Anal. Chem.*, 1976, **48**, 125.
3. S. J. Nagourney, V. C. Negro, D. C. Bogen, N. Latner and M. E. Cassidy, *Comput. Appl. Lab.*, 1984 **1**, 49.
4. J. R. Moody and R. M. Lindstrom, *Anal. Chem.*, 1977, **49**, 2264.

Table 11. ETAAS analysis of reference materials, $\mu\text{g}/\text{l}$.

Sample	Element	Wall		Platform	
		Found	Ref. value	Found	Ref. value
EPA TM-4	Mn	14 ± 1	15 ± 4	15 ± 1	15 ± 4
		68 ± 3	74 ± 7	70 ± 5	74 ± 7
	Fe	22 ± 2	22 ± 4	21 ± 5	22 ± 4
		75 ± 8	80 ± 11	79 ± 4	80 ± 11
	Pb	21 ± 4	24 ± 4	22 ± 2	24 ± 4
TM-4	Cd	2.4 ± 0.3	2.5*	2.4 ± 0.3	2.5*
		12 ± 1	12 ± 1	12 ± 1	12 ± 1
NBS SRM 1643	Mn	31 ± 1	<i>Cert. value</i> 29 ± 1	31 ± 3	<i>Cert. value</i> 29 ± 1
		74 ± 6	75 ± 1	79 ± 4	75 ± 1
	Pb	15 ± 1	20 ± 1	22 ± 2	20 ± 1
	Cd	8 ± 2	8 ± 1	9 ± 2	8 ± 1

*Uncertainty not available.

5. W. Slavin, G. R. Carnrick, D. C. Manning and E. Pruszkowska, *At. Spectrosc.*, 1983, **4**, 68.
6. H. L. Volchok and G. de Planque (eds.), *EML Procedures Manual*, U.S. Department of Energy Report HASL-300, 27th Ed., New York, 1984.
7. *Environmental Protection Agency Quarterly Newsletter*, Environmental Monitoring and Support Laboratory, Cincinnati, OH, 1983.
8. J. P. Matousek, *Prog. Anal. At. Spectrosc.*, 1981, **4**, 247.
9. R. D. Ediger, G. Peterson and J. D. Kerber, *At. Abs. Newsl.*, 1974, **13**, 61.
10. B. V. L'vov, *Spectrochim. Acta*, 1961, **17**, 761.
11. S. J. Nagourney and D. C. Bogen, in *Meteorological Aspects of Acid Rain*, C. M. Bhumralkar (ed.), pp. 145-154. Butterworth, Boston, 1984.
12. D. C. Bogen, S. J. Nagourney and C. C. Torquato, in *Meteorological Aspects of Acid Rain*, C. M. Bhumralkar (ed.), pp. 155-164. Butterworth, Boston, 1984.
13. G. R. Carnrick, W. Slavin and D. C. Manning, *Anal. Chem.*, 1981, **53**, 1866.
14. D. J. Hydes, *ibid.*, 1980, **52**, 959.
15. W. Slavin and D. C. Manning, *Prog. Anal. At. Spectrosc.*, 1982, **5**, 243.
16. W. Slavin, G. R. Carnrick and D. C. Manning, *Anal. Chem.*, 1984, **56**, 163.
17. B. V. L'vov, *Spectrochim. Acta*, 1978, **33B**, 153.
18. E. J. Czobik and J. P. Matousek, *Anal. Chem.*, 1978, **50**, 2.
19. R. E. Sturgeon, C. L. Chakrabarti and C. H. Langford, *ibid.*, 1976, **48**, 1972.
20. S. Callio, *At. Spectrosc.*, 1980, **1**, 80.
21. D. C. Manning and W. Slavin, *Anal. Chem.*, 1978, **50**, 1234.
22. S. J. Nagourney and D. C. Bogen, *U.S. Dept. Energy Environmental Rept. EML-390*, 1981, p. 241.
23. S. J. Nagourney, D. C. Bogen and V. C. Negro, *Pittsburgh Conference on Analytical Chemistry and Applied Spectroscopy*, 1983, Paper No. 459.
24. W. Slavin and D. C. Manning, *Anal. Chem.*, 1979, **51**, 261.
25. L. R. Hageman, J. A. Nichols, P. Viswanadham and R. Woodruff, *ibid.*, 1979, **51**, 1406.

2,6-DIACETYLPIRIDINE BIS(ARYLHYDRAZONE) DERIVATIVES AS ANALYTICAL REAGENTS FOR URANIUM

MARISSA BONILLA-ALVAREZ, MARGO PALMIERI, DEBRA DAVIS and JAMES S. FRITZ
Ames Laboratory and Department of Chemistry, Iowa State University, Ames, Iowa 50011, U.S.A.

(Received 16 September 1986. Accepted 12 December 1986)

Summary—The analytical properties of two compounds from a class of new complexing reagents for uranium have been investigated. The compounds, diacetylpyridine bis(furoylhydrazone) (H_2dapf) and diacetylpyridine bis(pyridylhydrazone) (H_2dapp), were synthesized and the extraction, resin sorption, and colorimetric properties of their metal complexes examined. The uranium- H_2dapf complex forms in solutions at $pH \geq 3$ and can be used to determine uranium colorimetrically. The system obeys the Lambert-Beer law between 0.72 and 10.8 ppm uranium with a molar absorptivity of 1.5×10^4 l. mole⁻¹. cm⁻¹ at 400 nm and 3.5×10^4 l. mole⁻¹. cm⁻¹ at 350 nm between pH 3 and 8. Interferences are masked with EDTA.

The reactivity of the uranyl ion with quinquedentate chelating hydrazone derivatives has been studied by research groups in Italy.¹⁻⁴ These studies have shown that bis(arylhydrazones) of 2,6-diacetylpyridine form stable chelates with UO_2^{2+} which have four 5-membered rings. 2,6-Diacetylpyridine bis(4-methoxybenzoylhydrazone) (H_2dapmb) forms $UO_2(Hdapmb)NO_3$ and $UO_2(H_2dapmb)(NO_3)_2$; these can be deprotonated to form $UO_2(dapmb)$.¹ Manganese(II), cobalt (II), nickel(II), copper(II) and zinc(II) derivatives of 2,6-diacetylpyridine bis(benzoylhydrazone) (H_2dapb) have been prepared and their structures characterized by X-ray and spectroscopic studies.²

Casoli *et al.*⁵ published a short paper on the chromatographic separation of uranyl and copper(II) complexes of H_2dapb , but no other analytical use has been made of these interesting chelating reagents. In the present work two hydrazones, 2,6-diacetylpyridine bis(furoylhydrazone) (H_2dapf) and 2,6-

diacetylpyridine bis(pyridylhydrazone) (H_2dapp), which form more water-soluble complexes with metal ions, have been prepared and characterized. Figure 1 gives the structure of the two hydrazones investigated. These are shown to be useful for the spectrophotometric determination of uranium(VI) and for the concentration of uranium(VI) by sorption of the hydrazone chelate on a small resin column.

EXPERIMENTAL

Synthesis of H_2dapf

To a 250-ml round-bottomed flask were added 0.05 mole of 2-furoic acid hydrazide and 0.025 mole of 2,6-diacetylpyridine (Aldrich) in 100 ml of absolute methanol. The mixture was heated for 3 hr at 40°, cooled and filtered. The precipitate collected was recrystallized from methanol as small white crystals. H_2dapf was synthesized by the method previously described,⁶ from 2,6-diacetylpyridine and nicotinic acid hydrazide (Aldrich). The compound 2,3-butanedione bis(furoylhydrazone) (H_2bdf) was synthesized from 2,3-butanedione and furoic acid (Aldrich) by a procedure analogous to that for H_2dapf .

The following procedures were used to characterize H_2dapf . The infrared spectrum was taken (KBr pellets). The mass spectrum was obtained on a Hewlett Packard 5995A GC/MS at 70 eV with direct insertion. The NMR spectrum of the sample dissolved in $CDCl_3$ containing TMS as internal standard was taken with a Jeol FX90Q FT-NMR spectrometer.

Complex formation studies

Two ml of $1 \times 10^{-3}M$ metal ion solution, 2 ml of $2 \times 10^{-3}M$ reagent in methanol and 2 ml of buffer solution were mixed together and diluted to volume. The pH was varied from 0 to 8. The intensity of the colour was used to determine the maximum formation of the complexes.

Spectra of selected complexes were taken with a Perkin-Elmer 552 UV-VIS Spectrophotometer at the pH corresponding to maximum complex formation. Solutions used in the measurement of molar absorptivity contained a two-fold molar excess of reagent.

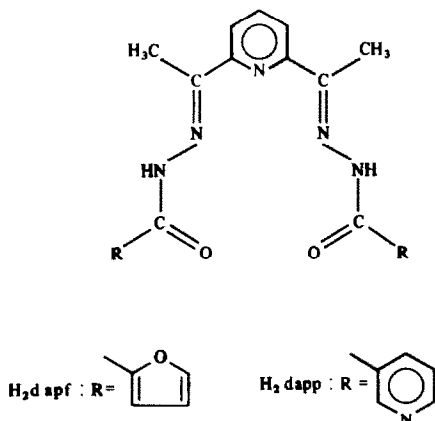


Fig. 1. Structure of H_2dapf and H_2dapp .

Solvent extraction and sorption studies of metal complexes

For the solvent extraction experiments H₂dapf was used because it was less soluble in aqueous media. The metal complex was formed in a 10:90 v/v methanol–water solution, which was buffered to give maximum complex formation. The solution, containing $8 \times 10^{-5}M$ metal ion and $1.6 \times 10^{-4}M$ H₂dapf, was extracted once with an equal volume of methylene chloride. The metal content of the two phases was then determined by established colorimetric methods.⁷

Sorption studies were done with H₂dapp because of its greater solubility in acidic aqueous solutions. A 25-ml volume of solution with a final concentration of $8 \times 10^{-5}M$ metal ion, $8 \times 10^{-4}M$ H₂dapp and buffer solution was made up. Ten-ml aliquots were passed through a conditioned gravitational-flow mini-column of 150–200 mesh XAD-4 resin which had been slurry-packed. The metal ion content of the eluates was determined colorimetrically.

Colorimetric determination of uranium

A sample aliquot containing between 18 and 270 μg of uranium was placed in a 30-ml beaker. To the sample were added 1.0 ml of 0.10M EDTA, 10.0 ml of methanol, 4.0 ml of $2 \times 10^{-3}M$ methanolic H₂dapf, and 1 ml of 1.0M triethanolamine (TEA) buffer. The apparent pH was adjusted to 6.0 (pH-meter) and the solution diluted with water to 25 ml. For the solutions analysed at a pH of 3.3, 2.5 ml of 0.10M formate buffer were used. The absorbance of the uranium complex was measured at 400 nm.

For the sorption experiments, the mini-column was washed with demineralized water adjusted to pH 6.0 with the TEA buffer. A 10-ml aliquot of the sample solution containing $1 \times 10^{-5}M$ uranium and H₂dapf in 56% methanol, with an apparent pH of 6.0, was passed through the column. The column was washed with 5 ml of water, and the complex eluted with 10 ml of 100% methanol. The eluate was collected in a 10-ml standard flask and the absorbance measured at 400 nm.

In the concentration experiment 200 ml of $2.0 \times 10^{-7}M$ uranium solution was placed in a 500-ml beaker containing 10 ml of methanol. Then 4.0 ml of $2 \times 10^{-3}M$ methanolic H₂dapf and 3 ml of the TEA buffer were added. The pH was adjusted to 6.0 and the solution was passed through the XAD-4 column. Five ml of demineralized water was passed through the column, and the uranium complex was eluted with 10 ml of methanol. The methanolic eluate was collected in a 25-ml standard flask, buffer was added, the solution was diluted to volume with methanol, and the absorbance measured and compared with that of a UO₂–H₂dapf solution of equivalent concentration.

RESULTS*Physical properties of the ligands and metal complexes*

The syntheses of H₂dapf and H₂dapp gave more than 90% yields. The solids and their solutions were

stable to light and could be kept for several months without discernible degradation. The physical characteristics for H₂dapf are given in Table 1. At pH >9, the ultraviolet spectrum of H₂dapf shifts to longer wavelengths. The physical properties of H₂dapp were given in a previous paper.³ These compounds, particularly H₂dapp, are much more soluble in aqueous solutions than H₂dapb. H₂dapp is very soluble in acidic solutions (pH \leq 1.7) owing to protonation of the pyridyl groups.

The metal complexes of H₂dapf and H₂dapp are yellow or yellow green. Table 2 shows the pH of maximum complex formation for the various metals tested. The structure of H₂dapf and H₂dapp allows for the formation of up to four chelate rings for each chelate molecule bound to the metal ion. Paolucci *et al.*³ proved by X-ray crystallography that H₂dapp forms a quinquecentate complex with UO₂²⁺. The large number of chelate rings gives greater complex stability than that observed for other ligands.

By Job's method, the ligand to metal ratio for the UO₂²⁺ and Tb³⁺ complexes was determined to be 1:1 for H₂dapf. This ratio agreed with the results obtained from X-ray crystallographic studies on the H₂dapp–UO₂²⁺ complex.^{3,4} In general, H₂dapf formed more stable complexes than did H₂dapp with most of the metals tested, as evidenced by the lower pH required for maximum colour formation. The H₂dapf complexes generally have higher molar absorptivity than the H₂dapp complexes. The low pH for the maximum formation of the uranium complexes with both ligands shows a selectivity for uranium relative to the lanthanide ions and bivalent ions such as those of Ni, Mn, Pb, Ag, Hg and Co. In studying the Ti(IV) complex of H₂dapf, it was found that the colour faded with time, making this complexing agent unsuitable for spectrophotometric determination of titanium.

Finally, the compound 2,3-butanedione bis(furoyl-hydrazone) (H₂bdf) was synthesized in order to investigate the effect of the pyridyl ring on the formation of the uranium complex. The uranyl–H₂bdf complex was more water-soluble than the complexes of H₂dapf or H₂dapp, being soluble in a 16:84 v/v methanol–water mixture. The uranium complex reached maximum formation at approximately pH 4.0. A higher pH was also needed for

Table 1. Characterization data of H₂dapf

Molecular weight	Melting range, °C	UV maxima, nm	IR maxima, cm ⁻¹	Major mass spectral lines, m/z (%)	¹ H NMR in CDCl ₃ (no. of H)
379	238–241	304 258	3310	77 (18)	8.4–8.2 (1H)
			3080	95 (100)	7.6 (1H)
			1660	104 (66.7)	7.4 (1H)
			1580	105 (15.7)	6.6 (1H)
			1550	132 (25.4)	2.5 (3H)
			1490	145 (15.4)	1.6 (1H)
			1435	188 (16.3)	
			1330	284 (14.5)	
				379 (1)	

Table 2. pH of maximum formation and molar absorptivity at peak maxima of the metal complexes of H₂dapf and H₂dapp*

Metal ion	H ₂ dapf			H ₂ dapp		
	pH _{max}	λ_{max} , nm	ϵ , l. mole ⁻¹ . cm ⁻¹	pH _{max}	λ_{max} , nm	ϵ , l. mole ⁻¹ . cm ⁻¹
Fe ³⁺	1	334	3.0×10^4			
Ti ⁴⁺	2	378	2.2×10^4			
Zr ⁴⁺	2	358	1.0×10^4			
UO ₂ ²⁺	3	354	3.5×10^4	4	346	2.1×10^4
		400	1.5×10^4		390	1.2×10^4
Cu ²⁺	4	350	2.0×10^4	5	341	1.5×10^4
Th ⁴⁺	4	350	3.2×10^4	2	353	2.7×10^4
		397	1.7×10^4			
Tm ³⁺	5	349	2.8×10^4	8	342	$< 1.0 \times 10^4$
Ni ²⁺	6	373	3.2×10^4	7	363	$< 1.0 \times 10^4$
Tb ³⁺	6	350	2.5×10^4			
Y ³⁺	6	352	2.8×10^4	8	341	$< 1.0 \times 10^4$
Hg ²⁺	7	353	2.0×10^4	7	349	$< 1.0 \times 10^4$
Mn ²⁺	7	348	2.2×10^4	8	338	$< 1.0 \times 10^4$
		382	1.3×10^4			
Ag ⁺	8	354	0.4×10^4	†		
Co ²⁺	8	352	3.5×10^4	7	331	1.1×10^4
Pb ²⁺	8	360	1.1×10^4			
		408	1.0×10^4			
Eu ³⁺	9	351	2.1×10^4			

*The samples were made up in 60% methanol and 40% water with an excess of complexing agent. The pH measured was the apparent pH.

†Ag⁺ was reduced by H₂dapp.

complete complex formation with Cu²⁺, Fe³⁺, Tm³⁺ and La³⁺. The formation of the uranyl-H₂bdf complex was slow, maximum absorbance being reached in 24 hr. For practical use, the absorbance should be measured after 60 min reaction time. The absorption spectrum of the uranium-H₂bdf complex showed a strong absorbance band with a molar absorptivity of 2.2×10^4 l. mole⁻¹. cm⁻¹ at 415 nm. A comparison of the molar absorptivities of the uranium complexes of H₂dapf and H₂bdf indicates that the pyridyl group of H₂dapf contributes little to the colour formation, and in fact causes a decrease in molar absorptivity and a blue shift.

Extraction and sorption properties of the metal complexes

Figure 2 gives the results of the solvent extraction experiments for the UO₂²⁺, Cu²⁺ and La³⁺ complexes. For efficient extraction the complex must be formed in 10:90 v/v methanol-water medium; extraction

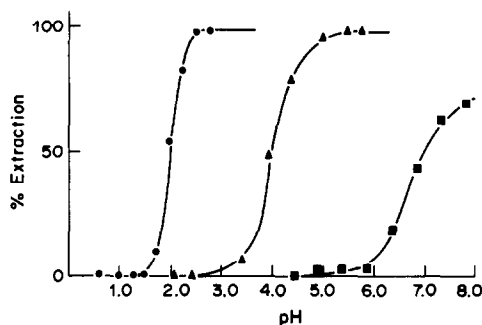


Fig. 2. Graph of % extraction of some H₂dapf complexes at different pH values. ●, U(VI), ▲, Cu(II), ■, La(III).

with organic phases containing H₂dapf had poor efficiency. A 2:1 ratio of H₂dapf to metal ion gave an efficient extraction (>99%) of the UO₂²⁺ and Cu²⁺ complexes. For 98% extraction of La at pH 7.6, a 10:1 molar ratio of H₂dapf to La³⁺ was required.

In the sorption of metal complexes onto an XAD resin from water, H₂dapp was used because of its higher solubility in water. A 10:1 H₂dapp to metal ion molar ratio was required for quantitative sorption of the metal complexes. Figure 3 shows the degree of sorption of the UO₂²⁺, Th⁴⁺, Cu²⁺ and La³⁺ complexes, as a function of pH. The order of sorption efficiency is the same as the order of complex stability.

Uranium colorimetric determination and interference study.

The yellow uranyl-H₂dapf complex formed instantaneously and remained stable for several hours.

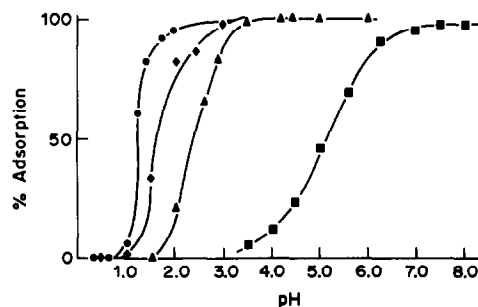


Fig. 3. Graph of % adsorption of some H₂dapp complexes on XAD-4 resin at different pH values. ●, U(VI), ◆, Th(IV), ▲, Cu(II), ■, La(III).

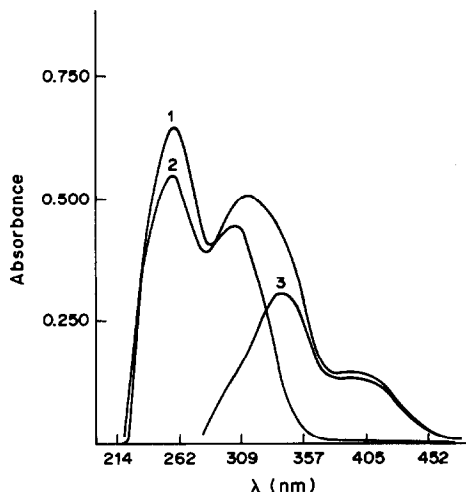


Fig. 4. UV-VIS spectra of: 1—Reagent, H_2dapf $2.5 \times 10^{-5}M$; 2— UO_2 - H_2dapf $1.0 \times 10^{-5}M$ vs. H_2O ; 3— UO_2 - H_2dapf $1.0 \times 10^{-5}M$ vs. reagent. Methanol content 24%, pH 2.8.

Figure 4 gives the spectra of H_2dapf and its uranyl complex at pH 2.8. The spectrum of the complex had two maxima, one at 340 nm and the other at 400 nm with molar absorptivities of 2.9×10^4 and 1.57×10^4 $l. mole^{-1}. cm^{-1}$ respectively. At 341 nm there was still considerable absorbance by the H_2dapf ligand. In addition, as the percentage of methanol in the solution was increased, the band at 341 nm shifted, causing an increase in absorbance at 341 nm. However, at 400 nm the absorptivity remained constant. Because of the dependence of molar absorptivity on

Table 3. Maximum allowable concentration of metal ions present in the determination of a $2.0 \times 10^{-5}M$ uranium solution* using EDTA as masking agent.

Metal ion	Max. allowable conc., M	Mole ratio metal/U
Al^{3+}	1.8×10^{-3}	91
Ca^{2+}	2.4×10^{-4}	12
Cd^{2+}	4.0×10^{-3}	200
Co^{2+}	4.9×10^{-4}	25
Cu^{2+}	3.0×10^{-3}	150
Fe^{3+}	1.2×10^{-5}	0.60
	$4.0 \times 10^{-4}†$	20
Hg^{2+}	2.0×10^{-3}	100
La^{3+}	3.3×10^{-3}	166
Mn^{2+}	2.0×10^{-3}	100
Na^+	1.2×10^{-3}	60
Ni^{2+}	4.8×10^{-4}	24
Pb^{4+}	1.4×10^{-3}	72
Th^{4+}	6.0×10^{-4}	30
Ti^{4+}	2.0×10^{-4}	10
Y^{3+}	2.0×10^{-3}	100
Zn^{2+}	3.4×10^{-4}	168
Zr^{4+}	1.2×10^{-4}	6.0

*Determinations were made at pH 6.0 (TEA buffer). Each solution contained 0.004M EDTA. The maximum allowable concentrations of metals gave a 3% or less deviation in the uranium analysis.

†Uranium determined at pH 3.3 (formic acid buffer). The Fe interference was corrected for by the preparation of a second blank.

the percentage of methanol in solution and the higher background at 341 nm, 400 nm was the preferred wavelength for analysis. At least 20% methanol is required to keep the uranyl- H_2dapf complex from precipitating. To maintain maximum absorptivity, the pH must be between 3.3 and 8.0. A pH between 3.3 and 4.0 was preferred for analysis to minimize interference from other elements which form complexes with H_2dapf at higher pH values.

Because H_2dapf forms complexes with many metals, there was considerable interference in the uranium determination from several other metal ions. At low pH values, Th^{4+} , Zr^{4+} , Fe^{3+} , Cu^{2+} and Ti^{4+} severely interfere with uranium when present in low concentrations. Many masking agents for these metals are either not particularly effective or they precipitate at low pH values. Low concentrations of lanthanide metals in solution are tolerated to a greater extent because at low pH values, only very slight complexation occurs between H_2dapf and lanthanides. The masking effect of EDTA on possible interferences was then tested at pH 6.0 to minimize precipitation of the EDTA in solution. Addition of EDTA to the solution eliminated interference from other metals with the exception of Fe^{3+} , Zr^{4+} and Ti^{4+} . Table 3 gives the maximum allowable concentrations of metal ions which can be present in solution at pH 6.0 without interference. EDTA masked Zr^{4+} and Ti^{4+} at low concentration, but was ineffective at higher interferent levels. The interference from Fe^{3+} after the addition of EDTA was due primarily to the absorption of the EDTA metal complex at the same wavelength. A method used to correct for Fe^{3+} interference required the preparation of two blanks, one containing sample and EDTA only, and the other the standard containing EDTA. Above a concentration of $4 \times 10^{-4}M$ Fe^{3+} , the iron began to form a complex with the H_2dapf and a second blank could no longer be used.

Resin sorption experiments were carried out to determine if the uranyl- H_2dapf complex could be concentrated from solution by using a resin column. A solution containing $2 \times 10^{-5}M$ uranium was passed through a resin column, and the complex was then eluted from the column with 100% methanol. The uranyl complex was sorbed with a 97.5% average recovery, which was within experimental error. A concentration experiment was then performed following the previous procedures. A 250-ml volume of solution of uranium was concentrated by a factor of 10, and an average recovery of 97% was attained. This experiment shows that H_2dapf is an effective chelating agent in analysis procedures requiring the preconcentration and determination of ultra-trace levels of uranium.

CONCLUSION

H_2dapf has some use as a colorimetric reagent for the determination of uranium. Other reagents such as

Arsenazo compounds⁸ and Br-PADAP⁹ are more sensitive for uranium than H₂dapf. With the addition of masking agents, these reagents are also selective for uranium. Because H₂dapf forms complexes with uranium at lower pH values than with the rare earths and many bivalent metal ions, some natural selectivity occurs. At higher pH values uranium can be determined without interference, by use of H₂dapf and EDTA. This complex is most useful, however, when preconcentration and determination of the uranium needs to be carried out. H₂dapf and its uranium complex can be concentrated and then eluted from a resin column. Many colorimetric reagents, such as the Arsenazo compounds, are irreversibly adsorbed on hydrophobic resins, making them useless for preconcentration procedures. The preconcentration of uranium with resin columns is preferable to solvent extraction, because the latter method can be time consuming. The masking of other metal ions present in a solution by EDTA in conjunction with the addition of H₂dapf to the sample, followed by sorption of the complex onto a resin, would allow selective preconcentration and determination of uranium.

Acknowledgements—This research was supported by the Institutional Supporting Research and Development Pro-

gram at Los Alamos National Laboratory which is operated by the University of California. The research was performed at Ames Laboratory which is operated by Iowa State University for the U.S. Department of Energy under Contract No. W-7405-Eng-82. We wish to thank Chin-Hsing Chou for his help in synthesis and characterization of the complexing agents and Robert Bachman and the University of Puerto Rico for the use of their equipment.

REFERENCES

1. G. Paolucci, G. Marangoni, G. Bandoli and D. Clemente, *J. Chem. Soc., Dalton Trans.*, 1980, 1304.
2. C. Lorenzini, C. Pelizzi, G. Pelizzi and G. Predieri, *ibid.*, 1983, 721.
3. G. Paolucci, G. Marangoni, G. Bandoli and D. Clemente, *ibid.*, 1980, 459.
4. G. Paolucci and G. Marangoni, *Inorg. Chim. Acta*, 1977, **24**, L5.
5. A. Casoli, A. Mangia and G. Predieri, *Anal. Chem.*, 1985, **57**, 563.
6. J. Curry, M. Robinson and D. Busch, *Inorg. Chem.*, 1967, **6**, 1570.
7. R. Phillips, *Ph.D. Dissertation*, Iowa State University, Ames, IA, 142.
8. *Gmelin Handbook of Inorganic Chemistry*, Uranium Supplement Vol. A7, Springer-Verlag, Berlin, 1982.
9. D. Johnson and T. Florence, *Talanta*, 1975, **22**, 253.

CHEMICAL REDUCTION AND SPECTROPHOTOMETRIC DETERMINATION OF SILVER, COPPER AND NICKEL

GHAZI AL-JABARI and BRUNO JASELSKIS

Department of Chemistry, Loyola University of Chicago, 6525 N. Sheridan Road, Chicago, Illinois 60626, U.S.A.

(Received 12 March 1986. Revised 3 December 1986. Accepted 12 December 1986)

Summary—Silver(I), copper(II) and nickel(II) can be reduced to the metallic state by formaldehyde at pH 11, chromium(II) in 2.5M sulphuric acid, and borohydride at pH 5.5–6.0, respectively. Reoxidation of these metals with iron(III) in the presence of Ferrozine enables their determination at concentration below 1 µg/ml by measurement of the absorbance of the iron(II)–Ferozine complex at 562 nm, with a precision better than 3%. The apparent molar absorptivities for silver, copper and nickel are 2.78×10^4 , 5.56×10^4 and 5.58×10^4 l. mole⁻¹. cm⁻¹, respectively. The average thickness of silver films on glass surfaces can be determined in the way.

Ferozine, 3-(2-pyridyl)-5,6-diphenyl-1,2,4-triazine-*p,p'*-disulphonic acid, monosodium salt monohydrate (FZ), is one of the most sensitive water-soluble iron chromogens currently available. It was first introduced by Stookey for trace analysis of ultrapure water.¹ Ferrozine has found wide acceptance² by clinical analysts in the determination of serum iron, iron-binding capacity,^{3–12} and of iron in seawater,¹³ plant nutrient solutions,¹⁴ plant materials,¹⁵ and in high-purity chemicals.¹⁶ It has also been used for the determination of cobalt(II),¹⁷ ruthenium(III), osmium(VIII),¹⁸ gold(III) and silver(I).¹⁹

In addition, iron(III) in the presence of Ferrozine has been used for the determination of chemical species able to reduce iron(III), such as ascorbic acid,²⁰ sulphur dioxide,²¹ nitrate and nitrite,²² sulphate,²³ tiron and substituted catechols,²⁴ molybdenum, vanadium, and arsenic,²⁵ and silver(I), gold(III) and mercury(II).²⁶

In this paper we describe a spectrophotometric method for the determination of micro amounts of silver(I), copper(II) and nickel(II), alone and in mixtures, after the reduction of these ions to the metallic state and reoxidation by iron(III) in the presence of Ferrozine.

EXPERIMENTAL

Apparatus

A Cary 14 spectrophotometer and Corning Model XII pH-meter were used. The amalgamated zinc reductor was prepared by treating analytical-grade 20-mesh metallic zinc with acidified mercuric chloride as described by Kolthoff.²⁷ A shortened 50-ml burette was filled with enough zinc to produce a column 15 cm long. The reductor was washed copiously with demineralized water. Cation- and anion-exchange columns were prepared by filling approximately 8 cm of shortened burettes with ion-exchange resins: AG-1-X8, 50–100 mesh, chloride-form anion-exchanger and AG-50W-X8, 20–50 mesh, sodium-form cation-exchanger.

All glassware was washed with 6M hydrochloric acid, and then demineralized water.

Reagents

All chemicals were analytical or primary standard grade. Ferrozine, 3-(2-pyridyl)-5,6-diphenyl-1,2,4-triazine-*p,p'*-disulphonic acid, monosodium salt monohydrate (Aldrich), was used to prepare an approximately 0.01M solution by dissolution of 1.42 g in 250 ml of demineralized water. Approximately 0.004M iron(III) solution was prepared by dissolving 0.484 g of ammonium ferric sulphate dodecahydrate in 0.1M sulphuric acid and diluted to 250 ml. Standard solutions (500 ml) of silver(I), nickel(II) and copper(II) were prepared by dissolving 0.4212 g of silver nitrate and 0.3715 g of nickel chloride hexahydrate in demineralized water and 0.1163 g of pure copper wire in dilute nitric acid; in the case of the silver and copper solutions, the nitrate was removed by evaporation till fuming, after addition of sulphuric acid, and the cooled residue was taken up in demineralized water and diluted to volume. The copper solution was standardized by iodimetric titration and the nickel solution gravimetrically by the dimethylglyoxime method.

Chromium(II) solution was prepared by passing approximately 0.02M chromium(III) sulphate through the amalgamated zinc reductor. Approximately 0.01M sodium borohydride was prepared by dissolving 40 mg of reagent in 100 ml of 0.05M sodium hydroxide. Chloroacetate buffer solution of pH 3.5 was prepared by dissolving 25 g of monochloroacetic acid in 900 ml of demineralized water and adjusting the pH to 3.5 by adding concentrated sodium hydroxide solution dropwise. An acetate buffer solution of pH 5.5 was prepared by adding concentrated sodium hydroxide solution dropwise to 0.5M acetic acid.

Procedures

Determination of elemental silver, copper and nickel. The silver, copper or nickel metal resulting from reduction of the corresponding metal ions is determined by adding 2 ml of 0.004M iron(III), 3 ml of 0.01M Ferrozine and 10 ml of chloroacetate buffer of pH 3.5, diluting to volume in a 50-ml standard flask and measuring the absorbance, after 5–10 min, at 562 nm against a blank prepared by using all the reagents except the ion being tested.

Determination of silver. For calibration, 0.050–0.500 ml aliquots of the 4.7×10^{-3} M standard silver solution are

placed in 50-ml standard flasks, and the reagents are added in the following order: approximately 0.1 ml of 36–40% formaldehyde solution, a few drops of 0.1M sodium hydroxide and, after 2 min, 2 ml of 0.004M iron(III), 3 ml of 0.01M Ferrozine and 10 ml of chloroacetate buffer. The solution is diluted to volume and the absorbance measured at 562 nm. This procedure is also used for analysis of solutions containing only silver.

In mixtures with copper and nickel, silver is determined by the procedure above except that the standard-addition method is used, with two or three standard additions.

Determination of copper. For calibration aliquots of nitrate-free standard copper solution are placed in 25-ml test-tubes and acidified with 5N sulphuric acid to yield a solution with approximately 2.5N acid concentration. The solutions are deaerated with nitrogen and chromium(II) is added directly from the Jones reductor. After the solutions have stood for 3 min under a nitrogen atmosphere, the excess of chromium(II) is destroyed by agitation with air by means of a "vortex" mixer. The solutions are transferred into 50-ml standard flasks already containing the requisite volumes of iron(III), Ferrozine and chloroacetate buffer solutions, and are diluted to volume with demineralized water. For analysis of samples containing nitrate or nitrite, the solution is acidified with dilute sulphuric acid and evaporated almost to dryness, then the residue is taken up in 2.5N sulphuric acid, ready for reduction.

Copper in mixtures containing silver is determined either after the precipitation and separation of silver chloride, or from the difference between the absorbance obtained for reduction of both ions by chromium(II) and that for the reduction of silver with formaldehyde. The difference procedure is applicable when the amount of silver is less, or not much greater, than that of copper.

Determination of nickel. For calibration, 0.100–0.500 ml aliquots of the 3.5×10^{-3} M standard solution are placed in 25-ml test-tubes. The pH is adjusted by addition of a few drops of 0.01M ammonium chloride or ammonium acetate-acetic acid buffer. Then, approximately 0.25 ml of alkaline sodium borohydride solution is added dropwise to each. The solutions are then acidified with acetic acid to pH 5.0–5.5, and the test-tubes are placed in a boiling water-bath for 20 min. After heating, the solutions are purged with nitrogen for 3 min and transferred into 50-ml standard flasks containing the required volumes of iron(III), Ferrozine, and chloroacetic acid buffer solutions. Nickel samples are analysed similarly.

When copper and silver are also present, the nickel is first separated by use of cation- and anion-exchange resins. The sample solution is first passed through the cation-exchanger, which is then treated with 9M hydrochloric acid, the eluate being placed on the anion-exchanger preconditioned with 9M hydrochloric acid; under these conditions, nickel passes through the anion-exchanger, and copper is retained. The copper is eluted with 3M hydrochloric acid, and the eluate is rendered chloride-free by addition of 1 ml of 3M sulphuric acid and evaporation almost to dryness. The residues are then analysed by the procedures used for each ion alone.

Analysis of silver-copper and German silver alloys

The sample (50–100 mg) is dissolved in approximately 4 ml of 3M nitric acid, then 3 ml of 2M sulphuric acid are added and the solution is evaporated till fuming. The residue is dissolved in 1 litre of demineralized water. A suitable aliquot (0.05–0.500 ml) is taken and the cations are determined by the standard-addition method.

Alternatively, 1–5 mg of sample is dissolved in 0.5 ml of 3M nitric acid, 0.5 ml of 2M sulphuric acid is added, the mixture is evaporated until fumes appear, then the residue is dissolved in a small amount of water. The silver in the silver alloy is reduced with 37% formaldehyde solution at pH 11–12 and at room temperature. After standing for 5 min the metallic silver is oxidized by addition of

approximately 15 mg of ammonium ferric sulphate, 40 mg of Ferrozine and 100 ml of 0.3M acetate buffer. The solution is diluted to volume in a 250-ml standard flask and the absorbance is measured against a blank prepared in a similar manner. The amount of silver in the sample is calculated by the equation $A_g = 107.9 \times 250A / 2.78 \times 10^4 = 0.970A$ mg, where A is the absorbance (1-cm path-length).

A sample weighing 1–2 mg is used for the determination of copper. The sample is dissolved in 0.5 ml of 3M nitric acid and the acid is evaporated after addition of 0.5 ml of 2M sulphuric acid. The residue is dissolved in 5 ml of 5M sulphuric acid. The solution is deaerated and approximately 10 ml of 0.02M chromous ion are added directly from the Jones reductor. The excess of chromous ion is destroyed by air and the metallic silver and copper are oxidized by addition of approximately 75 mg of ammonium ferric sulphate, 250 mg of Ferrozine and 100 ml of 0.3M acetate buffer. The mixture is accurately diluted to 1 litre with demineralized water and the absorbance is measured against a blank. The amount of copper is calculated from the absorbance corrected for the absorbance of the silver present, calculated from the silver determination and the sample weight:

$$Cu = 63.5 \times 1000 (A_{obs} - A_{Ag}) / 5.58 \times 10^4 = 1.131A \text{ mg}$$

German silver samples (1–2 mg) are treated like the silver alloys except that the residue from the evaporation is dissolved in 9M hydrochloric acid. This solution is passed through the anion-exchange resin and the eluate used for the nickel determination. Copper is then stripped with 3M hydrochloric acid. In both cases the hydrochloric acid is evaporated and the residues analysed by the procedures used for each ion alone, except that the amounts of chromous ion and borohydride used for the reduction of copper and nickel are increased. Metallic copper and nickel are analysed by the procedure used for silver alloys. [For nickel analysis the amount of iron(III) and Ferrozine used can be reduced by a factor of 3]. After the adjustment of pH the solution is accurately diluted to 1 litre and the absorbance measured.

Determination of average silver film thickness

Silver mirrors were deposited on the surfaces of glass microscope-slides by a procedure similar to those described in the CRC Handbook³³ and by Street.³⁴ The average thickness of these mirrors as a function of deposition time was investigated. Slides were removed from the silvering solution at various time intervals, washed gently with demineralized water and immersed in 20 ml of the 0.003M iron(III) solution. After 10 min all the silver had dissolved, and the solution was transferred into a 50-ml standard flask containing 5 ml of 0.02M Ferrozine and 10 ml of chloroacetate buffer and diluted to volume with water. The average thickness was calculated from the density of silver, the area of the mirror, and the observed absorbance.

RESULTS

Results for silver, copper and nickel alone are summarized in Table 1 and the results for the mixtures and alloys are summarized in Tables 2 and 3. The determination of the average thickness of silver mirrors on a glass surface as a function of the duration of chemical deposition of silver is summarized in Table 4.

DISCUSSION

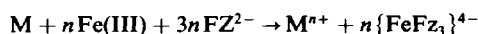
Reduction of silver, copper and nickel ions to the metallic state depends not only on the nature of the reducing agent, but also on the pH and time needed

Table 1. Determination of silver, copper and nickel individually

Metal	Amount in final 50 ml, μg	Absorbance*	Molar absorptivity, $10^4 \text{ l. mole}^{-1} \cdot \text{cm}^{-1}$
Silver	1.070	0.278 ± 0.006	2.80
	2.140	0.554 ± 0.003	2.79
	3.210	0.820 ± 0.001	2.76
			mean = 2.78 ± 0.03
Copper	0.465	0.410 ± 0.005	5.60
	0.930	0.820 ± 0.010	5.60
	1.400	1.250 ± 0.012	5.49
			mean = 5.56 ± 0.007
Nickel	0.367	0.350 ± 0.004	5.60
	0.550	0.525 ± 0.005	5.60
	0.734	0.692 ± 0.010	5.53
			mean = 5.58 ± 0.04

*Average and standard deviation of four determinations.

for the reaction. The rate of reoxidation of metals with iron(III) in the presence of Ferrozine depends on the particle size of the metals formed and on the pH, and the reaction is



The choice of reducing agent depends on the type of metal being determined, as summarized in Table 5.

The reduction of silver with formaldehyde is dependent on pH as shown in Fig. 1. Silver(I) at pH 11 is reduced in less than 5 min, but at lower pH the reduction is slow and incomplete. Ammoniacal or tert-butylamine solutions of silver nitrate have been

Table 2. Analysis of simulated samples of silver-copper and German silver alloys

Sample	Taken,* μg			Found,* μg		
	Ag	Cu	Ni	Ag	Cu	Ni
Simulated I	1.928	0.322	0.367	1.902	0.320	0.363
Simulated II	1.246	0.209	0.220	1.230	0.208	0.218
Simulated III	0.724	0.525	0.550	0.715	0.522	0.545
Ag alloy†	0.830	0.497	—	0.849	0.488	—
German silver‡	—	0.431	0.178	—	0.436	0.185

*In final solution measured.

†A 93.87 mg sample of silver alloy was dissolved and the solution diluted to 100 ml and aliquots of 0.500 and 0.050 ml were taken for the silver and copper determinations respectively.

‡A 68.00 mg sample of German silver was dissolved and the solution diluted to 1 litre, and aliquots of 0.500 and 1.00 ml were taken for the copper and nickel determinations respectively.

Table 4. Thickness of silver mirrors (area 15.30 cm^2)

Time, min	Absorbance	Calculated thickness, nm
2	0.867	20.8
4	2.450	48.8
6	2.900	69.6
8	3.320	79.7

used for formaldehyde determination.³³ Formaldehyde at pH 11 is quite specific for silver reduction and does not reduce copper(II), nickel(II) or iron(III). However, copper(II) can be reduced at pH above 12 on heating for 20 min at about 90° . Also, noble metals such as gold and platinum are partially reduced by formaldehyde and interfere.

Copper(II) is preferably reduced in 1.25M sulphuric acid by freshly prepared chromous sulphate as described by Zintl *et al.*^{29,30} In sulphuric acid the reduction proceeds quite smoothly to metallic copper, whereas in hydrochloric acid the reduction is slower and leaves some copper(I).²⁸⁻³⁰ The excess of chromous ion is readily oxidized by air. Chromous ion reduces silver(I) and iron(III), but nickel(II) is not reduced in acid media and does not interfere. Any nitrate and nitrite present must be removed by evaporation with sulphuric acid. Otherwise they are reduced by chromous ion to hydroxylamine, which causes reduction of iron(III), and a positive error, Silver in alloys containing copper is first determined by the formaldehyde reduction. Then copper and silver are both reduced with chromous ion and copper is determined by subtraction of the calculated absorbance for silver from the total absorbance for both copper and silver.

Nickel in German-silver is separated from copper by passing the sample through a cation-exchange resin followed by elution with 9M hydrochloric acid onto an anion-exchange resin.³¹ For the reduction it is essential to evaporate the acid and adjust the pH to 5-6. At pH > 6 the reduction of nickel is slow and at pH < 5 the decomposition of borohydride is fast, and consequently some of the nickel escapes reduction, giving values that are low. It has been reported that borohydride produces nickel boride^{35,36} but our tests, after heating the solutions, indicate that this side-reaction has a minimal effect on the determination of nickel. Borohydride decomposition at

Table 3. Analysis of mg samples of silver-copper and German silver alloys

Sample	Weight, mg	Final volume, l.	Absorbance	Amount of metal, mg		
				Taken	Found	Metal
German silver	2.19	1.0	1.193	1.38	1.36	Cu
	2.19	1.0	0.253	0.28	0.27	Ni
	1.60	1.0	0.870	1.01	0.99	Cu
Silver-copper alloy	4.80	0.2	0.553	0.42	0.43	Ag
	1.46	1.0	0.683 ^c	0.77	0.74	Cu

Table 5. Type of reducing agents used

Ion	Reducing agent	Optimum conditions	Remarks
Silver	Formaldehyde	pH 11	Fast. Formaldehyde is not oxidized by iron(III).
Copper	Chromium(II)	1.25M sulphuric acid	Moderately fast. Silver is also reduced, excess of chromous ion is oxidized by air.
Nickel	Sodium borohydride	pH 5.5	Moderately fast. Reductant destroyed on heating.

pH 5–6 requires heating for about 20 min. Borohydride reacts with copper(II) to produce not only metallic copper but also hydride. Thus, borohydride cannot be used for the determination of copper.

The spectrophotometric method involving reduction of the metal ions to the elemental state and reoxidation with iron(III) in the presence of Ferrozine provides a rather simple means to enhance the sensitivity for the determination of silver(I), copper(II) and nickel(II). These can be determined at concentrations of less than 1 $\mu\text{g/ml}$, even with 1-cm cells.

Copper and silver can both be reduced at concentrations as low as $4 \times 10^{-5} M$, but control of the pH is then fairly critical, and the reaction time has to be extended to 20 min, so preconcentration of such dilute solutions is preferable. The individual elements in pure solution can be determined with a relative precision of 3% or better. The precision and accuracy depend to a great extent on the absence of interferences. Nitrate and nitrite are to some extent reduced to a lower oxidation state by chromous ion and yield high absorbance values and halides stabilize the copper(I) state and yield low values for copper. Reduction of silver by formaldehyde is specific, and nitrate or sulphate do not interfere. However, when the copper to silver ratio is greater than 5, the results for silver are consistently higher by approximately 5% and the deviation increases with increase in the reduction time used.

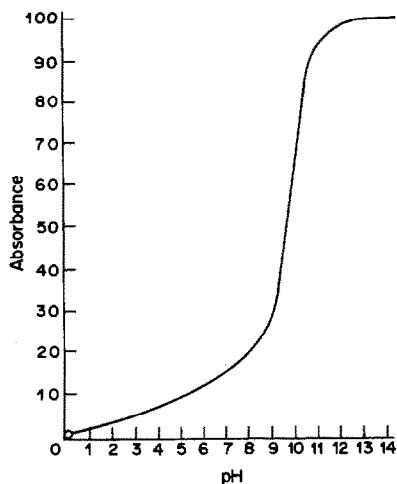


Fig. 1. Effect of pH on reduction of silver(I) with formaldehyde.

REFERENCES

1. L. L. Stookey, *Anal. Chem.*, 1970, **42**, 779.
2. C. R. Gibbs, *ibid.*, 1976 **48**, 1197.
3. J. P. Persijn, W. van der Slik and A. Riethorst, *Clin. Chem.*, 1971, **35**, 11.
4. P. Carter, *Anal. Biochem.*, 1971, **40**, 450.
5. H. Y. Yee and A. Zin, *Clin. Chem.*, 1971, **17**, 950.
6. E. Horak and F. W. Sunderman, *Am. J. Clin. Path.*, 1974, **62**, 133.
7. M. McArthur, J. Bygate and R. Chong-Kit, *Clin. Chem.*, 1975, **21**, 964.
8. J. Artiss, S. Vinogradov and B. Zak, *Clin. Biochem.*, 1981, **14**, 311.
9. S. Eskel, M. Haikonen and S. Raisanen, *Scand. J. Clin. Lab. Invest.*, 1983, **43**, 453.
10. J. Artiss, D. R. Strandberge and B. Zak, *Clin. Biochem.*, 1983, **16**, 334.
11. P. Carter, *Mikrochim. Acta*, 1972, 410.
12. R. Ruutu, *Clin. Chim. Acta*, 1974, **61**, 229.
13. J. Lewin and C. Chen, *Limnol. Oceanog.*, 1973, **18**, 590.
14. J. C. Brown, *Agron. J.*, 1972, **64**, 240.
15. C. Chen and J. Lewin, *J. Sci. Food Agric.*, 1972, **23**, 1355.
16. M. B. Kloster and C. C. Hach, *Anal. Chem.*, 1972, **44**, 1061.
17. S. K. Kundra, M. Katyal and R. P. Singh, *ibid.*, 1974, **46**, 1605.
18. *Idem*, *Curr. Sci.*, 1975, **44**, 548.
19. M. C. Mehra, M. K. Gadia and J. C. Landry, *J. Less-Common Metals*, 1982, **84**, 125.
20. B. Jaselskis and S. J. Nelepathy, *Anal. Chem.*, 1972, **44**, 379.
21. A. Attari and B. Jaselskis, *ibid.*, 1972, **44**, 1515.
22. S. J. Bajic and B. Jaselskis, *Talanta*, 1985, **32**, 115.
23. T. Akazawa, M. Kamaya and T. Murakami, *Kogakuin Daigaku Kenkyu Hokoku*, 1983, No. 54, 41.
24. N. Simonzadeh and B. Jaselskis, *Talanta*, 1984, **31**, 715.
25. G. J. Kellen and B. Jaselskis, *Anal. Chem.*, 1976, **48**, 1538.
26. M. K. Gadia and M. C. Mehra, *Microchem. J.*, 1978, **23**, 278.
27. I. M. Kolthoff, E. B. Sandell, E. J. Meehan and S. Bruckenstein, *Quantitative Chemical Analysis*, 4th Ed., p. 830. Macmillan, London, 1971.
28. J. J. Lingane and C. Auerbach, *Anal. Chem.*, 1951, **23**, 986.
29. E. Zintl, G. Rienacker and F. Schloffer, *Z. Anorg. Allgem. Chem.*, 1927, **168**, 97.
30. E. Zintl and G. Rienacker, *ibid.*, 1927, **161**, 374.
31. K. A. Kraus and G. E. Moore, *J. Am. Chem. Soc.*, 1953, **75**, 1460.
32. M. Matsuoka, M. Vokoi and T. Hayashi, *Denki Kagaku*, 1978, 325.
33. *CRC Handbook of Chemistry and Physics*, 30th Ed., C. D. Hogman (ed.), pp. 2537–2539. Chemical Rubber Publishing Co., Cleveland, Ohio, 1947.
34. K. W. Street, Jr. and A. Singh, *Anal. Lett.*, 1985, **18**, 529.
35. R. C. Wade, D. G. Holah, I. M. Hughes and B. C. Y. Hui, *Catal. Rev., Sci. Eng.*, 1976, **14**, 211.
36. H. Niederprum, *Angew. Chem. Int. Ed.*, 1975, **14**, 614.

HIGH-ENERGY COLLISIONAL SPECTROSCOPY IN QUALITATIVE AND QUANTITATIVE ANALYSIS OF DIESEL PARTICULATES

ANNA MARIA MACCIONI* and PIETRO TRALDI

Servizio di Spettrometria di Massa dell'Area di Ricerca del C.N.R., Corso Stati Uniti 4,
35020 Padova, Italy

LUCIO DORETTI

Servizio di Sicurezza del Lavoro e Protezione Sanitaria del C.N.R., Corso Stati Uniti 4,
35020 Padova, Italy

(Received 13 October 1986. Accepted 8 December 1986)

Summary—High-energy collisional spectroscopy provides a powerful analytical method for the characterization of polynuclear aromatic hydrocarbons present in diesel particulates. The absence of any need for extraction procedures and the large amount of information available from collisional spectra makes this technique of great interest. In particular, 3-methylcholanthrene can be determined from the daughter spectra of its molecular ion, with methylene iodide as internal standard.

Polynuclear aromatic hydrocarbons (PAHs) constitute an important class of chemical pollutants, many of which are known or suspected carcinogens and mutagens.^{1,2} The carcinogenicity of PAHs has been related to their structure, which determines the reactivity of the ultimate carcinogenic metabolites. For example, benzo(*a*)pyrene is a potent carcinogen, but the isomeric benzo(*e*)pyrene is a weak one.

In particular, 3-methylcholanthrene appears² to be a rapidly acting neoplastic agent and a potent hepatotumorigen; it has proved to be neoplastic or carcinogenic, by almost all routes tested, on chronic or repeated exposure of rats, mice, hamsters, guinea pigs, rabbits and dogs to it.

Several industrial sources of these compounds have been identified; an important source of PAHs in the air is known to be the exhaust gas of diesel engines. For these reasons, interest has recently grown in the analytical procedures used in identifying and determining PAHs in such matrices.

Mass spectrometry has proved to be a valuable tool in the qualitative and quantitative analysis of PAHs, owing to its sensitivity and specificity. Many analytical procedures have been proposed along this line, employing the classical gas chromatography/mass spectrometry (GC/MS) approach under different ionization conditions,³⁻⁷ or the more sophisticated (from the instrumental point of view) collisional methods.⁸⁻¹⁰ Among the latter, those linking negative-ion chemical ionization with collisionally-induced charge inversion gave interesting results.

High-energy collisions proved to be more diagnostic for isomer identification.⁹ Recently we have developed an analytical procedure for qualitative and quantitative analysis for anthracene and phenanthrene in diesel particulates with the aid of daughter spectra,^{10,11} without resorting to prior extraction procedures.¹²

Continuing our interest in the analysis of diesel particulates for PAHs, in the present paper we report a procedure for the qualitative and semi-quantitative analysis of the main PAHs, together with the determination of 3-methylcholanthrene in a diesel particulate.

EXPERIMENTAL

All mass spectrometric measurements were obtained with a VG ZAB 2F instrument operating under electron impact (EI) conditions (70 eV, 200 μ A). The samples were introduced by means of a direct inlet system; for quantitative analysis the diesel particulates were heated to 400° on the probe and a constant source temperature of 200° was used. Daughter (collisionally-activated decomposition, mass-analysed ion kinetic energy) spectra¹¹ were obtained by causing 8-keV ions to collide with nitrogen molecules in the second field-free region. The pressure in the collision cell was that required to reduce the main beam intensity to 60% of its usual value. These pressure conditions were accurately reproduced for all the measurements.

Positive-ion chemical ionization (PICI) data were obtained by using methane and ammonia as reagent gases, with the source operating in the chemical ionization (CI) mode (100 eV, 2 mA).

The exhaust particulates of a diesel engine were collected by means of a cyclone placed after the muffler and maintained at 200°; the engine used was an OM Tigrotto CO2D/1 with four cylinders in line, with a capacity of 4397 cm³.

"Washed" particulates, to be used as blanks in the determination of the calibration curve for the determination

*On leave from Istituto di Chimica Farmaceutica e Tossicologica dell'Università, Via Ospedale 72, 09100 Cagliari, Italy.

of 3-methylcholanthrene and the semi-quantitative analysis of the Supelco PAH Mixture, were obtained by successive extraction with solvents (benzene, toluene, acetone and chloroform). The extracted particulates were then introduced into the ion source and heated at 400° for 15 min (after this time, no trace of sample evaporation from the particulate was observed).

The standard 610-M PAH mixture (containing 16 polynuclear hydrocarbons in methanol/methylene chloride solution: acenaphthene, acenaphthylene, anthracene, benzo(*a*)anthracene, benzo(*a*)pyrene, benzo(*b*)fluoranthene, benzo(*ghi*)perylene, benzo(*k*)fluoranthene, chrysene, dibenzo(*a,h*)anthracene, fluoranthene, fluorene, indeno(1,2,3-*cd*)pyrene, naphthalene, phenanthrene, pyrene) was purchased from Supelco (Bellefonte, PA 16823, USA). The methylene iodide employed as internal standard for the determination of 3-methylcholanthrene, was an analytically pure sample purchased from Carlo Erba (Milano, Italy).

3-Methylcholanthrene was supplied by Aldrich Chemical Company, Inc., Milwaukee, Wis., USA.

RESULTS AND DISCUSSION

It has already been demonstrated³ that the extraction procedure for diesel particulates is not completely effective; in fact the direct introduction of the extracted diesel particulates into the ion source results in a consistent further release of PAHs, proving that severe recovery problems can arise from extraction procedures. Hence, direct introduction leads to better determination of the PAHs. By introduction of about 0.2 mg of diesel particulates by the direct inlet system into the ion source operating under EI conditions, the mass spectrum reported in Fig. 1 was obtained. It appears to be rather complicated, but peaks due to molecular ions of PAHs can easily be identified (m/z 202, fluoranthene and pyrene; m/z 228, benzo(*a*)anthracene and chrysene; m/z 268, 3-methylcholanthrene; m/z 252, benzo(*a*)pyrene, benzo(*b*)fluoranthene and benzo(*k*)fluoranthene, m/z 152, acenaphthylene).

The only means of confirming the presence of PAHs is the identification of their molecular peaks which have been employed for their quantitative analysis. This approach may give misleading results owing to the presence of interfering ionic species, isobaric with the molecular PAH ions. Furthermore,

isomeric PAHs (for example, anthracene and phenanthrene) cannot be distinguished and the quantitative data consequently lose specificity.

These ambiguities may be overcome by using collisional spectroscopy, for, by collision of selected ions with neutral molecules, it is possible to cause dissociation and so obtain daughter spectra which may be compared with the spectra obtained from authentic compounds.

Daughter spectra consequently can lead, in principle, to the unequivocal identification of PAHs. In some cases, as already shown¹² the characterization of isomeric PAHs is also possible. For example, in Fig. 2, the daughter spectrum (A) of the ion having m/z 268, obtained from diesel particulates, is compared with the daughter spectrum (B) from the molecular ion of 3-methylcholanthrene (m/z 268).

Similarly in Fig. 3, the daughter spectrum (A) of the ion having m/z 202, obtained from diesel particulates, is compared with the daughter spectrum (B) from the molecular ion of pyrene. It can be seen that the two pairs of spectra are practically identical, so proving the presence of 3-methylcholanthrene and pyrene in the diesel exhaust. Thus without prior extraction and time-consuming chromatographic runs, it is possible to obtain confirmation of the presence of these PAHs in a few seconds.

However, interfering ionic species, isobaric with molecular ions of the PAHs, are sometimes present, leading to the formation of rather complex collisional spectra.

Usually the PAHs are determined either by gas chromatography/mass spectrometry or by direct introduction of the diesel particulates into the mass spectrometer and analysis by multiple ion detection.

However, semi-quantitative data, leading to the mapping of the PAH mixture, can be rapidly obtained by simply introducing the diesel particulates into the ion source (at constant source and probe temperatures) and measuring the relative abundances of the PAH molecular ions. For example, by introducing a standard PAH mixture (Supelco 610-M) at constant source and probe temperatures (200° and 150°, respectively) under different ionization conditions, we have found that the relative abundances of

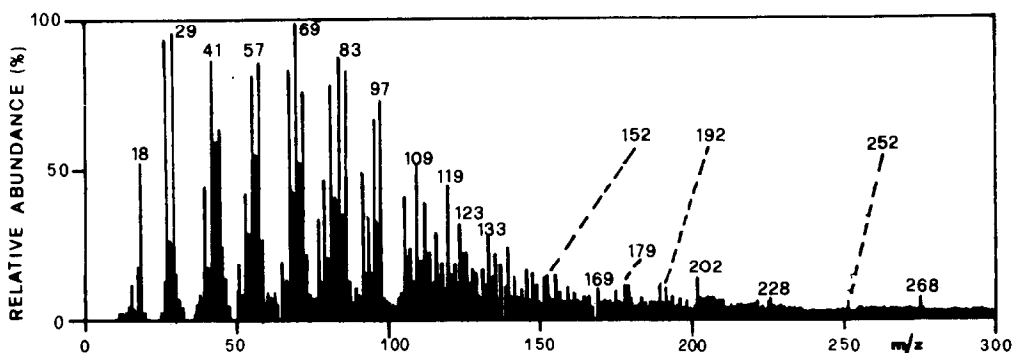


Fig. 1. 70 eV EI mass spectrum of a diesel particulate (ion source temperature 200°).

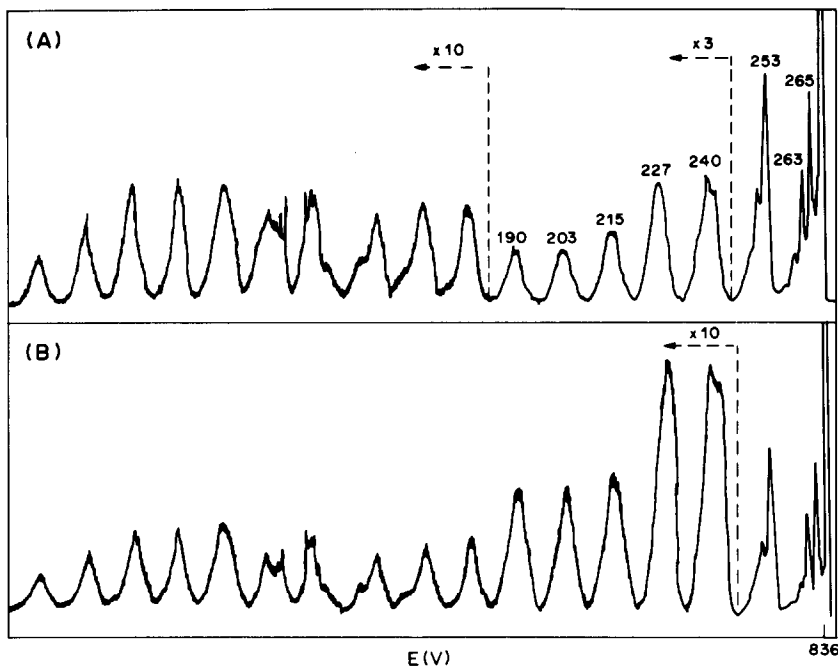


Fig. 2. Daughter spectra of: (A) ionic species at m/z 268 obtained by EI of a diesel particulate and (B) $[M]^{++}$ of 3-methylcholanthrene (m/z 268).

PAH molecular ions are linearly related to the PAH concentrations (see Table 1).

The best fit is obtained under PICI conditions (methane as reagent) with a correlation coefficient $R^2 = 0.9857$ (see Fig. 4). However, sufficiently high R^2 values are also obtained under EI and PICI (ammonia as reagent) conditions ($R^2 = 0.9403$ and 0.9593 , respectively), suggesting that the influence of the ionization method employed is only minor and proving that this semi-quantitative approach is gener-

ally correct because of the good reproducibility of such measurements ($\leq 10\%$ variation).

The daughter spectra are also useful for quantitative analysis, because they are both specific and sensitive. We have successfully employed this method for determination of compounds of interest in various complex matrices and have also tested its capabilities in the present case.

Owing to its carcinogenic properties, 3-methylcholanthrene was chosen as a model compound and

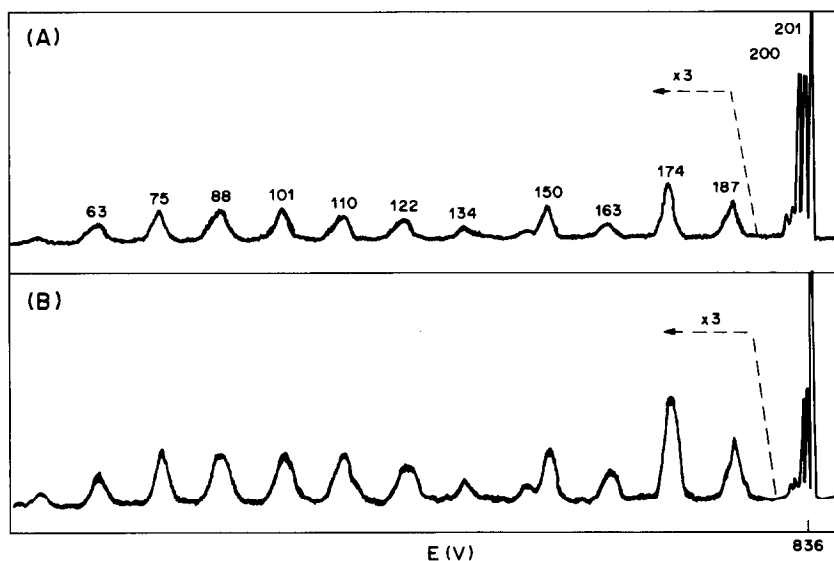


Fig. 3. Daughter spectra of: (A) ionic species at m/z 202 obtained by EI of a diesel particulate and (B) $[M]^{++}$ of pyrene (m/z 202).

Table 1. Relative abundances of ionic species due to molecular ions of PAHs present in the Supelco 610-M standard mixture, obtained under different ionization conditions (for chemical ionization data, the $[M + H]^+$ species were considered)

Compound	m/z for molecular ions	Ionization methods			Concentration, $10^{-3}M$
		EI	PICI (CH_4)	PICI (NH_3)	
Naphthalene	128	73	50	50	7.8
Acenaphthylene	152	100	100	100	13.2
Acenaphthene	154	31	37	30	6.5
Fluorene	166	5	7	5	1.2
Anthracene	178	5	6	8	1.1
Phenanthrene					
Fluoranthene	202	7	8	16	1.5
Pyrene					
Benzo(<i>a</i>)anthracene	228	6	6	5	0.9
Chrysene					
Benzo(<i>a</i>)pyrene					
Benzo(<i>b</i>)fluoranthene	252	15	10	10	1.6
Benzo(<i>k</i>)fluoranthene					
Benzo(<i>ghi</i>)perylene	276	12	5	7	1.1
Indeno(1,2,3- <i>c,d</i>)pyrene					
Dibenzo(<i>a,h</i>)anthracene	278	8	3	3	0.7

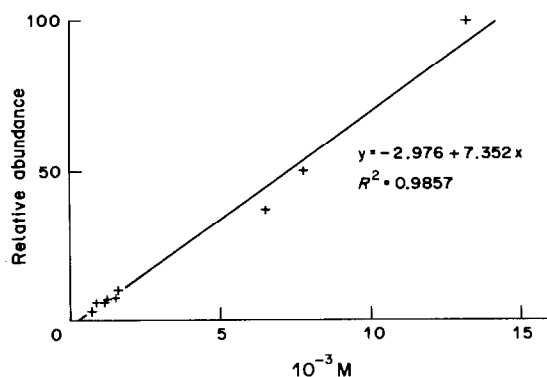


Fig. 4. Plot of relative abundances of ionic species due to $[M + H]^+$ ions of PAHs contained in the Supelco 610-M standard mixture obtained under PICI (CH_4) conditions, vs. PAH molar concentrations.

its determination was performed by means of the following steps:

- study of the collisional spectrum of $[M]^+$ of a pure sample of 3-methylcholanthrene;
- determination of the detection limit for the pure substance;
- determination of the detection limit for the pure substance present in a "washed" particulate;

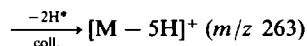
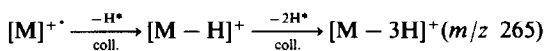
(d) choosing the instrumental standard and study of its collisional spectrum;

(e) choosing the collisionally-induced decomposition products of diagnostic value for 3-methylcholanthrene and for the instrumental standard, to be employed for single ion monitoring;

(f) calibration by introducing known amounts of the pure substance and an internal standard, supported on washed particulates into the ion source;

(g) introduction of a known amount of internal standard in a known amount of diesel particulate and, by peak-area ratio measurements, determination of the relative amount of 3-methylcholanthrene.

The daughter spectrum of $[M]^+$ of 3-methylcholanthrene is shown in Fig. 2. It contains diagnostic peaks at m/z 265 and 263, probably arising from multiple collision processes.



The detection limit for the pure substance was approximately 50 fg, which rises to 2 pg when it is added to a washed particulate. These values corre-

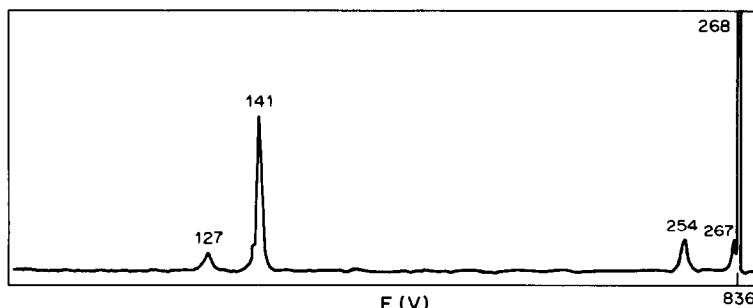


Fig. 5. Daughter spectrum of $[M]^+$ (m/z 268) of CH_2I_2 .

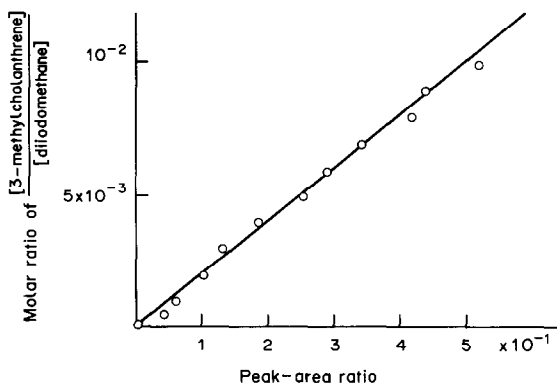


Fig. 6. Regression line for determination of 3-methylcholanthrene (plot of molar ratio [3-methylcholanthrene]/[CH₂I₂] vs. peak-area ratio).

spond to the amount of sample needed to give a signal-to-noise ratio of 10 for the peak at m/z 190.

As internal (instrumental) standard, a substance giving rise to abundant ionic species at m/z 268 was required, which had to be structurally unrelated to 3-methylcholanthrene, in order to avoid any overlapping of peaks for the collisionally-induced decomposition products. The use of methylene iodide, isobaric with 3-methylcholanthrene, as internal standard, solved the problem. In fact, its daughter spectrum, seen in Fig. 5, does not show any ions at m/z 265 and 263, but a particularly abundant collisionally-induced loss of I[•], leading to ions at m/z 141.

The calibration graph was obtained for "washed" particulates containing from 1.2 to 120 ng/mg 3-methylcholanthrene and a constant amount (12.3 $\mu\text{g}/\text{mg}$) of methylene iodide. Measurements were performed by single ion monitoring of the collisionally-induced decomposition products at m/z 265 for 3-methylcholanthrene and at m/z 141 for methylene iodide.

The results obtained were correlated by linear

regression analysis, leading to the calibration graph shown in Fig. 6 ($R^2 = 0.9935$). Introduction of 1.7 mg of the diesel particulate (the spectrum of which is shown in Fig. 1) and 12 μg of methylene iodide gave a peak-area ratio of 0.135 (mean of 5 determinations) corresponding to a molar ratio of 2.67×10^{-3} . The estimated amount of 3-methylcholanthrene present in the diesel particulate was thus 19.3 ng/mg.

This determination was possible because of the absence of isomers of 3-methylcholanthrene. If mixtures of isomers are present, further measurements would be necessary, as in the case of determination of anthracene and phenanthrene.¹²

Acknowledgements—The authors are grateful to Mrs. Liliana Vanuzzi for technical assistance and Dr. A. Di Lorenzo of the Istituto Motori del CNR, Naples, Italy, for collection of the diesel particulates. This research was partly supported by the Progetto Finalizzato Energetica, CNR-ENEA, of Italy.

REFERENCES

1. J. H. Weisburger, in *Toxicology, The Basic Science of Poisons*, L. J. Casarett and J. Doull (eds.), pp. 336–339. Macmillan, New York, 1975.
2. E. E. Sandmeyer, in *Patty's Industrial Hygiene and Toxicology*, 3rd Ed., G. D. Clayton and F. E. Clayton (eds.), pp. 3333–3368. Wiley, New York, 1981.
3. A. Di Lorenzo, *Adv. Mass Spectrom.*, 1980, **8B**, 1377.
4. N. Klempmeier and H. Binder, *Anal. Chem.*, 1983, **55**, 2104.
5. M. Oehme, *ibid.*, 1983, **55**, 2290.
6. G. Rhodes, R. P. Opsal, J. T. Meck and J. P. Reilly, *ibid.*, 1983, **55**, 280.
7. M. L. Lee and R. A. Hites, *J. Am. Chem. Soc.*, 1977, **99**, 2008.
8. B. Shushan and R. K. Boyd, *Org. Mass Spectrom.*, 1980, **15**, 445.
9. D. Zakett, J. D. Ciupek and R. G. Cooks, *Anal. Chem.*, 1981, **53**, 723.
10. J. D. Ciupek, D. Zakett, R. G. Cooks and K. V. Wood, *ibid.*, 1982, **54**, 2215.
11. R. G. Cooks (ed.), *Collision Spectroscopy*, Plenum Press, New York, 1978.
12. L. Doretto, A. M. Maccioni and P. Traldi, *Biomed. Environ. Mass Spectrom.*, 1986, **13**, 381.

METHODS FOR DETERMINING HYDROGEN IN STEELS

V. S. SASTRI

Physical Metallurgy Research Laboratories, Canada Centre for Mineral and Energy Technology,
555 Booth St., Ottawa, Ontario, Canada

(Received 2 June 1986. Accepted 6 December 1986)

Summary—The current status of methods for determining hydrogen in metals is reviewed. Methods based on vacuum techniques, carrier-gas techniques, secondary-ion mass-spectrometry and nuclear reactions are discussed.

The determination of hydrogen in metals has undergone extensive development in the last decade.¹ In 1974, an excellent book on determining gases in metals was published² and a few further reviews have appeared in the literature since.³⁻¹¹ This review summarizes the literature since 1974, with particular emphasis on steels.

In some metals (*e.g.* ferritic steels), hydrogen diffuses rapidly (Table 1) even at room temperature, as illustrated for Armco iron in Fig. 1.¹² It is obvious from this figure that appreciable losses of hydrogen occur even at room temperature and that it is necessary to store samples in liquid nitrogen to prevent losses.

In addition, because of the heterogeneous distribution of hydrogen in steels, samples of 5–20 g are considered necessary if hydrogen contents of 0.1–1.0 $\mu\text{g/g}$ (0.1–1.0 ppm) are to be determined with acceptable accuracy.

VACUUM TECHNIQUES

Classical techniques such as vacuum fusion and vacuum hot-extraction are still used to determine hydrogen in steels.¹³⁻²¹ The measurement technique used depends on the nature of the gases evolved on heating the steels. If hydrogen is the only gas evolved, the analysis may be performed by direct measurement of pressure with, for example, a McLeod gauge. When other gases are present, hydrogen may be determined by measuring the pressure after diffusion of the hydrogen through a palladium-silver tube into a calibrated volume. Alternatively, hydrogen may be determined by measuring the difference between the pressure of the total gas evolved and that of the gas remaining after oxidation of the hydrogen to water, which is then frozen out. Both methods are absolute and do not require the use of standards. Vacuum hot extraction analysis of steels is generally done at temperatures below the eutectoid temperature and, as

a result, low blank values are obtained and gettering problems minimized. Vacuum hot-extraction is generally considered more precise than vacuum fusion and, after considerable investigation, was the method eventually recommended by a task force committee of ASTM in 1969 for analysing steel.²²

Mass spectrometric analysis of the gaseous mixtures obtained on heating steels in vacuum hot-extraction is gaining prominence.²³⁻²⁵ Berkowitz *et al.*²³ developed a technique which uses the calibrated pumping speed of a vacuum system and a mass spectrometer to provide a dynamic analysis of gases evolved from the samples. The apparatus can accommodate five samples in a vacuum chamber, with provision for melting the samples individually. This arrangement saves time in evacuating the system. With Armco iron for example, hydrogen was released from the samples within 20 sec, thus minimizing hydrogen losses during the heating up period in the apparatus. Contrary to frequent practice, graphite crucibles were not used, and thus methane production was eliminated.

Martin *et al.*²⁶ made a critical evaluation of methods used for determining hydrogen in steel with the apparatus shown schematically in Fig. 2. The results obtained by mass spectrometric analysis, palladium-membrane and thermal conductivity techniques are compared in Table 2. For samples of HY80 the results obtained by mass spectrometry are in good agreement with those obtained by the palladium-membrane technique. However, there is poorer agreement with the results from thermal conductivity measurements, the differences amounting to as much as 1 ppm. The results for replicate samples of two other steels analysed by the palladium-membrane technique and two other methods (Table 3) were reproducible within 0.1 ppm. The values obtained by hot extraction combined with a palladium membrane for samples of vacuum-cast forgings are shown in Fig. 3. The hydrogen content decreased progressively from the centre of the forging to the surface.

Table 1. Diffusion coefficients of hydrogen (D)

Metal	$D, 10^{-4} \text{ cm}^2/\text{sec}$	
	Calculated	Experimental
α -Fe	51	6.4
γ -Fe	420	66

CARRIER-GAS METHODS

Carrier-gas methods of collecting hydrogen for analysis can be adapted to both fusion and hot extraction. In the carrier-gas fusion technique, a steel sample is melted inductively and the hydrogen released is swept into a thermal conductivity detector by nitrogen or argon.²⁷⁻³⁰ Carrier-gas techniques have been practised extensively in hot extraction methods.³¹⁻⁴² These techniques involve heating the samples to between 80° and 800° (temperatures far lower than their fusion temperatures) and passing the gas into a gas-chromatographic column. The advantage of this method is the ease with which the kinetics of hydrogen evolution as a function of temperature can be followed. It is important to note that the detection of hydrogen by thermal conductivity is quite sensitive, making it possible to detect 0.1 ppm of hydrogen. Automated commercial instruments have been developed, based on the principles of carrier-gas fusion, carrier-gas hot extraction and thermal conductivity detection. These instruments are used in routine analysis.⁴³⁻⁴⁸

ELECTROCHEMICAL METHODS

Koenig *et al.*⁴⁹ developed a method involving hot extraction, conversion of the hydrogen into water vapour by passing over heated copper(II) oxide and subsequent determination of the water vapour by amperometry. Hydrogen concentrations of 2-8 ppm in steel have been determined in this way, with a coefficient of variation of less than 0.9%. Berman and

other workers have determined the hydrogen content of high-strength steel by using coulometric hydrogen permeation techniques⁵⁰⁻⁵⁵ which have detection limits of 0.1 ppm. Permeation techniques have been found useful for *in situ* determination of hydrogen in steel structures, including ships and pipelines.

The determination of hydrogen by anodic dissolution of steels has been recently studied.^{56,57} The method depends on reacting a stable organic free radical, such as (2,2,6,6-tetramethyl-1-oxyl-4-piperidone) with atomic hydrogen released from steel during anodic dissolution.⁵⁷ This method could potentially yield the amounts of atomic and molecular hydrogen in steel samples. More detailed work on this system is needed before its usefulness can be established.⁵⁸

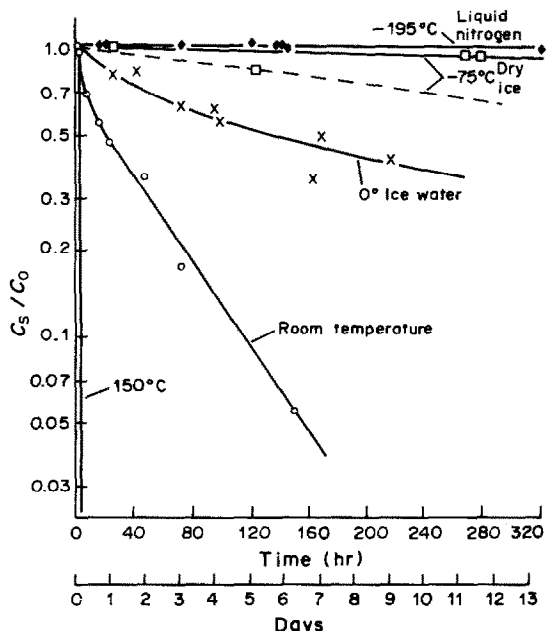


Fig. 1. Loss of hydrogen from iron samples: C_s , hydrogen content at time t ; C_0 , initial hydrogen content.

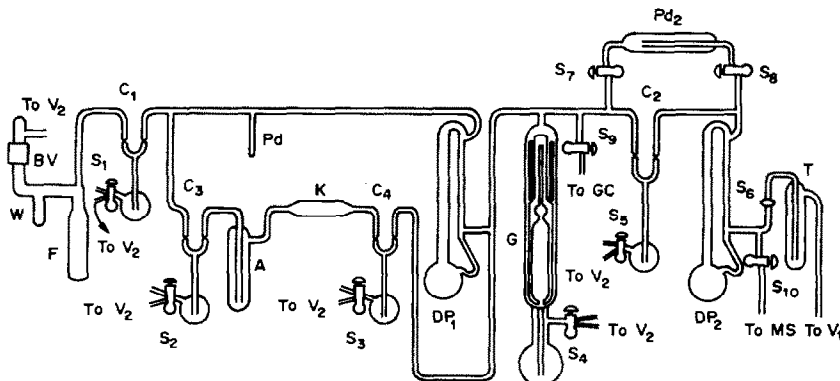


Fig. 2. Apparatus for determining hydrogen in steel.²⁶ Absorption trap; BV, ball valve; C_1 - C_4 , mercury cut-offs; DP_1 , DP_2 , mercury diffusion pumps; G, McLeod gauge; GC, gas chromatograph; K, catalyst; MS, mass spectrometer; Pd_1 , Pd_2 , palladium membranes; S_1 - S_{10} , stopcocks; T, trap; V_1 , V_2 , vacuum pumps; W, sample storage well.

Table 2. Comparison of hydrogen contents (ppm) obtained by various analytical methods (HY80 steel) (reproduced from J. F. Martin, R. C. Jakaes and L. M. Melnick, *Trans. Metall. Soc. AIME*, 1964, 230, 107, by permission. Copyright 1964, American Institute of Mining Metallurgical and Petroleum Engineers.)

Sample No.	Mass spectrometry	Palladium membrane	Thermal conductivity
1	6.08	5.63	5.31
2	5.69	5.48	4.41
3	5.09	4.92	5.52
4	2.22	1.99	2.26
5	5.39	5.25	4.27
6	2.36	2.18	1.98
7	1.73	1.66	1.85

NUCLEAR REACTION METHODS

Methods for hydrogen determination based on nuclear reactions, although of recent origin, are gaining importance. In nuclear reaction methods, a specimen is bombarded with an ion beam (6–12 MeV) and the γ -radiation yield monitored. Nuclear reactions of hydrogen with ^{15}N , ^{11}B , ^3He and ^{19}F have been used⁵⁹⁻⁶⁴ as non-destructive techniques to obtain the concentration profile of hydrogen in metals as a function of depth. Rauch *et al.*⁵⁹ used the nuclear reaction of hydrogen with ^{15}N ions to produce ^{12}C , ^4He and γ -radiation, in order to obtain the depth profile of hydrogen in an iron sample. The incident beam did not influence the hydrogen distribution in the sample, because the heating produced by the ion beam was very localized. Although no mention was made of the technique used for immobilizing the hydrogen in the sample, it is suspected that some form of cooling was used. With the microbeams currently available, lateral resolution of 0.1 mm, depth resolution of about 10 nm and accessible depths of 2–4 μm can be achieved. Increased activity in nuclear reaction methods is expected to continue although it will be hampered to some extent by the lack of commercially developed instruments.

Farrell and Lewis, using a nuclear microanalysis

technique following a nuclear reaction with deuterium,⁶⁵ determined the hydrogen content of 310 austenitic stainless steel in its near-surface layers. The results obtained were useful in throwing light on the mechanism by which hydrogen embrittles austenite.⁶⁵ The diffusion rate of hydrogen in stainless steels is many orders of magnitude lower than in ferritic steels and thus loss of hydrogen is not as great a problem for austenite samples. However, all steel samples should be cooled to minimize loss of hydrogen.

SPECTRAL METHODS

Hydrogen in steels has been determined spectrographically from red and infrared emission lines.⁶⁶ Kalinin applied emission spectroscopy to kinetic studies of hydrogen saturation in steel.⁶⁷ Although emission spectroscopy can be affected by spectral interference and there is a need for standards, this

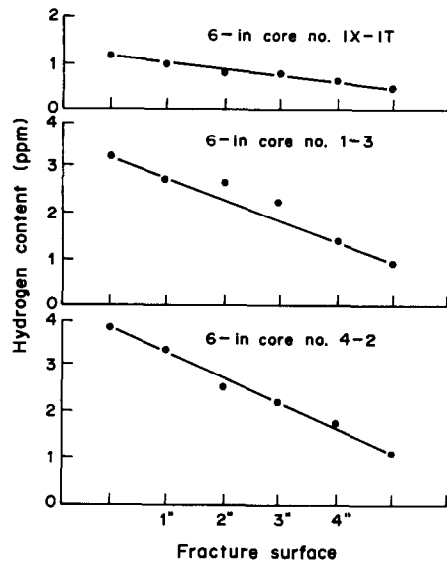


Fig. 3. Hydrogen contents as a function of distance from centre of vacuum-cast forgings.²⁶

Table 3. Comparison of reproducibility of hydrogen content (ppm) found by various methods (reproduced from J. F. Martin, R. C. Jakaes and L. M. Melnick, *Trans. Metall. Soc. AIME*, 1964, 230, 107, by permission. Copyright 1964, American Institute of Mining, Metallurgical and Petroleum Engineers.)

Sample	Mass spectrometry	Palladium membrane	Gas chromatography	Catalytic oxidation and absorption
AISI 316	1.70	1.63	1.62	1.67
	1.59	1.50	1.60	1.58
	1.60	1.49	1.42	1.54
	1.73	1.51	1.61	1.48
	1.50	1.57	1.73	1.66
3% SiFe	2.34	2.22	2.11	2.27
	2.29	2.09	2.36	2.22
	2.29	2.13	2.13	2.00
	2.28	2.03	2.21	2.24
	2.55	2.35	2.49	2.25

technique has been used in routine determination of hydrogen in carbon steels.⁶⁸

MISCELLANEOUS METHODS

Other methods for the detection of hydrogen in steels have been used with different degrees of success. One^{69,70} used neodymium tape on a degreased sample of AISI 4340 high-strength steel and heated it to 300°F for 1 hr to determine the location of hydrogen. After cooling, the neodymium tape was examined by electron microscopy for the presence of NdH₂. In this way a level of hydrogen as low as 0.001 ppm was detected.

MODERN SURFACE ANALYTICAL METHODS

In the last decade, many advances have been made in the application of surface analytical techniques such as laser mass spectrometry and secondary-ion mass-spectrometry (SIMS) to the study of hydrogen in metals. A brief discussion of these techniques applied to hydrogen in steels is given below.

Laser mass spectrometry

The distribution of hydrogen in steels electroplated with chromium was determined by localized fusion of the sample with a laser beam and subsequent analysis of the evolved gas by mass spectrometry.⁷¹ This method was used to determine bulk and surface hydrogen in 30 Kh GSNA steel. Zuev *et al.*⁷² also used this technique to determine the distribution of hydrogen in the region of non-metallic inclusions in steel.

The development of commercial laser microprobe mass spectrometry equipment with a sensitivity of 10⁻²⁰ g, coupled with a refrigerating stage, may make it possible to determine hydrogen distribution in steels.

SIMS

In this technique the surface of a sample is sputtered by a beam of caesium ions. The sputtered materials, including any hydrogen ions, are analysed in a mass spectrometer with detection limits as low as about 10 ng/g. Among other things, SIMS has been used⁷³ to study the distribution of molecular hydrogen in welds in steel. In combination with a suitable cooling stage, SIMS may prove useful in studying hydrogen distribution in steels.

CONCLUSIONS

Vacuum techniques still hold a prominent place among the many methods for determining hydrogen in metals, because they do not rely on standards. An

evaluation of the vacuum hot-extraction method coupled with mass spectrometry, palladium membrane, gas chromatography and catalytic oxidation and absorption techniques has shown that based on cost, maintenance, speed and accuracy of analysis, the palladium membrane technique is the method best suited for routine use. Commercial automated instruments based on carrier-gas techniques are satisfactory for routine analysis of steels, but they require calibration with metals containing known amounts of hydrogen. Techniques based on nuclear reactions appear promising for depth profiling of hydrogen in steels. It is appropriate to conclude that accurate determination of hydrogen in the different forms in which it can occur in steels is still a challenge to analytical chemists and will continue to be one in the foreseeable future.

REFERENCES*

1. H. K. Feichtinger, *Gase in Metallen Proc. Symp., Darmstadt, 1979*, Deutsche Gesellschaft für Metallkunde, Oberursel, FRG, 1979; G. Kraft (ed.), *Analysis of Non-metals in Metals*, de Gruyter, Berlin, 1981; D. Hirschfeld (ed.), *Gase in Metallen*, Deutsche Gesellschaft für Metallkunde, Oberursel, 1984.
2. L. Melnick, L. Lewis and B. Holt, *Determination of Gaseous Elements in Metals*, Wiley, New York, 1974.
3. V. L. Zueva, V. F. Isaev, Yu. A. Danielovich, T. A. Izmanova and V. G. Ignatev, *Proizvod. Ferrosplavov*, 1973, **2**, 101; *Chem. Abstr.*, 1975, **82**, 509095.
4. J. Bruch, *SEAIISI Q*, 1973, **2**, 39; *Chem. Abstr.*, 1977, **86**, 7573y.
5. *Idem*, *ibid.*, 1973, **2**, 43; *Chem. Abstr.*, 1976, **85**, 201684e.
6. A. Condylis, *Bull. Cercle Etud. Met.*, 1974, **12**, 567; *Chem. Abstr.*, 1974, **81**, 145028x.
7. L. A. De'Aeth, *Chem. Anal. (N.Y.)*, 1974, No. 40, 491; *Chem. Abstr.*, 1975, **83**, 125564g.
8. N. Yamaguchi, *Kinzoku*, 1974, **44**, No. 11, 13; *Chem. Abstr.*, 1975, **82**, 79930c.
9. M. Hanin, *Proc. Chem. Conf.*, 1976, **29**, 81; *Chem. Abstr.*, 1978, **88**, 57838a.
10. W. Thomich, *Fachber. Huettentrax. Metallweiter Verarb.*, 1977, **15**, 936; *Chem. Abstr.*, 1978, **88**, 145433V.
11. I. Taguchi, *Fushoku Boshoku Shinpojumu Shiryo*, 1980, **30**, 31; *Chem. Abstr.*, 1980, **83**, 125007j.
12. J. F. Martin, Private communication.
13. P. Boillot, M. Hanin and C. Maeder, *Hydrogene Met. Congres. Int.*, 1972, **2**, 381; *Chem. Abstr.*, 1975, **82**, 25435b.
14. A. Doughty and J. M. Mitchell, *Metall. Mater. Technol.*, 1973, **5**, 567; *Chem. Abstr.*, 1974, **81**, 114170 h.
15. T. S. Volkova, V. P., Karasev and L. G. Marukhno, *Metody Issled. Oprod. Gazov Met.*, 1973, 40; *Chem. Abstr.*, 1975, **83**, 37056 n.
16. M. H. Lloyd and C. E. A. Shanahan, *J. Iron Steel Inst.*, 1973, **211**, 615; *Anal. Abstr.*, 1974, **26**, 1536.
17. S. Hall, *Proc. Chem. Conf.*, 1974, **27**, 114; *Chem. Abstr.*, 1976, **85**, 103399w.
18. M. Martin, *Comm. Eur. Communities*, EVR 6159, Pt. 1, 1978; *Chem. Abstr.*, 1979, **91**, 116764k.
19. Centro Nacional Investigaciones Metalurgicas. *Rev. Soldadura*, 1979, **9**, 29; *Chem. Abstr.*, 1980, **92**, 208334u.
20. *Idem*, *ibid.*, 1979, **9**, 35; *Chem. Abstr.*, 1980, **92**, 68966z.
21. D. H. Kim and H. G. Ho, *Punsok Hwahak*, 1980, **1**, 8; *Chem. Abstr.*, 1980, **93**, 153994x.
22. Am. Soc. Test Mater., *Unpublished Committee E-3 Task Force Report*, March, 1969.

*Chemical Abstracts references are given for the reader's convenience in consulting material published in the less readily available journals.

23. B. J. Berkowitz, C. M. Preece and J. A. Strozier, *Scr. Metall.*, 1975, **9**, 803; *Chem. Abstr.*, 1975, **83**, 187887y.
24. R. Suzuki and K. Takimoto, *Japan Patent*, 80 40,921, 1980; *Chem. Abstr.*, 1980, **230**, 106459s.
25. P. Stokovszki, S. Larsson and K. E. Easterling, *Met. Sci.*, 1979, 597; *Chem. Abstr.*, 1980, **92**, 114542h.
26. J. F. Martin, R. C. Jakaes and L. M. Melnick, *Trans. Metall. Soc. AIME*, 1984, **230**, 107.
27. K. Hoshino, *Japan Patent*, 74 37,877, 12 October 1974; *Chem. Abstr.*, 1974, **84**, 129952a.
28. P. Boillot and M. Hanin, *Circ. Inf. Tech., Cent. Doc. Sider.*, 1975, **32**, 2479; *Chem. Abstr.*, 1976, **85**, 13374e.
29. T. Godai, T. Sugiyama, M. Sugino and M. Kondo, *German Patent*, 2,743,973, 6 April 1978; *Chem. Abstr.*, 1978, **89**, 70441f.
30. T. Sugiyama, S. Yamamoto, M. Yamada and M. Sugino, *Trends Steel Consumables Weld. Int. Conf.*, 1979, **1**, 299; *Chem. Abstr.*, 1980, **92**, 62757k.
31. W. Koch, E. Buechel and H. Lemm, *Thyssenforschung*, 1972, **4**, 144; *Chem. Abstr.*, 1974, **81**, 145337x.
32. A. Bargone, C. Fraccaro and E. Ramous, *Atti Ist. Veneto Sci.*, 1972, **130**, 467; *Chem. Abstr.*, 1974, **80**, 90731t.
33. A. V. Ivanchenko, *Zavodsk. Lab.*, 1973, **39**, 372; *Chem. Abstr.*, 1973, **79**, 95458c.
34. P. Boillot, *German Patent*, 2,237,487, 22 February 1973; *Chem. Abstr.*, 1973, **78**, 118933v.
35. G. Amati, S. Maneschi and N. Vantini, *German Patent*, 1,773,609; *Chem. Abstr.*, 1975, **83**, 125790c.
36. V. Rezl, B. Kaplanová and J. Janák, *Anal. Chem.*, 1975, **47**, 159.
37. B. Brule, M. Cornet and S. Talbot-Besnard, *Hydrogen Met., Proc. 2nd Int. Congr.*, 1978, **2**, 1F1, 1978; *Chem. Abstr.*, 1978, **89**, 20191t.
38. H. K. Feichtinger, *Qual. Control Eng. Alloys Role Met. Sci., Proc. Int. Symp.*, 1977, 29; *Chem. Abstr.*, 1979, **90**, 59541p.
39. A. Wutschel and K. Zimmerman, *Arch. Eisenhuettenwes.*, 1978, **49**, 313; *Chem. Abstr.*, 1978, **89**, 99148b.
40. L. N. Pankret'eva and P. A. Cherkasov, *Metall. Metody Ppovysh. Kach. Stali*, 1979, 240; *Chem. Abstr.*, 1980, **92**, 140102j.
41. V. G. Guglya and Gomez de Segura Urraco, *Zavodsk. Lab.*, 1980, **46**, No. 6, 490; *Chem. Abstr.*, 1980, **93**, 87997x.
42. A. Gomez Urraco and V. G. Guglya, *Izv. Vyssh. Uchebn. Zaved. Chern. Metall.*, 1980, **5**, 153; *Chem. Abstr.*, 1980, **93**, 36407x.
43. W. Schwartz and J. Gassner, *Berg-Huettenmaenn. Monatsh.*, 1972, **117**, 84; *Anal. Abstr.*, 1973, **24**, 141.
44. W. Koch, E. Buechel and H. Lemm, *Arch. Eisenhuettenwes.*, 1973, **44**, 301; *Anal. Abstr.*, 1973, **25**, 3088.
45. W. H. Herrnstein, *Electr. Furn. Conf. Proc.*, 1975, **32**, 156; *Chem. Abstr.*, 1976, **85**, 86701u.
46. R. B. Fricioni, G. H. Helling and K. E. Burke, *Proc. Natl. Open Hearth Basic Oxygen Steel Conf.*, 1976, **59**, 142; *Chem. Abstr.*, 1977, **87**, 94836y.
47. W. Thomich, *Hydrogen Met., Proc. 2 Int. Congr.* 1977, **1**, F11; *Chem. Abstr.*, 1978, **89**, 84242d.
48. K. H. Schmitz, E. Thiemann and W. Ansmann, in *Analysis of Non-metals in Metals, Proc. Int. Conf.*, 1980, G. Kraft (ed.), de Gruyter, Berlin, 1981.
49. P. Koenig, K. Schmitz and E. Thiemann, *Arch. Eisenhuettenwes.*, 1973, **44**, 41; *Anal. Abstr.*, 1973, **25**, 842.
50. D. A. Berman, W. Beck and J. J. DeLuccia, *Hydrogen Met., Proc. Int. Conf.*, 1973, 595; *Chem. Abstr.*, 1975, **83**, 21645t.
51. G. L. Powell, W. Beck and J. J. DeLuccia, *ibid.*, 585; *Chem. Abstr.*, 1976, **84**, 129923s.
52. V. M. Chistyakov, I. M. Verkhovskii, V. M. Androshchuk and M. M. Smyk, *Zavodsk. Lab.*, 1978, **44**, 641; *Chem. Abstr.*, 1978, **89**, 115183s.
53. J. J. DeLuccia and D. A. Berman, *MCIC Rep.* 1979, MCIC-79-40; *Proc. Tri-Serv. Conf. Corrosion*, 1978, 477; *Chem. Abstr.*, 1979, **91**, 179211y.
54. F. B. Mansfield, *Report SC 5128.2FR, NADC-77112-30*, 1978; *Chem. Abstr.*, 1979, **91**, 133401g.
55. F. B. Mansfield and D. K. Roe, *U.S. Patent*, 4,221,651, 24 June 1979; *Chem. Abstr.*, 1980, **93**, 227623z.
56. L. S. Vshivsteva and T. M. Ovchinnikova, *Zavodsk. Lab.*, 1975, **41**, 32; *Chem. Abstr.*, 1975, **83**, 21554n.
57. Yu. A. Klyachko, V. A. Gvazava, O. D. Larina and E. G. Pakhomova, *ibid.*, 1981, **47**, No. 1, 15; *Chem. Abstr.*, 1981, **94**, 113891a.
58. V. S. Sastri and B. McDonnell, Unpublished data.
59. F. Rauch, H. Baumann, U. Behrens, K. Bethge, H. Schwenk, B. Streb and W. Strohl, in *Analysis of Non-metals in Metals*, G. Kraft (ed.), p. 151. De Gruyter, Berlin, 1981.
60. E. Brauer, R. Doerr, R. Gruner and F. Rauch, *Corros. Sci.*, 1981, **21**, 449.
61. W. A. Lanford, *Proc. Workshop on The Analysis of Hydrogen in Solids*, 23-25 January, 1979, U.S. Dept. Energy, DOE/ER-0026, 1979, p. 75.
62. E. Ligeon, J. P. Bugeat, R. Danielou, J. Fontenille and A. Guivarch, *J. Radioanal. Chem.*, 1980, **55**, 367.
63. J. F. Singleton and N. E. W. Hartley, *ibid.*, 1979, **48**, 317.
64. B. R. Appleton, *Proc. Workshop on The Analysis of Hydrogen in Solids*, 23-25 January, 1979, U.S. Dept. Energy, DOE/ER-0026, 1979, p. 64.
65. K. Farrell and M. B. Lewis, *Scr. Metall.*, 1981, **15**, 661.
66. K. P. Andreeva and G. P. Startsev, *Metod. Issled. Oprod. Gazov. Met.*, 1973, 88; *Chem. Abstr.*, 1975, **83**, 52785t.
67. Yu. S. Kalinin and G. P. Kondrashova, *Fiz.-Khim. Metody Anal.*, 1977, **2**, 48; *Chem. Abstr.*, 1978, **89**, 167288z.
68. V. M. Arshanskaya and M. N. Kaldymova, *Zh. Met.*, 1972, 8K21; *Chem. Abstr.*, 1973, **79**, 87149h.
69. S. M. Toy and A. Phillips, *U.S. Patent*, 3,732,076; *Chem. Abstr.*, 1973, **79**, 13245q.
70. S. M. Toy, *Am. Soc. Test. Mater., Spec. Tech. Publ.*, STP453, 1974, 124; *Chem. Abstr.*, 1975, **82**, 34169v.
71. B. K. Zuev, Yu. A. Kulakov, L. L. Kunin, G. V. Mikhailova and A. Ya. Ryaboi, *Zavodsk. Lab.*, 1977, **43**, 456; *Chem. Abstr.*, 1977, **87**, 26703c.
72. B. K. Zuev, G. N. Kasatkin, Yu. A. Kulakov, L. L. Kunin and G. V. Mikhailov, *Zh. Analit. Khim.*, 1979, **34**, 1714; *Chem. Abstr.*, 1980, **92**, 68945s.
73. P. Stokovszki, S. Larsson and K. E. Easterling, *Met. Sci.*, 1979, **13**, 597.

A CONTINUOUS HYDRIDE-GENERATION SYSTEM FOR DIRECT CURRENT PLASMA ATOMIC-EMISSION SPECTROMETRY (DCP-AES)

DETERMINATION OF ARSENIC AND SELENIUM

PAUL EK and STIG-GÖRAN HULDÉN

Laboratory of Analytical Chemistry, Åbo Akademi, SF-20500 Åbo 50, Finland

(Received 9 June 1986. Revised 21 August 1986. Accepted 29 November 1986)

Summary—A continuously operating hydride-generation system has been developed for determination of volatile hydride-forming elements such as arsenic and selenium by d.c. plasma atomic-emission spectrometry. Arsenic and selenium are converted into their hydrides by reduction with sodium borohydride. The hydrides evolved are stripped from the liquid phase in a gas/liquid separator and are continuously fed into the d.c. plasma by a small argon stream. Under optimized operating conditions the detection limits ($3s$) obtained for arsenic and selenium are 0.3 and 0.5 $\mu\text{g/l.}$, respectively. The precision at the 5 $\mu\text{g/l.}$ level is better than 4% r.s.d. The measurement time, including sample introduction and three replicate measurements with 5-sec integration per sample is about 1 min. The effects of well known interferences such as copper and nickel have been investigated. For minimizing their interference continuous addition of 1,10-phenanthroline as masking agent has been found useful. The method has been tested by its use for analysing NBS standard reference materials.

The dual nature of arsenic and selenium, as essential elements in trace amounts^{1,2} and extremely toxic elements at slightly higher concentrations³ has increased the importance of reliable determination of these elements in biological and environmental materials. Among the analytical methods proposed for their determination at trace levels the hydride-generation technique in combination with atomic-absorption spectrometry (AAS) and more recently with inductively-coupled plasma atomic-emission spectrometry (ICP-AES) has become frequently used.⁴ A comprehensive review of the hydride-generation technique, including a number of approaches for determination of arsenic, selenium and similar elements in different materials, has been given by Godden and Thomerson.⁵

Although most of the hydride-generation/AAS applications are manual batch methods there has for a long time been an interest in development of automated systems⁶⁻¹⁰ based on the continuous flow principle. The analytical response in these continuously operating systems is measured in a steady state which allows a precise and accurate measurement of the intensity of the analytical line and of the background.

In the last few years such systems have also found increasing popularity in atomic-fluorescence¹⁰ and inductively-coupled plasma atomic-emission spectrometry.¹¹⁻¹⁶

Only a few papers involving d.c. plasma atomic-emission spectrometry in combination with hydride generation¹⁷⁻¹⁹ have been reported; however. To the best of our knowledge the first use of continuous hydride generation with d.c. plasma emission de-

tection was described by Panaro and Krull.¹⁸ In their system the analyte hydride was introduced directly into the conventional spray chamber of the DCP-instrument. The detection limit for arsenic was reported to 10-25 $\mu\text{g/l.}$, compared with 250 $\mu\text{g/l.}$ by direct DCP analysis without the hydride-formation step. The method also showed good agreement with both continuous and batch type hydride/AAS methods.

In the method proposed here the spray chamber of the spectrometer is by-passed and the analyte hydride is introduced through a gas/liquid separator directly into the d.c. plasma. This is made possible by a slight modification of the sample-introduction tube of the spectrometer.

The main aim of the present work was to develop a continuously operating hydride-generation system easily attachable to the DCP-spectrometer for determination of volatile hydride-forming elements in a wide range of materials. This report describes the application of the system to determination of arsenic and selenium in biological samples.

EXPERIMENTAL

Reagents

The chemicals used for preparation of the reagents and standards were of analytical reagent grade and were used without further purification. All solutions were made up in demineralized water from a Milli-Q system (Millipore Inc.)

Stock solutions of As(III) and Se(IV), 1000 mg/l., were prepared by dissolving 1.320 g of arsenic(III) oxide and 1.406 g of selenium dioxide in 20 ml of 6M hydrochloric acid and diluting to 1000 ml. Stock solutions of As(V) and Se(VI) were similarly prepared from $\text{Na}_2\text{HAsO}_4 \cdot 7\text{H}_2\text{O}$ and

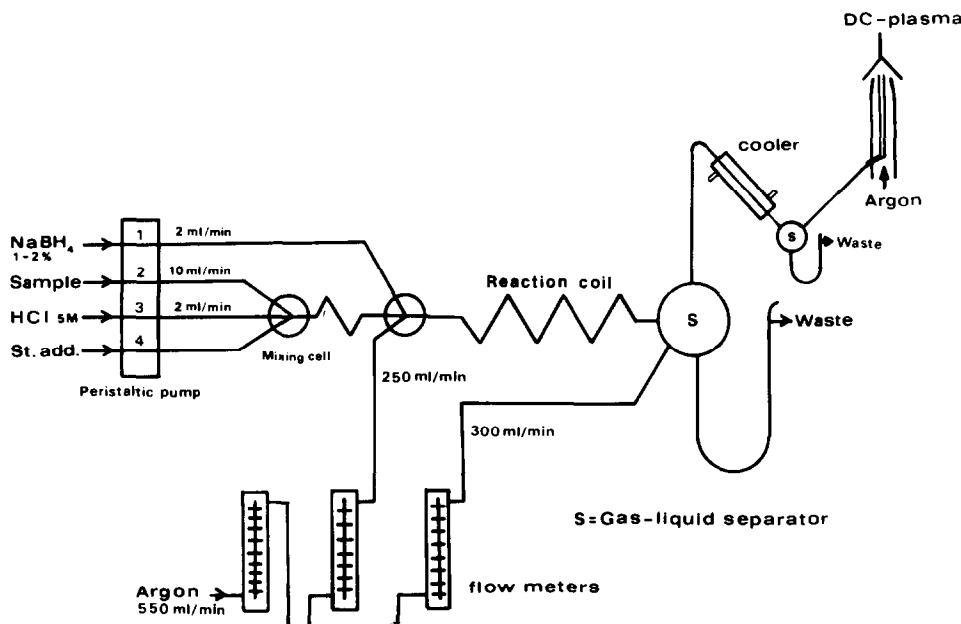


Fig. 1. Schematic diagram of the continuous DCP-hydride system.

$\text{Na}_2\text{SeO}_4 \cdot 10\text{H}_2\text{O}$. Standard working solutions of lower concentrations were made up by serial dilution with 0.1M hydrochloric acid. The standard solutions of lower concentration than $100 \mu\text{g/l}$. were prepared daily before use.

A 1% solution of sodium borohydride was prepared by dissolving 10 g of NaBH_4 pellets (Spectrosol R, BDH) and 4 g of sodium hydroxide in 100 ml of water. After filtration through a $0.45\text{-}\mu\text{m}$ membrane filter the solution was diluted to 1000 ml and stored in a polyethylene bottle in the dark, until use. The addition of alkali is necessary for minimizing hydrolysis of the sodium borohydride. The solution is stable for several days.

The test solutions were continuously acidified with 5M hydrochloric acid before mixing with the borohydride solution stream, as shown in Fig. 1.

A 0.1M 1,10-phenanthroline solution in 0.1M hydrochloric acid was prepared as masking agent for copper and nickel.

Apparatus

Plasma emission spectrometer. The instrument used for the measurements was a d.c. plasma atomic-emission spectrometer, the SpectraSpan III B (Spectrametrics, Inc., Andover, MA) operated in the sequential analysis mode. A detailed description of a similar instrument has been given elsewhere.^{20,21}

The DCP-spectrometer was equipped with a dynamic background compensator (DBC-33) for emission-line profiling and background-compensated measurements. To improve the collection, processing and presentation of analytical data from the spectrometer a Basic programmable microcomputer (HP-85, Hewlett Packard Co.) was interfaced to the spectrometer. The program software needed for the operation control has been evaluated by Sara.²² For control purposes the emission signals were also recorded graphically by a strip-chart recorder.

The continuous hydride-generator. The construction of the hydride-generation apparatus is schematically shown in Fig. 1. The module can be quickly and conveniently interfaced to the DCP-spectrometer.

In operation, the sample solution and the reagents, 5M hydrochloric acid and 1% sodium borohydride solution, are

pumped by a multichannel peristaltic pump (Gilson Minipuls 2, Medical Electronics) fitted with silicone-rubber tubing into two separate Teflon (PTFE) mixing cells.

An additional line (line 4 in the manifold), used for continuous standard-addition measurements or for the continuous addition of extra reagents (e.g., masking agents) to the sample stream, is also built into the system.

The mixing cells are connected through a short (10 cm long, 3.7 mm bore) mixing coil made of Teflon tubing. The sample solution is continuously acidified with the hydrochloric acid before it is combined and mixed with the reductant in the second cell. The rapid evolution of hydrogen at this stage causes formation of small gas pockets that segment the liquid stream during its passage through the reaction coil. The reaction coil is made of Teflon tubing with a bore of 3.7 mm and length of 1.5 m. The slow argon stream (flow-rate 0.25 l./min) further speeds up the transport of the gas-liquid mixture to the phase-separator.

Commercial grade argon (99.5%) is used as carrier gas. To obtain reproducible operating conditions the separate gas flows are controlled by three calibrated rotameters (Brooks Instrument B.V., Veenendaal). A second stream of argon (flow-rate 0.30 l./min) which emerges under the liquid level of the phase-separator is used to increase the efficiency of the stripping of the analyte hydride from the liquid. The phase-separator is described in detail in Fig. 2.

Before the gas stream enters the plasma it passes through a condenser for removal of moisture that otherwise could condense on the walls of the Teflon tube that connects the second phase-separator with the sample introduction tube. The condensed water is separated from the gas stream in the second phase-separator.

A specially designed sample introduction tube aligned in the optical path of the spectrometer delivers the analyte hydride directly into the excitation zone of the d.c. plasma (Fig. 3). The removable capillary tube is adjusted to be about 1 mm above the tip of the sample introduction tube. By removal of the upper part of the capillary tube and obstruction of the hydride inlet of the sample introduction tube, the DCP-spectrometer is conveniently changed from hydride operation to the conventional DCP-analysis mode. The remaining part of the capillary tube does not interfere

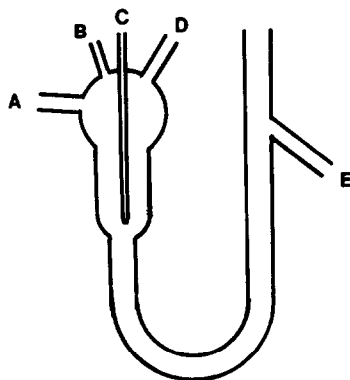


Fig. 2. The gas-liquid phase-separator: (A) inlet for hydride and carrier gas; (B) inlet for wash solution; (C) auxiliary carrier gas; (D) gas exit to d.c. plasma; (E) drain.

in the ordinary use of the DCP-spectrometer. The capillary tube, sample introduction tube, condenser and phase-separators are all constructed of borosilicate glass.

Analytical procedures

DCP-hydride analysis. The DCP-spectrometer is changed from the conventional analysis mode to hydride operation simply by connecting the hydride outlet tube to the sample introduction tube and inserting the small capillary tube as already described. The optimized operating conditions for arsenic and selenium are given in Table 1. Before the peristaltic pump is started the carrier-gas valves are opened and the argon and liquid flow-rates are set to the recommended values. The d.c. plasma is ignited and the analytical wavelength is located by aspirating a 1000 $\mu\text{g/l}$. standard solution and observing the steady-state signal on the strip-chart recorder. When the wavelength setting has been adjusted, a blank solution is introduced in order to set the base-line level. The spectrometer is then turned to the integration mode and the instrument is calibrated in the usual way by aspirating the high and low standards. The DCP-hydride system is then ready for use.

Sample preparation. For determination of arsenic and selenium by the hydride-generation technique selenium must be present as Se(IV) and arsenic preferably as As(III) in the sample solution. In most biological samples, however, these elements may exist as resistant organo-arsenic and organo-selenium compounds²³⁻²⁵ which require very harsh conditions for their destruction. Among the various procedures recommended in the literature for decomposition of different biological materials, wet digestions with nitric-perchloric acid^{19,24,26} and nitric-perchloric-sulphuric acid^{12,25,26} are perhaps the most frequently used. The decom-

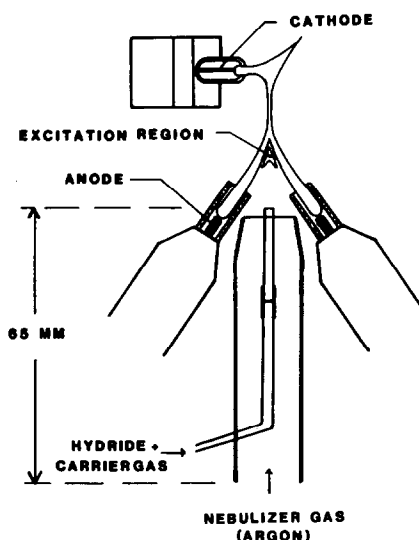


Fig. 3. Introduction of analyte hydride into d.c. argon plasma.

position method used in this work was modified essentially from the procedure reported by Verlinden²⁴ and the biological samples analysed were pretreated as follows. The samples (0.5–1.0 g) were accurately weighed into 50- or 100-ml standard flasks, then 10 ml of 65% nitric acid were added and the samples were left overnight at room temperature, to prevent foaming in the subsequent treatment. The flasks were then placed on a temperature- and time-controlled electrically heated sand-bath, their necks being fitted with 15-cm long borosilicate air-condensers to ensure effective reflux of acid vapours. To minimize the risk of charring, the temperature was first increased slowly to 140° during 2 hr. After cooling and addition of 5 ml of 70% perchloric acid the temperature of the solutions was raised to 210°. The samples were boiled at this temperature until their volumes were reduced to about 5 ml. The flasks were then removed from the sand-bath and allowed to cool. During this treatment arsenic and selenium are oxidized to their highest oxidation state. To reduce selenate to selenite 5 ml of concentrated hydrochloric acid were added and the solutions were boiled for 5 min. After cooling to room temperature the solutions were made up to volume and stored in polyethylene bottles until use. Reagent blanks were simultaneously prepared with the amounts of acids used in the decomposition procedure. The reagent blanks were used as low standards in the calibration of the DCP-hydride system.

Table 1. Operating conditions for determination of arsenic and selenium

DCP spectrometer		Hydride generator	
Power supply (d.c.)	7 A, 40 V	Sample flow	10.0 ml/min
Plasma gas (argon)	7 l./min	NaBH ₄ flow	2.0 ml/min
Nebulizer pressure	15 psig	NaBH ₄ conc.	1% (in
Sleeve pressure	50 psig		0.1 M NaOH)
Slit size:		HCl flow	2.0 ml/min
Entrance	300 × 200 μm (w × h)	HCl conc.	5.0 M
Exit	100 × 300 μm (w × h)	Carrier gas	argon
Photomultiplier voltage	300 V	Total flow:	550 ml/min
Integration time:		Reaction coil	250 ml/min
Direct mode	3 sec	Phase separation	300 ml/min
Integrated mode	3 × 5 sec		
Analytical wavelength:			
Arsenic	228.812 nm (193.696 nm)		
Selenium	196.026 nm		

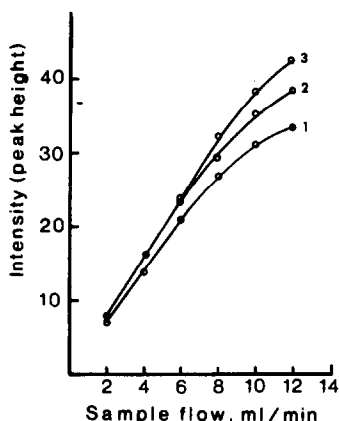


Fig. 4. Effect of the sample flow-rate on the sensitivity for 100 µg/l. As(III). Reductant (2% NaBH₄) flow: (1) 0.5 ml/min; (2) 1.0 ml/min; (3) 2.0 ml/min. For other parameters see Table 1.

Interference studies. The interference of Cu(II) and Ni(II) under the experimental conditions given in Table 1 was studied by analysing 10-µg/l. standard solutions of As(III) and Se(IV) spiked with known amounts of the interfering metal ions. To control the precision of the measurements an interferent-free standard solution of the analyte was analysed both before and after each test solution. This strategy was found necessary since at higher interferent concentrations [> 10 mg/l. Cu(II), > 100 mg/l. Ni(II)] the reaction coil became "poisoned" with accumulated metallic precipitates. The subsequent analysis of the interferent-free control solutions suffered from series signal depression. In such cases the coil was reconditioned by repeated washing with a 1:1 v/v mixture concentrated hydrochloric and nitric acids, and water, introduced into the system through line 1.

Since it was observed that copper and nickel interfered even at very moderate concentrations (see Fig. 8, later), the effect of 1,10-phenanthroline as masking agent was tested. A 0.1M 1,10-phenanthroline solution was therefore continuously added at a rate of 2 ml/min through line 4 to the sample stream. After recalibration of the system the analysis of the spiked test solutions was repeated.

RESULTS AND DISCUSSION

Optimization of operating conditions

To maximize the analytical sensitivity and precision the steps of the hydride-generation process

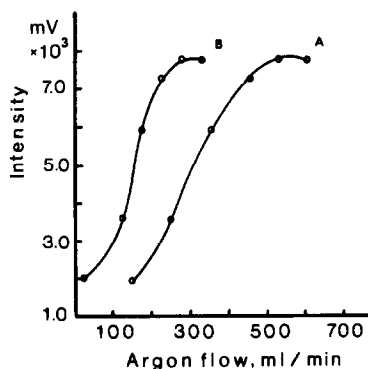


Fig. 5. Effect of carrier-gas flow-rate on sensitivity for 1000 µg/l. Se(IV). (A) total argon flow; (B) subflow through the reaction coil. Conditions: see Table 1.

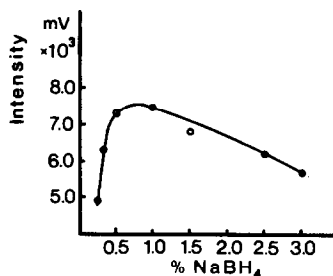


Fig. 6. Effect of NaBH₄ concentration on analyte signal. Analyte: 1000 µg/l. Se(IV) at 10.0 ml/min. NaBH₄ flow 2.0 ml/min. For other parameters see Table 1.

were examined in detail. The parameters investigated were the sample and carrier-gas flow-rates, the concentration and flow-rates of the sodium borohydride solution and hydrochloric acid, and the length and diameter of the reaction coil. Also different types of mixing cells, phase-separators and sample introduction tubes were developed and tested.

Figures 4–7 illustrate the effect of variation of a number of system parameters on the emission signal. Obviously the most critical are the rate of sample introduction and the flow-rate of the carrier gas.

Although theoretically the signal response is further increased at higher sample flow-rates, a sample introduction rate of 10 ml/min was selected to keep the sample consumption at a reasonable level. Because the pumping rate can be regulated and there is a constant ratio between the sample and the reagent flow-rates the sample consumption can easily be reduced to any desired level without affecting the solution conditions. Therefore, when the detection power is not critical but the available sample volume is limited, the possibility to reduce both sample and reagent consumption is an important benefit. Thus the sample flow-rate chosen will always be a compromise depending on the available sample volume and the concentration of the analyte.

The influence of the total carrier gas flow was studied over the range 150–650 ml/min. Above 650 ml/min gas flow the geometry of the DCP discharge was heavily distorted and at argon flows less

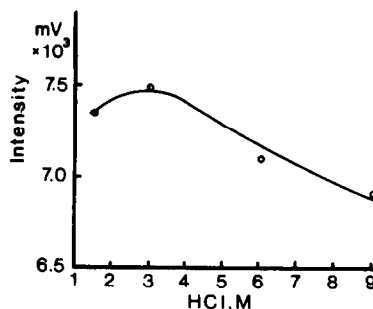


Fig. 7. Effect of HCl concentration on analyte signal. Analyte: 1000 µg/l. Se(IV) at 10.0 ml/min. HCl flow-rate 2.0 ml/min. The other parameters adjusted according to Table 1.

than 300 ml/min only a small fraction of the generated hydride entered the excitation region. The remainder was distributed around the plasma, resulting in very low emission signals. The best response was obtained at a total argon flow of 550 ml/min (Fig. 5, curve A).

The effects of sodium borohydride and hydrochloric acid on the analyte signal are plotted in Figs. 6 and 7. For generation of selenium hydride the optimal NaBH_4 and HCl concentrations are about 1% and 3–4M, respectively. Similar patterns have been observed by other workers using continuous hydride generation.^{8,9,11,14}

At higher NaBH_4 concentrations there is a distinct decrease of the emission signal. According to Thompson *et al.*¹¹ this is due to dilution of the analyte hydride or change in the plasma conditions by excess of hydrogen. Very high sodium borohydride levels (3–5%) caused some instability of the plasma but did not extinguish it.

One of the main purposes of the continuous introduction of hydrochloric acid is to permit uninterrupted production of hydrogen during the change of samples or standard solutions. This increases the stability of the system and reduces the analysis time. Another purpose is to adjust the pH of the sample or standard solution to about the same level before they are mixed with the reductant solution. Large differences in acidity between the sample solutions and standards will result in unequal hydrogen gas evolution, and this may affect the plasma position and cause shifts of the background. Although the signal response is somewhat lower at higher acidities we prefer to use 5M hydrochloric acid to ensure adequate levelling of the acidity of the samples and standards. The optimal conditions are summarized in Table 1.

Calibration, detection limits and precision

The performance of the method was assessed by analysis of laboratory standard solutions of As(III) and Se(IV). Calibration for both elements was done with the 1000 $\mu\text{g/l}$. solution as high standard and the blank solution as low standard. The linearity of calibration was established by analysing intermediate standards at 5, 10, 50, 100 and 500 $\mu\text{g/l}$. concentration.

The detection limits were taken as the concentrations corresponding to a net signal equal to three times the standard deviation of the blanks (determined with 10 replicates), and for arsenic and selenium were 0.3 and 0.5 $\mu\text{g/l}$. respectively. For both elements the precision (r.s.d.) at the 5- $\mu\text{g/l}$. level was 3–5% and at the 50- $\mu\text{g/l}$. level 1–3%. The analytical range¹⁰ for which the r.s.d. is < 10% is 1.5–1000 $\mu\text{g/l}$. At a sample introduction rate of 10 ml/min a stable and continuous emission signal is obtained within 10–15 sec after introduction of the analyte. Approximately the same time is required for the signal to reach the base-line level when the sample intro-

duction is interrupted. The sample throughput rate is thus about one sample or standard per minute for 5-sec integration and three replicate measurements per sample or standard.

Interferences from copper and nickel

One of the main drawbacks of the hydride-generation technique is the interference caused by a number of metal ions, especially transition metal ions of groups VIII and IB.^{27–33} These metal ions interfere in the liquid phase during the hydride-generation step. The interference is regarded as due to reduction of the interferent ions by sodium borohydride to finely dispersed metallic precipitates by which the evolved analyte hydride is captured and decomposed, forming insoluble metal arsenides and selenides.³⁰ In addition, interferences arising from the hydride-forming elements are also well known.^{27,34} Although the papers cited above all deal with interferences in hydride/AAS, similar interference effects have also been reported for the hydride/ICP^{13,16} and hydride/DCP^{17,19} methods. In hydride/AAS, however, processes occurring in the gas phase in the atomizer tubes,³⁵ e.g., molecule formation between analyte and matrix hydrides, result in incomplete atomization of the analyte. Owing to the high atomization and excitation temperature attainable in the DCP and ICP this type of gas-phase interference is very unlikely in these hydride systems.

Of the more common concomitants in biological and environmental matrices, copper and nickel are known as serious interferents in determination of arsenic and selenium by the hydride-generation method. Because the degree of the interferences seems to depend on the hydride-generator design and the reagent and acid concentrations,^{29,30} it is important to determine the threshold concentrations at which Cu(II) and Ni(II) start to interfere. Standard solutions of As(III) and Se(IV) (10 $\mu\text{g/l}$.) were therefore spiked with known amounts of the interfering metal ions and taken through the analytical procedure. Figure 8 shows the results. If a signal change of $> \pm 10\%$ between the interferent-free and the spiked solutions is taken as the criterion for interference,²⁷ copper and nickel begin to interfere in the deter-

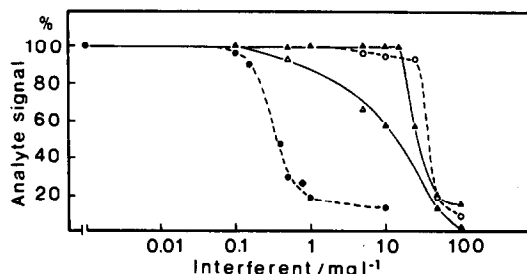


Fig. 8. Influence of copper and nickel concentration on analyte recovery. Conditions: see Table 1. (—●—) 10 $\mu\text{g/l}$. Se(IV) in presence of Cu(II); (△—△) 10 $\mu\text{g/l}$. Se(IV) in presence of Ni(II); (—○—) 10 $\mu\text{g/l}$. As(III) in presence of Cu(II); (▲—▲) 10 $\mu\text{g/l}$. As(III) in presence of Ni(II).

mination of Se(IV) at concentrations of *ca.* 160 and 750 $\mu\text{g/l}$, respectively. The effective hydrochloric acid and sodium borohydride concentrations were *ca.* 0.7M and 0.07%.

For As(III) 10% signal suppression was observed for 18 mg/l. Ni(II) and 25 mg/l. Cu(II), in good agreement with the results reported by Meyer *et al.*²⁹ and Welz and Melcher³⁰ for the hydride/AAS technique. The same authors have also shown that higher concentrations of copper and nickel can be tolerated if the determinations are done at higher acid concentrations (*e.g.*, 5M). Since it was not possible to achieve a such high effective acid concentration in our system, alternative methods for increasing the tolerance limit for the interferents were looked for.

Effect of masking

Besides use of standard additions^{8,31} or separation of the analyte by co-precipitation with lanthanum hydroxide, use of masking agents has also been proposed^{32,33} for dealing with the interference of copper and nickel. On account of the relatively high acidity normally required for hydride generation, especially for generation of hydrogen selenide, the choice of masking agent becomes critical.

Although the best masking effects are generally attained at rather high pH values there are some weakly basic reagents such as thiosemicarbazide and 1,10-phenanthroline which are also effective in acid solution.³⁶ The masking ability of a complexation reagent at different pH values can easily be judged from the α -coefficients calculated according to Ringbom.³⁶ For 0.01M 1,10-phenanthroline the $\log \alpha_{\text{M(L)}}$ values for Cu(II) and Ni(II) at pH 0 are relatively high, 2.6 and 4.2, respectively, indicating that these metal ions should be complexed by the reagent even at very low pH values. This has been confirmed in practice by Kirkbright and Taddia for masking copper and nickel in the determination of arsenic³² and recently by Chan and Baig³³ for masking Cu(II) and Ni(II) in determination of selenium.

Figure 9 shows that masking with 1,10-phenanthroline is satisfactory in the present hydride-generation system. In the determination of selenium the tolerance limit for Cu(II) is increased to at least 2 mg/l. and that for Ni(II) to 100 mg/l. Similarly a practically interference-free determination of arsenic is possible in the presence of at least 75 mg/l. Ni(II).

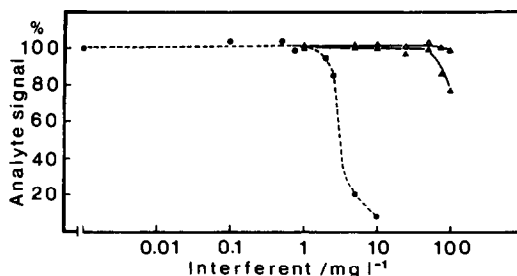


Fig. 9. The effect of on-line addition of 0.1M 1,10-phenanthroline as masking agent for copper and nickel in determination of arsenic and selenium. Conditions: see Table 1. (—●—) 10 $\mu\text{g/l}$. Se(IV) in presence of Cu(II); (—△—) 10 $\mu\text{g/l}$. Se(IV) in presence of Ni(II); (▲—▲) 10 $\mu\text{g/l}$. As(III) in presence of Ni(II).

The potential effects of even higher interferent concentrations were not tested because of the risk of obtaining metallic precipitates in the reaction coil tubing, and subsequent contamination of the system. On the other hand such experiments were not considered necessary because such high concentrations of copper and nickel are unlikely to occur in biological materials. Increasing the effective concentration of the masking agent, however, might allow still higher interferent concentrations to be tolerated.

Results for biological samples

The reliability of the method for analysis of real samples was tested by analysing certified reference materials, NBS 1573 Tomato Leaves and NBS 1577 Bovine Liver. About 500-mg samples (3 replicates of both materials) were accurately weighed out and treated according to the procedure described above. The results obtained are summarized in Table 2.

For arsenic in the tomato leaves the result is in satisfactory agreement with the certified value. No reliable results could be obtained for selenium in the tomato leaves or arsenic in the bovine liver because their concentrations in the prepared sample solutions were of the same order of magnitude as the detection limits. The value for selenium in the bovine liver was rather low, only about 72% of the certified value, but the precision was acceptable. Because of this low value, experiments were done to find whether losses might occur during the sample decomposition. Human scalp hair was used as test material because of limited availability of the bovine liver reference

Table 2. Determination of arsenic and selenium in NBS standard reference materials

Sample	Element	Test no.	Sample taken, mg/50 ml	Found		Certificate value, $\mu\text{g/g}$	Recovery, %
				$\mu\text{g/l.}^*$	$\mu\text{g/g}$		
NBS 1573 Tomato leaves	As	1	533.9	2.50 ± 0.28	0.23 ± 0.03	0.27 ± 0.05	85.2
		2	502.7	2.54 ± 0.25	0.25 ± 0.03		92.6
		3	614.3	3.28 ± 0.23	0.27 ± 0.02		100.0
NBS 1577 Bovine Liver	Se	1	501.6	7.94 ± 0.57	0.79 ± 0.06	1.10 ± 0.10	71.8
		2	466.4	7.48 ± 0.34	0.80 ± 0.03		72.7
		3	403.4	6.19 ± 0.36	0.77 ± 0.04		70.0

*Each value represents the mean \pm standard deviation obtained from three 5-sec integrations per replicate.

Table 3. Recovery of arsenic and selenium from a human scalp hair sample spiked with As(III) and Se(IV) before wet digestion in HNO₃ and HClO₄

Test no.	Sample taken, g/100 ml	Arsenic			Selenium		
		Added, µg/l.*	Found, µg/l.†	Recovery, %	Added, µg/l.*	Found, µg/l.†	Recovery, %
1	1.1074	—	1.6 ± 0.4	—	—	2.1 ± 0.2	—
2	0.8893	10.0	10.8 ± 0.1	93.1	10.0	10.2 ± 0.4	84.3
3	0.8892	10.0	11.5 ± 0.2	99.1	10.0	9.9 ± 0.2	81.8
4	1.1915	10.0	11.5 ± 0.4	99.1	10.0	10.9 ± 0.9	90.0

*Added as 1000-µl increments of 1000 µg/l. standard solutions of As(III) and Se(IV).

†Each value is the mean ± standard deviation based on three 5-sec integrations per replicate.

sample. The hair, obtained from the same person, was cleaned by washing with an acetone/alcohol mixture and rinsed with water. After drying, four 1-g portions of the hair were weighed into 100-ml standard flasks, 1.00 ml of a 1000 µg/l. standard solution of As(III) and Se(IV) was added to each flask and the samples were decomposed and analysed according to the procedure already described. The results (Table 3) show an acceptable recovery for arsenic, but the selenium values are again rather low.

The low selenium values are not a result of volatilization losses or incomplete reduction of Se(VI), since experiments with pure Se(IV) standard solutions digested and handled as above resulted in selenium recoveries between 98 and 102%. We believe that the negative systematic errors obtained for selenium in the hair samples as well as the bovine liver samples are caused by interference from endogenous copper in the sample matrix.

To test this hypothesis the hair and the NBS bovine liver samples were analysed for copper by the conventional DCP-AES technique. The mean copper content of the hair was found to be 21.4 ± 2.3 µg/g (3 replicates) corresponding to 0.20 ± 0.01 mg/l. in the sample solution. For NBS bovine liver the mean solution concentration of copper (4 replicates) was 1.67 ± 0.22 mg/l., equivalent to 209 ± 2 µg/g in the sample, which is in fair agreement with the certified value of 193 ± 10 µg/g. Comparison of these relatively high copper concentrations with the tolerance limit for copper (Fig. 8) shows that the low selenium recoveries must be attributed to the interference from copper. The tolerance limit for nickel is so much higher that interference from this element is unlikely.

Low values for selenium in NBS Bovine Liver have

also been observed by other workers using hydride/AAS methods. Egaas and Julshamn³¹ found a 17% suppression of the selenium signal which they explained as due to interference by copper and iron being present at concentrations above 1 mg/l. They compensated for the interferences by the method of standard additions. Subramanian and Meranger⁹ also reported a rather low recovery (84%) for selenium in NBS Bovine Liver.

In an attempt to increase the selenium recovery the bovine liver was analysed with on-line addition of 1,10-phenanthroline as masking agent. Table 4 shows that a recovery of 85–97% was thus obtained.

Conclusions

The results of this work show that continuous hydride-generation in combination with DCP-AES offers a convenient and sensitive method for determination of arsenic and selenium. The hydride-DCP method is about 100 times more sensitive than the conventional DCP-AES technique. The wide linear calibration range eliminates time-consuming dilutions. Interferences from transition metals such as copper and nickel can be reduced by masking with 1,10-phenanthroline.

REFERENCES

1. F. H. Nielsen, in *Advances in Nutritional Research*, Vol. 3, H. H. Draper (ed.), Chapter 6, Plenum Press, New York, 1980.
2. J. E. Spaltholtz, J. L. Martin and H. E. Ganther (eds.), *Selenium in Biology and Medicine*, AVI Publishing Co., Westport, CT, 1981.

Table 4. Determination of selenium in NBS 1577 Bovine Liver in the presence of 1,10-phenanthroline as masking agent for reducing interference by copper

Test no.	Sample taken, mg/50 ml	Selenium found		Certificate value, µg/g	Recovery, %
		µg/l.*	µg/g		
1	421.2	8.98 ± 0.12	1.07 ± 0.01	1.10 ± 0.10	97.3
2	271.5	5.17 ± 0.21	0.94 ± 0.02		85.4
3	346.2	6.70 ± 0.87	0.97 ± 0.09		88.2

*Each value represents the mean ± standard deviations from three 5-sec integrations per replicate.

3. B. A. Fowler, in *Toxicology of Trace Elements*, R. A. Goyer and M. A. Mehlman (eds.), Chapter 3, Hemisphere Publishing Co., Washington, DC, 1977.
4. W. B. Robbins and J. A. Caruso, *Anal. Chem.*, 1979, **51**, 889A.
5. R. G. Godden and D. R. Thomerson, *Analyst*, 1980, **105**, 1137.
6. K. T. Kan, *Anal. Lett.*, 1973, **6**, 603.
7. P. D. Goulden and P. Brooksbank, *Anal. Chem.*, 1974, **46**, 1431.
8. P. N. Vijan and G. R. Wood, *Talanta*, 1976, **23**, 89.
9. K. S. Subramanian and J. C. Méranger, *Analyst*, 1982, **107**, 157.
10. L. Ebdon and J. R. Wilkinson, *Anal. Chim. Acta*, 1982, **136**, 191.
11. M. Thompson, B. Pahlavanpour, S. J. Walton and G. F. Kirkbright, *Analyst*, 1978, **103**, 568.
12. P. D. Goulden, D. H. J. Anthony and K. D. Austen, *Anal. Chem.*, 1981, **53**, 2027.
13. D. D. Nygaard and J. H. Lowry, *ibid.*, 1982, **54**, 803.
14. E. de Oliveira, J. W. McLaren and S. S. Berman, *ibid.*, 1983, **55**, 2047.
15. E. Pruszkowska, P. Barrett, R. Ediger and G. Wallace, *At. Spectrosc.*, 1983, **4**, 94.
16. T. Nakahara, *Anal. Chim. Acta*, 1981, **131**, 73.
17. A. Miyazaki, A. Kimura and Y. Umezaki, *ibid.*, 1977, **90**, 119.
18. K. W. Panaro and I. S. Krull, *Anal. Lett.*, 1984, **17**, 157.
19. H. Hayrynen, L. H. J. Lajunen and P. Perämäki, *At. Spectrosc.*, 1985, **6**, 88.
20. J. Reednick, *Intern. Lab.*, 1979, May, 127.
21. R. J. Dellefield and T. D. Martin, *At. Spectrosc.*, 1982, **3**, 165.
22. R. Sara, in *The 9th Nordic Atomic Spectroscopy and Trace Element Conference (NASTEC)*, Reykjavik, Iceland, 1983, p. 62.
23. C. E. Stringer and M. Attrep, Jr., *Anal. Chem.*, 1979, **51**, 731.
24. M. Verlinden, *Talanta*, 1982, **29**, 875.
25. B. Welz and M. Melcher, *Anal. Chem.*, 1985, **57**, 427.
26. J. W. Jones, S. G. Capar and T. C. O'Haver, *Analyst*, 1982, **107**, 353.
27. A. E. Smith, *ibid.*, 1975, **100**, 300.
28. F. D. Pierce and H. R. Brown, *Anal. Chem.*, 1977, **49**, 1417.
29. A. Meyer, Ch. Hofer, G. Tölg, S. Raptis and G. Knapp, *Z. Anal. Chem.*, 1979, **296**, 337.
30. B. Welz and M. Melcher, *Analyst*, 1984, **109**, 569.
31. E. Egaas and K. Julshamn, *At. Abs. Newsl.*, 1978, **17**, 135.
32. G. F. Kirkbright and M. Taddia, *Anal. Chim. Acta*, 1978, **100**, 145.
33. C. C. Y. Chan and M. W. A. Baig, *Anal. Lett.*, 1984, **17**, 143.
34. B. Welz and M. Melcher, *Anal. Chim. Acta*, 1981, **131**, 17.
35. K. Dittrich, R. Mandry, Ch. Udelnow and A. Udelnow, *Z. Anal. Chem.*, 1986, **323**, 793.
36. A. Ringbom, *Complexation in Analytical Chemistry*, Interscience, New York, 1960.

SHORT COMMUNICATIONS

USE OF CHELEX 100 IN DETERMINATION OF BISMUTH IN SULPHIDE ORES, CONCENTRATES, METALS AND ALLOYS

J. S. ADSUL, C. C. DIAS, S. G. IYER and CH. VENKATESWARLU
Analytical Chemistry Division, Bhabha Atomic Research Centre, Bombay 400085, India

(Received 21 February 1986. Revised 18 December 1986. Accepted 16 January 1987)

Summary—In the determination of bismuth, Chelex 100 has been successfully employed for reducing the concentration of matrix and interfering elements from sulphide ores and concentrates and for separation of the matrix elements from bismuth in the analysis of high-purity copper, silver and silver-cadmium alloy.

Traces of bismuth in copper and nickel have been separated by use of a carboxylic acid ion-exchanger, ZeoKarb 226.¹ Blount *et al.*² have employed Chelex 100 in the determination of bismuth in silicate rocks. It was found in our laboratory that Chelex 100 (Batch No. 7949) exhibited very high sorption of bismuth and a few other metal ions from solutions at pH 1.0,³ but it was subsequently found that this batch of exchanger was bifunctional, whereas later batches (Nos. 14930 and 20958) were monofunctional.⁴ This communication describes further studies on the distribution of bismuth at still higher acidities with the monofunctional exchanger and the determination of bismuth in sulphide ores, concentrates and high purity copper, silver and silver-cadmium alloy.

EXPERIMENTAL

Bismuth solution

An approximately 50-mg/ml solution of bismuth in 0.5M nitric acid was prepared from the nitrate, and standardized;⁵ from this a working solution with 10 µg/ml bismuth concentration was prepared by suitable dilution.

Ion-exchanger

Chelex 100 (Batch No. 20958) was prepared in H⁺ form.³

Procedure

Lead and zinc ores and concentrates. Weigh accurately 0.5 g of sample into a 100-ml beaker. Wet it with water and add 20 ml of 20% v/v nitric acid. Boil gently until the volume is reduced to about 5 ml. Add 1 ml of concentrated perchloric acid and heat to fumes to remove excess of the acid. Cool, add 0.8 ml of concentrated nitric acid, dilute to about 30 ml, boil and filter through a Whatman No. 40 (9 cm) paper. Wash the residue with 20 ml of 0.25M nitric acid. Pass the combined filtrate and washings through the

ion-exchange column (0.9 × 5 cm) at a flow-rate of 1 ml/min. Wash the column with 50 ml of 0.25M nitric acid and reject the effluent. Elute bismuth from the column with 75 ml of 2M nitric acid at the same flow-rate and determine it spectrophotometrically.^{6*} If the bismuth content is very low (ppm range), determine it by AAS with hydride generation.⁷

Copper, silver and silver-cadmium alloy. Dissolve 1.0 g of sample in concentrated nitric acid and evaporate the solution just to dryness. Dissolve the residue in 2 ml of 40% v/v nitric acid, dilute to about 50 ml and proceed with the ion-exchange procedure as above.†

RESULTS AND DISCUSSION

Since the distribution ratios (K_d) for Hg(II), Au(III) and Mo(VI) are also high ($> 10^3$),³ that for bismuth was determined at various acidities by the batch method. From the results a nitric acid concentration of 0.25M seemed suitable for the quantitative sorption of bismuth, and the K_d values of other cations were determined at this acidity. The results in Table 1 show that bismuth cannot be separated from gold, molybdenum and mercury by Chelex 100 even at this acidity.

Table 1. Batch method K_d values (cation 1.00 mg/25 ml; 0.25 g of Chelex 100; 48 hr equilibration)

Cation	[HNO ₃],	
	M	K_d
Bi(III)	0.10	$> 10^4$
	0.20	6000
	0.25	2700
	0.30	1400
	0.40	550
	0.50	250
	1.0	15
	2.0	nil
Au(III)	0.25	$> 10^4$
Mo(VI)	0.25	$> 10^4$
Hg(II)	0.25	1950
In(III)	0.25	56
Fe(III)	0.25	30
Cu(II)	0.25	10
Ga(III)	0.25	10
Ag ⁺ , Zn ²⁺ , Cd ²⁺ , Pb ²⁺	0.25	< 10

*If the copper content of the aliquot used for the spectrophotometry is more than 1.0 mg, a turbidity appears, which may be centrifuged out.

†In the case of high-purity copper, dissolve the residue in 100 ml of 0.25M nitric acid containing 3 g of 1,10-phenanthroline. This is required because about 10 mg of copper will be retained on the column when 1.0 g of copper sample is taken.

Table 2. Ion-exchange separation of cations (100 mg) from 100 μg of Bi

Element	Amount retained on exchanger, mg
Ag	0.03
Pb	0.003
Cu	0.01*
Zn	0.002
Cd	0.005
Hg	89
Fe	4
Ga	nil
In	3.9
Mo	12.8

*But 10 mg will be retained from 1.0 g of copper.

In column experiments, it was found (Table 2) that bismuth was quantitatively retained along with substantial amounts of indium, iron(III), mercury(II) and molybdenum(VI), whereas only very small amounts of silver, lead, zinc, cadmium, copper and gallium were retained. It was therefore necessary to choose a sufficiently selective method for determination of bismuth. The spectrophotometric method based on the iodide complex was selected. Molybdenum, mercury, iron and indium do not interfere when present in less than 5 mg amounts; gold is not eluted from Chelex 100 with 2M nitric acid and hence will not interfere.

The procedure based on these findings was applied to a variety of samples, giving the results presented in Table 3. The same samples were analysed with use of ZeoKarb-226 for the ion-exchange separation and the results are included in the same table.

The results obtained establish the reliability of the method. The procedure uses smaller elution volumes than those required with a sulphonic acid type of ion-exchanger.⁸ It has been reported that when ZeoKarb-226 is used, bismuth is not completely eluted. No such effect was observed with Chelex 100.

Blount *et al.*² employed Chelex 100 at pH 2.0 for

separation of bismuth from other elements. It was observed in the present studies that a much higher acidity can be used without loss of bismuth. In the case of a few elements such as iron, copper and indium, which exhibit low K_d values, the portion retained on the exchanger is not easily washed out with 0.25M acid, possibly because of slow desorption kinetics.

To assess the recovery of bismuth from lead concentrates, standard additions of 50–200 μg of bismuth to 0.5 g sample of BAS 42 G were made. The recoveries were found to be quantitative within $\pm 5\%$. To examine the possibility of loss of bismuth in the analysis of lead concentrates rich in lead sulphide (which would be expected to yield some lead sulphate in the decomposition step), sulphuric acid was added to the spiked BAS 42 G sample to simulate this effect; the bismuth recovery fell to only 50%, so the method is not suitable for such samples. It should be possible to tolerate up to about 20% of copper in a sample without any change in the procedure, but in analysis of copper metal, it is necessary to add 1,10-phenanthroline to avoid sorption of copper on the exchanger.

Acknowledgement—The authors thank Dr. M. Sankar Das for his keen interest in this work.

REFERENCES

1. C. C. Dias, P. Murugaiyan and Ch. Venkateswarlu, in *Trace Analysis and Technological Development*, M. S. Das (ed.), p. 82. Wiley Eastern, New Delhi, 1983.
2. C. W. Blount, D. E. Leyden, T. L. Thomas and S. M. Guill, *Anal. Chem.*, 1973, **45**, 1045.
3. S. G. Iyer and Ch. Venkateswarlu, *Indian J. Chem.*, 1976, **14A**, 437.
4. *Idem, ibid.*, 1985, **24A**, 805.
5. W. F. Hillebrand, G. E. F. Lundell, H. A. Bright and J. I. Hoffman, *Applied Inorganic Analysis*, 2nd Ed., p. 238. Wiley, New York, 1955.
6. E. B. Sandell, *Colorimetric Determination of Traces of Metals*, 3rd Ed., p. 332. Interscience, New York, 1959.
7. K. C. Thompson and D. R. Thomerson, *Analyst*, 1974, **99**, 595.
8. G. Van Dyck and F. Verbeek, *Z. Anal. Chem.*, 1970, **249**, 89.

Table 3. Determination of Bi in ores, concentrates and some metals and alloys

Sample	Bi found			
	Chelex 100		ZeoKarb-226	
	Spectrophotometry, %	AAS, $\mu\text{g/g}$	Spectrophotometry, %	AAS, $\mu\text{g/g}$
Sulphide ore	0.14		0.13	
Zinc concentrate	0.075		0.073	
Lead concentrate	1.05		1.00	
Copper concentrate	0.17		0.15	
Copper screen		0.3		0.4
Silver screen		0.5		—
Cd–Ag alloy		63		55
Lead concentrate BAS 42 G	0.020			
(Bi certified value 0.020%)	0.021			
	0.019			
	0.019			

RAPID DETERMINATION OF MOLYBDENUM IN FERROMOLYBDENUM AND MOLYBDENUM ADDITIVES, WITH OXINE

OM P. BHARGAVA, PAUL G. BAILEY and GORD R. OVERHOLT
Stelco Inc., P.O. Box 2030, Hamilton, Ontario, Canada

(Received 5 November 1986. Accepted 12 December 1986)

Summary—A rapid method is presented for the gravimetric determination of molybdenum (as the oxinate) in ferromolybdenum and molybdenum additives. The sample is fused with a mixed flux of sodium peroxide and sodium carbonate in a zirconium crucible for complete decomposition. Leaching the cooled fusion cake with water provides instantaneous separation of molybdenum as sodium molybdate from iron(III) and other hydrous oxides. After filtration, the molybdenum is precipitated with oxine after addition of EDTA and oxalate to obviate interference from other metal oxinates, and determined gravimetrically. The precision and accuracy are comparable to those of referee methods.

Molybdenum is generally added to steel as ferromolybdenum or molybdic oxide. It forms complex carbides in steel, which are retained in solid solution on cooling from above the critical temperature. This induces remarkable hardenability. Analysis of these molybdenum additives is becoming more important both for quality in steel-making and on account of their high cost. The X-ray fluorescence method can be used for routine monitoring, but is subject to matrix interference and requires reference-type calibration standards and a complicated normalization procedure. Solution methods¹⁻³ use acid decomposition, e.g., with a combination of sulphuric, nitric and hydrofluoric acid, followed by heating till fuming. There is no provision for treatment of any insoluble residue, which may lead to low results. Further, the tedious acid decomposition is followed by treatment with sodium hydroxide^{1,2} or ammonia to separate molybdenum as sodium or ammonium molybdate. Sodium peroxide fusion in a zirconium crucible has been used in our laboratory for decomposition of various materials encountered in steel-making.⁴⁻⁶ Ferromolybdenum, molybdic acid *etc.* can similarly be decomposed, giving a completely clear melt. On leaching with water the cooled fusion cake produces sodium hydroxide *in situ*, simultaneously giving soluble sodium molybdate and precipitating iron(III) and other hydrous oxides. The advantages of complete decomposition, separation and speed ensue. The subsequent precipitation of molybdenum as oxinate in the presence of EDTA and oxalate to obviate interferences, as proposed by Přibil and Malát⁷ and applied in the British standard method¹ is attractive owing to its simplicity compared to the precipitation as lead molybdate² or the tedious separation as molybdenum sulphide and subsequent titration with permanganate as in the ASTM method.³

EXPERIMENTAL

Reagent

8-Hydroxyquinoline solution, 3%. Dissolve 3 g of 8-hydroxyquinoline in 12 ml of glacial acetic acid. Add 60 ml of water and warm to about 40°. Add ammonia solution until a slight precipitate forms. Just redissolve the precipitate by dropwise addition of glacial acetic acid, and dilute to 100 ml with water.

Procedure

Transfer an accurately weighed (0.3 ± 0.0001 g) portion of the finely ground sample into a 35-40 ml zirconium crucible containing 3 g of sodium peroxide. Cover the sample with 0.5 g of sodium carbonate and 1 g of sodium peroxide, and carefully mix. Slowly fuse over a low flame on a Méker burner, swirling the crucible until the melt is cherry red and clear. Increase the heat and continue the fusion for 30 sec to ensure complete decomposition. Remove from the heat and swirl the crucible until the melt solidifies on the walls of the crucible. After slight air-cooling of the crucible place it in a dry 600-ml beaker. Cover with a watch glass and add 20 ml of water to the crucible. After the effervescence ceases, empty the crucible contents into the beaker and wash the crucible with water. Remove any remaining residue from the crucible with a policeman. Rinse further with water. The volume should be approximately 100 ml. Place the beaker in a hot water-bath for 15-20 min. Cool, transfer the solution to a 250-ml standard flask, dilute to the mark with water, shake the flask well and let the precipitate settle. Filter by decantation about 150 ml through a dry Whatman No. 52 paper into a dry beaker. Pipette 100 ml of filtrate into a 500-ml tall beaker. Add about 100 ml of water, 10 ml of 1% EDTA solution and 3 g of ammonium oxalate. Warm to dissolve the oxalate, cool, and adjust the pH to 4.0 with hydrochloric acid (1 + 1) and ammonia solution (1 + 1), using a pH-meter. Bring to the boil, and add by pipette 20 ml of 8-hydroxyquinoline solution while keeping the mixture boiling. Digest for 5-10 min at 90° with occasional stirring. Collect the precipitate with a dried (125°) and weighed medium-porosity sintered-glass crucible, by suction. Use a policeman and hot water to transfer the last traces of the precipitate from the beaker. Wash 8-10 times with hot water. Dry at 125° for 4 hr. Cool in a desiccator and weigh the molybdenum oxinate. The conversion factor from weight of molybdenum oxinate to molybdenum is 0.5763.

RESULTS AND DISCUSSION

Sample decomposition and separation

As indicated above, the dissolution methods¹⁻³ use acid decomposition (nitric, sulphuric and hydrofluoric acid or *aqua regia*). This is quite time-consuming, especially the subsequent sulphurous acid fuming, heating to fumes with sulphuric acid, and requires constant attention and care by the analyst. Further, any undissolved residue is ignored, though it should be filtered off, ignited, fused with an alkaline flux, and taken up in solution, which should be united with the main solution. The preliminary separation of molybdenum from hydrous oxides is done in these methods by treatment with either sodium hydroxide or ammonia. In the present method the fusion of the sample with sodium peroxide accomplishes complete decomposition of the sample to yield sodium molybdate. The subsequent leaching with water generates sodium hydroxide, in which the sodium molybdate is soluble, whereas the hydrous oxides (except that of any aluminium) are precipitated.

Determination

The ASTM method³ was found to be further complicated as it requires additional separation of molybdenum as the sulphide from ammonium molybdate solution. This is followed by wet decomposition of the filter paper and the sulphide precipitate with nitric and sulphuric acid *etc.* The subsequent reduction, prior to permanganate titration, involves zinc amalgam, which is objectionable on grounds of occupational health and pollution. The lead molybdate procedure² is also quite tedious, requiring alkaline separation of a soluble molybdate, precipitation of lead molybdate in the presence of formate, carefully controlled ignition, dissolution in hydrochloric acid and reprecipitation of lead molybdate. The precipitation of molybdenum as the oxinate in the presence of EDTA and oxalate to eliminate interferences,^{1,7} is much more attractive and is successfully incorporated in the present method.

Table 1. Precision tests

Molybdenum content, %				
Stelco standard No. 3		MoO ₃ standard MP 816	BCS No. 231/4*	
A†	B†	A†	A†	B†
62.95	63.29	61.33	69.86	69.88
62.93	63.21	61.49	69.84	70.09
63.10	63.18	61.51	69.89	
63.04	63.02		69.88	
	63.17			
	63.14			
Mean				
63.00	63.18	61.44	69.87	69.99
Std. dev. (s)				
0.08	0.10	0.10	0.02	

*Certificate value 70.0%, range 69.8–70.1%, $s = 0.12\%$.

†Analyst.

The procedure described has been applied to our own works ferromolybdenum and molybdic acid standards and to a BCS ferromolybdenum reference standard. The results are recorded in Table 1. The method gives excellent precision and accuracy, and is rapid, simple, and of comparable accuracy to referee methods. The method has been in use in our laboratory for the last 6 years.

Acknowledgements—Our thanks are due to M. Gmitro for assistance in the experimental work and to Stelco Inc. for permission to publish this contribution.

REFERENCES

1. British Standards Institution, *B.S. Handbook No. 19*, British Standards House, London, 1970.
2. *Standard Methods of Analysis of Iron and Steel and Associated Materials*, 5th Ed., The United Steel Companies Ltd., Sheffield, 1961.
3. *Chemical Analysis of Metals and Metal Bearing Ores*, Vol. 03.05, *1984 Annual Book of ASTM Standards*, ASTM, Philadelphia, 1984.
4. O. P. Bhargava, *Analyst*, 1976, **101**, 125.
5. O. P. Bhargava, A. Alexiou and W. G. Hines, *Talanta*, 1978, **25**, 357.
6. O. P. Bhargava, M. Gmitro and W. G. Hines, *ibid.*, 1980, **27**, 263.
7. R. Přebil and M. Malát, *Collection Czech. Chem. Commun.*, 1950, **15**, 120.

PHTHALHYDRAZIDYLAZOACETYLACETONE AS A CHEMILUMINESCENT ACID-BASE INDICATOR

N. THANKARAJAN* and K. KRISHNANKUTTY

Department of Chemistry, University of Calicut, Kerala 673 635, India

(Received 17 June 1986. Accepted 12 December 1986)

Summary—Phthalhydrazidylazoacetylacetone, an azo derivative of luminol, has been shown to be superior to luminol as a chemiluminescent indicator for acid-base titrations.

Luminol (3-aminophthalhydrazide) has been used as a chemiluminescent indicator in various analyses, including acid-base titrations.¹ It has been pointed out that the relatively large amounts of luminol, hydrogen peroxide and catalyst [haemin, hexacyanoferrate(III), *etc.*] employed as indicator components in acid-base titrations have an appreciable buffer action and hence tend to cause lower precision of titration.² Further, since the chemiluminescence (CL) emission of luminol in alkaline medium persists only for <30 sec, alkali cannot be titrated directly with luminol as indicator. In the present investigation it was observed that these shortcomings of luminol can be overcome by using instead phthalhydrazidylazoacetylacetone,[†] which is an azo derivative of luminol.³ This new CL indicator produces with hydrogen peroxide alone, about five times more intense luminescence than luminol does with hydrogen peroxide and catalyst.³ Although many azo compounds have been used as indicators for various titrimetric analyses, this is the first report of an azo compound being used as a CL indicator.

EXPERIMENTAL

Synthesis of phthalhydrazidylazoacetylacetone

Luminol (0.88 g, 5 mmole) was diazotized with sodium nitrite and hydrochloric acid as usual. The resulting solution (~5 ml) was added slowly to a stirred solution of acetylacetone (0.5 ml, 5 mmole) in aqueous ethanol (10 ml, 70% v/v ethanol). Sodium acetate was added to maintain the apparent pH of the mixture between 7 and 8. After continued stirring for 1 hr the precipitated compound was filtered off, washed repeatedly with water, sucked dry and recrystallized twice from hot ethanol. Yellow needles, m.p. 312°. Found C 55.2%, H 4.5%, N 19.1%; C₁₃H₁₂O₄N₄ requires C 55.57%, H 4.98%, N 19.44%.

Preparation of indicator solution

Phthalhydrazidylazoacetylacetone³ (10 mg) was dissolved in ethanol (50 ml) and diluted to 100 ml with water.

Procedure for acid-base titration

In a typical titration, an aqueous solution of the base (10 ml) containing the indicator (0.2 ml) and hydrogen peroxide

(0.01% w/v; 0.5 ml) was titrated with an aqueous solution of the acid. A magnetic stirrer was used for mixing the solution. At the end-point the luminescence of the solution stopped abruptly. In titration in the opposite direction (acid solution, hydrogen peroxide and indicator, titrated with base), luminescence appeared suddenly at the end-point. Replicate titrations were done with 1, 0.1, 0.01 and 0.001*N* solutions of acids and bases. Blank titration corrections were applied. A semi-darkened room was found adequate for performing the titrations. Titrations could be done even in daylight if the flask was placed in a cardboard box with a hole in one side for observing the end-point.

RESULTS

It was found by pH-titration that at the end-point of the titrations the pH of the solution was between 7.5 and 8. More accurate results were obtained consistently with the azo dye indicator than with luminol (Table 1). Values obtained with phenolphthalein as indicator are shown for reference. To study the behaviour of the indicator in the presence of highly coloured components, titrations were done with Gentian Violet (0.003%) present in the test solution. The results of these titrations are also included in Table 1. The suitability of the indicator for titrations of carboxylic acids was also examined. The results are comparable with those obtained by using phenolphthalein (Table 2).

DISCUSSION

Phthalhydrazidylazoacetylacetone has been shown to exist predominantly in the hydrogen-bonded hydrazone-enol form.³ The greater CL efficiency of the azo indicator than that of luminol can thus be attributed to increased resonance interaction from extended conjugation of the hydrazone form, and to increased planarity of the system due to additional intramolecular hydrogen bonding.^{3,4} As expected, the CL emission maximum of the azo indicator (in aqueous alkali) is at longer wavelength (475 nm) than that of luminol (425 nm). In both cases, the emitting species has been shown to be the corresponding phthalic acid.^{3,4}

*Author for correspondence.

†Systematic name: 3[(2,3-dihydro-1,4-phthalazinedione)yl-5-azo]-2,4-pentanedione.

Table 1. Titration of 10 ml of 1, 0.1, 0.01 and 0.001M sodium hydroxide against hydrochloric acid of corresponding molarities

[HCl], M	Phenolphthalein, <i>ml</i>	Luminol, <i>ml</i>	Phthalhydrazidylazo- acetylacetone	
			Without Gentian Violet, <i>ml</i>	With Gentian Violet, <i>ml</i>
1	10.01	9.92	9.96	9.94
0.1	10.02	9.94	9.98	9.97
0.01	10.02	9.95	9.98	9.97
0.001	10.02	9.95	9.97	9.96

Table 2. Titration of 10 ml of 0.1N carboxylic acid with 0.1N sodium hydroxide

Acid	Phenolphthalein, <i>ml</i>	Phthalhydrazidylazo- acetylacetone, <i>ml</i>
Acetic	9.95	9.98
Butyric	9.94	9.97
Citric	9.92	9.96
Oxalic	9.98	10.01
Stearic	9.93	9.95
Tartaric	9.91	9.97

The CL of the azo indicator is enhanced by catalysts such as hexacyanoferrate(III), but as the emission is intense enough even without a catalyst, the latter can be avoided in titrations, so the buffer action by indicator components is reduced, and greater precision results. Thus, the variation of the titration values given in Table 1 is ± 0.02 ml for titrations using the azo indicator, and ± 0.04 ml for titrations using the luminol-catalyst indicator. Also, since the emission from the azo indicator persists for about 30 min, titrations can be done in both directions.

Luminol indicator solution is usually prepared in aqueous alkali, which introduces an additional error in acid-base titrations. However, the azo indicator can be prepared in aqueous ethanol and stored for several months without change. The concentration of the azo indicator needed for each titration is also considerably less than that of luminol.

The chief advantage of CL indicators is that they permit analysis of deeply coloured and turbid solutions. Excellent results were obtained with this indicator in determining saponification values of coloured oils and fats. The applicability of the indicator in other titrations is under investigation.

REFERENCES

1. U. Isacson and G. Wettermark, *Anal. Chim. Acta*, 1974, **68**, 339.
2. F. Kenny and R. B. Kurtz, *Anal. Chem.*, 1952, **24**, 1218.
3. N. Thankarajan, K. Krishnankutty and T. K. K. Srinivasan, *J. Indian Chem. Soc.*, in the press.
4. R. B. Brundrett, D. F. Roswell and E. H. White, *J. Am. Chem. Soc.*, 1972, **94**, 7536.

TRANSPORT OF ALKALI-METAL PICRATES THROUGH LIQUID MEMBRANES: COUPLED ACTION OF w/o MICROEMULSION DROPLETS AND LIPOPHILIC CROWN-ETHER CARRIERS

ARISTOTELIS XENAKIS, CLAUDE SELVE and CHRISTIAN TONDRE*

Laboratoire d'Etude des Solutions Organiques et Colloïdales (L.E.S.O.C.), Unité Associée au C.N.R.S.
No. 406, Université de Nancy I, B.P. 239, 54506 Vandoeuvre-les-Nancy Cedex, France

(Received 9 June 1986. Revised 9 January 1987. Accepted 16 January 1987)

Summary—The transport of potassium and sodium picrates is measured by a liquid membrane technique in the presence of two mobile carriers: water-in-oil microemulsion droplets and lipophilic crown-ethers. The fluxes are compared for two cases: (i) the crown-ether (dicyclohexano-18-crown-6) is assumed to be independent of the microemulsion droplet and (ii) the crown-ether (dodecano-18-crown-6) is assumed to be anchored in the droplet. A lower flux is observed when the microemulsion droplet and the crown-ether diffuse as a single entity. These results suggest that larger synergistic effects are obtained when the extractant can diffuse independently of the microemulsion droplet.

The use of water-in-oil (w/o) microemulsions in place of classical organic phases has recently been demonstrated in different liquid-liquid extraction systems.¹⁻³ The microemulsion phase (or reverse micellar phase depending on the terminology used) has appeared to be, at least in several cases, responsible for the enhanced extraction rates observed when surfactant molecules are present.⁴⁻⁶

We have previously used different model systems to perform transport experiments which have improved our understanding of the part that can be played by the microemulsion droplets in mass transfer processes.^{7,8} These experiments showed that water-in-oil microemulsions are capable of transporting alkali-metal picrates between two external water phases at a much faster rate than classical carrier molecules, but with the same flux for sodium as for potassium picrate.⁷ In contrast to the now classical water-in-oil-in-water double-emulsion systems, the water droplet here is not the receiving phase, but the mobile carrier.

While studying such transport by microemulsions used as liquid membranes, we tried to introduce ionic selectivity by adding crown-ether molecules to the microemulsion. When dicyclohexano-18-crown-6 (DC18C6) is added to the hydrocarbon continuous phase of a microemulsion made of n-decane/water/tetraethyleneglycol dodecyl ether (TEDGE)/hexanol-1-ol, two carriers can be considered to co-exist in the liquid membrane, the microemulsion "droplet" and the macrocycle. This situation results in (i) a synergistic effect^{7,8} and (ii) a larger transport rate for potassium picrate than for sodium picrate.⁷

Two of us had previously suggested⁷ that the

synergistic effect could be due to the large difference between the diffusion constants of the two kinds of mobile carrier. The rate-limiting step in these experiments is the diffusion of the carriers in the unstirred layers. Owing to the possible exchange of alkali-metal picrates between the two carriers during the transport process, the thickness of the diffusion layer operative for each carrier species was assumed to be less than that when there is only one carrier.

A point of particular interest would be to determine whether or not a synergistic effect is still present when the crown-ether molecule is anchored to the microemulsion "droplet" so that both species have to diffuse as a single entity.

We have attempted to check this by replacing the cyclohexyl groups of dicyclohexano-18-crown-6 by an alkyl chain with twelve carbon atoms so that the hydrophobic chain has the same chemical nature as the hydrophobic tail of the surfactant used (the crown-ether part of the molecule is already of the same chemical nature as the hydrophilic part of the surfactant). The surface properties of long-chain alkyl crown-ethers have been clearly demonstrated by Kuo *et al.*⁹ and we assume that the affinity of this crown-ether for the dispersed phase is considerably greater than that of the dicyclohexane crown-ether. Unfortunately, it is extremely difficult to determine experimentally the solubilization site of each crown-ether, because of the rather similar chemical nature of the different components involved in these systems.

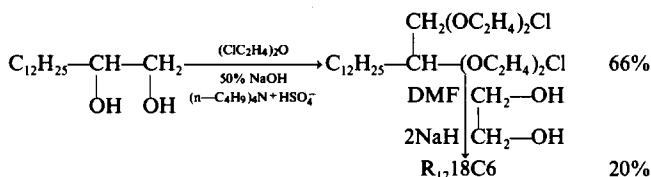
EXPERIMENTAL

Different synthetic routes have been explored for obtaining crown-ethers bearing an alkyl chain.¹⁰⁻¹³ The method of Ikeda *et al.*¹² starts from a 1,2-epoxyalkane and oligo ethylene glycols. The purification of the crude products

*Author to whom correspondence should be addressed.

requires an apparatus for molecular distillation that we do not have at our disposal. We tried the method used by Mizuno *et al.*,¹³ who prepared alkyl derivatives of 15-crown-5 and 12-crown-4. The chromatographic separation of the final product and of the brominated intermediary product appeared to be very difficult, both products having comparable polarities. In addition the method requires the expensive pentaethyleneglycol as a starting material. For these reasons, we have preferred to use a method derived from that described by Gehin¹⁴ for preparing chiral crown-ethers from sugars.

phases in the case of microemulsions has already been discussed.^{7,8} The composition of the microemulsion phase is given in Table I. The source and receiving phases in thermodynamic equilibrium with the microemulsion were found to contain 99% water. The initial picrate concentration in the source aqueous phase was $2 \times 10^{-3} M$. Either potassium or sodium picrate was used. When added to the system, the concentration of the crown-ether compounds in the liquid membrane was $10^{-2} M$. The experiments with microemulsions were usually run for 1–4 hr and the flux measurements were estimated to be reproducible within $\pm 10\%$.



The starting material is a diol, as in the methods of Cinquini and Tundo¹⁰ and Bowsher *et al.*¹¹ The first step is the condensation of di(2-chloroethyl) ether with tetradecane-1,2-diol by phase-transfer catalysis in the presence of tetrabutylammonium hydrogen sulphate. Di(2-chloroethyl) ether is both a reactant and the solvent for one of the phases, the other phase being 50% sodium hydroxide solution. The yield of the first step after chromatographic separation was 66%. The second step is the condensation of the dichloro product with ethane-1,2-diol. The latter was deprotonated by use of sodium hydride. *N,N*-Dimethylformamide was found to be a more convenient solvent than butanol¹⁴ (which can be deprotonated instead of the ethane-1,2-diol) or dioxan. It is a better solvent for the deprotonated diol and could favour the "template effect" of the sodium ions.¹⁵ The yield was 20% after purification on silica gel.

The ¹H NMR spectrum at 400 MHz in CDCl₃ was in accordance with the formula of the expected product (2-dodecyl-1,4,7,10,13,16-hexaoxacyclooctadecane = R₁₂18C6). Elemental analysis gave C 64.0%, H 11.1%; C₂₄H₄₈O₆·H₂O requires C 63.97%, H 11.18%.

The transport experiments were performed with a three-compartment glass cell in the shape of an inverted U, because the liquid membrane (either pure decane or a w/o microemulsion) had a lower density than the aqueous source and receiving phases. The cell is shown in Fig. 1, which also shows the connection of the flow-cell used for the spectrophotometric detection of the transported picrates.

The problem of thermodynamic equilibrium between the

RESULTS AND DISCUSSION

The results obtained are collected in Table 1, where the fluxes (mole/hr) of the two picrates are compared for different compositions of the liquid membrane. A distinct decrease in the flux is observed both for potassium and sodium picrate (but less for the latter) when DC18C6 is replaced by R₁₂18C6 in the microemulsion. At first glance, it seems that this observation cannot be attributed unambiguously to the anchoring of the R₁₂18C6 molecules to the microemulsion "droplets" because the alkyl chain is itself responsible for a decrease of the flux, which is reduced by a factor of 6–8 in pure decane. This is consistent with the earlier transport experiments by Bowsher *et al.*,¹¹ who reported that 18-crown-6 transported sodium picrate through a chloroform membrane 7 times as fast as C₁₀-18-crown-6 did, and potassium picrate 5 times as fast. On the other hand, the side-chain in macrocyclic carriers has practically no effect on the flux of amino-esters.¹⁶

Nevertheless, considering the orders of magnitude of the fluxes in decane and the microemulsion, the effect of the side-chain on the flux in decane should be almost undetectable for the microemulsion system.

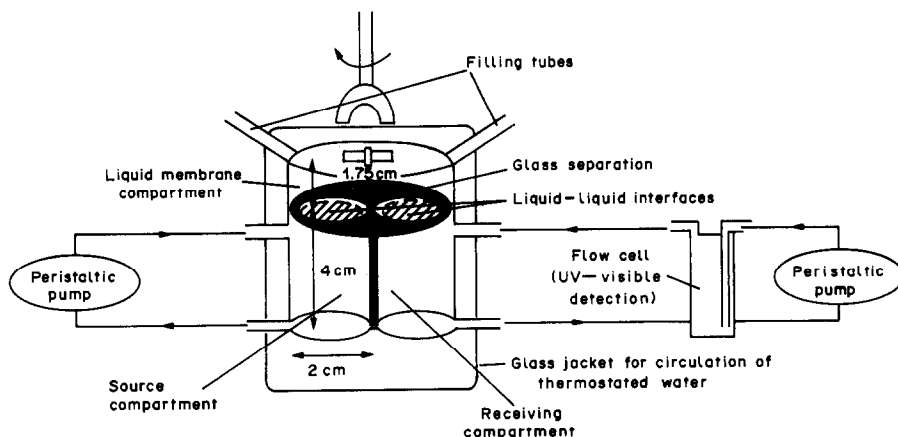


Fig. 1. Glass cell and arrangements for the transport measurements.

Table 1. Flux of potassium and sodium picrates, depending on the nature of the liquid membrane (interfacial area 3.14 cm²)

Liquid membrane	K ⁺ Pi ⁻ flux, mole/hr	Na ⁺ Pi ⁻ flux, mole/hr
R ₁₂ 18C6/Decane	7.0 × 10 ⁻⁸	~ 10 ⁻⁹
DC18C6/Decane	4.2 × 10 ⁻⁷	8.6 × 10 ⁻⁹
R ₁₂ 18C6/Microemulsion*	3.4 × 10 ⁻⁶ (1.3 × 10 ⁻⁶)	2.3 × 10 ⁻⁶ (0.2 × 10 ⁻⁶)
DC18C6/Microemulsion*	5.3 × 10 ⁻⁶ (3.2 × 10 ⁻⁶)	2.8 × 10 ⁻⁶ (0.7 × 10 ⁻⁶)
Microemulsion*	2.1 × 10 ⁻⁶	2.1 × 10 ⁻⁶

*The composition of the microemulsion (in weight %) was: 6.5% water, 74.8% decane, 4.7% hexan-1-ol, 14.0% TEDGE. Values in parentheses are obtained after deduction of the flux for the microemulsion alone (see text).

The results in Table 1 shows that in decane the flux is ~70 times larger for potassium picrate than for sodium picrate with R₁₂18C6 and ~50 times larger with DC18C6, and that changing the crown-ether from R₁₂18C6 to DC18C6 increases the flux 6-fold for potassium picrate and 8.6-fold for sodium picrate. Similar comparisons can be performed for the crown-ethers in the microemulsion after subtraction of the contribution of the microemulsion itself (values in parentheses in Table 1): the corresponding picrate flux ratios are 6.5 and 4.5 with R₁₂18C6 and DC18C6 respectively, and the increases on change from R₁₂18C6 to DC18C6 are 2.5-fold and 3.5-fold for the potassium and sodium picrates respectively. The picrate flux ratios for the two crown-ethers are reduced by a factor of about ten on changing from the decane to the microemulsion membrane. Because the flux ratio is practically unity for the microemulsion system without crown-ether, and the fluxes are much greater than in the crown-ether/decane system, we would expect a similar flux ratio (~1) for the crown-ether/microemulsion system. The fact that use of DC18C6 instead of R₁₂18C6 increases the fluxes by factors of 2.5–3.5 can thus be taken as indicating the contribution of another effect, which is presumably due to the anchoring of the R₁₂18C6 to the microdroplet. Nevertheless there is a considerable synergistic effect for potassium picrate with both crown-ethers in the microemulsion system since the fluxes obtained with it are about 50–100% greater than the sum of the fluxes measured independently for the microemulsion alone and for the crown-ether in decane. For sodium picrate however, the synergistic effect is much smaller (only about 10–30%), as expected from the well-known selectivity of 18C6 compounds for potassium ions.

The fact that a synergistic effect exists not only with DC18C6 but also with R₁₂18C6 suggests that although the latter is predominantly located in the

dispersed droplet phase, a small fraction of it may be present in the continuous organic phase.

These observations may have implications in the field of metal-ion recovery by liquid–liquid extraction processes, including liquid membrane techniques. Indeed, if microemulsions are used as transfer agents in conjunction with selective extractants to improve the transfer rate of metal-ions, it may be advantageous to choose a lipophilic extractant that is soluble in the continuous organic phase rather than interacting strongly with the microdroplets constituting the dispersed phase.

REFERENCES

- Jin-Guang Wu, Hong-Cheng Gao, Dian Chen, Tian-Zhu Jin, Sheng-Chong Li and Guang-Xian Xu, *Conf. Int. Solvent Extraction Chemistry, Liège, Belgium*, 1980, Paper 80-23.
- Idem*, *Sci. Sinica (Engl. Ed.)*, 1980, **23**, 1533.
- D. Bauer, P. Fourre and J. Lemerle, *Compt. Rend.*, 1981, **292**, 1019.
- K. Osseo-Asare and M. E. Keeney, *Sepr. Sci. Technol.*, 1980, **15**, 999.
- P. Fourre and D. Bauer, *Compt. Rend.*, 1981, **292**, 1077.
- P. Fourre, D. Bauer and J. Lemerle, *Anal. Chem.*, 1983, **55**, 662.
- C. Tondre and A. Xenakis, *Faraday Discuss. Chem. Soc.*, 1984, **77**, 115.
- Idem*, in *Surfactants in Solution*, Vol. 3, K. L. Mittal and B. Lindman (eds.), p. 1881. Plenum Press, New York, 1984.
- P. L. Kuo, I. Ikeda and M. Okahara, *Tenside Deterg.*, 1982, **19**, 204.
- M. Cinquini and P. Tundo, *Synthesis*, 1976, 516.
- B. Bowsher, B. Rest and B. Main, *J. Chem. Soc. Dalton Trans.*, 1984, 1421.
- I. Ikeda, S. Yamamura, Y. Nakatsuji and M. Okahara, *J. Org. Chem.*, 1980, **45**, 5355.
- T. Mizuno, Y. Nakatsuji, S. Yanagida and M. Okahara, *Bull. Chem. Soc. Japan*, 1980, **53**, 481.
- D. Gehin, *Thesis*, University of Nancy I, France, 1984.
- R. N. Greene, *Tetrahedron Lett.*, 1972, 1793.
- M. Sugiura and T. Yamaguchi, *Sepr. Sci. Technol.*, 1984, **19**, 623.

SPECTROPHOTOMETRIC DETERMINATION OF TUNGSTEN(VI) WITH RUTIN AND CETYLTRIMETHYLAMMONIUM BROMIDE

MINLIANG XU

Department of Chemistry, Central South University of Technology, Changsha, Hunan 410012,
People's Republic of China

GORDON A. PARKER*

Department of Chemistry, The University of Toledo, Toledo, Ohio 43606-3399, U.S.A.

(Received 19 November 1985. Revised 19 September 1986. Accepted 20 December 1986)

Summary—Tungsten(VI) reacts with rutin in the presence of cetyltrimethylammonium bromide to form a soluble yellow complex having maximum absorbance at 416 nm. The molar ratio of tungsten to rutin in the complex is 1:2. The molar absorptivity is 5.01×10^4 l. mole⁻¹. cm⁻¹. Beer's law is obeyed over the range 1×10^{-7} – 1×10^{-5} M tungsten(VI). Optimum solution conditions for the determination of tungsten in various sample matrices have been found and the interference of diverse ions has been examined.

Rutin, 3- $\{[6-o-(6\text{-deoxy-}\alpha\text{-L-mannopyranosyl})\text{-}\beta\text{-D-glucopyranosyl}]oxy\}$ -2-(3,4-dihydroxyphenyl)-5,7-dihydroxy-4H-1-benzopyran-4-one, has been used analytically for determination of thorium,¹ titanium,² uranium,³ vanadium,⁴ zirconium⁵ and molybdenum.⁶ Krunz and Pfendt⁷ have reported a spectrophotometric method for determination of tungsten with rutin in 50% methanol–water solution.

In recent years, systems containing a metal ion, an organic chromophore reagent and a surfactant have been used widely and effectively in spectrophotometric determination of trace amounts of metal ions. In these systems, the presence of the surfactant produces bathochromic and hyperchromic shifts in the absorption spectra and facilitates determination of the metal ions in aqueous solution. In the present paper, a sensitive spectrophotometric method for determination of tungsten with rutin and cetyltrimethylammonium bromide (CTMAB) in aqueous solution is presented.

EXPERIMENTAL

Reagents

Standard tungsten(VI) solution. Dissolve 0.330 g of reagent grade sodium tungstate dihydrate in distilled water, dilute the solution to 1 litre, and standardize it.

Rutin solution, 1.0×10^{-3} M. Dissolve 0.129 g of rutin in 200 ml of 50% ethanol.

CTMAB solution, 0.05 M. Acetate buffer pH 5.0. Dissolve 270 g of sodium acetate trihydrate in distilled water, add 60 ml of acetic acid and dilute to 1 litre with distilled water.

General procedure

Transfer an aliquot of the sample tungstate solution to a 25-ml standard flask, add 2.0 ml of rutin solution, 1 ml of CTMAB solution and 1 ml of acetate buffer, and dilute to volume with distilled water, and mix. Allow the sample to stand for 30 min at room temperature, then measure the

absorbance at 416 nm against a reagent blank, using 1.0-cm cells.

RESULTS AND DISCUSSION

Absorption spectra

The spectra of rutin and rutin–CTMAB, tungsten–rutin and tungsten–rutin–CTMAB mixtures are shown in Fig. 1. The absorption spectrum of the tungsten–rutin mixture is similar to that of the rutin solution alone. However, significant bathochromic and hyperchromic shifts are observed for the tungsten–rutin complex in the presence of CTMAB,

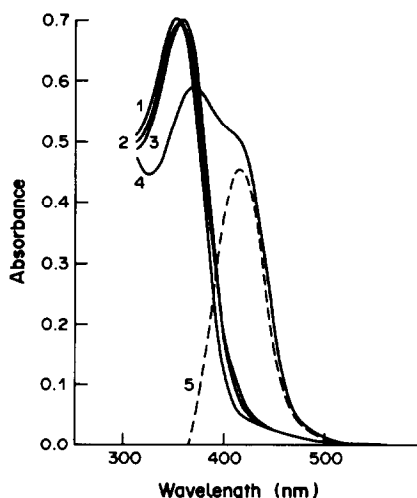


Fig. 1. Absorption spectra of 1, rutin (4×10^{-5} M); 2, W (8×10^{-6} M) + rutin (4×10^{-5} M); 3, rutin (4×10^{-5} M) + CTMAB (2×10^{-3} M); 4, W (8×10^{-6} M) + rutin (4×10^{-5} M) + CTMAB (2×10^{-3} M); 5, difference between curves 3 and 4.

*Author to whom correspondence should be addressed.

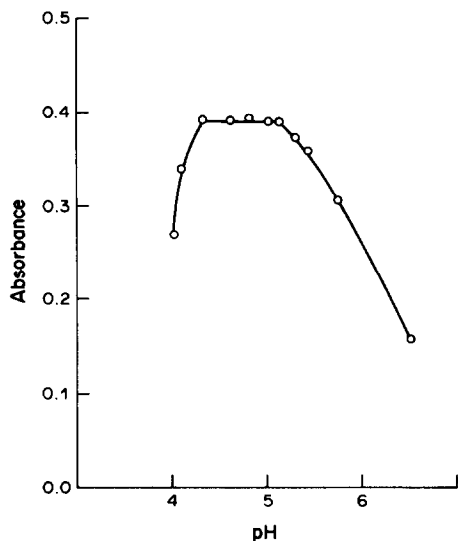


Fig. 2. Effect of pH on the absorbance of the tungsten-rutin-CTMAB complex at 416 nm.

the wavelength of maximum absorbance for the ternary system measured against a rutin blank solution being 416 nm.

Effect of pH

The effect of pH on the tungsten-rutin-CTMAB system was studied over the range 3–7. Figure 2 shows that the absorbance is constant and maximal from pH 4.4 to 5.1, and the wavelength for maximum absorbance is independent of pH within this range. The composition of the complex (tungsten: rutin = 1:2) is constant from pH 4.4 to 5.1. According to the literature,⁸ pK_a for rutin in aqueous methanolic medium is 9.17. At pH > 7, the colour of rutin solution is deeper yellow and the complex with tungsten is unstable.

Acetate buffer is used to maintain the optimum pH. It does not affect the absorbance but improves the stability of the colour of the complex.

Reagent concentrations

A fivefold molar excess of rutin is required for obtaining reproducible absorbance values.

The effect of the CTMAB concentration is interesting. At CTMAB concentrations $< 5 \times 10^{-5} M$, an opalescence or even turbidity appears owing to formation of insoluble ion-association complexes of rutin with CTMAB. At CTMAB concentrations $> 5 \times 10^{-5} M$, the solution remains transparent. The critical micelle concentration of CTMAB is reported to be $1 \times 10^{-3} M$ in aqueous solution.⁹ The absorbance of the tungsten-rutin-CTMAB system at 416 nm becomes maximal and constant at CTMAB concentrations above $\sim 1 \times 10^{-3} M$.

No yellow complex is observed at pH 5 for the tungsten-rutin system in aqueous solution in the absence of CTMAB, but there are bathochromic and hyperchromic shifts in the spectrum when CTMAB is

present. Krunz and Pfendt⁷ reported the tungsten-rutin complex in 50% methanol-water medium to have a molar absorptivity of $4.03 \pm 0.06 \times 10^4$ l.mole⁻¹.cm⁻¹ at the absorption maximum (405 nm). The molar absorptivity of the tungsten-rutin-CTMAB complex at 416 nm is 5.01×10^4 l.mole⁻¹.cm⁻¹.

Calibration graph

Beer's law is obeyed over the tungsten range $1 \times 10^{-7} - 1 \times 10^{-5} M$. At room temperature the colour development is complete after 20 min and the colour is stable for at least 24 hr.

Effect of diverse ions

The effect of other species on the determination of 37 μg of tungsten by means of the tungsten-rutin-CTMAB system was studied. Sulphate, nitrate, oxalate, chloride and fluoride (100 μg), EDTA (50 μg) and phosphate (20 μg) do not interfere, but tartrate (20 μg) does.

The following ions do not interfere with determination of tungsten when present at the mole ratio to tungsten stated in brackets: Mg²⁺, Ba²⁺, Zn²⁺, Cd²⁺, Co²⁺ and Ni²⁺ (250); Mn²⁺ (100); Sr²⁺ and Pb²⁺ (10); Ca²⁺ (2.5); Cu²⁺ and Hg²⁺ (1). Ions that do interfere when present at 1:1 mole ratio to tungsten are Al³⁺, Fe³⁺, Bi³⁺, Ti⁴⁺, ZrO²⁺, Th⁴⁺, VO₃⁻, CrO₄²⁻, MoO₄²⁻, and UO₂²⁺. Prior separation of tungsten by ion-exchange¹⁰ eliminates most of these interferences, although it is best if molybdenum is completely absent from the sample.

Analytical applications

The proposed method has been tested for determination of tungsten in selected samples. Typical results are given in Table 1. For the steel samples an

Table 1. Determination of tungsten in selected samples

Sample	W found, %		
	Proposed method ($n = 6$) \bar{x}	s	Accepted value*
Low alloy steel			
NBS SRM 1167	0.21	0.02	0.20
Tool steel ASTM A597	0.45	0.01	0.44
W(VI) solution† 1	1.28	0.02	1.29
2	14.6	0.2	14.7
Germinated seeds‡			
mustard 1	0.26		0.26
2	0.81		0.82
3	1.04		1.07
corn 1	0.015		0.015
2	0.14		0.14
3	0.22		0.21
pea 1	0.031		0.033
2	0.30		0.30

*Values by thiocyanate method¹¹ except for NBS sample, for which the certified value is given.

†Mother liquor from precipitation of lanthanum tungstate under varied conditions.

‡Seed germinated in solutions of varied W(VI) concentration, single samples.

ion-exchange separation preceded the complex formation and absorbance measurement. The saturated lanthanum tungstate solutions were used as received. For the germinated seed samples 1 g of plant material was first dried at 70° for 24 hr, then carbonized at 400°. The residue was digested with 20 ml of 0.5M sodium hydroxide, and the solution thus obtained was diluted to 100 ml with distilled water and 1.0–10.0 ml portions were taken for analysis. The values found are compared with either a certified value or with results from spectrophotometric measurements by the thiocyanate method.¹¹

Acknowledgement—The authors are indebted to Yanzhen He for her help and to Dr. N. L. Parinandi for providing the plant samples.

REFERENCES

1. R. W. Perkins and D. R. Kalkwarf, *Anal. Chem.*, 1956, **28**, 1989.
2. B. Dev and B. D. Jain, *Z. Anal. Chem.*, 1962, **190**, 316.
3. *Idem*, *J. Indian Chem. Soc.*, 1963, **40**, 117.
4. P. Szarvas and Z. Jarabin, *Anal. Chim. Acta*, 1959, **20**, 330.
5. B. S. Garg, R. P. Singh and M. Katyal, *Indian J. Appl. Chem.*, 1971, **34**, 17.
6. L. B. Pfendt, M. M. Krunz and T. J. Janjic, *Mikrochim. Acta*, 1980 **I**, 385.
7. M. M. Krunz and L. B. Pfendt, *Microchem. J.*, 1983, **28**, 162.
8. N. V. Chernaya, V. G. Matyashev and Yu. A. Omelchenko, *Vestn. Kiev. Politekh. Inst., Ser. Khim. Mashinostr. i Tekhnol.*, 1980, **17**, 45.
9. R. K. Chernova, L. N. Kharlamova, A. V. Belousova, E. G. Kulapina and E. G. Sumina, *Zh. Analit. Khim.*, 1978, **33**, 858.
10. R. S. Bottei and A. Trusk, *Anal. Chim. Acta*, 1963, **35**, 409.
11. A. G. Fogg, T. J. Jarvis, D. R. Marriott and D. T. Burns, *Analyst*, 1971, **96**, 475.

DOSAGE DES ACIDES FAIBLES EN MILIEU AMMONIUM QUATERNAIRE CONCENTRE

D. BAYLOCQ, W. KAYATA et F. PELLERIN

Laboratoire de Chimie Analytique, Faculté de Pharmacie de l'Université Paris Sud, 1 Rue J. B. Clément,
92296 Chatenay-Malabry, France

(Reçu le 26 avril 1986. Révisé le 23 juin 1986. Accepté le 28 novembre 1986)

Résumé—Le dosage des acides faibles est envisagé en milieu ammonium quaternaire concentré. Dans ce type de solvant, appauvri en liaison hydrogène, une complexation résultant d'une homoconjugaison ou d'une hétéroconjugaison est observée en présence de base et d'acide faible; celle-ci renforce l'acidité des couples acide-base conjugués et les rend directement titrables. Le procédé est applicable au dosage de la théobromine et de la théophylline par le nitrate d'argent en milieu acétate de tétrabutylammonium concentré. Ces composés sont titrables comme acides faibles et non comme base conjuguée.

Summary—The determination of weak acids in concentrated quaternary ammonium salt medium is proposed. In this type of solvent, which has few hydrogen bonds, complexation arises through homoconjugation or heteroconjugation in the presence of weak acids or bases; this enhances the acidity of the conjugate acid-base couples and makes them directly titratable. The procedure is applicable to determination of theobromine and theophylline with silver nitrate in concentrated tetrabutylammonium acetate medium. These compounds are titrated as weak acids and not as their conjugate bases.

L'emploi des sels fondus utilisés comme solvant en analyse inorganique a été développé pour les dosages de nombreux dérivés. De tels procédés sont inapplicables aux composés organiques du fait de la nécessité d'opérer le plus souvent à des températures incompatibles avec leur stabilité. L'utilisation de milieux tels que les solutions salines concentrées a alors pu être envisagée.

D'après plusieurs auteurs,¹⁻³ l'étude des solutions salines concentrées tend à prouver que leur comportement se rapproche de celui des solutions diluées.

Pellerin et Leroux-Mamo⁴ ont proposé un procédé de titrage des bases pures dans les solutions salines concentrées par formation de dérivés argentiques. Dans ces solvants appauvris en liaisons hydrogène (par rapport aux solutions diluées), la nature et la concentration en sel jouent un rôle essentiel dans les dosages des couples acide-base de caractère très faible.

Looy et Hammett⁵ furent parmi les premiers à mettre en évidence la complexation des anions dans un solvant pauvre en liaisons hydrogène pour former le complexe HA_2^- ou $A^-(HA)_{N+1}$ qui résulte d'une homoconjugaison⁵ ou le complexe RHA^- qui résulte d'une hétéroconjugaison.⁶

L'homoconjugaison et l'hétéroconjugaison renforcent le caractère acide des couples acido-basique lorsque ces composés sont conjugués, et les rendent directement titrables.

Différents facteurs⁷⁻⁹ influencent cette formation, en particulier la faible solvation des anions¹⁰ qui, en présence de leur acide conjugué deviennent suffisamment stables (grâce aux liaisons

Tableau 1

Composé	pK _a
Théophylline ¹⁴	8,77
Théobromine ¹⁴	10,05
Succinimide ¹⁵	9,50
	9,62

d'homoconjugaison) pour produire un changement profond dans les réactions acide-base.¹¹⁻¹³ Un autre facteur est la faible capacité des solvants à former des liaisons hydrogène qui favorisent la conjugaison.¹³

Dans les milieux salins concentrés, les titrages de la théobromine, du succinimide et de la théophylline par argentimétrie exigent d'alcaliniser fortement le milieu. En revanche, l'étude effectuée a montré que ces trois composés, dissous dans une solution d'ammonium quaternaire telle que l'acétate de tétrabutylammonium, sont titrables. La valeur de pK_a de ces composés (Tableau 1) montre une nette différence entre la théophylline et les deux autres composés. Il convient de noter que la théophylline et le succinimide sont solubles dans l'eau, alors que la théobromine est peu soluble.

Le choix d'un ammonium quaternaire et notamment l'acétate de tétrabutylammonium (ATBA) est fondé sur deux critères:

—son affinité pour l'eau qui permet de préparer des solutions très concentrées (2 g/ml) se rapprochant des propriétés des solvants des sels fondus;

—son emploi présente l'avantage d'opérer à la température ambiante ou toutefois inférieure à celle utilisée en milieu sel fondu.

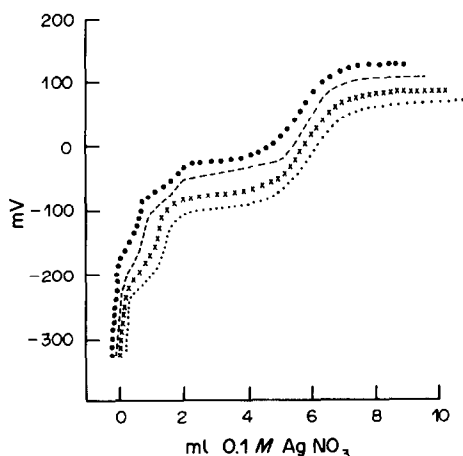


Fig. 1. Dosage potentiométrique de la théobromine en milieu aqueux de ATBA à concentration x (% p/v) par le nitrate d'argent: ●●● $x = 50\%$; --- $x = 60\%$; ××× $x = 80\%$; ··· $x = 100\%$.

PARTIE EXPERIMENTALE

Appareillage

Métrohm Titroprocesseur E 636; Dosimate E 635; électrode d'argent combinée, 6.0404.100 (1226); électrode de calomel combinée, 6.0202.000 (EA 120).

Réactifs

Acétate de tétrabutylammonium (Fluka), hydroxyde de sodium 1M (Prolabo), nitrate d'argent 0,1M (Prolabo).

RESULTATS

Dosage de la théobromine

La théobromine (TBH) est dosée par le nitrate d'argent en milieu acétate de tétrabutylammonium (ATBA) d'une part, en présence d'hydroxyde de sodium en excès (théobromine base) et d'autre part, en l'absence d'hydroxyde de sodium (théobromine acide).

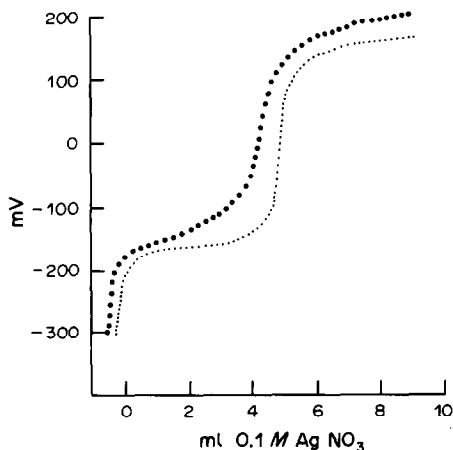
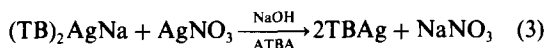
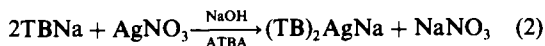
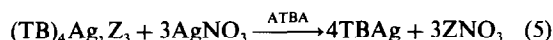
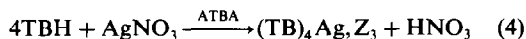


Fig. 2. Dosage potentiométrique de la théophylline en milieu aqueux de ATBA à concentration x (% p/v) par le nitrate d'argent (0,1 M): ●●● $x = 100\%$; ··· $x = 50\%$.

Dans le premier cas, l'apparition de deux points d'inflexion correspond successivement aux rapports argent/théobromine 0,5 et 1 selon les réactions (1-3) en milieu acétate de sodium concentré. Ceci confirme les résultats de Pellerin et Leroux-Mamo.⁴



Dans le second cas, en l'absence d'hydroxyde de sodium, les deux points d'inflexion (Fig. 1) correspondent successivement aux rapports argent/théobromine = 0,25 et 1, réactions (4) et (5):

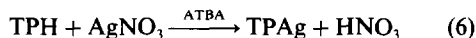


où $\text{Z} = \text{H}^+$ ou R_4N^+

Dosage de la théophylline

Le dosage de la théophylline (TPH) (Fig. 2) par le nitrate d'argent en milieu ATBA effectué à titre comparatif avec les milieux déjà étudiés, H_2O , CH_3COONa , KNO_3 , est exact et précis.

L'apparition d'un seul point d'inflexion correspond au rapport argent/théophylline = 1:



Dosage du succinimide

Le dosage du succinimide par le nitrate d'argent en milieu ATBA en présence d'hydroxyde de sodium donne un seul point d'inflexion et correspond au rapport argent/succinimide = 0,5 (comme en milieu aqueux); il est à remarquer que le complexe formé reste soluble dans le milieu de dosage. En revanche, en l'absence d'hydroxyde de sodium, ce rapport en milieu ATBA à 80% est égal à 1.

DISCUSSION

Le comportement des acides faibles varie selon les propriétés des acides eux-mêmes, mais aussi selon le milieu dans lequel ils ont été étudiés. La comparaison entre les travaux effectués par Pellerin et Leroux-Mamo⁴ en milieu acétate de sodium concentré et nos travaux effectués en milieu ATBA permet de mettre en évidence les points suivants:

—la formation de dithéobrominate d'argent en milieu salin concentré [CH_3COONa , $\text{CH}_3\text{COO}(\text{C}_4\text{H}_9)_4\text{N}$] alcalinisé par l'hydroxyde de sodium;

—la formation de tétrathéobrominate d'argent en milieu ATBA aqueux pour des concentrations supérieures à 80%;

—l'excès de nitrate d'argent ou le lavage à l'eau distillée transforme le dithéobrominate d'argent ou le tétrathéobrominate d'argent en monothéobrominate d'argent;⁴

—le complexe bis(succinimido-*N,N'*)argentate(I) de sodium monohydraté se forme en milieu aqueux alcalin¹⁶ aussi bien qu'en milieu salin concentré ($\text{CH}_3\text{COOR}_4\text{N}$).

Pour expliquer le rôle du milieu ammonium quaternaire, il est utile de le comparer avec d'autres milieux salins concentrés, comme l'acétate de sodium.

L'hypothèse que nous avons élaborée sur le mécanisme de la formation des complexes argentiques est la suivante: au fur et à mesure de la neutralisation de l'ion théobrominate par les ions argent, le complexe formé se combine avec une autre molécule de théobrominate, soit par une liaison covalente, comme dans le cas du bis(succinimido-*N,N'*)argentate(I) de sodium pentahydraté, soit par attraction électrostatique. Ceci a pour appui le fait qu'un acide (ou une base faible) en présence de sa base conjuguée (ou son acide conjugué) peut former un complexe (AH/A^-) par homoconjugaison. Celui-ci présente un caractère plus acide que l'acide de départ.

La faible solubilité du théobrominate d'argent, l'attraction entre le doublet électronique sur l'azote en position 2, l'atome d'argent électropositif et enfin le milieu salin concentré en acétate de tétrabutylammonium (ou acétate de sodium) justifient aussi cette conjugaison.

Cette explication confirme le passage de la formation du dithéobrominate au monothéobrominate d'argent.

En milieu ammonium quaternaire concentré (ATBA), la théobromine est dosée par potentiométrie avec le nitrate d'argent comme acide faible et non comme base conjuguée.

La formation successive de deux complexes théobrominate d'argent en milieu quaternaire, concentration minimum 0,8 mg/ml, avec les rapports argent/théobromine = 0,25 et 1, confirme l'existence d'un ordre moléculaire plus élevé qu'en milieu acétate de sodium à 5 mg/ml. Dans les milieux CH_3COONa , $\text{CH}_3\text{COOR}_4\text{N}$, cet ordre diminue en passant de la forme moléculaire à la forme ionique; dans les formes ioniques, les associations se font en partie entre les ions et les molécules du solvant, plutôt qu'entre les molécules d'acide elles-mêmes.

Les solutions salines concentrées exaltent l'acidité des acides faibles et cette exaltation est proportionnelle à la concentration en sel. Les sels d'ammonium quaternaire exaltent l'acidité des acides

faibles beaucoup plus que les autres sels (CH_3COOK , CO_3Na_2 etc.); bien que le cation R_4N^+ provoque une diminution de l'activité de H^+ . Mais, la grande affinité de ces sels pour l'eau, le fait que les sels R_4N^+ , leur donnent ce caractère particulier et laissent la porte ouverte à d'autres dosages d'acides faibles peu solubles en milieu aqueux et peu résistants à l'élévation de température.

Dans les solutions d'ammoniums quaternaires concentrés (ϵ , la constante diélectrique, tend vers zéro), l'eau est engagée avec les sels, les sels R_4N^+ augmentent le pontage (effet déshydratant). En d'autres termes, la solution est appauvrie en liaisons hydrogènes et celles-ci ne sont possibles qu'entre les molécules elles-mêmes.

Enfin, au cours du titrage, le nitrate d'argent forme avec une quantité équivalente de théobromine, un chélate par liaison covalente entre l'azote en position 2 et l'ion argent. La stabilisation de la charge de la fonction imide favorise la conjugaison entre le chélate formé et d'autres molécules de théobromine libres; ainsi, une molécule de théobrominate chélaté (théobromine argentique) fixe à son tour 3 autres molécules par attraction électrostatique et par liaison hydrogène pour former le tétrathéobrominate d'argent.

LITTÉRATURE

1. H. S. Harned et B. B. Owen, *The Physical Chemistry of Electrolyte Solutions*, 1st Ed., Reinhold, New York, 1943.
2. A. F. Scott, *J. Phys. Chem.*, 1931, **35**, 3379.
3. R. H. Stokes et R. A. Robinson, *J. Am. Chem. Soc.*, 1948, **70**, 1870.
4. F. Pellerin et G. Leroux-Mamo, *Ann. Pharm. Franc.*, 1971, **29**, No. 31, 153.
5. H. V. Looy et L. P. Hammett, *J. Am. Chem. Soc.*, 1959, **81**, 3872.
6. I. M. Kolthoff, M. K. Chantooni, Jr. et S. Bhowmik, *ibid.*, 1968, **90**, 23.
7. J. F. Coetzee et G. R. Padmanabhan, *J. Phys. Chem.*, 1965, **69**, 3193.
8. T. Jasinki, A. A. El-Harakany, F. G. Halaka et H. Sadek, *Croat. Chem. Acta*, 1978, **51**, 1.
9. I. M. Kolthoff, *Anal. Chem.*, 1974, **46**, 1992.
10. J. F. Coetzee et G. P. Cunningham, *J. Am. Chem. Soc.*, 1965, **87**, 2534.
11. G. A. Harlow et D. B. Bruss, *Anal. Chem.*, 1958, **30**, 1833.
12. H. B. van der Heijde, *Anal. Chim. Acta*, 1957, **16**, 392.
13. D. H. Morman et G. A. Harlow, *Anal. Chem.*, 1967, **39**, 1869.
14. *Merck Index*, 1st Ed., Merck, Rahway, New York, 1922.
15. H. F. Walton and A. A. Schilt, *J. Am. Chem. Soc.*, 1952, **74**, 4995.
16. W. Khayata, D. Bayloq, F. Pellerin et N. Rodier, *Acta Crystallog.*, 1984, **40C**, 765.

ANALYTICAL DATA

URANYL COMPLEXES OF α -CARBOXPOLYMETHYLENE-DIAMINETETRA-ACETIC ACIDS

A. MATILLA HERNANDEZ, S. GONZALEZ GARCIA and J. M. TERCERO MORENO
Departamento de Quimica Inorganica, Facultad de Farmacia, Universidad de Granada,
18071-Granada, Spain

M. CANDIDA T. A. VAZ and L. VILAS BOAS
Centro de Quimica Estrutural, Instituto Superior Tecnico, 1096 Lisboa Codex, Portugal

(Received 18 July 1986. Accepted 20 December 1986)

Summary—The uranyl complexes of *N,N,N',N'*-tetrakis(carboxymethyl)-2,3-diaminopropionic acid, *N,N,N',N'*-tetrakis(carboxymethyl)diaminobutyric acid, *N,N,N',N'*-tetrakis(carboxymethyl)ornithine and *N,N,N',N'*-tetrakis(carboxymethyl)lysine have been studied by potentiometry, with computer evaluation of the titration data by the MINQUAD program. Stability constants of the 1:1 and 2:1 metal:ligand chelates have been determined as well as the hydrolysis and polymerization constants at 25° in 0.1M potassium nitrate. Results are compared with those obtained for the uranyl complexes of the corresponding members of the series of the polymethylenediaminetetra-acetic acids.

We have recently prepared a new series of complexes, the α -carboxypolymethylenediaminetetra-acetic acids (cpdta) and studied their complexation reactions with some metal ions.¹⁻⁵ These acids have the general formula:



where $n = 1, 2, 3$ and 4 , and are respectively named α -carboxyethylenediaminetetra-acetic acid (CEDTA), *N,N,N',N'*-tetrakis(carboxymethyl)-1,3-diaminobutyric acid (DBT), *D,L-N,N,N',N'*-tetrakis(carboxymethyl)ornithine (OTC) and *N,N,N',N'*-tetrakis(carboxymethyl)lysine (LTC).

The asymmetry of these compounds may lead to some properties of possible interest as complex-forming agents, since the two complexing groups will behave differently, one being more powerful than the other.

In this work, we present results obtained for the formation in solution of complexes of the uranyl ion and the newly synthesized ligands.

The complexes formed by the uranyl ion and the parent polymethylenediaminetetra-acetic acids (pdta) have been thoroughly investigated and the influence of the length of hydrocarbon chain on the stability of the complex species formed has been discussed.⁶⁻⁸ The present study aimed to check the effects of the asymmetry of the ligands on the number and type of species formed and their stability. The potentiometric data were evaluated by computer with the MINQUAD program;^{9,10} we selected probable models for the series of complexes formed and calculated the corresponding stability constants.

EXPERIMENTAL

Reagents

All ligands were prepared by condensation of the corresponding diamino acid with monochloroacetic acid in alkaline medium.¹⁻⁵

Uranyl nitrate was analytical grade (Fluka), used without further purification. The stock UO_2^{2+} solutions were standardized gravimetrically. The potassium hydroxide solutions used as titrants were prepared under nitrogen from Merck "Titrisol" vials, with CO_2 -free demineralized water. The concentrations of these solutions and the absence of carbonate were checked regularly by potentiometric titration with standard hydrochloric acid.

Potentiometric measurements

A Crison digital potentiometer and Ingold electrodes were used. The measured potentials were converted into $[\text{H}^+]$ values according to the expression $E = K + \alpha \log[\text{H}^+]$. The experimental value of α , determined at 25°, was 59.2 ± 0.1 mV, in good agreement with the theoretical value of 59.15 (the drift of the liquid-junction potential during the measurements in the pH range of the titrations was found to be negligible and was not considered in the expression used). The cell constant K was calculated from a previous titration of hydrochloric acid with potassium hydroxide with end-point location by Gran's method.¹¹ The calibration was repeated before and after each titration.

The value of the ionic product of water (in 0.1M KNO_3) used in the calculations was 1.68×10^{-14} .

Method

Potentiometric titrations were performed on mixtures with $\text{UO}_2^{2+}/\text{cpdta}$ ratios of 1:1 and 2:1 at a range of ligand concentrations from 5×10^{-4} to 1.5×10^{-3} M. At concentrations below 5×10^{-4} M no polymeric species are formed, and at concentrations above 1.5×10^{-3} M the polymeric species precipitate as soon as the metal and ligand solutions are mixed.

The titrations were performed in a double-walled titration cell with the temperature controlled at $25.0 \pm 0.1^\circ$ by water

Table 1. Stability constants of the proton complexes of the ligands (25°, 0.1M KNO₃)

Ligand	β_{011}	β_{012}	β_{013}	β_{014}	β_{015}
CEDTA	1.182×10^{10}	3.580×10^{16}	7.707×10^{19}	4.227×10^{22}	6.796×10^{24}
DBT	1.680×10^{10}	5.079×10^{18}	3.807×10^{21}	6.425×10^{23}	5.900×10^{25}
OTC	3.022×10^{10}	3.254×10^{19}	2.415×10^{22}	4.677×10^{24}	3.196×10^{26}
LTC	2.455×10^{10}	5.248×10^{19}	7.413×10^{22}	1.778×10^{25}	1.288×10^{27}

Table 2. Hydrolysis constants of uranyl ion¹²

β_{10-1}	β_{20-2}	β_{30-3}	β_{30-5}	β_{40-7}
1.16×10^{-6}	1.26×10^{-6}	4.90×10^{-13}	3.47×10^{-17}	1.74×10^{-23}

circulated from a thermostat. The titrant was added from a Metrohm automatic burette.

After each addition of base, the equilibrium potential was reached within 30–180 sec.

RESULTS AND DISCUSSION

The MINIQUAD program, through a least-squares refinement, gives the formation constants of the complex species defined by:

$$\beta_{pqr} = \frac{[M_p L_q H_a(OH)_b]}{[M]^p [L]^q [H]^r}$$

where $r = b - a$, M is UO_2^{2+} and L the cpdta ligand, corresponding to the reaction:



The program also calculates an agreement factor, R , and other statistical parameters which allow comparison of the models proposed.

First, the protonation constants of the ligands were calculated (Table 1); the values obtained are in good agreement with those reported previously.¹⁻⁵ These constants, together with the hydrolysis constants of the uranyl ion (Table 2), were introduced as fixed data in the calculations for the different uranyl systems.

The potentiometric titrations of the cpdta show the increasing difference in nitrogen basicity as the chain lengths decrease,¹⁻⁵ as expected from electrostatic and hydrogen-bonding effects.

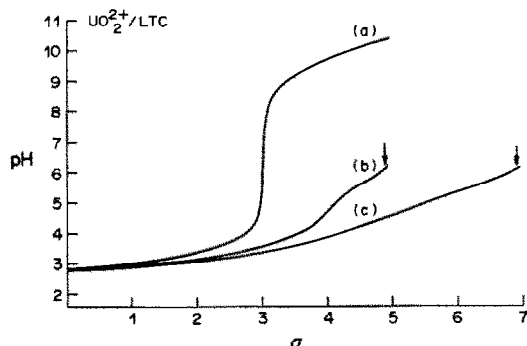
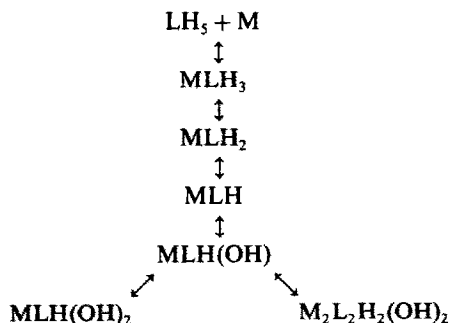


Fig. 1. Titration curves of LTC (a) and LTC-uranyl ion in molar ratios 1:1 (b) and 2:1 (c), at 25° and ionic strength 0.1M KNO₃; $C_{LTC} = 7.12 \times 10^{-4}M$; α = degree of neutralization; ↓ indicates precipitation.

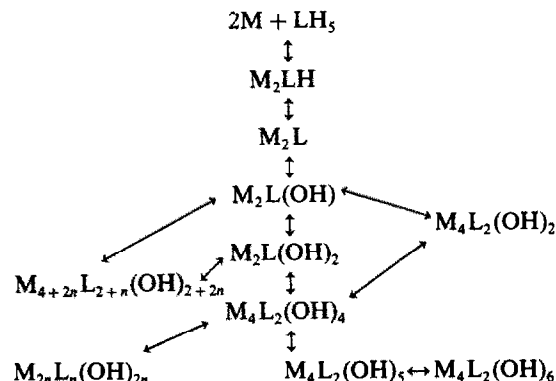
The behaviour of the titration curves of the different $UO_2^{2+}/cpdta$ systems is similar, and clearly suggests the formation of MLH and M_2L species (Fig. 1). However, it is not possible to rule out the presence of other protonated species or polynuclear hydrolysed species, and the value of the R parameter does indeed decrease when these are introduced into the model.

The number of possible complex species in the $UO_2^{2+}/cpdta$ system is high; the following equilibria are compatible with the titration curves.

1:1 species



2:1 species



The stability constants ($\log \beta$) of the complexes corresponding to the models for which the smallest values of R ($R < 0.004$) were obtained are given in Table 3. Species containing more than four UO_2^{2+} ions are rejected by the program. M_2LOH and $M_2L(OH)_2$ species, which may be intermediates for the formation of some other complexes, are also

Table 3. Stability constant of UO_2^{2+} -cpdta complexes for the best model obtained with the MINIQUAD program, with standard deviations in % (25° , $0.1M \text{KNO}_3$)

Ligand	$\log \beta_{113}$	$\log \beta_{112}$	$\log \beta_{111}$	$\log \beta_{110}$	$\log \beta_{11-1}$	$\log \beta_{220}$
CEDTA	23.04 ± 0.08	20.11 ± 0.03	17.06 ± 0.02	—	—	26.27 ± 0.05
DBT	25.00 ± 0.05	22.25 ± 0.04	19.39 ± 0.02	13.64 ± 0.03	7.33 ± 0.06	29.62 ± 0.40
OTC	25.17 ± 0.14	22.96 ± 0.06	19.91 ± 0.03	14.14 ± 0.06	7.73 ± 0.13	31.34 ± 0.22
LTC	25.32 ± 0.05	23.17 ± 0.01	20.05 ± 0.01	14.27 ± 0.02	7.73 ± 0.08	31.03 ± 0.14

	$\log \beta_{211}$	$\log \beta_{210}$	$\log \beta_{21-1}$	$\log \beta_{21-2}$	$\log \beta_{42-2}$	$\log \beta_{42-4}$	R
CEDTA	19.99 ± 0.02	16.53 ± 0.01	10.63 ± 0.29	—	26.32 ± 0.07	15.31 ± 0.39	0.0026
DBT	22.16 ± 0.01	18.61 ± 0.02	13.15 ± 0.13	7.62 ± 0.20	30.12 ± 0.13	19.21 ± 0.18	0.0035
OTC	22.99 ± 0.01	19.22 ± 0.02	—	—	31.86 ± 0.03	20.86 ± 0.04	0.0032
LTC	23.08 ± 0.01	19.42 ± 0.01	—	—	32.30 ± 0.02	21.15 ± 0.03	0.0035

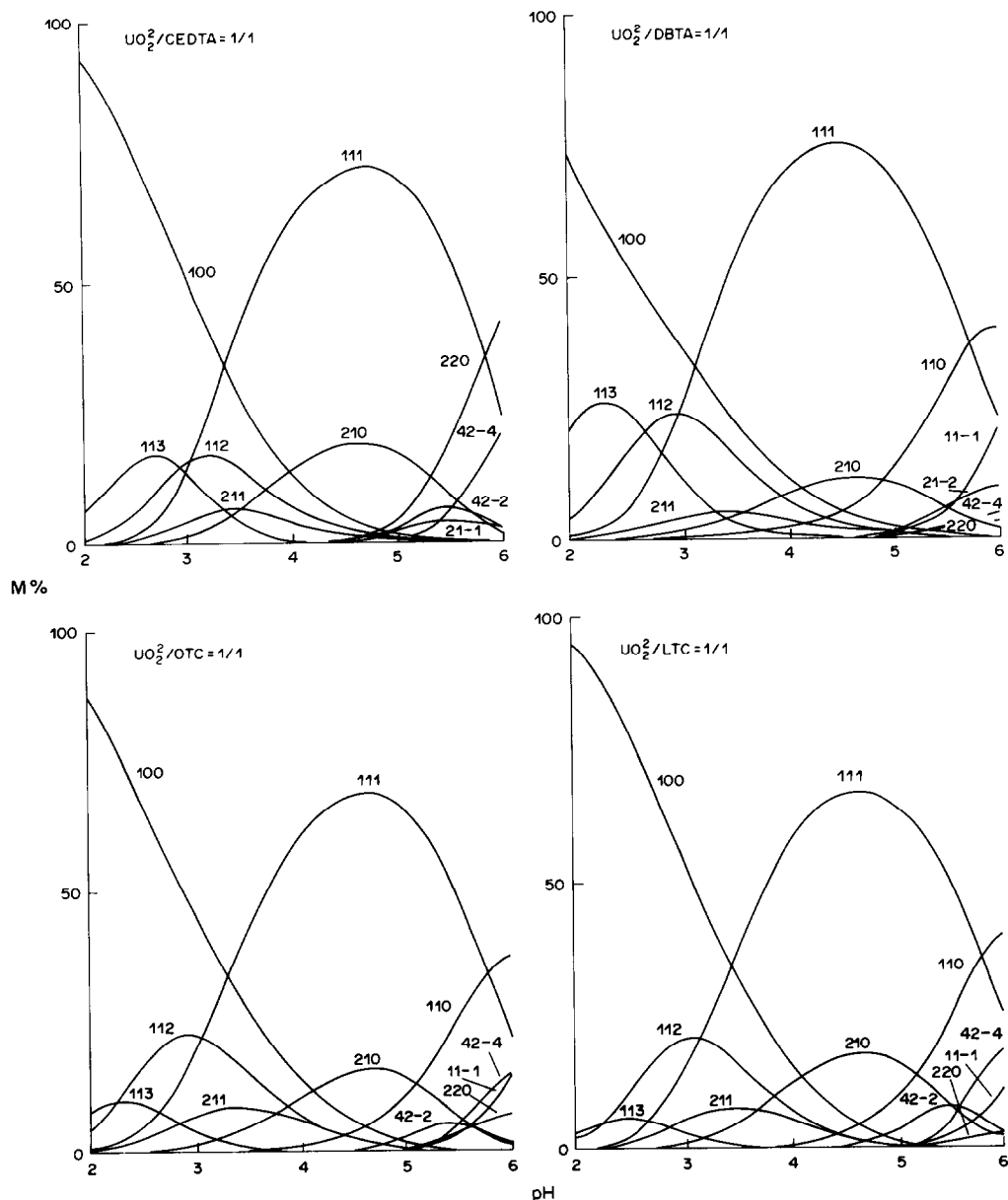


Fig. 2

Fig. 2(a). Fraction of the metal present in each complex as a function of pH, for the systems UO_2^{2+} /cpdta in 1/1 ratio.

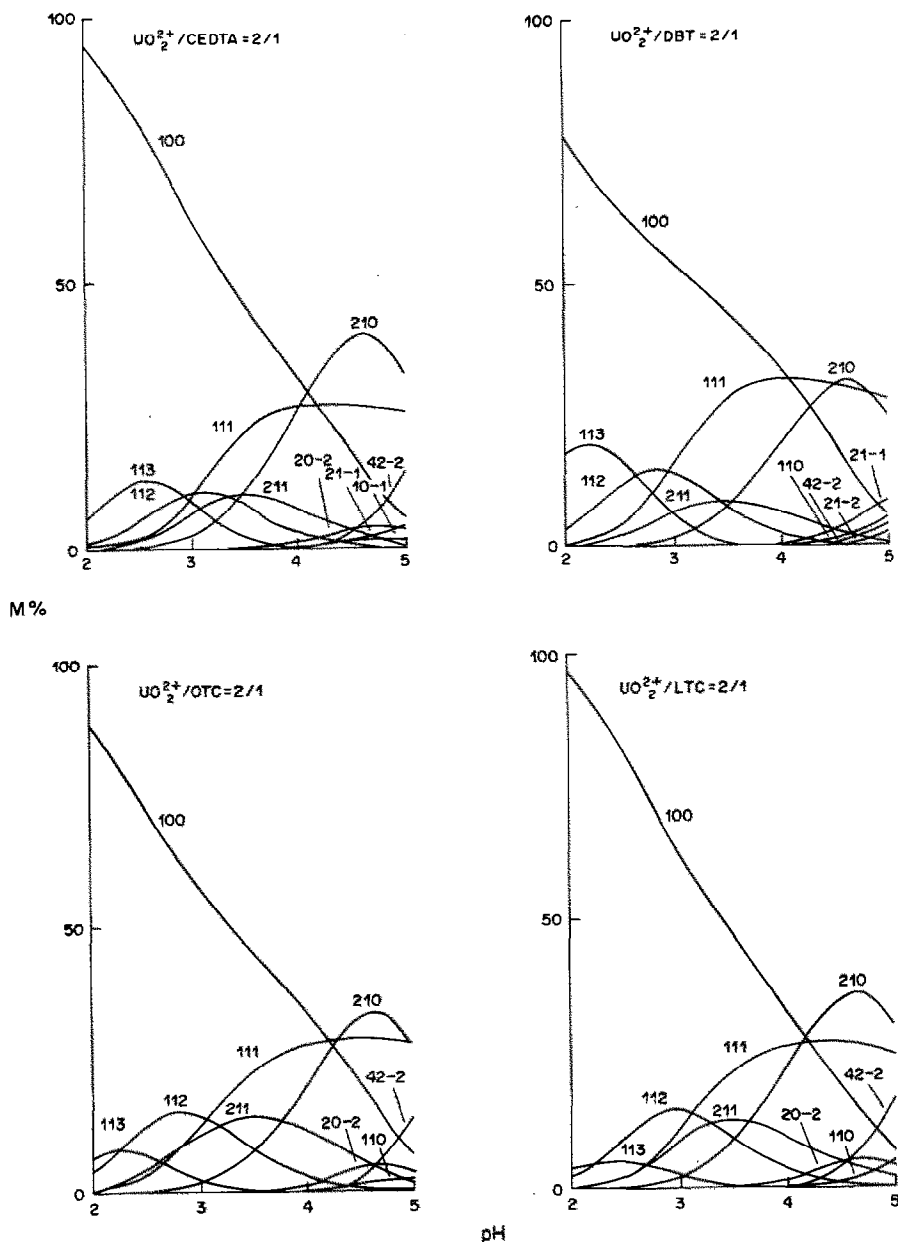


Fig. 2(b). Fraction of the metal present in each complex as a function of pH, for the systems $\text{UO}_2^{2+}/\text{cpdta}$ in 2/1 ratio.

rejected for some systems, and we take this to mean that their concentrations are too small compared to those of the other species present.

The stability constants follow a trend which correlates with that of the protonation constants of the ligands, *i.e.*, they are generally higher for the compounds with longer methylene chains. The difference is most marked from the first to the second member of the series, as expected from analogous differences in the values of β_{012} .

The distribution of the species is also different in the case of the first member of the series (CEDTA),

which does not form a normal ML complex, and the dimer M_2L_2 is more relevant above pH 5 than in the case of the higher homologues—see Fig. 2. The protonated complex MLH is the dominant species between pH 3 and 6 in all systems and it should be noted that the M_2L_2 complexes correspond to MLH dimers in which two UO_2^{2+} groups bonded to an iminodiacetic group of the ligand are bridged by two hydroxyl groups. The two protons will of course attach to the two remaining imino nitrogen atoms of the ligands.

Between pH 5 and 6 several other minor poly-

Table 4. Average difference between the conditional constants of the corresponding pdta and cpdta species

Ligands	$\Delta \log K'_{MLH}$
EDTA-CEDTA	0.764
PDTA-DBT	0.070
BDTA-OTC	0.027

nuclear species seem to coexist, but although the calculated constants are reproducible and the fitting parameters satisfactory, precipitates start to be formed in this pH range, depending on the concentration ratios of the metal and ligand, so a detailed discussion of differences and trends in the various systems is not warranted.

The stability constants given by the MINQUAD program for the $UO_2^{2+}/cpdta$ systems are always higher than those obtained for the corresponding $UO_2^{2+}/pdta$ systems. This does not indicate that the ability of the new ligands to complex the UO_2^{2+} ion is higher for the cpdta than for the pdta, since the basicity and the number of protons of the ligand must be taken into account. For this sort of comparison "conditional constants", as defined by Ringbom and Schwarzenbach,^{13,14} must be used.

The values of the conditional constants for the MLH species of CEDTA, DBT and OTC and for the corresponding UO_2^{2+} complexes formed with ethylenediaminetetra-acetic acid (EDTA), n-propanediaminetetra-acetic acid (PDTA) and n-butanediaminetetra-acetic acid (BDTA)⁸, were calculated by using the expression:

$$K'_{MLH} = \frac{[MLH]}{[M]' [L]'}$$

where $[M]'$ and $[L]'$ are the total concentrations of metal and protonated ligand not involved in MLH (i.e. the conditional concentrations).

The values of the conditional constants are pH-dependent and were calculated for a range of pH in which the MLH species are dominant (pH 3–5). The results are represented graphically in Fig. 3, and it can be seen that the trend is now reversed, i.e., the pdta form stronger complexes than the cpdta with UO_2^{2+} in this range of pH.

The difference is highest for EDTA and CEDTA, smaller for PDTA and DBT and within the error limits for BDTA and OTC. The decreasing difference on moving forward in the series, and the highest values for EDTA-CEDTA and PDTA-DBT show that the α -carboxyl substituent does not co-ordinate to UO_2^{2+} and, furthermore, decreases the stability of the complexes due to its effect on the basicity of the nitrogen atoms of the ligand. This effect is especially important if it is not compensated by a sufficiently long hydrocarbon chain.

These findings confirm that the uranyl ion has co-ordination number five in its equatorial plane for complexes formed with this type of ligand.^{15,16} Thus

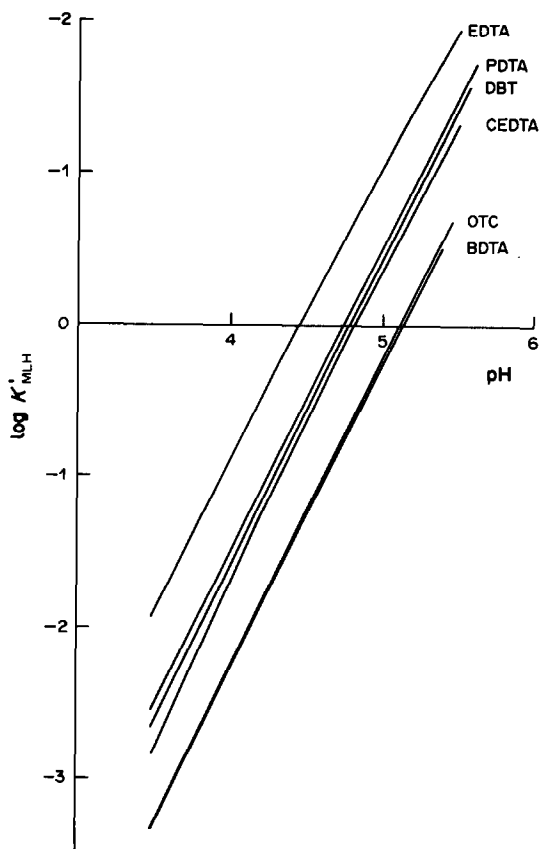


Fig. 3. Variation of $\log K'_{MLH}$ with pH for cpdta and pdta.

one of the carboxyl groups of the ligand cannot co-ordinate; on the contrary it decreases the stability of the complexes formed, by its negative inductive effect, particularly in the case of the first members of the series since both nitrogen atoms of the ligands are affected. For the higher members the effect is compensated and the presence of the α -carboxyl group becomes irrelevant with reference to complexation of the uranyl ion.

Acknowledgement—The authors thank Prof. J. J. R. Fraústo da Silva for help given in the interpretation and discussion of the results, and to the Spanish M.E.C. for a grant that enabled the research to be performed.

REFERENCES

1. S. Gonzalez Garcia, F. Sanchez Santos and M. F. Morales Ayala, *Ars Pharm.*, 1976, 17, 295.
2. S. Gonzalez Garcia, J. Niclos Gutierrez and A. Matilla Hernandez, *An. Quim.*, 1983, 79B, 24.
3. J. Niclos Gutierrez, S. Gonzalez Garcia, A. Matilla Hernandez and J. M. Tercero Moreno, *ibid.*, 1983, 79B, 517.
4. A. Matilla Hernandez, S. Gonzalez Garcia, J. Niclos Gutierrez and J. M. Tercero Moreno, *ibid.*, 1985, 81B, 297.
5. J. Niclos Gutierrez, S. Gonzalez Garcia, A. Matilla Hernandez and J. M. Tercero Moreno, *ibid.*, 1983, 79B, 525.
6. J. J. R. Fraústo da Silva and M. L. Simões Gonçalves, *Talanta*, 1968, 15, 609.

7. M. L. Simões Gonçalves, A. M. Almeida Mota and J. J. R. Fraústo da Silva, *ibid.*, 1983, **30**, 69.
8. *Idem*, *ibid.*, 1984, **31**, 531.
9. A. Sabatini, A. Vacca and P. Gans, *ibid.*, 1974, **21**, 53.
10. P. Gans, A. Sabatini and A. Vacca, *Inorg. Chim. Acta*, 1976, **18**, 237.
11. G. Gran, *Analyst*, 1952, **77**, 661.
12. S. Ahrlund, *Acta Chem. Scand.*, 1951, **5**, 199.
13. A. Ringbom, *Les complexes en chimie analytique*, Dunot, Paris, 1967.
14. G. Schwarzenbach and H. Flaschka, *Complexometric Titration*, Methuen, London, 1969.
15. J. J. R. Fraústo da Silva and M. L. Simões Gonçalves, *J. Inorg. Chem.*, 1970, **32**, 1313.
16. R. Graziani, B. Zarli, A. Cassol, G. Bombieri, E. Forsellini and F. Tondello, *Inorg. Chem.*, 1970, **9**, 2116.

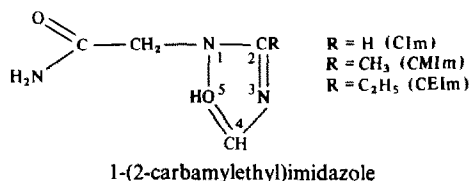
ACID-BASE IONIZATION EQUILIBRIA OF 1-(2-CARBAMYLETHYL) IMIDAZOLE AND ITS 2-METHYL AND 2-ETHYL DERIVATIVES

M. TERESA S. D. VASCONCELOS and ADÉLIO A. S. C. MACHADO
 Chemistry Department, Faculty of Science, University of Oporto, 4000 Oporto, Portugal

(Received 1 August 1986. Accepted 28 November 1986)

Summary—The acid and base ionization constants of 1-(2-carbamylethyl)-2-alkylimidazoles, as well as the acid ionization constants of acrylamide and acetamide, have been determined by potentiometry. Concentration constants at 10.0, 25.0 and 40.0° and $I = 0.1M$ (KNO_3) were measured. From plots of $\log K$ vs. $1/T$ the thermodynamic parameters (ΔH and ΔS) of the ionization reactions were calculated.

In 1-(2-carbamylethyl)imidazole (CIm) and its 2-methyl (CMIm) and 2-ethyl (CEIm) derivatives, two important co-ordinating groups in bio-inorganic chemistry, imidazole and amide, co-exist. To the best of our knowledge, no studies of the co-ordinating behaviour of simple ligands with both groups have been described in the literature. Hence a study of these complexing properties both in



solution¹ and in the solid state², was undertaken. In the solution study, the acid-base ionization equilibria of the ligands were studied (the compounds are amphiprotic). This note reports the concentration ionization constants found potentiometrically. The ionization constants were measured at different temperatures and ΔH and ΔS calculated. Simple amides (acetamide and acrylamide) were studied for comparison. A value of the ionization constant of acetamide was reported³ a long time ago. For acrylamide no value was found in the literature.

EXPERIMENTAL

General information on reagents, apparatus, procedure and calculations was given in a previous paper,⁴ and only details are presented here.

Chemicals

CIm was synthesized according to Dowbenko *et al.*,⁵ and CMIm and CEIm were prepared by a similar procedure.² The ligands were recrystallized twice from a mixture of methanol and acetone (m.p. CIm, 143–145° (lit.⁵ 143–145°); CMIm, 163–167°; CEIm, 119–122°). Acetamide and acrylamide (BDH) were recrystallized twice from the same mixture.

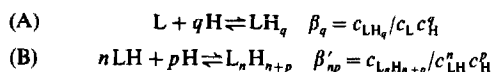
Procedure

Concentration constants in solutions with $I = 0.1M$ (KNO_3) were determined at 10.0 ± 0.2 , 25.0 ± 0.1 and

$40.0 \pm 0.2^\circ$ as before.⁴ Experimental data (about 20 points per titration) were collected for the following ligand concentration and pH ($= -\log [H^+]$) ranges: CIm $0.8-1.7 \times 10^{-2}M$, pH = 7.9–8.9; CMIm $1.0-1.2 \times 10^{-2}M$, pH = 8.9–9.7; CEIm $1.0-1.1 \times 10^{-2}M$, pH = 8.9–9.6; acetamide $9.0-18.5 \times 10^{-2}M$, pH = 9.3–10.4; acrylamide $1.4-15 \times 10^{-2}M$, pH = 9.4–10.5. In the last two cases pure solutions of the compounds were slightly acid (pH ca. 6) and sodium hydroxide was added to raise the pH to ca. 10.5 before titration with acid.

Calculations

Calculations were performed with the MINIQUAD program⁶ on an NCR 4100 ELLIOT computer with the following systems (LH = CIm, CMIm, CEIm)



The adjustment of the following models was attempted:

- (I) $L/LH/LH_2$, [A, $\log \beta_1 = pK_{a2}(LH_2^+)$, $\log (\beta_2/\beta_1) = pK_{a1}(LH_2^+)$], which allows for the amphiprotic character of the compounds;
- (II) LH/LH_2 [B, $\log \beta'_{11} = pK_{a1}(LH_2^+)$], in which the compounds were considered as monoprotic bases;
- (III) $LH/LH_2/LH_3$ [B, $\log \beta'_{11} = pK_{a2}(LH_3^{2+})$, $\log (\beta'_{12}/\beta'_{11}) = pK_{a1}(LH_3^{2+})$], in which the compounds were considered as diprotic bases;
- (IV) $LH/LH_2/L_2H_3$ [B, $\log \beta'_{11} = pK_{a1}(LH_2^+)$], which allows for association (β'_{21}) after protonation of the molecule.

Typical results of the adjustments obtained for CIm at 25.0° are presented in Table 1. At 10.0 and 40.0°, as well as for the other two imidazole derivatives, the results were similar. Table 1 shows that the best fit is obtained with model (I) (lowest R -factor). Any of the other models is rejected by the R -factor ratio test.⁷ Moreover, these other models do not satisfy the χ^2 test.⁸

For acetamide and acrylamide, only a model in which the compounds were considered monoprotic acids (system A) yielded results. Other constants were rejected when included in the model.

Values of K_w measured in the conditions used for the determinations were employed.⁴

RESULTS AND DISCUSSION

Ionization constants

The acid constant K_{a1} corresponds to protonation of the nitrogen atom at position 3 in the imidazole

Table 1. Comparison of typical data adjustments for different models (CIm, 25°)*

Model	$\log \beta_1$ (or β'_{11})	$\log \beta_2$ (or β'_{12})	$\log \beta_1/\beta_2$ (or β'_{23})	χ^2	$10^4 \times R$
(I)	11.619 (9)	18.216 (9)	6.598 (0.4)	9.6	0.4
(II)	6.586 (3)			28.1	5.0
(III)	6.550 (5)	13.406 (56)		26.4	2.3
(IV)	6.567 (4)	Rejected	22.980 (75)	26.0	2.9

*R, χ^2 given by MINIQAD; σ (standard deviation) refers to the last figure.

Model (I): $\log (\beta_2/\beta_1) = pK_{a1}(LH_2^+)$; $\log \beta_1 = pK_{a2}(LH_2^+)$

Model (II): $\log \beta'_{11} = pK_{a1}(LH_2^+)$

Model (III): $\log (\beta'_{12}/\beta'_{11}) = pK_{a1}(LH_3^{2+})$; $\log \beta'_{11} = pK_{a2}(LH_3^{2+})$

Model (IV): $\log \beta'_{11} = pK_{a1}(LH_2^+)$.

Table 2. Ionization constants of 1-(2-carbamylethyl) imidazoles ($I = 0.1M$)*

Ligand	Temp., °C	$\log \beta_1$	$\log \beta_2$	$\log \beta_2/\beta_1$
CIm	10.0	12.34 (2)	19.26 (2)	6.92 (3)
	25.0	11.657 (6)	18.261 (6)	6.604 (8)
	40.0	11.36 (2)	17.73 (2)	6.37 (3)
CMIm	10.0	12.65 (1)	20.56 (1)	7.91 (1)
	25.0	12.126 (6)	19.686 (6)	7.559 (8)
	40.0	11.89 (1)	19.18 (1)	7.29 (1)
CEIm	10.0	12.875 (7)	20.714 (6)	7.839 (9)
	25.0	12.211 (4)	19.728 (5)	7.517 (6)
	40.0	11.913 (9)	19.165 (9)	7.25 (1)

*Weighted averages of values obtained in 2-4 determinations; model(I); $\log \beta_1 = pK_{a2}(LH_2^+)$, $\log (\beta_2/\beta_1) = pK_{a1}(LH_2^+)$; σ as for Table 1.

ring of the compounds. The values of pK_{a1} (Table 2) show that the presence of the carbamylethyl groups as a substituent at position 1 is responsible for a rather large reduction of the basicity of the nitrogen atom at position 3 in CIm relative to that of imidazole (see pK_{a1} values in Fig. 1). This effect is opposite to that observed when the substituent at position 1 is the methyl group (1-MeIm), in which case a slight increase of basicity is observed. In CMIm, where besides the carbamylethyl group at position 1 there is a methyl group at position 2, the basicity is higher than that of both CIm and imidazole, similarly to the case for 2-MeIm. A similar situation was found for CEIm, although with slightly smaller pK_{a1} differences. The coherence of the differences in the pK_{a1} values is shown in Fig. 1.

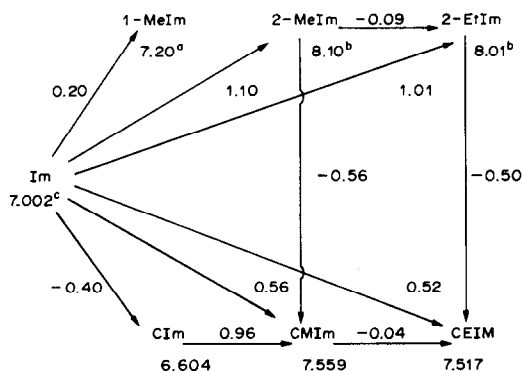


Fig. 1. Variations in pK_{a1} [at 25° and $I = 0.1M$ (KNO_3)] except when stated otherwise] with substitutions in imidazole at positions 1 and 2. Values of pK_{a1} are shown close to the formulae and their differences close to the lines. ^a $I = 0.15M$ (KNO_3). ^b $I = 0.2M$ (Na_2SO_4). ¹⁰ Reference 4.

The acid constant K_{a2} corresponds to deprotonation of the compounds. The assignment of the deprotonation to a definite atom of the molecules is difficult. For 1-(2-carbamylethyl)-2-alkylimidazoles the deprotonation cannot be assigned to the hydrogen atom at position 1, as it can in imidazole.⁴ Deprotonation in the amide group was contemplated and so acetamide and acrylamide were included in the study for the purpose of comparison. The value found (Table 3) for the pK_a of acetamide (13.40) is smaller than that (15.08) obtained by conductimetric measurements.³ However, in view of the value of the constant, the difference is not unexpected. Acrylamide (pK_a 13.05) is slightly more acidic than acetamide because of the electron-attracting effect of the vinyl group. In any case, the values of the acid constant found for these simple amides were smaller by more than a factor of 10 than the K_{a2} values found for the 1-(2-carbamylethyl)-2-alkylimidazoles, which suggests that in the latter compounds K_{a2} may not be due simply to deprotonation in the amide group. Indeed the measured constant is a macroscopic equilibrium constant which may be composed of several microscopic equilibrium constants. Deprotonations in the positions 2 and 4 (or 5) in the imidazole ring

Table 3. Ionization constants (pK_a) of simple amides* ($I = 0.1M$)

Temp., °C	Acrylamide	Acetamide
10.0	13.66 (2)	14.01 (2)
25.0	13.05 (1)	13.40 (1)
40.0	12.58 (3)	12.83 (1)

*Weighted averages of values obtained in 2-4 determinations; σ as for Table 1.

Table 4. Thermodynamic parameters for acid ionization constants of 1-(2-carbamylethyl) imidazoles, acetamide and acrylamide ($I = 0.1M$)*

Ligand	LH_2^+/LH			LH/L^-		
	ΔH , kJ/mole	ΔS , J.mole ⁻¹ .K ⁻¹	r	ΔH , kJ/mole	ΔS , J.mole ⁻¹ .K ⁻¹	r
Clm	31	-21	0.9986	56	-39	0.9806
CMIm	35	-27	0.9989	44	-88	0.9831
CEIm	33	-33	0.9996	55	-52	0.9826
Acetamide				61	-44	0.9990
Acrylamide				67	-33	0.9999

* r , correlation coefficient of linear least-squares adjustment.

may contribute to this macroscopic equilibrium constant, since complexes of deprotonated imidazole derivatives with metal bound at position 2 have been obtained¹¹ and the reactivity of the hydrogen atoms at positions 2 and 4 (or 5) in deuteration reactions of imidazole is explained by a mechanism which involves deprotonation.¹² Even if such deprotonation is not complete, hydrogen-bonding between the hydrogen atom in the 2 or 5 position and the oxygen of the amide group may favour deprotonation in the $-NH_2$ group, similar to that observed in complexes where the amide group is co-ordinated through its oxygen atom.¹³

Thermodynamic parameters

Values of ΔH and ΔS were obtained by linear least-squares adjustment of $\log K_{ai}$ vs. $1/T$ data (Table 4). The correlation coefficients are worse for the data corresponding to the deprotonation equilibria (LH/L^- in Table 4) of the imidazole derivatives than for their protonation equilibria (LH_2^+/LH). This situation is expected because the equilibrium constants corresponding to these deprotonations are very small.

The values of ΔH for the protonation reactions of the 1-(2-carbamylethyl)-2-alkylimidazoles are all smaller than the corresponding value for imidazole found by the same procedure ($\Delta H = 38$ kJ/mole).⁴ This is a consequence of the electron-withdrawing properties of the carbamyl group at position 1. The order of the ΔH values (Clm < CEIm < CMIm) is the same as that of the corresponding basic constants, which is a consequence of the electron-repelling properties of the alkyl groups at position 2 (H < Et < Me). This correlation also shows that the enthalpy contribution to K_{a1} is more important than the entropy contribution.

With respect to the values of ΔH for the deprotonation of the compounds, the values found for the 1-(2-carbamylethyl)-2-alkylimidazoles are a few kJ/mole smaller than for the simple amides. However, in view of the difficulties of the assignment of the deprotonation reaction to definite atoms in the molecules, no further comments seem worthwhile.

Acknowledgement—Financial support received from INIC (Lisbon) through Research Line No. 4A of CIQUUP is gratefully acknowledged.

REFERENCES

1. M. T. S. D. Vasconcelos, *Doctoral Thesis*, Faculty of Science of Oporto, Oporto, 1983.
2. M. C. R. M. P. Basto, *Doctoral Thesis*, Faculty of Science of Oporto, Oporto, 1984.
3. G. E. K. Branch and J. O. Clayton, *J. Am. Chem. Soc.*, 1928, **50**, 1580.
4. M. T. S. D. Vasconcelos and A. A. S. C. Machado, *Talanta*, 1986, **33**, 919.
5. R. Dowbenko, C. C. Anderson and W. H. Chang, *Ind. Eng. Chem. Prod. Res. Develop.*, 1971, **10**, 344.
6. P. Gans, A. Sabatini and A. Vacca, *Inorg. Chim. Acta*, 1976, **18**, 237.
7. M. Jaskólski and L. Lomozick, *Talanta*, 1985, **32**, 511.
8. A. Sabatini, A. Vacca and P. Gans, *ibid.*, 1974, **21**, 53.
9. N. C. Li, J. M. White and E. Doody, *J. Am. Chem. Soc.*, 1954, **76**, 6219.
10. M. Guntensperger and A. D. Zuberbühler, *Helv. Chim. Acta*, 1977, **60**, 2584.
11. R. J. Sunderg, R. F. Bryan, I. F. Taylor, Jr. and H. Taube, *J. Am. Chem. Soc.*, 1974, **96**, 381.
12. J. D. Vaughan, Z. Mughrabi and E. Chung Wu, *J. Org. Chem.*, 1970, **35**, 1141.
13. R. C. Martin, *Optical Properties of Transition Metal Ion Complexes of Amino Acids and Peptides*, in H. Siegel (ed.), *Metal Ions in Biological Systems*, Vol. 1, p. 129, Dekker, New York, 1974.

SECOND HARMONIC a.c. ANODIC STRIPPING VOLTAMMETRY OF METALS AT TRACE LEVEL

SIMULTANEOUS DETERMINATION OF LEAD AND THALLIUM, AND BISMUTH AND ANTIMONY

C. LOCATELLI,* F. FAGIOLI and C. BIGHI

Laboratory for Analytical Chemistry, Department of Chemistry, University of Ferrara,
Via L. Borsari 46, 44100 Ferrara, Italy

T. GARAI

Research Laboratory for Inorganic Chemistry, Hungarian Academy of Sciences, P.O.B. 132,
H-1502 Budapest, Hungary

(Received 26 November 1986. Accepted 6 February 1987)

Summary—Pairs of elements with very small differences in their half-wave potentials were determined at trace levels by second harmonic a.c. anodic stripping voltammetry. The simultaneous determination of lead and thallium as well as that of bismuth and antimony in 1M hydrochloric acid as supporting electrolyte was found to be possible in the range of concentration ratios: $7:1 \geq C_{\text{Pb}}:C_{\text{Tl}} \geq 1:36$ and $45:1 \geq C_{\text{Bi}}:C_{\text{Sb}} \geq 1:35$, with <5% relative error due to mutual interference. The limit of detection was $\sim 10^{-8}M$ for all four elements, and the precision and error were 2–3%. The simultaneous determination of these metals in mixtures with concentration ratios outside the quoted ranges is still feasible by the standard-addition technique.

Polarography has frequently been used for the simultaneous determination of depolarizers having only slightly different half-wave potentials (less than 150–200 mV apart). A considerable improvement in selectivity is attained by using modern voltammetric techniques such as a.c. or differential-pulse voltammetry^{1,2} in addition to proper choice of supporting electrolyte—a common approach suggested in the polarographic literature. The simultaneous determination of metals at trace levels, e.g., in biological matrices or environmental samples has aroused much interest in recent years.³ In view of the practical importance of this a systematic study was undertaken to evaluate the possibilities and limitations of the simultaneous determination of some pairs of metal ions.⁴ In this communication we report the simultaneous determination at trace levels of lead and thallium as well as of bismuth and antimony, which exhibit very small differences in half-wave potential in the commonly employed supporting electrolytes.

Klahre *et al.*⁵ determined lead and thallium in alkaline solution where the difference between the half-wave potentials of the two elements is sufficiently large.

Neeb and co-workers^{6–8} added complexing agents to eliminate interferences, and Dhaneshwar and Zarakpar⁹ determined lead and thallium in silicon as

well as in environmental particulate matter and rain water samples by using a tartrate-buffered medium at pH 4.5 in the presence of EDTA. Bruckenstein and Nagai¹⁰ developed an interesting method for determination of thallium in the presence of lead with a mercury film electrode and chemical stripping. Both lead and thallium were deposited on the working electrode simultaneously with mercury and the amalgam was then chemically oxidized by the excess of Hg(II) in the solution. The process was monitored chronopotentiometrically. Thallium was effectively separated from lead since the amalgam of the former reacted more rapidly with Hg(II) than did that of the latter.

Bismuth and antimony have been determined simultaneously by second harmonic a.c. polarography in 1M hydrochloric acid medium.¹¹ Gillain *et al.*¹² have determined bismuth and antimony in sea-water by differential-pulse anodic stripping voltammetry at a hanging mercury drop electrode, but optimized the instrumental parameters considering possible mutual interferences. Brihaye *et al.*¹³ have also determined bismuth and antimony in sea-water by the anodic stripping technique, and demonstrated the influence of sodium chloride concentration on the peak separation.

Petak and Koubova¹⁴ used anodic stripping voltammetry at a thin mercury-film carbon electrode for the determination of bismuth and antimony, after an ion-exchange separation.

*To whom correspondence should be addressed.

EXPERIMENTAL

Apparatus

Anodic stripping voltammetric analysis was done with an, AMEL model 471 multipolarograph equipped with a model 291/LF stirrer and a model 452/T timer. A conventional three-electrode cell was fitted with a long-lasting sessile-drop mercury electrode (LLSDME) with a drop-time of 240–300 sec, as the working electrode, and a saturated calomel electrode (SCE) and a platinum electrode were employed as the reference and auxiliary electrodes respectively.

The voltammetric cell was kept at $25.0 \pm 0.5^\circ$. Prior to analysis the solutions were deaerated by purging with pure nitrogen for about 20 min. During electrolysis the solutions were stirred with a Teflon-coated magnetic stirring bar. Standard additions were made with Eppendorf micropipettes with disposable plastic tips. A DIGITAL-MINC 11 desk computer was employed for all the linear regression and statistical calculations.

Reagents

All solutions were prepared with distilled water. The hydrochloric acid was Aristar grade (BDH). Aqueous stock solutions of lead(II), thallium(I), bismuth(III) and antimony(III) were prepared by dilution of 1000-mg/l BDH standard solutions.

The Teflon cell was rinsed periodically with concentrated nitric acid to minimize contamination.

RESULTS AND DISCUSSION

Hydrochloric acid (1M) was used as the supporting electrolyte. Lead(II), thallium(I), bismuth(III) and antimony(III) are reduced reversibly in this medium to yield the corresponding amalgams, the half-wave potentials (*V vs. SCE*) being -0.435 , -0.475 , -0.090 and -0.150 respectively.

Table 1 lists the experimental conditions for the determinations by first and second harmonic a.c. anodic stripping voltammetry. Attention was paid to

selecting the optimum demodulation phase angle (ϕ) to minimize the capacitive current.

Under these conditions, the peak-width measured at half-height ($W_{1/2}$) of the first harmonic and the peak-to-peak potential separation (ΔE_{p-p}) of the second harmonic voltamperograms were determined. For reversible electrode processes the theoretical values are $90/n$ mV for $W_{1/2}$ and $68/n$ mV for ΔE_{p-p} where n is the number of electrons involved in the electrode process (Table 2).¹ The experimental peak potentials of the first harmonic and the potentials corresponding to zero current of the second harmonic voltamperograms are also reported. Excellent agreement was found between the theoretical data (in brackets) and the corresponding experimental data.

The analytical calibration curves for both first and second harmonic a.c. anodic stripping voltammetry are described in Table 3. The standard-addition method was used in all cases and each point was the mean of five readings. The second harmonic calibration curves were calculated by using the peak current values at more positive or more negative potentials, as appropriate, than the half-wave potentials of both elements of each couple.^{1,11} The correlation coefficient (r) was excellent for all the regression functions, and the low relative standard deviation proved the good precision of the analytical procedure. The corresponding detection limit is also reported for each calibration curve.

The simultaneous determination of lead and thallium and of bismuth and antimony, was studied for various concentrations of the components.

Figures 1 and 2 show the typical first and the second harmonic voltamperograms obtained. The

Table 1. Experimental conditions for the determination of lead, thallium, bismuth and antimony in 1M HCl medium (first and second harmonic a.c. anodic stripping voltammetry)

	Pb(II)	Tl(I)	Bi(III)	Sb(III)
Deposition potential, <i>V vs. SCE</i>	-0.700	-0.700	-0.350	-0.350
Deposition time, <i>sec</i>	180	180	180	180
Rest time, <i>sec</i>	30	30	30	30
Scan-rate, <i>mV/sec</i>	10	10	10	10
Frequency (a.c.), <i>Hz</i>	100	100	100	100
Amplitude (a.c.), <i>mV</i>	10	10	10	10
ϕ first harmonic, <i>degrees</i>	270 + 87	270 + 82	270 + 83	270 + 86
ϕ second harmonic, <i>degrees</i>	270 + 71	270 + 68	270 + 67	270 + 69
Stirrer speed, <i>rpm</i>	800	800	800	800

Table 2. Experimental parameters* for first and second harmonic a.c. anodic stripping voltammetry in 1M HCl medium

	Pb(II)	Tl(I)	Bi(III)	Sb(III)
Peak potential, <i>V vs. SCE</i> (first harmonic)	-0.435 ± 0.005 (-0.435)	-0.480 ± 0.005 (-0.475)	-0.090 ± 0.005 (-0.090)	-0.150 ± 0.005 (-0.150)
Zero-current potential, <i>V vs. SCE</i> (second harmonic)	-0.440 ± 0.005 (-0.435)	-0.480 ± 0.005 (-0.475)	-0.085 ± 0.005 (-0.090)	-0.150 ± 0.005 (-0.150)
Peak-width at half-height, <i>mV</i>	43 ± 5 (45)	90 ± 5 (90)	27 ± 5 (30)	30 ± 5 (30)
Peak-to-peak separation, <i>mV</i>	34 ± 5 (34)	70 ± 5 (68)	20 ± 5 (23)	25 ± 5 (23)

*Mean ± confidence limits (95% probability).

Table 3. Calibration data* for a.c. anodic stripping voltammetric determinations

	First harmonic	Second harmonic
Pb(II)	$i_p = (-0.002 \pm 0.002) + (2.98 \pm 0.02) \times 10^6 c$ $r = 0.9999$; $s_r = 1.0\%$; D.L. = $6.7 \times 10^{-8} M$	$i_p = (-0.003 \pm 0.004) + (3.51 \pm 0.04) \times 10^5 c$ $r = 0.9996$; $s_r = 1.7\%$; D.L. = $5.7 \times 10^{-8} M$
	Range of concentrations $(0-2) \times 10^{-7} M$	
Tl(I)	$i_p = (0.003 \pm 0.004) + (2.33 \pm 0.02) \times 10^6 c$ $r = 0.9997$; $s_r = 1.4\%$; D.L. = $8.6 \times 10^{-8} M$	$i_p = (0.0005 \pm 0.0006) + (2.49 \pm 0.02) \times 10^5 c$ $r = 0.9993$; $s_r = 1.40\%$; D.L. = $8.0 \times 10^{-8} M$
	Range of concentrations $(0-3) \times 10^{-7} M$	
Bi(III)	$i_p = (-0.001 \pm 0.002) + (3.72 \pm 0.04) \times 10^6 c$ $r = 0.9996$; $s_r = 2.0\%$; D.L. = $5.4 \times 10^{-8} M$	$i_p = (-0.002 \pm 0.002) + (4.51 \pm 0.07) \times 10^5 c$ $r = 0.9991$; $s_r = 3.1\%$; D.L. = $4.4 \times 10^{-8} M$
	Range of concentrations $(0-2) \times 10^{-7} M$	
Sb(III)	$i_p = (0.001 \pm 0.002) + (1.91 \pm 0.02) \times 10^6 c$ $r = 0.9993$; $s_r = 2.2\%$; D.L. = $1.0 \times 10^{-8} M$	$i_p = (-0.004 \pm 0.005) + (2.33 \pm 0.03) \times 10^5 c$ $r = 0.9993$; $s_r = 2.3\%$; D.L. = $8.6 \times 10^{-8} M$
	Range of concentrations $(0-5) \times 10^{-7} M$	

The limit of detection (D.L.) is expressed according to the IUPAC recommendation¹⁶ and corresponds to a probability of 99%.

*Means $\pm 95\%$ probability confidence limits.

electroactive species are well resolved in the second harmonic voltamperograms, but not in the first harmonic voltamperograms, so the simultaneous determinations were done only by second harmonic a.c. voltammetry.

The experimental conditions were those in Table 1, except that the phase angles were set to $270^\circ + 68^\circ$ and $270^\circ + 69^\circ$ for the Pb/Tl and Bi/Sb combinations respectively. The peak currents measured for the mixture were compared with those calculated by using the corresponding equation for the calibration curve of the individual element (*cf.* Table 3), and the

relative errors were calculated for the element present at the lower concentration. These errors are plotted *vs.* the concentration ratios of the mixtures in Figs. 3 and 4.

The two arrows in Figs. 3 and 4 indicate the concentration ratio ranges for simultaneous determination of the two metals with a maximum experimental error of 5%. These ranges are $7:1 \geq C_{Pb}:C_{Tl} \geq 1:36$ and $45:1 \geq C_{Sb}:C_{Bi} \geq 1:35$. In these

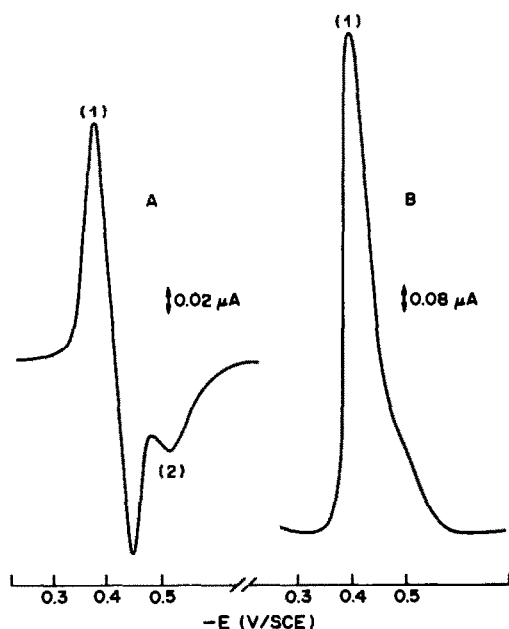


Fig. 1. Anodic stripping voltamperograms of (1) $5.1 \times 10^{-7} M$ lead, (2) $2.4 \times 10^{-7} M$ thallium. A, second harmonic, a.c.; B, first harmonic, a.c. Experimental conditions as in Table 1.

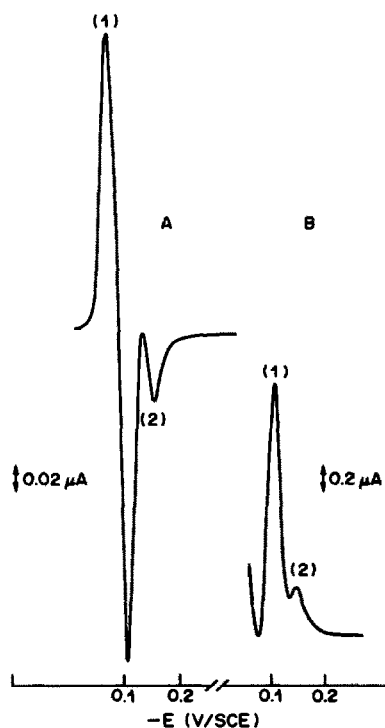


Fig. 2. Anodic stripping voltamperograms of (1) $5.1 \times 10^{-7} M$ bismuth, (2) $2.15 \times 10^{-7} M$ antimony. A, second harmonic, a.c.; B, first harmonic, a.c. Experimental conditions as in Table 1.

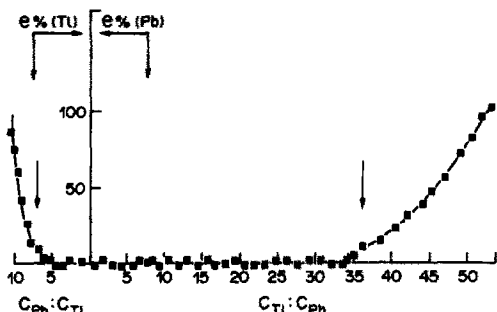


Fig. 3. Relationship between concentration ratios and relative errors ($e\%$) in determination of the element present at the lower concentration (lead and thallium mixture).

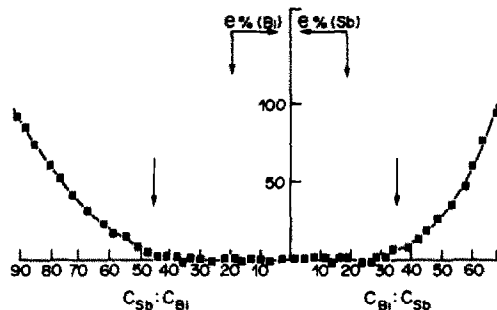


Fig. 4. Relationship between the concentration ratios and relative errors in the determination of the element present at the lower concentration (bismuth and antimony mixture).

ranges univariate and bivariate analyses of the experimental data were also performed. The interference of the second element is neglected in the univariate analysis, but taken into account in the bivariate analysis.

For both pairs of elements, the slopes obtained in the bivariate analysis were practically equal to those of the calibration curves (*cf.* Table 3) and the univariate analyses, showing that the mutual interferences were negligible, at least in the ranges of concentration ratios considered. This is confirmed by the negligible interferent slope coefficient of the bivariate regression functions (Tables 4 and 5). The precision, relative error and detection limits are also reported in Tables 4 and 5.

The precision, expressed as the relative standard

deviation (s_r), and the relative error (e), were about 2–3%, and the detection limits ($\sim 1 \times 10^{-8}M$) were low.

In practical analyses the following procedure was used, particularly for concentration ratios for which

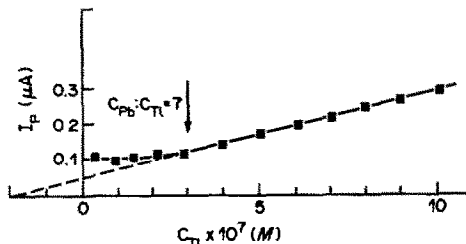


Fig. 5. Determination of thallium in a mixture with $c_{Pb} = 2.1 \times 10^{-6}M$ and $c_{Tl} = 1.87 \times 10^{-7}M$.

Table 4. Analysis of lead–thallium mixtures by second harmonic a.c. anodic stripping voltammetry (see footnotes to Table 3)

Determination of lead in the presence of thallium	Determination of thallium in presence of lead
Univariate analysis $i_p = (0.005 \pm 0.006) + (3.45 \pm 0.09) \times 10^5 c$ $r = 0.9995$; $s_r = 2.9\%$, $e = -1.7\%$ D.L. = $5.8 \times 10^{-8}M$	Univariate analysis $i_p = (-0.004 \pm 0.005) + (2.53 \pm 0.02) \times 10^5 c$ $r = 0.9993$; $s_r = 2.3\%$, $e = +1.6\%$ D.L. = $7.9 \times 10^{-8}M$
Bivariate analysis $i_p = -4.4 \times 10^{-4} + (3.40 \pm 0.02) \times 10^5 c_{Pb} + (2.5 \pm 1.9) \times 10^5 c_{Tl}$ $r = 0.9991$; $s_r = 1.3\%$; $e = -3.1\%$ D.L. = $5.9 \times 10^{-8}M$	Bivariate analysis $i_p = -6.8 \times 10^{-4} + (2.55 \pm 0.02) \times 10^5 c_{Tl} + (0.9 \pm 0.8) \times 10^5 c_{Pb}$ $r = 0.9994$; $s_r = 3.3\%$, $e = +2.4\%$ D.L. = $7.9 \times 10^{-8}M$

Table 5. Analysis of bismuth–antimony mixtures by second harmonic a.c. anodic stripping voltammetry (see footnotes to Table 3)

Determination of bismuth in presence of antimony	Determination of antimony in presence of bismuth
Univariate analysis $i_p = (0.002 \pm 0.003) + (4.41 \pm 0.03) \times 10^5 c$ $r = 0.9990$; $s_r = 1.6\%$, $e = -2.2\%$ D.L. = $4.5 \times 10^{-8}M$	Univariate analysis $i_p = (-0.004 \pm 0.005) + (2.31 \pm 0.05) \times 10^5 c$ $r = 0.9994$; $s_r = 1.4\%$, $e = -0.9\%$ D.L. = $8.7 \times 10^{-8}M$
Bivariate analysis $i_p = -1.4 \times 10^{-3} + (4.38 \pm 0.04) \times 10^5 c_{Bi} + (1.1 \pm 0.6) \times 10^5 c_{Sb}$ $r = 0.9992$; $s_r = 1.7\%$, $e = -2.9\%$ D.L. = $4.6 \times 10^{-8}M$	Bivariate analysis $i_p = -5.9 \times 10^{-4} + (2.25 \pm 0.05) \times 10^5 c_{Sb} + (2.3 \pm 0.5) \times 10^5 c_{Bi}$ $r = 0.9997$; $s_r = 1.4\%$, $e = -3.4\%$ D.L. = $8.9 \times 10^{-8}M$

Table 6. Recovery of the metal at lower concentration in the mixture (second harmonic a.c. anodic stripping voltammetry)

$c_M, 10^{-7}M$	$c_{M^*}, 10^{-7}M$	c_M/c_{M^*}	c_{M^*} found, $10^{-7}M$	Error, %
$c_{Tl} = 68.7$	$c_{Pb} = 1.34$	51.4:1	$c_{Pb} = 1.39$	+3.6
$c_{Tl} = 63.7$	$c_{Pb} = 1.35$	47.3:1	$c_{Pb} = 1.32$	-2.1
$c_{Tl} = 58.5$	$c_{Pb} = 1.35$	43.3:1	$c_{Pb} = 1.28$	-5.3
$c_{Pb} = 21.0†$	$c_{Tl} = 1.87$	11.2:1	$c_{Tl} = 1.78$	-4.8
$c_{Pb} = 17.6$	$c_{Tl} = 1.88$	9.4:1	$c_{Tl} = 1.94$	+3.4
$c_{Pb} = 15.8$	$c_{Tl} = 1.89$	8.4:1	$c_{Tl} = 1.82$	-3.6
$c_{Sb} = 81.2$	$c_{Bi} = 0.86$	94.4:1	$c_{Bi} = 0.90$	+4.4
$c_{Sb} = 67.7$	$c_{Bi} = 0.87$	77.3:1	$c_{Bi} = 0.95$	+8.2
$c_{Sb} = 53.6$	$c_{Bi} = 0.89$	60.1:1	$c_{Bi} = 0.87$	-2.7
$c_{Bi} = 94.7$	$c_{Sb} = 1.48$	64.1:1	$c_{Sb} = 1.37$	-6.8
$c_{Bi} = 82.4$	$c_{Sb} = 1.5$	54.8:1	$c_{Sb} = 1.52$	+1.8
$c_{Bi} = 69.1$	$c_{Sb} = 1.5$	45.4:1	$c_{Sb} = 1.59$	+4.3

†See also Fig. 5.

the calibration curves and the univariate and bivariate data analyses were no longer valid.

The element present at the higher concentration was determined by using the appropriate calibration curve (*cf.* Table 3), and the other was determined by addition of known amounts of standard solution to bring its concentration within the range of validity of the calibration curve and the uni- and bivariate analyses. An example is shown in Fig. 5 ($C_{Pb}:C_{Tl} = 11.2$). The thallium peak current was a non-linear function of the thallium concentration added until the concentration ratio came within the range for which mutual interference was effectively absent ($C_{Pb}:C_{Tl} \leq 7$, Fig. 3). The thallium was then easily determined by extrapolation in the usual way for standard additions methods. The limit of the linear domain was evaluated statistically according to the method of Liteanu *et al.*,¹⁵ using the *t*-test criterion. Some typical results are reported in Table 6. The error of the determinations was within experimental error in each case. The technique is applicable at any concentration ratio at which the peak for the minor

element is discernible in the voltamperogram. Thus lead can be determined in the presence of up to about 60-fold molar ratio of thallium and thallium in the presence of up to 15-fold molar ratio of lead.

For antimony and bismuth the corresponding limits are an approximately hundredfold excess of antimony can be tolerated in the determination of bismuth while an approximately seventyfold excess of bismuth still permits the determination of antimony.

The combination of second harmonic a.c. voltammetry and anodic stripping proves to be a powerful trace and ultratrace analytical technique for the simultaneous determination of species reversibly reducible at slightly different half-wave potentials.

REFERENCES

1. A. M. Bond, *Modern Polarographic Methods in Analytical Chemistry*. Dekker, New York, 1980.
2. T. Garai, Z. Nagy, F. Fagioli and C. Locatelli, *Anal. Sci.*, in the press.
3. F. Vydra, K. Štulík and E. Juláková, *Electrochemical Stripping Analysis*. Horwood, Chichester, 1976.
4. C. Locatelli, F. Fagioli, C. Bighi and T. Garai, *Talanta*, 1986, **33**, 243.
5. P. Klahre, P. Valenta and H. W. Nürnberg, *Vom Wasser*, 1978, **51**, 199.
6. R. Neeb, *Z. Anal. Chem.*, 1959, **171**, 321.
7. R. Neeb and I. Kiehnast, *ibid.*, 1968, **241**, 142.
8. W. Christmann, Z. Lukaszewski and R. Neeb, *ibid.*, 1980, **302**, 32.
9. R. G. Dhaneshwar and L. R. Zarapkar, *Analyst*, 1980, **105**, 386.
10. S. Bruckenstein and T. Nagai, *Anal. Chem.*, 1961, **33**, 1201.
11. F. Fagioli, F. Dondi and T. Garai, *Hung. Sci. Instr.*, 1983, **56**, 11.
12. G. Gillain, G. Duyckaerts and A. Disteche, *Anal. Chim. Acta*, 1979, **106**, 23.
13. C. Brihaye, G. Gillain and G. Duyckaerts, *ibid.*, 1983, **148**, 51.
14. P. Petak and V. Koubová, *Analyst*, 1978, **103**, 179.
15. C. Liteanu, I. C. Popescu and E. Hopirtean, *Anal. Chem.*, 1976, **48**, 2010.
16. IUPAC, *Spectrochim. Acta*, 1978, **33B**, 219.

DOSAGE SPECTROPHOTOMETRIQUE DES IONS CYANURE LIBRES PAR FORMATION DU COMPLEXE MIXTE BIS(BATHOPHENANTHROLINE) DICYANO FER(II)

M. MARIAUD et P. LEVILLAIN

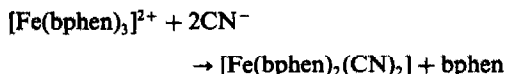
Laboratoire de Chimie Analytique, Faculté des Sciences Pharmaceutiques, 2 bis Boulevard Tonnellé, B.P. 3213, 37032 Tours Cedex, France

(Reçu le 13 janvier 1986. Révisé le 16 septembre 1986. Accepté le 6 février 1987)

Résumé—En milieu aqueux, les ions cyanure réagissent sur le complexe $[\text{Fe}(\text{bathophénanthroline})_3]^{2+}$ pour former le complexe mixte $[\text{Fe}(\text{bathophénanthroline})_2(\text{CN})_2]$ très fortement coloré et extractible par le chloroforme. Cette réaction a été utilisée pour doser les ions cyanure avec une bonne sensibilité et une excellente reproductibilité. De nombreuses interférences potentielles ont été étudiées.

Summary—Cyanide ions react in aqueous medium with $[\text{Fe}(\text{bathophenanthroline})_3]^{2+}$ to form the mixed-ligand complex $[\text{Fe}(\text{bathophenanthroline})_2(\text{CN})_2]$, which is strongly coloured and extractable into chloroform. This reaction can be used for determination of cyanide with good sensitivity and precision. Potential interferences have been studied.

La valeur élevée du nombre de publications relatives au dosage des ions cyanure libres en solution s'explique sans doute par la très grande toxicité de ces ions. Nombreuses et variées sont également les techniques proposées: potentiométrie, spectrophotométrie, etc. Comme cela a été indiqué récemment,¹ les techniques spectrophotométriques reposent, dans leur quasi totalité, sur la réaction de König.^{2,3} Or, il a été montré que les ions cyanure pouvaient réagir avec les complexes ferreux de la diphenyl-4,7 phénanthroline-1,10 (bathophénanthroline ou bphen), comme d'ailleurs avec les complexes de la phénanthroline-1,10 ou ceux de ces dérivés,⁴⁻⁷ pour former des complexes mixtes selon une réaction de type:



La coloration intense de complexe mixte formé et sa grande solubilité dans certains solvants organiques nous ont incités à étudier cette réaction en vue de la mise au point d'un dosage des ions cyanure. Une méthode utilisant la phénanthroline-1,10 a déjà été proposée,⁸ mais elle est longue et sa sensibilité est peu élevée.

PARTIE EXPERIMENTALE

Réactifs

Solutions d'ions cyanure, R₁. Elles sont préparées par dilution exacte et extemporanée d'une solution concentrée (renfermant 1 g de CN⁻ par litre) dont le titre précis est déterminé par argentimétrie en présence de *p*-diméthylaminobenzylidènerhodamine (Annexe 1 de la norme AFNOR T 90-107 de Mai 1975).

Solution tampon pH = 7 à 0,1M, R₂. A 10 ml d'une solution de KH₂PO₄ à 13,6 g/l., ajouter 15 ml d'une solution de Na₂HPO₄·2H₂O à 17,8 g/l.

Solution tampon pH = 7 à 0,01M, R₃. Elle est obtenue par dilution exacte de la solution R₂.

Solution de réactif colorant à 0,005M, R₄. Dissoudre 250 mg de bathophénanthroline dans environ 40 ml de méthanol. Dissoudre 69,5 mg de FeSO₄·7H₂O dans ~0,5 ml d'eau distillée. Ajouter à la solution de bathophénanthroline. Rincer et compléter à 50 ml avec du méthanol.

Solution d'hydroxyde de sodium, R₅. Ajouter 5 ml d'une solution de soude à 10M à 45 ml d'eau distillée. Mélanger avec 50 ml de méthanol.

Solution de Na₂SO₄·10H₂O à 32,2 g/l., R₆.

Papier séparateur de phases, Whatman 1 PS.

Technique opératoire

Technique A. Elle s'applique à des solutions renfermant de 1 à 20 mg/l. d'ions cyanure. Dans un tube à essais de 25 ml environ, bouchant hermétiquement, introduire 1 ml de la solution à doser, 1 ml de solution tampon (R₃) et 0,2 ml de réactif R₄. Porter 10 min au bain-marie à l'ébullition. Refroidir. Ajouter 1 ml de solution d'hydroxyde de sodium (R₅) et porter à nouveau au bain-marie à l'ébullition pendant 1 min. Refroidir. Ajouter 10 ml de solution de Na₂SO₄ (R₆) puis 5 ml de chloroforme. Agiter puis filtrer sur papier séparateur de phases. Mesurer l'absorbance des phases chloroformiques à 613 nm en réglant le 100% de transmission sur le blanc des réactifs. Préparer une gamme d'étalonnage en opérant de la même façon sur des solutions étalons renfermant de 1 à 20 mg d'ions cyanure par litre (R₁).

Technique B. Elle s'applique à des solutions de concentrations comprises entre 1 et 10 mg d'ions cyanure par litre. Elle est semblable à la technique A mais l'extraction est réalisée par 2 ml de chloroforme seulement.

Technique C. Elle s'applique à des solutions contenant de 0,1 à 2 mg d'ions cyanure par litre. Dans un tube à essais de 25 ml environ, bouchant hermétiquement, introduire 5 ml de solution à doser (ou de solutions étalons), 0,25 ml de solution tampon (R₃) et 0,2 ml de réactif R₄. Porter 10 min au bain-marie à l'ébullition. Refroidir. Ajouter 1 ml de solution d'hydroxyde de sodium (R₅). Porter au bain-marie à l'ébullition pendant 1 min. Refroidir et ajouter 10 ml de solution de Na₂SO₄ (R₆) puis 2 ml de chloroforme. Agiter, filtrer sur papier séparateur de phases. Mesurer l'absorbance des phases chloroformiques à 613 nm.

RESULTATS ET DISCUSSION

Extraction du complexe [Fe(bphen)₂(CN)₂]

Choix du solvant. Le solvant choisi doit être insoluble dans le milieu réactionnel et présenter un bon pouvoir solvant vis-à-vis du complexe mixte. Notre choix s'est porté sur le chloroforme qui remplit ces deux conditions.

Conditions d'extraction. Bien que non chargé et insoluble dans l'eau, le complexe mixte est difficile à extraire par le chloroforme, car il se présente, après réaction, sous forme d'une suspension colloïdale. L'extraction est facilitée par l'addition à la phase aqueuse de sels hydrophiles comme Na₂SO₄. Le rendement d'extraction atteint 100% lorsque la concentration de ce sel dans la phase aqueuse est au minimum égale à 0,05M. Une augmentation de cette dernière accélère le processus. C'est pourquoi la concentration optimale choisie est d'environ 0,08M.

Influence de la teneur en méthanol. Le complexe [Fe(bphen)₂]²⁺ qui sert de réactif est insoluble dans l'eau. Il est introduit dans le milieu réactionnel en solution dans le méthanol. Une partie de ce dernier est entraînée par le chloroforme au cours de l'extraction, ce qui modifie le spectre du complexe mixte formé. Ce dernier présente, en effet, un phénomène de solvatochromie très prononcé: son maximum d'absorption se situe à 613 nm dans le chloroforme et à 568 nm dans le méthanol.⁹ L'effet hypochrome est d'autant plus marqué que la concentration en méthanol de la phase aqueuse avant extraction est plus élevée (tableau 1). Pour éviter cet inconvénient, il convient de diluer le milieu réactionnel avec de l'eau distillée avant l'extraction afin que la teneur en méthanol reste inférieure à 10%. La dilution et l'addition de Na₂SO₄ sont réalisées en même temps par l'intermédiaire d'une solution aqueuse de ce sel.

Formation du complexe [Fe(bphen)₂(CN)₂]

Influence de la température. Comme le montrent les résultats du tableau 2, une élévation de température facilite la formation du complexe cyané en augmentant simultanément le rendement et la vitesse de la réaction. C'est pourquoi nous travaillons au bain-marie à l'ébullition.

Influence du pH. Comme le montre la figure 1:

—le rendement de la réaction atteint son maximum dès pH 6,5, ce qui laisse penser que les solutions de cyanures sont, du fait de leur très faible molarité, totalement dissociées;

Tableau 1. Position du maximum d'absorption du complexe en fonction du % de méthanol dans la phase aqueuse

Méthanol dans la phase aqueuse, % v/v	10	25	50	75
λ de la phase organique, nm	613	609	599	591

Tableau 2. Variation de l'absorbance de la phase organique en fonction de la température et du temps de chauffage de la phase aqueuse (technique A, solution de CN⁻ à 11,8 mg/l.)

Temps de chauffage, min	Absorbance		
	30°C	50°C	100°C
3	0,445	0,515	0,59
5	0,45	0,54	0,61
10	0,495	0,555	0,65
15	0,46	0,55	0,66
30	0,45	0,565	0,64
60	0,45	0,57	0,66

—le rendement de la réaction est indépendant de la nature du tampon pour des pH compris entre 6,5 et 9,4, à condition d'opérer dans une zone où le pouvoir tampon est suffisant. Pour des pH supérieurs à 10, le rendement diminue fortement sans doute à cause de la destruction du complexe [Fe(bphen)₂]²⁺.⁷ Le tampon phosphate, qui a donné les résultats les plus reproductibles, a été retenu et nous avons décidé de travailler à pH 7. En l'absence d'un apport extérieur important de protons ou de base, supérieur à la capacité tampon, les absorbances maximales ont été obtenues pour des concentrations finales en tampon comprises entre 0,0025 et 0,005M.

Influence des anions. Le dosage peut être perturbé par la réaction de certains anions avec le complexe [Fe(bphen)₂]²⁺ pour former une paire d'ions, qui peut être extraite par le chloroforme. L'absorption propre de cette paire d'ions, bien que faible à la longueur d'onde de lecture, entraîne une légère variation d'absorbance et fausse les résultats.

Dix huit anions, présents en solution à la molarité de 0,005 ont été étudiés. Ils se classent en deux groupes:

—le premier renferme des anions hydrophiles qui ne permettent pas l'extraction de la paire d'ions: F⁻,

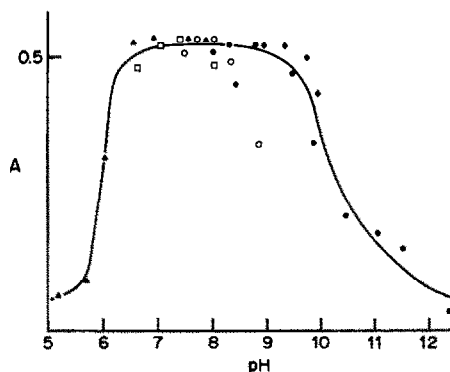


Fig. 1. Influence de la nature et du pH du tampon sur le rendement de la réaction (technique A—solution de cyanure à 9,5 µg/ml): ▲ tampon KH₂PO₄-Na₂HPO₄; □ borax-KH₂PO₄; ○ acide borique-NaOH; ◆ NH₃-(NH₄)₂SO₄; ● glycolle-NaOH.

SO_4^{2-} , HPO_4^{2-} , H_2PO_4^- , CH_3COO^- , HCO_3^- , CO_3^{2-} , citrate, tartrate;

—le deuxième renferme les ions qui permettent l'extraction totale (ClO_4^- , I^- , SCN^- , Br^- , NO_3^-) ou partielle (Cl^- , IO_3^- , oxalate, phthalate) de l'excès de réactif. Cette étape n'étant pas reproductible et pouvant donc fausser le dosage, il est nécessaire de détruire l'excès de réactif avant de procéder à l'extraction du complexe mixte à doser.

Le complexe $[\text{Fe}(\text{bphen})_3]^{2+}$ est instable en milieu alcalin.⁷ Nous avons donc choisi de le dénaturer par addition d'hydroxyde de sodium. Les essais ont été effectués en opérant en présence des anions du deuxième groupe, en concentration égale à 0,005M.

Quatre paramètres interviennent: la température, la durée du chauffage, la concentration en hydroxyde de sodium et la présence de méthanol. Une augmentation de chacun de ces paramètres se traduit par une accélération de dégradation du complexe $[\text{Fe}(\text{bphen})_3]^{2+}$.

Afin de ne pas augmenter exagérément le temps du dosage nous avons choisi d'opérer au bain-marie à l'ébullition, pendant 1 min. Dans ces conditions, le complexe est détruit en présence des ions Cl^- , IO_3^- , Br^- , oxalate, phthalate, dès que la concentration en NaOH devient supérieure à 0,08M. Une augmentation de cette concentration n'est pas efficace avec NO_3^- , ClO_4^- , SCN^- , I^- .

L'augmentation de la teneur en méthanol (11% v/v) permet, par contre, la dénaturation du complexe en présence des ions NO_3^- . Avec les ions plus fortement liés, il faut des conditions encore plus drastiques pour arriver à ce résultat. Pour un milieu réactionnel de concentration de NaOH égale à 0,15M, renfermant un pourcentage de méthanol voisin de 40%, il faut maintenir les solutions au bain-marie à l'ébullition pendant 1 min (I^-), 5 min (SCN^-), 10 min (ClO_4^-) pour obtenir la destruction du complexe $[\text{Fe}(\text{bphen})_3]^{2+}$. Mais, dans ces conditions, le complexe $[\text{Fe}(\text{bphen})_2(\text{CN})_2]$ est détruit en partie, ce qui rend impossible le dosage des ions cyanure par notre technique lorsque ces trois ions sont présents.

Etalonnage

Par la méthode dite de la régression simple,¹⁰ nous avons montré que, pour chacune des méthodes proposées, il existe une relation linéaire entre les absorbances des phases chloroformiques (A) et la concentration en ions cyanure (c) des solutions à doser. Si la concentration c est exprimée en mg d'ions cyanure par litre de solution à doser, les équations des droites sont données par les relations:

$$\begin{aligned} A &= 0,057c - 0,011 & \text{avec } r &= 0,9994 \text{ (technique A)} \\ A &= 0,144c - 0,042 & \text{avec } r &= 0,9998 \text{ (technique B)} \\ A &= 0,712c - 0,060 & \text{avec } r &= 0,9990 \text{ (technique C)} \end{aligned}$$

Les absorbances molaires apparentes, obtenues dans nos conditions opératoires, sont respectivement égales à $1,5 \times 10^3$ l.mole⁻¹.cm⁻¹ (technique A),

$3,7 \times 10^3$ l.mole⁻¹.cm⁻¹ (technique B), et $1,8 \times 10^4$ l.mole⁻¹.cm⁻¹ (technique C). L'absorptivité molaire apparente correspondant à la technique la plus sensible (technique C) est proche de celles calculées pour d'autres techniques spectrophotométriques, 2×10^4 l.mole⁻¹.cm⁻¹ par exemple pour la technique de Casassas et coll.¹

La déviation standard relative calculée sur 5 mesures, pour une solution renfermant 0,8 mg d'ions cyanure par litre, analysée par la technique C, est égale à 1,3%.

Etude de quelques interférences

Influence des anions. Nous avons montré que la présence de nombreux anions n'affecte pas le dosage des ions cyanure par les techniques proposées. Sur les 18 anions testés, 3 seulement sont gênants: les ions ClO_4^- , SCN^- , I^- . Les autres peuvent être présents jusqu'à une molarité égale à 0,005.

En effet, lors du dosage d'une solution d'ions cyanure de molarité égale à $3,8 \times 10^{-4}$, la déviation standard relative, obtenue pour la teneur en anions citée précédemment est la même que celle observée en l'absence de ces ions (1,3%).

Influence des cations. La présence de cations ne réagissant pas (ou peu) avec les agents complexants azotés ne perturbe pas la réaction: le dosage des ions cyanure en solution de molarité égale à $3,8 \times 10^{-4}$ est possible en présence des ions Pb^{2+} ou Mg^{2+} à une concentration égale à 10^{-3} M, ou Mn^{2+} jusqu'à une concentration égale à 5×10^{-4} M.

Par contre les ions pouvant former des complexes stables avec les ligands azotés interfèrent fortement. Pour une même molarité en cyanure, les ions Cu^{2+} , pour une concentration égale à 3×10^{-5} M, entraînent une inhibition de 33% de la réaction. De même, les ions Co^{2+} créent une inhibition totale pour une concentration égale à 2×10^{-4} M.

Les techniques décrites précédemment s'appliquent donc, *sans séparation préalable*, au dosage des ions cyanure libres. Le dosage des cyanures totaux pourrait être effectué classiquement après distillation en milieu acide.

Conclusion

Les techniques que nous préconisons permettent, sans séparation préalable, le dosage des ions cyanure libres lorsque leur concentration en solution est supérieure à 0,1 mg/l. Il est possible d'envisager leur application dans différents domaines (hydrologie, contrôle de pollution, analyse alimentaire, etc.).

La présence de nombreux anions n'est pas gênante, même à des teneurs très supérieures à celle des ions cyanure. Ces méthodes donnent d'excellents résultats sur le plan de la linéarité et sur celui de la reproductibilité. Elles sont rapides et d'une grande simplicité d'exécution. Par ailleurs la technique C est 100 fois plus sensible que la méthode antérieurement proposée par Schilt⁵ utilisant le complexe ferreux de la phénanthroline-1,10 non substituée.

LITTÉRATURE

1. E. Casassas, R. Rubio et G. Rauret, *Analyst*, 1984, **109**, 1159.
2. W. König, *J. Prakt. Chem.*, 1904, **69**, 105.
3. *Ibid.*, *Z. Angew. Chem.*, 1905, **69**, 115.
4. A. A. Schilt et T. W. Leman, *J. Am. Chem. Soc.*, 1967, **89**, 2012.
5. A. A. Schilt et J. Bacon, *Anal. Chem.*, 1969, **41**, 1669.
6. J. Burgess, *Inorg. Chim. Acta*, 1971, **5**, 133.
7. P. Levillain et R. Bourdon, *Bull. Soc. Chim. France*, 1972, 3309.
8. A. A. Schilt, *Anal. Chem.*, 1958, **30**, 1409.
9. P. Dubois, M. Mariaud et P. Levillain, *Bull. Soc. Chim. France*, 1978, **I**, 243.
10. D. Moccati, J. Lambert et G. Terrie, *Actualités de Chimie Thérapeutique*, 1976, 4ème Série 87.

AUTOMATED DETERMINATION OF LEAD IN URINE BY MEANS OF COMPUTERIZED FLOW POTENTIOMETRIC STRIPPING ANALYSIS WITH A CARBON-FIBRE ELECTRODE

HUANG HUILIANG,* DANIEL JAGNER and LARS RENMAN

Department of Technical Analytical Chemistry, Chemical Center, P.O. Box 124, S-221 00 Lund, Sweden

(Received 28 October 1986. Accepted 5 February 1987)

Summary—Five different digestion procedures have been investigated. In the recommended procedure 5 ml of concentrated hydrochloric acid–nitric acid mixture (1:1) were added to a 5-ml urine sample. After 1 min the sample was diluted to 100 ml with distilled water. The sample was divided into two 50-ml samples and to one of them a standard addition of 10 $\mu\text{g/l}$ lead(II) was made. The two samples were analysed fully automatically by means of computerized flow potentiometric stripping analysis, the main features of the procedure being mercury-film pre-coating, electrolysis of the sample for 90 sec and subsequent stripping in 1M calcium chloride/0.1M hydrochloric acid. Tin and copper were found not to interfere if present at concentrations below 50 mg/l. but high concentrations of tin had to be masked by the addition of copper in order to form a copper–tin intermetallic compound. Complexing agents used in lead poisoning therapy did not interfere with the determination. The lead concentration in a Seronorm® reference urine sample was found to be 93 $\mu\text{g/l}$. with a standard deviation of 8 $\mu\text{g/l}$. ($n = 5$), the certified value being 88 $\mu\text{g/l}$.

Elevated human concentrations of lead are normally determined by analysing whole blood samples. Because of the simple sampling procedure, however, preliminary investigations are often done on urine samples. Such samples are also analysed in epidemiological studies and for patients with lead poisoning who are under treatment with chelating agents.

Graphite-furnace atomic-absorption spectrometry is the most frequently used technique for the determination of lead in urine. Graphite-furnace spectrometers are, however, rather expensive and the possibility of using simpler instrumentation has therefore been investigated. Various reports suggest the use of anodic-stripping voltammetry^{1,2} and Jagner *et al.* have proposed the use of potentiometric stripping analysis.³ In the batch mode the latter technique was capable of determining lead in urine at concentrations down to 0.2 $\mu\text{g/l}$. The organic constituents of the urine sample caused problems, however, one of these being that the mercury film could not be formed *in situ*. Furthermore, the glassy-carbon electrode used as substrate for the mercury film had to be repolished frequently. Since the recently developed technique based on flow potentiometric stripping analysis with carbon-fibre electrodes ought to overcome these problems and at the same time increase the degree of automation of the analysis, it was decided to re-

investigate the determination of lead in urine. A major difference between the batch and flow procedures is that in the latter the electrolysis preconcentration step and the stripping step are performed in different solutions. Thus in changing from a batch procedure to a flow procedure the sample pretreatment must be re-investigated and the composition of a suitable stripping solution studied.

EXPERIMENTAL

Apparatus

Flow system. The flow system consisted of a peristaltic pump with which six different solutions could be drawn, in any order, into the flow-cell through magnetically-activated valves. The electrolysis potential, flow rate, and operation of the valves were under computer control. During stripping, the computer recorded the potential vs. time transient signal with a real-time sampling rate of 19.2 kHz.

The flow system and the computer program have been described in detail elsewhere.⁴

Electrode system. The working electrode was a carbon fibre with a diameter of approximately 10 μm , inserted perpendicular to the direction of flow into a PVC tube with an inner diameter of 0.5 mm. The counter-electrode was a platinum tube and the reference electrode a silver tube coated with silver chloride. All potentials given below are with respect to the Ag/AgCl electrode at the relevant chloride concentration in the solutions. The construction of the carbon-fibre electrode has been described elsewhere.⁵

Reagents

Mineral acids. All mineral acids used were of Suprapur grade (Merck).

Stock solutions of mercury(II) nitrate and lead(II) nitrate. Stock solutions were prepared by diluting the contents of

*Permanent address: Scientific Instrumentation Department, Xiamen (Amoy) University, Fujian Province, People's Republic of China.

Titrisol ampoules (Merck) with Millipore Q water to give solutions containing 4 g/l. mercury(II) or 4 g/l. lead(II).

Mercury coating solution. Stock mercury(II) nitrate solution was added to 5M calcium chloride and diluted with Millipore Q water to give a total concentration of 50 mg/l. mercury(II) and 2.5M calcium chloride.

Stripping solution. Hydrochloric acid was added to 5M calcium chloride and the mixture was diluted with Millipore Q water to give 0.1M hydrochloric acid/1M calcium chloride.

Samples

Urine samples were taken from laboratory personnel and acidified with 0.5M nitric acid. Seronorm[®] urine reference sample (batch 108) with a creatinine concentration of 1.5 g/l. was obtained from Nycomed AS, Oslo, Norway.

Sample pretreatment

Five different pretreatment procedures (previously used in connection with electrochemical stripping analysis of urine⁶) were tested on each urine sample.

1. **Hydrochloric acid treatment.** Ten ml of 1M hydrochloric acid were added to 10 ml of urine sample.

2. **Hydrochloric acid:nitric acid treatment.** A mixture of 2.5 ml of concentrated hydrochloric acid and 2.5 ml of concentrated nitric acid was added to 5 ml of urine sample. After 1 min, the mixture was diluted to 100 ml with Millipore Q water.

3. **Evaporation to dryness.** A mixture of 2.5 ml of concentrated hydrochloric acid and 2.5 ml of concentrated nitric acid was added to 10 ml of urine sample and the mixture was evaporated to dryness on a sand-bath. After cooling, the residue was dissolved in 100 ml of 0.5M hydrochloric acid.

4. **Ultraviolet treatment.** A mixture of 2.5 ml of concentrated hydrochloric acid and 2.5 ml of concentrated nitric acid was added to 10 ml of urine sample. The mixture was kept 25 cm below a 100-W ultraviolet source for 8 hr and then diluted to 100 ml with 0.5M hydrochloric acid.

5. **High-pressure digestion.** Concentrated nitric acid (2.5 ml) was added to 10 ml of urine sample and the mixture was held at 180° for 8 hr in a PTFE-coated bomb. After cooling, the mixture was diluted to 100 ml with 0.5M hydrochloric acid.

Addition of mercury(II) and lead(II)

Mercury(II) stock solution was added to 5 ml of the pretreated sample to yield a total mercury(II) concentration of 10 mg/l. To another 5-ml portion of the pretreated sample, mercury(II) and lead(II) stock solutions were added to yield total concentrations of 10 mg/l. and 10 µg/l., respectively. The two solutions were connected to two of the inlets of the flow potentiometric stripping analyser.

Flow potentiometric stripping procedure

After connection of the pretreated sample and the lead(II)-spiked pretreated sample to two inlets of the flow analyser the analytical procedure and the evaluation of the results were performed automatically. The main features of the analytical procedure were as follows (all flow-rates were 1 ml/min).

Mercury preplating. Fresh carbon fibres, or carbon fibres which had not been used previously on the day of analysis, were precoated with a film of mercury. In this procedure the mercury plating solution was allowed into the cell and a potential of -0.40 V was applied for 2 sec, after which the potential was disconnected for 1 sec. The potential was changed to -0.5 V and applied for 2 sec, then again disconnected for 1 sec. This procedure was repeated in steps of -0.1 V until a potential of -1.10 V was reached. The final precoating stage consisted of electrolysis at -1.10 V for 15 sec.

Mercury-film surface renewal. Prior to electrolysis of the sample, or the sample spiked with lead(II), the mercury film

was renewed by electrolysis for 10 sec at -1.10 V in the mercury plating solution.

Electrolysis of sample solutions. The sample solution was drawn into the cell and a potential of -0.10 V was applied for 2 sec in order to reoxidize trace lead(II) impurities in the mercury plating solution. A potential of -1.15 V was then applied for 90 sec, after which the stripping solution was passed into the cell for 30 sec. The potential vs. time stripping curve was then recorded for the potential interval from -1.15 to -0.20 V. The stripping solution was then electrolysed for 3 sec at -1.15 V and the background stripping curve was recorded over the same potential interval.

Graphical and digital presentation of the results. After differentiation, subtraction of the background, and digital filtration, the lead stripping peak was located by searching the potential interval from -0.35 to -0.55 V, and the peak was then integrated in the interval ± 0.06 V around the peak potential. The differentiated and filtered stripping curve was then displayed on the printer/plotter for the potential interval from -0.30 to -0.60 V. Filtering was achieved with an averaging filter of 30 mV and a Savitsky-Golay filter of 15 mV.⁴ The results from the analysis of the lead(II)-spiked sample were evaluated and displayed in the same way. Finally the lead(II) concentration in the sample was evaluated and reported, the normal equation for single standard-addition being used.

The mercury-film renewal procedure and subsequent electrolysis in the sample and in the spiked sample could be repeated any preset number of times. In the results reported below, the procedure was repeated five times in order to obtain information on the reproducibility. The mean value of the five standard-addition determinations and the relevant standard deviation were then obtained automatically.

RESULTS AND DISCUSSION

Comparison between sample pretreatment procedures

Forty different urine samples were subjected to the five different pretreatment procedures and then each was analysed five times for lead by the automated potentiometric stripping procedure. Four of the procedures (Nos. 2-5) yielded results that all agreed within one standard deviation, for the entire sample range, with lead concentrations from 3 to 15 µg/l. For five of the samples, the other pretreatment procedure (No. 1), yielded results which differed by more than three standard deviations from the average value obtained by the other four procedures. These five samples had in common that they were analysed immediately after sampling. After acidification with nitric acid and storage for one day these five samples yielded results in acceptable agreement with those obtained by the other four pretreatment procedures.

Two of the pretreatment procedures, ultraviolet irradiation and high-pressure digestion (Nos. 4 and 5), resulted in complete mineralization of the samples. That the much simpler method based on nitric acid/hydrochloric acid treatment (No. 2) yielded the same results as those obtained by these treatments strongly indicates that this procedure is sufficient for the flow potentiometric determination of lead in urine.

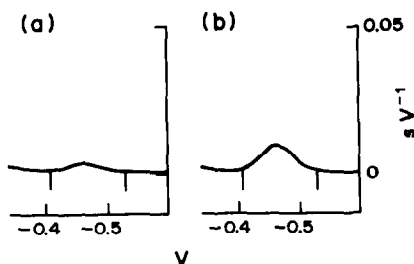


Fig. 1. Differential potentiometric stripping curves obtained in the analysis of urine reference sample (pretreatment procedure No. 2) (a) before and (b) after standard addition of 10 $\mu\text{g/l.}$ lead(II). Potentials were measured vs. Ag/AgCl in 2.1M chloride stripping solution.

Analysis of urine reference sample

The lead(II) concentration in urine reference sample BCR was determined by using the nitric acid/hydrochloric acid pretreatment procedure (No. 2). Figure 1(a) shows the potentiometric stripping curve obtained from this sample and Fig. 1(b) the stripping curve obtained from the sample spiked with lead(II). The value obtained for lead in the reference sample, 93 $\mu\text{g/l.}$ with a standard deviation of 8 $\mu\text{g/l.}$ ($n = 5$), is in good agreement with the certified value of 88 $\mu\text{g/l.}$

Effect of complexing agents

To investigate the effect of complexing agents frequently used in the treatment of lead poisoning, 1mM concentrations of Ca-EDTA and *D*-penicillamine were added to a urine reference sample prior to the nitric acid/hydrochloric acid treatment. The mean results differed from the certified value by less than one standard deviation.

Stability of the carbon-fibre electrode

Since urine contains a large number of organic compounds it is a very complicated matrix for electroanalytical measurements. Previous experiments using glassy carbon as substrate for the mercury film have shown that frequent repolishing of the electrode is necessary for analysis of urine samples. This has been attributed to the adsorption of organic material on those parts of the glassy carbon surface which are not covered by the mercury droplets constituting the mercury "film". The geometry of the carbon-fibre electrode seems to favour the formation of smaller mercury droplets and a more complete surface coverage. Thus a carbon fibre can be used for several hundred electrolysis/stripping cycles before it has to be replaced. This is at least a factor of ten more than for a glassy-carbon disc electrode.

Interferences and stripping medium composition

The two elements most likely to interfere with the lead stripping peak are copper and tin. The degree of interference from copper depends on the chloride

concentration of the stripping medium. At high chloride concentrations ($> 2M$) amalgamated copper is reoxidized to copper(I) complexes, shifting the peak potential in the negative direction and closer to the lead stripping peak. In the stripping medium used in this investigation, copper(II) interference with the lead stripping peak began at urine copper concentrations of approximately 100 mg/l. This is more than three orders of magnitude higher than the copper(II) concentrations normally occurring in urine.

After the nitric acid/hydrochloric acid pretreatment, any tin in the urine sample will be present as tin(IV). At the electrolysis potential used in this investigation tin(IV) is reduced very slowly. Total tin concentrations below 0.2 mg/l. in the urine do not interfere with the lead stripping peak. Interference from higher concentrations of tin(IV) can be eliminated by the addition of copper(II) to the urine sample. The Sn-Cu intermetallic compounds formed during electrolysis will completely mask the tin(IV) interference. For example, the addition of copper(II) at the 10 mg/l. level to the urine sample will completely mask the interference from up to 50 mg/l. tin(IV). Higher tin concentrations are unlikely to occur in urine.

Accuracy and precision

The accuracy of the method was tested by adding known amounts of lead to a urine sample, as well as by analysis of the urine reference sample. The nitric acid/hydrochloric acid pretreatment procedure (No. 2) was used and the results are summarized in Table 1. As can be seen, acceptable recoveries were obtained in the concentration range investigated, 5–100 $\mu\text{g/l.}$, but the precision is rather poor. This is due to the inherent imprecision of the standard-addition technique used.^{7,8}

CONCLUSIONS

Owing to the simplicity of the sample pretreatment procedure and the high degree of automation, computerized flow potentiometric stripping analysis would appear to be an attractive alternative to the graphite-furnace technique for the determination of lead in urine. The reliability of the carbon fibre as sensor makes the technique accessible to personnel

Table 1. Recoveries of lead(II) added to a urine sample prior to nitric acid/hydrochloric acid pretreatment

Lead(II) added, $\mu\text{g/l.}$	Lead(II) found,* $\mu\text{g/l.}$
0	6 ± 2
10	12 ± 4
20	26 ± 6
40	48 ± 6
60	60 ± 9
100	112 ± 12

*Mean ± 1 standard deviation ($n = 5$).

with limited experience in analytical chemistry. Since its installation does not demand access to ventilation or pressurized gases, the instrument can be used in a somewhat primitive laboratory environment or even in field investigations.

Acknowledgements—This work was supported by the Swedish Work Environment Fund and the Carl Trygger Research Foundation.

REFERENCES

1. T. R. Copeland, J. H. Christie, R. A. Osteryoung and R. K. Skogerboe, *Anal. Chem.*, 1973, **45**, 2171.
2. J. Golimowski, P. Valenta, M. Stoeppler and H. W. Nürnberg, *Z. Anal. Chem.*, 1978, **290**, 107.
3. D. Jagner, M. Josefson and S. Westerlund, *Anal. Chim. Acta*, 1981, **128**, 155.
4. L. Renman, D. Jagner and R. Berglund, *ibid.*, 1986, **188**, 137.
5. H. Huiliang, C. Hua, D. Jagner and L. Renman, *ibid.*, in press.
6. J. Wang, *Stripping Analysis: Principles, Instrumentation and Applications*, VCH Publishers, Deerfield Beach, 1985.
7. M. J. Gardner and A. M. Gunn, *Z. Anal. Chem.* 1986 **325**, 263.
8. B. Høyer and L. Kryger, *Talanta*, 1986, **33**, 883.

DETERMINATION OF CALCIUM AND MAGNESIUM IN LIMESTONE AND DOLOMITE BY ENTHALPIMETRIC FLOW-INJECTION ANALYSIS

WALACE A. DE OLIVEIRA and AFONSO S. MENDES

Instituto de Química, Universidade Estadual de Campinas, C.P. 6154, Campinas, SP, Brazil

(Received 11 July 1986. Revised 14 January 1987. Accepted 28 January 1987)

Summary—A flow-enthalpimetric method for the determination of calcium and magnesium in limestone and dolomite is described. Calcium is determined by measuring the heat evolved from the substitution reaction with Mg-EDTA. The amount of magnesium is calculated from the calcium content and the enthalpimetric signal for the reaction of the sample solution with disodium-EDTA, which gives the total concentration of calcium and magnesium. Analysis of reference materials and other samples indicates an error not exceeding 0.3% of CaO and MgO, and a sampling rate of 100 samples per hour.

Several methods are available for the determination of calcium and magnesium in limestone and dolomite. Conventional gravimetric procedures involve a number of laborious steps and are subject to cross-contamination of the precipitates (though fortunately this is to some extent compensatory). Atomic-absorption spectrometry is rapid and very useful for the determination of small amounts, but matrix effects may cause interferences. The development of new procedures for these determinations is desirable¹ because the increasing demand for more analytical results requires faster methods and automated procedures.

Thermometric and enthalpimetric methods have been proposed²⁻⁴ for the determination of calcium and magnesium in limestone and dolomite. These techniques have proved useful because they are simple and involve inexpensive instrumentation.

In this work, the application of enthalpimetric flow-injection analysis to the determination of calcium and magnesium is described. The use of precipitation and complexation reactions was investigated, to find the best choice for these determinations. The results obtained are compared with those found by other techniques.

EXPERIMENTAL

Apparatus

A recently described flow enthalpimeter⁵ was used. It consists of a peristaltic pump which impels the fluids through the injector and flow manifolds, which are placed in an insulated 8-litre water-bath. Temperature difference are measured with two thermistors connected in a d.c. Wheatstone bridge, the output voltage from which is registered on a strip-chart recorder.

Manifold

The manifold used is shown in Fig. 1. Polyethylene tubing of 0.5 mm bore was used for the sample, reagent and carrier

streams. Pulse dampers (D_1 and D_2), similar to those described earlier,⁶ were used for the reagent and carrier streams. The fluids pass through temperature equilibration coils E_1 - E_3 before passage through the injector block and the reactor and through a similar coil (E_4) after passage through the indicator flow-cell (Ti). All four coils are 1-m long 0.5-mm bore stainless-steel tubes. A home-made acrylic proportional injector⁷ (I) was used for introduction of 100 μ l of sample. The indicator (Ti) and reference (Tr) flow-cells had a volume of about 17 μ l and were home-made acrylic blocks modelled as T-connectors, with the thermistor mounted perpendicular to the fluid stream. The reactor (Rt) was made of Tygon tubing, 3.0-mm bore and 2 cm long, packed with glass beads (60-80 mesh) coated with silicone.

Procedure

About 1 g of sample (100-mesh, dried at 100° for 1 hr) was accurately weighed and transferred into a 100-ml porcelain cup, covered with a watch-glass. Small portions of distilled water were added to moisten the sample. About 15 ml of 6M hydrochloric acid were added, with stirring by a glass rod, followed by addition of 2 ml of concentrated nitric acid. The liquid was boiled off and the residue was dissolved in about 35 ml of hot distilled water. The cooled solution was filtered through a Whatman No. 40 paper into a 50-ml standard flask, the residue being washed with 1% v/v hydrochloric acid and the solution made up to volume with distilled water. For the determination of calcium, 5 ml of this solution were transferred into a 25-ml standard flask and the following solutions were added: 1 ml of 10% hydroxylamine hydrochloride solution, 5 ml of ammonium chloride buffer (pH 10; 34 g of ammonium chloride and 285 ml of concentrated ammonia solution diluted to 500 ml) and 1 ml of 40% v/v triethanolamine solution containing 6% potassium cyanide; the solution was made up to the mark with distilled water. The solution was mixed and introduced into the flow manifold shown in Fig. 1. The carrier was the pH-10 ammonium chloride buffer solution and the reagent was 0.2M Mg-EDTA in the same buffer. Calculations were performed by comparing the enthalpimetric signal for the sample with those for standard solutions of calcium, under the same experimental conditions. The procedure used for calcium was also employed for the determination of magnesium, except that a borate buffer (pH 9.2) was used and the reagent was 0.2M disodium-EDTA.

Analytical-reagent grade chemicals were used throughout.

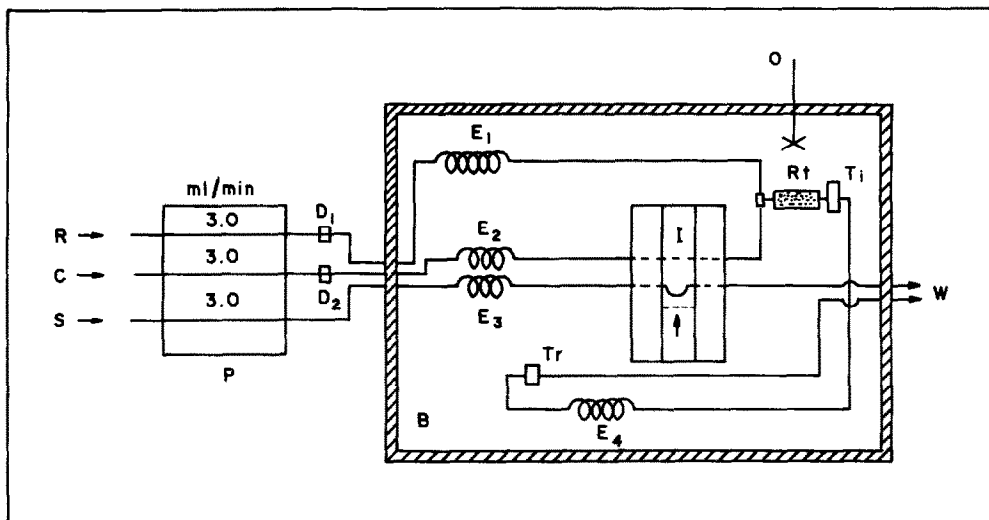


Fig. 1. Flow manifold for the determination of calcium and magnesium in limestone and dolomite. R, reagent; C, carrier; S, sample; P, peristaltic pump; D₁ and D₂, pulse dampers; E₁–E₄, equilibration coils; B, insulated water-bath; I, injector; Rt, reactor tube; T_i and T_r, indicator and reference thermistor cells; O, overhead stirrer; W, waste.

RESULTS AND DISCUSSION

Preliminary experiments

Initially an attempt was made to adapt conventional procedures to the flow-injection system. Calcium was precipitated in the presence of magnesium with 0.2M ammonium oxalate in pH-8 borate buffer, with the same buffer solution as carrier. Jordan and Billingham² have reported that thermo-

metric titration of calcium with oxalate, in the presence of magnesium, with these solutions permitted determination of calcium without interference from magnesium. Under these conditions magnesium gave quasi-isothermal titration curves. However, the results obtained with the flow enthalpimeter, as shown in Fig. 2, indicate that magnesium yields endothermic signals proportional to its concentration, and the signal for mixtures of calcium and magnesium is the

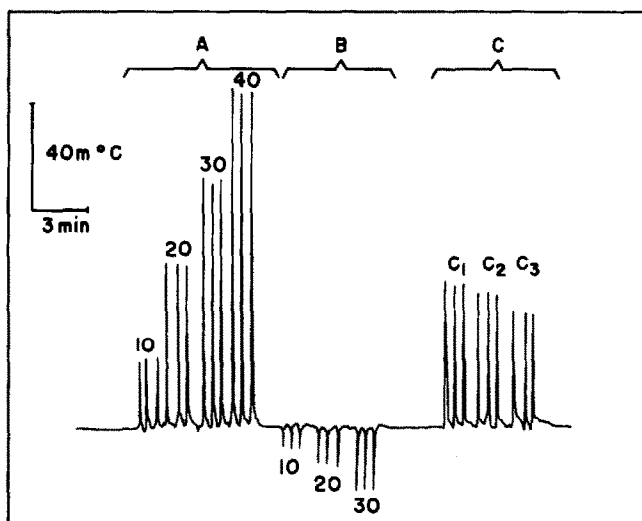


Fig. 2. Enthalpimetric signals for the reaction of oxalate with: A, standard solutions of calcium with concentrations (mM) shown above the peaks; B, standard solutions of magnesium with concentrations (mM) shown below the peaks; C, standard solutions of calcium with a concentration equal to 20mM, containing magnesium with concentrations equal to 5 (C₁), 10 (C₂) and 20mM (C₃).

sum of the individual signals for the components. This finding hindered the use of precipitation with oxalate for the purpose of this work. It is interesting to note the difference between the results of the thermometric titration and flow-injection enthalpimetry. Apparently, the experimental conditions prevailing in the flow-injection enthalpimetry have modified the kinetic behavior observed in thermometric titration.

The complexation reaction with EDTA has been used^{8,9} to determine calcium and magnesium by means of thermometric titration. The heat of complexation of calcium with EDTA is exothermic ($\Delta H = -23.4$ kJ/mole) and that of magnesium is endothermic ($\Delta H = 20.1$ kJ/mole). Preliminary experiments revealed that, under the working conditions of the flow enthalpimeter, the complexation of calcium and magnesium gives good enthalpimetric signals, proportional to their concentrations. When both calcium and magnesium are present in solution the magnitude of the resulting signal is a function of the concentration of the two elements. In this case also, the results of flow-injection enthalpimetry are different from those⁸ obtained by thermometric titration. Complexation with EDTA was used for the determination of the sum of calcium and magnesium, the exchange-reaction with Mg-EDTA for determining calcium. The magnesium content could then be calculated.

Determination of calcium

The substitution reaction between calcium and Mg-EDTA has been used¹⁰ for the thermometric determination of calcium. Besides avoiding the co-titration of magnesium, the substitution reaction yields an enthalpimetric signal which is 25% higher than that for the complexation reaction. Because of these advantages, the substitution reaction was chosen for the determination of calcium. It was found that the concentration of calcium, C_{Ca} (M), is linearly related to the enthalpimetric signal, S (degrees), by the equation $S = -a + bC_{Ca}$ with a correlation coefficient of 0.9993. The standard deviation (ten replicates) was 0.00041° for 20mM calcium and 0.00055° for 40mM calcium, corresponding to uncer-

Table 1. Effect of interferences on the enthalpimetric determination of calcium

Concentration taken, mM				Ca found, mM	Relative error, %
Ca	Mg	Al	Fe		
20.0	20.0	—	—	19.9	-0.5
20.0	—	0.4	—	20.1	+0.5
20.0	—	—	0.3	19.9	-0.5
20.0	—	0.4	0.3	20.0	0
20.0	20.0	0.4	0.3	20.1	+0.5

tainties of 0.10 and 0.14mM, respectively, at these concentration levels.

To study the effect of potential interferences, such as magnesium, aluminium and iron, synthetic samples containing these elements were analysed. The results are listed in Table 1 and show that the difference between the concentration taken and found is within the experimental error.

Table 2 shows the results for analysis of diverse samples from different parts of Brazil. Three reference materials are included in the table (IPT—Instituto de Pesquisas Tecnológicas, SP, Brazil, numbers 35, 48 and 46). The percentages of Fe_2O_3 and Al_2O_3 are also listed, when available. For the reference materials, the certified values are reported. For the other samples the reported values were obtained by using standard methods based on atomic-absorption and classic titrimetry. Each value is the average from three determinations encompassing the complete procedure, including the sample dissolution. Table 2 shows that the results for the enthalpimetric method are in good agreement with the accepted values, the average difference being 0.3% (absolute) CaO.

Determination of magnesium

It was observed that the magnitude of the enthalpimetric signal for the complexation reaction of calcium and magnesium with disodium-EDTA varies with the pH of the reaction medium. A borate buffer of pH 9.2 gave the best results.

The enthalpimetric signal of a solution containing calcium and magnesium, S_T , is the sum of the

Table 2. Comparison of results for the analysis of samples of limestone and dolomite

Sample	Fe_2O_3 , %	Al_2O_3 , %	CaO, %		MgO, %	
			Reported value	Enthalpimetric	Reported value	Enthalpimetric
IPT-35	0.14	0.24	53.8	53.3	0.7	0.8
IPT-48	0.17	0.17	31.0	31.4	21.2	21.7
IPT-46	2.34	4.7	60.9	60.6	6.2	5.9
CAL-OP	—	—	54.3	54.0	0.5	0.6
DAX-363	0.22	3.23	33.5	33.8	12.4	12.8
DAX-364	0.32	0.88	50.2	50.0	1.8	1.9
DAX-397	1.09	0.74	40.0	40.0	6.2	6.7
PI-AA	—	—	26.1	26.1	23.5	24.0
PQ-016	—	—	21.6	21.8	25.5	24.8
PQ-018	—	—	17.6	18.1	29.4	29.5
CIM-VO	—	—	51.9	51.8	2.7	2.5

contributions of the two elements, S_{Ca} and S_{Mg} ;

$$S_T = S_{Ca} + S_{Mg} \quad (1)$$

The experimental results have shown that the signals of each element can be represented by

$$S_{Ca} = a_1 C_{Ca} + b_1 \quad (2)$$

$$S_{Mg} = a_2 C_{Mg} + b_2 \quad (3)$$

where a_1 , a_2 , b_1 and b_2 are constants and C_{Ca} and C_{Mg} represent the concentrations of calcium and magnesium, respectively. Substituting equations (2) and (3) into equation (1) gives

$$C_{Mg} = \frac{S_T - a_1 C_{Ca} - b_1 - b_2}{a_2} \quad (4)$$

The values of a_1 , a_2 , b_1 and b_2 are obtained from calibration runs with standard solutions. Since C_{Ca} is known from its separate determination, C_{Mg} can be calculated with equation (4).

The signals for calibration with standard solutions of calcium and magnesium fitted equations (2) and (3) with correlation coefficients of 0.9999. The signals for blank runs in this case, as well as in the determination of calcium, were small, indicating that heat effects due to dissolution, neutralization and other factors are almost negligible. Interference from iron and aluminium was investigated and was not observed.

Results for the determination of magnesium in several samples of limestone and dolomite are shown in Table 2. These results indicate an average absolute difference between the reported and enthalpimetric

values equal to 0.3% of MgO. As can be seen from equation (4), the error in the concentration of magnesium depends on the uncertainties in determination of both C_{Ca} and S_T . The contribution due to the error in the measurement of S_T was found to be the larger. The absolute mean error for MgO is the same as that for CaO, although it would be expected to be larger, since the MgO value is obtained by difference; this apparent anomaly arises from the conversion factor from molarity to w/w concentration.

Although the precision and accuracy of the enthalpimetric method reported here are lower than those of classic methods, the enthalpimetric procedure is faster, allowing a sampling rate of 100 samples per hour. Also, the instrumentation required is simple and inexpensive.

REFERENCES

1. A. Hitchen and G. Zechanowitsch, *Talanta*, 1980, **27**, 269.
2. J. Jordan and E. J. Billingham Jr., *Anal. Chem.*, 1961, **33**, 120.
3. K. K. Chatterji, *J. Indian Chem. Soc.*, 1955, **32**, 366.
4. I. Sajó and B. Sipos, *Radex Rundsch.*, 1968, 178.
5. C. Pasquini and W. A. de Oliveira, *Anal. Chim. Acta*, 1984, **156**, 307.
6. R. S. Schifreen, C. S. Miller and P. W. Carr, *Anal. Chem.* 1979, **51**, 278.
7. H. Bergamin F^o, J. X. Medeiros, B. F. Reis and E. A. G. Zagatto, *Anal. Chim. Acta*, 1978, **101**, 9.
8. J. Jordan and T. G. Alleman, *Anal. Chem.*, 1957, **29**, 9.
9. H. Yoshida, T. Hattori, H. Arai and M. Taga, *Anal. Chim. Acta*, 1983, **152**, 257.
10. Z. Dancsi and F. Trischler, *Z. Anal. Chem.*, 1971, **256**, 129.

A NEW CHELATING ION-EXCHANGER CONTAINING *p*-BROMOPHENYLHYDROXAMIC ACID AS FUNCTIONAL GROUP—IV

COLUMN SEPARATIONS ON A HYDROXAMIC ACID RESIN

AJAY SHAH and SUREKHA DEVI*

Department of Chemistry, M.S. University, Baroda 390002, India

(Received 21 May 1986. Revised 20 January 1987. Accepted 27 January 1987)

Summary—A new chelating resin based on macroreticular acrylonitrile-divinylbenzene copolymer and containing hydroxamic acid functional groups has been synthesized. It is highly stable in acidic and alkaline solutions. The sorption characteristics of Cu(II), Cd(II), Pb(II), Zn(II), U(VI), Cr(VI), V(V), Co(II), Ni(II), Ca(II) and Mg(II) have been investigated over the pH range 1.0–6.0. The effect of various electrolytes at different ionic strengths on the K_d values for Cu(II), Cd(II), Pb(II) and Zn(II) has been studied systematically. Chromatographic separations of copper(II) and nickel(II) from cobalt(II), and of uranium(VI) from chromium(VI) by selective sorption at controlled pH, have been developed. The ion-exchanger can be used for purification of inorganic salts, and analysis of brass and bauxite.

The attention paid to removal of trace metals from industrial effluents and the degree of sophistication of separation methods have both increased enormously in recent years. Use of chelating resins for removal and separation of metal ions is of wide interest owing to its simplicity, elegance and range of variations.

The strong chelating power of hydroxamic acid ligands has been utilized in the manufacture of chelating resins containing these acids as functional groups. Poly(hydroxamic acid) resins have been synthesized from polymethacrylate,¹ Amberlite IRC-50,² Amberlite XAD-4 and styrene-divinylbenzene copolymer,^{3,4} and acrylonitrile-divinylbenzene copolymer.⁵⁻⁸ So far no poly(hydroxamic acid) resin based on *p*-bromophenylhydroxamic acid has been reported. Introduction of the bromo group at the *para*-position increases the basicity of the ligand and hence its chelating power and the distribution coefficients for various metal ions.

In this paper the synthesis and characterization of the *p*-bromophenylhydroxamic acid resin are reported, together with the conditions for the effective separation of copper(II) and lead(II), zinc(II) from cadmium(II), copper(II) and nickel(II) from cobalt(II), and uranium(VI) from chromium(VI). The resin has been applied to analysis of brass and bauxite, and purification of inorganic salts.

EXPERIMENTAL

Reagents

All chemicals used were of analytical grade. The acrylonitrile monomer was obtained from Fluka. Solvents were distilled prior to use.

Metal ion solutions

Metal solutions were prepared by dissolving appropriate amounts of the acetates of the metals in doubly distilled water and standardized by EDTA titration⁹ or spectrophotometrically.¹⁰

Synthesis of the chelating resin

Poly(acrylic acid), synthesized by the method reported earlier,⁸ was heated with *p*-bromophenylhydroxylamine at 75–80° for 18 hr. The *p*-bromophenylhydroxylamine was synthesized by partial reduction of *p*-bromonitrobenzene with zinc powder at 60° in the presence of ammonium chloride. The product was recrystallized from a mixture of petroleum ether (b.p. 40–60°) and benzene and then coupled with the poly(acrylic acid). The resulting polymer was washed thoroughly with methanol then with 2*M* hydrochloric acid and finally with demineralized water until free from chloride. A small portion was vacuum-dried prior to elemental and infrared analysis.

The water regain, true density, apparent density, void volume fraction, sodium exchange capacity, rate of exchange for sodium ion, rate of equilibration with metal ions, resin stability, effect of metal ion concentration on $t_{1/2}$, and the effect of different eluents were studied according to literature methods.^{11,12}

Metal ion capacity

The resin was equilibrated with acetate buffers (pH 1.0–6.0) for 12 hr. The buffer solutions were decanted and the resin samples (0.25 g) were equilibrated for 24 hr with 25 ml of 0.2*M* metal acetate solutions at appropriate pH. After 24 hr the metal ion concentration in the supernatant liquid was estimated. The results were cross-checked by eluting the chelated metal from the resin with 1*M* hydrochloric acid and determining it. Copper, chromium and uranium were determined spectrophotometrically,¹⁰ and the other metal ions by EDTA titration.⁹

K_d values for metal ions in the presence of electrolyte solutions

A 0.25-g portion of resin (H^+ form) was suspended in 50 ml of electrolyte solution of known concentration. The pH was adjusted to the value at which the resin shows maximum affinity for the metal ions. The mixture was

*Author for correspondence.

equilibrated for 24 hr. Then 2 ml of 5-mg/ml solution of the metal ion under study were added, and the pH was adjusted to 5.0, 4.0, 4.0 and 6.0 for Cu(II), Cd(II), Pb(II) and Zn(II) respectively. The solution was further equilibrated for 24 hr, with intermittent shaking, and then filtered. The solid was washed with demineralized water, and the filtrate and washings were combined and analysed for metal ion content. The procedure was repeated with 0.05–1M solutions of sodium chloride, sodium nitrate and sodium sulphate as electrolytes.

Chromatographic separations

A resin sample (H⁺ form) was equilibrated with buffer and packed into a chromatographic glass tube to form a bed \approx 17 cm in length and 0.5 cm in diameter. Mixtures of metals (10 mg of each per 25 ml) in the appropriate buffer were passed through the column at a flow-rate of 0.2 ml/min. During elution a flow-rate of 1 ml/min was used.

Analysis of brass

A 1-g sample of brass was dissolved in 5 ml of concentrated nitric acid and the solution evaporated just to dryness. The residue was dissolved in 5 ml of 0.1M hydrochloric acid and the solution filtered. The filtrate and washings were diluted to volume in a 100-ml standard flask with water. A 25-ml aliquot of this solution, adjusted to pH 5.0, was passed through the resin column at a flow-rate of 0.2 ml/min to separate the constituents of the brass.

Analysis of bauxite

A 1-g sample of bauxite was heated with 3 ml of concentrated nitric acid and 9 ml of concentrated hydrochloric acid. When dissolution seemed complete, the mixture was evaporated to dryness. The residue was dissolved in 5 ml of 0.1M hydrochloric acid. Silica was filtered off and the filtrate and washings were diluted to volume in a 100-ml standard flask with water. The silica was ignited, cooled, treated with a few drops of concentrated sulphuric acid and hydrofluoric acid and evaporated to dryness. The residue was fused with 0.8 g of potassium bisulphate, and the cooled melt was dissolved in dilute hydrochloric acid; no iron and aluminium were detected in this solution, indicating their quantitative dissolution in the *aqua regia* treatment. A 10-ml aliquot of the 100 ml of sample solution containing iron and aluminium was adjusted to pH 2.0 and passed through the resin column at a flow-rate of 0.2 ml/min.

RESULTS AND DISCUSSION

The infrared spectrum of the polyacrylonitrile-divinylbenzene copolymer showed a stretching band at 2260 cm⁻¹ (—C≡N), whereas the spectrum of the hydrolysed product exhibited stretching bands at 1720 and 920 cm⁻¹ (—COOH). The spectrum of the final product showed bands at 1650 cm⁻¹ (C=O), 2960 cm⁻¹ (O—H), 500 cm⁻¹ (C—Br), 3030 cm⁻¹ (benzene aromatic C—H stretching) and 1613–1471 cm⁻¹ (ring skeletal vibrations of —C=C). From the elemental analysis it was found that the conversion of carboxylic acid into hydroxamic acid was \sim 80% complete. The physicochemical properties of the resins are listed in Table 1. The reported sodium exchange capacities of the *p*- and *m*-chlorophenylhydroxamic acid resins are 5.24 and 5.16 meq/g (dry resin) respectively. The sodium exchange capacity of the *m*-bromophenylhydroxamic acid resin may be lower because of the less acidic character of the functional group. The resin exhibits cation-exchange capacity for sodium only at pH >10.5. The time

Table 1. Physicochemical properties

Moisture content, %	4.83
True density, g/cm ³	1.40
Apparent density, g/cm ³	0.60
Void volume fraction	0.57
Sodium exchange capacity meq/g (dry resin)	5.06
<i>t</i> _{1/2} for sodium exchange, min	8

required for 50% exchange is 8 min; complete exchange takes 12 hr.

The resin has high thermal stability. The capacity increases with temperature. A differential scanning calorimetry study showed that the resin decomposes at temperatures >385°. The resin can withstand repeated acid–base washing cycles, without change in sodium exchange capacity, indicating high chemical stability.

Metal ion capacity

The capacity as a function of pH, for the metals under study, is shown in Fig. 1. The resin exhibits good selectivity for these metals, the order of affinity being Ca(II) < V(V) < Mg(II) < Ni(II) < Co(II) < Pb(II) < U(VI) < Cd(II) < Zn(II) < Cu(II). The same order was observed¹³ for a macroreticular iminodiacetate resin, except for Mg(II), for which the affinity was less than that for Ca(II). It is expected that the metal capacities of the resin should increase with increasing stability of the metal complexes formed with the chelating resin. The capacities for the transition metal ions follow the Irving–Williams order, except for cobalt. The capacity of the resin for cobalt is higher than that for nickel. This may be due to aerial oxidation of cobalt(II) to cobalt(III), resulting in higher crystal-field stabilization energy for the cobalt complex than for the nickel complex. In the case of cadmium, lead, calcium and magnesium, purely electrostatic factors are involved. The hydrated-ion radius of cadmium is greater than that of zinc. This will result in lower electrostatic interaction between the metal and the co-ordinating group, lower complex stability and hence lower capacity. Calcium and magnesium, being alkaline-earth metals have less tendency to form co-ordination compounds.

From Fig. 1 it is clear that chromium can be separated from the other metal ions under study, at pH 5.0. It was found that the times needed for 50% exchange of 0.2M solutions of Cu(II), Cd(II), Pb(II), Zn(II), Cr(VI), U(VI) and V(V) are 6, 23, 14, 30, 23, 22 and 30 min respectively and that *t*_{1/2} is inversely proportional to the metal ion concentration.

Effect of different electrolytes on *K_d* values of metal ions

Table 2 shows that the distribution coefficients for Cu(II), Cd(II), Pb(II) and Zn(II) increase with decreasing concentration of sodium chloride, nitrate or sulphate. This is because the heavy-metal ions chelate with the hydroxamic acid groups in the resin, whereas

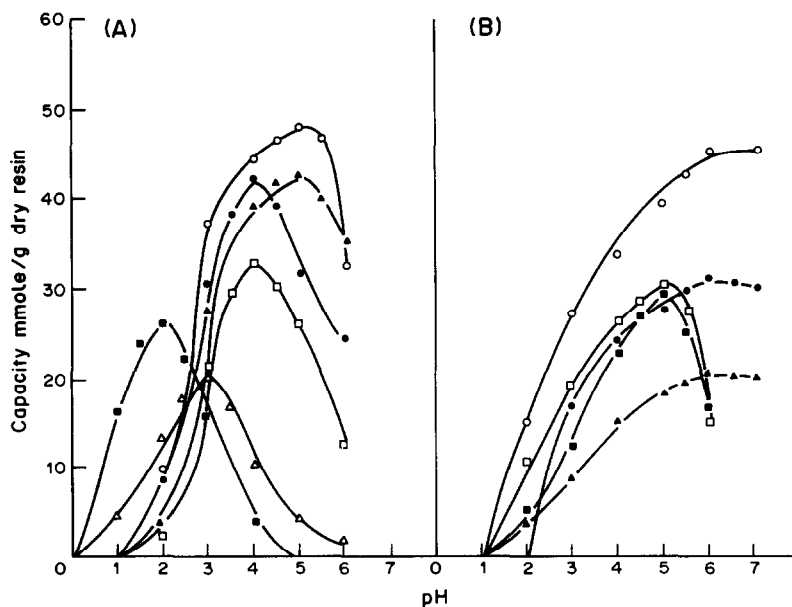


Fig. 1. Effect of pH on metal ion capacity. (A) \circ Cu(II), \bullet Pb(II), \square Cd(II), \blacksquare Cr(VI), \triangle V(V), \blacktriangle U(VI); (B) \circ Zn(II), \bullet Co(II), \square Ni(II), \blacksquare Mg(II), \blacktriangle Ca(II).

the background electrolyte is simply sorbed in the resin. The efficiency of exclusion of electrolyte (Donnan potential effect) increases with decreasing electrolyte concentration and thus favours increased K_d for heavy-metal ions. The electrolyte exclusion is found to be more efficient for counter-ions of low charge and co-ions of high charge. The decrease in K_d at 0.05M background electrolyte concentration is regarded as a deviation from ideal behaviour, similar to that reported for Au(III), Fe(III), Ga(III) and Tl(III) by Kraus *et al.*¹⁴

Study of eluents

The eluents tested were 1–6M hydrochloric acid, nitric acid, sulphuric acid, acetic acid, sodium chlo-

ride, 5–30% v/v perchloric acid (70%), and 0.25–1M tartaric acid. Of these, hydrochloric, nitric and sulphuric acids were found satisfactory but could give only 80% recovery for chromium(VI). Complete recovery of chromium from the resin was not achieved even after prolonged elution. Eluents made with mixed solvents (aqueous methanol or acetone) were useless.

Applications

Removal of iron from cobalt acetate. Iron(III) present in cobalt acetate can be removed by passage of a solution of the salt at pH 2 through a column of the resin; cobalt does not form the hydroxamic acid chelate at pH 2, and passes through the column. The

Table 2. Effect of different electrolytes on K_d values of metal ions

Metal	Concentration of electrolyte, M	K_d		
		Sodium chloride	Sodium nitrate	Sodium sulphate
Copper	1.0	109	126	256
	0.5	165	210	350
	0.1	330	554	1471
	0.05	223	257	490
Cadmium	1.0	58	20	74
	0.5	92	66	135
	0.1	123	148	193
	0.05	74	20	51
Lead	1.0	19	30	70
	0.5	42	70	87
	0.1	55	87	150
	0.05	19	19	30
Zinc	1.0	23	77	32
	0.5	30	128	69
	0.1	30	221	225
	0.05	11	40	32

iron can be eluted with 3M hydrochloric acid. A sample containing 0.02% of iron was purified in this way, the iron content being reduced to 0.0006%.

Analytical separations. Separations of copper(II) from lead(II) and zinc(II) from cadmium(II) (10 ml of 1 mg/ml solution of each metal ion) were performed at pH 5.0 by selective elution of lead with 6M sodium chloride and of copper with 1M nitric acid, and by gradient elution of zinc and cadmium with 0.5M hydrochloric acid. No cross-contamination was observed in either of the separations.

Separation of cobalt(II) from copper(II) and nickel(II) (10 ml of 1 mg/ml solution of each metal ion) was achieved by selective sorption of copper and nickel at pH 2 and their gradient elution with 0.25M tartaric acid. Effective separation of cobalt is achieved but copper and nickel are co-eluted.

The separation of chromium(VI) from uranium(VI) (10 ml of 1 mg/ml solution of each metal ion) was achieved at pH 5, at which uranium remains on the resin and chromium in the column effluent. The chelated uranium was quantitatively eluted with 25 ml of 1M nitric acid.

Analysis of bauxite. Bauxite solution was passed through the resin column at pH 2.0. Aluminium does not form the hydroxamic acid chelate at pH 2.0, and is thus separated from iron; the iron was eluted with 3M hydrochloric acid. The sample contained 1.6% iron, which was determined with 1.2% relative error.

Analysis of brass. Brass solution (25 ml) was passed

through the resin column at pH 5. Chelated zinc and copper were eluted with 0.1M nitric acid, followed by elution of iron with 3M hydrochloric acid. There was considerable overlap in the elution of zinc and copper.

Acknowledgement—The authors thank CSIR, New Delhi, for financial support during the research work.

REFERENCES

1. W. Kern and R. C. Schultz, *Angew. Chem. Int. Ed. Engl.*, 1957, **69**, 153.
2. G. Petrie, D. Locke and C. E. Meloan, *Anal. Chem.*, 1965, **37**, 919.
3. R. J. Phillips and J. S. Fritz, *Anal. Chim. Acta*, 1980, **121**, 225.
4. E. M. Moyers and J. S. Fritz, *Anal. Chem.*, 1977, **40**, 418.
5. F. Vernon and H. Eccles, *Anal. Chim. Acta*, 1976, **82**, 369.
6. *Idem, ibid.*, 1976, **83**, 187.
7. *Idem, ibid.*, 1977, **94**, 317.
8. A. Shah and S. Devi, *Analyst*, 1985, **110**, 1501.
9. A. I. Vogel, *Quantitative Inorganic Analysis*, 4th Ed., p. 325. Longmans, London, 1978.
10. E. B. Sandell, *Colorimetric Determination of Traces of Metals*, 3rd Ed., p. 444. Interscience, New York, 1959.
11. F. Helfferich, *Ion Exchange*, pp. 72–94. McGraw-Hill, New York, 1962.
12. R. Kunin, *Ion Exchange Resins*, p. 324. Wiley, London, 1958.
13. R. F. Hirsch, E. Gancher and F. R. Russo, *Talanta*, 1970, **17**, 483.
14. K. A. Kraus, D. C. Michelson and F. Nelson, *J. Am. Chem. Soc.*, 1959, **81**, 3204.

DESIGN AND EVALUATION OF AN ELECTROCHEMICAL SENSOR FOR DETERMINATION OF DISSOLVED OXYGEN IN WATER

S. QUINTAR DE GUZMAN, O. M. BAUDINO and V. A. CORTINEZ*

Department of Analytical Chemistry, Facultad de Química, Bioquímica y Farmacia,
Universidad Nacional de San Luis, 5700 San Luis, Argentina

(Received 27 January 1986. Revised 10 January 1987. Accepted 27 January 1987)

Summary—A voltammetric cell with a graphite-paste cathode and silver-wire anode was designed for dissolved oxygen determinations in water. Its most important features were evaluated in laboratory and field studies. Several advantages such as higher sensitivity, wider linear response interval, negligible interference due to carbon dioxide, and shorter response time, besides its low cost and simple construction, were found when it was compared with sensors having a platinum cathode.

The chemical methods used for dissolved oxygen (DO) determination in aqueous solutions are time-consuming and sometimes require expensive reagents. The instrumental methods available are faster and can be automated.

Electrochemical methods such as polarography, coulometry, voltammetry and amperometry have been reviewed by Brownman.¹ Polarographic analysis with the dropping-mercury electrode (DME) was the method that first simplified DO determination and up to the present is perhaps the most accurate instrumental method for laboratory analysis. However, the characteristics of the DME make it less useful in field work. Gold and platinum electrodes overcome some of the difficulties experienced with the DME, but themselves fail in some biological media in which the reduction produced by organic substances and even by certain ions lowers the selectivity. Clark² proposed the use of polymeric membranes (*e.g.*, polyethylene) permeable to oxygen, but impermeable to water and organic and inorganic solutes, to eliminate the difficulties above by thus keeping the electrodes out of close contact with such reducing substances.

Lately, papers have appeared on use of noble-metal electrodes and non-stoichiometric oxides and solid electrolytes³ and on a membraneless sensor consisting of a silver-amalgam cathode and a zinc or ion anode, the cathode surface being continuously cleaned by a rotating abrasive⁴ rod. Another membrane sensor has a spongy Pb:Hg (81:16) alloy anode to give a greater active surface, and a potassium hydroxide electrolyte containing primary alkylamine alcohols to suppress carbon dioxide.⁵ Finally, an optical sensor for DO has been developed.⁶

The cell described by Aiba⁷ has long been used in our laboratory for DO determination in natural waters. This sensor was chosen because it is strong,

simple, and easy to construct. However, the high cost of platinum as electrode material and its relatively slow response required a detailed performance evaluation, and simultaneously several modifications were tried.

Graphite was studied as the electrode material and a sensor using it as cathode was designed.

EXPERIMENTAL

Instrumentation

Potentiometric measurements were made with a Corning 110 pH-meter millivoltmeter (with ± 0.1 mV accuracy). Polarographic measurements were made with a Radiometer Polariter P04 polarograph, and voltammetric measurements with a conventional polarization source. Solutions were stirred whenever necessary, by means of a Metrohm Type E 402 magnetic stirrer.

Reagents

High-purity nitrogen was used for removing the DO from solutions. The oxygen used for the preparation of samples was also of high purity. Solutions with different oxygen concentrations were prepared by bubbling the gas for various times into 0.01M potassium chloride. Two aliquots were taken from each, one being used to determine the true oxygen concentration by the polarographic method,⁸ previously calibrated by the Winkler method,⁹ and the other to study the sensor performance. Measurements were made on stirred or unstirred solution at $25 \pm 0.5^\circ$. Spectral grade graphite powder was used to prepare the cathodes. High-quality liquid paraffin (checked by NMR) was used for paste preparation. All other reagents were of analytical grade.

Sensors

- (a) Aiba cell.⁷ [Fig. 1(a)].
- (b) An Aiba cell modified by replacing the external glass body with a threaded Teflon tube [Fig. 1(b)] to obtain a better fit of the platinum disk and an airtight seal to avoid the entrance of oxygen into the internal solution and make replacement of this solution easier.
- (c) Graphite-silver cell. The aluminium tube anode was replaced by a 1-mm thick silver wire about 5 cm long, wound round a Teflon tube as a support. A copper wire was passed through the centre of the tube, with its bottom end welded to a small copper disk attached to the base of the

*Author for correspondence.

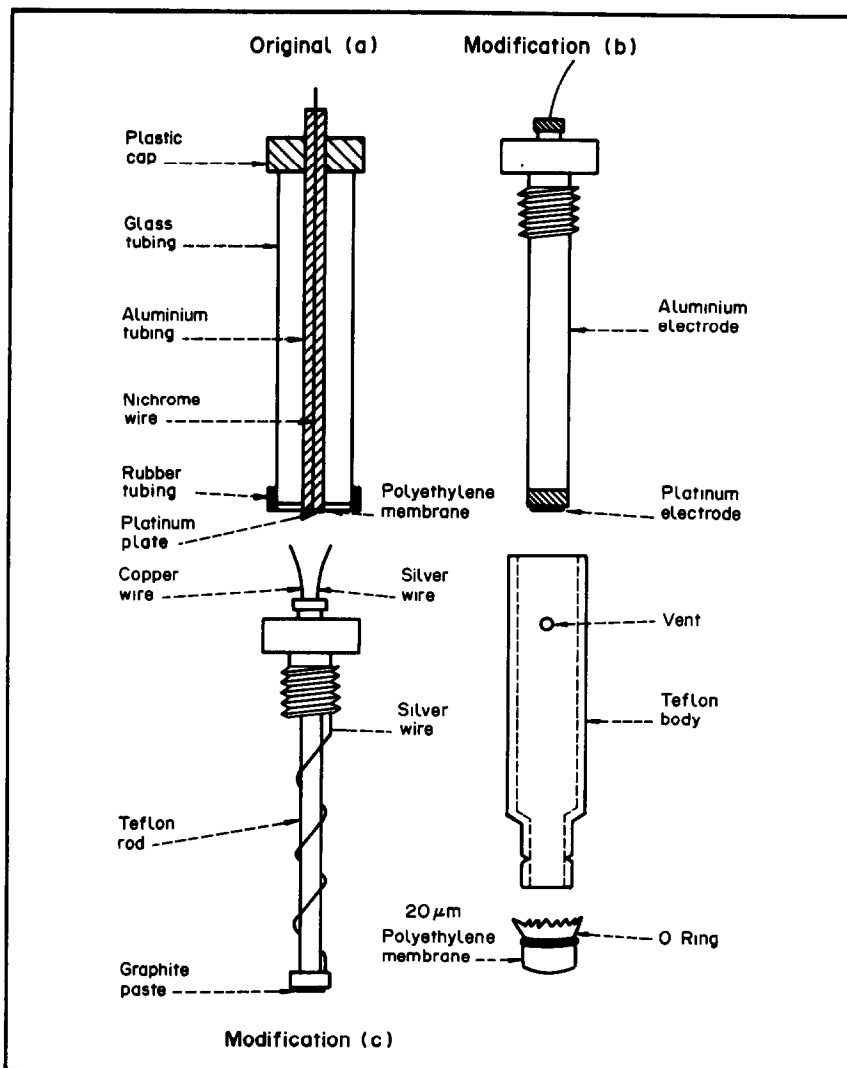


Fig. 1. Different designs of DO sensors used.

Teflon well containing the graphite paste, thus giving better electrical contact [Fig. 1(c)]. Between measurements, the probes were kept immersed in oxygen-free 0.1M potassium chloride. For the modified Aiba sensor, 0.01 and 0.1M potassium chloride solutions were used as internal electrolyte. For the other sensors a 2.0M solution of the same salt was used. The cathodes were covered with 15 and 20 μm thick polyethylene membranes, which later were replaced by a 20 μm thick Teflon FEP membrane.

(d) Graphite-aluminium cell, a device similar to modification (b) but with the platinum cathode replaced by graphite paste.¹⁰ It was tested with and without a protective membrane.

RESULTS AND DISCUSSION

Modified Aiba cell

With cell (b) the response time varied according to the oxygen concentration (Fig. 2). The potential reached constant values after 5 min for oxygen concentrations between 2 and 20 $\mu\text{g/ml}$, but for 0.5 $\mu\text{g/ml}$ the signal continued decreasing even after

20 min. When the cell was transferred from a solution of high oxygen concentration to one of low, the response of the cell was much slower.

The membrane thickness did not significantly affect the response time. The cell showed a linear response within a range of DO concentrations between 3 and 20 $\mu\text{g/ml}$. This was proved by performing two series of 15 trials each, with 15 and 20 μm thick membranes respectively. The average slopes obtained were 57 mV/decade with 8.6 mV/decade standard deviation and 62 mV/decade with 6.3 mV/decade standard deviation respectively. The slight differences in the values of average slopes can hardly be ascribed to the membrane thickness.

Although this device can be regarded as satisfactory in several of its features such as linear response and reproducibility, it showed some disadvantages: (i) relatively slow response, (ii) memory effect making it difficult to pass from concentrated to dilute solutions when making measurements, (iii)

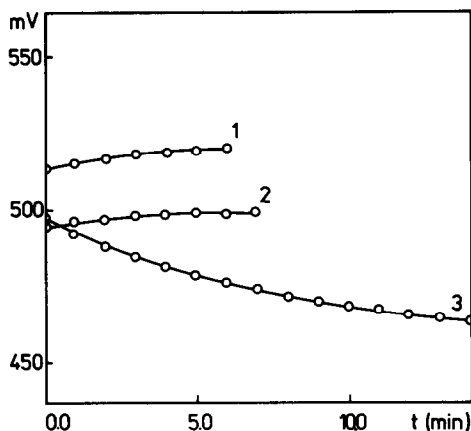


Fig. 2. Potential vs. time curves for the Pt/Al cell. DO concentration: 1, 2 $\mu\text{g/ml}$; 2, 20 $\mu\text{g/ml}$; 3, 0.5 $\mu\text{g/ml}$.

instability of the internal electrolyte solution (95% ethylene glycol saturated with potassium chloride, which had to be changed quite frequently).

Other sensors

The limitations of the modified Aiba sensor justified testing electrodes made with other materials and different internal electrolyte solutions by replacing the galvanic operating mode of the sensors by a voltammetric mode, which was expected to give shorter response time.

Graphite paste-aluminium cell. Carbon-paste electrodes are simple and practical, but the accuracy that can be attained with them in limiting-current measurements can hardly ever be equal to that obtained with noble-metal electrodes. Although graphite-paste electrodes have been widely used in anodic voltammetry,¹⁰ they have seldom been used for cathodic voltammetry, particularly in DO reduction. There is some information on use of pyrolytic and spectrographic graphite in rod form.^{11,12} It was decided to try a graphite-paste cathode.

The current-voltage curves obtained with this device, without the membrane, in both stirred and unstirred solutions, showed good definition. The performance was similar to that of the dropping-mercury electrode,¹³ with two plateaus due to oxygen reduction (Fig. 3). The response was linear from 0.5 to 20 $\mu\text{g/ml}$ DO. The average slope was 0.23 $\mu\text{g/decade}$ and the cell showed no change after one month of daily use.

The results showed the graphite-paste electrode has two advantages over platinum: lower cost and a considerable hydrogen overpotential which allows more flexibility in control of the applied potential and less risk of interference by carbon dioxide.¹⁴

Tests of the same sensor with the cathode covered with a 20 μm thick polyethylene membrane yielded poor results. The current-voltage curves were well defined but the sensitivity of measurement decreased rapidly with time. This was ascribed to the accumulation of aluminium hydroxide gel near the cathodic

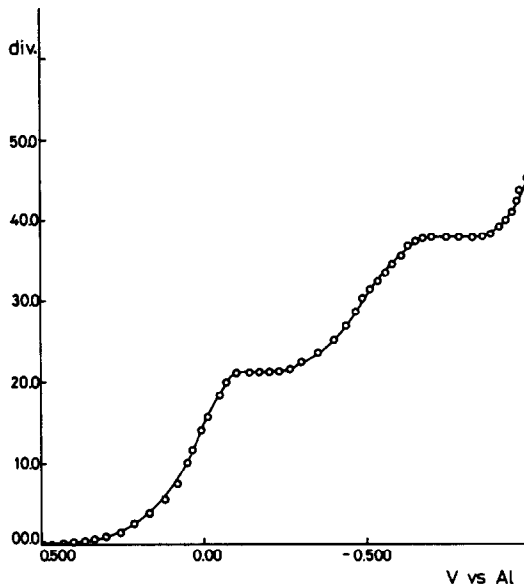


Fig. 3. Current vs. potential curve: graphite-paste cathode, 3 mm diameter; aluminium tubing anode. Sensitivity, 0.2 $\mu\text{A/divn.}$; no stirring, no membrane.

area because of the severe metal corrosion in chloride solutions. This difficulty could be solved neither by modifying the internal electrolyte pH nor by adding complexing agents.

Graphite paste-silver cell. Because of its undesirable features, the aluminium was replaced by silver wire as anode. This sensor showed a very well

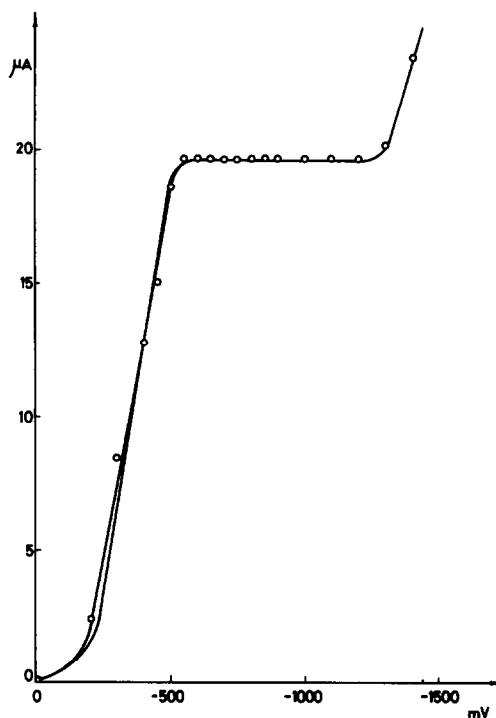


Fig. 4. Current vs. potential curve: graphite-paste cathode, 3 mm diameter; silver-wire anode, 1 mm diameter. Sensitivity 0.2 $\mu\text{A/divn.}$; 20 μm thick polyethylene membrane, stirring at 500 rpm.

Table 1. Linear response and sensitivity of the graphite paste-silver cell to oxygen dissolved in 0.1M KCl

Operating condition	Linear response		Sensitivity, $\mu A \cdot ml \cdot \mu g^{-1}$	n*	SD,† $\mu g/ml$
	interval, $\mu g/ml$				
Without stirring and with membrane	0.2-28		0.33	7	0.024
With stirring and with membrane	0.2-28		0.49	9	0.032

*n = number of trials.

†SD = standard deviation.

Table 2. Comparison of the graphite paste-silver (Gp-s) cell and Winkler methods

Origin of water	DO found, $\mu g/ml$	
	Gp-s cell	Winkler method
Tap water (San Luis City)	5.60	5.90
Tap water (San Luis City)	6.14	5.90
Lake (Cruz de Piedra)	6.77	6.22
Lake (Potrero de los Funes)	6.42	6.30
River (Río Grande)	6.24	5.97

defined response with a wider linear range than that of the other devices tested. Table 1 shows the linear response and sensitivity data for this cell. As expected, the current increased when the solution was stirred, the increase being large enough for operation with stirred solutions to be preferred. These results agree with those reported by others.²

Within the linear response range the time required to produce stable currents was 2 min, irrespective of oxygen concentration. Replacing the polyethylene membrane by a Teflon FEP membrane decreased the response time to 30 sec, while maintaining the other characteristics. With this cathode the plateau on the current-voltage curve (Fig. 4) was twice as wide with the silver cathode as with the gold or platinum one.¹⁵

The most outstanding features of the graphite paste-silver system, compared to the modified Aiba sensor, were (i) shorter time needed to produce a constant response, (ii) wider linear range, (iii) larger overpotential for hydrogen reduction than that obtained with platinum or gold cathodes.

Applications

The graphite paste-silver sensor was used to determine the DO concentration in natural waters of different origins. Potassium chloride solutions equilibrated with air were used for calibration, their oxygen content being obtained from the atmospheric pressure and tabulated data.⁹ To verify the accuracy of the values obtained, the same samples were analysed by the Winkler method.⁹ The results are shown in Table 2.

Acknowledgements—The authors wish to thank the late Dr. Carlos B. Marone for critical discussions, Dr. Domingo

F. Giménez for his helpful suggestions, and Mr. Esterino Bachetta for his efficient work in construction of the electrode bodies used in this work.

REFERENCES

1. A. Brownman, *Birmingham Univ. Chem. Eng.*, 1970, **21**, 1065.
2. L. C. Clark, Jr., R. Wolf, D. Granger and Z. Taylor, *J. Appl. Physiol.*, 1953, **6**, 189.
3. C. M. Masi, S. Pizzini, L. Manes and F. Toci, *Patents*, B.E. 894, 044(C1 G 01 N) 01 Dec. 1982; G.B. Appl. 81/24416 10 Aug. 1981; *Chem. Abstr.*, 1983, **98**, 154618t.
4. Ch. Perrin and H. Rhyn, *Inf. Chim.*, 1982, 231, 261; *Chem. Abstr.*, 1983, **98**, 113390u.
5. C. Farago and C. Rusu, *Patents Rom.* RO 67, 068(C1 G 01 N27/26) 30 Nov. 1979; Appl. 81, 357 08 Feb. 1975; *Chem. Abstr.*, 1983, **98**, 154606n.
6. Z. Zhang and W. R. Seitz, *Anal. Chem.*, 1986, **58**, 220.
7. S. Aiba, A. Humphrey and N. Mills, *Biochemical Engineering*, pp. 255-257. Academic Press, New York, 1964.
8. APHA, AWWA, WCPF, *Standard Methods for the Examination of Water and Wastewater*, 12th Ed., pp. 506-509. New York, 1965.
9. *Ibid.*, pp. 406-410.
10. R. N. Adams, *Electrochemistry at Solid Electrodes*, pp. 27 and 280-283. Dekker, New York, 1969.
11. A. Kozawa, V. E. Zilionis and R. J. Brodd, *J. Electrochem. Soc.*, 1970, **117**, 1470.
12. *Idem, ibid.*, 1970, **117**, 1474.
13. I. M. Kolthoff and J. J. Lingane, *Polarography*, 2nd Ed., Vol. 2, pp. 553. Interscience, New York, 1952.
14. C. D. Ferris, *Introduction to Bioelectrodes*, p. 131. Plenum Press, New York, 1974.
15. I. M. Kolthoff and J. Jordan, *J. Am. Chem. Soc.*, 1952, **74**, 4801.

POLAROGRAPHIC ADSORPTIVE WAVES OF ALKALINE-EARTH METAL COMPLEXES WITH THYMOLPHTHALEXONE

ZHANG QING* and HUANG YUYING

Department of Chemistry, Fuzhou University, Fuzhou, Fujian, China

(Received 6 August 1986. Revised 17 December 1986. Accepted 27 January 1987)

Summary—Sensitive derivative polarographic adsorption waves have been observed for alkaline-earth metal-TP complexes in 0.15M potassium hydroxide containing $3 \times 10^{-5}M$ thymolphthalexone (TP). The limit of detection for calcium, strontium and barium was $7.5 \times 10^{-7}M$ and for magnesium $4.0 \times 10^{-6}M$. The proposed method has been used successfully for determining trace amounts of calcium in natural waters and hair samples. The composition of the complex has been shown to be 1:1 alkaline-earth metal:TP and various experiments have confirmed that the wave is an adsorption wave. The reaction mechanism has been studied by a number of methods.

Alkaline-earth metal ions are very difficult to reduce at the dropping mercury electrode (DME) in aqueous solution and so they cannot be determined by conventional dc polarography. There is, however, a novel approach to improving the analytical sensitivity by making use of electro-reduction of the ligand in a complex formed between an alkaline-earth metal ion and a suitable dye or other organic reagent. Over the last few years, polarographic studies on the complexes of calcium and magnesium with murexide,¹ Eriochrome Black T,^{2,3} meso-tetra(4-trimethylammoniumphenyl)porphine⁴ and Alizarin Red S⁵ have been reported.

Although thymolphthalexone, 3,3-bis[*N,N*-bis(carboxymethyl)aminomethyl]thymolphthalein (TP), has been used as a reagent for the determination of rare-earth (RE)^{6,7} and alkaline-earth AE⁸ metals by spectrophotometry, nothing on the polarographic behaviour of its complexes with the alkaline-earth metals has been reported, though Zhang and Gao⁹ have reported on the polarographic behaviour of TP itself and of RE-TP complexes. No well-defined wave was observed for the RE-TP complexes.

We have used TP and its analogues as ligands forming complexes with the alkaline-earth metals, for polarographic determination of these metals. In this paper a sensitive polarographic adsorptive wave of the TP complexes of the alkaline-earth metals is reported, which can be used for analytical purposes. Rather satisfactory results have been obtained for the determination of calcium in natural waters and hair samples.

The adsorptive properties, composition and structure of the complexes and the mechanism of the electrochemical reduction have also been investigated.

*Present address: Division of Chemical and Physical Sciences, Deakin University, Waurn Ponds, Victoria 3217, Australia.

EXPERIMENTAL

Apparatus

A single-sweep polarograph and a voltammetric analyser were used, both in the three-electrode configuration, with an *x-y* recorder. A Metrohm Polarecord E506, with model 501 thermostat (set at $25 \pm 0.2^\circ$), was also used in the three-electrode configuration. A dropping mercury electrode was used as working electrode, except for the cyclic voltammetry, for which a hanging drop mercury electrode was used. All potentials were measured against an amalgamated silver electrode.

Reagents

Standard calcium, magnesium, strontium and barium solutions were prepared.¹⁰ The thymolphthalexone, analytical grade, was made by the Shanghai Third Chemical Reagent Co.; 0.1080 g of it was dissolved in distilled water containing 1 ml of 1M potassium hydroxide and the solution was diluted to give a $1.5 \times 10^{-3}M$ working solution. The solution was stable for at least one day when stored at room temperature. Other reagents were of analytical grade or better. Water distilled in a fused-silica still was used throughout. All solutions were stored in polyethylene bottles.

Procedure

Calibration graphs. Transfer an aliquot of the standard solution of an alkaline-earth metal into a 10-ml fused-silica standard flask, add 0.2 ml of $1.5 \times 10^{-3}M$ TP, 1.5 ml of 1M potassium hydroxide and dilute to the mark with water. Pour the solution into the polarographic cell and record the derivative polarogram, starting the potential scan at $-0.5V$.

Analysis of samples. Transfer 1.0 ml of water sample into a 10-ml standard flask, and continue as above. For analysis of hair, ash the sample as described elsewhere.¹¹

RESULTS AND DISCUSSION

Single-sweep polarography

Figure 1 shows derivative single-sweep polarograms of TP and its complexes with alkaline-earth metals in 0.15M potassium hydroxide. In this system TP has two small waves (P1 and P2) at about -0.65 and $-0.78V$. After the addition of small amounts of

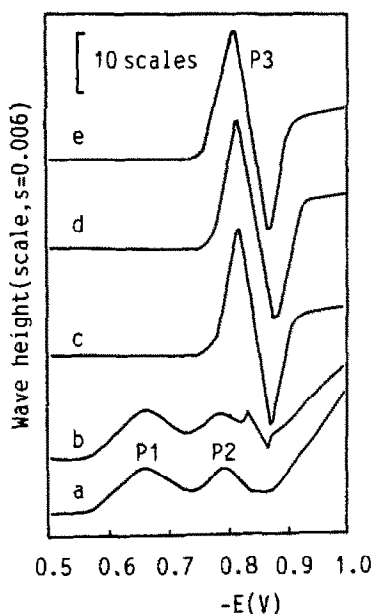


Fig. 1. Derivative single-sweep polarograms of the TP and AE-TP systems. a, $0.15M$ KOH + $3 \times 10^{-5}M$ TP; b, $a + 2 \times 10^{-5}M$ Mg^{2+} ; c, $a + 2 \times 10^{-5}M$ Ca^{2+} ; d, $a + 2 \times 10^{-5}M$ Sr^{2+} ; e, $a + 2 \times 10^{-5}M$ Ba^{2+} . JP-1A single-sweep, scan-rate 250 mV/sec, s = current multiplier.

Ca^{2+} , Sr^{2+} , Ba^{2+} or Mg^{2+} and TP, these waves are suppressed and a new wave (P3) appears at a potential about 60 mV more negative than P2 of TP; this is the reduction wave of the complex and can be used for analytical purposes. It is quite different from that of the RE-TP system.⁹

Further, we have found that the complexes of the alkaline-earth metals with other triphenylmethane dyes such as *o*-cresolphthalexone (OCP), Xylenol Orange (XO) and Methylthymol Blue (MTB), etc., give similar waves.

The potassium hydroxide concentration affects

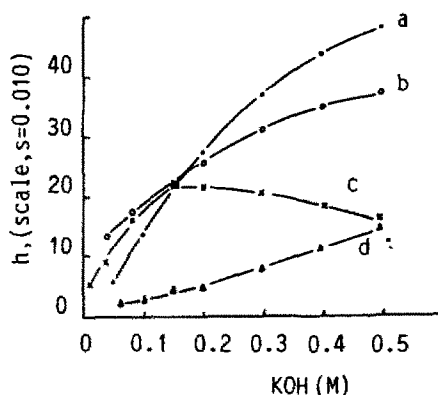


Fig. 2. Effect of KOH concentration on the peak height for $3 \times 10^{-5}M$ TP plus $2 \times 10^{-5}M$ AE: a, Ca^{2+} ; b, Sr^{2+} ; c, Ba^{2+} ; d, Mg^{2+} .

both the formation of the complex and the electrode processes (Fig. 2). In our experiments its concentration was kept at $0.15M$. At higher concentrations the blank value increases, so the linear range becomes narrower and the analytical sensitivity is decreased.

Ca^{2+} , Sr^{2+} , Ba^{2+} and Mg^{2+} do not give any reduction peak in $0.15M$ potassium hydroxide in the absence of TP. The height of the peaks at about -0.84 V for the AE-TP complexes is constant and maximal over the TP range 2.0×10^{-5} – $4.0 \times 10^{-5}M$. We chose $3 \times 10^{-5}M$ for further work.

Under the conditions selected, the peak heights for Ca^{2+} , Sr^{2+} , Ba^{2+} and Mg^{2+} complexes are a linear function of the metal-ion concentrations over the ranges shown in Table 1.

Table 1. Detection limits and linear ranges

	Detection limit, M	Linear range, M
Ca^{2+}	7.5×10^{-7}	2×10^{-6} – 3×10^{-5}
Sr^{2+}	7.5×10^{-7}	2×10^{-6} – 3×10^{-5}
Ba^{2+}	7.5×10^{-7}	2×10^{-6} – 3×10^{-5}
Mg^{2+}	4.0×10^{-6}	8×10^{-6} – 6×10^{-5}

Table 2. Analysis of various water and hair samples for calcium

Sample	Ca added, μg	Ca found, μg	Recovery,* %	Content,† ppm
Fuzhou running water, 1.0 ml	0	3.00		3.00 ± 0.10
	1.6	4.5	94	
	3.2	6.4	106	
	4.8	7.8	100	
Ming River water, 1.0 ml	0	6.00		6.00 ± 0.06
	1.6	7.7	106	
	3.2	8.9	91	
	4.8	10.4	92	
Hot-spring ground water, 1.0 ml	0	8.50		8.50 ± 0.16 §
	1.6	10.1	100	
	3.2	11.5	94	
	4.8	12.9	92	
Hair, 50.0 mg	0	97.5		1950 ± 45
	80	174	95	
	160	246	93	

*Mean of three determinations.

†Mean of ten determinations \pm standard deviation.

§Calcium level found by AAS: 8.2 ppm.

Interference studies

The effect of potential interferents was investigated with $8 \mu\text{g}$ of Ca^{2+} in 10 ml of solution. The amounts of other ions which did not interfere are as follows: large amounts of K^+ , Na^+ , Fe^{2+} and common anions; $800 \mu\text{g}$ of Be^{2+} , W(VI) , Mo(VI) , Bi^{3+} , Ti(IV) , Tl^+ , Al^{3+} , Cr(VI) , Sn(IV) , Mn^{2+} , Ce^{3+} , Ga^{3+} , V(V) , In^{3+} , Cu^{2+} , Zn^{2+} and Se(IV) ; $320 \mu\text{g}$ of Pb^{2+} ; $16 \mu\text{g}$ of Cd^{2+} and $4 \mu\text{g}$ of Fe^{3+} .

Because the sensitivity is the same for Ca-TP, Sr-TP and Ba-TP in this system, a determination actually measures the total of all three. It is interesting that up to a 5-fold amount of Mg^{2+} does not interfere in the determination of calcium. It is thus possible to determine the calcium content of natural waters and hair samples because their magnesium levels are normally lower than those of calcium.

Determination of calcium in water and hair

The method has been used for the determination of calcium in natural waters and human head hair samples. The results are shown in Table 2.

Adsorptive character of TP and AE-TP peaks

The following experiments were performed to verify the adsorptive character of the peaks for TP and its alkaline-earth metal complexes.

Temperature coefficient. The dependence of the peak heights and peak potentials of the Ca-TP system on temperature was examined over the range $9\text{--}50^\circ$. The peak height for Ca-TP had a temperature coefficient of $-4.4\%/ \text{deg}$ and the peak potential shifted by $+40 \text{ mV}$ when the temperature was increased from 9° to 50° . This behaviour is typical of an adsorptive reduction peak.

Relationship between peak height and the standing period before scanning. If a process is diffusion-controlled, the peak current will be independent of the standing time before scanning. In the case of adsorption, the peak current increases with increasing standing time, owing to accumulation

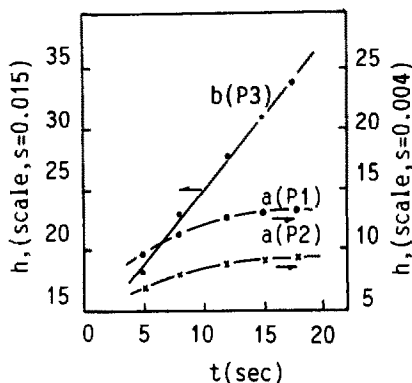


Fig. 3. The relationship between peak height and standing period. a, $0.15M$ KOH + $3 \times 10^{-5}M$ TP; b, a + $2 \times 10^{-5}M$ Ca^{2+} . P1, P2—the derivative polarographic waves of TP at -0.65 and -0.78 V respectively; P3—the derivative polarographic wave of Ca-TP.

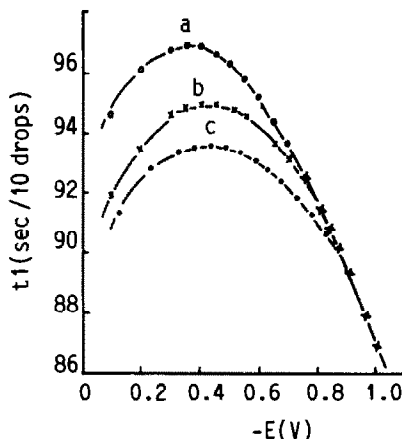


Fig. 4. Electrocapillary curves. a, $0.15M$ KOH; b, a + $6 \times 10^{-5}M$ TP; c, b + $4 \times 10^{-5}M$ Ca^{2+} .

of the adsorptive species.^{12,13} In performing linear-sweep polarographic experiments with the JP-1A and a DME, we can change the standing time before scanning by adjusting the variable resistance ($0.5\text{--}10 \times 10^6 \Omega$) which is connected in series with R73 of the JP-1A. When the head of mercury is adjusted so that the free mercury drop-time synchronizes with the knocking time, the area of each drop in different scans will be almost the same. The relationship between derivative peak height and the standing period in the TP and Ca-TP system is shown in Fig. 3. The peak heights for TP and Ca-TP both increase with increasing standing period before scanning. This is another characteristic feature of adsorptive waves.

Electrocapillary curves

These curves can give some information about the adsorption of a particular species. A solution containing TP and potassium hydroxide has an electrocapillary curve lower than that of the supporting electrolyte, $0.15M$ potassium hydroxide (see Fig. 4, a,b), owing to the adsorption of TP on the surface of the DME changing the surface tension of the mercury drop. The electrocapillary curve of a solution con-

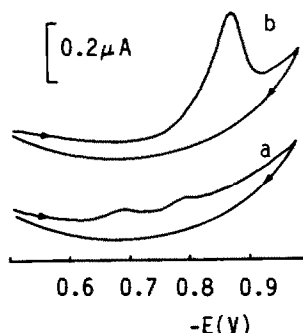


Fig. 5. Cyclic voltammograms. a, $0.15M$ KOH + $6 \times 10^{-5}M$ TP; b, a + $4 \times 10^{-5}M$ Ca^{2+} . Scan-rate 150 mV/sec .

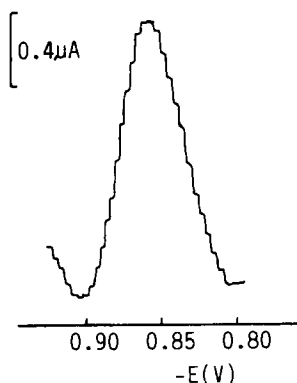


Fig. 6. Differential pulse polarogram for Ca-TP; 0.15M KOH + $6 \times 10^{-5}M$ TP + $4 \times 10^{-5}M$ Ca²⁺; scan-rate 4 mV/sec.

taining Ca-TP will be depressed further than that of the TP solution. This shows that the complex is adsorbed more strongly than TP (see Fig. 4, b,c). The change of capacitance of the TP solution relative to the electrolyte alone, clearly illustrates the adsorption of TP at the DME.

Cyclic voltammetry

The cyclic voltammetry of the systems was investigated with a Model 82-1 voltammetric analyser. Typical cyclic voltammetric curves are shown in Fig. 5. TP gives two indefinite cathodic peaks, P1 and P2, at about -0.69 and -0.81 V respectively, owing to its reduction. The peak of the Ca-TP complex, P3, appears at -0.87 V, and is due to reduction of the ligand in the complex. No peak was observed on the anodic branch, from which we conclude that the reduction of TP and the Ca-TP complex is irreversible.

Electron numbers involved in the electro-reduction

Zhang and co-workers^{14,15} proposed a simple method for measuring the electron numbers involved in the electro-reduction. We have used it here. For an adsorptive electrode process, the following equation can be derived:

$$W_{1/2} = 3.52 \frac{RT}{nF} = E_{pp}$$

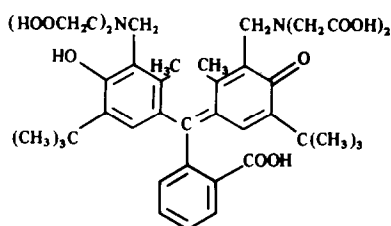
where $W_{1/2}$ is the width of the differential pulse polarographic peak at half height, and E_{pp} is the difference in the potentials of the positive and the negative peaks for the derivative single-sweep polarography of the adsorbed complex. E_{pp} or $W_{1/2}$ can be determined by experiment, so the electron number n can be calculated. We measured E_{pp} and $W_{1/2}$ for the derivative single-sweep polarograms (Fig. 1) and for the differential pulse polarograms (Fig. 6) of the AE-TP complexes respectively, and the results (six

determinations) were 0.048 and 0.050 V at 25° respectively. Substituting these results into the equation gives values of n for the reduction of AE-TP. In both cases $n = 2$. This indicates that two electrons are involved in the reduction of AE-TP, (which may take place in two single-electron steps.)

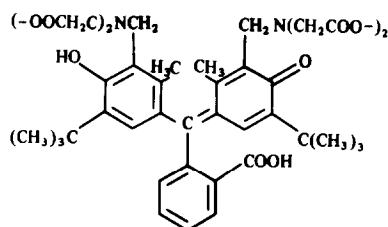
Composition of the electroactive complex

Under the analytical conditions TP (I) exists mainly in the form of H_2L^{4-} (II). The stoichiometry of the reaction between H_2L^{4-} and alkaline-earth metal ions (AE) has been determined by the polarographic linear method^{16,17} (see Fig. 7) and found to be 1:1.

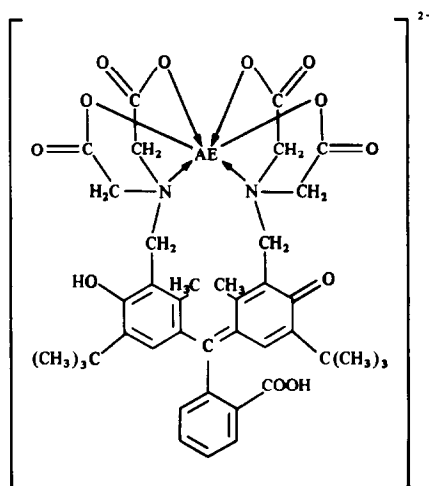
The complex may have structure III:



(I)



(II)



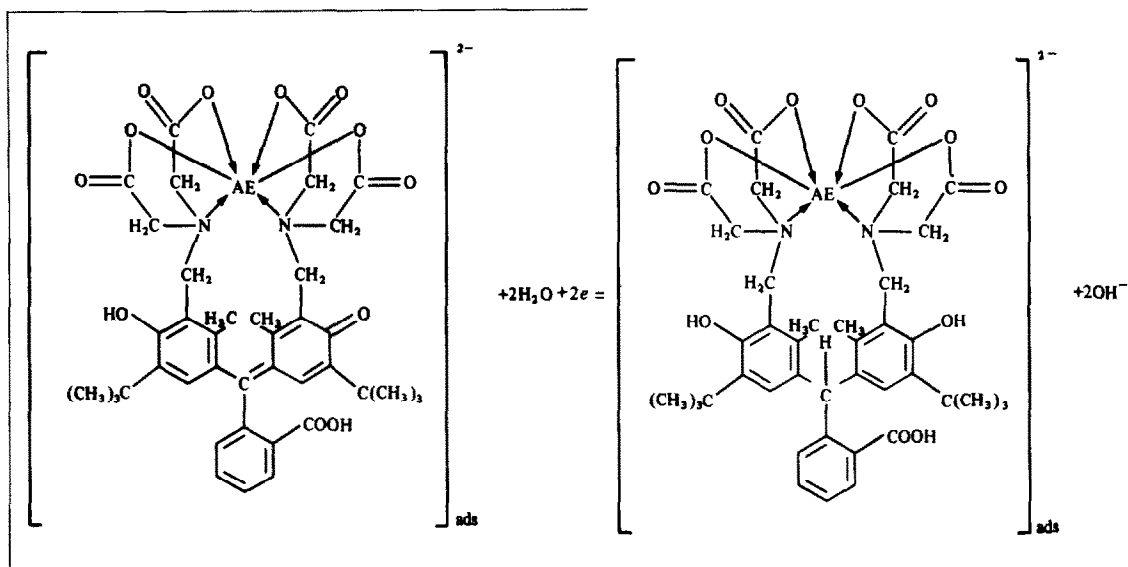
(III)

Electro-reduction mechanism

First H_2L^{4-} (II) and an AE metal cation form an electroactive complex $H_2(AE)L^{2-}$ (III) in solution. This complex diffuses to the electrode and is adsorbed on its surface. In single-sweep polarography the $C=C_6H_4=O$ group in the complex is reduced as soon as the scan potential reaches -0.84 V. The analytical sensitivity is greatly increased because of the adsorption on the electrode surface.

polarography. Linear relationships hold between peak height and concentration for these cations in a certain range.

It is concluded that the AE-TP complex is more strongly adsorbed than the ligand. The reaction scheme may be as follows:



CONCLUSION

In 0.15M potassium hydroxide medium, alkaline-earth metal ions (Ca^{2+} , Sr^{2+} , Ba^{2+} and Mg^{2+}) and thymolphthalexone (TP) can form an electroactive complex $H_2(AE)L^{2-}$, which gives a sensitive reduction peak at -0.84 V by derivative single-sweep

The electrode reaction of H_2L^{4-} corresponds to peaks P1 and P2, and the adsorbed complex is reduced to give peak P3, as shown in equation (3).

REFERENCES

1. D. Guo and E. Wang, *Fengxi Huaxue*, 1982, **10**, 277.
2. J. An, J. Zhou and X. Wen, *Talanta*, 1985, **32**, 479.
3. C. Meng, *Fengxi Huaxue*, 1985, **13**, 89.
4. D. Luo and Z. Zhao, *J. Wuhan Univ. (Natural Sci. Ed.)*, 1982, 100.
5. J. An and J. Zhou, *Huaxue Xuebao*, 1985, **43**, 524.
6. P. Danuta, *Chem. Anal. Warsaw*, 1962, **7**, 861.
7. *Idem, ibid.*, 1964, **9**, 111.
8. A. Bezděková and B. Buděšínský, *Collection Czech. Chem. Commun.*, 1965, **30**, 818.
9. M. Zhang and X. Gao, *Anal. Chem.*, 1984, **56**, 1917.
10. *Handbook of Purification and Preparation of Analytical Reagents for Metallurgy*, p. 188. Seventh Press, Peking, 1973.
11. J. An and Q. Zhang, *Environmental Sciences In China*, 1984, **4**, 75.
12. J. Koryta, *Collection Czech. Chem. Commun.*, 1953, **18**, 206.
13. J. An, Q. Zhang and X. Chen, *Fengxi Huaxue*, 1986, **14**, 62.
14. Z. Zhang and Q. Gao, *Huaxue Xuebao*, 1982, **40**, 523.
15. Z. Zhang and Y. Zhu, *ibid.*, 1983, **41**, 1021.
16. N. Li, L. Zhang and X. Gao, *Fengxi Huaxue*, 1973, **1**, 40.
17. N. Li and X. Gao, *ibid.*, 1974, **2**, 459.

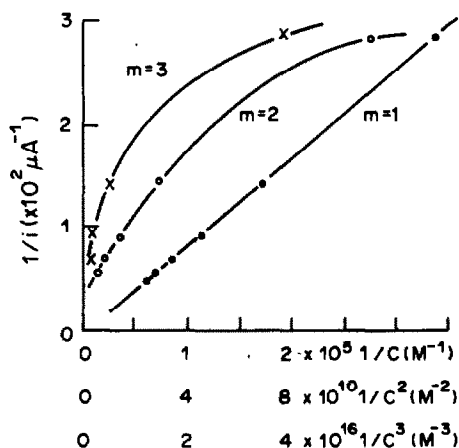


Fig. 7. Relation between $1/i$ and $1/C^n$.

ADSORPTIVE PRECONCENTRATION FOR VOLTAMMETRIC MEASUREMENTS OF TRACE LEVELS OF ZIRCONIUM

JOSEPH WANG,* PENG TUZHI† and KURIAN VARUGHESE

Department of Chemistry, New Mexico State University, Las Cruces, New Mexico 88003, U.S.A.

(Received 7 November 1986. Accepted 14 January 1987)

Summary—This paper describes an electrochemical stripping procedure for ultratrace measurements of zirconium, in which preconcentration is achieved by the adsorption of a zirconium–Solochrome Violet RS complex onto a hanging mercury drop electrode. Cyclic voltammetry was used to characterize the interfacial and redox behaviour. For a 10-min preconcentration time, the detection limit found was $2.3 \times 10^{-10}M$. Optimal experimental conditions were found to be use of a stirred acetate buffer (pH 4.6) solution with Solochrome Violet RS concentration $1.5 \times 10^{-6}M$, a preconcentration potential of -0.3 V and linear scan mode. A 60-fold enhancement of the response is obtained following 5-min preconcentration. With preconcentration for 60 sec, calibration plots for zirconium are linear for the 1.1×10^{-8} – $1.1 \times 10^{-7}M$ range. The relative standard deviation at $5.5 \times 10^{-8}M$ is 1.7%. Possible interferences by surface-active organic materials and other trace metals have been investigated. Zirconium added to a sea-water sample at the 10 ng/ml level was readily determined.

Few analytical techniques possess the sensitivity required for trace and ultratrace determination of zirconium. Since zirconium forms refractory compounds which are difficult to vaporize or dissociate, the sensitivity of atomic-absorption spectrometry is limited by the difficulty of generating free zirconium atoms.¹ Micromolar and nanomolar zirconium levels can be measured by X-ray fluorescence spectrometry² and inductively-coupled plasma atomic spectrometry³ respectively, both of which require costly instrumentation. The electrochemical behaviour of zirconium makes its voltammetric determination very difficult. Only indirect electroanalytical procedures have been suggested, allowing measurements of submicromolar and nanomolar concentrations of zirconium. Among these are recent polarographic assays based on the adsorptive wave of the zirconium–oxalic acid–cupferron–diphenylguanidine complex at the dropping mercury electrode,⁴ and the formation of molybdozirconophosphoric acid and subsequent measurement of its molybdenum content by its catalytic effects on the polarographic reduction of hydrogen peroxide.⁵

This work describes an extremely sensitive voltammetric procedure for the determination of ultratrace amounts of zirconium in which preconcentration is achieved by adsorption of the zirconium chelate with Solochrome Violet RS (SVRS) on the hanging mercury drop electrode. The ability of dihydroxyazo dyes to form electrochemically active chelates with zirconium has been known for many years.^{6,7} Combining the voltammetric activity of the

zirconium–dihydroxyazo dye complexes with their surface-active properties results in an effective adsorptive stripping procedure. Similar procedures based on the formation and interfacial accumulation of metal chelates of dihydroxyazo dyes have been developed recently for trace measurements of aluminium,⁸ titanium,⁹ thorium,¹⁰ and uranium.¹¹ Other ligands, such as catechol or dimethylglyoxime, can be employed for analogous trace measurements of vanadium,¹² iron,¹³ and nickel.¹⁴ As illustrated in the present study, subnanomolar concentrations of zirconium can be determined by using SVRS as chelating reagent, and carefully optimizing the operational conditions.

EXPERIMENTAL

Apparatus and reagents

The equipment used to obtain the voltamperograms, a PAR 264 voltammetric analyser with a PAR 303 static mercury drop electrode, has been described in detail before.⁸ All solutions were prepared from doubly-distilled water. A 1000 mg/l. zirconium stock solution (atomic-absorption standard, Aldrich) was used, and diluted as required for standard additions. A $10^{-4}M$ stock solution of SVRS was prepared daily. The supporting electrolyte was a 0.05M acetate buffer (pH 4.6). The sea-water used was unfiltered surface water collected at San Diego (CA) and stored frozen.

Procedure

The supporting electrolyte solution (10 ml), SVRS concentration $1.5 \times 10^{-6}M$, was pipetted into the polarographic cell, and purged with nitrogen for 8 min. The preconcentration potential (usually -0.30 V) was applied to a fresh mercury drop while the solution was stirred. Following the preconcentration period, the stirring was stopped, and after 15 sec the voltamperogram was recorded by applying a negative-going linear scan, terminated at -1.0 V. After the background stripping voltamperogram had been obtained, aliquots of the zirconium standard were introduced.

*Author for correspondence.

†On leave from: Chemistry Department, Hangzhou University, Hangzhou, China.

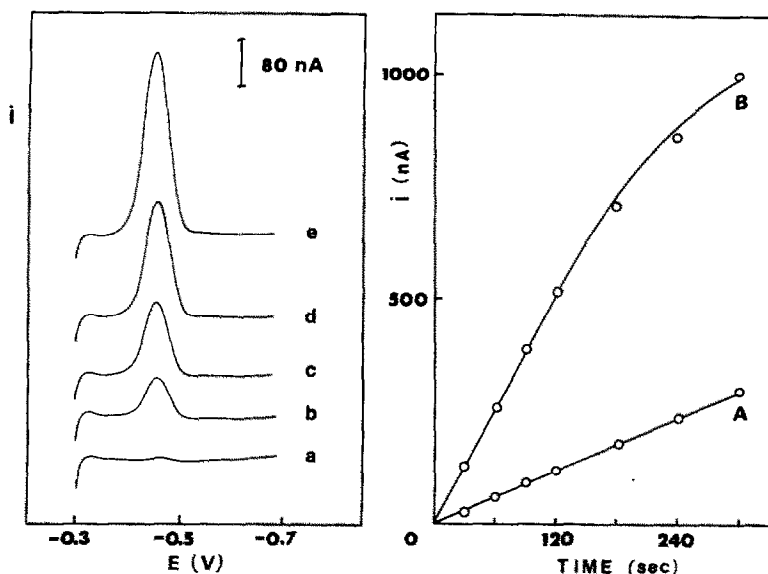


Fig. 1. Linear scan voltamperograms for 1 ng/ml zirconium after different pre-concentration periods: a, 0; b, 60; c, 120; d, 180; e, 300 sec. Pre-concentration at -0.30 V with 400 rpm stirring. Electrolyte, $0.05M$ acetate buffer (pH 4.6) containing $1.5 \times 10^{-6}M$ SVRS; scan-rate, 50 mV/sec. Also shown, current *vs.* pre-concentration time plots for 1 (A) and 4 (B) ng/ml Zr.

Throughout this operation, nitrogen was passed over the solution surface. All data were obtained at room temperature.

RESULTS AND DISCUSSION

Figure 1 shows linear scan voltamperograms for $1.1 \times 10^{-8}M$ (1 ng/ml) zirconium, in the presence of $1.5 \times 10^{-6}M$ SVRS, after different pre-concentration periods [0–300 sec (a–e)]. The chelate stripping peaks are well-defined, with a peak potential of -0.446 V and peak half-width of 53 mV. A rapid increase of the chelate peak is observed with increasing pre-concentration time, indicating an enhancement of the chelate concentration on the mercury surface. For example, 2- and 5-min pre-concentration periods yielded 24- and 60-fold enhancement of the peak current, respectively, relative to that obtained without pre-concentration (compare curves a, c, and e). As a result, zirconium can easily be determined at the sub-ng/ml level; such measurements are not feasible by conventional voltammetric methods (without pre-concentration, *e.g.*, curve a). Also shown in Fig. 1 are current *vs.* pre-concentration-time plots for 1 (A) and 4 (B) ng/ml zirconium. While the current peak at 1 ng/ml increases linearly with pre-concentration time (slope 1.02 nA/sec, correlation coefficient 1.000), that for 4 ng/ml exhibits deviation from linearity for pre-concentration periods longer than 180 sec (slope of initial linear portion 3.83 nA/sec, correlation coefficient 0.996); such deviation from linearity is expected for measurements limited by adsorption of the analyte.

Cyclic voltammetry was used to obtain a better understanding of the interfacial and redox processes.

Figure 2 shows repetitive cyclic voltamperograms for $1.5 \times 10^{-6}M$ SVRS recorded in the absence (A) and presence (B) of 25 ng/ml zirconium. The response was recorded following stirring for 60 sec at -0.1 V. The first scan (voltamperograms 1) shows two dis-

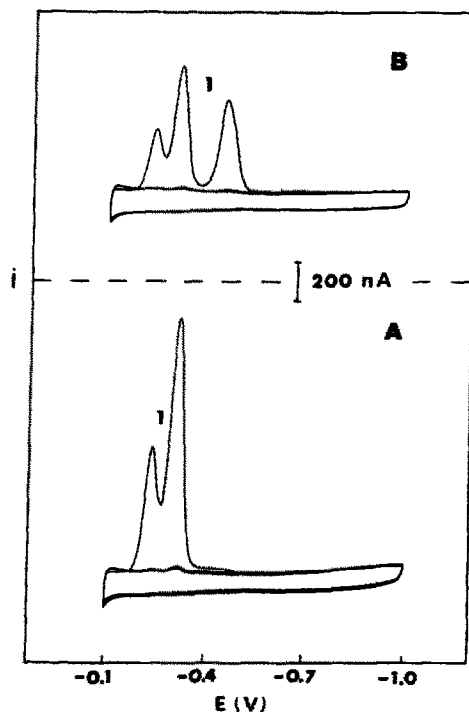


Fig. 2. Repetitive cyclic voltamperograms obtained following stirring for 60 sec at -0.1 V. A, Response for $1.5 \times 10^{-6}M$ SVRS; B, same as A but after addition of 25 ng/ml zirconium. Other conditions as for Fig. 1.

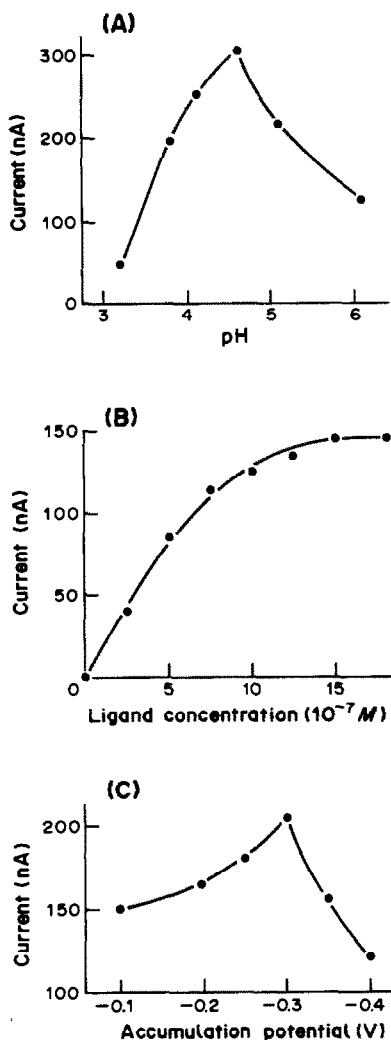


Fig. 3. Effect of pH (A), SVRS concentration (B), and preconcentration potential (C), on the adsorptive stripping current. Zirconium concentration, 5 (A), 2 (B), and 3 (C) ng/ml. Preconcentration time, 60 sec. Other conditions as for Fig. 1.

tinct cathodic peaks due to the reduction of the adsorbed dye at -0.23 and -0.31 V, and a separate reduction peak of the adsorbed Zr-SVRS chelate at -0.44 V. The chelate competes with the free dye for adsorption sites, resulting in lower dye peaks (compare A and B). No peaks are observed upon scanning in the positive direction. Subsequent scans yielded significantly smaller, but stable, reduction peaks, indicating that the dye and chelate are being rapidly desorbed from the surface. A similar adsorption-desorption behaviour has been observed for several metal chelates of SVRS. When a potential of -0.30 V was applied during the stirring period, only a single peak due to the reduction of the adsorbed chelate was observed (not shown). Under these conditions maximum adsorption density was observed after stirring for 60 sec. The maximum charge obtained by integrating the adsorbed-chelate reduction

peak was found to be $4.6 \mu C$, corresponding to an adsorbed layer of 7.8×10^{-10} mole/cm². The effect of potential scan-rate on the peak current and potential was also evaluated at maximum adsorption density. The plot of $\log(\text{peak current})$ vs. $\log(\text{scan-rate})$ was linear, with a slope of 0.630 over the 5–200 mV/sec range. The peak potential shifted negatively, from -0.410 to -0.480 V, upon increasing the scan-rate from 5 to 200 mV/sec, yielding a linear (peak potential) vs. $\log(\text{scan-rate})$ plot (correlation coefficient 0.997).

The suitability of various supporting electrolytes and azo dyes was examined. Small Zr-SVRS peaks were observed in phosphate buffer (pH 9), and in PIPES solutions of pH 9.4 and 11.4. Best results were obtained in acetate buffer (pH 4.6). A definite zirconium response was observed in the presence of Eriochrome Black T and Mordant Blue 9, but since SVRS yielded a zirconium peak about two and half times bigger, it was used in all subsequent work. The effect of other solution and instrumental conditions on the Zr-SVRS adsorptive stripping response is shown in Fig. 3. The solution pH has a pronounced effect on the magnitude of the chelate peak (curve A). The peak increases rapidly upon increasing the pH from 3.2 to 4.6, then a sharp decrease is observed at high pH values. A negative shift in the peak potential, from -0.35 to -0.53 V, was observed upon changing the pH from 3.2 to 6.1. As expected, the Zr-SVRS peak depends strongly on the SVRS concentration (curve B). The peak increases with the dye concentration, until it levels off at $1.5 \times 10^{-6} M$. This concentration was used in all subsequent trace measurements. The effect of the accumulation potential on the peak current was evaluated over the range from -0.1 to -0.4 V (curve C). The largest peak was observed for accumulation at -0.3 V. Accordingly, the potential was used for all further work. The increase in chelate peak upon changing the potential from -0.1 to -0.3 V is attributed, in part, to reduced competition on surface sites, because of desorption of the free dye (see cyclic voltammetric data). Other conditions affecting the Zr-SVRS adsorptive stripping peak include the mass-transport (during the preconcentration step) and the potential-time waveform (during the measurement step). For example, a stirring rate of 400 rpm resulted in a 4.5-fold enhancement of the response, compared to that obtained in a quiescent solution (5 ng/ml zirconium, 1 min preconcentration). The linear-scan stripping mode yielded slightly better signal-to-background characteristics than the differential pulse waveform. The latter resulted in a Zr-SVRS peak at -0.40 V, with half-width of 42 mV. As a result of its response characteristics and speed advantage, the linear scan mode was used throughout this study.

Response characteristics

Figure 4 shows voltamperograms obtained after increasing the zirconium concentration in 1-ng/ml ($1.08 \times 10^{-8} M$) steps (a–e). Well-defined stripping

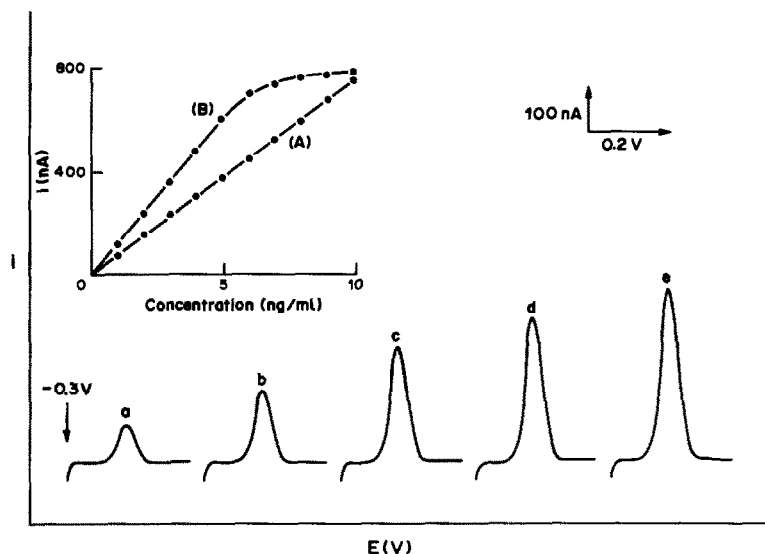


Fig. 4. Stripping voltamperograms obtained for solutions of increasing zirconium concentration, 1–5 ng/ml (a–e). Preconcentration for 60 sec. Other conditions as for Fig. 1. Also shown are calibration plots for 60 (A) and 120 (B) sec preconcentration.

peaks are observed when a 60-sec preconcentration period is used. These five measurements are from a set of ten concentration increments, up to 10 ng/ml. Also shown is the dependence of the stripping peak current on zirconium concentration, for different preconcentration periods. For 60-sec preconcentration (A) the response is linear over the entire 1–10 ng/ml range examined (slope $74 \text{ nA} \cdot \text{ml} \cdot \text{ng}^{-1}$, correlation coefficient 1,000). With preconcentration for 120 sec, the response is linear up to 6 ng/ml, and then it starts to level off as full surface coverage is approached (slope of the initial linear portion $117 \text{ nA} \cdot \text{ml} \cdot \text{ng}^{-1}$, correlation coefficient 0.999). Such curvature is consistent with a process that is limited by adsorption of the analyte.

Because of the effective preconcentration, associated with the interfacial accumulation of the zirconium–SVRS chelate, extremely low detection limits are obtained with short preconcentration times. The detectability was estimated from measurements of 1 ng/ml ($1.08 \times 10^{-8} M$) zirconium after preconcentration for 10 min; the resulting voltamperogram is shown in Fig. 5. The limit of detection—calculated from 3 times the noise—was found to be 22 pg/ml ($2.3 \times 10^{-10} M$). This value means that in the 10 ml of solution used, 220 pg can be detected. Hence, the signal enhancement associated with the accumulation of the Zr–SVRS chelate yields a substantial lowering of the detection limit compared to those of previously reported voltammetric measurements of zirconium.^{4,5} Adsorptive stripping procedures for measuring other metals have yielded similar detection limits.^{8–14} The adsorptive accumulation of the zirconium–SVRS chelate results in reproducible stripping peak currents. Eight successive measurements of 5-ng/ml zirconium yielded a mean

peak current of 222.5 nA, range 215–225 nA, and a relative standard deviation of 1.7% (conditions as for Fig. 1b).

Stripping measurements of trace metals based on chelate adsorption are subject to interference from

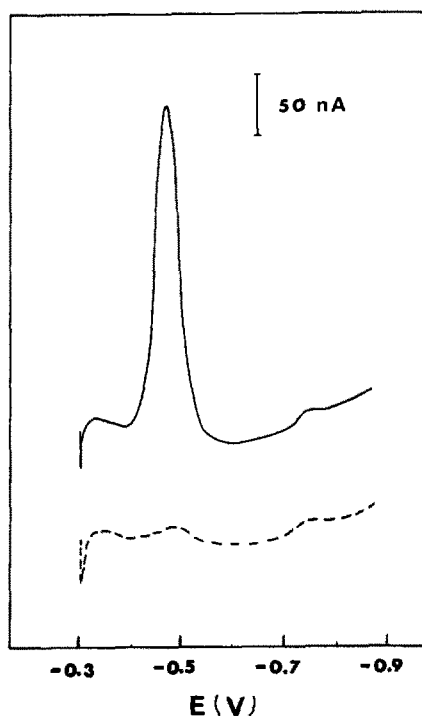


Fig. 5. Linear scan voltamperogram for 1 ng/ml ($1.1 \times 10^{-8} M$) zirconium following preconcentration for 10 min. The dotted line represents an analogous voltamperogram for the blank solution. Other conditions as for Fig. 1.

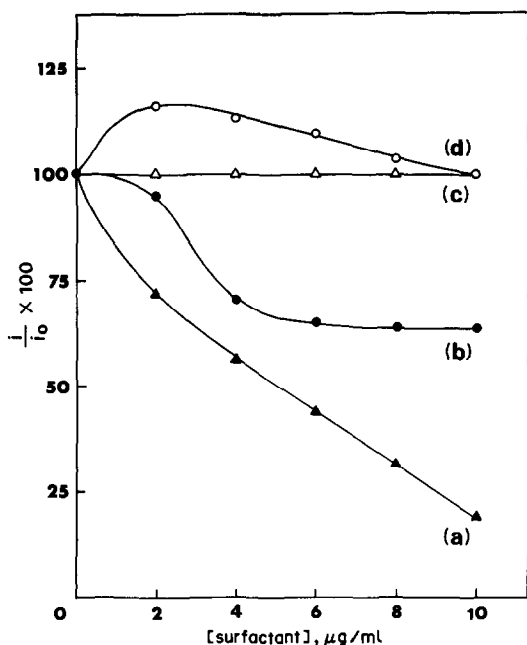


Fig. 6. Effect of humic acid (a), gelatin (b), camphor (c), and sodium dodecyl sulphate (a) on the 5-ng/ml zirconium response. Preconcentration for 60 sec. Other conditions as for Fig. 1.

two sources. First, co-existing metal ions that are also capable of forming chelates with SVRS may affect the Zr-SVRS response through overlapping response (*i.e.*, there is an increase in the Zr-SVRS signal) or by competition for adsorption sites (decrease in Zr-SVRS response). Secondly, organic surfactants may also compete with the chelate for space on the mercury surface. Figure 6 shows the effect of four model surfactants on the Zr-SVRS peak. Significant

depression of the peak current is observed upon addition of humic acid (a) and gelatin (b) (up to 82 and 38% reduction, respectively, at the 10 $\mu\text{g/ml}$ surfactant level). Some broadening of the Zr-SVRS peak accompanied these reductions. Humic acid is a natural chelating agent as well as a surface-active compound. Hence, the large current diminution observed in the presence of humic acid is attributed to both complexation and sorption effects. In contrast, similar additions of camphor (c) had no effect on the zirconium response, and sodium dodecyl sulphate (d) caused a slight enhancement (up to 15%) of the peak. The organic interference in metal-chelate adsorptive stripping measurements is commonly eliminated by ultraviolet irradiation.¹² The following metal ions were tested at the 15-ng/ml level and found not to affect the 5-ng/ml zirconium peak: Pb^{2+} , Cu^{2+} , Cd^{2+} , Zn^{2+} , Ag^+ , Fe^{3+} , Ni^{2+} , Hf^{4+} , Mn^{2+} , Al^{3+} and Bi^{3+} . The addition of Fe^{3+} at 15 ng/ml level resulted in the appearance of a new peak (*ca.* 0.15 V more negative than the Zr-SVRS peak), associated with reduction of the Fe-SVRS chelate.¹⁵ This peak separation is sufficient to permit simultaneous measurement of the two metals. Similar addition of Ti^{4+} resulted in a 50% diminution of the 5-ng/ml zirconium peak, and the appearance of an overlapping Ti-SVRS peak (*ca.* 0.07 V more positive than that for zirconium). Titanium, a member of the zirconium group, is known to yield a well-defined adsorptive stripping response in the presence of SVRS.⁹ (Another member of that group, hafnium, does not interfere at the 15-ng/ml level; see above.)

Figure 7 demonstrates the selectivity and sensitivity of the method when applied to an untreated sea-water sample (from a coastal source). Three 5-ng/ml concentration increments (b-d), yielded well-defined Zr-SVRS peaks, and a linear standard-

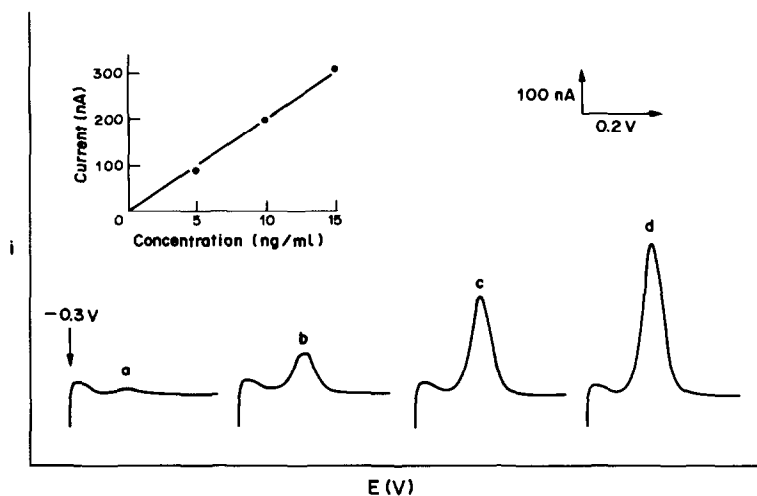


Fig. 7. Standard additions of zirconium to sea-water (8 ml of sea-water + 2 ml of buffer/ $1.5 \times 10^{-6} M$ SVRS). a, Voltamperogram for the sample following preconcentration for 60 sec; b-d, successive increments in zirconium concentration, each 5 ng/ml. Also shown is the resulting calibration plot over the 5-15 ng/ml range. Other conditions as for Fig. 1.

addition plot. The response of the original sample (a) indicates the absence of major interferences in the region of the zirconium peak. (The absence of zirconium response is expected because of the short, 60 sec, preconcentration time used, and the very low level of zirconium in sea-water.)

In conclusion, the method described provides a simple approach to the determination of zirconium at trace and ultratrace levels. The effective interfacial accumulation results in a substantial enhancement of the voltammetric response, hence permitting convenient quantification at the ng/ml level. Destruction of organic surfactants or removal of interfering metals may be required in some cases, depending on the complexity of the sample matrix.

Acknowledgement—This work was supported in part by the National Institutes of Health, Grant No. GM 30913-03.

REFERENCES

1. R. J. Seymour and C. B. Boss, *Anal. Chem.*, 1982, **54**, 1037.
2. E. Ricci, *ibid.*, 1980, **52**, 1708.
3. S. Greenfield, H. M. McGeachin and P. P. Smith, *Talanta*, 1976, **23**, 1.
4. Hua-Li and H. You-Hua, *ibid.*, 1984, **31**, 638.
5. Y. Castrillejo, R. Pardo, E. Barrado and P. Sanchez Batanero, *ibid.*, 1985, **32**, 407.
6. M. Ishibashi, T. Fujinaga and K. Izutsu, *J. Electroanal. Chem.*, 1959/60, **1**, 26.
7. G. W. Latimer, *Talanta*, 1968, **15**, 1.
8. J. Wang, P. A. M. Farias and J. S. Mahmoud, *Anal. Chim. Acta*, 1985, **172**, 57.
9. J. Wang and J. S. Mahmoud, *J. Electroanal. Chem.*, 1986, **208**, 383.
10. J. Wang and J. Zadeii, *Anal. Chim. Acta*, 1986, **188**, 187.
11. *Idem*, *Talanta*, 1987, **34**, 247.
12. C. M. G. van den Berg and Z. Q. Huang, *Anal. Chem.*, 1984, **56**, 2383.
13. *Idem*, *J. Electroanal. Chem.*, 1984, **177**, 269.
14. A. Braun and M. Metzger, *Z. Anal. Chem.*, 1984, **318**, 321.
15. J. Wang and J. S. Mahmoud, *ibid.*, in the press.

LIQUID-LIQUID EXTRACTION SEPARATION AND SEQUENTIAL DETERMINATION OF PLUTONIUM AND AMERICIUM IN ENVIRONMENTAL SAMPLES BY ALPHA-SPECTROMETRY*

K. SEKINE, T. IMAI and A. KASAI

Environmental Research Laboratory II, Japan Atomic Energy Research Institute, Tokai-mura, Ibaraki-ken 319-11, Japan

(Received 9 June 1986. Revised 8 September 1986. Accepted 23 December 1986)

Summary—A procedure is described by which plutonium and americium can be determined in environmental samples. The sample is leached with nitric acid and hydrogen peroxide, and the two elements are co-precipitated with ferric hydroxide and calcium oxalate. The calcium oxalate is incinerated at 450° and the ash is dissolved in nitric acid. Plutonium is extracted with tri-*n*-octylamine solution in xylene from 4*M* nitric acid and stripped with ammonium iodide/hydrochloric acid. Americium is extracted with thenoyltrifluoroacetone solution in xylene at pH 4 together with rare-earth elements and stripped with 1*M* nitric acid. Americium and the rare-earth elements thus separated are sorbed on Dowex 1 × 4 resin from 1*M* nitric acid in 93% methanol, the rare-earth elements are eluted with 0.1*M* hydrochloric acid/0.5*M* ammonium thiocyanate/80% methanol and the americium is finally eluted with 1.5*M* hydrochloric acid in 86% methanol. Plutonium and americium in each fraction are electro-deposited and determined by alpha-spectrometry. Overall average recoveries are 81% for plutonium and 59% for americium.

Plutonium-239 and -240 occur in environmental samples as the result of fall-out from nuclear detonations in the atmosphere; ²⁴¹Am is a decay product of ²⁴¹Pu, which is also a fall-out nuclide. Among the transuranic radionuclides, ²³⁹Pu, ²⁴⁰Pu and ²⁴¹Am are ecologically the most important because their concentrations are relatively high¹ and their radiotoxicities are in the highest group. In assessing the safety of disposal of high-level radioactive waste, they are also important radionuclides because of their physico-chemical properties. Further studies to clarify their environmental behaviour are required. One of their main characteristics is their strong interaction with soil and sediments.²

Many procedures have been described for the determination of plutonium and americium, in which the radiochemical separation is usually based on a combination of co-precipitation, ion-exchange and solvent extraction.³⁻⁵ Since ion-exchange separations can be rather slow, solvent extraction is more attractive. Thus Sill *et al.*⁶ developed a method for the simultaneous determination of the alpha-emitting nuclides of the elements from radium to californium in soil by liquid-liquid extraction with Aliquat-336. Bernabee *et al.*⁷ also reported a solvent extraction separation with di(2-ethylhexyl)phosphoric acid

(HDEHP) for determination of plutonium and americium.

In the present work, on soil samples, a procedure has been developed for sequential separation of plutonium and of americium with tri-*n*-octylamine and thenoyltrifluoroacetone. Americium is subsequently separated from the rare-earth elements by the method of Holm and Fukai,⁸ by ion-exchange in methanolic nitric acid media. The procedure has been tested on some certified reference samples of soils and sediments.

EXPERIMENTAL

Reagents

Thenoyltrifluoroacetone (TTA), 0.5*M*. Dissolve 45 g of TTA in 400 ml of xylene.

*Tri-*n*-octylamine (TOA) solution*. Dissolve 25 g of TOA in 250 ml of xylene.

Cresol Red solution. Dissolve 100 mg of Cresol Red in 26 ml of 0.01*M* sodium hydroxide and dilute the solution to 250 ml with water.

Methyl Red solution. Dissolve 100 mg of Methyl Red in 100 ml of ethanol.

Ammonium iodide-hydrochloric acid solution. Mix ammonium iodide solution (10.2 g in 200 ml of water) with concentrated hydrochloric acid in the ratio 29:71 v/v just before use.

Standard ²⁴⁴Cm solution. ²⁴⁴Cm, 7.415 × 10⁵ Bq/g, impurity <0.1%, from LMRI, France, was used.

Standard ²⁴²Pu solution. NBS SRM 4334-b(USA), 27.29 Bq/g, impurity <0.2%, was used.

Iron carrier solution (Fe 20 mg/ml). Dissolve 98 g of hydrated iron(III) chloride in 50 ml of concentrated hydrochloric acid and dilute the solution to 1 litre with water.

*Presented at the 33rd Annual Meeting of the Japan Society for Analytical Chemistry, Nagoya, October, 1984.

Calcium carrier solution (Ca 100 mg/ml). Dissolve 295 g of hydrated calcium nitrate in 500 ml of water.

Methanolic 1M nitric acid. Mix 35 ml of concentrated nitric acid with 465 ml of pure methanol.

Methanolic 0.1M hydrochloric acid/0.5M ammonium thiocyanate solution. Mix 50 ml of 1M hydrochloric acid and 50 ml of 5M ammonium thiocyanate with 400 ml of pure methanol.

Methanolic 1.5M hydrochloric acid. Mix 65 ml of concentrated hydrochloric acid with 430 ml of pure methanol and dilute to 500 ml with water.

Apparatus

The anion-exchange resin column used was made with Dowex 1 × 4 (100–200 mesh), bore 1 cm, volume 7 ml.

Pretreatment

Weigh the sample (about 50 g) into a porcelain dish and add ^{242}Pu and ^{244}Cm (to give an activity of ~ 1 dpm for each) as tracers. Ignite the sample in an electric furnace at 450° for at least 8 hr. Transfer the calcined sample to a 1-litre conical beaker, rinse the porcelain dish into the beaker with 200 ml of concentrated nitric acid and add 5 ml of 30% hydrogen peroxide. Boil the mixture for about 30 min on a hot-plate. Filter the solution while hot through a glass-fibre filter (Toyo GA-100), with suction, then wash the residue with three 25-ml portions of hot 8M nitric acid. Reserve the solution in a 1-litre beaker. Transfer the residue to a 200-ml Teflon decomposition vessel with 100 ml of 0.1M hydrofluoric acid solution in 10M nitric acid. Seal the vessel with its lid and heat it in an electric oven at 175° for 10 hr. Cool, remove the lid and filter the solution through a filter paper (Toyo No. 5C). Wash the residue with 8M nitric acid. Combine the filtrate and washings with the solution reserved in the 1-litre beaker and evaporate the mixture nearly to dryness. Add 20 ml of concentrated nitric acid and again evaporate nearly to dryness. Repeat this evaporation procedure once more. Dissolve the residue by heating with 50 ml of concentrated nitric acid plus 5 ml of 30% hydrogen peroxide, then heat further to decompose the peroxide completely. If a residue remains, filter the solution through a glass-fibre filter (GA-100). If the iron content is not enough for precipitation add 100 mg of iron(III) as carrier. Dilute the solution to 500 ml with water, and add 25 g of solid sodium hydroxide then 2.5M sodium hydroxide to raise the pH to about 10. Age the precipitate by heating.

Centrifuge, then discard the solution and dissolve the precipitate in a small volume of concentrated hydrochloric acid, and transfer the solution to a 1-litre beaker. Add 5 ml of 30% hydrogen peroxide and heat until all the precipitate has dissolved. Dilute the solution to 450 ml with water, add 500 mg of calcium carrier and 45 g of oxalic acid. After heating to dissolve the reagent, add ammonia solution to raise the pH to 1.5 to precipitate the calcium oxalate. Allow to settle overnight, filter off the precipitate on a Millipore membrane filter (pore size $3\ \mu\text{m}$) and wash the beaker and precipitate with small quantities of 0.1% ammonium oxalate solution. Dry and ignite the precipitate together with the filter in a crucible at 450° for 2 hr.

Extraction separation

Transfer the ash to a 100-ml beaker by rinsing with 10 ml of 8M nitric acid, add 0.5 ml of 30% hydrogen peroxide, cover the beaker with a watch-glass, and heat to dissolve the ash. Remove the watch-glass, evaporate the solution to about 1.5 ml and add 50 ml of 4M nitric acid.

Filter through a $3\text{-}\mu\text{m}$ membrane filter into a 50-ml separatory funnel, washing with a little 4M nitric acid. Shake the solution for 3 min with 10 ml of TOA solution. Drain the aqueous phase into a second separatory funnel and shake it with 10 ml of TOA solution for 3 min. Transfer

the aqueous phase to a 100-ml beaker. Combine the organic extracts, which contain the plutonium (Extract P).

To the aqueous phase add 1 drop of Cresol Red solution, and concentrated ammonia solution until the colour turns to yellow (the pH of the solution must be 1.5–2.0). Transfer the solution to a 100-ml separatory funnel and shake it with 10 ml of 0.5M TTA for 15 min to remove thorium. Drain the aqueous phase into a 100-ml separatory funnel and shake it with 10 ml of 0.5M TTA for 10 min. Drain the aqueous phase into a 100-ml separatory funnel and discard the two TTA phases. Add 5% ammonium acetate solution to the aqueous phase until the pH is 4.0 ± 0.2 (pH-paper), then shake it with 15 ml of 0.5M TTA for 5 min. Drain the aqueous phase and shake it with 15 ml of 0.5M TTA for 5 min. Discard the aqueous phase. Combine the two organic phases and strip the americium by shaking with two 25-ml portions of 1M nitric acid, for 5 min each. Shake the combined nitric acid extracts with 15 ml of xylene for 1 min. Transfer the aqueous phase to a 100-ml beaker and evaporate it to dryness. To the residue add 5 ml of concentrated nitric acid and 0.5 ml of 30% hydrogen peroxide. Evaporate the solution to dryness (Residue A).

Stripping of plutonium

Shake Extract P with 20 ml of 4M nitric acid for 3 min, then discard the aqueous phase. Shake the organic phase with two 20-ml portions of 10M hydrochloric acid for 3 min each, discarding the aqueous phases. Shake the organic phase with two 25-ml portions of ammonium iodide-hydrochloric acid solution for 3 min each time, to strip the plutonium. Discard the organic phase and shake the combined aqueous phases for 1 min with 15 ml of xylene. Transfer the aqueous solution to a 100-ml beaker and evaporate to dryness. To the residue add 5 ml of concentrated nitric acid and a few drops of 70% perchloric acid. Evaporate the solution to dryness.

Ion-exchange for americium

Dissolve Residue A, containing americium, in 15 ml of methanolic 1M nitric acid. Pass the solution through the conditioned ion-exchange resin column at a flow-rate of 0.5 ml/min. Wash the column with 40 ml of methanolic 1M nitric acid, then with 100 ml of methanolic hydrochloric acid/ammonium thiocyanate solution to remove rare-earth elements, and finally with 50 ml of methanolic 1M nitric acid to remove traces of iron. Elute the trivalent actinides into a 100-ml beaker with 60 ml of methanolic hydrochloric acid. Evaporate the solution to dryness. To the residue add 5 ml of concentrated nitric acid and 1 ml of 30% hydrogen peroxide. Evaporate the solution to dryness. To the residue add 3 ml of concentrated nitric acid and a few drops of 70% perchloric acid. Evaporate the solution to dryness.

Electro-deposition

To the residue containing plutonium or americium add 10 ml of 2M sulphuric acid, and heat to dissolve. Cool, add a drop of Methyl Red solution, and concentrated ammonia solution until the colour turns to yellow, then 2M sulphuric acid until the colour turns to pink, and then 1 drop in excess (pH 2–3). Transfer the solution to an electro-deposition cell, rinsing it with a little water. Deposit the plutonium or americium on a stainless-steel disc cathode at a current density of $0.57\ \text{A}/\text{cm}^2$ for 2 hr, with a platinum wire anode. Add 2 or 3 drops of concentrated ammonia solution and continue plating for 1 min. Remove the solution with a Komagome (or equivalent) pipette and switch off the power supply. Dismantle the cell. Rinse the disk with water and then with acetone. Ignite the disk at dull red heat in the flame of a Bunsen burner, then let it cool.

Alpha-spectrometry

Count the activity on the disc with a silicon barrier-layer detector coupled to a multichannel analyser, for $2\text{--}6 \times 10^5$ sec.

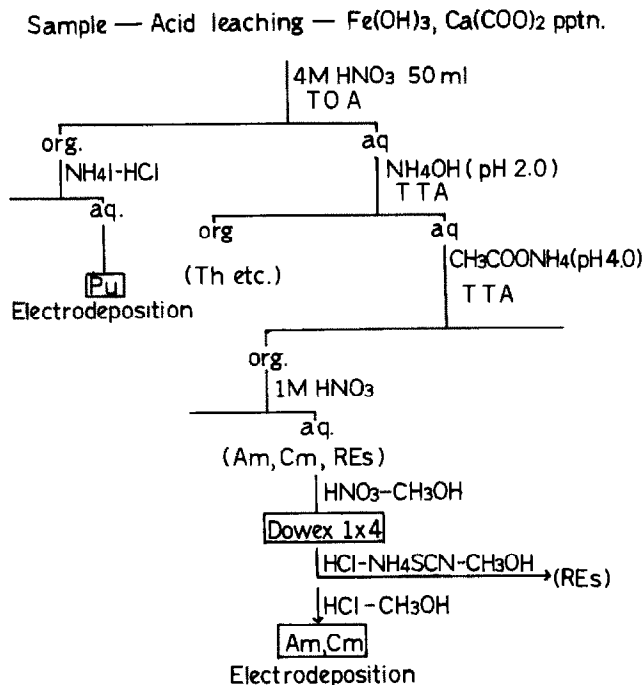


Fig. 1. Outline of procedure.

RESULTS AND DISCUSSION

In determining plutonium and americium in environmental samples it is important to separate them from natural α -nuclides, especially those of uranium and thorium. For separation of plutonium, extraction with TOA⁹ was adopted. The sequential separation of uranium, thorium and rare-earth elements by solvent extraction has already been established.¹⁰ Americium may be extracted along with rare-earth elements by TTA. The method of Holm and Fukai⁸ and of Yamato¹¹ was used for separation of americium from the rare-earth elements. The separation scheme is shown in Fig. 1.

Single co-precipitations with ferric hydroxide and calcium oxalate are considered sufficient, because the subsequent solvent extraction procedure is selective.

For electro-deposition a sulphuric acid-ammon-

ium sulphate electrolyte at about pH 2.0 was used because it gives high recovery of actinides and is simple to manipulate.¹²

Figure 2 shows the α -spectrum of plutonium separated from a standard soil sample. Peaks of ²⁴²Pu (added as tracer), ²³⁹Pu, ²⁴⁰Pu and ²³⁸Pu can be seen. Figure 3 shows the α -spectrum of americium separated from standard river sediment. Peaks for ²⁴¹Am and ²⁴⁴Cm (added as tracer) are also seen. These figures indicate that the procedures described achieve sufficient removal of uranium, thorium and other naturally occurring α -nuclides, and no serious interference has been encountered.

Because we could not obtain pure ²⁴³Am when this work was started, ²⁴⁴Cm was used as a radioisotopic tracer for ²⁴¹Am. As curium behaves like americium in the separation,¹¹ it is believed that the chemical recovery is correct. However, ²⁴³Am (e.g., NBS

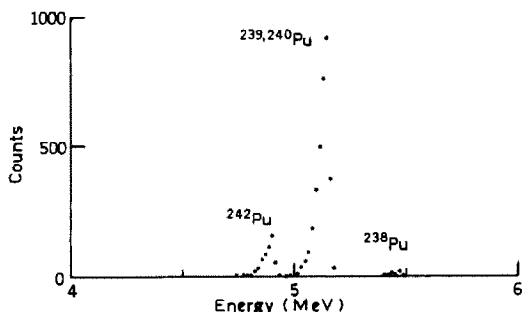


Fig. 2. Alpha-spectrum of Pu separated from NBS 4353 (Rocky Flats soil).

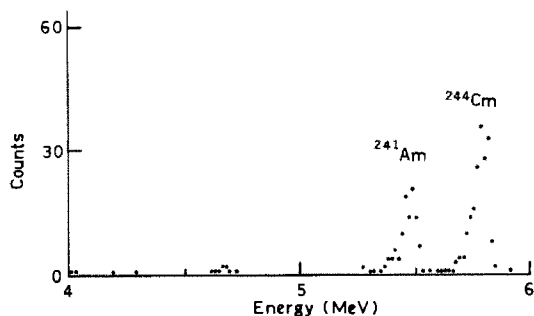


Fig. 3. Alpha-spectrum of Am fraction separated from NBS RM 45b (River sediment).

Table 1. Summary of the results

Sample	Nuclide	Present, mBq/g	Found, mBq/g
NBS 4353	Rocky Flats soil	$^{239,240}\text{Pu}$	8.03
		^{241}Am	7.2*, 5.7*, 7.9, 8.1
NBS 4350B	River sediment	$^{239,240}\text{Pu}$	1.25
		^{241}Am	1.3, 1.4, 1.4, 1.3
IAEA SD-N-1	Sediment	$^{239,240}\text{Pu}$	0.508
		^{241}Am	0.50*, 0.53
NBS 4355	Pervian soil	$^{239,240}\text{Pu}$	0.15
		^{241}Am	0.14
NBS 45b	River sediment	$^{239,240}\text{Pu}$	0.56
		^{241}Am	0.54
	Surface soil	$^{239,240}\text{Pu}$	0.49
		^{241}Am	0.46
		$^{239,240}\text{Pu}$	0.0076
		^{241}Am	0.008*
		$^{239,240}\text{Pu}$	0.004
		^{241}Am	0.004, 0.005
		$^{239,240}\text{Pu}$	1.3*, 1.3*, 1.4*
		^{241}Am	0.40, 0.44, 0.38
		$^{239,240}\text{Pu}$	1.8*
		^{241}Am	0.62

*By double $\text{HNO}_3\text{-H}_2\text{O}_2$ leaching.

4332B) is the preferred tracer and should be used when available.

The results for the determination of ^{239}Pu , ^{240}Pu and ^{241}Am in several standard reference materials, a standard material and a surface soil are presented in Table 1. For plutonium in the Rocky Flats Soil, values about 20% lower than the certified value were obtained by double leaching with nitric acid/hydrogen peroxide, but satisfactory values were obtained by decomposing the sample with nitric acid/hydrofluoric acid. Sill¹³ stated that treatment of the sample with nitric acid alone was grossly inadequate for dissolution of refractory compounds of plutonium. If refractory compounds of plutonium are known to be present, as in the Rocky Flats soil, treatment with nitric acid/hydrofluoric acid should be included in the procedure.

The NBS RM 45b river sediment was analysed to assess the spread of results given by the proposed method. There are no certified values for plutonium and americium in this material. Undisturbed surface soil (0–3 cm) at the site of JAERI was also analysed.

The chemical recovery for plutonium was 51–99%, average 81%, and for americium 21–86%, average 59%. The chemical yield for americium after plutonium extraction was about 70% and total americium recovery was about 60%.

The procedure is rapid and reliable; the separation by extraction takes about 2 days less than the ion-exchange method¹⁴ and the whole procedure takes 1

week, about a third of that for the LASL method.⁵ There is also less interference by other nuclides, such as ^{210}Po , than in the ion-exchange method.¹⁵

REFERENCES

1. R. W. Perkins and C. W. Thomas, in *Transuranic Elements in the Environment*, W. C. Hanson (ed.), DOE/TIC-22800, pp. 53–82. NTIS, Springfield, VA., 1980.
2. R. L. Watters, T. E. Hakonson and L. J. Lane, *Radiochim. Acta*, 1983, **32**, 89.
3. R. A. Wessman and L. Leventhal, *Analysis Methodology for Transuranics*, in *Transuranics in Natural Environments*, M. G. White and P. B. Dunaway (eds.), *USERDA Report NVO-178*, pp. 545–574. NTIS, Springfield, VA., 1978.
4. *Environmental Measurements Laboratory Procedures Manual, HASL 300*, with 8 supplements, J. H. Harley (ed.), New York, 1980.
5. D. Knab, *Los Alamos Scientific Laboratory Report, LA-7057*, 1978.
6. C. W. Sill, K. W. Pupal and F. D. Hindman, *Anal. Chem.*, 1974, **46**, 1725.
7. R. P. Bernabee, D. R. Percival and F. D. Hindman, *ibid.*, 1980, **52**, 2351.
8. E. Holm and R. Fukai, *Talanta*, 1976, **23**, 853.
9. Science and Technology Agency, *Manual for Plutonium Assay in Environmental Materials in Japan*, 1979.
10. H. Onishi and K. Sekine, *Talanta*, 1972, **19**, 473.
11. A. Yamato, *J. Radioanal. Chem.*, 1982, **75**, 265.
12. N. A. Talvitie, *Anal. Chem.*, 1972, **44**, 280.
13. C. W. Sill, *Health Phys.*, 1975, **29**, 619.
14. M. Thein, S. Ballestra, A. Yamato and R. Fukai, *Geochim. Cosmochim. Acta*, 1980, **44**, 1091.
15. T. Imai, K. Sekine and A. Kasai, unpublished work.

SHORT COMMUNICATIONS

FLUORESCENCE IN THIN LIQUID FILMS: A SIMPLE MODEL

R. VON WANDRUSZKA* and J. D. WINEFORDNER†

Department of Chemistry, University of Florida, Gainesville, Florida 32611, U.S.A.

(Received 3 October 1986. Accepted 6 February 1987)

Summary—A model is proposed to account for the effect of various parameters on the fluorescence characteristics of dyestuffs in thin films during drainage of the films.

We recently reported on an investigation of fluorescence emission from thin liquid films.¹ Fluorescent dyes were dissolved in surfactant solutions and thin films were drawn in metal frames from these. The films were excited with laser radiation and the fluorescence emission was monitored as a function of time.

EXPERIMENTAL

The experimental details were fully described earlier¹ and will only be summarized briefly here.

Surfactant solutions (sodium lauryl sulphate, tetradecyltrimethylammonium bromide, cetylpyridinium chloride and Brij 99) were prepared from analytical grade reagents. The dyes (Rhodamine B, Rhodamine 6G, Coumarin 440, Coumarin 450, Coumarin 540 and Oxazine 720) were of laser grade and other chemicals were of analytical grade. The films were formed in a thick-walled closed cell made of blackened brass, with a circular stainless-steel frame attached to the lid. The solution was drained from the bottom of this cell and measurements were started as the film formed. No special temperature control was implemented. A 1-mm² spot on the film was excited at 45° to the surface with radiation from an argon-ion laser (514.5 nm or broad-band ultraviolet radiation) and the fluorescence was measured (also at 45°) after dispersion with a double monochromator. The emission was monitored at a fixed wavelength over the lifetime of the film, and drainage profiles over periods extending from a few minutes to more than an hour were obtained (e.g., Fig. 1a).

RESULTS AND DISCUSSION

Previous work² on dyes in soap lamellae dealt with lightly doped films, having fluorescence intensities that were stable for several hours. Measurements were made of these relatively static films and the fluorescence emission intensity was observed to oscillate.

The present investigation was concerned with the highly mobile state of the film immediately after its

formation. The film was excited at a point near its middle, well above the wedge-shaped lower regions in which the drained solution accumulates. A strong periodicity was observed in the time-resolved emission, which showed certain similarities to Newtonian reflectance fringes. Unlike these, however, the signal was exponentially damped (Fig. 1) and appeared to be superimposed on a similarly decreasing background.

The periodicity arises from interference effects between the fluorescence emissions from the front and back surfaces of the film.^{1,2} There is a significant accumulation of dye molecules at the surfaces within

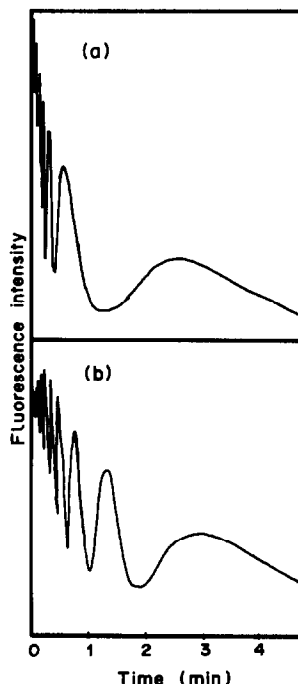


Fig. 1. Fluorescence drainage profiles of thin films containing dyes; (a) 1% tetradecyltrimethylammonium bromide and Coumarin 440; (b) 1% Brij 99 with Coumarin 440.

*On leave from Department of Chemistry, University of the Witwatersrand, Johannesburg, South Africa.

†Author to whom reprint requests should be sent.

seconds of film formation. Since these two main emitting regions of the film are separated by its thickness, constructive and destructive interference between the signals will occur alternately as the film drains. The resulting fluorescence fringe maxima are found to decrease with time, often after an initial sharp rise (Fig. 1b). The background decreases at a usually somewhat faster rate.

For an *a priori* treatment of the experimental results, we identify seven characteristics of the film-dye system, which we treat independently. We do not suggest that this represents an exhaustive list of variables or that the various parameters are not, in fact, related. The treatment aims to present a simple model consistent with experiment. The relevant characteristics are the following:

- (i) accumulation of dye in the film interior, between the surfaces;
- (ii) dye present in the film interior, between the surfaces;
- (iii) movement of dye from interior to the surface;
- (iv) rate of drainage of dye from the surfaces;
- (v) rate of drainage of dye from the interior;
- (vi) initial thickness of the film;
- (vii) rate of film thinning (drainage of bulk solution from film interior).

The experimental drainage profiles (Fig. 1) show sinusoidal oscillations with periods that appear to be exponentially expanding in time. Inspection suggests that the signal is exponentially damped and includes a similarly damped background. If it is assumed that the fluorescence signals arising from the film surfaces and from the film interior (background) are separable and additive, then a simple equation of the form

$$I(t) = I_b e^{-At} + I_s e^{-Bt} \sin(Ce^{-Dt}) \quad (1)$$

may be proposed, where $I(t)$ is the total time-dependent fluorescence; I_b and I_s are the initial emission intensities from the film interior and its surfaces, respectively; A is a parameter related to the rate of dye drainage from the interior; B describes the rate of dye drainage from the surfaces; C is related to the initial thickness of the film and D is related to the rate of thinning of the film.

This equation can be used to reproduce adequately some of the drainage profiles obtained. Notably, when the factor C (initial film thickness) is increased, the number of peaks within a typical observation period of 4 min increases. This is to be expected, since the number of instances when the film thickness passes through values corresponding to constructive (or destructive) interference of emission from its two opposing surfaces, increases with film thickness. Furthermore, a large value of B (rate of surface dye drainage) leads to a quickly damped signal, owing to the rapid drainage of dye from the film surfaces. The parameter D relates to the rate of film thinning, and the larger its value, the more closely spaced the peaks will be at the beginning of the profile. Again, this

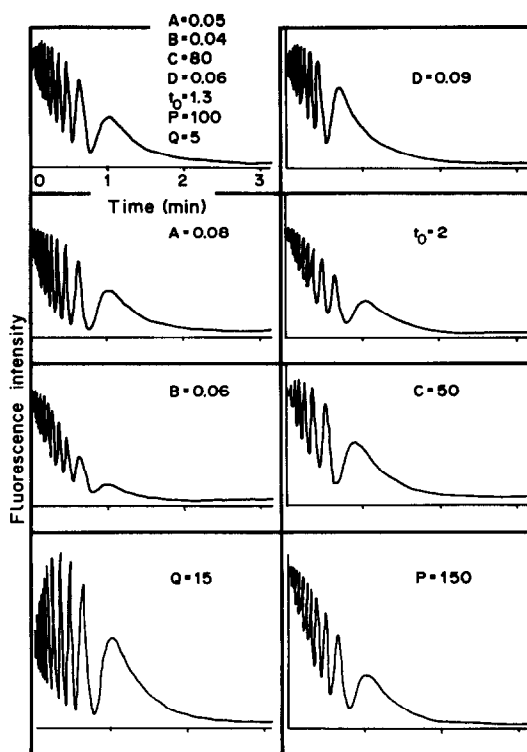


Fig. 2. Plot of equation (2); the top left profile has an arbitrarily assigned set of parameters and the others show the changes due to variations in individual parameters.

should be expected, since the instances of similar interference follow each other more quickly in a fast-draining film. Parameter A describes the loss of dye from the film interior and therefore the steepness of the background emission curve (the troughs of the oscillations). These considerations are illustrated in Fig. 2, which was generated with a more elaborate form of the equation (see later).

Some problems exist with the results obtained with equation (1). First, the oscillations are centred about a decreasing (background) curve, which causes the values in the later part of the profile to become negative. As a result, the trough of the last oscillation extends below the plateau reached when damping is complete. This is not consistent with the experimental profiles, which always show the lowest fluorescence intensities when oscillations have ceased. This problem can be overcome by adding 1 to the sine term, thus rendering it positive without affecting the oscillations.

Equation (1) is further deficient because it cannot generate the brief initial increase in oscillation amplitude that is often observed (Fig. 1b). Related to this is the problem that the amplitude damping calculated from the equation is often excessive and does not provide the required flexibility to match experimental results. This is probably because no account is taken of characteristic (iii), the movement of dye from the film interior to the surface during draining. A factor

related to surface dye enrichment must be included in the second term of the equation in order to modify the exponential damping factor. This variable must not only have a time dependence in order to have the desired effect, but must also have units of time so as to retain dimensional integrity.

In its expanded form, the equation becomes

$$I(t) = I_b e^{-At} + I_s \frac{t}{t_0} e^{-Bt} [\sin(Ce^{-Dt}) + 1] \quad (2)$$

where t_0 is a surface-enrichment time constant.

In the case of ionic surfactants, the exponential nature of the dye drainage from the film interior could be verified experimentally by rotation of the plane of polarization of the exciting radiation. In the experiments described above, vertically polarized light was used, *i.e.*, with the plane of polarization at 90° to the interference fringes. When the polarization was changed to horizontal (parallel to the fringes) by means of a compensator, no interference effects whatever were noted; the fluorescence signal consisted of a relatively smooth, exponentially decreasing curve,

not unlike the background noted above. Evidently, the surface orientation of dye molecules in ionic surfactant films is such that they are preferentially excited by vertically polarized radiation. Horizontal polarization mainly affects the randomly distributed dye molecules in the film interior. It should be noted that these results cannot be explained satisfactorily by consideration of penetration of the film by light of different polarization. Also, no such polarization effects were found with non-ionic surfactants (*e.g.*, Brij).

Equation (2) was generally successful in reproducing the experimental drainage profiles encountered with different surfactant/dye systems. The influence of the variables on the shapes of the curves, as explained above, was assessed through equation (2) and the resulting profiles are shown in Fig. 2.

REFERENCES

1. R. von Wandruszka and J. D. Winefordner, *Talanta*, 1986, **33**, 871.
2. P. Fromherz and R. Kotulla, *Ber. Bunsenges. Phys. Chem.*, 1984, **88**, 1106.

ANODIC-STRIPPING VOLTAMMETRIC DETERMINATION OF ARSENIC AT A COPPER-COATED GLASSY-CARBON ELECTRODE

S. JAYA, T. PRASADA RAO* and G. PRABHAKARA RAO
Central Electrochemical Research Institute, Karaikudi 623006, India

(Received 19 June 1986. Revised 2 January 1987. Accepted 27 January 1987)

Summary—The anodic-stripping voltammetric behaviour of arsenic(III) at a glassy-carbon electrode copper-coated *in situ* has been investigated. The effects of copper concentration, acidity, deposition potential and sweep rate on the stripping peak have been examined and criteria are given for the choice of experimental conditions. The procedure is applicable to the determination of 7.5–750 ng/ml of arsenic levels and is useful for the analysis of various types of water sample.

The widespread use of arsenic compounds in industry and the concern over their acute toxicity and possible carcinogenesis, have prompted the development of numerous analytical methods for their determination at trace levels.^{1,2} The voltammetric procedures utilize the reduction of As(III) to the element³⁻⁵ or the deposition of the element on gold,⁶ platinum⁶ or gold-coated electrodes.^{7,8} More recently, cathodic-stripping voltammetric determinations of arsenic have been developed which utilize a hanging mercury-drop electrode in the presence of selenium⁹ or copper.¹⁰ No studies have been reported so far on the stripping voltammetry of arsenic with the use of the glassy-carbon electrode (GCE), which is so widely used for the determination of mercury¹¹ and other metals.^{12,13} We have recently described the influence of copper on the deposition of mercury on a GCE,¹⁴ and the resultant development of a sensitive anodic-stripping voltammetric (ASV) procedure for the determination of mercury. This paper describes a simplified linear-scan ASV (LSASV) method for determining arsenic by utilizing a glassy-carbon electrode copper-coated *in situ*, and its possible application in monitoring polluted natural waters and sea-water samples.

EXPERIMENTAL

Reagents

All solutions were prepared with analytical grade reagents and conductivity water.

Arsenic(III) solution, 0.01M. Dissolve 1.30 g of sodium arsenite (NaAsO_2 , m.w. 129.9) in water and dilute to 100 ml. Standardize the solution by any convenient standard method. Dilute appropriate volumes of this stock solution as required, to obtain the required concentration of arsenic.

Copper(II) solution, 0.01M. Dissolve 0.624 g of copper(II) sulphate pentahydrate in water.

Perchloric acid, 10M.

Apparatus

Voltammetric studies were performed with a Wenking 75 M potentiostat and a Wenking potential-scan generator, with a 3-electrode cell assembly comprising a normal calomel reference electrode (NCE), a platinum-foil counter-electrode and a glassy-carbon (Tokai, Type V-10-50, 3 mm diameter) working electrode. A Digilog XY-2000 recorder was used.

Procedure

Transfer a suitable aliquot (up to 35 ml) of sample solution containing 0.38–37.5 μg of arsenic into a 50-ml standard flask, add 1 ml of copper solution and 10 ml of 10M perchloric acid and dilute to volume with water. Transfer the solution to the electrochemical cell and immerse the GCE. Electrolyse for 2 min at -0.6 V vs. NCE with stirring. Scan the potential anodically from -0.6 to 0.7 V at a rate of 140 mV/sec after a rest period of 30 sec.

RESULTS AND DISCUSSION

Preliminary studies on the deposition of arsenic on a GCE and its subsequent stripping revealed that this element is effectively not deposited from a 10^{-5}M solution (curve A, Fig. 1). Unlike mercury,^{14,15} arsenic is still not deposited either from higher concentrations or after repeated cycling. However, if copper is present in the analyte solution, arsenic is deposited and gives a distinct stripping signal (curve C, Fig. 1).

Curve B in Fig. 1 shows the stripping voltammogram obtained after the deposition of 10^{-4}M copper at -0.6 V for 2 min on a GCE. A single stripping peak (due to copper) occurs at 0.14 V. On addition of 10^{-5}M arsenic a stripping peak occurs at 0.36 V (curve C, Fig. 1) in addition to the one due to copper. Further, the height of the stripping peak at 0.36 V is linearly dependent on the concentration of arsenic in the test solution, and this forms the basis for the development of a sensitive LSASV procedure for determination of arsenic.

*Address for correspondence: Regional Research Laboratory, Industrial Estate P.O., Trivandrum 695 019, India.

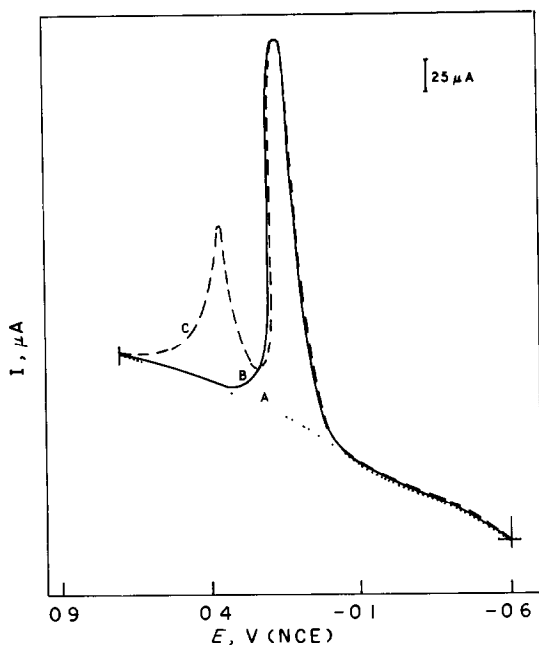


Fig. 1. Anodic stripping voltamperograms of $10^{-5}M$ arsenic(III) (curve A), $10^{-4}M$ copper (curve B) and $10^{-5}M$ arsenic + $10^{-4}M$ copper (curve C) in $2M$ $HClO_4$. Deposition potential $E_d = -0.6$ V vs. NCE; time of deposition $t_d = 2$ min.

The role of copper

Figure 2 shows the effect of the copper concentration on the stripping signal for $75 \mu g/ml$ arsenic obtained after deposition at -0.6 V for 2 min in $2M$ perchloric acid medium. The height of the stripping peak due to arsenic is constant for copper concentrations $\geq 8 \times 10^{-5}M$.

The deposition potential

The optimum deposition potential (E_d) was established by varying E_d from -0.5 to -0.8 V in steps of 0.05 V. As seen from Fig. 3 curve A, the stripping signal is at a maximum in the E_d range from -0.60 to -0.65 V. The decrease in the stripping signal at deposition potentials more negative than -0.65 V is due to the reduction of elemental arsenic to arsine.¹⁰

The scan-rate

Curve B in Fig. 3 shows the results obtained when the scan rate was varied from 50 to 400 mV/sec. The optimal scan-rate was in the range 100 – 180 mV/sec. Further, the arsenic stripping signal was found to be the same for successive determinations.

The optimum acidity was found to be 1 – $3M$ perchloric acid. A linear calibration graph passing through the origin on extrapolation was obtained for arsenic in the range 7.5 – 750 ng/ml. Five replicate determinations of 75 ng/ml arsenic gave results of

75.3 , 74.4 , 74.2 , 73.1 and 74.0 with a relative standard deviation of 3.5% .

Interference studies

The effect of various other cations on the LSASV determination of 75 ng/ml arsenic(III) was next investigated. Hundredfold amounts of zinc, cadmium, manganese and thallium and 10 -fold amounts of lead (relative to arsenic) do not interfere, but bismuth interferes seriously.

Analysis of sea-water samples

Sea-water samples collected from the Bay of Bengal were analysed for arsenic (Table 1), but none was found. The recoveries obtained on addition of known amounts of arsenic to the sea-water and to synthetic sea-water solutions were satisfactory (Table 1) and illustrate the potential usefulness of the procedure for the analysis of polluted sea-water. The arsenic concentration in the open sea is reported to be in the range 3 – 24 ng/ml.¹⁵

CONCLUSION

The procedure described is well suited to the determination of traces of arsenic(III) in sea-water with good precision. In view of its sensitivity, the pollution monitoring of arsenic is possible either after initial preconcentration as arsine or by using differential pulse ASV. However, the present pro-

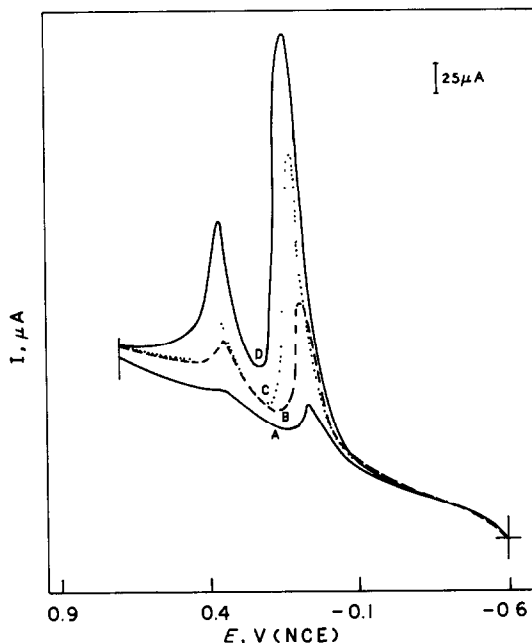


Fig. 2. Effect of copper concentration on the stripping voltamperograms of 75 ng/ml arsenic(III) in $2M$ $HClO_4$; $E_d = -0.6$ V vs. NCE, $t_d = 2$ min, curves A, B, C and D obtained with 10^{-6} , 3×10^{-5} , 5×10^{-5} and $8 \times 10^{-5}M$ copper respectively.

Table 1. Analysis of synthetic and Bay of Bengal sea-water samples

Sample taken, ml	Composition of synthetic sample, g/100 ml	Arsenic added, ng/ml	Amount of arsenic recovered, ng/ml	Recovery, %
35	None	20.0	19.0	95
			19.5	98
			20.6	103
35	Na (1.05), K (0.04) Mg (0.13), Ca (0.04) Cl (1.89)	20.0	19.2	96
			19.8	99
			20.2	101
30	Na (6.7), K (0.34) Mg (0.56), Ca (0.03) Cl (11.2)	20.0	19.5	98
			20.5	103
			20.1	101
15	Sea-water	20.0	19.8	99
			20.0	100
			20.5	103
30	Sea-water	10.0	9.2	92
			9.8	98
			10.6	106

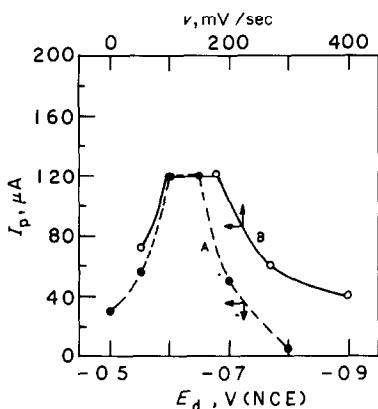


Fig. 3. Effect of deposition potential (curve A) and scan-rate (curve B) on the anodic-stripping current for arsenic(III); As(III) = 75 ng/ml, $E_d = -0.6$ V vs. NCE; $t_d = 2$ min, $Cu(II) = 10^{-4}M$.

cedure is more sensitive than the LSASV procedure developed by Forsberg *et al.*⁶ and can be used in monitoring arsenic in polluted natural and sea-water samples. The procedure is applicable only to determination of arsenic(III). It can be applied to determination of total inorganic arsenic if the samples are heated with hydrazine, hydrochloric acid and hydrobromic acid to reduce arsenic (V) to arsenic (III) as reported elsewhere.¹⁷

REFERENCES

1. Y. Talmi and C. Feldman, *The Determination of Traces of Arsenic*, in *Arsenical Pesticides*, E. A. Woolson (ed.), American Chemical Society, Washington, 1975.
2. D. W. Sundstrom and H. E. Klei, *Waste Water Treatment*, Prentice Hall, New Jersey, 1979.
3. D. J. Meyers and J. Osteryoung, *Anal. Chem.*, 1973, **45**, 267.
4. F. T. Henry, T. O. Kirch and T. M. Thorp, *ibid.*, 1979, **51**, 215.
5. F. T. Henry and T. M. Thorpe, *ibid.*, 1980, **52**, 80.
6. G. Forsberg, J. W. Laughlin, R. G. Megargle and S. R. Koirtyohann, *ibid.*, 1975, **47**, 1586.
7. P. H. Davis, G. R. Dulude, R. M. Griffin, W. R. Matson and E. W. Zink, *ibid.*, 1978, **50**, 137.
8. S. W. Lee and J. C. Meranger, *ibid.*, 1981, **53**, 130.
9. W. Holak, *ibid.*, 1980, **52**, 2189.
10. R. S. Sadana, *ibid.*, 1983, **55**, 304.
11. L. Sipos, P. Valenta, H. W. Nurnberg and M. Branica, *J. Electroanal. Chem.*, 1977, **77**, 263.
12. D. Jagner, *Anal. Chim. Acta*, 1979, **105**, 33.
13. F. Vydra, K. Štulík and E. Juláková, *Electrochemical Stripping Analysis*, Horwood, Chichester, 1976.
14. S. Jaya, T. Prasada Rao and G. Prabhakara Rao, in *Proc. Third International Symposium on Advances in Electrochemical Science and Technology*, Oxford-IBH Publishers, New Delhi.
15. *Idem*, *Analyst*, 1985, **110**, 1361.
16. R. C. Weast (ed.), *Handbook of Chemistry and Physics*, 59th Ed., CRC Press, Boca Raton, Florida, 1978.
17. R. S. Sadana, *Anal. Chem.*, 1983, **55**, 304.

A PVC MEMBRANE pH-SENSITIVE ELECTRODE BASED ON METHYLDIOCTADECYLAMINE AS NEUTRAL CARRIER*

HAI-LONG WU and RU-QIN YU

Department of Chemistry and Chemical Engineering, Hunan University, Changsha,
People's Republic of China

(Received 9 June 1986. Revised 27 November 1986. Accepted 27 January 1987)

Summary—A pH-sensitive PVC membrane electrode based on methyldioctadecylamine as neutral carrier has been prepared. It gives linear response over the pH-range 3.0–11.0 and a slope of -58.4 ± 0.3 mV/pH (at 20°). The electrode has fairly low resistance and good potential reproducibility. The selectivity and other characteristics of the electrode have been studied.

Although the classical glass-electrode pH-sensor exhibits outstanding potentiometric response characteristics and has for decades been used for routine pH measurements, there are limitations to its use under certain circumstances. For instance, it is difficult to measure pH values in hydrofluoric acid solution with a glass electrode. Miniaturization of glass electrodes for biological applications presents problems associated with their high resistance and fragility. Therefore, a non-glass pH-electrode is of considerable interest. Liquid-membrane electrodes responsive to pH have been studied by many investigators. LeBlanc *et al.*¹ prepared such an electrode, based on a proton-carrier, *p*-octadecyloxy-*m*-chlorophenylhydrazonemesoxalonitrile (OCPH), which was improved and applied in physiological studies by Poole-Wilson and co-workers.²⁻⁴ Simon and co-workers⁵⁻⁷ reported on several PVC membrane pH-electrodes based on neutral carriers, of which that based on tridodecylamine (TDDA) showed the best response characteristics.⁷ In our laboratory a number of organic compounds have been tested as possible hydrogen-ion carriers, and amines and other compounds capable of protonation have been found to produce a pH-sensitive response. Methyldioctadecylamine (MDODA) in particular showed promise. In this paper a pH-sensitive electrode based on this carrier is reported.

EXPERIMENTAL

Apparatus and reagents

Potentiometric and pH measurements were made with an Orion 901 Microprocessor Ionalyzer or a pHS-3 pH meter (Shanghai). The Ross glass pH-electrode, type 231 glass pH-electrodes (Shanghai) or PVC membrane pH-electrodes were used in conjunction with type 217 double-junction

reference electrodes (Shanghai) with 3M sodium nitrate solution in their outer compartments. The typical cell used was



For evaluation of the pH-electrodes secondary NBS standard buffers, phosphate-citrate-borate buffers (pH 2–13) and tris buffers (pH 7–10) were used.

Tri-*iso*-octylamine (Riedel de Haen), Amberlite LA-1 and LA-2 (Rohm and Haas), di-*iso*-octylamine and di-*n*-octylamine (Beijing Chem. Co.), and octadecylamine (Fluka) and various other primary amines were used as received. Dioctadecylamine, dihexadecylamine and ditetradecylamine were synthesized by similar procedures from the corresponding primary amines. Dimethyloctylamine and dimethyloctadecylamine were synthesized by reacting formaldehyde and the corresponding long-chain primary amine in formic acid medium, according to the procedure reported for synthesis of dimethyldodecylamine.^{8,9}

PVC membrane electrodes were prepared by standard procedures¹⁰ and conditioned in pure water for 10 hr. For activation they were left in contact alternately with dilute sodium hydroxide solution and hydrochloric acid. The activation procedure should be repeated if the electrode has been stored under dry conditions.

Demineralized water was used throughout.

Synthesis of dioctadecylamine (DODA)

Reflux 100 g of octadecylamine (ODA) with Raney nickel catalyst,¹¹ in a glycerol bath at 160–190° for 5–6 hr. After cooling, separate the catalyst residue and collect the clarified liquid, which is the crude DODA (yield about 50%). Treat the crude DODA with nitric acid, then separate the acid phase, neutralize it with sodium hydroxide and extract the DODA into benzene. Evaporate the benzene and purify the DODA by fractional crystallization from hot ethanol under nitrogen. Confirm the identity of the DODA by infrared spectroscopy¹² and the melting point (71.5–72.5°).

Synthesis of MDODA

Mix 4 g of DODA with 2 ml of 90% formic acid, add 1.2 ml of 35% formaldehyde solution and reflux the mixture at

*Taken in part from the M. S. Thesis of H.-L. Wu, Hunan University, 1985.

40° until bubbling ceases. Raise the temperature to 105° in a glycerol bath and continue refluxing for 4–5 hr. Add 100 ml of 1M hydrochloric acid and continue heating for 1 hr. Leave the mixture standing overnight. Make the solution strongly alkaline with sodium hydroxide. Extract repeatedly with hot benzene. Distil off the solvent from the combined benzene extracts, to obtain white solid MDODA. Confirm the identity of the MDODA by infrared spectroscopy.

RESULTS AND DISCUSSION

Quality of MDODA

Most of the methods reported for synthesis of long-chain tertiary amines require reactions at high temperature and pressure. The products obtained are usually mixtures of amines and require time-consuming fractionation by vacuum distillation. It has been shown that MDODA synthesized by the simplified procedure reported above is quite suitable for use in the preparation of electrode membranes. Elemental analysis of the product gave C 82.7%, H 14.4%, N, 2.6%; $C_{37}H_{77}N$ requires C 82.91%, H 14.48%, N 2.61%. The m.p. was 44–46°, in agreement with the literature.¹² The infrared spectrum matched that in the Sadtler Standard IR Spectra collection.¹²

Comparison of pH-electrodes based on different amines

Membranes were prepared from about 60 amines or other organic compounds containing functional groups capable of protonation and their potential

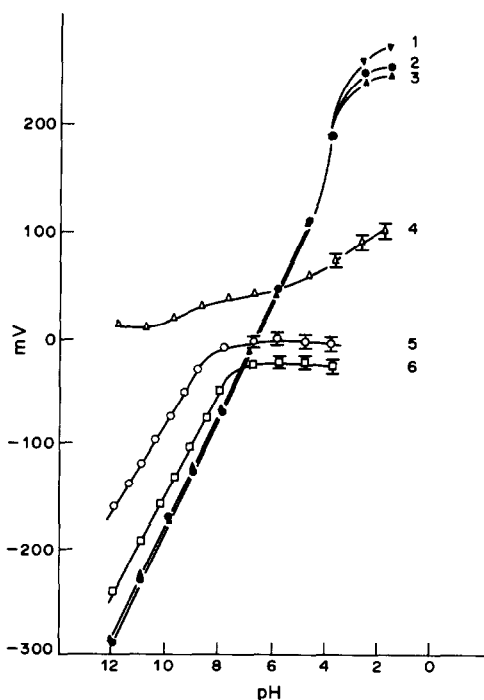


Fig. 1. Comparison of pH-response of the electrodes based on various symmetrical amines: 1—tri-iso-octylamine; 2—tri-n-octylamine; 3—trinonylamine; 4—tri-n-propylamine; 5—tri-n-butylamine; 6—tri-n-pentylamine.

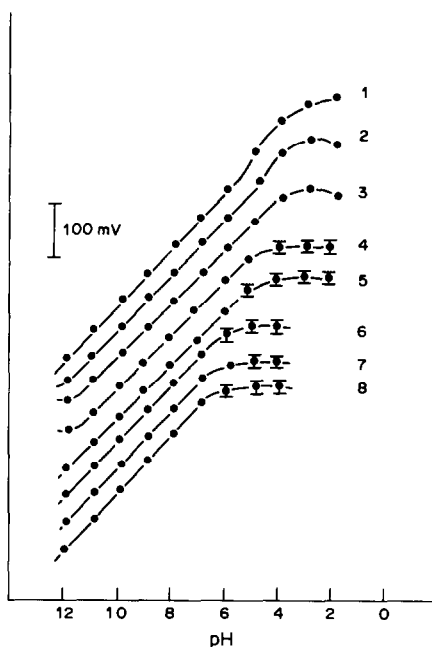


Fig. 2. Comparison of pH-response of electrodes based on some secondary amines: 1—Amberlite LA-1; 2—Amberlite LA-2; 3—dioctadecylamine; 4—dihexadecylamine; 5—ditetradecylamine; 6—dinonylamine; 7—di-iso-octylamine; 8—di-n-octylamine.

response characteristics were compared. Figures 1–3 show some of the results obtained. Long-chain tertiary amines with 24 or more carbon atoms and some secondary amines such as Amberlite LA-1 or La-2 are useful hydrogen-ion carriers. In this study MDODA was chosen for the preparation of PVC membrane pH-electrodes.

Optimization of membrane composition of the MDODA electrode

The membrane composition was optimized by using an orthogonal experimental design with the electrode slope as the function for optimization. The optimum composition found was 1.0% MDODA, 67.0% di-iso-octyl sebacate (DIOS), 31.7% poly(vinyl chloride) (PVC) and 0.3% sodium tetraphenylborate (NaTPB).

Potential-response characteristics of the MDODA electrode

The potential was a linear function of pH over the range 3.0–11.0. No super-Nernstian response was observed in the pH range 3.5–4.5, in contrast to the TDDA electrode.⁷

The potentiometric selectivity with respect to some clinically important ions such as Na^+ , K^+ and Ca^{2+} was determined by the fixed interference method and the values obtained were compared with those reported for the TDDA electrode (Table 1).

The MDODA and glass electrodes gave identical end-points for potentiometric titration of 0.1M sodium hydroxide with 0.5M hydrochloric acid.

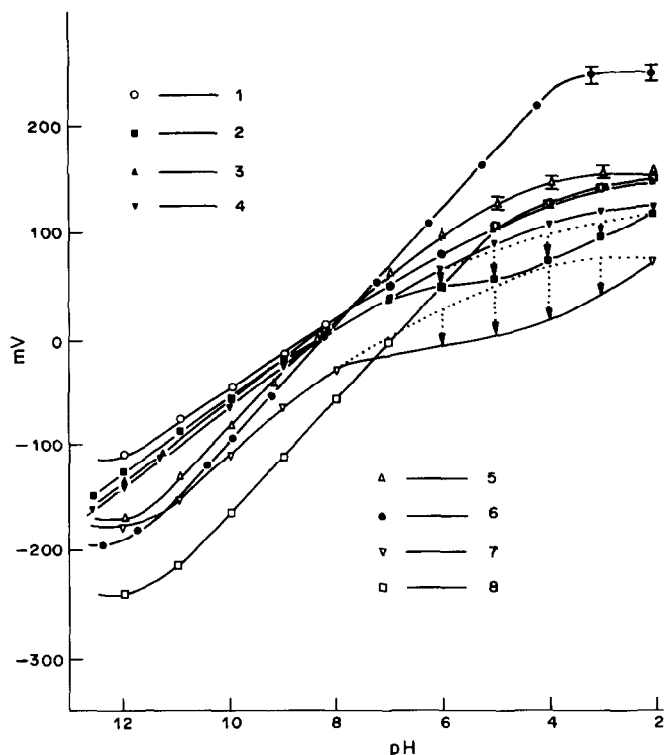


Fig. 3. Comparison of pH-response of electrodes based on primary amines and miscellaneous amines: 1—heptylamine; 2—dodecylamine; 3—tetradecylamine; 4—hexadecylamine; 5—octadecylamine; 6—methyl dioctadecylamine; 7—dimethyl octadecylamine; 8—dimethyl octadecylamine. Dashed line: initial potential readings; solid line: values of potential readings stabilized within ± 0.5 mV/min drift.

Table 1. Selectivity characteristics of the hydrogen-sensitive PVC membrane electrode*

Metal ion	$\log K_{H^+, M^{2+}}$	
	MDODA electrode	TDDA electrode ⁷
Na ⁺	-10.3	-10.4
K ⁺	-10.0	-9.8
Ca ²⁺	< -10.6	< -11.1

*Measured at the interfering ion concentration level of 1 M for both electrodes.

The MDODA electrode has excellent response characteristics in the pH range 8.5–6.5, which is of interest for biological studies.

The combined standard deviations for 3 measurements of each of 3 mixed serum samples were 0.006 pH for the glass electrode and 0.01 pH for the MDODA electrode.

The response of the MDODA electrode at $20 \pm 1^\circ$ gave standard deviations of 0.09 mV at pH 7.86 (static measurement over 13 hr, 52 variates) and 0.2 mV for alternating measurements on stirred solutions at pH 8.7 and 9.0 over 2 hr (11 variates).

The resistance of the electrode membrane was 1.49 ± 0.14 M Ω ($n = 6$) with a membrane area of about 50 mm² and a thickness of 0.4 mm. The resistance is much lower than that of a glass electrode and is favourable for electrode miniaturization.

The response time of the electrode is about 0.5 sec. The electrodes have a lifetime of at least 4 months.

Acknowledgement—This work was supported by the Science Foundation of the National Educational Committee of the People's Republic of China.

REFERENCES

- O. H. Le Blanc, Jr., J. F. Brown, Jr., J. F. Klebe, L. W. Niedrach, G. M. J. Slusarczuk and W. H. Stoddard, Jr., *J. Appl. Physiol.*, 1976, **40**, 644.
- S. M. Cobbe and P. A. Poole-Wilson, *J. Physiol.*, 1979, **289**, 3p.
- Idem*, *J. Med. Eng. Tech.*, 1980, **4**, 122.
- M. Clare-Harmon and P. A. Poole-Wilson, *J. Physiol.*, 1981, **315**, 1p.
- D. Erne, D. Ammann and W. Simon, *Chimia*, 1979, **33**, 88.
- D. Erne, K. V. Schenker, D. Ammann, E. Pretsch and W. Simon, *ibid.*, 1981, **35**, 178.
- P. Schulthess, Y. Shijo, H. V. Pham, E. Pretsch, D. Ammann and W. Simon, *Anal. Chim. Acta*, 1981, **131**, 111.
- J. E. Kirby, *U.S. Patent*, 2366534, 1945.
- R. A. Reck, H. J. Harwood and A. W. Ralston, *J. Org. Chem.*, 1947, **12**, 517.
- G. J. Moody, R. B. Oke and J. D. R. Thomas, *Analyst*, 1970, **95**, 910.
- S. W. Li and L. L. Fan (eds.), *Handbook of Practical Organic Chemistry*, p. 539. Shanghai Science and Technology Press, 1980.
- Sadtler Research Laboratories, Inc., *Standard Infrared Grating Spectra*, 30748K, 31306K, Philadelphia, 1974.

DETERMINATION OF COPPER, IRON, MANGANESE, LEAD AND CADMIUM IN AUTOMATICALLY WET-DIGESTED ANIMAL TISSUE BY GRAPHITE-FURNACE ATOMIC-ABSORPTION SPECTROMETRY WITH ZEEMAN BACKGROUND CORRECTION

H. VAN BEEK, H. C. A. GREEFKES and A. J. BAARS

Department of Analytical Chemistry and Toxicology, Central Veterinary Institute, P.O. Box 65,
8200 AB Lelystad, The Netherlands

(Received 5 December 1986. Accepted 21 January 1987)

Summary—An efficient wet digestion method is described which allows the determination of various elements in animal tissues. Copper, iron, manganese, lead and cadmium in one dilution of the digested sample can be determined by means of graphite-furnace atomic-absorption spectrometry, with Zeeman background correction. Tests with the National Bureau of Standards Bovine Liver SRM as reference gave analytical results, obtained with calibration graphs as well as by the standard-addition method, which agreed well with the certified values.

In analytical toxicology it is often necessary to analyse animal tissue for a number of elements. For such an analysis, digestion of the organic matter is a prerequisite, and a number of wet and dry ashing methods are known.^{1,2} A general disadvantage is the elaborate and time-consuming sample preparation, and multi-element determination in one digested sample is often not possible. This study reports the development of a method for automated wet digestion of animal tissues and organs by means of a Knapp device,³ followed by automated analysis for copper, iron, manganese, lead and cadmium in the same solution, by means of graphite-furnace atomic-absorption spectrometry with Zeeman background correction. The same digest can be analysed for zinc by flame atomic-absorption spectrometry.⁴

EXPERIMENTAL

Apparatus

An instrument for automated wet digestion, the Knapp device model VAO³ (Hans Kürner Analysentechnik, Rosenheim, F.R.G.), with a programmable temperature range from room temperature to 400° was used. The digestion tubes were long-necked Duran glass vessels, marked at 40-ml volume. Determinations were performed with a Perkin-Elmer Zeeman/3030 atomic-absorption spectrometer, HGA-600 graphite furnace, AS-60 autosampler and an Anadex Silent Scribe printer.

Copper, iron and manganese were determined with Perkin-Elmer hollow-cathode lamps, lead and cadmium with electrodeless discharge lamps as sources.

Reagents

All acids and reagents were of analytical grade (Merck). The solutions of the matrix modifiers, 5-g/l. magnesium nitrate hexahydrate and 40-g/l. ammonium dihydrogen

phosphate, in glass-distilled water, were purified by extraction into isobutyl methyl ketone with ammonium pyrrolidine dithiocarbamate.

Working standards were prepared from 1000-mg/l. atomic-absorption "Titrisol" solutions (Merck) with glass-distilled water and 1 ml of concentrated sulphuric acid in 40-ml digestion tubes.

Procedure

The tissue sample was cut, dried overnight in an oven at 100°, ground and homogenized. A 0.2–0.5 g sample was accurately weighed into a long-necked digestion tube, some pieces of carborundum and 6.5 ml of a sulphuric/perchloric/nitric acid mixture (concentrated acids, 2:1:10 v/v/v) were added and the tube was left to stand overnight at room temperature. The tube was placed in the Knapp digestion device, and the temperature programme was started; it gave heating at 170°, 210° and 240° for 20 min at each temperature, followed by heating at 280° for 40 min. This gave complete decomposition, with concomitant evaporation of the perchloric and nitric acids. After cooling, the sulphuric acid residue (ca. 1 ml) was diluted to 40 ml with glass-distilled water. Copper, iron, manganese, lead and cadmium were all determined in this solution.

RESULTS AND DISCUSSION

Sample preparation of biological tissue by the method reported in this study resulted in complete decomposition and a clear and colourless solution.

The long neck of the digestion tube acts as an air-condenser and the solution boils gently despite the high temperatures in the different steps of the digestion procedure.

Optimal analytical results were obtained with the spectrometer settings listed in Table 1 and the electrothermal programmes for the graphite furnace listed in Table 2.

Table 1. Spectrometric conditions for determination of copper, iron, manganese, lead and cadmium with a Perkin-Elmer Zeeman/3030 atomic-absorption spectrometer

Element	Wavelength, nm	Slit, mm	Sample volume, μ l	Graphite tube
Copper	324.8	0.7	10	Uncoated
Iron	344.1	0.2	10	Pyrocoated
Manganese	279.5	0.2	10	Uncoated
Lead	283.3	0.7	20	L'vov platform
Cadmium	228.8	0.7	20	L'vov platform

As reported by Smeyers-Verbeke *et al.*,^{5,6} the residual sulphuric acid after the digestion does not affect the sensitivity of the determination of copper and manganese. Although the 324.8 nm line used for copper gives an anomalous Zeeman pattern because the several isotopes split the line,⁷ this had no influence on the analytical results in the concentration range studied.

Samples containing more than 80 mg of copper per kg of dry material were analysed with application of an internal argon flow of 50 ml/min during the atomization step. For manganese exceeding 20 mg per kg of dry material, the alternative wavelength of 403.1 nm was used, which is less sensitive than the normally used 279.5 nm. In those cases the calibration curves were adjusted accordingly.

Pyrocoated tubes had to be used for optimum results to be obtained in the iron determination.

For lead and cadmium determination the L'vov platform was used, with matrix modifiers. Losses of lead and cadmium occurred at temperatures of 300°

and 500° respectively, if matrix modifiers were not added. Therefore, a 10- μ l portion of a mixture of ammonium dihydrogen phosphate and magnesium nitrate solutions (1:1) was added to the sample in the graphite tube, as recommended by Slavin *et al.*⁷ The pretreatment temperature of the graphite tube can be increased to 1000° and 900°, for lead and cadmium respectively, without any losses. When the L'vov platform is used a gentle two-step drying programme is necessary. If the tube is heated too fast the sample starts to splash and losses occur. The first drying step should be done at 10° below the boiling point of the solution, and the second step at 30–40° above it. The detection limits for lead and cadmium by this method are 1 and 0.5 ng/ml, respectively.

In contrast to the standard solutions, solutions prepared from biological samples tended to produce tailing peaks during atomization. For this reason peak area measurement had to be used instead of peak height. To optimize the peak area measurement the graphite furnace was cooled down before the

Table 2. Electrothermal programmes for determination of copper, iron, manganese, lead and cadmium in biological matrices with a Perkin-Elmer Zeeman/3030 atomic-absorption spectrometer

	Copper	Iron	Manganese	Lead	Cadmium
Dry 1					
Temperature (°C)	110	110	110	100	100
Ramp/hold (sec)	1/20	1/15	1/20	10/20	10/20
Dry 2					
Temperature (°C)				130	130
Ramp/hold (sec)				10/20	10/20
Pretreatment					
Temperature (°C)	900	1200	1000	1000	900
Ramp/hold (sec)	10/30	10/20	10/20	30/30	20/30
Cool					
Temperature (°C)	600	600	600	300	300
Ramp/hold (sec)	1/5	1/5	1/5	1/5	1/5
Atomize*					
Temperature (°C)	2300	2100	2200	1800	1600
Ramp/hold (sec)	0/4†	0/5†	0/4§	0/4†	0/4†
Clean					
Temperature (°C)	2650	2650	2650	2650	2650
Ramp/hold (sec)	1/5	1/5	1/5	1/5	1/5

*Peak area measurement.

†Internal gas flow reduction from 300 to 0 ml/min argon.

§Internal gas flow reduction from 300 to 50 ml/min argon.

Table 3. Analysis for copper, iron, manganese, lead and cadmium in NBS Bovine Liver No. 1577a

Element	Certified value, $\mu\text{g/g} \pm \text{SD}$	Value found,* $\mu\text{g/g}$	
		Calibration graph	Standard addition
Copper	158 ± 7	154 ± 2	159 ± 8
Iron	194 ± 20	197 ± 6	188 ± 37
Manganese	9.9 ± 0.8	10.0 ± 0.2	10.2 ± 0.5
Lead	0.135 ± 0.015	0.14 ± 0.01	0.14 ± 0.02
Cadmium	0.440 ± 0.060	0.42 ± 0.01	0.44 ± 0.02

*Mean \pm SD of 6 replicates.

atomization, otherwise the signal appeared too fast and the first part could not be integrated correctly.

The results of analysis of the NBS Bovine Liver SRM are presented in Table 3. Comparison of the results with the certified values and those obtained by the standard-addition method shows good agreement, and the variation in the results stays well within acceptable limits.

As also reported by Salisbury and Chan,⁸ an automated wet digestion method is time-saving and less hazardous than other methods. It can be left unattended during operation and it is not necessary to add acid to the hot digest, which is a potentially hazardous step. Clear and colourless solutions are produced from tissue samples, ready for subsequent analysis by graphite-furnace atomic-absorption spectrometry with Zeeman background correction.

The method presented in this study offers a pro-

cedure well adapted for routine determinations for a range of elements in animal tissue. In our experience, the method can also be applied for the analysis of plant samples.

REFERENCES

1. G. Middleton and R. E. Stuckey, *Analyst*, 1953, **78**, 532.
2. R. Bock, *A Handbook of Decomposition Methods in Analytical Chemistry*, Sections 5.1, 5.6, 5.7, 5.9 and 5.13. International Textbook Company, Glasgow, 1979.
3. G. Knapp, *Z. Anal. Chem.*, 1975, **274**, 271.
4. C. E. Mulford, *Atom. Abs. Newsl.*, 1966, **5**, 88.
5. J. Smeyers-Verbeke, G. Segebarth and D. L. Massart, *ibid.*, 1975, **14**, 153.
6. J. Smeyers-Verbeke, Y. Michotte, P. van den Winkel and D. L. Massart, *Anal. Chem.*, 1976, **48**, 125.
7. W. Slavin, G. R. Carnrick, D. C. Manning and E. Pruszkowska, *Atom. Spectrosc.*, 1983, **4**, 69.
8. C. D. Salisbury and W. Chan, *J. Assoc. Off. Anal. Chem.*, 1985, **68**, 218.

POTENTIOMETRIC TITRATION OF FULVIC ACIDS FROM LIGNITE, IN DIMETHYLFORMAMIDE AND DIMETHYLSULPHOXIDE MEDIA

JOSE M. ANDRES, C. ROMERO and JOSE M. GAVILAN

Instituto de Carboquímica, C.S.I.C. Pza. Paraíso No. 1, Ap. 589, 50004-Zaragoza, Spain

(Received 9 October 1985. Revised 10 December 1986. Accepted 16 January 1987)

Summary—Potentiometric titrations in dimethylformamide and dimethylsulphoxide have been performed in order to differentiate between the acidic groups of fulvic acids. With dimethylformamide as medium the best results have been obtained with potassium hydroxide as titrant, whereas both potassium hydroxide and tetrabutylammonium hydroxide yield good titrations in dimethylsulphoxide. The number of acidic groups differentiated depended on the solvent and titrant used; in the best case four sharp end-points were obtained. Titrations with potassium hydroxide are preferred.

Humic substances behave like weak-acid poly-electrolytes because of their carboxylic and phenolic functional groups. These groups in humic substances have frequently been studied by potentiometric titrations in water, but numerical end-point detection methods^{1,2} or numerical analysis by non-linear regression techniques^{3,4} must be used to distinguish between acidic groups of different strength, allowing the determination of up to four end-points in the best case.

The differentiation between acids of nearly equal strength in water can be achieved by using organic solvents which do not have the levelling properties of water, such as dimethylformamide (DMF)^{5,6} and dimethylsulphoxide (DMSO)^{7,8} both of which are good solvents of humic substances.

There are few reports on titrations of humic substances in those solvents. Wright and Schnitzer⁹ obtained a single inflection point in DMF, whereas Van Dijk¹⁰ was able to differentiate between carboxylic and phenolic groups by using high frequency conductometric titrations. Thompson and Chesters¹¹ used potentiometric titrations in DMF and obtained up to six inflections on the titration curve on different humic substances. In a more recent work,¹² titrations in DMSO containing known amounts of benzoic acid and phenol have been proposed.

In our laboratory we have started research into methods for determining the acidity of humic substances, and for differentiating between the acidic groups on the basis of acidic strength. Fulvic acids (FA) were chosen because of their solubility in a variety of solvents, and dimethylformamide and dimethylsulphoxide as being good enough media for potentiometric titrations. The results obtained in this preliminary work concerning total acidic hydrogen determination and differentiation of the acidic groups are shown in this paper.

EXPERIMENTAL

Preparation of fulvic acids

A lignite from Puentes de García Rodríguez (Coruña, Spain) was used. Its elemental analysis was: C 58.2%, H 7.1%, N 0.86%. The ash content was 30.1%. The humic substances were extracted with 0.5M sodium hydroxide. After centrifugation the extract was acidified with concentrated hydrochloric acid to pH 1 to precipitate the humic acids. The FA in solution were concentrated and purified by the method of Thurman and Malcolm¹³ on Amberlite XAD-8 resin, until the ash content was less than 1%. The solution of FA was lyophilysed and the FA were stored in a vacuum desiccator. The elemental analysis of the FA was: C 48.8%, H 3.8%, N 0.94%.

Apparatus

Titrations were done in 20-ml beakers, by adding the titrant in 0.02-ml increments. The titrated solution was protected by an atmosphere of nitrogen. The average titrant volume needed was kept to about 1 ml to avoid high concentrations of isopropyl alcohol in the titration mixture. The titration was monitored with a combined glass electrode with an internal Ag/AgCl reference electrode (Ingold pH electrode), the internal reference solution of which had been replaced by methanol saturated with potassium chloride. A (Crison 517) digital potentiometer was used. The use of Pt-calomel modified electrodes did not improve the performance of the system.

Reagents

The solvents used (DMF, DMSO and isopropyl alcohol; Merck, GR) were distilled and stored in a nitrogen atmosphere.

The potassium hydroxide and tetrabutylammonium hydroxide (TBAH) used for making the titrants were also Merck GR quality. Both were dissolved in isopropyl alcohol and standardized daily against benzoic acid. The titrant concentrations used were 0.2M for the potassium hydroxide and 0.2M and 0.08M for the TBAH.

Calculations

Two of the methods tested for numerical end-point determination made use of derivatives, which were calculated by fitting a third-degree polynomial to an interval of seven adjacent points centred at the desired point, and differentiating the expression obtained. Although this is a

more complicated procedure, it is better suited than the simpler use of the quotient of increments because it smoothes the curve, reducing the effect of experimental errors.

RESULTS AND DISCUSSION

Three methods were tested to determine the inflection points on the titration curve: the dE/dV , Gran I¹⁴ (dV/dE), and Gran II¹⁵ ($\exp[\pm nFE/RT]$) methods. Linearization of the branches was used in both Gran methods together with the correction for weak acids for more accurate determination of the inflection points.^{16,17} Gran II, though more accurate for simple acids, was too complex to deal with the mixture of acidic groups found in FA, so it was rejected. The dE/dV and dV/dE methods are similar in the plots they produce but the latter makes endpoint calculation easier and was the preferred method.

Three titrations were done with each combination of titrant and solvent, for different concentrations of FA ranging from 0.5 to 1.25 g/l. Even though the shape of the derivative curves is very sensitive to the concentration of FA titrated, the position of the calculated inflection points remained constant. The Pt-modified calomel electrode pair was tested in DMSO with potassium hydroxide as titrant but did not improve the sharpness of the titration curves.

Figure 1 shows the titration and derivative curves

obtained for the combinations of solvent and titrant tested. To make the comparison between curves easier, the potential or dV/dE is plotted *vs.* meq of base added per gram of FA. Table 1 shows the end-points obtained with each combination used, as well as the precision of the measurement. Information about potential ranges is included.

The results obtained show a great variation in the effect of choice of titrant on the differentiation between the acidic groups of FA. As shown in Table 1 and Fig. 1, the resolution of acidic groups is better by titration with potassium hydroxide than with TBAH, the former being able to titrate weaker acid groups than TBAH can. This could be attributed to the size of the TBA cation preventing access to hindered groups if the titration is regarded as combined cation-exchange and neutralization, but confirmation is necessary.

The total acidity values were higher for titrations in DMSO than in DMF, despite the more basic character of this solvent. However, Clare *et al.*¹⁸ have found that for several acids the acidity constants are higher in DMSO than in DMF, so several very weak groups could be titratable in DMSO, though not in DMF. On the other hand, FA could be considered as a polymer with a spatial structure which is affected by the solvent or by the degree of titration.^{19,20} This effect, together with the different solvation ability of the solvents tested, could account for the differences

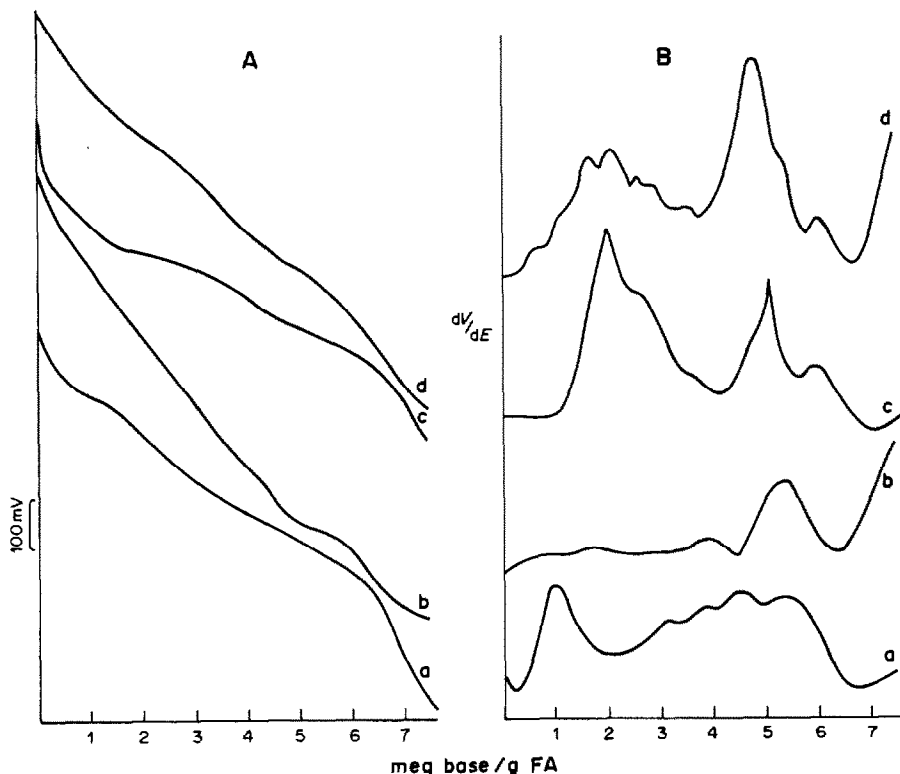


Fig. 1. Titration of FA in DMF or DMSO with KOH or TBAH in isopropyl alcohol. A, Potentiometric titration curves; B, dV/dE curves. Combination codes: a, DMF-KOH; b, DMF-TBAH; c, DMSO-KOH; d, DMSO-TBAH.

Table 1. End-points obtained for FA with various solvent-titrant combinations

Combination	$\delta E, mV$	End-points, <i>meq/g</i> (base/FA)				
DMF/KOH	815	0.20 [<0.10]	2.10 [<0.10]		6.80 [<0.10]	
DMF/TBAH	730			4.35 [<0.10]	6.30 [<0.10]	
DMSO/KOH	600	0.80 [0.18]		4.05 [0.13]	5.70 [0.25]	7.05 [<0.10]
DMSO/TBAH	770		3.35* [0.20]	3.85* [0.15]	5.85 [<0.10]	6.75 [<0.10]
Water						6.75†

*Indicates doubtful inflection point; values in brackets are standard deviations; †obtained by acid-base titration with potassium hydroxide.

in the inflection-points obtained in the two solvents. In addition, slight precipitation appeared in DMF when potassium hydroxide was used, indicating poorer solvation of the potassium salts of FA by DMF.

The intermediate values obtained could be attributed to clusters of acidic groups of nearly equal strength in a given solvent, but differing from one solvent to another. No attempt was made to attribute pK_a values to these groups either on the basis of the half-neutralization potential, or by comparison with benzoic acid, because of the dependence of the scale on the kind of group being titrated.^{7,18}

The values obtained in these non-aqueous titrations agree with those obtained for the exchangeable acidity by acid-base titration in water. This acidity is often considered to be the carboxylic acidity, which would suggest there is great deactivation of phenolic groups (salicylic or gallic acid type) present in FA or more likely there is an overestimation of the phenolic groups by the commonly accepted methods for humic substances (total acidity determined with barium hydroxide, minus carboxylic acidity).

This work shows the potential of non-aqueous titrations for differentiating acidic groups in FA, especially with potassium hydroxide as titrant. The method is being extended to other solvents or humic fractions in order to evaluate its usefulness.

REFERENCES

1. D. S. Gamble, *Can. J. Chem.*, 1970, **48**, 2662.
2. H. Davis and C. J. B. Mott, *J. Soil Sci.*, 1981, **3**, 379.
3. G. Sposito, K. M. Holtzclaw and D. A. Keech, *Soil Sci. Soc. Am. J.*, 1977, **41**, 1119.
4. P. A. Arp, *Can. J. Chem.*, 1983, **61**, 1671.
5. V. Z. Deal and G. E. A. Wyld, *Anal. Chem.*, 1955, **27**, 47.
6. R. H. Cundiff and P. C. Markunas, *ibid.*, 1956, **28**, 793.
7. R. Morales, *Anal. Chim. Acta*, 1969, **48**, 309.
8. J. Berčík, Z. Hladký and M. Cakrt, *Z. Anal. Chem.*, 1972, **261**, 113.
9. J. R. Wright and M. Schnitzer, *Trans. 7th Int. Congr. Soil Sci.*, 1960, **2**, 120.
10. H. Van Dijk, *Sci. Proc. Roy. Dublin Soc. Ser. A*, 1959-1964, **1**, 163.
11. S. O. Thompson and G. Chesters, *J. Soil Sci.*, 1969, **20**, 346.
12. K. Yonebayashi and T. Hattori, *Org. Geochem.*, 1985, **8**, 47.
13. E. M. Thurman and R. L. Malcolm, *Environ. Sci. Technol.*, 1981, **15**, 463.
14. G. Gran, *Acta Chem. Scand.*, 1950, **4**, 559.
15. *Idem*, *Analyst*, 1952, **77**, 661.
16. C. Liteanu and M. Mioscu, *Z. Anal. Chem.*, 1967, **13**, 1185.
17. J. W. Frazer, A. M. Kray, W. Selig and R. Lim, *Anal. Chem.*, 1975, **47**, 869.
18. B. W. Clare, D. Cook, E. C. F. Ko, Y. C. Mac and A. J. Parker, *J. Am. Chem. Soc.*, 1966, **88**, 1911.
19. G. Sposito and K. M. Holtzclaw, *Soil Sci. Soc. Am. J.*, 1977, **41**, 330.
20. E. M. Perdue, *Geochim. Cosmochim. Acta*, 1978, **42**, 1351.

SIGNAL PROCESSING WITH A SUMMING OPERATIONAL AMPLIFIER IN MULTICOMPONENT POTENTIOMETRIC TITRATIONS

A. PARCZEWSKI

Department of Analytical Chemistry, Jagiellonian University, Kraków, Poland

(Received 1 September 1986. Revised 6 October 1986. Accepted 16 January 1987)

Summary—It has been proved that application of two indicator electrodes connected to the ordinary titration apparatus through an auxiliary electronic device (a summing operational amplifier) significantly extends the scope of multicomponent potentiometric titrations in which the analytes are determined simultaneously from a single titration curve. For each analyte there is a corresponding potential jump on the titration curve. By application of the proposed auxiliary device, the sum of the electrode potentials is measured. The device also enables the relative sizes of the potential jumps at the end-points on the titration curve to be varied. The advantages of the proposed signal processing are exemplified by complexometric potentiometric titrations of Fe(III) and Cu(II) in mixtures, with a platinum electrode and a copper ion-selective electrode as the indicator electrodes.

Titration is one of the most widely used methods of quantitative analysis. Its popularity results from the accessibility and relatively low cost of equipment, ease of operation and minimal maintenance requirements. Moreover, titration techniques can easily be automated and computerized. In spite of the popularity and extensive development of titration techniques, their effectiveness and applicability can still be increased. This may be realized in the following ways: (a) finding better reagents and procedures of sample preparation, (b) finding and developing sensitive and selective analytical sensors and new ways of using them,^{1,2} (c) improving signal processing, (d) finding the best means of data acquisition and the methods of mathematical and statistical evaluation that yield maximum information. The present paper is concerned mainly with point (c).

One of the most attractive directions in which application of titration methods can be extended is multicomponent analysis in which solution components are determined simultaneously from a single titration curve. Such determinations are speedy, require only small amounts of sample, and may be easily automated, so their development becomes worth while. It has been shown theoretically³ that the practicability and efficiency of simultaneous determination of two or more cations or anions in solution from a single potentiometric titration curve may be significantly increased if two indicator electrodes are applied and the signals (electrode potentials) processed in a special way. The signal processing is realized by the use of a simple electronic device directly connected to a standard potentiometric titration apparatus. The device makes it possible to take full advantage of using two indicator electrodes in potentiometric titrations of multicomponent systems. The effectiveness of the device is demonstrated

by the potentiometric complexometric titration of mixtures of Fe(III) and Cu(II) in solution, with a platinum electrode and an ion-selective electrode for copper (CuISE).

THEORY

In conventional potentiometry the electromotive force E_- of a galvanic cell is the difference between the potentials of two electrodes immersed in the test solution: $E_- = E_1 - E_2$, where E_1 and E_2 denote the potentials of the indicator and reference electrodes, respectively. In potentiometric titration E_- is a function of the titrant volume, V , added to the sample solution: $E_- = E_-(V) = E_1(V) - E_2$. If two indicator electrodes are applied, then E_2 also depends on V : $E_2 = E_2(V)$. When a platinum electrode and a CuISE are applied in the complexometric titration of Fe(III) and Cu(II) in mixtures, the electrode potentials (mV) can be described approximately as follows, $E_1 = E_1^0 + 59 \log ([Fe^{3+}]/[Fe^{2+}] + L_1)$ and $E_2 = E_2^0 + 29.5 \log ([Cu^{2+}] + L_2)$, where L_1 and L_2 denote detection limits of the electrodes (for the sake of simplicity terms including selectivity coefficients have been omitted). During titration the concentrations of the ions indicated in these formulae change. The shapes of the functions $E_1(V)$ and $E_2(V)$ depend on such factors as the conditional stability constants of the complexes the titrant forms with the metal ions in solution, the concentration of the metals in solution, the sample volume and the titrant concentration, as well as on the electrode parameters.³ In order to take full advantage of using two indicator electrodes in the simultaneous determination of two or more metal ions (or anions) in mixtures, the sum of the electrode potentials, $E_+ = E_1 + E_2$, should be measured instead of the difference, E_- . A device which makes it

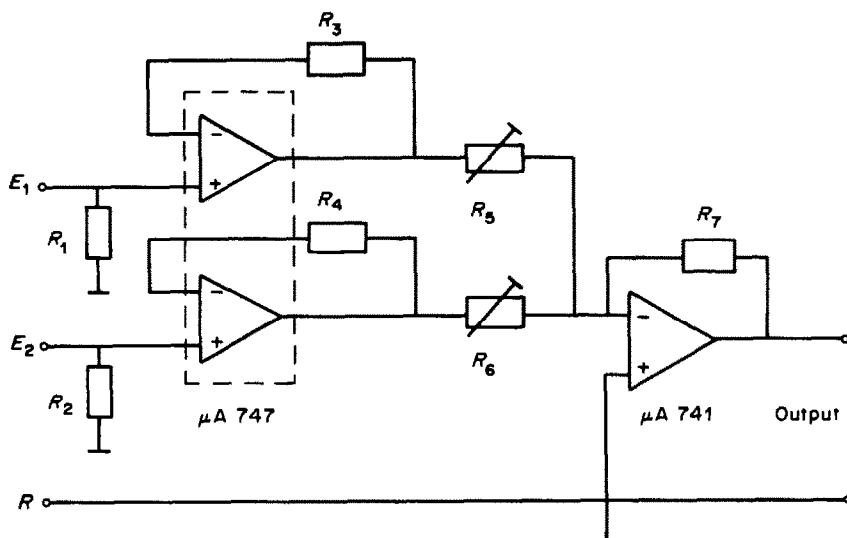


Fig. 1. The auxiliary device for multicomponent potentiometric titration with two indicator electrodes. The indicator electrodes are connected to inputs E_1 and E_2 and the reference electrode to R . The output is connected to a pH-meter (voltmeter). The resistances for the results presented here were:

$$R_1 = R_2 = 3.3 \text{ M}\Omega, R_3 = R_4 = 100 \text{ k}\Omega, R_7 = 10 \text{ k}\Omega \text{ (see Fig. 2 for } R_5 \text{ and } R_6).$$

possible to obtain the E_+ (V) titration curve is described below.

SUMMING OPERATIONAL AMPLIFIER

To obtain the titration curves ($E_+ = E_1 + E_2$) an electronic device (a summing operational amplifier) is proposed which is schematically presented in Fig. 1. The operational amplifiers indicated are adequate if electrodes of relatively low resistance are used. The device can be made more universal and its performance improved by application of high-quality (high input-impedance) operational amplifiers. This is especially important if liquid-membrane or glass electrodes are applied.

The device also enables the relative sizes of the potential jumps at the first and second end-points on the titration curve to be controlled without adjustment of the span selector on the recorder during titration. This is realized by appropriate selection of resistors R_5 and R_6 (Fig. 1) and makes automation and computerization of the titration easy. The reference electrode may be any suitable electrode connected to the test solution through an electrolyte bridge. It is very convenient to use a platinum wire electrode inserted inside the delivery tip of the burette,⁴ so that only the two indicator electrodes are immersed in the sample solution.

EXPERIMENTAL

All reagents were of analytical-reagent grade. Redistilled water was used in the preparation of sample solutions and buffers. The results concern the analysis of sample solutions (20 ml) each containing submilligram amounts of iron(III) and copper(II) in 0.02M acetate buffer of pH 3.5; 0.01M EDTA was used as the titrant.

A Radiometer RTS622 titrator (ABU12 autoburette with a 2.5-ml burette and TTA60 titration assembly) was used. The electrodes were a CuISE (DHN, Poland), a platinum electrode and a Radiometer SCE with a 1M potassium nitrate electrolyte bridge. The platinum electrode was pretreated by rinsing it in concentrated sulphuric acid and then immersing it in hot (ca. 50°) 3% potassium dichromate solution in 10% sulphuric acid for ca. 15 min. Then the electrode was kept in water for several hours. To avoid the

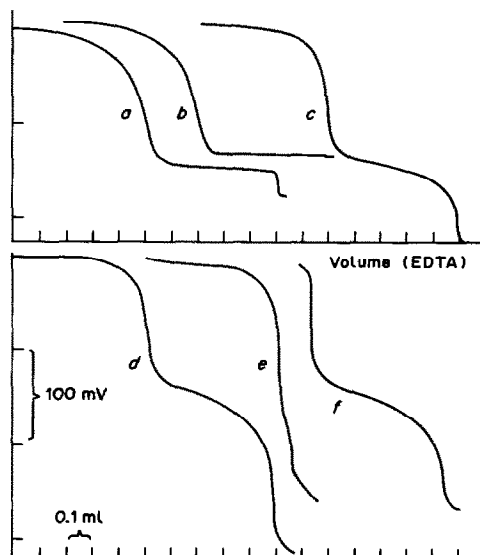


Fig. 2. Potentiometric compleximetric titration of Fe(III) and Cu(II) in mixture. Conventional titration [$E_-(V)$]: (a) Pt vs. SCE (KNO_3 bridge), (b) Pt vs. CuISE. Titration with use of the proposed auxiliary device and two indicator electrodes (Pt, CuISE) and SCE (KNO_3 bridge) as reference [$E_+(V)$]: (c) $R_5 = R_6 = R_7$, (d)-(f) $R_5 = R_6/2 = R_7/2$. The CuISE was connected to input E_1 (Fig. 1). The test solution contained 0.28 mg of Fe and 0.32 mg of Cu (a)-(d), 0.28 mg of Fe and 0.032 mg of Cu (e), and 0.028 mg of Fe and 0.32 mg of Cu (f).

possible influence of air, titrations were performed with the solution in an inert gas atmosphere.

The results are presented in Fig. 2.

RESULTS AND DISCUSSION

As shown in Fig. 2a, Fe(III) and Cu(II) can be determined from a single titration curve by using a platinum and a saturated calomel electrodes with conventional potentiometric titration apparatus. The shape of the titration curve depends significantly on the way in which the electrode has been pretreated (because of kinetic effects)^{5,6} and also on the concentration of traces of iron(II) in solution.³ A platinum electrode pretreated as described above gave the curve presented in Fig. 2a. The first potential jump on the curve indicates the end-point for titration of iron(III), and the second jump the end-point for copper(II). Figure 2b shows that substitution of a CuISE for the reference electrode results in a reduction of the potential jump at the second end-point (in some conditions the potential E_- at the second end-point may even change in the opposite direction to that observed when the SCE reference electrode is used³). Such behaviour occurs because both the Pt and the CuISE potentials change in the same direction during the titration, so the measured potential difference E_- changes less than for the Pt/SCE system, especially at the second end-point. However, by appropriate signal processing, namely measurement of the sum $E_+ = E_1 + E_2$ (+ constant) instead of E_- , the advantages of replacing the reference electrode by the CuISE can be exploited. This is shown in Fig. 2, where conventional titration curves (Fig. 2, a,b) are compared with those obtained by application of the proposed auxiliary device (Fig 2, c-f). It is seen from Fig. 2, d-f that by appropriate selection switching of resistance R_s (in the CuISE "channel") the ratio of the potential jumps on the titration curve can be easily and efficiently controlled. In consequence, precise determination of the end-points becomes possible

even if there is a much more of one component than the other in the sample, as seen in Fig. 2, e,f. The potential jump at the second end-point in Fig. 2e (which corresponds to the sum of the iron and copper) can be made still more distinct by selection of a lower value for resistance R_s . For example, with $R_s = R_0/4$ the apparent abrupt potential jump at the second end-point is ca. 100 mV and the determination of the end-point becomes very precise. When there is an abrupt change of the potentials of the indicating electrodes at the end-points, the determination of the solution components is easy. However, even small potential changes can be used in the determination of the sample components by appropriate numerical manipulation of the experimental data. Moreover, the device presented in Fig. 1 can be extended by adding other "channels" (inputs E_3, E_4, \dots) and used for titration of more than two solution components. With the use of appropriately selected electrodes and titrants the device may be successfully applied to titrations of mixtures of cations or anions, or both cations and anions can be determined together. The practical analytical procedures will be presented separately. The device will shortly be incorporated in commercial pH-meters in order to extend their capabilities as tools for the analyst.⁷

Acknowledgement—The investigations were supported financially within the scope of Project CPBP 01.17.

REFERENCES

1. R. Stępak, *Z. Anal. Chem.*, 1983, **315**, 629.
2. A. Parczewski and R. Stępak, *ibid.*, 1983, **316**, 29.
3. A. Parczewski, in preparation.
4. H. H. Willard, L. L. Merritt and J. A. Dean, *Instrumental Methods of Analysis*, Van Nostrand, New York, 1974.
5. L. Kékedy, *Surf. Technol.*, 1969, **4**, 269.
6. L. Kékedy and A. Popescu, *Talanta*, 1975, **22**, 135.
7. A. Parczewski and A. Karocki, in preparation.

ANALYTICAL DATA

ETUDE DE L'ADSORPTION DE SUBSTANCES ORGANIQUES SUR L'AMIANTE CHRYSOTILE PAR CHROMATOGRAPHIE EN PHASE GAZEUSE

H. MENARD

Département de Chimie, Université de Sherbrooke, Faculté des sciences Sherbrooke, Québec, Canada

Y. LEFEBVRE et J. KHORAMI

Institut de l'Amiante, Université de Sherbrooke, Sherbrooke, Québec, Canada

(Reçu le 12 juin 1986. Révisé le 20 août 1986. Accepté le 16 janvier 1987)

Résumé—La chromatographie en phase gazeuse a permis de mesurer les isothermes d'adsorption de molécules organiques sur des fibres d'amiante. Les résultats indiquent que l'adsorption mesurée pour ces molécules se situe à un niveau intermédiaire entre la physisorption et la chimisorption. L'adsorption relative des molécules étudiées, à une même température, est dans l'ordre toluène \geq THF \geq benzène \geq dichlorométhane.

Summary—The isotherms for adsorption of some organic molecules on asbestos fibres have been determined by gas chromatography. The results show that the adsorption mechanism lies somewhere between physisorption and chemisorption. The degree of adsorption at a given temperature, for the compounds studied, is toluene > tetrahydrofuran > benzene > dichloromethane.

Depuis quelques années, l'étude des propriétés de surface des matières particulières a permis de tirer des conclusions intéressantes au niveau de la toxicité.¹ Dans le cas de l'amiante notamment, plusieurs preuves ont été accumulées démontrant que celle-ci pouvait avoir des propriétés cancérigènes.^{2,3}

Le chrysotile appartient à une famille de minéraux, les serpentines, qui ont comme composition chimique idéale $3\text{MgO} \cdot 2\text{SiO}_2 \cdot 2\text{H}_2\text{O}$. Les fibres naturelles renferment cependant des quantités mineures et variables de métaux qui peuvent remplacer le Mg ou le Si dans la structure cristalline. Le chrysotile contient aussi d'autres impuretés comme la brucite, le talc et la magnétite.⁴

La surface hydroxylée de l'amiante est un adsorbant de type III, selon Kiselev et Yashin,⁵ et lui confère une grande affinité pour les molécules polaires et/ou aromatiques. Cette interaction que nous avons mesurée dans cette étude serait responsable en grande partie de la toxicité de l'amiante. Les impuretés métalliques en surface doivent aussi jouer un rôle important.⁶

Une étude sur les propriétés de surface de l'amiante, par chromatographie en phase liquide, a permis d'observer de fortes interactions avec les hydrocarbures aromatiques polycycliques.⁷ Nous étions aussi intéressés à savoir si la chromatographie en phase gazeuse donnerait des résultats comparables, dans le cas des molécules comme le benzène et le toluène.

CALCUL DE L'ISOTHERME D'ADSORPTION

La chromatographie en phase gazeuse sert au calcul de l'isotherme d'adsorption. Des perfectionnements récents ont permis d'augmenter sensiblement la précision des résultats obtenus, avec discussion des effets secondaires se produisant dans la colonne.⁸

A partir de l'équation de conservation de la masse de soluté dans une tranche élémentaire de la colonne on peut démontrer l'équation suivante:^{5,9}

$$\left(\frac{\partial n}{\partial p}\right)_T = \frac{V_n}{mRT} \quad (1)$$

où n est la quantité adsorbée, en $\mu\text{mole/g}$, p la pression partielle, m la masse d'adsorbant utilisée et V_n le volume net de rétention du soluté. En intégrant on obtient

$$n = \frac{1}{m} \int_0^p \frac{1}{RT} V_n dp \quad (2)$$

En addition à l'équation (2) on utilise le facteur de compressibilité j pour le gradient de pression à l'intérieur de la colonne.¹⁰ En assumant que la hauteur des pics, h , est proportionnelle à la pression partielle, cette dernière peut être calculée par

$$p = q_i h RT / S_{\text{pic}} F_{(0)} \quad (3)$$

où q_i est la quantité de soluté injectée, en moles, s_{pic} est l'aire sous le pic correspondant à cette injection et

$F_{(y_0)}$ est le débit du gaz vecteur à la température de la colonne. L'équation (3) peut être corrigée pour l'effet de sorption, *i.e.*, le changement de débit dû au transfert de masse,⁸

$$\frac{F_{(y_0)}}{F_{(0)}} = \frac{1 + K}{1 + K(1 - jy_0)} \quad (4)$$

où p_0 = pression à la sortie de la colonne, y_0 = fraction molaire = p/p_0 , K = coefficient de distribution de la masse du soluté (capacité), $F_{(y_0)}$ = débit corrigé pour l'effet de sorption: y_0 est évalué approximativement par l'équation (3). La valeur de $F_{(y_0)}$ est ensuite reportée dans (3) pour calculer la nouvelle valeur de p .

Cette correction doit aussi s'appliquer à la valeur du temps mort de la colonne: $t_{m,obs}$ est le temps mort observé, et t_m le temps mort corrigé.

$$t_m = t_{m,obs} F_{(0)} / F_{(y_0)} \quad (5)$$

L'effet total de la correction due aux équations (4) et (5) fut toujours inférieur à 5%.

CALCUL DE L'ENTHALPIE D'ADSORPTION

L'enthalpie isostérique différentielle est calculée à l'aide d'une équation dérivée de celle de Clausius-Clapeyron:

$$\Delta H_{st} = R \left[\frac{\partial \ln P}{\partial (1/T)} \right]_n$$

On effectue une régression linéaire sur des points interpolés à intervalles constants de n sur les isothermes d'adsorption en fonction de la température. On obtient alors une courbe de ΔH_{st} en fonction du recouvrement et on calcule $\Delta \bar{H}$, la moyenne dans un intervalle de recouvrement de 0.1 à 10 $\mu\text{mole/g}$.

On mesure l'isotherme par une série d'injections des solutés purs variant de 0.10 à 5.00 μl en utilisant la méthode du maximum du pic pour faire les calculs.⁹ Les pics furent enregistrés sur un intégrateur. Ceux-ci étaient surimposables à 5%, *i.e.*, on admet que la traînée d'un pic à plus haute concentration coïncide avec les sommets des pics à plus faible concentration. Le volume mort fut mesuré par injection de méthane pour chaque isotherme.

RESULTATS ET DISCUSSION

Les causes déterminantes affectant la reproductibilité des résultats sont: premièrement, l'erreur sur le volume de liquide injecté à l'aide des seringues, en moyenne 2%; deuxièmement le nombre peu élevé de plateaux théoriques que l'on peut obtenir avec une colonne remplie d'un matériau fibreux et hétérogène comme l'amiante. On obtient 20 plateaux pour la colonne utilisée dans cette expérience, (injection de 1.000 μl de benzène à 180° au débit optimum), et ce fait peut être responsable d'une erreur totale

d'environ 5%. Enfin les équations utilisées ici sont des équations simplifiées, que peuvent elles-mêmes introduire un certain pourcentage d'erreur.¹² Cette analyse concorde avec les résultats observés à la figure 1; les 3 isothermes sont reproductibles à 10%.

L'utilisation d'une colonne plus longue n'aurait pas augmenté significativement la précision, car il aurait alors fallu augmenter soit la chute de pression

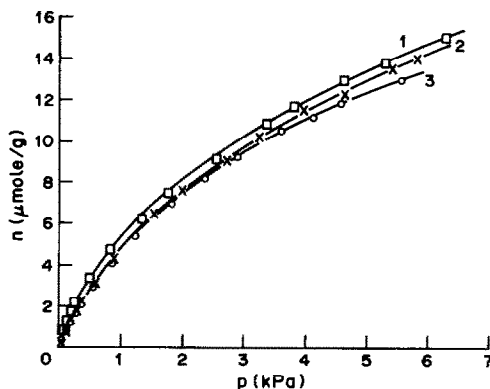


Fig. 1. Reproductibilité de l'adsorption du benzène sur l'amiante BC4-T à 180°C. Les courbes ont été obtenues en faisant varier le débit du gaz vecteur (ramené à TPN), et en changeant de colonne, courbe (1). (1) $m = 3.227$ g, $F_{(0)} = 6.07$ ml/min, $j = 0.6120$; (2) $m = 3.477$ g, $F_{(0)} = 6.20$ ml/min, $j = 0.6485$; (3) $m = 3.477$ g, $F_{(0)} = 7.45$ ml/min, $j = 0.6136$.

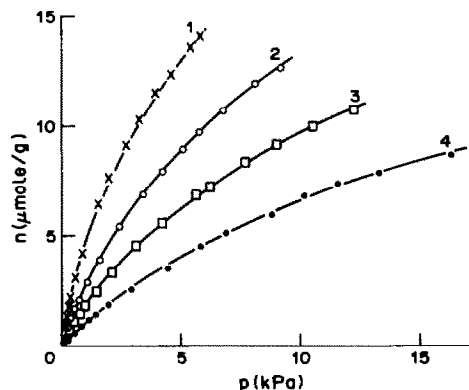


Fig. 2. Adsorption du benzène sur l'amiante BC4-T. (1) 180°C; (2) 200°C; (3) 220°C; (4) 240°C.

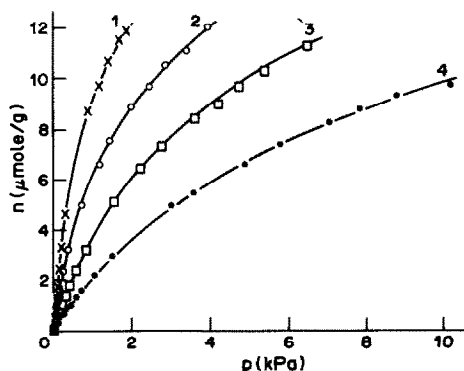


Fig. 3. Adsorption du toluène sur l'amiante BC4-T. (1) 180°C; (2) 200°C; (3) 220°C; (4) 240°C.

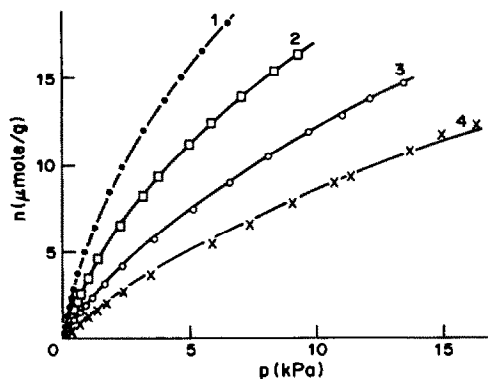


Fig. 4. Adsorption du dichlorométhane sur l'amiante BC4-T. (1) 120°C; (2) 140°C; (3) 160°C; (4) 180°C.

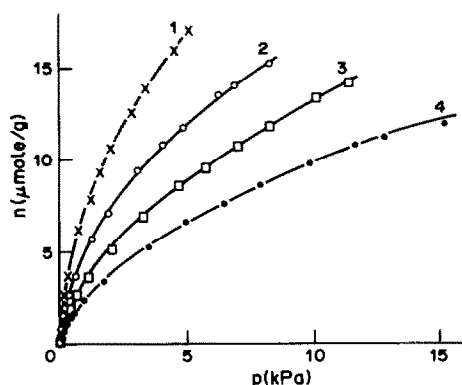


Fig. 5. Adsorption du THF sur l'amiante BC4-T. (1) 180°C; (2) 200°C; (3) 220°C; (4) 240°C.

qui était déjà assez élevée (environ une atmosphère) ou bien obtenir des temps de rétention plus longs, ceux-ci pouvant déjà aller jusqu'à environ 30 min pour les plus petites injections.

Les figures 2, 3, 4 et 5 montrent l'absorption du benzène, toluène, dichlorométhane et tétrahydrofurane à différentes températures. Dans tous les cas l'adsorption diminue régulièrement avec la température. Il faut noter que l'adsorption se produit à des températures assez élevées par rapport au point d'ébullition normal des substances étudiées. Ce type de comportement n'est pas très courant lorsque le phénomène étudié est de la physisorption.¹⁴

D'autre part les enthalpies isostériques mesurées sont nettement supérieures à l'enthalpie de la vaporisation (tableau 1), ce qui indique que les interactions adsorbant-adsorbant sont très importantes. De fait ces

Tableau 1. Enthalpie isostérique moyenne sur l'amiante BC4-T dans un intervalle de recouvrement de 0,1–10 μmole/g, à 210° et comparaison avec l'enthalpie standard de vaporisation ($\Delta H_{v,298}^0$)

Substance	$\Delta H_{st,483}^0$, kJ/mole	$\Delta H_{v,298}^0$, ¹³ kJ/mole
Benzène	58 ± 1	34.085
Toluène	70 ± 2	35.901
Dichlorométhane	43 ± 1*	31.683
Tétrahydrofurane	57 ± 2	—

*Valeur à 150°.

enthalpies isostériques se situent dans une zone intermédiaire entre la physisorption, (généralement moins de 40 kJ/mole), et la chemisorption, (généralement plus de 80 kJ/mole).¹⁵

Le tableau 2 donne les constantes de Henry pour les isothermes étudiés. La constante de Henry est la pente de l'isotherme à dilution infinie. On y voit que les valeurs données pour le THF décroissent moins vite avec la température de celles du toluène.

Comparaison à une même température, 180°, des isothermes d'adsorption pour les molécules étudiées montre que la séquence d'adsorption est toluène ≥ THF ≥ benzène ≥ dichlorométhane.

Remerciements—Les auteurs remercient pour l'appui financier le Conseil National de Recherches en Sciences Naturelles et en Génie du Canada et l'Institut de l'Amiante.

LITTÉRATURE

1. L. D. Scheel, C. H. Gorski, R. W. Vest, L. E. Steettler, W. C. Tripp et G. P. Gray, *J. Am. Ind. Hyg. Ass.*, 1971, **32**, 673.
2. B. T. Mossman et J. E. Craighead, *Env. Res.*, 1981, **25**, 269.
3. A. L. Reeves, H. E. Puro, R. G. Smith et A. J. Vorwald, *ibid.*, 1971, **4**, 496.
4. F. M. Kimmerle et P.-C. Aïtcin, *L'amiante chrysotile*, Chap. 8, Université de Sherbrooke, Canada, 1981.
5. A. V. Kiselev et Y. I. Yashin, *La chromatographie gaz-solide*, Chap. 4, Masson, Paris, 1969.
6. J. R. Dixon, D. B. Lowe, D. E. Richards, L. J. Cralley et H. E. Stokinger, *Cancer Res.*, 1970, **30**, 1068.
7. H. Ménard, L. Noël, F. M. Kimmerle, L. Tousignant et M. Lambert, *Anal. Chem.*, 1984, **56**, 1240.
8. J. R. Conder et C. L. Young, *Physicochemical Measurement by Gas Chromatography*, Chap. 9, Wiley, New York, 1979.
9. G. M. Dorris et D. G. Gray, *J. Coll. Int. Sci.*, 1979, **71**, 93.
10. A. B. Littlewood, *Gas Chromatography*, p. 23. Academic Press, New York, 1962.

Tableau 2. Constantes de Henry pour l'adsorption sur l'amiante BC4-T à différentes températures, calculées à partir de $\Sigma_{N_2} = 18.0 \pm 0.5$ m²/g

Substance	C_h , nmole/N			
	180°	200°	220°	240°
Benzène	0.39 ± 0.05	0.19 ± 0.02	0.12 ± 0.01	0.061 ± 0.004
Toluène	1.2 ± 0.1	0.63 ± 0.09	0.27 ± 0.02	0.135 ± 0.008
Dichlorométhane*	0.069 ± 0.005			
THF	0.8 ± 0.2	0.5 ± 0.1	0.28 ± 0.08	0.17 ± 0.04

*0.40 ± 0.04 à 120°; 0.22 ± 0.02 à 140°; 0.13 ± 0.01 à 160°.

11. S. Brunauer, P. H. Emmet et E. Teller, *J. Am. Chem. Soc.*, 1938, **60**, 309.
12. J. R. Conder, *Chromatographia*, 1974, **7**, 387.
13. R. C. Weast, *Handbook of Chemistry and Physics*, 61st Ed., CRC Press, 1981.
14. D. O. Hayward et B. M. W. Tapnell, *Chemisorption*, 2nd Ed., p. 3. Butterworths, London, 1964.
15. A. W. Adamson, *Physical Chemistry of Surfaces*, 4th Ed., p. 520. Wiley, New York, 1982.

ANNOTATION

IONIC STRENGTH DEPENDENCE OF FORMATION CONSTANTS—X

PROTON ACTIVITY COEFFICIENTS AT VARIOUS TEMPERATURES AND IONIC STRENGTHS AND THEIR USE IN THE STUDY OF COMPLEX EQUILIBRIA

SANTI CAPONE, ALESSANDRO DE ROBERTIS, CONCETTA DE STEFANO, SILVIO SAMMARTANO and
ROSARIO SCARCELLA

Istituto di Chimica Analitica dell'Università, Via dei Verdi, 98100 Messina, Italy

(Received 25 November 1986. Accepted 15 January 1987)

Summary—The activity coefficients of the proton were determined in aqueous solution in the presence of several background electrolytes at 10, 25, 37 and 45° and $0.01 \leq I \leq 1M$. The results indicate that the proton activity coefficients are fairly independent of the different salts used as background, in particular when ion-pair formation between cations and anions of the medium is taken into account. This result is in agreement with the findings of previous works in this series. Some previously published data were reanalysed for comparison, and showed excellent accordance with the present results. A general equation for calculating proton activity coefficients is reported.

When equilibria in solution are studied, one of the most important problems concerns the activity coefficients. Since individual activity coefficients are not accessible, some conventions have been adopted in defining them for electrolyte solutions. According to Brønsted¹ and Guggenheim,² it can be assumed that only linear interaction terms between pairs of ions of opposite charge cause deviations from the extended Debye-Hückel theory. On the basis of the Bjerrum³ and Davies⁴ model, as applied by some marine chemists (see, e.g., Garrels and Thompson⁵), the deviations from the extended Debye-Hückel theory are attributed to formation of ion-pairs and, in addition, the MacInnes convention⁶ [$\gamma_{K^+} = \gamma_{Cl^-} = \gamma_{\pm KCl}$] holds. The mole-fraction statistics model⁷ assumes the chloride ion to be unhydrated in aqueous solution. According to Platford,⁸ when ion-selective electrodes are employed, the liquid junction is assumed to be unaffected by transfer from the calibration solution to the experimental solution. None of these conventions has been applied extensively, but hybrid models have generally been used. For example, the Bjerrum model is often used in connection with the ion-selective electrode convention. Also the Brønsted-Guggenheim and Bjerrum models are often adopted together. Great success has been achieved by the constant-medium method,⁹ which assumes the activity coefficients to be constant when an inert electrolyte is added in sufficiently large (and constant) amount.

Extensive systematic work begun by us (and some

colleagues in other laboratories) some years ago showed that a general equation for the dependence of formation constants (and hence of activity coefficients) on ionic strength can be formulated if allowance is made for all interactions occurring in the solution under study. Very different types of systems have been studied: the protonation of several inorganic and organic acids;^{10,11} the formation of mixed-ligand¹² and mixed-metal¹³ complexes; the protonation of amines;¹⁴ the formation of La³⁺-carboxylate complexes;¹⁵ the formation of alkali and alkaline-earth metal complexes with carboxylates,¹⁶⁻²⁴ complexones,^{25,26} sulphate,²⁷ phosphate,²⁸ adenosine-5'-triphosphate,²⁹ hexacyanoferrate(II),³⁰ imines³¹ and polyphosphates;²⁶ the formation of alkali and alkaline-earth metal-low molecular-weight ligand complexes;³² the solubility product of some calcium compounds.³³ In addition, a great many literature values for several temperatures and ionic strengths have been analysed.^{34,35}

In this work we report a potentiometric study (with the proton-sensitive glass electrode) of proton activity coefficients in several media at temperatures in the range 10-50° and ionic strengths (*I*) in the range up to 1M. Alkali-metal nitrates, chlorides and perchlorates, alkaline-earth metal nitrates and chlorides, and tetra-alkylammonium chlorides and iodides were used as background electrolytes. Four sets of potentiometric apparatus were used in order to minimize systematic experimental errors.

EXPERIMENTAL

Materials

Lithium, sodium, potassium, rubidium and caesium chlorides and sodium and potassium nitrates (Erba or Fluka analytical grade) were dried in an oven at 110° or under reduced pressure, and used without further purification. Tetraethylammonium iodide (Et₄NI) and tetramethylammonium chloride (Me₄NCl) were Fluka puriss. and purified by recrystallization from methanol, according to Perrin.³⁶ Sodium perchlorate was Erba analytical grade; the concentration of its stock solution was determined by passing a known volume through a strong cation-exchange resin in H⁺ form and titrating the protons liberated. Magnesium, calcium, strontium and barium chlorides (Fluka purum) were dissolved in water and the solutions standardized by titration with EDTA.³⁷ Phthalic and malonic acids were Fluka puriss.; their purity, checked alkalimetrically, was >99%. Doubly distilled water and grade-A glassware were used for the preparation of all solutions.

Potentiometric apparatus

In order to avoid systematic errors, four sets of potentiometric apparatus were used: (a) an Orion 801A potentiometer with Metrohm glass-saturated calomel electrodes; (b) a Metrohm E600 potentiometer with Metrohm glass-saturated calomel electrodes; (c) a semiautomatic home-made potentiometer built with an Analog Devices millivoltmeter, Printel printer, and Mosteck logic circuits to add a pre-established volume of titrant and print the corresponding e.m.f. value; (d) an Amel 337 potentiometer with Metrohm glass electrode and Ingold saturated calomel electrode.

In all cases the titrant solution was delivered by an Amel model 882 dispenser, readable to 0.001 ml. The titration vessel was maintained within ±0.1° of the required temperature; magnetic stirring was employed; a stream of purified nitrogen pre-equilibrated with test solution was passed through the solution in order to exclude carbon dioxide and oxygen.

Procedure

A 25–50 ml volume of hydrochloric, nitric or perchloric acid (2.5–10mM) was titrated with a CO₂-free 0.2–0.5M standard solution of sodium or potassium hydroxide. In some cases the titrations were done in the presence of malonic or phthalic acid (2–8mM).

Since one of the major requirements for the present work was to have maximal constancy of e.m.f. readings (under the same experimental conditions), we used several new electrode couples, and during the work these couples were frequently replaced. The constancy of the e.m.f. was checked in two ways: (i) by measuring the e.m.f. with the electrode couple immersed in buffer solution, and (ii) by performing 5–10 titrations on the same day for the same system and measuring the standard potential of the hydrogen couple. In both cases the variations were 0.1–0.2 mV for a time lapse of 3 hr and 0.1–0.8 mV for a time lapse of 12 hr.

Calculations

The calculations for determining E° (and in some cases other analytical parameters of the titrations) were done with the non-linear least-squares computer programs ACBA,³⁸ ESAB³⁹ and/or ESAB2M.⁴⁰ The calculations for the refinement of the parameters for the dependence of the activity coefficients on ionic strength (see next section) were done by the non-linear least-squares computer program REGIS.⁴¹ Concentrations and activity coefficients are always expressed on the molar scale.

CALCULATION METHODS

Potentiometric readings obtained with the proton-sensitive glass electrode can be described by the equation

$$E = E^\circ + \frac{RT \ln 10}{F} \log a_{\text{H}} + j_{\text{a}} a_{\text{H}} \quad (1)$$

where E° is the standard potential of the electrode couple, a_{H} is the proton activity and j_{a} is the coefficient relating it to the junction potential ($E_{\text{j}} = j_{\text{a}} a_{\text{H}}$). Since $a_{\text{H}} = c_{\text{H}} f_{\text{H}}$ (c_{H} is the free proton concentration and f_{H} the activity coefficient for H⁺), equation (1) can be written (with $s = RT \ln 10/F$) as

$$E = E^\circ + s \log c_{\text{H}} + s \log f_{\text{H}} + j_{\text{a}} c_{\text{H}} + j_{\text{a}} f_{\text{H}} = E^\circ + s \log c_{\text{H}} \quad (2)$$

where*

$$E^\circ = E^\circ + s \log f_{\text{H}} + j_{\text{a}} a_{\text{H}} \approx E^\circ + s \log f_{\text{H}} \quad (3)$$

For the dependence of activity coefficients on ionic strength we can use a Debye-Hückel type equation

$$\log f_{\text{H}} = -A \sqrt{I} / (1 + \delta B \sqrt{I}) + CI + DI^{3/2} \quad (4)$$

where A , δ and B are constants of the Debye-Hückel theory, and C and D are empirical parameters. Since $A \sim 0.5$ and $\delta B \sim 1.5$ (by assuming $\delta = 5 \text{ \AA}$ for all ions), equation (4) can be written

$$\log f_{\text{H}} = -\sqrt{I} / (2 + 3\sqrt{I}) + CI + DI^{3/2} \quad (5)$$

The combination of equations (3) and (5) gives

$$E^\circ = E^\circ + s [-\sqrt{I} / (2 + 3\sqrt{I}) + CI + DI^{3/2}] \quad (6)$$

If we can assume that over a reasonable period E° is a constant for the potentiometric equipment used, a series of measurements of E° at different ionic strengths allows, through equations (5) and (6), the activity coefficients of H⁺, together with their dependence on ionic strength, to be determined.

In practice we adopted the following procedure. Five or six titrations were performed, in at most 4 hr, at different ionic strengths. Then we calculated E° values for each titration and recorded the differences $E^\circ(I) - E^\circ(I')$ (where I' is a reference ionic strength lying within the range studied). In this way all measurements became independent of the E° value and of the day on which the measurements were made. Therefore, instead of equations (5) and (6), the equations

$$\begin{aligned} & \log f_{\text{H}}(I) - \log f_{\text{H}}(I') \\ &= -[\sqrt{I} / (2 + 3\sqrt{I}) - \sqrt{I'} / (2 + 3\sqrt{I'})] \\ &+ C(I - I') + D(I^{3/2} - I'^{3/2}) \\ &= g(I, I') \end{aligned} \quad (7)$$

$$E^\circ(I) - E^\circ(I') = s[g(I, I')] \quad (8)$$

can be used.

*In our experimental conditions the term $j_{\text{a}} a_{\text{H}}$ is always less than 0.1 mV, so is neglected.

The dependence of the empirical parameters C and D on temperature (t , °C) was taken into account by a simple expansion⁴¹

$$C = C_{25} + C'_{25}(t - 25) + C''_{25}(t - 25)^2 \quad (9)$$

$$D = D_{25} + D'_{25}(t - 25) + D''_{25}(t - 25)^2 \quad (10)$$

In order to estimate the error in E° , and then in $\log f_{\text{H}}$, a simple variance propagation

$$\sigma^2(E^\circ) = \sigma^2(E) + \sum_i \left(\frac{\partial E^\circ}{\partial x_i} \right)^2 \sigma^2(x_i) \quad (11)$$

(where x_i are all parameters that can affect E° values) can be used. This calculation is necessary for comparing estimates of errors with experimental ones: the agreement between these errors confirms that the procedure adopted is correct and systematic errors are absent.

RESULTS AND DISCUSSION

The following sets of data were used in the calculations: (a1) E° values obtained from solutions of strong acids, in the presence of all the various backgrounds [389 titrations, 71 titration groups, 318 data points, $E^\circ(I) - E^\circ(I')$]; (a2) E° values obtained from solutions containing malonic or phthalic acid and strong acids, in the presence of alkali-metal or tetra-alkylammonium salt backgrounds (191 titrations, 32 titration groups, 159 data points); (a3) E° values obtained as for (a1) and (a2), in the simultaneous presence of two or three of the various background electrolytes (135 titrations, 27 titration groups, 108

data points); (b1) E° values obtained from some selected calibration curves from earlier work on the ionic-strength dependence of formation constants (366 titrations, 61 titration groups, 305 data points); (b2) as for b1, from some work on weak alkali-metal complexes (257 titrations, 47 titration groups, 210 data points). Therefore, 1100 data points in total were taken into account.

The calculations were done in the following ways: (c1) by taking into account groups (a1) . . . (b2) separately; (c2) by considering M^+ (alkali-metal and tetra-alkylammonium cations) and M^{2+} (alkaline-earth cations) separately; (c3) by taking into account groups (a1) . . . (b2) all together; (c4) by considering some backgrounds separately. In all cases equation (8) was found to fit the data quite satisfactorily and first-degree coefficients were sufficient for taking into account the dependence of the parameters C and D on temperature [equations (9) and (10)]. In the (c1) calculations, no significant differences could be observed among various (a1) . . . (b2) groups. In the (c3) calculations, a fairly good fit was obtained for all the data. Nevertheless, the (c2) and (c4) calculations revealed some significant differences. These differences can be attributed to three factors: (f1) different experimental errors (different purity of various salts); (f2) different degrees of dissociation of the different background electrolytes; (f3) specificity of $\log f_{\text{H}}$ in different backgrounds. Factor (f1) is not important, because in the worst case it can account for only 0.2–0.5% of the total difference. Factor (f2) must be important however. In fact, it is known that many salts used as background electrolytes in this

Table 1. Proton activity coefficients, calculated in different ways, at various temperatures and ionic strengths

I	f_{H}^a	f_{H}^b	f_{H}^c	f_{H}^d	f_{H}^e	f_{H}^a	f_{H}^b	f_{H}^c	f_{H}^d	f_{H}^e
	$t = 10^\circ$					$t = 25^\circ$				
0.01	0.912	0.911	0.912	0.913	0.912	0.911	0.910	0.911	0.912	0.911,
0.04	0.864	0.859	0.864	0.867	0.865	0.861	0.858	0.861	0.864	0.862
0.09	0.843	0.832	0.842	0.849	0.845	0.836	0.829	0.836	0.843	0.839
0.16	0.840	0.821	0.838	0.852	0.844	0.830	0.817	0.830	0.842	0.835
0.25	0.853	0.823	0.850	0.871	0.859	0.837	0.818	0.837	0.857	0.846
0.36	0.877	0.833	0.873	0.905	0.887	0.857	0.828	0.857	0.886	0.870
0.49	0.912	0.850	0.906	0.952	0.926	0.886	0.846	0.886	0.928	0.904
0.64	0.955	0.871	0.946	1.01	0.974	0.923	0.869	0.923	0.981	0.948
0.81	1.00	0.894	0.993	1.08	1.03	0.968	0.897	0.968	1.04	1.00
1.00	1.06	0.917	1.04	1.15	1.09	1.02	0.927	1.02	1.12	1.06
	$t = 37^\circ$					$t = 45^\circ$				
0.01	0.910	0.910	0.910,	0.911	0.911	0.910	0.910	0.910	0.911	0.910
0.04	0.858	0.856	0.859	0.862	0.860	0.857	0.855	0.857	0.860	0.858
0.09	0.831	0.827	0.832	0.838	0.834,	0.827	0.825	0.829	0.835	0.832
0.16	0.821	0.814	0.823	0.834	0.828	0.816	0.812	0.818	0.829	0.823
0.25	0.825	0.814	0.828	0.846	0.836	0.817	0.811	0.821	0.839	0.829
0.36	0.841	0.824	0.844	0.871	0.856	0.830	0.821	0.836	0.862	0.847
0.49	0.866	0.842	0.870	0.909	0.887	0.852	0.840	0.860	0.897	0.876
0.64	0.899	0.868	0.906	0.959	0.928	0.883	0.867	0.894	0.944	0.915
0.81	0.940	0.899	0.949	1.02	0.979	0.922	0.900	0.936	1.00	0.964
1.00	0.988	0.934	0.999	1.09	1.04	0.968	0.940	0.986	1.07	1.02

^a(c3) calculations.

^b(c4) calculations (KNO₃ + KCl).

^c(c2) calculations (M⁺), with correction for ion-pair formation.

^d(c2) calculations (M²⁺), with correction for ion-pair formation.

^e(c3) calculations, with correction for ion-pair formation.

Table 2. Proton activity coefficients, calculated from the data in previous work, at various temperatures and ionic strengths

$t = 10^\circ$									
I	f_H^a	f_H^b	f_H^c	f_H^d	f_H^e	f_H^f	\bar{f}_H^g		
0.01	0.913	0.913	0.912	0.912	0.912	0.912	0.912		
0.04	0.866	0.866	0.864	0.864	0.863	0.865	0.864 ₅		
0.09	0.847	0.847	0.842	0.843	0.841	0.845	0.844		
0.16	0.847	0.849	0.840	0.842	0.839	0.845	0.843		
0.25	0.864	0.868	0.853	0.856	0.852	0.861	0.857		
0.36	0.893	0.901	0.878	0.882	0.878	0.891	0.885		
0.49	0.933	0.947	0.913	0.920	0.915	0.933	0.923 ₅		
0.64	0.982	1.00	0.957	0.967	0.963	0.986	0.972		
0.81	1.04	1.07	1.01	1.02	1.02	1.05	1.03		
1.00	1.10	1.15	1.07	1.08	1.09	1.12	1.09 ₅		
$t = 25^\circ$									
I	f_H^h	f_H^a	f_H^b	f_H^i	f_H^c	f_H^d	f_H^e	f_H^f	\bar{f}_H^g
0.01	0.911	0.912	0.911	0.912	0.911	0.911	0.911	0.912	0.911 ₅
0.04	0.861	0.865	0.861	0.863	0.860	0.862	0.862	0.863	0.862
0.09	0.836	0.844	0.838	0.840	0.835	0.838	0.838	0.840	0.839
0.16	0.830	0.844	0.833	0.837	0.828	0.834	0.834	0.837	0.834 ₅
0.25	0.838	0.859	0.843	0.850	0.834	0.844	0.845	0.849	0.845
0.36	0.859	0.887	0.866	0.877	0.852	0.867	0.868	0.875	0.869
0.49	0.890	0.927	0.900	0.915	0.880	0.900	0.903	0.912	0.903
0.64	0.930	0.977	0.944	0.965	0.915	0.943	0.948	0.959	0.947
0.81	0.979	1.03	0.997	1.03	0.957	0.994	1.00	1.02	1.00
1.00	1.04	1.10	1.06	1.10	1.00 ₅	1.05	1.07	1.08	1.06
$t = 37^\circ$									
I	f_H^l	f_H^m	f_H^a	f_H^b	f_H^c	f_H^dG	f_H^e	f_H^f	\bar{f}_H^g
0.01	0.912	0.911	0.912	0.911	0.910	0.911	0.911	0.911	0.911
0.04	0.863	0.862	0.864	0.860	0.857	0.860	0.861	0.861	0.860
0.09	0.840	0.838	0.842	0.835	0.829	0.835	0.836	0.836	0.835
0.16	0.837	0.833	0.841	0.828	0.818	0.827	0.830	0.830	0.828
0.25	0.848	0.844	0.855	0.837	0.820	0.835	0.839	0.840	0.836
0.36	0.873	0.867	0.882	0.858	0.833	0.854	0.861	0.862	0.856
0.49	0.909	0.901	0.922	0.891	0.854	0.884	0.894	0.895	0.887
0.64	0.955	0.945	0.972	0.934	0.883	0.924	0.937	0.939	0.928
0.81	1.01	0.999	1.03	0.988	0.918	0.971	0.990	0.992	0.978
1.00	1.07	1.06	1.10	1.05	0.959	1.03	1.05	1.05	1.03 ₅
$t = 45^\circ$									
I	f_H^a	f_H^b	f_H^c	f_H^d	f_H^e	f_H^f	\bar{f}_H^g		
0.01	0.912	0.910	0.910	0.911	0.911	0.911	0.910 ₅		
0.04	0.863	0.858	0.856	0.859	0.860	0.860	0.859		
0.09	0.841	0.831	0.825	0.832	0.834	0.834	0.832		
0.16	0.839	0.822	0.812	0.823	0.827	0.826	0.824		
0.25	0.852	0.828	0.811	0.829	0.835	0.833	0.830		
0.36	0.879	0.846	0.820	0.846	0.856	0.853	0.848		
0.49	0.919	0.875	0.838	0.874	0.887	0.884	0.877		
0.64	0.969	0.914	0.863	0.911	0.929	0.925	0.915		
0.81	1.03	0.964	0.893	0.957	0.981	0.976	0.962 ₅		
1.00	1.10	1.02	0.929	1.01	1.04	1.04	1.02		

^aRef. 13; ^bRef. 11; ^cRef. 26; ^dRef. 26 (with calculations performed also on data of preceding works); ^eRef. 32; ^fRef. 35; ^gmean values; ^hRef. 34; ⁱRef. 15; ^lRef. 10; ^mRef. 12.

Table 3. Recommended f_H values at $10 \leq t \leq 45^\circ\text{C}$ and $0.01 \leq I \leq 1M$

I	f_H^*			
	10°	25°	37°	45°
0.01	0.912 ± 0.004	$0.911_5 \pm 0.003$	0.910 ± 0.003	0.910 ± 0.004
0.04	0.865 ± 0.006	0.862 ± 0.005	0.860 ± 0.005	0.859 ± 0.006
0.09	0.844 ± 0.007	0.839 ± 0.006	0.835 ± 0.007	0.832 ± 0.007
0.16	0.844 ± 0.009	0.835 ± 0.008	0.828 ± 0.009	0.823 ± 0.009
0.25	0.858 ± 0.010	0.846 ± 0.009	0.836 ± 0.010	0.829 ± 0.011
0.36	0.886 ± 0.011	0.869 ± 0.010	0.856 ± 0.011	0.848 ± 0.012
0.49	0.924 ± 0.013	0.904 ± 0.012	$0.887_5 \pm 0.012$	0.877 ± 0.013
0.64	0.972 ± 0.015	0.948 ± 0.013	0.929 ± 0.015	0.916 ± 0.016
0.81	1.03 ± 0.017	1.00 ± 0.015	0.979 ± 0.017	0.965 ± 0.018
1.00	1.09 ± 0.02	1.06 ± 0.017	1.04 ± 0.02	1.02 ± 0.03

* \pm Standard deviations.

work are not completely dissociated. In particular, potassium nitrate, among the alkali metal salts, forms a comparatively stable ion-pair (in 1M KNO₃, ~30% of the salt is associated). We repeated all the calculations, taking into account ion-pair formation for several alkali- and alkaline-earth metal salts.* With these corrections the more relevant differences disappeared or, at least, were minimized. Therefore, the residual differences can be attributed to factor (f₃). In Table 1 we report some details of the calculations. As can be seen, the proton activity coefficient in KNO₃ + KCl solutions (second column) are markedly lower than the mean values (first column), and the mean values calculated by taking into account ion-pair formation (last column) are considerably higher than the mean values. Moreover, the f_H values calculated for M⁺ and M²⁺ solutions (third and fourth columns) are slightly different (2.4% at $I = 0.25M$; ~10% at $I = 1M$). Errors in both the formation constants of the ion-pairs (we think a slight overestimate of the stability of some M²⁺ ion-pairs is probable) and the specificity factors can account for these differences; therefore we consider these differences as the limit of our approach to the determination of f_H values.†

Finally, we must estimate the errors in E° by equation (11). If we consider the probable errors in the variables‡ that can affect E° values, we can estimate $\sigma(E^\circ) = 0.15\text{--}0.30$ mV and $\sigma(f_H) = 0.5\text{--}1.5\%$. These errors are significantly lower than the differences in f_H discussed above.

As already mentioned, in some previous works we studied systematically the ionic-strength dependence of formation constants for several types of complexes. We reanalysed some of the data^{10-13,26,32,34,35} in order to find the activity coefficients of singly charged species and then of f_H . In Table 2 we report some of the results. Comparison of the last column f_H values in Table 1 with the last column f_H values in Table 2 (mean values) shows surprisingly good agreement. Therefore, we calculated new averages, reported in Table 3, as recommended f_H values. These values are described by the general equation

$$\begin{aligned} \log f_H = & -\sqrt{I}/(2 + 3\sqrt{I}) \\ & + [(0.335 - 2.3 \times 10^{-3}(t - 25))]I \\ & + [-0.109 + 1.8 \times 10^{-3}(t - 25)]I^{3/2} \end{aligned}$$

*The formation constants for ion-pair formation were taken from the literature.⁴²⁻⁴⁵ For NaCl, KCl, MgCl₂ and CaCl₂, some of us have recently performed a careful analysis of literature data⁴¹ and obtained fairly accurate values of the ion-pair stability constants. The lithium and tetra-alkylammonium salts were considered to be completely dissociated.

†To be correct, the limit of the equation used should also be taken into account. In fact, the simplifications (and assumptions) $A \sim 0.5$ and $dA = 1.5$ [equation (4)] can bias the f_H values, especially at low I values.

‡The following errors were considered: in E , 0.1–0.2 mV; in I , 0.1%; in t , 0.05–0.2°; in the concentrations of reagents, 0.1–0.2%.

$$= g_T(I). \quad (12)$$

The estimated errors (reported in Table 3, as standard deviations) range, at 25°, between 0.3 and 1.6% and are slightly higher at the other temperatures. These errors (but it would be better to call them variabilities, because they reflect specific different effects, rather than experimental and/or model errors) are sufficiently low to allow f_H , calculated by equation (12), to be used in several fields of solution chemistry. Some examples are as follows. If during a potentiometric titration there is variation of ionic strength, the E° value, calculated by separate calibration at a certain ionic strength I' , can be corrected, for a point with $I \neq I'$ by the equation

$$\begin{aligned} E^\circ(I) = E^\circ(I') + \frac{RT}{F} \left[\frac{-\sqrt{I}}{2 + 3\sqrt{I}} + \frac{\sqrt{I'}}{2 + 3\sqrt{I'}} \right. \\ \left. + C_T(I - I') + D_T(I^{3/2} - I'^{3/2}) \right] \\ = E^\circ(I') + j[g_T(I, I')] \end{aligned} \quad (13)$$

where $C_T = 0.335 - 2.3 \times 10^{-3}(t - 25)$ and $D_T = -0.109 + 1.8 \times 10^{-3}(t - 25)$. Equation (13) can be inserted in computer programs for the calculation of protonation constants and complex formation constants, such as MINIQUAD,⁴⁶ ACBA³⁸ or SUPERQUAD.⁴⁷ The same holds for calibrations with pH buffers:

$$\text{pH}(I) = \text{pH}(I') + g_T(I, I') \quad (14)$$

Many protonation constants have been reported in the literature as mixed constants

$$K_j^{\text{mixed}} = c_{H,A}/c_A a_H^j$$

related to concentration constants by the equations

$$\begin{aligned} K_j^{\text{mixed}} = K_j^{\text{conc}}/f_H^j \\ \log K_j^{\text{conc}} = \log K_j^{\text{mixed}} - j[g_T(I)] \end{aligned} \quad (15)$$

The errors associated with the use of equations (13)–(15) can be deduced from the errors in f_H reported in Table 3. For example, in the case of equation (15), we have $\sigma(\log K_j^{\text{conc}}) = j\sigma(\log f_H) = 0.43 j\sigma(f_H)/f_H$.

Acknowledgements—We thank CNR (Rome) and Ministero della Pubblica Istruzione for financial support, and Prof. C. Rigano for his helpful aid in calculations.

REFERENCES

1. J. N. Brønsted, *J. Am. Chem. Soc.*, 1922, **44**, 877; *Trans. Faraday Soc.*, 1927, **23**, 416.
2. E. A. Guggenheim, *Phil. Mag.*, 1935, **19**, 588; 1936, **22**, 322.
3. N. Bjerrum, *Trans. Faraday Soc.*, 1927, **23**, 433.
4. C. W. Davies, *Ion Association*, Butterworths, London, 1962.
5. R. M. Garrels and M. E. Thompson, *Am. J. Sci.*, 1962, **260**, 57.
6. D. A. MacInnes, *J. Am. Chem. Soc.*, 1919, **41**, 1086.
7. R. G. Bates, B. R. Staples and R. A. Robinson, *Anal. Chem.*, 1970, **42**, 867.

8. R. F. Platford, *J. Fish. Res. Bd. Can.*, 1965, **22**, 885; *J. Mar. Res.*, 1965, **23**, 55; R. F. Platford and T. Defoe, *ibid.*, 1965, **23**, 63.
9. F. J. C. Rossotti and H. Rossotti, *The Determination of Stability Constants*, McGraw-Hill, New York, 1961.
10. P. G. Daniele, C. Rigano and S. Sammartano, *Talanta*, 1983, **30**, 81.
11. S. Capone, A. De Robertis, C. De Stefano, S. Sammartano, R. Scarcella and C. Rigano, *Thermochim. Acta*, 1985, **86**, 273.
12. P. G. Daniele, C. Rigano and S. Sammartano, *Transition Met. Chem.*, 1982, **7**, 109.
13. P. G. Daniele, G. Ostacoli, C. Rigano and S. Sammartano, *ibid.*, 1984, **9**, 385.
14. P. G. Daniele, C. Rigano and S. Sammartano, *Talanta*, 1985, **32**, 78.
15. P. G. Daniele, A. De Robertis, C. Rigano and S. Sammartano, *Ann. Chim. (Rome)*, 1985, **75**, 115.
16. P. G. Daniele, C. Rigano and S. Sammartano, *ibid.*, 1980, **70**, 119; V. Cucinotta, P. G. Daniele, C. Rigano and S. Sammartano, *Inorg. Chim. Acta*, 1981, **56**, L45.
17. P. Amico, P. G. Daniele, C. Rigano and S. Sammartano, *Ann. Chim. (Rome)*, 1982, **72**, 1.
18. P. G. Daniele, A. De Robertis, C. De Stefano, C. Rigano and S. Sammartano, *ibid.*, 1983, **73**, 619.
19. P. G. Daniele, C. Rigano and S. Sammartano, *Thermochim. Acta*, 1981, **46**, 103.
20. *Idem, ibid.*, 1983, **62**, 101.
21. P. G. Daniele, A. De Robertis, S. Sammartano and C. Rigano, *ibid.*, 1984, **72**, 305.
22. A. De Robertis, C. De Stefano, R. Scarcella and C. Rigano, *ibid.*, 1984, **80**, 197.
23. A. De Robertis, C. De Stefano, C. Rigano, S. Sammartano and R. Scarcella, *J. Chem. Res.*, 1985, (S) 42, (M) 0629.
24. A. Casale, A. De Robertis and S. Sammartano, *Thermochim. Acta*, 1985, **95**, 15.
25. G. Arena, S. Musumeci, R. Purrello and S. Sammartano, *ibid.*, 1983, **61**, 129.
26. P. G. Daniele, C. Rigano and S. Sammartano, *Anal. Chem.*, 1985, **57**, 2956.
27. *Idem, Inorg. Chim. Acta*, 1982, **63**, 267.
28. *Idem, Ann. Chim. (Rome)*, 1982, **72**, 341; P. G. Daniele, M. Grasso, C. Rigano and S. Sammartano, *ibid.*, 1983, **73**, 495.
29. A. De Robertis, C. De Stefano, S. Sammartano, R. Cali, R. Purrello and C. Rigano, *J. Chem. Res.*, 1986, (S) 164, (M) 1301.
30. S. Capone, A. De Robertis, C. Rigano and S. Sammartano, *Thermochim. Acta*, 1986, **102**, 1.
31. S. Capone, A. De Robertis, C. De Stefano and R. Scarcella, *Talanta*, 1985, **32**, 675.
32. P. G. Daniele, A. De Robertis, C. De Stefano, C. Rigano and S. Sammartano, *J. Chem. Soc., Dalton Trans.*, 1985, 2353.
33. P. G. Daniele, S. Sonego, M. Ronzani and M. Marangella, *Ann. Chim. (Rome)*, 1985, **75**, 245.
34. P. G. Daniele, C. Rigano and S. Sammartano, *ibid.*, 1983, **73**, 741.
35. A. De Robertis, C. De Stefano, C. Rigano and S. Sammartano, *J. Chem. Res.*, 1986, (S) 194.
36. D. D. Perrin, W. L. F. Armarego and D. R. Perrin, *Purification of Laboratory Chemicals*, Pergamon Press, Oxford, 1966.
37. A. I. Vogel, *Quantitative Inorganic Analysis*, Longmans, London, 1955.
38. G. Arena, E. Rizzarelli, S. Sammartano and C. Rigano, *Talanta*, 1979, **26**, 1.
39. C. Rigano, M. Grasso and S. Sammartano, *Ann. Chim. (Rome)*, 1984, **74**, 537.
40. C. De Stefano, P. Princi, C. Rigano and S. Sammartano, *ibid.*, in press.
41. A. De Robertis, C. Rigano, S. Sammartano and O. Zerbinati, *Thermochim. Acta*, in press.
42. L. G. Sillén and A. E. Martell, *Stability Constants*, Chem. Soc. Special Publication No. 17, The Chemical Society, London, 1964; *Supplement No. 1*, Special Publication No. 25, London, 1971.
43. E. Högfeldt, *Stability Constants of Metal-Ion Complexes, Part A: Inorganic Ligands*, Pergamon Press, Oxford, 1982.
44. R. M. Smith and A. E. Martell, *Critical Stability Constants, Vol. 4, Inorganic Complexes*, Plenum Press, New York, 1976.
45. B. E. Conway, *Electrochemical Data*, Elsevier, Amsterdam, 1952.
46. A. Sabatini, A. Vacca and P. Gans, *Talanta*, 1974, **21**, 53.
47. P. Gans, A. Sabatini and A. Vacca, *J. Chem. Soc., Dalton Trans.*, 1985, 1195.

SOFTWARE SURVEY SECTION

Software package TAL-001-87

STATSTREAM

Contributor: Dr. A. Bangham, University of East Anglia, Norwich, Norfolk.

Brief description: STATSTREAM is a versatile and powerful tool for numerical analysis of data. It is invaluable to scientists, and can assist in the teaching of students. It can use pre-existing Apple files or Visicalc files. The program has 76 procedures including: enter and edit data, draw and annotate graphs, open or close text window, display disk file data, find the mean of a column of data, statistical tests, fit a non-linear function to data, generate pseudodata, etc. These can be used very simply by:

1. Calling the user-friendly menu-driven Statpack, which enables a variety of parametric and non-parametric tests to be performed after a single entry of data.
2. By using the 32 demonstration programs designed to teach the user all about statistics and fitting functions to data.
3. Writing straightforward BASIC programs to incorporate the desired procedures. Command procedures include: mean, standard deviation, standard error and confidence interval, Student's t test, ANOVA 1- and 2-way, F test, linear regression, correlation; chi-squared test, contingency tables; median, non-parametric confidence interval; sign test; Wilcoxon signed ranks test, Mann-Whitney, Kruskal-Wallis, Friedman t-test, F test; pseudodata generators for Gaussian, skewed noise etc.; minimization routines for non-linear function fitting and solving equations. Other command procedures can be added.

Potential users: Beginner to statistics and computing to professional statistician or research worker; teachers.

Fields of interest: Statistics and sciences.

This application and utility package has been written in (structured) BASIC for the Apple II microcomputer, to run under DOS 3.3. It is available on single-sided double density 5.25-in floppy disc. The memory required is 48K.

Distributed by Elsevier-Biosoft, 68 Hills Road, Cambridge, CB2 1LA, UK. Price US \$140, UK £80.

The minimum hardware configuration is a 48K Apple II. The program is easy to use, and there is extensive external documentation. The source code is available.

The package has been fully operational for 18 months, and is currently in use at around 200 sites. The distributor is willing to deal with user enquiries.

Software package TAL-002-87

TADPOLE

Contributor: Dr. T.H. Caradoc-Davies, Otago Hospital Board, Dunedin, New Zealand.

Brief description: TADPOLE is an easy-to-use general purpose numeric database management program with a built-in statistics package. Data files can contain up to 9999 records each with up to 60 fields, and each field can contain a real number with up to 6 significant figures. Data files can be up to 320K in size on a floppy disc and much larger on a hard disc. Statistics files can be either created by sorting selected fields from a data file or entered directly from the keyboard. TADPOLE can convert printout files from LOTUS 1-2-3 into either data or statistics file format for advanced analysis. Statistical tests available in TADPOLE include descriptive statistics such as means, standard errors, skewness, kurtosis,

median, frequency analysis including bar diagrams; parametric statistics such as Student's t, linear regression and ANOVA for equal and unequal groups; and non-parametric statistics such as contingency tables, chi-squared 2 x 2 and N x K, Fisher's exact test, McNemar's test, Mann Whitney U test, Wilcoxon signed-ranks matched-pairs test, Spearman's rank correlation test, and many more. The TADPOLE manual contains explanations of all the statistical procedures together with guidance on when a particular test is appropriate. To complement the explanations, the manual also contains examples and exercises on the different procedures.

Potential users: Students and research workers needing to use numeric database and statistics.

Fields of interest: Statistics, quantitative sciences.

This application program has been developed in BASIC for the IBM PC, XT, to run under DOS 1.1 or later. It is available on double-sided 5.25-in floppy disc. The memory required is 128K.

Distributed by Elsevier-Biosoft, 68 Hills Road, Cambridge, CB2 1LA, UK. Price US \$140, UK £80.

TADPOLE runs on an IBM PC with one or two disc drives, and on the XT. It is easy to use, with menus and screen based data entry, and it has a detailed instruction manual. The source code is available.

The package is fully operational, and has been used for about 16 months at over 200 sites. The distributor is willing to deal with user enquiries.

Software package TAL-003-87

MOLGRAF

Contributor: Dr. R.B. Barlow, University of Bristol, Bristol, and C. O'Donnell, Elsevier-Biosoft.

Brief description: MOLGRAF is a comprehensive package that can display, examine and experiment with three-dimensional maps of chemical compounds. It is suitable for teaching and research purposes wherever it is desirable to visualize a molecular structure. MOLGRAF includes all the basic features one expects: entry of new compounds using crystallographic co-ordinates and saving the data to disc; the ability to check, add, delete and correct data; calculation of bond lengths, bond angles and torsion angles. It also provides on disc the data for more than 200 compounds, including many common pharmaceuticals. Structures are displayed in high resolution graphics, and they may be rotated, expanded and moved across the screen. The images may be printed or plotted. Different compounds may be superimposed. MOLGRAF includes a routine called LECTURE which displays a sequence of images prepared in advance by the user, to illustrate a talk or presentation. The user can also build compounds by specifying only atom names, bond lengths, bond angles and torsion angles. The co-ordinates are calculated by the program.

Potential users: All kinds of chemists, pharmacologists, biochemists.

Fields of interest: Crystallography, study of 3-dimensional structures.

This application program in the area of molecular graphics has been developed in BASIC to run under PC-DOS 2.1 on the IBM PC, or DOS 3.3 on the Apple II series. It is available on 5.25-in floppy discs. The memory required is 256K (IBM) or 64K (Apple). The IBM requires a colour graphics card.

Distributed by Elsevier-Biosoft, 68 Hills Road, Cambridge, CB2 1LA, UK. Price US \$140, UK £80.

MOLGRAF is easy to operate, with a logical menu-driven program design, and clear data entry and editing procedures. There is an extensive user manual. The source code is not available.

The package has been fully operational for about 3 months, currently at 25 sites. The distributor is willing to deal with user enquiries.

Software package TAL-004-87

REFSYS

Contributor: J. Vickers, Dept. of Pathology, McMaster University, Canada.

Brief description: REFSYS is designed to store bibliographic references, and to provide a means of recalling and printing selected lists of the references in specified formats. REFSYS therefore enables the user to create a personal database of the literature references which he or she cites most frequently. It also provides a means of cross-referencing the references by subject categories. The modules include: Update - for the initial entry of the reference, for classifying the papers, for cross-referencing and for choosing authors for indexing; Print - for printing reference lists (all stored references or a selected list identified by their citations can be printed); Xref - for the cross-referencing of stored papers. It can handle up to 10000 papers with 100 categories.

Potential users: Scientists.

Fields of interest: Bibliographic storage and cross-referencing.

This application program has been developed in Turbo-Pascal for the IBM PC, to run under PC DOS 2.0 or later. It is available on 5.25-in floppy disc. The memory required is 256K minimum.

Distributed by Elsevier-Biosoft, 68 Hills Road, Cambridge, CB2 1LA, UK. Price US \$120 UK £70.

The minimum hardware configuration is an IBM PC or true compatible with one 360K floppy disc drive. A system with two floppy drives or a hard disc is recommended, however, because it will prove more flexible and have greater capacity. There is extensive external documentation. The source code is not available.

The package has been fully operational for 2 months, and is running at 5 sites. The contributor is not available for user enquiries.

Software package TAL-005-87

REFSCAN

Contributor: J. Vickers, McMaster University, Dept. of Pathology, Ontario, Canada; and H.L. Nelson, Millgrove, Ontario, Canada.

Brief description: REFSCAN is a supplementary program to REFSYS (TAL-004-87). The program scans through reference files and identifies all references which contain specified words, phrases, parts of words, numbers, or sequences of characters and numbers. Entire references are searched and information from the titles or lists of authors can be sought. REFSCAN stores the citation from each selected reference in a citation list file, which may then be reviewed by REFSYS and printed using any of the REFSYS formatting options. Refscan can also create, on printer or disc, a short list, which consists of a one-line summary of each selected reference, containing only the access number, part of the citation, the journal, page number and year. Optionally, each reference may be reviewed on screen as it is found, and it may then be included in or excluded from the citation list.

Potentials users: Scientists.

Fields of interest: Bibliographic storage etc.

This application program for the IBM PC or TI Professional is written in Turbo-Pascal to run under PC DOS 2.0 or later. It is available on 5.25-in floppy disc. The memory required is 256K minimum.

Distributed by Elsevier-Biosoft, 68 Hills Road, Cambridge, CB2 1LA, UK.

The minimum hardware configuration is an IBM PC or true compatible with one floppy disc drive (360K), or a TI Professional. There is extensive external documentation. The source code is not available.

The package has been fully operational for 1 month, at 5 sites. the contributor is not available for user enquiries.

Software package TAL-006-87

DADISP

Contributor: Elsevier-Biosoft.

Brief Description: DADISP is a powerful package for displaying and processing digital waveforms. It functions as the scientist's equivalent of a business spreadsheet. It can accept data in a wide variety of formats, including ASCII, Lotus PRN, 8-bit byte, 16-bit integer and IEEE 32-bit floating point. Data are displayed graphically on screen through up to 64 windows. DADISP can process data with more than 150 functions, including fast Fourier transforms, wave-form generation, statistical analyses, signal arithmetic and calculus, peak analysis, complex arithmetic, signal cursoring and editing, "signal spreadsheet" operations, etc. It supports user-defined functions through its macro definition facility, and it has command files for automating data analysis. It is capable of virtual signal management. DADISP window displays and menu-driven format make it exceptionally easy to use. A chain of processing steps is set up simply by typing in formulae; the results of each step are displayed in sequence, window by window. New data can be loaded into windows for instant re-evaluation of the worksheet. Worksheets can be saved, reloaded and applied to new tasks, enabling the user to build up a library of analysis templates. DADISP supports nine types of printer for hard copy output.

Potential users: Scientists, engineers.

Fields of interest: Analysis of waveforms in any discipline.

This application program in the field of data analysis has been developed to run on the IBM PC, XT, AT and compatibles, to run under DOS 2.0 or later, and is available on 5.25-in floppy disc. The memory required is 512K.

Distributed by Elsevier-Biosoft, 68 Hills Road, Cambridge, CB2 1LA, UK. Price US \$795, UK £550.

The minimum hardware configuration is a PC with an IBM colour graphics adaptor or IBM enhanced graphics adaptor or Hercules monochrome adaptor. An 8087 or 80287 co-processor is optional (automatically detected), as is a printer.

The program is easy to use; there is extensive external documentation. The package is fully operational. The distributor is willing to deal with user enquiries.

Software package TAL-007-87

MULTI-Q

Contributor: Z. Kruk, London Hospitals Medical College, Dept. of Pharmacology and Therapeutics, London, UK; and S. Day, Elsevier-Biosoft.

Brief description: MULTI-Q is a system for creating and presenting multiple choice tests on any topic. Questions can be entered and edited by using MULTI-Q or word-processing packages. A revision feedback option and a student scoring facility are included in the package. Questions consist of a stem with up to 9 true or false options depending on it. Besides a true or false answer, each option can have up to 9 lines (about 80 words) of feedback to provide further information, explanation, references etc. Each question is stored on disc with a unique name. MULTI-Q test papers consist of up to 50 questions selected from the whole range available, allowing complete flexibility in the range of knowledge tested. Optionally associated with each paper is an 'acceptable' score and comments relating to the paper as a whole. The question list, score and comments can all be edited in MULTI-Q or by a word-processor. Test papers are stored on disc along with the relevant questions. MULTI-Q can present the questions from a selected test paper either with feedback or without. At the end of the paper, the student's score is calculated and stored on disc, and displayed on screen together with the comments on the paper.

Potential users: Secondary- and tertiary-level teachers.

Fields of interest: General teaching.

This program is available in compiled BASIC for the IBM PC and the Apple II, to run under DOS 2.0 or later. It is available on 5.25-in floppy discs. The minimum memory required is 48K.

Distributed by Elsevier-Biosoft, 68 Hills Road, Cambridge, CB2 1LA, UK.

The program is easy to use and has menus and informative screen prompts for guidance. There is extensive external documentation. The source code is not available. The package will be available in early 1987; the contributor is not available for user enquiries.

Software package TAL-008-87

KINETIC EBDA LIGAND LOWRY

Contributor: G.A. McPherson, Dept. of Pharmacy, University of Vermont, Burlington, USA.

Brief description: KINETIC calculates association and dissociation rate constants for radioligands by using a weighted non-linear iterative curve-fitting technique. EBDA and LIGAND are for analysing equilibrium studies. EBDA performs the preliminary analysis of both saturation and competition studies, including conversion of dpm into concentrations, graphical transformation of data to provide initial estimates required by LIGAND and a number of other data analysis functions. LIGAND then uses disk files created by EBDA to obtain final parameter estimates by use of weighted non-linear curve-fitting techniques. LOWRY calculates protein concentrations measured by the standard technique of Lowry et al. A hyperbolic equation is used to fit the standard curve and calculate concentrations of unknown samples.

Potential users: Analytical chemists, biochemists, clinical chemists.

Fields of interest: Ligand binding analysis.

This application program has been developed in BASIC for the IBM PC to run under DOS 2.0 or later. It is available on 5.25-in double-sided floppy discs. The memory required is 256K.

Distributed by Elsevier-Biosoft, 68 Hills Road, Cambridge, CB2 1LA, UK. Price US \$140, UK £80.

The IBM PC requires a graphics card. The package is easy to use, and there is extensive external documentation. The source code is not available.

The software is fully operational, and has been in use for 2 months at about 30 sites. The contributor is not available for user enquiries.

Software package TAL-009/87

MKMODEL

Contributor: N. Holford, Dept. of Pharmacology, University of Auckland, New Zealand.

Brief description: MKMODEL contains a general non-linear regression program for use in pharmacokinetics, pharmacodynamics, ligand binding, and many other problems, and also a modelling worksheet for data transformation, descriptive statistics, and pharmacokinetic parameter estimation. There can be up to 25 parameters, 5 independent variables, 10 simultaneous data sets, and up to 100 total observations. There are: optional Bayesian parameter estimation, a choice of variance scale methods, and graphs with optional logarithmic axes and multiple curves. There is a facility for definition of models in BASIC. Non-linear regression avoids the biased and imprecise results obtained from linearizing transformations such as Lineweaver-Burke, Schild, Scatchard and Eadie-Hofstee plots. The extended least-squares method solves the problem of arbitrary weighting schemes required by ordinary least-squares methods to deal with real data. MKMODEL also features the DRUG library, which provides 15 models covering most common pharmacological data-analysis needs. Ligand binding experiments with one or two ligands and one or two binding sites can be characterized by law of mass action models. The modelling worksheet can be used to transform data, combine tables and obtain simple descriptive statistics.

Potential users: Biochemists, clinical chemists, pharmacologists.

Fields of interest: Pharmacology, biochemistry, kinetics.

This program has been developed in BASIC for the IBM PC to run under DOS 2.0 or later. It is available on 5.25-in floppy discs. The memory required is 128K minimum.

Distributed by Elsevier-Biosoft, 68 Hills Road, Cambridge, CB2 1LA, UK.

The IBM requires an IBM or Hercules graphics card. The program is extensively documented. The contributor is not available for user enquiries.

SPECTROPHOTOMETRIC DETERMINATION OF PARACETAMOL IN DRUG FORMULATIONS BY OXIDATION WITH POTASSIUM DICHROMATE

SALAH M. SULTAN

Chemistry Department, College of Science, King Saud University, Riyadh-11451, P.O. Box 2455,
Saudi Arabia

(Received 3 October 1986. Revised 4 February 1987. Accepted 13 February 1987)

Summary—A rapid spectrophotometric method for determination of paracetamol is described, based on oxidation with dichromate for 15 min in 6*M* sulphuric acid at 80°, and measurement (at 580 nm) of the chromium(III) formed. The method is applied to the determination of paracetamol in drugs prescribed for colds, coughs and flu. Of the common pharmaceuticals associated with paracetamol, only ascorbic acid and acetylsalicylic acid interfere. The results have been statistically compared with those obtained by the official (BP) and cerium(IV) methods.

Paracetamol (*N*-acetyl-*p*-aminophenol) is well known for its analgesic and antipyretic action. Several methods for its determination have been reported, including its assay in drug formulations. The majority of these are spectrophotometric,¹⁻¹⁵ most of which require lengthy treatments and lack suitability for routine analysis. For instance, the official pharmacopeia method¹⁶ requires a 60-min reflux period, and the recent cerium(IV) method¹⁷ requires heating of the reaction mixture for 90 min.

The present method is based on the oxidation of paracetamol by potassium dichromate in 6*M* sulphuric acid. It is simple, accurate and readily applied to the determination of paracetamol in drug formulations.

EXPERIMENTAL

Apparatus

Absorbance measurements were made with a Beckman model 35 spectrophotometer to which a Beckman model 24-25 ACC recorder was connected. Matched sets of W210/UU 10.00-mm cells were used throughout.

Reagents

Stock solutions were made from commercially available analytical or pharmaceutical grade chemicals and high-purity distilled water. Working solutions were prepared by appropriate dilution of the stock solutions. The 0.135*M* potassium dichromate solution was prepared in 12*M* sulphuric acid.

Paracetamol solution (1 mg/ml) was prepared from the pure crystalline powder made in the author's laboratory by the method described by Vogel.¹⁸ The material was checked by infrared and N.M.R. spectrometry and the melting point was found to comply with the B.P. requirements.¹⁶ The apparent purity was determined by the official method¹⁶ and found to be 100.7%. Paracetamol solutions (1 mg/ml) were also prepared from pharmaceutical-grade tablets and capsules. The pure stock solution was prepared by dissolving exactly 0.500 g in about 150 ml of warm water, stirring for 10 min and diluting to volume in a 500-ml standard flask after cooling. For assay of dosage forms, 10 tablets or capsules were mixed, crushed and carefully weighed. A

quantity of powder equivalent to 500 mg of paracetamol was weighed accurately and dissolved as described above. The solution was filtered through a Whatman No. 41 filter-paper, which was then washed with 20 ml of water, and the combined filtrate and washings were diluted to volume with water in a 500-ml standard flask after cooling to room temperature.

General procedure

Place 10.00 ml of potassium dichromate stock solution in a 50-ml standard flask. Add 15.0 ml of 12*M* sulphuric acid and the appropriate amount of paracetamol solution. Swirl the flask and its contents and dilute to the mark. Place the flask in a water-bath maintained at 80° and leave it there for 15 min. Cool under tap water, and measure the absorbance at 580 nm against a reagent blank treated similarly.

RESULTS AND DISCUSSION

Kinetics

In this method, potassium dichromate is used to oxidize paracetamol and the absorbance of the chromium(III) species produced, measured at 580 nm, is a measure of the paracetamol concentration. The optimum conditions were established by variation of such parameters as acid concentration, temperature and time of heating. The reaction is slow but can be accelerated by an increase in acid concentration as well as by heating. The effect of sulphuric acid concentration and time of heating at 80° are shown in Figs. 1 and 2 respectively; the general procedure was used but with 2.5 ml of dichromate solution instead of 10 ml. The spectral maxima at 580 and 430 nm are attributed to chromium(III) and chromium(VI) respectively, and there is a characteristic isosbestic point at 535 nm. Figure 1 shows that the chromium(III) absorbance increases as the acid concentration is increased; it reaches a maximum with 6*M* acid. Higher acidities do not result in greater absorbances. There is a small shift in λ_{\max} as the acid

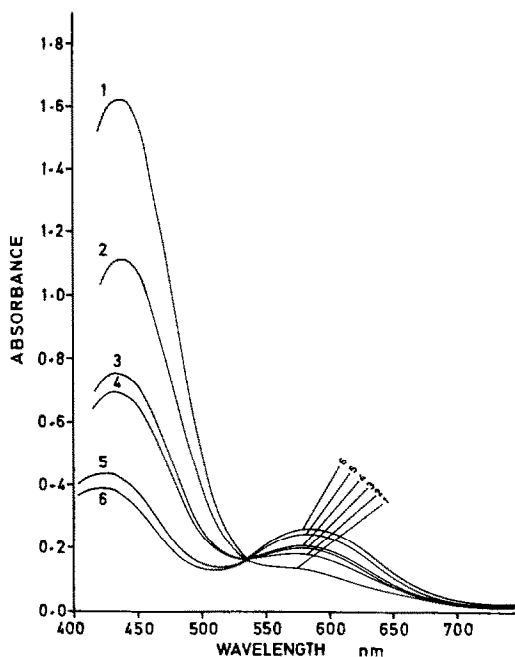


Fig. 1. Absorption spectra for reaction mixtures of 14 mg of paracetamol and 100 mg of potassium dichromate heated for 15 min at 80° in 50 ml of sulphuric acid of the molarity shown by the number by the curves.

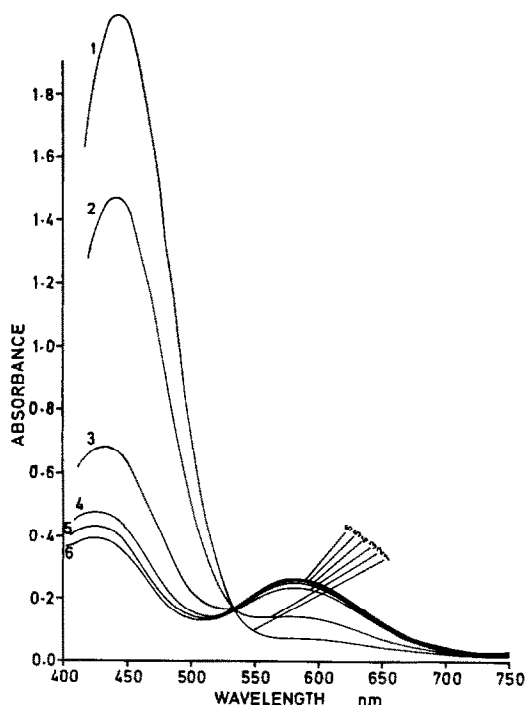
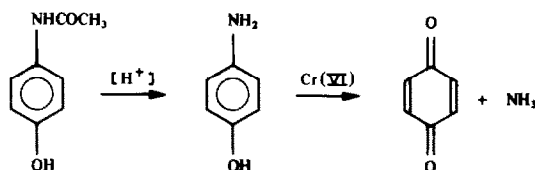


Fig. 2. Absorption spectra for a reaction mixture of 14 mg of paracetamol and 100 mg of potassium dichromate in 50 ml of 6M sulphuric acid heated at 80° for 0, 3, 6, 9, 12 and 15 min (curves 1, 2, 3, 4, 5, 6) before cooling and measurement.

concentration is increased. Figure 2 shows that the chromium(III) absorbance increases with heating time. The absorbance reaches a maximum after 15 min heating at 80°, and is stable thereafter for 48 hr. At higher temperatures there is a risk of unwanted chemical changes. The mechanism of paracetamol oxidation with dichromate is probably similar to that with cerium(IV):¹⁷ deacetylation to *p*-aminophenol in the first step, then oxidation to *p*-benzoquinone.



Analytical appraisal

Beer's law was found to be valid up to 400 $\mu\text{g/ml}$ paracetamol concentration in the final solution. The apparent molar absorptivity was 1620 $\text{l.mole}^{-1}.\text{cm}^{-1}$.

The method was applied to the determination of paracetamol in its pure form and in proprietary drugs supplied by different companies and containing other active ingredients as listed in Table 1. The results in Table 1 show that the method is successful for paracetamol determination and that excipients in the dosage forms do not interfere. Drugs such as phenylpropranolamine, phenyletoloxamine, phenylephrine, pheniramine, mepyramine, caffeine, codeine, noscapine, terpin, dimethindene maleate, ethenzamide, isometheptene mucate and octamylamine mucate displayed no interference when present with paracetamol. Ascorbic acid and acetylsalicylic acid caused a large positive error and gave rise to irreproducible results. This was manifested in analysis of Trimedil, Efferalgan, Prontopyrin and Veganin tablets. When ascorbic acid or acetylsalicylic acid was added to the dichromate reagent and left to react under the conditions of the experiment, a green colour absorbing at 580 nm was produced, not unexpectedly, confirming the reason for their interference being their reduction of the dichromate to chromium(III). Hydrochlorides should show positive interference because of oxidation of chloride by dichromate at the high acidity used; their apparent non-interference probably arises from the relatively small amounts present in the formulations tested.

A statistical comparison of paracetamol determination (in products containing neither ascorbic acid nor acetylsalicylic acid) by the dichromate method, official method¹⁶ and cerium(IV) method,¹⁷ for the same batch of material, is presented in Table 2. The student *t*-test values obtained indicate no significant difference between the three methods. The new method is simpler, quicker and more suitable for routine analysis.

Table 1. Results for determination of paracetamol in pharmaceutical products

Drug and supplier*	Nominal composition, mg	Paracetamol found, mg	Error, %
1 Paracetamol (laboratory made)	100 paracetamol (pure)	100.6	—
2 Paracetamol (Smith, France)	500 paracetamol	499	-0.2
3 Panadol (Winthrop, England)	500 paracetamol	499	-0.1
4 Triatussic (Wander, Switzerland)	200 paracetamol 5 mepyramine·HCl 4.2 pheniramine·HCl 12.5 phenylpropanolamine·HCl 20 noscipine 13 caffeine 90 terpin hydrate	200	+0.1
5 Trimedil (Zyma, Switzerland)	100 paracetamol 0.25 dimethindene maleate 15 <i>o</i> -(β -hydroxyethyl) rutoside 40 ascorbic acid 1.25 phenylephrine·HCl	125	+25.1
6 Efferalgan (Upsa, France)	330 paracetamol 200 ascorbic acid	425	+29.1
7 Sinutab (Warner, England)	200 paracetamol 25 phenylpropanolamine·HCl 22 phenyltoloxamine	297	-0.8
8 Revacod (The Arab Pharm. Manuf. Co., Jordan)	500 paracetamol 10 codeine phosphate	498	-0.4
9 Neopyrin-N (Knoll, Germany)	200 paracetamol 200 ethenzamide 10.72 isometheptene mucate 14.28 octamylamine mucate	198	-1.0
10 Veganin (Warner, England)	250 paracetamol 250 acetylsalicylic acid 6.8 codeine phosphate	469	+87.8
11 Prontopyrin (Mack, Germany)	200 paracetamol 250 aluminium acetylsalicylate 50 caffeine	222	+11.3
12 Revanin (The Arab Pharm. Manuf. Co., Jordan)	500 paracetamol	497	-0.4

*2-11 in tablet form; 12 in capsule form.

†Mean of 5 determinations; error calculated with reference to nominal content.

Table 2. Comparison of results for determination of paracetamol by the proposed method compared with the official method¹⁶ and the cerium(IV) method¹⁷

Drug name	Recovery*, %			<i>t</i> †
	Proposed method	Official method	Ceric sulphate method	
1 Paracetamol (laboratory made)	100.8 ± 0.4	100.7 ± 0.3	100.9 ± 0.6	0.61 0.84
2 Paracetamol (Smith)	99.9 ± 0.6	99.7 ± 0.7	100.1 ± 0.4	1.28 1.54
3 Panadol	99.8 ± 0.7	100.0 ± 0.6	101.0 ± 0.8	0.64 0.97
4 Triatussic	100.1 ± 0.6	100.2 ± 0.8	100.4 ± 0.6	0.35 0.98
5 Neopyrin	99.1 ± 0.7	98.9 ± 0.6	99.0 ± 0.3	0.86 0.44
6 Sinutab	99.2 ± 1.0	98.7 ± 0.4	98.9 ± 0.4	1.22 0.84
7 Revanin	99.6 ± 0.6	99.2 ± 0.2	99.1 ± 0.7	1.54 1.68
8 Revacod	99.6 ± 0.2	99.6 ± 0.3	99.8 ± 1.0	0.49 0.77

*Mean ± S.D. for 5 determinations, based on label claim.

†Theoretical value = 2.78 ($p = 0.05$).

Acknowledgements—The author thanks Mr. Yousif Asha for his technical assistance and the Research Center of the College of Science, King Saud University, for support.

REFERENCES

1. M. K. Srivastava, S. Ahmed, D. Singh and I. C. Shukla, *Analyst*, 1985, **110**, 735.
2. K. K. Verma, A. K. Gulati, S. Palod and P. Tyagi, *ibid.*, 1984, **109**, 735.
3. A. Z. D'Souza and K. G. Shenoy, *Can. J. Pharm. Sci.*, 1974, **36**, 47.
4. E. Kalatzis and I. Zarbi, *J. Pharm. Sci.*, 1976, **65**, 71.
5. M. C. Inamdar, M. S. Gore and R. V. Bhide, *Indian J. Pharm.*, 1974, **36**, 7.
6. C. T. Elcock and A. G. Fogg, *Analyst*, 1975, **100**, 16.
7. D. R. Davis, A. G. Fogg, D. T. Burns and J. S. Wragg, *ibid.*, 1974, **99**, 12.
8. S. F. Belal, M. A. H. Elsayed, A. Elwalily and H. Abdine, *ibid.*, 1979, **104**, 919.
9. M. A. H., Elsayed, S. F. Belal, A. Elwalily, and H. Abdine, *ibid.*, 1979, **104**, 620.
10. J. Wallace, *Anal. Chem.*, 1967, **39**, 531.
11. N. Elsayed, S. F. Belal, F. M. Abdel, and N. Abdine, *J. Assoc. Off. Anal. Chem.*, 1979, **62**, 549.
12. F. M. Plakogianis and A. M. Saad, *J. Pharm. Sci.*, 1975, **64**, 1547.
13. M. Mouton and M. Masson, *Ann. Pharm. Fr.*, 1960, **18**, 759.
14. R. M. Welch and A. H. Conney, *Clin. Chem.*, 1965, **11**, 1064.
15. J. B. Vaughan, *J. Pharm. Sci.*, 1969, **58**, 469.
16. *British Pharmacopeia 1980*, p. 326. H.M. Stationery Office, London, 1980.
17. S. M. Sultan, I. Z. Al Zamil, A. M. Aziz Alrahman, S. A. Altamrah and Y. Asha, *Analyst*, 1986, **111**, 919.
18. A. I. Vogel, *Elementary Practical Organic Chemistry*, Part 1, p. 242. Longmans, London, 1958.

DRUG DETERMINATION IN BIOLOGICAL FLUIDS—APPROACHES TO METHOD VALIDATION

ANIL C. MEHTA

Department of Pharmacy, The General Infirmary, Leeds, Yorkshire, England

(Received 16 July 1986. Revised 2 February 1987. Accepted 13 February 1987)

Summary—Procedures are described for the validation of analytical methods for the determination of drugs and metabolites in biological fluids.

The increasing emphasis on the pharmacokinetics, bioavailability, and therapeutic monitoring of drugs has placed a heavy burden on drug analysts. Reliable measurements of very low levels of drugs in complex matrices are frequently required. Because of the vast number of drugs already in use, and the increasing number of new drugs introduced every year, more and more methods for drugs and metabolite determination are being developed either for routine or research use. Most workers prefer chromatographic methods owing to their versatility, but immunoassays are also being developed, particularly for routine drug-monitoring. Existing methods often need major improvements to suit the requirements of the laboratory performing the assay. For evaluation of their suitability for producing reliable results, these methods must be thoroughly validated at the concentrations expected for real samples, before they are introduced into routine use. This is particularly important in drug analysis since the results are either used in vital preclinical or clinical studies, or in the diagnosis of illness and treatment of patients. In general, validation of an assay with respect to accuracy, precision, and specificity is required.¹⁻⁴ Other aspects needing to be considered include identification and handling of samples prior to analysis, stability of samples under various storage conditions, and the continuous assessment (quality control) of the method during its routine use.

SAMPLING AND STORAGE

In drug analysis the most commonly sampled body fluid is plasma or serum, because a good correlation between drug concentration and therapeutic effect is usually found. Urine analysis for drugs is used in connection with urinary excretion and bioavailability studies. Other body fluids (*e.g.*, saliva, cerebrospinal fluid) are also analysed for drugs, but less frequently.

The quality of analytical data depends critically on the validity of the sample and the adequacy of the sampling procedure. A non-representative sample is of no value, however carefully it has been analysed. It is essential that the samples are collected at the

correct time in relation to the dose, are adequately labelled, and preserved under appropriate conditions before being sent to the laboratory.^{5,6} Narayanan and Lin have reviewed devices available for sample collection.⁷ If the sample originates from a hospital, it should be accompanied by a request form containing adequate information about the patient and therapy, including co-administered drugs. For one-off assay, a reason for the assay request (*e.g.*, suspected toxicity) should also be stated. This means that the close co-operation of colleagues outside the laboratory is very important in any project involving drug analysis.

Drugs may be lost to the container or be degraded chemically, photochemically, or enzymatically during storage. Hence, an investigation of the stability of the drug and its metabolites in biological fluids during sample storage (temperature and duration) is a crucial part of method validation. The lack of information on stability may jeopardize subsequent investigations. Stability can be studied during the method development stage, by using a drug-free matrix suitably spiked, and eventually real samples. In general, samples that will be analysed within a few days should be stored at 4°; those that are to be stored for longer should be kept at -20°. For very long-term storage, freeze-drying should be considered. Provided it is available in sufficient quantity, the sample should be divided into aliquots before freezing, to minimize precipitation or degradation due to repeated freezing and thawing. Stock solutions of photodegradable drugs should be stored in amber-coloured containers. Adam,⁸ and Timm *et al.*⁹ have developed systematic procedures for investigating the stability of drugs in biological samples, based on statistical treatment of the experimental data.

CALIBRATION

Drug-free specimens of biological fluid (blanks) spiked with appropriate amounts of the drug should always be employed as calibration standards. Pure solutions (aqueous or methanolic) are not acceptable, because they differ greatly from the biological matrix.

At least six calibration points (excluding the blank) are needed for calibration. The concentrations of the calibration standards must cover the expected range of concentrations of the drug in the samples. Blank samples should be included in each calibration run in order to detect interference from substances other than the analyte which are present in the sample. If necessary, calibrations (including blanks) should be run in duplicate (or at even higher levels of replication) to improve the precision of the calibration line. Variation in the blank makes it imperative to run a calibration with every batch of samples. Any dubious points on the calibration line should be checked and no results falling outside the calibration range should be reported.

The calibration data should always be plotted by hand as well as subjected to linear regression analysis (if a linear response is obtained) and the slope, intercept, correlation coefficient, standard error of estimate (standard deviation about the regression line) and the standard deviations of slope and intercept should be calculated. The definitions and analytical interpretations of those parameters have been adequately reviewed elsewhere.^{2,3,10-12} Because of the ready availability of computer programs and calculators with facilities for statistical calculations, the task of calculating statistical parameters is not as difficult or time-consuming as it used to be.

ACCURACY AND PRECISION

Accuracy refers to the difference between a result (or mean) and the true or known value. Precision (or reproducibility) refers to the variation or scatter of the data around the mean. Accuracy can be determined by replicate analysis of samples containing known amounts of the drug. The deviation from the true values serves as a record of the method's accuracy. Usually three concentrations (a low, an intermediate and a high value within the analytical range) are tested to determine whether or not accuracy is concentration-dependent. It should be noted that outside the linear calibration range, the accuracy decreases rapidly. It also decreases rapidly as the limit of detection is approached. The within-day precision can be determined by duplicate measurement of drug levels at three different concentrations, in at least 10 samples for each concentration. Similarly day-to-day precision is measured by analysis on at least 10 separate days. The results are expressed as the standard deviation at each level or the coefficient of variation (CV). Although a CV value of 10% should be acceptable as the minimum acceptable precision, higher precision (CV < 10%) should be aimed at, particularly in the middle of the calibration range. For day-to-day precision experiments, each sample representing a particular concentration should be separately stored frozen, and thawed each day for analysis. If lyophilized serum is used, the same recommended reconstitution procedure should be

used each time; alternatively, the contents of a sufficient number of vials should be reconstituted and mixed and then treated as a liquid sample. It must be emphasized that good precision does not necessarily imply good accuracy: a systematic error may lead to precise but inaccurate results.

SENSITIVITY AND LIMIT OF DETECTION

The term sensitivity is sometimes misused to denote the limit of detection (LOD). A method is said to be sensitive if a small change in concentration (c) causes a large change in instrumental response (x), that is, when the derivative dx/dc is large. The sensitivity is thus defined as the slope of the calibration line and, provided the plot is linear, can be measured at any point on it. On the other hand the LOD of a method is calculated by using the section of plot near the origin and is arbitrarily defined as the lowest concentration or amount of analyte which can be distinguished from the blank with a stated degree of confidence (usually 99%), *e.g.*, the mean blank value plus three times the standard deviation (s) of the blank. The blank is also called the background or the noise. Some workers prefer to report the limit of quantification (or determination) rather than the LOD, using a higher multiple of s , *e.g.*, the mean blank value plus $10s$, because this gives a much more realistic estimate of the level at which the analyte can be determined in the sample. Because of the uncertainty of measured values at or near the LOD, quantitative interpretation should be limited to values at or above the limit of quantification.

The value of a , the intercept of the calibration line on the y -axis, can be used as the blank since it gives a more accurate estimate of the blank than a single measured value does. For more detailed statistical treatment of the LOD, the articles by McAinsh *et al.*¹³ and Mitchell and Garden¹⁴ should be consulted.

Because of the different approaches to calculating the LOD^{2,12,15,16} it is essential that the method used should be specified in all publications. The volume of sample needed to achieve the stated LOD should also be given. However, published LOD values should be considered only as typical, because the LOD is governed by instrumental and procedural factors. It varies with different batches of blank control (plasma, urine, *etc.*), type of sample (*e.g.*, presence of other drugs), and type and condition of instrument. For these reasons the LOD should not be rigidly fixed at the time the method is validated. It is necessary to reassess it whenever changes in conditions affecting it are suspected. If the concentration apparently obtained happens to fall below the LOD, the result should not be reported as zero, but rather as "non-measurable" or "non-detectable", or as < LOD.

It is seldom advisable to use an instrument constantly at its highest sensitivity setting or to work near the LOD of a method. High sensitivity of the

instrument cannot always achieve better detection limits, because a concomitant increase in noise level would result in only a small increase in overall signal-to-noise ratio. The LOD value can often be improved by judicious choice of experimental conditions, *e.g.*, by adjusting the size of the sample, the reconstitution solvent, or the injection volume.

SPECIFICITY

The specificity of the assay for the parent drug and its major metabolites should be thoroughly investigated in the method development phase. The constituents of biological fluids and the presence of other drugs, if any, should not interfere with the determination. Specificity can be incorporated into a work-up step (*e.g.*, selective extraction) and/or the analytical technique (*e.g.*, chromatographic separation and use of specific detectors). Each laboratory should determine the specificity of its own assay methods and any limitation of specificity in a method should be mentioned in the description of the method. It would also be sensible to reinvestigate a published method before putting it to a new use, particularly with regard to specificity, since a method which works in one situation may give rise to problems (or even fail) in another.

Yosselson-Superstine¹⁷ has reviewed assay methods for eight of the most commonly monitored drugs (digoxin, gentamicin, phenobarbitone, phenytoin, procainamide, quinidine, salicylate and theophylline) in plasma together with studies dealing with interferences of other drugs with these assays, and has suggested how to eliminate some of these potential sources of interference. The suggestions are mainly based on the preference of one analytical technique over another or change of experimental conditions.

EXTRACTION EFFICIENCY AND RECOVERY

Recovery experiments are particularly useful in testing the various stages of an analytical method and for assessing losses in sample processing, *e.g.*, in solvent extraction. Extraction conditions should always be optimized by using the relevant biological fluid. Ideally, several recovery experiments should be performed by adding varying amounts of authentic standard to a blank specimen. Spiking should cover the highest and the lowest concentrations expected in the unknowns, because recovery may vary with concentration. The recovery is calculated as

$$\text{recovery} = \frac{\text{amount found}}{\text{amount added}} \times 100\%$$

Absolute recovery can be determined by comparing the average peak height or area for extracted plasma or urine samples at each standard concentration of drug, with that for unextracted samples of identical concentrations made up in reconstitution fluid (preferably the mobile phase in the case of

HPLC). In recovery studies, since the weighed amount of the drug is taken as the true amount, it is imperative that the spiked samples are prepared very carefully, in the expectation that the variances of the sample preparation (weighing, preparation of solutions, *etc.*) will be small in comparison to the total variance of the overall method.

The accuracy, precision and LOD of the method are greatly influenced by the recovery of the drug to be determined. The overall recovery for a standard taken through the entire assay procedure should be reproducible and preferably >75%. If recovery is low (say 60%) but reproducible, it may still be acceptable; if, however, it is low, variable, and unpredictable, the reason for this should be investigated and eliminated, or an alternative approach to isolating the drug should be sought. Good recovery is aided by keeping the method as simple as possible, by efficient solvent extraction, and by preventing adsorption losses.

INTERNAL STANDARDS

During sample preparation an accurately known amount of a known compound (internal standard) is added to the sample at the earliest possible stage, in the expectation that any procedural loss of sample will be accompanied by an equivalent loss of internal standard. The ratio of the detector response (peak height or area) for the drug and the internal standard is then used in calibration and assay. The use of an internal standard, however, does not lessen the importance of careful analytical work. Workers in the toxicological laboratory prefer external to internal standards during screening, to avoid the masking of an unknown peak by the internal standard.

Ideally an internal standard should have physicochemical and chromatographic properties close to those of the test compound. Also it should be stable and easily available. If a derivative of the analyte is to be prepared, the internal standard should be capable of giving a derivative in the same way. For these reasons most internal standards are compounds structurally similar to the drug to be assayed. Some workers prefer to use a second drug within the structurally related class (*e.g.*, benzodiazepines) as an internal standard so that they have two methods instead of one. However, in employing such a method in drug-level monitoring, it has to be ascertained that the second drug (the internal standard) is not already part of the patient's therapeutic regime. If a mass spectrometer is being used as a detector (as in GC-MS work), a stable isotope labelled form of the drug can be used as an internal standard.

In HPLC, whenever sample preparation is simple and recoveries are high there is a tendency to dispense with an internal standard altogether. Such practice requires careful control of injection volume, however, and a valve injector is preferred. However, such a device does not compensate for errors arising from

changes in column or detector performance and the internal standard technique still offers better precision. It should be noted that the concentration-dependent variations in recovery cannot be compensated by using an internal standard, because doing so assumes constant recovery over the entire calibration range. Guidelines are available^{2,3,18} for the proper application of the internal standard technique in the determination of drugs in biological material.

METHOD COMPARISON

The performance of a newly developed (or modified) method can be assessed by comparing the results obtained by it with those found with a comparison (or reference) method of known accuracy and precision. GLC and HPLC are often used as reference methods since they are less susceptible to interferences from other drugs and endogenous substances. Sometimes, however, it is not possible to conduct method comparison studies, particularly for a less frequently used or newly developed drug, simply because a widely accepted reference method is not available.

Linear regression analysis is the preferred statistical method for comparing two analytical methods. It is widely used for this purpose, but it must be stressed that the accuracy and precision of the new method should be established before comparing it with the reference method. A reasonable number of samples (30–40) from different patients, covering the concentration range of interest in a roughly uniform manner, are analysed in duplicate by the candidate method and the reference method. It is preferable to use the same set of calibration standards for both methods. If this is not possible, both sets of standards should be analysed by both methods to obtain a measure of any difference between them. Data pairs are plotted as points on a scatter diagram, with the abscissa (x -axis) for the reference method (assumed to be more precise, *i.e.*, smaller random errors in the x -values) and the ordinate (y -axis) for the candidate method. The scatter diagram provides a visual first impression of the type of relationship between the two methods. The slope and intercept may give some indication of the type of systematic errors. For example a new method based on fluorimetry may give higher values for the drug if the metabolites or the blank contribute to the fluorescence signal. If the relationship between the two methods is linear over the concentration range investigated, the linear regression of y on x is calculated and the intercept and slope are determined. Further statistical tests are applied to see whether the intercept differs significantly from zero, or the slope from unity.¹² Such tests are performed by determining the confidence limits for the slope and the intercept, generally at 95% significance level. The ideal regression plot would be a straight line, passing through the origin, with a slope of 1. If the slope deviates from unity or the

regression line does not pass through the origin, the candidate method is biased with respect to the reference method. In such a situation professional judgement must be used to decide whether or not the bias is acceptable. If it is constant, a correction factor can be applied, but if it is variable, it becomes a component of the reproducibility and the correction factor procedure will not be useful. It should be borne in mind that statistics cannot decide whether the new method is acceptable or not. It can only provide estimates of the type and size of the errors, to guide the analyst in making the decisions.

In addition to the scientific criteria of accuracy and precision, the two methods may also be compared on the basis of cost, and ease and speed of operation. In developing an analytical method it may be prudent to try the simplest approach (the method having fewest steps) first. This means that direct analysis would be preferable to use of derivatives, because any procedure involving extra analytical steps would lower its precision and increase the cost and analysis time. Several studies of method comparison can be cited in the literature, for instance, a newly developed fluorescence polarization immunoassay system (Abbot TDx) for phenobarbitone, phenytoin, carbamazepine and theophylline has been evaluated by comparing it with the well-established techniques (GC, HPLC, EMIT) for the measurement of these drugs.¹⁹

QUALITY CONTROL

Once the assay has been established for routine use, its performance should be regularly monitored to update information regarding its characteristics and to ensure that it continues to work satisfactorily. This is done by using an internal quality control (QC) scheme, which is defined as the long-term and continuing assessment of accuracy and precision of an assay for a particular drug with a view to minimizing within-laboratory variation and improving assay precision. The procedure most widely used for the continuing evaluation of assay performance involves the construction of QC charts. Many schemes for constructing such charts have been suggested.^{12,20,21} The most commonly used control chart consists of a central line representing the mean (μ) of 20–30 earlier determinations of the drug (standard deviation s) in control material (QC sample) preferably performed on separate occasions, and two pairs of limit lines at $\mu \pm 2s$ (warning line) and $\mu \pm 3s$ (action line), which approximate to the 95% and 99% confidence limits respectively. Each day a result (the mean of duplicates) of QC sample is plotted on the chart. When the process is under control, the day-to-day results are normally distributed about μ . A result outside the warning line indicates that something is wrong. Such a result need not be rejected but should be checked for instrumental or procedural errors. Two successive values of the QC sample falling outside the action line indicate that the process is no longer under

statistical control. In this case the results are rejected and the process is investigated for its unusual behaviour and any faults are rectified. QC charts provide a long-term picture of the accuracy and precision of the method and identify trends and outliers in the analysis.

If the method is to be used for routine drug monitoring, it is useful to participate in a large scheme involving many laboratories (external QC scheme) provided the drug in question is included in such a scheme. External QC schemes²² for some of the routinely monitored drugs are available (e.g., Heath-control scheme for antiepileptics). Serum samples are periodically sent to the participant for assay, and the scheme co-ordinator (after receiving a result) reports that laboratory's performance together with a summary of the results from all participants.

When a batch of samples is analysed, calibration standards are included in the run to allow a standard curve to be constructed. This will secure meaningful results even if the instrument response changes for some reason. In addition to this a number of separately prepared QC samples are analysed along with actual samples at intervals depending on the total number of actual samples. As a rough guide one control every ten samples or two per small batch should suffice. Once the number of controls per batch has been decided, it should be maintained. Like calibration standards, QC samples are prepared by adding known amounts of drug to blank specimens. For a relatively stable drug, at least 20 ml of blank specimen can be spiked with the drug and 1-ml aliquots transferred to vials and stored at low temperatures. QC materials based on serum or urine are commercially available for many drugs which are assayed routinely for therapeutic or toxicological purposes.

Controls should be run in duplicate at three concentrations corresponding to levels below, within, and above the therapeutic range, particularly for methods with limited linear range (e.g., GC with electron-capture detection). For methods with linear concentration-response relationships over a wider range, two concentrations, one at the high end and one at the low end of the range (a high and a low QC) are adequate. The sample results are acceptable if the QC results are within 10% of the known values or within $\pm 3s$ of the means previously determined from replicate analyses. Besides control samples, a few randomly chosen test samples should also be analysed in duplicate to check precision within the batch. It is true that in the smaller laboratories quality control increases the work load, but in the long run it does improve the quality of results, and increases the individual's confidence in the assay.

Because of the pioneering efforts of clinical chemists, the importance of quality control has already been established for many drugs which are routinely measured in clinical laboratories. Several reviews are available that describe in detail the principles

and practice of quality control in clinical chemistry.^{4,20,21,23-25}

CONCLUSION

The validation procedure described in this paper represents the minimum amount of work which should be done to gain confidence in the ability of an analytical method to produce meaningful results. The extent to which a method needs to be validated is a matter of professional judgement. Each investigator should decide for himself which parameters are more relevant to the particular assay and modify the validation procedure accordingly. In addition to a valid method, the skill and dedication of the analyst are equally important for the production of reliable data and hence the success of the project involving drug analysis.

REFERENCES

1. A. P. De Leenheer and H. J. C. F. Nelis, *Analyst*, 1981, **106**, 1025.
2. E. Reid (ed.), *Blood Drugs and other Analytical Challenges*. Horwood, Chichester, 1978.
3. E. Reid (ed.) *Trace Organic Sample Handling*. Horwood, Chichester, 1981.
4. J. Chamberlain, *Analysis of Drugs in Biological Fluids*. CRC Press, Boca Raton, 1985.
5. A. C. Mehta, *Talanta*, 1986, **33**, 67.
6. P. A. Toseland, in *Clarke's Isolation and Identification of Drugs*, A. C. Moffat (ed.) 2nd Edn, p. 111. Pharmaceutical Press, London, 1986.
7. S. Narayanan and F. C. Lin, in *Therapeutic Drug Monitoring and Toxicology by Liquid Chromatography*, S. H. Y. Wong (ed.), p. 79. Dekker, New York, 1985.
8. H. K. Adam, in *Trace Organic Sample Handling*, E. Reid (ed.), p. 291. Horwood, Chichester, 1981.
9. U. Timm, M. Wall and D. Dell, *J. Pharm. Sci.*, 1985, **74**, 972.
10. R. B. Davis, J. E. Thompson and H. L. Pardue, *Clin. Chem.*, 1978, **24**, 611.
11. K. A. Connors, *A Textbook of Pharmaceutical Analysis*, 3rd Ed., p. 581. Wiley, New York, 1982.
12. J. C. Miller and J. N. Miller, *Statistics for Analytical Chemistry*. Horwood, Chichester, 1984.
13. J. McAinsh, R. A. Ferguson and B. F. Holmes, in *Trace Organic Sample Handling*, E. Reid (ed.), p. 311. Horwood, Chichester, 1981.
14. D. G. Mitchell and J. S. Garden, *Talanta*, 1982, **29**, 921.
15. J. N. Miller, *Anal. Proc.*, 1982, **19**, 114.
16. G. L. Long and J. D. Winefordner, *Anal. Chem.*, 1983, **55**, 712A.
17. S. Yosselson-Superstine, *Clin. Pharmacokinetics*, 1984, **9**, 67.
18. P. Haefelfinger, *J. Chromatog.*, 1981, **218**, 73.
19. K. F. Loomis and R. M. Frye, *Am. J. Clin. Path.*, 1983, **80**, 686.
20. J. Williams, in *Therapeutic Drug Monitoring*, B. Widdop (ed.), p. 95. Churchill Livingstone, Edinburgh, 1985.
21. *Quality Control in Clinical Chemistry*, Wellcome Diagnostics, Dartford, 1982.
22. J. Page and A. Richens, *Syva Monitor (The Bulletin of Therapeutic Drug Monitoring)*, 1982, No. 11, 1.
23. Provisional Recommendation on Quality Control in Clinical Chemistry, *Clin. Chem.*, 1976, **22**, 1922.
24. Approved Recommendation on Quality Control in Clinical Chemistry, *J. Clin. Chem. Clin. Biochem.*, 1983, **21**, 877.
25. D. Burnett and J. Williams, in *Clarke's Isolation and Identification of Drugs*, A. C. Moffat (ed.), 2nd Ed., p. 118. Pharmaceutical Press, London, 1986.

SPECTROPHOTOMETRIC DETERMINATION OF BROMIDE (AND IODIDE) IN A FLOW SYSTEM AFTER OXIDATION BY PEROXODISULPHATE

ANNIKA CARLSSON, ULLA LUNDSTRÖM and ÅKE OLIN*

Department of Analytical Chemistry, University of Uppsala, P.O.B. 531, S-751 21 Uppsala, Sweden

(Received 14 November 1986. Revised 20 January 1987. Accepted 13 February 1987)

Summary—The peroxodisulphate method for the determination of bromide has been modified. A flow-injection system for the spectrophotometric finish has been developed and the size of the ion-exchange column in the preconcentration step has been scaled down. The sum of bromate and iodate produced in the oxidation is determined by treating the oxidized sample with iodide in hydrochloric acid. The iodate is separately determined by applying the reaction in acetic acid. The working range of the spectrophotometric finish is 1–15 μ M and the limit of determination (10σ) is 0.7 μ M for iodate and for iodate plus bromate. The enrichment factor in the preconcentration step is 50, yielding a limit of determination of 15 nM for bromide in natural waters. Eighteen samples of water from the Baltic, with salinity ranging from 3 to 33‰ have been analysed. A Br/Cl ratio of $(1.53 \pm 0.02) \times 10^{-3}$ was found. A comparative study of the original and the new preconcentration step has been made with three river waters, rich in humic substances. The results agreed within $\pm 1.5\%$.

The concentration of bromide in fresh water is often very low ($< 1\mu$ M), which necessitates a preconcentration step before the final determination of the bromide. Recently a procedure was presented in which bromide was enriched on an ion-exchanger.^{1,2} After elution, the bromide was oxidized by peroxodisulphate to bromate, which was subsequently treated with iodide; the absorbance of the tri-iodide formed was measured. The method has been used in a study of the bromide concentration in precipitation, surface and ground waters.³ Although the method worked well even for concentrations of bromide $< 0.05\mu$ M, certain inconveniences became apparent during this work. First, the consumption of sample in the spectrophotometric finish was too great, and only one measurement per sample could be made. Secondly, the sample volumes required in the preconcentration step were large, particularly at low concentrations of the analyte. This is a definite drawback when specimens have to be transported to the laboratory. In order to remedy these disadvantages, the procedure has been changed to include a spectrophotometric finish in a flow system, and the preconcentration system has been scaled down.

Various papers⁴⁻⁶ have dealt with the spectrophotometric determination of bromide and iodide by the flow-injection technique. However, none of the methods proposed offers advantages over the peroxodisulphate method,¹ particularly not for low concentrations and waters containing large amounts of humic substances. Thus the original method¹ was adhered to.

EXPERIMENTAL

Most of the equipment and chemicals used were the same as described earlier.^{1,2} Only major changes will be mentioned here.

Chemicals

Sodium peroxodisulphate (Fluka, *p.a.*) was used in place of the corresponding potassium salt in order to avoid precipitation of potassium perchlorate.

The ion-exchange resin, Dowex 1 \times 8 (100–200 mesh), was used only once and rinsed in the columns first with 40 ml of 1M sodium hydroxide and then with 30 ml of 2M bromide-free hydrochloric acid, followed by distilled water until the effluent was neutral. For the smaller resin volume (0.5 ml) used in the scaled-down enrichment, the corresponding volumes were 10 and 7 ml.

All solutions were made from analytical grade chemicals with demineralized and distilled water.

Apparatus

The sum of the bromate and iodate concentrations produced was determined by treating an aliquot of the oxidized sample with iodide and hydrochloric acid in a flow system. The iodate was determined by treating a second aliquot with iodide and acetic acid in the same flow system. The absorbance of the iodine formed was measured at 355 nm with a Beckman DU spectrophotometer rebuilt to provide digital and recorder read-outs.

The flow system (Fig. 1) consisted of a peristaltic pump (Gilson), a valve (FIA-05, Bifok), a manifold (Chemifold type III, Tecator) and a 1-cm flow-through cuvette. The flow-rate of the carrier stream was 2.6 ml/min and the sample and reagent streams were propelled at 0.6 ml/min. Teflon tubing (0.7 mm bore) was used throughout for transportation of the streams. The lengths of the mixing coils are given in Fig. 1. For small samples the injector loop (200 μ l) was filled by a separate pump at a low flow-rate (0.5 ml/min.) An injection volume of 200 μ l was used throughout.

The solutions were deaerated by passing nitrogen through them. Oxidation of iodide by oxygen diffusing through the tube walls was found to be negligible.

*Author for correspondence.

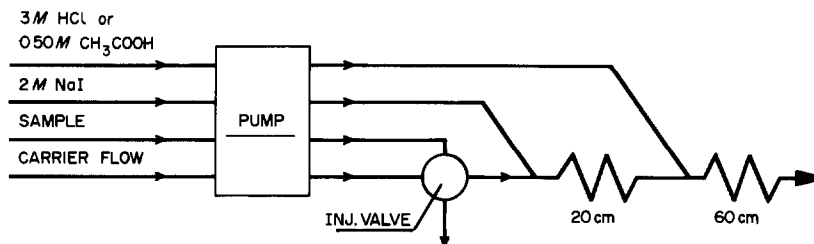


Fig. 1. Schematic diagram of the flow-injection system.

Appropriate concentrations of the reagent streams were found by running the flow system in the steady-state mode with $10\mu\text{M}$ test solutions of bromate or iodate. The influence of the hydrochloric acid and sodium iodide concentrations, and of the length of the reaction coil, on the reaction between bromate and iodide was examined. With a 60 cm reaction coil the absorbance reached a limiting value when the concentrations of both reagents were 2M or greater. This indicates that the reaction between bromate and iodide is complete under these conditions. With the same reaction coil and 2M sodium iodide reagent, it was found that the reaction between iodate and iodide went to completion with 0.5M acetic acid as the acidic reagent stream.

The ion-exchange columns for the scaled-down enrichment had the following dimensions: the cylindrical funnel at the top was 50 mm long and 24 mm wide. The tube holding the resin was 95 mm long and 7 mm in bore, and was drawn out to a tip 2 mm in bore.

The eluate from the small columns was oxidized by the peroxodisulphate in a 10-ml graduated test-tube fitted with a ground-glass stopper held in place by a clip.

Procedures

The iodide reagent stream was always 2M sodium iodide. The acid reagent stream was 3M hydrochloric acid for determination of bromate plus iodate and 0.50M acetic acid for determination of iodate. An injected sample with $10\mu\text{M}$ bromate or iodate concentration yields a peak absorbance of about 0.4.

Without preconcentration. Perform the oxidation as described earlier.¹ Use a carrier stream with the following composition: 0.040M sodium sulphate, 0.072M sodium dihydrogen phosphate, and 0.008M sodium hydrogen phosphate. If the sample contains a high concentration of electrolytes it may be necessary to match the carrier stream to the sample with respect to these electrolytes. Calibrate with standard bromide solutions (which may also need to be matched to the sample in electrolyte concentration).

Preconcentration with the normal column. Pretreat the resin as described earlier.² Measure out 2.0 ml of resin in a graduated 10-ml cylinder and transfer it to the ion-exchange column. Wash it with sodium hydroxide solution and hydrochloric acid as described above. Place the sample in a suitable size of standard flask, invert the flask with its neck in the wide mouth of the ion-exchange column, and let the sample pass through the resin under gravity. Elute with three 3-ml portions of 2M sodium perchlorate and wash with 2 ml of distilled water. Oxidize the bromide (plus iodide) in the eluate with 5 ml of peroxodisulphate solution as described earlier. Dilute the oxidized solution to volume in a 25-ml standard flask and inject $200\mu\text{l}$ into a carrier stream of composition 0.128M sodium chloride, 0.592M sodium perchlorate, 0.040M sodium sulphate, 0.072M sodium dihydrogen phosphate and 0.008M disodium hydrogen phosphate. Calibrate with standard bromide solutions carried through the whole procedure. Include blanks as a check on the purity of the chemicals. Measure the absorbance at 355 nm.

Preconcentration with the small column. Proceed as above but use 0.5 ml of resin. Elute with three 0.8-ml portions of 2M sodium perchlorate and rinse with 0.5 ml of distilled water. Oxidize with 0.5 ml of peroxodisulphate solution of twice the normal concentration and dilute to volume in a 4.0-ml standard flask. Inject $200\mu\text{l}$ into a carrier stream of composition 0.20M sodium chloride, 1.00M sodium perchlorate, 0.050M sodium sulphate, 0.090M sodium dihydrogen phosphate and 0.010M disodium hydrogen phosphate. Calibrate and determine the blank as above. To increase the stability of the baseline the acid reagents may be made 1M in sodium perchlorate.

Obviously, the procedures above must be modified when the sample matrix contains components which will absorb radiation of 355 nm wavelength, or react to yield iodine after the oxidation step.

RESULTS AND DISCUSSION

The flow system has been designed to measure low concentrations of the halates. Two reagent streams are necessary since oxidation of iodide to iodine by oxygen cannot be avoided in acid solution. A large loop-volume is used in order to decrease the dispersion, which is about 1.3. The high concentrations of the reactant streams together with use of a long reaction coil ensures that the reaction between the halates and iodide goes almost to completion. Linear calibration graphs were obtained for bromate and iodate when the system was run in either the flow-injection mode or in the steady-state mode. The slopes of the graphs were the same for the reaction of iodate in 3M hydrochloric acid or in 0.50M acetic acid and for reaction of bromate in 3M hydrochloric acid. Bromate did not react with iodide in 0.50M acetic acid. The standard deviation of the absorbance readings was 0.002 ($n = 30$) and independent of the value of the absorbance. The standard deviation of the blank was also 0.002 ($n = 14$). The limit of determination (taken as the concentration corresponding to 10 times the standard deviation of the absorbance) is $0.7\mu\text{M}$.

The analytical results reported here are based on three consecutive injections of the sample. The injection frequency is 60 per hr. When a preconcentration step is needed, it should be possible to analyse about 40 samples per day if the enrichment is run overnight.

The performance of the equipment was tested by analysing mixtures of known amounts of bromate and iodate. Some data are collected in Table 1. Similar results were obtained for oxidation mixtures

of bromide and iodide. The data reflect the relative error of the method, which is about 1% at the $10\mu\text{M}$ level and about 4% at a concentration of $2\mu\text{M}$. Since the iodate concentration is obtained directly, the precision for iodide is better than that for bromide, the concentration of which is obtained by difference. This does not affect the precision of the determination of bromide in natural waters, because their bromide concentration is several orders of magnitude greater than the iodide concentration.

Since the absorbance signal was found to be somewhat sensitive to differences between the electrolyte content of the oxidized sample and the carrier stream, the composition of the carrier stream was matched to that of the sample. It was also found necessary to use fairly well defined amounts of ion-exchange resin.

As an application of the procedure without preconcentration, 18 samples of water from the Baltic were analysed in duplicate for bromide. The salinity of the samples ranged from 3 to 33‰ and the chloride content was determined according to Mohr.⁷ A sample volume yielding a bromate concentration of about $9\mu\text{M}$ in the final solution was used. This led to a chloride concentration of about 0.005M in the oxidized sample. Separate measurements showed that sodium chloride concentrations in the range 0–0.1M did not affect the absorbance signal. The untreated samples showed no absorbance at 355 nm, so the calibration graph could be established by use of standard bromide solutions. The mean value of the bromide to chloride ratio was $(1.53 \pm 0.02) \times 10^{-3}$, which is close to the almost invariant value, 1.54×10^{-3} , obtained for the oceans.⁸ The values fell in the range $(1.49\text{--}1.57) \times 10^{-3}$. The precision of the analytical results indicates that the observed variation in the quotient is real. Morris and Riley,⁸ and Kremling,⁹ have reported a systematic change of the ratio with chloride concentration in the Baltic. Our data are too few to confirm this observation, however.

It is interesting to note that the very simplest model of the composition of the water in the Baltic, which regards it as a mixture of sea-water and fresh water, predicts significant deviation from the ratio 1.54×10^{-3} to occur only at very low salinities. From data³ obtained for river water in northern Sweden, where the ratio is close to 1.0×10^{-3} , it can be calculated that at a salinity of 3‰ the ratio would still be 1.54.

Table 1. Analytical results for mixtures of known amounts of bromate and iodate

IO_3^- taken, μM	BrO_3^- taken, μM	$\text{IO}_3^- + \text{BrO}_3^-$ found, μM	IO_3^- found, μM	BrO_3^- calculated, μM
9.00	1.00	10.0	8.92	1.1
8.00	2.00	10.0	8.02	2.0
6.00	4.00	10.1	6.06	4.0
5.00	5.00	10.1	5.12	5.0
4.00	6.00	10.1	4.08	6.0
2.00	8.00	10.1	2.08	8.0

Table 2. Determination of bromide in three strongly humic river waters

Sample	Exchanger bed volume, ml	Sample volume, ml	Bromide, μM	Mean, μM
1	2.0	500	0.155	0.158 $s = 0.003$
	2.0	1000	0.160	
	0.5	75	0.155	
	0.5	125	0.162	
2	2.0	250	0.522	0.522 $s = 0.005$
	2.0	500	0.529	
	0.5	50	0.519	
	0.5	75	0.518	
3	2.0	100	1.30	1.32 $s = 0.02$
	2.0	250	1.32	
	0.5	15	1.31	
	0.5	25	1.34	

The enrichment step on the small ion-exchange beds was tested by passing 25–200 ml portions of 0.010M sodium chloride through the columns. Each portion contained 125 nmoles of bromide. The amount of bromide accumulated was determined by the procedure for large columns described above, and the recovery was found to be $100 \pm 1\%$. The result is in agreement with the estimate² of the largest permissible volume, $v = 2.8/[C] = 280$ ml.

Table 2 presents results from an application of the procedures to the duplicate determination of bromide in three river waters which contained large amounts of dissolved humic substances. Enrichment was performed with 2.0 and 0.5 ml of ion-exchange resin. The agreement between the analytical results obtained with the various bed and sample volumes is satisfactory. The results seem to indicate that somewhat higher results are obtained when the sample volume is increased. On the other hand this shows that the accumulation step works well.^{2,3} The observed variations may well be caused by errors in the correction applied for the blank and the iodide present. Although these corrections are small, errors of the order of a few per cent may be introduced when the absorbance is low.

For natural waters no net iodide signal is generally observed. This is to be expected since the iodide to bromide ratio is less than 10^{-3} . However, measurement of the iodide signal is still included since a substantial signal indicates a failure in the procedure. As an example, incomplete removal and destruction of humic substances might occur.

CONCLUSIONS

The introduction of a flow-injection system into the spectrophotometric finish of the peroxodisulphate method should reduce the risk of accidental determination errors caused, for instance, by oxidation of iodide by oxygen. A spurious result is difficult to identify in the original method, since only one measurement can be made. Furthermore, when no pre-

concentration step is necessary, the analysis time will be shortened. The scaling down of the enrichment step is a valuable asset in survey work when transportation of the samples to a laboratory is necessary. The sensitivity of the method is moderately diminished by working with a flow system. With a 200-ml sample a bromide concentration of about $0.025\mu\text{M}$ can be determined with a relative error less than 10%. However, for certain waters, such as rain water, this sensitivity is not sufficient. Methods other than spectrophotometry must apparently be sought and used for the determination of very low bromide concentration and analysis of small sample volumes.

Acknowledgements—Thanks are due to Dr. S. Fonzelius at the Oceanographical Laboratory of the Swedish Meteor-

ological and Hydrological Institute for providing the water samples from the Baltic.

REFERENCES

1. U. Lundström, *Talanta*, 1982, **29**, 291.
2. U. Lundström, Å. Olin and F. Nydahl, *ibid.*, 1984, **31**, 45.
3. U. Lundström and Å. Olin, *Water Res.*, 1986, **20**, 751.
4. M. Miyazaki, N. Okubo, K. Hayakawa and T. Umeda, *Chem. Pharm. Bull.*, 1984, **32**, 3702.
5. T. Anfält and S. Twengström, *Anal. Chim. Acta*, 1986, **179**, 453.
6. O. F. Kamson, *ibid.*, 1986, **179**, 475.
7. I. M. Kolthoff, E. B. Sandell, E. J. Meehan and S. Bruckenstein, *Quantitative Chemical Analysis*, 4th Edn. Macmillan, New York, 1969.
8. A. W. Morris and J. P. Riley, *Deep-Sea Res.*, 1966, **13**, 699.
9. K. Kremling, *Kiel. Meeresforsch.*, 1972, **28**, No. 2, 99.

DESIGN AND CHARACTERIZATION OF AN INTENSIFIED DIODE ARRAY DATA-ACQUISITION SYSTEM FOR SPECTROMETRIC MEASUREMENTS

MARY RYAN-HOTCHKISS* and J. D. INGLE, JR.†

Department of Chemistry, Oregon State University, Corvallis, Oregon 97331, U.S.A.

(Received 25 November 1986. Accepted 13 February 1987)

Summary—A computer-based data-acquisition system for an intensified diode array (IDA) detector is described. A unique combination of hardware and software provides many data-acquisition and calculation options useful for multiple-wavelength spectrometric measurements. The data-acquisition system is used to evaluate critically many characteristics of the IDA detector, including the dependence of the light and dark signals and noise on experimental variables, and the linearity, memory effects and resolution.

The usefulness of an intensified diode array (IDA) detector and data-acquisition system for multiple-wavelength equilibrium and kinetics-based luminescence measurements has been demonstrated in recent papers.¹⁻⁴ This paper is concerned with the construction of an IDA data-acquisition system and the critical evaluation of the characteristics of the IDA. The new data-acquisition system was constructed to provide versatility and options uniquely suited to our purposes (monitoring of reactions involving fluorescent species). Important features include the ability to store signals from specific diodes to save memory, the ability to scan unused diodes at higher rates to reduce the integration time, the ability to control both integration times and times between scans, and the calculation of means, standard deviations and rates of change of signals from different wavelength ranges.

The IDA has not previously been well characterized. Therefore a thorough study of its characteristics (e.g., signal-to-noise ratio, linearity) was made so that its limitations can be understood and it can be used under optimal conditions as a precise analytical instrument, and the data-acquisition system can be properly designed.

EXPERIMENTAL

Intensified diode array spectrometer

A Tracor Northern (Middleton, WI) TN-1710-21 IDA detector was used in conjunction with a Tracor Northern TN-1150 F/3 holographic grating spectrograph. The detector contains a microchannel plate (MCP) intensifier followed by a phosphor and finally a Reticon (Sunnyvale, CA) RL512EC/17, 512-element diode array (DA) (photodiodes 50 μm wide and 0.45 mm high). Photons striking the photocathode of the MCP intensifier are converted into

photoelectrons which are then amplified into electron packets; these in turn strike the phosphor to produce a burst of photons which then strike the individual photodiodes in the DA. The spectral response in the visible range is determined by the MCP photocathode (S-25). At wavelengths shorter than about 400 nm, the response is controlled by a scintillator placed in front of the photocathode. The scintillator is used to convert ultraviolet into visible radiation since the glass fibre optic faceplate of the intensifier prevents direct monitoring of ultraviolet-region photons.

The IDA detector face is placed at the focal plane of the spectrograph to provide a spectrometer system with coverage from 200 to 840 nm (1.25 nm/diode). The spectrograph and IDA detector were used in place of a conventional emission monochromator and photomultiplier tube (PMT), as previously described,¹ to observe fluorescence radiation from a sample cell in a spectrofluorimeter. A thermoelectric cooler is used to reduce the dark signal from the DA.

The IDA detector is supplied with some signal-processing electronics. The user (the commercial data-acquisition system was not purchased) must supply (1) a TTL clock signal (IDA CLOCK) which determines the frequency at which the diodes are interrogated and (2) a logic-0 start signal [IDA BEGIN SCAN (BS)] which determines when the interrogation starts and hence the integration time. The output signals available are the video signal, a voltage pulse with amplitude proportional to the signal accumulated by a diode, and an end of scan (EOS) signal which is high only during the interrogation.

Since the signal-processing electronics require about 2.5 μsec to pass the voltage peak for each diode, the maximum clocking rate of the array is about 400 kHz. This means that 512 diodes can be interrogated in about 1.3 msec (512/400000). This is the minimum integration time as determined by the speed of the signal-processing electronics which accompany the detector. The diode array itself may be clocked at rates up to 10 MHz.⁵

Data-acquisition system

Figure 1 is a schematic diagram showing the components and interconnections of the IDA computer-controlled data-acquisition system. This system consists of a computer, a control module, and the IDA with its intensifier gain control. The computer used is a DEC (Maynard, MA) PDP 11/20 computer with a T-4002 Tektronix (Beaverton, OR) graphics terminal and a 4601 Tektronix hard-copy unit. The control module consists of 4 printed circuit (PC) boards

*Present address: Tektronix, Inc., P.O. Box 500, Beaverton, OR 97077, U.S.A.

†To whom correspondence should be addressed.

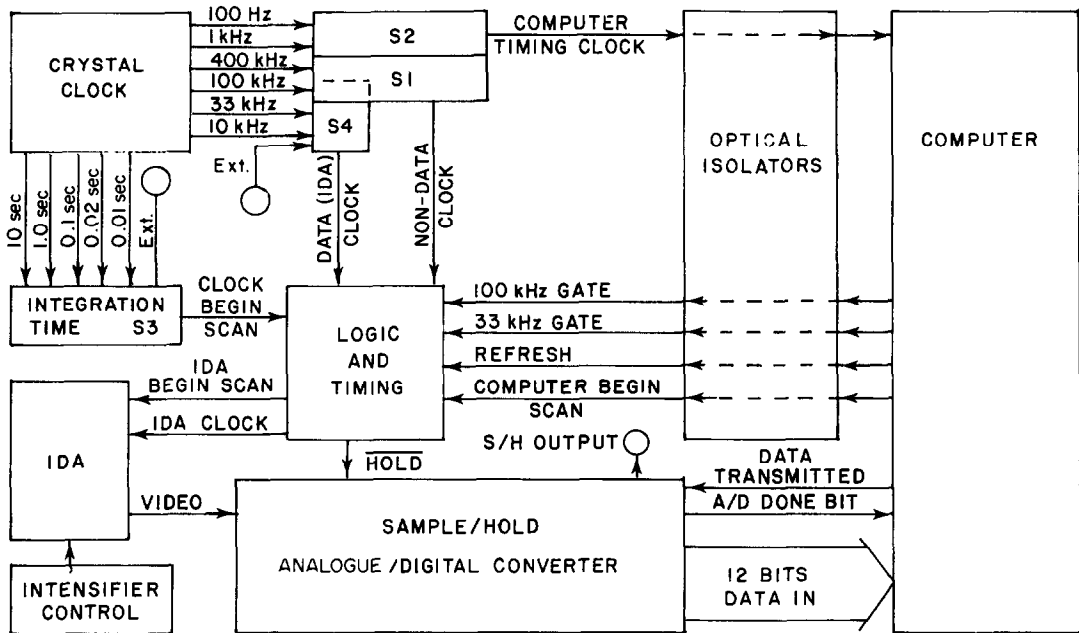


Fig. 1. IDA data-acquisition system.

(crystal clock; logic and timing; sample and hold and analogue-to-digital converter (S/H-ADC); optical isolation) which are mounted in a vector cage in separate metal boxes with appropriate switches, connectors, and power supplies. Complete circuit diagrams are available upon request.

The control module (a) allows integration times to be controlled by the computer, (b) digitizes analogue signals for computer storage, (c) allows synchronization between data-generation by the IDA and data-storage by the computer, (d) provides for refresh scanning between computer-controlled scans, and (e) provides optical isolation to provide immunity from noise for signals coming from the computer. As seen in Fig. 1, an external pulse train, the COMPUTER TIMING CLOCK signal, is input to the computer through S2 for computer-timed integration times. The computer triggers the IDA BA signal and initiates the scan with the COMPUTER BEGIN SCAN (COMP BS) signal. The output of the S/H is digitized with a 12-bit ADC, and a 12-bit binary number is transmitted to the computer through its parallel input port. Synchronization of data generation and storage is provided by the 33-kHz GATE and 100-kHz GATE signals with the logic and timing circuitry, and by the ADC DONE BIT and DATA TRANSMITTED signals. The frequency of the IDA CLOCK signal during the refresh scans is selected by S1 and is called NON-DATA CLOCK. When the computer is not timing a data-scan, the REFRESH signal allows scanning at repetition rates determined by S3. Optical isolation is used for the 5 signal lines shown in Fig. 1.

Stand-alone mode

The system was also designed to operate without a computer, in which case the spectra are displayed on an oscilloscope. The stand-alone mode is useful for optimization because the spectra are displayed in real time. In this case, the control module allows selection of the IDA integration time (time between BS pulses) through S3 and IDA clocking frequency through S4. The video signal output by the IDA is sampled during the appropriate portion of each cycle, and is output at the sample and hold (S/H) OUTPUT for display on an oscilloscope. The oscilloscope is triggered by the BS signal.

Control module components

The crystal clock PC board is based on a standard design and provides the various frequencies (indicated in Fig. 1) required for timing and synchronization. All lines carrying signals between the computer and the control module are isolated with TIL111 optical isolators, except the DATA TRANSMITTED line. This minimizes excess noise on the analogue input line to the ADC and false triggering by the COMPUTER TIMING CLOCK signal.

The S/H-ADC PC board is used to sample the video signal, output a stable voltage level to the ADC, and convert that voltage level into a 12-bit binary number. The components on this board were carefully chosen to provide the speed and accuracy required in this application. The S/H ADC board consists of the S/H, inverting amplifier and ADC. A flip-flop (SN7474) was connected to the ADC READY SIGNAL output of ADC to provide a logic-1 DONE BIT signal for the computer. The Computer Labs (Greensboro, NC) HTC-0300 S/H tracks on a high and holds on a low signal-input to the HOLD input. It settles to within 0.01% error for a 10-V change with only a 300-nsec wide pulse to HOLD. In this application the HTC-0300 is used in the S/H mode since it is normally left in the HOLD condition.

The ADC is a Datal Systems, Inc. (Canton, MA) Model ADC-EH 12 B3. The Computer Labs MAS-1202 ADC can be directly substituted for the Datal ADC. The ADC converts voltages between 0 and 10 V into a 12-bit binary number in $2 \mu\text{sec}$. It clears on a high and starts a conversion on the falling edge of a logic-1 TTL signal input to the START CONVERSION input. An Analog Devices AD528J (Norwood, MA) operational amplifier, in the inverting amplifier mode, between the S/H and ADC, has a time constant of $0.15 \mu\text{sec}$ and a slew rate of $50 \text{ V}/\mu\text{sec}$ and gain of unity. A gain of 1.31 was chosen to provide 10 V to the ADC when the IDA is saturated (the maximum signal provided by a photodiode). The layout of this board and the grounding were carefully planned to minimize interaction of analogue signals with digital or external signals.

The circuitry on the logic and timing board is a group of independent circuits which provide several functions which will be discussed separately. The first function provided is

the capability to allow the control module or the computer to determine integration times and to provide refresh scans. A few logic gates and a monostable (74121) (a) allow the control module to initiate scans at the integration times selected at S3 when the computer is not connected, (b) allow the computer to determine integration times when the computer is used and (c) provide for refresh scans when the computer is used but is not timing an integration, at a rate selected by S3 (typically 50 Hz). Either the CLOCK BS signal from S3 or the COMP BS signal (a 10 μ sec logic-0 pulse) from the computer triggers a monostable to produce the 2 μ sec logic-0 IDA BS signal. When the computer is connected, the logic state of the REFRESH signal from the computer determines whether the COMPUTER BS or the CLOCK BS signal triggers the IDA BS signal.

The second function provided by the logic and timing board is the ability to gate a faster IDA clock frequency when data are not being stored, to allow a scan to be completed in less than 15 m sec when under computer control. In addition, synchronization between generation of data by the IDA and storage of the data by the computer is provided. When the PDP 11/20 is storing data, at least 24 μ sec are required per data point. The IDA CLOCK frequency when interfaced to the computer was chosen to be 33.3 kHz (i.e., 4 MHz divided by 120) because that frequency allows 30 μ sec per data point and is easily obtained from the 4-MHz frequency. For simplicity this signal is usually referred to as 33 kHz. With this IDA CLOCK frequency, about 15 msec are required to scan the complete 512-element DA and thus 15 msec is the minimum integration time. A few logic gates allow a faster frequency to be gated in after the data from the pertinent channels have been stored. This allows shorter integration times when signals from diodes towards the end of the array are not stored. In addition, the logic gates and timing signals allow the IDA CLOCK signal to be gated to the IDA at precise times to synchronize data-generation by the IDA and data-storage by the computer.

The circuit works as follows. When the computer is not connected, the DATA CLOCK signal from S4 (typically 33 kHz) is gated through to become the IDA CLOCK. If the computer is connected, the logic states of the 33-kHz GATE signal and the 100-kHz GATE signals from the computer (and controlled by software) determine whether the DATA CLOCK signal from S4 (typically 33 kHz) or the NON-DATA CLOCK signal from S1 (typically 100 kHz) becomes the IDA CLOCK. The 33-kHz clock is used when the computer is storing data, and the 100-kHz clock is used during REFRESH or to finish clocking through the diodes (without data-storage) at a more rapid rate.

With these gates and signals, integration times as short as 5.3 msec can be obtained if the data from only the first few diodes in the array are stored. However, if the portion of the spectrum desired falls on the diode array at the end that is interrogated last, the minimum integration time would be about 15 msec. In this situation, if only one portion of the spectrum was desired, the detector could be turned upside down with respect to the spectrograph, so that the desired wavelengths would be at the end interrogated first.

The third function provided by the logic and timing PC board is a variable delay and pulse-width signal to trigger the S/H and a variable-width pulse to start the ADC. The IDA video signal, which has a pulse height proportional to the amount of light integrated on the photodiode, peaks at about 1 μ sec after a falling transition of the IDA CLOCK signal and is only about 1 μ sec wide. Thus a very narrow trigger signal is necessary to trigger the S/H at the peak of the pulse.

The IDA CLOCK signal is input to a monostable (SN 74121) to generate a 0.50 μ sec logic-1 DELAY pulse on the falling edge of the IDA CLOCK signal, which then triggers another monostable (2 NAND gates) to generate a 0.45 μ sec logic-1 HOLD AND ADC START pulse. This is illustrated

in the timing diagram in Fig. 2. The DELAY and HOLD signals are chosen so that the S/H tracks only in the region near the peak of the video signal. The ADC is cleared by a high from HOLD and is started on its falling edge. Two μ sec later, the ADC conversion is complete and the END OF CONVERSION signal from the ADC triggers the DONE BIT signal to go high. When the computer senses the DONE BIT, it stores the 12-bit binary number and sends out the short-duration DATA TRANSMITTED signal which clears the DONE BIT. This process is repeated for each data point. The time required by the S/H and ADC to process the information for one data point is only 3 μ sec. The ADC and S/H are triggered and the DONE BIT is set whenever the IDA CLOCK signal is active, even when the IDA is not being interrogated and the computer is not storing data.

Software

Listings of the BASIC and assembly language software and their flow-charts are available from the authors. Here we only describe what the program does.

When the program is started, it prompts the operator to specify the values of several parameters, including the integration time (t), the number of sets (spectra) to be accepted, the number of scans (s) added in each set, the time between sets, and the portion of the spectrum to be stored (the number of leading diodes to ignore and the number of data points to acquire per scan).

The user also selects a number of display and calculation options, shown in Table 1, with the 16 switch registers (SR) on the front of the computer. These selections are implemented by various interactive BASIC subroutines, which may call other BASIC or assembly language subroutines. Once the spectral data are stored, any of the calculation options may be applied to the data. Both the ability to store only a portion of the spectrum and to store each partial spectrum adjacent in memory, rather than in a pre-assigned 512-word block of memory, was incorporated to conserve memory. Assembly language subroutines are used where their conciseness and speed are useful, such as for the control signals.

Important points with respect to the interaction of hardware and software are discussed below. The states of four of the control signals throughout the program are illustrated in Fig. 3. The letters in the figure are correlated with the discussion below. (A) The levels of the four control signals are initialized by the BASIC program and are re-initialized on each loop through the program. When the operator requests a scan the following sequence of events occurs. (B) REFRESH goes low. The program times a 5-msec delay to allow the current refresh scan to finish. (C) The integration time is begun and the 100-kHz GATE is closed with a high level. This holds the IDA CLOCK signal low. (D) The

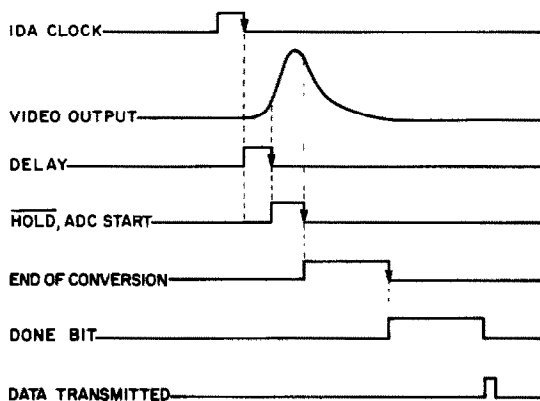


Fig. 2. S/H-ADC circuit waveforms.

Table 1. Program options

Option name	Purpose of function
DISPLAY	Plot any requested set (spectrum) on TEK terminal
CROSSHAIR	Displays crosshair on screen, which can be moved with joystick, and feeds back crosshair location on the display (indicates diode number, wavelength and signal for diode)
SCALE	Allows the display to be made larger or smaller in the x or y direction
SUBTRACT	Adds or subtracts any two requested sets
SUB DURING ACCEPT	Subtracts the second scan from the first as it is being stored in the same locations
ROUGH PLOT	To save time only every fifth point is plotted
CHANGE REGIONS	Sets up regions for CALC REGIONS
CALC REGIONS	Calculates and prints the sum, mean, standard deviation of regions and rate of change between stored sets. A region can be 1-512 diodes and up to ten regions can be chosen
CALCULATE	Difference in the signals in a specified wavelength range between two consecutive spectra is calculated and printed for rate measurements
PRINT	Prints out the value of each data point in a region
STORE HERE	Stores next spectra accepted in a specified region of memory
CALIBRATE	Allows wavelength calibration for display and region calculations

COMP BS pulse is given for the clearing scan. This scan is used to remove light- or dark-signals accumulated on the detector before the integration time. At this point the ADC DONE BIT is cleared by the DATA TRANSMITTED signal. Since the IDA CLOCK is still being held low, the DONE BIT cannot be reset in this period. (E) The 33-kHz GATE is opened, the IDA is clocked and the ADC is started at the 33-kHz rate required by the computer for data-storage. (F) The program begins looking for the DONE BIT. Since the IDA CLOCK was inactive during (D) and the DONE BIT has been cleared, the first DONE BIT which is sensed after (E) is known to be generated by the first negative edge of the 33-kHz IDA CLOCK.

The amount of time required to perform the clearing scan must be exactly the same as the amount of time used during a data scan, so that each diode will have exactly the same integration time. To do this the same number of points is counted for the clearing scan, before the faster 100-kHz CLOCK is gated in, as is used for the data scan. During the clearing scan the data points are not stored. (G) The 33-kHz GATE is closed, the 100-kHz GATE is opened and the remaining diodes are clocked through at 100 kHz and the points are not counted or stored. (H) When the integration time is over, steps (C), (D) and (E), now labelled (I), (J), and (K), are repeated. That is, (I) the 100-kHz GATE is closed, (J) the COMP BS signal is sent and (K) the 33-kHz GATE is opened. (L) The program begins looking for the DONE BIT and starts taking data after the second DONE BIT since the signal from the first diode appears on the video line after the second IDA CLOCK transition from the IDA BS

signal. The program counts the number of points which will not be stored, and then counts and stores the data points which were requested. (M) After the requested points have been stored, the 33-kHz GATE is closed and the 100-kHz GATE opens to clock through the rest of the diodes.

Three different situations may arise at this point, depending on the number of sets and scans per set requested by the operator. (1) If more than one scan per set is requested, steps (H)-(N) are repeated for each additional scan and the data are added to the previous sum stored in the memory. (2) If more than one set is requested, the REFRESH signal goes high at (N), allowing refresh scans at intervals determined by S2. The computer determines the time between sets. Then steps (B)-(N) are repeated for each additional set. If all the requested scans and sets have been accepted, the REFRESH signal goes high at (N), allowing refresh scans to occur.

RESULTS AND DISCUSSION

Experimental studies were conducted to evaluate the performance characteristics of the IDA. The signal and noise expression are first reviewed as they provide the framework in which to discuss the results.

The total signal (N_T), in counts observed from a given group of diodes, is made up of three components as shown in equation (1).

$$N_T = N_0 + N_d + N_L \quad (1)$$

N_0 is the offset signal in counts and is the signal observed with zero integration time (extrapolated) and represents the counts due to the DC offset voltage on the video line. The offset voltage is normally set to a slightly positive value since the ADC is unipolar. The offset signal is given by

$$N_0 = n_0 sc \quad (2)$$

where n_0 is the offset signal per diode in counts, s the number of scans added together in one set, and c the number of channels for which signals are added together. N_d is the net dark-current signal in counts obtained when no light impinges on the detector, and is given to a first approximation by

$$N_d = tcsGd \quad (3)$$

where t is the integration time (sec) per scan, d the

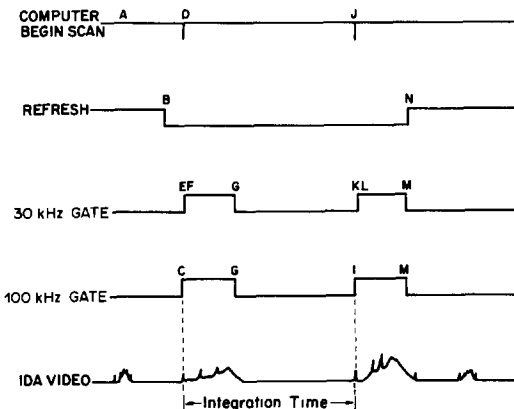


Fig. 3. Sequence of control signals from the computer and the resultant IDA VIDEO spectra.

dark-signal (electrons per sec) per channel, and G the gain factor for the electronics (counts per electron). It is assumed that d is the same for all the photodiodes. The value of d depends on the temperature of the DA and on the intensifier gain.

N_L is the net light-signal in counts, and given to a first approximation by

$$N_L = tcsmRG\Phi \quad (4)$$

where m is the gain of the intensifier-DA combination or the number of electron-hole pairs produced at the DA per photoelectron generated at the intensifier photocathode, R the responsivity of the intensifier photocathode (photoelectrons per photon) and Φ the incident light level per channel (photons per sec). Here it is assumed that Φ is constant with time and that Φ , m and R are identical for all channels.

The net dark-current signal is found by subtracting N_0 from the total dark signal ($N_{dt} = N_0 + N_d$). The net light-signal is found by subtracting N_{dt} from N_T for the same integration time t .

Noise may be attributed to variations in the read-out process, the dark-signal, and the photon-signal. The total noise, σ_T , is given by

$$\sigma_T = (\sigma_R^2 + \sigma_d^2 + \sigma_L^2)^{1/2} \quad (5)$$

where σ_R is the read-out noise (counts), including reset noise of the diodes in the DA and electronic noise from the IDA electronics and the data-acquisition and read-out circuitry, σ_d the dark-noise (counts) and σ_L the photon-noise (counts).

If there is no flicker noise in the light- or dark-signals, then only shot noise in these signals need be considered. The shot noise in these signals is proportional to the square root of the signal and if the read-out noise is random the following expressions apply:

$$\sigma_R = (cs\sigma_r^2)^{1/2} \quad (6)$$

$$\sigma_d = (tcsG^2d)^{1/2} \quad (7)$$

$$\sigma_L = [tcsR(mG)^2\Phi]^{1/2} \quad (8)$$

where σ_r is the read-out noise (in counts per channel per scan) and σ_{dt} is the noise in the total dark-signal [$\sigma_{dt} = (\sigma_d^2 + \sigma_R^2)^{1/2}$].

The signal-to-noise ratio (S/N) of the total measurement is presented by equations (9) and (10) if equations (2)-(4) are valid:

$$S/N = N_L/\sigma_T = N_L/(\sigma_R^2 + \sigma_d^2 + \sigma_L^2)^{1/2} \quad (9)$$

$$S/N = tcsmRG\Phi/[tcsR(mG)^2\Phi + tcsG^2d + cs\sigma_r^2]^{1/2} \quad (10)$$

To evaluate the validity of these signal, noise and S/N equations, c , t and s were varied, and mean signals and standard deviations were calculated. In most cases, 30 measurements were made for a given set of experimental conditions, to calculate means and standard deviations. In addition, memory effects,

spectral resolution, the effect of cooling the DA, and the effects of the intensifier gain on the data were evaluated. Unless otherwise stated, a Heath (Benton Harbor, MI) model EU-701-50 optically-stabilized tungsten light-source was used for light measurements.

Memory effects

Although diode arrays are normally considered not to exhibit lag (*i.e.*, all of the signal is read in one interrogation cycle), it was observed that after a large dark-signal had accumulated, several scans were required to reach a constant level for successive identical dark-signal integration periods. For example, the first spectrum obtained after a clearing spectrum, after the array was saturated with a dark-signal, was 3% higher than the average of nine subsequent spectra with identical integration times. This lag is not seen when a REFRESH signal is used to scan the diode array continuously every 20 msec until the computer takes control and provides timing and data storage. The REFRESH signal prevents the initial high value because the array is not allowed to be saturated with dark-signal. Lag has also been observed with other diode arrays^{6,7} and the Tracor Northern data-acquisition system provides for refresh scans when data are not being taken.

Whereas the signal which is carried over from a saturating dark-signal is removed after two scans, a longer lasting and larger effect is seen with light-signals. For example, when the intensifier was on, the slit briefly exposed and a light-signal allowed to saturate the array, it was found that five or more 2-sec scans were required to reach a stable baseline value after the exposure was terminated. Five sets of two 1-sec scans had the same effect. The ultraviolet-detecting regions of the array stabilized faster than the visible-detecting regions. These symptoms indicate that a longer lived component of the phosphor between the MCP intensifier and the DA may be causing the apparent lag of light-signals. The ultraviolet-detecting regions appeared to stabilize faster, because the light levels were lower there. If it was assumed that the decay was exponential, the half-life of the residual phosphorescence was found to be between 1 and 3 sec. One of the components of the phosphor is known to have a life time of about 30 msec and a longer lived component has also been observed by Tracor Northern.⁸ Cooling could cause the phosphorescence to persist longer.

Intensifier characteristics

The intensifier requires about 0.3 sec to reach 90% of its maximum gain once the switch is turned on. The combination of intensifier turn-off time and phosphor decay means that the diode array requires about 1 sec to go from full-scale signals with the intensifier on, to dark-levels with the intensifier off. The intensifier may be used as a shutter to prevent light signals from reaching the array before the

experiment, but sufficient time should be allowed for the intensifier to be fully operative at the beginning of the experiment.

The gain of the intensifier varies by a factor of about 50 between settings of 0.0 and 10.0 on the intensifier control potentiometer. When the light-signals are much larger than dark-signals, the relative standard deviation (RSD) of the light-signals is not significantly affected by the magnitude of the gain, but the intensifier may still be affecting the S/N of light-signals even when this effect is independent of the magnitude of the gain. It has been predicted for very large gains that the S/N is degraded by a factor of about 2 by a channel plate electron multiplier.⁹

There is a small dark-signal and noise contribution from the intensifier, which is greater at higher gains. This is due to thermal electrons from the intensifier photocathode, which are collected and amplified by the MCP intensifier. At an intensifier setting of 0.0, the dark-current signal and noise are the same whether the intensifier is on or off. With the intensifier switched on at the maximum gain setting of 10, and a 1-sec integration time, the dark-signal is ≈ 10 counts higher than the ≈ 180 count dark-current signal obtained with the intensifier off, and σ_d is about 8 counts, compared to about 4 counts with the intensifier off. Thus d in equations (3) and (7) must be determined for a given intensifier setting, and σ_d does not strictly equal $(tcsG^2d)^{1/2}$ since part of the dark-current noise arises from the dark-current generated in the DA and part from dark-current originating from the intensifier.

The intensifier degrades the resolution by a factor of about 2, according to the manufacturer's specifications. The maximum possible resolution, based only on the diode size of $50 \mu\text{m}$, is 20 line-pairs/mm. The specified resolution with the intensifier is 8 line-pairs/mm at 50% MTF (modulation transfer function), or 2.5 channels (3.1 nm with the spectrograph used). The measured resolution of the combination of IDA plus spectrograph fitted with the narrowest entrance slit (0.05 mm), for a mercury pen lamp placed in the sample cell of the fluorimeter, was 3.5 channels FWHM, or 4.4 nm.

Cooling characteristics

Tracor Northern specify 0° as the typical lower temperature limit obtainable with the Peltier effect thermoelectric cooler. Removing the heat generated by one side of the Peltier cooler allows it to cool more efficiently and attain lower temperatures. An aluminium water-cooled collar was constructed which fitted snugly around the portion of the IDA where the diode array and thermoelectric cooler were mounted. Tap water was continuously circulated through the collar at a constant rate, about 1–2 l./min, to remove the heat generated by the electronics and the cooler. With the collar the dark current stabilized in about 1 hr, in contrast to the several hr required without the collar. The dark-signal was about 80 counts per sec

when the collar was used, and 180 counts per sec when it was not. The dark-signal of photodiode arrays is known to be approximately doubled by a 7° temperature increase.^{5,10,11} Since the dark-current decreases by more than a factor of 2 with water cooling, the temperature of the array is about -10° when tap water is circulating through the cooling collar. At normal operating temperatures with the thermoelectric cooler on continuously, and with the collar cooled with tap water, a dark-signal equivalent to about 2% of saturation (80 counts out of 4095 at saturation) is accumulated per sec.

Dependence of signal levels on experimental variables

The characteristics of dark-signals and light-signals with respect to integration time, number of scans summed, and number of diodes summed were studied. The dark-signal was a non-linear function of the integration time. Figure 4 illustrates the curvature in the dark-signal graph at two different temperatures, viz. with and without the thermoelectric cooler operating. The curvature becomes significant when the dark-signal is equivalent to about 25% of the saturation level. The non-zero intercepts in Fig. 4 are due to an offset level of about 80 counts. The rapidity with which the dark-signal accumulates at room temperature, as shown in curve B, underscores the necessity for cooling the array, especially when working at low signal levels that require long integration times. The non-linearity of the dark-signals is rarely mentioned in the literature but has been observed.^{11,12} When the cooler is on, equation (3) is only valid up to an integration time of about 12 sec.

When the dark-signal reaches about 25% of full scale, the net light-signal is also a non-linear function of integration time. However, the non-linearity is not related to approach to saturation, as is shown by curve C in Fig. 5. Curve C was obtained at a light level high enough for the light-signals to approach

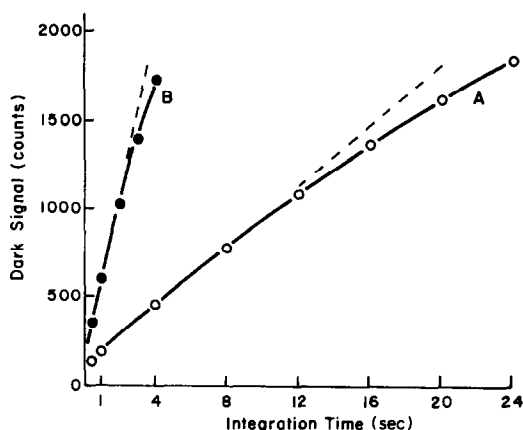


Fig. 4. Dependence of the dark-signal on integration time. (A) At approximately -10° , with use of the thermoelectric cooler. (B) At nearly room temperature, without the thermoelectric cooler. The dashed lines are straight lines for comparison.

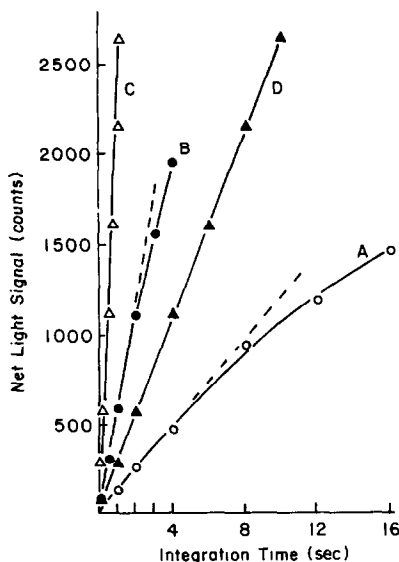


Fig. 5. Dependence of net light-signal on integration time at various light levels: A, with thermoelectric cooler; B and C, without thermoelectric cooler; D, same as curve C with the time axis expanded by a factor of 10 (e.g., a point at 4 sec corresponds to one at 0.4 sec). Light source: Hg-Xe lamp with a scatterer in the fluorimeter sample cell. Neutral density filters were used to vary the light intensity for A, B and C. Intensifier setting 2.5.

saturation before the dark-signals reached 5% of saturation.

Other experiments, with neutral density filters, indicated that for a constant integration time, the net light-signal is proportional to the incident light level. Thus the non-linear relation to integration time, discussed above, is due to processes in the DA and is not caused by the manner in which the signal is processed or sampled, or by the intensifier. The IDA is a linear light-detector with respect to light intensity, but all light measurements and dark-current measurements must be made with the same integration time for a correct net light-signal to be obtained.

The effect, on the signal magnitude, of adding together multiple scans in a set or several channels in a region was also examined. The total signal magnitude from c diodes increases in direct proportion to the number of scans obtained under identical conditions, for either dark- or light-signals. However, the individual response to the same amount of incident light or of dark-signal varies considerably from channel to channel both in terms of slight variations from diode to diode and larger deviations exhibited by some individual diodes. These variations are reproducible. The dark-signal for any one of the 512 diodes varied by less than 30% from the average dark-signal. Uniform illumination of the IDA with white light indicated that the diode-to-diode response varied by up to about 50% around the mean value, regardless of the intensifier gain. Thus in equation (3),

cd should be replaced by

$$\sum_{i=1}^c d_i$$

where d_i is the dark-current for any individual diode i , and in equation (4), $cmk\Phi$ should be replaced by

$$\sum_{i=1}^c m_i R_i \Phi_i$$

where m_i , R_i , and Φ_i are the gain, intensifier photocathode responsivity, and incident-light signal, respectively, for the i th diode.

The variation in response to light-signals could be due to non-uniformity in the photocathode responsivity, microchannel plate gain, phosphor emission, diode responsivity, or diode size. Tests which could differentiate between the effects of the photocathode, microchannel plate, or phosphor were not performed, because these components are in a sealed evacuated assembly.

Although the channel-to-channel variation does not affect the usefulness of the detector for quantitative measurements, it does affect the quality and usefulness of the spectra obtained. Variations may make it difficult to determine the maximum of an unknown peak for qualitative purposes. In addition, the spectra appear noisier than the signals really are. A corrected spectrum, free from detector distortion, can be obtained by use of the ratio of signal from each channel in a spectrum, to the relative response of the channel when the detector is uniformly illuminated.

Dependence of noise on experimental variables

The dependence of the standard deviation (SD) of the dark- and light-signals on t , n and c is shown in Table 2. All measurements except those at $t = 16$ sec were made so that the dark-signal was less than 25% of saturation, to ensure that N_L and N_d were proportional to t . All light measurements were made so that σ_L was $\gg \sigma_{d+1}$, and with uniform illumination of the intensifier photocathode.

The variation of the SD of the dark-signal with t , s and c agrees well with that predicted by theory [equations (6) and (7)] over the range of variation shown in Table 2. For the scan and channel number studies, σ_{di} is primarily due to read-out noise, and for the integration-time study, $\sigma_d \approx \sigma_r$ at $t = 7$ sec and σ_d is not measurable below $t = 2$ sec.

The SD of the dark-signal increases dramatically above 8 sec when the water-cooled collar is not used, because the drift in signal over the time required to collect 30 measurements is comparable to the SD. For $t = 16$ sec, $\sigma_d = 20$ counts without the cooling collar and 6 counts with the collar. Besides reducing the magnitude of the dark-signal, the additional cooling evidently stabilizes the temperature and the dark-signal. This becomes more evident and important at long integration times. Without the cooling collar, the theoretically predicted square

Table 2. Dependence of noise on experimental variables

Type	Variable*	Range	Slope†	SD§	RSD§, %
σ_d	t	2.0–16 sec	0.60	6	0.4
σ_d	s	1–50	0.52	27	0.5
σ_{dt}	c	1–100	0.50	33	0.2
σ_L	t	0.5–16 sec	0.49	22	1.2
σ_L	s	1–50	0.52	73	0.2

* $t = 1$ sec, $s = 1$, $c = 1$ except where variable is changed.

†Slope of plot of log of σ_d or σ_L vs. log of magnitude of variable, where 0.50 is the theoretical value from equations (7) and (8).

§SD in counts and RSD at maximum magnitude of variable in range.

root improvements in S/N were not obtained with integration times longer than 8 sec.

In most cases the SD of the dark-signal will not be limiting, because the noise inherent in the light-signals is much greater than the SD of the dark-signal. However, when work at very low signal levels and with long integration times is necessary, the temperature-related instability of the dark-signal can introduce unacceptable uncertainties into the total measurement. In these cases use of the water-cooled collar is recommended.

The fact that σ_{dt} is proportional to $s^{1/2}$ and $c^{1/2}$ means that ensemble averaging and multiplexing are applicable. Therefore, from equation (10), the S/N for low light levels increases in proportion to the square root of the number of scans or the number of channels added together ($\sigma_L < \sigma_{dt}$).

Table 2 also illustrates that the dependence of σ_L on t and s (ensemble averaging) agrees well with that predicted by equation (8). These square root relationships were observed when the stable tungsten lamp was used, but were not observed in all cases when scattering or fluorescence radiation studies with a xenon-mercury arc lamp as the excitation source. With this source, flicker noise and drift are obvious, and for longer integration times σ_L is 2 or 3 times greater than with the tungsten lamp.

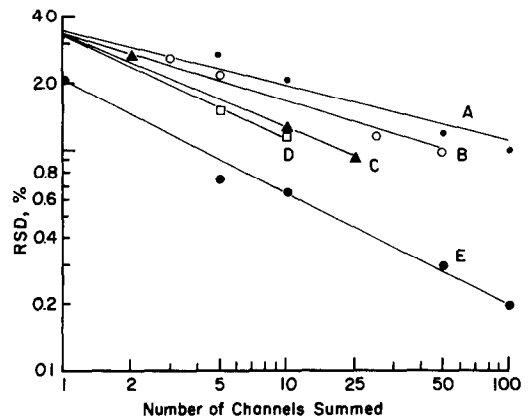
The SD of the light-signal did not vary with $c^{1/2}$ although according to equation (10) it should. Since the specified resolution of the intensifier is 2.5 channels, adjacent channels are not totally independent. Thus it is not surprising that adding together the signals from adjacent channels does not give the expected square root improvement in S/N. Curve A in Fig. 6 shows the change in RSD as signals from a greater number of channels are added together. The signal was obtained from the scattered light from a deuterium lamp in the tungsten light-source module. The scatter spectrum was relatively flat in the region used in the calculations. The slope of -0.27 indicates that the improvement in RSD is much less than that seen for the dark-signal in Curve E, Fig. 6. This result is independent of the intensifier gain. To investigate more fully the non-independence of channels, the data used for curve A were used to generate curves B, C and D by averaging the signals from non-adjacent channels. For curve B, every second channel

in a group was summed, for C every fifth channel and for D every tenth channel. Curves B, C, and D show that as the distance between the channels used increases the improvement in S/N approaches the square root dependence. Other studies confirmed the non-independence of the diodes. The SD of the sum of the signals from two channels was not equal to the square root of the sum of the variances of the signals from the individual channels if the channels were less than 7 diodes apart.

Other S/N considerations

The read-out noise of 3.5 counts is limiting for measurement of low light levels ($\sigma_d < \sigma_r$) when the integration time is less than about 7 sec and lower intensifier gain settings are used. At the highest intensifier gain, σ_d is greater than σ_r for integration times longer than about 1 sec owing to the increased dark-current noise originating from the intensifier. The SD of the data-acquisition circuitry was found to be only 1.2 counts with a stable voltage source attached to the S/H input and thus is insignificant compared to the read-out noise generated by the IDA and its electronics.

On the basis of the specified saturation charge⁵ of 3.2 pC of the DA used in this work and saturation at 4095 counts, one count is equivalent to about 4.9×10^3 electrons. Thus, the 3.5 counts of read-out noise of the IDA represent about 1.7×10^4 electrons. Read-out noise of the order of 1000 electrons has been reported^{7,11} for some DA and amplifier combinations. If such a DA-amplifier system was used with the intensifier used in this work, there would be



PLOT	SIGNAL	SLOPE	CHANNEL SEPARATION	SYMBOL
A	Light	-0.27	0	•
B	Light	-0.31	1	○
C	Light	-0.43	4	▲
D	Light	-0.45	9	□
E	Dark	-0.51	0	●

Fig. 6. Dependence of relative standard deviation of light and dark-signals on the number of channels summed. Conditions: 1 sec integration time, 4.5 intensifier gain setting. Signal level about 1600 counts for net light-signals.

insignificant improvement in the S/N at higher intensifier gains and longer integration times, since the dark-signal noise originating from the intensifier would be limiting as it is with the present system. Possibly, use of another intensifier photocathode with lower dark-current would improve S/N.

At the highest intensifier gain, $\sigma_L \approx (2N_L)^{1/2}$. This would indicate that one photoelectron from the intensifier photocathode is equivalent to 2 counts if the variation in the intensifier gain is insignificant, or 1 count if the variation in gain doubles the shot noise. The fact that 1 photoelectron is equivalent to 2 counts or about 10^4 electrons at the DA is also consistent with the calculations based on the nominal gain of the intensifier and the quantum efficiency of the DA. If the read-out plus dark-current noise (σ_{dt}) were one count, 1 photoelectron could be detected with an S/N = 1 or 2. Since $\sigma_{dt} = 8$ counts at full intensifier gain and $t = 1$ sec, the present system can detect a minimum of 4–8 photoelectrons (S/N = 1). This could be improved by first reducing σ_d and then σ_r . The read-out noise in recent commercial IDA systems is specified as about 1500 electrons. This allows the use of the resolving power of a 14-bit ADC, and the detection (S/N = 1) of about 1 photoelectron or 10 photons.

Equations (9) and (10) indicate that if σ_d or σ_r is comparable to or greater than σ_L (or d is comparable to $mk\Phi$), the gain of the intensifier, m , should be increased to improve the S/N, but once σ_L is dominant, a larger gain yields no improvement in S/N. This is tempered by the fact that at the larger intensifier gains σ_d is also increased by increasing m . For very low light levels, the S/N is improved by using nearly maximum intensifier gain and long integration times. At maximum intensifier gain with $t = 1$ sec and $s = c = 1$, $\sigma_L > \sigma_D$ if $N_L > \approx 60$ counts. The S/N

should also be improved by using the S series Reticon DA for which the individual diodes are over 5 times higher than those of the EC series DA used in this work.

Acknowledgement—Acknowledgement is made to the NSF (Grants # CHE-76-16711, CHE-79-21293 and CHE-84-01784) for partial support of this research, and one of us (M.R.-H.) gratefully acknowledges an NSF graduate fellowship and an American Chemical Society, Division of Analytical Chemistry Summer Fellowship sponsored by General Motors Research Laboratory. Presented in part at the 1979 Pittsburgh Conference, Cleveland, Ohio, the 1980 Pittsburgh Conference, Atlantic City, New Jersey, and the 184th ACS National Meeting, Kansas City, Missouri, 1982.

REFERENCES

1. M. A. Ryan, R. J. Miller and J. D. Ingle, Jr., *Anal. Chem.*, 1978, **50**, 1772.
2. M. A. Ryan and J. D. Ingle, Jr., *Talanta*, 1981, **28**, 225.
3. *Idem*, *Luminescence Measurements with an Intensified Diode Array*, in *Multichannel Detectors*, Y. Talmi (ed.), Vol. 2, pp. 155–170. American Chemical Society, Washington, DC, 1983.
4. D. F. Marino and J. D. Ingle, Jr., *Anal. Chem.*, 1981, **53**, 645.
5. *Reticon C Series Solid State Line Scanners*, Reticon Corp., Sunnyvale, CA, 1976.
6. R. G. Tull, J. P. Choisser and E. H. Snow, *Appl. Optics*, 1975, **14**, 1182.
7. Y. Talmi and K. W. Bush, *Guidelines for the Selection of Four Optoelectronic Image Detectors for Low-Light Level Applications*, in *Multichannel Detectors*, Y. Talmi (ed), Vol. 2, pp. 130. American Chemical Society, Washington, DC, 1983.
8. D. Osten, Tracor Northern Corp., personal communication, Middleton, WI, 1979.
9. P. Schagen, in *Advances in Image Pickup and Display*, B. Kazan (ed.), Vol. 1, pp. 1–69. Academic Press, New York, 1974.
10. J. F. McNall and K. Nordsieck, *An Intensified Self-Scanned Array Detector System that is Photon Limited*, preprint, University of Wisconsin, Madison WI.
11. R. W. Simpson, *Rev. Sci. Instrum.*, 1979, **50**, 730.

COMPARATIVE STUDY OF ANALYTICAL INDUCTIVELY- COUPLED ARGON-PLASMA DISCHARGES USING DIFFERENT OUTER GASES

G. ZARAY, J. A. C. BROEKAERT*, R. G. BÖHMERT† and F. LEIS

Institut für Spektrochemie und angewandte Spektroskopie, Postfach 778, D-4600 Dortmund 1,
Federal Republic of Germany

(Received 23 December 1986. Accepted 12 February 1987)

Summary—The analytical capabilities of high power (2–4 kW) ICPs with argon as inner and intermediate gas and different outer gases (argon, nitrogen, oxygen and air) were studied under optimum and compromise operating conditions. Under the optimum conditions, the lowest detection limits for elements with sensitive atom lines (C, B, Zn) or ion lines (Mg, Mn, Fe, Cr, Ti, V) were achieved with argon as outer gas and an observation height of 13 mm. Under compromise conditions (3 kW, aerosol gas gauge-pressure 3 bar) the lowest detection limits for the atom lines were also found with a pure argon plasma at an observation height of 13 mm. For ion lines, however, the argon/oxygen and argon/nitrogen plasmas and an observation height of 8 mm were better. The detection limits were poorer in the presence of an aluminium matrix; under the optimum operating conditions, the relative increase in detection limit was smaller with the argon/oxygen and argon/air ICPs than with the pure argon or argon/nitrogen ICPs. It was found that the interferences arising from an easily ionizable matrix are lower with a diatomic gas than with argon as outer gas. The interferences when the argon/nitrogen, argon/oxygen and argon/air plasmas are used are similar and practically independent of the nebulizer-gas pressure applied.

With respect to the use of diatomic gases, ICP sources can be divided into two groups. In the first, one of the three argon gas streams is partly or completely replaced by a stream of a diatomic gas.^{1–31} ICPs using only diatomic gases^{32–39} form the second group. In their early work on inductively-coupled plasma optical-emission spectrometry (ICP-OES), Greenfield and co-workers^{1–10} used diatomic gases both as outer gas and aerosol gas and studied the effect of N₂, O₂, H₂ and air on the analytical capabilities of the ICP. They found that high-power plasmas with diatomic gases in the outer gas flow have a smaller diameter than an argon plasma operated at the same power. This was explained as due to absorption of energy in dissociation of the diatomic gases. They further reported a substantial reduction in the continuum radiation when diatomic gases (especially nitrogen) were used in the outer stream. The optimum power itself was found to depend on the torch dimensions and on the type of the outer gas (e.g., the Greenfield torch with nitrogen as outer gas: 0.8–2.6 kW). When optimizing for each line, Greenfield and Burns¹⁰ concluded that for an argon plasma with nitrogen as outer gas, the signal-to-background ratios are higher than those obtained with an argon plasma. Montaser and co-workers^{11–13}

reported that the highest net line emission at any forward power and observation height was found when the outer gas was argon containing 5–15% v/v nitrogen. However, owing to the higher background intensities in these plasmas, the detection limits were higher than those observed for argon plasmas. Indeed, under the compromise conditions found for 20 lines, the detection limits and signal-to-background ratios of ion and atom lines having high excitation energies in an argon plasma (1.2 kW, observation height 15 mm) were superior to those obtained with the argon plasma (2.5 kW, observation height 10 mm) with nitrogen as outer gas. This disagrees with the results of Greenfield and co-workers. However, it should be noted that the torch, the analytical lines and the operating conditions were quite different.

Many authors^{14–22} have discussed the analytical applications of the argon/nitrogen plasmas, but few have studied the argon/oxygen or argon/air plasmas. Zeeman *et al.*²³ performed diagnostic studies with a 9-MHz argon/air ICP, and Ohls and Sommer^{24–26} studied the analytical performance of 3-kW argon/air, argon/oxygen and argon/nitrogen plasmas. They found that the argon/air and the argon/oxygen plasmas give higher sensitivities and lower detection limits for most analytical lines than the argon/nitrogen plasma does.

Recently, Choot and Horlick²⁷ demonstrated that argon ICPs, in which a 1:9 v/v mixture of a diatomic gas and argon was used as outer gas, showed superior

*To whom correspondence should be sent.

†On leave from the University of Pretoria, Republic of South Africa.

signal-to-noise ratios. The best signal-to-noise ratios were obtained at an observation height lower than that used with the conventional argon plasmas. Signal-to-noise ratios for ion lines measured with the optimized mixed-gas plasmas were 3–4 times those obtained with the argon plasma, but the signal-to-noise ratios for atom lines were hardly improved.

The diatomic gases have also been used as aerosol carrier gas for argon ICPs. The use of nitrogen as aerosol carrier gas impoverished the detection limits for all elements tested.^{11,12} With an argon/hydrogen mixture as aerosol carrier gas, the signal-to-background ratios for most analytical lines were increased.^{28,29} By inclusion of 0.5–5% v/v oxygen in the aerosol gas, the background intensities in the analysis of organic solutions can be reduced to the level obtained with aerosols of aqueous solutions.^{30,31} Recently, ICP discharges for spectrochemical purposes have been operated entirely with diatomic gases.^{32–36} The detection limits for the air and the oxygen ICPs are on average poorer by factors of 1–30 and 2–100, respectively, than those obtained with the argon ICP.

The influence of easily ionizable elements (EIE) on analyte emission in argon ICPs has been studied by many groups.^{37–47} Some papers focus on nebulization effects, whereas others study the overall interferences as a function of carrier-gas flow, power and observation height. Axial intensity distributions for atom and ion lines in the presence of EIE matrices were measured with the aid of a photodiode array^{43–45} or a movable mask outside the entrance slit of the monochromator.⁴⁶ In general, the addition of EIE enhances emission in the lower regions of the aerosol injection channel for both atom and ion lines. The emission intensities for both atom and ion species were found to be decreased in the upper regions of the channel.⁴⁴ The interferences of EIE in argon ICPs with a diatomic gas as outer gas have been studied much less than those experienced in the case of argon ICPs. Watson and Steele⁴⁸ found that with a 5.5-kW argon/nitrogen ICP and an observation height of

10 mm, the intensities of different atom and ion lines in the presence of sodium (1–30 g/l) increased. However, at an observation height of 15 mm, there was a significant decrease for all the analytical lines investigated. Choot and Horlick²⁷ found that in the argon/nitrogen and argon/oxygen ICPs, the influence of potassium on a calcium ion line was lower than that in a pure argon ICP.

Because the high-power argon ICPs with diatomic gases as outer gas are particularly robust (which is attractive for routine work), and all comparisons up to now have been made with different instrumentation or within a limited range of rf power, it was decided to compare the analytical capabilities of argon/nitrogen, argon/oxygen, argon/air and argon ICPs operating in the same Greenfield torch, with the same nebulizer and the same spectrometer. Further, the rf power and the aerosol carrier gas pressure were varied within a wide range. The results of a comprehensive study of the influence of the outer gas, forward power, observation height and gauge pressure of the aerosol argon on the background, net analyte emission, signal-to-background ratios and detection limits are presented here. The influence of EIE on the net line intensities and the influence of an aluminium matrix on the detection limits obtained with the optimized operating parameters are reported.

EXPERIMENTAL

ICP emission spectrometric instrumentation

A high-power ICP-system and a computer-controlled emission spectrometer were used. Argon, nitrogen, oxygen and air were used as the outer gas. A concentric glass nebulizer was operated at a gauge pressure of 2.0–3.5 bar, with free aspiration. At this pressure the nebulizer gas flow-rates were 1–1.8 l./min. The procedure involved aspiration of sample for 15 sec, then integration of the signal over a 10-sec period, and finally rinsing for 30 sec with demineralized water. The background signals were estimated from on-line measurements on demineralized water.

Table 1. Instrumental and operational parameters

<i>ICP</i>	
High-frequency generator	FS-10 (Kontron-Linn), maximal output power 10 kW; frequency 27.12 MHz; free-running with power stabilization; forward power used in this work 2–4 kW.
Torch	As described by Greenfield <i>et al.</i> ⁴⁹ Outer gas flow 25 l./min; intermediate gas flow 8 l./min (argon)
Nebulization	Pneumatic concentric glass nebulizer (Meinhard Assoc.), operated at 2–3.5 bar with free sample aspiration; nebulization chamber as described by Scott <i>et al.</i> ⁵⁰
<i>Spectral apparatus</i>	
Illumination	Three-lens system, 4 × 4 mm observation zone located centrally in the ICP, 6–10 and 11–15 mm above the rf-coil and selected at the intermediate image. ⁵¹
Polychromator	A 1-m Paschen-Runge vacuum spectrometer (modified Baird Spectrovac 1000) with computer-controlled displacement of the entrance slit; grating constant 1/1440 mm; width 50 mm; height 30 mm; entrance slit-width 25 μm, exit slit-width 89 μm, wavelength range 173–385 nm 2nd order, 346–767 nm 1st order; photomultipliers 1 P 28, R 166; computer Modcomp II. Analytical lines (nm): Zn I (213.8), B I (249.7), Fe II (259.9), Cr II (267.7), Mg II (279.5), Mn II (293.3), V II (310.2), Cu I (324.7), Ti II (337.2). Integration time 10 sec.

The experimental facilities, operating conditions and analytical lines used are given in Table 1.

N.B. All pressures reported are gauge pressures.

Preparation of solutions

The analyte solution contained nine elements (Zn, B, Fe, Cr, Mg, Mn, V, Cu, Ti) and was prepared from stock solutions (Titrisol, Merck). A matrix solution of aluminium was prepared from the pure metal (99.997%, Aluisse, Switzerland). For dissolution, 1 g of the aluminium was heated in a PTFE beaker with 20 ml of demineralized water, 3 drops of 1% mercuric chloride solution (to accelerate the dissolution) and 20 ml of concentrated hydrochloric acid. After cooling, the solution was accurately diluted to 100 ml. No contamination problems were encountered, as the measurements for the comparison study—which was the aim of the work—could be made with relatively high analyte concentrations (50 µg/ml). All test solutions were finally adjusted to have a hydrochloric acid concentration of 0.15M.

RESULTS AND DISCUSSION

Effect of the type of outer gas, the forward power and the argon carrier-gas flow-rate on the background intensities, net line intensities and line-to-background ratios

In Fig. 1, the background intensities, net line intensities and line-to-background ratios of three analytical lines having very different excitation energies (Zn I 213.8 nm, Mn II 293.3 nm, Cu I 324.7 nm) and measured at an observation height of 13 mm are shown as a function of the forward power and the aerosol gas pressure. It can be seen from Fig. 1(a) that the background intensities increase with the forward power (2–4 kW). In contrast to the ICPs with diatomic gases as outer gas, the background of the pure argon plasma is particularly low at all three wavelengths investigated. The net line intensities also increase with increasing power except for the Cu 324.7 nm line in the argon/air plasma, which shows a maximum at 2.5 kW. The highest net intensities for all three analytical lines were obtained at 2–3.5 kW for the argon/air plasma and 4 kW for the argon/oxygen plasma. The line-to-background ratios for all three analytical lines increase with power in the range 2–4 kW for the argon/oxygen ICP and decrease for the argon/nitrogen ICPs. With the argon/air plasma, the line-to-background ratios for Zn I (213.3 nm) and Mn II (293.3 nm) practically do not change with power, but for Cu I (324.7 nm), a decrease is found. With the argon plasma, increasing the power from 2 to 3 kW is favourable for the Zn I line, but disadvantageous for the Cu I and Mn II lines.

In most cases the background intensities decrease when the aerosol gas pressure is increased from 2.0 to 3.5 bar [Fig. 1(b)]. With the argon/air and argon/nitrogen plasmas the net line intensities and line-to-background ratios for the three analytical lines investigated then increase. The analytical lines with high excitation energy (Zn I 213.8 nm and Mn II 293.3 nm) both reach a maximum at an aerosol gas pressure between 2.5 and 3.0 bar, for the

argon/oxygen plasma. For the argon plasma, however, increasing the aerosol gas pressure leads to a considerable deterioration of the net line intensities and line-to-background ratios.

For the analytical lines with low excitation energy, such as Cu I 324.7 nm, the net intensity and line-to-background ratio increase with increasing aerosol gas pressure in the argon/oxygen plasma and reach a maximum at 2.5 bar in the argon plasma.

At an aerosol gas pressure of 2 bar, the highest net line intensities for the three analytical lines are obtained with the argon plasma, but at all higher gas pressures investigated they are obtained with the argon/air plasma. As nebulization effects become smaller with increasing aerosol gas pressure, it appears that argon ICPs with diatomic gases as outer gas are especially favourable with respect to matrix effects.

Power of detection under optimum and compromise operating conditions

To optimize the operating conditions for the argon ICPs with different outer gases, the line-to-background ratios for the nine analytical lines were measured at varying forward power (2–4 kW) and aerosol gas pressure (2–3.5 bar) for observation heights of 8 and 13 mm. The optimum power and aerosol carrier-gas pressure for the simultaneous determination of the nine elements were determined as the mean of the values giving the optimum line-to-background ratios for each individual line and element (Table 2). They were practically the same at both observation heights, and the values were Ar/Ar 2.0 kW, 2.0 bar; Ar/N₂ 2.5 kW, 3.5 bar; Ar/O₂ 4.0 kW, 3.5 bar; Ar/air 3.0 kW, 3.5 bar. The argon ICPs with diatomic gases as outer gas were found to need a higher power and aerosol gas pressure than the argon ICP.

The detection limits c_L were calculated according to Kaiser and Specker⁵² from the line-to-background intensity ratios as $c_L = 0.01c (I_U/I_X) 3\sqrt{2}$, where I_U is the intensity of the spectral background, I_X the net line intensity for an analyte concentration c , $3\sqrt{2}$ is the probability factor, and 0.01 corresponds to a relative standard deviation of 1% for I_U . The values obtained for the nine elements under optimum operating conditions for observation heights of 8 and 13 mm are listed in Table 3. These values are often higher than the literature values.¹⁵ This is related to the use of a polychromator possessing exit slits with widths of 89 µm, resulting in a lower practical resolution and consequently a decrease in power of detection. It can be seen that the detection limits of the argon plasma at an observation height of 13 mm are superior to those of the other plasmas at both observation heights.

Under optimum operating conditions, the mean of the detection limits for the argon/nitrogen, argon/oxygen and argon/air plasmas is respectively 2, 4 and 8 times higher than that for the argon plasma.

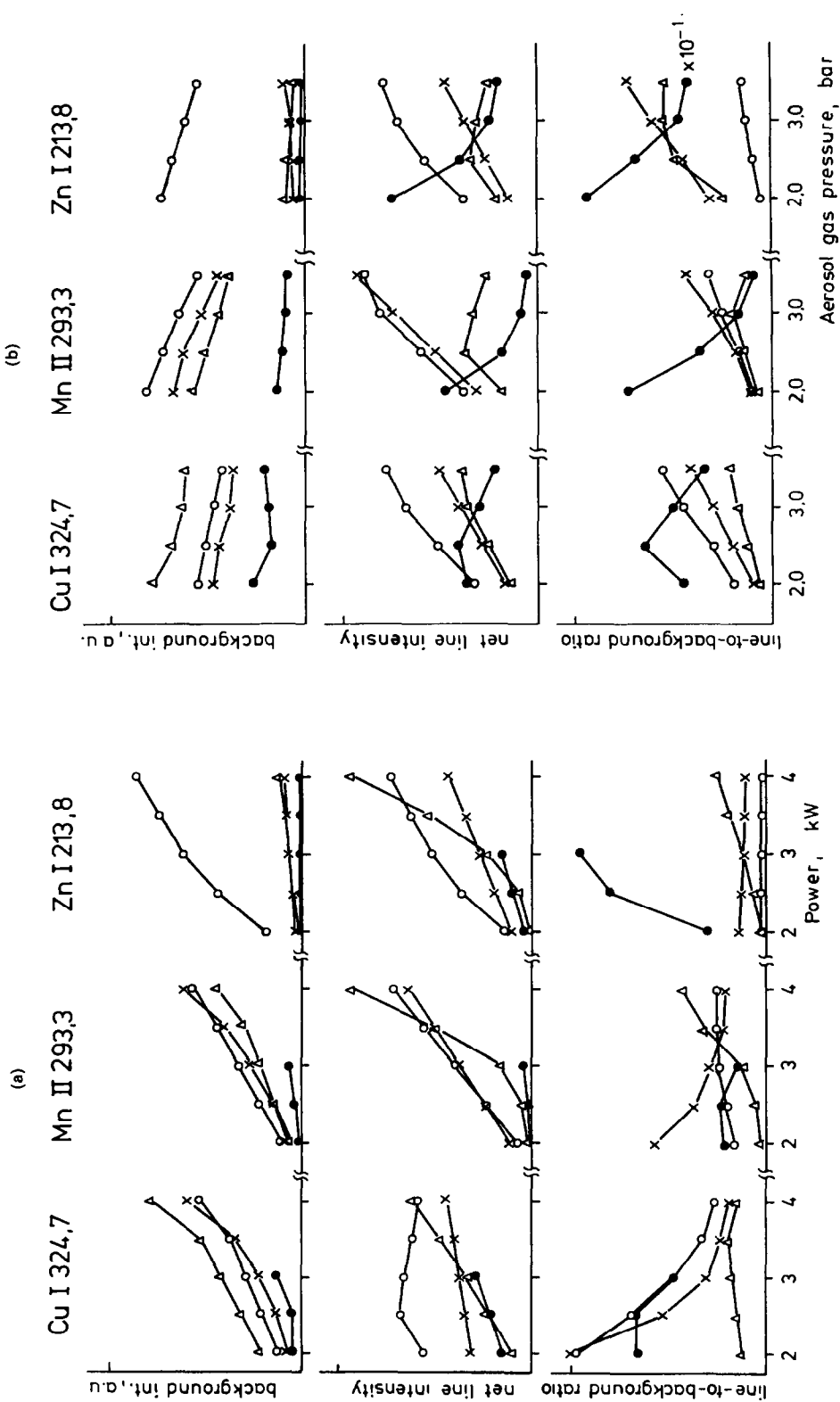


Fig. 1. Influence of (a) forward power and (b) aerosol gas pressure on background intensities, net line intensities and line-to-background ratios, arbitrary units (a.u.). Observation height 13 mm; outer gases (●) Ar; (×) N₂; (○) O₂; (△) forward power 3 kW.

Table 2. Optimum power and aerosol carrier-gas pressure values for the nine analytical lines in argon, argon/nitrogen, argon/oxygen and argon/air ICPs

Element line, <i>nm</i>	Ar/Ar		Ar/N ₂		Ar/O ₂		Ar/air	
	<i>kW</i>	<i>bar</i>	<i>kW</i>	<i>bar</i>	<i>kW</i>	<i>bar</i>	<i>kW</i>	<i>bar</i>
B I 249.7	2.0	2.5	2.5	3.5	4.0	3.5	3.0	3.5
Cu I 324.7	2.0	2.0	2.0	3.5	3.5	3.5	2.0	3.5
Zn I 213.8	2.5	2.0	4.0	3.5	4.0	3.5	4.0	3.5
Cr II 267.7	2.0	2.0	3.0	3.5	4.0	3.5	4.0	3.5
Fe II 259.9	2.0	2.0	2.5	3.5	4.0	3.5	4.0	3.5
Mg II 279.5	2.0	2.0	3.0	3.5	4.0	3.5	4.0	3.5
Mn II 293.3	2.0	2.0	2.0	3.5	4.0	3.5	3.5	3.5
Ti II 337.2	2.0	2.0	2.0	3.5	3.5	3.5	2.0	3.5
V II 310.2	2.5	2.0	2.0	3.5	4.0	3.5	3.0	3.5
<i>Mean values:</i>	2.0	2.0	2.5	3.5	4.0	3.5	3.0	3.5

The highest difference is found for the Zn atom line, for which the detection limit in the argon/air plasma is 112 times that in the argon ICP. The detection limits in the four plasmas were also determined under compromise conditions (3 kW, aerosol gas pressure 3 bar) at observation heights of 8 and 13 mm. It is clear from Table 4 that at an observation height of 8 mm, the argon/oxygen plasma gives the best power of detection. These results agree with the observations of Ohls and Sommer.²⁶ It should, however, be noted

that for the atom lines investigated, the lowest detection limits are still those in the argon plasma at an observation height of 13 mm.

Despite the fact that the net intensities in the argon/air plasma for all the analytical lines investigated are higher than those in the other ICPs studied, the detection limits obtained with the argon/air ICP are much closer to those with the other plasmas. From records of the background spectrum between 200 and 500 nm under compromise working

Table 3. Detection limits for argon, argon/nitrogen, argon/oxygen and argon/air ICPs under optimum operating conditions

Element line, <i>nm</i>	Detection limits, $\mu\text{g/ml}$							
	Observation height 8 mm				Observation height 13 mm			
	Ar/Ar	Ar/N ₂	Ar/O ₂	Ar/air	Ar/Ar	Ar/N ₂	Ar/O ₂	Ar/air
B I 249.7	0.07	0.08	0.11	0.22	0.02	0.06	0.18	0.27
Cu I 324.7	0.02	0.01	0.08	0.04	0.004	0.007	0.06	0.01
Zn I 213.8	0.005	0.01	0.03	0.45	0.004	0.02	0.05	0.55
Cr II 267.7	0.06	0.03	0.08	0.10	0.03	0.04	0.12	0.19
Fe II 259.9	0.04	0.02	0.06	0.06	0.01	0.02	0.09	0.11
Mg II 279.5	0.002	0.001	0.003	0.005	0.0006	0.002	0.006	0.006
Mn II 293.3	0.08	0.06	0.08	0.09	0.03	0.07	0.22	0.24
Ti II 337.2	0.06	0.05	0.05	0.04	0.01	0.04	0.02	0.03
V II 310.2	0.06	0.02	0.06	0.08	0.02	0.03	0.09	0.08

Table 4. Detection limits for argon, argon/nitrogen, argon/oxygen and argon/air ICPs under compromise operating conditions

Element line, <i>nm</i>	Detection limits, $\mu\text{g/ml}$							
	Observation height 8 mm				Observation height 13 mm			
	Ar/Ar	Ar/N ₂	Ar/O ₂	Ar/air	Ar/Ar	Ar/N ₂	Ar/O ₂	Ar/air
B I 249.7	0.08	0.09	0.07	0.15	0.03	0.09	0.37	0.32
Cu I 324.7	0.08	0.02	0.02	0.04	0.01	0.03	0.05	0.02
Zn I 213.8	0.09	0.07	0.06	0.51	0.02	0.14	0.15	0.62
Cr II 267.7	0.89	0.08	0.10	0.17	0.27	0.11	0.44	0.27
Fe II 259.9	0.39	0.03	0.07	0.10	0.06	0.03	0.27	0.15
Mg II 279.5	0.02	0.002	0.003	0.005	0.005	0.003	0.007	0.007
Mn II 293.3	0.91	0.12	0.09	0.11	0.51	0.29	0.51	0.32
Ti II 337.2	0.33	0.05	0.04	0.05	0.14	0.05	0.04	0.05
V II 310.2	0.92	0.11	0.09	0.13	0.61	0.15	0.29	0.12

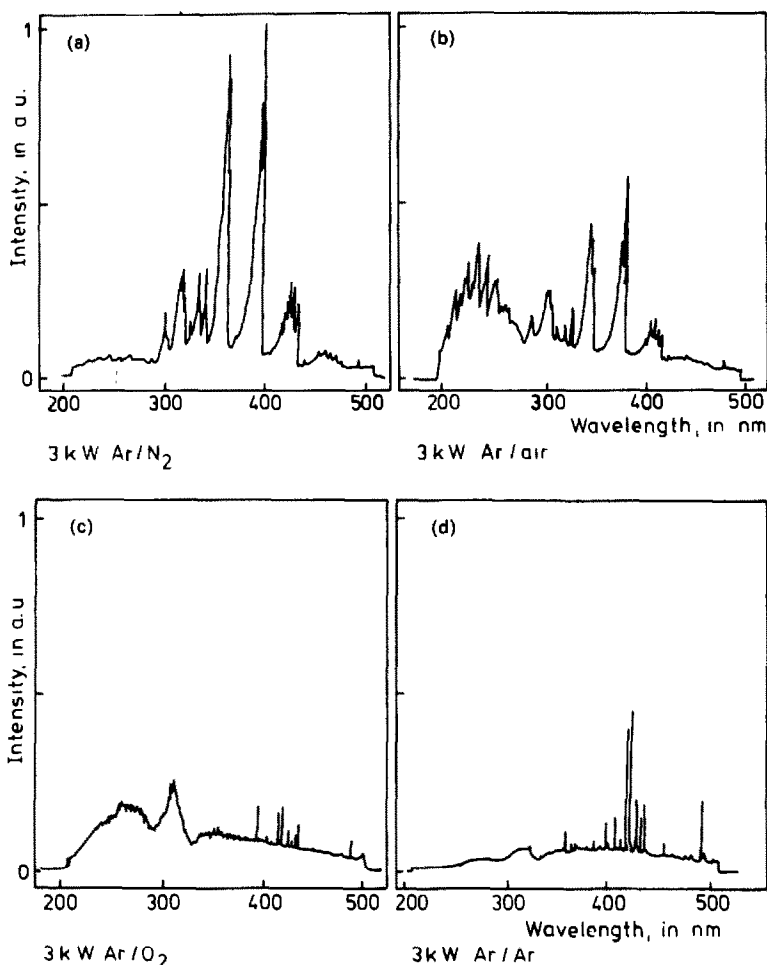


Fig. 2. Emission spectrum of argon ICPs with different outer gases operated at 3 kW with aspiration of demineralized water at aerosol gas pressure 3 bar. Observation height 13 mm; wavelength range 200–500 nm; (a) nitrogen, (b) air, (c) oxygen, (d) argon.

conditions and at an observation height of 13 mm above the load coil (Fig. 2), it can be seen that the argon plasma has the lowest background continuum intensities and is almost free from molecular bands, with the exception of the OH band. However, N_2 and N_2^+ occur with the argon/nitrogen ICP, and N_2 , N_2^+ , CN and γ -NO bands with the argon/air plasma. In the argon/air plasma the γ -NO band system extends over the wavelength range 200–280 nm, where many elements have their most sensitive emission lines. Therefore, the detection limits for these elements are poorer than those obtained by use of other gases. The argon/nitrogen plasma does not display intense molecular bands between 200 and 280 nm yet the background continuum intensities measured are greater by a factor of 2–4 than those obtained with the pure argon plasma. The argon/oxygen plasma has no clearly resolved molecular bands in the whole spectral range studied but exhibits a substantially higher background continuum between 200 and 280 nm than that of the argon or the argon/nitrogen ICP. It should be noted that the intensity of the different

molecular band systems changes considerably with the gas flow-rates and observation heights.

Interferences caused by the presence of aluminium as matrix

The effect of aluminium at a concentration of 10.0 mg/ml on the net line intensities of the same nine elements at a concentration of 50 μ g/ml and on the background intensities was measured for the four ICPs operated under optimum conditions. The following trends were observed.

1. In the presence of an aluminium matrix, the net line intensities are decreased, except for the atom lines observed in the pure argon ICP.

2. In the presence of an aluminium matrix, the spectral background intensities are increased, except for the argon/nitrogen ICP at wavelengths between about 260 and 300 nm (Fig. 3).

The background intensity at 213.8 nm increases considerably owing to broadening of the Al I 213.0

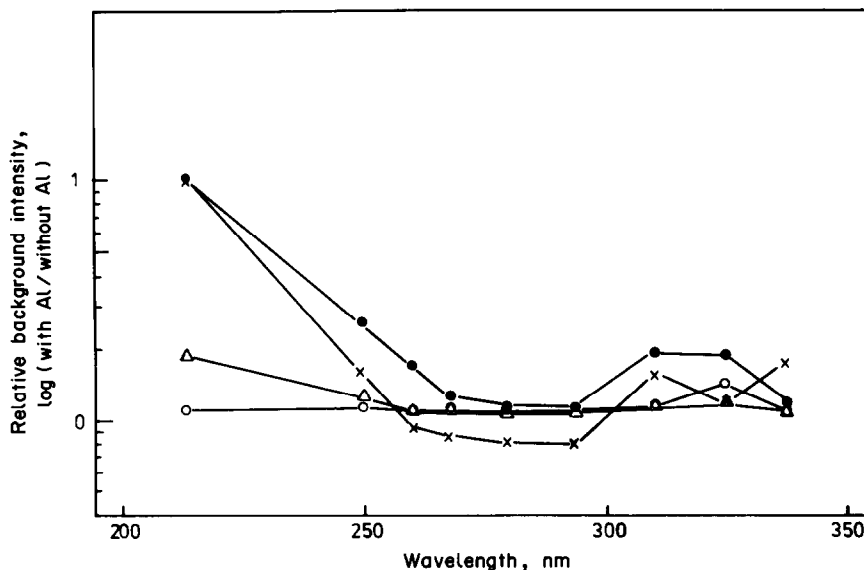


Fig. 3. Influence of an aluminium matrix on background intensities between 213 and 337 nm for argon ICPs with different outer gases. Observation height 13 mm. Outer gas: (●) Ar, 2 kW, 2 bar; (×) N₂, 2.5 kW, 3.5 bar; (△) O₂, 4 kW, 3.5 bar; (○) air, 3 kW, 3.5 bar.

and 214.6 nm lines.⁵³ The detection limits in the presence of an aluminium matrix are listed in Table 5. In all cases, they are higher than in the absence of aluminium, the relative increases under optimized conditions for the argon, argon/nitrogen, argon/oxygen and argon/air plasmas being 104, 81, 38 and 34%, respectively. However, it should be noted that the last two plasmas are operated at higher power, which may contribute to a reduction of the matrix effect.

Interference effect of sodium on the observed emission of the analyte elements

The net line intensities and background intensities in the four plasmas were measured for 50- μ g/ml analyte solutions containing sodium at the 1000- μ g/ml level. In Fig. 4, the ratios of the net intensities for Cu I 324.7 nm, Zn I 213.8 nm and Mn II 293.3 nm with and without sodium present are

shown as a function of the aerosol carrier-gas pressure and for observation heights of 8 and 13 mm, respectively. The measurements were made at the optimum power level for each type of ICP (Table 2). From the results the following conclusions may be drawn.

1. The interference effect of sodium is much larger for the argon plasma than for the argon ICPs with a diatomic gas as outer gas.

2. In the argon ICP the extent of the interference increases with aerosol gas pressure at both observation heights, except for spectral lines of high excitation energies such as Zn I 213.8 nm and Mn II 293.3 nm. Here, a maximum is reached (in the lower region of the plasma) at about 3 bar pressure. In the case of the argon plasmas with a diatomic gas as outer gas, the influence of the aerosol gas pressure on the extent of interference is substantially smaller and in some cases negligible.

Table 5. Detection limits for argon, argon/nitrogen, argon/oxygen and argon/air ICPs under optimum operating conditions with and without aluminium matrix

Element line, nm		Detection limits, μ g/ml							
		Without Al matrix				With Al matrix			
		Ar/Ar	Ar/N ₂	Ar/O ₂	Ar/air	Ar/Ar	Ar/N ₂	Ar/O ₂	Ar/air
B	I 249.7	0.02	0.06	0.18	0.27	0.06	0.09	0.23	0.33
Cu	I 324.7	0.004	0.007	0.06	0.01	0.02	0.01	0.09	0.03
Zn	I 213.8	0.004	0.02	0.05	0.55	0.05	0.08	0.09	0.66
Cr	II 267.7	0.03	0.04	0.12	0.19	0.04	0.06	0.18	0.33
Fe	II 259.9	0.01	0.02	0.09	0.11	0.03	0.04	0.09	0.14
Mg	II 279.5	0.0006	0.002	0.006	0.006	0.003	0.005	0.007	0.01
Mn	II 293.3	0.03	0.07	0.22	0.24	0.04	0.09	0.25	0.28
Ti	II 337.2	0.01	0.04	0.02	0.03	0.03	0.06	0.09	0.09
V	II 310.2	0.02	0.03	0.09	0.08	0.04	0.05	0.11	0.12

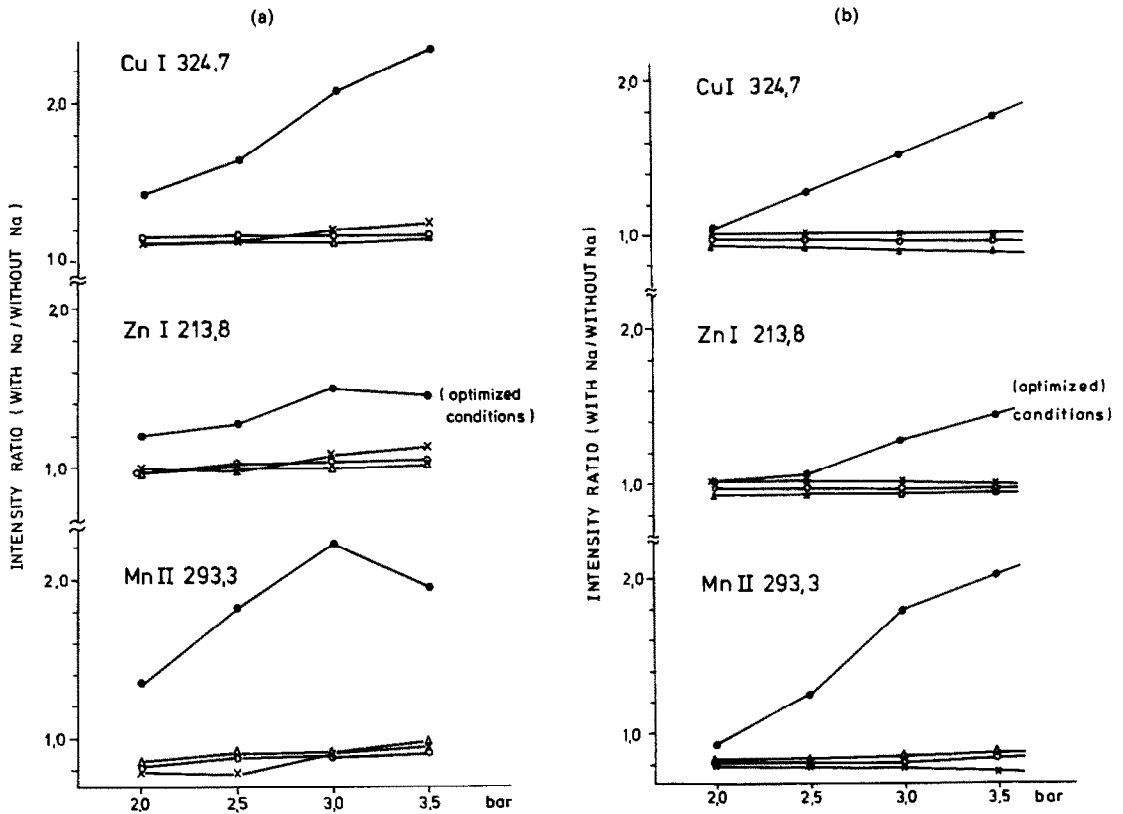


Fig. 4. Interference of sodium for argon ICPs with different outer gases as a function of aerosol gas pressure. (●) Ar 2 kW; (×) N₂ 2.5 kW; (△) O₂ 4 kW; (○) air; 3 kW. Observation height (a) 8 mm, (b) 13 mm.

3. As known from the literature cited, the interferences also depend on the observation height; for the argon plasmas with a diatomic gas as outer gas, however, the influence of this parameter on the matrix effect is not as critical as for the argon ICP.

4. As expected, the interferences differ from one line or element to another. In the argon plasma, at both observation heights, the enhancements for Zn I 213.8 nm were found to be half those for Cu I 324.7

nm and Mn II 293.3 nm. In the argon ICPs with diatomic gases as outer gas there is a signal depression, except for the Cu and Zn atom lines, at an observation height of 8 mm.

5. It seems that the interference effect of sodium at the optimum power is minimal for the argon plasma at an aerosol gas pressure of 2 bar and an observation height of 13 mm, and for the argon ICPs with a diatomic gas as outer gas, at 3.5 bar and 8 mm. The

Table 6. Relative changes in background intensities at optimum power as a function of aerosol gas pressure and observation height

Element line, <i>nm</i>	Aerosol gas pressure, <i>bar</i>	Observation height 8 mm				Observation height 13 mm			
		Ar/Ar	Ar/N ₂	Ar/O ₂	Ar/air	Ar/Ar	Ar/N ₂	Ar/O ₂	Ar/air
Cu I 324.7	2.0	0.95	3.8	0.84	-0.84	6.8	-2.9	0.54	-1.1
	2.5	11	-15	0.93	0.32	6.2	3.1	1.3	1.5
	3.0	3.2	-18	2.4	0.64	12	6.5	1.5	2.2
	3.5	1.1	8.6	3.6	1.9	3.5	18	2.5	10
Zn I 213.8	2.0	74	2.7	6.2	1.4	62	-5.5	2.9	1.8
	2.5	92	-4.1	6.8	1.1	37	0.0	3.5	1.4
	3.0	44	-4.7	11	0.65	77	0.0	6.6	0.93
	3.5	5.5	5.6	14	1.1	68	4.1	0.54	2.9
Mn I 293.3	2.0	2.2	2.6	2.8	0.73	7.8	0.83	0.74	0.45
	2.5	8.9	-11	1.3	0.92	7.7	5.7	0.82	1.7
	3.0	0.96	-16	3.5	2.5	13	0	0.63	-0.24
	3.5	-2.8	11	5.2	1.1	0	16	2.1	5.2

extent of the interference is then similar to the values reported by Boumans and de Boer³⁹ for an argon ICP.

The relative changes of the background intensities when sodium is present are given in Table 6 for the wavelengths 213.8, 293.3 and 324.7 nm. The results for different aerosol gas pressures and observation heights show that the background intensities usually increase in the presence of sodium. The extent of the changes in the case of the argon, argon/nitrogen, argon/oxygen and argon/air plasmas were from -3 to +93%, -19 to +18%, +0.5 to +15% and -1 to +10%, respectively. For the argon and the argon/oxygen plasmas, the highest changes in the background intensities were at 213.8 nm and for the argon/nitrogen and argon/air plasmas at 324.7 nm. Only for the argon/nitrogen plasma was a depression of the background intensity observed, at 293.3 and 324.7 nm.

CONCLUSIONS

1. The best detection limits under optimized conditions for both atom and ion lines are obtained with an argon ICP at an aerosol pressure of 2 bar, a forward power of 2 kW, and an observation height of 13 mm.

2. Under compromise operating conditions (3 kW, aerosol gas pressure 3 bar), the lowest detection limits for atom lines are obtained with an argon plasma and an observation height of 13 mm. For ion lines, however, the argon/oxygen and argon/nitrogen plasmas, with an observation height of 8 mm, give better values. The optimum observation zone for the argon ICPs with a diatomic outer gas is lower than that for the argon plasma.

3. The spectral background intensities in the wavelength region 200–500 nm are lowest for an argon ICP. With air or nitrogen as outer gas, the background intensities are substantially higher and intense γ -NO, N₂, N₂⁺ and CN, or N₂ and N₂⁺ molecular bands, respectively, occur. The argon/oxygen ICP has a low spectral background only in the wavelength region 320–500 nm.

4. With diatomic gases as outer gas, the influence of EIE on both atom and ion lines is lower than that with argon as outer gas. For the argon/nitrogen, argon/oxygen and argon/air ICPs under optimum analytical conditions, the extent of this interference is similar and practically independent of the aerosol gas pressure in the range 2–3.5 bar.

5. For the four plasmas under optimum operating conditions, the aluminium matrix causes a depression of the net signal (except for atom lines in the argon plasma). In general, aluminium increases the background, and consequently poorer detection limits are achieved. The deterioration of the detection limits with the argon/oxygen and argon/air ICPs is less than that with the argon or argon/nitrogen ICPs.

Acknowledgements—The work was supported by the "Ministerium für Wissenschaft und Forschung des Landes Nordrhein-Westfalen" and by the "Bundesministerium für Forschung und Technologie" (Bonn). G. Zaray thanks the Alexander-von-Humboldt-Foundation (Bonn, Bad God- esberg) for the grant of a Research Fellowship.

REFERENCES

1. S. Greenfield, *Proc. Soc. Anal. Chem.*, 1965, **2**, 111.
2. S. Greenfield, P. B. Smith, A. E. Breeze and N. M. D. Chilton, *Anal. Chim. Acta*, 1968, **41**, 385.
3. S. Greenfield and P. B. Smith, *ibid.*, 1971, **57**, 209.
4. S. Greenfield, *Metron Rovigo*, 1971, **3**, 224.
5. R. M. Dagnall, D. J. Smith, T. S. West and S. Greenfield, *Anal. Chim. Acta*, 1971, **54**, 397.
6. S. Greenfield and P. B. Smith, *ibid.*, 1972, **59**, 341.
7. S. Greenfield, H. M. McGeachin and P. B. Smith, *Talanta*, 1976, **23**, 1.
8. S. Greenfield, I. L. Jones, H. M. McGeachin and P. B. Smith, *Anal. Chim. Acta*, 1975, **74**, 225.
9. S. Greenfield and H. M. McGeachin, *ibid.*, 1978, **100**, 101.
10. S. Greenfield and D. T. Burns, *ibid.*, 1980, **113**, 205.
11. A. Montaser and J. Mortazavi, *Anal. Chem.*, 1980, **52**, 255.
12. A. Montaser, V. A. Fassel and J. Zalewski, *Appl. Spectrosc.*, 1981, **35**, 292.
13. A. Montaser and V. A. Fassel, *ibid.*, 1982, **36**, 613.
14. J. A. C. Broekaert, F. Leis and K. Laqua, *Talanta*, 1981, **28**, 745.
15. A. Aziz, J. A. C. Broekaert and F. Leis, *Spectrochim. Acta*, 1982, **37B**, 369.
16. I. B. Brenner, A. E. Watson, T. W. Steele, E. A. Jones and M. Goncalves, *ibid.*, 1981, **36B**, 785.
17. G. L. Moore, P. J. Humphries-Cuff and A. E. Watson, *ibid.*, 1984, **39B**, 915.
18. L. Ebdon, M. R. Cave and D. J. Mowthorpe, *Anal. Chim. Acta*, 1980, **115**, 179.
19. *Idem*, *ibid.*, 1980, **115**, 171.
20. L. Ebdon and M. R. Cave, *Analyst*, 1982, **107**, 172.
21. K. Ohls and D. Sommer, *Z. Anal. Chem.*, 1979, **296**, 241.
22. *Idem*, *ibid.*, 1979, **295**, 337.
23. P. B. Zeeman, S. P. Terblanche, K. Visser and F. H. Hamm, *Appl. Spectrosc.*, 1978, **32**, 572.
24. K. Ohls and D. Sommer, *ICP Inf. Newsl.*, 1979, **4**, 532.
25. *Idem*, *Developments in Atomic Plasma Spectrochemical Analysis*, R. Barnes (ed.), p. 321. Heyden, London, 1981.
26. *Idem*, *ICP Inf. Newsl.*, 1984, **9**, 555.
27. E. H. Choot and G. Horlick, *Spectrochim. Acta*, 1986, **41B**, 889, 907, 925, 937.
28. P. Schramel, R. Fisher, A. Wolf and S. Hasse, *ICP Inf. Newsl.*, 1981, **6**, 401.
29. P. Schramel and Xu. Li-qiang, *Z. Anal. Chem.*, 1984, **319**, 229.
30. B. Magyar, P. Lienemann and S. Wunderli, *GIT Fachz. Lab.*, 1982, **26**, 541.
31. B. Magyar, P. Lienemann and H. Vonmont, *Spectrochim. Acta*, 1986, **41B**, 27.
32. R. M. Barnes and G. A. Meyer, *Anal. Chem.*, 1980, **52**, 1523.
33. R. M. Barnes and S. Nikdel, *Appl. Spectrosc.*, 1976, **30**, 310.
34. *Idem*, *J. Appl. Phys.*, 1976, **47**, 3.
35. G. A. Meyer and M. D. Thompson, *Spectrochim. Acta*, 1985, **40B**, 195.
36. G. A. Meyer and R. M. Barnes, *ibid.*, 1985, **40B**, 893.
37. G. F. Larson, V. A. Fassel, R. H. Scott and R. N. Kniseley, *Anal. Chem.*, 1975, **47**, 238.
38. J. M. Mermet, *Spectrochim. Acta*, 1975, **30B**, 383.

39. P. W. J. M. Boumans and F. J. De Boer, *ibid.*, 1975, **30B**, 309.
40. *Idem*, *ibid.*, 1976, **31B**, 355.
41. G. R. Kornblum and L. De Galan, *ibid.*, 1977, **32B**, 455.
42. R. N. Savage and G. M. Hieftje, *Anal. Chem.*, 1980, **52**, 1267.
43. G. Horlick and M. W. Blades, *Appl. Spectrosc.*, 1980, **34**, 229.
44. M. W. Blades and G. Horlick, *Spectrochim. Acta*, 1981, **36B**, 881.
45. H. Kawaguchi, T. Ito, K. Ota and A. Mizuike, *ibid.*, 1980, **35B**, 199.
46. S. R. Koirtjohann, J. S. Jones, C. P. Jester and D. A. Yates, *ibid.*, 1981, **36B**, 49.
47. L. M. Faires, C. T. Apel and T. M. Niemczyk, *Appl. Spectrosc.*, 1983, **37**, 558.
48. A. E. Watson and T. W. Steele, *ICP Inf. Newsl.*, 1980, **5**, 553.
49. S. Greenfield, I. Jones and C. T. Berry, *Analyst*, 1964, **89**, 713.
50. R. H. Scott, V. A. Fassel, R. N. Kniseley and D. E. Nixon, *Anal. Chem.*, 1975, **46**, 75.
51. J. A. C. Broekaert, F. Leis and K. Laqua, *Spectrochim. Acta*, 1979, **34B**, 73.
52. H. Kaiser and H. Specker, *Z. Anal. Chem.*, 1956, **149**, 46.
53. G. F. Larson and V. A. Fassel, *Appl. Spectrosc.*, 1979, **33**, 592.

A GRAPHICAL DERIVATIVE APPROACH TO THE PHOTOMETRIC DETERMINATION OF LUTETIUM AND PRASEODYMIUM IN MIXTURES

F. GARCIA SANCHEZ, M. HERNANDEZ LOPEZ and J. C. MARQUEZ GOMEZ

Department of Analytical Chemistry, Faculty of Sciences, The University, 29071-Malaga, Spain

(Received 1 September 1986. Accepted 12 February 1987)

Summary—The reaction of lanthanides with 1,4-dihydroxyanthraquinone has been examined and optimum conditions have been found for the separate spectrophotometric determination of Lu and Pr. A graphical method based on use of first and second derivative spectra has been developed for analysis of binary mixtures of the two, in concentration ratios from 1:5 to 5:1. Linear calibration curves were obtained between 1 and 10 $\mu\text{g/ml}$.

Individual lanthanides are usually determined by either physical methods such as emission spectrography or a combination of chemical and physical methods (such as neutron-activation analysis, or chemical processing followed by X-ray fluorescence spectrometry). Where the total lanthanide content in rocks and minerals is required, gravimetric methods can be used. Lanthanide determination at trace levels is still very difficult because of interelement interferences or lack of sensitivity when instrumental analytical techniques are directly used without prior sample treatment.

Isotope-dilution mass spectrometry,^{1,2} neutron-activation analysis^{3,4} and ICP-AES interfaced with HPLC⁵ are used for lanthanide determination. Isotope-dilution mass spectrometry provides high sensitivity but the selectivity is rather poor, and Pr, Tb, Ho and Tm cannot be detected because these elements do not have more than one multiple stable isotope.

The chief problem in quantitative analysis for the rare-earth elements is generally selectivity. Many reagents have been suggested for the spectrophotometric determination of lanthanides but none is specific and even the most selective requires extractive separation to remove interfering elements. Reagents suggested for the spectrophotometric determination of total lanthanide content include Alizarin Red S, aluminon, Xylenol Orange, Arsenazo I, Arsenazo III, PAN and PAR. None is specific for lanthanides as a group and their selectivity is poor. Until now, the reagent studied here, 1,4-dihydroxyanthraquinone, has not been reported as a ligand for the spectrophotometric determination of lanthanides.

The most recent approach to improvement of the selectivity of spectrophotometric methods is the use of derivative techniques of various kinds for resolution of overlapping spectral bands.

This paper reports a method based on use of the first and second derivative spectra of the

praseodymium and lutetium complexes of 1,4-dihydroxyanthraquinone. The method is an extension of that used in the simultaneous determination of acetaminophen and sodium salicylate.⁶

EXPERIMENTAL

Apparatus

Spectral measurements were made with a Shimadzu UV-240 Graphicord recording spectrophotometer and 1-cm fused-silica cells. The spectra were obtained with a bandwidth of 0.5 nm and a scan-speed of 3 nm/sec with recording on a 10 nm/cm scale. First and second derivative spectra were obtained with a Shimadzu derivative spectrum attachment (model OPI-2 optional program/interface) capable of taking 1st-4th order derivatives with $\Delta\lambda$ values of 1, 2 and 4 nm.

Reagents

Stock lanthanide solutions (~ 9 g/l.) were prepared from the 99.99% pure oxides (Merck or Sigma). The oxide was dissolved in concentrated hydrochloric acid, then excess of the oxide was added and the surplus was filtered off. The solution had a pH of 4-5. The solutions were standardized by titration with EDTA, Xylenol Orange being used as indicator.

1,4-Dihydroxyanthraquinone (DHA) was recrystallized from methanol (analytical reagent grade) and a $10^{-3}M$ solution prepared in the same solvent.

Procedure

Place 4 ml of DHA solution and a portion (≤ 1 ml) of sample solution (pH 4.5-6.5, containing 1-100 μg of lutetium and praseodymium) in a 10-ml standard flask. Dilute to volume with water and methanol to give a final 90% v/v methanol concentration. Record the first and second derivative spectra between 530 and 590 nm against a reagent blank, using the following fixed instrumental parameters: $\Delta\lambda = 4$ nm, scan speed = 3 nm/sec.

Determine Lu from the first derivative spectrum by measuring $dA/d\lambda$ at the isodifferential point for Pr (559.5 nm) and comparing the value with a calibration graph. Determine Pr from the second derivative spectrum by measuring $d^2A/d\lambda^2$ at the isodifferential point for Lu (564 nm) and comparing the value with the appropriate calibration graph. The wavelengths of the isodifferential points quoted are those we obtained, but they should be established independently for other instruments or conditions as part of the calibration procedure.

Preparation of calibration graphs. Prepare a series of lutetium solutions covering the range 1–10 $\mu\text{g/ml}$ and a similar series of praseodymium solutions. Treat the solutions as above and record the first and second derivative absorption spectra for each series, with all the spectra of a given order superimposed on the same chart paper. Use the first derivative curves to locate an isodifferential point (on the base-line) for each series of solutions; these points correspond to the wavelengths of maximal absorption in the fundamental spectra (555.5 nm for lutetium and 559.5 nm for praseodymium). Plot the lutetium first derivative amplitudes at 559.5 nm against concentration to obtain a calibration graph free from interference by praseodymium. Similarly plot the praseodymium second derivative amplitudes at 564 nm (the isodifferential wavelength for lutetium) against concentration.

RESULTS AND DISCUSSION

Solvent effects on spectral data

Figure 1 shows the absorption spectra of DHA and its complex with lutetium in DMF and 90% v/v methanol media. A considerable red-shift on chelation is observed, with both media. The absorbance difference between the spectra of the complex and the free ligand is maximal near 560 nm.

The effect of various solvents on the absorption spectra of the ligand and complex is shown in Table 1. The wavelengths of maximum absorption are affected only slightly by solvent polarity, but the effect on the molar absorptivity of the complex is very important in selection of the solvent. In DMF the absorbance decreases by 50% in 30 min, and methanol is the best solvent since it gives both good sensitivity and adequate stability.

After the selection of methanol, the influence of water was studied. The absorbance decreases increasingly rapidly as the water content is raised above 10%, so 90% v/v methanol medium is essential.

Photometric conditions

DHA reacts with lutetium and praseodymium to form purple complexes with absorption maxima at 555.5 and 559.5 nm, respectively, in 90% methanolic medium. Chelate formation is very rapid and the absorbance remains constant (within 2%) for at least 4 hr. For complete chelation, a fourfold molar excess of ligand is sufficient. The composition of the complexes was established as 1:1 by the molar ratio method.

Selectivity of lutetium determination

All the lanthanides react with DHA under the same conditions to form purple complexes. Table 2 shows that there are considerable variations in the molar absorptivities, and with increase in atomic number there is a progressive blue shift in the absorption maxima. The nature of the spectra makes it impossible to use them directly to determine the individual lanthanides in mixtures without prior separation.

Table 1. Spectral characteristics of DHA (R) and its lutetium complex (C) in different aqueous mixtures

Organic solvent	Content, % v/v	λ_a , nm		log ϵ^*	
		R	C	C	R
<i>N,N</i> -DMF	90	480	566	4.06	2.39
ethanol	90	480	558	3.96	0.0
methanol	90	478	555.5	4.06	0.0
acetonitrile	90	478	550	3.59	0.0
acetone	90	478	559	3.72	0.0
dioxan	90	480	558	2.94	0.0
dioxan	60	476	560	3.12	0.0
dioxan	40	480	560	2.64	0.0
dioxan	20	480	560	3.12	2.39
methanol	50	480	555.5	3.62	0.0

*At λ_{max} of the complex; units $\text{l. mole}^{-1} \cdot \text{cm}^{-1}$.

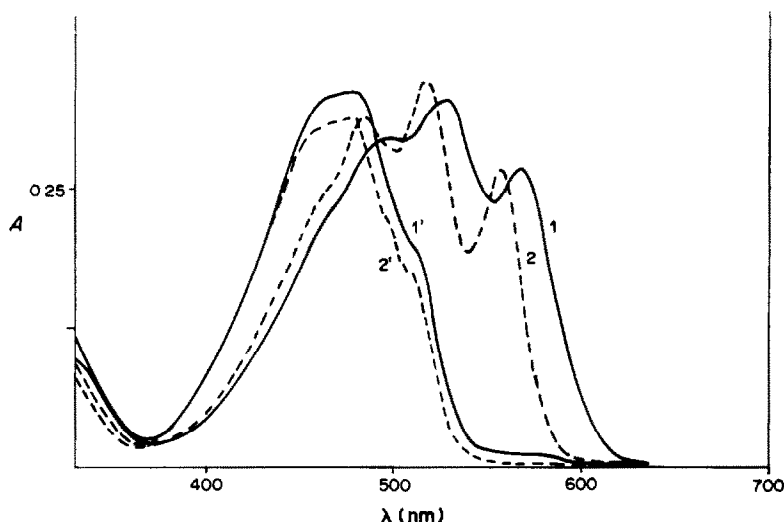


Fig. 1. Absorption spectra of DHA (1', 2') and its lutetium complex (1, 2) in 90% v/v methanol (2, 2') and *N,N*-dimethylformamide (1, 1'). $[\text{Lu}] = 2.3 \times 10^{-5} M$; $[\text{DHA}] = 4 \times 10^{-4} M$.

Table 2. Spectral shifts in the lanthanides series

	λ_{\max} , nm	$\log \epsilon_{\max}$
Ce	561.5	3.70
Pr	559.5	3.80
Nd	559	3.81
Sm	558.2	4.03
Gd	557.7	3.70
Tb	557	4.10
Dy	556.2	3.94
Ho	557	3.97
Er	556.7	4.03
Tm	557	3.99
Lu	555.5	4.07

The derivative spectra, however, may provide ways of increasing the selectivity. Figure 2 shows the first derivative spectra for series of solutions containing increasing amounts of lutetium or praseodymium. The isodifferential point for the praseodymium series, corresponding to the absorption maximum, is at 559.5 nm, and that for lutetium at 555.5 nm. These points are of analytical interest because in a mixture of the two lanthanides lutetium can be determined by measurement of the first derivative spectrum at 559.5 nm, where the contribution from the praseodymium is zero. Figure 3 shows that the second derivative spectrum similarly allows determination of praseodymium by measurement at 555.5 nm.

Selection of instrumental variables

The dependence of the derivative spectra on the

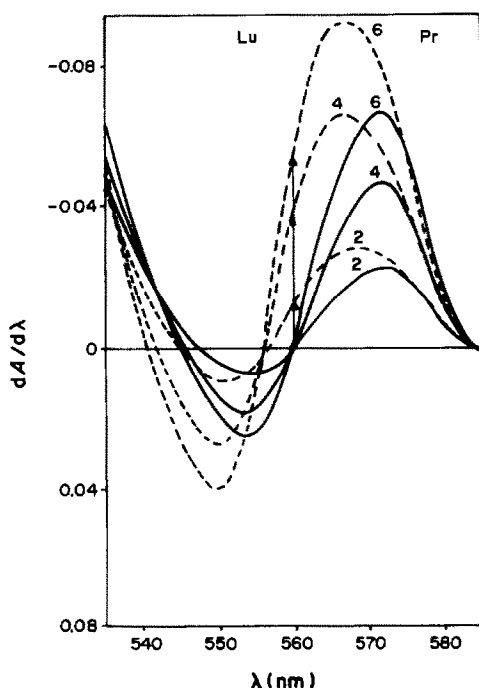


Fig. 2. First derivative absorption spectra of Lu-DHA and Pr-DHA standard solutions. [DHA] = $4 \times 10^{-4} M$. Numbers indicate concentrations in $\mu\text{g/ml}$.

instrumental parameters in the cases studied follows the general pattern for derivative spectroscopy.⁸ The main instrumental parameters affecting the shape of the derivative spectra are the wavelength scanning speed (v_{scan}), the wavelength increment over which the derivative is obtained ($\Delta\lambda$), the response-time (t_r), and the derivative order. In general, high v_{scan} and $\Delta\lambda$ values give large amplitudes but low resolution, while high t_r values give small amplitudes but good signal-to-noise (S/N) ratios. However, these general trends are restricted by the interdependence of the three parameters. Thus, $\Delta\lambda$ must be $\leq \delta\lambda$ (where $\delta\lambda$ is the peak width at half height) if good resolution is needed, and the scan-speed and response-time must satisfy the condition $v_{\text{scan}(\max)} = \delta\lambda/t_r$ if drift effects and distorted derivative spectra are to be avoided. The derivative order should be the lowest needed to achieve the analytical objective, since the S/N ratio worsens with increasing derivative order. In the present work, moderate values of v_{scan} (3 nm/sec) and $\Delta\lambda$ (4 nm) were employed; response-times were automatically selected by the OPI attachment in accord with the v_{scan} used.

Calibration graphs, sensitivity and precision

All the methods used gave linear graphs of absorbance, $dA/d\lambda$ and $d^2A/d\lambda^2$ vs. lutetium and/or praseodymium concentration (in $\mu\text{g/ml}$), with intercepts all close to zero.

The sensitivity of the method is expressed as the analytical sensitivity, $S_A = S_s/m$, where S_s is the standard deviation of the analytical signal and m is the slope of the calibration graph. The detection limit, C_L , and determination limit, C_Q , are reported as defined by IUPAC.¹⁰ C_Q is used to establish the lower limit of the linear dynamic range. The precision, expressed as the relative standard deviation from 11 replicate samples containing 4.0 $\mu\text{g/ml}$ of Lu and 4.0 $\mu\text{g/ml}$ of Pr respectively, is given in Table 3, and deteriorates with increase in derivative order (as expected from increasing S/N degradation with derivative order).

Simultaneous determination of lutetium and praseodymium in binary mixtures

The absorption maximum of the DHA-Lu complex is at 555.5 nm, too close to that of the DHA-Pr complex (559.5 nm) for resolution of the mixture even by the traditional method of measurement of the total absorbance at two wavelengths and use of simultaneous equations to calculate the concentration of the individual components.¹¹ Derivative spectrophotometry enhances the detectability of minor spectral features, and its ability to discriminate between closely related spectral shapes makes it useful in several areas of analytical spectrometry.¹² Several approaches, generally based on trial and error methods, have been used for quantitative evaluation of the derivative spectra of solutions containing mixtures of analytes.

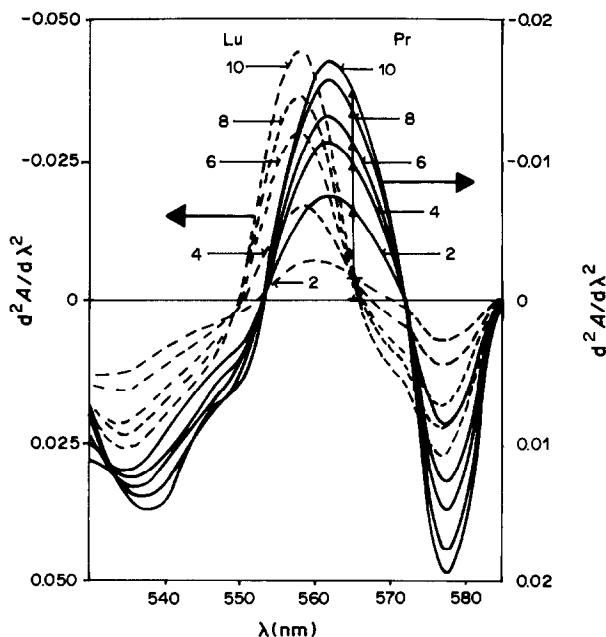


Fig. 3. Second derivative absorption spectra of Lu-DHA and Pr-DHA standard solutions. [DHA] = $4 \times 10^{-4}M$. Numbers indicate concentrations in $\mu\text{g/ml}$.

The method used in this paper is based on the assumptions that Beer's law is obeyed in the concentration range studied and that for a mixture the amplitude of a derivative spectral band is equivalent to the sum of the amplitudes of the component derivative bands.

The first derivative spectrum is simply the plot of the gradient, $dA/d\lambda$, of the absorption envelope, as a function of λ , and passes through zero at the wavelength of maximum absorption in the fundamental spectrum. When the spectra of binary mixtures of two components of concentration c_1 and c_2 are recorded

Table 3. Characteristics of the analytical methods

Method		Sensitivity, S_A , $\mu\text{g/ml}$	$C_1(k=3)$, $\mu\text{g/ml}$	Linear dynamic range, $\mu\text{g/ml}$	R.S.D., %
Lu	Normal photometry	0.044	0.08	0.26–10	0.2
	1st derivative	0.036	0.07	0.24–10	0.9
	2nd derivative	0.114	0.20	0.68–10	1.2
Pr	Normal photometry	0.170	0.24	0.8–10	0.3
	1st derivative	0.087	0.17	0.5–10	0.9
	2nd derivative	0.120	0.36	1.2–10	1.2

Table 4. Analysis of binary mixtures of lutetium and praseodymium

Method	Lu:Pr, w/w	Lutetium, $\mu\text{g/ml}$		Praseodymium, $\mu\text{g/ml}$	
		Taken	Found*	Taken	Found*
1st derivative	1:4	4.00	$4.00 \pm 0.2_5$		
	1:2.5	4.00	$4.00 \pm 0.1_8$		
	1:1	4.00	$4.00 \pm 0.2_4$		
	2:1	4.00	$4.10 \pm 0.1_9$		
	2.5:1	10.00	$9.70 \pm 0.1_6$		
2nd derivative	5:1	20.00	$19.80 \pm 0.2_9$		
	5:1			4.00	$4.00 \pm 0.2_2$
	2:1			2.00	$1.90 \pm 0.0_9$
	1:1			4.00	$4.00 \pm 0.1_3$
	1:2.5			10.00	$9.65 \pm 0.1_8$
	1:5			20.00	$20.49 \pm 0.1_5$

*Three determinations; standard deviation calculated from $0.59 \times$ range.

with a path-length b , the following equations can be written:

$$\text{(at } \lambda_1) \quad A_1 = \epsilon_1 bc_1 + \epsilon_2 bc_2$$

and

$$\frac{dI/d\lambda_1}{I} = -bc_1 d\epsilon_1/d\lambda_1 - bc_2 d\epsilon_2/d\lambda_1$$

$$\text{(at } \lambda_2) \quad A_2 = \epsilon'_1 bc_1 + \epsilon'_2 bc_2$$

and

$$\frac{dI/d\lambda_2}{I} = -bc_1 d\epsilon'_1/d\lambda_2 - bc_2 d\epsilon'_2/d\lambda_2$$

where ϵ_1 and ϵ_2 are the molar absorptivities of compounds 1 and 2 at λ_1 , and ϵ'_1 and ϵ'_2 those at λ_2 ; I is the band intensity.

When $d\epsilon_1/d\lambda_1 = 0$ (corresponding to a maximum in the zero order spectrum) the contribution of component 1 to the overall derivative amplitude is zero and, consequently, component 2 may be measured free of interference from component 1. The same applies to component 1 when $d\epsilon_2/d\lambda = 0$.

In a broad sense, optimal conditions should be obtained if the first derivative amplitude of compound 1 is zero when the first derivative for compound 2 is maximal. This condition is satisfied if the first derivative spectrum of 1 and the second derivative spectrum of 2 pass through zero at the same wavelength.

These considerations are of analytical interest for predicting whether two overlapping bands can be measured satisfactorily by using the isodifferential approach. Only a few data on the fundamental spectra of the overlapping compounds are needed, *viz.* the maximum absorbance (A), the band half-width at half maximum height (B), and the wavelength (C) of the absorption maximum.

Resolution of the overlapping spectra of a mixture of two compounds is simplified when the overlapping bands are both Gaussian. In that case the intensities of the bands (1 and 2) as functions of wavelength (x) are given by

$$I_1(x) = A_1 \exp[-(x - C_1)^2/2B_1^2]$$

$$I_2(x) = A_2 \exp[-(x - C_2)^2/2B_2^2]$$

The first derivative of band 1 is

$$\frac{dI_1(x)}{dx} = \frac{-A_1(x - C_1)}{B_1^2} \exp\left[-\frac{(x - C_1)^2}{2B_1^2}\right]$$

and the second derivative of band 2 is

$$\frac{d^2 I_2(x)}{dx^2} = \frac{A_2}{B_2^2} \left[\frac{(x - C_2)^2}{B_2^2} - 1 \right] \exp\left[-\frac{(x - C_2)^2}{2B_2^2}\right]$$

Maximum sensitivity and precision are obtained in the isodifferential derivative method when the first derivative amplitude for one component and the second derivative amplitude for the second component are zero at the same wavelength.

$$d^2 I_2(x)/dx^2 = 0$$

when

$$(x - C_2)/B_2 = 1,$$

and

$$dI_1(x)/dx = 0$$

when

$$x = C_1$$

These conditions occur simultaneously when $C_1 - C_2 = B_2$.

This implies that the best conditions for evaluating amplitudes for component 2 at the isodifferential point of component 1 are obtained when the separation between the band maxima ($C_1 - C_2$) is equal to B_2 , the band half-width at half maximum height for component 2. Conversely, when $C_1 - C_2 = B_1$ the evaluation of component 1 at the isodifferential point for component 2 is optimal.

By use of these principles, lutetium and praseodymium may be determined in mixtures over a wide range of concentration. Figure 3 shows that the first derivative spectra of the praseodymium and lutetium complexes have distinct isodifferential points at 559.5 and 555.5 nm, corresponding to the wavelength of the absorption maxima of the two complexes in the zero derivative spectra. Lutetium can be determined precisely and sensitively by measurement of the first derivative amplitude for the mixture at the praseodymium isodifferential point.

The first derivative is not adequate for the determination of praseodymium because its amplitude is small at 555.5 nm, the isodifferential point for lutetium. However, the second derivative allows accurate determination of praseodymium by measurement of the derivative amplitudes at 565 nm.

The results obtained for the determination of each ion in various binary mixtures are shown in Table 4. It can be seen that the proposed methods give satisfactory results for the analysis of the binary mixtures tested. Presumably analogous methods could be applied to other suitable binary combinations of the lanthanides.

Acknowledgement—We thank the Comision Asesora de Investigacion Cientifica y Tecnica for supporting this study (Project No. 3007/83 C02-02).

REFERENCES

1. J. H. Jolly, *Rare Earth Elements and Yttrium; Mineral Facts and Problems*, Bureau of Mines, U.S. Department of the Interior, Washington DC, 1975.
2. A. Masuda, N. Nakamura and T. Tanaka, *Geochim. Cosmochim. Acta*, 1973, **37**, 239.
3. S. F. Marsh, *Anal. Chem.*, 1967, **39**, 641.
4. J. J. McCowan and R. P. Larsen, *ibid.*, 1961, **33**, 1003.
5. K. Yoshida and H. Haraguchi, *ibid.*, 1984, **56**, 2580.
6. D. Y. Tobias, *J. Assoc. Off. Anal. Chem.*, 1983, **66**, 1450.

7. A. I. Busev, V. G. Tiptsova and V. M. Ivanov, *Handbook of the Analytical Chemistry of Rare Elements*, Ann Arbor-Humphrey, Ann Arbor, Mich., 1970.
8. J. Medinilla, F. Ales and F. García Sánchez, *Talanta*, 1986, **33**, 329.
9. *Anal. Chem.*, 1980, **52**, 2242.
10. F. García Sánchez and C. Cruces Blanco, *ibid.*, 1986, **58**, 73.
11. M. García Vargas, M. Milla, I. Antequera and J. A. Pérez Bustamente, *Anal. Chim. Acta*, 1985, **171**, 313.
12. M. A. Kovany and A. A. Seif, *J. Assoc. Off. Anal. Chem.*, 1984, **67**, 138.

ETUDE ANALYTIQUE DES PRODUITS LOURDS DU PETROLE—V

BROMATION DES RESIDUS LOURDS PETROLIERS AU MOYEN D'UN REACTIF ORIGINAL, LE TRIBROMURE DE TETRABUTYLAMMONIUM, ET ESSAIS PRELIMINAIRES DE DETERMINATION D'UN INDICE DE BROME APPLICABLE AUX FRACTIONS LOURDES

P. L. DESBENE*, J. BERTHELOT, M. OUCHEFOUN, C. GUETTE et J. J. BASSELIER
Laboratoire de Chimie Organique Structurale, UA 455, Université P. et M. Curie, Bat.F, 4 Place Jussieu
75230 Paris Cedex 05, France

R. BOULET
Département des Mesures Physiques, Institut Français du Pétrole, 1 à 4 Avenue du Bois Préau, 92500
Rueil-Malmaison, France

A. DESBENE-MONVERNAY
ITODYS, LA 34, Université de Paris VII, 2 Place Jussieu, 75005 Paris, France

(Reçu le 19 décembre 1986. Accepté le 6 février 1987)

Résumé—On rapporte une méthode originale de détermination de l'indice de brome applicable aux produits lourds du pétrole. Cette méthode, qui fait appel au tribromure de tétrabutylammonium comme agent bromant et à un dosage électrochimique, est développée dans le cas d'un résidu atmosphérique Boscan. Par un dosage en retour des ions tribromures en excès et un dosage direct des ions bromures formés on peut aisément distinguer la part correspondant aux réactions d'addition du brome aux liaisons multiples de celle ayant trait aux réactions de substitution sur les composés aromatiques (phénols, amines, etc.). La sensibilité et la reproductibilité de cette méthode s'avèrent satisfaisantes, sa mise en oeuvre aisée.

Summary—A new method of bromine number determination appropriate to heavy-ends petroleum is reported. This method, which uses an electrochemical titration and tetrabutylammonium tribromide as reagent, has been tested on Boscan atmospheric residues. The titration of the unreacted tribromide ions and of the bromide ions produced enables the proportion of the bromine addition to multiple bonds and the proportion of substitution reactions with aromatic compounds (phenols, amines, etc.) to be estimated. The sensitivity and reproducibility of this easy method are both good.

En raison de leur extrême complexité les produits lourds pétroliers restent mal connus malgré les nombreuses investigations menées ces dix dernières années¹ avec des techniques d'analyse parfois très performantes (R.M.N. ¹H et ¹³C, rayons X, etc.). De nombreuses questions simples demeurent sans réponse satisfaisante. Ainsi malgré tous les efforts développés on ne peut aujourd'hui avancer une valeur précise quant à la masse moléculaire moyenne de tels composés, les valeurs proposées variant dans des proportions extrêmement importantes selon la technique utilisée.¹ De même le taux de métaux présents sous forme porphyrinique est une question encore totalement ouverte.²⁻⁵ Enfin des caractéristiques telles que le degré d'insaturation ou une approche de celui-ci, l'indice de brome, ne peuvent être actuellement fournies. En effet les méthodes de détermination de cet indice de brome faisant appel, par exemple, à une titration par une solution de bromure-bromate⁶ ne

sont applicables qu'aux fractions légères (fractions pétrolières dont 90% de la masse distille avant 325°).

Ayant récemment développé un nouvel agent de bromation de doubles et triples liaisons, le perbromure de tétrabutylammonium (TBABr₃)^{7,8} et mis au point une méthode analytique de l'indice de brome,^{9,10} nous rapportons dans ce mémoire les premiers résultats montrant la fiabilité de l'adaptation d'une telle méthode aux résidus lourds du pétrole.

PARTIE EXPERIMENTALE

Dosage

Les mesures ont été effectuées à l'aide d'une microélectrode en platine tournant à 500 tours par minute (type Tacussel EM-EDI Pt D2), commandée par une unité d'asservissement de type Contravit (Tacussel), et plongeant dans une cellule munie d'un agitateur magnétique. L'électrode auxiliaire est une grille de platine. Les potentiels sont mesurés par rapport à une référence (Ag/Ag⁺, 0,01M). On introduit dans la cellule 25 ml d'acétonitrile 0,1M en perchlorate de tétrabutylammonium (Bu₄NClO₄), puis à l'aide d'une microseringue les diverses prises d'essai (250 μl

*Auteur pour correspondance.

chacune) du mélange réactionnel. Les courbes $i = f(E)$ ont été enregistrées sur une table traçante IFELEC IF 3802 couplée à un potentiostat PAR EGG 173 gouverné par un générateur de signaux PAR EGG 175, dans l'intervalle de -1 V à $+1,3$ V. L'ensemble du dosage électrochimique est effectué sous atmosphère inerte d'argon à température ambiante.

Les analyses centésimales, quant à elles, ont été réalisées par le Centre de Microanalyse du CNRS que nous tenons à remercier.

Réactifs

La fraction pétrolière utilisée est un résidu atmosphérique d'un brut Vénézuélien (Boscan). Le TBABr₃ commercialisé pur et prêt à l'emploi par Janssen Chimica est lavé en milieu chloroformique par une solution aqueuse de bicarbonate. Par contre le cyclohexène de qualité pur pour analyse (Fluka), le styrène de qualité pur pour analyse (Fluka), l'acétonitrile de qualité "99 + % spectrophotometric grade" (Janssen Chimica) et le sel de fond Bu₄NClO₄ *purum* (Fluka) sont utilisés tels quels.

RESULTATS ET DISCUSSION

Le nouvel agent bromant utilisé, le perbromure de tétrabutylammonium (TBABr₃) se présente sous forme d'un solide orange, cristallisé ($F = 84^\circ$), stable et possédant un degré constant de brome actif. Il agit en particulier, dès la température ambiante, en solution dans le chloroforme, sur les doubles et triples liaisons,^{7,8} en fixant deux atomes de brome et en libérant un ion bromure.^{9,10}

Il est d'autre part connu que les perbromures réagissent sur les composés présentant un atome d'hydrogène actif.^{11,12} Pour notre part nous avons récemment montré que le TBABr₃ réagit avec les phénols¹³ et les amines aromatiques¹⁴ pour conduire avec d'excellents rendements et de façon stéréospécifique aux dérivés monobromés correspondants.

Aussi un indice de brome et une estimation précise de la part d'addition sur les liaisons multiples et de substitution de phénols et/ou d'amines aromatiques, présents dans une matrice complexe, pouvant ils être obtenus en opérant avec un excès d'agent bromant et en dosant:

- d'une part les ions Br⁻ formés
- d'autre part les ions Br₃⁻ qui n'ont pas réagi.

Pour ce faire il est nécessaire d'être en possession d'une méthode de dosage précise, reproductible et facile à mettre en oeuvre, applicable à la matrice pétrolière. Compte tenu de sa complexité et de sa forte absorption dans les domaines ultra-violet, visible et infra rouge, nous nous sommes tout na-

tuellement tournés vers les méthodes électrochimiques et avons choisi parmi celles-ci la technique d'ampérométrie.

Nous avons tout d'abord envisagé le dosage des ions Br⁻ et Br₃⁻ dans le cas d'une réaction modèle effectuée dans le chloroforme, solvant compatible avec la matrice pétrolière.

Etude de la bromation du styrène dans le chloroforme

Conformément à notre méthode de détermination d'indice de brome rapportée précédemment pour des composés éthyléniques,⁷ le dosage des ions Br⁻ (vagues d'oxydation $E_{1/2} = +0,39$ et $+0,75$ V *vs.* Ag/Ag⁺) et Br₃⁻ (vague de réduction $E_{1/2} = +0,025$ V *vs.* Ag/Ag⁺ et vague d'oxydation $E_{1/2} = +0,71$ V *vs.* Ag/Ag⁺) est effectué sous argon en milieu acétonitrile/Bu₄NClO₄ 0,1M en utilisant une micro-électrode de platine tournante. Le styrène, modélisant la fraction pétrolière, doit être solubilisé dans un solvant compatible avec cette dernière. L'acétonitrile ne pouvant être retenu, nous avons fait appel à un tiers solvant. Parmi les divers solvants possibles, notre choix s'est porté sur le chloroforme qui permet dans le cas des doubles et triples liaisons la bromation rapide par TBABr₃.⁷⁻¹⁰

Comme mentionné plus haut il est connu que les tribromures réagissent avec les composés présentant un atome d'hydrogène actif.^{11,12} De tels composés étant susceptibles de se trouver dans les fractions lourdes du pétrole nous avons décidé, afin de garder des conditions opératoires constantes, d'opérer, dès la mise en oeuvre de la réaction témoin, dans du chloroforme additionné d'oxyde de magnésium. La fonction de ce dernier composé est de piéger les éventuels protons libérés au cours d'un dosage effectué sur la matrice pétrolière.

Après avoir vérifié que le styrène ne donne pas de vague d'oxydo-réduction dans le domaine de potentiel exploré, de -1 V à $+1,3$ V *vs.* Ag/Ag⁺, nous procédons alors au dosage de la manière suivante.

Au temps $t = 0$ on ajoute du styrène à une solution de TBABr₃ 0,1M dans le chloroforme contenant de l'oxyde de magnésium de façon à avoir un mélange équimoléculaire des deux réactifs. On suit l'évolution de la réaction en prélevant un échantillon de 250 μ l du mélange réactionnel qu'on dispose dans la cellule d'électrolyse contenant 25 ml d'acétonitrile 0,1M en Bu₄NClO₄. Les courbes voltammétriques obtenues en fonction du degré d'avancement de la réaction de bromation sont rapportées dans la figure 2.

Des courbes $i-E$ précédentes et des droites de calibration (*cf.* tableau 1) on peut déduire l'évolution des concentrations en Br⁻ et Br₃⁻ en fonction du temps, comme représenté sur la figure 3.

La réaction de bromation apparaît achevée en 20 min. Elle consiste apparemment en la fixation d'une molécule de brome sur la double liaison du styrène et en la libération d'un ion bromure par ion perbromure. En ce qui concerne la vague d'oxydation située vers $+0,7$ V *vs.* Ag/Ag⁺, qui résulte de la

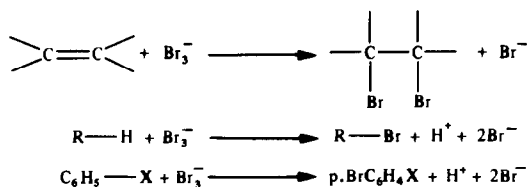


Fig. 1. Bromations par TBABr₃ (X = OH, NH₂).

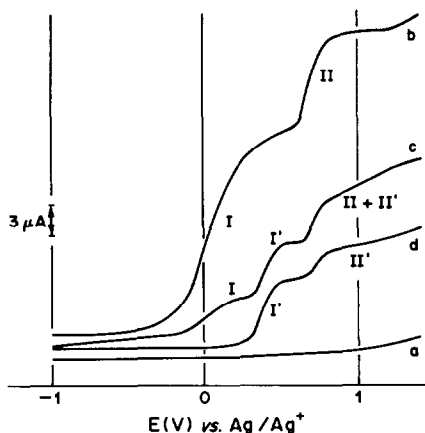
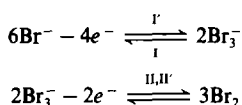


Fig. 2. Evolution des courbes voltammétriques lors de la bromation du styrène par TBABr₃ dans le chloroforme (vitesse d'enregistrement = 50 mV/sec):

(a) sel support; (b) *t* = 0 min; (c) *t* = 2 min; (d) *t* = 20 min.



présence des ions Br⁻ et Br₃⁻, on note un bon accord entre la valeur du courant de diffusion observée expérimentalement et la valeur calculée à partir des concentrations en Br⁻ et Br₃⁻ (figure 4).

Le dosage des ions Br⁻ et Br₃⁻ pouvant être effectué au cours d'une réaction de bromation par TBABr₃ dans le chloroforme, solvant compatible avec la matrice pétrolière, nous avons décidé d'entreprendre un tel dosage sur une fraction pétrolière lourde.

Détermination de l'indice de brome d'une fraction pétrolière lourde par dosage électrochimique des ions Br⁻ et Br₃⁻ après bromation par le TBABr₃

La fraction pétrolière lourde retenue pour cette étude est constituée par un résidu atmosphérique Boscan (Venezuela).

Nous avons tout d'abord vérifié que la fraction pétrolière ne donnait pas lieu à des vagues d'oxydo-réduction dans la zone de potentiel explorée (de -1 V à +1,3 V vs. Ag/Ag⁺).

Pour ce faire et conformément au protocole décrit ci-dessus pour la réaction témoin, la fraction pétrolière est d'abord dissoute dans du chloroforme contenant de l'oxyde de magnésium. Une fraction aliquote de cette solution est prélevée et diluée par de

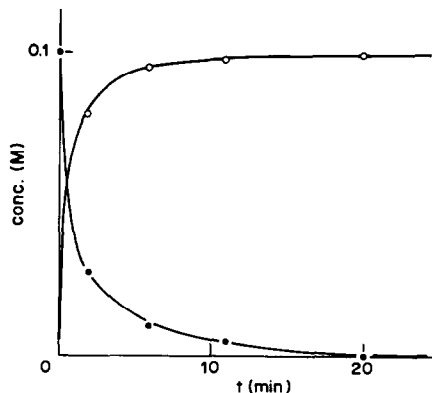


Fig. 3. Evolution des concentrations en Br₃⁻ (●) et Br⁻ (○) dans le mélange réactionnel au cours de la bromation du styrène par TBABr₃.

l'acétonitrile 0,1 M en sel support (Bu₄NClO₄). Après filtration sur membrane Millipore 0,45 µm on procède à l'enregistrement des courbes. Manifestement (cf. figure 5a), le pétrole ne donne lieu, dans ces conditions, à aucune vague parasite et en conséquence ne peut pas perturber le dosage des ions Br⁻ et Br₃⁻.

Nous avons donc dans un second temps procédé, selon le schéma opératoire décrit ci-dessus, à l'enregistrement des courbes voltammétriques du mélange réactionnel au cours de la bromation du résidu

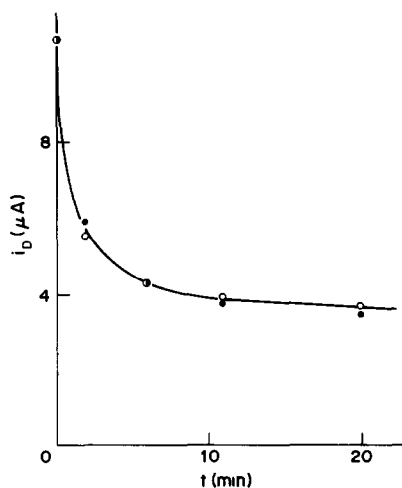


Fig. 4. Comparaison des intensités *i*_D^{II+II'} (points expérimentaux ● et calculés ○) au cours de la bromation du styrène.

Tableau 1. Expressions analytiques des droites de calibration *i*(µA) = pente × *C*(mM) obtenues par régression linéaire à partir de 6 manipulations indépendantes

Réactif	Vague	<i>E</i> _{1/2} , V vs. Ag/Ag ⁺	Pente ± limite de confiance à 95%	Coefficient de corrélation
Br ₃ ⁻	Red (I)	+ 0,025	40,0 ± 2,1	0,995
	Ox (II)	+ 0,71	24,6 ± 0,9	0,999
Br ⁻	Ox (I')	+ 0,39	17,7 ± 0,5	0,999
	Ox (II')	+ 0,75	9,0 ± 0,1	0,999

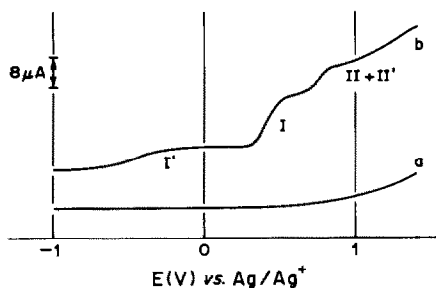
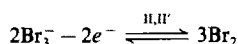
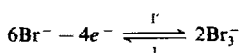


Fig. 5. Courbes voltammétriques (vitesse d'enregistrement 50 mV/sec) relatives à la bromation d'un résidu atmosphérique Boscan par TBABr₃: (a) 100 μl échantillon de résidu atmosphérique Boscan témoin; (b) 100 μl échantillon de résidu atmosphérique Boscan mis en présence de TBABr₃ (rapport massique: TBABr₃/pétrole = 1,75).



atmosphérique Boscan par TBABr₃ (rapport massique TBABr₃/pétrole = 1,75). La courbe voltammétrique obtenue après un temps de réaction de 20 min est représentée par la figure 5b.

L'enregistrement des courbes *i*-*E* pour des temps de réaction supérieurs à 20 min n'indique aucune modification du milieu réactionnel. En conséquence la bromation de la fraction pétrolière par TBABr₃ est une réaction rapide dans le chloroforme à température ambiante.

Les dosages effectués tant sur les ions Br₃⁻ restant après bromation, que sur les ions Br⁻ formés lors de la bromation du résidu atmosphérique Boscan sont rassemblés dans le tableau 2, tandis que dans le tableau 3 nous avons fait figurer à titre de comparaison les résultats obtenus par analyse élémentaire.

L'examen de ces deux tableaux appelle quelques commentaires.

—Tout d'abord à la lecture du tableau 2, il apparaît, compte tenu des limites de confiance mentionnées, qu'il n'y a pas d'équivalence entre la valeur de la concentration des ions Br₃⁻ restant dans la cellule d'électrolyse [(0,88 ± 0,01) × 10⁻³ M], soit une consommation de 0,29 ± 0,01 mmole de Br₃⁻ par litre de solution, et celle de la concentration en ions Br⁻ formés [(0,37 ± 0,01) × 10⁻³ M]. Ceci indique simplement que les ions tribromures ne s'additionnent pas exclusivement sur les liaisons multiples présentes

Tableau 2. Dosages effectués sur les ions Br₃⁻ restants et Br⁻ formés lors de la bromation du résidu atmosphérique Boscan

		Solution chloroformique de départ (TBABr ₃ dans 22,5 ml de CHCl ₃)	Après addition de 1,815 g de RA Boscan
[Br ₃ ⁻]	Concentration dans la cellule d'électrolyse*†	1,17 × 10 ⁻³ M	0,88 × 10 ⁻³ M
	Limite de confiance à 95%†	—	± 0,01 × 10 ⁻³ M
[Br ⁻]	Concentration dans la cellule d'électrolyse*†	—	0,37 × 10 ⁻³ M
	Limite de confiance à 95%†	—	± 0,01 × 10 ⁻³ M
Brome fixé sur le RA	Taux*	—	12,4%
	Limite de confiance à 95%†	—	± 0,8%

*Déterminée à partir des droites de calibration rapportées dans le tableau 1.

†Valeur moyenne et limite de confiance obtenues à partir de 6 manipulations indépendantes.

Tableau 3. Résultats de l'analyse élémentaire d'un RA Boscan

	C, %	H, %	N, %	O, %	S, %	Br, %	V, %	Ni, %
Analyse centésimale*	82,0	10,1	0,8	1,0	5,6	—	0,123	0,012 ₅
	0,4	0,2	0,2	0,3	0,6	—	0,022	0,001 ₃
Analyse centésimale d'un RA soumis à TBABr ₃ §	71,1	8,2	0,7	1,5	5,6	11,8	0,101	0,013 ₅
	0,5	0,4	0,1	0,4	0,5	0,7	0,022	0,003 ₂
Formule brute fictive d'un RA*‡	C ₁₀₀ H ₁₄₈ N _{0,8} O _{0,9} S _{2,6}							
Formule brute fictive d'un RA soumis à TBABr ₃ ‡‡	C ₁₀₀ H ₁₃₉ N _{0,8} O _{1,7} S _{2,9} Br _{2,4}							

*Analyse centésimale moyenne déduite de 7 analyses indépendantes; sur la ligne inférieure figurent les limites de confiance à 95%.

†RA Boscan soumis pendant 30 min à l'action de TBABr₃ (TBABr₃/pétrole = 1,75).

§Analyse centésimale moyenne déduite de 5 manipulations indépendantes; sur la ligne inférieure figurent les limites de confiance à 95%.

‡Calculée en prenant arbitrairement comme base 100 atomes de carbone.

dans le résidu atmosphérique Boscan mais réagissent également sur d'autres sites, tels que les phénols et les amines aromatiques contenus dans la matrice pétrolière, selon des réactions de substitution. Ce comportement n'a rien d'extraordinaire puisque nous avons mis récemment en évidence de telles réactions de substitution lors d'études sur des molécules modèles.^{13,14}

—Sur la base de réactions compétitives d'addition aux doubles liaisons et de réactions de substitution on peut donc évaluer à partir des mesures électrochimiques le taux de brome fixé sur la matrice pétrolière (*cf.* avant-dernière ligne du tableau 2). Ainsi à partir de six bromations indépendantes par TBABr₃ une valeur moyenne de 12,4 g de brome fixé par 100 g de résidu atmosphérique peut être retenue comme indice de brome pour le résidu atmosphérique Boscan (en se souvenant que pour une réaction de substitution la disparition d'une mole de Br₃⁻ fait apparaître deux équivalents de Br⁻ tandis que la réaction d'addition aux liaisons multiples se traduit par l'apparition d'une mole de Br⁻ par mole de Br₃⁻ consommée). De plus comme le mentionne la dernière ligne du tableau 2 une précision de l'ordre de 0,8% peut être retenue pour cette détermination (limite de confiance à 95%).

—Il est alors instructif de rapprocher cette valeur moyenne déterminée par voie électrochimique (12,4 ± 0,8%) de celle obtenue à partir de 5 analyses centésimales indépendantes et rapportée dans le tableau 3 (11,8 ± 0,7%). On voit qu'aux erreurs expérimentales près il y a bon accord entre le taux de brome déterminé par voie électrochimique et celui obtenu à partir de l'analyse centésimale. On doit également noter que la précision obtenue à partir de la méthode électrochimique avoisine celle de l'analyse centésimale. Cette concordance confère à notre méthode de dosage électrochimique une fiabilité certaine. Cette dernière méthode de dosage présente toutefois de nombreux avantages sur l'analyse centésimale.

—Tout d'abord une plus grande souplesse d'utilisation permettant un suivi en continu.

—Ensuite et surtout, grâce au double dosage

(d'une part sur les Br₃⁻ qui ont réagi, d'autre part sur les Br⁻ apparus), la méthode électrochimique permet de distinguer, comme nous l'avons mentionné précédemment, la bromation résultant de l'addition aux liaisons multiples de celle correspondant à une substitution sur un noyau aromatique. L'analyse centésimale, mesure globale, est bien évidemment incapable de fournir un tel distinguo.

—Il apparaît de plus à la lecture du tableau 3 que la réaction de bromation ne s'accompagne d'aucune démetalation. Les teneurs tant en nickel qu'en vanadium demeurent, aux erreurs expérimentales près, inchangées après bromation. Par contre il semble que la réaction de bromation s'accompagne d'une légère oxydation.

—Enfin il doit être remarqué, comme le font ressortir les formules brutes fictives mentionnées dans le tableau 3, qu'à une telle teneur en brome (environ 12%) correspond seulement une faible bromation totale (addition + substitution) de la matrice pétrolière: 2,4 atomes de brome pour 100 atomes de carbone.

La méthode de dosage électrochimique du brome fixé sur la matrice pétrolière s'avérant, en plus de ses qualités intrinsèques (rapidité et facilité de mise en oeuvre), fiable et précise, nous nous sommes attachés, dans un dernier temps, à démontrer que la matrice pétrolière, milieu chimique fort complexe, n'entravait ni la réaction de bromation, ni le dosage de composés oléfiniques connus pour subir une réaction de bromation totale par TBABr₃.^{7,8}

Dosage de composés oléfiniques au sein d'un résidu atmosphérique; cas du styrène et du cyclohexène

Nous avons donc cherché à montrer la validité de notre méthode de détermination d'indice de brome dans des fractions pétrolières lourdes en procédant au dosage de quantités connues d'oléfiniques mises en solution dans la matrice pétrolière. Les deux oléfiniques retenues pour ces tests exploratoires sont d'une part le styrène, d'autre part le cyclohexène.

Nous avons dans un premier temps procédé à des

Tableau 4. Dosage d'ajouts de styrène dans du résidu atmosphérique Boscan par une solution de TBABr₃ initialement 1,67 mM dans la cellule électrochimique et dont le titre est abaissé à 1,34 mM après action sur le pétrole

[styrène] ajoutée, mM	Σ[styrène] ajoutée, mM	[Br ⁻] apparue, mM	[styrène] dosée correspondant à l'ajout, mM	[styrène] totale dosée, mM
0	0	0,33*	0	0
0,025	0,025	0,38	0,05	0,05
0,025	0,05	0,40	0,02	0,07
0,05	0,10	0,44	0,04	0,11
0,10	0,20	0,53	0,09	0,20
0,20	0,40	0,76	0,23	0,43
0,20	0,60	1,02	0,26	0,69
0,20	0,80	1,19	0,17	0,86

*Correspondant aux ions Br⁻ libérés lors de la bromation de la matrice pétrolière avant ajout de styrène.

Tableau 5. Dosage d'ajouts de cyclohexène dans du résidu atmosphérique Boscan à l'aide d'une solution de TBABr₃ initialement 1,60mM dans la cellule électrochimique, et dont le titre est abaissé à 1,26mM après action sur le pétrole

[cyclohexène] ajoutée, mM	Σ[cyclohexène] ajoutée, mM	[Br ⁻] apparue, mM	[cyclohexène] dosée correspondant à l'ajout, mM	[cyclohexène] totale dosée, mM
0	0	0,34*	0	0
0,05	0,05	0,40	0,06	0,06
0,05	0,10	0,46	0,06	0,12
0,10	0,20	0,56	0,10	0,22

*Correspondant aux ions Br⁻ libérés lors de la bromation de la matrice pétrolière avant ajout de cyclohexène.

ajouts d'oléfine dans la matrice pétrolière ayant déjà réagi avec un excès de TBABr₃.

Les résultats obtenus pour le styrène sont consignés dans le tableau 4, tandis que ceux relatifs au cyclohexène sont mentionnés dans le tableau 5. Pour ces deux exemples, seuls sont rapportés, par souci de clarté, les résultats des dosages effectués sur les ions Br⁻ formés, mais des résultats tout aussi satisfaisants sont obtenus lorsqu'on effectue le calcul à partir des ions tribromures consommés.

L'examen de ces deux tableaux révèle que si l'accord est moyen pour le styrène (cf. tableau 4), il s'avère bon pour le cyclohexène (cf. tableau 5), un bon accord étant observé entre les valeurs expérimentales (cf. colonne 4) obtenues par dosages des ions Br⁻ et les quantités effectivement ajoutées (cf. colonne 1).

De même l'estimation de la quantité totale d'oléfine ajoutée (cf. colonne 5) obtenue à partir du dosage des ions Br⁻ est en bon accord avec la valeur effective de l'ajout total (cf. colonne 2).

Enfin il est à noter que le seuil de sensibilité de notre méthode de dosage peut être estimé à $5 \times 10^{-5}M$ dans la cellule électrochimique soit $5 \times 10^{-3}M$ dans le milieu réactionnel. Il va de soi que pour une telle concentration, la précision de la mesure n'est pas excellente.

Dans un second temps nous avons additionné d'abord l'oléfine dans la matrice pétrolière puis procédé à son dosage par ajout d'un excès de TBABr₃. Un tel protocole opératoire impose bien entendu le recours à un blanc indépendant effectué sur la matrice pétrolière, en l'occurrence ici un résidu atmosphérique Boscan. Les résultats obtenus dans ces conditions sur six manipulations indépendantes

effectuées respectivement sur le styrène et le cyclohexène sont rapportés dans le tableau 6.

La lecture de ce tableau met en évidence qu'un accord satisfaisant existe entre les concentrations effectives dans la cellule électrochimique en styrène ($0,35 \times 10^{-3}M$) et en cyclohexène ($0,25 \times 10^{-3}M$) et celles trouvées expérimentalement, $[\text{styrène}] = 0,35 \times 10^{-3}M$ et $[\text{cyclohexène}] = 0,26 \times 10^{-3}M$ compte tenu de la précision expérimentale exprimée à l'aide des limites de confiance à 95%, respectivement $\pm 0,03 \times 10^{-3}M$ pour le styrène et $\pm 0,02 \times 10^{-3}M$ pour le cyclohexène.

Ainsi il apparait clairement qu'une matrice pétrolière aussi visqueuse et complexe qu'un résidu atmosphérique Boscan n'altère pas de façon significative la détermination, par la méthode décrite, de l'indice de brome correspondant aux oléfines additionnées.

CONCLUSION

Nous venons de montrer que l'utilisation d'un dosage électrochimique des ions Br⁻ et Br₃⁻ à l'issue de la bromation par les ions tribromures des fractions lourdes du pétrole constitue une approche rapide, reproductible et fiable pour déterminer l'indice de brome de telles fractions.

Nous nous proposons d'appliquer de façon systématique la méthode décrite dans cet article aux fractions pétrolières plus légères, donc moins rebutantes (fuel oil, essences issues de différents procédés de crackage, essence légère etc.) pour lesquelles un degré d'insaturation a pu être déterminé, notamment par couplage GC-MS. Une étude de modélisation

Tableau 6. Dosages de quantités connues de styrène et de cyclohexène additionnées à une matrice pétrolière (RA Boscan); comparaison des titres théoriques et expérimentaux dans la cellule d'électrolyse

	Styrène, mM	Cyclohexène, mM
Concentration théorique	0,35	0,25
Concentration expérimentale*	0,35	0,26
Limite de confiance à 95%*	±0,03	±0,02

*Moyenne et limite de confiance obtenues à partir de 6 manipulations indépendantes.

basée sur des composés présents dans les fractions lourdes est également poursuivie.

LITTÉRATURE

1. J. Bunger, *Chemistry of Asphaltenes*, American Chemical Society, Washington, 1961.
2. J. Goulon, C. Esselin, P. Friant, C. Berthé, J. F. Muller, J. L. Poncet, R. Guillard, J. C. Escallier et B. Neff, *Symposium international sur la caractérisation des huiles lourdes et des résidus pétroliers*, Lyon, 25-27 Juin 1984, Technip Edit., p. 158.
3. C. Berthé, J. F. Muller, D. Cagnant, J. Guimblot et J. P. Bonnelle, *ibid.*, p. 164.
4. J. C. Reynolds, W. R. Biggs, J. C. Fetzer, E. J. Gallegos, R. H. Fish, J. J. Komlenic et B. K. Wines, *ibid.*, p. 153.
5. P. L. Desbène, D. Richard, D. Lambert, J. J. Basselier, R. Boulet et A. Huc, *Analisis*, 1986, **14**, 148.
6. *Norme NF: M07-017*.
7. M. Fournier, F. Fournier et J. Berthelot, *Bull. Soc. Chim. Belg.*, 1984, **93**, 157.
8. J. Berthelot et M. Fournier, *Can. J. Chem.*, 1986, **64**, 603.
9. J. Berthelot, A. Desbène-Monvernay, J. J. Basselier et P. L. Desbène, *Analisis*, accepté pour publication.
10. A. Desbène-Monvernay, J. Berthelot et P. L. Desbène, *J. Chem. Educ.*, sous presse.
11. A. Marquet, J. Jacques et B. Tchoubar, *Bull. Soc. Chim. France*, 1962, **90**, et références citées.
12. *Idem, ibid.*, 1964, 511 et références citées.
13. J. Berthelot, C. Guette, M. Ouchefoun, P. L. Desbène et J. J. Basselier, *J. Chem. Res.*, 1986, 381.
14. J. Berthelot, C. Guette, M. Essayegh, P. L. Desbène et J. J. Basselier, *Synth. Comm.*, 1986, **16**, 1641.

SHORT COMMUNICATIONS

USE OF *N*-BENZYL-2-NAPHTHOHYDROXAMIC ACID AS A HIGHLY SELECTIVE REAGENT FOR SOLVENT EXTRACTION AND SPECTROPHOTOMETRIC DETERMINATION OF VANADIUM(V)

BASANT SAHU*

Department of Chemistry, Ravishankar University, Raipur (MP), India

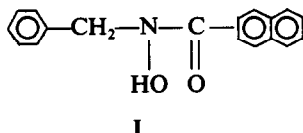
USHA TANDON

Department of Chemistry, Government Science College, Raipur (MP), India

(Received 17 January 1986. Revised 24 December 1986. Accepted 5 February 1987)

Summary—*N*-Benzyl-2-naphthohydroxamic acid extracts vanadium(V) selectively and quantitatively into chloroform from 2–8.5*M* hydrochloric acid in the presence of Mo(VI), Zr(IV) and Ce(IV). The extraction takes place quickly and gives a stable reddish-violet extract which shows an absorption maximum at 505 nm with molar absorptivity of $(5.34 \pm 0.05) \times 10^3$ l.mole⁻¹.cm⁻¹. The optimum range for the determination is 2.2–7.4 ppm of vanadium(V) in the final solution. The method has been used for the determination of vanadium in steels.

Efforts made to improve the sensitivity and selectivity of hydroxamic acids as reagents for vanadium by substituting groups on the nitrogen atom or the phenyl rings had led to a few hydroxamic acids¹⁻⁵ which are superior to *N*-phenylbenzohydroxamic acid (PBHA), the best known and most widely used reagent for vanadium(V). For example, *N*-benzylbenzohydroxamic acid (BBHA) is more selective than PBHA. We have found that *N*-benzyl-2-naphthohydroxamic acid (B-2-NHA) I, extracts vanadium(V) selectively and quantitatively into chloroform from hydrochloric acid in the presence of Mo(VI), Zr(IV) and Ce(IV), which seriously interfere in almost all the procedures based on use of other *N*-arylhydroxamic acids. It also gives higher sensitivity. This communication describes an assessment of B-2-NHA for the solvent extraction and spectrophotometric determination of vanadium(V).



EXPERIMENTAL

Reagents

N-Benzyl-2-naphthohydroxamic acid (m.p. 130°) was prepared and purified by the method reported elsewhere.⁶ A 0.1% solution was prepared in alcohol-free chloroform. Stock solutions of vanadium were prepared from ammo-

nium metavanadate in glass-distilled water and standardized titrimetrically.⁷ Solutions of diverse ions were prepared as recommended by West.⁸ All chemicals used were of analytical grade whenever possible.

Procedure for extraction and determination of vanadium

Transfer a suitable aliquot of solution containing 40–200 µg of vanadium(V) to a separating funnel, and add water and concentrated hydrochloric acid to give a final volume of 10–15 ml and acid concentration of 2–8*M* (optimum is 4–5*M*). Add 10 ml of reagent solution in chloroform and shake the mixture for at least 2 min, allow the phases to separate, and collect the reddish-violet organic phase. Repeat the extraction with two 2-ml portions of reagent solution in chloroform, then wash the aqueous solution with two 2-ml portions of pure chloroform. Dry the combined extracts and washings over anhydrous sodium sulphate (1–2 g), and transfer to a 25-ml standard flask, washing the sodium sulphate with chloroform and adding the washings to the flask. Dilute to volume with chloroform and measure the absorbance in a 1-cm cell at 505 nm against pure chloroform.

Procedure for steel samples

Dissolve 0.3–0.5 g of steel in about 5 ml of 3*M* sulphuric acid with gentle heating. Add a little concentrated nitric acid (0.5–1 ml) and heat to fumes. Cool, dilute to about 10 ml with water, heat to about 80° and oxidize the vanadium by addition of 0.05*N* permanganate solution. Cool, make up to volume in a 100-ml standard flask, and take a suitable aliquot for analysis as already described. Alternatively treat 20–50 mg of steel in the same way, but omit the final dilution to 100 ml, and use the whole solution for the extraction step.

RESULTS AND DISCUSSION

The reddish-violet V(V)–B-2-NHA complex extracted into chloroform from 4.5*M* hydrochloric acid has an absorption maximum at 505 nm. As the reagent does not absorb at this wavelength, pure

*Present address: Department of Chemistry, C.M.D. Post, Graduate College, Bilaspur (MP), India.

Table 1. Survey of interferences

Ions	Tolerance limit, mg	Ions	Tolerance limit, mg
Al(III)	40	Pb(II)*	70
Ba(II)	140	Pr(III)	130
Bi(III)	50	Th(IV)	60
Cu(II)	50	Ti(IV)	5
Cd(II)	100	Tl(III)*	2.5
Cr(III)	40	U(VI)	50
Co(II)	20	W(VI)†	5
Fe(III)	25	Zn(II)	20
Li(III)	70	Zr(IV)	70
Mn(II)	25	Acetate	60
Mg(II)	150	Fluoride	25
Mo(VI)	50	Chloride	120
Ni(II)	30		

*Repeated extraction.

†Repeated extraction with 0.3% reagent solution, phosphoric acid as masking agent.

chloroform can be used as the blank for all absorbance measurements.

The intensity of the colour is dependent on the acidity but is constant over the range 2.0–8.5*M* hydrochloric acid. The influence of other factors was investigated with an acid concentration of 4.5*M*.

The volume of the aqueous phase may be varied from 5 to 30 ml without affecting the final absorbance. Chloroform, in which the complex is freely soluble, is the most suitable solvent for the extraction. The absorbance remains constant for at least a week if the extract is kept in a cool dark place.

The molar ratio of reagent to vanadium must be at least 6:1 for full colour development, but can be up to 90:1 without adverse effect on the colour. The recommended conditions give a minimum mole ratio of ~9:1.

Beer's law holds at 505 nm over the concentration range 1.8–8.8 ppm of vanadium in the chloroform solution. The optimum working range for determination, based on Sandell's recommendation,⁹ is 2.2–7.4 ppm. The molar absorptivity (ϵ) of the complex at 505 nm is $(5.34 \pm 0.05) \times 10^3$ l. mole⁻¹. cm⁻¹.

Effect of diverse ions

Various amounts of diverse ions were added to a fixed amount (87.4 μ g) of vanadium(V) and the colour was developed according to the recommended procedure. The tolerance limit was calculated as the amount of foreign ion which would cause a change of 2% in the absorbance. The limits found are listed

Table 2. Determination of vanadium(V) in B.C.S. steels

B.C.S. Steels	Certified value, %	V found,* %
Cr-V, No. 224 Low alloy steel	0.242	0.239 \pm 0.003
No. 252 High speed steel	0.460	0.457 \pm 0.002
No. 241/1	1.570	1.567 \pm 0.006

*Average \pm standard deviation of four determinations, sample weights 25–48 mg for No. 224, 23–33 mg for No. 252, and 20–21 mg for No. 241/1.

in Table 1. Phosphoric acid and sulphuric acid are tolerated up to 0.67*M* and 0.15*M*, respectively.

PBHA and many other *N*-arylhydroxamic acids give coloured complexes with cerium(IV) and molybdenum(VI) which are extractable from fairly concentrated hydrochloric acid, and these complexes cause serious interference in the determination and vanadium(V). However, B-2-NHA does not give coloured extracts with Ce(IV), Mo(VI) or Zr(IV) under the conditions recommended for vanadium(V), so these ions do not interfere. This shows the remarkable selectivity of B-2-NHA for vanadium(V). However, titanium(IV) forms a yellow complex with B-2-NHA and is tolerated only in very small amounts.

Determination of vanadium in steels

Typical results for some standard steels are given in Table 2.

Acknowledgements—The authors are thankful to Prof. S. G. Tandon, Head of Chemistry Department, Ravishankar University, Raipur, for providing laboratory facilities and useful suggestions. One of them (BS) is thankful to U.G.C., New Delhi, for a Teacher Fellowship award.

REFERENCES

1. U. Priyadarshini and S. G. Tandon, *Analyst*, 1961, **36**, 544.
2. S. G. Tandon and S. C. Bhattacharya, *Anal. Chem.*, 1961, **33**, 1267.
3. D. C. Bhura and S. G. Tandon, *Anal. Chim. Acta*, 1971, **53**, 379.
4. S. A. Shahid Abbasi, *Anal. Chem.*, 1976, **48**, 714.
5. A. K. Mazumdar and G. Das, *Anal. Chim. Acta*, 1964, **31**, 147.
6. B. R. Sahu and U. Tandon, *J. Chem. Eng. Data*, 1983, **28**, 433.
7. A. I. Vogel, *Quantitative Inorganic Analysis*, 3rd Ed., pp. 265, 646. Longmans, London, 1961.
8. P. W. West, *J. Chem. Educ.*, 1951, **18**, 528.
9. E. B. Sandell, *Colorimetric Determination of Traces of Metals*, 3rd Ed. Interscience, New York, 1959.

SPECTROPHOTOMETRIC DETERMINATION OF IRON BY EXTRACTION OF THE IRON(II)-5,5-DIMETHYL-1,2,3- CYCLOHEXANETRIONE-1,2-DIOXIME-3-THIOSEMI- CARBAZONE COMPLEX

F. SALINAS, T. GALEANO DIAZ and J. C. JIMENEZ SANCHEZ

Department of Analytical Chemistry, Faculty of Sciences, University of Extremadura,
06071 Badajoz, Spain

(Received 21 February 1986. Revised 17 November 1986. Accepted 3 February 1987)

Summary—The iron (II)-5,5-dimethyl-1,2,3-cyclohexanetrione-1,2-dioxime-3-thiosemicarbazone complex can be extracted from a medium of high acidity into amyl alcohol. Measurement of the absorbance at 550 nm gives a determination limit for iron of 0.015 µg/ml. The method has been applied to the determination of iron in water, wine, beer and fruit juice.

We have already described the synthesis and analytical properties of 5,5-dimethyl-1,2,3-cyclohexanetrione-1,2-dioxime-3-thiosemicarbazone (DCDT) and its application to the determination of iron in strongly acidic medium.¹ Extraction of the Fe(II)-DCDT complex into amyl alcohol increases the sensitivity of the method, and can be applied to the determination of iron in water, wine, beer and fruit juice. This application, along with an improved procedure for synthesis of the reagent, forms the subject of this paper.

EXPERIMENTAL

Reagents

All chemicals were of analytical reagent grade or better. Stock standard iron(II) solution (1.002 g/l.) was standardized by titration with potassium dichromate and diluted further as required.

Synthesis of DCDT

Dissolve 5 g of 5,5-dimethyl-1,3-cyclohexanedione in a solution of 2.5 g of potassium hydroxide in 15 ml of water. Add 2.46 g of potassium nitrite, cool the solution in a freezing mixture, and keep it at <0° during the subsequent procedure. With continuous stirring add concentrated hydrochloric acid until a slight excess is present. Then add cold ethanol until all the yellow product has dissolved, and mix with a solution of 2.48 g of hydroxylamine hydrochloride in water, neutralized with sodium carbonate. Filter off the white precipitate of 5,5-dimethyl-1,2,3-cyclohexanetrione-1,2-dioxime obtained and wash it with water.

Add a solution of 1.4 g of thiosemicarbazide in 70 ml of 5% v/v hydrochloric acid to a solution of 2.5 g of the dioxime in 70 ml of ethanol. Collect the yellow precipitate (which appears after a few minutes) and wash it with 1:1 v/v ethanol-water mixture (yield 80%).

The m.p., infrared spectrum and elemental analysis confirm the identity of the product. It is used as a 0.5% solution in dimethylformamide.

Procedures for determination of iron

Place in a separatory funnel 100 ml of sample solution containing between 1.5 and 45 µg of iron, and add 15 ml of concentrated hydrochloric acid and 1 ml of reagent

solution. After 5 min add 10 ml of amyl alcohol and shake the mixture vigorously for 1 min. Separate the organic phase and centrifuge it. Measure its absorbance at 550 nm against water.

Analysis of water. Filter the water immediately after sampling and acidify it with 8 ml of concentrated hydrochloric acid per litre. Boil a 100-ml portion for 10 min, and determine iron as above.

Analysis of fruit juice. Filter the juice and acidify it with a few drops of concentrated hydrochloric acid. Analyse a known volume containing 1.5-45 µg of iron by the procedure above, measuring the absorbance against a blank prepared by similar treatment of the same volume of the juice, but with omission of the reagent.

Analysis of wines. Analyse as for fruit juice, but omit the filtration.

Analysis of beer. Degas the sample and analyse as for water.

RESULTS AND DISCUSSION

As already reported,¹ iron(II) and iron(III) form a violet complex with DCDT, with maximum absorption at 550 nm. The stoichiometry of the iron(II)-DCDT complex is 3:1 (reagent:Fe). Iron(III) is reduced by the reagent and gives the iron(II) complex. The optimum acidity range for complex formation is between $H_0 = -2.8$ and $\text{pH} = 1$ (H_0 is the Hammett acidity function²). At least a 10-fold molar excess of reagent is necessary. The molar absorptivity at 550 nm is 8.9×10^3 l.mole⁻¹.cm⁻¹.

Various solvents have been tested for extraction of the Fe(II)-DCDT complex, and amyl alcohol was found the best. The effect of acidity on the distribution of DCDT between hydrochloric acid and amyl alcohol is shown in Fig. 1. The extraction of DCDT was decreased by protonation of the DCDT at negative values of H_0 and by dissociation at $\text{pH} > 6$.

The effect of acidity on extraction of the Fe(II)-DCDT complex was also studied with 20 µg of iron(II) in 10 ml of aqueous phase at the desired

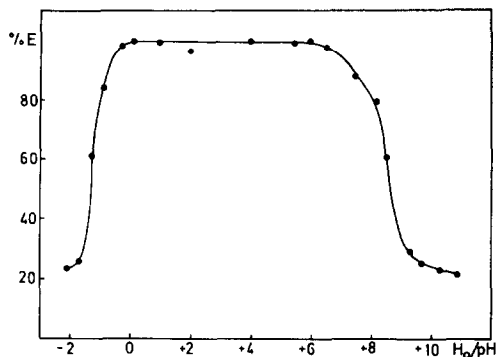


Fig. 1. Effect of acidity on the extraction of DCDT (initial concentration $3.9 \times 10^{-3} M$).

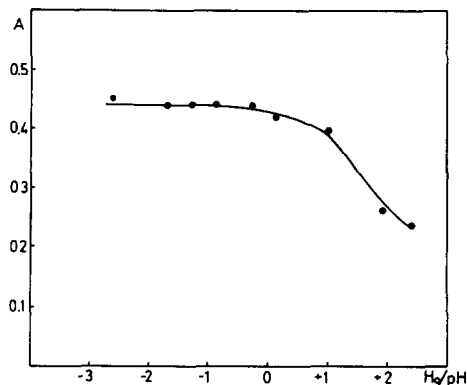


Fig. 2. Effect of acidity on extraction of the Fe(II)-DCDT complex.

acidity, 1 ml of reagent solution, and 10 ml of amyl alcohol. The results are shown in Fig. 2. At H_0 values more negative than -3 the phase separation is not satisfactory.

Table 1. Tolerance for foreign ions in determination of 20 μg of iron

Maximum permissible w/w ratio of foreign ion to Fe(II)	Ions tested
2	Co(II), Te(IV), Pd(II)
5	Ni(II)
25	Mo(VI), Cu(II), BO_2^-
100	Hg(II), Sn(II), Ag(I), Cr(III), Cr(VI)*, Al(III), Be(II), W(VI), Zn(II), Cd(II), Pb(II), Bi(III), As(III), Mn(II), Ti(IV), Sb(III), Ca(II), Ba(II), Mg(II), V(V)*, PO_4^{3-} , F^- , SO_4^{2-} , NO_3^- , Br^- , IO_3^- *, BrO_3^- *, ClO_3^- *
> 100	

*In presence of 1 ml of 10% ascorbic acid solution.

Table 2. Determination of iron in water ($\mu g/ml$)*

Sample	DCDT	1,10-Phenanthroline method†
Guadiana river	0.104–0.107	0.102
Well water	0.087–0.089	0.087
Tap water	0.096–0.102	0.094

*Range of 3 determinations.

†With 5.0-cm path-length.

Table 3. Determination of iron in fruit juices ($\mu g/ml$)*

Sample	DCDT method	AAS
Apple juice	0.53–0.55	0.50
Tomato juice	0.58–0.60	0.62
Lemon juice	0.45–0.46	0.44
Orange juice	0.46–0.48	0.50

*Range of 3 determinations.

Table 4. Determination of iron in wine and beer ($\mu g/ml$)*

Sample	DCDT method	AAS
Dry sherry	1.64–1.66	1.69
Beer	0.11–0.13	0.12

*Range of 3 determinations.

We chose 1:10 volume ratio of isoamyl alcohol to sample, a shaking time of 1 min and 1 ml of 0.5% reagent solution as optimal.

The extraction constant, determined by the method of Román Galán *et al.*³ was 2.8×10^{15} and the method confirmed the stoichiometry of the complex.

The extract obeys Beer's law over a wide range of concentration. The detection limit⁴ is $0.005 \mu g/ml$ and the determination limit⁵ $0.015 \mu g/ml$. The relative error (11 determinations, 20 μg of iron, 95% confidence level) is 0.5%.

In the determination of 20 μg of iron, foreign ions can be tolerated at the levels given in Table 1.

Applications

The results obtained in the determination of iron in water, fruit juice, wine and beer are given in Tables 2–4, with those obtained with 1,10-phenanthroline or atomic-absorption spectrometry.

Acknowledgements—We thank the Comisión Asesora de Investigación Científica y Técnica del Ministerio de Educación y Ciencia de España for supporting this study (Project No. 2903–83).

REFERENCES

1. F. Salinas, J. C. Jiménez Sánchez and T. Galeano Díaz, *Anal. Chem.*, 1986, **58**, 824.
2. M. A. Paul and F. A. Long, *Chem. Rev.*, 1957, **57**, 1.
3. T. Román Galán, A. Arrebola Ramirez and M. Román Ceba, *Talanta*, 1980, **27**, 545.
4. *Pure Appl. Chem.*, 1976, **105**, 45.
5. *Anal. Chem.*, 1980, **52**, 2242.

HYDRODYNAMIC VOLTAMMETRY AT TUBULAR ELECTRODES—III

DETERMINATION OF TRACES OF BISMUTH BY DIFFERENTIAL-PULSE ANODIC-STRIPPING VOLTAMMETRY AT A GLASSY-CARBON TUBULAR ELECTRODE WITH *IN SITU* MERCURY PLATING

WAN ZHEN and CHEN QIANG

Department of Chemistry, Xiamen University, Xiamen, People's Republic of China

(Received 20 December 1985. Revised 1 August 1986. Accepted 20 December 1986)

Summary—An equation for the current in differential-pulse anodic-stripping voltammetry at tubular electrodes is derived. Application of a glassy-carbon tubular electrode to determination of traces of bismuth in environmental water samples by differential-pulse anodic-stripping voltammetry is described. In hydrochloric acid medium, the stripping peak current is proportional to the concentration of bismuth in the range 2–100 ng/ml, with a deposition time of 3–10 min. The detection limit is 0.5 ng/ml.

Tubular electrodes have been studied by Blaedel and co-workers¹⁻³ and anodic stripping voltammetry (ASV) with thin mercury films deposited on various forms of carbon has been widely used for trace metal analysis, and recently for on-line analysis.⁴ Lieberman and Zirino⁵ have used a very high flow-rate in a tubular mercury-coated graphite electrode to detect zinc in sea-water at concentrations of $1 \times 10^{-9}M$, with 5-min deposition. Schieffer and Blaedel^{6,7} used a pair of tubular glassy-carbon thin mercury-film electrodes in series for measurement of trace amounts of heavy metals in tap water; the metals were first collected on the upstream electrode, then stripped from it and collected on the downstream electrode.

In this paper, we derive an equation for differential-pulse anodic-stripping voltammetry (DPASV) which expresses the dependence of the differential-pulse anodic-stripping current on parameters such as flow-rate, pulse amplitude, bulk concentration of electroactive species, etc., and confirm it experimentally. We have designed a glassy-carbon tubular electrode flow-through cell and applied it to continuous determination of trace bismuth in tap and ground water by DPASV. In 0.06M hydrochloric acid medium, the stripping peak current of bismuth can be obtained at -0.11 V (vs. Ag/AgCl) and is linearly related to bismuth concentration over the range 2–100 ng/ml, with 3–10 min deposition. This method has many advantages such as high sensitivity and stability and can be applied to continuous and on-line analysis. The bismuth content of environmental water samples has been measured.

THEORY

Blaedel and Klatt² have derived a simple equation for the diffusion current at tubular electrodes:

$$i = 5.31 \times 10^5 n D^{2/3} X^{2/3} V_f^{1/3} C_0 \quad (1)$$

where C_0 is the bulk concentration of electroactive species, D the diffusion coefficient, X the length of the tubular electrode, and V_f the volumetric flow-rate.

In DPASV, by analogy with Hubbard and Anson's treatment,⁸ the electrolysis current is given by

$$i = -nFV \frac{dC_R}{dt} \quad (2)$$

where n is the number of electrons involved in the electrode reaction, F the Faraday constant, V the volume of the metal thin film, and C_R the bulk concentration of reactant R. For differential-pulse voltammetry, when the pulse amplitude is ΔE and the duration of the potential pulse is δ , if the potential scan-rate is slow and δ is small, Δi can be expressed by

$$\Delta i = -nFV \frac{\Delta C_R}{\Delta t} = nFV \frac{C_1 - C_2}{\delta} \quad (3)$$

where C_1 and C_2 are the concentrations of reactant R on the surface of the electrode when the potentials applied are E and $E + \Delta E$, respectively.

We suppose that before the deposition potential is applied, the concentration of R on the surface of the electrode (C_R^*) is zero, and that after a deposition time t_{dep}

$$C_R^* = it_{dep}/nFV \quad (4)$$

For convenience, we will write

$$\exp \left[\frac{nF}{RT} (E - E_{1/2}) \right] = \theta_1 \quad (5)$$

so in the stripping process

$$C_1 = C_R^*/(1 + \theta_1) \quad (6)$$

before the pulse is applied. Similarly, for the situation

after application of a potential pulse ΔE , we can write

$$\exp\left[\frac{nF}{RT}(E - E_{1/2} + \Delta E + \delta v)\right] = \theta_2 \quad (7)$$

where v is the potential scan-rate. If $\Delta E \gg \delta v$, equation (7) can be approximated to

$$\exp\left[\frac{nF}{RT}(E - E_{1/2} + \Delta E)\right] = \theta_2 \quad (8)$$

so

$$C_2 = C_R^*/(1 + \theta_2) \quad (9)$$

From equations (3), (6) and (9), Δi can be expressed as a function of θ_1 and θ_2 by

$$\Delta i = nFV \left(\frac{1}{1 + \theta_1} - \frac{1}{1 + \theta_2} \right) C_R^*/\delta \quad (10)$$

On the other hand, combining (1) and (4) gives

$$C_R^* = 5.31 \times 10^5 nD^{2/3} X^{2/3} V_f^{1/3} C_0 t_{\text{dep}}/nFV \quad (11)$$

From equations (10) and (11), Δi can be expressed by

$$\Delta i = 5.31 \times 10^5 nD^{2/3} X^{2/3} V_f^{1/3} t_{\text{dep}} C_0 \times \left(\frac{1}{1 + \theta_1} - \frac{1}{1 + \theta_2} \right) / \delta \quad (12)$$

When $E = E_{1/2} - \frac{1}{2}\Delta E$, Δi will be maximal and expressed by

$$(\Delta i)_p = 5.31 \times 10^5 nD^{2/3} X^{2/3} V_f^{1/3} t_{\text{dep}} C_0$$

$$\times \left\{ \frac{1}{1 + \exp\left[\frac{-nF}{2RT}\Delta E\right]} - \frac{1}{1 + \exp\left[\frac{nF}{2RT}\Delta E\right]} \right\} / \delta \quad (13)$$

If $\Delta E \leq nF/RT$ the peak current equation for DPASV at tubular electrodes will be:⁹

$$(\Delta i)_p = 1.33 \times 10^5 n^2 F \times (\Delta E/\delta) D^{2/3} X^{2/3} V_f^{1/3} t_{\text{dep}} C_0 / RT \quad (14)$$

but if δv approximates to ΔE , $(\Delta i)_p$ can be expressed as

$$(\Delta i)_p = 1.33 \times 10^5 n^2 F D^{2/3} X^{2/3} V_f^{1/3} t_{\text{dep}} C_0 \times (\Delta E + \delta v) / \delta RT \quad (15)$$

EXPERIMENTAL

Apparatus

A model F-78 pulse polarograph was used. The output was fed into a recorder (model XWT-204, Dahua Meter Factory, Shanghai).

A schematic diagram of the cell is shown in Fig. 1. The body, made from Teflon, is in two parts, each with a 1-mm diameter hole drilled through its centre. The upper block contains a silver-silver chloride reference electrode. Four stainless-steel bolts (not shown in the figure) hold the blocks together and compress the O-ring and three anion-exchange membrane washers on the lower block to provide a leak-free liquid bridge between the working and reference electrodes. The working electrodes are glassy-carbon tubular electrodes, made by drilling a 1.0-mm diameter hole in a rod (The Man-made Crystalline Institute of Beijing) and cutting

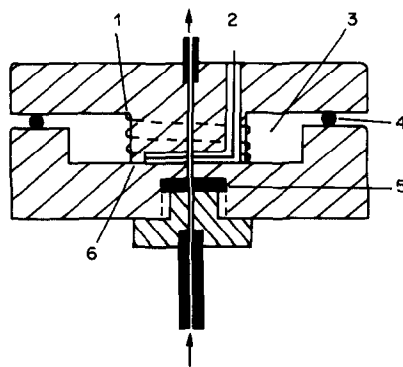


Fig. 1. Glassy-carbon tubular electrode flow-through cell. 1, Ag/AgCl electrode; 2, Pt wire counter-electrode; 3, 1M KCl; 4, O-ring; 5, tubular electrode; 6, anion-exchange membranes.

it into suitable lengths, typically 2.0 mm. The polishing procedure is that described by Schieffer and Blaedel.⁶ Siphoning was used for solution flow.

Reagents

All chemicals used were of analytical-reagent grade and doubly distilled water was used.

Standard bismuth solution. Bismuth powder (1.000 g) was dissolved in 10 ml of concentrated nitric acid and the solution was diluted to 1000 ml. This 1000- $\mu\text{g/ml}$ stock solution was further diluted as required.

Mercuric nitrate solution. Mercuric nitrate (0.3426 g) was dissolved in 100 ml of water.

Procedure

Transfer 1.25 ml of $1 \times 10^{-3}M$ mercuric nitrate, 0.75 ml of 2M hydrochloric acid and 2 ml of standard 1- $\mu\text{g/ml}$ bismuth solution into a 25-ml standard flask, and dilute to the mark with water. Place this solution in the cell, set the deposition potential at -0.5 V, pulse amplitude at 50 mV, and the flow-rate (V_f) at 0.6 ml/min. After deposition, scan the potential from -0.5 to $+0.2$ V and 10 mV/sec. The differential pulse anodic stripping peak is at -0.11 V.

RESULTS AND DISCUSSION

Cyclic voltammetry

A 6- $\mu\text{g/ml}$ bismuth solution was examined by d.c. cyclic voltammetry. The difference between the an-

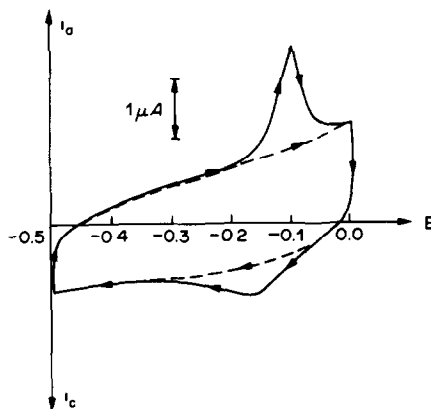


Fig. 2. A typical cyclic voltammetric curve for bismuth: 6 ppm Bi (III), 0.06M HCl, V_f 0.6 ml/min, v 10 mV/sec.

Table 1. Dependence of peak current on scan-rate

Scan-rate, mV/sec	1	2	5	10
$(\Delta i)_p, \mu A$	0.97	1.06	1.13	1.30

odic and cathodic peak potentials ($E_{p,a} - E_{p,c}$) was 35 mV, so this electrode process on the glassy-carbon tubular electrode with *in situ* mercury-plating is reversible. The height of the anodic peak being greater than that of the cathodic peak shows that bismuth can be deposited on the electrode easily. A typical cyclic voltammetric curve is shown in Fig. 2.

Experimental conditions

Electrolyte. Hydrochloric acid is used as the electrolyte. Changing its concentration from 0.04 to 0.60M has no effect on the peak current, and 0.06M was chosen as the acid concentration of the medium.

Hg(NO₃)₂ concentration. Mercuric nitrate was chosen for *in situ* mercury plating, and the stripping currents were found constant over the range from 4×10^{-6} to 5×10^{-4} M mercuric nitrate. The concentration chosen for use was 5×10^{-5} M.

Deposition potential. Peak currents were independent of deposition potential in the range from -0.3 to -1.0 V, and -0.5 V was selected for practical use.

Scan-rate. The peak current could not be measured at scan-rates of 100 and 50 mV/sec because the scan was too fast. The peak heights slowly increased as the scan-rate was increased from 1 to 10 mV/sec (Table 1), in accordance with equation (15); 10 mV/sec was chosen for its higher sensitivity.

Pulse intervals. The diffusion layer thickness will increase as the pulse interval increases, and the diffusion current will become smaller. It was found that the peak current decreased as the pulse intervals

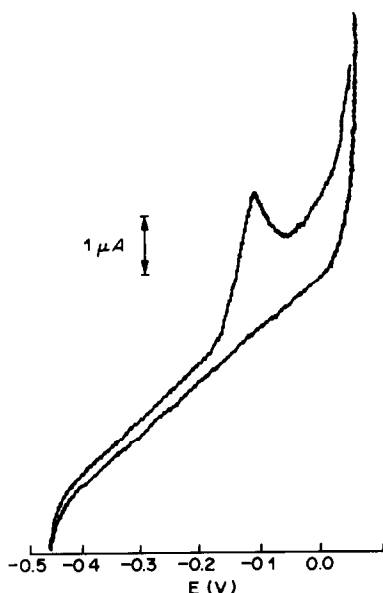


Fig. 3. A typical DPASV curve for bismuth and a blank: 1, blank; 2, 80 ng/g Bi(III); 0.06M HCl; t_{dep} 3 min; v 10 mV/sec; pulse amplitude 50 mV; pulse interval 0.5 sec.

were increased from 0.5 to 5.0 sec. A 1-sec pulse interval was chosen because it gave a good peak shape and higher sensitivity.

Pulse amplitude. The peak heights were found to be a linear function of the pulse amplitude.

Deposition time. The peak heights were linearly related to deposition time in the range from 1 to 15 min, and 3 and 10 min deposition times were chosen for 10^{-8} and 10^{-9} g/ml bismuth, respectively.

Flow-rate. The dependence of $(\Delta i)_p$ on $V_f^{1/3}$ was linear and 0.6 ml/min was chosen as the flow-rate.

Electrode length. The dependence of $(\Delta i)_p$ on $X^{2/3}$ was linear, and in good agreement with expectation.

Calibration graph and detection limit

The graph of $(\Delta i)_p$ vs. bismuth concentration was linear and passed through the origin. The detection limit was 0.5 ng/ml with a deposition time of 15 min. Figure 3 shows typical DPASV curves for bismuth and a blank.

Interferences

The effect of foreign substances was studied with an 80-ng/ml bismuth solution. Co(II), Mn(II), Ni(II), W(VI), Pb(II), Mo(VI), Cr(VI), Se(IV) and Ti(IV) at 8 μ g/ml do not interfere with the stripping peak of bismuth. Higher levels of Cu(II) can be dealt with by removal of the copper and bismuth with "thiol cotton", and their differential elution with 0.2M hydrochloric acid (copper) and 2M hydrochloric acid (bismuth).¹⁰

Water analysis

Untreated water samples can be directly analysed. Transfer 20 ml of environmental water sample, 0.75 ml of 2M hydrochloric acid and 1.25 ml of 1×10^{-3} M mercuric nitrate into a 25-ml standard flask, and dilute to the mark with doubly distilled water. Determine the bismuth content by the standard additions method, with anodic stripping at -0.11 V. Results are shown in Tables 2 and 3. Relative standard

Table 2. Analysis of water samples (mean and standard deviation of 6 results)

Sample	Bi content, ng/ml	s.d. ng/ml
I	2.0	0.11
II	1.7	0.09
III	5.2	0.07
IV	4.5	0.11

Table 3. Recovery of 10 ng/ml bismuth added to samples

Sample	Bi content,* ng/ml	Bi found,* ng/ml	Recovery, %
V	5.1	14.9	98
VI	1.5	12.0	105
VII	6.7	17.3	106
VIII	2.7	12.2	95

*Means of 3 determinations.

deviations are less than 5.6% and percentage recoveries are in the range 95–106%.

REFERENCES

1. W. J. Blaedel, C. L. Olson and L. R. Sharma, *Anal. Chem.*, 1963, **35**, 2100.
2. W. J. Blaedel and L. N. Klatt, *ibid.*, 1966, **39**, 879.
3. W. J. Blaedel and G. W. Schieffer, *J. Electroanal. Chem.*, 1977, **80**, 252.
4. J. Wang, *Am. Lab.*, 1983, 15, No. 7, 14.
5. S. H. Lieberman and A. Zirino, *Anal. Chem.*, 1974, **46**, 20.
6. G. W. Schieffer and W. J. Blaedel, *ibid.*, 1977, **49**, 49.
7. *Idem*, *ibid.*, 1978, **50**, 99.
8. A. T. Hubbard and F. C. Anson, *ibid.*, 1966, **38**, 58.
9. J. A. Plambeck, *Electroanalytical Chemistry: Basic Principles and Applications*. Wiley, New York, 1982.
10. Mu-ying Yu, Gui-qui Liu and Qinhan Jin, *Talanta*, 1983, **30**, 265.

ARTIFACTS OF THE DECALIN-MOLECULAR SIEVE SYSTEM IN THE ANALYSIS OF MINERAL WAXES

MUHAMMAD NAZIR and MUHAMMAD KHURSHID BHATTY
PCSIR Laboratories, Lahore-16, Pakistan

FRANK D. GUFFEY
Western Research Institute, Laramie, Wyoming 82071, U.S.A.

(Received 10 September 1986. Revised 3 February 1987. Accepted 10 February 1987)

Summary—Analysis of commercial paraffin waxes by use of molecular sieves and decalin has been shown to give misleading results because of the formation of additional compounds. The source and the nature of these compounds have been investigated and it has been found that they are polymers of partially dehydrogenated decalin. Care should be taken when using this solvent in such analyses.

Several procedures for the analysis of commercial mineral waxes have been reported.¹⁻⁴ In our work on correlation of wax constituents as the basic feedstock for production of fatty acids or alcohols, the correct composition of these compounds had to be determined, and we used the procedure of Washall *et al.*⁴ because of its simplicity and ease of operation. In doing so, however, we encountered artifacts in the form of additional compounds in the unabsorbed portion of the waxes. The source and nature of these additional compounds were investigated and are described in this communication.

EXPERIMENTAL

Materials

Waxes. Several refined commercial paraffin waxes were used but only the results for the wax with m.p. 52.5° are described.

Decalin. Freshly distilled commercial decalin, which was a mixture of the *cis* and *trans* forms, was used.

Molecular sieve (5A, $\frac{1}{16}$ -in. pellets, Alltech Associates). Activated by heating in a vacuum oven at 250° for 6 hr and stored in a desiccator for later use.

Apparatus

A Hewlett-Packard model 5700 gas chromatograph was coupled directly to a Kratos AEI MS-12 mass-spectrometer. Data were collected with a Finnigan INCOS 2300 system.

Procedure

A mixture of molecular sieve (10 g), decalin (10 ml) and wax (0.5 g) was heated at 180° for 24 hr, then cooled and filtered through a sintered-glass funnel. The molecular sieve was extracted in a Soxhlet extractor with a mixture of benzene and propanol-2 (100 + 50 ml) for 6 hr. The filtrate and extract were combined, and the solvent was removed, leaving a brownish mass. A blank experiment without the addition of wax was conducted in a similar way.

A 0.1- μ l portion of a cyclohexane solution of unabsorbed material from the wax was injected into the column. The brownish mass from the blank experiment was applied to the probe tip, as a saturated solution in cyclohexane. The solvent was removed by a stream of nitrogen. The ion source

temperature was maintained at 280°. A Dexsil 300 SCOT column programmed to rise in temperatures from 150° to 300° at 2°/min was used for the gas chromatographic separations. Helium at a flow-rate of 5 ml/min was used as the carrier gas. The injection port and the transfer lines were maintained at 350° and 310° respectively.

For recording the mass spectra and acquisition of data the experimental conditions were as follows.

Ionizing voltage	70 V
Accelerating voltage	4 kV
Filament current	100 μ A
Scan-rate	2 sec/decade
Scan time	2 sec
Hold	1 sec
Cycle time	6 sec
Acquisition	Downward scan

RESULTS AND DISCUSSION

The unabsorbed material from the waxes was brown and fluorescent, and showed strong absorption in the ultraviolet region. It was analysed by gas chromatography-mass spectrometry. The reconstructed ion-current chromatogram, when compared with the chromatogram of the original wax sample,

Table 1. Characteristic peaks in the spectra of the components of the unabsorbed material derived from waxes

Peak*	Base peak, <i>m/z</i>	Molecule ion peak, <i>m/z</i>
1	135	270
2	135	270
3	131	270
4	131	268
5	145	268
6	131	268
7	145	268
8	158	266
9	158	266
10	165	262

*In order of appearance on chromatogram.

Table 2. Summary of results of the mass spectrometric probe analysis of the molecular sieve-decalin extract

m/z	Relative intensity	Molecular formula	No. of rings	No. of double bonds
262	0.93	C ₂₀ H ₂₂	4	6
264	0.51	C ₂₀ H ₂₄	4	5
266	1.09	C ₂₀ H ₂₆	4	4
268	2.04	C ₂₀ H ₂₈	4	3
270	1.48	C ₂₀ H ₃₀	4	2
396	0.02	C ₃₀ H ₃₆	6	7
400	0.03	C ₃₀ H ₄₀	6	5
404	0.02	C ₃₀ H ₄₄	6	3

* $100X/(Y - Z)$, where X is the measured intensity, and Y is the total ionization and Z the ionization sum for $m/z = 0-85$.

Table 3. Ions in the mass spectrum of the molecular sieve-decalin extract from mass 128 to mass 138

m/z	Relative intensity*	Isotope-corrected intensity	Molecular formula	No. of rings	No. of double bonds
128	1.72	1.67	C ₁₀ H ₈	2	5
129	2.85	2.66	C ₁₀ H ₉	2	
130	2.02	1.71	C ₁₀ H ₁₀	2	4
131	5.13	4.90	C ₁₀ H ₁₁	2	
132	1.17	0.60	C ₁₀ H ₁₂	2	3
133	0.62	0.49	C ₁₀ H ₁₃	2	
134	0.60	0.53	C ₁₀ H ₁₄	2	2
135	1.80	1.77	C ₁₀ H ₁₅	2	
136	1.06	0.86	C ₁₀ H ₁₆	2	1
137	1.07	0.95	C ₁₀ H ₁₇	2	
138	0.11	0.00	C ₁₀ H ₁₈	2	0

*See footnote to Table 2.

showed at least ten additional peaks, the characteristics of which are shown in Table 1. The components causing these peaks are unusual in wax samples, since they do not represent a homologous series but only a change in the degree of unsaturation.

The filtrate, the washings and the extract from the blank experiment, when evaporated, gave a brownish semi-solid mass which was fluorescent and showed absorption in the ultraviolet region similar to that exhibited by the unabsorbed material from the waxes. The reconstructed ion-current chromatogram for the molecular sieve extract (direct introduction probe technique) had a large number of peaks. The characteristics of some of them are recorded in Table 2. These peaks had the same molecular weight and fragmentation pattern as those in Table 1. Moreover, these peaks could possibly originate from compounds having a carbon skeleton containing multiples of ten carbon atoms, or a bicyclic compound containing ten carbon atoms and having varying degrees of unsaturation. This observation confirmed that the source of the additional peaks present in the unabsorbed material from the waxes was not the transformed products of the waxes but had its origin in the decalin-sieve system.

To explain the formation of these compounds, it is proposed that decalin becomes dehydrogenated under the influence of a molecular sieve at elevated temperatures. The presence of ions with an even m/z

(Table 3) supports the hypothesis that there are dehydrogenated species in the mixture. The suggested dehydrogenation is analogous to some reactions of decalin which have been described earlier.⁵ The dehydrogenated intermediates may polymerize in a similar manner to dialins.^{6,7} The newly formed C—C bond may be between two α -positions or an α and a β -position to form a linear dimer, or two molecules may condense to form a polynuclear compound. The ionic species having m/z 135, which may have the structure shown in Fig. 1, could be formed by the fragmentation of the molecule ion of a linear dimer. The other ionic species, having m/z 131 might have formed part of a symmetrical molecule with a molecular weight (m.w.) of 262 but does not because the

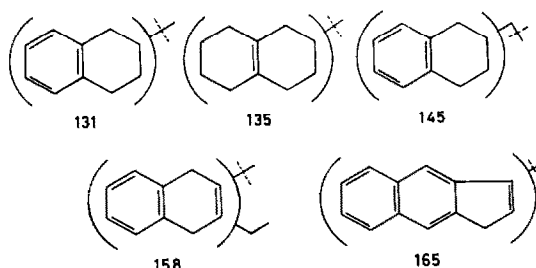


Fig. 1. Possible partial structures of ions in the spectra of the additional compounds formed in the decalin-molecular sieve system.

parent ion m.w. is 268. The remaining ionic species, having m/z 145, 158 and 165, which may have the structures shown in Fig. 1, cannot arise from the fragmentation of symmetrical molecule ions, but could originate from compounds containing cyclohexane rings separated by one or more carbon atoms.⁸ The formation of such compounds may result from the rupture of one cyclohexane ring and generation of free radicals as proposed by Bredael and Vinh.⁹

On the basis of these observations it is therefore proposed that under the experimental conditions described,⁴ decalin (in the presence of molecular sieves) polymerizes to form at least the dimer and trimer. For this reason it is felt that care must be taken in the application of this procedure for the analysis of mineral waxes.

Acknowledgements—M. Nazir is thankful to the Council for International Exchange of Scholars, Washington D.C.

20036, for the award of a Fulbright-Hays Scholarship and to the Pakistan Council of Scientific and Industrial Research (PCSIR) for allowing him to take up this scholarship.

REFERENCES

1. J. G. O'Connor F. H. Buro and M. S. Norris, *Anal. Chem.*, 1962, **34**, 82.
2. J. V. Brunnock, *ibid.*, 1966, **38**, 1648.
3. V. R. Sista and G. C. Srivastava, *ibid.*, 1976, **48**, 1583.
4. T. A. Washall, S. Blittman and R. S. Mascieri, *J. Chromatog. Sci.*, 1970, **8**, 663.
5. F. Radt, *Elsevier Encyclopedia of Organic Chemistry*, Vol. 12B, p. 84. Elsevier, New York, 1948.
6. F. Radt, *op. cit.*, p. 57.
7. N. D. Scott and J. F. Walker, *Ind. Eng. Chem.*, 1940, **32**, 312.
8. H. Budzikiewicz, C. Djerassi and D. H. Williams, *Mass Spectrometry of Organic Compounds*, p. 88. Holden-Day, San Francisco, 1967.
9. P. Bredael and T. H. Vinh, *Fuel*, 1979, **58**, 211.

PHOTOMETRIC DETERMINATION OF SELENIUM WITH FERROCENE

MINORI KAMAYA, TETSURO MURAKAMI and EIZEN ISHII

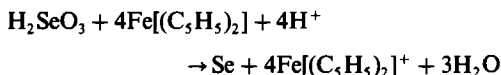
Department of Industrial Chemistry, Kogakuin University 1-24-2, Nishi-Shinjuku, Shinjuku-Ku 162,
Tokyo, Japan

(Received 16 September 1986. Revised 27 January 1987. Accepted 6 February 1987)

Summary—A sensitive spectrophotometric method for the determination of selenium has been developed. The method depends on a redox reaction between selenious acid in 8M hydrochloric acid and a chloroform solution of ferrocene. One mole of selenious acid produces 4 moles of ferricenium ions, which are then oxidized by bromine water. The resulting iron(III) is reduced to iron(II) and determined with 1,10-phenanthroline. The relative standard deviation for 20 µg of selenium was 1.1%. The apparent molar absorptivity of the final solution, referred to selenious acid, is $4.23 \times 10^4 \text{ l. mole}^{-1} \text{ cm}^{-1}$ at 512 nm. This method has been used to determine selenium in copper metal.

The determination of selenite with 3,3'-diaminobenzidine¹⁻³ and related reagents⁴⁻⁷ is well established. However, these reagents are unstable to light and air.⁸ Also, primary amines are carcinogenic⁹ and their selenite complexes have low molar absorptivities.

Valsov *et al.*¹⁰ reported a photometric determination of selenious acid with ferrocene, based on a redox reaction between selenious acid and ferrocene in a strong acid solution (6M hydrochloric acid).



The ferricenium ion has an absorption maximum at 620 nm and the molar absorptivity corresponding to selenious acid is about $2 \times 10^3 \text{ l. mole}^{-1} \text{ cm}^{-1}$. Such a low sensitivity is not suitable for the determination of trace amounts of selenium.

Chemical multiplication methods have recently attracted much attention for increasing the sensitivity of analytical procedures. Attempts have been made to achieve chemical multiplication for the photometric determination with 1,10-phenanthroline of the iron(III) formed from the oxidative decomposition of ferricenium ions. The proposed method has been applied to the determination of selenium in copper metal, selenite first being separated from copper(II) by co-precipitation with arsenic.

EXPERIMENTAL

Reagents

Standard selenious acid solution, $1 \times 10^{-3}\text{M}$. Dissolve 0.1290 g of commercially available selenious acid in water and dilute to 1 litre. Prepare a $1 \times 10^{-5}\text{M}$ solution by diluting the stock solution with water.

Chloroform solution of ferrocene, $2 \times 10^{-3}\text{M}$. Add 20 ml of $1 \times 10^{-2}\text{M}$ methanol solution of ferrocene and 20 ml of concentrated hydrochloric acid to 100 ml of chloroform,

and shake the mixture in a separating funnel. Any ferricenium ion in the ferrocene is transferred into the aqueous phase. Repeat the extraction. The chloroform solution can be used for up to three days after preparation.

Concentrated hydrochloric acid. Pass the acid through a column of IRA-900 anion-exchange resin to remove iron(III).

Buffer solution, pH 6.0. Dissolve 13.75 g of sodium nitrilotriacetate in water, adjust the pH to 6.0 with phosphoric acid and dilute the solution to 500 ml.

1,10-Phenanthroline, $5 \times 10^{-3}\text{M}$. Dissolve 0.59 g of 1,10-phenanthroline dihydrochloride in water and dilute the solution to 500 ml.

Hydroxylamine solution. Dissolve 1 g of hydroxylamine hydrochloride in water and dilute the solution to 100 ml.

Sodium arsenite solution. Dissolve 3.47 g of sodium arsenite in water and dilute the solution to 200 ml. This solution contains 10 mg of arsenic per ml.

Sodium phosphinate solution. Dissolve 125 g of sodium phosphinate monohydrate ($\text{NaPH}_2\text{O}_2 \cdot \text{H}_2\text{O}$) in water and dilute the solution to 250 ml.

Washing solution. Mix 10 ml of the sodium phosphinate solution and 250 ml of hydrochloric acid (1 + 1). This solution is used for washing the arsenic precipitate.

Apparatus

A Hitachi, Model 200-10, double-beam spectrophotometer and a Hirma, Model 6C, photoelectric digital spectrophotometer were used, with 1-cm cells.

Procedure

Add 10 ml of concentrated hydrochloric acid freed from iron(III) by treatment with the anion-exchange resin to 5 ml of sample solution containing selenious acid ($\text{Se} < 20 \mu\text{g}$). Shake the mixture with 5 ml of the chloroform solution of ferrocene in a separating funnel for 15 min. The ferricenium ion passes into the aqueous phase from the chloroform solution of ferrocene. Evaporate the aqueous phase to about 5 ml, add 2 ml of bromine water and evaporate to dryness in a beaker, dissolve the residue in 1 ml of 0.1M nitric acid, add 1 ml of hydroxylamine hydrochloride solution, 4 ml of 1,10-phenanthroline solution and 5 ml of buffer solution (pH 6.0) and dilute with water to 25 ml. Measure the absorbance at 512 nm in 1-cm cells after 30 min.

Copper analysis procedure. Dissolve the sample in 140 ml

of mixed acid ($\text{HNO}_3:\text{HClO}_4:\text{H}_2\text{O} = 2:5:3$ v/v). Dilute with water to volume in a 200-ml standard flask, take a 20-ml aliquot, add 30 ml of water, 50 ml of concentrated hydrochloric acid, 1 ml of arsenite solution (10 mg of arsenic) and 20 ml of sodium phosphinate solution in that order. Boil the solution for 10 min, filter off the precipitate on filter paper, and wash with washing solution. Dissolve the precipitate off the filter paper with 5 ml of hot nitric acid (1 + 2) and wash the paper with 5 ml of hot water. Evaporate the solution and washings to dryness and dissolve the residue in 3 ml of water. Pass the solution through a column (8 mm bore, 100 mm in height) of CG-120 cation-exchange resin to remove copper(II). Wash the column with two 1-ml portions of water and add 10 ml of hydrochloric acid to the eluate. Determine selenium by the procedure above.

RESULTS AND DISCUSSION

Blank value

Chemical multiplication procedures are very useful for the determination of trace amounts of some elements. However, there may be a disadvantage in that the blank value is also increased. Here the blank values from the reagents were almost negligible, but that from the concentrated hydrochloric acid had to be decreased by pretreating the acid with a strong anion-exchange resin. Valsov *et al.*¹⁰ used a homogeneous solution (acetic acid-methanol-hydrochloric acid) as the medium for the ferrocene-selenite reaction. We found that shaking an aqueous selenite solution with a chloroform solution of ferrocene gave a blank that was only 40% of that obtained by the method of Valsov *et al.*¹⁰

Effect of concentration of hydrochloric acid

The reaction of ferrocene with selenious acid in methanol-hydrochloric acid-acetic acid is complete in a few minutes. However, when the two-phase system is used with the same concentration of hydrochloric acid, the time required to attain constant absorbance is 40 min. The effect of the acid concentration of the aqueous phase on the reaction rate was examined by measuring the absorbance of the aqueous phase after shaking the extraction system for 20 min. Figure 1 shows that the absorbance begins to

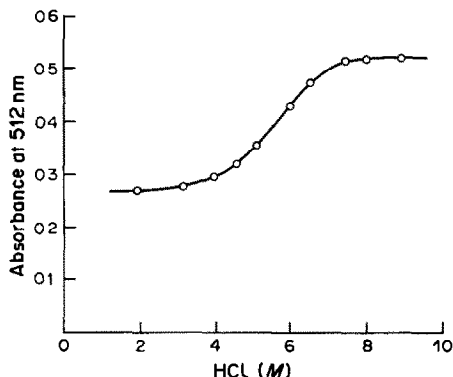


Fig. 1. Effect of acid concentration: 5 ml of $5 \times 10^{-5}M$ selenite, 5 ml of $2 \times 10^{-3}M$ ferrocene in chloroform, 20 min shaking time.

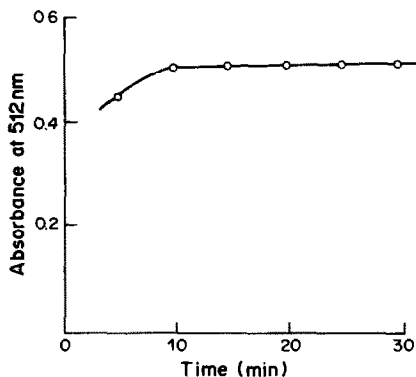


Fig. 2. Effect of shaking time: 5 ml of $5 \times 10^{-5}M$ selenite, 5 ml of $2 \times 10^{-3}M$ ferrocene in chloroform, 10 ml of 12M hydrochloric acid.

increase at 4M acid and reaches a constant value at $>7M$ acid.

The shaking time needed for equilibration also depends on the acidity and was found to be 10 min for 8M and 40 min for 6M hydrochloric acid medium (Fig. 2).

Effect of amount of ferrocene

As shown in Fig. 3, a constant absorbance was obtained when more than 5 ml of $1.6 \times 10^{-3}M$ ferrocene solution was used. The concentration of ferrocene is then 40 times greater than that of selenious acid.

Effect of other ions

The effect of various ions on the determination of selenium was examined. Cations such as copper(II) and iron(III) interfere with the reaction of ferrocene and selenious acid. Oxidizing anions, such as dichromate, chlorate and nitrite lead to positive errors.

Since both tellurite and selenite react with ferrocene and release ferricinium ion in acid solution, selenite should be separated from tellurite. Two methods^{11,12} have been proposed for the separation.

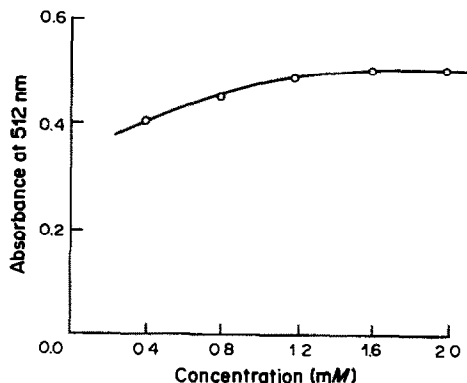


Fig. 3. Effect of ferrocene concentration: 5 ml of $5 \times 10^{-5}M$ selenite, 10 ml of 12M hydrochloric acid, 5 ml of ferrocene solution, 20 min shaking time.

Table 1. Determination of selenium (five replicates) in copper

Sample	Proposed method		3,3'-Diaminobenzidine method ³	
	Se, ppm	c.v., %	Se, ppm	c.v., %
A	197	3.2	200	3.8
B	0.41	16	0.36	10

Marbinya and Kapantsyah¹¹ reported that tellurite is sorbed on a column of IRA-900 anion-exchange resin from 8M hydrochloric acid, but selenite is not. We found this method useful for separation of selenite from a 30-fold mole ratio of tellurite. The traces of tellurium in ordinary samples of copper metal, however, have negligible effect on the determination of selenium even without a separation.

Calibration graph

The calibration graph showed that Beer's law is obeyed for up to 20 μg of selenium, with the reagent solution as reference. The molar absorptivity found was $4.23 \times 10^4 \text{ l. mole}^{-1} \cdot \text{cm}^{-1}$ at 512 nm and the coefficient of variation (estimated for 20 μg of selenium) was 1.1%. The absorbance of the reagent blank was 0.142 (water as reference) in 1-cm cells at 512 nm.

Determination of selenium in copper metal

The proposed method was used to determine trace amounts of selenium in copper metal. Prior separation of selenite from copper(II) was necessary and the method of co-precipitation with arsenic was employed. The co-precipitation gave good recovery of selenium and the arsenite did not interfere with the ferrocene-selenious acid reaction. However, if a high concentration of copper(II) solution containing selenious acid and arsenite was treated with sodium phosphinate in acid medium, traces of copper were

adsorbed on the precipitated arsenic, leading to a large error. This copper(II) was therefore removed with a cation-exchange resin. For sample A, 1 g was dissolved and a tenth of the solution used for analysis. For sample B, a 50-g portion was dissolved in 350 ml of mixed acid and a tenth of the solution used for analysis.

The results (Table 1) showed good agreement with those found by the 3,3'-diaminobenzidine method.³

REFERENCES

1. T. Danzuka and K. Ueno, *Anal. Chem.*, 1958, **30**, 1370.
2. C. L. Luke, *ibid.*, 1959, **31**, 572.
3. *Industrial Analysis of Copper and Alloys*, p. 176. Nippon Shindo Kyokai, 1962.
4. K. Hirai, O. Yui, Y. Nishikawa and T. Shigematsu, *Bunseki Kagaku*, 1973, **22**, 712.
5. O. Yui, K. Hirai, Y. Nishikawa and T. Shigematsu, *ibid.*, 1977, **26**, 91.
6. T. Murakami and E. Ishii, *Kogyokagaku Zasshi*, 1963, **66**, 1652.
7. *Idem, ibid.*, 1965, **68**, 1865.
8. K. L. Cheng, K. Ueno and T. Imamura, *CRC Handbook of Organic Analytical Reagents*. CRC Press, Florida, 1982.
9. R. W. Weeks, Jr. and B. J. Dean, *Am. Ind. Hyg. Assoc. J.*, 1978, **39**, 758.
10. V. A. Valsov, V. T. Solomatin, S. P. Gubin, A. P. Rysev and G. P. Tikhonov, *Izv. Akad. Nauk SSSR, Ser. Khim.*, 1965, No. 4, 921.
11. M. V. Marbinya and E. E. Kapantsyah, *Izv. Akad. Nauk Armyanskoi SSR*, 1965, **18**, 18.
12. A. Iguchi, *Bull. Chem. Soc. Japan*, 1958, **31**, 748.

DETERMINATION OF HYDROGEN PEROXIDE WITH *N,N*-DIETHYLANILINE AND 4-AMINOANTIPYRINE BY USE OF AN ANION-EXCHANGE RESIN MODIFIED WITH MANGANESE-TETRAKIS(SULPHOPHENYL)PORPHINE, AS A SUBSTITUTE FOR PEROXIDASE

YUTAKA SAITO*, MASAKI MIFUNE, SUZUYO NAKASHIMA, JUNICHI ODO and YOSHIMASA TANAKA
Faculty of Pharmaceutical Sciences, Okayama University, 1-1-1 Tushima-Naka, Okayama 700, Japan

MASAHIKO CHIKUMA

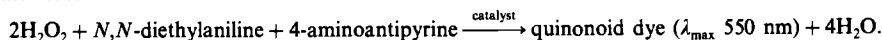
Osaka College of Pharmacy, 2-10-65 Kawai, Matsubara-City 580, Japan

HISASHI TANAKA

Faculty of Pharmaceutical Sciences, Kyoto University, Sakyo-Ku, Kyoto 660, Japan

(Received 3 October 1986. Revised 11 December 1986. Accepted 1 February 1987)

Summary—Amberlite IRA 900 anion-exchange resin modified with manganese-tetrakis(sulphophenyl)-porphine has been used as a catalyst instead of peroxidase for the determination of hydrogen peroxide by the reaction



The apparent molar absorptivity for hydrogen peroxide was $1.1 \times 10^4 \text{ l. mole}^{-1} \cdot \text{cm}^{-1}$, coefficient of variation 0.7%. This value is approximately 84% of that obtained by the use of peroxidase as catalyst. Similar conditions to those in the enzymatic reaction were suitable for use of the modified resin as catalyst, and the results show it to be a good substitute for peroxidase in this reaction system.

We have demonstrated¹ that an anion-exchange resin (Amberlite IRA 900) modified with manganese-tetrakis(sulphophenyl)porphine (I; Fig. 1) can act like peroxidase as a catalyst in the determination of hydrogen peroxide by formation of a dye from 4-aminoantipyrine (AAP) and phenol, as in reaction (1).² However, a large excess of phenol is required to obtain sensitivity comparable to that given by peroxidase, because a large amount of the phenol is adsorbed on the modified resin. However, if a cationic chromogen, *N,N*-diethylaniline (DEA), is used instead of peroxidase [reaction (2)] satisfactory sensitivity for the determination of hydrogen peroxide is obtained, since there is no adsorption of this chromogen on the resin.

EXPERIMENTAL

Materials

Tetrakis(sulphophenyl)porphine (Tokyo Kasei Co., Ltd.) was used without further purification, for preparation of the modified resin. Other reagents were of analytical or reagent grade. The chromogenic reagent solution was a 1:1:3 v/v mixture of AAP (1 mg/ml), DEA (1 mg/ml) and borate buffer (pH 7.0, 0.05M).

Preparation of the resin

An aqueous solution of I was prepared and used to modify the Amberlite IRA 900 resin as described pre-

viously.³ The absorption spectrum of the solution agreed with that reported by Harriman and Porter.⁴

Apparatus

The absorption spectra and the absorbances were measured on a Shimadzu UV-180 double-beam spectrophotometer with a 10-mm fused-silica cell.

Procedure

The chromogenic reagent solution (5.0 ml) and the modified resin (100 mg) were added to the sample solution (1.0 ml) containing 5–20 µg of hydrogen peroxide, and the mixture was incubated at 37° for 20 min. The absorbance of the supernatant solution was measured at 550 nm against the reagent blank. Measurements were also made on comparison solutions⁵ consisting of 5.0 ml of pH 7.0 phosphate buffer containing 2.5 units of peroxidase, 500 µg of AAP, 500 µg of DEA and appropriate amounts of hydrogen peroxide.

RESULTS AND DISCUSSION

Selection of optimal conditions

In optimization of the conditions, 1.0 ml of hydrogen peroxide solution (20 µg/ml) was used in all tests.

pH. The absorbance of the dye produced in reaction (2) reached a maximum at around pH 7 in borate, acetate and Tris buffers, as shown in Fig. 2. It is of interest that the absorbance of the dye formed at a given pH differed considerably from buffer to buffer. In phosphate buffer the absorbance was only 70% of that obtained in borate buffer. This indicates

*To whom correspondence should be addressed.

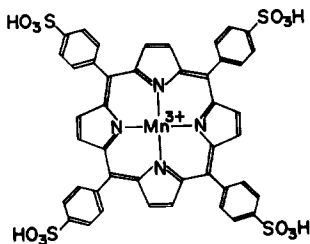
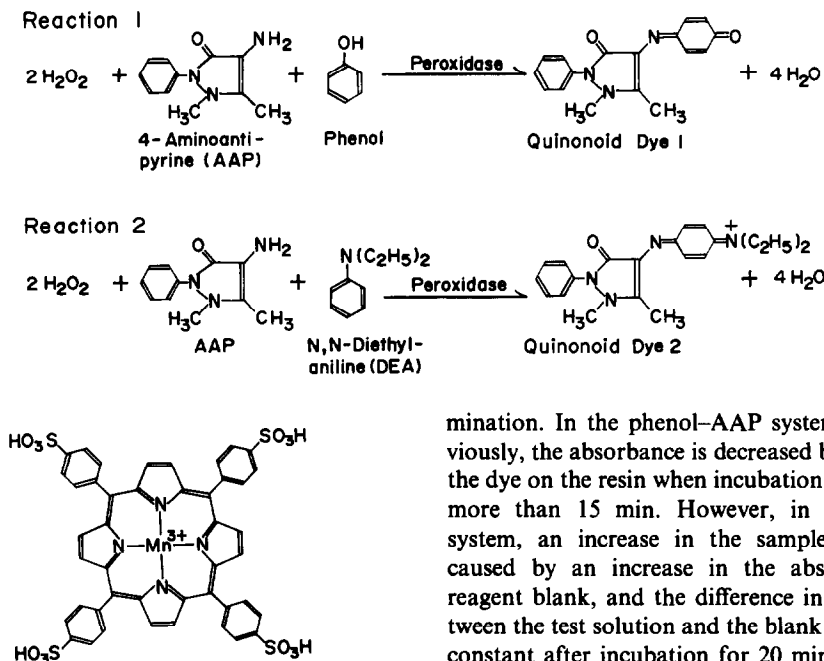


Fig. 1. Structure of manganese-tetrakis(sulphophenyl)-porphine complex.

that the presence of a large amount of phosphate inhibits the peroxidase-like activity of the modified resin, probably by co-ordination as an axial ligand to Mn^{3+} . In the present study, therefore, we chose 0.05M borate buffer of pH 7.0, which is also the optimal value for the use of peroxidase.

Incubation temperature and time. As shown in Fig. 3, the maximum absorbance of the dye was obtained when the incubation was done at 35–37°. We selected 37°, the optimal temperature for the reaction of peroxidase. Figure 4 shows that reaction (2) reached equilibrium after 20–30 min. Residual hydrogen peroxide in the reaction mixture was hardly detectable even after incubation for 10–15 min, indicating that hydrogen peroxide was consumed in formation of the quinonoid dye. We therefore judged incubation for 20 min to be enough for the deter-

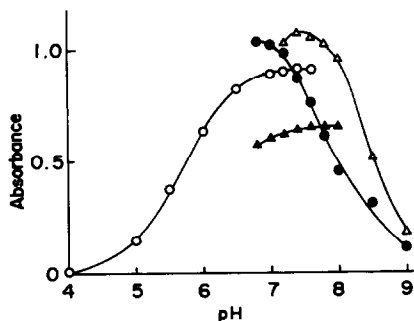


Fig. 2. Effects of pH and buffers. ● borate buffer; ○ acetate buffer; △ Tris buffer; ▲ phosphate buffer.

mination. In the phenol–AAP system reported previously, the absorbance is decreased by adsorption of the dye on the resin when incubation is continued for more than 15 min. However, in the DEA–AAP system, an increase in the sample absorbance is caused by an increase in the absorbance of the reagent blank, and the difference in absorbance between the test solution and the blank becomes almost constant after incubation for 20 min. This indicates that the quinonoid dye formed in the present system is not adsorbed on the modified resin.

Quantity of DEA. The effect of amount of DEA on the absorbance was examined in the presence of 1.0 mg of AAP, with the results shown in Fig. 5. In the previous work² a large excess of phenol (> 10 times the amount of AAP) was required because of its adsorption on the modified resin. However, in the present system, a weight of DEA equal to that of the AAP is sufficient.

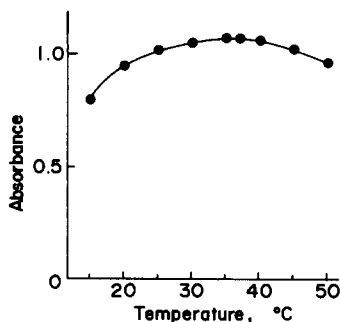


Fig. 3. Effect of incubation temperature.

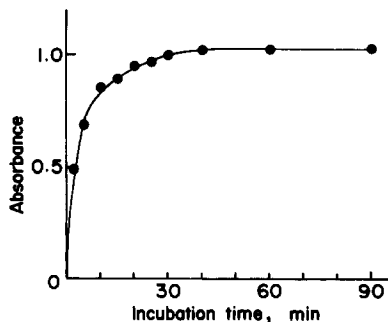


Fig. 4. Effect of incubation time.

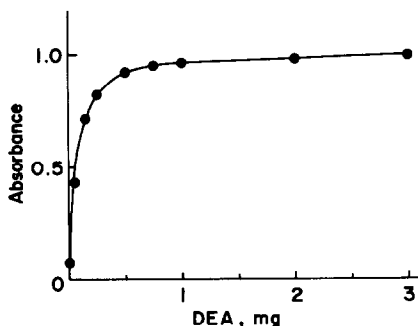


Fig. 5. Effect of quantity of DEA.

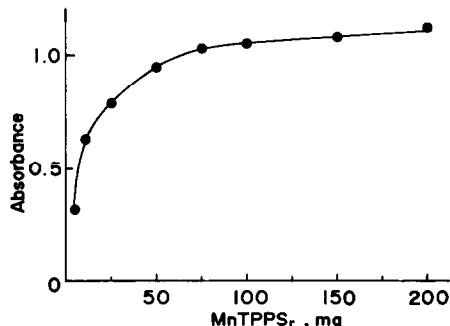


Fig. 6. Effect of quantity of resin.

Table 1. Effect of foreign substances*

Substance	Added, μg	Error,* %	Substance	Added, μg	Error,* %
Heparin	0.4	+1.1	Fe^{3+}	20	-3.9
NaF	400	+0.8	Br^-	1000	+7.4
EDTA	40	0.0		100	+0.5
Glycine	100	+2.2	CO_3^{2-}	1000	+29.3
Ascorbic acid	40	-0.5		100	+1.4
K^+	1000	+1.4	PO_4^{3-}	1000	-18.7
Ca^{2+}	1000	+1.7		100	-2.4

*In determination of 20 μg of hydrogen peroxide incubated for 20 min at 37°C in 0.05M borate buffer (pH 7.0).

Quantity of resin. The absorbance of the quinonoid dye reaches a maximum and constant value when more than 100 mg of modified resin is added to the DEA-AAP system, as shown in Fig. 6, whereas a large amount of the resin causes the absorbance of the phenol-AAP system² to decrease.

Repeated use of the resin

In an attempt to confirm that the resin accelerates reaction (2) catalytically, the effect of repeated use of the resin on the absorbance of the resulting dye was examined. Practically constant absorbance was obtained for the dye produced in ten consecutive cycles of use of the same portion of resin and no decrease in absorbance because of no adsorption of dye on the resin was observed. This result strongly suggests that the resin behaves as a catalyst which may be comparable to immobilized peroxidase.

Calibration graphs

Both the modified resin and the peroxidase method give linear response up to 20 μg of hydrogen peroxide. The relative standard deviation found was 0.7% for 20 μg of hydrogen peroxide ($n = 10$). The apparent molar absorptivity obtained with the resin system was $1.1 \times 10^4 \text{ l. mole}^{-1} \cdot \text{cm}^{-1}$, in contrast to $1.3 \times 10^{-4} \text{ l. mole}^{-1} \cdot \text{cm}^{-1}$ for the peroxidase method.

Interferences

The results of the interference tests are summarized in Table 1. Of the inorganic ions tested, only iron(III) interfered seriously, but the interference was tolerable with less than 20 μg . Up to 100 μg of carbonate,

phosphate or bromide can be tolerated. Usual doses of anticoagulants, 0.02 ml of serum and 1.5 mg of albumin did not interfere seriously, indicating that the present method could be applicable for the determination of hydrogen peroxide liberated in serum. Ascorbic acid, which causes serious interference in the determination of hydrogen peroxide with peroxidase,⁶ did not interfere in amounts up to 40 μg .

CONCLUSION

The results obtained indicate that the DEA-AAP system is better than the phenol-AAP system for the determination of hydrogen peroxide with the modified resin as catalyst. The resin is very stable and a good substitute for peroxidase.

Acknowledgement—This work was supported in part by a Grant-in-Aid for Scientific Research from the Ministry of Education, Science and Culture, Japan.

REFERENCES

1. Y. Saito, M. Mifune, J. Odo, Y. Tanaka, M. Chikuma and H. Tanaka, *Reactive Polym.*, 1986, 4, 243.
2. Y. Saito, S. Nakashima, M. Mifune, J. Odo, Y. Tanaka, M. Chikuma and H. Tanaka, *Anal. Chim. Acta*, 1985, 172, 285.
3. Y. Saito, M. Mifune, S. Nakashima, Y. Tanaka, M. Chikuma and H. Tanaka, *Chem. Pharm. Bull.*, 1986, 34, 5016.
4. A. Harriman and G. Porter, *J. Chem. Soc. Faraday Trans. II*, 1979, 75, 1532.
5. P. Kabasakalian, *Clin. Chem.*, 1974, 20, 606.
6. P. Sharp, *Clin. Chim. Acta*, 1972, 40, 115.

THE USE OF 2,3-DICHLORO-5,6-DICYANO-*p*-BENZOQUINONE FOR THE SPECTROPHOTOMETRIC DETERMINATION OF SOME CARDIOVASCULAR DRUGS

A. S. ISSA, M. S. MAHROUS, M. ABDEL SALAM and N. SOLIMAN
Pharmaceutical Chemistry Department, Faculty of Pharmacy, University of Alexandria,
Alexandria, Egypt

(Received 9 October 1986. Revised 4 December 1986. Accepted 14 January 1987)

Summary—Some basic cardiovascular drugs containing secondary or tertiary amino groups are determined spectrophotometrically. The method is simple and sensitive; it is based on the interaction of the drugs, as *n*-electron donors, with 2,3-dichloro-5,6-dicyano-*p*-benzoquinone (DDQ) as a π -acceptor. The highly coloured radical anion exhibits maximum absorption at 460 nm. The drugs determined are pindolol, dipyridamole, hydralazine hydrochloride, quinidine sulphate, prenylamine lactate and tolazoline hydrochloride. Beer's law is obeyed for these drugs. The procedure is sensitive enough to permit unit dose assay of the individual drugs in their pharmaceutical formulations. The assay results are in accord with the pharmacopoeial assay results.

The cardiovascular drugs investigated are of diverse chemical types, and many chemical methods have been reported for their evaluation.

Pindolol, which is a β -adrenergic blocking drug, is determined in its pure form or in pharmaceutical preparations spectrophotometrically in 0.1M hydrochloric acid medium at 264 nm.¹ It may also be determined spectrofluorometrically in ethanol medium by its excitation at 263 nm and emission at 305 nm.²

Tolazoline, which is a peripheral vasodilator drug, is determined spectrophotometrically in alcohol at 257 nm,³ or at 250 nm after its alkaline hydrolysis to phenylacetic acid.⁴ It can also be determined colorimetrically by formation of an ion-pair complex with Methyl Orange.⁵

The antihypertensive drug hydralazine has been determined by direct spectrophotometric measurement at 239, 260, 302 and 315 nm,^{6,7} and also by reaction with *p*-dimethylaminobenzaldehyde.⁸ Hydralazine has been determined fluorometrically in sulphuric acid medium.⁹

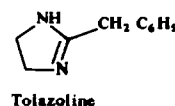
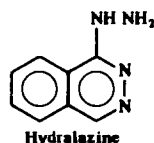
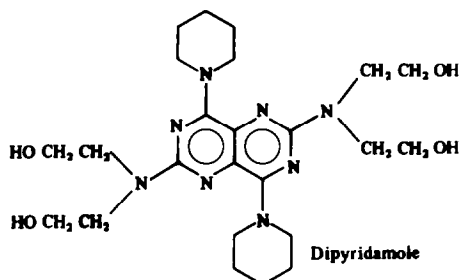
Dipyridamole, which is a coronary vasodilator drug, has been determined simultaneously with oxazepam by application of the orthogonal function method to absorbance measurement at two pH values.¹⁰ The drug has also been determined fluorometrically in methyl alcohol¹¹ or in hexane-isoamyl alcohol mixture.¹²

Another coronary vasodilator, prenylamine, has been colorimetrically determined with α,α -diphenyl- β -picrylhydrazyl (absorbance measurement at 520 nm).¹³ It has also been determined fluorometrically after reaction with sodium anthracene-2-sulphonate.¹⁴

Many spectrophotometric¹⁵⁻¹⁷ and fluorometric¹⁸⁻²⁰ methods have been reported for the determination of the antiarrhythmic drug quinidine.

2,3-Dichloro-5,6-dicyano-*p*-benzoquinone (DDQ) has been used for the detection of some drugs having an imidazoline ring in their molecules,²¹ and for the spectrophotometric determination of some alkaloids,²² some antimalarials²³ and some tranquillizers and antidepressants.²⁴ Formation of the radical anion in the reactions has been established by electron-spin resonance measurements, for the alkaloids, tranquillizers and antidepressants.^{22,24}

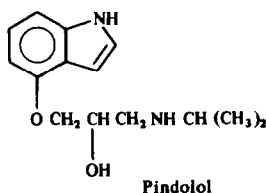
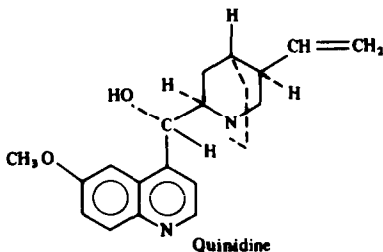
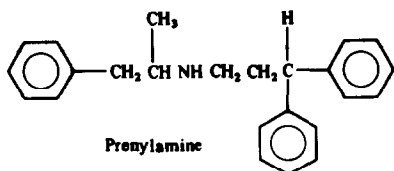
In the research described here, the reagent was utilized to develop a simple, sensitive and accurate method for the spectrophotometric determination of some cardiovascular drugs, namely pindolol, dipyridamole, quinidine sulphate, hydralazine hydrochloride, prenylamine lactate and tolazoline hydrochloride, either in their pure form or in their tablet preparations.



EXPERIMENTAL

Materials and reagents

Pharmaceutical grade pindolol (Sandoz), dipyridamole (Boehringer), quinidine sulphate (Misr), hydralazine hydro-



chloride (CIBA), prenylamine lactate (Hoechst) and tolazoline hydrochloride (CID).

DDQ reagent; a freshly prepared 0.2% solution of 2,3-dichloro-5,6-dicyano-*p*-benzoquinone (EGA Chemie, West Germany) in acetonitrile.

Preparation of standard solutions

For drug salts. An accurately weighed amount of the drug salt [hydralazine hydrochloride (183.2 mg \equiv 150.0 mg of base), quinidine sulphate (120.6 mg \equiv 50.0 mg of base), tolazoline hydrochloride (61.4 mg \equiv 50.0 mg of base) or prenylamine lactate (127.8 mg \equiv 100.0 mg of base)] was dissolved in about 40 ml of water. The solution was made alkaline with ammonia solution and extracted by shaking with four successive 20-ml portions of chloroform. The extracts were pooled by filtration through a filter paper containing anhydrous sodium sulphate into a 100-ml standard flask and made up to volume with chloroform.

For drug bases. A 0.5 mg/ml chloroform solution of pindolol or dipyridamole was prepared.

Calibration graphs

A 20 ml-portion of standard solution was diluted to 100 ml with chloroform. Serial volumes of this solution in the range 0.4–3 ml were transferred to 5-ml standard flasks, and the solvent was evaporated by heating in a water-bath at 70°. Each residue was dissolved in 2 ml of acetonitrile, then 2 ml of DDQ reagent were added. The volume was brought to 5 ml with acetonitrile and the absorbance was measured, after 15 min, at 460 nm (430 nm for dipyridamole) against a reagent blank prepared simultaneously.

Analysis of tablets

For drug salts. Ten tablets were finely powdered and mixed. An accurately weighed quantity equivalent to the drug base concentration mentioned in preparation of standard solutions was transferred to a 100-ml standard flask and extracted with 80 ml of water by vigorous shaking for 15 min. The solution was then made up to volume with water, mixed and filtered. In a separatory funnel, a 50-ml portion of the filtrate was made alkaline to litmus paper with ammonia solution and extracted with four successive 10-ml portions of chloroform, which were pooled, dried and diluted accurately to 50 ml with chloroform as for the

standard solution. The procedure was then completed as for the calibration graph.

For drug bases. An accurately weighed quantity of powdered tablets equivalent to 50 mg of pindolol or dipyridamole was transferred to a 100-ml standard flask and shaken for 15 min with 50 ml of chloroform. The solution was then made up to volume with chloroform, mixed and filtered. The procedure was completed as for the calibration graphs.

RESULTS AND DISCUSSION

Each of the drugs tested reacts with DDQ in acetonitrile to give an intensely orange-red product, exhibiting an absorption maxima at 460 nm, except for dipyridamole, for which the maximum at 430 nm is used (Fig. 1).

The electron-spin resonance investigations^{22,24} have proved that a charge-transfer complex is formed by the interaction of the drug base as an *n*-donor and DDQ as a π -acceptor. This reaction is enhanced by polar solvents such as methanol or acetonitrile, which promote complete electron transfer from the donor to the acceptor, resulting in formation of the DDQ radical anion as the major chromophore.

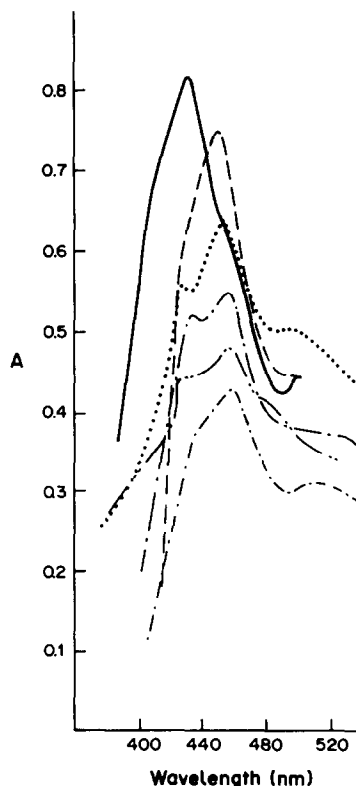


Fig. 1. Absorption curves for DDQ colour reaction. — Pindolol (22 μ g/ml); - - - dipyridamole (37 μ g/ml); tolazoline (48 μ g/ml); — prenylamine (88 μ g/ml); - - - quinidine (31 μ g/ml); hydralazine (70 μ g/ml).

Table 1. Assay results for some cardiovascular drugs by use of DDQ reagent

Drug name	DDQ method	Official method	t †	F §
	Mean recovery,* %	Mean recovery,* %		
Prenylamine lactate BP 1980	99.6 ± 0.8	99.7 ± 1.0	0.24	1.48
Segontine (Hoechst) 60 mg/tab.	98.7 ± 0.9	99.3 ± 0.6	1.67	1.81
Quinidine sulphate BP 1980	100.3 ± 0.5	100.0 ± 0.7	1.04	2.41
Lab. prep. tab.* 200 mg/tab.	99.3 ± 0.7	99.7 ± 1.1	0.81	2.56
Tolazoline hydrochloride BP 1980	100.2 ± 1.0	100.3 ± 0.6	0.16	3.30
Lab. prep. tab.* 50 mg/tab.	99.9 ± 0.7	100.5 ± 0.9	1.58	1.93
Hydralazine hydrochloride USP XX	99.9 ± 0.6	100.1 ± 0.4	0.82	2.91
Lab. prep. tab.* 25 mg/tab.	101.4 ± 0.8	101.2 ± 0.4	0.38	3.43
Pindolol‡	100.4 ± 0.5	100.1 ± 0.6	0.80	1.47
Visken (Sandoz) 5 mg/tab.	101.4 ± 0.8	101.0 ± 1.2	0.86	2.16
Dipyridamole‡	99.0 ± 0.4	99.9 ± 0.6	1.25	1.66
Persantin (Boehringer) 75 mg/tab.	100.9 ± 1.1	100.8 ± 0.8	0.26	1.81

*Mean and standard deviation (9 results) calculated with respect to nominal content in sample.

†Theoretical $t = 1.75$.

§Theoretical $F = 3.44$.

*Laboratory prepared tablets; the tablet filler is composed of lactose 90, starch 7, talc 2.7 and magnesium stearate 0.3 parts.

‡Assayed by the BP 1980 non-aqueous titration method with Crystal Violet as indicator, for comparison.

The influence of various factors on the colour development was studied to determine the optimal conditions, *viz.* reagent concentration and choice of solvent. Maximum absorption was obtained when 2 ml of 0.2% DDQ solution were used in a total volume of 5 ml. Non-polar solvents (benzene, carbon tetrachloride or chloroform) were found to be unsuitable, but polar solvents such as methanol or acetonitrile were found ideal, as they provide a high yield of DDQ radical. In these solvents the colour attains maximum intensity in about 15 min and remains stable for a further 30 min.

The calibration graphs are linear over the concentration ranges 8–40 $\mu\text{g/ml}$ for pindolol and quinidine, 10–50 $\mu\text{g/ml}$ for dipyridamole, 12–60 $\mu\text{g/ml}$ for tolazoline, 20–100 $\mu\text{g/ml}$ for prenylamine and 32–160 $\mu\text{g/ml}$ for hydralazine, in the final solution measured.

The molar absorptivities were 4.8×10^3 l.mole⁻¹.cm⁻¹ for pindolol, 1.07×10^3 for hydralazine, 5.73×10^3 for quinidine, 2.33×10^3 for tolazoline, 1.03×10^4 for dipyridamole and 3.13×10^3 for prenylamine.

Results obtained for determination of the chosen drugs in their tablet formulations were compared with results obtained by the official BP 1980 methods²⁵ for prenylamine lactate, quinidine sulphate and tolazoline hydrochloride and the USP method²⁶ for hydralazine hydrochloride. For pindolol and dipyridamole, for which there are no official methods, the BP 1980 non-aqueous titration method with Crystal Violet as indicator was used (Table 1). The calculated t and F values indicate that the proposed and the official methods are equally accurate.

Compared with the official methods the DDQ method is simple, fast and more sensitive, and seems useful for the analysis and quality control of these cardiovascular drugs in tablet preparations.

REFERENCES

1. M. E. Mohamed, M. S. Tawakkol and H. Y. Aboul-Enin, *Spectrosc. Lett.*, 1982, **15**, 609.
2. *Idem*, *J. Assoc. Off. Anal. Chem.*, 1983, **66**, 273.
3. V. Georgescu, *Farmacia (Bucharest)*, 1968, **16**, 371.
4. E. Farkas, *Pharmazie*, 1966, **21**, 600.
5. J. Vachek and E. Svátek, *Cesk. Farm.*, 1964, **13**, 463.
6. S. G. Solomonova, N. M. Turkevich and N. V. Kurinnaya, *Farm. Zh. (Kiev)*, 1973, **28**, 42.
7. *The National Formulary*, 13th Ed., p. 349. Mack, Easton, Pa., 1970.
8. B. Wesley-Hadžiya and F. Abffy, *Croat. Chem. Acta*, 1958, **30**, 15.
9. D. V. Naik, B. R. Davis, K. M. Minnet and S. G. Schulman, *J. Pharm. Sci.*, 1976, **65**, 274.
10. M. A. Korany and R. Haller, *J. Assoc. Off. Anal. Chem.*, 1982, **65**, 144.
11. H. Wullen, E. Stainier and M. Luyckx, *J. Pharm. Belg.*, 1966, **21**, 409.
12. J. M. Steyn, *J. Chromatog.*, 1979, **164**, 487.
13. S. Salman and N. Bayrakdar, *Eczacılık Bull. (Turkey)*, 1983, **25**, 30.
14. D. Westerlund, K. O. Borg and P. O. Lagers, *Acta Pharm. Suecica*, 1972, **9**, 47.
15. J. D. Endiz, *J. Assoc. Off. Anal. Chem.*, 1963, **46**, 637.
16. R. N. Bhattacharya and G. K. Ganguly, *J. Pharm. Pharmacol.*, 1954, **6**, 191.
17. S. Bruno, *Farmaco Ed. Sci.*, 1955, **10**, 922.
18. P. Brockman, V. R. Severin and L. Moeseke, *Pharm. Tijdschr. Belg.*, 1963, **40**, 113.
19. J. Eisenbrand, *Z. Anal. Chem.*, 1961, **179**, 170.
20. B. B. Brodie and S. Udenfriend, *J. Pharmacol. Exp. Ther.*, 1943, **78**, 154.
21. K. A. Kovar and M. Abdel-Hamid, *Arch. Pharm.*, 1984, **317**, 246.
22. M. E. Abdel-Hamid, M. Abdel-Salam, M. S. Mahrous and M. M. Abdel-Khalek, *Talanta*, 1985, **32**, 1002.
23. A. S. Issa, M. S. Mahrous, M. Abdel-Salam and M. Abdel-Hamid, *J. Pharm. Belg.*, 1985, **40**, 5, 339.
24. M. Abdel-Salam, A. S. Issa, M. Mahrous and M. E. Abdel-Hamid, *Anal. Lett.*, 1985, **18**, 1391.
25. *British Pharmacopoeia*, Her Majesty's Stationary Office, London, 1980.
26. *The United States Pharmacopoeia XX*, Mack, Easton, Pa., 1980.

ANALYTICAL DATA

COLOUR SPECIFICATION OF PYRIDINE-2-ALDEHYDE AND 6-METHYLPYRIDINE-2-ALDEHYDE *p*-NITROPHENYLHYDRAZONES AS INDICATORS FOR pH DETERMINATION

A. M. CAMEAN FERNANDEZ and M. GUZMAN CHOZAS*

Department of Bromatology, Toxicology and Applied Chemical Analysis, Faculty of Pharmacy,
University of Seville, 41012 Seville, Spain

(Received 20 October 1985. Revised 20 March 1986. Accepted 27 January 1987)

Summary—The physicochemical properties, chromaticity co-ordinates and chromatic parameters for pyridine-2-aldehyde *p*-nitrophenylhydrazone and 6-methylpyridine-2-aldehyde *p*-nitrophenylhydrazone (proposed as new indicators for colorimetric pH measurements) are reported. The sensitivity and rapidity of colour change have been evaluated in terms of specific colour discrimination (SCD), pH of maximum colour change and half band-width of change of SCD (in terms of pH). The chromatic separations calculated from the co-ordinates obtained by the CIE 1976 recommendations (CIELUV or CIELAB) and the LABHNU 1977 colour space are compared and correlated with the standard deviation of colour matching.

In spite of the number of acid-base indicators that have been proposed, full reports on their properties are scanty, especially for indicators covering the high pH range (10–14). The most suitable approach to spectrophotometric evaluation of colour changes in the transition range is through the CIE chromaticity systems.

Konopik and Leberl^{1,2} reported that some azo and hydroxyazo dyes are suitable for colorimetric determination of high pH values. Chugreeva³ proposed phenylhydrazones as indicators for alkaline medium, and the *p*-nitrophenylhydrazones have been reported to be the best compounds for this purpose.^{4,5} Pyridine-2-aldehyde *p*-nitrophenylhydrazone (2-PANPH) and 6-methylpyridine-2-aldehyde *p*-nitrophenylhydrazone (6-Me-2-PANPH) have been proposed as colorimetric pH indicators.^{6,7} The present paper reports their physicochemical properties and colour change characteristics.

EXPERIMENTAL

Apparatus

All pH measurements were made with a Phillips PW 9408 digital pH-meter and a Beckman PHI-70 pH-meter with a glass-Ag/AgCl combined electrode and Enduraglass electrodes. The pH-meters were calibrated with standard buffers and calcium hydroxide solution. All absorption spectra were recorded on Pye-Unicam SP 800 and Perkin-Elmer Coleman 55 spectrophotometers equipped with 1.0-cm glass cells.

Reagents

Reagent-grade chemicals and doubly-distilled water were used throughout. 2-PANPH and 6-Me-2-PANPH were prepared as reported earlier.^{6,7} The products were recrystallized from ethanol and tested for purity by TLC.⁸ Their analytical characteristics agreed with those reported earlier.^{6,7} The chemical shifts of the n.m.r. spectra agreed well with the literature data.^{9,10}

The indicator solutions ($4.0 \times 10^{-5} M$) were prepared in 2:3 v/v ethanol-water mixture, adjusted to an ionic strength of 0.1 with potassium chloride.

Buffer solutions of Na₂B₄O₇-NaOH (pH 9.20–10.80), Na₂HPO₄-NaOH (pH 10.90–12.00), NaOH-KCl (pH 12.00–13.00), as recommended by Bates and Bower,¹¹ were used.

Procedure

The ionization constants were determined spectrophotometrically by the methods of parallel straight lines,¹² concurrent straight lines¹³ and the Ågren-Sommer method¹⁴ and recalculated from the complementary chromaticity parameters.^{15,16}

The stability of the indicator solutions was determined by periodical spectrophotometric measurements at the absorption maxima.

The pH of the indicator solutions was measured and the absorbances or transmittances were recorded over the range 380–770 nm, at pH-intervals of 0.2 in the transition range. The weighted ordinate method¹⁷ was applied for estimation of the trichromatic stimuli *X*, *Y* and *Z* by use of the CIE distribution functions¹⁸ of standard illuminant C. The proportional *x*, *y* chromatic co-ordinates were calculated from the trichromatic stimuli.

RESULTS AND DISCUSSION

The absorption spectra of the indicator solutions at different pH values clearly demonstrate the sharpness

*Author for correspondence.

Table 1. Spectral characteristics

Indicator	Medium	λ_{\max} , nm	Log ϵ *	λ_{isos} , nm
2-PANPH	pH 10.2	405	4.553	450
	pH 14.0	545	4.602	
6-Me-2-PANPH	pH 10.2	420	4.278	450
	pH 13.0	550	4.307	

* ϵ units were $\text{l. mole}^{-1} \cdot \text{cm}^{-1}$.

of absorbance change with increase in pH. The spectral characteristics are given in Table 1.

The indicator solutions were stable for about a month. In acid medium the absorbance decreased by 3% in 24 hr for 2-PANPH and by 5% in 30 hr for 6-Me-2-PANPH. At pH 13, 2-PANPH was stable for only 1 hr and 6-Me-2-PANPH for 4 hr.

Table 2 lists the visual transition characteristics of both indicators. The $\text{pH}_{1/2}^*$ values were found from absorbance *vs.* pH graphs for measurements at 545 nm for 2-PANPH and 550 nm for 6-Me-2-PANPH. The transition intervals of $1.0 \times 10^{-4} M$ 6-Me-2-PANPH solutions in various solvents were determined; *N,N*-dimethylformamide narrows the transition interval and shifts it towards lower pH values. In acetone-water (2:3 v/v) medium the transition interval is widened. The *pK* values were determined at $20 \pm 1^\circ$, in ethanol-water (2:3) at ionic strength 0.1.

Colour change evaluation

The colour transition for both indicators was evaluated through the *x-y* CIE 1931 chromaticity co-ordinates¹⁷ at pH-intervals of 0.2 (Table 3). These co-ordinates were converted by simplified transformations in the "perceptually more uniform chromatic spacing" (P.M.U.C.S.) co-ordinates which give rise to the CIE-1960 UCS diagram (Fig. 1); the colour change goes from the yellow to the reddish-purple zones.

The sensitivity and rapidity of the colour changes were evaluated in terms of the SCD (specific colour discrimination) values,¹⁹ which were easily obtained from the P.M.U.C.S. co-ordinates.²⁰ The SCD values, together with the pH of maximum colour change

Table 3. Chromaticity co-ordinates for the colour-change of the indicators*

pH	2-PANPH			6-Me-2-PANPH		
	<i>x</i>	<i>y</i>	<i>Y</i>	<i>x</i>	<i>y</i>	<i>Y</i>
10.2	0.357	0.400	96.2	0.342	0.375	96.9
10.4	0.357	0.399	95.7	0.343	0.373	96.0
10.6	0.358	0.398	94.7	0.343	0.372	94.7
10.8	0.358	0.396	93.2	0.343	0.369	92.5
11.0	0.359	0.394	91.3	0.344	0.365	89.4
11.2	0.361	0.389	88.0	0.345	0.358	85.1
11.4	0.363	0.383	83.5	0.347	0.349	79.1
11.6	0.366	0.373	77.0	0.348	0.336	71.6
11.8	0.370	0.360	69.0	0.350	0.319	62.9
12.0	0.376	0.341	59.2	0.352	0.299	54.0
12.2	0.382	0.317	49.0	0.353	0.278	45.9
12.4	0.388	0.290	39.7	0.354	0.257	39.3
12.6	0.391	0.262	32.1	0.353	0.239	34.3
12.8	0.392	0.237	26.5	0.352	0.225	30.9
13.0	0.389	0.216	22.7	0.351	0.214	28.6
13.2	0.385	0.200	20.2			
13.4	0.381	0.189	18.7			
13.6	0.377	0.181	17.7			
13.8	0.375	0.175	17.1			
14.0	0.373	0.172	16.7			

* $c_{\text{HI}} = 4.0 \times 10^{-5} M$; EtOH-H₂O (2:3); $\mu = 0.1$.

(pH_{mcc}) and the half band-width of change of SCD, in pH units ($\Delta\text{pH}_{1/2\text{SCD}}$) are listed in Table 4, along with those for other indicators reported in the literature.^{20,21} The SCD/pH plot shows a single peak (at pH 12.4–12.6), and the absence of humps proved that no significant impurities were present. The SCD values of 6-Me-2-PANPH are of the same order as those of phenolsulphamphthalein (at pH 7.0–8.0), Cresol Red and Thymol Blue. The sensitivity of 2-PANPH, as demonstrated by its SCD values, is at least as good as that of the sulphamphthalein indicators. The rate of colour change, as shown by the half band-width of colour change, was lower by a factor of 2–3 than that of some indicators of the family of phthaleins, sulphonphthaleins and sulphamphthaleins.^{20,21} The pH_{mcc} values fall very close to the corresponding *pK*₁ values, and 2-PANPH may be regarded as a "reference indicator".

In accordance with Stiles's proposals,²² colour-difference formulae (ΔE) are applied, following the

Table 2. Estimated pH intervals of colour change

Indicator and medium	pH interval of colour change†	$\text{pH}_{1/2}^*$	<i>pK</i> ₁ (<i>n</i>)‡	<i>pK</i> ₁ (<i>n</i>)§
2-PANPH				
EtOH-H ₂ O (2:3)	10.2–13.5	12.50	12.59 ± 0.01 (4)	12.51 ± 0.02 (6)
6-Me-2-PANPH				
EtOH-H ₂ O (2:3)	10.8–13.2	12.10	12.22 ± 0.02 (7)	12.18 ± 0.06 (5)
Acetone-H ₂ O (2:3)	10.4–13.5			
DMF-H ₂ O (2:3)	10.6–12.7			

†From visual observations ($c_{\text{HI}} = 1.0 \times 10^{-4} M$).

‡Mean \pm SD resulting from the application of the several spectrophotometric methods to *n* replicates.

§Mean \pm SD calculated from the complementary chromaticity parameters (*n* replicates).

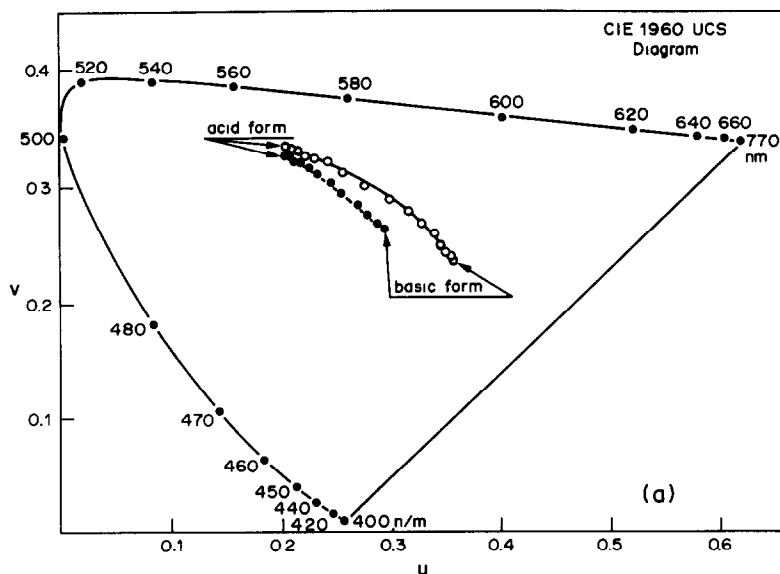


Fig. 1. Chromatic co-ordinates (u, v) on the CIE 1960 UCS diagram¹⁸ of ethanol-water (2:3) solutions of 2-PANPH (○) and 6-Me-2-PANPH (●) at different pH values ($c_{HI} 4.0 \times 10^{-5} M$; $\mu = 0.1$). For the transition intervals, $pH_1 = 10.2$ for both indicators; $pH_{final} = 14.0$ for 2-PANPH and 13.0 for 6-Me-2-PANPH.

CIE recommendations, owing to their significance in practice. Bhuchar *et al.*²¹ earlier compared the $\Delta E_{ab}^*/\Delta pH$ values with the $1000\Delta\sigma/\Delta pH$ values, calculated according to PMUCS recommendations, for sequential pH values of indicator solutions. They concluded that ΔE^* has the same significance for the colour change as the standard deviation $\Delta\sigma$ does for colour matching.

Recently, Richter²³ has defined a new uniform colour space called LABHNU 1977, with the object of attaining uniformity for the CIELUV and CIELAB 1976 systems. Co-ordinates were obtained

from the expressions

$$L^* = 116(Y/Y_n)^{1/3} - 16$$

$$A^* = 500(A' - A'_n) Y^{1/3}$$

$$B^* = 500(B' - B'_n) Y^{1/3}$$

where $X_n = 98$, $Y_n = 100$ and $Z_n = 118$ are the colour stimuli for standard illuminant C (CIE 1931 recommendations), and X , Y and Z are the tristimuli as obtained for an indicator solution at a particular pH. The A' and B' co-ordinates may be obtained from

Table 4. Colour changes of various indicators

Indicator	pH_{mcc}	pK_1	SCD at maximum colour change	Half band-width of change of SCD in pH units	$pH_{mcc} - pK_1$
Phenolphthalein	10.26		45.0	0.40	
<i>o</i> -Cresolphthalein	9.00		71.0	0.40	
Thymolphthalein	10.50		35.0	0.50	
	10.90		30.0	0.40	
Phenol Red	7.68		35.0	0.85	
	8.32	8.05	16.0	0.85	+0.27
Cresol Red	7.90		23.0	0.90	
	8.70	8.46	19.0	0.80	+0.24
Thymol Blue	8.90		27.0	0.90	
Congo Red	5.05		17.0	0.72	
Phenolsulphamphthalein	7.65	7.96	25.4	1.10	-0.31
	8.15	7.82	32.6	0.55	+0.33
<i>o</i> -Cresolsulphamphthalein	8.05	8.32	36.0	1.57	-0.27
	8.20	8.22	39.0	0.70	-0.02
2-PANPH	12.60	12.59	38.1	1.40	+0.01
6-Me-2-PANPH	12.40	12.22	25.3	1.50	+0.18

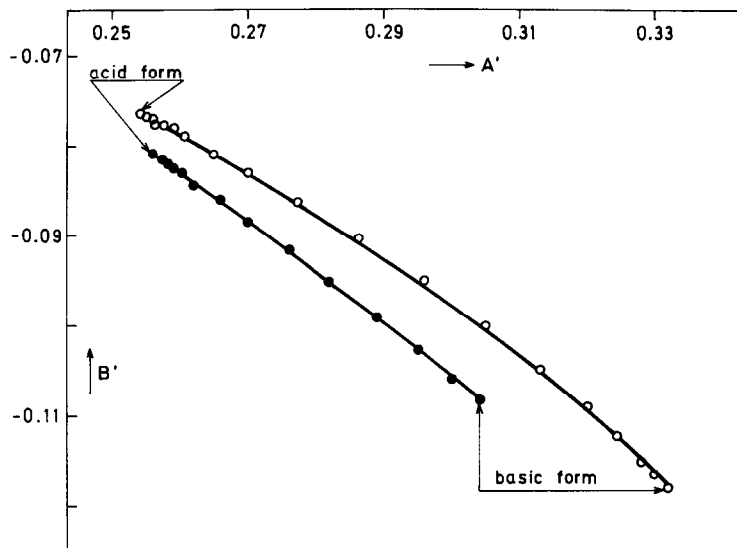


Fig. 2. Change of colour co-ordinates $A'B'$ (LABHNU²³ mode) of the $4.0 \times 10^{-5}M$ ethanol-water (2:3) solutions of 2-PANPH (○) and 6-Me-2-PANPH (●) at different pH values ($\mu = 0.1$). For transition intervals see caption to Fig. 1.

the CIE-xy 1931 co-ordinates:

$$A' = 1/4(x/y + 1/6)^{1/3}$$

$$B' = -1/12(z/y + 1/6)^{1/3}$$

In Fig. 2 the colour co-ordinates A' and B' [$c_{HI} = 4.0 \times 10^{-5}M$; 35% w/w ethanol in water; $I = 0.1$] of the indicators proposed are plotted for the first time in LABHNU space. The $\Delta E_{AB}^*/\Delta pH$ values calculated according to the LABHNU system gave linear correlation with those calculated according to the CIELAB system, with slopes of 1.020 and 0.997 for 2-PANPH and 6-Me-2-PANPH, respectively. Thus the diverse colour-difference formulae are shown to be fully equivalent to the unit standard deviation method for colour matching. The values of pH_{mcc} and $\Delta pH_{1/2SCD}$ (or $\Delta pH_{1/2\Delta E^*/\Delta pH}$) would not change considerably if compared with those obtained in accordance with PMUCS calculations (Table 4) and CIELAB recommendations, mainly with the latter. The pH_{mcc} values for both systems were 12.4 (2-PANPH) and 12.2 (6-Me-2-PANPH) and $\Delta pH_{1/2\Delta E^*/\Delta pH}$ values of 1.50 units were obtained for both indicators.

REFERENCES

1. N. Konopik and O. Leberl, *Monatsh. Chem.*, 1948, **79**, 586.
2. *Idem, ibid.*, 1949, **80**, 420.
3. N. V. Chugreeva, *Zh. Analit. Khim.*, 1960, **15**, 391.
4. M. Kambe, Y. Hasegawa and E. Shindo, *Bunseki Kagaku*, 1964, **13**, 1218.
5. M. Kambe, E. Shindo and M. Morito, *ibid.*, 1967, **16**, 1015.
6. J. Carrillo and M. Guzmán, *Microchem. J.*, 1979, **24**, 234.
7. M. Guzmán, A. M. Cameán and J. Bautista, *ibid.*, 1982, **27**, 1.
8. E. Denti and M. Luboz, *J. Chromatog.*, 1965, **18**, 325.
9. F. Venien and M. Lefevre, *Org. Magn. Reson.*, 1973, **5**, 113.
10. G. S. Karabatsos, F. M. Vane, R. A. Taller and N. Hsi, *J. Am. Chem. Soc.*, 1964, **86**, 3351.
11. R. G. Bates and V. E. Bower, *Anal. Chem.*, 1956, **28**, 1322.
12. P. Maroni and J. P. Calmon, *Bull. Soc. Chim. France*, 1964, 519.
13. R. S. Stearns and G. W. Wheland, *J. Am. Chem. Soc.*, 1947, **69**, 2025.
14. L. Sommer, *Folia Fac. Sci. Natn. Univ. Purkynianae (Brno)*, 1964, **5**, 1.
15. C. N. Reilley and E. M. Smith, *Anal. Chem.*, 1960, **32**, 1233.
16. K. Vytrás, *Chem. Zvesti*, 1974, **28**, 252.
17. Report of the Committee on Colorimetry, *J. Opt. Soc. Am.*, 1944, **34**, 633.
18. G. Wyszecki and W. S. Stiles, *Color Science*, 2nd Edn, Wiley, New York, 1982.
19. V. M. Buchar and S. R. Das, *J. Opt. Soc. Am.*, 1964, **54**, 817.
20. M. Buchar and A. K. Agrawal, *Analyst*, 1982, **107**, 1439.
21. V. M. Buchar, V. P. Kukreja and S. R. Das, *Anal. Chem.*, 1971, **43**, 1847.
22. W. S. Stiles, *Rev. d'Optique*, 1949, **28**, 215.
23. K. Richter, *Color Res. Appl.*, 1980, **5**, 25.

A SURVEY OF THE DETERMINATION OF THE PLATINUM GROUP ELEMENTS

SILVE KALLMANN

Ledoux & Company, 359 Alfred Avenue, Teaneck, NJ 07666, U.S.A.

(Received 6 August 1986. Revised 19 March 1987. Accepted 4 April 1987)

Summary—The platinum-group metals (PGMs), Ru, Rh, Pd, Os, Ir and Pt, are widely used as catalysts in petroleum and chemical processes. They find wide applications in automotive exhaust-gas control converters and are of immense importance to the electronics industry. They are found in many items of jewellery and serve to an increasing extent as a form of investment. The PGMs are extracted in minute quantities from a limited number of ores, found mainly in S. Africa and the USSR. They are concentrated and separated from each other by elaborate chemical processes. Because of their great intrinsic value (Pt \$650 per oz; Rh \$1400 per oz), the recycling of the PGMs from literally hundreds of different forms of scrap is an essential factor in the overall management of the PGM economy. In this survey emphasis is placed on the need to tailor the analytical method according to (a) the environment in which the PGMs occur, (b) the individual PGM concentrations, and (c) the desired sensitivity and precision. The factors which determine the choice of chemical, physicochemical and/or instrumental approaches are discussed. They are further commented on in extensive presentations of dissolution and separation techniques and methods for the final measurement of individual PGMs. Appendices are provided which present the compositions and sources of the products most frequently encountered in PGM analysis, along with information on methods of decomposition, separations required, type of separation, and final determination.

SAMPLING¹⁻³

The sampling of homogeneous substances containing precious metals is comparatively simple. Minerals, ores and concentration products should be in powdered form, preferably finer than 200-mesh. They can be sampled by conventional techniques with such sampling equipment as sieves, riffles and screens. Sampling may be manual or automatic. Homogeneous metals and alloys can be sampled by taking swarf, chips, millings, or sawings.

The sampling of heterogeneous substances is more complicated. Electronic scrap can be alloyed with copper, nickel, or sometimes lead, to produce homogeneous alloys which can be sampled by the conventional sampling procedures mentioned above; alternatively the material can be melted with aluminium, leading to a friable alloy which can be crushed to a powder suitable for normal sampling methods. Some heterogeneous substances can be burned to a powder. Solutions containing precious metals can be evaporated or treated with zinc or aluminium, and the residues ignited prior to sampling. Powdered material containing precious metals is often referred to as "sweeps".

DECOMPOSITION

Low-grade material

Geochemical exploration samples, ores, residues and sweeps.^{2,6,7,9-12} These substances contain one or more of the platinum-group metals (PGMs), often in acid-

insoluble form. To remove the matrix elements and isolate the PGMs, it is often advantageous to employ some form of fire-assay concentration. It must, however, be borne in mind that the traditional fire-assay methods involving the lead collection system are suitable for isolating gold and silver, less so for isolating platinum and palladium, and only to a very limited extent for isolating rhodium, ruthenium, iridium and osmium. This is largely due to the high melting points of the PGMs and their inability to form alloys with gold and silver that are suitable for subsequent chemical treatment. Therefore, a brief outline of the fire-assay procedure should suffice.

An assay ton* (29.166 g), or a fraction thereof, of sample is taken for analysis and mixed with a suitable flux containing a large proportion of lead monoxide and various proportions of compounds such as sodium carbonate, potassium carbonate, borax, silica, potassium nitrate, or organic substances, such as starch or flour. The ratio of the various components depends on whether the sample (a) contains an excess of basic components, in which case more silica is added, (b) contains an excess of acidic components (additional carbonate or borax is then required), (c) is high in copper (more PbO is then used), (d) tends to oxidize the flux components, requiring addition of organic reducing substances, (e) reduces too much PbO to lead, in which case potassium nitrate is added as an oxidizing agent.

Optimum conditions, as indicated by the fluidity of the melt and the weight of lead button desired, are ensured by a judicious balancing of the weights of sample and the various flux reagents. The PGMs, together with silver and gold, are collected in the resulting lead button. The matrix elements react with

*One mg per assay ton is equivalent to 1 troy oz per ton.

the flux components to form a slag which is subsequently discarded, unless additionally reworked for the recovery of trace amounts of precious metals retained in it.

If the lead button obtained is of proper weight (30–60 g) and comparatively clean, the scorification step may be omitted. However, when the lead button weighs more than 60 g or is known or suspected to retain base metals, it should be transferred to a fireclay dish called a scorifier. More lead is added, and a little silica, and the mixture is melted in an oxidizing atmosphere for about 30 min at about 900°. Much of the lead then oxidizes to form a glassy slag which further extracts impurities. The lead button is next placed on a preheated cupel prepared from bone ash or magnesite. On heating in a muffle furnace at a temperature of about 800–850° in an oxidizing environment, the resulting lead oxide is absorbed into the cupel or is volatilized. A bead of precious metals remains. This cupellation step is only feasible when the bead contains an adequate amount of silver, either present in the original sample or added to the sample-fusion charge, to collect the PGMs. Osmium is largely volatilized during the cupellation step. For further treatments of the silver bead, see below. For a chemical treatment of the lead button, see the section on separations, below.

Other fire-assay collection media have been suggested for determining small amounts of platinum-group elements. They involve the use of iron-nickel-copper alloys and tin.^{2,12,13} Because of the lower fusion temperature required, copper alone has also been suggested as a collector of the precious metals.^{14–17} However, none of the methods above has yet found general acceptance. On the other hand, the collection of PGMs into nickel sulphide (fusion of the sample with a mixture of borax, sodium carbonate, nickel carbonate and sulphur) is being used to an increasing extent.^{18–20} This approach has many advantages over the conventional lead-based fire-assay systems. A new technique involving the collection of PGMs into copper sulphide has recently been described,²¹ and has several advantages over the nickel sulphide technique. First of all, in the copper sulphide method gold is also quantitatively collected. Another advantage is the possibility of dissolving the copper sulphide in hydrobromic acid, thus allowing the separation of the PGMs from large amounts of silver and lead. In both the nickel sulphide and copper sulphide collection schemes the matrix elements are removed by acid treatments and the precious metals contained in the acid-insoluble residue are eventually determined instrumentally or, where justified, gravimetrically.

Automotive exhaust and petroleum reforming catalysts.^{22–27} For the most exacting requirements, the samples are decomposed by an acid treatment with sulphuric acid alone or mixed with phosphoric acid. The final determination is either spectrophotometric or by some other instrumental technique. In the

opinion of the writer, fire-assay procedures are less suitable for decomposing catalysts, whether automotive or reforming, since the normal fire-assay fluxes cannot successfully cope with the large alumina content of these catalysts.²⁸ Other investigators, however, claim quantitative recoveries of platinum metals by fire-assay procedures.^{27,29,30}

Metals and alloys containing small amounts of PGMs. Fire-assay procedures are often applicable but in many instances a chemical attack can be used to greater advantage. Typical are copper metal and alloys containing the PGMs originating in electronic scrap. This type of sample can be dissolved in dilute nitric acid and the solution evaporated with sulphuric acid. Sometimes, the sample can be directly decomposed with sulphuric acid. A subsequent treatment with formic acid will aid in the precipitation of platinum and palladium. An additional precipitation of a small amount of copper as sulphide, with either hydrogen sulphide or sodium thiosulphate, ensures complete recovery of even trace amounts of platinum and palladium.³¹ In the case of rhodium, this precipitation is quantitative only if the rhodium is first converted into chloride complexes by boiling with hydrochloric acid. This approach is not applicable to ruthenium, since this element is largely volatilized during the heating with sulphuric acid. In addition, the method cannot be applied to iridium, since iridium sulphate is sufficiently stable to resist quantitative precipitation with formic acid, hydrogen sulphide or thiosulphate. More efficient is the dissolution of copper base alloys in fuming perchloric acid and subsequent precipitation of all the PGMs with formic acid from a dilute perchloric acid medium.³¹

Intermediate concentrations of PGMs in powdered form (individual elements up to 25%)

In many instances, the PGMs are soluble in *aqua regia*. If a small residue remains, it may be solubilized by fusion with sodium peroxide, or the precious metals in it may be recovered by one of the fire-assay procedures. It must, however, be remembered that rhodium, iridium and ruthenium do not alloy with silver. On the other hand, small amounts of rhodium and iridium can be collected into gold. Upon treatment with *aqua regia*, gold and rhodium dissolve while iridium remains insoluble.^{32,33}

High concentration of PGMs

Platinum-base alloys, Pt 80%, containing 0–5% of Pd, Rh, Ru, Ir, Au or Ag. These alloys are usually soluble in *aqua regia*. Any insoluble silver chloride must be filtered off and re-treated for the recovery of occluded PGMs. The separation of these elements from each other and their final measurements will be described later.

Platinum-base alloys containing more than 10% of Ir or Rh. These alloys are insoluble in *aqua regia* at atmospheric pressure but can be dissolved in it at elevated temperatures in high-pressure systems.³⁴

More convenient is preliminary fusion of the sample with zinc and dissolution of the melt in hydrochloric acid.⁷ A black powder remains, containing the platinum metals in elemental form, ready for an attack by acids or by other appropriate means, prior to distillation (Os and Ru), chlorination (Rh, Ir), or chemical separations such as by bromate hydrolysis (Pt, from Ir and Rh).

Also of considerable value is a fusion of the sample with lead. The resulting lead alloy can be dissolved in dilute nitric acid, leaving a residue containing PGMs. A small amount of rhodium must, however, be recovered from the nitric acid filtrate. If the lead alloy is decomposed with perchloric acid all PGMs and also silver and gold, can be precipitated as metals by the use of formic acid.^{31,35}

Pt–Rh and Pt–Ir alloys, if in finely divided form, can also be solubilized by mixing the sample with 10 times its weight of sodium chloride and heating at 800° in a stream of chlorine.⁷

Palladium-base alloys. These usually contain silver and often varying amounts of platinum, gold and ruthenium. Dental alloys may also contain non-precious metals such as tin, indium, gallium, zinc or copper. These alloys can sometimes be decomposed with nitric acid, but more often require the use of *aqua regia*. Any undissolved ruthenium must be fused with sodium peroxide, dissolved and added to the main sample solution. The separation and determination of the PGMs in palladium-base alloys will be described later.

Pure PGMs

Platinum and palladium are soluble in *aqua regia*; rhodium is solubilized by fusion with sodium pyrosulphate; ruthenium is strongly attacked by hypochlorites; Ru, Rh, Os and Ir are rendered soluble by fusion with sodium peroxide and dissolution of the cooled melt in hydrochloric acid.

SEPARATIONS

Separation from matrix elements

Separations involving fire-assay products. The lead button obtained as described above is treated with dilute nitric acid. After filtration, the insoluble residue contains all the gold, ruthenium and iridium, most of the platinum, but only part of the palladium and rhodium. The insoluble residue is therefore best suited for the determination of ruthenium, iridium and, where required, of gold. The determination of the other platinum group elements by the lead button–nitric acid dissolution method is complex. Thus, when a lead button containing Au, Ag, Pt, Pd, Rh, Ir, Ru and/or Os is dissolved in dilute nitric acid, most of the osmium is volatilized. Silver and part of the palladium and rhodium are dissolved together with the lead. If the silver content of the sample is significant, some platinum will also dissolve. When

the insoluble residue is treated with *aqua regia*, gold, platinum, residual palladium and part of the rhodium dissolve, while iridium, ruthenium and residual rhodium remain insoluble. Recently an alternative treatment of the lead button was described,³⁵ based on the dissolution of the lead button in perchloric acid with the addition of acetic acid. Subsequently, the PGMs were precipitated with formic acid. More recent tests indicate that the acetic acid can be entirely omitted, and if the lead button contains only small amounts of PGMs the dissolution can be speeded up by the addition of about 0.25 g of arsenious oxide. The method can be extended to major concentrations of all the PGMs.³¹ Most surprisingly, no Ru is lost during the heating step with perchloric acid, since the Ru apparently remains as an Ru–Pb alloy.

If the lead button has been subjected to cupellation (see fire-assay methods, above), the silver bead containing PGMs is treated with dilute nitric acid to dissolve the silver and most of the palladium. Platinum will also dissolve if the sample contains at least an equivalent amount of gold. The silver bead naturally must be large enough to hold any rhodium, ruthenium, and iridium mechanically (minimum ratio of Ag to PGM 1000:1). These three elements, together with gold, remain insoluble in dilute nitric acid and can be determined instrumentally after fusion of the insoluble residue with sodium peroxide and acidification of the leached melt with hydrochloric acid. In another recently introduced fire-assay technique, cupellation is interrupted when the weight of the lead button has been reduced to less than 1 mg. This lead bead is then analysed for the PGMs by standard optical emission spectrometry techniques.³⁶ Platinum and palladium can also be determined instrumentally after removal of the silver by precipitation as the chloride. If present in sufficient quantities, platinum and palladium can be determined gravimetrically after precipitation with ammonium chloride (Pt) or dimethylglyoxime (Pd). Also of interest is the selective extraction of the palladium dimethylglyoxime complex with chloroform.³⁷

Other separation schemes. These are justified only if other elements interfere with the final determination of individual platinum group elements. With modern instrumentation it is often possible to make final measurements without the necessity for any separations. In other instances, limited separation schemes may suffice. Thus, the PGM content of a solution can be determined efficiently by plasma techniques without the removal of modest concentrations of alkali metals (e.g., from sodium peroxide fusions) or copper (from dissolution of Cu₂S).²¹ Similarly, small amounts of copper or nickel do not interfere with the precipitation of platinum by ammonium chloride or the precipitation of palladium by dimethylglyoxime (DMG). On the other hand, the gravimetric determination of a PGM presupposes the absence of all other elements when the final weighing form is the PGM itself. Of the many ion-exchange

methods suggested in the past, only the separation of PGMs from base metals by cation-exchangers (such as Dowex-1) is used to any extent.¹¹ Thus, in weakly acid medium, base metals are retained, while the PGMs, owing to the strength of their chloride complexes, pass into the effluent. Unfortunately, there is slight retention of palladium, probably as palladium(IV). One other cation-exchange procedure deserves to be mentioned. Strelow³⁸ recently described a method for the separation of all the PGMs from large amounts of base metals, with the strongly acidic cation-exchange resin Ag5QW \times 4. This method is based on the formation of stable PGM-thiourea complexes which are sorbed by the resin.

Various possibilities of applying solvent extraction techniques to separations of PGMs from base metals and from each other have been discussed by Freiser.³⁹ Another technique which has not yet been fully investigated is based on cellulose chromatography.^{11,40}

Only a few other separation schemes can be cited here. Platinum and palladium in trace amounts can be collected by freshly precipitated tellurium.^{25,26} Palladium can be separated from large amounts of silver and/or lead by its precipitation from dilute nitric acid solution with dimethylglyoxime.³¹ Small amounts of Pd(DMG)₂ can be extracted with chloroform.¹¹ All the PGMs can be separated from the matrix elements by precipitating the former with hypophosphite and a mercurous salt in a slightly acid medium⁴¹ or with hydrazine hydrate or aluminium in an alkaline medium.³¹ Sodium nitrite can also be used; it is one of the most effective reagents for complexing the PGMs and precipitating gold and base metals.^{2,42}

Separation of PGMs from silver and gold

The separation from silver is achieved by precipitation of silver chloride. It must, however, be remembered that the precipitate has a tendency to occlude PGMs, particularly palladium, so it must be purified. This can be done by fire-assay or by converting AgCl into soluble AgClO₄ by fuming with perchloric acid. There are many schemes for separating the PGMs from gold, amongst which precipitation of the latter with oxalic acid appears to be the most quantitative.² There are also ion-exchange resins suitable for the separation of PGMs from gold.⁴³

Separation of the PGMs from each other

As in the case of the separation of the PGMs from base metals, there is an increasing tendency to avoid at any cost chemical separation of the precious metals from each other. Since there exist comparatively few mutual interferences of the precious metals in their determination by atomic-absorption spectrometry (AAS) or plasma techniques, the belief is widespread that, with good instrumentation, time and money could be saved by eliminating chemical separations altogether by relying strictly on instrumental

measurements. Nothing could be further from reality. First of all, the precision obtainable by AAS or plasma techniques is rarely better than 1% and may be as poor as 5–10%, particularly when the sample and standard solutions cannot be closely matched. Also, in most instrumental methods the sensitivity varies to a great extent from one PGM to another. For instance, the sensitivity for rhodium by both AAS and by PES (plasma emission spectrometry) is very high, whereas that of AAS for iridium is wholly unsatisfactory and that of plasma emission just about acceptable. This will be discussed further below in the section on instrumental methods. It is for this reason that the chemical separations, which admittedly are considerably slower and which also require a thorough knowledge of the chemistry of the precious metals, cannot be entirely avoided.

Separation of platinum and palladium. If platinum is the predominant element, the usual procedure consists of precipitating the platinum with ammonium chloride and determining the palladium in the filtrate by precipitation with dimethylglyoxime. The platinum usually retains a little palladium and must therefore be reprecipitated. A small amount of platinum is soluble in the ammonium chloride medium and must be determined by AAS or plasma techniques, usually after destruction of the ammonium chloride with nitric acid.

If palladium is the predominant element, or the sample contains at least 100 mg of palladium, prior precipitation of the palladium with dimethylglyoxime is more effective. Platinum is determined in the palladium filtrate after the alcohol has been boiled off and the organic matter destroyed by evaporation with nitric and perchloric acids. Subsequently, the platinum is precipitated with ammonium chloride or other agents such as hydrazine or hydrogen sulphide. The separation of platinum from palladium can also be achieved in conjunction with the bromate hydrolysis scheme described later.

Separation of platinum from iridium and/or rhodium. This is a modification suggested by German analysts⁴⁴ of a method originally introduced by Gilchrist.^{45,46} Rhodium and iridium are separated from platinum by the interaction of sodium bromide with sodium bromate in a very dilute hydrochloric acid solution. The reaction takes up protons and liberates bromine, until a pH of 6.5 is reached. At this pH rhodium and iridium are quantitatively precipitated, while palladium and platinum stay in solution. In the original Gilchrist version the palladium accompanied the rhodium and iridium, because the pH was adjusted to 7. The pH adjustment is automatic in the German version, whereas the adjustment in the original method requires considerable skill. To achieve a quantitative separation it is advisable to reprecipitate the rhodium plus iridium. Platinum is recovered from the combined filtrates by precipitation with zinc and the addition of hydrochloric acid. The platinum sponge is filtered off and dissolved in *aqua regia* and

the metals are eventually precipitated with ammonium chloride. The hydrated oxides of rhodium and iridium are dissolved in acid and the metals determined instrumentally.

Separation of rhodium from iridium. This is one of the most difficult analytical tasks. No entirely satisfactory method is available. Copper, silver and antimony powders have been suggested by some and rejected by others.^{2,7,47-50} The precipitation of rhodium with titanium trichloride, originally proposed by Gilchrist,⁴⁵ though tedious and lengthy, is probably as good as any other method. This then is one area where modern instrumentation can come to the rescue of the chemically inclined precious-metals analyst.

Separation of ruthenium and osmium from the other PGMs. Ru and Os in their octavalent state form volatile compounds which give clean separations from the other PGMs. The oxidation to this state can best be achieved in an alkaline medium. This can be done by fusing the finely divided sample with sodium peroxide in a zirconium crucible. Beamish describes a number of distillation procedures. For the simultaneous removal of both metals, oxidation with sodium bromate, bromic acid, perchloric acid, chlorine, bismuthate, permanganate, ceric oxide, lead dioxide or peroxydisulphate can be used.² For selective distillation of osmium tetroxide, nitric acid has been recommended.² The present writer prefers the distillation of the osmium from a hydrochloric acid medium with sodium chlorate and absorption of the resulting OsO_4 in a sodium hydroxide solution containing some ethanol as reductant. Use of a 1-2*M* hydrochloric acid medium prevents the loss of any ruthenium during the distillation of the osmium. After removal of the osmium, an excess of sulphuric acid is added to the sample solution, which is then evaporated until light fumes appear. A small amount of perchloric acid introduced into the distillation flask will then effect instantaneous oxidation of the ruthenium to the tetroxide, which distils. The RuO_4 is passed into a train consisting of several flasks containing 6*M* or 4*M* hydrochloric acid, which will reduce the RuO_4 to non-volatile RuCl_3 . Other PGMs can be recovered in the sample solution after the distillation of the Os and Ru.

DETERMINATION OF THE PLATINUM GROUP ELEMENTS

The question whether an element should be determined chemically or by an instrumental technique is a fundamental one for which there is no easy answer. Ideally, the goal is to obtain an analytical result as fast as possible, as precisely and accurately as possible, with equipment which is as cheap as possible, and with personnel requiring the minimum amount of training and/or supervision. Obviously, there have to be choices and compromises. Generally speaking,

chemical methods are more precise, instrumental methods more rapid. Errors in gravimetric measurements are usually of the same absolute magnitude, those in instrumental measurements are usually of the same relative magnitude. Thus, a 1-mg error in a gravimetric procedure causes a relative error of only 1 part per thousand if 1 g of the element determined is present. The error is 1 part per hundred (1%), if 100 mg of the element determined is present, and 1 part in ten (10%), if only 10 mg of the element is present. Since the concentration of an element in solution which can be determined instrumentally is more or less constant, the analytical errors are constant and relate to the concentration of the element in the original sample. A typical 1-2% relative error in measurements is intolerable if the concentration of a PGM in the sample is 50% or more. The same error may be tolerable when the concentration of an element is less than 10%. Since the relative error in a typical gravimetric procedure for the same concentration range is 1%, a generalization can be made that instrumental methods should be used optimally in the 10% range or lower, while gravimetric measurements, if applicable, are best suited for the >10% range. The errors inherent in spectrophotometric methods are similar to those of instrumental methods requiring the preparation of solutions, namely AAS and PES (plasma emission spectrometry) techniques. Spectrophotometric methods have the additional disadvantage that in most instances they require the removal of virtually all other elements, particularly other precious metals.

Determination of platinum group elements by chemical methods

Platinum. Earlier researchers disapproved of the ammonium chloride precipitation of platinum because of (a) the slight solubility of $(\text{NH}_4)_2\text{PtCl}_6$ and (b) the occlusion of small amounts of other PGMs in the precipitate.^{2,45} These objections, however, are no longer valid, since solubility losses and impurity gains can be monitored effectively by modern instrumentation, and corrections applied. The precipitate is ignited to the metal, which is a convenient weighing form. The method is well suited for amounts of platinum greater than 100 mg, particularly for the determination of platinum in platinum-base alloys. Another effective precipitation agent for platinum is formic acid. It should be used in 4.5*M* sulphuric acid medium. The platinum sponge obtained can be directly ignited and weighed, as long as the solution contains no other PGM. Other precipitating agents are hydrogen sulphide, zinc, magnesium and hydrazine. As a rule, the platinum sponge thus obtained is either purified, or dissolved, and the platinum finally precipitated as $(\text{NH}_4)_2\text{PtCl}_6$. Other precipitants have been described by Beamish and van Loon.⁵⁰

Small amounts of platinum (1-75 mg) can be determined with good precision by the spectrophotometric stannous chloride method.^{51,52} This

method is particularly suited to the determination of platinum in reforming and automotive catalysts, since large amounts of alumina and acids, such as hydrochloric, sulphuric and phosphoric, do not interfere. If the final determination is based on the differential spectrophotometric principle, precisions of 0.5% relative can be achieved.⁵³ Palladium interferes in the determination and must be removed by a dimethylglyoxime-chloroform extraction. The small but significant effect of rhodium and the slight effect of iridium can be compensated for by preparing platinum standard solutions containing matching amounts of the interfering elements. Other reagents suitable for the spectrophotometric measurement have been described by Beamish,² Beamish and van Loon,⁵⁰ and more recently by Gorda *et al.*⁵⁴ Diaminobenzoic acid, originally proposed in 1971,⁵⁵ has recently been proposed for the determination of platinum in automotive catalysts.⁵⁶ For the determination of 0.1–100 mg of platinum by instrumental methods, see below. Prior separation or concentration schemes may or may not be required.

Palladium. Dimethylglyoxime (DMG) has been used for more than 70 years as a precipitating agent for amounts of palladium ranging from a few mg to 1000 mg.⁵⁷ Its value lies in its specificity and the fact that the Pd-DMG product is of definite composition, and hence can be used as the weighing form. There is no interference from the other PGMs, but more than milligram amounts of gold do interfere. Normally, a 1% solution of the reagent in ethanol or methanol is used. An aqueous solution of the sodium salt of DMG is used if alcohol interferes in subsequent treatments of the Pd-DMG filtrate. A great many other dioximes have been suggested over the years. None, however, has been shown to be superior to DMG.² Two reagents used in the past, nitrosonaphthol⁵⁸ and potassium iodide⁵⁹ are now largely replaced by the dioximes. Beamish lists a number of other reagents suitable for gravimetric purposes;² their use, however, is limited to special situations and can hardly be justified in view of the recent developments in the instrumental field.

There are a number of possibilities for determining trace amounts of palladium spectrophotometrically.² The present writer prefers furildioxime. Its complex with palladium can be extracted with chloroform and measured directly, without back-extraction.³¹ For milligram amounts of palladium, the palladium iodide complex looks attractive.⁶⁰ Recent developments in spectrophotometric methods for palladium are discussed by Chang and Zhou.⁶¹

Rhodium. The anhydrous trichloride, RhCl_3 , obtained by chlorination, can be converted into metallic rhodium by ignition, first in air and then under hydrogen, producing an excellent weighing form. Iridium, which also forms an acid-insoluble trichloride, interferes. In the absence of other H_2S -group elements, hydrogen sulphide is also an excellent precipitant for rhodium. If rhodium has

been separated from platinum and palladium by the bromate hydrolysis technique, the precipitate, after thorough washing with ammonium chloride solution, can also be converted into the metal by ignition first in air and then under hydrogen.⁷ The metal, however, must be treated with hot dilute hydrochloric acid for removal of residual alkali metal. Again, iridium interferes. It was mentioned above that the separation of the two elements is difficult. It is therefore now a common practice to determine the sum of the two elements gravimetrically, then the lesser component instrumentally. Several other precipitating agents are available.^{2,50}

For trace amounts of rhodium, spectrophotometric methods using either stannous chloride⁶² or bromide⁶³ are available. Both methods tolerate small amounts of iridium, but no other PGM. Again, Beamish lists several other reagents which may be of interest.² Since the sensitivity for rhodium is one of the highest in both emission and absorption spectrometry, most precious-metals analysts now opt for an instrumental approach.

Iridium. Chlorination to give the anhydrous trichloride and subsequent conversion into the metal can be applied in the same way as for rhodium. Similarly, the product obtained by bromate hydrolysis can be converted into the metal. There is a scarcity of specific precipitating agents for iridium in an acid medium. Reducing agents which easily precipitate the other PGMs are useless for iridium, since small but significant amounts of the iridium are merely reduced to a lower oxidation state.

For trace amounts of iridium there are several spectrophotometric procedures which, unfortunately, are not particularly attractive.² They may be of limited interest to those who do not have plasma equipment. The most selective method is based on the production of a purple colour by heating with a mixture of perchloric, sulphuric, phosphoric and nitric acids.⁶⁴ The detection limit, however, is only 20 μg per ml of mixed acid.² A procedure for determination of iridium in the presence of moderate amounts of platinum (as in Pt-Ir catalysts) is based on the reddish colour developed in hydrochloric or sulphuric acid medium on addition of sodium hypochlorite,^{7,65} but rhodium interferes. The instrumental approach involving plasma techniques is far superior (see below).

Ruthenium and osmium. These two elements have many characteristics in common, *e.g.*, they can be separated from matrix elements and other PGMs by distillation of the tetroxides. For the gravimetric determination of both elements precipitation with hydrogen sulphide is feasible, or both elements can be precipitated by hydrolysis at a pH of about 6–6.5.⁷ The ruthenium products can be filtered off on paper, but the osmium products must be collected in a Gooch crucible on a pad of asbestos, or on a Munroe-type platinum crucible, before ignition in a stream of hydrogen.

For trace amounts of both elements the spectrophotometric determination based on the thiourea complexes appears attractive. The ruthenium colour is blue⁶⁶ and that of osmium is red.^{2,67} Other spectrophotometric reagents have been mentioned by Beamish.² Owing to the position of Fe and Ru in the Periodic Table it should be of interest that most reagents suitable for spectrophotometric determinations of iron(II) also form coloured compounds with ruthenium.

Determination of the platinum group elements by instrumental methods

The instrumental methods introduced during the last 20 years have undoubtedly revolutionized the repertoire of the precious-metals analytical chemist. In 1966, Lewis mentioned atomic-absorption spectrometry, introduced by Walsh,¹⁸ on the last page of Beamish's classical monograph.² In the same monograph Beamish gave a brief outline of potential applications of neutron activation and mass spectroscopy and prophetically predicted "each of these methods may contribute much to the analytical field. As with all analytical methods, they are subject to limitations." At that time, spectrochemical and X-ray fluorescence (XRF) methods were to some extent already used in precious-metals laboratories and therefore were more prominently featured in Beamish's monograph.

The question whether a PGM should be determined by a chemical procedure or by an instrumental technique has already been touched on above. There is no single correct answer to this question. The expression "it all depends", although usually considered a cliché, is most appropriate here. Let us then consider the various factors which may influence the chemist in deciding whether to use a chemical or an instrumental approach, or possibly both.

Type and concentration of elements to be determined. For the trace to low range (0.01% or less) the PGMs are preferably determined instrumentally or, where applicable, by spectrophotometry (generally considered a chemical technique). For the low to medium range (1–10%), there are many instances where a chemical approach may be justified, e.g., the gravimetric determination of palladium with dimethylglyoxime, the gravimetric determination of rhodium and/or iridium after chlorination, the gravimetric determination of osmium or ruthenium after distillation. In this range an instrumental error of 2% relative is reflected in an uncertainty of 0.02–0.2% absolute in the final PGM result. In the high range (10–100%), chemical methods generally have the advantage over instrumental methods, primarily because of their superior precision. Even so, if matrix matching is possible and statistical data indicate that a precision of 1% can be achieved, many analysts may prefer instrumental measurement of the PGMs, particularly if lengthy separations can be avoided.

Equipment available. Instruments are expensive.

DCP, ICP and XRF instruments cost \$75,000 or more, AAS equipment somewhat less. For the occasional user, the purchase of such instruments, therefore, can scarcely be justified. If the work load of the laboratory, however, consists of often recurring analytical requirements, the acquisition of appropriate instrumentation should be seriously considered. The case for the introduction of instrumentation becomes even more compelling, if more than one PGM must be determined in the same sample. Also of primary importance is the question whether the preparation of the sample solution is simple and the instrumental measurements relatively free from matrix interferences.

Personnel available. The use of instrumentation requires personnel of a higher calibre than that commonly found in a fire-assay laboratory. Though many of the operations with instruments have been simplified and even automated, there has to be someone in the organization who is capable of trouble-shooting when the equipment misbehaves and someone who is capable of determining which parameters of a method are essential. A sound knowledge of the analytical chemistry of precious metals, as well as that of base metals, is a prerequisite for ensuring optimum use of an instrument as the final measuring device.

Standards. It should be remembered that all instrumental methods, unlike most chemical methods, merely compare the concentration of an element in the sample with that in a reference material of known composition. The instrumental method used may tolerate small, moderate, or even large deviations between the concentrations of matrix elements in standards and samples. If the time required to prepare matching standards becomes excessive, a chemical procedure may be more attractive.

The most important instrumental techniques

X-Ray fluorescence.^{70,71} XRF was developed from X-ray emission (XRE), in which the sample is directly exposed to radiation with an energy greater than the excitation threshold of the element under study. The method is based on measurement of the secondary X-rays emitted by the constituents of a sample excited by primary X-rays. The inner electron shells of the atom lose one or more electrons, which are then replaced by the outer shell electrons. There is an accompanying loss of energy by the replacement electrons, which is emitted as radiation. The resulting line spectrum is characteristic for each element. Though the intensity of the emitted lines of XRF is only a small fraction of that of XRE, recent advances in electronics have reduced much of the sensitivity advantage of XRE. The main advantage of XRF is its simplicity. Two different types of XRF instrument are available; energy-dispersive and wavelength-dispersive.

Considerable progress in the instrumentation, particularly with regard to the energy sources, the

precision of the dispersion systems and the electronic quality of the detection and measuring devices, allows rapid analysis for the PGMs with excellent precision. Multi-channel spectrometers facilitate the simultaneous determination of all the PGMs, and of gold, silver, and many base metals.

The main advantage of XRF over the various atomic emission or absorption techniques (OES, DCP, ICP, AAS) described below, is that it is non-destructive, allowing recovery of the original sample after the determination. Its main disadvantage is that for quantitative work standards with the same chemical composition and physical characteristics as the sample must be available or prepared. If solid samples are to be analysed, facilities are required for preparing a set or sets of PGM-bearing alloys with highly polished surfaces. One laboratory⁷¹ routinely analyses platinum alloys containing 5–10% of palladium and/or rhodium, another⁷⁰ determines the PGMs in a tin button⁷² obtained by the fire-assay technique mentioned earlier. A solution technique used by another organization⁷³ simplifies the preparation of standards, but at the expense of sensitivity. Microgram amounts of all precious metals have been determined by absorbent-pad-and-cellulose pellet techniques.⁷⁴ Computer programs have been designed to correct for the positive or negative effects of other PGMs or those of base metals on the result for the PGM being determined. As far as sensitivity is concerned, with wavelength-dispersive instruments, the radiation of the *K*-lines of Ru, Rh, Pd and Ag is 2–3 times more intense than that of the *L*-lines of Os, Ir, Pt and gold.

Optical emission spectroscopy (OES). This technique is particularly well suited for the determination of impurities in pure PGMs. In addition, when combined with preconcentration techniques based on chemical or fire-assay principles, it allows determination of platinum and palladium concentrations in complex matrices down to 0.03 $\mu\text{g/g}$ or 0.001 oz/ton.³¹ In this particular procedure 20 mg of gold is used as a collector and the Pt and Pd content of the gold is compared with that of gold standards containing known quantities of the two PGMs. With minor variations, the method can be applied to the determination of trace amounts of rhodium and iridium.

The direct current (dc) arc is the most useful spectral source. It is produced by passing a current of 2–30 A between two electrodes, one of which contains the sample. Although the high-voltage ac and interrupted dc arcs are useful for some applications, they have largely been replaced by newer techniques, such as AAS and PES. One attractive feature of OES with photographic recording is its capability of providing simultaneously qualitative and/or quantitative information on many elements (typically 20–40 or more).⁷⁵

Spark-source mass-spectroscopy (SSMS). SSMS is a semiquantitative technique with ultrahigh sensitivity, which has detection limits in the low $\mu\text{g/g}$ and ng/g ranges. When used instead of OES for final

measurements, it allows determination of the PGM content of complex matrices at the 1 ng/g level.³¹ In this technique the sample is sparked in a vacuum by a high-energy radiofrequency spark to produce positive ions of the sample elements. A double-focusing spectrometer separates the ions according to their "mass-to-charge" ratio, first in an electrostatic, then in a strong magnetic field. The ions thus separated are recorded photographically on an ion-sensitive photoplate or are measured by means of photomultipliers. Accelerator mass spectrometry has recently been used to determine the isotopic composition of osmium in terrestrial samples.⁷⁶

Flame atomic emission and absorption spectrometry. In FAES and in FAAS the sample solution is subjected to a high-energy thermal environment provided by a flame, which evaporates the solvent and produces excited-state atoms, which return to the ground-state or other lower energy state and emit light. In FAES the emission spectrum is measured. This technique cannot be applied to PGMs because the flame is unable to provide the energy needed for excitation of the PGMs. In FAAS, some of the ground-state PGM atoms are excited by resonance absorption light of specific wavelength from a suitable source containing the analyte element. The fraction of light absorbed increases with the number of PGM atoms present, thus providing quantitative measurement of the amount of the PGM.

FAAS has largely replaced spectrophotometry as the work-horse in the precious-metals analytical laboratory. There are several reasons for this. (a) FAAS is virtually element-specific. Thus a PGM which cannot be determined spectrophotometrically at all in the presence of certain other PGMs or base metals, can often be determined with comparative ease by FAAS. (b) In many instances, there is no interference by moderate concentrations of base metals, and even where there is, it can be dealt with by the standard-addition technique. The limitations to the use of FAAS in precious-metals analysis mainly arise from the sensitivity, which is poor for some PGMs, particularly iridium. The relative concentrations of PGMs required to match the AAS response of a reference unit concentration of silver are: Pd 4, Rh 5, Ru 9, Os 100, Ir 150, Pt 38, Au 5. A relative value of 40 or more would indicate that the element should not be handled by FAAS (Os, Ir), unless present in substantial quantities or isolated from the matrix. It must also be remembered that FAAS is a solution technique and therefore requires that the element(s) can be dissolved with relative ease, and without introducing too much extraneous matter. This is obviously difficult, if not impossible, in the case of many samples containing the PGMs in a complex matrix.^{11,50,77,78}

Electrothermal atomic-absorption spectrometry (ETAAS). This technique supplements FAAS, inasmuch as it offers greatly enhanced sensitivity. This can be explained as follows. In FAAS, the sample

passes through the observation zone so rapidly that the effective lifetime of the absorbing atom is very brief, only a few thousandths of a second. In ETAAS, on the other hand, the residence time of atoms in the light-beam is 100–1000 times longer, thereby providing correspondingly greater sensitivity. Unfortunately, the precision is much poorer because of the small volume of sample solution (5–50 μl) used and the difficulties encountered in reproducible sampling and control of the atomization conditions. In addition, since ETAAS also generally relies on the preparation of solutions of samples and standards, it is subject to the same dissolution limitations as FAAS. Attempts have been made to use solid samples, but with limited success. An interesting application of ETAAS for geochemical exploration work was recently described,⁷⁹ in which diantipyryl-methane was used for isolating the PGMs by extraction into chloroform.

Plasma emission spectrometry (PES). Plasma emission spectrometry is a variant of atomic emission spectrometry (AES), based on use of a plasma for excitation. It is based on the principle that in high-intensity electromagnetic fields gases become conductors and complex electric charge-transfer phenomena occur, called gas discharges. The result of a gas discharge is the production of an ionized gas at very high temperature, containing electrons, positive ions and neutral atoms and molecules, called a plasma.

Plasmas are increasingly used as a spectral excitation source for determining the PGMs. Generally, the sample is introduced in the form of a solution that is atomized by the carrier gas in various fashions. Two types of plasma are used: the direct current plasma (DCP) and the inductively-coupled plasma (ICP). Lasers are also used as an excitation source.

Instrumentation for both techniques has been developed rapidly during the last few years. Moderately priced instruments are readily available, based on the sequential principle (measurement of one PGM at a time). There are also more expensive instruments based on the use of multichannel detectors (ICP) or cassettes (DCP) allowing the simultaneous determination of all the PGMs, as well as of silver, gold and many base metals. There is even a fast sequential DCP instrument.^{80–84}

Though FAAS has certain advantages over the arc and spark emission methods for PGM analysis, it is decidedly inferior to PES in sensitivity and linear dynamic range. Also, the PES methods tolerate the presence of moderate amounts of alkali-metal salts, and this will often permit use of fusion of a sample with alkaline fluxes such as sodium peroxide and sodium carbonate.

The linear dynamic ranges ($\mu\text{g/ml}$) of DCP for the eight precious metals at interference-free wavelengths are Ru 0.5–50, Rh 0.1–50, Pd 0.1–30, Ag 0.4–60, Os 0.5–100, Ir 0.5–5, Pt 0.3–75, Au 0.3–100. The corresponding ranges of ICP are similar, but

depend to some extent on the instrumentation used and the availability of interference-free wavelengths.

Inductively-coupled plasma–mass spectrometry. This technique (ICP–MS) has recently been introduced, but not yet fully examined as to its suitability for PGM determinations.⁸⁵ However, effective means have been devised to extract ions from the plasma (which is at atmospheric pressure) and introduce them (at greatly reduced pressure) into a quadrupole mass spectrometer for mass resolution and detection. ICP–MS may be of interest to laboratories having no access to SSMS. Laser MS instruments have also been built, but are still in the experimental stage.

Inductively coupled plasma–atomic fluorescence spectrometry. This technique (ICP–AFS) has recently been advocated as an efficient tool for PGM analysis.⁸⁶ In atomic fluorescence, the plasma does not function as an excitation source but solely as an atomization cell to produce ground-state (or low-energy excited state) atoms. Excitation is mainly by resonance absorption of light from an external light-source, and the fluorescence emitted by return to a lower energy state is viewed at an angle to the excitation beam. The sensitivity of the method is said to be comparable to that of FES techniques. The cost of the equipment compares favourably with that of AAS.

Activation analysis. Gamma rays, charged particles, and particularly neutrons react with isotopes of the PGMs to produce radioactive nuclides. The characteristic radiation emitted by the nuclides produced can be used for detection and determination of the PGMs. In some instances, neutron-activation analysis is more sensitive than any other technique. Though instrumental NAA (INAA) can be applied effectively to gold and silver determinations, in the case of the PGMs some separation or concentration is necessary, either before or after the irradiation.^{50,87}

Controlled-potential coulometry (CPC). In controlled-potential coulometry, the substance is electrolysed at a working electrode with the potential controlled or kept constant during the electrolysis by means of a potentiostat. The current is integrated with an electronic integrator or coulometer. A reference electrode and a two-electrode electrolysis cell are employed.

For the analyst, the manipulation of the technique resembles that of conventional titrations, except that the amount of “titrant” used is measured by means of current and the operations are inherently semi-automatic. This technique has been shown to be very effective for the determination of all the PGMs, as well as of gold and silver.⁸⁸ Unfortunately, it has not yet received the attention from precious-metal analysts that it richly deserves.

Other instrumental techniques that are of value to the PGM analyst for specific applications include polarography, differential pulse polarography, anodic stripping voltammetry, ion-selective electrode potentiometry and most recently, ion-chromatog-

raphy. The applicability of this latter technique to PGM analysis was recently discussed by Heberlin.⁸⁹

CONCLUSIONS

Up to twenty years ago the chemical repertoire for the analysis of PGMs was largely limited to gravimetric methods (including fire-assay), enhanced to a limited extent by various spectrophotometric methods. The analysis of substances rich in PGMs always involved extensive and often tedious separation schemes to isolate the elements to be determined, before a final gravimetric method could be applied. In many respects, the introduction of instrumental methods of analysis has lessened the burden on precious-metals analysts, by reducing the need for extensive chemical separations. On the other hand, the availability of these techniques has led to tightened accuracy requirements and to the extension of the analytical repertoire to additional elements and to a variety of products not previously encountered.

Only a limited number of PGM materials can be analysed by purely instrumental techniques. Though in instrumental methods random errors can sometimes be limited to 1% relative, systematic errors are often significantly greater, unless standard samples of the same composition, both chemical and physical, are available and employed.

Although the 1% relative error (at best) of the instrumental approach may be acceptable when the content of an element is 10% or less, for higher concentrations of an element a 1% error is in most instances intolerable. Where a higher degree of precision is required or when the PGMs are present in trace amounts, the precious-metals analyst has to take recourse to chemical methods, some involving gravimetry, others preconcentration steps. It should be pointed out that chemical methods, whether based on some form of classical or neoclassical form of fire-assay or on wet chemical techniques, can often be extensively modified by instrumental measurement of the solubility of certain precipitates or of the contamination of final products. It is thus possible to

streamline or revitalize many older procedures which previously had suffered from such defects. This clearly demonstrates, in the case of PGM analysis, the "Interdependence of Chemical and Instrumental Methods".⁹⁰

APPENDIX

CONDENSED OUTLINE OF METHODS OF ANALYSIS APPLICABLE TO THE PLATINUM GROUP METALS

Table 1 lists the common designation and composition of important PGM-bearing substances. In the case of minerals, the formulae will often correspond only roughly to the actual result of an analysis.

Table 1 also provides each substance with a code number which is used to identify it in Table 2. In addition, Table 1 lists the constituents of each substance for which methods of analysis are included in Table 2. Although the determination of other elements may occasionally be required for various special purposes, only those for PGMs are included. Thus, the entry Pt-Re catalyst following the sample code 25 signifies that only methods suited to the determination of Pt will be found in Table 2.

As pointed out repeatedly in the text, the choice of a procedure for determining any particular element depends considerably on the environment in which this element occurs, the equipment available for its isolation and final determination, and also on the experience of the analyst. Different substances must be decomposed in different ways and necessitate the execution of different separations. Procedures which are suited to the determination of a PGM in a specific substance may not be applicable to its determination in a sample of different origin. This is particularly so in the case of sweeps, which have wide ranging base-metal compositions and precious metal contents ranging from below 1 ppm to 20–30%. In the case of referee analysis, the analyst is also frequently asked to determine just one or two PGMs, with the remaining PGMs not to be determined at all. No attempt is therefore made to provide methods covering all eventualities. The procedure which is best suited for the determination of a specific PGM may be identified by locating the code number in the second column of Table 2. The remaining columns of this table will then provide information concerning the decomposition of the sample, the nature and some details of the separations that must be made, and the final isolation and determination of the element sought. A reasonable estimate of the composition of most PGM-bearing substances can be obtained by a preliminary XRF scan.

Table 1. List of important PGM-bearing substances often analysed

No.	Name of PGM substance	Approximate composition	Associated compounds	Analyse for
1	Native platinum concentrate	Pt 75–85%; OsIr 1–4% raw ore about 7 ppm Pt	Au, Pd, Rh, Pd, Rh olivine mineral	Pt, Pd, Au, Ir, Rh
2	Osmiridium	Os:Ir:Ru:Pt 3.5:3:1.0:0.6	Native Pt	Os, Ir, Pt, Ru
3	Sperrylite	PtAs ₂ ; Pt 50–55%	Ni–Cu sulphides	Pt, Rh
4	Cooperite	PtS; Pt 82%, Pd 2.5%	Minerals of of Merensky Reef	Pt, Rd, Rh
5	Braggite	Pt ₂ PdNiS ₄	see No. 4	Pt, Pd, Rh
6	Stibiopalladinite	Pd ₃ Sb and Pd ₇ Sb ₃	see No. 4	Pd, Pt
7	Laurite	RuS ₂	see No. 4 sands of Borneo	Ru, Os
	<i>PGM-metals or sponge</i>	Ru, Rh, Pd, Os, Ir, or Pt		
8	99.999%		—	Purity
9	99.99%		—	Purity
10	99.9%		—	Purity
11	99%		—	Purity
	<i>PGM salts</i>			
12	Ru-salts, pure	RuCl ₃ ·3H ₂ O	—	Ru
13	Rh-salts, pure	RhCl ₃ , Rh(NO ₃) ₃ ·nH ₂ O	—	Rh
14	Pd-salts, pure	PdCl ₂ , Pd amines	—	Pd
15	Os-salts, pure	OsO ₄	—	Os
16	Ir-salts, pure	Na ₂ IrCl ₆ ·6H ₂ O	—	Ir
17	Pt-salts, pure	H ₂ PtCl ₆ , Pt amines		Pt
	<i>PGM solutions</i>			
18	Solutions of substances 12–17			elements of substances 12–17
19	Ru-soln.	pure or impure	waste or recovery	Ru
20	Rh-soln.	pure or impure	waste or recovery	Rh
21	Pd-soln.	pure or impure	waste or recovery	Pd
22	Ir-soln.	pure or impure	waste or recovery	Ir
23	Pt-soln.	pure or impure	waste or recovery	Pt
	<i>Catalysts</i>			
24	Pt catalyst	Pt 0.3–0.8%	on alumina	Pt
25	Pt–Re catalyst	Pt 0.3–0.6%	on alumina	Pt
26	Pt–Pd catalyst	Pt 0.03–0.15% Pd 0.02–0.12%	on alumina	Pt, Pd
27	Pt–Rh catalyst	Pt 0.03–0.25% Rh 0.005–0.03%	on alumina	Pt, Rh

continued

Table 1—*continued*

No.	Name of PGM substance	Approximate composition	Associated compounds	Analyse for
28	Pt-Pd-Rh catalyst	Pt 0.03-0.20% Pd 0.03-0.15% Rh 0.005-0.05%	on alumina	Pt, Pd, Rh
29	Pt-Pd monolith	see No. 26	on cordierite	Pt, Pd
30	Pt-Rh monolith	see No. 27	on cordierite	Pt, Rh
31	Pt-Pd-Rh monolith	see No. 28	on cordierite	Pt, Pd, Rh
32	Pt-Ir pellets	Pt 0.30%-Ir 0.30%	on alumina	Pt, Ir
33	Pt catalyst	Pt 0.3-15%	on carbon	Pt
34	Pd catalyst	Pt 0.25-20%	on carbon	Pd
35	Pt-Pd catalyst	Pt 0.15-15% Pd 0.15-20%	on carbon	Pt, Pd
36	Ru catalyst	Ru 0.5-10%	on carbon	Ru
37	Ru catalyst	Ru 0.25-0.60%	on alumina	Ru
38	Ru residue	Ru 0.15-0.50%	on various organics	Ru
39	Rh catalyst	Rh 0.5-4%	on carbon	Rh
<i>Residues</i>				
40	Rh residue	Rh 0.20-0.60%	on various organics	Rh
41	Anode slime Se > 5%	Ag 5-50%; Au 0.1-0.5%; Pt 3-10 ppm; Pd 10-100 ppm	often high Cu, Pb, Sn, Sb	Pt, Pd (Ag, Au)
42	Anode slime Se 20-30%	similar to No. 40	similar to No. 40	Pt, Pd (Ag, Au)
43	Electronic scrap	Ag, Au, Pt, Pd, Rh; any one 0.01-1%	powder left after ignition	Pt, Pd (Ag, Au)
44	Electronic scrap	Ag, Au, Pt, Pd, Rh; any one 0.0-1%	usually collected in copper	Pt, Pd (Ag, Au)
45	Ruthenium paste	Ru 3-10%; Ag 5-20% Pd 3-8%; Pt, Au low	high in Pb, Bi SiO ₂ ; for making resistors	Ru, Ag, Pd Au, Pt
46	Ag-Pd paste	Ag: Pd 7:3	usually on barium titanate for making capacitors	Pd(Ag)
47	Copper anodes	Ag, Au, Pt, Pd	upon electrolysis anode slime remains; see 40, 41	Pt, Pd (Ag, Au)
<i>Alloys</i>				
48	Pt-Rh	Rh 5-10%	balance is Pt	Pt, Rh
49	Pt-Ir	Ir 5-20%	balance is Ir	Pt, Ir
50	Pt-Pd	Pd 40-60%	HNO ₃ production "gettering alloy"	Pt, Pd
51	Jewellery scrap	Pt 80-90%, Pd 0-10% Rh 0-10%, Ru 1-5% Ir 0.25-8%, Au 0-5% Ag 0.25-3%	various precious metals are melted with platinum to form solid soln.	Pt, Pd Ir, Rh Ir, Rh, Ru (Ag, Au)

continued

Table 1—continued

No.	Name of PGM substance	Approximate composition	Associated compounds	Analyse for
52	Dental alloy	Ag 10–50%, Pd 10–60% Pt 0–2%, Ru 0–0.5%	often contains Cu, Sn, In, Zn, Ga	Pd, Pt Ru(Ag)
53	Dental alloy	Ag 5–15%, Au 50–60% Pd 3–10%, Pt 3–7%	always contains Cu	Pd, Pt (Ag, Au)
54	Pt–Ni	Pt 20–45%	Ni is used to melt heterogeneous Pt material	Pt
55	Pt–Co	Pt 20–45%	Co serves the same purpose as nickel	Pt
56	Ir–Ni	Ir 20–35%	Ni is used to melt heterogeneous Ir scrap	Ir
57	PtPd–Rh concentrate	Pt 18–35%, Pd 7–15% Rh 0.8–3% Fe 20–50%, Pb 0.5–3%	Recovery of the PGMs from automotive catalyst	Pt, Pd, Rh
<i>Examples of "sweeps" compositions</i>				
58	Example No. 1	Rh 2.5%; Pd 0.015%; Pt 0.72% Ru 3.5%; also Au, Ag each	Majors: Pb, Bi, Cu	Pt, Pd, Rh (Ag, Au)
59	Example No. 2	Pd 2.5%; Pt 0.1%; Ag 0.25%	Majors: Al, Si, Zr Minors: Fe, Ni, Zn	Pt, Pd (Ag)
60	Example No. 3	Pd 10.5%; Ag 12.3%; Pt 0.12%; Au 0.27%	Majors: Ba, Ti Minors: Zr, Nb, Sr	Pt, Pd (Ag, Au)
61	Example No. 4	Au 2.8%; Ag 3.2% Pt 0.14%; Pd 1.3%	Majors: Cu, Pb, Al Minors: Fe, Zn, Zr	Pt, Pd (Ag, Au)
62	Example No. 5	Au 0.04%; Pt 0.07% Pd 3.25%; Rh 0.05% Ir 0.18%; Ru 0.10% Ag 1.25%	Majors: Si, Al, Cu, Pb, MgO. Minors: Fe, Ni, Cr, Ti, Sn Zn, Ba	Pt, Pd Rh, Ru, Ir, (Ag, Au)
63	Example No. 6	Pt 15%; Pd 1% Rh 0.15%	Majors: Fe, Ni Minors: Cr, Si	Pt, Pd Rh
64	Example No. 7	Pd 35%; Pt 2%; Rh 1.5%; Ru 0.04%; Ir 0.07%;	Majors: Si, Fe, Pb	Pd, Pt, Rh, Ru
65	Example No. 8	Rh 17%; Pt 0.20%; Pd 0.48%	Majors: Si, Al, Fe	Rh, Pd Pt
66	Example No. 9	Ru 12%; Ir 0.15%; Pt 0.05%; Pd 1.24%	Majors: Si, Pb, Bi Fe, Zn	Ru, Ir Pt, Pd
67	Example No. 10	Au 0.18%; Ag 2.4%; Pt 0.75%; Pd 3.4%	Majors: Al, Cu, Pb Si, Zn	Pd, Pt (Ag, Au)

Table 2. Procedures for the analysis of PGM substances (n.a. = not applicable; coll. = collector)

Element(s) determined	Material code (see Table 1)	Decomposition with	Separation required from	Type of separation	Final determination	References
Ru, Os, Ir, Pt	2	Zn, then Na ₂ O ₂ fusion	all matrix elements	distillation	Os, Ir grav. Ru, Pt PES	2,7
Ru	8	n.a.	n.a.	n.a.	SSMS	91,92
Ru	9, 10, 11	n.a.	n.a.	n.a.	OES	75,93,94
Ru, Os	7	fire-assay Cu ₂ S, NiS	all matrix elements	Na ₂ O ₂ fusion of acid-insol.	PES	18-22
Ru	12	convert into metal	n.a.	n.a.	grav. + OES	
Ru	18, 19, pure Ru < 100 mg	n.a.	n.a.	n.a.	PES	20
Ru	18, 19, pure Ru < 100 mg	pptn. with H ₂ S or hydrolysis at pH 6	n.a.	n.a.	grav.	7
Ru	19, impure Ru < 100 mg	n.a.	n.a.	n.a.	PES	20
Ru	19, impure Ru > 100 mg	(a) n.a. (b) n.a.	n.a. matrix and all PGMs	n.a. distillation	PES grav.	20 7
Ru	36, 38	ignition and Na ₂ O ₂ fusion	n.a.	n.a.	PES	20
Ru	37	(a) Na ₂ O ₂ fusion (b) fire-assay	n.a. Pb	n.a. fusion of HNO ₃ -insol. with Na ₂ O ₂	PES PES	20 20
Ru, Pd, Pt (Ag, Au)	45	Pb, NiS, Cu ₂ S	HCl, HBr, HClO ₄	distil Ru	PES	18-21,35
Ru, Rh, Pd, Ir (Ag, Au)	51	<i>aqua regia</i>	n.a.	fusion of residue with Na ₂ O ₂	PES	20
Ru	62	see 62, Pd, Pt, Rh, Ru, Ir (Ag, Au)				
Ru, Ir, Pt, Pd	66	Na ₂ O ₂ fusion	isolation of ruthenium	distillation	grav. or PES	7,20
Rh, Ir, Pd(Au)	1	<i>aqua regia</i>	insol.	filt., Na ₂ O ₂ fusion of residue	AAS, PES	20
Rh, Pt, Pd	3, 4, 5 (a) ore (b) mineral	lead fire-assay <i>aqua regia</i>	matrix filtration	collection in gold Na ₂ O ₂ fusion of residue	OES grav. or PES	2,7,50,75,93,94 2,20

Rh	8	n.a.	n.a.	n.a.	SSMS	91,92
Rh	9, 10, 11	n.a.	n.a.	n.a.	OES	75,93,94
Rh	13	conversion into metal	n.a.	n.a.	grav. + OES	2,7,75,93,94
Rh	18, 20, pure Rh < 100 mg	(a) direct	n.a.	n.a.	AAS, PES	11,20
Rh	18, 20, pure Rh > 100 mg	(b) convert into metal	n.a.	n.a.	grav.	2,7
Rh	20, impure Rh < 100 mg	convert into metal	n.a.	n.a.	grav. + OES	2,7,75,93,94
Rh	20, impure Rh < 100 mg	n.a.	n.a.	n.a.	AAS, PES	20
Rh	20, impure Rh > 100 mg	n.a.	n.a.	n.a.	grav.	7
Rh	27	see 27, Pt, Rh	all base metals and other PGMs	precipitate + chlorinate		
Rh	28	see 28, Pt, Pd, Rh				
Rh	30	see 30, Pt, Rh				
Rh	31	see 31, Pt, Pd, Rh				
Rh	39, 40	ignition Na ₂ O ₂ fusion	n.a.	n.a.	AAS, PES	7,20
Rh	43, 44	see Pt, Pd, Rh (Ag, Au)				
Rh, Pt	48	(a) direct (b) <i>aqua regia</i> (c) <i>aqua regia</i>	n.a. n.a. Rh from Pt	n.a. n.a. hydrol. pptn.	XRF Rh, AAS, PES grav. or PES	71 11,20 44-46
Rh	57	see 57, Pt, Pd, Rh				
Rh, Pt, Pd	58	Pb, NiS, Cu ₂ S collection	removal of collector	dissolve collector. Na ₂ O ₂ fusion of acid-insol.	PES	18-21
Rh	62	see 62, Pd, Pt Rh, Ru, Ir (Au, Ag)				
Rh	63	see 63 Pt, Pd, Rh				
Rh	64	see 64, Pd, Pt, Rh, Ru				
Rh, Pt, Pd	65	Pb, NiS, Cu ₂ S collection	removal of collector	fusion of acid-insol. with Na ₂ O ₂ , pptn. with Zn, chlorination	Rh, grav. Pt, Pd, PES	2,7,11,18-21
Pd, Pt	4, 5, 6	fire-assay	collect with Au		OES, PES	2,7,36,75,93,94

continued

Table 2—continued

Element(s) determined	Material code (see Table 1)	Decomposition with	Separation required from	Type of separation	Final determination	References
Pd	8	n.a.	n.a.	n.a.	SSMS	91,92
Pd	9, 10	n.a.	n.a.	n.a.	OES	75,93,94
Pd	11	n.a.	n.a.	n.a.	by difference OES	75,93,94
Pd	14	(a) convert into metal (b) dissolve in dil. HCl	n.a. n.a.	n.a. pptn. with DMG	grav. + OES grav.	2,7,75,93,94 2,7,11,50
Pd	18, 21 pure Pd > 100 mg	n.a.	n.a.	(a) pptn. with DMG (b) direct	grav. AAS, PES	2,7,11,50 11,20
Pd	18, 21 pure Pd > 100 mg	n.a.	n.a.	pptn. with DMG	grav.	2,7,11,50
Pd	21 impure Pd < 100 mg	n.a.	n.a.	(a) pptn. with DMG (b) direct	grav. AAS, PES	2,7,11,50 11,20
Pd	21 impure Pd > 100 mg	n.a.	n.a.	pptn. with DMG	grav.	2,7,11,50
Pd	26	see 26, Pt, Pd				
Pd	28	see 28, Pt, Pd				
Pd	29	see 29, Pt, Pd				
Pd	31	see 31, Pt, Pd, Rh				
Pd	34	ignition, <i>aqua regia</i>	filtration		<10%, PES, AAS >10%, DMG grav.	11,20 2,7,11,50
Pd	35	ignition, <i>aqua regia</i>	filtration	treatment of insol. by fire-assay	<3%, PES, AAS >3%, DMG grav.	11,20 2,7,11,50
Pd	41, 42	(a) H ₂ SO ₄ decomposition (b) lead fire-assay	Ag pptn., filtration, fuse, scorify and cupel		AAS, PES AAS, PES	11,20 7,11,20
Pd	43, 44	see 43, 44, Pt, Pd, Rh (Au, Ag)				
Pd	45	see 45, Ru, Pd, Pt(Ag, Au)				
Pd, Pt(Ag, Au)	47	H ₂ SO ₄ decomp. or Pb fire-assay <i>aqua regia</i>	collection into silver separation of Pt and Pd	HNO ₃ parting	AAS, PES	2,7,11,20,44
Pd, Pt	50			DMG pptn. of Pd	Pd, Pt grav.	2,7,41

Pd, Pt, Ru(Ag)	52	HNO ₃	Pd from Ag by AgCl pptn.	Pd from Pt, Ru with DMG	Pd(Ag) grav. Pt, Ru PES	2,7,11,50 20
Pd, Pt(Au, Ag)	53	<i>aqua regia</i>	pptn. of Ag as AgCl	pptn. of Au with oxalic acid oxalic acid	Pt or Pd > 5%, AAS, PES >5%, grav.	11,20 2,7,11
Pd	57	see 57, Pt, Pd, Rh				
Pd	58	see 58, Rh, Pt, Pd				
Pd, Pt(Ag)	59	Ag-bead collection HNO ₃ treatment	removal of Ag	pptn. as AgCl	AAS, PES	7,11,20
Pd, Pt(Ag, Au)	60	(a) as for 59 above (b) Pb-button collection	removal of lead	HClO ₄ dissol. HCOOH pptn.	Pd(Ag) grav. Pt(Au) AAS, PES	7,11,35 11,20
Pd, Pt(Ag, Au)	61	(a) as for 60(b) above (b) Cu ₂ S coll.	removal of matrix coll.	HClO ₄ dissol. HBr dissol.	AAS, PES AAS, PES	11,20,35 11,20,21
Pd, Pt, Rh, Ru, Ir(Ag, Au)	62	Pb-button or Cu ₂ S collection	removal of matrix coll.	HClO ₄ , HBr HBr	AAS, PES	11,20,21,35
Pd	63	see 63, Pt, Pd, Rh				
Pd, Pt, Ru, Rh	64	<i>aqua regia</i> , Na ₂ O ₂ fusion of residue	separate Pd	DMG pptn.	Pd grav.	2,7,11,50
Pd	65	see 65, Rh, Pt, Pd		acidify, fusion	Pt, Ru, Rh, PES	11,20
Pd, Pt, Ir	66	NiS, Cu ₂ S	remove Ru	dissolve in HCl or HBr, fume residue with HNO ₃ + HClO ₄	AAS, PES	18-21
Pd, Pt (Ag, Au)	67	(a) Ag bead coll. (b) Pb-button coll.	remove Ag remove Pb	dissolve in HNO ₃ dissolve in HClO ₄	AAS, PES AAS, PES	2,7,11,20 11,20,35
Ir	2	see 2, Ru, Os	Ru, Os	Use residue from distill.	PES	20
Ir	8	n.a.	n.a.	n.a.	SSMS	91,92
Ir	9, 10, 11	n.a.	n.a.	n.a.	OES	75,93,94
Ir	16	conversion into metal	n.a.	n.a.	grav. + OES	2,7,11,75,93,94
Ir	18, 22 pure < 10%	(a) conversion into metal (b) n.a.	n.a. n.a.	n.a. n.a.	grav. PES	2,7,11,50 20
Ir	18, 22 pure > 10%	convert into metal	n.a.	n.a.	grav. + OES	2,7,11,75,93,94
Ir	22, impure < 10%	n.a.	n.a.	n.a.	PES	20

Table 2—continued

Element(s) determined	Material code (see Table 1)	Decomposition with	Separation required from	Type of separation	Final determination	References
Ir	22, impure > 10%	n.a.		bromate hydrol. + chlorination	grav. + OES	2,7,11,75,93,94
Ir, Pt	32	(a) HF or H ₂ SO ₄ (b) NaOH or Na ₂ O ₂	Ir, Pt soln. Ir, Pt, pptc.	plus oxidant plus reductant	PES PES	20,31 20,31
Ir, Pt	49	(a) n.a. (b) <i>aqua regia</i> (c) chlorination (d) Zn-fusion HCl dissoln.	n.a. Ir < 5% heat with pressure IrCl ₃ insol. insol. <i>aqua regia</i> dissoln.	n.a. bromate hydrol.	XRF Pt grav. Ir PES grav. Pt grav. Ir PES	71,73 44-46 20 7 44-46 20
Ir	56	chlorination	IrCl ₃ insol.	NiCl ₂ sol.	grav.	7
Ir	62	see Pd, Pt Rh, Ru Ir(Ag, Au)				
Ir, Pt, Pd	66	Cu ₂ S, NiS collection	HBr or HCl dissolution	acid-insol., expel RuO ₄ with HClO ₄	PES	18-21
Pt	4, 5, 6	see 4, 5, 6 Pd, Pt				
Pt	8	n.a.	n.a.	n.a.	SSMS	91,92
Pt	9, 10	n.a.	n.a.	n.a.	OES	75,93,94
Pt	11	n.a.	n.a.	n.a.	OES by diff.	
Pt	17	convert into metal	n.a.	n.a.	grav. + OES	2,7,75,93,94
Pt	18, 23, pure Pt < 100 mg	n.a.	n.a.	(a) n.a. (b) NH ₄ Cl or N ₂ H ₄ , HCl pptn.	AAS, PES	11,20 2,7,41
Pt	18, 23, impure Pt > 100 mg	n.a.	n.a.	pptn.	grav.	2,7,41
Pt	18, 23, pure Pt > 100 mg	see 18, 23 pure				
Pt	18, 23, impure Pt > 100 mg	see 18, 23 pure				
Pt	24, 25	H ₂ SO ₄ -H ₃ PO ₄	pptn. of Pt	use H ₂ S, HCOOH or Na ₂ S ₂ O ₃	spectrophot. or AAS, PES	22,23 11,20
Pt, Pd	26	see Pt, 24, 25	separation of Pt and Pd	DMG-CHCl ₃ extraction	Pt spectrophot. Pd AAS, PES	22,23 11,20

Pt, Rh	27	H ₂ SO ₄ -H ₃ PO ₄	treatment of insol. by fire-assay Au collection	oxalic acid pptn. of Au Pt, Pd recovery in filtrate	Pt spectroph. Rh AAS, PES	22,3 11,20
Pt, Pd, Rh	28	see 27, above	see 27	see 27, also DMG-CHCl ₃ extraction	Pt spectroph. Pd, Rh AAS, PES	22,23 11,20
Pt, Pd	29	see 26, above				
Pt, Rh	30	see 27, above				
Pt, Pd, Rh	31	see 28, above				
Pt	33	ignite, dissolve in <i>aqua regia</i>	recover residue Pt fire-assay	n.a.	(a) <50 mg phot. (b) >50 mg grav.	22,23 2,7,11,50
Pt	35	see 35, Pd			(a) <100 mg PES (b) >100 mg grav. AAS, PES	11 2,7,11,50 11,20
Pt	41, 42	see 41, 42, Pd	see 41, 42, Pd	see 41, 42, Pd	AAS, PES	11,18-21
Pt, Pd, Rh (Ag, Au)	43	Pb, NiS or Cu ₂ S collect.	collector removal	HCl, HBr or HClO ₄ treat.	AAS, PES	
Pt	45	see 45, Ru, Pd Pt(Ag, Au)				
Pt	47	see 47, Pd, Pt Ag, Au				
Pt	48	see 48, Rh, Pt				
Pt, Pd, Rh, Ir Ru(Au, Ag)	51	<i>aqua regia</i> (a) (b)	sep. & Pt from others n.a.	bromate hydrol. n.a.	Pt grav. others, PES others, PES	2,7,11,44-46 20 20
Pt	52	see 52, Pd, Pt Ru(Ag)				
Pt	53	see 53, Pd, Pt (Ag, Au)				
Pt	54	<i>aqua regia</i>	pptn. of Pt	use HCOOH	grav.	2,7,11,50
Pt	55	see preceding entry				
Pt, Pd, Rh	57	(a) Cu ₂ S, NiS (b) <i>aqua regia</i>	insol. insol.	fuse insol. fuse insol.	Pt, Pd, grav. Rh, PES, AAS	2,7,11,50 11,20
Pt	58	see 58, Rh, Pt, Pd				
Pt	59	see 59, Pd, Pt(Ag)				

continued

Table 2—continued

Element(s) determined	Material code (see Table 1)	Decomposition with	Separation required from	Type of separation	Final determination	References
Pt	60	see 60, Pd, Pt(Ag, Au)				
Pt	61	see 61, Pd, Pt (Ag, Au)				
Pt	62	see 62, Pd, Pt, Ir Rh, Ru,(Ag, Au)				
Pt, Pd, Rh	63	(a) Cu, S, NiS (b) Pb-button	dissolve acid-insol.		Pt grav. Pd, Rh PES, AAS	2,7,11 18-21
Pt	64	see 64, Pd, Pt Ru, Rh				
Pt	65	see 65, Rh, Pt, Pd				
Pt	66	see 66, Pd, Pt, Ir				
Pt	67	see 67, Pd, Pt(Ag, Au)				
Pt	1	see 1, Rh, Ir, Pd(Au) use <i>aqua regia</i> solution			grav.	2,7,11,50

REFERENCES

1. C. O. Ingamells, *General Sampling Theory*, paper presented at IPMI Conference on Precious Metals, Morristown, N.J., 1978, and San Francisco, Cal., 1980.
2. F. E. Beamish, *The Analytical Chemistry of the Noble Metals*. Pergamon Press, Oxford, 1960.
3. G. F. Williams, *Sampling—Poor Relation*, paper presented at IPMI, New England Chapter Meeting, Newport, I.E., 1984.
4. P. M. Gy, *Sampling of Particulate Materials—Theory and Practice*, Elsevier, Amsterdam, 1979.
5. Gesellschaft Deutscher Metallheuten und Bergleute, *Analyse der Metalle*, Vol. 3. Springer, Berlin, 1975.
6. E. A. Smith, *The Sampling and Assay of the Precious Metals*, 2nd Ed. Griffin, London, 1947.
7. T. J. Walsh and E. A. Hausman, in *Treatise on Analytical Chemistry*, I. M. Kolthoff and P. J. Elving, (eds.) Part II, Vol. 8, 379. Wiley, New York, 1963.
8. J. Sarins, *Sampling of Unusual Precious Metal Bearing Materials*, paper presented at 10th annual IPMI meeting, Lake Tahoe, Nev., 1986.
9. E. E. Bugbee, *A Textbook of Fire Assaying*. Wiley, New York, 1957.
10. A. McGuire, *Classical Fire Assaying*, paper presented at 1st IPMI Seminar on Sampling and Assaying, Morristown, N.J., 1978.
11. F. E. Beamish and J. C. van Loon, *Analysis of Noble Metals*. Academic Press, New York, 1977.
12. G. H. Faye and W. R. Inman, *Anal. Chem.*, 1961, **33**, 278.
13. J. Whitney, *X-Ray Fluorescence Analyses of Precious Metal Concentrates Melted With Tin*, paper presented at Eastern Analytical Symposium, New York, 1982.
14. R. de Nève, *Analysis of Precious Metals Combining Classical Collection Procedures With Modern Instrumentation*, paper presented at 10th annual IPMI meeting, Lake Tahoe, Nev., 1986.
15. L. M. Banbury and F. E. Beamish, *Z. Anal. Chem.*, 1965, **211**, 178.
16. K. C. Agrawal and F. E. Beamish, *ibid.*, 1965, **211**, 265.
17. L. M. Banbury and F. E. Beamish, *ibid.*, 1966, **218**, 263.
18. R. V. D. Robert, E. van Wyk and R. Palmer, *Natl. Inst. Met. Rep. S. Afr. Rept.*, No. 1371, 1971.
19. M. M. Kruger and E. van Wyk, *ibid.*, No. 1432, 1972.
20. S. Kallmann and C. Maul, *Talanta*, 1983, **20**, 21.
21. S. Kallman, *ibid.*, 1986, **33**, 75.
22. *Idem*, *ibid.*, 1976, **23**, 579.
23. S. Kallmann and P. Blumberg, *ibid.*, 1980, **27**, 827.
24. R. J. Van Duyn and E. J. Gapper, *Interlaboratory Assessment Study*, AC Spark Plug Division of General Motors, Part I, 1976, Part II, 1977.
25. N. M. Potter, *Anal. Chem.*, 1976, **48**, 531.
26. P. Palmer and G. Streichert, *Natl. Inst. Techn., Rep. S. Afr. Rept.*, No. 8, 1971.
27. J. Sarins, *Spent Auto Catalysts, Sample Preparation and Analysis*, paper presented at the IPMI New England Chapter Meeting, Newport, R.I., 1984.
28. S. Kallmann, *Sampling and Analysis of Automotive Catalysts*, paper presented at the Platinum Symposium of IPMI, Washington, D.C., 1985.
29. A. Davies, *The Analysis of Precious Metal Bearing Catalysts*, paper presented at the 10th annual IPMI meeting, Lake Tahoe, Nev., 1986.
30. D. Hunt, *An Investigation into the Collection of Noble Metals By Fire Assay With Particular Reference to the Texas Gulf Project*, paper presented at the 10th annual meeting of IPMI, Lake Tahoe, Nev., 1986.
31. S. Kallmann, Ledoux & Co, unpublished laboratory notes.
32. M. M. Schnepfe and F. S. Grimaldi, *Talanta*, 1969, **16**, 591.
33. *Idem*, *ibid.*, 1969, **16**, 1641.
34. E. W. Wichers, W. G. Schlecht and C. L. Gordon, *J. Res. Natl. Bur. Stds.*, 1944, **33**, 451.
35. A. Diamantatos, *Analyst*, 1986, **111**, 213.
36. *Annual Book of ASTM Standards*, Part 42, E 400, 351, 1982.
37. J. G. Fraser, F. E. Beamish and W. A. E. McBride, *Anal. Chem.*, 1954, **26**, 495.
38. C. H. S. W. Weinert and F. W. E. Strelow, paper presented at 2nd International Symposium on the Analytical Chemistry in the Exploration, Mining and Processing of Materials, Pretoria, 1985.
39. H. Freiser, *Solvent Extraction of Metal Chelates*, paper presented at IPMI meeting, San Francisco, Cal., 1980.
40. S. T. Payne, *Analyst*, 1960, **85**, 698.
41. W. R. Schoeller and A. R. Powell, *The Analysis of Minerals and Ores of the Rarer Elements*, 3rd Ed. Griffin, London, 1955.
42. R. Gilchrist, *J. Res. Natl. Bur. Stds.*, 1938, **20**, 745.
43. R. C. Mallet, E. J. Ring, H. R. Middleton, M. Dubois and T. W. Steele, *Natl. Inst. Techn., Rep. S. Afr. Rept.*, No. 17, 1973.
44. Gesellschaft Deutscher Metallhuetten und Bergleute, *Edelmetall-Analyse*. Springer, Berlin, 1964.
45. R. Gilchrist, *J. Res. Natl. Bur. Stds.*, 1932, **9**, 547.
46. R. Gilchrist and E. Wichers, *J. Am. Chem. Soc.*, 1935, **57**, 2565.
47. A. D. Westland and F. E. Beamish, *Anal. Chem.*, 1954, **26**, 739.
48. T. J. Walsh and F. A. Meier, Engelhard Industries, unpublished work, 1930.
49. G. G. Tertipis and F. E. Beamish, *Anal. Chem.*, 1980, **32**, 486.
50. F. E. Beamish and J. C. van Loon, *Recent Advances in the Analytical Chemistry of the Noble Metals*. Pergamon Press, Oxford, 1972.
51. G. H. Ayres, *Anal. Chem.*, 1953, **25**, 1626.
52. G. H. Ayres and A. S. Meyer, Jr., *ibid.*, 1951, **23**, 299.
53. S. Kallmann, *Talanta*, 1976, **23**, 579.
54. A. Timmegowda, H. Sankegowda and N. M. M. Gowda, *Anal. Chem.*, 1984, **56**, 358.
55. L. D. Johnson and G. H. Ayres, *ibid.*, 1966, **38**, 1218.
56. Meffert, Degussa, Work Rhein Felden, private communication, 1986, 11/86.
57. L. Duparc, *Compt. Rend. Soc. Phys. Hist. Nat.*, 1912, **29**, 20.
58. W. Schmidt, *Z. Anorg. Chem.*, 1913, **80**, 335.
59. F. E. Beamish and J. Dale, *Ind. Eng. Chem., Anal. Ed.*, 1938, **10**, 697.
60. R. Kaltenbach, Engelhard Corp., private communication, 1986.
61. Chang Yun Po and Zhou Nan, *Talanta* 1986, **33**, 939.
62. G. H. Ayres, B. L. Tuffly and J. S. Forester, *Anal. Chem.*, 1955, **27**, 1742.
63. S. S. Berman and R. Ironside, *Can. J. Chem.*, 1958, **36**, 1151.
64. G. H. Ayres and Q. Quick, *Anal. Chem.*, 1950, **22**, 1403.
65. H. Robinson, Engelhard Industries, Assay Laboratory, Newark, New Jersey, unpublished work, 1945.
66. G. H. Ayres and F. Young, *Anal. Chem.*, 1950, **22**, 1277.
67. L. Tschugaeff, *Compt. Rend.*, 1918, **167**, 235.
68. A. Walsh, *Spectrochim. Acta*, 1955, **7**, 108.
69. L. S. Birks, *X-Ray Spectrochemical Analysis*, 2nd Ed. Interscience, New York, 1969.
70. R. Jenkins, *An Introduction to X-Ray Spectrometry*, Heyden, New York, 1976.
71. K. Heim, Johnson Matthey, private communication, 1983.
72. J. Whitney, *X-Ray Fluorimetric Spectrometry—Some Precious Metals Applications*, paper presented at the Analytical Seminar of the New England Chapter of IPMI, Newport, Rhode Island, 1984.
73. H. M. Lueschow, Degussa, Wolfgang, West Germany, private communication, 1985.

74. P. R. Oumo and E. Nieboer, *Analyst*, 1979, **104**, 1037.
75. C. L. Lewis, in reference 2, p. 487ff.
76. U. Fehn, R. Teng, D. Elmore and P. W. Kubik, *Isotopic Composition of Osmium in Terrestrial Samples Determined By Accelerator Mass Spectrometry, University of Rochester Report*, UR-NSRL-304, 1986.
77. Perkin Elmer, *Analytical Methods for Atomic Absorption Spectrometry*, Revised Ed., 1982.
78. S. Kallmann and E. W. Hobart, *Anal. Chim. Acta*, 1970, **51**, 120.
79. D. J. Nicholas, *The Rapid Separation and Analysis of the Primary Platinum Group Elements, Gold and Silver*, paper presented at the 2nd International Symposium on Analytical Chemistry in the Exploration, Mining and Processing of Materials, Pretoria, S.A., 1985.
80. T. J. Hanson and R. D. Ediger, *Am. Lab.*, 1980, **12**, No. 3, 116.
81. Beckman, *Atomic Spectroscopy By Plasma Emission, Techn. Bulletin T-1630-AS-8533*.
82. J. Skwarto, A. Savolainen, G. Olear, B. Marvelle and H. Griffin, *Multielement Analysis of Fire Assay Collection Beads By Multichannel DCP Spectrometer*, paper presented at the seminar of the New England Chapter of IPMI, Newport, Rhode Island, 1984.
83. R. Brown, V. Luciano and D. Leighty, *Analysis of Precious Metals Using Inductively Coupled Plasma (ICP) Spectroscopy*, paper presented at the seminar of the New England Chapter of IPMI, Newport, Rhode Island, 1984.
84. A. Kettrup and M. Grothe, *Applications of Multi-element DCP Emission Spectrometry to the Investigation of Ion-Exchangers with High Affinity for Noble Metals*, paper presented at the 2nd International Symposium on Analytical Chemistry in the Exploration, Mining and Processing of Materials, Pretoria, South Africa, 1985.
85. R. S. Houk, *Plasma Ionization Techniques for Elemental Analysis By Mass Spectrometry*, paper presented at the 2nd International Symposium on Analytical Chemistry in the Exploration, Mining and Processing of Materials, Pretoria, South Africa, 1985.
86. R. Lancione, *Precious Metal Analysis by Inductively Coupled Plasma-Atomic Fluorescence Spectrometry*, paper presented at the Eastern Analytical Symposium, New York, 1983.
87. A. Egan, Atomic Energy of Canada Limited, private communication, 1986.
88. J. E. Harrar and M. C. Waggoner, *Pap. Surf. Finish.*, 1981, **68**, 41.
89. S. Heberlin, paper presented at the IPMI Western Regional Analytical Symposium, San Jose, Cal., 1987.
90. S. Kallmann, *Interdependence of Instrumental and Classical Chemical Methods of Analysis of Precious Metals*, paper presented at the Eastern Analytical Symposium, New York, 1983.
91. A. J. Ahearn, *Mass Spectrometric Analysis of Solids*. Elsevier, Amsterdam, 1966.
92. J. Franzen and K. D. Schuy, *Z. Anal. Chem.*, 1967, **225**, 295.
93. ASTM Committee E-2, *Methods for Emission Spectrographic Analysis*, 7th Ed., 1982.
94. A. J. Lincoln and J. C. Kohler, *Anal. Chem.*, 1962, **34**, 1247.

A NEW TYPE OF ZEEMAN-EFFECT ATOMIC-ABSORPTION SPECTROPHOTOMETER

JING SHI-LIAN*, LI SHAO-YUAN, WANG RONG-RONG, MA YI-ZAI, YU CHU-MING, YAN YAN,
ZHANG DONG-HUA, SUN JINA and ZHANG ZHONG-MING
Technology Laboratory, Institute of Environmental Chemistry, Academia Sinica, Beijing,
People's Republic of China

(Received 6 February 1985. Revised 9 March 1987. Accepted 3 April 1987)

Summary—A new type of Zeeman-effect atomic-absorption spectrophotometer has been developed. It uses fast heating of a special atomizer made from a pyro-coated graphite tube lined with tungsten-tantalum alloy, for easier determination of refractory and rare-earth elements. A boxcar integrator is used, and the atomic absorption, background absorption and atomization temperature can be recorded. By means of the Zeeman effect, the instrument can correct for background absorbance up to 2.0.

Zeeman-effect atomic-absorption spectrophotometers (ZAAS) can simultaneously correct for background absorption and change in the light-intensity from the hollow-cathode lamp. Hence they bring the high sensitivity of the graphite furnace technique into full play, and make the results accurate and reliable. Much attention has therefore been paid to instruments of this kind, which may be regarded as the third generation of atomic-absorption spectrophotometers.¹

Our first Zeeman-effect model, the ZM-I,² had much the same specifications as the Zeeman-effect instruments made abroad. On the basis of our experience with the ZM-I and investigation of the advantages and weaknesses of various Zeeman-effect models,³ a new model—the ZM-II—has been developed.

The ZM-II is designed to use the model QR-1 graphite-furnace power-supply made in this laboratory, which can raise the temperature of the graphite furnace at a rate of up to 6000°/sec. It is also equipped with a new version of the graphite furnace, the graphite tube being lined with tungsten-tantalum alloy. The sensitivity and reproducibility thus obtained for determining refractory and rare-earth elements are superior to those of the ZM-I.

Operating principle

The general operational principle of the ZM-II is shown in Fig. 1, as a block diagram.

When the instrument works in the Zeeman mode, the power supply to the deuterium lamp is disconnected from the circuit, and the signal which would

otherwise be provided to the deuterium lamp is connected to the power supply of the hollow-cathode lamp by means of the summing amplifier. The hollow-cathode lamp (HCL) then emits light under rigorous control by the rotating artificial-quartz Rochon prism, *i.e.*, when the polarization plane of the Rochon prism is parallel with or perpendicular to the applied magnetic field, the lamp source emits pulsed light beams P_{\parallel} or P_{\perp} , respectively. Thus these two kinds of light beam, P_{\parallel} and P_{\perp} , have exactly the same wavelength but different planes of polarization. They pass alternately through the graphite furnace, which is placed between the poles of a 9-kG magnet. During atomization, these two light beams are modulated by the Zeeman effect, with the modulation related to the concentration of the analyte in the graphite-furnace atomization cell. The beam P_{\parallel} can be absorbed by both the background and the atomic vapour of the sample, but the beam P_{\perp} is absorbed only by the background. Therefore, electronic subtraction of the one signal from the other produces the net atomic absorption of the sample.⁴ After Zeeman modulation, these two light beams P_{\parallel} and P_{\perp} pass through the monochromator, which selects the analyte resonance line and removes the stray light. The photomultiplier converts the light received through the monochromator slit into an electronic signal. After processing of this signal by the electronic circuit, the atomic-absorption and background absorption are recorded.

Optical system of the ZM-II ZAAS

The optical system of the ZM-II ZAAS is shown in Fig. 2. Figure 2a shows the optical system for the deuterium-lamp correction mode. When the instrument operates in the Zeeman mode (Fig. 2b), the Rochon prism together with lenses L_1 and L_2 replaces

*Author for correspondence. Current address: Research Center for Eco-Environmental Sciences, Academia Sinica, P.O. Box 934, Beijing, China.

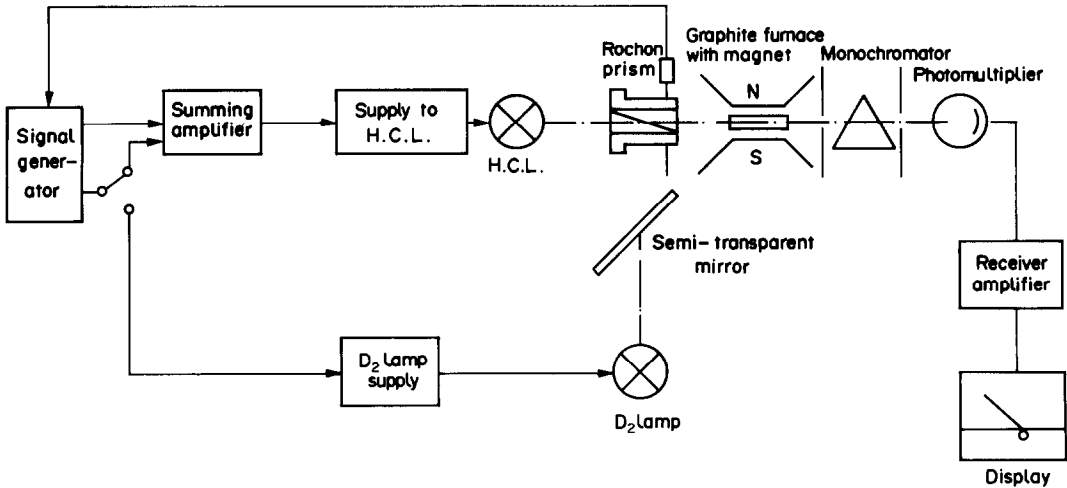


Fig. 1. Block diagram of spectrometer.

the semi-transparent mirror M_1 and lens L_2 , and the graphite furnace takes the place of the burner, with the same optical axis as the burner, as shown in Fig. 2b. The optical aperture is 16.8 mm, the angle of acceptance 3.5° and the transmission efficiency 13.9% at 250 nm.

Electronic circuit of the ZM-II ZAAS

A schematic diagram of the electronic circuit of the ZM-II ZAAS is shown in Fig. 3. Briefly, it consists of two parts, the lamp supply and the receiver-amplifier.

The lamp supply consists of the Zeeman signal

generator, multivibrator, signal generator for modulation and demodulation, summing amplifier, hollow-cathode lamp supply and deuterium lamp supply.

The circuit of the hollow-cathode lamp supply plays two roles. One is to make the lamp emit light only according to the position of the rotating Rochon prism, and the other is to produce the demodulation signal and correction signal. The demodulation signal is used to demodulate the atomic-absorption signal plus the background signal, as well as the background signal only. The correction signal serves to guarantee outstanding background-correction capability.

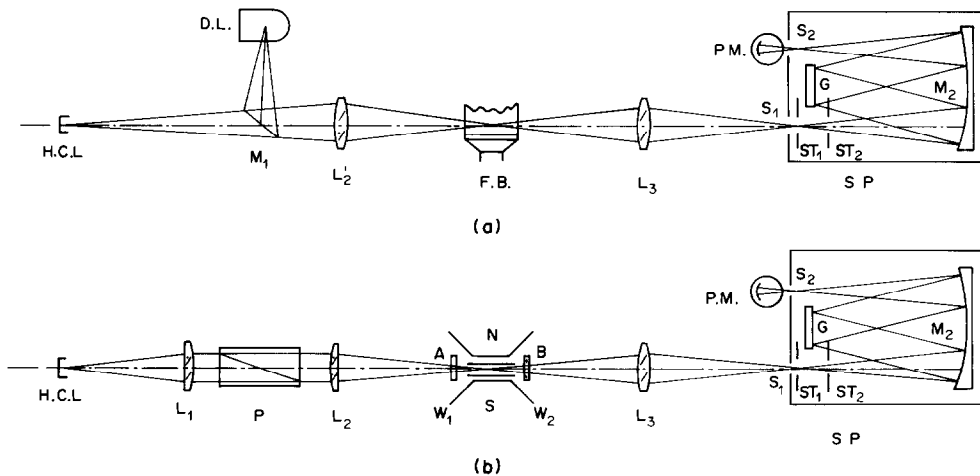


Fig. 2. The optical layout of the ZM-II ZAAS:

H.C.L.	hollow-cathode lamp	S_1, S_2	slits
L_1	collimating lens	G	grating
L_2	convergent lens	M_1	semi-transparent mirror
P	Rochon prism	M_2	collimating/convergent mirror
AB	graphite tube	P.M.	photomultiplier
W_1, W_2	quartz window	ST_1, ST_2	diaphragms
L_3	convergent lens	D.L.	deuterium lamp
SP	monochromator	F.B.	burner

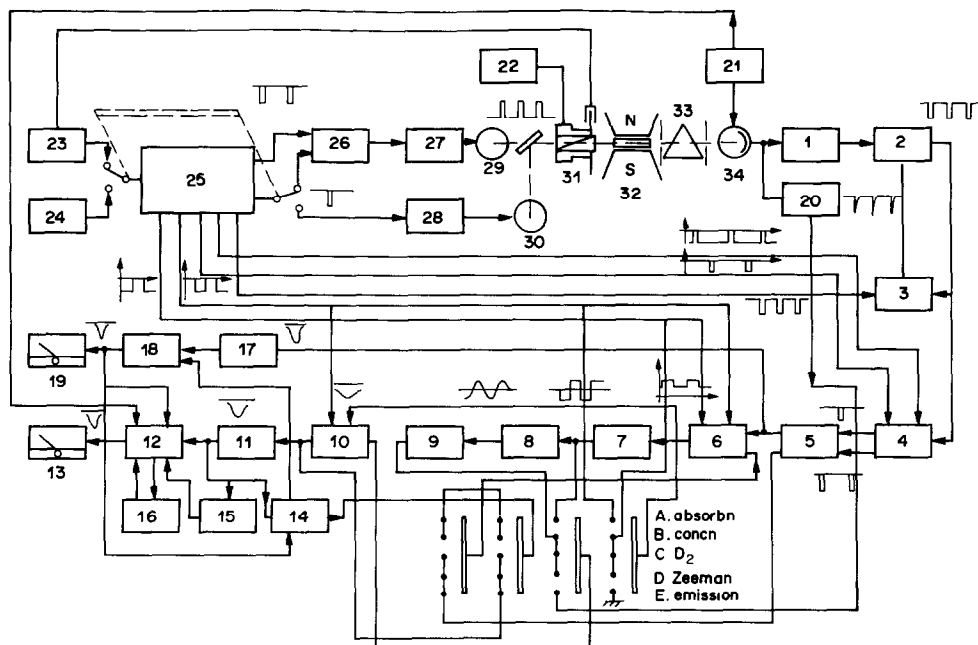


Fig. 3. The electronic circuit diagram of the ZM-II ZAAS:

- | | |
|-------------------------|--------------------------------|
| 1 pre-amplifier | 16 peak-holder |
| 2 main amplifier | 17 logarithmic amplifier |
| 3 feedback corrector | 18 BKG output |
| 4 demodulator | 19 BKG display |
| 5 response | 20 emission amplifier |
| 6 connecting circuit | 21 H.V. supply |
| 7 logarithmic amplifier | 22 power supply of motor |
| 8 band-pass filter | 23 Zeeman signal generator |
| 9 expander | 24 multivibrator |
| 10 synchronous detector | 25 modulation signal generator |
| 11 output stage | 26 summing amplifier |
| 12 selector of output | 27 E.L. supply |
| 13 absorption display | 28 deuterium lamp supply |
| 14 automatic resetter | 29 element lamp |
| 15 integrator | |

The receiver-amplifier unit consists of pre-amplifier, main amplifier, feedback corrector, demodulator, response circuit, connecting circuit, logarithmic amplifier, band-pass filter, expander, synchronous detector, output stage of the background signal and output-mode selector.

First, the photomultiplier signal is amplified by the pre-amplifier and main amplifier. Then the demodulator detects the electric signal corresponding to the light-intensity of beams P_{\parallel} and P_{\perp} , representing atomic-absorption plus background absorption, and background absorption only, respectively. The response circuit has a suitable time-constant and smooths the signal. The connecting circuit then uses these two kinds of signal to form a new signal which alternately represents light-beams P_{\parallel} and P_{\perp} . Finally, the signal passes through the logarithmic amplifier, band-pass filter, expander, synchronous detector and output stage. The feedback corrector is used to keep the output of the main amplifier at zero, when no light-beam is arriving at the photomultiplier, and therefore can correct the dark-current of the photo-

multiplier, and reduce the disturbance produced by radiation from the furnace and background absorption. The band-pass filter is used to alleviate any disturbance produced by radiation from the graphite furnace during atomization, as well as the background absorption. The background signal comes from P_{\perp} , and passes through a logarithmic amplifier to the background output stage.

RESULTS AND DISCUSSION

To test and check the characteristics of the model ZM-II atomic-absorption spectrophotometer, the major parameters, such as noise, linearity, background-correction accuracy and sensitivity, were determined with As, Cd, Pb, Cu, V, Y and Ba.

A special pyrolytically-coated graphite tube (WTaPT) lined with tungsten-tantalum alloy is used, which makes it easy to determine refractory and rare-earth metals with the ZM-II AAS. The WTaPT tube consists of a pyrolytically-coated graphite tube

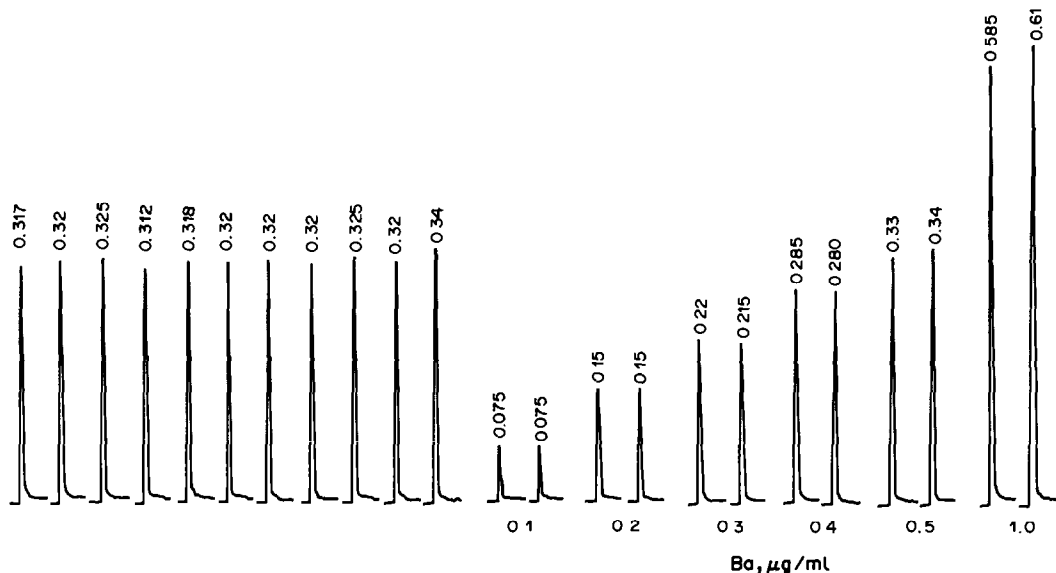


Fig. 4. The determination of 0.5 $\mu\text{g/ml}$ Ba at 553.5 nm (10- μl sample, H.V. 300 V, lamp current 10 mA, slit 0.5 mm, heating rate 3000 $^\circ\text{/sec}$, dry for 20 sec at 20 A, ash for 15 sec at 42 A, atomize for 8 sec at 440/190 A, response 0.01 sec).

with a small tungsten-tantalum cylinder inside it. The useful lifetime of the WTaPT is fairly long; it can be used for at least 100 yttrium determinations, with an argon flow-rate of 1.5 l./min. Repetitive determinations of 0.5 ppm yttrium had a relative standard deviation of 2.4%, and no memory effects were observed, which is important since it is well known

that one of the difficulties in determination of refractory and rare-earth elements is the memory effect due to reaction with the graphite tube to form metallic carbides, resulting in tailing of the atomic-absorption signal, so the atomization time needed is rather long, and the atomization temperature rather high. Generally speaking, the random variation for deter-

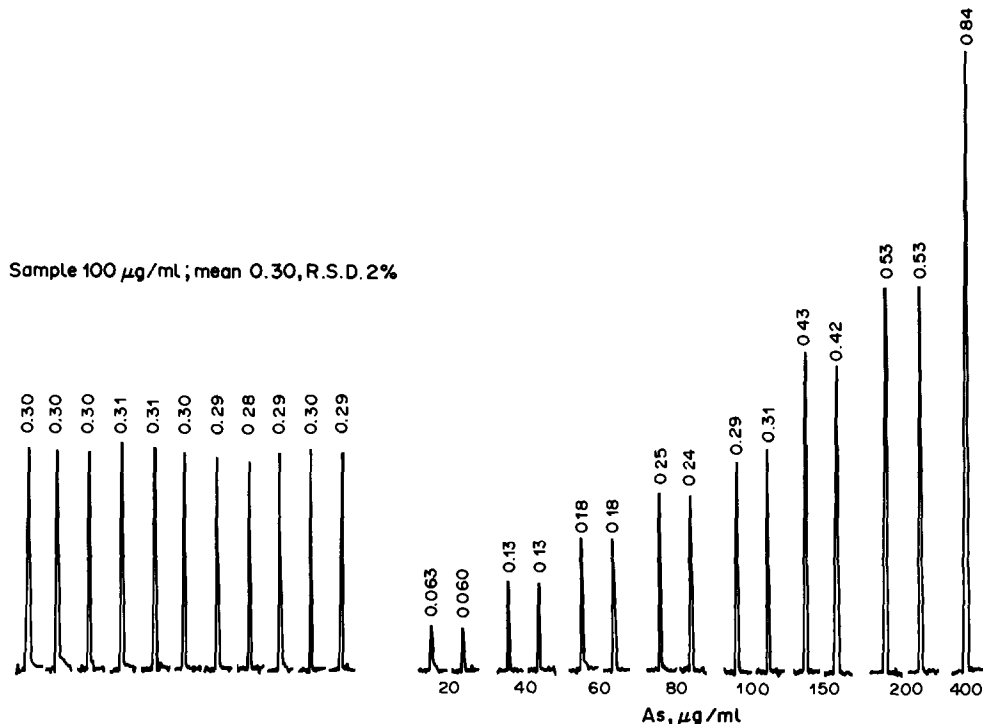


Fig. 5. Determination of 100 ng/ml As at 189.0 nm (10- μl sample, H.V. 610 V, lamp current 6 mA, slit 0.5 mm, heating rate 1400 $^\circ\text{/sec}$, dry for 20 sec at 22 A, ash for 15 sec at 42 A, atomize for 5 sec at 420/150 A, response 0.01 sec).

Table 1. Results for several elements

Wavelength, nm	Characteristic mass,* pg	Maximum absorbance	Noise	R.S.D.,†%	Concn., ng/ml	Volume, μl
As 189.0	11	1.2		2.9	50	5
As 193.7	15	0.95		1.8	50	10
Cd 228.8	0.75	0.72		2.5	1	10
Pb 283.3	16	0.87				
Cu§ 324.7			0.0006			
V‡ 314.8	12	1.2				
Y 410.2	250	2.0		4.6	500	5
Rb 780.0	3.9	1.3		1.9	20	10

*For 0.0044 absorbance.

†For 11 replicates.

‡Determined by means of WTaPGT; the other elements by conventional pyro-coated graphic tube.

§Wavelength = 324.7 nm, spectral bandwidth 1.0 nm, lamp current 7.5 mA.

Table 2. Background correction for Cd 228.8 nm line in presence of various amounts of NaCl

NaCl, μg	Background absorbance	Correction to Cd line absorbance
9	1.4	0.005
12	1.8	0.005
15	2.1	0.011

mination of rare-earth elements by other ZAAS methods ranges from 5 to 10%, whereas it is reduced to 3–6% with the ZM-II instrument. The corresponding results for determination of yttrium with our model ZM-I instrument displayed a pronounced memory-effect, requiring the graphite furnace to be reheated once or twice after each determination in order to clear the residual yttrium out of the furnace. Furthermore, after preparation of a calibration curve, the graphite furnace in the ZM-I model could not be used to analyse samples, because the useful life of the furnace was already over. Even when the furnace had not been damaged by making the calibration curve, lower concentrations of the analyte in

samples could not be determined, owing to the serious memory effect. Figures 4 and 5 show the performance for barium and arsenic respectively.

The other characteristics such as noise, sensitivity, range of linearity, reproducibility, are listed in Table 1 and the background-correction accuracy is shown in Table 2.

In conclusion, from the results obtained and the discussion above, it is evident that the ZM-II ZAAS has distinct advantages for the determination of refractory and rare-earth elements and gives as good a performance as that of commercially available ZAAS instruments.

REFERENCES

1. M. T. C. de Loos-Vallebereg and L. de Galan, *Spectrochim. Acta*, 1978, **33B**, 495.
2. Institute of Environmental Chemistry, *Yuanzhi Guangpu Fenxi (Atomic Spectroscopy)*, 1981, **1**, No. 2, 34.
3. Jing Shi-lian, Wang Rong-rong, Yu Chu-ming, Yan Yan and Ma Yi-zai, *Huanjing Kexue (J. Environmental Science)*, 1984, **5**, No. 3, 41.
4. H. Koizumi and K. Yasuda, *Spectrochim. Acta*, 1976, **31B**, 523.

AN ELECTROCHEMICAL STRIPPING METHOD FOR THE SELECTIVE DETERMINATION OF TRACES OF SILVER

RUDOLF PŘIBIL*

Institute of the Physics of the Atmosphere, Czechoslovak Academy of Sciences, Boční II,
141 31 Prague 4, Czechoslovakia

MADELEINE ŠTULÍKOVÁ

Lečkova 1521, 149 00 Prague 4, Czechoslovakia

(Received 7 January 1987. Accepted 23 February 1987)

Summary—A method has been developed for the determination of traces of silver in the presence of large concentrations of interfering metals, particularly copper, involving reduction of the silver on a glassy-carbon electrode modified by an adsorbed layer of previously deposited hydrogen.

Previous attempts to determine silver by electrochemical stripping in the presence of copper have been hampered by the closeness of the deposition potentials of these two metals¹ and primarily by the fact that intermetallic compounds are formed on the electrode surface, so that even at very low concentrations multiple peaks are formed and the copper peak begins to coalesce with the silver peak.¹ Attempts to solve this problem have included the use of a.c. techniques,^{2,3} precise control of the electrolysis potential⁴ and the use of various base electrolytes, notably ammoniacal solutions,^{1,5} as well as the addition of complexing agents such as EDTA and related compounds^{5,6} to the base electrolyte and the use of a platinum ring-disk electrode.⁷ Even in the absence of copper, the determination of trace amounts of silver in complex matrices such as ores, metallurgical concentrates and similar samples requires preliminary separation of silver.⁷ Nonetheless, completely satisfactory results have not been obtained with any of these techniques, especially in the presence of a large excess of copper. This paper describes a procedure based on the observation that the deposition potential of silver at a glassy carbon electrode is shifted to more positive potentials if the deposition step is preceded by polarization of the electrode at the potential of hydrogen evolution. This phenomenon has been observed for platinum (and platinum black) electrodes in studies primarily concerned with hydrogen deposition and adsorption phenomena.^{8,9} However, so far, only limited analytical use seems to have been made of this process at platinum electrodes¹⁰ and no study of this phenomenon at glassy-carbon electrodes has been described.

EXPERIMENTAL

Apparatus

All the voltamperograms were recorded on an OH 104 polarograph (Radelkis, Hungary) with a three-electrode system. A rotating glassy-carbon disk electrode, consisting of a glassy-carbon rod 5 mm in diameter (G.C. 20, Tokay Electrode Manufacturing Co., Japan), pressure-fitted in a Teflon holder, was employed as the working electrode. This electrode was polished with metallographic paper to a mirror-like finish. The rotation rates used were 960 and 2100 rpm (the latter for very low concentrations). A saturated calomel reference electrode, connected with the solution by a salt bridge filled with 3M ammonium nitrate, and a platinum wire auxiliary electrode were used in a conventional electrolysis cell that could hold 50–100 ml of solution. The solution was deaerated with nitrogen and protected from contact with air in the usual manner.

Reagents

All the chemicals used were of *p.a.* purity (Lachema, Czechoslovakia) and the ammonia solution was prepurified by isothermal distillation. Doubly distilled water from an all-silica apparatus was employed in the preparation of all solutions.

Procedure

At the beginning of each experimental day, the electrode was immersed in the base electrolyte and its potential commutated four times between -0.8 and $+1.6$ V (*vs.* SCE) at 30-sec intervals. Between individual measurements, the electrode surface was cleaned (pretreated) by electrolysis in the sample solution at a potential of $+1.6$ V for 30 sec. No mechanical treatment of the glassy-carbon electrode was used except for occasional wiping with fine filter paper.

Deposition and stripping

Anodic-stripping analysis with the unactivated electrode was performed in the usual manner. The solution was deaerated by a stream of nitrogen and the rotating electrode was set to a predetermined deposition potential for the required period of time. The deposit was then stripped by a linear anodic potential sweep starting from the deposition potential, with a scan-rate of 4.00 V/sec and continuous electrode rotation.

*To whom correspondence should be addressed. Current address: Analytical Laboratory, Institute of Geological Sciences, Charles University, Albertov 6, Prague 1, Czechoslovakia.

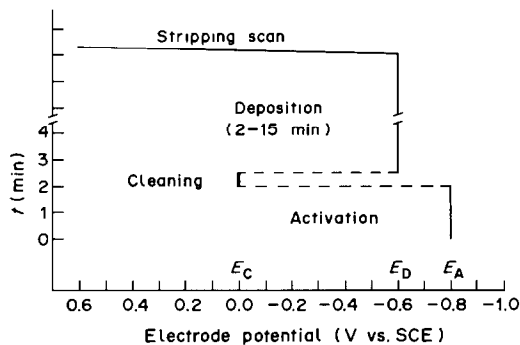


Fig. 1. Schematic depiction of the overall electrochemical procedure. E_A —activation potential, E_C —cleaning potential, E_D —deposition potential (2–15 min), electrode rotation rate 960 rpm.

The stripping analysis with the hydrogen-activated electrode was done as follows. After pretreatment, the electrode was maintained at an activation potential of -0.8 V for a 2-min period, during which hydrogen ions and certain other substances present in the solution were discharged. The electrode was then kept for 30 sec at a cleaning potential, E_C (usually 0.0 V), at which all the substances deposited, except hydrogen, were stripped from the electrode. This procedure yielded the hydrogen-activated electrode.

Silver was then deposited at a potential of -0.5 V for 2–15 min, depending on the silver concentration. The deposit was anodically stripped by a linear potential sweep, starting at the deposition potential, with a scan rate of 4.00 V/sec, with continuous electrode rotation. The overall electrochemical procedure is depicted schematically in Fig. 1.

RESULTS AND DISCUSSION

In general, the deposition potential of silver on both hydrogen-activated and unactivated electrodes in ammoniacal base electrolytes depends on the concentration of silver in the solution. The deposition potential at which the stripping peak is maximal shifts by approximately 50 mV towards more negative values for a decrease of one order of magnitude in the silver concentration.

The shift of the silver deposition potential towards more positive potentials as a result of previous deposition of hydrogen on a glassy-carbon electrode was observed to occur with various base electrolytes containing ammonium nitrate, in slightly acidic, neutral and alkaline solutions. However, an alkaline base electrolyte ($0.15M$ ammonium nitrate/ $0.75M$ ammonia) seemed to be the most favourable for removal of interference from copper and was used in subsequent experiments. Hydrogen activation of the electrode is complete after polarization of the electrode for 30 sec at -0.8 V in the sample solution containing the base electrolyte. Although the use of longer polarization times or more negative potentials seems to have no further effect in enhancing the electrode activity, a 2-min activation period was used in subsequent experiments. The difference between the deposition potentials on hydrogen-activated and unactivated

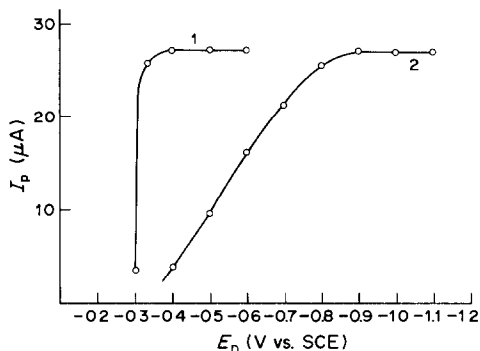


Fig. 2. Dependence of the silver stripping-peak height on the deposition potential at hydrogen-activated and unactivated electrodes. Base electrolyte $0.15M$ $NH_4NO_3/0.75M$ NH_3 , 1—Hydrogen-activated electrode, $E_A = -0.8$ V, $E_C = 0.0$ V; 2—unactivated electrode. $C_{Ag} = 5 \times 10^{-7}M$; electrode rotation rate 960 rpm.

rotating glassy-carbon electrodes in the base electrolyte is depicted in Fig. 2.

The first experiments were made in order to confirm that the presence of deposited hydrogen is essential for the shift in the silver deposition potential to more positive values. To this end, a pure silver solution in the base electrolyte was analysed and the electrode activation potential E_A was varied. It was found that if the value of E_A was more positive than the potential of hydrogen evolution, no electrode activation and therefore no shift in the silver deposition potential was observed. Similarly, an electrode activated at negative potentials (-0.8 V) loses its activity after polarization to sufficiently positive potentials, *i.e.*, the electrode activity decreases as the cleaning potential E_C is increased to more positive potentials. This dependence is depicted in Fig. 3. It is interesting to compare the shape of this dependence with that of the anodic wave recorded in the base electrolyte in the absence of depolarizer, also depicted

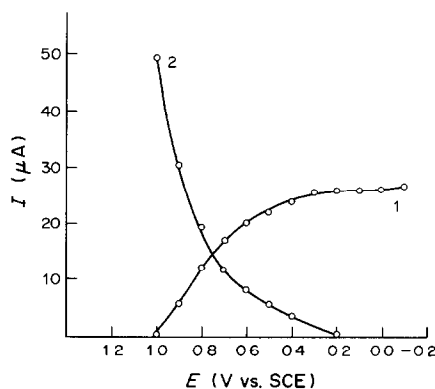


Fig. 3. 1—Dependence of the silver stripping-peak height on the value of E_C , and 2—the current–voltage relationship in the base electrolyte in the absence of depolarizer (hydrogen stripping). Base electrolyte $0.15M$ $NH_4NO_3/0.75M$ NH_3 , $C_{Ag} = 5 \times 10^{-7}M$ (curve 1), $t_D = 5$ min. Other conditions as for Fig. 2 (curve 1).

in Fig. 3, and attributed to the removal of hydrogen from the electrode surface.

At higher silver concentrations in solution (1–5 μM) the deposition of silver on the hydrogen-activated electrode proceeds even if the electrode is disconnected from the circuit. The stripping peak thus obtained is of the same height as that obtained by electro-deposition under the same conditions. This phenomenon can be accounted for by measurement of the electrode potential at equilibrium in the base electrolyte, which indicates that the electrode with deposited hydrogen assumes a sufficiently negative potential for quantitative deposition of silver if the latter is present in sufficiently high concentrations.

It follows from the discussion above that a species formed on the electrode, most probably hydrogen, is relatively firmly adsorbed on the electrode surface and takes part in the process of reduction and deposition of silver on the electrode. The silver stripping peaks obtained at the hydrogen-activated electrode are sharp and have very good reproducibility.

The observed shift in the silver deposition potential at a hydrogen-activated glassy-carbon electrode offers a means of removing interference from copper or large quantities of other more electronegative metals encountered in silver analysis.

Special attention was paid to copper, as the most common interfering metal in analysis for silver. The effect of copper was first studied by addition of increasing concentrations of copper to a pure silver solution in the base electrolyte. It was found that at $8 \times 10^{-7} M$ silver concentration, up to $10^{-4} M$ copper has very little influence on the silver peak. At very low

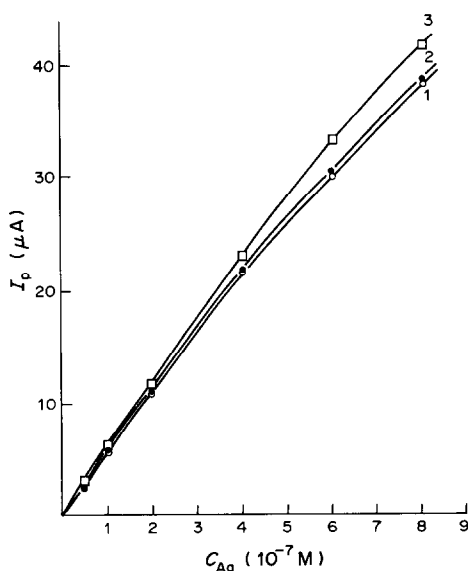


Fig. 4. Concentration dependence of the silver stripping-peak height in the presence and absence of copper. Base electrolyte $0.15M NH_4NO_3/0.75M NH_3$. $C_{Cu^{2+}}$: curve 1—0, curve 2— $10^{-5}M$, curve 3— $10^{-4}M$. Other conditions as for Fig. 3.

Table 1. The accuracy and precision of the ASV determination of silver with an activated glassy-carbon electrode in synthetic solutions containing copper, base electrolyte $0.15M NH_4NO_3/0.75M NH_3$, $E_A = -0.8 V$, (2 min), $E_C = 0.0 V$ (30 sec), $E_D = -0.5 V$, electrode rotation rate 960 rpm

C_{Ag} , $\mu g/ml$	C_{Cu} , $\mu g/ml$	t_D , min	C_{Ag} (found),* $\mu g/ml$	Standard deviation, $\mu g/ml$
5.39	63.5	10	5.43	0.03
	635 6345		5.47	0.04
10.79	63.5	10	10.83	0.06
	635		10.80	0.05
			11.28	0.08
53.9	63.5	5	54.1	0.6
	635		54.1	0.5
	6345		54.2	0.5
107.9	63.5	2	108.8	1.0 ₃
	635		109.8	1.2
	6354		110.1	1.3

*Averages of eight determinations.

silver concentrations, the effect of copper is somewhat greater (see Table 1). Nevertheless, no stripping peak of copper is observed and the shape of the silver peak is not distorted. The effect of relatively large amounts of copper on the concentration dependence of the silver stripping peak is depicted in Fig. 4. The dependence obtained for pure silver solutions is curved at higher silver concentrations but its general shape is not affected by the presence of copper. However, the presence of $1 \times 10^{-4} M$ copper causes a 10–15% increase in the height of the silver stripping peak. The reason for this interference is not quite clear, as copper in silver-free solutions under identical experimental conditions yields no stripping peak. It seems most probable that slight co-deposition of

Table 2. Comparison of the determination of silver in soil and sedimentary rock samples by AAS* and stripping at a hydrogen-activated electrode (samples ground, and extracted with nitric acid; stripping conditions as for Fig. 3)

Sample	Silver content found, ppm		
	Stripping	AAS ⁽¹⁾	AAS ⁽²⁾
1	0.23	0.21	0.18
2	0.57	0.56	0.63
3	1.10	0.93	1.05
4	1.35	1.36	1.41
5	1.53	1.52	1.49
6	1.59	1.62	1.66
7	2.41	2.35	3.16
8	3.16	3.24	3.05
9	4.63	4.57	5.02
10	6.83	6.90	6.69
11	7.61	7.63	8.05

*AAS analyses performed in the Analytical Laboratory of the Institute of Geological Sciences, Charles University, Prague (1) and the Analytical Laboratory of the Central Geological Institute in Prague (2).

copper occurs simultaneously with the deposition of silver on the electrode. This relatively small interference can be avoided in a solution containing higher silver concentrations ($\geq 10^{-7}M$) by using a more positive deposition potential, E_D , of -0.4 V instead of -0.5 V, which is the value generally used for all silver concentrations. It was demonstrated that a potential of -0.4 V is still sufficient for quantitative deposition of silver in this concentration range.

Table 1 gives the results for the determination of silver in synthetic solutions containing various amounts of copper and silver, with evaluation by means of a calibration curve.

The method has been applied to determination of silver in nine samples of sedimentary rocks and soil which were also analysed by flame atomic-absorption spectrometry. The results are shown in Table 2.

REFERENCES

1. U. Eisner and H. B. Mark, Jr., *J. Electroanal. Chem. Interfacial Electrochem.*, 1970, **24**, 345.
2. F. Vydra, M. Štulíková and P. Peták, *ibid.*, 1972, **40**, 99.
3. M. Štulíková and F. Vydra, *ibid.*, 1973, **42**, 127.
4. E. Ya. Neiman, G. M. Dolgoplova and L. M. Trukhacheva, *Zavodsk. Lab.*, 1971, **37**, 887.
5. F. Billand, M. F. Hutin, P. Bourret and D. Burneh, *Anal. Biol. Clin. (Paris)*, 1977, **35**, 51.
6. S. Rubel, E. Stryjewska and J. Colimovski, *Chem. Anal. (Warsaw)*, 1979, **24**, 247.
7. P. Peták and F. Vydra, *Anal. Chim. Acta*, 1973, **65**, 171.
8. S. H. Cadle and S. Bruckenstein, *Anal. Chem.*, 1971, **43**, 1858.
9. S. Szabo and F. Nagy, *J. Electroanal. Chem. Interfacial Electrochem.*, 1976, **70**, 357.
10. Z. Boguszewska, M. Krasiejko and B. Palmovska-Kus, *Talanta*, 1986, **33**, 155.

APPLICATION OF PERSONAL COMPUTERS IN THE ANALYTICAL LABORATORY—III ASV ANALYSIS

DRORA KAPLAN*

Department of Electrical and Computer Engineering, Ben-Gurion University of the Negev,
Beer Sheva, 84105, Israel

DAN RAPHAELI and SAM BEN-YAAKOV

Department of Electrical and Computer Engineering, Ben-Gurion University of the Negev, Beer Sheva,
84105, Israel

(Received 15 September 1986. Revised 8 February 1987. Accepted 21 February 1987)

Summary—Automatic operation and data-processing of ASV analysis is achieved by interfacing a general-purpose polarograph to a personal computer. The software package, written in SUPER BASIC, includes graphic routines that are used to display the voltamperograms and calibration curve, and as an interface with the operator. Data-processing can be done manually, interactively or automatically. In the last of these modes, peak position and height are evaluated by first correcting for baseline drift and then fitting the peaks to a Gaussian function. It is found that this procedure is relatively insensitive to noise. The system is used routinely in the analysis of treated domestic wastewater and soils irrigated by effluents. The flexibility of the programming and the feature of interactive work are important in this connection, which calls for careful examination of peaks distorted by matrix interferences.

The proliferation of inexpensive microprocessors and peripheral devices is revolutionizing the analytical laboratory by automating many operational, control and computational tasks which hitherto have been performed manually. Indeed, many commercially available analytical instruments are microprocessor-based "smart machines", which free the operator from the need to execute routine operations such as graphical evaluation of peak heights in voltammetric analysis. This type of instrument is extremely useful in the research and industrial laboratory when used for routine analysis of a large number of samples. However, since these machines are usually "black boxes" to the user, in terms of knowledge of the program(s) used, the use of microprocessor-based instrumentation could prove to be of no advantage to the researcher. For example, assessment of interferences due to matrix and other effects could be difficult or even impossible, if the instruments are not programmed to comment on the integrity of the response.¹ Careful data-evaluation and subsequent tuning of the data-processing algorithms is especially important when large matrix effects are expected.

The need for more sophisticated data-evaluation and processing became apparent when we approached the problem of analysis for heavy metals in domestic sewage waters by anodic stripping voltammetry (ASV).² The study of metal speciation and formation of organometallic complexes in these solutions called for a careful examination of calibration plots obtained by the method of standard additions.

The analysis is done on samples which have been subjected to various treatments, such as enzyme and acid digestion. It became clear that manual evaluation of strip-chart recorder data was impractical. It was also felt that commercially available microprocessor-based instruments for voltammetric analysis were not flexible enough to handle the problems of heavy interference, and were also very expensive. A decision was therefore made to extend the approach we had already used for potentiometric analysis³ and data-acquisition,⁴ to the problem at hand. The basic philosophy behind this approach has already been discussed;³ it is based on the application of a general-purpose, low-cost personal computer which is interfaced to electrodes and auxiliary devices, such as a motor-driven burette, through a general-purpose interface controller. In this paper we describe our adaptation of this approach to ASV instrumentation.

INTERFACE DESIGN

The present interface controller is an improved design of the one described earlier.³ It comprises 16 analogue inputs, 16 digital I/O lines and 16 uncommitted control relays (Fig. 1). The main difference between this and the earlier design is the replacement of the analogue to frequency digit (A/F) converter digitization scheme by a commercially available dual-slope analogue to digital (A/D) converter (Analog Devices Model AD7552). The resolution of the converter is 12 bits plus sign, which is comparable to the resolution of 1 part in 10⁴ (unipolar) obtained ear-

*To whom correspondence should be addressed.

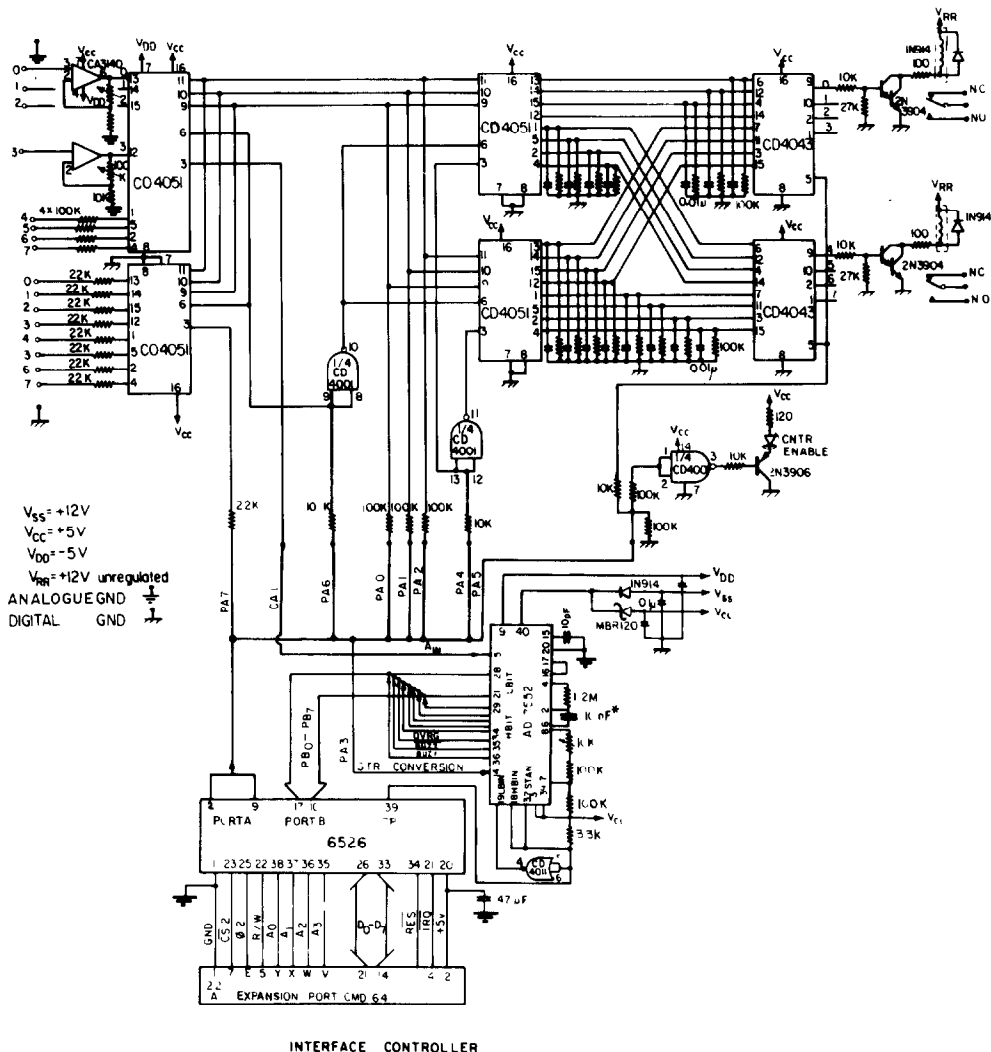


Fig. 1. Circuit diagram of interface controller used in present study.

lier.³ For a full-scale range of ± 2 V, as used here, the resolution is 0.5 mV, thought to be ample in the present application. The dual-slope type A/D converter is an integrating converter similar to the digitizer used earlier³ and has similar noise suppression characteristics. The main disadvantage of the present design of interface controller is the need for additional computer I/O lines to service the A/D con-

verter. The additional I/O lines, as well as the original lines required to control the interface controller, were derived from a dedicated Peripheral Interface Adaptor (PIA), type 6526, that was connected to the main base of the personal computer used (Commodore model CMD 64). A different type of peripheral adaptor may be required if a different kind of personal computer is used.

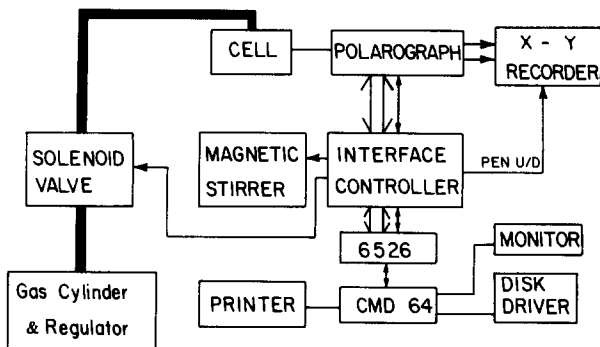


Fig. 2. ASV instrumentation system.

HARDWARE AND SOFTWARE

The present ASV instrumentation system (Fig. 2) comprises a CMD64 general-purpose personal computer, a 1514 diskette driver, an MPS801 line-printer (all from Commodore Business Machines, Inc.), the interface controller described above, an *X-Y* plotter (type 3086, Yew Co.), and a polarograph (E 1224) developed and built at the Department of Electrical and Computer Engineering, Ben-Gurion University. Design details of the polarograph have been described elsewhere.^{5,6} The instrument can be operated in the d.c. sweep, d.c. pulse, and differential pulse modes. The last mode was used in this study. The interface controller is used to perform the following tasks. (1) To sample the polarograph output voltage signal, which is proportional to the working electrode current. (2) To sample the working electrode potential. (3) To initialize the potentiostat sweep. (4) To turn the magnetic stirrer on and off. (5) To actuate the solenoid valve used to control the flow of the purge gas (CO₂) through the sample.

It is also envisaged that the interface controller will eventually be used to control motor-driven burettes to perform automatic calibration by standard additions.³ Signal sampling is synchronized to the internal operation of the polarograph, which in turn is synchronized to the power-line frequency. The benefit of synchronization to the power-line frequency was discussed earlier.⁶

The menu-driven software package developed for this application is organized in a number of basic blocks (Fig. 3): file management, polarograph control, automatic data-processing, manual data-processing, and input-output tasks. The program is written in SUPER BASIC, which includes high-level language graphic commands. These are used for plotting the voltamperograms, calibration curves, *etc.* on the monitor screen and the dot matrix printer.

The processing of the voltamperograms includes peak detection, baseline interpolation and peak-height determination. These can be performed either automatically or in an interactive mode. In the latter mode, which is akin to the approach described by others,¹ the beginning, maximum and tail of each peak are marked by the operator by placing the cursor on corresponding points of the voltamperogram displayed on the monitor screen. Once these features are identified, the program will continue to process it. First, the baseline is restored by fitting a second-order polynomial to the data points on the two sides of the peak. The fitted baseline is then subtracted from the peak data-points to produce a zero baseline peak. The data-points around the peak are then processed for estimation of the peak value. Details of the algorithms used for this are given below.

In the automatic mode, peak detection is done by a subroutine which examines the derivative of the voltamperogram. It was found, however, that peak

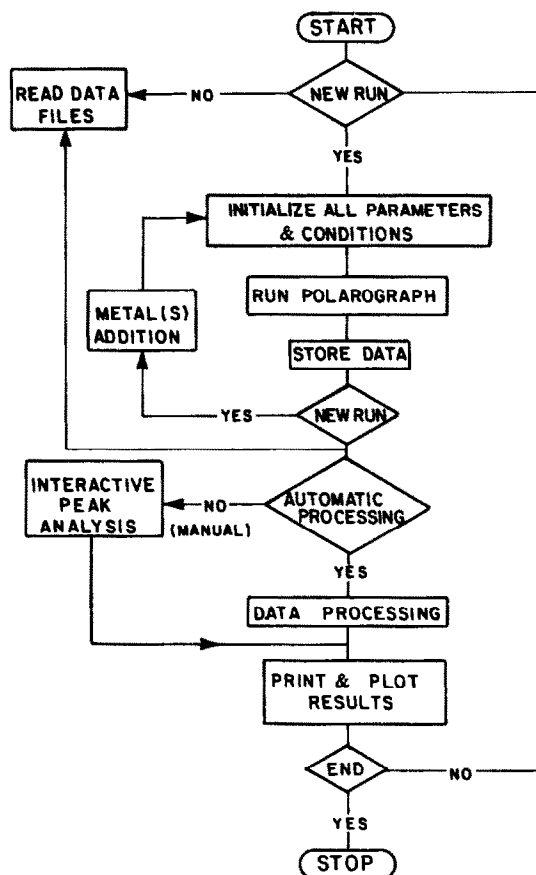


Fig. 3. Flow diagram of supervisory program.

marking could be unreliable if the digital differentiation was performed on the raw data, because of its inherent sensitivity to noise. We have therefore inserted digital filtering of the raw voltamperogram data before the peak identification procedure. The digital filter is similar to the one described earlier.⁷ Once the potentials of a peak's main features are identified (start, maximum and end), the baseline fitting and peak-height algorithms are operated on the original (unfiltered) data to estimate the peak-height.

EXPERIMENTAL

Sampling

Soil and plant samples from the area of Beer Sheva, Israel, were analysed for Zn, Cd, Pb and Cu content. Samples of cultivated soils (from a depth of 30–40 cm) which had been irrigated with water from a local well, and leaves of plants grown on these soils, were collected in acid-washed glass dishes. In the laboratory the samples were dried at 70° for 48 hr to remove moisture and 0.25-g portions of the dried samples were subjected to acid digestion (concentrated sulphuric acid at 400° for 2 hr or until a clear solution was obtained) to remove organic compounds. After the digested samples had cooled to room temperature, the pH was adjusted to 4.5 and the volume to 100 ml with distilled and demineralized water (DDW), and the concentrations of Zn, Cd, Pb and Cu were determined by ASV. All reagents and chemicals used were of analytical

grade, and appropriate blanks were run for all chemicals used.

ASV operating mode

Differential pulse anodic stripping voltametry (DPASV) was used to determine the concentration of Zn^{2+} , Cd^{2+} , Pb^{2+} and Cu^{2+} in samples from various sources. The test solution was placed in a 100-ml PTFE beaker fitted with a PTFE cover through which the electrodes and the tube carrying the oxygen-purging gas (CO_2) were inserted. The solution was stirred with a PTFE-coated stirring bar. A calomel electrode filled with saturated potassium chloride solution served as a reference electrode, and a coiled platinum wire was used as an auxiliary electrode. The working electrode was a hanging mercury drop electrode (HMDE, Metrohm type E410). The analysis consisted of the following steps: (a) plating the working electrode (WE) at -1400 mV for 120 sec in a stirred solution flushed with CO_2 , (b) rest period, without stirring or flushing, for 30 sec at the deposition potential, (c) scanning from -1400 to $+300$ mV ($E_{pulse} = 50$ mV, $E_{step} = 10$ mV, $T = 640$ msec) and recording the current on an X - Y plotter and/or saving the data on a diskette, (d) stripping the WE at $+300$ mV in stirred and flushed solution, (e) starting again from step (a). Steps (a)–(d) are controlled by the microcomputer. A fresh mercury drop was used for each plating/stripping cycle. Calibration was done by making standard additions of increasing concentrations of the cations to each sample.

RESULTS AND DISCUSSION

A typical voltamperogram as seen on the monitor screen and plotted on the dot matrix printer is depicted in Fig. 4(a). Examination of small details is facilitated by the zoom operation (Fig. 4, b, c) which enables the operator to investigate a small section of the voltamperogram by specifying the starting and end potentials of the section. Vertical scaling is done automatically. Following the automatic peak-identification procedure, all recognized peak shoulders and peak points are marked on the screen for inspection by the operator (Fig. 5). Another graphic feature is the presentation of a family of voltamperograms generated by the standard-addition procedure (Fig. 6). The resulting calibration data can also be graphed and, if required, recalculated after manual elimination of one or more points.

Proposed algorithms for baseline fitting and peak-height estimation were tested with experimental voltamperograms and a synthetic voltamperogram of the form:

$$y = 10[\exp(-1.69 \times 10^{-3} x)] + 500\{\exp[-0.001(x + 800)^2]\} + GN[RND(TI) - 0.5] \quad (1)$$

where the last term permits the addition of random noise [RND(TI)] at different levels (GN), and the base of the exponent is e .

The first question to explore was the influence of noise on the baseline fitting. It was found that the uncertainty of the fitted baseline was of the same order of magnitude as the added noise level, as intuitively expected. Another question to be investigated was the best form of the function to be

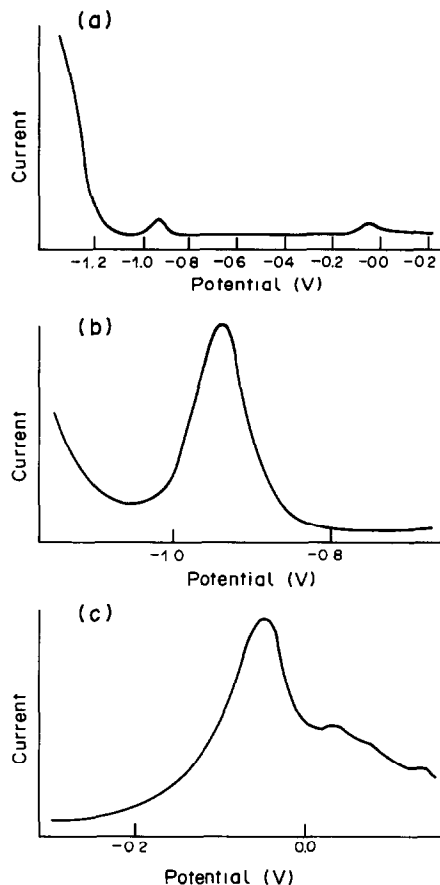


Fig. 4. Sample voltamperogram of plant material (acid digested wheat leaves) without any metal addition: (a) complete scan, (b) enlarged 1st peak (ca. 6 ng/ml), (c) enlarged 2nd peak (8 ng/ml).

used for peak fitting. Previous investigators¹ suggested fitting a parabola to the peak data-points. Another possibility is to use a Gaussian function. Although more complex in form, the Gauss function can be converted into a second-order polynomial by a log transformation:

$$y = A \exp\left[-\frac{(x - x_0)^2}{2}\right] \quad (2)$$

$$\ln y = \ln A - \frac{(x - x_0)^2}{2} \quad (3)$$

$$\ln y = \ln A - \frac{x^2 + 2x_0x - x_0^2}{2} \quad (4)$$

$$\ln y = ax^2 + bx + c \quad (5)$$

where $a = -1/2$; $b = x_0$; $c = \ln A - x_0^2/2$. Hence, by fitting equation (5) to the data, the coefficient a , b and c can be estimated and A , x_0 and x^2 derived. It was found, however, that direct application of the log transformation of equation (3) did not yield accurate results, owing to the finite resolution with which the calculations were done by the CMD 64 computer (which had a 9-digit mantissa and an exponent range

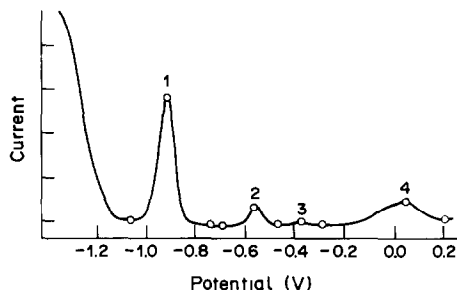


Fig. 5. Display of peak features after automatic processing.

of ± 38). The difficulty stems from the fact that the peak potential of some peaks (e.g., for Zn) is relatively large compared to the peak width. The accuracy of fit was improved markedly if a linear transformation of the form

$$x_j = x_i - x_0 \quad (6)$$

preceded the curve fitting of equation (5). With this algorithm and a second-order polynomial fit⁸ we compared the Gaussian and parabolic fits for an experimental voltamperogram peak with added noise (Table 1). As the results of these tests seemed to indicate that a Gaussian fit was superior to a parabolic one, we adopted the former for implementation in the peak-height estimation routine.

The synthetic voltamperogram, equation (1), was used to test alternative procedures for processing the voltamperograms for peak-height estimation after baseline correction. Since the theoretical value of the synthetic peak height is 500 [equation (1), at $x = -800$] deviations from this value are indicative of deficient algorithms, and lack of robustness in the presence of noise. The following six procedures were tested on the synthetic voltamperogram without added noise.

1. The signal was passed through the digital filter, the baseline was fitted, and the peak height estimated as the maximum distance between the restored baseline and voltamperogram curve (calculated value 480.5).

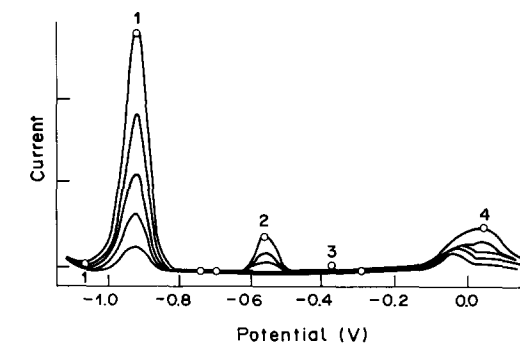


Fig. 6. Voltamperogram family (sample as in Fig. 4) obtained after standard addition of (a) 0, (b) 10, (c) 20, (d) 40, (e) 60 ng/ml concentration of (1) Zn^{2+} , (2) Cd^{2+} , (3) Pb^{2+} , (4) Cu^{2+} .

2. As for 1 but without passing the signal through a digital filter (calculated value 489.2).

3. Interactive mode without baseline fitting (estimated value 492.4).

4. Interactive work with baseline fitting (estimated value 490.9).

5. Baseline in fitting and Gauss fitting of peak (calculated value 495.7).

6. Same as 5 but after passing the signal through a digital filter (calculated value 483.7).

These results imply that: (a) the peak height is reduced by about 3% by use of the digital filter; (b) Gauss fitting improves the accuracy, presumably by smoothing the quantized data; (c) automatic peak-height processing can restore the peak value to within 1% of the true value.

The robustness of the algorithm in the presence of noise was tested by adding random noise to the synthetic voltamperogram and processing the data by the baseline restoration and Gauss fitting routines. Results for 2, 10 and 40% noise levels (relative to peak height) were 500.3 ± 0.07 , 499.6 ± 5.6 ; 514.6 ± 23.6 respectively (mean ± 2 standard deviations; 10 deviates). The results seem to suggest that the proposed algorithms are highly effective, even in the presence of a relatively high noise level such as might

Table 1. Comparison of (A) Gaussian and (B) parabolic fittings for a measured voltamperogram peak with added noise of 0.05 (RND -0.5) for three runs (a, b, c).

Fitting Peak	Original sample, I_p	Sample + noise								
		a		b		c		Average		
		I_p	%*	I_p	%*	I_p	%*	I_p	%*	
A	1	0.51	0.569	110	0.500	96	0.508	98	0.526	101
	2	0.113	0.095	84	0.139	123	0.147	136	0.127	112
	3	0.391	0.373	95	0.402	103	0.395	101	0.390	100
	4	0.400	0.420	105	0.434	109	0.412	103	0.422	105
B	1	0.508	0.549	108	0.566	111	0.499	98	0.538	106
	2	0.111	0.155	140	0.163	147	0.134	108	0.151	136
	3	0.362	0.316	87	0.332	92	0.425	117	0.358	96
	4	0.390	0.430	110	0.445	114	0.429	110	0.435	112

*Deviation from noise-free value, %.

Table 2. Comparison of calibration data obtained for (A) manual, (B) interactive, and (C) automatic data-processing modes for a sample of plant material; numbers in brackets are standard deviations (5 replicates)

	Metal	Voltage, mV	Intercept on x-axis, ng/ml	Correlation coefficient	Slope of standard addition graph
(A)	Zn	-900.0	-6.75	0.9953	20.3
	Cu	+100.0	-10.32	0.9946	125.5
(B)	Zn	-936.8	-6.36 (0.19)	1.0000	18.74 (0.03)
	Cu	+28.7	-8.49 (0.64)	0.9742	118.7 (0.13)
(C)	Zn	-935.6	-6.54 (0.19)	1.0000	18.46 (0.03)
	Cu	+33.2	+20.31 (0.15)	0.9631	57.03 (0.15)

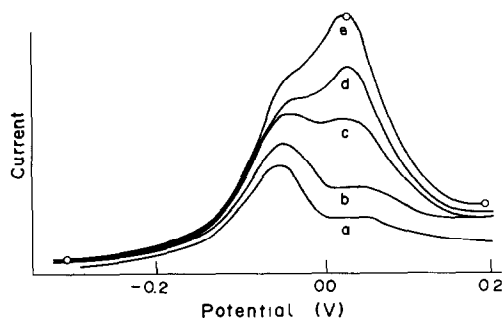


Fig. 7. Voltamperogram of the Cu^{2+} peak after the standard addition of: (a) 0, (b) 10, (c) 30, (d) 50, (e) 70 ng/ml Cu^{2+} .

be encountered near the detection threshold of the instrument.

Manual, interactive and automatic data-processing were compared by applying them to one voltamperogram. The resulting peaks obtained for zinc by the three operational modes are in good agreement for the metal concentration and other parameters (Table 2). However, a large discrepancy was found between the manual and interactive modes on the one hand, and the automatic mode on the other, for the copper peak. As shown in Figs. 4–6 the zinc peak is sharp and regular but that for copper is very irregular. The copper peak changes shape when known amounts of copper are added (Fig. 7). In the voltamperogram for the original sample, only a shoulder is detected in the copper region, because of peak overlap [Fig. 4(c) and Fig. 7(a)]. On increasing the copper concentration by standard addition there is a

gradual change in the signal shape and the shoulder for copper is converted into a detectable peak. The shoulder can be detected when the manual or interactive mode is used for data processing but not by the automatic mode, which would include it in the baseline correction. For the specific example shown here (Fig. 7), the signal for copper was detected as a separate peak only after addition of at least 30 ng of copper per ml. This explains the discrepancy with copper concentrations found by the different processing modes, and demonstrates the importance of the interactive data-processing option in addition to the automatic mode.

Acknowledgements—This study was financed by a grant from the European Economic Community and the Israeli National Council for Research and Development, Ministry of Science.

REFERENCES

1. A. M. Bond and I. D. Heritage, *Anal. Chem.*, 1985, **57**, 174.
2. D. P. H. Laxen and R. M. Harrison, *Water Research*, 1981, **15**, 1053.
3. S. Ben-Yaakov, R. Raviv, H. Guterman, A. Dayan and B. Lazar, *Talanta*, 1983, **29**, 267.
4. H. Guterman and S. Ben-Yaakov, *Comp. Appl. Lab.*, 1983, **3**, 203.
5. B. Lazar and S. Ben-Yaakov, *J. Electroanal. Chem.*, 1980, **108**, 143.
6. S. Ben-Yaakov and H. Guterman, *ibid.*, 1981, **125**, 41.
7. R. Raviv and S. Ben-Yaakov, *Biotech. Bioeng.*, 1985, **27**, 1136.
8. P. R. Bevington, *Data Reduction and Error Analysis for the Physical Scientist*. McGraw-Hill, New York, 1969.

DIRECT FLAME ATOMIC-ABSORPTION DETERMINATION OF MINOR ELEMENTS IN ARGILLITES

E. KLAOS*, R. TALKOP and V. ODINETS

Institute of Chemistry, Estonian Academy of Sciences, Tallinn, Estonian SSR, USSR

(Received 24 March 1986. Revised 25 October 1986. Accepted 21 February 1987)

Summary—The possibility of direct atomic-absorption determination of minor elements in argillites without preliminary concentration and separation is studied. The possibility is examined of producing an analytical flame zone in which free analyte atoms can be produced by use of chemical additives, such as potassium thiocyanate for molybdenum, and potassium thiocyanate plus dodecylamine hydrochloride for vanadium.

Argillite is a variety of oil shale consisting of 10–20% organic matter, 20–40% clay material, and 50–55% aleurite, and cannot be readily analysed.

The direct atomic-absorption methods for determining minor elements have been developed for substances less complex than argillites.^{1–3} With complex materials, separation from matrix elements or the use of matrix-matched standards or the method of standard additions becomes necessary. However, for trace elements the available methods of eliminating matrix effects are often unreliable and not effective. Systematic errors are possible owing to incompleteness of extraction.

The development of direct matrix-independent methods seems likely to be the most effective approach to the flame atomic-absorption spectrophotometric analysis of argillites. The present work is a study of this possibility.

EXPERIMENTAL

Apparatus

A Pye-Unicam SP-1900 spectrophotometer with a single-slot burner (100 mm path-length) was used.

Reagents

All the reagents were of analytical grade. The standard solutions of Mo, V, Co, Ni and Cu were prepared according to Price.⁴ The solutions of AlCl_3 (50 mg/ml) and KCNS (10%), citric, tartaric, and ascorbic acids (3%) were prepared by dissolving the required amounts in demineralized water.

Buffer I ($\text{NH}_4\text{Cl} + \text{LaCl}_3 + \text{MgCl}_2$). Prepared by dissolving 10 g of NH_4Cl , 6.5 g of La_2O_3 and 10 g of MgCl_2 in 100 ml of concentrated hydrochloric acid in a 1-litre standard flask and diluting to the mark with demineralized water.

Dodecylamine hydrochloride solution (2%) in ethanol.

Argillite solution. Prepared by heating a 1-g sample with 20 ml of concentrated hydrofluoric acid, 10 ml of concentrated perchloric acid and 6 ml of concentrated nitric acid in a platinum dish until perchloric acid fumes were evolved, then cooling, rinsing down with a little demineralized water,

heating again until the perchloric acid was completely removed, cooling, taking up the residue with 40 ml of hydrochloric acid (1 + 1), and finally diluting to volume in a 100-ml standard flask with demineralized water.

Procedure

Aliquots of the argillite and additive solutions were placed in 25-ml standard flasks and diluted to the mark with demineralized water. Calibration solutions were matched with the sample solutions in acid and additive contents. The solutions were aspirated into the flame and the atomic absorption was measured under the conditions given in Table 1.

RESULTS AND DISCUSSION

Flame composition and observation height

The effects of flame composition and observation height on the absorption signals for the refractory elements molybdenum and vanadium are more complex than those for copper, nickel and cobalt. The absorption signals of Mo and V depend very strongly on which flame zone is chosen for measurements.

Thus (Fig. 1), changes in acetylene flow-rate from 1.30 to 2.00 l./min result in approximately tenfold increase in the molybdenum absorbance. The maximum absorbance is obtained with an acetylene flow-rate of 1.80–1.90 l./min and an observation height of 6.5–7.0 mm, presumably because these conditions correspond to the optimal carbon to oxygen ratio in the flame. At observation heights of 10 mm or more the signal decreases and then disappears completely, probably because of diffusion of aerial oxygen into the flame, and thermal expansion of the combustion products. Vanadium behaves similarly. In contrast, for copper (and nickel and cobalt) the absorbance does not vary much in the flame profile, over a wide range of acetylene flow-rates.

Effects of additives

Molybdenum. The possibility of using additives to produce a flame zone which would contain reproducible concentrations of free analyte atoms from

*To whom all correspondence should be addressed.

Table 1. Instrumental conditions

	Mo	Co	Ni	Cu	V
Wavelength (nm)	313.3	240.7	232.0	324.8	318.3
Slit-width (mm)	0.4	0.4	0.4	0.8	0.4
Burner	—air—acetylene—			—N ₂ O—acetylene—	
Observation height (cm)	0.6	0.8	0.7	0.5	0.7
Air flow (l./min)	4.5	4.5	4.5	4.5	—
N ₂ O flow (l./min)	—	—	—	—	5.0
Acetylene flow (l./min)	1.6	1.0	1.0	0.8	4.2
Lamp current (mA)	24	12	8	4	28
Integration period (sec)	4	4	4	4	4

both standard and argillite sample solutions was studied.

Figure 2 shows the apparent molybdenum content found in argillite samples, as a function of observation height, in the absence (A) and presence (B) of

aluminium chloride as additive. The true content (C) was determined by the standard-additions method and confirmed by X-ray fluorescence. Without additive present, there was a large positive error with any combination of observation height and acetylene

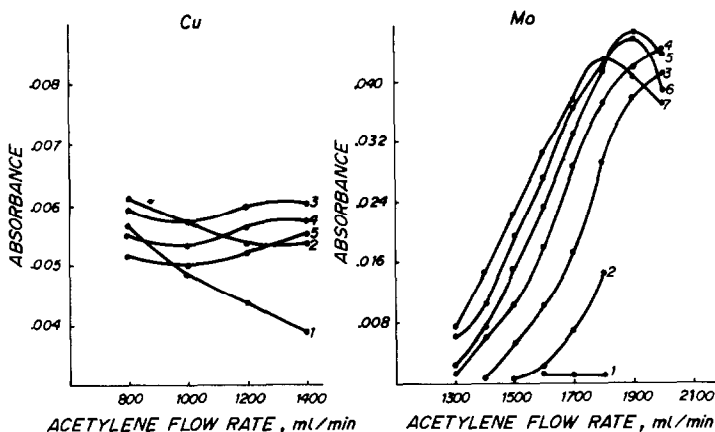


Fig. 1. Influence of acetylene flow-rate on the absorbance of molybdenum (8 μ g/ml) and copper (0.6 μ g/ml) at various observation heights *h*: 1—15 mm; 2—10 mm; 3—9 mm; 4—8 mm; 5—7 mm; 6—6.5 mm; 7—6 mm.

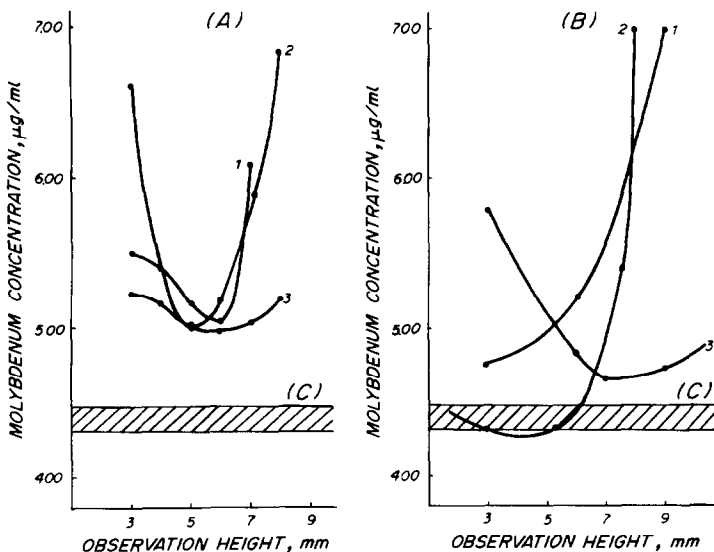


Fig. 2. Plots of the Mo contents detected in argillites, vs. observation height in the absence (A) and presence (B) of AlCl₃. Air flow-rate, 4.5 l./min; acetylene flow-rate, 1—1.4 l./min; 2—1.6 l./min; 3—1.9 l./min.

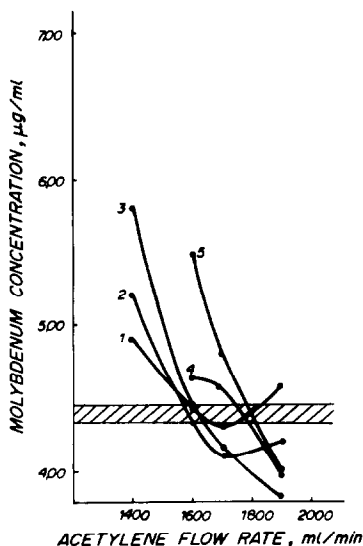


Fig. 3. Plots of the Mo contents detected in argillites, vs. observation height in the presence of KCNS (0.6%). Observation height, 1—4 mm; 2—5 mm; 3—6 mm; 4—7 mm; 5—8 mm.

flow-rate. The addition of 5 mg/ml of AlCl_3 reduced this enhancement effect to an acceptable level under certain conditions, namely an observation height of 6 mm and acetylene flow-rate of 1.60 l./min.

The addition of potassium thiocyanate is of special interest. The presence of 0.3% KCNS in the argillite solution gives a broader range of acceptable conditions. As shown in Fig. 3, the optimal observation height is 4 mm above the burner, with an acetylene flow-rate of 1.60–1.80 l./min. With an acetylene flow-rate of 1.60 l./min, satisfactory results can be obtained at any observation height between 4 and 6 mm above the burner. These conditions have been tested with almost 300 argillite samples, and enriched fractions and technological solutions, and found satisfactory. Typical results are given in Table 2 for use of AlCl_3 and in Table 3 for use of KCNS.

It is also of interest that the addition of KCNS raises the sensitivity for Mo in the air–acetylene flame nearly to that in the N_2O –acetylene flame in the absence of KCNS.

Kirkbright *et al.*⁵ have proposed that the high degree of atomization of some refractory elements in the N_2O –acetylene flame is at least partly due to the strongly reducing atmosphere formed by long-lived CN and NH radicals, and is not due only to reaction with carbon, as is usually suggested for air–acetylene flames.

The efficiency of the KCNS buffer in the air–acetylene flame seems to result from changes in the reaction mechanism in the analytical flame zone:

Table 2. Recovery of standard additions of Mo to argillites; buffer AlCl_3

Sample	Mo in sample solution, $\mu\text{g/ml}$	Mo added, $\mu\text{g/ml}$	Observation height above burner, mm	C_2H_2 flow-rate, l./min	Mo found, $\mu\text{g/ml}$	Recovery of Mo added, %
Argillite 1	0.52	0.50	3	1.4	0.55	110
				1.6	0.51	102
				1.9	0.64	128
			6	1.4	0.59	118
				1.6	0.50	100
				1.9	0.54	108
Argillite 2	1.23	1.00	3	1.4	1.08	108
				1.6	1.02	102
				1.9	1.27	127
			6	1.4	1.16	116
				1.6	0.99	99
				1.9	1.07	107
Mineral fraction	2.71	2.50	3	1.4	2.80	112
				1.6	2.56	102
				1.9	3.29	132
			6	1.4	3.03	121
				1.6	2.53	101
				1.9	2.83	113
Quartz fraction	0.49	0.50	3	1.4	0.53	106
				1.6	0.51	102
				1.9	0.61	122
			6	1.4	0.56	112
				1.6	0.49	98
				1.9	0.52	104
Organic fraction	5.48	5.00	3	1.4	5.37	107
				1.6	5.11	102
				1.9	6.31	126
			6	1.4	5.72	114
				1.6	5.72	114
				1.9	5.30	106

Table 3. Recovery of standard additions of Mo to argillites; buffer KCNS

Sample	Mo in sample solution, $\mu\text{g/ml}$	Mo added, $\mu\text{g/ml}$	Observation height above burner, mm	C_2H_2 flow-rates, l./min	Mo found, $\mu\text{g/ml}$	Recovery of Mo added, %
Argillite 1	0.52	0.50	4	1.4	0.56	112
				1.6	0.51	102
				1.9	0.52	104
			6	1.4	0.64	128
				1.6	0.49	98
				1.9	0.43	86
Argillite 2	1.23	1.00	4	1.4	1.17	117
				1.6	1.02	102
				1.9	1.11	111
			6	1.4	1.34	134
				1.6	1.01	101
				1.9	0.81	81
Mineral fraction	2.71	2.50	4	1.4	3.00	120
				1.6	2.44	98
				1.9	2.72	109
			6	1.4	3.32	133
				1.6	2.46	98
				1.9	2.02	81
Quartz fraction	0.49	0.50	4	1.4	0.53	106
				1.6	0.48	96
				1.9	0.52	104
			6	1.4	0.58	116
				1.6	0.49	98
				1.9	0.47	94
Organic fraction	5.48	5.00	4	1.4	5.41	108
				1.6	5.12	102
				1.9	5.21	104
			6	1.4	6.34	127
				1.6	5.08	102
				1.9	4.45	89

There is increased formation of CN and NH radicals and a decrease in the carbon effect. Thus, attempts to remove chemical interferences should not necessarily be confined to use of a higher temperature flame (with its intrinsic risk of ionization effects). An alternative would be to search for buffers that would affect the complex reactions in low-temperature flames. As an example, calculation of the carbon "oxidation degree" (Z)⁶ of ascorbic, citric, and tartaric acids places them in the sequence tartaric acid ($Z = 1.5$), citric acid ($Z = 1.0$), and ascorbic acid ($Z = 0.66$), which is also the sequence in which their suppressant effect on

the Mo absorption signal increases (Table 4). The higher the Z value, the lower the chance of free carbon being formed by thermal decomposition of the compounds, which would explain the suppression sequence, if the interference was due to interaction with carbon.

Vanadium. Vanadium compounds are difficult to dissociate in the flame, so high-temperature flames are generally used. The determination of vanadium in the N_2O -acetylene flame is influenced by many elements, and ionization effects may also occur. The standard solutions have to be matched in

Table 4. Depressive effect of some acids (3% solutions) on Mo absorbance

Medium	Carbon oxidation degree, Z	Mo absorbances					
		C_2H_2 -air			C_2H_2 - N_2O		
		Mo concentration ($\mu\text{g/ml}$)			Mo concentration ($\mu\text{g/ml}$)		
		2	4	8	2	4	8
Aqueous solution	—	0.006	0.012	0.024	0.016	0.032	0.064
Tartaric acid	1.51	0.004	0.008	0.016	0.012	0.024	0.048
Citric acid	1.00	0.002	0.003	0.006	0.009	0.018	0.035
Ascorbic acid	0.66	0.000	0.001	0.002	0.007	0.014	0.028

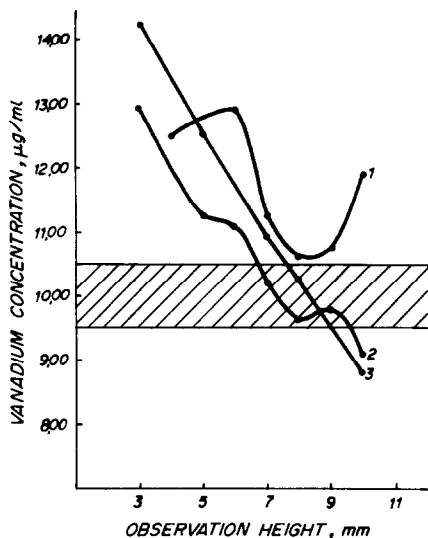


Fig. 4. The V contents detected in argillite in the presence of buffer I. N_2O flow-rate, 5 l./min; acetylene flow-rate, 1—4.2 l./min; 2—4.4 l./min; 3—4.8 l./min.

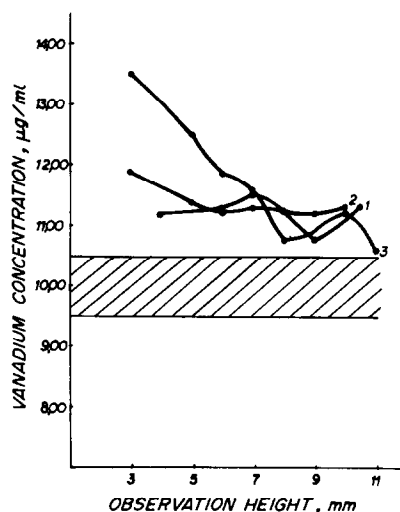


Fig. 5. The V contents detected in argillite in the presence of ethylene glycol. N_2O flow-rate, 5 l./min; acetylene flow-rate, 1—4.2 l./min; 2—4.4 l./min; 3—4.8 l./min.

composition to the test solutions. However, properly chosen additions may improve the situation considerably.

Figure 4 shows that the presence of a mixture of $MgCl_2 + NH_4Cl + LaCl_3$ (each at 0.5 mg/ml concentration)³ results in some flame zones which offer true results for determination of vanadium. With an acetylene flow-rate of 4.40 l./min any observation height from 7 to 9 mm above the burner will give acceptable results.

The recommended⁷ addition of ethylene glycol is of no use with such complex substances as argillites, as shown in Fig. 5.

Studies of surfactants (such as dodecylamine hydrochloride, cetyltrimethylammonium bromide, and sodium laurate) reveal (*e.g.*, Fig. 6) that the necessary

freedom from interference is provided in flame zones which are much higher than that for the maximal absorption signal for vanadium. However, addition of 0.06% KCNS together with 0.1% dodecylamine hydrochloride allows vanadium to be reliably determined by the calibration method at an observation height of 6 mm, *i.e.*, in the zone for maximum sensitivity (Fig. 7). Typical results are given in Table 5.

Hence, the addition of KCNS for Mo and of KCNS plus surfactant for V enables various analytical forms of standard and sample solutions to be used. Matrix matching of the standard and sample solution is not necessary.

To summarize, a proper choice of additives providing for high reliability in determining trace elements

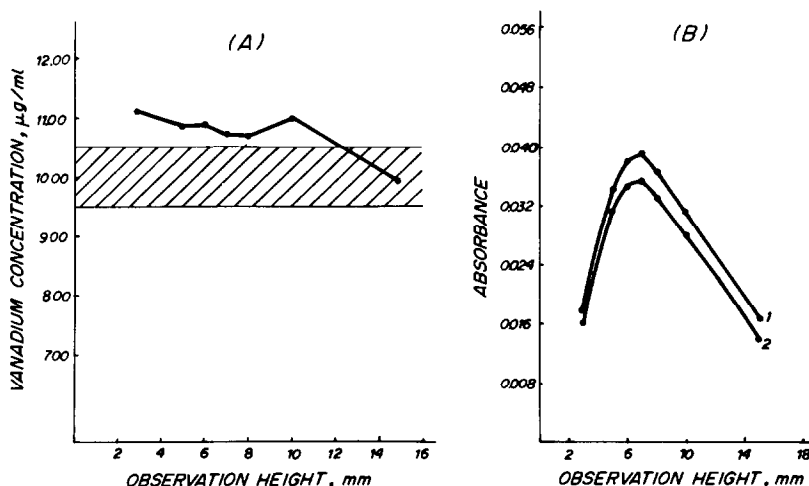


Fig. 6. (A) The V contents detected in argillite in the presence of dodecylamine hydrochloride (0.1%). N_2O flow-rate, 5 l./min; acetylene flow-rate, 4.6 l./min. (B) Plot of V absorption signal in pure solution (1) and argillite solution in the presence of dodecylamine hydrochloride (2) vs. observation height.

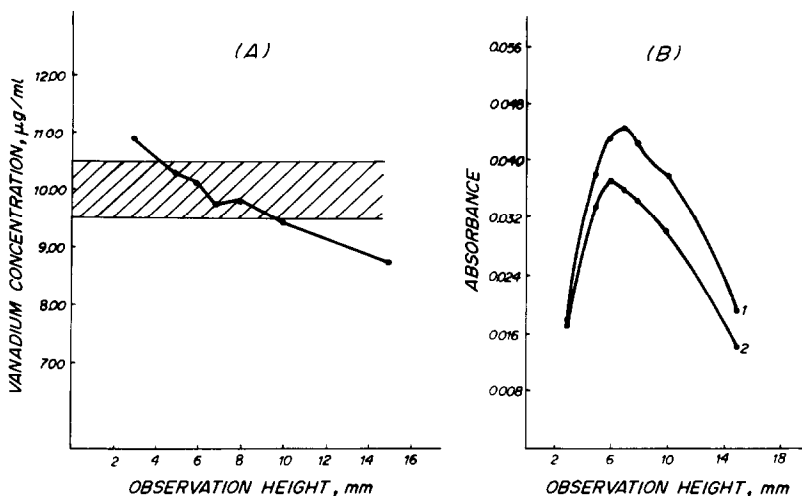


Fig. 7. (A) The V contents detected in argillite in the presence of addition of KCNS (0.6%) + dodecylamine hydrochloride (0.1%). N_2O flow-rate, 5 l./min; acetylene flow-rate, 4.6 l./min. (B) Plots of the V absorption signal in pure solution (1) and argillite solution in the presence of KCNS (0.6%) + dodecylamine hydrochloride (0.1%) additive (2), vs. observation height.

Table 5. Recovery of standard additions of V to argillites; buffer KCNS

Sample	V in sample solution, $\mu\text{g/ml}$	V added, $\mu\text{g/ml}$	Observation height above burner, mm	N_2O flow-rates, l./min	V found, $\mu\text{g/ml}$	Recovery of V added, %
Argillite 3	7.81	7.50	5	4.2	9.22	123
				4.4	8.23	110
				4.8	8.96	119
			7	4.2	8.20	109
				4.4	7.61	101
				4.8	8.02	107
			9	4.2	7.80	104
				4.4	7.07	94
				4.8	7.03	94
Argillite 4	9.68	10.00	5	4.2	12.27	123
				4.4	11.10	111
				4.8	11.83	118
			7	4.2	10.91	109
				4.4	9.90	99
				4.2	10.53	105
			9	4.2	10.46	105
				4.4	9.48	95
				4.8	9.41	94
Mineral fraction	11.04	11.00	5	4.2	14.96	136
				4.4	12.76	116
				4.8	13.97	127
			7	4.2	12.43	113
				4.4	10.83	98
				4.8	11.11	101
			9	4.2	12.00	109
				4.4	8.17	74
				4.8	8.10	74
Organic fraction	11.95	12.00	5	4.2	13.19	110
				4.4	12.71	106
				4.8	13.30	111
			7	4.2	13.10	109
				4.4	11.80	98
				4.8	12.38	103
			9	4.2	12.31	103
				4.4	11.64	97
				4.8	11.60	97

is very useful in development of direct methods of completely matrix-independent atomic-absorption analysis of compounds such as argillites.

REFERENCES

1. P. Sutcliffe, *Analyst*, 1976, **101**, 949.
2. E. F. Pereverzeva, *Nauchn. Tr. NII Tsvet. Met.*, 1977, **43**, 39.
3. I. Sire, I. Collin and I. A. Voinovitch, *Spectrochim. Acta*, 1978, **33B**, 31.
4. W. I. Price, *Analytical Atomic Absorption Spectrometry*. Heyden, London, 1972.
5. G. F. Kirkbright, M. K. Peters and T. S. West, *Talanta*, 1967, **14**, 789.
6. E. M. Sedykh, Yu. I. Belyaev and E. V. Sorokina, *Zh. Analit. Khim.*, 1980, **35**, 2348.
7. S. L. Sachdev, J. W. Robinson and P. W. West, *Anal. Chim. Acta*, 1967, **37**, 156.

NEW LIQUID-MEMBRANE ELECTRODES FOR DIRECT DETERMINATION OF ATROPINE IN PHARMACEUTICAL PREPARATIONS*

SAAD S. M. HASSAN†, M. A. AHMED and F. S. TADROS

Department of Chemistry, Faculty of Science, Ain Shams University, Cairo, Egypt

(Received 23 October 1986. Accepted 12 December 1986)

Summary—Solutions of atropinium 5-nitrobarbiturate in *n*-octanol and atropinium picrolonate in *p*-nitrotoluene are used as novel liquid ion-exchangers in electrodes that respond to the atropine cation. The performance characteristics of the two electrodes are almost identical: the response is linear for 10^{-5} – $10^{-2}M$ atropine with a slope of 56.5 ± 1 mV/concentration decade. The static response times are 30–90 sec and the potential readings are stable over the pH range 3–8. There is negligible interference from a number of inorganic and organic cations, and some common excipients. In the direct determination of 1–200 $\mu\text{g/ml}$ of atropine, the average recovery with both electrodes is 98% (mean standard deviation 1.7%). Atropine has been determined in some pharmaceutical preparations with an average recovery of 98% (standard deviation 1.9%), the results being in agreement with those obtained by standard methods.

Atropine has been determined spectrophotometrically by a number of chromogenic reactions. Some organic dyes such as Bromothymol Blue,¹ Bromophenol Blue,² and tetrabromophenolphthalein ethyl ester³ react with atropine to form coloured complexes extractable into organic solvents. Complexation of atropine with ammonium bis(aniline) tetrakis(isothiocyanato)chromate(III),⁴ and ammonium reineckate,⁵ followed by measurement of the absorbance of the complex solutions, has been suggested. Nitration of atropine followed by alkylation,⁶ or simultaneous nitration and condensation with nitromethane in the presence of methanolic benzyltrimethylammonium hydroxide and dimethylformamide⁷ gives coloured products. Chromogenic reactions with reduced molybdophosphoric acid,⁸ citric acid–acetic anhydride,⁹ *cis*-aconitic anhydride,¹⁰ and *p*-aminobenzaldehyde¹¹ have also been described. Most of these methods, however, require strictly controlled reaction conditions and involve a time-consuming prior extraction or precipitation step.

The commonly used titrimetric methods for determination of atropine are mainly based on the release of the base from its salts, extraction, and titration with acids, with visual indicators.¹² Extraction of the base followed by dissolution in sulphuric acid and titration with sodium hydroxide (Methyl Red as indicator) has been recommended by both the United States and British Pharmacopoeias.^{13,14} Conductometric,¹⁵ thermometric,¹⁶ potentiometric,¹⁷ hetero-

metric,¹⁸ and turbidimetric¹⁹ titrations have also been suggested. Reactions with copper or lead picrate,^{20,21} and ammonium reineckate,²² isolation of the products, treatment with excess of alkaline EDTA and acidic potassium chromate followed by complexometric and iodometric titrations of the excess of reagents, respectively, have been proposed. Many of these methods involve several steps and suffer from severe interference by basic, redox and metallic species.

Membrane electrodes for atropine based on the use of tetraphenylborate²³ and reineckate²⁴ as counterions in liquid and poly(vinyl chloride) matrices have been developed and shown to be simple and convenient monitoring sensors. We have previously described some liquid-membrane electrode systems for direct determination of strychnine,²⁵ caffeine,²⁶ ephedrine,^{27,28} and lidocaine,²⁹ based on suitable ion-pairing reagents. It has been reported that protonated atropine and some other protonated alkaloids can form stable water-insoluble ion-pair complexes with 5-nitrobarbituric³⁰ and picrolonic acids.³¹ The photomicrographs and melting points of these derivatives have been utilized for identification of the alkaloids. We have prepared two liquid-membrane electrodes based on atropinium 5-nitrobarbiturate and atropinium picrolonate ion-pair complexes as novel electroactive species. These were characterized and found suitable for determination of atropine in some pharmaceutical preparations.

EXPERIMENTAL

Apparatus

Potentiometric measurements were made at $25 \pm 1^\circ$ with an Orion model 901 microprocessor "Ionalyzer" with atropinium 5-nitrobarbiturate and atropinium picrolonate

*Based on a paper presented at the 30th IUPAC Congress, Manchester, 9–13 September 1985.

†To whom correspondence should be addressed. Present address: Department of Chemistry, Qatar University, Doha, Qatar.

liquid-membrane electrodes in conjunction with an Orion model 90-02 Ag/AgCl double-junction reference electrode with 10% potassium nitrate solution in the outer compartment. An Orion model 91-02 combined glass-calomel electrode was used in the pH adjustment.

Reagents

All reagents used were of analytical-reagent grade. Doubly distilled water and solvents were used throughout. Atropine and its salts, 5-nitrobarbituric acid and picrolonic acid were obtained from Sigma Chemical Co. (St. Louis, Mo). Atropinium sulphate injections and "Isopto" atropine eye-drops were obtained from El-Nile Pharmaceutical Company (Egypt) and Alcon Pharmaceutical Company (Belgium), respectively.

Procedure

The atropinium 5-nitrobarbiturate was prepared by mixing 20 ml of 1M aqueous atropine hydrochloride with 20 ml of 1M ethanolic 5-nitrobarbituric acid solution. After stirring for 15 min, the yellowish precipitate was filtered off on a porosity-3 sintered-glass crucible, washed twice with doubly distilled water, followed by ethanol, dried at 100° for 1 hr, then ground to fine powder. The atropinium picrolonate was prepared similarly from atropine hydrochloride and picrolonic acid. Elemental analysis and the infrared spectra of the products confirmed that 1:1 compounds had been formed.

An Orion liquid-membrane body (model 92) was used as the electrode assembly with an Orion 92-81-04 porous membrane. The organic ion-exchanger used was a 0.05M solution of either atropinium 5-nitrobarbiturate in *n*-octanol or atropinium picrolonate in *p*-nitrotoluene. The aqueous reference solution was a mixture of equal volumes of 0.02M atropine hydrochloride and 0.02M potassium chloride. Both electrodes were preconditioned by soaking in a solution of 10⁻³M atropine hydrochloride for 2 days after preparation, and stored in the same solution when not in use. Potentiometric selectivity-coefficient data were obtained by the mixed-solution method as described previously.^{25-29,32,33}

A calibration graph for determination of atropine in pharmaceuticals was prepared by taking around 20 ml each of 10⁻⁵-10⁻²M aqueous atropine hydrochloride (the most usable range of concentration) solutions in 100-ml beakers. The atropine liquid-membrane electrode and the reference electrode were immersed in the stirred solutions, and the emf readings recorded after stabilization. A plot of emf *vs.* the logarithm of the atropine concentration was used for subsequent determination of atropine in other solutions.

Atropine was determined in pharmaceutical ampoules and injections by transferring the contents of 5 ampoules (1 ml each, 1% atropine) or 5-ml samples of 0.5-1% atropine eye-drops to a 100-ml beaker, diluting to ~50 ml with demineralized water, adjusting the pH to 4-6, if necessary, diluting to 100 ml with demineralized water, and shaking. A suitable aliquot (say 20 ml) of the solution was transferred to a 100-ml beaker and the emf of the electrode systems was measured.

RESULTS AND DISCUSSION

Performance characteristics of the electrode systems

Atropinium 5-barbiturate and atropinium picrolonate were prepared and their lipophilic solutions were tested for their response to atropine. The efficiency of various solvents for the first compound decreases in the order *n*-octanol > *p*-nitrotoluene > nitrobenzene > benzyl alcohol, and for the second decreases in the order: *p*-nitrotoluene > nitrobenzene > *o*-dichlorobenzene > chlorobenzene. The performance of two sets of liquid-membrane electrodes prepared from 0.005-0.01M solutions of the atropine compounds in these solvents were evaluated according to IUPAC recommendations.³² The typical cell used for potentiometric measurements was

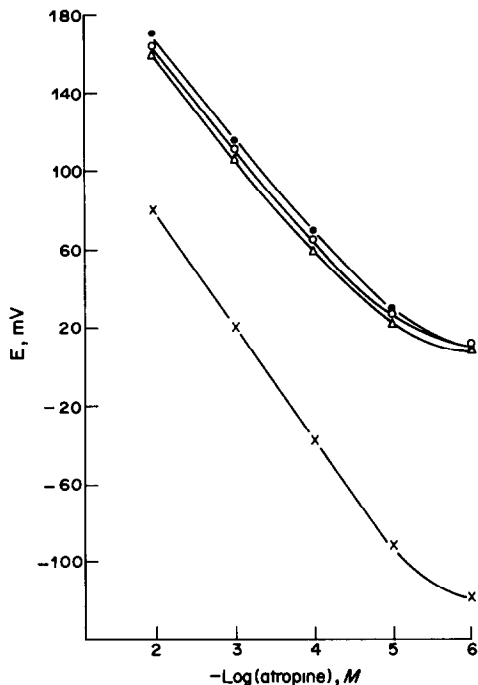
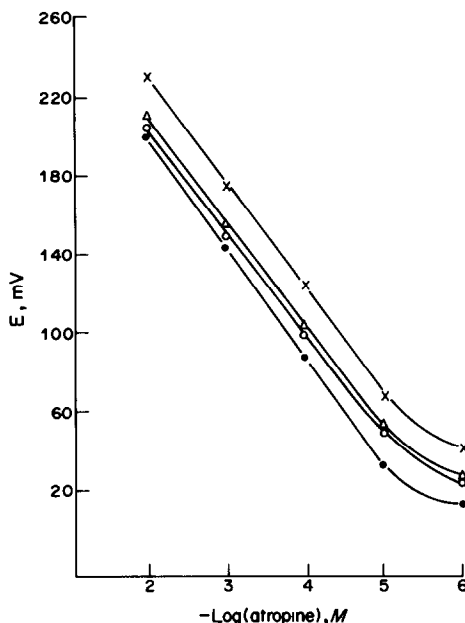
Ag-AgCl 0.01M KCl 0.01M aqueous atropine hydrochloride	atropine complex in organic solvent	porous membrane	atropine in aqueous test solution	Ag-AgCl reference electrode
--	--	--------------------	---	-----------------------------------

Table 1. Selectivity coefficients of atropinium 5-nitrobarbiturate and atropinium picrolonate liquid-membrane electrodes

Interfering substance (B)	$K_{atrop,B}^{pot}$	
	Atropinium 5-nitrobarbiturate in <i>n</i> -octanol	Atropinium picrolonate in <i>p</i> -nitrotoluene
Aminobenzoic acid	7.2×10^{-2}	3.7×10^{-2}
Aminopropanol	9.1×10^{-2}	8.5×10^{-2}
Ethanolamine	3.5×10^{-2}	3.0×10^{-2}
Diethylamine	4.2×10^{-2}	3.7×10^{-2}
Dibutylamine	5.3×10^{-3}	6.6×10^{-3}
Triethanolamine	5.1×10^{-1}	2.8×10^{-1}
Tetraethylammonium chloride	5.9×10^{-1}	4.4×10^{-1}
Piperidine	1.5×10^{-2}	2.5×10^{-2}
Glycine	2.4×10^{-2}	5.1×10^{-2}
Cysteine	1.3×10^{-2}	2.1×10^{-2}
Urea	2.5×10^{-2}	3.4×10^{-2}
Succinamide	2.1×10^{-3}	1.7×10^{-3}
Ammonium chloride	1.6×10^{-3}	3.1×10^{-3}
Strychnine	2.9	2.5
Caffeine	2.1	1.8
Nicotine	1.8	1.7

Table 2. Response characteristics of the atropinium 5-nitrobarbiturate liquid-membrane electrode made with different membrane solvents

Parameter	n-Octanol	<i>p</i> -Nitrotoluene	Nitrobenzene	Benzyl alcohol
Slope, $mV/\log C$	57.5	46.6	46.0	45.0
Std. devn., $mV/\log C$	0.8	1.5	2.0	2.5
Corr. coeff., r	0.9997	0.9977	0.9983	0.9976
Intercept, mV	194	260	249	249
Lower limit of linear range, M	10^{-5}	10^{-5}	10^{-5}	10^{-5}
Detection limit, M	5×10^{-6}	5×10^{-6}	7×10^{-6}	8×10^{-6}

Fig. 1. Effect of the membrane solvent on the response of the atropinium 5-nitrobarbiturate liquid membrane electrode: (x) n-octanol; (Δ) nitrobenzene; (\circ) benzyl alcohol; (\bullet) *p*-nitrotoluene.Fig. 2. Effect of the membrane solvent on the response of the atropinium picrolonate liquid membrane electrode: (\bullet) *p*-nitrotoluene; (Δ) nitrobenzene; (\circ) *o*-dichlorobenzene; (\times) chlorobenzene.

Least-squares analyses of the data are given in Tables 1 and 2.

The results obtained show that atropinium 5-nitrobarbiturate in n-octanol and atropinium picrolonate in *p*-nitrotoluene give fairly stable and sensitive membranes for potentiometric measurement of atropine. The overall performance characteristics of the two electrode systems are almost identical and all the results shown below were obtained with both electrodes. At $25 \pm 1^\circ$, the electrodes give a linear

response for 10^{-5} – $10^{-2}M$ atropine with an average slope of 56.5 ± 1 mV/concentration decade. Typical calibration curves are shown in Figs. 1 and 2. The lower limit of detection (IUPAC definition) offered by both electrodes is $5 \times 10^{-6}M$. Their static response times are almost the same; steady potentials were attained after successive immersion of both electrodes in 10^{-2} , 10^{-3} , 10^{-4} and $10^{-5}M$ aqueous atropine hydrochloride solutions for 30, 45, 72 and 180 sec, respectively. The useful lifetime of both electrodes is

Table 3. Response characteristics of the atropinium picrolonate liquid membrane electrode made with different membrane solvents

Parameter	<i>p</i> -Nitrotoluene	Nitrobenzene	<i>o</i> -Dichlorobenzene	Chlorobenzene
Slope, $mV/\log C$	55.7	51.4	50.0	47.7
Std. dev., $mV/\log C$	1.0	1.5	2.0	2.0
Corr. coeff., r	0.9999	0.9967	0.9988	0.9980
Intercept, mV	311	308	302	322
Lower limit of linear range, M	10^{-5}	10^{-5}	10^{-5}	10^{-5}
Detection limit, M	5×10^{-6}	4×10^{-6}	6×10^{-6}	6×10^{-6}

Table 4. Determination of atropine with atropinium 5-nitrobarbiturate and picrolonate liquid-membrane electrodes

Sample	Amount added, $\mu\text{g/ml}$	5-Nitrobarbiturate electrode			Picrolonate electrode		
		Recovery,* %	Std. devn., %	Recovery,* %	Std. devn., %	Recovery,* %	Std. devn., %
Atropine base	15	97.8	1.8	98.2	1.4		
	10	98.3	1.9	98.2	1.4		
	5	98.6	1.7	98.5	1.8		
Atropine sulphate	200	98.8	1.7	98.0	1.8		
	175	98.4	1.8	98.5	1.9		
	100	98.5	1.6	98.5	1.6		

*Average of 3 measurements.

Table 5. Determination of atropine in some pharmaceutical preparations with the atropinium 5-nitrobarbiturate and picrolonate liquid-membrane electrodes

Preparation	Atropine, nominal, mg/ml	USP method			5-Nitrobarbiturate electrode			Picrolonate electrode		
		Recovery,* %	Std. devn., %	Recovery,* %	Std. devn., %	Recovery,* %	Std. devn., %	Recovery,* %	Std. devn., %	
Atropine sulphate† injection	1	98.2	2.4	97.9	2.0	98.0	1.8			
Isopto atropine§ eye-drops	10	98.6	2.1	98.2	2.0	98.1	2.0			
Isopto atropine§ eye-drops	5	97.8	2.0	98.3	1.8	98.3	1.9			

*Average of 3 measurements.

†El-Nile Pharmaceutical Company (Egypt).

§Alcon Pharmaceutical Company (Belgium).

about 2 months. During this period, the potentials are reproducible within ± 4 mV and the variation of the slope of the calibration plots does not exceed 3 mV/concentration decade.

The interference of organic compounds such as amines, amides, amino-acids and carboxylic acids and also inorganic cations and anions was assessed. The responses of the electrode systems are not affected noticeably by the presence of most common cations and anions such as K^+ , Na^+ , Mg^{2+} , Ca^{2+} , Cd^{2+} , Cu^{2+} , NO_3^- , Cl^- , SO_4^{2-} , acetate, oxalate and maleate at 0.01M concentration. Potentiometric selectivity coefficients ($K_{atrop,B}^{pot}$) were determined by the mixed solution method as described previously.^{25-29,32,33} The atropine concentrations were varied from 10^{-3} to 10^{-5} M while the concentration of the competing species was kept at 10^{-3} M. The two electrodes behave similarly and suffer negligible interference from many basic compounds (Table 3). The electrodes do respond, however, to some alkaloids such as nicotine, caffeine and strychnine.

The responses of the electrodes are practically unaffected by changes in pH over the range 3.2–8.1. At higher pH values, the potential markedly decreases because of the progressive loss of the positive charge of the atropinium cation. In general, the overall performance characteristics of the proposed electrode systems are similar to those of the atropinium tetraphenylborate and reineckate electrode systems.^{23,24}

Determination of atropine

Table 4 presents the results obtained from direct potentiometric determination of pure atropine and atropinium sulphate in aqueous solutions by use of the proposed electrodes and the calibration graph method. The average recovery for triplicate analysis of 6 samples containing 5–200 μ g of atropine per ml is 98.4% (std. devn. 1.7%), typical for a direct potentiometric technique. The electrodes were also used for determination of atropine in some pharmaceutical preparations. Additives and diluents commonly used in drug formulations, such as acacia, Tween-80, ethylene glycol, carboxymethylcellulose, cocoa butter and paraffin oil, at concentration levels as high as 1000 times that of the atropine, have no significant effect on the response of either electrode system.

The results obtained for determination of 0.1–1% of atropine in some injections and eye-drops show an average recovery of 98.1% (std. devn. 1.9%) referred to the nominal values (Table 5). These results are in good agreement with those obtained by the United States and British Pharmacopoeia standard procedure (average recovery 98.2%, std. devn. 1.9%) which involves conversion of atropine salts into the free base, extraction, dissolution in standard sulphuric acid, and back-titration of the excess of acid with standard sodium hydroxide, with Methyl Red as indicator.^{13,14}

The electrode systems reported here provide a rapid, inexpensive and reliable method for direct determination of atropine, with minimum sample preparation and high selectivity. A detection limit of 5×10^{-6} M (~ 1.5 μ g/ml) along with the short static response time, stability in various matrices and applicability to coloured and turbid solutions add to the usefulness of these electrodes in pharmaceutical analyses.

REFERENCES

1. D. M. Shingbal, *Indian J. Pharm.*, 1973, **35**, 160.
2. M. Turowska, W. Czabajaska and J. Lutowski, *Herba Pol.*, 1972, **18**, 242.
3. M. Tsubouchi and S. Hara, *Agri. Biol. Chem. (Tokyo)*, 1971, **35**, 1315.
4. I. Grecu and S. Barbu, *Farmacia (Bucharest)*, 1972, **20**, 21.
5. J. Weyers and M. Skora, *Diss. Pharm.*, 1962, **14**, 201.
6. I. Nir-Grosfeld and E. Weissenberg, *Drug Stand.*, 1957, **25**, 180.
7. J. Bartos and P. Balleydier, *Chim. Anal. (Paris)*, 1971, **53**, 384.
8. D. Carvalho, A. B. Prado, H. C. Silva and L. Larini, *Rev. Fac. Farm. Odont. Araraquara*, 1972, **6**, 1.
9. Y. A. Beltagy, *Pharmazie*, 1976, **31**, 483.
10. M. Palumbo and S. Sacca, *Farmaco, Ed. Prat.*, 1962, **17**, 65.
11. O. A. Akopyan, *Aptechn. Delo*, 1958, **7**, 19.
12. L. Nyitray, *Acta Pharm. Hung.*, 1964, **34**, 159.
13. *The United States Pharmacopoeia*, XXth Rev., p. 39. Mack Publishing Co., Easton, Pa, 1980.
14. *British Pharmacopoeia*, Vol. I, p. 40. The University Press, Cambridge, 1980.
15. H. Piasecka, *Farmacja Pol.*, 1975, **31**, 123.
16. E. J. Greenhow and L. E. Spencer, *Analyst*, 1973, **98**, 98.
17. N. P. Dzyuba and M. S. Shraiber, *Aptechn. Delo*, 1957, **6**, 17.
18. M. Bobtelsky and I. Barzily, *Anal. Chim. Acta*, 1963, **28**, 82.
19. A. I. Sichko, *Khim.-Farm. Zh.*, 1978, **12**, 140.
20. S. Rolski, M. Gajewska and E. Matusak, *Farmacja Pol.*, 1969, **25**, 111.
21. M. Gajewska, *Chem. Anal. (Warsaw)*, 1973, **18**, 313.
22. Y. A. Beltagy, *Pharmazie*, 1977, **32**, 51.
23. E. P. Diamandis, E. Athanasiou-Malaki, D. S. Papanstathopoulos and T. P. Hadjiioannou, *Anal. Chim. Acta*, 1981, **128**, 239.
24. S. S. M. Hassan and F. S. Tadros, *Anal. Chem.*, 1984, **56**, 542.
25. S. S. M. Hassan and M. B. Elsayes, *ibid.*, 1979, **51**, 1651.
26. S. S. M. Hassan, M. A. Ahmed and M. M. Saoudi, *ibid.*, 1985, **57**, 1126.
27. S. S. M. Hassan and G. A. Rechnitz, *ibid.*, 1986, **58**, 1052.
28. S. S. M. Hassan and M. M. Saoudi, *Analyst*, 1986, **111**, 1367.
29. S. S. M. Hassan and M. A. Ahmed, *J. Assoc. Offic. Anal. Chem.*, 1986, **69**, 618.
30. L. G. Chatten and P. J. Barry, *Can. J. Pharm. Sci.*, 1968, **3**, 40.
31. W. Warren and R. Weiss, *J. Biol. Chem.*, 1907, **3**, 327.
32. IUPAC Analytical Chemistry Division, Commission on Analytical Nomenclature, Recommendations for Nomenclature of Ion Selective Electrodes, *Pure Appl. Chem.*, 1976, **48**, 127.
33. T. S. Ma and S. S. M. Hassan, *Organic Analysis Using Ion Selective Electrodes*. Academic Press, London, 1982.

SHORT COMMUNICATIONS

DETERMINATION OF FREE ACIDITY IN ANTIMONY CHLORIDE SOLUTIONS

S. C. SOUNDAR RAJAN

Process Control Laboratory, Zinc Smelter, Visakhapatnam 530015, India

(Received 8 August 1983. Revised 28 October 1986. Accepted 24 March 1987)

Summary—A method for the determination of free acid in antimony(III) chloride solutions is described. The total acid is determined by titration in the presence of tartrate as masking agent, and the bound acidity is calculated from the antimony content of the same aliquot, determined by titration with bromate. This method is simple and rapid compared to the earlier potentiometric techniques.

Determination of free acid by direct titration is not possible in the presence of hydrolysable cations.¹ Sometimes the problem can be solved by converting the hydrolysable ion into a complex or precipitate, e.g., by adding potassium fluoride to complex aluminium and iron¹⁻³ or sodium dihydrogen phosphate to precipitate iron.⁴ If no protons are liberated during this reaction, as in the complexation of copper with thiourea,⁵ the total acid present will be the free acidity. If protons are liberated, however, it is necessary to determine the total acidity thus obtained, and then determine the metal ion independently and apply a correction for the acid liberated. The difference is the free acidity. Other techniques tried include conductometric titration,⁶ and addition of oxalate and titration to a preselected pH.⁶⁻⁸

In our laboratories, during the course of studies on recovery of antimony from residues such as antimony dross, a need arose for accurate determination of free hydrochloric acid in antimony(III) chloride solutions. Since antimony does not form simple complexes with neutral ligands,⁹ it is difficult to avoid liberation of acid due to antimony complexation. The differential method of determining total acidity and bound acidity¹⁰ appears to be the most convenient method of determination of the free acidity in antimony(III) chloride solutions, and simpler than the potentiometric titration after addition of potassium oxalate.⁸ In the present investigations, tartrate was used as complexing agent for determination of total acidity; the solution was then used for determination of the antimony content by titration with potassium bromate;¹¹ the free acid concentration was calculated from the results.

EXPERIMENTAL

Reagents

Sodium hydroxide, 0.48M. Standardized by titration with potassium hydrogen phthalate.

Potassium sodium tartrate solution, 0.1 g/ml. Fifty g of the salt were dissolved in about 400 ml of water. A drop of

phenolphthalein indicator solution was added and the solution was titrated with 1M hydrochloric acid until the pink colour disappeared; 0.1M sodium hydroxide was then added until the pink colour just reappeared. The solution was then diluted to 500 ml with distilled water.

Potassium bromate solution, 0.01667M.

Methyl Orange solution in water, 1 mg/ml.

Antimony(III) chloride. Supplied by Polypharm, India, and used as received.

Procedure

Transfer (by safety pipette) 1 or 2 ml of the sample solution in a 250-ml conical flask and dilute it to about 50 ml; a white turbidity will appear. Add 20 ml of the tartrate solution and warm if necessary to obtain a clear solution, then titrate with sodium hydroxide to a phenolphthalein end-point that is stable for at least 2 min. Note the volume of sodium hydroxide. A premature fading end-point often occurs because some tartaric acid is precipitated when the tartrate solution is added to the highly acidic sample solution, and goes into solution slowly as the titration proceeds.

To the titrated solution add 15 ml of concentrated hydrochloric acid followed by 2 or 3 drops of Methyl Orange indicator and titrate with potassium bromate until the indicator colour is discharged.¹¹

1 ml of 1M NaOH \equiv 36.45 mg of HCl

1 ml of 0.01667M KBrO₃ \equiv 6.09 mg of Sb

\equiv 5.48 mg of HCl

1 g/l. Sb \equiv 0.898 g/l. HCl

RESULTS AND DISCUSSION

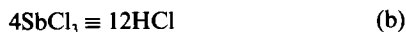
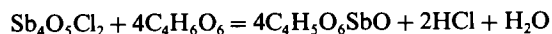
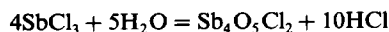
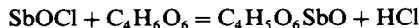
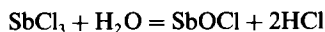
It is difficult to prepare a synthetic solution of known concentration of antimony(III) chloride in hydrochloric acid because antimony(III) chloride is highly deliquescent, fuming, and highly reactive, so a known quantity cannot be accurately weighed. An aqueous solution cannot be accurately made either. To overcome this problem, experiments were conducted as follows. A known quantity of 100–200 g/l. hydrochloric acid was taken in a conical flask and titrated with sodium hydroxide. To known portions of the acid, various quantities of antimony chloride (weighed approximately) were added. These mixtures

Table 1

HCl taken, ml	SbCl ₃ added, mg (approx.)	NaOH needed, ml	KBrO ₃ needed, ml	Antimony found, mg	Total acidity, g/l.	Acidity due to antimony, g/l.	Free acidity, g/l.
1		12.4	—	—	217	—	217
1	100	14.8	8.0	48.7	259	44	215
1	150	16.3	12.0	73.1	285	66	219
1	200	18.0	18.4	112.1	315	101	214
1	300	20.2	24.8	151.0	354	136	218
2	200	30.6	18.9	115.1	536	104	216
2	300	32.2	24.4	148.6	563	134	215
							Mean 216.3
							Std. devn. 1.9

were then analysed by the procedure described. The free acidity calculated was compared with that of the original hydrochloric acid. The results are presented in Table 1.

From the results, it can be inferred that hydrolysis of antimony chloride involves liberation of 3 moles of hydrogen chloride per mole of antimony(III) chloride. The hydrolysis products of antimony(III) chloride are said to vary from SbOCl to Sb₄O₅Cl₂ depending on the extent of dilution.¹² For these two extremes, the hydrolysis and complexation reactions can be written as follows:



This is in quite good agreement with the observed results.

Acknowledgements—The author thanks Dr. Y. L. Mehta and Dr. B. R. L. Row for their interest in the work. The

assistance from Shri Gopal Krishnan Pandey, Shri Karan Singh Bolia and Kumari Maju Rani Chaudhary is also acknowledged.

REFERENCES

1. I. M. Kolthoff and V. A. Stenger, *Volumetric Analysis*, Vol. II, 2nd Ed., pp. 110–112. Interscience, New York, 1947.
2. T. Eder, *Z. Anal. Chem.*, 1940, **119**, 399.
3. T. J. I. Craig, *J. Soc. Chem. Ind.*, 1911, **30**, 184.
4. C. C. Ahlum, *J. Chem. Soc.*, 1906, **89**, 470.
5. G. Ortner, *Z. Anal. Chem.*, 1938, **112**, 96.
6. W. J. Blaedel and J. J. Panos, *Anal. Chem.*, 1950, **22**, 910.
7. G. L. Booman, M. C. Elliott, R. B. Kimball, F. O. Cartan and J. E. Rein, *ibid.*, 1958, **30**, 284.
8. P. Pakalns, *Anal. Chim. Acta*, 1981, **127**, 263.
9. J. D. Smith, in *Comprehensive Inorganic Chemistry*, J. C. Bailon, H. J. Emeleus, S. Nyholm and A. F. Dickenson (eds.), p. 580. Pergamon Press, Oxford, 1973.
10. F. J. Welcher (ed.), *Standard Methods of Chemical Analysis*, 6th Ed., Vol. IIA, p. 586. Van Nostrand, Princeton, 1963.
11. A. I. Vogel, *A Text Book of Quantitative Inorganic Analysis*, 3rd Ed., p. 386. Longmans, London, 1961.
12. J. W. Mellor, *A Comprehensive Treatise on Inorganic and Theoretical Chemistry*, Vol. IX, p. 473. Longmans, London, 1929.

A FACILE AND SENSITIVE SPECTROPHOTOMETRIC DETERMINATION OF ASCORBIC ACID

AMIR BESADA

Microanalytical Research Laboratory, National Research Centre, Dokki, Cairo, Egypt

(Received 4 June 1986. Revised 3 March 1987. Accepted 13 March 1987)

Summary—A simple and sensitive procedure for the spectrophotometric determination of ascorbic acid is described. It involves formation of ferroin when ascorbic acid reacts with a mixture of iron(III) and 1,10-phenanthroline, and measurement of the absorbance at 510 nm. The procedure has been applied to assay of pharmaceutical preparations of vitamin C. The average error did not exceed 0.3%.

Ascorbic acid is essential for the formation of collagen and intercellular material. It also influences the formation of haemoglobin and maturation of erythrocytes. It is used primarily for the prevention and treatment of scurvy.

Several reagents have been used for direct or indirect spectrophotometric determination of ascorbic acid, including 2,6-dichlorophenolindophenol,¹ diazotized 4-methoxy-2-nitroaniline,² dimethoxydiquinone,³ 2,4-dinitrophenylhydrazine,⁴ phenylhydrazinium chloride,⁵ 4-nitrobenzenediazonium fluoroborate,⁶ 2,3,5-triphenyltetrazolium chloride,⁷ the ferricinium cation,⁸ phosphomolybdic acid⁹ and ammonium molybdate.¹⁰ For a broad collection of older methods, the reader is referred to the literature cited by Sebrell.¹¹

In the present paper, a simple, rapid, accurate and broadly applicable spectrophotometric procedure is described, based on measurement of the tris(1,10-phenanthroline)iron(II) complex (ferroin) produced by reaction of ascorbic acid with a mixture of iron(III) and 1,10-phenanthroline.

EXPERIMENTAL

Apparatus

A Shimadzu UV-240 recording spectrophotometer with 1-cm cell was used.

Reagents

All reagents, unless otherwise stated, were of analytical grade and doubly distilled water was always used.

Ascorbic acid standard aqueous solution, 20 mg/l. Prepared daily.

1,10-Phenanthroline-iron(III) colour reagent. Prepared by mixing 0.198 g of 1,10-phenanthroline monohydrate, 2 ml of 1M hydrochloric acid and 0.16 g of ferric ammonium sulphate and diluting with water to 100 ml.

Procedures

For pure ascorbic acid. Transfer an aliquot of sample solution (containing 20–120 µg of ascorbic acid) to a 25-ml standard flask, add 1 ml of the 1,10-phenanthroline-iron(III) reagent, mix and let stand for ca. 1 min. Dilute to

the mark with water and record the absorbance of the solution at 510 nm against a reagent blank (use 1-cm cells). Find the concentration of ascorbic acid from a calibration graph constructed under the same conditions.

Analysis of tablets and capsules. Extract the ground tablet or capsule contents with several portions of distilled water, filter through a Whatman No. 5 filter paper into a suitable size of standard flask and dilute to volume with water. Pipette an adequate aliquot and apply the procedure described above.

Analysis of injection ampoules. Transfer the ampoule contents quantitatively to a suitable size of standard flask, dilute to the mark with water and apply the general procedure.

RESULTS AND DISCUSSION

The method is based on oxidation of ascorbic acid to dehydroascorbic acid by iron(III) in the presence of 1,10-phenanthroline, with consequent formation of ferroin. The apparent molar absorptivity (*i.e.*, referred to ascorbic acid) is $2.2 \times 10^4 \text{ l. mole}^{-1} \text{ cm}^{-1}$, twice that for ferroin ($1.1 \times 10^4 \text{ l. mole}^{-1} \text{ cm}^{-1}$), as expected from the stoichiometry of the reaction. Full colour development is achieved within 1–2 min at room temperature. The effect of pH is shown in Fig. 1. Stoichiometric reaction and maximum colour intensity were obtained at pH 1.5–6.5. The composition of the colour reagent provided an acidity lying in this range (pH of the final solution was 5.5) and adjustment of the pH of the ascorbic acid test solution was not necessary. The decrease in absorbance at pH values outside this range may be due to incomplete oxidation of ascorbic acid at low pH or aerial oxidation at high, or to partial decomposition of ferroin by protonation or hydrolysis. Under the conditions given in the procedure, the ferroin is stable for at least 24 hr. The colour reagent is stable for many weeks.

Besides being simple and rapid, the proposed method has some advantages over some other procedures. For example, the reaction with ceric sulphate is not stoichiometric and varies with time, acidity and

Table 1. Determination of ascorbic acid in some pharmaceutical preparations

Name	Company	Ascorbic acid, μg	
		Nominal	Found*
Supervine (capsules)	Alexandria Co., for Pharmaceuticals & Chem. Ind., Alexandria	20.00	19.9 ₇
Vitacid "C" (tablets)	CID Laboratories, Giza, Cairo	20.00	19.9 ₈
Civamin (ampoules)	Misr Co., for Pharmaceutical Ind., Mataria, Cairo	15.00	15.0 ₂

*Mean of 3 determinations.

temperature.¹² The method proposed by Aly⁸ based on use of the ferricinium cation requires careful pH adjustment, a filtration, and measurement in a chloroform medium, and the error reported was 4%. The colour produced in the reaction with 4-methoxy-2-nitroaniline fades within 10 min.² The method of Eldawy *et al.*, which is based on an uncharacterized coloured product, involves a tedious preparation of the diquinone and the colour produced is stable only in the dark.³

Triplicate calibration showed that the absorbance was linearly related to amount of ascorbic acid taken, over the range 20–120 μg , with reproducibility of the absorbance to ± 0.001 .

Although the method is not selective for ascorbic acid, ten-fold amounts of the following species (which are sometimes added to commercial vitamin C preparations) do not interfere: nicotinic acid, nicotinamide, urea, thiourea, methionine, starch, glucose, fructose, mannose, sucrose, maltose, aspartic acid, tartaric acid, glutamic acid, citric acid and calcium,

magnesium and copper(II) ions. The non-interference of these compounds, particularly those having reducing properties, is presumably due to the very short time needed for the analysis, and the use of oxidation at room temperature. These very mild conditions make the procedure more selective. Multivitamin medical formulations containing ascorbic acid and vitamins A (12,500 I.U.), D₁ (1000 I. U.), B₁ (5 mg), B₂ (5 mg), B₆ (1 mg), nicotinamide (50 mg) and calcium pantothenate (10 mg) have been successfully analysed for ascorbic acid without any interference (Table 1).

Sodium metabisulphite is added to some vitamin C preparations as an antioxidant, usually at 0.1% level. It also will react with the iron(III)–phenanthroline system, but the amount present is so small that the resulting signal is less than the experimental error of the absorbance measurement, and can be ignored.

REFERENCES

1. L. P. Pepkowitz, *J. Biol. Chem.*, 1943, **151**, 405.
2. M. Schmall, C. W. Pifer and E. G. Wollish, *Anal. Chem.*, 1953, **25**, 1486.
3. M. Eldawy, A. S. Tawfik and S. Elshabouri, *ibid.*, 1975, **47**, 461.
4. J. J. Roe and C. A. Kuether, *Science*, 1942, **95**, 77.
5. N. Wahba, D. A. Yassa and R. S. Labin, *Analyst*, 1974, **99**, 397.
6. K. Istvan and F. Gustane, *Acta Pharm. Hung.*, 1967, **37**, 127.
7. H. M. Hashmi, A. S. Adil, A. Viegas and I. Ahmad, *Mikrochim. Acta*, 1970, 457.
8. M. M. Aly, *Anal. Chim. Acta*, 1979, **106**, 379.
9. A. D. Vleeschauer, W. Deschacht and H. Hendrick, *Mededel. Landbouwhogeschool Opzoekingsstat. Staat Gent*, 1961, **26**, 149.
10. E. S. Elenaey and R. Soliman, *Talanta*, 1979, **26**, 1164.
11. W. H. Sebrell, *The Vitamins*, 2nd Ed., Vol. I, p. 305. Academic Press, New York, 1967.
12. G. G. Rao and G. S. Sastry, *Anal. Chim. Acta*, 1971, **56**, 325.

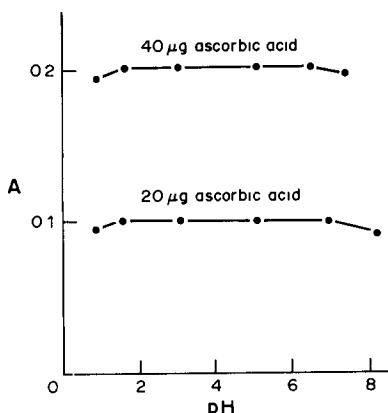


Fig. 1. Effect of pH on the absorbance.

THERMOMETRIC TITRATION OF CADMIUM WITH SODIUM DIETHYLDITHIOCARBAMATE, WITH OXIDATION BY HYDROGEN PEROXIDE AS INDICATOR REACTION

TOSHIAKI HATTORI and HITOSHI YOSHIDA*

Department of Chemistry, Faculty of Science, University of Hokkaido, 060 Sapporo, Japan

(Received 28 November 1986. Revised 17 February 1987. Accepted 13 March 1987)

Summary—A new method of end-point indication is described for thermometric titration of cadmium with sodium diethyldithiocarbamate (DDTC). It is based on the redox reaction between hydrogen peroxide added to the system before titration, and the first excess of DDTC. Amounts of cadmium in the range 10–50 μ moles are titrated within 1% error.

Thermometric titration is a widely applicable and simple analytical method. However, when the temperature change accompanied by a titration reaction is small, determination of the end-point often becomes difficult. Many attempts have been made to increase the clarity of the end-point, namely use of a catalytic reaction (so-called catalytic thermometric titration),¹ the heat of dilution of excess of titrant,² combination of reactions with markedly different enthalpy changes for sequential titration,^{3–5} and addition of a dispersing agent when a precipitation reaction is employed.⁶

Sodium diethyldithiocarbamate (DDTC) is a very useful reagent for the thermometric titration of Cu^{2+} , Pb^{2+} , Ni^{2+} , Cd^{2+} , Zn^{2+} , Ag^+ and Tl^+ .⁷ However, in the titration of low concentrations of these, especially Cd^{2+} and Zn^{2+} , the accompanying temperature change is insufficient for the end-point to be accurately located.

In this work we investigated a new method for sharpening the end-point by means of the large heat of reaction of the oxidation of DDTC with hydrogen peroxide.

EXPERIMENTAL

Apparatus

The differential thermometric titration apparatus described in detail previously was used.⁶

Reagents

All reagents used were of guaranteed reagent grade. A 0.1M cadmium solution was prepared from the nitrate and standardized with 0.5M EDTA solution by thermometric titration. A 0.1M DDTC solution was prepared daily by dissolving 5.62 g of sodium *N,N*-diethyldithiocarbamate trihydrate in 250 ml of distilled water. The solution was standardized with a standard zinc solution by thermometric titration.⁷ The hydrogen peroxide solution (2.5M) was standardized by iodimetry.

Procedure

One of the twin burettes is filled with 0.1M DDTC, and the other (the reference burette) with distilled water. The sample solution containing 10–50 μ moles of cadmium is placed in a 100-ml Dewar flask, 5 ml of 1M acetate buffer (pH 5.5) are added, the mixture is diluted to 49 ml with distilled water, and 1 ml of 2.5M hydrogen peroxide is added. In the reference flask 50 ml of distilled water are placed. When they are at same temperature, the two solutions are simultaneously titrated with the twin burette system at the rate of 0.1 ml/min. The concentration of cadmium is determined from the inflection point in the titration curve and corrected for a blank titration.

RESULTS AND DISCUSSION

Typical titration curves

A cadmium solution (0.4mM) was titrated with 0.1M DDTC. As shown in curve a in Fig. 1, the temperature change after the equivalence point is so small that the detection of the end-point is often difficult. However, curve b, obtained in the presence of hydrogen peroxide, has a large temperature change after the equivalence point and the end-point detection is very easy. The curve shows that the heat of the redox reaction of DDTC with hydrogen peroxide is several times larger than that of chelation of DDTC with cadmium.

Effect of oxidizing reagents

Iodine, chlorate, bromate, iodate, periodate and chloramine-T were also tested as reagents for oxidizing DDTC, but only bromate proved suitable for the indicator reaction. The heat of oxidation of DDTC with iodine was smaller than that with hydrogen peroxide, and the amount of DDTC consumed by cadmium appeared to increase with increase in the concentration of iodine added. DDTC was hardly oxidized at all with chlorate. Iodate, periodate and chloramine-T gave a large temperature change early in the titration, and no end-point for cadmium could

*Author for correspondence.

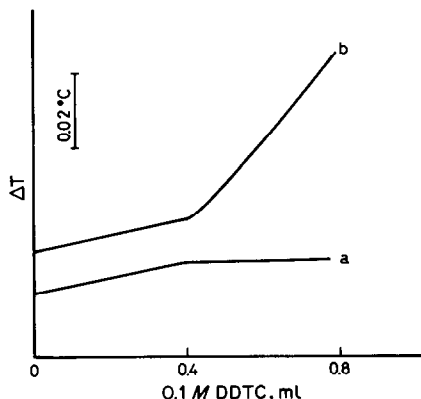


Fig. 1. Typical curves for thermometric titration of cadmium with 0.1M DDTC: a, 0.4mM cadmium at pH 5.5; b, a + 0.05M hydrogen peroxide.

be detected. Bromate gave much the same titration curve as hydrogen peroxide did.

Effect of hydrogen peroxide concentration

Figure 2 shows the thermometric titration curves for cadmium in the presence of various concentrations of hydrogen peroxide. The slope after the equivalence point increases with hydrogen peroxide concentration. At hydrogen peroxide concentrations $> 0.05M$, the final slope remains almost unchanged.

Effect of pH

Figure 3 shows the titration curves for a blank solution containing hydrogen peroxide, at various pH values. These curves correspond to those observed after the equivalence point for cadmium titration. The slopes increase with pH in the range from 4.1 to 5.5, and after the addition of DDTC has been stopped the slopes still increase slowly. These phenomena are presumably due to the decomposition of DDTC consisting of stepwise reactions, the first being fast and the subsequent ones slower. A slight rise in

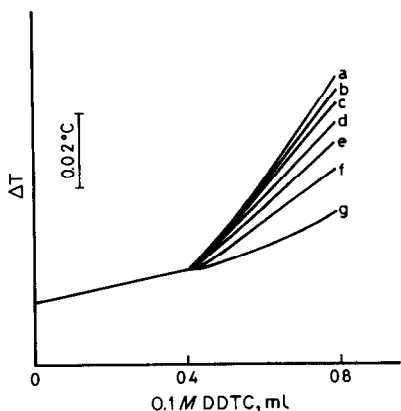


Fig. 2. Effect of concentration of hydrogen peroxide on the shape of the thermometric titration curve for 0.4 mM cadmium at pH 5.5. $[H_2O_2]$, M: a, 0.2; b, 0.1; c, 0.05; d, 0.02; e, 0.01; f, 0.005; g, 0.002.

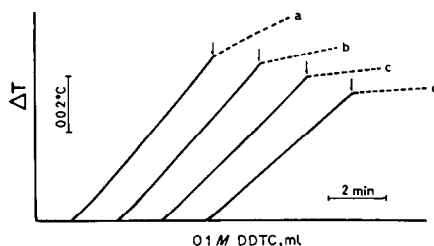
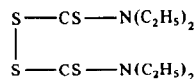


Fig. 3. Effect of pH on the heat of reaction of 0.05M hydrogen peroxide with 0.1M DDTC. pH: a, 5.5; b, 5.0; c, 4.6; d, 4.1. Arrows indicate the point at which the burette was turned off.

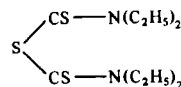
temperature after the end-point was also observed when hydrogen peroxide was not present.⁷ These slow rises decrease in slope with increase in pH, and are due to the slow decomposition of the excess of DDTC to the diethylammonium ion and carbon disulphide.

Oxidation products of DDTC

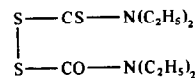
The products of oxidation of DDTC with hydrogen peroxide were investigated. They were prepared by using the conditions for the blank titrations, at various pH values. The products were extracted with chloroform, and separated by thin-layer chromatography on silica gel with benzene-ethyl acetate mixture. The chief product was tetraethyl thiuram disulphide (I), which was identified by infrared spectroscopy. Minor products were tetraethyl thiuram monosulphide (II) and diethylcarbonyl diethylthiocarbonyl disulphide (III), which were identified by high-resolution electron-impact mass spectroscopy and infrared spectroscopy. The amount of these products decreased with increasing pH. The aqueous phases from the extraction were found to contain sulphate after heating, in almost the same amount as that calculated by difference from the total amount of DDTC added and the amount equivalent to the organic oxidation products. Changing the pH for the oxidation changed the ratios between the various products.



I



II



III

Table 1. Determination of cadmium (mean and r.s.d. of 5 results)

Taken, μmoles	Found, μmoles	r.s.d., %
10.1	10.0	0.9
20.3	20.3	0.5
30.4	30.4	0.4
40.6	40.6	0.4
50.7	50.7	0.2

Determination of cadmium and some heavy metals

Table 1 shows results for the thermometric titration of cadmium. The relative standard deviations are $\leq 1\%$ for 10–50 μmoles of cadmium (0.2–1.0 mM). Some heavy metals which form relatively stable complexes with DDTc, such as Cu^{2+} , Pb^{2+} , Ni^{2+} and Zn^{2+} , can also be determined by this method. In the titration curve for copper(II) considerable curvature is observed before the end-point, because copper(II) catalyses the decomposition of hydrogen peroxide. However, copper can be determined satisfactorily if 1 ml of 0.1M EDTA is added to the titrand to mask the copper; the Cu-EDTA complex undergoes ligand exchange with DDTc but does not cause decomposition of the peroxide.

CONCLUSION

A new technique for increasing the clarity of the end-point in thermometric titration with DDTc has been developed. It is based on addition of hydrogen peroxide to the titrand, and its oxidation of excess of titrant after the equivalence point. This direct thermometric titration is simpler and more rapid than the indirect complexometric titration with indication by the manganese(II) catalysed hydrogen peroxide-resorcinol reaction.⁸

Acknowledgements—This work was supported in part by a Grant-in-Aid for Scientific Research from the Ministry of Education, Science and Culture of Japan.

REFERENCES

1. E. J. Greenhow, *Chem. Rev.*, 1977, **77**, 835; T. F. A. Kiss, *Talanta*, 1983, **30**, 771.
2. G. A. Vaughan and J. J. Swithenbank, *Analyst*, 1967, **92**, 364.
3. J. Jordan and T. G. Alleman, *Anal. Chem.*, 1957, **29**, 9.
4. K. Doi and M. Tanaka, *Anal. Chim. Acta*, 1974, **71**, 464.
5. H. Yoshida, T. Hattori, H. Arai and M. Taga, *ibid.*, 1983, **152**, 257.
6. T. Hattori and H. Yoshida, *Anal. Sci.*, 1986, **2**, 209; *Talanta*, 1986, **33**, 167.
7. T. Hattori, S. Kusumi, T. Suzuki, M. Taga and H. Yoshida, *Bunseki Kagaku*, 1987, **36**, 125.
8. H. Weisz and T. Kiss, *Z. Anal. Chem.*, 1970, **249**, 302.

FIRE-ASSAY COLLECTION OF GOLD AND SILVER BY COPPER

ANDREAS DIAMANTATOS

Rand Refinery Limited, Box 565, Germiston, South Africa

(Received 21 May 1986. Revised 7 January 1987. Accepted 16 January 1987)

Summary—Gold and silver are very effectively collected in copper after fire-assay fusion at 1200°. The resultant copper button is dissolved in perchloric acid and the parting solution is diluted with an equal volume of water. Both gold and silver are precipitated in the copper perchlorate medium by reduction with formic acid or hydroquinone. The two noble metals are collected, dissolved in acids, and determined by atomic-absorption spectrometry. The proposed procedure is simple, relatively rapid, and has been successfully applied to ores, concentrates, furnace products, and copper alloys. Recoveries compare favourably with those obtained by the classical lead cupellation method.

Copper has been recommended by Beamish and his co-workers as a collector for platinum and palladium,¹ for iridium,² and for rhodium.³ There is no published paper on the fire-assay collection of gold and silver by copper. These two precious metals are usually determined in ores and concentrates by the traditional lead cupellation technique. Although their collection in molten lead is essentially complete, the subsequent removal of lead by cupellation introduces certain losses and errors for gold^{4,5} and for silver,⁶⁻⁸ which are compensated for by applying corrections. Moreover, the lead method is not applicable to samples with relatively large proportions of base metals.^{9,10} If the copper content of the sample is fairly high, slag retention and cupel absorption of gold and silver are appreciable; a high concentration of iron is detrimental because this metal cannot be removed during the cupellation but remains stuck on top of the cupel in the form of a ring scoria, invariably retaining some of the gold and silver; with samples containing zinc, the loss of gold and silver in the slag during the fusion process is high. The lead method is also inadvisable for gold-bearing samples containing osmiridium, because spitting takes place during cupellation, causing losses of gold and silver and contamination of the surrounding samples. Nickel sulphide collection, as an alternative to the lead method, gives low and erratic results for gold,¹¹⁻¹⁴ and silver cannot be determined in the nickel chloride parting solution.¹⁵

These problems led to the decision to examine the possibilities of extending the copper collection technique¹⁻³ to gold and silver. This paper demonstrates the high efficiency of copper as a collector of gold and silver, and describes a novel procedure for the recovery of the two noble metals from the copper assay buttons.

EXPERIMENTAL

Apparatus and reagents

The fusions were done in a fire-assay electric furnace, with

fireclay pots, size No 3. A Varian-Techtron AA375 atomic-absorption spectrophotometer was used for the absorption measurements.

The flux for fire-assay was prepared by mixing 40 g of cupric oxide (powdered), 25 g of borax, 60 g of soda ash, 10 g of silica and 2.0 g of graphite (powdered).

Procedures

Preparation of copper button. The accurately weighed sample (1-30 g) is roasted on a thin silica bed at 750° to convert the sulphides into oxides. The roasted sample is mixed with 30 g of flux in a cellophane bag (cooking bag 28 × 18 cm) and then the bag is folded fairly tightly to form a small packet which is placed in the fusion pot over a 30-g portion of flux and finally covered completely with the remainder of the flux (77 g). The pot is inserted in the fire-assay furnace, preheated to 1200°, and kept at this temperature for 1.5 hr. Carefully, and without shaking, the pot is removed from the furnace and allowed to cool for ca. 1 hr. The fireclay pot is then broken to free the copper button and any adhering slag is removed by tapping.

Analysis of copper button. The clean copper button (ca. 30 g) is placed in an 800-ml beaker and 300 ml of 70% perchloric acid are added and boiled for ca. 2 hr until all the copper has dissolved. The beaker is removed from the hot plate and allowed to cool to about 100°. The parting solution is diluted with 300 ml of water, with stirring. The diluted solution is brought to the boil and formic acid (20 ml) or 0.25 g of hydroquinone (dissolved in a little water) is added slowly and with stirring. The gentle boiling is continued for 1 hr. After cooling in water for 15-20 min, the mixture is left to stand for 1.5 hr in the dark to ensure complete precipitation of silver, and the precipitate is then filtered off on a 45-mm diameter 0.45- μ m pore-size filter in a Millipore filter apparatus. After three or four washes with water, the filter disc and precipitate are transferred to the original 800-ml beaker, 40 ml of *aqua regia* are added and the mixture is boiled until the filter membrane is completely dissolved. The solution is evaporated to dryness in the presence of a little sodium chloride, then 20 ml of concentrated hydrochloric acid and 5 or 6 drops of 100-volume hydrogen peroxide are added and the solution is boiled gently to dissolve all the gold and silver. The solution is cooled and transferred to an appropriate size of standard flask (to give concentrations of 5-20 ppm of gold and 1-5 ppm of silver) and diluted to volume with 3M hydrochloric acid to prevent any precipitation of silver chloride. The atomic-absorption of gold and silver is measured at 242.8 and 328.1 nm, respectively, and interpreted from the absorption values for standard solutions of the two metals.

RESULTS AND DISCUSSION

Preliminary investigations were undertaken to establish the optimum proportions of flux constituents, particularly those of cupric oxide and graphite, which after fusion with the sample would produce copper buttons capable of collecting gold and silver quantitatively and be of reasonable size (*ca.* 30 g), thus avoiding large buttons which would increase considerably the time necessary for dissolution by the parting acid. Accordingly, a number of fire-assay fluxes were salted with 20 mg each of gold and silver and fused to produce copper buttons as described above. The experimental data and the weights of the buttons are shown in Table 1.

To check the efficiency of collection, each of the fusion slags was individually ground, mixed with lead flux and analysed by the classical lead assay. Only trace amounts of gold (< 20 μ g) and silver (< 15 μ g) were retained in the slags.

Furthermore, the lower part of the pot wall, which had been attacked by the flux during fusion, was also ground and analysed by the lead fire-assay but neither gold nor silver was detected. As flux 5 (Table 1) appears the most advantageous, it was chosen for all further experiments.

Behaviour of silver and gold during parting the copper button with perchloric acid

A 30-g copper button containing 40 mg of silver, added as the powdered metal, was boiled with 300 ml of 70% perchloric acid in an 800-ml beaker. The dissolution of the button was complete after boiling for approximately 2 hr. After cooling to *ca.* 100°, the blue copper perchlorate parting solution was diluted with 300 ml of water, reboiled for 4–5 min and then cooled completely. This diluted solution was clear, and only a small white residue, which was identified as silica, was left undissolved at the bottom of the beaker. After filtration with a Millipore apparatus, the filter disc and residue were analysed. No silver was detected, thus indicating complete dissolution of silver by the parting acid and no retention of the precious metal by the siliceous residue.

Analogous tests were done with copper buttons containing 10 mg of gold, added as metal powder. The hydrogen evolved during the dissolution of copper by the perchloric acid reduced part of the gold (~3.7 mg) to the metal, which floated as a brown

sponge in the parting solution. When this test was repeated on copper buttons containing gold added as sulphide (leached copper–nickel matte), no partial precipitation of gold took place but the noble metal dissolved completely in the perchloric acid. It is evident that the behaviour of gold during the parting is dependent on the nature of the starting materials.

Precipitation of gold and silver in the copper–perchloric acid parting solution

Factors which could affect the completeness of precipitation of gold and silver in the copper perchlorate medium were investigated. Copper perchlorate parting solutions (300 ml) containing 10 mg of silver were diluted with 300 ml of water. These diluted solutions were brought to the boil and formic acid (98–100%, 10 ml) or 0.25 g of hydroquinone (dissolved in 20 ml of water) was added, with stirring. The gentle boiling was continued for 45 min. After cooling in water for 15 min, the solutions were allowed to stand in the dark for different periods of time ranging from 15 min to 2 hr, and then filtered with the Millipore apparatus. Analysis showed no silver in the filtrates from the solutions which had been left standing for more than 1 hr. A similar procedure was applied for gold. Not even trace amounts of gold could be detected in any filtrate tested. A boiling time of 1 hr and standing time of 1.5 hr were considered safer and are therefore recommended. Precipitations were performed under these conditions with different amounts of reductant. Analysis of the filtrates showed that 10 ml of formic acid or 0.25 g of hydroquinone sufficed for complete precipitation of at least 10 mg of each noble metal.

The effect of perchloric acid concentration on the precipitation was also studied. Copper perchlorate parting solutions were diluted with different volumes of water (300, 400 and 500 ml) and then treated with the reductants as before. Neither gold nor silver was found to be unprecipitated at any of three acid concentrations examined. To avoid inconveniently large working volumes, dilution of the parting solution with an equal volume of water (300 ml) was adopted.

Behaviour of foreign elements

It was found that iron, nickel, chromium, lead, zinc, cobalt, bismuth and tellurium in copper–

Table 1. Copper buttons

Flux	Composition of flux					Weight of copper button, g
	Cupric oxide, g	Borax, g	Soda ash, g	Silica, g	Graphite, g	
1	65	25	60	10	3.5	52
2	45	25	60	10	3.5	38
3	40	25	60	10	3.0	35
4	45	25	60	10	2.0	32
5	40	25	60	10	2.0	30
6	40	25	60	20	2.0	30

Table 2. Accuracy and precision

Gold, mg		Silver, mg	
Added	Recovered	Added	Recovered
9.98	10.02	10.01	9.98
	9.95		9.92
	9.96		10.04
5.52	5.50	3.00	2.98
	5.46		3.00
	5.46		2.94
	5.52		2.98
0.424	0.417	1.04	1.08
	0.419		1.02
	0.422		1.02
	0.415		1.04
0.106	0.105	0.520	0.514
	0.101		0.520
	0.101		0.514
0.053	0.056	0.130	0.132
	0.047		0.125
	0.050		0.128

perchloric acid solutions, were not precipitated either by formic acid or hydroquinone; platinum, palladium and rhodium were. Selenium was precipitated by hydroquinone but not by formic acid. However, the platinum metals and selenium do not interfere in the determination of gold and silver by atomic-absorption spectrometry (AAS), if a uranium buffer solution is added.¹⁶

Accuracy and precision

To assess the accuracy and reproducibility of the method, copper fluxes salted with known milligram and microgram quantities of gold and silver were fused at 1200° as described, and the copper assay buttons analysed. The results given in Table 2 show good accuracy and precision.

Analysis of various samples and comparison with the classical lead cupellation

A number of samples of different origins, compositions and ratios of noble metal content, were analysed for gold and silver by the copper collection

Table 3. Comparison of copper and lead assay methods

Sample	Method	Results, µg/g	
		Gold	Silver
Gold ore (30 g)	Copper	18.3	15.8
	Lead	18.5	15.7
Concentrate (10 g)	Copper	1.77×10^3	202
	Lead	1.75×10^3	196
Carbon leader (5 g)	Copper	1.13×10^3	142
	Lead	1.15×10^3	148
Refinery borax slag (5 g)	Copper	857	3.23×10^3
	Lead	848	3.15×10^3
Jeweller's sweeps (0.5 g)	Copper	2.88×10^4	3.07×10^4
	Lead	2.86×10^4	3.08×10^4

Average of three determinations.

and lead collection methods. Only one fusion was used for the lead assay. For comparative purposes and to eliminate any errors which might have arisen from the use of different final measurement techniques, all measurements were done by AAS. Thus the gold-silver precipitates derived after formic acid reduction in the copper method and the gold-silver prills derived after cupellation in the lead method, were brought into solution with *aqua regia* and then converted into 3M hydrochloric acid solutions in which the two noble metals were determined by AAS. The results listed in Table 3 show that the copper collection procedure yields recoveries which compare favourably with those obtained by the lead method.

CONCLUSION

The copper fire-assay quantitatively collects gold and silver from ores and concentrates. It is widely applicable and useful for determining gold and silver in materials that cannot be taken through the traditional lead assay. Of particular interest is the analytical treatment of the copper collector. Once the copper assay button is obtained, the dissolution of copper and the recovery of gold and silver from the copper-perchloric acid parting solution are accomplished with ease. This treatment itself represents a novel and attractive method for determining gold and silver in copper alloys.

Acknowledgement—The author wishes to thank the General Manager of Rand Refinery for permission to publish this work.

REFERENCES

- L. M. Banbury and F. E. Beamish, *Z. Anal. Chem.*, 1965, **211**, 178.
- K. C. Agrawal and F. E. Beamish, *ibid.*, 1965, **211**, 265.
- L. M. Banbury and F. E. Beamish, *ibid.*, 1966, **218**, 263.
- C. H. Coxon, C. J. Verwey and D. N. Lock, *J. S. Afr. Inst. Mining Met.*, 1962, **62**, 546.
- N. N. Popova, E. P. Zdorova and M. A. Kondulinskaya, *Zavodsk. Lab.*, 1974, **40**, 1061.
- G. H. Faye and W. R. Inman, *Anal. Chem.*, 1959, **31**, 1072.
- Y. Nakamura and K. Fukami, *Bunseki Kagaku*, 1957, **6**, 687.
- R. Le Houillier and N. Rheume, *Can. Metall. Q.*, 1984, **23**, 427.
- V. S. Dillon, *Assay Practice on the Witwatersrand*, Parrow, Cape Times, 1952.
- K. Yaguchi and J. Kuneko, *Bunseki Kagaku*, 1972, **21**, 601.
- R. V. D. Robèrt, E. Van Wyk, R. Palmer and T. W. Steele, *Nat. Inst. Metall., Repub. S. Afr., Rept.*, No. 1371, 1971.
- A. P. Kuznetsov, Y. N. Kukushkin and D. F. Makarov, *Zh. Analit. Khim.*, 1974, **29**, 2155.
- A. Diamantatos, *Anal. Chim. Acta*, 1977, **94**, 49.
- E. L. Hoffman, A. J. Naldrett, J. C. Van Loon, R. G. V. Hancock and A. Manson, *ibid.*, 1978, **102**, 157.
- K. Dixon, E. A. Jones, S. Rasmussen and R. V. D. Robèrt, *Nat. Inst. Metall., Repub. S. Afr., Rept.*, No. 1714, 1975.
- R. C. Mallett, D. C. G. Pearton, E. J. Ring and T. W. Steele, *Talanta*, 1972, **19**, 181.

ANALYTICAL DATA

STUDIES ON FLUORESCEIN—V*

THE ABSORBANCE OF FLUORESCEIN IN THE ULTRAVIOLET, AS A FUNCTION OF pH

HARVEY DIEHL and NAOMI HORCHAK-MORRIS

Department of Chemistry, Iowa State University, Ames, Iowa 50011, U.S.A.

(Received 3 October 1986. Accepted 21 December 1986)

Summary—The ultraviolet absorption spectrum of an aqueous solution of highly-purified yellow fluorescein at ionic strength 0.10 has been measured at various pH values in the range from 0.15 to 8.70. The maxima at 227, 249 and 295 nm change little with pH, but the maximum found at 437 nm in acid medium changes greatly in absorbance and position on addition of alkali, resolving first into two maxima, at 455 and 475 nm, and finally becoming a single large maximum (at $\text{pH} \geq 8$) at 490 nm. A unique feature of the absorption at 437 nm is that all four prototropic forms of fluorescein, H_3Fl^+ , H_2Fl , HFl^- and Fl^{2-} , absorb at this wavelength. The total absorbance at this wavelength first falls rapidly as the pH rises from 0.15, reaching a minimum at pH 3.63, then increases to a maximum at pH 5.3, and finally falls to steady value at $\text{pH} > 8.0$. The absorbance as a function of pH is defined by seven constants: three dissociation constants ($K_{\text{H}_3\text{Fl}} = 6.61 \times 10^{-3}$, $K_{\text{H}_2\text{Fl}} = 3.98 \times 10^{-5}$, $K_{\text{HFl}} = 4.36 \times 10^{-7}$) and four molar absorptivities ($\epsilon_{\text{H}_3\text{Fl}} = 4.94 \times 10^4$, $\epsilon_{\text{H}_2\text{Fl}} = 1.20_5 \times 10^4$, $\epsilon_{\text{HFl}} = 2.16 \times 10^4$ and $\epsilon_{\text{Fl}} = 7.61 \times 10^3 \text{ l. mole}^{-1} \text{ cm}^{-1}$). Solutions of yellow fluorescein in water undergo rapid deterioration on exposure to daylight or fluorescent lighting but are stable in the dark.

Three sets of values for the acid dissociation constants of fluorescein, calculated from absorption data, have been reported, as follows,

	$\text{p}K_{\text{H}_3\text{Fl}}$	$\text{p}K_{\text{H}_2\text{Fl}}$	$\text{p}K_{\text{HFl}}$
Zanker and Peter, ¹ water-dioxan mixtures; no attention to ionic strength	1.95	5.05	7.0
Lindqvist, ² water only; ionic strength 0.01 as far as possible	2.2	4.4	6.7
Vig, ³ water only; ionic strength 1.0	2.25	5.1	7.1

It was Zanker and Peter who established the existence of the four prototropic forms of fluorescein, H_3Fl^+ , H_2Fl , HFl^- , Fl^{2-} , but unfortunately they did not appreciate the great internal changes in structure and acid strength the fluorescein molecule undergoes on passing from a solvent of high dielectric constant to one of low. Lindqvist rejected their values for the dissociation constants on the basis that they were not applicable to his own work on the flash photolysis of fluorescein in purely aqueous medium, and repeated the absorption measurements at an ionic strength kept as close as possible to 0.01. Only the final values obtained by Vig have been reported (Bannerjee and Vig,⁴ p. 447, column 1, line 7), in a paper which deals with the polarography of fluorescein. Through the courtesy of Professor S. K. Vig, we have obtained photocopies of the appropriate pages of his dissertation³ and learned the details of his work, so far unpublished.

Although in general agreement, the three sets of values appear to differ by more than would be expected from experimental error and the differences in ionic strength.

To calculate values for the dissociation constants a considerable volume of data from a family of absorption spectra as functions of pH is required, and is not available in the papers of Zanker and Peter and of Lindqvist, where a few selected spectra at widely separated pH values are given together with summaries in the form of plots of absorbance at selected wavelengths as functions of pH. Vig's dissertation gives a family of some 15 spectra at different pH values, but all on a single figure; the reproduction made available to us was small in size and unfortunately the individual curves carried no identification, making interpretation impossible.

What makes all this frustrating is that of the four prototropic forms only one, at first sight, appears associated exclusively with a single absorption band—the protonated species, H_3Fl^+ , with the absorption band at 437 nm. The differences in the dissociation constants of fluorescein are small and the absorption bands associated with the other three species overlap not only with each other but also to a considerable degree with the band at 437 nm. This creates problems which a careful reading of the papers cited reveals have neither been fully realized nor resolved. All the workers concerned are vague as to the precise wavelengths at which the absorbances were measured, and in the work of Lindqvist and of Vig, absorbances at an isobestic point are used without justification. Some very serious discrepancies in repeating our own earlier measurements of the ab-

*Part IV—H. Diehl, *Talanta*, 1986, **33**, 935.

Table 1. Molar absorptivity of yellow fluorescein; concentration $2.407 \times 10^{-5}M$; ionic strength, 0.10; λ_{\max} = wavelength of maximum absorption (nm); ϵ_{\max} = molar absorptivity ($l.mole^{-1}.cm^{-1}$)

pH 1.10		pH 4.60		pH 7.72	
λ_{\max}	ϵ_{\max}	λ_{\max}	ϵ_{\max}	λ_{\max}	ϵ_{\max}
227	4.24×10^4	229	4.24×10^4	237	4.05×10^4
249	2.62×10^4	274	1.31×10^4	282	1.31×10^4
295	0.57×10^4	310	0.49×10^4	320	0.86×10^4
437	4.72×10^4	*		*	

*Undergoes extensive change with pH; see text.

sorption spectra alerted us to another source of trouble: the fairly rapid deterioration of stock solutions of fluorescein on exposure to daylight or fluorescent lighting.

EXPERIMENTAL

Reagents

Yellow fluorescein. The preparation procedures followed were those described earlier.⁵

Buffers. Buffers in the pH range 1–4 were prepared from hydrochloric acid, dilutions being made with 0.10M potassium chloride to maintain constant ionic strength. The pH of the buffers was measured before and after addition of the fluorescein stock solution, by use of a Hach Expanded Range pH-meter with a Beckman glass electrode. The pH meter was standardized against standard buffer solutions of pH 1.68 and 3.56, prepared from potassium tetraoxalate and potassium hydrogen tartrate, respectively, according to the NBS prescriptions.

Standard solutions. An accurately weighed quantity of 0.8 g of yellow fluorescein was dissolved in 250 ml of 0.1024M sodium hydroxide. The pH was adjusted to 7 with 0.10M hydrochloric acid, and the solution was diluted to 1 litre with 0.10M potassium chloride and labelled Stock Solution I, $2.407 \times 10^{-3}M$. A volume of 100.0 ml of this solution was diluted to 1 litre with 0.10M potassium chloride, giving Stock Solution II, $2.407 \times 10^{-4}M$. After it was discovered that solutions of fluorescein deteriorate on exposure to daylight or fluorescent lighting, these stock solutions were stored in the dark. For the absorbance measurements, a 10.0-ml portion of Stock Solution II was taken, the buffer added, the pH measured, and dilution to 100.0 ml made with 0.1M potassium chloride. Thus in every case, the concentration of the fluorescein was $2.407 \times 10^{-5}M$ and the ionic strength 0.10. The ionic strengths of the four solutions of pH < 1 (made by adding just the necessary volume of 1M hydrochloric acid) were, of course, greater than 0.10, but no record was kept of the actual ionic strength.

Absorption measurements

Absorption measurements were made with a Perkin-Elmer model 320 spectrometer with a 1-cm fused-silica cell, over the range from 195 to 700 nm. The absorption spectra and related individual measurements (digital read-out with the wavelength drive shut off) at wavelengths slightly displaced on either side of the absorption maxima were made promptly with minimum exposure to light. Although there was no deterioration of the pH-7 solutions stored in the dark (no change in absorbance observable in 6 days), preparation and measurement of the final solutions was completed within 36 hr.

RESULTS AND DISCUSSION

Maxima in the absorbance were found (at pH 1.00) at 226, 247, 295 and 435 nm. The first three of these

maxima change little with pH, Table 1. On the other hand, the maximum at 437 nm undergoes extensive change with pH. Our goal being to relate absorbance to the dissociation steps of fluorescein, our attention was devoted to this maximum. The effect of increasing pH on the characteristics of this absorption band is reported in Table 2. The measurements were made in two series, the first 18 values for pH 0.15–3.40, and the other 22 for pH 3.60–8.70. Note that there is not a completely smooth variation of A with pH (owing to experimental error) in the pH-region 2.0–3.2, where there is overlap of the bands.

Deterioration of fluorescein in solution on exposure to light

After discovering and confirming that our stock solution of fluorescein was undergoing relatively rapid decrease in absorbance, tests were made that showed that the deterioration was caused by exposure to light and that solutions of pH 7 stored in the dark were stable. More extensive tests showed that exposure in Pyrex standard flasks 6 ft below an 80-W fluorescent lighting tube decreased the absorbance by 20% in 6 days, 35% in 10 days and 54% in 6 weeks. In a further experiment with $2.407 \times 10^{-5}M$ fluorescein at pH 1.05, the absorbances at the maxima at 228, 250, 296 and 437 nm all deteriorated at the same rate, indicating a general breakdown of the molecule.

The absorption band with a maximum at 437 nm at pH 1.00 shifts to longer wavelengths with increasing pH and decreases in height; a shoulder appears between 475 and 490 nm at pH 1.80, and grows with increasing pH, and at pH 4.80 separate maxima are present, at 455 and 475 nm; this band finally becomes, at pH ≥ 8 , a single major peak at 490 nm. Table 2 gives the absorbances at five wavelengths for each of 40 values of pH between 0.15 and 8.70; these values were obtained with the wavelength drive turned off and thus with the best precision obtainable from the spectrometer. The measurements were made at the wavelengths specified and not at the absorption maxima. The absorbance at 464 nm was recorded because earlier workers had observed and made use of an isosbestic point at this wavelength.

A unique feature of yellow fluorescein is that all four of the prototropic forms, H_3Fl^+ , H_2Fl , HFl^- ,

Table 2. Absorbance of yellow fluorescein at five wavelengths in the visible spectrum as a function of pH; concentration $2.407 \times 10^{-5}M$; ionic strength 0.10; path length 1.0 cm

Line No.	pH	[H ⁺]	A ₄₃₇	A ₄₅₅	A ₄₆₄	A ₄₇₅	A ₄₉₀
1	0.15	7.009E-1	1.187	0.490	0.185	0.033	0.000
2	0.65	2.239E-1	1.169	0.318	0.096	0.015	0.000
3	0.70	1.995E-1	1.162	0.370	0.100	0.019	0.000
4	0.90	1.295E-1	1.145	0.368	0.104	0.026	0.000
5	1.00	0.100E-1	1.135	0.346	0.105	0.025	0.000
6	1.25	5.620E-2	1.095	0.370	0.109	0.027	0.010
7	1.50	3.162E-2	1.031	0.285	0.098	0.030	0.015
8	1.80	1.585E-2	0.968	0.299	0.092	0.033	0.018
9	1.95	1.122E-2	0.854	0.360	0.135	0.050	0.030
10	2.05	8.912E-3	0.804	0.294	0.094	0.053	0.031
11	2.10	7.940E-3	0.830	0.265	0.110	0.045	0.020
12	2.35	4.466E-3	0.643	0.260	0.108	0.060	0.034
13	2.40	3.981E-3	0.667	0.210	0.092	0.058	0.034
14	2.90	1.259E-3	0.456	0.182	0.108	0.090	0.050
15	2.98	1.047E-3	0.392	0.194	0.123	0.103	0.062
16	3.10	7.943E-4	0.395	0.195	0.127	0.110	0.065
17	3.22	6.025E-4	0.364	0.190	0.139	0.126	0.069
18	3.40	3.981E-4	0.346	0.212	0.161	0.150	0.089
19	3.60	2.512E-4	0.343	0.257	0.216	0.209	0.120
20	3.80	1.585E-4	0.347	0.294	0.258	0.254	0.143
21	4.00	1.000E-4	0.367	0.355	0.323	0.322	0.180
22	4.05	8.913E-5	0.367	0.358	0.326	0.326	0.182
23	4.25	5.623E-5	0.390	0.415	0.386	0.390	0.217
24	4.60	2.512E-5	0.427	0.506	0.482	0.491	0.277
25	4.80	1.585E-5	0.458	0.582	0.563	0.579	0.340
26	5.15	7.080E-6	0.474	0.639	0.628	0.656	0.426
27	5.50	3.162E-6	0.468	0.660	0.664	0.713	0.542
28	5.78	1.660E-6	0.446	0.659	0.682	0.757	0.680
29	6.00	1.000E-6	0.419	0.649	0.692	0.796	0.829
30	6.30	5.012E-7	0.359	0.620	0.704	0.865	1.107
31	6.50	3.162E-7	0.322	0.601	0.710	0.905	1.276
32	6.82	1.514E-7	0.263	0.569	0.717	0.965	1.533
33	6.92	1.202E-7	0.241	0.557	0.720	0.988	1.633
34	7.15	7.080E-8	0.222	0.548	0.723	1.011	1.762
35	7.40	3.981E-8	0.216	0.545	0.724	1.017	1.753
36	7.72	1.906E-8	0.205	0.538	0.725	1.027	1.796
37	7.88	1.318E-8	0.194	0.533	0.728	1.043	1.858
38	8.25	5.623E-9	0.193	0.532	0.729	1.044	1.864
39	8.50	3.162E-9	0.192	0.533	0.731	1.049	1.879
40	8.70	1.995E-9	0.189	0.530	0.729	1.049	1.882

and Fl^{2-} , absorb at 437 nm. At this wavelength the absorbance falls rapidly as the pH rises from 0.15, reaches a minimum at 3.63, then rises to a maximum at pH 5.3, and thereafter falls, reaching a steady value at pH 8.0. Assuming that the system conforms to the Beer-Lambert and additivity laws, this function is defined by

$$A_{437} = A_{\text{H}_3\text{Fl}}^{\rightarrow} \alpha_{\text{H}_3\text{Fl}} + A_{\text{H}_2\text{Fl}}^{\rightarrow} \alpha_{\text{H}_2\text{Fl}} + A_{\text{HFl}}^{\rightarrow} \alpha_{\text{HFl}} + A_{\text{Fl}}^{\rightarrow} \alpha_{\text{Fl}}$$

the A terms marked by the superscript arrows (redundancy markers) being the working absorptivities of the respective forms and related to the molar absorptivities by multiplying the latter by the molar concentration of the fluorescein. The α terms are the fractions of the fluorescein present in the respective prototropic forms and are determined by the three dissociation constants, $K_{\text{H}_3\text{Fl}}$, $K_{\text{H}_2\text{Fl}}$, K_{HFl} . The system is thus defined by seven constants. The experimental data in Table 2, column 4, are fitted closely by

$$A_{437} = 1.190\alpha_{\text{H}_3\text{Fl}} + 0.290\alpha_{\text{H}_2\text{Fl}} + 0.520\alpha_{\text{HFl}} + 0.1833\alpha_{\text{Fl}}$$

The α values are calculated by using $K_{\text{H}_3\text{Fl}} = 6.607 \times 10^{-3}$; $K_{\text{H}_2\text{Fl}} = 3.981 \times 10^{-5}$; $K_{\text{HFl}} = 4.364 \times 10^{-7}$.

The values for the seven constants were obtained by a series of approximations which are described in the following paper⁶ of this series. The standard deviation of the differences between the observed and calculated values of the absorbance is 0.0136. The concentration of fluorescein being $2.407 \times 10^{-5}M$ throughout the measurements, the molar absorptivities of the four prototropic forms are: $\epsilon_{\text{H}_3\text{Fl}} = 4.94 \times 10^4$, $\epsilon_{\text{H}_2\text{Fl}} = 1.205 \times 10^4$, $\epsilon_{\text{HFl}} = 2.16 \times 10^4$, $\epsilon_{\text{Fl}} = 7.61 \times 10^3 \text{ l. mole}^{-1} \cdot \text{cm}^{-1}$.

REFERENCES

1. V. Zanker and W. Peter, *Chem. Ber.*, 1958, **91**, 972.
2. L. Lindqvist, *Arkiv Kemi*, 1960, **16**, 79.
3. S. K. Vig, *Reduction of Fluorescein at DME*, Ph.D. Dissertation, Delhi University, 1967.
4. N. R. Bannerjee and S. K. Vig, *Indian J. Chem.*, 1971, **9**, 444.
5. R. Markuszewski and H. Diehl, *Talanta*, 1980, **27**, 937.
6. H. Diehl, to be submitted.

PRELIMINARY COMMUNICATIONS

FLUOROMETRIC DETERMINATION OF CYANIDE WITH 2,3-NAPHTHALENEDIALDEHYDE AND TAURINE

Akira Sano*, Masaaki Takezawa and Shoji Takitani

Faculty of Pharmaceutical Sciences, Science University of Tokyo,
12, Ichigaya-funagawara-machi, Shinjuku-ku, Tokyo 162, Japan

(Received 10 March 1987. Accepted 8 April 1987)

Summary - A method is proposed for the fluorometric determination of cyanide based on a fluorogenic reaction with 2,3-naphthalenedialdehyde and taurine at basic pH. As little as 10 pmole of cyanide in 500 μ l of sample can be determined.

A fluorometric method for determination of cyanide with *o*-phthalaldehyde (OPA) and taurine was proposed in our previous study.¹ We suggested that the sensitivity of the method could be improved by using 2,3-naphthalenedialdehyde (NDA) as a reagent instead of OPA. Recently, Roach and Harmony² reported that primary amino compounds could be converted into fluorescent 1-cyano-2-alkylbenzisoindoles by using NDA and cyanide, with higher sensitivity than that obtained with OPA and 2-mercaptoethanol. The present work aimed at using the NDA reaction (Fig. 1) for determining cyanide.

NDA can be synthesized by the method of Ried and Bodem³ or Carlson *et al.*⁴

In borate-phosphate buffer (pH 7-11), cyanide gives an immediate green fluorescence with NDA and primary amino compounds such as taurine, alanine, methylamine and 2-amino-ethanol. Taurine was chosen as reagent for the same reason as described in the previous paper.¹ After examination of the various reaction conditions such as NDA and taurine concentrations and the pH, the following procedure is recommended. To 500 μ l of aqueous sample solution add 500 μ l of a 0.6mM taurine/4mM NDA solution in 0.05M borate-0.1M phosphate buffer (pH 9.0). Measure the fluorescence intensity at 460 nm with excitation at 418 nm.

Fluorescence excitation and emission spectra of the product are shown in Fig. 2. Excitation is maximal at 418 nm and emission at 460 nm. The fluorescence was stable for at least 1 hr at room temperature.

The calibration graph for cyanide was linear in the range from 2×10^{-8} to 1×10^{-5} M. The relative standard deviations ($n = 10$) were 2.0% for 1×10^{-7} M cyanide and 1.6% for 4×10^{-6} M.

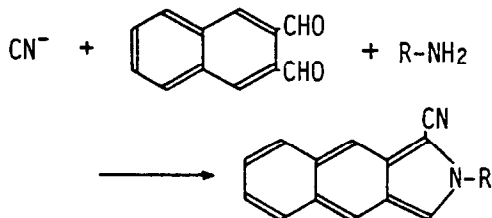


Fig. 1. Fluorogenic reaction of cyanide with NDA and primary amino compounds.

A 1000-fold molar ratio (to cyanide) of common anions and cations such as nitrate, sulphate, thiocyanate, calcium, magnesium and zinc did not interfere in the determination of $1 \times 10^{-6} \text{ M}$ cyanide. Sulphite, sulphide and thiols⁵ also react with NDA and taurine to form fluorescent compounds. The molar tolerance ratios of sulphite, sulphide and *N*-acetyl-cysteine were found to be 1, 100 and 10, respectively. Arginine also reacts with NDA,⁵ and its tolerance ratio was found to be 1000. The interference caused by sulphite, sulphide and thiols may be removed by masking with *N*-ethylmaleimide.^{1,5} If necessary, a micro-diffusion method⁶ may be applicable to avoid the interferences.

To test the utility of the method, cyanide added to natural water collected from Sotobori in Shinjuku-ku (Tokyo) was determined. For 0.05 and 2 nmole of cyanide added to 500 μl of water sample, 99-101% recoveries were obtained.

The sensitivity of the method is greater than that of the other fluorometric methods based on using *p*-benzoquinone,⁶ pyridoxal,⁷ pyridine-barbituric acid⁸ and OPA,¹ and the procedure is simpler. Determination of cyanide in biological fluids is of interest,^{6,9,10} and the application of the method for this purpose is under study.

Acknowledgement - The authors are grateful to Dr. T. Miura, Hokkaido University for supplying the NDA.

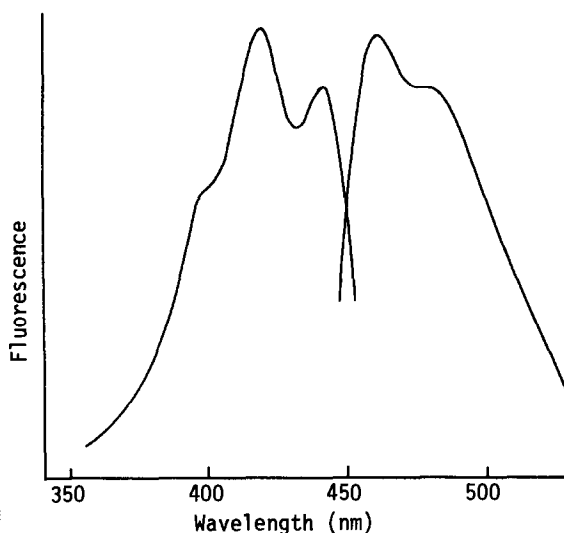


Fig. 2. Fluorescence excitation and emission spectra of $1 \mu\text{M}$ cyanide complex.

REFERENCES

1. A. Sano, M. Takezawa and S. Takitani, *Anal. Sci.*, 1986, 2, 491.
2. M.C. Roach and M.D. Harmony, *Anal. Chem.*, 1987, 59, 411.
3. W. Ried and H. Bodem, *Chem. Ber.*, 1956, 89, 708.
4. R.G. Carlson, K. Srinivasachar, R.S. Givens and B.K. Matuszewski, *J. Org. Chem.*, 1986, 51, 3978.
5. T. Miura, M. Kashiwamura and M. Kimura, *Bunseki Kagaku*, 1981, 30, 765.
6. A. Ganjeloo, G.E. Isom, R.L. Morgan and J.L. Way, *Toxicol. Appl. Pharmacol.*, 1980, 55, 103.
7. S. Takanashi and Z. Tamura, *Chem. Pharm. Bull.*, 1970, 18, 1633.
8. T. Toida, S. Tanabe and T. Imanari, *ibid.*, 1981, 29, 3763.
9. F.L. Rodkey and H.A. Collison, *Clin. Chem.*, 1977, 23, 1969.
10. P. Lundquist, H. Rosling and B. Sörbo, *ibid.*, 1985, 31, 591.

QUANTITATIVE ANALYSIS BY SURFACE-ENHANCED RAMAN SPECTROMETRY
ON SILVER HYDROSOLS IN A FLOW-INJECTION SYSTEM

J.J. Laserna*, A. Berthod[†] and J.D. Winefordner

Department of Chemistry, University of Florida,
Gainesville, FL 32611, U.S.A.

(Received 21 April 1987. Accepted 17 June 1987)

The enormous increase in Raman-scattering cross-section produced by adsorption of molecules on rough surfaces, provides an analytical technique, known as Surface Enhanced Raman Scattering (SERS),^{1,2} of sensitivity comparable to that of conventional molecular adsorption or fluorescence spectrometry, with the additional major advantage of the selectivity inherent in vibrational spectroscopy.

SERS by molecules adsorbed on silver hydrosols is of particular interest because of the simplicity of the substrate preparation, characterization and manipulation.^{3,4} However, the degree of enhancement is strongly dependent on the particle size and previous surface coverage of the colloidal suspension, and this imposes a rather severe restriction on the ultimate analytical usefulness of SERS. In fact, the rather poor precision of the measurements has not only prevented generalized quantitative analytical applications, but also adversely affected the reliability of the results in investigation of the effects of experimental variables on SERS signals.

In a previous communication,⁴ it was shown that silver hydrosols, properly prepared at room temperature, could provide satisfactory precision if activated by partial coagulation with electrolytes. In this communication, quantitative analytical applications of SERS are reported. Good reproducibility (-3% RSD) is provided by the automated preparation and delivery of the sample to the measurement cell in a flow-injection system. Aminobenzoic acid (PABA) and 9-aminoacridine (AA) were employed as model compounds.

EXPERIMENTAL

The Raman system has already been described.³ A special flow-through cell was constructed, consisting of a fused-silica tube (3 mm long, 0.5 mm bore) connected to a flow-injection chamber by Teflon tubing (0.5 mm bore). The flow-injection chamber (volume 1.2 ml), placed after the 6-port sample injector, ensured homogeneity and reproducible mixing of the sample. Two peristaltic pumps were used to pump and mix the 0.002M sodium tetrahydroborate and 0.001M silver nitrate and push the resulting silver hydrosol through the system. A diagram of the FIA manifold is shown in Fig. 1. Solutions of AA were prepared in ethanol, and solutions of PABA in water-ethanol (60:40 v/v) mixture. All experiments were performed at room temperature.

*Department of Analytical Chemistry, Faculty of Sciences, University of Málaga, 29071 Málaga, Spain.

†Laboratoire des Sciences Analytiques, Université de Lyon 1, 69622 Villeurbanne, France.

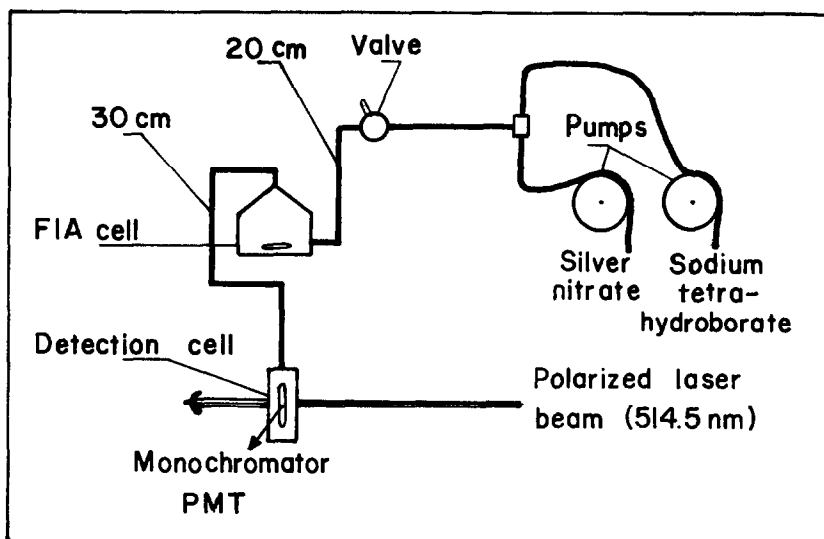


Fig. 1. The FIA manifold

RESULTS AND DISCUSSION

The SERS spectra of PABA and AA, obtained by stopping the flow when the analyte reaches the sample cell, are shown in Fig. 2. The PABA spectrum presents the same vibrational features as the spectra obtained under static conditions and reported elsewhere.^{4,5} The SERS spectrum of AA is reported here for the first time. Both spectra were obtained by injecting 20 μ l of the acidified sample into the hydrosol stream. The same spectra were obtained with neutral samples, but the concentration had to be increased at least tenfold for the signal-to-noise ratio to be as high as for the acidic samples. Thus, as under static conditions, a high analytical sensitivity requires activation of the silver hydrosol with electrolyte (in this case an acid).

Activation of the colloidal silver particles was slow, as indicated by the strong influence of flow-rate on the height of the peaks. A total flow-rate of 2 ml/min resulted in a small peak for PABA. The peak height increased with decreasing flow-rate, but if the flow-rate was too low (e.g., \sim 0.3 ml/min), the peak height decreased again as a result of excessive coagulation and deposition of the sol-adsorbate system on the walls of the tubing.

SERS signals for six successive injections of 10- μ g/ml PABA are shown in Fig. 3. The relative standard deviation of the peak height was 3.2%, showing the good precision achieved with the system. There was a linear relationship between SERS peak signal and PABA concentration over the range 4-100 μ g/ml. However, after repetitive injection of samples, a residual signal was obtained for a blank of acidified solvent, apparently because of contamination of the flow-cell walls with silver particles carrying an adsorption layer of analyte: the spectrum obtained by stopping the flow after a blank injection was the SERS spectrum of PABA. The increased blank signal was found to be a cumulative effect, requiring the cleaning of the whole system with nitric acid (40% v/v) after about 3 hr of running (10-15 injections).

The system reported here seems to overcome many of the precision problems associated with SERS in colloidal suspensions. It not only allows the effect of experimental variables to be studied reliably, but permits quantitative analytical applications to be developed. In addition, the problem of decomposition, frequently associated with the intense laser

fields employed in SERS experiments, is avoided because of the continuous renewal of sample by flow through the cell.

Fig. 2. SERS spectra for (a) 10- $\mu\text{g/ml}$ PABA and (b) 4- $\mu\text{g/ml}$ AA; both solutions were made 0.027M in nitric acid, and the analytes adsorbed on silver hydrosol.

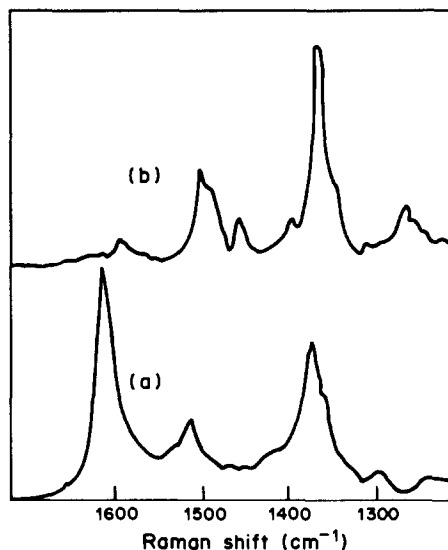
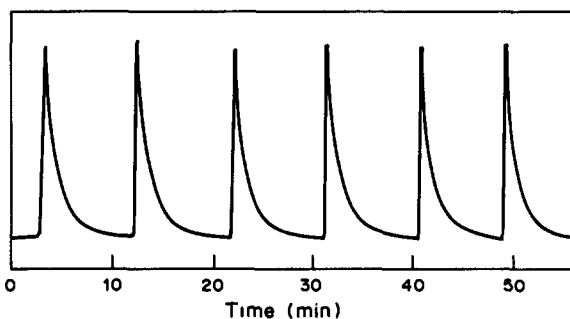


Fig. 3. SERS signals from injection of 20 μl of PABA (sample as in Fig. 2). Raman shift fixed at 1605 cm^{-1} . Flow-rate 0.7 ml/min.



Acknowledgement - Research supported by NIH 5-R01-GM11373-23.

REFERENCES

1. H. Metiu, Prog. Surface Sci., 1984, 17, 153.
2. J.I. Gersten and A. Nitzén, Surface Sci., 1985, 158, 165.
3. E.L. Torres and J.D. Winefordner, Anal. Chem., in the press.
4. J.J. Laserna, E.L. Torres and J.D. Winefordner, Anal. Chim. Acta, in the press.
5. J.S. Suh, D.P. Dilella and M. Moskovits, J. Phys. Chem., 1983, 87, 1540.

COMPUTER-ASSISTED OPTIMIZATION OF HPLC WITH POST-COLUMN REACTION FOR THE DETERMINATION OF AMINO-ACIDS

S. AL-NAJAFI*, C. A. WELLINGTON†, A. P. WADE‡, T. J. SLY§ and D. BETTERIDGE¶
The Chemistry Department, University College Swansea, Singleton Park, Swansea, Wales

(Received 11 February 1986. Revised 16 March 1987. Accepted 3 April 1987)

Summary—Computer-assisted optimization of a high-performance liquid chromatograph and associated post-column reactor is reported for the determination of six amino-acids. First six, then seven, experimental variables were considered. Non-standard experimental conditions were found which gave significantly improved colour development in the ninhydrin reaction. The composite modified simplex method for experimental optimization and a novel system-response function facilitated rapid and simultaneous improvement of separation, sensitivity and analysis time. The approach described is directly applicable to many similar systems.

The reaction of 1,2,3-indanetrione monohydrate (ninhydrin) with amino-acids to form Ruhemann's purple has been used extensively for routine analysis ever since the classic work of Moore and Stein¹ and Spackman *et al.*² The recommended experimental conditions for the reaction (pH, temperature, ninhydrin and stannous chloride concentrations, *etc.*) seem highly dependent on the amino-acid(s) under study.¹⁻⁴ Until now, all investigations of the reaction have been univariate in nature, and so have not rigorously considered possible interaction of experimental variables. A limited multivariate study⁵ indicated that, for some groups of amino-acids, the standard conditions^{1,2} did not yield the highest intensity of colour. This was considered worthy of further investigation.

For this study, a set of six amino-acids (glycine, methionine, phenylalanine, tryptophan, isoleucine and leucine) was chosen. These were considered to be representative of five general classes of amino-acids in that they were, respectively, a simple aliphatic, a sulphur-containing amino-acid, an aromatic, an amino-acid containing more than one nitrogen atom, and finally two isomers.

The apparatus used was a high-performance liquid chromatograph (HPLC) coupled with a post-column reactor (PCR) (see Fig. 1). It was decided to optimize the reaction in the PCR and, at the same time,

improve the chromatographic separation of the amino-acids. The HPLC and the PCR cannot be considered as independent systems since (i) the flow-rate and composition of the effluent from the column affect both the chemical reaction and the physical dispersion characteristics in the PCR, and (ii) the PCR itself causes broadening of the bands eluted from the column. Combination of two non-independent analytical systems is likely to double the number of experimental variables to be considered. A novel aspect of the work reported here is the optimization of the complete HPLC/PCR apparatus as a *single system*.

Initially, six experimental variables were considered; these were the pH, temperature, solvent composition (% propan-1-ol), ninhydrin and stannous chloride concentrations of the PCR reagent stream, and the pH of the HPLC eluent. Starting conditions for the optimization were the best of those obtained by "trial and error". Then, in a seven-variable study, the PCR temperature was held constant and the HPLC eluent flow-rate and composition were added to the variables listed above. The length of the PCR and the colour reagent flow-rate were not readily variable.

Optimization of relevant experimental systems

The hazards of univariate optimization methods (in which each variable in turn is changed while all others are held constant) are now well documented.⁶⁻⁹ Multivariate methods, which search by simultaneously changing more than one factor, are better able to deal with interacting variables and are usually more efficient.⁹ They are to be preferred for the optimization of chemical systems which have several variables. Modified simplex optimization⁶ is one such multivariate method which has been extensively and

*Present address: The Chemistry Department, College of Education, University of Mosul, Mosul, Iraq.

†Author for correspondence.

‡Present address: The Chemistry Department, Michigan State University, East Lansing, MI 48824, U.S.A.

§Present address: Dearborn Chemicals, Foundry Lane, Widnes, Cheshire, England.

¶Present address: British Petroleum Research Centre, Chertsey Road, Sunbury-on-Thames, Middlesex, England.

effectively used in analytical chemistry.¹⁰ Many variants on the basic algorithm exist.^{8,9,11-19} The version used in this work was the Composite Modified Simplex (CMS) method of Betteridge *et al.*^{8,9} which has been implemented on a variety of microcomputers.⁷

Deming²⁰ noted that the systems which change the order in which components are eluted from a column can complicate the optimization process: at low eluent pH, peak A may be eluted before peak B (good chromatography); at medium pH they may be co-eluted (bad chromatography); their order may be reversed at a higher pH (good chromatography). This good-bad-good sequence indicates a valley on the optimization response surface. If several pairs of components change their elution order the response surface may be highly complex.²¹ Though this hinders the search for the global optimum, a good optimization method is usually still able to obtain a substantial improvement over conditions selected by "trial and error", and do so within a reasonable number of experiments.

Several groups have applied simplex optimization to HPLC and PCR systems separately. Betteridge and co-workers developed an HPLC/PCR system for carbohydrates;²² they then sought the optimum concentrations for acrylonitrile and alkali in the PCR, and rapidly improved the sensitivity of the method by a factor of three.²³ Deming *et al.* optimized two variables of a gas-liquid chromatography system, for samples containing up to five components.²⁴ Berridge optimized two- and three-variable HPLC systems for samples containing up to four components.²⁵ Rainey and Purdy optimized HPLC systems with two variables (two- and seven-component samples) and four variables (five-component sample).²⁶ Recently, Crouch and Ratanathanawongs used the CMS to optimize a PCR specific for phenols.²⁷ Berridge has recently thoroughly dealt with the subject of automated chromatographic optimization.²⁸

Choice of system response function

Optimization of any analytical technique requires that some response be chosen which indicates the merit of a given set of experimental conditions.^{8,9} Response functions combine two or more analytical responses to give a single weighted merit value. For chromatographic systems, this must reflect the perceived quality of the chromatogram produced. Several "chromatographic response functions" (CRFs) have been reported.^{24-26,29-31} Response functions have also been used in simplex optimizations of other analytical techniques.^{8,9,32,33} In this work, a system response function (SRF) was chosen which considered both the separation and the post-column reaction with a view to finding conditions which would maximize resolution and sensitivity, and minimize the time per analysis.

Consider a sample containing j components. Let t_i be the time taken for the i th component acid to traverse the system, Δt_i the time elapsed between the detection of two consecutive components ($\Delta t_i = t_i - t_{i-1}$), and h_i the height of the i th peak. By definition, the time of injection is $t_0 = 0$. The baseline width (in min) of the i th peak, W_i , increases with residence time and is dependent on the prevailing experimental conditions. The chosen ideal separation in time for two peaks, $\Delta t_{i(\text{ideal})}$, is then defined as

$$\Delta t_{i(\text{ideal})} = cW_i$$

where c is a constant which defines the degree of peak separation.* Thus $c = 0$ would indicate total overlap (no chromatographic separation); $c = 1$ corresponds to adjacent peaks being just separated on the baseline (good chromatography).

The system response function (SRF) is then given by

$$\text{SRF} = \sum_{i=1}^j h_i / [(\Delta t_i - \Delta t_{i(\text{ideal})})^2 + 1]$$

The divisor is minimal (unity) when all peak maxima are separated by c baseline peak-widths, *i.e.*, $\Delta t_i = \Delta t_{i(\text{ideal})}$. The SRF value is decreased by too long an analysis time *and* by too much peak overlap. Higher h_i values will enhance the function value and will result from improved post-column reactor performance (more intense colour, less dispersion) and from decreased analysis time (less band broadening). The relative significance of separation quality, analysis time and sensitivity assumed by this function may be modified by inclusion of appropriate weighting factors defined by the user.

EXPERIMENTAL

Reagents

All chemicals were reagent grade. Doubly distilled water was used throughout. A potassium dihydrogen phosphate buffer solution (0.01M, in 1% propan-1-ol, adjusted to pH 2.7 with phosphoric acid) was prepared. Amino-acid stock solutions were prepared in the phosphate buffer: glycine 0.025M, L-methionine 0.05M, L-isoleucine 0.05M, L-leucine 0.05M, L-phenylalanine 0.05M, L-tryptophan 0.05M, and a mixture containing equal volumes of each. The HPLC eluent was 0.01M phosphate buffer as above, adjusted to the required pH with phosphoric acid or potassium hydroxide. The reagent solution contained appropriate concentrations of ninhydrin and stannous chloride dihydrate in 0.1M phosphate buffer. After addition of the stannous chloride dihydrate, this solution was left for 1 hr in an ice-bath to allow any precipitation to occur. All solutions were filtered (Whatman No. 1 or No. 42 filter papers) and stored at below 5° in the dark. Solutions were degassed in an ultrasonic bath for at least 20 min prior to use.

Apparatus

The apparatus was set up as in Fig. 1. The HPLC apparatus was composed of a pump (Altex model 110A single-head), a sampling valve (Rheodyne type 7125, 20- μ l loop, Rheodyne Inc., Cotati, USA) and a 5- μ m octadecyl-silica column (ODS-Hypersil, length 250 mm, bore 4.6 mm). The column and eluent reservoir were kept at 50° in a water-bath. The eluent reservoir was fitted with a condenser to eliminate evaporation of solvent. Eluent was drawn through

* c is related to the resolution, R_s , after post-column reaction, by $R_s = 2cW_i / (W_i - W_{i-1})$, for i from 2 to j .

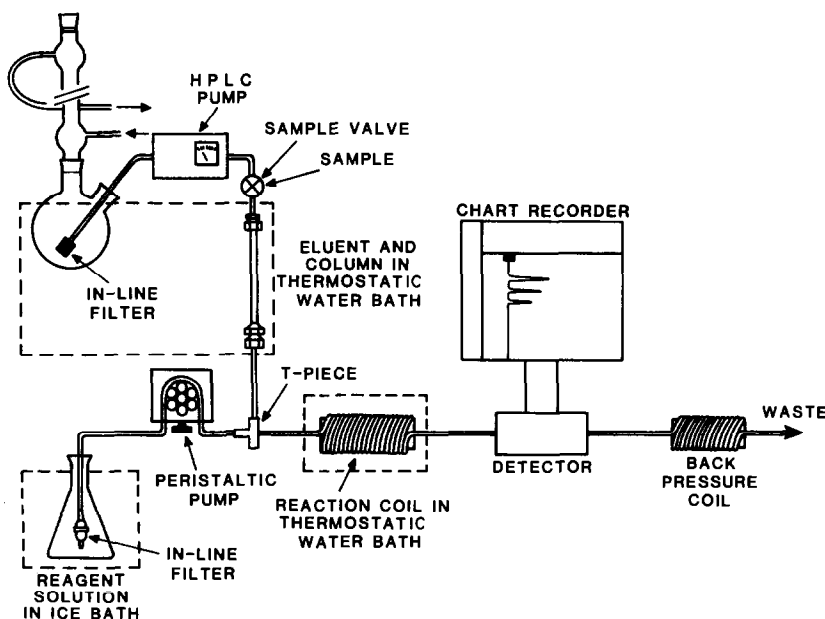


Fig. 1. Schematic diagram of the HPLC/PCR apparatus. Hatched enclosures indicate temperature control by water-bath.

a stainless-steel gauze in-line filter. A minimal length of 0.2-mm bore stainless-steel tubing was used to connect the injection valve to the column. The PCR reagent stream was drawn through an in-line tube filter (Gradko) by a peristaltic pump (LKB Multiplex model 2115). The PCR reaction coil was a fixed length of stainless-steel tube (2 m, 0.508 mm bore) which was set in a helical groove on a 75-mm diameter aluminium cylinder placed in a thermostatically controlled water-bath ($\pm 0.1^\circ\text{C}$). The photometric detector had a path-length of 1.2 mm and used a green LED light-source and a phototransistor detector mounted transversely on a clear plastic tube. Its design and construction have been reported elsewhere.³⁴ The emission of the LED (maximum 565 nm, bandwidth 15 nm) closely matched the absorbance maximum of the purple product (570 nm) in wavelength. The polytetrafluoroethylene (PTFE) back-pressure coil was 3.75 m long, with a bore of 0.5 mm. The connecting tubing after the column was a minimal length of 0.8-mm bore PTFE. Optimization calculations were done on a Commodore SuperPET 9000 microcomputer system. Software was written in BASIC and is available from its authors.⁷

Method

Each day, before use, the column was flushed with redistilled water for 1 hr to remove any propan-1-ol. Then, for each set of experimental conditions, the required HPLC eluent and reagent solution were prepared and 50 ml of the appropriate eluent mixture were passed through the column to ensure equilibrium with the stationary phase. Then 20 μl of each amino-acid solution and of the mixture were separately injected into the column, with 3–5 replicate injections for each. In the six-variable study, the eluent flow-rate was fixed at 1 ml/min. The column effluent merged at a T-piece with a 0.44-ml/min stream of ninhydrin reagent solution. The reagent flow-rate was kept slow to minimize post-column band-broadening. The product was detected photometrically downstream and the resultant trace recorded. Before going to waste, the solution passed through a "back-pressure" coil. This raised the pressure in the PCR to minimize bubble formation from the heated solvent and thus decrease the noise evident on the trace. The peak heights and times from injection to detection were recorded and averaged. After use, the apparatus was flushed

with doubly distilled water for at least 30 min and then with propan-1-ol for at least 20 min to reduce the risk of damage to the pump seals and column from precipitated stannous phosphate.

Optimization

To start the optimizations, it was necessary to define the system response function and enter the following data into the microcomputer:

- the system variables to be considered,
- a range for each variable, within which the search is constrained,
- an estimate of the measurement precision for the variables,
- the size for each variable in the initial simplex,
- a set of conditions for the initial experiment.

The values are shown in Table 1. For an n -variable optimization, $n + 1$ experiments are required to set up the first simplex. After the initialization data had been entered, the

Table 1. Range and measurement precision for each variable

Variable	Range	Measurement precision
PCR temperature ($^\circ\text{C}$)*	83–20	0.1
Propan-1-ol in reagent solution (% v/v)	0–100	0.05
Concentration of ninhydrin in reagent solution (M)	0.0028–0.2806	0.0001
Concentration of stannous chloride in reagent solution (M)	0–0.0443	0.0001
HPLC eluent pH	2.4–6.5	0.05
Reagent solution pH	10.0–2.5	0.05
HPLC eluent flow-rate (ml/min)†	0.1–2.5	0.01
Propan-1-ol in HPLC eluent (% v/v)†	0–100	0.05

*Value fixed for seven-variable optimization.

†Value fixed for six-variable optimization.

program calculated the sets of experimental conditions to be used for the initial $n + 1$ (here seven and eight) experiments. These experiments were performed by the operator and the results were entered. The program then calculated conditions for the next experiment, and this was done, the results being entered and a new set of conditions computed to continue the optimization. Optimization was halted when several experiments ceased to give further improvement in system response. This interaction of operator and computer has also been reported elsewhere.⁷⁻⁹ The operator had no previous computer experience but found the optimization program easy to use. Minor code modifications were required to facilitate the automatic calculation of the response from the time and peak-width data.

The system response function used a value of $c = 1.5$, to preclude insufficient penalization of conditions giving too much overlap. In the six-variable case, peak-widths were calculated from t_r , by use of an experimentally determined first-order relation $W_i = 0.0914t_r$. In the seven-variable case the peak-widths were measured by hand from the chart-recorder trace and entered directly into the microcomputer.

The search limits were chosen from experimental considerations. For example, the maximum PCR temperature was set at 83° to protect the detector flow-cell from damage and minimize the formation of vapour bubbles from the organic solvent component.

RESULTS

Tables 2-4 indicate the experiments done and the full sets of results obtained in the six-variable study. The complete data sets for the seven-variable study are given elsewhere²⁵ and, for reasons of brevity, are not repeated here. The findings for both studies (initial and final experimental conditions, responses,

times per analysis and improvement in sensitivity for each amino-acid) are summarized in Tables 5 and 6.

Six-variable system

A total of 25 experiments was performed. No change in elution order was observed. An order of magnitude increase in the response function was achieved. This corresponded to sensitivity increases between 8-fold and 44-fold for individual amino-acids. The sensitivities for isoleucine and leucine under the conditions of best overall response (experiment 15) were improved by factors of 30.3 and 18.7 respectively. For these two amino-acids, the conditions for experiment 16 were even more favourable, giving 45.7-fold and 28.6-fold increases. An average detection limit of better than 10nM was obtained. The residence time of the slowest eluting component was reduced from 16.1 min to 10.3 min. Figure 2 shows the trace obtained for the mixture under the best conditions found (experiment 15). Acceptable separation was obtained for all components except the leucine-isoleucine isomeric pair.

Confirmatory experiments. Most workers use ninhydrin at about pH 5. Since the best response was found at pH 7.6, two further experiments were desirable. First, experiment 15 was repeated. The response obtained was in good agreement with the previous value of 1656. Then the same conditions were tried, but with the reaction at pH 5.1-5.15. This resulted in a response of only 728 and confirmed that the higher pH was preferable.

Table 2. Experimental conditions and response function values for the six-variable system

Expt. No.	PCR temp., °C	PCR propanol, %	PCR ninhydrin, M	PCR SnCl ₂ , mM	HPLC pH	PCR reag. pH	Response SRF	pH of reaction
1	74.0	1.00	0.1684	4.4	2.60	6.70	170	5.65
2	64.1	1.00	0.1684	4.5	2.60	6.60	44	5.50
3	69.5	1.80	0.1684	4.4	2.55	6.70	61	5.20
4	69.5	1.30	0.2133	4.4	2.45	6.75	69	5.05
5	69.5	1.30	0.1853	5.8	2.50	6.70	91	5.50
6	69.3	1.30	0.1853	5.0	3.10	6.70	104	6.25
7	69.0	1.30	0.1854	4.9	2.80	6.60	117	—
8	80.1	1.25	0.1809	4.7	2.70	6.75	239	6.05
9	82.2	1.40	0.1876	4.9	2.70	6.85	283	6.20
10	82.2	0.90	0.2058	5.4	2.85	6.90	532	6.40
11	82.2	0.65	0.1882	6.2	3.25	7.10	604	6.75
12	82.2	0.25	0.1923	6.0	3.90	7.35	1222	7.00
13	82.2	0.00	0.1987	6.9	4.35	7.80	1141	7.25
14	82.2	0.00	0.2002	7.1	4.70	8.05	1206	7.40
15	83.0	0.00	0.2198	7.9	5.25	8.10	1656	7.60
16	83.0	0.00	0.2359	9.9	6.55	8.90	1606	8.60
17	83.0	0.00	0.2223	9.9	6.50	9.15	1332	—
18	83.0	0.00	0.2437	9.8	6.50	9.25	1282	8.80
19	83.0	0.50	0.2408	9.5	6.50	8.80	1557	8.25
20	83.0	0.16	0.2466	9.7	6.45	8.70	1649	8.15
21	83.0	0.00	0.2646	11.6	6.45	9.65	1387	8.40
22	83.0	0.19	0.2172	8.1	5.25	7.70	1515	7.35
23	83.0	0.16	0.2377	7.7	5.20	7.45	1449	7.20
24	83.0	0.20	0.1904	5.3	4.75	6.75	706	6.00
25	83.0	0.07	0.2462	10.0	6.00	8.95	1240	8.00
Confirmatory experiment:								
26	83.0	0.00	0.2198	7.9	5.25	5.10	728	5.15

Table 3. Average peak heights (*mm*) for each amino-acid (six-variable study)

Expt. No.	Glycine	Methionine	Isoleucine	Leucine	Phenylalanine	Tryptophan
1	186	203	29	49	67	35
2	48	52	6.5	13	20	11.7
3	62	84	12.5	22	24.5	18.5
4	89	72	12.5	26	23.3	11.5
5	104	110	14	29	33	18
6	106	122	13.5	22.5	47	24
7	130	156	22.5	31	51	30
8	310	238	12.7	32	38	17
9	422	262	8.3	18	22	11.5
10	705	600	20.3	34	62	25
11	683	843	39	149	317	161
12	1195	1083	385	748	935	1160
13	1275	860	177	613	900	1255
14	1250	1140	172	410	880	1243
15	1473	1617	880	915	1082	1555
16	1298	1412	1324	1402	973	1407
17	1102	1125	1050	1155	695	1130
18	1093	1083	1041	1139	658	1057
19	1353	1360	1117	1303	850	1283
20	1432	1473	1170	1302	993	1337
21	505	412	322	393	287	500
22	1368	1437	777	980	937	1310
23	1310	1429	633	850	907	1160
24	680	860	66	193	540	608
25	1120	1167	740	980	680	1235
Confirmatory experiment:						
26	598	893	292	478	478	530

Table 4. Average time from injection to detection (*min*) for each amino-acid (six-variable study)

Expt. No.	Glycine	Methionine	Isoleucine	Leucine	Phenylalanine	Tryptophan
1	3.00	4.20	5.80	6.20	8.90	16.15
2	3.00	4.20	5.77	6.10	8.80	16.10
3	3.00	4.17	5.70	6.20	9.05	16.70
4	3.10	4.20	6.00	6.40	9.00	16.95
5	3.00	4.10	5.70	6.30	8.95	16.55
6	3.00	3.97	5.15	5.45	8.10	14.00
7	3.07	4.10	5.30	5.67	8.05	14.00
8	3.00	4.13	5.55	6.10	8.47	15.30
9	3.05	4.13	5.57	6.07	8.50	15.35
10	3.03	4.13	5.50	5.90	8.30	14.60
11	3.05	4.00	5.00	5.30	7.35	12.13
12	2.95	3.87	4.83	5.07	7.23	11.25
13	3.03	3.87	4.77	5.03	7.07	11.00
14	2.97	3.70	4.50	4.75	6.97	10.60
15	3.00	3.70	4.33	4.55	6.93	10.27
16	3.00	3.77	4.30	4.47	6.80	9.90
17	2.97	3.70	4.23	4.37	6.67	9.83
18	3.00	3.70	4.27	4.50	6.77	9.87
19	3.00	3.77	4.27	4.47	6.67	9.77
20	3.00	3.80	4.33	4.55	6.83	10.00
21	3.02	3.83	4.37	4.60	6.83	10.10
22	3.00	3.80	4.27	4.47	6.90	10.10
23	2.97	3.75	4.25	4.45	6.83	10.02
24	3.00	3.73	4.35	4.67	6.90	10.33
25	3.05	3.85	4.35	4.53	6.87	9.90
Confirmatory experiment:						
26	3.00	3.70	4.30	4.50	6.90	10.30

Table 5. Initial and best conditions, time per analysis and response function values

Experiment No.	Six variables		Seven variables	
	1 (Initial)	15 (Best)	1 (Initial)	15 (Best)
Temperature (°C)	74.0	83.0	83.0*	83.0*
Propan-1-ol in reagent stream (% <i>v/v</i>)	1.00	0.00	0.00	0.80
Ninhydrin in reagent stream (M)	0.1684	0.2198	0.1853	0.2178
SnCl ₂ in reagent stream (M)	0.0044	0.0079	0.0058	0.0080
HPLC eluent pH	2.60	5.25	4.50	4.65
Reagent stream pH	6.70	8.10	7.00	8.70
HPLC eluent flow-rate (ml/min)	1.00*	1.00*	1.00	0.90
Propan-1-ol in HPLC eluent (% <i>v/v</i>)	1.00*	1.00*	1.00	1.00
Reagent stream flow-rate (ml/min)	0.44*	0.44*	0.44*	0.44*
Slowest component (<i>t</i> , min)	16.15	10.27	10.75	12.00
pH after detector (reaction pH)	5.65	7.60	6.70	8.20
SRF	170	1656	1210	5332

*Values not varied.

Table 6. Sensitivity (peak height, *mm*) improvements for each amino-acid

Experiment No.	Six variables		Seven variables	
	1 (Initial), <i>mm</i>	15 (Best), <i>mm</i>	1 (Initial), <i>mm</i>	15 (Best), <i>mm</i>
Glycine	186	1473	925	1825
Methionine	203	1617	793	1808
Isoleucine	29	880	93	1600
Leucine	49	915	104	1595
Phenylalanine	67	1082	458	1335
Tryptophan	35	1555	650	1593
SRF	170	1656	1210	5332

Seven-variable system

For these experiments the temperature of the column and reaction coil was fixed at 83°, the upper experimental boundary. This was on the basis of the findings of the six-variable optimization, and because higher temperatures are likely to decrease longitudinal dispersion and enhance reaction rates.³⁶⁻³⁸ Nineteen experiments were done. No change in elution order was observed. Figure 3 shows the trace for the best conditions found. The optimum pH for the ninhydrin reaction was 8.2 and represented a further improvement over the conditions arrived at by the six-variable study.

DISCUSSION

The performance of both the six- and seven-variable systems was markedly and rapidly improved by CMS. An eluent flow-rate of 1 ml/min and reagent flow-rate of 0.44 ml/min fixed the time spent in the PCR by each amino-acid at about 20 sec. This must

be compared with the many minutes that commercial amino-acid analysers assign to the ninhydrin reactions. Acceptable colour formation was achieved (Figs. 2 and 3).

The seven-variable study gave rise to further improvements in sensitivity over that obtained in the six-variable study. Trends in the response due to variables common to both optimizations were the same for all variables except one. Such agreement has been noted elsewhere.⁷ The exception was the concentration of propan-1-ol in the reagent stream, which was thought to have a comparatively minor effect over the range studied.

The isoleucine-leucine isomeric pair was only partially separable with this apparatus. Optimization methods can only make the best of the chosen analytical apparatus and method. A more appropriate system specification or design can result in substantial gains in performance, which can then be further improved by experimental optimization.⁸

The behaviour of the amino-acids was examined for each individually, and the problem of estimation

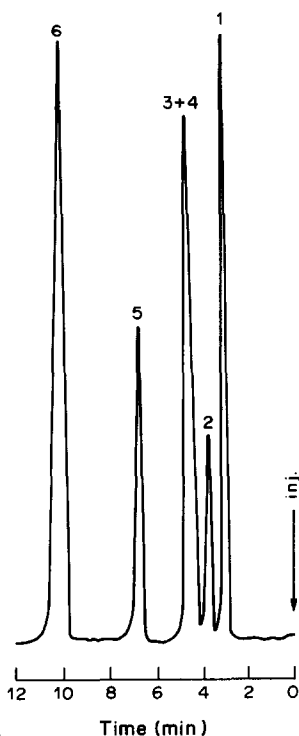


Fig. 2. Trace obtained for the amino-acid mixture under the best conditions found by the six-variable optimization. Column ODS (C_{18} , 250×4.6 mm); eluent $0.01M$ phosphate buffer containing 1% v/v propan-1-ol; pH = 5.25; flow-rate 1.0 ml/min; temperature $50^\circ C$. Post-column conditions: $0.2198M$ ninhydrin reagent in $0.1M$ phosphate buffer at pH 8.10; $0.0079M$ stannous chloride with no propanol in reagent solution; reaction temperature $83^\circ C$. Peaks: 1 = glycine; 2 = methionine; 3 + 4 = isoleucine and leucine; 5 = phenylalanine; 6 = tryptophan.

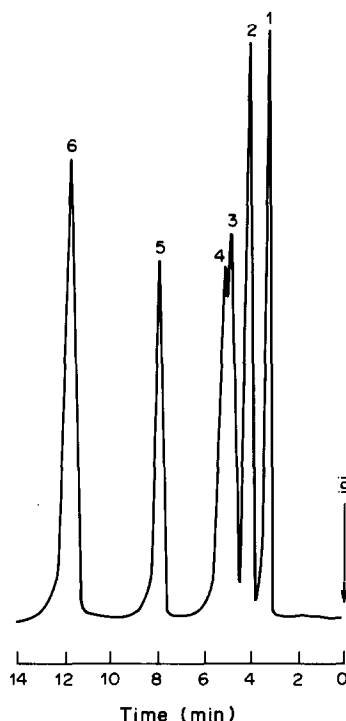


Fig. 3. Trace obtained for the amino-acid mixture under the best conditions found by the seven-variable optimization. Column ODS (C_{18} , 250×4.6 mm); eluent $0.01M$ phosphate buffer containing 1% v/v propan-1-ol; pH = 4.65; flow-rate = 0.9 ml/min; temperature $50^\circ C$. Post-column conditions: $0.2178M$ ninhydrin reagent in $0.01M$ phosphate buffer at pH 8.70; $0.0080M$ stannous chloride; 0.8% v/v propan-1-ol in reagent solution; reaction temperature $83^\circ C$. Peaks: 1 = glycine; 2 = methionine; 3 = isoleucine; 4 = leucine; 5 = phenylalanine; 6 = tryptophan.

of the width and height of overlapping peaks during the optimization was thus avoided. In other systems such care might not be possible or desirable. An improved approximation for the relationship of peak-width to time would then be useful. Also, a PCR working at higher pressure and temperature would further enhance the sensitivity⁴ and decrease vapour-bubble problems.

Calculations indicated that the sample dispersion for this HPLC/PCR system was approximately double that for a similar HPLC/PCR system for phenols recently reported by Crouch and Ratanathanawongs.²⁷ These workers used an air-segmented PCR, and were able to show that band-broadening in the PCR was minimal. This was not the case with the unsegmented reactor used here. However, the absence of air bubbles simplified the experimental system.

CONCLUSIONS

Rapid computer-assisted optimization of an HPLC separation and subsequent determination of a selected group of amino-acids post-column reaction with ninhydrin has been readily achieved by use of

the composite modified simplex method and a system response function based on sensitivity, analysis time and chromatographic resolution. This work has shown that none of the previously published sets of conditions for the ninhydrin reaction gives the highest sensitivity attainable. Moreover, for optimization purposes, HPLC/PCR systems can be successfully treated as a single experimental system.

Acknowledgements—The authors thank the Iraqi government for an M.Sc. studentship to S.A., and The British Petroleum Company for funding the research of A.P.W. and T.J.S. Thanks are due to A. F. Taylor and R. S. Rowles for helpful comments on the manuscript.

REFERENCES

1. S. Moore and W. H. Stein, *J. Biol. Chem.*, 1951, **192**, 663.
2. D. H. Spackman, W. H. Stein and S. Moore, *Anal. Chem.*, 1958, **30**, 1190.
3. Y. P. Lee and T. Takahashi, *Anal. Biochem.*, 1966, **14**, 71.
4. N. G. Anderson, R. H. Stevens and J. W. Holleman, *ibid.*, 1968, **26**, 104.
5. A. G. Howard and A. P. Wade, unpublished work, 1981.
6. S. L. Morgan and S. N. Deming, *Anal. Chem.*, 1974, **46**, 1170.

7. D. Betteridge, T. J. Sly, A. P. Wade and J. E. W. Tillman, *ibid.*, 1983, **55**, 1292.
8. D. Betteridge, A. G. Howard and A. P. Wade, *Talanta*, 1985, **32**, 709.
9. *Idem*, *ibid.*, 1985, **32**, 723.
10. S. N. Deming and S. L. Morgan, *Anal. Chim. Acta*, 1983, **150**, 183.
11. W. Spendley, G. R. Hext and F. R. Himsforth, *Technometrics*, 1962, **4**, 441.
12. J. A. Nelder and R. Mead, *Computer J.*, 1965, **7**, 308.
13. P. G. King, S. N. Deming and S. L. Morgan, *Anal. Lett.*, 1975, **8**, 369.
14. M. W. Routh, P. A. Swartz and M. B. Denton, *Anal. Chem.*, 1977, **49**, 1422.
15. P. B. Ryan, R. L. Barr and H. D. Todd, *ibid.*, 1980, **52**, 1460.
16. E. R. Aberg and A. G. T. Gustavsson, *Anal. Chim. Acta*, 1982, **144**, 39.
17. L. G. Sabate and X. Tomas, *J. High Res. Chrom., Chrom. Commun.*, 1984, **7**, 104.
18. P. F. A. van der Wiel, *Anal. Chim. Acta*, 1980, **122**, 421.
19. P. F. A. van der Wiel, R. Maassen and G. Kateman, *ibid.*, 1983, **153**, 83.
20. S. N. Deming, private communication, 6th Summer School of Automated Chemical Analysis, Brighton, UK, July 1983.
21. C. A. Wellington and K. Ahmad, *Anal. Proc.*, 1984, **21**, 144.
22. D. Betteridge, N. G. Courtney, T. J. Sly and D. G. Porter, *Analyst*, 1984, **109**, 91.
23. D. Betteridge and T. J. Sly, unpublished work, 1981.
24. S. L. Morgan and S. N. Deming, *J. Chromatog.* 1975, **112**, 267.
25. J. C. Berridge, *ibid.*, 1982, **244**, 1.
26. M. L. Rainey and W. C. Purdy, *Anal. Chim. Acta*, 1977, **93**, 211.
27. S. K. Ratanathanawongs and S. R. Crouch, *ibid.*, 1987, **197**, 277.
28. J. C. Berridge, *Techniques for the Automated Optimization of HPLC Separations*, Wiley, New York, 1985.
29. R. Cela and J. A. Perez-Bustamante, *Comput. Appl. Lab.*, 1983, No. 2, 137.
30. H. J. G. Debets, B. L. Bajema and D. A. Doornbos, *Anal. Chim. Acta*, 1984, **151**, 131.
31. J. L. Glajch, J. J. Kirkland, K. M. Squire and J. M. Minor, *J. Chromatog.*, 1980, **199**, 57.
32. R. M. Belchamber, D. Betteridge, J. Cruickshank, P. Davison and A. P. Wade, *Spectrochim. Acta*, 1986, **41B**, 503.
33. D. Betteridge, A. F. Taylor and A. P. Wade, *Anal. Proc.*, 1984, **21**, 373.
34. T. J. Sly, D. Betteridge, D. Wibberley and D. G. Porter, *J. Automatic Chem.*, 1982, **4**, 186.
35. S. Al-Najafi, *M.Sc. Thesis*, University of Wales, 1984.
36. D. Betteridge, A. P. Wade and C. Z. Marczewski, *Anal. Chim. Acta*, 1984, **165**, 227.
37. C. L. M. Stults, A. P. Wade and S. R. Crouch, *ibid.*, 1987, **197**, 301.
38. C. D. Crowe, H. W. Levin, D. Betteridge and A. P. Wade, *ibid.*, in the press.

CONTROL OF VOLTAMMETRIC EXPERIMENTS BY MEANS OF THE COMMODORE 64 MICROCOMPUTER

MIKAEL WASBERG

Åbo Akademi, Laboratory of Analytical Chemistry, Biskopsgatan 8, SF-20500, Åbo, Finland

PÉTER SÁRKÁNY

Technical University of Budapest, Department of General and Analytical Chemistry, Gellért tér 4, H-1111 Budapest, Hungary

(Received 20 March 1987. Accepted 10 April 1987)

Summary—An electronic interface for the Commodore 64 microcomputer suitable for generation of voltammetric waveforms and for data acquisition has been built. Used together with analogue voltammetric instruments the interface makes updating of the measurement techniques possible. Also, fast A/D-conversion and a floppy disk drive make the system useful as a universal data-acquisition unit in the laboratory. The system has been tested together with an amperometric detector in the square-wave voltammetric determination of paracetamol and iodide.

Microcomputers are today used in virtually all commercial chemical instruments. There are, however, many older analogue instruments in the laboratory that are fully capable of handling the required measurements but lack the convenience and efficiency provided by computer-control. This is the case with most smaller instruments manufactured before about 1980. Furthermore, even if controlled by a microcomputer, a commercial instrument has dedicated software which is usually difficult to alter. A data-acquisition and control system of the kind described here is programmable and can be moved from one instrument to another. The use of larger computers in the evaluation and storing of experimental chemical data is important.¹⁻³ The link between an instrument and larger computers can also be provided by a desktop computer.

Voltammetric instruments are rather simple from an electronic point of view, since the quantity measured is a current produced in response to a voltage signal. This also means that the computer-control of such an instrument is straightforward. By using one analogue/digital (A/D) and one D/A-converter it is possible to control the voltage applied in the measurement cell and acquire the electrical current data. A computer interface of this kind can be built in the laboratory by a chemist with some knowledge of digital and analogue electronics. The construction of a versatile analogue voltammetric instrument would, on the other hand, be both expensive and time-consuming, even if done by an expert. By interfacing the computer to an already available analogue instrument it is possible to obtain a voltammetric system capable of performing a wide range of different pulse measurements. Square-wave voltammetry is a technique which has gathered interest in recent years. The cost of a commercial instrument capable of per-

forming square-wave voltammetry is high, and cheap instrumentation is required for the technique to grow.⁴ Some authors have modified commercial instruments to allow new pulse measurements to be made, by using hardware circuits^{5,6} or a computer⁷ to generate the waveforms. Others have used laboratory-built analogue circuitry⁸⁻¹⁰ in their systems.

As a result of developments in microelectronics microcomputer production has increased considerably. Computers ranging from home-computers to very powerful professional systems are available. A home-computer, of the type used in this work, can be considered a toy in comparison with the more powerful professional systems. This is true as regards the data-processing capabilities, but the small computers are still useful for data-acquisition and simple control tasks. The cost of home-computers is also very low, and owing to their widespread use, a wide range of software is available. Further, cheap add-on units such as standardized serial and parallel communication interfaces, printers, floppy-disk drives and plotters are available. Home-computers are also well documented, *e.g.*, a full description of the operating system is usually available. This is of importance when modifying existing software for a special control task.

In this work a Commodore 64 (C64) home-computer was equipped with a simple interface and connected to an amperometric detector. A C64 computer was used because it was available in the laboratory. However, certain features of this computer make it well suited for laboratory interfacing. One is the availability of an expansion port with decoded I/O-control signals ready for use. Additionally, two programmable 16-bit timers are available inside the computer, which makes the generation of potential

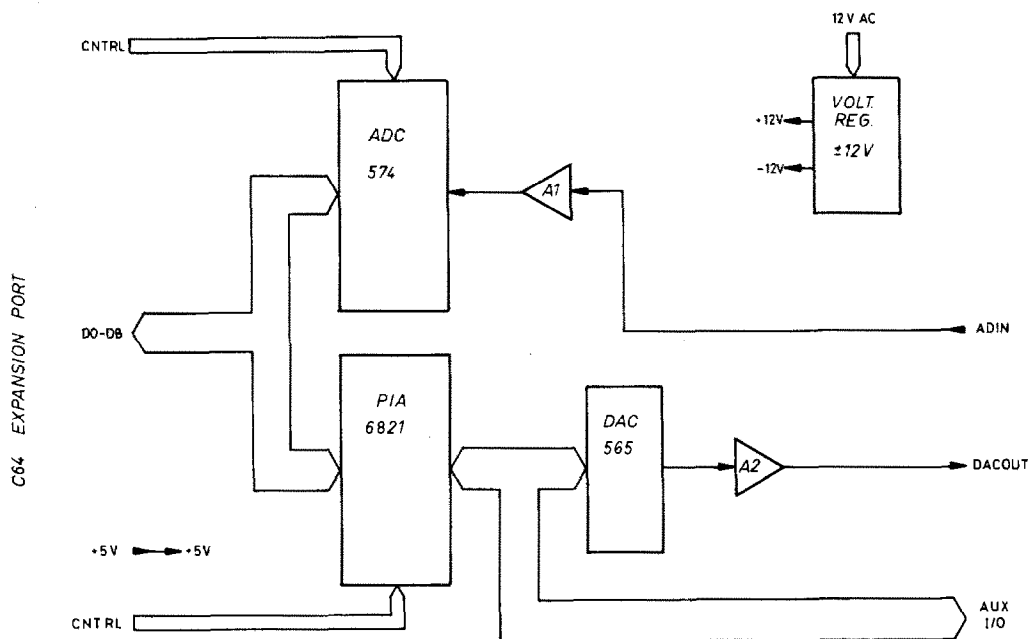


Fig. 1. Schematic drawing of the interface unit, which comprises an A/D converter (ADC), a peripheral interface adapter (PIA), and a D/A converter (DAC), on a single circuit board. The ADC and the PIA are directly connected to the computer data-bus while the data to the DAC are passed through the PIA. Amplifier A1 is the input amplifier of the ADC and A2 is a current/voltage converter used to produce an analogue output voltage. A small power supply generates +12 V and -12 V for the ADC and DAC.

waveforms simple. Further, the non-maskable interrupt of the C64 is not ordinarily used and hence it is possible to let the timers use this interrupt mode. There is also a real-time clock inside the C64, which makes generation of longer time delays easy.

Some advantages of this system are the low price, simple interfacing because the control signals needed already exist inside the computer, reasonably good graphics capability, BASIC high-level language for data manipulation, and convenient floppy-disk data-storage. To test the system a program which generates square-wave waveforms was developed and tested in the determination of iodide and paracetamol with carbon-paste and polymer-modified carbon electrodes.

DESCRIPTION OF THE SYSTEM

The computer

The computer system consists of a Commodore 64 home-computer, one floppy-disk unit and a matrix printer. The computer is equipped with 64 kbyte of RAM and a BASIC-interpreter in ROM. The memory-configuration depends on the software used. In this case the BASIC interpreter and operating system occupied about half of the memory space and the rest (32 kbyte) of the memory was used for program and data storage. For mass storage of data a 160-kbyte floppy-disk drive was used. Further, the computer has a graphics capability with a resolution of 320×200 points.

The interface unit

The interface unit consists of one circuit board, which is connected to the computer's extension port. In Fig. 1 a schematic drawing of the interface is shown. The computer data bus is directly connected to the A/D converter (ADC) and a peripheral interface adapter (PIA). The D/A converter, DAC receives its data through the PIA. Amplifier A1 is a bandwidth-limited input-amplifier for the ADC and amplifier A2 is a current/voltage converter which produces the required voltage signal from the current output of the DAC. A ± 12 V voltage-regulator unit, powered by a separate transformer, supplies the ADC and DAC with power. The +5 V voltage is taken from the computer's power supply. The ADC is a fast converter (Analog Devices AD574), with a conversion time of about $25 \mu\text{sec}$, and its resolution is 12 bits. The DAC (Analog Devices AD565) is also a fast device with 12 bits resolution. Both converters have an on-chip voltage reference. The input range of the ADC is from +10 V to -10 V, and the output range of DAC is from +5 V to -5 V. The PIA and the ADC occupy 4 and 2 addresses, respectively, in the memory space of the computer.

Control-signals for data transfer are generated inside the C64. The ADC is started through writing a dummy byte to the even address of the converter and the two data-bytes of a conversion are input through reading the two addresses. Data to the DAC are channelled through the PIA, which has two bidirectional parallel I/O-ports. A hold-latch (not

shown in Fig. 1), is used for temporary storage of the low-byte output to the DAC. The remaining four I/O-bits of the PIA are drawn to an edge connector and can be used for on/off-control.

Software

The software which is needed for square-wave voltammetry is written both in BASIC and in assembly language. Because of the short pulses used in pulse voltammetry, the control program for potential-generation and data-acquisition has to be written in assembly language.¹¹ Parameter-selection and data-presentation are, on the other hand, conveniently handled by a BASIC program. A short BASIC program has been written with which parameters for a run are input to the computer and measurement data are plotted on the screen. Hard copies of the data are obtained by output of the current-code to the DAC, which in turn is connected to a pen-recorder. This is also done by a BASIC program. At the beginning of a run the following parameters are chosen: start potential, end potential, pulse heights (forward and reverse), pulse length, current-measurement point, and number of current measurements. After this the parameters are converted for use by the assembly program and saved in a table. To start a run the two timers are initiated and the interrupt is enabled, and one of the timers is started. Waveform-generation and data-acquisition are then handled by the assembly routine. Since the control routines are interrupt-routines their execution is completely transparent to the BASIC program. The remaining task for the BASIC program is then to plot the measurement data, which are stored in a memory-buffer by the assembly routine.

Pulse-generation and data acquisition

Execution is much faster for assembly routines than for routines written in BASIC, but assembly language programming is slow because of its elementary character and a large part of the program development is concerned with debugging of the program. However, it is the only way to handle fast computer-control problems. For this reason all data-transfers to and from the interface are controlled by assembly-language subroutines which can also be called from a BASIC program. Accurate timing is of great importance when generating pulse waveforms. The use of programmable timers simplifies the programming, especially if the control can be handled by interrupt routines initiated by the timers. The time between a timer interrupt-request and the actual execution of the routine is not immediate, nor is the delay constant. The time difference, which depends on the instruction the processor is currently executing when an interrupt is requested, is of the order of a few μsec and the total delay is some tens of μsec . The relative accuracy of the timing will then depend on the length of the time intervals chosen. In square-wave voltammetry the shortest time measured is

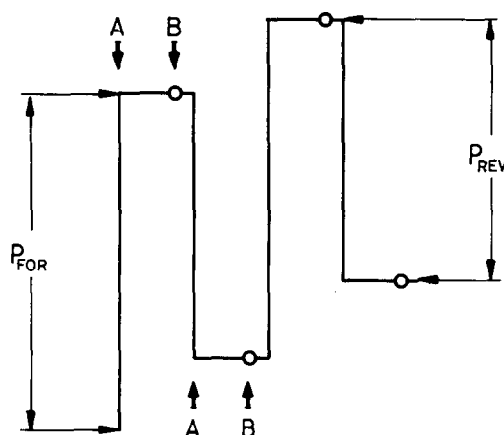


Fig. 2. Two square-wave period with forward pulse P_{FOR} and reverse pulse P_{REV} . Arrows A and B indicate when the two timers generate interrupts. A timer-A interrupt causes the potential to change and a timer-B interrupt starts the current sampling.

about 1 msec. A variation of 10 μsec in the timing will then cause a relative error of 0.1%, which is still acceptable. This estimation is valid for the C64 and similar computers working with a clock frequency of about 1 MHz. More accurate timing can be achieved with fast microcontrollers or by using hardware circuits.

In Fig. 2 two periods of a square-wave waveform are shown. P_{FOR} in the figure is the forward pulse height and P_{REV} is the reverse pulse height. The assembly program written for the generation of this waveform makes use of these two parameters and two timing parameters which determine the pulse length and current-measurement point. Arrows A and B in Fig. 2 indicate the time at which the two timers of the C64 generate interrupts. The timers are 16-bit counters which count down once every 980 nsec. The longest time interval which can be generated is then 64.2 msec. Timer A is used to create the pulse length, while timer B creates the current-measurement delay. Timer A is started from the BASIC program. After counting down to zero an interrupt is generated. The interrupt-routine determines whether timer A or timer B caused the interrupt. A timer-A interrupt causes timer B to be started, outputs the current potential value and calculates the new potential. A timer-B interrupt causes the current to be measured and the measurement data to be stored in a memory-buffer. The potential value which is to be output is generated by alternately adding the forward pulse height and subtracting the reverse pulse height to and from the last potential value. A pulse-counter in the interrupt-routine keeps track of the number of pulses which are output and the run is stopped when a predetermined number of pulses have been output. In this way the scan-speed is determined by the pulse length and by the difference between forward and reverse pulse height.

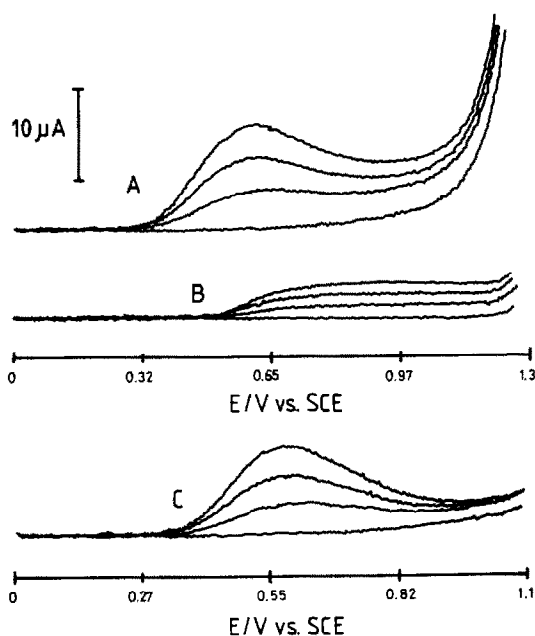


Fig. 3. Square-wave voltamperograms for paracetamol in acetate buffer (pH 4.7). (A): forward current, (B): reverse current and (C) difference current. Concentrations: 0, 9.9, 19.6 and 29.1 ppm. Pulse height: 200 mV. Pulse-length: 60 msec. Scan-rate: 42 mV/sec. The current was measured 16 times, starting 5 msec before the end of the pulse. Average values were plotted and the electrode used was a polymer-modified carbon type.

If the reverse pulse height is zero a staircase waveform is generated, with two current measurements on each step.

RESULTS AND DISCUSSION

To test the system the interface was connected to an amperometric detector normally used in HPLC-experiments. The detector was laboratory built and consisted of a potentiostat, an I/E-converter unit and a filter unit. The DAC-output of the interface was directly connected to the input of the potentiostat and the output of the I/E-converter was connected to the ADC-input. A filter capacitor in the feedback loop of the I/E-converter was replaced by a smaller one to improve the response. Measurements were then made with solid electrodes in static solutions. Iodide was determined with a carbon-paste electrode and paracetamol with a Radelkis polymer-modified carbon electrode.

In Fig. 3 square-wave voltamperograms for the oxidation of paracetamol are shown. Experimental data are given in the figure. Oxidation of the amino group gives rise to a forward current peak while only a small wave is generated by the reverse pulse. The absence of reverse peaks indicates an irreversible charge-transfer and the signal from the reverse pulses is caused by the forward reaction taking place at the lower potential of the reverse pulse. The concen-

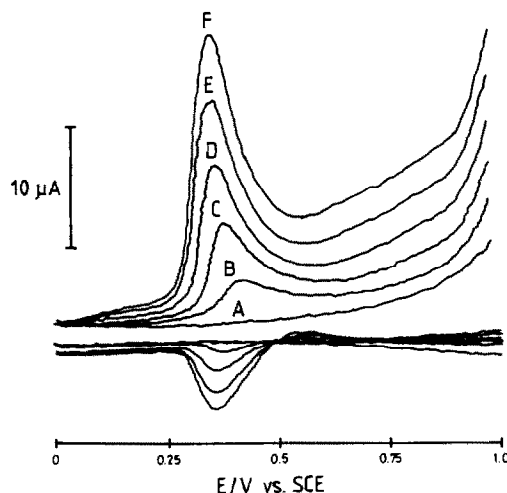


Fig. 4. Forward and reverse square-wave voltamperograms for iodide-iodine in acetate buffer (pH 4.7). Concentrations: 0, 22.1, 44.3, 66.4, 88.5 and 110.6 ppm (A-F). Pulse height: 300 mV. Pulse length: 63 msec. Scan-rate: 40 mV/sec. The current was measured 3 times, starting 3 msec before the end of the pulse. The electrode used was a carbon-paste electrode.

tration of oxidizable paracetamol near the electrode surface, and thus also the reverse current, is lower because of the forward pulses. In Fig. 4, on the other hand, both a forward and a reverse peak are seen in the determination of iodide. The charge-transfer is thus more reversible for the iodide oxidation. The forward peaks which are due to the oxidation of the iodide also show a concentration dependence. The shift to lower peak potentials with increasing iodide concentration is probably caused by conversion of the iodine produced into the tri-iodide ion I_3^- . The reverse signal, which is a result of the reduction of iodine, has a peak potential which does not show any clear concentration dependence. It is evident that it is useful to be able to study both the forward and reverse current when an electrode reaction is investigated.

The voltamperograms obtained with the amperometric detector have a noisy appearance, probably because of the direct measurement method used. Usually the voltage-converted current signal is sampled or integrated before plotting or A/D-conversion.^{6,8,10,12} A numerical method to filter staircase voltammetric data has also been used.⁹ This, however, requires a fast computer if smoothing is to be done in real time. The amperometric detector used here did not provide any current-sampling circuits, but the remaining 4 digital I/O-lines of the computer interface can be used to control sample-and-hold circuits or analogue integrators. Only two control lines are needed to control the PAR 174 sample-and-hold circuits, for example.

Acknowledgement—The financial support of the Academy of Finland and the Hungarian Academy of Science is gratefully acknowledged.

REFERENCES

1. P. G. Barker, *Computers in Analytical Chemistry*, Pergamon Press, Oxford, 1983.
2. S. S. Shukla and J. F. Rusling, *Anal. Chem.*, 1984, **56**, 1347A.
3. E. Ziegler, *Anal. Chim. Acta*, 1983, **147**, 77.
4. S. A. Borman, *Anal. Chem.*, 1982, **54**, 705A.
5. L. L. Jackson, C. Yarnitsky, R. A. Osteryoung and J. Osteryoung, *Chem. Biomed. Environm. Instr.*, 1980, **10**, 175.
6. A. Lavy-Feder and C. Yarnitsky, *Anal. Chem.*, 1984, **56**, 678.
7. P. Barrett, L. J. Davidowski and T. R. Copeland, *Anal. Chim. Acta*, 1980, **122**, 67.
8. J. H. Christie, L. L. Jackson and R. A. Osteryoung, *Anal. Chem.*, 1976, **48**, 242.
9. L. L. Miaw, P. A. Bodreau, M. A. Pichler and S. P. Perone, *ibid.*, 1978, **50**, 1988.
10. E. B. Buchanan, Jr. and W. J. Sheleski, *Talanta*, 1980, **27**, 955.
11. R. L. Sing, S. W. McGeorge and E. D. Salin, *ibid.*, 1983, **30**, 805.
12. M. S. Krause, Jr. and L. Ramaley, *Anal. Chem.*, 1969, **41**, 1365.

DIAGRAMMES POTENTIEL-NIVEAU D'ACIDITE DANS LES MILIEUX H₂O-H₃PO₄-I

SYSTEMES ELECTROCHIMIQUES NE FAISANT PAS INTERVENIR LE PROTON

C. LOUIS et J. BESSIERE

Laboratoire de Chimie et d'Electrochimie Analytique, Faculté des Sciences, Université de Nancy 1,
B.P. 239, 54506 Vandoeuvre les Nancy, France

(Reçu le 19 décembre 1986. Accepté le 10 avril 1987)

Résumé—La variation des potentiels normaux de systèmes oxydo-réducteurs ne faisant pas intervenir le proton est étudiée en fonction de la concentration du milieu acide phosphorique (1 à 14M). Le couple ferricinium/ferrocène est le système de comparaison. Les systèmes envisagés sont ceux mettant en jeu les espèces du cuivre, du cadmium, de l'étain, du zinc, de l'argent, du plomb, du mercure, du bismuth, ainsi que les systèmes hexacyanoferrate(III)/hexacyanoferrate(II) et iode/iodure. Un intérêt particulier est porté au cas du fer. L'ensemble des résultats est présenté sous la forme d'un diagramme potentiel-concentration de H₃PO₄ (ou potentiel-niveau d'acidité).

Summary—The conditional potentials of redox systems not involving protons have been studied as a function of phosphoric acid concentration (1-14M), with the ferricinium/ferrocene couple as the comparison system. The following systems were considered: Cu(II)/Cu, Cd(II)/Cd, Sn(II)/Sn, Zn(II)/Zn, Ag(I)/Ag, Pb(II)/Pb, Hg(II)/Hg, Bi(III)/Bi and particularly Fe(III)/Fe(II) and Fe(II)/Fe. The hexacyanoferrate(III)/hexacyanoferrate(II) and iodine/iodide couples were also studied. The results are presented as a potential-H₃PO₄ concentration diagram (or potential-acidity level diagram).

Dans les solutions aqueuses diluées, les diagrammes potentiel-pH permettent d'interpréter un grand nombre de phénomènes d'oxydo-réduction et en particulier de préciser les conditions de stabilité des espèces (possibilité de dismutation, réactivité vis à vis du solvant ou d'autres solutés).

Notre but est d'établir les diagrammes potentiel-pH généralisé dans les milieux H₂O-H₃PO₄ (1 à 14M). Ils sont indispensables pour préciser les conditions de milieux compatibles avec l'existence d'une espèce à un degré d'oxydation donné. Or, pour l'extraction d'espèces ioniques à partir des milieux H₂O-H₃PO₄ par l'utilisation de solvants non-miscibles, de résines échangeuses d'ions ou par flottation ionique, le choix des composés chimiques convenables est directement lié au degré d'oxydation de l'espèce à extraire. Ils permettent également de déterminer les réactifs susceptibles d'amener une espèce au degré d'oxydation souhaité, de définir les conditions de titrage *in situ* et d'apporter des précisions sur la corrosion des métaux.

Afin de faciliter la présentation des résultats, nous examinerons dans une première partie les systèmes électrochimiques ne faisant pas intervenir le proton. Dans ce cadre, nous envisagerons l'oxydation des métaux dans les milieux phosphoriques, seuls ou en présence d'espèces susceptibles de conduire à la formation de composés insolubles. Le fer sera étudié plus particulièrement. Les systèmes non-métalliques engageant les hexacyanoferrates et les iodures seront

également envisagés. L'étude des systèmes électrochimiques faisant intervenir le proton: uranium, vanadium, arsenic fera l'objet d'une deuxième partie. L'ensemble des résultats sera présenté sous la forme d'un diagramme potentiel-concentration de H₃PO₄.

RAPPEL THEORIQUE: SOLVATATION ET PROPRIETES D'OXYDO-REDUCTION

Lorsque l'on passe du milieu de référence (solution infiniment diluée dans l'eau) aux différents milieux envisagés, les deux constituants du système de comparaison: ferricinium/ferrocène subissent la même variation de solvation. Mais, pour la plupart des espèces en solution, la solvation est nettement modifiée selon la composition du milieu. Nous allons rappeler comment se traduisent les variations de solvation au niveau des propriétés d'oxydo-réduction.

Considérons la réaction d'oxydo-réduction:



A l'équilibre, en solution aqueuse suffisamment diluée, le potentiel du couple A/B est donné à 298 K par

$$E_{H_2O} = E_{H_2O}^0 + \frac{0.059}{n} \log \frac{[A]}{[B]} \quad (2)$$

Dans un milieu H₂O-H₃PO₄ concentré en acide, une relation analogue peut être écrite, à condition de faire

intervenir les activités (A) = $f_A[A]$ et (B) = $f_B[B]$ des espèces A et B.

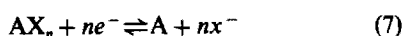
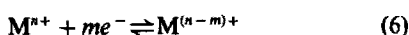
$$E_{\text{H}_2\text{O}/\text{H}_3\text{PO}_4} = E_{\text{H}_2\text{O}}^0 + \frac{0.059}{n} \log \frac{f_A}{f_B} + \frac{0.059}{n} \log \frac{[A]}{[B]} \quad (3)$$

Le couple redox A/B est donc caractérisé en milieu $\text{H}_2\text{O}-\text{H}_3\text{PO}_4$ par un potentiel conditionnel:

$$E_{\text{H}_2\text{O}/\text{H}_3\text{PO}_4}^0 = E_{\text{H}_2\text{O}}^0 + 0.059 \log \frac{f_A}{f_B} \quad (4)$$

Son écart avec le potentiel normal dans l'eau ne dépend que des coefficients d'activité f_A et f_B des espèces A et B.

Dans le cas particulier des réactions d'oxydo-réduction:



l'expression (4) prend les formes:

$$E_{\text{H}_2\text{O}/\text{H}_3\text{PO}_4}^0 = E_{\text{H}_2\text{O}}^0 + \frac{0.059}{n} \log f_{\text{M}^{n+}} \quad (8)$$

$$E_{\text{H}_2\text{O}/\text{H}_3\text{PO}_4}^0 = E_{\text{H}_2\text{O}}^0 + \frac{0.059}{n} \log \frac{f_{\text{M}^{n+}}}{f_{(\text{M}^{n-m})+}} \quad (9)$$

$$E_{\text{H}_2\text{O}/\text{H}_3\text{PO}_4}^0 = E_{\text{H}_2\text{O}}^0 + \frac{0.059}{n} \log \frac{1}{(f_{X^-})^n} \quad (10)$$

L'effet de changement de milieu sur les caractéristiques de ces couples redox peut donc être envisagé comme résultant de la variation de solvation de l'espèce en solution si l'autre constituant du système est un solide (ou un gaz) en solution saturée [relations (8) et (10)] ou de la variation relative de solvation des espèces oxydées et réduites en solution [relation (9)].

EXPERIMENTAL

Réactifs

Acide phosphorique, acide sulfurique, acide fluorhydrique, fluorure d'ammonium, fluorure de potassium, fer (poudre), argent (poudre), zinc (grenaille) de qualité RP sont utilisés sans purification préalable.

Les solutions de cations métalliques destinées aux études polarographiques (Cu^{2+} , Sn^{2+} , Cd^{2+} , Pb^{2+} , Zn^{2+}) sont obtenues soit par attaque du métal, soit par dissolution d'oxyde ou de carbonate dans les milieux phosphoriques convenables. Les solutions de Fe(II) sont préparées par dissolution de poudre de fer dans les différents milieux phosphoriques. Les solutions de Fe(III) sont obtenues par oxydation des solutions de Fe(II) à potentiel contrôlé (+700 mV vs. ECS dans H_3PO_4 0,1M) sur une électrode cylindrique de platine de grande surface.

Matériel

Les mesures potentiométriques à intensité nulle ont été faites au moyen du millivoltmètre Aries 10000 Tacussel. Les tracés polarographiques ont été obtenus sur le polarographe PRG 3 Tacussel. Pour les tracés voltampérométriques sur électrode solide, réalisés avec un ensemble Tipol EPL 2 Tacussel, un montage classique à trois électrodes a été utilisé.

Méthodes

Le dégazage des milieux réactionnels est obtenu par passage d'azote. L'électrode au calomel saturé placée dans un compartiment séparé contenant H_3PO_4 0,1M est utilisée comme électrode de référence. L'électrode auxiliaire est constituée par un fil de platine. Les électrodes de travail sont l'électrode de platine EDI Controvit Tacussel (diamètre 1 mm) ou un fil de platine (diamètre 0,8 mm) serti dans du verre ou du Teflon, l'électrode de carbone vitreux EDI Controvit Tacussel (diamètre 3 mm) ou un barreau de carbone vitreux (diamètre 2 mm) serti dans du verre. Leur vitesse de rotation est de 600 tours/min.

RESULTATS ET DISCUSSION

Oxydation des métaux dans les milieux phosphoriques

Les réactions de l'acide phosphorique avec les métaux sont importantes. Il est en effet utilisé pour le traitement des surfaces métalliques.¹ Le plomb, le cuivre seul ou en alliage² présentent une résistance à la corrosion qui a permis de résoudre une partie des problèmes posés par le traitement et le stockage des produits de l'industrie de l'acide phosphorique. Le fer, l'argent, le zinc (sous forme d'amalgame solide) sont utilisés comme réducteur dans les milieux phosphoriques. Les métaux biologiquement toxiques comme le cadmium doivent être éliminés des acides phosphoriques destinés à la production des engrais et des phosphates alimentaires.

Les espèces ioniques mises en jeu dans les systèmes redox engageant le cuivre, l'étain, le cadmium et le zinc sont réductibles à l'électrode à goutte de mercure. Les systèmes sont rapides et la réaction correspond à l'échange de deux électrons. Les potentiels normaux dans l'eau et dans les différents milieux phosphoriques sont donnés dans le Tableau 1 et présentés par la Figure 1. Ils sont calculés à partir des potentiels de demi-vague de réduction en tenant compte de la variation des courants de diffusion avec la concentration de l'acide. La correction n'est significative que pour les milieux de concentration >8M. Le pouvoir réducteur du cuivre, de l'étain, du cadmium et du zinc diminue lorsque la concentration de l'acide augmente. Cependant, l'ordre des potentiels normaux qui existe en milieu aqueuse:

$$E_{\text{Zn}^{2+}/\text{Zn}}^0 < E_{\text{Cd}^{2+}/\text{Cd}}^0 < E_{\text{Sn}^{2+}/\text{Sn}}^0 < E_{\text{Cu}^{2+}/\text{Cu}}^0$$

est conservé dans tout le domaine de concentration de l'acide.

D'un point de vue thermodynamique, seul le cuivre n'est pas oxydé par les protons du milieu, quelle que soit sa concentration. Ceci explique la résistance à la corrosion du cuivre en présence d'acide phosphorique même concentré. Sur électrode de cuivre, l'étendue du domaine d'électroactivité (Fig. 2) est de 700 mV pour les concentrations d'acide <11,5M et de 1 V environ dans les milieux plus concentrés. La limite en oxydation est légèrement inférieure au potentiel normal du système Cu^{2+}/Cu . La limite en réduction, qui correspond à la réduction du proton, indique que la surtension de H^+ sur électrode de cuivre est plus

Tableau 1. Potentiels normaux dans les milieux $H_2O-H_3PO_4$: Systèmes électrochimiques ne faisant pas intervenir le proton (mV vs. Fc^+/Fc)

	H_2O	H_3PO_4, M	2,0	5,5	8,0	11,5	14,0
		$H_3PO_4, \%$ $P_2O_5, \%$	18,0 13,0	42,5 30,8	56,5 40,9	72,5 52,7	83,0 60,0
$R_0(H)$			-0,2	-1,9	-3,2	-6,1	-8,9
H^+/H_2	-400		-387	-290	-205	-40	+120
O_2/H_2O	+829		+841	+942	+1020	+1197	+1371
ECS dans $H_3PO_4 (0,1M)$			-50	+40	+115	+265	+380
Zn^{2+}/Zn	-1160		-1100	-1000	-930	-818	-672
Cd^{2+}/Cd	-800		-700	-600	-530	-418	-272
Sn^{2+}/Sn	-530		-550	-450	-360	-218	-52
Pb^{2+}/Pb	-520		-480	-420	-350	-268	-152
AgI/Ag	-552		-470	-440	-410	-350	-300
$AgBr/Ag$	-329		-370	-300	-240	-130	-50
$AgCl/Ag$	-178		-120	-80	-45	+30	+105
$BiPO_4/Bi$	-593		-160	-75	-5	+135	+220
Cu^{2+}/Cu	-60		-70	0	+70	+182	+278
Fe^{3+}/Fe^{2+}	+370		+120	+149	+190	+294	+360
I_2/I^-	+134		+168	+184	+185		
Hg_2HPO_4/Hg	-24		+250	+330	+405	+525	+620
Ag^+/Ag	+400		+440	+495	+550	+680	+775
$Fe(CN)_6^{3-}/Fe(CN)_6^{4-}$	-40		+330	+500	+650	+930	+1230

importante que sur électrode de platine,³ l'écart variant de 400 à 700 mV.

Les systèmes Ag^+/Ag , $AgCl/Ag$, $AgBr/Ag$ et AgI/Ag ont été étudiés par potentiométrie à intensité nulle sur électrode d'argent.^{3,4} Ils obéissent à la loi de Nernst dans tout le domaine de concentration d'acide, à l'exception de AgI/Ag dans les milieux phosphoriques concentrés (14M) où une oxydation rapide de I^- par Ag^+ a lieu. Leurs potentiels normaux, donnés dans le Tableau 1 et présentés par la Figure 1, mettent en évidence la diminution du caractère réducteur de l'argent lorsque la concentration de H_3PO_4 augmente et la modification de son comportement en présence des différents halogénures. L'oxydation électrochimique de l'argent en milieu phosphorique et la réduction du proton limitent le domaine d'électroactivité sur électrode d'argent. Son étendue (Figure 2) est de 1400 mV dans les milieux dilués en acide et de 1200 mV dans les milieux concentrés. La surtension du proton est nettement plus importante que sur électrode de platine, l'écart variant de 900 à 600 mV lorsque la concentration d'acide passe de 2 à 14M. Les potentiels pris par le système Hg_2Cl_2/Hg dans les milieux phosphoriques ont été comparés à ceux de l'électrode au calomel saturé aqueuse plongée directement dans le milieu acide fréquemment utilisée comme électrode de référence⁵⁻¹⁰ et de l'électrode ECS placée dans un compartiment séparé contenant H_3PO_4 0,1M qui

nous a servi d'électrode de référence (Tableau 2). L'étendue du domaine d'électroactivité sur électrode à goutte de mercure est voisine de 1,4 V quelle que soit la concentration de l'acide. La surtension des protons sur mercure est la plus importante de celles qui ont été observées. L'écart avec l'électrode de platine est d'environ 900 mV.

Les caractéristiques polarographiques du système du plomb montrent qu'il est rapide et que l'échange est de deux électrons dans tout le domaine de concentration d'acide. Les potentiels normaux, déterminés à partir des potentiels de demi-vague de réduction sont donnés dans le Tableau 1 et présentés par la Figure 1. D'un point de vue thermodynamique, le plomb est donc oxydé par les protons du milieu et ses propriétés réductrices diminuent lorsque la concentration d'acide augmente.

Le mercure, la plomb ainsi que le bismuth forment dans les milieux phosphoriques des phosphates peu solubles. L'étude des caractéristiques électrochimiques de systèmes Hg_2HPO_4/Hg et $BiPO_4/Bi$ a conduit à la détermination des fonctions basiques $R_0(H_2PO_4^-)$, $R_0(HPO_4^{2-})$, $R_0(PO_4^{3-})$.¹¹ L'analyse par diffraction des rayons X des phosphates de plomb montre que seule la forme $PbHPO_4$ précipite dans les milieux $H_2O-H_3PO_4$ de concentration 2 à 8M, et qu'en milieu plus concentré, c'est la forme $Pb(H_2PO_4)_2$ qui précipite. L'analyse polarographique des solutions saturées a conduit à la détermination de

Tableau 2. Système Hg_2Cl_2/Hg , dans les milieux $H_2O-H_3PO_4$; électrode ECS *in situ*; électrode ECS aqueuse, mV vs. ECS aqueuse placée dans un compartiment séparé contenant H_3PO_4 (0,1M)

H_3PO_4, M	1,0	2,0	5,5	8,0	11,5	14,0
ECS <i>in situ</i>		-68	-130	-168	-225	-280
ECS aqueuse	-40	-57	-93	-114	-125	-125

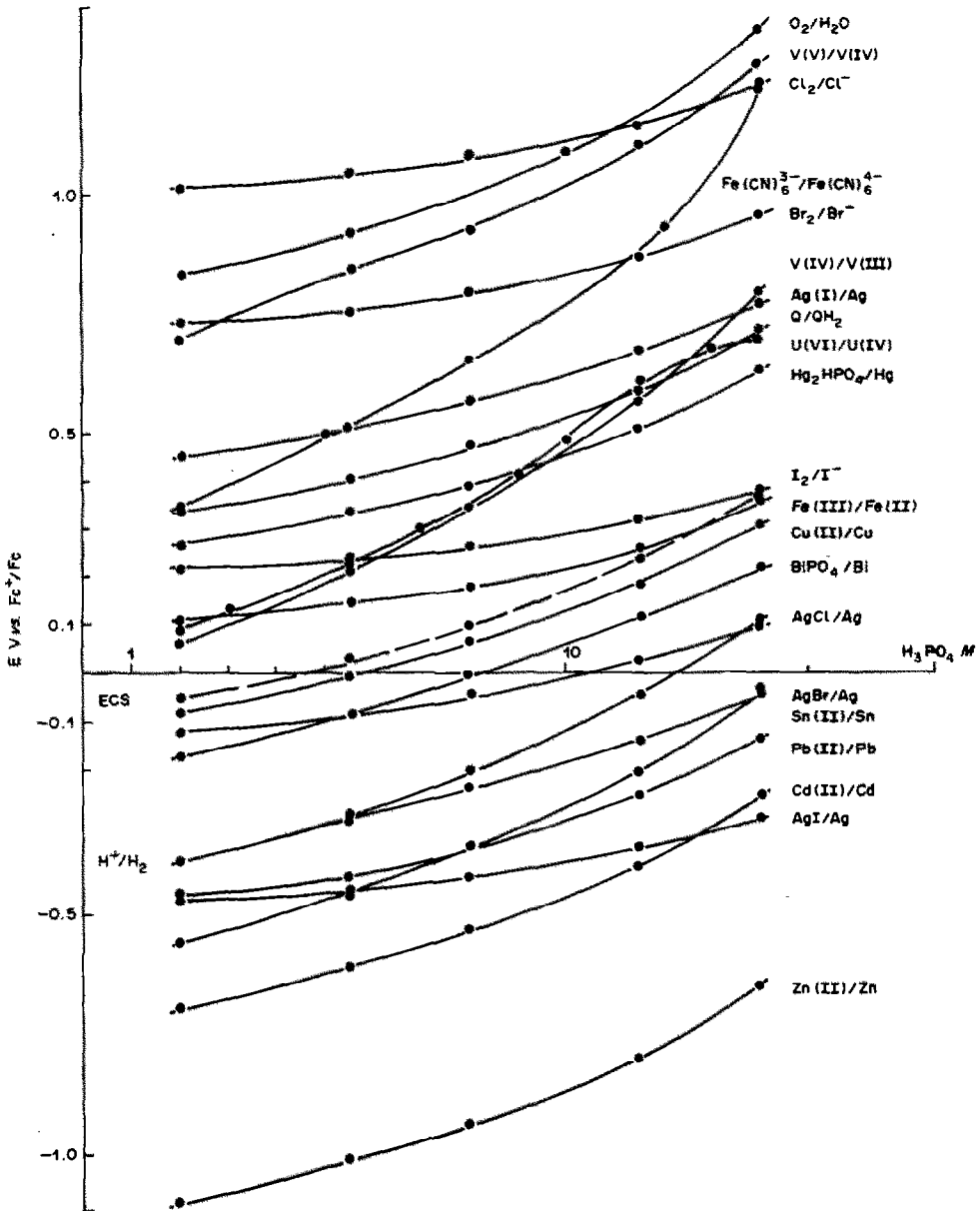


Fig. 1. Diagrammes potentiel-concentration de H_3PO_4 : V vs. Fe^{3+}/Fe^{2+} .

valeurs de solubilité cohérentes avec celles calculées à partir des fonctions basiques et des coefficients d'activité des espèces Pb^{2+} .

Le fer est présent dans les phosphates naturels à des teneurs qui varient selon leur origine de 0,1 à 2%.^{8,12,13} Dans les milieux phosphoriques industriels, il se trouve sous la forme $Fe(III)$ ou $Fe(II)$ selon le vieillissement des solutions, leur exposition à l'air, leur température. En raison des propriétés oxydo-

réductrices du système $Fe(III)/Fe(II)$, sa présence conditionne les propriétés d'extraction d'espèces minérales comme l'uranium et le vanadium soit parce qu'il a une influence directe sur leur degré d'oxydation, soit parce que le collecteur utilisé s'associe préférentiellement aux espèces du fer avant de se combiner avec l'espèce à extraire ou qu'il est oxydé par les ions ferriques. Les propriétés réductrices du $Fe(II)$ ont été utilisées à des fins analytiques dans les milieux phosphoriques concentrés.^{7,14-21}

Notre but est de compléter les données thermodynamiques de Baes,⁵ Marcus⁶ et de Rao et Sagi⁷ et de déterminer ainsi l'évolution de la réactivité des couples redox $Fe(III)/Fe(II)$ et $Fe(II)/Fe$ dans tout le domaine de concentration d'acide.

Les espèces* Fe^{3+} et Fe^{2+} sont électroactives dans

* Cette représentation est purement formelle et n'implique pas que les espèces ferriques et ferreuses sont sous forme cationique quelle que soit la concentration d'acide. Le comportement électrophorétique des espèces ferriques²² montre qu'elles restent sous forme cationique en solution H_3PO_4 diluée, sont neutres en milieu H_3PO_4 3M, anioniques en milieu H_3PO_4 5M.

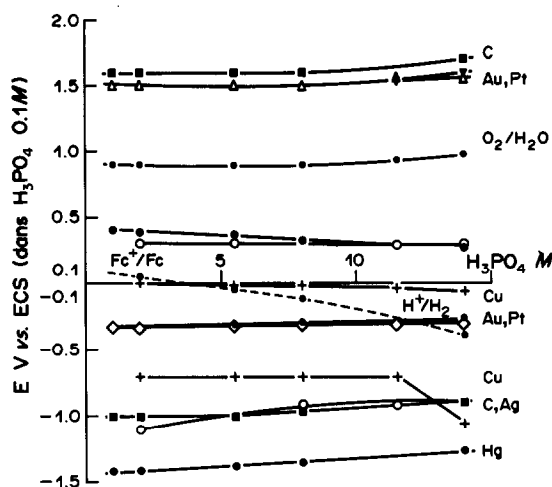


Fig. 2. Limites des domaines d'électroactivité dans le milieu $\text{H}_2\text{O}-\text{H}_3\text{PO}_4$ (V vs. ECS aqueuse dans H_3PO_4 $0,1M$) pour les électrodes de carbone $\blacksquare-\blacksquare-\blacksquare$; d'or, $-\triangle-\triangle-\triangle$; de platine, $-\nabla-\nabla-\nabla$; de mercure, $-\bullet-\bullet-\bullet$; d'argent, $-\circ-\circ-\circ$; de cuivre, $-+-+-+-$.

tout le domaine de concentration d'acide sur électrode de platine, de carbone vitreux et sur électrode à goutte de mercure. Cependant, le système n'est rapide que sur mercure. Les résultats de l'analyse des tracés polarographiques sont rassemblés dans le Tableau 3.

La variation des potentiels normaux du système $\text{Fe}^{3+}/\text{Fe}^{2+}$ met en évidence l'accroissement du caractère oxydant de Fe^{3+} avec l'augmentation de la concentration d'acide. L'évolution des propriétés réductrices de Fe^{2+} sera mise à profit pour déterminer les potentiels normaux du système $\text{UO}_2^{2+}/\text{U}^{4+}$ dans les milieux de concentration 3 à $6M$ en H_3PO_4 . Le courant de diffusion limite est, pour les espèces du fer, divisé par 6 lorsque la concentration d'acide passe de 2 à $14M$. L'étude en fonction de la température montre qu'il n'est pas possible de compenser cette diminution du courant de diffusion limite par une élévation de la température de 298 à 323 K.

Il importe de savoir si les sulfates qui sont présents dans les solutions industrielles à des teneurs comprises entre 0,1 et $0,3M$ ont un effet sur la réactivité

du fer vis à vis de l'uranium. Nous avons vérifié, dans tout le domaine de concentration d'acide et pour une concentration de sulfate allant jusqu'à $0,5M$ (ajouté sous forme de K_2SO_4) que les polarogrammes du couple redox $\text{Fe}^{3+}/\text{Fe}^{2+}$ ne sont modifiés ni en ce qui concerne les potentiels de demi-vague, ni en ce qui concerne les courants de diffusion limite. Ces résultats ont été confirmés par des mesures potentiométriques à intensité nulle sur électrode de platine. L'addition de sulfate à des concentrations supérieures à $1M$ sous forme de K_2SO_4 ou de H_2SO_4 , entraîne une modification du niveau d'acidité donc une variation du potentiel du système $\text{Fe}^{3+}/\text{Fe}^{2+}$ mais qui n'est pas due à un effet de complexation.

Afin d'analyser l'influence des ions fluorure sur la réactivité de Fe(II) vis à vis de U(VI) , nous avons examiné l'évolution du pouvoir oxydant de Fe(III) avec la teneur en fluorure en particulier dans le milieu H_3PO_4 $5,5M$ où l'addition de HF n'entraîne pas la formation d'acide monofluorophosphorique.^{23,24} L'évolution du potentiel pris par une électrode de platine plongeant dans différents mélanges de Fe^{2+} et Fe^{3+} met en évidence une faible complexation de Fe^{3+} . En toute rigueur, l'évolution du potentiel ne peut être analysée que dans le domaine de concentration en fluorure inférieure à $0,5M$. Au delà, la composition du milieu change et son niveau d'acidité varie selon que l'on ajoute l'espèce fluorure sous la forme HF ou KF . La baisse de potentiel est d'autant plus importante que le rapport $F_{\text{total}}^-/\text{Fe}^{3+}$ est grand. Ces résultats sont confirmés par potentiométrie à une électrode spécifique des fluorures. Le potentiel pris par cette électrode dans le milieu H_3PO_4 , $5,5M/\text{HF}$ $0,3M$ ne varie pas lorsque Fe^{3+} est introduit à la concentration $0,05M$. Le rapport F^-/Fe^{3+} est égal à 6 et le complexe ne se forme pas. La formation quantitative de FeF^{2+} aurait entraîné une variation de potentiel de 5 mV décelable au moyen de l'électrode utilisée. Dans les solutions concentrées en fluorure, les ions Fe^{3+} sont complexés. Ce résultat confirme les déterminations faites par Plazanet et Lamache⁹ par voltampérométrie cyclique. Dans les milieux phosphoriques industriels pour lesquels la teneur en Fe(III) est de l'ordre de $0,1M$, la concentration en HF est insuffisante pour que la totalité des ions ferriques soit complexée. Globalement, le

Tableau 3. Caractéristiques polarographiques du système $\text{Fe}^{3+}/\text{Fe}^{2+}$ dans les milieux $\text{H}_2\text{O}-\text{H}_3\text{PO}_4$

[H_3PO_4], M	$E_{1/2} = E^0$, mV vs. Fc^+/Fc	Pente, mV/decade	$n =$ 59/pente	I/C , $\mu\text{A} \cdot \text{l. mmole}^{-1}$	
				25°C	50°C
0 (H_2O)	+370	—	—	—	—
1,0	+115	—	—	—	—
2,0	+120	60	0,98	1,16	1,74
5,5	+149	58	1,02	0,75	0,97
8,0	+190	61	0,97	0,54	0,86
10,0	+240	—	—	—	—
11,5	+294	60	0,98	0,31	0,52
14,0	+360	58	1,02	0,20	0,34

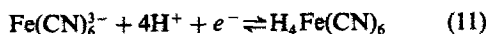
pouvoir réducteur de Fe(II) n'est pas modifié par la présence de fluorure.

Le fer métal, très fréquemment utilisé comme réducteur dans les milieux phosphoriques industriels, est oxydé par les mélanges $H_2O-H_3PO_4$ pour donner des solutions de Fe(II) dont la concentration peut atteindre 0,5M. La cinétique d'attaque dépend du degré de pureté du métal, de son état de division, du mode d'agitation, de la température et de la concentration en acide.⁸ Ces solutions sont stables vis à vis de l'oxygène, l'apparition de Fe(III) ne se fait à température ambiante, en milieu non agité, qu'après plusieurs heures. La poudre de fer permet de réduire de nombreuses espèces en milieu phosphorique, en particulier U(VI) et Fe(III). Du fer métal a été ajouté progressivement à des solutions de Fe(III) 0,05M préparées par oxydation électrochimique de solutions de Fe(II) dans H_3PO_4 5,5 et 11,5M. La variation de potentiel à intensité nulle a été suivie sur électrode de platine. D'après la Figure 3, il apparaît que le fer métal réduit l'espèce en solution et très peu le proton. L'excès de fer métal nécessaire est de l'ordre de 4% en milieu phosphorique 5,5M et de 12% dans le milieu 11,5M dans le cas de milieux réactionnels simplement agités par passage d'azote. Les conditions d'agitation influent en effet notablement sur la formation d'hydrogène au cours de la réaction entre le fer métal et le Fe(III). Du plus, lorsque le fer métal est encore présent dans le milieu, il impose un potentiel nettement réducteur (-300 mV vs. ECS) qui est voisin de celui du système H^+/H_2 .

Systèmes non métalliques

Le système redox hexacyanoferrate(III)/hexacyanoferrate(II) a été étudié dans les milieux phosphoriques⁴ car il peut intervenir en tant qu'indicateur électrochimique et l'insolubilité des composés qu'il donne en présence de nombreux ions métalliques présente un intérêt analytique. Les propriétés oxydantes de $Fe(CN)_6^{3-}$ ont été utilisées pour des dosages, en particulier de Fe(II), en milieu concentré en H_3PO_4 .²⁵ Ce système est rapide et obéit à la loi de Nernst dans tout le domaine de concentration de H_3PO_4 . Les valeurs de son potentiel normal sont données dans le Tableau 1. Leur augmentation pour une variation de concentration de H_3PO_4 de 2 à 14M est la plus importante observée parmi tous les systèmes redox envisagés. Ceci est lié au fait que $Fe(CN)_6^{4-}$, contrairement à $Fe(CN)_6^{3-}$, présente des propriétés basiques dans l'eau.

Dans les milieux concentrés en acide, l'équilibre d'oxydo-réduction est probablement:



et non plus:



L'étude électrochimique du système I_2/I^- dans les milieux phosphoriques a été menée essentiellement pour définir ses conditions d'utilisation comme indi-

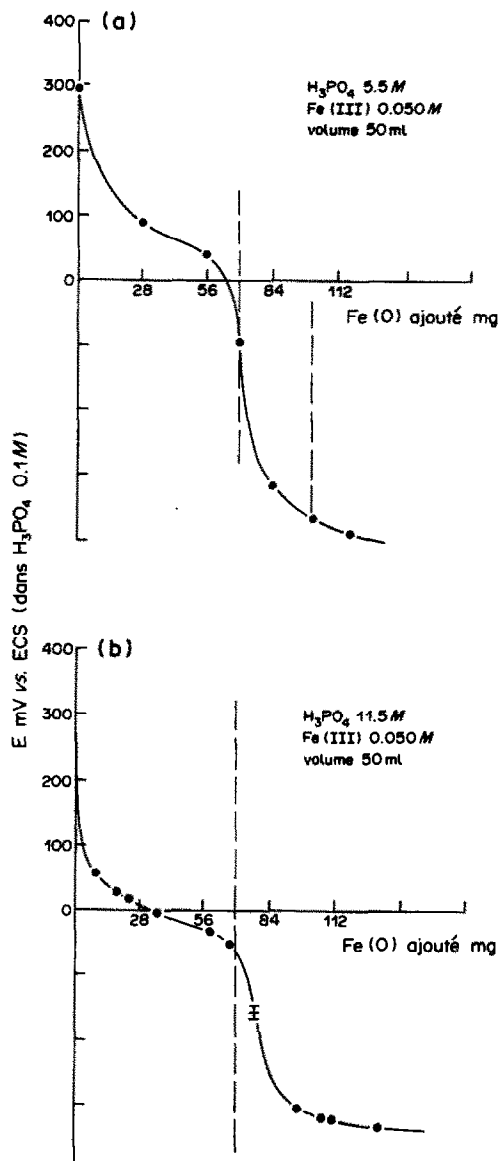


Fig. 3. Réduction de Fe(III) par Fe: (a) dans H_3PO_4 5,5M, (b) dans H_3PO_4 11,5M.

cateur électrochimique.²⁶ En outre, la présence d'iode catalyse un certain nombre de réactions redox à cinétique lente et les conditions de catalyse sont fonction de la position relative des différents systèmes sur l'échelle de potentiel. Le système redox I_2/I^- obéit à la loi de Nernst dans le domaine de concentration phosphorique 1 à 8M. Les valeurs de son potentiel normal sont données dans le Tableau 1.

CONCLUSION

Les données thermodynamiques caractérisant dans les milieux phosphoriques les systèmes redox ne faisant pas intervenir le proton ainsi que les phénomènes aux électrodes sont résumés sous la forme de deux diagrammes (Figures 1 et 2). Les potentiels

redox croissent avec la concentration d'acide et leurs variations sont d'amplitude voisine. Nous verrons qu'elles sont en général moins marquées que celles des systèmes redox faisant intervenir le proton. Ces premiers résultats permettent de disposer d'une série de tampons de potentiel dans les milieux phosphoriques. Ils conduisent au calcul des coefficients d'activité de transfert de solvation des anions et des cations mis en jeu.²⁷

LITTÉRATURE

1. T. Saji, *Kinzoku Hyomen Gijutsu*, 1977, **28**, 2.
2. E. Pelliti, *Phosphoric Acid*, A. V. Slack (ed.), Vol. 1, Part 2, p. 779. Dekker, New York, 1968.
3. C. Louis et J. Bessière, *Anal. Lett.*, 1980, **13**, 937.
4. N. Benlakhdim, *Thèse de Doctorat de 3^e Cycle*, Nancy, 1981.
5. C. F. Baes, Jr., *J. Phys. Chem.*, 1956, **60**, 805.
6. Y. Marcus, *ibid.*, 1958, **62**, 1314.
7. G. G. Rao et S. R. Sagi, *Talanta*, 1962, **9**, 715.
8. D. Mastef, *Thèse de Docteur Ingénieur*, Nancy, 1977.
9. C. Plazanet et M. Lamache, *Electrochim. Acta*, 1981, **26**, 45.
10. K. Elkacemi, B. Tyburce et S. Belcadi, *ibid.*, 1982, **27**, 729.
11. C. Louis et J. Bessière, *Can. J. Chem.*, 1985, **63**, 908.
12. F. Habashi, *2nd Intern. Congr. Phosphorus Compounds, Proceedings*, p. 629, 1980.
13. J. R. Lehr, *Phosphoric Acid*, A. V. Slack (ed.), Vol. 1, Part 2, p. 635. Dekker, New York, 1968.
14. G. G. Rao et S. R. Sagi, *Talanta*, 1963, **10**, 169.
15. G. G. Rao et L. S. A. Dikshitulu, *ibid.*, 1963, **10**, 295.
16. *Idem, ibid.*, 1963, **10**, 1023.
17. N. K. Murty, V. Satyanarayana et Y. P. Rao, *ibid.*, 1977, **24**, 757.
18. N. B. Mazumdar, K. Chatterjee et S. N. Das, *J. Indian Chem. Soc.*, 1975, **52**, 419.
19. N. K. Murty, Y. P. Rao et V. Satyanarayana, *ibid.*, 1978, **55**, 686.
20. N. K. Murty et P. M. D. Murty, *Talanta*, 1982, **29**, 234.
21. N. K. Murty, V. Satyanarayana et N. Rukmini, *J. Indian Chem. Soc.*, 1978, **55**, 770.
22. E. Jdid, J. Bessière et P. Blazy, *Compte-rendu de fin d'étude d'une recherche financée par le Ministère de la Recherche et de la Technologie, Action Concertée VRSS No. 807 0423, No. 807 0423*, 1982, INPL-CRVM, Nancy.
23. W. Lange et E. Muller, *Ber. Deut. Chem. Ges.*, 1930, **63**, 1058.
24. Y. Israel et B. Paschkes, *Mikrochim. Acta*, 1981 **II**, 69.
25. N. K. Murty et V. Satyanarayana, *J. Indian Chem. Soc.*, 1976, **53**, 712.
26. M. Bruant, DEA, Nancy, 1982.
27. C. Louis et J. Bessière, *Can. J. Chem.*, 1986, **64**, 608.

DIAGRAMMES POTENTIEL-NIVEAU D'ACIDITE DANS LES MILIEUX H₂O-H₃PO₄-II

SYSTEMES ELECTROCHIMIQUES FAISANT INTERVENIR LE PROTON

C. LOUIS et J. BESSIERE

Laboratoire de Chimie et d'Electrochimie Analytique, Faculté des Sciences, Université de Nancy I,
 B.P. 239, 54506 Vandoeuvre les Nancy, France

(Reçu le 19 décembre 1986. Accepté le 10 avril 1987)

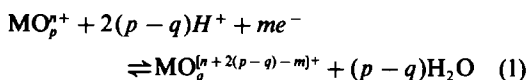
Résumé—La variation des potentiels normaux de systèmes oxydo-réducteurs faisant intervenir le proton est étudiée en fonction de la concentration du milieu acide phosphorique (1 à 14M). Le système de comparaison est le couple ferricinium/ferrocène. Les systèmes envisagés sont ceux mettant en jeu les espèces de l'uranium, du vanadium et de l'arsenic. Les interactions uranium-fer et uranium-argent sont étudiées ainsi que l'influence des sulfates et des fluorures sur le potentiel normal du couple U(VI)/U(IV).

Summary—The conditional potentials of redox systems involving protons, such as those of uranium, vanadium and arsenic, have been studied as a function of phosphoric acid concentration (1-14M) with ferricinium/ferrocene as comparison system. The influence of sulphate and fluoride on the conditional potential of the U(VI)/U(IV) couple, and uranium-iron and uranium-silver interactions are considered.

Dans le cadre des travaux ayant pour but d'établir les diagrammes potentiel-niveau d'acidité dans les milieux H₂O-H₃PO₄, une première partie a été consacrée à l'étude de systèmes électrochimiques ne faisant pas intervenir le proton. Parmi les systèmes qui font intervenir le proton, les couples H⁺/H₂ et 1,4 benzoquinone/hydroquinone ont déjà étudiés pour la détermination de la fonction d'acidité R₀(H).¹ Nous allons envisager à présent les systèmes de l'uranium, du vanadium et de l'arsenic.

RAPPEL THEORIQUE

Dans le cas de tels systèmes, la réaction d'oxydo-réduction est de la forme:



et le potentiel conditionnel est donné par la relation (à 298 K):

$$E_{\text{H}_2\text{O}/\text{H}_3\text{PO}_4}^{\circ} = E_{\text{H}_2\text{O}}^{\circ} + 2(p-q) \frac{0,059}{m} \log a_{\text{H}^+} - \frac{0,059}{m} (p-q) \log a_{\text{H}_2\text{O}} + \frac{0,059}{m} \log \frac{f_{\text{MO}_p^{q+}}}{f_{\text{MO}_q^{(n+2(p-q)-m)+}}} \quad (2)$$

*Des tests de migration électrophorétique ont montré que la charge globale des espèces U(VI) et U(IV) change avec la concentration de l'acide.^{17,18} Les espèces U(VI) sont cationiques lorsque la concentration de H₃PO₄ est inférieure à 1 mole/l. En milieu 5.5 mole/l, U(VI) et U(IV) sont anioniques.

L'effet de changement de milieu sur les caractéristiques de tels couples redox peut donc être envisagé comme résultant non seulement de la variation relative de solvation des espèces oxydées et réduites en solution mais aussi du niveau d'acidité et de l'activité en eau du milieu.

RESULTATS ET DISCUSSION

Uranium

Les travaux de mise au point des procédés d'extraction de l'uranium à partir de l'acide phosphorique sont à l'origine de nombreuses données caractérisant les espèces de l'uranium dans ces milieux.²⁻⁹ Cependant, elles sont souvent difficiles à comparer ou divergentes. Notre but a donc été d'établir les grandeurs thermodynamiques relatives aux systèmes de l'uranium en fonction de la concentration de l'acide en précisant en particulier l'évolution de la réactivité de U(VI) vis à vis de Fe(II) en l'absence ou en présence d'ions sulfate ou fluorure.

Dans les milieux acides perchlorique et sulfurique dilués,^{10,11} les niveaux d'oxydation U(VI), U(IV) et U(III) ont été mis en évidence; dans les milieux acides concentrés,^{10,11} la réduction de U(VI) se fait jusqu'à U(IV) seulement. En milieu chlorhydrique,^{12,13} la réduction de U(VI) conduit aux espèces U(V) puis U(IV). En milieu nitrique dilué,¹⁴ les niveaux d'oxydation sont U(VI), U(V) et U(IV), tandis qu'en milieu concentré,¹⁴ la réduction de U(VI) est limitée au niveau d'oxydation U(V). Dans les milieux phosphoriques, différents auteurs s'accordent sur le fait que la réduction de U(VI) ne se fait pas au delà de U(IV).^{6-9,15,16*} Les arguments invoqués font appel à la spectrophotométrie visible et à l'électrochimie. Les

solutions d'uranium(VI) possèdent dans tout le domaine de concentration d'acide envisagé un spectre caractéristique. Après leur réduction par voie chimique ou électrochimique, ces solutions présentent le spectre caractéristique de l'uranium(IV). La réduction de U(VI), réalisée à potentiel contrôlé sur nappe de mercure dans les milieux phosphoriques 2,0, 5,5 et 11,5M met en évidence un échange de deux électrons.

Dans les solutions phosphoriques résultant du traitement des phosphates minéraux, les deux formes U(VI) et U(IV) peuvent être présentes. Or, les composés utilisés pour l'extraction liquide-liquide ou la flottation ionique¹⁷ sont en général spécifiques de l'une ou l'autre forme. On est donc amené à oxyder ou à réduire l'uranium présent dans ces milieux. Dans les procédés industriels, le fer métal est le réducteur le plus fréquemment utilisé. Au laboratoire, à côté des méthodes électrochimiques déjà mentionnées, la réduction de l'uranium(VI) peut être également obtenue sur amalgame de zinc. Comme dans les milieux chlorhydriques,¹⁹ l'argent est un réducteur de U(VI) dans les milieux phosphoriques, mais la quantitativité de la réaction dépend de la concentration de l'acide. Les propriétés réductrices de Fe(II) vis à vis de U(VI) dans les milieux phosphoriques ont été mises à profit pour le dosage de l'uranium.^{5,20-22} Les phosphites sont également des réducteurs de U(VI). Les solutions de U(IV) qui présentent la particularité d'être très stables vis à vis de l'oxydation par l'air,²³ peuvent être oxydées par le chlorate de sodium, et l'eau oxygénée. Dans les milieux phosphoriques concentrés, le bichromate de potassium est un oxydant de Mn(II), V(IV), Ce(III) et Fe(II),²⁴⁻²⁷ comme le permanganate de potassium, c'est un oxydant de U(IV).^{28,29} Certains composés de type quinone ont des propriétés oxydo-réductrices vis à vis de l'uranium.

Des valeurs des potentiels normaux du système redox U(VI)/U(IV) ont déjà été données pour des domaines limités de concentration d'acide. Le caractère partiel des résultats de Baes³ (H₃PO₄ 1 à 5M en présence de H₂SO₄ 0,36M) et de Marcus⁴ (H₃PO₄ 1 à 6M) ainsi que les problèmes soulevés par la méthode mise en oeuvre par Rao et Sagi⁵ (potentiométrie à intensité nulle sur électrode de platine) nous ont conduit à reprendre ces déterminations.

Electroactivité des espèces U(VI) et U(IV). L'espèce U(IV) est électroactive aux électrodes de platine et de carbone vitreux. Elle donne un signal anodique situé à +900 mV pour une concentration d'acide de 5,5M et à +850 mV pour une concen-

tration d'acide de 11,5M, l'électrode de référence étant l'électrode au calomel saturée aqueuse. Dans les deux cas, la variation du courant limite avec la vitesse de rotation de l'électrode obéit au critère de Levich. L'espèce U(VI) n'est pas électroactive sur électrode de platine. Sur électrode de carbone vitreux, les réductions de U(VI) et des protons se font à des potentiels trop voisins pour que la vague cathodique de l'uranium soit bien définie. Pour une concentration de H₃PO₄ de 5,5M, il existe un écart de près de 1,5 V entre les signaux correspondant à l'oxydation de U(IV) et à la réduction de U(VI). Le potentiel pris par une électrode platine plongeant dans un milieu phosphorique contenant les espèces de l'uranium est donc mal défini, le courant d'échange étant très faible. Ceci explique les difficultés rencontrées pour obtenir des potentiels stables et reproductibles dans ce cas.⁵

L'espèce U(IV) n'est pas électroactive à l'électrode de mercure. Mais le signal de réduction de l'espèce U(IV) a permis d'analyser l'évolution du mécanisme de la réduction de U(VI) en fonction de la concentration d'acide.^{6-9,15,16} Dans les milieux phosphoriques de concentration inférieure à 1M, deux vagues de réduction sont observées.^{8,15} Dans les milieux plus concentrés, la réduction de U(VI) est caractérisée par une seule vague polarographique (Tableau 1).

L'analyse des tracés polarographiques nous conduit comme Issa *et al.*^{8,15} à conclure à une réduction irréversible au niveau de l'électrode mettant en jeu deux électrons dans les milieux phosphoriques de concentration supérieure à 1M, plutôt qu'à un mécanisme de réduction réversible de U(VI) en U(V) suivi de la dismutation de U(V)⁷ analogue à celui qui a été montré dans le cas des milieux perchloriques.³⁰ Les caractéristiques d'électroactivité des espèces U(VI) et U(IV) dans les milieux phosphoriques donnent les conditions dans lesquelles il est possible de les transformer ou de les doser par des méthodes électrochimiques mais ne permettent pas une détermination directe aisée du potentiel normal du couple U(VI)/U(IV). Nous avons donc utilisé les systèmes Fe(III)/Fe(II) et Ag(I)/Ag comme indicateurs potentiométriques. Le calcul des constantes d'équilibre de la réaction de réduction de U(VI) par Fe(II) dans les milieux de concentration d'acide inférieure à 7M et de la réaction de réduction de U(VI) par Ag dans les milieux plus concentrés donne accès aux valeurs des potentiels normaux du système U(VI)/U(IV) dans tout le domaine de concentration envisagé.

Tableau 1. Caractéristiques des polarogrammes correspondant à la réduction de U(VI) dans les milieux H₂O-H₂PO₄

[H ₃ PO ₄], M	$E_{1/2}$, mV vs. Fe ³⁺ /Fe	Pente, mV	$an =$ 59/pente	i_D/C (25°C), $\mu A \cdot l. mmole^{-1}$
2,0	-250	-60	0,98	-2,12
5,5	-105	-55	1,07	-1,40
8,0	-10	-53	1,11	-1,03
11,5	+190	-85	0,69	-0,65
14,0	+365	-85	0,69	-0,41

Tableau 2. Variation de l'écart des potentiels normaux des couples U(VI)/U(IV) et Fe(III)/Fe(II) en fonction de la concentration de H₃PO₄

[H ₃ PO ₄], M	d_1	$d_2 - d_1$	pK_1	$E_{U(VI)/U(IV)}^{\circ} - E_{Fe(III)/Fe(II)}^{\circ}$, mV
3,00	0,117	0,115	-0,02	1
3,50	0,175	0,100	-0,02	22
3,60	0,190	0,088	-1,00	30
4,00	0,087	0,035	-1,18	36
4,00	0,227	0,080	-1,35	41
4,50	0,285	0,065	-1,92	58
4,60	0,300	0,065	-1,99	60
5,00	0,350	0,057	-2,36	71
5,50	0,398	0,045	-2,83	85
5,75	0,450	0,038	-3,62	97
6,30	0,475	0,031	-3,55	107
6,90	0,530	0,025	-3,97	119

Etude de la réaction de réduction de U(VI) par Fe(II). Alors que la réduction de U(VI) par le fer métal est rapide pour toutes les concentrations d'acide, la réduction de U(VI) par Fe(II) n'est quantitative et rapide que pour les concentrations d'acide supérieures à 7M. Pour les concentrations d'acide comprises entre 2 et 7M, elle est équilibrée et cinétiquement lente. Dans ce domaine de concentration, nous avons repris le principe d'une détermination spectrophotométrique⁴ de la constante d'équilibre.

Une solution de Fe(II), préparée en milieu phosphorique 11,5M à partir de fer métal est oxydée quantitativement par addition d'acétate d'uranyle. Après contrôle spectrophotométrique de la réduction complète de l'uranium en milieu phosphorique 11,5M, des milieux de concentration d'acide comprise entre 3 et 6M sont préparés par dilution. Après mise en équilibre, la concentration de U(IV) est évaluée par spectrophotométrie à 660 nm (d_1). Comme le coefficient d'absorption molaire de U(IV) varie avec la concentration d'acide, la concentration de U(IV) à l'équilibre est déterminée dans un milieu donné par comparaison avec la concentration de U(IV) totale (d_2) obtenue après addition de fer en excès dans le même milieu réactionnel. Les valeurs d_1 et d_2 sont déterminées indépendamment par rapport à un témoin H₃PO₄ de même concentration. Dans le cas où l'écart des deux valeurs est faible, ($d_2 - d_1$) est déterminé directement par spectrophotométrie différentielle.

Le pK de la réaction d'oxydo-réduction:



est lié aux valeurs d_1 et d_2 par la relation:

$$pK_1 = 3 \log[(d_2 - d_1)/d_1] \quad (4)$$

Le potentiel normal du système U(VI)/U(IV) est donc:

$$E_{U(VI)/U(IV)}^{\circ} = E_{Fe(III)/Fe(II)}^{\circ} - \frac{3 \times 0,059}{2} \log[(d_2 - d_1)/d_1] \quad (5)$$

Les résultats expérimentaux et le calcul de l'écart des potentiels normaux des systèmes U(VI)/U(IV) et

Fe(III)/Fe(II) sont donnés dans le Tableau 2. Les potentiels normaux du couple redox U(VI)/U(IV) dans le domaine de concentration d'acide phosphorique 3 à 14M sont donnés dans le Tableau 3 et Figure 1.

Etude de la réaction de réduction de U(VI) par Ag. En milieu concentré en acide phosphorique, la réduction de U(VI) par Fe(II) est quantitative. Le système Fe(III)/Fe(II) ne peut donc plus être utilisé comme indicateur potentiométrique pour la détermination du potentiel normal du système U(VI)/U(IV). Nous avons donc utilisé l'argent métal dont les propriétés réductrices sont moins marquées que celles de l'espèce Fe(II). La réaction



est très peu quantitative en milieu phosphorique 8M. En milieu phosphorique 14M au contraire, la quantitativité est presque réalisée mais dans tous les cas, la cinétique de la réaction est lente.

De l'argent en poudre fine est introduit dans des solutions de U(VI) pour différentes concentrations d'acide. Les milieux réactionnels sont maintenus en agitation sous courant d'azote à température constante. La quantité d'uranium(IV) formée est déterminée par spectrophotométrie à 660 nm jusqu'à ce que l'équilibre soit atteint. La quantité de Ag⁺ présent dans le milieu à l'équilibre est contrôlée par potentiométrie à intensité nulle sur électrode d'argent. La constante K_2 de la réaction (6) dépend des potentiels normaux des systèmes redox U(VI)/U(IV) et Ag(I)/Ag selon la relation:

$$E_{U(VI)/U(IV)}^{\circ} = E_{Ag(I)/Ag}^{\circ} - (0,059/2) pK_2 \quad (7)$$

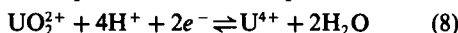
Les résultats expérimentaux et le calcul de l'écart des potentiels normaux des systèmes mis en jeu sont donnés dans le Tableau 4. Les potentiels normaux du couple redox U(VI)/U(IV) dans le domaine de concentration d'acide phosphorique 3 à 14M sont donnés dans le Tableau 3 et Figure 1.

Potentiels normaux du système redox U(VI)/U(IV) dans les milieux H₂O-H₃PO₄. Le pouvoir oxydant de l'uranium(VI) augmente avec la concentration d'acide beaucoup plus rapidement que dans le cas de

Tableau 3. Potentiels normaux du système redox U(VI)/U(IV) dans les milieux H₂O-H₃PO₄

[H ₃ PO ₄], M	$E_{U(VI)/U(IV)}^{\circ}$, mV vs. Fc ⁺ /Fc	[H ₃ PO ₄], M	$E_{U(VI)/U(IV)}^{\circ}$, mV vs. Fc ⁺ /Fc
3,0	+127	6,5	+274
3,5	+152	8,0	+357
4,0	+172	9,0	+420
4,5	+195	10,0	+493
5,0	+214	10,5	+533
5,5	+234	11,5	+616
6,0	+252	13,0	+679
		14,0	+706

systèmes redox n'engageant pas formellement le proton. Ceci est dû à l'intervention du niveau d'acidité dans l'expression du potentiel normal apparent correspondant à l'équilibre électrochimique:



en plus de la variation due à la solvation des espèces UO₂²⁺ et U⁴⁺. L'expression du potentiel normal apparent est en effet:

$$E_{H_2O/H_3PO_4}^{\circ} = E_{H_2O}^{\circ} - 2 \times 0,059 R_o(H) + (0,059/2) \log f_{UO_2^{2+}}/f_{U^{4+}} - 0,059 \log a_{H_2O} \quad (9)$$

où $E_{H_2O}^{\circ} = -0,066$ V vs. Fc⁺/Fc.

En ce qui concerne les milieux de concentration d'acide inférieure à 6M, l'accord est bon avec les résultats de Baes³ et de Gyves et Bessière.² L'écart existant avec les résultats de Marcus⁴ n'a pas d'interprétation immédiate cependant l'allure de la variation est analogue. Pour les milieux concentrés en acide, l'écart existant avec les résultats de Rao et Sagi⁵ est très important. L'accroissement avec la concentration d'acide du pouvoir oxydant de U(VI) donné par ces auteurs est très faible. Ceci est dû essentiellement à la mauvaise réponse de l'électrode de platine en présence des espèces UO₂²⁺ et U⁴⁺ en raison de la lenteur de ce système électrochimique.

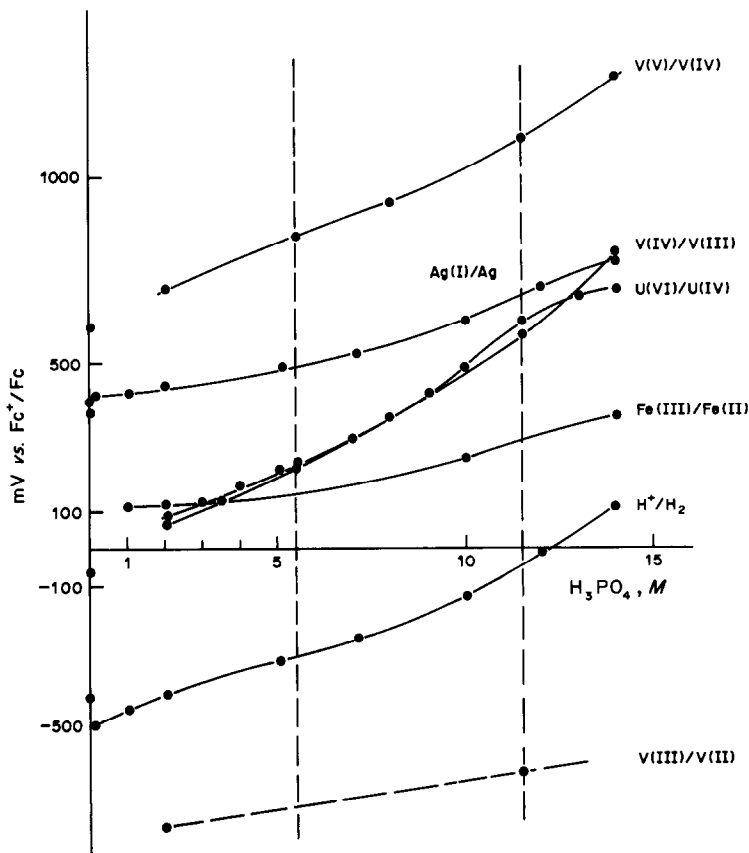


Fig. 1. Diagramme potentiel-concentration de H₃PO₄: systèmes de l'uranium, du vanadium, du fer et de l'argent dans les milieux H₂O-H₃PO₄ (1 à 14M).

Tableau 4. Variation de l'écart des potentiels normaux des couples U(VI)/U(IV) et Ag(I)/Ag en fonction de la concentration de H₃PO₄

[H ₃ PO ₄], M	DO _{660 nm}		U(IV)eq, mM	pK ₂	E ^o _{U(VI)/U(IV)} - E ^o _{Ag(I)/Ag} , mV
	U(IV), 0,025M	U(IV)eq.,			
8,0	1,03	0,05	1,21	6,5	-196
9,0	1,01	0,12	2,97	5,3	-160
10,0	1,01	0,295	7,30	4,0	-122
10,5	1,07	0,45	10,5	3,5	-105
11,5	1,08	0,88	20,4	2,1	-64
13,0	1,12	0,92	20,5	2,1	-63
14,0	1,10	0,85	18,3	2,3	-69

Influence des espèces sulfate et fluorure sur les caractéristiques d'oxydo-réduction du système U(VI)/U(IV). Afin de préciser le rôle des ions sulfate sur les interactions uranium-fer, nous avons déterminé le potentiel normal du système de l'uranium en présence de sulfate en utilisant les indicateurs potentiométriques Fe(II) et Ag. Les expériences menées en présence de SO₄²⁻ 0,5M dans les milieux H₃PO₄ 5,5 et 11,5M, montrent qu'il n'y a pas d'effet des ions sulfate sur le potentiel du couple UO₂²⁺/U⁴⁺. Puisque dans les mêmes conditions, les ions sulfate ne modifient pas le potentiel du couple Fe³⁺/Fe²⁺, leur présence n'intervient pas sur la réactivité du fer sur l'uranium dans ces milieux.

L'analyse potentiométrique (électrode spécifique des fluorure) et spectrophotométrique des espèces U(VI) et U(IV) (0,05M) dans le milieu H₃PO₄ 5,5M-HF 0,3M montre que la présence de fluorure à cette concentration provoque la complexation de l'espèce U(VI) seule. Pour des concentrations plus élevées de fluorure, le composé insoluble UF₄ se forme. Dans ces conditions, le pouvoir oxydant de U(VI) est renforcé. Comme d'autre part le pouvoir réducteur de Fe(II) est légèrement accru, l'amélioration de la réactivité de Fe(II) sur U(VI) en milieu H₃PO₄ 5M-HF 1M observée par Plazanet et Lamache⁶ résulte de l'action des fluorures, non pas sur le couple Fe(III)/Fe(II) seul, mais sur les deux systèmes redox en présence.

Vanadium

Comme l'uranium, le vanadium est présent à l'état de traces dans les phosphates naturels³¹⁻³³ et dans les milieux phosphoriques industriels. Il peut être récupéré par extraction liquide-liquide.^{34,35} Les problèmes posés par les conditions de stabilisation de degrés d'oxydation donnés afin de réaliser des extractions sélectives nous ont conduits³⁶ à étudier l'évolution des propriétés oxydoréductrices des espèces du vanadium avec la concentration en acide. De plus, ces systèmes, engageant des espèces électroactives et douées de caractéristiques spectrophotométriques différenciées,^{36,37} sont susceptibles de constituer de bons indicateurs pour la détermination des potentiels normaux de systèmes redox dans un large domaine de potentiel. Sur le plan analytique,³⁸ pro-

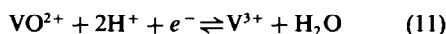
pose de titrer les espèces du vanadium par Fe(II) en suivant les réactions par voie électrochimique.

Les espèces du vanadium correspondant aux niveaux d'oxydation (V), (IV), (III), (II) sont mises en évidence dans les milieux phosphoriques et les potentiels normaux des couples correspondants sont déterminés par potentiométrie à intensité nulle sur électrode de platine et étude des tracés polarographiques.³⁶

Les espèces VO₂⁺ et VO²⁺ sont électroactives à l'électrode de carbone vitreux³⁹ et à l'électrode de platine poli. L'équilibre électrochimique:



obéit à la loi de Nernst dans tout le domaine de concentration envisagé. Les espèces VO²⁺ et V³⁺ sont électroactives aux électrodes de platine et de mercure. Contrairement au cas du système VO₂⁺/VO²⁺, le potentiel correspondant à l'équilibre:



se stabilise difficilement. L'addition de traces de Fe(III)³⁸ permet néanmoins la détermination précise des potentiels normaux de ce système. L'espèce V²⁺ peut être produite par réduction électrochimique de V³⁺ à l'électrode de mercure. Cependant, elle n'est pas stable et est lentement oxydée par le milieu. Ce phénomène peut être catalysé électrochimiquement en mettant une électrode de platine en contact avec la nappe de mercure. Un dégagement d'hydrogène se produit alors à l'électrode de platine. Le système électrochimique V³⁺/V²⁺ correspondrait à l'équilibre simple:



Puisqu'il est bien défini sur électrode de mercure, son potentiel normal a pu être évalué dans les milieux phosphoriques de concentration 5,5 et 11,5M.

Les variations des potentiels normaux des trois systèmes redox VO₂⁺/VO²⁺, VO²⁺/V³⁺, V³⁺/V²⁺ avec la concentration de l'acide sont données dans le Tableau 5 et présentées par la Figure 1.

Ces résultats mettent en évidence le caractère fortement oxydant de l'espèce VO₂⁺ dans tout le domaine de concentration de H₃PO₄. Il apparaît également que les potentiels normaux des systèmes UO₂²⁺/U⁴⁺ et

Tableau 5. Potentiels normaux des systèmes V(V)/V(IV), V(IV)/V(III), V(III)/V(II) dans les milieux H₂O-H₃PO₄

[H ₃ PO ₄], M	E°, mV vs. Fc ⁺ /Fc		
	VO ₂ ⁺ /VO ²⁺	VO ²⁺ /V ³⁺	V ³⁺ /V ²⁺
0 (H ₂ O)	+600	-63	-655
2,0	+700	+70	-750
5,5	+840	+220	—
8,0	+930	+350	—
11,5	+1120	+570	-600
14,0	+1280	+800	—

VO²⁺/V³⁺ sont très voisins, quelle que soit la concentration de l'acide. L'accroissement du pouvoir oxydant des espèces VO₂⁺ et VO²⁺ avec la concentration de H₃PO₄ est beaucoup plus marqué que celui de V³⁺. Ceci est lié au fait que les équilibres d'oxydo-réduction mettant en jeu les deux premières espèces font également intervenir le proton alors que ce n'est pas le cas pour le système V³⁺/V²⁺ dont l'évolution avec la concentration d'acide est analogue à celle du système Fe³⁺/Fe²⁺.

Arsenic

Dans la formule générale des apatites Ca₁₀F₂(PO₄)₆, PO₄ peut être remplacé par AsO₄. L'arsenic est donc normalement présent dans les phosphates naturels à des teneurs variables selon leur origine: par exemple, 3,5 à 96,5 ppm d'arsenic pour des phosphates d'origine américaine.⁴⁰ La teneur en arsenic des acides phosphoriques industriels est de l'ordre 0,02 à 1,16 g/l, pour des acides de concentration comprise entre 3,5 et 7M.³² Elle doit être considérablement réduite lorsque ces acides sont utilisés pour la préparation des phosphates destinés à l'industrie alimentaire ou à l'industrie des engrais.⁴¹ Ceci peut être réalisé en particulier par flottation ionique.^{17,42}

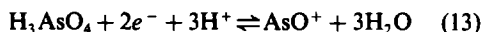
L'espèce As(III) est réductible en As à l'électrode à goutte de mercure, mais l'espèce As(V) n'est pas électroactive. Le système redox As(V)/As(III) est donc lent. La variation de son potentiel normal a été déterminée jusqu'à une concentration d'acide de 8M en utilisant le système I₃⁻/I⁻ comme indicateur potentiométrique et ampérométrique.⁴² Ses valeurs sont données dans le Tableau 6.

Le potentiel normal du système As(V)/As(III) augmente avec la concentration de H₃PO₄, mais la variation, voisine de celle observée pour système Fe(III)/Fe(II), est inférieure à celle à laquelle on

Tableau 6. Potentiels normaux du système redox As(V)/As(III) dans les milieux H₂O-H₃PO₄

[H ₃ PO ₄], M	E° _{As(V)/As(III)} , mV vs. Fc ⁺ /Fc
0 (H ₂ O)	+150
2,0	+228
5,5	+281
8,0	+335

pouvait s'attendre. Ceci pourrait suggérer que la réaction d'oxydo-réduction mise en jeu est non pas:



mais:



CONCLUSION

Les potentiels normaux des systèmes redox mettant en jeu les espèces de l'uranium, du vanadium et de l'arsenic ont été déterminés dans les milieux H₂O-H₃PO₄ par des méthodes directes: polarographie, potentiométrie à intensité nulle ou par l'intermédiaire d'indicateurs potentiométriques: Fe(III)/Fe(II), Ag(I)/Ag, I₃⁻/I⁻. Leurs variations avec la concentration d'acide, ainsi que celles des systèmes H⁺/H₂ et 1,4 benzoquinone/hydroquinone sont présentées par la Figure 1 de notre publication précédente.⁴³ Le renforcement de leurs propriétés oxydantes est plus marqué que celui des systèmes redox ne faisant pas intervenir le proton. Il résulte des variations du niveau d'acidité et de la solvation relative des espèces mises en jeu, les deux facteurs intervenant de manière antagoniste: le terme activité de l'eau ne devient significatif que dans les milieux les plus concentrés en acide. Ces données thermodynamiques conduisent au calcul des coefficients d'activité de transfert de solvation des espèces en jeu.⁴⁴ Ils permettent d'interpréter ou de prévoir les réactions d'oxydo-réduction (diagrammes potentiel-niveau d'acidité), l'évolution des propriétés de solubilité y compris celles des phosphates et devraient également intervenir dans la prévision des réactions mises en jeu dans les processus de séparation comme l'extraction liquide-liquide et la flottation ionique.

LITTÉRATURE

1. C. Louis et J. Bessière, *Can. J. Chem.*, 1985 **63**, 908.
2. J. de Gyves et J. Bessière, 14^e Congrès latino-américain de Chimie, février 1981, San Jose, Costa Rica.
3. C. F. Baes, Jr., *J. Phys. Chem.*, 1956, **60**, 805.
4. Y. Marcus, *ibid.*, 1958, **62**, 1314.
5. G. G. Rao et S. R. Sagi, *Talanta*, 1962, **9**, 715.
6. C. Plazanet et M. Lamache, *Electrochim. Acta*, 1981, **26**, 45.
7. K. Elkacemi, B. Tyburce et S. Belcadi, *ibid.*, 1982, **27**, 729.
8. I. M. Issa, R. M. Issa et L. A. Shalaby, *Z. Anal. Chem.*, 1960, **176**, 257.
9. S. Belcadi et K. Elkacemi, 2nd International Congress on Phosphorus Compounds Proceedings, p. 735, 1980.
10. L. Sipos, L. J. Jeftic et M. Branca, *Electroanal. Chem. Interfac. Electrochem.*, 1971, **32**, 35.
11. H. G. Heal, *Nature*, 1946, **157**, 225.
12. W. E. Harris et I. M. Kolthoff, *J. Am. Chem. Soc.*, 1945, **67**, 1484.
13. I. M. Kolthoff et W. E. Harris, *ibid.*, 1946, **68**, 1175.
14. M. A. Ghandour, R. P. Abo-Doma et E. A. Goma, *Electrochim. Acta*, 1982, **27**, 159.
15. M. Issa, M. Tharwat et Y. A. Elewady, *ibid.*, 1972, **17**, 1065.

16. K. Elkacemi et S. Belcade, *Journées d'Electrochimie*, Bruxelles, 55, 1981.
17. E. Jdid, J. Bessière et P. Blazy, *Compte-rendu de fin d'étude d'une recherche financée par le Ministère de la Recherche et de la Technologie, Action Concertée VRSS N° 807 0422, N° 807 0423*, INPL-CRVM, Nancy.
18. P. de Donato, D.E.A. Nancy, 1983.
19. N. Birnbaum et S. M. Edmonds, *Ind. Eng. Chem., Anal. Ed.*, 1940, 12, 155.
20. G. G. Rao et L. S. A. Dikshitulu, *Talanta*, 1963, 10, 1023.
21. A. Hitchen et G. Zechanowitsch, *ibid.*, 1980, 27, 383.
22. N. K. Murty et Y. P. Rao, *J. Indian Chem.*, 1976, 14A, 1023.
23. J. M. Schreyer, *U.S. Atom. En. Commiss. Rept.*, ORNL 1747.1, 1954.
24. G. G. Rao et P. K. Rao, *Talanta*, 1963, 10, 1251.
25. *Idem*, *ibid.*, 1964, 11, 703.
26. G. G. Rao, P. K. Rao et S. B. Rao, *ibid.*, 1964, 11, 825.
27. T. M. Mizoguchi et H. Ishii, *ibid.*, 1978, 25, 311.
28. G. G. Rao et P. K. Rao, *ibid.*, 1964, 11, 1031.
29. G. G. Rao, P. K. Rao et M. A. Rahman, *ibid.*, 1965, 12, 953.
30. M. Mastragostino et J. M. Saveant, *Electrochim. Acta*, 1968, 13, 751.
31. D. Mastef, *Thèse de Docteur-Ingénieur*, Nancy, 1977.
32. F. Habashi, *2nd International Congress on Phosphorus Compounds Proceedings*, p. 629, 1980.
33. J. R. Lehr, dans *Phosphoric Acid*, A. V. Slack (ed.), Vol. 1, Part 2, Dekker, New York, 1968.
34. B. F. Warner, dans *Solvent extraction Chemistry*, D. Dyrssen, J. O. Liljenzin et J. Rydberg (eds.), p. 635. North-Holland, Amsterdam, 1967.
35. A. K. De, S. M. Khopkar et R. A. Chalmers, *Solvent Extraction of Metals*, Van Nostrand-Reinhold, London, 1970.
36. N. Benlakhdim, *Thèse de Doctorat de 3° Cycle*, Nancy, 1981.
37. Z. El Abbassi et S. Belcade, *Journées d'Electrochimie*, Paris, 3.3 1983.
38. G. G. Rao et L. S. A. Dikshitulu, *Talanta*, 1963, 10, 295.
39. P. K. Agasyan, E. R. Nikolaeva et V. M. Khasykov, *J. Anal. Chem. USSR*, 1980, 35, 452.
40. J. R. Van Wazer, dans *Phosphorus and its Compounds*, J. R. Van Wazer (ed.), Vol. 2, p. 973. Interscience, New York, 1961.
41. T. L. Hurst, dans *Phosphorus and its Compounds* J. R. Van Wazer (ed.), Vol. 2, p. 1214. Interscience, New York, 1961.
42. M. Bruant, D.E.A. Nancy, 1982.
43. C. Louis et J. Bessière, *Talanta*, 1987, 34, 763.
44. *Idem*, *Can. J. Chem.*, 1986, 64, 608.

SOLVENT EXTRACTION OF LITHIUM AND SODIUM WITH 4-BENZOYL OR 4-PERFLUOROACYL-5-PYRAZOLONE AND TOPO

SHIGEO UMETANI*, KOHJI MAEDA, SORIN KIHARA and MASAKAZU MATSUI
Institute for Chemical Research, Kyoto University, Uji, Kyoto 611, Japan

(Received 26 May 1986. Revised 30 July 1986. Accepted 10 April 1987)

Summary—The synergic solvent extraction of lithium and sodium into benzene or cyclohexane with 4-benzoyl or 4-perfluoroacyl-5-pyrazolone and trioctylphosphine oxide (TOPO) has been investigated. Quantitative extraction (>99%) of lithium, which is one of the most poorly extractable metal ions, can be achieved with 1-tolyl-3-methyl-4-perfluoroacyl-5-pyrazolone and TOPO. The extraction of sodium is somewhat poorer than that of lithium under the same conditions. The perfluoroacyl group at the 4-position of the pyrazolone ring enhances the extraction and increases the maximum percentage extracted. Cyclohexane is found to be suitable for a quantitative extraction as an organic phase when the reagents are soluble in it. Improved separation of lithium and sodium can be attained when they are extracted into benzene.

Alkali-metal ions usually form complexes of low stability owing to their single charge and relatively large ionic radius. The solvent extraction of alkali-metal ions with crown ethers has been widely investigated.¹⁻³ Although alkali-metal ions form stable complexes with crown ethers, it is difficult to achieve their quantitative extraction, especially for lithium. β -Diketones have also been applied for the extraction of alkali-metals.⁴⁻⁷ It was found that the alkali-metal ions are extractable into so-called active solvents, which have a co-ordinating oxygen atom, such as ethers, esters and alcohols, and are also extractable with the combination of a β -diketone and an auxiliary reagent such as TOPO or tributyl phosphate. The order of the efficiency with which the alkali-metals are extracted by β -diketones is $\text{Li}^+ > \text{Na}^+ > \text{K}^+ > \text{Rb}^+ > \text{Cs}^+$, which is also the order in which their ionic radii increase.

4-Acyl-5-pyrazolones are a type of β -diketone and are known to be versatile extracting reagents, having two oxygen atoms as co-ordinating centres. According to the Pearson concept, the pyrazolones are hard bases and thus expected to form stable chelates with hard acids such as the alkaline-earth and rare-earth metal ions. We have synthesized a number of 4-acyl-5-pyrazolones and investigated their use for solvent extraction of metals.⁸ In the course of these studies, it was found that lithium, though one of the most poorly extractable metal ions, could be almost quantitatively extracted with the pyrazolones and TOPO as an auxiliary ligand.⁹

In the present investigation, 4-benzoyl and 4-perfluoroacyl-5-pyrazolones were examined as

synergic extractants (in combination with TOPO) in the expectation that the electron-attracting effect of the perfluoroalkyl group might enhance the stability of its metal-ion chelates in the presence of a Lewis base such as TOPO, and result in a higher distribution ratio for alkali-metal ions.

EXPERIMENTAL

Reagents

4-Benzoyl and 4-fluoroacyl derivatives of 1-aryl-3-methyl-5-pyrazolone were prepared according to the method of Jensen from 1-aryl-3-methyl-5-pyrazolone and benzoyl chloride or the corresponding perfluoroacyl anhydride.¹⁰ The crude products were recrystallized twice from dioxan-water or ethanol-water mixtures and dried under reduced pressure. TOPO was obtained commercially and used without further purification. Caesium hydroxide solution was prepared by dissolving the oxide in water. The other chemicals were pure or reagent-grade materials. Water was demineralized and distilled.

Apparatus

Flame emission measurements were made with a Hitachi Polarized Zeeman Atomic-Absorption Spectrophotometer, model 180-80. The pH measurements were performed with a Hitachi-Horiba F-7ss pH-meter, equipped with a glass electrode.

Solvent extraction procedure

An aqueous phase prepared from 10 ml of alkali-metal solution ($< 1 \times 10^{-4} M$) and 0.01M caesium acetate as buffering agent was adjusted to the desired pH with hydrochloric acid or caesium hydroxide solution, placed in a 30-ml centrifuge tube and mechanically shaken with an equal volume of benzene or cyclohexane containing the required amount of the pyrazolone and TOPO, for 1 hr at 25°. Preliminary experiments showed that equilibrium was reached within 15 min. The phases were then centrifugally separated, and the pH of the aqueous phase was measured again and taken as the equilibrium value.

The concentration of alkali-metal ion in the aqueous phase was determined by flame spectrophotometry. The

*Author for correspondence.

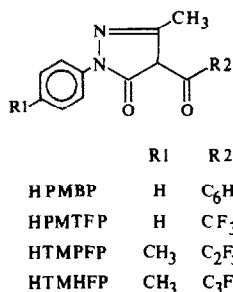


Fig. 1. 4-Acyl-5-pyrazolones studied.

concentration of alkali-metal ion in the organic phase was determined in the same way after stripping with hydrochloric acid. The sum of the metal concentrations in the two phases agreed well with the initial concentration.

RESULTS AND DISCUSSION

4-Acyl-5-pyrazolones

The 4-acyl-5-pyrazolones synthesized in this work (Fig. 1) and their abbreviations are as follows. 1-Phenyl-3-methyl-4-benzoyl-5-pyrazolone (HPMBP), 1-phenyl-3-methyl-4-trifluoroacetyl-5-pyrazolone (HPMTFP), 1-tolyl-3-methyl-4-pentafluoropropionyl-5-pyrazolone (HTMPFP) and 1-tolyl-3-methyl-4-heptafluorobutyl-5-pyrazolone (HTMHFP). The identity of these compounds was confirmed by elemental analysis, summarized in Table 1 together with the melting points. Attempts to synthesize 1-phenyl-3-methyl-4-pentafluoropropionyl-5-pyrazolone and 1-phenyl-3-methyl-4-heptafluorobutyl-5-pyrazolone were unsuccessful. Introducing a methyl group into the 1-phenyl group made it possible to synthesize 4-pentafluoroacetyl and 4-heptafluoroacetyl derivatives of 5-pyrazolone.

Data processing

In the synergic extraction of a univalent metal ion (M^+) such as an alkali-metal ion, the extraction equilibrium can be expressed by



where HA and L stand for 4-acyl-5-pyrazolone and TOPO respectively and subscript o indicates species in the organic phase. In this treatment, side-reactions

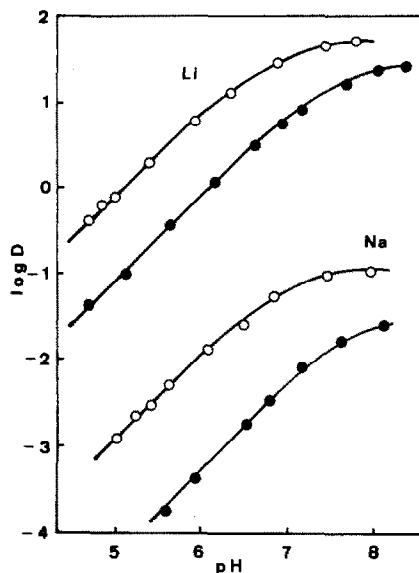


Fig. 2. Extraction of lithium and sodium into cyclohexane (○) or benzene (●) with 0.05M HPMBP and 0.1M TOPO.

such as complex formation between M^+ and acetate are assumed to be absent. The synergic extraction constant, $K_{ex,s}$, is defined as

$$K_{ex,s} = \frac{[MAL_{s,o}][H^+]}{[M^+][HA]_o[L]_o^s} = \frac{D[H^+]}{[HA]_o[L]_o^s} \quad (2)$$

where D is the distribution ratio of the alkali-metal ion. The slope of a plot of $\log D$ vs. $\log [L]_o$ at constant $[HA]_o$ and pH gives s , the number of TOPO molecules attached to MA.

Dependence of the distribution on pH

In the present work, the pH of the aqueous phase was controlled with caesium acetate and caesium hydroxide, preliminary experiments having indicated that the extraction of caesium is negligible under the conditions used.

Figure 2 shows the distribution of lithium and sodium with the combination of HPMBP and TOPO, as a function of pH. Without any adduct-forming reagent such as TOPO, the extraction of lithium and

Table 1. Element analysis of the compounds studied

Reagent	Calculated (found), %			m.p., °C
	C	H	N	
HPMBP	73.37 (73.5)	5.07 (5.0)	10.07 (10.2)	92-92.5 (92) ¹⁰
HPMTFP	53.34 (53.6)	3.33 (3.3)	10.36 (10.6)	146 (146) ¹⁰
HTMPFP	50.31 (50.5)	3.32 (3.1)	8.38 (8.4)	115
HTMHFP	46.89 (47.0)	2.89 (2.7)	7.29 (7.3)	101

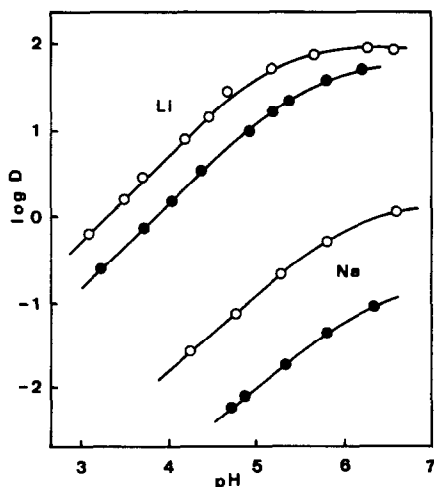


Fig. 3. Extraction of lithium and sodium into cyclohexane (O) or benzene (●) with 0.05M HPMTFP and 0.1M TOPO.

sodium is negligible. As seen in the figure, $\log D$ increases linearly with pH and then comes close to a constant value. The slopes of the linear part of the plots are very close to 1, the theoretical value according to equation (1). Lithium was extracted from more acidic media than sodium and its distribution constant was much higher than that of sodium. When cyclohexane was employed as the organic solvent, the synergic effect and distribution constant were both higher for lithium and sodium.

The dependence on pH was also examined for the 4-perfluoroacyl-5-pyrazolone/TOPO system. The results for HPMTFP are illustrated in Fig. 3. The acid dissociation constants (pK_a) of some 4-acyl-5-pyrazolones have been determined by the liquid-liquid distribution method.¹¹ The pK_a of HPMTFP in 0.1M sodium perchlorate medium is 2.56, much lower than that of HPMBP, which is 3.92. Both lithium and sodium could be extracted from much more acidic media with the HPMTFP/TOPO system than with the HPMBP/TOPO system. This enhancement is attributed to the much greater acidity of

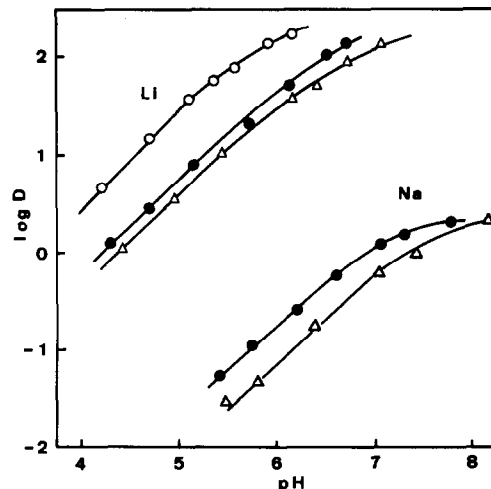


Fig. 4. Extraction of lithium and sodium with 0.1M TOPO and acylpyrazolone: O 0.002M HTMPFP in cyclohexane; ● 0.05M HTMPFP in benzene; △ 0.05M HTMHFP in benzene.

HPMTFP, which results in greater dissociation of the reagent in aqueous solution and stabilizes the adduct formation between the alkali-metal pyrazolonates and TOPO.

The extraction of lithium and sodium with HTMPFP or HTMHFP was also examined and is illustrated in Fig. 4. Although it was expected that HTMPFP and HTMHFP would exhibit stronger acidity than HPMTFP owing to their longer perfluoroalkyl substituents, they did not enhance the degree of extraction of lithium and sodium. The HTMPFP concentration used was 0.02M, for it is only slightly soluble in cyclohexane. HTMHFP is not soluble in cyclohexane.

The $pH_{1/2}$ values, and the approximate maximum percentages extracted are summarized in Table 2. The maximum percentage extracted could not be determined exactly, because the aqueous phase became cloudy at pH values higher than those illustrated in Figs. 2-4. Quantitative extraction (>99%) of lithium could be achieved with the HTMPFP/TOPO

Table 2. Extraction parameters for MAL_2

Reagent	$pH_{1/2}^*$ (Li)	$\log K_{ex}$		R, %		α
		Li	Na	Li	Na	
HPMBP						
benzene	6.10	-2.68	-5.88	96	3	1590
cyclohexane	5.07	-1.50	-4.54	98	9	1100
HPMTFP						
benzene	3.84	-0.48	-3.64	98	9	1450
cyclohexane	3.29	0.32	-2.56	98.9	50	760
HTMPFP						
benzene	4.22	-0.92	-3.54	99.3	66.6	420
cyclohexane	3.59†	0.11	—	99.5	—	—
HTMHFP						
benzene	4.38	-1.08	-3.95	99.3	68.1	740

* $[HA]_0 = 0.05M$, $[TOPO]_0 = 0.1M$.

† $[HA]_0 = 0.02M$, $[TOPO]_0 = 0.1M$.

and HTMHFP/TOPO systems. Though only a small percentage of sodium was extractable with the HPMBP/TOPO system, > 60% extraction was achieved with the HTMPFP/TOPO and HTMHFP/TOPO systems. For all the extraction systems, greater extraction and higher distribution constants were achieved with cyclohexane as the organic solvent.

Dependence of distribution on the TOPO concentration

To clarify the composition of the extracted species, the dependence of the distribution ratio on the TOPO concentration was examined at constant pH and pyrazolone concentration. The plots of $\log D$ vs. $\log [\text{TOPO}]_0$ for the lithium/HPMTPF system at pH 4.3 (benzene as organic phase) and 3.5 (cyclohexane) had slopes of almost 2, indicating that the extracted species is MAL_2 . The slopes were also ~ 2 for the corresponding sodium systems at pH 5.7 (benzene) and 4.5 (cyclohexane). The same slopes were obtained for the other extraction systems.

The extraction constants, $K_{\text{ex},s}$, defined in equation (2), were obtained and are summarized in Table 2. The values were calculated not from $\log D$ vs. pH plots but from the linear part of $\log D$ vs. $\log [\text{TOPO}]_0$ plots, since the extraction does not follow equation (2) at high TOPO concentrations. The extraction constants decrease according to the ligand used, in the order $\text{HPMTPF} > \text{HTMPFP} > \text{HTMHFP} > \text{HPMBP}$ for lithium and $\text{HTMPFP} > \text{HPMTPF} > \text{HTMHFP} > \text{HPMBP}$ for sodium. Obviously the perfluoroalkyl substituents increase the extraction constants compared with those for use of 4-benzoyl-5-pyrazolone, but increasing their chain-length does not always increase $K_{\text{ex},s}$. The maximum percentage

extracted decreases with ligand in the order $\text{HTMHFP} > \text{HTMPFP} > \text{HPMTPF} > \text{HPMBP}$, which is also the order in which the length of perfluoroalkyl substituent decreases.

Separation of lithium and sodium

The separation factor, α , is defined as

$$\alpha = \frac{D_{\text{Li}}}{D_{\text{Na}}} = \frac{K_{\text{ex},s(\text{Li})}}{K_{\text{ex},s(\text{Na})}}$$

and its values are summarized in Table 2. The best separation was obtained with the HPMBP/TOPO/benzene system, only a few percent of the sodium being extracted at the pH at which lithium was almost quantitatively extracted. Larger α values are obtained with benzene as the organic phase. Increasing the acidity of the pyrazolone does not seem to increase α .

REFERENCES

1. P. R. Danesi, H. Meider-Gorican, R. Chiarizia and G. Scibona, *J. Inorg. Nucl. Chem.*, 1975, **37**, 1479.
2. A. Sadakane, T. Iwachido and J. Tôei, *Bull. Chem. Soc. Japan*, 1975, **48**, 60.
3. Y. Takeda and H. Goto, *ibid.*, 1979, **52**, 1920.
4. R. F. Apple and J. C. White, *Talanta*, 1966, **13**, 43.
5. T. V. Healy, *J. Inorg. Nucl. Chem.*, 1968, **30**, 1025.
6. *Idem*, *ibid.*, 1969, **31**, 499.
7. M. Munakata, S. Niina and N. Shimoji, *Bunseki Kagaku*, 1974, **23**, 1506.
8. S. Umetani, M. Matsui, J. Tôei and T. Shigematsu, *Anal. Chim. Acta*, 1980, **113**, 315.
9. S. Umetani, K. Sasayama and M. Matsui, *ibid.*, 1982, **134**, 327.
10. B. Jensen, *Acta Chem. Scand.*, 1959, **13**, 1668.
11. S. Umetani and M. Matsui, *Bull. Chem. Soc. Japan*, 1983, **56**, 3426.

STUDIES OF TWO-PHASE EQUILIBRIA BY LIQUID-LIQUID SEGMENTED FLOW EXTRACTION OF DITHIOCARBAMIC ACIDS INTO VARIOUS SOLVENTS

KENNETH BÄCKSTRÖM, LARS-GÖRAN DANIELSSON, FOLKE INGMAN and ZHAO HUAZHANG*
Department of Analytical Chemistry, The Royal Institute of Technology, S-100 44 Stockholm, Sweden

(Received 27 November 1986. Revised 2 April 1987. Accepted 9 April 1987)

Summary—A method for the study of two-phase equilibria by extraction in liquid-liquid segmented flow is presented. The main advantage of the method is the very rapid equilibration achieved. In many cases a contact time of 5 sec is sufficient. By performing the measurements needed on-line with the extraction the total residence time of a substance studied in the system can be kept below 10 sec. This makes it possible to study two-phase equilibria of moderately unstable compounds. Other advantages are the semi-enclosed design, which minimizes contact with solvent fumes and increases the speed of operation after the system has been set up. The system has been used for a study of the two-phase equilibria of dithiocarbamic acids. The dithiocarbamates are often used for the separation and preconcentration of metals, and co-extraction of the reagent can cause severe interference in the final determination. By means of the extraction constants presented, the extraction of diethyldithiocarbamic acid and pyrrolidinedithiocarbamic acid into Freon 113, carbon tetrachloride, methyl isobutyl ketone and chloroform can be estimated.

Solvent extraction is one of the most often used methods for separation and preconcentration in the analytical laboratory.^{1,2} Studies of two-phase equilibria in the various systems of analytical interest have therefore been a frequent preoccupation for analytical chemists for many years and generally performed by shaking two phases of suitable composition in a separatory funnel for a period considered (or determined) to be long enough for equilibrium to be reached. The equilibration time depends on the efficiency of droplet formation from the two phases,³ and the reaction rates and diffusion coefficients in the two phases. After equilibration the funnel is left for some minutes for the phases to separate and the concentration of the species of interest is then measured in one or both of the phases. Thus studies of two-phase equilibria were relatively tedious, and often involved the handling of considerable volumes of potentially harmful solvents.

These studies can be made with less solvent and in a semi-enclosed system, by use of liquid-liquid segmented flow, a possibility which was pointed out some years ago.^{4,5} The systems devised are, however, not suitable for work with compounds such as the dithiocarbamic acids, that cannot be obtained in solid form and are more or less unstable in any solvent.⁶ However, as recently shown, the attainment of equilibrium in liquid-liquid segmented flow can be very rapid.⁷ Provided that some simple guidelines concerning the design of the flow system are followed and

that no slow chemical reactions are involved, equilibrium in the segmented flow can be reached after only a few seconds. As the effective volume of the phase separator and the connection to the detector can be kept small (< 15 μ l) the total residence time in the system will be very short.^{8,9} This opens the possibility of studying the two-phase equilibria of moderately unstable compounds.

The dithiocarbamates are often used for extractive separation and preconcentration of metal ions prior to determination. As these reagents are fairly non-selective and react with many transition elements, they have mainly found use in conjunction with highly selective instrumental methods such as atomic-absorption spectrophotometry and atomic-emission spectrometry, with flames or plasmas. Among the various dithiocarbamates, pyrrolidinedithiocarbamate (PDC) and diethyldithiocarbamate (DDC) have been preferred for analytical work.^{2,10} Surprisingly, relatively little work has been done on the two-phase equilibria of these reagents. One reason for this is the poor stability of the dithiocarbamates in aqueous solutions of low pH.^{10,11} As the co-extraction of dithiocarbamic acids can constitute an interference both in spectrophotometry, mass spectrometry and atomic spectroscopy, especially with the graphite furnace, a closer study of their distribution is warranted. By determining the extraction constants for the dithiocarbamic acids in relevant systems it should be made possible to estimate in advance the risks for interference from co-extracted reagent. In earlier distribution studies carbon tetrachloride¹¹⁻¹⁴ and chloroform^{12,14-16} were used as the organic phase. In this study we have also included 1,1,2-trichloro-1,2,2-

*Permanent address: Centre of Structure and Element Analysis, China University of Science and Technology, Hefei, Anhui, People's Republic of China.

trifluoroethane (Freon 113) and methyl isobutyl ketone (MIBK). The former is less toxic than chloroform or carbon tetrachloride and the latter is more suitable for atomic spectrometry with flames or plasmas.

EXPERIMENTAL

Apparatus

The two extraction manifolds used are shown in Fig. 1. Flows were maintained with the aid of peristaltic pumps (Gilson Minipuls, France) fitted with Tygon pump tubes (Technicon, USA). When Freon 113 was used the displacement bottle was omitted and this solvent was pumped directly, through Solvaflex tubing (Technicon, USA). The segmentor was an ordinary T-piece, 0.7 mm bore, made of poly(vinylidenedifluoride) (PVDF). Phase separation was achieved with a membrane phase-separator of the type previously described.⁸ The membrane was 0.2- μ m pore-size Fluoropore (Millipore, USA). In all cases restrictors were chosen such that practically complete phase separation was obtained. Photometric measurements were made with an LKB 2151 variable-wavelength detector (LKB, Sweden) equipped with a 10- μ l flow-cell with 10-mm path-length. The wavelength of maximum absorbance in the range 330–360 nm was found for each solvent-dithiocarbamate combination and subsequently used for the measurements.

The pH of the aqueous outflow was measured with a pH-meter (Metrohm Herisau, Switzerland). The electrode couple, a glass electrode and a double-junction reference electrode, was standardized with NBS buffers. Flow-rates were measured, by use of a stop-watch and a balance, for each set of experiments.

Reagents

All chemicals were of analytical grade and used as purchased, except for the Freon 113 for which the technical grade was satisfactory. The pH for extraction was adjusted with nitric acid and acetate and phosphate buffers. Sodium nitrate was used for ionic strength adjustments. The ammonium pyrrolidinedithiocarbamate and diethylammonium diethyldithiocarbamate solutions had a concentration of 3.2 g/l, unless stated otherwise.

Procedure

The basic arrangement for the extraction experiments is shown in Fig. 1(a). The organic phase and dithiocarbamate reagent are brought together to give segmented flow. The pH of the aqueous phase is then adjusted through the addition of a buffer or nitric acid. This order of addition is chosen in order to minimize the residence time for the dithiocarbamic acids in aqueous solution. The dithiocarbamic acid formed is distributed between the phases during transport through the extraction coil. After passage through a suitable length of tubing, equilibrium is reached,

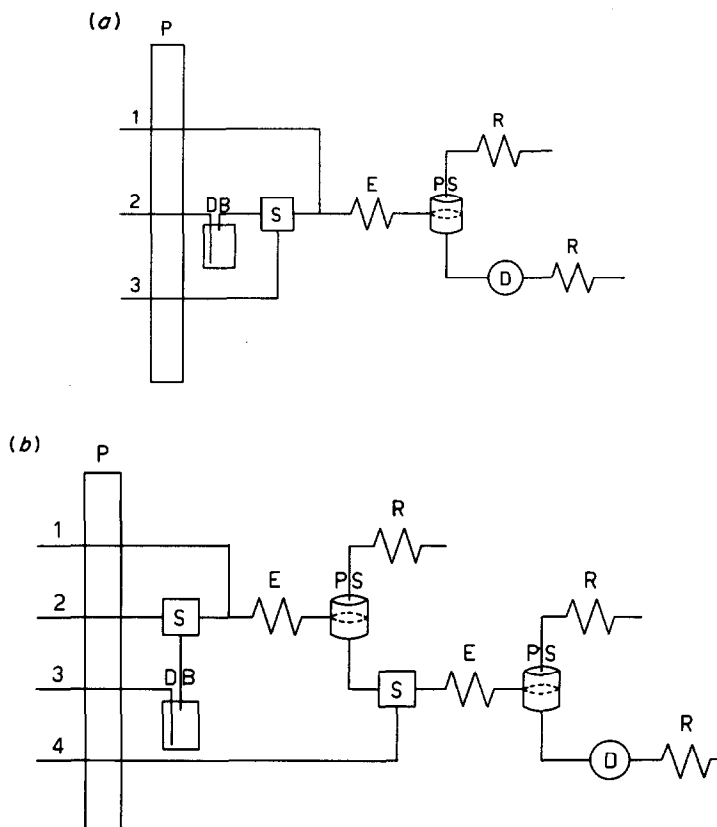


Fig. 1. Manifolds for the extraction of dithiocarbamic acids from an aqueous into an organic phase (a) 1, pH-adjusting solution (buffer or HNO_3) (approximate flow-rate 0.7 ml/min); 2, water feed to displacement bottle delivering organic solvent (0.9 ml/min); 3, aqueous solution of the extractant (0.7 ml/min); P, peristaltic pump; DB displacement bottle; S segmentor; E, extraction coil (Teflon), 1 m long, 0.35 mm bore; PS, phase separator; D, photometric detector; R, restrictor. (b) The organic solution of the extractant is produced in-line: 1, 0.14M HNO_3 (approximate flow-rate 0.7 ml/min); 2, aqueous solution of the extractant (0.7 ml/min); 3, water feed to displacement bottle delivering organic solvent (0.9 ml/min); 4, pH-adjusting solution (buffer or HNO_3) (0.7 ml/min); other symbols as for (a).

and the two phases are separated and the organic phase is led to the detector, where its absorbance is measured. Meanwhile, the aqueous phase is collected for pH measurement, performed as soon as possible after the run.

THEORY

The dithiocarbamic acid, HX, is distributed between the phases according to the distribution constant:

$$K_d = [\text{HX}]_o / [\text{HX}] \quad (1)$$

The distribution of dithiocarbamate between the phases is also influenced by the pH of the aqueous phase:

$$K_{\text{HX}} = [\text{HX}] / [\text{H}][\text{X}] \quad (2)$$

Equations (1) and (2) give an expression for the extraction of dithiocarbamic acid:

$$K_e = [\text{HX}]_o / [\text{H}][\text{X}] = K_d K_{\text{HX}} \quad (3)$$

When extractions are studied by means of absorbance measurements on only the organic phase, it is necessary to transform absorbance values into concentrations. For dithiocarbamic acids this cannot be done in the usual way because they cannot be obtained in solid form,⁶ and they are all more or less unstable in organic solvents.

If the possibility of dimerization in the organic phase is regarded as negligible,¹⁶ the total concentration of dithiocarbamic acid (calculated as if it were all present in the organic phase) can be expressed by:

$$\begin{aligned} C_o &= [\text{HX}]_o + ([\text{HX}] + [\text{X}])/r \\ &= [\text{HX}]_o (1 + 1/rK_d + 1/rK_{\text{HX}}K_d[\text{H}]) \quad (4) \end{aligned}$$

where r is the phase flow-ratio Q_o/Q_{aq} . If the extraction is done at a pH low enough for the last term in (4) representing $[\text{X}]$, to be neglected, maximal concentration of HX in the organic phase will be reached:

$$[\text{HX}]_{o,\text{max}} = C_o / (1 + 1/rK_d) \quad (5)$$

The concentration of dithiocarbamate in the aqueous phase is given by:

$$[\text{X}] = (C_o - [\text{HX}]_o - [\text{HX}]/r)r \quad (6)$$

From equations (1), (5) and (6) we obtain:

$$[\text{X}] = r(1 + 1/rK_d)([\text{HX}]_{o,\text{max}} - [\text{HX}]_o) \quad (7)$$

Inserting equation (7) into (3), using Beer's law and taking logarithms, we obtain:

$$\begin{aligned} \log [A/A_{\text{max}} - A] \\ = -\text{pH} + \log K_e + \log r + \log(1 + 1/rK_d) \quad (8) \end{aligned}$$

where A is the absorbance of the organic phase. Thus plotting $\log[A/A_{\text{max}} - A]$ vs. pH will give a straight line with slope -1 . From the hydrogen-ion concentration at $A = A_{\text{max}}/2$, $[\text{H}]_i$, and K_{HX} for the dithiocarbamic acid, the extraction constant can be calculated:

$$K_e = (1/H_i - K_{\text{HX}})/r \quad (9)$$

Once K_e has been evaluated the assumption leading to equation (5) can easily be checked.

RESULTS AND DISCUSSION

Initially, experiments were performed to elucidate the influence of the length of the extraction tubing and hence the phase contact time on the extraction. With a constant total flow-rate of about 2.1 ml/min, extractions were performed in the manifold shown in Fig. 1a with varying lengths of extraction coil. The results obtained for Freon 113 are shown in Fig. 2. As can be seen, the extraction is very rapid, and is complete after passage of the reaction mixture through about 1 m of extraction coil. This is equivalent to a phase-contact time of 2.5 sec. As expected, the rate of extraction is not affected by the pH of the aqueous phase since protonation/deprotonation reactions are very fast. Interestingly, calculations of K_e based on results obtained with extraction coils shorter than 1 m gave results corresponding to those obtained when the system was allowed to reach equilibrium. However, under non-equilibrium conditions the need for constancy of flow-rates will be more stringent.

It can also be seen from Fig. 2 that increasing the phase-contact time has no effect on the absorbance of the extract. Thus, no significant degradation of the dithiocarbamic acid in the organic phase takes place during this time (about 5 sec). The time elapsed between separation of the phases and absorbance measurement was kept at 2 sec or less. Thus, degradation of the dithiocarbamic acid after separation is not likely, especially since the rate of degradation should decrease after the separation.^{17,18} Results similar to those in Fig. 2 were also obtained with MIBK as the organic phase. In the further work a 1 m length of tubing was used throughout for the extraction.

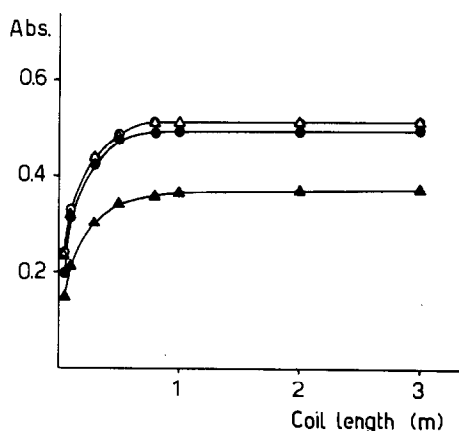


Fig. 2. Absorbance of the organic phase (Freon 113) as a function of the length of the extraction coil. Flow conditions as in Fig. 1(a): 0.14M HNO₃ as pH-adjusting solution; extractant: ○ HDDC; △ HPDC; 2M acetate buffer (pH = 3.4) as pH-adjusting solution; extractant: ● HDDC; ▲ HPDC.

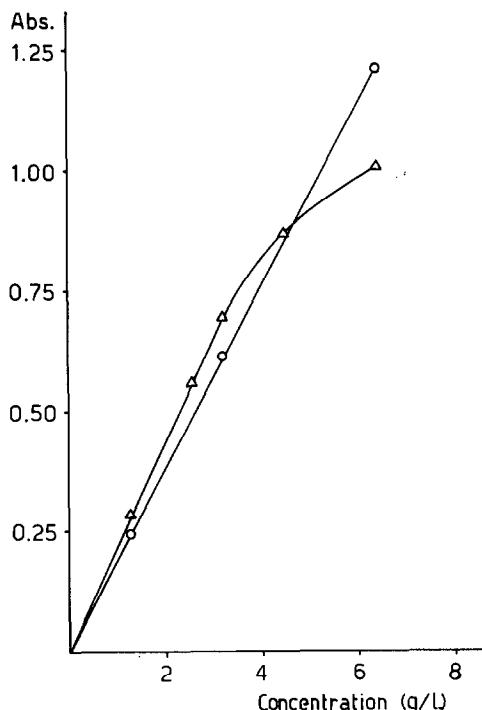


Fig. 3. Absorbance of the organic phase (Freon 113) as a function of the initial concentration of extractant (g/l.) in the aqueous solution. Flow conditions as in Fig. 1(a). Extractant: ○ HDDC; △ HPDC.

To ascertain whether the solubilities of the dithiocarbamic acids in the different organic solvents were sufficient, some experiments with various concentrations of dithiocarbamates were performed, with the manifold shown in Fig. 1(a) and 0.14M nitric acid for pH adjustment. Freon 113 was used as organic phase, previous experience having shown that this is the solvent in which the dithiocarbamic acids are least soluble. The results, given in Fig. 3, show that for HDDC the solubility is sufficient in the concentration range tested, but for HPDC the effects of limited solubility can be seen. To give an acceptable safety margin, the concentration of APDC used was decreased to 0.64 g/l. in the case of extraction into Freon 113.

For each solvent-dithiocarbamate combination the determination of K_e was started by establishing the pH-absorbance relationship. With decreasing pH more dithiocarbamic acid is extracted, and the absorbance increases until finally a steady A_{max} is established, as shown in Fig. 4. With a strongly acidic aqueous phase the absorbance was sometimes lower than A_{max} , probably because of degradation of the dithiocarbamic acid. For all combinations tested in this work A_{max} could be established by using 0.28M nitric acid for pH adjustment. After establishment of A_{max} a number of buffers were introduced into the system in rapid succession, under constant flow conditions, and the corresponding pH and absorbance values were found. These data were then treated according to equation (8) and the equation for the

best line through the points was found by linear regression. The intersection of this line and the line $\log[A/(A_{max} - A)] = 0$ gives the pH_i value, which thus represents the pH for 50% of maximal extraction. From these values, the measured phase flow-ratios, and literature values for the acidity constants of the dithiocarbamic acids,¹⁹ K_e values could be calculated according to equation (9).

To ascertain that the values obtained correspond to true equilibrium conditions, measurements were also performed by extracting the dithiocarbamic acids from organic solvents into water. The organic solutions of dithiocarbamic acids were produced in-line with the measurement system in the manifold shown in Fig. 1(b). Phase flow-ratios were in these cases based on the measured outflows from the second separator, to avoid possible errors due to losses of organic phase in the first separator.

The slopes found for the plots of $\log[A/(A_{max} - A)]$ vs. pH were all in the range between -0.96 and -1.06 and were not significantly different from the theoretical value of -1. This good agreement with theory is a further indication that no disturbing decomposition of the dithiocarbamates takes place over the range of pH studied. The assumption leading to equation (5) can be erroneous if the pH is too high in the determination of A_{max} , especially if K_d is low. Thus the largest risk in this case is connected with the Freon 113-HPDC combination. A rough calculation shows, however, that at the pH used for A_{max} determination only 0.2% of the dithiocarbamate was

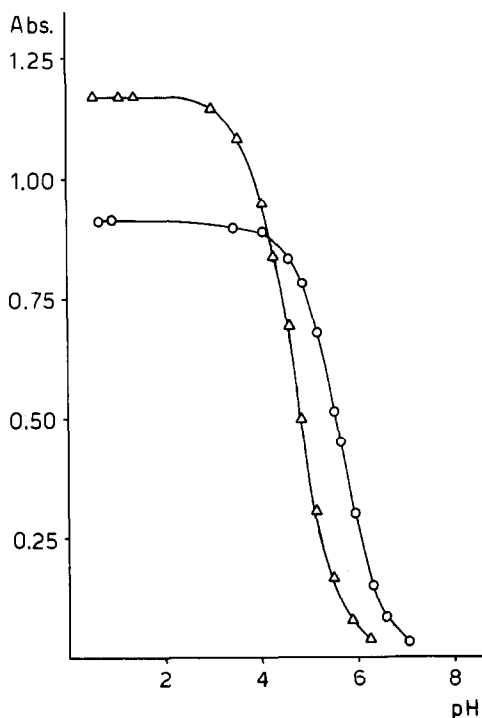


Fig. 4. Absorbance of the organic phase (CCl_4) as a function of pH during extraction. Flow conditions as in Fig. 1(a). Extractant: ○ HDDC; △ HPDC.

Table 1. Logarithms of two-phase equilibrium constants for some solvent-dithiocarbamate combinations

Solvent	Dithiocarbamic acid							
	HPDC				HDDC			
	K_c	$s_{\log K}$	K_d	Lit. values	K_c	$s_{\log K}$	K_d	Lit. values
Freon 113*	3.88	0.01	0.63	—	5.00	0.01	1.65	—
Freon 113†	3.93	0.03	0.68	—	5.03	0.03	1.68	—
CCl ₄ *	4.80	0.03	1.55	—	5.75	0.03	2.40	6.21 ^{11,14} , 5.74 ¹² , 5.79 ¹³
CCl ₄ †	4.72	0.09	1.47	—	5.83	0.07	2.48	—
CCl ₄ §	—	—	—	—	5.70	0.03	2.35	—
MIBK*	5.07	0.03	1.82	—	6.00	0.06	2.65	—
CHCl ₃ *	6.10	0.02	2.85	6.13 ¹⁵ , 6.0 ¹⁶	6.78	0.03	3.43	6.72 ¹² , 6.77 ¹³ , 7.0 ¹⁶
CHCl ₃ †	—	—	—	—	6.76	0.04	3.41	—

*Normal extraction with the manifold in Fig. 1(a).

†Back-extraction with the manifold in Fig. 1(b).

§Normal extraction with the manifold in Fig. 1(a) and constant ionic strength $I = 0.1M$.

present in anionic form in the aqueous phase. Thus the approximation is justified.

Initially extractions were performed without adjustment of the ionic strength, which therefore varied with pH from very low values to the strength of the diluted buffer, 0.1M. As most of the experiments were performed at a pH higher than $\log K_{HX}$ for the buffer, the stability constants of the dithiocarbamic acids given by Aspila *et al.*¹⁹ were recalculated to an ionic strength of 0.1M. A set of experiments performed at a constant ionic strength of 0.1M gave results close to those obtained earlier. Furthermore, evaluation of K_c for each run, by use of equation (3), showed no trend in the results obtained at different pH and hence at different ionic strength. By using in our calculations K_{HX} values valid for 0.1M ionic strength we can obtain K_c values for this medium. The K_c values found are shown in Table 1, together with the corresponding K_d values. The standard deviations were obtained from the evaluation of pH_i by linear regression. Results found in the literature are also given. Generally the correspondence is quite good, considering the difficulties caused for the earlier workers by the poor stability of the dithiocarbamic acids.

As expected, the extractability of the dithiocarbamic acids into different solvents increases in the order Freon 113 < carbon tetrachloride < MIBK < chloroform. For three of the solvents K_d is approximately ten times greater for HDDC than for HPDC. With chloroform, however, a much smaller difference in K_d was found. This behaviour can probably be explained as due to the formation of association compounds in the organic phase. Such effects have been found by Imura *et al.*^{20,21} A closer study of this behaviour is the aim of further research.

CONCLUSIONS

The concept of extraction in liquid-liquid segmented flow has proved to be very suitable for the study of two-phase equilibria, especially for work with relatively unstable compounds. After the experi-

mental system has been established, the system produces data rapidly. Furthermore, relatively small amounts of solvents are needed and the system is semi-enclosed. The precision of the data obtained is more than adequate for analytical purposes.

The results obtained for the two-phase equilibria of the dithiocarbamic acids show that the amount of reagent co-extracted when these reagents are used for separation of metals can be considerable, especially at low pH. This fact should be taken into consideration when designing separation schemes in conjunction with determination methods that might be disturbed by the excess of reagent. The results also explain the varying ease with which metals can be stripped from dithiocarbamate extracts in different solvents.²² By correct choice of solvent and pH of extraction the amount of co-extracted reagent can in most cases be reduced to insignificant levels.

Acknowledgements—The financial support given by the Swedish National Board for Technical Development is gratefully acknowledged. We also thank the Ministry of Education of the People's Republic of China for providing an allowance for Zhao Huazhang.

REFERENCES

1. G. H. Morrison and H. Freiser, *Solvent Extraction in Analytical Chemistry*. Wiley, New York, 1957.
2. J. Stary, *The Solvent Extraction of Metal Chelates*. Pergamon Press, Oxford, 1964.
3. H. Freiser, *Acc. Chem. Res.*, 1985, **17**, 126.
4. P-A. Johansson, B. Karlberg and S. Thelander, *Anal. Chim. Acta*, 1980, **114**, 215.
5. J. F. M. Kinkel and E. Tomlinson, *Int. J. Pharm.*, 1980, **6**, 261.
6. G. D. Thorn and R. A. Ludwig, *The Dithiocarbamates and Related Compounds*. Elsevier, Amsterdam, 1962.
7. L. Nord, K. Bäckström, L-G. Danielsson, F. Ingman and B. Karlberg, submitted to *Anal. Chim. Acta*.
8. K. Bäckström, L-G. Danielsson and L. Nord, *Anal. Chim. Acta*, 1985, **169**, 43.
9. *Idem, ibid.*, 1986, **187**, 255.
10. A. Hulanicki, *Talanta*, 1967, **14**, 1371.
11. H. Bode, *Z. Anal. Chem.*, 1954, **142**, 414.
12. F. Neumann, *Dissertation*, Hannover University of Technology, 1959.
13. J. Stary and K. Kratzer, *Anal. Chim. Acta*, 1968, **40**, 93.

14. J. Starý, M. Kyrš and M. Marhol, *Separation Methods in Radiochemistry*, p. 34. Academia, Prague, 1975.
15. W. Likussar and D. F. Boltz, *Anal. Chem.*, 1971, **43**, 1273.
16. K. I. Aspila, C. L. Chakrabarti and V. S. Sastri, *ibid.*, 1975, **47**, 945.
17. H. Bode and F. Neumann, *Z. Anal. Chem.*, 1959, **169**, 410.
18. S. Bajo and A. Wyttenbach, *Anal. Chem.*, 1979, **51**, 376.
19. K. I. Aspila, C. L. Chakrabarti and V. S. Sastri, *ibid.*, 1973, **45**, 363.
20. H. Imura and N. Suzuki, *J. Radioanal. Nucl. Chem.*, 1985, **88**, 63.
21. H. Imura, S. Matsomura and N. Suzuki, *Bull. Chem. Soc. Japan*, 1986, **59**, 621.
22. B. Magnusson and S. Westerlund, *Anal. Chim. Acta*, 1981, **131**, 63.

ANALYTICAL PROPERTIES OF 2-NITRO-5,6-DIMETHYL-1,3-INDANEDIONE DITHIOSEMICARBAZONE

Y. LINGAPPA, K. HUSSAIN REDDY and D. VENKATA REDDY

Department of Chemistry, Sri Krishnadevaraya University, Anantapur 515 003, India

(Received 1 September 1986. Revised 3 February 1987. Accepted 3 April 1987)

Summary—The synthesis, characterization and analytical properties of 2-nitro-5,6-dimethyl-1,3-indanedione dithiosemicarbazone (NDIDT) are described. NDIDT is used as a chromogenic reagent for the rapid spectrophotometric determination of cobalt(II), palladium(II) and osmium(VIII). The spectrophotometric method developed for cobalt has been used in the analysis of alloys.

Thiosemicarbazones have been frequently employed as chromogenic reagents for the spectrophotometric determination of inorganic ions and their analytical potentialities have been reviewed.^{1,2} Monothiosemicarbazones with an electron-donating group in the α -position and α -bisthiosemicarbazones have been widely studied.² β -Dithiosemicarbazones have been found potentially useful for the spectrophotometric determination of inorganic ions.³⁻⁶ In this paper, the analytical properties of 2-nitro-5,6-dimethyl-1,3-indanedione dithiosemicarbazone (NDIDT) and its utility for the rapid spectrophotometric determination of cobalt(II), palladium(II) and osmium(VIII) are presented.

EXPERIMENTAL

Synthesis of NDIDT

2-Nitro-5,6-dimethyl-1,3-indanedione was prepared according to the literature procedure.⁷ A hot solution of 3 g of 2-nitro-5,6-dimethyl-1,3-indanedione in 150 ml of methanol was added dropwise to a stirred solution of 3 g of thiosemicarbazide dissolved in 100 ml of 3M hydrochloric acid. An orange-red product separated and was purified by washing with methanol (m.p. 220–222°, yield 65%). Found: C 43.1%, H 4.0%, N 27.0%. Calculated for C₁₃H₁₅N₇O₂S₂: C 42.75%, H 4.17%, N 26.74%. A solution of NDIDT ($5 \times 10^{-3}M$) was prepared in 50% aqueous dimethylformamide solution.

Stock cobalt(II) solution ($1 \times 10^{-2}M$) was prepared from cobalt(II) chloride hexahydrate and standardized.⁸ Stock solutions of palladium(II) and osmium(VIII) were prepared and standardized as described earlier.^{9,10}

Buffer solutions were prepared from 1M hydrochloric acid + 1M sodium acetate (pH 0.5–3.0), and 0.2M sodium acetate + 0.2M acetic acid (pH 4.0–7.0).

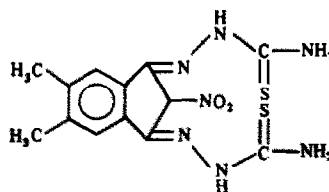
Reactions with cations and anions

The test solutions were prepared in 25-ml standard flasks with 25–200 μ g of the test ion, 3.0 ml of $5 \times 10^{-3}M$ NDIDT, 2.5 ml of dimethylformamide, 10 ml of buffer and dilution to volume with water. The spectrum was measured over the region 350–650 nm with a reagent blank as reference.

General procedure for determination of cobalt, palladium and osmium

Samples were prepared in 25-ml standard flasks with 10 ml of buffer (pH 5.0 for Co, 4.5 for Pd, 6.5 for Os), metal ion (Co 6–60 μ g, Pd 10–95 μ g, Os 19–190 μ g), 2.5 ml of dimethylformamide, 3 ml of $5 \times 10^{-3}M$ NDIDT and dilu-

tion to volume with water. The absorbances were measured at 420 nm for Co, 480 nm for Pd, 490 nm for Os, against a reagent blank as reference.



Structure of NDIDT

RESULTS AND DISCUSSION

Solubility

The solubility of NDIDT in several solvents was determined by Wittemberger's method.¹¹ NDIDT is soluble in dimethylformamide (28 g/l.), dimethylsulphoxide (12 g/l.), ethyl acetate (0.6 g/l.) and methyl isobutyl ketone (0.3 g/l.) and sparingly soluble in water, chloroform, carbon tetrachloride and cyclohexanone.

Stability

A $5 \times 10^{-3}M$ solution of NDIDT is stable for a day in 1:1 v/v water–dimethylformamide mixture and for a week in 1:1 v/v ethanol–water mixture.

Spectral characteristics

The infrared spectrum was obtained (KBr discs) and bands (cm^{-1}) were assigned to the stretching vibrations of $-\text{NH}$ (3311), $>\text{C}=\text{N}$ (1631), $>\text{C}=\text{S}$ (1145).

The NMR spectrum was obtained in DMSO-*d*₆ with tetramethylsilane as reference. The peaks (τ) were assigned as follows: 2.18 (C–H protons, aromatic), 6.48 (CH₃ protons of indane ring), 7.59–7.76 (NH and NH₂ protons). The ultraviolet absorption spectra of NDIDT at various pH values are shown in Fig. 1. The dissociation constants were determined by the Phillips and Merritt method¹² at 25° and ionic strength 0.1. The average results obtained were $\text{p}K_1 = \text{p}K_2 = 9.8$ ($>\text{C}=\text{S}$ group thione–thiol tautomerism).¹³

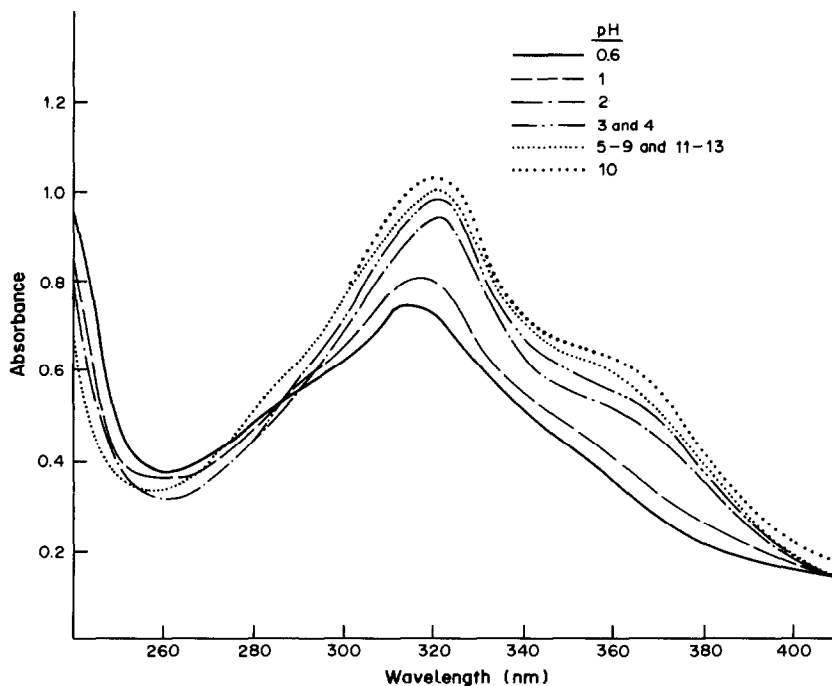


Fig. 1. Absorption spectra of $2 \times 10^{-5}M$ NDIDT at different pH values.

Qualitative tests

The most important results are summarized in Table 1. NDIDT gives chelating reactions, *e.g.*, with Co(II) and Pd(II), and redox reactions with Cr(VI), IO_3^- and BrO_3^- which involve a two-electron mechanism in accordance with general redox behaviour of bithiosemicarbazones.^{5,14} By analogy with earlier reports,^{14,15} the oxidation products may be

Determination of cobalt(II), palladium(II) and osmium(VIII)

The order of addition of metal ion, buffer and NDIDT is immaterial provided dimethylformamide

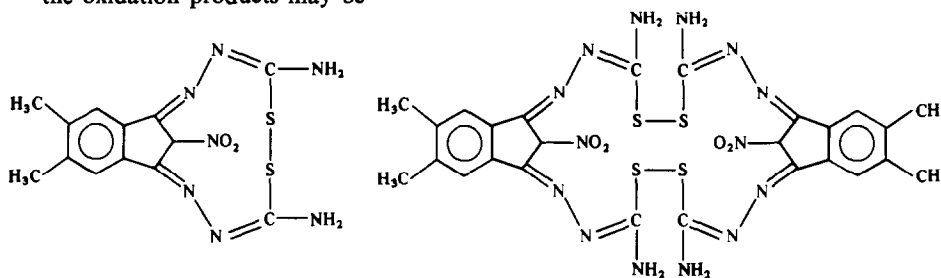


Table 1. Analytical characteristics of NDIDT reactions

Ion	pH/medium	λ_{max} , nm	ϵ , $l. \text{mole}^{-1}. \text{cm}^{-1}$	Stoichiometry, M:NDIDT	Colour
Co(II)	4-6	420	1.5×10^4	1:2	Brown
Ni(II)	8-9	430	1.0×10^4	1:2	Yellow
Cu(II)	4-6	420	1.2×10^4		Red
Ru(III)	4-6	440	5.0×10^3		Brown
Pd(II)	2-6	480	1.6×10^4	1:2	Orange-red
Os(VIII)	6-8	420-490	1.3×10^4	1:4	Brown
Pt(IV)	1-6				Yellow*
Au(III)	3-6	420	8.0×10^3		Yellowish-red
Cr(VI)	HClO_4	370	3.0×10^3	2:3	Red
BrO_3^-	0.8-1.6M				
	HClO_4	360	6.5×10^3	1:3	Red
IO_3^-	1.0-2.0M				
	HClO_4	470	2.0×10^4	1:3	Yellow

*Precipitate.

Table 2. Physicochemical and analytical characteristics of complexes

Characteristic	NDIDT complex of		
	Cobalt	Palladium	Osmium
Moles of reagent required per mole of metal ion	5	10	10
Beer's law range (ppm)	0.24–2.40	0.42–3.83	0.76–7.61
Optimum concentration range (ppm)			
(Ringbom plot)	0.94–2.24	0.85–3.83	2.28–6.85
Stability constant	3.50×10^9	1.45×10^9	
Mean absorbance \pm s.d.*	0.302 ± 0.004	0.287 ± 0.007	0.337 ± 0.0046

*In the determination of 1.18 ppm Co(II), 2.13 ppm Pd(II) or 4.56 ppm Os(VIII).

Table 3. Tolerance limit of cations in the determination of cobalt (1.4 ppm), palladium (1.7 ppm) and osmium (3.8 ppm)

Metal ion	Tolerance limit, ppm		
	Co	Pd	Os
Uranium(VI)	950	950	950
Thorium(IV)	400	930	460
Zinc(II)	30	770	130
Manganese(II)	220	660	110
Iridium(III)	150	190	65
Nickel(II)	2	120*	35*
Iron(III)	180†	110†	110* (70)§
Chromium(III)	70	100	50
Aluminium(III)	55	50	65
Cobalt(II)	—	50*	50*
Rhodium(III)	150	40	40
Copper(II)	—	25*	15*
Zirconium(IV)	—	15	70
Osmium(VIII)	6‡	7‡	—
Platinum(IV)	3	3	2
Gold(III)	2	2	1
Ruthenium(III)	1	2	1
Palladium(II)	—	—	1

*In the presence of 4000 ppm of EDTA.

†In the presence of 1100 ppm of NaF.

‡In the presence of 130 ppm of thiourea.

§In the presence of 200 ppm of phosphate.

—Interferes seriously.

(DMF) is added before the NDIDT. In aqueous media the metal complexes are precipitated, but they are soluble in 10% v/v DMF medium. The reactions are quite rapid and require no heating for full colour development. Important characteristics of the Co, Pd and Os complexes are summarized in Table 2. The stoichiometry and stability constants were determined by the Job and mole-ratio methods.

Interferences

The tolerance limits for various anions (<2% error) in determination of 1.4 ppm Co(II), 1.7 ppm Pd(II) or 3.8 ppm Os(VIII) respectively are: fluoride (1500, 3000, 3000), chloride (700, 2350, 4200), bromide (320, 320, 320), iodide (500, 0, 250), tartrate (1200, 600, 600), citrate (400, 1900, 1500), phosphate (380, 760, 300), nitrate (800, 830, 830), sulphate (1540, 1540, 1920), thiocyanate (2, 460, 460), oxalate (180, 700, 700) thiourea (80, 150, 0), thiosulphate (90, 90, 90), tetraborate (600, 620, 600), chlorate (80, 152, 40) EDTA (0, 5500, 5200), chromate (11, 18, 22), molybdate (130, 680, 630), tungstate (940, 990, 940), vanadate (20, 20, 20). Bromate and iodate interfere

Table 4. Analysis of samples for cobalt

Sample	Composition, %	Cobalt certified value, %	Cobalt content† by the present method, %
BCS 483	10.8 W; 3.21 Cr; 0.54 V; 0.29 Mn; 0.17 Mo; Rest Fe*	1.94	1.94 ± 0.002
JSS 607-6 High-speed steel SKH-3	16.96 W; 4.14 Cr; 0.86 V; 0.32 Si; 0.30 Mo; 0.30 Mn; 0.75 C; 0.012 P; 0.006 S, Rest Fe*	4.72	4.72 ± 0.008
High-speed steel	18.5 W; 5.5 Mo; 4.15 Cr; 0.4 Mn; 0.35 S; 0.05 S; Rest Fe*	9.25	9.25 ± 0.02
Eligiloy M-1712	20 Cr; 15 Nim; 15 Fe; 7 Mo; 2 Mn; 0.15 C; 0.05 Be	40.0	40.0 ± 0.1

*Masked with sodium fluoride (1000 ppm).

†Average \pm s.d. of five determinations.

seriously in all three methods. The tolerance limits for metal ions are presented in Table 3.

Analysis of a cobalt alloy

A 0.1–0.5 g sample was dissolved in a mixture of 10–15 ml of concentrated hydrochloric acid and 2 ml of concentrated nitric acid. The solution was evaporated nearly to dryness. The residue was dissolved in 10–20 ml of 1M hydrochloric acid, and the solution was diluted and filtered into a 10-ml standard flask and made up to volume with water. A known volume was suitably diluted to bring the cobalt concentration into the upper end of the calibration range, and a fraction analysed by the procedure already described. The results obtained are given in Table 4.

Acknowledgements—The authors thank the authorities of CDRI, Lucknow, India for providing the elemental analysis and NMR data for NDIDT.

REFERENCES

1. R. B. Singh, B. S. Garg and R. P. Singh, *Talanta*, 1978, **25**, 619.
2. K. H. Reddy and D. V. Reddy, *Quart. Chem. Rev.*, 1985, **I**, 47.
3. M. Guzmán, D. Pérez-Bendito and F. Pino, *Anal. Chim. Acta*, 1976, **83**, 259.
4. J. J. Berzas Nevado, J. A. Muñoz Leyva and M. Román Ceba, *Talanta*, 1976, **23**, 257.
5. K. H. Reddy and D. V. Reddy, *Analyst*, 1983, **108**, 1247.
6. *Idem*, *Anal. Lett.*, 1984, **17**, 1275.
7. D. R. Buckle, M. J. Morgan, J. W. Ross, H. Smith and B. A. Spicer, *J. Med. Chem.*, 1973, **16**, 1334.
8. A. I. Vogel, *A Text Book of Quantitative Inorganic Analysis*, 4th Ed., p. 389. Longmans, London, 1975.
9. K. H. Reddy and D. V. Reddy, *Indian J. Chem.*, 1983, **22A**, 723.
10. K. H. Reddy, K. G. Reddy and D. V. Reddy, *Mikrochim. Acta*, 1985, **II**, 319.
11. W. Wittemberger, *Chemische Laboratoriumstechnik*, 4th Ed., p. 101. Springer, Vienna, 1950.
12. J. P. Phillips and L. L. Merritt, *J. Am. Chem. Soc.*, 1948, **70**, 410.
13. B. A. Gingras, R. S. Somarjai and C. H. Bayley, *Can. J. Chem.*, 1961, **39**, 973.
14. M. Román Ceba, J. A. Muñoz Leyva and J. J. Berzas Nevado, *Analyst*, 1978, **103**, 963.
15. *Idem*, *Anal. Quim.*, 1978, **74**, 1075.

UTILIZATION OF CHARGE-TRANSFER COMPLEXATION IN THE SPECTROPHOTOMETRIC DETERMINATION OF SOME MONOSACCHARIDES THROUGH THEIR OSAZONE INTERMEDIATES

MAGDA AYAD, SAIED BELAL*, AFAF ABOU EL KHEIR and SOBHI EL ADL

Pharmaceutical Chemistry and Pharmaceutical Analytical Chemistry Department, College of Pharmacy,
Zagazig and Alexandria Universities, Zagazig and Alexandria, Egypt

(Received 21 February 1986. Revised 3 March 1987. Accepted 13 March 1987)

Summary—Monosaccharide osazones are utilized in the spectrophotometric determination of their parent compounds through charge-transfer complexation with two-electron acceptor reagents. The molar combining ratio and the optimum complexation conditions have been studied. The method has been used to analyse for glucose and fructose and in determining blood glucose.

Glucose and fructose are widely used in current medical practice as plasma substitutes and body fluid compensatory agents, and other hexoses such as galactose and mannose are of use as diagnostic aids. Several procedures have been reported for their assay in ampoules or biological fluids, including titrimetric,^{1,2} potentiometric,^{3,4} polarographic,⁵ fluorimetric,⁶ atomic-absorption spectrophotometric,⁷ spectrophotometric,⁸⁻¹⁴ NMR,¹⁵ GC¹⁶⁻¹⁸ and HPLC¹⁹⁻²¹ methods. Many of the colorimetric methods depend on the reducing action of the sugar molecule on chromogenic reagents such as the cupric ion,²² silver salts,²³ mercury salts,^{24,25} halogens in alkaline media,²⁶ ferricyanide,²⁷ periodate,²⁸ ceric salts,²⁹ tetrazolium salts,³⁰ aromatic nitro-compounds,³¹ phosphomolybdate,³² mineral acid,³³ anthrone,³⁴ phenolic compounds in mineral acid,³⁵⁻³⁷ or aromatic amines.³⁸ Condensation of hexoses with phenylhydrazine to form a hydrazone or an osazone has also been utilized,³⁹ and claimed⁴⁰ to give true values for glucose in biological fluids.

Charge-transfer complexation reactions are now finding wide use in the determination of electron-donating nitrogenous bases, the reagents being the σ -acceptor iodine⁴¹⁻⁴⁸ or some π -acceptors (polyhalo- or polycyanoquinones)⁴⁹⁻⁵² in organic solvents. In earlier work,⁵³ we determined corticosteroid drugs by charge-transfer complexation of their extractable phenylhydrazones. Condensation of monosaccharides with phenylhydrazine to form the osazones results in the introduction of basic centres, making possible charge-transfer complexation reactions with electron-accepting reagents, as described here.

EXPERIMENTAL

Reagents

Standard aqueous solutions (1 mg/ml) of D(+)-glucose, D(-)-fructose, D(+)-mannose, D(+)-galactose, dextrose and laevulose were prepared and diluted tenfold to give 100- μ g/ml working solutions.

Phenylhydrazine hydrochloride solution (50 mg/ml) and 10⁻³M chloroform solutions of iodine and chloranil were prepared.

Preparation of osazones

To 10 ml of aqueous solution containing 10-15 mg of the monosaccharide, 5 ml of phenylhydrazine hydrochloride solution were added and the mixture was heated in a glycerol bath at 110° for 10 min, cooled, transferred to a 100-ml separatory funnel and extracted by shaking for 1-2 min each time with 5 successive 10-ml portions of ethyl acetate. The extracts were all filtered through anhydrous sodium sulphate into a 50-ml standard flask and the volume made up to the mark with ethyl acetate.

Colour development

Procedure A. A 1.8-ml volume of the osazone extract was transferred into a 10-ml standard flask, treated with 2 ml of iodine solution, allowed to stand for 30 min and then diluted to volume with chloroform. The absorbance of the resulting solution was measured in a 1-cm cell at 305 nm against a reagent blank prepared in the same manner.

Procedure B. A portion of the osazone extract (equivalent to 0.3-1.4 mg of the parent carbohydrate) was transferred into a 10-ml standard flask, treated with 5 ml of chloranil solution and left at room temperature for 45 min or in a water-bath at 45° for 15 min, then diluted to volume with chloroform. The absorbance of the resulting solution was measured at 440 nm in a 1-cm cell against a reagent blank prepared in the same manner.

The concentration equivalent to parent monosaccharide in the final measured solution was calculated from the calibration results obtained by applying the same procedure to an appropriate range of standard solutions of the parent compound.

Application to injections

To a volume of sample containing about 20 mg of glucose or fructose, 5 ml of phenylhydrazine hydrochloride solution were added and the assay was completed as above.

*Present address: College of Medicine and Allied Sciences, King Abdulaziz University, Jeddah, Saudi Arabia.

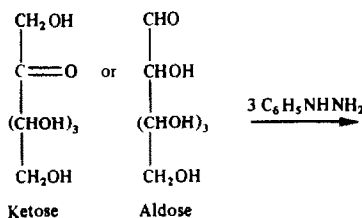
Determination of glucose in blood

To a centrifuge tube containing 4 ml of isotonic solution ($\text{Na}_2\text{SO}_4 \cdot 10\text{H}_2\text{O}$, 30 g/l., a 1.5-ml sample of blood or 1.0 ml of diabetic blood sample (or other body fluids to be analysed) was transferred followed by 0.1 ml of 10% sodium tungstate solution. The mixture was centrifuged for 10 min, and 1 ml of the supernatant liquid was treated with 5 ml of phenylhydrazine hydrochloride solution to form the osazone, which was then extracted with three 5-ml portions of ethyl acetate. The three extracts were filtered through anhydrous sodium sulphate, and evaporated to dryness in a 10-ml standard flask. The residue was dissolved in 1 ml of ethyl acetate, and the colour was developed and the determination completed as above.

RESULTS AND DISCUSSION

Osazone formation

Phenylhydrazine condenses with aldose and ketose monosaccharides to give yellow osazones.



The osazones are measurable spectrophotometrically but with low sensitivity. Their potential basicity initiated our study of their participation in charge-transfer complexation reactions, with the aim of increasing the sensitivity and accuracy of determination of the parent sugars.

An excess of phenylhydrazine is heated with the sugar for 10 min at 110° or 20 min in a boiling water-bath, for quantitative reaction. Ethyl acetate will give complete extraction of the osazone, but then has to be dehydrated by filtration through anhydrous sodium sulphate. A blank run in the same manner has zero absorbance when measured against ethyl acetate, showing that the excess of phenylhydrazine is not extracted.

A Job plot⁵⁵ showed that the combining ratio of osazone (donor) and acceptor was 1:2, as expected from the structural formula of the osazone. It is assumed that the reactive basic centre is the $-\text{NHC}_6\text{H}_5$ group in view of the weak basicity of the $>\text{C}=\text{N}-$ grouping.

Osazone-iodine interaction

Mixing the osazone extract with iodine resulted in a change of the iodine colour from violet to yellow. This is attributed to charge-transfer between the n -donor osazone and the σ -acceptor iodine, followed by the formation of an ion-association complex with tri-iodide anions. The following reaction scheme is suggested.

The absorption spectrum of the products has a high-intensity band with a maximum at about 305 nm and a low-intensity band with a maximum at about

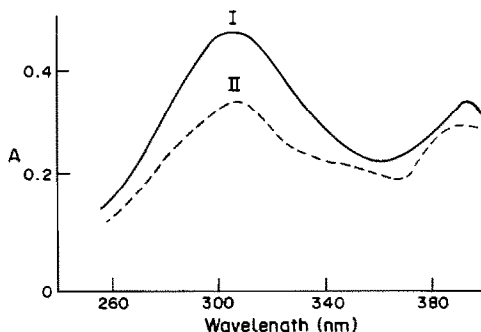
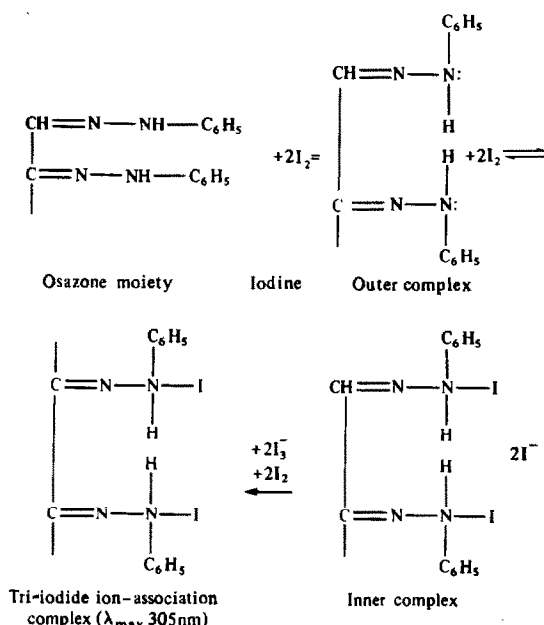


Fig. 1. Absorption spectra of carbohydrate osazone-iodine complexes. I—Dextrose (0.093 mg/ml). II—Fructose (0.083 mg/ml).

360 nm (Figs. 1 and 2), which is characteristic of n -donor-iodine charge-transfer complexes.^{41,46,47,54}

Osazone-chloranil interaction

Mixing the osazone extract with a chloroform solution of chloranil resulted in development of a red colour. This is considered due to charge-transfer between the π -acceptor chloranil and the n - or π -donor osazone which, owing to the polarity of the medium, yields a coloured radical-ion complex.



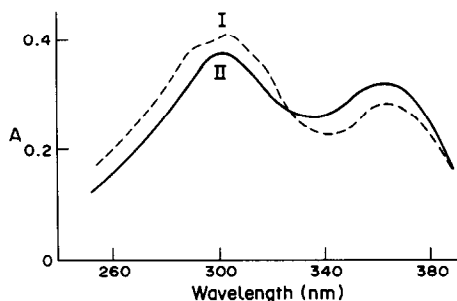
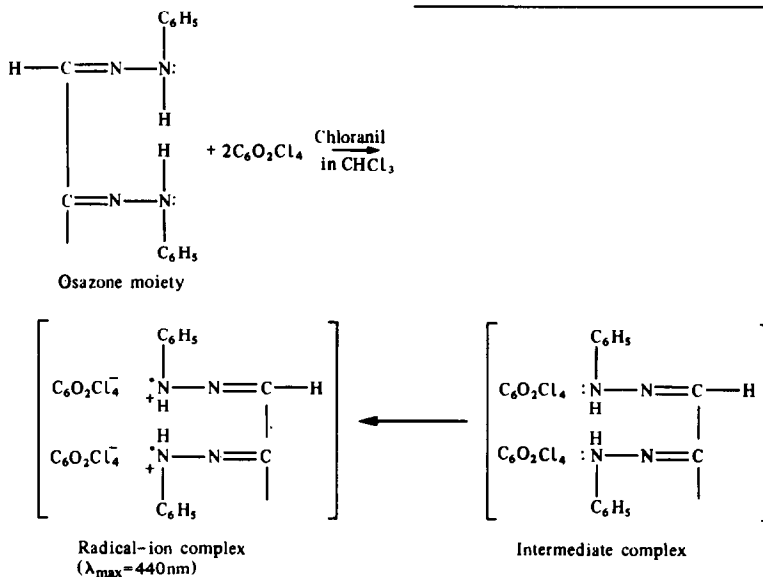


Fig. 2. Absorption spectra of osazone-iodine complexes. I—Mannose (0.096 mg/ml). II—Galactose (0.096 mg/ml).

From consideration of similar cases for basic drugs,^{49,50,53} the following scheme is suggested.



The final reaction product has an absorption maximum at 440 nm (Figs. 3 and 4), which is characteristic of the chloranil radical ion. The latter pairs with the osazone cation resulting from loss of 2 electrons per molecule of osazone, and thus modifies the wavelength of maximum absorption. The possibility of a

substitution reaction between chloranil and the secondary amino ($\text{C}_6\text{H}_5-\text{NH}-$) moiety of the osazone is excluded by the non-aqueous conditions used and the absence of the alkaline buffer necessary for such a reaction.^{51,52}

Conformity to Beer's law

A linear relationship was obtained for amounts of parent monosaccharide in the range 2–12 mg. Disaccharides such as maltose and lactose gave weak and unsatisfactory reaction, indicating the poor donor activity of their osazones.

Determination

The applicability of the procedure for determination of glucose and fructose in ampoules was

assessed with pure drugs and two commercial injections, by the standard-addition technique (Table 1). The samples were also assayed by the official method⁵⁶ and/or the conventional phosphomolybdate³² method (Table 2). The results in Table 1 indicate that the proposed method is fairly accurate

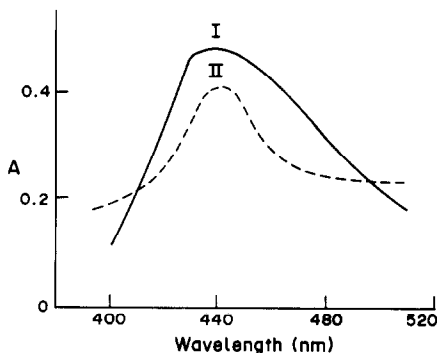


Fig. 3. Absorption spectra of carbohydrate osazone-chloranil complexes. I—Dextrose (0.138 mg/ml). II—Fructose (0.131 mg/ml).

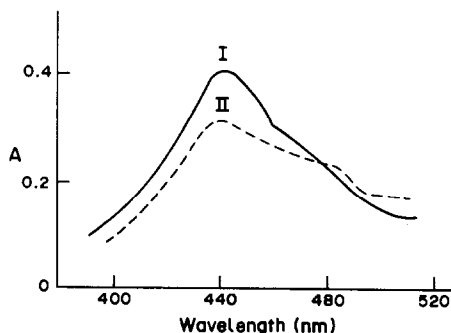


Fig. 4. Absorption spectra of osazone-chloranil complexes. I—Mannose (0.13 mg/ml). II—Galactose (0.13 mg/ml).

Table 1. Determination of pure glucose, pure fructose and their injections, by the proposed method and the B.P. 1953 method

	Recovery,* %		
	Official method	Iodine acceptor	Chloranil acceptor
Glucose	100.0 ± 0.7	99.7 ± 0.5	99.8 ± 0.4
<i>t</i> -test (2.3)		1.34	1.12
<i>F</i> -test (6.39)		1.96	3.06
Fructose	100.0 ± 0.8	99.6 ± 0.6	99.9 ± 0.5
<i>t</i> -test (2.3)		1.49	0.45
<i>F</i> -test (6.39)		1.77	2.56
Glucose injection (dextrose injection)	100.0 ± 0.7	99.8 ± 0.4	99.7 ± 0.4
<i>t</i> -test (2.3)		1.49	1.60
<i>F</i> -test (6.39)		3.06	3.06

*Mean ± standard deviation of 5 determinations, calculated on nominal amount taken, sample weights 2-4 g for BP method, 15-20 mg for proposed method. The figures in parentheses are the tabulated values of *t* and *F*.

and as precise as the official method, since the calculated *t* and *F* values do not exceed the tabulated values. The proposed procedure also gave good results in the determination of blood glucose, as compared with the commonly used phosphomolybdate method (Table 3). The proposed method possesses advantages over the phosphomolybdate method in that it is more sensitive, yields a stable chromophore, gives zero blank readings, and uses simple reagents. It is suggested for use in clinical laboratories for

determining blood glucose in normal and diabetic patients.

The proposed procedure for assay of glucose and fructose injections is simple, accurate, precise and more sensitive than the official methods [E.P. 1953 (Fehling titrimetry), B.P. 1980 and USP 1980 (polarimetry)], which require 2-5 g quantities of the monosaccharide. Thus, the proposed charge-transfer methods are suggested for use in pharmaceutical quality control laboratories.

Table 2. Analysis of glucose and fructose injections by the proposed method and the phosphomolybdate method

	Recovery,* %		
	Phosphomolybdate method	Iodine acceptor	Chloranil acceptor
Dextrose ampoule	100.0 ± 0.5	99.9 ± 0.4	100.0 ± 0.5
<i>t</i> -test (2.3)		0.56	0.18
<i>F</i> -test (6.39)		1.56	1.0
Laevulose ampoule	100.2 ± 0.7	100.0 ± 0.4	100.0 ± 0.5
<i>t</i> -test (2.3)		0.11	0.04
<i>F</i> -test (6.39)		3.06	1.96

*Mean ± standard deviation, calculated on nominal amount taken. Figures in parentheses are the tabulated values of *t* and *F*.

Table 3. Determination of blood glucose by the proposed method and the phosphomolybdate method (standard-addition technique)

	Recovery, %		
	Phosphomolybdate method	Iodine acceptor	Chloranil acceptor
	99.0	99.5	99.5
	99.6	100.0	101.0
	99.2	100.0	99.6
	101.0	100.0	100.0
	100.0	101.0	101.0
*Mean ± SD	99.8 ± 0.8	100.0 ± 0.6	100.0 ± 0.8
<i>t</i> (2.3)		0.75	0.55
<i>F</i> (6.39)		1.70	1.0

*Mean ± standard deviation; recovery calculated on standard amount of glucose added to the blood. The figures in parentheses are the tabulated values of *t* and *F*.

REFERENCES

1. Keyu Ma, *Shipin Kexue (Beijing)*, 1982, **27**, 57.
2. V. Ya. Zakharans, V. V. Elkin, Yu. R. Laurs and V. E. Egert, *Zh. Analit. Khim.*, 1983, **38**, 491.
3. Chung Chiun Liu, J. P. Weaver and A. K. Chen, *Bioelectrochem. Bioenerg.*, 1981, **8**, 379.
4. A. Palanivel and P. Riyazuddin, *Curr. Sci.*, 1984, **53**, 647.
5. M. Mareck, J. Bacilek and J. Jary, *J. Apic. Res.*, 1980, **19**, 255; *Chem. Abstr.*, 1981, **94**, 172969e.
6. R. G. Fulcher, P. J. Wood and S. H. Yiu, *Food Tech., (Chicago)*, 1984, **39**, 101.
7. Yaozu Chen and Chenxi Yang, *Huaxue Xueba*, 1982, **40**, 1066; *Chem. Abstr.*, 1983, **98**, 83079e.
8. M. J. Koziol, *Anal. Chim. Acta*, 1981, **128**, 195.
9. M. Porro, S. Viti, G. Antoni and P. Neri, *Anal. Biochem.*, 1981, **118**, 301.
10. S. Honda, Y. Nishimura, M. Takashi, H. Chiba and K. Kakehi, *ibid.*, 1982, **119**, 194.
11. G. L. Hosfield, S. A. Sippel and D. D. Curtin, *J. Am. Soc. Hortic. Sci.*, 1982, **107**, 61.
12. E. P. Diamandis and T. P. Hadjiioannou, *Analyst*, 1982, **107**, 1471.
13. G. Halliwell, M. Sakajoh and T. Dunn, *Enzyme Microbiol. Technol.*, 1983, **5**, 37.
14. M. Lever, T. A. Walmsley, R. S. Visser and S. J. Royde, *Anal. Biochem.*, 1984, **139**, 205.
15. A. Yamasaki, *Bunseki*, 1983, 262.
16. H. Kouchi, *J. Chromatog.*, 1982, **241**, 305.
17. D. E. Willis, *J. Chromatog. Sci.*, 1983, **21**, 132.
18. P. J. Harris, R. J. Henry, A. B. Blakeney and B. A. Stone, *Carbohydr. Res.*, 1984, **127**, 59.
19. B. Fournet, J. Parente, Y. Leroy and J. Montreuil, *Spectra 2000*, 1982, **9**, No. 73, 28.
20. G. K. Grimble, H. H. Barker and R. H. Taylor, *Anal. Biochem.*, 1983, **128**, 442.
21. M. Petchey and M. J. C. Crabbe, *J. Chromatog.*, 1984, **307**, 180.
22. A. V. Ablov and D. G. Batyr, *Zh. Analit. Khim.*, 1960, **15**, 112.
23. R. J. Ferrier and P. M. Collins, *Monosaccharide Chemistry*, Penguin Books, London, 1972.
24. A. Abou El Kheir, *Z. Lebensm. Unters. Forsch.*, 1974, **155**, 29.
25. W. Wiegrebe, E. Roesel, W. Sasse and H. Keppel, *Arch. Pharm.*, 1969, **302**, 22.
26. G. L. Miller and A. L. Burton, *Anal. Chem.*, 1959, **54**, 158.
27. R. I. Matales, *Nature*, 1960, **187**, 241.
28. J. M. Bailey, *J. Lab. Clin. Med.*, 1959, **54**, 158.
29. A. A. Forist and J. C. Speck, Jr., *Anal. Chem.*, 1955, **27**, 1166.
30. A. Carruthers and A. E. Wootton, *Intern. Sugar J.*, 1955, **62**, 193.
31. R. T. Bottle and G. A. Gilbert, *Analyst*, 1958, **83**, 403.
32. A. M. Asatoor and E. J. King, *Biochem. J.*, 1954, **56**, XLIV.
33. B. Mendel, A. Kemp and D. K. Myers, *Biochem. J.*, 1954, **56**, 739.
34. R. Johnson, *Nature*, 1953, **171**, 176.
35. A. W. Devor, *Anal. Chem.*, 1952, **24**, 1626.
36. W. Chefurka, *Analyst*, 1955, **80**, 485.
37. M. R. Shetlar and Y. F. Masters, *Anal. Chem.*, 1957, **29**, 402.
38. A. Borrow and E. G. Jeffreys, *Analyst*, 1956, **81**, 598.
39. J. A. P. Stroes and H. A. Zondnag, *Clin. Chim. Acta*, 1963, **8**, 152.
40. N. Wahba, S. Hanna and M. M. El-Sadr, *Analyst*, 1956, **81**, 430.
41. A. M. Taha, A. K. S. Ahmed, C. S. Gomaa and H. El Fatatry, *J. Pharm. Sci.*, 1974, **63**, 1853.
42. C. S. Gomaa and A. M. Taha, *ibid.*, 1975, **64**, 1398.
43. S. I. I. Henry, D. G. Erich and S. D. Anthony, *ibid.*, 1977, **66**, 767.
44. S. Belal, M. Abdel-Hady Elsayed, M. E. Abdel-Hamid and H. Abdine, *Analyst*, 1980, **105**, 774.
45. M. S. Rizk, M. I. Walsh and F. A. Ibrahim, *ibid.*, 1981, **106**, 1163.
46. A. M. Taha, N. A. El-Rabbat and F. A. Fattah, *ibid.*, 1980, **105**, 568.
47. *Idem*, *J. Pharm. Belg.*, 1980, **35**, 1437.
48. C. N. R. Rao, S. N. Bhat and P. C. Dwivedi, *Appl. Spectrosc. Rev.*, 1972, **5**, 1.
49. A. Taha and G. Rücker, *Arch. Pharm., (Weinheim)*, 1977, **310**, 485.
50. S. Belal, M. A. Abdel Hady, M. E. Abdel Hamid and H. Abdine, *J. Pharm. Sci.*, 1981, **70**, 1927.
51. F. Al Sulimany and A. Townshend, *Anal. Chim. Acta*, 1973, **66**, 195.
52. T. S. Al Ghabsha, S. A. Rahim and A. Townshend, *ibid.*, 1976, **85**, 189.
53. M. A. Ayad, S. Belal, S. M. El Adl and A. A. El Khair, *Analyst*, 1984, **109**, 1417.
54. R. Foster, *Organic Charge Transfer Complexes*, pp. 61, 191. Academic Press, London, 1969.
55. P. Job, *Ann. Chim. (Paris)*, 1936, **16**, 97.
56. N. Wahba, S. Hanna and M. M. El Sadr, *Analyst*, 1956, **81**, 430.

OXYDATION VANADIQUE DE L'IODOMETHYLATE DE *p*-CHLOROBENZYL-4 DIMETHOXY-6,7 ISOQUINOLEINE EN MILIEU SULFURIQUE AQUEUX

E. POSTAIRE, C. VIEL et M. HAMON

Faculté des Sciences Pharmaceutiques et Biologiques de Paris-sud, 3 rue J. B. Clément,
92290 Chatenay-Malabry, France

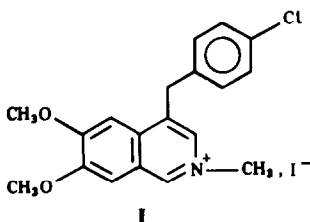
A. GOND

Laboratoires BIOMED, Boulevard Brune, 75005 Paris, France

(Reçu le 29 janvier 1987. Accepté le 13 mars 1987)

Résumé—Afin de vérifier la part prise dans l'oxydation vanadique respectivement par les groupements étheroxyde et le doublet électronique de l'azote de benzylisoquinoléines, les auteurs ont étudiés l'oxydation sulfovanadique de l'iodométhylate de *p*-chlorobenzyl-4 diméthoxy-6,7 isoquinoléine. Dans le milieu réactionnel ont été identifiés des produits tels que les acides et aldéhydes *p*-chlorobenzoyques, le chloro-4 phényl-2 éthanone-2 ol-1, l'acide *p*-chlorophényl-3 propionique, l'acide *p*-chlorophényl-3 cétro-2 propionique, l'acide hydroxy-5 *p*-chlorobenzylidène-4 δ valérolactone-2 acétique et son ester méthylique, et l'acide *p*-chlorobenzyl-3 méthylamino-4 butène-2 oïque. En tenant compte de la structure chimique de ces molécules, une hypothèse de mécanisme réactionnel est proposée.

Des travaux récents ont pu mettre en évidence une oxydabilité accrue par le pentoxyde de vanadium des benzyl-4 isoquinoléines par rapport aux benzyl-1 isoquinoléines.¹ Il a ainsi pu être vérifié que le doublet électronique libre de l'azote, en formant des complexes initiaux avec le vanadium,²⁻⁵ joue un rôle prédominant dans l'oxydation de molécules azotées. Des modifications liées à l'acidité du milieu ont également pu être mises en évidence: au fur et à mesure de l'élévation de la concentration en ions hydrogène, le doublet de l'azote devient de moins en moins disponible pour former une liaison avec le vanadium. L'étude de l'oxydation vanadique d'un ammonium quaternaire: l'iodométhylate de *p*-chlorobenzyl-4 diméthoxy-6,7 isoquinoléine (I) a donc été réalisée pour déterminer l'influence de la complète indisponibilité du doublet de l'azote. Seul l'iodure (I) a pu être obtenu facilement par synthèse, les essais de formation du sulfate ou du méthylsulfate n'ayant donné aucun résultat.



PARTIE EXPERIMENTALE

Reactif

La solution sulfovanadique⁶ 0,1M en milieu acide sulfurique environ 0,72M est étalonnée par titrage avec une

solution de sulfate de fer et d'ammonium. La synthèse de l'iodométhylate I a été réalisée par addition d'un excès (2 fois) d'iodure de méthyle à une solution éthanolique de la base et chauffage à reflux. L'iodométhylate précipite et après séparation, est recristallisé dans l'éthanol ($F = 224^\circ$).

Mode opératoire d'oxydation

Dans une fiole jaugée de 50 ml sont introduits 50 à 100 μ l de l'iodure I, 30 ml de solution sulfovanadique puis soit, pour une réaction en milieu sulfurique 2,5M, 10 ml d'acide sulfurique 8M et un volume suffisant d'acide sulfurique 2,5M pour obtenir 50 ml soit, pour une réaction en milieu sulfurique 5M, 16 ml d'acide sulfurique 13M, et un volume suffisant d'acide sulfurique 5M pour obtenir 50 ml.

Le contenu de la fiole jaugée est transvasé dans un erlenmeyer surmonté d'un réfrigérant, puis placé dans un bain marie à 100°. La cinétique de la réaction est suivie par dosage du pentoxyde de vanadium. Pour cela, une partie aliquote du mélange réactionnel est prélevée à temps déterminé jusqu'à oxydation complète de la molécule, et l'excès de V_2O_5 est déterminé par titrage potentiométrique avec du fer(II) (électrodes platine et calomel).

Dosage des composés volatils

Le dioxyde de carbone et le formaldéhyde ont été identifiés et dosés par chromatographie en phase gazeuse selon la technique de l'espace de tête avec détection par ionisation de flamme après réduction dans un four à méthanation.⁷ L'appareil utilisé est un chromatographe en phase gazeuse Perkin-Elmer Sigma 3B.

Caractérisation des produits d'oxydation par couplage de la chromatographie en phase gazeuse à la spectrométrie de masse

Le milieu réactionnel a été extrait par l'éther, le solvant évaporé et le résidu analysé par la technique du couplage chromatographie en phase gazeuse-spectrométrie de masse (CG-SM). Le chromatographe, équipé d'une colonne capillaire en pyrex SE 30 de 25 m de long et de 0,3 mm de diamètre intérieur, est couplé à un spectromètre de masse Hewlett Packard HP 5992 B. Le débit d'hélium utilisé comme gaz vecteur est de 2 ml/min, la température de

l'injecteur est de 180°, celle du four est programmée de 100 à 280° (8°/min). La tension d'accélération du spectromètre de masse est de 1800 V et l'énergie d'impact électronique 70 eV.

RESULTATS ET DISCUSSION

Etude de l'influence des différents paramètres sur l'oxydation

De nombreux paramètres influencent la cinétique de la réaction: température, acidité et rapport oxydant/produit. Tous ces paramètres agissent dans le même sens que lors de l'oxydation de I. L'influence de l'acidité du milieu (acide sulfurique 2,5M ou 5M) ne se fait sentir qu'au niveau de la vitesse de la réaction qui est supérieure en milieu acide 5M. Le nombre de moles d'oxydant (VO_2^+) consommées par une mole d'iodure I est identique: $30 \pm 0,5$ pour 2,5M acide et 30 ± 3 pour 5M. La consommation d'oxydant est donc plus faible que pour la *p*-chlorobenzyl-4 diméthoxy-6,7 isoquinoléine, qui réduit 37 moles de VO_2^+ par mole.¹

Les dosages de I par chromatographie liquide montrent que sa disparition est complète respectivement en 30 min et en 3 hr pour les solutions sulfovanadiques 5M et 2,5M de ce composé.

CARACTERISATION ET DOSAGE DES PRODUITS D'OXYDATION

Dioxyde de carbone

En raison du blocage du doublet de l'azote et de la plus faible consommation en ions VO_2^+ , le nombre de molécules de dioxyde de carbone formées par mole d'iodométhylate est plus faible pour ce dernier que pour la base correspondante.¹ En effet, la valeur moyenne trouvée est de 5 moles de dioxyde de carbone par mole d'iodométhylate au lieu de 7 pour la base.

Formaldéhyde

Les résultats obtenus mettent en évidence l'oxydation des méthoxyles particulièrement réactifs dans ce cas. Comme pour l'étude des cinétiques de

réaction, on note une nette influence de la concentration en acide du milieu et par la suite, on constate que la concentration en formaldéhyde est maximale (0,4 mole/mole) après 3 hr en milieu 2,5M alors qu'elle n'est que de 0,2 mole/mole après 1 hr en milieu 5M.

*Acide et aldéhyde *p*-chlorobenzoiques*

L'aldéhyde et l'acide *p*-chlorobenzoiques, déjà mis en évidence lors de l'oxydation de la base¹ ont été identifiés par leur spectre de masse après séparation par chromatographie en phase gazeuse. Les temps de rétention sont respectivement de 2,3 et 6,8 min. Les spectres observés sont identiques à ceux reportés dans la littérature.¹

Chloro-4 phényl-2 éthanone-2 ol-1 2

Le composé élué avec un temps de rétention de 4,2 min présente un spectre de masse (Tableau 1) dont la fragmentation pour les masses inférieures à 140 est identique à celle de l'acide ou de l'aldéhyde *p*-chlorobenzoique. Le pic moléculaire ($m/z = 170$) subit une fragmentation classique des dérivés hydroxyméthylés⁸ avec formation des ions correspondant à la perte d'un radical OH^\cdot ($m/z = 153$) et CH_2 ($m/z = 139$).

*Acide *p*-chlorophényl-3 propionique 3*

Le spectre de masse de ce composé obtenu (Tableau 1) dont le $t_R = 6,24$ min est caractéristique des dérivés chlorobenzylés et des acides carboxyliques.⁸ Comme pour la majorité des acides carboxyliques aliphatiques, le pic moléculaire ($m/z = 184$) est peu abondant. Le pic le plus caractéristique, $m/z = 60$, provient d'une migration d'hydrogène. Les pics à $m/z = 156$ et 139 correspondent à la perte des groupements CO et COOH respectivement. La chaîne latérale subit une coupure benzylique avec une formation d'un chlorotropylium ($m/z = 125$). La perte d'une molécule d'acide chlorhydrique donne un pic $M - 36$ ($m/z = 89$) classiquement observé dans ce cas. L'ion à $m/z = 63$ résulte de l'élimination d'une molécule d'acétylène de l'ion tropylium ($m/z = 44$).⁹

Tableau 1. Principales fragmentations des composés fournis lors d'oxydation sulfovanadique de l'iodométhylate de PV₂†

Composé	m/z (abondance relative)
2	75(26), 111(57)*, 139(100)*, 153(13)*, 170(21)*
3	60(12), 63(12), 89(21), 125(100)*, 139(6)*, 156(5) 184(23)*
4	63(5), 89(6), 125(100)*, 198(21)*
5	52(20), 59(59), 63(28), 89(89), 123(17)*, 124(43)* 127(10)*, 251(100)*, 310(85)*
6	63(6), 89(10), 125(100)*, 181(6)*, 194(5)*, 239(8)*
7	52(25), 59(6), 63(36), 89(57), 123(8)*, 124(19)*, 127(81)*, 251(81)*, 296(100)*

*Les fragments chlorés sont suivis d'un astérisque afin de ne pas alourdir outre mesure le tableau en donnant les fragments et abondances isotopiques dues au ³⁷Cl.

†Seules les abondances supérieures ou égales à 5% ont été prises en considération.

Acide *p*-chlorophényl-3 céto-2 propionique 4

Le spectre de masse obtenu pour le composé élué à 6,2 min (Tableau 1) présente une fragmentation très proche de celle observée pour le composé précédent. Les pics à $m/z = 125$, 89 et 63 permettent de conclure à une structure chlorobenzyle. L'identification de la chaîne latérale est liée à la présence d'un pic moléculaire peu abondant ($m/z = 198$), et de pics correspondant à la perte des groupements COOH ($m/z = 153$) et CO-COOH ($m/z = 125$), caractéristiques des acides α -cétoniques.⁸ Le pic à $m/z = 125$ correspond à l'ion tropylium précédemment décrit.

Ester méthylique de l'acide hydroxy-5 *p*-chlorobenzylidène-4 δ -valérolactone-2 acétique 5

Au temps de rétention 13,2 min nous avons obtenu un spectre dont les principales fragmentations permettent d'envisager une structure correspondant à l'ester méthylique de l'acide hydroxy-5 *p*-chlorobenzylidène-4 δ -valérolactone-2 acétique. La fragmentation initiale correspond à la perte d'un groupement H₃CO-CO ($m/z = 59$); l'ion de $m/z = 251$ constitue le pic de base. Cet ion est ensuite coupé en deux entités ($m/z = 127$, 124) qui subissent une fragmentation propre (Schéma 1).

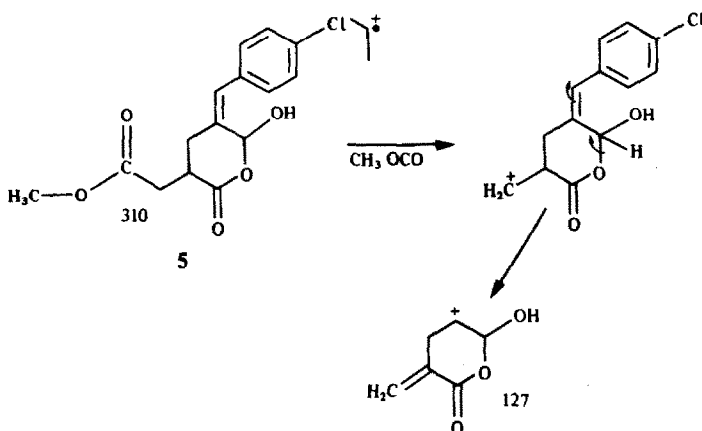


Schéma 1

L'ion de $m/z = 124$ va conduire à un intermédiaire chlorotropylium ($m/z = 123$) qui donne ultérieurement l'ion $m/z = 89$. L'ion $m/z = 127$ perd dans un premier temps le groupement hydroxyle ($m/z = 110$) puis un méthylène ($m/z = 96$). Le fragment lactonique se décarboxyle ensuite pour donner¹⁰ un ion de masse 52 (Schéma 2).

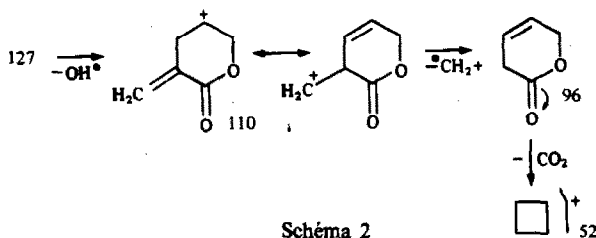


Schéma 2

Acide *p*-chlorobenzyl-3 méthyl amino-4 butène-2 oïque 6

Le composé élué en 14,1 min présentant un pic moléculaire de masse 239 a été identifié comme l'acide *p*-chlorobenzyl-3 méthyl amino-4 butène-2 oïque (Tableau 1). On observe un pic de base de faible abondance à $m/z = 239$ et une fragmentation correspondant à la structure chloro-4 benzylique ($m/z = 125$, 89, 63) et acide ($m/z = 195$, 194). La perte d'une masse 58 par l'ion moléculaire ($m/z = 181$) peut être attribuée aux fragments $\cdot\text{CH}_2\text{-NH-CH}_3$ et $\cdot\text{CH-COOH}$ (Schéma 3).

Acide hydroxy-5 *p*-chlorobenzylidène-4 δ -valérolactone-2 acétique 7

Ce composé élué en 15,6 min a été facilement identifié grâce à l'étude préalablement réalisée pour l'ester méthylique de l'acide correspondant 5. Son spectre de masse (Tableau 1) présente effectivement une analogie profonde avec ce composé. La différence de 14 unités de masse correspond au remplacement du groupement méthyle par un hydrogène acide. Seules les abondances relatives sont différentes de

celles observées pour l'ester méthylique (pour les masses inférieures à 296).

PROPOSITION D'UN MECANISME REACTIONNEL

Les structures établies précédemment permettent de proposer un mécanisme réactionnel pour l'oxydation sulfovanadique de l'iodométhylate du PV₂.

Oxydation du méthoxyle en 6 (Schéma 4)

Le doublet électronique de l'azote étant bloqué par la formation d'un ammonium quaternaire, n'est de ce fait plus disponible pour une éventuelle formation du

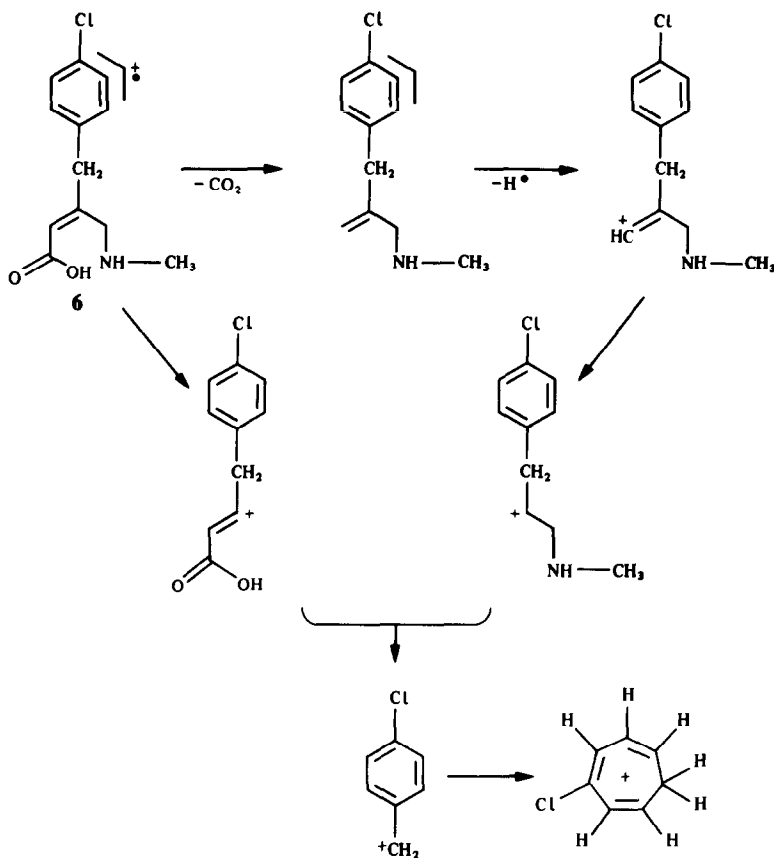


Schéma 3

complexe vanadique initial. Seule reste possible une réaction de l'ion VO_2^+ au niveau de l'un des doublets libres des oxygènes des groupements méthoxylés. Des deux méthoxyles en 6 et 7, il est vraisemblable que c'est le méthoxyle en 6, celui qui est conjugué avec l'azote quaternaire, qui subit une rupture homolytique pour conduire à un intermédiaire de type semiquinonique⁸ par perte d'un radical méthyle. Ce dernier réagit avec l'eau pour former du méthanol qui subit ensuite l'oxydation classique avec consommation de 4 équivalents de vanadium. Les groupements carbonylés sont connus pour réagir facilement avec le vanadium pentavalent et *à fortiori* un radical déjà plus oxydé. La réaction se poursuit donc à ce niveau avec rupture de la liaison carbonée en 6-7 et formation d'un acide ester 10.

Or les acides éthyléniques sont susceptibles d'être oxydés par les solutions vanadiques comme le montrent Morette *et al.*¹¹ dans le cas de l'acide oléique. *A fortiori*, il est possible d'envisager cette réaction pour un acide α -éthylénique dans lequel la conjugaison peut renforcer cette oxydabilité. Il se forme sans doute un aldéhyde 11 qui est oxydé ensuite en acide 12.

Formation du dialdéhyde 13 (Schéma 5)

La formation de ce dialdéhyde fait correspondre l'ouverture de la partie hétérocyclique de l'ion iso-

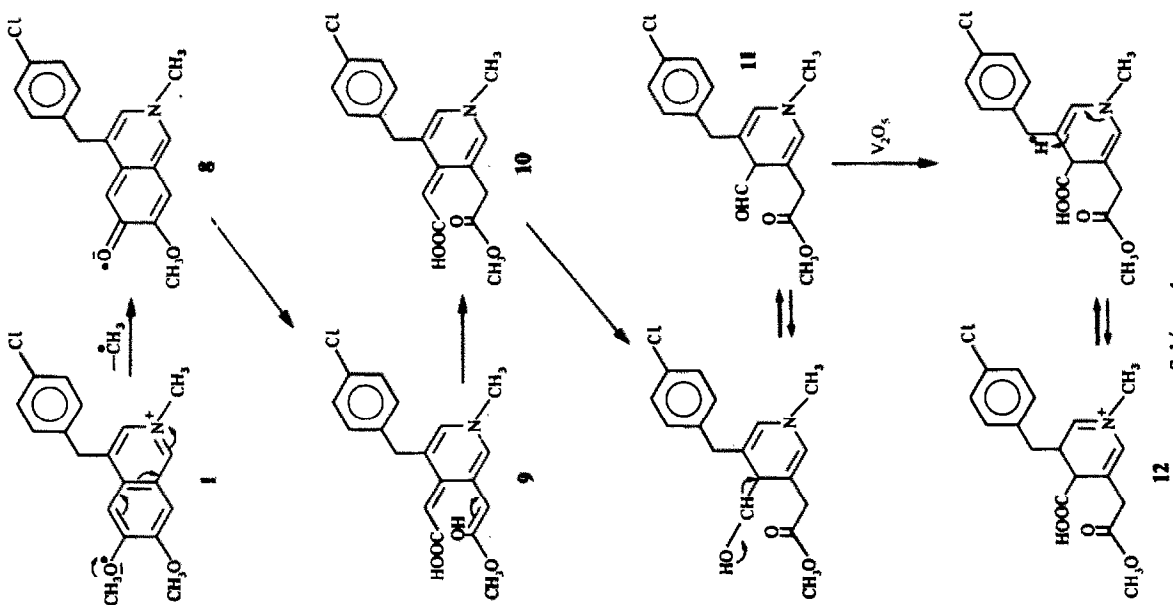
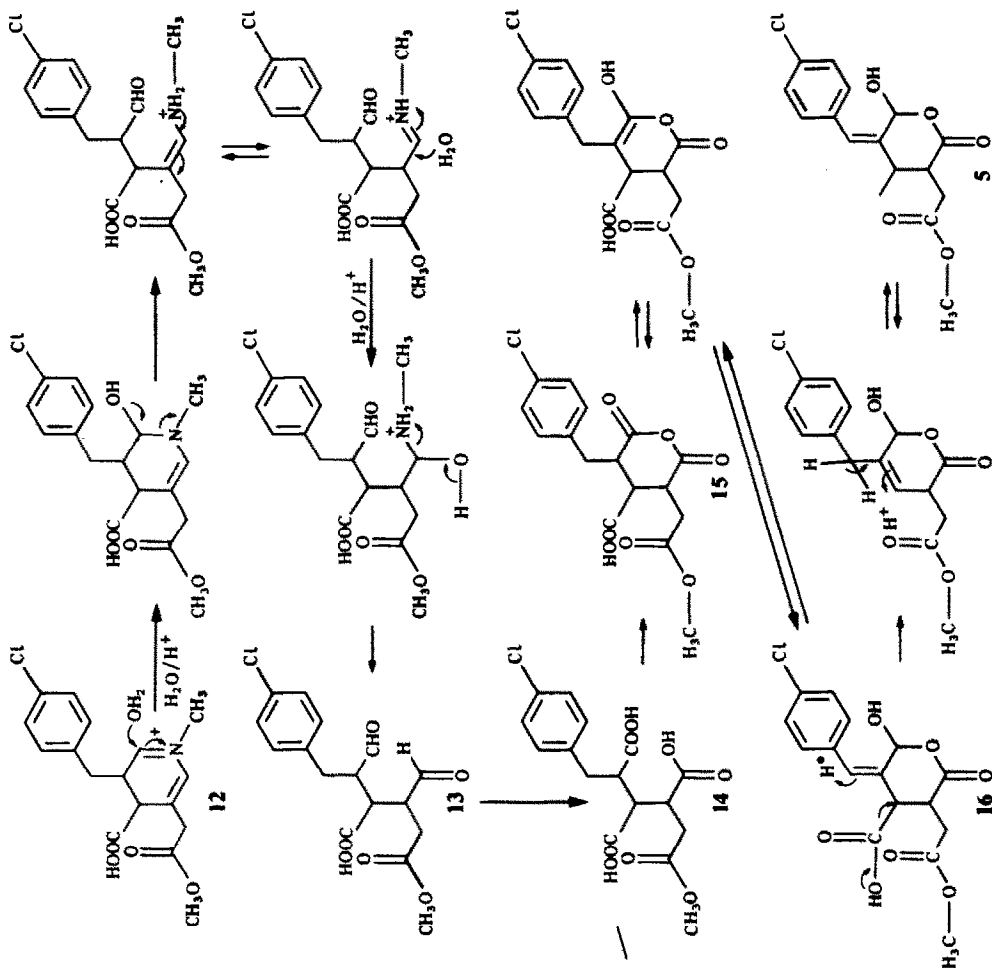
quinolénum 12 par une hydrolyse acide, ainsi que nous le proposons sur le Schéma 5.

Le dialdéhyde 13 ainsi formé s'oxyde de nouveau en diacide correspondant 14, qui s'anhydride partiellement 15 puis perd le groupement carboxylique de l'acide β -éthylénique intermédiairement formé 16. Ceci conduit à l'ester méthylique de l'acide hydroxy-5 *p*-chlorobenzylidène-4 δ -valérolactone-2 acétique 5 et, par hydrolyse à l'acide correspondant, 7, qui ont tous deux été isolés.

Formation de l'acide méthylamino-4 butène-2 oïque substitué 6

La conjugaison avec le carbonyle de la diénamine 12 permet d'expliquer la formation de cet acide (Schéma 6).

L'aldéhyde 17, comme dans l'hypothèse précédente, s'oxyde en acide carboxylique correspondant 18 dont la décarboxylation, ainsi que l'oxydation de la liaison ester déjà décrites conduisent au diacide 19. Contrairement à l'acide succinique, l'acide méthylsuccinique est oxydé par le pentoxyde de vanadium, et il est donc tout à fait logique que des structures de type $\text{HOOC-RCH-CH}_2\text{-COOH}$ s'oxydent dans de telles conditions. Le produit ultime obtenu est l'acide *p*-chlorobenzyl-3 méthyl amino-4 butène-2 oïque 6 qui a, lui aussi, été identifié comme intermédiaire d'oxydation.



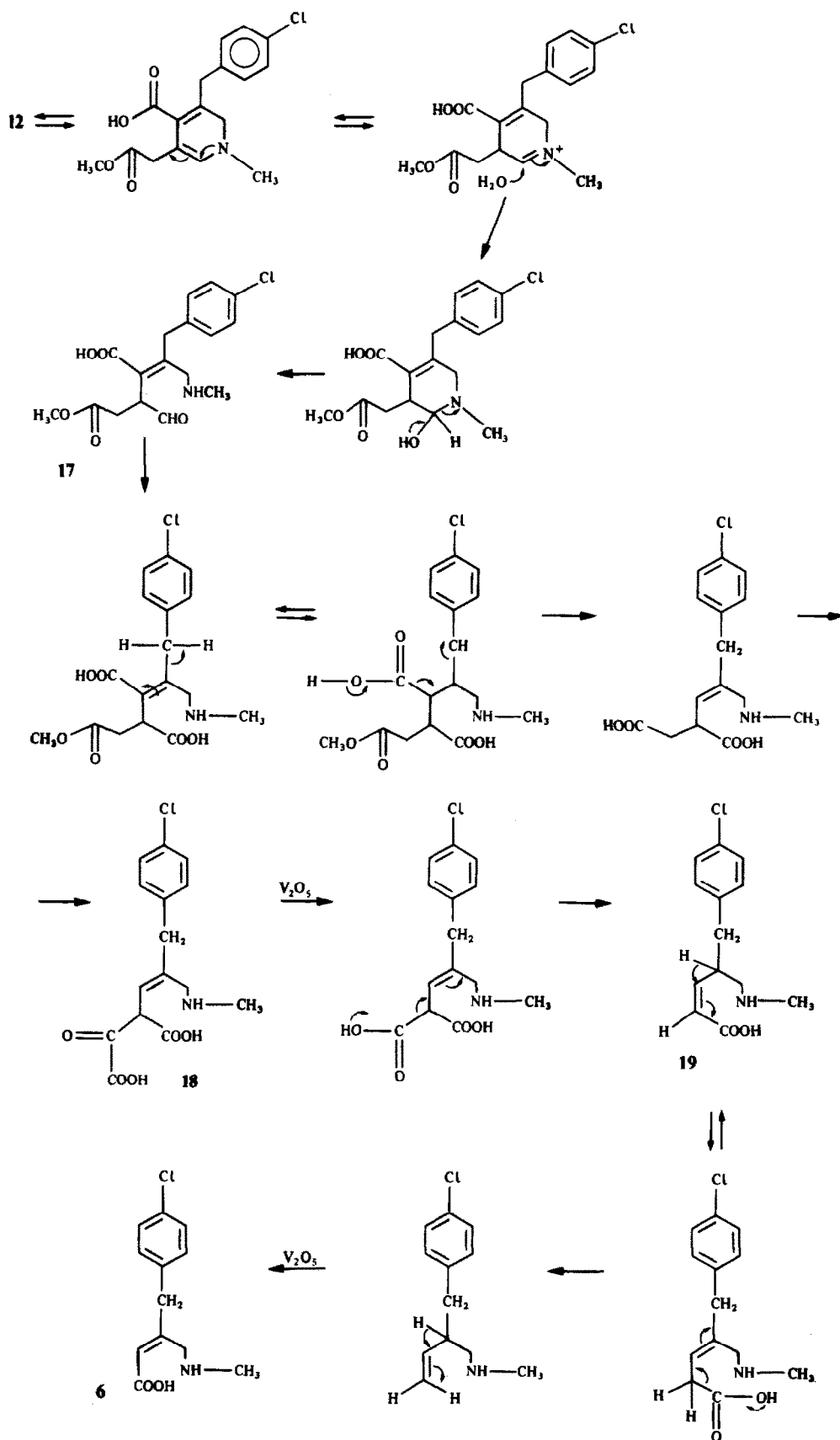


Schéma 6

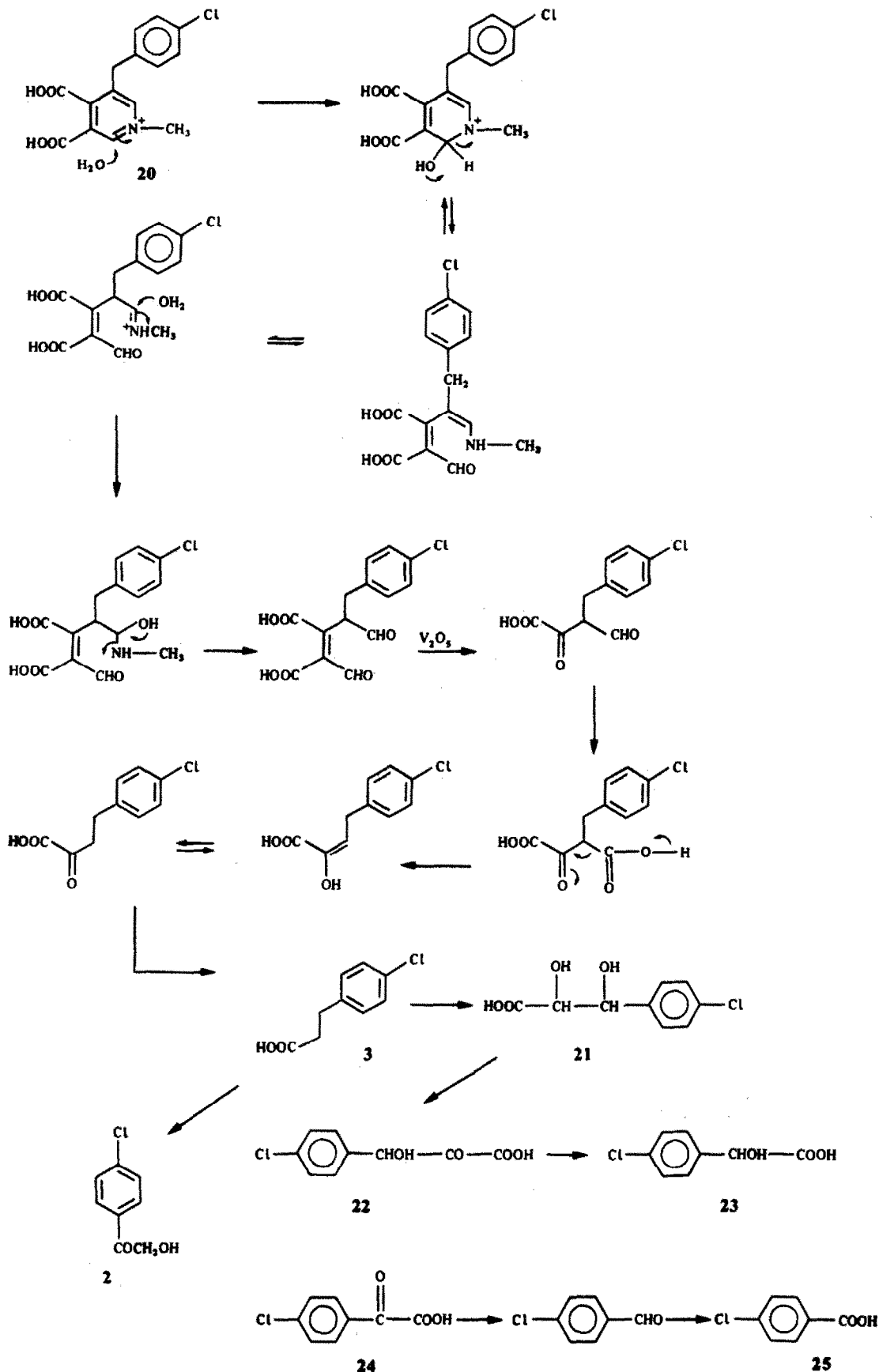


Schéma 7

Oxydation concomitante des deux méthoxyles

L'hypothèse de l'oxydation concomitante des deux méthoxyles conduit comme nous l'avons noté précédemment à la formation d'un acide pyridine dicarboxylique **20** qui, ensuite, subit une oxydation analogue à celle que nous avons mise en évidence (Schéma 7). L'acide *p*-chlorophényl-3 propionique **3** s'oxyde à son tour en un acide chlorocinnamique. La double liaison peut s'oxyder entraînant, comme dans l'oxydation permanganique, la formation d'un α -glycol **21**. Celui-ci peut s'oxyder soit au niveau du carbone 2, soit au niveau du carbone 3. Dans le cas de l'oxydation en 2 il y a formation d'un acide cétonique β -hydroxylé **22** qui subit une oxydation, au niveau de la liaison céto acide en donnant l'acide carboxylique hydroxylé **23**, puis l'acide α -cétonique **24**, et enfin l'acide *p*-chlorobenzoïque **25**, ultime étape de l'oxydation.

Une oxydation en 3 est également plausible, compte tenu du caractère électroattracteur du carboxyle et du caractère donneur du chlore diminuant l'électrophilie du noyau. Elle conduirait à un acide α -cétonique se décarboxylant spontanément en α -cétol **2** qui a été isolé. En effet, les cétols primaires sont beaucoup plus oxydables que les céto acides.¹²

L'oxydation de l'acide *p*-chlorocinnamique peut également conduire à la formation de l'acide *p*-chlorophényl-3 céto-2 propionique également mis en évidence **4**.

CONCLUSION

Les résultats obtenus comparés à ceux mis en évidence dans l'oxydation du PV₂¹ témoignent d'une

oxydation moindre de ce composé dérivé ammonium quaternaire, dans lequel aucune disponibilité de l'azote n'est initialement envisageable. L'isolement de produits d'oxydation possédant un nombre d'atomes de carbone nettement supérieur à celui de l'acide succinique¹ confirme le rôle secondaire mais non négligeable du doublet libre de l'azote lors de l'oxydation vanadique.

LITTÉRATURE

1. E. Postaire, M. Tsitini-Tsamis, M. Hamon et C. Viel, *Talanta*, 1983, **30**, 193.
2. B. Galeffi et M. Postel, *Nouv. J. Chim.*, 1984, **8**, 481.
3. S. Miyake, K. Saitoh et N. Suzuki, *Chromatographia*, 1985, **20**, 417.
4. F. Preuss, E. Fuchslocher et W. S. Sheldrick, *Z. Naturforsch.*, 1985, **40b**, 363.
5. G. Schmid, D. Kampmann, W. Meyer, R. Boese, P. Paetzold et K. Delpy, *Chem. Ber.*, 1985, **118**, 2418.
6. M. J. Waechter, J. Likforman et M. Hamon, *Analisis*, 1977, **5**, 34.
7. E. Postaire, J. E. Hila, A. Assamoi, D. Pradeau, C. Dauphin et M. Hamon, *ibid.*, 1985, **13**, 463.
8. H. Budzikiewicz, C. Djerassi et D. Williams, *Interpretation of Mass Spectra of Organic Compounds*, Holden Day, San Francisco, 1964.
9. R. M. Silverstein, G. C. Bassler et T. C. Morill, *Spectrometric Identification of Organic Compounds*, Wiley, New York, 1981.
10. Q. N. Porter, *Mass Spectrometry of Heterocyclic Compounds*, p. 263. Wiley, New York, 1985.
11. A. Morette et G. Gaudefroy, *Bull. Soc. Chim. France*, 1954, 956.
12. Vinh Chon Thanh, *Thèse de doctorat*, Université Paris Sud, 1973.

SHORT COMMUNICATIONS

A WET CHEMICAL METHOD FOR THE ESTIMATION OF CARBON IN URANIUM CARBIDES

V. CHANDRAMOULI, R. B. YADAV and P. R. VASUDEVA RAO

Radiochemistry Programme, Indira Gandhi Centre for Atomic Research, Kalpakkam 603 102, India

(Received 26 March 1986. Revised 25 March 1987. Accepted 10 April 1987)

Summary—A wet chemical method for the estimation of carbon in uranium carbides has been developed, based on oxidation with a saturated solution of sodium dichromate in 9M sulphuric acid, absorption of the evolved carbon dioxide in a known excess of barium hydroxide solution, and titration of the excess of barium hydroxide with standard potassium hydrogen phthalate solution. The carbon content obtained is in good agreement with that obtained by combustion and titration.

The conventional procedure for the determination of carbon in uranium carbides involves combustion of the carbide in a stream of oxygen at about 900° and estimation of the evolved carbon dioxide by manometric,¹ gas chromatographic,² conductometric³ or gravimetric⁴⁻⁶ methods. As part of a programme on the development of wet chemical methods for the characterization of nuclear fuel materials, a detailed study of the oxidation of uranium carbide with different oxidizing agents was undertaken to evolve a procedure for the estimation of carbon in uranium carbides.

550 mm, bore 6 mm, filled with barium hydroxide solution to a height of about 250 mm; the absorption tube contains some glass beads to increase the absorption efficiency.

Reagents

Tungsten carbide was obtained from Powder Metals and Alloys Ltd., Bombay. Uranium carbide was prepared by reduction of uranium dioxide with carbon at 1600° in a molybdenum-wire resistance furnace. The products obtained were characterized by X-ray diffractometer. All other chemicals used were of analytical grade.

A saturated solution of sodium dichromate (~90 g/l) was prepared in sulphuric acid (1 + 1). A standard solution of potassium hydrogen phthalate was prepared by dissolving an accurately weighed amount of potassium hydrogen phthalate in distilled water. Barium hydroxide solution (~0.25M) was prepared by dissolving solid barium hydroxide in boiling water, cooling and filtering off any residue. This solution was standardized by titration with the standard potassium hydrogen phthalate solution, with phenolphthalein as indicator.

EXPERIMENTAL

A schematic diagram of the apparatus used is given in Fig. 1. The carbon dioxide is absorbed in a tube of height

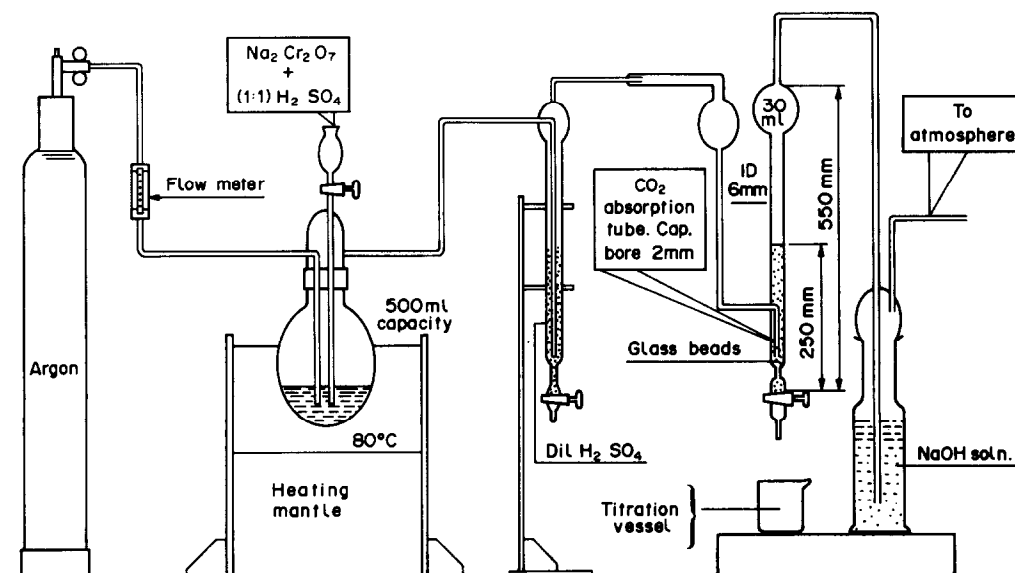


Fig. 1. Apparatus for the wet chemical method.

Table 1. Carbon* in a UC/UC₂ mixture determined by use of sodium dichromate in sulphuric acid, as a function of acid concentration

3M H ₂ SO ₄		6M H ₂ SO ₄		9M H ₂ SO ₄	
Carbide, mg	Carbon found, %	Carbide, mg	Carbon found, %	Carbide, mg	Carbon found, %
38.80	1.47	44.41	3.73	25.37	5.76
39.55	1.75	56.33	3.96	43.71	5.83
72.41	1.57	69.16	3.24	64.24	5.75

*Carbon found by combustion method $5.83 \pm 0.11\%$.

Procedures

Wet chemical oxidation. An accurately weighed amount (40–80 mg) of uranium carbide was transferred into the round-bottomed flask (Fig. 1), 15 ml of the saturated sodium dichromate solution were added and the flask was heated at $\sim 90^\circ$ for 30 min, the carbon dioxide evolved being swept by argon (flow-rate 25 ml/min) through a trap containing a very dilute solution of sulphuric acid into a known excess of barium hydroxide solution in the absorption tube. The excess of barium hydroxide was titrated with standard potassium hydrogen phthalate solution, with phenolphthalein as indicator.

Combustion method. An accurately weighed amount (about 50 mg) of calcium carbonate or tungsten carbide or uranium carbide was transferred into a clean and dry silica boat, and loaded into a quartz combustion tube, then heated in a stream of oxygen (flow-rate 25 ml/min) at 900° (resistance furnace). The carbon dioxide evolved was absorbed and estimated as above.

RESULTS AND DISCUSSION

Combustion method

Calcium carbonate was used to standardize the combustion method. The carbon content found (12 replicates) was 12.03%, standard deviation 0.09%, corresponding to a recovery of $100.3 \pm 0.8\%$. The carbon content of the tungsten carbide was determined in order to check the standardization. The value found (6 replicates) was 6.01%, s.d. 0.07%, the theoretical value being 6.1%.

Wet chemical method

The effect of different oxidizing agents such as potassium permanganate, potassium dichromate and ceric sulphate, all in sulphuric acid medium, was studied. When oxidation was attempted by adding solid potassium permanganate followed by concentrated sulphuric acid, the permanganate sublimed on warming, and this method was therefore unsuitable.*

The solubility of ceric sulphate, even in 6M sulphuric acid, is low, and even a saturated solution gave very low recovery of carbon (only 5% of the expected value).

Treatment of uranium carbide with solid potassium dichromate and a 1:1 v/v mixture of concen-

trated phosphoric acid and sulphuric acid gave $4.12 \pm 0.10\%$ carbon (5 replicates, mean \pm s.d.), which agreed well with the value obtained by the combustion method ($4.13 \pm 0.07\%$). (The particular sample used was an old batch, and contaminated with oxygen, hence the lower carbon content.) However, the separate addition of the reagents was cumbersome. Potassium dichromate solution in sulphuric acid was tried, but the solubility of potassium dichromate in concentrated sulphuric acid is low, and use of potassium dichromate solution in 6M and 12M sulphuric acid gave only 64% and 34% recovery respectively. This approach was therefore also unsuitable.

The solubility of sodium dichromate is high even in concentrated sulphuric acid, hence quantitative oxidation was obtained with sodium dichromate solution in sulphuric acid. The carbon content found for a UC/UC₂ mixture with this reagent was $4.92 \pm 0.08\%$ (5 replicates) which compared well with the values obtained by the combustion method ($4.91 \pm 0.07\%$, 5 replicates).

The effect of the sulphuric acid concentration on the recovery was studied. The results are given in Table 1 and clearly show that the higher the acid concentration, the more complete the recovery of the carbon as carbon dioxide. With 8M sulphuric acid medium the carbon recovery was only 95–96%, but was quantitative with $\geq 9M$ sulphuric acid.

CONCLUSIONS

Of all the oxidizing agents tried, sodium dichromate was found to be the most suitable, owing to its high solubility even in concentrated sulphuric acid. This oxidizing mixture may be used for determining carbon (present as organic compounds) in solutions of uranium carbide dissolved in concentrated nitric acid, and also for determining carbon in organic compounds.⁷ The sulphuric acid concentration used must be at least 9 M.

*WARNING: Mixtures of potassium permanganate and concentrated sulphuric acid yield manganese heptoxide, Mn₂O₇, which is extremely explosive, and should never be heated [Ed.].

Acknowledgements—The authors are thankful to Dr. C. K. Mathews, Head, Radiochemistry Programme, Indira Gandhi Centre for Atomic Research, Kalpakkam for his encouragement and keen interest in this work.

REFERENCES

1. D. Crossley and G. Philips, *UKAEA Rep.*, AERE-3790, 1961.
2. P. S. Sankaran, N. Balachander, Y. S. Sayi, P. Venkataramana and P. R. Natarajan, *Z. Anal. Chem.*, 1983, **315**, 496.
3. G. H. Rizvi, P. R. Sethuraman, P. Venkataramana and P. R. Natarajan, *BARC/I-348*, 1975, Bhabha Atomic Research Centre, Trombay.
4. H. J. Kavanaugh, J. W. Dehlby and A. P. Lovell, *Los Alamos Rept.* LA-7981, 1979.
5. W. C. Dietrich, *Report*, No. Y-1456, Nuclear Technology Chemistry and Chemical Engineering, Union Carbide Corporation, Nuclear Division, 1964.
6. V. K. Manchanda and M. S. Subramaniam, *Z. Anal. Chem.* 1978, **290**, 302.
7. D. D. Van Slyke, *Anal. Chem.* 1954, **26**, 1706.

SPECTROPHOTOMETRIC AND TITRIMETRIC DETERMINATION OF CATECHOLAMINES

FATMA BASYONI SALEM*

Faculty of Pharmacy, Mansoura University, Mansoura, Egypt

(Received 21 December 1984. Revised 16 March 1987. Accepted 3 April 1987)

Summary—Ammonium metavanadate is used to determine adrenaline, noradrenaline, isopropylnoradrenaline and methyl dopa by titrimetric and photometric procedures. Oxidation of these catecholamines produces aminochrome derivatives which can be measured spectrophotometrically at 485 nm. Beer's law is obeyed over the ranges 0.09–0.90 mg for adrenaline, 0.07–0.65 mg for noradrenaline, 0.07–0.75 mg for isopropylnoradrenaline and 0.10–0.95 mg for methyl dopa.

A variety of methods have been used for determination of catecholamines in pharmaceutical dosage forms, including titrimetry, spectrofluorometry, gas chromatography and polarography.¹⁻⁵

The methods (spectrophotometric and titrimetric) described in this paper depend on oxidation of the catecholamines with ammonium metavanadate in acid medium.

1 mg of catecholamine in a 10-ml standard flask; add 0.5–1 ml of 0.02M ammonium vanadate, dilute to the mark with 0.01M acetic acid, and let stand for 20–25 min. Measure the absorbance at 485 nm against a blank prepared in the same way; construct calibration graphs covering the ranges 0.09–0.90 mg for adrenaline, 0.07–0.65 mg for noradrenaline, 0.07–0.75 mg for isopropylnoradrenaline hydrochloride and 0.1–0.95 mg for methyl dopa.

Assay of pharmaceutical dosage forms. Apply the procedures above to sample solutions prepared as instructed in the B.P.⁷ and U.S.P.⁸

EXPERIMENTAL

Reagents

Ammonium metavanadate solution, 0.02M, prepared by dissolving 2.34 g of NH_4VO_3 in water and diluting to 1 litre, and standardized iodometrically.⁶

Standard solutions, 0.02M, of adrenaline, noradrenaline, methyl dopa and isopropylnoradrenaline hydrochloride were freshly prepared by dissolving 3.67, 3.38, 4.77 and 4.04 g respectively in 1 litre of 0.01M acetic acid.

Procedures

Direct titration. Transfer an accurately measured volume of solution containing 1.0–38 mg of catecholamine into a 100-ml beaker, add 15 ml of concentrated hydrochloric acid and dilute to about 50 ml with distilled water. Add 3 drops of indicator and titrate with 0.02M ammonium vanadate (magnetic stirring is recommended) until the indicator colour is discharged. Titrate a blank under the same conditions. Alternatively, detect the end-point potentiometrically, with platinum and calomel electrodes.

Indirect titration. Add a known volume of sample solution containing 1.0–38 mg of catecholamine to a measured and excessive volume of 0.02M ammonium vanadate in an iodine flask. Add 15 ml of concentrated hydrochloric acid, dilute to 50 ml with distilled water, add 10 ml of 20% potassium iodide solution and titrate the liberated iodine with 0.02M sodium thiosulphate, using starch as indicator. Titrate a blank in the same way.

Spectrophotometric determination. Place an accurately measured volume of sample solution equivalent to about

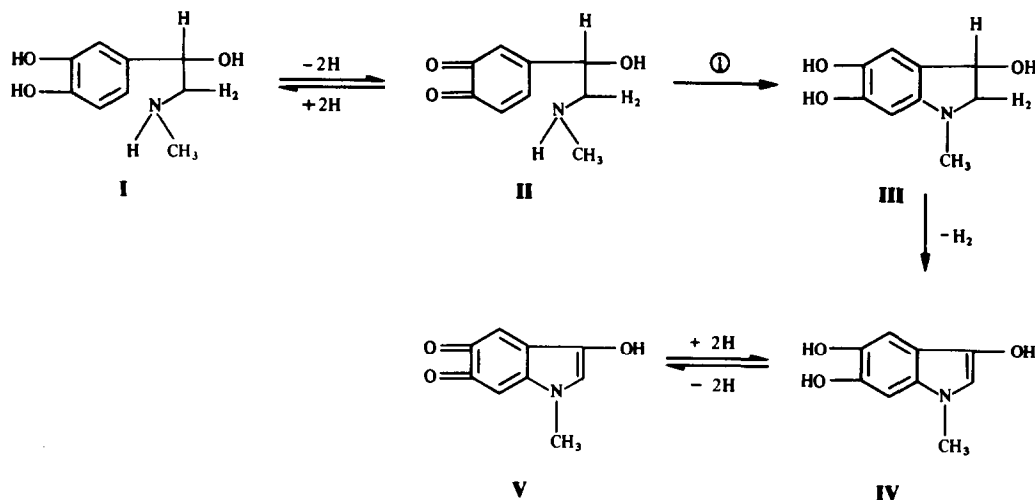
RESULTS AND DISCUSSION

Table 1 gives the results of titrimetric and spectrophotometric determination of the four catecholamines tested. Methyl Red, Methyl Orange, indigotine and amaranth were used as indicators, and gave a very sharp change at the equivalence point, being oxidized by the first excess of titrant. The potentiometric titration also gives good results but is slow, taking 20–30 min for completion, because of the slow equilibration of the electrodes. Heating to accelerate the procedure gives rise to errors because catecholamines are easily decomposable by heat.^{9,10} The main advantage of the potentiometric method is its applicability to catecholamine solutions of high concentration, which are difficult to titrate with use of visual indicators, because they are highly coloured.

The catecholamines are oxidized to the corresponding aminochromes, and the equivalence point in the titration corresponds to the reaction of 4 moles of ammonium vanadate per mole of catecholamine; the reaction can be expressed by Scheme 1.

The absorption spectra of the catecholamines show an absorption maximum at 280 nm. Oxidation by ammonium vanadate yields two absorption maxima, at 300 and 485 nm, owing to the production of aminochrome derivatives (Fig. 1). The reaction in acetic acid medium is slow, but although the reaction

*Present address: Department of Chemistry, College of Science, Girls Colleges General Adm. In Dammam, Dammam P.O. Box 838, Saudi Arabia 31113.



Scheme 1. Possible oxidation products of adrenaline (I). The products shown are adrenoquinone (II); leucoadrenochrome (III); 3,5,6-trihydroxy-1-methylindole (IV) and its *o*-quinone state (V) postulated by Harley-Mason.⁹

Table 1. Determination of catecholamines

Taken, mg	Recovery \pm standard deviation,* %				Purity by standard method \pm s.d. %
	Visual titration	Potentiometric titration	Back-titration	Spectrophotometry	
Adrenaline	1.8-36.0 0.09-0.90	99.4 \pm 0.3	99.4 \pm 0.3	99.4 \pm 0.2	99.4 \pm 0.4 99.4 \pm 0.1
Noradrenaline	1.7-30.4 0.07-0.65	98.9 \pm 0.2	98.9 \pm 0.3	98.9 \pm 0.3	98.9 \pm 0.3 98.9 \pm 0.2
Isopropylnoradrenaline	1.3-37.2 0.08-0.74	98.9 \pm 0.3	98.9 \pm 0.3	98.9 \pm 0.2	98.9 \pm 0.2 98.9 \pm 0.2
Methyldopa	2.2-38.2 0.10-0.95	98.9 \pm 0.2	98.9 \pm 0.2	98.9 \pm 0.2	98.9 \pm 0.2 98.9 \pm 0.2

*For each catecholamine ten evenly spaced amounts in the stated range were analysed by the method stated, each amount 6 times for the titrimetric methods and 10 times by spectrophotometry. The standard deviation quoted is the highest for the given series.

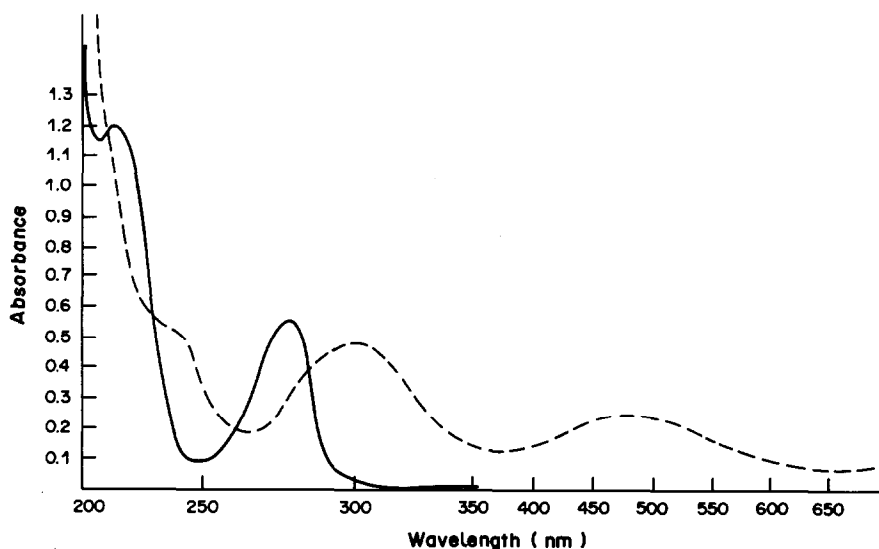


Fig. 1. (—) Absorption spectrum of adrenaline in acetic acid. (---) Absorption spectrum of adrenaline in presence of ammonium vanadate.

Table 2. Determination of catecholamines in pharmaceuticals

Sample*	Catecholamine content	Recovery \pm standard deviation, † %				Standard method
		Visual titration	Potentiometric titration	Back-titration	Spectrophotometry	
1. Adrenaline ampoules	Adrenaline 1mg/ml	99.0 \pm 0.2	99.0 \pm 0.3	99.0 \pm 0.2	99.0 \pm 0.5	99.4 \pm 0.2
2. Epiphrin ophthalmic solution	Adrenaline 2% of base	99.0 \pm 0.1	99.9 \pm 0.2	99.0 \pm 0.3	98.9 \pm 0.3	99.2 \pm 0.3
3. Artenerol ampoules	Noradrenaline 1 mg/ml	98.6 \pm 0.2	98.6 \pm 0.3	98.6 \pm 0.2	98.6 \pm 0.2	98.6 \pm 0.2
4. Prenasma tablets	Isoprenaline sulphate§ 20.0 mg/tablet	98.0 \pm 0.1	98.1 \pm 0.3	98.0 \pm 0.5	97.9 \pm 0.6	98.1 \pm 0.3
5. Aleudrin tablets	Isoprenaline sulphate 20.0 mg/tablet	98.1 \pm 0.3	98.2 \pm 0.3	98.0 \pm 0.2	98.2 \pm 0.2	98.3 \pm 0.3
6. Aldomet tablets	Methyldopa 250 mg/tablet	98.7 \pm 0.2	98.9 \pm 0.3	98.7 \pm 0.1	98.7 \pm 0.5	98.7 \pm 0.0,

*1,4, Misra, Egypt; 2, Allergan Pharmaceuticals; 3, Hoechst; 5, Boehringer; 6, Merck, Sharp & Dohme.

†Calculated relative to the nominal content.

§Isopropylnoradrenaline sulphate.

sequence is complicated the absorbance remains constant over a 10-min period, between 20 and 30 min after preparation of the solution. Beer's law is obeyed at 485 nm. The *N*-haloimides have been used as the oxidant in an analogous spectrophotometric method (at pH 7.4)¹.

The aminochromes produced were characterized by thin-layer chromatography, with a butanol-acetic acid-water mixture.¹¹

The methods have been applied to the analysis of commercial preparations and typical results are given in Table 2.

REFERENCES

1. A. A. Abou Ouf, W. I. Mohamed and F. B. Salem, *Analyst*, 1981, **106**, 949.
2. S. Honda, Y. A. Araki, M. Takahashi and K. Kakehi, *Anal. Chim. Acta*, 1983, **149**, 297.
3. A. E. Ciarlone, B. W. Fry and R. L. Parker, *Microchem. J.*, 1981, **26**, 436.
4. B. Y. Lin and K. L. Cheng, *Anal. Chim. Acta*, 1980, **120**, 335.
5. M. A. Korany and A.-A. M. Wahbi, *Analyst*, 1979, **104**, 149.
6. A. I. Vogel, *Text-Book of Quantitative Inorganic Analysis*, 3rd Ed., p. 381. Longmans, London, 1961.
7. *British Pharmacopoeia, 1973 and 1980*, HMSO, London.
8. *United States Pharmacopoeia XX and National Formulary XV*, United States Pharmacopoeial Convention, Washington, 1980.
9. J. Harley-Mason, *J. Chem. Soc.*, 1950, 1276.
10. N. A. El-Rabbat and N. M. Omar, *J. Pharm. Sci.*, 1978, **67**, 779.
11. E. Stahl, *Thin-Layer Chromatography*, 2nd Ed., p. 499. Allen & Unwin, London, 1969.

THE URANIUM-XYLIDYL BLUE I COMPLEX AND ITS APPLICATION IN LINEAR SWEEP POLAROGRAPHY

ZAOFAN ZHAO, XIAOHUA CAI and PEIBIAO LI

Department of Chemistry, University of Wuhan, Wuhan, People's Republic of China

(Received 16 October 1986. Revised 1 December 1986. Accepted 3 April 1987)

Summary—The linear sweep polarographic wave of the uranium–Xylidyl Blue I complex in ethylenediamine–1,10-phenanthroline–hydrochloric acid medium has been studied. The complex, corresponding to $\text{UO}_2(\text{XBI})_2^{2-}$ with $\log \beta' = 9.09$ (by polarography), 8.81 (by spectrophotometry), is strongly adsorbed on the surface of the mercury electrode. The polarographic wave is attributed to the reduction of Xylidyl Blue I in the complex. The method is very sensitive with a detection limit of $3 \times 10^{-8} M$. The wave height is proportional to the concentration of uranium over the range 8×10^{-8} – $7 \times 10^{-6} M$. Solvent extraction is used to separate possible interferences. The recommended procedure has been applied to the determination of trace amounts of uranium in ores.

In our previous paper,¹ the linear sweep polarography (LSP) of the thorium complex with Xylidyl Blue I (XBI) was reported: this paper deals with the LSP of the uranium–XBI complex. In recent years, the polarography of uranium complexes with some polarographically-active organic compounds has received special attention. Donoso *et al.*² described the oscillography of the cupferron–uranium complex and proposed a sensitive method for the determination of uranium. The method was further improved by Xiao³ and used successfully for determination of traces of uranium in minerals. Gao⁴ studied the polarography of the uranium–thenoyl-trifluoroacetone complex and the mechanism of the polarographic wave.

Xylidyl Blue I has been widely used for the spectrophotometric determination of magnesium.⁵ We have found that a sensitive LSP wave related to the concentration of uranium appears in the presence of XBI in a medium containing ethylenediamine (en) and 1,10-phenanthroline (phen). Under optimum conditions the detection limit is $3 \times 10^{-8} M$. The relationship between the peak height and uranium concentration is linear over the range 8×10^{-8} – $7 \times 10^{-6} M$. The LSP wave of the complex is attributed to reduction of the XBI in the complex. The molar ratio of U:XBI in the complex was found to be 1:2, conditional formation constant $\log \beta' = 9.09$ (by polarography), 8.81 (by spectrophotometry). The complex was shown to be strongly adsorbed on the surface of the mercury electrode. The method has been used for the determination of uranium in minerals with good results, after separation of interfering ions by solvent extraction.

EXPERIMENTAL

Reagents

Stock solution of uranium ($10^{-2} M$ in $0.3 M$ acetic acid– $0.2 M$ hydrochloric acid medium) was prepared from

uranyl acetate and diluted working solutions with $0.1 M$ hydrochloric acid to give $10^{-4} M$ and $10^{-5} M$. Xylidyl Blue I (First Chemicals Co., Tianjing, China) was used, without further purification, as a $1 \times 10^{-3} M$ solution in water. All reagents were of analytical grade.

Apparatus

A JP-1A oscillograph (Chendu Instrumental Factory, China), JMJ-1 polarograph (Wuhan Electronic Instrumental Factory China), model PAR 303 SDME (EG&G PARC, USA) and a PO4 Polariter (Radiometer, Denmark) were used for the polarographic measurements. The settings on the JP-1A oscillograph were: drop-time 7 sec, scan-rate 250 mV/sec, potential scan range 500 mV in the negative direction, mercury-column height 50 cm, and mercury flow-rate 2.0 mg/sec. A three-electrode system was used with a dropping mercury (DME) working electrode, a platinum counter-electrode and a saturated calomel (SCE) reference electrode. The values of potential were referred to the SCE. The electrolytic cell was a 10-ml beaker.

All experiments were performed at room temperature. It was not necessary to remove dissolved oxygen from the solutions.

Procedure

To the sample solution (8×10^{-8} – $7 \times 10^{-6} M$ uranium) add 0.3 ml of $10^{-3} M$ XBI, 0.5 ml of $2 \times 10^{-3} M$ phen, 1.5 ml of 10% v/v en solution and 0.4 ml of $0.5 M$ hydrochloric acid. The pH is then about 10.5. Make up to 10 ml with distilled water, mix thoroughly and let stand for a few minutes. Record the derivative linear sweep polarogram from -0.5 to -1.0 V (*vs.* SCE) and measure the height of the peak at -0.86 V (*vs.* SCE). The solution is stable for at least 90 min.

Analysis of ores

Weigh 0.2 g of sample into a 50-ml beaker and add 4–5 g of a 1:1:1 w/w mixture of ammonium chloride, nitrate and fluoride. Heat until vapour is no longer evolved. Cool, add 1 ml of perchloric acid and 5 ml of distilled water and heat to dissolve the residue. Filter into a 150-ml separating funnel and wash the filter with a little water. Add 15 ml of $0.5 M$ hydrochloric acid, 5 ml of 10% ammonium nitrate solution, and a volume of 20% v/v tributyl phosphate solution (in carbon tetrachloride) equal to that of the aqueous phase. Shake the mixture for 2 min. Discard the aqueous phase. Add 30 ml of distilled water to the separating funnel and shake it. Discard the organic phase. Transfer the aqueous

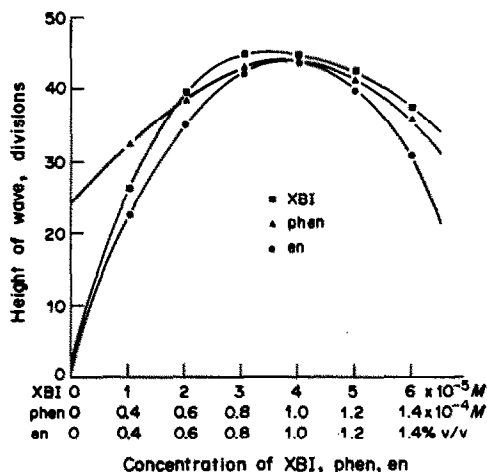


Fig. 1. Effect of concentration of various components on the wave height for $10^{-6} M$ uranium.

phase to a 50-ml beaker and evaporate it to dryness. Add 5 ml of distilled water and heat to dissolve the residue. Complete the determination by the procedure described above. Run a calibration curve.

RESULTS AND DISCUSSION

Optimum conditions

The reason for use of the en-HCl buffer solution was indicated in our previous paper.¹ 1,10-Phenanthroline (phen), a surface-active substance, is used because it can be adsorbed at the surface of the DME, depress the background and improve the wave shape. Because of the low solubility of XBI in acidic solution, a weakly alkaline medium is preferred for the polarographic determination. The effects of XBI, phen and en concentrations on the peak height are shown in Fig. 1. Their optimum concentrations

are $3 \times 10^{-5} M$, $1 \times 10^{-4} M$ and 1% v/v respectively. Figure 2 shows the variation of the peak height with pH of the solution. The optimum pH is about 10.5, which is maintained with en-hydrochloric acid buffer solution.

Formation of the uranium-XBI complex

Under the selected conditions, the red uranium-XBI complex is rapidly formed. The d.c. polarograms of XBI and its uranium complex are similar to those for the thorium complex¹ and clearly show a new wave, related to the uranium-XBI complex, appearing at about $-0.86 V$. When LSP is used, the polarographic wave of XBI splits into three peaks; in the presence of uranium, two of these decrease and a new and larger LSP peak appears at almost the same potential as that of the third peak for XBI. As with thorium,¹ the height of the new polarographic peak is proportional to the concentration of

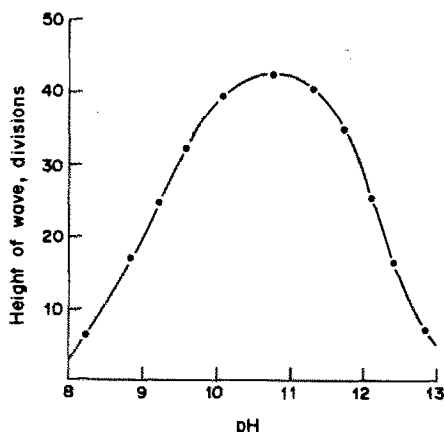


Fig. 2. Effect of pH on the wave height.

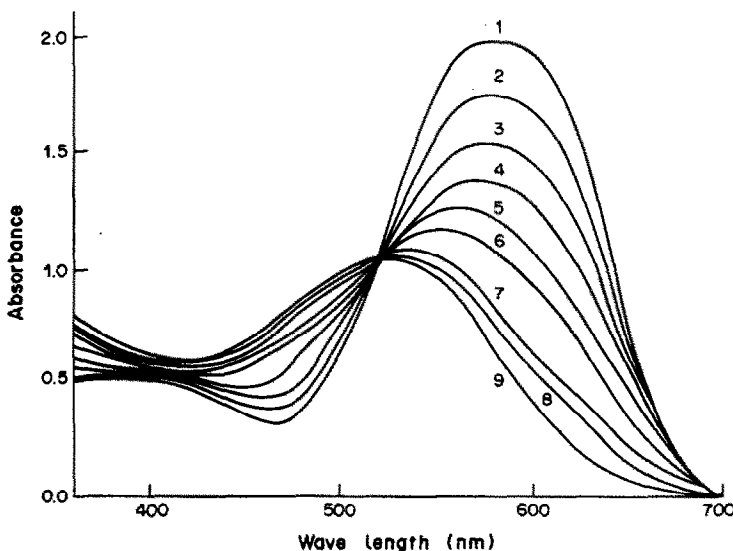


Fig. 3. Absorption spectra. $10^{-4} M$ XBI-30% (v/v) ethanol-1% v/v en (pH 10.5)-U. Concentration of U: 1, 0M; 2, $2 \mu M$; 3, $4 \mu M$; 4, $6 \mu M$; 5, $8 \mu M$; 6, $20 \mu M$; 7, $40 \mu M$; 8, $80 \mu M$; 9, $120 \mu M$.

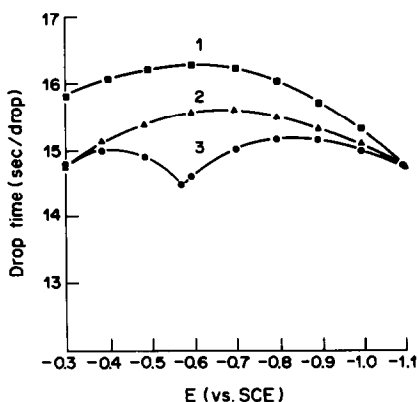


Fig. 4. Electrocapillary curves. 1, 1% (v/v) en- $10^{-4}M$ phen (pH 10.5); 2, 1 plus $3 \times 10^{-5}M$ XBI; 3, 2 plus $10^{-6}M$ U.

the metal ion, so there is no doubt that this peak must be ascribed to the uranium-XBI complex.

Furthermore, as can be seen from Fig. 3, the formation of the complex is accompanied by a decrease of the absorbance at 590 nm and appearance of a new absorption band at 470 nm. This is similar to formation of the XBI-Mg complex⁶. The change in absorbance at 470 nm is too small to be useful for the spectrophotometric determination of uranium, but decrease in the absorbance at 590 nm can be used for indirect determination of uranium, with linearity over the uranium concentration range up to $8 \times 10^{-6}M$ (apparent molar absorptivity 1×10^5 l. mole⁻¹. cm⁻¹). The sensitivity of the spectrophotometric method cannot compare with that of the polarographic determination, however.

The ratio of uranium to XBI in the complex, and the conditional formation constant, were determined by means of a log-log plot. The results are U:XBI = 1:2, $\log \beta' = 9.09$ (by polarography), 8.81 (by spectrophotometry).

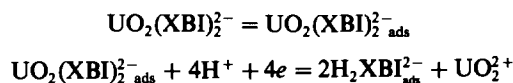
Properties of the polarographic wave of the complex

The electrocapillary curves for various solutions are shown in Fig. 4, and show that XBI and its uranium complex are strongly adsorbed on the surface of the mercury electrode. With the uranium-XBI complex, there is a sharp notch appearing at -0.56 V (vs. SCE), indicating that an adsorption mechanism is involved. The peak current (i_p) of the polarographic wave was found to be proportional to the rate of potential scan, another feature characteristic of an adsorption mechanism.⁷ Various

small amounts of surfactants, such as Triton X-100, sodium dodecyl sulphate, sodium tetraphenylborate *etc.*, strongly depress the wave height and split the wave, which also indicates the adsorptive nature of the wave. Furthermore, the slope of the $\log i$ vs. $\log t$ curve is 0.5, which is much larger than the value for a diffusion-controlled process.⁸ The d.c. limiting current is proportional to the height of the mercury column.

All these facts indicate that the polarographic wave of the uranium-XBI complex is an adsorptive reduction wave in which the complex is more strongly adsorbed than the ligand and reduced at a more negative potential.

The peak potential of the uranium-XBI complex is related to pH ($\partial E_p/\partial \text{pH} = 60$ mV/pH), in the same way as that for the ligand alone. The mechanism of the reduction of XBI at the mercury electrode has been thoroughly studied.⁹ The first reduction wave is attributed to reduction of its azo-group ($-\text{N}=\text{N}-$) to a hydrazo-group ($-\text{NH}-\text{NH}-$). Hence the electrode reaction for reduction of the uranium-XBI complex may be:



Interferences

In the presence of $10^{-3}M$ DCTA, up to 1000-fold Pb(II), 100-fold Cu(II), Zn(II), Cd(II), Fe(III), Fe(II), Mo(VI), Mn(II), In(III), Ge(IV), Sb(III), Pd(II), V(V), and 50-fold Tl(I), Sn(IV), Nb(V), Ta(V), Se(VI) have no effect on the determination of uranium; up to 20-fold lanthanide and 10-fold Th(IV), Bi(III), Cr(III) have little effect on the complex wave, and up to 1000-fold SiO_3^{2-} , PO_4^{3-} , NO_3^- , NO_2^- , F^- , Br^- , I^- do not interfere

Application

Several ore samples were analysed by the procedure described. The results agree well with the certified values and therefore validate the proposed procedure (Table 1).

REFERENCES

1. Z. F. Zhao, X. H. Cai, P. B. Li and H. D. Yang, *Talanta*, 1986, **33**, 623.
2. G. Donoso N., M. A. Santa Ana V. and I. Chadwick W., *Anal. Chim. Acta*, 1968, **42**, 109.
3. S. S. Xiao, *Fenxi Huaxue*, 1973, **1**, 22.
4. W. W. Gao, *ibid.*, 1981, **9**, 411.
5. C. K. Mann and J. H. Yoe, *Anal. Chem.*, 1956, **28**, 202.
6. V. Svoboda and V. Chromý, *Anal. Chim. Acta*, 1971, **54**, 121.
7. R. A. Osteryoung, G. Lauer and F. C. Anson, *Anal. Chem.*, 1962, **34**, 1833.
8. S. J. Dong and E. K. Wang, *Huaxue Tongbao*, 1965, **2**, 103.
9. Z. F. Zhao, X. H. Cai and P. B. Li, unpublished work.

Table 1. Determination of uranium in ores*

Sample	Found, %	Ref. values, %
1	0.0078 ± 0.0005	0.0081
2	0.0021 ± 0.0003	0.0020
3	0.207 ± 0.008	0.206
4	0.281 ± 0.009	0.295

*All the samples were from Institute of Geology and Mineral Resources of Yichang, China.

ANALYTICAL DATA

DETERMINATION OF STABILITY CONSTANTS FOR ALKALINE-EARTH AND ALKALI METAL ION COMPLEXES OF GLYCINE BY SPECTROPHOTOMETRY

LEO HARJU

Department of Chemistry, Åbo Akademi, SF-20500 Åbo 50, Finland

(Received 26 May 1986. Revised 27 March 1987. Accepted 10 April 1987)

Summary—The complex equilibria between alkaline-earth and alkali metal ions with glycine were studied by a spectrophotometric method. The following stability constant (concentration) values valid at 25° and ionic strength 1.0M were found: $K_{\text{HL}} = 10^{9.57}$, $K_{\text{LL}} = 10^{-1.2}$, $K_{\text{BaL}} = 10^{-0.40}$, $K_{\text{SrL}} = 10^{0.14}$, $K_{\text{CaL}} = 10^{0.55}$, $K_{\text{MgL}} = 10^{1.17}$.

The study of the metal complexes of amino-acids has long been of interest for co-ordination chemists and biochemists. Many equilibrium data for the glycine complexes can be found in the compilations of stability constants,¹⁻³ but not for the alkaline-earth and alkali metal ion complexes, for which very few literature data can be found. The reason for this is obvious; these complexes are of very low stability and it is difficult to determine their stability constants by the conventional methods. In this work the stability constants are determined by a spectrophotometric method similar to that used earlier⁴ for the alkali-metal ion complexes of NTA (nitrilotriacetic acid).

Glycine (aminoacetic acid, aminoethanoic acid) is a bidentate ligand which co-ordinates through the nitrogen atom of the amino group and one carboxylate oxygen atom. At neutral pH values, glycine adopts the zwitterionic structure typical of amino-carboxylic acids:



EXPERIMENTAL

For rapid determination of the stability constants, a titration procedure was used. The hydrogen-ion concentration and the absorbance were measured simultaneously for a solution that was gradually neutralized by addition of tetramethylammonium hydroxide.

An Orion 801 pH/mV-meter was used for the potential measurements and the electrode system was calibrated in terms of hydrogen-ion concentrations instead of activities, according to a procedure described earlier.⁵ Thus all constants determined in this work are concentration constants.

The spectrophotometric measurements were made with a Varian DMS 90 spectrophotometer equipped with an Epson MX-80 printer for data output. Absorbance measurements were made at 8 programmed fixed wavelengths, in the double-beam mode. For accurate measurements a fused-silica flow-through cell with an optical path-length of 10 mm was used. The reproducibility of the absorbance measurements was very good, repeated readings usually agreeing to within 0.001.

The titration cell and spectrophotometric cell were kept at $25 \pm 0.1^\circ$. The ionic strength derived from the metal salts

was calculated, and if necessary tetramethylammonium chloride (which is non-complexing) was added to bring the ionic strength to 1.0M. Glycine *pro analysi* (Merck, Darmstadt) was used for the experiments. The chloride salts of the metal ions were also of *pro analysi* grade (Merck) and used without further purification.

RESULTS AND DISCUSSION

Absorbance curves

Glycinate, GLY^- , absorbs light in the ultraviolet region at wavelengths shorter than 250 nm (Fig. 1). A suitable analytical wavelength is chosen where the difference between the absorbance of the non-protonated and protonated species is sufficiently large to enable accurate spectrophotometric measurements and determinations of stability constants.

Figure 2 presents curves of the absorbance (at 225 nm) for glycine in the presence of tetramethylammonium, sodium, lithium, barium, strontium, calcium and magnesium ions as a function of the negative logarithm of the hydrogen ion concentration. The absorbance curves in the figure are

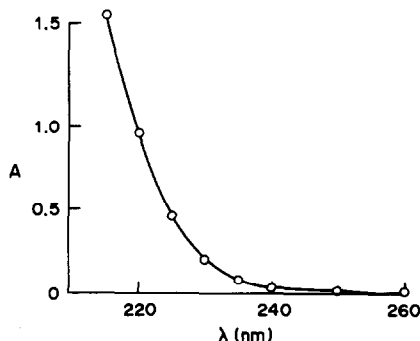


Fig. 1. The absorbance curve of $1.80 \times 10^{-2}M$ glycine solution at $-\log [\text{H}] = 10.970$ and $I = 1.0$ [$(\text{CH}_3)_4\text{NCl}$].

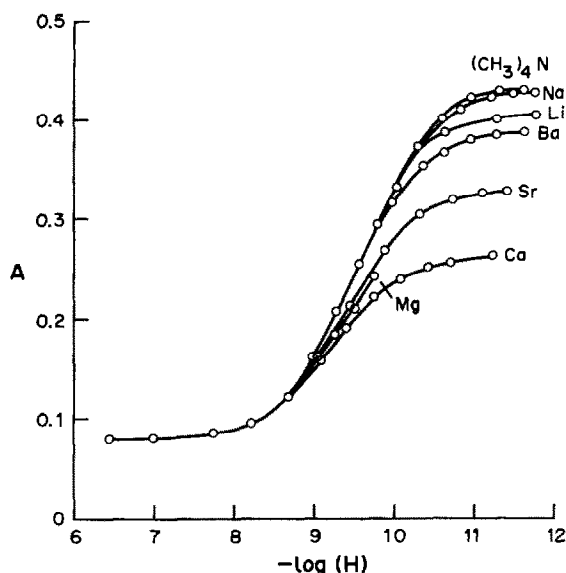


Fig. 2. The absorbance of $2.00 \times 10^{-2} M$ glycine plotted as a function of $-\log [H]$ in the presence of $1.0 M (CH_3)_4N^+$, $1.0 M Na^+$, $1.0 M Li^+$, $0.333 M Ba^{2+}$, $0.333 M Sr^{2+}$, $0.333 M Ca^{2+}$ and $0.050 M Mg^{2+}$. $\lambda = 225 \text{ nm}$. $V_0 = 50.00 \text{ ml}$. $-\log [H]$ was adjusted with $(CH_3)_4NOH$.

corrected for slightly different background absorbances. The background absorbances of tetramethylammonium chloride and the metal salt solutions were independent of pH in the regions used for the calculation of the stability constants. The shape of the absorbance curve in the presence of tetramethylammonium ions shows that one proton is liberated from the amino group at pH 9–10. For the metal ions the series of curves shows decreasing absorbance due to an increasing degree of complex-formation.

Protonation of glycine

For the protonation of the amino group in aminoacids the general reaction is (signs of charges are omitted for simplicity)



and the corresponding equilibrium constant

$$K_{HL}^{H,L} = \frac{[HL]}{[H][L]} \quad (1)$$

(Notations defined by Ringbom and Harju^{6,7} are used in this work.) The total analytical concentration of the ligand, C_L , is defined by the general equation

$$C_L = [L] + [HL] + \dots + [H_n L] \quad (2)$$

Because the calculations are made at pH values above 7, and the difference between the first and second protonation constants of glycine is greater than 10^6 , terms containing H_2L and higher complexes in the equation above can be omitted in the calculations in this work.

The molar absorptivity for the free ligand, ϵ_L , was determined from Beer's law:

$$\epsilon_L = \frac{A_{\max} - A_{bg}}{C_L} \quad (3)$$

where A_{\max} is the absorbance for a solution in which the ligand is present only in non-protonated form, L^- , and A_{bg} is the background absorbance for a solution in which all the ligand is in monoprotinated form HL . A_{bg} was mainly due to absorption by the inert salt present and was determined in the pH region 6–7. Because a titration procedure was used, volume corrections had to be applied to C_L , A_{\max} and A_{bg} in the calculations.

The free ligand concentration is calculated from

$$[L] = \frac{A - A_{bg}}{\epsilon_L} \quad (4)$$

where A is the absorbance measured at different experimental pH values.

The first protonation constant can readily be calculated from equations (1), (2) and (4). The results for K_{H-GLY} at three wavelengths are given in Table 1. The amounts of hydroxide ion consumed during the titration are not used in the calculations.

At shorter wavelengths and higher absorbances, better precision was, of course, obtained. At 225 nm the standard deviation was as low as 0.0018 for

Table 1. Spectrophotometric determination of K_{H-GLY} at the wavelengths 230, 227 and 225 nm: $C_{GLY} = 0.0200 M$, $I = 1.0 M$ $[(CH_3)_4NCl]$; initial volume 50.00 ml; $\epsilon_L^{230} = 7.25$, $\epsilon_L^{227} = 12.72$, $\epsilon_L^{225} = 18.07 \text{ l.mole}^{-1} \text{ cm}^{-1}$; $A_{bg}^{230} = 0.090$; $A_{bg}^{227} = 0.122$; $A_{bg}^{225} = 0.147$

$-\log [H]$	Volume, ml	A_{230}	$\log K_{HL}$	A_{227}	$\log K_{HL}$	A_{225}	$\log K_{HL}$
9.068	50.25	0.124	9.572	0.183	9.561	0.233	9.566
9.201	50.30	0.133	9.565	0.198	9.562	0.254	9.568
9.308	50.35	0.140	9.574	0.211	9.566	0.273	9.569
9.412	50.40	0.149	9.561	0.225	9.567	0.294	9.564
9.507	50.45	0.156	9.568	0.239	9.562	0.313	9.564
9.605	50.50	0.164	9.567	0.252	9.569	0.332	9.568
9.698	50.55	0.172	9.560	0.265	9.569	0.351	9.566
9.798	50.60	0.179	9.569	0.279	9.566	0.370	9.568
9.897	50.65	0.187	9.558	0.292	9.563	0.388	9.568
10.011	50.70	0.194	9.566	0.305	9.565	0.407	9.567
Mean values \pm std. devn.			9.566 \pm 0.005		9.565 \pm 0.003		9.567 \pm 0.002

Table 2. Spectrophotometric determination of K_{Ba-GLY} : $C_{GLY} = 0.0200M$; $C_{Ba} = 0.333M$; $I = 1.0M$; $\lambda = 225$ nm; $\epsilon_L = 18.07$ l.mole⁻¹.cm⁻¹; $A_{bg} = 0.068$; $V_0 = 50.0$ ml; $\alpha_{Ba(Cl)} = 10^{0.051}$

-log [H]	OH ⁻ added,		log K_{Ba-GLY}	
	ml	A		
10.349	0.85	0.346	-0.427	
10.626	0.92	0.358	-0.342	
10.959	1.02	0.373	-0.397	Average -0.397
11.259	1.16	0.378	-0.402	Std. devn. ± 0.033
11.628	1.50	0.380	-0.415	

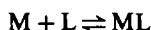
log K_{HL} . At very high absorbances, stray light affects the readings and the validity of Beer's law.

The optimal range for the determination of the first protonation constant is around the point of half-neutralization, in this case at log [H] ~ 9.6 , and small errors in the absorbance will then have minimal effects on the calculated ratio [HL]/[L].

In the compilation *Critical Stability Constants*, Martell and Smith recommend a log K_{HL} value of 9.63 ± 0.06 , at 25° and $I = 1.0M$. This is in satisfactory agreement with $K_{HL} = 10^{9.57}$ obtained in this work.

Alkaline-earth and alkali metal ion complexes of glycine

For the formation of 1:1 metal-ion-glycine complexes the general reaction is



and the corresponding stability constant

$$K_{ML}^{M,L} = \frac{[ML]}{[M][L]} \quad (5)$$

The free ligand concentration was calculated from equation (4). The concentrations of [ML] and [M] were obtained from the equations

$$C_L = [L] + [HL] + [H_2L] + [ML] \quad (6)$$

$$C_M = [M] + [ML] \quad (7)$$

$$K_{HL}^{H,L} = \frac{[HL]}{[H][L]} \quad (8)$$

A volume correction (as already explained) has to be applied to the total analytical concentrations of the metal ion (C_M) and of the ligand (C_L). In equation (6) the formation of H_2L complexes can be omitted because of the low stability of this species, and hence its negligible concentration at high enough pH.

The formation of chloride and hydroxo complexes with the alkaline-earth metal ions was considered

by means of the $\alpha_{M(Cl)}$ and $\alpha_{M(OH)}$ side-reaction coefficients as defined by Ringbom:⁶

$$\alpha_{M(Cl)} = 1 + [Cl] K_{MCl}^{M,Cl} \quad (9)$$

$$\alpha_{M(OH)} = 1 + [OH] K_{MOH}^{M,OH} \quad (10)$$

The calculation of the $\alpha_{M(Cl)}$ coefficients was based on the following stability constants for chloride complexes: $K_{MgCl} = 0.34$,⁸ $K_{CaCl} = 0.60$,⁹ $K_{SrCl} = 0.62$,¹⁰ $K_{BaCl} = 0.2$.⁹ The value for K_{SrCl} was corrected to ionic strength 1.0M before the calculations.

The stability constants for hydroxo complexes were taken from *Critical Stability Constants*.² At the experimental pH values used in this work the interfering effects of hydroxo complexes are negligible. For instance the formation of barium hydroxo complexes affects mainly the fourth decimal in the logarithm of the stability constants given in Table 2.

Table 2 presents the results of determination of K_{Ba-GLY} based on equations (3) and (5)–(8). The optimal range for the determination of equilibrium constants of alkaline-earth and alkali metal ion complexes of glycine is above pH 10, where the interference of proton complexes is low.

Table 3 summarizes the stability constants for the alkaline-earth, alkali metal and proton complexes determined in this work by the spectrophotometric method. The absorbance curves recorded in the presence of sodium and potassium lay very close to the curve of the uncomplexed ligand. Thus the estimation of stability constants would be very uncertain, and no values are reported for the glycine complexes of these metal ions.

The influence of the spectrophotometric error on the precision of the method can be estimated theoretically either by differentiation, or numerically by use of simple computer programs. For instance, for the determination of the protonation constant, a precision of 0.0005 in the absorbance measurements corresponds to an error in log K_{HL} of 0.003 at 225 nm, 0.004 at 227 nm and 0.008 at 230 nm. These values are calculated at -log [H] values close to the half-titration point and are in satisfactory agreement with the relative standard deviations reported in Table 1.

For the alkaline-earth metal ion complexes only a few values can be found in the literature. For magnesium, Hopgood and Leussing¹¹ have obtained the constant $10^{1.34}$ ($I = 0.5M$), and Murphy and Martell¹²

Table 3. Logarithmic stability constants (and standard deviations) for the proton, lithium and alkaline-earth metal ion complexes of glycine determined at $I = 1.0M$ and 25°C

Species	log K	Species	log K
HL	9.567 ± 0.002	CaL	0.55 ± 0.01
LiL	-1.2 ± 0.1	SrL	0.14 ± 0.01
MgL	1.17 ± 0.02	BaL	-0.40 ± 0.03

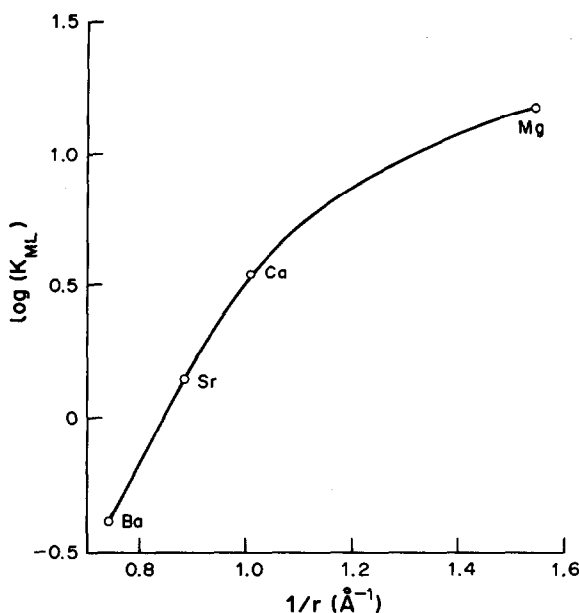


Fig. 3. The logarithm of the stability constants, $\log K_{M-GLY}$ plotted as a function of the reciprocal of the ionic radius for the alkaline-earth metal ions.

found $10^{2.23}$ ($I = 0.16M$, 30°) by utilizing potentiometric pH measurements. By using an ion-exchange method, Schubert and Lindenbaum¹³ found $K_{Sr-GLY} = 10^{0.6}$ at $I = 0.16$. For calcium complexes with glycine, Daniele *et al.*¹⁴ reported the formation constants $K_{Ca-GLY}^{Ca, GLY} = 10^{1.05}$ and $K_{CaHGLY, H}^{Ca, GLY, H} = 10^{8.80}$, determined by a pH-method at $I = 0.25M$. From the co-ordination chemistry point of view, the high stability constant reported for the protonated species, $CaHGLY$, seems doubtful. The corresponding constant for the protonated calcium complex with EDTA, a hexadentate aminocarboxylic acid, for instance, is $10^{3.18}$ and for the protonated nitrilotriacetic acid and iminodiacetic acid calcium complexes no values have been reported.²

The values obtained by the various authors are difficult to compare because of variations in the experimental conditions. In general, the stability constants reported here are somewhat lower than those in the literature, even though the differences in ionic strength and temperature have been allowed for where known. In some papers the medium and ionic strength are not clearly stated.

Figure 3 shows the relationship between the stability constants of the alkaline-earth metal ions and the reciprocals of the ionic radii (crystal, co-ordination number 6). For barium, strontium and calcium there is an almost linear relationship between $\log K_{ML}$ and the reciprocal of the ionic radii. This indicates that the complexes are mainly held together by electrostatic forces. Magnesium shows a different behaviour; owing to its small size it shows a more covalent character.

The complexation of glycine with alkaline-earth and alkali metal ions occurs mainly through the

nitrogen donor atom of the amino group. Because the protonation of the amino group occurs at about pH 9.5, the degree of complexation is strongly dependent on the pH of the solution. Because the ligand is bidentate, water molecules are also bound to the metal ion to satisfy the co-ordination requirements. In the presence of additional ligands the formation of mixed-ligand chelates is very probable.

CONCLUSION

Stability constants for the alkaline-earth metal ion complexes of amino-acids have previously been determined mainly by potentiometric methods with glass electrodes. These methods give good results for complexes of medium stability, but if very weak complexes are formed they cannot yield very accurate values of stability constants. The spectrophotometric method described in this work is very useful for the study of weak complexes, as the absorbances depend linearly on the concentration of the components in the system. K_{ML} values as low as $10^{-1.2}$ have been determined in this way.

The titration procedure used is relatively fast and the calculations are simple. There is no need for a set of buffers, which may introduce interfering reactions into the system studied. The electrodes are not removed from the solution during a set of experiments.

The degree of precision for the spectrophotometric method presented is high because the ratio of $[HL]/[L]$ and $[ML]/[L]$ is obtained directly from the absorbance data, and modern spectrophotometers permit very accurate absorbance measurements.

REFERENCES

1. L. G. Sillén and A. E. Martell, *Stability Constants of Metal-Ion Complexes*, The Chemical Society, London, Special Publications Nos. 17 and 25, 1964 and 1971.
2. A. E. Martell and R. M. Smith, *Critical Stability Constants*, Vols. 1, 4, 5. Plenum Press, New York, 1974, 1976, 1982.
3. D. D. Perrin, *Stability Constants of Metal-Ion Complexes, Part B, Organic Ligands*. Pergamon Press, Oxford, 1979.
4. L. Harju, *Finn. Chem. Lett.*, 1985, 235.
5. A. Ivaska and L. Harju, *Talanta*, 1975, **23**, 1051.
6. A. Ringbom, *Complexation in Analytical Chemistry*. Wiley-Interscience, New York, 1963.
7. A. Ringbom and L. Harju, *Anal. Chim. Acta*, 1972, **59**, 33.
8. B. Elgquist and M. Wedborg, *Mar. Chem.*, 1978, **6**, 243.
9. S. K. Patil and H. D. Sharma, *Can. J. Chem.*, 1969, **47**, 3851.
10. L. Šúcha, J. Čadek, K. Hrábek and J. Veselý, *Collection Czech. Chem. Commun.*, 1975, **40**, 2020.
11. D. Hopgood and D. L. Leussing, *J. Am. Chem. Soc.*, 1969, **91**, 3740.
12. C. B. Murphy and A. E. Martell, *J. Biol. Chem.*, 1957, **226**, 37.
13. J. Schubert and A. Lindenbaum, *J. Am. Chem. Soc.*, 1952, **74**, 3529.
14. P. G. Daniele, A. De Robertis, C. De Stefano, S. Sammartano and C. Rigano, *J. Chem. Soc. Dalton Trans.*, 1985, 2353.

SOFTWARE SURVEY SECTION

Software package TAL-010/87

JESS

(Joint Expert Speciation System)

Contributors: Dr. Peter May, Murdoch University, Murdoch 6150, Western Australia; and Dr. Kevin Murray, National Chemical Research Lab., CSIR, PO Box 395, Pretoria, South Africa.

Brief description: JESS is a long-term international collaborative project to produce computing tools for solution chemistry research (modelling natural-water, physiological, or industrial systems and determining model parameters such as formation constants). A library of portable mutually compatible FORTRAN77 routines is thus being developed to perform common tasks in (i) numerical analysis, (ii) database management, (iii) intercomputer data transfer, (iv) associated text processing and (v) assisting inexperienced workers by use of artificial-intelligence techniques.

The first stage of the JESS project, now completed, has been the development of some 100 routines, called the "Common Interface". These facilitate low-level data manipulations that would otherwise be tedious to do in portable FORTRAN. They provide uniform access to the underlying operating system, creating a powerful interface which, as far as possible, ensures the portability of JESS programs.

Many important issues lying outside the scope of the FORTRAN77 standard have been addressed. A carefully selected character set has been defined, encompassing 94 symbols most frequently adopted by the various National Standards organizations. General methods of performing I/O (both to VDU and file), that work on the largest possible number of computers, have been determined and implemented. Standardized ways of checking user responses, sorting data, list processing, generating random numbers and obtaining the time and date have been achieved by writing a set of about a dozen system-specific routines (so far including VAX, SPERRY, DATA GENERAL, HONEYWELL MULTICS, PRIME, ICL 2900, all UNIX machines and an AMIGA microcomputer).

Potential users: analytical, physical and inorganic solution chemists.

Fields of interest: chemical modelling, electrochemistry, bioinorganic chemistry, environmental chemistry.

This library of programs in the area of chemical equilibria in solution has been developed for a wide variety of machines (at least 32-bit), and is written in portable FORTRAN77. It is available on 2400-ft magnetic tape recorded in ASCII at 1600 bpi. The memory required is 500 Kb.

Researchers in solution chemistry, especially those interested in participating with future JESS development, can arrange to obtain copies of the code by contacting the authors.

The coding has been fully operational for over a year, and there is extensive external documentation. The source code is available, and the contributors are willing to deal with enquiries.

Software package TAL-011/87

LU4D

Contributors: F. Garcia Sanchez and A.L. Ramos Rubio, Department of Analytical Chemistry, Faculty of Sciences, The University, Malaga-29071, Spain.

Brief description: The program LU4D.OY allows the acquisition of an excitation synchronous matrix to allow selection of the optimum $\Delta\lambda$ for a synchronous fluorimetric analysis. The program can also obtain excitation, emission or synchronous spectra at different elapsed times and plot these in a 3-dimensional plot. This mode is useful for the study of time-dependent processes, and for selection of optimum values of λ_{exc} , λ_{em} or $\Delta\lambda$. The additional option of chart displacement, which allows production of a 3D image with a variable angle of view for the spectra collected, allows the observation of the same spectra as if scanned in several different positions. The program can also operate in a phosphorescence mode.

Potential users: analytical chemists, chromatographers, molecular luminescence spectroscopists.

Fields of interest: analytical and environmental chemistry.

This application program has been developed for the Perkin-Elmer 3600 Data Station in the language OBEY, running under PECLS-II (PETOS). It is available on 5.25-in double-sided floppy disc. The hardware required includes the LS-5, 3600 DS, Epson FX-85, and RS232C interface. The memory required is 64 Kb.

Distributed by the contributors.

The program is self-documenting and user-friendly. Design is complete and the software has been fully operational for 6 months. The source code is available.

DETERMINATION OF ALKALINE-EARTH METALS IN FOETUS BONES BY INDUCTIVELY- COUPLED PLASMA ATOMIC-EMISSION SPECTROMETRY

KUNIO SHIRAIISHI, HISAO KAWAMURA and GI-ICHIRO TANAKA

Division of Radioecology, National Institute of Radiological Science, 3609 Isozaki, Nakaminato,
Ibaraki 311-12, Japan

(Received 23 October 1986. Revised 16 January 1987. Accepted 27 May 1987)

Summary—Alkaline-earth metals in human bone samples have been determined simultaneously by inductively-coupled plasma atomic-emission spectrometry (ICP-AES). Results obtained by atomic-absorption spectrometry for Mg, Sr and Ba, and complexometry for Ca, have been compared with those by ICP-AES for a laboratory-control bone sample. Accuracy and precision were examined by analysing the IAEA animal bone standard (H-5). Agreement with the certified values to within 5% was obtained. The concentrations of the elements in foetal bone have also been determined.

Analysis for alkaline-earth metals in the human body and in environmental samples is important for the estimation of internal and external dosimetry.¹ The metabolism of two elements, calcium and strontium, as bone seekers is considered to be important in the assessment of dosage from radionuclides in the environment.² Measurements of strontium and calcium in human bones have been made routinely in our laboratory for the national radioactivity surveillance programme in Japan. Moreover, Japanese data in relation to the "Reference Man" of the International Committee of Radiation Protection (ICRP)³ are being collected and reported.^{2,4,5} Alkaline-earth metals in human bones have been studied with different aims and by different analytical methods. A detailed AAS investigation of strontium and barium in man has been reported by Schroeder *et al.*⁶ Calcium and magnesium have been measured by AAS, with reference to human metabolism.⁷ Neutron-activation analyses for strontium and barium in bone,⁸ and for calcium and magnesium⁹ have been reported. Ancient human skeletons have also been analysed by neutron-activation analysis.¹⁰

Although ICP-AES has recently been used for simultaneous multielement analysis of environmental materials,¹¹⁻¹³ its application to human bone samples has not been reported previously. It has two major advantages: low detection limits for alkaline-earth metals¹⁴ and simultaneous determination of strontium and calcium, *i.e.* the strontium-to-calcium ratio is obtained without difficulty.

In this paper, simultaneous determination of four alkaline-earth metals, calcium, magnesium, strontium and barium, in human bones by ICP-AES is described. Concentrations of the four elements in foetal bones are also reported.

EXPERIMENTAL

Apparatus

A Shimadzu ICPQ-1012W inductively-coupled plasma atomic-emission spectrometer was used. The instrument and operating parameters employed are given in Table 1. A Perkin-Elmer model 5000 atomic-absorption spectrophotometer equipped with a deuterium and tungsten background corrector was used with an air-acetylene flame and an HGA 400 graphite-furnace atomizer. The hollow-cathode lamps used were obtained from Hamamatsu Photonics, Hamamatsu, Japan. Magnesium was determined with an air-acetylene flame at 285.2 nm. Strontium was determined with an air-acetylene flame at 460.7 nm, with sample solutions containing 3000 µg/ml calcium.⁴ Barium was determined with a pyrocoated graphite tube at 553.6 nm by the method of standard additions. Temperatures for drying, ashing and atomizing were 130, 1500 and 2700°, respectively. Argon gas purge was provided at a flow-rate of 50 ml/min.

Reagents

Freshly purified water was prepared from tap water with a Barnstead D-2794 outfit. Nitric and hydrochloric acid "for trace element analysis" were obtained from Wako Chemicals, Tokyo. The "Specpure" materials, calcium carbonate, magnesium oxide, strontium carbonate and barium carbonate, were obtained from Johnson Matthey Chemicals. Yttrium oxide (99.999% pure) was obtained from Research Chemicals, Phoenix, AZ, U.S.A. Stock solutions (1000 µg/ml) were prepared by dissolving these standard materials in hydrochloric acid and diluting with purified water.

Reference materials

Laboratory-control bone sample, National Institute of Radiological Sciences (NIRS) human bone sample was used for comparison of two analytical methods, ICP-AES and AAS, with the assistance of complexometry for calcium. The Animal Bone (H-5), issued by the International Atomic Energy Agency (IAEA), was analysed only by ICP-AES. Approximately 0.38 g of the ash was weighed and treated as described in the following section. Samples were diluted

Table 1. Operating parameters

Operating frequency	27.120 MHz
Operation power	1.2 kW
Argon gas flow-rate, carrier	1.0 l/min
coolant	11.5 l/min
plasma	1.5 l/min
Nebulizer	Concentric
Observation height above load coil	1.5 cm (nominal)
Sample uptake rate	2.5 ml/min (demineralized water)
Polychromator	
Grating	Holographic, 2700 grooves/mm
Mount	Paschen-Runge
	1.0 m focal length
Reciprocal linear dispersion	0.37 nm/mm
Entrance slit width	20 μ m
Exit slit width	50 μ m
Integration time	20 sec
Analytical lines	
Species and wavelength (nm)	Ca (I) 422.67
	Mg (I) 383.83
	Sr (II) 407.77
	Ba (II) 455.40
Data acquisition system	
Processor	MELCOM 70/L
Program	QC-5D

to give approximately the calcium and phosphorus concentrations corresponding to the matrix concentrations of the standard solution used for ICP-AES analysis. Four replicate analyses were made.

Sample preparation

Foetus bone samples were obtained in 1982-1983 during the course of a national radioactivity surveillance programme in Japan. Sample materials were ashed in a muffle furnace at 550°. The procedure has already been reported⁴ and may be summarized as follows. The sample treatment was conducted in a clean-hood. A 400-mg portion of bone ash was digested in a beaker with 2 ml of concentrated nitric acid on a Thermolyne HP-11415B ceramic top hot-plate until a white residue was obtained. The residue was dissolved in 5 ml of 1M hydrochloric acid, transferred to a 50-ml borosilicate glass standard flask and diluted to volume so that the final acid concentration was 0.1M. In the case of the NIRS human bone sample, the sample solution (50 ml) was run through an anion-exchange resin column (Bio-Rad 1 \times 8, 50-100 mesh). The phosphate-free eluate was analysed for strontium by AAS and for calcium by complexometry.^{4,15}

ICP-AES measurement

Standard solutions. Six groups of standard solutions were prepared, the concentrations being as shown in Table 2. Solutions A and B were used in preparing calibration curves for calcium and magnesium. The matrix-matching method was used for standard solutions C, D and E. The calibration curve of calcium was obtained at three concentration levels. Magnesium, strontium and barium were measured by using four or five different standard solutions (including one of

zero concentration). Yttrium (1 μ g/ml) was used as internal standard.

Interference by the matrix elements. The effects of calcium and phosphorus on the strontium and barium measurements were checked with model solutions¹³ containing 0, 250, 500 and 1000 μ g/ml calcium and phosphorus. Each contained 1 μ g/ml or 0.1 μ g/ml of both strontium and barium. Analytical curves were constructed by use of standard solutions containing strontium and barium at four different concentrations (including one of zero concentration). The standard solutions contained no matrix-elements in this experiment. Yttrium (1 μ g/ml) was added to both standard and sample solutions as internal standard.

Test for tolerable range of deviation in matrix concentration level between sample and standard solutions. The NIRS bone sample solution (50 ml, untreated by anion-exchange) was diluted four times to make the calcium and phosphorus concentrations correspond to the matrix contents shown in Table 2.

Before analysis of bone samples, model solutions of different matrix and analyte concentrations were prepared with aliquots of the NIRS bone sample solution, instead of by changing the matrix element concentrations in the standard solutions.¹⁶ The concentration ratio of test to standard solution was varied from 0.5 to 2.0. The working curves were obtained with the standards shown in Table 2.

Spike test for recovery of alkaline-earth metals. The NIRS bone sample was used and two levels of spike were chosen. One was 10, 0.5 and 0.02 μ g/ml for magnesium, strontium and barium, respectively, approximately half the levels in the NIRS bone sample, and the other was double or half this level. For calcium, relatively low concentration levels (100 and 150 μ g/ml) were chosen for the standard calibration range used.

Table 2. Standard solutions used for bone analysis

Element	Standard solution, μ g/ml				
	A	B	C	D	E
Ca	1000	500	850	850	850
P	350	350	350	350	350
Mg	0	100	10	25	50
Sr	0	0	1	5	10
Ba	0	0	1	0.5	0.25

RESULTS AND DISCUSSION

Interferences

Interference by the major matrix components, calcium and phosphorus, was checked against the model solutions without matrix-matching and the results are shown in Table 3. The matrix effect was evaluated from the ratio of the concentration obtained to that

Table 3. Effects of major elements on 1 $\mu\text{g/ml}$ and 0.1 $\mu\text{g/ml}$ of strontium and barium

Element	Relative concentration of each element*							
	Strontium				Barium			
	Matrix concentration, $\mu\text{g/ml}$				Matrix concentration, $\mu\text{g/ml}$			
	0	250	500	1000	0	250	500	1000
Ca	100	100	101	103	100	99	99	99
	(100)†	(116)	(131)	(159)	(100)	(106)	(110)	(116)
P	100	101	101	101	100	101	101	102
	(100)†	(103)	(104)	(104)	(100)	(104)	(104)	(104)
Na	100	99	99	98	100	98	99	97
Mg	100	98	98	98	100	99	99	97
K	100	98	98	98	100	98	97	97

*Mean of three determinations.

†0.1 $\mu\text{g/ml}$ strontium and barium.

with a zero concentration of the matrix. When the strontium and barium concentrations were 1 $\mu\text{g/ml}$, little influence was shown by calcium and phosphorus concentrations in the range 0–1000 $\mu\text{g/ml}$. However, in the case of 0.1 $\mu\text{g/ml}$ strontium and barium, the matrix effects (shown in parentheses in Table 3) increased with increase of matrix concentration. The effect of calcium on the measured strontium concentration was marked, indicating an apparent 60% increase at 1000 $\mu\text{g/ml}$. Since the concentrations of calcium, strontium and barium in the human bone sample were approximately 850, 0.4 and 0.02 $\mu\text{g/ml}$, respectively, there was spectral interference by calcium. Strontium and barium cannot be measured without matrix matching. The presence of phosphorus slightly influenced the measurement of strontium and barium concentrations, the error for solutions containing 0.1 $\mu\text{g/ml}$ being less than 4%.

Table 4 shows that the alkaline-earth metals can be determined with not more than 4% relative error when the difference in matrix concentration between sample and standard solutions is not more than 20%

of the sample matrix concentration. The result for calcium at a sample to standard matrix-ratio of 2.0 was low because this ratio was outside the range used in the calibration programme.

Recovery test for the NIRS sample

The results of a recovery test made with the NIRS bone sample are shown in Table 5. All four alkaline-earth metals showed good recovery, that for barium being high because of the low concentration and spectral interference (see Table 3).

Comparison of two methods

The NIRS bone sample solution which had not been treated with the anion-exchange resin was directly analysed by ICP-AES. Its magnesium and barium contents were also measured by AAS. Calcium and strontium in the phosphate-free eluate treated obtained after treatment of the same solution with the ion-exchange resin were measured by AAS and complexometry, respectively. The results are compared in Table 6. The ratio of the result obtained

Table 4. Effects of the matrix concentration ratio between samples and standards in the determination of alkaline-earth metals in NIRS human bone sample

Element	Relative concentration of each element					
	Total matrix concentration ratio*					
	0.5	0.8	1.0	1.2	1.5	2.0
Ca	100	99	100	102	100	90†
Mg	93	97	100	104	103	100
Sr	94	98	100	102	101	96
Ba	104	99	100	100	98	103

*Total matrix concentration of sample solutions divided by that of the standard.

†Outside the calibration range.

Table 5. Recovery of added elements (ICP-AES)

Element	Concentration of sample, $\mu\text{g/ml}$	Added, $\mu\text{g/ml}$		Recovery range, %	
		A	B	A	B
Ca	853	150	100	99–100	100–103
Mg	10.2	10	5	100–104	102–107
Sr	0.395	0.5	1	98–101	99–100
Ba	0.025	0.02	0.05	105–109	101–102

*Three determinations.

Table 6. Comparison between the two methods of measuring alkaline-earth metal content* in human bone

Element	ICP-AES	AAS & complexometry
Ca, mg/ml	3.41 ± 0.02	3.29 ± 0.02
Mg, µg/ml	40.8 ± 0.2	41.0 ± 0.6
Sr, µg/ml	1.57 ± 0.03	1.47 ± 0.03
Ba, ng/ml	98 ± 2	94 ± 15

*A 400-mg portion of bone ash was dissolved in 50 ml of 0.1M HCl and analysed four times.

by the two methods (ICP-AES/AAS or complexometry), was found to vary from 104 to 107% because of loss during the anion-exchange step.¹⁵ The eluate was also analysed by ICP-AES and values corresponding to those found by AAS and complexometry were obtained.

Accuracy and precision

The results for IAEA H-5 are shown in Table 7. The calcium, magnesium and strontium concentrations found were in good agreement (±3%) with the certified values. For barium, the result was about 6% high, but fell within the IAEA certified range and had better reproducibility.

The relative standard deviation in repetitive measurements for IAEA H-5 was 0.5, 0.6, 0.4 and 0.5% for Ca, Mg, Sr and Ba, respectively.

Detection limits for these elements were as follows: Ca 0.3, Mg 0.007, Sr 0.0003 and Ba 0.0005 µg/ml. Those for magnesium, strontium and barium were estimated as three times the standard deviation ob-

Table 7. Analytical results for alkaline-earth metals of IAEA animal bone H-5 by ICP-AES

Element	Present results*	Certified content
Ca, mg/g	217 ± 1	212 ± 8
Mg, mg/g	3.61 ± 0.03	3.55 ± 0.09
Sr, µg/g	99 ± 1	96 ± 8
Ba, µg/g	84 ± 2	79 ± 13

*Mean and standard deviation of four determinations.

tained in the measurements of the 0-µg/ml standard solution containing matrix elements. For calcium, the standard deviation in measuring a solution containing 1000 µg/ml calcium was used.

Foetal bone analysis

Samples from eight foetal skeletons were analysed, and the results are shown in Table 8. The mean calcium concentration in the ashed foetal bone was found to be 371 mg/g. This result is close to that given (37.47%) in our previous report.⁵ Although the strontium concentration seems to decrease after six lunar months, it is unclear from these results (owing to the small numbers of samples analysed) whether this is a real effect. The mean strontium concentration measured was 64.8 µg/g, derived from a distribution of values lower than those yielding the earlier reported value of 86.4 µg/g.⁵ The measured strontium-to-calcium concentration ratio was 0.175 mg Sr/g Ca because of the lower strontium concentration, but a similar result has also been reported.⁵ The mean magnesium concentration was 6.42 mg/g, but for

Table 8. Concentration of alkaline-earth metals in foetus bones

Age, Lunar months	Sex	Bone	Element concentration*					Sr-to-Ca ratio, mg Sr/g Ca
			Calcium, mg	Magnesium, mg	Strontium, µg	Barium, µg		
4	M	Long bone	362†	6.45	86.1	1.8	0.238	
		Miscellaneous	331†	6.59	80.0	3.8	0.241	
5	F	Vertebra	362‡	6.42	81.9	5.5	0.226	
		Long bone	375‡	7.09	84.3	5.0	0.225	
		Pelvis	379‡	6.47	83.2	3.1	0.220	
6	M	Miscellaneous	373†	6.44	83.2	5.2	0.223	
		Vertebra	351‡	6.82	57.0	2.5	0.162	
		Long bone	370†	7.09	47.2	2.0	0.128	
7	F	Flat bone	376‡	5.68	84.8	0.8	0.225	
		Long bone	365‡	7.03	69.7	3.9	0.191	
8	M	Miscellaneous	358†	6.43	63.6	3.6	0.178	
		Long bone	377†	5.95	78.6	3.7	0.208	
9	F	Pelvis	381†	5.92	81.2	4.0	0.214	
		Vertebra	369†	7.21	49.6	2.5	0.134	
9	M	Long bone	375†	7.05	50.5	3.4	0.135	
		Pelvis	388†	6.87	54.4	2.3	0.141	
		Miscellaneous	379†	7.01	51.8	6.2	0.137	
10	M	Vertebra	381‡	5.69	49.3	2.2	0.129	
		Long bone	389†	5.63	49.2	2.1	0.127	
		Rib	384‡	5.60	49.1	1.6	0.128	
Overall mean	Range	Vertebra	372†	6.12	53.0	10.0	0.143	
		Long bone	359†	6.53	48.7	8.3	0.136	
		Pelvis	384†	5.57	53.3	3.9	0.139	
			371	6.42	64.8	3.8	0.175	
			331-388	5.57-7.09	47.2-86.1	0.8-10.0	0.127-0.241	

*Per gram of ash.

†Mean of two determinations.

‡One determination, mean of three measurements.

adult bone a value of 5.3 mg/g has been reported.¹⁰ The mean barium concentration was found to be 3.8 $\mu\text{g/g}$. This result, despite a relatively large variation, is in agreement with the literature values of 4.7,¹⁷ and 7.0 ± 4.0 ,⁸ $\mu\text{g/g}$. The intraskeletal element distribution in the foetus bones was not clear in this work, owing to the small number of samples analysed.

In conclusion, it may be stated that alkaline-earth metals in human bone samples can be simultaneously determined by the ICP-AES by the matrix-matching and internal standard method. The Sr-to-Ca concentration ratio can also be easily obtained by this procedure.

Acknowledgement—The authors would like to thank Miss Masako Ouchi for her help in processing the data.

REFERENCES

1. ICRP Task Group of Committee 2, *Alkaline Earth Metabolism in Adult Man*, ICRP Publ. 20, Pergamon Press, Oxford, 1973.
2. *Idem*, *Report of the Task Group on Reference Man*, ICRP Publ. 23, Pergamon Press, Oxford, 1975.
3. G. Tanaka, H. Kawamura and Y. Nakahara, *Health Phys.*, 1979, **36**, 333.
4. G. Tanaka, H. Kawamura and E. Nomura, *ibid.*, 1981, **40**, 601.
5. H. Kawamura, G. Tanaka and K. Shiraishi, *ibid.*, 1986, **50**, 159.
6. H. A. Schroeder, I. H. Tipton and A. P. Nason, *J. Chron. Dis.*, 1972, **25**, 491.
7. P. Plenge and O. J. Rafaelsen, *Acta Psychiat. Scand.*, 1982, **66**, 361.
8. E. M. Sowden and S. R. Stutch, *Biochem. J.*, 1957, **67**, 104.
9. P. Braetter, D. Gawlik, J. Lausch and U. Roesick, *J. Radioanal. Chem.*, 1977, **37**, 393.
10. G. C. Goode, C. M. Howard, A. R. Wilson and V. Parsons, *Anal. Chim. Acta*, 1972, **58**, 363.
11. M. Abdullah, K. Fuwa and H. Haraguchi, *Spectrochim. Acta*, 1984, **39B**, 1129.
12. K. A. Wolnik, J. I. Rader, C. M. Gaston and F. C. Frick, *ibid.*, 1985, **40B**, 245.
13. K. Shiraishi, G. Tanaka and H. Kawamura, *Talanta*, 1986, **11**, 861.
14. P. W. J. M. Boumans and R. M. Barnes, *ICP Inform. Newslett.*, 1978, **3**, 445.
15. G. Tanaka, A. Tomikawa, H. Kawamura and Y. Ohyagi, *Nippon Kagaku Zasshi*, 1968, **89**, 175.
16. K. Shiraishi, H. Kawamura and G. Tanaka, *Anal. Sci.*, 1985, **1**, 321.
17. H. Kawamura, G. Tanaka and Y. Ohyagi, *Spectrochim. Acta*, 1973, **28B**, 318.

A COMPARISON OF TWO DIGESTION PROCEDURES FOR THE DETERMINATION OF SELENIUM IN BIOLOGICAL MATERIAL

LENA HANSSON, JEAN PETERSSON and ÅKE OLIN

Department of Analytical Chemistry, University of Uppsala, P.O. Box 531, S-751 21 Uppsala, Sweden

(Received 28 January 1987. Revised 20 April 1987. Accepted 10 May 1987)

Summary—Two digestion procedures have been tested on samples of flour, blood and urine for application in the determination of selenium by hydride-generation atomic-absorption spectrometry. The first utilizes a mixture of concentrated nitric, perchloric and sulphuric acids and the second a mixture of magnesium nitrate hexahydrate, concentrated nitric acid and 6*M* hydrochloric acid. The accuracy of the procedures was tested by analysis of standard reference materials and by comparison with results from neutron-activation analysis. It was found that the "magnesium method" can replace the more common procedure, which includes perchloric acid, for the sample types investigated in this paper.

Selenium is an element both essential and detrimental to living organisms. As such it has received great attention from workers in diverse fields such as biochemistry, agriculture and medicine. The importance of selenium for the health of man and livestock is well documented.¹⁻³ In many reports the effects on human health are discussed, and it is indicated that too low an intake of the element may cause illness. On the other hand selenium becomes toxic at higher concentrations.⁴ The ambivalence of selenium in living organisms, together with the small range of beneficial selenium concentrations in plant material or biological liquids and tissues, *etc.*, calls for precise methods for determination of the element. Stringent demands are made on the final determination step as well as on the digestion procedure chosen for destruction of the organic matter. The design of a digestion procedure for selenium is not trivial, since different specimens may react diversely with a given digestion mixture, and hence false information on the selenium content may be obtained. Factors that influence the outcome of the digestion step are the destructive power of the mixture of reagents used, the resistance of the selenium compounds involved to oxidation, and the volatility of the selenium species originally present or formed in the digestion.⁵⁻⁷

The most common digestion method for biological materials utilizes the high oxidation potential of hot concentrated perchloric acid,⁸⁻¹⁴ which is often used together with other concentrated acids such as nitric, sulphuric or phosphoric. However, perchloric acid is inconvenient to work with owing to the hazard of explosions if it is incorrectly handled.^{15,16} In particular, its use in laboratories with a high turnover of staff should be avoided. Also, more stringent requirements are continually appearing for the materials and construction of fume-hoods used for digestions in-

volving perchloric acid. Hence there is a need for testing alternative digestion procedures which do not use this acid. One way to open out biological material without use of perchloric acid is combustion in oxygen in a closed system.¹⁷ Excellent results have been obtained in the determination of selenium by Knapp *et al.*,¹⁸ but their equipment is specialized and not suitable for routine analysis.

This work describes the destruction of flours, human whole blood and urine by use of magnesium nitrate^{19,20} combined with nitric acid^{21,22} and hydrochloric acid and the subsequent determination of selenium in the digests by hydride-generation atomic-absorption spectrometry (HG-AAS) in a flow system. Results obtained with this method are compared with those from a procedure which utilizes a mixture of concentrated nitric, perchloric and sulphuric acids, hereafter called the three-acid mixture. Standard reference materials have been analysed and in a few instances samples have been subjected to neutron-activation analysis (NAA).

EXPERIMENTAL

Apparatus

The HG-AAS apparatus, which has been described elsewhere,²² consisted of a Varian AA5 atomic-absorption spectrophotometer connected to a flow-injection system (Bifok, Sweden). The spectrophotometer was equipped with a selenium electrodeless discharge lamp (Westinghouse). Peak heights were evaluated with an integrator (Shimadzu C-R3A).

The digestion vessels were heated in a temperature-programmed aluminium block made in the laboratory. A temperature regulator (MDV, ERO Electronics, Italy) interfaced with a calculator (HP-41 CV) was used to control the temperature programme.

Reagents

All reagents used were of analytical grade. A standard solution of selenium(IV), 1 g/l., was prepared from an ampoule of selenium dioxide in dilute nitric acid (Merck).

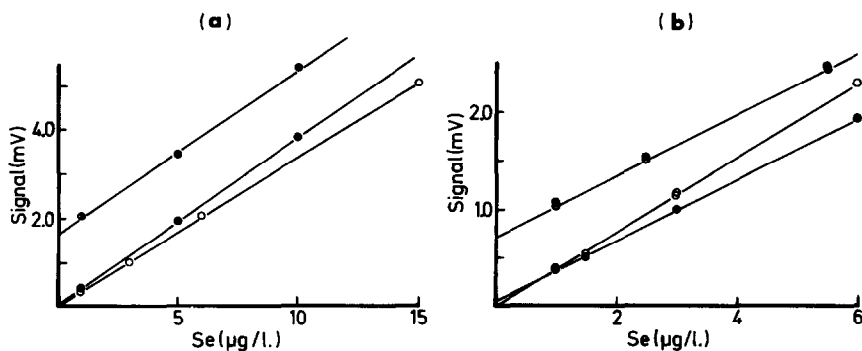


Fig. 1. Calibration and standard addition curves for ○ selenite in dilute hydrochloric acid; ● selenite added to digested reagent blank; ⊗ selenite added to digested sample. (a) Method A: 10 ml of concentrated nitric acid, 5 g of magnesium nitrate, and 1 ml of 1:1 v/v hydrochloric acid; diluted to 50 ml. (b) Method B: 20 ml of three-acid mixture; diluted to 50 ml.

The selenium(VI) standard solution, 1 g/l., was prepared from sodium selenate decahydrate. Further standards were obtained by dilution of these solutions. A small addition of hydrochloric acid was made to prevent adsorption.

The three-acid mixture was composed of the concentrated acids in the proportions nitric:perchloric:sulphuric 20:5:2 v/v.

The reference materials were SRM 1567 wheat flour (NBS) and Seronorm 105 and 108 (Nycomed AS, Oslo, Norway).

Sample pretreatment

The North American wheat grains Durum and North Spring were ground into flour by a Turmix mill, and passed through 30 and 60 mesh sieves. Swedish wheat flour, potato flour, and Canadian buckwheat flour were analysed as supplied by the manufacturer. A batch of about 400 ml of human whole blood was divided into several small portions and stored in a freezer until used. A portion of the whole blood was freeze-dried and sent for determination of selenium content by neutron-activation analysis.

Digestion procedures

Two digestion procedures were applied to the samples. In method A two versions were used, one for samples of low organic content and the other for samples with high organic content.

A. Nitric acid–magnesium nitrate digestion. Put the sample in a 50-ml glass tube and add 2 or 5 g of magnesium nitrate hexahydrate, 5 or 10 ml of concentrated acid, and 1 ml of 6M hydrochloric acid. Insert the tube into the aluminium block and apply the temperature programme of 50° for 1 hr, 85° for 1 hr, 105° for 1 hr, 125° for 2 hr, 175° for 2 hr, 225° for 2 hr, 300° for 2 hr and 500° for 3 hr. Cool the tube, and add 9 or 12 ml of 6M hydrochloric acid to dissolve the magnesium oxide formed and to adjust the hydrochloric acid concentration to about 4M. Then heat at 130° for 1 hr to reduce any selenate to selenite. Dilute the digest so that the selenium concentration falls within the working range of the HG–AAS finish.

The larger reagent amounts are recommended for samples with a high organic content.

B. Nitric–perchloric–sulphuric acid digestion. Add 20 ml of the three-acid mixture to the sample in a 50-ml Kjeldahl flask. Boil in a heating stand until the sulphuric acid starts to reflux. Cool, add 6 ml of 6M hydrochloric acid and heat again until the sulphuric acid starts to reflux. Cool and dilute to an appropriate volume.

RESULTS AND DISCUSSION

The general performance of the HG–AAS flow system used in this work has been described earlier together with its application to bovine liver samples.²² To facilitate the present discussion some data on the performance of the equipment will be repeated here. The precision is better than 1% for selenium at a concentration of 6 µg/l. and about 3% at 1 µg/l. This means that the limit of detection for pure selenium solutions is about 0.1 µg/l. The working curve is linear up to at least 15 µg/l. and the characteristic mass (1% absorption, 0.6 ml injection volume) is 30 pg.

Evaluation of the absorption signal

Reagent-matched calibration solutions were prepared by addition of known amounts of selenite to portions of the blank after digestion. Figure 1a,b shows calibration curves obtained in this way from blank solutions from procedures A and B. The curve for selenite in dilute hydrochloric acid is included as a reference. Standard-additions curves are also shown. It can be seen that the three-acid mixture

Table 1. The recovery (%) of selenite and selenate added to blanks and samples before digestion by methods A and B (see text for details)

Sample	Method A			Method B		
	Recovery, %	<i>s</i>	<i>n</i>	Recovery, %	<i>s</i>	<i>n</i>
Blank + Se(IV)	101	5.2	12	104	4.5	3
Blank + Se(VI)	101	5.2	6	103	3.5	3
Sample + Se(IV)	100	2.3	8	105	2.8	4
Sample + Se(VI)	100	7.7	4	103	9.5	4

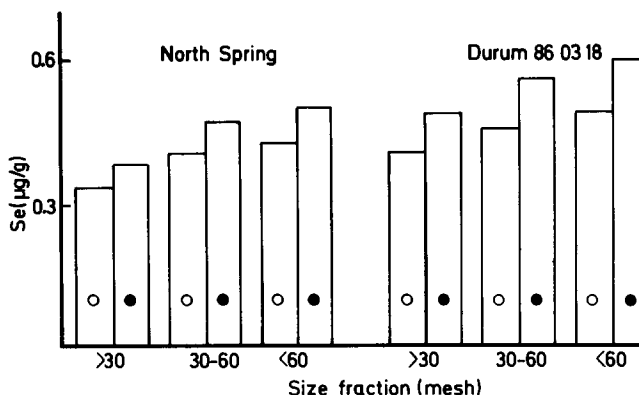


Fig. 2. Selenium concentrations obtained for three different size fractions of the North American wheat flours North Spring and Durum 860318 after digestion with 10 ml of 1:1 v/v nitric acid and 5 g of magnesium nitrate. ○ Without and ● with addition of 1 ml of 1:1 v/v hydrochloric acid. Each result represents the mean of two determinations.

decreased the selenium signal to about 80% of that for the reference solution, whereas the magnesium nitrate–nitric acid reagent slightly enhanced it. It can also be noted that the standard-additions curves are parallel to the “reagent” calibration curves for both methods, indicating that there was no interference from sample components. This was the case for all matrices studied in this investigation.

The slopes of the analytical curves may vary from time to time depending, *e.g.*, on the effectiveness of the sodium tetrahydroborate reagent, but the relative slopes (that is, the ratios between the slopes of the “reagent” curves and the “reference” curve) are fairly constant. For the conditions used in the experiments presented in Fig. 1 the relative slopes are 106% ($s = 3\%$, $n = 21$) for method A and 82% ($s = 5\%$, $n = 7$) for method B.

The method of standardization described above

results in a calibration curve that corrects for the blank. Neither method A or B gave blank signals distinguishable from the noise. Nevertheless the analytical curve had an intercept on the y -axis, the size and precision of which greatly influenced the analytical result from samples giving signals close to the limit of detection. This intercept exhibited a standard deviation of about $20 \mu\text{V}$, representing an absorbance of 0.0004 or a selenium concentration of $0.05 \mu\text{g/l}$. This means that the practical limit of detection is about $0.15 \mu\text{g/l}$. ($3s$) and the limit of determination about $0.5 \mu\text{g/l}$. ($10s$). For some specimens in this investigation these limits were approached.

Recovery studies

The recoveries of selenite and selenate added to blanks and samples before digestion were determined for both destruction procedures. The results are given

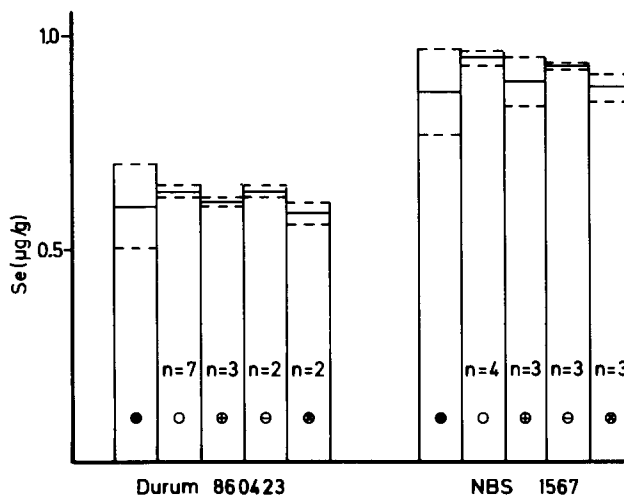


Fig. 3. Selenium concentration in NBS 1567 wheat flour and Durum 860423 digested with 5 g of magnesium nitrate and ○ 10 ml of 1:1 v/v nitric acid; ⊖ 10 ml of 1:1 v/v nitric acid and 1 ml of 1:1 v/v hydrochloric acid; ⊕ 10 ml of concentrated nitric acid; ○ 10 ml of concentrated nitric acid and 1 ml of 1:1 v/v hydrochloric acid. The samples were also analysed by ● NAA (Studsвик Energiteknik AB, Sweden). The ranges are shown.

Table 2. Selenium concentration in flour samples

Sample	Amount, g	Method A				Method B				NAA†
		Mean, µg/g	RSD, %	CI, µg/g	n	Mean, µg/g	RSD, %	CI, µg/g	n	Result, µg/g
Potato flour	1.0	<0.003								
Wheat flour	0.8	0.011	12.7	0.007–0.015	3	0.012	4.2	0.010–0.014	3	
Buckwheat	0.7	0.034	10.0	0.031–0.037	9	0.031	4.2	0.029–0.033	8	
Durum 860318	0.4	0.615	0.7	0.606–0.624	3	0.583	4.0	0.525–0.641	3	
Durum 860423	0.4	0.635	1.6	0.625–0.645	7	0.544	1.9	0.527–0.561	4	0.6 ± 0.1
North Spring	0.4	0.509	1.2	0.494–0.524	3					
NBS 1567*	0.2	0.951	1.2	0.933–0.969	4	0.953	3.5	0.869–1.037	3	0.87 ± 0.1

*Certified 1.1 ± 0.2 µg/g.

†Studsvik Energiteknik AB, Sweden.

CI = Confidence interval (95%).

in Table 1. The specimens digested were blood and various kinds of flour. The additions usually ranged from 15 to 30 ng of selenium, giving concentrations between 0.6 and 1.2 µg/l in the solutions. In method B, 20 ml of the three-acid mixture were used and in method A conditions varied slightly, but with no detectable effect on the recovery. According to the data in Table 1 there is no evidence that selenite or selenate was lost in the digestions.

Analytical results

Flour samples. Methods A and B have earlier been used to digest liver samples.²² Very satisfactory results were obtained with method A, using 10 ml of 100% nitric acid together with 5 g of magnesium nitrate hexahydrate for a 0.1–0.2 g dry-weight sample. However these amounts of reagents may yield blanks too high for the accurate determination of selenium in samples low in selenium. Therefore, the use of 10 ml of 1:1 concentrated nitric acid (70%) was tested for flour samples weighing 0.3–0.8 g, but the results were low. It was then found that a small addition of hydrochloric acid to the digestion mixture led to higher recoveries of selenium. The same increase in recovery was obtained when 2–15 mmoles of hydrochloric acid were added. The reason for this behaviour is not known at present. In addition, 10 ml of concentrated nitric acid instead of the 1:1 acid gave higher yields, and the presence of a small amount of hydrochloric acid further improved the digestion in this case also.

In method B, 20 ml of the three-acid mixture were used. This amount is supposed to digest at least 1.6 g of organic material.¹⁴ When the reagent volume was reduced to 10 ml for samples weighing 0.1–1.0 g, low and varying results were observed. This is attributed to the small final volume of sulphuric acid remaining after digestion. This volume is thought not to be able to hold the selenium, but to lose an unpredictable fraction of it.

Figure 2 shows the effect of hydrochloric acid on the analytical results for the wheat flours North Spring and Durum. Three different size fractions were analysed for each grain and method A was applied with 10 ml of 1:1 nitric acid with or without addition of 1 ml of 1:1 hydrochloric acid. It can be seen that the addition of hydrochloric acid gave enhanced recovery of selenium. If the same volume of concentrated nitric acid was used instead of 1:1 nitric acid the effect of added hydrochloric acid was still observed although it was not as marked. This can be seen in Fig. 3 where results are given from the analyses of another grinding of Durum sieved through a 60 mesh sieve and from the analysis of NBS SRM 1567 wheat flour. These samples were also analysed by NAA. It is seen that all digestion reagents chosen yielded selenium concentrations that fall within the range reported from the NAA.

Table 2 summarizes the results from the determination of selenium in flours of differing selenium content. Ten ml of concentrated nitric acid, 5 g of magnesium nitrate hexahydrate and 1 ml of 1:1 hy-

Table 3. Selenium concentration in blood, serum and urine samples

Sample	Amount, g	Method A				Method B				NAA†
		Mean, µg/g	RSD, %	CI, µg/g	n	Mean, µg/g	RSD, %	CI, µg/g	n	Result, µg/g
Whole blood	0.5	0.088	1.1	0.087–0.089	12	0.082	0.9	0.080–0.084	3	
Whole blood*	0.2	0.424	2.0	0.410–0.438	4					0.4 ± 0.1
Seronorm 105§	0.5	0.086	2.6	0.084–0.088	7	0.082	4.5	0.078–0.086	6	
Seronorm 108‡	1.0	0.049	2.0	0.048–0.050	8	0.047	4.0	0.044–0.050	5	

*Freeze-dried whole blood. The experimentally determined dry weight was 20.9%, giving a selenium concentration of 0.089 µg/g in the original sample.

†Studsvik Energiteknik AB, Sweden.

‡Human urine with certified value 49 µg/l.

§Human serum with certified value 90 ± 6 µg/l.

CI = Confidence interval (95%).

drochloric acid were used for the digestion in method A and 20 ml of the three-acid mixture were used in method B. These are the amounts of reagent that we recommend for selenium determination in flours. The sample weight should not exceed 0.8 g for trouble-free digestion in method A ("boiling over", incomplete digestion). In method B the sample weight should not exceed 1 g, in order to avoid excessive charring when the nitric acid oxidation is complete. Charring may lead to losses of selenium,^{7,10} and for some flours large sample sizes may lead to copper concentrations in the test solution that interfere in the HG-AAS step.²² From Table 2 it can be seen that procedure A is well suited to replace procedure B as digestion method when selenium is to be determined. Unfortunately the analyses of NBS SRM 1567, wheat flour, are not completely satisfactory. In this reference material the selenium concentration found is often below the certified mean value,^{12,13,20,21,23-28} but results in agreement with the certified value have been obtained by some workers.^{8,18,29} Our result is consistent with the NAA result but nevertheless we believe that our methods fail to some extent to yield quantitatively the selenium in SRM 1567 and possibly in flour in general.

Blood and urine samples. It is generally sufficient to digest 0.5 g of whole blood, plasma or serum to obtain a satisfactory absorption signal when the test solution is diluted to 25 ml. For urine, 1 g is often required. In these sample types the organic matter is only a minor component, and reduced amounts of reagents can be used in the destruction procedures. For optimal performance, 5 ml of concentrated nitric acid, 2 g of magnesium nitrate hexahydrate and 1 ml of 1:1 hydrochloric acid were taken for the digestion by procedure A. The effect of hydrochloric acid is not as pronounced as for flour samples. For procedure B, 20 ml of the three-acid mixture are recommended in order to diminish the risk of losses. Table 3 gives the results from the determination of selenium in whole blood. The results from the analyses of the reference materials Seronorm human serum batch 105 and Seronorm human urine batch 108 are also included. A portion of freeze-dried blood was subjected to NAA and the result is given in Table 3. The selenium concentrations found in the reference materials as well as the NAA result confirm that procedures A and B both give accurate results. It is also seen that there was no loss of selenium when the blood was freeze-dried.

The iron in whole blood results in an iron concentration of about 10 mg/l. in the test solutions. Interference from iron(III) in determination of 2 µg/l. of selenium was separately investigated and found to be absent for iron(III) concentrations up to 50 mg/l.

CONCLUSION

For selenium determination in flour, blood and urine samples the two methods described in this

paper give results in close agreement to NAA. Method A is recommended since it avoids the use of perchloric acid. The digestion is rather time-consuming but no supervision is necessary, and it can be performed overnight. When method B is used, it is advisable to take no less than 20 ml of the three-acid mixture.

Acknowledgement—Katarina Lagerström is thanked for making the blood analyses.

REFERENCES

1. R. J. Shamberger, in *Mineral Elements '80. Proceedings*, Part II, pp. 501-509. Hanasaari Culture Center, Helsinki, 1981.
2. W. Mertz, *ibid.*, pp. 381-398. Hanasaari Culture Center, Helsinki, 1981.
3. K. Jaakkola, P. Kurkela, A. U. Arstila and H. M. Larni, *ibid.*, pp. 225-233. Hanasaari Culture Center, Helsinki, 1981.
4. W. C. Cooper and J. R. Glover, in *Selenium*, R. A. Zingaro and W. C. Cooper (eds.), Chapter 11, Van Nostrand-Reinhold, New York, 1974.
5. M. Verlinden, *Talanta*, 1982, **29**, 875.
6. B. Welz, M. Melcher and J. Nève, *Anal. Chim. Acta*, 1984, **165**, 131.
7. R. Bock and D. Jacob, *Z. Anal. Chem.*, 1964, **200**, 6.
8. H. Narasaki and M. Ikeda, *Anal. Chem.*, 1984, **56**, 2059.
9. B. T. G. Ting, A. Nahapetian, V. R. Young and M. Janghorbani, *Analyst*, 1982, **107**, 1495.
10. *Official Method of Analysis of the A.O.A.C.*, W. Horwitz (ed.), 12th Ed., p. 455. A.O.A.C., Washington, 1975.
11. B. Irsch and K. Schäfer, *Z. Anal. Chem.*, 1985, **320**, 37.
12. J. W. Jones, S. G. Capar and T. C. O'Haver, *Analyst*, 1982, **107**, 353.
13. H. A. M. G. Vaessen, A. Ooik and J. Zuydendorp, *Z. Lebensm.-Unters. Forsch.*, 1985, **181**, 189.
14. *Kungl. Lantbrukstyrelsens Kungörelser m.m.*, 1950, No. 9.
15. T. T. Gorsuch, *The Destruction of Organic Matter*, pp. 22-24. Pergamon Press, Oxford, 1970.
16. H. Diehl, *Talanta*, 1966, **13**, 867.
17. R. Bock, *A Handbook of Decomposition Methods in Analytical Chemistry*, pp. 162-163. International Textbook Company, London, 1979.
18. G. Knapp, S. E. Raptis, G. Kaiser, G. Tölg, P. Schramel and B. Schreiber, *Z. Anal. Chem.*, 1981, **308**, 97.
19. F. Nakata, Y. Yasui, H. Matsuo and T. Kumamaru, *Anal. Sci.*, 1985, **1**, 417.
20. D. C. Reamer and C. Veillon, *Anal. Chem.*, 1981, **53**, 1192.
21. H. Han, G. Kaiser and G. Tölg, *Anal. Chim. Acta*, 1981, **128**, 9.
22. J. Pettersson, L. Hansson and Å. Olin, *Talanta*, 1986, **33**, 249.
23. M. H. Hahn, R. W. Kuennen, J. A. Caruso and F. L. Fricke, *J. Agric. Food Chem.*, 1981, **29**, 792.
24. M. H. Hahn, K. A. Wolnik and F. L. Fricke, *Anal. Chem.* 1982, **54**, 1048.
25. A. Meyer, Ch. Hofer, G. Knapp and G. Tölg, *Z. Anal. Chem.*, 1981, **305**, 1.
26. K. A. Wolnik, F. L. Fricke, M. H. Hahn and J. A. Caruso, *Anal. Chem.*, 1981, **53**, 1030.
27. M. Yamamoto, M. Yasuda and Y. Yamamoto, *ibid.*, 1985, **57**, 1382.
28. H. Narasaki, *Z. Anal. Chem.*, 1985, **321**, 464.
29. J. Piwonka, G. Kaiser and G. Tölg, *ibid.*, 1985, **321**, 225.

FLUORIMETRIC DETERMINATION OF GALLIUM IN A NICKEL ALLOY AND ALUMINIUM WITH N-OXALYLAMINE(SALICYLALDEHYDE HYDRAZONE)

FERNANDO DE PABLOS, GUILLERMINA GALAN* and JOSE GOMEZ ARIZA

Department of Analytical Chemistry, Faculty of Chemistry, University of Seville, 41012-Seville, Spain

(Received 17 November 1986. Revised 15 April 1987. Accepted 10 May 1987)

Summary—A fluorimetric determination of gallium, based on the formation of the fluorescent chelate with *N*-oxalylamine(salicylaldehyde hydrazone) (OSH)-Ga(III), is proposed. The complex has excitation and emission maxima at 395 and 475 nm, respectively. The detection limit is 3 ng/ml and Ga can be determined up to 277 ng/ml. The method has been applied to the determination of gallium in a nickel alloy and aluminium. Extraction with *n*-butyl acetate from 6*M* hydrochloric acid medium has been used to separate Ga from the interfering elements in the alloys.

Gallium is considered one of the rare elements. It occurs to the extent of a few parts per million in most silicate rocks and minerals, where, as a result of the similar ionic radii and ionization potentials, it tends to be camouflaged by aluminium.¹

The increasing use of gallium compounds in the electronics industry and their antitumor activity²⁻⁴ are reasons for needing sensitive analytical methods for determining this element.

Several methods have been used for determination of gallium in various samples: neutron-activation analysis for pure metals and geological samples,⁵ coal and spinach,⁶ bauxite,^{7,8} coal ash,⁸ semiconductors;⁹ polarography for ores and metals;¹⁰ potentiometric stripping analysis for biological materials;¹¹ differential pulse anodic stripping voltammetry for ores;¹² X-ray fluorescence for synthetic mixtures of chromium and gallium;¹³ inductively-coupled plasma emission for silicon-germanium-gallium¹⁴ and aluminium¹⁵ alloys; atomic-absorption spectrometry for alloys of iron and nickel,¹⁶ ores,¹⁷ aluminium and aluminium alloys,¹⁸ semiconductors,¹⁹ and orchard leaves, river sediments, soils and rocks.²⁰ Spectrophotometric²¹⁻²³ and fluorimetric²¹⁻²² methods involving the use of organic reagents have also been extensively used for determining gallium in different kinds of samples.

It is remarkable that many of these methods involve prior separation steps, the most usual being the extraction of gallium chloride from 6*M* hydrochloric acid²² with an appropriate organic solvent, such as diethyl ether,^{24,25} di-isopropyl ether,²⁶ methyl isobutyl ketone,²⁷ and *n*-butyl acetate.²²

N-Oxalylamine(salicylaldehyde hydrazone) (OSH), described previously²⁸ as a fluorimetric reagent for

aluminium, yields a fluorescent chelate with gallium. In this paper a sensitive method for determining gallium with it is described. The content of gallium in a nickel alloy and aluminium has been determined by the proposed method.

EXPERIMENTAL

Apparatus

Fluorescence measurements were made with a Perkin-Elmer LS-5 spectrofluorimeter, equipped with a xenon lamp source, 1.0-cm fused-silica cells and a Perkin-Elmer 561 recorder. The fluorescence data are given without spectral correction. An ultrathermostatic water-bath circulator (Colora KS) was used for temperature control. A Perkin-Elmer 554 spectrophotometer and a Crison-501 digital pH-meter with a combined glass-Ag/AgCl electrode were used.

Reagents

OSH was synthesized as previously described²⁸ and used as a 2.0 g/l. solution in dimethylformamide. A stock solution of gallium was prepared from the chloride and standardized by titration with EDTA. Working solutions were prepared by appropriate dilutions.

A buffer solution (pH 2.3) of potassium mono-chloroacetate-mono-chloroacetic acid (0.25*M*) was used.

Procedure

Into a 25-ml standard flask place a sample containing not more than 2 µg of gallium, add 0.3 ml of OSH solution and 12.2 ml of dimethylformamide and adjust the pH with 5 ml of buffer solution; dilute to volume with distilled water. Measure the fluorescence at 475 nm with excitation at 395 nm, against a reagent blank, at 25°.

Determination of gallium in aluminium

Dissolve a 1-g sample (accurately weighed) in 30 ml of 6*M* hydrochloric acid. Cool the solution and add 15% titanium chloride solution dropwise until the solution becomes permanent light violet. Wait a few minutes. Transfer the solution into a 100-ml separating funnel and extract the gallium by shaking the solution with 25 ml of *n*-butyl acetate for 1 min. Discard the aqueous layer and wash the extract with two 3-ml portions of 6*M* hydrochloric acid. Strip the gallium from the organic phase with two 15-ml portions of distilled water. Transfer the aqueous solution

*Present address: Department of Bromatology, Toxicology and Applied Chemical Analysis, Faculty of Pharmacy, University of Seville, 41012-Seville, Spain.

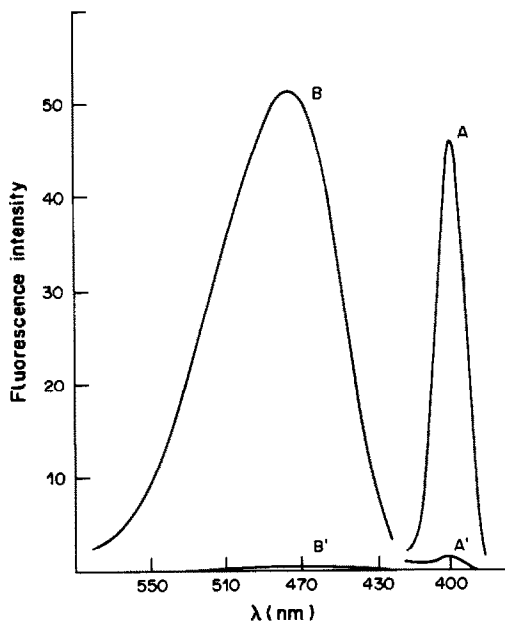


Fig. 1. Uncorrected excitation (A, A') and emission (B, B') spectra of complex (A, B) and free ligand (A', B'), at pH 3.8. $C_{Ga} = 1.4 \times 10^{-6} M$; $C_R = 7.7 \times 10^{-5} M$.

to a 50-ml beaker and add 0.1 g of sodium chloride. Evaporate the solution to dryness, dissolve the residue in water and dilute it to volume in a 25-ml standard flask. Determine the gallium content by the recommended procedure, using fluoride as masking agent.

Determination of gallium in nickel alloy

Weigh accurately about 1 g of sample, transfer it into a beaker, heat it first with 5 ml of concentrated hydrochloric acid and then with 10 ml of concentrated nitric acid and 2 ml of bromine, and evaporate the solution nearly to dryness, on a sand-bath. After cooling, add 2 ml of concentrated sulphuric acid and heat until copious white fumes are evolved. Cool again, then take up the residue with about 25 ml of 1.5M hydrochloric acid and filter the solution through a Whatman No. 41 filter paper into a 100-ml standard flask. Wash the beaker and filter paper with 1.5M hydrochloric acid to make up the volume to the mark. Transfer a 50-ml aliquot into a beaker and evaporate the solution nearly to dryness. Add 30 ml of 6M hydrochloric acid then 15% titanium chloride solution dropwise until its colour persists in the mixture, and wait several minutes. Transfer the solution to a 100-ml separating funnel and extract the gallium by shaking with 25 ml of n-butyl acetate for 1 min. Discard the aqueous layer and wash the extract with two 3-ml portions of 6M hydrochloric acid. Strip the gallium with two 15-ml portions of distilled water. Transfer these aqueous phases to a beaker, then add 0.1 g of sodium chloride and evaporate to dryness. Dissolve the residue in water and dilute it to volume in a 25-ml standard flask. Determine the gallium content by the recommended procedure.

RESULTS AND DISCUSSION

Study of the Ga(III)-OSH complex

Gallium forms a complex with OSH, the absorption spectrum of which has its maximum at 382 nm.

The complex exhibits an intense yellow-greenish fluorescence and the maximal emission occurs at 475 nm, with excitation at 395 nm. Figure 1 shows the uncorrected excitation and emission spectra.

The maximal emission is reached immediately and remains constant for at least 18 hr. The relative fluorescence intensity of the complex [$1 \mu\text{g/ml}$ Ga(III)] is 22 times that of $0.1 \mu\text{g/ml}$ quinine sulphate in 0.05M sulphuric acid.

Because of the low solubility of the reagent a mixture of water and dimethylformamide is used. The influence of the dimethylformamide content on the fluorescence intensity was examined, the most suitable concentration being found to be 50% v/v.

Influence of pH. The effect of pH on the absorbance and fluorescence of the chelate was determined (*N.B.*, throughout this paper "pH" is used to denote the pH-meter reading). As can be seen in Fig. 2(a), the absorbance is not affected by the pH in the range 5.0–6.5; for this reason an acetic acid-acetate buffer solution (pH 4.5) was selected for the preparation of samples with a final pH of about 5.5. The fluorescence intensity is constant in the pH range 2.7–3.3 [Fig. 2(b)]. A buffer solution of monochloroacetic acid-monochloroacetate (pH 2.3) was

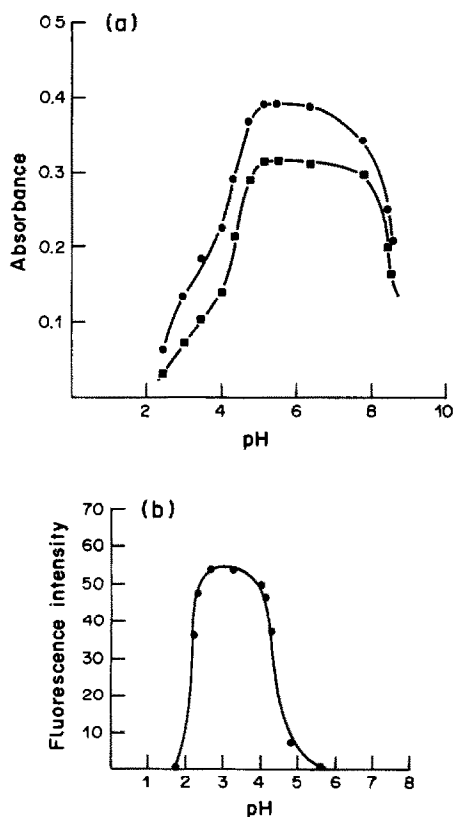


Fig. 2. Influence of pH on the Ga(III)-OSH complex. $C_{Ga} = 4.4 \times 10^{-6} M$; $C_R = 9.7 \times 10^{-4} M$. (a) Absorbance-pH plot, ● 382 nm, ■ 400 nm; (b) relative fluorescence-pH plot, $\lambda_{ex} = 395 \text{ nm}$, $\lambda_{em} = 475 \text{ nm}$.

Table 1. Effect of other species on the determination of gallium (29.7 ng/ml) with OSH

Foreign species	Tolerance, ng/ml
Cl ⁻ , I ⁻ , NO ₃ ⁻ , SO ₄ ²⁻	15000
Ca(II)	12000
Ag(I)	8000
Ni(II)	6000
Mg(II), Tl(I), Hg(II)	4000
Co(II), Cd(II), Pb(II), BICIN*	1000
Pd(II), Y(III), Mn(II)	400
Br ⁻ , F ⁻ , SCN ⁻ , S ₂ O ₃ ²⁻ , tartrate	300
Zn(II), Ti(IV), Bi(III)	200
Fe(III), V(V), AsO ₄ ³⁻ , Cr(III), Mo(VI), U(VI), citrate	100
Zr(IV)	50
EDTA, PO ₄ ³⁻ , Cu(II), Sb(III)	30
In(III)	20
Sn(II)	15
Al(III)	<10

*N,N-Bis(2-hydroxyethyl)glycine.

used to ensure the pH of the samples fell within the desired interval.

Stoichiometry of the complex. The mole-ratio²⁹ and continuous variations³⁰ methods were used to determine the composition of the complex. Both methods showed a 1:3 metal:reagent ratio.

Calibration range, sensitivity and precision

The conditions for determining gallium with OSH were optimized. The most suitable concentration of the reagent was found to be $1.16 \times 10^{-4} M$ (for 200 ng/ml gallium). There was a linear relationship between the gallium concentration and the fluorescence intensity over the range 3–277 ng/ml. The detection limit³¹ was 3 ng/ml.

The precision of the method was studied by analysing eleven 29.7 µg/ml gallium replicates; the maximum relative error ($P = 0.05$) was $\pm 2\%$.

Effect of foreign ions

To assess the possible analytical applications of the method, the effects of other species on the determination of gallium with OSH were studied. Table 1 summarizes the tolerance limits for the ions tested (concentrations giving less than $\pm 5\%$ error in the determination of 29.7 ng/ml gallium).

Indium and aluminium, which yield fluorescent complexes with OSH, give strong interference, but

Table 3. Determination of gallium in alloys (range of 3 determinations)

Sample	Present, %	Found, %
Aluminium BCS 195g*	0.009	0.0093; 0.0086; 0.0092
Nickel BCS-346†	0.005	0.0051; 0.0053; 0.0052

*Al 99.85, Si 0.03, Fe 0.-08, Cu 0.001, Mn 0.001, Ti 0.002, V 0.004, Zn 0.015%.

†Ni 60.2, Co 15, Ti 5, Cr 3, Al 5.5, Mo 3, V 1, Pb 0.0021, Bi 0.0010, Ag 0.0035, Se 0.0009, Te 0.0012, Sb 0.0047, As 0.0050, Cd 0.00004, Sn 0.0091, Zn 0.0029, Mg 0.014, TI 0.0002, Ca 0.0036, In 0.0019%.

most ions tested can be tolerated at fairly high concentrations.

The influence of several masking agents was tested. The results are shown in Table 2. By addition of fluoride the tolerance level for Al(III) and In(III) can be increased and BICIN and tartrate are useful for masking Zn(II), Co(II) and Fe(III).

Determination of gallium in alloys

The proposed method was used for determining gallium in two alloys: BCS 195 g and BCS 346. Because of the complexity of the samples and their low level of gallium a prior separation from interfering ions was necessary; the method proposed by Busev *et al.*²² was used.

For determining gallium in BCS 195 g, fluoride (300 ng/ml) was added to prevent the interference of the small amounts of aluminium that contaminated the initial gallium extract. The results are shown in Table 3.

Conclusions

Several organic reagents have been proposed for the fluorimetric determination of gallium. In Table 4, OSH is compared with some of the most frequently used reagents. OSH compares favourably in sensitivity with all of them except sulphonaphthol-resorcinol. An extraction step is necessary with most of these reagents. The method with OSH is performed in homogeneous medium and the fluorophore is yielded instantaneously; heating is not necessary and the complex remains stable for a long time. For determining gallium in a complex matrix with OSH a prior separation from the interferents cannot be avoided, but this applies to most of the methods listed in the bibliography.

Table 2. Elimination of interferences by addition of masking agents

Foreign ion	Amount tolerated, ng/ml		Masking agent (ng/ml)
	Without masking agent	With masking agent	
Al(III)	<10	80	fluoride (300)
In(III)	20	100	fluoride (300)
Zn(II)	200	500	BICIN (1000)
Co(II)	1000	2000	BICIN (1000)
Fe(III)	100	300	tartrate (300)

Table 4. Characteristics of reagents for fluorimetric determination of gallium

Reagent	Sensitivity, ng/ml	Experimental conditions	Applications	References
Lumogallion	15	pH 2.2; incubate at 80° for 20 min; extract with isoamyl alcohol	biological material	32, 33
Rhodamine B	10	6M hydrochloric acid; extract with benzene:ether (9:1)	zinc, indium, bauxite	34-37
8-Hydroxyquinoline	50	pH 3.9-5.5; extract with chloroform	germanium	38, 39
Sulphonaphtholresorcinol	1	pH 3	semiconductor materials	40, 41
Solochrome Black	10	pH 4.7 extract with amyl alcohol		
OSH	3	pH 2.7-3.3	alloys	this work

REFERENCES

- P. J. Jeffery, *Chemical Methods of Rock Analysis*, 1st Ed., p. 238, Pergamon Press, Oxford, 1970.
- M. M. Hart and R. H. Adamson, *Proc. Natl. Acad. Sci. U.S.A.*, 1971, **68**, 1623.
- R. C. Hayes, *J. Nucl. Med.*, 1970, **18**, 740.
- R. A. Zweidinger and L. Barnett, *Anal. Chem.*, 1973, **45**, 1563.
- I. P. Alimarin, Y. V. Yakovlev and V. P. Kolotov, *Zh. Analit. Khim.*, 1983, **38**, 208.
- J. St-Pierre and L. Zikovsky, *Can. J. Chem.*, 1982, **60**, 2278.
- S. G. Chen and H. T. Tsai, *J. Radioanal. Chem.*, 1983, **78**, 263.
- H. C. Wu, S. G. Chen and H. T. Tsai, *J. Chin. Chem. Soc. (Taipei)*, 1983, **30**, 235; *Anal. Abstr.*, 1984, **46**, 8B47.
- K. P. Rudolph, J. Flachowski, A. Lange and J. Dubnack, *Isotopenpraxis*, 1983, **19**, 225.
- J. Chen and Y. Deng, *Fenxi Huaxue*, 1982, **10**, 459; *Anal. Abstr.*, 1983, **44**, 6B76.
- D. Jagner, *Trends Anal. Chem.*, 1983, **2**, 53.
- K. Han, *Fenxi Huaxue*, 1982, **10**, 558; *Anal. Abstr.*, 1983, **44**, 6B77.
- R. Govil and S. K. Kataria, *X-Ray Spectrom.*, 1982, **11**, 144.
- I. Hayashi, H. Hara and Y. Goshi, *Bunseki Kagaku*, 1984, **33**, T9.
- J. A. C. Broekaert, F. Leis and G. Dinçler, *Analyst*, 1983, **108**, 717.
- T. F. Rybina, M. S. Dymova and N. N. Alekseeva, *Zavodsk. Lab.*, 1983, **49**, No. 4, 40.
- C. Huang, *Fenxi Huaxue*, 1983, **11**, 135; *Anal. Abstr.*, 1983, **45**, 6B150.
- M. N. Gorlova and N. D. Veller, *Zavodsk. Lab.*, 1982, **48**, No. 12, 31.
- K. Kuga, S. Ooyu, E. Kitazume and K. Tsujii, *Bunseki Kagaku*, 1984, **33**, E29.
- H. Han and Z. Ni, *Fenxi Huaxue*, 1983, **11**, 571; *Anal. Abstr.*, 1984, **46**, 7H4.
- F. D. Snell, *Photometric and Fluorimetric Methods of Analysis*, Part I, pp. 497-534. Wiley, New York, 1978.
- A. I. Busev, V. G. Tipsova and V. M. Ivanov, *Analytical Chemistry of Rare Elements*, pp. 276-290. Mir, Moscow, 1981.
- Z. Marczenko, *Spectrophotometric Determination of Elements*, pp. 267-273. Horwood, Chichester, 1976.
- C. L. Luke and M. E. Campbell, *Anal. Chem.*, 1956, **28**, 1340.
- W. Geilmann, H. Bode and E. Kunkel, *Z. Anal. Chem.*, 1955, **48**, 161.
- H. Omishi and E. B. Sandell, *Anal. Chim. Acta*, 1955, **13**, 159.
- K. Henning and H. Specker, *Anal. Chem.*, 1968, **241**, 81.
- F. de Pablos, J. L. Gómez Ariza and F. Pino, *Analyst*, 1986, **111**, 1159.
- J. H. Yoe and A. L. Jones, *Ind. Eng. Chem., Anal. Ed.*, 1944, **16**, 111.
- P. Job, *Ann. Chim. (Paris)*, 1928, **9**, 113.
- J. D. Ingle, Jr., *J. Chem. Educ.*, 1974, **51**, 100.
- N. B. Lebed and R. P. Panteler, *Zh. Analit. Khim.*, 1965, **20**, 59.
- R. A. Zweidinger, L. Barnett and C. G. Pitt, *Anal. Chem.*, 1973, **45**, 1563.
- G. N. Lypka and A. Chow, *Anal. Chim. Acta*, 1972, **60**, 65.
- G. I. Kuchmistaya, *Zavodsk. Lab.*, 1961, **27**, 377.
- K. Nishimura and T. Iwai, *Bunseki Kagaku*, 1964, **13**, 518.
- V. Gluck and S. Ioan, *Rev. Chim. (Bucharest)*, 1962, **13**, 551.
- E. B. Sandell, *Anal. Chem.*, 1947, **19**, 63; J. Collat and L. Rogers; *ibid.*, 1955, **27**, 961.
- C. L. Luke and M. E. Campbell, *ibid.*, 1956, **28**, 1340, 1588.
- A. Lukin and E. A. Bozhevol'nov, *J. Anal. Chem., USSR*, 1960, **15**, 45.
- V. A. Nazarenko, S. Y. Vinkovetskaya and R. V. Ravitskaya, *Zh. Analit. Khim.*, 1958, **13**, 327; *Ukr. Khim. Zh.*, 1962, **28**, 726.
- I. Ladenbauer, J. Korkis and F. Hecht, *Mikrochim. Acta*, 1955, 1076.
- G. Oshina, *Bunseki Kagaku*, 1958, **7**, 549.

COMPLEXES OF VANADYL AND URANYL IONS WITH THE CHELATING GROUPS OF HUMIC MATTER

M. L. SIMÕES GONÇALVES and A. M. MOTA

Centro de Química Estrutural, Instituto Superior Técnico, Av. Rovisco Pais, 1096 Lisboa, Portugal

(Received 31 December 1986. Revised 10 April 1987. Accepted 10 May 1987)

Summary—The uranyl and vanadyl complexes formed with salicylic, phthalic and 3,4-dihydroxybenzoic acids have been studied by potentiometry in order to determine the stability constants of the M_mL_n species formed in solution, and the constants for the hydrolysis and polymeric complexes, at 25.0°, in 0.10, 0.40 and 0.70M sodium perchlorate. MINQUAD was used to process the data to find the best models for the species in solution, and calculate the formation constants. The uranyl-salicylic acid system was also studied by spectrophotometry and the program SQUAD used to process the data obtained. The best models for these systems show that co-ordination of the uranyl ion by carboxylate groups is easier than for the vanadyl ion, whereas the vanadyl ion seems to form more stable complexes with phenolate groups. Both oxo-cations seem to tend to hydrolyse rather than form complexes when the L:M ratios are greater than unity. Although the change in the constants with ionic strength is small, the activity coefficients of the salicylate and phthalate species have been calculated at ionic strengths 0.40 and 0.70M, along with the interaction parameters with Na^+ , from the stability constants found for the species ML and H_2L , according to the Brønsted-Guggenheim expression.

A large proportion of soil organic matter consists of quite complex polymeric molecules referred to as humic matter, with aromatic rings containing carboxylic and phenolic groups as the principal chelating groups. Phthalate, salicylate and dihydroxybenzoate are therefore good models for the binding sites of fulvic and humic acids.^{1,2} EPR studies with vanadyl ion and humic matter support this, since in many cases there is evidence of ionic co-ordination where carboxylate and phenolate groups are involved.¹ On the other hand, it seems that catechol functional groups are probably the structural components of humic matter responsible for the reduction of environmentally mobile metavanadate VO_3^- to VO^{2+} , followed by chelation of vanadium.¹ Uranyl ion is also easily co-ordinated by oxygen-donor ligands such as carboxylate or phenolate groups, and the two oxo-cations UO_2^{2+} and VO^{2+} have a tendency to form hydrolysed complexes in natural water conditions.

CALCULATIONS

Stability constants

The program MINQUAD^{3,4} was used to seek the best model to explain the experimental results obtained by potentiometry. This program yields: (a) the formation constants of the complexes, by a non-linear least-squares refinement by the Gauss-Newton method; (b) statistical information which provides a sound basis for deciding which model best fits the experimental points. For the models chosen in this work the stability constant of each complex will be reported together with its standard deviation and the

agreement factor R defined as:⁵

$$R = \left[U / \sum_{i=1}^n (C_M^2 + C_L^2 + C_H^2) \right]^{1/2}$$

where U is the sum of squared residuals for all the mass-balance equations, n is the number of experimental points and C_M , C_L and C_H represent the experimental values for the total concentration of metal, ligand and hydrogen ion respectively. A model is acceptable if the agreement factor is less than 0.004, which is the permitted deviation from a calculated R based on the experimental errors.⁶ The choice of the best model depends not only on the statistical data but also on chemical knowledge of the system (some models that appear to be good statistically might not be chemically acceptable) and on comparison with similar systems.⁷ From the models that are chemically and statistically allowed, if there is no reason to prefer one of them, the model with the lowest number of species should be chosen (Occam's razor). If there are still two or more candidate models, other techniques besides potentiometry should be used to obtain more information about the system.

The formation constants of the species are defined as

$$\beta_{m,n,p} = \frac{[M_m L_n H_b(OH)_a]}{[M]^m [L]^n [H]^p}$$

where $p = b - a$, corresponding to the reaction:



For simplicity, charges are omitted and solvation of the species is not considered. Each species is defined by three numbers— m, n, p —which represent the number of metal ions, ligand ions and the difference between the numbers of protons (H^+) and hydroxide ions (OH^-) in the complex.

To determine stability constants from spectrophotometric data, the program SQUAD was used.⁸⁻¹⁰ This program refines simultaneously a set of molar absorptivities and stability constants of the species in solution, from a non-linear least-squares refinement of function U , by using the Newton-Raphson method, where

$$U = \sum_{i=1}^{NS} \sum_{k=1}^{NW} \left(A_{ik} - \sum_{j=1}^{NC} C_{ij} \epsilon_{jk} b_i \right)^2$$

NS is the number of solutions for which the absorbance A_{ik} has been measured, NW is the number of wavelengths selected (≥ 1), NC is the number of species which contribute to the absorption of radiation, ϵ_{jk} is the molar absorptivity of species j at wavelength k , b_i (cm) is the optical path-length ($b = 1$ cm in this work), and C_{ij} is the concentration of species j in solution i .

Activity coefficients

As the Brønsted-Guggenheim expression is valid for the determination of the activity coefficients of charged species for ionic strengths less than $1.0M$,¹¹ this equation has been used:

$$\log f_E = -A |Z_E|^2 \left(\frac{\sqrt{I}}{1 + \sqrt{I}} \right) + B_{E-X}(I)I \quad (1)$$

where A is ~ 0.511 at 25° , Z_E the charge of the species E , I the molal ionic strength, and B the summation of the interaction parameters between the species E and the counter-ions in solution. In the presence of a supporting electrolyte, the counter-ion comes from the electrolyte and will be represented by X . B_{E-X} can be related to the ionic strength through the Pitzer expression:¹²

$$B_{E-X}(I) = B_{E-X}(\infty) + [B_{E-X}(0) - B_{E-X}(\infty)]F(I) \quad (2)$$

where

$$F(I) = [1 - (1 + 2\sqrt{I} - 2I)\exp(-2\sqrt{I})]/(4I) \quad (3)$$

with $F(0) = 1$ and $F(\infty) = 0$.

Interaction parameters determined experimentally for inorganic cations and anions have been reported,¹² but there is very little information for ions of organic molecules.

In this work the interaction parameters at ionic strengths 0 and ∞ , $B(0)$ and $B(\infty)$, were calculated for the anions salicylate and phthalate from the interaction parameters with Na^+ given by the Brønsted-Guggenheim expression for 0.4 and 0.7M sodium perchlorate medium. In this expression the f_{L2-} value was obtained at these ionic strengths from

the ratio of β_{ML} (or β_{H_2L}) values at $\mu = 0.1M$ and the molar ionic strength considered ($\mu = 0.4M$ or $0.7M$):

$$(\beta_{ML})_\mu / (\beta_{ML})_{0.1} = (f_M f_L)_\mu / (f_M f_L)_{0.1} \quad (4)$$

$$(\beta_{H_2L})_\mu / (\beta_{H_2L})_{0.1} = (f_H^2 f_L)_\mu / (f_H^2 f_L)_{0.1} \quad (5)$$

Molar values (μ, M) are converted into molal (I, m) by using a factor f extrapolated for the ionic strengths 0.10, 0.40 and 0.70M from the values presented in Table II.1 of reference 12:

$$0.100M \rightarrow 0.101m;$$

$$0.400M \rightarrow 0.409m;$$

$$0.700M \rightarrow 0.725m$$

The activity coefficients f_M and f_H have been calculated at the different ionic strengths from equation (1) with B values determined from equation (2) and tabulated values for $B(0)$ and $B(\infty)$. Since the activity coefficient f_{L2-} could not be determined from equation (1) at $\mu = 0.10M$ because the $B(I)$ values are not known, the Davies expression was used instead:

$$\log f_{L2-} = -A |Z_{L2-}|^2 \left(\frac{\sqrt{I}}{1 + \sqrt{I}} - 0.3I \right)$$

Figure 1 shows $\log f$ values obtained from the Brønsted-Guggenheim, Davies and Debye-Hückel [$\log f_E = -A |Z_E|^2 \sqrt{I}/(1 + \sqrt{I})$] expressions for the hydrogen, uranyl and vanadyl ions. From comparison of the curves it can be concluded that, for

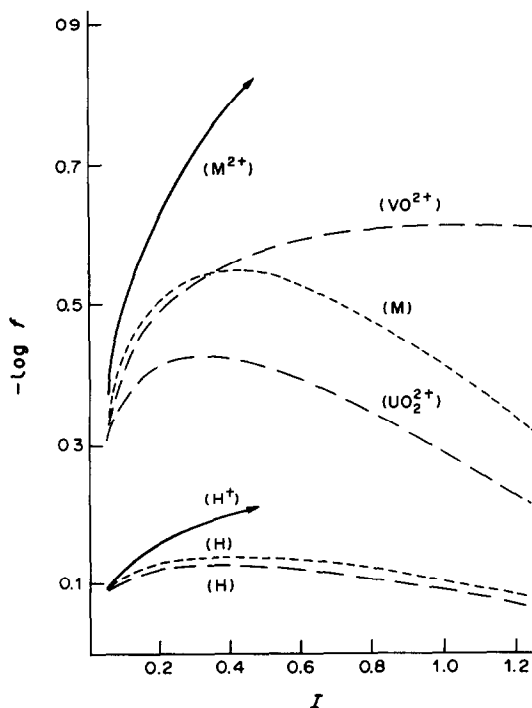


Fig. 1. Curves of logarithm of activity coefficients vs. ionic strength for H^+ , VO_2^+ and UO_2^{2+} cations, calculated by means of the Debye-Hückel (—), Davies (---) and Brønsted-Guggenheim expressions (-·-·-).

each cation, the activity coefficients tend to the same value for low ionic strengths, as expected, and at $\mu = 0.1M$ the activity coefficients obtained by the Davies and Brønsted-Guggenheim theories are in quite good agreement, so that calculation of f_{L_2} by the Davies expression at $\mu = 0.1M$ should be satisfactory. Equations (4) and (5) also require that the activity coefficients of neutral species should be approximately unity, which is only valid if formation of dipoles can be neglected. For the ligands considered, this approximation is probably valid because they are small, with very little charge separation.

Hydrolysis constants

The hydrolysis constants β_{xy}^c of the reaction $xM + yH_2O \rightleftharpoons M_x(OH)_y + yH^+$ at a given ionic strength were calculated from values of the thermodynamic constants— β_{xy}^T —and the activity coefficients of the species calculated from equation (1) at the relevant ionic strength.

$$\log \beta_{xy}^c = \log \beta_{xy}^T + 0.511\Delta Z^2 \left(\frac{\sqrt{I}}{1 + \sqrt{I}} \right) + bI \quad (6)$$

$$\Delta Z^2 = (2x - y)^2 + y - 4x \quad (7)$$

$$b = xB_{M-x} - yB_{H-x} - B_{xy-x} \quad (8)$$

where X represents ClO_4^- , M the metal ion (vanadyl or uranyl), H the proton and xy the hydrolysed species $M_x(OH)_y$.

For the hydrolysis of the vanadyl ion, b is calculated at each ionic strength from equation (8), taking values for $B(0)$ and $B(\infty)$ from the literature.¹²

For the hydrolysis of uranyl ion, b is extrapolated from the b values given at other ionic strengths in perchlorate medium.¹²

EXPERIMENTAL

Reagents

All the reagents were commercial products of analytical grade and used without further purification. The purity of the ligands was confirmed by potentiometric titration.

The uranyl nitrate stock solution was standardized gravimetrically.¹³ Vanadyl perchlorate stock solutions, approximately $0.1M$, were prepared under a nitrogen atmosphere from vanadyl sulphate and barium perchlorate, and the solution obtained was acidified with perchloric acid to pH 1.0 to avoid the oxidation of V(IV) to V(V). The vanadyl stock solution was standardized by titration with permanganate, and the perchloric acid concentration was checked by titration with a strong base, with interpretation by Gran's method¹⁴ for the acid pH range.

The potassium hydroxide titrant solutions were prepared under nitrogen from Merck "Titrisol" concentrates, and CO_2 -free demineralized water. The concentrations of these solutions and the absence of carbonate was checked regularly by potentiometric titration with standard hydrochloric acid.

Potentiometric measurements

All the measurements were made at 25° in sodium perchlorate medium. A Corning-Eel 112 digital potentiometer was used with Corning electrodes (pH triple purpose, Ag/AgCl internal, and calomel reference electrodes, both No. 476022). The reference electrode was filled with

sodium chloride solution, to avoid precipitation of potassium perchlorate.

The potential readings were converted into $\log[H^+]$ values according to the expression $E = Q + \alpha \log[H^+] + j_H[H] + j_{OH}[OH]$. This assumes a linear variation of the liquid-junction potential with $[H]$ at acidic pH values and with $[OH]$ at alkaline pH values. In the pH range 2.5–11, $j_H[H] + j_{OH}[OH]$ can be considered as equal to zero. The Q value which is constant in the experimental conditions used, was calculated from a previous titration of hydrochloric acid in the appropriate medium, with potassium hydroxide, by Gran's method.^{14,15} The calibration was repeated before and after each series of titrations at regular intervals during the day. The j_{OH} value necessary for the determination of pH values higher than 11 was obtained at each ionic strength from a previous titration of potassium hydroxide in the appropriate medium with hydrochloric acid, for the pH range 12.0–12.8.¹⁵

The ionic product of water was determined at each ionic strength from the titration of hydrochloric acid, in the appropriate medium, with sodium hydroxide, with use in the basic pH range (pH ~ 10.5) of the Q value determined for the acidic pH range (pH ~ 3). It should be pointed out that this is valid only if the asymmetry potential of the glass electrode and the liquid-junction potential do not change significantly in the pH range 2.5–11. The K_w values obtained at 25° are in good agreement with those reported previously for the same ionic strength.¹⁶

For the determination of the stability constants of phenolic groups with $K_{HL} > 11$, experimental conditions were chosen such that (a) the ligand and titrant concentrations were sufficiently high to yield significant variations of pH between consecutive experimental points ($\Delta pH \geq 0.05$), (b) the ionic strength was kept constant, (c) the concentrations of HL and L were not negligible [C_L and $C_{HL} \geq 0.05(C_L + C_{HL})$], and (d) alkaline error was avoided (pH ≥ 12.5). Basic solutions of the ligands were used immediately after their preparation in the dark, to prevent decomposition. The ligand and metal concentrations ranged between 0.25×10^{-3} and $4 \times 10^{-3}M$, with a metal:ligand ratio ranging from 0.25 to 2.

The titrations were performed with use of a double-walled titration cell under nitrogen, at a temperature controlled at $25.0 \pm 0.1^\circ$ by circulation of water. The titrant was added from a Metrohm 655 Dosimat automatic burette, provided with soda-lime guard-tubes. Oxygen must be rigorously excluded during the vanadyl titration to prevent the oxidation of VO^{2+} to VO_2^+ , which becomes easier as the pH increases.

Spectrophotometric measurements

All the measurements were made at 25° in $0.1M$ sodium perchlorate medium. A Perkin Elmer 4.5 spectrophotometer was used, and the spectra of the uranyl ion in the absence and presence of ligand were recorded in the visible range (350–800 nm), with a halogen-lamp source, a bandwidth of 1 nm, and glass 1-cm cells. In the wavelength range considered, salicylic acid does not absorb.

The absorbance was measured at 374 nm because at this wavelength and at pH 3–6.5 the uranyl ion absorbs very little, and uranyl ion in the presence of salicylic acid shows a plateau with an absorbance that changes significantly with pH.

The molar absorptivity of the hydrolysed uranyl-ion species was determined from measurements of the absorbance of 20 uranyl solutions with concentrations in the range 0.5×10^{-3} – $10^{-3}M$, at pH 3–5.5. At 374 nm only $M_3(OH)_3$ absorbs [$\epsilon_{M_3(OH)_3} = 57 \pm 5$].

In the study of the system uranyl ion + salicylic acid, 40 solutions were prepared with high $C_L:C_M$ ratios (10–20) in order to minimize the amounts of hydrolysis products present, and to increase formation of organic complexes. The metal concentration range was varied in the range

0.25×10^{-3} – $10^{-3}M$. The pH (potentiometrically measured) was adjusted with sodium hydroxide to between 3.8 and 6.5.

RESULTS AND DISCUSSION

In the study of complex formation between uranyl or vanadyl ions and salicylic, phthalic and 3,4-dihydroxybenzoic acids, the stability constants considered to have fixed values were: (a) the ionization constants of the ligands and the ionic product of water, listed in Table 1 and determined from experimental values, (b) the hydrolysis constants for the oxo-cations, given in Table 2.

It should be pointed out that the pH range used in the study of the vanadyl systems is restricted by the precipitation of $VO(OH)_2$, beginning at pH ~ 4.5 at the concentration used. To prevent this precipitation, the $C_L:C_M$ ratio should be increased to > 20 , but in these conditions potentiometry is not a good technique for studying the system.

The precipitation of hydrolysed uranyl species is detected at pH ~ 6.0 , the $M_x(OH)_y$ species having

Table 1. Stability constants of the proton complexes of the ligands and the ionic product of the water at three different ionic strengths—0.10, 0.40, 0.70M in $NaClO_4$. $T = 25^\circ$

Acid		0.10M	0.40M	0.70M
Phthalic	$\log \beta_{HL}$	4.90	4.74	4.70
	$\log \beta_{H_2L}$	7.65	7.43	7.39
Salicylic	$\log \beta_{HL}$	13.0	13.0	13.0
	$\log \beta_{H_2L}$	15.82	15.73	15.84
3,4-DHB	$\log \beta_{HL}$	12.5	12.5	12.5
	$\log \beta_{H_2L}$	21.19	21.09	21.12
	$\log \beta_{H_3L}$	25.50	25.36	25.40
	K_w	1.70×10^{-14}	1.80×10^{-14}	1.86×10^{-14}

Table 2. Hydrolysis constants of the uranyl and vanadyl ions at three different ionic strengths—0.10, 0.40 and 0.70M ($NaClO_4$); $T = 25^\circ$

		0.10M	0.40M	0.70M
Vanadyl	β_{10-1}	1.72×10^{-6}	2.69×10^{-6}	4.50×10^{-6}
	β_{20-2}	1.72×10^{-7}	2.69×10^{-7}	4.50×10^{-7}
Uranyl	β_{10-1}	1.11×10^{-6}	1.17×10^{-6}	1.35×10^{-6}
	β_{20-2}	1.61×10^{-6}	1.46×10^{-6}	1.40×10^{-6}
	β_{30-5}	7.11×10^{-17}	4.85×10^{-17}	4.30×10^{-17}

Table 3. Stability constants for vanadyl and uranyl systems with phthalic acid for the best model obtained with MINQUAD ($T = 25^\circ$; $\mu = 0.10, 0.40$ and $0.70M$ in $NaClO_4$)

	I_M	$\log \beta_{111}$	$\log \beta_{110}$	$\log \beta_{120}$	$\log \beta_{22-2}$	R
VO^{2+}	0.10	6.28 ± 0.08	3.97 ± 0.01	6.39 ± 0.06	1.75 ± 0.03	0.0002
	0.40	6.10 ± 0.07	3.68 ± 0.01	5.85 ± 0.06	0.27 ± 0.03	0.0002
	0.70	6.97 ± 0.09	3.61 ± 0.02	6.48 ± 0.07	0.74 ± 0.04	0.0002
UO_2^{2+}	0.10	—	4.742 ± 0.008	7.73 ± 0.03	2.37 ± 0.006	0.0022
	0.40	—	4.464 ± 0.006	7.38 ± 0.02	1.93 ± 0.05	0.0010
	0.70	—	4.43 ± 0.001	6.97 ± 0.04	1.58 ± 0.08	0.0032

Table 4. Stability constants for the uranyl system with salicylic acid for the best models obtained with MINQUAD ($T = 25^\circ$; $\mu = 0.10M$ $NaClO_4$)

	$\log \beta_{111}$	$\log \beta_{110}$	$\log \beta_{11-1}$	$\log \beta_{120}$	R
	14.68 ± 0.04	12.041 ± 0.003	6.10 ± 0.02	—	0.0010
	14.61 ± 0.04	12.041 ± 0.003	—	22.07 ± 0.03	0.0013

a high concentration for all the systems studied at pH > 4.0 , as can be seen from the distribution curves presented later in the text.

Phthalate complex systems

For the uranyl and vanadyl systems with phthalic acid the same types of species were obtained (Table 3), with the exception of MHL, which seems to be formed with vanadyl ion for pH < 4.5 , but not with uranyl ion for pH > 3.0 . This might be due to the higher affinity of uranyl ion for carboxylate groups and to the stereochemistry of these groups in vicinal positions in the molecule. From the distribution curves (Fig. 2) it can be seen that the dominant species is ML at practically all the pH values studied. The ML_2 species always has a low concentration, and the hydrolysis dimer $M_2L_2(OH)_2$ becomes important at pH values higher than 4.5, which seems to indicate that both oxo-cations form hydrolysis species rather than species with $L:M > 1$. The monomer MLOH is always rejected when included in the model with its dimer.

Salicylate complex systems

For both oxo-cations, the ML species seems to be the dominant organic complex (Fig. 3), MHL having some importance for pH < 4 , mainly for the uranyl system. This is in accordance with the higher affinity of the uranyl ion for carboxylate groups. For higher pH values the vanadyl system forms MLOH but for the uranyl system there is some ambiguity in the species formed (Table 4). Indeed, a distinction between ML_2 and MLOH is not possible statistically or in terms of concentration, since for the models including $ML + MLOH$ or $ML + ML_2$ the species MLOH or ML_2 exist in similar percentage in the experimental conditions used (pH < 6 and ligand to metal ratio from 1 to 2). On the other hand, the co-existence of both species is rejected by the program.

In order to obtain more information spectrophotometric experiments have been done. The data have been analysed by program SQUAD with β_{ML} intro-

duced as a fixed value (given by potentiometry) and β_{MLOH} or β_{ML_2} as a constant to be refined.

Comparing the values obtained by spectrophotometry (A) and by potentiometry (B):

$$(A) \log \beta_{\text{MLOH}} = 6.25 \pm 0.04 \quad \log \beta_{\text{ML}_2} = 21.3 \pm 0.1$$

$$(B) \log \beta_{\text{MLOH}} = 6.10 \pm 0.02 \quad \log \beta_{\text{ML}_2} = 22.0 \pm 0.03$$

it can be seen that the agreement in the results is better when the species MLOH is considered, and so it seems that $\text{ML} + \text{MLOH}$ represents a better model than $\text{ML} + \text{ML}_2$.

However, it is worthwhile to emphasize that from a chemical point of view it is not possible to distinguish between the MLOH or ML_2 species, since at $\text{pH} > 4.0$ the uranyl ion has a high tendency to be hydrolysed but on the other hand, owing to the high affinity of the uranyl ion for the carboxylate groups, the ML_2 species is also possible.

The stability constants for the vanadyl and uranyl

systems with salicylic acid are reported in Table 5 for the three different ionic strengths.

3,4-Dihydroxybenzoate complex systems

This ligand, with three co-ordinating groups (one carboxylate and two phenolate), presents a higher number of possible species in solution. However, for the vanadyl system and in the pH range studied, only two species are detected— M_2L and ML (Table 6)—where one of the two metal ions is bound to the carboxylate group and the other to two phenolate groups in the M_2L species and one metal ion is bound to two phenolate groups in the ML species. In practically all of the pH range studied, M_2L is the dominant species (Fig. 4), which confirms the high affinity of vanadyl ion for carboxylate and phenolate groups. For the highest pH values used it is possible that other species such as ML_2 or hydrolysis products such as MLOH are also formed. In fact these species

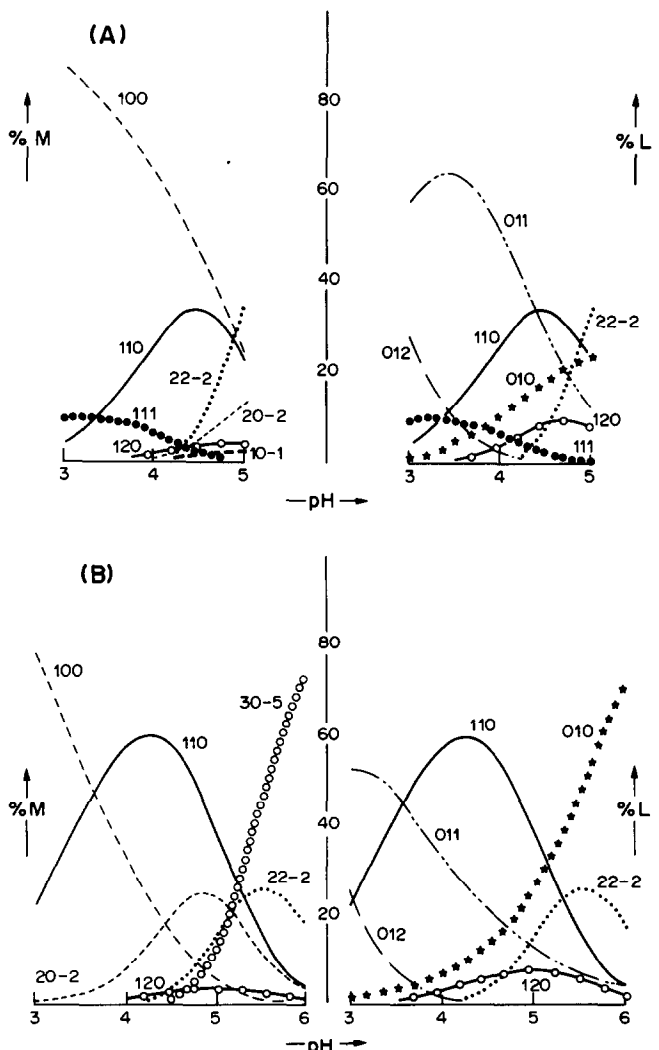


Fig. 2. Distribution curves for the concentration of metal or ligand of the species in solution, as a function of pH, for the vanadyl (A) and uranyl (B) systems with phthalic acid ($\mu = 0.70\text{M NaClO}_4$).

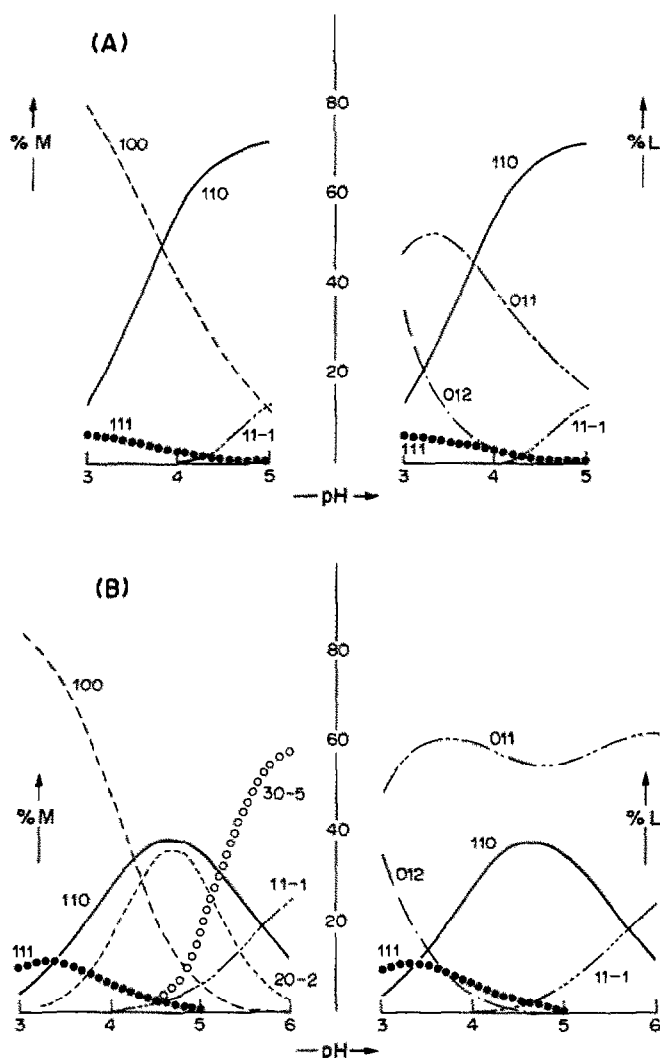


Fig. 3. Distribution curves for the concentration of metal or ligand of the species in solution, as a function of pH, for the vanadyl (A) and uranyl (B) systems with salicylic acid ($\mu = 0.70M$ NaClO_4).

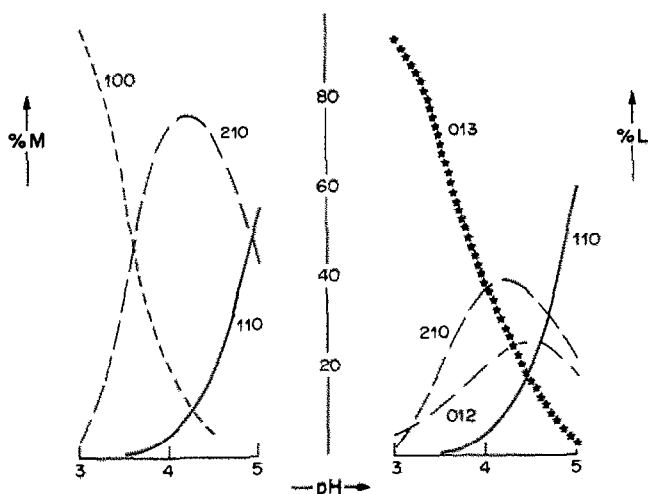


Fig. 4. Distribution curves for the concentration of metal or ligand of the species in solution, as a function of pH, for the vanadyl system with 3,4-dihydroxybenzoic acid ($\mu = 0.70M$ NaClO_4).

Table 5. Stability constants for the vanadyl and uranyl systems with salicylic acid for the best model obtained with MINQUAD; $T = 25^\circ$; $\mu = 0.10, 0.40$ and $0.70M$ (NaClO_4)

	I_M	$\log \beta_{111}$	$\log \beta_{110}$	$\log \beta_{11-1}$	R
VO^{2+}	0.10	14.68 ± 0.06	12.683 ± 0.004	6.54 ± 0.02	0.0009
	0.40	14.88 ± 0.05	12.518 ± 0.002	6.07 ± 0.01	0.0003
	0.70	15.25 ± 0.05	12.562 ± 0.003	6.62 ± 0.01	0.0003
UO_2^{2+}	0.10	14.68 ± 0.04	12.041 ± 0.003	6.10 ± 0.02	0.0010
	0.40	15.56 ± 0.05	11.969 ± 0.004	5.58 ± 0.04	0.0017
	0.70	15.41 ± 0.06	12.004 ± 0.004	6.32 ± 0.03	0.0021

Table 6. Stability constants for the vanadyl system with 3,4-dihydroxybenzoic acid for the best model obtained by MINQUAD; $T = 25^\circ$; $\mu = 0.10, 0.40$ and $0.70M$ (NaClO_4)

I_M	$\log \beta_{110}$	$\log \beta_{210}$	R
0.10	16.632 ± 0.008	20.827 ± 0.006	0.0015
0.40	16.342 ± 0.004	20.651 ± 0.005	0.0009
0.70	16.241 ± 0.006	20.763 ± 0.003	0.0009

are not rejected by the program MINQUAD but their concentrations are less than 2%, so there is no certainty about their presence.

Although for the uranyl system the M_2L species still occurs, there is some ambiguity, from potentiometric results, about the other species present in solution (Table 7). For $\text{pH} < 4.5$, ML_2H_4 or MLH_2

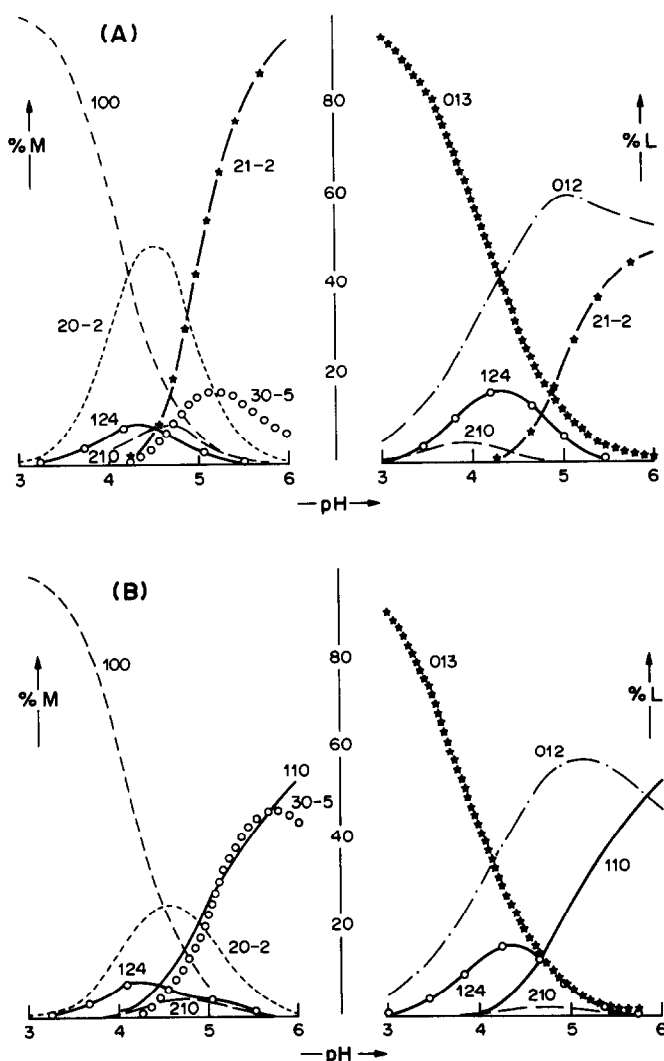


Fig. 5. Distribution curves for the species assumed to be in solution, as a function of pH, of two models (A and B) for the uranyl system with 3,4-dihydroxybenzoic acid ($\mu = 0.70M$ NaClO_4). A—model assuming the complex species 124, 210, 21-2; B—model assuming the complex species 124, 210, 110.

Table 7. Stability constants of the uranyl system with 3,4-dihydroxybenzoic acid for the best models obtained by MINIQUAD ($T = 25^\circ$; $\mu = 0.70M$ NaClO₄)

$\log \beta_{124}$	$\log \beta_{112}$	$\log \beta_{110}$	$\log \beta_{210}$	$\log \beta_{21-2}$	R
48.41 ± 0.09		14.95 ± 0.04			0.0043
	24.02 ± 0.09	15.20 ± 0.04			0.0043
48.35 ± 0.08		14.92 ± 0.02	17.88 ± 0.08		0.0030
48.36 ± 0.07			18.23 ± 0.03	9.16 ± 0.03	0.0030
	23.89 ± 0.08		18.51 ± 0.02	9.22 ± 0.04	0.0035
	23.95 ± 0.08	16.04 ± 0.03	18.02 ± 0.05		0.0028

Table 8. Activity coefficients for salicylate and phthalate ions calculated for 0.40 and 0.70M NaClO₄ media, from β_{H_2L} or β_{ML} ($M = UO_2^{2+}$ or VO_2^{2+}); $T = 25^\circ$

Medium	$f_{\text{salicylate}}$		$f_{\text{phthalate}}$	
	$\mu = 0.40M$	$\mu = 0.70M$	$\mu = 0.40M$	$\mu = 0.70M$
NaClO ₄ (H ⁺)	0.33	0.40	0.25	0.21
NaClO ₄ (VO ₂ ²⁺)	0.36	0.44	0.27	0.25
NaClO ₄ (UO ₂ ²⁺)	0.35	(0.33)	0.22	0.18
Mean value	0.35 ± 0.02	0.42 ± 0.02	0.25 ± 0.03	0.21 ± 0.03

could exist as well as M₂L. In the first two complexes the metal ion is bound to the carboxylate group, the phenolic groups undergoing no dissociation. Micera *et al.*¹⁷ verified from solid-state studies with the uranyl ion and 2,6-dihydroxybenzoic acid that the metal ion is co-ordinated to two carboxylate groups, which might suggest that with 3,4-dihydroxybenzoic acid the species ML₂H₄ would be the one present in solution. The existence of this species, not found in the vanadyl system, can be explained by the higher affinity of the uranyl ion for carboxylate groups and the lower affinity for phenolate groups, compared with the vanadyl ion. It should be pointed out that in all models considered and for pH < 4.5, the organic complex concentrations are minor relative to those of the hydrolysis products of the cation (Fig. 5).

For pH > 4.5, the potentiometric data can be explained by the formation of one of the species ML or M₂L(OH)₂. When both are introduced simultaneously in the same model, one of them is rejected, depending on the experimental conditions used. The models including M₂L(OH)₂ or ML have similar R factors, so the statistical data are not helpful. However, from a chemical point of view, the existence of ML seems most probable, though further information from other methods should be obtained.

The results obtained suggest that for the systems studied, (a) the uranyl ion is more easily bound than the vanadyl ion to carboxylate groups, but the vanadyl ion is more easily bound to phenolate, (b) the complexes of both cations hydrolyse rather than form complexes when the ligand:metal ratio is > 1.

Dependence of the stability constants on ionic strength

Since the stability constants do not vary much with change in the ionic strength, speciation studies for sea-water and estuarine conditions can be done with the same set of constants.

However, more accurate results for a given ionic strength could be obtained if it were possible to know the activity coefficients of the species present in solution.

In this work it was possible to determine the activity coefficient of the deprotonated species L²⁻ ($f_{L^{2-}}$) for salicylic and phthalic acid at ionic strength 0.4 and 0.7M, from experimental values for β_{H_2L} or β_{ML} determined at the three ionic strengths, 0.1, 0.4 and 0.7M.

The results presented in Table 8 show quite good agreement for the values obtained with the different cations (H⁺, UO₂²⁺ and VO₂²⁺), except for the value for ionic strength 0.70M for the uranyl ion-salicylic acid system. From the average values for $f_{\text{salicylate}}$ and $f_{\text{phthalate}}$ at $\mu = 0.40$ and 0.70M, B_{L-Na} values were calculated at these ionic strengths for each ligand, from equation (1). From these values and equation (2), $B(0)$ and $B(\infty)$ can be determined (Table 9).

It is now possible to calculate B_{L-Na} for any ionic strength from equation (2) and therefore the activity coefficient from equation (1). This is very important in speciation studies because it allows good estimates to be made of β_{H_2L} or β_{ML} at any ionic strength, and of the stability constants of other salicylate or phthalate neutral complexes with metal ions of known activity coefficients.

Table 9. Interaction parameters B_{L-Na} for salicylate and phthalate ions at 0.40M, 0.70M, 0 and ∞ ionic strengths ($T = 25^\circ$; NaClO₄ medium)

	Salicylate	Phthalate
B_{L-Na} (0.4M)	0.83	0.48
B_{L-Na} (0.7M)	0.78	0.37
B_{L-Na} (0)	1.16	1.06
B_{L-Na} (∞)	0.64	0.12

The determination of $\log f_L$ at $\mu = 0.1M$ from equation (1) with values for $B(0)$ and $B(\infty)$ from Table 9 gives -0.429 for phthalate ion (which agrees with the Davies value within $\pm 1\%$), and -0.397 for salicylate (which agrees with the Davies value within $\pm 4\%$). The bigger difference observed for salicylate might be due to the error in β_{HL} (which affects β_{ML}), calculated at high pH (which is unfavourable for potentiometric determination). It should also be pointed out that calculation of $B(\infty)$ and/or $B(0)$ might involve large errors arising from the quotient of small quantities in the expression:

$$B(\infty) = \frac{[B(0.4)F(0.7) - B(0.7)F(0.4)]}{[F(0.7) - F(0.4)]}$$

Finally it should be emphasized that, in order to obtain reliable interaction parameters B_{L-Na} , very accurate values of stability constants should be used.

REFERENCES

1. N. D. Chasteen, *Biol. Magnet. Resonance*, 1981, **3**, 53.
2. F. Cariati, L. Erre, G. Micera and A. Panzanelli, *Inorg. Chim. Acta*, 1983, **80**, 57.
3. A. Sabatini, A. Vacca and P. Gans, *Talanta*, 1974, **21**, 54.
4. P. Gans, A. Sabatini and A. Vacca, *Inorg. Chim. Acta*, 1976, **18**, 237.
5. A. Sabatini, A. Vacca and M. A. Gristina, *Coord. Chem. Rev.*, 1972, **8**, 45.
6. A. Sabatini and A. Vacca, *ibid.*, 1975, **16**, 161.
7. M. S. Gonçalves, A. M. Mota and J. F. Silva, *Talanta*, 1984, **31**, 531.
8. D. J. Leggett and W. A. McBryde, *Anal. Chem.*, 1975, **47**, 1065.
9. D. J. Leggett, *ibid.*, 1977, **49**, 276.
10. D. J. Leggett, S. L. Kelly, L. R. Shiue, Y. T. Wu, D. Chang and K. M. Kadashi, *Talanta*, 1983, **30**, 579.
11. M. Whitfield, *Activity Coefficients in Electrolyte Solution*, Vol. II, R. Pytkowicz (ed.), CRC Press, Boca Raton, 1979.
12. C. J. Baes, Jr. and R. E. Mesmer, *The Hydrolysis of Cations*, J. Wiley, New York, 1976.
13. W. Hillebrand, G. E. F. Lundell, H. Bright and J. Hoffman, Jr., *Applied Inorganic Analysis*, 2nd Ed., Wiley, New York, 1953, p. 468.
14. G. Gran, *Analyst*, 1952, **77**, 661.
15. L. Pehrsson, F. Ingman and A. Johansson, *Talanta*, 1976, **23**, 769.
16. R. M. Smith and A. E. Martell, *Critical Stability Constants*, Vol. 4, Plenum Press, New York, 1976.
17. G. Micera, L. S. Erre, F. Cariati, D. A. Clemente, A. Marzotto and M. B. Cingi, *Inorg. Chim. Acta*, 1985, **109**, 135.

DIRECT DETERMINATION OF METALS IN MILLIGRAM MASSES AND MICROLITRE VOLUMES BY DIRECT-CURRENT ARGON-PLASMA EMISSION SPECTROMETRY WITH SAMPLE INTRODUCTION BY ELECTROTHERMAL VAPORIZATION

PETER G. MITCHELL*

Department of Chemistry, New Mexico State University, Las Cruces, New Mexico 88003, U.S.A.

JOSEPH SNEDDON†

Department of Chemistry, University of Lowell, Lowell, Massachusetts 01854, U.S.A.

(Received 26 March 1986. Revised 9 April 1987. Accepted 10 May 1987)

Summary—The development of an electrothermal vaporization and direct-current argon-plasma emission spectrometric system which allowed the determination of metals in microlitre volumes and milligram masses is described. For the five metals investigated, the concentration detection limits were comparable to those for conventional pneumatic nebulization of solutions, and the mass detection limits were superior. The use of an ashing stage was found to reduce enhancement by sodium in the determination of copper and manganese by the plasma method. The system was shown to give accurate results for complex biological, nutritional, water and geological samples.

The direct-current argon plasma (DCP) has become widely used and accepted as an excitation source for ultratrace and trace metal determination in a variety of materials by emission spectrometry. This is due, in part, to its availability, ease of operation and inherent multi-element capability, and the long linear dynamic range, low detection limits, high sample throughput, good accuracy and acceptable precision attainable with it.¹⁻⁵ However, a limitation is that the sample is almost always introduced as a solution by a pneumatic nebulizer. Pneumatic nebulization of solutions has a rather low efficiency (~15%)⁶ and a relatively high sample requirement (uptake rate ~1.0 ml/min). However, the use of an organic solvent to improve the efficiency can perturb the plasma and reduce the accuracy. The decomposition of solid samples for trace metal analysis often results in a solution that is too dilute for the metal concentrations to be within the analytical capability of the DCP and may introduce error through contamination. Any concentration steps thus necessitated will lengthen the analysis.

In recent years, the separation of the vaporization-excitation step has been shown to give improvement in signal and accuracy, particularly for direct analysis of solid samples, which can have a high background continuum and weak analyte signal owing to incomplete atomization and scattering from particles. Sample introduction into the inductively-coupled plasma (ICP) has been achieved by means of an electrothermal vaporizer⁷⁻⁹ and laser ablation,¹⁰⁻¹²

and into the microwave-induced plasma (MIP) by using a spark discharge.¹³ Introduction of solid samples into the DCP has been achieved by laser ablation.^{14,15} This paper describes the development and use of an electrothermal vaporizer (ETV) for the introduction of microlitre volumes and milligram masses of sample into the DCP for emission spectrometric determination of copper and manganese in complex biological, nutritional, water and geological samples. The ETV-DCP emission system has been shown to give good results for the determination of gold¹⁶ and mercury¹⁷ in solid algal cells.

EXPERIMENTAL

Apparatus

A Spectraspan V direct-current plasma emission spectrometer was used. A detailed description and operating conditions of this system are available elsewhere.^{1,2,14,15} Sample introduction was achieved by using an Allied Instrumentation Laboratories 455 temperature-controlled furnace with the modifications described below.

Reagents

All chemicals were of analytical reagent grade. High-purity demineralized water was used in the preparation of all solutions. Glassware was washed with dilute nitric acid and before use was rinsed with demineralized water. Surface water was collected from the Rio Grande River, Las Cruces, New Mexico in an acid-washed 1-litre plastic bottle, made 0.04M in hydrochloric acid and stored at -4° until required. The caudal epididymis was cut from bovine testes and the sperm flushed out with a 0.9% sodium chloride solution by retrograde flushing of the vas deferens. The sperm cells were washed twice with 0.9% sodium chloride solution and finally suspended in 0.9% sodium chloride solution and stored at -4° until required. A detailed description of this procedure is given elsewhere.¹⁸ Dried powdered milk, "Infamil" (Mead Johnson, Evansville, IN) was digested in a Teflon-lined metal acid-digestion bowl

*Present address, Department of Cell Biology, Vanderbilt University, Nashville, Tennessee 37232 U.S.A.

†Author to whom correspondence should be addressed.

(Parr, Moline, IL). Two ml of concentrated nitric acid, 1 ml of milk and 1 ml of 30% hydrogen peroxide were heated in the bowl at 145° for 2 hr. This process resulted in complete decomposition of all milk solids.¹⁹ Five U.S. Geological Survey (USGS) solid standards were obtained for manganese determination. These standards had been analysed for 42 metals at Los Alamos National Laboratories by nuclear and atomic-absorption spectrometry methods.²⁰

Procedure

The DCP emission spectrometer was set at the analyte emission line with pneumatic nebulization of an aqueous sample containing the analyte of interest. The nebulizer was then removed and the plasma sample-introduction tube connected to the electrothermal vaporizer by 20 cm of 1/4-in. bore Tygon tubing. The argon flow-rate, ETV power programme, detector voltage and chart recorder variables were set. The required volume or mass of sample was placed in a micro-boat which was then inserted in the ETV cuvette. The ETV programme was initiated and the peak height recorded digitally and on a chart recorder.

RESULTS AND DISCUSSION

Design criteria

The main objective in modifying the electrothermal vaporizer for sample introduction was to achieve efficient transfer of the transient population of free analyte atomic species in the vapour phase into the DCP. Ideally, this modification would limit diffusion and condensation of the analyte. Several authors have described modifications to commercial electrothermal vaporizers (Allied Instrumentation Laboratory,^{21,22} Perkin-Elmer HGA 74,²³ and HGA 500²⁴) for introduction into an ICP. Initial experiments involved removing the quartz windows on each side of the electrothermal vaporizer and directly connecting one window port to the chimney of the DCP by means of a glass or tygon connector and the other to the argon supply. However, when a sample was vaporized, the glass or tygon would melt or become distorted after several trials, owing to the heat transferred from the vaporizer. To overcome this problem, the quartz windows of the atomizer were replaced by inserts made of boron nitride, chosen because of its high thermal stability (up to ~3000°) mechanical strength, chemical inertness and machinability. The boron nitride inserts were machined to fit tightly in

the electrothermal vaporizer, and had a 0.093-in. diameter hole drilled along the long axis, to allow passage of the argon flow. The dimensions are shown in Fig. 1. The exit hole of the connector to the DCP was periodically checked and cleaned to ensure that no sample condensation occurred in it.

Initially, experiments were performed with a relatively low flow of argon (0.1–0.2 l./min) through the vaporizer. This argon flow was joined by a Y-connection to the higher flow of argon (1 l./min) used to sustain the plasma. The signals from this system were poor, however, possibly because of back-pressure from the plasma argon-flow not allowing entrance of the slow flow from the vaporizer, or more likely because of dilution of the sample vapour with the support gas. The Y-connector was, therefore, connected directly to the plasma. At low argon flow-rates of <0.4 l./min, the plasma image was weak and diffuse. The flow through the vaporizer was next raised to 0.6 l./min to sustain a well defined plasma. This system produced very sharp emission signals at the 324.7 nm emission line from μ l copper samples. However, it was found that if the sample was dried and immediately vaporized, the graphite tube of the vaporizer would oxidize easily and require frequent replacement. This was because there were still appreciable amounts of oxygen in the vaporizer. Delaying the drying/vaporization steps by at least 30 sec was found to purge the sample chamber of oxygen and minimize this problem.

The system was further simplified by replacing one of the inserts by the original quartz window and using the purge-gas entrance port for entry of the argon. The purge-gas relief valve was completely closed, and the argon passed through the electrothermal vaporizer tube and then through the boron nitride insert, to the DCP.

A constant flow of argon was critical for reproducible results to be obtained with the DCP, since flow variations changed the position of the plasma image with respect to the entrance slit. A flow regulator (Dwyer Instruments, Inc., Houston, Tex.) was therefore introduced between the electrothermal vaporizer control module and the sample chamber.

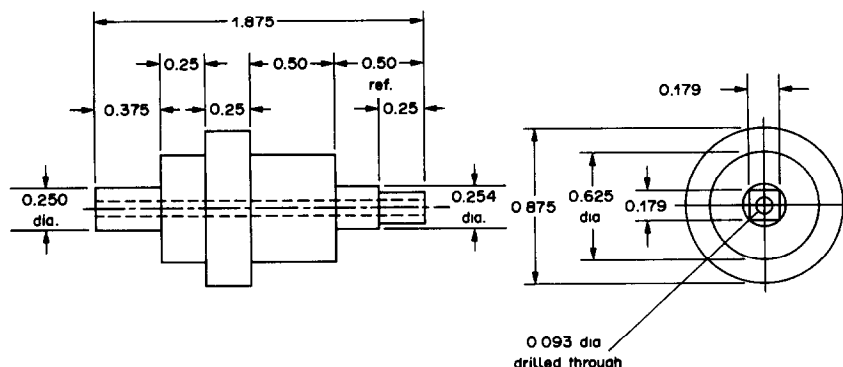


Fig. 1. Dimensions (inches) of insert for ETV and DCP interface.

Table 1. Selected detection limits for pneumatic nebulization-DCP* and ETV-DCP spectrometry†

Element	Emission wavelength, nm	Pneumatic nebulization detection limit,	Absolute pneumatic nebulization detection limit,	ETV-DCP detection limit,	Absolute ETV-DCP detection limit,
		$\mu\text{g/l.}$	ng	$\mu\text{g/l.}$	ng
Copper	324.7	2	2	6	0.1
Gold	267.6	8	8	30	0.7
Magnesium	279.6	2	2	20	0.4
Manganese	257.6	3	3	25	0.5
Zinc	213.9	10	10	30	0.7

*Based on a nebulized volume of 1.0 ml.

†Based on a 20 μl volume.

Detection limits

Detection limits were estimated by analysing a blank (20 μl of demineralized water) ten times and calculating the standard deviation of the peak height. The detection limit was defined as the analyte concentration equal to three times the standard deviation, the concentration being extrapolated from a calibration graph. Table 1 gives the detection limits found for copper, gold, magnesium, manganese and zinc with the ETV-DCP system and, for comparison purposes, those for conventional pneumatic nebulization-DCP spectrometry. The concentration detection limits for the ETV-DCP system were poorer by a factor of 2–10 than those for pneumatic nebulization-DCP spectrometry, but the mass detection limits were superior by a factor of 5–60. The poorer concentration detection limits could be due to excessive dilution of the sample vapour by the plasma-support argon flow. In Table 2, the mass detection limits obtained by ETV-DCP spectrometry for copper, gold, magnesium, manganese and zinc are compared with published detection limits for ETV-ICP and ETV-MIP. To compare the systems directly, the published detection limits were normalized to 20- μl volumes (the actual volumes ranged from 5 to 50 μl , depending on the system). The DCP and MIP absolute detection limits are similar within an order of magnitude, but the ICP absolute detection limits are generally superior by 1–2 orders of magnitude. This correlates with the detection limits obtained with pneumatic nebulization of solutions into an ICP being generally superior to those obtained with a DCP. It is worth noting that detection limits for different ETV-plasma spectrometry systems cannot be directly compared, on account of the different

operating conditions. The object of Table 2 is to show trends rather than absolute values. Of course, the detection limits for ETV sample introduction can always be improved at the expense of analysis time by successive additions and drying of aliquots of analyte. The apparent detection limit will be lowered, but the matrix will be concomitantly concentrated, which could affect the analysis.

Effect of sodium on copper and manganese emission signals

When a solution containing an analyte in the presence of an easily ionized element (EIE) is directly introduced into the DCP, an enhancement often occurs.^{1,2,32,33} At present, this is not fully understood, although Miller *et al.*³³ have proposed a model for this enhancement. The enhancement of emission by an EIE can be beneficial if it is reproducible and/or can be allowed for by standard techniques such as matrix-matching or standard additions, but otherwise is a disadvantageous interference. To find which was the case when the sample was introduced into the DCP by electrothermal vaporization, the effect of increasing amounts of sodium from 0.1 to 25 μg on the signal from 20 ng of copper, at the 324.7 nm emission line, was examined as shown in Fig. 2. When the sample was dried and vaporized, pronounced enhancement of the copper emission signal was obtained. However, when an ashing step of heating at 800° for 120 sec was introduced between the drying and vaporizing steps, the enhancement did not occur. An examination of the peaks obtained for 20 ng of copper in the presence of increasing amounts of sodium is shown in Fig. 3. The copper emission signal appeared approximately 7 sec after the electrothermal

Table 2. Selected absolute detection limits* for ETV-DCP, ETV-ICP and ETV-MIP spectrometry

Element	Emission wavelength, nm	ETV-DCP, This work	ETV-MIP		ETV-ICP						
			Ref. 25	Ref. 26	Ref. 23	Ref. 25	Ref. 27	Ref. 28	Ref. 29	Ref. 30	Ref. 31
Copper	324.7	0.1	0.33	—	—	0.02	0.004	—	0.1	—	—
Gold	267.6	0.7	—	—	—	—	—	—	—	0.002	0.02
Magnesium	279.6	0.4	—	0.048	0.02	—	—	—	—	0.0002	—
Manganese	257.6	0.5	—	—	—	—	0.002	0.04	—	0.002	0.002
Zinc	213.9	0.7	0.33	—	0.12	0.01	0.02	0.40	0.2	0.004	0.04

*Volumes normalized to 20 μl .

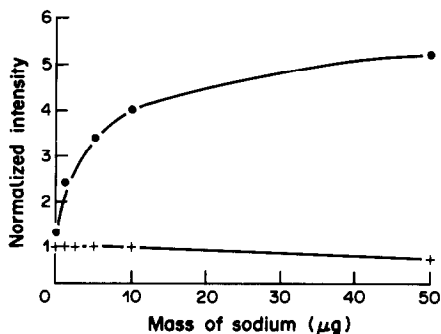


Fig. 2. Enhancement by sodium for 20 ng of copper introduced into the DCP by ETV, ●—without ashing and +—with ashing.

vaporization was started. However, there was a separate peak at an appearance time of approximately 5 sec, which grew in intensity with increasing amount of sodium, and for 50 μg of sodium overlapped the copper peak. The ashing temperature was held constant at 800° and the ashing time and the power applied at the vaporization stage were both varied, for 50 ng of copper in the presence of 50 μg of sodium, with the results shown in Fig. 4. The maximum power available and applied to the ETV was 35%, which gives a temperature increase of about 800°/sec, whereas an applied power of 26% gives about 400°/sec temperature increase. With ashing at maximum power for 45 sec, a signal consisting of three unresolved peaks occurs. Ashing for 90 sec at maximum power separates one of the peaks from the other two; ashing for 90 sec at 26% power still separates this peak but not quite so well. To separate or isolate the copper emission peak, a high power and long ashing time are required, otherwise an enhancement of the copper signal by sodium can occur.

The use of the ETV for introduction of sample vapour into the DCP thus involves an additional variable (the ashing step) which can be used to separate the copper emission signal from an interference signal. The nature of the interference peak is unknown but its cause is undoubtedly due to sodium or sodium chloride. Blank runs with sodium but no copper (Figs. 3 and 4) gave a small peak at the same appearance time as the interferent peaks, and this could be due to a structured background as reported elsewhere.³⁴ The peak cannot be due to emission from sodium or sodium chloride, which do not give an emission signal at 324.7 nm. A similar series of experiments to that illustrated in Fig. 3, with monitoring of the sodium emission line at 589.0 nm, confirmed that the first peak was not due to sodium or sodium chloride. A possible cause of the interferent peak may be the formation of copper(I) chloride (b.p. 1490°) by decomposition of copper(II) chloride (at 993°). A copper(I) chloride peak should occur before the copper emission peak because of the difference in boiling point (b.p. for copper 2336°). The supply of solid may be exhausted by the increase

in vapour pressure before the boiling point is reached. This effect has been noted previously with halide salts.³⁵ A possible explanation of the double interferent peak would be concomitant formation of a mixed halide salt *e.g.*, CuNaCl_2 , which should have a lower boiling point than copper(II) chloride.

When increasing amounts of sodium up to 50 μg were added to 100 ng of manganese, a similar enhancement to that for copper was obtained, as

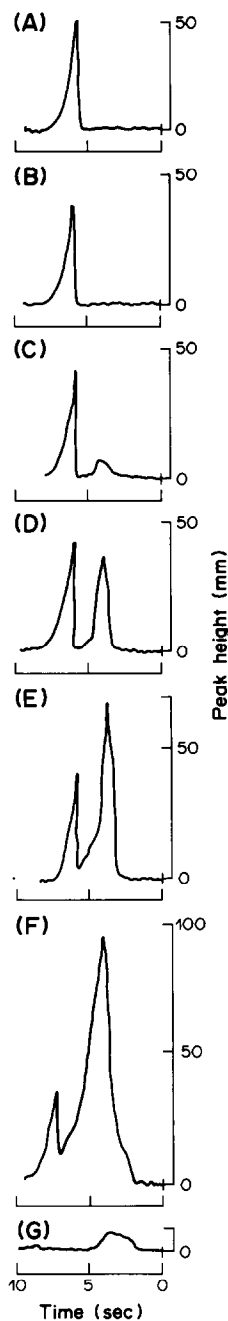


Fig. 3. Effect of increasing sodium concentration on 20 ng of copper. A—20 ng Cu, B—20 ng Cu + 0.5 μg Na, C—20 ng Cu + 2.5 μg Na, D—20 ng Cu + 5 μg Na, E—20 ng Cu + 10 μg Na, F—20 ng Cu + 50 μg Na, G—50 μg Na.

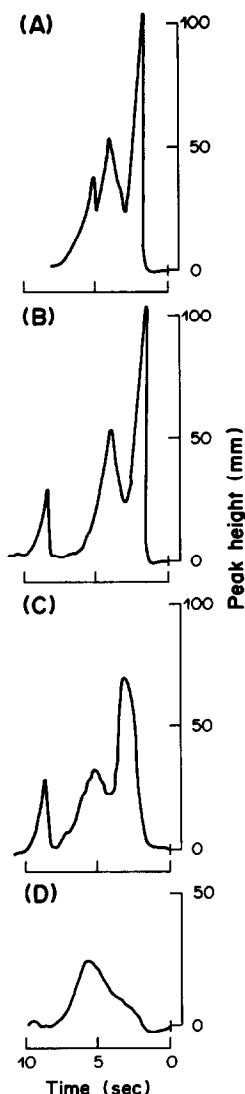


Fig. 4. Effect of ashing time and applied power on peak shape and appearance time for 50 ng of copper + 50 μg of sodium (A—C). A—45 sec ash and 35% power B—90 sec ash and 35% power, C—90 sec ash and 26% power, D—50 μg Na at 90 sec ash and 26% power.

shown in Fig. 5. With up to 5 μg of sodium present, no peaks appeared before the manganese peak, but with 44 μg of sodium present, the signal consisted of three peaks, as shown in Fig. 6. The same amount of sodium in a blank run gave no comparable signal (Fig. 6). When ashing at 800° for 120 sec was introduced, up to 50 μg of sodium did not significantly affect the manganese emission signal (Fig. 5).

The nature of the three peaks produced by 44 μg of sodium and 100 ng of manganese when the ashing step is not used, is not clear. One of the peaks will be due to manganese and the other two may be due to manganese(II) chloride and a double halide salt, analogously to the proposed mechanism for the three

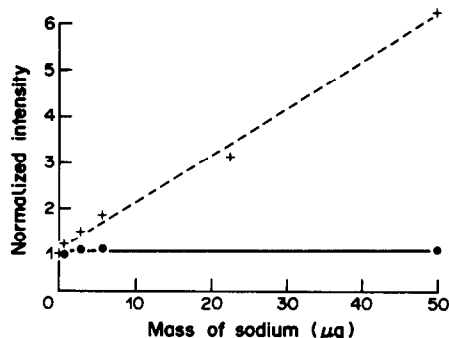


Fig. 5. Enhancement by sodium for 20 ng of manganese introduced into the DCP by ETV, +—without ashing and ●—with ashing.

peaks observed for copper, but it is not clear which is which. Work on solving this problem is continuing.

Application of ETV—DCP to samples

To evaluate the use of the ETV—DCP system, a series of copper and manganese determinations was performed on a variety of samples.

NBS SRM 2670 urine. The urine standard consists of two different samples: for normal levels and clinically elevated levels of copper, respectively. The direct analysis of urine by conventional pneumatic nebulization into a flame or plasma results in poor precision owing to build up of salts, dissolved solids and organic matrix in the nebulizer orifices. Analysis by conventional electrothermal atomization AAS of undiluted urine is difficult owing to molecular and particulate interferences. To test the ETV—DCP emission system, the standard urine was dissolved in 2.0 ml of demineralized water instead of the recommended 20.0 ml. This resulted in a final sodium chloride concentration of 2.6%. Copper standards in the 1.0–5.0 $\mu\text{g}/\text{ml}$ range were therefore prepared in 2.6% sodium chloride medium. The high salt concentration caused significant enhancement of the copper emission signal, making it large enough for the integration mode of the plasma computer module to be used instead of measurement of peak heights from the start of vaporization in the ETV. Integration for 6 sec was used. A linear calibration graph was obtained and triplicate determinations of copper in the standard urine gave the results shown in Table 3, which were in good agreement with the certified values.

Rio Grande water. One litre of Rio Grande water was collected, acidified, and filtered to remove suspended material. It was found that without an ashing stage, the signal for a given manganese concentration was substantially higher for the river water than for an aqueous standard. Use of an optimized ashing programme gave a relatively broad peak for both aqueous standards and water samples, before a sharper peak which was used for measurement. Signal vs. concentration plots of 5, 10, 15 and 20 μl of

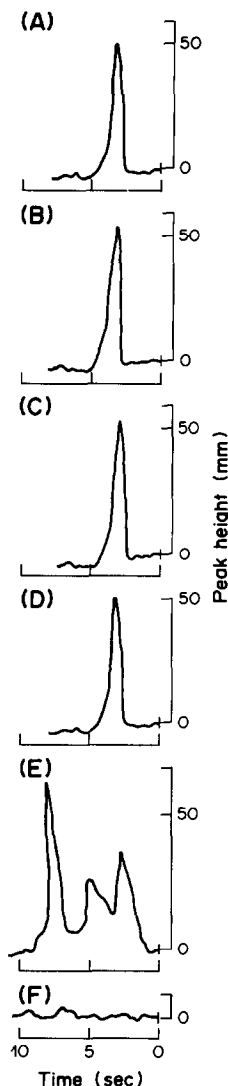


Fig. 6. Effect of increasing sodium concentration on 100 ng of manganese. A—100 ng Mn, B—100 ng Mn + 0.4 μg Na, C—100 ng Mn + 2.4 μg Na, D—100 ng Mn + 5.1 μg Na, E—100 ng Mn + 44 μg Na, and F—44 μg Na.

10- $\mu\text{g}/\text{ml}$ manganese solution [as manganese(II) chloride] added to 40 μl of the water sample and to 40 μl of demineralized water and diluted with 15, 10, 5 and 0 μl of demineralized water, respectively, had similar slopes (0.62 and 0.58 mm/ng, respectively). Extrapolation analysis gave a manganese concentration of 0.6 $\mu\text{g}/\text{ml}$ in the river water. Analysis by conventional flame AAS¹⁹ at 279.5 nm, with aqueous standards, gave a manganese concentration of 0.5 $\mu\text{g}/\text{ml}$.

Canned infant-milk. If no ashing step was used, the milk matrix caused signal enhancement. When ashing was used and the power was increased by 5% increments, it was found that the peak height of the copper signals from 20 μl of 10- $\mu\text{g}/\text{ml}$ aqueous copper standard [copper(II) nitrate] did not decline significantly until the ashing power exceeded 30%, as shown in Fig. 7. Over the same power range, the copper signal from 20 μl of milk decreased significantly, but the signal for copper in the milk matrix was still enhanced relative to that for the corresponding aqueous standard. To match the enhancement effect, an ionization buffer (5 μl of 10 mg/ml caesium solution) was added to each 20- μl injection and a lower ashing power of 26% was used to prevent loss of caesium before completion of ashing of the organic

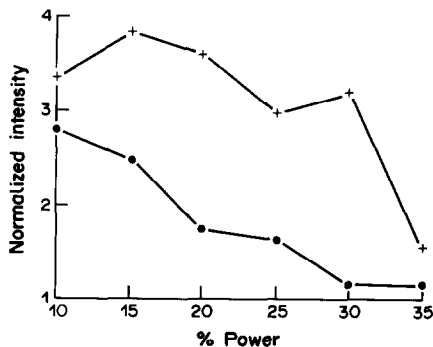


Fig. 7. Emission intensity of copper as a function of power applied to the ETV, ●—milk matrix and +—aqueous solution.

Table 3. Comparison of ETV-DCP emission spectrometry with certified values

Element	Sample	Certified value	ETV-DCP emission spectrometry value
Cu, $\mu\text{g}/\text{ml}$	NBS-SRM 2670 normal urine	1.3 \pm 0.2	1.2 \pm 0.1
Cu, $\mu\text{g}/\text{ml}$	NBS-SRM 2670 elevated urine	3.7 \pm 0.3	3.5 \pm 0.1
Mn, $\mu\text{g}/\text{g}$	USGS Geological Standard, Number 4	140 \pm 20	140 \pm 20
Mn, $\mu\text{g}/\text{g}$	USGS Geological Standard, Number 5	250 \pm 40	280 \pm 20
Mn, $\mu\text{g}/\text{g}$	USGS Geological Standard, Number 2	930 \pm 70	960 \pm 100
Mn, $\mu\text{g}/\text{g}$	USGS Geological Standard, Number 6	1010 \pm 40	1000 \pm 50
Mn, mg/g	USGS Geological Standard, Number 3	22.1 \pm 1.0	22.3 \pm 2.0

matrix. The vaporization temperature was increased to a maximum of 2800° because at lower power settings for the ashing the copper peak for the milk matrix was broader than that for the aqueous standards. With this temperature programme, a calibration plot for 10 μ l of milk spiked with 1, 2, 4 and 6 μ l of 5- μ g/ml copper solution (nitrate) gave a slope of 2.00 mm/ng, that for the corresponding aqueous standards being 1.90 mm/ng. This analysis gave the copper concentration in the milk as 1.7 μ g/ml. Flame AAS analysis of an acid digest of the milk gave a concentration of 1.8 μ g/ml.¹⁹

Bull sperm. It has been shown for several tissues that manganese is a modulator of adenylate cyclase,^{34,35} which is implicated in several different sperm cell processes, including energy metabolism and maturation. Casillas and Hoskins¹⁸ have demonstrated stimulation of spermatozoal adenylate cyclase by manganese. Changes in manganese concentration during the course of sperm maturation have not been reported. Attempts were made to determine manganese in bull sperm by electrothermal atomization AAS, but were unsuccessful, mainly because of the presence of high salt concentrations and molecular absorption. As already mentioned, the ETV-DCP system can be applied to complex matrices containing high salt concentrations. A sperm sample from the caudal epididymis of bovine testes was suspended in 0.9% sodium chloride solution and analysed by addition of 0, 5, 10 and 15 μ l of 616- μ g/ml manganese (nitrate) solution to 20- μ l portions of the suspension and diluted to the same volume with 20, 15, 10 and 5 μ l of demineralized water, followed by ETV-DCP analysis. The concentration found was 1.5 μ M in the suspended sperm (equivalent to 0.32 nmole/10⁹ cells).

United States Geological Survey standards. The determination of manganese was first attempted by adding some of the powdered standard directly to a micro-boat and applying maximum power. This procedure left a round ball of unvolatilized material in the micro-boat and caused some instability of the plasma. Samples were therefore diluted 1:20 with powdered cellulose in a ball mill. Direct volatilization of about 5 mg of these diluted samples appeared to leave very little residue, and decreased the plasma instability. Analysis of the five USGS standards for manganese in this way gave the results shown in Table 3; these were in good agreement with the certified values. A blank containing only cellulose gave no manganese signal.

CONCLUSION

The use of an electrothermal vaporizer for introduction of microlitre volumes or microgram masses of samples for determination of copper and manganese by DCP emission spectrometry has been shown to give good results. For certain determinations, matrix matching or addition of an

ionization-suppression buffer to the standards improves the accuracy. It is possible to remove enhancement of the copper and manganese signal by sodium by means of an ashing step. Detection limits are comparable to those for pneumatic nebulization of the sample but have the advantage that microlitre volumes or microgram samples may be used.

Acknowledgement—J. S. was supported, in part, by Grant RR-08136 for Minorities Biomedical Research Support, Division of Research Resources, National Institutes of Health and Grant GM-07667 from Minority Access Research Careers, National Institutes of Health.

REFERENCES

1. B. Greene, A. Uranga and J. Sneddon, *Spectrosc. Lett.*, 1985, **18**, 425.
2. M. Rodriguez and J. Sneddon, *Atom. Spectrosc.*, 1986, **7**, 64.
3. H. Matusiewicz and D. F. S. Natusch, *Acta Chim. Acad. Sci. Hung.*, 1981, **108**, 103.
4. R. J. Dellefield and T. D. Martin, *Atom. Spectrosc.*, 1982, **3**, 165.
5. R. J. Decker, *Spectrochim. Acta*, 1980, **35B**, 19.
6. L. Ebdon and S. Sparkes, *ICP Inf. Newslett.*, 1986, **12**, 1.
7. W. M. Blakemore, P. H. Casey and W. R. Collie, *Anal. Chem.*, 1984, **56**, 1376.
8. J. Sneddon and F. Bet-Pera, *Trends Anal. Chem.*, 1986, **5**, 110.
9. D. R. Hull and G. Horlick, *Spectrochim. Acta*, 1984, **39B**, 843.
10. M. Thompson, J. E. Goulter and F. Sieper, *Analyst*, 1982, **106**, 32.
11. J. W. Carr and G. Horlick, *Spectrochim. Acta*, 1982, **37B**, 1.
12. T. Ishizaka and Y. Uwamino, *ibid.*, 1983, **38B**, 519.
13. D. J. C. Helmer and J. P. Walters, *Appl. Spectrosc.*, 1984, **38**, 392.
14. P. G. Mitchell, J. A. Ruggles, J. Sneddon and L. J. Radziemski, *Anal. Lett.*, 1985, **18**, 1723.
15. P. G. Mitchell, J. Sneddon and L. J. Radziemski, *Appl. Spectrosc.*, 1986, **40**, 274.
16. B. Greene, P. G. Mitchell and J. Sneddon, *Spectrosc. Lett.* 1986, **19**, 101.
17. P. G. Mitchell, B. Greene and J. Sneddon, *Mikrochim. Acta*, 1986, **I**, 249.
18. E. R. Casillas and D. D. Hoskins, *Ann. Rev. Biochem.*, 1980, **49**, 1980.
19. J. L. Munro and J. Sneddon, *Atom. Spectrosc.*, 1987, **8**, 92.
20. E. S. Gladney, D. R. Perin, J. W. Owens and D. Knabb, *Anal. Chem.*, 1979, **51**, 1557.
21. Y. Y. Cheung, G. F. Kirkbright and R. D. Snook, *Anal. Chim. Acta*, 1982, **140**, 213.
22. H. Matusiewicz and R. M. Barnes, *Appl. Spectrosc.* 1984, **38**, 745.
23. A. Aziz, J. A. C. Broekaert and F. Leis, *Spectrochim. Acta*, 1982, **37B**, 369.
24. G. Crabi, P. Cavalli, M. Achilli, G. Rossi and N. Omenetto, *Atom. Spectrosc.*, 1982, **3**, 81.
25. K. Chiba, M. Kurosawa, K. Tanabe and H. Haraguchi, *Chem. Lett.*, 1984, 75.
26. A. Aziz, J. A. C. Broekaert and F. Leis, *Spectrochim. Acta*, 1982, **37B**, 381.
27. R. M. Barnes and P. Fodor, *ibid.*, 1983, **38B**, 1191.
28. H. M. Swaidan and G. D. Christian, *Anal. Chem.*, 1984, **56**, 120.
29. G. F. Kirkbright and R. D. Snook, *Appl. Spectrosc.*, 1983, **37**, 11.

30. S. E. Long, R. D. Snook and R. F. Browner, *Spectrochim. Acta*, 1985, **40B**, 553.
31. A. M. Gunn, D. L. Millard and G. F. Kirkbright, *Analyst*, 1978, **103**, 1066.
32. M. H. Miller, D. Eastwood and M. S. Hendrick, *Spectrochim. Acta*, 1984, **39B**, 13.
33. M. H. Miller, E. Keating, D. Eastwood and M. S. Hendrick, *ibid.*, 1985, **40B**, 593.
34. D. D. Nygaard, *Anal. Chem.*, 1979, **51**, 881.
35. C. F. Baur and D. F. S. Natusch, *ibid.*, 1981, **53**, 2020.
36. E. M. Ross and A. G. Gilman, *Ann. Rev. Biochem.*, 1980, **49**, 553.
37. G. D. Aurbach, *Ann. Rev. Physiol.*, 1982, **44**, 653.

A SIMPLE AND RAPID FLUORIMETRIC METHOD FOR THE MICRODETERMINATION OF ISONICOTINIC ACID HYDRAZIDE

P. C. IOANNOU

Laboratory of Analytical Chemistry, Chemistry Department, University of Athens, 104 Solonos St.,
Athens 10680, Greece

(Received 3 October 1986. Revised 7 April 1987. Accepted 10 May 1987)

Summary—A simple, rapid and sensitive fluorimetric method has been developed for the micro-determination of isonicotinic acid hydrazide, based on its formation of a hydrazone with 2-hydroxy-1-naphthaldehyde in acidic medium, in the presence of excess of scandium ions, and the consequent formation of a strongly fluorescent complex (λ_{ex} 430 nm, λ_{em} 510 nm) between the hydrazone and scandium in weakly acidic medium. Kinetic and equilibrium procedures for isonicotinic acid hydrazide determination are proposed. A calibration graph linear up to 5.00 $\mu\text{g/ml}$ is obtained by both procedures, with a mean relative error of about 2.0%. The detection limit for the kinetic procedure is 0.4 ng/ml and for the equilibrium procedure about 0.2 ng/ml.

Hydrazones are a very significant class of organic compounds with several applications in analytical chemistry.^{1,2} Their most important property is the ability to form stable chelates with transition metals; some of the products are coloured or strongly fluorescent, and have been used for the spectrophotometric and fluorimetric determination of the corresponding metal ions. These products may also be used for determination of the compounds that can react to form hydrazones (*e.g.*, carbonyl compounds, hydrazides). Many hydrazones and hydrazides are physiologically active and are used for the treatment of disease such as tuberculosis, leprosy and mental disorder. The development of simple, sensitive and rapid methods for their determination is of importance. One of the most important hydrazides, which is used for the treatment of tuberculosis and has drastically reduced the morbidity and mortality of the disease, is isonicotinic acid hydrazide (INH). Various analytical techniques have been applied for its determination in biological fluids and drugs. Fluorimetry is one of the most sensitive and simple techniques for INH determination. Most fluorimetric methods for INH^{3-5} have been based on its reaction with aldehydes to produce hydrazones which fluoresce under particular conditions, *e.g.*, in the presence of reducing agents or metal ions. The fluorimetric methods reported are sensitive but time-consuming, and require some preliminary treatment.

The present work describes a fluorimetric method for determination of INH, based on its reaction with 2-hydroxy-1-naphthaldehyde (HNA) in the presence of excess of scandium, and the consequent formation of the strongly fluorescent HNAINH-Sc complex. The method developed is simple, rapid, selective, and more sensitive than the other fluorimetric methods.

EXPERIMENTAL

Apparatus

A model 512 Perkin-Elmer double-beam fluorescence spectrophotometer with a 150-W xenon lamp was used in the ratio mode to compensate for variations in the light-source intensity. The instrument settings were: dynode voltage 750 V; excitation wavelength 430 nm with a bandwidth of 20 nm; emission wavelength 510 nm with a bandwidth of 20 nm. Finpipette microsyringes were used for transfer of small sample and reagent volumes.

Reagents

All solutions were prepared in demineralized distilled water from reagent grade materials, unless otherwise stated.

Standard INH solution, 1000 ppm, in water. Prepared from INH obtained from Sigma. When stored at 4°, the stock solution was stable for several weeks. Working solutions were prepared daily by appropriate dilution with water.

HNA solution, 0.01M, in acetonitrile. Prepared from HNA obtained from Fluka. This solution was stable at room temperature for several weeks.

Scandium solution, 0.02M. "Specpure" scandium oxide (Johnson Matthey, 0.2758 g) was dissolved by warming in a minimal volume of concentrated hydrochloric acid with addition of several drops of concentrated nitric acid, and the solution was diluted to volume in a 100-ml standard flask with water. A 0.01M working solution with pH 1.1-1.2 was prepared by appropriate dilution with water and a few drops of saturated sodium hydroxide solution.

Stock acetate buffer solution, 0.1M, pH 5.10-5.20. Prepared by dissolving 2.06 g of anhydrous sodium acetate in 100 ml of water, adjusting to pH 5.10-5.20 with 1M hydrochloric acid and diluting with water to 250 ml.

Working buffer solution, apparent pH 6.00-6.10. Prepared by mixing one volume of the stock acetate buffer solution with one volume of acetonitrile.

Procedures

Kinetic procedure. Transfer 20 μl of the INH sample or standard solution into the cuvette. Add 100 μl of scandium working solution, then 50 μl of HNA solution, and start the stirrer. After exactly 60 sec, rapidly inject 2.00 ml of working

buffer solution to stop the reaction, and measure the fluorescence intensity.

Equilibrium procedure. Transfer 20 μl of the INH sample or standard solution into a 10-ml test-tube. Add 100 μl of scandium working solution, then 50 μl of HNA solution, and agitate the tube vigorously in an ultrasonic bath for 10 min. Then add 2.00 ml of the working buffer solution, stir the mixture and measure the fluorescence intensity.

RESULTS AND DISCUSSION

In acidic water-acetonitrile solution INH forms with excess of HNA the weakly fluorescent 2-hydroxy-1-naphthaldehyde isonicotinoyl hydrazone (HNAINH), which gives a strong yellowish green fluorescence in weakly acidic solution in the presence of scandium (λ_{ex} 430 nm, λ_{em} 510 nm). The excitation and emission spectra of the complex are shown in Fig. 1. Under the same conditions INH-Sc, HNA-Sc, and HNAINH do not exhibit fluorescence. The effect of various parameters on the formation of HNAINH and the HNAINH-Sc complex have been studied and the reaction conditions optimized.

Optimum conditions for HNAINH formation

Effect of hydrochloric acid concentration. Because of the catalytic effect of hydrogen ions on hydrazone formation the influence of acidity on the reaction between INH and HNA was examined. The reaction was performed at different hydrochloric acid concentrations in the presence of scandium. After the reaction was completed, the working buffer solution was added, the pH was adjusted to 5.9–6.1, if necessary, and the fluorescence intensity of the HNAINH-Sc complex was measured.

From the results obtained, it was concluded that a hydrochloric acid concentration of at least 0.06M in the INH-Sc-HNA mixture is necessary for complete condensation. Increasing the acid concentration to 0.28M does not affect the yield of the reaction product.

Effect of standing time. Figure 2 shows that in the absence of scandium the condensation between INH

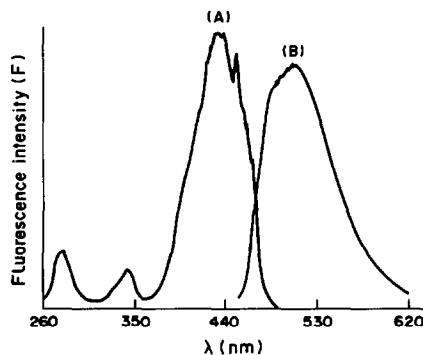


Fig. 1. Excitation (A) and emission (B) spectra of HNAINH-Sc complex solution (uncorrected): $[\text{INH}] = 3.4 \times 10^{-6}\text{M}$, $[\text{Sc}] = 4.6 \times 10^{-4}\text{M}$, $[\text{HNA}] = 2.3 \times 10^{-4}\text{M}$, pH = 6.0, standing time 15 min. Other conditions as in procedure.

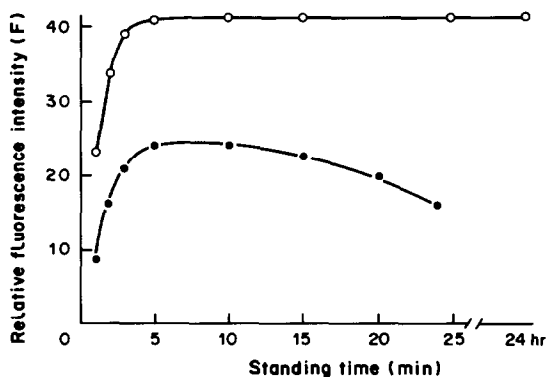


Fig. 2. Effect of standing time in the absence (●) and in the presence (○) of scandium. $[\text{INH}] = 7.0 \times 10^{-7}\text{M}$, $[\text{Sc}] = 4.6 \times 10^{-4}\text{M}$, $[\text{HNA}] = 2.3 \times 10^{-4}\text{M}$.

and HNA is completed in about 10 min with stirring (about 30 min without stirring), but the HNAINH then begins to decompose. The presence of scandium does not affect the reaction time but stabilizes the hydrazone by complexation and the complex has much stronger fluorescence, which permits measurement at a fixed time, before the condensation step is complete.

Effect of scandium concentration. The fluorescence intensity for $7.0 \times 10^{-7}\text{M}$ INH increases with increase in scandium concentration up to $2.5 \times 10^{-4}\text{M}$ and becomes constant at higher scandium concentrations. Use of 100 μl of a $1.0 \times 10^{-2}\text{M}$ scandium solution with a pH of about 1.1–1.2 gives the desired acidity in the condensation step and a final scandium concentration of about $5.0 \times 10^{-4}\text{M}$.

Effect of HNA concentration. Because of the large excess of HNA needed and the possibility of a high blank signal in the measurement of low INH concentrations, the effect of HNA excess at three INH concentrations was examined. As expected, the effect of HNA excess is more significant at low INH concentration. A concentration of $2.5 \times 10^{-4}\text{M}$ HNA was chosen as the best compromise because it gives practically maximum fluorescence at all three INH concentrations (Fig. 3).

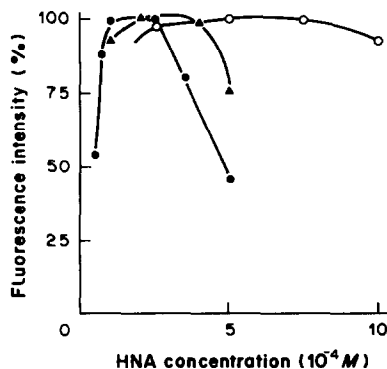


Fig. 3. Effect of HNA concentration. $[\text{INH}]$, 10^{-6}M : (●) 0.07, (▲) 0.7, (○) 7.0. $[\text{Sc}] = 5.0 \times 10^{-4}\text{M}$. Other conditions as in the procedure.

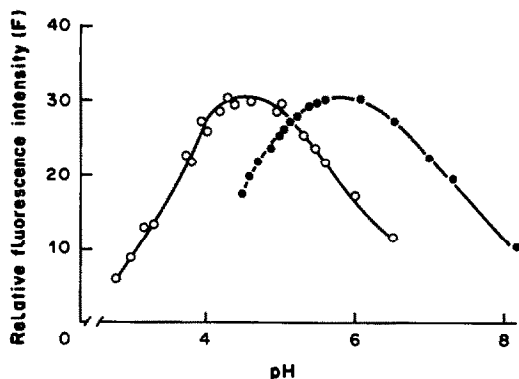


Fig. 4. Effect of "pH" on the fluorescence intensity of the HNAINH-Sc complex in the absence (○) and in the presence (●) of acetate buffer solution (0.05M). [INH] = $4.6 \times 10^{-6}M$, [Sc] = $4.6 \times 10^{-4}M$, [HNA] = $2.3 \times 10^{-4}M$.

Optimum conditions for the HNAINH-Sc fluorescence measurements

Effect of the apparent pH ("pH"). The effect of "pH" on the fluorescence intensity of the HNAINH-Sc complex in the absence and presence of acetate buffer was studied (Fig. 4). To the INH-Sc-HNA solution, after complete reaction (10 min time, with stirring), 10 μ l of 1.0M sodium hydroxide were added to neutralize the mixture, then 2.0 ml of water-acetonitrile solution (1:1, v/v) at different "pH" values were added and the fluorescence intensity was measured. The study was repeated with acetate present by addition of the stock buffer solution instead of the water-acetonitrile mixture, and without neutralization with sodium hydroxide. The optimum "pH" range in the absence of acetate buffer solution was found to be 4.3-4.9. In the presence of acetate buffer the optimum "pH" increased to 5.6-6.2, but the fluorescence intensity did not change. An aqueous 0.1M acetate buffer solution

of pH 5.0-5.2 was found to be satisfactory to establish a "pH" value of 5.9-6.1 after dilution with an equal volume of acetonitrile.

Effect of acetonitrile concentration. Because of the low solubility of HNAINH and its scandium complex in water, a mixed aqueous-organic solvent is required. Acetonitrile was chosen as the best of the common solvents (acetone, ethanol, dimethylformamide) because of its higher enhancement of the fluorescence intensity, its lower toxicity, higher purity and stability (in comparison with dimethylformamide), its excellent extractive power for INH and the low solubility in it of interfering metal ions. The fluorescence intensity of the complex was maximal at an acetonitrile concentration of about 50% v/v.

Stability of the complex. The fluorescence intensity of the complex, measured after the buffer solution had been added, decreased by 15% in the first 2 min, and then remained stable for at least 48 hr.

Analytical applications

The relationship between the fluorescence intensity and INH concentration was studied under the optimum conditions established for the kinetic and equilibrium procedures. A linear calibration graph was obtained for the range up to 5.00 μ g/ml. Results for the determination of INH in pure aqueous solutions are given in Table 1. They indicate that in the range 0.0025-5.00 μ g/ml INH can be determined by the two procedures with a mean relative error of about 2.0%. Three replicate determinations at each of the 0.0025, 0.025, 0.250, 2.50 μ g/ml INH levels had relative standard deviations of 4.5, 2.4, 2.0 and 1.5% respectively, for the kinetic procedure and 4.0, 1.7, 1.7 and 1.2%, respectively for the equilibrium procedure. As Table 1 shows, there is no significant difference in the accuracy and reproducibility of the results obtained by the two procedures. Use of the

Table 1. Analytical results for INH aqueous solutions

Taken, μ g/ml	Found (range)*, μ g/ml		Relative error, %	
	Equilibrium procedure	Kinetic procedure	Equilibrium procedure	Kinetic procedure
0.0025	0.0025 (0.0001)	0.0024 (0.0003)	0.0	-4.0
0.0050	0.0049 (0.0001)	0.0051 (0.0005)	-2.0	2.0
0.0075	0.0077 (0.0001)	0.0076 (0.0004)	2.6	1.3
0.0100	0.0099 (0.0001)	0.0099 (0.0003)	1.0	1.0
0.0250	0.0240 (0.0006)	0.0245 (0.0010)	-4.0	-2.0
0.0500	0.0513 (0.0008)	0.051 (0.004)	2.6	2.4
0.0750	0.0757 (0.0008)	0.074 (0.002)	0.9	-1.0
0.1000	0.0997 (0.0002)	0.1000 (0.0010)	0.3	0
0.250	0.239 (0.007)	0.248 (0.010)	-4.4	-0.8
0.500	0.514 (0.014)	0.505 (0.018)	2.8	1.0
0.750	0.753 (0.010)	0.745 (0.007)	0.4	-0.7
1.000	0.993 (0.010)	1.001 (0.010)	-0.7	0.1
1.25	1.20 (0.03)	1.19 (0.03)	-4.0	-4.8
2.50	2.54 (0.03)	2.59 (0.07)	1.6	3.5
3.75	3.86 (0.07)	3.76 (0.03)	2.9	0.3
5.00	4.91 (0.10)	4.96 (0.06)	-1.8	0.7

*Average of 3 measurements on single sample.

Table 2. Interference study for INH determination at a concentration of 0.100 $\mu\text{g/ml}$ ($7.0 \times 10^{-7}M$)

Foreign species	Tolerance molar ratio, [interferent]/[INH]
Fe(III)	10
Cu(II)	1
Ni(II)	1000
Co(II)	1000
Ca ²⁺	> 1000
Mg ²⁺	> 1000
Al ³⁺	1000
F ⁻	100
CN ⁻	100
PO ₄ ³⁻	100
Hydrazine	500
Creatinine	> 1000
Urea	> 1000
Glucose	> 1000
Galactose	> 1000
Pyruvic acid	25
Lactic acid	> 1000
L-Alanine	> 1000
Formaldehyde	10

equilibrium procedure removes the need for precise timing control. On the other hand, the kinetic procedure is less time-consuming, with fewer manipulation steps. The detection limits (defined as three times the standard deviation of the mean blank) are 0.4 ng/ml for the kinetic method and 0.2 ng/ml for the equilibrium procedure.

Interferences

As the proposed fluorimetric method for INH determination is very sensitive and could be applied in clinical analysis, an interference study of organic compounds likely to be present in biological fluids was made. The effect of interfering ions on the determination of INH at 0.1 $\mu\text{g/ml}$ concentration was also examined. The tolerance limit was taken as the concentration that did not cause more than $\pm 5\%$ change in the fluorescence intensity. The results sum-

marized in Table 2 show that most of the metals and organic compounds tested do not interfere. Copper(II) and iron(III) decrease the fluorescence of the complex and are tolerated only at 1:1 and 10:1 molar ratio to INH, respectively. Aluminium, which also forms a fluorescent complex with HNAINH, does not interfere, because scandium reacts much faster and is used in excess. Carbonyl compounds, such as pyruvic acid and formaldehyde, decrease the fluorescence intensity because of their interaction with INH and are tolerated to a limited extent (25- and 10-fold molar ratio to INH, respectively). Acetylisoniazide, which is the main metabolite of INH in blood serum, did not react under the recommended conditions.

Conclusions

The method is fairly simple, rapid and highly sensitive, and the measurements can be performed with very small samples. A feature of the method is that the condensation of INH with HNA, catalysed by hydrogen ions, is more complete in the presence of scandium, and the hydrazone formed is stable for a long time. Another advantage of the proposed method is the accuracy and reproducibility obtained with both the procedures. The method is suitable for routine measurements of INH in biological fluids. Its application for INH determination in blood serum and for the determination of acetylator phenotype is being examined.

REFERENCES

1. M. Katyal and Y. Dutt, *Talanta*, 1975, **22**, 151.
2. R. B. Singh, P. Jain and R. P. Singh, *ibid.*, 1982, **29**, 77.
3. E. M. Scott and R. C. Wright, *J. Lab. Clin. Med.*, 1967, **70**, 355.
4. J. N. Miceli, W. A. Olson and W. W. Weber, *Biochem. Med.*, 1975, **12**, 348.
5. T. Uno and A. Taniguchi, *Bunseki Kagaku*, 1971, **20**, 997.
6. P. C. Ioannou and P. A. Siskos, *Talanta*, 1984, **31**, 253.

HYDROXIDE COMPLEXES OF LANTHANIDES—VIII* LANTHANUM(III) IN PERCHLORATE MEDIUM

J. KRAGTEN and L. G. DECNOP-WEEVER

Laboratorium voor Analytische Chemie der Universiteit van Amsterdam, Nieuwe Achtergracht 166,
1018 WV Amsterdam, The Netherlands

(Received 17 March 1987. Accepted 10 May 1987)

Summary—From the precipitation borderline in the pLa' – pC_H diagram the stability constants for (mononuclear) lanthanum–hydroxide species have been established. The presence of polynuclear species could not be demonstrated and seems unlikely. The values found were $\log^* \beta_1 = -8.6$, $\log^* \beta_2 = -17.9$, $\log^* \beta_3 = -27.3$ and $\log^* K_{s0} = 22.8$. The data refer to precipitates prepared under CO_2 -free conditions at room temperature ($21.5 \pm 0.5^\circ$) in sodium perchlorate medium with an ionic strength of 1.

Hydroxide-complex formation by lanthanum has been studied by many workers and therefore was not examined earlier in our series. However, it became apparent during our work that the earlier lanthanum data were questionable, especially with reference to polycomplexes.

Most investigators started with concentrated lanthanum solutions and restricted their studies to small areas in the pM' – pH diagram where the $LaOH^{2+}$ -ion is present only as a minor species and where the evidence for higher forms and polyhydroxides appears to be rather speculative, coming mainly from better fits of curves.

Similarly to other lanthanides, lanthanum has a great affinity for carbonate ions and the tendency for carbonate precipitation seems to be stronger than for hydroxide precipitation. Even after prolonged purging with nitrogen gas the formation of minor amounts of La–carbonate ions cannot be excluded, and allowance for this can serve as well as postulation of polycomplexes in obtaining better fits of curves.

Consequently there is a fair diversity in the literature values of the first constant $\log^* \beta_1$.^{1–8} The values of the solubility product $\log^* K_{s0}$ ^{9–16} (Table 1) agree better, although some relate to the formation of lanthanum carbonate rather than lanthanum hydroxide.¹⁷ In other cases the concentration of the counterion is not negligible; correction is difficult because of lack of reliable side-reaction coefficients.

The formation of polycomplexes has been mentioned but the data are not consistent.⁷ Reuben and Fiat¹⁸ investigated with ¹⁷O-NMR the hydration of lanthanum ions in the concentration region 0.01–2M and concluded that no polyhydroxides are formed.

We believe that the formation of carbonate complexes has been mistaken for polynuclear hydroxide complex formation and that this has led to sug-

gestions of minor amounts of $La_2(OH)_2$, $La_3(OH)_3$, $La_5(OH)_5$ and/or $La_6(OH)_6$.

Our current conclusion is that if polycomplexes are formed their concentration is so small that their presence can be neglected for practical analytical applications.

Values for $\log^* \beta_2$, $\log^* \beta_3$ and $\log^* \beta_4$ have not been found in the literature, although it has been recognized that formation of soluble hydroxides takes place extensively at higher pH values.¹⁷ Ivanov-Emin *et al.*¹⁹ investigated the formation of amphoteric complexes but could not demonstrate their presence.

Our experiments were designed to cover a wide range of concentration and pH (Fig. 1) and were done in sodium perchlorate medium ($I = 1.0$ at $21.5 \pm 0.5^\circ$) in a nitrogen atmosphere in a glove-box. All manipulations were standardized for reasons discussed before.^{20–23} The precipitate was formed as described for ytterbium.^{23,24} The pC_H values were determined with a pH-meter calibrated in pC_H units.²²

RESULTS AND CONCLUSIONS

The ascending branch of the borderline of the precipitation region for La (Fig. 1) consists of a slightly bent line connected by a curve from pC_H 9 to pC_H 10 with a straight horizontal part at higher pC_H values. According to the theory^{20–22} in which straight-line segments determine the borderline of precipitation, we can assign equation (4) (see Table 2) to the horizontal part of the borderline. The best fit corresponds to $pLa' = 4.49 \pm 0.05$. The ascending branch can be represented by a straight line. From regression analysis a slope of 2.5 can be deduced for $pC_H < 9.4$. Polycomplexes, if formed at all, will be present as only minor components at lanthanum levels of 0.1M or lower, because the slope is lower than 3.

As the slope of the ascending branch (2.5 ± 0.1) differs significantly from the integer values 3 and 2

*Part VII: *Talanta*, 1984, 31, 731.

Table 1

Reference	$\log * \beta_1$	$\log * K_{\infty}$	Polycomplexes $\log * \beta_{sp}$	Medium	Remarks
1	-10.94	—		$I = 0.3$; NaClO ₄ ; 25°	Pot. titn.
2	-7.4	—		$I = 0.1$; (H, Li)ClO ₄ ; 25°	Radiochem. detection
3	-9.1	—		$I = 0.05$; NaCl, ClO ₄ ; 25°	Pot. titn. of 0.005M La; CO ₂ -free; La ³⁺ predominates
4	-10.04	—		$I = 3$; LiClO ₄ ; 25°	pH determ.; 0.1-0.4M La; pH 7.0-7.5; CO ₂ -free
5	-8.3	—		$I = 0.1$	
6	-8.4	—		$I = 0.1$; La-nitrate; 20°	Titn. with NaOH, glass electr.
7	-10.12	—	La ₂ (OH) ₉ : 9.98 La ₃ (OH) ₆ : 71.43 or La ₆ (OH) ₁₀ : 78.75		
8	-10.0	—		$I = 0.001$; sulphate; 25°	pH determ.; aged ppte.
8	-8.12	23		$I = 0.05$; sulphate; 25°	pH determ.; aged ppte.
9	-8.5	20.3		$I = 0$	Empirical relation
9	-8.8	20.3		$I = 0.05$	Empirical relation
9	-9.9	20.3		$I = 3.0$	Empirical relation
10	—	23.5		$I = 0.1$; 25°	Pptn. titn.; sol. product not temp. dependent after correction for presence of LaOH
		23.2			
11	—	19.4			
12	—	20.5			
13	—	22.8		0.38M NaNO ₃	Fresh ppte.
14	—	23.1			Fresh ppte.
15	—	23.2		$I = 0.05$; sulphate; 25°	pH determ.; aged ppte.
16	—	22.8		$I = 0$; sulphate	pH determ.; 0.001-0.0001M, pH 4-7; aged ppte. (24 hr)
		20		$I = 0.01$	pH determ.; 0.001-0.0001M, pH 4-7; aged ppte. (24 hr)

Table 2

Equation	p	q	Slope ($np - q$)	Equation for the borderline segment
1	1	0	3	$pLa' = 3pC_H - \log *K_{30}$
2	1	1	2	$pLa' = 2pC_H - \log *K_{30} - \log *β_1$
3	1	2	1	$pLa' = pC_H - \log *K_{30} - \log *β_2$
4	1	3	0	$pLa' = -\log *K_{30} - \log *β_3$

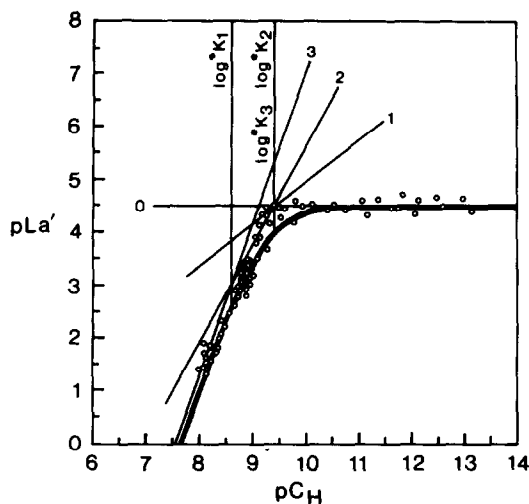


Fig. 1. The solid curve—the borderline of precipitation of $La(OH)_3$ —was constructed with the values given in Table 3. The numbers 0, 1, 2, 3 correspond to the slopes of the straight-line segments (equations 1–4, Table 2) approximating the exact envelope curve. The circles denote the experimental results.

Table 3

$\log *K_1 = -8.6 (-8.55)$	$\log *β_1 = -8.6 (-8.55)$
$\log *K_2 = -9.4 (-9.38)$	$\log *β_2 = -17.9 (-17.93)$
$\log *K_3 = -9.4 (-9.38)$	$\log *β_3 = -27.3 (-27.31)$
$\log *K_{30} = 22.8$	

corresponding to the straight-line segments [equations (1) and (2) in Table 2], it can be concluded that in this region both La^{3+} and $LaOH^{2+}$ are in equilibrium with the precipitate. It implies that the vertical line separating the predominance regions must end somewhere in the middle of the ascending branch.

From the sharp bend near pC_H 9.5 it follows that the $La(OH)_2^+$ ion is present only in minor amounts. This implies that the corresponding straight-line segment with slope of 1 should not contribute to the real curve. Its most likely locus passes through the intersection point of the segments with slopes 0 and 2. A higher position would reverse the sequence of $\log *K_i$ values (the pC_H values of the intersection points correspond to the $\log *K_i$ values). At a lower position the line would push down the (real) precipitation line.

For the best fit to the experimental points it is necessary to take into account that the experimental

errors are different for the horizontal branch where the error is dominant in the vertical direction, and the ascending branch where the error is oriented horizontally.

The best fit was found with the equation

$$[La']_{\max} = 10^{-(3pC_H - 22.80)} + 10^{-(2pC_H - 14.25)} + 10^{-(pC_H - 4.87)} + 10^{-4.50}$$

The separate terms correspond to the equations in Table 2, from which the corresponding equilibrium constants can be deduced (Table 3).

It is difficult to discuss the accuracy of the individual constants, but we can make the following statement from our experiments. The position of the envelope curve is uncertain within 0.1 log unit in the X -direction in the ascending branch and in the Y -direction in the horizontal branch.

The $\log *K$ values given in Table 3 lead to the best fit to our experimental results assuming "fresh precipitate" (30-min equilibration) and CO_2 -free conditions.

The $\log *K_i$ -values are independent of each other, but $\log *K_{30}$ is not, because it is strongly dependent on the height of the horizontal part and $\log *β_3$, the sum of the $\log *K$ -values. The error in $\log *K_1$ is estimated to be 0.2, the errors in $\log *K_2$ and $\log *K_3$ to be 0.1, and in $\log *K_{30}$ to be 0.2.

The different values of the equilibrium constants $\log *β$ are correlated. It has to be emphasized, however, that whatever set is taken it is the position of the precipitation borderline which determines the combination of values. The set in Table 3 gives the best fit to our data. At $pC_H \leq 13$ no amphoteric character could be found.

Our results for $\log *K_1$ agree well with literature data in Table 1 in cases of similar ionic strengths, the absence of complexing ions such as sulphate, and determination under strictly CO_2 -free conditions. The same holds for $\log *K_{30}$. The low slope of the ascending branch is evidence that polycomplex formation can be rejected.

Acknowledgement—We are indebted to Mr. Ernest van Beckhoven for his valuable contributions to the experimental work.

REFERENCES

1. U. K. Frolova, V. N. Kumok and V. V. Serebrennikov, *Izv. Vys. Ucheb. Zaved. SSSR, Khim. Khim. Tekhnol.*, 1966, 9, 176.

2. R. Guillaumont, B. Désiré and M. Galin, *Radiochem. Radioanal. Lett.*, 1971, **8**, 189.
3. L. N. Usherenko and N. A. Skorik, *Russ. J. Inorg. Chem.*, 1972, **17**, 1533.
4. T. Amaya, H. Kakihana and M. Maeda, *Bull. Chem. Soc. Japan*, 1973, **46**, 1720.
5. K. Kraus, *Proc. Int. Conf. Geneva*, 1955, **7**, 245.
6. E. J. Wheelwright, F. H. Spedding and G. Schwarzenbach, *J. Am. Chem. Soc.*, 1953, **75**, 4196.
7. G. Biedermann and L. Ciavatta, *Acta Chem. Scand.*, 1961, **15**, 1347.
8. T. Moeller, *J. Phys. Chem.*, 1946, **50**, 242.
9. C. F. Baes, Jr. and R. E. Mesmer, *The Hydrolysis of Cations*, pp. 129–138. Wiley-Interscience, New York, 1976.
10. C. C. Melocke and F. Vratny, *Anal. Chim. Acta*, 1959, **20**, 415.
11. N. N. Mironov and A. I. Odnosevtev, *Zh. Neorgan. Khim.*, 1957, **2**, 2022.
12. V. I. Ermolenko, *Thesis*, Kiev, 1960; *Izd. ANUSSR, Kiev*, 1962, **3**, 148.
13. D. M. Ziv and I. A. Shestakova, *Radiokhimiya*, 1965, **7**, 175.
14. E. Sadolin, *Z. Anorg. Chem.*, 1927, **160**, 133.
15. T. Moeller and N. Vogel, *J. Am. Chem. Soc.*, 1951, **73**, 4481.
16. L. I. Buchenko, P. N. Kovalenko and M. M. Evstifeev, *Russ. J. Inorg. Chem.*, 1970, **15**, 1666.
17. D. I. Ryabchikov and V. A. Ryabukhin, *Analytical Chemistry of Yttrium and the Lanthanide Elements*, pp. 58 and 272. Ann Arbor-Humphrey Science Publishers, London, 1970.
18. J. Reuben and D. Fiat, *J. Chem. Phys.*, 1969, **51**, 4909, 4918.
19. B. N. Ivanov-Emin, E. N. Siforova, M. Mekes Fischer and V. Mel'yado Kampos, *Zh. Neorgan. Khim.*, 1966, **11**, 475.
20. J. Kragten and L. G. Decnop-Weever, *Talanta*, 1978, **25**, 147.
21. *Idem, ibid.*, 1979, **26**, 1105.
22. *Idem, ibid.*, 1980, **27**, 1047.
23. *Idem, ibid.*, 1982, **29**, 219.
24. *Idem, ibid.*, 1983, **30**, 134.

PIEZOELECTRIC DETECTORS COATED WITH LIQUID-CRYSTAL MATERIALS

ADAM MIERZWINSKI and ZYGFRYD WITKIEWICZ

Institute of Chemistry, Military Technical Academy, 01 489 Warsaw 49, Poland

(Received 9 June 1986. Revised 9 March 1987. Accepted 9 April 1987)

Summary—The usefulness of liquid crystals as coating materials for quartz resonators in piezoelectric detectors of air-pollution has been tested. The concentration characteristics of the detector with respect to benzene, toluene, chlorobenzene, *o*- and *m*-dichlorobenzene, nitrobenzene, and *o*-, *m*- and *p*-diethylbenzene have been determined with the use of 4-pentyl-4'-cyanodiphenyl, 4-pentyl-4'-propylazobenzene, 4-propyl-4'-methylazoxybenzene, and cholesteryl oleylcarbonate as coating materials. The effects of the quantity of coating material and of temperature on the sensitivity of the piezoelectric detector have been tested. The influence of the ordered structure of the liquid-crystal coating materials on the selectivity of the detector is discussed. Experiments have been performed to test the usefulness of the detector with liquid-crystal coating for detecting organophosphorus pesticides (DDVP and Phosdrin).

Monitoring of gaseous pollutants in atmospheric air is one of the most important problems of protection of the natural environment. However, despite their many advantages, the analytical instruments available still do not meet all requirements, so research continues for design of simple, cheap, sensitive and reliable detectors of air pollution. In recent years much attention has been paid to piezoelectric detectors,¹ which allow the detection of many chemical substances, including ammonia, nitrogen oxides, sulphur dioxide, aromatic and aliphatic hydrocarbons, and organophosphorus pesticides.

It has been estimated² that the theoretical detection limit with piezoelectric detectors is in the pg range. In practice it is lower, however, and depends on the relationship between the variation of the quartz resonator vibration frequency (Δf) and the mass (Δm) of substance deposited on its surface.³

$$\Delta f = a \Delta m \quad (1)$$

where a is a constant for given conditions of measurement.

To increase the sensitivity and selectivity of piezoelectric detectors the resonators are coated with substances that interact physically or chemically with the substances to be detected. High-boiling liquids and solids may be used as these coating materials. The former are commonly the substances used as stationary phases in gas chromatography and usually interact physically, and hence less selectively, with the pollutants to be detected. The solid coating materials usually react chemically with one of the substances present in the air tested and thus produce high selectivity. However, these materials have the disadvantage that detectors coated with them have very long recovery (desorption) times.

At present, research concentrates on finding coating materials that give good selectivity together with

rapid response and recovery. It is therefore of interest to examine liquid crystals as coating materials.

Liquid crystals are liquids with molecules which interact to yield ordered systems exhibiting the anisotropy associated with crystals. There are two principal types of liquid crystal: lyotropic and thermotropic. Lyotropic liquid crystals exist only in solution and arise from interaction of the solvent and solute. Thermotropic liquid crystals are mesomorphic phases, the existence or decay of which depends on changes in temperature. The liquid-crystal structure, known also as the mesophase, exists in a certain temperature range above the melting point but below the clearing point, *i.e.*, the transition to the isotropic liquid.

The properties of liquid crystals are due to the structure of their molecules. Depending on this structure and the character of the intermolecular interactions, three principal mesomorphic structures may be formed: smectic, nematic and cholesteric. There are several types of the smectic structure, and the cholesteric is a modification of the nematic.⁴ Figure 1 shows schematically the types of structural ordering in liquid crystals. In nematics (*b*) there is no ordering apart from the parallel orientation of the molecules. In smectics (*a*) besides the parallel orientation of the long axes of molecules there is stratification, with the long axes oriented vertically or at a certain angle to the plane of the layers. In the cholesterics (*c*) the molecules have their long axes plane parallel within a layer, but successive layers are rotated with respect to the axis orientation.

Thermotropic liquid crystals have found wide application in display devices, and are also used as stationary phases in gas chromatography,⁵ where they exhibit high selectivity for positional and geometric isomers, since their ordered structure dissolves molecules of different shape in different ways. It

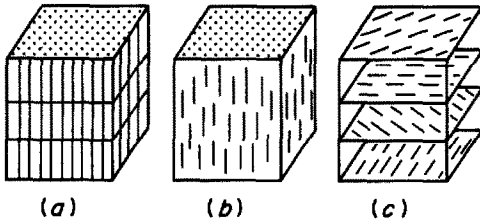


Fig. 1. Mesomorphic structures of liquid crystals: (a) smectic, (b) nematic, (c) cholesteric.

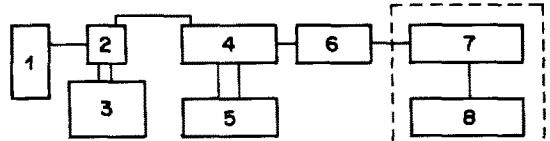


Fig. 2. Block diagram for instrument lay-out: 1—generator for standard gaseous mixtures, 2—detector cell, 3—thermostat, 4—quartz generator, 5—power supply, 6—frequency counter, 7—digital-to-analogue converter, 8—recorder.

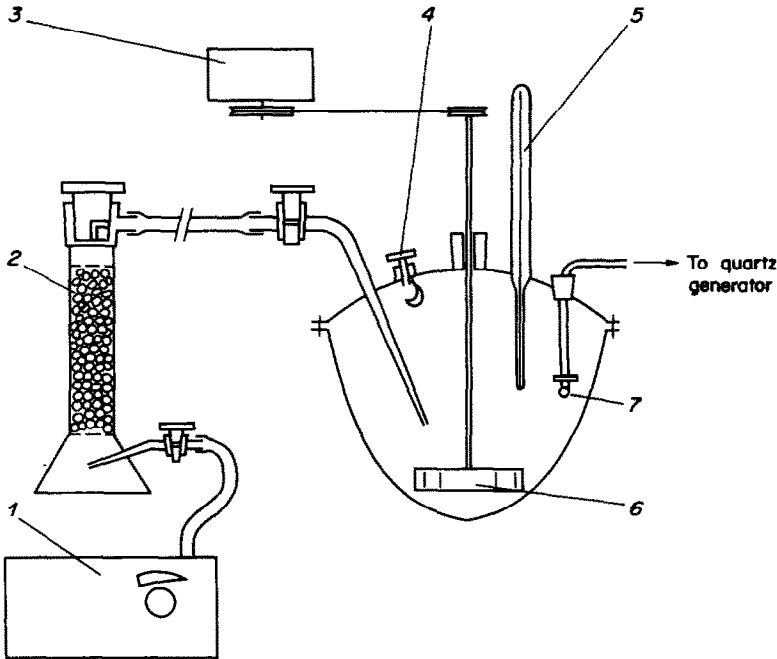


Fig. 3. Block diagram for generator of standard gaseous mixtures (static method): 1—membrane pump, 2—drying tube, 3—mixer motor, 4—electrically heated injector, 5—thermometer, 6—mixer, 7—quartz crystal resonator sensor of the piezoelectric detector.

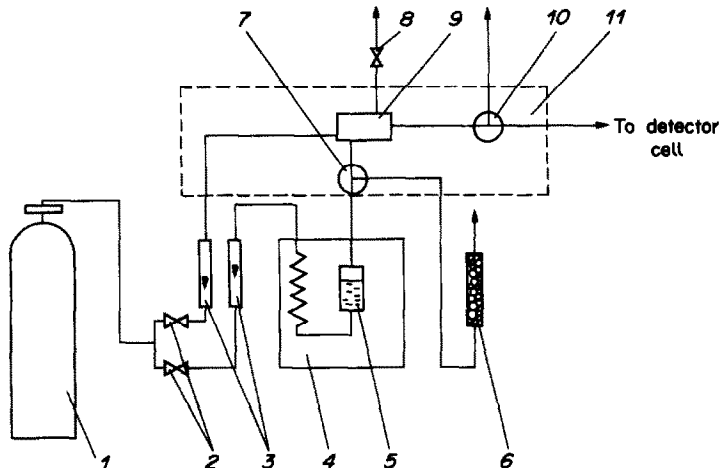


Fig. 4. Block diagram for generator of standard gaseous mixtures (dynamic method): 1—gas cylinder of carrier gas, 2,8—needle valves, 3—flowmeters, 4—thermostat, 5—evaporation device, 6—active-carbon filter, 7,10—valves, 9—mixer, 11—air thermostat.

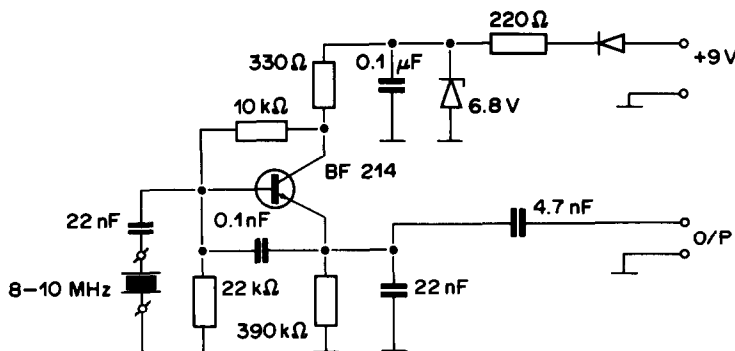


Fig. 5. Circuit diagram for quartz generator.

might therefore be expected that liquid crystals would prove to be good coating materials for piezoelectric detectors of air pollution. The studies made so far⁶ have shown that piezoelectric detectors coated with liquid crystals are stable, sufficiently sensitive and give a wide range of linear response.

EXPERIMENTAL

The measuring system

The tests were done with the set-up presented in Fig. 2. Both static and dynamic methods were used for preparation of the standard gas mixtures.

In the static method a precisely determined volume of analyte was injected into a 500-ml flask provided with a high-speed stirrer and electric heater. The heater ensured rapid evaporation, and the agitator accurate mixing of the substance with the diluent gas. The concentration (c) of the analyte was found from the formula $c = V_x \rho_x / V_k$ where V_x is the volume and ρ_x the density of the analyte, and V_k the volume of the flask. The temperature of the flask was kept constant within 0.1° . After each measurement the analyte was removed from the apparatus by passage of large amounts of pure gas until the detector response returned to its initial value.

In the dynamic method the analyte was removed from an evaporator equipped with a ceramic frit, by passage of carrier gas at a flow-rate of 5 l/hr. The desired concentration (c) was obtained by diluting the initial stream of gas

mixture with pure gas:

$$c = \frac{c_0 Q_1}{Q_1 + Q_2}$$

where c_0 is the concentration in the initial stream, corresponding to saturation at the temperature used, Q_1 is the flow-rate of the carrier gas through the evaporator and Q_2 the flow-rate of the diluent gas. The evaporator was placed in a thermostat controlled to 0.1° . The gas ducts and the dilution system were in an air thermostat controlled to 0.5° .

The static sample-preparation procedure (Fig. 3) was used to determine the partition coefficients of the test substances between the coating material and the gas phase, this coefficient being taken as the measure of the coating-material efficiency. The remaining tests were performed with the dynamic system of preparing the gas mixtures (Fig. 4). The sorption-desorption kinetics will be reported in a subsequent paper.

The quartz resonator, the probe of the detector, was operated as the frequency-determining element in the circuit shown in Fig. 5. The quartz resonators used (OMIG, Warsaw) were AT-cut and characterized by a basic frequency of 8.273 MHz. The frequency was measured to ± 1 Hz with a PFL-22 frequency meter (ZOPAN, Warsaw).

Coating materials and test substances

The liquid crystals used gave the mesophase at normal temperatures. Their properties are given in Table 1. Three were nematics (PCB, PPAB, PMAOB) and the fourth cholesteric (OLWCh).

Table 1. Characteristics of the liquid-crystal coating materials

Coating material	Chemical formula	Molecular weight	Density, g/cm^3	Temperature of phase transition, † K
4-cyano-4'-n-pentylidiphenyl (PCB)	<chem>N#C-C6H4-C6H4-C5H11</chem>	249	1.03*	K 295.5 N 310 I
4-n-pentyl-4'-propylazobenzene (PPAB)	<chem>C5H11-C6H4-N=N-C6H4-C3H7</chem>	290	1.06*	K 290 N 317 I
4-propyl-4'-methylazoxybenzene (PMAOB)	<chem>C3H7-C6H4-N=N-C6H4-CH3</chem>	254	1.04*	K 273 N 323 I
cholesteryl oleylcarbonate (OLWCh)	<chem>H3C-(CH2)7-CH=O</chem> <chem>Ch-O-C(=O)-O-(CH2)7-CH=O</chem>	702	0.91	K 293 Ch 309 I

*Values obtained by interpolation.

†Transition temperature from crystalline state (K) to liquid crystal state (N or Ch) and then to isotropic liquid (I).

Table 2. Characteristics of the compounds detected

Compound	Molecular weight	Boiling point, K	Vapour pressure at 293 K, Pa	Abbreviation
benzene	78.12	353	1.013×10^4	B
toluene	92.14	384	2.933×10^3	T
chlorobenzene	112.56	405	1.173×10^3	ChB
<i>o</i> -dichlorobenzene	147.01	453	133.3	<i>o</i> -DChB
<i>m</i> -dichlorobenzene	147.01	446	145.3	<i>m</i> -DChB
nitrobenzene	123.12	484	20.0	NB
<i>o</i> -diethylbenzene	134.21	457	139.0	<i>o</i> -DEB
<i>m</i> -diethylbenzene	134.21	454	151.0	<i>m</i> -DEB
<i>p</i> -diethylbenzene	134.21	457	140.0	<i>p</i> -DEB
DDVP	220.98	343 (at 133 Pa)	1.59	DDVP
Phosdrin	224.15	380 (at 13.3 Pa)	0.29	Phosdrin

The liquid crystals were dissolved in *n*-hexane to give 1.0 $\mu\text{g/ml}$ concentration. The solution was applied to the centre of the quartz resonator with a microsyringe, and the coated resonator was placed flat in an oven (at 323 K) and left there for 30 min. The amount of coating material on the resonator surface was expressed in terms of the change of frequency (Δf_x) of its vibration:

$$\Delta f_x = f - f_x \quad (2)$$

where f and f_x are the vibration frequencies (Hz) of the resonator before and after coating. It has been found that the operation of the detector is stable and the results are reproducible if the coating material completely covers both electrodes of the resonator. If this condition is not fulfilled, there is high drift of the base-line because spreading of the coating material over the resonator surface increases f (and hence decreases Δf_x). If the quartz resonator electrodes are only 50% covered, the drift is about 10 Hz/hr, depending on the distribution of the coating, but not more than 1 Hz/hr for the completely covered electrodes.

The test substances used are listed, along with their major properties, in Table 2.

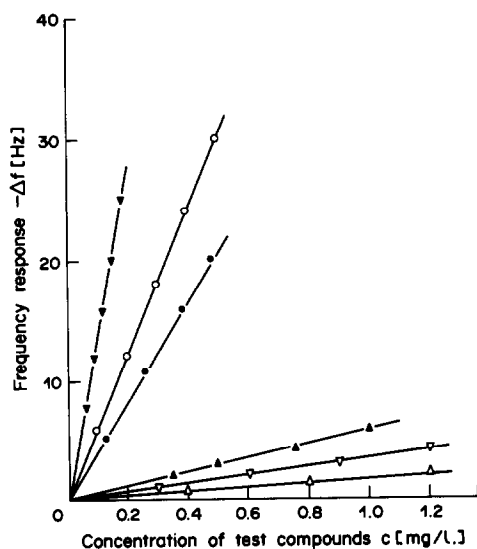


Fig. 6. Plots of frequency response vs. concentration of test compounds. Coating material PMAOB, $\Delta f_x = 1800$ Hz, carrier gas dry air, $T = 293$ K, Δ —benzene, ∇ —toluene, \blacktriangle —chlorobenzene, \circ —*o*-dichlorobenzene, \bullet —*m*-dichlorobenzene, \blacktriangledown —nitrobenzene.

RESULTS AND DISCUSSION

The static method of preparing gas mixtures was used in determining the detector response $\Delta f = \phi(c)$ to benzene and its derivatives, for all the coating materials used. The response was linear over the concentration ranges tested. Equilibrium between the coating material and the gas phase was established in 2–3 min, depending on the coating and test substance. Figure 6 shows the response to benzene and its derivatives for the detector coated with PMAOB.

After removal of the test vapours from the flask and desorption of the analyte from the coating, the detector returned to its original frequency. No drift of the base-line was observed. At this stage we did not investigate the desorption kinetics, since the concentration of test substance in the flask varied in accordance with the exponential dilution law. The desorption processes were investigated with the dynamic method of preparing the gas mixture, and will be described in a subsequent paper.

The sensitivity (S) of the detector was measured as the slope of the response graph:

$$S = \frac{\Delta f}{c} \quad (3)$$

The formula:

$$K_{y/x} = \frac{S\rho_x}{\Delta f_x} \quad (4)$$

was used for calculating the partition coefficient of the test substance between the coating material and the gas phase; this equation is applicable only if the mass sensitivity of the system is identical for the analyte and the coating. In the frequency range used, this appeared to be the case.

Table 3 summarizes the partition coefficients found. They increase with the boiling point of the test substance, which is in accordance with the results of Karasek and co-workers.^{7,8}

Interesting results were obtained for the diethylbenzene positional isomers, which differ only slightly in boiling point and vapour pressure. Some liquid-

Table 3. Partition coefficients of test compounds between coating material and air at 293 K (confidence limits for $P = 0.95$)

Test compound	Coating material			
	PCB	PPAB	PMAOB	OLWCh
B	$(5.6 \pm 0.8) \times 10^2$	$(5.8 \pm 1.1) \times 10^2$	$(5.9 \pm 1.0) \times 10^2$	$(2.9 \pm 0.6) \times 10^2$
T	$(1.81 \pm 0.25) \times 10^3$	$(1.61 \pm 0.28) \times 10^3$	$(1.72 \pm 0.27) \times 10^3$	$(9.5 \pm 1.6) \times 10^2$
ChB	$(5.55 \pm 0.66) \times 10^3$	$(4.49 \pm 0.63) \times 10^3$	$(4.67 \pm 0.64) \times 10^3$	$(2.33 \pm 0.34) \times 10^3$
<i>o</i> -DChB	$(3.69 \pm 0.29) \times 10^4$	$(2.99 \pm 0.24) \times 10^4$	$(3.32 \pm 0.25) \times 10^4$	$(1.59 \pm 0.17) \times 10^4$
<i>m</i> -DChB	$(2.55 \pm 0.19) \times 10^4$	$(2.34 \pm 0.18) \times 10^4$	$(2.60 \pm 0.23) \times 10^4$	$(1.23 \pm 0.14) \times 10^4$
NB	$(9.55 \pm 0.53) \times 10^4$	$(7.52 \pm 0.42) \times 10^4$	$(7.84 \pm 0.42) \times 10^4$	$(2.88 \pm 0.19) \times 10^4$
<i>o</i> -DEB	$(3.44 \pm 0.27) \times 10^4$	$(2.84 \pm 0.23) \times 10^4$	$(3.07 \pm 0.21) \times 10^4$	$(2.27 \pm 0.18) \times 10^4$
<i>m</i> -DEB	$(2.72 \pm 0.22) \times 10^4$	$(2.28 \pm 0.18) \times 10^4$	$(2.59 \pm 0.22) \times 10^4$	$(1.91 \pm 0.15) \times 10^4$
<i>p</i> -DEB	$(4.18 \pm 0.32) \times 10^4$	$(3.11 \pm 0.24) \times 10^4$	$(3.11 \pm 0.21) \times 10^4$	$(2.46 \pm 0.19) \times 10^4$

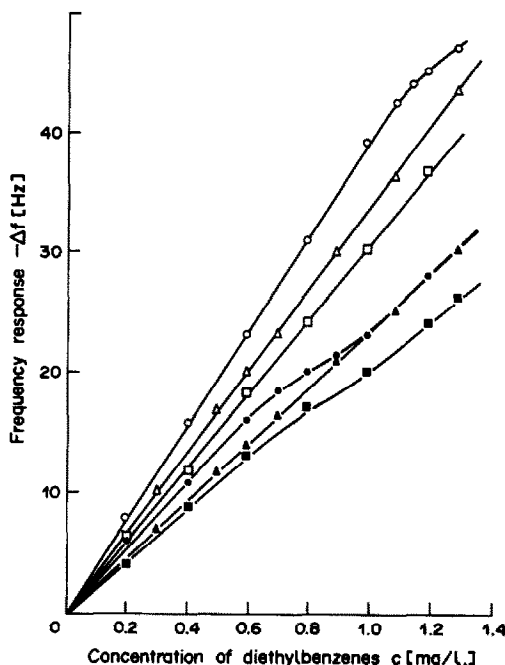


Fig. 7. Plots of frequency response vs. concentration of diethylbenzenes. Coating material PCB, $\Delta f_x = 900$ Hz, $T = 298$ K, \triangle —*o*-DEB, \square —*m*-DEB, \circ —*p*-DEB. Coating material PMAOB, $\Delta f_x = 900$ Hz, $T = 298$ K, \blacktriangle —*o*-DEB, \blacksquare —*m*-DEB, \bullet —*p*-DEB.

crystal coatings gave different sensitivities for these isomers, whereas other coating materials gave almost identical responses. For instance, Carbowax 400 ($f_0 = 8.265$ MHz, $\Delta f_x = 500$ Hz) gave $\Delta f = 9$ Hz for all the diethylbenzene isomers at a concentration of $0.69 \mu\text{g/ml}$. With a PCB coating $\Delta f_x = 900$ Hz; however, the Δf values were 20 Hz for *o*-DEB, 17 Hz for *m*-DEB and 24 Hz for *p*-DEB (see also Table 3 and Fig. 7). This points to the effect of liquid-crystal structure on the process of dissolution of the test substance in the coating material. These effects are most manifest when the detector is operated at a temperature slightly above the melting point of the mesogenic substance. The use of PCB as coating material gave a sensitivity 15% higher for *p*-diethylbenzene than for *o*-diethylbenzene although the boiling points of these compounds differ by only

0.3 K. However, PMAOB as coating material gave the same sensitivity for *m*- and *o*-diethylbenzene though the boiling point of the former is 2.3 K lower than that of the latter. This suggests that the shape of the analyte molecule determines the sensitivity of the detector with a liquid-crystal coating and supports the supposition that the liquid crystal preserves the extensive ordering of its molecules when it forms a coating on the resonator surface.

When the concentration of the analyte in the gas phase in contact with the coated resonator exceeds a certain level, the ordering of the coating molecules decreases. This is shown by the curvature of the calibration graphs for *p*- and *m*-diethylbenzene (Fig. 7), in qualitative agreement with the results obtained by Oweimreen⁹ and with the general behaviour of liquid crystals, which cease to have an ordered structure when the quantity of a non-mesomorphic component exceeds a certain level.

The effect of the shape of the analyte molecule on the sensitivity of the detector decreases with the operating temperature of the detector (Fig. 8), probably because of lowering of the ordering parameter with temperature.¹⁰ Lowering of the separability of isomers, as a result of the decreased ordering of the liquid-crystal structure, is also observed in gas chromatography.^{11,12}

According to equation (4) the sensitivity of the piezoelectric detector for a given substance can be

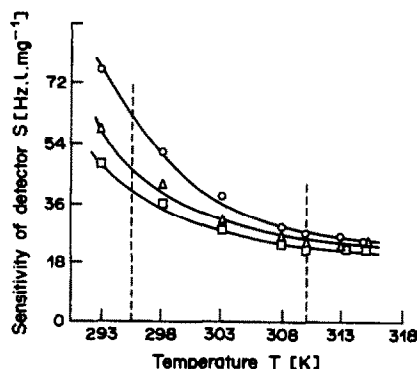


Fig. 8. Temperature effect on sensitivity of detector for diethylbenzene isomers. Coating material PCB, $\Delta f_x = 1800$ Hz, \triangle —*o*-DEB, \square —*m*-DEB, \circ —*p*-DEB.

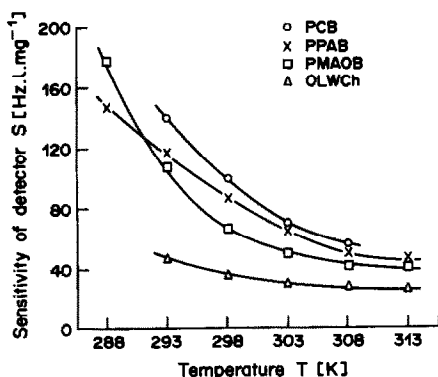


Fig. 9. Variation of detector sensitivity with temperature for liquid crystals as coating materials. Test substance—nitrobenzene (0.2 mg/l.) in dry air as carrier gas, dynamic method ($Q = 0.5$ l./min).

raised by increasing the quantity of coating material applied, *viz.*

$$S = \frac{K_{y/x} \Delta f_x}{\rho_x} \quad (5)$$

and this has been shown to hold over a wide range. This indicates that there is no surface effect such as formation of adsorption layers of the analyte on the surface of the coating material.

It has been found that piezoelectric detectors can be used for detecting organophosphorus pesticides in air even in the presence of high concentrations of other substances commonly present in atmospheric air, as shown in Table 4, which lists the sensitivities of the PCB-coated detector for various compounds.

On the basis of the results obtained we have designed a threshold-signalling device. The device uses a high-frequency generator and a quartz resonator. At a preselected concentration of the analyte the vibration decays in the generator system, and this decay activates the light or sound signalling block. Selectivity is achieved primarily by varying the quantity of coating material on the resonator. The maximum quantity of the coating material that may be deposited on the resonator surface depends largely on the kind of quartz generator used, and on its

physicochemical properties. The change in the mass of substance deposited on the resonator surface should not change the frequency by more than 1%, or the relation of vibration frequency to mass will cease to be linear; non-linearity may also be caused by the oscillator electronics however.

If the quantity of coating increases the vibration frequency by more than about 3000 Hz the dynamic characteristics of the detector deteriorate, because a longer time is needed to establish equilibrium between the gas phase and the coating material.

The dynamic characteristics of the detector are also influenced by the temperature of operation. The mass transport processes are accelerated by increase in temperature, which leads to faster response and recovery of the detector. For example, raising the temperature from 293 to 298 K halves the response and recovery time, *e.g.*, from 60 to 30 sec for PPAB. On the other hand, increasing the temperature decreases the sensitivity of the detector, because of the dependence of the partition coefficient on temperature, as described by the Littlewood formula¹³

$$K_{y/x} = \frac{\rho_x RT}{\gamma p_x^0 M_x}$$

where ρ_x is the density of the coating material, R the universal gas constant, T the absolute temperature of operation of the detector, M_x the molecular weight of the coating material, p_x^0 the vapour pressure of the analyte and γ the activity coefficient of the analyte in the coating material.

The temperature dependence of the sensitivity of different liquid-crystal coatings with respect to nitrobenzene is presented in Fig. 9.

If the resonator cell in the signalling device is not kept at constant temperature, the variation of the detector sensitivity with temperature must be compensated for in the measuring system.

One of the principal problems in use of liquid crystals as coating materials for quartz resonators is the effect of the acoustic wave on their structure. The experiments described in the present work have shown that in the systems used the liquid-crystal

Table 4. Sensitivity of the PCB-coated detector for various test compounds ($\Delta f_x = 2400$ Hz; $T = 298$ K)

Compound	Change in		Sensitivity, (S)
	Concentration, $\mu\text{g/l.}$	frequency (Δf), Hz	
benzene	5000	6	0.0012
toluene	5000	26	0.0052
chlorobenzene	1000	16	0.016
ethanol	5000	11	0.0022
ethyl acetate	5000	10	0.0020
nitrobenzene	240	38	0.1583
sulphur dioxide	5000	4	0.0008
ammonia	5000	0	—
petrol	5000	7	0.0014
DDVP	25	83	3.32
Phosdrin	25	141	5.64

ordering is at least partly preserved. More detailed studies are necessary, however, to allow the determination of the effect of the acoustic wave.

CONCLUSIONS

The use of liquid crystals as coating materials for piezoelectric detectors provides:

- (1) detection of many chemical substances down to $\mu\text{g/l}$. levels;
- (2) detection with sensitivities which depend only on the shape of the analyte molecules;
- (3) linear response characteristics over a wide range of analyte concentration;
- (4) optimization of the detector sensitivity by variation of the quantity of coating material. However, compensation of the variation of sensitivity with resonator operation temperature is a problem still to be solved.

REFERENCES

1. I. F. Alder and I. I. McCallum, *Analyst*, 1983, **108**, 1169.
2. W. H. King, Jr., *Anal. Chem.*, 1964, **36**, 1735.
3. G. Z. Sauerbrey, *Z. Physik*, 1959, **155**, 206.
4. E. Bialecka-Floriańczyk, *Wiad. Chem.*, 1984, **38**, 109.
5. Z. Witkiewicz, *J. Chromatog.*, 1982, **251**, 311.
6. A. Mierzwiński and Z. Witkiewicz, *Chem. Anal., Warsaw*, 1985, **30**, 429.
7. F. W. Karasek, P. Guy, H. H. Hill Jr. and J. M. Tiernay, *J. Chromatog.*, 1976, **124**, 179.
8. F. W. Karasek and I. M. Tiernay, *ibid.*, 1974, **89**, 31.
9. G. A. Oweimreen, *Mol. Cryst. Liq. Cryst.*, 1981, **68**, 257.
10. H. Kluder and C. L. de Ligny, *J. Solution Chem.*, 1982, **11**, 169.
11. D. E. Martire, A. Nokolic and K. L. Vasanth, *J. Chromatog.*, 1979, **178**, 401.
12. Z. Witkiewicz and S. Popiel, *ibid.*, 1978, **154**, 60.
13. A. B. Littlewood, *Gas Chromatography*, Academic Press, New York, 1970.

SENSITIVE LUMINESCENCE ANALYSIS FOR INORGANIC IONS

L. E. ZEL'TSER, SH. TALIPOV and N. G. VERECHAGINA
Department of Chemistry, Tashkent State University, 700095 Tashkent, USSR

(Received 29 January 1986. Revised 20 March 1987. Accepted 3 April 1987)

Summary—Use of excitation by powerful monochromatic light sources (including lasers) and of selective quasilinear radiation spectra of organoluminophores in metal complexes in non-aqueous media is proposed for more efficient luminescence analysis of inorganic substances.

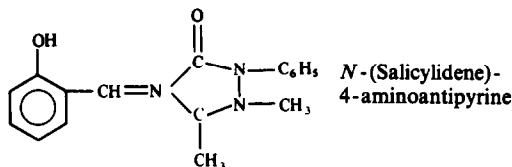
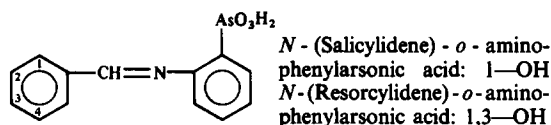
The practical use of luminescence analysis started in the middle of this century. Only about 70 fluorescent reactions were known in 1957, but the last two decades have seen a rapid advance in this field.¹⁻⁵

Besides having low detection limits and high sensitivity, chemical luminescence analysis is relatively simple and requires only inexpensive equipment,⁶ and fluorescence reactions are now available for almost all the elements.^{5,7}

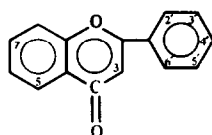
The current development of the technique is largely due to the demands of analysis of high-purity substances, semiconductor materials and environmental samples.

Here we outline some possibilities for improving luminescence analysis for some metal ions with organic reagents (Fig. 1).

1. Azomethines



2. Flavanols



3,5,3',4',-OH,7-glucose: quercetin-7-glucoside
3,5,7,3',4',5'-OH: myricetin
3,5,7,4',5'-OH, 3'-glucose: myricetin-3'-glucoside
3,5,7,4'-OH: kaempferol
3-OH,5,7,4'-OCH₃: trimethoxykaempferol

Fig. 1. Organic luminescence reagents.

EXPERIMENTAL

Reagents

Standard solutions of the metal ions (1 $\mu\text{g/ml}$) were prepared by dissolving the 99.9% pure metals (Ga, In, Al, Zr, Hf and Mg) in dilute hydrochloric acid. Acetate buffer solutions (pH 3–4.5) were prepared by adding 0.2M sodium acetate to 100 ml of 0.1M acetic acid. Demineralized doubly-distilled water was used for all solution.

Hydroxyflavonols and nitrogenous bases were extracted from plants;^{8,9} hydroxyazomethines were synthesized by the literature procedures.¹⁰ The other hydroxyazo compounds used were commercially available (Merck and Chemapol). All reagents were purified by recrystallization and their purity was checked. Standard solutions of the organic reagents (0.1%) were prepared in acetone or dimethylformamide that had been purified by the standard techniques and showed no fluorescence.

Apparatus

All the measurements were made with a Hitachi-512 spectrophotofluorimeter equipped with a high-pressure xenon tube, and with a Russian ISP-51 luminescence spectrometer with an FEP-1 photomultiplier and a DRSh-250 or SVDSH-120 mercury lamp. For measurements at room temperature standard 1-cm "suprasil" silica cells were used. For measurements at liquid-nitrogen temperatures (77 K) the sample was placed in a 3-mm diameter silica test-tube capped with a silica window and inserted in an ultraviolet-transparent silica Dewar flask.

Low-temperature laser-excited luminescence spectra were obtained with an LGP-21 nitrogen laser and an ISP-51 spectrograph equipped with an FEP-1 photomultiplier. Laser radiation at 337.1 nm with an average power of 4 mW, in the form of pulses with a duration of 10 nsec and a frequency of 100 Hz, was reflected by a mirror downwards along the axis of the silica test-tube in the silica Dewar flask. The emitted radiation was directed into the entrance slit of the ISP-51 and detected by an FEU-39 photomultiplier with correction for its spectral sensitivity.

Table 1. Comparison of various methods of fluorometric determination of Al, Sc, Zr, Hf

Element	Reagents	Detection limits, ng/ml			
		Room temperature	Glassy media*, 77 K	Solid adsorbents†	Polymer films†
Zr	Quercetin-3-glucoside	8.0	0.5	2.0	2.0
	Quercetin-7-glucoside	3.3	0.1	0.5	0.5
Hf	Myricetin	8.0	0.5	3.0	2.0
	Myricetin-3-glucoside	2.0	0.1	0.4	0.5
Sc	Myricetin	5.4	—	1.0	2.0
	Trimethoxykaempferol	0.66	—	0.2	0.2
Al	Kaempferol	3.0	—	1.0	1.0
	Trimethoxykaempferol	0.1	0.55	0.6	0.2

*Concentration by freezing the solvent.

†Concentration by extraction.

RESULTS AND DISCUSSION

The excitation and radiation spectra of organic metal-complex luminophores are similar in properties (*e.g.*, for Ga, Al and In, Zr and Hf and others), and usually consist of broad, shallow overlapping bands, which is why they are non-selective.^{11,12} The method of low-temperature luminescence (LL) and the use of solid supports (polymer films and solid adsorbents) improve the resolution of the radiation spectra and increase the luminescence intensity (Table 1). Conventional methods of low-temperature luminescence excitation by polychromatic radiation sources (mercury or deuterium lamps) use low radiation power and hence the LL signal is also weak. What is more, the spectral range available from the line spectra of mercury sources does not always coincide with the optimum excitation region of the metal complexes. Above all, it is not possible to use the small differences that exist in the relative efficiency of excitation of complexes of inorganic ions that are similar in structure and properties. The polychromatic excitation sources do not provide sufficiently selective excitation. The advantages of laser excitation for the analysis of organic compounds are well understood¹³⁻¹⁵ but are not so clear-cut for the determination of inorganic ions.¹⁶ However, the high stability and monochromaticity of the radiation, the possibility of temporal resolution of

the spectra according to the duration of the luminescence, and the concentration of the excitation light on a small area should provide high efficiency and selectivity of both excitation and radiation.

Examination of the relative efficiency of LL excitation of some groups of organic metal complexes (Table 2) shows that the highest efficiency with minimum interference from the other complexes is observed for excitation of the salicylal-4-aminoantipyrine complexes of Al at 337 nm, Ga at 416 nm and In at 452 nm, and of the quercetin-7-glucoside complexes of Zr at 337 nm and Hf at 416 nm. The excitation efficiency of xenon and halogen sources is roughly equal. With excitation by polychromatic mercury sources the difference in excitation efficiency of the luminophores is too small for exploitation.

Laser excitation ensures high efficiency of excitation and radiation and also increases the selectivity (Table 2). By using the virtually line-source radiation typical of laser excitation we obtained a specific quasi-line spectrum of the Zr complex differing from that of the Hf complex, and a similar effect for the Al-Ga-In system (Fig. 2).

When frozen sample solutions were exposed to laser illumination, even for several hours, under the chosen analytical conditions, no new quasi-lines and radiation intensity changes appeared, as the laser-induced destruction or photochemical processes

Table 2. Effectiveness of the excitation of organic luminophores, by various excitation sources on the basis of their metal complexes with Al, Ga, In, Zr, Hf

Complex	Effectiveness of excitation, %								
	Xenon lamp			Halogen lamp			Hg lamp		N laser§
	337 nm	416 nm	452 nm	337 nm	416 nm	452 nm	366 nm	436 nm	
R ₁ -Al*	78.2	4.2	0.7	76.3	5.4	3.9	12.0	7.4	100.0
R ₁ -Ga*	5.4	76.0	4.8	5.2	74.9	4.4	10.2	11.8	6.5
R ₁ -In*	3.2	5.2	74.0	2.8	6.3	77.4	8.0	13.7	4.1
R ₂ -Zr†	75.8	32.1	5.8	74.2	29.5	4.2	15.2	5.7	100.0
R ₂ -Hf†	3.2	73.9	42.3	2.8	72.5	40.2	0.9	22.1	12.5

*LL of complexes of Al at 345 nm was taken as 100%.

†LL of complexes of Zr at 330 nm was taken as 100%.

§Conventional; differs from other sources of excitation.

R₁—salicylidene-4-aminoantipyrine; R₂—quercetin-7-glucoside.

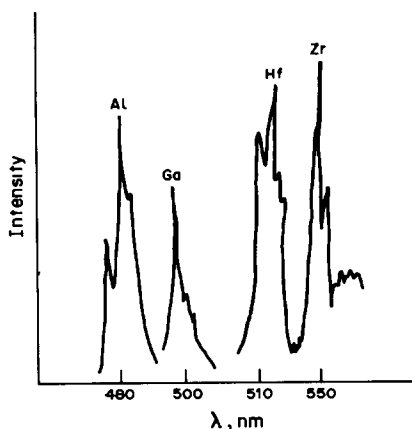


Fig. 2. The low-temperature luminescence spectra of complex compounds of Al, Ga, Zr, and Hf with laser excitation. $C_R = 1 \times 10^{-4} M$, $C_{Me} = 1 \times 10^{-6} M$, pH = 0, DMF 60% v/v.

expected¹⁷ for organic compounds did not occur. Thus, the use of monochromatic excitation sources, especially lasers, significantly increases the selectivity and efficiency of excitation and hence radiation of the complexes examined. Table 3 shows that in this way detection limits for Al, Ga and In with azomethines and azo-reagents and for Zr and Hf with quercetin-7-glucoside are lowered by a factor of 10–100 and that the selectivity is much better than with polychromatic excitation.

The Shpol'skii effect has already gained general recognition in organic analysis.¹⁸ This interesting phenomenon is not clearly understood for organoluminophores in metal complexes and is hardly used in the determination of inorganic ions, though it offers strong possibilities for improving the performance characteristics of inorganic luminescence analysis. It is known that discrete spectra are obtained for aromatic molecules in a crystalline organic matrix. In choosing such a matrix for complexes we have taken into account both the nature of the complex molecule and of the matrix, the solvating

Table 4. Analytical use of the Shpol'skii spectra of the Zr and Hf complexes with polyhydroxyflavonols

Metal ions	Detection limits, ng/ml	Tolerance levels (concentration ratio), w/w
Zr*	0.1–1	Sc, Th (100); Hf (500); Al, Fe, Cu (2500)
Hf*	1–3	Zr (600); Ni, Co (1000); Al, Fe, Cu (2500)
Al†	10	Ga (300); Mo, W, Zn, Mg (3000); In (3500)
Ga†	1	Al (500); Mg, W, Zn, Mg (2000); In (3000)

*With quercetin-7-glucoside.

†With salicylidene-4-aminoantipyrine.

action of the solvent and its influence on the complex structure, *i.e.*, its activating effect on the radiation of organoluminophores. The system consists of crystalline frozen solvent and a radiating molecule or complex compound.

Convenient solvents as matrices for Al, Ga and In complexes with hydroxyazomethines include a mixture of acetic acid and propyl alcohol (3:1 for Al and 1:3 for Ga) in the presence of 20% v/v dimethylformamide (DMF), and a 20% v/v mixture of *n*-butane with 1:3 *n*-octane-DMFA mixture for Zr and Hf complexes with polyhydroxyflavonols.

Intense lines (at 480 nm for Al, 505 nm for Ga, 550 nm for Zr and 510 nm for Hf) appear when these media are used (Fig. 2). The high solvating ability of DMF, propyl alcohol and acetic acid are likely to favour further localization of the *n,p*-electrons of quenching groups by increasing the hydrogen-bond strength in the photo-excited state in non-aqueous media. Fluorimetric measurement of the narrow lines typical of these ions decreases the detection limit and improves the selectivity (Tables 1, 3, 4). Some characteristic features of the luminescence methods developed on the basis of low-temperature luminescence and quasi-linear Shpol'skii spectra are given in Table 5. The results show promise for the use of powerful monochromatic sources of excitation (including lasers), solid matrices made by freezing non-aqueous

Table 3. Improvement of the determination characteristics for Al, Ga, In, Zr, Hf by use of various excitation sources

Metal ion	Detection limits, % (wavelengths, nm)			Selectivity factor		
	Xenon lamp	Hg lamp	N laser	Xenon lamp	Hg lamp	N laser
Al*	5×10^{-4} (345)	1×10^{-3} (336)	5×10^{-5} (337)	Ga (1500) In (800)	Ga, In (100)	Ga (2000) In (2500)
Ga*	5×10^{-6} (416)	1×10^{-4} (436)	—	Al (1000) In (800)	Al, In (100)	—
In*	3×10^{-6} (460)	1×10^{-4} (436)	—	Al (1500) Ga (1000)	Ga, Al (100)	—
Zr†	1.2×10^{-4} (370)	1×10^{-3} (436)	2×10^{-6} (337)	Hf (300) Fe, Ti, Cu (500)	Hf (50); Fe, Ti, Cu (100)	Hf (1500); Fe, Ti, Cu (800)
Hf†	1×10^{-4} (416)	1×10^{-3} (436)	—	Zr (500); Fe, Ti, Cu (800)	Zr (100); Fe, Ti, Cu (150)	—

*With resorcyldene-4-aminoantipyrine.

†With quercetin-7-glucoside.

Table 5. Basic characteristics of luminescence methods for determination of elements

Sample	Element	Reagent	Excitation sources	Fluorometric method	Detection limits, ng/ml
Minerals	Ga	R ₃	Hg lamp	LL* in C ₃ H ₇ OH; CH ₃ COOH	0.1
	In	R ₇	xenon lamp	LL in C ₃ H ₇ OH; DMF	0.01
	Sc	R ₆	xenon lamp	LL in DMSO	0.06
	Al	R ₅	Hg lamp	LL in C ₃ H ₇ OH; CH ₃ COOH; HCl	0.01
	Zr	R ₄	xenon lamp	LLS† in DMF, n-octane	0.001
	Hf	R ₄	Hg lamp	LL in DMF	
Mineral water	Be	R ₁	laser	LLL§ in DMF	0.0001
	Al	R ₈	xenon lamp	LL in C ₃ H ₇ OH; CH ₃ COOH; HCl	0.004
	Ga	R ₄	xenon lamp	LL in C ₃ H ₇ OH; CH ₃ COOH	0.01
	Zr	R ₆	laser	LLL in DMF; n-octane	0.0008
Semiconductors (high-purity substances)	Ga	R ₅	laser	LLL in C ₃ H ₇ OH; CH ₃ COOH; DMF	0.0005
	In	R ₆	xenon lamp	LL in DMF	0.006
	Zr	R ₄	laser	LLL in DMF, n-octane; TBF	0.0008
	Hf	R ₄	xenon lamp	LLS in DMF; n-octane	0.001
	Be	R ₂	laser	LLL in DMSO	0.0003
	Sc	R ₆	xenon lamp	LL in DMSO	0.03

*LL—low-temperature luminescence.

†LLS—low-temperature luminescence in matrix by Shpol'skii.

§LLL—laser-induced low-temperature luminescence.

solutions, and selective Shpol'skii spectroscopy as applied to organoluminophores in metal complexes, to improve the characteristics of the luminescence analysis method.

REFERENCES

- D. P. Shcherbov and R. N. Plotnikova, *Zavodsk. Lab.*, 1976, **42**, 1429.
- A. P. Golovina and L. V. Levshin, *Chemical Luminescence Analysis of Inorganic Substances*, Khimiya, Moscow, 1978.
- C. E. White and R. J. Argauer, *Fluorescence Analysis: A Practical Approach*, Dekker, New York, 1970.
- J. D. Winefordner, S. G. Schulman and T. C. O'Haver, *Luminescence Spectrometry in Analytical Chemistry*, Wiley-Interscience, New York, 1972.
- J. D. Winefordner (ed.), *Spectroscopic Methods of Determining Trace Elements*, Mir, Moscow, 1979.
- W. F. Pickering, *Modern Analytical Chemistry*, p. 32. Dekker, New York, 1977.
- C. A. Parker, *Photoluminescence of Solutions*, p. 300. Mir, Moscow, 1972.
- S. P. Pakidina, A. S. Sadikov and P. Denliev, *Dokl. Akad. Nauk UzSSR*, 1962, No. 8, 34.
- A. S. Sadikov, *Chemistry of anabasis aphylla Alkaloids*, p. 56. Tashkent, 1956.
- A. I. Busev, *Synthesis of New Organic Reagents for Inorganic Analysis*, p. 82. Moscow State University, 1972.
- L. E. Zel'tser, Sh. Talipov and L. A. Morozova, *Zh. Analit. Khim.*, 1980, **35**, 1747.
- L. E. Zel'tser, L. A. Archipova, Sh. Talipov and Kh. Chikmatov, *ibid.*, 1983, **38**, 811.
- R. I. Personov, E. I. Al'shiks, L. A. Bykovskaya and B. M. Kharlamov, *Zh. Exper. i Teoret. Fiz.*, 1973, **65**, 1825.
- V. I. Vershinin, I. V. Kuzovenko, G. I. Baranov and A. M. Sozikov, *Zh. Analit. Khim.*, 1981, **36**, 981.
- T. F. van Geel and J. D. Winefordner, *Anal. Chem.*, 1976, **48**, 335.
- T. Vo-Dihn and U. P. Wild, *J. Luminescence*, 1973, **6**, 296.
- R. I. Personov, *Izv. Akad. Nauk SSSR, Ser. Fiz.*, 1960, **24**, 620.
- E. V. Shpol'skii, *Usp. Fiz. Nauk*, 1963, **80**, 255.

SOME ANALYTICAL ASPECTS OF THE MEASUREMENT OF HEAVY-ATOM KINETIC ISOTOPE EFFECTS

PIOTR PANETH

Institute of Applied Radiation Chemistry, Technical University of Łódź, Zwirki 36, 90-924 Łódź, Poland

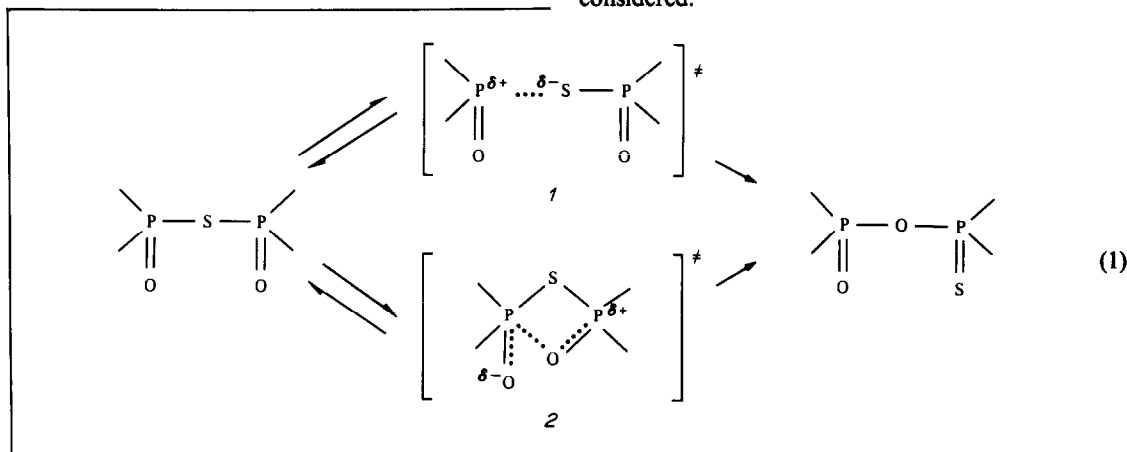
(Received 4 March 1986. Accepted 4 March 1987)

Summary—Measurements of the kinetic isotope effects of heavy atoms are discussed from an analytical point of view. The discussion includes the choice of isotope, the procedure for measurement, and methods for increasing the kinetic isotope effect. The procedures most commonly used and newly developed techniques are presented and their advantages and disadvantages considered.

Heavy-atom kinetic isotope effects have become a very useful tool for studying mechanisms of chemical¹⁻⁵ and biochemical⁶⁻⁹ reactions. The development of this technique has been stimulated by the progress made in analysis of stable and radioactive isotopes, because the effects are very small and require a high precision of measurement. A review of kinetic isotope effects was published earlier by Melander and Saunders.¹⁰

The purpose of this article is to describe the analytical aspects of the measurement of heavy-atom kinetic isotope effects. No attempt has been made to cover the literature on kinetic isotope effects of heavy atoms, and references are given only to articles reviewing a particular problem.

In the literature. If neither approach is possible there is still the chance that alternative models can be distinguished intuitively, *e.g.*, it may be predicted that for one model the isotope effect will be small (secondary), whereas for the other it will be large (primary). In such cases it is considered best to follow the kinetic isotope effects due to two different atoms involved in the reaction centre (successive labelling procedure).¹² This is best achieved when these atoms have opposite kinetic isotope effects for different reaction models. As an example consider the kinetic isotope effects of oxygen and sulphur on the Michalski rearrangement.^{13,14} It was known from kinetic studies¹⁵ that the reaction is complex and that the first, irreversible, unimolecular step is rate-determining. Two alternative structures for the transition state were considered:



Values of isotope effects are meaningful only when they can be compared with the theoretical predictions for different mechanisms. To make such theoretical predictions¹¹ it is usually necessary to know some of the properties of the reacting molecules and to assume a transition state structure. Sometimes it is possible to use data for analogous reactions available

If the reaction proceeds through transition state 1 then the sulphur kinetic isotope effect will be large, and the phosphoryl-oxygen atoms will exhibit small, secondary, isotope effects. If it proceeds through transition state 2 the sulphur isotope effect will be small and the oxygen isotope effect will be dominant. Thus the two heavy atom kinetic isotope effects can be used for differentiation of the two possible structures for the transition state.

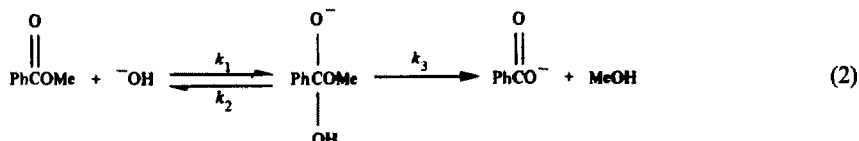
CHOICE OF STABLE OR RADIOACTIVE ISOTOPES

In studying kinetic isotope effects of carbon, sulphur and chlorine we can choose whether to work with stable (^{13}C , ^{34}S , ^{37}Cl) or radioactive (^{14}C , ^{35}S , ^{36}Cl) isotopes. There are several factors which favour using stable isotopes. The first is the necessity to synthesize labelled substrates when using radioactive material, whereas the natural abundance (Table 1) of heavy isotopes frequently allows the measurement of isotope effects by means of natural polyisotopic reagents. The higher precision of mass spectrometry compared with radiochemical measurement is often used as an argument for using stable isotopes, but is less decisive nowadays, as a precision of 0.2–0.3% can easily be reached with liquid scintillation techniques.¹⁶

In radioisotope work, special care should be taken with samples which can be contaminated with natural polyisotopic material before analysis. For example contamination of $^{14}\text{CO}_2$ with the natural abundance CO_2 present in the atmosphere can cause a large change in the specific activity of the sample. The same is true for ^{13}C -enriched CO_2 . In contrast, natural abundance samples are much less sensitive to contamination.

CHOICE OF ISOTOPIC COMPOSITION

The choice of isotopic composition is not an independent problem because the method of measurement and the type of isotope may determine the level of enrichment needed. Radioactive isotopes are normally studied at trace levels, but the method of two independent kinetic runs requires highly enriched material. The method of isotopic competition, with stable isotopes, gives greater freedom in the choice of isotopic levels. When measurements are performed by means of routine mass spectrometry it can be found from simple statistical analysis that the error is minimal at an enrichment of 50%. From results obtained by Capriolli *et al.*¹⁸ it can be concluded that the range 10–90% is still acceptable. The application of isotopically substituted compounds is sometimes the only way to measure isotope effects with a mass spectrometer. The procedure called remote labelling was introduced for stable isotopes by O'Leary and Marlier.¹⁹ Its advantages are presented by using the example of the hydrolysis of methyl benzoate:

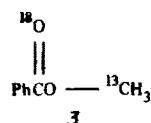


It is not easy to measure the carbonyl-oxygen isotope effect because of the difficulties of its conversion into carbon dioxide for both substrate and product. The procedure involving conversion into methanol, on the

Table 1. Isotopic composition¹⁷ of some elements commonly used in studies of heavy atom kinetic isotope effects

Element	Mass number	Isotopic composition, atom %
C	12	98.90
	13	1.10
N	14	99.634
	15	0.366
	16	99.762
O	17	0.038
	18	0.200
	28	92.23
	29	4.67
Si	30	3.10
	32	95.02
	33	0.75
	34	4.21
Cl	36	0.02
	35	75.77
	37	24.23
Br	79	50.69
	81	49.31

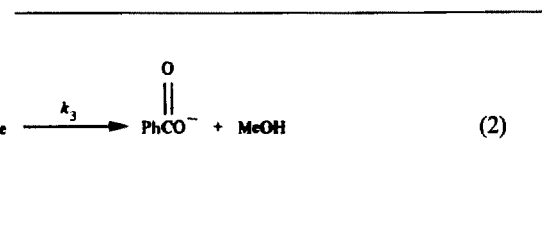
other hand, is simple. The isotope effect calculated from the isotopic composition of methanol after a high and low fraction of conversion represents the methyl-carbon kinetic isotope effect (k_{12}/k_{13}) and can easily be measured. If a doubly labelled compound such as that presented below (3) is synthesized and the same isotopic compositions are measured, then the isotope effect obtained ($k_{12,16}/k_{13,18}$) reflects both the methyl-carbon and carbonyl-oxygen kinetic isotope effects.



From the rule of geometric means it follows that:²⁰

$$k_{12,16}/k_{13,18} \cong (k_{12}/k_{13})(k_{16}/k_{18}) \quad (3)$$

and k_{16}/k_{18} can be calculated from the two measured isotope effects. The method has been applied to radioactive isotopes.²¹ The rule of geometric means holds for reactions with complex mechanisms²² when



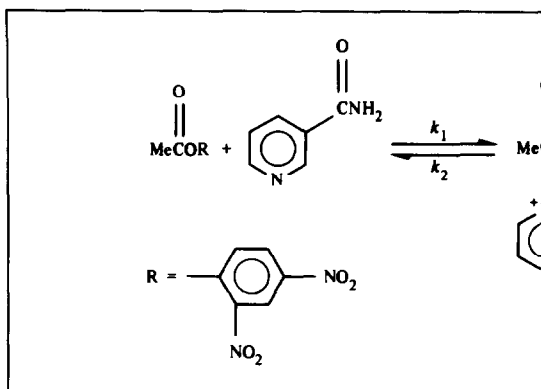
both isotopic positions are occupied by heavy atoms, but can fail if one position is occupied by a hydrogen atom.²³

ISOTOPIC COMPETITION AND INDEPENDENT KINETIC RUNS

Traditionally, methods of measuring kinetic isotope effects are divided into two groups. When both isotopic species react in the same solution, the isotopic composition of the reagents is constantly changing because of their different reaction rates. Comparison of isotopic ratios during the course of reaction is the basis of the commonly used method called isotopic competition. Alternatively, when the isotopes are not mixed (are in different solutions) the specific rates can be compared directly from separate (independent) kinetic runs. The distinction is somewhat artificial as we can deal with the kinetics of two isotopes in one solution. The easiest way is to use material doubly labelled with radioisotopes. Two separate solutions containing different isotopes can, on the other hand, be compared directly, e.g., spectrophotometrically. No reports of these possibilities have previously been published.* The latter, however, provides the basis for the so-called equilibrium perturbation method.²⁴ If the difference (Δf) between the extents of reaction for isotopically different substances ($\Delta f = f_L - f_H$) is directly measured, then a plot of the type shown in Fig. 1 can be constructed. The maximum difference, which corresponds to a value of f around 0.63 for the heavy atom, depends only on the magnitude of the isotope effect α :

$$\Delta f_{\max} = \alpha^{1/(1-\alpha)} - \alpha^{\alpha/(1-\alpha)} \quad (4)$$

Equation (4) is identical with that obtained by



Cleland²⁴ for apparent kinetic isotope effects in enzymic reactions. The method of isotopic competition suffers from the necessity for isotopic synthesis. The heavy-atom kinetic isotope effects are very small and the differences between the extents of reaction for isotopically different species are also very small. For a typical range of heavy-atom kinetic

*The first report of such direct spectrophotometric comparison of two solutions containing different isotopic species seems to be that for the ¹⁵N/¹⁴N kinetic isotope effect, by J. W. Burgner and W. J. Ray,⁴⁸ at the Steenback Symposium on Enzyme Stereochemistry. 1-3 July 1985, Madison, WI, U.S.A.

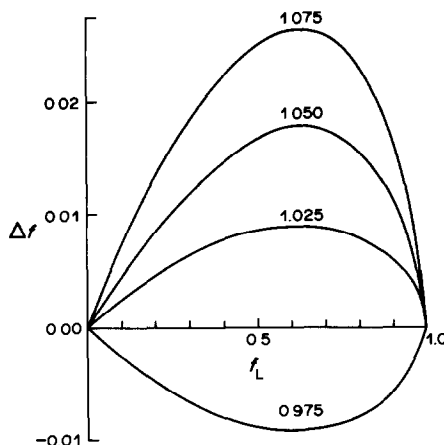


Fig. 1. Dependence of the difference $\Delta f = f_L - f_H$ on the extent of reaction.

isotope effects, 0.975–1.075, the maximum differences are not greater than 0.025 (Fig. 1), which is of the order of magnitude of the precision usually obtained in measuring the extent of reaction.

In spite of these problems this method has been used²⁵⁻²⁷ from time to time since Mitton and Schowen²⁸ first applied it in 1968 to the measurement of the oxygen isotope effect. Up to the present the only analytical method giving sufficient precision for the purpose is spectrophotometry.

The papers published by Rosenberg and Kirsch^{26,29} are interesting from an analytical point of view. They dealt with the reaction of nicotinamide with 2,4-dinitrophenyl acetate

and measured the kinetic isotope effect of the ether-oxygen atom by two methods: isotopic competition and independent runs. The values obtained, 1.043 ± 0.007 and 1.040 ± 0.002 , respectively, are in good agreement and can be used as an argument for the applicability of the method of independent kinetic runs to the measurement of heavy-atom kinetic isotope effects.

As substituted or highly enriched isotopic material is frequently unavailable, the papers of Rosenberg and Kirsch can serve as an example of the application of labelled material in the method of independent measurements. They performed their studies at two isotopic levels: $x_H = 0.38$ and 0.77 (x_H is the isotopic mole fraction of the heavy species) and corrected the

results by means of the equation:

$$k_{16}/k_{18} = [(k_{16}/k_{18})_{\text{ex}} - 1 + a_{\text{H}}]/x_{\text{H}}. \quad (6)$$

It should be noted that equation (6) is exactly correct for reciprocals of isotope effects, but the values of heavy-atom kinetic isotope effects are close enough to unity for the isotope effects to be used instead of their reciprocals without great change in the results.

MEASUREMENT OF THE CONCENTRATION OF RADIOACTIVE ISOTOPES

Early radiochemical studies of kinetic isotope effects used ionization chambers³⁰ for measurements of the activity of gases containing a radioisotope (e.g., $^{14}\text{CO}_2$). Nowadays, liquid scintillation counting is in common use and two different techniques have been developed. In the first, two radioisotopes are present in one sample and these isotopes must have distinctive β^- emission spectra. It is possible, for example, to measure the content of ^3H ($E_{\beta^-} = 0.018$ MeV) and ^{14}C ($E_{\beta^-} = 0.159$ MeV) in the same sample provided that the tritium is used in so large an excess that the contribution of ^{14}C in the channel corresponding to ^3H may be neglected. It is not possible, on the other hand, to measure ^{35}S ($E_{\beta^-} = 0.167$ MeV) and ^{14}C together as the spectra are too similar. This technique suffers from poor precision,^{31,32} but positive results have been reported.²¹ Calculation of the activity ratio from the kinetics of radioactive decay³³ rather than from multiple counting of a sample seems to be promising.

The second technique is the application of liquid scintillation counting for measurement of the specific activity of one radioisotope. Specific activity corresponds to the ratio of radioisotope to stable isotopes if the radioisotope is present at trace level, which is usually the case. Counting rates in the range 10^5 – 10^6 /min are used in order to obtain high precision. The resulting errors in kinetic isotope effects are 0.003–0.004. There are two different ways of making such measurements: in the first,³⁴ an external standard is used, and in the second,¹⁶ an internal standard is employed. The first method is in more frequent use.

SELECTION OF THE APPROPRIATE MASS SPECTROMETER

Once the decision to work with stable isotopes and the isotopic competition method (the most frequent choice) has been taken there remains a further problem, the type of mass spectrometer to be used. The costs of isotope-ratio and routine mass spectrometers are similar nowadays. Isotope-ratio mass spectrometers give high precision of the order of 0.01%. The early models were equipped with two detectors arranged in the following way: one receives a signal corresponding to one isotope, usually the heavier, and the other receives all signals in the vicinity. This

arrangement is subject to error if there are other ions in this part of the spectrum. Newer spectrometers have two or three (or even more) detectors placed exactly on the path of the designated ions. The natural abundance of heavy isotopes is usually too low for measurements to be made with routine mass spectrometers. Methods of conversion³⁵ into suitable gaseous forms, first developed in the 1950s, are still being investigated. The conversion itself can be a considerable source of error, so isotope-ratio mass spectrometers are especially useful when one of the reagents (preferably the product) is itself gaseous. Furthermore, isotope-ratio spectrometers are designed for measurement of one particular gas. The change to another gas is usually expensive if the appropriate collector is bought, or very inconvenient if the geometry of one collector is to be changed.

An attractive alternative is a recently developed method of measurement with a routine mass spectrometer. The main problem with such measurements is the selection of an appropriate time for the collection of ions with the given mass number and the provision of a computer which is sufficiently fast to collect the data. Routine spectrometers, unlike isotope-ratio spectrometers, are equipped with only one detector. Ion beams of different mass-to-charge ratio are focused on this detector in turn. When too little time is devoted to the collection of ions with the appropriate m/z value the total charge collected is low and subject to large statistical error. Good results have been obtained when the ion currents for any number of scans from a few hundred³⁶ to a few hundred thousand³⁷ have been accumulated in a computer. The greater the difference between isotopic abundances the larger the number of scans required. Kwart, who developed this method, reported^{37–40} errors of about 0.002 for kinetic isotope effects. The currents due to molecular ions are usually measured. Problems connected with instability and background are more serious with this method than with measurements by means of isotope-ratio mass spectrometers.

DETERMINATION OF THE COURSE OF REACTION

If we denote the isotopic ratio of the substrate by S and that of the product by R and the extent of reaction by f , the kinetic isotope effect is given by the equation:

$$\begin{aligned} k_{\text{L}}/k_{\text{H}} &= \ln(1 - f_{\text{L}})/\ln[(1 - f_{\text{L}})S/S_0] \\ &= \ln(1 - f_{\text{L}})/\ln(1 - f_{\text{L}}R/S_0). \end{aligned} \quad (7)$$

To evaluate the kinetic isotope effect from this equation we must measure the isotopic ratio of the substrate at the beginning of the reactions, S_0 (S at time $t = 0$), and at least one pair of values of f_{L} and R , or f_{L} and S , where R and S correspond to the extent of reaction f_{L} . These equations are based on the extent of reaction for the light isotope. It is equal

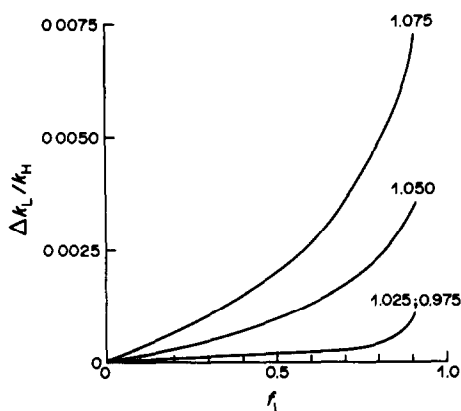


Fig. 2. Dependence of the error in k_L/k_H on the extent of reaction.

to the chemical extent of reaction, f , (*i.e.*, for both isotopes) only when the heavier species is present at trace level. The relation between different extents of reaction is presented in the equation:

$$f = f_L x_L + f_H x_H \quad (8)$$

where x represents the isotopic mole fraction.

Sometimes it is more convenient to follow the course of reaction of the heavier isotope, *e.g.*, radiochemically. In this case:

$$k_L/k_H = \ln(1 - f_H S_0/R) / \ln(1 - f_H). \quad (9)$$

If both isotopic species are present in comparable amounts, the appropriate form of equation (7) is:

$$\frac{k_L}{k_H} = \frac{\ln(1-f)}{\ln[1-fR(1+S_0)/S_0(1+R)]}. \quad (10)$$

It is not usually necessary, however, to rewrite equation (7) in the form of (9) or (10). Figure 2 illustrates the error in the kinetic isotope effect caused by the use of f_L instead of f_H and *vice versa* (f always lies between the two). As can be seen, up to an extent of reaction of 0.4, the shift of the calculated value is within experimental error.

Furthermore, the difference $f_L - f_H$ is always smaller than the precision of determination of f (Fig. 1) and isotope effects are not very sensitive to the value of the extent of reaction. It is sometimes not possible to measure the extent of reaction with reasonable precision. In such a situation we can use the approximation which results from the first form of equation (7) or from equation (9) for $f_i \rightarrow 0$:

$$k_L/k_H = S_0/R. \quad (11)$$

From this equation the kinetic isotope effect can be calculated on the basis of the isotope ratios of the substrate at the beginning of the reaction and of the product formed immediately after initiation of the reaction. This method of evaluating kinetic isotope effects has often been used but because the substrate and the product are different chemical substances, care must be taken in comparing S_0 with R (especially,

when a routine mass spectrometer is used). If there are no side-reactions it can be calculated from an isotope balance that $S_0 = R_\infty$ where R_∞ is the isotopic ratio of the product after the completion of reaction ($f_i = 1$). Whenever this is the case it is much safer to compare R with R_∞ .

HOW TO INCREASE KINETIC ISOTOPE EFFECTS

When measuring heavy atom kinetic isotope effects, more especially the secondary effect, an increase in this small effect is desirable in order to make its value (in terms of deviation from unity) larger than its standard deviation. One possibility is to decrease the temperature of reaction. From the typical dependence of kinetic isotope effects on temperature⁴¹ it can be predicted that their values increase with decrease of temperature (secondary isotope effects can, however, exhibit an atypical dependence).^{41,42} If the mechanism of reaction, rather than the particular reactant, is of interest (few substrates are studied with different substituents), then the substrate for which the reaction has the largest activation energy should be chosen.

Whenever possible, the heaviest of the isotopes of an element should be used, for instance ¹⁴C instead of ¹³C or ³⁶S instead of ³⁴S. The relation that holds for kinetic isotope effects for different isotopes of the same element is defined by the equation:

$$r = \ln(k_L/k_{H2}) / \ln(k_L/k_{H1}) \approx \left(\frac{k_L}{k_{H2}} - 1 \right) / \left(\frac{k_L}{k_{H1}} - 1 \right). \quad (12)$$

It has been predicted theoretically^{43,44} and confirmed experimentally^{14,15} that the r -value is usually smaller than the ratio $(H2 - L)/(H1 - L)$, where $H1$, $H2$ and L are the mass numbers of the three isotopes, $H2$ being the heaviest and L the lightest, so for equally spaced isotopes ($H2 - H1 = H1 - L$) the isotope effect can be doubled.

CONCLUSIONS

The scheme presented overleaf summarizes commonly used procedures. The wider the line the more frequent the use of the combination.

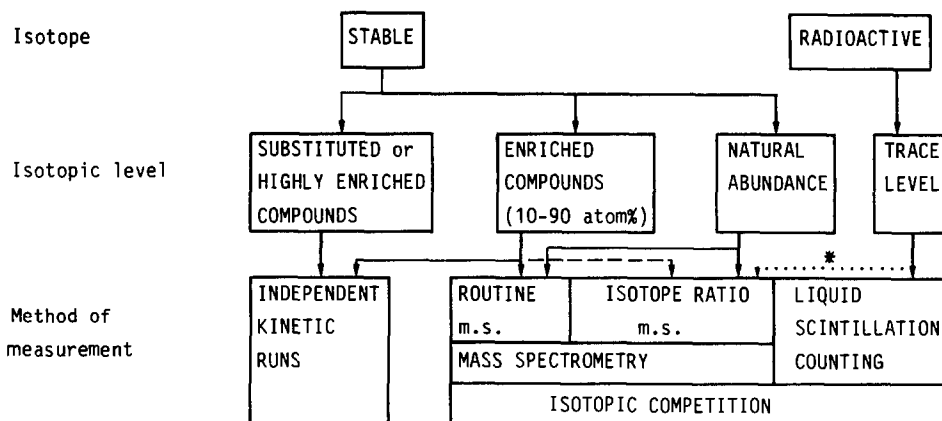
The complications caused by the complexity of a reaction⁴⁶ are illustrated by considering a reaction of the type



and treating it as an elemental reaction



This becomes the case when the concentration of the intermediate I is sufficiently low ($k_1 \ll k_2$). We can then evaluate the kinetic isotope effect by using equation (11). This gives good results up to an f value of about 0.1 (*e.g.*, for $f = 0.1$ and $k_L/k_H = 1.05$



the error caused by the use of this approximation is 0.0026). When the true reaction scheme is represented by (13) the kinetic isotope effect obtained from S_0/R is equal to

$$k_L/k_H = \frac{\left(\frac{x}{\alpha_2} - \frac{1}{\alpha_1}\right)[xf - 1 + (1-f)^2]}{(x-1) \left\{ \frac{[1 - (1-f)^{1/\alpha_1}]x}{\alpha_2} - \frac{[1 - (1-f)^{2/\alpha_2}]}{\alpha_1} \right\}} \quad (15)$$

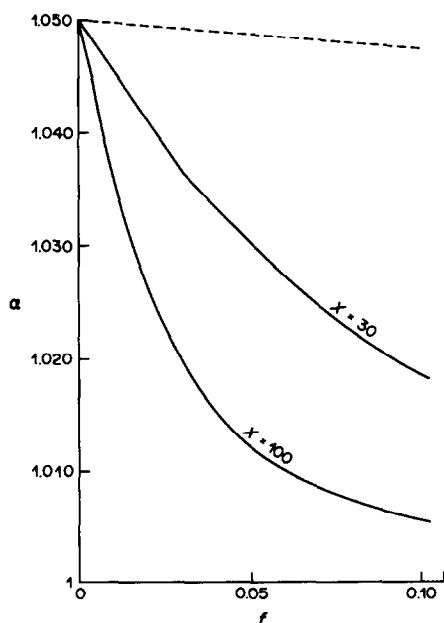


Fig. 3. Dependence of an experimental kinetic isotope effect on the extent of reaction calculated by means of equation (11) for consecutive reactions, $\alpha_1 = 1$, $\alpha_2 = 1.05$. The dotted line illustrates the change in the value caused by adopting the assumptions inherent in equation (11); $x = 30$ and 100 correspond to a relative accumulation of the intermediate (at its maximum concentration) equal to 3 and 1%, respectively.

where $\alpha_1 = k_{1L}/k_{1H}$; $\alpha_2 = k_{2L}/k_{2H}$; $x = k_{2L}/k_{1L}$; $f = 1 - e^{-k_1 t}$.

If the first reaction step is isotopically insensitive ($\alpha_1 = 1$) and the second step has a large isotope effect then the experimental kinetic isotope effect estimated by using equation (11) is incorrect. An example of such a case is illustrated in Fig. 3. As can be seen, the lower the concentration of the intermediate I , the larger the difference. In such cases the comparison of values measured for different (but still small) degrees of conversion f can indicate whether the reaction is complex or simple.

The complication introduced by the complexity of a reaction has certain advantages. The presence of unsuspected intermediates may be detected by using the dependence of the kinetic isotope effect on the extent of reaction at small degrees of conversion.

The possibility of isotopic exchange between substrates and products must be examined as its intervention can result in lowering or even masking the isotope effect.

Acknowledgement—I would like to thank the Editors of *Talanta* for help in revising the manuscript.

REFERENCES

1. L. Melander, *Isotope Effects on Reaction Rates*, Ronald Press, New York, 1960.
2. J. Bigeleisen and M. Wolfsberg, *Adv. Chem. Phys.*, 1958, 1, 15.
3. A. Fry, in C. J. Collins and N. S. Bowman (eds.), *Isotope Effects in Chemical Reactions*, Van Nostrand Reinhold, New York, 1970.
4. P. Krumbiegel, *Isotopieeffekte*, Akademie-Verlag, Berlin, 1970.
5. A. Maccoll, *Ann. Rep. Prog. Chem., Sect. A*, 1975, 71, 77.
6. M. H. O'Leary in R. L. Schowen and R. Gandour (eds.), *Transition States of Biochemical Processes*, Plenum Press, New York, 1978.
7. *Idem*, in E. E. van Tamelen (ed.), *Bioorganic Chemistry*, Vol. 1, Academic Press, New York, 1977.
8. *Idem*, in W. W. Cleland, M. H. O'Leary and D. B. Northrop (eds.), *Isotope Effects on Enzyme-Catalyzed*

- Reactions, Univ. Park Press, Baltimore, Maryland, 1977.
9. *Idem*, *Methods in Enzymology*, 1980, **64**, 83.
 10. L. Melander and W. H. Saunders, Jr., *Reaction Rates of Isotopic Molecules*, Wiley, New York, 1980.
 11. L. B. Sims and D. E. Lewis, in E. Buncl and C. C. Lee (eds.), *Isotopes in Organic Chemistry*, Vol. 6, Chap. 4. Elsevier, New York, 1984.
 12. A. Fry, *Pure Appl. Chem.*, 1964, **8**, 409.
 13. W. Reimschuessel and P. Paneth, *Anal. Chem. Symp. Ser. (Stable Isotopes)*, 1982, **11**, 49.
 14. *Idem*, *J. Am. Chem. Soc.*, 1985, **107**, 1407.
 15. J. Michalski, W. Reimschuessel and R. Kaminski, *Phosphorus Sulfur*, 1987, **30**, 257.
 16. J. McKenna, J. M. McKenna and P. S. Taylor, *J. Chem. Res. Synop.*, 1980, 281; S. M. Husain, J. McKenna and J. M. McKenna, *ibid.*, 1980, 280.
 17. N. E. Holden, R. L. Martin and I. L. Barnes, *Pure Appl. Chem.*, 1984, **56**, 675.
 18. R. H. Capriolli, W. F. Fies and M. S. Story, *Anal. Chem.*, 1974, **46**, 453A.
 19. M. H. O'Leary and J. F. Marlier, *J. Am. Chem. Soc.*, 1978, **100**, 2582; 1979, **101**, 3300.
 20. J. Bigeleisen, *J. Chem. Phys.*, 1955, **23**, 2264.
 21. G. R. Stark, *J. Biol. Chem.*, 1971, **246**, 3064.
 22. P. Paneth, *J. Chim. Phys. Phys.-Chim. Biol.*, 1986, **83**, 217.
 23. M. H. O'Leary, H. Yamada and C. J. Yapp, *Biochemistry*, 1981, **20**, 1476.
 24. W. W. Cleland, *Isotope Effects on Enzyme-Catalyzed Reactions*, p. 153. Univ. Park Press, Baltimore, Maryland, 1977.
 25. D. G. Gorenstein, Y. Lee and D. Kar, *J. Am. Chem. Soc.*, 1977, **99**, 2264; D. G. Gorenstein, *ibid.*, 1972, **94**, 2523.
 26. S. Rosenberg and J. F. Kirsch, *Anal. Chem.*, 1979, **51**, 1375.
 27. J. L. Kutz and J. Lee, *J. Am. Chem. Soc.*, 1980, **102**, 5427.
 28. C. G. Mitton and R. L. Schowen, *Tetrahedron Lett.*, 1968, 5803.
 29. S. Rosenberg and J. F. Kirsch, *Anal. Chem.*, 1979, **51**, 1379.
 30. M. L. Bender and D. F. Hoeg, *J. Am. Chem. Soc.*, 1957, **79**, 5649.
 31. E. T. Bush, *Anal. Chem.*, 1964, **36**, 1083.
 32. R. J. Herborg, *ibid.*, 1964, **36**, 1079.
 33. R. Kaminski and P. Paneth, unpublished work.
 34. B. W. Palmer and A. Fry, *J. Am. Chem. Soc.*, 1970, **92**, 2580.
 35. J. H. Beynon, *Mass Spectrometry and its Application to Organic Chemistry*, Elsevier, Amsterdam, 1960.
 36. W. Reimschuessel and P. Paneth, *Org. Mass Spectrom.*, 1980, **15**, 302.
 37. H. Kwart and J. J. Stanulonis, *J. Am. Chem. Soc.*, 1976, **98**, 4009.
 38. H. Kwart and D. A. Benko, *ibid.*, 1979, **101**, 1277.
 39. H. Kwart, D. A. Benko, J. Streith, D. J. Harris and J. L. Shuppiser, *ibid.*, 1978, **100**, 6502.
 40. H. Kwart and W. E. Barnette, *ibid.*, 1977, **99**, 614.
 41. W. A. Van Hook in C. J. Collins and N. S. Bowman (eds.), *Isotope Effects in Chemical Reactions*, Van Nostrand Reinhold, New York, 1970.
 42. P. C. Vogel and M. J. Stern, *J. Chem. Phys.*, 1971, **54**, 779.
 43. J. Bigeleisen, *J. Phys. Chem.*, 1952, **56**, 823.
 44. P. Paneth, *J. Chem. Phys.*, 1985, **82**, 3705.
 45. M. J. Stern and P. C. Vogel, *ibid.*, 1971, **55**, 2007.
 46. P. Paneth, *J. Am. Chem. Soc.*, 1985, **107**, 7070.
 47. P. E. Yankwich, A. Promislow and R. F. Nystrom, *ibid.*, 1954, **76**, 5893.
 48. J. W. Burgner II and W. J. Ray, in P. A. Frey (ed.), *Mechanisms of Enzymatic Reactions: Stereochemistry*. Elsevier, New York, 1986.

SHORT COMMUNICATIONS

IODIMETRIC DETERMINATION OF ORGANOLEAD COMPOUNDS

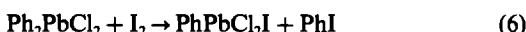
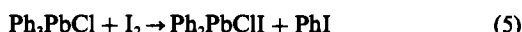
D. AMIN and TALAL A. K. AL-ALLAF*

Department of Chemistry, College of Science, University of Mosul, Mosul, Iraq

(Received 30 October 1985. Revised 25 April 1986. Accepted 27 May 1987)

Summary—A sensitive, rapid and accurate titrimetric method has been developed for the determination of 50–5000 μg of ethyl-lead or phenyl-lead compounds, based on their oxidation with a chloroform solution of iodine, removal of the excess of iodine, oxidation of the resulting iodide with bromine, and iodometric titration of the iodate formed. The coefficient of variation does not exceed 1.2% for amounts >1000 μg of the organolead compound, but increases to 2.8% for the 50- μg level. The ethyl- and phenyl-lead compounds can be determined independently in mixtures.

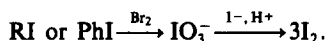
Organolead compounds have been determined by polarographic,¹ atomic-absorption,² colorimetric,³ X-ray spectrophotometric,⁴ potentiometric⁵ and titrimetric⁶ methods, but some of these methods have various drawbacks, including lack of selectivity and sensitivity. The method described here is simple and rapid, needs no complicated apparatus, and can be applied to the determination of alkyl and phenyl compounds in mixtures, independently. It is based on the reaction of the organolead compounds with a chloroform solution of iodine:



where



The method continues with removal of the excess of iodine, oxidation of the resulting iodide (in the aqueous or organic phase) by bromine water to iodate and iodometric titration:⁷



It should be noted that the alkyl iodide products are transferred to the aqueous layer and then oxidized with bromine to iodate. However, the phenyl iodide products remain in the organic layer, where they are oxidized with bromine, the iodate formed being transferred into the aqueous layer.

EXPERIMENTAL

Reagents

Tetraphenyl-lead was prepared as described by Gilman *et al.*⁸ and converted into triphenyl-lead chloride and diphenyl-lead dichloride by passing dry hydrogen chloride into its refluxing solution in chloroform.⁹ Tetraethyl-lead (kindly supplied by the Petroleum Authorities at Kirkuk Establishments, Iraq) was distilled under reduced pressure (78°/10 mmHg) and converted into triethyl-lead chloride and diethyl-lead dichloride as described by Heap and Saunders.¹⁰ Triethyl-lead acetate was prepared by heating tetraethyl-lead and glacial acetic acid under reflux.¹¹

Stock solutions, 1 mg/ml, of the ethyl-lead and phenyl-lead compounds were prepared in ethanol and chloroform respectively, and diluted as required. Sodium thiosulphate solutions, 0.001 and 0.01M, were standardized against 0.0002 and 0.002M potassium iodate solutions. The iodine solution was prepared by dissolving 0.600 g of pure iodine in 500 ml of dry chloroform. Solutions of bromine water (saturated), formic acid (80%), sodium sulphite (1%) and starch (1%), were also prepared.

Procedures

Determination of ethyl-lead compounds. In a 100-ml separating funnel, place a suitable volume (0.5–5 ml) of sample solution containing 0.05–5.0 mg of tetraethyl-lead, triethyl-lead acetate, triethyl-lead chloride or diethyl-lead dichloride, and 10 ml of iodine solution. Stopper the funnel and shake it for 2 min. Add 40 ml of distilled water, mix well and separate the organic layer. Remove the last traces of iodine from the aqueous layer by extraction with 10 ml of chloroform. Transfer the aqueous phase (containing iodide) quantitatively to a 100-ml conical flask. Add 2 ml of bromine water and stir for 2 min. Destroy the excess of bromine by addition of 2 ml of formic acid solution, add about 0.5 g of potassium iodide, and titrate the liberated iodine with 0.01M thiosulphate (for less than 1.0 mg of the ethyl-lead compound, use 0.001M thiosulphate), using starch as indicator. Run a blank determination (the average blank value is 0.05 ml of 0.01M thiosulphate). One ml of 0.01M thiosulphate is equivalent to 269.5 μg of tetraethyl-lead, 549 μg of triethyl-lead chloride, 588 μg of triethyl-lead acetate or 1120 μg of diethyl-lead dichloride.

Determination of phenyl-lead compounds. Transfer a suitable volume (0.5–5 ml) of sample solution containing 0.05–5.0 mg of tetraphenyl-lead, triphenyl-lead chloride or

*Author to whom correspondence should be addressed.

Table 1. Accuracy and precision of the method (5 replicates)

Compound	Amount taken, μg	Recovery, %	Coeff. of variation, %
Tetraphenyl-lead	50	100.2	1.3
	1000	99.9	0.2
	5000	99.2	0.4
Triphenyl-lead chloride	50	98.3	1.1
	1000	100.0	0.0
	5000	99.4	0.3
Diphenyl-lead dichloride	50	98.5	1.4
	1000	100.0	0.3
	5000	99.6	0.5
Tetraethyl-lead	50	99.0	1.0
	1000	100.0	0.1
	5000	99.3	0.3
Triethyl-lead chloride	50	98.0	2.1
	1000	99.1	0.9
	5000	98.5	1.2
Triethyl-lead acetate	50	97.8	1.8
	1000	99.3	1.1
	5000	97.0	1.0
Diethyl-lead dichloride	50	98.1	2.8
	1000	99.8	1.0
	5000	98.2	0.7

diphenyl-lead dichloride, to a 100-ml separating funnel, add 10 ml of iodine solution and shake the mixture for 2 min. Add 10 ml of distilled water and 1 ml of sodium sulphite solution and shake until the mixture is colourless. Drain the organic layer into another separating funnel, add 10 ml of water and 2 ml of bromine water to it and shake the mixture for 2 min. Discard the organic layer and transfer the aqueous phase quantitatively to a 100-ml conical flask. Complete the determination as for ethyl-lead compounds. One ml of 0.01M thiosulphate is equivalent to 429 μg of tetraphenyl-lead, 394.6 μg of triphenyl-lead chloride or 360 μg of diphenyl-lead dichloride.

RESULTS AND DISCUSSION

Preliminary investigations showed that the tetraethyl-lead and phenyl-lead compounds react with iodine in 1:2 molar ratio [equations (1, 4–6)], whereas the triethyl-lead compounds react in 1:1 ratio [equation (2)] and diethyl-lead dichloride in 2:1 ratio [equation (3)].

The solutions of the organolead compounds react quantitatively with a chloroform solution of iodine within 2 min, and a reaction time of up to 30 min has no effect on the results. It was found that 10 ml of 0.12% iodine solution can oxidize up to 5 mg of organolead compound.

In determination of the ethyl-lead compounds, the reaction products containing iodine were extracted quantitatively into the aqueous phase when the ratio of organic to aqueous phase was 1:4. However, low results were obtained when the organic to aqueous phase volume-ratios were 1:3, 1:2 and 1:1, the recoveries being 92, 55 and 32%, respectively.

The phenyl-lead reaction products were extracted quantitatively into the organic layer, and the phase-volume ratio had no significant effect on the results.

The method has been applied successfully to the determination of 1 mg of an ethyl-lead compound in the presence of 10 mg of a phenyl-lead compound with an error of less than 1.5%. Similarly, 1 mg of a phenyl-lead compound can be determined in the presence of 10 mg of an ethyl-lead compound with a similar error. The results in Table 1 indicate the reliability of the method.

The ethyl-lead procedure can be used to analyse gasoline for tetraethyl-lead and gives results comparable to those obtained by the standard method of Hein *et al.*⁶ Five replicate analyses of a gasoline gave a mean tetraethyl-lead concentration of 768 $\mu\text{g}/\text{ml}$, compared with 762 $\mu\text{g}/\text{ml}$ by the standard method and 778 $\mu\text{g}/\text{ml}$ reported by the manufacturer. The coefficient of variation was 0.6%.

REFERENCES

1. *ASTM Standard*, D 1269-61, Part 17, American Society for Testing and Materials, Philadelphia, 1973.
2. *ASTM Standard*, D 3237-79, Part 25, p. 112. American Society for Testing and Materials, Philadelphia, 1979.
3. *ASTM Standard*, D 3348-79, Part 25, p. 253. American Society for Testing and Materials, Philadelphia, 1979.
4. *IP Standards for Petroleum and its Products*, Part 1, Section 2, p. 1032. Institute of Petroleum, London, 1971.
5. S. M. Farroha, A. E. Habboush and N. Issaq, *Analyst*, 1984, **109**, 1531.
6. F. Hein, A. Klein and H. J. Mesece, *Z. Anal. Chem.*, 1939, **115**, 177.
7. T. Leipert, *Mikrochemie*, 1959, 266.
8. H. Gilman, L. Summers and R. W. Leeper, *J. Org. Chem.*, 1952, **17**, 630.
9. H. Gilman and H. D. Robinson, *J. Am. Chem. Soc.*, 1959, **51**, 3112.
10. R. Heap and B. C. Saunders, *J. Chem. Soc.*, 1949, 2983.
11. G. C. Robinson, *J. Org. Chem.*, 1963, **28**, 843.

USE OF AN ION-SELECTIVE MEMBRANE ELECTRODE FOR THE DETERMINATION OF THE ACTIVE COMPONENTS IN INTESTOPAN

M. S. IONESCU and M. LAZARESCU

Institute of Chemical and Pharmaceutical Research, 74351-Sos. Vitan 112, Bucharest-3, Romania

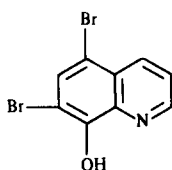
A. IONESCU and G. E. BAIULESCU

National Institute of Chemistry, 77207-Spl. Independentei 202, Bucharest-6, Romania

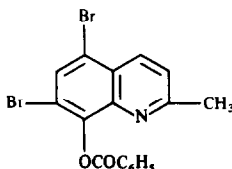
(Received 14 September 1984. Revised 16 April 1986. Accepted 4 February 1987)

Summary—The conditions for the determination of broxyquinoline and brobenzoxaldine, the active components of "Intestopan", by use of ion-selective membrane electrodes are described. Broxyquinoline is determined directly through precipitation with CuSO_4 , and brobenzoxaldine is first hydrolysed in alkaline solution and the product precipitated with CuSO_4 . In both cases the CuSO_4 in excess is determined by potentiometric titration at pH 5.6 with EDTA, a Cu^{2+} -selective electrode being used for end-point detection.

8-Hydroxyquinoline and its halogenated derivatives have found many applications in pharmaceutical practice, because of their antibacterial and antiseptic properties. A 5:1 w/w mixture of broxyquinoline (I) and brobenzoxaldine (II) is the active principle of the drug "Intestopan", an intestinal antiseptic with potent antibacterial and amoebicidal activity which does not upset the balance of the normal intestinal flora.



Broxyquinoline (I)
(5,7-dibromo-8-hydroxyquinoline)



Brobenzoxaldine (II)
(2-methyl-5,7-dibromo-8-hydroxyquinolinyl benzoate)

These two compounds have been determined in pharmaceutical formulations (tablets, ointments, etc.) by thin-layer chromatography^{1,2} or spectrophotometrically.³ Copper(II)-selective membrane electrodes have been used in potentiometric titration of 8-hydroxyquinoline derivatives with cupric salts.⁴⁻⁶

The method proposed in this paper involves chelation of broxyquinoline with Cu^{2+} , followed

by potentiometric titration of excess of Cu^{2+} with EDTA. Brobenzoxaldine is hydrolysed to 2-methyl-5,7-dibromo-8-hydroxyquinoline which is then similarly determined.

EXPERIMENTAL

Apparatus

A Radiometer ABU 12 autoburette, TTT 2 titrator and SBR 2c recorder were used with an Orion 94-29 Cu^{2+} -selective membrane electrode as indicator electrode and a Radiometer K401 saturated calomel electrode as reference. For pH measurement a Radiometer glass-calomel electrode system (G202C and K401 electrodes) was used.

Reagents

All reagents were of analytical grade, and I and II were synthesized and purified by us.

Determination of broxyquinoline (in pure form)

The broxyquinoline (0.15–0.20 mmole) is dissolved in 30 ml of acetone and 15 ml of distilled water and 5.00 ml of 0.05M copper(II) sulphate are added. The pH is adjusted to 5.6 with 30 ml of 0.05M acetate buffer and excess of copper is potentiometrically titrated with 0.05M EDTA.

1 ml of 0.05M $\text{CuSO}_4 \equiv 30.3$ mg of I

Determination of brobenzoxaldine (in pure form)

The brobenzoxaldine (0.20–0.25 mmole) is dissolved in 30 ml of acetone, 10 ml of 0.1M sodium hydroxide are added and the sample is hydrolysed by refluxing on a hot water-bath for 30 min. After cooling to room temperature, the sample is quantitatively transferred to a 100-ml beaker with 25 ml of 2:1 v/v acetone–water mixture, the pH is adjusted to 6.0 with 0.1M hydrochloric acid and then to 5.6 with 15 ml of 0.05M acetate buffer (pH 5.6). At least 7 ml of 0.05M copper sulphate (accurately measured) are added, the mixture is mechanically stirred for a few minutes and the excess of copper is potentiometrically titrated with EDTA, as described above.

1 ml of 0.05M $\text{CuSO}_4 \equiv 42.2$ mg of II

Analysis of "Intestopan" tablets

At least five tablets of the sample batch are finely powdered and a portion of the mixed powder equivalent to

about 100 mg of I and 20 mg of II is accurately weighed and dissolved in 30 ml of acetone. The mixture is hydrolysed and titrated as described for brobenzoxaldine assay to yield the volume of copper solution equivalent to the sum of I and II.

Another portion of the powder equivalent to about 100 mg of I is accurately weighed and analysed as described for determination of pure broxyquinoline, to yield the amount of I present. The content of II is then calculated by difference.

RESULTS AND DISCUSSION

8-Hydroxyquinoline and its derivatives form copper complexes which have stability constants related to the basicity of the chelating molecule and any steric effects caused by substituents. The dibrominated compounds are more acidic than the parent compound,^{7,8} so their copper complexes should be less stable than the parent 8-hydroxyquinoline complex ($\log \beta_2 = 24.64$ for broxyquinoline, 26.22 for oxine). However, because of the much greater basicity of the EDTA anion, at pH 5–6 the side-reaction coefficient for protonation of EDTA is very much greater than that for protonation of the substituted 8-hydroxyquinolines, and the conditional stability of the Cu-EDTA complex is consequently lower than that of the substituted 8-hydroxyquinoline complexes (otherwise the method would not work). The possible interaction of excess of EDTA with the precipitate will be very slow because of the two-phase reaction system, and would not affect location of the end-point. The results obtained are presented in Table 1. The relative standard deviation was 1.0%. All determinations were performed in acetone–water (2:1 v/v) mixture. Other organic solvents (e.g., dioxan, methanol) were tested but in these solvents the copper(II) chelates are produced as a gel which is deposited on the Cu^{2+} -electrode surface and affects the electrode response. The presence of water in the reaction medium is essential, since the Cu^{2+} -selective electrode does not work properly in completely non-aqueous medium.

For choosing the pH for the potentiometric titration, we took into account the effect of pH on the potential jump at the equivalence point. Although the jump increases with pH, the hydrolysis of the benzoate ester in alkaline medium starts even at room temperature, which causes interference in the determination of broxyquinoline in presence of brobenzoxaldine. As a compromise we chose pH 5.6, adjusted with acetate buffer.

2-Methyl-5,7-dibromo-8-hydroxyquinoline benzoate is hydrolysed in alkaline medium to 2-methyl-5,7-dibromo-8-hydroxyquinoline by heating with

Table 1. Determination of broxyquinoline in pure form

Weight, mg		
Taken	Found	Recovery, %
59.9	60.8	101.5
60.7	61.6	101.5
62.6	62.7	100.1
64.0	63.3	98.9
64.2	64.8	100.9
66.4	65.9	99.2
67.9	67.1	98.8
68.7	68.8	100.1
69.2	68.8	99.4
73.5	73.0	99.3

Table 2. Determination of brobenzoxaldine in pure form

Weight, mg		
Taken	Found	Recovery, %
40.4	40.6	100.5
44.6	44.0	98.7
65.5	65.0	99.2
92.8	91.8	98.9
118.7	119.0	100.3
145.0	144.2	99.4
154.0	153.1	99.4
163.2	163.0	99.9
173.4	171.9	99.1
180.3	181.0	100.4

0.1M sodium hydroxide on a boiling water-bath for 30 min. The results obtained for pure brobenzoxaldine are given in Table 2. The relative standard deviation (rsd) was 0.7%.

Some of the excipients and diluents commonly used in preparation of tablets (magnesium stearate, stearic acid, gelatine, talc, lactose, corn starch) were investigated and found not to affect the determination. Replicate analysis of Intestopan tablets (Sandoz Ltd., Basle) gave a mean recovery of 99.6% for broxyquinoline (rsd 1.1%) and 99.8% for brobenzoxaldine (rsd 1.6%).

REFERENCES

1. M. Amin and U. Jakobs, *Z. Anal. Chem.*, 1974, **268**, 119.
2. A. Gyeresi and E. Man, *Rev. Med. (Târgu Mures)*, 1978, **24**, 176.
3. N. Nin'o, *Tr. Nauchn-Issled, Khim. Farm. Inst.*, 1972, **7**, 417.
4. D. J. Stoeber, *Pharm. Weekbl.*, 1972, **107**, 201.
5. G. J. Van Rassum and G. den Boef, *Anal. Chim. Acta*, 1972, **61**, 144.
6. E. Vinkler, F. Klivenyi and S. M. Gati, *Acta Pharm. Hung.*, 1972, **42**, 141.
7. A. N. Sevastyanov and N. P. Rudenko, *Vestn. Mosk. Univ., Ser. II*, 1967, **22**, 110.
8. D. A. Knyasev, *Zh. Analit. Khim.*, 1964, **19**, 273.

SPECTROPHOTOMETRIC DETERMINATION OF TITANIUM WITH *N-m*-TOLYL-*N*- PHENYLHYDROXYLAMINE AND ITS APPLICATION TO ENVIRONMENTAL SAMPLES

SADANOBU INOUE*, SUWARU HOSHI and MUTSUYA MATSUBARA

Department of Environmental Engineering, Kitami Institute of Technology, Kitami-shi, 090 Japan

(Received 10 February 1987. Accepted 27 May 1987)

Summary—*N-m*-Tolyl-*N*-phenylhydroxylamine is proposed for the spectrophotometric determination of titanium. The reagent forms a yellow chloroform-soluble complex with titanium in media with a hydrochloric acid concentration of at least 9*M*. The apparent molar absorptivity at 380 nm is 7.4×10^3 l.mole⁻¹.cm⁻¹. The optimum final concentration range is 0–54 µg of titanium in 10 ml of chloroform. The complex contains the metal and reagent in 1:2 ratio. The proposed method has been successfully applied to the determination of titanium in coal, coal fly-ash, pond sediment and asphalt.

N-Benzoyl-*N*-phenylhydroxylamine is well known as a specific reagent for the spectrophotometric determination of vanadium in 4–8*M* hydrochloric acid, and many of its derivatives, such as *N*-cinnamoyl-*N*-phenylhydroxylamine¹ and *N*-benzoyl-*N*-*o*-tolylhydroxylamine,² have also been used for the determination of vanadium. Furthermore, *N*-benzoyl-*N*-phenylhydroxylamine reacts with titanium in strongly acidic media to form a yellow complex which can be extracted with chloroform, and has been used for the spectrophotometric determination of titanium.^{3–5} Some other hydroxylamines such as the *N*-benzoyl-*N*-methyl-,⁶ *N*-acetyl-salicyloyl-*N*-phenyl,⁷ *N*-cinnamoyl-*N*-phenyl⁸ and *N*-benzoyl-*N*-tolyl-⁸ derivatives, also have been proposed for the spectrophotometric determination of titanium.

In a systematic investigation of *N*-benzoyl-*N*-phenylhydroxylamine derivatives and their analytical applications, it was found that *N-m*-tolyl-*N*-phenylhydroxylamine formed a yellow complex with titanium in strongly acidic media. On the basis of this colour reaction, an extraction-spectrophotometric method has been developed for determination of titanium with higher sensitivity than that with *N*-benzoyl-*N*-phenylhydroxylamine⁴ or its derivatives such as *N*-benzoyl-*N*-methylhydroxylamine.⁶ Furthermore, the method is superior in selectivity to the hydrogen peroxide,⁹ tiron¹⁰ and diantipyrylmethane methods,¹¹ and the procedure for determination of titanium is very simple. The method has been applied satisfactorily to several environmental samples.

EXPERIMENTAL

Reagents

A standard solution (3.75×10^{-2} *M*) of titanium was prepared by dissolving 0.7491 g of high-purity titanium

oxide which had been heated at 1000° for 1 hr, in 20 ml of concentrated sulphuric acid together with 10 g of ammonium sulphate, with heating, and then diluting to 250 ml with sulphuric acid (1 + 19).

N-m-Tolyl-*N*-phenylhydroxylamine was prepared from *m*-toluoyl chloride and phenylhydroxylamine as described previously.¹²

Chloroform was freed from alcohol and saturated with water by shaking with distilled water.

All other reagents used were of analytical grade.

Apparatus

A Hitachi model 200-10 spectrophotometer with 10-mm silica cells, and a Hitachi-Horiba F-7AD pH meter were used.

General procedure

Place a volume of solution containing up to 54 µg of titanium in a separating funnel and add about 40 mg of tin(II) chloride dihydrate, followed by enough concentrated hydrochloric acid to give a concentration of 10*M*. Then add 10 ml of a 1 mg/ml solution of the reagent in chloroform. Shake the mixture vigorously for about 3 min and allow the phases to separate. Measure the absorbance of the extract at 380 nm *vs.* chloroform.

Samples

The National Bureau of Standards (NBS) Coal SRM-1632b and Coal fly ash SRM-1633a, National Institute for Environmental Studies (NIES, Japan) Certified Reference Pond Sediment, and asphalt samples which were obtained from asphalt-surfaced roads in Kitami and Abashiri were used to evaluate the accuracy and precision of the method. The asphalt samples were obtained as a core, 9.8 cm in diameter. A 5.0-cm thickness of the upper part of the core was ground in iron and porcelain mortars to pass a 60-mesh sieve. The standard reference samples of coal and fly-ash, and the asphalt samples were dried under vacuum at ambient temperature for 24 hr. The standard reference sample of pond sediment was dried in an oven at 110° for 4 hr.¹³

Analysis of environmental samples

Portions of about 0.08–0.1 g of these samples (accurately weighed) were taken in 50-ml PTFE beakers and treated with a mixture of 5 ml of concentrated hydrofluoric acid and 5 ml of concentrated nitric acid at 150° on a hot-plate, and evaporated to dryness. Then a mixture of 10 ml of concen-

*Author for correspondence.

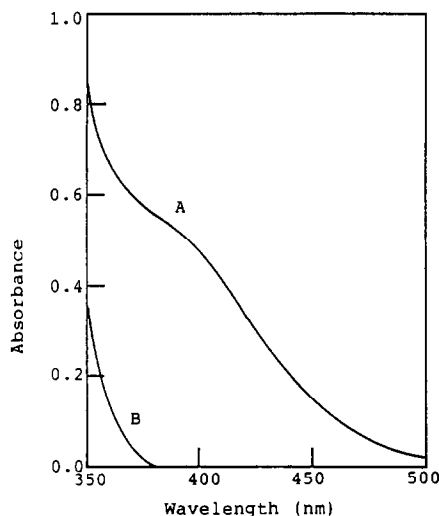


Fig. 1. Absorption spectra of *N-m-tolyl-N-phenylhydroxylamine* and its titanium complex, in chloroform. A—complex with 35.9 μg of titanium; B—0.1% reagent solution; reference, chloroform.

trated nitric acid and 10 ml of concentrated perchloric acid was added to each and the samples were digested, with the beaker covered by a PTFE lid, at 250° on a hot-plate for about 6 hr until a pale yellow solution was obtained, then evaporated to dryness at 150°. The residues were dissolved in about 10 ml of 6*M* hydrochloric acid with gentle heating. After cooling, the samples were diluted to volume with 6*M* hydrochloric acid in standard flasks. An aliquot of each sample digest was transferred to a separating funnel and titanium was determined as described above.

RESULTS AND DISCUSSION

Absorption spectra

The absorption spectra of the reagent and the titanium-*N-m-tolyl-N-phenylhydroxylamine* complex in chloroform are shown in Fig. 1. The absorption of the complex extracted into chloroform from a solution $>9M$ in hydrochloric acid increases continuously towards the ultraviolet from 500 nm, and the spectrum shows a discernible shoulder in the vicinity of 380 nm. The most suitable wavelength for spectrophotometric work seemed to be 380 nm, since the reagent solution in chloroform (1 mg/ml) scarcely

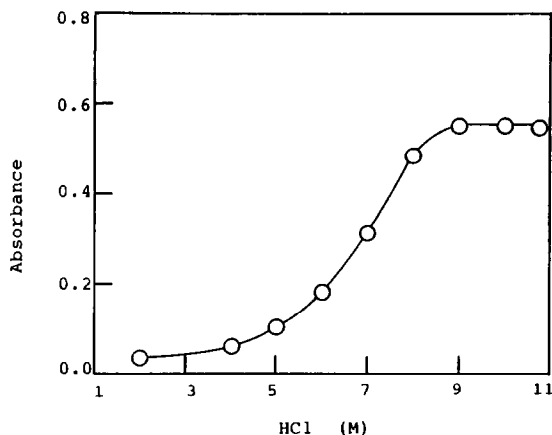


Fig. 2. Effect of hydrochloric acid concentration on absorbance. Titanium 35.9 μg ; $V_{\text{org}} = V_{\text{aq}} = 10$ ml; wavelength 380 nm.

absorbs at 380 nm. The apparent molar absorptivity of the complex at 380 nm is $7.4 \times 10^3 \text{ l. mole}^{-1} \cdot \text{cm}^{-1}$.

Effect of acidity and reagent concentration

The effect of acidity on the extraction of titanium is shown in Fig. 2. The maximum absorbance was obtained when the hydrochloric acid concentration was above 9*M*, and the colour remained unchanged for at least 24 hr at room temperature. A large excess of the reagent can be used even for a small amount of titanium, because it has no effect on the colour.

Beer's law

The colour system obeys Beer's law for up to 54 μg of titanium in 10 ml of chloroform. The method is more sensitive than the *N-benzoyl-N-phenylhydroxylamine*⁴ and hydrogen peroxide⁹ methods, although it has lower sensitivity than the tiron¹⁰ and dantipyrylmethane¹¹ methods. The relative standard deviation of the absorbance at 380 nm was 0.3% (10 replicates with 36 μg of titanium).

Effect of diverse ions

The effects of diverse ions on the absorbance obtained for the titanium complex were studied. The presence of 0.5 mg of chromium(VI), iron(III),

Table 1. Analytical results

Sample	Certified value, %	Found by proposed method, %	Found by AAS, %
Coal			
NBS SRM 1632b	0.0454 \pm 0.0017	0.0446 (5 detns.), rsd 1.4%	—
Coal fly ash			
NBS SRM 1633a	0.8	0.79 (5 detns.), rsd 0.9%	—
Pond sediment			
NIES No. 2	0.64*	0.58 (9 detns.), rsd 2.9%	—
Asphalt			
(Kitami city)	—	0.42 (8 detns.), rsd 5.0%	0.49 (8 detns.), rsd 4.9%
Asphalt			
(Abashiri city)	—	0.26 (8 detns.), rsd 5.7%	0.30 (8 detns.), rsd 6.8%

*Reference value.

molybdenum(VI), tungsten(VI), vanadium(V), zirconium(IV) and niobium(V) causes interference with 36 μg of titanium. However, in the presence of tin(II) chloride, only niobium(V) can be considered a serious interference. The presence of 10–20 mg of common anions such as citrate, oxalate, tartrate, EDTA, phosphate and fluoride did not interfere in determination of 36 μg of titanium.

Composition of the complex

The molar ratio method showed the molar ratio of titanium to reagent to be 1:2.

Application to environmental samples

The method was applied to the determination of titanium in coal (NBS SRM 1632b), fly-ash (NBS SRM 1633a), pond sediment (NIES, No. 2) and asphalt samples. The results obtained are compared in Table 1 with the certified values or those obtained by an independent method (atomic-absorption spectrometry) and gave good agreement with them. The relative standard deviations (rsd) for the asphalt samples were larger than those for the NBS reference materials, possibly because of inhomogeneity in the asphalt samples.

Acknowledgements—The authors are grateful to Dr. K. Okamoto of the National Institute for Environmental Studies, Japan Environment Agency, for providing the NIES sample.

REFERENCES

1. U. Priyadarshini and S. G. Tandon, *Analyst*, 1961, **86**, 544.
2. A. K. Majumdar and G. Das, *Anal. Chim. Acta*, 1964, **31**, 147.
3. J. E. Schwarberg and R. W. Moshier, *Anal. Chem.*, 1962, **34**, 525.
4. K. Tanaka and N. Takagi, *Bunseki Kagaku*, 1963, **12**, 1175.
5. B. K. Afghan, R. G. Marryatt and D. E. Ryan, *Anal. Chim. Acta*, 1968, **41**, 131.
6. H. K. L. Gupta and N. C. Sogani, *J. Indian Chem. Soc.*, 1963, **40**, 15.
7. C. P. Savariar and J. Joseph, *Anal. Chim. Acta*, 1969, **47**, 347.
8. N. K. Dutt and T. Seshadri, *Indian J. Chem.*, 1968, **6**, 741.
9. A. Weissler, *Ind. Eng. Chem., Anal. Ed.*, 1945, **17**, 695.
10. D. N. R. Nichols, *Analyst*, 1960, **85**, 452.
11. H. Ishii, *Bunseki Kagaku*, 1967, **16**, 110.
12. S. Inoue, H. Inai, S. Hoshi and M. Matsubara, *Anal. Sci.*, 1985, **1**, 423.
13. Y. Iwata, K. Matsumoto, H. Haraguchi, K. Fuwa and K. Okamoto, *Anal. Chem.*, 1981, **53**, 1136.

INFLUENCE OF THE NATURE OF ORGANIC PHASE EMULSIONS ON SENSITIVITY IN ATOMIC-ABSORPTION DETERMINATIONS

M. T. VIDAL and M. DE LA GUARDIA*

Department of Analytical Chemistry, Faculty of Chemistry, University of Valencia, Valencia, Spain

(Received 9 May 1985. Revised 7 April 1987. Accepted 27 May 1987)

Summary—The influence of the nature of organic phase emulsions on sensitivity in atomic-absorption determinations has been studied for the copper-APDC chelate extracted into various solvents. Oil-in-water emulsions containing 10% of organic phase emulsified with non-ionic and anionic surfactants were introduced into the flame and the atomic-absorption of copper was measured. An attempt was made to relate the effect on sensitivity to the physical properties of the different emulsions but no correlation was found. Rheological properties such as aspiration rate and nebulization efficiency did not differ significantly for different emulsified organic solvents. Enrichment of the waste solution proved the most important parameter for predicting an increase in sensitivity.

In analysis by atomic spectrometry the use of organic solutions sometimes provides notable increases in sensitivity.¹⁻³ Different increases in sensitivity have been found with different solvents, and attempts have been made to find correlations between the enhancement factors and the physical properties of the organic solvents.

Allan⁴ attributed the increased sensitivity primarily to an increase in the amount of solution reaching the flame and suggested that this increase might be the result of an increased uptake rate, the formation of a finer aerosol and the more rapid evaporation of solvent to produce smaller droplets. He also suggested that viscosity, surface tension and vapour pressure might be controlling factors in the physical process of nebulization.

Cresser⁵ suggested that the causes of the sensitivity enhancement are differences in viscosity, changes in droplet size distribution, increased solvent volatility, increases in flame temperature, flame radical effects and changes in atomizer geometry. However, no theoretical treatment of the phenomenon was made.

Recently, the use of emulsions has been proposed for use in the preparation of samples and standards for the direct determination of metallic elements in liposoluble matrices^{6,7} and also for improving the aspiration characteristics of organic extracts.^{8,9} This technique allows direct analysis and the use of aqueous solutions for standard preparation. The oil-in-water emulsions increase the sensitivity relative to that for aqueous solutions.

The increase in sensitivity obtained with emulsified systems seems to depend more on the presence of an organic phase than on the addition of a surfactant, since, as Kornahrens *et al.*¹⁰ have shown, the sensi-

tivity for determinations on aqueous phases is sometimes raised by these agents. These authors explain this by extending the theory of aerosol ionic redistribution proposed by Borowiec *et al.*¹¹ to suggest that in the nebulization process, smaller droplets are formed by stripping of the surface layers of existing drops, where there is already an analyte-rich double layer produced by accumulation of surfactant molecules at the air-water interface, hence giving analyte-enriched smaller drops and analyte-deficient larger drops.

The purpose of the present work was to determine the reasons for the increase in sensitivity when emulsions are used, in order to establish criteria for choosing the emulsion composition. The determination of copper after its liquid-liquid extraction with APDC into several solvents was chosen as the test system.

EXPERIMENTAL

Apparatus

A double-beam Pye Unicam SP 1900 spectrophotometer equipped with a copper hollow-cathode lamp was used, with the following operating conditions, which provided maximum sensitivity for all systems studied.

Wavelength 324.8 nm
Lamp current 4 mA
Band-width 0.15 nm
Air flow 4.5 l./min
Acetylene flow 700 ml/min
Observation height 0.8 cm

The physical properties of the emulsions were measured with a PAAR density-meter model DMA 35, a Brookfield viscometer model IVF and a stalagmometer.

Reagents

"DILUT-IT" 1000-ppm standard copper solution. A freshly prepared 1% aqueous solution of ammonium pyrolydinethiocarbamate (APDC), purified by extraction

*Author for correspondence.

with methyl isobutyl ketone (MIBK). The surfactants used were Masso and Carol Nemol K 38 (condensate of nonylphenol with 10 ethylene oxide units), Hoechst Emulsogen LBH (mixture of anionic surfactants and solvents) and a 1% aqueous solution of Tergitol XD (condensation product of ethylene oxide and propylene oxide, Union Carbide).

Procedure

One ml of 1% APDC solution was added to 50 ml of copper solution in a separatory funnel and 20 ml of organic solvent were added. After mechanical shaking for 5 min, the two phases were allowed to settle and were separated.¹² When MIBK, ethyl acetate and isobutyl acetate were used as extractants, mutually saturated solvent and aqueous phase were used.

The emulsions stabilized with LBH were prepared by mixing 10 ml of the organic phase with 3 ml of surfactant, followed by slow addition of distilled water to form a gel, and more water to make the total volume 100 ml. When isobutyl acetate, ethyl acetate or MIBK was used, no gel was formed and these emulsions were quite unstable. For this reason, we tried to obtain emulsions stabilized with another type of surfactant. These emulsions were prepared by using 0.25 g of Nemol K 38 plus 25 ml of 1% Tergitol XD solution, adding 10 ml of organic extract and then distilled water to make up to 100 ml.

The standards used were emulsions prepared in the same way, but with 10 ml of pure organic solvent and the copper introduced in the aqueous phase.

Samples prepared in this manner were introduced into the air/acetylene flame and the absorbances measured.

RESULTS AND DISCUSSION

The slopes of the calibration curves obtained with the emulsified standards were compared with those obtained for aqueous solutions (Table 1). Only the stabilized isobutyl acetate and MIBK emulsions gave higher sensitivity than that for aqueous solutions. These results suggest that the nature of the organic solvent is the main factor affecting the sensitivity.

Physical properties of emulsified organic phases

To try to identify the reason for the changes in sensitivity found in the determination of copper, these changes have been compared with the differences in physical properties of the pure solvents and the emulsions. The properties of the pure solvents

were taken from published data and those of the emulsions were determined with commercial instrumentation.

Table 2 shows that no obvious relationship can be deduced between the physical properties studied and the variation in sensitivity obtained in the copper determination. It can only be observed that the properties of the emulsions varied much less than those of the pure solvents, because the emulsions contained only 10% of the organic phase.

Effect on the transport properties

The properties studied were the aspiration rate, which is related to the sample viscosity, the efficiency of nebulization (the fraction of total sample solution which reaches the flame) and the relative concentration of the waste solution (defined as the ratio of absorbance of the waste solution, on nebulization, to the original absorbance of the emulsion).

Table 3 shows that the aspiration rates are all quite similar and have no direct relationship to the sensitivity for copper. Moreover, the ratios are lower than that for aqueous solutions by about 21–27%, which should lead to a corresponding decrease in sensitivity unless other factors also affect the results.

There were marked differences in the efficiency of nebulization for different emulsions, and it varied between 2 and 3 times that for aqueous solution; however, there was no such increase in sensitivity. The increased nebulization efficiency is partly offset by the lower aspiration rate, and there will also be complications caused by variation in atomization efficiency.

The only parameter which seemed related to the change in sensitivity was the change in apparent concentration of the waste. The increase in sensitivity was higher as the apparent concentration of the waste decreased.

The absorbance values of the samples and the waste showed changes that depended on the nature of the organic solvent in the emulsified phase. Isobutyl acetate and MIBK gave increased sensitivity and

Table 1. Calibrations equations for copper in oil-in-water emulsions made with various solvents and stabilizers

Stabilizer	Run*	Solvent	Calibration equation
LBH	1	Benzene	$Y = 0.001 + 0.075 X$
	1	Xylene	$Y = 0.003 + 0.074 X$
	1	MIBK	$Y = 0.004 + 0.097 X$
	2	Cyclohexane	$Y = 0.003 + 0.086 X$
	2	White spirit	$Y = 0.006 + 0.087 X$
	2	Carbon tetrachloride	$Y = 0.001 + 0.069 X$
	3	Ethyl acetate	$Y = 0.003 + 0.068 X$
Tergitol XD plus Nemol	1	Isobutyl acetate	$Y = 0.003 + 0.102 X$
	1	Ethyl acetate	$Y = 0.008 + 0.070 X$
K 38	1	MIBK	$Y = 0.004 + 0.103 X$

*The calibration data were obtained in different runs, during which data for aqueous standards were also obtained, the corresponding equations being: Run 1 $Y = 0.004 + 0.080 X$, Run 2 $Y = 0.006 + 0.088 X$, Run 3 $Y = 0.005 + 0.070 X$.

Table 2. Physical properties of pure solvents and oil-in-water emulsions stabilized with LBH

Solvent	Density, g/cm^3				Viscosity, cP		Surface tension, $dyne/cm$		
	Pure solvent	Emulsion			Pure solvent	Emulsion	Pure solvent	Emulsion*	
		\bar{x}	s	n				x	s
Isobutyl acetate	0.863	0.986	6×10^{-4}	3	0.8	1.9	23.0	26.3	0.4
MIBK	0.801	0.981	5×10^{-4}	4	0.52	2.0	26.9	26.5	0.4
White spirit	0.840	0.977	0.002	5	1.0	2.0	25.7	30.1	0.5
Cyclohexane	0.779	0.976	—	4	0.76	1.4	27.4	29.7	0.3
Ethyl acetate	0.898	0.995	6×10^{-4}	4	1.37	1.1	23.5	27.0	1.0
Benzene	0.879	0.981	0.002	3	0.65	1.8	28.8	29.3	0.3
Xylene	0.86–0.88	0.984	5×10^{-4}	5	0.63–0.81	1.6	28.4–30.1	28.6	0.3
Carbon tetrachloride	1.594	1.056	—	3	0.91	1.9	25.5	30.0	0.5

*Ten independent determinations.

Table 3. Transport properties of water and of emulsified organic phases stabilized with (a) LBH, (b) Tergitol XD plus Nemo K 38 (s estimated from three measurements)

Solvent	Aspiration rate, ml/min	Efficiency of nebulization, %	Relative absorbance of the waste, %	Δs^*
Water	6.6	7.7	100	1.0
Isobutyl acetate	4.8 ($s = 0.09$)	20 ($s = 1$)	68 ($s = 0.03$)	1.24
Isobutyl acetate	5.2 ($s = 0.06$)	19.3 ($s = 1.5$)	64 ($s = 4$)	1.28
MIBK	4.9 ($s = 0.03$)	17.3 ($s = 0.6$)	77 ($s = 3$)	1.21
MIBK	5.1 ($s = 0.06$)	19 ($s = 0$)	53 ($s = 3$)	1.29
White spirit	5.1 ($s = 0$)	11 ($s = 0$)	99 ($s = 5$)	0.99
Cyclohexane	5.0 ($s = 0$)	16 ($s = 0$)	103 ($s = 2$)	0.98
Ethyl acetate	4.9 ($s = 0.06$)	20 ($s = 1$)	95 ($s = 3$)	0.97
Ethyl acetate	5.1 ($s = 0$)	17 ($s = 0$)	87 ($s = 6$)	0.86
Benzene	5.1 ($s = 0.06$)	15.3 ($s = 0.6$)	101 ($s = 7$)	0.94
Xylene	5.2 ($s = 0.05$)	11.3 ($s = 0.3$)	97 ($s = 2$)	0.93
Carbon tetrachloride	4.8 ($s = 0.06$)	17.3 ($s = 0.6$)	114 ($s = 4$)	0.78

*Sensitivity relative to aqueous medium.

depletion of the apparent copper content of the waste, whereas carbon tetrachloride produced the reverse effect.

CONCLUSIONS

It is clearly difficult to establish a direct relationship between the increase in sensitivity for emulsified systems and the physical or transport (aspiration rate and efficiency of nebulization) properties. However, the model proposed by Kornahrens *et al.*¹⁰ seems to offer an explanation of the data, the effect being related to the manner in which the analyte is distributed between the large and small droplets of the aerosol.

We suggest that collection of the waste and determination of its absorbance relative to that of the original emulsion is the best way to assess the value of a given organic solvent as a means of improving sensitivity.

REFERENCES

1. M. S. Cresser, *Solvent Extraction in Flame Spectroscopy Analysis*, Butterworths, London, 1978.
2. A. B. Volynsky, B. Ya. Spivakov and Yu. A. Zolotov, *Talanta*, 1984, **31**, 449.
3. A. S. Attiyat and G. D. Christian, *Anal. Chem.*, 1984, **56**, 439.
4. J. E. Allan, *Spectrochim. Acta*, 1961, **17**, 459.
5. M. S. Cresser, *Prog. Anal. Atom. Spectrosc.* 1982, **5**, 35.
6. V. Berenguer, J. L. Guiñon and M. de la Guardia, *Z. Anal. Chem.*, 1979, **294**, 416.
7. A. Salvador M. de la Guardia and V. Berenguer, *Talanta*, 1983, **30**, 986.
8. M. de la Guardia and V. Berenguer, *Afinidad*, 1982, **39**, 377.
9. M. de la Guardia and M. T. Vidal, *Talanta*, 1984, **31**, 799.
10. H. Kornahrens, K. D. Cook and D. W. Armstrong, *Anal. Chem.*, 1982, **54**, 1352.
11. J. A. Borowiec, A. W. Boorn, J. H. Dillard, M. S. Cresser, R. F. Browner and M. J. Matteson, *Anal. Chem.*, 1980 **52**, 1054.
12. M. de la Guardia and M. T. Vidal, *Atom. Spectrosc.*, 1983, **4**, 39.

SEPARATION OF TRACE AMOUNTS OF INDIUM, GALLIUM AND ALUMINIUM FROM EACH OTHER BY CATION-EXCHANGE CHROMATOGRAPHY ON AG50W-X4 RESIN

FRANZ W. E. STRELOW*

National Chemical Research Laboratory, Council for Scientific and Industrial Research, P.O. Box 395,
Pretoria 0001, Republic of South Africa

TJAART N. VAN DER WALT

Atomic Energy Corporation, Private Bag X256, Pretoria 0001, Republic of South Africa

(Received 4 February 1987. Accepted 28 March 1987)

Summary—Traces and minor amounts of indium, gallium and aluminium can be separated from gram amounts of thallium and from each other by cation-exchange chromatography on a column containing as little as 2 g of AG50W-X4, a cation-exchange resin with low cross-linking. An elution sequence of 0.1M HBr in 40% acetone [for Tl(III)], 0.2M HBr in 80% acetone for In, 0.3M HCl in 90% acetone for Ga and 3M aqueous HCl for Al is used. The separations are very sharp and even 10- μ g amounts of In, Ga and Al in synthetic mixtures are recovered quantitatively, with a standard deviation of 0.3 μ g. The separation factors between neighbouring ions are extremely large (>5000).

The trivalent ions of the group IIIA elements Al, Ga, In and Tl form anionic complexes with chloride and bromide which increase markedly in stability with increase in atomic weight of the metal. The best current ion-exchange procedure using a single column for the sequential separation of all four elements, is based on this fact. It is a cation-exchange procedure which employs the sequence 0.1M hydrochloric acid in 50% aqueous acetone, 0.5M hydrochloric acid in 50% aqueous acetone, 2.0M hydrochloric acid in 70:30 v/v acetone-water mixture and 3.0M aqueous hydrochloric acid for the elution of Tl, In, Ga and Al, respectively.¹ The separations are quite sharp and recoveries quantitative for 1–100 mg amounts of all four elements.

However, the method has the disadvantage that it uses rather large columns because aluminium is not very strongly retained from the reagent selected for the elution of gallium ($D_{Al} = 75$) and, with small columns, an early breakthrough can be expected for large amounts of aluminium. From 0.5M hydrochloric acid in 90% acetone medium aluminium is retained much more strongly ($D_{Al} = 1250$), but gallium shows a significant amount of tailing when an 8% cross-linked resin is used. Furthermore, special treatment is required for the gallium eluate when accurate results are required, because a small percentage of gallium is lost during evaporation of the eluates containing large concentrations of hydrochloric acid and acetone.¹

For separating trace amounts of indium, gallium and aluminium from gram amounts of thallium it would be preferable to use small columns. It has been

shown that by use of a resin of lower cross-linkage, tailing can be diminished quite significantly or even completely eliminated.^{2,5} Furthermore, the distribution coefficient of indium and the separation factor between indium and thallium (III) can be increased quite considerably by using hydrobromic acid-acetone mixtures instead of hydrochloric acid-acetone as eluting agents.⁶ In addition, the separation factor between indium and gallium can also be increased, according to published distribution coefficients.⁷ Based on these facts a new and improved separation procedure has been developed which can separate trace and also milligram amounts of Al, Ga and In from 2 g of thallium on a column containing only 2 g of AG50W-X4 resin.

EXPERIMENTAL

Reagents and apparatus

The reagents were analytical grade, and the distilled water was further purified by passage through an Elgastat demineralizer. Solutions containing 500 ppm of indium, gallium and aluminium in 0.1M nitric acid were prepared by appropriate dilution from more concentrated solutions which had been standardized by complexometric titration. Solutions containing lower concentrations of these elements were prepared by further dilution when required.

The resin was the AG50W-X4 sulphonated polystyrene cation-exchanger of 100–200 mesh particle size marketed by Bio-Rad Laboratories, Richmond, California. It was used in the hydrogen form. Borosilicate glass tubes (11.5 mm bore and 200 mm long) joined to a wider upper part (20 mm bore and 100 mm long) served as columns. The columns were fitted with a No. 1 porosity sintered-glass disc and a burette tap at the bottom, and a B19 ground-glass sleeve at the top to hold a dropping-funnel as a reservoir.

The columns were filled with a slurry of resin until the settled resin had a volume of 8.7 ml in water (\equiv 2.0 g of dry resin). The columns were cleaned by passage of 100 ml of

*To whom correspondence should be addressed.

Table 1. Relevant cation-exchange distribution coefficients

Species	0.10M HBr in 40% acetone	0.20M HBr in 80% acetone	0.30M HCl in 90% acetone	Aqueous 3.0M HCl
Tl(III)	0.3	0.3	<0.5	0.5
In	4400	1.1	<0.5	0.6
Ga	>10 ⁴	>10 ⁴	1.2	1.8
Al	>10 ⁴	>10 ⁴	>5000	3.2

4.0M hydrochloric acid and then equilibrated by passage of three 10-ml portions of 0.1M hydrobromic acid.

Atomic-absorption measurements were made with a Varian-Techtron AA-5 instrument. An automatic Aimer Central Fractionator was used to collect fractions for the preparation of elution curves.

Distribution coefficients

Portions of dry AG50W-X4 resin (2.500 g) were equilibrated for 24 hr in a mechanical shaker at 20° with 250 ml of a solution containing 0.67 mmole (2 meq) of the tervalent ions and the concentrations of acetone and hydrobromic or hydrochloric acid shown in Table 1. After equilibration the resin was separated from the aqueous phase by filtration with a short and wide glass column with a No. 1 porosity sintered-glass disc at the bottom. The resin was transferred into the columns and washed with demineralized water and the aqueous phase was retained. The sorbed ions were eluted with 3M hydrochloric acid and the eluate was collected. The amounts of elements in both phases were determined by suitable methods and distribution coefficients calculated from the analytical results. Relevant coefficients are shown in Table 1.

Separation of Tl(III)-In-Ga-Al

A mixture containing 2 g of Tl(III), 5 mg each of indium and gallium and 10 mg of aluminium in 100 ml of 0.1M hydrobromic acid (free acid) containing a small amount of bromine was prepared and passed through an equilibrated 2-g resin column as described above. The elements were washed onto the resin with small amounts of 0.10M hydrobromic acid containing 40% v/v acetone and thallium(III) was eluted with the same reagent, 100 ml in all being used. Indium was then eluted with 100 ml of 0.20M hydrobromic acid containing 80% v/v acetone, followed by gallium with 100 ml of 0.30M hydrochloric acid containing 90% v/v

acetone and finally aluminium with 100 ml of aqueous 3.0M hydrochloric acid. A flow-rate of 2.5 ± 0.5 ml/min was maintained, and 10-ml fractions were collected from the beginning of the sorption step, by an automatic fractionator. After removal of the acetone, the amounts of the elements in each fraction were determined by atomic-absorption spectrometry after suitable dilution. Standard conditions and the air-acetylene flame were used for thallium and indium. For gallium and aluminium the nitrous oxide-acetylene flame was used after addition of 2000 ppm of potassium as ionization suppressor. Scale expansion was used for very small amounts. The experimental elution curve is shown in Fig. 1.

Quantitative separations of synthetic mixtures

A series of columns containing 2 g (8.7 ml) of AG50W-X4 resin was prepared as described above. Amounts of 2.607 g of thalious nitrate ($\equiv 2.000$ g of thallium) were weighed out accurately in quadruplicate and appropriate volumes of standard solutions of indium, gallium and aluminium containing 5 mg of each of these elements were added, together with about 20 ml of concentrated hydrobromic acid and a few drops of bromine. The solutions were evaporated to dryness on the water-bath with occasional stirring, and the dry salts were dissolved in 10 ml of 1M hydrobromic acid plus about 60 ml of demineralized water. A few ml of bromine water were added to ensure that any thallium reduced was reoxidized to thallium(III), but a large excess of bromine (indicated by light yellow colour of solution) was avoided. After cooling, the volumes were adjusted to about 100 ml with demineralized water and the solutions passed through the ion-exchange columns. The elements were washed onto the columns quantitatively with a few small amounts of 0.10M hydrobromic acid containing 40% v/v acetone and thallium(III) was eluted with the same reagent (100 ml in total). The indium was eluted with 60 ml

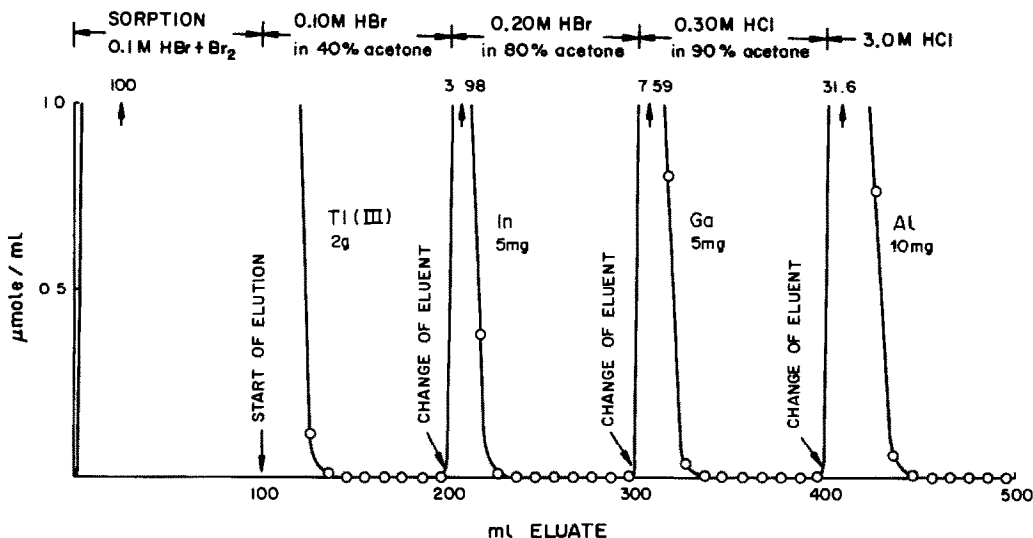


Fig. 1. Elution curve for Tl(III)-In-Ga-Al: 8.7 ml ($\equiv 2$ g) of G50W-X4 resin, 100-200 mesh (83×11.5 mm). Flow-rate 2.5 ± 0.5 ml/min.

Table 2. Results for quantitative separations of synthetic mixtures* from 2 g of thallium

Taken	Found		
	In	Ga	Al
In, Ga and Al			
5.00 mg of each	5.00 ± 0.01 mg	5.01 ± 0.02 mg	5.00 ± 0.01 mg
1000 µg of each	1000 ± 3 µg	999 ± 3 µg	999 ± 3 µg
100 µg of each	100 ± 1 µg	99 ± 2 µg	100 ± 2 µg
10 µg of each	10.0 ± 0.3 µg	9.8 ± 0.3 µg	10.0 ± 0.3 µg

*Averages of quadruplicate analyses.

of 0.2M hydrobromic acid containing 80% v/v acetone, gallium with 80 ml of 0.30 M hydrochloric acid containing 90% acetone and aluminium with 70 ml of 3.0M aqueous hydrochloric acid, at a flow-rate of 2.5 ml/min. The eluates containing the three minor components were kept separate, and after evaporation to dryness (after addition of 80 ml of demineralized water to the gallium fraction), the residues were dissolved in 5M nitric (In and Ga) or hydrochloric acid (Al) and the solutions made up to an appropriate volume with 0.5M acid. Triplicate amounts of the elements were measured out together with the mixtures but kept separate and used for comparison. The elements were determined by flame atomic-absorption spectrometry after suitable dilution. The air-acetylene flame and 303.9 nm line were used for the determination of indium and the nitrous oxide-acetylene flame and the 294.4 and 309.3 nm lines for the determination of gallium and aluminium, respectively. For the last two elements 2000 ppm of potassium was added as ionization suppressor, to samples and standards.

The separation procedure was repeated with 1000-µg, 100-µg and 10-µg amounts of indium, gallium and aluminium. In the case of the 100-µg amounts the final determinations were made on a volume of 10 ml, and considerable scale expansion had to be used for the 10-µg amounts.

RESULTS AND DISCUSSION

The results of the quantitative separations are presented in Table 2. The method described provides an excellent means for the quantitative separation of the group IIIA elements (from Al to Tl) in a single column run, and especially for the separation of traces or minor amounts of indium, gallium and aluminium from gram amounts of thallium. A column containing only 2 g of resin is required, instead of the 20-g resin column used previously.¹ This makes it possible to use considerably smaller elution volumes. Though only amounts of 2 g of thallium were separated in the work described above, the extremely large separation factors of the other elements from thallium (Table 1) suggest that the separation of even as much as 10 g of thallium on a 2-g resin column should present no problems. For trace amounts of the other elements even a 1-g resin column should be quite sufficient. The distribution coefficient for indium increases from 240 to 4400 when the 0.10M hydrochloric acid containing 50% v/v acetone used previously¹ is replaced by 0.10M hydrobromic acid containing 40% v/v acetone, and the separation factor for the thallium(III)-indium pair is enhanced from 480 to > 10⁴. Similarly, the separation factors of 390 and 150 for the indium-gallium and gallium-aluminium pairs are enhanced to values of > 10⁴ and > 5 × 10³, respectively. The use of a 4% cross-linked

resin makes it possible to elute gallium with considerably lower concentrations of hydrochloric acid because the tailing observed with the 8% cross-linked resin disappears almost completely. Because gallium can be eluted quantitatively with 80 ml of 0.30M hydrochloric acid containing 90% v/v acetone in the procedure described above, as compared with 300 ml of 2.0M hydrochloric acid containing 70% v/v acetone used previously,¹ the special step to separate gallium from excess of hydrochloric acid and acetone to avoid small losses (1-2%) of gallium becomes unnecessary. When 80 ml of demineralized water are added to the gallium fractions, direct evaporation can be used without any observable losses.

The separations are very sharp and the recoveries quantitative. Tailing is practically non-existent, even with a 100-200 mesh resin. This is demonstrated by the elution curve, which has been enlarged in the vertical scale to show the sharpness of the tail ends. After an elution volume of 30 ml the indium concentration in the eluate had disappeared below the detection limit of the atomic-absorption method (<0.05 ppm). For gallium and aluminium this happened with elution volumes of 50 and 40 ml, respectively. The larger elution volumes used for the quantitative separations include a considerable safety margin to ensure quantitative recovery.

Though this has not been investigated experimentally, there seems to be little doubt that the sequential separation scheme described can just as well be applied for separating trace or micro amounts of gallium and aluminium from gram amounts of indium by sorption from the hydrobromic acid-acetone mixture used for the elution of indium, or for the separation of traces of aluminium from gram amounts of gallium.

REFERENCES

1. F. W. E. Strelow and A. H. Victor, *Talanta*, 1972, 19, 1019.
2. F. W. E. Strelow, *ibid.*, 1980, 27, 727.
3. A. H. Victor and F. W. E. Strelow, *Anal. Chim. Acta*, 1982, 138, 285.
4. F. W. E. Strelow and T. N. van der Walt, *S. Afr. J. Chem.*, 1984, 37, 149.
5. T. N. van der Walt, F. W. E. Strelow and R. Verheij, *Solvent Extr. Ion Exchange*, 1985, 3, 723.
6. F. W. E. Strelow, C. H. S. W. Weinert and M. D. Boshoff, *S. Afr. J. Chem.*, 1973, 26, 118.
7. F. W. E. Strelow, M. D. Hanekom, A. H. Victor and C. Eloff, *Anal. Chim. Acta*, 1975, 76, 377.

EVALUATION OF VOLUME AND MATRIX EFFECTS FOR THE GENERALIZED STANDARD ADDITION METHOD

JOHN H. KALIVAS

Department of Chemistry, Idaho State University, Pocatello, ID 83209, U.S.A.

(Received 20 February 1987. Revised 20 June 1987. Accepted 2 July 1987)

Summary—A volume-dependent problem in use of the generalized standard addition method (GSAM) is evaluated. It is shown both mathematically and experimentally how to correct the deficiency. The revised GSAM was applied with direct current plasma spectroscopy in the presence of a salt and an acetone matrix effect.

Interferences are a common and severe problem that may render a chemical analysis invalid. In general, interferences are classified as physical, chemical and spectral. Physical interferences are caused by the effects of physical properties of the sample solution on physical processes involved in the analytical measurements. The viscosity, surface tension, and vapour pressure of the sample solution are physical properties that commonly cause interferences in atomic absorption (AA) and atomic emission (AE).¹⁻⁴ For AA and AE, the signal intensity can be enhanced by any change in a physical property that will increase the sample uptake rate.^{1-3,5} Organic solvents are often used in this way to achieve improved sensitivity.⁵ Similarly, the signal intensity can be depressed by a physical change that decreases the uptake rate.⁴⁻¹⁰ For AA and AE, many applications require acid dissolution of samples.^{9,10} A difference in acidity between samples and standards can result in a viscosity effect and change the sensitivity of the analysis. Chemical interferences are those chemical interactions between the analyte and other substances present in the sample solution that can influence the analyte signal. A common example in AA and AE is the effect of an easily ionizable concomitant element,^{5,9-13} which can cause signal enhancement by suppression of ionization of the analyte. When the amount of an easily ionizable element is known or varies between samples, the degree of enhancement can vary. Another example is the formation of a thermally stable compound, as shown by the effect of phosphate on the AA or AE signal for calcium.⁶⁻⁸ These problems can be dealt with by the deliberate addition of ionization buffers or releasing agents to swamp the chemical interactions. Spectral interferences are those which arise when a sensor is not completely specific for the analyte, and are quite common in most spectroscopic methods of analysis.

Physical and chemical effects can be combined and identified as sample matrix effects. Interferences can

therefore be considered to have two components: spectral and sample matrix effects. Spectral interferences cause a parallel shift in a calibration curve, whereas sample matrix effects change the slope. Thompson *et al.*¹⁴ called these effects translational and rotational respectively.

The standard addition method (SAM)^{15,16} can be used to correct for sample matrix effects. Bader¹⁵ has investigated various types of the SAM. The first type of interest is that in which increasing amounts of standard are added to aliquots of the sample and the mixtures are diluted to the same total volume (method 1). In the second type, the spikes are added to sample aliquots, without dilution, so the total volume increases (method 2); the responses are then multiplied by the ratio of total to initial volume to correct for dilution. Unfortunately, in method 2 the matrix concentration is decreased by the spikes, creating a non-linear sample matrix effect which may or may not be transformed into a linear effect by volume correction. Therefore, an important requirement for completely reliable use of the SAM is that all sample aliquots, unspiked and spiked, be diluted to a constant volume. This ensures that any sample matrix effects should be the same throughout,^{16,17} and in effect a calibration graph is prepared with *exact* matrix-matching of the sample and standards. Other requirements are that the response for the analyte should be zero when its concentration is zero, the response is a linear function of the concentration of analyte, and the sample matrix effects are independent of the ratio of the analyte and matrix.¹⁸ Figure 1 shows how the SAM can be used to correct for matrix effects when the volume remains constant. The figure also shows that the SAM cannot be used when both spectral interferences and matrix effects are present.

Saxberg and Kowalski¹⁹ generalized the standard addition method (GSAM) to incorporate spectral interference corrections as well as matrix effects, and Lorber²⁰ revised it to an unbiased format. The

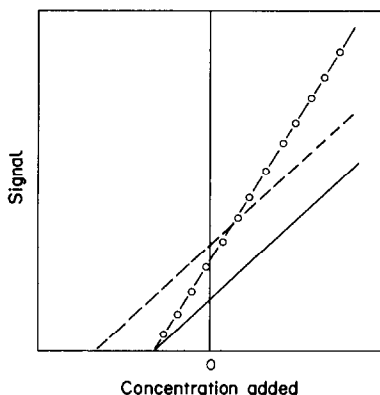


Fig. 1. Effect of spectral interference (---) and sample matrix effect (—○—) on the true SAM calibration graph (—).

GSAM has been applied to spectrophotometry,²¹⁻²⁴ inductively-coupled plasma atomic-emission spectrometry,^{25,26} flame photometry,²⁷ and stripping voltammetry.^{28,29} Accurate results were obtained because sample matrix effects were absent. The interferences present were of a spectral origin which can be volume-corrected. When matrix effects are non-linear functions of the matrix concentrations, it is especially important to keep the volume constant. This study will show the importance of maintaining constant volume in the GSAM to ensure equivalent matrix effects throughout. Recently, Araújo *et al.*²⁷ proposed a flow-injection analysis/GSAM procedure that would create standard additions with a constant degree of dilution holding sample matrix effects constant.

THEORY

For simplicity, single-component determination will serve as an example for the proposed method. Extension of the procedure to multicomponent analysis will be made after development of the single-component determination. A measured analytical signal at any sensor, r , is a function not only of the analyte concentration, c , but also of the overall sample matrix effect, M , and can be estimated as

$$r = ck + cM \quad (1)$$

where k is the sensitivity coefficient. The type and magnitude of M will dictate the final slope of the calibration graph. It is important to note that M is a function of volume. More specifically, equation (1) can be written as

$$r_0 = c_0 k + c_0 \frac{m}{v} \quad (2)$$

where r_0 is the initial response for a sample aliquot that has been diluted to a total volume v , c_0 is the initial concentration of the analyte at volume v , and M has been rewritten as m/v to represent the volume-dependency of the matrix effect. Because the volume will be held constant, m/v will not change during the

standard additions and can be incorporated into k to give

$$r_0 = c_0 k' \quad (3)$$

which is similar to the usual form of the SAM.^{16,17} After the s th standard addition of the analyte, equation (3) becomes

$$r_s = c_s k' \quad (4)$$

where c_s is the total analyte concentration after the s th addition. The change in response with change in concentration is given by

$$\Delta r_s = \Delta c_s k' \quad (5)$$

Therefore, when the volume is held constant the true form of the SAM is maintained and sample matrix effects are corrected.

However, when the volume is allowed to vary, the GSAM and SAM will not be acceptable. Volume-correcting the initial response (q_0) and the response (q_s) after the s th addition results in

$$q_0 \equiv v_0 r_0 = n_0 k + n_0 \frac{m}{v_0} \quad (6)$$

$$q_s \equiv v_s r_s = n_s k + n_s \frac{m}{v_s} \quad (7)$$

where n_0 is the initial absolute amount (*i.e.*, number of moles) of analyte, v_0 is the initial volume, v_s is the volume and n_s the total amount of analyte present after the s th spike. Equation (7) can be expanded to give

$$q_s = (n_0 + \Delta n_s)k + (n_0 + \Delta n_s) \frac{m}{v_s} \quad (8)$$

Again, considering the change in response results in

$$\Delta q_s = \Delta n_s k + \left(n_0 \frac{m}{v_s} - n_0 \frac{m}{v_0} \right) + \Delta n_s \frac{m}{v_s} \quad (9)$$

This equation shows that the matrix effect cannot be included in the sensitivity coefficient when the volume is allowed to vary. Therefore, the GSAM will not correct for matrix effects as claimed.^{19-24,27} When the volume is held constant, equation (9) reduces to equation (5) because m/v_s is equal to m/v_0 . The last term in equation (9) may then be incorporated into the first term, as was done in equation (3).

For multicomponent analysis, volume-correcting the response complicates the matter further. However, diluting to constant volume and expanding equation (2) for multicomponent analysis yields

$$r_{0,l} = \sum_{n=1}^l c_{0,n} k_{n,l} + \sum_{n=1}^l c_{0,n} M_n; \quad l = 1, \dots, p \quad (10)$$

where $r_{0,l}$ is the initial response of the l th sensor (of p sensors used), $c_{0,n}$ is the initial concentration of the n th component (of the l components present) and $k_{n,l}$ is the sensitivity coefficient of the l th sensor for the n th component. Since the volume is held constant,

equation (10) is reduced to

$$r_{0,l} = \sum_{n=1}^t c_{0,n} k'_{n,l} \quad (11)$$

Considering the change in response gives

$$\Delta r_{s,l} = \sum_{n=1}^t \Delta c_{s,n} k'_{n,l} \quad (12)$$

where $\Delta c_{s,n}$ is the amount of component n added in the s th standard addition. In matrix notation

$$\Delta \mathbf{R} = \Delta \mathbf{C} \mathbf{K} \quad (13)$$

where $\Delta \mathbf{R}$ is $s \times p$, $\Delta \mathbf{C}$ is $s \times t$ and \mathbf{K} is $t \times p$. This is analogous to Jochum *et al.*'s equation (10),²¹ with the volume held constant. The reader should refer to Jochum *et al.*²¹ for the solution to the calibration matrix \mathbf{K} of sensitivity coefficients to obtain the individual component concentrations.

If a chemical species simultaneously causes a chemical interference and a spectral interference, the model of the GSAM just given is not applicable. A quadratic model for the GSAM with interaction terms in the concentrations could be used.^{19,30,31} Volume corrections should not be used here either.

Common concerns in use of the SAM are the size and number of additions that should be made. Franke *et al.*³² and Ratzlaff³³ have concluded that a single addition of the largest amount possible can be used, provided the response is within the linear dynamic range. Ratzlaff noted that too large an addition may change the matrix effect, thereby altering the slope.

EXPERIMENTAL

Apparatus and computation

A Beckman SpectraSpan VI Direct Current Plasma (DCP) Spectrometer was used for all measurements. The DCP is equipped with a SpectraJet III electrode system and a cross-flow nebulizer. Argon pressure to the electrodes was 50 psig and 25 psig to the nebulizer. Instrument control, data manipulation, storage, and graphics output were provided by a Data Spar Controller computer and commercial software. Measurement values were transferred to the Idaho State University HP-1000 computer for subsequent data analysis.

Reagents

Single-element stock solutions were prepared with metal nitrates of reagent grade and distilled demineralized water. Stock solutions were used to prepare standards for standard additions and test sample solutions. All stock solutions were approximately 1000 ppm. Reagent grade acetone and an approximately 5M solution of lithium chloride were used to produce a matrix effect. Wavelengths used for analysis were Zn 202.548 nm (ion), Ni 243.789 nm (ion) and Co 236.379 nm (ion). All dilutions were done with distilled demineralized water.

Procedures

Zn determination. Four test samples were prepared in 100-ml standard flasks, with 5.0, 12.5, 15.0 and 17.5 ml of the zinc stock solution and 20 ml of the lithium chloride stock solution, and dilution to volume. Four more test samples were similarly prepared, with 10 ml of acetone instead of the lithium chloride solution.

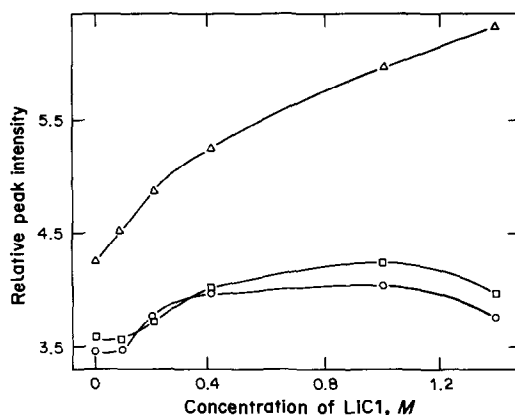


Fig. 2. Enhancement effect of LiCl on signal for 50-ppm Zn. Lines: 213.856 nm atomic (Δ), 202.548 nm ionic (\circ), 206.200 nm ionic (\square).

To investigate the effect of varying the volume a standard 150-ppm zinc solution was used for spiking. Four 10-ml test samples were prepared with a zinc concentration of 50.0 ppm in 1M lithium chloride medium. Standard additions of 3, 6 and 9 ml of the 150-ppm zinc stock solution were made. Four more samples were prepared in 10% v/v acetone medium instead of in 1M lithium chloride.

Zn, Ni and Co determinations. Ten test samples were prepared in 100-ml standard flasks with 5.0 ml of zinc solution, 2.0 ml each of the nickel and cobalt solution, and 10.0 ml of acetone. Additions of 7.5, 10.0 and 12.5 ml of zinc solution were made to three flasks, 3.5, 5.0 and 6.5 ml of nickel solution to another three flasks, and 3.5, 5.0 and 6.5 ml of cobalt solution to a further three flasks. All solutions were then diluted to volume.

RESULTS AND DISCUSSION

Previous investigations have suggested that the presence of easily ionizable elements in the sample solution can cause emission-line enhancement in a DCP.^{11,12} Line enhancement has been shown to occur for both singly ionized and neutral atoms of the same element.^{12,34} Figure 2 shows the enhancement effect on a zinc atom line and two zinc ion lines. The enhancement is not due to a background shift. This is verified by the spectral scan of the Zn 213.856 nm line (50 ppm zinc) shown in Fig. 3. If a background shift was present, GSAM would not evaluate the results correctly. Responses must be background-corrected for the GSAM. The enhancement is attributed to a chemical process which is not the concern of this paper.

Table 1 lists the estimated recovery values for zinc in the 1M lithium chloride and 10% acetone sample matrices. With either chemical or physical interference, acceptable results are obtained only when the volume is held constant, as predicted from the equations given above. The large error with the lithium chloride matrix is due to dilution of the sample matrix by successive additions. The volumes used here are similar in magnitude to those used in previous GSAM applications.²¹⁻²⁵ The incremental changes in the volume-corrected responses for each

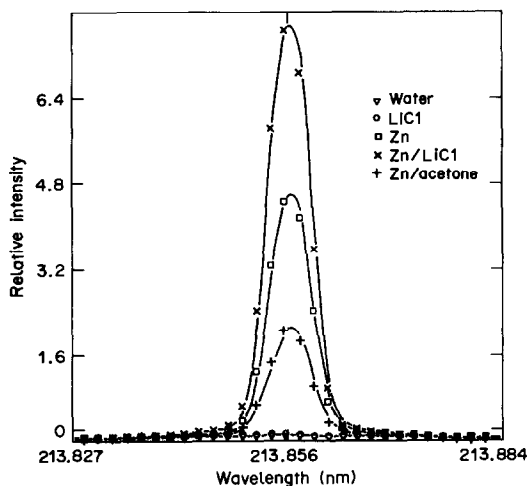


Fig. 3. Spectral scans for the Zn 213.856 nm line. Concentrations were LiCl 2M, Zn 50 ppm, and acetone 10% v/v.

addition are shown in Table 2. If dilution is not a problem, the volume-corrected responses should be equal within experimental error. The volume corrected responses are seen to be slightly decreasing. This stems from the fact that the lithium chloride concentration levels used yield responses which are located on a relatively flat portion of the matrix effect curve, as shown in Fig. 2.

In contrast, 10% acetone causes a depression in the intensity of the zinc line as shown in Figs. 3 and 4. Dilution of the acetone sample matrix with each addition results in a continual increase in the incremental changes of the volume-corrected responses listed in Table 2. Thus, for a simple one-component determination the volume must be held constant for acceptable results to be obtained. Table 3 lists the

Table 1. Results of determination of 50.0 ppm zinc in LiCl and acetone matrices with $\Delta v = 0$ and $\Delta v \neq 0$

Matrix	Zinc found, ppm	Relative error, %
LiCl		
$\Delta v = 0$	52.0	4
$\Delta v \neq 0$	58.5	17
Acetone		
$\Delta v = 0$	51.6	3
$\Delta v \neq 0$	35.6	28

*Relative error = 100 ((true - calcd.)/true).

Table 2. Incremental volume-corrected response changes for zinc in LiCl and acetone matrices

Matrix	Δq^*	Addition
LiCl	342	1
	295	2
	297	3
Acetone	173	1
	201	2
	217	3

*Arbitrary units.

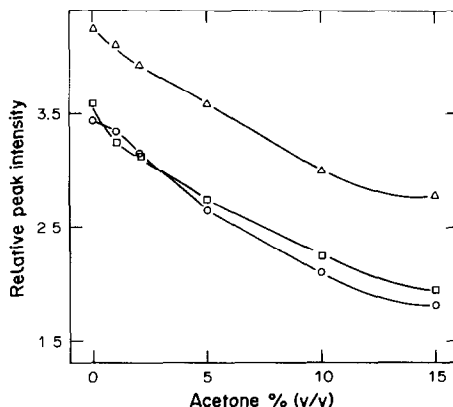


Fig. 4. Depressant effect of acetone on signal for 50-ppm Z. Lines: 213.856 nm atomic (Δ), 202.548 nm ionic (\circ), 206.200 nm ionic (\square).

results for the three-component solution in the presence of 10% acetone. Good estimates are obtained by using a constant-volume GSAM procedure.

The volume limitation of the GSAM could be reduced by using smaller volumes for the standard additions. This assumption will be valid for some matrix effects, depending on their magnitude. For instance, if only one standard addition of 3 ml is used for the zinc/lithium chloride system, the relative error is reduced to 8% from 17%. This is again due to the analysis system corresponding to the relatively flat portion of the matrix effect curve shown in Fig. 2. On the other hand, when a single 3-ml addition is used with the acetone matrix, the relative error is only reduced to 21% from 28%. Although, there is less matrix dilution with the smaller volume, it shifts the matrix effect to a more steeply rising part of the enhancement shown in Fig. 4. Thus, when the volume is allowed to vary, the size of the additions may directly affect the magnitude of the matrix effect. Because the types and magnitudes of matrix effects for a given sample are not always known, it is clearly advisable to use a constant-volume GSAM, which will correct for the interferences at all times.

In conclusion, simple volume-corrected responses cannot be used unless sample matrix effects are not present, or volume changes are negligible. If the sample cannot be subdivided because of the nature of the analysis, micropipettes which can reproducibly dispense volumes of 5 μ l or less can be used in conjunction with concentrated standards to make successive additions to the same solution with mini-

Table 3. Results of zinc, nickel and cobalt determination in acetone matrix with $\Delta v = 0$

Element	Taken, ppm	Found, ppm	Relative error, %
Zn	50.2	48.6	3
Ni	20.0	19.0	5
Co	20.1	19.4	4

mal effect on the matrix concentration (provided the sample volume is large enough, say > 5 ml). Moran and Kowalski³⁵ have suggested using standard additions of solid material, in order to keep the volume constant and minimize the variance of the analyte estimates.

Acknowledgements—The author is grateful to Bonnie Root for her preparation of this paper and Lorie Juhl for assistance with the experimental procedures, and would like to thank John Knutson and Don Hooper of Gould AMI for instrumental assistance.

REFERENCES

1. J. A. Dean and T. C. Rains (eds.), *Flame Emission and Atomic Absorption Spectrometry*, Vol. 1. Dekker, New York, 1969.
2. *Idem*, *op. cit.*, Vol. 2. Dekker, New York, 1971.
3. G. F. Kirkbright and M. Sargent, *Atomic Absorption and Fluorescence Spectroscopy*, Academic Press, New York, 1974.
4. R. K. Skogerboe and S. J. Freeland, *Appl. Spectrosc.*, 1985, **39**, 925.
5. G. D. Christian, *Analytical Chemistry*, 4th Ed., Wiley, New York, 1986.
6. C. Monder and N. Sells, *Anal. Biochem.*, 1967, **20**, 215.
7. W. F. Ulrich and J. Ramirez-Muñoz, *Am. Soc. Test. Mater., Spec. Tech. Publ.*, 1969, No. 443, 90.
8. R. E. Dickson and C. M. Johnson, *Appl. Spectrosc.*, 1966, **20**, 214.
9. E. E. Angino and G. K. Billings, *Atomic Absorption Spectrometry in Geology*, 2nd Ed., Elsevier, New York, 1972.
10. W. B. Barnett, *Anal. Chem.*, 1972, **44**, 695.
11. D. D. Nygaard and T. R. Gilbert, *Appl. Spectrosc.*, 1981, **35**, 52.
12. D. D. Nygaard, *Anal. Chem.*, 1979, **51**, 881.
13. D. D. Nygaard and D. A. Leighty, *Appl. Spectrosc.*, 1985, **39**, 353.
14. M. Thompson, S. J. Walton and S. J. Wood, *Analyst*, 1979, **104**, 299.
15. M. Bader, *J. Chem. Educ.*, 1980, **57**, 703.
16. M. J. Cardone, *J. Assoc. Off. Anal. Chem.* 1983, **66**, 1257.
17. D. A. Skoog and D. M. West, *Fundamentals of Analytical Chemistry*, 4th Ed., p. 590. Saunders College Publishing, New York, 1982.
18. L. Pszonicki, *Talanta*, 1977, **24**, 613.
19. B. E. Saxberg and B. R. Kowalski, *Anal. Chem.*, 1979, **51**, 1031.
20. A. Lorber, *ibid.*, 1985, **57**, 952.
21. C. Jochum, P. Jochum and B. R. Kowalski, *ibid.*, 1981, **53**, 85.
22. M. Raymond, C. Jochum and B. R. Kowalski, *J. Chem. Educ.*, 1983, **60**, 1072.
23. B. Vandeginste, J. Klaessens and G. Kateman, *Anal. Chim. Acta*, 1983, **150**, 71.
24. J. H. Kalivas and B. R. Kowalski, *Anal. Chem.*, 1983, **55**, 532.
25. *Idem*, *ibid.*, 1981, **53**, 2207.
26. E. A. G. Zagatto, A. O. Jacintho, F. J. Krug, B. F. Reis, R. E. Bruns and M. C. V. Araújo, *Anal. Chim. Acta*, 1983, **145**, 169.
27. M. C. V. Araújo, C. Pasquini, R. E. Bruns and E. A. G. Zagatto, *ibid.*, 1985, **171**, 337.
28. R. W. Gerlach and B. R. Kowalski, *ibid.*, 1982, **134**, 119.
29. B. Høyer and L. Kryger, *ibid.*, 1985, **167**, 11.
30. P. Kościelniak and A. Parczewski, *Mikrochim. Acta*, 1984 **II**, 359.
31. P. Kościelniak, *ibid.*, 1984 **II**, 369.
32. J. P. Franke, R. A. deZeeuw and R. Hakkert, *Anal. Chem.*, 1978, **50**, 1374.
33. K. L. Ratzlaff, *ibid.*, 1979, **51**, 232.
34. H. L. Felkel, Jr. and H. L. Pardue, *ibid.*, 1978, **50**, 602.
35. M. G. Moran and B. R. Kowalski, *ibid.*, 1984, **56**, 562.

SPECTROPHOTOMETRIC DETERMINATION OF CHLORIDE IN Pt-Al₂O₃/SiO₂ CATALYSTS WITH Hg(SCN)₂-Fe³⁺ REAGENT*

V. J. KOSHY and V. N. GARG†

Research Centre, Indian Petrochemicals Corporation Limited, P.O. Petrochemicals,
Baroda-391 346, India

(Received 25 April 1985. Revised 4 June 1987. Accepted 20 June 1987)

Summary—A method is described for the determination of chloride in Pt-Al₂O₃/SiO₂ catalysts, based on its extraction with alkali followed by reaction with Hg(SCN)₂-Fe³⁺ reagent and spectrophotometric measurement at 460 nm. Beer's law is obeyed in the concentration range 5-75 µg of chloride in 25 ml of aqueous solution. The molar absorptivity is 1.99×10^3 l.mole⁻¹.cm⁻¹. The rapid colour development, excellent reproducibility and absence of interference from the species most often present in the catalysts are the advantages of the method.

The Pt-Al₂O₃ reforming catalysts mostly contain platinum/sulphide species¹ along with traces of metallic precursors, finely dispersed on highly stable chlorinated alumina.² The chlorinated alumina provides an acidic function, and control of the chloride content of the catalyst is of major importance.^{3,4} It is observed⁵ that chloride is slowly leached out of the catalysts by traces of moisture present in the process feed. Deactivation of the catalyst occurs as a result of chloride-water imbalance.^{6,7} This causes problems in industrial reforming units.^{6,7} Determination of chloride in these catalysts is therefore very important in order to (1) quantify the maximum chloride level for optimum process efficiency, (2) measure the decrease in chloride content as a function of traces of moisture, and (3) assess the degree of catalyst deactivation and selectivity as a function of the chloride present.

The most popular procedure^{8,9} for determining traces of chloride is based on spectrophotometric measurement of the colour produced by interaction of Cl⁻ with an Hg(SCN)₂-Fe³⁺ mixture. The method has been applied for determining chloride in high-purity water,¹⁰ boiler water,¹¹ biological material,¹² uranium,¹³ cement stone,¹⁴ sea-water¹⁵ and naphtha¹⁶ but not so far for determining chloride in catalysts. The purpose of the present work was to assess its utility for catalyst analysis.

EXPERIMENTAL

Apparatus

Absorbance measurements were made with a Varian Superscan-3 spectrophotometer with matched 1-cm silica cells. The instrument was calibrated for photometric linearity with a series of potassium chromate solutions. The wavelength calibration was checked with a holmium oxide filter as standard.

Flame atomic-absorption measurements were made with a Varian Techtron Model 1200 spectrophotometer. The following operating conditions were used:

Lamp current	3 mA
Flame	air-acetylene
Wavelength	328.1 nm
Spectral band-pass	0.2 nm
Optimum working range	2-10 µg/ml

Reagents

Doubly distilled water and analytical reagent grade acids and salts were used throughout unless otherwise stated.

Sodium chloride solution, 1000 µg/ml. Weigh 0.412 g of sodium chloride (dried at 110° under vacuum) to the nearest mg, dissolve it in water and dilute to volume in a 250-ml standard flask. Prepare working solutions by dilution of this solution with water.

Mercuric thiocyanate solution. Dissolve 1.5 g of mercuric thiocyanate in 250 ml of methanol by stirring for 30 min at 40°, and store in an amber-coloured bottle.

Ferric ammonium sulphate solution. Dissolve 5.0 g of ferrous ammonium sulphate in 30 ml of water, add 38 ml of concentrated nitric acid with low chloride content (0.00005%) and boil the solution for half an hour. Transfer the solution into a 100-ml standard flask and dilute to the mark with water.

Silver nitrate solution, 0.01M. Dissolve 1.699 g of silver nitrate (previously dried at 100°) in 1000 ml of water.

Sodium sulphide solution, ~4 mg/ml. Dissolve 3.0 g of sodium sulphide monohydrate in 100 ml of water. Standardize the solution with standard iodine and thiosulphate solutions before dilution or use. Dilute the solution as and when required.

Spectrophotometric determination of chloride in presence of sulphide

Pipette a portion of sample containing up to 75 µg of chloride and 500 µg of sulphide into a 100-ml conical flask. Add 5 ml of 2M sodium hydroxide and 5 ml of 30% hydrogen peroxide solution. Boil the solution for 5 min, and then evaporate it to 5 ml. Transfer the solution into a 25-ml standard flask. Add 2 ml of mercuric thiocyanate solution and 5 ml of ferric ammonium sulphate solution, and dilute to the mark with water. After at least 10 but not more than 30 min, measure the absorbance at 460 nm against a similarly treated blank.

*I.P.C.L. Communication No. 104.

†Author to whom correspondence should be addressed

Prepare a calibration graph by treating standards containing 5–75 μg of chloride by the procedure described.

Spectrophotometric determination of chloride in catalysts

Weigh 0.2 g of catalyst to the nearest 0.1 mg into a 100-ml round-bottomed flask. Add 5 ml of 30% hydrogen peroxide solution and 20 ml of 1M sodium hydroxide. Digest the mixture under reflux for 30 min. Cool and filter through a fluted filter paper (Whatman No. 41) into a 100-ml standard flask. Digest the residue with 10 ml of 1M sodium hydroxide and filter into the same flask; repeat this step, then dilute to the mark with water. Pipette 3 ml of the solution into a 25-ml standard flask, add 2 ml of mercuric thiocyanate solution and 5 ml of ferric ammonium sulphate solution, dilute to the mark with water, and measure the absorbance at 460 nm after 30 min, against a similarly treated blank.

Determination of chloride by atomic absorption

Take 20 ml of the 100-ml catalyst digest (prepared as above) in a 100-ml beaker and adjust the pH to about 2.5 with concentrated nitric acid. To do this, find the volume of acid needed to adjust the pH of another 20-ml aliquot, using narrow range pH paper (pH 2.0–4.5) for testing the pH, and add the same volume of acid to the test sample. Add exactly 2 ml of 0.01M silver nitrate and 10 ml of acetone–water mixture (1:3 v/v). Heat on a steam-bath for 30 min. Cool and filter off the precipitate on a Whatman No. 42 paper. Wash the precipitate four times with dilute nitric acid (1 + 5), collecting the filtrate and washings in a 50-ml standard flask, and dilute to the mark with water. Measure the amount of silver in this solution by flame AAS under the experimental conditions given above. Calculate the chloride content of the digest. Prepare a calibration graph by taking 20-ml aliquots of standard solutions containing 2–10 $\mu\text{g}/\text{ml}$ chloride through the procedure.

RESULTS AND DISCUSSION

Analytical characteristics of the spectrophotometric method

The apparent molar absorptivity for chloride was calculated to be $1.99 \times 10^3 \text{ l. mole}^{-1} \cdot \text{cm}^{-1}$ at 460 nm. The calibration graph was linear from 0.2 to 3.0 μg of chloride per ml of final aqueous solution. The lower detection limit for chloride was $0.04 \pm 0.02 \mu\text{g}/\text{ml}$ in the final solution, which is good enough for the determination of chloride in catalysts. The precision of the procedure, expressed as the relative standard deviation (RSD) for 10 independent determinations of 0.6 $\mu\text{g}/\text{ml}$ chloride in the final solution was found to be 1.5%.

Effect of diverse ions

This spectrophotometric method is prone to interference from both cations and anions since there are many species⁹ which (a) yield insoluble sulphides and/or thiocyanates, e.g., lead, copper, antimony(III), silver, mercury(I), (b) form complexes with thiocyanate ions, e.g., mercury(II), cadmium, zinc, antimony(III), (c) give coloured solutions, e.g., copper, bismuth, molybdenum (yellow or orange), ruthenium (pink), iridium (pink), osmium (blue), (d) form complexes with ferric ions in acid solution, e.g., fluoride, metaphosphate, oxalate.

In the Pt–Al₂O₃/SiO₂ reforming/isomerization catalysts, in addition to platinum and other species

such as PtS and chloride, certain metal additives (so-called promoters^{2,17}) are also incorporated at trace levels to increase the activity and selectivity. These are rhodium, rhenium, rubidium, ruthenium, iridium, antimony, copper, molybdenum, calcium, vanadium, nickel *etc.* The recommended procedure was used to study the interference of these ions and others most often present in the catalysts, in analysis of aqueous solutions containing 2 $\mu\text{g}/\text{ml}$ chloride. A concentration that did not cause more than 0.001 change in absorbance was taken as the tolerance limit. The values found for several species are shown in Table 1.

The major interference is from sulphide and is caused by precipitation of mercuric sulphide. Yamamoto *et al.*¹⁸ mentioned such interference in the Hg(SCN)₂–Fe³⁺/1,10-phenanthroline system in nitrobenzene. We did not expect this interference because the digestion with alkali should not decompose PtS. However, traces of sulphide were present in the alkaline extract from partially or completely deactivated catalysts. This may be attributed to partial accumulation of sulphur on the catalyst during processing of sulphur-containing feedstocks, as found by Menon and Prasad¹ during their studies on the role of sulphur in reforming reactions. On a deactivated catalyst sulphur seems to be present in two forms: (a) irreversibly chemisorbed PtS_(s) species formed during selective presulphiding; (b) reversibly sorbed sulphur present as PtS_(s)S_(r). This concept has been confirmed by Barbier,¹⁹ Parera *et al.*,²⁰ Guzzi *et al.*²¹ and Jossens and Peterson.²² It is very likely that this

Table 1. Interference levels of foreign ions in the spectrophotometric determination of 2.0 ppm chloride*

Species	Added as	Tolerance,* ppm
Sulphide	Na ₂ S · 9H ₂ O	0.3
Lithium	LiNO ₃	200
Potassium	KNO ₃	180
Lead	Pb(NO ₃) ₂	150
Cadmium	3CdSO ₄ · 8H ₂ O	15
Tin	Sn(SO ₄) ₂ · 2H ₂ O	30
Aluminium	Al(NO ₃) ₃ · 9H ₂ O	80
Cobalt	Co(NO ₃) ₂ · 6H ₂ O	7
Manganese	Mn(NO ₃) ₂ · 4H ₂ O	13
Zinc	Zn(NO ₃) ₂ · 4H ₂ O	100
Nickel	Ni(NO ₃) ₂ · 6H ₂ O	60
Calcium	Ca(NO ₃) ₂ · 4H ₂ O	7
Barium	Ba(NO ₃) ₂	12
Magnesium	Mg(SO ₄) ₂ · 7H ₂ O	40
Rhenium	Re ₂ O ₇ †	17
Rhodium	Rh(NO ₃) ₃ · 2H ₂ O	12
Rubidium	RbNO ₃	16
Iridium	Ir ₂ (SO ₄) ₃ · 4H ₂ O	6
Osmium	Os metal†	8
Vanadium	VOSO ₄ · 5H ₂ O	30
Bismuth	Bi(NO ₃) ₃ · 5H ₂ O	6
Silicate	Na ₂ SiO ₃ · 5H ₂ O	60
Copper	CuSO ₄ · 5H ₂ O	70
Molybdate	(NH ₄) ₆ Mo ₇ O ₂₄ · 4H ₂ O	0.8
Phosphate	Na ₃ PO ₄ · 12H ₂ O	70

*In the final solution.

†Dissolved in HNO₃.

Table 2. Determination of chloride in presence of sulphide in synthetic solution*

Sulphide present, μg	Chloride added, μg	Absorbance at 460 nm \dagger	Chloride found, μg
100	5.0	0.012 ± 0.001	5 ± 0.5
	30.0	0.071 ± 0.002	30 ± 1
	60.0	0.144 ± 0.001	61 ± 0.5
250	5.0	0.012 ± 0.001	5 ± 0.5
	30.0	0.071 ± 0.001	30 ± 0.5
	60.0	0.143 ± 0.001	60 ± 0.5
500	5.0	0.011 ± 0.002	4.5 ± 1.0
	30.0	0.071 ± 0.000	30 ± 0.0
	60.0	0.143 ± 0.001	60 ± 0.5

*In 25 ml of final solution.

 \dagger Average and range for three determinations.

reversibly sorbed sulphur is leached out during the extraction with alkali in the work described here.

In any case it was necessary to study the interference from sulphide and work out a possible way to eliminate it. An attempt was made to oxidize sulphide to sulphate with alkaline hydrogen peroxide. Synthetic solutions containing 5–60 μg of chloride and various amounts of sulphide (100–500 μg) were prepared and the chloride was determined. The results are summarized in Table 2.

The interference due to aluminium and silicate is interesting. These ions were found to impart red and pale yellow colours, respectively, and thus affect the absorbance of the iron(III) thiocyanate complex. It is difficult to see why such colour reactions should occur, and it seems likely that the interference was due to the presence of trace impurity of chloride (or bromide or iodide) in the aluminium nitrate and sodium silicate used, which were able to develop the colour even in the absence of added chloride.

Chloride determination in catalysts

On the basis of the observations above, attempts were made to determine chloride in three types of Pt–Al₂O₃/SiO₂ catalyst, *viz.* fresh, deactivated and regenerated. The catalysts are available in the extruded form and are heterogeneous in nature, so care was taken to ensure proper sampling. The procedure used was successive division of 100 g of catalyst down to a mass of approximately 10 g. This sample was then ground to a fine powder in a high-speed agate

ball-mill to provide a homogeneous representative sample for analysis. The chloride was extracted with various alkaline solutions, *e.g.*, ammonia or sodium hydroxide solutions having concentrations ranging from 0.1 to 6.0M. Extraction was very poor in the case of ammonia. It was not quantitative in 0.6M sodium hydroxide, but improved steadily as the sodium hydroxide concentration increased and was quantitative with a 1.0M solution. The chloride values obtained for various catalyst samples by this method are given in Table 3. For each sample the complete procedure, starting from extraction, was repeated five times and the absorbance was measured in triplicate. The standard deviation of the absorbances was about 0.002, which is quite satisfactory.

Since no standard catalyst sample with certified chloride value was available, a series of recovery experiments was performed. Initially, attempts were made to incorporate known amounts of chloride in catalyst samples by impregnation, but were unsuccessful. It was difficult to achieve the desired final level of chloride by addition of known amounts hydrochloric acid during the impregnation. Generally, the chloride in a calcined alumina-supported catalyst is incorporated^{23–26} in the impregnation step by means of chloroplatinic acid and hydrochloric acid, which is used to control the metal deposition. The impregnation depends upon many factors, for instance the number of hydroxyl groups present (which changes with the temperature of calcination), the time and temperature of impregnation, and concentration of chloride in solution.^{23–26} Most of this information is patented. The usefulness of the method was then corroborated by a recovery study involving the addition of standard chloride solution to an analysed catalyst sample and its analysis by the procedure described. The recoveries obtained are given in Table 4. In view of the low absorbances, and the resultant error in obtaining recovery values by difference, the results are acceptable.

Besides the recovery experiments, a correlation programme was also applied to the same catalyst samples by using an indirect flame AAS method.²⁷ The chloride was precipitated with a definite amount of silver nitrate solution in water–acetone media and the unconsumed silver nitrate was determined by AAS. Acceptable agreement was observed between

Table 3. Determination of chloride in some catalysts

Catalyst	Chloride found, * %	
	Proposed method	AAS
A Fresh Pt/Al ₂ O ₃ ·SiO ₂	0.42 ± 0.00	0.43 ± 0.02
B Deactivated Pt/Al ₂ O ₃ ·SiO ₂	0.35 ± 0.01	0.34 ± 0.02
C Regenerated Pt/Al ₂ O ₃ ·SiO ₂	0.44 ± 0.02	0.41 ± 0.03
D Fresh Pt/Al ₂ O ₃	0.69 ± 0.02	0.71 ± 0.02
E Fresh Pt–Re/Al ₂ O ₃	0.74 ± 0.02	0.72 ± 0.03
F Deactivated Pt–Re/Al ₂ O ₃	0.48 ± 0.01	0.48 ± 0.03
G Fresh Pt/zeolite	0.38 ± 0.01	0.40 ± 0.02
H Deactivated Pt/zeolite	0.26 ± 0.01	0.25 ± 0.04

*Average \pm standard deviations for 5 sets (3 aliquots analysed per set).

Table 4. Recovery of chloride added to catalyst sample solutions

Catalyst	Chloride found in solution, μg	Chloride added, μg	Total chloride found, μg	Recovery of added chloride, μg
A	27.5	10	39	11.5
		20	49.5	22
		30	58.5	31
B	21	10	31	10
		20	42.5	21.5
		30	52	31
C	25.5	10	35	9.5
		20	45	19.5
		30	54.5	29
D	42.5	10	54.5	12
		20	62	19.5
		30	73.5	31
E	45	10	56	11
		20	65	20
		30	75	30
F	28.5	10	40	11.5
		20	50	21.5
		30	58.5	30
G	23	10	31.5	8.5
		20	43	20
		30	54	31
H	16	10	26.5	10.5
		20	37	21
		30	46.5	30.5

the results obtained by the two techniques (AAS and spectrophotometry). Undoubtedly, the latter method is faster and simpler than AAS, which cannot be adopted in routine use.

The accuracy of the extraction of chloride from catalysts with alkali could not be properly assessed by adding known amounts of inorganic analyte to untreated catalyst samples. However, it is certain that if the extractions were not reproducible, the final results for the chloride content would have shown very high standard deviations. Hence we presume that the extraction of chloride present in the catalyst is either quantitative or fractional but highly reproducible.

Acknowledgements—We thank the Management of IPCL for their keen interest in this work and kind permission to publish this work. We also thank Mr. H. K. Taviyad and Mr. A. R. Shah for their technical assistance in various phases of this work. The critical comments and suggestions of Dr. R. A. Chalmers are gratefully acknowledged.

REFERENCES

- P. G. Menon and J. Prasad, *Proc. 6th International Cong. on Catalysts*, London, 1976, Vol. 2, 1061.
- J. H. Sinfelt, in *Catalysis, Science and Technology*, J. R. Anderson and M. Boudart (eds.), Vol. 1, p. 256. Springer-Verlag, Heidelberg, 1981.
- N. S. Figoli, M. R. Sad, J. N. Beltramini, E. L. Jablonski and J. M. Parera, *Ind. Eng. Chem. Prod. Res. Dev.*, 1980, **19**, 545.
- R. J. Verderoane, C. L. Pieck, M. R. Sad and J. M. Parera, *Appl. Catalysis*, 1986, **21**, 239.
- O. Svajji, *Int. Chem. Eng.*, 1972, **12**, 55.
- Nat. Petr. Ref. Assoc., Question and Answer Session, *Oil Gas J.*, 1966, 30 April 250.
- Idem*, *ibid.*, 1966, 15 August 88.
- D. M. Zall, D. Fisher and M. Q. Garner, *Anal. Chem.*, 1956, **28**, 1665.
- D. F. Boltz, W. J. Holland and J. A. Howell, in *Colorimetric Determination of Non-metals*, D. Boltz and J. A. Howell (eds.), p. 83. Wiley, New York, 1978.
- R. D. Rodabaugh and G. T. Upperman, *Anal. Chim. Acta*, 1972, **60**, 434.
- T. M. Florence and Y. J. Farrar, *ibid.*, 1971, **54**, 373.
- V. Kulhanek and C. Fiser, *Collection Czech. Chem. Commun.*, 1966, **31**, 1890.
- Chi-Fen Chu and Shaw-shii Wu, *J. Chin. Chem. Soc.*, 1974, **21**, 223; *Chem. Abstr.*, 1975, **82**, 105940c.
- V. G. Dragan, Z. G. Aboimova and V. M. Kravstov, *Sb. Tr. Nauchno-Issled. Inst. Prom. Stroit. Ufa*, 1974, **14**, 163; *Chem. Abstr.*, 1976, **84**, 139896z.
- T. Kanou and S. Sugito, *Nippon Kaisui Gakkai-Shi*, 1977, **31**, 179; *Chem. Abstr.*, 1978, **89**, 225635y.
- A. B. Carel and M. J. Whitaker, *Oil Gas J.*, 1982, **80**, No. 10, 269.
- Handbook of Catalyst Manufacture—Chemical Technology Review*, W. Sittig (ed.), No. 98, Noyes Data Corporation, New York, 1978.
- Y. Yamamoto, T. Kumamaru, A. Tatehata and N. Yamada, *Anal. Chim. Acta*, 1970, **50**, 433.
- J. Barbier, *Struct. Surf. Sci. Catal.*, 1982, **11**, 293; *J. Catal.*, 1982, **78**, 352.
- J. M. Parera, C. R. Apesteguia, J. F. Plaza de los Reyes and T. F. Garetto, *React. Kinet. Catal. Lett.*, 1980, **15**, 107; *Appl. Catal.*, 1981, **1**, 159; 1982, **4**, 5.
- Z. Schay, K. Matuzek and L. Guzzi, *Appl. Catal.*, 1984, **10**, 173.
- L. W. Jossens and E. E. Peterson, *J. Catal.*, 1982, **76**, 265.
- L. D. Sharma, P. K. Sinhamahapatra, H. R. Sharma, R. P. Mehrotra and G. Balamalliah, *ibid.*, 1977, **48**, 404.
- E. Santacesaria, D. Gelosa and S. Carra, *Ind. Eng. Chem. Prod. Res. Dev.*, 1977, **16**, 45.
- E. Santacesaria, S. Carra and I. Adami, *ibid.*, 1977, **16**, 41.
- A. A. Castro, O. A. Scelza, E. R. Benvenuto, G. T. Baronetti and J. M. Parera, *J. Catal.*, 1981, **69**, 222.
- M. Garcia-Vargas, M. Milla and J. A. Pérez-Bustamente, *Analyst*, 1983, **108**, 1417.

ULTRASENSITIVE AND SELECTIVE MEASUREMENTS OF TIN BY ADSORPTIVE STRIPPING VOLTAMMETRY OF THE TIN-TROPOLONE COMPLEX

JOSEPH WANG* and JAVAD ZADEBI

Department of Chemistry, New Mexico State University, Las Cruces, NM 88003, U.S.A.

(Received 24 April 1987. Accepted 20 June 1987)

Summary—Trace levels of tin can be determined by voltammetry after controlled adsorptive preconcentration of the tin-tropolone complex on a hanging mercury drop electrode. The resulting adsorptive stripping procedure offers better sensitivity and selectivity than conventional stripping methods for tin. Optimal conditions include $4 \times 10^{-6}M$ tropolone in a stirred acetate buffer (pH 4.0), a preconcentration potential of -0.40 V, and differential-pulse stripping. For an 8-min preconcentration period, the detection limit is $2.3 \times 10^{-10}M$ (28 ng/l.). Linear calibration plots of i_p vs. C are obtained at low concentrations, with linear plots of $1/i_p$ vs. $1/C$ at high concentrations. The relative standard deviation (at the $6\text{-}\mu\text{g/l.}$ level) is 2.6%. The response is not affected by the presence of lead, cadmium, indium and thallium, which commonly interfere severely in analogous anodic stripping measurements. Results are reported for river and orange-juice samples.

Considerable interest has developed in the determination of tin in environmental, biological or food samples. Depending on the specific matrix, tin levels from subnanomolar to micromolar may be present. Anodic stripping voltammetry, the most sensitive electroanalytical technique, has been extensively applied for over 20 years to the measurement of trace tin.^{1,2} The detection limits lie in the low nanomolar range but there are serious interferences due to overlapping stripping peaks of lead, cadmium, indium and thallium. Various approaches have been employed to improve the selectivity of tin measurement by stripping voltammetry. These include prior separation,³ flow or medium-exchange schemes^{4,5} or the addition of surfactants.^{6,7}

This paper reports a highly sensitive and selective stripping approach for determining tin, following controlled interfacial accumulation of its complex with tropolone (2-hydroxy-2,4,6-cycloheptatrienone) at the hanging mercury drop electrode. It has been shown recently⁸ that the addition of tropolone to an acetate supporting electrolyte significantly enhances the polarographic response of tin. The effect has been attributed to the adsorption of the tin-tropolone complex at the surface of the dropping mercury electrode. When a stationary mercury electrode is used the complex can be accumulated over substantially longer times and trace levels of tin can then be measured by adsorptive stripping voltammetry.⁹

Stripping voltammetry following adsorption of a metal chelate is currently becoming a more widely accepted analytical tool, as it extends the scope of stripping voltammetry to include more important

elements, and also offers an effective alternative method for measuring other metals. Likewise, the adsorption approach offers important advantages over conventional stripping measurements for tin. The results of a detailed investigation into the adsorption stripping method for tin in the presence of tropolone are reported below.

EXPERIMENTAL

Apparatus and reagents

The equipment used to obtain the voltamperograms, a PAR 264A voltammetric analyser with a PAR 303 static mercury drop electrode, has been described in detail.^{10,11} A medium-size hanging mercury drop electrode (HMDE), with a 0.16 cm^2 surface area was employed. All solutions were prepared from twice-distilled water. A 1000 ppm stock tin solution (VW0768-3, VWR Scientific) was used, and diluted as required for standard additions. Tropolone was purchased from Aldrich; a $4 \times 10^{-4}M$ stock solution was prepared daily. The supporting electrolyte was $0.1M$ acetate buffer (pH 4.0). River water (Rio Grande) was unfiltered surface water collected at Las Cruces, NM. The canned orange juice sample (Texsun) was diluted hundred-fold with twice-distilled water; a $10\text{-}\mu\text{l}$ aliquot of this solution was added to the supporting electrolyte present in the cell. All measurements were made at room temperature.

Procedure

Add 0.10 ml of the $4 \times 10^{-4}M$ tropolone solution to 10.0 ml of acetate buffer electrolyte in the polarographic cell and deaerate it by passage of nitrogen for 8 min. Switch on the magnetic stirrer (400 rpm) and the preconcentration potential (usually -0.4 V). After the selected preconcentration period switch off the stirrer, wait 15 sec and record the voltamperogram by applying a negative-going differential pulse scan, terminating at -1.0 V. This gives the background scan. Add suitable small portions of standard tin solution and construct a calibration curve from the peaks on the voltamperograms. Repeat the entire cycle on a fresh mercury drop.

*Author for correspondence.

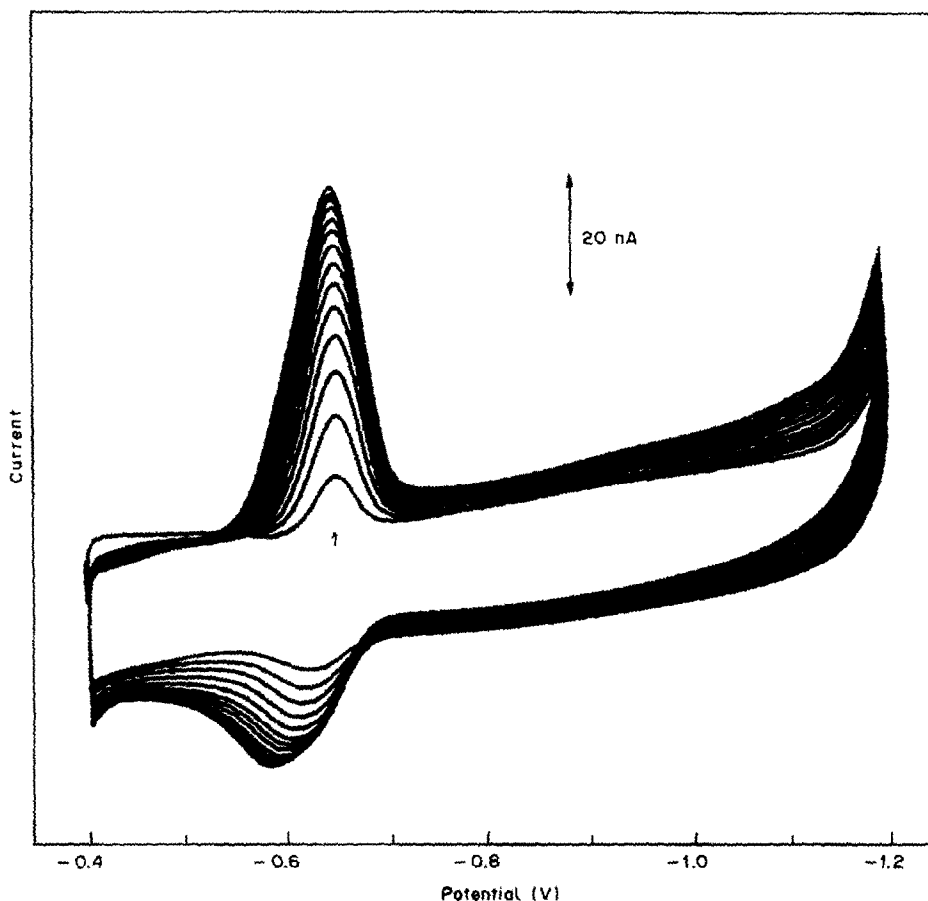


Fig. 1. Repetitive cyclic voltamperograms for 25 $\mu\text{g/l.}$ tin in an acetate buffer (pH 4.0) containing $4 \times 10^{-6} M$ tropolone. Scan rate: 20 mV/sec. Total time for these scans was ca. 19 min.

RESULTS AND DISCUSSION

Interfacial and redox behaviour

Figure 1 shows a set of repetitive cyclic voltamperograms obtained with the HMDE placed in a quiescent acetate buffer solution containing 25 $\mu\text{g/l.}$ tin and $4 \times 10^{-6} M$ tropolone. The cathodic and anodic peak currents associated with the redox reaction of the tin ($\text{Sn}^{2+} + 2e^- \rightleftharpoons \text{Sn}$) in its complex with tropolone, increase in magnitude as more and more of the complex has time to diffuse to the electrode and be adsorbed on its surface. Hence, the peak current with the adsorbed complex at saturation level on the electrode is several times greater than that for the species only in solution (estimated from the first scan, designated as 1). The irreversible nature of the redox process of the adsorbed complex is indicated by the shape and separation of the reduction and oxidation peaks ($b_{1/2,c} = 84 \text{ mV}$, $b_{1/2,a} = 132 \text{ mV}$; $\Delta E_p = 66 \text{ mV}$). The maximum charge, obtained by integrating the reduction current at saturation, ("cut and weigh" method), was found to be $0.27 \mu\text{C}$. Division of the charge by the conversion factor (nFA) gives an estimated coverage of the adsorbed complex layer of

$9.3 \times 10^{-11} \text{ mole/cm}^2$. Because the adsorbed layer contains both tin complex and free tropolone, the area occupied by a single complex molecule cannot be estimated. The effect of the potential-scan rate (V) on the peak current was explored at maximum adsorption density (after 120 sec stirring at -0.4 V). The height of the reduction peak for the complex increased with increase in the scan rate. The plot of $\log i_p$ vs. $\log V$ was linear, with a slope of 0.829 (correlation coefficient, 0.999), over the range 1–200 mV/sec. The plot of E_p vs. $\log V$ was also linear over the same range, with a correlation coefficient of 0.999. There was also a gradual increase in the cathodic current at ca. -1.1 V , which has been attributed to the adsorption and reduction of the free tropolone.⁸ When the potential was scanned over a wider range, from -0.2 to -1.2 V , an additional peak appeared at -0.35 V , associated with the $\text{Sn}^{4+} + 2e^- \rightleftharpoons \text{Sn}^{2+}$ redox process of the complex. While this peak also exhibited adsorption enhancement, the Sn–tropolone peak at -0.64 V was more useful analytically and was used throughout this work.

Adsorption of the tin–tropolone complex can be used as an effective preconcentration step, prior to

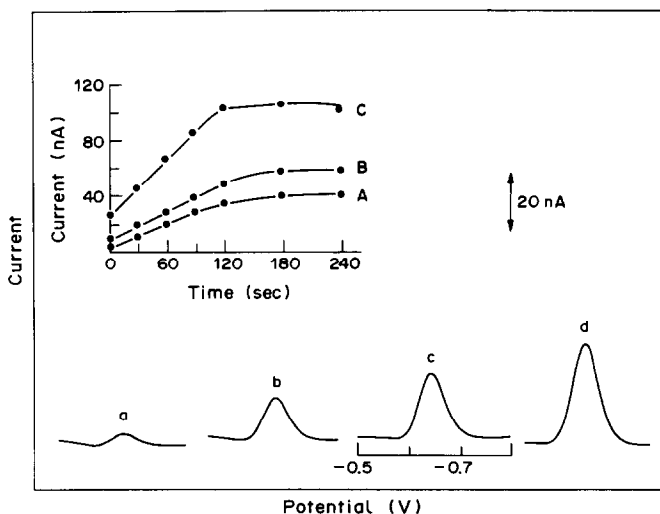


Fig. 2. Effect of preconcentration period on the stripping voltamperogram for $0.5 \mu\text{g/l.}$ tin. Preconcentration period: (a) 0, (b) 30, (c) 60, (d) 120 sec. Preconcentration potential: -0.4 V ; differential pulse waveform with scan rate 5 mV/sec and amplitude 50 mV . Inset are current-time plots for different tin concentrations: (A) 0.5 ; (B) 1 ; (C) $4 \mu\text{g/l.}$ Electrolyte: acetate buffer at pH 4.0 containing $4 \times 10^{-6} \text{ M}$ tropolone.

voltammetric measurement, and makes possible a highly sensitive determination. For example, Fig. 2 shows differential pulse voltamperograms for $0.5 \mu\text{g/l.}$ ($4.2 \times 10^{-9} \text{ M}$) tin, after different preconcentration periods from zero to 120 sec (a–d). The longer the preconcentration time, the more metal complex is adsorbed on the surface, and the larger is the peak-current. For example, with preconcentration for 120 sec, there is a 10-fold enhancement of the peak current relative to that obtained without preconcentration (a vs. d). As a result, excellent signal-to-background characteristics are obtained which permit convenient measurement at the subnanomolar concentration level. Also shown in Fig. 2 (inset) are plots of peak-current vs. preconcentration time at three levels of tin: 0.5 (A), 1 (B) and 4 (C) $\mu\text{g/l.}$ In all three cases the current increases linearly with time at first (up to 120 sec) and then levels off [the slopes of the initial linear portions are 0.21 (A), 0.30 (B) and 0.59 (C) nA/sec ; correlation coefficients, 0.997 (A), 0.995 (B,C)].

The adsorptive stripping response depends strongly on the solution pH (Fig. 3A). For example, increasing the pH from 3 to 4 results in a sharp increase in the peak-height; a gradual decrease in response is observed as the pH is raised further. A negative shift in the peak potential, from -0.54 to -0.75 V , accompanies the increase of pH from 3 to 6. The concentration of tropolone has a pronounced effect on the adsorptive stripping response (Fig. 3B). The stripping peak for $12 \mu\text{g/l.}$ tin increases linearly with increase in the ligand concentration up to $2 \times 10^{-6} \text{ M}$, above which it starts to level off. The dependence of the stripping peak current on the preconcentration potential was examined over the range from 0.0 to -0.60 V (Fig. 3C). A small and

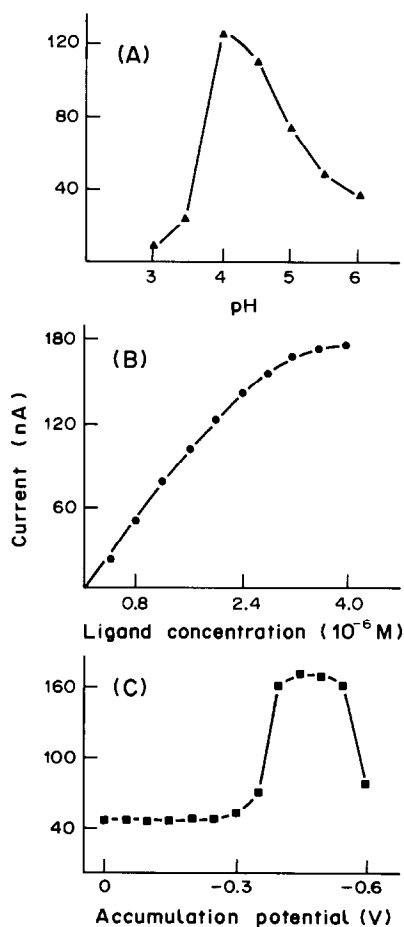


Fig. 3. Effect of pH (A), tropolone concentration (B) and preconcentration potential (C) on the stripping peak current. Tin concentration, 10 (A), 12 (B) and 8 (C) $\mu\text{g/l.}$ Preconcentration time, 60 (A,B) and 90 (C) sec. Preconcentration potential -0.45 V (A). Other conditions as for Fig. 1.

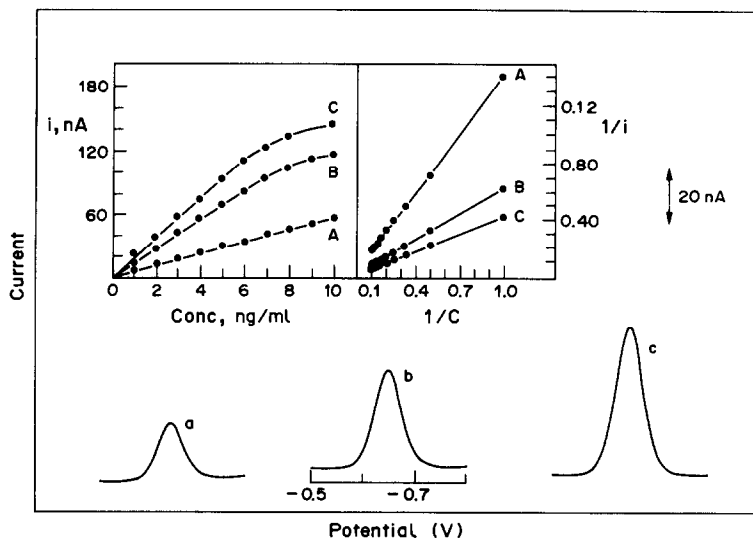


Fig. 4. Stripping voltamperograms for solutions of increasing tin concentration, 1–3 $\mu\text{g/l}$. (a–c). Preconcentration for 30 sec. Other conditions as for Fig. 2. Also shown are the resulting i_p vs. C and $1/i_p$ vs. $1/C$ plots following 0 (A), 30 (B) and 60 (C) sec preconcentration.

stable peak was observed in the region from 0.0 to -0.30 V; substantially larger (4-fold) peaks were obtained following preconcentration over the range from -0.40 to -0.55 V. A sharp decrease in response was observed at potentials more negative than -0.55 V. Optimal conditions, used for all subsequent work, were acetate buffer solution (pH 4.0), $4 \times 10^{-6}M$ tropolone, and a preconcentration potential of -0.40 V.

The magnitude of the stripping current peak is also affected by mass-transport (during the preconcentration) and by the voltammetric waveform used to measure the surface-bound complex. A $1 \mu\text{g/l}$ tin solution and 120 sec preconcentration period were employed to evaluate these effects: a 3-fold peak enhancement was obtained when the solution was stirred at 400 rpm (compared to a quiescent solution) and a differential pulse waveform yielded a slightly better signal-to-background ratio than linear scan measurements did.

ANALYTICAL UTILITY

The preconcentration effect associated with adsorption of the tin–tropolone complex results in an extremely low detection limit: the limit estimated from measurements of $0.7 \mu\text{g/l}$ tin, following an 8-min preconcentration (other conditions as in Fig. 2), and assuming a signal-to-noise ratio of 3, was 28 ng/l . ($2.3 \times 10^{-10}M$). This value means that in the 10 ml of solution used, 280 pg of tin can be detected. Compared to conventional stripping procedures for tin^{4,12} the adsorptive approach lowers the detection limit by 1–2 orders of magnitude. The adsorptive stripping detection limit is substantially lower than that obtained by flame atomic-absorption spec-

troscopy (AAS), and is comparable to that attained by the more costly electrothermal AAS.¹² Differential pulse polarographic measurements of the tin–tropolone complex permit detection of about $1 \mu\text{g/l}$ tin.⁸

Quantitative evaluation is based on measurement of the peak current. Figure 4 illustrates the response for successive increases of $1 \mu\text{g/l}$ in tin concentration with a 30-sec preconcentration period (a–c). Well-defined peaks are observed. These three peaks were part of a series of ten concentration increments, up to $10 \mu\text{g/l}$ tin. The resulting calibration plots, obtained with different preconcentration periods, are also shown in Fig. 4. As expected for processes limited by adsorption of the analyte, the response is linear only for very dilute solutions and/or short preconcentration periods, e.g., below $7 \mu\text{g/l}$ with 30-sec preconcentration. Non-linearity is observed for higher levels of tin. Reciprocal calibration plots, of $1/i_p$ vs. $1/C$, also shown in Fig. 4, can be used to extend the linear range over the entire range examined. Statistical treatment of the data plotted in Fig. 4 (inset) is given in Table 1. The reproducibility was estimated from a series of 14 successive measurements on a $6 \mu\text{g/l}$ tin solution (60-sec preconcentration). The mean peak current was 103.7 nA, with a range of 99–108, and a relative standard deviation of 2.6%.

The major drawback of conventional anodic stripping measurements of tin is the poor resolution in the presence of lead, cadmium, indium and thallium. The selective co-ordination, associated with the adsorption approach, offers a very promising voltammetric method for a highly selective determination of tin in the presence of these metals. For example, Fig. 5 compares measurements of $10 \mu\text{g/l}$ tin in the

Table 1. Linear regression statistics for data plotted in Fig. 4

Equation of response	Preconcentration time, sec	Concentration range, $\mu\text{g/l.}$	r^2	a, nA	$b, \text{nA.l.}\mu\text{g}^{-1}$
$i_p = a + bC$	0	1-10	0.996	3.1	5.4
	30	1-7	0.997	4.9	13.0
	60	1-6	0.998	6.6	17.7
$1/i_p = a + b/C$	0	1-10	0.999	0.004	0.135
	30	1-10	0.999	0.002	0.060
	60	1-10	0.999	0.002	0.040

presence of similar levels of lead and cadmium, by the adsorptive approach (A) and conventional stripping anodic stripping voltammetry (B). It is obvious that tin cannot be measured selectively by conventional stripping voltammetry, owing to severe peak overlap. In contrast, no effect of lead and cadmium on the tin peak-height is observed in the analogous adsorptive stripping measurements. Besides the substantial improvement in selectivity, it is clear from Fig. 5 that the adsorption strategy offers improved sensitivity and overall detectability compared to conventional stripping measurements [A(a) vs. B(a)]. The effects of a wide range of other metals, present at the $10\text{-}\mu\text{g/l.}$ level, on the response for $5\text{-}\mu\text{g/l.}$ tin was evaluated for a 30-sec preconcentration period. No change in peak-height for the tin-tropolone complex was observed in the presence of silver, zinc, nickel, bismuth, thallium, chromium or indium; gallium and copper enhanced the tin peak by 6 and 3%, respectively, while a 3% peak depression was observed in the presence of iron. Titanium yielded an overlapping response, with E_p ca. 75 mV more negative than the tin peak. In general, therefore, no major interference is caused by the presence of other metal ions. In contrast, organic surfactants that compete with the complex for the

surface sites cause a substantial depression of the tin response (ca. 17 and 90% at the 1 mg/l. level for gelatin and dodecyl sodium sulphate, respectively for $6\text{-}\mu\text{g/l.}$ tin, with 45-sec preconcentration). Hence, destruction of organic surfactants by ultraviolet irradiation is recommended for samples containing relatively high levels of these materials. Similar surfactant interferences are expected to occur in analogous anodic stripping measurements.^{2,13}

The suitability of this method for the determination of tin in environmental and food samples is illustrated in Fig. 6. Three successive standard additions (of 1.0 or $0.5\text{-}\mu\text{g/l.}$ tin) to samples of a river water (A) and a diluted orange juice (B) respectively, resulted in well-defined adsorptive stripping peaks (curves b-d). The tin peak for the original sample (curve a) can thus be evaluated by means of the resulting standard-addition calibration plots (also shown in Fig. 6). These plots are linear with correlation coefficients of 0.999. The inherent sensitivity of the method permits significant sample dilution (B) or use of short preconcentration periods (A). The tin peak is not affected by overlapping signals, as it often is in analogous anodic stripping measurements. Definite tin peaks were observed for a similar analysis

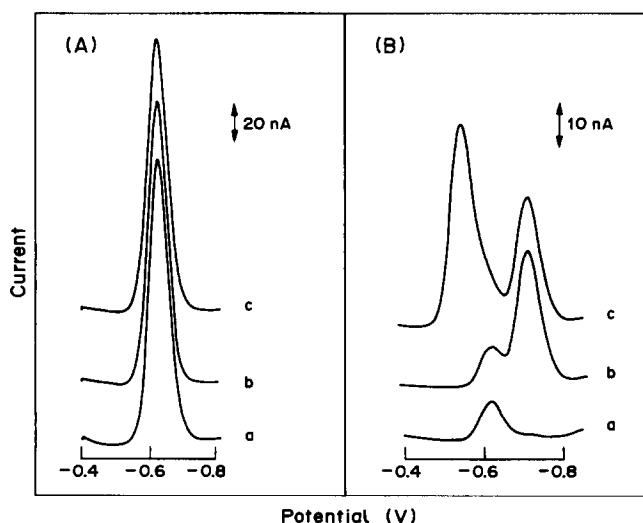


Fig. 5. Measurements of tin in the presence of lead and cadmium by (A) adsorptive stripping voltammetry and (B) differential pulse anodic stripping voltammetry. (a) $10\text{-}\mu\text{g/l.}$ lead; (c) same as (b) but after addition of $10\text{-}\mu\text{g/l.}$ lead; (c) same as (b) but after addition of $10\text{-}\mu\text{g/l.}$ cadmium. Preconcentration for 60 sec at -0.4 (A) and -1.2 (B) V. Other conditions as for Fig. 2, except that tropolone was not present in B.

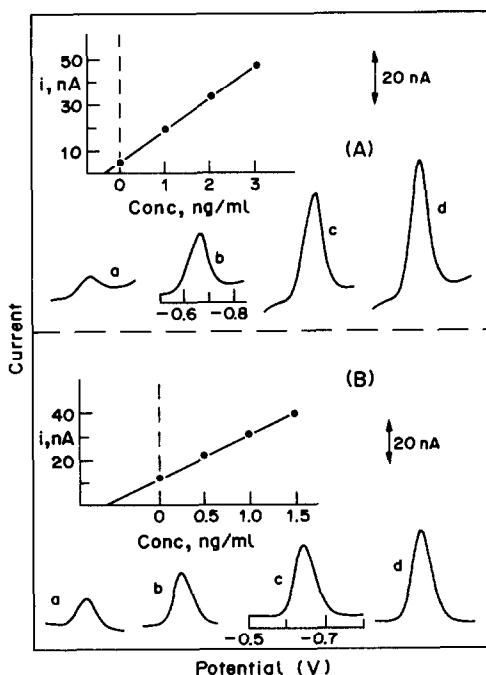


Fig. 6. Measurements of tin in river water (A) and canned orange juice (B). (a) Voltamperogram for the sample; (b-d) successive concentration increments of 1 (A) and 0.5 (B) $\mu\text{g/l}$. tin. Samples were as follows: (A) 9 ml of natural water + 1 ml of supporting electrolyte containing $4 \times 10^{-6}M$ tropolone; (B) a 10- μl aliquot of the hundredfold diluted orange juice added to 10 ml of supporting electrolyte solution, containing $4 \times 10^{-6}M$ tropolone. Preconcentration for 60 (A) and 30 (B) sec. Other conditions as for Fig. 2.

of a canned Coca-Cola sample. A similar assay of a canned tomato juice sample was less successful because of interference from non-electroactive surfactants, competing for adsorption sites.

When the method is applied to environmental samples, it is not at present clear which fraction of the tin is actually being measured. Because the adsorption approach is based on detection principles fundamentally different from those of conventional anodic stripping voltammetry, it may well not give the same result, depending on the nature of the tin species present. Further investigation is being made of this important question, with respect to tin species (organic and inorganic) in particular, and the distribution of other metals currently being measured by the adsorption approach, in general.

Acknowledgement—This work was generously supported by the National Institutes of Health (Grant No. GM 30913-04).

REFERENCES

1. F. Vydra, K. Štulík and B. Juláková. *Electrochemical Stripping Analysis*, Horwood, Chichester, 1976.
2. J. Wang, *Stripping Analysis: Principles, Instrumentation and Applications*. VCH Publishers, Deerfield Beach, 1985.
3. T. M. Florence and Y. J. Farrar, *J. Electroanal. Chem.*, 1974, **51**, 191.
4. E. Desimoni, F. Palmisano and L. Sabbatani, *Anal. Chem.*, 1980, **52**, 1889.
5. S. Mannino, *Analyst*, 1984, **109**, 905.
6. J. H. Mendez, R. C. Martinez and M. E. G. Lopez, *Anal. Chim. Acta*, 1982, **138**, 47.
7. J. Georges and M. Mermet, *ibid.*, 1986, **185**, 363.
8. G. Weber, *ibid.*, 1986, **186**, 49.
9. J. Wang, *Am. Lab.*, 1985, **17**, No. 5, 41.
10. J. Wang, D. B. Luo, P. A. M. Farias and J. S. Mahmoud, *Anal. Chem.*, 1985, **57**, 158.
11. J. Wang, D. B. Luo and P. A. M. Farias, *J. Electroanal. Chem.*, 1985, **185**, 61.
12. T. R. Copeland and R. K. Skogerboe, *Anal. Chem.*, 1974, **46**, 1275A.
13. J. Wang and D. B. Luo, *Talanta*, 1984, **31**, 703.

DETERMINATION OF VISCOSITY WITH AN OPEN-CLOSED FLOW-INJECTION SYSTEM

A. RIOS, M. D. LUQUE DE CASTRO and M. VALCARCEL

Department of Analytical Chemistry, Faculty of Sciences, University of Córdoba, Córdoba, Spain

(Received 31 December 1986. Revised 22 April 1987. Accepted 20 June 1987)

Summary—A flow-injection configuration for the determination of the viscosity of water-miscible samples is proposed. The method is based on the use of an open-closed flow-injection system involving a trapped sample (carrier) and injection of a dye plug. The behaviour of the plug is monitored photometrically by a detector included in the circuit. The parameters of the multipeak recording obtained are related to the viscosity, which can be determined in the range 1–28 cp with an r.s.d. of about $\pm 1\%$.

The food industry makes frequent use of rheological measurements, particularly of viscosity. This physical parameter, used to characterize a liquid rheologically, can be defined as the internal friction of the liquid (*i.e.*, its resistance to flow).¹ Viscosity is evaluated through the viscosity coefficient, η , measured in poise (p). There are several experimental procedures available for its determination, *e.g.*, flow through tubes (Ostwald viscometer), descent of a solid through liquids, rotational and vibrational viscometers. By their similarity to unsegmented flow systems (especially those used in flow-injection analysis, FIA) some of the devices used (*e.g.*, the Ostwald viscometer) for measuring viscosity, constitute a potential tool for the study or determination of the viscosity of Newtonian liquids (laminar flow regime). Some papers on this topic have been published in the last few years, the earliest being a communication by Betteridge and Růžička² in 1976. These authors used a single-channel FIA system to study the influence of viscosity on the photometric signals obtained for different glycerol-water mixtures into which a dye was injected. Later, Betteridge *et al.* proposed an automatic microcomputer-controlled viscometer based on an FIA system,³ and applied it to the measurement of viscosity and diffusion coefficients.⁴ The system was in effect a modified Ostwald viscometer and involved measurement of the time required by the sample to travel a fixed distance (the flow was gravity-based). These authors compared and discussed the advantages of photometric (use of a dye) and conductimetric (use of a salt) detection for this type of measurement.

The present paper reports the use of an FIA configuration based on the trapping of a bolus within an open-closed system, including a peristaltic pump, an injection valve and a photometric detector. The circuit is opened between introduction of consecutive samples, to flush the system. The atypical signals obtained provide valuable information.⁵ These systems were used earlier for individual and simultaneous determinations,^{5,6} development of amplifi-

cation and dilution methods,^{5,7} speciation studies^{8,9} and calculation of stoichiometries.¹⁰ The viscosity of a sample dramatically affects the dispersion or dilution of a plug injected into a closed system; this effect, shown in the multipeak recording, allows the convenient determination of viscosity, from the different parameters characterizing the FIA signal, by use of conventional instrumentation.

EXPERIMENTAL

Apparatus

A Pye-Unicam SP-500 single-beam spectrophotometer equipped with a Hellma 178.12QS flow-cell (inner volume 18 μ l) and connected to a Radiometer REC-80 recorder was used as detector. A Gilson Minipuls-2 peristaltic pump and two Rheodyne 5041 injection valves were also used.

Reagents

A Bromocresol Green stock solution was prepared by dissolving 0.100 g of the dye in 25 ml of $10^{-2}M$ borax solution. Aqueous sucrose solutions were prepared as required.

Configuration

The manifold used is shown in Fig. 1. The sample for viscosity determination acts as a carrier and circulates continuously in the system. The selecting valve is a 6-way valve with one channel blocked off and the others arranged so that in the "open" position the valve allows the sample to be driven to the detector, and then to waste through W_2 . Once the sample has filled the system, the valve S is turned to the closed position, connecting the sample flow (channel 1) to waste through W_1 , and allowing continuous circulation of the liquid in channel 2 with the aid of pump P' (or one of the lines of pump P). The dye (Bromocresol Green) is then injected through valve V_1 . The plug of dye passes through the detector as many times as required (multi-detection with a single detector) to become completely homogenized with the liquid trapped in channel 2. The process is monitored photometrically at 617 nm.

RESULTS AND DISCUSSION

Viscosity measurements on substances flowing through tubes are based on Poiseuille's law, *i.e.* $q = \pi pr^4/8 \eta l$, where q is the flow-rate, p the difference in pressure between the ends of the tube, r the tube

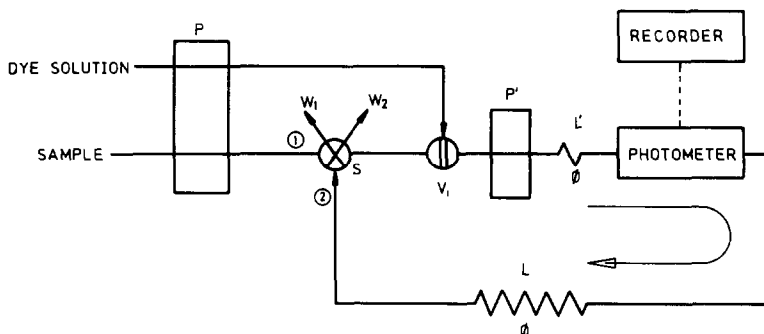


Fig. 1. Open-closed flow-injection manifold used for the determination of viscosity.

radius, l its length, and η the viscosity. Nevertheless, absolute viscosities are seldom determined, because they require prior knowledge of the values of the variables in the expression above. Thus, it is much commoner to determine relative viscosities by use of water or sucrose solutions as reference standards. Viscometers are usually calibrated with sucrose solutions, the viscosity of which varies exponentially with concentration. Sucrose solutions of known viscosity were used as reference standards in the present work.

Interference by refracted light

In the proposed configuration (Fig. 1), the sample acts as the carrier and the dye is injected. Otherwise the result would be the occurrence of negative peaks and a complex multippeak recording, resulting from

the appearance of a series of parasitic peaks, as shown in Fig. 2. According to Betteridge *et al.*,¹¹ these peaks are due to the difference in refractive index of the sample and carrier solutions when the sample-carrier interfaces pass through the photometric detector. When the refractive index of the injected plug is higher than that of the carrier solution, the incident radiation is refracted by the sample-carrier interface towards the cell walls and so does not interfere in the detection. Nevertheless, we have found that not all of the refracted radiation is directed away from the phototube (Fig. 2).

Taking these facts into account, we elected to use the manifold shown in Fig. 1, in which the sample is used both as the carrier and as the medium for the injected solution, the latter consisting of the sample

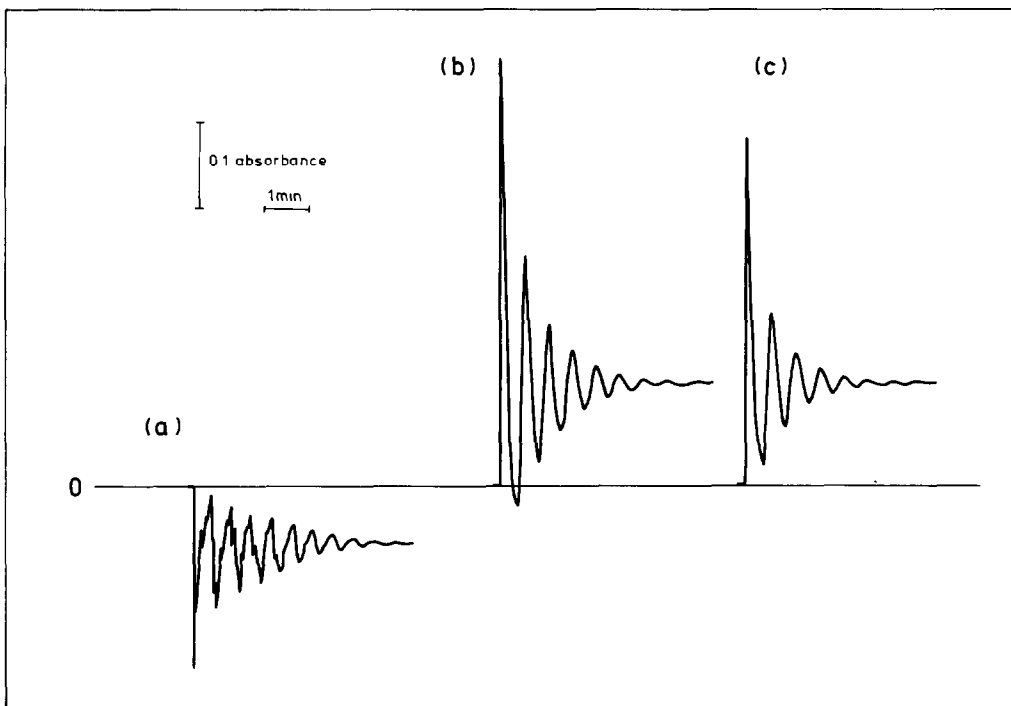


Fig. 2. Multippeak recordings: (a) by normal FIA (injection of a viscous substance into an aqueous solution of dye), (b) by reverse FIA, (c) by reverse FIA and equalization of the viscosity of the sample and the carrier.

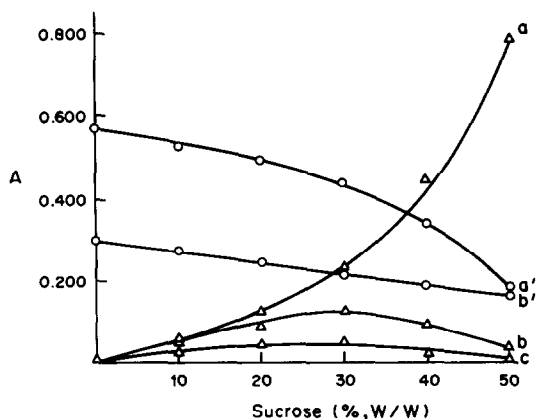


Fig. 3. Influence of viscosity (O) and refractive index (Δ) on the absorbance of sucrose at different concentrations (a, a', first peaks; b, b', second peaks; c, third peak).

plus 1% v/v of a 4-g/l. Bromocresol Green solution. In this way the refractive index of the carrier and injected plug is made practically identical, and the contribution of this to the signals obtained can be determined by injecting an aqueous 1% (v/v) solution of the Bromocresol Green. The contribution of these two physical parameters (viscosity and refractive index) to the signal is illustrated in Fig. 3. The nature of these contributions is different, because the latter is a purely optical effect, whereas the former affects the hydrodynamic characteristics of the system, determining the rate of homogenization with the liquid enclosed in the circuit. As can be seen from Fig. 3, the contribution of refraction to the signal dramatically decreases from the first to the second peak.

Kinetics of the process

As viscosity is a measure of the internal resistance to flow in a liquid, the configuration proposed in this paper may be used in the study of the kinetics of dispersion of the injected dye when the viscosity of the carrier solution is changed. Although the envelopes of the maxima and minima of the recording obtained define the kinetic profiles of the process, they also allow the following characteristic parameters to be obtained.

(a) The rate constant of the dilution process, k_v (first order): $v = k_v[\text{dye}]$. In this case, the equation $\log(A_t - A_\infty) = \log(A_0 - A_\infty) - 0.434k_v t$ (where A_0 , A_t and A_∞ are the initial absorbance, absorbance at time t and absorbance at equilibrium, respectively) is obeyed. The plot of $\log(A_t - A_\infty)$ as a function of time is a straight line with slope $-0.434k_v$.

(b) The average rate of dye dilution between successive peaks, \bar{v} , can be calculated from the expression $(A_2 - A_1)/(t_2 - t_1)$, where the absorbances and corresponding residence times are indicated by the subscripts.

(c) The overall time required to attain equilibrium, t_∞ , which is a measure of the kinetics of the process.

(d) An overall constant, k_η , the sum of the absorbances at all maxima and minima, characteristic for each carrier solution viscosity under the given working conditions. It is a kinetic parameter that is also dependent on η .

Kinetic equation

The influence of the different variables on the overall process (especially the FIA variables) can be determined through their respective partial reaction orders, obtained from the plot of $\log \bar{v}$ vs. \log (variable). The results can be used to establish the overall kinetic equation of the process, which in an unsegmented flow technique such as FIA, is also a function of the geometric and hydrodynamic characteristics of the system. In this case, the equation obtained is of the form:

$$\bar{v} = k_v C / \eta + k'_v q^{3/2} L^{-2/3} V_i$$

where k_v and k'_v are rate constants, C is the molar concentration of Bromocresol Green, q is the flow-rate (ml/min), L the reactor length (cm, bore constant at 0.5 mm) and V_i the injected volume (μl). The second term on the right-hand side includes the influence of the FIA variables on the overall process considered in the first term (dilution of a dye in a solution of given viscosity). It is noteworthy that q and V_i have a positive influence on \bar{v} , but the influence of L is negative. The values of the FIA variables (Fig. 1) used to study the effect of η and the dye concentration on \bar{v} were, $q = 2.9$ ml/min; $V_i = 30$ μl ; $L = 80$ cm; $L' = 15$ cm, $\phi = 0.5$ mm. As demonstrated above, the process is first order with respect to C and inverse first order with respect to η .

Effect of temperature

Temperature is the variable which has the greatest influence on viscosity. By studying the effect of this variable on parameters such as t_∞ and k_v (inversely and directly proportional to viscosity, respectively) it is possible to quantify this influence. Figure 4 shows

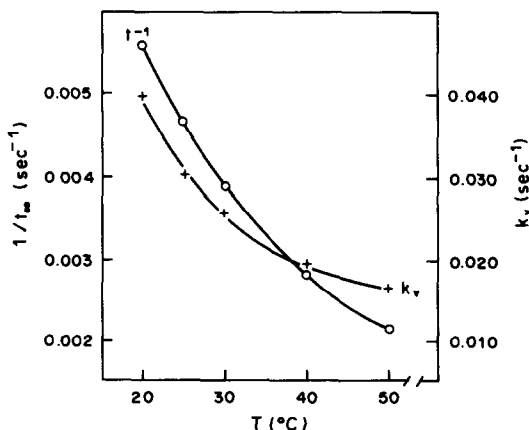


Fig. 4. Variation of the time needed for the attainment of equilibrium as a function of the rate constant (k_v) and temperature.

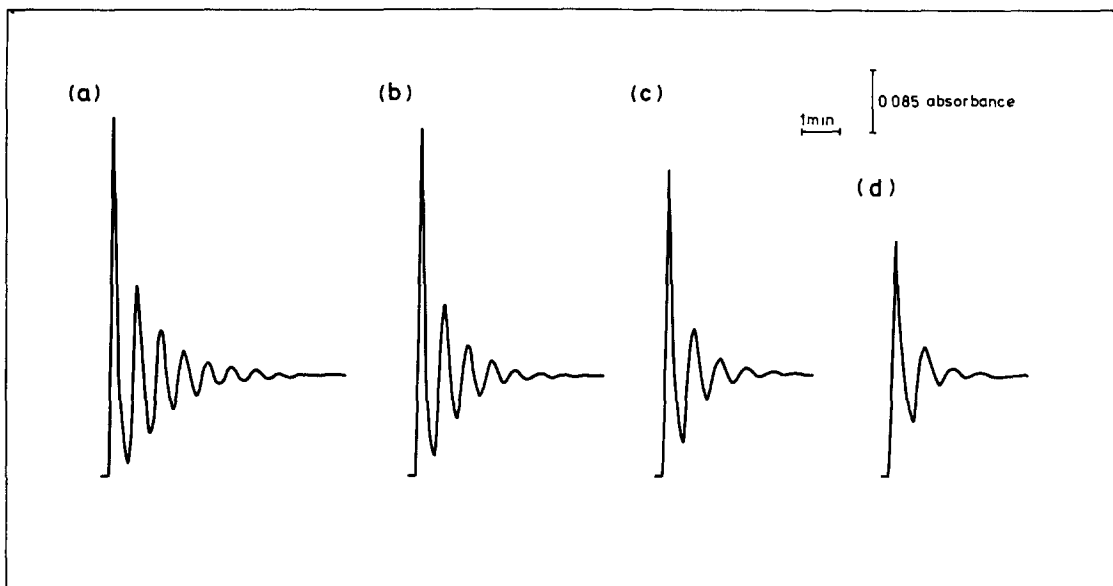


Fig. 5. Recordings for sucrose samples of different viscosities; (a) 1.5 cp; (b) 2.0 cp; (c) 3.2 cp; (d) 6.2 cp.

the variation of these parameters with temperature (T), which satisfies an exponential equation of the type $\eta = a \exp(b/T)$, where a and b are constants and a logarithmic plot of viscosity against the reciprocal of the temperature is linear.

$$\log(1/t_{\infty}) = 1.38 \times 10^3/T - 6.95$$

$$\log k_v = 1.40 \times 10^3/T - 6.27$$

The slopes and intercepts of the lines should give b and a , respectively.

Determination of viscosity

It is possible to determine the viscosity of a sample from the parameters defined above. The recordings obtained for sucrose solutions of different viscosities appear in Fig. 5. The viscosity of the samples must lie between 1.005 cp (distilled water) and 28 cp. More viscous samples cause unacceptably high pressures in the flow system. According to the kinetic equation, the order with respect to viscosity is -1 (the rate decreases with increasing viscosity), but the recordings in Fig. 5 show that the time required for the

attainment of equilibrium (t_{∞}) decreases with increase in viscosity. This apparent contradiction may be attributed to increasing thickness of the wall-film with increasing viscosity, and presumably more efficient mixing with the carrier stream.

The salient features of the determination of viscosity from the different parameters are summarized in Table 1. All the parameters conform to linear equations, thus making possible the direct determination of viscosity from any of them. The parameters based on a single absorbance measurement (conventional FIA peaks at different residence times: A_1 , A_2 and A_3) show poorer regression coefficients and less favourable determinations than do those achieved through measurements based on the overall kinetics of the process. Nevertheless, measurements based on these parameters provide higher sampling frequencies as they do not require the complete recording to be obtained. The determination of viscosity from \bar{v} suffers from the shortcoming of a regression similar to that of the determinations based on A_i , and viscosities determined from t_{∞} are subject to imprecise measurements of the final absorbance

Table 1. Features of the determination of viscosity from different parameters obtained with the open-closed flow system used

Parameter measured	Equation of the calibration curve*	Regression coefficient	r.s.d., † %	Samples/hr
A_1	$A_1 = 0.0413\eta + 0.590$	0.9866	± 2.04	75
A_2	$A_2 = 0.0382\eta + 0.334$	0.9705	± 1.89	45
A_3	$A_3 = 0.0246\eta + 0.247$	0.9347	± 1.82	30
\bar{v}	$\bar{v} = -6.71 \times 10^{-4}\eta + 7.6 \times 10^{-3}$	0.9852	± 1.37	45
k_v	$k_v = 4.95 \times 10^{-3}\eta + 9.4 \times 10^{-3}$	0.9986	± 0.92	15
k_{η}	$k_{\eta} = -0.125\eta + 1.683$	0.9991	± 1.21	20
t_{∞}	$t_{\infty} = -49.4\eta + 463$	0.9978	± 1.60	15

* η = viscosity (cp); \bar{v} = average rate between the first two maxima (sec^{-1}); k_v in sec^{-1} ; t_{∞} in sec; at 20°C.

†For $\eta = 3.2$ cp (11 samples).

(the equilibrium is considered to have been attained when the absorbance is within the range $A \pm 0.005$). The measurement of k_η (sum of the maximum and minimum absorbances, with values higher or lower, respectively, than that corresponding to $A \pm 0.005$) is an intermediate method between the single measurement of A_i and the use of the typically kinetic parameters defined as a function of the time (\bar{v}, k_v, t_∞), and its measurement involves the application of an amplification method providing good regression coefficients and precision.

As the sensitivity of the two methods, expressed in identical units, is comparable, only the following comparisons can be made.

Sensitivity of the determination based on absorbance measurements:

$$k_\eta \gg A_1 > A_2 > A_3.$$

Sensitivity of the determinations based on time measurements:

$$k_v \gg \bar{v} > t_\infty.$$

Thus, we may conclude that viscosity determinations based on the measurement of k_v and k_η are the most advantageous (the former increases and the latter decreases with increasing viscosity).

CONCLUSIONS

The use of an open-closed flow-injection system

for viscosity measurements is an easy way of automating control of this physical parameter. The large amount of information provided by these systems allows the manipulation of a variety of parameters directly related to viscosity. The monitoring is done photometrically and the instrumentation used is the same as that employed in control or research laboratories. The contribution of refraction effects to the observed signals is conveniently eliminated, so the signals depend on sample viscosity alone.

REFERENCES

1. H. G. Muller, *An Introduction to Food Rheology*, Heinemann, London, 1973.
2. D. Betteridge and J. Růžička, *Talanta*, 1976, **23**, 409.
3. D. Betteridge, W. C. Cheng, E. L. Dagless, P. David, T. B. Goad, D. R. Deans, D. A. Newton and T. B. Pierce, *Analyst*, 1983, **108**, 1.
4. *Idem, ibid.*, 1983, **108**, 17.
5. A. Ríos, M. D. Luque de Castro and M. Valcárcel, *Anal. Chem.*, 1985, **57**, 1803.
6. *Idem, Anal. Chim. Acta*, 1986, **179**, 463.
7. A. Ríos, F. Lázaro, M. D. Luque de Castro and M. Valcárcel, *ibid.*, in the press.
8. J. Ruz, A. Ríos, M. D. Luque de Castro and M. Valcárcel, *Talanta*, 1986, **33**, 199.
9. A. Ríos, M. D. Luque de Castro and M. Valcárcel, *Quim. Anal.*, in the press.
10. *Idem, J. Chem. Educ.*, 1986, **63**, 552.
11. D. Betteridge, E. L. Dagless, B. Fields and N. F. Graves, *Analyst*, 1978, **103**, 897.

CONTINUOUS FLOW DETERMINATION OF CHLORIDE IN THE NON-LINEAR RESPONSE REGION WITH A TUBULAR CHLORIDE ION-SELECTIVE ELECTRODE

HIROKAZU HARA* and YOSHIKI WAKIZAKA

Laboratory of Chemistry, Faculty of Education, Shiga University, Otsu, Shiga 520, Japan

SATOSHI OKAZAKI

Department of Chemistry, Faculty of Science, Kyoto University, Kyoto 606, Japan

(Received 28 April 1986. Revised 20 September 1986. Accepted 18 June 1987)

Summary—A microcomputer-aided continuous-flow system was constructed for the determination of chloride in the non-linear electrode-response region from 10 to 0.1 mg/l. Interpolation by spline function was used to calculate the concentration from the measured potential. As few as four points were enough to obtain a practical calibration curve, plotted as E vs. $\log c$. The interferences of bromide and iodide (at weight ratios <0.1 to chloride) could be removed by adding colloidal silver chloride continuously in the flow stream. Analysis of rain and snow containing 0.07–8.8 mg/l. chloride showed fairly good agreement with that by ion-chromatography.

Recently the analysis of atmospheric precipitation has become more and more important in environmental chemistry, in connection with air pollution and acid rain.

Although methods such as spectrophotometry and ion-chromatography are often used for rain water analysis, the use of ion-selective electrodes does not seem to have been fully exploited.¹⁻³ One reason for this is that the concentrations of ionic species in rain water are usually lower than the linear response ranges of the electrodes.

The most significant characteristic of rain water is that the concentration of its chemical contents varies widely during the rainfall. For example, the concentration of chloride is usually several mg/l. at the beginning and below 1 mg/l. towards the end. A concentration change of two orders of magnitude may be observed. Because ion-selective electrodes have a wide dynamic range, they can be used advantageously in rain water analysis, if their detection limits are sufficiently low. With the silver chloride based chloride ion-selective electrode, the detection limit of 0.1 mg/l. is usually low enough for chloride determination in rain water.

Recently, a few papers on the continuous flow determination of chloride by means of a chloride ion-selective electrode have appeared⁴⁻⁶ but the problem of determination in the non-linear calibration range has not been dealt with.

In this paper, a system for continuous flow determination of chloride is described. The possible inter-

ference of bromide and iodide is removed by the silver chloride pretreatment reported previously.⁷ A microcomputer is used for data-acquisition, calibration and calculation of results. Several interpolation methods are compared and it is concluded that a spline function serves best.

EXPERIMENTAL

Apparatus

Electrodes. An Orion 94-17B solid-state chloride ion-selective electrode was used for the batchwise determination. A tubular chloride ion-selective electrode was made from copper pipe, 2 cm long and 0.28 cm in bore. Its inner surface was first plated with silver, which was then electro-oxidized in 0.1M potassium chloride to form a silver chloride layer. This electrode was used in combination with an Orion double-junction reference electrode (Model 90-02). The outer filling solution was 1M sodium nitrate in 30% v/v methanol.

Measurement of potential. The electrode potentials at room temperature ($20 \pm 3^\circ$) were measured with 0.1 mV precision by an Orion Model 701A digital pH/mV meter and recorded by an analogue pen recorder (Rikadenki Model R-10), and also transmitted every 0.6 sec to an NEC PC8801 Mk II microcomputer through an 8-bit parallel interface.

Flow system. A schematic diagram of the flow system is shown in Fig. 1. Sample or standard solution was mixed with colloidal silver chloride solution to remove bromide and iodide impurities and then passed through the tubular electrode. The colloidal silver chloride was formed by mixing solutions I and II:

I: $n \times 2.93 \times 10^{-4}M$ $AgNO_3$ + 500 mg/l. Tween 80 (polyoxyethylene sorbitan mono-oleate) + 0.17M $NaNO_3$ in 95% v/v methanol.

II: $n \times 2.93 \times 10^{-4}M$ $NaCl$ + 500 mg/l. Tween 80 + 0.17M $NaNO_3$ in 95% methanol solution.

*Author for correspondence.

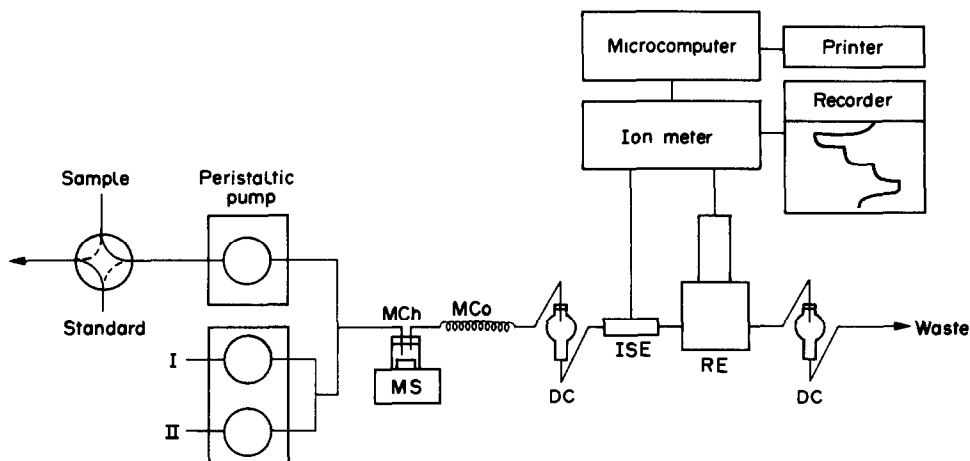


Fig. 1. Schematic diagram of continuous flow system (MS, magnetic stirrer; MCh, mixing chamber; MCo, mixing coil; DC, drop chamber; ISE, tubular chloride ion-selective electrode; RE, reference electrode). Compositions of solutions I and II are given in the text.

The Tween 80 was added to stabilize the colloid.⁷ The value of n was 1, 2 or 4. The flow-rate was 3.0 ml/min for sample solution and 0.6–0.7 ml/min for the colloidal solution unless otherwise stated. The flow-rates of solutions I and II were adjusted to be the same (within 1%).

The mixing chamber contained about 0.2 ml of solution and a magnetic stirring bar 6 mm long. The mixing coil was a Teflon tube 2.7 m long and 1 mm in bore. The drop chamber was used to reduce electrical noise.⁸

Ion-chromatograph. Ion-chromatographic measurements were made at the Shiga Prefecture Institute of Public Health and Environmental Science with a Dionex 2020i ion-chromatograph.

Sampling of rain water. Rain water was collected with a large funnel, diameter 30 cm.

Reagents

Analytical-reagent grade inorganic salts were used without further purification. Distilled demineralized water was used throughout. The composition of the silver plating solution was 36 g/l. silver cyanide, 60 g/l. potassium cyanide and 15 g/l. potassium carbonate.⁹

Principle of the system

Standard chloride solutions were measured, starting with the most dilute. Equilibrium potentials were recorded after the potential change was less than 0.15 mV/min. From the data set of equilibrium potential and logarithm of the chloride concentration, the third order spline function was calculated to express the potential as a function of $\log [\text{Cl}^-]$ (in mg/l.).¹⁰ The spline function is one of the interpolation methods used in various fields.^{11–13} The concentration of chloride in the sample was calculated by solving the non-linear equation numerically, by an interval-halving method

(Brent method^{14,15}) with 0.03 and 10 mg/l. as the initial values.⁸ The whole procedure was programmed in BASIC.

RESULTS AND DISCUSSION

Effect of methanol

In the flow system, the sample was inevitably diluted by addition of the colloidal silver chloride solution and ionic-strength adjuster. To compensate for the resultant decrease in concentration organic solvents were added.¹⁶ Table 1 shows the effect of addition of increasing proportions of methanol. It should be noted that the final concentrations decreased as the volume of methanol added was increased. Because the calibration graph is curved in the two concentration ranges examined, the dilution decreases the potential difference between the pairs of standard solutions, but this is partly offset by the effect of the methanol on the electrode response.

Effect of silver chloride

In our previous paper,⁷ the interference of bromide, iodide and sulphide in the low concentration range was examined and found to be much lower than expected from the solubility products. For bromide, the selectivity coefficient was estimated to be between 10 and 100. Addition of colloidal silver

Table 1. Effect of methanol on electrode sensitivity

[MeOH], % v/v	0	10	20	30	40	60	80	90
$\Delta E1$	22.1	23.1	25.6	27.4	27.7	27.3	23.9	19.0
$\Delta E2$	49.3	51.6	51.2	52.7	52.4	54.0	50.7	47.5

$\Delta E1$: difference between potentials for 0.1 and 1 mg/l. Cl^- , mV; $\Delta E2$: difference between potentials for 1 and 10 mg/l. Cl^- , mV; (the concentrations are those corresponding to the concentration of the standards before dilution with methanol), Orion 94-17B chloride ion-selective electrode. Ionic strength adjusted by adding 0.5 ml of 2M KNO_3 to 20 ml of sample.

Table 2. Effect of silver chloride on the interference from bromide or iodide

Sample	[Cl ⁻] found, mg/l.		
	a*	b*	c*
0.1 mg/l. Cl ⁻ + 0.1 mg/l. Br ⁻	0.100	0.100	0.100
+ 0.01 mg/l. I ⁻	0.104	0.108	0.100
1.0 mg/l. Cl ⁻ + 0.1 mg/l. Br ⁻	1.04	1.05	1.04
+ 0.1 mg/l. I ⁻	1.02	1.03	1.01
10 mg/l. Cl ⁻ + 1 mg/l. Br ⁻	10.8	10.4	10.4
+ 1 mg/l. I ⁻	10.5	10.3	10.2

*Concentrations of silver nitrate and sodium chloride for a, b and c were 1, 2 and $4 \times 2.93 \times 10^{-4} M$, respectively. Values were measured by spline interpolation.

chloride was found to remove the interference from bromide in stream waters. Though the concentration of bromide in rain water is usually below 0.01 mg/l.,¹⁷ which is too low to give an appreciable effect, we have experienced interference with some of the rain water samples. Table 2 shows that the interference was completely removed when the concentration of colloidal silver chloride used was higher than $5.86 \times 10^{-4} M$ (10 times the molarity of 1 mg/l. bromide). About 4% and 2% positive error was expected if there was complete ion-exchange from silver chloride to silver bromide or iodide, respectively.⁷ Thus the limitation of the suppression system is that the molar ratio of bromide or iodide to chloride must be small enough, since a positive error in the measured chloride concentration is inevitably incurred after the ion-exchange.

Calibration graph

The calibration graph for the system is shown in Fig. 2, together with the batchwise calibration graph for use of the AgCl/Ag₂S-based Orion chloride ion-selective electrode. There is little difference between these calibration graphs, and the homemade elec-

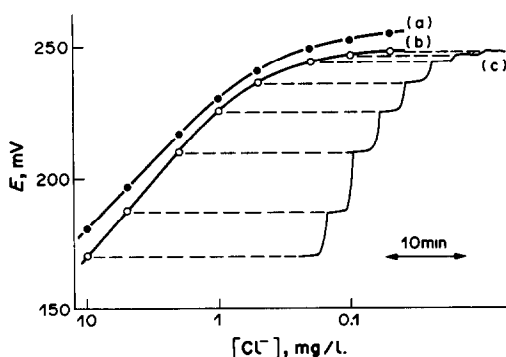


Fig. 2. Calibration curves and continuous flow record for chloride ion-selective electrodes in the non-linear range. (a) Orion 94-17B solid-state chloride ion-selective electrode. (b) Tubular chloride ion-selective electrode. (c) Continuous flow record of tubular chloride ion-selective electrode response.

trode is equal to the commercial electrode at least in terms of sensitivity.

The tubular electrode is more suitable for a flow system than the usual stick-type electrode, because it can be incorporated within the flow system without need for a flow cell.¹⁸⁻²⁰ It took about 1.5 min for newly introduced solution to reach the electrode surface and then 2.5 min to reach the equilibrium potential (constant to within 0.1 mV). The response time was somewhat slower than that (~ 2 min) of the Orion chloride electrode.

Precision and accuracy

The relative standard deviation increased as the chloride concentration decreased (Table 3), on account of the curvature of the calibration graph. No concentration dependence of the standard deviation was observed. The relative error of an individual value at 0.1 mg/l. was about $\pm 10\%$. The data indicate that the detection limit is about 0.1 mg/l.

Interpolation

To determine the concentration from the observed potential in the non-linear region, several interpolation methods have been devised and used. Jain and Schultz²¹ divided the methods into three groups, (1) graphical methods, (2) methods based on the non-ideal behaviour of the electrodes, (3) method based on non-linear calibration with least-square splines. The graphical method is not suitable for on-line measurement. Method 2 was adopted by Jain and Schultz, who expressed the non-ideal behaviour of the electrode by the potential function derived by Midgley, in which the solubility product of silver chloride was taken into consideration.²² There are two major reasons why we did not adopt method (2). One is that a single potential function could not apply to the calibration graph over such a wide concentration range as in this study (see Fig. 2), and a linear relationship to potential holds only over a very low concentration range of chloride.⁵ The other reason is that the solubility product of silver chloride in our system is different from that in a purely aqueous medium, because of the addition of methanol and ionic strength adjuster. Moreover, the Marquardt

Table 3. Precision and accuracy of five successive measurements*

Run	[Cl ⁻], mg/l.							
	0.05	0.1	0.2	0.5	1	2	5	10
1	0.037	0.091	0.207	0.528	1.00	1.98	4.94	9.92
2	0.037	0.104	0.210	0.496	1.00	2.14	4.98	9.92
3	0.055	0.112	0.223	0.492	0.989	2.05	5.16	10.1
4	0.030	0.091	0.210	0.512	0.989	1.92	5.00	9.55
5	0.037	0.112	0.190	0.488	1.02	2.01	4.92	9.88
mean	0.039	0.102	0.208	0.503	1.00	2.02	5.00	9.88
rsd, %	24	10	5.7	3.3	1.3	4.1	1.9	2.0
error, %	-22	2.0	4.0	0.6	0.0	1.1	0.0	-1.2

*Potentials of standard solutions for calibration was constructed were 247.6, 246.6, 243.8, 235.2, 224.5, 209.7, 187.6 and 169.9 mV for the eight solutions from 0.05 to 10 mg/l. respectively.

method used²¹ requires too much calculation time on an 8-bit microcomputer BASIC system.

Method 3 was adopted by Frazer *et al.*, but their method was too complicated and needed sophisticated devices for controlling a titration procedure.¹³ The spline function was believed to be suitable to describe correctly the curvature of the calibration graph. To implement spline interpolation with an 8-bit microcomputer, it is much easier to take $\log c$ as ordinate and E as abscissa, since the concentration can then be obtained directly from the measured potential. With $\log c$ as abscissa, however, it is necessary to solve the non-linear function of E vs. $\log c$ numerically to obtain a good approximation of the concentration. The interval-halving method (Brent method^{14,15}) was used for the purpose. The calculation time is as long as 20–30 sec, depending on the final concentration.

Table 4 compares the spline interpolation methods and an n th order polynomial by using the data obtained. If eight points were used for the calibration, the relative error was less than $\sim 5\%$ for all three interpolation methods, and arises from the error in measurement rather than in interpolation. In the spline interpolation of $\log c$ vs. E , the relative error depends on both the number and location of the

measurement points, and at least six properly spaced points are necessary to construct a practical calibration curve (case C). In contrast, in the spline interpolation of E vs. $\log c$, the relative error is $< 5\%$ irrespective of the number of measurement points unless there are less than four, which is too few for construction (case H) of a reasonable calibration graph. Figure 3 shows that for four calibration points, the use of $\log c$ as ordinate gives an abnormal shape of calibration curve, whereas with $\log c$ as abscissa the shape is normal (and coincident with a manual plot). This result clearly demonstrates that spline interpolation can give rise to completely different plots that cannot be interconverted by rotation and inversion. This fact should be noted together with the observation that oscillation might occur if the points are not appropriately sited. It was concluded that four points would be enough to construct a calibration curve as accurate as that prepared with eight points as demonstrated in case G of Table 4. To verify this conclusion, a comparison was made as shown in Table 5. The values for 0.05 and 0.08 mg/l. were obtained by extrapolation in the case of the four-point calibration. No significant difference in relative error was observed. Interpolation by n th order polynomial gave reasonable results

Table 4. Comparison of various interpolation methods for the determination of chloride in the non-linear response range

Case	No. of points	Concns., mg/l.	Range of relative errors, %*		
			Spline ($E, \log c$)	Spline ($\log c, E$)	n th Polynomial (n)
A	8	0.05, 0.1, 0.2, 0.5, 1, 2, 5, 10	-1.2 to +4.0	-1.2 to +4.0	-1.2 to +5.1 (5)
B	6	0.05, 0.1, 0.2, 0.5, 2, 10	-6.8 to +12	-2.3 to +4.0	-2.5 to +4.0 (5)
C	6	0.05, 0.1, 0.2, 0.5, 1, 10	-1.2 to +4.0	-1.1 to +4.3	-1.1 to +4.8 (5)
D	5	0.05, 0.1, 0.2, 1, 10	-16 to +28	-1.1 to +4.5	-1.2 to +4.0 (4)
E	5	0.05, 0.1, 0.5, 2, 10	-47 to +98	-2.3 to +3.5	-2.0 to +4.0 (4)
F	4	0.05, 0.2, 1, 10	-46 to +89	-1.1 to +4.5	-2.9 to +9.4 (3)
G	4	0.1, 0.5, 2, 10	-20 to +18	-4.9 to +1.2	-3.4 to +16 (3)
H	3	0.1, 1, 10	-30 to +43	-19 to +7.1	-4.4 to +10 (2)

*Range of seven relative errors for chloride from 0.1 mg/l. to 10 mg/l.

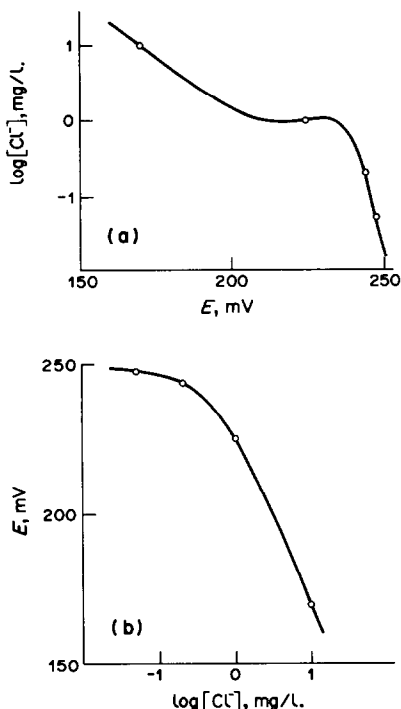


Fig. 3. Calibration curves obtained by spline function: (a) $\log c$ as a function of E ; (b) E as a function of $\log c$.

provided at least five points were used. Spline interpolation is often superior to the n th order polynomial interpolation, especially as the latter is more susceptible to unnecessary oscillation.¹²

Analysis of rain and snow

Analysis of rain and snow was performed, with eight-point calibration. The results agreed fairly well with those of ion-chromatography, the relative difference being within 10% for 12 samples with chloride concentration >0.75 mg/l.

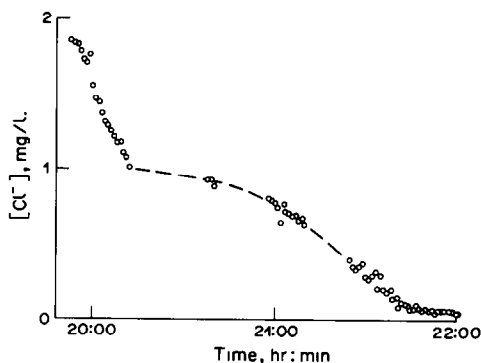


Fig. 4. Continuous monitoring of rain-water: Dashed line indicates amount of rainfall was below sampling rate (1 ml/min) during this period. Concentration and flow-rate of AgNO_3 and NaCl : $1.17 \times 10^{-3} M$ and 0.19 ml/min.

Rain water was continuously monitored with the system and the results are shown in Fig. 4. Although the amount of rainfall sometimes became less than the sampling rate (1 ml/min), the decrease in chloride concentration was clearly demonstrated. The drift of the standard electrode potential was 0.5 mV/hr during the measurement.

This system will be more useful and practical if the flow-rate can be arranged to vary automatically with the amount of rainfall, and the whole system modified to be portable. The non-linear calibration by the spline function can be used advantageously for other electrode systems, especially in the low concentration range.

Acknowledgement—We are indebted to Messrs. Y. Tanaka and S. Ichiki of the Shiga Prefecture Institute of Public Health and Environmental Science for their offer of rain and snow water samples together with the ion-chromatography data for them.

Table 5. Comparison of spline interpolations from four and eight measurement points

[Cl ⁻] taken, mg/l.	Four points*		Eight points*	
	[Cl ⁻] found, mg/l.	Error, %	[Cl ⁻] found, mg/l.	Error, %
0.050	0.068	36	0.040	-20
0.080	0.093	16	0.091	14
0.100	0.107	7	0.109	9
0.200	0.229	15	0.222	11
0.400	0.446	12	0.442	11
0.500	0.520	4	0.522	4
0.800	0.834	4	0.863	8
1.00	1.06	6	1.09	9
2.00	2.00	0	2.00	0
4.00	3.91	-2	3.98	-1
5.00	4.90	-2	5.00	0
10.0	10.2	2	10.2	2

*Concentration of standards were 0.1, 0.5, 2 and 10 mg/l. for four-point calibration and 0.05, 0.1, 0.2, 0.5, 1, 2, 5 and 10 mg/l. for eight-point calibration. Interpolation with $\log c$ as abscissa and E as ordinate.

REFERENCES

1. R. C. Harris and H. H. Williams, *J. Appl. Meteor.*, 1969 **8**, 299.
2. T. B. Warner and D. J. Bressan, *Anal. Chim. Acta*, 1972, **63**, 165.
3. J. Slanina, W. A. Lingerak and F. Bakker, *ibid.*, 1980, **117**, 91.
4. M. Vandeputte, L. Dryon and D. L. Massart, *ibid.*, 1977, **91**, 113.
5. K. Tomlinson and K. Torrance, *Analyst*, 1977, **102**, 1.
6. M. Trojanowicz and R. Lewandowski, *Z. Anal. Chem.*, 1981, **308**, 7.
7. H. Hara, Y. Wakizaka and S. Okazaki, *Analyst*, 1985, **110**, 1087.
8. *Idem*, *Anal. Chem.*, 1986, **58**, 1502.
9. T. Matsuno and S. Asakura, *Denki Kagaku* 2nd Ed., p. 213. Dainihon Tosho, Tokyo, 1981.
10. I. Anzai, *I/O*, 1985, **10**, 217.
11. C. A. deBoor, *Practical Guide to Splines*, Springer-Verlag, New York, 1978.
12. K. Ichida and F. Yoshimoto, *Spline Kansuu to Sono Ouyou*, Kyoiku Shuppan, Tokyo, 1979.
13. J. W. Frazer, D. J. Balaban, H. R. Brand, G. A. Robinson and S. M. Lanning, *Anal. Chem.*, 1983, **55**, 855.
14. G. E. Forsythe, M. A. Malcolm and C. B. Moler, *Computer Method for Mathematical Computation*, Prentice-Hall, New York, 1977.
15. M. Gen and K. Ida, *Kagaku-Gijyutsu Keisan Program Shu*, p. 109. Kogaku Tosho Shuppan, Tokyo, 1983.
16. G. J. Kakabadse, *Ion-Selective Electrode Rev.*, 1981, **3**, 127.
17. A. Sakuragawa, K. Tamura and S. Utsumi, *Bunseki Kagaku*, 1986, **35**, 95.
18. K. Hiiro, A. Kawahara and T. Tanaka, *Nippon Kagaku Kaishi*, 1980, 1447.
19. S. Alegret, J. Alonso, J. Bartroli, J. M. Paulis, J. L. F. C. Lima and A. A. S. C. Machado, *Anal. Chim. Acta*, 1984, **164**, 147.
20. H. L. Lee and M. E. Meyerhoff, *Analyst*, 1985, **110**, 371.
21. R. Jain and J. S. Schultz, *Anal. Chem.*, 1984, **56**, 141.
22. D. Midgley, *ibid.*, 1977, **49**, 1211.

PERIODIC TRENDS IN SENSITIVITY AND ITS DEPENDENCE ON THE PROPERTIES OF PYROLYTIC AND NON-PYROLYTIC GRAPHITE IN GRAPHITE-FURNACE ATOMIC-ABSORPTION SPECTROMETRY

CHAN-HUAN CHUNG*, ETSURO IWAMOTO† and YUROKU YAMAMOTO‡§
Department of Chemistry, Faculty of Science, Hiroshima University, Hiroshima 730, Japan

(Received 31 January 1987. Revised 12 May 1987. Accepted 5 June 1987)

Summary—The sensitivities for metal determination by GFAAS in the peak-height and integration modes were examined with pyrolytic graphite (PG) and non-pyrolytic graphite (NPG) tubes for 34 elements. It was found that there are periodic trends of the mole sensitivity and the elements can be classified according to whether their sensitivity of determination is enhanced by use of (a) the PG tube (alkali, alkaline-earth and transition metals); (b) the NPG tube (semi-metals); about equally by both tubes (Mg, Zn, Cd, and Pb). The mole sensitivity pM for atomic-absorption spectrometry (AAS) was defined as $pM = -\log(m_h/A_w)$ where m_h is the weight of an element corresponding to 1% absorption and A_w is the atomic weight. It was found that the pM values for graphite furnace AAS have a periodic trend similar to that for flame AAS and atomic-fluorescence spectrometry.

Important furnace-tube properties that govern the sensitivity in graphite-furnace atomic-absorption spectrometry (GFAAS) include permeability to gases and reactivity with analyte elements in such processes as reduction, and formation of carbides and lamellar compounds.¹ Of the modifications proposed for improvement in the quality of furnace tubes, coating with a thin layer of pyrolytic graphite is now popular. However, the pyrolytic graphite (PG) tube is not always superior to the non-pyrolytic graphite (NPG) tube, the effect varying greatly from element to element.²⁻¹⁷ Thus there is an improvement in sensitivity for molybdenum^{6,17} but a deterioration in sensitivity for volatile selenium.^{2,3} The dependence of sensitivity on the nature of the graphite surface has been well explored for some elements, but few systematic studies based on the periodic table have been reported.

In GFAAS the sensitivity (m_h) is usually reported as the weight of element required to give 1% absorption (*i.e.*, 0.0044 absorbance) and is evaluated by means of the equation

$$m_h = 0.0044m/A_h \quad (1)$$

where m is the weight of element giving a peak absorbance A_h . Slavin and Carnrick¹⁸ developed the concept of "characteristic mass" in terms of the number of picograms of element needed to give an integrated absorbance signal equivalent to 0.0044 sec,

and suggested that the characteristic masses for Cd, Al, As, Pb, Se, and Tl are remarkably stable and independent of experimental conditions and matrix. However, those values are still governed by the atomic weights of the elements, in addition to the resonance-line oscillator strengths and the ground-level populations.¹

We therefore propose the concept of "mole sensitivity" pM , defined as

$$pM = -\log m_h/A_w \quad (2)$$

where A_w is the atomic weight. When there are no effects caused by differences in the atomizer and instrument used, it is expected that the pM values will be a "characteristic" parameter.

The purpose of the present work was to examine the relation between sensitivity and position in the periodic table, and its dependence on the qualities of the tube surface. It was found that the semi-metallic elements of groups III, IV, V, and VI give better sensitivity with non-pyrolytic graphite, and that the periodic trends in the mole sensitivity are nearly the same for GFAAS, flame atomic-absorption spectrometry (FAAS), and atomic-fluorescence spectrometry (AFS).

EXPERIMENTAL

Apparatus

The experiments were performed with a Perkin-Elmer model 5000 atomic-absorption spectrometer, an HGA-500 power supply for the atomization program and a model AS-40 sample introduction system. Tungsten and deuterium background correctors were used. Hamamatsu TV hollow-cathode lamps were used as the light-sources. The peak height (A_h) and integrated (A_i) absorbances were auto-

*Present address: Laboratory of Anhui Geological Bureau, Hefei, Anhui, People's Republic of China.

†Authors for correspondence.

§Present address: Fukui Institute of Technology, Gakuen 3-618, Fukui 910, Japan.

Table 1. Instrumental parameters

Step	Drying	Ashing	Atomization	Conditioning
Temperature, °C	200	variable	2450	2700
Ramp time, sec	40	30	0	1
Hold time, sec	5	5	5	2
Recorder setting			-2	
Internal gas flow, ml/min	300	300	0	300

matically printed out and displayed by a Perkin-Elmer Data System 10. Argon was used as purge gas. The standard program for determination with maximum-power heating is listed in Table 1. Pyrolytic graphite (PG, Perkin-Elmer, part No. 4559-4) and non-pyrolytic graphite (NPG, Perkin-Elmer, part No. 070699) tubes were used throughout. Although even 100 firings hardly degraded the graphite surface with regard to sensitivity, usually tubes with fewer than 70 firings were used. The same PE 5000 instrument conditions were used with both tube materials. A CHINO recording pyrometer was used to calibrate the temperature settings.

Reagents

All chemicals used were of the highest purity commercially available. A stock solution, 1000 mg/l., for each element was prepared as follows. Solutions of Li, Na, K, Sc, Ga, Cs, Ba, and Hg were prepared from the chlorides. Solutions of As, Se, Te, and Sb were prepared from As_2O_3 , SeO_2 , TeO_2 , and potassium antimony tartrate, respectively. The SeO_2 and TeO_2 were dissolved in hydrochloric acid and the As_2O_3 in a minimum amount of 10M sodium hydroxide. The solutions of other metals used were 1000-mg/l. certified standard solutions for AAS, which were standardized by EDTA titration (Wako Pure Chemical Industries, Ltd. and Katayama Chemical Industries, Ltd.). Sample solutions were prepared by serial dilution of the stock solutions with distilled demineralized water just before use. All sample solutions were made 0.05M in hydrochloric acid. Sulphuric acid and nitric acid media were also used for some elements. Sample volumes introduced into the furnace were 20–50 μ l.

RESULTS AND DISCUSSION

The absorbances for 34 elements were measured with PG and NPG tubes, to find their sensitivities. The amounts taken all corresponded to linear sections of the calibration graphs. The results are given in Table 2 together with the appearance temperatures (T_{app}). The change in the tube surface makes little difference in the appearance temperature and so the average T_{app} values are given in Table 2. The integrated absorbances are taken as the absorbance summation multiplied by one-sixtieth of a second, $\Sigma A_j \times 1/60$. The absorbances A_1 and A_2 are the means of 3–5 measurements at the best ashing temperature for each element. Relative standard deviations for all the elements were less than 5%.

Periodic trends of PG and NPG effects

To prevent diffusion of atomic vapour through the tube walls, coating the tube with a layer of pyrolytic graphite was advocated by L'vov.¹ This layer is impermeable to gases, non-porous and resistant to oxidation, and has a high thermal conductivity.^{1,19} The effects of these properties of the PG tube on analytical sensitivity in GFAAS have been in-

vestigated and compared with those of the NPG tube. Thompson *et al.*,⁴ Manning *et al.*,^{8,9} Sturgeon and Chakrabarti,¹⁰ and Slavin *et al.*¹¹ all reported that the coating increases the sensitivity for many refractory-oxide or carbide-forming elements such as Mo, Ti, and V, whereas significant improvements in sensitivity are not observed for elements which do not form stable carbides or oxides. However, various investigators differed in the results they reported for some elements such as Al^{8–12} and volatile elements.^{2,3,12,14} Fernandez and Iannarone¹² reported the analytical sensitivities obtained for 26 elements by using PG and NPG tubes in the maximum-power heating mode. They observed significant sensitivity improvements with the PG tube even for the relatively volatile elements Se and Te.

It has also been pointed out that the sensitivity strongly depends on the quality of the pyrolytic graphite coating and that this varies during the lifetime of the tube.^{11,20–22} Thus, a strict comparison of sensitivity between PG and NPG requires instrumental and analytical conditions that are as identical as possible. In this connection, the PE-5000 spectrometer and its associated automatic instruments seem adequate for the purpose.

The periodic trends of effects of the PG or NPG tubes on the sensitivities for 34 elements, obtained in this work with respect to peak height and integrated absorbances, are shown in Fig. 1.

The criterion for superiority of the effect of a tube on sensitivity was that the *other* tube gave an absorbance that was less than 90% of that obtained with the "superior" tube.

It is well known that some elements, especially those in the right-hand side of the periodic table, are best atomized from a medium other than hydrochloric acid. Table 3 gives the sensitivity for Ba, Zn, Ga, Ge, As, and Se in various matrices. It is worthwhile noting that the superiority of the PG or NPG tubes for most of the elements is independent of the kind of acid medium, although nitric acid (0.05M) and sulphuric acid (0.025M) significantly lower the sensitivity for Se with NPG tubes and lead to superiority of the PG tube. The use of sodium nitrate and hydroxide as matrix modifiers for Ge^{23,24} and of the graphite-cloth ribbon for As³ to increase the sensitivity leads to about the same performance for both types of surface.

There is a general tendency for PG tubes to give higher sensitivity for elements in the left-hand groups of the periodic table, *i.e.*, those that are more metallic

Table 2. Spectral lines, appearance temperatures, absorbances and sensitivity ratios of 34 elements in 0.05M hydrochloric acid medium with pyrolytic graphite (PG) and non-pyrolytic graphite (NPG) tubes

Element	λ /bandpass, nm	T_{app} , K	Amount taken, ng	A_i		A_h		Sensitivity ratios (PG/NPG)	
				PG	NPG	PG	NPG	A_i	A_h
Li	670.8/0.7	1600	0.12	0.386	0.162	1.36	0.68	2.2	2.0
Na	589.5/0.7	1290	0.04	0.436	0.073	1.40	0.14	6.0	10.0
Mg	285.2/0.7	1760	0.032	0.193	0.198	1.37	1.40	1.0	1.0
Al	309.3/0.7	2310	1.8	0.258	0.544	0.97	0.88	0.5	1.1
K	766.5/0.7	1050	0.04	0.691	0.390	1.58	0.87	1.8	1.8
Ca	422.7/0.7	2160	0.16	0.580	0.460	1.00	0.70	1.3	1.4
Sc	391.2/0.7	2510	3.0	0.595	0.067	1.63	0.14	8.9	11.6
Ti	365.3/0.7	2600	9.0	0.544	0.092	1.65	0.15	5.9	9.7
V	318.4/0.7	2490	8.0	0.570	0.060	1.03	0.10	9.5	10.3
Cr	357.9/0.7	1910	0.5	0.407	0.273	1.10	0.34	1.5	3.2
Mn	279.5/0.2	1610	0.2	0.222	0.243	1.10	0.60	0.9	1.8
Fe	248.3/0.2	1700	0.6	0.252	0.251	0.88	0.34	1.0	2.6
Co	240.7/0.2	1670	1.2	0.449	0.355	0.95	0.36	1.3	2.6
Ni	232.0/0.2	1680	1.6	0.546	0.260	0.83	0.26	2.1	3.2
Cu	324.7/0.7	1280	0.7	0.409	0.278	0.98	0.26	1.5	3.8
Zn	213.9/0.7	1100	0.05	0.110	0.106	0.49	0.48	1.0	1.0
Ga	294.4/0.7	1530	8.0	0.123	0.244	0.42	0.49	0.5	0.8
Ge	265.1/0.7	2190	150	0.040	0.565	0.21	1.51	0.1	0.1
As	193.7/0.7	1770	5.0	0.010	0.147	0.16	0.63	0.1	0.3
Se	196.0/0.7	1470	10	0.063	0.292	0.47	1.25	0.2	0.4
Sr	460.7/0.4	2230	0.3	0.535	0.002	0.83	0.07	267	11.2
Mo	313.3/0.7	2450	1.6	0.486	0.160	1.05	0.25	3.0	4.2
Ag	328.1/0.7	1120	0.24	0.167	0.059	1.01	0.35	2.8	2.9
Cd	228.8/0.7	875	0.12	0.173	0.176	1.11	1.03	1.0	1.1
Sn	224.6/0.7	1600	4.0	0.130	0.340	0.38	0.60	0.4	0.6
Sb	217.6/0.2	1470	5.0	0.116	0.312	0.47	1.26	0.4	0.4
Te	214.3/0.2	950	5.0	0.107	0.474	0.35	1.24	0.2	0.3
Cs	852.1/4.0	1350	3.0	0.287	0.160	1.04	0.56	1.8	1.9
Ba	553.6/0.2	2370	2.0	0.460	0.148	0.82	0.14	3.1	5.9
Eu	459.4/0.2	2200	1.5	0.343	0.028	1.18	0.10	12.3	11.8
Au	242.8/0.7	1220	1.2	0.222	0.226	1.33	0.71	1.0	1.9
Hg	253.6/0.7	400	450	0.060	0.927	0.38	1.02	0.1	0.4
Pb	283.3/0.7	1110	1.8	0.149	0.160	0.89	0.86	0.9	1.0
Bi	223.1/0.7	960	2.4	0.106	0.155	0.66	0.89	0.7	0.7

in character, and NPG tubes give higher sensitivity for semi-metallic elements in the right-hand groups, and their effects are similar for the intermediate elements.

The first group includes mainly the alkali and alkaline-earth metals and some transition elements. The alkaline-earth metals and most transition metals in this group tend to form stable carbides²⁵ which are poorly atomized. Of these metals, Mn, Fe, and Au show comparable integration sensitivities with both types of tube, indicating that the decrease in peak absorbance is compensated by the broadening of the peak profile.

The metals (Mg, Zn, Cd, and Pb) for which the sensitivity is independent of the nature of the tube give sharp narrow peaks. These metals, except for magnesium, are relatively volatile and their atomization begins at lower temperatures (Table 2). These results indicate that these metals hardly interact with carbon. Aluminium behaves uniquely: the sensitivity with an NPG tube is comparable to that with a PG tube for the peak-height mode but for the integration mode is twice that obtained with a PG tube. The

residence time of Al_2O_3 on the NPG wall is prolonged. Sturgeon *et al.*²⁶ pointed out that in general, elements having relatively high volatility give sharp narrow peaks, whereas elements having relatively low volatility give broader peaks. Our observations for this group support this view.

The group for which NPG tubes give higher sensitivity includes volatile elements. Matousek²⁷ suggested that the NPG surface enhances the sensitivity for Se, Te, As, and Sb by the beneficial effect of retardation of release of the dimers which are their atomizing species at low temperatures. In the present study considerably increased sensitivity with the NPG tube was obtained for all the elements of this group, compared to that with the PG tube. Organic compounds of As and Se extracted into a chloroform-carbon tetrachloride mixture also showed much higher sensitivity with the NPG than the PG tube.^{2,3} In determination of these elements, loss by vaporization during the ashing step causes lower sensitivity^{5,28-30} and many attempts have been made to overcome this problem. For the determination of selenium it has been empirically demon-

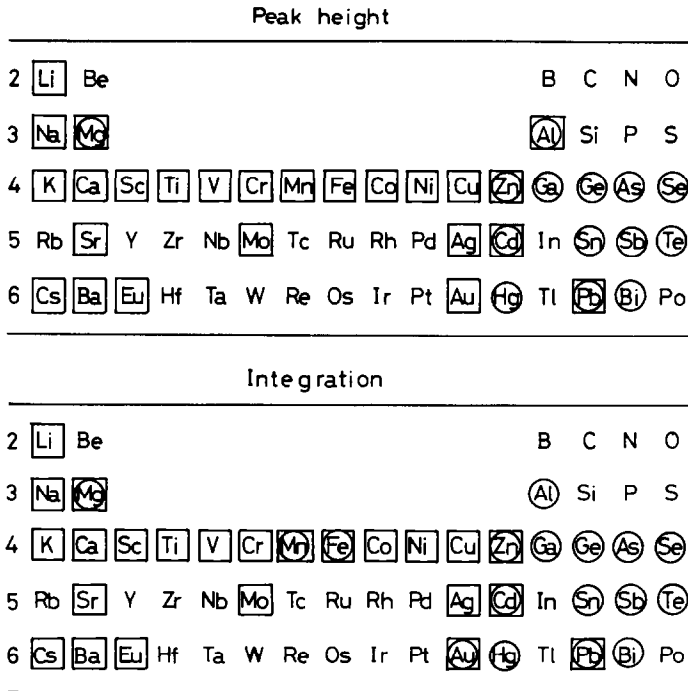


Fig. 1. Periodic trends of the sensitivities obtained with pyrolytic graphite (PG) and non-pyrolytic graphite (NPG) tubes for 34 elements with respect to peak-height (A_h) and integrated (A_i) absorbances. \square = PG/NPG > 1; \circ = PG/NPG < 1; \boxtimes = PG/NPG \sim 1.

Table 3. Matrix effects on the sensitivity for Ba, Zn, Ga, Ge, As, and Se

	Amount taken, ng	Matrix ^a	A_h		Sensitivity ratio for A_h , (PG/NPG)	m_n^b , g	pM
			PG	NPG			
Ba	2	HCl	0.82	0.14	5.9	1.1×10^{-11}	13.10
	2	HNO ₃	0.84	0.16	5.3	1.0×10^{-11}	13.14
	2	H ₂ SO ₄	0.84	0.16	5.3	1.0×10^{-11}	13.14
Zn	0.05	HCl	0.49	0.48	1.0	4.5×10^{-13}	14.16
	0.05	HNO ₃	0.62	0.63	1.0	3.5×10^{-13}	14.27
	0.05	H ₂ SO ₄	0.58	0.72	0.8	3.1×10^{-13}	14.32
Ga	2	HCl	0.10	0.12	0.8	7.3×10^{-11}	11.98
	2	HNO ₃	0.16	0.48	0.3	1.8×10^{-11}	12.59
	2	H ₂ SO ₄	0.16	0.28	0.6	3.1×10^{-11}	12.35
Ge	20	HCl	0.0	0.22	0.0	4.0×10^{-10}	11.26
	20	HNO ₃	0.22	0.61	0.4	1.4×10^{-10}	11.70
	20	H ₂ SO ₄	0.05	0.48	0.1	1.8×10^{-10}	11.60
	20	NaCl	0.06	0.32	0.2	2.8×10^{-10}	11.42
	2	NaNO ₃	0.43	0.42	1.0	2.0×10^{-11}	12.56
	2	NaOH	0.37	0.36	1.0	2.4×10^{-11}	12.49
As	5	HCl	0.16	0.63 ^d	0.3	3.5×10^{-11}	12.33
	5	HCl*	1.37	1.16	1.2	1.6×10^{-11}	12.67
	5	HNO ₃	0.54	1.16 ^d	0.5	1.9×10^{-11}	12.60
	5	H ₂ SO ₄	0.61	0.89 ^d	0.7	2.5×10^{-11}	12.47
Se	5	HCl	0.25	0.63	0.4	3.5×10^{-11}	12.35
	5	HCl*	0.18	0.72	0.3	3.1×10^{-11}	12.41
	5	HNO ₃	0.25	0.23	1.1	8.8×10^{-11}	11.95
	5	HNO ₃	0.15	0.49	0.3	4.5×10^{-11}	12.24
	5	H ₂ SO ₄	0.16	0.12	1.3	1.4×10^{-10}	11.75
	5	H ₂ SO ₄ *	0.22	0.44	0.5	5.0×10^{-11}	12.20

^aThe concentration is 0.05M except for H₂SO₄ (0.025M). The concentrations marked by an asterisk are 0.001M for HCl and HNO₃, and 0.0005M for H₂SO₄.

^bThe weight of element which gives a peak height absorbance of 0.0044, calculated for the system of higher sensitivity.

^cFrom Ref. 3 (using the graphite-cloth ribbon).

^dFive times the A_h values obtained by using 1 ng of As.

Table 4. Sensitivities for 34 elements in 0.05M hydrochloric acid

Element ^a	$m_{h, g}^b$	Sensitivity		Element ^a	$m_{h, g}^b$	Sensitivity	
		pM	pM _c			pM	pM _c
Li	3.9×10^{-13}	13.21	11.91	Ge*	4.4×10^{-10}	11.22	9.92
Na	1.3×10^{-13}	14.25	12.95	As*	3.5×10^{-11}	12.33	11.03
Mg*	1.0×10^{-13}	14.40	13.10	Se*	3.5×10^{-11}	12.35	11.05
Al	8.2×10^{-12}	12.52	11.22	Sr	1.6×10^{-12}	13.74	12.44
K	1.1×10^{-13}	14.54	13.24	Mo	6.9×10^{-12}	13.15	11.85
Ca	7.0×10^{-13}	13.77	12.47	Ag	1.1×10^{-12}	14.01	12.71
Sc	8.1×10^{-12}	12.74	11.44	Cd	4.8×10^{-13}	14.37	13.07
Ti	2.4×10^{-11}	12.30	11.00	Sn*	2.9×10^{-11}	12.61	11.31
V	3.4×10^{-11}	12.17	10.87	Sb*	1.8×10^{-11}	12.84	11.54
Cr	2.0×10^{-12}	13.42	12.12	Te*	1.8×10^{-11}	12.86	11.56
Mn	8.0×10^{-13}	13.84	12.54	Cs	1.3×10^{-11}	13.02	11.72
Fe	3.0×10^{-12}	13.27	11.97	Ba	1.1×10^{-11}	13.10	11.80
Co	5.6×10^{-12}	13.03	11.73	Eu	5.6×10^{-12}	13.43	12.13
Ni	8.5×10^{-12}	12.84	11.54	Au	4.0×10^{-12}	13.69	12.39
Cu	3.1×10^{-12}	13.31	12.01	Hg*	1.9×10^{-9}	11.01	9.71
Zn	4.5×10^{-13}	14.16	12.86	Pb	8.9×10^{-12}	13.37	12.07
Ga*	7.2×10^{-11}	11.99	10.69	Bi*	1.2×10^{-11}	13.24	11.94

^aSensitivities for elements marked by an asterisk were obtained by using a non-pyrolytic graphite tube and the others by using a pyrolytic graphite tube.

^bThe weight of element which gives a peak height absorbance of 0.0044.

strated that the addition of a matrix modifier such as nickel(II)²⁸ or copper (II)²⁹ to the sample is effective for reducing the volatility. Quite recently we found that the use of a graphite-cloth ribbon, which is placed inside the graphite tube and on which the sample is deposited, greatly enhances the sensitivity for selenium² and arsenic³ and reduces interferences from concomitant foreign ions. This enhancement was attributed to recondensation of the analyte element on the ribbon during atomization and to formation of stable lamellar compounds because of the greatly increased graphite surface area available for reaction. As stated earlier, techniques such as the use of matrix modifiers for increasing sensitivity leads to the sensitivity being independent of the surface nature of the tubes used (Table 3) since the interaction of the analyte with the modifiers becomes more important than that with the graphite surface.

It has been claimed that the porous nature of NPG, which causes the loss of analytes due to penetration into the graphite, is a disadvantage.¹ However, no periodic trend to support such claims is observed in Fig. 1. Recent kinetic studies³¹ have also shown that the dissipation constant obtained from the tail of the absorbance signals does not depend on the weight of analyte but is influenced by surface effects on the graphite wall. Periodic trends observed in this study indicate that the effect of the PG and NPG tubes on the sensitivity depends on the chemical properties of the analyte element. Therefore, the most important property of the graphite tube is the degree to which it tends to form carbide and lamellar compounds with the analyte rather than its permeability to gases.

Comparison of the pM values for various analytical techniques

The mole sensitivity defined by equation (2) was calculated by using the absolute sensitivity obtained

by using whichever tube gave the larger absorbance in the peak-height mode (Table 2). The absolute sensitivities and pM values are given in the last two columns of Table 4. Even a 10% difference between the absorbances for a given amount of analyte results in only a difference of 0.05 in pM. The pM values for Ba, Zn, Ga, Ge, As, and Se in various matrices are given in Table 3. Nitric acid produces the largest increase (0.44) in pM for Ge, relative to the hydrochloric acid values.

For comparison of the mole sensitivity for the various techniques measuring concentration rather than weight, we define the mole sensitivity involving concentration (pM_c) as

$$pM_c = -\log C/A_w \quad (3)$$

where C is the concentration (g/ml) corresponding to 1% absorption. The pM_c values for GFAAS were calculated on the basis of a sample volume of 50 μ l, and are given in the last column in Table 4.

In Figure 2 the pM_c values are plotted for determination of the first long-period elements by GFAAS, FAAS and AFS. The data for the latter two were obtained from Koch *et al.*³² The pM_c values for AFS were calculated by using the limits of determination,³² in g/ml, defined as $10s_{bl}$, where s_{bl} is the standard deviation of the blank signal. The data obtained with the Perkin-Elmer HGA-74 graphite furnace³² were also compared. The greatest sensitivity for each element was obtained with the Perkin-Elmer HGA 500 graphite furnace in this work. The vertical lines for Zn, Ga, Ge, As, and Se show the dependence of pM_c on the acid matrix. It is worth noting that the periodic trends of pM_c for the three methods are very similar, and characteristic of the elements. The maximum sensitivities are seen with K, Mn, Zn, and Se for all the methods. It is interesting that the sensitivity for Zn, Ga, Ge, As, and Se obtained with the

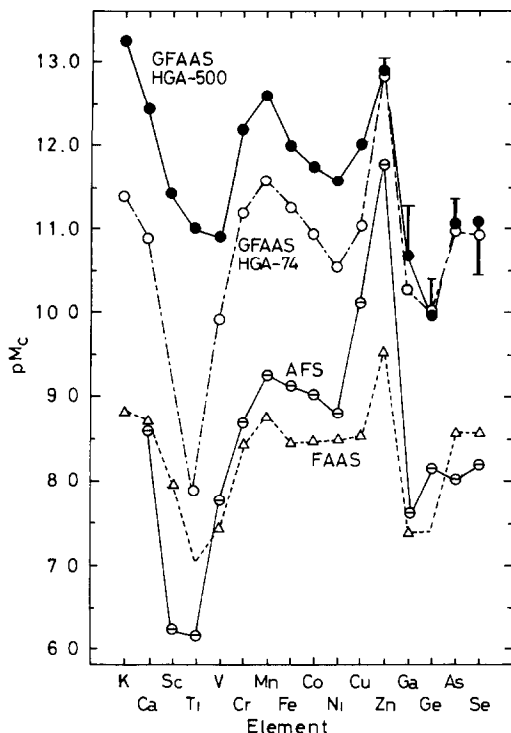


Fig. 2. Periodic trends of the mole sensitivity of the fourth-period elements for GFAAS (HGA 500 from this work, and HGA-74 data from Ref. 32), FAAS (data from Ref. 32) and AFS (data from Ref. 32).

HGA-500 in the present work is in good agreement with that obtained with the HGA-74. This is because these elements were determined by using the NPG tube. It is clear that the mole sensitivity for other metals was markedly improved by using the maximum-power heating mode and the PG tube in place of the NPG tube.

Acknowledgements—This research was supported in part by Grants-in-Aid for Scientific Research (Nos. 57470031, 58540363 and 58030061) from the Ministry of Education, Science and Culture.

REFERENCES

1. B. V. L'vov, *Atomic Absorption Spectrochemical Analysis*, Hilger, London, 1970.

2. C. H. Chung, E. Iwamoto, M. Yamamoto, Y. Yamamoto and M. Ikeda, *Anal. Chem.*, 1984, **56**, 829.
3. E. Iwamoto, C. H. Chung, M. Yamamoto and Y. Yamamoto, *Talanta*, 1986, **33**, 577.
4. K. C. Thompson, G. R. Godden and D. R. Thomerson, *Anal. Chim. Acta*, 1975, **74**, 289.
5. J. Korečková, W. Frech, E. Lundberg, J.-Å. Persson and A. Cedergren, *ibid.*, 1981, **130**, 267.
6. J. P. Erspamer and T. M. Niemczyk, *Anal. Chem.*, 1982, **54**, 538.
7. *Idem, ibid.*, 1982, **54**, 2150.
8. D. C. Manning and R. D. Ediger, *At. Absorpt. Newsl.*, 1976, **15**, 42.
9. D. C. Manning, F. J. Fernandez and G. E. Peterson, *Ind. Res.*, 1977, **19**, 82.
10. R. E. Sturgeon and C. L. Chakrabarti, *Anal. Chem.*, 1977, **49**, 90.
11. W. Slavin, D. C. Manning and G. R. Carrick, *ibid.*, 1981, **53**, 1504.
12. F. J. Fernandez and J. Iannarone, *At. Absorpt. Newsl.*, 1978, **17**, 117.
13. K. Kuga and K. Tuji, *Bunseki Kagaku*, 1978, **27**, 441.
14. T. M. Vickrey and M. S. Buren, *Anal. Lett.*, 1980, **13**, 1465.
15. J. Fazakas, *ibid.*, 1982, **15**, 573.
16. D. Littlejohn, I. Duncan, J. Marshall and J. M. Ottaway, *Anal. Chim. Acta*, 1984, **157**, 291.
17. J. Sneddon and V. A. Fuavao, *ibid.*, 1985, **167**, 317.
18. W. Slavin and G. R. Carrick, *Spectrochim. Acta*, 1984, **39B**, 271.
19. S. A. Clyburn, T. Kantor and C. Veillon, *Anal. Chem.*, 1974, **46**, 2213.
20. J. R. Montgomery and G. N. Peterson, *Anal. Chim. Acta*, 1980, **117**, 397.
21. G. Volland, G. Kölblin, P. Tschöpel and G. Tölg, *Z. Anal. Chem.*, 1977, **284**, 1.
22. M. Hoenig, F. Dehairs and A.-M. de Kersabiec, *J. Anal. At. Spectrom.*, 1986, **1**, 449.
23. Y. Mino, S. Shimomura and N. Ota, *Anal. Chim. Acta*, 1979, **107**, 253.
24. K. Dittrich, R. Mandry, W. Mothes and J. G. Judelevic, *Analyst*, 1985, **110**, 169.
25. B. V. L'vov, *Spectrochim. Acta*, 1978, **33B**, 153.
26. R. E. Sturgeon, C. L. Chakrabarti and P. C. Bertels, *Anal. Chem.*, 1975, **47**, 1250.
27. J. P. Matousek, *Prog. Anal. At. Spectrosc.*, 1981, **4**, 247.
28. R. D. Ediger, *At. Absorpt. Newsl.*, 1975, **14**, 127.
29. T. Kamada and Y. Yamamoto, *Talanta*, 1980, **27**, 473.
30. A. Cedergren, I. Lundberg, E. Lundberg, D. C. Baxter and W. Frech, *Anal. Chim. Acta*, 1986, **180**, 373.
31. C. H. Chung, *Anal. Chem.*, 1984, **56**, 2714.
32. O. G. Koch, P. O. LaFleur, G. H. Morrison, A. Jackwerth, A. Townshend and G. Tölg, *Pure Appl. Chem.*, 1982, **54**, 1565.

THE DETERMINATION OF FORMATION CONSTANTS OF WEAK COMPLEXES BY POTENTIOMETRIC MEASUREMENTS: EXPERIMENTAL PROCEDURES AND CALCULATION METHODS

ALESSANDRO DE ROBERTIS, CONCETTA DE STEFANO and SILVIO SAMMARTANO

Istituto di Chimica Analitica dell'Università, Salita Sperone, Loc. Papardo, 98010 S. Agata di Messina, Messina, Italy

CARMELO RIGANO

Dipartimento di Matematica dell'Università, Viale A. Doria 6, 95125 Catania, Italy

(Received 14 January 1987. Revised 5 May 1987. Accepted 5 June 1987)

Summary—Experimental and calculation procedures for the study of weak complexes by the pH-measurement technique are described. An algorithm for the calculation of formation constants, together with a computer program in FORTRAN and BASIC versions, is reported. The problems of studying weak interactions are discussed. Simulated titration curves and experimental data for K^+ -thiodiacetate complexation were used to check the proposed method.

Weak complexes are often important in defining rigorously the composition of natural fluids.¹ In sea-water, blood plasma, urine and numerous other fluids the formation of weak species is highly probable because of their high concentrations of alkali and alkaline-earth metal ions. Monocarboxylates form [ML] species with Li^+ , Na^+ and K^+ , having mean stability constants (± 3 standard deviations) of 1.5 ± 0.5 , 1.1 ± 0.4 and 1.1 ± 0.6 ($I = 0$, $T = 37^\circ$), respectively.²⁻⁴ Dicarboxylates form [ML]⁻ species with Li^+ , Na^+ and K^+ with mean stability constants of 15 ± 5 , 9 ± 3 and 9 ± 4 ($I = 0$, $T = 37^\circ$), respectively, and [MLH] species having stabilities comparable to those of the monocarboxylate complexes.^{4,5} Citrate forms [ML]²⁻ species with stability constants of 32, 20 and 16 ($I = 0$, $T = 37^\circ$) for Li^+ , Na^+ and K^+ , respectively,⁶⁻⁹ and protonated [MLH]⁻ species more stable than the simple dicarboxylate complexes. NTA, EDTA, pyrophosphate, triphosphosphate,¹⁰ ATP^{11,12} and hexacyanoferrate(II)^{13,14} form stronger alkali-metal complexes than the simple carboxylates do. Sulphate¹⁵ and phosphate¹⁶ show complexing abilities towards alkali metals comparable to those of dicarboxylate ligands. Many other complexes (NH_4^+ carboxylates, phosphate and sulphate,^{17,18} Mg^{2+} and Ca^{2+} monocarboxylates,^{2,19} and amine and amino-acid complexes^{4,20}) in biofluids have stability constants < 100 . Moreover, some ligands form polynuclear weak complexes [pyrophosphate, triphosphosphate,¹⁰ ATP and hexacyanoferrate(II)¹¹⁻¹³] and hexacyanoferrate(II) forms heteropolynuclear species with alkali-metal ions.¹⁴ Weak alkali-metal complexes have been reviewed.²¹

The determination of low stability constants is, therefore, an important problem. In the last five years

we, together with colleagues from other laboratories, have studied potentiometrically (using mainly the pH glass electrode, but in some cases other ion-selective electrodes) several systems^{2-20,22-26} in which weak complexes are formed, with the aim of understanding the complexing ability of alkali and alkaline-earth metal ions towards low molecular-weight ligands. In these studies we met three main problems: (i) the choice of a suitable reference background that complexes neither the ligand nor the metal under study; (ii) the choice of a model for the dependence of activity coefficients on ionic strength, because high and variable concentrations often make the constant ionic medium method unsuitable; (iii) the choice of a suitable calculation method.

As regards the first problem, it has been shown^{4,10,27-33} that tetra-alkylammonium salts (A_4N^+) are suitable for *O*-donor ligands (including some inorganic ligands such as sulphate and phosphate), and potassium salts for *N*-donor ligands. It is impossible to predict that there will be no interactions. This is particularly so for multiply charged ions, e.g., hexacyanoferrate(II) interacts with all cations, including alkali-metal¹³ and tetra-alkylammonium³⁴ ones, but even the singly charged ClO_4^- ion, which is widely used in background media, shows some complexing ability.³⁵ Another difficulty arises from the possibility of weak interactions between protonated amines and anions.³⁶ The assumption of non-interaction should be verified for each ligand studied. The ions of background medium may also be associated and so complicate the calculation of ionic strength. As regards the dependence of activity coefficients and hence stability constants on ionic strength, studies on several systems^{4,10,27-33,37} have demonstrated that activity coefficients may be

calculated by a simple Debye–Hückel type equation. We have used two methods of calculation. (a) Some well-known computer programs were modified to take into account the variations of ionic strength.³⁸ (b) New algorithms were derived that simplified the calculations and took into consideration the specific problems of dealing with weak complexes. The program WECO²⁵ was written for calculating low stability constants of complexes formed by monoprotic acids. A more powerful program, ES2WC, was written to cope with polyfunctional ligands and polynuclear complexes and this has been applied to several systems.⁴

This work describes experimental procedures and calculation methods to be followed in studying the formation of weak complexes. Particular attention is paid to the assumptions to be made in this type of investigation. The calculations have been checked with simulated data and applied to experimental data for thiodiacetate–potassium weak complex formation. Calculations have been performed on a personal computer and the results compared with those from a general computer program.

EXPERIMENTAL

Reagents

Thiodiacetic acid [H₂(tda)], Fluka pract. 95% (HPLC), was twice recrystallized from a water–ethanol mixture: its purity, checked by alkalimetric titration, was always >99.5%. Potassium chloride solution was prepared from the salt (C. Erba >99.8%) dried in an oven at 110°. Potassium hydroxide stock solution was prepared from ampoules of concentrate (C. Erba) and standardized against potassium hydrogen phthalate, Fluka puriss. Tetraethylammonium iodide, Fluka puriss., was recrystallized from methanol.

Apparatus

The free hydrogen-ion concentration, c_H , was measured at 25 ± 0.2° with a Metrohm E600 potentiometer and glass and saturated calomel electrodes from the same firm. The glass electrode was calibrated by titrating hydrochloric acid with standard potassium hydroxide solution under the same conditions as the solutions under study, either in separate titrations or by using the initial portion of a titration in which an excess of strong acid is added to the solution under study. In the latter case, some programs can calculate E^0 simultaneously with the formation constants.

A thermostatic bath was used to control the temperature of the test cell.

Procedure

Full details have been published elsewhere.⁴ It is important to exclude oxygen and carbon dioxide, so the cell was fitted with a cover and purified nitrogen bubbled through the test solution. A series of alkalimetric titrations of solutions containing the ligand in the protonated form (and also a strong acid when necessary to complete the protonation of the ligand or when internal standardization of the electrodes is required) is carried out in the presence of different metal ions.

METHOD OF CALCULATION

Choice of conditions

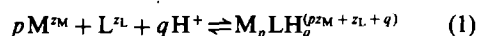
The choice of a background medium that does not interact with the ligand and the method under study

is critical, because the definition of interaction is subjective. No absolute methods are available for identifying completely dissociated electrolytes, but from practical experience of mainly conductometric and spectroscopic measurements it is possible to define a lower limit for the stability constant of a weak interaction. We assume that the interaction can be neglected if $\beta < 0.1$. As regards the association of the background medium, the majority of alkali-metal and alkaline-earth metal chlorides, nitrates and perchlorates are completely dissociated in solution or the extent of their association is known (*e.g.*, the association between K⁺ and NO₃⁻ has been studied by several methods and a reasonable value for the formation constant has been estimated⁷). It must be stressed, however, that in our method we deal with a hybrid reference state, lying between the classical constant ionic medium³⁹ reference state (in which all interactions except those between the ligand and the metal under study are neglected) and the pure water reference state (in which all possible interactions in the solution have to be taken into account). Our method approaches the latter reference state, but it would be incorrect to say that it is equivalent to it. All assumptions and experimental conditions should be clearly reported in work dealing with equilibria in solution, particularly when the complexes are weak.

There are two ways of carrying out the titrations: (i) at constant high ionic strength with $I = T_M + T_{M'}$, where M' is the cation of the background medium, or (ii) the ionic strength may be allowed to vary so that its effect on the formation constants can be studied. The second method has the advantage of being able to accommodate wide ranges of concentration of ligand (even if this is highly charged). Figure 1 shows a flow-chart of the processes and decisions involved in studying weak complexes.

The algorithm

For the general formation reaction



the formation constants and the mass-balance equations are written as follows (setting the stoichiometric coefficient of the ligand equal to unity)

$$\beta_{pq} = [M_p LH_q][M]^{-p}/[L][H]^q \quad (2)$$

$$\left. \begin{aligned} T_M &= [M] + [L]\Sigma p\beta_{pq}[M]^p[H]^q \\ T_L &= [L](1 + \Sigma\beta_{pq}[M]^p[H]^q) \\ T_H &= [H] + [L]\Sigma q\beta_{pq}[M]^p[H]^q \end{aligned} \right\} \quad (3)$$

When the formation of weak complexes is neglected

$$\left. \begin{aligned} T_L &= [L](1 + \Sigma\beta'_{pq}[H]^q) \\ T_H &= [H] + [L]\Sigma q\beta'_{pq}[H]^q \end{aligned} \right\} \quad (4)$$

where primes indicate conditional quantities. The average number of protons bound to the ligand is

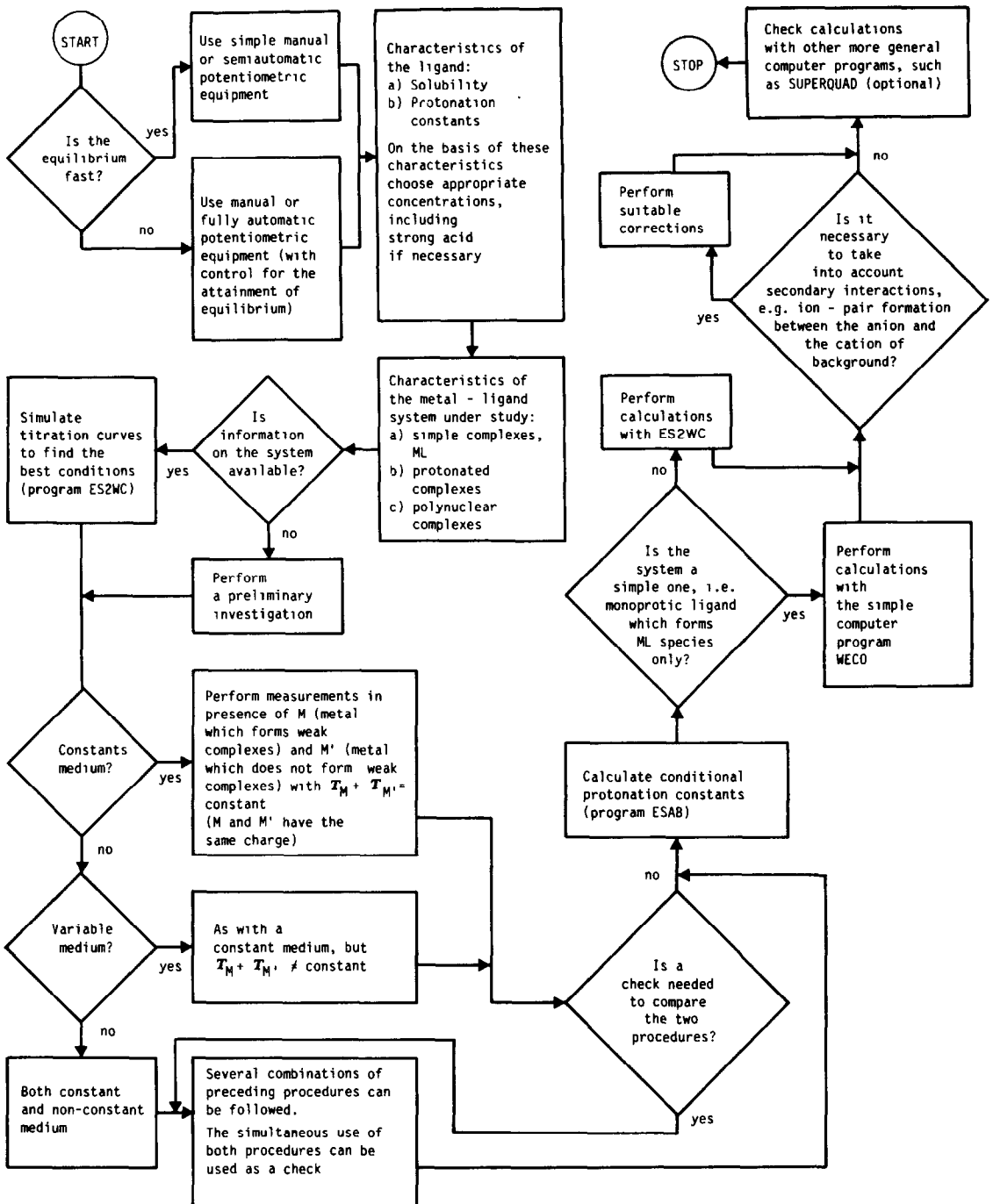


Fig. 1. Flow chart for the experimental procedure to be followed in the study of weak complexes by the pH-measurement method.

defined by

$$\bar{n}_{exp} = \frac{T_H - [H]}{T_L} \quad (5)$$

From the mass-balance equations (3) or (4),

$$\bar{n} = \frac{\sum q \beta_{pq} [M]^q [H]^q}{1 + \sum \beta_{pq} [M]^q [H]^q} \quad (6)$$

$$\bar{n}' = \frac{\sum q \beta'_{oq} [H]^q}{1 + \sum q \beta'_{oq} [H]^q} \quad (7)$$

As a first step, the conditional protonation constants are simply calculated from primary experimental data by appropriate computer programs;^{40,41} \bar{n}' is then obtained at $k = 2q_{max} - 1$ values of $[H]$ corresponding to characteristic points of the titration curve given by

$$\left. \begin{aligned} [H]_j &= \beta'_{o(j-1)/2} / \beta'_{o(j+1)/2} & j \text{ odd} \\ [H]_j &= [\beta'_{o(j+2)/2} / \beta'_{o(j-2)/2}]^{-1/2} & j \text{ even} \end{aligned} \right\} \quad (8)$$

for $j = 1, 2, \dots, q_{\max}$ (q_{\max} = maximum number of protons bound to the ligand); \bar{n}' is a quasi-experimental quantity, $\bar{n}' \cong n_{\text{exp}}$, and \bar{n} [equation (6)] is a calculated one. Therefore, the β_{pq} values can be calculated by minimizing the residual square sum over nk points (n = number of titrations) instead of all the experimental data

$$U = \sum_i (\bar{n}_i - \bar{n}'_i)^2 \quad (i = 1 \dots nk) \quad (9)$$

When dealing with weak complexes, the constant ionic medium method is often unsuitable and we need a relationship for the dependence of formation constants on ionic strength. A systematic study performed on several systems^{4,10,27-33,37} has shown that a Debye-Hückel type equation is valid for all complexes in the range $0 \leq I \leq 1M$. I' is the ionic strength of the reference state.

$$\begin{aligned} \log \beta_{pq}(I) = \log \beta_{pq}(I') & - z_{pq}^* \left(\frac{\sqrt{I}}{2 + 3\sqrt{I}} - \frac{\sqrt{I'}}{2 + 3\sqrt{I'}} \right) \\ & + C_{pq}(I - I') + D_{pq}(I^{3/2} - I'^{3/2}) \end{aligned} \quad (10)$$

where

$$C_{pq} = c_0 p_{pq}^* + c_1 z_{pq}^* \quad (11)$$

$$D_{pq} = dz_{pq}^* \quad (12)$$

$$z_{pq}^* = pz_M^2 + z_L^2 + q - (pz_M + z_L + q)^2 \quad (13)$$

and

$$p_{pq}^* = p + q \quad (14)$$

In some cases it is also advisable to take into account the dependence of β_{pq} on temperature. This can be done by expanding $\log \beta_{pq}$ (and the parameters for the dependence on ionic strength) about the point θ :

$$\begin{aligned} \log \beta_{pq}(T) = \log \beta_{pq}(\theta) + \Sigma(a_{pq})_i (T - \theta)^i \\ = \log \beta_{pq}(\theta) + F(T) \end{aligned} \quad (15)$$

$$\chi(T) = \chi(\theta) + \Sigma(a_\chi)_i (T - \theta)^i \quad (16)$$

where $\chi = c_0, c_1$ or d , with $T_{\min} < \theta < T_{\max}$.

By considering equations (10)–(16) we obtain the general relationship

$$\begin{aligned} \log \beta_{pq}(I, T) = \log \beta_{pq}(I', \theta) + G(I, T) + F(T) \quad (17) \\ G(I, T) = -z_{pq}^* \left(\frac{\sqrt{I}}{2 + 3\sqrt{I}} - \frac{\sqrt{I'}}{2 + 3\sqrt{I'}} \right) \\ + \{p_{pq}^* [c_0(\theta) + \Sigma(a_{c_0})_i (T - \theta)^i] \\ + z_{pq}^* [c_1(\theta) + \Sigma(a_{c_1})_i (T - \theta)^i]\} (I - I') \\ + z_{pq}^* [d(\theta) + \Sigma(a_d)_i (T - \theta)^i] (I^{3/2} - I'^{3/2}) \end{aligned} \quad (18)$$

At the end we have for \bar{n} and \bar{n}' the general functions:

$$\begin{aligned} \bar{n}_k = f[\beta_{pq}(\theta, I'), c_0, (a_{c_0})_i, c_1, (a_{c_1})_i, \\ d, (a_d)_i, ([M], [H], I, T)_k] \end{aligned} \quad (19)$$

$$\bar{n}'_k = f[(\beta'_{0q}, [H], I, T)] \quad (20)$$

Equations (19) and (20) can be used in the least-squares refinement by minimizing function (9). In equation (19) the quantity $[M]$ is not experimentally accessible by the pH-measurement method. However, when $T_M \gg T_L$ we can assume $[M] = T_M$; if this assumption is not valid, $[M]$ can be calculated iteratively.

Computer programs

On the basis of the algorithm above, computer programs have been written in FORTRAN (ES2WC1) and BASIC (ES2WC2). We used the Gauss-Newton⁴² least-squares method to refine the parameters of equation (19) by minimizing the error-squares sum [equation (9)]. In ES2WC, MAIN performs the majority of the calculations and subroutine GAUSSC resolves the system of linear equations (*i.e.*, calculates the shifts). The special features of the program are as follows.

The program can refine the parameters for the dependence on ionic strength, c_0, c_1 and d [equations (10)–(14)], as well as the formation constants. The dependence of all the parameters on temperature can also be calculated [equations (15)–(18)]. For the damping of the shifts we used the well-known Levenberg-Marquardt algorithm.^{43,44} The system of normal equations is solved by the Compact Gauss Method⁴⁵ (GAUSSC). During the refinement procedure β_{pq} can assume negative values: the program then sets $\beta_{pq} = 10^{-10}$ and another refinement cycle is performed. This procedure can avoid divergence, particularly when bad initial estimates are chosen. The program is written in a compact form and needs no particular experience for its use. Core requirements and calculation times are suitable for running ES2WC1 and ES2WC2 on personal computers: ES2WC1 (IBM PC, operating system MSDOS 3.10, compiler FORTRAN 2.00) needs 82 kbyte (single precision) or 92 kbyte (double precision). Listings of ES2WC1 and ES2WC2 are available on request.

RESULTS AND DISCUSSION

The calculation method described here has been successfully applied to several systems. Now we will examine in detail some features of this method with the aim of demonstrating its rigorosity. The first point to be examined concerns the choice of the $(2q_{\max} - 1)$ values of $[H]$ to obtain the \bar{n}' values. By calculating the error in pH generated by the errors in β_{pq} (using the rules of error propagation) we can deduce the best choice of $[H]$ values. Figure 2 shows $\epsilon(\text{pH})$ (error in pH due to a given error in β_{pq} , chosen arbitrarily) as a function of pH. As can be seen, the

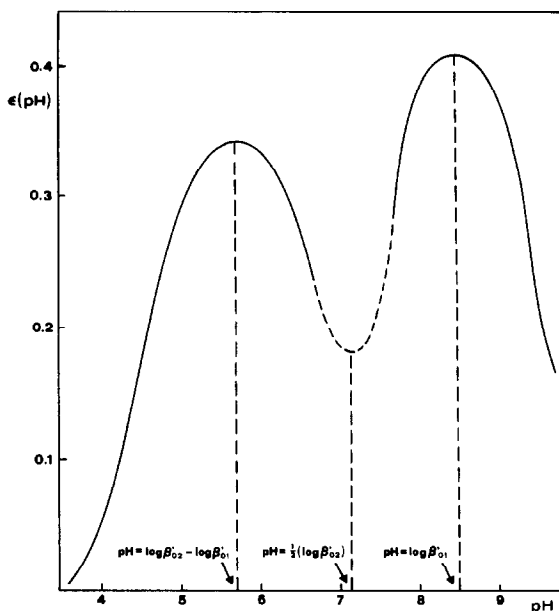


Fig. 2. Behaviour of the function $\epsilon(\text{pH}) = f[\epsilon(\beta)]$ for a diprotic ligand, where ϵ indicates a generic variation.

curve for a diprotic ligand shows three characteristic points (two maxima and one minimum), corresponding to the $[\text{H}^+]$ values from equation (8). In practice, q_{max} points [odd j in equation (8)] are sufficient for simple systems, as revealed by simulated experiments (see below).

Simulated data (details available on request) were used to check the performance of the ES2WC program. The simulated experiments were made up as follows: (a) six hypothetical systems; (b) calculation of five (or twenty) titration curves for each system [at five different ionic strengths (and at four different temperatures for one system)] by means of computer program ES4EC;⁴⁶ (c) calculation of β'_{0j} values by means of the computer program ESAB⁴¹ ($\log \beta'_{0j}$ values were rounded to ± 0.005); (d) calculation by ES2WC of β_{pq} and the parameters for the dependence on ionic strength and temperature. The calculated values were very close to those used to construct the simulated experiments: $\log \beta$ values were reproduced within ± 0.01 and the coefficients c_0 , c_1 and d within 4, 7 and 15% respectively. Small differences can be attributed to the rounding of conditional protonation constants and to the use of initial total metal concentrations instead of free concentrations.

All calculations were performed for $(2q_{\text{max}} - 1)$ and q_{max} points, with the same results in both cases. Calculation times for all 6 systems were < 4 min on the Honeywell Lev. 6, mod. 43 (operating system GCOS 6 mod 400, release 3.0; ES2WC1) and on the IBM PC (ES2WC2) 48 min in double precision and 23 min in single precision. After taking into account that 87% of the total time was spent on one system (4), in which 27 parameters were refined, these ex-

cution times can be considered satisfactory. Calculations in single and double precision resulted in the same refined values. In one system (5) some formation constants became negative for two cycles and setting $\beta = 10^{-10}$ avoided divergence.

The possibility of determining the formation constants of polynuclear species by the pH-measurement technique must be considered separately. Some authors have affirmed that the pH-measurement method is not suitable for such systems, but simulations indicate that both $[\text{M}_2\text{L}]$ and $[\text{MM}'\text{L}]$ complexes can be studied by this method. This can be shown by considering the effect of neglecting the formation of binuclear species, *i.e.*, β_{20} in equation (6), for a system of HL, H_2L , ML and M_2L complexes. This leads to the equality $\beta_{10} + \beta_{20}[\text{M}] = \beta'_{10}$ (where β'_{10} is a conditional constant); unless $[\text{M}]$ is constant, this equality is invalid, and therefore determining \bar{n} is sufficient for calculating β_{20} .

Another fundamental point to be discussed in analysing the present method of determining low

Table 1. Results for the potentiometric investigation of the H-K-thiodiacetate system

ESAB calculations				
$\log \beta'_{01}$	$\log (\beta'_{02}/\beta'_{01})$	$\log \beta'_{01}$	$\log (\beta'_{02}/\beta'_{01})$	I, M
Et_4N^+		K^+		
(± 0.003)	(± 0.003)	(± 0.004)	(± 0.003)	
4.297	3.177	4.262	3.193	0.012
4.202	3.136	4.184	3.159	0.042
4.163	3.132	4.104	3.103	0.091
4.128	3.115	4.055	3.108	0.159
4.129	3.117	4.002	3.046	0.248
4.142	3.142	3.956	3.028	0.354
4.159	3.163	3.962	3.026	0.478
4.199	3.211	3.945	3.040	0.627
4.240	3.249	3.954	3.053	0.785
—	—	3.951	3.054	0.975

ES2WC calculations at $I' = 0.25\text{M}$

	C	D
$\log \beta_{01} = 4.118 \pm 0.004$	0.99	-0.37
$\log \beta_{02} = 7.240 \pm 0.004$	1.60	-0.56
$\log \beta_{10} = 0.32 \pm 0.01$	0.99	-0.37
$\log \beta_{11} = 3.88 \pm 0.02$	1.60	-0.56

SUPERQUAD calculations at $I' = 0.25\text{M}$

	C	D
$\log \beta_{01} = 4.126 \pm 0.004$	1.03	-0.40
$\log \beta_{02} = 7.248 \pm 0.016$	1.62	-0.57
$\log \beta_{10} = 0.40 \pm 0.04$	0.95	-0.40
$\log \beta_{11} = 4.07 \pm 0.08$	1.47	-0.60

Formation constants at different ionic strengths

I, M	$\log \beta_{01}$		$\log \beta_{02}$		$\log \beta_{10}$		$\log \beta_{11}$	
	(a)	(b)	(a)	(b)	(a)	(b)	(a)	(b)
0.00	4.49	4.49	7.77	7.77	0.69	0.78	4.4	4.6
0.04	4.22	4.22	7.36	7.37	0.42	0.51	4.0	4.2
0.16	4.12	4.13	7.24	7.24	0.32	0.41	3.9	4.1
0.36	4.13	4.14	7.28	7.28	0.33	0.41	3.9	4.1
0.64	4.20	4.21	7.42	7.43	0.40	0.46	4.1	4.2
1.00	4.31	4.31	7.61	7.62	0.51	0.53	4.3	4.3

(a) ES2WC; (b) SUPERQUAD

stability constants is related to the choice of a suitable model for the ionic strength dependence of formation constants. Obviously, the equations proposed [(10)–(14) and (18)] cannot be tested with simulated data alone. Statistical analysis of experimental data also demonstrates the validity of our approach.²⁵ Moreover, in this work we performed some measurements on the system $K^+ - H^+ - \text{thiodiacetate (tda)}$ and calculated β_{pq} , together with the parameters for the ionic strength dependence of β_{pq} , by means of both ES2WC and, for comparison, the general computer program SUPERQUAD⁴⁷ (modified by us to take account of the dependence of ionic strength). The results in Table 1 show two interesting features. (i) There is good agreement between ES2WC and SUPERQUAD. (ii) The dependence of the formation constants on the ionic strength can be expressed by equation (10) and the *C* and *D* parameters for this system are in agreement with several previous results. It is our opinion that the results for the ionic strength dependence of formation constants can be used as a check for the correctness of the ionic interaction model.

The conclusions of this work are: (a) the proposed method is quite simple as regards both the experimental and calculation procedure; (b) the method is rigorous and allows parameters for the dependence on temperature and ionic strength to be determined together with formation constants; (c) the calculation procedure implies a preliminary smoothing of experimental data (through calculation of conditional protonation constants) that allows a better control of the data (avoiding accidental errors); (d) the instrumentation needed to follow the present procedure (potentiometric equipment and a personal computer) is relatively inexpensive.

Acknowledgements—We thank the C.N.R. (Rome) and the Ministero della Pubblica Istruzione for financial support.

REFERENCES

1. E. A. Jenne (ed.), *Chemical Modeling in Aqueous Systems*, American Chemical Society, Washington D. C., 1979.
2. P. G. Daniele, A. De Robertis, C. De Stefano, C. Rigano and S. Sammartano, *Ann. Chim. (Rome)*, 1983, **73**, 619.
3. A. De Robertis, C. De Stefano, S. Sammartano, R. Scarcella and C. Rigano, *J. Chem. Res.*, 1985, 42 (S), 629 (M).
4. P. G. Daniele, A. De Robertis, C. De Stefano, S. Sammartano and C. Rigano, *J. Chem. Soc., Dalton Trans.*, 1985, 2353.
5. P. G. Daniele, C. Rigano and S. Sammartano, *Thermochim. Acta*, 1983, **62**, 101.
6. G. Arena, R. Cali, M. Grasso, S. Musumeci, S. Sammartano and C. Rigano, *ibid.*, 1980, **36**, 329.
7. P. G. Daniele, C. Rigano and S. Sammartano, *Ann. Chim. (Rome)*, 1980, **70**, 119.
8. V. Cucinotta, P. G. Daniele, C. Rigano and S. Sammartano, *Inorg. Chim. Acta*, 1981, **56**, L45.
9. P. G. Daniele, G. Ostacoli, C. Rigano and S. Sammartano, *Transition Met. Chem.*, 1984, **9**, 385.
10. P. G. Daniele, C. Rigano and S. Sammartano, *Anal. Chem.*, 1985, **57**, 2956.
11. R. Cali, S. Musumeci, C. Rigano and S. Sammartano, *Inorg. Chim. Acta*, 1981, **56**, L11.
12. A. De Robertis, C. De Stefano, S. Sammartano, R. Cali, R. Purrello and C. Rigano, *J. Chem. Res.*, 1986, 164 (S), 1301 (M).
13. S. Capone, A. De Robertis, S. Sammartano and C. Rigano, *Thermochim. Acta*, 1986, **102**, 1.
14. S. Capone, A. De Robertis, C. De Stefano and R. Scarcella, *J. Chem. Res.*, 1986, 412 (S).
15. P. G. Daniele, C. Rigano and S. Sammartano, *Inorg. Chim. Acta*, 1982, **63**, 267.
16. P. G. Daniele, M. Grasso, C. Rigano and S. Sammartano, *Ann. Chim. (Rome)*, 1983, **73**, 495.
17. P. Amico, P. G. Daniele, C. Rigano and S. Sammartano, *ibid.*, 1981, **71**, 659.
18. A. De Robertis, C. De Stefano, S. Sammartano and R. Scarcella, *J. Chem. Res.*, 1985, 322 (S).
19. A. Casale, A. De Robertis and S. Sammartano, *Thermochim. Acta*, 1985, **95**, 15.
20. S. Capone, A. De Robertis, C. De Stefano and R. Scarcella, *Talanta*, 1985, **32**, 675.
21. D. Midgley, *Chem. Soc. Rev.*, 1975, **4**, 549.
22. P. G. Daniele, C. Rigano and S. Sammartano, *Thermochim. Acta*, 1981, **46**, 103.
23. *Idem*, *Ann. Chim. (Rome)*, 1982, **72**, 341.
24. P. G. Daniele, A. De Robertis, S. Sammartano and C. Rigano, *Thermochim. Acta*, 1984, **72**, 305.
25. A. De Robertis, C. Rigano and S. Sammartano, *ibid.*, 1984, **74**, 343.
26. A. De Robertis, C. De Stefano, R. Scarcella and C. Rigano, *ibid.*, 1984, **80**, 197.
27. P. G. Daniele, C. Rigano and S. Sammartano, *Transition Met. Chem.*, 1982, **7**, 109.
28. *Idem*, *Talanta*, 1983, **30**, 81.
29. *Idem*, *ibid.*, 1985, **32**, 78.
30. P. G. Daniele, A. De Robertis, C. Rigano and S. Sammartano, *Ann. Chim. (Rome)*, 1985, **75**, 115.
31. S. Capone, A. De Robertis, C. De Stefano, S. Sammartano, R. Scarcella and C. Rigano, *Thermochim. Acta*, 1985, **86**, 273.
32. P. G. Daniele, S. Sonogo M. Ronzani and M. Marangella, *Ann. Chim. (Rome)*, 1985, **75**, 245.
33. A. De Robertis, C. De Stefano, C. Rigano and S. Sammartano, *J. Chem. Res.*, 1986, 194 (S).
34. F. Ferranti and A. Indelli, *J. Solution Chem.*, 1974, **3**, 619.
35. L. Johansson, *Coord. Chem. Rev.*, 1974, **12**, 241.
36. S. Capone, A. Casale, A. Curro, A. De Robertis, C. De Stefano, S. Sammartano and R. Scarcella, *Ann. Chim. (Rome)*, 1986, **76**, 441.
37. P. G. Daniele, C. Rigano and S. Sammartano, *ibid.*, 1983, **73**, 741.
38. P. Amico, P. G. Daniele, C. Rigano and S. Sammartano, *ibid.*, 1982, **72**, 1.
39. F. J. C. Rossotti and H. Rossotti, *The Determination of Stability Constants*, McGraw-Hill, New York, 1961.
40. G. Arena, E. Rizzarelli, S. Sammartano and C. Rigano, *Talanta*, 1979, **26**, 1.
41. C. Rigano, M. Grasso and S. Sammartano, *Ann. Chim. (Rome)*, 1984, **74**, 537.
42. L. C. W. Dixon, *Nonlinear Optimization*, English Univ. Press, London, 1972.
43. K. Levenberg, *Quart. Appl. Math.*, 1944, **2**, 164.
44. D. W. Marquardt, *J. Soc. Indust. Appl. Math.*, 1963, **11**, 431.
45. I. S. Berezin and N. P. Zhidkov, *Computing Methods*, Vol. 2, Pergamon, Oxford, 1965.
46. A. De Robertis, C. De Stefano, S. Sammartano and C. Rigano, *Anal. Chim. Acta*, 1986, **191**, 385.
47. P. Gans, A. Sabatini and A. Vacca, *J. Chem. Soc., Dalton Trans.*, 1985, 1195.

DETERMINATION OF SOLUBLE CHROMIUM IN SIMULATED PWR COOLANT BY DIFFERENTIAL-PULSE ADSORPTIVE STRIPPING VOLTAMMETRY

K. TORRANCE and C. GATFORD

Central Electricity Generating Board, Central Electricity Research Laboratories, Kelvin Avenue,
Leatherhead, Surrey, England

(Received 2 March 1987. Accepted 5 June 1987)

Summary—An analytical method has been developed for the determination of dissolved chromium at concentrations less than $2 \mu\text{g/l}$. in PWR coolant by differential-pulse adsorptive stripping voltammetry at a hanging mercury drop electrode. Concentrations above $2 \mu\text{g/l}$. can be determined by appropriate dilution of the sample. The method is based on measurement of the current associated with reduction of a chromium(III)-DTPA (diethylenetriaminepenta-acetic acid) complex adsorbed at the surface of the mercury drop. The effects of boric acid, pH, DTPA concentration, accumulation potential and time were investigated together with the oxidation state of the chromium. No interference was observed from other transition metal ions expected to be present in PWR coolant. No alternative chemical technique of similar sensitivity was available for comparison with the results obtained in solutions containing $<1 \mu\text{g/l}$. chromium. Recoveries from simulated coolant solutions were greater than 95% and the relative standard deviations for single determinations were in the range 12–25%. The statistical limit of detection at the 95% confidence level was $0.023 \mu\text{g/l}$. This method of analysis should prove valuable in corrosion studies and is uniquely capable of following the changes in soluble chromium concentration in PWR coolant that follow operational changes in the reactor.

The boric acid solution used as the coolant in the primary circuit of a pressurized water reactor (PWR) contains trace amounts of metals derived from the materials of construction. Periodic analysis is required to assess the concentrations of the metals present in soluble and insoluble forms. In the initial stages of operation of a reactor, a wide inventory of these metals will be taken in order to characterize the chemical behaviour of the system during certain operational procedures, such as start-up and shut-down. For this purpose, methods of analysis are required for the major elements (iron, chromium and nickel) derived from the austenitic steels and nickel-rich alloys used in construction, and these methods should take into consideration procedures for both soluble and insoluble forms of the elements. Current procedures for the analysis of insoluble material after collection on a membrane filter are satisfactory but the determination of low concentrations of soluble metals in the presence of the high concentrations of boric acid added to the coolant is difficult. A new method is proposed here for the determination of soluble chromium at concentrations relevant to PWR coolant, for which no alternative direct method has been found in the literature.

Under normal operating conditions, the concentrations of soluble chromium are considerably below $1 \mu\text{g/l}$. These levels have been measured, after preconcentration on ion-exchange membrane filters, by X-ray fluorescence or ^{51}Cr γ -spectrometry. Chromium at concentrations $<1 \mu\text{g/l}$. can be determined by graphite-furnace atomic-absorption spectrometry,

but the presence of lithium and boric acid severely reduces the accuracy and for practical purposes the limit of detection is about $1 \mu\text{g/l}$. Ion-chromatography has the potential for determining low concentrations of Cr(III) but no detailed reports on this measurement in the presence of boric acid are available.

Anodic-stripping voltammetry, with its amalgam concentration stage, is potentially the most sensitive electrochemical technique, but chromium has low solubility in mercury and only limited success has been reported. An alternative accumulation technique¹ involves concentration of chromium(VI) on a platinum electrode coated with an ion-exchange material; the accumulated ions are then reduced in a voltammetric sweep. However, the background currents limit the application to chromium greater than $1 \mu\text{g/l}$. and the procedure has not become generally adopted.

The adsorption stripping voltammetric technique described here is based on an effect first reported by Tanako and Ito² in which both Cr(VI) and Cr(III), in a supporting electrolyte containing ethylenediaminetetra-acetic acid (EDTA) and nitrate, gave high polarographic currents attributable to catalytic reoxidation of Cr(II) by nitrate. This reaction was further investigated by Zarebski,³ who defined the analytical conditions for the pulse polarographic determination of Cr(VI) and Cr(III) and found that diethylenetriaminepenta-acetic acid (DTPA) was more suitable than EDTA. For the conditions described, Zarebski reported limits of detection of 5

and 1 $\mu\text{g/l.}$ for Cr(VI) and Cr(III), respectively. Golimowski *et al.*⁴ introduced adsorptive pre-concentration of the Cr(III)-DTPA complex at a hanging mercury drop and reported a detection limit of 0.02 $\mu\text{g/l.}$ for chromium in natural waters.

In previously described work on the determination of nickel and cobalt⁵ and soluble iron⁶ in simulated coolant, adsorption stripping voltammetry has proved to be very successful and the sensitivity reported for chromium in natural waters⁴ suggested that it would be suitable for the measurement of the very low concentrations expected in PWR coolant.

EXPERIMENTAL

Reagents

All reagents used were of analytical grade unless otherwise stated. All solutions were stored in polyethylene bottles unless otherwise stated.

DTPA solution, 0.1M. Prepared by dissolving recrystallized Fluka DTPA in demineralized water containing 2 moles of sodium hydroxide per mole of DTPA.

Sodium nitrate solution (2.5M). Prepared from material recrystallized twice from a 12:1 v/v water/methanol mixture.

Ammonium acetate solution, pH 6.2. Ammonium acetate solution was prepared by adding appropriate volumes of isothermally distilled ammonia solution and "Aristar" acetic acid (BDH) to demineralized water to give an acetate concentration of 0.5M. The pH was measured and adjusted to 6.2 by the addition of further ammonia solution.

Chromium(VI) solutions. A stock solution of 100 $\mu\text{g/l.}$ Cr(VI) was prepared by dissolving potassium dichromate in demineralized water, and diluted daily to give 100 $\mu\text{g/l.}$ and 50 $\mu\text{g/l.}$ Cr(VI) standards.

Chromium(III) solutions. A stock solution of 100 mg/l. Cr(III) was prepared by dissolving potassium dichromate in daily with demineralized water to give 100 $\mu\text{g/l.}$ and 50 $\mu\text{g/l.}$ Cr(III) standards.

Boric acid solutions. A boric acid solution containing 6000 mg/l. boron was prepared by dissolving high-purity boric acid (Borax Consolidated Ltd.) in demineralized water, and diluted as required to give the concentrations of boron relevant to PWR coolant.

Lithium solutions. A solution containing 200 mg/l. lithium was prepared from reagent-grade lithium hydroxide (Fisons, SLR-grade). Portions of this solution were added to boric acid solutions to give the concentrations of lithium (0.2–2 mg/l.) relevant to PWR coolant.

Bromine water. A saturated solution of bromine in water was prepared by adding reagent-grade bromine to demineralized water in a dark glass reagent bottle until excess of bromine was present after the mixture had been shaken and allowed to stand overnight. Portions of this saturated bromine water were diluted hundredfold with demineralized water each day.

Interferent solutions. Solutions containing cobalt, nickel, manganese(II) and iron(III) were prepared by dilution of BDH "Spectrol" standard solutions (1000 mg/l.) of these ions. Standard iron(II) solutions in 0.05M sulphuric acid were prepared daily, as required, from ammonium ferrous sulphate.

Isothermally distilled ammonia solution. Polyethylene beakers, one half-filled with demineralized water and the other half filled with 0.88 (s.g.) ammonia solution were left in a sealed desiccator for a week, at the end of which the beaker originally containing the water contained pure ammonia solution, the concentration of which was determined by titration with hydrochloric acid.

Demineralized water. Obtained by continuously circulating water (purified by reverse osmosis) through a mixed cation/anion exchange column, to yield a product with a conductivity at 25° of the order of 0.06–0.07 $\mu\text{S/cm.}$

Voltammetric conditions and peak current measurement

An EG&G Princeton Applied Research Model 264 Polarographic Analyzer and Model 303 Static Mercury Drop Electrode assembly were used in conjunction with a Model RE0089 X-Y recorder.

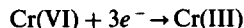
The electrode assembly was controlled by a micro-processor in the analyser, programmed to give a purge time of 8 min during which oxygen in the solution was removed by passage of nitrogen (99.999% pure), an accumulation time at a selected voltage, and a voltage scan between the accumulation voltage and a second selected voltage. For the determination of chromium an accumulation voltage of -0.9 V and final voltage of -1.35 V were selected, and a scan-rate of 5 mV/sec. The deposition times were varied between 30 and 120 sec, depending on the concentration of metal ions in the sample. In every case a "medium" drop (2.5 mg) was used with a pulse (amplitude 50 mV) every 0.5 sec, in the differential-pulse stripping mode. A cracked-junction reference half-cell⁵ was used, filled with 3M potassium chloride.

The chromium peak at -1.15 V rises from a curved base-line, and if the peak heights are measured from a straight line drawn tangentially to the base-line on either side of the peak, the results have a negative bias, especially for small peaks (*i.e.*, with low concentrations or short accumulation times). Bias-free results are obtained from peak-height measurements made from a smooth curve drawn between the troughs on either side of the peak, and this procedure was followed throughout. The contour of this curve was obtained from voltamperograms of the reagent blank solution containing boric acid.

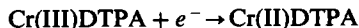
RESULTS AND DISCUSSION

Chromium oxidation state and peak current

The first stage of the stripping analysis involves adsorptive accumulation of chromium as a Cr(III)-DTPA complex on the surface of the mercury electrode at -0.9 V . Cr(VI), diffusing as chromate from the bulk solution to the electrode surface, is reduced at this potential, since



has $E_{1/2} = -0.2\text{ V}$. In the presence of the DTPA ions already in the structured ionic interface of the electrode, the Cr(III) ions are rapidly complexed and adsorbed on the mercury surface. The exact nature of this complex is unknown; but at the pH of the bulk solution it seems by analogy with the aluminium and iron(II) complexes to be mainly CrDTPA^{2-} with some CrHDTPA^- . After accumulation of the adsorbed complex, the voltage is scanned from -0.9 to -1.35 V , resulting in reduction of the adsorbed complex,



(charges on the complexes are omitted for simplicity). It is the current associated with this reduction at $E_{1/2} = -1.15\text{ V}$ which is measured for analytical purposes. The role of the nitrate ion is considered to be re-oxidation of the Cr(II) at the electrode surface

to Cr(III), thus making further adsorbed complex immediately available for enhancement of the reduction current.²⁻⁴

In the polarographic determination of chromium Zarebski³ reported that there was a difference in the reduction current for Cr(III) and Cr(VI) solutions of equal concentration and concluded that it was not possible to determine the soluble chromium content of a sample without first separating the oxidation states. The opposite conclusion was reached by Golimowski *et al.*,⁴ who used a differential pulse adsorption stripping procedure and found that the peak currents were the same for equal concentrations of Cr(III) and Cr(VI). Clearly this aspect required further investigation and experiments were done to compare the relative sensitivities of the peak currents for the two oxidation states.

The peak currents at -1.15 V were measured for solutions that were identical except for the oxidation state of the chromium. In solutions containing $1 \mu\text{g/l.}$ chromium and 250 mg/l. boron, buffered to pH 5.4, the ratio of the peak currents Cr(VI):Cr(III) was 1.2:1. In another test, at pH 5.8, with $0.1 \mu\text{g/l.}$ chromium and 300 mg/l. boron, the Cr(VI):Cr(III) peak-current ratio was 1.4:1. These results agree with the observations of Zarebski,³ confirming that a differential pulse voltammetric determination of soluble chromium must take into consideration the oxidation state of the metal. The most obvious method, other than physical separation of the Cr(VI) and the Cr(III), is to treat the sample so that only one oxidation state is present. Reduction of chromium to the lower oxidation state was not considered after it was observed that the peak currents in Cr(III)-DTPA solutions decreased significantly with time. For example, the peak current for a solution containing 600 mg/l. boron, 1.2 mg/l. lithium and $0.2 \mu\text{g/l.}$ Cr(III) decreased by 15% over the first 5 min after the addition of DTPA. In a corresponding solution containing $0.2 \mu\text{g/l.}$ Cr(VI) the decrease over the same time period was 6% (Fig. 1). Although dependence of peak current on time is undesirable, the change for the Cr(VI) solution was considered to be acceptable and only the oxidative pretreatment of solutions was investigated thoroughly.

Choice of oxidizing agent

It was intended to treat a sample containing soluble chromium, in an undefined oxidation state, with an oxidizing reagent that would give a final solution containing only Cr(VI). Two oxidants, hydrogen peroxide and bromine, were investigated because their reduced forms were known to cause no interference in the subsequent voltammetric analysis. Bromine, added as bromine water, was the better of the two, since it is reduced at potentials much more positive than the accumulation potential (-0.9 V), whereas hydrogen peroxide is reduced at between -0.9 and -1 V. An injection of bromine water into

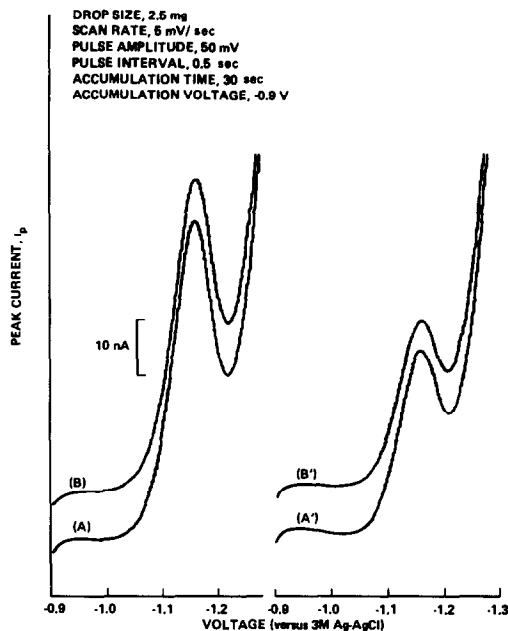


Fig. 1. Comparison of peak currents of $0.2 \mu\text{g/l.}$ Cr(VI) and Cr(III) in a solution containing 600 mg/l. of boron and 1.2 mg/l. of lithium. (A) and (B) Cr(VI) 1.7 and 5 min after the addition of DTPA and (A') and (B') Cr(III) for the same conditions.

test Cr(VI) solution produced no significant change in the peak current (Fig. 2).

Preliminary experiments confirmed that Cr(III) in boric acid solutions containing up to 1000 mg/l. boron was completely oxidized to Cr(VI) by boiling with bromine water. To make the procedure as simple as possible and, ideally, omit a boiling step, the effects of bromine concentration, oxidation time and temperature were investigated. It was found that the addition of 2 ml of a 100-fold dilution of saturated bromine water to 50 ml of 1-mg/l. Cr(III) solution and heating for 15 min at 60° in a water-bath gave $>95\%$ oxidation. The efficiency of the oxidation

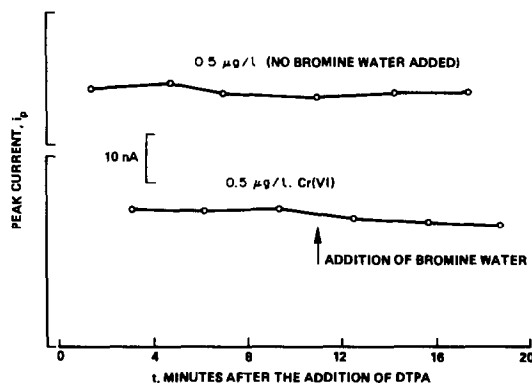


Fig. 2. Effect of the addition of bromine water to an analytical solution containing $0.5 \mu\text{g/l.}$ Cr(VI).

Table 1. Comparison of peak currents, i_p , of 1- $\mu\text{g/l. Cr(VI)}$ and oxidized Cr(III) solutions

Dilution of saturated bromine water*	i_p, nA	
	Oxidized Cr(III)	Cr(VI)
1:100	115	117
1:300	130	138
1:1000	109	123

*Two ml of diluted bromine water added per 50 ml of Cr solution (containing 1500 mg/l. boron).

procedure at low chromium concentrations was demonstrated by comparison of the peak currents for solutions initially containing Cr(III) or the same concentration of Cr(VI) (Table 1).

Effect of nitrate concentrations

The catalytic effect of oxy-anions in polarography is well established. The effects of nitrate on the reduction of Cr(III)-EDTA and -DTPA complexes^{2,3} and of nitrate and bromate on DTPA complexes⁴ have been reported. In our experiments these catalytic effects were confirmed as occurring in boric acid solutions (boron 600 mg/l.) containing 1 $\mu\text{g/l. Cr(III)}$. The peak current doubled when the nitrate concentration was increased from 0.05 to 1.0M and approximately doubled again on increase of nitrate concentration from 1.0 to 1.5M. A nitrate concentration of 0.5M was chosen as a compromise between higher sensitivity and the level of chromium impurity introduced with this reagent (0.04 $\mu\text{g Cr/mole NaNO}_3$).

Effect of pH

This effect was measured over the pH range 4.6-7.6 for 0.5M nitrate, for 10 $\mu\text{g/l. Cr(VI)}$, 600 mg/l. boron and optimum DTPA concentration. The current was highest at pH 6 and was reduced by 50% by a pH change of ± 0.8 . The ammonium acetate solution recommended in the analytical procedure was chosen to give pH 6 ± 0.2 in the analytical solution.

Effect of DTPA concentration

This was investigated with 0.5 $\mu\text{g/l. Cr(VI)}$, 0.5M nitrate and 500 mg/l. boron at pH 5.8. The peak current increased by 80% as the DTPA concentration was increased from 0.5×10^{-3} to $2.5 \times 10^{-3} M$ then remained constant up to $5 \times 10^{-3} M$ DTPA. In most of the experiments a concentration of $2 \times 10^{-3} M$ was used.

Effects of accumulation potential and time

The current associated with the different pulse reduction peak at -1.15 V is dependent on the accumulation potential and a gradual increase in peak current (i_p) was observed as the potential was reduced from -0.6 to -0.9 V. The latter value was subsequently used throughout.

The effect of accumulation time was investigated

with a simulated coolant solution containing 750 mg/l. boron, 20 $\mu\text{g/l. Fe(III)}$, 25 $\mu\text{g/l. Ni}$, 5 $\mu\text{g/l. (each) Co(II) and Mn(II)}$ and 0.4 $\mu\text{g/l. Cr(VI)}$. The transition metal ions were added because it is known^{5,7} that complexes similar to the species of interest can compete for the adsorption sites on the mercury drop and alter the accumulation characteristics. A plot of peak current vs. accumulation time was pseudo-linear for times up to 300 sec. For most of the determinations in this work, the accumulation times used were ≤ 50 sec; longer times were not necessary, because of the high sensitivity.

Time-dependence of peak currents

With both Cr(III) and Cr(VI) solutions there were kinetic effects that produced a decrease in peak current with time. The changes were greater in the Cr(III) solutions and this was the main reason for selecting an oxidative pretreatment of the sample. However, the kinetic effects in Cr(VI) solution cannot be ignored and must introduce imprecision, particularly when long accumulation periods are used.

The influences of variations in pH, temperature, concentration of boric acid, and the concentrations and order of addition of reagents were studied in an effort to identify the source of the slight time-dependence of the peak current. Variation of these parameters did not significantly alter the time-dependence but it was clearly shown that the changes in peak current depended on the time elapsed after the addition of DTPA. Possibly the Cr(VI) was being reduced by traces of oxidizable impurities introduced with the DTPA and any progressive partial reduction to Cr(III) in the bulk solution would bring about a corresponding decrease in the peak current.

To obtain reproducible analysis by using a standard-addition procedure, the DTPA was introduced after nitrogen had been passed through the test solution for 8 min, and the peak current was measured after a fixed interval, with the shortest accumulation time commensurate with the chromium

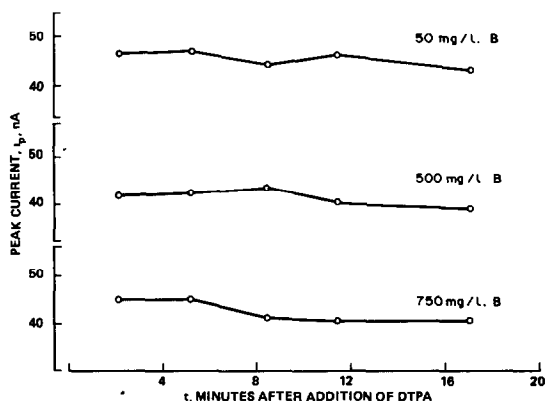


Fig. 3. Variation of peak current with time for solutions containing 0.1 $\mu\text{g/l. Cr(VI)}$ at three concentrations of boron as boric acid.

Table 2. Effects of some transition metal ions

Interferents	[Cr], $\mu\text{g/l.}$	
	Taken	Found
—	0.18*	0.16, 0.18
Fe(II) etc.	0.18*	0.14, 0.14
Fe(III) etc.	0.18*	0.17, 0.19
Fe(II) etc.	0.18†	0.17, 0.18
—	0.88†	1.00, 0.87
Fe(II) etc.	0.88†	0.86, 0.84

*0.25 ml of 100-fold dilution bromine water per 20 ml.

†1.0 ml of 100-fold dilution bromine water per 20 ml.

concentration in the sample. At chromium concentrations $\geq 0.2 \mu\text{g/l.}$ in the sample, accumulation for 30 sec was sufficient and the analysis could be completed in less than 6 min after the addition of DTPA. The absence of bias in the recovery tests (see Table 3) suggests that any kinetic errors introduced are small. This is confirmed by the consistency of the peak current in the 4–6 min period after DTPA addition, for solutions containing $0.1 \mu\text{g/l.}$ Cr(VI) at three concentrations of boric acid and pH 5.8 (Fig. 3).

Effect of some transition metal ions

The effect of transition metal ions known to be present in PWR coolant was investigated at both the oxidation and voltammetric stages. Interference at the voltammetric stage was not observed and the peak current sensitivity was the same in the presence and absence of Fe, Ni, Co and Mn ions.

The potential for interference from transition metal ions at the oxidation stage only arises when the sample contains chromium(III). In this case, any Fe(II) present will compete for oxidant, and may cause incomplete conversion of Cr(III) into Cr(VI). The effect of a mixture of $40 \mu\text{g/l.}$ Fe(II) or Fe(III), $10 \mu\text{g/l.}$ Ni, $5 \mu\text{g/l.}$ Co and $5 \mu\text{g/l.}$ Mn(II) on recovery tests for simulated coolant containing 1500 mg/l. boron and either 0.18 or 0.88 $\mu\text{g/l.}$ chromium(III) is shown in Table 2, for two concentrations of bromine water.

With the lower concentration of bromine water the chromium recovery was slightly lowered by the presence of $40 \mu\text{g/l.}$ Fe(II), but use of the higher concentration of bromine water eliminated this effect.

Calibration

The calibration procedure best suited to this form of voltammetric analysis is standard addition, but requires a linear relationship between peak current and concentration, for a specified accumulation period. This is particularly important when adsorption saturation of the mercury drop is a possibility.

Analysis of a simulated coolant solution containing 500 mg/l. boron and 1.2 mg/l. lithium and increasing concentration of chromium(VI) (added by micro-

pipette) gave the voltamperograms shown in Fig. 4. The peak currents were measured after an accumulation period of 30 sec at -0.9 V. Regression analysis of the corrected peak currents for 10 concentrations in the range $0.1\text{--}1.0 \mu\text{g/l.}$ gave the equation $i_p = 231c + 13$ where c is the chromium concentration ($\mu\text{g/l.}$) and i_p is in nA.

Analytical procedure, accuracy and precision

Simulated coolant solutions containing known concentrations of chromium(III) were prepared and five replicate portions analysed by the following procedure, which was shown to be suitable for the determination of $\leq 2 \mu\text{g/l.}$ chromium in the presence of up to 1500 mg/l. boron.

Exactly 20 ml of sample and 0.2 ml of 1M sodium hydroxide were added to a clean polyethylene bottle, followed by 1 ml of 100-fold dilution of saturated bromine water. The sealed bottle was heated in a water-bath at 60° for 15 min, then cooled to room temperature before addition of 0.2 ml of 0.5M sulphuric acid. A 5-ml portion of this oxidized sample was added to the polarographic cell, together with 2.8 ml of 0.5M ammonium acetate (pH 6.2) and 2 ml of 2.5M sodium nitrate. The contents of the cell were then deaerated for 8 min before addition of 200 μl of 0.1M Na_2DTPA . After a further 30-sec gas purge, the chromium complex was accumulated for 30 sec at -0.9 V and then a voltamperogram recorded between -0.9 and -1.35 mV/sec. The concentration was determined from a single standard addition large

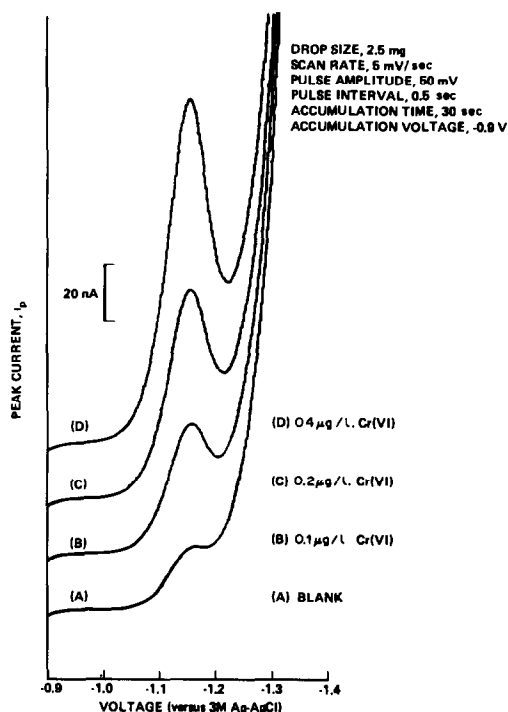


Fig. 4. Voltamperograms of analytical solution containing 250 mg/l. boron and 0.6 mg/l. lithium and Cr(VI).

Table 3. Accuracy and precision of analysis of simulated coolant (5 determinations)

Chromium, $\mu\text{g/l.}$			Boron, mg/l.
Added		Found \pm s.d.	
Cr(III)	Cr(VI)		
2.0		2.0 ± 0.24	1500
0.2		0.20 ± 0.04	1500
0.41		0.40 ± 0.10	600
	0.40	0.39 ± 0.06	600
Blank		0.019 ± 0.005	

enough for the peak current to be approximately doubled. In every case a reagent blank was necessary.

The results are shown in Table 3. In one case, the chromium was added as Cr(VI) to assess the effect of the oxidation procedure on the accuracy and precision.

The mean recoveries agree well with the added concentrations of chromium and have relative standard deviation in the range 12–25%. These precisions are poorer than those obtained from a similar analysis for nickel and cobalt,⁵ partly because of the single standard-addition method used.⁶ However, the oxidation stage and the small but appreciable time-dependence of the peak current will also contribute to the standard deviation. The statistical limit of detection at the 95% confidence level can be expressed as $4.65\sigma_B$, where σ_B is the standard deviation of the

blank, and so from the results in Table 3 the limit of detection is $0.023 \mu\text{g/l.}$

Any significant reduction in this figure would depend to some extent on reducing the amount of chromium in the reagents, particularly the sodium nitrate solution. However, the method is sufficiently sensitive to prove valuable in determining the variations in soluble chromium that accompany operational changes in the reactor and thus contribute to the overall efficiency of the chemical control of the primary coolant circuit.

Acknowledgements—The authors wish to acknowledge the helpful suggestions made by Mr. G. I. Goodfellow during the course of this work, which was carried out at the Central Electricity Research Laboratories of the CEGB Technology Planning and Research Division and is published by permission of the Central Electricity Generating Board.

REFERENCES

1. J. A. Cox and P. J. Kulesza, *Anal. Chim. Acta*, 1983, **154**, 71.
2. N. Tanaka and T. Ito, *Bull. Chem. Soc. Japan*, 1966, **39**, 1043.
3. J. Zarebski, *Chem. Anal. (Warsaw)*, 1977, **22**, 1037.
4. J. Golimowski, P. Valenta and H. W. Nürnberg, *Z. Anal. Chem.*, 1985, **322**, 315.
5. K. Torrance and C. Gatford, *Talanta*, 1985, **32**, 273.
6. *Idem*, *Analyst*, 1986, **111**, 359.
7. J. Wang, P. A. M. Farias and J. S. Mahmoud, *J. Electroanal. Chem. Interfacial Electrochem.*, 1985, **195**, 165.

THE ROLE OF THIOUREA AS ADDITIVE FOR SOLVING MEDIUM-MODIFICATION PROBLEMS IN POTENTIOMETRIC STRIPPING ANALYSIS

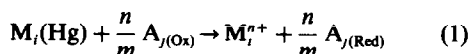
C. LABAR and L. LAMBERTS

Laboratoire de Chimie Analytique et de Spectrométrie de Masse, Facultés Universitaires Notre-Dame de la Paix, 61, rue de Bruxelles, B 5000 Namur, Belgium

(Received 2 August 1984. Revised 15 May 1987. Accepted 27 May 1987)

Summary—Thiourea (TU) has been studied as a possible additive for medium modification in order to modulate ion sensitivity in PSA (potentiometric stripping analysis). TU has three effects: (a) chelation with the metal ion and/or oxidizing agent; (b) specific adsorption at the mercury thin-film electrode (in the $10^{-4}M$ TU range); (c) diffusional electron transfer during the electro-deposition and redissolution steps in a PSA measurement. These effects were studied by PSA, ASV (anodic stripping voltammetry) and CA (chronoamperometry). For TU concentrations higher than $10^{-3}M$, electron-transfer by the additive is the predominant factor affecting sensitivity; this effect depends upon the value of the ion-stripping potential. For TU concentrations lower than $10^{-3}M$, complexation with the metal ion and/or oxidizing agent is the main factor affecting sensitivity. Appropriate choice of the concentration of TU therefore makes it possible to enhance or to lower the specific ion sensitivity, and even to mask an ion with respect to other ions. Examples are given for Zn^{2+} , Cu^{2+} , Cd^{2+} , Tl^+ , Bi^{3+} , and an extensive study was performed with Pb^{2+} .

Potentiometric stripping analysis (PSA)^{1,2} is similar to conventional voltammetric stripping analysis (VSA) in that the analyte is preconcentrated by potentiostatic deposition on a mercury electrode, but different from it in the method of signal generation. In PSA the amalgamated species $M_i(Hg)$ is reacted with excess of a suitable oxidant $A_{j(Ox)}$, such as mercury(II) or dissolved oxygen:



and the redox couple $M_i(Hg)/M_i^{n+}$ determines the potential of the mercury electrode until all the amalgamated metal has been oxidized, the change in the potential signal being recorded as a function of time. The analytical parameters in PSA are thus the "stripping potential", $E_{s, M_i(Hg)}$, and the "stripping time", $t_{s, M_i(Hg)}$, the first being characteristic of the nature of the redox couple and the second proportional to the activity of the M_i^{n+} analyte. PSA offers significant advantages over VSA because such factors as high solution resistivity and irreversible redox couples present fewer problems: however, a consequence of the type of PSA signal generation is that all M_i^{n+} analytes give approximately (and theoretically) the same response to the technique (identical sensitivity).

Both PSA and VSA are normally restricted to relatively noble metals when performed in aqueous solutions. Recently, PSA has been extended to more electropositive elements, such as alkali and alkaline-earth metals, by proper choice of solvent,³ and the use of matrix-exchange techniques coupled with flow-injection analysis during the electro-deposition

and reoxidation steps has given rise to various studies⁴ involving rather sophisticated instrumentation. It has also been demonstrated^{5,6} that the PSA parameters are affected by the competitive effects of diffusion of $A_{j(Ox)}$, equilibria in the bulk solution (e.g., complexation of $A_{j(Ox)}$ and/or M_i^{n+}) and interfacial specific adsorption of the electrolyte anions at the working electrode. By governing these effects, it is possible to affect, without practical modification of the analysis scheme and with conventional commercial instrumentation, both the sensitivity and the qualitative and quantitative determination of M_i^{n+} , and in some cases to avoid interference problems arising with various real samples.

The simplest analytical approach thus consists of performing at least the reoxidation step in a medium free from complexation and specific adsorption, making no appreciable contribution to the capacitance background curve of the chronopotentiometric response, and inactive with respect to reaction (1). The first three demands are met by using perchlorate medium,^{6,7} but this lowers the sensitivities for M_i^{n+} analytes to a level unacceptable in trace element analysis and does not deal with certain interference problems.^{4,8} It is thus of interest to study the effect of certain additives to a given electrolyte medium in PSA. Thiourea (TU) has been chosen for trial for various reasons: it forms complexes with most common cations (particularly heavy metal ions⁹) determined by PSA, its adsorption behaviour at the mercury-aqueous solution interface is different from that of most neutral organic surfactants,^{10,11} and it has been widely used as an additive in VSA studies.^{12,13}

EXPERIMENTAL

Instruments

PSA determinations were done with the Radiometer ISS 820¹⁴ and/or Tecator Striptec 1067–1069 systems; the analytical procedures for cleaning the electrodes, testing the reference electrode (SCE) for Hg(II) leakage, conservation of the glassy-carbon (gC) electrode, mercury pre-coating and finding the factor for electrode surface irregularities, have already been described.^{5,6,14,15}

Specific adsorption phenomena were studied with the EG&G Princeton Applied Research 384-4B polarographic analyser system in the anodic stripping voltammetry mode, as already described.⁶

Potential cycles in PSA were simulated with the Tacussel SGCV 512 instrumental system (SG 510 wave generator, PRGS 5 differential-pulse polarograph, S 223 Servogor BBC Goertz X-Y-t recorder, coupled to a Radiometer TTA 80 three-electrode assembly). All potentials are quoted *vs.* SCE.

Reagents

All chemicals were of analytical reagent grade; triply-distilled water was used and the usual cleaning procedures for trace element analysis were followed;¹⁶ the thiourea was purified as described earlier by Nyman and Parry.¹⁷ All stock solutions were prepared and diluted with special care to minimize relative errors.¹⁸ All experiments were done at 20 ± 0.1°.

RESULTS

PSA experiments

Preliminary PSA experiments done with a chloride electrolyte medium showed that the competitive effect of complexation and co-adsorption with chloride obscured the effect of TU addition on the PSA parameters. A perchlorate medium (0.10M perchloric acid, 0.500M sodium perchlorate, 1.349 × 10⁻⁴M mercury(II), M_T²⁺ in the 10⁻⁶M range) was therefore used instead, since it gives^{6,7} no specific adsorption of perchlorate anions at the interface and no strong complexation between perchlorate and M_T²⁺ or A_{J(Ox)}. Table 1 shows the effect of addition of TU, at various concentrations, to this reference medium, on the conventional PSA parameters for TI⁺ as analyte.

TI⁺ is complexed neither by TU nor perchlorate,⁹ in contrast, Hg(II) undergoes strong complexation with TU.⁹ Consequently, E'_{s, TI(Hg)} remains approximately constant for all TU concentrations whereas E'_{s, Hg(Hg)} undergoes a cathodic shift of 0.510 V when the medium is made 0.178M in TU, as theoretically predicted.^{19,20} Lowering the A_{J(Ox)} activity enhances the sensitivity of detection of the analyte, s'_{TI(Hg)}, to a

maximum at a TU concentration of ~10⁻³M; higher TU concentration reduces the sensitivity by adsorption of the additive, eventually to a value lower than that for the TU-free medium. In this simple case, the factors acting on the PSA parameters are the complexation of A_{J(Ox)} and specific adsorption of TU, at concentrations higher than 10⁻³M. Note finally that E'_{s, TI(Hg)} remains, in all media, in the -0.6 V range (Table 1).

Interpretation becomes more difficult if M_T²⁺ is also complexed, as can be the case for Pb²⁺. It is made even more difficult by the disparity in the published values for the stability constants of certain complexes. Thus for the Pb-TU complexes there apparently is a choice ranging from β₁ = 2, β₂ = 8, β₃ = 25, β₄ = 40, to β₁ = 25, β₂ = 1.3 × 10³, β₃ = 5.0 × 10⁴ and β₄ = 2.0 × 10⁸.²¹ However, the problem is more apparent than real in this case, as comparison of the values given by Ringbom do not agree with those given in the original paper²² from which they were said to be taken, those values being β₁ = 4, β₂ = 11, β₃ = 10, β₄ = 110, in fair agreement with those selected by Smith and Martell²³ and those recently reported by Crow²⁴ (β₁ = 4–7, β₂ = 11–30, β₃ = 40–95, β₄ = 80–110, these being the ranges for five independent methods of calculation, with means 6, 20, 56 and 98 respectively). The values of the stability constants will also depend on the ionic strength and nature of the medium. A HALTAFALL²⁵ calculation of the distribution of species in a mixture with total concentrations C_{Hg} = 1.35 × 10⁻⁴M, C_{Pb} = 10⁻⁶M and C_{TU} = 10⁻⁶–1M, with the "Smith and Martell" constants²³ gives the following predominance regions (species concentration at least about 50% of total metal ion concentration): Hg²⁺ at C_{TU} < 2 × 10⁻⁴M, Hg(TU)₂²⁺ at C_{TU} = 1 × 10⁻⁴–3 × 10⁻³M, Hg(TU)₃²⁺ at C_{TU} = 3 × 10⁻³–1 × 10⁻²M, and Hg(TU)₄²⁺ at C_{TU} > 1 × 10⁻²M. For lead, the predominant form is free Pb²⁺ until C_{TU} exceeds ~0.1M. The variation in sensitivity for lead, as a function of C_{TU} (Fig. 1), suggests that at C_{TU} < 3 × 10⁻⁴M the behaviour of s'_{Pb(Hg)} is essentially the same as that of s'_{TI(Hg)} in the absence of adsorption, both being affected by the same factors. At C_{TU} between 3 × 10⁻⁴M and ~8 × 10⁻³M, the formation of Hg-TU complexes and adsorption occur simultaneously, the latter factor being predominant, as in the case of TI⁺. At still higher TU concentrations, above about 10⁻²M,

Table 1. Effect of thiourea on the PSA parameters of TI(I)

[TU] added, M	E' _{s, TI(Hg)} , V vs. SCE	E' _{s, Hg(Hg)} , V vs. SCE	Sensitivity, s' _{TI(Hg)} * sec. μg.l. ⁻¹
—	-0.580	+0.270	(0.750 ± 0.020) × 10 ⁶
3.84 × 10 ⁻⁵	-0.620	+0.205	(0.834 ± 0.060) × 10 ⁶
3.71 × 10 ⁻⁴	-0.610	+0.070	(1.04 ± 0.06) × 10 ⁶
2.78 × 10 ⁻³	-0.600	-0.020	(1.15 ± 0.06) × 10 ⁶
3.71 × 10 ⁻²	-0.620	-0.130	(0.924 ± 0.073) × 10 ⁶
1.04 × 10 ⁻¹	-0.630	-0.200	(0.848 ± 0.042) × 10 ⁶
1.78 × 10 ⁻¹	-0.600	-0.240	(0.600 ± 0.084) × 10 ⁶

*Sensitivity is defined as the slope of the calibration graph s'_{TI(Hg)} = f([TI(I)]).^{1,3}

$\text{Hg}(\text{TU})_4^{2+}$ will become increasingly predominant, and complexation of the lead will also begin to be significant, leading to the further changes in the sensitivity curve.

Such an interpretation is only qualitative, and thus is not entirely satisfactory; it cannot be quantitatively deduced from the PSA results, since these cannot indicate the effect of adsorption on the two separate steps of the PSA cycle (electro-deposition and stripping). PSA parameters are not directly related to fundamental adsorption phenomena,^{5,7} as evidenced by the fact that the electrochemical characteristics of M_i^{n+} (such as half-wave potential and the sensitivity as measured by differential-pulse polarography^{12,26}) behave normally with adsorption of TU.

ASV experiments

The adsorption of TU and its derivatives has been the subject of several studies,^{7,11,12,27-30} leading to the general conclusion that TU behaves quite differently from most other organic surfactants at the mercury-aqueous solution interface.⁷ Nevertheless, no experiments have been performed on its adsorption under PSA conditions.

To elucidate the actual effect of TU, ASV experiments were performed under PSA conditions (cathodic electro-deposition of the same duration at identical potential, followed by sweeping the potential to the anodic region at the same speed). Figure 2(b), based on results similar to those given in Fig. 2(a), shows that TU, in perchlorate medium, undergoes both adsorption and diffusion-controlled electron-transfer in the potential range from -0.6 to -0.2 V (*vs.* SCE). Both mechanisms occur for TU concentrations in the $10^{-4}M$ range (*cf.* TU adsorption as visualized in PSA measurements in the $10^{-3}M$ TU range, with a maximum surface coverage seeming to be attained at $\sim 3 \times 10^{-3}M$ TU). The new fact that emerges here is that TU behaves as an electroactive species during the two steps of a PSA

experiment, for TU concentrations lower than approximately $3 \times 10^{-4}M$.

PSA simulation of experiments by chronoamperometric methods

The electron-transfer undergone by TU leads to the idea of discriminating current responses due to $\text{M}_i^{n+}/A_{j(\text{Ox})}$ (or $\text{M}_i/A_{j(\text{Red})}$) from those due to TU. The main fundamental method for doing this seems to be potential-step chronoamperometry (CA) with potential reversal.³¹ The typical waveform applied to the gC(Hg) working electrode [Fig. 3(a)] leading to the idealized current response [Fig. 3(b)] must be adapted to the potential-time data pairs of PSA and ASV experiments for a given M_i^{n+} species. For instance, with Pb^{2+} in perchlorate medium, potential E_1 corresponds to -0.950 V (PSA/ASV deposition potential), time τ_1 to 240 sec (PSA/ASV electrolysis time), potential E_2 to -0.400 V (value corresponding to $E'_{\text{Pb}(\text{Hg})}$ in PSA or to the final redissolution potential in ASV) and τ_2 to 60 sec (redissolution time needed in PSA and ASV to reach the base-line of the capacitance background curve in the media studied, with M_i^{n+} in the $10^{-6}M$ range^{1,3,5}).

Figure 3(c) gives the actual form of the CA response for a given TU concentration along with designation of the information conveyed (i_{Ox} and i_{Red} , corresponding to the initial redissolution and electro-deposition currents). Considering the double-step waveform as a superposition of two potentiostatic components acting respectively during 240 and 300 sec,³¹ and using the theory applicable to this type of working electrode,^{30,32,33} it is seen that the conventional criterion for a stable electrochemical system,³¹ *i.e.*,

$$-\frac{i_{\text{Ox}}}{i_{\text{Red}}} \frac{2\tau_1}{\tau_2} = 0.293 \quad (2)$$

is not met: i_{Ox} is much larger than that predicted by theory and the CA current ratio is more negative than

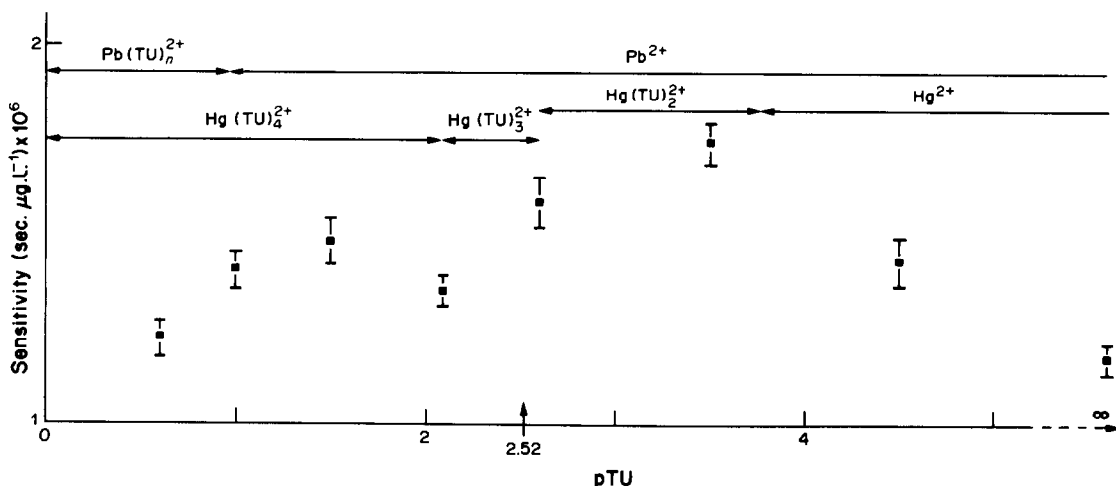


Fig. 1. Evolution of PSA sensitivity with pTU; Pb^{2+} -TU systems; predominance regions shown for metal species.

the ideal, where both the Ox and Red species are stable during the observation period.^{32,33} Hence these species produce kinetic complications in the system considered here.

The nature of the kinetics and the identity of the species effectively responsible for the effects observed can be elucidated by the following CA experiments.

At constant M_i^{n+} and $A_{j(Ox)}$ activity, with E_1 characteristic of the electro-deposition potential range for the more common ions determined by PSA (-0.950 V),

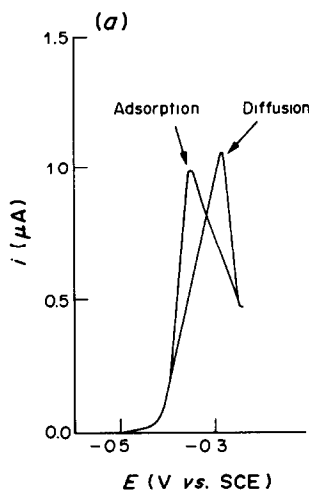


Fig. 2(a). ASV: diffusion and adsorption peaks of TU in perchlorate medium, at $[TU] = 1.16 \times 10^{-4} M$: diffusion: $E_p = -0.354$ V; $i_p = 460$ nA; adsorption: $E_p = -0.292$ V; $i_p = 395$ nA.

variations of the CA ratio with the redissolution potential E_2 can be measured from experiments such as those illustrated in Fig. 4. In this figure, two TU activities have been selected: "below" ($3.34 \times 10^{-5} M$) and "above" ($4.09 \times 10^{-1} M$) those needed for adsorption of the additive. In both cases i_{Ox} is greater than i_{Red} , but, with the higher TU concentration, the potentials are closer together and more cathodic. The additive thus has more marked effect on the PSA stripping step, enhanced by the more cathodic value of E_2 (i.e., $E'_{s, M_i(Hg)}$).

Moreover, when similar experiments are done over the whole TU activity range covered by the earlier PSA experiments, the behaviour of the CA ratio is in general similar to the behaviour of the PSA sensitivity (Fig. 5) for redissolution potentials E_2 characteristic of the $E'_{s, M_i(Hg)}$ range for the more common ions studied by PSA (from -0.6 to -0.2 V). This indicates a correspondence between the PSA sensitivity (global analytical result of the two steps of the PSA measurement) and the CA reoxidation current (for the same set of experimental conditions: E_1 , E_2 , τ_1 , τ_2). Hence, after complexation (in solution) and adsorption (at the interface) have taken place (at TU concentrations $< 3 \times 10^{-4} M$), TU acts mainly as an electron-donor and progressively substitutes its faradaic current for the $M_i(Hg)$ faradaic current and $A_{j(Red)}$ capacitive reoxidation current. In this situation, the electron-donor capacity of TU is enhanced by the more cathodic value of E_2 (in the CA experiments) or $E'_{s, M_i(Hg)}$ (in the corresponding PSA experiments): the nature of M_i^{n+} and $A_{j(Ox)}$, through the

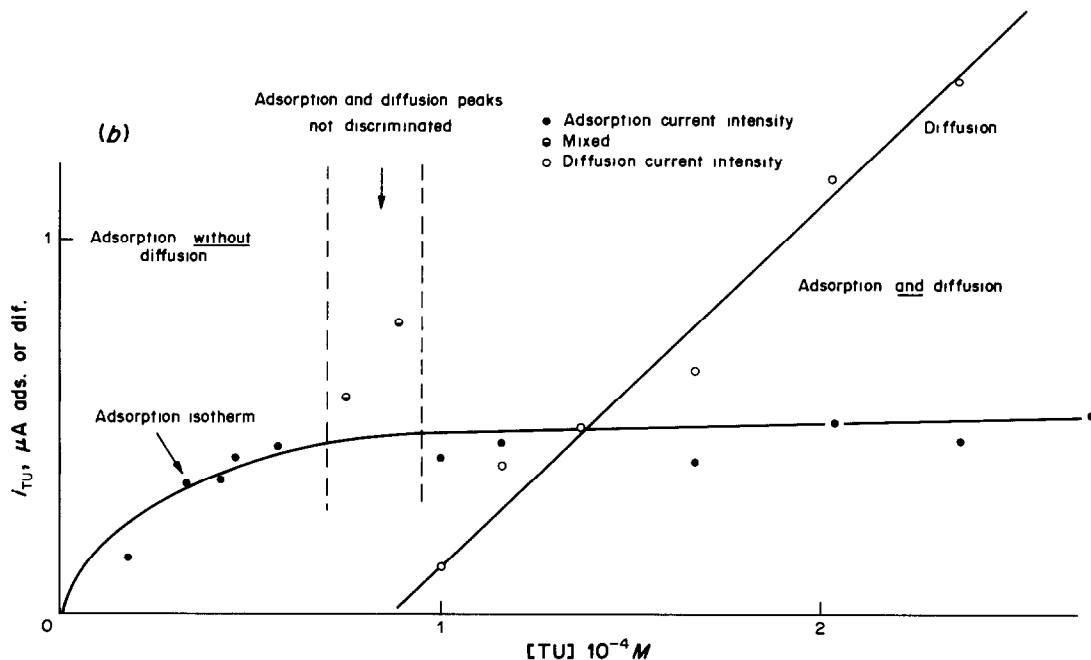


Fig. 2(b). Behaviour of TU at the DME solution interface in perchlorate medium, $[TU]$ in the $10^{-4} M$ range. Conditions: electro-deposition, -0.950 V, 60 sec; redissolution, $E_i = -0.600$ V, $E_f = -0.200$ V; deaeration, 240 sec; drop time, 1 sec; scan increment, 0.002 V; electrode conditioning, 30 sec; electrode equilibration, 60 sec, pulse height, 0.050 V; cyclic; background suppression; DPP mode.

corresponding values of $E'_{s, M_i(Hg)}$, consequently induces the actual electron-donor activity of TU.

This argument rests on the hypothesis that the $M_i(Hg)$ and $A_{j(Red)}$ redissolution faradaic currents are negligible compared to the TU reoxidation effect. Measurements of the CA ratio at various M_i^{n+} activities for constant $A_{j(Ox)}$ and TU concentrations fixed in the adsorption range, with $E_1 = -0.950$ V and $E_2 = -0.400$ V, demonstrate this hypothesis for the current component $M_i(Hg)$. Incidentally, such experiments can be used for a rather tedious determination of M_i^{n+} , with relative standard deviation 0.9%. Changing the $A_{j(Ox)}$ activity leads to linear calibration graphs such as those illustrated in Fig. 6, but with different slopes, as can be theoretically predicted.²⁴ Finally, changing the TU activity over the whole range covered by the PSA experiments

leads to Fig. 6: $\delta i_{Ox}/\delta[M_i^{n+}]$ and $\delta i_{Red}/\delta[M_i^{n+}]$ both increase with TU activity. This behaviour is independent of the selected E_1-E_2 potential pair (in the range previously mentioned).

This confirms that the TU electron-donor mechanism during the stripping step is entirely responsible for the change in PSA sensitivity over this range of TU activity.

Analytical implications and conclusions

It has been demonstrated that for TU concentration $> 3 \times 10^{-4} M$ and $E'_{s, M_i(Hg)}$ between -0.6 and -0.2 V, TU is responsible for the main component of the chronoamperometric reoxidation currents; TU also forms in those conditions a chemical bond with the $M_i(Hg)$ film.²⁶ TU thus governs the PSA sensitivity. The effect is enhanced by cathodic displace-

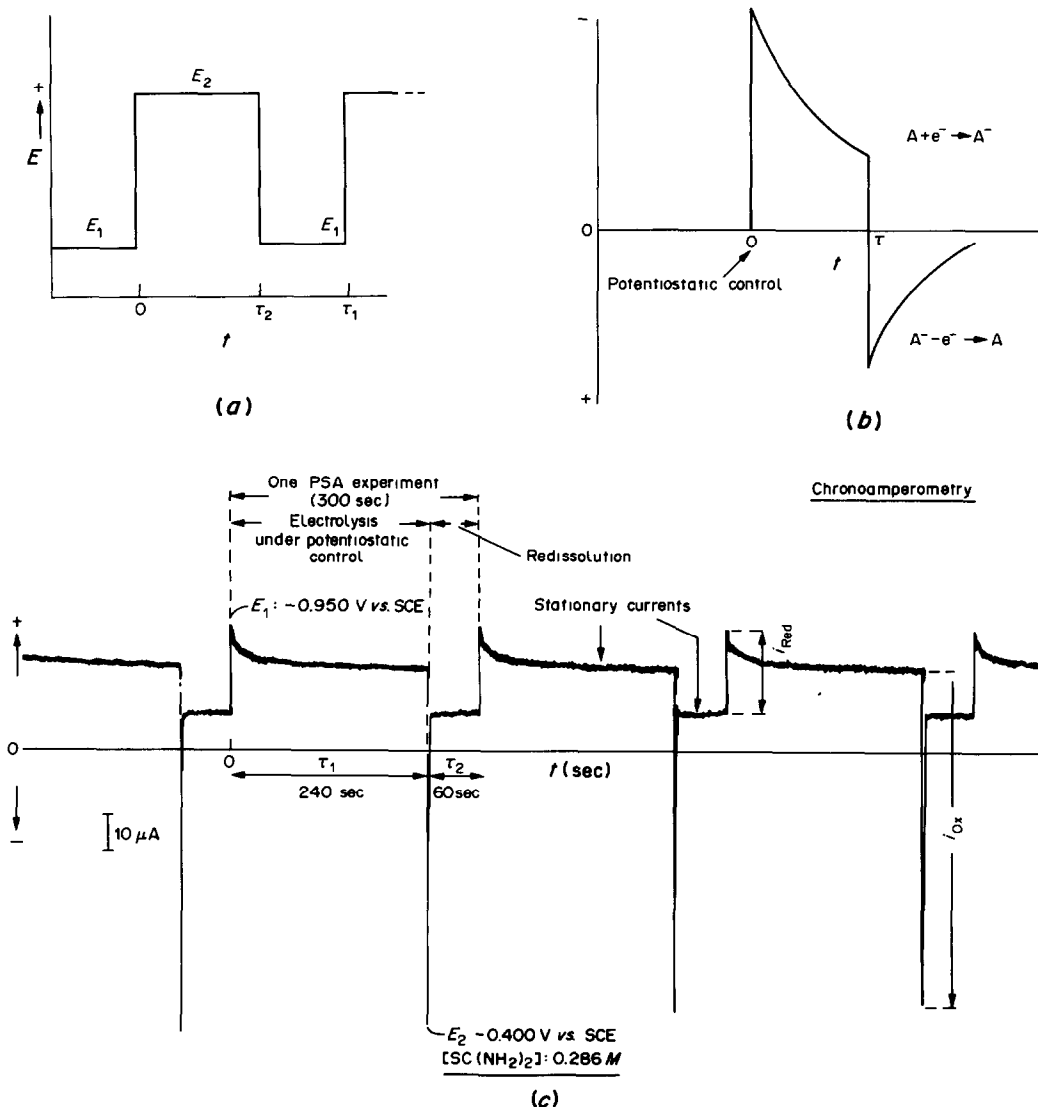


Fig. 3. CA: double potential step chronoamperometry as simulation of PSA experiments: (a) waveform injected at the working electrode; (b) typical current response for a stable, reversible electrochemical system; (c) actual experiment in perchlorate media as described in the text; [TU] = 0.286M.

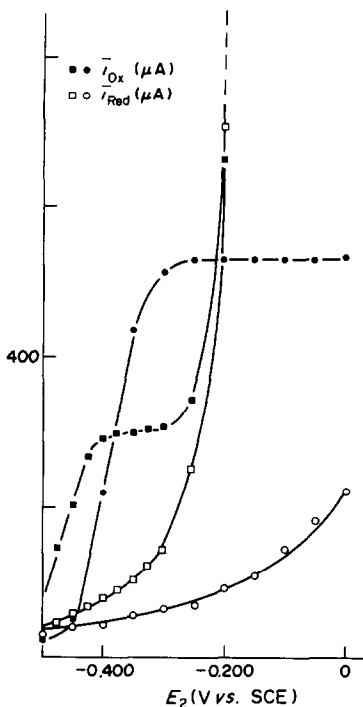


Fig. 4. Variations of i_{Ox} with i_{Red} with E_2 , at fixed M_i^{n+} and $A_{j(Ox)}$ activities, for $E_1 = -0.95$ V and two TU concentrations, $3.34 \times 10^{-3}M$ (○, ●) and $0.409M$ (□, ■).

ment of $E'_{s, M_i(Hg)}$ (to an extent dependent on the complexation data for M_i^{n+} and $A_{j(Ox)}$), whereas the $A_{j(Ox)}$ and M_i^{n+} activities (in the range studied in the PSA experiments) cannot affect the general behaviour of TU.

This suggests direct analytical applications for enhancing or lowering the sensitivity in PSA metal-ion determinations.

For M_i^{n+} ions with $E'_{s, M_i(Hg)}$ more cathodic than -0.6 V (outside the TU electron-donor potential range), the two parameters affecting PSA sensitivity are *complexation* and *specific adsorption*. Complexation of $A_{j(Ox)}$ enhances the sensitivity by lowering the corresponding activity gradient at the electrode interface;² complexation of M_i^{n+} lowers the sensitivity by reducing the stripping time, which is proportional to the M_i^{n+} free ion activity.⁵ Moreover, the sensitivity should show an abrupt change in the TU adsorption range (TU concentration $\sim 3 \times 10^{-4}M$). This is illustrated in Table 1 (for Tl^+) and in Table 2 (for Cu^{2+}), two metal ions having different TU complexation constants and characterized by $E'_{s, M_i(Hg)}$ values outside the TU electron-donor potential range.

For M_i^{n+} ions with $E'_{s, M_i(Hg)}$ more anodic than -0.2 V (at the upper limit of the TU electron-donor potential range), an additional parameter, the *electroactivity of TU* must be taken into account and this last factor is largely preponderant for TU concentrations $> 3 \times 10^{-4}M$. This is illustrated by Bi^{3+} (Table 2): this species has an $E'_{s, Bi(Hg)}$ value of -0.117 V, due to complexation with TU; two effects thus lower Bi^{3+} PSA sensitivity: (1) specific adsorption at a TU concentration of $\sim 3 \times 10^{-4}M$ and (2) TU oxidation at higher TU concentrations. This ion is finally completely masked in PSA experiments performed in media with TU concentration $> 3 \times 10^{-3}M$ (Table 2).

For M_i^{n+} ions with $E'_{s, M_i(Hg)}$ between -0.6 and -0.2 V, the three parameters play independent roles. The final effect on PSA sensitivity at TU concentrations $> 3 \times 10^{-4}M$ is a function of the actual $E'_{s, M_i(Hg)}$ value and thus of the nature of the $M_i^{n+}/A_{j(Ox)}$ couple. In this respect, Pb^{2+} has been systematically studied in this work (Table 2).

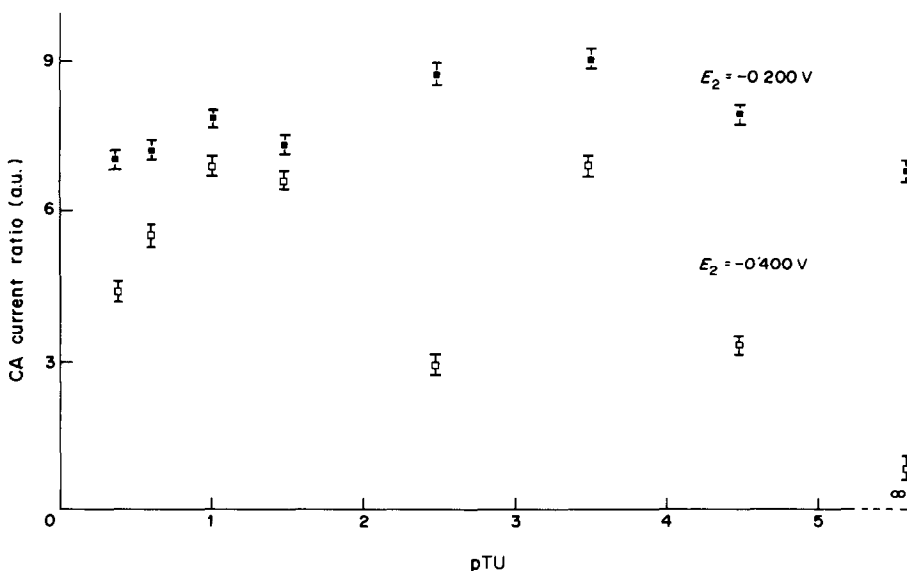


Fig. 5. Evolution of the CA ratio with TU concentration in perchlorate medium, at fixed M_i^{n+} and $A_{j(Ox)}$ activities and for $E_1 = -0.950$ V. Two E_2 values are illustrated, $E'_{s, Pb(Hg)} = -0.460$ V.

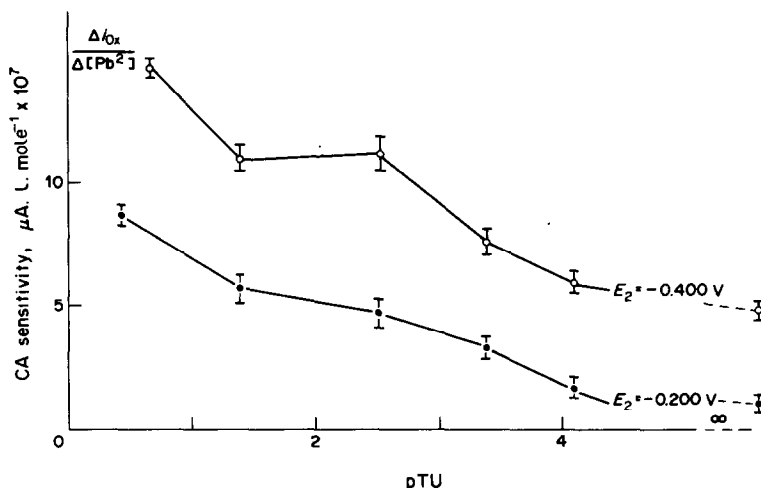


Fig. 6. Variation of redissolution CA sensitivity with thiourea activity, at fixed M_i^{n+} , $A_{j(Ox)}$, $E_1 = -0.950$ V, and for two redissolution potential values E_2 , -0.400 V and -0.200 V. Note that $E'_{s, Pb(Hg)} = -0.460$ V.

Table 2. Effect of thiourea on stripping potential and detection sensitivity of metal ions* in Cl^- medium, in potentiometric stripping analysis

M_i^{n+}	[TU], M	$E'_{s, M_i(Hg)}$, V vs. SCE	$E'_{s, Hg(Hg)}$, V vs. SCE	Sensitivity, $s'_{M_i^{n+}(Hg)}$, sec. $\mu g. l.^{-1}$
Zn(II)	0	-1.080	0.065	$(7.00 \pm 0.39) \times 10^5$
	0.133	-1.080	-0.200	$(1.05 \pm 0.22) \times 10^5$
Cd(II)	0	-0.700	0.065	$(1.54 \pm 0.14) \times 10^6$
	0.133	-0.705	-0.214	$(1.68 \pm 0.10) \times 10^6$
Tl(I)	0	-0.610	0.065	$(9.63 \pm 0.41) \times 10^6$
	0.133	-0.655	-0.210	$(2.31 \pm 0.19) \times 10^6$
Cu(II)	0	-0.217	0.072	$(5.09 \pm 0.27) \times 10^6$
	0.133	-0.630	-0.210	$(5.29 \pm 0.23) \times 10^6$
Pb(II)	0	-0.470	0.072	$(4.62 \pm 0.51) \times 10^6$
	0.133	-0.480	-0.210	$(6.62 \pm 0.35) \times 10^6$
Bi(III)	0	-0.117	0.060	$(2.89 \pm 0.25) \times 10^6$
	0.133	not observed	-0.198	—

*The metal ions are listed according to their $E'_{s, M_i(Hg)}$ values in presence of thiourea.

The electroactivity of TU is a quite general phenomenon: it must consequently be considered in other electrochemical techniques used for trace metal determinations (e.g., ASV and DPP). As the effect of the additive depends on the nature of M_i^{n+} ($E'_{s, M_i(Hg)}$ value), this can explain some apparent discrepancies often encountered in electrochemical studies.^{5,28,32,34} Conclusions such as attribution of contradictory behaviour (e.g. enhancement or lowering of M_i^{n+} DPP signal with addition of TU) solely to TU adsorption at the DME interface,³⁵⁻³⁷ must now be reconsidered in the light of the results of this study.

Acknowledgements—The authors thank Professor P. Claes (Université Catholique de Louvain-la-Neuve), P. Nangniot (Faculté des Sciences Agronomiques de l'Etat à Gembloux) and G. Patriarche (Université Libre de Bruxelles) for experiments made with specific instrumentation and for helpful discussions. They also thank Mrs. Van Eenoo and Mr. S. Pochet for technical assistance and help in writing the manuscript.

REFERENCES

- D. Jagner and A. Graneli, *Anal. Chim. Acta*, 1976, **83**, 19.
- D. Jagner, *Analyst*, 1982, **107**, 593.
- J. F. Coetzee, A. Hussam and T. R. Petrick, *Anal. Chem.*, 1983, **55**, 120.
- A. Hu, R. E. Dessey and A. Graneli, *ibid.*, 1983, **55**, 320.
- C. Labar and L. Lamberts, *Anal. Chim. Acta*, 1981, **132**, 23.
- Idem*, unpublished work.
- M. Gonze, *Ph.D. Thesis*, Université Libre de Bruxelles, Brussels, 1985.
- H. Eskinsson and D. R. Turner, *Anal. Chim. Acta*, 1984, **161**, 293.
- L. G. Sillén, *Stability Constants*, Suppl. No. 1, Spec. Pubn. No. 25, Chemical Society, London, 1972.
- L. Lorenz and G. Krüger, *Z. Phys. Chem. Leipzig*, 1962, **221**, 231.
- C. Buess-Herman, *J. Electroanal. Chem.*, 1985, **186**, 27.
- H. Yoshida, S. Tanaka and M. Taga, *Bunseki Kagaku*, 1980, **29**, 479.
- H. W. Nürnberg, *Thalassia Yugoslavica*, 1980, **16**, 95.
- D. Jagner, *Anal. Chem.*, 1978, **50**, 1924.

15. D. Jagner and S. Westerlund, *Anal. Chim. Acta*, 1980, **117**, 159.
16. T. C. O'Haver, *Chemical Aspects of Element Analysis, in Trace Analysis*, J. D. Winefordner, (ed.), Wiley, New York, 1976.
17. C. J. Nyman and E. P. Parry, *Anal. Chem.*, 1958, **30**, 1255.
18. R. B. Lam and T. L. Isenhour, *ibid.*, 1980, **52**, 1158.
19. S. D. Brown and B. R. Kowalski, *ibid.*, 1979, **51**, 2133.
20. A. Hussam and J. F. Coetzee, *ibid.*, 1985, **57**, 581.
21. A. Ringbom, *Complexation in Analytical Chemistry*, Interscience, New York, 1963.
22. T. J. Lane, J. A. Ryan and E. F. Britten, *J. Am. Chem. Soc.*, 1958, **80**, 315.
23. A. E. Martell and R. M. Smith, *Critical Stability Constants*, Plenum Press, New York, 1974–1976.
24. D. R. Crow, *Talanta*, 1983, **30**, 659.
25. N. Ingri, W. Kokołowicz, L. G. Sillén and B. Warnquist, *ibid.*, 1967, **14**, 1261; errata, 1968, **15**, No. 3, ix.
26. N. Meurée and L. Gierst, *Collection Czech. Chem. Commun.*, 1971, **36**, 389.
27. R. V. Ivanov and O. G. Ivanova, *Electrokhimiya*, 1979, **15**, 1474; 1980, **18**, 2017.
28. A. Batana, R. C. Rocha Fo, L. A. Avaca and E. R. González, *Electrochim. Acta*, 1980, **25**, 679.
29. R. Parsons, R. Peat and R. M. Reeves, *J. Electroanal. Chem.*, 1975, **62**, 151.
30. F. D. Koppitz, J. W. Schultze and D. Rolle, *ibid.*, 1984, **170**, 5.
31. A. J. Bard and L. A. Faulkner, *Electrochemical Methods, Fundamentals and Applications*, 1st Ed., p. 138. Wiley, New York, 1980.
32. R. Parsons and A. Stockton, *J. Electroanal. Chem.*, 1970, **25**, 10.
33. M. Dorten, Z. Stojek and Z. Kublick, *ibid.*, 1984, **163**, 11.
34. R. Parsons and P. Symons, *Trans. Faraday Soc.*, 1968, **64**, 1077.
35. J. Wang and D.-B. Luo, *Talanta*, 1984, **31**, 703.
36. J. Wang and B. A. Freiha, *ibid.*, 1983, **30**, 317.
37. J. Kirchnerová and W. C. Purdy, *Anal. Lett.*, 1980, **13**, 1031.

LIQUID-LIQUID EXTRACTION OF METAL IONS BY THE 6-MEMBERED N-CONTAINING MACROCYCLE HEXACYCLEN

S. ARPADJAN, M. MITEWA and P. R. BONTCHEV*

Department of Chemistry, University of Sofia, 1126 Sofia, Bulgaria

(Received 26 June 1986. Revised 29 April 1987. Accepted 27 May 1987)

Summary—The nitrogen-containing analogue of 18-crown-6, 1,4,7,10,13,16-hexa-azaoctadecane (hexacyclen) was studied as a reagent for complexation and extraction of some metal ions. It was found that with this reagent and methyl isobutyl ketone, metal ions such as silver(I), mercury(II), copper(II), platinum(II) and palladium(II) can be quantitatively extracted and separated from iron(III) and some other metal ions.

During the last years a number of macrocyclic compounds (crown ethers) have been successfully applied in liquid-liquid extraction.¹⁻¹³ Up till now, mainly oxygen-containing crown ethers are used for alkali and alkaline-earth metal ion extraction.¹ Only a few papers are dedicated to transition-metal ion extraction—with thiacycrown ethers,^{2-4,6,10} O,N-containing macrocycles^{7,8,11,12} and O-crowns.^{5,9,13}

In the present paper results concerning metal-ion extraction with 1,4,7,10,13,16-hexa-azaoctadecane (hexacyclen) are reported in connection with its analytical application, based on liquid-liquid extraction of ion-pairs formed between the positively-charged hexacyclen complexes and suitable anions, followed by an AAS determination. Since the hexacyclen molecule exhibits remarkable flexibility and pronounced donor properties¹⁴ it might be expected that this N-analogue of 18-crown-6 would be a good extracting agent for a number of metal ions that prefer nitrogen as a donor atom in co-ordination processes.

EXPERIMENTAL

Reagents and apparatus

All reagents used were of analytical grade. The commercially available trisulphate of the hexa-aza ion (hexacyclen $\cdot 3\text{H}_2\text{SO}_4$ Aldrich) was used. "Free" ligand solution ($5 \times 10^{-3}M$) was prepared from hexacyclen $\cdot 3\text{H}_2\text{SO}_4$ by boiling with barium carbonate. The standard solutions for Zn(II), Cd(II), Pb(II), Mn(II), Co(II), Ni(II), Ag(I) and Hg(II) were those produced by BDH as standards for atomic-absorption spectrometry (1000 $\mu\text{g}/\text{ml}$ in 0.2M nitric acid). The metal salts used for preparation of the other stock metal ion solutions ($5 \times 10^{-3}M$) were TiNO_3 , FeCl_3 , CuCl , FeSO_4 , $(\text{NH}_4)_2\text{SO}_4 \cdot 6\text{H}_2\text{O}$, $(\text{NH}_4)_2\text{PtCl}_4$, $(\text{NH}_4)_2\text{PtCl}_6$ and $(\text{NH}_4)_2\text{PdCl}_4$. The working solutions ($5 \times 10^{-5}M$) were prepared from the stock solutions by dilution with redistilled water. The counter-ion solutions— $5 \times 10^{-4}M$ picric acid (Pic) and $5 \times 10^{-4}M$ sodium dodecylbenzenesulphonate (DBSA, surfactant counter-ion) were freshly prepared from corresponding stock solutions.

The acidity of the aqueous phase was regulated with 0.01M acetate buffer solution for pH 5 and 6, and 0.01M

borate buffer for pH 9. The other pH values used, in the ranges 3-5 and 6-9, were adjusted with 0.01M hydrochloric acid, acetic acid or ammonia solution. The extraction of Pd(II) and Hg(II) was studied in the pH range 3-11, the pH being adjusted to 9-11 by means of 0.01M sodium hydroxide. The pH values were measured with a Radelkis OP-208 pH-meter after estimation of the extraction equilibrium.

Atomic-absorption spectrometry (AAS) was performed with a double-beam spectrometer (Pye Unicam SP 1950, acetylene/air flame) at the best signal-to-noise ratio for each metal.

All measurements were obtained at constant ionic strength (0.1M NaClO_4).

Metal ion extraction

To 2.00 ml of the metal-ion solution ($5 \times 10^{-5}M$) in a 50-ml glass-stoppered tube, the following solutions were added: 1 ml of sodium perchlorate, 2 ml of $5 \times 10^{-4}M$ Pic or DBSA, 2 ml of the buffer (or other pH-adjusting) solution and 2 ml of $5 \times 10^{-3}M$ hexacyclen. Distilled water was then added to give a total volume of 10.0 ml.

Most of the experiments were done at ambient temperature. To find the influence of temperature on the formation of the complexes to be extracted, some of the reaction solutions were first heated at 90° (water-bath) for 30 min, cooled to ambient temperature and then extracted. The extraction was performed with 10.0 ml of methyl isobutyl ketone (MIBK). The metal-ion concentrations in the aqueous and organic phases were determined by AAS.

The extraction of Cu(I) was studied with freshly prepared solutions of CuCl, in order to prevent their disproportionation.

RESULTS AND DISCUSSION

The extraction of Ag(I), Tl(I), Zn(II), Cd(II), Hg(II), Pb(II), Fe(III), Fe(II), Mn(II), Co(II), Ni(II), Cu(II), Cu(I), Pt(II), Pt(IV) and Pd(II) with hexacyclen was studied under various conditions. First the extraction time to be used in the next batch of studies was determined. For this purpose the metal-ion concentrations were monitored for the extraction systems M^{n+} -hexacyclen-Pic and M^{n+} -hexacyclen-DBSA after preliminary heating [only Ag(I) was studied at ambient temperature] after 5, 15 and 30 min extraction. The results obtained are shown in Table 1. It is evident that after 30 min practically total extraction

*Author for correspondence.

Table 1. Time-dependence of metal-ion extraction (%) after preliminary heating ($\mu = 0.1M$ NaClO_4)

M^{n+}	pH	M^{n+} -hexacyclen-Pic			M^{n+} -hexacyclen-DBSA		
		Extraction time			Extraction time		
		5 min	15 min	30 min	5 min	15 min	30 min
Ag(I)*	6	48 ± 5	72 ± 3	99 ± 1	40 ± 5	68 ± 3	99 ± 1
Cu(I)	4	10 ± 3	43 ± 2	98 ± 3	12 ± 3	50 ± 3	99 ± 1
Cu(II)	5	73 ± 4	82 ± 3	98 ± 1			
Hg(II)	5	77 ± 4	99 ± 1	>99.5	77 ± 4	99 ± 1	>99.5
Pd(II)	9	42 ± 5	56 ± 3	>99.5	40 ± 4	62 ± 3	>99.5
Pt(II)	3	18 ± 3	50 ± 4	98 ± 1	16 ± 3	54 ± 3	98 ± 1

*At ambient temperature.

is realized in both systems, the only exception being Hg(II), for which 15 min shaking leads to 99% extraction.

The dependence of extraction on acidity was studied in the pH range 3–9 both at ambient temperature and after preliminary heating (extraction time 30 min). The data obtained are given in Table 2 and show that the systems used are suitable for liquid-liquid extraction of Ag(I), Hg(II), Cu(I), Cu(II), Pt(II), Pt(IV) and Pd(II). For these ions the extraction over a wide pH range with both Pic and DBSA as counter-ions was studied (see Figs. 1–7). It should be mentioned that only for Ag(I) and Hg(II) is quantitative extraction at ambient temperature realized. Heating Ag(I) solutions with the reagent leads to partial reduction to Ag. In spite of the fact that according to Figs. 5 and 6 the separation of Cu(II) and Cu(I) at pH 7–8 seems possible, our efforts in this direction failed, because of the partial disproportionation of Cu(I), leading to higher results for Cu(II).

The correlation of the extraction data with the ionic radii of the corresponding metal ions shows that

the tendency for co-ordination by the *N*-donor groups is more important for complexation than the ionic dimensions are, and is maybe the crucial factor. It follows, however, from this fact, that in the com-

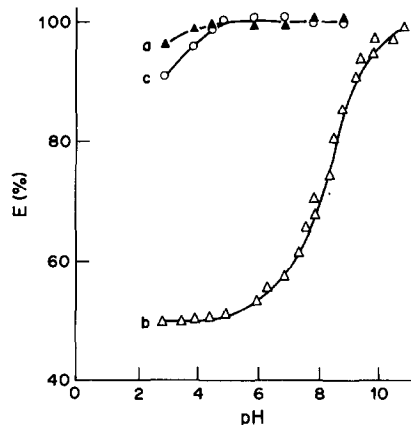


Fig. 2. Extraction vs. pH plot for palladium(II). (a) Pd(II) with Pic after heating; (b) Pd(II) with Pic at 20°C; (c) with DBSA after heating.

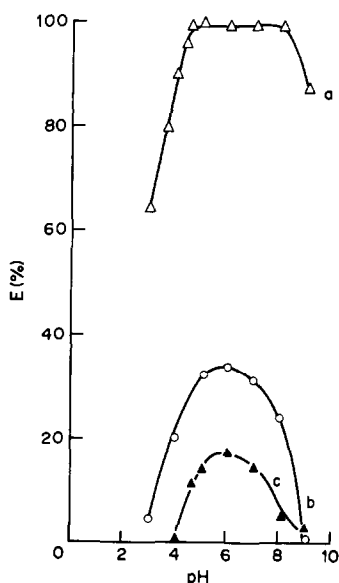


Fig. 1. Extraction vs. pH plot for silver(I). (a) Ag(I) with Pic at 20°C; (b) Ag(I) with DBSA after heating; (c) Ag(I) with Pic after heating.

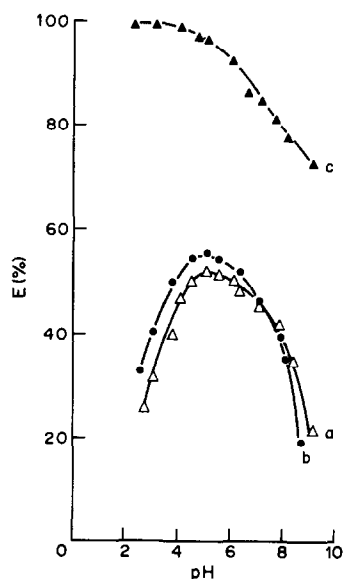


Fig. 3. Extraction vs. pH plot for platinum(II). (a) Pt(II) with Pic at 20°C; (b) Pt(II) with DBSA at 20°C; (c) Pt(II) with Pic after heating.

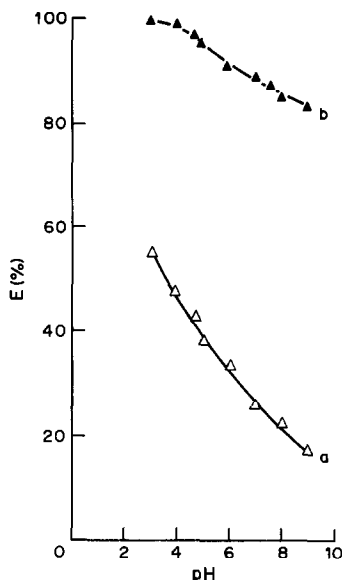


Fig. 4. Extraction vs. pH plot for platinum(IV), (a) Pt(IV) with Pic at 20°C; (b) Pt(IV) with Pic after heating.

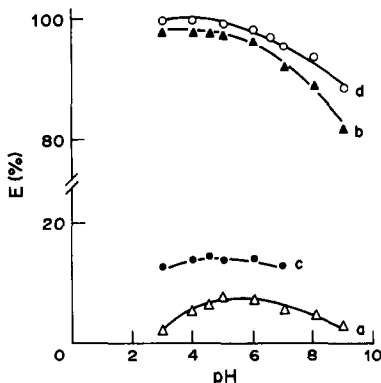


Fig. 5. Extraction vs. pH plot for copper(II), (a) Cu(II) with Pic at 20°C; (b) Cu(II) with Pic after heating; (c) Cu(II) with DBSA at 20°C; (d) Cu(II) with DBSA after heating.

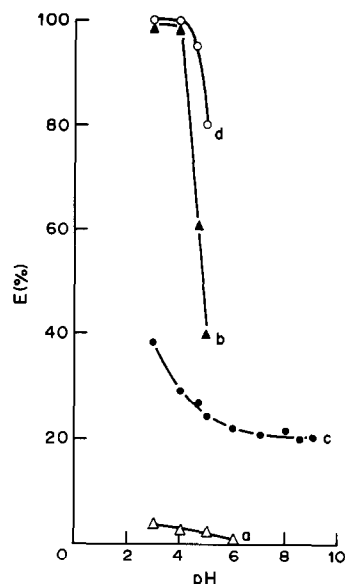


Fig. 6. Extraction vs. pH plot for copper(I), (a) Cu(I) with Pic at 20°C; (b) Cu(I) with Pic after heating; (c) Cu(I) with DBSA at 20°C; (d) Cu(I) with DBSA after heating.

plexes of Cu(II), Pt(II), Pt(IV), Pd(II), Cu(I), Hg(II) and Ag(I), which have ionic radii ranging from 0.72 to 1.26 Å, the flexible macrocyclic molecule forms complexes with quite a different structure.

The data presented in Table 1 indicate that both the complex formation with hexacyclen and the extraction of the complexes are not fast enough. This is confirmed also by the data presented in Figs. 2–6, showing that the metal is completely extracted only after complexation at higher temperatures. Ag(I) should not be heated, as already mentioned above, and Hg(II) is extracted quantitatively even without preliminary heating (Fig. 7). At least in the case of Pt(II) and Pd(II) the low complex formation rate can be related to the well known inertness of their

Table 2. pH-Dependence of metal-ion extraction (%) at different temperatures in the presence of picric acid ($\mu = 0.1M$); all data are average values (and range) from 3–6 experiments

M^{n+}	Ionic radius, Å ¹⁵	20°C			After preliminary heating		
		pH 3	pH 5	pH 9	pH 3	pH 5	pH 9
Ag(I)	1.26	65 ± 4	99 ± 1	87 ± 5	0	14 ± 2	3 ± 1
Cd(II)	0.97	<1	18 ± 2	10 ± 2	<0.5	17 ± 2	17 ± 2
Co(II)	0.72	0	<1	<1	0	7 ± 1	3 ± 1
Cu(I)	0.96	4 ± 1	2 ± 1	0	98 ± 3	40 ± 5	0
Cu(II)	0.72	2 ± 1	8 ± 1	3 ± 1	98 ± 2	98 ± 1	82 ± 4
Fe(II)	0.74	0	0	0	0	0	0
Fe(III)	0.64	0	0	0	0	0	0
Hg(II)	1.10	94 ± 2	>99.5	86 ± 2	98 ± 2	>99.5	96 ± 2
Mn(II)	0.80	0	0	24 ± 4	0	0	24 ± 3
Ni(II)	0.69	0	4 ± 1	2 ± 1	0	23 ± 3	3 ± 1
Pb(II)	1.20	0	0	0	0	0	0
Pd(II)	0.80	50 ± 3	52 ± 3	88 ± 4	90 ± 2	95 ± 2	>99.5
Pt(II)	0.80	32 ± 2	52 ± 3	21 ± 2	98 ± 1	97 ± 2	72 ± 4
Pt(IV)	0.65	55 ± 3	37 ± 3	17 ± 2	98 ± 2	95 ± 2	83 ± 3
Tl(I)	1.47	0	0	0	0	0	0
Zn(II)	0.74	0	8 ± 2	5 ± 1	0	8 ± 2	6 ± 1

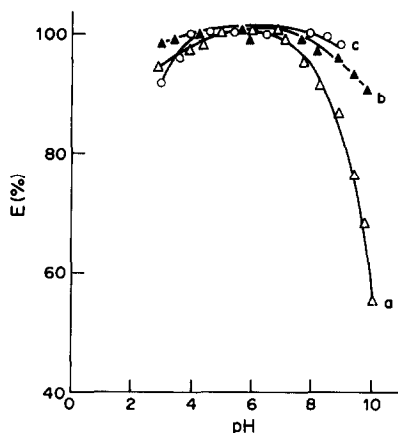


Fig. 7. Extraction vs. pH plot for mercury(II), (a) Hg(II) with Pic at 20°C; (b) Hg(II) with Pic after heating; (c) Hg(II) with DBSA after heating.

Table 3. Separation of metal ions from iron(III) [extraction of Ag(I) and Hg(II) at ambient temperature, all other ions after preliminary heating]

M:Fe(II)	pH	R, %
Ag(I):Fe(III) = 1:3	5	99 ± 1
Ag(I):Fe(III) = 1:10	5	90 ± 2
Ag(I):Fe(III) = 1:10 ²	5	68 ± 3
Cu(II):Fe(III) = 1:10 ²	5	90 ± 3
Hg(II):Fe(III) = 1:10 ³	5	98 ± 2
Hg(II):Fe(III) = 1:10 ⁴	5	80 ± 3
Pd(II):Fe(III) = 1:10 ⁴	5	98 ± 1
Pd(II):Fe(III) = 1:10 ⁵	5	85 ± 5
Pt(II):Fe(III) = 1:10 ³	3	98 ± 2
Pt(II):Fe(III) = 1:10 ⁴	3	97 ± 3

complexes, while in the other cases it might be connected with larger deformations of the ligand in the course of the complexation process.

The results thus obtained show that extraction with hexacyclen can be used for separation of copper, silver, mercury, platinum and palladium from iron,

zinc, lead, manganese, etc. This was confirmed by direct experiments, the results of which are presented in Table 3. The separation is obtained by preliminary heating of the sample with the reagent on a water-bath for 30 min, followed by a 30-min extraction (15 min in the case of mercury). The recovery percentage ($R\%$) for the metal ion is a measure of the efficiency of the separation. It can be seen that some of the recoveries are rather poor. Effective separation from iron is realized for platinum and palladium at $M:Fe = 1:10^4$, for mercury at $1:10^3$, for copper at $1:10^2$ and for silver at 1:5.

REFERENCES

1. E. Blasius and K. P. Janzen, in *Topics in Current Chemistry*, F. Vögtle (ed.), Vol. 98, p. 163. Springer-Verlag, Berlin, 1981.
2. D. Sevdic and H. Meider, *J. Inorg. Nucl. Chem.*, 1977, **39**, 1403.
3. *Idem, ibid.*, 1977, **39**, 1409.
4. D. Sevdic, L. Fakete and H. Meider, *ibid.*, 1980, **42**, 885.
5. Y. Takeda, M. Nemoto and S. Fujiwara, *Bull. Chem. Soc. Japan*, 1982, **55**, 3438.
6. K. Saito, Y. Masuda and E. Sekido, *Anal. Chim. Acta*, 1983, **151**, 447.
7. Yu. A. Zolotov, V. P. Ionov, N. V. Nizieva and A. A. Formanovsky, *Dokl. Akad. Nauk USSR*, 1984, **277**, 1145.
8. E. I. Morosanova, E. D. Matveeva, Yu. G. Bundel, V. A. Bodnya and Yu. A. Zolotov, *ibid.*, 1984, **277**, 1151.
9. A. Sanz-Medel, D. Blanco Gomis, E. Fuente and S. A. Jimeno, *Talanta*, 1984, **31**, 515.
10. K. Saito, Y. Masuda and E. Sekido, *Bull. Chem. Soc. Japan* 1984, **57**, 189.
11. E. I. Morosanova, Yu. A. Zolotov, V. A. Bodnya and A. A. Formanovsky, *Mikrochim. Acta*, 1984 **III**, 389.
12. Yu. A. Zolotov, E. I. Morosanova, S. G. Dmitrienko, A. A. Formanovsky and G. V. Ivanov, *ibid.*, 1984 **III**, 399.
13. J. Hasegawa, H. Tanabe and S. Yoshida, *Bull. Chem. Soc. Japan*, 1985, **58**, 3649.
14. R. W. Hay, B. Jeragh, S. F. Lincoln and G. H. Searle, *Inorg. Nucl. Chem. Lett.*, 1978, **14**, 435.
15. L. Ahrens, *Geochim. Cosmochim. Acta*, 1952, **2**, 155.

EXTRACTION OF AROMATIC ORGANIC COMPOUNDS BY POLYURETHANE FOAM

L. SCHUMACK and A. CHOW

Department of Chemistry, University of Manitoba, Winnipeg, Manitoba, Canada

(Received 10 September 1986. Revised 25 March 1987. Accepted 27 May 1987)

Summary—The mechanism of extraction of organic compounds by open-cell polyurethane foam has been investigated through a detailed study with simple aromatic compounds. Comparison with identical extractions into diethyl ether suggests that the basic extraction mechanism is an ether-like solvent extraction process. The addition of salt increases the extraction and changing the dielectric constant of the aqueous solution also affects the extraction. For organic compounds which have a group capable of hydrogen bonding, some additional factor appears to influence the extraction. This appears to be hydrogen bonding with the polyurethane foam; it is stronger with polyether foam and reduced by the presence of a strong intramolecular hydrogen-bonding group placed *ortho* to the hydrogen-bonding group. Thermodynamic studies support these conclusions.

Since their origin, polyurethane polymers have been applied to a variety of tasks. In 1970, Bowen¹ first used foamed polyurethane for the extraction from aqueous media of a variety of metal species such as mercury(II), gold(III), iron(III), antimony(V), molybdenum(VI), rhenium(III) and uranium(VI) as well as benzene and phenol. Because of the large sorption capacities (0.5–1.5 mole/kg), Bowen deduced that the extraction was not a surface phenomena but that absorption into the bulk of the polyurethane must occur. The possibility of a solvent extraction mechanism and the similarity between extraction by foam and by diethyl ether was reported. Considerable further research has dealt with the extraction of various inorganic compounds and metal species, a summary of which can be found in several reviews^{2,3} and books.^{4,5}

Only a few papers have discussed the mechanism of the extraction process. Gesser and co-workers^{6,7} described the extraction of Ga(III), regarding the polyurethane foam extraction as similar to an ether-type solvent extraction in which the neutral HGaCl_4 species was extracted. Later work by Lo and Chow⁸ also found the foam-extraction of antimony to be similar to that into an organic solvent. This view of the extraction mechanism was further supported by Korkisch *et al.*⁹ who examined the extraction of uranium and found the salting-out effects to be similar to those in the liquid–liquid extraction of uranium by ethers. More evidence was presented by Braun *et al.*,¹⁰ who used Mössbauer spectroscopy to show the similarity between diethyl ether extraction and the extraction by polyurethane foam.

An alternative mechanism was postulated by Hamon *et al.*¹¹ for the extraction of cobalt and other metals. This mechanism, known as the “cation-chelation mechanism”, consisted of having the negatively-charged metal complexes solvated within

the polymer matrix, with accompanying cations strongly solvated within “crown ether” type structures within the polymer configuration. Since only the polyether-type foam can form these “crown ether” type structures, it is a much better extractor than the polyester-type polyurethane foam. Further research^{12–14} also supports this mechanism.

Some work has been done on the extraction of organic compounds by polyurethane foam since Bowen's publication. Gesser *et al.*¹⁵ extracted polychlorinated biphenyls from water, by using foam plugs placed in a chromatographic column. It was found that organochlorine pesticides were extracted along with the polychlorinated biphenyls and a detailed study of the factors affecting the extraction and recovery of these compounds was made by Musty and Nickless.¹⁶ The uncoated foams gave better extraction than those coated with chromatographic greases, indicating an absorption mechanism. Later, Gough and Gesser¹⁷ looked at the extraction and recovery of phthalate esters from aqueous media. They found that a column containing foam plugs could remove these phthalates at the $\mu\text{g/l.}$ level and that these compounds could be recovered by elution with acetone and hexane. There was no attempt to define the mechanism involved. Recent work by Ahmad *et al.*¹⁸ looked at extraction by polyurethane foam as a means of separating different carboxylic acids in aqueous solution.

Although there has been some speculation as to the mechanism of extraction for inorganic compounds, to date there has been very little work done on the mechanism of extraction of organics by untreated open-cell polyurethane foam. The present investigation looked at the extraction of simple aromatic compounds with the intention of determining whether the extraction by solvent extraction, cation-chelation or another mechanism.

EXPERIMENTAL

Apparatus

Ultraviolet absorbance measurements were made with a Unicam SP500 series 2 or a Varian Series 634S spectrophotometer. Sodium concentration was measured with a Waters Millipore ILC-1 Ion/Liquid Chromatograph with a Wisp 710B, a model 430 conductivity detector and a 740 data module with Waters Millipore IC Pak cation and guard columns. Ethanol concentration was measured with a Hewlett-Packard 5710A gas chromatograph with a flame-ionization detector, equipped with a glass column packed with Waters Porapak P.

The solutions were equilibrated with the foam in borosilicate glass squeezing-cells mounted within a thermostatically controlled ($25.0 \pm 0.1^\circ$) cabinet. This equipment was designed to produce repetitive solution-mixing and foam-squeezing at a rate of 30 ± 0.5 cycles/min and is described elsewhere.¹⁹

Reagents

All chemicals were of reagent grade unless otherwise indicated. Pure water was obtained from a Barnstead Nanopure II water purification system fed with water purified by reverse osmosis.

Two types of polyurethane foam were used. The polyester foam was obtained as Dispo T. M. plugs from Canlab, Winnipeg and the polyether plugs were cut from a foam pad obtained from a local department store. The cleaning process for both foam types consisted of soaking for 1 hr in 1M hydrochloric acid with occasional squeezing; rinsing with pure water; soaking for 1 hr in 95% ethanol with occasional squeezing; rinsing overnight in pure water; extracting with acetone for 3 hr in a Soxhlet apparatus; drying overnight in a vacuum desiccator before use.

General procedure

Preliminary experiments showed that 1 hr of squeezing was enough for equilibrium to be attained for the compounds studied. Simple aromatic compounds were used because they had several desirable properties such as good ultraviolet absorption for easy detection, enough polarity to dissolve sufficiently in 10% ethanol solution, and reasonable extraction into the foam. The 10% ethanol in water medium was chosen because it was able to dissolve the compounds tested, did not give severe evaporation problems and gave larger extraction values than higher ethanol concentrations did. Sample solutions were prepared by diluting 1 ml of an organic stock solution to 100 ml with 10% ethanol solution. The ultraviolet absorbance (A) of the sample solutions was measured before addition of the foam and again after the squeezing period. The values obtained were corrected by means of the values from a blank run simultaneously. The degrees of extraction (E) and the distribution coefficients were then calculated;

$$E = [(A_{\text{initial}} - A_{\text{final}}) / A_{\text{initial}}] \times 100\%$$

$$D = \frac{E}{(100 - E)} \times \frac{\text{volume of solution}}{\text{weight of foam}}$$

the units used being litres for volume of solution and kg for weight of foam. Several trials were run simultaneously and the standard deviations were calculated.

The wavelength used for absorbance measurements was that for the highest absorbance (λ_{max}). They were either taken from the Sadtler Handbook²⁰ or the D.M.S. UV atlas,²¹ or determined experimentally by scanning from 500 to 200 nm with the Varian spectrophotometer.

For many of the compounds an extraction was performed with diethyl ether and compared with the foam extraction. The ether extraction consisted of extracting the organic compound from 20 ml of sample solution with 10 ml of diethyl ether at 25° .

RESULTS AND DISCUSSION

Extraction time

Preliminary experiments showed that extraction equilibrium was attained within 1 hr. Further experiments indicated that a 5-ppm solution of *m*-nitrophenol in 10% ethanol reached equilibrium after 4 min of squeezing with the foam. The same results were obtained with 0.25-g pieces of either polyether or polyester foam. For 0.40-g pieces of polyester foam the time for equilibrium to be reached increased to 6 min. The extraction with diethyl ether extraction reached equilibrium within 15 min. According to Hamon *et al.*¹¹ the cation-chelation mechanism can take up to 18 hr to reach equilibrium for 0.05-g foam pieces. Thus the extraction time for organics is similar for polyurethane foam and for diethyl ether extraction, and is more rapid than would be expected for a cation-chelation mechanism.

General survey

The results of the general survey and for the diethyl ether extraction are shown in Table 1. In the solvent extraction with diethyl ether, more than 99% extraction was obtained in some cases; because of the relative volumes of the two phases, the amount of solute left in the aqueous phase was too small for accurate measurement in these cases, so the distribution coefficient is recorded as being greater than a value arbitrarily selected as the highest measurable. The distribution coefficients obtained in the foam experiments generally paralleled those of the ether experiments. This supports the suggestion that the extraction mechanism with the polyurethane foam is similar to that with ether. The reason for the negative values of D reported for the pyridine/foam systems is not known; since it means that the absorbance of the aqueous phase is greater after the extraction than before it, it is perhaps due to extraction of a degradation product of the foam into the aqueous phase, but this was not investigated.

Effect of salts on the extraction

The extraction of *m*-nitrophenol by foam from various salt solutions gave the results shown in Table 2. Korkisch *et al.*⁹ found that the salting-out efficiency of cations in the extraction of uranium by polyurethane foam was in the order $\text{NH}_4^+ < \text{Ca}^{2+} < \text{Al}^{3+}$. The results in Table 2 show that a singly-charged cation (K^+) had less effect on the extraction than a doubly-charged cation (Ca^{2+}).

It was found that the effect of the alkali-metal ions on the extraction increased as the charge-density on the ion increased. This is consistent with a solvent-extraction mechanism, as an ion with a larger charge density should be more strongly solvated, thus reducing the number of solvent molecules available to solvate the organic compound, which would therefore be forced out of the solvent phase into the foam. The solvation numbers for the cations examined are

Table 1. Extraction of organic compounds from 10% v/v ethanol by polyurethane and diethyl ether

Compound	Number of trials	λ_{\max} , nm	Concentration, ppm	$D \pm \text{std. devn.}$		
				Polyether, l./kg	Polyester, l./kg	Solvent extraction
Azobenzene	4	314	5	$(3.8 \pm 0.6) \times 10^3$	$(3.3 \pm 0.2) \times 10^3$	> 500
Aniline	8	230	6	20 ± 3	26 ± 6	14
Benzaldehyde	4	244	4	41 ± 1	45 ± 1	30
Benzonitrile	4	230	6	56 ± 1	53 ± 2	74
Toluene	4	261	100	$(8 \pm 5) \times 10^2$	$(8 \pm 5) \times 10^2$	> 450
Acetophenone	4	240	50	38 ± 2	40 ± 1	58
<i>m</i> -Dinitrobenzene	4	233	5	121 ± 3	167 ± 12	67
Nitrobenzene	4	251	10	124 ± 2	116 ± 3	120
Benzene	4	254	500	$(4.7 \pm 1.8) \times 10^2$	$(4.4 \pm 3.2) \times 10^2$	> 340
Biphenyl	4	247	8	$(6.5 \pm 0.4) \times 10^3$	$(5.9 \pm 0.9) \times 10^3$	> 340
Benzophenone	4	252	9	$(1.20 \pm 0.04) \times 10^3$	$(1.09 \pm 0.03) \times 10^3$	
Ethyl benzoate	4	230.5	5	$(2.6 \pm 0.1) \times 10^2$	188 ± 2	200
Phenyl ether*	4	258	50	$(2.97 \pm 0.09) \times 10^3$	$(2.2 \pm 0.2) \times 10^3$	> 330
Chlorobenzene	4	264	100	$(6.8 \pm 1.6) \times 10^2$	$(5.6 \pm 1.1) \times 10^2$	
Pyridine	4	256	10	-9 ± 3	-4 ± 3	2
<i>p</i> -Nitroaniline	4	382	5	275 ± 6	193 ± 3	36
<i>o</i> -Nitroaniline	4	281	10	264 ± 6	208 ± 11	
Triphenylphosphine	4	223	5	$(5.8 \pm 0.2) \times 10^2$	$(5.4 \pm 0.8) \times 10^2$	

Conditions: $25.0 \pm 0.1^\circ$; polyether 0.25-g pieces; polyester 0.40-g pieces; 1 hr extraction time.

*Extraction from 20% ethanol.

reported²² to be 5.4, 8.4 and 14.0 for K^+ , Na^+ and Li^+ respectively, the reference ion, Cl^- , being assumed to have a solvation number of 4. The degree of extraction also increased with the amount of salt added, which is also characteristic of a solvent-extraction mechanism, since the amount of "free" solvent molecules will decrease with increase in amount of preferentially solvated ions. The decrease in extraction when sodium perchlorate is added to the system is interesting, but the reason for it has not been discovered. Both ion-chromatography and gravimetric analysis showed that no sodium perchlorate is extracted.

The effect of pH on the extraction

Compounds such as benzoic acid, *m*-nitrophenol and aniline, which can be involved in equilibria with protons, were extracted into the foam only at pH-values at which they were in the neutral form. For compounds such as nitrobenzene, which exist as the

neutral species irrespective of pH, change in the acidity had no effect on the degree of extraction. Thus the extraction mechanism involves neutral species and there is no evidence for a mechanism requiring ionic species. This observation is also consistent with a solvent-extraction mechanism.

Effect of ethanol concentration on the extraction

It was found, as shown in Table 3, that as the aqueous phase was made less polar by increasing its ethanol content, the degree of extraction decreased. When a compound of low dielectric constant is distributed between a phase which has a low dielectric constant and another which has a high dielectric constant, the degree of extraction should increase with increase in the polarity of the polar phase. A compound with a high dielectric constant such as ethanol should not be extracted at all, and this was confirmed experimentally. These observations are

Table 2. Effect of salts on the extraction of 5 ppm *m*-nitrophenol

Salt	Concentration, M	$D \pm \text{std. devn.}, l./kg$	
		Polyether	Polyester
LiCl	3.00	$(1.94 \pm 0.03) \times 10^3$	$(6.0 \pm 0.5) \times 10^2$
NaCl	0.50	$(6.5 \pm 0.11) \times 10^2$	$(2.6 \pm 0.12) \times 10^2$
NaCl	1.00	$(8.0 \pm 0.1) \times 10^2$	$(2.9 \pm 0.04) \times 10^2$
NaCl	1.50	$(9.3 \pm 0.3) \times 10^2$	$(3.6 \pm 0.12) \times 10^2$
NaCl	2.00	$(1.26 \pm 0.1) \times 10^3$	$(4.9 \pm 0.3) \times 10^2$
NaCl	3.00	$(1.55 \pm 0.06) \times 10^3$	$(5.4 \pm 0.3) \times 10^2$
KCl	3.00	$(8.7 \pm 0.2) \times 10^2$	$(3.4 \pm 0.1) \times 10^2$
$NaClO_4$	3.00	$(4.1 \pm 0.1) \times 10^2$	$(2.0 \pm 0.1) \times 10^2$
None	0.00	$(5.5 \pm 0.1) \times 10^2$	$(2.3 \pm 0.06) \times 10^2$
$CaCl_2$	1.00	$(1.11 \pm 0.06) \times 10^3$	$(3.7 \pm 0.1) \times 10^2$
Na_2SO_4	1.00	$(1.53 \pm 0.01) \times 10^3$	$(4.7 \pm 0.2) \times 10^2$

Conditions: $25.0 \pm 0.1^\circ$; polyether = 0.25-g pieces; polyester = 0.40-g pieces; 1 hr extraction time; three trials for each value.

Table 3. Effect of ethanol concentration on extraction

Compound	Ethanol concentration, % v/v	$D \pm \text{std. devn.}, l./\text{kg}$	
		Polyether	Polyester
<i>m</i> -Nitrophenol	0	550 \pm 12	229 \pm 6
	10	441 \pm 10	180 \pm 6
	20	282 \pm 16	143 \pm 12
	30	145 \pm 10	77 \pm 6
Benzoic acid	0	100 \pm 12	29.6 \pm 0.9
	10	111 \pm 6	30.4 \pm 2.3
	20	60 \pm 8	8 \pm 5
	30	10 \pm 10	0 \pm 0.3
Phenol	0	88 \pm 1	40 \pm 2
	10	79 \pm 1	34 \pm 1
	20	47 \pm 4	26 \pm 1

Conditions: 25.0 \pm 0.1°; polyether = 0.25-g pieces; polyester = 0.40-g pieces; 1 hr extraction time; *m*-nitrophenol (5 ppm) λ = 229 nm; benzoic acid (10 ppm) λ = 228 nm; phenol (40 ppm) λ = 270 nm.

again consistent with a solvent-extraction mechanism.

Hydrogen bonding

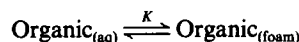
It was found that for many compounds an additional factor was involved in the extraction mechanism. The compounds listed in Table 4 all contain a phenolic or a carboxylic group, and unlike the compounds listed in Table 1 they all have larger distribution coefficients for extraction by polyether foam than by polyester foam, though for *o*-nitrophenol, *o*-methoxyphenol and salicylaldehyde the difference was small. This effect may be due to hydrogen bonding between the phenolic or carboxylic group and the foam. Such bonding would be stronger with the polyether foam and very weak with the polyester. This bonding is prevented by the presence of a strongly electron-donor group *ortho* to the

hydrogen-bonding group, as in *o*-nitrophenol, salicylaldehyde, and *o*-methoxyphenol, where intramolecular hydrogen bonding can take place. For the *para* and *meta* nitrophenols the distribution coefficients are much greater for the polyether foam than for the polyester foam, whereas for the *ortho* compound the coefficients are similar for the two types of foam. This cannot be attributed to a difference in dipole moment, because the dipole moment gradually increases for the compounds in the order *ortho* < *meta* < *para*. Induction effects due to the position of the nitro group should be minimal owing to the distance between that group and the phenol group, so it may be concluded that the strong intramolecular hydrogen bonding is responsible for preventing formation of a hydrogen bond with the polyurethane foam.

The hydrogen bonding is probably stronger with the polyether foam, since ethers are much better than esters at forming hydrogen bonds. This is reasonable, because the ether group is easier to protonate than an ester group²³ and the ability of a group to form hydrogen bonds is indicated by its protonation constant.

Effect of temperature on the extraction

The degree of extraction of azobenzene and *m*-nitrophenol was measured at various temperatures, by use of a jacketed temperature-controlled squeezing cell. For the equilibrium



the equilibrium constant, K , with standard enthalpy change ΔH° and standard entropy change ΔS° is given by

$$\ln K = -\Delta H^\circ/RT + \Delta S^\circ/R$$

Table 4. Extraction of compounds containing an —OH group

Compound	Number of trials	$\lambda_{\text{max}}, \text{nm}$	Concentration, ppm	$D \pm \text{std. devn.}, l./\text{kg}$		
				Polyether	Polyester	Solvent extraction
Benzoic acid	8	228	10	112 \pm 7	30 \pm 2	18
Phenol	8	270	40	79 \pm 1	34 \pm 1	37
Salicylic acid	4	235	10	206 \pm 15	21 \pm 3	7
Pyrogallol	4	267	10	54 \pm 30	-3 \pm 5	5
Hydroquinone	4	293.5	40	21 \pm 10	8 \pm 8	
Catechol	4	277.5	10	60 \pm 9	26 \pm 5	10
Resorcinol	4	275	10	53 \pm 4	28 \pm 2	6
<i>p</i> -Nitrophenol	4	311	8	407 \pm 7	165 \pm 3	100
<i>m</i> -Nitrophenol	4	229	10	470 \pm 10	183 \pm 6	170
<i>o</i> -Nitrophenol	4	272	10	128 \pm 4	122 \pm 2	120
2,6-Dinitrophenol	4	253	10	179 \pm 12	213 \pm 16	57
2,4-Dinitrophenol	4	258	10	382 \pm 23	276 \pm 13	93
2,4-Dihydroxybenzoic acid	4	256	10	292 \pm 12	36 \pm 6	6
3,5-Dihydroxybenzoic acid	4	241	10	142 \pm 8	12 \pm 3	2
<i>o</i> -Tert-butylphenol	4	271	30	(4.84 \pm 0.15) $\times 10^3$	(1.32 \pm 0.1) $\times 10^3$	> 500
2,6-Di-tert-butylphenol	4	270	50	(2.63 \pm 0.09) $\times 10^3$	(1.90 \pm 0.25) $\times 10^3$	> 700
2,4-Di-tert-butylphenol	4	258	10	(2.15 \pm 0.14) $\times 10^4$	(9.8 \pm 0.4) $\times 10^3$	
Salicylaldehyde	4	255	5	104 \pm 3	82 \pm 5	70
<i>o</i> -Methoxyphenol	4	274.5	20	47 \pm 3	33 \pm 3	24

Conditions; 25.0 \pm 0.1°; polyether = 0.25-g pieces; polyether = 0.40-g pieces; 1 hr extraction time.

Table 5. Thermodynamic data for extraction

Compound	Foam type	ΔH° , kJ/mole	ΔS° , J.mole ⁻¹ .deg ⁻¹
Azobenzene	Polyether	-20 ± 2	5 ± 5
	Polyester	-23 ± 1	-3 ± 5
<i>m</i> -Nitrophenol	Polyether	-19 ± 2	2 ± 4
		-22 ± 1	-4 ± 4
	Polyester	-30 ± 1	-50 ± 3
		-31 ± 1	-55 ± 2
Polyester	-21 ± 2	-21 ± 1	
	-28 ± 5	-28 ± 2	

Conditions: extraction from 10% ethanol; azobenzene (5 ppm) $\lambda = 314$ nm; *m*-nitrophenol (10 ppm) $\lambda = 230$ nm; all values ± standard deviation calculated from slope; temperature range 25°–75°.

Assuming no chelation or precipitation and that the compounds exist only as neutral species, then K is equivalent to D . Thus by plotting $\ln D$ vs. $1/T$, the values of ΔH° and ΔS° can be obtained (Table 5). The ΔS° values for azobenzene are almost the same for extraction into either polyether or polyester foam. Thus the organic compound has approximately the same degree of freedom in the polymer as in the aqueous solution, which is consistent with a solvent-extraction mechanism. With *m*-nitrophenol there is a decrease in entropy for both the polyether and polyester foam extractions, with the change larger for the polyether system. This entropy change is believed to be due to hydrogen bonding reducing the freedom of movement of the organic compound in the polymer. The bonding of the organic compound with the polyether foam is apparently much stronger than reported previously. The strength of the hydrogen bond with the foam can be estimated as about 10 kJ/mole by subtracting the enthalpy change ΔH° for the polyester system from that for the polyether system. Although this calculation is only valid if it can be assumed that there is no hydrogen bonding between the organic compound and the polyether foam, it at least gives a rough idea of the value. The calculation is useful as the intramolecular hydrogen bonding in *o*-nitrophenol, salicylaldehyde and *o*-methoxyphenol has been calculated to have a bond strength of 30,²⁴ 30,²⁵ and 10.²⁶ kJ/mole, respectively, which is greater than or equal to the estimated polyurethane hydrogen-bonding strength.

The hydrogen bonding between the foam and the organic compound should occur for groups other than -OH which are capable of hydrogen bonding. A few amines were surveyed but any hydrogen bonding was not strong enough to be detected within the experimental error of the work. Future work with thiol compounds could be used to look for evidence of this hydrogen bonding.

CONCLUSIONS

The extraction of organic compounds by polyurethane foam appears to occur generally by an ether-like solvent-extraction mechanism. This conclu-

sion is supported by the short time required for extraction equilibrium to be achieved and the evidence of the salting-out phenomenon. It was found that the addition of inert salts increases the extraction efficiency and that changing the polarity of the raffinate phase also affects the extraction. Varying the pH showed no evidence of a mechanism requiring an ionic species. All observations were consistent with a solvent-extraction mechanism. However, when the compound contained a group capable of hydrogen bonding, such as -OH, an additional factor appeared to be involved. This factor is probably hydrogen bonding between the polyurethane and the group on the organic compound. Strong intramolecular hydrogen bonding in the organic compound will negate this hydrogen bonding, and occurs whenever a group such as -NO₂ is *ortho* to the -OH group. Because ester groups form weaker hydrogen bonds than ether groups, this bond is weaker in the polyester foam system.

The solvent-extraction mechanism, modified by hydrogen bonding wherever applicable, may explain the extraction of all organic compounds by polyurethane foam. Future studies on aliphatic organic compounds will be used to examine this.

Acknowledgement—This work was supported by the Natural Sciences and Engineering Research Council of Canada.

REFERENCES

1. H. J. M. Bowen, *J. Chem. Soc. A*, 1970, 1082.
2. T. Braun and A. B. Farag, *Anal. Chim. Acta*, 1978, **99**, 1.
3. T. Braun, *Cellular Polym.*, 1984, **3**, 81.
4. T. Braun, J. D. Navratil and A. B. Farag, *Polyurethane Foam Sorbents in Separation Science*, CRC Press, Boca Raton, 1985.
5. G. J. Moody and J. D. R. Thomas, *Chromatographic Separation and Extraction with Foamed Plastics and Rubbers*, Dekker, New York, 1982.
6. H. D. Gesser, E. Bock, W. G. Baldwin, D. W. McBride and W. Lipinsky, *Sepr. Sci.*, 1976, **11**, 317.
7. H. D. Gesser and G. A. Horsfall, *J. Chim. Phys. Phys.-Chim. Biol.*, 1977, **74**, 1072.
8. V. S. K. Lo and A. Chow, *Anal. Chim. Acta*, 1979, **106**, 161.
9. J. Korkisch, I. Steffan and J. D. Navratil, *Radioact. Waste Manage.*, 1982, **6**, 349.

10. M. N. Abbas, A. Vertes and T. Braun, *Radiochem. Radioanal. Lett.*, 1982, **54**, 17.
11. R. F. Hamon, A. S. Khan and A. Chow, *Talanta*, 1982, **29**, 313.
12. G. J. Moody, J. D. R. Thomas and M. A. Yarmo, *Anal. Proc.*, 1983, **20**, 132.
13. R. Caletka, R. Hausbeck and V. Krivan, *Talanta*, 1986, **33**, 219.
14. *Idem, ibid.*, 1986, **33**, 315.
15. H. D. Gesser, A. Chow, F. C. Davis, J. F. Uthe and J. Reinke, *Anal. Lett.*, 1971, **4**, 883.
16. P. R. Musty and G. Nickless, *J. Chromatog.*, 1974, **100**, 83.
17. K. M. Gough and H. D. Gesser, *ibid.*, 1975, **115**, 383.
18. S. R. Ahmad, H. S. Rathore, I. Ali and S. K. Sharma, *J. Indian Chem. Soc.*, 1985, **62**, 786.
19. L. J. Schumack, *M.Sc. Thesis*, University of Manitoba, 1986.
20. *The Sadtler Handbook of Ultraviolet Spectra*, W. W. Simons (ed.), Heyden, London, 1978.
21. *D.M.S. U.V. Atlas of Organic Compounds*, Verlag Chemie, Weinheim, 1966.
22. E. S. Amis and J. F. Hinton, *Solvent Effects on Chemical Phenomena*, Vol. I, p. 52. Academic Press, New York, 1973.
23. J. March, *Advanced Organic Chemistry*, 3rd Ed., p. 220. Wiley, New York, 1985.
24. T. Schaefer and T. A. Wildman, *Can. J. Chem.*, 1979, **57**, 450.
25. T. Schaefer, R. Sebastian, R. Laatikainen and S. R. Salman, *ibid.*, 1983, **62**, 326.
26. T. Schaefer, *J. Phys. Chem.*, 1975, **79**, 1888.

SHORT COMMUNICATIONS

DETERMINATION OF MOLECULAR NITROGEN BY ELECTRON-IMPACT INDUCED FLUORESCENCE

DAVID A. RADSPINNER* and E. L. WEHRY†

Department of Chemistry, University of Tennessee, Knoxville, TN 37996, U.S.A.

(Received 10 April 1987. Accepted 19 May 1987)

Summary—When a sample of nitrogen gas is bombarded by 100-eV electrons, fluorescent emission from the nitrogen molecular ion, N_2^+ , is observed. The intensity of this fluorescence can be related to the pressure (or molar concentration) of the parent molecule, N_2 . The limit of detection for N_2 by means of electron-impact induced fluorescence is 5.0×10^{-8} mmHg (1.6×10^9 molecules/cm³ or 2.7×10^{-12} mole/l.). The fluorescence signal is linearly related to N_2 pressure over a range of four orders of magnitude, and relative standard deviations of less than 2% are observed for replicate measurements.

Bombardment of a compound in the gas phase with monoenergetic electrons can produce ionization, electronic excitation, and/or fragmentation of the parent molecule. Any fragment species has the possibility of being formed in electronically (as well as vibrationally and rotationally) excited states. The electronically excited parent molecules, molecular ions, and fragments so produced may exhibit radiative decay (fluorescence or phosphorescence).¹⁻³

The use of electrons (rather than photons) to excite fluorescence or phosphorescence has two potential advantages in chemical analysis. First, molecular electronic excitation by electron impact (EI) is not governed by the selection rules associated with optical absorption phenomena. Hence, EI can be used to populate excited molecular states that may be inaccessible by photon absorption, either because the absorption cross-sections are very small or the allowed absorption transitions are situated in spectral regions for which no practical photon sources exist. Second, if the parent molecule is itself non-fluorescent (irrespective of the excitation technique used), it may undergo fragmentation by EI to produce luminescent products. Accordingly, it is possible to extend the analytical applicability of molecular fluorescence spectrometry to non-fluorescent analytes by EI-induced fragmentation followed by measurement of the fluorescence or phosphorescence of the fragment species.^{2,4}

That EI is widely used as an ionization technique in mass spectrometry means that molecular ionization, excitation, and fragmentation phenomena induced by EI have been studied extensively and are reasonably well understood. Although the potential

applicability of EI-induced fragmentation and excitation in molecular fluorescence spectrometry has been evident for some time,^{2,4} few analytical applications of the principle have yet been reported.

We report here the detection and determination of molecular nitrogen by means of the fluorescence of N_2^+ induced by 100-eV electrons. EI of N_2 produces electronically excited parent molecules, molecular ions (N_2^+) and nitrogen atoms, the fluorescence of which can be detected and utilized for analytical purposes. The limits of detection, linear dynamic range and precision of the measurements are reported.

EXPERIMENTAL

The apparatus used for producing electron-impact induced fluorescence from nitrogen consists of an electron source, a vacuum chamber and a photon detection system.

The vacuum chamber comprises a cross of ca. 33×51 cm dimensions, with a volume of approximately 8 l. The chamber is differentially pumped by 2 Balzers TSU 331 turbomolecular pumps having pumping speeds of 300 l/sec for N_2 . The pressure in the chamber is 3×10^{-8} mmHg or less (as measured by a Bayard-Alpert ionization gauge) in the absence of sample. When samples are admitted into the chamber, the sample pressure is measured with a capacitance manometer.

The two compartments of the vacuum chamber are separated from each other by the lens assembly of an electron gun constructed to the design of Erdman and Zipf.⁵ The gun uses a thoria-coated iridium filament (Troynics, Kenil, N.J.) mounted on a vacuum translator (to permit adjustment and optimization of the filament-to-grid distance). The filament is generally operated at 3-4 A d.c. and -100 V. Electron-lens elements, consisting of gold-coated copper plates separated by ruby spheres, guide the electron beam to the electron-sample interaction region. Beam currents of the order of 1 mA (6×10^{15} electrons/sec) are produced by this gun.

Samples are admitted directly into the vacuum chamber through a metering valve. Fluorescence is collected through a fused-silica viewpoint at 90° to the electron beam, col-

†Present address: Department of Chemistry, Wabash College, Crawfordsville, IN 47933.

*To whom correspondence should be addressed.

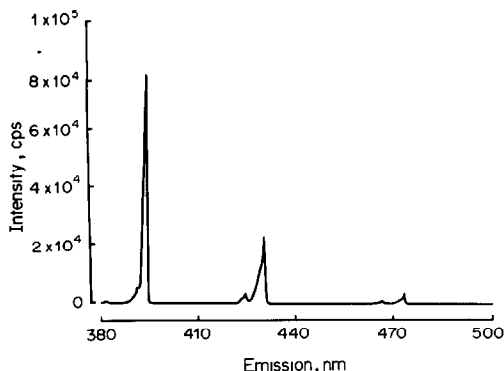


Fig. 1. Electron-impact induced fluorescence spectrum of nitrogen. All features are portions of the "main system" of the fluorescence spectrum of the nitrogen molecular ion.

limited, and focused by two lenses onto the entrance slit of Kratos GMA 201 0.25-m grating monochromator. The fluorescence is detected with an RCA 8850 photomultiplier operated at 1.75 kV. Fluorescence signals are processed by EGG ORTEC photon-counting electronics and, after digital-to-analogue conversion, are plotted by an X-Y recorder. Fluorescence spectra are not corrected for the wavelength-dependence of the photomultiplier response.

RESULTS AND DISCUSSION

The visible portion (380–500 nm) of the EI-induced fluorescence spectrum of nitrogen at 4×10^{-4} mmHg is shown in Fig. 1. The spectrum is dominated by two features, at 391.9 nm and 427.8 nm, which have been assigned to the (0,0) and (0,1) components, respectively, of the $B^2\Sigma_u^+ \rightarrow X^2\Sigma_g^+$ transition of N_2^+ .^{6,7} All quantitative results reported here were obtained by using the emission feature at 391.9 nm.

The dependence of the EI-induced N_2^+ fluorescence signal on N_2 pressure is shown in Fig. 2. The linear dynamic range extends over nearly four decades of nitrogen pressure, from 1×10^{-7} to 9×10^{-4} mmHg

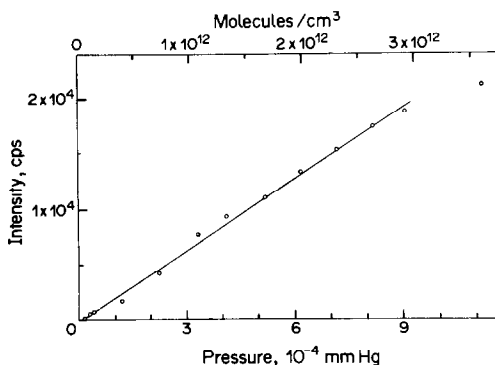


Fig. 2. Analytical calibration curve for N_2^+ fluorescence at 391.9 nm as a function of N_2 pressure.

(i.e., N_2 molecular densities ranging from 3×10^9 to 2×10^{13} molecules/cm³, or molar concentrations of 5×10^{-12} – 5×10^{-8} mole/l.). The calibration curve exhibits negative deviation from linearity at pressures greater than 9×10^{-4} mmHg, primarily because of collisional self-quenching phenomena.

The limit of detection for N_2 (defined as the pressure of N_2 producing a fluorescence signal equal to three times the standard deviation of the signal observed in the absence of any sample in the chamber) was 5.0×10^{-8} mmHg, (1.6×10^9 molecules/cm³ or 2.7×10^{-12} mole/l.). This limit of detection is virtually equal to the minimum background pressure attainable in the vacuum chamber. Thus, the capabilities of the vacuum system, rather than the photon-detection sensitivity of the instrumentation, establish the limit of detection. In this gas-phase fluorescence measurement (as in the vast majority of conventional liquid-solution fluorometric determinations⁸), the detection capabilities are ultimately "background-limited".

EI-induced fluorescence measurements exhibit good precision. For example, at a sample pressure of 1.11×10^{-4} mmHg, ten replicate measurements produced a mean N_2^+ fluorescence signal of 7781 cps with a standard deviation of 146 cps (i.e., a relative standard deviation of 1.9%). The factor limiting the precision of these measurements was the current-stability of the DC electron gun (no standard addition or internal standardization techniques were used in these measurements). In view of the extended linear range of the analytical calibration curve (Fig. 2), standard addition techniques could be employed if desired.

Acknowledgements—This work was supported by the National Science Foundation (Grant CHE-8317000). Participation of D. A. R. was made possible by a Summer Undergraduate Program in Chemical Analysis, supported by the National Science Foundation (CHE-8605166).

REFERENCES

1. R. N. Compton and J. N. Bardsley, in *Electron-Molecule Collisions*, I. Shimamura and K. Takayanagi (eds.), p. 275. Plenum Press, New York, 1984.
2. M. L. Robin, G. K. Schweitzer and E. L. Wehry, *Appl. Spectrosc. Rev.*, 1981, **17**, 165.
3. T. A. Miller and R. S. Freund, *Adv. Magn. Reson.*, 1977, **9**, 49.
4. C. A. Gierczak, M. A. Heindorf and J. Allison, *Anal. Chem.*, 1984, **56**, 2966.
5. P. W. Erdman and E. C. Zipf, *Rev. Sci. Instrum.*, 1982, **53**, 225.
6. R. W. B. Pearse and A. G. Gaydon, *The Identification of Molecular Spectra*, 3rd Ed., Wiley, New York, 1963.
7. R. G. Bennett and F. W. Dalby, *J. Chem. Phys.*, 1959, **31**, 434.
8. F. E. Lytle, *J. Chem. Educ.*, 1982, **59**, 915.

GALVANIC STRIPPING DETERMINATION OF TRACE AMOUNTS OF LEAD

S. JAYA, T. PRASADA RAO and G. PRABHAKARA RAO
Central Electrochemical Research Institute, Karaikudi-623 006, India

(Received 27 September 1985. Revised 4 June 1987. Accepted 27 June 1987)

Summary—A galvanic stripping procedure for rapid determination of trace amounts of lead with a glassy-carbon electrode is described. The method is useful for determining lead at 1–200 ng/ml concentration.

Recently we have demonstrated the potentiality of potentiometric stripping analysis^{1,2} for determining lead and thallium, for which the $E_{1/2}$ values are quite close.³ Galvanic stripping analysis (GSA), which we described recently,⁴ is analogous to PSA except that the stripping is done by a galvanic couple in the absence of any externally impressed emf or oxidant in solution; the galvanic couple used is formed between bare glassy-carbon and an amalgam film, which together constitute the electrode. During our electrochemical phase-formation studies of lead on a glassy-carbon electrode (GCE)⁵ it was noticed that the deposition of lead occurred non-uniformly, *i.e.*, at selected spots, by electrocrystallization processes. This fact has been used in developing a sensitive procedure for the determination of lead by stripping the deposited lead (in the absence of an impressed emf or oxidant) by means of the localized galvanic couples between the lead deposited on the GCE and the uncovered portions of the GCE.

EXPERIMENTAL

Reagents

All solutions were prepared with analytical grade chemicals and conductivity water.

Lead(II) solution, 0.1M.

Sodium chloride, 5M.

Acetate-acetic acid buffer (pH 5), 1.0M.

Apparatus

A conventional three-electrode cell with a glassy-carbon working electrode (Tokai & Co., 3 mm diameter), a platinum foil counter-electrode and a normal calomel reference electrode were used. A Wenking model (Model LB 75) potentiostat coupled with a Wenking scan generator (Model VSG 72) was used for controlling the potential. An XY/t recorder (Digitronic Model 2000 series) was used to record curves of potential *vs.* time. All the potentials were calculated with respect to the NCE and the measurements were made at room temperature.

Procedure

Transfer a suitable volume (up to 40 ml) of sample solution containing ≤ 200 ng/ml lead into a 50-ml standard flask. Add 5 ml each of the sodium chloride and acetate buffer solutions and dilute to volume with conductivity water.

Transfer the solution to the electrochemical cell and deaerate it by passage of nitrogen for 15 min. Apply a

potential of -1.2 V for 5 min to deposit lead, then apply the GSA step by recording the potential output as a function of time, with the potentiostat in the open-circuit mode, *i.e.*, with the counter-electrode disconnected from the cell. The time taken for stripping is the GSA signal. Prepare a calibration graph covering the range 1–200 ng/ml lead, by applying the procedure to standard solutions.

RESULTS AND DISCUSSION

Preliminary studies indicated that the lead deposited on the glassy carbon electrode from acetate-buffered chloride medium at -1.2 V for 5 min dissolves again (Fig. 1, curves B and C) without application of an external emf or a chemical oxidant (as required with a mercury-film GCE).⁴ The experiments designed to investigate the driving force behind this dissolution, as described elsewhere,⁴ revealed that there is a current flow between the counter- and working electrodes, when the applied potential used in the deposition step is removed; the current presumably arises because a localized galvanic cell is formed between the uncovered and the lead-covered portions of the GCE (there is an impedance of the

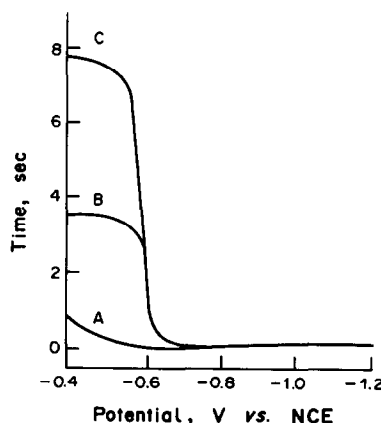


Fig. 1. Galvanic stripping curves recorded for (A) 0, (B) 20 and (C) 200 ng/ml lead (0.1M acetate buffer + 0.5M sodium chloride, total volume 50 ml, deposition potential -1.2 V, deposition time 5 min).

Table 1. Effect of supporting electrolyte (concentration of lead = 20 ng/ml; $E_d = -1.2$ V vs. NCE; $t_d = 5$ min)

Supporting electrolyte	Stripping time, sec
Hydrochloric acid, 0.1M	0.35
Monochloroacetic acid, 0.1M	0.36
Citrate buffer, pH 5, 0.1M	0.07
Acetate buffer, pH 5, 1M	1.60
Potassium nitrate, 0.1M	3.10
Sodium chloride, 0.50M	3.00
Acetate buffer + sodium chloride, 0.1M + 0.5M	3.50

order of 10^{11} ohm between the working electrode and the NCE in the external circuit). In contrast, the lead amalgam formed on a hanging-drop mercury electrode in the same medium (acetate buffer containing chloride) is stable for about 15 min under various hydrodynamic conditions, in open circuit. This difference in behaviour is considered to confirm the view that the dissolution of lead from the GCE is due to internal galvanic action. Further confirmation was provided by the observation that the magnitude of the stripping signal was independent of the stirring rate during stripping. The stripping was also accompanied by evolution of hydrogen (as shown by experiments similar to those described earlier⁴).

Effect of supporting electrolyte

The galvanic stripping of lead (20-ng/ml level) in a variety of supporting electrolytes gave $E-t$ curves with no clear-cut break-points when perchlorate or carbonate media were used. On the other hand, with nitrate, acetate, chloride, citrate and acetate-chloride media, characteristic $E-t$ curves were obtained, with the stripping time proportional to the concentration of lead in the initial solution. The results obtained by depositing lead on the GCE from various media (20 ng/ml lead) at -1.2 V, then recording the $E-t$ signal, are shown in Table 1, from which it is clear that the stripping signal is highest for acetate-chloride medium, followed by nitrate, chloride and then acetate. Hence, acetate-chloride medium was used in subsequent studies.

Choice of electrode material

Of the various electrode materials tested, viz. glassy-carbon graphite, mercury-film coated graphite, and mercury-film coated glassy carbon, the first gave the highest galvanic stripping signal in determination of 20 ng/ml lead. Hence, glassy carbon was chosen as the electrode material.

Effect of sodium chloride

Various amounts of sodium chloride were added to 0.1M acetate buffer solutions for use in determination of 20 ng/ml of lead. The results in Table 2 show that the stripping signal increases with increasing sodium chloride concentration up to 0.4M, then remains constant on further increase to 1M chloride concen-

Table 2. Effect of sodium chloride concentration (concentration of lead = 20 ng/ml; $E_d = -1.2$ V vs. NCE; 0.1M acetate buffer, pH 5; $t_d = 5$ min)

[NaCl], M	Stripping time, sec
0	1.60
0.1	1.60
0.3	2.65
0.4	3.50
0.5	3.50
0.7	3.40
1.0	3.45

tration. Hence 0.5M sodium chloride was chosen as optimal.

Effect of pH

The effect of changing the pH of the 0.1M acetate buffer + 0.5M sodium chloride supporting electrolyte (curve A in Fig. 2) shows that the optimum pH lies in the range 4–6; hence pH 5 was chosen as the working pH.

Effect of deposition potential and time

As seen from curve B in Fig. 2, the maximum analytical signal is obtained with deposition potentials more negative than -1.1 V.

Table 3 shows that the stripping signal is directly proportional to the time of deposition, suggesting possible extension of the procedure to determination of still lower concentrations of lead by use of longer deposition times.

Calibration graph and precision

Calibration graphs with two linear sections, one passing through the origin, were obtained for

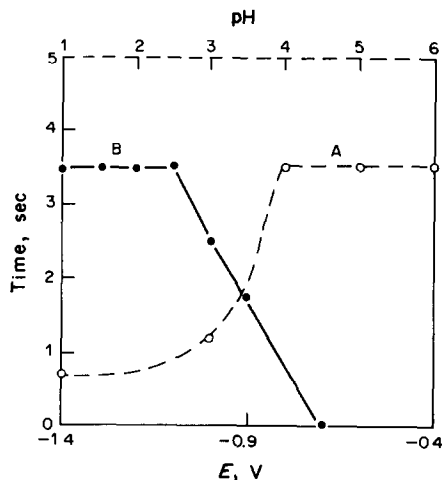


Fig. 2. Effect of pH (curve A) and deposition potential (curve B) on the galvanic stripping signal for 20 ng/ml lead (0.1M acetate buffer + 0.5M sodium chloride, time of deposition 5 min).

Table 3. Effect of deposition time (concentration of lead = 20 ng/ml; $E_d = -1.2$ V vs. NCE; 0.1M acetate buffer + 0.5M NaCl; pH 5)

Deposition time, min	Stripping time, sec
1	0.74
2	1.42
4	2.80
8	5.60

1–200 ng/ml lead, with a deposition time of 5 min. The slope changed at ~ 10 ng/ml lead concentration. The coefficient of variation for 10 replicate determinations of 20 ng/ml lead was found to be 2%.

Analyses of synthetic samples corresponding to sea-water, deep-sea water and Great Salt Lake water, to which 20 ng of lead per ml had been added, gave results correct within $\pm 1.5\%$.

Acknowledgement—The authors thank Professor K. I. Vasu, Director, CECRI, Karaikudi, for his keen interest and permission to publish these results.

REFERENCES

1. D. Jagner, *Analyst*, 1982, **107**, 593.
2. S. Jaya and T. P. Rao, *Rev. Anal. Chem.*, 1982, **6**, 343.
3. S. Jaya, T. P. Rao and G. P. Rao, *Talanta*, 1985, **32**, 1061
4. *Idem*, *Anal. Lett.*, 1985, **18**, 1441.
5. *Idem*, *Bull. Electrochem.*, 1986, **2**, 65.

A RAPID SPECTROPHOTOMETRIC METHOD FOR DETERMINATION OF PIPERAZINE

SALWA R. EL-SHABOURI*, FARDOUS A. MOHAMED and ABDEL-MABOUD I. MOHAMED
Department of Pharmaceutical Chemistry, Faculty of Pharmacy, University of Assiut, Assiut, Egypt

(Received 31 January 1986. Revised 30 April 1987. Accepted 27 May 1987)

Summary—A spectrophotometric method has been developed for the determination of piperazine and its salts (citrate, phosphate, and tartrate) without prior separation, based on the interaction of piperazine or any of its salts with phenothiazine and *N*-bromosuccinimide in aqueous methanol. The products exhibit absorption maxima at 448, 595 and 645 nm. Measurements are made at 595 nm. Beer's law is obeyed in the concentration range 0.5–5 µg/ml for piperazine salts and 0.5–3 µg/ml for piperazine hexahydrate. The method is rapid, simple and successful for analysis of some pharmaceutical preparations.

Piperazine is a potent anthelmintic drug used for treatment of threadworms and roundworms in both humans and animals. Various techniques have been used for assay of piperazine and its salts in the pure form and different dosage forms. They include non-aqueous titration,^{1,2} gravimetry,^{3,4} near infrared spectrophotometry,^{5,6} colorimetry,^{7–11} complexometry,¹² liquid chromatography¹³ and polarography.¹⁴

Phenothiazine and bromine have been used for detection of secondary amines by production of blue to blue-green colours.¹⁵ The chemistry of this reaction has been suggested to involve the reaction of phenazathionium perbromide (formed from bromine and phenothiazine) with the secondary amine to give a thiazine dye. In this work, the principle of the reaction is used to determine piperazine and its salts with phenothiazine and *N*-bromosuccinimide (NBS).

EXPERIMENTAL

Reagents

All chemicals and solvents used were of analytical grade.

Phenothiazine solution, 0.12 mg/ml, in methanol. Prepared fresh daily.

NBS solution, 0.1 mg/ml, in distilled water. Prepared fresh daily.

Standard piperazine solution. Prepared by dissolving 100 mg of piperazine hexahydrate, tartrate, citrate or phosphate (100% purity calculated on a dry basis), in 100 ml of distilled water. Working standards covering the range 10–100 µg/ml are made by further dilution.

Procedure

Pipette 0.5 ml of a working standard or sample piperazine solution into a 10-ml standard flask. Add 0.5 ml of phenothiazine solution and 1 ml of NBS solution. Mix well and heat on a boiling water-bath for 30 sec, then cool to room temperature. Make up to volume with ethanol. Measure the absorbance in 1-cm cells against a reagent blank at 595 nm.

For greater precision use 50-ml flasks and five times the volumes of the various reagents, and shake the flasks during the heating period.

For piperazine phosphate tablets. Weigh and powder 20 tablets. Transfer an accurately weighed quantity equivalent to 50 mg of piperazine phosphate to a 100-ml standard flask. Add 70 ml of distilled water, agitate gently for 5 min, then dilute to volume with distilled water. Filter through a dry paper and reject the first portion of filtrate. Pipette 5 ml of further filtrate and dilute it to volume in a 50-ml standard flask with distilled water. Apply the procedure to 0.5 ml of this solution.

For elixir. Transfer an accurately measured volume of elixir, equivalent to 30 mg of piperazine citrate, to a 100-ml standard flask, dilute it to volume with distilled water and mix well. Pipette 10 ml of this solution into a 50-ml standard flask and dilute it to volume with distilled water. Apply the procedure to 0.5 ml of this solution.

RESULTS AND DISCUSSION

Piperazine and its salts (citrate, phosphate or tartrate) react with phenothiazine and NBS in aqueous methanol to form intensely blue products which exhibit three absorption peaks at 448, 595 and 645 nm (Table 1). Figure 1 shows the absorption spectra of the product from piperazine phosphate and of a reagent blank. Measurement at 595 nm is recommended.

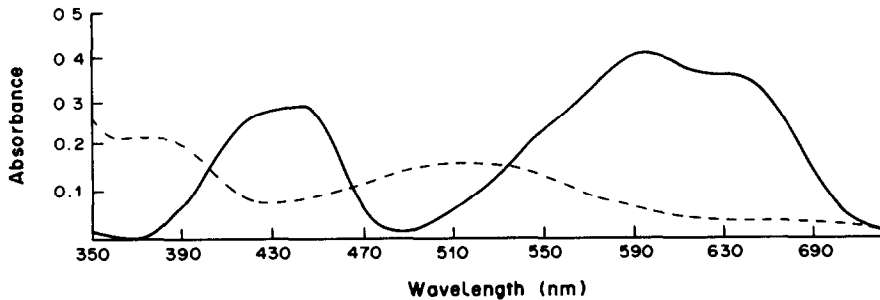
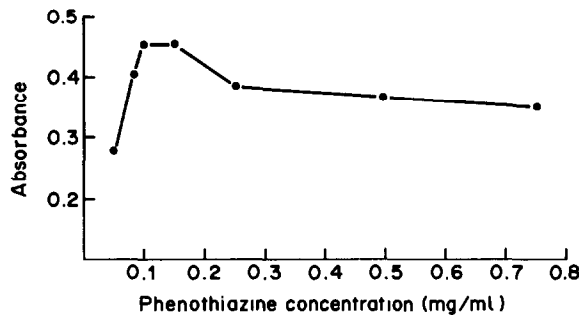
The optimum concentration of phenothiazine for maximum colour intensity was 6 µg/ml in the reaction mixture, which corresponds to addition of 0.5 ml of the phenothiazine reagent (Fig. 2) when a 10-ml standard flask is used. The NBS concentration is rather critical; concentrations below or above 0.01 mg/ml in the reaction mixture, which corresponds to 1 ml of NBS reagent per 10 ml, markedly decrease the sensitivity and the reproducibility of the method (Fig. 3). This can be attributed to the production of other oxidation products of phenothiazine by the action of NBS in a similar manner to that reported for bromine.¹⁶

At room temperature the blue colour developed immediately and remained stable for 20 min. Heating

*Author to whom correspondence should be addressed.

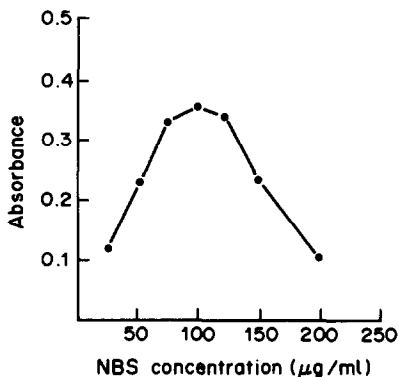
Table 1. Spectral data for reaction of piperazine and its salts with phenothiazine and NBS

Piperazine compound	$\epsilon, 10^4 \text{ l. mole}^{-1} \cdot \text{cm}^{-1}$			Beer's law range at 595 nm, $\mu\text{g/ml}$
	440 nm	595 nm	645 nm	
Hexahydrate	1.69	2.25	2.02	0.5–3.0
Phosphate	1.61	2.18	1.96	0.5–5.0
Citrate	1.73	2.35	2.12	0.5–5.0
Tartrate	1.62	2.20	1.98	0.5–5.0

Fig. 1. Absorption spectra of the piperazine phosphate (4 $\mu\text{g/ml}$) product (—) and reagent blank (---).Fig. 2. Effect of phenothiazine concentration on the absorbance of the piperazine phosphate (3 $\mu\text{g/ml}$) product.

for 0.5–2 min in a boiling water-bath increased in the absorbance by about 10%. Further heating, slightly decreased the absorbance. Heating for 30 sec in a boiling water-bath is recommended.

Water, ethanol, methanol, 2-propanol, dioxan, acetone and dimethyl sulphoxide were tested as diluents for the reaction mixture for piperazine and its salts. Water is unsuitable as it produces turbidity owing to precipitation of phenothiazine. The wavelength for maximal absorption is not affected by the choice of solvent, but the molar absorptivity is dependent on it (Table 2). Ethanol is preferred as diluent.

Fig. 3. Effect of NBS concentration on the absorbance of the piperazine phosphate (3 $\mu\text{g/ml}$) product.Table 2. Effect of different solvents on absorbance (at 595 nm) of the reaction product of piperazine tartrate (3 $\mu\text{g/ml}$) with phenothiazine and NBS

Solvent	Absorbance
Ethanol	0.283
Methanol	0.243
2-Propanol	0.268
Dioxan	0.268
Acetone	0.277
Dimethyl sulphoxide	0.261

Table 3. Assay of piperazine and its salts alone and in pharmaceutical preparations by the proposed ("10-ml") method and an official method

Sample	Nominal piperazine content, g	Proposed method			Official method, found,* %
		Found,* %	Added, g	Recovery,* %	
Piperazine hexahydrate	—	—	—	99.1 ± 0.6	99.3 ± 0.8†
Piperazine phosphate Tablets	0.3/tablet	99.6 ± 1.1 $t = 1.96, F = 0.45‡$	0.5/tablet	99.5 ± 1.0 99.4 ± 1.0	99.6 ± 0.7§ 98.9 ± 1.6§
Piperazine citrate Elixir	14/100 ml	92.2 ± 1.1 $t = 1.47, F = 0.71‡$	10/100 ml	98.9 ± 1.1 99.3 ± 0.8	99.4 ± 0.9§ 91.7 ± 1.3†
Piperazine tartrate	—	—	—	98.9 ± 0.4	—

*Average of 10 determinations, ± standard deviation.

†BP (1980) method.

§U.S.P. (1980) method.

‡Theoretical values at 95% confidence limit: $t = 2.26, F = 3.18$.

The reaction is strongly pH-dependent, the blue colour being completely discharged on addition of a few drops of 0.1N acid or alkali. The use of phosphate or McIlvaine's citric acid-phosphate buffers¹⁷ in the pH range 6–8 also lowers the molar absorptivity.

Beer's law is obeyed at 595 nm over the concentration range of 0.5–3 µg/ml for piperazine hexahydrate and 0.5–5 µg/ml for piperazine salts.

The reproducibility of the method was checked by ten replicate determinations at the 3-µg/ml level for piperazine hexahydrate, citrate, phosphate or tartrate, and the standard deviation was found to be between 1.3 and 2.4%. Table 3 shows the results for application of the proposed method for the determination of piperazine and its salts in the bulk drugs and some commercial preparations.

In the t - and F -tests, there were no significant differences between the calculated and theoretical values (95% confidence) for comparison of the proposed method with the official methods (Table 3), indicating similar precision and accuracy.

Under the reaction conditions used, other secondary amines such as morpholine, piperidine *etc.* give a positive reaction, but this is also the case with the official gravimetric method. However, the problem of interferences does not arise in the analysis of the commercially available plain dosage forms. Commonly encountered pharmaceutical additives in the dosage forms, such as lactose, mannitol, starch, gum acacia and tragacanth do not interfere. On the other hand, hexamine, citric acid, sodium citrate and sodium bicarbonate in the amounts found in pharmaceutical preparations decrease the recovery of piperazine in analysis by the proposed method, which is therefore not suitable for assay of effervescent formulations which contain these compounds.

The proposed method is simpler, faster and more sensitive than the BP and USP official methods, and the method does not require the prior extraction needed in some other methods.^{8,9}

REFERENCES

1. *U.S. Pharmacopeia XX and National Formulary XV*, pp. 629–633, U.S. Pharmaceutical Convention, Rockville, MD, 1980.
2. S. A. Soliman, H. Abdine and M. Morcos, *Can. J. Pharm. Sci.*, 1976, **11**, 136.
3. *British Pharmacopoeia*, pp. 353, 557, 807, HMSO, London, 1980.
4. G. R. Bond, *Anal. Chem.*, 1960, **32**, 1332.
5. *Official Methods of Analysis of the Association of Official Analytical Chemists*, 12th Ed., Section 38.206, AOAC, Arlington, VA, 1975.
6. A. A. Abou-Ouf, M. I. Walash, M. S. Rizk and A. F. Ibrahim, *J. Assoc. Off. Anal. Chem.*, 1979, **62**, 1138.
7. S. Belal, A. M. El-Sayed, M. E. Abdel Hamid and H. Abdine, *J. Pharm. Sci.*, 1981, **70**, 127.
8. M. S. Risk, M. I. Walash and F. A. Ibrahim, *Analyst*, 1981, **106**, 1163.
9. M. Muralikrishna, M. Krishnamurthy and N. S. Rao, *ibid.*, 1984, **109**, 1277.
10. A. M. Wahbi, M. Abou-Nassif and E. A. Gad-Kariem *ibid.*, 1984, **109**, 1513.
11. S. R. El-Shabouri, M. M. Amer, A. M. Taha and P. Y. Khashaba, *Bull. Pharm. Sci., Assiut University*, 1983, **6**, 226.
12. M. S. Tawakkol, S. A. Ismaiel and M. M. Amer, *Pharmazie*, 1976, **31**, 609.
13. F. L. Fricke and S. M. Walters, *J. Assoc. Off. Anal. Chem.*, 1966, **49**, 1230.
14. J. D. McLean and O. L. Daniels, *ibid.*, 1971, **54**, 556.
15. H. Bröll and G. Fischer, *Microchim. Acta*, 1962, 249.
16. A. R. Katritzky and A. J. Boulton, *Advances in Heterocyclic Chemistry*, Vol. 9, pp. 389–393. Academic Press, New York, London, 1968.
17. J. R. Geigy, *Documenta Geigy, Scientific Tables*, 6th Ed., p. 314. Basle, Switzerland, 1962.

ANALYTICAL DATA

FORMATION CONSTANTS FOR THE COMPLEXES OF 2-MERCAPTO-3-PHENYLPROPANOATE WITH NICKEL(II) AND HYDROGEN IONS

MONTERRAT FILELLA*, NURIA GARRIGA and ALVARO IZQUIERDO

Departament de Química Analítica, Universitat de Barcelona, 08028 Barcelona, Spain

(Received 21 July 1986. Revised 21 May 1987. Accepted 29 May 1987)

Summary—The system formed by 2-mercapto-3-phenylpropanoate (MPP), nickel(II) and hydrogen ions in 30% (v/v) ethanol-water at 25° and $I = 100mM$ (nitrate) has been characterized by means of glass-electrode potentiometry. Protonation constants for 2-mercapto-3-phenylpropanoate and formation constants for the complexes $Ni_3(MPP)_4^{2-}$ and $Ni(MPP)_2^{2-}$ are reported.

The formation and composition of several stable complexes formed by mercapto-acids with metals have been reported in the literature. Mercapto-acids have been recommended as reagents for sensitive colorimetric methods and as powerful masking agents in spectrophotometric analysis and complexometric titrations. More recently, these ligands have been proposed as simple models for the study of the co-ordination of metal ions with biologically interesting organic molecules.

Although mercaptoacetic and 2-mercapto-3-phenylpropanoic acids have been the most commonly used mercapto-acids, little information is available about derivatives containing an aryl substituent. Nevertheless, our preliminary studies have indicated that these aryl-substituted ligands may also have useful analytical applications^{1,2} and that, as a consequence, the determination of their complexing activity with metal ions might be of interest.

In a previous investigation on the complex equilibria between nickel(II) and 2-mercapto-2-phenylacetic acid,³ the formation of a mixture of the polynuclear complexes $M_3L_4^{2-}$ and $M_2L_3^{2-}$ and the mononuclear ML_2^{2-} was found. The formation of polynuclear species between mercapto-acids and nickel(II) has long been known⁴⁻⁷ and is mainly due to the presence of the sulphur atom, which acts as a strong electron-donor, as well as a strong π -electron acceptor, thus favouring the formation of complexes with sulphur bridges between two or more metal ions.

In the present work the system formed by nickel(II) and 2-mercapto-3-phenylpropanoic acid has been examined in order to continue the study of the influence of the presence of aryl substituents on the complexing activity of 2-mercapto-acids. No study of complexation by this ligand appears in the literature, probably owing to its not being commercially available, its insolubility in water (which necessitated

study in 30% v/v ethanol-water), and the poor stability of its solutions.

EXPERIMENTAL

Materials

2-Mercapto-3-phenylpropanoic acid was prepared from 2-mercapto-3-phenylpropenoic acid previously obtained as described by Campaigne and Cline,⁸ by reduction of the double bond with sodium amalgam,⁹ acidification, and extraction with diethyl ether. Recrystallization from petroleum ether (b.p. 30–50°) yielded a product with m.p. 47–48°. (Found: C 59.3%, H 5.5%, S 17.5%. $C_9H_{10}O_2S$ requires C 59.32%, H 5.53%, S 17.59%). The purity of the reagents was periodically tested by iodometric titration.¹⁰ Freshly prepared solutions were used for each titration.

A standard stock solution of nickel was prepared from its nitrate (Merck) and made slightly acid with dilute nitric acid (Merck). The metal concentration was determined gravimetrically with dimethylglyoxime.¹¹

Potassium hydroxide solutions were freshly prepared under nitrogen from potassium hydroxide pellets (Merck) and standardized against potassium hydrogen phthalate (Merck).

All solutions were prepared from demineralized doubly distilled water, boiled and cooled under nitrogen, and absolute ethanol (Merck) so that all of them contained 30% v/v ethanol. To control the ionic strength they were made up to a nitrate concentration of 100mM by the addition of potassium nitrate (Merck).

High-grade nitrogen (S.E.O.) was passed successively through a vanadate solution,¹² concentrated sodium hydroxide solution, water and background electrolyte, kept at 25°, prior to use. A purified nitrogen atmosphere was maintained in the vessel during the titrations, and all solutions were thoroughly flushed with nitrogen before use.

Method

Formation constants for the nickel complexes were determined by potentiometric titrations in a double-walled vessel, kept at $25 \pm 0.05^\circ$ by circulation of water.

The free hydrogen-ion concentration was measured with a Radiometer PHM84 pH-meter equipped with a wide-range glass electrode, Radiometer G202B, and a calomel reference electrode, Radiometer K401, with an agar-agar/potassium chloride salt bridge.

The electrode system was calibrated in terms of hydrogen-ion concentration by performing strong acid vs. strong base titrations. The logarithm of the autoprotolysis constant of

*Author for correspondence.

Table 1. Summary of the titration data used for calculating stability constants

System	Titration	No. of points	C_{Ni} , mM	C_{MPP} , mM	$-\log[H]$ range
MPP-H ⁺	1	40		2.015	2.3-11.0
	2	51		4.034	2.4-11.2
	3	45		4.218	2.8-10.9
	4	51		4.260	2.3-11.1
	5	40		4.528	2.2-11.2
	6	59		6.054	2.9-11.3
	7	61		8.273	2.3-11.3
Ni ²⁺ -MPP-H ⁺	1	45	0.212	0.833	3.3-6.9
	2	47	0.306	1.319	3.3-7.6
	3	35	0.408	1.667	3.0-9.9
	4	51	1.019	3.973	2.9-6.5
	5	54	2.038	8.270	2.8-6.2
	6	52	3.058	11.873	2.8-6.1
	7	47	4.062	16.253	2.6-6.2
	8	51	6.116	24.898	2.4-6.0

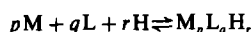
the medium under the experimental conditions was found to be 14.20.

Experimental solutions containing ligand, metal and nitric acid were titrated, the hydrogen-ion concentration being varied by adding potassium hydroxide. Acid solutions containing the metal ion were titrated with base to check the acid concentration and to allow the E° value to be calculated. Before the titrations reached the equivalence point, an aliquot of ligand solution was added and the titration continued.

The total metal-ion concentration was kept constant by adding, after each addition of titrant, an equal volume of metal ion solution with a concentration twice that of the metal ion in the cell.

Data treatment

The general equilibria involving metal M^{2+} , ligand L^{2-} (i.e., deprotonated 2-mercapto-3-phenylpropanoic acid, MPP) and H^+ ions can be written as:



The associated overall formation constant is denoted by β_{pqr} .

The complexation titration data were processed with the ESTA computer program library.^{13,14} The initial models were obtained from the shapes of the formation curves, $\bar{Z}_M(-\log[A])$, and the deprotonation curves, $\bar{Q}(-\log[H])$, \bar{Z}_M being defined as:

$$\bar{Z}_M = \frac{T_L - [A] \left(1 + \sum_n \beta_{LH_n} [H]^n \right)}{T_M}$$

where $[A] = (T_H - [H] + [OH]) / \sum_n n \beta_{LH_n} [H]^n$, T_L = total ligand concentration, T_M = total metal concentration and T_H = total hydrogen-ion concentration.

\bar{Q} is defined as:

$$\bar{Q} = \frac{T_H^* - T_H}{T_M}$$

where T_H^* = calculated total concentration of protons in the system at the observed $-\log[H]$, ignoring the presence of all metal complexes.

Initial estimates of the formation constants were obtained by using the BETA task of the ESTA library, which calculates values for the formation constant of a single species from the emf reading at each titration point, supposing that this particular species is the only one present in the system.

A set of possible models was deduced from plots of experimental formation and deprotonation curves, and from the BETA task of ESTA. For each model, four different criteria for model selection were applied simultaneously. (i) Search for the minimum value of the objective function being minimized. (ii) Search for the best fit between experimental and calculated formation and deprotonation curves. Both functions have proved to be very sensitive to species composition and provide a good tool for studying the degree to which trends correspond in the calculated and observed data.¹⁵ (iii) Calculation of the degree of formation of each species. It is important to check that all the proposed species exist in significant concentration over a reasonable range of data. (iv) Application of chemical knowledge.

Formation constants were refined by using the ESTA optimization module. Its weighted objective function may be minimized with respect to either emf or total electrode-ion concentration. The weighting for each titration point was based on the standard deviations of the titration volume (0.005 ml) and emf (0.1 mV). The objective functions shown in Tables 2 and 3 are based on emf residuals.

The computer programs MINQUAD^{16,17} and SUPERQUAD¹⁸ were also used for comparison purposes. The same weighting as in ESTA was used in SUPERQUAD.

All calculations were done with a VAX 11/750 computer.

Table 2. Protonation constants determined in this study at 25° and $I = 100.0mM$ NO_3^- (30% v/v ethanol-water): number of points = 473, number of titrations = 7

Program	$\log \beta_{011}$	$\log \beta_{012}$	Complementary information†	
ESTA	10.533 ± 0.001*	14.490 ± 0.002	$U = 17.4$	$R = 0.004$ ($R_{lim} = 0.001$)
MINQUAD	10.528 ± 0.002	14.477 ± 0.003	$U = 6.38E-07$	$R = 0.005$
SUPERQUAD	10.533 ± 0.002	14.492 ± 0.003	sigma = 4.36	

*Standard deviations given by the programs.

† U , in ESTA output: $[\sum w(emf^o - emf^c)^2] / (N - n_p)$ where N = no. of points, n_p = no. of refined parameters; in MINQUAD output: $\sum (T_i^o - T_i^c)^2$ where T_i = total concentrations. Sigma = sample standard deviation from SUPERQUAD output. R = Hamilton R factor; R_{lim} = Hamilton R -limit.

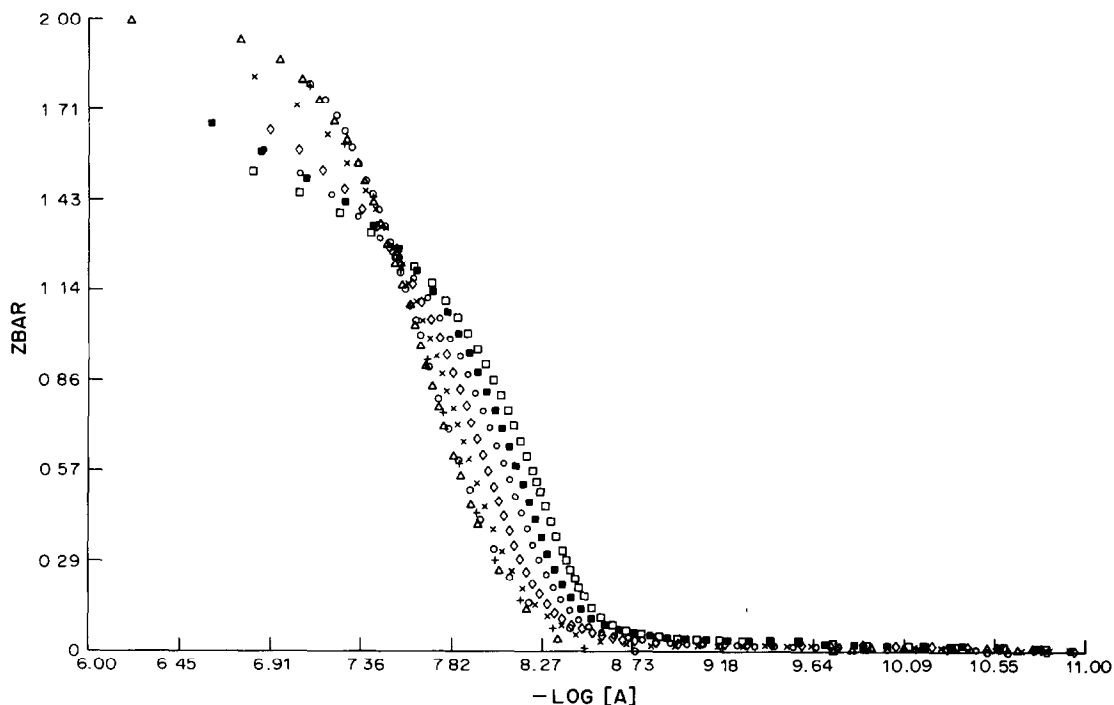


Fig. 1. Ni^{2+} -MPP- H^+ experimental formation curves. Different symbols refer to different titrations (i.e., from left to right, titrations 1-8).

RESULTS AND DISCUSSION

2-Mercapto-3-phenylpropanoate has two protonation constants that can be assigned to the thiol and carboxylate groups. As shown in Table 1, seven protonation titrations were done with initial ligand concentrations of 2-8mM. A satisfactory fit between

the parameters and the data was indicated by reasonable values obtained for the ESTA objective function and the MINIQAD and SUPERQUAD outputs. Values for the protonation constants are presented in Table 2.

The system Ni^{2+} -MPP- H^+ was studied by doing

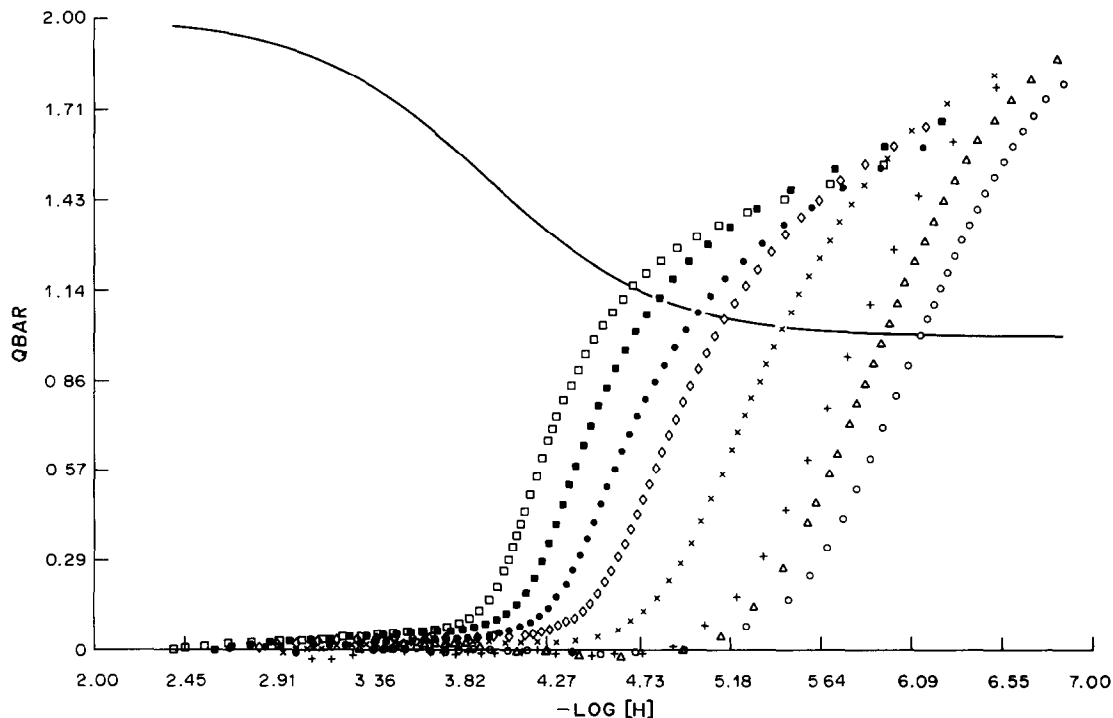


Fig. 2. Ni^{2+} -MPP- H^+ experimental deprotonation curves. The symbols have the same meaning as in Fig. 1. A plot of \bar{n} vs. $-\log[\text{H}]$ appears as a solid line.

Table 3. Formation constants determined in this study at 25°C and $I = 100.0\text{mM NO}_3^-$ (30% v/v ethanol-water): number of points = 382, number of titrations = 8

Model	Program	$\log\beta_{111}$	$\log\beta_{340}$	$\log\beta_{120}$	Complementary information	
A	ESTA		37.086 ± 0.006	15.185 ± 0.004	$U = 19.8$	$R = 0.007$ ($R_{\text{lim}} = 0.002$)
	MINIQUAD		37.092 ± 0.010	15.161 ± 0.016	$U = 1.77\text{E-}06$	$R = 0.004$
B	ESTA	11.663 ± 0.014	37.202 ± 0.005	15.208 ± 0.002	$U = 7.92$	$R = 0.004$ ($R_{\text{lim}} = 0.002$)
	MINIQUAD	11.549 ± 0.050	37.195 ± 0.015	15.178 ± 0.015	$U = 1.45\text{E-}06$	$R = 0.003$

Table 4. Literature formation constants of nickel complexes of similar ligands

Ligand	p	q	r	$\log\beta_{pqr}$	Conditions	Reference	
Mercaptoacetic acid	4	6	0	49.84	25°	4	
	1	2	0	13.04	0.1M KCl		
	1	1	0	6.2	20°	5	
	3	4	0	33.267	0.1M NaClO ₄		
	2	3	0	22.68			
	4	6	0	49.849			
	1	2	0	13.009			
		1	3	0	14.987		
		3	4	0	32.219	25°	6
		4	6	0	49.157	0.5M KNO ₃	
	1	2	0	12.759			
2-Mercaptopropanoic acid	1	1	0	6.052	25°	7	
	3	4	0	30.709	0.5M KNO ₃		
	1	2	0	13.144			
2-Mercapto-2-phenylacetic acid	3	4	0	40.437	25°	3	
	2	3	0	28.819	1M NaClO ₄ (50% v/v ethanol-water)		
	1	2	0	16.717			

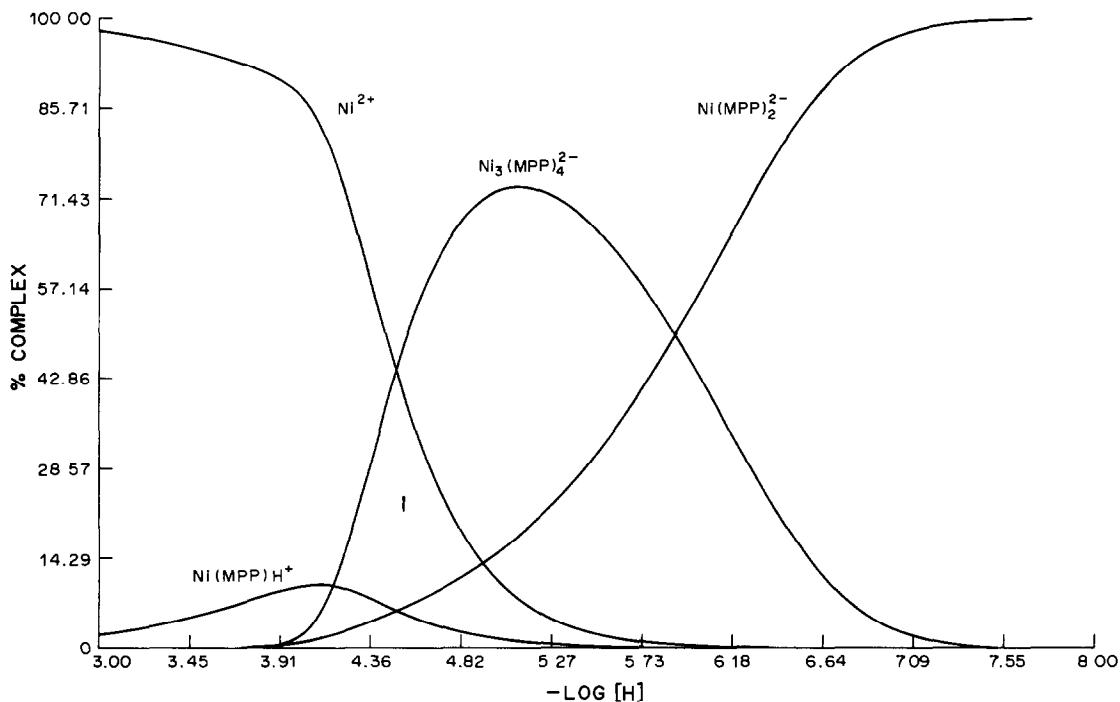


Fig. 3. Species distribution as a function of $-\log[\text{H}]$. Ligand concentration = 16.0mM ; metal concentration = 4.0mM .

eight titrations with initial metal concentrations of 0.2–6mM (Table 1). The upper concentrations used were limited by the insolubility of the ligand or the metal complex.

Analysis of the formation curves (Fig. 1) and of the deprotonation curves (Fig. 2) suggests that not only mononuclear species are formed in the Ni^{2+} –MPP– H^+ system, since not all the points fall on a single curve. This was confirmed by the fact that the species 340 was found to account for 75% of the nickel at $\text{pH} \cong 5.0$ in the titrations with higher metal and ligand concentrations, 120 being the major species at higher pH values irrespective of component concentration. No evidence was found for the formation of the following species, which were also tested in the search for the best model: 130, 112, 122, 121, 11-2, 11-1, 12-2, 12-1, 230, 460, 342 and 341.

The inclusion of the species 111 causes a relatively large improvement in the fit (ESTA weighted sum of squared residuals changing from 19.8 to 7.9; MINQUAD sum of squared residuals changing from 1.77E-06 to 1.45E-06) but its extent of formation is low, gradually ranging from 1% in titrations 1 and 2 to 10% in titrations 7 and 8. Therefore, although the existence of the complex 111 is highly probably, the inclusion of the species in the final model should be considered at least doubtful.

The inclusion of the species 110 results in a very slight improvement of the fit (ESTA weighted sum of squared residuals changing from 19.8 to 16.6; MINQUAD sum of squared residuals changing from 1.77E-06 to 1.71E-06). As the species was found to be formed only to a maximum of 8% in titrations 1 and 2, it was not considered further. Moreover, simultaneous optimization of the complexes 111 and 110 results in the rejection of the latter whichever computer program is used.

Two models proved, eventually, to fit the experimental data, namely model A which includes only the species 340 and 120, and model B which also includes the species 111. Values for the formation constants are given in Table 3. Program SUPERQUAD was not applied to the data since it cannot handle addition of more than one titrant.

Values reported in the literature for the formation constants for complexes of similar ligands with

nickel(II) are shown in Table 4. Comparison of these values with those obtained in the present work confirms the previously stated trend³ towards complex stabilization when an aryl substituent is present in the ligand molecule.

Figure 3 shows the species distribution for the Ni^{2+} –MPP– H^+ system computed from the constants reported in Table 3 (model B) for total concentrations of 16mM 2-mercapto-3-phenylpropanoate and 4mM nickel(II).

Acknowledgements—We are much indebted to Dr. M. A. Hughes, Inorganic Chemistry Laboratory (Oxford) for her valuable suggestions. This research was supported by CAYCIT grant 657/81.

REFERENCES

1. A. Izquierdo, M. D. Prat and M. Filella, *Microchem. J.*, 1985, **32**, 191.
2. A. Izquierdo and N. Garriga, *Talanta*, 1985, **32**, 669.
3. E. Casassas, M. Filella, A. Izquierdo, D. Prat and R. Rodríguez, *Polyhedron*, 1985, **4**, 1951.
4. D. L. Leussing, R. E. Laramy and G. S. Alberts, *J. Am. Chem. Soc.*, 1960, **82**, 4862.
5. D. D. Perrin and I. G. Sayce, *J. Chem. Soc. (A)*, 1967, 82.
6. H. F. de Brabander, L. C. van Poucke and Z. Eeckhaut, *Anal. Chim. Acta*, 1974, **70**, 401.
7. H. F. de Brabander, A. M. Goeminne and L. C. van Poucke, *J. Inorg. Nucl. Chem.*, 1975, **37**, 799.
8. E. Campaigne and R. E. Cline, *J. Org. Chem.*, 1956, **21**, 32.
9. C. Ravazzoni and R. Valerio, *Ann. Chim. (Roma)*, 1962, **52**, 305.
10. D. L. Leussing and I. M. Kolthoff, *J. Electrochem. Soc.*, 1953, **100**, 334.
11. A. I. Vogel, *A Textbook of Quantitative Inorganic Analysis*, 4th Ed., p. 447. Longman, London, 1978.
12. L. Meites, *Polarographic Techniques*, p. 89. Interscience, New York, 1965.
13. K. Murray and P. M. May, *ESTA: Equilibrium Simulation for Titration Analysis*, UWIST, Cardiff, 1984.
14. P. M. May, K. Murray and D. R. Williams, *Talanta*, 1985, **32**, 483.
15. G. Berthon, P. M. May and D. R. Williams, *J. Chem. Soc., Dalton Trans.*, 1978, 1433.
16. A. Sabatini, A. Vacca and P. Gans, *Talanta*, 1974, **21**, 53.
17. P. Gans, A. Sabatini and A. Vacca, *Inorg. Chim. Acta*, 1976, **18**, 237.
18. *Idem*, *J. Chem. Soc., Dalton Trans.*, 1985, 1195.

SULPHA-DRUG SENSITIVE MEMBRANE ELECTRODES AND THEIR ANALYTICAL APPLICATIONS

SHOU-ZHOU YAO*, JING SHIAO and LI-HUA NIE

New Material Research Institute, Department of Chemical Engineering, Hunan University, Changsha,
People's Republic of China

(Received 21 March 1986. Revised 20 July 1986. Accepted 27 June 1987)

Summary—Cetyltriocetylammmonium sulphathiazole, sulphadoxine and sulphadimethoxine membrane electrodes are proposed for the potentiometric determination of sulpha-drugs. The construction and basic characteristics of the electrodes are discussed.

A number of methods have been suggested for the determination of sulpha-drugs, such as titrimetry,¹ spectrophotometry,² chromatography,³ polarography⁴ and Raman spectrometry.⁵ Some of these methods have shortcomings in selectivity or accuracy, or require expensive apparatus. Ion-selective electrodes have several well known advantages and have been extensively developed as electrochemical sensors in the last two decades. The only electrode sensitive to sulpha-drugs given so far in the literature was that developed by Hazemoto *et al.*⁶ This electrode was based on the ion-pair complex of the iron(II)-bathophenanthroline chelate with the sulpha-anion, embedded in a liquid membrane. The electrode has a limited linear response range down to 1mM and contains nitrobenzene as membrane solvent, which is toxic. More recently, results for the determination of some sulpha-drugs by potentiometric titration with an Hg(II), Cu(II) or Ag(I) ion-sensitive membrane electrode as indicator have been reported,⁷⁻¹¹ but the methods lack selectivity and sensitivity, and can be used only for titration of the drugs at rather high concentrations. Baiulescu *et al.*⁸ have made an effort to prepare an electrode sensitive to sulphamethoxazole for use in sulpha-drug determinations by direct potentiometry, but without much success, the electrode function being linear over only a narrow range of activities and non-reproducible, and the response slope being only 33 mV/decade.

In the work described in this paper, a new type of membrane electrodes sensitive to sulpha-drugs in anionic form was constructed, and various factors influencing the electrode functions were studied. It was found that electrodes made with cetyltriocetylammmonium sulphathiazole or sulphadoxine as electro-active material gave the best response. The electrodes can be successfully applied in the potentiometric determination of sulpha-drugs.

EXPERIMENTAL

Apparatus and reagents

The emf values were measured at room temperature, in stirred solutions, with a PXJ-1B model digital pH/mV-meter (Jiangsu Electroanalytical Instrument Factory) a sulpha-drug ion-selective electrode as indicator electrode, and a saturated calomel electrode (model 232, Shanghai Deikuong Electronic Factory) as reference electrode (with 1M sodium nitrate in the outer compartment). The pH measurements were made with a glass-calomel electrode pair (models 231 and 232, Shanghai Deikuong Electronic Factory).

All reagents used were of analytical grade, except the cetyltriocetylammmonium iodide and cetyltributylammmonium iodide, which were synthesized¹² in our laboratory, and the tris(hydroxymethyl)aminomethane, which was a biochemical reagent. Doubly distilled water was used throughout.

Preparation of standard solutions

Buffer solution. Fifty ml of 0.5M sulphuric acid were added to 66 ml of 1M tris(hydroxymethyl)aminomethane and the mixture was diluted to 1 litre. The buffer had pH 8.63 and ionic strength 0.05M.

Standard sulpha-drug solutions. Sodium sulphathiazole (0.1387 g) was dissolved in water and the solution diluted to volume in a 50-ml standard flask, to give a 0.01M standard solution. Working standards were made by successive dilution of the 0.01M solution with the tris buffer. A standard sodium sulphadiazine series was prepared in a similar manner. As the other sulpha-drugs tested cannot be dissolved directly in water, they were first dissolved in an appropriate amount of 1M sodium hydroxide, then the solutions were adjusted to pH 8-9 with 1M sulphuric acid, and diluted with appropriate amounts of the tris buffer, taking into account the ionic strength due to the salts produced during neutralization.

Preparation of the ion-pair complexes

Cetyltriocetylammmonium sulphathiazole. Cetyltriocetylammmonium iodide (0.11 g) was dissolved in 15 ml of chloroform. The solution was shaken in a separating funnel for 15 min with 15 ml of 0.01M sodium sulphathiazole, then the chloroform solution of the ion-pair complex was separated, and treated repeatedly with the sodium sulphathiazole solution until no iodide was found (test with silver nitrate solution) in the aqueous layer. The organic layer was filtered through a dry filter, dried with anhydrous sodium sulphate, and evaporated to dryness, resulting in a yellowish product.

Cetyltriocetylammmonium sulphamethoxine, sulphadimethoxine, and ion-pair complexes of other quaternary ammonium cations with sulpha-drug anions were prepared in a similar way as above.

*Author for correspondence.

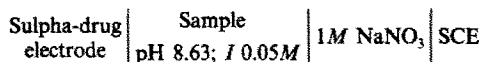
Electrode construction

At one end of a PVC tube (12 mm outer diameter, 8 mm inner diameter, *ca.* 75 mm long) a shallow hole of 1.5 mm depth and 10 mm diameter was bored. A copper disk (1.3–1.4 mm thick, 10 mm diameter) was inserted into the hole, with an outlet wire soldered on the inner side. The outer side of the copper disk was electroplated with platinum or gold. Platinum plating conditions: Pt(NH₃)₂Cl₂ 3–6 g/l., KCl 20 g/l., DMSO 10–20% (v/v), pH 6–8, current density 1 A/dm², room temperature. Gold plating conditions: K₆[Au(SO₃)₂HY] 6 g/l., K₂Na₂Y 2.5 g/l. (Y = EDTA), K₂SO₄ 2 g/l., K₂HPO₄ 2 g/l., CdCl₂ 0.05 g/l., pH 9.5, current density 0.5 A/dm², room temperature, graphite anode.

A 0.34-ml portion of 0.005M solution of the ion-pair complex in dibutyl phthalate was mixed with 2.4 ml of 5% PVC solution in tetrahydrofuran. Two drops (24 drops = 1 ml) of the mixed solution were spread on the outer surface of the electrode disk and dried, this step being repeated twice more. A transparent uniform membrane was thus formed on the metal surface. The electrode was preconditioned in 0.001M sulpha-drug solution for 1–2 hr, and was then ready for use. When not in use, the electrode can be stored in air.

Measuring cell

The emf measurements were made at constant pH and constant ionic strength, and the junction potential was kept constant. The following cell was used:



Procedure

Twenty sulpha-drug tablets were weighed and finely powdered. A portion of the powder, equivalent to about 0.5 mmole of the sulpha-compound, was weighed out accurately, dissolved in a minimum amount of 1M sodium hydroxide, transferred to a 50-ml standard flask and diluted to volume with the tris buffer, then analysed (after 25- or 50-fold dilution), by a standard-addition method or a calibration curve method.

For the analysis of tablets containing sulphamethoxazole and trimethoprim (co-trimoxazole, abacin), the sample solution was left for 2 hr on a water-bath (*ca.* 50°) to let the undissolved trimethoprim settle. After filtration, the filtrate was analysed for sulphamethoxazole as described above.

RESULTS AND DISCUSSION

Comparison of electroactive materials

The effect of divers electroactive materials (based on the ion-pair complexes of quaternary ammonium salts with various sulpha-drugs) on the electrode

function has been studied. The characteristic performances of electrodes made with the ion-pair complexes of anionic species of some sulpha-compounds with cetyltrialkylammonium salts containing alkyl groups of different carbon chain length, are listed in Table 1. It is seen that the electrode based on the ion-pair complex of cetyltrioctylammonium with sulphathiazole or sulphadoxine shows the best response characteristics, giving a linearity range from 1×10^{-5} to $1 \times 10^{-2}M$ with a nearly Nernstian anionic response slope of *ca.* 58 mV/concentration decade, the detection limit being $2.5 \times 10^{-6}M$. The electrode made with cetyltrioctylammonium-sulphadimethoxine as electroactive material gives nearly the same electrode performance. However, the electrode made with the ion-pair complex with cetyltributylammonium gives only sub-Nernstian slope of 46–50 mV/concentration decade with a shorter linearity range down to only *ca.* $10^{-4}M$, and the electrodes made with cetyltrimethylammonium ion pairs cannot be used successfully for sulpha-drug determinations.

It is evident that the effect of increasing molecular weight of the long carbon-chain system (quaternary ammonium ions in this case) here plays an important role in the improvement of the electrode performance, and the order is cetyltrioctylammonium > cetyltributylammonium > cetyltrimethylammonium. Our tests with a benzalkonium (dodecyltrimethylbenzylammonium) salt has shown that it is inappropriate for the purpose. Similar phenomena have been observed in our studies on the phenytoin ion-selective electrodes, where the electrode performances are in the order cetyltrioctylammonium > dodecyltriheptylammonium > cetyltrimethylammonium > tetra-butylammonium.¹²

Response to divers sulpha-drugs

As sulpha-drugs contain a common sulphanil group in their structure, it is of importance to test the response of a given sulpha-drug-sensitive electrode toward divers sulpha-drugs. The response characteristics of the cetyltrioctylammonium-sulphathiazole, sulphadoxine and sulphadimethoxine electrodes are listed in Table 2. It can be concluded from the experimental results that the electrodes tested re-

Table 1. Comparison of electroactive materials

Ion-pair complex		Slope, –mV/log C	Linearity range, M	Detection limit, M
Anionic species	Cationic species			
Sulphadoxine	CTMA	12.0 ± 3.0	10^{-3} – 10^{-2}	
	CTBA	46.5 ± 1.5	10^{-4} – 10^{-2}	2×10^{-5}
	CTOA	57.7 ± 0.6	10^{-5} – 10^{-2}	2.5×10^{-6}
Sulphadimethoxine	CTMA	12.0 ± 3.5	10^{-3} – 10^{-2}	
	CTBA	47.0 ± 1.3	2×10^{-4} – 10^{-2}	5×10^{-5}
	CTOA	57.6 ± 0.5	10^{-5} – 10^{-2}	5×10^{-6}
Sulphathiazole	CTMA	17.0 ± 2.4	10^{-3} – 10^{-2}	
	CTBA	50.0 ± 0.9	10^{-4} – 10^{-2}	1×10^{-5}
	CTOA	58.0 ± 0.6	10^{-5} – 10^{-2}	2.5×10^{-6}

Sodium sulphathiazole sample solution. Slopes are given as average values from 3 parallel measurements. Membrane concentration $5 \times 10^{-3}M$.

Table 2. Response characteristics of some sulpha-drug sensitive electrodes to divers sulpha-drugs other than sulphathiazole

Electrode	Sulpha-drug	Slope, -mV/log C	Linearity range, M	Detection limit, M
CTOA-sulphathiazole	Sulphamethoxazole	58.0 ± 1.0	3 × 10 ⁻⁵ -10 ⁻²	1 × 10 ⁻⁵
	Sulphadoxine	54.3 ± 0.6	10 ⁻⁴ -10 ⁻²	2 × 10 ⁻⁵
	Sulphadimethoxine	50.7 ± 0.4	10 ⁻⁴ -10 ⁻²	1 × 10 ⁻⁵
	Sulphacetamide	44.0 ± 1.0	10 ⁻³ -10 ⁻²	
	Sulphadiazine	43.0 ± 1.5	10 ⁻³ -10 ⁻²	
	Sulphanilamide	20.0 ± 1.5	10 ⁻³ -10 ⁻²	
CTOA-sulphadoxine	Sulphamethoxazole	55.5 ± 1.5	3 × 10 ⁻⁵ -10 ⁻²	1 × 10 ⁻⁵
	Sulphadoxine	53.5 ± 0.6	5 × 10 ⁻⁵ -10 ⁻²	2 × 10 ⁻⁵
	Sulphadimethoxine	50.0 ± 0.4	10 ⁻⁴ -10 ⁻²	2 × 10 ⁻⁵
	Sulphacetamide	46.0 ± 0.6	10 ⁻³ -10 ⁻²	
	Sulphadiazine	47.0 ± 1.5	10 ⁻³ -10 ⁻²	
	Sulphanilamide	21.0 ± 3.0	10 ⁻³ -10 ⁻²	
CTOA-sulphadimethoxine	Sulphamethoxazole	54.7 ± 2.3	6 × 10 ⁻⁵ -10 ⁻²	2 × 10 ⁻⁵
	Sulphadoxine	54.0 ± 0.6	7 × 10 ⁻⁵ -10 ⁻²	1 × 10 ⁻⁵
	Sulphadimethoxine	50.3 ± 0.6	10 ⁻⁴ -10 ⁻²	1 × 10 ⁻⁵
	Sulphacetamide	42.0 ± 1.7	10 ⁻³ -10 ⁻²	
	Sulphadiazine	40.0 ± 0.6	10 ⁻³ -10 ⁻²	
	Sulphanilamide	23.0 ± 2.5	10 ⁻³ -10 ⁻²	

Values are given as average values from 2 or 3 measurements.

spond to all sulpha-drugs tested, except sulphaguanidine and trimethoprim, which are only slightly soluble in the basic medium used. Sulphathiazole shows the best response characteristics (in the sense of response slope, linear response range, and detection limit) of the sulpha-drugs tested, and sulphanilamide gives the worst.

It is noteworthy that the cetyltriocetylammmonium-sulphadoxine electrode and the cetyltriocetylammmonium-sulphadimethoxine electrode response to sulphadoxine and sulphadimethoxine with a narrower linearity range and lower response slope than the cetyltriocetylammmonium-sulphathiazine or sulphamethoxazole electrodes. The electrode responses toward different sulpha-drugs are in the main similar for the various electrodes tested, deteriorating in the order sulphathiazole, sulphamethoxazole > sulphadoxine, sulphadimethoxine > sulphacetamide, sulphadiazine > sulphanilamide.

As the cetyltriocetylammmonium-sulphathiazole, sulphadoxine and sulphadimethoxine electrodes can all respond to a number of sulpha-drugs, it is therefore possible to use them as general-purpose indicator electrodes in the potentiometric determinations of sulpha-drugs.

Influence of substrate metal

Coated-wire electrodes have been widely used in analytical practice. However, in some cases, it is difficult to make electrodes of this type that have the same electrode performance, even if they were made in parallel under the same conditions. The liquid-membrane electrodes suggested in the literature for sulpha-drugs require an internal reference electrode with an internal reference solution and an organic solvent such as nitrobenzene has to be used for the liquid-membrane, and such a construction is more or less complicated and needs careful handling so that it

is not tipped over. To avoid all these inconveniences, the sulpha-drug sensitive electrodes proposed in this paper are of all-solid-state construction. Neither a liquid membrane nor an internal reference electrode is needed, and the electrode is convenient to use. Electrodes made under the same conditions yield nearly the same performances, the average response slope for the cetyltriocetylammmonium-sulphathiazole electrodes being -58.0 ± 0.6 mV/decade (gold-plated) or -56.8 ± 1.8 mV/decade (copper substrate) with linearity range 1×10^{-5} - 1×10^{-2} M. Electrode performances with copper, gold-, and platinum-plated metal substrates are listed in Table 3. It has been found that the gold- or platinum-plated metal substrates exhibit better electrode response and can be used for at least 3 months, with the electrode slope remaining constant and the reproducibility in emf measurements being better than ± 1 mV for five successive measurements in 10^{-4} - 10^{-2} M sulphathiazole solutions, whereas the electrode made with a copper substrate exhibits a shorter life-span and poorer reproducibility in emf measurements (± 2 mV under the same conditions as above), and darkens at the interface of the substrate metal with the electroactive material.

As a conventional gold- or platinum-plating bath is not stable enough or uses poisonous cyanide, and a relatively high concentration of the expensive metal salt is needed, we have suggested new plating methods, with plating baths which are stable for several months and easy to operate, with less than 0.5 g of the expensive metal salt being needed. They yield a poreless layer on the copper substrate.

It is sufficient to use 5 or 6 drops of the mixed liquid to prepare the electroactive membrane (dried after each 1 or 2 drops), and membranes that are too thick (9 drops) yield slower responses and higher membrane resistances. If the electroactive membrane

Table 3. Comparison of electrode substrates*

Usage time, months		1	2	3
Gold or platinum	Slope, $-mV/\log C$	58.0 ± 0.6	58.0 ± 0.6	57.9 ± 0.9
	Linearity range, M	10^{-5} – 10^{-2}	10^{-5} – 10^{-2}	3×10^{-5} – 10^{-2}
	Detection limit, M	2.5×10^{-6}	3×10^{-6}	7×10^{-6}
Copper	Slope, $-mV/\log C$	56.8 ± 1.8	56.0 ± 1.5	50.0 ± 1.5
	Linearity range, M	10^{-5} – 10^{-2}	10^{-4} – 10^{-2}	10^{-4} – 10^{-2}
	Detection limit, M	2×10^{-6}	8×10^{-5}	8×10^{-5}

*Electroactive material: cetyltriocetylammmonium sulphathiazole. Measured in sodium sulphathiazole solutions (pH 8.63, $I = 0.05M$).

is too thin (less than 4 drops applied), the potential readings tend to drift.

Effect of pH

The effect of pH on the response of the cetyltriocetylammmonium-sulphathiazole electrode at different sodium sulphathiazole concentrations (ionic strength $0.05M$) was studied. The potential observed was not affected by pH variation in the range from 8.0 to 11.5, so the direct potential measurements for calibration of the electrode were done at pH 8.63 (tris buffer). For the cetyltriocetylammmonium-sulphadoxine electrode and the cetyltriocetylammmonium-sulphadimethoxine electrode, the pH ranges in which the potential remains constant are 8.0–12.0 and 8.2–12.0 respectively. Outside these ranges, the potential tends to higher values and is not stable.

Selectivity

Sulpha-drugs may be determined by potentiometric titration with Ag(I), Hg(II) or Cu(II), with end-point detection by use of the appropriate ion-selective electrode.⁷⁻¹¹ However, many other substances interfere and have to be removed or masked

Table 4. Selectivity coefficients for the cetyltriocetylammmonium sulphathiazole electrode (mixed-solution method)

Interferent	C_j	K_{ij}
Sodium acetate	1×10^{-3}	5.2×10^{-3}
Sodium chloride	1×10^{-4}	2.5×10^{-2}
Sodium sulphate	1×10^{-2}	5.1×10^{-5}
Ampicillin	1×10^{-3}	1.6×10^{-3}
Urea	1×10^{-4}	1.3×10^{-3}
Sodium borate	1×10^{-4}	3.7×10^{-2}
Sodium aminosulphonate	1×10^{-3}	1.4×10^{-3}
Sodium dl- α -aminopropionate	1×10^{-3}	1.3×10^{-3}
Streptomycin sulphate	1×10^{-3}	8.0×10^{-5}
Sodium citrate	1×10^{-3}	3.6×10^{-3}
Sodium glutamate	1×10^{-3}	5.0×10^{-3}
Sodium benzoate	1×10^{-3}	1.4×10^{-2}
Disodium orthophosphate	1×10^{-3}	6.3×10^{-3}
Sodium oxalate	1×10^{-3}	1.5×10^{-3}
Potassium bicarbonate	1×10^{-3}	7.8×10^{-3}
Glucose	1×10^{-2}	1.8×10^{-3}
Potassium bromide	3×10^{-4}	3.0×10^{-2}
Potassium iodide	2×10^{-4}	3.6×10^{-2}
Sodium sulphide	4×10^{-4}	6.3×10^{-4}
Potassium thiocyanate	2×10^{-4}	0.2
Potassium cyanide	1×10^{-3}	5.0×10^{-2}

Primary ion-sulphathiazole (sodium salt).
Solution pH 8.63, $I = 0.05M$.

beforehand. Interference by some of these substances and other compounds, with the response of the cetyltriocetylammmonium-sulphathiazole electrode, were studied by the mixed-solution method. The results obtained are listed in Table 4. The selectivity coefficients are listed in Table 5. It is seen that no significant interference is caused by sulphide, chloride, bromide, iodide, phosphate, carbonate, oxalate and cyanide, which are severe interferents in the titrations with Ag(I), Hg(II) or Cu(II).

Table 5 shows that the selectivity coefficients are, in the main, of the same order of magnitude for the electrodes tested and decrease in the order sulphathiazole, sulphamethoxazole > sulphadoxine, sulphadimethoxine > sulphacetamide, sulphadiazine > sulphanilamide, *i.e.*, in nearly the same order as the electrode response discussed above.

Response time

The sulpha-drug sensitive electrodes of all-solid-state construction exhibit fast dynamic response, which is a most important factor in direct potentiometry. The response time is less than 15 sec in $\geq 10^{-5}M$ solutions and 20–25 sec in 10^{-6} – $10^{-7}M$ solutions.

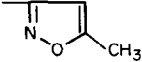
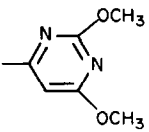
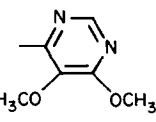
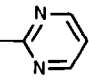
Membrane concentration effect

The effect of different concentrations of the electroactive material in the dibutyl phthalate plasticizer, on the electrode performance, was investigated. The results showed that the optimum membrane concentration is $0.005M$. When higher or lower membrane concentration was used, the linearity range was narrower, the response slope smaller, and the membrane resistance greater, resulting in less stable potential readings.

Applications to sulpha-drug determination

The cetyltriocetylammmonium-sulphathiazole electrode was used in the direct potentiometric determination of sulpha-drugs at mg/ml or lower concentration level. The results for sulphadiazole, sulphamethoxazole, sulphadiazine and sulphacetamide determinations gave an average recovery of 99.3% with standard deviation 1.3%. The electrode can also be applied to the determination of sulpha-drugs in pharmaceutical tablets and solutions. The sulpha-drug content can generally be determined

Table 5. Selectivity coefficients of some sulpha-drug sensitive electrodes toward different sulpha-drugs (mixed-solution method)

Sulpha-drug (Name and R*)	K_{ij}		
	CTOA-ST	CTOA-SDM'	CTOA-SDM
Sulphamethoxazole (SMZ) 	1.00	0.99	0.99
Sulphadimethoxine (SDM) 	0.93	0.96	1.02
Sulphadoxine (SDM') 	1.08	1.02	1.05
Sulphacetamide (SA) —COCH ₃	0.18	0.30	0.13
Sulphadiazine (SD) 	0.14	0.25	0.13
Sulphanilamide (SN) —H	0.05	0.06	0.03

Primary ion—sulphathiazole (sodium salt). K_{ij} values are given as average values from 3 parallel measurements. $C_j = 10^{-4}M$. Solution pH = 8.63. $I = 0.05M$. CTOA = cetyltriocetylammmonium.

*General formula for sulpha-drugs: $H_2NC_6H_4SO_2NHR$.

without preliminary filtration or other separation treatment. The results are in good agreement with those obtained by the pharmacopoeial method. The mean relative standard deviations were 0.9–5.7% (Table 6). The electrode can also be applied to the determination of sulphamethoxazole in a mixture

with trimethoprim, which is widely used and known as co-trimoxazole.

In the standard-addition method, a small error in potential may give rise to a relatively large error in the concentration found. In order to minimize the error in determination, a modified method proposed

Table 6. Analysis of pharmaceutical preparations

Pharmaceutical preparation	Nominal content	Found	
		Electrode method	Pharmacopoeial method
Sulphadiazine tablet	0.5 g/tablet	0.498 ± 0.012	0.508 ± 0.002
Co-trimoxazole tablets*	0.4 g/tablet (sulphamethoxazole)	0.392 ± 0.013	0.407 ± 0.003
Sultrin tablets†	0.171 g/tablet (sulphathiazole)	0.170 ± 0.002	No result
Sulphacetamide sodium ophthalmic solution	15% (sulphacetamide sodium)	14.79 ± 0.09	14.85 ± 0.09

*Each tablet contains 0.08 g of trimethoprim and 0.4 g of sulphamethoxazole.

†Each tablet contains 0.171 g of sulphathiazole and 0.013 g of urea.

by Carmack and Freiser¹³ for direct potentiometry by use of a calibration curve was employed. The potential measurements were repeated several times. Results with large deviations were rejected and the mean values calculated.

REFERENCES

1. A. L. Singh, Q. S. Usmani and I. C. Shukla, *Indian J. Pharm. Sci.*, 1980, **42**, 118.
2. S. Belal, A. S. Soliman and M. Bedair, *J. Drug Res.*, 1983, **14**, 1.
3. A. Bye and G. J. Land, *J. Chromatog.*, 1977, **139**, 181.
4. L. Faith, J. Cincarová and A. Felingová, *Farm. Obz.*, 1980, **49**, 395.
5. S. Satos, S. Higuchi and S. Tanaka, *Anal. Chim. Acta*, 1980, **120**, 209.
6. N. Hazemoto, N. Kamo and Y. Kobatake, *J. Pharm. Sci.*, 1976, **65**, 435.
7. M. Ionescu, S. Cilianu, A. A. Bunaciu and V. V. Coşofreş, *Talanta*, 1981, **28**, 383.
8. G. E. Baiulescu, G. Kandemir, M. S. Ionescu and C. Cristescu, *ibid.*, 1985, **32**, 295.
9. S. S. M. Hassan and M. M. Habib, *Microchem. J.*, 1981, **26**, 181.
10. F. Maleski and R. Staroscik, *Anal. Chim. Acta*, 1982, **139**, 353.
11. S. S. M. Hassan and M. H. Eldesouki, *J. Assoc. Off. Anal. Chem.*, 1981, **64**, 1158.
12. S. Yao and Y. Tang, *Acta Pharm. Sinica*, 1984, **19**, 454.
13. G. D. Carmack and H. Freiser, *Anal. Chem.*, 1977, **49**, 1577.

A TRIMETHOPRIM-SELECTIVE MEMBRANE ELECTRODE

SHOU-ZHOU YAO*, JING SHIAO and LI-HUA NIE

New Material Research Institute, Department of Chemical Engineering, Hunan University, Changsha,
People's Republic of China

(Received 21 March 1986. Revised 20 July 1986. Accepted 27 June 1987)

Summary—An electrode selective for trimethoprim is based on the ion-pair complex of trimethoprim with silicotungstate, and gives rapid response to change in trimethoprim concentration over the range 3×10^{-5} – $2 \times 10^{-2} M$ with a response slope of 51.0 ± 1.5 mV/decade. No significant interferences are caused by sulpha-drugs. The electrode can be used for the potentiometric determination of trimethoprim.

Trimethoprim, 2,4-diamino-5-(3,4,5-trimethoxybenzyl)pyrimidine, is now widely used in conjunction with sulpha-drugs, most commonly sulphamethoxazole, because the antimicrobial activity is greater than when the sulpha-drug is used alone. Non-aqueous titrimetry,^{1,2} HPLC or ultraviolet spectrophotometry^{1,3,4} have been suggested for the determination of trimethoprim alone or mixed with sulphamethoxazole. The titrimetric method suffers from lack of selectivity, and other basic substances may cause interference. The other methods require expensive instrumentation. We have found that the sulpha-drug may be determined potentiometrically in pharmaceutical preparations containing trimethoprim, by use of an electrode sensitive to the sulpha-drug. In the present paper, a trimethoprim-selective electrode is reported and proposed for use in pharmaceutical analysis.

EXPERIMENTAL

Apparatus and reagents

The apparatus used was the same as that previously reported,⁵ except that the trimethoprim ion-selective electrode was used as indicator electrode. All reagents used were of analytical grade. Doubly distilled water was used throughout.

Preparation of solutions

Buffer solution. Sodium hydroxide solution (1 M, 50 ml) was mixed with 428 ml of 1 M acetic acid and the mixture diluted to 1 litre. The buffer had pH 4 and ionic strength 0.05 M.

Standard trimethoprim solution. Trimethoprim (0.2903 g) was dissolved in the minimum amount of 36% acetic acid solution, and the solution was adjusted to pH 4 with sodium hydroxide solution, and diluted to volume in a 50-ml standard flask with the buffer, to give a 0.02 M standard solution. Standard series were prepared by successive dilution to 10^{-2} – $10^{-6} M$ with the buffer.

Preparation of the electroactive component

Trimethoprim silicotungstate was prepared by mixing 20 ml of 0.02 M silicotungstic acid and 40 ml of 0.01 M trimethoprim. The precipitate was filtered off on a porosity-4 sintered-glass crucible, washed several times with water and dried under vacuum. Other trimethoprim compounds (e.g., dipicrylamine, phosphotungstate) were prepared similarly.

Preparation of the electrode

The electrode of solid-state type was prepared as described previously.⁵ The electroactive membrane had a thickness of ca. 0.1 mm.

The PVC-membrane trimethoprim silicotungstate electrode was prepared essentially as before.⁶ A 0.1 M potassium chloride solution was used as the internal reference solution. An Ag/AgCl electrode was used as internal reference electrode.

The electrode was preconditioned in 0.001 M trimethoprim solution for 3 hr.

Procedure

For the analysis of trimethoprim tablets, twenty tablets were weighed and finely powdered. A portion of the powder, equivalent to about 0.5 mmole of trimethoprim, was weighed out accurately, dissolved in a minimum amount of 36% acetic acid, and the solution was adjusted to pH 4 with dilute sodium hydroxide solution, and diluted to volume in a 50-ml standard flask with the acetate buffer solution. A 1 or 2 ml portion was pipetted, made up accurately to 50 ml with the buffer, and analysed by a standard-addition method.

For the analysis of tablets containing trimethoprim and sulphamethoxazole (co-trimoxazole, abacin), after treatment with acetic acid solution and adjustment to pH 4, the sample solution was diluted to ca. 30 ml with the acetate buffer, and left for ca. 2 hr on a water-bath (ca. 60°) for the undissolved sulphamethoxazole to settle. After filtration, the filtrate was analysed for trimethoprim as above.

Determination in a single drop with an inverted electrode

The trimethoprim ion-selective electrode was placed upside down as shown in Fig. 1, with a saturated calomel electrode fixed at a distance of ca. 1 mm above it. After the electrode pair had been washed and wiped dry, the solution under test was placed on the electrode surface with a 50- μ l microsyringe. Potential measurements were performed repeatedly on the sample solution and on two standard

*Author for correspondence.

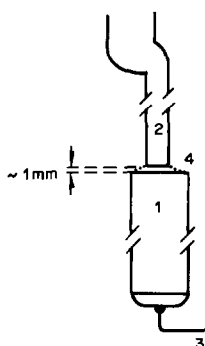


Fig. 1. Single-drop method using an inverted solid-state trimethoprim ion-selective electrode. 1—Trimethoprim ion-selective electrode; 2—SCE; 3—outlet; 4—sample solution drop.

solutions having trimethoprim concentrations bracketing that of the sample.

RESULTS AND DISCUSSION

Electrode performance

Electrodes made with the trimethoprim salts of different anions as electroactive material were prepared and their performances were compared. All experiments were made in stirred trimethoprim acetate solutions at pH 4 and ionic strength of 0.05M. The electrodes tested were of all-solid-state type. Results for the trimethoprim silicotungstate, dipicrylaminate, and phosphomolybdate membrane electrodes are shown in Fig. 2. It is seen that the trimethoprim silicotungstate electrode yields the best response toward trimethoprim, linear from 2×10^{-2} to $3 \times 10^{-5}M$ with a slope of 51.0 ± 1.5 mV/concentration decade and a detection limit of $10^{-5}M$.

PVC membrane electrodes were also prepared in order to compare the performances of the various electrode types. No significant differences were found

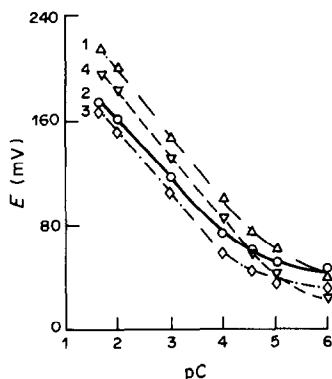


Fig. 2. Calibration curves (pH = 4, $I = 0.05M$). Trimethoprim silicotungstate (1), trimethoprim dipicrylaminate (2), and trimethoprim phosphotungstate (3) electrodes (solid-state). PVC membrane trimethoprim silicotungstate electrode (4).

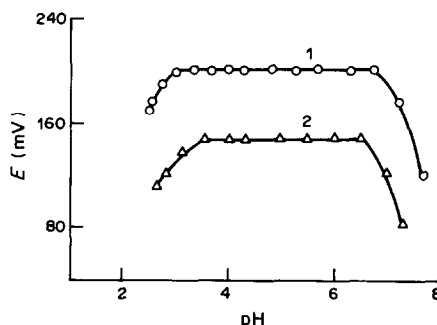


Fig. 3. Effect of pH on the potential of the trimethoprim ion-selective electrode. Membrane concentration: 1— $10^{-2}M$; 2— $10^{-3}M$ ($I = 0.05M$).

between the linearity ranges and the response slopes of the two types, but the solid-state type is easier to make and more convenient to handle, because the internal reference electrode and the internal reference solution are eliminated. Electrodes made under the same conditions gave practically the same electrode function.

Sulpha-drugs are amphoteric. As we have succeeded in preparing electrodes sensitive for sulpha-drugs in anionic form,⁵ attempts were made to obtain an electrode sensitive for the cationic sulpha-drug species, but without success: electrodes made with the compounds tested, such as those of sulphadimethoxine, sulphaguanidine and sulphadiazine with silicotungstate, phosphotungstate, tetraphenylborate and dipicrylaminate, responded rather poorly to sulpha-drugs in cationic form, and the electrode function was linear over only a narrow concentration range, with a response slope which was very low, 20–30 mV/concentration decade. The reason for this is that sulpha-drugs can be dissolved only at relatively low pH (< 1.5–0.5), where the interference of the hydrogen ion cannot be neglected. However, some of these electrodes, such as the sulphadimethoxine tetraphenylborate electrode, the sulphadiazine dipicrylaminate electrode and the sulphadimethoxine phosphomolybdate electrode, can give satisfactory response to trimethoprim with a slope of 44–50 mV/concentration decade and a linearity range from 2×10^{-2} to $10^{-4}M$.

Influence of pH

Figure 3 shows the influence of pH on the response of the trimethoprim silicotungstate electrode at different trimethoprim concentrations ($I = 0.05M$). The pH range where the potential remains constant is 3.5–6.5. At pH > 7, trimethoprim tends to precipitate, causing the potential to decrease. The potential also decreases at pH < 3. The direct potential measurements for calibration of the electrode were made at pH 4 (acetate buffer).

Table 1. Selectivity coefficients (mixed-solution procedure)

Interferent	$-\log C_i$	$-\log K_{ij}$
Sulphadimethoxine	4	1.64
Sulphaguanidine	4	1.60
Sulphadiazine	4	1.50
Sulphanilamide	4	1.96
Sulphacetamide	4	1.72
Sulphamethoxazole	4	1.77
Sodium chloride	2	3.10
Potassium chloride	2	2.85
Potassium bromide*	3	2.41
Potassium iodide*	3	2.43
Potassium thiocyanate*	3	2.52
Ammonium sulphate	2	2.96
Calcium chloride	2	3.51
Glutamic acid*	3	2.80
Alanine	3	3.25
Urea*	3	2.59
Oxalic acid	3	2.20
Citric acid	3	2.41
Chlorpheniramine	5	-0.50
Glycopyrrolate	5	-0.49
Atropine sulphate	5	-1.28
Glucose	1%	No interference
Starch	0.5%	No interference

Trimethoprim silicotungstate solid-state electrode, pH = 4, $I = 0.05M$.

*Separate-solution procedure.

Selectivity

Selectivity coefficients for 23 substances were determined with the trimethoprim ion-selective electrode. The results (Table 1) shows that the electrode has rather good selectivity for trimethoprim, and most sulpha-drugs do not interfere significantly. Therefore, it is possible to determine trimethoprim even in the presence of other sulpha-drugs, *e.g.*, in co-

trimoxazole. It is seen that no significant interferences are caused by several inorganic compounds, amino-acids and pharmaceutical ingredients such as starch and glucose, but chlorpheniramine, atropine and glycopyrrolate are likely to cause interference. However, these substances will rarely be contained in the same pharmaceutical preparation as trimethoprim.

Response time and life-span

The response characteristics of the all-solid-state electrode were evaluated with trimethoprim acetate solutions of different concentrations but identical acidity (pH 4) and ionic strength ($I = 0.05M$), the emf being recorded as a function of time. The response time of the electrode in $10^{-6}M$ solution is about 1 min, in 10^{-4} – $10^{-5}M$ solution 15–30 sec, and in 10^{-2} – $10^{-3}M$ solutions < 10 sec.

The electrode can be used for at least 3 months with practically unimpaired performance.

Applications to trimethoprim determination

The trimethoprim silicotungstate membrane electrode was applied to the potentiometric determination of trimethoprim. The results are listed in Tables 2 and 3.

For the standard addition method, a computer program was written for use with double and multiple addition techniques, based on the following equation, and an $R-x$ correlation table was compiled for convenience:

$$R = \frac{\Delta E_i}{\Delta E_m} = \frac{\log\left(\frac{100+x}{100+1}\right)}{\log\left(\frac{100+mx}{100+m}\right)}$$

Table 2. Determination of trimethoprim

Standard-addition method			Single-drop method		
Taken, mg	Found, mg	Error, %	Taken, μg	Found, μg	Error, %
1.50	1.55	3.3	12.0	12.3	2.5
2.60	2.70	3.8	17.0	16.5	2.9
4.40	4.30	2.3	26.0	27.0	3.8
5.20	5.30	1.9	32.0	31.5	1.6
5.80	5.55	4.3	41.0	42.0	2.4

Table 3. Analysis of pharmaceutical preparations

Pharmaceutical preparation	Standard-addition method	Single-drop method	Pharmacopoeial method ¹
Co-trimoxazole (trimethoprim 0.08 g/tablet; sulpha methoxazole 0.4 g/tablet)	0.0805, 0.0791	0.083	
	0.0770, 0.0810	0.079	
	0.0792	0.081	
	Average: -0.0794	Average: 0.081	
Trimethoprim tablet (0.1 g/tablet)	0.1007, 0.0940	0.099	0.098
	0.0997, 0.1025	0.095	0.095
	0.0997	0.100	0.099
	Average: 0.0993	Average: 0.098	Average: 0.097

where $x = C_s/C_x$, $m = 100 V_s/V_x$ (m is an integer from 1 to 100), $\Delta E_1 = E_1 - E_x$, $\Delta E_m = E_m - E_x$. This is applicable for any number (m) of additions of V_s ml of a solution of known concentration C_s to V_x ml of solution of unknown concentration C_x . As C_s/C_x is usually between 25 and 200, and V_s/V_x is between 0.01 and 0.05, the value of x was set at 20–250 in steps of 0.1. Results were processed on an IBM personal computer.

A distinct advantage of the all-solid-state electrode construction is that it can be adapted for analysis of only one or two drops of sample solution by keeping the electrode inverted and injecting the sample into the limited space between the indicator electrode and the reference electrode, to form a miniature detection cell. Because no stirring is involved, the emf reading is stable, and the reproducibility is good. Results for

the determination of trimethoprim in aqueous samples and pharmaceutical preparations by this technique are listed in Tables 2 and 3. It is seen that the proposed method is applicable to determinations at μg level.

Acknowledgement—This work was supported by the Science Fund of the Chinese Academy of Sciences.

REFERENCES

1. *U.S. Pharmacopeia*, XX, pp. 744–751. American Pharmaceutical Association, Washington, D.C., 1980.
2. W. Messerschmidt, *Pharm. Ind.*, 1979, **41**, 1082.
3. R. O. Singletary, Jr. and F. D. Sancilio, *J. Pharm. Sci.*, 1980, **69**, 144.
4. M. A. Korany, A. M. Wahbi, M. A. Elsayed and S. Mandour, *Anal. Lett.*, 1984, **17**, 1373.
5. S. Z. Yao, J. Shiao and L.-H. Nie, *Talanta*, 1987, **34**, 977.
6. S. Z. Yao and G. H. Liu, *ibid.*, 1985, **32**, 1113.

DIODE-ARRAY DETECTORS IN FLOW-INJECTION ANALYSIS

MIXTURE RESOLUTION BY MULTI-WAVELENGTH ANALYSIS

M. BLANCO*, J. GENE, H. ITURRIAGA, S. MASPOCH and J. RIBA

Departamento de Química, División de Química Analítica, Facultad de Ciencias, Universidad Autónoma de Barcelona, 08193 Bellaterra (Barcelona), Spain

(Received 30 June 1986. Revised 27 May 1987. Accepted 27 June 1987)

Summary—The application of diode-array spectrophotometers to multi-component analysis by flow-injection analysis is reported. Two different aspects are considered: (a) the obtainment of a reproducible spectrum corresponding to the maximum of the FIA peak, and (b) the mathematical treatment involved in determining the mixture of components. The spectrum is recorded by two different procedures according to the type of injection system used. The mixtures are resolved with the aid of three different treatments: (a) a linear equation system, (b) a multi-component analysis program (Hewlett-Packard) and (c) a graphical method (multi-wavelength linear regression analysis). All three procedures have been applied to the determination of Fe(II) and Fe(III) with a mixture of 1,10-phenanthroline and sulphosalicylic acid.

Flow-injection analysis (FIA) is an analytical technique of well-known potential, and its application to simultaneous determination of several analytes in the same sample is a subject of growing interest.¹ One of the ways to increase its potential in the resolution of complex mixtures is the use of image detectors. Diode-array spectrophotometers are image detectors capable of completely recording an ultraviolet-visible spectrum in about 0.1 sec. Despite their increasing use as HPLC detectors and their potential advantages,² they have only very recently begun to be used in FIA. For example, Vithanage and Dasgupta³ have applied diode-array detectors (DADs) to the study of proton-ligand and metal-ligand equilibria occurring in the FIA-peak gradient zone. Valcárcel *et al.* have reported the simultaneous determination of Fe(II) and Cu(II) with a mixture of specific chromogenic reagents,⁴ the metal concentrations being calculated by means of a linear equation system. The use of DADs results in faster analyses thanks to the possibility of making several simultaneous measurements at various wavelengths. Although there are a number of procedures available for optimization of the wavelengths to be used,⁵⁻⁸ the resolution of mixtures on the basis of a few linear equations is inapplicable to systems having extensive spectral overlap.

Derivative spectra are known to be more selective than absorption spectra⁹ (zeroth-derivative). This increased selectivity has been exploited in the determination of a given component in a sample by making measurements at a single wavelength. Diode-array detectors considerably facilitate the obtainment of derivative spectra. The application of a multi-

component analysis program to these spectra has allowed the resolution of mixtures of analytes with strongly overlapped spectra and the cancellation of matrix effects.¹⁰⁻¹² Derivative spectra have recently been applied to the resolution of a quaternary mixture by use of a combined FIA-DAD system.¹³

The aim of this work was to expand the use of DADs in the simultaneous determination of several species by FIA by exploiting all the information obtainable from the absorption and derivative spectra of each analyte.

Multi-component analysis with an FIA-DAD system involves two essential aspects, namely (a) the recording of the spectrum under conditions of maximum sensitivity and reproducibility, and (b) the mathematical treatment of the information gathered, to resolve the analyte mixture.

This paper reports two different procedures for spectrum recording, and three methods for treating the results, namely: (a) the resolution of a system consisting of one equation per analyte; (b) multi-component analysis (MA) by a computation program supplied by Hewlett-Packard; (c) multi-wavelength linear regression analysis (MLRA), a linear regression graphical method. All three procedures have been applied to the simultaneous determination of Fe(II) and Fe(III) by use of a mixture of 1,10-phenanthroline and sulphosalicylic acid as chromogenic reagent. The results obtained by the three methods are compared and discussed.

EXPERIMENTAL

Reagents

Stock iron solutions containing 1000 ppm Fe(II) and Fe(III) were prepared by dissolving $\text{Fe}(\text{NH}_4)_2(\text{SO}_4)_2 \cdot 6\text{H}_2\text{O}$

*To whom all correspondence should be addressed.

and $\text{FeNH}_4(\text{SO}_4)_2 \cdot 12\text{H}_2\text{O}$, respectively, in 0.05M sulphuric acid and standardized both titrimetrically with a standard dichromate solution and *p*-diphenylaminesulphonate as indicator and gravimetrically by weighing as Fe_2O_3 . Working solutions were prepared by appropriate dilution with degassed distilled water. The concentration of the Fe(II) solution was checked daily by titration with standard dichromate solution.

1,10-Phenanthroline (Phen) solution 0.5%. Prepared from 1,10-phenanthroline hydrochloride.

Sulphosalicylic acid solution (SSA), 2.5%.

Acetate buffer, 1M, pH 5.7. Adjusted with sodium hydroxide.

The stock reagent solutions were used to prepare those injected into the manifolds, as follows.

Manifold A: 1 mM Phen, 15 mM SSA, 0.2M acetate buffer.
Manifold B: 10 mM Phen, 25 mM SSA, 0.2M acetate buffer.

All solid reagents used were of analytical grade.

Apparatus and manifolds

A Hewlett-Packard 8451A diode-array spectrophotometer furnished with a 128-K RAM HP-82909A module, an HP-9121 floppy disk drive, an HP-98155A keyboard and an HP-7440A plotter was used as the detection and data-processing system. An HP-82940 GPI/O interface was used to control the automatic injection valve. Other equipment included a Gilson Minipuls-2 peristaltic pump and a Hellma 178.712-QS flow-cell (inner volume 18 μl , optical path length 10 mm).

An automatic Tecator V-200 and a manual Rheodyne 5020 injection valve were used in manifolds A and B, respectively. All reaction coils and sample loops were made from PTFE tubing of 0.5 mm bore.

Normalized standard spectra

Three pure standard solutions of each component of the mixture, with a concentration lying in the linear concentration range and giving absorbance readings lower than 1.0, were prepared. The batch solutions were injected in triplicate and a spectrum for each standard was obtained by averaging the three spectra obtained. A normalized spectrum for unit concentration was obtained for each component by regression of the absorbance *vs.* concentration. These normalized spectra were used as references for resolution of mixtures.

RESULTS AND DISCUSSION

Recording of spectra

The HP-8415A spectrophotometer is capable of recording a whole spectrum (190–820 nm) in 0.1 sec every 0.7 sec. Such a high recording speed allows a vast amount of information to be gathered from an FIA peak, yet a mixture can be resolved from a single spectrum. In order to ensure the greatest possible sensitivity and reproducibility, the spectrum was recorded at the maximum of the FIA peak. The first few attempts at recording spectra at high speed failed because of the poor reproducibility of the results obtained in successive injections. The reproducibility was improved by increasing the integration time, T_1 , the period over which the spectrophotometer is continuously measuring the spectrum, the end of which is marked by delivery of the spectrum. Obviously, since FIA signals are transient peaks, T_1 should be as short as possible. Relative standard deviations not

greater than 1% were achieved for integration times of 0.3 sec or longer. Thus, a T_1 of 0.4 sec, symmetrically distributed about the residence time of the FIA peak, was chosen for further experiments.

Flow-injection analysis is characterized by the fact that the dispersion of the sample in the manifold is a reproducible function of time. Thus, the reproducibility of the sample image obtained at a given time will depend chiefly on the reproducibility of the time elapsed between image recording and the reference time. Every FIA recording features two points that are eligible as a reference time, namely sample injection and sample arrival at the detector. A suitable computer program facilitates recording of spectra under preselected conditions (wavelength range, time interval, integration time, *etc.*).

The simplest approach uses sample injection as the reference time. Obviously, the injection should be synchronized as accurately as possible with the triggering of the program handling the spectrum recording, in order to ensure reproducibility; this is made possible by the use of an automatic valve, the control scheme of which is depicted in Fig. 1(A).

A suitable alternative is to record the spectra once a preselected time has elapsed after arrival of the sample at the detector. This needs no synchronization, so the analyst can inject the sample manually and then execute the recording program.

A computer-controlled injection system (manifold A) allows the recording of spectra in both ways, whereas a manual system (manifold B) can only cope with the second of the two.

Figure 2 shows the flow diagrams of the programs used to control the recording of the spectra. FIAREC1 uses the first few injections to calculate the residence time, T_R ; the spectrum is recorded from further successive injections at $T_R - (T_1/2)$ sec after each.

FIAREC2 employs the first few injections to calculate the time elapsed between the start and the maximum of the FIA peak, T' , the spectrum being subsequently recorded at $T' - (T_1/2)$ sec after arrival of the sample at the detector.

FIAREC1 and FIAREC2 were used in conjunction with manifolds A and B, respectively.

Data treatment

The analytes were determined by processing the information abstracted from the spectra of the mixtures, by three different procedures, as follows.

(a) By solving a system of two linear equations based on the absorbances of the two complexes, measured at their respective absorption maxima (510 and 486 nm). The equations concerned were:

Manifold A

$$A_{510} = 0.0682[\text{Fe}^{2+}] + 0.0255[\text{Fe}^{3+}]$$

$$A_{486} = 0.0634[\text{Fe}^{2+}] + 0.0280[\text{Fe}^{3+}]$$

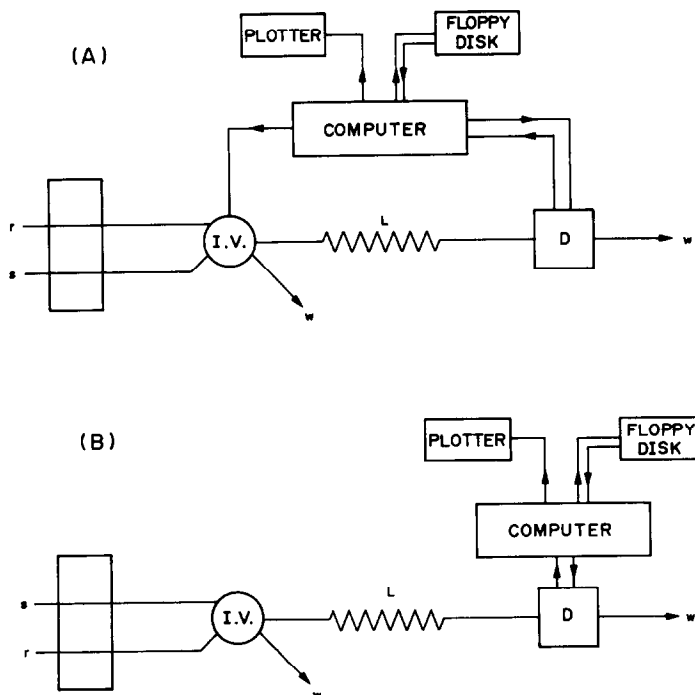


Fig. 1. Schemes of the flow-injection manifolds. S = sample; I.V. = injection valve; L = reaction coil; D = diode-array detector; W = waste. (A) $V_{in} = 120 \mu\text{l}$; flow-rate 0.95 ml/min; $L = 270 \text{ cm}$; $T_R = 39 \text{ sec}$, (B) $V_{in} = 8 \mu\text{l}$; flow-rate 1.07 ml/min; $L = 50 \text{ cm}$ $T_R = 7 \text{ sec}$. In manifold A the sample is injected into the reagent stream (normal FIA mode) while in manifold B the reagent is injected into the sample stream (reverse FIA mode).

Manifold B

$$A_{510} = 0.1658[\text{Fe}^{2+}] + 0.0538[\text{Fe}^{3+}]$$

$$A_{486} = 0.1548[\text{Fe}^{2+}] + 0.0562[\text{Fe}^{3+}]$$

(b) By use of the multi-component analysis (MA) program supplied as part of the Hewlett-Packard spectrophotometer bundled software. This is written in machine code and is therefore modifiable only by experienced programmers. It uses spectra from pure standards of accurately known concentration as reference, and yields the analyte concentrations that give the best least-squares fit between the calculated spectrum and that obtained for the mixture. This program was applied to the absorption spectrum and the first, second and third-derivative spectra over the selected wavelength ranges. The derivative spectra were run with the aid of the bundled software.

(c) By application of a graphical linear regression method known as multi-wavelength linear regression analysis (MLRA). For simultaneous spectrophotometric determination of several components in a mixture to be achieved, each species must absorb according to Beer's law, and the absorbances must be additive. For a binary mixture, both conditions can be summed up in the equation

$$A_m = a_1 d C_1 + a_2 d C_2 \quad (1)$$

where a_1 and a_2 are the molar absorptivities of the

two species, d is the optical path-length and C_1 and C_2 are the respective concentrations.

The molar absorptivities at each wavelength can be calculated from the absorbance of a pure standard solution of each component:

$$A_{s_i} = a_i d C_{s_i} \quad (i = 1 \text{ or } 2) \quad (2)$$

where A_{s_i} is the standard absorbance at each wavelength and C_{s_i} the corresponding concentration.

If the same cell is used to measure both species, and $C_{s_1} = C_{s_2} = 1$, appropriate substitution and rearrangement gives

$$A_{s_1}/A_m = (1/C_1) - (C_2/C_1)(A_{s_2}/A_m) \quad (3)$$

Plotting the values obtained at different wavelengths as A_{s_1}/A_m vs. A_{s_2}/A_m gives a straight line with slope and intercept which allow calculation of C_1 and C_2 .

Optimization of manifold parameters

Because of the lower molar absorptivity of the Fe(III) complex, the optimization was aimed at increasing the sensitivity of the determination of the ferric ion. This was accomplished by applying the univariate method.

The sensitivity of the reaction between Fe(III) and SSA increases with pH, but the injection of Fe(II) yields a signal when alkaline media are used. A pH of 5.7 was therefore chosen as a compromise. It

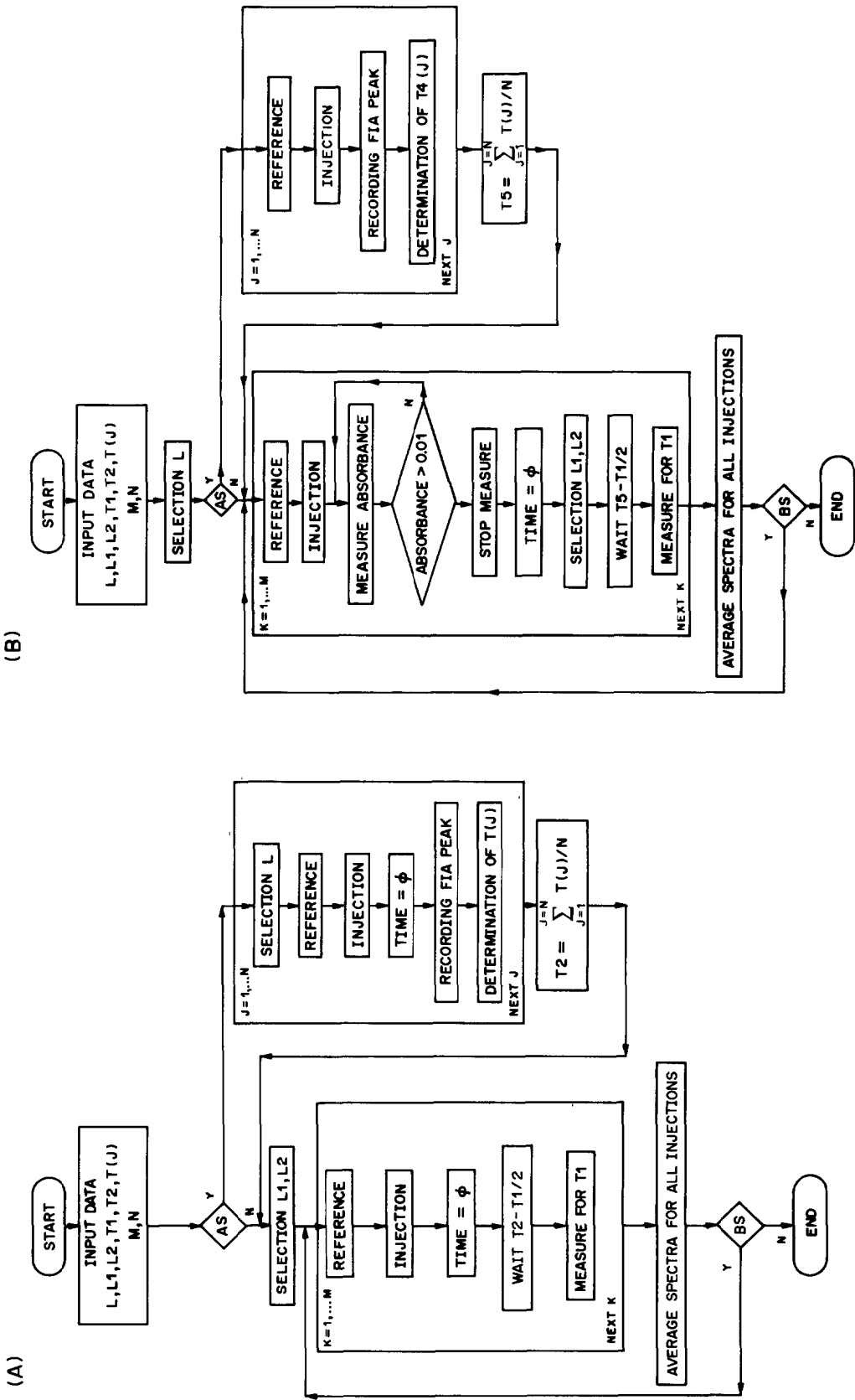


Fig. 2. Flow chart of programs for recording of spectra. A: FIAREC1; B: FIAREC2. See Table 1 for definition of variables.

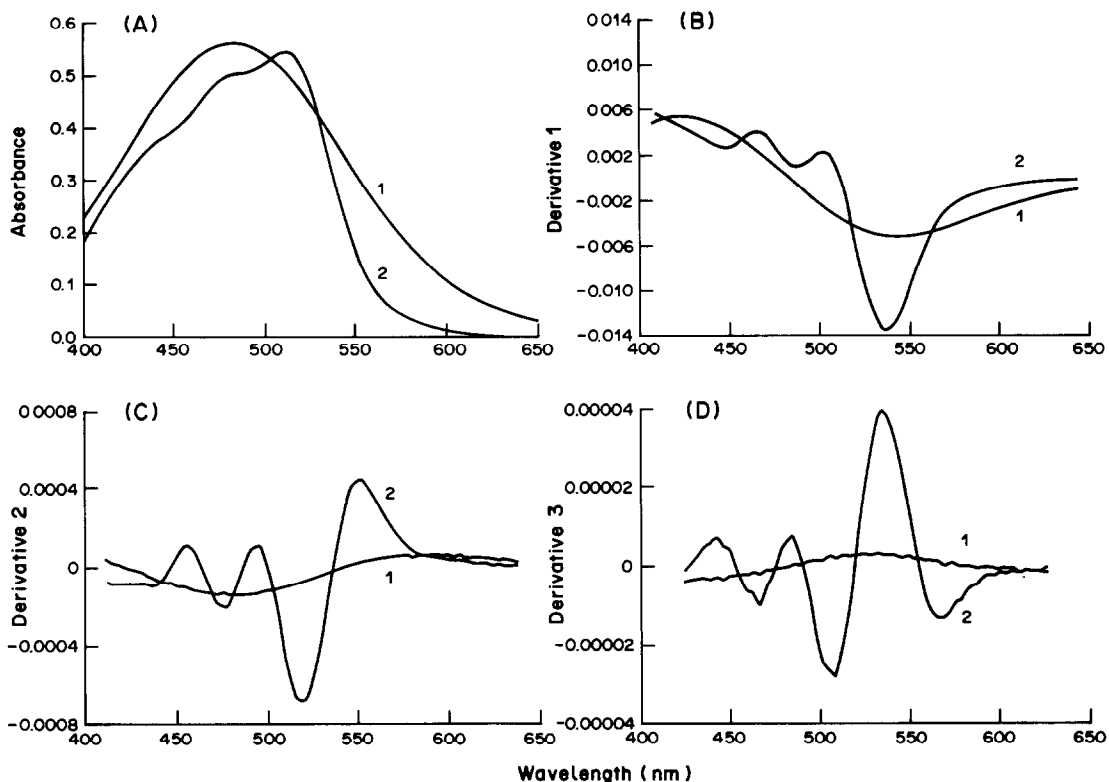


Fig. 3. Spectra obtained for 20 ppm of Fe(III) (1) and 8 ppm Fe(II) (2) with a normal nFIA manifold. A, absorption spectra; B, first-derivative spectra; C, second-derivative spectra; D, third-derivative spectra.

should be pointed out that the volume injected into the manifold was kept rather low in order to avoid the appearance of double peaks.

Mixture resolution

A series of 12 mixed solutions containing various amounts of Fe(II) and Fe(III) in the ranges 0.25–15.5 and 3–20 ppm, respectively, and [Fe(II)]/[Fe(III)] ratios from 0.6 to 40, were prepared for manifold A. Similarly, another set of 14 solutions with Fe(II) and Fe(III) contents in the ranges 0.5–5.2 and 1–12.4 ppm, respectively, in ratios from 0.25 to 16, were prepared for manifold B. The conventional and the first, second and third-derivative spectra (Fig. 3A–D)

were processed over the whole wavelength range covered (400–650 nm).

The results obtained in the resolution of the Fe(II)–Fe(III) mixtures (Tables 2 and 3) are shown as the correlation between the concentrations taken and found, for the different calculation procedures used.

The real achievement of this work is not the accurate calculation of the concentration of a given species in the presence of a higher concentration of another, but rather the possibility of simultaneously determining both under all types of conditions.

As would be expected from the degree of spectral overlap, the classical method of mixture resolution based on a linear equation system resulted in substan-

Table 1. Definition of variables used by FIAREC1 and FIAREC2

Variable	Meaning
AS	'Y' if residence time must be determined
BS	'Y' if another sample or standard is injected
L	Wavelength of maximum sample absorbance
L1, L2	Lower and upper limit of the useful wavelength range
M	Number of averaged spectra
N	Number of injections used for measuring residence time
T(J)	Residence time for each injection
T2	Average residence time
T1	Integration time
T4(J)	Time interval between start and maximum of FIA peak
T5	Average T4

Table 2. Least-squares statistical data for fits of calculated *vs.* added concentrations (manifold A)

	Fe ³⁺			Fe ²⁺		
	Intercept $\pm s$	Slope $\pm s$	Correlation coeff. (R^2)	Intercept $\pm s$	Slope $\pm s$	Correlation coeff. (R^2)
	Linear equations					
	-0.33 ± 0.97	1.06 ± 0.09	0.937	0.10 ± 0.08	0.95 ± 0.01	0.998
	Multicomponent analysis					
Absorption spectrum	0.32 ± 0.37	0.97 ± 0.03	0.988	-0.12 ± 0.08	1.02 ± 0.01	0.998
First derivative	0.45 ± 0.50	0.97 ± 0.05	0.978	-0.05 ± 0.08	0.99 ± 0.01	0.999
Second derivative	0.10 ± 0.56	1.00 ± 0.05	0.976	-0.03 ± 0.07	0.99 ± 0.01	0.999
Third derivative	0.02 ± 0.65	1.01 ± 0.06	0.967	0.01 ± 0.07	0.98 ± 0.01	0.999
	MLRA					
400–600 nm	0.42 ± 0.40	0.96 ± 0.04	0.986	-0.15 ± 0.09	1.02 ± 0.01	0.998
420–580 nm	0.24 ± 0.40	0.97 ± 0.04	0.987	-0.11 ± 0.08	1.01 ± 0.01	0.999

tial errors and hence in poor precision, as can be seen from the deviation from linearity and the low correlation coefficient obtained.

The use of a calculation program (MA) operating throughout the visible spectrum provides better results for the slope, intercept and precision. However, deviations from linearity are still significant and the slope is rather low for Fe(III) and high for Fe(II).

The application of the MA program to the derivative spectra results in considerably improved results, particularly for Fe(II). The precision achieved is virtually independent of the spectral mode and the best slope and intercept are obtained for the first and second-derivative spectra.

Although the use of derivative spectra also improves the slope and intercept for Fe(III), increasing the derivative order results in poorer precision as a result of the concomitantly decreasing spectral signal.

It should be noted that manifold B yields more precise results than manifold A, probably because of the greater sensitivity it produces.

The MLRA treatment, as applied to the whole wavelength range, yields similar results to those obtained by multicomponent analysis, but has two significant advantages, namely the resolution procedure is straightforward and transparent to the analyst—whereas that of MA is obscure and inaccessible—and (most important), it makes

selection of the most suitable wavelength range for resolution of the mixture quite a simple task. The reliability of mixture resolution has been reported to depend strongly on the wavelength range selected,¹⁰ but up till now the selection has been made empirically.

The MLRA program provides the user with the wavelength range that gives the best linearity of response. This is illustrated in Fig. 4 for a mixture containing 0.52 ppm Fe(II) and 8.32 ppm Fe(III). In this case, deviations from linearity are observed only near the ends of the wavelength range, where the absorbance values are significantly smaller. This is consistent with the finding¹³ that one of the requisites for accurate mixture resolution with the aid of the MA program is that all species to be determined must absorb significantly in the selected wavelength range. Narrowing of the spectral interval to 420–580 nm results in a better fit, as can be seen from Tables 2 and 3. This range narrowing also resulted in slight improvements in the results obtained by MA from the absorption spectra, though not from the derivative spectra. No other wavelength range assayed yielded better results.

CONCLUSIONS

This paper demonstrates the possibility of accomplishing simultaneous determinations by FIA with

Table 3. Least-squares statistical data for fits of calculated *vs.* added concentrations (manifold B)

	Fe ³⁺			Fe ²⁺		
	Intercept $\pm s$	Slope $\pm s$	Correlation coeff. (R^2)	Intercept $\pm s$	Slope $\pm s$	Correlation coeff. (R^2)
	Linear equations					
	-0.09 ± 0.26	1.12 ± 0.04	0.983	0.17 ± 0.09	0.88 ± 0.03	0.986
	Multicomponent analysis					
Normal spectrum	0.03 ± 0.08	0.95 ± 0.01	0.998	0.06 ± 0.02	1.036 ± 0.006	0.9996
First derivative	0.09 ± 0.06	1.02 ± 0.01	0.999	0.06 ± 0.03	0.994 ± 0.009	0.9991
Second derivative	0.08 ± 0.08	1.04 ± 0.01	0.999	0.06 ± 0.03	0.99 ± 0.01	0.999
Third derivative	0.02 ± 0.15	1.07 ± 0.02	0.994	0.06 ± 0.03	0.99 ± 0.01	0.999
	MLRA					
400–600 nm	0.02 ± 0.08	0.95 ± 0.01	0.998	0.05 ± 0.02	1.04 ± 0.006	0.9996
420–580 nm	0.04 ± 0.07	0.96 ± 0.01	0.999	0.05 ± 0.02	1.029 ± 0.006	0.9996

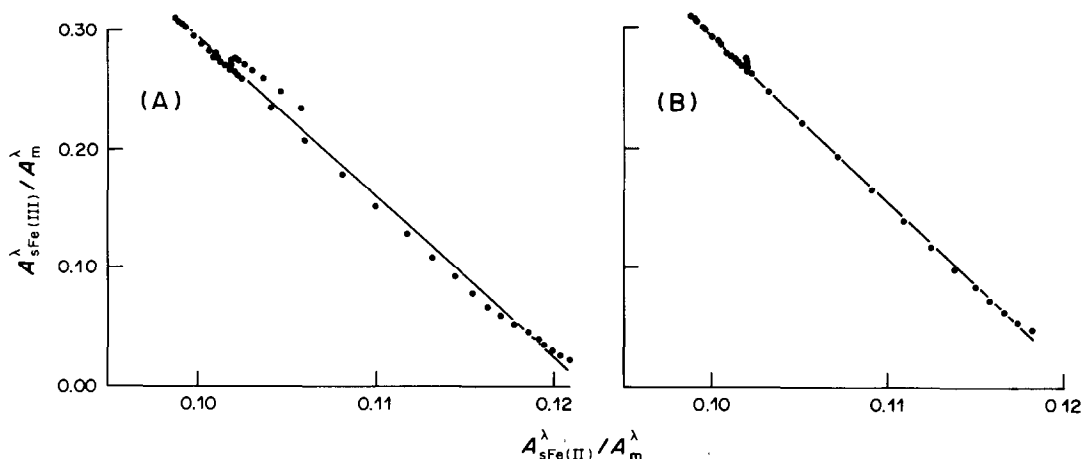


Fig. 4. MLRA plot for a mixture of 8.32 ppm Fe(II) and 0.52 ppm Fe(III). Data obtained with manifold B. (A) Wavelength range, 400–650 nm; Fe(III) found, 8.22 ppm; Fe(II) found, 0.60 ppm; regression coefficient, $r^2 = 0.997$. (B) Wavelength range, 420–580 nm; Fe(III) found, 8.26 ppm; Fe(II) found, 0.58 ppm; regression coefficient, $r^2 = 0.9994$. Absorbance measurements made at 4-nm intervals.

the aid of a diode-array detector. Most of the reproducibility problems encountered in working at high spectrum-recording speeds are overcome by both procedures proposed, which afford a reproducibility of the order of 1% at absorbance values not greater than 1.5.

As can be seen from Tables 2 and 3, the resolution of mixtures with highly overlapped spectra yields poorly correlated results by the linear-equation method, but the MA and MLRA programs result in better fittings. The results provided by both MA and MLRA when applied to the absorbance spectrum are comparable in accuracy and precision, but, the best fittings are obtained by MA and the first and second-derivative spectra obtained by use of manifold B.

The most outstanding features of the MLRA program are probably its transparency to the user and the possibility of selecting the wavelength range best suited to the particular mixture to be resolved.

Acknowledgement—The authors are grateful to the CAICYT (Project No. 821/84) and the Fundación Roviralta for financial support.

REFERENCES

1. M. D. Luque de Castro and M. Valcárcel Cases, *Analyst*, 1984, **109**, 413.
2. A. F. Fell, *Anal. Proc.*, 1980, **17**, 266.
3. R. S. Vithanage and P. K. Dasgupta, *Anal. Chem.*, 1986, **58**, 326.
4. F. Lázaro, A. Rios, M. D. Luque de Castro and M. Valcárcel, *Anal. Chim. Acta*, 1986, **179**, 279.
5. S. D. Frans and J. M. Harris, *Anal. Chem.*, 1985, **57**, 2680.
6. M. R. Ditusa and J. Schilt, *J. Chem. Ed.*, 1985, **62**, 541.
7. A. T. Pilipenko, L. I. Savranskii and A. N. Mas'ko, *Zh. Analit. Khim.*, 1985, **40**, 232.
8. E. J. Meehan, in *Treatise on Analytical Chemistry*, 2nd Ed., P. J. Elving, E. J. Meehan and I. M. Kolthoff (eds.), Part 1, Vol. 7, pp. 96–104. Wiley, New York, 1981.
9. P. Levillain and D. Fompeydie, *Analisis*, 1986, **14**, 1.
10. D. T. Rossi and H. L. Pardue, *Anal. Chim. Acta*, 1985, **175**, 153.
11. T. R. Matton, P. McSwiggen and S. A. George, *Metal Finishing*, 1985, **83**, 83.
12. Y. R. Tahboub and H. L. Pardue, *Anal. Chem.*, 1985, **57**, 38.
13. M. Blanco, J. Gené, H. Iturriaga and M. Maspocho, *Analyst*, 1987, **112**, 619.

DETERMINATION OF TRACES OF Zn, Cd, Pb AND Cu IN WHITE SUGAR BY ANODIC STRIPPING VOLTAMMETRY AND A MODIFIED OXYGEN-FLASK COMBUSTION TECHNIQUE

THURAYA M. KARADAKHI, FADHIL M. NAJIB and FAHMI A. MOHAMMED*
Department of Chemistry, College of Science, University of Salahaddin, Erbil, Iraq

(Received 27 September 1984. Revised 11 March 1987. Accepted 27 June 1987)

Summary—Anodic stripping voltammetry with a hanging-drop mercury electrode is used for determination of traces of Zn, Cd, Pb and Cu in white sugar. The sample (1.5 g) is decomposed by ignition in oxygen in a specially modified system.

Anodic stripping voltammetry (ASV) is a very sensitive and selective technique for trace metal analysis of sugars. A mercury electrode,⁷⁻¹⁰ either hanging drop (HMDE) or thin-film (TFME), is used.

The present work was a study of the best conditions for determination of traces of zinc, cadmium, lead and copper in refined white sugar by ASV with the HMDE. It also included development of a modified method for the oxygen-flask combustion of sugar samples large enough for trace-metal analysis.

The original Hempel technique¹¹ has undergone various modifications in the past¹²⁻²⁰ but has not been specifically modified for dealing with large sugar samples.

EXPERIMENTAL

Apparatus

A model 174 A polarograph (Princeton Applied Research, PAR) was used in conjunction with a model RE 0074 X-Y recorder and model 9323 HMDE kit, and an Ingold model PT-800 platinum wire auxiliary electrode. The calomel reference electrode was a PAR model 9331, used in a model 9332 salt-bridge consisting of a thin polypropylene tube closed at the end with a piece of polymer, which deteriorated and was later replaced by a piece of polyether sulphone (I.C.I.). The electrodes and nitrogen inlet were assembled in a PAR model 9301 polarographic cell.

The HMDE was cleaned according to Oehme,²¹ and the capillary tube was siliconed with PAR 9356 solution.

The modified combustion flask

A 10-litre round-bottomed flask is used, fitted with a 34/35 socket. The modified sample holder is shown in Fig. 1. It consists of a borosilicate glass cup (1) 25 mm high and 18 mm in diameter, with many holes (2-3 mm diameter) all round its wall, and a slightly rounded bottom. It is attached to a tube (2) to form an S-bend to prevent molten sugar from passing down the tube. This tube is 83 mm long and 7 mm in bore, and fused into the stopper (6) of the flask. Two insulated copper-wire leads (1-mm diameter single electrical wire in an ordinary insulator) are connected at one

end by a 16-mm length of platinum wire (0.3-0.5 mm diameter), which is bent in a U-shape and sealed into a borosilicate tube 75 mm long and 7 mm in bore (3) so that only 10-12 mm of it (5) is outside the tube. The tube is sealed into the stopper (6) so that the platinum wire is about 10 mm from the bottom of the sample cup. The tube carrying the cup is led out of the stopper at a right angle and carries a tap (7) near the end. The two wire leads are connected externally (4) to a 10-V d.c. power supply and a switch.

Reagents

Triply distilled mercury (99.999% pure, Fluka), analytical grade chemicals from BDH or Fluka, and distilled demineralized water were used throughout. The buffers and supporting electrolytes were further purified by electrolysis with a large-area mercury pool as cathode.²²

Standard stock solutions 1000 ppm. Zinc, cadmium, lead and copper were dissolved in the minimum necessary volume of nitric acid (1+1)²³ and the solutions were diluted to the appropriate volume and stored in polythene bottles.²⁴ Solutions for calibration were prepared daily by dilution of the stock solutions.

Alkaline pyrogallol solution.²⁵

Procedures

Sample decomposition. N.B. The ignition must be done behind a transparent safety board. Wrap the sugar sample (up to 1.5 g) in a piece of filter paper as usual for oxygen-flask combustion, and place the product in the cup, with the paper fuse coming out through one of the holes and touching the platinum wire. Place 25 ml of 0.5M nitric acid in the flask, insert the sample holder, invert the assembly and clamp it vertically in place. Connect the leads to the 10-V d.c. power supply, and the oxygen tube to a vacuum pump. Apply the vacuum for 5-10 min. Close the tap and connect the tube to a safety bottle half-filled with distilled water, and thence to an oxygen cylinder. Open the tap to admit oxygen into the flask at a slow and constant rate (~0.5 l./min). Switch on the 10-V supply for a few seconds until the fuse has started to burn. The sample will then begin to burn and continue burning while oxygen is admitted continuously at a rate sufficient to maintain steady combustion. The rate of addition of oxygen is controlled by means of the tap—too fast a flow causes splashing in the wash bottle, and overvigorous combustion. When the combustion is complete, close the tap and leave the flask for 30 min, shaking it periodically in the last 10 min to complete the absorption of combustion products. At this stage a

*Present address: Chemistry Department, College of Education, University of Salahaddin, Erbil, Iraq.

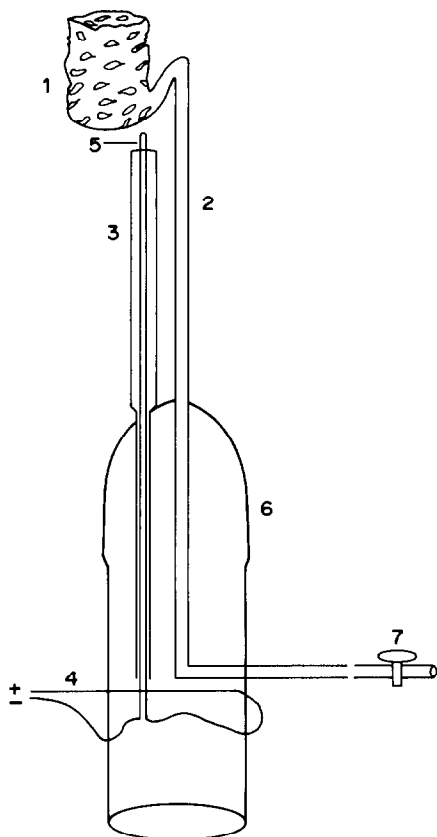


Fig. 1. The modified sample holder for use in combustion. 1, Sample cup; 2, O₂ - inlet; 3, tube protecting wire leads; 4, wire leads; 5, Pt-wire; 6, ground glass stopper of the flask; 7, tap.

further 1.5 g of sample can be burned if desired, and the procedure can be repeated, with the same absorbent, as many times as required to bring the concentration of any metal to a measurable level. Finally the solution is transferred quantitatively to a 100-ml standard flask and made up to the mark for analysis.

ASV determination. Pipette 50 ml of sample solution into the ASV cell. This solution should be about 0.1M in nitric acid and contain not more than 50 μg each of Cl, K and Ca, 1.5 μg each of As, Sb, Bi, Co and Ni, and 4.5 μg of Fe. Add solid sodium acetate carefully until the pH is 4 (pH-meter). Assemble the ASV cell with the three electrodes, and the nitrogen inlet. Pass nitrogen (freed from oxygen by passage through the alkaline pyrogallol solution) through the test solution for 5 min, then maintain a blanket of nitrogen over the solution surface throughout the analysis. Form the hanging mercury drop by turning the micrometer syringe three divisions. Start the stirrer at a suitable speed, keeping the drop steady in place. Deposit the metals at -1.2 V for 5 min. Stop the stirrer, and allow 30 sec rest time, during which the sensitivity, pen position *etc.* can be adjusted. Scan the potential in the positive direction in the differential mode at 10 mV/sec with a modulation amplitude of 25 mV. Measure the stripping current (*i*) for the sample before and after the addition of each of five successive 0.01-ml portions of a mixture containing 100 μg/ml zinc and copper and 10 μg/ml cadmium and lead. Pass nitrogen through the solution for 1 min after each addition. Plot the *i* values *vs.* the volume of standard mixture of the metal ions added.

*During the revision of this paper, the use of this method was independently reported by Wang *et al.*²⁷

RESULTS AND DISCUSSION

From Fig. 2 it seems in general that the best sensitivity is obtained at pH 3.6-4.2.

For selection of the supporting electrolyte, a criterion used in column chromatography,²⁶ but not previously employed* in the same manner in ASV, was chosen, namely the resolution (R_s) given by the formula

$$R_s = \frac{E_{p_2} - E_{p_1}}{0.5(W_1 + W_2)} = \frac{E_{p_2} - E_{p_1}}{0.85(b_{(1/2)_1} + b_{(1/2)_2})} \quad (1)$$

where E_{p_1} and E_{p_2} are the peak potentials of two adjacent peaks, for which W_1 and W_2 are the baseline widths and the $b_{(1/2)}$ values are the peak-widths at half-height (Fig. 3). For complete resolution, R_s should not be less than 1.5.

Table 1 shows the R_s values obtained with various supporting electrolytes, together with the E_p values, and Table 2 shows the values for other characteristics. The best overall values of R_s were obtained with potassium hydroxide or sodium acetate solutions as supporting electrolyte.

It is obvious from equation (1) that R_s can be improved by an increase in E_p or by narrowing of the peaks by changing from one supporting electrolyte to another.

The effect of the electrolytes on the sensitivity of measurement is indicated by the values of i_p (given in Table 2) for 10 ng/ml of each metal ion in the mixture.

The seven supporting electrolytes examined can be divided into two groups. Those in the first group (potassium hydroxide and sodium acetate) are suitable for all four metal ions, separately or in a mixture. Of the others, which form the second group, sodium citrate, and potassium hydroxide + sodium sulphate, or potassium nitrate or sodium tartrate all give high sensitivity for copper and zinc, but the first, second and third of these are not suitable for zinc because of the very broad peaks they give (large $b_{1/2}$ values). For the same reason sodium citrate is unsuitable for copper.

Another supporting electrolyte useful for zinc is the mixture of potassium hydroxide and sodium perchlorate, but it is not useful for copper, which gives two unresolved peaks and overlaps with the lead peak.

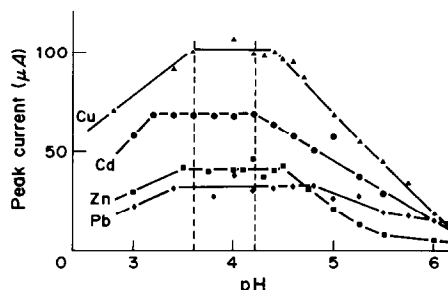


Fig. 2. Effect of pH on sensitivity.

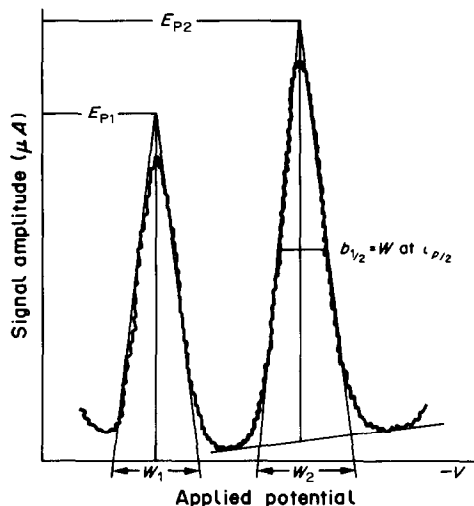


Fig. 3. Measurement of various parameters for two adjacent peaks.

Most of the supporting electrolytes gave low sensitivity for cadmium and poorer resolution of the lead and cadmium peaks, but gave satisfactory reproducibility.

The final factor in choosing the supporting electrolyte was the correlation coefficient of the calibration

graph, which proved best for the sodium acetate buffer, which was therefore the chosen supporting electrolyte.

The optimal instrument settings and other conditions were established as those given in the experimental section.

Interferences

Mutual interference of the four metals of interest was investigated by increasing the concentration of one of them to 500 $\mu\text{g/ml}$ and examining its effect on the determination of the other three at the 2- $\mu\text{g/ml}$ level. For copper and zinc as analytes the maximum error was not more than 10%. Lead was affected by all three of the other metals but the error reached 20% only at interferent levels > 500 $\mu\text{g/ml}$. Cadmium was similarly affected by copper and lead but not zinc.

In refined sugar, the concentrations of these metals, except for cadmium, are usually the same within an order of magnitude. Their concentrations may be up to two orders of magnitude greater than that of cadmium.

These findings suggest that for calibration and standard addition it would be best to use mixtures of all four ions. This was confirmed experimentally and it was found that good straight lines could be ob-

Table 1. Values of E_p and R_s for the supporting electrolytes used

No.	Electrolyte	E_p, V				R_s for pairs of peaks		
		Zn	Cd	Pb	Cu	Zn-Cd	Cd-Pb	Pb-Cu
1	Na acetate	-0.98	-0.575	-0.410	0.0	3.5	1.5	3.2
2	Na citrate	-1.01	-0.600	-0.455	-0.063	2.8	1.3	2.4
3	KOH	-0.98	-0.565	-0.375	+0.03	3.9	1.7	3.5
4	KOH + Na ₂ SO ₄	-1.01	-0.575	-0.395	+0.01	3.4	1.5	3.0
5	KOH + KNO ₃	-1.01	-0.565	-0.380	+0.03, -0.10	2.9	1.5	3.2
6	KOH + NaClO ₄	-1.06	-0.580	-0.465	+0.02	3.5	0.9	*
7	KOH + Na tartrate	-1.01	-0.590	-0.425	-0.03	3.2	1.4	3.0

*Overlap with the unresolved peaks for Cu.

Table 2. Effect of supporting electrolytes (numbered as in Table 1) on the selectivity and sensitivity of the ASV method

Metal ion		Electrolyte						
		1	2	3	4	5	6	7
Zn ²⁺	$b_{1/2}, mV$	60	86	60	93	93	58	65
	$i_p, \mu A$	28.3	12.0	29.3	64	29.4	35	37
	CV, %	0.1	0.6	1	1	2	1	10
Cd ²⁺	$b_{1/2}, mV$	55	58	55	60	60	60	55
	$i_p, \mu A$	10.6	10.8	12.3	5.8	6.8	9.8	7.7
	CV, %	0.1	0.7	0.7	4	1	4	6
Pb ²⁺	$b_{1/2}, mV$	55	58	55	63	60	58	55
	$i_p, \mu A$	7.2	11.2	13.7	11.1	9.6	6.6	14.3
	CV, %	0.3	0.6	0.6	1	5	5	0.6
Cu ²⁺	$b_{1/2}, mV$	65	95	60	68	60	*	70
	$i_p, \mu A$	19.5	28.8	25.3	40.8	30.8	*	43.8
	CV, %	0.2	1	0	0	4	*	0.8

*Two unresolved peaks.

Table 3. Interference effects (deviation for 2-ng/ml analyte concentration)

Groups		Analysis mode*	Zn	Cd	Pb	Cu	
1	Ca ²⁺ , Na ⁺ , K ⁺ , Cl ⁻	A	Error, %	1	6	1	2
			CV, %	1	7	3	2
2	Bi ³⁺ , Sb(III), As(III)	A	Error, %	6	13	11	>50†
			CV, %	8	9	7	8
		B	Error, %	2	5	4	9
			CV, %	5	7	6	8
3	Ni ²⁺ , Co ²⁺ , Fe ³⁺	A	Error, %	8	9	4	39
			CV, %	7	7	8	7
		B	Error, %	2	5	2	2
			CV, %	5	6	6	5

*A = calibration graph; B = standard-addition.

†A *t*-test ($(\bar{X} - \mu) = ts/\sqrt{N}$) showed that the difference ($\bar{X} - \mu$) is not significant at the 95% confidence level ($N = 2$) except at this value.

tained in both cases with $r = 0.92$ for zinc, 0.97 for cadmium, 0.99 for lead and 0.95 for copper.

For the purpose of this study, interferences from other ions likely to be found in refined sugar were considered in three groups and examined for group 1 ions at 1- $\mu\text{g/ml}$ level and for groups 2 and 3 ions at 30 ng/ml. The ions in the last two groups are usually expected to be present only at ultratrace level. Table 3 shows that the effect can be considerably reduced by using the standard-addition method instead of a calibration graph.

The recommended procedures have been applied to samples of refined white sugar, and Table 4 shows the results, together with those of a comparison of the modified oxygen-flask method with dry ashing³⁵ and wet digestion as a means of destruction of the organic matter. Direct analysis without destruction of the organic matter (Direct I) was also compared with the method of Cormier *et al.*,⁵ (Direct II).

The accuracy of the three decomposition methods was tested by determining the recovery of 250 μg of metal ion added to 1.5 g of sugar sample.

Since the method of determination was always the same, the difference in the reproducibility of the methods should be mainly due to the method of destruction. Paired-comparison by the *t*-test showed

that there was no significant difference between the performance of the three methods (95% confidence level).

However, the oxygen-flask method allowed use of smaller samples and was much faster. The recommended method can be performed with a 1.5-g sample in only 40–50 min, compared to a 50-g sample-size and up to about 24 hr analysis time for the other two methods.

The recovery showed good accuracy for zinc by all three methods. Lower accuracy, though still within experimental error, was obtained in only three cases, namely for cadmium by the oxygen-flask method, lead by wet digestion and copper by dry ashing.

Direct analysis of sugar solutions, *i.e.*, without destruction of the organic matter, gave low results by both the recommended procedure and the method of Cormier *et al.* Possible reasons are that in the direct method only the free metal ion is measured, and that the high sugar concentration might disturb the ASV to a considerable extent.

This problem, however, was not pursued. It is considered that destruction of the organic matter is necessary, and best achieved by the recommended procedure.

Extensive work with the recommended oxygen-

Table 4. Comparison of methods (\bar{X} = mean of five determinations CV = coefficient of variation multiplied by $\sqrt{2}$, R = recovery for 250 μg of added analyte)

Method		Zn	Cd	Pb	Cu
O ₂ -flask	\bar{X} , $\mu\text{g/g}$	0.88	0.0029	0.20	1.15
	CV, %	6	7	14	11
	R , %	100	90	100	99
Dry-ashing	\bar{X} , $\mu\text{g/g}$	0.81	0.002	0.21	0.78
	CV, %	13	14	6	10
	R , %	100	98	100	92
Wet digestion	\bar{X} , $\mu\text{g/g}$	1.01	0.0024	0.13	1.25
	CV, %	6	16	7	13
	R , %	101	97	91	100
Direct I	\bar{X} , $\mu\text{g/g}$	0.046	Nil	0.014	0.029
	CV, %	3	—	10	6
Direct II	\bar{X} , $\mu\text{g/g}$	0.039	Nil	0.01	0.02
	CV, %	6	—	7	9

flask method showed that use of more than 1.5 g of sample or ignition in air or with too slow a rate of oxygen flow resulted in imperfect burning, melting of the sugar and sometimes loss of sample by unburned sugar falling through the holes in the cup. Too fast a flow of oxygen, which would be needed for a larger sample size, caused over-vigorous burning and ejection of some of the sample; such conditions were thought to be unsafe for the flask, although no hazard was experienced during several trials. It is certainly much safer to repeat the whole procedure with two (or more) 1.5-g samples, but without changing the absorbent. Either a 5 or 10-litre flask can be used, but it is probably safer to use the larger size.

Acknowledgement—The authors wish to thank Dr R. A. Chalmers for assistance in revision of the paper.

REFERENCES

1. P. Pommez and M. A. Clarke, *Proc. 1972 Tech. Session Cane Sugar Refining Research*, 40.
2. W. Mauch and E. Farhoudi, *Sugar Technol. Rev.*, 1980, 7, 118.
3. ICUMSA, 15th Session 1970, p. 172, London.
4. ICUMSA, 16th Session, 1974, p. 224, Ankara.
5. R. Cormier, L. H. Mai and A. D'Antico, *Proc. 1976 Tech. Session Cane Sugar Refining Research*, p. 162.
6. P. Pommez and R. Corneir, *Proc. 1979 Tech. Session Cane Sugar Refining Research*, p. 123.
7. W. D. Ellis, *J. Chem. Educ.*, 1973, 50, 131A.
8. J. P. Franke, *Potential of ASV for the Toxicological Analysis of Heavy Metals*, Doctoral Dissertation, University of Groningen.
9. T. R. Copeland, J. H. Christie, R. A. Osteryoung and R. K. Skogerboe, *Anal. Chem.*, 1973, 45, 2171.
10. G. E. Batley and T. M. Florence, *J. Electroanal. Chem.*, 1974, 55, 23.
11. W. Z. Hempel, *Z. Angew. Chem.*, 1892, 13, 393.
12. A. M. G. Macdonald, *Analyst*, 1961, 86, 3.
13. *Idem*, in *Advances in Analytical Chemistry and Instrumentation*, C. N. Reilley (ed.), Vol. 4, p. 75. Wiley, New York, 1965.
14. A. M. Ure, *Anal. Chim. Acta*, 1975, 76, 1.
15. M. L. Dow, *J. Assoc. Off. Anal. Chem.* 1970, 53, 1040.
16. H. Mohadjerani and E. Hauser, *Fleischwirtschaft, Chem. Abstr.*, 1976, 56, 258; 1976, 84, 162983j.
17. W. H. Gutenmann and D. J. Lisk, *J. Agric. Food Chem.*, 1960, 8, 306.
18. W. H. Gutenmann, L. E. Saint John, D. L. Berry, E. D. Jones and D. J. Lisk, *ibid.*, 1961, 9, 50.
19. L. L. Farley and A. Winkler, *Anal. Chem.*, 1963, 35, 772.
20. T. Fukasawa and T. Yamane, *Anal. Chim. Acta*, 1980, 113, 123.
21. M. Oehme, *ibid.*, 1979, 107, 67.
22. I. M. Kolthoff and P. J. Elving, *Treatise on Analytical Chemistry*, 1st Ed., Part 1, Vol. 4, Chap. 50. Wiley, New York, 1967.
23. C. R. Parker, *Water Analysis by Atomic Absorption Spectroscopy*, Varian Techtron, 1972.
24. G. Tölg, *Talanta*, 1972, 19, 1489.
25. A. I. Vogel, *A Textbook of Quantitative Inorganic Analysis*, 3rd Ed., Longmans, London, 1961.
26. J. A. Dean, *Chemical Separation Methods*, Van Nostrand-Reinhold, New York, 1969.
27. J. Wang, D. B. Luo and B. Freiha, *Talanta*, 1986, 3, 397.
28. A. W. Mann and R. L. Deutscher, *Analyst*, 1976, 101, 652.
29. M. J. Pinchin and J. Newham, *Anal. Chim. Acta*, 1977, 90, 91.
30. E. A. Schonberger and W. F. Pickering, *Talanta*, 1980, 27, 11.
31. T. M. Florence and G. E. Batley, *J. Electroanal. Chem.*, 1977, 75, 791.
32. H. N. Heckner, *Z. Anal. Chem.*, 1978, 293, 110.
33. J. Gardiner and M. J. Stiff, *Water Research*, 1975, 9, 517.
34. I. Vartires, M. Borda, N. Bonciocat and N., Totir, *Rev. Chim. (Bucharest)*, 1979, 30, 791.
35. H. Jönsson, *Z. Lebensm. Unters. Forsch.*, 1976, 160, 1.
36. K. Tomobe and T. Nagasaka, *Seitol Gijutsu Kenkyu Kaishi*, 1978, 28, 1; *Chem. Abstr.*, 1979, 91, 41141.

DETERMINATION OF MERCURY BY DIFFERENTIAL-PULSE ANODIC-STRIPPING VOLTAMMETRY WITH VARIOUS WORKING ELECTRODES

APPLICATION TO THE ANALYSIS OF NATURAL WATER SEDIMENTS

MIROSLAV HÁTLE*

Department of Analytical Chemistry, Charles University, Albertov 2030, 128 40 Prague 2, Czechoslovakia

(Received 15 April 1987. Accepted 27 June 1987)

Summary—Four types of working electrode (glassy-carbon and gold rotating-disk electrodes and two types of gold-film electrode) have been used in determination of traces of mercury by differential-pulse anodic-stripping voltammetry, and the analytical parameters of the procedures compared. The technique has been applied to the analysis of river sediments. The lowest limit of detection (0.02 µg/l.) was obtained with the gold rotating-disk electrode. Two procedures have been found optimal for analyses of sediment samples; determination with the gold rotating-disk electrode and solution-exchange after the pre-electrolysis, and determination with the gold-film electrode prepared *in situ* in the sample extract. The sample pretreatment involved a separation of the 0.45–63 µm fraction, mineralization with a mixture of hydrochloric and nitric acids (3:1 or 1:3) under atmospheric pressure in a fused silica vessel, followed by irradiation with ultraviolet light, after addition of hydrogen peroxide (to destroy organic matter). The most serious interference is from iron; this can be prevented by adding fluoride or pyrophosphate. The procedure is an alternative to the AAS determination of the total mercury content in sediments, especially with heavily polluted samples (mercury concentrations up to 0.01%).

Electrochemical stripping analysis has been used for the determination of mercury much less often than for that of cadmium, lead and some other heavy metals, for which differential-pulse anodic-stripping voltammetry (DPASV) with a hanging mercury drop electrode (HMDE) or a mercury film electrode (MFE) has been used routinely for a great variety of natural samples.^{1,2} The main reason for this is that mercury can be determined easily and with good sensitivity by flameless AAS methods (the cold vapour method and various procedures utilizing amalgamation preconcentration of mercury), and there are the well-known difficulties when solid electrodes are used for electrochemical determinations of mercury.

Glassy-carbon electrodes have been mainly used in recent determinations of mercury in water³⁻⁵ and in air;⁶ gold electrodes have been applied to the analysis of waters,⁷⁻⁹ urine,¹⁰ fish^{11,12} and the atmosphere.¹³

Among the important locations where mercury is accumulated and which may serve as indicators of general mercury pollution, are the bottom sediments in natural aquatic ecosystems.¹⁴ Flameless AAS has

so far been most often used for the determination of mercury in river and reservoir sediments,^{15,16} but electrochemical stripping analysis may be a useful alternative, especially with strongly industrially polluted sediments with higher mercury concentrations, where the somewhat higher limit of detection of the electrochemical method is unimportant.

Sediments are materials with a very wide range of compositions and the extracts obtained after sample decomposition by concentrated acids may contain large concentrations of elements interfering in the DPASV determination of mercury. The most serious interference can be expected from iron, which is commonly present in sediments at concentrations several orders of magnitude higher than those of other metals. The average natural concentration of iron in the pelitic fraction of sediments corresponds roughly to the level in the geochemical shale standard,¹⁷ *i.e.*, 4.7%. For this reason, the present paper deals in some detail with interferences by iron and some other elements in the DPASV determination of mercury.

EXPERIMENTAL

Instruments

The DPASV measurements were made with a three-electrode circuit, the instrument used being a PA-4 polarographic analyser permitting partial automation of electro-

*Present address: City of Prague Planning Board, Environmental Studio (AŽP ÚHA), Hradčanské nám. 8, 118 54 Prague 1, Czechoslovakia.

chemical stripping measurements, with an XY 4105 plotter and a rotating-disk electrode (RDE) (Laboratorní Přístroje, Czechoslovakia). The working electrodes were a gold rotating-disk electrode (AuRDE), prepared by pressing a gold rod into a PTFE mantle,¹⁸ and a glassy-carbon rotating-disk electrode (GC-RDE), obtained from Laboratorní Přístroje, which was used directly or served as the support for preparation of a gold-film electrode (AuFE). The active surface area of each electrode was 7.3 mm². A saturated silver-silver chloride electrode was used as the reference electrode and was connected with the test solution by a bridge filled with the base electrolyte, which was exchanged before each measurement. All the potentials in this work are referred to this electrode. A platinum wire served as the counter-electrode. The electrolysis vessels were made of fused silica and had volumes ranging from 20 to 50 ml. The optimal instrumental parameters were found experimentally: potential scan-rate, 10 mV/sec; pulse amplitude and frequency, +50 mV and 0.2 sec, respectively; RC time constant, 100 msec; electrode rotation rate, 1500 rpm; pre-electrolysis time, $t_D = 40-480$ sec; rest period before the stripping step, 10 sec. These parameters were used for all the measurements, unless stated otherwise. When the GC-RDE and the gold electrodes were used at low mercury concentrations, the test solutions were deaerated by passage of nitrogen that had been freed from traces of oxygen by bubbling through an acidic solution of a chromium(II) salt and then an alkaline solution of sodium anthraquinone-2-sulphonate; the absorption solutions were continuously regenerated by amalgamated granular zinc. Traces of mercury vapour present in the nitrogen from the oxygen scrubber were absorbed by bubbling the gas through a concentrated solution of potassium permanganate in sulphuric acid. The measurements were made at laboratory temperature and all the solutions were allowed to attain this temperature prior to measurement.

Chemicals

A stock 1 mg/ml solution of mercuric ions was prepared by dissolving 1 g of purified mercury in several ml of nitric acid, boiling off oxides of nitrogen, and diluting to 1 litre with redistilled water. The solution concentration was periodically checked by complexometric titration. Solutions of lower concentration were prepared immediately before measurement by diluting the stock solution with redistilled water. A stock 1 mg/ml solution of gold(III) was prepared¹⁹ by dissolving 100 mg of pure gold (Safina, Czechoslovakia) in a small amount of *aqua regia*, evaporating to dryness, dissolving the residue in 5 ml of concentrated hydrochloric acid and diluting with redistilled water to 100 ml. Solutions of the other metals (Cu, Cd, Pb, As, Zn, Ni, Co, Bi, Se, Mn, Fe, Cr) and of the masking agent ions (F^- , $P_2O_4^{2-}$) were prepared at 1 mg/ml concentration from *p.a.* salts (Lachema, Czechoslovakia).

Dilute solutions of mineral acids (perchloric, nitric, hydrochloric) in the range 0.1–1M and their mixtures were used as the base electrolytes for DPASV, since the sediment decomposition procedures used *aqua regia* or the Lefort mixture (hydrochloric acid–nitric acid, 1:3 v/v) and subsequent dilution by factors of 50 and 100. A 0.1M potassium thiocyanate solution was also used as the base electrolyte in measurements with the GC-RDE. The solutions for the base electrolytes and for the sample mineralization were prepared from semiconductor grade hydrochloric or nitric acid, or *p.a.* chemicals (Lachema, Czechoslovakia). For measurements close to the limit of determination, the base electrolytes were freed from traces of mercury by passage through a thin layer of a selective sorbent based on a 2,3-epithiopropylmethacrylate (ETPMA) and ethylenedimethacrylate (EDMA) copolymer, prepared at the Department of Polymers, Institute of Chemical Technology, Prague.²⁰ The water used was distilled twice in fused silica apparatus.

Electrode preparation and activation

Before use, the GC-RDE and the AuRDE were rubbed down with wet metallographic papers Carbimet Nos. 320 and 400 (Buehler Ltd., USA) and then polished with an aqueous suspension of alumina (VEB Chemiewerk, GDR, grades 1 and 3) and finally on "Microcloth" (Buehler, Ltd., USA). The electrodes were rinsed with redistilled water and activated by cyclic polarization in 0.1M perchloric acid (ten cycles from –0.5 to +0.5 V for the GC-RDE and twenty cycles from –0.2 to +1.8 V for the AuRDE; the latter electrode was always maintained for 10 sec at –0.2 V and for 30 sec at +1.8 V). The AuRDE was then cyclically polarized from –0.2 V to +1.8 V with a potential scan-rate of 200 mV/sec, until the voltamperograms were reproducible. The electrodes were stored dry and the activation procedure above was always repeated after their prolonged storage. The gold-film electrodes (AuFE) were prepared by depositing gold on the GC-RDE while it was rotating, either before the determination, in which case 0.1M hydrochloric or perchloric acid containing Au(III) was used, or *in situ*, during the determination, by adding Au(III) to the test solution, analogously to the preparation of an MFE.²¹ In the first method, the electrolysis current was integrated and the amount of the gold deposited was calculated. The cleaning and activation procedures applied between individual determinations will be discussed later together with the measurement reproducibility.

Sampling of sediments and sample pretreatment

Representative (mixed) samples were taken from the upper layers (0–5 cm) of river sediments with a plastic core-sampler²² 50 mm in diameter. The samples were transferred to 1-litre polyethylene bottles and treated immediately. The wet samples were sieved on two nylon sieves in two steps and the fraction with particle size below 63 μ m was separated, as is most often recommended for the determination of heavy metals.¹⁴ The lower size limit was 0.45 μ m, determined by the pore size of the membrane filter used for the removal of water from the sample by pressure filtration (Sartorius SM 16510 apparatus, FRG). The samples were then dried at laboratory temperature and stored in glass bottles fitted with ground-glass stoppers. Samples of 0.1–0.2 g of the dry sediment were mineralized in 5 ml of *aqua regia* or the Lefort mixture in sealed silica ampoules, by heating with an infrared lamp to a maximum of 60° for 60 min. This procedure has given better results than the decomposition at 110° in a PTFE autoclave with a steel mantle. The autoclave decomposition led to more complete destruction of organic matter, but caused very high blank values (up to several μ g/l.), apparently arising from adsorption of mercury on the PTFE, either from the atmosphere or from previous experiments. Liberation of the adsorbed mercury during the decomposition procedure was not suppressed by prolonged leaching of the Teflon vessel with concentrated acids.

After the decomposition step the extract was allowed to cool and was diluted to 50 ml with redistilled water. The remaining organic matter, which would interfere in the DPASV determination (causing depression of peak height, an increase in the residual current and electrode passivation), was removed by oxidative photolysis, which is often used in sample treatment prior to electrochemical stripping determination.²³ To do this, the extract was diluted by a factor of 5 or 10 and a 50-ml portion plus 200 μ l of 30% hydrogen peroxide solution was sealed in a silica ampoule, which was then exposed to ultraviolet radiation from a low-pressure lamp (RVK 400 W, Tesla, Czechoslovakia), while being cooled with air so that the solution temperature did not exceed 60°. An irradiation time of 2 hr was sufficient. Decompositions with the Lefort mixture yielded extracts with lower residual organic matter levels and thus an irradiation time of 1.0–1.5 hr was sufficient.

RESULTS AND DISCUSSION

The DPASV determination of mercury was studied on all four types of working electrode. With the GC-RDE, the highest sensitivity was obtained with 0.1M potassium thiocyanate as supporting electrolyte, which is in agreement with the literature.²⁴⁻²⁶ The stripping peak ($E_p = +0.04$ V) is well developed and about twice as high as that obtained in a non-complexing medium (e.g., with perchloric acid).²⁷ In chloride solutions the sensitivity is decreased, apparently owing to the formation of mercurous chloride, which passivates the electrode.²⁶ In the determination of mercury on a GC-RDE, an increase in the sensitivity has often been observed^{28,29} in the presence of other metals, especially when mercury is co-deposited with copper or cadmium. We have found that the maximum sensitivity is attained with a five-fold ratio of cupric ions to mercury or a ten-fold ratio of cadmium ions. Higher ratios of copper lead to a decrease in the sensitivity, whereas higher ratios of cadmium are without further effect. The optimal pre-electrolysis potential is -1.0 V.

In determinations with the AuRDE, the best results were obtained by using 0.1M perchloric acid containing a small amount of hydrochloric acid. This electrolyte has been recommended for the stripping step after solution-exchange, in determinations of mercury in media with high chloride contents, e.g., sea-water⁸ or mineralized biological samples,¹² with gold electrodes. Analogous conditions are encountered in analyses of sediment extracts after decomposition with hydrochloric acid. Solutions with high concentrations of chloride irreversibly damage the electrode surface at positive potentials, owing to dissolution of gold.³⁰ However, the addition of a small amount of hydrochloric acid to the perchloric acid is necessary, as the mercury stripping peak is then shifted to more negative potentials where the residual current is lower and the peak distortion smaller. It has been verified experimentally that the optimal hydrochloric acid concentration is 3mM, which ensures a sufficient shift of the peak ($E_p = +0.68$ V) without damaging the AuRDE, even at the very positive potentials ($+1.8$ V) at which the AuRDE is cleaned and activated. The optimal pre-electrolysis potential is $+0.2$ V. The solution-exchange after pre-electrolysis was done manually.

At the end of the pre-electrolysis time t_D (and the rest period) the electrode system was switched off and the potential scan-rate set to zero. The reference electrode and the counter-electrode were rinsed with distilled water and the outside Teflon body of the AuRDE (not the active surface!) was wiped carefully with a piece of tissue paper. The sample solution was then replaced by a similar volume of pure base electrolyte. The electrode system was then switched on again and the stripping stage executed under normal conditions (scanned at 10 mV/sec). The whole procedure took 30 sec and was always done under the

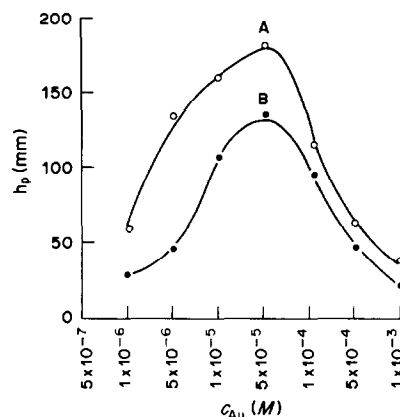


Fig. 1. Dependence of the mercury stripping peak height on the concentration of Au(III) in 0.1M HCl, for the preformed AuFE. $E_{D(Au)} = -0.5$ V, $t_{D(Au)} = 240$ (A) and 480 (B) sec, RDE rotation rate 1500 rpm. DPASV of mercury in 0.1M HClO₄, $E_{D(Hg)} = 0.0$ V, $t_{D(Hg)} = 360$ (A) and 120 (B) sec, $c_{Hg} = 10$ μ g/l. (A) and 50 μ g/l. (B). Sensitivity, 10 nA/mm; experimental points are the averages of three determinations.

same conditions. The AuRDE was reactivated in the exchange-solution.

With the AuFE prepared prior to the determination, factors affecting the sensitivity of measurement were studied, primarily the thickness of the gold film, which depends, for a given rotation speed and temperature on the Au(III) concentration in the solution, and the time and potential of the deposition. Figure 1 gives the dependence of the mercury stripping peak height on the Au(III) concentration; the optimal concentration is $c_{Au} = 5 \times 10^{-5}$ M. The effect of the electrolysis time and potential at this Au(III) concentration is depicted in Fig. 2; the optimal values are $t_{D(Au)} = 240$ sec and $E_{D(Au)} = -0.5$ V, with a rotation rate of 1500 rpm. For determining the lowest mercury concentrations, close to the limit of determination, the sensitivity is highest when gold films only a few monolayers thick are used ($c_{Au} = 5 \times$

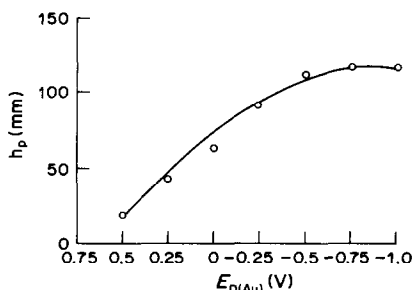


Fig. 2. Dependence of the mercury stripping peak height on the electro-deposition potential of gold ($E_{D(Au)}$) for the preformed AuFE. $c_{Au(III)} = 5 \times 10^{-5}$ M in 0.1M HCl, $t_{D(Au)} = 240$ sec, RDE rotation rate 1500 rpm. For the conditions of DPASV of mercury see Fig. 1; $t_{D(Hg)} = 240$ sec; $c_{Hg} = 10$ μ g/l.; experimental points are the averages of three determinations.

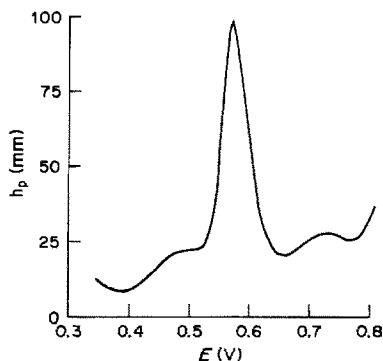


Fig. 3. A typical stripping curve for mercury on the pre-formed AuFE. For details of the electrode preparation see Fig. 2; $E_{D(Au)} = -0.5$ V. The DPASV determination in $0.1M$ $HClO_4/3mM$ HCl , $c_{Hg} = 30 \mu g/l$, $t_{D(Hg)} = 120$ sec, $E_{D(Hg)} = 0.0$ V. Sensitivity 10 nA/mm.

$10^{-6}M$). If the mercury concentration amounts to several tens of $\mu g/l$, it is more suitable to use a thicker gold film corresponding to several tens of monolayers ($c_{Au} = 5 \times 10^{-4}M$ or $10^{-4}M$), which is mechanically more stable. Figure 3 shows a typical recording for the determination of mercury under these conditions; in $0.1M$ perchloric acid/ $3mM$ hydrochloric acid the E_p value is $+0.58$ V. If the chloride concentration is higher the solution must be exchanged after the pre-electrolysis, as in measurement with the AuRDE.

The conditions for the preparation of the AuFE *in situ* are identical with those above. The optimal concentration of Au(III) in the test solution is $5 \times 10^{-5}M$, with $E_D = -0.5$ V. At gold concentrations above $1 \times 10^{-4}M$ the mercury stripping peak splits. Compared with the AuFE prepared prior to analysis, the electrode prepared *in situ* gives a somewhat poorer sensitivity, apparently owing to a stronger interaction between gold and mercury during their co-deposition on the GC-RDE surface and a lower efficiency of the stripping of the mercury from the bulk of the gold film. The AuFE prepared *in situ* is also more strongly affected by interferences (iron and residual organic matter) than the other gold electrodes. On the other hand, the procedure is less time-consuming and there is no danger of damage to the gold film during manipulation, or problems with aging and passivation of the film, which is formed anew during each determination.

Cleaning and reactivation procedures between individual determinations are necessary for the attainment of reproducible results. Decrease in the sensitivity, and gradual passivation of the electrode surface, during repeated determinations without reactivation are especially pronounced with the AuRDE (Fig. 4). The reactivation procedures and the relative standard deviation estimates are listed in Table 1 for the electrodes studied.

The calibration plot parameters in the region of the lowest mercury concentrations and the limits of

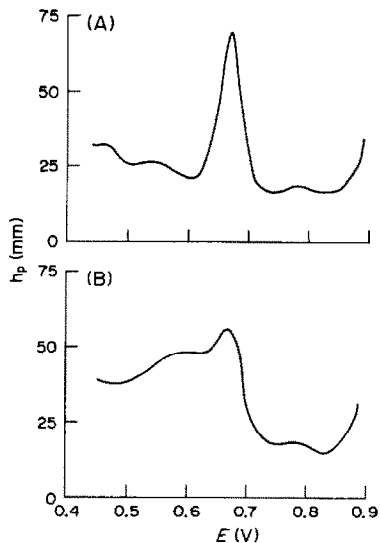


Fig. 4. The decrease in the sensitivity of the AuRDE over ten DPASV cycles without reactivation of the electrode. For conditions see Fig. 3; $c_{Hg} = 10 \mu g/l$, $E_{D(Hg)} = +0.2$ V. A—1st DPASV cycle after activation for 60 sec at $+1.8$ V in the base electrolyte; B—10th cycle. Sensitivity 10 nA/mm.

determination are given in Table 2. The limits of determination were calculated from the calibration slopes.³¹ The plots are linear up to approximately 200, 40, 80 and $100 \mu g/l$ for the GC-RDE, AuRDE,

Table 1. Reactivation procedures and the reproducibility of DPASV of mercury

Electrode	Procedure	$s_{rel}(\%)$
GC-RDE	A	15.1
GC-RDE	B	13.6
GC-RDE	C	9.9
GC-RDE	D	3.5
AuFE (preformed)	A	17.2
AuFE (preformed)	E	3.3
AuFE (<i>in situ</i>)	F	4.2
AuFE (<i>in situ</i>)	G	2.7
AuRDE	A	23.1
AuRDE	H	3.5

Conditions: 10 measurements; GC-RDE— $0.1M$ $KSCN$, pH 2, $+200 \mu g/l$ $Cu(II)$, $c_{Hg} = 40 \mu g/l$; AuRDE, AuFE— $0.1M$ $HClO_4/3mM$ HCl , $c_{Hg} = 10 \mu g/l$.

Pretreatment and reactivation: A—repeated measurements with no treatment; B—60 sec repolishing with damp filter paper (Filtrak 390) and 30 sec polarization at $+0.5$ V; C—polarization for 30 sec at $+0.5$ V without mechanical treatment; D—60 sec repolishing with Al_2O_3 suspension and 30 sec polarization at $+0.5$ V; E—60 sec polarization at $+0.8$ V in $0.1M$ $HClO_4$ without mechanical treatment; F—removal of the Au film (mechanical), followed by 60 sec repolishing of GC-RDE with Al_2O_3 suspension and 60 sec polarization at $+1.2$ V; G—dissolution of the Au film, followed by 60 sec polarization at $+1.2$ V without mechanical treatment; H—60 sec polarization at $+1.8$ V without mechanical treatment. If not stated otherwise, the polarization reactivation was done in the test solution.

Table 2. Parameters of the calibration plots ($I = a.c_{Hg} + b$) in the DPASV determination of mercury

Electrode	Number of measurements, n	$a \pm s_a$, $nA \cdot l. \mu g^{-1}$	$b \pm s_b$, nA	Corr. coeff., r	Limit of detn., $\mu g/l.$
GC-RDE (A)	7	18.3 ± 1.3	-80 ± 47	0.9877	13.9
GC-RDE (B)	7	15.9 ± 0.3	-15 ± 8	0.9988	3.2
AuRDE	9	1034 ± 21	79 ± 5	0.9988	0.02
AuFE (preformed)	9	138.5 ± 1.7	83 ± 8	0.9995	0.3
AuFE (<i>in situ</i>)	9	95.6 ± 1.3	44 ± 31	0.9993	1.8

Conditions: GC-RDE—0.1M KSCN, pH 2 (A); 0.1M KSCN, pH 2 + 100 $\mu g/l.$ Cu(II) (B); $E_D = -1.0$ V, $t_D = 360$ sec, $c_{Hg} = 0-60$ $\mu g/l.$, reactivation for 30 sec at +0.5 V after repolishing. AuRDE—0.1M HClO₄/3mM HCl; $E_D = +0.2$ V, $t_D = 480$ sec, $c_{Hg} = 0.0-0.4$ $\mu g/l.$, reactivation for 60 sec at +1.8 V. Preformed AuFE—film preparation: 0.1M HCl, $c_{Au} = 5 \times 10^{-5}M$, $E_{D(Au)} = -0.5$ V, $t_{D(Au)} = 240$ sec, 1500 rpm; determination: 0.1M HClO₄/3mM HCl, $E_{D(Hg)} = 0.0$ V, $t_{D(Hg)} = 360$ sec, $c_{Hg} = 0-8$ $\mu g/l.$, reactivation for 60 sec at +0.8 V in 0.1M HClO₄. AuFE *in situ*—0.1M HClO₄/3mM HCl, $c_{Au} = 5 \times 10^{-5}M$, $E_D = -0.5$ V, $t_D = 480$ sec, $c_{Hg} = 5-40$ $\mu g/l.$, reactivation for 60 sec at +1.2 V.

preformed AuFE and AuFE prepared *in situ*, respectively.

Interference removal and determination in sediment samples

On the basis of the experiments above, two electrodes were selected for practical application: the AuRDE, because of the low limit of determination, and the AuFDE prepared *in situ*, for higher mercury concentrations, because of the simple procedure without the solution-exchange which is necessary with the AuRDE. Both electrodes yielded good reproducibility, provided they were properly reactivated. A summary of interferences is presented in Table 3.

Considering the values in Table 3 and the concentrations of these elements common in sediments, there is no danger of interference from most of the elements examined. An exception is iron, which commonly occurs at the 1-100 mg/l. level in the sediment extracts. Under the given conditions, iron is reduced on the gold electrode and the E_p value for the DPV peak is +0.54 V, so this peak strongly interferes with the mercury stripping peak. This effect is strongest with the AuFE prepared *in situ*, in media with high chloride concentration, which cause the mercury peak to shift towards more negative potentials. These effects have been verified with solutions simulating the composition of sediment extracts and with real samples. The interference can be suppressed by ex-

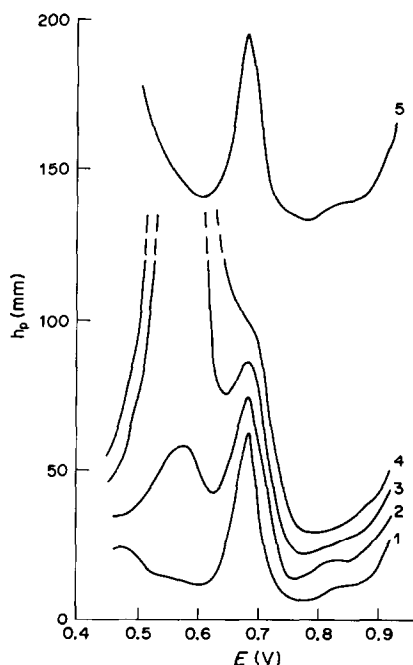


Fig. 5. Interference of iron in DPASV of mercury on the AuRDE and suppression of the interference by addition of fluoride. For conditions see Fig. 4; reactivation of the AuRDE for 60 sec at +1.8 V; 1—without iron, 2,3,4—1, 5, 10 mg/l. Fe(III), respectively, 5—10 mg/l. Fe(III)/500 mg/l. F⁻. Sensitivity 10 nA/mm.

Table 3. Maximum permissible concentrations of the interfering metals in the DPASV determination of mercury*

Element	$c_{max}, mg/l.$	
	AuRDE	AuFE <i>in situ</i>
Cd(II), Pb(II), Zn(II), Co(II), Ni(II), Mn(II)	100	50
Cu(II)	10	3
As(III), Bi(III), Cr(III)	1	0.5
Ag(I), Se(IV)	0.5	0.2
Fe(III)	0.5	0.1

*0.1M HClO₄/3mM HCl, $c_{Hg} = 10$ $\mu g/l.$

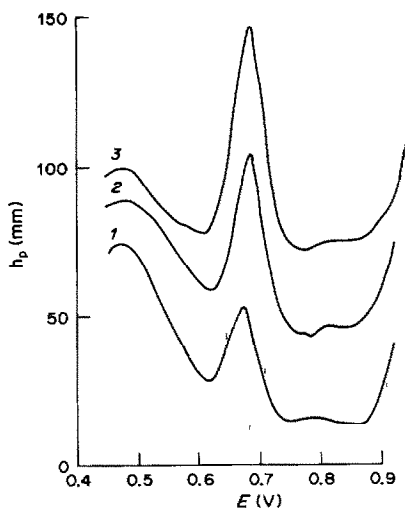


Fig. 6. Determination of mercury in a sediment extract by DPASV on the AuRDE with medium-exchange. Test solution: *aqua regia* diluted 50-fold, ultraviolet-irradiated for 2 hr; $t_D = 120$ sec, $E_D = +0.2$ V. Exchange for 0.1M $\text{HClO}_4/3\text{mM HCl} + 100$ mg/l. fluoride after the pre-electrolysis. Electrode reactivation for 60 sec at $+1.8$ V. Sensitivity 5 nA/mm. 1—Sample, 2—1st standard addition (5 $\mu\text{g/l.}$), 3—2nd standard addition (10 $\mu\text{g/l.}$).

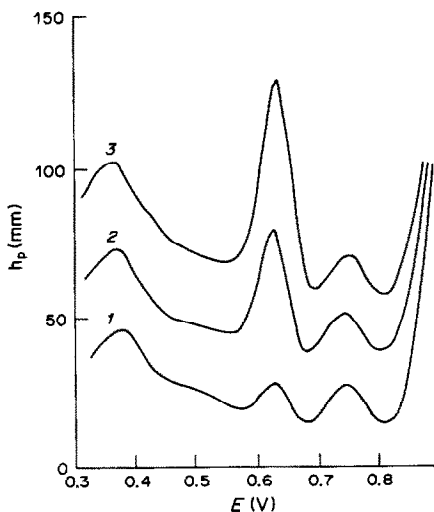


Fig. 7. Determination of mercury in a sediment extract by DPASV on the AuFE formed *in situ*. Test solution: Lefort mixture diluted 50-fold + 500 mg/l. F^- , ultraviolet-irradiated for 2 hr; $t_D = 480$ sec, $E_D = -0.5$ V, $c_{\text{Au}} = 5 \times 10^{-3}$ M. Electrode reactivation for 60 sec at $+1.2$ V. Sensitivity, 25 nA/mm. 1—Sample, 2—1st standard addition (10 $\mu\text{g/l.}$), 3—2nd standard addition (20 $\mu\text{g/l.}$).

changing the solution for a pure base electrolyte after the pre-electrolysis, or by masking the iron; for the latter purpose, addition of pyrophosphate or fluoride yielded the best results (Fig. 5). For typical iron concentrations in the extracts, the optimal concentrations are 100 mg/l. pyrophosphate and 500 mg/l.

Table 4. Recovery test for the samples decomposed in Lefort mixture, followed by the DPASV determination of mercury with the AuRDE

Taken, $\mu\text{g/g}$	Found, $\mu\text{g/g}^*$	Recovery, %
0 (blank)	4.8	—
5	10.4	112
10	15.3	105

*The values are the averages of three determinations.

fluoride. In determinations with the AuRDE with solution-exchange, the residues of iron can be masked by addition of these reagents at concentrations about a fifth of these just quoted.

Typical recordings for the determination of mercury in a sediment extract are given in Fig. 6 for the AuRDE and solution-exchange and in Fig. 7 for the AuFE prepared *in situ*, without solution-exchange. The mercury was determined by double standard-addition. The accuracy of the procedure was tested by recovery tests from spiked dilute *aqua regia* (1:10). For $c_{\text{Hg}} = 10 \mu\text{g/l.}$, the mean relative error of six determinations was -4.8% ($s_r = 7.3\%$) for the AuRDE and -7.4% ($s_r = 11.4\%$) for the AuFE prepared *in situ*. For $c_{\text{Hg}} = 1 \mu\text{g/l.}$, the corresponding values were -9.5% ($s_r = 12.9\%$) with the AuRDE.

The whole procedure for the mercury determination was verified by the recovery test for which the results are given in Table 4. A standard mercury solution was added by micropipette, prior to decomposition, to the silica mineralization vessel containing a 0.2-g sample of sediment. The recovery of the mercury added was found from the difference between the value found and a value corresponding to the mercury originally present in the sediment.

REFERENCES

- H. W. Nürnberg, *Pure Appl. Chem.*, 1982, **54**, 853.
- Idem*, *Sci. Total Environ.*, 1984, **37**, 9.
- K. Kritsotakis, N. Laskowski and H. J. Tobschall, *Intern. J. Environ. Anal. Chem.* 1979, **6**, 203.
- K. Kritsotakis, P. Rubischung and H. J. Tobschall, *Z. Anal. Chem.*, 1979, **296**, 358.
- S. Jaya, T. P. Rao and G. P. Rao, *Analyst*, 1985, **110**, 1361.
- M. Taddia, *Microchem. J.*, 1978, **23**, 64.
- L. Sipos, J. Golimowski, P. Valenta and H. W. Nürnberg, *Z. Anal. Chem.*, 1979, **298**, 1.
- L. Sipos, H. W. Nürnberg, P. Valenta and M. Branica, *Anal. Chim. Acta*, 1980, **115**, 25.
- I. Gustavsson, *J. Electroanal. Chem.*, 1986, **214**, 31.
- M. Leu and H. Seiler, *Z. Anal. Chem.*, 1985, **321**, 479.
- J. Golimowski and I. Gustavsson, *Sci. Total Environ.*, 1983, **31**, 89.
- R. Ahmed, P. Valenta and H. W. Nürnberg, *Mikrochim. Acta*, 1981 **I**, 171.
- H. Braun, M. Metzger and H. Vogg, *Z. Anal. Chem.*, 1984, **317**, 304.
- W. Salomons and U. Förstner, *Metals in the Hydro-cycle*, Springer Verlag, Berlin, 1984.
- R. Breder, *Z. Anal. Chem.*, 1982, **313**, 395.
- F. Maruta, S. Watanabe, N. Inomata and H. Mukai, *Niigata Rikagaku*, 1983, **9**, 37; *Chem. Abstr.*, 1984, **100**, 126602z.

17. K. K. Turekian and K. H. Wedepohl, *Bull. Geol. Soc. Am.*, 1961, **72**, 175.
18. P. Beran and F. Opekar, *Chem. Listy*, 1974, **68**, 305.
19. J. Lexa and K. Štulík, *Talanta*, 1983, **30**, 845.
20. V. Maroušek, P. Novák, M. Hejtmánek, V. Dvořák, L. Salát and J. Kálal, *4th Meeting of Czech. Chemists*, High Tatras, 20–25 October, 1985, Paper No. 5 V 43.
21. T. M. Florence, *J. Electroanal. Chem.*, 1970, **27**, 273.
22. L. Håkanson and L. Jansson, *Principles of Lake Sedimentology*, p. 32. Springer Verlag, Berlin, 1983.
23. W. Dorten, P. Valenta and H. W. Nürnberg, *Z. Anal. Chem.*, 1984, **317**, 264.
24. M. Štulíková and F. Vydra, *J. Electroanal. Chem.*, 1973, **42**, 127.
25. K. Štulík and M. Štulíková, *Anal. Lett.*, 1973, **6**, 441.
26. R. Bilewicz, Z. Stojek and Z. Kublik, *J. Electroanal. Chem.*, 1979, **96**, 29.
27. P. Kiekens, M. Mertens, C. Laire and E. Temmerman, *Analyst*, 1983, **108**, 1082.
28. L. Luong and F. Vydra, *J. Electroanal. Chem.*, 1974, **50**, 379.
29. R. Bilewicz and Z. Kublik, *Anal. Chim. Acta*, 1983, **152**, 203.
30. J. N. Gaur and G. M. Schmid, *J. Electroanal. Chem.*, 1970, **24**, 279.
31. R. K. Skogerboe and L. C. Grant, *Spectrosc. Lett.*, 1970, **3**, 215.

END EFFECTS IN FLOW-ANALYSIS AND PROCESS SYSTEMS

SPAS D. KOLEV and ERNŐ PUNGOR

Institute of General and Analytical Chemistry, Technical University of Budapest, Gellért tér 4,
 H-1502 Budapest XI, Hungary

(Received 15 December 1986. Accepted 27 June 1987)

Summary—The “end effects” in flow-analysis and process systems are investigated theoretically on the basis of the axially-dispersed plug-flow model. Three-section systems consisting of reactor, fore- or after-section and additional section are used. In the additional section back-mix flow is assumed to exist. The corresponding Peclet number has been found to be 0.01. The difference between the system responses to a delta-function input signal for finite and infinite length of the fore- or after-section is studied. Both the statistical moments of the system responses and the actual response curves are used for that purpose. The results can be used to evaluate the length of the fore- and after-sections needed in real flow-analysis and process systems in order that the phenomena taking place downstream or upstream of these two sections, respectively, will not play an important role in the system response.

The hydrodynamic modelling of flow analysis and process systems is based on the fact that the performance of the whole physical system is mainly governed by certain sections of it. For that reason only these are included in the physical model and corresponding mathematical model. Quite often, however, various processes that occur in those sections but are not included in the model may considerably affect the performance of the system, *e.g.*, the shape and magnitude of the response in stimulus-response experiments.¹ The deviation of the real behaviour of the system from that predicted by the model constitutes the so-called “end effect”. Obviously the development of an adequate mathematical model of a flow-analysis or process system is closely related to identification of the conditions under which the end effects can be neglected.

The systems considered in this investigation are usually composed of tubular elements so it is very convenient to describe the flow pattern by the axially-dispersed plug-flow model:¹

$$\partial c / \partial t = D_L \partial^2 c / \partial x^2 - u \partial c / \partial x \quad (1)$$

(the symbols are defined in Table 1). In this case the problem is reduced to investigation of the requirements for assuming that the fore- and the after-sections of the system (Fig. 1a) which are included in the model have infinite lengths.

THEORETICAL CONSIDERATIONS

The model system will be regarded as consisting of three main sections, analogously to the one considered earlier,² as shown in Fig. 1a. The fore-section or after-section are regarded as having “infinite”

length and being part of the reactor and there is an additional section which represents those parts of the real system which are not included in the mathematical model. The end effects produced by the dispersion processes in the additional section will be considered separately according to whether they occur downstream of the after-section (Fig. 1b) or upstream of the fore-section (Fig. 1c). In both cases a delta-function input is assumed for simplicity.

When the end effects originating downstream of the after-section are investigated it is convenient to place both the injection and the detection points in the reactor (Fig. 1b). The mathematical description

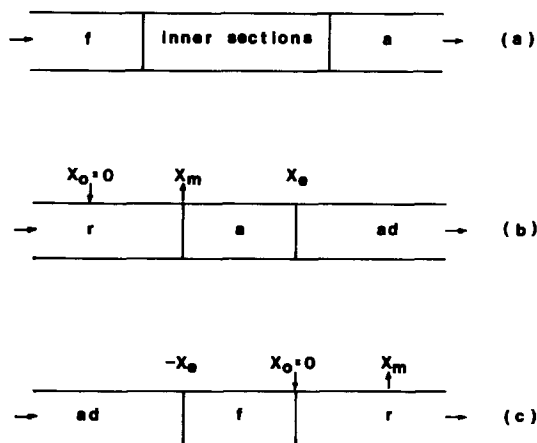


Fig. 1. Schemes of multi-sectional flow systems: (a) general scheme of a flow-analysis or process system; (b) and (c) schemes for investigation of the “end effects” downstream of the measurement point and upstream of the injection point, respectively.

consists of the following set of partial differential equations in dimensionless quantities and variables:²

$$\frac{\partial C_r}{\partial \theta} + \gamma_r \frac{\partial C_r}{\partial X} - \frac{\gamma_r}{P_r} \frac{\partial^2 C_r}{\partial X^2} = \gamma_r \delta(\theta) \delta(X + X_o) \quad (X \leq X_m) \quad (2)$$

$$\frac{\partial C_a}{\partial \theta} + \gamma_a \frac{\partial C_a}{\partial X} - \frac{\gamma_a}{P_a} \frac{\partial^2 C_a}{\partial X^2} = 0 \quad (X_m \leq X \leq X_e) \quad (3)$$

$$\frac{\partial C_{ad}}{\partial \theta} + \gamma_{ad} \frac{\partial C_{ad}}{\partial X} - \frac{\gamma_{ad}}{P_{ad}} \frac{\partial^2 C_{ad}}{\partial X^2} = 0 \quad (X_e \leq X) \quad (4)$$

The corresponding initial and boundary conditions are:

$$C_r(X, 0) = C_a(X, 0) = C_{ad}(X, 0) = 0$$

$$C_r(X_m^-, \theta) = C_a(X_m^+, \theta)$$

$$C_r(X_m^-, \theta) - \frac{1}{P_r} \frac{\partial C_r(X_m^-, \theta)}{\partial X} = C_a(X_m^+, \theta) - \frac{1}{P_a} \frac{\partial C_a(X_m^+, \theta)}{\partial X}$$

$$C_a(X_e^-, \theta) = C_{ad}(X_e^+, \theta)$$

$$C_a(X_e^-, \theta) - \frac{1}{P_a} \frac{\partial C_a(X_e^-, \theta)}{\partial X} = C_{ad}(X_e^+, \theta) - \frac{1}{P_{ad}} \frac{\partial C_{ad}(X_e^+, \theta)}{\partial X}$$

and $C_r(-\infty, \theta)$ and $C_{ad}(\infty, \theta)$ must be finite.

The solution of equations (2)–(4) in the Laplace domain for $X_o = 0$ is

$$\overline{C_m} = \frac{\{q_a + q_{ad} - (q_{ad} - q_a) \exp[-2P_a q_a (X_e - 1)]\} \exp[P_r (0.5 - q_r)]}{\{(q_a + q_{ad})(q_r + q_a) - (q_{ad} - q_a)(q_r - q_a) \exp[-2P_a q_a (X_e - 1)]\}} \quad (5)$$

The statistical moments of the output signal about the origin can be calculated¹ from

$$\mu_i = (-1)^i \lim_{p \rightarrow 0} (d^i \overline{C_m} / dp^i) \quad (6)$$

The equations obtained for the mean (μ_1) and the variance (σ^2) of the output signal are as follows:

c	Concentration (kmole/m ³)
c_M	$= \left[\int_0^\infty vc \, dt \right] / V_t$: integral average concentration in the test-section (kmole/m ³)
C	$= c/c_M$: dimensionless concentration
\overline{C}	Laplace transform of C
d	Diameter (m)
D_L	Axial dispersion coefficient (m ² /sec)
E	Relative error
L	$= x_m - x_o$: length of the test-section (m)
n	Number of points of the response curve used for calculation of E : [equation (15)]
p	Laplace complex variable
P	$= uL/D_L$: Peclet number
q	$= [p/(\gamma P) + 0.25]^{0.5}$
t	Time (sec)
u	Linear flow-rate (m/sec)
v	Volumetric flow-rate (m ³ /sec)
V_t	$= \pi L d^2/4$: volume of the test-section (m ³)
V	$= \pi L d^2/4$: volume of the test-section if the diameter is d (m ³)
x	Axial position (m)
X	$= x/L$: dimensionless axial position
y_i	Positive root of equation (11)
γ	$= V_t/V$
δ	Dimensionless Dirac delta-function
θ	$= vt/V_t$: dimensionless time
μ_i	i th moment of the response curve about the origin [equation (14)]
σ^2	$= \int_0^\infty C(\theta - \mu_1)^2 d\theta$: variance of the response curve

*Subscripts a and ad refer to the after-section and the additional section, respectively (Fig. 1); subscripts f and r refer to the fore-section and the reactor, respectively; subscripts o and m refer to the beginning and the end of the test-section; subscript e refers to the beginning of the additional section; subscript ∞ refers to the case of an infinitely long after-section.

$$\sigma^2 = \mu_2 - \mu_1^2 = \frac{3}{\gamma_r^2 P_r^2} + \frac{3}{\gamma_a^2 P_a^2} + \frac{2}{\gamma_r P_r \gamma_a P_a} + \frac{2}{\gamma_r^2 P_r} + \frac{2}{\gamma_{ad} P_{ad}} - \frac{2}{\gamma_a P_a} + \left\{ \frac{2}{\gamma_{ad} P_{ad}} + \frac{1}{\gamma_r P_r} + \frac{1}{\gamma_a P_a} + 2 - 0.5 \left(\frac{1}{\gamma_{ad} P_{ad}} - \frac{1}{\gamma_a P_a} \right) \exp[-P_a (X_e - 1)] \right\} \exp[-P_a (X_e - 1)] \quad (8)$$

$$\mu_1 = \frac{1}{\gamma_r} + \left(\frac{1}{\gamma_{ad} P_{ad}} - \frac{1}{\gamma_a P_a} \right) \exp[-P_a (X_e - 1)] + \frac{1}{\gamma_r P_r} + \frac{1}{\gamma_a P_a} \quad (7)$$

For convenience it will be assumed that the diameters of the sections (Fig. 1) are all equal, *i.e.*, $\gamma_r = \gamma_a = \gamma_{ad} = 1$. In this case, if the Peclet number of the additional section is equal to that of the after-section then the assumption of infinite length for the after-section is valid and there will be no end effects. The strongest end effects would be expected when the hydraulic conditions in the additional section resemble those in an ideally mixed tank.³ This condition will exist if the corresponding Peclet number is zero, but this value cannot be used for calculations because the Peclet number very often appears in the denominator [*e.g.*, in equations (7) and (8)]. For that reason it is necessary to find a value for the Peclet number such that the corresponding response curve will be practically identical with that for an ideally mixed tank, which for delta-function input is described by the equation¹

$$C = \exp[-\theta] \tag{9}$$

Physically, a closed vessel (*i.e.*, a vessel for which fluid moves in and out by plug-flow alone)¹ with small Peclet number, resembles a perfectly mixed tank. For delta-function input the behaviour of such a vessel is described by:²

$$C = \exp[0.5P(1 - \theta/2)] \sum_{i=1}^{\infty} (2y_i^2 \cos y_i + Py_i \sin y_i) \times \exp[-y_i^2\theta/P]/(y_i^2 + P^2/4 + P) \tag{10}$$

where y_i is the *i*th positive root of

$$\tan y = Py/(y^2 + P^2/4) \tag{11}$$

For $C > 0.01$ and $P \leq 0.01$ the concentration profiles calculated by means of equations (9) and (10), Fig. 2, are identical within 0.33% error. Later, the hydraulic regime corresponding to $P = 0.01$ will be considered as back-mix flow.

If the length of the after-section is increased, the end effects obviously decrease. For a given set of Peclet numbers of the sections of the system there is some critical length of the after-section at which the

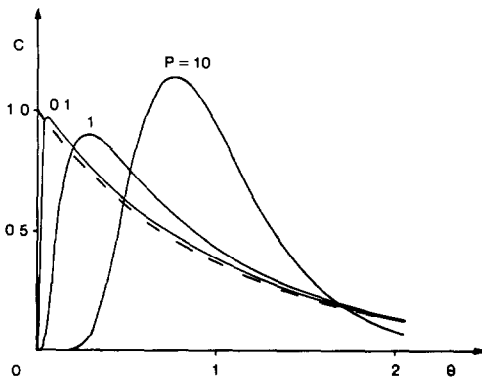


Fig. 2. Response curves for different values of the Peclet number of a closed vessel (—), and the response curve for an ideally mixed tank (---).

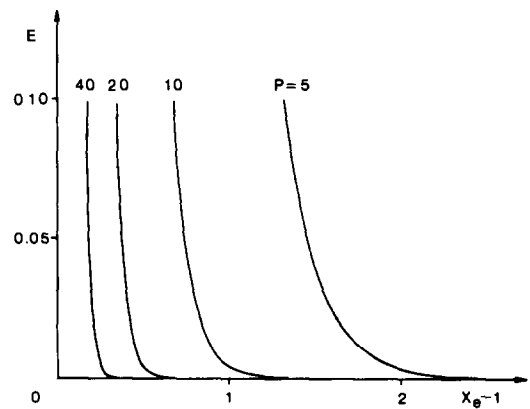


Fig. 3. Error in assuming infinite length for the after-section (the mean is used); $P = P_a = P_r$; $P_{ad} = 0.01$.

error caused by the end effects will not exceed some previously selected value. For longer lengths the end effects can be neglected. Two approaches can be applied for determining the critical length. They correspond to the two most frequently used methods for processing response curves, *viz.* the method using the statistical moments of the response curves, and the method of curve-fitting.

According to the first approach the mean and variance of the response curve are calculated for infinite length and a given finite length of the after-section. The relative error introduced assuming infinite length of the after-section is then calculated as a function of the real length.

$$E = |\mu_{1\infty} - \mu_1|/\mu_1 \quad \text{or} \quad E = |\sigma_{\infty}^2 - \sigma^2|/\sigma^2 \tag{12}$$

The dependence of E on the length of the after-section in the special case of equal Peclet numbers for the reactor and the after-section corresponds to having both the injection and detection performed within the section being investigated. The results obtained are presented in Figs. 3 and 4. Figure 5 illustrates the influence of the after-section length on the relative

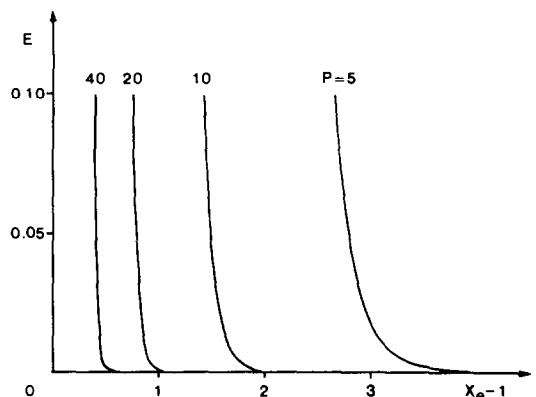


Fig. 4. Error in assuming infinite length for the after-section (the variance is used); $P = P_a = P_r$; $P_{ad} = 0.01$.

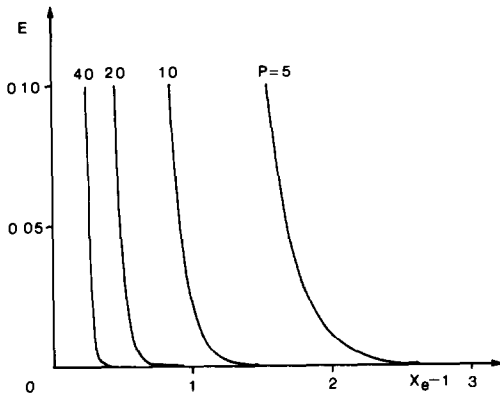


Fig. 5. Error in determining the reactor Peclet number on the basis of assumption of infinite vessel length; $P = P_a = P_r$; $P_{ad} = 0.01$.

error in determination of the reactor Peclet number when the end effects are neglected. In this case, for a given value of P_r the mean is calculated from equation (7). This value is then used in equation (13) to find the Peclet number of the reactor, on the assumption that the reactor is an infinitely long tube.¹

$$P_{r_{\infty}} = 2/(\mu_1 - 1) \quad (13)$$

Similar investigations using the variance instead of the mean have been reported by Bischoff and Levenspiel³ and the results obtained are in good agreement with those presented in Fig. 4.

Figures 3 and 4 show that the influence of the end effects on the relative error [equation (12)] increases if moments of higher order are used. This is explained by the fact that back-flow in the additional section makes the concentration in the tail region of the response curve approach zero more slowly. The influence of the tail on the statistical moments of the curve greatly increases with increase in their order:

$$\mu_1 = \int_0^{\infty} C\theta^1 d\theta \quad (14)$$

This means that when the statistical moments of the output signal are used (e.g., parameter identification, determination of sample frequency in flow injection analysis⁴) the result is very sensitive to the end effects. Furthermore, the tail of the experimental response curve contains the least accurate information, so the errors associated with the computation of the corresponding moments can be quite large. For these reasons, when experimental response curves are processed the necessary information should be extracted, whenever possible, without using the tail portion. A suitable option for this is curve-fitting. In that case another criterion for determination of the critical length should be used, namely that it is that length over which the portion of response curve used is identical, within some previously determined error, with the corresponding portion of the curve calculated on the basis of an infinitely long tube. This is

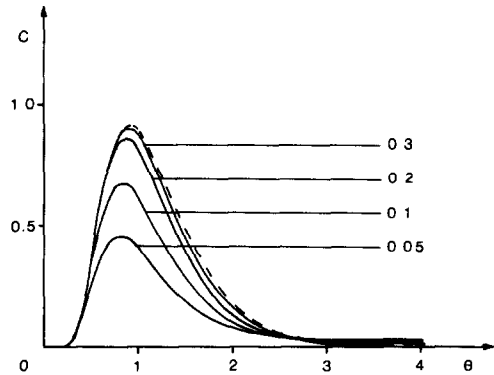


Fig. 6. Response curves obtained for different finite values of the after-section length (—) and for infinite after-section length (---); $P_a = P_r = 10$; $P_{ad} = 0.01$.

the second approach for determining the critical length. Figure 6 illustrates the influence of the after-section length on the shape and magnitude of the response curve.

The inverse Laplace transform of \bar{C}_m [equation (5)] is performed numerically by its expansion into a series of Chebyshev polynomials of the first kind for $P_r \leq 5$ and into a Fourier sine series for $P_r > 5$.⁵

In the present investigation the portion of the response curve used lies between the two points corresponding to a concentration equal to 5% of that at the peak maximum. The influence of the after-section length on the mean relative error [equation (15)] between response curves calculated for that and for infinite length is illustrated in Fig. 7.

$$E = \frac{1}{n} \sum_{i=1}^{i=n} |C_{i\infty} - C_i|/C_i \quad (15)$$

It can be seen that according to the second approach the "critical" lengths are reduced to a considerable extent in comparison with the corresponding values determined by the first approach (Figs. 3–5). This result is very important in practice, because it is quite often inconvenient or not even possible to use a very long after-section, as would

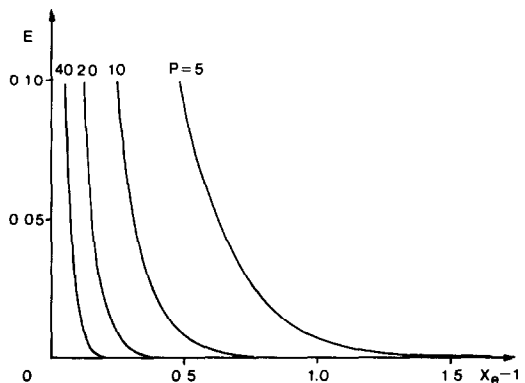


Fig. 7. Error in assuming infinite length for the after-section (the response curve is used); $P = P_a = P_r$; $P_{ad} = 0.01$.

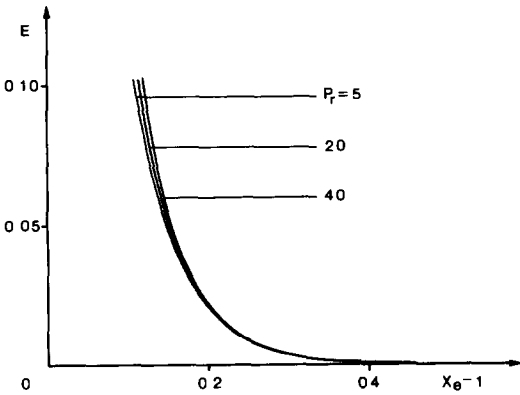


Fig. 8. Error in assuming infinite length for the after-section, for different values of P_r ; $P_a = 20$, $P_{ad} = 0.01$.

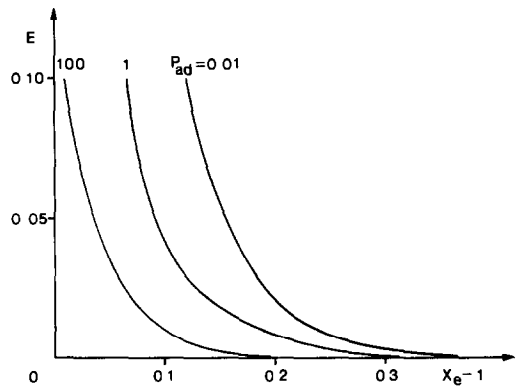


Fig. 10. Error in assuming infinite length for the after-section, for different values of P_{ad} ; $P_a = P_r = 20$.

be required by the first approach, for small Peclet numbers. The response curves obtained when such long after-sections are used are practically indistinguishable from those calculated for after-sections only half as long.

The dependence of the relative error [equation (15)] on the values of the Peclet numbers of the reactor and the after-section are presented in Figs. 8 and 9. These results show that the "critical" length of the after-section depends mainly on its Peclet number.

The end effects due to dispersion processes upstream of the fore-section will be investigated with a three-sectional system (Fig. 1c) similar to that already discussed (Fig. 1b). This system is described by the following set of partial differential equations:

$$\frac{\partial C_{ad}}{\partial \theta} + \gamma_{ad} \frac{\partial C_{ad}}{\partial X} - \frac{\gamma_{ad}}{P_{ad}} \frac{\partial^2 C_{ad}}{\partial X^2} = 0; \quad (X \leq -X_e) \quad (16)$$

$$\frac{\partial C_r}{\partial \theta} + \gamma_r \frac{\partial C_r}{\partial X} - \frac{\gamma_r}{P_r} \frac{\partial^2 C_r}{\partial X^2} = \gamma_r \delta(\theta) \delta(X + X_o); \quad (-X_e \leq X \leq 0) \quad (17)$$

$$\frac{\partial C_r}{\partial \theta} + \gamma_r \frac{\partial C_r}{\partial X} - \frac{\gamma_r}{P_r} \frac{\partial^2 C_r}{\partial X^2} = 0 \quad (0 \leq X) \quad (18)$$

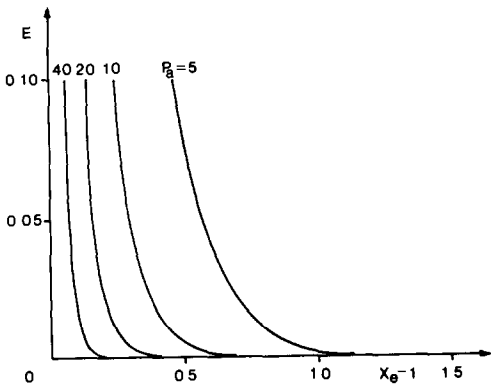


Fig. 9. Error in assuming infinite length for the after-section, for different values of P_a ; $P_r = 20$, $P_{ad} = 0.01$.

The initial and boundary conditions are analogous to those of equations (2)–(4). The Laplace domain solution for $X_o = 0$ is

$$\begin{aligned} \bar{C}_m = & \{q_r + q_{ad} - (q_{ad} - q_r) \exp[-2P_r q_r X_c]\} \\ & \times \exp[P_r(0.5 - q_r)] / \{(q_r + q_{ad})(q_r + q_r) \\ & - (q_{ad} - q_r)(q_r - q_r) \exp[-2P_r q_r X_c]\} \quad (19) \end{aligned}$$

Equations (5) and (19) are identical with the exception that q_r and q_a are interchanged. This means that the conclusions made for the end effects occurring downstream of the measurement point (Fig. 1b) are valid for the end effects originating upstream of the injection point (Fig. 1c). For that reason it can be concluded that the "critical" lengths of the fore- and after-sections are equal.

In practice the flow pattern in the additional sections very often differs from back-mix flow. This situation is illustrated in Fig. 10. It can be seen that with increase in P_{ad} the influence of the end effects is strongly diminished and the corresponding "critical" length becomes much more shorter in comparison with the value calculated for $P_{ad} = 0.01$.

CONCLUSIONS

On the basis of the results obtained in this study the following conclusions can be drawn.

- (1) For Peclet numbers equal to or less than 0.01 back-mix flow exists.
- (2) The "critical" lengths of the fore- and after-sections of a given flow-analysis or process system are equal.
- (3) When curve-fitting is used for processing experimental response curves, the "critical" length is reduced considerably in comparison with that found when the statistical moments of the curves are utilized for obtaining the necessary information.
- (4) When the flow pattern in the additional sections deviates from back-mix flow, the "critical" length becomes shorter.

REFERENCES

1. O. Levenspiel and K. B. Bischoff, *Adv. Chem. Eng.*, 1963, **4**, 95.
2. S. D. Kolev and E. Pungor, *Anal. Chim. Acta*, 1986, **185**, 315.
3. K. B. Bischoff and O. Levenspiel, *Chem. Eng. Sci.*, 1962, **17**, 245.
4. L. R. Snyder, *Anal. Chim. Acta*, 1980, **114**, 3.
5. S. D. Kolev and E. Pungor, *Anal. Chim. Acta*, 1987, **194**, 61.

OXYDATION VANADIQUE DE LA QUININE ET DE QUELQUES ANALOGUES

APPLICATION AU DOSAGE D'UN NOUVEL ANTIPALUDEEN: LA MEFLOQUINE

A. ASSAMOI et M. HAMON

Laboratoire de Chimie Analytique, Faculté des Sciences Pharmaceutiques et Biologiques, 3, rue J. B. Clément, F 92 290 Chatenay Malabry, France

M. CHASTAGNIER et M. CHAIGNEAU

Laboratoire des gaz, Faculté des Sciences Pharmaceutiques et Biologiques, 4 avenue de l'Observatoire, F 75 270 Paris Cédex 06, France

(Reçu le 9 mai 1987. Accepté le 20 juin 1987)

Résumé—L'oxydation vanadique de la méthoxy-6 quinoléine montre la possibilité de la formation d'un complexe initial entre le cation vanadique VO_2^+ et l'oxygène éther-oxyde. L'ouverture de la molécule au niveau de l'homocycle conduit alors principalement à l'acide pyridone-2 carboxylique-3. Dans le cas de la quinine ou de la méfloquine, l'attaque initiale se situe préférentiellement au niveau de la fonction alcool secondaire qui permet dans un premier temps, la formation d'acides quinoléine carboxyliques-4. Le dérivé acide provenant de la méfloquine est, contrairement à celui de la quinine, totalement résistant à l'oxydation vanadique, et cette propriété permet une consommation reproductible de réactif et l'établissement d'un dosage simple de ce nouvel antimalarique.

Summary—Oxidation of 6-methoxyquinoline with vanadate shows the possibility of initial complex formation between the dioxovanadium(V) ion VO_2^+ and the etheral oxygen atom. The opening of the homocycle yields mainly 2-pyridone-3-carboxylic acid. In the case of quinine or mefloquine, the VO_2^+ ion preferentially forms a pentagonal chelate with the secondary alcohol function. Oxidation of this complex initially produces quinoline-4-carboxylic acids. The acid that results from mefloquine is stable in the reaction solution and this property allows a reproducible consumption of reagent and a quantitative determination of this new antimalarial drug.

Lors de précédents travaux dans notre laboratoire sur les dérivés de l'isoquinoléine^{1,2} et du chromanne³ il a été remarqué que la présence d'un ou plusieurs groupements éther-oxyde sur une molécule favorise considérablement l'oxydation de celle-ci par le pentaoxyde de vanadium.

L'objet de ce travail est donc l'étude dans les mêmes conditions expérimentales de l'oxydation de certains dérivés quinoléiniques porteurs de ce groupement; la quinoléine est en effet à la fois un isomère de position de l'isoquinoléine et l'analogue azoté du déhydro chromanne.

Notre choix a porté initialement sur la méthoxy-6 quinoléine en raison du fait que la quinine, molécule d'intérêt thérapeutique, porte également un substituant méthoxyle dans cette position.

Nous avons ensuite étendu cette étude à la quinine, à la quinidine et à la dihydroquinidine, mais aussi et surtout à un antimalarique de synthèse: la méfloquine dont la structure est voisine de celle de la quinine. Le point commun réside en la présence en position 4 d'un groupement alcool secondaire qui permet de relier la fragment quinoléique à un hétérocycle azoté entièrement hydrogéné. Cette structure est susceptible de favoriser une oxydation rapide en raison

de la possibilité de la formation initiale d'un chélate pentagonal stable entre l'oxygène de la fonction alcool, l'azote pipéridinique ou quinuclidinique et le cation vanadique VO_2^+ .

PARTIE EXPERIMENTALE

Réactifs

Solution sulfovanadique 0,2M (exprimé en cations vanadique VO_2^+). Dans un récipient contenant 300 ml d'une solution d'hydroxyde de sodium 1M, introduire 19 g de pentaoxyde de vanadium et porter à ébullition jusqu'à dissolution totale. Après refroidissement, transvaser dans une fiole jaugée de 1000 ml, y ajouter lentement 420 ml d'acide sulfurique 8M, 200 ml d'acide sulfurique 9M et après refroidissement compléter avec de l'eau distillée. La concentration en acide sulfurique de réactif ainsi préparé est de 5M.

Solution de sulfate de fer(II) et d'ammonium 0,1M.

Mode opératoire général

Une prise d'essai comprise entre 20 et 200 μ moles de produit organique est introduite dans une fiole conique rodée de 100 ml. Cinquante ml de solution sulfovanadique y sont ajoutés et l'ensemble porté au bain marie bouillant sous réfrigérant à reflux. La cinétique de la réaction est suivie par dosage du vanadium(V) en excès, en prélevant à des temps déterminés une partie aliquote du mélange réactionnel, jusqu'à oxydation complète de la molécule. Le dosage est effectué à l'aide de la solution de sulfate de fer(II)

et d'ammonium avec indication potentiométrique du point d'équivalence (électrodes platine-calomel). Pour l'étude du mécanisme réactionnel de l'oxydation, la quantité de substance à oxyder et le volume de réactif indiqués précédemment, sont multipliés par 5 dans le but d'isoler plus facilement des quantités suffisantes de composés réactionnels.

Microdosage de la méfloquine

Une prise d'essai voisine de 11,5 mg de chlorhydrate de méfloquine est exactement pesée et dissoute dans 100 ml d'eau distillée. La dissolution est facilitée dans une cuve à ultra-sons. La méfloquine se trouve alors à une concentration d'environ 1mM. Dans une fiole conique rodée de 50 ml contenant exactement 10 ml de solution sulfovanadique, ajouter une quantité de produit comprise entre 1 et 20 μ moles. Un témoin contenant seulement le même volume de réactif est préparé et l'ensemble porté au bain marie bouillant.

Le dosage est effectué, après 7 hr d'oxydation sur la totalité du contenu de chaque fiole, à l'aide de la solution titrée de sulfate de fer(II) et d'ammonium, avec indication potentiométrique du point d'équivalence (électrodes platine-calomel).

Les résultats sont exprimés en μ moles d'ions VO_2^+ réduits.

Dosage du dioxyde de carbone

Le dioxyde de carbone libéré au cours de l'oxydation est recueilli et dosé sur une cuve à mercure selon la méthode gazométrique de Chaigneau.⁴ Le dosage est effectué à l'aide d'une solution concentrée d'hydroxyde de potassium qui permet de capter le gaz.

Isolement et identification de l'hydroxy-6 quinoléine

Après environ 3 hr, temps au bout duquel la formation du formaldéhyde est maximale, la solution issue de

l'oxydation de la méthoxy-6 quinoléine est extraite par l'acétate d'éthyle après réduction de l'excès de vanadium(V) par du bisulfite de sodium et élévation du pH à 2 par une solution d'hydroxyde de potassium. Après évaporation du solvant organique, le résidu est repris par une solution d'hydroxyde de sodium 1M. La solution aqueuse alcaline est rincée plusieurs fois à l'éther, puis réacidifiée et extraite à nouveau par l'acétate d'éthyle. L'évaporation complète du solvant laisse apparaître un produit blanc-mat qui est ensuite cristallisé dans un mélange de méthanol et d'acétone (1:1). L'analyse élémentaire fournit les résultats C 73,8%; H 4,97%; N 9,9%. Le spectre de masse effectué en impact électronique à 70 eV conduit à un schéma de fragmentation qui confirme la structure du dérivé (schéma 1).

Isolement et identification de l'acide méthoxy-6 quinoléine carboxylique-4 ou acide quininique

La solution réactionnelle obtenue en fin d'oxydation de la méthyl-6 quinoléine est extraite par l'acétate d'éthyle dans les mêmes conditions décrites précédemment. L'évaporation du solvant organique fait apparaître un produit incolore ($F = 256-257^\circ$) dont l'analyse élémentaire fournit les résultats C 51,9%; H 3,8%; N 10,1%.

L'étude spectrale (spectre infra rouge et spectre de masse) a permis de confirmer que ce produit est l'acide pyridone-2 carboxylique-3 que nous avons déjà isolé lors de l'oxydation de l'hydroxy-8 quinoléine.⁵

Isolement et identification de l'acide méthoxy-6 quinoléine carboxylique-4 ou acide quininique

Ce dérivé est isolé quantitativement en début d'oxydation de la quinine, de la quinidine ou de la dihydroquinidine. La solution réactionnelle obtenue après environ 6 hr de réaction est extraite par l'éther après réduction de l'excès de vanadium(V) par le sulfite acide de sodium et élévation du pH à 2.

Le produit jaune pâle obtenu après évaporation du solvant est recristallisé dans un mélange de méthanol et d'acétone (1:1). L'identification est faite dans un premier temps par la mesure du point de fusion ($280-281^\circ$) et l'analyse élémentaire (C 64,9%; H 4,4%; N 7,0%), conforme aux données de la littérature.^{6,7} L'étude de la fragmentation de masse n'ayant à notre connaissance jamais été réalisée, nous avons confirmé par ce moyen la structure du produit isolé. Le spectre de masse est effectué en impact électronique (70 eV). L'étude de la fragmentation est proposée dans le schéma 2.

Identification de l'acide hydroxy-6 quinoléine carboxylique-4

Au cours de l'oxydation de la quinine, de la quinidine ou de la dihydroquinidine, cet acide peut être identifié en même temps que l'acide quininique précédemment isolé. Sa concentration étant très faible dans l'extrait étheré, son identification a nécessité l'emploi de la spectrométrie de masse couplée à la chromatographie en phase gazeuse (colonne de silice fondue, $25 \times 0,3$ cm, remplie d'une phase OV1; gaz vecteur, hélium; four système à programmation).

Le schéma 3 donne la fragmentation du spectre de masse obtenu après injection de l'extrait étheré.

Isolement et identification de l'acide bis(trifluorométhyl)-2,8 quinoléine carboxylique-4

Au cours de l'oxydation de la méfloquine, ce dérivé apparaît dans la solution sulfovanadique sous forme de petits flocons blancs. Après récupération sur un filtre en verre fritté (No. 3) et lavage à l'eau distillée, le produit est cristallisé dans un mélange d'eau et d'acétone (3:7).

Le spectre de masse obtenu en impact électronique donne une confirmation de la structure du produit; on observe notamment la présence de pics à $m/z = 50, 69$ et 119 qui correspondent respectivement aux fragments caractéristiques CF_2^+ , CF_3^+ et $(\text{CF}_3\text{CF}_2)^+$ (schéma 4).

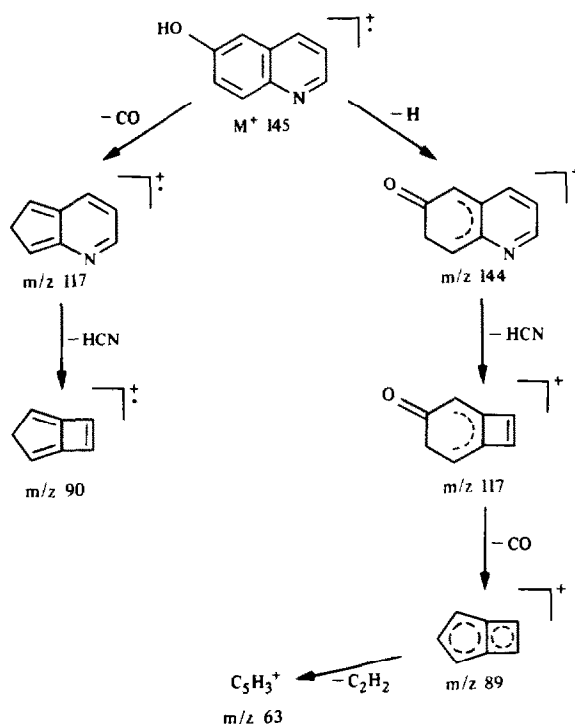


Schéma 1

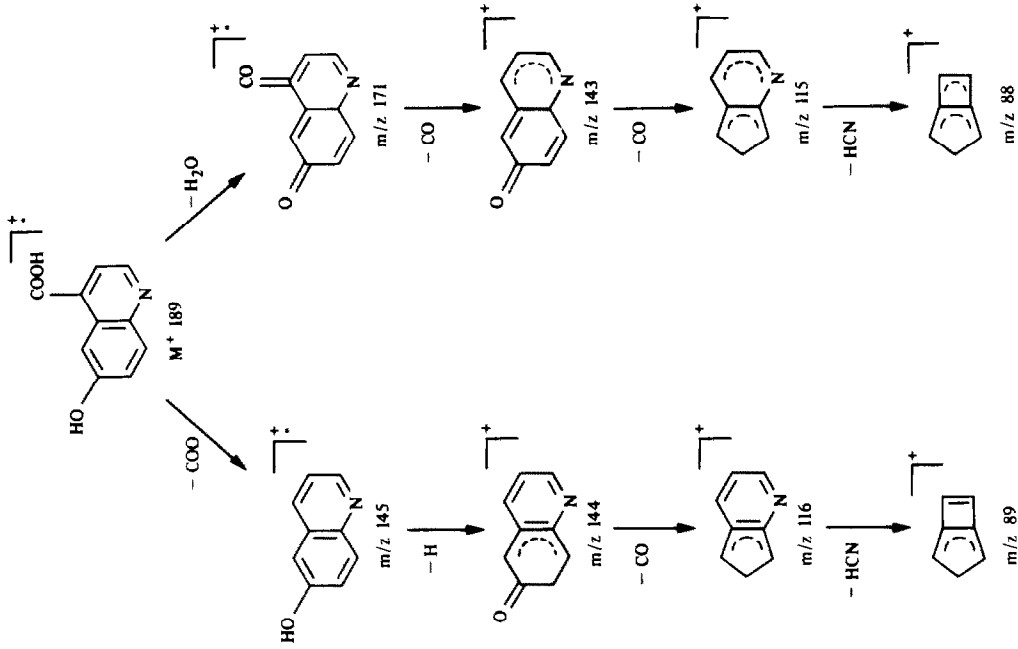


Schéma 3

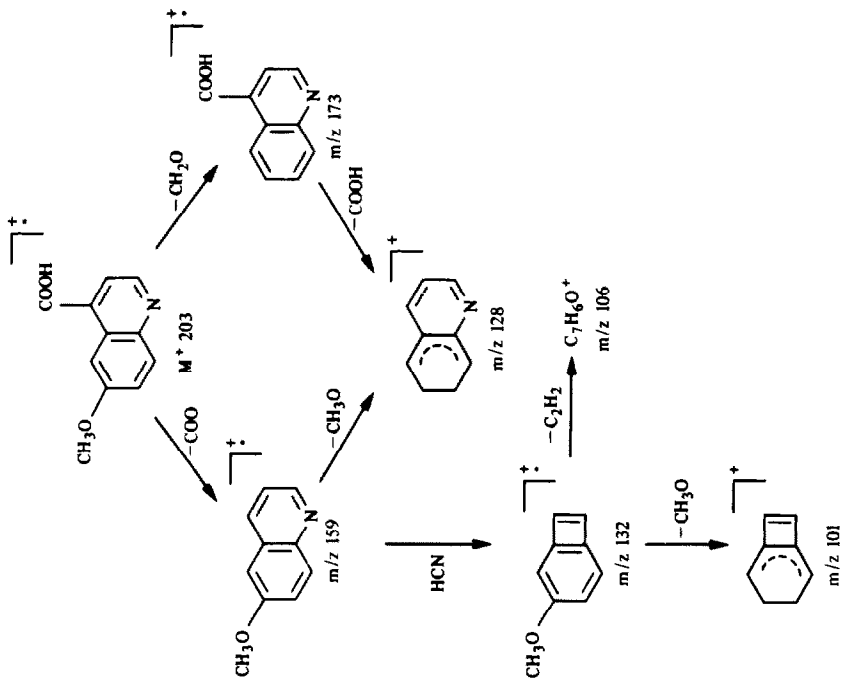
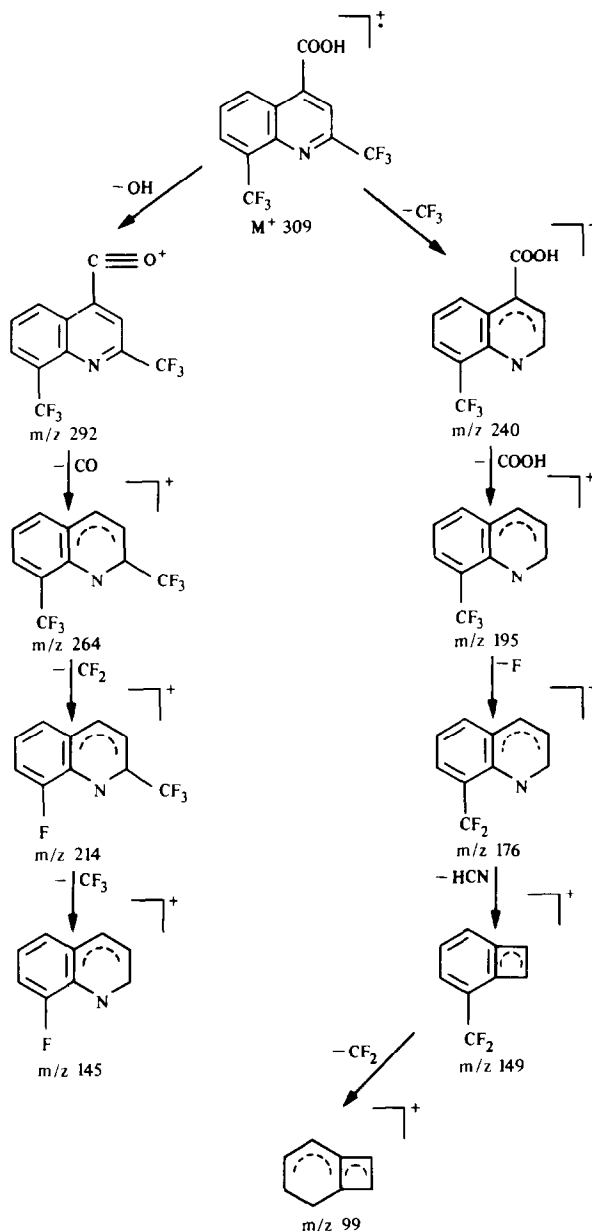


Schéma 2



RESULTATS ET DISCUSSION

Oxydation de la méthoxy-6-quinoléine

L'étude préalable du dérivé le plus simple: la méthoxy-6-quinoléine a permis de préciser les conditions optimales d'oxydation. En effet, nous avons

Tableau 1. Variation de la quantité de réactif consommée en fonction du rapport molaire

Rapport molaire	50	100	200	300	400	500
Réactif consommé (mole/mole)	22,8	26,0	28,7	30,2	31,9	32,3

noté, comme dans le cas de l'oxydation des dérivés du chromanne,³ une évolution de la consommation du réactif en fonction du rapport molaire oxydant-produit (tableau 1).

Le rapport molaire est défini comme étant le rapport existant entre la quantité de réactif vanadique et la quantité de produit oxydé, exprimées en moles. Dans ce contexte, un rapport élevé indique un grand excès de réactif dans le milieu réactionnel.

Les résultats du tableau 1 montrent la nécessité de réaliser les essais en grand excès de réactif pour obtenir une oxydation complète de la molécule. Pour des rapports molaires supérieurs à 500, la variation de la consommation devient négligeable, mais dans ces

conditions il devient difficile de déterminer avec précision la quantité de réactif réduite. Le tableau 1 montre que cette quantité est alors d'environ 32 moles des cations vanadique par mole de produit.

L'étude cinétique de la réaction révèle un temps relativement long: 72 hr. Cependant le dosage spectrofluorimétrique de la méthoxy-6 quinoléine résiduelle en fonction du temps indique une extinction totale de la fluorescence après 24 hr d'oxydation. Ces deux observations traduisent une plus grande résistance des produits intermédiaires, vis à vis du réactif vanadique.

Le dosage du formaldéhyde montre par chromatographie en phase gazeuse (méthode de l'espace de tête et réduction en méthane)⁸ qu'il apparaît rapidement. Le maximum (0,8 mole/mole) de la teneur est déterminé après seulement 3 hr d'oxydation. Ceci montre que l'attaque initiale de l'ion VO_2^+ s'effectue au niveau du groupement méthoxyle. La déméthylation rapide de la molécule est également confirmée par l'identification dans le milieu de l'hydroxy-6 quinoléine.

En fin de réaction, la présence de l'acide pyridone-2 carboxylique-3 indique que l'oxydation du dérivé hydroxylé conduit ensuite à l'ouverture du cycle benzénique. Cette dernière réaction explique les quantités importantes de dioxyde de carbone libéré (5,4 mole/mole).

Il convient de remarquer qu'un certain nombre d'autres oxydants: permanganate de potassium,^{9,10} acide nitrique,^{11,12} oxydent la quinoléine ou ses dérivés substitués sur l'homocycle avec formation de l'acide pyridine dicarboxylique-2,3. Ce diacide n'a pu être identifié au cours de cette étude, en effet son oxydation par le pentoxyde de vanadium conduit à la formation de l'acide pyridone-2 carboxylique-3.

Ceci montre par rapport à l'action des oxydants usuels, l'action particulière du vanadium(V).

Oxydation de la quinine et des dérivés de structure voisine

L'oxydation des dérivés d'intérêt thérapeutique permet d'observer cependant que l'attaque initiale de l'ion VO_2^+ est susceptible de porter sur un site autre que le groupement méthoxyle. En effet, que ce soit dans le cas de la quinine ou de la méfloquine, la formation rapide d'un dérivé acide issu de la rupture au niveau du groupement fonctionnel alcool secondaire, explique une grande sensibilité de celui-ci vis à vis de l'oxydant.

L'étude parallèle de la quinine et de la quinidine n'a pas montré une influence notable de l'isomérisation optique. Par contre, l'oxydation de la dihydroquinidine a permis d'observer des différences significatives, tant au niveau de la quantité de réactif

consommé qu'au niveau des quantités de formaldéhyde et de dioxyde de carbone formés.

En effet, la dihydroquinidine réduit 32,2 moles par mole de produit soit un défaut d'environ 8 moles par rapport à la quinine (40,3 mole/mole) ou à la quinidine (40,4 mole/mole).

De même, nous pouvons noter la libération d'une quantité de formaldéhyde (0,86 mole/mole) ou de dioxyde de carbone (9,1 mole/mole) inférieure d'environ une unité à celle de la quinine (respectivement 1,6 et 10,2 mole/mole) ou de la quinidine (1,6 et 10,2 mole/mole).

Ces différences s'expliquent par la réactivité du groupement vinylique présent dans le cas de la quinine ou de la quinidine. Si l'oxydation de ces molécules a permis d'observer là encore, une évolution de la consommation de réactif en fonction du rapport molaire jusqu'à une valeur très élevée de celui-ci, et un temps de réaction relativement long (72 hr), celle de la méfloquine, réalisée dans les mêmes conditions opératoires, n'a pas montré une influence notable de ces deux paramètres. En effet, la méfloquine réduit 14 moles de réactif par mole après 7 hr d'oxydation quelque soit le rapport molaire.

Le temps de réaction relativement court et la régularité de la quantité de réactif consommée peuvent s'expliquer par la grande stabilité du dérivé réactionnel: acide bis(trifluorométhyl)-2,8 quinoléine carboxylique-4, formé au cours de la réaction. En effet, ce dérivé est totalement réfractaire au réactif vanadique, contrairement à l'acide quininique formé de façon semblable dans le cas de la quinine, de la quinidine ou de la dihydroquinidine et dont la structure, s'apparente à celle de la méthoxy-6 quinoléine précédemment étudiée.

Cette observation importante au niveau de l'oxydation de la méfloquine a rendu possible l'établissement d'un dosage vanadimétrique simple et précis de cette molécule.

Dans le cas de la quinine ou de ses homologues, la nécessité de réaliser les oxydations avec un très grand excès de réactif diminue de façon notable la reproductibilité du dosage, comme le montrent les valeurs des coefficients de variations obtenus après 10 essais (quinine: 7,2%; méfloquine: 0,9%).

De plus, le temps d'oxydation trop long ne permet pas une méthode rapide de dosage de la quinine ou de ses homologues.

Application au microdosage de la méfloquine dans une forme galénique

Appliquée à la matière première, la méthode montre une bonne reproductibilité, la droite de régression établie entre 1 et 20 μ moles présente un coefficient de corrélation $r = 0,9999$.

La forme galénique choisie est la comprimé de méfloquine dosé à 50 mg.* Le comprimé est pulvérisé dans 10 ml de méthanol. Après filtration et évaporation partielle, le résidu est déposé sur une plaque de silice GF 254, puis chromatographié (solvant:

*Nous remercions les laboratoires Roche qui ont bien voulu nous procurer la matière première et le médicament terminé: *LARIAM®.

méthanol-ammoniac 25%, 100:1,5). Après migration sur environ 10 cm, la tache correspondant à la méfloquine ($R_f = 0,3$) est récupérée et éluee par trois fois 25 ml de méthanol. La phase organique est ensuite évaporée et le résidu dosé par le réactif vanadique.

Les points de gamme d'étalonnage sont déterminés dans les mêmes conditions chromatographiques. Le rendement quantitatif de l'extraction est vérifié en déposant sur la plaque chromatographique des quantités connues de méfloquine.

La technique est ensuite comparée à la méthode spectrophotométrique classique fondée sur l'absorption moléculaire. Les résultats obtenus montrent l'absence de différences significatives entre les deux méthodes et une précision légèrement plus grande de la technique proposée. La teneur par rapport à la valeur théorique $91,5\% \pm 0,88$ ($n = 5$) pour la méthode proposée et de $92,5\% \pm 1,2$ ($n = 5$) pour le dosage spectrophotométrique.

CONCLUSION

L'oxydation de la méthoxy-6 quinoléine conduit à l'ouverture de l'homocycle de la molécule, après déméthylation préalable. La quinine ou la méfloquine présente par contre une structure qui favorise la réalisation d'un chélate pentagonal, plus stable, au niveau du groupement fonctionnel alcool secondaire

dont la rupture et l'oxydation conduisent à la formation d'acides quinoléine carboxyliques-4.

Dans le cas de la méfloquine, le dérivé acide formé dans le milieu réactionnel ne subit par la suite aucune attaque du cation vanadique. Cette propriété entraîne une consommation de réactif moins importante mais plus reproductible et permet ainsi de réaliser un dosage simple et précis de ce nouvel antimalarique dans une forme galénique.

L'avantage de la méthode que nous proposons réside essentiellement dans la possibilité de réaliser des dosages même dans des laboratoires ne possédant qu'un équipement restreint.

LITTÉRATURE

1. M. Tsitini-Tsamis, M. Chaigneau, M. Hamon et J. Likforman, *Analisis*, 1980, **8**, 428.
2. M. J. Wachter et M. Hamon, *Ann. Pharm. Fr.*, 1976, **34**, 281.
3. J. E. Hila, M. Tsitini-Tsamis, M. Hamon et J. P. Delcroix, *Analisis*, 1982, **10**, 220.
4. M. Chaigneau, *Bull. Soc. Chim. France*, 1970, **37**, 4133.
5. A. Assamoi, *Thèse de l'Université de Paris Sud.*, 1986.
6. W. Koenigs, *Annalen*, 1906, **347**, 143.
7. Z. Skraup, *ibid.*, 1879, **197**, 352.
8. E. Postaire, J. E. Hila, A. Assamoi, D. Pradeau, C. Dauphin et M. Hamon, *Analisis*, 1985, **13**, 463.
9. R. Goutarel, M. M. Janot, V. Prelog et W. I. Taylor, *Helv. Chim. Acta*, 1950, **33**, 150.
10. P. C. Guha et R. K. Maller, *Current Sci. (Calcutta)*, 1944, **13**, 206.
11. S. Carboni, *Gazz. Chim. Ital.*, 1955, **85**, 1194.
12. W. Stix et S. A. Bulbatsch, *Ber.*, 1932, **65**, 11.

SPECTROPHOTOMETRIC REACTION-RATE METHOD FOR THE DETERMINATION OF NITRITE IN WATERS WITH PYRIDINE-2-ALDEHYDE 2-PYRIDYLHYDRAZONE

R. MONTES and J. J. LASERNA

Department of Analytical Chemistry, Faculty of Sciences, University of Málaga, 29071 Málaga, Spain

(Received 26 March 1986. Revised 21 April 1987. Accepted 5 June 1987)

Summary—A method for the kinetic determination of submicrogram amounts of nitrite has been developed, based on its acceleration of the rate of bromate oxidation of pyridine-2-aldehyde 2-pyridylhydrazone in acidic medium. The reaction is monitored spectrophotometrically at 372 nm. A comparative study with hydrochloric acid and perchloric acid media shows that the analytical parameters are affected by the type of acid used. Within-day precision, based on ten replicate determinations, was better than 0.011 $\mu\text{g/ml}$, which corresponds to 2.2–1.5% relative standard deviation at the concentrations examined. Application of this method in the determination of nitrite in water has been discussed. The recovery of nitrite from drinking waters ranges from 90 to 117% and the average relative standard deviation for nitrite determinations in polluted river water is 3.2%. Large amounts of nitrate and ammonium ions do not interfere. However, there is interference by Cu^{2+} , Pd^{2+} and electroactive substances. Major advantages for the method are simplicity, absence of a reagent blank, and the wide determination range.

Nitrite is an active form of the nitrogen cycle, resulting from incomplete oxidation of ammonia or from reduction of nitrates. Under ordinary conditions nitrite levels in waters are low (down to 0.1 $\mu\text{g/ml}$), but the increasing use of nitrite as a preservative in the food industry and a corrosion inhibitor in industrial process water results in these levels occasionally being exceeded as a result of uncontrolled wastes. Nitrite has been reported to cause methenoglobinaemia¹ and is a well known precursor of carcinogenic *N*-nitrosamines.²⁻⁴ Because of these properties analytical methods for nitrite are of interest for application to environmental samples.

Ion-chromatography,⁵ chemiluminescence,^{6,7} voltammetry,^{8,9} amperometry,¹⁰ potentiometry,^{10,11} flow-injection,^{12,13} and volumetry¹⁴ have been used for the determination of nitrite. However, the most widely used methods are spectrophotometric,¹⁵⁻¹⁷ most of them based on diazotization reactions.¹⁸⁻²⁰ Approved methods for nitrite in water²¹ belong to this latter category and are characterized by high sensitivity (minimum determinable concentration 0.003 $\mu\text{g/ml}$). Interferences by oxidizing and reducing agents,²² as well as long reaction times and large sample volumes, are common drawbacks of these methods.

To date, only a few kinetic methods for nitrite have been published.^{23,24} Utsumi *et al.*²³ reported a method based on the kinetic effect of nitrite on the colour-fading of the iron(III) thiocyanate complex in dilute nitric acid solution in the presence of iodide. The proposed method gives accurate results for nitrite concentrations ranging from 0.0005 to 10 $\mu\text{g/ml}$, but no precision data were reported. As a result of use of the fixed-time method, the determination at low

concentrations requires up to 24 min of reaction time. Koupparis *et al.*²⁴ reported an automatic kinetic determination of nitrite in waters, with a stopped-flow analyser, based on the diazotization of sulphanimide, the product being coupled with *N*-(1-naphthyl)ethylenediamine dihydrochloride. The method has limited sensitivity (the calibration graph is linear from 0.125 $\mu\text{g/ml}$ nitrite), but compares favourably with the Technicon AutoAnalyzer method in terms of rate of analysis, precision and accuracy.

The bromate oxidation of pyridine-2-aldehyde 2-pyridylhydrazone in acidic medium has been used for the kinetic determination of palladium and cobalt.^{25,26} The present report describes the application of this reaction for kinetic determination of nitrite. The reaction is monitored spectrophotometrically and nitrite in the range 0.04–4 $\mu\text{g/ml}$ is determined with a relative standard deviation of 1.5%. The method has been applied satisfactorily to the determination of nitrite in water.

EXPERIMENTAL

Apparatus

A Shimadzu model 240 S Graphicord spectrophotometer, fitted with a controlled-temperature cell-holder, was used throughout. The kinetic curves were registered by monitoring the changes in absorbance at 372 nm with time. The range of absorbance units was kept constant at 1.5 in all the experiments.

Reagents

All solutions were prepared from distilled demineralized water and analytical grade chemicals. The working solutions were all kept in a water-bath at 25°.

Pyridine-2-aldehyde 2-pyridylhydrazone (PAPH) was purchased from Ega-Chemie and used without purification.

Solutions ($1.5 \times 10^{-3} M$) were prepared in $0.1 M$ perchloric acid and $0.1 M$ hydrochloric acid. These solutions are stable for at least two weeks.

Potassium bromate was recrystallized twice from water. A stock solution ($0.100 M$) was prepared by dissolving 16.70 g of it in 1 litre of water.

Standard nitrite solution, $0.250 M$, was prepared by dissolving 1.725 g of sodium nitrite, dried at 110° for 1 hr, in 100 ml of water containing a few drops of chloroform as preservative. The solution was protected from light. Working standards were prepared daily.

A chromic nitrate solution (Cr^{3+} 5 g/l.) was also prepared.

Procedures

Water samples were collected in May 1986 from the River Guadalhorce, near a meat product dump and stored in polyethylene bottles which had previously been washed several times with dilute nitric acid. The bottles were filled and emptied repeatedly with the river water before a sample was retained. All samples were filtered through a Whatman No. 1 filter paper before analysis. Most analyses were performed within 3 hr of sample collection. Otherwise, samples were stored at 4° for a maximum of 48 hr.

Determination of nitrite in perchloric acid medium. Into a 25-ml standard flask, introduce an aliquot of sample containing 1.1–23 μg of nitrite and 1.0 ml of $1.5 \times 10^{-3} M$ PAPH. Add 6.5 ml of $5 M$ perchloric acid, 1.0 ml of $0.012 M$ potassium bromate, and dilute to volume with demineralized water. Monitor the absorbance at the absorption maximum of PAPH ($\lambda = 372$ nm, $\epsilon = 2.5 \times 10^4$ l.mole $^{-1}$.cm $^{-1}$) against water, starting 30 sec after the addition of bromate. Find the initial rate ($\Delta A/\Delta t$) at the start of monitoring.

Determination of nitrite in hydrochloric acid medium. Into a 25-ml standard flask, introduce an aliquot of sample containing 1.2–100 μg of nitrite, 3 ml of 5-g/l. Cr^{3+} solution, and 1.0 ml of $1.5 \times 10^{-3} M$ PAPH. Add 1.0 ml of $1.5 M$ hydrochloric acid, 1.0 ml of $0.075 M$ potassium bromate, and dilute to volume with demineralized water. Monitor the absorbance as above.

RESULTS AND DISCUSSION

Nitrite has been found to increase the rate of bromate oxidation of PAPH in acidic medium. This reaction can be followed spectrophotometrically by monitoring the disappearance of the organic reagent, at 372 nm. Although the kinetics of the indicator reaction has been studied,^{25,26} it was decided to re-investigate the reaction to find the experimental conditions leading to maximum sensitivity. The reaction rate is found to depend on the initial concentration of all three reactants. In addition, preliminary information indicates that the type of acid used has a strong effect on the rate. Perchloric acid and hydrochloric acid have been used in this work. As the optimum conditions are different for the two acids, two methods for nitrite have been developed.

Oxidation in perchloric acid medium

The effect of the initial concentrations of the reactants on the reaction is summarized in Fig. 1. The reaction rate in the absence of nitrite was zero in all cases. The reaction was zero order with respect to perchloric acid for concentrations above $1.0 M$, and a concentration of $1.3 M$ was chosen for further studies. The reaction rate and the sensitivity increased with

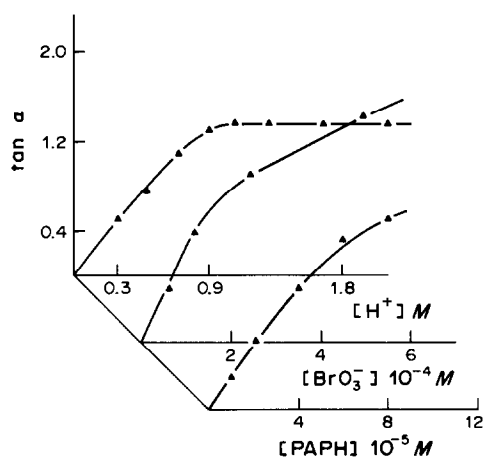


Fig. 1. Effect of initial concentrations of reactants on reaction rate in perchloric acid medium. Nitrite concentration $0.46 \mu g/ml$.

increasing concentration of bromate and reagent. For bromate concentrations $> 5 \times 10^{-4} M$ the reaction rate at 30 sec decreased, but this resulted more from measurement of the rate in the latter stages of the reaction than from a real decrease in reaction rate. PAPH concentrations $> 8 \times 10^{-5} M$ lead to kinetic curves difficult to characterize (poor precision in rate measurements) because the absorbance is outside the best sensitivity range of the apparatus. The combination of $4.8 \times 10^{-4} M$ bromate and $6 \times 10^{-5} M$ PAPH gives an adequate compromise between precision and sensitivity.

Oxidation in hydrochloric acid medium

The effect of hydrochloric acid concentration on the reaction rate was studied with the optimum bromate and PAPH concentrations just mentioned. The results are shown in Fig. 2. In this case, the reaction rate in the presence of nitrite could be distinguished from the background reaction only for acid concentrations lower than $0.2 M$. An acid con-

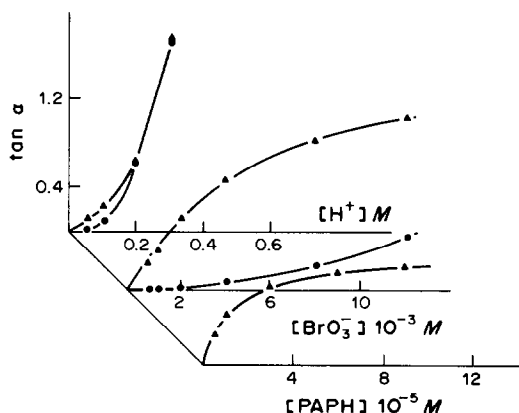


Fig. 2. Effect of initial concentrations of reactants on reaction rate in hydrochloric acid medium. (▲) Reaction rate in the presence of $0.46 \mu g/ml$ nitrite. (●) Reaction rate in the absence of nitrite.

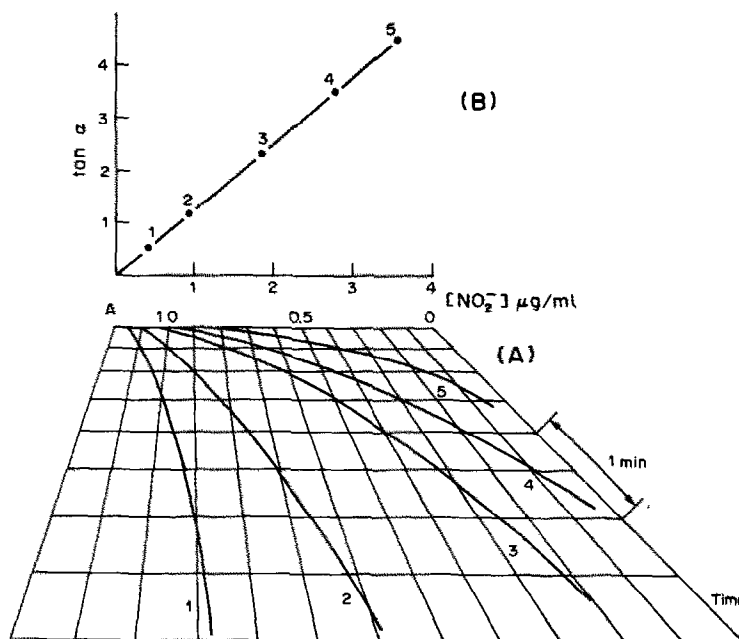


Fig. 3. (A) Typical kinetic curves obtained in the calibration with method II. (B) Calibration curve. Nitrite concentrations, $\mu\text{g/ml}$: (1) 0.46; (2) 0.92; (3) 1.84; (4) 2.76; (5) 3.68.

centration of $0.06M$ was chosen since this ensured the absence of a background signal.

The rates of the nitrite and blank reactions increased with increasing concentration of bromate (Fig. 2). Although the maximum rate difference was at $[\text{BrO}_3^-] = 7 \times 10^{-3}M$, a concentration of $3 \times 10^{-3}M$ was selected because this is the maximum concentration at which there was no blank reaction. The optimum PAPH concentration was found to be $6 \times 10^{-5}M$. Although at all other PAPH concentrations studied there was no background reaction (Fig. 2), this concentration gave maximum precision of rate measurement.

Analytical parameters

Under the chosen experimental conditions, linear calibration plots for nitrite, passing through the origin, were obtained over the range $0.04\text{--}0.92 \mu\text{g/ml}$ nitrite for the perchloric acid method (henceforth called method I) and $0.04\text{--}4.0 \mu\text{g/ml}$ nitrite for the hydrochloric acid method (method II). Figure 3 shows typical kinetic curves obtained for calibration with method II. Statistical analysis of the calibration data gave the results in Table 1. The limit of detection could not be calculated according to the usual recommendations,²⁷ because of the absence of a blank reaction in both kinetic methods. The limits of de-

Table 1. Statistical profile of calibration

Method	Regression equation ^a	r	Slope RSD, %	Intercept RSD, %	LOD, ^b $\mu\text{g/ml}$	LCL, ^c $\mu\text{g/ml}$	UCL, ^d $\mu\text{g/ml}$
I	$\tan \alpha = 3.63[\text{NO}_2^-] + 0.053$	0.999	3.22	47.0	0.021	0.013	0.046
II	$\tan \alpha = 1.22[\text{NO}_2^-] + 0.052$	0.999	1.53	49.0	0.037	0.023	0.081

^aConcentration of nitrite in $\mu\text{g/ml}$.

^bLimit of detection.

^cLower confidence limit of the LOD, 95% confidence limit.

^dUpper confidence limit of the LOD, 95% confidence limit.

Table 2. Effect of diverse species on determination of $0.46 \mu\text{g/ml}$ nitrite, Method II

Tolerance limit, $\mu\text{g/ml}$	Species
1000	$\text{Li}^+, \text{Na}^+, \text{K}^+, \text{Rb}^+, \text{NH}_4^+, \text{Be}^{2+}, \text{Mg}^{2+}, \text{Ca}^{2+}, \text{Sr}^{2+}, \text{Ba}^{2+}, \text{Zn}^{2+}, \text{Cd}^{2+}, \text{Pb}^{2+}, \text{Cr}^{3+}, \text{Al}^{3+}, \text{Se(IV)}, \text{Mo(VI)}, \text{HCO}_3^-, \text{NO}_3^-, \text{ClO}_4^-, \text{IO}_4^-, \text{CO}_3^{2-}, \text{SO}_3^{2-}, \text{SO}_4^{2-}, \text{S}_2\text{O}_8^{2-}, \text{PO}_4^{3-}, \text{EDTA}$
500	$\text{F}^-, \text{ClO}_3^-, \text{ClO}_2^-, \text{IO}_3^-$
100	$\text{Co}^{2+}, \text{Ni}^{2+}, \text{Hg}^{2+}, \text{Fe}^{2+}$
50	Bi^{3+}
10	$\text{Ag}^+, \text{Fe}^{2+}, \text{S}^{2-}$
1	$\text{Pd}^{2+}, \text{Cu}^{2+}, \text{I}^-, \text{Br}^-, \text{S}_2\text{O}_3^{2-}, \text{H}_2\text{O}_2, \text{ascorbate}$

Table 3. Recovery of nitrite from drinking water (10-ml sample)

Sample	Nitrite added, $\mu\text{g/ml}$	Method I				Method II				Standard method			
		Nitrite found, $\mu\text{g/ml}$	Recovery, %	RSD, %	Nitrite found, $\mu\text{g/ml}$	Recovery, %	RSD, %	Nitrite found, $\mu\text{g/ml}$	Recovery, %	RSD, %	Nitrite found, $\mu\text{g/ml}$	Recovery, %	RSD, %
1	0.092	0.085	92	6	0.082	90	12	0.034	38	15			
1	0.460	0.466	103	6	0.542	118	6	0.401	87	1			
1	0.680	0.633	94	4	0.746	110	4	0.620	91	1			
2	0.091	0.082	90	4	0.088	97	0	0.089	98	3			
2	0.446	0.446	104	1	0.495	111	3	0.450	101	1			
2	0.652	0.635	97	4	0.708	109	5	0.654	100	1			
3	0.356	0.347	98	6	0.370	104	1	0.207	58	11			
3	0.560	0.547	98	3	0.574	103	4	0.418	75	11			

^aAverage of three determinations.^bRelative standard deviation of the recovery.

tection in Table 1 are defined as the minimum concentration that can be measured and reported with 99% confidence that the nitrite concentration is greater than zero.²⁸ Although the procedure employed allows the limit of detection to be determined for various matrices, the data in Table 1 are reported for demineralized water to assist in method comparison. Table 1 also indicates that the sensitivity (calibration slope) of method I is three times that of method II. However, the linear range of concentration response for method II covers two orders of magnitude. The relative standard deviation of ten replicate analyses of a 0.46 $\mu\text{g/ml}$ standard was 2.2% for method I and 1.5% for method II. Between-day precision for ten measurements made over two weeks showed relative standard deviations of 4.0% and 3.4%, respectively. The order of reagent addition is not critical with respect to precision and the reaction can be started by addition of either acid or bromate.

Effect of foreign species

Forty-five foreign species were examined as potential interferents. The concentrations at which the species caused an error of no more than 6% in the rate for 0.46 $\mu\text{g/ml}$ nitrite in method II are listed in Table 2. As observed, 27 ions (including nitrate and ammonium) can be tolerated at the 1000 $\mu\text{g/ml}$ level. Electroactive substances cause interference when present at the 50 $\mu\text{g/ml}$ level, as expected from the nature of the analytical reaction. Metal ions forming complexes with the reagent (Pd^{2+} and Cu^{2+}) decrease its concentration in solution, causing negative interferences. The interference from Cu^{2+} (up to 100 $\mu\text{g/ml}$) can be eliminated by addition of 1000 $\mu\text{g/ml}$ EDTA.

The selectivity of method I is similar to that expressed in Table 2 except for chlorate, the tolerance for which is lower (limit 1 $\mu\text{g/ml}$) as a result of the higher acidity of the medium. However, this acidity increases the tolerance for copper (tolerance limit 100 $\mu\text{g/ml}$) since it facilitates destruction of the Cu-PAPH complex. Chloride causes positive interference in method I, presumably because the chlorine produced destroys PAPH, and only 1 $\mu\text{g/ml}$ can be tolerated.

Water analysis

The study above indicated that both methods could be used for the determination of nitrite in waters. The recovery for drinking waters spiked with nitrite at about ten times natural levels is shown in Table 3, which includes the data given by an alternative method based on the nitrite reaction with sulphanic acid and phenol in hydrochloric acid medium (Zambelli reagent) and spectrophotometric measurement of the colour.²⁹ The first two samples were mineral waters, and the third tap water. In samples 2 and 3, method I requires removal of the chloride interference. This can be done by dropwise addition of 3.8 g/l. silver nitrate solution until precip-

Table 4. Analysis of polluted waters by the kinetic method in hydrochloric acid medium (10-ml sample)

Sample	Nitrite added, $\mu\text{g/ml}$	Kinetic method		Standard method		t^d
		Nitrite found, ^a $\mu\text{g/ml}$	Recovery, ^{b,c} %	Nitrite found, ^a $\mu\text{g/ml}$	Recovery, ^{b,c} %	
1	—	0.360 ± 0.009		0.360 ± 0.003		0
	1.150	1.529	101 (1)	1.484	98 (1)	
2	—	0.320 ± 0.008		0.330 ± 0.006		0.72
	1.150	1.489	101 (2)	1.454	98 (0)	
3	—	0.268 ± 0.005		0.275 ± 0.005		2.09
	1.150	1.375	97 (2)	1.392	98 (2)	
4	—	0.283 ± 0.009		0.289 ± 0.001		1.15
	1.150	1.381	96 (2)	1.430	99 (1)	
5	—	0.290 ± 0.017		0.285 ± 0.001		0.60
	1.150	1.405	97 (1)	1.423	99 (2)	

^aAverage of three determinations \pm standard deviation.

^bAverage of three determinations.

^cIn parenthesis, relative standard deviation of the recovery, %.

^d t calculated for the difference between the means of paired observations ($t > 2.77$ needed to indicate a significant difference between the kinetic and standard methods; 95% confidence level).

itation of AgCl is complete, followed by centrifugation and decantation of the supernatant liquid. This treatment is not necessary for sample 1, as the chloride concentration is less than $1 \mu\text{g/ml}$. In method II all samples were analysed directly without any pretreatment. The results in Table 3 indicate that both methods give satisfactory recovery and precision. However, the standard method gave low results with sample 3, probably as a result of the hypochlorite incorporated in the drinking water, which is known to interfere with this method.²⁹

Method II was applied to the determination of nitrite in polluted river water, with 10-ml samples. The results are shown in Table 4, where the sample number is an arbitrary designation for the sampling site in the river stream. Some samples gave low results when method II was applied directly. However, the interference was found to be eliminated when Cr^{3+} (3 ml of 5-g/l. solution) was added to the water sample. Therefore, as a precaution, addition of Cr^{3+} to all samples is recommended (but note that it will not prevent interference by ascorbic acid). The results in Table 4 indicate that the relative standard deviation of the direct determinations by the kinetic method ranged from 5.9% to 1.9%, with an average of 3.2%. This value takes into account all the replicate analyses performed and is a good indicator of the precision expected for the method. Student's t -test for the difference between the means of paired observations by the kinetic and standard methods, Table 4, indicates no significant differences between the two methods.

Although the recovery study indicated that the treatment with silver should not affect the results obtained with method I, systematically low results were obtained for polluted waters. The reason for this could not be established, because the exact nature of the discharge was not known. However, the polluted water presumably contained species capable of oxidizing nitrite under the conditions of method I, since the accuracy of method II was satisfactory.

Conclusions

The results obtained by the kinetic method for the determination of nitrite in water are dependent on the type of acid used. The hydrochloric acid method, though less sensitive at low nitrite concentrations, is better suited than the perchloric acid method when variable nitrite concentrations are expected, as in polluted waters. The kinetic method is at least one order of magnitude less sensitive than established polarographic⁹ and chemiluminescence⁷ methods, but is more rapid than spectrophotometric or polarographic procedures and comparable in speed to chemiluminescence. The small sample volume required and the wide determination range are other relevant characteristics of the method.

REFERENCES

1. F. P. Swann, *J. Sci. Food Agric.*, 1975, **26**, 1761.
2. T. Panalaka, J. R. Iyengan and N. P. Sen, *J. Assoc. Off. Anal. Chem.*, 1973, **56**, 621.
3. W. Lijinski and S. S. Epstein, *Nature*, 1970, **225**, 21.
4. D. Jenkins, *Prog. Water Technol.*, 1977, **8**, 31.
5. Z. Iskandarani and D. J. Pietrzyk, *Anal. Chem.*, 1982, **54**, 2601.
6. R. C. Doerr, J. B. Box, Jr., L. Lakritz and W. Fiddler, *ibid.*, 1981, **53**, 381.
7. R. D. Cox, *ibid.*, 1980, **52**, 332.
8. B. D. Seiler and J. P. Avery, *Anal. Chim. Acta*, 1980, **119**, 277.
9. S. K. Chang, R. Kozeniauskas and G. H. Harrington, *Anal. Chem.*, 1977, **49**, 2272.
10. J. E. Newbery and M. P. Lopez de Haddad, *Analyst*, 1985, **110**, 81.
11. V. Simeonov, G. Andreev and A. Stoianov, *Z. Anal. Chem.*, 1979, **297**, 418.
12. L. Anderson, *Anal. Chim. Acta*, 1979, **110**, 123.
13. M. F. Giné, H. Bergamin F., E. A. G. Zagatto and B. F. Reis, *ibid.*, 1980, **114**, 191.
14. K. K. Verma and A. K. Gulati, *Talanta*, 1983, **30**, 279.
15. S. J. Bajic and B. Jaselskis, *ibid.*, 1985, **32**, 115.
16. K. Nagashima, M. Matsumoto and S. Suzuki, *Anal. Chem.*, 1985, **57**, 2065.
17. M. Nakamura, T. Mazuka and M. Yamashita, *ibid.*, 1984, **56**, 2242.
18. S. Flamerz and W. A. Bashir, *Analyst*, 1985, **110**, 1513.

19. A. Chaube, A. K. Baveja and V. K. Gupta, *Talanta*, 1984, **31**, 391.
20. Q. F. Wu and P. F. Liu, *ibid.*, 1983, **30**, 375.
21. *Standard Methods for the Examination of Water and Wastewater*, 14th Ed., M. C. Rand, A. E. Greenberg, M. J. Taras and M. A. Franson (eds.), American Public Health Assoc., Washington, D.C., 1976.
22. G. Norwitz and P. N. Keliher, *Analyst*, 1985, **110**, 689.
23. S. Utsumi, T. Okutani, A. Sakuragawa and A. Kenmotsu, *Bull. Chem. Soc. Japan*, 1978, **51**, 3496.
24. M. A. Koupparis, K. M. Walczak and H. V. Malmstadt, *Analyst*, 1982, **107**, 1309.
25. R. Montes and J. J. Laserna, *ibid.*, 1985, **110**, 1339.
26. J. J. Laserna and R. Montes, *Mikrochim. Acta*, 1985, **II**, 457.
27. L. H. Keith, W. Crummet, J. Deegan, Jr., R. A. Libby, J. K. Taylor and G. Wentler, *Anal. Chem.*, 1983, **55**, 2210.
28. United States Environmental Protection Agency. Guidelines Establishing Test Procedures for the Analysis of Pollutants, *Federal Register*, Vol. 49, p. 198, 26 October, 1984.
29. J. Rodier, *Analysis of Water*, p. 123. Keter, Jerusalem, 1975.

DETERMINATION OF SEVERAL TRACE ELEMENTS IN SILICATE ROCKS BY AN XRF METHOD WITH BACKGROUND AND MATRIX CORRECTIONS

J. PASCUAL*

Instituto de Edafología y Biología Vegetal, C.S.I.C. c/Serrano, 115 Dpdo, 28006 Madrid, Spain

(Received 2 August 1985. Revised 14 September 1985. Accepted 13 March 1987)

Summary—An X-ray fluorescence method for determining trace elements in silicate rock samples was studied. The procedure focused on the application of the pertinent matrix corrections. Either the Compton peak or the reciprocal of the mass absorption coefficient of the sample was used as internal standard for this purpose. X-Ray tubes with W or Cr anodes were employed, and the W $L\beta$ and Cr $K\alpha$ Compton intensities scattered by the sample were measured. The mass absorption coefficients at both sides of the absorption edge for Fe (1.658 and 1.936 Å) were calculated. The elements Zr, Y, Rb, Zn, Ni, Cr and V were determined in 15 international reference rocks covering wide ranges of concentration. Relative mean errors were in many cases less than 10%.

XRF spectrometry has been widely used for the determination of trace elements in a diversity of matrices, such as environmental samples,^{1,2} alloys,³ etc. In the present work it was applied to silicate rocks. A homogeneous sample is essential, and to achieve this some researchers have used fusion with borates,^{4,5} but this introduces problems from dilution. For this reason, many workers have compressed the samples into briquettes. In any case, the samples should always be "infinitely" thick, so that the fluorescence intensities of the different elements do not change with sample thickness. To obtain the net peak intensity, it is necessary to subtract the spectral background contribution. Feather and Willis⁶ used blank samples, free from the elements to be determined, to assess the background. Although this method has the advantage of requiring measurement of only one position on the spectrum, it is less accurate than those methods based on the measurement of the background at both sides of the peak of interest. Franzini *et al.*⁷ proposed a method for matrix corrections which takes into account the effect of major sample components. However, most work mentions the use of either the Compton peak, or the reciprocal of the mass absorption coefficient of the sample, as an internal standard.^{8,9}

Background correction

Figure 1 shows the typical shape of the signal obtained for a given line in the absence of spectral interference. To eliminate background curvature effects¹⁰ it is best to assume that the background

signal is linear in the vicinity of the line of interest and to take the background correction as the mean of the background signals at positions either side of the maximum signal and equidistant from it (in terms of 2θ).

Matrix correction

The Compton peak is the result of sample-scatter of the radiation from the X-ray tube. The relationship between the concentration C_i and the fluorescence intensity I_i of the analyte is

$$C_i = kI_i\mu_{\lambda_i} \quad (1)$$

where k is an instrumental constant and μ_{λ_i} the mass absorption coefficient of the sample at the measurement wavelength λ_i for the fluorescence radiation. If there is no absorption edge of a major element between the wavelength λ_i and the wavelength of measurement of the Compton peak intensity I_C , there is an inverse relationship between μ_{λ_i} and I_C .¹¹⁻¹³

$$\mu_{\lambda_i} = f_i \left(\frac{1}{I_C} \right) \quad (2)$$

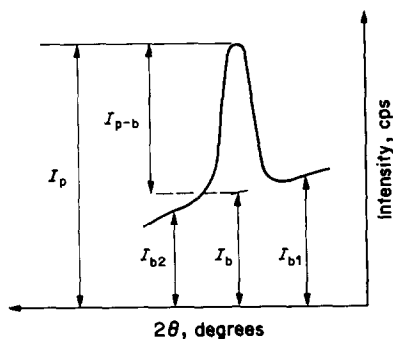


Fig. 1. Background correction method. Background intensity $I_b = (I_{b1} + I_{b2})/2$. Net peak intensity $I_{p-b} = I_p - I_b$ (see text).

*Present address: Construcciones Aeronáuticas S.A., Laboratorio Central de Garantía de Calidad, Factoría de Getafe, Getafe, Madrid. Correspondence address: Dr J. Pascual, c/Ferraz, 73, 28008 Madrid.

Comparison of these two equations has led to the conclusion that the matrix correction can be made by use of either μ_{λ_i} or I_C .¹⁴⁻¹⁹ If there is no absorption edge of any major element between the analyte line and the Compton peak, I_C can be used as internal standard, and if there is an absorption edge, the reciprocal of μ , calculated at the wavelength side corresponding to the analyte line, is used as internal standard.

EXPERIMENTAL

Standard samples

The 15 reference rocks analysed covered a wide range of matrices and compositions, and were: AGV-1 (andesite), BCR-1 (basalt), GSP-1 (granodiorite), PCC-1 (peridotite), BR (basalt), GA (granite), Mica Fe (biotite), Mica Mg (phlogopite), BX-N (bauxite), DR-N (diorite), DT-N (kyanite), UB-N (serpentine), JB-1 (basalt) and JG-1 (granodiorite).

Sample preparation

The samples were prepared by compression in a Herzog HTP-20 press. First a ring (external and internal diameters 50 and 40 mm) was made from approximately 6 g of borax, by application of a load of 10 tons for a period of 30 sec. Two or three drops of a 20% w/w solution of elvacite in acetone were added as binder to 4 g of the powdered sample, and this mixture was introduced into the borax support and compressed under a load of 25 tons for 60 sec. The sample disc thus obtained was placed in a sample holder (without a Mylar window) presenting a sample surface 36 mm in diameter to the radiation used.

Analysis

A Philips PW 1410 sequential semi-automatic spectrometer, with a two-sample changer, was used. Seven trace elements were determined: Zr, Zn, Ni, Cr, Y, Rb and V. An X-ray tube with a tungsten anode was used for the first four, and another tube with a chromium anode for the rest. The 2θ settings corresponding to the $K\alpha$ (and tungsten $L\beta$ Compton) analytical lines measured are listed in Table 1. An LiF (200) analyser crystal, a fine collimator (150 μ m) and window discrimination were used in all cases.

The same counting time (100 sec) was used for both the peak and the background. Whenever possible, background measurements were made at two angular positions for 50 sec each.

The $K\alpha$ fluorescence lines of Zr, Y and V are spectrally interfered with by the $K\beta$ lines of Sr, Rb and Ti respectively.

Table 1. Experimental settings

2θ , degrees	Line	X-ray tube (anode)*	Detector†
22.46	Zr $K\alpha$	W	S
38.00	W $L\beta C$		F + S
41.70	Zn $K\alpha$		F + S
48.57	Ni $K\alpha$		F + S
—	Fe K edge		—
69.27	Cr $K\alpha$		F
23.70	Y $K\alpha$	Cr	S
26.50	Rb $K\alpha$		S
—	Fe K edge		—
70.25	Cr $K\alpha C$		F
76.84	V $K\alpha$		F

*W (50 kV, 45 mA); Cr (60 kV, 40 mA).

†F = flow counter; S = scintillator counter.

The overlap factors were calculated by the conventional method,²⁰ from the $K\alpha$ lines of the interfering elements, and found to be 0.0257, 0.121 and 0.0200, in the order mentioned.

The sample weight corresponding to "infinite" thickness was found experimentally by comparing the Zr $K\alpha$ line intensities for samples (of the same material) weighing 2.5, 3.0, 3.5 and 4.0 g, and it was found that 4 g of sample was enough.

To check the instrumental drift, a reference sample was run after every 4 samples.

RESULTS AND DISCUSSION

The mass absorption coefficients of the reference rocks were calculated at both sides of the Fe K edge (1.744 Å) for the wavelengths corresponding to the Ni $K\alpha$ (1.658 Å) and Fe $K\alpha$ (1.936 Å) lines. Thin and Leroux's method²¹ and the concentrations of the major and minor elements in the rocks^{22,23} were employed. The intensities corresponding to the W $L\beta$ and Cr $K\alpha$ Compton peaks were also measured as recorded in Table 2. The relationship between the mass absorption coefficients (μ_{λ_i}) and the relative Compton intensities (R_C), obtained by a least-squares fit, was of the type:

$$\log \mu_{\lambda_i} = a_i - b_i \log R_C \quad (3)$$

where a_i and b_i are constants. Although the correlation is satisfactory in both cases, it is better for the tungsten/nickel combination, for two reasons: (1) the $\mu_{Ni, K\alpha}$ range is 2.3 times that for $\mu_{Fe, K\alpha}$, and (2) the tungsten Compton peak is at shorter wavelength than the chromium Compton peak, so the incoherent scattering has a greater effect.

For samples of unknown composition, the mass absorption coefficient on the wavelength side, corresponding to the Compton peak, can be calculated by measuring R_C and applying equation (3). The mass absorption coefficient on the other side of the Fe K absorption edge can then be calculated, without

Table 2. Calculated mass absorption coefficients and relative Compton peak intensities on either side of the Fe K edge

Reference sample	$\mu_{Ni, K\alpha}$, cm^2/g	$R_{W, L\beta C}$ *	Reference sample	$\mu_{Fe, K\alpha}$, cm^2/g	$R_{Cr, K\alpha C}$ *
DT-N	42.0	1.321	UB-N	57.5	1.696
GH	49.6	1.082	PCC-1	58.9	1.298
JG-1	52.3	1.029	BX-N	59.4	1.390
GA	54.1	1.005	DT-N	63.9	1.147
UB-N	56.8	0.981	GH	72.3	1.049
PCC-1	57.3	0.935	JG-1	73.9	1.017
GSP-1	59.3	0.903	GA	74.2	1.018
AGV-1	65.7	0.823	GSP-1	76.6	0.989
DR-N	73.1	0.730	AGV-1	77.0	0.999
JB-1	74.0	0.725	DR-N	77.5	1.027
Mica Mg	74.6	0.720	Mica Mg	78.2	0.946
BCR-1	84.1	0.631	Mica Fe	79.1	0.984
BR	88.3	0.575	BCR-1	80.3	0.961
BX-N	93.4	0.570	JB-1	81.5	0.951
Mica Fe	113	0.441	BR	88.8	0.877

*W $L\beta$ and Cr $K\alpha$ Compton peak intensities relative to the values for GA and GSP-1 respectively.

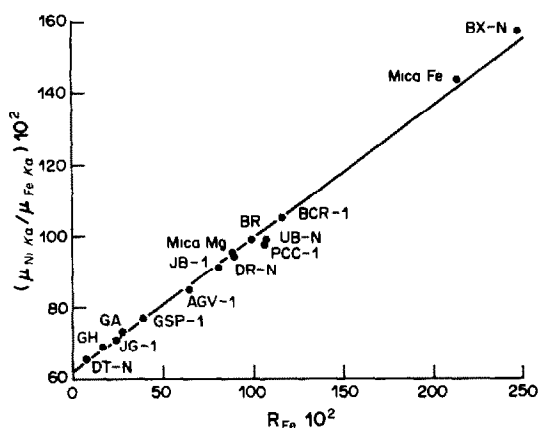


Fig. 2. Relationship between $\mu = \text{Ni } K\alpha / \text{Fe } K\alpha$ and emission intensities of iron, relative to values for BR.

having to change the X-ray tube, by making use of the relationship.

$$\mu_{\text{Ni}, K\alpha} / \mu_{\text{Fe}, K\alpha} = c + dR_{\text{Fe}} \quad (4)$$

where c and d are two constants and R_{Fe} is the emission intensity of Fe. Figure 2 shows this relationship for the reference rocks under study. The emission intensities were measured for the $K\beta$ line with an LiF (200) crystal and normalized relative to the values for BR.

The matrix corrections which were pertinent, according to the procedure explained in the theoretical section, were used in the construction of calibration curves. As stated in Table 1, a tungsten X-ray tube was used for the determination of Zr, Zn, Ni and Cr. $R_{\text{W}, L\beta C}$ was used as internal standard for the first three, and the reciprocal of $\mu_{\text{Fe}, K\alpha}$ was used for Cr, since the Fe absorption edge is located between the W $L\beta$ Compton peak and the Cr $K\alpha$ line of the analyte. A similar procedure was followed for the determination of Y, Rb and V, for which a chromium X-ray tube was employed. The reciprocal of $\mu_{\text{Ni}, K\alpha}$ was used as internal standard for the first two, and $R_{\text{Cr}, K\alpha C}$ was used for V. The corresponding calibration curves, concentration ranges and relative mean errors are recorded in Table 3. It was convenient to use two working curves for Ni, according to its range of

concentration. Blank tests showed the presence of Cr at impurity level in the tungsten X-ray tube, and this was taken into account in the calibration curve for this element. For K_2CO_3 , CaCO_3 , Al_2O_3 and MgO blanks, 35, 31, 38 and 37 ppm of Cr were obtained.

The analytical results which correspond to the elements under study are recorded in Table 4. There is good agreement between the literature data and the findings in this work, in view of the errors normally tolerated in this type of determination.²⁵ Results are reported as "nd" (not determined) if (1) the concentrations of the elements they refer to are outside the working ranges given in Table 3 or (2) the intensities (in the case of unknown concentrations) are outside the corresponding range. Some of the results in Table 4 deviate fairly considerably from the "recommended" values, which might be regarded as raising a question about the latter. Table 5 gives the "minimum detectable limits" (C_{MDL})²⁶ calculated from the results for peak and background for a reference sample of known concentration (C_{RS}):

$$C_{\text{MDL}} = \frac{1.645 C_{\text{RS}}}{I_{\text{p-b}}} \left(\frac{2 I_{\text{b}}}{t_{\text{b}}} \right)^{1/2} \quad (5)$$

where I_{b} and t_{b} are the intensity and counting time of the background and $I_{\text{p-b}}$ the peak intensity correcting for background. The sensitivities (S), calculated as

Table 3. Working curves $C_i = mX_i + b$

Analyte (i)	Range, ppm	m	X_i	b	E_i^*
Zr	100-500	136	$R_i / R_{\text{W}, L\beta C}$	11	5.1
Zn	30-1350	64.1	$R_i / R_{\text{W}, L\beta C}$	8.2	10
Ni	3-35	117	$R_i / R_{\text{W}, L\beta C}$	-4.1	8.4
Ni	135-2500	128	$R_i / R_{\text{W}, L\beta C}$	-27	5.6
Cr	10-2500	5.46	$R_i \mu_{\text{Fe}, K\alpha}$	3.2	15
Y	20-70	0.45	$R_i \mu_{\text{Ni}, K\alpha}$	2.5	9.1
Rb	5-1500	4.16	$R_i \mu_{\text{Ni}, K\alpha}$	2.6	6.7
V	20-450	199	$R_i / R_{\text{Cr}, K\alpha C}$	20	13

*Relative mean error, %.

Table 4. Determination of some trace elements in international reference rocks (concentration in ppm)

Reference sample	Zr		Zn		Ni		Cr		Y		Rb		V	
	This work	Other values*†	This work	Other values*†	This work	Other values*†	This work	Other values*†	This work	Other values*†	This work	Other values*†	This work	Other values*†
AGV-1	227	230	83	86	17	15	16	10	21	19	74	67	113	125
BCR-1	200	185	118	125	12	10	31	15	32	40	54	47	416	420
GSP-1	492	500	103	105	9	9	12	12	29	29	249	250	45	54
PCC-1	nd	—	47	41	2505	2400	2331	2800	nd	—	8	0.3	52	29
BR	261	250	147	150	287	260	323	380	30	30	53	47	248	240
GA	136	150	73	80	8	7	13	12	20	21	173	175	34	38
GH	146	150	66	85	4	3	14	6	72	70	380	390	9	5
BX-N	246	520	86	60	196	200	291	300	nd	120	13	—	431	310
DR-N	131	125	145	145	20	16	46	42	29	30	70	70	218	230
DT-N	327	370	31	28	14	16	252	240	nd	—	12	—	153	160
UB-N	nd	8	80	92	1990	2000	2208	2300	nd	11	8	6	71	75
JB-1	140	155	82	84	115	135	383	400	20	26	48	41	181	210
JG-1	112	110	44	40	8	8.2	65	53	31	31	171	185	27	24
Mica Fe	nd	800	1350	1300	36	35	92	90	61	25	2032	2200	147	135
Mica Mg	nd	20	296	290	105	110	161	100	nd	—	1254	1300	82	90

**"Usable value" from Abbey.²⁴

†Mica Fe and Mica Mg data are quoted from Flanagan.²³

Table 5. Minimum detectable limit (C_{MDL}) for 100-sec background counting time, and sensitivity (S) for the elements determined

Element	Reference sample	C_{RS} , ppm	I_{p-b} , cps	I_b , cps	C_{MDL} , ppm	S , cps/ppm
Zr	GA	150	542.59	587.90	1.6	3.6
Zn	GA	80	756.83	495.29	0.55	9.5
Ni	Mica Fe	35	207.12	290.30	0.67	5.9
Cr	BX-N	200	1366.1	328.13	0.62	6.8
Y	BX-N	300	1612.0	254.02	0.69	5.4
Rb	GSP-1	29	38.789	156.19	2.2	1.3
V	GSP-1	250	310.74	136.14	2.2	1.2
	BR	240	187.64	129.22	3.4	0.78

Table 6. Mean, standard deviation and confidence level (four determinations)

Element	Reference sample (RS)	C_{RS} , ppm	Mean, ppm	Std. devn., ppm	t
Zr	AGV-1	230	243	4.9	< $t_{99\%}$
Zn	AGV-1	86	83	0.82	> $t_{99\%}$
Ni	DR-N	16	20	0.82	> $t_{99\%}$
Cr	BX-N	200	199	3.6	< $t_{90\%}$
Y	DR-N	42	48	1.4	> $t_{99\%}$
Rb	GA	21	20	1.5	< $t_{90\%}$
V	GA	175	173	4.3	< $t_{90\%}$
	UB-N	75	95	6.3	> $t_{99\%}$

I_{p-b}/C_{RS} , are also given. Finally, the analytical validity of the method was tested statistically.²⁷ Table 6 compares the experimental values of Student's t with the tabulated critical values for confidence levels of 90 and 99%. It can be said that the method is generally adequate, especially if we can take into account that the values given are based on measurements made several weeks after the calibration curves had been obtained. Furthermore, the X-ray tubes were changed several times during this period of time.

REFERENCES

1. R. F. Coleman, *Anal. Chem.*, 1974, **46**, 989A.
2. J. V. Gilfrich, P. G. Burkhalter and L. S. Birks, *Anal. Chem.*, 1973, **45**, 2002.
3. N. M. Sine and C. L. Lewis, *Talanta*, 1965, **12**, 389.
4. I. L. Thomas and M. T. Haukka, *Chem. Geol.*, 1978, **21**, 39.
5. J. T. Hutton and S. M. Elliot, *ibid.*, 1980, **29**, 1.
6. C. E. Feather and J. P. Willis, *X-Ray Spectrom.*, 1976, **5**, 41.
7. M. Franzini, L. Leoni and M. Saitta, *ibid.*, 1972, **1**, 151.
8. K. K. Nielson, *Adv. X-Ray Anal.*, 1979, **22**, 303.
9. G. Andermann and J. W. Kemp, *Anal. Chem.*, 1958, **30**, 1306.
10. L. Leoni and M. Saitta, *Rend. Soc. Ital. Mineral. Petrol.*, 1976, **32**, 497.
11. R. C. Reynolds, *Am. Mineral.*, 1963, **48**, 1133.
12. *Idem, ibid.*, 1967, **52**, 1493.
13. M. Franzini, L. Leoni and M. Saitta, *X-Ray Spectrom.*, 1976, **5**, 84.
14. J. C. Mills, K. E. Turner and C. B. Belcher, *ibid.*, 1981, **10**, 131.
15. R. Vié le Sage, J. P. Quisefit, R. Dejean and de la Bâtie and J. Faucherre, *ibid.*, 1979, **8**, 121.
16. R. D. Giauque, R. B. Garret and L. Y. Goda, *Anal. Chem.*, 1979, **51**, 511.
17. J. T. Wilband, *Am. Mineral.*, 1975, **60**, 320.
18. L. Leoni and M. Saitta, *X-Ray Spectrom.*, 1977, **6**, 181.
19. E. A. Th. Verdurmen, *ibid.*, 1977, **6**, 117.
20. L. Leoni and M. Saitta, *ibid.*, 1976, **5**, 29.
21. Tran Phuc Thinh and J. Leroux, *X-Ray Spectrom.*, 1979, **8**, 85; 1981, **10**, v.
22. S. Abbey., *ibid.*, 1978, **7**, 99.
23. F. J. Flanagan, *Geochim. Cosmochim. Acta*, 1973, **37**, 1189.
24. S. Abbey, *Geol. Surv. Can Pap.*, 1983, 83-15.
25. W. B. Stern, *X-Ray Spectrom.*, 1976, **5**, 56.
26. R. Jenkins, R. W. Gould and D. Gedcke, *Quantitative X-Ray Spectrometry*, Dekker, New York, 1981.
27. K. Eckschlager, *Errors Measurement and Results in Chemical Analysis*, Van Nostrand, London, 1969.

SHORT COMMUNICATIONS

AN INDIRECT COMPLEXOMETRIC METHOD FOR DETERMINATION OF TIN IN ALLOYS

N. RUKMANI DESIKAN and M. VIJAYAKUMAR

Defence Metallurgical Research Laboratory, Kanchanbagh, P.O. Hyderabad 500258, India

(Received 1 September 1986. Revised 27 May 1987. Accepted 5 June 1987)

Summary—A simple and fast complexometric method for the determination of tin in alloys is presented. It is based on the initial complexation of tin with EDTA and its subsequent decomposition with mercaptosuccinic acid. Interference of ions normally encountered in determination of tin was studied. The method has been used for the analysis of alloys such as bronzes, solders, white metal and titanium base alloys.

Numerous methods for the determination of tin in a variety of materials are available.^{1,2} The titrimetric procedures are preferred because of their speed and simplicity in routine analysis. Favoured methods of this type are the indirect ones based on the initial formation of the tin(IV) EDTA complex, followed by its selective decomposition and titration of the EDTA released. Oxalate,^{3,4} fluoride,⁵ citric acid and tartaric acid,⁶ lactic acid⁷ and gallic acid⁸ have been reported as releasing agents. Recently, use of a totally different type of reagent based on the ability of thiols, for example, thioglycolic and mercaptopropionic acid, to form tin complexes was reported from our laboratory.⁹ In the present paper, the results of investigations on the use of mercaptosuccinic acid, which has greater complexing ability, in the routine determination of tin in alloys are presented.

EXPERIMENTAL

Reagents

EDTA solution, 0.02M, standardized with standard copper solution in dilute ammonia medium (pH 7.5-8.0) with murexide as indicator. Standard zinc solution (0.02M) prepared by dissolving the metal in dilute hydrochloric acid, adjusting the pH to 5.0-5.5 with sodium hydroxide and acetic acid, then diluting to 1000 ml. Mercaptopropionic acid solution, 0.7% Xylenol Orange solution, 0.1%.

Procedure

A 200-500 mg sample is dissolved by heating with 10-20 ml of concentrated hydrochloric acid and 2-4 ml of concentrated nitric acid on a hot-plate. The cooled solution is diluted to volume in a 100-ml standard flask with distilled water. A suitable aliquot containing 5-50 mg of tin is taken in a 250-ml conical flask, excess of EDTA is added and the pH is adjusted to 5-5.5 with saturated hexamine solution. The excess of EDTA is back-titrated with the zinc solution, with Xylenol Orange as indicator. Then 10 ml of the thiol solution are added for every 10 mg of tin present and the EDTA released is titrated with the zinc solution.

RESULTS AND DISCUSSION

EDTA forms both Sn(II) and Sn(IV) complexes. Thiols release EDTA from the tin-EDTA complex by

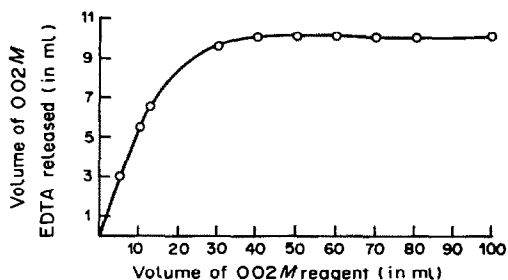


Fig. 1

reduction of Sn(IV) to Sn(II), and/or complexation of Sn(II). Figure 1 shows the amount of EDTA released as a function of the volume of 0.02M mercaptosuccinic acid added to 10 ml of 0.02M Sn(IV)-EDTA solution, from which it is clear that at least a 4:1 mercaptosuccinic acid:tin ratio is required for complete release of EDTA from the complex. It is

Table 1. Determination of tin in alloys

Alloy	Tin, %		
	Certified range	Found*	Relative standard deviation, %
Leaded bronze BCS 364	(9.25-9.45) (mean 9.35)	9.35	0.6
White metal (Lead base) BCS 177/1	(10.3-10.5) (mean 10.4)	10.40	0.03
Phosphor bronze BCS 374	9.68-9.89 (mean 9.8)	9.79	0.4
Ounce metal NBS 124 d	4.48-4.64 (mean 4.56)	4.57	0.8
Solder NBS 127 b	39.3 ± 0.1 (mean 39.3)	39.3	0.3
Tin-base BCS 178/1	86.0-86.4 (mean 86.2)	86.2	0.1
Titanium-base NBS 176	2.47 ± 0.01 (mean 2.47)	2.43	0.1

*Average of ten determinations.

therefore recommended to use 1 ml of 0.04M (0.7%) mercaptosuccinic acid solution per mg of tin present. Ions normally encountered in the analysis of alloys for tin, such as Cu(II), Ni, Pb, Zn, Co(II), Cd, Hg(II), Fe(III), Al, Sb(III), Bi, Ti(IV), Zr, V(IV), and lanthanides have been examined for potential interference. Cu(II), Hg(II) and Bi(III) were found to interfere, but Cu(II) can be masked with thiourea.¹⁰ Interference by Hg(II) and Bi(III) cannot be avoided, however. Other ions were found not to interfere.

The procedure has been utilized successfully for the analysis of various tin-containing alloys such as bronzes, solders, white metal and Ti-base alloys. The results are presented in Table 1.

The method is simple and fast, and the Sn-EDTA complex is decomposed at room temperature.

Acknowledgement—The authors thank Dr. P. Rama Rao,

Director, DMRL, Hyderabad, for his permission to publish this work.

REFERENCES

1. M. Farnsworth and J. Pekola, in *Treatise on Analytical Chemistry*, I. M. Kolthoff, P. J. Elving and E. B. Sandell (eds.), Part II, Vol. 3, 327. Interscience, New York, 1961.
2. K. Kodama, *Quantitative Inorganic Analysis*, p. 203. Interscience, London, 1963.
3. J. Kinnunen and B. Wennerstrand, *Chemist-Analyst*, 1957, **46**, 34.
4. *Idem ibid.*, 1957, **46**, 92.
5. M. Goldstein and G. Kober, *Z. Anal. Chem.*, 1976, **279**, 287.
6. S. Raoot and K. N. Raoot, *Indian J. Technol.*, 1983, **21**, 442.
7. Y. C. Chen, C. V. Hsiao and G. C. Fang, *Acta Chem. Sinica*, 1964, **30**, 330.
8. Linchow Steel Works, *Fen Hsi Hua Hsueh*, 1978, **6**, 161; *Chem. Abstr.*, 1980, **92**, 173893w.
9. K. N. Raoot and S. Raoot, *Talanta*, 1984, **31**, 469.
10. O. B. Budevsky and L. Simova, *ibid.*, 1962 **9**, 769.

DETERMINATION OF CHLORIDE IN SULPHURIC ACID BY POTENTIOMETRIC MERCURIOMETRIC TITRATION

F. G. BĂNICĂ and E. DIACU

Bucharest Polytechnic, Dept. of Analytical Chemistry, Spl. Independenței 313, Bucharest, Romania

(Received 16 February 1987. Accepted 27 June 1987)

Summary—The chloride content of concentrated sulphuric acid is determined by mercuriometric titration in 80% v/v methanol medium, with a mercury pool as indicator electrode. The method is simple, fast, accurate and reasonably sensitive (limit of detection 4.5 µg/ml), and suitable for routine application.

The chloride content of sulphuric acid is important with regard to corrosion of steel equipment in chemical plants. The recommended methods for determination of chloride in sulphuric acid are based on precipitation of silver chloride¹ and are turbidimetric, titrimetric or gravimetric, according to the chloride content. However, these methods have some disadvantages connected with the intense turbidity and/or colour of many technical grades of sulphuric acid. Also the solubility of silver chloride is high enough to vitiate this method for determination of very low contents of chloride, characteristic of many samples of sulphuric acid. This is why other methods are sought, such as use of the chloride ion-selective electrode.²

Our goal was to find a titrimetric method appropriate for routine analysis in plant laboratories. Because mercurous chloride is less soluble than silver chloride, the mercurous ion was selected as precipitating reagent. Potentiometric end-point determination was chosen since it avoids any problems caused by the optical properties of the sample.

Although potentiometric mercuriometric titration of chloride was proposed a long time ago,³ it seems to be almost completely forgotten (see e.g., Williams⁴). However, this method is very promising for use in sulphuric acid analysis.

EXPERIMENTAL

Reagents

All reagents used were of analytical grade. A 0.005M mercurous nitrate solution was used as titrant. This solution was prepared daily by dilution of a 0.05M stock solution standardized and stored according to known procedures.⁵

Apparatus

The potentiometric titrations were performed in 100-ml cells, with a mercury pool microelectrode⁶ as indicator and a double-junction calomel electrode (filled with saturated potassium nitrate solution) as reference. The e.m.f. of the cell was measured by a high input impedance digital millivoltmeter. The titrant was added from a microburette.

Procedure

Since the precision required in the chloride assay is not high, the sample is taken by volume, not by weight.

Five ml of sulphuric acid are diluted with 5 ml of water in the titration cell, then 25 ml of methanol are added and the solution is titrated with 0.005M mercurous nitrate, either automatically or manually. In the manual titration, the end-point is directly indicated by attainment of the e.m.f. previously found to correspond to the equivalence point for a synthetic sample (290 mV for our equipment).

The mercurous nitrate solution is standardized by using it to titrate a solution containing 5 ml of pure sulphuric acid (or 0.5M nitric acid), 5 ml of water, 1 ml of 0.01M standard sodium chloride solution and 25 ml of methanol.

RESULTS AND DISCUSSION

The effect of sulphuric acid in aqueous solutions

During the titration of chloride in the presence of an excess of sulphate, both mercurous chloride and sulphate can precipitate. From the values of the solubility products,⁷ the solubilities of these compounds are readily calculated: $S_{\text{Hg}_2\text{Cl}_2} = 6.9 \times 10^{-7}M$; $S_{\text{Hg}_2\text{SO}_4} = 8.6 \times 10^{-4}M$. Mercurous chloride is also much less soluble than silver chloride ($S_{\text{AgCl}} = 1.33 \times 10^{-5}M$) but this advantage is partly offset by the relatively low solubility difference between mercurous sulphate and chloride, especially as the solubility of mercurous sulphate in sulphuric acid is decreased somewhat by the common-ion effect. Consequently, the potential-jump at the end-point will be small. The potential difference between the points corresponding to 99 and 101% of the equivalence volume is only about 20 mV for a sample of $3 \times 10^{-4}M$ chloride in 1M sulphate medium, as shown by a simple computation based on the Nernst equation applied to an electrode of the second kind.

The experimental data (Fig. 1) confirm this conclusion. The small potential-jump observed (curve 1) does not allow precise determination of the end-point. However, comparison of curves 1 and 2 in Fig. 1 (the second being recorded for chloride titration in the absence of sulphuric acid), demon-

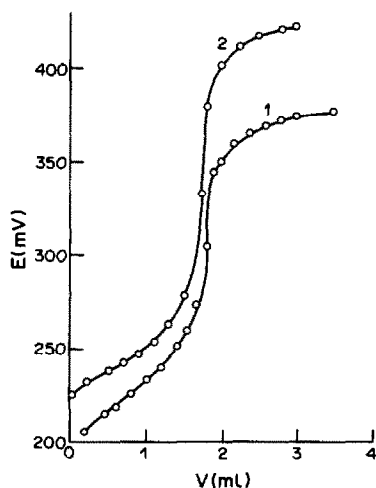


Fig. 1. Titration of chloride ($4 \times 10^{-4}M$) with mercurous nitrate in aqueous solution containing (1) $0.8M$ H_2SO_4 ; (2) $0.01M$ HNO_3 .

states the absence of any noticeable effect of sulphate on the equivalence volume.

The effect of solvent composition

Although titration in aqueous medium led to satisfactory results, an attempt was made to increase the potential-jump at the equivalence point by selective modification of the solubilities of mercurous chloride and sulphate by use of water-alcohol mixtures (Fig. 2, curves 2-4). Comparison with curve 1 (obtained in aqueous solution) shows that the end-point is much better defined in mixed solvents, without change in the equivalence volume.

The curves in Fig. 2 show a strong decrease of the solubility of mercurous chloride in the presence of an alcohol, whereas the solubility of mercurous sulphate is only slightly modified. The different behaviour of the two compounds may be due to the higher degree of hydration of chloride compared with the bulky sulphate ion. The partial replacement of water by another solvent strongly decreases the degree of solvation of chloride and this effect, combined with the lower dielectric constant, drastically reduces the solubility of mercurous chloride.

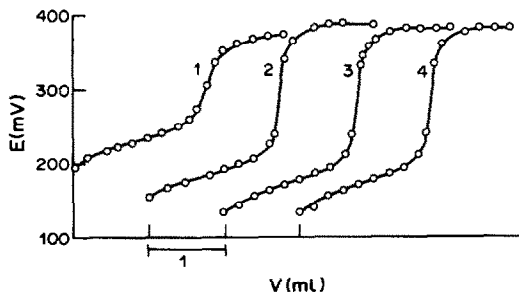


Fig. 2. The effect of alcohols on the titration curves: 2 ml of $0.01M$ $NaCl$ and 4 ml of 98% sulphuric acid were added to a mixture of x ml of water + $(50 - x)$ ml of alcohol; x : (1) 0; (2) 10 (methanol); (3) 10 (ethanol); (4) 6 (n-butanol).

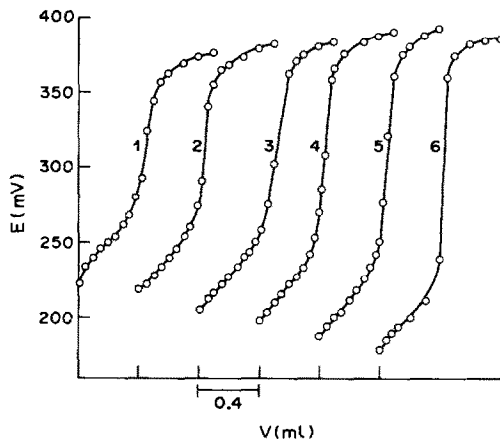


Fig. 3. The effect of water-alcohol ratio: 30 ml of solution containing 1 g of H_2SO_4 and $177.5 \mu g$ of Cl^- . Methanol, % v/v: (1) 0; (2) 15; (3) 35; (4) 50; (5) 65; (6) 80.

From a practical point of view, the most convenient titration curves are obtained in presence of ethanol or methanol (Fig. 2). Further experiments were performed in water-methanol mixtures.

The effect of the water-methanol ratio

Figure 3 shows that use of higher alcohol contents improves the shape of the titration curve and increases the potential-jump at equivalence, but the equivalence volume remains constant. Hence the methanol content was made as high as conveniently possible, 80% v/v.

The effect of sulphuric acid content in water-methanol mixtures

Figure 4 shows that when chloride is titrated in a water-methanol (1:4) mixture containing $0.01M$ nitric acid or a large amount of sulphuric acid, the sulphate ion does not modify the equivalence volume.

Titration of several solutions containing the same quantity of chloride ($178 \mu g$) and various quantities of sulphuric acid (0.4-8.0 g) gave only a fairly small variation of the equivalence volume with sulphuric acid concentration (relative standard deviation, 4%).

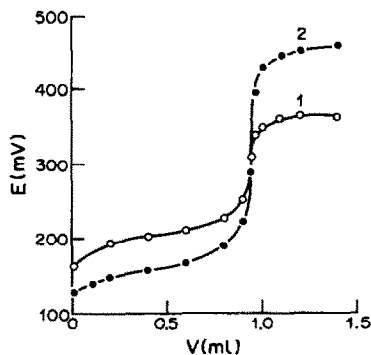


Fig. 4. Influence of sulphuric acid on the titration curve in 80% (v/v) methanol. The sample contains $355 \mu g$ of Cl^- and (1) 4 g of H_2SO_4 ; (2) $0.01M$ HNO_3 .

Table 1. The correlation of the equivalence volume, V_e , and the chloride content in the sample, m

$m, \mu\text{g}$	35.5	71	142	213.5	355	532	710
V_e, ml	0.08	0.17	0.36	0.54	0.90	1.37	1.73
		Line $V_e = a + bm$			Line $V_e = b'm$		
Intercept		$a = 0.0052$			$a' = 0$		
		$s_a = 0.017$					
Slope		$b = 0.00248,$			$b' = 0.00249,$		
		$s_b = 4.6 \times 10^{-5}$			$s'_b = 6.4 \times 10^{-5}$		
Standard devn. of V_e		$s_0 = 0.0284$			$s'_0 = 0.064$		
Correlation coeff.		0.9991			—		
Sum of squares of residuals		$S = 0.00402$			$S' = 0.00511$		
Degrees of freedom		$n = 5$			$n' = 6$		
Differences		$S' - S = 0.0011$			$n' - n = 1$		
		$F = (S' - S)/s_0^2 = 0.269; F(95\%, 1; 5) = 6.61$					

Table 2. Determination of added chloride in p.a. sulphuric acid (98%)

Cl^- added, $\mu\text{g/ml}$	7.1	71	177	248	355	710
Cl^- found, $\mu\text{g/ml}$	7.7	73	174	243	358	711

The equivalence potential was constant (290 mV) at sulphuric acid concentrations higher than 0.1 g/ml.

The titration is satisfactory over a wide range of sulphuric acid concentration (0.01–0.3 g/ml), but it is recommended to use at least 0.1 g/ml sulphuric acid, to avoid variations in the equivalence potential.

Standardization of the mercurous nitrate solution

It is recommended to use the same titration procedure for the standardization of the titrant and the analysis of samples. However, if sufficiently pure sulphuric acid is not available, an alternative standardization procedure must be employed. Figure 4 suggests the possibility of standardization with a dilute nitric acid solution containing chloride.

Five solutions prepared by adding 1 ml of concentrated sulphuric acid and 1 ml of 0.01M sodium chloride to 5 ml of water and 25 ml of methanol, were titrated with mercurous nitrate solution. The mean equivalence volume and standard deviation were 0.906 ± 0.010 ml. Five solutions similarly prepared but with 1 ml of 0.5M nitric acid instead of the sulphuric acid were titrated with the same solution, the corresponding values being 0.908 ± 0.008 ml. A t -test showed that the mean values obtained are statistically identical ($t_{\text{found}} = 0.37; t_{(95\%, 8)} = 1.86$) and either method can be used for standardization of the titrant.

Validation of the method

First, the linear correlation of the equivalence volume and the chloride content was checked with synthetic samples (Table 1). The results show that the two parameters are directly proportional.

Next, the method of Currie⁸ was applied to find the limits of the analytical procedure. If the standard deviation of the blank is taken as that of the intercept of the correlation graph, s_a (Table 1), the decision

(L_c), detection (L_D) and determination (L_Q) limits for chloride are $L_c = 2.2, L_D = 4.5, L_Q = 13.5 \mu\text{g/ml}$.

The precision of the method was assessed by the determination of known amounts of chloride added to pure 98% sulphuric acid (Table 2). Additionally, technical grade 98% sulphuric acid was doped with sodium chloride to contain 25 $\mu\text{g/ml}$ chloride. Five replicate determinations gave a mean value of 24.5 $\mu\text{g/ml}$ with standard deviation 1.2 $\mu\text{g/ml}$ (values corrected for background).

Finally, the ability of less-skilled staff to use the method was tested. After 10 minutes of training, a laboratory assistant performed ten analysis of technical grade sulphuric acid, the first under supervision and the others independently. The end-point was directly determined from the e.m.f. value. Each titration took about 4 min. The samples had previously been analysed by an expert, by recording the whole titration curve. The two series of values agreed very well, the deviation not exceeding 2%.

CONCLUSIONS

The method described permits the fast and fairly accurate determination of chloride concentrations higher than 4.5 $\mu\text{g/ml}$ in concentrated sulphuric acid. Although not as sensitive as the ion-selective electrode method,² the mercurometric titration meets all requirements for routine determinations.

REFERENCES

1. F. J. Welcher (ed.), *Standard Methods of Chemical Analysis*, Vol. II A, p. 542. Van Nostrand, New York, 1962.
2. K. D. Brown and G. A. Parker, *Analyst*, 1982, **107**, 1510.
3. E. Muller, *Z. Elektrochem.*, 1924, **30**, 420.
4. W. J. Williams, *Handbook of Anion Determination*, p. 291. Butterworths, London, 1979.
5. C. L. Wilson and D. W. Wilson (eds.), *Comprehensive Analytical Chemistry*, Vol. IB, p. 234. Elsevier, Amsterdam, 1960.
6. R. Kalvoda, *Anal. Chim. Acta*, 1958, **18**, 132.
7. L. Meites (ed.), *Handbook of Analytical Chemistry*, McGraw-Hill, New York, 1963.
8. L. A. Currie, *Anal. Chem.*, 1968, **40**, 586.

ANALYTICAL DATA

ACIDITY CONSTANTS OF BENZIDINE IN AQUEOUS SOLUTIONS

G. B. REARTES, S. J. LIBERMAN and M. A. BLESÁ

Comisión Nacional de Energía Atómica, Avenida del Libertador 8250, Buenos Aires 1429, Argentina

(Received 17 June 1986. Revised 1 June 1987. Accepted 20 June 1987)

Summary—The acidity constants of benzidine (Bz) in aqueous solutions determined potentiometrically at 25° were $K_{a1} = (1.11 \pm 0.08) \times 10^{-5}$, $K_{a2} = (1.45 \pm 0.12) \times 10^{-4}$. The apparent mixed constants in 0.1M sodium nitrate are $K_{a1} = (5.37 \pm 0.28) \times 10^{-6}$ and $K_{a2} = (1.14 \pm 0.09) \times 10^{-4}$. The ultraviolet spectra were recorded as a function of pH and analysed with these constants to obtain the absorption spectra of H_2Bz^{2+} , HBz^+ and Bz; the corresponding wavelengths of maximal absorption are 247, 273 and 278 nm, and molar absorptivities 1.63×10^4 , 1.76×10^4 and 2.26×10^4 l.mole⁻¹.cm⁻¹.

Benzidine (Bz), (4,4'-diaminobiphenyl, C₁₂H₁₂N₂), has a number of analytical applications.^{1,2} In particular, it forms a complex with copper and oxalic acid with molar absorptivity 2.49×10^4 l.mole⁻¹.cm⁻¹ at 246 nm, which is used for determining oxalic acid in mixtures of decontamination reagents in nuclear reactors.³

The spectral properties of aqueous Bz solutions at various pH values are not adequately described in the literature. We report here such a study, in conjunction with a re-examination of the potentiometric determination of the acidity constants of H_2Bz^{2+} and HBz^+ , in an attempt to resolve the discrepancies in the values reported in the literature.⁴⁻⁷ The molar absorptivities of free Bz and its diprotonated form H_2Bz^{2+} were also measured, and the value for that of the monoprotated species HBz^+ was estimated. The electronic transitions involved are discussed briefly.

EXPERIMENTAL

Reagents

All reagents were analytical grade and the solutions were prepared with doubly distilled water. The benzidine (RPL, Belgium, p.a. quality) was used without further purification. It was tested for purity by potentiometric titration with perchloric acid in glacial acetic acid. No purification to above 98% could be achieved by repeated recrystallization.

Potentiometric titrations of aqueous 10^{-3} M Bz solutions in 0.1M sodium nitrate at $25.00 \pm 0.05^\circ$ were done with a Metrohm 636 automatic titrator. The pH-meter was standardized with standard buffer solutions at pH values (conventional activity scale) of 4.00 ± 0.02 , 7.00 ± 0.02 and 9.00 ± 0.02 at 25°. The solutions were deaerated with nitrogen and titrated with 0.012M nitric acid in 0.1M sodium nitrate. The low solubility of Bz prevented the use of higher concentrations of the reagent. All experiments were performed in duplicate.

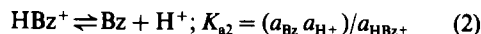
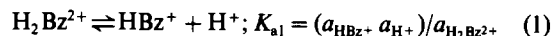
The absorption spectra (240-330 nm) of 10^{-4} - 10^{-5} M Bz in 0.1M sodium nitrate solution acidified with sulphuric acid

were measured at room temperature (22-25°) and various pH values, with a Zeiss DM4 spectrophotometer and fused-silica cells of 0.5 and 1 cm optical path, against 0.1M sodium nitrate as reference.

RESULTS AND DISCUSSION

Figure 1 shows the potentiometric titration curves of 1.001×10^{-3} M Bz. The lack of distinct steps is typical of acids with relatively close (and rather high) K_{a1} and K_{a2} values.

For the evaluation of K_{a1} and K_{a2} equations (1) and (2) were considered:



together with the mass-balance relationships (3) and (4):

$$c_0 = ([Bz] + [HBz^+] + [H_2Bz^{2+}]) \frac{(V_a + V_0)}{V_0} \quad (3)$$

$$[H^+] = \frac{c_a V_a - [HBz^+](V_a + V_0) - 2[H_2Bz^{2+}](V_a + V_0)}{V_a + V_0} \quad (4)$$

where a_i and $[i]$ are the activity and concentration of species i , c_0 and c_a are the initial concentrations and V_0 and V_a the volumes of Bz and nitric acid. From these, equation (5) is derived:

$$y = 1/K_{a1} K_{a2} + x/K_{a2} \quad (5)$$

where:

$$y = \left(\frac{c_a V_a - (V_a + V_0)(a_{H^+}/\gamma_{H^+})}{(V_a + V_0)(a_{H^+}^3/\gamma_{H^+}) + (2c_0 V_0 - c_a V_a) a_{H^+}^2} \right) \times \left(\frac{\gamma_{H_2Bz^{2+}}}{\gamma_{Bz}} \right) \quad (6)$$

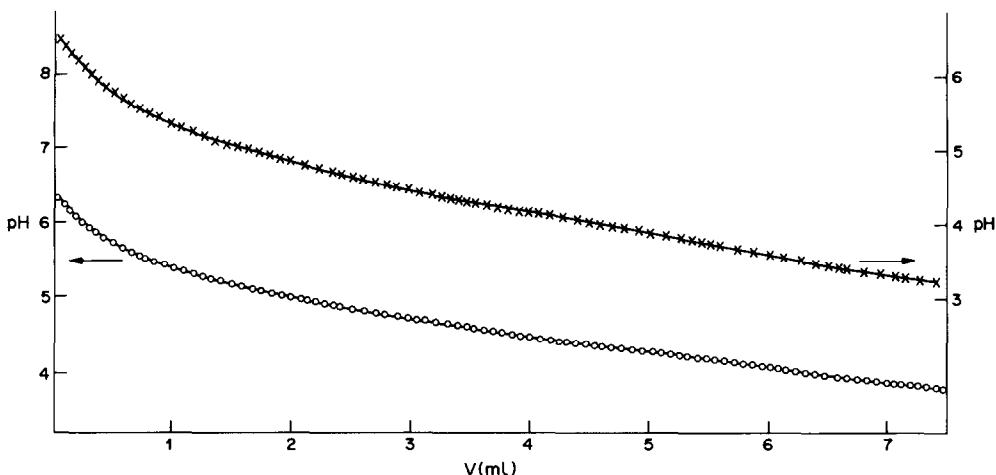


Fig. 1. Potentiometric titration of $1.001 \times 10^{-3} M$ benzidine solutions with $0.012 M$ HNO_3 at 25° ; \times and \circ correspond to independent runs.

and

$$x = \left(\frac{(V_a + V_0)(a_{H^+}/\gamma_{H^+}) + (c_0 V_0 - c_a V_a)}{(V_a + V_0)(a_{H^+}^2/\gamma_{H^+}) + (2c_0 V_0 - c_a V_a)a_{H^+}} \right) \times \left(\frac{\gamma_{H_2Bz^{2+}}}{\gamma_{Bz}} \right) \quad (7)$$

The activity coefficient γ_{H^+} at $I = 0.1$ was taken to be 0.761, as suggested by Tamamushi⁸ from conductance data, in agreement with the Bates-Guggenheim (pH) convention.⁹

The activity coefficients for the protonated species $\gamma_{H_2Bz^{2+}}$ and γ_{HBz^+} were calculated from the Davies equation (8),¹⁰ in view of the lack of the thermo-

dynamic data needed to use more accurate expressions:

$$\log \gamma_i = -B z_i^2 \{ [\sqrt{I}/(1 + \sqrt{I})] - 0.3 I \} \quad (8)$$

where z_i is the charge on species i , I is the ionic strength and B is equal to 0.505 at 25° .

Figure 2 shows experimental results plotted according to equation (5). From the slope and intercept, the values $K_{a1} = (1.11 \pm 0.08) \times 10^{-5}$ and $K_{a2} = (1.45 \pm 0.12) \times 10^{-4}$ are obtained. The corresponding apparent mixed constants in $0.1 M$ sodium nitrate are $K_{a1} = (5.37 \pm 0.28) \times 10^{-6}$ and $K_{a2} = (1.14 \pm 0.09) \times 10^{-4}$. These values should be preferred to the older figures reported in the

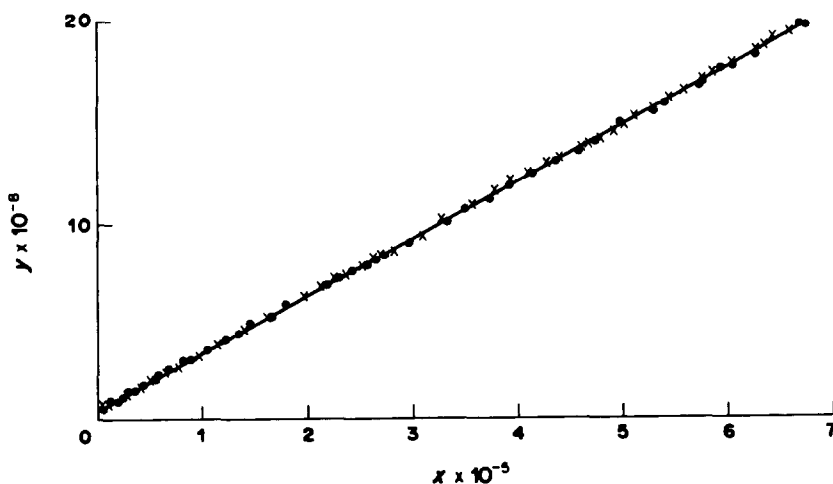


Fig. 2. Evaluation of acidity constants K_{a1} and K_{a2} at 25° according to equation (5); \times and \circ correspond to independent runs.

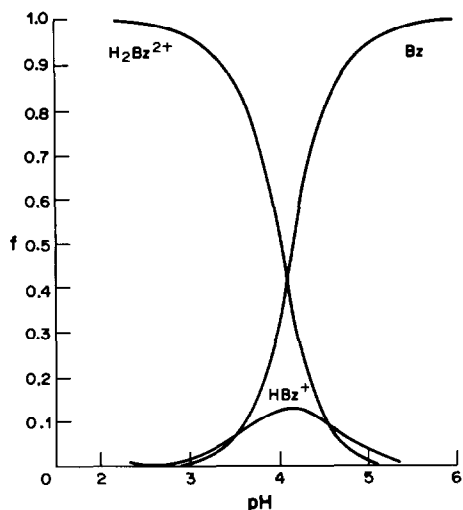


Fig. 3. Distribution of species in benzidine solutions showing the fraction f corresponding to each species as a function of pH at 25° in 0.1M NaNO₃.

literature⁴⁻⁷ for the apparent constants; the values range from 1.05×10^{-5} to 2.19×10^{-5} for K_{a1} and from 1.78×10^{-4} to 3.31×10^{-4} for K_{a2} . These earlier papers do not give much detail about the calculation procedures.

Figure 3 shows the distribution of Bz species as a function of pH. At pH 2.25 H_2Bz^{2+} is the only species, while at pH 6.00 free Bz predominates. HBz^+ is never predominant, reaching only 9.5% of the total at pH 4.50.

Figure 4 shows some of the experimental molar absorptivities obtained for solution in 0.1M sodium nitrate media at various pH values. A maximum at 247 nm for pH 2.28 can be observed to correspond to

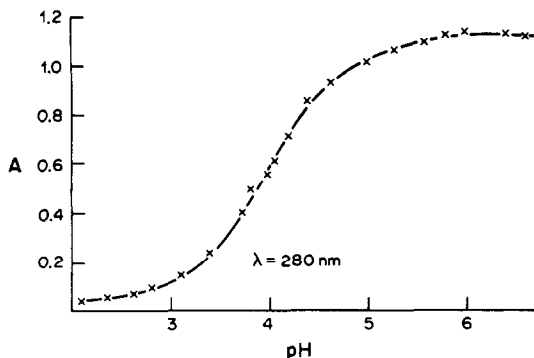


Fig. 5. Absorbance of $10^{-4}M$ benzidine in 0.1M NaNO₃ solution in 0.5-cm cells as a function of pH at $\lambda = 280$ nm; \times experimental data, — calculated.

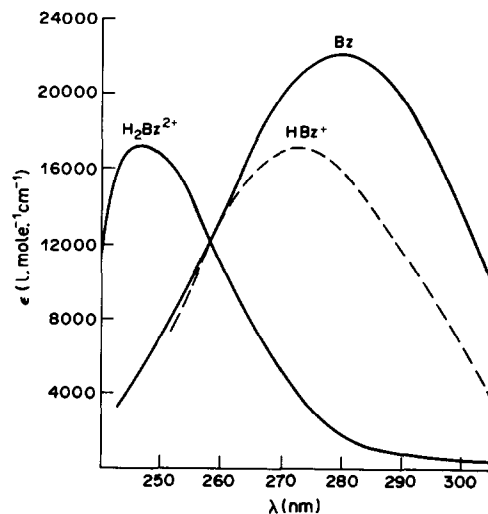


Fig. 6. Molar absorptivities of benzidine species in 0.1M NaNO₃ as a function of wavelength.

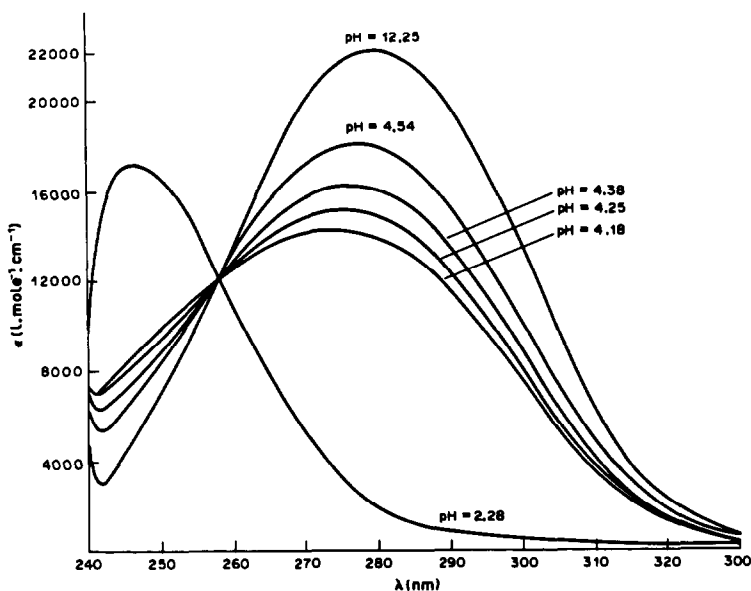


Fig. 4. Molar absorptivities obtained from the spectra of $10^{-4}M$ benzidine at various pH values in 0.1M NaNO₃.

H_2Bz^{2+} , with $\epsilon_{\text{H}_2\text{Bz}^{2+}} = 1.633 \times 10^4 \text{ l. mole}^{-1} \cdot \text{cm}^{-1}$. Molar absorptivities at pH values down to 1.80 had the same values. The maximum shifts to longer wavelengths as the pH increases, and is at 278 nm, ($\epsilon = 2.259 \times 10^4 \text{ l. mole}^{-1} \cdot \text{cm}^{-1}$) for free Bz. There is an isosbestic point at 258 nm. The value for ϵ_{Bz} from this work is in agreement (within 10%) with the values given in the literature for water-methanol solution.¹¹

The absorption spectrum of the monoprotated ion was computed by using the mixed apparent potentiometric K_{a1} and K_{a2} values, and the absorptivities of Bz and H_2Bz^{2+} at each wavelength (from the spectra at pH 2.28 and 12.25 respectively), and analysing the spectra in the intermediate pH range. A least-squares procedure was used to compute a value for ϵ_{HBz^+} that would minimize U in equation (9) for each species:

$$U = A^2 - (l \sum \epsilon_i c_i)^2 \quad (9)$$

where l is the cell path-length.

The goodness of the fit is checked in Fig. 5, which shows the absorbance A of $10^{-4} M$ Bz solutions in $0.1 M$ sodium nitrate in 0.5-cm cells as a function of pH at 280 nm, where Bz has its maximum. The curve was calculated according to the Lambert-Beer law and $\epsilon_{\text{Bz}} = 2.24 \times 10^4$, $\epsilon_{\text{H}_2\text{Bz}^{2+}} = 6.2 \times 10^2$ and $\epsilon_{\text{HBz}^+} = 1.672 \times 10^4 \text{ l. mole}^{-1} \cdot \text{cm}^{-1}$, calculated by the procedure above. The points in the plot are data from Fig. 4. The agreement is acceptable; similar results were obtained for other wavelengths.

The spectra of H_2Bz^{2+} , HBz^+ and Bz are shown in Fig. 6; small differences from the data shown in Fig. 4 reflect the use of a large number of spectral runs in the fitting procedure. The absorption maximum for the monoprotated species at 273 nm ($\epsilon_{\text{HBz}^+} = 1.76 \times 10^4 \text{ l. mole}^{-1} \cdot \text{cm}^{-1}$ between the max-

ima for free Bz (at 278 nm) and H_2Bz^{2+} (at 247 nm). The band corresponds to a $\pi \rightarrow \pi^*$ transition (E -band), the position being determined by the auxochromic effect of the $-\text{NH}_2$ substituents. Upon protonation of one group, only a modest shift (from 278 to 273 nm) is observed, compatible with the influence of the remaining non-protonated NH_2 group. There is however a substantial decrease in the intensity (see Fig. 6). When the second $-\text{NH}_2$ group is protonated, the maximum shifts to 247 nm, reflecting the more difficult interaction of the nitrogen non-bonding electrons with the π -electrons of the aromatic nucleus. Related systems such as aniline, anilinium and benzene exhibit similar trends.¹²

REFERENCES

1. F. J. Welcher, *Organic Analytical Reagents*, Vol. II, pp. 275-328. Van Nostrand, Princeton, 1950.
2. Z. D. Draganic, *Anal. Chim. Acta*, 1971, **28**, 394.
3. G. B. Reartes, S. J. Liberman and M. A. Blesa, *XVI Congreso Argentino de Quimica*, Córdoba, Sept. 1982. Abstract Sec. 8-8.
4. P. H. Grantham, E. R. Weisburger and J. H. Weisburger, *J. Org. Chem.*, 1961, **26**, 1008.
5. R. C. Weast, (ed.), *CRC Handbook of Chemistry and Physics*, Ed., Chemical Rubber Co., Cleveland, Ohio, 1980.
6. W. M. Clark, B. Cohen and H. D. Gibbs, *U.S. Public Health Repts.*, 1926, Suppl. No. 54, 61.
7. N. S. Hush, *J. Chem. Soc.*, 1953, **I**, 684.
8. R. Tamamushi, *Bull. Chem. Soc. Japan*, 1974, **47**, 1921.
9. R. G. Bates and E. A. Guggenheim, *Pure Appl. Chem.*, 1960, **1**, 163.
10. C. W. Davies. *Ion Association*, Butterworths, London, 1962.
11. *Ultraviolet Spectral Data*, Sadtler Research Laboratories, Philadelphia, Pa. U.S.A.
12. R. M. Silverstein, *Spectrometric Identification of Organic Compounds*, p. 101. Wiley, New York; 1963.

ANALYSIS OF THE CCRMP Oka-2 RARE-EARTH REFERENCE MINERAL OF THE BRITHOLITE–APATITE SERIES BY ELECTROTHERMAL ATOMIC-ABSORPTION AND INDUCTIVELY-COUPLED PLASMA ATOMIC-EMISSION SPECTROMETRY*

J. G. SEN GUPTA

Geological Survey of Canada, Ottawa, Ontario, Canada

(Received 28 October 1986. Revised 4 June 1987. Accepted 20 June 1987)

Summary—The lanthanides and yttrium in the Canadian Certified Reference Materials Project (CCRMP) new rare-earth mineral reference material, Oka-2, were determined by electrothermal atomic-absorption and inductively-coupled plasma atomic-emission spectrometry (ICPAES) after sample decomposition with acids and separation of the rare-earth metals from phosphate and other matrix elements by precipitation as fluorides and oxalates. Thorium, yttrium and the common major and minor elements were determined by ICPAES after sample decomposition by fusion with lithium meta- and tetraborates and dissolution of the melt in a mixture of dilute nitric acid and ethylenediaminetetra-acetic acid solution. For comparison purposes, silicon, phosphorus, calcium, magnesium and iron were also determined by other methods. The results obtained are compared with other CCRMP values and with those obtained previously for a similar rare-earth mineral from the same geographical area. Oka-2 is considered to be a thorian intermediate member of the britholite–apatite series.

In 1964 the analysis of a thorian intermediate member of the britholite–apatite series from Oka, Quebec (henceforth referred to as Oka-A) by ion-exchange separation and conventional chemical and X-ray fluorescence methods was reported.¹ Later, nine lanthanides were determined in four rare-earth minerals, including Oka-A, and some rocks by a method based on fluoride and oxalate separations of the lanthanides, followed by their co-precipitation with hydrous ferric oxide and ultimate determination by flame atomic-absorption (AAS) or atomic-emission spectrometry (AES).² Subsequently, this method, and an additional method involving an emission spectrometric finish after co-precipitation of the lanthanides with silica and hydrous ferric and aluminium oxides, were used to determine trace amounts of the rare-earth elements in 24 international reference rocks.³ In recent years electrothermal AAS (ETAAS) finishes have been applied in the determination of many of the rare-earth elements in silicate rocks and related materials, after suitable separations as described above.^{4–7} This work resulted in an invitation to participate in a Canadian Certified Reference Materials Project (CCRMP) interlaboratory programme for the certification of thorium and the

rare-earth elements in a britholite mineral, designated Oka-2, taken from a massive deposit in the same area as the Oka-A mineral.¹ This paper gives the results obtained for these elements, as well as for the matrix elements, by using ETAAS, inductively-coupled plasma atomic-emission spectrometry (ICPAES) and other finishes.

EXPERIMENTAL

Apparatus and reagents

The AAS equipment, auxiliary apparatus and preparation of standard solutions of rare-earth elements are described in previous papers.^{6–8} The operating parameters for the Varian GTA-95 graphite-tube atomizer are given in Table 1. Other required AAS instrumental parameters were as reported previously.^{7,8}

For ICPAES determinations, a Jobin-Yvon Model JY 48 simultaneous instrument was used. The spectral lines used are listed in Table 2. In most cases, synthetic standard solutions were prepared from high-purity 1000- $\mu\text{g}/\text{ml}$ commercial solutions.

A Beckman Model B spectrophotometer with matched 10-mm cells was used for the spectrophotometric determination of phosphorus.

Determination of yttrium and the rare-earth elements after decomposition with acids

Ce, Pr, Nd, Tb, Ho, Er, Tm and Lu by electrothermal AAS. The powdered sample (1 g) was decomposed in a covered 100-ml platinum dish by heating with concentrated hydrofluoric and nitric acids, and the solution was evaporated to dryness to remove silica.² The salts were heated with concentrated hydrofluoric acid and the resultant fluorides of calcium, magnesium, thorium, yttrium and the rare-earth elements were separated from phosphate by filtration (11-cm No. 40 Whatman paper) and washed with hot 2% v/v nitric acid.

*Invited paper presented at CASALS 86—Congress on Advances in Spectroscopy and Laboratory Science, held in Toronto, Ontario, 6–9 October, 1986. Government of Canada copyrights reserved. Geological Survey of Canada contribution 32186.

Table 1. Operating parameters for electrothermal AAS determination of the rare-earth elements

Element	Step number	Temperature, °C	Time, sec	Argon gas flow, l./min
Ce, Pr, Nd, Tb,	1	75	15	3
Ho, Er, Tm and	2	90	60	3
Lu	3	120	10†	3
	4	850	10	3
	5	1800	10	3
	6	1800	2	0
	7	2700‡	1.3	0*
	8	2700‡	2	0*
	9	2800‡	5§	3

*Read command initiated.

†60 sec for Lu in a tantalum foil-lined furnace.

‡2600° for Lu as above.

§1 sec for Lu as above.

The paper containing the precipitate was transferred back to the platinum dish and heated first with concentrated nitric acid, then with concentrated perchloric acid to destroy the paper and convert the salts into perchlorates. After evaporation of the solution to dryness, the salts were warmed with 10% v/v nitric acid containing 5% hydrogen peroxide, and the solution was stirred, then filtered (7-cm Whatman No. 40 paper) and the paper was washed with hot 10% v/v nitric acid–5% hydrogen peroxide solution. Any insoluble material remaining was decomposed by transferring the paper back to the platinum dish and repeating the nitric–perchloric acid treatment. The resulting residue was ultimately dissolved as described and the solution was added to the initial nitric acid–hydrogen peroxide solution. After a double methyl oxalate and a single hydrous ferric oxide separation and conversion of the salts into nitrates by heating with nitric acid and hydrogen peroxide, as described previously,^{2,4,6} the solution was evaporated to dryness. The salts were dissolved in 1M nitric acid by warming and the solution was diluted to volume with 1M nitric acid in a 25-ml standard flask.

By use of the wavelengths reported previously,⁷ the operating parameters shown in Table 1 and a 10- μ l volume, the solution was analysed for holmium and lutetium by ETAAS. Thulium and erbium were determined after two-fold dilution of the sample solution with 0.1M nitric acid;

cerium, praseodymium and terbium were determined after fourfold dilution in a similar manner, and neodymium was determined after a hundredfold dilution. Except for lutetium, which was atomized from a furnace lined with tantalum foil, the elements were atomized from a pyrolytically-coated graphite furnace. Standard solutions (5- μ g/ml Ho, 1- μ g/ml Lu, 0.2- μ g/ml Er, 1000- μ g/ml Ce, 100- μ g/ml Pr, 5- μ g/ml Tb and 10- μ g/ml Nd in 0.1M nitric acid) were used for calibration. The standard lutetium solution contained approximately the same concentrations of Y, Th and other rare-earth elements as the sample solution.

Y, La, Ce, Sm, Eu, Gd, Dy and Yb by ICPAES. Cerium and lanthanum were determined by ICPAES at the wavelengths given in Table 2, in two solutions obtained after 200- and 100-fold dilutions of the sample solution with 10% v/v nitric acid, and the mean of two results was taken. The remaining rare-earth elements were determined in both of these diluted solutions, and also after 50-fold dilution of the sample solution with 10% v/v nitric acid, and the mean of these results was taken. The instrument was calibrated at the appropriate wavelengths with synthetic standard solutions of the rare-earth elements that bracketed the analyte concentrations in the diluted sample solutions.

Determination of Th, Y and the common elements by ICPAES after decomposition by fusion

The sample (0.5 g) was mixed with 1.5 g of a flux consisting of 2 parts of LiBO₂ and one part of Li₂B₄O₇ and fused in a graphite crucible at 1000° for 30 min. The melt was poured into a beaker containing ~150 ml of water and 10 ml each of concentrated nitric acid and 0.8% diammonium ethylenediaminetetra-acetate solution. After being stirred with a magnetic stirrer to dissolve the salts, the solution was transferred to a 250-ml standard flask, diluted to volume with water, and then filtered through a dry 11-cm Whatman No. 40 paper and stored in a plastic bottle. Thorium was determined by ICPAES, at 283.73 nm, after tenfold dilution of the solution with water. Two synthetic solutions containing 1- and 10- μ g/ml thorium and approximately similar concentrations of yttrium, the rare-earth elements, lithium meta- and tetraborate and diammonium EDTA as the sample solutions were used for calibration. Yttrium and common major and minor elements were determined by ICPAES in the undiluted sample solution, at the spectral lines given in Table 2. Some synthetic and "in-house" reference material solutions were used to prepare calibration curves.

For comparison purposes, calcium, magnesium and iron were determined by AAS in an air–acetylene flame after 12.5-fold dilution of the sample solution and addition of sufficient strontium nitrate solution to give a final strontium

Table 2. Wavelengths used for ICPAES determinations

Element*	Wavelength, nm	Element	Wavelength, nm
Na	588.99	Co	228.62
Mg ₁	279.08	Ni	231.60
Mg ₂	383.83	Cu	324.75
Al	308.22	Zn	213.86
Si ₁	251.61	Sr	407.77
Si ₂	288.16	Y	371.03
P	178.29	Zr	343.80
K	766.49	Ba	233.53
Ca ₁	317.93	La	333.75
Ca ₂	315.89	Ce	413.77
Ti	337.20	Sm	359.26
V	292.40	Eu	381.97
Cr	267.72	Gd	335.05
Mn ₁	257.61	Dy	353.17
Fe ₁	259.94	Yb	328.94
Fe ₂	261.19	Th	283.73

*Subscript 1 or 2 after the symbol indicates that the corresponding wavelength is the most or least sensitive, respectively.

Table 3. Determination of thorium, yttrium and the rare-earth elements (%) in Oka-2

Constituent	Found* (this work)	Standard deviation (s)	Range of CCRMP values	Number of contributing laboratories	Methods used [¶]	Mean of CCRMP values $\pm 2s$
ThO ₂	3.38†	0.045	3.11–3.57	25	A, B, C, D, E, F, G,	3.34 \pm 0.25
Y ₂ O ₃	0.50‡ 0.40†	0.010 0.007	0.27–0.37	4	A, E, F, H	0.31 \pm 0.08
La ₂ O ₃	5.84‡	0.055	5.51–6.21	11	A, D, E, F, H	5.8 \pm 0.5
CeO ₂	15.5‡ 15.4§	0.100 0.145	12.87–16.02	12	A, D, E, F, H	14.4 \pm 1.8
Pr ₆ O ₁₁	1.70§	0	1.37–2.18	9	A, D, F, H	1.8 \pm 0.5
Nd ₂ O ₃	7.70§	0.12	6.11–7.68	10	A, D, F, H	6.7 \pm 1.0
Sm ₂ O ₃	1.30‡	0	0.86–1.21	11	A, D, F, H	1.0 \pm 0.2
Eu ₂ O ₃	0.30‡	0	0.20–0.37	12	A, D, F, H	0.26 \pm 0.09
Gd ₂ O ₃	0.73‡	0.005	0.28–0.80	10	A, D, F, H	0.6 \pm 0.3
Tb ₂ O ₃	0.053§	0.001	0.033–0.076	10	A, D, F, H	0.06 \pm 0.03
Dy ₂ O ₃	0.26‡	0.007	0.131–0.318	9	A, D, E, F, H	0.19 \pm 0.11
Ho ₂ O ₃	0.0094§	0.0001	0.0186–0.0282	4	D, F, H	0.023 \pm 0.008
Er ₂ O ₃	0.0122§	0.0003	0.0053–0.1000	3	A, D, F, H	0.06 \pm 0.04 ^a
Tm ₂ O ₃	0.0011§	0	0.0017–0.0034	3	D, F, H	0.003 \pm 0.002
Yb ₂ O ₃	0.0108‡	0.0003	0.0076–0.0171	5	D, E, F, H	0.013 \pm 0.008
Lu ₂ O ₃	0.0010	0	0.0006–0.0017	6	D, F,	0.0012 \pm 0.0007

*Mean of 5 values.

†Determined by ICPAES after fusion of the sample with lithium meta- and tetraborates.

‡Determined by ICPAES after preconcentration by fluoride and oxalate precipitations.

§Determined by ETAAS after preconcentration as described above.

||Determined by ETAAS in a tantalum foil-lined furnace after preconcentration as described above.

¶A—X-ray fluorescence spectrometry; B—spectrophotometry; C—gamma-ray spectrometry; D—neutron activation analysis; E—ICPAES; F—direct coupled plasma emission spectrometry; G—titrimetry; H—inductively-coupled plasma mass spectrometry.

^aMean $\pm s$.

concentration of $\sim 1500 \mu\text{g/ml}$.⁹ Silica, in a suitable aliquot, was determined gravimetrically after dehydration by evaporation with perchloric acid, ignition, and treatment of the residue with hydrofluoric acid and perchloric acid, and a correction was applied for silica not recovered from the filtrate. Phosphorus was determined spectrophotometrically by the molybdenum blue method¹⁰ in the solution obtained after fusion of the silica residue with sodium carbonate, dissolution of the melt in water, filtration, and addition of the filtrate to the original filtrate from the separation of the impure silica. The concentration of phosphorus in the final solution measured was $\sim 1 \mu\text{g/ml}$.

Determination of total water and carbon dioxide

Total water and carbon dioxide were determined by volatilization and non-dispersive infrared absorptiometry.¹¹ A 0.2-g sample was mixed with 1 g of a 1:1 mixture of vanadium pentoxide and tungsten trioxide in a nickel boat and heated at 950° in a silica tube in an electric furnace. The evolved gases were carried in a current of nitrogen to two Beckman Model 864 infrared analysers, connected to an integrator where the signals (mV) were displayed digitally. The instrument was calibrated with "in-house" reference materials.

Determination of fluorine

The sample (0.1 g) was mixed with 0.5 g of vanadium pentoxide and heated in a combustion furnace at 1050°. The evolved gas was swept out by a carrier gas (water vapour at 60°, saturated with oxygen) at a flow-rate of 1 ml/min and absorbed in 50 ml of a 0.003M sodium bicarbonate/0.0024M sodium carbonate buffer. The fluorine content of this solution was determined by ion-chromatography in a Dionex System 12 analyser.

RESULTS AND DISCUSSION

The results for thorium, yttrium and the rare-earth elements by ETAAS and ICPAES are given in Table 3. In the absence of a similar type of rare-earth reference mineral, the recoveries of the rare-earth elements were monitored by analysing the CCRMP reference syenite rock, SY-3, which was taken through the entire procedure used for Oka-2 and for which the thorium and most rare-earth element contents are known.¹² Table 3 also shows the range of results obtained during the CCRMP interlaboratory certification programme after extreme outliers, and any results more than two standard deviations away from the mean had been deleted by using the "trimmed mean" approach described by Steele *et al.*¹³ and Gladney and Goode.¹⁴ In most cases, the results of the present work fall within the range of the "trimmed" CCRMP values and are in relatively good agreement with the final "trimmed mean" values.

Table 4 shows that the results obtained for the common major and minor elements by ICPAES and for water, carbon dioxide and fluorine are in reasonably good agreement, where applicable, with those obtained by other investigators during the interlaboratory certification programme. The results obtained for silica and phosphorus and for total iron, magnesium and calcium also agree fairly well with those obtained by gravimetric, spectrophotometric and flame AAS methods, respectively.

Table 4. Comparison of results for common elements in Oka-2

Constituent	Found, %, this work*				CCRMP values, %
	ICPAES†	Standard deviation	Other methods	Standard deviation	
SiO ₂	15.3	0.2	14.9‡	0.1	14.72, 14.9
TiO ₂	0.33	0.01			0.24
Al ₂ O ₃	1.00	0			0.82
Fe ₂ O ₃ total	5.40	0.05	5.28§	0.03	5.83, 5.4
MnO	0.56	0.01			0.51
MgO	1.26	0.01	1.20§	0	1.24
CaO	22.1	0.2	21.6§	0.2	22.4, 23.2
Na ₂ O	0.49	0.01			0.36, 0.45, 0.30
K ₂ O	0.42	0.01			0.35
H ₂ O total	1.10	0			
CO ₂	1.20	0			
P ₂ O ₅	11.4	0.9	11.46¶	0	11.9
F	1.68	0			
BaO	0.13	0.002			
CoO	0.006	0.0001			
Cr ₂ O ₃	0.013	0.0001			
CuO	0.036	0.001			
NiO	0.017	0.002			
SrO	0.85	0.01			
V ₂ O ₅	0.09	0			
ZnO	0.024	0.0004			
ZrO ₂	0.074	0.001			

*Mean of five values (a standard deviation of zero means that the five results were identical within experimental error).

†All results by ICPAES except for water, carbon dioxide and fluorine.

‡Gravimetric value.

§Flame AAS value.

¶Spectrophotometric value.

Table 5 shows that Oka-2 contains significantly less phosphorus, calcium, thorium and fluorine than does the earlier Oka-A mineral but more silica, aluminium, iron and magnesium. However, the rare-earth content and specific gravity (determined with a pycnometer) are only slightly higher than those of Oka-A. X-Ray powder diffraction studies of unignited Oka-A and Oka-2 samples, made with a Phillips diffractometer with nickel-filtered copper radiation, indicated that the Oka-A britholite is totally metamict and that the only identifiable

contaminant it contains is apatite. In Oka-2 some non-metamict britholite diffraction spacings were observed and the major contaminants identified were mica and apatite with very minor amounts of calcite and magnetite. The presence of several per cent of apatite in Oka-A, even after a series of magnetic and gravity separations from gangue minerals, was reported previously.¹ Because there are other impurities in Oka-2 in addition to apatite, some differences in the compositions of the common elements in the two samples is to be expected.

Table 5. A comparison of specific gravities and partial compositions of britholite, fluorapatite and the Oka-2 and Oka-A rare-earth minerals

	Britholite* (Greenland)	Oka-2† (this work)	Oka-A*	Fluorapatite*
Sp. gr.	4.446	3.95	3.86	3.203
SiO ₂	16.71	15.3	12.28	—
P ₂ O ₅	6.48	11.4	16.96	41.87
CaO	11.28	22.1	28.84	55.16
Σ Rare-earths	60.54	33.8	33.43	—
ThO ₂	—	3.38	5.62	—
MgO	—	1.26	0.20	—
Fe ₂ O ₃ total	—	5.40	0.14	—
Al ₂ O ₃	—	1.00	0.47	—
Na ₂ O	—	0.49	0.21	—
TiO ₂	—	0.33	0.09	—
H ₂ O total	—	1.10	0.54	—
F	—	1.68	2.10	—

*Concentrations (%) reported previously.¹

†Concentration in %.

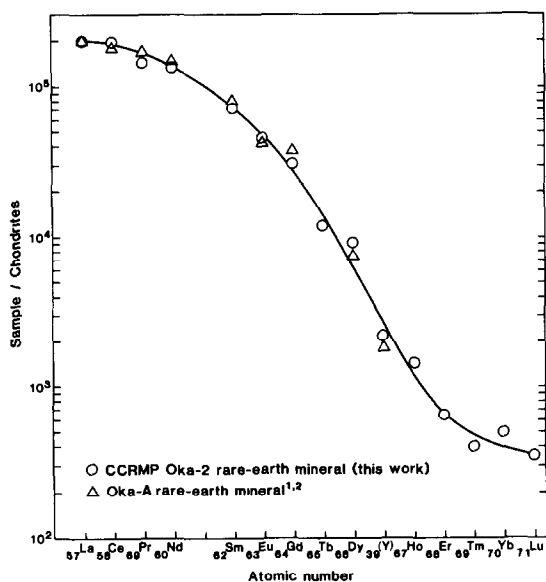


Fig. 1. Chondrite-normalized yttrium and rare-earth element pattern for Oka-A and Oka-2 rare-earth minerals.

However, from X-ray powder diffraction patterns and the compositions shown in Table 5, it appears that there is less apatite in Oka-2 than in Oka-A, and that like britholite, Oka-2 contains more silica than phosphorus. Therefore, although Oka-2 can be placed one step closer to britholite than can Oka-A it is still considered to be an intermediate member of the britholite-apatite series.

Figure 1 shows the abundances of yttrium (normalized to the average chondritic abundance data given by Haskin *et al.*¹⁵) and the rare-earth elements (normalized to the average CI chondritic abundance values given by Evensen *et al.*¹⁶) for the Oka-A and Oka-2 minerals. The abundance for yttrium is plotted between that for dysprosium and holmium because of the similarity in properties and ionic radii of the three

elements. The rare-earth distribution in the samples is found to be highly fractionated with respect to chondrites, lighter rare earths being much more enriched than the heavier ones. The similarity of the abundance patterns for the rare earths in the two samples is indicated by the single curve in Fig. 1. The curve is reasonably smooth, which indicates the reliability of the analytical data.

Acknowledgements—The author wishes to thank various members of the GSC Chemical Laboratories for providing ICPAES results and the values for water, carbon dioxide and fluorine in Oka-2; A. C. Roberts for X-ray powder diffraction studies; C. W. Smith, the Coordinator of the CCRMP, for providing and permitting the use of additional CCRMP values; and Elsie M. Donaldson for critical reading of the manuscript. The interpretation of CCRMP values as embodied in this paper is that of the author.

REFERENCES

1. M. R. Hughson and J. G. Sen Gupta, *Am. Mineral.*, 1964, **49**, 937.
2. J. G. Sen Gupta, *Talanta*, 1976, **23**, 343.
3. *Idem*, *Geostds. Newsl.*, 1977, **1**, 149.
4. *Idem*, *Talanta*, 1981, **28**, 31.
5. *Idem*, *Geostds. Newsl.*, 1982, **6**, 241.
6. *Idem*, *Talanta*, 1984, **31**, 1053.
7. *Idem*, *ibid.*, 1985, **32**, 1.
8. *Idem*, *ibid.*, 1984, **31**, 1045.
9. S. Abbey, *Geol. Surv. Can.*, 1968, Paper 68-20.
10. D. F. Boltz and C. H. Lueck, in *Colorimetric Determination of Nonmetals*, D. F. Boltz (ed.), p. 29. Interscience, New York, 1958.
11. J. L. Bouvier and S. Abbey, *Can. J. Spectrosc.*, 1980, **25**, 126.
12. S. Abbey, *Geol. Surv. Can.*, 1983, Paper 83-15.
13. T. W. Steele, A. Wilson, R. Goudvis, P. J. Ellis and A. J. Radford, *Geostds. Newsl.*, 1978, **2**, 71.
14. E. S. Gladney and W. E. Goode, *ibid.*, 1981, **5**, 31.
15. L. A. Haskin, M. A. Haskin, F. A. Frey and T. R. Wildeman, in *Origin and Distribution of the Elements*, L. H. Ahrens (ed.), p. 889. Pergamon Press, Oxford, 1968.
16. N. M. Evensen, P. J. Hamilton and R. K. O'Nions, *Geochim. Cosmochim. Acta*, 1978, **42**, 1199.

SOFTWARE SURVEY SECTION

Software package TAL-012787

ENZFITTER

Contributor: Dr. R. J. LEATHERBARROW, Imperial College of Science and Technology, London

Brief description: ENZFITTER fits two sets of experimental data by non-linear regression (Marquardt algorithm) to one of several different equations provided. If the equation required is not on the list below, it can be added with the easy-to-use integrated equation editor. The results are presented in tabular and graphic form, with a presentation quality screen-dump facility available for Epson-compatible printers and the Hewlett Packard Laserjet. Extra sets of data and transformed/derivative plots of the same data can be shown on screen at the same time. Graphs can be drawn side-by-side for comparison. To distinguish data sets, a variety of symbols and semi-continuous lines can be selected, and labels can be added (including some Greek alphabet characters). ENZFITTER can be set up to perform weighting, removal of outlying data, and to run in batch mode (performing several analyses automatically, without user intervention). All results can be sent to a printer. It provides sophisticated entry and editing facilities and will read ASCII files, including LOTUS 1-2-3 PRN. ENZFITTER is presented in menu form, with windows and context-sensitive help.

The equations that can be fitted are: linear regression; pK_a determination; Michaelis-Menten kinetics; ligand binding (1 or 2 sites); single, double or triple exponential decay; first order rate equation; Hill equation. Transformed/derivative plots fitted are: residuals; Scatchard; Eadie; Lineweaver-Burk; semi-logarithmic; linearize pK_a .

Potential users: Scientists.

Fields of interest: Enzyme kinetics, chemistry, biochemistry.

This application program has been developed for the IBM PC and is written in Turbo Pascal, to run under DOS 2.0 or later. It is available on 5.25-in double-sided floppy discs. The memory required is 384K minimum.

Distributed by Elsevier-Biosoft, 68 Hills Road, Cambridge, CB2 1LA.

The IBM requires an IBM CGA or EGA, or a Hercules graphics card. The program has extensive external documentation. The source code is not available. The software is fully operational, and is in use at over 60 sites. The publisher is willing to deal with enquiries.

Software package TAL-013/87

COMPUTERIZED QUALITY CONTROL

Contributor: T.F. HARTLEY, Institute of Medical and Veterinary Science, Adelaide, Australia; and M.R. MASSON, Dept. of Chemistry, University of Aberdeen, Meston Walk, Old Aberdeen, AB9 2UE.

Brief description: The computer programs published in the book T.F. Hartley, Computerized Quality Control: Programs for the analytical laboratory, Ellis Horwood, Chichester, 1987, originally written for a Labtam computer, have been converted to run on several other machines. The topics covered are: Calibration graphs, including linear calibration graphs, and non-linear calibration graphs fitted by cubic spline or by a partial sigmoid equation; Batch quality control, including an operating characteristic curve program and a geometric mean regression program; Between-batch quality control, including programs to implement a computerized cusum V-mask, and to use that and the Trigg tracking signal to produce a summary report on between-batch quality-control data; and a Gaussian error generator. The programs are all written in an open readable format, and are fully described and explained in the book. The program organization closely follows the accompanying description of the technique and the equations. Memory requirements for the programs and data files are modest compared with those of commercial packages.

The discs include, in addition to the programs given in the book, an additional program that is a menu-driven combination of the between-batch quality control programs.

Potential users: Analytical chemists, clinical chemists.

Fields of interest: Clinical laboratories, analytical laboratories.

These programs were developed for a Labtam 3000 computer, but they have been converted to run on IBM PC and compatibles, Apple II, and Acorn BBC computers. They are written in BASIC. The programs all run in less than 32 K of memory. They are available on 5.25-in floppy disc, in appropriate formats. An 80-column card is recommended for the Apple, and a BBC B+ or Master is more suitable than a BBC B, because screen displays are designed for 80-columns. No graphics card is required, because the displays use "line-printer" type graphics.

Distributed by Ellis Horwood Ltd., Market Cross House, Cooper Street, Chichester, West Sussex PO19 1EB, UK. Price £20.00 + postage and packing.

The programs are documented mainly in the book, but a manual for the additional program is included with the disc. The source code is provided.

The programs are fully operational, and in regular use. The contributors are willing to deal with enquiries.

Talanta

The International Journal of Pure and Applied Analytical Chemistry



The illustration of a Greek balance from one of the Hope Vases is reproduced here by kind permission of Cambridge University Press

Editor-in-Chief

DR R.A.CHALMERS, Department of Chemistry, University of Aberdeen, Old Aberdeen, Scotland

Assistant Editors

DR J.R.MAJER, University of Birmingham, England

DR I.L.MARR, University of Aberdeen, Scotland

DR D.MIDGLEY, Central Electricity Research Laboratories, Leatherhead, England

Computing Editor

DR MARY R.MASSON, University of Aberdeen, Scotland

Regional Editors

PROFESSOR I.P.ALIMARIN, Vernadsky Institute of Geochemistry and Analytical Chemistry, U.S.S.R. Academy of Sciences, Kosygin St., 19, Moscow V-334, U.S.S.R.

PROFESSOR E.BLASIUS, Institut für Analytische Chemie und Radiochemie der Universität des Saarlandes, D-6600 Saarbrücken 15, G.F.R.

PROFESSOR J.S.FRITZ, Department of Chemistry, Iowa State University, Ames, IA 50010, U.S.A.

PROFESSOR T.HORI, Department of Chemistry, Kyoto University, Kyoto, Japan

DR M.PESEZ, Roussel-Uclaf, 102 et 111 route de Noisy, F-93, Romainville (Seine), France

PROFESSOR E.PUNGOR, Institute for General and Analytical Chemistry, Technical University, Gellért tér 4, 1502 Budapest XI, Hungary

PROFESSOR J.D.WINEFORDNER, Department of Chemistry, University of Florida, Gainesville, FL 32611, U.S.A.

Consulting Editor

DR M.WILLIAMS, Oxford, England

Editorial Board

Chairman: PROFESSOR J.D.WINEFORDNER

DR J.R.MAJER

DR M.R.MASSON

DR R.A.CHALMERS

DR I.L.MARR

DR D.MIDGLEY

Dr M.Williams

Annual Subscription Rates (1987)

Annual institutional subscription rate (1987) DM 1100.00; 2-year institutional rate (1987/88) DM 2090.00; personal subscription rate for those whose library subscribes at the regular rate (1987) DM 228.00. Prices are subject to amendment without notice.

Microform Subscriptions and Back Issues

Back issues of all previously published volumes are available in the regular editions and on microfilm and microfiche. Current subscriptions are available on microfiche simultaneously with the paper edition and on microfilm on completion of the annual index at the end of the subscription year.

Publishing Office

Pergamon Journals Ltd, Journals Production Unit, Hennock Road, Marsh Barton, Exeter, Devon EX2 8NE, England (Tel. Exeter (0392) 51558; Telex 42749).

Subscription and Advertising Offices

North America: Pergamon Journals Inc., Maxwell House, Fairview Park, Elmsford, NY 10523, U.S.A.

Rest of the World: Pergamon Journals Ltd, Headington Hill Hall, Oxford OX3 0BW, England (Tel. Oxford (0865) 64881).

Copyright © 1987 Pergamon Journals Limited

It is a condition of publication that manuscripts submitted to this journal have not been published and will not be simultaneously submitted or published elsewhere. By submitting a manuscript, the authors agree that the copyright for their article is transferred to the publisher if and when the article is accepted for publication. However, assignment of copyright is not required from authors who work for organizations which do not permit such assignment. The copyright covers the exclusive rights to reproduce and distribute the article, including reprints, photographic reproductions, microform or any other reproductions of similar nature and translations. No part of this publication may be reproduced, stored in a retrieval system or transmitted in any form or by any means, electronic, electrostatic, magnetic tape, mechanical, photocopying, recording or otherwise, without permission in writing from the copyright holder.

Photocopying information for users in the U.S.A. The Item-fee Code for this publication indicates that authorization to photocopy items for internal or personal use is granted by the copyright holder for libraries and other users registered with the Copyright Clearance Center (CCC) Transactional Reporting Service provided the stated fee for copying, beyond that permitted by Section 107 or 108 of the U.S. Copyright Law is paid. The appropriate remittance of \$3.00 per copy per article is paid directly to the Copyright Clearance Center Inc., 27 Congress Street, Salem, MA 01970.

Permission for other use. The copyright owner's consent does not extend to copying for general distribution, for promotion, for creating new works or for resale. Specific written permission must be obtained from the publisher for such copying.
The Item-fee Code for this publication is: 0039-9140/87 \$3.00 + 0.00

PAPERS RECEIVED

- Spectrophotometric determination of primary aromatic amines with 4-*N*-methylaminophenol and 2-iodylbenzoate as reagent:** KRISHNA K. VERMA, SUNIL K. SANGHI and ARCHANA JAIN. (1 July 1987)
- Analysis of mixtures of various amino-acids and sulphonamides in pharmaceutical preparations with *N*-bromocaprolactam:** ASHUTOSHI SRIVASTAVA and ANITA GUPTA. (1 July 1987)
- A comparative study of the chelation reaction of *N*-benzoyl-*N*-phenylhydroxylamine with Sn(II) and Sn(IV):** HE CHUN XIANG and ZHOU NAN. (1 July 1987)
- Optical fibre detector for flow-injection analysis: Determination of palladium(II) in ore:** XU YANJUN, CHEN XINGGUO, LIU MANCANG and HU ZHIDE. (1 July 1987)
- On the formation of the ternary complex of Mo(VI)-NH₂OH-Br-PADAP and its application in spectrophotometric determination of molybdenum:** ZE-XING HUANG, SHU-QIONG HE and CAI-XIA LIN. (1 July 1987)
- Differential pulse polarographic determination of the herbicides atrazine, prometryne and simazine:** M. T. LIPPOLIS and V. CONCIALINI. (15 July 1987)
- Hydrometallurgical processing of molybdenite ores:** KAMIN KHAN and TAJ ALI. (15 July 1987)
- Extraction-spectrophotometric determination of molybdenum(VI) and application to molybdenite ores:** KAMIN KHAN and TAJ ALI. (15 July 1987)
- Complete model of flow-through porous electrodes composed of screens normal to the flow direction:** ROMAN E. SIODA. (15 July 1987)
- Study of the vanadium-catalysed perphenazine-bromate reaction: Kinetic determination of perphenazine and vanadium:** P. VIÑAS, C. PIQUERAS, M. HERNANDEZ CORDOBA and C. SANCHEZ-PEDREÑO. (15 July 1987)
- Evaluation of certain pharmaceuticals with hexa-aminocobalt(III) tricarbonatocobaltate(III)—I: Determination of some *N*-substituted phenothiazine derivatives:** M. I. WALASH, F. BELAL and F. A. ALY. (15 July 1987)
- Ion-selective electrode determination of some halo-organometallic compounds:** RAMADAN M. RAMADAN and WAGIHA H. MAHMOUD. (15 July 1987)
- Preconcentration and voltammetric measurement of mercury with a crown-ether modified carbon-paste electrode:** JOSEPH WANG and MOJTABA BONAKDAR. (15 July 1987)
- Analytical sonochemistry: A review:** P. LINARES, F. LAZARO, M. D. LUQUE DE CASTRO and M. VALCARCEL. (15 July 1987)
- Extraction-spectrophotometric method for determination of aluminium in silicates:** N. L. BANERJEE and B. C. SINHA. (15 July 1987)
- Determination of organotins in natural waters by toluene extraction and graphite-furnace AAS:** S. C. APTE and M. J. GARDNER. (22 July 1987)
- Spectrophotometric determination of diphenylamine, pyrrole and indole—a kinetic study:** MOHSIN QURESHI, IFTEKHAR AHMAD KHAN, HINA KHAN and ANNEES AHMAD. (22 July 1987)
- Determination of manganese in steels by atomic-absorption spectrophotometry:** L. P. PANDEY, P. DASGUPTA, N. N. CHATTERJEE and S. N. JHA. (6 August 1987)
- Aliphatic monoamines, diamines, polyamines: An HPLC method for their identification and separation: Study of separation factors in homologous series:** M. C. GENNARO, E. MENTASTI, C. SARZANINI, V. PORTA. (31 July 1987)
- Higher order derivative spectrophotometric determination of mercury(II) as the ternary complex with iodide and Pyronine G:** SAJI MATHIEW, RUGMINI SUKUMAR, T. PRASADA RAO and A. D. DAMODARAN. (31 July 1987)
- Micellar systems in flow-injection analysis: Determination of gadolinium with 1-(2-pyridylazo)-2-naphthol in the presence of Triton X-100:** B. MORENO CORDERO, J. HERNANDEZ MENDEZ and J. L. PEREZ PAVON. (31 July 1987)
- Some observations on the Kerr effect in suspensions of bentonite:** JAMES B. KING and ROGER STEPHENS. (31 July 1987)
- Substitution complexometric determination of cadmium in the presence of zinc in homogeneous water-organic medium:** ASSEN KAROLEV. (31 July 1987)
- Substitution complexometric determination of magnesium in homogeneous water-dioxan medium, based on MgEDTA decomposition with 8-hydroxyquinoline and back-titration with calcium.** ASSEN KAROLEV. (31 July 1987)
- Ion-pair formation applied to pharmaceutical analysis—II: Paired-ion chromatography:** J. MARTINEZ CALATAYUD. (31 July 1987)
- Neutralization indicators in acetonitrile: pK values and chromatic parameters of transition ranges:** J. BARBOSA, M. ROSES and V. SANZ-NEBOT. (10 August 1987)
- To and fro FIA—II: Determination of glucose with a two-pump reversed-flow procedure:** JUN'ICHI TOEI. (10 August 1987)
- A new colorimetric reagent for submicrogram determination of cyanide:** SULBHA AMLATHE, SWETA UPADHYAY and V. K. GUPTA. (10 August 1987)
- Solvent extraction of Cd(II) with *N*-cyclohexyl-*N*-nitrosohydroxylamine and 4-methylpyridine into methyl isobutyl ketone:** G. RAURET, L. PINEDA, R. CASAS, R. COMPAÑO and A. SANCHEZ-REYES. (10 August 1987)
- Interference in atomization of Ag, Bi, Cd, Sn, Tl traces by AAS/ETA in presence of In³⁺ and HBr:** I. G. YUDELEVICH, D. A. KATSKOV and T. S. PAPINA. (10 August 1987)
- Determination of two metals from a single potentiometric titration curve: The application of two indicator electrodes:** A. PARCZEWSKI. (10 August 1987)
- Simultaneous determination of CO₂ and SO₂ in wine by gas-diffusion/flow-injection analysis:** P. LINARES, M. D. LUQUE DE CASTRO and M. VALCARCEL. (10 August 1987)

PAPERS RECEIVED

- Complexation equilibria between niobium(V) and 4-(4H-1',2',4'-triazolyl-3'-azo)-2-methylresorcinol: Extraction-spectrophotometric determination of niobium in pyrochlore-bearing rocks:** MA. J. SANCHEZ, A. FRANCISCO, F. JIMENEZ and F. GARCIA MONTELONGO. (1 June 1987)
- Solvent extraction studies of metal ions—I: Synergic effect of acetylacetonone on thiocyanate-induced extraction of iron(III) from water with triphenylphosphine oxide in chloroform as extractant:** T. S. LOBANA and C. K. SHARMA. (4 June 1987)
- Determination of fluorine and chlorine in geological materials by induction-furnace pyrohydrolysis and standard-addition ion-selective electrode measurement:** T. DENIS RICE. (4 June 1987)
- Stability of complexes of cysteine with Be(II), Mn(II), Co(II), Ni(II), Zn(II), Cd(II) and Pb(II):** A. K. ROUL and R. K. PATNAIK. (4 June 1987)
- On the stabilization of Nb(V)-solutions by Zr(IV) and Hf(IV):** E. SØRENSEN and A. B. BJERRE. (4 June 1987)
- Determination of residual aromatic amine hydrochlorides in process samples of di-isocyanate used in polyurethane manufacture: A comparison of electroanalytical methods:** PAOLO UGO, SALVATORE DANIELE, GINO BONTEMPELLI and ANTONIO BECCARI. (10 June 1987)
- Study on multicomponent spectrophotometric computing analysis with information theory:** LONG-BIAO YING, CHI-ZHEN ZHOU and YI-YING LIU. (10 June 1987)
- Polarographic study of the dipropylidithiophosphonate complexes of Pd(II), Pb(II), Cd(II) and Zn(II) ions:** ZHIVKO I. DENCHEV and NIKOLA K. NIKOLOV. (10 June 1987)
- A highly sensitive spectrophotometric method for determination of iodine in natural water.** FENG-SAN ZHAO. (10 June 1987)
- Chemical interferences in the determination of calcium, revisited:** M. O. OMOJOLA, S. A. THOMAS and J. Y. OLAYEMI. (12 June 1987)
- Simultaneous determination of ammonium and potassium ions by capillary type isotachopheresis:** KEIICHI FUKUSHI and KAZUO HIRO. (16 June 1987)
- The role of α -alumina in the determination of phosphate ions by column chromatography:** J. E. DAVIES, R. GAZESKOWIAK and J. MENDHAM. (16 June 1987)
- On the influence of the adsorption of electroactive species on the polarographic determination of stability constants:** M. C. MONTEMAYOR and E. FATAS. (16 June 1987)
- Some more evidence of the new organization effect of spectral line intensity ratio fluctuations of different elements:** BO THELIN. (19 June 1987)
- Determination of antimony in rocks and minerals by atomic-absorption spectrometry:** N. K. ROY and A. K. DAS. (19 June 1987)
- Stability of reduced molybdosilicic acids (MSA):** J. MIGDALSKI and Z. KOWALSKI. (19 June 1987)
- A cheap and versatile data-acquisition system for multiple ion-selective electrodes:** P. C. HAUSER, D. J. ANEAR, T. J. CARDWELL, R. W. CATTRALL and I. C. HAMILTON. (22 June 1987)
- The mass spectrometric behaviour of pentachlorophenyl β -carbonylenolate phosphine nickel(II) complexes: An example of thermal generation of nickel(III) species detected under mass spectrometric conditions:** B. CORAIN, B. LONGATO, A. M. MACCIONI, B. PELLI, P. TRALDI and F. R. KREISSL. (22 June 1987)
- A new electrochemical method at the liquid/liquid interface for determination of barium and strontium:** ZHISHENG SUN and ERKANG WANG. (24 June 1987)
- A study of the chemiluminescence of some acidic triphenylmethane dyes:** G. N. CHEN and C. S. HUNG. (24 June 1987)
- Determination of metals at trace levels as dibenzylidithiocarbamate complexes by reversed-phase HPLC:** C. BAIOCCHI, A. MARCHETTO, G. SAINI and G. PETTITI. (24 June 1987)
- Spectrophotometric microdetermination of bismuth in organic compounds after oxygen flask combustion:** H. N. A. HASSAN, M. E. M. HASSOUNA and Y. A. GAWARGIOUS. (26 June 1987)
- Ion-pair formation applied to pharmaceutical analysis—I: Non-chromatographic methods:** J. MARTINEZ CALATAYUD. (26 June 1987)
- The influence of carbon dioxide in the determination of oxygen in copper by reduction fusion:** LI MANLING, TANG MEIER, SUN ZHENGCAI, WU LINGYE, TANG SUNMING, WANG GUOWEI, HE HUANNAN, YAN RONGHUA, ZHAO GUANDI and LU QINGREN. (26 June 1987)
- Study on a new catalytic polarographic system for determination of trace amount of tungsten:** DEZHONG DAN and JUN RE. (29 June 1987)
- Investigations of partition of salicylic acid between aqueous and different organic phases at various temperatures—I:** AZRA IMTIAZ, GHULAM NABI and ISHTIAQ HUSSAIN. (29 June 1987)
- First derivative spectrophotometric determination of salicylic acid in aspirin:** ABDEL-AZIZ M. WAHBI, HAMAD A. AL-KHAMEES and AHMAD M. A. YOUSSEF. (29 June 1987)
- Synthesis and characterization of some chromogenic crown ethers as optical potassium-ion sensors:** S. M. S. AL-AMIR, D. C. ASHWORTH, R. NARAYANASWAMY and R. E. MOSS. (29 June 1987)

PAPERS RECEIVED

- Determination of antimony in lead, zinc concentrates and other smelter products:** S. S. MURTI, S. C. S. RAJAN and J. SUBRAHMANYAM. (5 May 1987)
- Sensitive and selective spectrophotometric method for the determination of micro amounts of palladium with 5,6-dimethyl-1,3-indanedione-2-oxime:** D. MALLIKARJUNA RAO, K. HUSSAIN REDDY and D. VENKATA REDDY. (11 May 1987)
- Oxydation vanadique de la quinine et de quelques analogues: Application au dosage d'un nouvel antipaludéen la méfloquine:** A. ASSAMOI, M. CHASTAGNIER, M. CHAIGNEAU and M. HAMON. (9 May 1987)
- Sorption of protons and metal ions from aqueous solutions by a strong anionic-exchange resin loaded with sulphonated azo-dyes:** MARIA PESAVENTO, ANTONELLA PROFUMO and RAFFAELA BIESUZ. (9 May 1987)
- Fibre optic biosensor for ethanol, based on use of an internal enzyme:** B. S. WALTERS, T. J. NIELSEN and M. A. ARNOLD. (20 May 1987)
- Chemical measurements with optical fibres for process control:** G. BOISDE, F. BLANC and J. J. PEREZ. (20 May 1987)
- A new fibre-optic based ion sensor:** F. V. BRIGHT, G. E. POIRIER and G. M. HIEFTJE. (20 May 1987)
- Towards a fluorescent chemoreceptive lipid membrane-based optrode:** U. J. KRULL, R. S. BROWN, R. F. DEBONO and B. D. HOUGHAM. (20 May 1987)
- Electrochromic dyes, enzyme reactions and antigen-antibody interactions in fluorescence optic sensor (optrode) technology:** N. OPITZ and D. W. LÜBBERS. (20 May 1987)
- Fibre optic sensor for CO₂ determination:** C. MUNFHOLM, D. R. WALT and F. P. MILANOVICH. (20 May 1987)
- Optical fibre sensing of fluoride ions in a flow-stream:** R. NARAYANASWAMY, D. A. RUSSELL and F. SEVILLA III. (20 May 1987)
- Solid-state instrumentation for use with optical fibre chemical sensors:** A. J. GUTHRIE, R. NARAYANASWAMY and N. A. WELTI. (20 May 1987)
- Fibre optic biosensors based on fluorescence energy transfer:** D. MEADOWS and J. S. SCHULTZ. (20 May 1987)
- An optical ionic-strength sensor based on polyelectrolyte association and fluorescence energy transfer:** L. M. CHRISTIAN and W. R. SEITZ. (20 May 1987)
- Fibre-optics based time-resolved fluorimetry for immunoassays:** R. D. PETREA, M. J. SEPANIAK and T. VO-DINH. (20 May 1987)
- A multi-element optical waveguide sensor:** R. R. SMARDZEWSKI. (20 May 1987)
- Optic and fibre-optic sensor for vapours of polar solvents:** H. E. POSCH, J. PUSTERHOFER and O. S. WOLFBEIS. (20 May 1987)
- A simple spectrophotometric method for determination of isoxsuprinehydrochloride in pharmaceuticals:** C. V. RAJESWARI, D. V. NAIDU, N. V. S. NAIDU and P. R. NAIDU. (20 May 1987)
- Chemical and electrochemical activation of the nitration of naphthalene by N₂O₅ in aprotic media:** ABDELLATIF BOUGHRIET, CLAUDE BREMARD and MICHEL WARTEL. (20 May 1987)
- Liquid-liquid distribution behaviour of ion-associates with aromatic sulphonic acid dyes, and a method for prediction of extraction constants:** SHOJI MOTOMIZU, HIROSHI AKIYAMA and MITSUKO OSHIMA. (20 May 1987)
- Estimation of thallium(III) with hydrogen peroxide: A photochemical redox method:** A. RAMA MOHANA RAO, M. S. PRASADA RAO, KARRI V. RAMANA and S. R. SAGI. (25 May 1987)
- Determination of orotic acid (vitamin B₁₃) in milk by differential pulse polarography (DPP):** L. CALVO, J. RODRIGUEZ, F. VINAGRE and A. SANCHEZ. (25 May 1987)
- Colorimetric methods for the determination of manganese—I. Assessment of methods:** BARRY CHISWELL, GUY RAUCHLE and MARK PASCOE. (27 May 1987)
- Spectrophotometric determination of gallium in alloys and fly-ashes with pyridoxal derivatives of thiocarbohydrazide and carbohydrazide:** F. J. BARRAGAN DE LA ROSA, R. ESCOBAR GODOY and J. L. GOMEZ ARIZA. (27 May 1987)
- Determination of free elemental sulphur in petroleum products:** DODDABALLAPUR K. PADMA. (27 May 1987)
- On the determination of total dissolved tin in natural waters by direct hydride generation and non-dispersive atomic-fluorescence spectrometry:** ALESSANDRO D'ULIVO. (27 May 1987)
- Normal-phase high-performance liquid chromatographic determination of phenols:** S. N. LANIN and YU. S. NIKITIN. (27 May 1987)
- Derivative ultraviolet-visible absorption spectrophotometry and its analytical applications:** F. SANCHEZ ROJAS, C. BOSCH OJEDA and J. M. CANO PAVON. (29 May 1987)
- Determination of water in organic solvents by flow-injection analysis with Karl Fischer reagent and a biamprometric detection system:** CHEN LIANG, PAVEL VÁCHA, WILLEM E. VAN DER LINDEN. (29 May 1987)

PAPERS RECEIVED

- Potential of a new solvent extraction procedure for flow-injection analysis:** JUN-ICHI TOEI. (16 March 1987)
- X-Ray photoelectron spectroscopic analysis of lead accumulated in aquatic bryophytes:** M. SOMA, H. SEYAMA and K. SATAKE. (16 March 1987)
- Study of polarographic behaviour of magnesium ion in aqueous solution by means of modified reverse pulse polarography:** MINORU HARA and NOBORU NOMURA. (17 March 1987)
- Hydroxide complexes of lanthanides—VIII: Lanthanum(III) in perchlorate medium:** J. KRAGTEN and L. G. DECNOP-WEEVER. (17 March 1987)
- Kinetic determination of Hg(II) in different materials, based on its inhibitory effect on a catalysed process:** C. SANCHEZ-PEDREÑO, M. I. ALBERO and M. S. GARCIA. (17 March 1987)
- Simultaneous determination of platinum(II) and palladium(II) as their glyoxal bis(4-phenyl-3-thiosemicarbazone) complexes by reversed-phase high-performance liquid chromatography with spectrophotometric detection:** SUWARU HOSHI, SIN KATOH, TAKASHI KOTANI, SADANOBU INOUE and MUTSUYA MATSUBARA. (17 March 1987)
- Interpretation of selectivity and detection limit of liquid ion-exchanger electrodes:** MAGDALENA MAJ-ZURAWSKA, TOMASZ SOKALSKI and ADAM HULANICKI. (17 March 1987)
- Determination of copper in the presence of a large excess of bismuth by differential pulse anodic stripping voltammetry without preliminary separation:** ALEKSANDER CISZEWSKI. (20 March 1987)
- Control of voltammetric experiments by the Commodore 64 microcomputer:** MIKAEL WASBERG and PÉTER SÁRKANY. (20 March 1987)
- Application of la spectrophotométrie atomique a l'analyse du vins: Système de génération d'hydrures:** C. BALUJA-SANTOS and A. GONZALEZ-PORTAL. (20 March 1987)
- Detection and spectrophotometric determination of novalgin in tablets with potassium iodate:** SAIDUL ZAFAR QURESHI, TAUSIFUL HASAN and AHSAN SAEED. (20 March 1987)
- Determination of indicator transition and its use in the titration of weak bases:** SHOJI INAGAKI, KATSUMI SUMIDA, SHIGERU YOSHIDA and SHINGO HIROSE. (20 March 1987)
- Study of the physicochemical properties of dantrolene aqueous solutions by differential pulse polarography:** M. H. LIVERTOUX, Z. JAYYOSI and A. M. BATT. (23 March 1987)
- Extraction-spectrophotometric determination of iron(II) by ternary complex formation with Pyrocatechol Violet and cetyltrimethylammonium bromide:** M. TAREK M. ZAKI, W. H. MAHMOUD and A. Y. EL-SAYED. (23 March 1987)
- Complexation of nicotinic and quinaldonic acids with some metal ions of biological interest:** W. G. HANNA, M. ZAKY and M. M. MOAWAD. (23 March 1987)
- Complexation of R-acid azo dye derivatives with some lanthanide ions:** M. ZAKY, W. G. HANNA, A. L. EL-ANSARY and M. M. MOAWAD. (23 March 1987)
- Complexometric determination of mercury(II) with 2-imidazolidinethione as a selective masking agent:** B. NARAYANA and M. R. GAJENDRAGAD. (25 March 1987)
- Indirect determination of mercury by flame atomic-absorption spectrometry and use of Reinecke's salt:** M. ORTUNO MOLINS and V. BERENQUER NAVARRO. (25 March 1987)
- Radiometric determination of uranium accumulated in bacterial cells:** M. CHWISTEK, J. CHMIELOWSKI and I. TOMZA. (25 March 1987)
- The calculation of equilibrium concentrations—III: ES4EC1: A FORTRAN program for computing distribution diagrams and titration curves:** CONCETTA DE STEFANO, PIETRO PRINCI, CARMELO RIGANO and SILVIO SAMMARTANO. (25 March 1987)
- Determination of pentachlorophenol by flow-injection analysis with spectrophotometric detection:** M. RODRIGUEZ-ALCALA, P. YAÑEZ-SEDEÑO and L. MA. POLO DIEZ. (30 March 1987)
- Studies on fluorescein—VI: Absorbance in the ultraviolet of the various prototropic forms of yellow fluorescein in water solution:** HARVEY DIEHL. (1 April 1987)
- Sensitive spectrophotometric determination of trace arsenic as the arsenomolybdic acid—Malachite Green complex in the presence of non-ionic surfactant:** ZHAO FENSAN. (1 April 1987)
- Periodate determination with a chemiluminescence emission detector and F.I.A. technique—application to ethylene glycol determination:** N. P. EVMIRIDIS. (1 April 1987)
- Thermodynamic stability constants of lanthanide complexes of 2-hydroxy-3,4-dimethoxyacetophenone:** BHAGWAN S. GARG, RESH B. BASNET and SHEO RAJ SINGH. (1 April 1987)

PAPERS RECEIVED

Spectrophotometric quantitation of ornidazole and its formulations: MAHMOUD M. A. HASSAN, AHMAD I. JADO and BAHAA-EL-DIN M. EL-SHAZLY. (27 February 1987)

Spectrophotometric evaluation of the acidity constants of 4-aminoazobenzene in mixtures of aliphatic amides with water: Estimation of the medium effect on the 4-aminoazobenzene system: ANTONIO G. GONZALEZ, AGUSTIN G. ASUERO and MARIA A. HERRADOR. (26 February 1987)

Determination of Mo(VI) in tap and sea waters by means of differential pulse polarography and co-flotation: J. L. HIDALGO, M. A. GOMEZ, M. CABALLERO, R. CELA and J. A. PEREZ-BUSTAMANTE. (27 February 1987)

The determination of soluble chromium in simulated PWR coolant by differential pulse adsorption stripping voltammetry: K. TORRANCE and C. GATFORD. (2 March 1987)

Instrumental neutron activation determination of phosphorus in biological materials by bremsstrahlung measurement: S. BAJO and A. WYTTENBACH. (6 March 1987)

Extraction-spectrophotometric determination of selected rare-earth elements in the presence of other elements in the system Ln^{3+} -hexa-aza 18 crown 6-Erythrosin A: W. SZCZEPANIAK, W. CISZEWSKA and B. JUSKOWIAK. (9 March 1987)

A computational method for the potentiometric evaluation of ionization constants: A. GUSTAVO GONZALEZ, DANIEL ROSALES, JOSE L. GOMEZ ARIZA and A. GUIRAUM PEREZ. (9 March 1987)

Improvement of Smets' method in electrothermal atomic-absorption spectrometry: XIUPING YAN, ZHIJUN LIU and TIEZHENG LIN. (9 March 1987)

Influence of the solvent on metal-amino-acid complexes: F. REY, A. VARELA, J. M. ANTELO and F. ARCE. (9 March 1987)

Simultaneous determination of potassium and ammonium ions with multiple ion-selective electrodes: SCOTT A. GLAZIER, MARK A. ARNOLD and JEFFERY P. GLAZIER. (10 March 1987)

Determination of glibenclamide in human plasma by high-pressure liquid chromatography: SADEQ OTHMAN, OMAR SHAHEEN, IBRAHEEM JALAL, ABDULLAH AWIDI and WALID AL-TURK. (10 March 1987)

Fluorometric determination of cyanide with 2,3-naphthalenedialdehyde and taurine: AKIRO SANO, MASAOKI TAKEZAWA and SHOJI TAKITANI. (10 March 1987)

GLC Microdetermination of indomethacin in capsules: CH. SURYAPRAKASA SASTRY, A. RAMA MOHANA RAO, A. G. K. MURTHY and C. V. S. V. GOPALA KRISHNA. (10 March 1987)

PAPERS RECEIVED

- Catalytic determination of trace amounts of cobalt by flow-injection analysis:** YOU-XIAN YUAN and YUE-JUN WANG. (14 January 1987)
- The determination of formation constants of weak complexes by potentiometric measurements: Experimental procedures and calculation methods:** ALESSANDRO DE ROBERTIS, CONCETTA DE STEFANO, CARMELO RIGANO and SILVIO SAMMARTANO. (14 January 1987)
- Action of inadequate operating conditions of ion-exchange units on boiler feed-water quality:** K. M. E. HASHEM, F. A. E. A. ALI, A. GHORAB and G. DARWISH. (16 January 1987)
- The determination of brominated vegetable oils in soft drinks made in Nigeria:** NKEMFULU U. EZEKWE. (16 January 1987)
- Sequential potentiometric micro-scale determination of chlorides and phosphates:** AGOSTINO PIETROGRANDE and MIRELLA ZANCATO. (21 January 1987)
- Utility of iodine and 7,7,8,8-tetracyanoquinodimethane in the determination of terfenadine:** MOHAMED E. ABDEL-HAMID and MUSTAFA A. ABUIRJEIE. (21 January 1987)
- Stability constants and molar absorptivities of complexes of Au(III), Pt(IV), Pd(II), Os(VIII) and Cu(II) with 4-methoxybenzaldehyde-4-phenyl-3-thiosemicarbazone:** KINTHADA M. M. S. PRAKASH, L. D. PRABHAKAR and D. VENKATA REDDY. (17 January 1987)
- Analytical properties of *o,o'*-diaminoazobenzene: Spectrophotometric determination of Pd(II):** L. VICH, J. M. ESTELA, V. CERDA, E. CASASSAS and S. HERNANDEZ. (26 January 1987)
- Liquid chromatography/electrochemistry investigations on 4-(2-pyridylazo)resorcinol as chelating agent for simultaneous determination of metal ions:** JI HUAMIN, CAO SHUYING and WANG ERKANG. (26 January 1987)
- Complexometric determination of beryllium and aluminium with 5-hydroxy-2-methyl-1,4-naphthoquinone:** C. R. JOSHI and S. V. CHALGERI. (28 January 1987)
- A comparison of two digestion procedures for the determination of selenium in biological material:** LENA HANSSON, JEAN PETERSSON and ÅKE OLIN. (28 January 1987)
- Oxydation vanadique de l'iodométhylate de parachlorobenzyl-4 diméthoxy-6,7 isoquinoléine en milieu sulfurique aqueux:** E. POSTAIRE, C. VIEL, M. HAMON and A. GOND. (29 January 1987)
- Characterization of iminodiacetic acid chelating filter papers by electrophoresis and other techniques:** I. NUKATSUKA and RYOEI ISHIDA. (29 January 1987)
- "Electrochemical masking" of large concentrations of titanium in EDTA solution in DPASV:** ALEKSANDER CISZEWSKI and ZENON LUKASZEWSKI. (30 January 1987)
- Periodic view of the mole sensitivity and dependences of sensitivities in peak height and integration modes on the properties of pyrolytic and non-pyrolytic graphite in graphite-furnace atomic-absorption spectrometry:** CHAN-HUAN CHUNG, ETSURO IWAMOTO and YUROKU YAMAMOTO. (31 January 1987)
- Determination of metal ions as 8-hydroxyquinolinate complexes by reversed-phase liquid chromatography:** CHEN-WEN WHANG, LONG-CHUEN WU and LAIN-CHING CHOU. (2 February 1987)
- Separation of trace amounts of indium, gallium and aluminium from gram amounts of thallium and from each other by cation-exchange chromatography on AG50W-X4 resin:** FRANZ W. E. STRELOW and TJAART N. VAN DER WALT. (4 February 1987)
- Stripping voltammetry of lipoic acid and lipoamide with use of the catalytic hydrogen wave:** SHUNITZ TANAKA and HITOSHI YOSHIDA. (10 February 1987)
- Spectrophotometric determination of titanium with *N-m*-tolyl-*N*-phenylhydroxylamine and its application to environmental samples:** SADANOBU INOUE, SUWARU HOSHI and MUTSUYA MATSUBARA. (10 February 1987)
- pH Determination with acid-base indicators: Implications for optical fibre probes:** T. E. EDMONDS, N. J. FLATTERS, C. F. JONES and J. N. MILLER. (10 February 1987)
- Analysis of polynuclear aromatic hydrocarbons in shale oil and diesel particulates:** YULIN L. TAN. (13 February 1987)
- Extraction and spectrophotometric determination of bismuth as iodobismuthite complexes by use of amides, amidines and hydroxyamidines:** ABHA GOLWELKER, K. S. PATEL and R. K. MISHRA. (13 February 1987)
- Simple kinetic-thermometric determination of submicrogram quantities of ruthenium based on its catalytic effect on the Ce(IV)-As(III) reaction:** F. BORRULL, P. RAMIREZ DE LA PISCINA, N. HOMS and V. CERDA. (16 February 1987)
- Determination of chloride in sulphuric acid by potentiometric mercurometric titration:** F. G. BĂNICĂ and E. DIACU. (16 February 1987)
- A novel separation of Cu²⁺ from some alkali and transition metal ions by a modified anion-exchange resin:** NOOMAN A. KHALAF, G. S. NATARAJAN and V. A. JOSHI. (18 February 1987)
- Spectrophotometric determination of bismuth with semi-Xylenol Orange and its application in metal analysis:** ZHOU NAN, YU REN-QING, YAO XU-XHANG and LU ZHI-REN. (18 February 1987)
- Application of reverse pulse polarography to the determination of substances which form films electrochemically on the mercury electrode:** J. M. LOPEZ FONSECA, A. OTERO and J. C. GARCIA MONTEAGUDO. (20 February 1987)
- On Ingamells' sampling constant:** G. J. LYMAN. (20 February 1987)
- Estimation of pH and autoprotolysis constants in mixtures of aliphatic amides with water:** AGUSTIN G. ASUERO, MARIA A. HERRADOR and ANTONIO G. GONZALEZ. (23 February 1987)

PAPERS RECEIVED

- Diagrammes potentiel-niveau d'acidité dans les milieux $H_2O-H_3PO_4$ -I: Systèmes électrochimiques ne faisant pas intervenir le proton:** C. LOUIS and J. BESSIERS. (19 December 1986)
- Diagrammes potentiel-niveau d'acidité dans les milieux $H_2O-H_3PO_4$ -II: Systèmes électrochimiques faisant intervenir le proton:** C. LOUIS and J. BESSIERS. (19 December 1986)
- Etude analytique des produits lourds de pétrole-V. Bromation des résidus lourds pétroliers au moyen d'un réactif original, le tribromure de tétrabutyl ammonium. Essais préliminaires de détermination d'un indice de brome applicable aux fractions lourdes:** P. L. DESBENE, J. BERTHELOT, M. OUCHEFOUN, C. GUETTE, J. J. BASSELIER, R. BOULET and A. DESBENE-MONVERNAVY. (19 December 1986)
- Etude des complexes fluorés et chlorés du cadmium dans les mélanges eau-HF:** REJEAN BEAUDOIN and HUGHES MENARD. (19 December 1986)
- Etude des propriétés adsorbantes de fibres d'amiante modifié chimiquement et de fibres proposées comme substitut à l'amiante, par chromatographie en phase gazeuse:** Y. LEFEBVRE, M. LAMBERT, J. KHORAMI, H. MENARD. (19 December 1986)
- Détermination de cobalt au niveau de ng/ml basée sur son effet catalytique sur la réaction hydrazine-peroxyde d'hydrogène:** M. CALULL, M. R. MARCE, N. HOMS, P. RAMIREZ DE LA PISCINA and F. BORRULL. (19 December 1986)
- A comparative study of analytical inductively-coupled argon-plasma discharges using different outer gases.** G. ZARAY, J. A. C. BROEKAERT and F. LEIS. (23 December 1986)
- Extraction and spectrophotometric determination of iron(II) with *N*-phenylcinnamohydroxamic acid:** ABERRA FURA and B. S. CHANDRAVANSHI. (23 December 1986)
- Phase composition analysis of aluminium hydroxide by thermoanalysis and infrared spectrometry:** Z. S. WITTMANN, E. KÁNTOR, K. BÉLAFI, L. PÉTERFY and L. P. FARKAS. (24 December 1986)
- Effect of acetate buffer and temperature on the kinetics of the metal exchange reaction between Cu(II) and the europium(III)-ethylene glycol-bis(2-aminoethyl ether tetra-acetate complex):** E. R. SOUAYA and M. L. ISKANDER. (24 December 1986)
- Study of the complex formation of uranyl(VI) with di(2-ethylhexyl) phosphoric acid with different diluents:** E. R. SOUAYA, F. M. EL-ZAWAWY, F. EL-SHAHAAT and L. H. KHALIL. (24 December 1986)
- Determination of trace palladium by FIA:** CHEN XINGGUO, LIU MANCANG and HU ZHIDE. (31 December 1986)
- Oxidation of thiols by *N*-metallo-*N*-halogeno aryl sulphonamides—an analytical investigation:** A. S. ANANDA MURTHY, S. ANANDA MURTHY and D. S. MAHADEVAPPA. (31 December 1986)
- Determination of viscosity with an open-closed flow-injection system:** A. RIOS, M. D. LUQUE DE CASTRO and M. VALCARCEL. (31 December 1986)
- Complexes of vanadyl and uranyl ions with the chelating groups of humic matter:** M. L. SIMOES GONÇALVES and A. M. MOTA. (31 December 1986)
- An electrochemical stripping method for the selective determination of traces of silver:** RUDOLF PŘIBIL and MADELEINE ŠTULÍKOVÁ. (7 January 1987)
- AAS determination of copper extracted with a liquid chelating exchanger and its application to human blood:** SHUVENDU S. BHATTACHARYYA and ARABINDA K. DAS. (7 January 1987)
- Polarographic determination of bismuth—sensitization in the presence of nioxime:** C. GONZALEZ PEREZ and M. I. GONZALEZ MARTIN. (7 January 1987)
- A fibre optic sensor based on an ion-exchange membrane out of phase: The determination of Be in Berylco alloy:** XU YANJUN, LIU MANCANG and HU ZHIDE. (31 December 1986)
- The effect of complexing agents on the extraction of lanthanides by di(2-ethylhexyl)phosphoric acid:** S. N. BHATTACHARYYA and K. M. GANGULY. (9 January 1987)
- Determination of hafnium in presence of zirconium by the Methylthymol Blue—hydrogen peroxide method:** STANISLAW KICIAK. (9 January 1987)
- Investigation of the flow gradient function by using a multifunction pump delivery system:** JUN-ICHI TOEI. (9 January 1987)

PAPERS RECEIVED

- Ionic strength dependence of formation constants—X: Proton activity coefficients at different temperatures and ionic strengths and their use in the study of complex equilibria:** SANTI CAPONE, ALLESSANDRO DE ROBERTIS, CONCETTA DE STEFANO, SILVIO SAMMARTANO and ROSARIO SCARCELLA. (25 November 1986)
- A note on the sharpness index of single donor–acceptor titrations:** A. G. ASUERO and G. GONZALEZ. (25 November 1986)
- Design and characterization of an intensified diode-array data-acquisition system for spectrometric measurements:** MARY ANDRIEU RYAN and J. D. INGLE, JR. (25 November 1986)
- Studies of two-phase equilibria using liquid–liquid segmented flow: Extraction of dithiocarbamic acids into various solvents:** KENNETH BÄCKSTRÖM, LARS-GÖRAN DANIELSSON, FOLKE INGMAN and ZHAO HUAZHANG. (28 November 1986)
- Thermometric titration of cadmium ion with sodium diethyldithiocarbamate with oxidation by hydrogen peroxide as indicator reaction:** TOSHIAKI HATTORI and HITOSHI YOSHIDA. (28 November 1986)
- Kinetics and analytical applications of the ruthenium(III) catalysed bromate oxidation of bordeaux—III: The catalytic determination of ruthenium:** J. T. AYODELE, B. G. COOKSEY and J. M. OTTAWAY. (28 November 1986)
- Second harmonic a.c. anodic stripping voltammetry of metals at trace level: Simultaneous determination of lead and thallium, and bismuth and antimony:** C. LOCATELLI, F. FAGIOLI, T. GARAI and C. BIGHI. (26 November 1986)
- Hydrallazine-selective PVC membrane electrode based on the hydrallazine–tetraphenylborate ion-pair:** S. S. BADAWY, A. F. SHOUKRY, M. S. RIZK and M. M. OMAR. (5 December 1986)
- Application of factor analysis to the study of the succinylfluorescein forms present in methanol–water aqueous buffer solutions:** F. AMAT-GUERRI, M. E. MARTIN, J. SANZ and R. MARTINEZ-UTRILLA. (5 December 1986)
- Simplified analytical method for trace levels of dimethyl sulphide in freshwater:** DOUGLAS A. HOLDWAY and JEROME O. NRIAGU. (10 November 1986)
- Determination of copper, iron, manganese, lead and cadmium in automatically wet-digested animal tissue, by graphite-furnace atomic-absorption spectrometry with Zeeman background correction:** H. VAN BEEK, H. V. A. GREEFKES and A. J. BAARS. (5 December 1986)
- A note on the buffer index of a polyprotic acid:** A. G. ASUERO. (5 December 1986)
- Spectrophotometric determination of ethambutol hydrochloride in pharmaceutical preparations, with cupric chloride as a chromogenic agent:** UTPAL SAHA, ARUN K. SEN and JIBAN GANGULY. (5 December 1986)
- Review of methods for the determination of lanthanides in geological samples:** CHIRAN J. KANTIPULY and ALAN D. WESTLAND. (5 December 1986)
- Iopanoate ion-selective electrodes with long carbon-chain quaternary ammonium and phosphonium ions:** S. Z. YAO, D. Z. LIU and L. H. NIE. (5 December 1986)
- Extraction chromatographic separation of gallium, indium and thallium:** FAN BIWEI and KONG QINGCHUN. (10 December 1986)
- End-effects in flow analysis and process systems:** SPAS D. KOLEV and ERNŐ PUNGOR. (15 December 1986)
- Determination of semimicro amounts of calcium in the presence of other alkaline-earth metals:** NIRMAL MAITRA, ALBERT W. HERLINGER and BRUNO JASELSKIS. (15 December 1986)
- Solid–liquid separation after liquid–liquid extraction: Spectrophotometric determination of cobalt in vitamins, alloys and ore by extraction of its 3-hydroxy-2-methyl-1,4-naphthoquinone-4-oxime complex into molten naphthalene:** R. K. SHARMA and S. K. SINDHWANI. (17 December 1986)
- Distribution studies of some metal ions in nitric acid media in aqueous and aqueous-organic solutions on quaternary amine styrene–butadiene phenol–formaldehyde anion-exchange resin:** A. S. ABOUL-MAGD, F. H. KAMAL, M. M. B. EL-SABBAH and E. A. HASSAN. (17 December 1986)
- Researches on chemically modified electrodes—XXIV: Preparation and characterization of a nafion polymer-film modified electrode containing Fe(II)–phen complex:** ZILING LU and SHAOJUN DONG. (17 December 1986)

PAPERS RECEIVED

- Sulphur distribution in inorganic polysulphides:** MIECZYŚLAW WROŃSKI. (20 October 1986)
- Ionizations of polyfunctional substances: Determination of thermodynamic macroscopic constants and thermodynamic parameters:** JULIO CASADO, MARIA N. MORENO, JOSE LUIS GONZALEZ and M. ANGELES DEL ARCO. (20 October 1986)
- New liquid membrane electrodes for direct determination of atropine in pharmaceutical preparations:** SAAD S. M. HASSAN, M. A. AHMED and F. SH. TADROS. (23 October 1986)
- Separation and determination of selenium(IV) and molybdenum(VI) in mixtures by selective precipitation with potassium thiocarbonate:** M. YUSUF, A. C. SARKI, S. B. IDRIS, G. A. AYOKO and K. SINGH. (23 October 1986)
- Determination of alkaline-earth metals in foetus bones by inductively-coupled plasma atomic-emission spectrometry:** KUNIO SHIRAIISHI, HISAO KAWAMURA and GI-ICHIRO TANAKA. (23 October 1986)
- The analysis of the CCRMP OKA-2 rare-earth reference mineral of the britholite-apatite series by electrothermal atomic-absorption and inductively coupled plasma atomic-emission spectrometry:** J. G. SEN GUPTA. (28 October 1986)
- Determination of tin, bismuth, antimony, indium, gallium and arsenic by atomic-absorption spectrophotometry:** K. VENKAJ, P. P. NAIDU and T. J. P. RAO. (28 October 1986)
- Automated determination of lead in urine by means of computerized flow potentiometric stripping analysis using a carbon fibre electrode:** HUANG HUILIANG, DANIEL JAGNER and LARS RENMAN. (28 October 1986)
- Synthesis, characterization and analytical properties of 3-amino-5,6-di(2-pyridyl)-1,2,4-triazine:** S. K. CHOUDHURY and S. K. SINDHWANI. (29 October 1986)
- Separation of bismuth from gram amounts of thallium and silver by cation-exchange chromatography in nitric acid:** E. MEINTJES, F. W. E. STRELOW and A. H. VICTOR. (29 October 1986)
- Spectrophotometric determination of zinc with hydrazidazol in the presence of Triton X-100 and its application in metal analysis:** NAN ZHOU, YUAN-XIANG GU, ZHI-REN LU and WEI-YONG CHEN. (29 October 1986)
- Rapid determination of molybdenum in ferro-molybdenum and molybdenum additives as molybdo-oxinate complex:** OM P. BHARGAVA, PAUL G. BAILEY and GORD R. OVERHOLT. (5 November 1986)
- Protonation and solvent extraction of *N-p*-tolylbenzohydroxamic acid in hydrochloric acid medium:** RAMA PANDE and S. G. TANDON. (5 November 1986)
- Simultaneous spectrophotometric determination of erbium and praseodymium with 1-(2-pyridylazo)-2-naphthol in the presence of octylphenol polyethyleneglycol ether (TX-100):** J. HERNANDEZ MENDEZ, B. CORDERO MORENO and J. L. PEREZ PAVON. (5 November 1986)
- Gas chromatographic studies of copper, nickel and palladium chelates of bis(isovaleroylacetone)ethylenedi-imine:** M. Y. KHUHAWAR and A. G. M. VASANDANI. (5 November 1986)
- Adsorptive preconcentration for voltammetric measurements of trace levels of zirconium:** JOSEPH WANG, PENG TUZHI and KURIAN VARUGHESE. (7 November 1986)
- Abridgement and study of methods based on the linearization of potentiometric titration data in acid-base determinations:** M. C. PASCUAL MARTI, P. CAMPINS FALCO and R. MICO ALBERT. (7 November 1986)
- Catalytic spectrophotometric determination of trace amounts of copper(II) with 3-hydroxy-2-naphthoic acid:** E. CASASSAS, A. IZQUIERDO-RIDORSA and L. PUIGNOU. (10 November 1986)
- Ion chromatographic analysis of mixtures of ferrous and ferric iron:** CARL O. MOSES, ALAN T. HERLIHY, JANET S. HERMAN and AARON L. MILLS. (24 October 1986)
- Spectrophotometric determination of bromide (and iodide) in a flow system after oxidation by peroxodisulphate:** ANNIKA CARLSSON, ULLA LUNDSTRÖM and ÅKE OLIN. (14 November 1986)
- Analytical application of retention of organic anions on a non-ionic adsorbent:** KRYSZYNA BRAJTER, EWA OLBRYCH-ŚLESZYŃSKA and MIECZYŚLAW STAŚKIEWICZ. (17 November 1986)
- Fluorimetric determination of gallium in nickel-alloy and aluminium with *N*-oxalylamine(salicylaldehyde hydrazone):** FERNANDO DE PABLOS, GUILLERMINA GALAN and JOSE GOMEZ ARIZA. (17 November 1986)
- Quantitative approximation for the selectivity of analytical spectrophotometric procedures not following Beer's law:** V. PERIS MARTINEZ, J. V. GIMENO ADELANTADO, A. PASTOR GARCIA and F. BOSCH REIG. (20 November 1986)
- Indirect atomic-absorption spectrophotometric method for determination of phosphorus in steel by use of the bismuth phosphomolybdate complex:** R. RAMCHANDRAN and P. K. GUPTA. (20 November 1986)

PAPERS RECEIVED

- A novel Urushi matrix chloride ion-selective field-effect transistor:** SHIN-ICHI WAKIDA, MASATAKA YAMANE and KAZUO HIRO. (10 August 1987)
- Influence of trace impurities contained in nitrobenzene on potential response of liquid anion-sensitive electrodes:** Z. MALÁ and J. ŠENKÝŘ. (10 August 1987)
- Potential response of liquid ion-exchange membrane electrodes with a weak acid anion as primary ion and its dependence on pH:** Z. MALÁ and J. ŠENKÝŘ. (10 August 1987)
- The determination of nitrate and sulphate in 50% sodium hydroxide solution by ion-chromatography:** JARL M. PETTERSEN, HANNE G. JOHNSEN and WALTER LUND. (10 August 1987)
- Simultaneous spectrophotometric determination of furazolidone and berberine in dosage forms:** S. M. HASSAN, F. BELAL and M. SULTAN. (10 August 1987)
- Evaluation of new asymmetric derivatives of thiocarbonylhydrazide as spectrophotometric analytical reagents:** FERNANDO ALVAREZ, FERNANDO DE PABLOS and JOSE LUIS GOMEZ ARIZA. (10 August 1987)
- Photometric and amperometric flow-injection determination of psychotropic drugs: Triazolam and clonazepam:** R. M. ALONSO, R. M. JIMENEZ, A. CARAVAJAL, J. GARCIA, F. VINCENTE and L. HERNANDEZ. (10 August 1987)
- Solvent and reversed-phase extraction chromatographic separation of niobium, zirconium and hafnium with Aliquat 336:** N. R. DAS and P. CHATTOPADHYAY. (10 August 1987)
- Measurements at nanomolar levels of psychoactive drugs in urine by adsorptive stripping voltammetry:** LUCAS HERNANDEZ, ANTONIO ZAPARDIEL, JOSE ANTONIO PEREZ LOPEZ and ESPERANZA BERMEJO. (10 August 1987)
- New system of a polarographic complex adsorptive wave for the determination of trace tellurium:** LU GUANHAN, HAN QIYI and HE ZHIKE. (10 August 1987)
- Analytical applications of some flotation techniques: A review:** M. CABALLERO, R. CELA and J. A. PEREZ BUSTAMANTE. (10 August 1987)
- Determination of arsenic and antimony in biological materials by solvent extraction and neutron activation:** W. M. MOK and C. M. WAI. (20 June 1987)
- Metal ion-chromatography on silica-immobilized 2-pyridinecarboxaldehyde phenylhydrazine:** NINUS SIMONZADEH and A. A. SCHILT. (23 July 1987)
- Studies on direct determination of trace organophosphates in chlorine-containing water by an enzymic method:** DU TINFA and ZHOU SHIGUANG. (10 August 1987)
- Extraction-polarography of metalhydroxamates—individual and simultaneous determination of traces of molybdenum and tungsten:** S. K. BHOWAL and MITA BHATTACHARYYA. (14 August 1987)
- A solvent-independent correlation between the free energies of solvation of gaseous alkali-metal ions and their electro-negativities:** RISHI K. VARSHNEY and PUSHKIN M. QURESHI. (14 August 1987)
- Determination of uranium at trace level by radiochemical neutron-activation analysis employing radioisotopic yield evaluation:** A. R. BYRNE and L. BENEDIK. (14 August 1987)
- Effect of various mixed aquo-organic solvents on the stability constants of metal complexes with ω -benzoyl-2-hydroxy-4-methoxy-3-methylacetophenone (BHMMA):** B. S. GARG and RANJANA DIXIT. (18 August 1987)
- Fluorescence drainage profiles of thin liquid films:** RAY VON WANDRUSZKA and JAMES D. WINEFORDNER. (18 August 1987)
- Ion-selective electrodes in organic analysis: Determination of xanthates:** WING HONG CHAN, ALBERT W. M. LEE and KAM TONG FUNG. (18 August 1987)
- The influence of atomization pressure on the behaviour of aluminium in electrothermal atomic-absorption spectrometry:** JÁNOS FAZAKAS and MICHEL HOENIG. (21 August 1987)
- Spectrophotometric determination of NO_2^- and NO_3^- :** ZHAO XINWEI, KOU ZONGYAN and HU ZHIDE. (21 August 1987)
- Determination of the sum of rare earth elements by flow-injection analysis with Arsenazo III, 4-(2-pyridylazo)resorcinol, Chromazurol S and 5-bromo-2-(2-pyridylazo)-5-diethylaminophenol as spectrophotometric indicators:** D. B. GLADILOVICH, V. KUBÁŇ and L. SOMMER. (21 August 1987)
- Utility of 7,7,8,8-tetracyanoquinodimethane and sodium acetate for the colorimetric determination of some benzothiadiazine diuretics:** ABDEL-MABOUD I. MOHAMED. (24 August 1987)
- A novel and specific solid-state detection and semiquantitative determination of catechol and *o*-nitrophenol, and some of their kinetic parameters:** PUSHKIN M. QURESHI, K. M. SHAMSUDDIN and SYED ALI. (26 August 1987)
- Improvements on methodological search with non-aqueous media:** A. GUSTAVO GONZALEZ. (28 August 1987)
- Towards a donor-acceptor approach to ion-exchange—I: Correlation between the ion-exchange properties of stannic tellurite: Explanation of the selectivity sequence of oxoanions:** S. ASHFAQ NABI, RIFAQAT A. K. RAO and PUSHKIN M. QURESHI. (4 September 1987)
- Electrochemical reduction behaviour of ruthenium(III)-salicylaldehyde thiosemicarbazone system:** R. PALANIAPPAN and AGNES PAUL. (4 September 1987)
- Extraction of several benzoic and phenylacetic acid derivatives and their complexation with lanthanides:** YUKO HASEGAWA, YOKO MORITA, MASAKO HASE and TOMOMI ISHIZAWA. (4 September 1987)
- Determination of selenium(IV) and tellurium(IV) by differential pulse polarography:** B. V. TRIVEDI and N. V. THAKKAR. (4 September 1987)
- Biamperometric titrations of anions with chloranilic acid—I: Phosphate:** M. A. MALLEA, S. QUINTAR DE GUZMAN and V. A. CORTINEZ. (10 September 1987)
- A new indirect spectrophotometric procedure for determination of sulphur dioxide:** ABDULHAMEED LAILA. (10 September 1987)
- The uranyl-chloro-substituted benzoic acid-Rhodamine B-benzene extraction system:** RESAT APAK, FIKRET BAYKUT and ADNAN ADYIN. (10 September 1987)

- Analytical determination of dimethyl sulphoxide by complex formation with pentacyanoferrate(III):** HENRIQUE E. TOMA, DENISE OLIVEIRA and AMERICO T. MEENOCHITE. (10 September 1987)
- Luminescence characteristics of dibenzofuran and several polychlorinated dibenzofurans and dibenzo-*p*-dioxins:** I. M. KHASAWNEH and J. D. WINEFORDNER. (10 September 1987)
- Rapid decomposition and rapid dissolution methods for silicate rocks with lithium tetraborate/lithium sulphate fusion:** NOBUTAKA YOSHIKUNI. (14 September 1987)
- Dosage potentiométrique des acides aminés par le cuivre II, à l'aide d'une électrode indicatrice de cuivre:** ELIAN LATI, CHANTAL DAUPHIN and MICHEL HAMON. (31 August 1987)
- 3,3',4',5,7-Pentahydroxyflavylium chloride: A selective spectrophotometric reagent for determination of aluminium and tin:** C. A. NWADINIGWE and B. C. IGWE. (14 September 1987)
- Comparative study of IBMK and DIBK as extracting solvents in strongly acidic media: Effect of mutual solubility of solvents on the extraction of Cu(PCD)₂ and its kinetic stability:** MASAHIKO MURAKAMI and TAKEO TAKADA. (14 September 1987)
- High-performance liquid chromatography of micellar solubilization complexes—IV: Reversed-phase ion-pair chromatography of 3,5-diBr-PADAP-Triton-X-100 complexes:** YOU-XIAN YUAN and YUE-JUN WANG. (14 September 1987)
- A comparison of glassy-carbon and carbon-polymer composite electrodes incorporated into electrochemical detection systems for high-performance liquid chromatography:** J.-M. KAUFFMANN, C. R. LONDERS, G. J. PATRIARCHE and MALCOLM R. SMYTH. (14 September 1987)
- Molecular emission spectrometry in a low-pressure electrical discharge:** T. YU and J. D. WINEFORDNER. (15 September 1987)
- Extraction and determination of zinc from pharmaceutical analysis samples:** BHANU RAMAN and V. M. SHINDE. (15 September 1987)
- Determination of lead in fly-ash from a garbage incinerator by atomic-absorption and X-ray fluorescence spectrometry:** MARIT ANDERSSON, CHRISTINA ERIKSON and ÅKE OLIN. (17 September 1987)
- Studies on catalytic kinetic spectrophotometric determination of iron:** DAI CUO-ZHONG, JIANG ZHI-LIANG and LI CHANG-WEI. (23 September 1987)
- Preparation, characterization and performance of surface-loaded chelating resins for ion-chromatography:** P. M. M. JONAS, D. J. EVE and J. R. PARRISH. (23 September 1987)
- Extraktion von Ginsenosiden mit Ammoniak und Kohlensäure unter erhöhtem Druck:** J. R. KIM and H. LENTZ. (23 September 1987)
- Determination of arsenic in ores, concentrates and related materials by continuous hydride generation atomic-absorption spectrometry after separation by xanthate extraction:** ELSIE M. DONALDSON and MAUREEN E. LEAVER. (23 September 1987)
- Solution nebulization of aqueous samples into the tubular electrode-torch capacitatively-coupled microwave plasma:** B. M. PATEL, J. P. DEAVOR and J. D. WINEFORDNER. (23 September 1987)
- Solvent effect on the liquid-liquid distribution of lead(II) with monothiothenoyltrifluoroacetone:** TAKAHARU HONJO, AKIKO IKAZAKI, KIKUO TERADA and TOSHIYASU KIBA. (23 September 1987)
- Anodic-stripping voltammetric determination of trace lead with a nafion/crown-ether film electrode:** SHAOJUN DONG and YUDONG WANG. (23 September 1987)
- Photometric determination of malathion with molybdenum:** U. VENKATADRI NAIDU, P. RAMA DEVI, K. SESHIAH and G. R. K. NAIDU. (29 September 1987)

PUBLICATIONS RECEIVED

Flow-Injection Analysis: Principles and Applications: M. VALCARCEL and M. D. LUQUE DE CASTRO, Ellis Horwood, Chichester 1987. Pages x + 400. £49.50.

The book has been translated from the Spanish and consists of thirteen chapters. The first two chapters consist of a general discussion and classification of automatic methods of analysis and define the position of flow-injection analysis in the complex of analytical methods. The third chapter describes analyte zone dispersion as the theoretical background of FIA. Chapter 4 and 5 discuss in detail the FIA instrumentation, including the present commercial instruments. Chapters 6-10 are concerned with various experimental techniques that are systematically treated, from simple single-channel measurements, through multi-channel and closed-loop analyses, measurement involving intermittent pumping and zone merging, to gradient and titration techniques and kinetic measurements. On-line separations (distillation, dialysis, ion-exchange, extraction, etc.) are also discussed in detail. The applications of FIA to the two most important fields, namely, clinical and environmental analysis, are treated in Chapters 11 and 12 and the book is completed by an outline of the features, present trends and the future of FIA.

The book contains a wealth of concrete data, often summarized in figures and tables, and is a very good source of references to the original literature. Great care has also been exercised in its editing and technical preparation so that it is virtually free of printers' errors.

This is certainly the most extensive treatment of flow-injection analysis to date and, in fact, often transcends the scope suggested by the title, as many general aspects of automatic analysis are also discussed. The most important part of the book is the description of experimental techniques and applications (Chapters 6-12), from which all practising analysts, those with experience in flow analysis and novices alike, will benefit. The first three chapters suffer a little from a tendency to over-classification and over-definition, which necessarily leads to somewhat subjective conclusions and in places obscures the principal questions. The homogeneity and readability of the theoretical treatment has perhaps been affected in several places by too great emphasis being placed on the polemics that have accompanied the development of FIA. Of course, the lack of a unified treatment reflects the fact that the theoretical background of FIA and, indeed, of all flow methods is far from complete.

The book makes an important contribution to the rapidly expanding field of flow analysis and will be useful for all analysts, particularly those active in the fields of clinical and environmental analysis, as well as for undergraduate and graduate students of chemistry.

KAREL ŠTULÍK

Organic Pollutants in Water: T. H. (MEL) SUFFET and MURUGAN MALAIYAND. (Editors), American Chemical Society, 1987. Pages XV + 797. \$109.95 (U.S. & Canada), \$131.95 (elsewhere).

The conventional methods for analysing drinking waters typically account for only 10% of their total organic contents. Biological testing of waters sometimes reveals levels of toxicity that cannot be explained on the basis of the chemical analyses. Also, the more sophisticated analytical methods are being questioned because of their cost, selectivity and artifacts. In this book a great deal of expertise has been marshalled into the battle against these problems in order that we may achieve an adequate means of assessing the quality of natural and drinking waters.

The book begins with a summary of the USA Environmental Protection Agency Priority Pollutants Protocol and Master Analytical Scheme procedures, and goes on to explain in detail the merits of the modern developments in biological testing, sampling methods, and the various concentration and extraction procedures, including use of reverse osmosis, solid sorbents, supercritical fluid carbon dioxide, and continuous liquid/liquid extraction. It is also meticulous in its assessment of the difficulties associated with these techniques: their recovery efficiencies, artifacts, awkward manipulations, and their cost. It examines the question of how to tackle the as yet unidentified toxic substances which some waters appear to contain. And it gives examples of statistical methods for assessing and comparing complex sets of data.

Although the book was developed from a symposium at the 188th meeting of the American Chemical Society, and retains the lay-out of a conference proceedings, with individual papers (now called chapters) retaining the formal pattern of introduction, experimental, etc., a unified approach to the subject has been achieved. This is due to the very high standard of both the review and the specialized papers, and also the willingness of each contributor to discuss the problems as well as the attributes of his method. The result is that one can "read" this book and gain an understanding of the relative merits of the techniques. This self-critical approach is infectious and readers may find themselves taking a fresh look at their own procedures—even those in unrelated fields. It should help to generate new ideas.

B. I. BROOKES

Detectors for Liquid Chromatography: E. S. YEUNG (Editor), Wiley-Interscience, New York 1986. Pages VI + 366. £52.75.

The book consists of nine chapters devoted to various detector types: refractive index (E. S. Yeung), absorption (R. B. Green), FTIR (J. Jinno), indirect absorbance (M. D. Morris), fluorimetric (M. J. Sepaniak and C. N. Kettler), polarimetric (E. S. Yeung), those based on electrical and electrochemical measurements (S. G. Weber), mass-spectrometric (J. B. Crowther, T. R. Covey and J. D. Henion) and miscellaneous (E. S. Yeung). Although there exist specialized monographs on liquid chromatography detection, e.g. R. P. W. Scott, *Liquid Chromatography Detectors*, Elsevier, 1977 and 1986 or T. M. Vickrey (ed.), *Liquid Chromatography Detectors*, Dekker, New York, 1983, the publication of this new book is justified, as the field is developing very rapidly and there is constant need for new sensitive detectors, both selective and universal.

The reader will find in the book a compact and lucid explanation of the principles of detection, elements of the instrumentation, main advantages and drawbacks, and examples of some important applications. The detectors are critically discussed and future trends outlined.

The most important contribution of the book to the field lies in the treatment of the newest detection techniques, such as FTIR, LC-MS, multiwavelength spectrometry, infrared absorption and intracavity absorption, as well as photoacoustic and thermal lens spectroscopy with laser radiation sources. It is also useful that the detectors are discussed from the point of view of their miniaturization, necessary for their application to micropacked and open tubular column HPLC, and from the viewpoint of use in supercritical fluid chromatography, as these belong among the major directions of future development of high-performance chromatography.

A certain shortcoming of the book is the absence of a chapter on the general requirements placed on detectors and their principal properties. These topics are only discussed to a certain extent in Chapter 7 on electrochemical detection. Conductometric detectors are discussed in two chapters, Chapter 7, where they belong, and in Chapter 9, but the symbols have not been unified. The problems of reaction detection might perhaps have been discussed more generally.

The book will be useful for all analysts using HPLC, as well as for advanced courses in separation sciences.

V. PACÁKOVÁ

Computer Supported Spectroscopic Databases: J. ZUPAN (Editor), Ellis Horwood, Chichester, 1986. Pages viii + 165. £28.50.

The book is one of the titles in the Ellis Horwood series in Analytical Chemistry. There are eight chapters which discuss the possibilities for and problems associated with computer-assisted spectrum interpretation. The first part of the book deals with various aspects of database organization, with one chapter devoted to an evaluation of the current status of computer-assisted structure elucidation, one to a discussion of problems in the management of chemical databases, and one to a demonstration of the advantages in a hierarchical database organization. Following this general discussion, information systems based on specific types of spectroscopy are presented. Two chapters deal with infrared spectra, one with mass spectra and one with nuclear magnetic resonance spectra. Finally, chapter eight surveys the problems in multispectroscopy expert systems. The book gives a thorough survey of useful approaches and of a number of widely used search and interpretation systems. It is well organized with an index and several clear illustrations. Further, since the book contains many suggestions as regards the future development of computerized retrieval and interpretation systems, I believe it would be a valuable source of information both for potential users of such systems and for researchers who either supply the experimental data or are engaged in software development.

LARS KRYGER

Clinical Specimens: D. HAWCROFT and T. HECTOR, Wiley, Chichester, 1987, Pages xvii + 123. £9.95 (soft cover), £28.00 (cloth bound).

This book is one of the titles in the ACOL (Analytical Chemistry by Open Learning) series and introduces the range of human specimens that can be considered in clinical analysis. The main part of the book discusses the range of clinical specimens (blood, urine, saliva and many more) available, their roles, origins, and characteristics with an indication of their individual importance in diagnosis. It also considers the techniques used to obtain representative samples of these materials, and the problems involved in sampling, transport, storage and analysis. There is also a good discussion on hazards associated with collecting blood specimens. Further coverage includes discussion on how the composition of biofluids is influenced by factors such as age, sex, diet, stress and physical activity.

In the latter part of the book some common type of biopsy specimens (body tissues) used in clinical investigations are considered together with the methods employed for their removal and problems involved in their analysis.

At the end of each chapter a summary is given emphasising the important points covered in the chapter and at the end of the book revision questions (and answers) are provided. On the whole, the book is written in clear, simple and informal style; it is relatively free of errors, and is recommended to newcomers to medical laboratory work.

A. C. MEHTA

Diagnostic Enzymology: D. HAWCROFT, Wiley, Chichester, 1987. Pages xxi + 280. £11.50 (soft cover), £32.00 (cloth bound).

This book is also one of the texts in ACOL series and deals with enzyme methodology in the diagnosis of human illness. The book begins with a detailed discussion of the general properties of enzymes, followed by the spectroscopic and non-spectroscopic techniques used for measuring their activity, and the problems associated with obtaining reproducible and meaningful results. There is also a chapter on quality control in enzyme assays. The book culminates with a discussion on clinical applications of enzyme assays. The diagnostic value of the assays is highlighted with specific examples of disease states (e.g., enzyme assays in diagnosis of liver disease). Further references on enzyme literature are provided at the end of the book.

The general format of the book is in accordance with the other ACOL titles (or units as they are generally called), viz. summary at the end of each chapter, and self-assessment questions (and answers) provided throughout the book. I am not quite sure why Tables are referred to as Figures (although they are referred to as Tables in appendices!) and indexes are ignored in these books. A small criticism of this particular book is that it seems to be more biochemically oriented and there is no mention of enzyme-based drug assays such as EMIT, RIA, or FIA. Nevertheless, the book is already thick for its price and there is a lot of information in it. It is neatly presented, the diagrams are clear, and there are hardly any errors. It should be very useful to technical staff working in clinical chemistry laboratories.

A. C. MEHTA

PAPERS RECEIVED

- A rapid spectrophotometric method for the determination of carbon monoxide in ambient air: P. SELVAPATHY, T. V. RAMAKRISHNA and R. PITCHAI. (6 April 1987)
- Potentiometric titration of fulvic acids from lignite, in acetone, acetonitrile and propan-2-ol: JOSE M. ANDRES and CLEMENTE ROMERO. (6 April 1987)
- Electrochemical behaviour of some substituted benzophenone oximes: I. GURRAPPA and S. JAYARAMA REDDY. (8 April 1987)
- Spectrophotometric study and analytical applications of rare-earth-kojic acid complexes: The direct determination of Nd, Ho and Er in mixed rare-earths: SHI-FU ZHOU and ZHONG LI. (8 April 1987)
- Studies on chelating resins—III: An alternative way to represent metal-resin complex equilibria: O. SZABADKA. (8 April 1987)
- Determination of mercury by differential-pulse anodic-stripping voltammetry with various working electrodes and its application in analysis of natural water sediments: MIROSLAV HÁTEL. (15 April 1987)
- Ion-pair liquid-solid extraction for the preconcentration of trace metal ions: Optimization of experimental conditions: VALERIO PORTA, EDOARDO MENTASTI, CORRADO SARZANINI and MARIA CARLA GENNARO. (18 April 1987)
- Determination of arsenic in ores, concentrates and related materials by graphite-furnace atomic-absorption spectrometry after separation by xanthate extraction: ELSIE M. DONALDSON. (18 April 1987)
- Spectrophotometric determination of iron(III), in blood and pharmaceutical products, with 1-hydroxy-2,3-diaminopropane-tetra-acetic acid (HPDT): MA. TERESA SEVILLA ESCRIBANO, JOSE MA. PINILLA MACIAS and LUCAS HERNANDEZ HERNANDEZ. (18 April 1987).
- Separation of amino-alcohols by HPLC with a ternary mobile phase containing nickel(II) chelate additives: GRZEGORZ BAZYLAK and JOANNA MASZOWSKA. (18 April 1987)
- Conditional stability constant determination of metal aquatic fulvic acid complexes: DANIEL T. HAWORTH, MARK R. PITLUCK and BRUCE D. POLLARD. (18 April 1987)
- The effect of surfactants on the dissociation constants of phenothiazine derivatives: An alkalimetric determination of diethazine and chlorpromazine: P. RYCHLOVSKÝ and I. NĚMCOVÁ. (14 April 1987)
- Room-temperature phosphorimetry of polyaromatic hydrocarbons using organized media and paper substrate: A comparative study: G. RAMIS RAMOS, I. M. KHASAWNEH, M. C. GARCIA-ALVAREZ-COQUE and J. D. WINEFORDNER. (14 April 1987)
- Flow-injection determination of ethanol in whole blood by use of immobilized enzymes: J. RUZ, M. D. LUQUE DE CASTRO and M. VALCARCEL. (14 April 1987)
- Quantitative analysis by surface-enhanced Raman spectrometry on silver hydrosols in a flow-injection configuration: J. J. LASERNA, A. BERTHOD and J. D. WINEFORDNER. (21 April 1987)
- Identification and determination of volatiles derived from phenol-formaldehyde materials. ROMAN GRZESKOWIAK and GRAHAM D. JONES. (21 April 1987)
- Determination of molecular nitrogen by electron-impact-induced fluorescence: DAVID A. RADSPINNER and E. L. WEHRY. (10 April 1987)
- A spectrophotometric study on the complex formation of 3-(1-naphthyl)-2-mercaptopropenoic acid with nickel(II), palladium(II) and hydrogen ions: ALVARO IZQUIERDO and JOSE LUIS BELTRAN. (21 April 1987)
- Three-dimensional synchronous fluorescence spectrometry for the analysis of three-component alkaloid mixtures: F. GARCIA SANCHEZ, A. L. RAMOS RUBIO and C. CRUCES BLANCO. (21 April 1987)
- Separation of some transition-metal ions and preconcentration of Pt(IV) and Cr(III) on alumina-immobilized diethylenetriaminepenta-acetic acid by ligand exchange: D. K. SINGH and PALLAVI MEHROTRA. (22 April 1987)
- The interaction between sodium dodecyl sulphate (SDS) and Eriochrome Azurol B (ECAB) or Chrome Azurol S (CAS) studied by means of NMR and spectrophotometry: ZHENG YONGXI and CHU JINJING. (24 April 1987)
- Determination of amodiaquine in pharmaceuticals and plasma by reaction with periodate and spectrophotometry or by high-performance liquid chromatography: KRISHNA K. VERMA and SUNIL K. SANGHI. (24 April 1987)
- Electrochemical reduction of methylparathion: T. N. REDDY and S. J. REDDY. (24 April 1987)
- Electrochemical determination of metronidazole: P. SIVA SANKAR and S. JAYARAMA REDDY. (24 April 1987)
- Multiparametric curve fitting—XIII: Reliability of formation constants determined by analysis of potentiometric titration data: MILAN MELOUN, MICHAL BARTOŠ and ERIK HÖGFELDT. (27 April 1987)
- Studies on the extraction of Ni(II), Fe(II), Fe(III) and V(IV) with bis(4-hydroxypent-2-ylidene)diaminoethane: Separation and spectrophotometric determination of iron, nickel and vanadium: F. IK NWABUE and E. N. OKAFO. (27 April 1987)
- Direct polarographic determination of Ce(III) in aqueous medium: J. LOPEZ PALACIOS and M. BARRERA. (27 April 1987)
- Solvent extraction equilibria of the 3-(2-furyl)-2-mercaptopropenoic acid complex of nickel(II) as an ion-pair with diphenylguanidium: A. IZQUIERDO, M. D. PRAT and A. GARBAYO. (24 April 1987)
- Ultrasensitive and selective measurements of tin by adsorptive stripping voltammetry of the tin-tropolone complex: JOSEPH WANG and JAVID ZADEH. (24 April 1987)
- Mass-transfer coefficient for a normal circular cylinder placed in a circular flow tube: ROMAN E. SIODA. (24 April 1987)
- Modification of a Beckman model 501 autosampler for pre-column derivative-formation: T. J. BYDALEK, D. A. COX and L. R. DREWES. (5 May 1987)
- Separation of oxyanions of sulphur by single-column ion-chromatography: A. BEVERIDGE, W. F. PICKERING and J. SLAVEK. (5 May 1987)
- Spectrophotometric determination of some antiamoebic and anthelmintic drugs with metol and chromium(VI): C. S. P. SASTRY, M. ARUNA and A. RAMA MOHANA RAO. (5 May 1987)
- Studies on non-aqueous porphines—I: Synthesis of $\alpha,\beta,\gamma,\delta$ -tetra-(4-methylphenyl) porphine and spectrophotometric study of its reaction with palladium: ZE-XING HUANG, SHU-QIONG HE, JIN-TONG LU and TIAN-FU HUANG. (5 May 1987)

Studies on non-aqueous porphines—II: Synthesis of $\alpha,\beta,\gamma,\delta$ -tetra-(4-acetyloxyphenyl)porphine and spectrophotometric study of its colour reaction with copper(II): ZE-XING HUANG, SHU-QIONG HE, DONG-JIN WANG, TIAN-HU CHEN and CHANG-MING JIN. (5 May 1987)

Room-temperature phosphorescence of 3- and 5-substituted indoles: CATHERINE HAUSTEIN, WILLIAM D. SAVAGE, CHE F. ISHAK and RONALD T. PFLAUM. (5 May 1987)

Formation constants of trivalent lanthanide ions and β -diketonehydrazones in 75% dioxan-water medium: BASHEIR A. EL-SHETARY, MOHAMED S. ABDEL-MOEZ, SHAKER LABIB STEFAN and MAHMOUD M. MASHALY. (5 May 1987)

Ion-chromatography using pH detection and CO₂ removal: HIDEHARU SHINTANI and PERNEANDU K. DASGUPTA. (5 May 1987)

Study on a coated carbon rod PVC thallium ion-selective electrode and its application to the determination of thallium in rocks and minerals: DEZHONG DAN and YALAN DONG. (5 May 1987)

SUBJECT INDEX

Absorbance, of fluorescein, ultraviolet	739
Absorptiometry, ion-exchanger, Sensitivity of	239
Acid-base ionization equilibria, of 1-(2-carbamylethyl)imidazoles	525
Acidity constants, of benzidine	1039
Adsorption isotherms, Determination by GC	589
Advances in voltammetry	41
Air pollution, piezoelectric detectors	865
Alkali metals, stability constants of complexes.	817
—, Determination by atomic ionization	191
— picrates, Transport through membranes	509
Alkaline-earth metals, Determination, by plasma AES	823
—, —, polarographic	555
—, —, Stability constants of complexes	817
Aluminium, Separation from In and Ga	895
Americium, Determination, by alpha-spectrometry	567
Amino-acids, Detection, by fluorescence	438
—, Determination, by HPLC.	749
Analysis, of diesel particulates	483
—, of high-purity substances.	123
—, of inorganic substances	873
—, of paraffin waxes	661
—, potential stripping, Role of thiourea	945
Analytical chemistry, in the USSR.	1
—, of transplutonium elements	31
—, Teaching in the USSR.	9
Anion-exchange, for enrichment of U	433
— resin, for determination of Se(IV) and Se(VI)	435
—, —, modified, as catalyst	667
Antimony chloride solutions, Determination of free acid	729
Aromatic organic compounds, Extraction of	957
Arsenic, Determination, by AES	495
—, —, by ASV	574
Ascorbic acid, Determination, spectrophotometric	731
Assay, of enzyme effectors	201
Atomic-absorption spectrometry (AAS), Determination of elements	179, 715
—, —, of Rb, Sr and Ba	427
—, —, flameless (FAAS), Analysis of high-purity substances	147
—, —, Atomizer for	259
—, —, Determination, of Ge	341
—, —, —, of lanthanides and Y.	1043
—, —, —, of metals	580
—, —, —, of Mn, Fe, Pb and Cd	465
—, —, —, of Mo	271
—, —, —, of Se	337
—, —, Effect of graphite on sensitivity	927
—, —, —, of sample pretreatment	141
—, —, —, new Zeeman-effect spectrometer	699
—, —, —, with tungsten-coil atomizer	197
—, —, Sensitivity of	892
— ionization, Determination of alkali metals	191
Atropine, Determination, with membrane electrode	723
Azo dyes, Co-ordination of silver ions	449
Barium, Determination by AAS	427
Benzidine, Activity constants.	1039
Bismuth, Complexes with dicarboxylic acids	375
—, Determination, by ASV	657
—, —, spectrophotometric and by AAS	503
—, Separation from Tl and Ag	401
— and antimony, Determination by ASV	529
Block copolymers, Identification by TLC	167
—, —, Molecular-weight distribution	161

Bromide and iodide, Determination, spectrophotometric	615
Bromine number, new method for	645
Cadmium, Determination by ASV	995
—, — by FAAS	465, 580
—, Titration, thermometric	733
Calcium, Determination by flow-injection analysis (FIA)	543
—, —, spectrofluorimetric	423
Calculation, of formation constants	933
Calibration, Microcomputer-assisted	283
Carbon, Determination, wet-chemical	807
Cardiovascular drugs, Determination, spectrophotometric	670
Catalytic kinetic methods, for Pt metals	69
Catecholamines, Determination	810
Cation-exchanger, for concentration of Sc, Zr, Hf and Th	103
1-(2-Carbamylethyl)imidazoles, Acid-base ionization equilibria	525
Chelex 100 resin, Separation of Bi	503
Chloride, Determination, mercurimetric	1035
—, —, spectrophotometric	905
—, —, with ion-selective electrode	921
<i>p</i> -Chlorobenzyl-4-dimethoxy-6,7-isoquinoline iodomethylate, Oxidation of	799
Chromatography, gas (GC), Determination of adsorption isotherms	589
—, —, Pulse-circulation	227
—, gel-permeation, Molecular-weight distribution of polymers	161
—, high-pressure liquid (HPLC), Ionization detector for	461
—, ———, of amino-acids	749
—, ———, of Pd	223
—, ion, of metal ions	415
—, ion-exchange, of Bi, Tl and Ag	401
—, ———, of In, Ga and Al	895
—, ———, on hydroxamic acid resin	547
—, ———, on macroreticular resins	361
—, thin-layer (TLC), Identification of block copolymers	167
—, ———, with low-volatility mobile phases	183
Chromium, Determination by adsorptive stripping voltammetry	939
Clofibrate, Determination, spectrophotometric	365
Cobalt, Determination of ultratraces	277
—, —, spectrophotometric	367, 369
Cobalt(II), Determination, spectrophotometric	789
—, Extraction of	303
Colour specification, of pH indicators	673
Complexes, Formation in aqueous solution	385
—, ternary, Use in photometry	313
Components, volatile, Determination of	51
Computers, personal, Application in analysis	709
Computer-assisted optimization, of HPLC	749
Co-ordination compounds, Determination of metals	77
Copper, Determination, by ASV	995
—, —, by FAAS	580
—, —, spectrophotometric	293, 479
Cyanide, Determination, fluorimetric	743
— ions, Determination, spectrophotometric	535
Data-acquisition system	619
Detectors, for flow-injection analysis	987
—, for HPLC	461
—, piezoelectric	865
Diesel particulates, Analysis of	483
Digestion procedures, for Se	829
Dithiocarbamic acids, Extraction	783
Drugs, analytical methods for	609
Electrochemical sensor, for oxygen	551
Electrode, glassy-carbon, for ASV	574, 657
—, ion-selective, for Ag and Au	111
—, ———, for chloride	921
—, ———, for Cu	407
—, ———, for Intestopan analysis	887
—, ———, for sulpho-drugs	977
—, ———, for Trimethoprim	983
—, liquid-membrane, for atropine	723
—, metallized-membrane, for sulphur compounds	453
—, pH-sensitive	577
Electromigration, of radionuclide ions	375

Elements, Determination, by AAS	179, 715
—, —, by XRF	1027
—, Extraction of	175
—, transplutonium, Analytical chemistry of	31
Emulsions, Effect of AAS	892
End effects, in flow analysis	1009
Enzyme effectors, Assay of	201
Extraction, of aromatic organic compounds	957
—, of Co(II)	303
—, of dithiocarbamic acids	783
—, of elements	175
—, of Li	779
—, of metals	953
—, of metal complexes	211
—, of Se	337
—, of Zr and Hf	331
Fluorescein, Absorbance in the ultraviolet	739
Fluorescence, in thin liquid films	571
—, of U(VI) complexes	207
Flow analysis, End effects in	1009
— injection analysis (FIA), Detectors for	987
—, —, of bromide and iodide	615
—, —, of Ca and Mg	543
—, —, system, Determination of viscosity	915
—, —, for Raman spectroscopy	745
— potentiometric stripping analysis, Determination of Pb	539
Formation constants, Dependence on ionic strength	593
—, of 2-mercapto-3-phenylpropanoate complexes	971
—, of weak complexes	933
Free acid, Determination in SbCl ₃ solutions	729
Fulvic acid, Titration, potentiometric	583
Gallium, Determination, fluorimetric	835
—, Separation from In and Al	895
Galvanic stripping, Determination of Pb	965
Germanium, Determination, by FAAS	341
Gold, Determination, by ion-selective electrode	111
—, Fire-assay collection	736
Graphite, Effect on FAAS	927
— furnace, for atomic-fluorescence spectrometry	290
— platform atomizer, for FAAS	259
Hafnium, Concentration by cation-exchange	103
—, Extraction with polyurethane foam	331
Heavy atoms, kinetic isotope effects	877
High-purity substances, Analysis of	123, 147
Histidine and histamine, Determination, fluorimetric	325
Hydride generation system, for AES	495
Hydrogen, Determination in steels	489
Hydrogenation enthalpimetry	283
Hydrogen peroxide, Determination, spectrophotometric	667
Indicator, for acid-base titrations	507
—, for pH, Colour specifications	673
Indium, Separation from Ga and Al	895
Inductively-coupled plasma discharges	629
Infrared spectrometer, interfacing to microcomputer	243
Inorganic substances, Luminescence analysis	873
Insecticides, Determination, spectrophotometric	372
Intelligence systems, for spectral analysis	21
Interfacing, infrared spectrometer to microcomputer	243
Intestopan, Electrodes for determination	887
Iodide, Determination, kinetic	351
— and bromide, Determination, spectrophotometric	615
Ion-exchange resins, for anion-chromatography	361
—, —, absorptiometry, Sensitivity of	239
Ion-exchanger, chelating, new	547
Iron, Determination, by FAAS	465, 580
—, —, spectrophotometric	655
Isonicotinic acid hydrazide, Determination, fluorimetric	857
Kinetic isotope effects, of heavy atoms	877
Lanthanides, Determination by FAAS and plasma AES	1043
—, chelates, Stability order	445

Lanthanum(III), Stability constants of complexes	861
Laser plasma-source mass spectrometry, Theory of	61
— ultramicroscopy, Analysis of suspensions	133
Lead, Determination, by ASV	995
—, —, by FAAS	465, 580
—, —, by flow potentiometric stripping analysis	539
—, —, by galvanic stripping	965
— and thallium, Determination by ASV	
Lithium, Extraction of	779
Louis Gordon Memorial Award	No. 6, III; No. 10, III
Luminescence analysis, of inorganic substances	873
Lutetium, Determination, spectrophotometric	639
Magnesium, Determination, by flow-injection analysis	543
Manganese, Determination by FAAS	465, 580
—, —, kinetic spectrophotometric	321
—, Speciation of	307
Matrix, Alloys, Determination of Co	367
—, —, — of Sn	1033
—, — and Al, Determination of Ga	835
—, Animal tissues, Determination of metals	580
—, Argillites, Determination of minor elements	715
—, Barite, Determination of Rb, Sr and Ba	427
—, Biological fluids, Determination of drugs	609
—, — material, Determination of Se	829
—, Britholite-apatite, Determination of rare earths	1043
—, Catalysts, Determination of chloride	905
—, Drugs, Determination of paracetamol	605
—, Ferromolybdenum, Determination of Mo	505
—, Foetus bones, Determination of alkaline-earth metals	823
—, Hair, Determination of Se	337
—, Lake water, Determination of metals	465
—, Limestone and dolomite, Determination of Ca and Mg	543
—, Metals, Determination of oxygen	153
—, — and alloys, Determination of Bi	503
—, Natural waters, Determination of elements	179
—, —— sediments, Determination of Hg	1001
—, Petroleum residues, Determination of bromide number	645
—, Pharmaceuticals, Determination of atropine	723
—, PWR coolant, Determination of Cr	939
—, Rocks, Determination of W	215
—, Sea-water, Determination of U	433
—, Silicate rocks, Determination of Sc	345
—, —, — of trace elements	1027
—, Steel, Determination of hydrogen	489
—, Sulphide ores and concentrates, Determination of Bi	503
—, Sulphuric acid, Determination of chloride	1035
—, Uranium carbide, Determination of C	807
—, Urine, Determination of Pb	539
—, Water, Determination of dissolved oxygen	551
—, —, — of nitrite	1021
—, —, — of Se	337
—, —, Speciation of Mn	307
Metals, chelates, Determination by HPLC	223
—, complexes, Extraction of	211
—, Determination, by co-ordination compounds	77
—, —, by plasma AES	849
—, Extraction of	953
—, ions, Extraction of	303
—, —, Separation by ion-chromatography	415
—, noble, Determination, spectrophotometric	87
6-Methoxyquinoline, Oxidation of	1015
Metoprolol tartrate, Determination, titrimetric	296
Microcomputer, Interfacing with infrared spectrometer	243
Microcomputer-assisted calibration	283
Mobile phases, low volatility, for TLC	183
Molecular weight distribution, of block copolymers	161
Molybdenum, Determination of ultratraces	271
—, —, with oxine	505
Molybdenum(VI), Determination, spectrophotometric	419
Monosaccharides, Determination, spectrophotometric	793
Nickel, Determination, spectrophotometric	479
Nickel(II), Formation constants of complexes	971
Nitrite, Determination, kinetic spectrophotometric	1021

Nitrogen, Determination, emission-spectrometric	253
—, molecular, Determination, fluorimetric	963
<i>N</i> -Nitrosamines, Determination by TLC	441
Nomifensine maleate, Determination, spectrophotometric	287
Organolead compounds, Determination, iodometric	885
Oxidation, of <i>p</i> -chlorobenzyl-4-dimethoxy-6,7-isoquinoline iodomethylate	799
Oxprenolol hydrochloride, Determination, titrimetric	296
Oxygen, Determination in metals	153
—, electrochemical sensor for	551
Palladium, Determination, by HPLC	223
—, —, polarographic	219
Paracetamol, Determination, spectrophotometric	605
Paraffin waxes, Analysis of	661
Particulates, Effect on ASV signals	231
Pharmacia Prize	No. 6, III
Pharmacokinetics and the analytical chemist	355
Photometry, Use of ternary complexes	313
Piperazine, Determination, spectrophotometric	968
Plasma discharges, inductively-coupled	629
Platinum metals, Determination, catalytic kinetic	69
—, Survey of methods	677
Plutonium, Determination by alpha-spectrometry	567
Polarography, Determination of alkaline-earth metals	555
—, differential-pulse, Determination of Pd	219
—, linear-sweep, Determination of U	813
Polyurethane foam, for extraction of aromatics	957
—, — of Zr and Hf	331
Potential acidity diagrams	763, 771
Praseodymium, Determination, spectrophotometric	639
Protonation constants, of acids and bases	411
Pulse-circulation GC	227
Radionuclide ions, Electromigration	375
Reagent, Antipyrine, for extraction	175
—, <i>N</i> -Benzyl-2-naphthohydroxamic acid, for V(V)	653
—, Bis(8-quinolyl)disulphide, for elements	179
—, <i>p</i> -Chloromandelic acid, for Mo(VI)	419
—, Chlorpromazine, for iodide	351
—, Constant Calcein Blue, for Ca	423
—, 2,6-Diacetylpyridine bis(arylhydrazine), for U	473
—, <i>O,O</i> -Dialkyldithiophosphoric acid, for extraction	211
—, Diantiprylmethane, for extraction	175
—, 2,3-Dichloro-5,6-dicyano- <i>p</i> -benzoquinone, for drugs	670
—, 2-(3,5-Dichloro-2-pyridylazo)-5-dimethylaminophenol, for Co	369
—, 1,4-Dihydroxyanthraquinone, for Lu and Pr	639
—, 5,5-Dimethyl-1,2,3-cyclohexanetrione-1,2-dioxime-3-thiosemicarbazone, for Fe(II)	655
—, Ferrocene, for Se	664
—, Ferron, for Cu	293
—, Hexacyclen, for extraction	953
—, 3-Hydroxy-4 <i>H</i> -pyran-4-ones, for lanthanides	445
—, Hydroxylamine hydrochloride, for clofibrate	365
—, 9-Isothiocyanatoacridines, for amino-acids	438
—, Malachite Green, for Mo(VI)	419
—, 8-Mercaptoquinoline, for elements	179
—, 3-Methyl-2-benzothiazoline hydrazone hydrochloride, for insecticides	372
—, Mordant Blue 9, for U	247
—, 2,3-Naphthalenedialdehyde, for cyanide	743
—, 2-Nitro-5,6-dimethyl-1,3-indanetrione dithiosemicarbazone, for Co(II), Pd(II) and Os(VIII)	789
—, <i>N</i> -Oxalylamine(salicylaldehyde hydrazone), for Ga	835
—, Oxine, for Mo	505
—, Phthalhydrazidylazoacetylacetone, as indicator	507
—, Pyridine-2-aldehyde 2-pyridylhydrazone, for nitrite	1021
—, 1-(2-Pyridylazo)2-naphthol, for Pd, Co, Ni and Cu	223
—, Rhodanine derivatives, for noble metals	87
—, Rutin, for W(VI)	512
—, Salicylaldehyde guanylhydrazone, for Mn	321
—, Sodium diethyldithiocarbamate, for Cd	733
—, Taurine for cyanide	743
—, Tetrabutylammonium tribromide, for bromine number	645
—, Thymolphthalexone, for alkaline-earth metals	555
—, Tiron, for Co	277
—, <i>N-m</i> -Tolyl- <i>N</i> -phenylhydroxylamine, for Ti	889

—, Trihydroxyfluorones, for W	215
—, Tropolone, for Sn	909
—, Xylidyl Blue I, for U	813
Redox systems, Potentials of	763, 771
Rubidium, Determination by AAS.	427
Sample pretreatment, Effect on FAAS	141
Scandium, Concentration by cation-exchange	103
—, Determination, fluorimetric	345
Selectivity and sensitivity, of metal determination	77
Selenium, Determination by AES	495
—, — by FAAS	337
—, —, spectrophotometric	664
—, Digestion procedures	829
Selenium(IV) and selenium(VI), Determination in mixtures	435
Sensitivity, of ion-exchanger absorptiometry	239
Signal processing, in potentiometric titrations	586
Silver, Determination by ASV	705
—, — by ion-selective electrode.	111
—, —, spectrophotometric	479
—, Fire-assay collection	736
— ion, Co-ordination by azo dyes.	449
Software, for thermal titrations	381
— survey, DADISP	602
—, DATABANK	288
—, JESS	821
—, LABMASTER	299
—, LABROM	300
—, LU4D	822
—, MKMODEL	603
—, MOLGRAF	600
—, MULTI-Q	602
—, NUMBERMASTER	300
—, PAPERBASE de Luxe	301
—, REFSCAN	601
—, REFSYS	601
—, SIGNWRITER	300
—, STATSTREAM	599
—, TADPOLE	599
Soviet Union, Analytical chemistry in	1
—, Teaching of analytical chemistry	9
Speciation, of Mn in water	307
Spectral analysis, artificial intelligence systems for	21
Spectrometry, Data-acquisition system for	619
Spectrometry, alpha, Determination of Pu and Am	567
—, atomic-fluorescence (AFS), Graphite furnace for	290
—, —, tungsten-coil atomizer for	197
—, emission, Determination of nitrogen	253
—, fluorescence, Determination of molecular nitrogen	963
—, —, — of nomifensine maleate	287
—, high-energy collisional, Determination of diesel particulates	483
—, mass (MS), spark-source and plasma-source	61
—, plasma atomic-emission (AES), Determination of alkaline-earth metals	823
—, —, —, Determination of As and Se	495
—, —, —, — of lanthanides and Y	1043
—, —, —, — of metals	849
—, Raman, surface-enhanced	745
—, second-derivative fluorescence	325
—, X-ray fluorescence (XRF), Determination of trace elements	1027
Stability constants, of complexes	385
—, —, of glycine complexes	817
—, —, of La(III) complexes	861
—, —, of uranyl complexes	519
—, —, of vanadyl and uranyl complexes	839
Standard-addition method, Effect of volume and matrix	899
Strontium, Determination by AAS.	427
Sulpha-drugs, Determination by ion-selective electrode	977
Sulphate, Determination by pH-titration.	397
Sulphides, organic, Complexes with Pd(II)	219
Sulphur compounds, Determination by ion-selective electrode	453
Survey of methods, for Pt group elements	677
Suspensions, Analysis by laser-ultramicroscopy	133
Talanta Advisory Board	No. 2, V
Thiourea, Role in potential stripping analysis	945

Thorium, concentration by cation-exchange	103
Tin, Determination by adsorptive stripping voltammetry	909
—, —, complexometric	1033
Titanium, Determination, spectrophotometric	889
Titration, of catecholamines	810
—, complexometric, of Sn	1033
—, coulometric, Determination of protonation constants	411
—, iodometric, of organolead compounds	885
—, pH, of sulphate	397
—, potentiometric, of chloride	1035
—, —, of fulvic acids	583
—, —, of weak acids	515
—, —, Signal processing	586
—, thermometric, of Cd	733
—, —, Software for	381
Trimethoprim, Determination by selective electrode	983
Tungsten, Determination, spectrophotometric	215, 513
— coil atomizer, for FAAS	197
Uranium, Determination by adsorptive stripping voltammetry	247
—, —, polarographic	813
—, —, spectrophotometric	433, 473
Uranium(VI), Determination by fluorescence	207
Uranyl complexes, Stability constants	519, 839
Validation, of methods for drugs analysis	609
Vanadium(V), Determination, spectrophotometric	653
Vanadyl ion, Oxidation of 6-methoxyquinoline	1015
—, —, Stability constants of complexes	839
Viscosity, Determination in flow-injection system	915
Volatile components, Determination of	51
Voltammetry, adsorptive stripping, Determination of Cr	939
—, —, — of U	247
—, —, — of Zr	561
—, Advances in	41
—, anodic stripping (ASV), Determination of Ag	705
—, —, — of Bi	657
—, —, — of Bi/Sb and Pb/Tl	529
—, —, — of Hg	1001
—, —, — of Zn, Cd, Pb and Cu	995
—, —, —, Effect of particulates	231
—, —, —, Use of Personal computer	709
—, computer-controlled	757
Weak acids, Titration, potentiometric	515
Yttrium, Determination by FAAS and plasma AES	1043
Zeeman background correction, for FAAS	580
— effect, new type of AA spectrometer	699
Zinc, Determination by ASV	995
Zirconium, Concentration by cation-exchange	103
—, Determination by adsorptive stripping voltammetry	561
—, Extraction with polyurethane foam	331

PUBLICATIONS RECEIVED

Quantitative Analysis of Catecholamines and Related Compounds: A. M. KRSTULOVIĆ (Editor), Ellis Horwood, Chichester, 1986. Pages 384. £47.50.

The heart of this book is a multi-section chapter on HPLC methodology for the determination of the biogenic amines. The simplicity and sensitivity of the HPLC technique, which has recently come to the fore as the method of choice for estimating the trace amounts of catecholamines and associated materials in biological fluids and tissues, are clearly presented in a very well-organized text. The favoured detection systems (electrochemical and fluorometric) are discussed at length. The seven sections cover the fundamentals of HPLC, sample preparation and handling, electrochemical detection (with full details of detector design) involving dual-electrode systems in combination with microbore columns and the use of reversed-phase and ion-exchange packing materials, assays of the enzymes involved in catecholamine metabolism, fluorescence detection following the formation of phthalaldehyde derivatives, and automated analyses by use of trihydroxyindole oxidation products. Other methods covered include GLC and GLC/MS, radioenzymatic assays, immunoassay procedures (including that for chromogranin), and immunofluorescence and fluorescence assays. An introductory chapter on the biochemistry of neurotransmitters and their role in disease processes, together with a final one on tissue analysis, complete a text compiled by 25 scientists representing 18 laboratories around the world. The volume overall provides a clear, comprehensive and detailed picture of current analytical procedure for an important group of natural products, together with a refreshing amount of chemical and biochemical background material.

A. B. TURNER

Inductively Coupled Plasma Emission Spectroscopy: P. W. J. M. BOUMANS (Editor), Wiley-Interscience, New York, 1987. Part 1, pages xi + 584, £71.75. Part 2, pages xiii + 486, £64.20.

As a pioneer in ICP studies Dr Paul Boumans is uniquely qualified to edit the two-volume treatise, *Inductively Coupled Plasma Emission Spectroscopy*. Part 1 deals with methodology, instrumentation and performance, while Part 2 is concerned with applications and fundamentals. It is surprising that a field so important and extensive as emission spectroscopy with inductively coupled plasma sources has had to wait so long for a definitive work and so the publication of the treatise is timely. Chapter one gives an easy introduction to atomic-emission spectrometry with an outline of, for instance, spectroscopic instrumentation, the basis of quantitative analysis, together with information on sample introduction and excitation sources. The section on a guide to the literature on emission spectroscopic analysis is useful but it is a pity that the RSC publication *Annual Reports on Analytical Atomic Spectroscopy* (latterly *Journal of Analytical Atomic Spectrometry*) is only mentioned in a bibliographical list and not in the main text. There is a chapter on plasma sources other than ICPs and then one devoted to the ICP itself, which also gives brief mention of the related techniques of ICP-AFS and ICP-MS. The bulk of the volume is the chapter on Basic Concepts and Characteristics of ICP-AES. Here, Boumans discusses at length detection limits, precision, accuracy, dynamic range, multielement capability, line selection and optimization of ICP operating conditions. There are chapters, jointly written with G. M. Hieftje, on torches for ICPs and with J. A. C. Broekaert on the important topic of sample introduction, then Boumans brings his experience to bear with a chapter on line selection and spectral interferences. The final two chapters of the volume are the only ones not contributed to by the editor, and these deal with spectrometers and detection and measurement.

The first half of Part 2 deals with applications and there are sections on metals and industrial materials, geological, environmental, agriculture and food, biological, clinical and organic samples. These chapters are written by different authors and so reflect their experience. With some exceptions, notably the chapter on biological and clinical materials by Maessen, there is a lack of information in tabular form, but there are ample references for those willing to search.

The remainder of the volume is concerned with fundamentals. There is a chapter on the direct analysis of solids, describing the multitude of methods that have been used to investigate this difficult problem. Browner describes in theoretical terms his work with aerosol generation and transport, and Boulos and Barnes describe plasma modelling and computer simulation. There are chapters by Mermet and Blades on spectroscopic diagnostics and excitation mechanisms and discharge characteristics. The volume ends with a chapter by Broekaert and Tölg on the status and trends in elemental trace determinations.

Two of the stated aims of the volume are to fill an essential gap in the AES literature and to provide a critical and tutorial survey of more than 20 years of research, development, and application in the field of ICPs and related plasma sources. In both of these it succeeds admirably.

G. B. MARSHALL

Photometric Determination of Traces of Metals, 4th Ed., Part IIA: Individual Metals, Aluminum to Lithium: HIROSHI ONISHI, Wiley-Interscience, New York, 1986. Pages xix + 885. £143.70.

This long-awaited companion to Part I, published in 1978, was inevitably delayed by the death in 1984 of Professor E. B. Sandell, the author of the first three editions, and co-author of Part I. It is a great pity that he did not see Part IIA (to which he contributed material) come to fruition, but it will be a lasting memorial to his many contributions to analytical chemistry, and spectrophotometric analysis in particular. The book contains an enormous amount of practical information, with useful footnotes (appearing in the guise of references) in the style of Hillebrand, Lundell, Bright and Hoffman's classic "Applied Inorganic Analysis". For each element there is a thorough survey of the separation methods available for concentrating traces of the element and/or removing interferences, followed by a review of the reagents available for the determination of the element, and finally applications to various types of sample, with full details of procedures recommended by the author. The work is thorough, scholarly and comprehensive. Part IIB will be as eagerly awaited.

R. A. CHALMERS

PUBLICATIONS RECEIVED

Non-ionic Surfactants—Chemical Analysis: JOHN CROSS (Editor), Dekker, New York, 1987. Pages x + 417. Price \$82.75 U.S. and Canada; \$99.25 elsewhere.

This book is in three parts: a short introduction to non-ionic surfactants (part A) is followed by analytical methods specific to oxyalkylated surfactants (part B), and more than half of the book is devoted to separational and instrumental methods of analysis (part C).

The opening chapter, "Introduction to non-ionic surfactants" (John Cross), deals with the characteristics and general properties of various categories of non-ionic surfactants. Chapter 2, "Metal ion complexes of polyoxyalkylene chains" (John Cross), deals with the formation of a complex between a polyether chain and an inorganic ion (Ba^{2+} , K^+ , Na^+) followed by a reaction of the complexed ion with a relatively large anion to produce a salt which will either precipitate out from the aqueous solution, or can be readily extracted by a less polar solvent. Rapid progress is shown to have been made in this field of study but a concise picture of the reaction between the oxyethylate chains and metal ions has not yet emerged. Chapter 3, "Trace analysis of non-ionic surfactants" (Phillip Crisp) is concerned mainly with the preconcentration of surfactants by solvent extraction before analysis, and by forming complexes in aqueous media and then extracting with solvents for analysis by chromatographic, spectroscopic, or other methods. Critical assessments of up-to-date methods are made and recommendations given. It is regrettable that the use of such hazardous solvents as benzene and halohydrocarbons continues. Chapter 4, "Potentiometry of Oxyalkylates" (Gwilym Moody and John Thomas), describes the fabrication and operation of poly(vinyl chloride) membrane ion-selective electrodes, which were originally designed for the determination of barium ions, but which were found to give a linear response to the logarithm of the concentration of oxyalkylates. The characteristic break in the linearity of the curves provides a useful and simple determination of the critical micelle concentration. The oxyalkylate/barium sensors have potential use for on-line industrial and environmental monitoring.

Chapter 5, "Determination of total oxyethylene content by fission techniques" (John Cross), confines itself to analytical methods based on the fission of oxyethylene chains into discrete recognizable fragments, using such cleavage agents as hydriodic acid, hydrogen bromide, mixed acid anhydrides, acetyl and Lewis acids. Some methods are suitable for the determination of the total ethylene oxide content, whilst others are suitable for determining oxyethylene/oxypropylene ratios in copolymers.

The remainder of the book deals with description and applications of separational and instrumental methods of analysis of non-ionic surfactants: these include gas-liquid chromatography (John Cross), high performance liquid chromatography (Nissim Garti, Vered Kaufman and Avraham Aserin), thin-layer and paper chromatography (Fredric Rabel), nuclear magnetic resonance spectrometry (Antony Montana), infrared spectroscopy and mass spectrometry (Georgi Rauscher). The book ends with a chapter on "Aspects of quality and process control" (John Cross) dealing with a range of chemical and physical tests used in maintaining quality control of manufactured products.

The book is well-written, comprehensive, informative and reasonably up-to-date: the layout is good and the number of typographical errors is small. Each author has written with authority, each topic has a good introduction, and experimental methods are described in detail and assessed critically. No single method of analysis is perfect or adequate, and the need for internal standardization is emphasized. The problems and pitfalls in analyses are treated seriously and ways of overcoming or avoiding these are described. The complex formulation of non-ionic surfactants for industrial, domestic and personal use, requires a combination of several complementary methods and instrumental techniques, of the types described in this book, before a good qualitative and quantitative analysis can be achieved. Anyone working with, or having an interest in, the manufacture, use or environmental effects of non-ionic surfactants, will benefit considerably from reading this book.

J. B. CRAIG

Handbook of Polycyclic Aromatic Hydrocarbons, Vol. 2: ALF BJØRSETH and THOMAS RAMDAHL (Editors), Dekker, New York, 1985. Pp. x + 416. \$95.00 (U.S. and Canada); \$114.00 (all other countries).

It would be natural to ask how this volume relates to the first, published in 1983—does it repeat some of the same material? Does it follow the same pattern? Is it useful on its own without the first volume? The editors state that they found it necessary to update some important areas and add new information on selected topics. I think the second volume is much more than just a supplement—it is a complement to the first. Whereas the first devoted much space to the analytical and sampling methodology this concentrates on the findings resulting from applying these methods. There is an introductory chapter on the sources of PAHs followed by three on detailed reports of the emissions of PAHs from coal-burning boilers, combustion of biomass, and automobile engines. There is also some coverage of nitrogen-containing PAHs and of occupational exposure to them. Analytical methodology is not ignored, but is reviewed in two chapters, one on GC methods, and one on HPLC methods, usefully supplemented by one on reference materials. Finally, there is a chapter on some PAH chemistry—dealing with atmospheric reactions of these compounds.

This volume, like the first, is set from camera-ready copy, but on better quality paper than the first. It is well presented and illustrated. I would expect it to find a wider readership than the first because it deals with environmental aspects as well as with the analytical methods.

IAIN L. MARR

PUBLICATIONS RECEIVED

Modern Analysis of Antibiotics: A. ASZALOS (Editor), Dekker, New York, 1986. Pages xvi + 535, \$107.50.

There are 14 chapters in this book. Half of them deal with chemical analysis and the remainder with biological assays of antibiotics. The chemistry section includes chapters (reviews) on gas chromatographic analysis, ultraviolet and light absorption spectrometry, infrared spectrometry, mass spectrometric analysis, electron spin resonance spectroscopy, thin-layer chromatography, high-performance liquid chromatography, and thermal analysis. Each chapter provides an up-to-date account of methods that were developed in the last 5-7 years and have proved to be valuable tools in the laboratory. Procedures are described in reasonable detail so that sufficient information about them is available without consultation of other sources. The emphasis is on quality control, safety, and stability evaluations of bulk and formulated antibiotics derived from natural, synthetic, and semisynthetic sources. In the HPLC chapter, body fluid and tissue analyses are also discussed. All the chapters have an extensive list of references.

The biological section includes chapters, among others, on microbiological and immunological assays. These chapters should interest analytical chemists because chemical assays (in particular HPLC) for antibiotics are frequently correlated with microbiological assays (to test the biological activity of the drug), and immunological assays (RIA, EMIT, *etc.*) are now routinely performed in many chemical laboratories.

On the whole the book is well presented. It contains numerous tables, figures, and structures. The index is comprehensive. The book would be a valuable source of information for anyone involved in the analysis of antibiotics.

A. C. MEHTA

Assessment and Control of Biochemical Methods: T. HECTOR, Wiley, Chichester, 1986. Pages xvii + 150. £9.95.

This book is one of the titles in the ACOL (Analytical Chemistry by Open Learning) series and deals with the problems associated with selecting and evaluating biochemical assays. It is specially designed for either private study or for specific units in courses leading to BTEC, RSC, or other qualifications. The level is that of senior technician.

The book takes the reader through the process of method selection, testing, quality control, and assessment. Examples are taken from assays used in clinical laboratories. At the end of each chapter a summary is given emphasizing the important points covered in the chapter and a list of objectives which should have been achieved. Self-assessment questions are provided throughout the book to enable the learner to check his/her progress. The answers are discussed at the end of the book.

There is a good discussion on basic statistics, accuracy, precision, method comparison, calibration and control materials (mainly serum), and internal and external quality control. With accuracy and precision it would have been nice to have some discussion on other analytical parameters such as sensitivity and limit of detection. The book is written in simple, unambiguous and informal style; the diagrams are clear and there are hardly any errors, except on p. 119 where iceteric should read icteric. Unfortunately there is no index.

Overall the book is quite suitable for its intended audience. It would also be useful for technical staff working in pharmaceutical or clinical chemistry laboratories. The price is reasonable by today's standards.

A. C. MEHTA

Ultratrace Analysis of Pharmaceuticals and other Compounds of Interest: SATINDER AHUJA (editor), Wiley-Interscience, New York, 1968. Pages xvi + 384. £57.50.

This text was written in response to a perceived need for a means of evaluating methodologies at the limits of trace analysis. It covers a wide range of analyses performed at submicrogram levels, principally of pharmaceuticals, together with some carried out at microgram levels with animal feeds, animal-derived foods, and in forensic work.

The first half of the book deals with the techniques involved, and comprises chapters by leading authorities on gas and liquid chromatography (including derivatization procedures), selected ion-monitoring, GC-MS and LC-MS, thin-layer chromatography (including HPTLC and reversed-phase systems), and atomic spectroscopy.

Applications form the second half of the book, starting with the quality control of drugs and the inert substances used in their formulation. Examples are drawn from many classes of pharmaceutical compounds, and the treatment here appears somewhat cursory, although it does not aim to provide in-depth assessment of specific areas of work. Metabolic and toxicological studies are then reviewed, and the final chapters deal with drug analysis in animal feeds (both in the areas of toxicological testing and medicated feedstuffs), regulatory analysis of drug residues in foods derived from animals, and drug analysis in forensic science, including postmortem toxicology.

A. B. TURNER

PUBLICATIONS RECEIVED

Separation and Spectrophotometric Determination of Elements: ZYGMUNT MARCZENKO, Ellis Horwood, Chichester, 1986. Pages 678. £69.50.

The determination of low element concentrations by precise and comparatively low cost photometric absorption methods continues to be of great value and this new book by Professor Marczenko fully lives up to the reputation of his earlier work on the topic. The book begins with a chapter on separation and preconcentration of elements which deals in detail with solvent extraction, precipitation, flotation, volatilization and ion-exchange, including use of chelating resins. Use of periodic table charts to illustrate the range of applications of various reagents is a useful feature. Chapter 2 covers principles and practice of spectrophotometric analysis and deals clearly and concisely with the basis of colour, Beer's law and causes of deviation therefrom, various expressions concerning sensitivity of methods, errors, masking and the development of specific methods. The section closes with an excellent summary of the basic colour-forming reactions, with examples. Chapter 3 surveys the most commonly used reagents with masterly pinpointing of the salient features of each. There follows part 2 of the book in which the elements, both metallic and otherwise, are dealt with in alphabetical order by name. For each element (or group, *e.g.*, alkali metals) there is a section on methods of separation (precipitation, solvent extraction, ion-exchange and other relevant techniques) followed by methods of determination. Here two or three tried and trusted procedures are described in detail for immediate use in the laboratory. Other methods of value are mentioned briefly but with very comprehensive referencing up to early 1986. Surfactant enhancement techniques and use of newer reagents such as porphyrins are well covered. Under "Carbon" are described methods for cyanide, thiocyanate, cyanate, hexacyano-ferrates, carbon monoxide and carbon disulphide; under "Oxygen," methods for ozone and hydrogen peroxide. The chapter on fluorine analysis, a subject of particular interest to your reviewer, gives an excellent balanced account of popular methods. Some minor errors were noted including a lapse in structure printing on pp. 101 and 103 but the book as a whole is a masterpiece of lucid condensation of a great mass of material and translation editor Dr. Mary Masson is to be congratulated on ensuring that Professor Marczenko's well constructed work has appeared in first-rate and enjoyable English. For those who still enjoy a little chemistry with their analysis this book is a delight and can be warmly recommended.

M. A. LEONARD

PUBLICATIONS RECEIVED

Kennzahlen der Verfahrenstechnik: HANS WETZLER, Hüthig Verlag, Heidelberg, 1985. Pp. 167.

The use of characteristic numbers in the context of the technological application of heat and mass transfer mechanisms is rapidly growing and constantly being refined.

In this book 400 of the most popular characteristic numbers are listed alphabetically together with their definitions and physical application. It also contains an extensive up to date bibliography.

The book is written primarily in German but it does contain a brief English translation of all comments and explanations. Even though the alphabetical order is derived from the German version of the characteristic numbers this does not normally cause problems, because with few exceptions the English and German nomenclature correspond to each other. It would have been nice to include cross references for the very few cases where they do not. The English translations are sometimes a bit awkward but generally understandable.

In summary it can be said that this book is a very compact source of reference and useful beyond the stage of a pure dictionary because it also gives equations for application of the characteristic numbers. Considering it was written by a German primarily for Germans, it is still useful to English-speaking scientists from student to expert levels because of its compactness and wide coverage.

KLAUS WIBBELMANN

PUBLICATIONS RECEIVED

Nuclear Magnetic Resonance Spectroscopy: D. A. R. WILLIAMS, Wiley, New York, 1986. Pages xix + 272. Hard cover £28.00; Soft cover £9.95.

The intention of this book (one of the series "Analytical Chemistry by Open Learning") is to provide an introduction to the practice of NMR spectroscopy at a basic level for those studying for B.Tech., levels IV and V and similar qualifications. It deliberately avoids the more general theoretical treatment necessary for progression to advanced study and in this sense is unsuitable as a general elementary book. However, in its declared objectives it succeeds admirably and it will be useful up to senior technician level. The numerous self-assessment questions, lists of objectives, and worked examples make it particularly suitable for students working with minimum supervision or without access to specialist teaching staff.

The severe curtailment of theoretical material does lead, perhaps inevitably, to some unevenness of treatment. For example, the explanation of FT spectra seems very inadequate in contrast to a very detailed account of signal/noise enhancement methods. Again, the understandable desire to minimize complications has resulted in oversimplification to the point of occasional inaccuracy. The use of α and β to designate nuclear spin states is the reverse of normal convention and could lead to confusion if the student consults other texts.

Figures, including spectra, are very well reproduced, though additional labelling would have been helpful in some cases. There are a number of typographical errors of a minor nature. On the whole this is a useful and worthwhile book which fills a gap in the range of teaching material in this topic.

D. G. WILLIAMSON

Fourier Transform Infrared Spectrometry: P. R. GRIFFITHS and J. A. DE HASETH, 2nd Ed., Wiley, New York, 1986. Pages xv + 656. £76.75.

This book is divided into two almost equal halves, the first dealing with operational aspects of Fourier transform spectrometry, the second with advances in the diverse applications to which this powerful technique lends itself.

Full treatments are given of the basic optical and computational requirements of FTIR and their recent developments and refinements towards higher efficiency, resolution, and sensitivity. Although a highly technical subject, this is written in an eminently readable manner, with many instructive diagrams.

The applications of FTIR spectrometry to analysis and chemical research in general range from the well-established to the newly-developing. Amongst others, individual chapters are devoted to quantitative analysis, surface analysis, studies of biochemical and biomedical processes, atomic-emission spectrometry, time-dependent studies and time-resolved spectrometry, studies of polymers, the well-established gas chromatography interface, and the developing interface with high performance liquid chromatography.

Selected references to pertinent reports in the literature are included at the end of each chapter of an excellent book.

Pollutants and their Ecotoxicological Significance: Edited by H. W. NÜRNBERG, J. Wiley, Chichester, 1985. Pages xi + 515. Price £49.50.

Pollution—environment—ecology: an emotive combination of three terms always sure to catch the attention of the media and the public, yet which of our young scientists are trained to cover this field? Our new graduates do not have the background necessary to cross the many interdisciplinary boundaries encountered in such studies, and current trends in training tend to take them into ever narrower specializations. This first-rate compilation of thirty essays, compiled by the late Hans Nürnberg, will be welcomed by any reader attempting to cope with the many unknowns and imponderables in environmental studies, so far removed from the (almost) ideal model systems usually chosen for investigation in the laboratory.

The topics, grouped for convenience under four headings—Atmosphere, Aquatic Environment, Terrestrial Environment and Man, and Regulatory and General Aspects—range from chemistry (SO₂, strong acids, halocarbons, carcinogens, heavy metals, hydrocarbons, organochlorines) through physics of transport and diffusion, the botany of plants as bio-indicators and the zoology of aquatic systems, birds eggs and pesticides, to aspects of human biology, geography and legislation.

The compiler aimed to present "a comprehensive treatment of the subject exemplified by instructive examples and based on experience, expertise and recent findings of experts..." This he has indeed achieved, with the co-operation of his many colleagues in Western Europe. It is perhaps a little disappointing that only one contribution is from a British author. I would have wished for at least a chapter on UK legislation to complement the one on German regulations. On the other hand, all the authors and the editor are to be congratulated on presenting a fascinating, informative and readable survey of this complex topic. It deserves to be widely consulted, not just by researchers but by all those concerned about the future of our environment and what can be and is being done to preserve it for the future. This book will stand as a fitting memorial to Hans Nürnberg—a man who believed in combining research in analytical chemistry with its application outside the laboratory.

IAIN L. MARR

Fleet Street Editor: D. CLARE, J. WARMISHAM, F. DART, S. MERCER and P. BITTON, Mirrorsoft, London, 1986. (2 discs) £39.95. Admin Xtra: (1 disc) £14.95. Available for the BBC-B, B+ and Master 128, in 40 and 80-track versions.

The title of this piece of software, which may suggest some sort of computer game, conceals a most useful and valuable package. Described as "the first of a new generation of one-step publishing packages", it allows graphics and text to be combined together and printed out by a dot-matrix printer. The facilities offered include a graphics library of illustrations, symbols and typefaces, a drawing package that allows modification of items from the graphics library or creation of new illustrations, and a word processor that allows text (in 2 sizes of type and 10 founts in all) to wrap around the graphics on a page. These facilities allow the creation of "panels" which can then be combined in various ways to make up the page for printing.

I have been aware for some time of a need for some way of producing printed hand-outs for students, incorporating illustrations along with the text (particularly desirable in chemistry), and *Fleet Street Editor* meets this need admirably. Also, the ability to print large text—either the normal double height founts, or the larger letters available in the graphics library—could be utilized profitably for production of material for "poster sessions" at meetings and conferences.

The Admin Xtra supplementary disc further enhances the usefulness of the package by allowing conversion of graphics between the various screen modes of the BBC microcomputer, so aiding the incorporation of chemical illustrations produced by other programs. It also allows printing of enlarged single panels for "posters", and viewing of previously created panels, and includes a database program especially designed for cataloguing discs.

In both the main package and the supplementary disc, most of the applications are ikon-driven. The whole system has been programmed in a thoroughly professional fashion, and, despite its complexity, is easy to learn to use. The printed pages produced look professional, yet are refreshingly different from duplicated typescript or the normal printed page. The handbook is nicely produced in a loose-leaf binder, and it provides the detailed information required in a most helpful way. One suggestion—I would like to have had a reference card summarizing the main points of operation, to save having to refer to the manual for minor points.

Overall, I think this is an excellent package offered at a most competitive price.

MARY MASSON

Computer Aids to Chemistry: G. VERNIN and M. CHANON, Editors, Ellis Horwood, Chichester, 1986. Pages 411. £49.50.

The wide variety of topics covered in this book reflects the importance of computers as aids in most branches of chemistry today. The chapter titles give an idea of the range of coverage: Computer-aided organic synthesis, Teaching chemistry with microcomputers, Computer graphics: a new tool in chemical education, Kinetics, Multivariate analysis of chemical data sets with factorial methods, Computer aids to crystallography, Mass spectra and Kováts' indices databank of volatile aroma compounds, and Online access to chemical information. Although there are many other applications of computers in chemistry, I think the editors have succeeded admirably in their aim to select topics that illustrate most of the types of chemical problems that computers are used to solve. The wide range of topics may seem reminiscent of a Conference Proceedings, but the text shows no resemblance to such a publication. Each chapter goes into some detail, so that the reader will acquire considerable depth of knowledge. This book can be recommended for reading by senior undergraduate and postgraduate students, as a guide to what is being done in chemistry with computers at the present time, and many of their teachers would find it a stimulating introduction to chemical applications of modern computer systems.

MARY MASSON

CORRIGENDA

In the paper by Akira Sano, Masaaki Takezawa and Shoji Takitani, *Talanta*, 1987, **34**, 743, the following corrections should be made.

Page 743, lines 12–14 from the bottom should read:

concentrations and the pH, the following procedure is recommended. To 500 ml of aqueous sample solution add 500 μ l of 0.6 mM taurine solution in 0.05M borate–0.1M phosphate buffer (pH 9.0) and 500 μ l of 0.4 mM NDA solution in the same buffer. Measure the fluorescence

Page 744, line 11 should read:

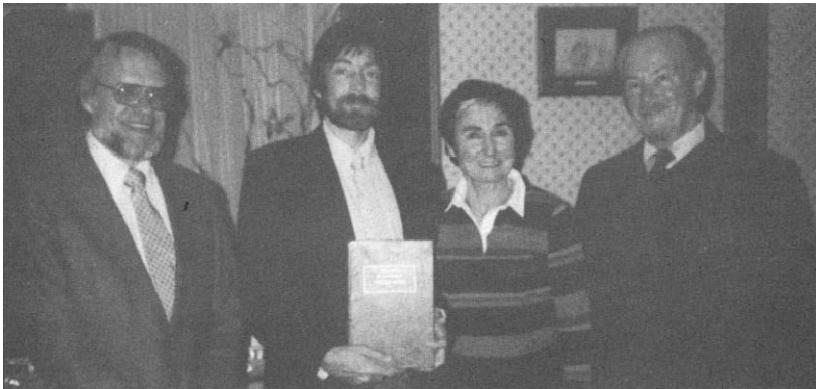
and its tolerance ratio was found to be 100.

LOUIS GORDON MEMORIAL AWARD

The Louis Gordon Memorial Award for 1985 was presented to Professor Ben Freiser by Professor J. W. Winefordner at the 1987 Pittsburgh Conference



Professor Freiser and Professor Winefordner



**Professor Winefordner, Professor B. Freiser and
his parents (Professor Henry Freiser and Mrs. Freiser)**

NOTICE

1st INTERNATIONAL SYMPOSIUM ON SEPARATION OF CHIRAL MOLECULES

PARIS, 31 May–2 June 1988

ORGANIZATION

Société Française de Chimie (S.F.C.)
Congress department: G. PERREAU
250, rue Saint-Jacques
75005 PARIS (France)
Tel.: (1) 43.25.20.78

SCIENTIFIC ORGANIZATION

Analytical Chemistry Division of S.F.C.
10, rue Vauquelin, 75231 PARIS Cedex 05 (France)
Tel.: (1) 47.07.08.71
D. BAUER (Chairman)
F. GUYON (Secretary)—Tel.: (1) 42.34.82.62

The 3 days meeting will consist of several sessions with a main topic: how to separate chiral molecules on the analytical or preparative scale. Various techniques will be presented. It will be pointed out how they are complementary. In addition, we propose invited introductory lectures dealing with subjects of general interest, such as importance of chiral molecules for "high-tech" chemistry, chiral molecules in pharmacology, current status of physical methods in analysis of chiral molecules.

4 sessions will be organized on the following subjects:

- Direct separation: static and dynamic crystallizations.
- Crystallization by diastereoisomer formation.
- Chromatographic methods (GC, LC) based on chiral separative phases (CSP) or not.
- Enzymatic separations.

Each session will consist of plenary lectures, oral and poster communications. Panels will be organized on specific topics.

A one-page definitive abstract (300 words in French or English) of a proposed paper should be sent no later than 5th October 1987 to the scientific organization (address above). Acceptance will be notified to authors by the end of November 1987.

The official languages for the meeting will be French or English.

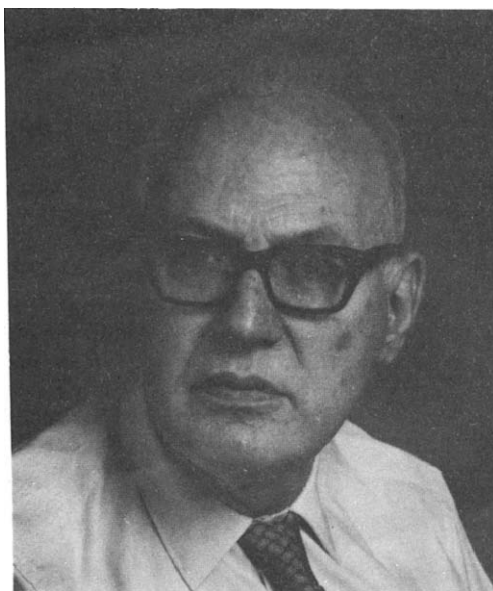
EDITORIAL

This issue contains a review paper on the determination of the platinum group metals. We draw special attention to it because of the large number of papers on spectrophotometric reagents for these metals that already clutters up the literature and continues to increase. Like copper, cobalt and most transition metals, the platinum group metals (and silver and gold) readily form coloured complexes with a wide diversity of organic compounds. The consequence is that it is rather easy to manufacture still more such reagents, and write papers about them, without bothering to think about whether it is really worthwhile doing so except for the purpose of training research students. There are now some thousands of these reagents, most of which are variations on a theme, with no real advantages over the many others available for the same purpose. It is even questionable whether the work on such reagents can properly be called research at all, since in many ways it is akin to using a well established chemical reaction and merely changing the final method of measurement from say spectrophotometry in the visible region to spectrometry in the ultraviolet, or exchanging one buffer for another. The importance of the review paper referred to is that it should give prospective workers in this field some idea of where new methods would really be useful, acquaint them with what has been done already, and warn them that the nature of these metals is such that the preliminary chemistry of decomposition and adjustment of oxidation state is more important than the final determination method. After all, if the metal is present in an oxidation state that will not give the desired (or expected) reaction with the selected reagent, the result obtained will be incorrect, and probably expensively so. For that reason, referees and editors should firmly reject all papers that do not give detailed procedures for producing the required oxidation states (free from polynuclear or mixed-ligand or hydrolysed species) and not simply rely on use of simulated samples prepared by starting with solutions of the correct kind. Those who wish to work in fields so narrow that they are the scientific equivalent of battery farming are welcome to do so, of course, but they should not expect to publish the results—publication is a privilege, not a right.

R. A. CHALMERS

THE PHARMACIA PRIZE

Pharmacia AB (Uppsala, Sweden) and the Editorial Board and Publisher of *Talanta* take great pleasure in announcing that the Pharmacia Prize for 1985–1986 (for the paper published in *Talanta* that was judged to be the best contributed from an industrial laboratory) has been awarded to Silve Kallmann, Ledoux and Company, Teaneck, NJ, U.S.A., for his paper “Analysis of sweeps: The cuprous sulphide collecting system” (*Talanta*, 1986, 33, 75).



THE RONALD BELCHER MEMORIAL AWARD FOR 1988

Applications are invited for the Ronald Belcher Memorial Award, in commemoration of the late Professor Belcher's outstanding contributions to analytical chemistry, international relations and understanding, his interest in student welfare, and continued association with *Talanta* from his conception of the journal in 1957 right up to his death. The award takes the form of a travel grant of US\$1000 to enable a young analytical scientist to undertake travel abroad and is made in even-numbered years. Candidates may be of either sex and any nationality, but must be under 30 years of age at the time of application, and not have had more than one year of post-doctoral experience. Applications may be sent by the candidates themselves, or on their behalf by a responsible senior (e.g., Head of Department, research supervisor), and must be submitted by the end of the year preceding the award. They must include a brief curriculum vitae, a short statement of the purpose of travel and the places to be visited, a testimonial of ability, and a recommendation from a senior research worker.

Applications for the 1988 award should be sent to either

Dr. R. A. Chalmers
Department of Chemistry
University of Aberdeen
Old Aberdeen, Scotland

or

Professor J. D. Winefordner
Department of Chemistry
University of Florida
Gainesville, Florida 32611, U.S.A.

to arrive before 31 December 1987.

NOTICE

1988 Winter Conference on Plasma Spectrochemistry

San Diego, California
3-9 January, 1988

Papers describing original work with plasma spectrochemical applications, fundamentals, and novel instrumentation developments are solicited for the 1988 Winter Conference on Plasma Spectrochemistry to be held 3-9 January 1988 at the San Diego Princess resort and Convention Center in San Diego, California. Titles and 50-word abstracts are due by 2 July 1987.

Sponsored by the ICP Information Newsletter, this fifth in a series of biennial meetings will feature developments in plasma spectrochemical analysis as performed with inductively coupled plasma, dc plasma, microwave plasma, or glow and hollow-cathode discharge sources. Ten symposia organized and chaired by recognized experts will be presented in lecture and poster sessions along with six plenary and 15 invited lectures. Thirty expert short courses will be taught at introductory and advanced levels. A three-day exhibition of spectroscopic instrumentation and chemicals, electronics, glassware, publications and software supporting plasma spectroscopy will complement the scheduled sessions.

For details, contact Dr. Ramon M. Barnes, Conference Chairman, Department of Chemistry, GRC Towers, University of Massachusetts, Amherst, MA 01003-0035, U.S.A. Telephone (413) 545-2294.

EDITORIAL

This issue contains a fresh batch of contributions to the Software Survey feature. To avoid the risk of this material being lost when the journal comes to be bound, the contributions have been treated in the same way as the other features, and given regular page numbers, and not supplementary page numbers. This will also facilitate indexing. The success of this feature, which offers a very convenient format for display of software that is available for various purposes, depends on a regular flow of material, and contributions will be welcome. Readers wishing to contribute are invited to complete and submit a Software Description Form (found at the end of this issue).

NOTICES

CAC—88

4th INTERNATIONAL CONFERENCE ON CHEMOMETRICS IN ANALYTICAL CHEMISTRY

Amsterdam, The Netherlands
18–20 May 1988

The influence of chemometrics in analytical chemistry is unmistakable and the application of chemometric techniques in daily and analytical practice is of growing importance. The theme of this 4th CAC conference will be "Chemometrics in Analytical Chemistry, with emphasis on practical applications, theoretical developments, and chemometric software".

The scientific programme will include invited plenary lectures, keynote lectures, and submitted research papers.

Topics

- Application and development of formal techniques for design, optimization and evaluation of analytical procedures and results.
- Sampling
- Application of systems theory, operations research, information theory, statistics and other chemometric techniques in analytical chemistry.
- Computerized signal-, image-, and data analysis/processing, optimum filtering, parameter estimation, time series analysis, calibration, curve resolution.
- Multivariate data analysis, pattern recognition, cluster analysis, principal-components analysis, factor analysis, etc.
- Expert systems/artificial intelligence. Data retrieval/library searching, management systems.
- Mathematical modelling and computer simulation of analytical processes.
- Robotics, automation
- Education in chemometrics.

Final date for receipt of abstracts: 15 January 1988.

Registration and information:

Secretariat, CAC-88, Laboratory for Analytical Chemistry, University of Amsterdam, Nieuwe Achtergracht 166, 1018 WV Amsterdam, The Netherlands [telephone: (020)-5256541, Dr. Smit].

INTERNATIONAL SEMINAR ON ANALYTICAL TECHNIQUES IN MONITORING THE ENVIRONMENT

ISAME

Department of Chemistry, Sri Venkateswara University, College of Engineering, Tirupati-517 502,
India

10–12 January, 1989

OBJECTIVES

This International Seminar intends to focus on the state-of-the-art and the progress made in developing analytical methods for use in monitoring the environment.

SESSIONS

1. Electroanalytical methods
2. Spectral methods
3. Radioanalytical methods
4. Chromatographic methods

Scientific sessions of the Seminar will include plenary lectures, invited and contributed papers as well as posters. Exhibition of scientific equipment will also be arranged. Efforts will be made to print Extended Abstracts.

Abstracts of papers to be sent in duplicate before April 30 1988, Preliminary Registration by 1 January 1988, to the address shown above.

PUBLICATIONS RECEIVED

Radiochemical Methods: W. GEARY, Wiley, Chichester, 1986. Pages 229. £9.95

This book (in the ACOL—Analytical Chemistry by Open Learning—series) is aimed at those “who wish to study in a more flexible way than traditional institute attendance or to augment such attendance”. After an introduction, there are chapters on radioisotopes and labelled compounds, practical aspects, radioanalytical methods, new applications (which includes reprints of three research publications) a repeat of all the self-assessment questions but with responses, and five useful tables of units. The inclusion of the research papers displays clearly the necessity to understand the basics of radiochemistry before tackling more complex problems. The use in each chapter of an overview, followed by explanation, self-assessment questions, summary, and objectives, is an excellent concept. The style of writing and layout of text are good, and there are few errors. In the text, tables are labelled as figures.

The theory and techniques are explained in a reasonably satisfactory way, but there are several statements with little or no supporting evidence or explanation: a “distance learner” would, for example, find it difficult to comprehend why one would choose a detector of low resolution, rather than one of high resolution, to resolve complex mixtures of photopeaks. The author’s decision to use an inherently faulty expression to predict whether or not a particular isotope is radioactive, rather than to provide a simple table or chart of stable and unstable isotopes, seems open to question.

On balance, the book is reasonably good value for money, but distance or other learners might require tutorial assistance to meet all the objectives of the book. It should be considered as a useful introduction to the subject of radiochemical methods, but reference should be made to the text-books quoted in the bibliography before the commencement of any practical work.

J. B. CRAIG

PAPERBASE De Luxe: A. DURHAM, Wight Scientific, London, 1985. £90. Available for MS-DOS, PC-DOS and CP/M computers.

Many database programs are available for personal computers, and most of these would be eminently suitable for storing a bibliographic reference collection, so is there a place for a specialized program like this one? Testing the program for this review has convinced me that there are indeed many advantages in the specialized approach. A major one is the use of sequential ASCII files, with fields delimited by commas, to store the data, rather than the usual random access files: this allows great flexibility in the amount of information that can be stored, since only the space actually needed for each reference is used. Even more important is the program’s ability to print out references in the correct format for any journal. A section of the program uses a question-and-answer session to produce and store the code needed for any particular format, but also codes are already included on the disc for many of the most popular journals. It would be a great joy to editors if this facility became more widely used by the scientific community. The information is stored as four “lines” of data; first, the names of the author(s) and year of publication; second, the title of the publication; third, the journal, volume, first page and last page numbers, keywords; and fourth, any link to an abstract in another file, and any comments. Lines may be as long as is needed, or left blank if the information is not required. The searching, selecting and sorting facilities would be expected in any database program: here they can be used for authors’ names, or for keywords in the title of the paper or the keyword list. An EDIT program is included, although the ASCII files can also be edited by most word-processor programs. In the past, I have looked at main-frame bibliographic packages with a view to utilizing them, but concluded that a card-index was still superior for my purposes. This system I will certainly use, and will encourage postgraduate students to use; the only remaining problem is that it is difficult to take the computer to the library, so paper or cards would still be needed to transfer the information. I suppose the next step is to get a hand-held computer to take to the library, then transfer the data collected to the main database on the PC by an RS232 link.

MARY MASSON

Solubility and Related Properties (Drugs and the Pharmaceutical Sciences Series, Volume 28); KENNETH C. JAMES. Dekker, New York, 1986. \$69.75 (U.S. and Canada), \$83.50 (elsewhere). Pages ix + 425.

This book attempts to cover the subject of solubility with a practical approach, and with particular reference to choices of solvents for use in pharmaceutical and related applications. It has two basic aims: to enable the reader to select the most suitable solvent for the purpose he has in mind; and to provide information from which the reader can estimate solubilities that have not been determined experimentally. Topics covered include solutions and solubility, the liquid state, qualitative treatment of solubility, ideal solutions, regular solutions, “nearly regular” solutions, solute–solute and solvent–solvent interactions, solute–solvent complexation, the distribution law, and aqueous solubilities. Besides the practical approach, a great deal of theoretical material is included.

MARY MASSON

Chemometrics: M. A. SHARAF, D. L. ILLMAN and B. R. KOWALSKI, Wiley, New York, 1986. Pages xi + 332. £51.00.

The publication of two new journals on chemometrics this year must signal confidence by publishers that the topic is becoming well established, but surely these authors' reference to a "new science" being born is a little extravagant. The present book aims to introduce the field of chemometrics to advanced students of chemistry, with an admission that it was not possible for the descriptions of the seven major concepts to be complete in a volume of this size. The main topics referred to are Sampling Theory, Fundamentals of Experimental Design and Optimization, Signal Detection and Manipulation, Calibration and Chemical Analysis, Resolution of Analytical Signals, Exploratory Data Analysis, and An Introduction to Control and Optimization. Much of the material is quite familiar as the subject of several books (or chapters in books) on statistics for analytical chemistry. I liked the way some of the topics were presented, but I think I would prefer some of the other available texts for use with students. The other material, particularly that on signal resolution and pattern recognition, is less familiar and therefore potentially more useful. However, I found the treatment rather uneven: some parts, particularly the longer descriptive sections, were excellent, while others were difficult to follow, making it difficult to grasp the real aim of the technique being expounded. The preface states "The treatments are focused on chemistry with mathematical derivations avoided as much as possible." This should *not* be taken to mean that *mathematics* is avoided as much as possible: there are many mathematical expressions and equations given, and the reader would need to be well acquainted with probability theory, matrix algebra, and calculus to make full use of this book. I think that in some instances, the inclusion of mathematical derivations might have made the mathematics easier for non-mathematicians to follow. However, the book does offer a useful compact introduction to many of the concepts and techniques of chemometrics, and each chapter has an extensive bibliography which would be most valuable to a reader who wanted to delve further into the subject.

MARY MASSON

SIGNWRITER: A. DURHAM, Wight Scientific, London, 1986. IBM PC version tested: £80 + VAT, \$120. Also available for Apricot, BBC, Amstrad.

SIGNWRITER is a software package designed to allow the user to produce posters with the use of a dot-matrix printer. Dot-matrix print-out is usually rather like newspaper photographs, but the programmers have ensured that the lettering produced by SIGNWRITER is an intense solid black, by using three passes of the printer head (except in the fast draft-printing mode). It is quick and very easy to input text to the program and lay it out on the page to look like a real professional job. The printing takes much longer, but needs no supervision. Printing can be done sideways to allow for signs wider than the standard 80-column paper. Characters can be any size that will fit onto the paper, and the bigger they are, the better the shapes appear. A full set of the usual keyboard characters is provided, and there is also an on-screen DESIGN program that lets the user modify existing characters, or design new ones from scratch. SIGNWRITER would be ideal for producing textual material for poster presentations at conferences, and conference organisers would find it invaluable for making the many signs that are usually required. Highly recommended.

MARY MASSON

COPS: P. F. A. VAN DER WIEL, B. G. M. VANDENGINSTE and G. KATEMAN, Elsevier Scientific Software, Amsterdam, 1986. Available for Apple II series and IBM-PC, IBM-PC AT. Dfl. 975, \$405. Manual only (no listings) Dfl. 100.00, \$41.50. The IBM-PC version was tested.

Most analytical chemists must know about simplex optimization; it is a technique that is quite easy to describe and discuss in qualitative terms. However, it has not been particularly easy to actually use simplex optimization in the laboratory. However, the availability of COPS (Chemometrical OPTimization by Simplex) means that there is no longer a valid excuse for avoiding use of this powerful and potentially time-saving method. The programs (driver program, input program, modified simplex program, super-modified simplex program, and a utility program) are written in Pascal. Both the source code and compiled programs are provided on the disc; the compiled programs will run without Pascal in the machine. The package ran without any trouble on a "PC-compatible" that is not particularly compatible. A model response surface is provided as part of the package; this allows the user to become familiar with operation of the programs without having to collect data for a real system, and it also makes COPS a useful tool for teaching. However, use for doing a real optimization is also convenient; the program may be halted at any time and the current data saved to disc, ready for reloading whenever required. The package is easy to use, and to learn to use. The handbook, which includes the source code listings when obtained with the software, is well produced, and includes examples of the use of the programs. The background theory is well presented, and there is a useful bibliography.

MARY MASSON

NAME OF JOURNAL TALANTA

P E R G A M O N
SOFTWARE DESCRIPTION FORM

Title of software package: _____

It is: [] Application program [] Utility [] Other _____

Specific area _____
(e.g. stability constants, calibration, pattern recognition, optimization)

Software developed for [name of computer(s)] _____

in [language(s)] _____

to run under [operating system] _____
and available on:

[] Floppy disk/diskette.

Size _____ Density _____ [] Single-sided [] Double-sided

[] Magnetic tape.

Size _____ Density _____ Character set _____

Distributed by: _____

Minimum hardware configuration required: _____

Memory required: _____ User friendly?: [] Yes [] No

Documentation: [] None [] Minimal [] Self-documenting
[] Extensive external documentation

Source code available: [] Yes [] No

Level of development: [] Design complete [] Coding complete

[] Fully operational [] Collaboration would be welcomed

Is software being currently used? [] Yes [] No

If yes, how long? _____ If yes, how many sites? _____

Contributor is willing to deal with enquiries?: [] Yes [] No

(continued)

RETURN COMPLETED FORM TO:

Dr. M. R. Masson
Department of Chemistry
University of Aberdeen
Old Aberdeen, Scotland

[This Software Description Form may be photocopied without permission]

Description of what software does
[200 words maximum; use separate sheet if necessary]:

Potential users: _____

Fields of interest: _____

#####

Name of contributor: _____

Institution: _____

Address: _____

Telephone number: _____

#####

Reference No. [Assigned by Journal Editor] _____

[The information below is not for publication.]

Would you like to have your program:

Reviewed? []Yes []No []Not at this time
Marketed and distributed? []Yes []No []Not at this time

[This Software Description Form may be photocopied without permission]

NOTICES

X CONFERENCE ON ANALYTICAL ATOMIC SPECTROSCOPY (CANAS)

Toruń, Poland, 5-12 September 1988

This conference and the VII Polish Spectroanalytical Conference with international participation will be organized by the Commission of Analytical Atomic Spectrometry of the Committee of Analytical Chemistry of the Polish Academy of Sciences and by the Nicholas Copernicus University in Toruń. The Conference will take place at the Campus of the Nicholas Copernicus University in Toruń, Poland, from 5 till 9 September 1988.

The Conference will cover the following branches of spectroscopy:

- physical aspects of analytical atomic spectroscopy
- optical emission spectroscopy and excitation sources
- atomic-absorption and fluorescence spectroscopy
- X-ray spectroscopy
- inorganic mass spectrometry
- electron and ion spectrometry
- instrumental neutron-activation analysis
- lasers in analytical atomic spectroscopy
- application of spectroscopy in trace analysis
- speciation analysis
- surface analysis

All correspondence concerning the Conference should be addressed to:

Dr J. Fijałkowski
Institute of Nuclear Chemistry and Technology
ul. Dorodna 16
03-195 Warszawa
Poland

5TH INTERNATIONAL WORKSHOP ON TRACE ELEMENT ANALYTICAL CHEMISTRY IN MEDICINE AND BIOLOGY

Neuherberg, FRG, 15-18 April 1988

The main scientific topics will be:

- (I) Trace element analysis
 - (1) Analysis of trace elements, especially new trace elements such as Ge or Pt.
 - (2) Solid sample analysis
 - (3) New developments in the decomposition of biological materials
- (II) Speciation analysis of trace elements
 - (1) Methodical aspects of the identification of trace element compounds in biological matrixes
 - (2) Coupling of different analytical methods for speciation analysis
- (III) Trace elements in the bio-medical field
 - (1) Diagnosis, therapy, therapy-control
 - (2) Homeostatic control mechanism
 - (3) Bioavailability
 - (4) Supplementation

The most important aspect will be to cover different problems within special sessions in order to deal with all new points of view and to initiate fruitful discussions among the participating experts. The invited papers will deal with modern developments and latest scientific findings in these special fields. The Workshop will consist of a number of invited papers on specific problem areas followed by an extended discussion period in which all participants will be invited to take part. Short contributed papers (oral or poster presentation) are also solicited for the Workshop.

Call for Papers

Included in this circular is a Provisional Application Form. Preliminary title and some catchwords must be delivered by *30 June 1987*.

Abstracts of papers intended as contributions to the Workshop must be submitted in English (three copies), to the Chairman of the Organizing Committee by *30 November 1987*.

Provisional Application Form

PLEASE PRINT

Surname:

First name(s):

Title:

Institution:

.....

.....

Street:

ZIP code:

Country:

I intend to participate in the 5th Workshop

I intend to submit a paper on:

.....

.....

Catchwords:

Name:

Address:

Date: Signature:

Address for Correspondence

Gesellschaft für Strahlen und Umweltforschung mbH
Institut für Ökologische Chemie
AG "Spurenelementanalytik"

Dr P. Schramel
Ingolstädter Landstraße 1
D-8042 Neuherberg
Federal Republic of Germany

NOTICES

SELENIUM IN MEDICINE AND BIOLOGY

SECOND CONGRESS ON TRACE ELEMENTS IN MEDICINE AND BIOLOGY AVORIAZ (France), 15-18 March 1988

This Congress, held under the auspices of the Association des Internes et Anciens Internes du C.H.U. de Grenoble, the Association Française d'Etude et de Recherche sur les éléments traces essentiels, and the Centre d'Etude et de Recherche sur les oligoéléments et les vitamines will have four sessions, on Biological functions, metabolism and requirements; Biological parameters for assessing selenium status and selenium supplementation; Selenium and human diseases (I); Selenium and human (II) or animal diseases. Three hours will be left free each afternoon, for skiing. The deadline for offer of oral communications, posters and workshops is 15 January 1988. Further information and registration forms may be obtained from:

CONGRÈS OLIGOÉLÉMENTS:
SÉLÉNIUM
Laboratoire de Biochimie C
C.H.R.U.G.—BP 217 X
38043 GRENOBLE CEDEX FRANCE

ElectroFinnAnalysis

An International Conference on Electroanalytical Chemistry 6-9 June 1988 Turku-Åbo, Finland

The scientific programme will consist of invited plenary lectures, keynote lectures, submitted research papers and posters. The programme will be divided into the following sessions, where the speakers mentioned have promised to give their contributions:

1. *Instrumentation*
Prof. L. R. Faulkner, University of Illinois at Urbana-Champaign, Illinois, USA
Prof. J. J. Kanakare, University of Turku, Turku, Finland
2. *Industrial applications*
Prof. E. Pungor, Technical University, Budapest, Hungary
Dr. J. Asplund, Nobel Chemicals AB, Karlskoga, Sweden
Dr. P. M. Bersier, Ciba-Geigy Ltd, Basel, Switzerland
3. *Pharmaceutical applications*
Prof. W. F. Smyth, Queen's University, Belfast, Northern Ireland
Dr. J. Reust, Sandoz Ltd, Basel, Switzerland
4. *Clinical applications*
Prof. W. Simon, Swiss Federal Institute of Technology, Zürich, Switzerland
Dr. A. Lewenstam, Åbo Akademi, Turku, Finland
5. *Electrochemical sensors*
Prof. J. Janata, University of Utah, Utah, USA
Prof. I. Lundström, Linköping Technical University, Linköping, Sweden
6. *Electrochemical flow analysis*
Dr. E. Hansen, Technical University of Denmark, Lyngby, Denmark
Dr. M. Trojanowicz, University of Warsaw, Warsaw, Poland

Participants wishing to present a paper should submit an abstract, in English, of about 250 words before December 31, 1987 to

Dr. Ari Ivaska
 Laboratory of Analytical Chemistry
 Åbo Akademi
 SF-20500 Turku (Åbo)
 FINLAND
 Telephone 358-21-654420; telex aabib sf 62301
 from whom further information can be obtained.

ISM-11
11th International Symposium on Microchemical Techniques

Wiesbaden
 28 August–1 September 1989

Like preceding Symposia, ISM-11 will cover both pure and applied aspects of analytical chemistry related to micro- and trace-analysis. Special attention will be paid to the application of modern instrumental techniques in the field of trace-analysis.

Plenary and keynote lectures will be presented by invited speakers. For the general sessions, contributions are requested for presentation in either oral or poster sessions.

The Gesellschaft Deutscher Chemiker will be responsible for the detailed organization of the Congress.

**I am interested in attending the
 11th International Symposium on Micro-
 chemical Techniques 1989 at Wiesbaden**

Please send me all relevant circulars

 (Title)

 (Initials) (Name)

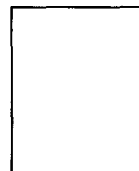
 (Institution)

 (Street)

 (Zip) (City)

 (Country)

POSTCARD



**Gesellschaft
 Deutscher Chemiker
 Abt. Tagungen
 P.O. Box 90 04 40
 D-6000 Frankfurt/Main 90
 (Fed. Rep. Germany)**

NOTICES

FESTSTOFF COLLOQUIUM WETZLAR

SOLID SAMPLING COLLOQUIA

3RD INTERNATIONAL COLLOQUIUM
WETZLAR FRG
10-12 OCT 1988

SOLID SAMPLING FOR OPTICAL ATOMIC SPECTROSCOPY

OBJECTIVES

This series of meetings intends to focus on the state-of-the art and progress of solid sampling with optical atomic spectroscopic methods. It will consist of invited and contributed papers, possibly also posters with discussion time for themes of particular importance.

MAIN TOPICS

- Theory and instrumentation
- Methodology and procedures
- Biological and medical applications
- Food applications
- Environmental applications
- Product and quality control

Details from:

Dr. M. Stoepler
KFA Jülich—ICH-4-
Postfach 1913
D-5170 Jülich, FRG

32nd IUPAC CONGRESS

Stockholm 2-7 August 1989

Organized by the Swedish National Committee for Chemistry
The Royal Swedish Academy of Sciences

SCIENTIFIC PROGRAMME

Section I Large-Scale Separation of Biological Macromolecules, Cells and Particles.

- Recovery of bioproducts directly from crude homogenates.
- Chromatographic techniques, conventional and HPLC.
- Affinity purification techniques.
- Electrokinetic techniques.
- Automation and control of separation processes in biotechnology.

Section II Atmospheric and Marine Chemistry.

- Atmospheric chemistry.
- Air-sea interface chemistry.
- Marine chemistry.
- Marine biochemistry.
- Analytical air and sea chemistry.

- Section III Chemical Communication and Interaction between Organisms.**
—The chemistry of exocrine chemical signals.
—Structure-activity relationships.
—Chemical application for pest control.
- Section IV Solid State Chemistry-Frontiers in the Chemistry of Inorganic Materials.**
—New preparative routes to inorganic materials
—Low-dimensional solids.
—Extended defects and grossly non-stoichiometric solids.
—The chemistry of new electronic, magnetic and superconducting materials.
—The chemistry of high-performance ceramics and superhard materials.
- Section V Structure and Dynamics of Macromolecules.**
—Dynamic aspects of protein structures.
—Computational chemistry.
—Protein engineering.
—Interaction between macromolecules.
—Folding.
- Section VI Electron Transfer Reactions.**
—Mechanisms of electron transfer reactions of organic molecules.
—Organic syntheses using electron transfer mediated steps.
—Photoelectrochemistry, photochemistry and chemiluminescence.
—Conducting and superconducting organic materials.
—Electron transfer and toxicity.
- Section VII Chemistry and Biochemistry of Bile Acids.**
—Analytical chemistry of bile acids.
—Physical chemistry of bile acids.
—Biosynthesis and metabolism of bile acids.
—Inborn and acquired defects in bile acid biosynthesis.

Details from:

IUPAC
c/o Stockholm Convention Bureau
Box 6911
S-102 39 Stockholm, Sweden

SAC 89

CAMBRIDGE, ENGLAND, 30 JULY–5 AUGUST 1989
INTERNATIONAL CONFERENCE ON ANALYTICAL CHEMISTRY
ANALYTICAL DIVISION ROYAL SOCIETY OF CHEMISTRY

The scientific programme will be organized around plenary, invited and contributed papers and posters covering the whole field of analytical chemistry. As at previous Conferences, special symposia on particular analytical themes will be organised by RSC Groups and the East Anglia Region of the Analytical Division. The programme will include Workshops, where research workers can demonstrate new apparatus and techniques. Update Courses are also planned, to provide all-day tutorial and practical demonstration sessions. These will be held on the Wednesday, as an alternative to scientific or cultural visits.

Details from:

The Secretary, Analytical Division,
Royal Society of Chemistry,
Burlington House,
London W1V 0BN, UK.

6th INTERNATIONAL SYMPOSIUM ON ISOTACHOPHORESIS AND CAPILLARY ZONE ELECTROPHORESIS

Vienna 21–23 September, 1988

Österreichische Gesellschaft für Mikrochemie und Analytische Chemie
Institute for Analytical Chemistry of the University of Vienna

The programme will include all aspects of electrophoresis in capillaries, i.e. isotachopheresis, high performance zone electrophoresis and electrokinetic chromatography. The programme will comprise lectures and poster presentations. Symposium language is English. It is intended to publish the proceedings of the symposium in a special issue of "Journal of Chromatography".

Details from:

E. Kenndler
Institute for Analytical Chemistry,
University of Vienna, Währinger Straße 38,
A-1090 Vienna, Austria
Phone: (0222) 34 46 30–47 or 53

Vth INTERNATIONAL SYMPOSIUM ON BIOLUMINESCENCE AND CHEMILUMINESCENCE

Florence, Bologna-Italy, 25–29 September, 1988

The Symposium in Florence will cover the fundamental aspects and the most recent applications of Bioluminescence and Chemiluminescence in clinical sciences, biotechnology, genetics, microbiology, phagocytosis, immunoassay, environmental monitoring.

The Symposium will consist of Invited Lectures, Short Communications, Poster Sessions and Workshops. "ALMA MATER STUDIORUM SAECULARIA NONA": the meeting will include a special Symposium on 27 September 1988 in Bologna as part of the Celebration to mark the Foundation of the University of Bologna in the XIth Century.

Further information is available from:

Prof. Mario Pazzagli
Endocrinology Unit
University of Florence
Viale Morgagni, 85
50134 FLORENCE, Italy

Deadline for Abstracts: 15th March 1988

CHROMATOGRAPHIC COURSE AT KENT STATE UNIVERSITY

FUNDAMENTALS OF CHROMATOGRAPHIC ANALYSIS,
KENT STATE UNIVERSITY, 7–11 DECEMBER, 1987

The course, sponsored by Nicolet Instrument Corporation in cooperation with KSU's Chemistry Department and the University Conference Bureau, will be given for the fifth consecutive year.

An overview of chemical separations by chromatographic methods will be presented. The course is different from other programs in that the material will include gas, liquid and thin-layer methods stressing the three techniques as complementary rather than competing processes. The program will blend fundamental information on theory and instrumentation with applications. Accompanying laboratory sessions will provide intensive hands-on training in the various techniques discussed in the lectures.

The lecturers will be Dr. Roger K. Gilpin, Course Director and Department Chairman at Kent State University, Dr. Neil D. Danielson, Associate Professor at Miami University, and Mr. Ronald L. Lewis of Nicolet Instrument Corporation.

Additional information can be obtained from

Carl J. Knauss,
Chromatographic Course Coordinator,
Chemistry Department, Kent State University,
Kent, Ohio 44242,
or by calling 216/672-2327.

LIST OF CONTENTS

JANUARY

SOVIET UNION HONOUR ISSUE

Current Analytical Chemistry in the USSR

- | | |
|---|---|
| R. A. Chalmers | V Foreword |
| Yu. A. Zolotov | 1 Analytical chemistry in the Soviet Union |
| Ye. N. Dorokhova | 9 Analytical chemistry teaching in the USSR |
| M. E. Elyashberg, V. V. Serov
and L. A. Gribov | 21 Artificial intelligence systems for molecular spectral analysis |
| B. F. Myasoedov | 31 Recent advances in the analytical chemistry of the transplutonium elements |
| Kh. Z. Brainina | 41 Advances in voltammetry |
| R. V. Golovnya | 51 Determination of volatile components of systems not in thermodynamic equilibrium |
| G. I. Ramendik, B. M. Manzon,
D. A. Tyurin, N. E. Benyaev
and A. A. Komleva | 61 Perspectives in the development of the theory of spark-source and laser-plasma source mass-spectrometry |
| K. B. Yatsimirskii and L. P. Tikhonova | 69 Catalytic kinetic methods for the determination of platinum metals |
| A. T. Pilipenko and L. I. Savransky | 77 Selectivity and sensitivity of metal determination by co-ordination compounds |
| S. B. Savvin and R. F. Gur'eva | 87 5-Azo derivatives of rhodanine and its analogues in the analytical chemistry of the noble metals |
| I. P. Alimarin, V. I. Fadeeva,
G. V. Kudryavtsev, I. M. Loskutova
and T. I. Tikhomirova | 103 Concentration, separation and determination of scandium, zirconium, hafnium and thorium with a silica-based sulphonic acid cation-exchanger |
| O. M. Petrukhin, E. N. Avdeeva,
Yu. V. Shavnya, V. P. Yankauskas,
R. M. Kazlauskas, A. S. Bychkov
and Yu. A. Zolotov | 111 Ion-selective electrodes for gold and silver determination |
| G. G. Devyatykh and Yu. A. Karpov | 123 The analysis of solid and liquid high-purity substances |
| G. G. Devyatykh, Yu. A. Karpov,
V. A. Krylov and O. P. Lazukina | 133 Laser-ultramicroscopic method of determining suspended particles in high-purity liquids |
| B. V. L'vov, L. K. Polzik
and L. F. Yatsenko | 141 The effect of thermal sample pretreatment on the absorption signal in graphite furnace AAS |
| I. G. Yudelevich, L. V. Zelentsova
and N. F. Beisel | 147 Atomic-absorption methods for analysis of high-purity substances |
| L. L. Kunin, A. A. Bogdanov
and V. I. Rodionov | 153 Determination of oxygen in fusible metals by use of solid electrolyte cells |
| V. V. Nesterov, O. I. Kurenbin,
V. D. Krasikov and B. G. Belenkii | 161 Determination of molecular-weight distribution and average molecular weights of block copolymers by gel-permeation chromatography |
| E. S. Gankina, I. I. Efimova,
J. J. Kever and B. G. Belenkii | 167 Identification of block copolymers and determination of their purity by thin-layer chromatography |
| B. I. Petrov and V. P. Zhivopistsev | 175 Liquid-liquid extraction of elements by antipyrine and diantipyrilmethane salts from non-aqueous solutions or in systems without an organic solvent |
| Yu. A. Bankovsky, M. V. Vircavs,
O. E. Veveris, A. R. Pelne
and D. K. Vircava | 179 Preconcentration of microamounts of elements in natural waters with 8-mercaptoquinoline and bis(8-quinoly) disulphide for their atomic-absorption determination |

V. G. Berezkin and S. L. Bolotov	183	Thin-layer chromatography with mobile phases of low volatility
V. I. Chaplygin, Yu. Ya. Kuzyakov, O. A. Novodvorsky and N. B. Zorov	191	Determination of alkali metals by laser-induced atomic-ionization in flames
V. N. Muzgin, Yu. B. Atnashev, V. E. Korepanov and A. A. Pupyshev	197	Electrothermal atomic-absorption and atomic-fluorescence spectrometry with a tungsten-coil atomizer
I. F. Dolmanova, T. N. Shekhovtsova and V. V. Kutcheryaeva	201	Assay of enzyme effectors
G. I. Romanovskaya, V. I. Pogonin and A. K. Chibisov	207	Fluorescence determination of trace amounts of uranium(VI) in various materials by a repetitive laser technique
V. F. Toropova, A. R. Garifzyanov and I. E. Panfilova	211	Steric and hydrophobic effects of substituents in extraction of metal complexes with <i>O,O</i> -dialkyldithiophosphoric acids
V. A. Nazarenko, V. P. Antonovich and N. A. Veschikova	215	Photometric determination of tungsten in rocks with trihydroxyfluorones
H. C. Budnikov, V. N. Maystrenko and Yu. I. Murinov	219	Electrochemical investigation of palladium complexes with organic sulphides and their use in extraction differential pulse polarography
Yu. S. Nikitin, N. B. Morozova, S. N. Lania, T. A. Bol'shova, V. M. Ivanov and E. M. Basova	223	Liquid chromatography of palladium and non-ferrous metal chelates with 1-(2-pyridylazo)-2-naphthol
V. P. Chizhkov, S. S. Pavlov, N. V. Sterkhov, V. M. Ravikovich, E. F. Litvin and E. A. Varyvonchik	227	Pulse circulation gas chromatography on capillary columns

<i>Papers Received</i>	i
<i>Publications Received</i>	ii
<i>Questionnaire: Software Survey Section</i>	iii

FEBRUARY

Editorial	III	
<i>Talanta Advisory Board</i>	V	
T. U. Aualiitia and W. F. Pickering	231	The effect of inorganic particulates on the ASV signals of Cd, Pb and Cu
Kazuhisa Yoshimura and Hirohiko Waki	239	Enhancement of sensitivity of ion-exchanger absorptiometry by using a thick ion-exchanger layer
M. J. Adams and G. J. Ewen	243	Interfacing an analogue infrared spectrometer to a microcomputer
Joseph Wang and Javad M. Zadeii	247	Adsorptive stripping voltammetric measurements of trace levels of uranium following chelation with Mordant Blue 9
G. T. Abou Zeid, J. B. Headridge and C. White	253	An apparatus for the emission spectrometric determination of nitrogen released into an argon gas stream by chemical reactions in solution
C. L. Chakrabarti, S. B. Chang, P. W. Thong, T. J. Huston and Shaole Wu	259	Studies of atomization from a graphite platform in graphite-furnace atomic-absorption spectrometry
Scott P. Ericson, Michael L. McHalsky and Bruno Jaselskis	271	Ultratrace molybdenum determination in biological samples by graphite-furnace atomic-absorption spectrometry
Kenji Isshiki and Eiichiro Nakayama	277	Determination of ultratrace amounts of cobalt by catalysis of the iron-hydrogen peroxide reaction with an improved continuous-flow analysis system
D. W. Rogers and B. J. Siedman	283	Hydrogenation enthalpimetry—I. Microcomputer-assisted calibration and data-acquisition

Short Communications

Abdel-Aziz M. Wahbi, Mohammad A. Abounassif, El-Rasheed A. Gad-Kariem and Hassan Y. Aboul-Enein	287	Spectrophotometric and fluorimetric determination of nomifensine maleate
D. Goforth and J. D. Winefordner	290	A graphite-tube furnace for use in laser-excited atomic-fluorescence spectrometry
S. P. Arya, J. L. Malla and Veena Slathia	293	A selective spectrophotometric method for determination of copper with ferron
Saeed Ahmad, R. D. Sharma and I. C. Shukla	296	Microdetermination of oxprenolol hydrochloride and metoprolol tartrate with ammonium metavanadate
Software Survey Section	299	Databank; Labmaster; Labrom; Numbermaster; Signwriter; Paperbase De Luxe
<i>Papers Received</i>	i	
<i>Publications Received</i>	ii	
<i>Errata</i>	iv	
<i>Notes for Authors</i>	v	
<i>Questionnaire: Software Survey Section</i>	vii	

MARCH

S. K. Gogia, D. Singh, O. V. Singh and S. N. Tandon	303	Study on the synergistic extraction of cobalt(II) with lower fatty acids in the presence of heterocyclic amines and some metal ion separations
Barry Chiswell and Mazlin Bin Mokhtar	307	Speciation of manganese in fresh water—I. Use of EPR studies
S. Koch und G. Ackermann	313	Untersuchungen zur Anwendung ternärer Komplexe in der Photometrie—IV. Das Chelat FeY^- ($\text{H}_4\text{Y} = \text{EDTE}$) als Reagens für Phenole
F. Salinas, J. J. Berzas Nevado and P. Valiente	321	Kinetic spectrophotometric determination of nanogram levels of manganese by use of the salicylaldehyde guanylhydrazone-hydrogen peroxide system
M. C. Gutierrez, S. Rubio, A. Gómez-Hens and M. Valcárcel	325	Simultaneous determination of histidine and histamine by second-derivative synchronous fluorescence spectrometry
Liu Jin-Chun and Arthur Chow	331	Extraction of zirconium and hafnium thiocyanate with polyurethane foam
M. Ejaz and M. A. Qureshi	337	Extraction and preconcentration of selenium from aqueous solutions and its determination in water and hair samples by atomic-absorption spectrophotometry
Yoshiki Sohrin, Kenji Isshiki, Tooru Kuwamoto and Eiichiro Nakayama	341	Determination of germanium by graphite-furnace atomic-absorption spectrometry
F. García Sánchez, C. Cruces Blanco and A. Heredia Bayona	345	Non-aqueous fluorimetric determination of scandium in silicate rocks
P. Viñas, M. Hernández Córdoba and C. Sánchez-Pedreño	351	Kinetic determination of iodide, based on the chlorpromazine-bromate reaction
Anil C. Mehta	355	Pharmacokinetics and the analytical chemist
Ali S. Al-Omair and Samuel J. Lyle	361	Some ion-exchange resins for anion-chromatography
<i>Short Communications</i>		
Y. K. Agrawal and D. R. Patel	365	Spectrophotometric determination of clofibrate
B. V. Rao, V. G. Radha Menon and K. C. Sarojam	367	Spectrophotometric determination of cobalt in iron-, cobalt- and nickel-base alloys

Masaaki Nakamura, Yutaka Sakanashi, Hiroaki Chikushi, Fumiaki Kai, Shigeya Sato, Toshie Sato and Sumio Uchikawa	369	Synthesis of 2-(3,5-dichloro-2-pyridylazo)-5-dimethylaminophenol and its application to the spectrophotometric determination of cobalt
C. S. P. Sastry and D. Vijaya	372	Spectrophotometric determination of some insecticides with 3-methyl-2-benzothiazolinone hydrazone hydrochloride
<i>Analytical Data</i>		
F. Rösch, Tran Kim Hung, M. Milanov and V. A. Khalkin	375	Electromigration of carrier-free radionuclide ions. Bismuth complexes in aqueous solutions of oxalic, fumaric and succinic acids
<i>Papers Received</i>	i	
<i>Publications Received</i>	ii	
<i>Notice</i>	iii	
<i>Questionnaire: Software Survey Section</i>	v	

APRIL

Richard C. Graham	381	Design of software for thermal titrations
Robert Fournaise et Christian Petitfaux	385	Etude de la formation des complexes en solution aqueuse—III. Nouvelle méthode d'affinement des constantes de stabilité des complexes et des autres paramètres des titrages protométriques
Béla Noszál and Mária Juhász	397	Determination of sulphate by pH titration
E. Meintjies, F. W. E. Strelow and A. H. Victor	401	Separation of bismuth from gram amounts of thallium and silver by cation-exchange chromatography in nitric acid
Adam Hulaniccki and Tadeusz Krawczyński vel Krawczyk	407	Behaviour of a chalcocite copper ion-selective electrode in solutions of iron(III) ions
Stanisław Glab, Elżbieta Skrzydlewska and Adam Hulaniccki	411	Determination of protonation constants by coulometric titration
Nancy E. Fortier and James S. Fritz	415	The effect of temperature on single-column ion-chromatography of metal ions
Shigeya Sato, Mari Iwamoto and Sumio Uchikawa	419	Extraction and spectrophotometric determination of molybdenum(VI) with Malachite Green and <i>p</i> -chloromandelic acid
Geraldine M. Huitink	423	Constant Calcein Blue: an indicator for spectrofluorometric calcium determination
J. G. Sen Gupta	427	Determination of rubidium, strontium and barium in barite by atomic-absorption spectrometry after dissolution in disodium ethylenediamine-tetra-acetate
<i>Short Communications</i>		
Rokuro Kuroda, Koichi Oguma, Noriko Mukai and Masatoshi Iwamoto	433	Anion-exchange enrichment and spectrophotometric determination of uranium in sea-water
Morio Nakayama, Tomoo Tanaka, Motoko Tanaka, Masahiko Chikuma, Kazuo Itoh, Hiromu Sakurai, Hisashi Tanaka and Terumichi Nakagawa	435	Sequential collection of selenium(IV) and selenium(VI) by the use of an anion-exchange resin loaded with bismuthiol-II sulphonic acid
C. Sârbu, C. Mărutoiu, M. Vlassa and C. Lîteanu	438	Direct fluorescent detection of chromatographically separated amino-acids by means of 9-isothiocyanatoacridines
O. R. Idowu and O. O. P. Faboya	441	New derivatives of <i>N</i> -nitrosamines
<i>Analytical Data</i>		
Rajja Petrola, Paula Lampén and Seppo Lindroos	445	Stability order of the lanthanide chelates of two disubstituted 3-hydroxy-4 <i>H</i> -pyran-4-ones in aqueous solution

**J. Katona-Balázs, G. Molnár,
Zs. Nemes-Vetéssy and K. Burger** 449 Potentiometric study of silver ion co-ordination by azo dyes

Papers Received i

Questionnaire: Software Survey Section iii

MAY

The Ronald Belcher Memorial Award III

**Jan Langmaier, František Opekar
and Věra Pacáková** 453 Application of a metallized membrane electrode for the determination of gaseous sulphur compounds after reductive pyrolysis

S. Yamada, C. Sakane and T. Ogawa 461 A sub-microlitre two-photon ionization detector for high-performance liquid chromatography

**Stuart J. Nagourney, Merrill Heit
and Donald C. Bogen** 465 Electrothermal atomic-absorption spectrometric analysis of lake waters for Mn, Fe, Pb and Cd

**Marissa Bonilla-Alvarez,
Margo Palmieri, Debra Davis
and James S. Fritz** 473 2,6-Diacetylpyridine bis(arylhydrazone) derivatives as analytical reagents for uranium

Ghazi Al-Jabari and Bruno Jaselskis 479 Chemical reduction and spectrophotometric determination of silver, copper and nickel

**Anna Maria Maccioni, Pietro Traldi
and Lucio Doretto** 483 High-energy collisional spectroscopy in qualitative and quantitative analysis of diesel particulates

V. S. Sastri 489 Methods for determining hydrogen in steels

Paul Ek and Stig-Göran Huldén 495 A continuous hydride-generation system for direct current plasma atomic-emission spectrometry (DCP-AES). Determination of arsenic and selenium

Short Communications

**J. S. Adsul, C. C. Dias, S. G. Iyer
and Ch. Venkateswarlu** 503 Use of Chelex 100 in determination of bismuth in sulphide ores, concentrates, metals and alloys

**Om P. Bhargava, Paul G. Bailey
and Gord R. Overholt** 505 Rapid determination of molybdenum in ferromolybdenum and molybdenum additives, with oxine

N. Thankarajan and K. Krishnankutty 507 Phthalhydrazidylazoacetylacetone as a chemiluminescent acid-base indicator

**Aristotelis Xenakis, Claude Selve
and Christian Tondre** 509 Transport of alkali-metal picrates through liquid membranes: coupled action of w/o microemulsion droplets and lipophilic crown-ether carriers

Minliang Xu and Gordon A. Parker 512 Spectrophotometric determination of tungsten(VI) with rutin and cetyltrimethylammonium bromide

D. Baylocq, W. Kayata et F. Pellerin 515 Dosage des acides faibles en milieu ammonium quaternaire concentré

Analytical Data

**A. Matilla Hernandez,
S. Gonzalez Garcia,
J. M. Tercero Moreno, M. Candida
T. A. Vaz and L. Vilas Boas** 519 Uranyl complexes of α -carboxypolymethylenediaminetetra-acetic acids

**M. Teresa S. D. Vasconcelos
and Adélio A. S. C. Machado** 525 Acid-base ionization equilibria of 1-(2-carbamylethyl) imidazole and its 2-methyl and 2-ethyl derivatives

Papers Received i

Publications Received ii

Notices iii

Questionnaire: Software Survey Section v

JUNE

Pharmacia Prize	III
Louis Gordon Memorial Award	IV
C. Locatelli, F. Fagioli, C. Bigli and T. Garai	529
	Second harmonic a.c. anodic stripping voltammetry of metals at trace level. Simultaneous determination of lead and thallium, and bismuth and antimony
M. Mariaud et P. Levillain	535
	Dosage spectrophotométrique des ions cyanure libres par formation du complexe mixte bis(bathophénanthroline) dicyano fer(II)
Huang Huiliang, Daniel Jagner and Lars Renman	539
	Automated determination of lead in urine by means of computerized flow potentiometric stripping analysis with a carbon-fibre electrode
Wallace A. de Oliveira and Afonso S. Mendes	543
	Determination of calcium and magnesium in limestone and dolomite by enthalpimetric flow-injection analysis
Ajay Shah and Surekha Devi	547
	A new chelating ion-exchanger containing <i>p</i> -bromophenylhydroxamic acid as functional group—IV. Column separations on a hydroxamic acid resin
S. Quintar de Guzman, O. M. Baudino and V. A. Cortinez	551
	Design and evaluation of an electrochemical sensor for determination of dissolved oxygen in water
Zhang Qing and Huang Yuying	555
	Polarographic adsorptive waves of alkaline-earth metal complexes with thymolphthalexone
Joseph Wang, Peng Tuzhi and Kurian Varughese	561
	Adsorptive preconcentration for voltammetric measurements of trace levels of zirconium
K. Sekine, T. Imai and A. Kasai	567
	Liquid-liquid extraction separation and sequential determination of plutonium and americium in environmental samples by alpha-spectrometry
<i>Short Communications</i>	
R. von Wandruszka and J. D. Winefordner	571
	Fluorescence in thin liquid films: a simple model
S. Jaya, T. Prasada Rao and G. Prabhakara Rao	574
	Anodic-stripping voltammetric determination of arsenic at a copper-coated glassy-carbon electrode
Hai-Long Wu and Ru-Qin Yu	577
	A PVC membrane pH-sensitive electrode based on methyldioctadecylamine as neutral carrier
H. van Beek, H. C. A. Greefkes and A. J. Baars	580
	Determination of copper, iron, manganese, lead and cadmium in automatically wet-digested animal tissue by graphite-furnace atomic-absorption spectrometry with Zeeman background correction
José M. Andrés, C. Romero and José M. Gavilan	583
	Potentiometric titration of fulvic acids from lignite, in dimethylformamide and dimethylsulphoxide media
A. Parczewski	586
	Signal processing with a summing operational amplifier in multi-component potentiometric titrations
<i>Analytical Data</i>	
H. Ménard, Y. Lefebvre et J. Khorami	589
	Etude de l'adsorption de substances organiques sur l'amiante chrysotile par chromatographie en phase gazeuse
<i>Annotation</i>	
Santi Capone, Alessandro De Robertis, Concetta De Stefano, Silvio Sammartano and Rosario Scarcella	593
	Ionic strength dependence of formation constants—X. Proton activity coefficients at various temperatures and ionic strengths and their use in the study of complex equilibria
Software Survey Section	599
	STATSTREAM; TADPOLE; MOLGRAF; REFSYS; REFSCAN; DADISP; MULTI-Q; KINETIC EBDA LIGAND LOWRY; MKMODEL
<i>Papers Received</i>	i
<i>Notices</i>	iii
<i>Questionnaire: Software Survey Section</i>	v

JULY

Salah M. Sultan	605 Spectrophotometric determination of paracetamol in drug formulations by oxidation with potassium dichromate
Anil C. Mehta	609 Drug determination in biological fluids—approaches to method validation
Annika Carlsson, Ulla Lundström and Åke Olin	615 Spectrophotometric determination of bromide (and iodide) in a flow system after oxidation by peroxodisulphate
Mary Ryan-Hotchkiss and J. D. Ingle, Jr.	619 Design and characterization of an intensified diode array data-acquisition system for spectrometric measurements
G. Zaray, J. A. C. Broekaert, R. G. Böhmer and F. Leis	629 Comparative study of analytical inductively-coupled argon-plasma discharges using different outer gases
F. García Sánchez, M. Hernández Lopez and J. C. Marquez Gomez	639 A graphical derivative approach to the photometric determination of lutetium and praseodymium in mixtures
P. L. Desbène, J. Berthelot, M. Ouchefoun, C. Guette, J. J. Basselier, R. Boulet and A. Desbène-Monverney	645 Étude analytique des produits lourds du pétrole—V. Bromation des résidus lourds pétroliers au moyen d'un réactif original, le tribromure de tétrabutylammonium, et essais préliminaires de détermination d'un indice de brome applicable aux fractions lourdes
<i>Short Communications</i>	
Basant Sahu and Usha Tandon	653 Use of <i>N</i> -benzyl-2-naphthohydroxamic acid as a highly selective reagent for solvent extraction and spectrophotometric determination of vanadium(V)
F. Salinas, T. Galeano Díaz and J. C. Jiménez Sánchez	655 Spectrophotometric determination of iron by extraction of the iron(II)–5,5-dimethyl-1,2,3-cyclohexanetrione-1,2-dioxime-3-thiosemicarbazone complex
Wan Zhen and Chen Qiang	657 Hydrodynamic voltammetry at tubular electrodes—III. Determination of traces of bismuth by differential-pulse anodic-stripping voltammetry at a glassy-carbon tubular electrode with <i>in situ</i> mercury plating
Muhammad Nazir, Muhammad Khurshid Bhatti and Frank D. Guffey	661 Artifacts of the decalin–molecular sieve system in the analysis of mineral waxes
Minori Kamaya, Tetsuro Murakami and Eizen Ishii	664 Photometric determination of selenium with ferrocene
Yutaka Saito, Masaki Mifune, Suzuyo Nakashima, Junichi Odo, Yoshimasa Tanaka, Masahiko Chikuma and Hisashi Tanaka	667 Determination of hydrogen peroxide with <i>N,N</i> -diethylaniline and 4-aminoantipyrine by use of an anion-exchange resin modified with manganese-tetrakis(sulphophenyl)porphine, as a substitute for peroxidase
A. S. Issa, M. S. Mahrous, M. Abdel Salam and N. Soliman	670 The use of 2,3-dichloro-5,6-dicyano- <i>p</i> -benzoquinone for the spectrophotometric determination of some cardiovascular drugs
<i>Analytical Data</i>	
A. M. Cameán Fernández and M. Guzmán Chozas	673 Colour specification of pyridine-2-aldehyde and 6-methylpyridine-2-aldehyde <i>p</i> -nitrophenylhydrazones as indicators for pH determination
<i>Papers Received</i>	i
<i>Questionnaire: Software Survey Section</i>	iii

AUGUST

Editorial	III
Silve Kallmann	677 A survey of the determination of the platinum group elements
Jing Shi-lian, Li Shao-yuan, Wang Rong-rong, Ma Yi-zai, Yu Chu-ming, Yan Yan, Zhang Dong-hua, Sun Jina and Zhang Zhong-ming	699 A new type of Zeeman-effect atomic-absorption spectrophotometer

Rudolf Přibil and Madeleine Štulíková	705	An electrochemical stripping method for the selective determination of traces of silver
Drora Kaplan, Dan Raphaeli and Sam Ben-Yaakov	709	Application of personal computers in the analytical laboratory—III. ASV analysis
E. Klaos, R. Talkop and V. Odinets	715	Direct flame atomic-absorption determination of minor elements in argillites
Saad S. M. Hassan, M. A. Ahmed and F. S. Tadros	723	New liquid-membrane electrodes for direct determination of atropine in pharmaceutical preparations
<i>Short Communications</i>		
S. C. Soundar Rajan	729	Determination of free acidity in antimony chloride solutions
Amir Besada	731	A facile and sensitive spectrophotometric determination of ascorbic acid
Toshiaki Hattori and Hitoshi Yoshida	733	Thermometric titration of cadmium with sodium diethyldithiocarbamate, with oxidation by hydrogen peroxide as indicator reaction
Andreas Diamantatos	736	Fire-assay collection of gold and silver by copper
<i>Analytical Data</i>		
Harvey Diehl and Naomi Horchak-Morris	739	Studies on fluorescein—V. The absorbance of fluorescein in the ultraviolet, as a function of pH
<i>Preliminary Communications</i>		
Akira Sano, Masaaki Takezawa and Shoji Takitani	743	Fluorometric determination of cyanide with 2,3-naphthalenedialdehyde and taurine
J. J. Laserna, A. Berthod and J. D. Winefordner	745	Quantitative analysis by surface-enhanced Raman spectrometry on silver hydrosols in a flow-injection system
<i>Papers Received</i>	i	
<i>Publications Received</i>	iii	
<i>Questionnaire: Software Survey Section</i>	v	

SEPTEMBER

S. Al-Najafi, C. A. Wellington, A. P. Wade, T. J. Sly and D. Betteridge	749	Computer-assisted optimization of HPLC with post-column reaction for the determination of amino-acids
Mikael Wasberg and Péter Sárkány	757	Control of voltammetric experiments by means of the Commodore 64 microcomputer
C. Louis et J. Bessière	763	Diagrammes potentiel-niveau d'acidité dans les milieux $H_2O-H_3PO_4$ —I. Systèmes électrochimiques ne faisant pas intervenir le proton
C. Louis et J. Bessière	771	Diagrammes potentiel-niveau d'acidité dans les milieux $H_2O-H_3PO_4$ —II. Systèmes électrochimiques faisant intervenir le proton
Shigeo Umetani, Kohji Maeda, Sorin Kihara and Masakazu Matsui	779	Solvent extraction of lithium and sodium with 4-benzoyl or 4-perfluoroacyl-5-pyrazolone and TOPO
Kenneth Bäckström, Lars-Göran Danielsson, Folke Ingman and Zhao Huazhang	783	Studies of two-phase equilibria by liquid-liquid segmented flow extraction of dithiocarbamic acids into various solvents
Y. Lingappa, K. Hussain Reddy and D. Venkata Reddy	789	Analytical properties of 2-nitro-5,6-dimethyl-1,3-indanedione dithiosemicarbazone
Magda Ayad, Saied Belal, Afaf Abou El Kheir and Sobhi El Adl	793	Utilization of charge-transfer complexation in the spectrophotometric determination of some monosaccharides through their osazone intermediates
E. Postaire, C. Viel, M. Hamon et A. Gond	799	Oxydation vanadique de l'iodométhylate de <i>p</i> -chlorobenzyl-4 diméthoxy-6,7 isoquinoléine en milieu sulfurique aqueux

Short Communications

V. Chandramouli, R. B. Yadav and P. R. Vasudeva Rao	807	A wet chemical method for the estimation of carbon in uranium carbides
Fatma Basyoni Salem	810	Spectrophotometric and titrimetric determination of catecholamines
Zaofan Zhao, Xiaohua Cai and Peibiao Li	813	The uranium–Xylidyl Blue I complex and its application in linear sweep polarography
<i>Analytical Data</i> Leo Harju	817	Determination of stability constants for alkaline-earth and alkali metal ion complexes of glycine by spectrophotometry
Software Survey Section	821	JESS; LU4D
<i>Papers Received</i>	i	
<i>Publications Received</i>	ii	
<i>Notice</i>	iii	
<i>Questionnaire: Software Survey Section</i>	v	

OCTOBER

Louis Gordon Memorial Award	III	
Kunio Shiraishi, Hisao Kawamura and Gi-ichiro Tanaka	823	Determination of alkaline-earth metals in foetus bones by inductively-coupled plasma atomic-emission spectrometry
Lena Hansson, Jean Pettersson and Åke Olin	829	A comparison of two digestion procedures for the determination of selenium in biological material
Fernando de Pablos, Guillermina Galan and Jose Gomez Ariza	835	Fluorimetric determination of gallium in a nickel alloy and aluminium with <i>N</i> -oxalylamine(salicylaldehyde hydrazone)
M. L. Simões Gonçalves and A. M. Mota	839	Complexes of vanadyl and uranyl ions with the chelating groups of humic matter
Peter G. Mitchell and Joseph Sneddon	849	Direct determination of metals in milligram masses and microlitre volumes by direct-current argon-plasma emission spectrometry with sample introduction by electrothermal vaporization
P. C. Ioannou	857	A simple and rapid fluorimetric method for the microdetermination of isonicotinic acid hydrazide
J. Kragten and L. G. Decnop-Weever	861	Hydroxide complexes of lanthanides—VIII. Lanthanum(III) in perchlorate medium
Adam Mierzwinski and Zygfryd Witkiewicz	865	Piezoelectric detectors coated with liquid-crystal materials
L. E. Zel'tser, Sh. Talipov and N. G. Verechagina	873	Sensitive luminescence analysis for inorganic ions
Piotr Paneth	877	Some analytical aspects of the measurement of heavy-atom kinetic isotope effects
<i>Short Communications</i> D. Amin and Talal A. K. Al-Allaf	885	Iodimetric determination of organolead compounds
M. S. Ionescu, M. Lazarescu, A. Ionescu and G. E. Baiulescu	887	Use of an ion-selective membrane electrode for the determination of the active components in Intestopan
Sadanobu Inoue, Suwaru Hoshi and Mutsuya Matsubara	889	Spectrophotometric determination of titanium with <i>N</i> - <i>m</i> -tolyl- <i>N</i> -phenyl-hydroxylamine and its application to environmental samples
M. T. Vidal and M. de la Guardia	892	Influence of the nature of organic phase emulsions on sensitivity in atomic-absorption determinations
Franz W. E. Strelow and Tjaart N. van der Walt	895	Separation of trace amounts of indium, gallium and aluminium from each other by cation-exchange chromatography on AG50W-X4 resin

<i>Publications Received</i>	i
<i>Notices</i>	iii
<i>Questionnaire: Software Survey Section</i>	vii

NOVEMBER

John H. Kalivas	899	Evaluation of volume and matrix effects for the generalized standard addition method
V. J. Koshy and V. N. Garg	905	Spectrophotometric determination of chloride in Pt-Al ₂ O ₃ /SiO ₂ catalysts with Hg(SCN) ₂ -Fe ³⁺ reagent
Joseph Wang and Javad Zadeii	909	Ultrasensitive and selective measurements of tin by adsorptive stripping voltammetry of the tin-tropolone complex
A. Ríos, M. D. Luque De Castro and M. Valcárcel	915	Determination of viscosity with an open-closed flow-injection system
Hirokazu Hara, Yoshiki Wakizaka and Satoshi Okazaki	921	Continuous flow determination of chloride in the non-linear response region with a tubular chloride ion-selective electrode
Chan-Huan Chung, Etsuro Iwamoto and Yuroku Yamamoto	927	Periodic trends in sensitivity and its dependence on the properties of pyrolytic and non-pyrolytic graphite in graphite-furnace atomic-absorption spectrometry
Alessandro De Robertis, Concetta De Stefano, Silvio Sammartano and Carmelo Rigano	933	The determination of formation constants of weak complexes by potentiometric measurements: experimental procedures and calculation methods
K. Torrance and C. Gattford	939	Determination of soluble chromium in simulated PWR coolant by differential-pulse adsorptive stripping voltammetry
C. Labar and L. Lamberts	945	The role of thiourea as additive for solving medium-modification problems in potentiometric stripping analysis
S. Arpadjan, M. Mitewa and P. R. Bontchev	953	Liquid-liquid extraction of metal ions by the 6-membered N-containing macrocycle hexacyclen
L. Schumack and A. Chow	957	Extraction of aromatic organic compounds by polyurethane foam
<i>Short Communications</i>		
David A. Radspinner and E. L. Wehry	963	Determination of molecular nitrogen by electron-impact induced fluorescence
S. Jaya, T. Prasada Rao and G. Prabhakara Rao	965	Galvanic stripping determination of trace amounts of lead
Salwa R. El-Shabouri, Fardous A. Mohamed and Abdel-Maboud I. Mohamed	968	A rapid spectrophotometric method for determination of piperazine
<i>Analytical Data</i>		
Montserrat Filella, Núria Garriga and Alvaro Izquierdo	971	Formation constants for the complexes of 2-mercapto-3-phenylpropanoate with nickel(II) and hydrogen ions
<i>Papers Received</i>	i	
<i>Publications Received</i>	ii	
<i>Corrigenda</i>	iii	
<i>Questionnaire: Software Survey Section</i>	v	

DECEMBER

Shou-zhou Yao, Jing Shiao and Li-hua Nie	977	Sulpha-drug sensitive membrane electrodes and their analytical applications
---	-----	---

Shou-zhou Yao, Jing Shiao and Li-hua Nie	983	A trimethoprim-selective membrane electrode
M. Blanco, J. Gené, H. Iturriaga, S. Maspoch and J. Riba	987	Diode-array detectors in flow-injection analysis. Mixture resolution by multi-wavelength analysis
Thuraya M. Karadakhi, Fadhil M. Najib and Fahmi A. Mohammed	995	Determination of traces of Zn, Cd, Pb and Cu in white sugar by anodic stripping voltammetry and a modified oxygen-flask combustion technique
Miroslav Hátle	1001	Determination of mercury by differential-pulse anodic-stripping voltammetry with various working electrodes. Application to the analysis of natural water sediments
Spas D. Kolev and Ernő Pungor	1009	End effects in flow-analysis and process systems
A. Assamoi, M. Hamon, M. Chastagnier et M. Chaigneau	1015	Oxydation vanadique de la quinine et de quelques analogues. Application au dosage d'un nouvel antipaludéen: la méfloquine
R. Montes and J. J. Laserna	1021	Spectrophotometric reaction-rate method for the determination of nitrite in waters with pyridine-2-aldehyde 2-pyridylhydrazone
J. Pascual	1027	Determination of several trace elements in silicate rocks by an XRF method with background and matrix corrections
<i>Short Communications</i>		
N. Rukmani Desikan and M. Vijayakumar	1033	An indirect complexometric method for determination of tin in alloys
F. G. Bănică and E. Diacu	1035	Determination of chloride in sulphuric acid by potentiometric mercurometric titration
<i>Analytical Data</i>		
G. B. Reartes, S. J. Liberman and M. A. Blesa	1039	Acidity constants of benzidine in aqueous solutions
J. G. Sen Gupta	1043	Analysis of the CCRMP Oka-2 rare-earth reference mineral of the britholite-apatite series by electrothermal atomic-absorption and inductively-coupled plasma atomic-emission spectrometry
Software Survey Section	1049	ENZFITTER; Computerized Quality Control
<i>Papers Received</i>	i	
<i>Notices</i>	iii	
<i>Questionnaire: Software Survey Section</i>	v	

THE LOUIS GORDON MEMORIAL AWARD

The Editorial Board and Publisher of *Talanta* take great pleasure in announcing that the Louis Gordon Memorial Award for 1986 (for the paper judged to be the best written of those appearing in *Talanta* during the year) will be made to Dr Anil C. Mehta, of the General Infirmary, Leeds, England, for his paper "Sample pretreatment in the trace determination of drugs in biological fluids" (*Talanta*, 1986, 33, 67).



ERRATA

In the paper by Om P. Bhargava, *Talanta*, 1975, **22**, 471, the last line of the procedure should read $26.98 \times M/S \dots$

In the paper by B. Rozanska and E. Lachowicz, *Talanta*, 1986, **33**, 1072, an acknowledgement was omitted at the end. It should read:

Acknowledgement—This work was supported in part by the research programme C.P.B.P.-01.17.

FOREWORD

As pointed out by one of the contributors to this special issue of *Talanta*, there is a semipermeable information barrier between scientists in the Soviet Union and those in the rest of the world, many of the latter either being ignorant of the developments in research in the Soviet Union, or at any rate choosing not to acknowledge them. This state of affairs is contrary to the scientific tradition that knowledge and exchange of information should transcend all frontiers, and to a large extent is due to the language barrier, which has not yet been satisfactorily tunnelled by computers. Some Soviet journals—but all too few—are available in translation (and at a price) in the rest of the world, whereas the major journals in other languages circulate widely in the Soviet Union. The purpose of this issue, then, is partly to try to improve this situation, but mainly to give readers some idea of the quality and scope of the enormous range of analytical research being conducted in the Soviet Union. In addition, it provides an introduction to the ways in which analytical chemistry is organized and taught there, which contrast very markedly with the situation in many other parts of the world and will give many of us food for thought. In spite of the information barrier, the names of many of the contributors to this issue will already be familiar to all our readers, particularly that of the doyen of Soviet analytical chemistry, Professor I. P. Alimarin, one of the two Soviet Union recipients of the *Talanta* Gold Medal (the other being Professor B. V. L'vov). The Publisher and Editorial Board of *Talanta* take great pleasure in presenting this issue as a tribute to the skill and ability of the analytical chemists of the Soviet Union.

R. A. CHALMERS

TALANTA ADVISORY BOARD

The Editorial Board and the Publisher of *Talanta* take pleasure in welcoming the following new members of the Advisory Board of the journal.

D. T. E. HUNT D. MALJKOVIĆ N. OMENETTO
L. SOMMER E. L. WEHRY, JR

The Editorial Board and the Publisher also wish to record their sincere thanks for the help given by

G. M. HIEFTJE G. WERNER

who retire from the Advisory Board.

DR D. T. E. HUNT was born in Aberystwyth, Wales in 1950 and graduated in Chemistry in 1971 from Imperial College, London. He subsequently obtained a Master's degree in Physical Oceanography at the Marine Science Laboratories of the University College of North Wales. Research work, undertaken during tenure of a Demonstratorship at the same institution, involved heavy-metal adsorption and silicon chemistry in fresh and saline waters and led to a Ph.D. degree in 1978. Since then he has worked at the Water Research Centre's Medmenham Laboratory. Formerly Head of the Analytical Development Section, he is now Head of Environmental Chemistry—Inorganics. His interests include trace element determination and water analysis in general, trace element speciation and its effects on toxicity and analytical quality control. He is an author of over 40 papers and technical reports, and is co-author with the late A. L. Wilson of the second edition of *The Chemical Analysis of Water, General Principles and Techniques*, published by the Royal Society of Chemistry in 1986. For some years he chaired the Department of the Environment's Analytical Quality Control (Harmonised Monitoring) Committee, and he is a member of the Department's Standing Committee of Analysts for the water cycle.



D. T. E. HUNT

PROFESSOR DARKO MALJKOVIĆ was born on 12 July 1935 at Osijek, Croatia, Yugoslavia. He obtained his B.Sc (Chemical Engineering), M.Sc. (Physical Chemistry) and Ph.D. (Solvent Extraction studies) from the University of Zagreb. From 1960 to 1965 he worked as Assistant in the Department of Petroleum Refining of the University of Zagreb, then successively as Lecturer (1965–1969), Assistant Professor (1969–1976) and Associate Professor (1976–1979). Since 1979 he has been associated with the Laboratory of Chemistry and Non-Ferrous Metallurgy in the Faculty of Metallurgy and the Laboratory of Analytical Chemistry in the Faculty of Natural Sciences and Mathematics in the University of Zagreb, as Associate Professor (1979–1981) and Professor (1981 onwards). His research interests are in sample preparation for X-ray emission

spectrometry, and separation by solvent extraction and paper chromatography, on which he has published more than 40 papers. He is a member of the Croatian Chemical Society (and was a member of its Executive Board, and Head of the Section of Analytical Chemistry from 1981 to 1984. He has been a member of the Executive Board of the Yugoslav Academy of Sciences and Arts Scientific Council for Petroleum since 1981, and Editor-in-Chief of the Council's publications. He is a member of the Advisory Boards of *Croatica Chemica Acta* and *Metalurgija* (Sisak).



D. MALJKOVIĆ

NICOLÒ OMENETTO graduated in chemistry at the University of Padova in 1964. During 1965–68 he was granted a joint fellowship from the University of Pavia and the European Community Centre in Ispra (Varese) for the development of spectroscopic methods of analysis. He was appointed at the University of Pavia in 1969 and remained there until 1979 when he became associated with the Joint Research Centre of the European Community in Ispra (Varese). He has also spent 3 years (1971–73 and 1978–79) at the University of Florida, Gainesville (USA) working with Prof. Winefordner. Since 1980, he has held the summer position of Distinguished Visiting Professor in analytical spectroscopy at the University of Florida. N. Omenetto is a member of the Italian Chemical Society (Division of Analytical Chemistry) and of the Society of Applied Spectroscopy. He is now the European Editor of *Applied Spectroscopy (Atomic Spectroscopy)* and serves on the Editorial Boards of *Spectrochimica Acta (Part B)*, *CRC Critical Reviews in Analytical Chemistry*, *Progress in Analytical Atomic Spectroscopy* and *Journal of Analytical Atomic Spectroscopy*. His research interests have been directed towards the theory and application of atomic and molecular spectroscopic methods to analytical chemistry, in particular to the use of the laser-induced fluorescence and ionization techniques in atmospheric pressure flames and plasmas, to the characterization of scattering, to the possibility of local sensing of physical parameters such as temperature, number density and quantum efficiency for combustion diagnostics, and to the study of saturation effects in laser induced fluorescence. In this and related fields, he has published more than 100 papers and has lectured to many International Conferences in Atomic Spectroscopy. He is the Editor of the book *Analytical Laser Spectroscopy* (Wiley, 1979).



N. OMENETTO

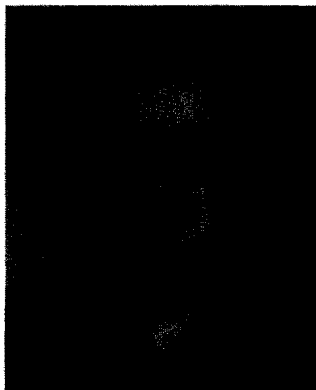
PROFESSOR LUMÍR SOMMER was born 19 January 1929 in Opava (Czechoslovakia), graduated in Chemistry and Physics in 1952 at the Faculty of Science, J. E. Purkyně University, Brno (Rer. Nat. Doctor) and received his D.Sc. (in Chemistry) in 1964 from the Technical University in Prague. From 1964 he has served as full Professor of Analytical Chemistry in the Department of Analytical Chemistry of Brno University, as vice-head of this Department from 1961 till 1973 and as Dean of the Faculty of Science from 1962 to 1965. For many years he has been the director of various internal and inter-university research projects in analytical chemistry, has taught undergraduate and graduate topics of analytical chemistry in Brno University, lectured at universities in the USSR, Germany (DDR and BRD), Hungary, Poland, Bulgaria, India, Italy, Sweden and Great Britain and spent one year as visiting professor at Dalhousie University (1969/70) in Halifax (Canada). He has published more than 150 papers on analytical and solution co-ordination chemistry; his main research interests are in organic analytical reagents, complex equilibria in solutions, analytical spectrometry (UV + VIS), molecular and atomic-absorption spectrometry, emission spectrometry, fluorimetry, trace analysis and environmental analysis. He is a titular member of Commission V.I. (Analytical Reactions and Reagents) of IUPAC and the recipient of the Silver Medal of Brno University, Memory Medal of the High School of Mines, Ostrava and the Gregor Mendel Award for Science, *etc.*



L. SOMMER

EARL L. WEHRY, JR was born in Reading, Pennsylvania on 13 February 1941. He received the B.S. degree from Juniata College (Huntingdon, Pennsylvania) in 1962 and the Ph.D. under the direction of L. B. Rogers at Purdue University in 1965. From 1965 to 1970, he was a member of the chemistry faculty at Indiana University (Bloomington). Since 1970, he has been a member of the chemistry faculty at the University of Tennessee (Knoxville), where he is now Professor of Chemistry. Dr Wehry's research interests are concentrated in the general areas of spectroscopy, photochemistry, and trace organic analysis. Current research activities include: applications of low-temperature and molecular fragmentation techniques to analytical fluorescence spectrometry; analytical applications of laser-excited fluorescence; the analytical chemistry of polycyclic aromatic compounds; the chemical fate of environmental pollutants; and the chemical properties of electronically excited molecules. He is the editor of the four-volume monograph series *Modern Fluorescence Spectroscopy*, and has published approximately 100 research papers. From 1980 to 1986, he was author of the biennial fundamental review article on "Molecular Fluorescence, Phosphorescence, and Chemiluminescence Spectrometry" published in *Analytical Chemistry*. He is a member of the Editorial Board of *Analytical Letters*. Professor Wehry was co-recipient (with Professor Gleb Mamantov and Dr Arlene Garrison) of the William F. Meggers Award of the Society of Applied Spectroscopy in 1982. He received an award as "Outstanding Scholar" from the University of Tennessee chapter of the Phi Kappa Phi honor society in 1985, and was named a University of Tennessee Chancellor's Research Scholar in 1986. He is a member

of the American Chemical Society, Society for Applied Spectroscopy, Optical Society of America, Inter-American Photochemical Society, American Association for the Advancement of Science, Sigma Xi, and Phi Lambda Upsilon.



E. L. WEHRY, JR

AUTHOR INDEX

- Abdel Salam M. 670
 Abou Zeid G. T. 253
 Aboul-Enein H. Y. 287
 Abounassif M. A. 287
 Ackermann G. 313
 Adams M. J. 243
 Adsul J. S. 503
 Agrawal Y. K. 365
 Ahmad S. 296
 Ahmed M. A. 723
 Al-Allaf T. A. K. 885
 Al-Jabari G. 479
 Al-Najafi S. 749
 Al-Omair A. S. 361
 Alimarin I. P. 103
 Amin D. 885
 Andrés J. M. 583
 Antonovich V. P. 215
 Arpadjan S. 953
 Arya S. P. 293
 Assamoi A. 1015
 Atnashev Yu. B. 197
 Aualitita T. U. 231
 Avdeeva E. N. 111
 Ayad M. 793
- Baars A. J. 580
 Bäckström K. 783
 Bailey P. G. 505
 Baiulescu G. E. 887
 Bănică F. G. 1035
 Bankovsky Yu. A. 179
 Basova E. M. 223
 Basselier J. J. 645
 Baudino O. M. 551
 Bayloqç D. 515
 van Beek H. 505
 Beisel N. F. 147
 Belal S. 793
 Belenkii 161, 167
 Ben-Yaakov S. 709
 Benyaev N. E. 61
 Berezkin V. G. 183
 Berthelot J. 645
 Berthod A. 745
 Berzas Nevado J. J. 321
 Besada A. 731
 Bessière J. 763, 771
 Betteridge D. 749
 Bhargava O. P. 505
 Bhatti M. K. 661
 Bigli C. 529
 Blanco M. 987
 Blesa M. A. 1039
 Bogdanov A. A. 153
 Bogen D. C. 465
 Böhmer R. G. 629
 Bolotov S. L. 183
 Bol'shova T. A. 223
 Bonilla-Alvarez M. 473
 Bontchev P. R. 953
 Boulet R. 645
 Brainina Kh. Z. 41
 Broekaert J. A. C. 629
 Budnikov H. C. 219
 Burger K. 449
 Bychkov A. S. 111
- Cai X. 813
 Caméan Fernández A. M. 673
 Capone S. 593
- Carlsson A. 615
 Chaigneau M. 1015
 Chakrabarti C. L. 259
 Chandramouli V. 807
 Chang S. B. 259
 Chaplygin V. I. 191
 Chastagnier M. 1015
 Chibisov A. K. 207
 Chikuma M. 435, 667
 Chikushi H. 369
 Chiswell B. 307
 Chizhkov V. P. 227
 Chow A. 331, 957
 Chu-ming Y. 699
 Chung C.-H. 927
 Cortinez V. A.
 Cruces Blanco C. 345
- Danielsson L.-G. 783
 Davis D. 473
 Decnop-Weever L. G. 861
 De Robertis A. 593, 933
 De Stefano C. 593, 933
 Desbène P. L. 645
 Desbène-Monvernay A. 645
 Desikan N. R. 1033
 Devi S. 547
 Devyatkykh G. G. 123, 133
 Dong-hua Z. 699
 Diacu E. 1035
 Diamantatos A. 736
 Dias C. C. 503
 Diehl H. 739
 Dolmanova I. F. 201
 Doretta L. 483
 Dorokhova Ye. N. 9
- Efimova I. I. 167
 Ejas M. 337
 Ek P. 495
 El Adl S. 793
 El Kheir A. A. 793
 El-Shabouri S. R. 968
 Elyashberg M. E. 21
 Ericson S. P. 271
 Ewen G. J. 243
- Faboya O. O. P. 441
 Fadeeva V. I. 103
 Fagioli F. 529
 Filella M. 971
 Fortier N. E. 415
 Fournaise R. 385
 Fritz J. S. 415, 473
- Gad-Kariem E.-R. A. 287
 Galan G. 835
 Galeano Díaz T. 655
 Gankina E. S. 167
 Garai T. 529
 García Sánchez F. 345, 639
 Garg V. N. 905
 Garifzyanov 211
 Garriga N. 971
 Gattford C. 939
 Gavilan J. M. 583
 Gené J. 987
 Gtáb S. 411
 Goforth D. 290
 Gogia S. K. 303
 Golovnya R. V. 51
- Gomez Ariza J. 835
 Gómez-Hens A. 325
 Gonçalves M. L. S. 839
 Gond A. 799
 Gonzalez Garcia S. 519
 Graham R. C. 381
 Greefkes H. C. A. 580
 Gribov L. A. 21
 de la Guardia M. 892
 Guette C. 645
 Guffey F. D. 661
 Gur'eva R. F. 87
 Gutierrez M. C. 325
 Guzmán Chozas M. 673
- Hamon M. 799, 1015
 Hansson L. 829
 Hara H. 921
 Harju L. 817
 Hassan S. S. M. 723
 Hátle M. 1001
 Hattori T. 733
 Headridge J. B. 253
 Heit M. 465
 Heredia Bayona A. 345
 Hernández Córdoba M. 351
 Hernández Lopez M. 639
 Horchak-Morris N. 739
 Hoshi S. 889
 Huazhang Z. 783
 Huiliang H. 539
 Huitink G. M. 423
 Hulanicki A. 407, 411
 Huldén S.-G. 495
 Hung T. K. 375
 Huston T. J. 259
- Idowu O. R. 441
 Imai T. 567
 Ingle J. D. Jr 619
 Ingman F. 783
 Inoue S. 889
 Ioannou P. C. 857
 Ionescu A. 887
 Ionescu M. S. 887
 Ishii E. 664
 Issa A. S. 670
 Isshiki K. 277, 341
 Itoh K. 435
 Iturriaga H. 987
 Ivanov V. M. 223
 Iwamoto E. 927
 Iwamoto M. 419
 Iwamoto M. 433
 Iyer S. G. 503
 Izquierdo A. 971
- Jagner D. 539
 Jaselskis B. 271, 479
 Jaya S. 574, 965
 Jiménez Sánchez J. C. 655
 Jin-Chun L. 331
 Jina S. 699
 Juhász M. 397
- Kai F. 369
 Kalivas J. H. 899
 Kallmann S. 677
 Kamaya M. 664
 Kaplan D. 709
 Karadakhli T. M. 995

- Karpov Yu. A. 123, 133
 Kasai A. 567
 Katona-Balázs J. 449
 Kawamura H. 823
 Kayata W. 515
 Kazlauskas R. M. 111
 Kever J. J. 167
 Khalkin V. A. 375
 Khorami J. 589
 Kihara S. 779
 Klaos E. 715
 Koch S. 313
 Kolev S. D. 1009
 Komleva A. A. 61
 Korepanov V. E. 197
 Koshy V. J. 905
 Kragten J. 861
 Krasikov V. D. 161
 Krawczyński vel Krawczyk T. 407
 Krishnankutty K. 507
 Krylov V. A. 133
 Kudryavtsev G. V. 103
 Kunin L. L. 153
 Kurenbin O. I. 161
 Kuroda R. 433
 Kutcheryaeva 201
 Kuwamoto T. 341
 Kuzyakov Yu. Ya. 191
- Labar C. 945
 Lamberts L. 945
 Lampén P. 445
 Langmaier L. 453
 Lanin S. N. 223
 Laserna J. J. 745, 1021
 Lazarescu M. 887
 Lazukina O. P. 133
 Lefebvre Y. 589
 Leis F. 629
 Levillain P. 535
 Li P. 813
 Liberman S. J. 1039
 Lindroos S. 445
 Lingappa Y. 789
 Liteanu C. 438
 Litvin E. F. 227
 Locatelli C. 529
 Loskutova I. M. 103
 Louis C. 763, 771
 Lundström U. 615
 Luque De Castro M. D. 915
 L'vov B. V. 141
 Lyle S. J. 361
- Machado A. A. S. C. 525
 Maccioni A. M. 483
 Maeda K. 779
 Mahrous M. S. 670
 Malla J. L. 293
 Manzon B. M. 61
 Mariaud M. 535
 Marquez Gomez J. C. 639
 Mărutoiu C. 438
 MasPOCH S. 987
 Matilla Hernandez A. 519
 Matsubara M. 889
 Matsui M. 779
 Maystrenko V. N. 219
 McHalsky M. L. 271
 Mehta A. C. 355, 609
 Meintjies E. 401
 Ménard H. 589
 Mendes A. S. 543
 Mierzwinski A. 865
 Mifune M. 667
- Milanov M. 375
 Mitchell P. G. 849
 Mitewa M. 953
 Mohamed A.-M. I. 968
 Mohamed F. A. 968
 Mohammed F. A. 995
 Mokhtar M. B. 307
 Molnár G. 449
 Montes R. 1021
 Morozova N. B. 223
 Mota A. M. 839
 Mukai N. 433
 Murakami T. 664
 Murinov Y. I. 219
 Muzgin V. N. 197
 Myasoedov B. F. 31
- Nagourney S. J. 465
 Najib F. M. 995
 Nakagawa T. 435
 Nakamura M. 369
 Nakashima S. 667
 Nakayama E. 277, 341
 Nakayama M. 435
 Nazarenko V. A. 215
 Nazir M. 661
 Nemes-Vetéssy Zs. 449
 Nesterov V. V. 161
 Nie L. 977, 983
 Nikitin Yu. S. 223
 Noszál B. 397
 Novodvorsky O. A. 191
- Odinets V. 715
 Odo J. 667
 Ogawa T. 461
 Oguma K. 433
 Okazaki S. 921
 Olin Á. 615, 829
 Oliveira W. A. de 543
 Opekar F. 453
 Ouchefoun M. 645
 Overholt G. R. 505
- Pablos F. de 835
 Pacáková V. 453
 Palmieri M. 473
 Paneth P. 877
 Panfilova I. E. 211
 Parczewski A. 586
 Parker G. A. 512
 Pascual J. 1027
 Patel D. R. 365
 Pavlov S. S. 227
 Pellerin F. 515
 Pelne A. R. 179
 Petitfaux C. 385
 Petrola R. 445
 Petrov B. I. 175
 Petrukhin O. M. 111
 Pettersson J. 829
 Pickering W. F. 231
 Pilipenko A. T. 77
 Pogonin V. I. 207
 Polzik L. K. 141
 Postaire E. 799
 Prabhakara Rao G. 574, 965
 Prasada Rao T. 574, 965
 Příbil R. 705
 Pungor E. 1009
 Pupyshev A. A. 197
- Qiang C. 657
 Qing Z. 555
 Quintar de Guzman S. 551
 Qureshi M. A. 337
- Radha Menon V. G. 367
 Rads spinner D. A. 963
 Ramendik G. I. 61
 Rao B. V. 367
 Raphaeli D. 709
 Ravikovich V. M. 227
 Reartes G. B. 1039
 Reddy D. V. 789
 Reddy K. H. 789
 Renman L. 539
 Riba J. 987
 Rigano C. 933
 Rios A. 915
 Rodionov V. I. 153
 Rogers D. W. 283
 Romanovskaya G. I. 207
 Romero C. 583
 Rong-rong W. 699
 Rösch F. 375
 Rubio S. 325
 Ryan-Hotchkiss M. 619
- Sahu B. 653
 Saito Y. 667
 Sakanashi Y. 369
 Sakane C. 461
 Sakurai H. 435
 Salem F. B. 810
 Salinas F. 321, 655
 Sammartano S. 593, 933
 Sánchez-Pedreño C. 351
 Sano A. 743
 Sârbu C. 438
 Sárkány P. 757
 Sarojam K. C. 367
 Sastri V. S. 489
 Sastry C. S. P. 372
 Sato S. 369, 419
 Sato T. 369
 Savransky L. I. 77
 Savvin S. B. 87
 Scarcella R. 593
 Schumack L. 957
 Sekine K. 567
 Selve C. 509
 Sen Gupta J. G. 427, 1043
 Serov V. V. 21
 Shah A. 547
 Sharma R. D. 296
 Shavnaya Yu. V. 111
 Shekhovtsova T. N. 201
 Shiao J. 977, 983
 Shiraiishi K. 823
 Shukla I. C. 296
 Siedman B. J. 283
 Singh D. 303
 Singh O. V. 303
 Shao-yuan L. 699
 Shi-lian J. 699
 Skrzydlewska E. 411
 Slathia V. 293
 Sly T. J. 749
 Sohrin Y. 341
 Soliman N. 670
 Sneddon J. 849
 Soundar Rajan S. C. 729
 Sterkhov N. V. 227
 Strelow F. W. E. 401, 895
 Štulíková M. 705
 Sultan S. M. 605
- Tadros F. S. 723
 Takezawa M. 743
 Takitani S. 743
 Talkop R. 715

- Talipov Sh. 873
 Tanaka G. 823
 Tanaka H. 435, 667
 Tanaka M. 435
 Tanaka T. 435
 Tanaka Y. 667
 Tandon S. N. 303
 Tandon U. 653
 Tercero Moreno J. M. 519
 Thankarajan N. 507
 Thong P. W. 259
 Tikhomirova T. I. 103
 Tikhonova L. P. 69
 Tondre C. 509
 Toropova V. F. 211
 Torrance K. 939
 Traldi P. 483
 Tuzhi P. 561
 Tyurin D. A. 61

 Uchikawa S. 369, 419
 Umetani S. 779

 Valcárcel M. 325, 915
 Valiente P. 321
 Varughese K. 561
 Varyvonchik E. A. 227
 Vasconcelos M. T. S. D. 525
 Vasudeva Rao P. R. 807
 Vaz M. C. T. A. 519

 Venkateswarlu Ch. 503
 Verechagina N. G. 873
 Veschikova N. A. 215
 Veveris O. E. 179
 Victor A. H. 401
 Vidal M. T. 892
 Viel C. 799
 Vijaya D. 372
 Vijayakumar M. 1033
 Vilas Boas L. 519
 Viñas P. 351
 Vircava D. K. 179
 Vircavs M. V. 179
 Vlassa M. 438

 Wade A. P. 749
 Wahbi A.-A. M. 287
 Waki H. 239
 Wakizaka Y. 921
 Walt T. N. van der 895
 Wandruszka R. von 571
 Wang J. 247, 561, 909
 Wasberg M. 757
 Wehry 963
 Wellington C. A. 749
 White C. 253
 Winefordner J. D. 290, 571, 745
 Witkiewicz Z. 865
 Wu H.-L. 577
 Wu S. 259

 Xenakis A. 509
 Xu M. 512

 Yadav R. B. 807
 Yamada S. 461
 Yamamoto Y. 927
 Yan Y. 699
 Yankauskas V. P. 111
 Yao S. 977, 983
 Yatsenko L. F. 141
 Yatsimirskii K. B. 69
 Yi-zai M. 699
 Yoshida H. 733
 Yoshimura K. 239
 Yu R.-Q. 577
 Yudelevich I. G. 147
 Yuying H. 555

 Zadeii J. M. 247, 909
 Zaray G. 629
 Zelentsova L. V. 147
 Zel'tser L. E. 873
 Zhao Z. 813
 Zhen W. 657
 Zhivopistsev V. P. 175
 Zhong-ming Z. 699
 Zolotov Yu. A. 1, 111
 Zorov N. B. 191